hexagon:2611.01302v1

Nonunique continuation after blow-up for the forced Navier–Stokes equations

27 November 2026

Abstract

This manuscript gives a proof of non-uniqueness of Leray–Hopf solutions for the Navier–Stokes equations after a singularity, with compactly supported and smooth forcing. We construct a one-parameter family of solutions, all with zero initial data, identical until a singularity forms. After the singularity is formed, the solutions are different. They are all of Leray–Hopf type, satisfy the energy identity, and are smooth outside the singular point $(x, t) = (0, 0)$.

The construction is based on the matching of an anisotropic self-similar background profile with a forward one, satisfying compatibility conditions that ensure smoothness across $t = 0$. Both profiles have stress-type errors in a gluing region, which are corrected with a convex-integration-style approach using Craik–Criminale waves. The mechanism for non-uniqueness is the instability of the forward self-similar profile.

An announcement about this manuscript can be found in https://caolab97.github.io/NS-non-uniqueness-after-blowup/ANNOUNCEMENT.pdf

Contents

Introduction

Consider the incompressible Navier–Stokes equations on $\mathbb{R}^3$ with viscosity $\nu = 1$,

$$\partial_t u + u \cdot \nabla u = \Delta u - \nabla p + F, \qquad \operatorname{div} u = 0. \tag{1}$$

This manuscript gives a proof of the following Theorem.

Main Theorem. *There exist $T_{\text{in}} > 0$, a force $F \in C_c^\infty(\mathbb{R}^3 \times \mathbb{R})$ and solutions $u^{(a)}$, $a \in [-1, 1]$, of (1) with zero initial data $u^{(a)}(x, -T_{\text{in}}) = 0$ such that:*

(i) Blow-up happens only at $(x, t) = (0, 0)$, and the solution is smooth elsewhere:

$$u^{(a)} \in C^\infty\big((\mathbb{R}^3 \times [-T_{\text{in}}, T_{\text{out}}]) \setminus \{(0, 0)\}\big), \qquad \lim_{t \uparrow 0} \|u^{(a)}(t)\|_{L^\infty(\Omega)} = \infty$$

for every ball $\Omega \subset \mathbb{R}^3$ containing the origin.

(ii) The solutions exist until a common time $T_{\text{out}} > 0$ independent of a. All solutions $u^{(a)}$ are identical for $t \le 0$, and they are different for $t > 0$: $u^{(a)}(t) \neq u^{(b)}(t)$ for $a \neq b$ and $0 < t \le T_{\text{out}}$.

(iii) The solutions are in the Leray–Hopf class and satisfy the energy identity

$$\tfrac{1}{2}\|u^{(a)}(t)\|_{L^2}^2 + \int_s^t \|\nabla u^{(a)}(\tau)\|_{L^2}^2 \, d\tau = \tfrac{1}{2}\|u^{(a)}(s)\|_{L^2}^2 + \int_s^t \int_{\mathbb{R}^3} F \cdot u^{(a)} \, dx \, d\tau$$

for all $-T_{\text{in}} \le s \le t \le T_{\text{out}}$.

History of global well-posedness and singularities. The study of (1) goes back almost two centuries. The Cauchy problem for (1) is locally well posed [40, 25]; for local well-posedness in critical spaces see [25, 35, 36]. The next natural question is whether these solutions extend globally in time [24].

The history of this problem is intimately related to the attempts to prove global well-posedness for (1). Although these attempts did not reach that goal, they were fundamental for our understanding of fluids and for the development of their mathematical theory. Leray showed that a suitable notion of weak solution yields global solutions of (1) [40]. Hopf extended these results [28], and the resulting global weak solutions in the energy class are called Leray–Hopf solutions. The advantage of these solutions is that they are known to exist globally; however, their uniqueness was an important open problem. Later, Caffarelli, Kohn and Nirenberg proved that if a suitable weak solution becomes singular, its singular set has zero one-dimensional parabolic Hausdorff measure [10]; that is, singularities cannot occupy too large a set in space-time.

Regarding singularity formation, a classical route to construct singularities with $F = 0$ is to look for self-similar singularities, that is, solutions of the form

$$u(x, t) = \frac{1}{\sqrt{-t}} U\Big(\frac{x}{\sqrt{-t}}\Big), \qquad t < 0, \tag{2}$$

with the blow-up time fixed at $t = 0$. This ansatz comes from the natural isotropic scaling of (1): if u solves (1) (say, with force $F = 0$), then for every $\lambda > 0$

$$u_\lambda(x,t) = \lambda\, u(\lambda x, \lambda^2 t)$$

is also a solution. However, for the unforced equations, Nečas, Růžička and Šverák ruled out nonzero profiles $U \in L^3(\mathbb{R}^3)$ [41]; see also [45]. Despite this obstruction, self-similarity has been very successful for singularity formation in other fluid equations. Elgindi [22] (see also [23]) proved finite-regularity self-similar blow-up for the three-dimensional Euler equations, and Chen and Hou proved smooth blow-up for the three-dimensional axisymmetric Euler equations with boundary [11, 12]. These works suggested a new approach: construct approximate self-similar profiles numerically with neural networks, in settings not covered by obstructions such as [41, 15], and then establish the existence of an exact profile nearby by a computer-assisted proof [48].

A second route, which does not rely on self-similarity, was initiated by Córdoba and Martínez-Zoroa. They proved finite-regularity singularity formation with forcing for the three-dimensional Euler equations [17] and, with Zheng, for the hypodissipative Navier–Stokes equations [18]. This approach was later followed by Alpöge and Buckmaster, who released a manuscript which proves singularity formation for the Euler equations with forcing [4]. One day later, OpenAI released a manuscript removing the forcing from that construction [43].

OpenAI also released a second manuscript constructing singularities for the forced Navier–Stokes equations (1) [42] (see also the exposition by Lei and Ren [37, 38]). The ideas extracted from a careful understanding of [42] have been fundamental for the present work. We also mention the more recent proof of singularity formation for the unforced Navier–Stokes equations by Alpöge and Buckmaster [3]. It follows the route of [11, 12, 48]: a discretely self-similar profile is found numerically and its existence is established by a computer-assisted proof.

Non-uniqueness. A classical problem in the study of (1) has been to understand uniqueness of weak solutions. When a solution is classical, uniqueness follows from weak–strong uniqueness, and therefore non-uniqueness can only happen after a singularity. For this reason, none of the works in this area covers the case of smooth solutions, since Navier–Stokes singularities were not known to exist.

One remarkable achievement in this direction is the work of Buckmaster and Vicol showing that sufficiently weak solutions of the Navier–Stokes equations are not unique [8]. Their proof uses convex-integration techniques that were introduced in the study of fluids by De Lellis and Székelyhidi [21]. Cheskidov and Luo also used convex integration to obtain non-uniqueness in $L^p_t L^\infty_x$ for $1 \le p < 2$, arbitrarily close to the $L^2_t L^\infty_x$ uniqueness criterion [13].

A different route for non-uniqueness was the one initiated by Jia and Šverák [33, 34] (see also the numerical work of Guillod and Šverák [27]), where they proposed a route based on self-similar ansätze like the one in (2), just in this case for $t > 0$, using an instability of the self-similar profile to generate bifurcating solutions that start from singular data. Vishik proved non-uniqueness for the forced two-dimensional Euler equations along these lines, using an unstable vortex [46, 47]. That route was carried out successfully by Albritton, Bruè and Colombo in the case with force [1], and, combined with computer assistance to remove the force, by Hou, Wang and Yang [29]. Coiculescu and Palasek proved non-uniqueness from critical data in BMO^{-1} [14]. Recently, there have been different proofs of unforced non-uniqueness in stronger scenarios or removing computer assistance [31, 9, 30, 6].

We remark, however, that none of those works covers the case of smooth solutions. That route is prior to Navier–Stokes singularity formation, and we know that solutions are unique while they

remain classical, so a singularity is needed in order to get non-uniqueness from smooth data. We also mention the work of Dahne and Šverák, where non-uniqueness is proved to arise from a singularity for the complex Ginzburg–Landau equation, also following a self-similar structure [20].

Overview of the proof

Our construction of the common past adapts the backward blow-up mechanism of [42]. We start by describing the construction of the top order profile. As in [42], we use an anisotropic version of the self-similar ansatz (2). Write r for the distance to the symmetry axis and z for the axial coordinate. With the blow-up time at $t = 0$, one defines the self-similar variables $R = r/(-t)^{1/2}$ and $Z = z/(-t)^{1/2-h}$ and looks for an axisymmetric background profile of the form

$$u_\theta = \frac{1}{(-t)^{1/2+h}}\,\bar{U}_\theta(R,Z), \qquad u_z = \frac{1}{(-t)^{1/2+h}}\,\bar{U}_z(R,Z), \qquad u_r = \frac{1}{(-t)^{1/2}}\,\bar{U}_r(R,Z), \tag{3}$$

up to lower order terms, with $h > 0$ a small parameter (see Figure 1(a) for an illustration). The difference with the isotropic ansatz (2) is that the axial scale $(-t)^{1/2-h}$ is larger than the radial scale $(-t)^{1/2}$, and the swirl and axial velocities are larger than the radial velocity by a factor $(-t)^{-h}$. Finding an exact self-similar solution of (1) of the form (3) is forbidden due to [16].

Since we are proving non-uniqueness, we also need a forward profile for $t > 0$, of the same form with $-t$ replaced by t. Moreover, those profiles will satisfy the following properties.

(i) They are axisymmetric (since (3) is independent of the angle).

(ii) Due to the anisotropic scaling, they locally look, at top order, like a vortex column (see Figure 1(c)).

(iii) They satisfy the top order self-similar equations close to the axis and far away, making errors only in a gluing region (see Figure 1(b)).

(iv) In the gluing region, the profile is asked to support instabilities (satisfying the Leibovich–Stewartson conditions [39]). Moreover, the error is of the type $\operatorname{div}(T \otimes e_r + e_r \otimes T)$, and one asks that the instabilities of the vortex column can be generated in the direction of T.

(v) The forward and backward profiles have to satisfy a compatibility condition to have smoothness across $t = 0$. Since the behaviour at $t = 0$ is given by the behaviour at infinity of the self-similar profiles, this corresponds to a certain matching of asymptotics.

(vi) The forward profile moreover needs to support an instability that grows faster than any other perturbation, to be able to prove non-uniqueness of solutions.

These profiles are constructed in Chapter 1.

In Chapter 2, we correct two types of errors: (A) the ones that are subdominant in the scaling (3), generated by the fact that (iii) only asks the profile to solve the top order equation, and (B) the error $\operatorname{div}(T \otimes e_r + e_r \otimes T)$ from (iv). Regarding correction (A), one employs a series expansion around the top order profile, whose successive terms remove these errors to all orders. Correction (B) is done via a convex-integration technique [21, 5]. That convex-integration technique is based on a quasiperiodic arrangement of Craik–Criminale type waves [19] (see [2, 26] for rigorous results on those waves). Craik–Criminale waves grow due to the Leibovich–Stewartson instability of the vortex column and grow in frequency, so eventually they also decay due to the effect of the dissipation (see Figure 1(d)). Therefore, time-localization comes naturally from the actual dynamics of how the

perturbation evolves around the leading order profile, which, at top order, is a vortex column. The amplitude of the Craik–Criminale waves is fixed as one would do in convex integration, imposing that the top order of the average of $w \otimes w$, where w is the wave, cancels the top order of the stress tensor. Further errors are treated with one of three approaches: (i) the introduction of forced Craik–Criminale waves at integer multiples of their original frequency, (ii) a small perturbation of the initially chosen amplitudes that allows us to correct a next order term, or (iii) a correction of the axisymmetric part of the background that deals with the axisymmetric errors (zero frequency in the phase) with zero average. Thanks to the quasiperiodic arrangement, a zero average over the arrangement means a zero average both in time and in the radius: these errors can be integrated in time, and all their radial moments vanish. This is crucial to avoid pressure jumps, since the pressure correction then stays compactly supported and the field outside the waves is not modified. We adapt the backward completion of [42, Sections 5–10], choosing the corrections on both sides of $t = 0$ together so that they match away from the origin. After localizing in space, this gives a single velocity and pressure (B, p_B), whose Navier–Stokes residual is a smooth force f with fixed compact spatial support.

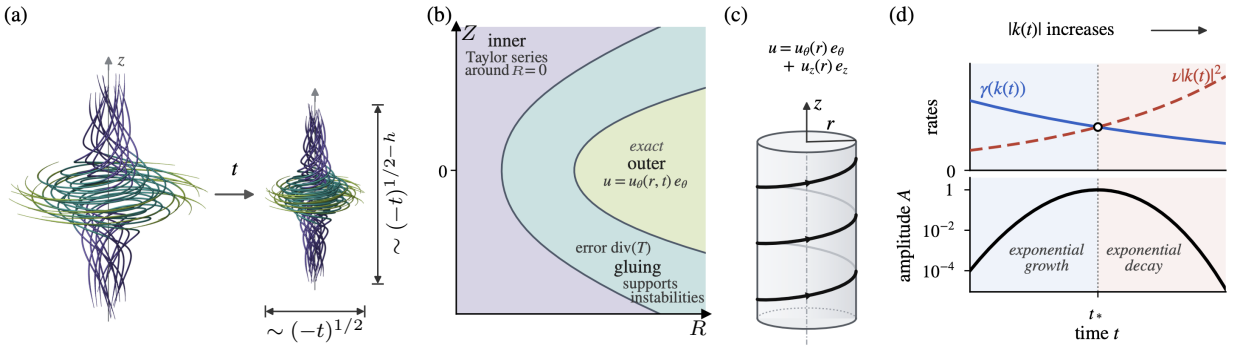

Figure 1: The Navier–Stokes blow-up of [42]. (a) 3D Navier–Stokes background solution with its rates of concentration. (b) Inner, gluing, and outer region for the background. Vortex column instability: (c) Exact vortex column. (d) Amplitude of a Craik–Criminale wave of frequency k, with the unstable Euler eigenvalue $\gamma(k)$ in blue and the dissipation $\nu|k|^2$ in red.

After Theorem 2, one has a background B whose leading part is self-similar both for $t < 0$ and for $t > 0$. It generates a solution of Leray–Hopf type that can be continued after the blow-up and that, due to (vi), supports instabilities for $t > 0$. Near the singular time we seek the forward branches in the form

$$u^{(a)} = B + aV + w_a, \qquad -1 \le a \le 1, \qquad \text{with } V = w_a = 0 \text{ for } t \le 0.$$

Here V must solve the linearized equation about the completed background B, including the oscillations that make the force smooth. Due to the anisotropic self-similar structure of the background, the instability V follows an evolution of the type $t\partial_t V \sim t^{-h}\lambda_0 V$, where λ_0 is the eigenvalue. This contrasts with the evolution $t\partial_t V \sim \lambda_0 V$ typical of isotropic self-similar instabilities, and means that in physical variables the mode grows like $\exp(-\lambda_0 t^{-h}/h)$ instead of t^{λ_0} (notice that the function equal to $\exp(-\lambda_0 t^{-h}/h)$ for $t > 0$ and to 0 for $t \le 0$ is smooth at $t = 0$).

In Chapter 3, we construct V from the unstable eigenvalue λ_0 of the forward profile given by (vi). It gives an approximate solution of the linearized equation around B, based on a Gaussian wave packet at the right position and frequency that maximize its growth rate.

Correcting its residual with an inverse of the linearized operator gives an exact mode V. To construct w_a, we need that no perturbation grows faster than V, which amounts to estimates on the full linearized evolution around B, including the Craik–Criminale corrections. We show that it grows at most at the rate of V (up to an arbitrarily small ε). This gives an inverse G, mapping to functions decaying at a rate $\frac{3}{2}\Lambda_*$, where $\Lambda_* = \operatorname{Re}\lambda_0/h$ is the rate of V, and w_a is the fixed point of

$$w_a = -G\,\mathbb{P}\operatorname{div}\big((aV + w_a)\otimes(aV + w_a)\big),$$

where $\mathbb{P}$ is the Leray projector. Since the quadratic term decays faster than V, w_a is of size a^2, and on a common interval $0 < t \le t_*$,

$$\|w_a(t) - w_b(t)\|_2 \le \tfrac{1}{2}|a-b|\,\|V(t)\|_2.$$

Thus the leading difference $(a-b)V(t)$ separates the branches, see (3.12.9).

Since $q_a = aV + w_a$ solves an equation with zero external force, all the branches have the same force as B. Parabolic smoothing and the decay of V and w_a as $t \downarrow 0$ show that q_a and its pressure correction vanish to infinite order at $t = 0$, so their extension by zero to $t \le 0$ is smooth. The energy identities of B for $t < 0$ and of $u^{(a)}$ for $t > 0$ add up across $t = 0$, since both have the same strong L^2 trace at $t = 0$. Finally, we continue the branches on a short regular interval after t_*, where they remain distinct, and multiply the background by a cutoff in time. This makes the solutions vanish near $t = -T_{\mathrm{in}}$ and produces the force F of (3.14.1), which is smooth and has compact support in space-time.

Remark. A natural question, given the recently released manuscript [3] proving unforced blow-up for Navier–Stokes, is whether non-unique Leray–Hopf solutions can originate in the unforced scenario. As described above, that could be done by combining the backward discretely self-similar profile of [3] with a forward one that (i) satisfies the compatibility condition, so that the solution is smooth across $t = 0$, and (ii) supports an instability. If those conditions were to hold in [3], then the natural strategy would be to use a computer-assisted approach as in [3] to prove the existence of the forward profile, combined with an extra computer-assisted proof to show the existence of the instability. However, it is currently uncertain whether (i) and (ii) hold numerically from the publicly released data, and it is also uncertain what amount of computational power would be required to find those solutions at the required precision and to perform the computer-assisted proof.

Contents

Introduction **i**

1 Construction of the forward–backward background **1**
1.1 Similarity variables, leading fields and radial histories 1
1.2 Main statement 2
1.3 Notation and scope conventions 11
1.4 Backward profile identities and moment corrections 12
1.5 Construction hypotheses and order of parameter choices 14
1.5.1 Leading profile requirements 14
1.5.2 Order of the parameter choices 17
1.6 Compatible leading profiles on the two sides of zero 21
1.6.1 Coordinates, radial primitives and stress 21
1.6.2 The slice chart and smooth joining across $t = 0$ 25
1.6.3 Outer profiles with one heat tail 27
1.6.4 Canonical pressure, the regular core and moment corrections 47
1.6.5 Strict stress inequalities and the reserved radial layout 79
1.7 The backward heat profile 80
1.8 The backward member and the class $\mathcal{O}^\flat$ 82
1.8.1 Edge weights 82
1.8.2 The outer collar of the backward member 83
1.8.3 An integrable majorant for the backward datum 87
1.8.4 Datum, exterior and reserved patches 88
1.8.5 The backward core and the interior cone 90
1.9 The forward leading system and a convergent axis construction 108
1.9.1 Actual histories and the integrated equations 108
1.9.2 The axis theorem 109
1.9.3 Divergence and Cartesian regularity 112
1.10 A positive linear profile and one decreasing exit 112
1.11 Nonlinear continuation on a fixed radial interval 114
1.11.1 The norm and the actual difference equations 115
1.11.2 Initial data on an amplitude-independent disk 116
1.11.3 A contraction with two derivative placements 116
1.11.4 Same radius, identification, and signs 117
1.12 An active protected collar and delayed angular insertion 117
1.12.1 Shear and admissibility 118
1.12.2 Flat activation with actual histories 118
1.12.3 Remove the core before we insert the calibrated shape 120

1.12.4 The delayed shape and its positive margin 121
1.12.5 The outlet interface 123
1.13 The actual outer connection and its heat exterior 124
1.13.1 A finite reference with the actual axis pressure 125
1.13.2 The slow entrance and its finite wait 126
1.13.3 A bounded pulse with two exact returns 127
1.13.4 Scalarization of the velocity and its primitive 130
1.13.5 A scalar power segment with a controlled primitive deficit 130
1.13.6 The regular and fast heat modes 132
1.13.7 Positive shooting to the exact regular coefficient 133
1.13.8 The full angular lift and a positive primitive bridge 134
1.13.9 Endpoint regularity and the full canonical tail estimates 137
1.13.10 The full cone at the wing and the outer support 139
1.13.11 The pressure root is solved before the energy root 140
1.13.12 Fixed-h parameter choices and identification of all histories 142
1.13.13 A late restoration which leaves the calibrated future unchanged 143
1.14 Actual prefix data and the true affine pulse inlet 145
1.14.1 One explicit finite pretemplate, with its parameter endpoint 146
1.14.2 The $G = 0$ wait and its fixed-physical-coordinate data 147
1.14.3 Actual fixed-λ turnoff data and affine memories 148
1.14.4 Moving primitive corrections and their actual small targets 150
1.14.5 The actual heat correction: late-scale bounds and exact bookkeeping . . . 151
1.14.6 The actual affine return data 153
1.14.7 Outputs and other source estimates 153
1.15 Actual future realization and inlet order 154
1.15.1 Exact terminal power model and its actual histories 154
1.15.2 The complete heat-tail integral and the added leg 156
1.15.3 The actual scalar coefficient map and the same fast mode 157
1.15.4 A rank-one actual primitive correction, with all inlet germs fixed 159
1.15.5 The actual central memory, hold, and scalar source 171
1.15.6 Scope and remaining source interfaces 177
1.15.7 An exact model ordering calculation 177
1.15.8 The mixing identity and a uniform cutoff under the actual order condition 179
1.15.9 Actual transfer by the rank-one primitive construction 179
1.15.10 The actual inverse, flat endpoints, and source floor 180
1.15.11 Scope 185
1.16 Pulse response for the selected member 185
1.16.1 The fixed-coordinate pulse identities and their response 185
1.16.2 The flat central pulse with ordinary angular derivatives 194
1.17 Actual primitive and source corridors 197
1.17.1 Source and primitive reserves on the actual corridor 197
1.18 Uniform finite-order pressure bounds 207
1.19 Strict shear with the specified histories 212
1.19.1 Strictifying the shear while keeping the actual histories 213
1.19.2 The geometric loop lemma 215
1.20 The admissible cover and the positivity of the leading stress 221
1.20.1 Inputs 221
1.20.2 The algebraic core 223

1.20.3 Constant history shifts . . . 223
1.20.4 The prefix . . . 224
1.20.5 Verification of the admissible cover for the selected member . . . 224
1.20.6 The outer corridor and the terminal faces . . . 273
1.21 The selected curved inner weight and protected domain . . . 275
1.21.1 The joint cutoff gauge and the same finite algorithms . . . 276
1.22 The protected leading core and its angular regularity . . . 277
1.22.1 Order-zero compatibility on the collars . . . 280
1.22.2 Termination and interpolation on the endpoint collars . . . 282
1.23 The actual aggregate weight . . . 282
1.24 One-sided regularity of the leading fields . . . 292
1.24.1 The actual late pressure corridor . . . 294
1.24.2 Weights on the two tubes and generic radial primitives . . . 295
1.24.3 The backward side: one saturation rectangle and the weight $c_b\zeta$ . . . 296
1.25 Endpoint geometry and parameter maps . . . 298
1.25.1 The endpoint geometry and one-sided calculus . . . 298
1.25.2 Nondegeneracy on the closed angular interval . . . 300
1.25.3 The actual leading endpoint jets along the full radial path . . . 303
1.26 The protected hold and the selected spectrum . . . 308
1.26.1 The protected hold and its quantitative margins . . . 308
1.26.2 The selected physical frozen spectrum . . . 309
1.27 The source family and its quantitative bounds . . . 311
1.27.1 A radius-independent product bound . . . 311
1.27.2 Source bounds on all columns before spectral selection . . . 311
1.27.3 The large derivative and the five histories . . . 318
1.27.4 A noncircular choice of the spectral source parameters . . . 320
1.28 The positive moment ladder and the weighted profile bootstrap . . . 321
1.28.1 Notation . . . 321
1.28.2 Angular Hardy inequality and the multiplier ladder . . . 322
1.28.3 The Leray ladder . . . 324
1.28.4 The weighted profile bootstrap . . . 325
1.29 Conditional physical resolvent estimates . . . 329
1.29.1 From the scalar pencil to a true velocity resolvent . . . 330
1.29.2 Algebraic simplicity of the selected band . . . 334
1.29.3 High axial frequency and the viscosity bridge . . . 343
1.29.4 The far-angular physical space . . . 348
1.30 Full-frequency spectral selection for one member . . . 353
1.30.1 Inputs and precise output . . . 354
1.30.2 Source choices before any spectral conclusion . . . 355
1.30.3 Centered parameter and all-Z global form budget . . . 356
1.30.4 The model and its strict normalized margins . . . 361
1.30.5 Exhaustive frequency exclusion, with $\alpha\to 0$ . . . 363
1.30.6 True-domain compact comparison and large centered imaginary parameter 365
1.30.7 Centered Fredholm count and the pre-control simple branch . . . 366
1.30.8 Actual away-center rank, with the real old power slope . . . 367
1.30.9 Actual width IVT and discrete angular gap . . . 368
1.30.10 Physical complex centering and quadratic curvature without losing the winner . . . 369

1.30.11 Physical pressure, full resolvent exclusion and adjoint . . . 370
1.30.12 Required finite weighted spectral data for this same member . . . 371
1.30.13 One parameter order, replacements, and exact scope . . . 372
1.30.14 Actual all-Z B1/B2, not a compact-chart substitution . . . 373
1.30.15 Far angular labels: actual F4 and its parameter order . . . 374
1.30.16 Compact strain, small viscosity, true shifts and F1/F2 . . . 375
1.30.17 Last spectral and leading-field hypotheses and their scope . . . 377
1.30.18 Actual-member admission of the retained model . . . 377
1.30.19 Typed local Green, determinant and physical control interfaces . . . 383
1.31 Consequences of the spectral selection theorem . . . 406
1.31.1 Frozen comparison and signed layers . . . 406
1.32 Selection of the same leading member . . . 409
1.32.1 Radial placement and the pressure-class correction . . . 409
1.33 The selected physical two-band shift . . . 411
1.34 Leading propagation from frozen physical estimates . . . 412
1.34.1 Block coordinates . . . 414
1.34.2 Phase-space toolkit . . . 416
1.34.3 Low axial frequencies: the packet comparison . . . 419
1.34.4 High axial frequencies and very far angular labels . . . 422
1.34.5 The two block lemmas . . . 424
1.35 Finite physical reference profiles and kernel calculus . . . 427
1.36 The Gram metric of the leading field . . . 431
1.36.1 A viscosity-uniform finite-time metric . . . 431
1.37 Proof of the main statement . . . 436

2 Craik–Criminale perturbations and a smooth Navier–Stokes force 438
The leading pair supplied by Theorem 1 . . . 438
2.1 The local packet ansatz . . . 444
2.2 Main statement . . . 445
2.3 Notation and hypotheses for the completion . . . 450
2.3.1 Slow coefficients, mean and oscillations . . . 450
2.3.2 Leading coefficients used in the completion . . . 451
2.3.3 Tip coordinates, slice jets, and the heat exterior . . . 456
2.3.4 Finite-stage estimates and the backward completion . . . 461
2.4 From the leading stress to a smooth force . . . 462
2.4.1 Weights, cutoffs and the common trace . . . 463
2.4.2 The single smooth force and the same strong trace . . . 463
2.5 The selected relative source interface . . . 464
2.6 Slow completion and its edge weights . . . 466
2.6.1 Positive-order support and the full pressure hull . . . 466
2.6.2 The exact forward coefficient equations . . . 467
2.6.3 A full-rectangle inner inverse . . . 468
2.6.4 Five linear moments and compact positive-order profiles . . . 477
2.6.5 Conservation closes the stress primitives . . . 481
2.6.6 The one exceptional outer viscosity coefficient . . . 482
2.6.7 Borel realization on divergence potentials . . . 483
2.6.8 The signed stress bound and one edge cutoff . . . 486
2.7 The full radial endpoint data and the joint physical atlas . . . 486

2.7.1 Backward pressure saturation and finite transfer 487
2.8 One-sided regularity at the initial slice away from the tip 496
2.9 Endpoint regularity of the selected data 505
2.9.1 Finite algorithms in the common cutoff gauge 508
2.10 The same gauge and finite construction 508
2.11 Axis regularity and the slow force at the joining time 510
2.11.1 Axis regularity in Cartesian coordinates 510
2.11.2 Cutoffs preserve the actual endpoint jets 511
2.11.3 Extension of the slow force through the origin 512
2.12 The pulse clock and the choice of schedule 513
2.12.1 All auxiliary orders for the actual schedule 515
2.13 Separated packets, Gaussian inversion, and the actual covariance 531
2.13.1 The full half-space atlas and the coefficient classes 531
2.13.2 A fixed separated graph and compatible covering maps 533
2.13.3 Rounded phases and the moving normal plane 535
2.13.4 The Gaussian inverse and positive homogeneous pulse 537
2.13.5 Exact curls and the physical linear remainder 539
2.13.6 Positive leading amplitudes and all six covariance entries 541
2.13.7 Signed cross corrections using the original amplitude 543
2.13.8 Finite complex harmonics and their complete residual 544
2.13.9 Weighted radial mixing on the same cover 547
2.13.10 The finite-source radial primitives on both time sides 549
2.13.11 Output for the finite mean–wave stage 550
2.14 The mean equations and the finite iteration 551
2.14.1 The fixed reference and the coefficient conventions 551
2.14.2 Shifted radial primitives and the complete radial response 552
2.14.3 The current auxiliary response 556
2.14.4 Three actual state integrals and the five protected rows 558
2.15 The finite packet and mean corrections 563
2.15.1 The canonical tensor and its explicit flat remainder 563
2.15.2 Initialization on the actual slow reference 564
2.15.3 One paired wave–mean step 568
2.15.4 Finite return and compatible actual states 572
2.16 The inventory of the mean–wave stage 574
2.17 Derivative bounds on the whole profile hull 579
2.17.1 The bridge with an arbitrary physical prefactor 579
2.17.2 Quantitative axis bounds for the slow sum 579
2.17.3 Why the finite errors vanish near the axis 581
2.17.4 The finite-state and finite-residual estimates 581
2.18 The physical limit, the initial trace, and localization 582
2.18.1 Finite states and a derivative loss independent of the stage 582
2.18.2 Heat-exterior radii and the spatial support of the background 583
2.18.3 Cutoffs which keep the exact divergence 587
2.18.4 A locally finite sum 589
2.18.5 The ordinary residual and its smooth extension 590
2.18.6 A strong local trace on a fixed physical ball 592
2.18.7 Compact spatial localization without an initial defect 592
2.18.8 The singular cusp and the energy identity 594

2.18.9 The output of the admissible-source construction 594
2.19 The forward base 598
2.20 The joint physical completion 599
2.20.1 Backward stage estimates and finite time locality 603
2.21 Energy and past blowup for the background 606
2.22 The completed-source envelope 607
2.23 The clock of the completed packet field 612
2.23.1 The pulse clock and its contrast 612
2.24 Completion of the selected member 614
2.25 Proof of the main statement 615

3 Nonunique continuations from zero initial velocity 618
Input from the smooth completion 618
3.1 Energy solutions and the physical linearization 624
3.2 Main statement 625
3.3 Linear inputs for this background 626
3.3.1 A sufficient criterion for branching 627
3.3.2 Canonical coordinates and physical normalization 628
3.4 Full-frequency propagation for the completed field 629
3.4.1 Weighted Hodge control and the high Gram estimate 630
3.4.2 Transported total-frequency filters 634
3.4.3 Propagation transfer for the two applications 636
3.5 The full propagator without a shift 639
3.6 Physical reference columns for the selected spectral pair 639
3.6.1 Fixed-chart quantization and profile identities 639
3.7 Finite prepared columns and their two-band bounds 647
3.7.1 Actual radial and coefficient domains of the preparation 647
3.7.2 The raw pressure pair and its operator domains 653
3.7.3 Mixed frozen-parameter and radial-moment macro domain 656
3.8 The prepared-shifted propagator and its Green operator 681
3.8.1 The fixed reference and the completed shift 681
3.9 Removal of the physical shift and an exact real mode 683
3.9.1 Typed OUTPUT bounds and finite graph localization 684
3.9.2 The finite profile algebra and the fixed masks 690
3.9.3 Exact two-column algebra 708
3.9.4 A right inverse of the unshifted completed operator 711
3.10 The centered Gaussian and a global physical packet 742
3.11 A faster inverse from the full propagator 747
3.11.1 The L^2 inverse by Duhamel 747
3.11.2 Forced physical smoothing and one uniform Sobolev inverse 748
3.12 The abstract branching argument 750
3.13 Joining at the singular time and continuation on a regular interval 752
3.14 Proof of the main statement 754

Bibliography 756

Chapter 1

Construction of the forward–backward background

The target of the three parts is a real one-parameter family for viscosity one on $\mathbb{R}^3$. It starts from rest at a common negative time under one smooth force of compact space-time support, follows the same solution into blow-up at zero and separates at every positive time of a common interval. In this part the two endpoint charts, including their actual partial moment histories, are compared in the paragraph on p. 306.

We select the leading flows on the two sides of this slice together. A local change in swirl changes the pressure through a radial integral extending to infinity. The two flows must therefore agree at the joining slice in their pressure and radial moments as well as in their velocity. A protected forward annulus leaves room to select a growing frozen mode while preserving those quantities. Part 2 completes this pair on both sides. Part 3 uses its forward spectral data to construct a growing mode of the linearization about the completed background. Starting with the radial histories and the heat exterior, we construct the regular core and its pressure, then verify the endpoint, stress and frozen spectral estimates for the same member.

1.1 Similarity variables, leading fields and radial histories

Write $x = (x_1, x_2, z) \in \mathbb{R}^3$, $r = (x_1^2 + x_2^2)^{1/2}$, $e_r = (x_1, x_2, 0)/r$, $e_\theta = (-x_2, x_1, 0)/r$ and $e_z = (0, 0, 1)$ for $r > 0$. For $0 < h < 1/2$ and $\varepsilon \in \{-1, +1\}$, the native coordinates on the half-space $\varepsilon t > 0$ are

$$q - z^2 q^{2h} = \varepsilon t, \qquad \xi = r q^{-1/2}, \qquad \eta = z q^{-1/2+h}, \qquad d = 1 - \eta^2, \quad L = 1 - 2h\eta^2.$$

Here $q = q_\varepsilon(t, z)$ is the unique root with $q > |z|^{2/(1-2h)}$. Its range gives $\xi \geq 0$ and $|\eta| < 1$. Set $\mathcal{D} = [0, \infty) \times [-1, 1]$. Smoothness on $\mathcal{D}$ means smoothness in its interior with continuous one-sided derivatives of every order on its faces, locally in ξ. A swirl profile E_ε, axial profile U_ε, radial profile V_ε and pressure profile P_ε represent the physical fields

$$B_\varepsilon^0 = q^{-1/2} \frac{V_\varepsilon}{\xi} e_r + q^{-1/2-h}(E_\varepsilon e_\theta + U_\varepsilon e_z), \qquad p_\varepsilon^0 = q^{-1-2h} P_\varepsilon. \tag{1.1.1}$$

Unless the side is displayed, the letters E, U, V, P and their histories refer throughout a formula

to a single ε. The histories are

$$\begin{pmatrix} M \\ I \\ J \\ S \\ C_p \end{pmatrix}(\xi,\eta) = \int_0^{\xi} \begin{pmatrix} \rho U \\ \rho^2 E \\ \rho^2 U E \\ \rho(U^2 - \frac{1}{2}E^2) \\ E^2/\rho \end{pmatrix}(\rho,\eta)\, \mathrm{d}\rho. \tag{1.1.2}$$

Thus all five vanish at the axis. The pressure normalization is $\lim_{\xi\to\infty} P(\xi,\eta) = 0$ and the axis pressure is $\Pi(\eta) = P(0,\eta)$. Radial balance and incompressibility then give

$$\begin{aligned} \Pi(\eta) &= -\int_0^{\infty} E(\rho,\eta)^2 \frac{\mathrm{d}\rho}{\rho}, & P(\xi,\eta) &= \Pi(\eta) + C_p(\xi,\eta), \\ V(\xi,\eta) &= \frac{\eta\xi^2 U - (1-2h)\eta M - dM_\eta}{L}. \end{aligned} \tag{1.1.3}$$

For an axisymmetric velocity B and pressure p write $D_B = \partial_t + B_r\partial_r + B_z\partial_z$ and $\Delta_r = \partial_r^2 + r^{-1}\partial_r$. The reduced equations retain incompressibility, radial pressure balance, and the following two tangential momentum expressions:

$$\mathcal{R}_\theta = D_B B_\theta + r^{-1}B_r B_\theta - (\Delta_r - r^{-2})B_\theta, \qquad \mathcal{R}_z = D_B B_z + \partial_z p - \Delta_r B_z. \tag{1.1.4}$$

For the fields (1.1.1), define their integrated stress $T_0 = (T_{0,\theta}, T_{0,z})$ at $r > 0$ by the regular radial primitives

$$\begin{aligned} q^{-1-h}T_{0,\theta}(\xi,\eta) &= -r^{-2}\int_0^r r'^2 \mathcal{R}_\theta(r',z,t)\, \mathrm{d}r', \\ q^{-1-h}T_{0,z}(\xi,\eta) &= -r^{-1}\int_0^r r' \mathcal{R}_z(r',z,t)\, \mathrm{d}r'. \end{aligned}$$

Equivalently one may evaluate these formulas at $q = 1$, $(r,z,t) = (\xi,\eta,\varepsilon(1-\eta^2))$ and extend to the faces by their one-sided limits. Put $H = \xi E$, $F = E/\xi$, and write $\mathbf{S} = (S_\theta, S_z) = (\xi\partial_\xi F, \partial_\xi U)$ for the two components of the tangential shear. The scalar history S in (1.1.2) will always be written without boldface.

1.2 Main statement

Theorem 1 (The selected pair of leading fields)**.** The endpoint comparison underlying (ii)–(iii) is proved in the paragraph on p. 306. The box comparison needed in (vii) is given in the paragraph on p. 432. Both use the selected member of this statement. There exist $\lambda, h, C, \sigma, \Delta, c_{\mathrm{heat}} > 0$ and an integer $m \geq 30$, with

$$0 < h < \lambda/6 < 1/120, \qquad C > 1, \qquad 0 < \sigma < 5, \qquad \Delta = C^\sigma,$$

and, for each $\varepsilon = \pm 1$, real-valued functions $E_\varepsilon, U_\varepsilon, V_\varepsilon, P_\varepsilon \in C^\infty(\mathcal{D})$ for which all eight assertions below hold simultaneously. In particular the spectral and evolution estimates use the forward field defined by these very profiles. Unless a uniformity is specified, constants may depend on the chosen profiles and parameters.

(i) *Reduced equations, axis conditions and moments.* The velocity and pressure are given by (1.1.1), with histories, pressure normalization and radial velocity given by (1.1.2)–(1.1.3). On $\{r > 0,\ \varepsilon t > 0\}$ they satisfy, writing $(B,p) = (B_\varepsilon^0, p_\varepsilon^0)$,

$$\begin{aligned} r^{-1}\partial_r(rB_r) + \partial_z B_z = 0, & \qquad \partial_r p = B_\theta^2/r, \\ \mathcal{R}_\theta = -r^{-2}\partial_r(r^2 q^{-1-h}T_{0,\theta}), & \quad \mathcal{R}_z = -r^{-1}\partial_r(r q^{-1-h}T_{0,z}). \end{aligned} \tag{1.2.1}$$

The stress vanishes outside the radially bounded active set specified in (iv); thus the reduced equations have zero tangential residual on each open stress-free region. The physical fields extend smoothly in Cartesian coordinates through $r = 0$. In native variables, E_ε/ξ, U_ε, V_ε/ξ^2 and P_ε are smooth functions of (ξ^2, η) at $\xi = 0$, and $E_\varepsilon(\xi, \eta) > 0$ for $\xi > 0$.

For every $(z, t) \in \mathbb{R}^2$ with $\varepsilon t > 0$ the moments satisfy

$$\int_0^\infty r(B^0_\varepsilon)_z(r, z, t)\, \mathrm{d}r = 0, \qquad \int_0^\infty r^2\big[(B^0_\varepsilon)_\theta(r, z, t) - c_{\mathrm{heat}} r^{-1-2h}\big]\, \mathrm{d}r = 0. \tag{1.2.2}$$

Both integrals converge. Write $\boldsymbol{M} = (M, I, J, S, C_p)$ and let $\Delta\boldsymbol{M}$ be its value at the outlet of a compact radial modification minus the value there before the modification, at the same η. For the loop together with its five restoration bumps, and for the spectral modification together with its associated return, $\Delta\boldsymbol{M} = 0$ at the respective completed outlet. For the pressure correction alone, if Π_{ref} and p_0 are its incoming and prescribed axis pressures, respectively, then

$$\Delta\boldsymbol{M} = (0, 0, 0, 0, \Pi_{\mathrm{ref}} - p_0), \qquad p_0 + C_{p,\mathrm{new}} = \Pi_{\mathrm{ref}} + C_{p,\mathrm{ref}}$$

at the outlet. On partial intervals the five integrals always use the modified profiles. The explicit forward and backward stresses are (1.9.2)–(1.9.3) and (1.4.3)–(1.4.4), respectively.

(ii) *One exterior coefficient and full leading endpoint jets.* There exists $\xi_{\mathrm{heat}} < \infty$ such that on $\xi > \xi_{\mathrm{heat}}$ both U_ε and V_ε vanish. The physical swirl there equals a function $K_\varepsilon(r, t)$ satisfying $\partial_t K_\varepsilon = (\Delta_r - r^{-2})K_\varepsilon$. With the same c_{heat} on both time sides,

$$E_\varepsilon(\xi, \eta) = c_{\mathrm{heat}} \xi^{-1-2h}(1 + O(\xi^{-2})) \quad (\xi \longrightarrow \infty).$$

The differentiated heat estimates of (1.13.35) and Lemma 1.7.1 apply, uniformly on the closed angular interval, at every fixed finite derivative order.

For $z \neq 0$ set

$$\widetilde{Q} = |z|^{2/(1-2h)}, \qquad \widetilde{\xi} = r/\sqrt{\widetilde{Q}}, \qquad \widetilde{\eta} = t/\widetilde{Q}.$$

The slice representatives of both leading velocities, pressures and all five histories have equal derivatives of every order at $\widetilde{\eta} = 0$, on the full radial path. Explicitly, if g has weight w, then

$$\widetilde{g}_\varepsilon(\widetilde{\xi}, \widetilde{\eta}) = |\eta|^{2w/(1-2h)} g_\varepsilon(\xi, \eta), \qquad \partial^k_{\widetilde{\eta}} \widetilde{g}_-(\cdot, 0) = \partial^k_{\widetilde{\eta}} \widetilde{g}_+(\cdot, 0) \quad (k \geq 0).$$

Here w means that the physical scalar is $q^{-w} g$. For either sign of z, use $\operatorname{sgn}\eta = \operatorname{sgn} z$, $\xi = \widetilde{\xi}|\eta|^{1/(1-2h)}$ and $\widetilde{\eta} = \varepsilon(1 - \eta^2)|\eta|^{-2/(1-2h)}$. The equality holds for every $\widetilde{\xi} \geq 0$, with one-sided derivatives at zero. The weights of $(V/\xi, E, U, M, I, J, S, C_p, P)$ are respectively $(\frac{1}{2}, \frac{1}{2} + h, \frac{1}{2} + h, h - \frac{1}{2}, h - 1, 2h - \frac{1}{2}, 2h, 1 + 2h, 1 + 2h)$. On $\mathbb{R}^2_{z,t} \setminus \{(0, 0)\}$ there is a positive smooth cutoff gauge

$$\widetilde{q} = q_- \quad (t \leq 0), \qquad \widetilde{q} = q_+/L_{\mathrm{cut}}(\eta_+) \quad (t \geq 0).$$

Here L_{cut} is smooth and positive on $[-1, 1]$. Near each endpoint it equals the positive branch $\lambda_{\mathrm{ch}}(\pm 1) = 1$ of $\eta_+^2 \lambda_{\mathrm{ch}}^{1-2h} = 1 + \lambda_{\mathrm{ch}}(1 - \eta_+^2)$. The continuation of the backward chart into this collar obeys $q_- = q_+/\lambda_{\mathrm{ch}}$. This is one smooth physical function across $t = 0$ away from $z = 0$.

Here the history weights are those of (1.6.4) and the transition of the native charts is (1.6.16), with the slice weights and equality of all derivatives as in Definitions 1.6.4 and 1.6.5. The forward exterior has the two differentiated heat expansions (1.13.34) and (1.13.35). The backward exterior and its moments are those of Lemma 1.8.7.

(iii) *Protected core and exact correction domains.* For each side there exist positive functions $\xi_{a,\varepsilon}, \xi_{p,\varepsilon} \in C^\infty([-1,1])$. On an open collar of each angular endpoint put $l = \lambda_{\mathrm{ch}}(\eta)$ and $\eta_b = l^{1/2-h}\eta$. Using the constant continuations of the backward entry and pulse radii, the two graphs obey

$$\xi_{j,-}(\eta_b)^2 = l\,\xi_{j,+}(\eta)^2, \qquad j \in \{a,p\}.$$

Thus both ξ/ξ_a and ξ/ξ_p agree in the two charts throughout the collars. We suppress ε on these graphs. There are common levels $1 < \Xi_{\mathrm{need}} < \Xi_{\mathrm{cut}} < \Xi$ and the following derivative estimates in the coordinate $\varpi = (\xi/\xi_a(\eta))^2$. For one $r_G > 0$, each integer $j \ge 0$ has a finite constant C_j with

$$\sup_{0\le\varpi\le\Xi,\ \eta\in[-1,1]} \left|\partial_\varpi^j \partial_\eta^k G(\varpi,\eta)\right| \le C_j r_G^{-k} (k!)^{3/2} \qquad (k \ge 0), \tag{1.2.3}$$

for all four pullbacks G of $E/\xi, U, V/\xi^2, P$ by $(\varpi,\eta) \mapsto (\xi_a(\eta)\sqrt{\varpi}, \eta)$, on each side. The angular functions extend to a fixed neighborhood of $[-1,1]$; the radius r_G is the same for every fixed radial order j. There is one smooth cutoff $\chi_{\mathrm{cut}}(\varpi) \in [0,1]$ equal to one on $[0, \Xi_{\mathrm{need}}]$ and zero on $[\Xi_{\mathrm{cut}}, \infty)$, of Gevrey order $3/2$, meaning $\|\chi_{\mathrm{cut}}^{(k)}\|_\infty \le AB^k (k!)^{3/2}$ for some $A, B > 0$ and all $k \ge 0$.

On the backward side $\xi_{a,-} = \xi_a^0$ is constant and there is an analytic rectangle $0 \le \xi \le \xi_{\mathrm{an}}$ before the loop. For one angular neighborhood $U_b \supset [-1,1]$ and one $r_b > 0$, every fixed radial derivative of $F_- = E_-/\xi$, U_-, V_-/ξ^2 and P_- has angular bounds $C_j r_b^{-k} k!$ there. The final member equals the analytic core and first collar on this whole rectangle. The shared levels obey

$$\Xi \le e^{t_{\mathrm{act}}}, \qquad \xi_a^0 \sqrt{\Xi} \le \xi_{\mathrm{an}} < \xi_-^{\mathrm{loop}}, \qquad \Xi_{\mathrm{cut}} < e^{y_s},$$

where $t_{\mathrm{act}} > 0$ is the logarithmic length of the activation interval, ξ_-^{loop} the first radius of the backward shear modification, and $y_s > 0$ the endpoint of the collar on which the strict inequalities in (iv) hold for $0 < 2\log(\xi/\xi_a) \le y_s$; the protected rectangle also precedes I_{pos}. The derivative support of the shared termination cutoff is compactly contained in this strict positive collar and has a positive minimum of the native weight. These are the feasible choices of (1.22.1).

The moving logarithmic coordinate $y_p = 2\log(\xi/\xi_p(\eta))$ reserves the untouched power intervals

$$I_{\mathrm{pos}}:\ -14 < y_p < -9, \qquad I_{\mathrm{mean}}:\ -8 < y_p < -3.$$

On these unchanged patches

$$H(\xi,\eta) = c(\eta)\xi^{-2\mu(\eta)}, \qquad c(\eta) > 0, \qquad 0 < \nu_c \le \mu(\eta) \le \lambda,$$

and U is radially constant; on I_{pos} it is zero. For either interval choose two axial and three swirl bumps in C_c^∞ of its y_p coordinate, nonnegative, nonzero and with strictly ordered disjoint supports in each group. For a group $b_1, \dots, b_l$ and exponents $s_1, \dots, s_l$ its radial moment matrix is

$$B_{ij}(\eta) = \int_0^\infty \xi^{s_i} b_j(2\log(\xi/\xi_p(\eta)))\ \mathrm{d}\xi.$$

For $(s_1, s_2) = (1, 1-2\mu)$ and $(s_1, s_2, s_3) = (2, -2-2\mu, -2\mu)$, respectively, $\sup_{[-1,1]} \|B^{-1}\| < \infty$. These are the linear moment blocks on the positive-order and mean intervals. For the nonlinear five-history maps, the variables are the two axial and three swirl bump amplitudes and the output is the outlet change $\Delta \boldsymbol{M}$ from (i). At the selected amplitudes on the early restoration

reserve and on the late reserve selected in Lemma 1.27.5a, the absolute Jacobian determinants have strictly positive minima on $[-1,1]$. The five trial columns are defined before the choice of their angularly supported amplitudes. Let $\mathcal{P}(A)$ be the left side minus the right side of the pulse energy equation (1.6.26), with its incoming moments and outgoing energy evaluated on this member. Its positive root A_p satisfies $\mathcal{P}'(A_p) \ge 2^{-3/2}$.

For the selected member the exponent equation and the stopping level are transverse, and the two-return matrix and the two-row Jacobian of Lemma 1.15.5 have bounded inverses on their selected branches. The circle reparametrization of the loop has strictly positive angular derivative. The resulting pulse, return, stop, shot and loop parameters are smooth in η up to both ends of $[-1,1]$. Section 1.25.2 verifies these assertions for this member.

The later meridional and spectral returns are retained when defining the full pressure hull. In the squared radial coordinate used only to describe these sets, that hull is covered by the two tubes

$$K_0 = \{\xi_p(\eta)^2 e^{-14.5}/2 \le \xi^2/2 \le R_o e^{-0.5}\},$$
$$K_{\mathrm{ext}} = \{\eta \in K_1,$$
$$\xi_p(\eta)^2 e^{-14.5}/2 \le \xi^2/2 \le R_+\},$$

Here χ is the angular cutoff of Lemma 1.15.26; $K_1 \Subset K_2 \Subset \{\chi = 0\}$ are the nested angular sets of Proposition 1.24.2, with K_1 containing the angular support of the spectral modification. $R_o(\eta)$ is the outlet graph of the returned pulse in that proposition and R_+ is a constant upper bound for the squared radial coordinate $\xi^2/2$ at the last spectral return. On these tubes the azimuthal integrated stress satisfies $T_{0,\theta} \ge cH > 0$, where $H = \xi E$. The tube K_{ext} has the stated angular restriction. The backward side satisfies all leading clauses (B1)–(B6) of Hypothesis 1.5.5. Its pre-loop core matches the reference velocity and all five histories at $X_{\mathrm{match}} = \xi_{\mathrm{match}}^2/2$. Its native strict cone, weight, moments, two reserved power patches, terminal multiplier and pressure hull refer to the actual backward member. These are leading geometric data for the later slow pressure rows; the positive-order velocity and pressure supports need not end at the same radius.

The protected radii and angular bounds are those of Proposition 1.22.4. Proposition 1.22.7 gives the order-zero slice jets on $0 \le \varpi \le \Xi$. The five-history return has the local inverse of Lemma 1.27.5 on a power gap and the global angular determinant bound of Lemma 1.27.5a on the selected late gap. With its returns included, the six-real spectral control map has the invertible Jacobian of Lemma 1.30.36 at the admitted parameters. These choices follow the order in Section 1.5.2. The forward supports have the radial order (O1)–(O8), with the early positions in Lemma 1.20.49 and the full order in Section 1.32, including the pre-pulse banks and the spectral layers with their returns. The central wing ends at (1.13.52) and the outer component at the edge of (1.15.2). On the backward side the protected slots and the terminal edge satisfy Lemma 1.8.8(S3)–(S4) and Lemma 1.8.7(S2).

(iv) *Strict stress margins and radial inverse weights.* For $\xi > 0$ define $a = -\xi F_\xi/F$, $b = \xi U_\xi/E$ and $(p_1, p_2) = F^{-1}(T_0 - \mathbf{S})$, so $\mathbf{S} = F(-a, b)$ and $T_0 = F((p_1, p_2) - (a, -b))$. Put

$$t_s = -b/a, \quad v = a + b^2/a, \quad P_c = p_1 + t_s p_2, \quad J_c = p_2 - t_s p_1.$$

Define $\mathcal{A}_\varepsilon = \{(\xi,\eta) \in \mathcal{D} : T_0(\xi,\eta) \ne 0\}$ for each side. There are $c_s > 0$ and $0 < \delta_c < 2$ independent of the point such that on $\mathcal{A}_\varepsilon$ one has $F, a, v - 2 \ge c_s$ and, for $n = (n_\theta, n_z) = T_0/|T_0|$,

$$n_\theta + t_s n_z \ge \delta_c, \qquad (v-2)(n_z - t_s n_\theta)^2 \le (2 - \delta_c)(n_\theta + t_s n_z)^2.$$

These are the normalized strict margins of Proposition 1.19.6 and (1.5.1) for the final profiles after the spectral returns. On every compact subset of $\mathcal{A}_\varepsilon$ the four quantities

$$a, \qquad v-2, \qquad P_c - v, \qquad 2(P_c-v)^2 - (v-2)J_c^2 \tag{1.2.4}$$

have strictly positive infima. In particular the shear and the stress direction $n = T_0/|T_0|$ satisfy there

$$-|\mathbf{S}|^2 < 2FS_\theta < 0, \qquad n\cdot\mathbf{S} < 0, \qquad (n\cdot\mathbf{S})^2 > |\mathbf{S}|^2 + 2FS_\theta.$$

Indeed $|\mathbf{S}|^2 = F^2 av$ and $T_0\cdot\mathbf{S} = -F^2 a(P_c - v)$. Expressing T_0/F in the orthogonal directions $(1, t_s)$ and $(-t_s, 1)$ reduces the last inequality to the fourth gap in (1.2.4).

On each side there exists $\mathsf{W} \in C^\infty(\mathcal{D})$ with $0 \le \mathsf{W} \le e^{-2}$, supported between the inner and terminal zero faces of the corresponding profile, and positive on the pressure tubes in (iii). The active set is $\{\mathsf{W} > 0\}$. It equals $\mathcal{A}_\varepsilon$ and lies in $\{\xi \ge \xi_a(\eta),\ \xi \le \xi_{\max}\}$ for a finite $\xi_{\max}$. For every mixed derivative order j there are finite C_j, N_j such that, with $\mathcal{L}_W = 1 + \log(1/\mathsf{W})$,

$$|T_0| \ge c\mathsf{W}, \qquad |D^j T_0| + |D^j \mathsf{W}| \le C_j \mathsf{W}\mathcal{L}_W^{N_j} \quad \text{on } \{\mathsf{W} > 0\}. \tag{1.2.5}$$

Here D^j is any fixed word in $\xi^{-1}\partial_\xi$ and $\partial_\eta|_\xi$; $T_0 = 0$ where $\mathsf{W} = 0$. Every positive power of W extends flatly by zero. On I_{mean} the weight has a positive lower bound. On the forward side set $X = \xi^2/2$. Let X_{mid} be the least starting radius $X_{1,i}$ of the terminal radial splices of the weight, in the X coordinate. Let H_{heat} denote the numerator of the matched homogeneous heat swirl, including its fast component, in the same chart as $H_+ = \xi E_+$. For $X \ge X_{\mathrm{mid}}$ and every word D^j as above there are constants C_j, N_j for this member such that

$$|D^j(H_+ - H_{\mathrm{heat}})| \le C_j\, \mathsf{W}\, \mathcal{L}_W^{N_j}.$$

The right side is extended by zero at $\mathsf{W} = 0$, including points where a radial and an angular terminal face meet. On the compact middle region $y_a = 2\log(\xi/\xi_a) \ge y_{\mathrm{col}}$, $X \le X_{\mathrm{mid}}$, for a fixed inner collar width $y_{\mathrm{col}} > 0$, the forward weight has a positive lower bound. This forward estimate follows from Lemma 1.23.8a and the proof of (W3) in Proposition 1.23.8.

At the inner edge let $y_a = 2\log(\xi/\xi_a(\eta))$. Define $f(s) = e^{-1/s^2}$ for $s > 0$ and $f(s) = 0$ otherwise, and denote by $\sigma_{\mathrm{step}}(s) = f(s)/(f(s) + f(1-s))$ the transition from zero to one. For some $0 < \kappa_{\mathrm{act}} < 1$,

$$T_0 = e(y_a)\mathcal{B}, \qquad e = (1-\kappa_{\mathrm{act}})\sigma_{\mathrm{step}}(y_a/t_{\mathrm{act}}), \qquad \mathcal{B}_\theta \ge b_* > 0, \quad |\mathcal{B}| \le b^*.$$

The edge weight is $w_{\mathrm{in}} = c_{\mathrm{in}} e$; both components of T_0 have the bound in (1.2.5) with this weight.

In particular the backward outer edge has the actual multiplier germ required for the order-one stress bound. With $B = \xi_{b,-}^2/2$, $u = 1 - \xi^2/(2B)$ and $\kappa = 1 - e^{-3}$,

$$E_-(\xi,\eta) = c_{\mathrm{heat}}\xi^{-1-2h}\mathcal{H}_-(4d/\xi^2)\, m(\xi^2/2), \qquad m = 1 - \rho_w \Psi(\xi^2/(2B)), \quad 0 < \rho_w < 1.$$

Here $\Psi(s) = 1 - \sigma_{\mathrm{step}}((s-e^{-3})/\kappa)$, $\mathcal{H}_-(z) = \Gamma(1+h)^{-1}\int_0^\infty e^{-v}v^h(1+zv)^{-h}\,\mathrm{d}v$ for $z \ge 0$, and $m = 1$ beyond the edge. For every $j \ge 0$, on its inner terminal collar,

$$|(\xi^{-1}\partial_\xi)^j(1-m)| \le C_j e^{-\kappa^2/u^2} u^{-N_j}.$$

More precisely $T_{0,\theta} = e^{-\kappa^2/u^2}u^{-3}b_\theta$ and $T_{0,z} = e^{-\kappa^2/u^2}u^3 b_z$, with smooth b_θ, b_z and $b_\theta(0,\eta) > 0$. This is the specific outer germ (O4) and the terminal stress factorization of Lemma 1.8.2; it is retained by all later leading edits.

Fix the subtraction bank as part of the choice of profile data, before selecting a source or its derivative order. For definiteness take $b_0(y) = c_0 f(y+7)f(-4-y)$ with $c_0^{-1} = \int_{\mathbb{R}} f(y+7)f(-4-y)\,\mathrm{d}y$, where f was defined above. Thus $b_0 \in C_c^\infty((-8,-3))$, $b_0 \geq 0$ and $\int b_0 = 1$. Put

$$\chi_m(\xi,\eta) = \int_\xi^\infty \frac{2}{\rho^2} b_0(2\log(\rho/\xi_p(\eta)))\rho\,\mathrm{d}\rho.$$

For each $k \in \mathbb{N}_0$ let $g \in C^\infty(\mathcal{D})$ have support in the fixed radial hull of (iii)–(iv), vanish on $\{\mathsf{W} = 0\}$, and satisfy $|D^j g| \leq A_j \mathsf{W}\mathcal{L}_W^{N_j}$ on $\{\mathsf{W} > 0\}$ for each word of length $j \leq k$ and some finite $A_j, N_j \geq 0$. Then

$$\mathcal{I}_m g(\xi,\eta) = \int_\xi^\infty g(\rho,\eta)\rho\,\mathrm{d}\rho - \chi_m(\xi,\eta)\int_0^\infty g(\rho,\eta)\rho\,\mathrm{d}\rho \tag{1.2.6}$$

satisfies $|D^j\mathcal{I}_m g| \leq A'_j \mathsf{W}\mathcal{L}_W^{N'_j}$ on $\mathcal{A}_\varepsilon$ for $j \leq k$, with $A'_j \leq C_{k,N}\max_{i\leq k} A_i$ and $N'_j = \max_{i\leq j} N_i$. Here $C_{k,N}$ depends on the selected data and the exponents $N = (N_i)_{i\leq k}$. Any other fixed non-negative normalized $b_0 \in C_c^\infty((-8,-3))$ gives the same estimate, with additional dependence on $\|b_0\|_{C^{k-1}}$ for $k \geq 1$. The function $b(\xi,\eta)\int_0^\infty g(\rho,\eta)\rho\,\mathrm{d}\rho$ obeys bounds of the same form for every fixed smooth b supported in I_{mean}, with constants also depending on its derivatives.

The native inner-edge factor is (1.23.3). The backward terminal multiplier satisfies (O4) of Definition 1.5.2, with the factorization in Lemma 1.8.2. The aggregate weights have properties (W1)–(W5) of Proposition 1.23.8 in their native coordinates, with the backward slot and pressure rectangle specified in Lemma 1.24.4, and the derivative bounds of Lemma 1.23.9. For a derivative Z commuting with radial integration at fixed native coordinates, the moving-bank commutator is exactly $[Z,\mathcal{I}_m]g = -(Z\chi_m)\int_0^\infty g(\rho,\eta)\rho\,\mathrm{d}\rho$ as in (1.24.2).

(v) *The physical frozen instability of this same forward member.* For $y \in \mathbb{R}^2$, $Z \in \mathbb{R}$, let $\mathcal{Q} = q_+(1,Z)$, $R = |y|$ and $\langle R\rangle = (1+R^2)^{1/2}$. Define

$$\mathcal{U}_0(y,Z) = R\Omega(R,Z)e_\theta + W(R,Z)e_z, \qquad R\Omega = \mathcal{Q}^{-1/2-h}E_+(R/\sqrt{\mathcal{Q}}, Z\mathcal{Q}^{-1/2+h}),$$

with $W = \mathcal{Q}^{-1/2-h}U_+(\xi,\eta)$ and $\mathcal{U}_1 = \mathcal{Q}^{-1/2}(V_+(\xi,\eta)/\xi)e_r$, where $(\xi,\eta) = (R/\sqrt{\mathcal{Q}}, Z\mathcal{Q}^{-1/2+h})$. Values on the axis are taken by smooth extension. Below the spatial L^2 norms at fixed Z use Lebesgue measure on $\mathbb{R}^2_y$. For every $j,l \geq 0$,

$$|\partial_Z^l\partial_R^j\Omega(R,Z)| \leq C_{j,l}\langle R\rangle^{-2-2h-j}.$$

The axial profile is zero for $R \geq \xi_U\sqrt{\mathcal{Q}(Z)}$, for a finite ξ_U. There is one all-Z constant $C_{\mathfrak{B}}$ for the following profile and dilation bounds:

$$\begin{gathered}
|\nabla_y^i\partial_Z^j\mathcal{U}_0| + |\partial_Z^j\Omega| \leq C_{\mathfrak{B}} \quad (i+j\leq 2),\\
|\mathcal{U}_1| + |\nabla_y\mathcal{U}_1| + |\partial_Z\mathcal{U}_1| \leq C_{\mathfrak{B}},\\
\langle R\rangle^2|\nabla_y\mathcal{U}_0| + R(|\Omega| + |W| + |\partial_Z\Omega|) \leq C_{\mathfrak{B}},\\
\|\Omega(\cdot,Z)\|_2 + \|W(\cdot,Z)\|_2 + \|\nabla_y\mathcal{U}_0(\cdot,Z)\|_2 \leq C_{\mathfrak{B}},\\
|y\cdot\nabla_y f| + |Z\partial_Z f| \leq C_{\mathfrak{B}} \quad (f = \Omega, W, \nabla_y\mathcal{U}_0).
\end{gathered}$$

For $n \in \mathbb{Z}$ and $k \in \mathbb{R}$ let

$$\mathsf{H}_n = \{v \in L^2(\mathbb{R}^2_y;\mathbb{C}^3) : v(R_\varphi y) = e^{in\varphi}\widehat{R}_\varphi v(y) \text{ in } L^2 \text{ for every } \varphi\},$$
$$X_{n,k} = \{v \in \mathsf{H}_n : \nabla_y \cdot v_h + ikv_3 = 0 \text{ in distributions}\}.$$

Here $v_h = (v_1, v_2)$, R_φ is planar rotation, and $\widehat{R}_\varphi = \operatorname{diag}(R_\varphi, 1)$. P_k is the horizontal Fourier multiplier with symbol $I - \zeta \otimes \zeta/|\zeta|^2$, $\zeta = (\zeta_h, k) \neq 0$; its restriction to H_n is the orthogonal projection onto $X_{n,k}$. For $\nu \geq 0$ the frozen generator on $X_{n,k}$ is

$$A_{\nu,n}(Z,k)v = -P_k[(\mathcal{U}_0 \cdot \nabla_k)v + (v_h \cdot \nabla_y)\mathcal{U}_0] + \nu(\Delta_y - k^2)v, \qquad \nabla_k = (\nabla_y, ik). \tag{1.2.7}$$

Its domain is $X_{n,k} \cap H^2$ for $\nu > 0$ and all of $X_{n,k}$ for $\nu = 0$. Write $s(A) = \sup\{\Re z : z \in \operatorname{spec} A\}$. The supremum of $s(A_{0,n}(Z,k))$ over $(n,Z,k) \in \mathbb{Z} \times \mathbb{R}^2$ is a number $\lambda_c > 0$ attained precisely at $(m,0,0)$ and $(-m,0,0)$. On a neighborhood of $(0,0)$ the m sector has an algebraically simple eigenvalue $\lambda(Z,k)$, with $\lambda_0 = \lambda(0,0)$ and $\Re\lambda_0 = \lambda_c$. Its $-m$ counterpart is $\overline{\lambda(Z,-k)}$. For some $c_g, c, c_C, c_*, C_* > 0$ and $g = c_g\Delta$,

$$\lambda_c - g \geq c\Delta, \qquad \sup_{z \in \operatorname{spec} A_{0,m}(0,0)\setminus\{\lambda_0\}} \Re z \leq g, \qquad \sup_{\substack{n \neq \pm m \\ (Z,k)\in\mathbb{R}^2}} s(A_{0,n}(Z,k)) \leq \lambda_c - \delta_{\mathrm{ang}},$$

where $\delta_{\mathrm{ang}} \geq c_C\Delta d_m^2 > 0$. Here d_m is the selected width in Theorem 1.30.1. On that neighborhood,

$$c_*(Z^2 + k^2) \leq \lambda_c - \Re\lambda(Z,k) \leq C_*(Z^2 + k^2).$$

Let $r_0 > 0$ be the center radius of the spectral layer at $Z = 0$. There exist $0 < c_A \leq C_A$ and $C_q > 0$ with the following properties. The physical complex derivatives, evaluated at the pole, obey

$$\begin{gathered}
\lambda_Z = \lambda_k = \lambda_{Zk} = 0, \qquad a_m = m/r_0, \\
-C_A\Delta \leq a_m^2 \Re\lambda_{kk}/h^2 \leq -c_A\Delta, \quad |a_m^2\lambda_{kk}/h^2| \leq C_A\Delta, \\
q_G = a_m^2 C_q/\Delta > 0, \qquad \frac{\lambda_{kk}}{h^2}q_G^2 + \left(\frac{1}{h} - 1\right)q_G - \lambda_{ZZ} = 0, \\
b_d = \frac{1}{2h} - \frac{1}{2}, \qquad X_G = -\frac{\Re\lambda_{kk}}{2h^2}q_G > b_d, \qquad X_G - \frac{b_d}{2} - \sqrt{X_G^2 - b_d X_G} \leq \frac{1}{16}.
\end{gathered} \tag{1.2.8}$$

The Riccati identity in (1.2.8) is an equality in $\mathbb{C}$. The conjugate label has the conjugate data.

The true physical resolvent, pressure and adjoint have the contour and weighted profile bounds of Proposition 1.28.8 and Corollary 1.28.9. In particular, on a fixed pole chart, right and adjoint eigenvectors can be normalized by $\langle e, e^\sharp\rangle = 1$ so that

$$\|\partial_Z^l\partial_k^j e\|_{H^6_{7-j}} + \|\partial_Z^l\partial_k^j e^\sharp\|_{H^6_{7-j}} \leq C \qquad (0 \leq j \leq 5,\ 0 \leq l \leq 17).$$

Here H^s_w consists of the distributions with finite norm $\sum_{|\alpha|\leq s}\|\langle y\rangle^w\partial_y^\alpha f\|_2$, and $\langle e, e^\sharp\rangle$ is the $L^2(\mathbb{R}^2;\mathbb{C}^3)$ pairing. For parameter derivatives on a fixed space, extend $A_{0,n}$ by zero on $(I - P_k)\mathsf{H}_n$. On a compact phase rectangle about the origin there are positively oriented contours, uniform on that rectangle, isolating the selected eigenvalue and the complementary spectrum as in Definition 1.28.7. For z on those contours the resolvent and its adjoint satisfy

$$\|\partial_Z^l\partial_k^j(z - A_{0,\pm m})^{-1}\|_{H^s_{w+j}\cap\mathsf{H}_{\pm m}\to H^s_w\cap\mathsf{H}_{\pm m}} \leq C \quad (l \leq 17,\ \lceil w\rceil + j \leq m - 1)$$

for every fixed integer $s \ge 0$, real $w \ge 0$ and integers $j, l \ge 0$ in the displayed ranges; the constant may depend on s, w, j, l and the rectangle. At the last available horizontal weight the derivatives are taken strongly on each datum and the displayed norm bounds the resulting operator (Proposition 1.28.8). Integration of $(2\pi i)^{-1}(z-A)^{-1}\,\mathrm{d}z$ around the simple eigenvalue defines its Riesz projection. That projection and the resolvent on its complementary invariant subspace obey the same bounds. The physical Leray multiplier on each selected angular sector also obeys $\|\partial_k^j P_k f\|_{H^s_w} \le C\|f\|_{H^s_{w+j}}$ for $\lceil w\rceil + j \le m-1$, by Corollary 1.28.5(a).

(vi) *Uniform frozen data for later evolution.* There are $\nu_0 > 0$, $N_{\mathrm{far}} > \max(m, 2)$, $g_{\mathrm{far}} < g_1 < \lambda_c$, $C_F, M_{\mathrm{far}} < \infty$, and compactly phase-supported shifts $S_{\nu,\pm m} = d_0\chi_\pm P_{\nu,\pm m}$, zero on the other angular sectors. Here $d_0 > 0$; $0 \le \chi_\pm \le 1$ are smooth compactly supported functions on the simple-eigenvalue charts, equal to one near $(0,0)$ and satisfying $\chi_-(Z,k) = \chi_+(Z,-k)$. Their supports are compactly contained in one open rectangle U about the pole, symmetric in k, whose closure lies in the weighted contour rectangle of (v). On $\overline{U}$ the real Hessian of $\Re\lambda$ is negative definite and $|\ell_0 P_{0,m}(Z,k)e_0 - 1| \le 1/2$, where $P_{0,m}(0,0) = e_0\ell_0$ and $\ell_0 e_0 = 1$. On each support $P_{\nu,\pm m}$ is the Riesz projection onto the continuation of that simple eigenvalue at viscosity ν. The following norms are operator norms on $X_{n,k}$:

$$\begin{aligned} \|e^{\tau(A_{\nu,n}(Z,k)-S_{\nu,n}(Z,k))}\| &\le C_F e^{g_1\tau} \quad (|n| < N_{\mathrm{far}},\ \tau \ge 0), \\ \|(z - A_{\nu,n}(Z,k))^{-1}\| &\le M_{\mathrm{far}} \qquad (|n| \ge N_{\mathrm{far}},\ \Re z \ge g_{\mathrm{far}}), \end{aligned} \tag{1.2.9}$$

uniformly in $(Z,k) \in \mathbb{R}^2$ and $0 \le \nu \le \nu_0$. Extend the shifts by zero on $(I - P_k)\mathsf{H}_n$, so $S_{\nu,n} = P_k S_{\nu,n} P_k$. On the common space H_n they have uniformly bounded norms, are strongly Borel measurable in (ν, Z, k), are norm continuous at $\nu = 0$, and satisfy $\sup_{Z,k}\|S_{\nu,n} - S_{0,n}\| \to 0$ as $\nu \downarrow 0$. There are also $0 < d_* \le 1$ and a smooth function $\delta(R) \in [d_*, 1]$, equal to one near the axis and outside an annulus, and $\gamma < g_1$ such that

$$\sup_{R,Z}\left\{\frac{|2\Omega - \delta(2\Omega + R\Omega_R)|}{2\sqrt{\delta}} + \frac{|W_R|}{2}\right\} < \gamma.$$

These are the all-phase frozen estimates; the subsequent leading and completed evolution estimates use this same source.

(vii) *Independent leading evolution and its Gram metric.* For $t > 0$, put $s = -t^{-h}/h$, $\rho = t^h$, $y = x_h/\sqrt{t}$, $Z = z/t^{1/2-h}$ and let P_ρ be the orthogonal projection onto $X_\rho = \{v \in L^2(\mathbb{R}^2_y \times \mathbb{R}_Z; \mathbb{C}^3) : \mathrm{div}_y\, v_h + \rho\partial_Z v_3 = 0\}$. The unshifted operator $U_{\mathrm{lead}}(s,\sigma) : X_{\rho(\sigma)} \to X_{\rho(s)}$ maps the initial value of v at σ to its value at s, where $w(x,t) = t^{-1/2-h}v(y,Z,s)$ solves

$$\partial_t w - \Delta w + \mathbb{P}\big[(B^0_+ \cdot \nabla)w + (w \cdot \nabla)B^0_+\big] = 0, \qquad \mathrm{div}\, w = 0.$$

$\mathbb{P}$ is the orthogonal projection onto divergence-free fields in physical $L^2(\mathbb{R}^3; \mathbb{C}^3)$. To define the shifted evolution $U^\sharp_{\mathrm{lead}}$, subtract $P_\rho T^*_\rho S_{\rho,n} T_\rho P_\rho v$ from the right-hand side of the equation for $\partial_s v$ in sector n. Here $S_{\rho,n}$ acts by multiplication in (Z,k), and the axial Gaussian transform with phase measure $\mathrm{d}Z\,\mathrm{d}k/(2\pi\rho)$ is

$$(T_\rho v)(y,Z,k) = (\pi\rho)^{-1/4}\int_{\mathbb{R}} e^{-(z'-Z)^2/(2\rho) - ik(z'-Z)/\rho} v(y,z')\,\mathrm{d}z'.$$

There are $g_2 < \lambda_c$, $C, T_0 < \infty$ such that

$$\|U^\sharp_{\mathrm{lead}}(s,\sigma)\|_{2\to 2} \le Ce^{g_2(s-\sigma)} \qquad (\sigma \le s \le -T_0). \tag{1.2.10}$$

For every $\epsilon > 0$ there are $C_\epsilon, T_\epsilon < \infty$ with

$$\|U_{\mathrm{lead}}(s,\sigma)\|_{2\to 2} \le C_\epsilon e^{(\lambda_c+\epsilon)(s-\sigma)} \qquad (\sigma \le s \le -T_\epsilon).$$

Both estimates are uniform over all angular sectors and all ancient initial times.

The leading field also supplies the fixed finite-time Gram constants used in the completion estimates. Fix a family of box half-lengths $L_{\mathrm{box}}(Q) \ge 0$ with $L_{\mathrm{box}}(Q) + L_G = o(\log(1/Q^h))$ as $Q \downarrow 0$, where L_G is the fixed horizon below. The starting times satisfy $|\theta| \le L_{\mathrm{box}}(Q)$, and the coefficients are taken on the whole interval $[\theta, \theta + L_G]$. For Q sufficiently small put $t = Q + Q^{1+h}\theta$, $y = x/\sqrt{Q} \in \mathbb{R}^3$, $\rho = Q^h$, $B_0(y,\theta) = Q^{1/2+h} B_+^0(\sqrt{Q}y, Q + Q^{1+h}\theta)$, $P = \mathbb{P}$, $Q_\perp = I - P$ and $(G_0)_{ij} = \partial_{y_j}(B_0)_i$. One may fix a smooth physical approximation S_{app} of the two-band shift, of the form $P\,\mathrm{Op}_{\mathrm{AW}}(S_{\mathrm{sm}})P$, where $\mathrm{Op}_{\mathrm{AW}}(S_{\mathrm{sm}})$ is the Gaussian analysis, multiplication by S_{sm} and synthesis just defined, transferred to the box coordinates. The smooth finite-rank radial symbol S_{sm} has compact phase support and is chosen as in (1.36.2)–(1.36.3), with $\|S_{\mathrm{app}}\|_{H^{-j}\to H^j} \le C_j$ at each required finite order. For the whole-space extension

$$A_{\mathrm{ext}} = -B_0 \cdot \nabla - G_0 + 2Q_\perp G_0 P + (G_0 - G_0^\top)Q_\perp + \rho\Delta - S_{\mathrm{app}},$$

there are a fixed rate $g_G < \lambda_c$, a finite horizon L_G, and a positive self-adjoint operator $M(\theta)$ on $L^2(\mathbb{R}^3;\mathbb{C}^3)$ commuting with P. In terms of the propagator U_{ext} generated by A_{ext} in box time,

$$M(\theta) = I + c\int_0^{L_G} e^{-2g_G r} U_{\mathrm{ext}}(\theta + r, \theta)^* U_{\mathrm{ext}}(\theta + r, \theta)\, \mathrm{d}r \quad (c > 0).$$

It satisfies $I \le M \le C_M I$ and, as a quadratic-form inequality on $H^1(\mathbb{R}^3;\mathbb{C}^3)$ at interior box times,

$$\langle u, (\partial_\theta M + A_{\mathrm{ext}}^* M + M A_{\mathrm{ext}})u\rangle \le 2g_G\langle u, Mu\rangle + C_M\|Q_\perp u\|_2^2 - 2\rho\|\nabla u\|_2^2. \tag{1.2.11}$$

For every bounded real Lipschitz vector field $W : \mathbb{R}^3 \to \mathbb{R}^3$ and every bounded real Lipschitz function $b : \mathbb{R}^3 \to \mathbb{R}$,

$$\|[M, W\cdot\nabla]\|_{2\to 2} \le C_M(\|W\|_\infty + \|\nabla W\|_\infty),$$
$$\|[b, M]\|_{2\to H^1} \le C_M(\|b\|_\infty + \|\nabla b\|_\infty).$$

The constants g_G, L_G, c, C_M are fixed before the box-length family. For each such family they apply at every stated start once Q is below a threshold that may depend on the family. Lemma 1.36.1 also gives the fixed-box form estimate with zero viscosity when its propagator and coefficient hypotheses hold. The same C_M applies to every such W and b. For the unshifted leading equation the same construction, with $S_{\mathrm{app}} = 0$, gives the Gram inequality at any fixed rate $\lambda_c + \epsilon$. The horizon and constants are chosen from the leading propagator and leading jets before the completed clock is estimated.

(viii) *The schedule reserved for completion.* With $T_g = 4 + \sqrt{2}$ (the larger eigenvalue of $\left(\begin{smallmatrix} 3 & 1 \\ 1 & 5 \end{smallmatrix}\right)$), use the common physical gauge in (ii) and fix, for all sufficiently large band indices ℓ,

$$Q_\ell = 2^{-\ell}, \quad \rho_\ell = Q_\ell^h, \quad S_\ell = \ell^{6/5}, \qquad i(\ell) = \left\lfloor \frac{(1+h)\ell\log 2 - (6/5)\log\ell}{\log T_g} \right\rfloor.$$

Then $c_i = T_g^{i(\ell)} Q_\ell^{1+h} \asymp S_\ell^{-1}$, $|i(\ell+1) - i(\ell)| \le C$, and for every fixed $B, N, M, c > 0$,

$$Q_\ell^{-B} S_\ell^N e^{-cS_\ell} = O(Q_\ell^M).$$

1.3 Notation and scope conventions

The similarity chart and the leading profile use the following notation.

Symbol	Definition
x, r, θ, z, t	Physical point, cylindrical coordinates and time measured from blow-up.
$\hat{t}$, q	Compactification scale $\hat{t} - z^2\hat{t}^{2h} = \lvert t\rvert$. In profile formulas $q = \hat{t}$ unless explicitly used for another local quantity or the physical cutoff gauge.
$\hat{\xi}, \hat{\zeta}$	Tip variables $r/\sqrt{\hat{t}}, z/\hat{t}^{1/2-h}$.
$R, Z, \mathcal{Q}$	Normalized physical coordinates and scale in (1.6.10).
h, ω	Scaling parameter h and exponent $\omega = (1-6h)/4$ in (1.6.1).
d, L	The functions $1-\eta^2$, $1-2h\eta^2$.
$u, p, \mathbf{f}$	Physical velocity, pressure and force.
$\widehat{\mathcal{U}}_P, \widehat{\mathcal{P}}_P$	Leading hatted velocity and pressure. The algebraic variables are $F = \widehat{\Lambda}_P$, $H = \hat{\xi}^2 F$, $U = \widehat{\mathcal{U}}_{P,z}$, $V = \hat{\xi}\widehat{\mathcal{U}}_{P,r}$, $P = \widehat{\mathcal{P}}_P$.
$\mathfrak{M}_1, \mathfrak{M}_2, \mathfrak{M}_3, \mathfrak{M}_4$	Histories from the axis, (1.9.1).
$\mathcal{K}, \mathcal{B}, \mathcal{C}$	Core coefficients: $\mathcal{K} = (1-2h)\eta\mathfrak{M}_1 + d\mathfrak{M}_{1\eta}$, $\mathcal{B} = 1 + 2\mathcal{K}/\hat{\xi}^2$, $\mathcal{C} = dU - (\frac{1}{2}-h)\eta$.
$\widehat{\mathcal{T}}_{P,\theta}, \widehat{\mathcal{T}}_{P,z}$	Integrated leading stresses, not the physical force.
$\mathfrak{a}, \mathfrak{b}, \mathfrak{v}, \mathfrak{t}$	Shear quantities (1.12.1).
κ, ε	Core strain and nonlinear swirl amplitude.
$b_c, c, \phi, g_\beta, H_{\mathrm{lin}}$	Scale function, analytic amplitudes and linear core.
g, φ	Analytic pressure-aligned and smooth calibrated angular shapes. We do not assume a Gevrey bound for φ.
$\gamma, c_{\mathrm{a}}, a_{\mathrm{p}}$	Growing exponent $3/5$, activation size and power amplitude $\varepsilon c_{\mathrm{a}}$.
$\frac{\hat{\xi}_{\mathrm{e}}^2}{2}, B, \ell, \mathcal{R}$	Exit, fixed core-removal radius, protected width and remote matching scale.
$\sigma, \mu, N_{\mathrm{sh}}$	Outer amplitude normalization, slow-decay exponent and finite shear-loop frequency.
$\Lambda_{\mathrm{rad}}, \Lambda_\eta$	Axis coefficient majorant parameters.
$\varrho, \mathcal{G}_\varrho$	Axial Gevrey radius and norm (1.11.2).
Q, ρ_Q, S_ℓ	Frozen band scale $2^{-\ell}$, Q^h, and $\ell^{6/5}$. ρ in band calculations means ρ_Q. We hold a band scale fixed under differentiation.
$\mathsf{R}, \mathsf{Z}, \mathsf{T}$	Band coordinates $r/Q^{1/2}, z/Q^{\frac{1}{2}-h}, t/Q$, distinct from R, Z in the theorem.
$g_h, g_f, c_{\mathrm{bank}}, k_f$	Regular and fast heat modes and their positive coefficients. The two modes belong to the leading profile.
$\mathsf{W}, \mathcal{L}_W$	Positive aggregate support weight and $1 + \log(1/\mathsf{W})$. W is not a wave velocity.

Each proof defines its temporary integration variables and coefficients. A constant C_j can depend on a fixed derivative order j. It never asserts a bound uniform over all orders. One Gevrey radius applies to one fixed constructed field and the specified rectangle. We do not assert that it applies to all outer calibrations, all slow coefficient orders, or all values of h.

Weights, coordinates and profile parameters. W is the aggregate weight in product form, Definition 1.23.6 and (1.23.6); $y_a = 2\log(\hat{\xi}/\hat{\xi}_a(\eta))$ and $y_p = 2\log(\hat{\xi}/\hat{\xi}_p(\eta))$ are the activation and pulse-entry variables, with the radial order (1.23.5). In Section 1.20, tags (J1)–(J9) are the inputs of Section 1.20.1, and (I1)–(I6) are the quoted inputs of the activation zone. The endpoint calculus uses the class $\mathcal{S}$ of Definition 1.25.3. e_{end} and Y_{end} are the endpoint pulse amplitude and length (1.15.32); $e_{\mathrm{out}}(\eta)$ denotes only the normalized future energy of Section 1.13. In parts of Section 1.26

(the main edit, the late widths J_d, and Section 1.30.19) d also denotes the late layer width; elsewhere $d = 1 - \eta^2$.

1.4 Backward profile identities and moment corrections

We use the backward profile variables of [42]. The following identities fix the signs, integration constants and cone used in this chapter. In the backward chart write $\xi = \hat{\xi}$, $\eta = \hat{\zeta}$, $d = 1 - \eta^2$, $L = 1 - 2h\eta^2$ and $\partial_\ell = (\xi/2)\partial_\xi$. Put $H = \xi E$, $F = E/\xi$ and $l = \partial_\ell \log H$. The five integrals M, I, J, S, C_p are defined in (1.1.2). The pressure profile in this section is $P = P_{\mathrm{ax}} + C_p$.

Lemma 1.4.1 (Backward transport, stress and matching)**.** *Set $W = 1 - 2((1-2h)\eta M + dM_\eta)/\xi^2$ and $H_c = (\frac{1}{2} - h)\eta + dU$. Define*

$$\begin{aligned} S_q &= -Wl - h(1 - 2\eta U) - H_c(\log E)_\eta, \\ S_n &= -W\partial_\ell U - (\tfrac{1}{2} + h)(1 - 2\eta U)U - H_c U_\eta - dP_\eta + (2 + 4h)\eta P + 2\eta\partial_\ell P. \end{aligned} \tag{1.4.1}$$

The regular solutions of

$$\partial_\ell Q_s + (1 + l)Q_s = S_q, \qquad \partial_\ell N_s + N_s = S_n \tag{1.4.2}$$

are given for $\xi > 0$ by

$$\begin{aligned} Q_s &= -W + \frac{2}{\xi^2 H}\big[(1-h)I - (\tfrac{1}{2} - h)\eta I_\eta - dJ_\eta + (4h-1)\eta J\big], \\ N_s &= -WU + \frac{2}{\xi^2}\big[(\tfrac{1}{2} - h)(M - \eta M_\eta) + 4h\eta S - dS_\eta\big] + (2 + 4h)\eta P - dP_\eta. \end{aligned} \tag{1.4.3}$$

With $a_s = 2 - 2l$, $b_s = \xi U_\xi/E$ the integrated stress is

$$p_s = \frac{\xi^2}{2L}(Q_s, N_s/E), \qquad T_0 = F\big[p_s - (a_s, -b_s)\big]. \tag{1.4.4}$$

If $\mathcal{R}_\theta, \mathcal{R}_z$ denote the reduced tangential momentum residuals (transport plus pressure gradient minus radial viscosity), then

$$\mathcal{R}_\theta = -r^{-2}\partial_r(r^2 q^{-1-h} T_{0,\theta}), \qquad \mathcal{R}_z = -r^{-1}\partial_r(r q^{-1-h} T_{0,z}). \tag{1.4.5}$$

In particular the stress-free regular equations are

$$-L(F_{\xi\xi} + 3F_\xi/\xi) = FS_q, \qquad -L(U_{\xi\xi} + U_\xi/\xi) = S_n, \qquad P_\xi = E^2/\xi. \tag{1.4.6}$$

Suppose two pairs have the same P_{ax}, agree on $\xi \geq \xi_* > 0$ and have identical five histories at ξ_*. Then their stresses, pressures and radial velocities agree for $\xi \geq \xi_*$. On a compact radial interval in $(0, \infty)$ on which both $E \geq e_0 > 0$, write $\|\cdot\|_k$ for the supremum over the rectangle of its angular derivatives through order k. With $\mathbf{m} = (M, I, J, S, C_p)$,

$$\|\Delta(Q_s, N_s, p_s)\|_k \leq C\big(\|\Delta(U, E)\|_{k+1} + \|\Delta\mathbf{m}\|_{k+1}\big). \tag{1.4.7}$$

The constant depends on k, h, e_0, the radial interval, and common bounds at order $k+1$ for the two data and the axis pressure.

Proof. For any weight b, differentiating $q - z^2 q^{2h} = -t$ at fixed physical radius gives

$$\partial_t(q^b f) = \frac{q^{b-1}}{L}[-bf + \partial_\ell f + (\tfrac{1}{2} - h)\eta f_\eta], \qquad \partial_z(q^b f) = \frac{q^{b-1/2+h}}{L}[2b\eta f - 2\eta\partial_\ell f + df_\eta].$$

Insert the radial velocity of (1.1.3) into the material derivatives of $ru_\theta = q^{-h}H$ and $u_z = q^{-1/2-h}U$. The angular transport divided by r and the axial transport plus $\partial_z(q^{-1-2h}P)$ are, respectively, $-q^{-3/2-h}ES_q/L$ and $-q^{-3/2-h}S_n/L$. The radial viscous fluxes have profiles $E_\xi - E/\xi = -Fa_s$ and $U_\xi = Fb_s$. The two radial divergences in (1.4.5) applied to the inviscid flux $q^{-1-h}Fp_s$ give the opposite of these transport terms by (1.4.2). This proves the stress formula, and applying the radial viscous operators to $E = \xi F$ and U gives (1.4.6).

The integrating factors in (1.4.2) are $\xi^2 H$ and ξ^2. The regular primitives are therefore

$$Q_s = \frac{2}{\xi^2 H}\int_0^\xi HS_q\,\rho\,\mathrm{d}\rho, \qquad N_s = \frac{2}{\xi^2}\int_0^\xi S_n\,\rho\,\mathrm{d}\rho.$$

At a regular positive axis $H = \xi^2 F$ with $F(0) > 0$, so a nonzero homogeneous constant is singular. To obtain (1.4.3), differentiate its right sides after multiplication by their integrating factors. Use $\partial_\xi(\xi^2 W)/(2\xi) = 1 - (1-2h)\eta U - dU_\eta$, $J_\xi = \xi UH$, $S_\xi = \xi(U^2 - E^2/2)$ and $P_\xi = E^2/\xi$. The resulting derivatives are $2\xi HS_q$ and $2\xi S_n$, and both primitives vanish at zero. Beyond a matching radius the five integrands agree, so their differences are constant there, including their angular derivatives. Their common values determine P, V and T_0 by the displayed formulas. Finally the only variable denominators in (1.4.3) and (1.4.4) are powers of E times fixed positive factors. The product rule and the identity $1/E_2 - 1/E_1 = -\Delta E/(E_2E_1)$ give (1.4.7). □

Lemma 1.4.2 (The shear cone and its compact test)**.** *For $a_s > 0$ set $t_s = -b_s/a_s$, $v_s = a_s(1 + t_s^2)$, $P_c = p_1 + t_s p_2$ and $J_c = p_2 - t_s p_1$. Define the relaxed cone by*

$$P_c > 2, \qquad v_s < \mathcal{U}(P_c, J_c), \qquad \mathcal{U}(P, J) = P + \frac{J^2}{4} - |J|\sqrt{\frac{P-2}{2} + \frac{J^2}{16}}. \tag{1.4.8}$$

On $v_s > 2$ the cone is called admissible. There it is equivalent to $P_c > v_s$ and $2(P_c - v_s)^2 > (v_s - 2)J_c^2$. If $p_2 = wp_1$, then on any compact set of triples (a_s, b_s, w) satisfying

$$a_s > 0, \qquad a_s - b_s w > 0, \qquad 2b_s w + b_s^2/a_s + (a_s - 2)w^2 < 2, \tag{1.4.9}$$

one threshold on p_1 suffices for the relaxed cone at every point.

Proof. As a polynomial in v, $2(P - v)^2 - (v - 2)J^2$ has smaller root $\mathcal{U}(P, J)$ and larger root at least P. For $P > 2$ its smaller root lies in $(2, P]$, as follows by rationalizing $\mathcal{U} - 2$. This proves the equivalence and gives the relaxed test at $v_s \le 2$. Put $c = 1 - b_s w/a_s$, $j = w + b_s/a_s$. Then $P_c = cp_1$, $J_c = jp_1$ and

$$2c^2 - (v_s - 2)j^2 = (1 + b_s^2/a_s^2)[2 - 2b_s w - b_s^2/a_s - (a_s - 2)w^2].$$

Both c and the displayed quantity have positive minima on the compact set. Dividing the quadratic test by p_1^2 changes its limiting value by $-4cv_s/p_1 + 2v_s^2/p_1^2$, uniformly tending to zero. Increasing p_1 also makes $cp_1 > \max(2, v_s)$ uniformly. □

Lemma 1.4.3 (Power moments and small corrections)**.** *Suppose that on a reserve $U = u(\eta)$ and $E = e(\eta)x^\alpha$, where $x = (\xi/\xi_*)^2$, $e > 0$, and $\alpha \notin \{-1/2, 1/2, 3/2\}$. Two smooth nonnegative nonzero axial bumps and three such swirl bumps, with strictly ordered disjoint radial supports within each group, give an invertible differential for the five histories at the exit. The assertion persists uniformly in any smooth compact parameter family for which these hypotheses hold.*

Proof. With $\rho_* = \xi_*^2/2$, changing variables in (1.1.2) divides (M, I, J, S, C_p) by $(\rho_*, \rho_*^{3/2}, \rho_*^{3/2}, \rho_*, 1)$ to give the unit-scale histories. Subtract uI from J and $2uM$ from S before differentiating. After nonzero row scalings the axial weights are $1, x^{\alpha+1/2}$, and the swirl weights are $x^{1/2}, x^{\alpha}, x^{\alpha-1}$. For distinct exponents s_i, a nonzero sum of m powers x^{s_i} has at most $m-1$ positive zeros. Divide by the least power, differentiate, and apply Rolle's theorem and induction. Hence $\det(x_j^{s_i})$ has constant nonzero sign for $0 < x_1 < \cdots < x_m$. Integrating this determinant against the product of the bumps preserves its strict sign. This proves invertibility of both blocks. Compactness and the cofactor formula bound the inverse and its fixed derivatives. If two exponents in a two-row block differ by $\lambda \downarrow 0$, subtracting the limiting row and dividing by λ gives a $\log x$ row with a strictly larger weighted average on the second support. The resulting inverse loss is $O(\lambda^{-1})$ for fixed separated bumps and exponents in a compact interval.

The full change of the five rows is exactly $Bc + Q(c, c)$, since the integrands have degree at most two. For a prescribed defect b take $\beta = \|B^{-1}\|$, $k_Q = \|Q\|$ in the chosen C^k parameter norm as operators on functions. If $8\beta^2 k_Q \|b\| \le 1$, iteration of $c \mapsto B^{-1}(b - Q(c, c))$ preserves the ball of radius $2\beta\|b\|$ and contracts distances there by at most $1/2$. Its geometric convergence gives the unique small solution. Smallness in C^0 suffices for smooth data: $B + Q(c, \cdot) + Q(\cdot, c)$ has inverse given by its convergent Neumann series after factoring out B. Difference quotients in each parameter therefore converge to the implicit derivative, and successive differentiation gives all higher derivatives. A fixed C^k bound follows by the same iteration at that order whenever its displayed smallness condition holds. □

The flat step and its primitives. For the flat step we use $g(s) = e^{-1/s^2}$ for $s > 0$, $g(s) = 0$ for $s \le 0$, and $\sigma(s) = g(s)/(g(s) + g(1-s))$. The following exact primitive is useful at an edge. For $c > 0$, a fixed real j and a smooth coefficient b on a closed collar,

$$\int_0^s e^{-c/u^2} u^{-j} b(u, \eta)\, \mathrm{d}u = \tfrac{1}{2} e^{-c/s^2} s^{3-j} \int_0^\infty e^{-cv} (1 + s^2 v)^{(j-3)/2} b\big(s(1 + s^2 v)^{-1/2}, \eta\big)\, \mathrm{d}v. \tag{1.4.10}$$

Indeed $v = u^{-2} - s^{-2}$. Every fixed derivative of the last integrand is bounded on the collar by e^{-cv} times a polynomial in v. Its integral is smooth up to $s = 0$, with value $b(0, \eta)/c$ there.

Internal constructions. The backward axis construction is Theorem 1.8.10: the core, frozen reference, first collar and outer join are Lemmas 1.20.33, 1.20.34, 1.20.40 and 1.20.41; continuation and admissibility use Proposition 1.20.38, Theorem 1.20.36 and Lemma 1.20.37. The prefix and pulse coefficients are Lemmas 1.8.17 and 1.8.18, and the backward interior is Proposition 1.8.16. The backward completion starts from these leading data.

1.5 Construction hypotheses and order of parameter choices

1.5.1 Leading profile requirements

The leading construction verifies the admissible cover and the six backward leading-profile properties stated below. Positive-order slow coefficients and the packet iteration are constructed after this leading member is fixed.

Hypothesis 1.5.1 (Admissible cover). The comparison field with the selected axis pressure satisfies (Cov1), and its relation to the physical field is (Cov2) of Hypothesis 1.20.4.

These conditions collect pointwise cone statements of the main text. Theorem 1.20.54 reduces (Cov1) for the forward member to the finite list (R1)–(R7). The quiet-power part (the wait from

$y_p = -W$ to the pulse) and the strict-entry collar are proved there, and (Cov2) is Proposition 1.20.56. The zone conditions (R3)–(R4) between the activation collar and the growth arc are proved in Proposition 1.20.17 and Theorem 1.20.28, for the modified activation of Definition 1.20.22. Proposition 1.20.29 gives a conditional obstruction to a single late termination near a transverse zero of Z_R off the drift root. The quantitative inputs (R5)–(R7) and (I1)–(I6) are traced to their proofs in Theorem 1.20.58, which proves Hypothesis 1.5.1. The clause $p_{1,r} > 0$ at the drift root is Lemma 1.6.45.

The Fourier–Bessel and angular Hardy positive ladder is Corollary 1.28.5, and the weighted profile bootstrap of Section 1.30.12 is Proposition 1.28.8 with Corollary 1.28.9.

Definition 1.5.2 (The profile class $\mathcal{O}^\flat$)**.** Fix $h \in (0, 1/100)$, $\lambda > 0$, $C > 1$ and two radii $0 < \hat\xi_a < \hat\xi_b$ in the chart $\hat\xi = r/\sqrt{\bar t}$ of (1.6.2). For $\hat\xi_a < \hat\xi < \hat\xi_b$, put $d_a = 2\log(\hat\xi/\hat\xi_a)$, $d_b = 2\log(\hat\xi_b/\hat\xi)$ and $\delta = \min\{1, d_a, d_b\}$. A leading profile (E, U, Π) on $[0,\infty) \times [-1,1]$ belongs to $\mathcal{O}^\flat(h, \lambda, C, \hat\xi_a, \hat\xi_b)$ if the following conditions hold.

(O1) *Regularity, residual and stress direction.* Write $F = E/\xi$, $\xi = \hat\xi$, $H = \xi E$ and T_0 as in (1.4.4). The functions $F, U, \Pi, V_0/\xi^2$ are smooth in (ξ^2, η) up to the axis on every bounded rectangle, with one-sided derivatives at its boundaries, and $F > 0$. For $0 \le \xi \le \xi_{\mathrm{an}}$, with some $\xi_{\mathrm{an}} \in (\xi_a, \xi_b)$, these functions and each fixed radial derivative extend holomorphically in η to a common neighborhood of $[-1,1]$. The pressure is $\Pi(\xi,\eta) = -\int_\xi^\infty E^2 \,\mathrm{d}\rho/\rho$, where E is evaluated at (ρ,η). Thus $\Pi_\xi = E^2/\xi$. The reduced tangential residuals are (1.4.5). The stress is zero for $\xi \le \xi_a$ and $\xi \ge \xi_b$ and nonzero for $\xi_a < \xi < \xi_b$. In particular the regular core satisfies (1.4.6). On $[\xi_a, \xi_b] \times [-1,1]$ the quantities $F, a_s, v_s - 2$ have positive lower bounds and $n = T_0/|T_0|$ extends smoothly from the interior. For some $0 < \kappa < 2$ it satisfies

$$n_\theta + t_s n_z \ge \kappa, \qquad (v_s - 2)(n_z - t_s n_\theta)^2 \le (2-\kappa)(n_\theta + t_s n_z)^2. \tag{1.5.1}$$

At ξ_a the direction is parallel to $(a_s, -b_s)$; at ξ_b it equals $(1,0)$ and $b_s = 0$.

(O2) *(edge weight)* there are $s_0 > 0$, $a_a, a_b > 0$, functions $\varphi_a, \varphi_b \in C^\infty([0, s_0])$ with $\varphi_*(0) = 0$ and $\varphi_*' > 0$, and a smooth weight ζ, positive for $\hat\xi_a < \hat\xi < \hat\xi_b$ and zero elsewhere, such that

$$\zeta = g_a(\tfrac{\hat\xi^2}{2}) \exp(-a_a/\varphi_a(d_a)^2) \ (d_a \le s_0), \qquad \zeta = g_b(\tfrac{\hat\xi^2}{2}) \exp(-a_b/\varphi_b(d_b)^2) \ (d_b \le s_0),$$

with g_a, g_b smooth and bounded above and below by positive constants on these collars, $0 \le \zeta \le 1$ (rescale ζ and its comparison constants if necessary), and (1.5.2) holds:

$$|T_0| \ge c\zeta, \qquad |\partial^\alpha T_0| \le C_\alpha \zeta \delta^{-m_\alpha} \qquad \text{for } \hat\xi_a < \hat\xi < \hat\xi_b, \quad |\eta| \le 1; \tag{1.5.2}$$

(O3) *Moments, exterior and reserves.* Set $H_{\mathrm{pow}}(\xi) = \xi c_\infty (\xi/\sqrt{2})^{-1-2h}$ with $c_\infty > 0$ independent of η. For every η the integrals converge and satisfy

$$M(\infty,\eta) = J(\infty,\eta) = S(\infty,\eta) = 0, \qquad \int_0^\infty (H - H_{\mathrm{pow}})\,\xi \,\mathrm{d}\xi = 0. \tag{1.5.3}$$

For some $\xi_v \in (\xi_a, \xi_b)$ one has $U = V_0 = 0$ for $\xi \ge \xi_v$. On $\xi \ge \xi_b$ one has $E = c_\infty(\xi/\sqrt{2})^{-1-2h}\mathcal{H}_-(4d/\xi^2)$, the backward heat solution of Lemma 1.7.1. There are two fixed open intervals in the squared radial coordinate, $\xi_a^2/2 < \inf I_{\mathrm{pos}} < \sup I_{\mathrm{pos}} < \inf I_{\mathrm{mean}} < \sup I_{\mathrm{mean}} < \xi_v^2/2$. On both reserves the final leading profile has

$$U = 0, \qquad E = c_{\mathrm{patch}}(1+\eta^2)^{-1}(\xi/\sqrt{2})^{-1-2\lambda}, \tag{1.5.4}$$

with the same constant $c_{\mathrm{patch}} > 0$.

(O4) *(outer multiplier)* on the outer collar $d_b \le s_0$ one has $U = V_0 = 0$ and

$$E = c_\infty(\hat\xi/\sqrt{2})^{-1-2h}\mathcal{H}(4d/\hat\xi^2)\, m(\tfrac{\hat\xi^2}{2}),$$

where $\mathcal{H} = \mathcal{H}_-$ is given by (1.7.1). The function m is smooth, depends on $\frac{\hat\xi^2}{2}$ only, equals 1 for $\hat\xi \ge \hat\xi_b$, and

$$|(\hat\xi^{-1}\partial_{\hat\xi})^j(1-m)| \le C_j\, e^{-a_b/\varphi_b(d_b)^2}\delta^{-N_j} \qquad \text{for every } j.$$

Remark 1.5.3 (Backward construction). The local history, cone and correction identities are established in Section 1.4. Theorem 1.8.10(i) supplies the analytic rectangle for the backward slow construction.

Remark 1.5.4 (Native-weight requirements). Clauses (O2) and (O4) specify more than smoothness and flatness: Lemma 1.8.1 supplies the derivative and primitive bounds used in Lemma 1.24.4, and (O4) specifies the flat multiplier for the order-one viscosity term at the outer edge. These properties are verified for the selected weight.

Hypothesis 1.5.5 (The backward member is in the class $\mathcal{O}^\flat$). In the backward chart, with $\tau = -t$ and side label $\varsigma = -1$, the backward leading member of the selected family has the following properties.

(B1) *Core.* Let $(E^\natural, U^\natural, \Pi^\natural)$ be the backward member before the strictifying modulation of Section 1.19 and its returns, and put $\hat\xi_{\mathrm{ref}} = \hat\xi_i(CP_*)^5$, $\hat\xi_{\mathrm{match}} = e^{-5/2}\hat\xi_{\mathrm{ref}}$. On $[0, \frac{\hat\xi^2_{\mathrm{match}}}{2}]$ this pre-loop member is the profile of Theorem 1.8.10 (the analogue of [42, Prop. 4.10], proved here) for the datum Π_0 of Lemma 1.8.6, with the parameters chosen in the order of Remark 1.8.12. Put $X = \hat\xi^2/2$, $X_{\mathrm{match}} = \hat\xi^2_{\mathrm{match}}/2$, $X_{\mathrm{ref}} = \hat\xi^2_{\mathrm{ref}}/2$ and $X_{p,b} = \hat\xi^2_{p,b}/2$. At X_{match} all five histories equal those of the reference pair integrated from the axis with datum Π_0. On $[X_{\mathrm{match}}, X_{\mathrm{ref}}]$ the fields are $U = 4\beta$, $E = P_* f(\beta)(X/X_{\mathrm{ref}})^{1/10}$. The pre-loop fields follow the template (S3) of Lemma 1.8.8 on $[X_{\mathrm{match}}, X_{p,b}]$ except for the three-swirl heat compensation supported in $X_{p,b}e^{(-20,-15)}$. The five histories on that interval are integrated through this correction. From $X_{p,b}$ onward the member uses the axial pulse and its returns, flattening and A11, then the added power leg with its rank-one bump, the drive and the spliced heat wing of Lemma 1.8.7 in their prescribed radial positions. The final member agrees with it on $[0, \frac{(\hat\xi^{\mathrm{loop}}_-)^2}{2}]$ for some $\frac{(\hat\xi^{\mathrm{loop}}_-)^2}{2} \in (\frac{\hat\xi^2_a}{2}, \frac{\hat\xi^2_{\mathrm{match}}}{2})$, the inner end of the loop of Proposition 1.8.16, and the analytic collar endpoint is taken in $(\frac{\hat\xi^2_a}{2}, \frac{(\hat\xi^{\mathrm{loop}}_-)^2}{2})$.

(B2) *Strict cone.* Inequality (1.5.1) holds on $[\frac{\hat\xi^2_a}{2}, \frac{\hat\xi^2_b}{2}] \times [-1,1]$ for the $\varsigma = -1$ integrated stresses of the final member, and F, a_s and $v_s - 2$ have positive lower bounds there.

(B3) *Weight.* Clause (O2) holds with $\varphi_a = \mathrm{id}$ and $\varphi_b(s) = (1-e^{-s})/\kappa$, where $\kappa = 1 - e^{-3}$.

(B4) *Moments and exterior.* The moments and heat exterior of (O3) hold, including (1.5.3) with c_∞ independent of β.

(B5) *Reserved patches.* The unchanged patches satisfy (1.5.4) with $I_{\mathrm{pos}} = \frac{\hat\xi^2_{p,b}}{2}e^{(-14,-9)}$ and $I_{\mathrm{mean}} = \frac{\hat\xi^2_{p,b}}{2}e^{(-8,-3)}$, where $\frac{\hat\xi^2_{p,b}}{2} = \frac{\hat\xi^2_{s,b}}{2}e^T\lambda^{-60}$ is the backward pulse entry.

(B6) *Outer multiplier.* Clause (O4) holds on the outer collar, with $m = 1 - \rho\Psi(\frac{\hat\xi^2}{2}/B)$.

Remark 1.5.6 (Backward suppliers). For (B1), apply Theorem 1.8.10(i),(iii) to the datum of Lemma 1.8.6 in the order of Remark 1.8.12. Its outlet collar has the reference fields, its five outlet integrals equal the reference integrals, and both axis pressures are Π_0. Integrating the five densities in (1.1.2) from that outlet therefore gives the reference histories through $X_{p,b}e^{-20}$. The native layout in the proof of Lemma 1.8.8 places only the three-swirl bank between this point and the pulse. On the bank the histories include the partial density changes. At its outlet the full changes in (I, S, C_p) are $(0, -\Delta S_f, -\Delta C_{p,f})$ by (1.14.16), and $U = 0$ keeps M, J fixed there. The first untouched collar of the final member follows from the support of the modulation and its returns in Proposition 1.8.16.

For (B2), the five ranges are supplied by Proposition 1.8.16, Lemma 1.8.19, Lemma 1.8.20, Lemmas 1.8.3 and 1.8.4, and Lemma 1.8.2. Their backward coefficients and parity are Lemmas 1.8.17, 1.8.18 and 1.8.15, under the smallness (1.6.18) and the pulse inputs (P1)–(P2). The angular stress numerator on this side is

$$(\varsigma\tfrac{\hat{\xi}^2}{2} + \mathcal{K})H - \varsigma(1-h)\mathfrak{M}_2 + \varsigma(\tfrac{1}{2}-h)\eta\mathfrak{M}_{2\eta} - d\mathfrak{M}_{3\eta} + 2(h-(\tfrac{1}{2}-h))\eta\mathfrak{M}_3, \qquad \varsigma = -1.$$

Thus the forward cone inequalities do not transfer without these backward coefficient calculations.

For (B3)–(B6), the outer weight and terminal bounds are Lemma 1.8.2, the exterior is Lemma 1.8.7, and the protected patches are Lemma 1.8.8. In the existential selection (B3) choose the specific scalar weight of Section 1.24.3; its two edge germs and comparison with the actual stress are checked there. Their support layout places the loop in $y_p < -W + 1$ and the restoration returns in $-25 < y_p < -20$ (Section 1.20.5).

1.5.2 Order of the parameter choices

The construction uses this order. Each selection uses only constants from previous steps.

1. We fix chart supports, plateau/phase reserves, T_d, T_0, all finite moment-correction profiles, the same wait coefficient 60, and the protected central hold layout. We select λ, then h, then ν_c/h as in (1.6.18).

2. We set $T_f = T_0/\lambda$ and construct the normalized central and outer future profiles with one set of bounds over their compact tiny-memory family. These profiles include all heat, A10/A11, and primitive corrections. We reserve strict ordering and the same exact heat sector.

3. We select the flat-logit interpolation after its finite component bounds. We select Y_0 large to satisfy the central-pressure smallness inequality of Lemma 1.6.19 and the other stated conditions. We solve (1.6.25), the exact geometry (1.6.23), the same coefficient (1.6.21), and the one root (1.6.26). The backward length is $L_b = \lambda Y_{\mathrm{end}}$, not an independently frozen earlier length. We include each specified endpoint compensation one time.

4. We fix the field tolerance τ_b (proof of Lemma 1.6.36). We use uniform C^2 pressure bounds to fix the C^1 approximation scales (ε_p, w, the mollifier; the pressure-bank target must be less than $\tau_b/10$) and the same $G^{3/2}$ majorant of the $p_0(R)$ family. The backward datum Π_0 is now fixed. We select the axial tolerance ε_u (Lemma 1.6.36), then the moment tolerance ε_m, the endpoint offset j_0 with $j_0 \le .05$, $K_{\mathrm{geo}}K_{\mathrm{ax}}j_0 \le \frac{1}{2}j_\sharp$ and $K_{\mathrm{ch}}j_0 \le \varepsilon_u/8$ (proof of Lemma 1.6.14, Section 1.6.4), the backward thresholds δ_* and σ_*, then the small axial gauges, $B_{\mathrm{r}0}$, $\frac{\hat{\xi}_i^2}{2} = B_{\mathrm{r}1}$ and δ_Z (Definition 1.20.22), then the core majorant (condition (D) of paragraph 1.6.4.3, Lemma 1.6.39), which fixes ρ_0 and Λ_{core}; it bounds the data u, s_0, b, χ, ζ, a' chosen before it. Then Λ and T_s above the thresholds of both sides, and the matching geometry and moment-correction bounds with uniform control on this family (Remark 1.8.12). We select C

after these uniform leading-data and first-strain/spectral-feasibility bounds. This selection includes the leading admission threshold $C_{0,\mathrm{lead}}(Y_0)$ and the pressure/core thresholds. For the backward outer join, the C^2 constants are taken over the uniform family $K_{\mathrm{part}}b_2 \le 1$ of Corollary 1.20.39; they are fixed before C, and the late controls are subsequently chosen in that family. We construct the core for that member's $p_0(R)$. At this stage also impose the fixed-$\hat{\xi}$ angular bound of order two on the three-E bank used in Lemma 1.8.15(b), by (1.14.15) with $k = 2$.

5. For this selected C (which includes the thresholds (C) of Theorem 1.20.28), we fix $y_*(C)$ and the axial-termination template $y_1(\eta), \omega_0$ of Definition 1.20.22, common to both members. Then we select $\kappa_{\mathrm{act}}(C)$, then $t_{\mathrm{act}}(C) \le \min\{y_*(C)/8, \kappa_{\mathrm{act}}(C)^2\}$, then the interpolation width $\omega_2(C)$. At each step, we fix the previous controls and use the minimum forward/backward endpoint tolerances for the next control. We fix the higher leading-data jets after these controls. These higher jets can have bounds that depend on C. The first-derivative budgets for the previous selection have one bound for all late widths. We also impose the finite angular budget $b_2 = t_{\mathrm{act}} + \kappa_{\mathrm{act}}(1 + \omega_0^{-1})$ of Corollary 1.20.39, including the stricter upper bounds required by Lemma 1.20.41. Its constants are fixed before the late controls, and the uniform family $K_{\mathrm{part}}b_2 \le 1$ supplies the C^2 bounds used in the preceding choice of C. We do not assert one more increase of C with those controls fixed.

6. With $\Delta = C^{\sigma}$, we select and freeze the capped-loop frequency. This fixes the leading member before the spectral layers, and with it the background jet bound K_S of Hypothesis 1.30.12(e) (Lemma 1.30.13). This K_S may depend on C and N_{sh}, and on no later choice. The pole model supplies the robust curvature interval and C_q. We select the envelope to control its nonvanishing contributions. The early C selection includes the persistent retained-slope margins of (1.26.2).

   We use the stated model maximum and curvature interval. We prove the pre-control true-domain comparison and simple branch before we calculate the physical response rank. We then select the target-dependent cutoff, total-variation allowances, and $J_C, N_0, K_{\mathrm{fin}}$.

   Next, we select one late m and solve its width equation by the intermediate value theorem. We apply the exact physical centering/curvature controls and all five returns. We fix the physical leading fields. Only after this step, we select N_{far} and prove its all-Z and small-viscosity inputs.

7. We prove the full-radial endpoint data and positive saturated pressure hull, together with the curved inner weight and protected solved-cover cutoff of Lemma 1.21.1. We construct the same slow coefficients and independent slow Borel background, then the one physical atlas and its 6/5 factorial estimates. We use one uncut mean initialization and its finite cycles, followed by one joint packet/mean diagonal. The finite demand list includes velocity and pressure jets on the two sides, P1's macro domains, and clock/source tails. It also includes P2's output and graph estimates and physical four-jet prefix estimates. Each later longer prefix estimates this same completed field.

8. We give the physical leading propagation proof from the frozen inputs. Its leading Gram and the selected completion give the completed clock and unshifted propagation estimates. We construct the finite stress and macro. Then we construct the coarse prepared shift and shifted physical inverse, then the finite-kernel/P2 local rows.

   We calculate the macro and b_0 with all their terms. Only after these inputs, we select critical masks and the scalar-blend parameter κ_{crit} (distinct from κ_{act}), then ancient thresholds. Part 3

uses the exact mode and the faster physical inverse to construct the nonlinear continuations on one forward interval for all $a \in [-1, 1]$.

At a regular time in this forward interval, Part 3 bounds the data of all continuations and fixes a common terminal interval. A single time cutoff then prepares the background from rest at a negative initial time and switches off the common force before the terminal endpoint. In step 6 the source-cone allowances of Theorem 1.30.1 ((1.30.8)) are fixed with the cutoff and total-variation allowances, before the late integer m.

All parameters by step. The table records the leading and completion parameters and the later choices that depend on them. A parameter is selected only after every parameter in an earlier row, and within a row in the order listed. Each constraint is an upper or lower bound whose constants come from earlier rows or from earlier entries of the same row.

Step	Parameters (in order)	Main constraints
1	M_d, T_d; chart supports, reserves, T_0, turn length T, mixing band $\eta_c \geq 2\eta_a$, central hold; P_*; $K_{\mathrm{wt}} = C_w/c_w$, q_*, K_{pre}, C_{pre}, K_{geo}, K_{ax}, c_j; λ; h; ν_c	$P_* > e^{T_d}$; (1.6.18) and (λ1)–(λ9); $h < \lambda/6$; $\nu_c < h/10$
2	$T_f = T_0/\lambda$; B_h; L_o; normalized future (s_γ, K_H, K_P)	lower bounds on L_o (Section 1.6.3)
3	χ; K_f; Y_{min}; Y_0; Y_{end}, $L_b = \lambda Y_{\mathrm{end}}$; $\Theta(Y_0)$, $m_\pm$; Π_0	$m_R \leq (\frac{1}{2} - h)/64$ (Lemma 1.6.19); Θ, m_- do not depend on $\frac{\hat{\xi}_i^2}{2}$; Y_{min} includes $\|\delta_{\mathrm{mem}}\|_{C^1} \leq \lambda^{30}$ (Lemma 1.15.19(4), Lemma 1.8.20(P3))
4	τ_b; ε_p, w, mollifier; ε_u; ε_m; j_0; δ_*, σ_*; central offset(s), drift u, s_0, b; B_{r0}, $\frac{\hat{\xi}_i^2}{2} = B_{\mathrm{r1}}$; δ_Z; $r_e, \underline{e}_e, K_-$; core majorant $(\varrho_d, M_{\mathfrak{D}})$, ρ_0, Λ_{core}; Λ; T_s; C, $\Delta = C^\sigma$; $p_0(R)$ and the core	ε_p relative to m_- and τ_b; $w < 4\eta_c$; $K_{\mathrm{geo}}K_{\mathrm{ax}}j_0 \leq \frac{1}{2}j_\sharp$, $K_{\mathrm{ch}}j_0 \leq \varepsilon_u/8$; $\|u - G\|_{C^1} \leq \varepsilon_u/4$; Λ-thresholds (Λ_{core} of Proposition 1.6.42, Lemma 1.20.24, Theorem 1.20.28, Proposition 1.20.53); C-thresholds ($C_{\mathrm{core}}(\Lambda)$ of (1.6.65), Theorem 1.20.28, Lemma 1.6.36, $C_{0,\mathrm{lead}}(Y_0)$, $K_{\mathrm{sc}}(Y_0)/R_{\mathrm{master}}$, Remark 1.20.55)
5	$y_*(C)$; Υ, y_1, $\omega_0 = y_*/4$; κ_{act}; t_{act}; ω_2; higher jets	(late) of Theorem 1.20.28; $K_{\mathrm{part}}b_2 \leq 1$ and the b_2 bounds of Lemma 1.20.41; $t_{\mathrm{act}} \leq \min\{y_*(C)/8, \kappa_{\mathrm{act}}^2\}$; $K_I\omega_2 \leq \frac{1}{4}$ ($\frac{1}{20}$ backward)
6	loop data $d_0, \mu_{\max}, \delta_L, \zeta$ of Lemma 1.19.2, one choice for both sides ((J1)–(J2) of Lemma 1.19.4; (J2) uses the members fixed in step 5); then loop frequency N_{sh}; background jet bound K_S of Hypothesis 1.30.12(e) (Lemma 1.30.13); pole interval, rounding, L_ζ; c_{cut}; $J_C, N_0, K_{\mathrm{fin}}$; m (with d_m by the intermediate value theorem and ℓ_m); N_{far}	$N_{\mathrm{sh}} \geq N_*$; $d\Delta \leq C^{-1}$; $\ell_m \leq (r_0 L_\zeta/\alpha_*)d_m$

7	levels $\Xi_{\mathrm{need}} < \Xi_{\mathrm{cut}} < \Xi$; weight W (its support radius $\frac{\hat\xi_W^2}{2}$ is the maximum of step-4 radii, Proposition 1.23.8(W4)); $\frac{\hat\xi_{\mathrm{all}}^2}{2}$; c_n; $J_{\mathrm{src}} = 80$, $J_{\mathrm{prep}} = 72$; δ_n; R_*, localization $a < b < R_*$, χ_{loc}, $\mathcal{O}$	(1.22.1); $\hat\xi_{\mathrm{all}} > \hat\xi^+_{\mathrm{lead}}, \frac{\hat\xi_W^2}{2}, \frac{\hat\xi_P^2}{2}, B$
8	κ_{crit}, masks, ancient thresholds, common forward interval, regular terminal interval, negative initial time and time cutoff	one nonlinear threshold for $\lvert a\rvert \le 1$ and one cutoff for all continuations

Absolute constants: $\varkappa = 10^{-5}$, $c_1 = \frac{3}{8}$, J_{src}, J_{prep}, and the core norm constants $s = \frac{3}{2}$, $R_0 \in (4.1, 10)$, $Y_{\mathrm{buf}} \in (4, 4.1]$ (paragraph 1.6.4.3). In this order each constraint uses only parameters fixed before the parameter it selects.

Symbols with one meaning in the order. The following renames remove symbols that had two meanings in the parameter order:

- $K_{\mathrm{wt}} := C_w/c_w$ in (1.6.18) and Lemmas 1.8.15, 1.8.19. In the parameter order K_w keeps only its meaning as the outer coefficient $A_w f(\beta) e^{(\lambda-h)L_o}$. In the spectral bulk-form allowance (Lemma 1.30.4 and its proof) K_w is the local C^2 bound of the control templates. The core bound for $|w_Y - Z_R/(2Lb)|$ is K_{wY}.
- The core regularizer constant is σ_*. $\sigma_b(\nu)$ denotes only the prefix energy ratio of the pulse.
- The stop-map templates are $\kappa_{\mathrm{st}}, \delta_{\mathrm{st}}$. $\kappa_0 = \kappa_{\mathrm{act}}$ in the backward member. Other uses of κ_0 (Lemma 1.20.14, the propagation part) are local and do not enter the order.
- The axial-termination templates are Υ, Υ^b. In (1.22.1), Ξ, Ξ_{need} and Ξ_{cut} are levels of the scaled radius ϖ. Elsewhere Ξ has unrelated local meanings ($Q_{\mathrm{lin}}(-W)$ in the central source, a Gaussian vector in the propagation part), and none of them enters the order.
- The central pressure comparison constants are $c_{\mathrm{P}}, C_{\mathrm{P}}$. c_0 is the source floor and $C_0(\cdot)$ a threshold on C.
- B denotes the outer edge of the backward member. $\frac{\hat\xi_b^2}{2} = B_{\mathrm{r0}}$ is the termination radius, except where $\frac{\hat\xi_b^2}{2}$ is the backward chart radius in endpoint-chart comparisons ($\frac{\hat\xi_b^2}{2} = \lambda_{\mathrm{ch}} \frac{\hat\xi_f^2}{2}$; Section 1.6.1, Subsection 1.25.1 and the other endpoint charts), and in Section 1.24.3, where $\frac{\hat\xi_b^2}{2} = B$.
- K_{ax} is the constant of Lemma 1.6.16.

The local core proof permits each fixed

$$0 < h < 10^{-2}, \qquad 0 < \kappa \le 10^{-6}. \tag{1.5.5}$$

It imposes no upper bound on h/κ. The scalar component lemmas in Section 1.13 have their own conditional geometry and smallness choices. Their scalar $\mu \le h/10$ is not a constraint on the variable outer exponent of the selected relative family. Their pressure-root argument also does not select that family.

We do not enlarge the selected matching radius after Δ to remove a radius-independent angular error. We do not enlarge C after we freeze its member-dependent activation controls. The local core and bridge constants can depend on their fixed component data. Later constants can depend on the actual selected source and its higher norms. We do not impose one Gevrey radius on all selected members.

For one fixed member, one positive axial radius must apply to each fixed radial derivative order on the protected rectangle. Section 1.11 treats the scalar component. For the selected variable-scale core, Proposition 1.22.4 gives one positive angular radius for all fixed radial orders. The auxiliary radius used for packet oscillations is a separate parameter.

1.6 Compatible leading profiles on the two sides of zero

Main result. We construct one family of compatible leading fields on the two sides of zero. The family has strict stress margins, a regular axis, and a reserved central interval. It includes the canonical pressure and five radial primitives. We select the outer continuation first. Its complete integrals give the targets for the pulse and core corrections.

Section 1.26 modifies the reserved interval and the specified moment correction regions. We then fix the leading member.

1.6.1 Coordinates, radial primitives and stress

We write $x = (x_1, x_2, z)$, $r = (x_1^2 + x_2^2)^{1/2}$, and θ for the cylindrical angle. We take cylindrical vector components in the moving frame (e_r, e_θ, e_z). Their angular mean

$$\langle v\rangle_\theta(r,z) = \frac{1}{2\pi}\int_0^{2\pi} v(r,\theta,z)\,\mathrm{d}\theta$$

is a componentwise mean, not an average of Cartesian vectors. The forward and backward descriptions use the same physical cylindrical coordinates (r, z). Each description has its own similarity chart. We fix

$$0 < h < 10^{-2}, \qquad \omega = \frac{1-6h}{4}, \tag{1.6.1}$$

with the selection of h after λ as specified below, and we put $d = 1 - \hat\zeta^2$. Constants can depend on this fixed h. We do not assert uniform estimates when $h \downarrow 0$. The two charts are

$$t = \pm\hat t(1-\hat\zeta^2), \qquad z = \hat\zeta\hat t^{1/2-h}, \qquad \hat\xi = \frac{r}{\hat t^{1/2}}. \tag{1.6.2}$$

Here $\hat t \asymp |t| + |z|^{2/(1-2h)}$. The minus sign gives the backward chart on $t \le 0$. The plus sign gives the forward chart on $t \ge 0$. We call these two charts the *tip charts*. When we compare them, we write $(\hat t_b, \hat\xi_b, \hat\zeta_b)$ for the backward chart and $(\hat t_f, \hat\xi_f, \hat\zeta_f)$ for the forward chart. In some later formulas $\hat\xi_b$ is the name of a bridge or bump radius. The text gives this meaning at each such use.

The two tip charts are different on the two sides of $t = 0$. Subsection 1.6.2 gives one chart, the *slice chart*, on the two sides of $t = 0$ for $z \ne 0$. In this chart, smooth joining across $t = 0$ is equality of one-sided jets at $\widetilde\eta = 0$ (Lemma 1.6.6).

Tip coordinates and profile conventions. On each time side use its own concentration scale $\hat t$, radius $\hat\xi$, and axial coordinate $\hat\zeta$:

$$\hat t - z^2\hat t^{2h} = \sigma t, \qquad \hat\xi = \frac{r}{\hat t^{1/2}}, \qquad \hat\zeta = \frac{z}{\hat t^{1/2-h}}, \qquad t = \sigma\hat t(1-\hat\zeta^2).$$

Here $\sigma = -1$ on the backward side and $\sigma = +1$ on the forward side. We choose the root $\hat{t} > |z|^{2/(1-2h)}$ for $t \neq 0$. We use $q = \hat{t}$, $\eta = \hat{\zeta}$, and the radius $\hat{\xi}$ as calculation variables, with side subscripts when both charts occur. The native profiles $\widehat{\mathcal{U}}_P$, $\widehat{\mathcal{P}}_P$, and $\mathfrak{M}$ take $\hat{\xi}$ as their radial argument. For a scalar function g of the radial polynomial argument, its value at radius $\hat{\xi}$ is $g(\hat{\xi}^2/2, \eta)$. With arguments suppressed, g denotes this function of $\hat{\xi}$, and $g_{\hat{\xi}}$ is its radial derivative. The radial measure is $\hat{\xi}\,\mathrm{d}\hat{\xi}$. The corresponding logarithmic radial operator is $\frac{1}{2}\hat{\xi}\partial_{\hat{\xi}}$. Angular derivatives of the profiles below are taken at fixed $\hat{\xi}$.

Leading fields and radial histories. The primary velocity and pressure profiles are $\widehat{\mathcal{U}}_P$ and $\widehat{\mathcal{P}}_P$. Writing $E = (\widehat{\mathcal{U}}_P)_\theta$, $U = (\widehat{\mathcal{U}}_P)_z$, $P = \widehat{\mathcal{P}}_P$, and $V = \hat{\xi}(\widehat{\mathcal{U}}_P)_r$, the physical fields are

$$u_r^{\mathrm{lead}} = q^{-1/2}(\widehat{\mathcal{U}}_P)_r = V/r, \qquad (u_\theta^{\mathrm{lead}}, u_z^{\mathrm{lead}}) = q^{-1/2-h}(E, U), \qquad p^{\mathrm{lead}} = q^{-1-2h}P.$$

We use $H = \hat{\xi}E$ and $F = E/\hat{\xi} = H/\hat{\xi}^2$. Quotients at the axis are understood by regular extension. The five radial histories, with zero constants at the axis, are

$$\mathfrak{M}[\widehat{\mathcal{U}}_P](\hat{\xi}, \hat{\zeta}) = \int_0^{\hat{\xi}} \begin{pmatrix} \rho\widehat{\mathcal{U}}_{P,z} \\ \rho^2\widehat{\mathcal{U}}_{P,\theta} \\ \rho^2\widehat{\mathcal{U}}_{P,z}\widehat{\mathcal{U}}_{P,\theta} \\ \rho(\widehat{\mathcal{U}}_{P,z}^2 - \frac{1}{2}\widehat{\mathcal{U}}_{P,\theta}^2) \\ \widehat{\mathcal{U}}_{P,\theta}^2/\rho \end{pmatrix} (\rho, \hat{\zeta})\,\mathrm{d}\rho = (M, I, J, S, C_p)^{\mathsf{T}}.$$

Their derivatives with respect to $\hat{\xi}$ are $(\hat{\xi}U, \hat{\xi}^2E, \hat{\xi}^2UE, \hat{\xi}(U^2 - \frac{1}{2}E^2), E^2/\hat{\xi})$. The axis pressure Π is separate: $P = \Pi + C_p$. Incompressibility gives

$$V = \frac{\eta\hat{\xi}^2U - (1-2h)\eta M - dM_\eta}{L}, \qquad d = 1 - \eta^2, \qquad L = 1 - 2h\eta^2.$$

Rotation, shear, and stress. The normalized angular velocity is $\widehat{\Lambda}_P = F$, so $u_\theta^{\mathrm{lead}}/r = q^{-1-h}\widehat{\Lambda}_P$. The normalized shear has tangential components

$$\widehat{\mathcal{S}}_P = (\hat{\xi}\partial_{\hat{\xi}}\widehat{\Lambda}_P, \partial_{\hat{\xi}}U) = F(-a_s, b_s), \qquad a_s = -\hat{\xi}F_{\hat{\xi}}/F, \qquad b_s = \hat{\xi}U_{\hat{\xi}}/E,$$

where the divided formulas are used where $F > 0$. The normalized stress $\widehat{\mathcal{T}}_P = (\widehat{\mathcal{T}}_{P,\theta}, \widehat{\mathcal{T}}_{P,z})$ splits into transport (including the pressure contribution) and radial viscosity: $\widehat{\mathcal{T}}_P = \widehat{\mathcal{T}}_P^{\mathrm{tr}} + \widehat{\mathcal{S}}_P$. Its physical stress is $q^{-1-h}\widehat{\mathcal{T}}_P$; it is not itself the momentum residual. The normalized reduced tangential residual is

$$-((\partial_{\hat{\xi}} + 2/\hat{\xi})\widehat{\mathcal{T}}_{P,\theta},\ (\partial_{\hat{\xi}} + 1/\hat{\xi})\widehat{\mathcal{T}}_{P,z}),$$

with physical prefactor $q^{-3/2-h}$. In particular the backward transport formula is not the forward one: for the pullback of an auxiliary scalar function $g(\hat{\xi}^2/2, \eta)$,

$$\partial_t(q^\gamma g) = -\sigma q^{\gamma-1}\mathsf{T}_\gamma g, \qquad \partial_z(q^\gamma g) = q^{\gamma-1/2+h}\mathsf{Z}_\gamma g,$$
$$\mathsf{T}_\gamma g = L^{-1}(-\gamma g + (\tfrac{1}{2} - h)\eta g_\eta + \tfrac{1}{2}\hat{\xi}g_{\hat{\xi}}), \qquad \mathsf{Z}_\gamma g = L^{-1}(2\gamma\eta g + dg_\eta - \eta\hat{\xi}g_{\hat{\xi}}).$$

Only the explicit time sign changes; spatial operators and physical viscosity do not.

Joining coordinates. For $z \neq 0$, the common slice variables are

$$\widetilde{Q} = |z|^{2/(1-2h)} = q|\eta|^{2/(1-2h)}, \qquad \widetilde{\xi} = \frac{r}{\sqrt{\widetilde{Q}}}, \qquad \widetilde{\eta} = \frac{t}{\widetilde{Q}} = \sigma(1-\eta^2)|\eta|^{-2/(1-2h)}.$$

Thus $\eta = \pm 1$ in a tip chart corresponds to $\widetilde{\eta} = 0$ in the slice chart. On the extended endpoint overlap, $q_b = q_f/\lambda_{\mathrm{ch}}$, $\hat{\xi}_b = \lambda_{\mathrm{ch}}^{1/2}\hat{\xi}_f$, and $\eta_b = \lambda_{\mathrm{ch}}^{1/2-h}\eta_f$, where $\lambda_{\mathrm{ch}} = (\eta_b/\eta_f)^{2/(1-2h)}$. For a quantity $q^{-w}g$, the profile in slice coordinates is $\widetilde{g} = |\eta|^{2w/(1-2h)}g$; we match the two one-sided jets of this profile, not the native tip-chart derivatives. The separate physical cutoff gauge is $\widetilde{q} = q_b$ backward and $\widetilde{q} = q_f/L_{\mathrm{cut}}$ forward, with $L_{\mathrm{cut}} = \lambda_{\mathrm{ch}}$ on the endpoint collars.

The symbols E and U denote the swirl and axial velocity profiles. We set $H = \hat{\xi}E$ and $F = H/\hat{\xi}^2$. We use five radial primitives, which we call *histories*. The axis data fix their integration constants. Those constants do not change at an interface:

$$\begin{aligned} M_{\hat{\xi}} &= \hat{\xi}U, \quad I_{\hat{\xi}} = \hat{\xi}^2E, \quad J_{\hat{\xi}} = \hat{\xi}^2UE, \\ S_{\hat{\xi}} &= \hat{\xi}(U^2 - \tfrac{1}{2}E^2), \quad (C_p)_{\hat{\xi}} = E^2/\hat{\xi}, \quad P = \Pi + C_p. \end{aligned} \tag{1.6.3}$$

The canonical pressure datum is $\Pi = -\int_0^\infty E(\rho^2/2,\eta)^2\,\mathrm{d}\rho/\rho$. Each profile g has a *weight* w (Definition 1.6.4). With this weight, $\hat{t}^{-w}g(\hat{\xi}^2/2,\hat{\zeta})$ is the same function of (r,z,t) in the two tip charts. The weights of the leading profiles and histories are

g	E	U	H	M	I	J	S	C_p	P
w	$\frac{1}{2}+h$	$\frac{1}{2}+h$	h	$h-\frac{1}{2}$	$h-1$	$2h-\frac{1}{2}$	$2h$	$1+2h$	$1+2h$

(1.6.4)

The weight of the radial primitive $\int_0^{\hat{\xi}} \rho g(\rho^2/2,\hat{\zeta})\,\mathrm{d}\rho$ is $w-1$, because $\hat{t}\hat{\xi}\,\mathrm{d}\hat{\xi} = r\,\mathrm{d}r$ does not depend on the chart.

This rule and (1.6.3) give the table. The rule applies to the constants of integration as well as to the derivatives, because the axis data fix the constants. In particular one regular heat coefficient c in $H \sim c(\hat{\xi}^2/2)^{-h}$ is the same in the two charts, because $\hat{t}^{-h}(\hat{\xi}^2/2)^{-h} = (r^2/2)^{-h}$.

The forward chart. For $t > 0$, $\hat{t} = \hat{t}(z,t)$ in (1.6.2) is the unique positive solution of

$$\hat{t} - z^2\hat{t}^{2h} = t, \qquad \hat{\xi} = \frac{r}{\hat{t}^{1/2}}, \qquad \hat{\zeta} = z\hat{t}^{-1/2+h}. \tag{1.6.5}$$

With $\hat{t}_0 = |z|^{2/(1-2h)}$, the left side is zero at $\hat{t}_0$ when $z \neq 0$, and its derivative on $[\hat{t}_0,\infty)$ is at least $1-2h > 0$. For $z = 0$, $\hat{t} = t$. Thus $t = \hat{t}(1-\hat{\zeta}^2)$, $|\hat{\zeta}| < 1$. We set

$$d(\hat{\zeta}) = 1 - \hat{\zeta}^2, \qquad L(\hat{\zeta}) = 1 - 2h\hat{\zeta}^2. \tag{1.6.6}$$

In particular $L \geq .98$ on $[-1,1]$. We extend the profiles in $\hat{\zeta}$ to a fixed, slightly larger symmetric compact interval $K_{\hat{\zeta}} = [-1-\epsilon_{\hat{\zeta}}, 1+\epsilon_{\hat{\zeta}}]$ on which $L > 0$. We fix this interval after the core strain κ. Lemma 1.10.1 gives a zero-free complex tube of radius $m_c/4$ about $[0,1]$ for b_c, where $m_c = 3\kappa/((1+\kappa)(2h+3\kappa))$. We take $0 < \epsilon_{\hat{\zeta}} < \min(m_c/16, 1/16)$.

The square map then sends the related tube about $[-1,1]$ into that zero-free tube. We do not specify a pole location.

Direct implicit differentiation gives

$$\begin{aligned} \hat{t}_t &= L^{-1}, & \hat{t}_z &= 2\hat{\zeta}\hat{t}^{1/2+h}/L, \\ \hat{\xi}_t &= -\hat{\xi}/(2\hat{t}L), & \hat{\xi}_z &= -\hat{\zeta}\hat{\xi}\hat{t}^{-1/2+h}/L, \\ \hat{\zeta}_t &= -(\tfrac{1}{2}-h)\hat{\zeta}/(\hat{t}L), & \hat{\zeta}_z &= d\hat{t}^{-1/2+h}/L. \end{aligned} \tag{1.6.7}$$

The determinant of $(\hat t,\hat\zeta)\mapsto(z,t)=(\hat\zeta\hat t^{1/2-h},dq)$ is $-Lq^{1/2-h}$. Thus the endpoint analysis does not divide by d. The endpoints $\hat\zeta=\pm1$ describe the initial half-space boundary, not the physical angular variable θ.

For given profiles H,U, we define

$$\mathfrak{M}_1[\widehat{\mathcal{U}}_P](\hat\xi,\hat\zeta)=\int_0^{\hat\xi}\rho U(\rho^2/2,\hat\zeta)\,\mathrm{d}\rho,\qquad V=\frac{\hat\zeta\hat\xi^2U-(1-2h)\hat\zeta\mathfrak{M}_1-d\mathfrak{M}_{1\hat\zeta}}{L}.\tag{1.6.8}$$

Their leading physical velocity is

$$u_\theta^{\mathrm{lead}}=\hat t^{-1/2-h}\widehat{\mathcal{U}}_{P,\theta},\qquad u_z^{\mathrm{lead}}=\hat t^{-1/2-h}\widehat{\mathcal{U}}_{P,z},\qquad u_r^{\mathrm{lead}}=\hat t^{-1/2}\widehat{\mathcal{U}}_{P,r}=\frac{V}{r}.\tag{1.6.9}$$

The values at $r=0$ are understood through the regular Cartesian extension established in Section 1.9. This field is divergence-free. It is an input to the construction. It solves the leading equations. The stress remains to be corrected. For normalized variables $R\ge0$, $Z\in\mathbb{R}$, we define

$$\mathcal{Q}-Z^2\mathcal{Q}^{2h}=1,\qquad\hat\zeta=Z\mathcal{Q}^{-1/2+h},\qquad\hat\xi=\frac{R}{\sqrt{\mathcal{Q}}}.\tag{1.6.10}$$

For the selected, fixed leading profiles, we put

$$\mathcal{H}(R,Z)=\mathcal{Q}^{-1/2-h}\frac{H(\hat\xi^2/2,\hat\zeta)}{\hat\xi},\quad\mathcal{U}(R,Z)=\mathcal{Q}^{-1/2-h}U(\hat\xi^2/2,\hat\zeta),\quad\mathcal{V}(R,Z)=\mathcal{Q}^{-1/2}\frac{V(\hat\xi^2/2,\hat\zeta)}{\hat\xi}.\tag{1.6.11}$$

The *leading data* consist of the physical fields, axis pressure, and these five histories. A *moment correction* changes the profiles on a compact support to match specified radial integrals. We give its support and targets at each application. A radial *future* is the continuation beyond a specified outlet. Its complete energy and pressure integrals include all later corrections and the heat tail. They differ from partial histories inside a correction region.

In the Navier–Stokes equation, f denotes the external force. The quantities Q_s,N_s, and S_q occur in the stress equations defined below. The term *source data* denotes the leading data when they enter those equations. The *completion* adds slow terms, the tangential mean, principal and higher waves, curl corrections, and the summation remainder. It also applies the spatial localization and its divergence correction. This use of completion does not refer to a normed space.

Stress and cone conventions. We define the stress variables by $\ell_r=\frac12\hat\xi\partial_{\hat\xi}\log H$, $a_s=2(1-\ell_r)$, $b_s=\hat\xi\partial_{\hat\xi}U/E$, $p_1=\hat\xi^2Q_s/[2(1-2h\hat\zeta^2)]$, $w=N_s/(EQ_s)$ and $p_s=(p_1,p_1w)$. For $a_s>0$, we set $t_s=-b_s/a_s$, $v_s=a_s+b_s^2/a_s$, $P_c=p_1+t_sp_1w$ and $J_c=p_1w-t_sp_1$. For $v_s>2$, the exact relaxed/admissible cone criterion is $P_c>\max(2,v_s)$ and $2(P_c-v_s)^2>(v_s-2)J_c^2$. For $v_s\le2$, we use its relaxed branch.

In particular $b_s=0$, $0<a_s\le2$ and $p_1>2$ give the strict relaxed cone for all w. For bounded w, the large-p_1 sufficient tests used below are

$$a_s-b_sw>0,\qquad2b_sw+b_s^2/a_s+(a_s-2)w^2<2.$$

We apply them with strict margins before we select the finite radial scale. On a forward main pulse the response estimates (1.16.14) and (1.6.32) control the errors from $(a_s,b_s,w)=(2,-R,2R)$ in their respective charts. At that triple the first expression is $2+2R^2$ and the second is $-7R^2/2$. On the backward main pulse the derivative of its shape contributes to w even at $\beta=0$. Lemmas 1.8.18 and 1.8.20 retain that term and give strict gaps in both tests. On an unedited power wait with $b_s=0$ and $a_s=2+2\nu$ the second test reads $2\nu w^2<2$. We impose the stronger bound $2\nu w^2<1$ below.

1.6.2 The slice chart and smooth joining across $t = 0$

This subsection gives one chart on the two sides of $t = 0$ for $z \neq 0$. In this chart, the comparison of the two sides is a comparison of one-sided jets at one hypersurface. We use it for all two-sided statements in this paper. The slice chart degenerates at $z = 0$. Near $z = 0$ we keep the tip charts (1.6.2).

Definition 1.6.1 (Slice chart)**.** For $z \neq 0$ we put

$$\widetilde{Q} = |z|^{2/(1-2h)}, \qquad \widetilde{\xi} = \frac{r}{\sqrt{\widetilde{Q}}}, \qquad \widetilde{\eta} = \frac{t}{\widetilde{Q}}. \tag{1.6.12}$$

We write $\widetilde{Q}$, not Q, because Q is the dyadic band scale used to index the packet scales. In Cartesian variables $x = (x_1, x_2, z)$, the map $(x, t) \mapsto (x_1, x_2, \widetilde{Q}, \widetilde{\eta})$ is a real-analytic diffeomorphism of $\{z > 0\}$ onto its image. The same holds on $\{z < 0\}$. The inverse is $z = \pm\widetilde{Q}^{1/2-h}$, $t = \widetilde{Q}\widetilde{\eta}$. The map keeps the sign of t: $\widetilde{\eta} < 0$ if and only if $t < 0$. Also $\widetilde{\xi}^2 = r^2/\widetilde{Q}$ is a smooth function of r^2 for each fixed $\widetilde{Q} > 0$.

Lemma 1.6.2 (Conversion from the tip charts)**.** *Let $\sigma = -1$ in the backward chart and $\sigma = +1$ in the forward chart. Then*

$$\widetilde{Q} = \hat{t}|\hat{\zeta}|^{2/(1-2h)}, \qquad \widetilde{\xi} = \hat{\xi}|\hat{\zeta}|^{-1/(1-2h)}, \qquad \widetilde{\eta} = \sigma(1 - \hat{\zeta}^2)|\hat{\zeta}|^{-2/(1-2h)}. \tag{1.6.13}$$

On $0 < |\hat{\zeta}| \le 1$ the map $\hat{\zeta} \mapsto \widetilde{\eta}$ is real-analytic and strictly monotone in $|\hat{\zeta}|$. It maps $0 < |\hat{\zeta}| \le 1$ onto $\{\sigma\widetilde{\eta} \ge 0\}$, with $|\hat{\zeta}| = 1$ to $\widetilde{\eta} = 0$. At $\hat{\zeta} = \pm 1$ its derivative is $d\widetilde{\eta}/d\hat{\zeta} = -2\sigma\hat{\zeta}$. Thus $d|\hat{\zeta}|/d\widetilde{\eta} = \frac{1}{2}$ in the backward chart and $-\frac{1}{2}$ in the forward chart at $\widetilde{\eta} = 0$.

Proof. We substitute (1.6.2) into (1.6.12). This gives $|z|^{2/(1-2h)} = |\hat{\zeta}|^{2/(1-2h)}\hat{t}$, $r/\sqrt{\widetilde{Q}} = \hat{\xi}|\hat{\zeta}|^{-1/(1-2h)}$ and $t/\widetilde{Q} = \sigma\hat{t}(1 - \hat{\zeta}^2)/(\hat{t}|\hat{\zeta}|^{2/(1-2h)})$. For $s = |\hat{\zeta}|$,

$$\frac{d}{ds}\big[(1 - s^2)s^{-2/(1-2h)}\big] = -\frac{2s^{-1-2/(1-2h)}}{1 - 2h}(1 - 2hs^2) < 0 \qquad (0 < s \le 1),$$

because $1 - 2hs^2 \ge 1 - 2h > 0$. At $s = 1$ the factor $1 - s^2$ is zero, so the derivative there is -2. □

Lemma 1.6.3 (Range of the tip charts)**.** *The backward formula in (1.6.13) is also defined for $|\hat{\zeta}| > 1$, and there it gives $t > 0$. On $1 \le |\hat{\zeta}| < (2h)^{-1/2}$ it increases in $|\hat{\zeta}|$ from 0 to*

$$c_h = \Big(\frac{1}{2h} - 1\Big)(2h)^{1/(1-2h)}.$$

Thus the backward chart, extended to $|\hat{\zeta}_b| < (2h)^{-1/2}$, is a real-analytic chart on $\{\widetilde{\eta} < c_h\}$, $z \neq 0$. We write $\hat{\zeta}_b(\widetilde{\eta})$ for its inverse with $\operatorname{sgn}\hat{\zeta}_b = \operatorname{sgn} z$.

In the same way the forward chart is a chart on $\{\widetilde{\eta} > -c_h\}$, and $\hat{\zeta}_f(\widetilde{\eta})$ is its inverse. As $h \to 0$, $c_h \to 1$. For $h = 0.005$ and $h = 0.01$, c_h is about 0.945 and 0.905.

Proof. For $s = |\hat{\zeta}| > 1$ the backward formula is $(s^2 - 1)s^{-2/(1-2h)}$. Its derivative is $2s^{-1-2/(1-2h)}(1 - 2hs^2)/(1 - 2h)$, because $2 - 2/(1 - 2h) = -4h/(1 - 2h)$. This is positive for $s^2 < 1/(2h)$ and zero at $s^2 = 1/(2h)$, where the value is c_h. The forward case is the same with the sign of $\widetilde{\eta}$ changed. □

Definition 1.6.4 (Weight and slice profile)**.** A tip-chart auxiliary scalar function g has *weight* w if the physical quantity is $\hat{t}^{-w} g(\hat{\xi}^2/2, \hat{\zeta})$. Its *slice profile* is

$$\widetilde{g}(\widetilde{\xi}^2/2, \widetilde{\eta}) = |\hat{\zeta}|^{2w/(1-2h)} g(\hat{\xi}^2/2, \hat{\zeta}), \tag{1.6.14}$$

where $(\hat{\xi}, \hat{\zeta})$ and $(\widetilde{\xi}, \widetilde{\eta})$ satisfy (1.6.13). A profile can also depend on $\hat{t}$, on the angle θ and on auxiliary variables. Then the same definition applies, with $\hat{t} = \widetilde{Q}|\hat{\zeta}|^{-2/(1-2h)}$.

The identity $\hat{t}^{-w} g = \widetilde{Q}^{-w} \widetilde{g}$ follows from $\hat{t} = \widetilde{Q}|\hat{\zeta}|^{-2/(1-2h)}$. Thus the slice profile of a physical quantity does not depend on the tip chart. In slice variables the histories (1.6.3) have the same form, with $\widetilde{\xi}$ for $\hat{\xi}$, because $\hat{t}\hat{\xi}\, \mathrm{d}\hat{\xi} = \widetilde{Q}\widetilde{\xi}\, \mathrm{d}\widetilde{\xi}$.

Definition 1.6.5 (Equal slice jets)**.** Let g_b and g_f be a backward and a forward profile of the same weight w. Suppose that $\widetilde{g}_b$ is smooth up to $\widetilde{\eta} = 0$ from $\widetilde{\eta} \le 0$, and $\widetilde{g}_f$ from $\widetilde{\eta} \ge 0$. Here and below, one-sided smoothness means that every mixed derivative on the interior extends continuously to its closed side. We say that g_b and g_f have *equal slice jets* if

$$\partial_{\widetilde{\eta}}^k \widetilde{g}_b(\,\cdot\,, 0) = \partial_{\widetilde{\eta}}^k \widetilde{g}_f(\,\cdot\,, 0) \qquad (k \ge 0) \tag{1.6.15}$$

for each fixed value of the other slice variables. Here each side uses its one-sided derivatives.

By Lemma 1.6.2, one-sided smoothness in $\hat{\zeta}$ up to $\hat{\zeta} = \pm 1$ is the same as one-sided smoothness in $\widetilde{\eta}$ up to $\widetilde{\eta} = 0$.

Lemma 1.6.6 (Gluing across $t = 0$)**.** *Let $V \subset \mathbb{R}^4$ be open, with $V \cap \{z = 0\} = \emptyset$. Put $V_\pm = V \cap \{\pm t \ge 0\}$ and $\Sigma = V \cap \{t = 0\}$. Let $G_\pm \in C^\infty(V_\pm)$ up to the boundary in this sense.*

(a) If $\partial_t^k G_+ = \partial_t^k G_-$ on Σ for all $k \ge 0$, then the function G equal to $G_\pm$ on $V_\pm$ is C^∞ on V.

(b) Let $G_- = \widetilde{Q}^{-w} \widetilde{g}_b$ and $G_+ = \widetilde{Q}^{-w} \widetilde{g}_f$, with one-sided smooth slice profiles. Then G is C^∞ on V if and only if g_b and g_f have equal slice jets.

Proof. (a) Let $F_\pm \in C^\infty(V_\pm)$ satisfy $\partial_t^k F_+ = \partial_t^k F_-$ on Σ for all k. We prove that the joined function F is C^1 and that its first derivatives are joined functions of the same type. Induction on the order then gives $F \in C^\infty(V)$. We apply this to $F_\pm = G_\pm$.

(i) The functions F_+ and F_- agree on Σ. Thus F is continuous.

(ii) Let ∂ be a derivative in a variable of x. For $\epsilon > 0$ the fundamental theorem of calculus at $t = \pm\epsilon$ and the limit $\epsilon \to 0$ show that $\partial F_\pm$ on Σ is the derivative of $F_\pm|_\Sigma$ along Σ. These restrictions are equal, so $\partial F_+ = \partial F_-$ on Σ, and ∂F exists on Σ.

(iii) We take a point of Σ. By the mean value theorem, the difference quotients of F in t converge to $\partial_t F_+$ from above. From below they converge to $\partial_t F_-$. The hypothesis with $k = 1$ makes these limits equal. Thus $\partial_t F$ exists on Σ.

(iv) The pairs $(\partial_t F_+, \partial_t F_-)$ and $(\partial F_+, \partial F_-)$ satisfy the hypothesis again. For the first pair this is the hypothesis with $k + 1$. For the second pair, $\partial_t^k \partial F_\pm = \partial\, \partial_t^k F_\pm$, and step (ii) applied to $\partial_t^k F_\pm$ gives equality on Σ. By step (i) for these pairs, the first derivatives of F are continuous.

(b) At fixed (x_1, x_2, z) the variables $\widetilde{Q}$ and $\widetilde{\xi}$ do not depend on t, and $\widetilde{\eta} = t/\widetilde{Q}$. Thus

$$\partial_t^k G_\pm = \widetilde{Q}^{-w-k}\, \partial_{\widetilde{\eta}}^k \widetilde{g} \qquad (\widetilde{g} = \widetilde{g}_f \text{ or } \widetilde{g}_b).$$

Also $G_\pm \in C^\infty(V_\pm)$, because the slice chart is a diffeomorphism that keeps the sign of t and composition preserves the one-sided derivatives by the chain rule. At $t = 0$ the hypothesis of (a) is thus (1.6.15). Conversely, if G is C^∞, its one-sided t-derivatives agree on Σ, and the same formula gives (1.6.15). □

We apply the lemma to scalar functions of (x,t). A scalar slice profile that is smooth as a function of $(\widetilde{\xi}^2,\widetilde{\eta})$ for $\widetilde{\xi}\ge 0$ gives a smooth function of x, because $\widetilde{\xi}^2$ is a smooth function of r^2. The Cartesian components of the vector fields are scalars of this type by the regular-axis structure of Section 1.9. The lemma does not change that structure. It uses no extension operator and no comparison chart.

Remark 1.6.7 (The chart change). For $0\le\widetilde{\eta}<c_h$, a forward point has forward coordinates and extended backward coordinates (Lemma 1.6.3). The composition of the two conversions (1.6.13) is

$$\hat{t}_b=\hat{t}_f/\lambda_{\mathrm{ch}},\quad \hat{\xi}_b=\lambda_{\mathrm{ch}}^{1/2}\hat{\xi}_f,\quad \hat{\zeta}_b=\lambda_{\mathrm{ch}}^{1/2-h}\hat{\zeta}_f,\qquad \lambda_{\mathrm{ch}}=(\hat{\zeta}_b/\hat{\zeta}_f)^{2/(1-2h)}. \tag{1.6.16}$$

Equality of $\widetilde{\eta}$ gives the chart equation $\hat{\zeta}_f^2\lambda_{\mathrm{ch}}^{1-2h}=1+\lambda_{\mathrm{ch}}(1-\hat{\zeta}_f^2)$. Implicit differentiation gives $\lambda_{\mathrm{ch}}(\pm1)=1$, $\lambda'_{\mathrm{ch}}(\pm1)=\mp4/(1-2h)$ and $\frac12-h-h\lambda_{\mathrm{ch}}(1-\hat{\zeta}_f^2)=\frac12-h\hat{\zeta}_b^2$. For an explicit two-sided backward formula of weight w, we choose its smooth expression in slice variables on both sides of the joining slice. Its forward value is $g_f(\hat{\xi}^2/2,\hat{\zeta})=\lambda_{\mathrm{ch}}^w g_b(\lambda_{\mathrm{ch}}\hat{\xi}^2/2,\lambda_{\mathrm{ch}}^{1/2-h}\hat{\zeta})$ by Lemma 1.6.8(b). The symbol ℓ is the dyadic band index ($Q_\ell=2^{-\ell}$), so we write the chart change as λ_{ch}. We use it only in explicit formulas for forward quantities on the endpoint collars, for example the chart speed (1.15.26).

Lemma 1.6.8 (Design objects as one slice function)**.** *Let g_b be a backward object of weight w. Suppose that $\widetilde{g}_b$ is the restriction to $\widetilde{\eta}\le0$ of a function $\widetilde{g}$ that is C^∞ on $\{|\widetilde{\eta}|<\epsilon\}$, with $0<\epsilon<c_h$. The forward profile $g_f=|\hat{\zeta}|^{-2w/(1-2h)}\widetilde{g}$ near $\hat{\zeta}=\pm1$ is the* slice continuation *associated with the chosen extension $\widetilde{g}$.*

(a) The objects g_b and g_f have equal slice jets, and $\widetilde{Q}^{-w}\widetilde{g}$ is C^∞ across $t=0$ for $z\ne0$.

(b) Suppose that g_b is a formula in $(\hat{t}_b,\hat{\xi}_b,\hat{\zeta}_b)$ that is defined and smooth for $|\hat{\zeta}_b|$ near 1 on the two sides of 1. Choose $\widetilde{g}$ to be this formula expressed in slice variables on the two-sided collar. Then $g_f(\hat{\xi}^2/2,\hat{\zeta})=\lambda_{\mathrm{ch}}^w g_b(\lambda_{\mathrm{ch}}\hat{\xi}^2/2,\lambda_{\mathrm{ch}}^{1/2-h}\hat{\zeta})$ there.

(c) A one-sided smooth forward profile g'_f has equal slice jets with g_b if and only if g'_f-g_f has zero $\hat{\zeta}$-jets at $\hat{\zeta}=\pm1$.

Proof. Part (a) is Lemma 1.6.6(b) for the single function $\widetilde{g}$. For (b), changing coordinates in the chosen extension gives the identity on the open collar by Lemma 1.6.3 and Remark 1.6.7. Any other smooth extension agrees with it to all orders at the joining slice by (a). For (c), the factor $|\hat{\zeta}|^{2w/(1-2h)}$ is smooth and positive, and $\hat{\zeta}_f\mapsto\widetilde{\eta}$ is a diffeomorphism at ±1. □

For the following explicit design objects we use the two-sided formulas in part (b). Examples are the joint gauge (Lemma 1.21.2), the shear phase (1.6.66), the moving radius graphs $\hat{\xi}_s,\hat{\xi}_p,\hat{\xi}_a,\sqrt{2R_o}$ and the bump variable $y=2\log(\hat{\xi}/\hat{\xi}_p(\hat{\zeta}))$. A moving radius graph $\hat{\xi}_*(\hat{\zeta})$ converts like $\hat{\xi}$, so it has weight $-1/2$, and $2\log(\hat{\xi}/\hat{\xi}_*)=2\log(\widetilde{\xi}/\widetilde{\xi}_*)$ has weight 0. A function of the fixed tip radius $\mathfrak{r}=\hat{\xi}$ is not one slice function.

In slice variables $\mathfrak{r}=\widetilde{\xi}\,|\hat{\zeta}|^{1/(1-2h)}$, and the two tip charts give different $\widetilde{\eta}$-derivatives of $|\hat{\zeta}|$ (Lemma 1.6.2). For a bump $b(\mathfrak{r})$ the backward and forward first jets thus differ by $\mathfrak{r}b'(\mathfrak{r})/(1-2h)$. For this reason we take the moving moment bumps to be functions of y.

1.6.3 Outer profiles with one heat tail

Keep R_g fixed while varying the exponent and pulse length in the genuine exponent transition. On the distinct fixed-λ bridge, the paragraph on p. 32 sets the transported growth radius. This gives

the central and outer components one heat tail with the prescribed endpoint graphs. A translation of the full growing profile to a rapidly moving pulse entrance would introduce a negative term in the growing-region stress equation.

1.6.3.1 Fixed geometry and the backward reference

We first fix the angular supports, plateau reserves, and radial bump templates. We fix a smooth nondecreasing step σ_{off} that is zero on $(-\infty, 0]$ and one on $[1, \infty)$. For the parameter $M_d > 0$, the slow turnoff duration is $T_d = e^{M_d} + 10$. In the turnoff coordinate $\zeta \geq 0$, we define

$$k(\zeta) = 1 - \sigma_{\mathrm{off}}\left(\frac{\log(1+\zeta)}{M_d}\right), \qquad e_d = \frac{\|\sigma'_{\mathrm{off}}\|_\infty}{M_d}. \tag{1.6.17}$$

We extend k by one for $\zeta \leq 0$. Flatness of the step gives a smooth extension. Direct differentiation gives $|k'(\zeta)| \leq e_d/(1+\zeta)$. The cutoff is zero for $\zeta \geq e^{M_d} - 1$, so the last eleven units of this stage have $k = 0$.

Thus a sufficiently large M_d makes e_d small before the selection of λ. The bounded phase shifts used below change this derivative bound only by the fixed geometric factor.

We fix also the radial cutoff shape $0 \leq \zeta_g \leq 1$, equal to one on a neighbourhood of 0 and zero on a neighbourhood of $[1, \infty)$. Its width is selected later. Put

$$Z_{g,j} = \|\zeta_g^{(j)}\|_\infty \quad (j = 1, 2), \qquad C_{\mathrm{germ}} = 12e\left(2 + \frac{5}{2}Z_{g,1} + \frac{1}{2}Z_{g,2}\right).$$

These constants depend only on the early radial cutoff shape.

We put $N = 60$ and select the model amplitude $P_* > e^{T_d}$. Thus $T_d > 10$, and P_* is not a small parameter. We select the bridge exponent $\lambda_{\mathrm{br}} > 0$ after these fixed constants. Throughout this construction, we write $\lambda = \lambda_{\mathrm{br}}$ and impose

$$\lambda P_*^2 (T_d + 1)^2 \ll 1, \qquad 60\lambda \log(1/\lambda) \ll 1, \qquad K_{\mathrm{wt}}^2 \lambda (3 + \log(1/\lambda))^2 \leq \tfrac{1}{2}. \tag{1.6.18}$$

Here $K_{\mathrm{wt}} = C_w/c_w$ is formed from the wait constants of Lemma 1.8.17(c), the backward form of [42, (A.27)] (Lemma 1.8.19). It is not the outer coefficient $K_w = A_w f(\beta) e^{(\lambda - h)L_o}$, which depends on L_o. K_{wt} depends only on M_d, T_d, P_* and the turnoff output. It is bounded uniformly for $0 < \lambda \leq \lambda_0$ and for all later choices (h, L_o, Y_0, C). Indeed c_w multiplies the explicit factor λ and is free of h (Lemma 1.8.19), and C_w enters through the pressure on the wait, whose constants are uniform in λ (Lemma 1.8.15(b)). So the third condition is an upper bound on λ (since $\lambda \log^2(1/\lambda) \to 0$). It is stronger than the first condition by the factor $(3 + \log(1/\lambda))^2$. With $P_* > e^{T_d}$ and $T_d > 10$, the first condition gives $\lambda < e^{-20}$, $h < \lambda < e^{-2T_d}$ and $P_* < \lambda^{-1/2}$. We also impose the following upper bounds on λ. All their constants are fixed before λ.

(λ1) $2\lambda(T + 60\log(1/\lambda)) \leq \log 2$, with T the turn length of the prefix template (Lemma 1.20.45).

(λ2) $\lambda(2^{32} e^T K_{\mathrm{pre}} C_{\mathrm{pre}})^2 W_{\mathrm{hi}}^2 \leq \frac{1}{8}$, where W_{hi} is the supremum over $0 < h \leq 10^{-2}$ and $0 \leq \nu \leq \lambda_0$ in Lemma 1.20.45(i).

(λ3) With $W = 60\log(1/\lambda)$, impose

$$\tfrac{1}{4}(e^{2\lambda W} - 1) + \lambda e^{2\lambda W} M_\sigma \leq \tfrac{1}{200}$$

where M_σ is the larger of the variable-prefix supremum in Lemma 1.14.2 and $\sup_{|\beta| \leq 1} |\sigma_b(\beta)|$ for the backward model. The latter finite template integrals in (1.14.11) are uniformly bounded on $|\beta| \leq 1$ ($G = 4\beta$, $f \geq 1/2$), so the left side tends to zero with λ. The complete future contribution is controlled separately by (1.6.30).

($\lambda 4$) $K_{\mathrm{geo}}\lambda \le \frac{1}{2}$, so that $1 + K_{\mathrm{geo}}\lambda + \epsilon_R \le 2$ in Lemma 1.6.14 once $\epsilon_R \le \frac{1}{2}$.

($\lambda 5$) $\lambda \le \lambda_0 \le \frac{1}{20}$ (Lemma 1.15.5, Remark 1.20.55), and $C_{11}\lambda^{28}$ is at most half the radius of the A11 small-data ball, where $C_{11}\lambda^{30(1-\lambda)}$ is the model bound of Lemma 1.15.5; both constants are template constants (Step 6 of the proof of Lemma 1.6.10). At this stage also impose $K_{11}\lambda^{28} \le \lambda/24$, where K_{11} bounds the model contribution in (1.8.6). It uses the same uniform inverse and the fixed C^1 bump norms.

($\lambda 6$) $\lambda \le \lambda_A$, the threshold of Lemma 1.8.17, whose constants depend only on the template, T_d, P_* and C_Π.

($\lambda 7$) $111\, e^{T/10}\lambda^{29.5} \le 1$, with T as in ($\lambda 1$) (Lemma 1.8.4). Fix the drive length $\delta > 0$ with the radial template. In the same choice of λ require $2C_0C_2^2e^{T/5}\lambda^{56} \le 1$, using the slope and stress-ratio constants in the last paragraph of Lemma 1.8.20. The normalized power and flattening bounds in (P2) there are uniform after the specified lower bound on L_o, and the final scale absorbs the heat-edit errors.

($\lambda 8$) The three upper bounds of Lemma 1.20.48 on the near-endpoint buffer: $\lambda(1 + S_{\mathrm{ph}} + K_M^*) \le \frac{1}{2}(\frac{1}{2} - h)\eta_a c_f$; $2\lambda(2K_\sigma + T + 60\log(1/\lambda)) \le \frac{1}{2}$, which gives both conditions of part (b) there because $z_p - z_e \le T + 60\log(1/\lambda)$ and $\frac{1}{2} < \log 2$; and $\lambda W_\sharp^2 \le \frac{1}{8}$. All their constants are fixed with the bridge template, before λ (Lemma 1.20.48; κ_1 is bounded uniformly for $\lambda \le \lambda_0$). The first two are of the form $\lambda\log(1/\lambda) \le c$, the third of the form $\lambda \le c$.

In addition to ($\lambda 1$)–($\lambda 8$), we impose

$$C_{\mathrm{germ}}\lambda \le \frac{1}{2e}. \tag{$\lambda 9$}$$

This preserves strict decreasing swirl in Lemma 1.17.9. Its constant is independent of the later width, angular cutoff, h, ν_c, L_o, Y_0 and absolute radius. Then we select $h < \lambda_{\mathrm{br}}/6$ to satisfy the finite backward plateau bound. We select $0 < \nu_c < h/10$ with ν_c/h sufficiently small. In particular $\nu_c < \lambda_{\mathrm{br}}/60$.

We select the post-pulse angular-flattening length $T_f = T_0/\lambda$. If $\theta = 1-\sigma(\lambda y/T_0)$, its logarithmic radial slope is

$$\ell_r = -\lambda - (\lambda/T_0)\sigma'(\log 2 - J_0).$$

We select the fixed T_0 large on the fixed chart band. Then $-3\lambda/2 \le \ell_r \le -\lambda/2$, and the true backward source obeys

$$S_{q,b} = -\ell_r - h + 2(\tfrac{1}{2} - h)\beta^2\theta/(1+\beta^2) \ge \lambda/3.$$

All fixed angular derivatives of H/H_{base} stay bounded independently of T_f. Integration bounds the local flattening contribution by CH^2/λ. The outer power length selected below controls the complete later heat-tail contribution. We do not assume a bound independent of h.

After that selection the actual downstream energy and pressure bounds are $|S| + |S_\beta| \le CH^2/\lambda$ and $|P| + |P_\beta| \le CE^2$. Lemmas 1.15.4 and 1.15.3 keep the local and complete contributions. The preceding pulse decay makes the corresponding cone error $O(E/\lambda^2)$ sufficiently small. This gives a fixed-width chart band before λ is selected, rather than a band of width $O(\lambda)$ whose derivatives would invalidate (1.6.18). The flattening and complete-tail estimates are those of Lemmas 1.15.4 and 1.15.3.

After the model A11 equilibrium outlet (R_A, H_A) from Lemma 1.15.5, we insert a λ-power leg of scalar logarithmic length L_o. This leg precedes the fixed λ-to-h transition and terminal wing.

The model ratio stays $I/(\frac{\hat{\xi}^2}{2}H) = (1-\lambda)^{-1}$ on this added leg. With the fixed transfer $J > 0$ and the complete postdrive energy constant K_S, the exact laws are

$$c_B = H_A R_A^h J e^{-(\lambda-h)L_o}, \qquad \frac{S(R_A)}{H_A^2} = \frac{1-e^{-2\lambda L_o}}{8\lambda} + e^{-2\lambda L_o} K_S.$$

We select one finite L_o after h, the central hold and scalar templates, and the fixed outer transition and wing. It gives $e^{-2\lambda L_o} K_S \le (8\lambda)^{-1}$, the actual inlet ordering in Proposition 1.15.25, separation from all central deviations, and the necessary central and outer postdrive amplitude bounds. These are lower bounds on L_o. None reselects the earlier λ.

The positive-corridor construction proves the full primitive corridor and outer source. Inlet ordering alone does not prove them. We fix this length before χ, Y_0 and the selected C.

We use the actual A10/A11 block and the explicit heat replacement of Proposition 1.15.8. We keep its power entrance, same c_B, k_f and terminal edge fixed. A compact rank-one H correction inside the new leg cancels the complete heat-edit primitive discrepancy. Thus the actual future has total $\Delta I_{\mathrm{ren}} = 0$.

We keep its energy and pressure changes and their quadratic terms. A disjoint pre-pulse correction with three E bumps has target $(0, -\Delta S_f, -\Delta C_{p,f})$. Its first target is zero because the primitive discrepancy is zero after its correction. On the full-target protected collars, the corrected pressure thus equals the analytic pre-heat pressure.

The actual drive ratio can differ from its model by $O(C^{-p})$. Its positive model margin controls that difference. We use no new inverse entrance radius and do not reset I.

In the backward construction, we first fix the pulse root of the complete pre-heat model and its analytic pressure datum. We then change the swirl and compensate for that change. For a later swirl edit $E_0 \mapsto E_0 + e$ on the region $U = 0$, its exact changes are

$$dI = \int \hat{\xi}\, e\, \hat{\xi}\, \mathrm{d}\hat{\xi}, \qquad dS = -\int (E_0 e + e^2/2)\, \hat{\xi}\, \mathrm{d}\hat{\xi}, \qquad dC_p = \int (E_0 e + e^2/2)\big(\tfrac{\hat{\xi}^2}{2}\big)^{-1} \hat{\xi}\, \mathrm{d}\hat{\xi}.$$

The disjoint pre-pulse three-E correction solves the opposite full nonlinear target.

If the future swirl-energy integral increases by dT, its S change is $-dT$ and the correction contributes $+dT$. The original pulse root still satisfies the actual energy equation. We solve no second backward root. The forward actual-field normalization below includes these same contributions.

On the endpoint germ, in slice variables (Definition 1.6.4), its unique positive root is the selected model root. A11's two-row matrix and its quantitative inverse/source estimates are those of Lemma 1.15.5. Propositions 1.15.8 and 1.15.9 prove the actual zero-primitive heat construction and single correction. In a partial fixed-λ correction extension χ_b, we keep the uncancelled root increment $-2\nu(1-\chi_b)\Delta S_f/H_p^2$. The selected scale makes it small. We assert exact preservation of the model root on the full-target protected endpoint collars.

1.6.3.2 Same heat and exact inlet maps

For the central component, we use the scalar radial construction up to the interval of the primitive blend with the heat continuation. We call this the *scalar construction before the lift*. The scalar primitive precedes the blend in (1.13.57). The lifted primitive and wing occur after it.

The formula for H includes the derivative of the blending cutoff. In particular, we do not extend the lift backward to the central pulse entrance. See Lemma 1.17.7.

We insert a fixed finite scalar ν_c-power hold of length B. It comes after the actual axial and primitive-memory returns and before its heat drive.

We reserve its first part for the spectral construction. We keep a disjoint next part for the five-moment correction. The exact hold map is

$$\begin{aligned} R_h' &= R_h e^{B}, \qquad G' = G e^{-\nu_c B}, \\ r' &= (1-\nu_c)^{-1} + [r-(1-\nu_c)^{-1}] e^{-(1-\nu_c)B}, \\ T_{\mathrm{hold}} := -\Delta S &= \frac{G^2(1-e^{-2\nu_c B})}{8\nu_c}, \\ C_{p,\mathrm{hold}} &= \frac{G^2(1-e^{-(1+2\nu_c)B})}{4R_h(1+2\nu_c)}. \end{aligned} \tag{1.6.19}$$

We include the hold before we solve the same heat and energy roots. The heat coefficient has the exact form

$$c = G R_h^h e^{(h-\nu_c)B} K_{\mathrm{old}}(R_h e^{B}, r'). \tag{1.6.20}$$

The stable scalar drive and heat shot have this exact coefficient as their target. The shot is not an unaccounted perturbation of c. With the normalized reference ratio fixed, K_{old} is independent of the amplitude and is bounded below by a positive constant on the selected family. Thus at the selected central hold scale R_h the actual linear coefficient equation is solved by

$$G = \frac{c_B}{R_h^h e^{(h-\nu_c)B} K_{\mathrm{old}}(R_h e^{B}, r')}.$$

This linear coefficient equation gives the amplitude. The normalized central amplitude has a strictly positive lower bound after all finite geometry and pulse parameters are fixed, before C is enlarged. It can be very small. The full radial profile gives the central pressure m_R through its canonical integral.

Later admitted primitive-memory corrections leave the inlet H and terminal heat pair fixed, so they do not change this coefficient equation. The constructed family includes their energy and pressure contributions.

Let $R := (CP_*)^{10}$ denote the same large model scale, so that $\frac{\hat{\xi}_{\mathrm{ref}}^2}{2} = \frac{\hat{\xi}_i^2}{2} R$. The selected backward future supplies, with its actual normalized tail factor,

$$c_B = K_B R^{\frac{1}{2}+h} e^{-(\lambda-h)(Y_{\mathrm{end}}+L_o)}, \qquad L_b = \lambda Y_{\mathrm{end}}. \tag{1.6.21}$$

Here c_B is the coefficient in $H \sim c_B(\hat{\xi}/\sqrt{2})^{-2h}$. We use the forward coefficient convention. If we write the backward heat formula with its original constant c_{old}, we get the same physical trace coefficient

$$C_{\mathrm{tr}} = 2^{\frac{1}{2}+h} c_{\mathrm{old}} = 2^h c_B, \qquad c_B = c_{\mathrm{bank}} = \sqrt{2}\, c_{\mathrm{old}}.$$

Thus we measure K_B in (1.6.21) in this coefficient convention, with that fixed conversion. It excludes the separately displayed factor $e^{-(\lambda-h)L_o}$. If we match equal symbols without this conversion, we get different physical heat traces. We fix all future ordering parameters, the hold, and the tiny-memory family before we select the large C.

The distinct hold radius obeys $R_h = k_h R$, with the normalized factor k_h fixed after the future geometry and Y_0, before C. We do not identify it with the model scale R or the pulse comparison graph R_o. The coefficient maps include all such fixed factors. We normalize the central and outer components to this same c_B. They have the same actual heat pair.

Sector convention for the growth radius. Write $X = \hat{\xi}^2/2$ and let $R_{g,b} = \hat{\xi}^2_{s,b}/2$ be the backward growth-turn inlet. On the scalar central sector and on the entire genuine exponent transition use $R_g = R_{g,b}$. On the separate fixed-λ phase bridge use the cutoff $\tau = \rho_s$ of (1.25.4) and set $R_g = R_{g,b}\ell^{-\tau}$, $\ell = \lambda_{\mathrm{ch}}$. Here $\tau = 0$ at the inner end and $\tau = 1$ on open collars of both endpoints. The backward $R_{g,b}$ is scalar at every angle. We choose the outlet R_o first as in Section 1.15.7, and define $\rho = \tau_f = \log(R_o/R_g) - Y_0$. Thus $\partial_\eta \log R_o = \rho' + \partial_\eta \log R_g$. Fixed-$X$ source derivatives use the full outlet slope; derivatives of a memory ratio use ρ'. On the endpoint collars $R_o = R_e/\ell$, $X_p = X_{p,b}/\ell$, $\rho' = 0$. On the positive collar $\ell'(1) = -4/(1-2h)$, so these equalities also identify the first derivatives of the physical graphs. At the same outgoing comparison graph $R_o = R_g e^{Y_0+\tau_f(\eta)}$, we write

$$H_c = c_B R_o^{-h} K_c, \quad H_w = c_B R_o^{-h} K_w, \quad H_{\mathrm{out}} = (1-\chi)H_c + \chi H_w.$$

The ratios and their necessary finite derivatives are bounded on the fixed normalized tiny-memory family. The length L_o gives actual $H_c(R_o) \le H_w(R_o)/2$ and puts the outer heat-edit region beyond all central deviations and the hold. The primitive order on the full radial domain and its mixture source have their own proofs. Here we use only the same exact heat pair and inlet ordering.

The prefix gives explicit incoming primitive and energy ratios. The scalar finite pretemplate $F(y;\nu)$ ends at $T_b(\nu)$ with value $F_b(\nu)$. We put $\gamma = 3/5$, $r_a = (1+\gamma)^{-1}$, $\sigma_a = -1/(4\gamma)$, and

$$r_b(\nu) = \frac{r_a + \int_0^{T_b} e^y F(y;\nu)\,dy}{e^{T_b}F_b}, \qquad \sigma_b(\nu) = \frac{\sigma_a - \frac{1}{2}\int_0^{T_b} F(y;\nu)^2 dy}{F_b^2}, \tag{1.6.22}$$

$$W = 60\log(1/\nu), \qquad r_p = \frac{1}{1-\nu} + \left(r_b - \frac{1}{1-\nu}\right) e^{-(1-\nu)W},$$

$$\sigma_p = e^{2\nu W}\sigma_b - \frac{e^{2\nu W}-1}{4\nu}.$$

Here $r = I/(\frac{\hat{\xi}^2}{2}H)$ and $\sigma = 2S/H^2 = S/(\frac{\hat{\xi}^2}{2}E^2)$. These formulas integrate (1.6.3). No history is reset.

They give $|\sigma_p| + \nu|\sigma_p'| \le C(T_d + 1 + \log(1/\nu))$. We set

$$\frac{\hat{\xi}_p^2}{2} = R_g e^{T_b(\nu)}\nu^{-60}, \quad Y = Y_0 + \tau_f - T_b + 60\log\nu, \quad H_p = H_{\mathrm{out}}e^{\nu Y}, \quad H_a = H_p e^{\nu W}/F_b. \tag{1.6.23}$$

The length Y can vary in the transition and is constant on both endpoint collars. For the unedited template the primitive exit map is

$$\mathcal{F}(\nu,\eta) = \frac{1}{1-\nu} + \left(r_b(\nu) - \frac{1}{1-\nu}\right) e^{-(1-\nu)(Y_0+\tau_f(\eta)-T_b(\nu))}. \tag{1.6.24}$$

The long wait cancels from this formula. The complete futures admit these inlet memories. We use a central $\delta I\zeta$ correction before the hold and an outer A11 correction with the actual target. The two corrections leave the inlet H germ and terminal heat pair unchanged. We keep their canonical energy and pressure contributions.

This inverse and cutoff argument uses the actual component inlet maps on the admitted finite-scale domain specified below in Remark 1.6.9. The same inlet graph $R_o = R_g\exp(Y_0+\rho(\eta))$ and component geometries are selected before χ, not solved from the mixed field. We write $H_c = cR_o^{-h}K_c(\epsilon,\eta)$ and $H_w = cR_o^{-h}K_w(\epsilon,\eta)$, with the admitted memory variables understood. Proposition 1.15.25 gives the actual bounds $0 < m \le K_c, K_w \le M$, $K_c \le K_w/2$ and $|\log(K_c/K_w)| \le B$ with the same m, M, B on that domain.

The factor $e^{(\lambda-h)L_o}$ in K_w is scalar and does not increase this logarithmic derivative bound. We select a flat logit cutoff on a fixed angular band, for example $\chi = \mathrm{logistic}(a[-t^{-2} + (1-t)^{-2}])$ for $0 < t < 1$, extended by its flat endpoint values. We increase a to dominate the fixed bound on $\partial_\eta \log(H_w/H_c)$. Thus $\omega = (1-\chi)H_c/H_{\mathrm{out}}$ decreases and $-\dot\omega \geq k\omega(1-\omega)$, where a dot denotes $(\frac{1}{2} - h)\eta\partial_\eta$.

The exact derivative is $-\dot\omega = \omega(1-\omega)[\dot{\log}(\chi/(1-\chi)) - \dot{\log}(K_c/K_w)]$. In the prefix and bridge estimates, G denotes the axial template coefficient in $U = Gk$. Lemma 1.6.14 gives this template in physical coordinates. It is different from the central swirl amplitude G in (1.6.19). The notation $G = 0$ labels angles where the axial template coefficient is zero.

We select this mixing cutoff after the fixed h and component templates, but before Y_0. It uses the uniform bound B. It is distinct from the earlier $G = 2$ bridge and growth-rise cutoffs. The actual weight ω can vary with $\epsilon(C, Y_0)$ and thus across the family.

We hold it fixed only during the given member's ν solve. Its primitive/germ corrections keep the component inlet values. We define ν by the actual equation

$$\mathcal{F}(\nu, \eta) = \omega\mathcal{F}(\nu_c, \eta) + (1-\omega)\mathcal{F}(\lambda, \eta). \tag{1.6.25}$$

On the fixed-λ bridge $\chi = 1$, so (1.6.25) sets $\nu = \lambda$. Its two sides there describe the raw power template. The actual primitive after the pre-pulse taper is (Inlet); it is this corrected inlet that is used by the outer flattening. For large fixed Y_0, $\mathcal{F}_\nu$ has a lower bound. Monotonicity also holds at the flat ends. In the coordinate $x = \mathcal{F}$, the fixed-ν angular derivative has second x derivative $O(\mathrm{poly}(Y_0)e^{-(1-\lambda)Y_0})$.

This constant times $[\mathcal{F}(\lambda) - \mathcal{F}(\nu_c)]^2\omega(1-\omega)$ bounds its interpolation defect. The term $-\dot\omega[\mathcal{F}(\lambda) - \mathcal{F}(\nu_c)]$ dominates. The factor $\omega(1-\omega)$ is necessary to get this comparison at the flat ends.

1.6.3.3 Stress estimates, pressure, and pulse normalization

The outer pre-A10 chart band has source q_w. The scalar central inlet has source q_c. Their values are

$$q_w = (k-1)\left[\lambda - h + \frac{2(\frac{1}{2} - h)\beta^2}{1+\beta^2}\right] \geq q_* > 0, \qquad k = \dot{\log} R_o \geq 2, \qquad q_c = h - \nu_c > 0.$$

The full outer-active band uses the exact chart geometry of (1.15.26). Thus q_* does not depend on the later h, L_o. The second formula uses the central field before the lift.

It would not hold for a raw lifted inlet. The mixture identity is

$$h - \nu + c_{\mathrm{mix}} = \omega q_c + (1-\omega)q_w + \dot\chi(H_w - H_c)/H_{\mathrm{out}} + (\nu - \bar\nu)(v_o - 1), \quad \bar\nu = \omega\nu_c + (1-\omega)\lambda.$$

Ordering makes the third term nonnegative. The outer stress reserve controls the last term, which is at most $C\lambda^2\omega(1-\omega)$, independently of a small central h reserve. Thus $Q_{\mathrm{out}} \gtrsim h\omega + q_*(1-\omega)$ and $\nu/Q_{\mathrm{out}} \leq C(\nu_c/h + \lambda)$.

In the $G = 0$ band, $S_{q,g}$ is the source on the growth interval. The source on the negative-power wait is $S_{q,w}$. Their formulas are

$$\begin{aligned} S_{q,g} &= \gamma + h + c_{\mathrm{mix}} + \dot\nu[Y_0 + \tau_f - T_b - \nu T_b' - (\log F_b)'], \\ S_{q,w} &= h - \nu + c_{\mathrm{mix}} + \dot\nu(Y_0 + \tau_f - y). \end{aligned}$$

We select Y_0 after the finite template derivatives. During the wait the actual prefix, rather than a crude $1/\nu$ future bound, gives $|\sigma| \leq C(T_d + 1 + y)$ and $|\sigma_\nu| \leq C(T_d + 1 + y)^2$. The fixed-$\hat\xi$ derivative includes $y_\nu = -T_b'$, not W'.

At a contact point, the source barrier $Q \geq cq$ results from $[1 - c(1-\nu)]q + c\dot{\nu} > 0$, because $q_y = -\dot{\nu}$. Canonical pressure is

$$P/E^2 = -\frac{1 - e^{-(1+2\nu)L}}{2(1+2\nu)} + e^{-(1+2\nu)L}(P/E^2)_{\text{out}}.$$

Its angular derivative includes the actual outgoing graph and future pressure derivatives, all multiplied by the displayed exponential. The actual expression $N_s = 4h\eta S/\frac{\hat{\xi}^2}{2} - d\partial_\eta(S/\frac{\hat{\xi}^2}{2}) + (2+4h)\eta P - dP_\eta$ gives

$$|w| \leq CE\left[T_d + 1 + y + Q^{-1} + (T_d + 1 + y)^2/Y_{\min}\right] + \text{exponentially small terms.}$$

For $\nu \geq \lambda/2$, the source has a fixed outer reserve and (1.6.18) ensures the wait cone inequality $2\nu w^2 < 1$. For $\nu \leq \lambda/2$, the actual amplitude carries $e^{-(\lambda-\nu)(Y_{\text{end}}+W(\lambda))}$, and this controls the fixed inverse powers of h after we select Y_0. The same heat coefficient fixes the amplitude used here.

The pulse has $U/E = A_p\Phi(\nu y)$ and two compact corrections follow it to return M, J to their specified values. For the original backward pulse with shape R_0 and amplitude Amp_b, we set $K_{\text{pulse}} = \int e^{-2\xi}R_0(\xi)^2\,\mathrm{d}\xi$, $\Phi = R_0/(2\sqrt{K_{\text{pulse}}})$ and $A_p = 2\sqrt{K_{\text{pulse}}}\,\text{Amp}_b$. Then $A_p\Phi = \text{Amp}_b R_0$ is the same physical pulse. We normalize only its notation.

With $\int e^{-2\xi}\Phi^2 d\xi = 1/4$, its single energy root is

$$\frac{A_p^2}{4} + \nu\sum_j K_j(A_p\beta_j + \gamma_j)^2 = \frac{1 - e^{-2\nu Y}}{4} - \nu\sigma_p + 2\nu e^{-2\nu Y}\tau_f^{\text{en}}. \tag{1.6.26}$$

We solve the return coefficients from the incoming histories. On the genuine $G = 0$ transition, $M = J = 0$ at the pulse inlet. Hence the affine offsets γ_j vanish and the displayed equation reduces to $A_p^2[1/4 + \nu\sum K_j\beta_j^2]$ on the left. On the outer sector, we keep the affine constants γ_j.

Here σ_p denotes the actual prefix ratio with the specified endpoint corrections. The scalar formula from the transition does not apply there. Each heat, primitive and moment-correction contribution occurs one time in σ_p or τ_f^{en}. The root is transverse on the selected compact family.

For a graph $f(\eta)$ write $\dot{f} = (\frac{1}{2} - h)\eta\,\partial_\eta f$. Differentiating $X_p = R_g e^{T_b(\nu)}\nu^{-60}$ gives

$$v_p = \log\dot{X}_p = \log\dot{R}_g + (T_b'(\nu) - 60/\nu)\dot{\nu}.$$

On the genuine exponent transition $R_g = R_{g,b}$ and $T_b = T$ are constant, so $v_p = -60\dot{\nu}/\nu$. This gives the phase contribution $60/Y_{\min}$ in the variable-exponent estimate below. On the fixed-λ bridge $v_p = \log\dot{R}_g = -\dot{\tau}\log\ell - \tau\log\dot{\ell}$. In particular, at $\eta = 1$, $R_g = R_{g,b}/\ell$ and $\ell'(1) = -4/(1-2h)$ give $v_p(1) = 2$. At fixed X the derivative of $\Phi(\lambda\log(X/X_p))$ is $-\lambda v_p\Phi'$, as used in the affine pulse estimate. Lemma 1.16.8 first establishes a positive denominator. It uses the fixed-coordinate identities, complete canonical histories, and prefix estimates. On the genuine variable-ν sector it first gives $Q \geq c[q_{\text{out}} + \dot{\nu}(Y - y)] > 0$ through the full pulse, then gives $w = 2(U/E) + o(1)$ on the main window.

The explicit errors are those of Lemmas 1.16.3 and 1.16.6. On the genuine exponent transition these bounds include the phase term $60/Y_{\min}$ and the RE_η term. For $\nu \geq \lambda/2$, the true source floor is fixed positive and the nonlinear cost is $O(K_{\text{pre}}\lambda^{29})$. For $\nu \leq \lambda/2$, the actual heat-coefficient factor $e^{-(\lambda-\nu)Y_{\text{end}}}$ controls the late inverse-h and inverse-ν_c constants after they have been fixed.

Proposition 1.15.20 supplies K_f before Y_0. The selected scale controls the early-correction constant $K_{\text{sc}}(Y_0)$. These constants do not enter the earlier selection of λ. The quiet/return proof below uses this proved main window and these actual source and future inputs. The fixed-λ affine sector uses its genuine incoming memories and the correction residual. Lemma 1.16.8 gives these quantities.

1.6.3.4 Uniform bounds for the future profile and return intervals

Remark 1.6.9 (Parameter domain and remaining source conditions). These estimates use fixed normalized geometry and one inlet graph. They use positive bounds and uniform first derivatives for the component ratios, together with transverse root margins. They also use a compact family of small incoming memories with the stated heat-tail and fast-mode exposure bounds. The independent parameter domain is the product of this memory set and $0 < \epsilon = R_b^{-1} \le \epsilon_0$.

We analyze the stop in $\epsilon^{1/5}$ down to zero. The estimates apply to normalized radial, angular and logarithmic-scale derivatives. They do not assume pointwise compactness of all angular jets on this open scale interval. We evaluate the matched-memory map for $Y_0 \ge Y_{\min}$ on this domain.

Along the constructed family, $R_b = x_b(\varepsilon)e^B k_h(Y_0)R$ with $R = (CP_*)^{10}$, so ϵ varies with C, Y_0. After we fix Y_0, we select $C \ge C_0(Y_0)$ to satisfy the heat-compensation, small-correction, memory and finite-scale conditions. A lower bound on R_b alone does not establish all these conditions, and we do not assert any threshold uniform before Y_0. At fixed ϵ, the other normalized dependence on Y_0 is the exponentially small matched memory. The uniform scale bounds control finite-scale dependence.

Lemma 1.6.10 realizes the leading heat, memory and A11 data with the relative support arrangement specified below. Sections 1.6.4 and 1.26 impose the pressure, regular-core and spectral conditions for the selected scale C.

The variable-Y argument applies only where $G = 0$ and $|\eta| \ge \eta_a > 0$. Lemma 1.6.13 treats the central band with ordinary angular derivatives under its stated hypotheses. Division by η in the variable-exponent argument does not give this result.

Tags (I1)–(I17) refer to the inputs of Section 1.15.4.1; the ledger is Proposition 1.15.20.

In fixing the finite hold geometry we reserve its first part for the central spectral layers and a disjoint, later part for five fixed radial bumps. In $X = \xi^2/2$ choose the three swirl supports so that every X_i in the ith support satisfies $2X_1 < X_2 < X_3$. For example, beyond the last layer choose narrow intervals centered at $X_*, 3X_*, 5X_*$, and the two axial intervals centered at $2X_*, 4X_*$. These centers and the outlet buffer are fixed multiples of R_h. Choose the finite hold length B_h to contain them before the drive. Lemma 1.15.6 allows every fixed B_h. This choice precedes L_o, Y_0, C and the spectral integer.

Lemma 1.6.10 (Realization of the leading radial continuation). *Fix the templates, λ, $h < \lambda/6$, $\nu_c < h/10$ satisfying (1.6.18), the hold length B_h with its downstream scalar deficit and shot templates, and the normalized supports $R_m = a_m \max R_o$, $R_h = a_h R_m$ with $a_m > 1$, $a_h > 2$. Let $L_o \ge L_*$, where*

$$L_* := \max\Big\{\underbrace{\tfrac{1}{\lambda-h}\log^+\tfrac{2K_c^+}{A_w f_-}}_{(1.6.29)},\ \underbrace{\tfrac{1}{2\lambda}\log^+(8\lambda K_S)}_{(1.15.5)},\ \underbrace{\log^+\tfrac{4M_c}{e^\delta k_A}}_{\text{Lemma 1.15.7}},\ \log 4,\ \underbrace{\tfrac{1}{\lambda-h}\log^+\tfrac{B_c E_{A,\max}}{\varepsilon_c}}_{\text{Proposition 1.15.22}},\ L_{\mathrm{gap}}\Big\}, \tag{1.6.27}$$

with L_{gap} the finite threshold of Lemma 1.17.3. Fix χ by Lemma 1.15.26. Then there is $Y_{\min}$ such that for each $Y_0 \ge Y_{\min}$ there is $C_{0,\mathrm{lead}}(Y_0, L_o) < \infty$ with the following property. For every $C \ge C_{0,\mathrm{lead}}$ there are actual central and outer futures such that:

(R1) (Same heat pair.) Both components end in the same exact heat field with pair (c, k_f). Here k_f is the actual fast coefficient of the central shot, and c is given by the coefficient law (1.15.3).

(R2) (Central chain.) The memory return on $[R_m, 2R_m]$ restores $I/(\frac{\hat\xi^2}{2}H) = (1-\nu_c)^{-1}$ exactly. The hold and the stop/shot map of Lemma 1.15.6 apply at $R = R_h e^{B_h}$, with $k_- \le K_{\mathrm{old}} \le k_+$. The central inlet coefficient is (1.6.28). The central component satisfies the source and relative axial estimates of Proposition 1.15.22.

(R3) (Outer chain.) A11 has a unique small root with C^1 bound $O(\|u\|_{C^1})$. The actual heat future H^a of Proposition 1.15.8 is positive, keeps the inlet germ, (c, k_f) and the terminal edge, and has zero total primitive increment. At the A11 outlet (R_A, H_A), the complete increments satisfy, for $j = 0, 1$,

$$\frac{|\partial_\eta^j \Delta S|}{H_A^2} + \frac{R_A |\partial_\eta^j \Delta C_p|}{H_A^2} \le \frac{K}{R_A}, \qquad R_A \asymp R_o.$$

Here the derivative is in the native angular variable of the member and K may depend on the fixed geometry.

(R4) (Order.) $K_w = A_w f(\beta) e^{(\lambda - h)L_o}$ and $K_c \le K_w/2$ on the chart band.

(R5) (Early restoration.) The three-swirl bank solves (1.14.16) with a unique small coefficient vector. Its first row is zero and its supports preserve the inlet germs and heat pair. On the native backward chart and the full-compensation forward collars its energy row preserves the model pulse root. On the intermediate extension the root retains the residual in (1.14.18).

(R6) (Uniform ledger.) Proposition 1.15.20 holds with one K_f for all $Y_0 \ge Y_{\min}$ and $C \ge C_{0,\mathrm{lead}}(Y_0, L_o)$.

No claim is made that $\sup_{Y_0} C_{0,\mathrm{lead}}(Y_0, L_o) < \infty$.

Proof. We verify the hypotheses of each cited result in the order (1.15.11). For each threshold we record the stage at which it is imposed. A threshold imposed at a stage may use only constants from earlier stages.

Step 1 (central scalar map; stage C). Lemma 1.15.6 requires fixed $0 < \nu_c < h/10$ and a fixed scalar post-hold drive; both are fixed. Its initial datum $W(1) = a^{-1} - (1 - \nu_c)^{-1} > 0$ ($a = 1 - h$, $h > \nu_c$) requires the exact reference ratio at the end of the hold. The memory return $I = i_s + p\zeta(\frac{\hat\xi^2}{2}/R_m)$ gives $I = i_s = \frac{\hat\xi^2}{2} H_s/(1 - \nu_c)$ on $2R_m \le \hat\xi^2/2 \le R_h e^{B_h}$ (I8), and the hold map (1.6.19) preserves $r' = (1-\nu_c)^{-1}$ when $r = (1-\nu_c)^{-1}$. Hence K_{old} is evaluated at the Y_0-independent reference r_{ref}, which is the reason its constants do not depend on the memory. The lemma applies for $R = R_h e^{B_h} \ge R_*$. Since $R_h = k_h(Y_0)R$ and $R \asymp (CP_*)^{10}$ (Section 1.6.3), this is a lower bound on C at fixed Y_0. It gives $k_- \le K_{\mathrm{old}} \le k_+$, with $k_\pm$ depending only on h, ν_c and the drive. In particular $k_\pm$ does not depend on L_o, Y_0, C.

Step 2 (coefficient formulas; exact). On $[R_o, R_h e^{B_h}]$ the central H is $A_c(\frac{\hat\xi^2}{2})^{-\nu_c}$ outside the compact memory support, where $\zeta' = 0$. Combining this with $c = G\, R^h K_{\mathrm{old}}(R)$ at $R = R_h e^{B_h}$ (Lemma 1.15.6) gives

$$K_c = \frac{H_c(R_o) R_o^h}{c} = \frac{(R_o/R_h)^{h-\nu_c} e^{-(h-\nu_c)B_h}}{K_{\mathrm{old}}(R_h e^{B_h})}. \tag{1.6.28}$$

The outer coefficient law (1.15.3) $c = H_A R_A^h J e^{-(\lambda-h)L_o}$, $J = p(\delta)e^{h\delta}/(1-\rho)$, together with the chart transfers $H_A^b = a_A H_e$, $R_A^b = k_A R_e$, $R_o = R_e/\ell$, $H_w(R_o) = \ell^h H_e f(\beta)$, gives $K_w = A_w f(\beta) e^{(\lambda-h)L_o}$ with $A_w = (a_A k_A^h J)^{-1}$. The constants $a_A, k_A, J, \delta, \rho$ are fixed before L_o (Section 1.15), and K_{old} does not involve L_o.

Step 3 (ordering; stage L_o). Lemma 1.15.24 requires $K_{\mathrm{old}} \ge k_-$ for all large R_h, which holds by Step 1. With $K_c^+ = \sup (R_o/R_h)^{h-\nu_c} e^{-(h-\nu_c)B_h}/k_-$ and $f_- = \min f(\beta)$,

$$L_o \ge \frac{1}{\lambda - h} \log^+ \frac{2K_c^+}{A_w f_-} \tag{1.6.29}$$

gives $K_c \le K_c^+ \le \frac{1}{2}A_w f_- e^{(\lambda-h)L_o} \le K_w/2$ on the band. All constants here are fixed before L_o. Proposition 1.15.25 shows that the actual corrections keep the inlet H germs, so the actual K_c, K_w are the model ones and (R4) holds.

Step 4 (fast mode; stage L_o, then C). Lemma 1.15.7 requires the central geometry to be fixed, which it is (independent of L_o; proof of Proposition 1.15.22), and $b_s \le M_c R_o$, with M_c the supremum of the fixed ratio b_s/R_o. It also requires $R_0 \ge 4M_c R_o$. Since $R_0/R_o = e^{\delta} k_A e^{L_o}$ in the backward chart (Section 1.15), the third entry of (1.6.27) suffices. The conclusion (1.15.13) is uniform in the large radius.

Step 5 (actual heat future; stage C). Proposition 1.15.8 needs the terminal separation $B > e^4 R_0$, which is (1.15.1), fixed with ρ before L_o; $L_o \ge \log 4$; and (1.15.13), from Step 4. Its positivity requires a large radius, i.e. a lower bound on C at fixed Y_0, L_o. This gives (R3) except for A11.

Step 6 (A11; stages λ and $Y_{\min}$). Lemma 1.15.5 requires a bounded normalized ratio and derivative at the flattening inlet. The Jacobian of the two ordered translates is $2A_1B_1(e^{-(1+2\lambda)d_*} - e^{(1-\lambda)d_*})$, which is bounded away from 0 on $0 \le \lambda \le 1/20$ and the quantitative implicit function theorem has a fixed data ball $\mathcal{B}$. The target is $u = u_{\text{model}} + u_{\text{mem}}$. Here $\|u_{\text{model}}\|_{C^1} \le C\lambda^{30(1-\lambda)} \le C\lambda^{28}$ for $\lambda \le 1/15$, which is placed in $\frac{1}{2}\mathcal{B}$ at stage λ (condition (λ5) after (1.6.18)). Also $\|u_{\text{mem}}\|_{C^1} \le C\|\delta_{\text{mem}}\|_{C^1}$, which is placed in $\frac{1}{2}\mathcal{B}$ for $Y_0 \ge Y_{\min}$ by Lemma 1.15.19(4). Increase $Y_{\min}$ at fixed λ so the memory contribution to (1.8.6) is at most $\lambda/24$.

Step 7 (central source; stages L_o, $Y_{\min}$, C). Proposition 1.15.22 needs: the reference and the stop/shot of Step 1; the memory support $[R_m, 2R_m]$ after all axial returns and before $R_h > 2R_m$. The returns $c_j\psi(y - Y + d_j)$ (1.16.17) lie in the pulse interval $\frac{\hat{\xi}^2}{2} \le R_o < R_m$, and $R_h > 2R_m$ since $a_h > 2$; the amplitude threshold on L_o (fifth entry of (1.6.27)), in which $E_{A,\max}$ is controlled by $C_{\text{pre}}\lambda^{30}$ from (1.15.36) and so does not depend on L_o; $C\epsilon_I \ll \min(h, \nu_c)$, which holds for $Y_0 \ge Y_{\min}$ by (I8); and a last radius threshold, a lower bound on C.

Step 8 (early restoration; stage C). Lemma 1.15.9. The rows have radial powers $\frac{1}{2}, -\frac{1}{2} - \lambda, -\frac{3}{2} - \lambda$. For three ordered disjoint nonnegative bumps the Jacobian is $\iiint \det[x_j^{a_i}] \prod_j \psi_j(x_j)\,dx$, by multilinearity in the columns. Lemma 1.25.7 gives a positive determinant for increasing exponents. Here the exponents are decreasing, so reversing the three rows gives a negative determinant. In the early-bank units of (1.14.15), the target $(0, -\chi_b\Delta S, -\chi_b\Delta C_p)$ is $O_{L_o,Y_0}(R_{\text{master}}^{-1})$ by Step 5 and the fixed ratios of the two sets of units. The quantitative inverse function theorem gives a unique small solution above a scale threshold depending on (L_o, Y_0). The zero first row preserves the A11 primitive target. Since $H_{\text{out}}^2 = H_p^2 e^{-2\nu Y}$, the change of the right side of the pulse equation is $-2\nu(1-\chi_b)\Delta S/H_p^2$. It vanishes on the full-compensation set, including the native backward chart.

Step 9 (same inlet fields and heat pair). The central amplitude is solved linearly from the outer c (Section 1.15). The central shot targets c exactly (Step 1), and the outer heat collar uses the central shot's (c, k_f) (Lemma 1.15.7). Every correction (memory return, A11, heat collar, rank-one bump, early restoration) has support strictly after R_o, or on the pre-pulse reserve, and keeps the inlet H germ. This gives (R1).

Step 10 (ledger). After χ is fixed, Proposition 1.15.20 gives K_f. Its domain contains the physical family for $Y_0 \ge Y_{\min}$ (Step 6 and Lemma 1.15.19). This gives (R6).

Thresholds. $Y_{\min}$ is the maximum of the finitely many lower bounds from Steps 6, 7 and Lemma 1.15.19, including $\|\delta_{\text{mem}}\|_{C^1} \le \lambda^{30}$ (Lemma 1.15.19(4) with $r_1 = \lambda^{30}$; (P3) of Lemma 1.8.20). $C_{0,\text{lead}}(Y_0, L_o)$ is the maximum of the lower bounds from Steps 1, 4, 5, 7 and 8, and of $\epsilon \le \epsilon_*$ in the stop lemma. Each is finite at fixed (Y_0, L_o).

Non-circularity. Every entry of (1.6.27) uses only constants fixed before L_o: k_- (Step 1), the central geometry ratios, B_h, A_w (a_A, k_A, J), f_-, K_S (independent of L_o, Section 1.15), M_c, B_c, ε_c, and $E_{A,\max} \le C\,C_{\text{pre}}\lambda^{30}$. The cutoff χ uses $B_* = \sup|\log(K_c/K_w)|$, which is independent of L_o

because the factor $e^{(\lambda-h)L_o}$ is scalar. K_f uses χ and L_o. $Y_{\min}$ uses K_f and the constants of Steps 6–7. $C_{0,\mathrm{lead}}$ uses Y_0, L_o. Every L_o-threshold is monotone, so enlarging L_o to the maximum keeps all of them (proof of Proposition 1.15.22). No threshold is reset after a later choice. □

Lemma 1.6.11 (Uniform future integrals before the selection of pulse length)**.** *We use the inputs constructed in Lemma 1.6.10. We fix the selected normalized geometry of the full future and its actual small-memory family. Then the complete normalized energy and pressure integrals have one C^1 bound before the selection of Y_0. Constants can depend on fixed h, ν_c, T, T_f, B, L_o and all fixed angular and radial templates (precisely, on the data to the left of K_f in (1.15.11)), but not on Y_0 or the sufficiently large normalized future scale.*

If $R_b = x_b(\varepsilon)e^B k_h(Y_0)R$ with $R = (CP_*)^{10}$, we impose its threshold on R_b and keep the factor $k_h(Y_0)$. We select the master C only after Y_0. It must satisfy $C_0(Y_0)$ and each admissibility condition in that remark.

Proof. This is Proposition 1.15.20: items (1)–(2) give the C^1 bound K_f of the complete normalized energy and pressure integrals, independent of Y_0, of C and of the inverse scale ϵ, and item (3) applies it along the whole physical family $Y_0 \ge Y_{\min}$. The master scale is selected after Y_0, at the threshold $C_0(Y_0, L_o)$ of that proposition. For the native backward model we also include its complete normalized future energy and its ordinary β derivative in K_f. Indeed, at the flattening inlet $H_o = H_e/(1+\beta^2)$, so $H_o/H_e \ge 1/2$. Lemmas 1.15.4 and 1.15.3 bound the outward integral divided by H_e^2 and its angular derivative before Y_0 is chosen. With $Y = Y_{\mathrm{end}} = Y_0 + \rho(1) - T_b(\lambda) + 60\log\lambda$, increase the lower bound on Y_0 until

$$e^{-2\lambda Y}(\tfrac14 + 2\lambda K_f) \le \tfrac{1}{200}, \qquad e^{-2\lambda Y}K_f \le 1, \qquad Y \ge 4(\xi_m+2)/\lambda + 8\max_j(1+|d_j| + \operatorname{diam}\operatorname{supp}\psi). \tag{1.6.30}$$

Here ξ_m bounds the support of the fixed main template and d_j are the two return offsets in (1.16.15). These are finite length conditions after L_o, K_f and λ have been fixed. □

Lemma 1.6.12 (Contiguous quiet, late, and return control)**.** *We assume the estimates of Lemma 1.16.8 and Proposition 1.15.20. We work on the selected $G = 0$ transition with $|\eta| \ge \eta_a > 0$. Then the main pulse estimate extends through the full quiet interval and the two actual returns, with a strict relaxed-cone margin. This statement does not give the central ordinary-angular estimate at $\eta = 0$.*

Proof. Let $\beta = 1/2 - \nu \ge \beta_* = 1/2 - \lambda$, and put $y_m = (\xi_m+2)/\nu$, $y_{m,\max} = (\xi_m+2)/\nu_c$. We select

$$Y_{\min} \ge 4y_{m,\max} + 8\max_j(1 + |d_j| + \text{return support radius}_j).$$

Lemma 1.16.8 gives the actual main-window value $|w(y_m)| \le \epsilon_m$ and establishes the denominator before this proof divides by it. We increase the uniform constant K_f to at least one.

Lemma 1.16.2 gives the canonical fixed-coordinate identities. We first make the incoming memory and nonlinear corrections sufficiently small. The actual source coefficient then satisfies $Q \ge c(q_{\mathrm{out}} + \dot\nu Y)$ through $Y/2$ and $Q \ge cq_{\mathrm{out}}$ on the remaining interval. We first get these Q bounds from the specified U. We use the stable M, J equations and the exact algebraic $Q - Q_{\mathrm{lin}}$ expression.

The early normalized-memory bounds and late decay do not use N_s or w. Thus we derive the denominators below without an assumption of the quiet cone. Here $q_{\mathrm{out}} \ge ch\omega + q_*(1-\omega) > 0$. We set $q_{\mathrm{floor}} = \min(ch, q_*) > 0$. We assume no lower bound on $\dot\nu$ at a flat end.

On a quiet interval $U = 0$, but M, J can be nonzero. The exact identity and its normalized version are

$$(N_s)_y + N_s = \eta E^2 + 4(\tfrac12 + h)\eta P - dP_\eta, \qquad n_y + \beta n = EL, \quad n = N_s/E,$$

where $L = \eta + 4(\frac{1}{2} + h)\eta(P/E^2) - dP_\eta/E^2$. The actual canonical formula is

$$\frac{P}{E^2} = -\frac{1}{2(1+2\nu)} + e^{-(1+2\nu)(Y-y)}\left[\frac{1}{2(1+2\nu)} - 2\tau_P\right].$$

At fixed $\hat{\xi}$, $(\dot{Y} - y) = \log \dot{R}_{\text{out}}$.

We differentiate this formula and include the derivative of E^2. Lemma 1.6.11 then gives

$$|L| \le K_{\text{geo}}(1 + q(y) + |\dot{\nu}|) + K_f \mathcal{P}(Y) e^{-(1+2\nu)(Y-y)}, \qquad q(y) = q_{\text{out}} + \dot{\nu}(Y - y).$$

Here and below $\mathcal{P}$ is a fixed polynomial in $Y_{\max}$ and fixed inverse ν_c, source-floor and template constants, not a constant selected after Y. Because $Y = Y_0 + \rho - T_b - W$ and $\nu \in [\nu_c, \lambda]$ is in a fixed interval, $Y_{\max} - Y_{\min} \le C_{\text{fixed}}$. One increase of Y_0 thus makes all these polynomial-times-exponential bounds small.

Explicitly $\log \dot{E} = q + \nu - h$ and $[-1/(2(\dot{1} + 2\nu))] = \dot{\nu}/(1+2\nu)^2$. On the early half $|\dot{\nu}| \le 2q/Y$. The local coefficient K_{loc} depends only on fixed geometry and η_a. It does not depend on late h, ν_c-dependent future derivative norms. On the late half the finite compact-family bound of $\dot{\nu}$ enters $\mathcal{P}$, and exponential decay in Y controls it. Late heat constants occur only in the attenuated future term.

For $t = y - y_m$ and $y \le Y/2$, the ratios $Q(s)/Q(y)$ stay bounded for $y_m \le s \le y$. Exact convolution and $(1 - e^{-2\nu t})/(2\nu) \le t$ give

$$\begin{aligned} |w(y)| \le{}& K\epsilon_m e^{-\beta_* t} + K_{\text{loc}} E_m (1 + q_{\text{out}}^{-1}) t e^{-\beta_* t} \\ &+ K_f \mathcal{P}(Y) e^{-cY_{\min}}, \qquad E_m = e_p e^{-(1/2+\nu)(\xi_m+2)/\nu}. \end{aligned}$$

For $\nu \ge \lambda/2$, the actual mixing weights give $q_{\text{out}} \ge q_0 > 0$, and the amplitude produced by the wait controls this term. For $\nu \le \lambda/2$, the same heat-coefficient identity gives $e_p \le K e_{\text{end}} e^{-\lambda Y_{\text{end}}/2}$. This controls the fixed inverse h and ν_c factors once we select those parameters. This estimate uses the amplitude determined by the construction.

For $y \ge Y/2$ before the returns, $y - y_m \ge Y_{\min}/4$. We solve the same equation from y_m with the actual outlet floor. The future forcing now can have order one relative to E^2, but the exponentially small $E(y)$ multiplies it. More explicitly, with $\alpha = 1/2 + \nu$, $b = 1 + 2\nu$,

$$\int_{y_m}^{y} e^{-\beta(y-s)} E(s) e^{-b(Y-s)} ds = E(y) e^{-b(Y-y)}[1 - e^{-(y-y_m)}].$$

This identity uses $\alpha + \beta = 1$ and is at most $e_p e^{-\alpha Y/2}$ on the late half. Direct convolution gives

$$|w| + |m| + |\dot{m}| \le (1 + K_f)\mathcal{P}(Y) e^{-c_{\text{late}} Y_{\min}}, \qquad m = M/(\tfrac{\hat{\xi}^2}{2} E),$$

with fixed $c_{\text{late}} > 0$ smaller than $\beta_*/8$ and $\nu_c/4$. On a quiet interval, $m_y + \beta m = 0$ with its actual nonzero entry. Its fixed-$\hat{\xi}$ angular derivative adds only polynomial factors.

The normalized $J/(\frac{\hat{\xi}^2}{2} HE)$ has quiet decay rate $1/2 - 2\nu > 0$ (and $J/(\frac{\hat{\xi}^2}{2} H)$ has rate $1 - \nu$). The corresponding estimate for J controls the nonlinear correction to Q. We reset no moments before the return equations.

Those equations have row entries proportional to

$$e^{(1/2-\nu)(Y-d_j)} L(1/2 - \nu), \quad e^{(1/2-2\nu)(Y-d_j)} L(1/2 - 2\nu), \qquad L(a) = \int e^{as} \psi(s) ds > 0.$$

The absolute value of their factored determinant contains $|e^{\nu d_2} - e^{\nu d_1}|$, bounded below by $c\nu$. Thus for the actual zero incoming M, J, $c_j = A_p \beta_j$ and

$$|\beta_j| + |\dot{\beta}_j| + |\partial_y R_j| \le \mathcal{P}(Y) e^{-c_{\mathrm{ret}}(Y_{\min} - \xi_m/\nu_c)}, \qquad c_{\mathrm{ret}} < 1/2 - 2\lambda.$$

We keep derivatives of the exponents and moving centers.

Finite-interval convolution on each return support then gives

$$|b_s| + |w| + |Q - Q_{\mathrm{lin}}|/q_{\mathrm{floor}} \le (1 + K_f)\mathcal{P}(Y) e^{-c' Y_{\min}}.$$

After the second return $M = J = 0$ and their angular derivatives are zero. Their energy contribution stays in (1.6.26). They do not change pressure because they change U only.

On quiet portions $a_s = 2 + 2\nu, b_s = 0$, and these bounds give $2\nu w^2 < 1$. On returns they give a small perturbation of $a_s = 2 + 2\nu, b_s = w = 0$. Thus the relaxed cone has strict margins on the quiet and return intervals. The main estimate covers the adjoining phase window through y_m, so there is no gap. We then select the physical scale to control the finite-p and viscous errors with only these fixed quantities. □

1.6.3.5 The flat central pulse with ordinary angular derivatives

Lemma 1.6.13 (Central pulse, quiet, and returns through $\eta = 0$)**.** *We use the selected central component before the lift on an open band $\chi = 0$. It has the actual scalar prefix and the admitted complete future from Remark 1.6.9. After the parameter selections below, the pulse, quiet intervals, and actual returns have uniform strict relaxed-cone margins. All angular estimates use ordinary ∂_η and cover $\eta = 0$.*

This is not an extension of an estimate that contains $1/\eta_a$ to the central plane. Here $\eta = z q^{h-\frac{1}{2}}$ and $\eta_z = q^{h-\frac{1}{2}}(1-\eta^2)/(1-2h\eta^2)$, so $\eta = 0$ is the regular plane $z = 0$ at positive time, not the cylindrical axis. The cylindrical axis is $r = 0$, equivalently $\hat{\xi} = 0$, and the core theorem with $H = \hat{\xi}^2 F$ supplies its Cartesian regularity separately.

Proof. We apply Lemma 1.16.9 to the same corrected central component. Lemmas 1.6.10 and 1.6.11, with Proposition 1.15.20, provide its complete future on the fixed normalized-geometry and actual matched-memory domain. The same finite prefix and wait of Lemmas 1.14.1 and 1.14.2 give

$$H = A_c(\hat{\xi}/\sqrt{2})^{-2\nu}, \qquad I = \frac{A_c\big(\frac{\hat{\xi}^2}{2}\big)^{1-\nu}}{1-\nu} + K_c, \qquad \nu = \nu_c,$$

with scalar $A_c, K_c, \frac{\hat{\xi}_p^2}{2}, H_p, e_p, r_p, \sigma_p$. Thus $H_\eta = E_\eta = (\frac{\hat{\xi}_p^2}{2})_\eta = \nu_\eta = 0$ at fixed $\hat{\xi}$ on the pulse.

The actual incoming data satisfy $M_p = J_p = 0$, $r_p \le r_{\mathrm{eq}} = (1-\nu)^{-1}$ and $|r_p - r_{\mathrm{eq}}| \le K\nu^{60(1-\nu)}$. No primitive constant is reset. We keep the selected outlet graph ρ, its endpoint germs and bounded ordinary derivative, together with the stated C^1 bounds for τ_S, τ_P. Their angular derivatives can be nonzero at $\eta = 0$. In particular, the hypothesis includes non-even ρ.

We write $y = 2\log(\hat{\xi}/\hat{\xi}_p)$ and use the actual positive energy root A_p and its two-return coefficients:

$$R = U/E = A_p(\eta)\Phi(\nu y) + \sum_j c_j(\eta)\psi(y - Y + d_j), \qquad c_j = A_p\beta_j.$$

We set $a = 1 - \nu$, $q = h - \nu$, $m = M/(\frac{\hat{\xi}^2}{2}E)$ and $j = J/(\frac{\hat{\xi}^2}{2}HE)$. Then

$$Q_{\mathrm{lin}} = q/a + (1-h)(r_{\mathrm{eq}} - r_p)e^{-ay} \ge q/a \ge ch.$$

The ordinary-angular identity of (1.16.30) is

$$Q - Q_{\mathrm{lin}} = E[2(\tfrac{1}{2} - h)\eta m + dm_\eta - dj_\eta + 2(h - (\tfrac{1}{2} - h))\eta j]. \tag{1.6.31}$$

The stable history equations in the cited proof bound this correction by KE. The heat-coefficient inlet amplitude obeys $e_p \le K_{\mathrm{env}} e_{\mathrm{end}} e^{-(\lambda-\nu)Y_{\mathrm{end}}}$, with $\nu < h/10 < \lambda/2$. We select Y so that $Ke_p \le q/(4a)$. Then $Q \ge 3q/(4a)$ before we estimate N_s or w.

The same actual root contains the return energies and scalar σ_p. It satisfies $|(A_p)_\eta| \le K_f \mathcal{P}(Y_{\max}) e^{-c_\nu Y_{\min}}$. We impose no parity or $O(|\eta|)$ bound on this derivative.

The canonical S, P identities in that proof keep all moving-outlet boundary terms. Scalar H on the pulse does not imply that these angular derivatives vanish. On the main template and its adjoining phase window $y \le y_m = (\xi_m + 2)/\nu$, (1.16.31) gives

$$|w - 2R| \le K_\Phi[\nu/h + |(A_p)_\eta|/h + |r_p - r_{\mathrm{eq}}|/h] + K_{\mathrm{cen}} e_p/h. \tag{1.6.32}$$

The constant K_Φ depends only on the fixed finite C^3 template.

The constant K_{cen} can contain $1/\nu$ and the fixed future constants. It is uniform for all sufficiently large later Y. These identities use ordinary derivatives throughout and do not divide by η.

The parameter order is unchanged. First we select ν/h small after the original template and prefix constants. The wait controls the incoming memory. We then select Y so that the root-derivative and amplitude terms are small.

These terms include $e_p/(\nu h)$ when it occurs in K_{cen}. We also impose $Y_{\min} \ge 4(\xi_m + 2)/\nu$ plus the fixed return offsets. The convolution and actual return estimates in that lemma give $2\nu w^2 < 1$ on quiet intervals. They give strict relaxed-cone margins on the two returns.

After the last return, $M = J = 0$ with all angular derivatives. Their energy stays in this same root and their pressure contribution is zero because they change only U. These are estimates for the same fields on the central open band. We can take the overlap with the variable-sector argument at $\eta_c/2 \le |\eta| < \eta_c$, where $\chi = 0$ and $\dot\nu = 0$.

The positive root, return solution and histories coincide there, so no new angular gluing is necessary. Higher same-member jets are finite. We infer no higher-jet bound from the C^1 future bound.

For this fixed Y, with $L_{\mathrm{geom}} = 1 - 2h\eta^2$,

$$\inf_{\mathrm{pulse}} \tfrac{\hat\xi^2}{2} Q/L_{\mathrm{geom}} \ge ch^{\frac{\hat\xi_p^2}{2}} \longrightarrow \infty$$

as $C \to \infty$ with Y fixed. We first fix the finite w and control norms. We then select C to meet this finite-p threshold and the viscosity bound. It must also meet each condition $C \ge C_0(Y)$ in Remark 1.6.9.

Then we select the activation parameters for this member. We do not increase C to reduce e_p. This proves the stated central estimate. The next sections establish the remaining admissibility conditions. □

1.6.3.6 The fixed-λ buffer and exact endpoint obligations

All large-amplitude and ν transitions lie where $G = 0$. We use a fixed-width buffer to connect this region to the decreasing endpoint angular profile and keep the stress sign. Lemma 1.6.14 proves its fixed-coordinate identities. Let

$$K = K_b \lambda_{\mathrm{ch}}^{h-\lambda}/(1+\beta^2), \qquad H = K(\hat\xi_s/\sqrt{2})^{-2\lambda} F_\lambda(2\log(\hat\xi/\hat\xi_s)), \quad U = Gk(2\log(\hat\xi/\hat\xi_s)).$$

The backward pretemplate F_λ starts with the γ-power, passes through a plateau, and equals $F_T(\lambda)e^{-\lambda(z-T)}$ on the power germ $z \ge T$. Thus the coefficient there is

$$H_w(R_o)R_o^\lambda = KF_T(\lambda)e^{\lambda T}.$$

We write $\frac{\hat\xi_s^2}{2} = \frac{\hat\xi_{s,b}^2}{2}e^s$, $s = -\rho_s \log\lambda_{\rm ch}$. First we increase G from zero to 2 with $s = 0$. Then we change s to $-\log\lambda_{\rm ch}$ with $G = 2$. Then we increase G to the exact $G_e = 4\lambda_{\rm ch}\eta$.

We arrange $\dot s \le 2 + \epsilon$ on the phase-change band. A negative $\dot s$ gives a positive contribution to this source. The growth source is

$$\gamma + h + 2((\tfrac12 - h)\gamma + h)\eta G + \gamma dG' + \frac{(\frac12 - h)\eta - dG}{(\frac12 - h)\eta}[\log\dot K - (\lambda + \gamma)\dot s].$$

At the limiting endpoint with $G = 2$ and $\dot s = 2$ its reserve is $1.1 - .4h > 0$.

Fixed small bands and smooth flat cutoffs keep a uniform reserve, and $(\frac12 - h)\eta - dG$ stays outward. The slow turnoff is inside the plateaus of the two profiles. We fix the phase spread smaller than the original plateau-before-turnoff reserve. Then $H/H_{\rm chart} = 1 + O_{C^1}(\lambda)$ there, and the actual complete outward pressure differs by $O_{C^1}(\lambda E^2) + O(C_{\rm geo}/R)$. After the negative turn the two fields have the same power germ $H = KF_T(\lambda)e^{\lambda T}(\hat\xi/\sqrt{2})^{-2\lambda}$.

We keep the incoming histories after U becomes zero. The negative-turn source is

$$S_q = \ell_r + h + \log\dot K - (\lambda + \ell_r)\dot s + \ell_r K_M/\tfrac{\hat\xi^2}{2}, \qquad K_M = (1 - 2h)\eta M + dM_\eta. \tag{1.6.33}$$

The chart reserve controls the fixed bound on $K_M/\frac{\hat\xi^2}{2}$ times $|\ell_r| \le C\lambda$. The fixed-coordinate proof below keeps this term, the incoming histories and the complete pressure through the slow turnoff. The changes in I, S stay in the normalization.

On the last flat-λ band, Lemmas 1.14.3, 1.14.4, and 1.14.5 construct the true incoming histories, primitive taper, and heat-compensation correction. Their supports are outside the genuine ν transition. The affine returns of (1.14.19) keep their nonzero incoming M, J. The full energy Gram equation keeps all mixed square terms.

Proposition 1.14.6 keeps the actual bridge residual $-2\lambda(1 - \chi_b)\Delta S_f/H_p^2$, which the selected scale makes sufficiently small. The residual vanishes with all jets on the protected collars where the full correction target is restored. Only there does Lemma 1.16.5 give exact equality with the jointly rebuilt backward root. The late A11 target is that same actual canonical primitive.

The new rank-one correction has zero complete primitive discrepancy. We do not correct it a second time. Lemma 1.16.8 gives the bridge pulse estimate and its quiet/return cone bounds. Thus the chart transformation (1.6.16) applies to this jointly rebuilt member on its full radial prefix. Lemma 1.25.10 identifies its two leading jets there.

Lemma 1.6.14 (The bridge in fixed physical coordinates)**.** *For the selected fixed-width near-endpoint buffer, the complete edited reference has the strict relaxed cone during its slow axial turnoff. The constants used to select M_d, T_d, P_* come from fixed chart and normalized model geometry. The later radius controls the heat-correction errors, whose constants do not enter these earlier selections. We do not assert strict admissibility at all points where $U_y = 0$.*

Proof. We work on the positive turnoff buffer, where $\eta \ge \eta_a > 0$, and reflect at the other end. We put $y = 2\log(\hat\xi/\hat\xi_{s,b})$, independent of η, and $z = y - s(\eta)$. On the same plateau containing each k' support, we absorb the scalar plateau normalization into P_1. The actual fields are

$$\begin{aligned} &E = P_1 f(\eta)e^{-y/2}, && f \ \text{ proportional to } (K/K_b)e^{-\lambda s}, \\ &U = Gk(y - s), && U_\eta|_{\hat\xi} = G'k - Gk's', \qquad U_y = Gk'. \end{aligned} \tag{1.6.34}$$

Thus $(\log f)' = K'/K - \lambda s'$.

In particular the endpoint identities are

$$\begin{aligned} \dot{\log} K &= (\tfrac{1}{2} - h) - 2h + 2\lambda, \quad \dot{s}_e = 2, \\ \dot{\log} f &= (\tfrac{1}{2} - h) - 2h, \\ (\log f)' &= ((\tfrac{1}{2} - h) - 2h)/(\tfrac{1}{2} - h), \quad s_e' = 2/(\tfrac{1}{2} - h). \end{aligned}$$

Dots mean $(\frac{1}{2} - h)\eta\partial_\eta$, not ordinary derivatives. Let C_{ph} denote a fixed phase-spread bound. This bound is distinct from the heat-error constant C_{geo} that we define next. The fixed buffer has $\dot{s} \le 2 + \epsilon_{\mathrm{geo}}$ and a fixed lower bound.

We can thus fix its width so $(\log f)' \ge c_f > 0$ and $(\frac{1}{2} - h)\eta - dG \ge c_v > 0$, with the same constants for all later sufficiently small λ, h. Also $G, G', s', f, 1/f$ have fixed bounds. There is no angular cutoff of width $O(\lambda)$.

We select one fixed-radius section after each growth turn and before each k' support. The plateau reserve and bounded phase spread ensure it exists. We shift y by its scalar value to a coordinate $\tau = 0$ at that section. For $\tau = y - y_0$, we replace P_1 by $P_1 e^{-y_0/2}$, so that $E = P_1 f e^{-\tau/2}$ in this proof.

This leaves all fixed-$\hat{\xi}$ angular derivatives unchanged. At this section, fixed growth-turn and chart factors give positive lower and upper bounds for P_1/P_*, independently of T_d. The section is only a fixed distance past the growth turn. This is an evaluation of the same prefix, not an independent normalization of K_b at the distant wait inlet.

No $e^{\lambda T_d}$ factor is hidden. Before the section $k = 1$, so the actual ideal histories are

$$M = G\tfrac{\hat{\xi}^2}{2}, \qquad J = GI, \qquad S/\tfrac{\hat{\xi}^2}{2} = G^2 - \left(\tfrac{\hat{\xi}^2}{2}\right)^{-1} \int_0^{\frac{\hat{\xi}^2}{2}} E(x,\eta)^2/2 \, dx.$$

Thus, with $m = M/\frac{\hat{\xi}^2}{2}$ and $n = S/\frac{\hat{\xi}^2}{2}$,

$$|m_0| + |m_{0,\eta}| \le K_{\mathrm{geo}}, \qquad |n_0| + |n_{0,\eta}| \le K_{\mathrm{geo}}(1 + E_0^2). \tag{1.6.35}$$

The growth arc has $H \sim \left(\frac{\hat{\xi}^2}{2}\right)^\gamma$, and its swirl integral divided by $\frac{\hat{\xi}_0^2}{2} E_0^2$ is a fixed constant.

Only a bounded short turn and plateau precede this same section. Differentiation of their single smooth moving-phase template keeps the boundary densities and gives the same bound. The incoming integral bound does not depend on the next length T_d. All earlier exact-history returns target this reference. No integration constant is reset.

On the pure growth arc the actual $I = \frac{\hat{\xi}^2}{2} H/(1+\gamma)$, $M = G\frac{\hat{\xi}^2}{2}$, $J = GI$ give $Q = S_{q,\gamma}/(1+\gamma)$. The source has a fixed positive lower bound. Its exact equation $Q_y + (1 + \ell_r)Q = S_q$ across the bounded γ-to-zero turn and short plateau yields $0 < q_0 \le Q_0 \le K_{\mathrm{geo}}$. This is a true incoming-primitive calculation, not an equilibrium assumption. Here Q is the leading stress-equation coefficient. The selected radius controls the finite-scale errors.

We next verify the complete-pressure input for this same future. Let P_e be the chart of the rebuilt backward model with phase $s_e = -\log \lambda_{\mathrm{ch}}$. Beyond the same section the two fields have passed the two growth turns. On their plateaus $H/H_e = e^{\lambda(s_e - s)}$.

On the next negative turns $|\ell_r| \le \lambda$ gives the same $1 + O_{C^1}(\lambda)$ comparison. After the two turns both fields equal $KF_T(\lambda) e^{\lambda T} (\hat{\xi}/\sqrt{2})^{-2\lambda}$ on their common power germ. The backward model has fixed angular factors $f_b(\beta)^\vartheta$ with $0 \le \vartheta \le 1$, and a nonincreasing bounded H envelope outward from this plateau. Direct integration of $H^2/(4\frac{\hat{\xi}^4}{4})$ and its β derivative gives

$$|P_b| + |P_{b,\beta}| \le K E_b^2.$$

The normalized scalar model terminal shape has the same bound. The constant is independent of T_d, P_*, Y_0 and later small λ, h: no $1/h$ energy estimate is used for pressure. The exact chart law and its fixed-$\hat\xi$ derivative are

$$P_e = \lambda_{\rm ch}^{1+2h} P_b(\lambda_{\rm ch}\tfrac{\hat\xi^2}{2}, \beta), \tag{1.6.36}$$
$$P_{e,\eta} = \lambda_{\rm ch}^{1+2h}\left[(1+2h)\frac{\lambda'_{\rm ch}}{\lambda_{\rm ch}}P_b + \beta' P_{b,\beta} + \frac{\lambda'_{\rm ch}}{\lambda_{\rm ch}}\frac{\hat\xi_b^2}{2}\frac{P_{b,\hat\xi_b}}{\hat\xi_b}\right], \qquad \frac{\hat\xi_b^2}{2}\frac{P_{b,\hat\xi_b}}{\hat\xi_b} = E_b^2/2.$$

Here $\beta = \lambda_{\rm ch}^{\frac12-h}\eta$. In slice variables the first identity is $\widetilde P_e = \widetilde P_b$, because P has weight $2(\frac12+h) = 1+2h$ (Remark 1.6.7).

The second identity is the chain rule for the first one at fixed $\hat\xi$. We keep it, because the estimate below uses the forward η-derivative. In particular $|P_e| + |P_{e,\eta}| \le K_e E_e^2$. The last term is the actual moving-radius boundary term.

We integrate the relative density difference on the plateau and short turn. The identity $\int_{(\frac{\hat\xi^2}{2})}^{\infty} x^{-2}dx = (\frac{\hat\xi^2}{2})^{-1}$ gives this bound for the actual edited reference:

$$|P - P_e| + |\partial_\eta(P - P_e)| \le (K_{\rm geo}\lambda + \epsilon_R)E_e^2, \qquad \epsilon_R \le C_{\rm geo}/R. \tag{1.6.37}$$

No duration factor occurs. At support endpoints that move, the *difference* density vanishes because the power germs agree. This does not remove the raw boundary term in (1.6.36).

The two-E I/C_p taper and A11 family have zero total C_p and thus no earlier pressure effect. Their energy contributions stay in the pulse normalization. The exact heat edit and its three-E compensation extension have the normalized C^1 $O(C_{\rm geo}/R)$ bound. In the protected chart collar the total compensation is exact. In the buffer, we include its error.

Only the later selection of R controls the constant $C_{\rm geo}$, which can depend on the fixed heat/future geometry. The pressure-class repair and core five-moment correction keep the physical pressure of this edited reference past their supports. Thus this comparison uses the same histories and future as (1.6.35), not a factorized example.

We put $B = 1 + 2(\frac12 - h)\eta m + d m_\eta$. The exact axial numerator is

$$N_s = BU - (\tfrac12 - h)m + (\tfrac12 - h)\eta m_\eta + 4h\eta n - d n_\eta + 4(\tfrac12 + h)\eta P - dP_\eta.$$

The incoming bounds and actual pressure give $|N_s(0)|/E_0^2 \le K$ when $P_1 \ge 1$. On this annulus $|\eta| \ge \eta_a$, so the usual weighted incoming bound also holds.

In the fixed coordinate,

$$m_\tau = U - m, \qquad n_\tau = U^2 - E^2/2 - n, \quad P_\tau = E^2/2, \tag{1.6.38}$$
$$Q_\tau + Q = h(1 + 2\eta U) + ((\tfrac12 - h)\eta - dU)(\log f)'.$$

The source is at least $q_* > 0$. Thus $Q \ge q_*(1 - e^{-\tau}) + q_0 e^{-\tau} \ge q_{\min} > 0$.

Direct differentiation cancels the EE_η terms and gives

$$(N_s)_\tau + N_s = BU_\tau + (\tfrac12 + h)U + (\tfrac12 - h)\eta U_\eta + 2(\tfrac12 + h)\eta U^2 - dUU_\eta \tag{1.6.39}$$
$$+ \eta E^2 + 4(\tfrac12 + h)\eta P - dP_\eta.$$

Substitution of (1.6.34) keeps the phase term $-((\frac12 - h)\eta - dU)Gk's'$. We keep this term, not omit it, and $K_{\rm geo}|k'|$ bounds it. Direct convolution bounds m, m_η.

No k'' bound is necessary here. With $|k'| \le K_{\mathrm{geo}} e_d/(1+\tau)$ and $0 \le \tau \le T_d + C_{\mathrm{ph}}$, the actual convolution yields

$$\frac{|N_s|}{E^2} \le K\left[1 + \tau + \frac{e^\tau - 1}{P_1^2}\right].$$

The last term comes from the bounded geometric coefficients. The selection $P_1^2 \ge K_{\mathrm{geo}} e^{T_d + C_{\mathrm{ph}}}$ gives $|N_s|/E^2 \le K(1+\tau)$.

Thus $a_s = 2$, $b_s = 2U_\tau/E$, $w = N_s/(EQ)$ satisfy

$$|b_s w| \le K e_d, \qquad b_s^2 \le K e_d^2 e^{T_d + C_{\mathrm{ph}}}/P_1^2.$$

We use the total normalized axial deviation j_{eff} of the actual edited reference from the turnoff template, Definition 1.6.15 below. Its core part contains the endpoint offset j_0: $u - G_e = \lambda_{\mathrm{ch}}^{\frac12+h} j_0$ exactly, because $(\frac12 + h) + (\frac12 - h) = 1$. We have $j_{\mathrm{eff}} \le K_{\mathrm{geo}} K_{\mathrm{ax}}(j_0 + \varepsilon_u)$, with K_{ax} the constant of Lemma 1.6.16, where ε_u is the axial mismatch tolerance of Lemma 1.6.36 (Lemma 1.6.16; the bound on $|b_s w|$ below is Lemma 1.6.17).

With the pressure error included, the same convolution gives

$$|b_s w| \le K\big[e_d + j_{\mathrm{eff}}(1 + T_d + C_{\mathrm{ph}})\big](1 + K_{\mathrm{geo}}\lambda + \epsilon_R), \qquad b_s^2 \le K(e_d^2 + j_{\mathrm{eff}}^2) e^{T_d + C_{\mathrm{ph}}}/P_1^2.$$

We have $(1+T)^2 e^{-T} \le 4/e < 1.48$ for $T \ge 0$. Thus the j_{eff} term is at most $1/8$ if $1 + K_{\mathrm{geo}}\lambda + \epsilon_R \le 2$ and

$$j_{\mathrm{eff}}^2 e^{T_d + C_{\mathrm{ph}}} \le c_j := \big(1.48\,(16K)^2\big)^{-1}.$$

We first select the fixed geometry, then M_d, T_d so that $K e_d \le 1/8$.

We next select $P_* > e^{T_d}$ with its fixed normalization multiplier, so that $P_1^2 \ge K_{\mathrm{geo}} e^{T_d + C_{\mathrm{ph}}}$. Then we select λ, a smaller h, the future, and Y_0, in this order. The endpoint offset j_0 is selected in Step 4 of Section 1.5.2, after the backward datum Π_0 and the tolerance ε_u are fixed (Remark 1.8.12). It is subject to $K_{\mathrm{geo}} K_{\mathrm{ax}} j_0 \le \frac12 j_\sharp$, where $j_\sharp := \min\{\sqrt{c_j}\, e^{-(T_d + C_{\mathrm{ph}})/2},\ 1,\ q_*/(4K_{\mathrm{geo}})\}$. These constants are fixed here. We apply the same threshold, $K_{\mathrm{geo}} K_{\mathrm{ax}} \varepsilon_u \le \frac12 j_\sharp$, when we select ε_u. Then $j_{\mathrm{eff}} \le j_\sharp$. This gives $j_{\mathrm{eff}}^2 e^{T_d + C_{\mathrm{ph}}} \le c_j$, and it also gives the hypothesis $j_{\mathrm{eff}} \le \min\{1, q_*/(4K_{\mathrm{geo}})\}$ of Lemma 1.6.17. We select R last to control ϵ_R. Thus

$$a_s - b_s w > 1, \qquad 2 - 2b_s w - b_s^2/a_s - (a_s - 2)w^2 > 1.$$

These are strict relaxed-cone inequalities.

After we fix P_1, T_d and all finite geometry, we bound w. This bound can depend on P_1. We increase the radius for the finite-p threshold and use $\frac{\hat\xi^2}{2} Q \ge q_{\min} \frac{\hat\xi_{\mathrm{start}}^2}{2}$. When $U_\tau = 0$ we get $a_s = 2$ and $v_s = 2$, so we make no strict-admissibility assertion at that face. □

The deviation j_{eff} and the turnoff cone. *Inputs.* Lemma 1.6.14: fields (1.6.34), incoming histories (1.6.35), the Q equation and floor $q_{\min}$ (1.6.38), the N_s identity (1.6.39), $|k'| \le K_{\mathrm{geo}} e_d/(1+\tau)$ and $0 \le \tau \le T_d + C_{\mathrm{ph}}$ (proof of Lemma 1.6.14), $P_1^2 \ge K_{\mathrm{geo}} e^{T_d + C_{\mathrm{ph}}}$, pressure comparison (1.6.37), and $H/H_e = 1 + O_{C^1}(\lambda)$ (Section 1.6.3, proof of Lemma 1.6.14). Endpoint core germ $u = \lambda_{\mathrm{ch}}^{\frac12+h}(4\beta + j_0)$, $\beta = \lambda_{\mathrm{ch}}^{\frac12-h}\eta$, $0 \le j_0 \le .05$ (Lemma 1.6.38, proof of Lemma 1.6.38), $\lambda_{\mathrm{ch}} = \ell$ (Section 1.6.1). Exact endpoint template $G_e = 4\ell\eta$ (Section 1.6.3). "We select the tiny central and endpoint axial offsets first" (Section 1.6.4). Axial mismatch tolerance ε_u in the normalized C_η^1 norm (Lemma 1.6.36, proof of Lemma 1.6.36). The order of Remark 1.8.12, in which j_0 is chosen after h: $\cdots \ll j_0 \ll \varepsilon_m \ll h \ll \lambda \ll P_*^{-1} \ll M_d^{-1}$.

The endpoint core axial profile satisfies $u - G_e = \ell^{\frac12+h}(4\ell^{\frac12-h}\eta + j_0) - 4\ell\eta = \ell^{\frac12+h} j_0$ because $(\frac12 + h) + (\frac12 - h) = 1$. The deviation from the turnoff template includes this term.

Definition 1.6.15. Let I_{off}^{+} be the closed positive turnoff buffer in the fixed-λ sector beyond the exponent transition, selected in Section 1.6.3. Set $I_{\mathrm{off}} = I_{\mathrm{off}}^{+} \cup (-I_{\mathrm{off}}^{+})$. Here $|\eta| \ge \eta_a$ is a lower bound on the buffer. The endpoint chart is taken on the near-endpoint interval selected in Section 1.15.7, where $1 \le \lambda_{\mathrm{ch}} \le 2$. On I_{off} let the template be $U_{\mathrm{tmp}} = Gk(y-s)$, $m_{\mathrm{tmp}} = G$ and $n_{\mathrm{tmp}} = G^2 - (\frac{\hat\xi^2}{2})^{-1} \int_0^{\frac{\hat\xi^2}{2}} E^2/2$ before the section (proof of Lemma 1.6.14). Let $\delta U = U - U_{\mathrm{tmp}}$ on the band $0 \le \tau \le T_d + C_{\mathrm{ph}}$, and let $\delta m_0, \delta n_0$ be the history deviations at the section $\tau = 0$. Put

$$j_{\mathrm{eff}} := \sup_{\eta \in I_{\mathrm{off}}} \Big[\sup_{\tau} \big(|\delta U| + |\partial_\tau \delta U| + |\partial_\eta \delta U| \big) + |\delta m_0| + |\partial_\eta \delta m_0| + |\delta n_0| + |\partial_\eta \delta n_0| \Big].$$

Lemma 1.6.16 (Size of j_{eff})**.** *In the selected construction, $\delta U \equiv 0$ on the band: the fields (1.6.34) are the actual fields of the edited reference before the strictification of Subsection 1.6.5 (the capped loop acts later and may be active on the turnoff buffer I_{off}; it is not part of this reference, and the spectral edits lie on the central hold), and the core, its activation and the $G_i \to G$ interpolation precede the section. Let $\varepsilon_{\mathrm{ax}}$ be the normalized $C^1_\eta C^0_{\hat\xi}$ size of $U - U_{\mathrm{tmp}}$ on $[0, \frac{(\hat\xi_0(\eta))^2}{2}]$, where $\frac{\hat\xi_0^2}{2}$ is the section radius. Then $j_{\mathrm{eff}} \le K_{\mathrm{geo}} \varepsilon_{\mathrm{ax}}$. On the endpoint collars $\varepsilon_{\mathrm{ax}} \ge \ell^{\frac12 + h} j_0$, and $\varepsilon_{\mathrm{ax}} \le K_{\mathrm{ax}}(j_0 + \varepsilon_u)$.*

Proof. $\delta M(\frac{\hat\xi_0^2}{2}) = \int_0^{\frac{\hat\xi_0^2}{2}} (U - U_{\mathrm{tmp}})\,\mathrm{d}x$, so $|\delta m_0| \le \varepsilon_{\mathrm{ax}}$. The fixed-$\hat\xi$ η-derivative adds the moving-endpoint density, which is bounded by the same C^1_η quantity times the fixed bound on $(\log \frac{\hat\xi_0^2}{2})'$. $\delta S = \int (U - U_{\mathrm{tmp}})(U + U_{\mathrm{tmp}})$, and the E-part of S is the actual one in both, so $|\delta n_0| + |\partial_\eta \delta n_0| \le K_{\mathrm{geo}} \varepsilon_{\mathrm{ax}}$. The core part of the mismatch is j_0 plus the core error controlled by Λ (proof of Lemma 1.6.36). The interpolation and termination parts are within ε_u. □

Lemma 1.6.17 (Turnoff cone with deviation)**.** *Assume the inputs, $j_{\mathrm{eff}} \le \min\{1, q_*/(4K_{\mathrm{geo}})\}$, and $P_1^2 \ge K_{\mathrm{geo}} e^{T_d + C_{\mathrm{ph}}}$. Then there is K_3, depending only on the fixed geometry ($K_{\mathrm{geo}}, C_{\mathrm{ph}}, q_{\min}, f^{\pm 1}$), such that on the band*

$$|b_s w| \le K_3 \big[e_d + j_{\mathrm{eff}}(1 + T_d + C_{\mathrm{ph}}) \big](1 + K_{\mathrm{geo}}\lambda + \epsilon_R), \qquad b_s^2 \le K_3 (e_d^2 + j_{\mathrm{eff}}^2)\, e^{T_d + C_{\mathrm{ph}}}/P_1^2.$$

If $\delta U \equiv 0$ (Lemma 1.6.16), the first bound improves to $|b_s w| \le K_3 e_d (1 + j_{\mathrm{eff}} + K_{\mathrm{geo}}\lambda + \epsilon_R)$.

Proof. At fixed η, $E^2 = P_1^2 f^2 e^{-\tau}$. The Q source changes by at most $K_{\mathrm{geo}} j_{\mathrm{eff}} \le q_*/4$, so $Q \ge q_{\min}/2$. In $(N_s)_\tau + N_s = S_{\mathrm{geo}} + S_{\mathrm{pr}}$ (1.6.39), $|S_{\mathrm{geo}}| \le K(1 + j_{\mathrm{eff}})^2$, since $U, U_\eta, U_\tau, m, m_\eta$ are bounded by $K_{\mathrm{geo}}(1 + j_{\mathrm{eff}})$. Also $|S_{\mathrm{pr}}| \le KE^2$. The pressure error contributes at most $(K_{\mathrm{geo}}\lambda + \epsilon_R) K E^2$, because $E_e \le KE$ on the band. Further, $|\delta N_s(0)| \le K j_{\mathrm{eff}}$. Using $\int_0^\tau e^{-(\tau-\sigma)}\,\mathrm{d}\sigma = 1 - e^{-\tau}$ and $\int_0^\tau e^{-(\tau-\sigma)} e^{-\sigma}\,\mathrm{d}\sigma = \tau e^{-\tau}$,

$$|N_s|/E^2 \le K\big[1 + \tau + j_{\mathrm{eff}} + (1 + j_{\mathrm{eff}})^2 (e^\tau - 1)/P_1^2 + (K_{\mathrm{geo}}\lambda + \epsilon_R)\tau\big],$$

and $(e^\tau - 1)/P_1^2 \le 1$. Since $b_s = 2U_\tau/E$ and $|U_\tau| \le K_{\mathrm{geo}} e_d/(1+\tau) + j_{\mathrm{eff}}$, we get $|b_s w| = 2|U_\tau||N_s|/(E^2 Q)$, which gives the first bound after $(1+\tau)/(1+\tau) \le 1$ and $\tau \le T_d + C_{\mathrm{ph}}$. The second follows from $1/E^2 = e^\tau/(P_1^2 f^2)$. If $\delta U \equiv 0$, then $U_\tau = U_{\mathrm{tmp},\tau} = Gk'$, and the factor $K_{\mathrm{geo}} e_d/(1+\tau)$ multiplies the whole bracket. □

Corollary 1.6.18 (Cone and parameter order)**.** *With $a_s = 2$ on the plateau (proof of Lemma 1.6.14), $|b_s w| \le \frac14$ and $b_s^2 \le \frac12$ give $a_s - b_s w \ge \frac74 > 1$ and $2 - 2b_s w - b_s^2/a_s - (a_s - 2)w^2 \ge \frac54 > 1$. These hold if $K_3 e_d(1 + K_{\mathrm{geo}}\lambda + \epsilon_R) \le \frac18$ and $K_3 j_{\mathrm{eff}}(1 + T_d + C_{\mathrm{ph}})(1 + K_{\mathrm{geo}}\lambda + \epsilon_R) \le \frac18$. The second condition is implied by*

$$j_{\mathrm{eff}}^2\, e^{T_d + C_{\mathrm{ph}}} \le c_j := \big(1.48 \cdot (16 K_3)^2\big)^{-1},$$

because $(1+T)^2e^{-T} \le 4/e < 1.48$. *This is the condition "*$j_{\mathrm{eff}}^2 e^{T_d+C_{\mathrm{ph}}} \ll 1$*". The same two conditions also give* $b_s^2 \le \frac{1}{2}$*: by Lemma 1.6.17 and* $P_1^2 \ge K_{\mathrm{geo}} e^{T_d+C_{\mathrm{ph}}}$, $b_s^2 \le K_3(e_d^2+j_{\mathrm{eff}}^2)/K_{\mathrm{geo}}$*; here* $K_3 e_d^2 \le 1/(64K_3)$ *and, since* $j_{\mathrm{eff}} \le \sqrt{c_j}$, $K_3 j_{\mathrm{eff}}^2 \le 1/(378K_3)$, *so* $b_s^2 \le 0.019/(K_3K_{\mathrm{geo}}) \le \frac{1}{2}$ *once* $K_3, K_{\mathrm{geo}} \ge 1$ *(we enlarge these constants if necessary). It is achievable without circularity:* $K_3, T_d, C_{\mathrm{ph}}, K_{\mathrm{geo}}, K_{\mathrm{ax}}, q_*$ *are fixed before* λ*, and first* ε_u *and then* j_0 *are selected later. The selections are* $K_{\mathrm{geo}}K_{\mathrm{ax}}j_0 \le \frac{1}{2}j_\sharp$*, with* $j_\sharp = \min\{\sqrt{c_j}e^{-(T_d+C_{\mathrm{ph}})/2}, 1, q_*/(4K_{\mathrm{geo}})\}$ *and* c_j *as just displayed. This selection is made at the position of "*j_{eff}*" in the proof of Lemma 1.6.14. The same bound holds for* $K_{\mathrm{geo}}K_{\mathrm{ax}}\varepsilon_u$ *when* ε_u *is selected in Lemma 1.6.36. By Lemma 1.6.16 these selections give* $j_{\mathrm{eff}} \le j_\sharp$*. This gives the display, and it also gives the hypothesis* $j_{\mathrm{eff}} \le \min\{1, q_*/(4K_{\mathrm{geo}})\}$ *of Lemma 1.6.17. Smaller* j_0 *harms nothing. There are two other uses: Lemma 1.6.38 needs* $j_0 \le .05$*, and the drift bound of Section 1.6.4 needs* $K_{\mathrm{ch}}j_0 \le \varepsilon_u/8$*. The endpoint margin* $|Z_R(\sigma)| \ge 2(5P_*^2/8-7)$ *is* j_0*-independent. The central drift root uses the separate central offset* u_0 *(Section 1.6.4).*

1.6.4 Canonical pressure, the regular core and moment corrections

The preceding construction fixes the radial continuation and its canonical pressure. We now approximate the axis pressure in a Gevrey class. We construct the regular core for that datum and restore the specified radial integrals. We then connect this core to the outer profile. We arrange the pressure and moment corrections to keep the later radial continuation and its pulse normalization unchanged.

1.6.4.1 Pressure regularity and Gevrey approximation

We fix Y_0 and all finite geometry before the selected large scale. Proposition 1.18.4 gives a scale threshold and a constant $K_P(Y_0)$. For each larger scale, the complete ideal reference pressure $\Pi_{\mathrm{ref}} = -\int_0^\infty H^2/(4\frac{\hat\xi^4}{4})\,\hat\xi\,\mathrm{d}\hat\xi$ has C^2 norm at most $K_P(Y_0)$. Its proof keeps the shot's second stable derivative and the integrated second moving-edge derivative of the narrow wing.

It includes all quadratic mixture and connector terms and the two- and three-row moment corrections. The width of its radial integration region offsets the height $R_b^{1/5}$ of the normalized wing derivative. We assert no uniform pointwise C^2 field bound there. The normalized future integral has the stronger before-Y_0 estimate of Proposition 1.18.3.

The complete prefix constant can depend on this fixed Y_0. The pressure functional depends on the fixed swirl, so it does not use an axial pulse-root regularity result to prove its own input. The same coefficient bounds give a positive scale-uniform correction amplitude e_* at fixed Y_0. We select the C^1 approximation tolerance relative to it.

The pressure of the heat tail can fail to belong to a Gevrey class of order $s < 2$. In fact its endpoint asymptotic coefficients can grow factorially. We use only $K = 1$ pressure approximation. Its inputs are the uniform C^2 bound of Proposition 1.18.4 and the central parity of Proposition 1.6.33. We use no central C^1 or C^K convergence in the scale. The complete endpoint jets are analytic.

The full correction to C_p cancels the backward heat edit where $\chi_b = 1$. Thus, on the full-compensation endpoint collars ($\chi_b = 1$), the complete backward datum is the analytic model Π_0. Differentiated full-path integrals with tail dominators then give the forward jets. In slice variables Π has weight $2(\frac{1}{2}+h)$, and

$$\partial_{\widetilde\eta}^k \widetilde\Pi_{\mathrm{ref}}(0^+) = \partial_{\widetilde\eta}^k \widetilde\Pi_0(0) \qquad (k \ge 0), \qquad \widetilde\Pi = |\eta|^{(1+2h)/(\frac{1}{2}-h)}\Pi. \tag{1.6.40}$$

Here $\widetilde\Pi_0$ is real-analytic across $\widetilde\eta = 0$, because Π_0 is analytic in η_b (Lemma 1.6.3).

In the forward chart, (1.6.40) states that Π_{ref} has the jets of $\lambda_{\mathrm{ch}}^{1+2h}\Pi_0(\lambda_{\mathrm{ch}}^{\frac{1}{2}-h}\eta)$ at $\eta = \pm 1$. This is a cancellation of the full canonical integral, not a regularity claim about its tail alone.

1.6.4.2 The central pressure before smoothing

Lemma 1.6.19 (Central pressure interval from the actual swirl)**.** *We fix the selected central templates, $0 < \nu = \nu_c \le h/10 < \lambda$, the finite turn, wait $W = 60\log(1/\nu)$ and hold, and the admitted scalar heat future before the selection of Y_0. For the actual complete central reference, we define*

$$m_R = -\Pi_{\mathrm{ref}}(0) = \int_0^\infty \frac{H(\frac{\hat\xi^2}{2},0)^2}{4\frac{\hat\xi^4}{4}}\,\hat\xi\,\mathrm{d}\hat\xi.$$

There are constants $0 < c_{\mathrm{P}} \le C_{\mathrm{P}} < \infty$, independent of the later Y_0 and of sufficiently large C, such that

$$c_{\mathrm{P}} e_p(C,Y_0)^2 \le m_R \le C_{\mathrm{P}} e_p(C,Y_0)^2. \tag{1.6.41}$$

The constants can depend on the fixed ν, h and templates.

By Lemma 1.6.20 and Theorem 1.6.29, one can select Y_0 first, and then a large-scale threshold, so that

$$0 < m_- \le m_R \le (\tfrac12 - h)/64 < m_+ := (\tfrac12 - h)/32 < (\tfrac12 - h)/8.$$

This bound applies to the actual canonical integral before the pressure-class smoothing and correction. We do not use smoothing to get it.

Proof. On a fixed flat-central band $\chi = 0$ the selected component is the unlifted scalar power $H_c(\frac{\hat\xi^2}{2}) = A_c(\hat\xi/\sqrt{2})^{-2\nu}$ before its actual primitive-memory correction and later heat drive. The pulse entry $\frac{\hat\xi_p^2}{2} = R_g e^{T_b+W}$ is scalar. The comparison outlet $R_o = R_g e^{Y_0+\rho(\eta)}$ may be curved, but it evaluates the same physical field, and

$$Y = Y_0 + \rho - T_b - W, \quad H_p = A_c(\hat\xi_p/\sqrt{2})^{-2\nu}, \quad e_p = H_p/\hat\xi_p, \quad H_{\mathrm{out}} = H_p e^{-\nu Y}.$$

Thus e_p is scalar on this band.

We write $b_c = 1 + 2\nu$ and $e_a = H_a/\sqrt{2R_g}$. The exact finite prefix gives

$$B_c := \frac{e_a}{e_p} = \frac{e^{T_b/2+(.5+\nu)W}}{F_b}, \tag{1.6.42}$$

which is fixed before Y_0. The positive-growth power, finite turn and negative-power wait contribute the complete pressure integral

$$\begin{aligned} P_{\mathrm{pre}} &= e_a^2 D_{\mathrm{pre}}, \\ D_{\mathrm{pre}} &= \frac12 + \frac12\int_0^{T_b} e^{-y}F(y;\nu)^2\,dy + e^{-T_b}F_b^2\frac{1-e^{-b_cW}}{2b_c}. \end{aligned} \tag{1.6.43}$$

In particular the unmodified growth arc $R_g/e \le \frac{\hat\xi^2}{2} \le R_g$ contributes $c_{\mathrm{arc}}e_a^2$, where $c_{\mathrm{arc}} = \frac52(1 - e^{-1/5}) > 0$. The specified outer heat-compensation extension is supported outside this flat-central band.

We can omit corrections with zero total C_p increment only in the complete pressure calculation. Partial histories must include them. We include the nonzero central memory edit below.

The exact pulse swirl contributes

$$P_{\mathrm{pulse}} = e_p^2\frac{1-e^{-b_cY}}{2b_c} \le \frac{e_p^2}{2b_c}. \tag{1.6.44}$$

The main amplitude and the actual axial return coefficients change U, not H. They do not change this pressure functional. Their nonzero energy contributions stay in the one actual energy root. There is no pressure factor proportional to the pulse length.

We next show that the full actual central future satisfies

$$0 < H(\tfrac{\hat{\xi}^2}{2}, \eta) \le K_H H_{\mathrm{out}}(\eta), \qquad \tfrac{\hat{\xi}^2}{2} \ge R_o(\eta), \tag{1.6.45}$$

with K_H fixed independently of Y_0, C. On the central angular band $d \ge d_{\min} > 0$. Scalar power holds and the deficit drive have negative logarithmic H slopes and do not increase H. Their output satisfies the amplitude and radius bounds (1.13.28), $2a_* \le R_b \le C_h a_*$ and $c_h G_0 \le G \le C_h G_0$, with deficit $C_b \asymp hGR_b^{4/5}$.

For the actual scalar shot, we write $y = g_* - H_b$, $z = i - I_b$. The stable system has $y' + a_s y = \beta_s z + q$, $z' = y$, zero initial difference, $a_s \ge 1/3$, $|q| \le CC_b/W_s$ and $|\beta_s| \le C/R_b$, where $W_s = \epsilon_s R_b$. Its stable kernel gives

$$\sup|y| \le CC_b/W_s + C(W_s/R_b)\sup|y|.$$

The fixed small ϵ_s absorbs the last term. This proves $|g_*| \le G(1 + CR_b^{-1/5}) \le K_s G$.

After the shot, the positive actual heat solution stays decreasing. The homogeneous equation $2xg_*'' + xg_*' + hg_* = 0$ gives $g_*'' < 0$ wherever $g_*' = 0$ and $g_* > 0$. Thus its initially negative derivative cannot become positive. We do not replace this field estimate with a bound on an unexposed modal fast coefficient.

The lift satisfies $H_L = d^{-h} g_*(\tfrac{\hat{\xi}^2}{2}/d) \le d_{\min}^{-h} K_s G$. The central wing subtracts a nonnegative term from H_L. On the actual radial primitive blend, the positive added velocity is $\chi_b' \Delta$, with $|\Delta| \le CC_b$ and $|\chi_b'| \le C/W_s$. It is bounded by $CC_b/W_s \le KG$.

These are the estimates for the constructed blend and primitive gap in (1.13.57), (1.13.56) and (1.13.61). They prove (1.6.45) for the reference shot, blend, wing and tail. Their constants do not depend on their scale or on the earlier pulse length. We include the actual hold pressure $G_h^2(1 - e^{-b_c B})/(4R_h b_c)$. Because $R_h \ge R_o$ and $G_h \le H_{\mathrm{out}}$, the same pressure scale bounds it without a fixed-R_h/R assumption when Y_0 varies.

The central E edit can be nonzero on the flat-central band. We give its formula here. We fix, before Y_0 and heat-coefficient calibration, the equilibrium-reference point $r_{\mathrm{ref}} = 1/(1-\nu)$ in the admitted central family. It is strictly less than the heat ratio $1/(1-h)$, with

$$\frac{1}{1-h} - r_{\mathrm{ref}} = \frac{h - \nu}{(1-h)(1-\nu)} \asymp h.$$

Thus it has the necessary actual deficit $w_d \asymp h\tfrac{\hat{\xi}^2}{2}$, and the same scalar drive/shot construction applies.

This does not replace the heat coefficient after calibration. The actual incoming prefix memory relative to this reference is

$$\delta I = (r_b - r_{\mathrm{ref}})\tfrac{\hat{\xi}_p^2}{2} H_p e^{-(1-\nu)W}, \qquad \frac{\delta I}{R_o H_{\mathrm{out}}} = (r_b - r_{\mathrm{ref}}) e^{-(1-\nu)(Y+W)}.$$

This is a nonzero primitive constant. We remove it on the scalar central strip before the protected hold on a scalar interval $[R_m, 2R_m]$, at a fixed ratio to $\max R_o$, by

$$I_{\mathrm{new}} = i_s + \delta I\, \zeta(\tfrac{\hat{\xi}^2}{2}/R_m), \qquad \delta H = \frac{\delta I}{R_m}\zeta'(\tfrac{\hat{\xi}^2}{2}/R_m).$$

With $G_m = H_s(R_m)$, the normalized error satisfies $\epsilon_I = |\delta I|/(R_m G_m) \le K_I e^{-(1-\nu)Y_0}$. We select an initial $Y_{\min}$ so this lies in the fixed admitted small-memory range. Then $|\delta H| \le C\epsilon_I G_m$ keeps

(1.6.45) after a fixed enlargement of K_H. The corrected field and primitive equal the reference pair after the correction support. The correction leaves the next heat pair unchanged.

The signed actual pressure change is

$$\Delta C_{p,I} = \int \frac{2H_s\delta H + (\delta H)^2}{4\frac{\hat{\xi}^4}{4}}\,\hat{\xi}\,\mathrm{d}\hat{\xi}, \qquad |\Delta C_{p,I}| \le C\frac{H_{\mathrm{out}}^2}{R_o}(\epsilon_I + \epsilon_I^2).$$

We keep the cross and quadratic terms and include its energy contribution in the same pulse normalization. In contrast, the mixture's power-germ correction is identically zero on $\chi = 0$, because the component and target there have the same actual power and primitive germ. This specific fact does not eliminate the preceding nonzero memory edit.

The full actual bound (1.6.45) includes that edit. Integration gives

$$P_{\mathrm{future}} \le \frac{K_H^2 H_{\mathrm{out}}^2}{4R_o} = \frac{K_H^2}{2}e_p^2 e^{-b_c Y}. \tag{1.6.46}$$

Thus no factor $k_h(Y_0)$ or support length occurs. The formula for the memory correction identifies a contribution included in (1.6.46).

The combined bounds prove (1.6.41) with

$$c_{\mathrm{P}} = c_{\mathrm{arc}}B_c^2, \qquad C_{\mathrm{P}} = D_{\mathrm{pre}}B_c^2 + \frac{1}{2b_c} + \frac{K_H^2}{2}.$$

These constants are independent of the next Y_0. They can be large for the fixed small ν.

We now use the actual heat-coefficient envelope, not an independent selection of e_p:

$$\frac{e_p}{e_{\mathrm{end}}} = \frac{K_c}{K_{w,\mathrm{end}}}e^{-(\lambda-\nu)Y_{\mathrm{end}}}(\nu/\lambda)^{60(.5+\nu)} \cdot e^{(.5+\nu)(T_b(\lambda)-T_b(\nu))}e^{(\nu-h)(\rho_c-\rho_{\mathrm{end}})}.$$

An exact coefficient formula gives the necessary uniformity. Before the selection of Y_0, we select R_m at a fixed ratio to $\max R_o$. We select $R_h > 2R_m$ at a fixed ratio to R_m.

We leave an open power buffer after the memory support, as in Lemma 1.6.10. Then R_h/R_o ranges over a fixed positive compact interval even though R_h/R_{master} grows with Y_0. After the real memory edit the hold inlet is $G_h = A_c R_h^{-\nu}$ with reference ratio $r_{\mathrm{ref}} = 1/(1-\nu)$. The exact hold/coefficient law gives

$$K_c = \frac{H_{\mathrm{out}}R_o^h}{c_B} = \frac{(R_o/R_h)^{h-\nu}e^{-(h-\nu)B}}{K_{\mathrm{old}}(R_h e^B, r_{\mathrm{ref}})}.$$

The drive has the stated normalized radius and amplitude bounds. Together with the shot's exact regular-coefficient target, they give

$$K_{\mathrm{old}} = \frac{G_{\mathrm{bank}}}{G_{\mathrm{afterhold}}}\left(\frac{R_b}{R_{\mathrm{afterhold}}}\right)^h,$$

because the specified regular coefficient is $c_{\mathrm{bank}} = G_{\mathrm{bank}}R_b^h$. The two positive ratio bounds in (1.13.28) thus give positive lower and upper bounds for K_{old} independently of Y_0, C. The fixed outer postpulse coefficient law also gives positive lower and upper bounds for $K_{w,\mathrm{end}}$.

Its A10/A11 and drive templates precede Y_0, and the real memory/heat controls keep the inlet H and regular coefficient. Thus $K_c/K_{w,\mathrm{end}}$ has a bound independent of Y_0, C. This bound does not

use outer ordering at the central plane or a convergence rate uniform in Y_0. The actual endpoint wait gives $e_{\mathrm{end}} \le K_{\mathrm{pre}}\lambda^{30}$, so

$$e_p \le K_{\mathrm{env}}K_{\mathrm{pre}}\lambda^{30}(\nu/\lambda)^{60(.5+\nu)}e^{-(\lambda-\nu)Y_{\mathrm{end}}}.$$

We select Y_0 sufficiently large, before the core and selected C, that

$$C_{\mathrm{P}}K_{\mathrm{env}}^2K_{\mathrm{pre}}^2\lambda^{60}(\nu/\lambda)^{60(1+2\nu)}e^{-2(\lambda-\nu)Y_{\mathrm{end}}} \le (\tfrac{1}{2}-h)/64.$$

This establishes the upper bound for the actual pressure. The limit $C\to\infty$ alone would not establish it. The lower bound $m_- \le m_R$ is proved after Corollary 1.6.30. □

For this now fixed Y_0 we do not use a limit $C\to\infty$. We use an exact identity for e_p and two bounds that are uniform in C. These statements are Proposition 1.6.27, Theorem 1.6.29 and Corollary 1.6.30 below. They need one input on the backward outlet. It follows from the normalization of the backward model.

Lemma 1.6.20 (The backward outlet is a template quantity)**.** *Let $R := (CP_*)^{10}$, so that $\frac{\hat\xi_{\mathrm{ref}}^2}{2} = \frac{\hat\xi_i^2}{2}R$, and put $s_b := \big(\hat\xi_{s,b}/\hat\xi_{\mathrm{ref}}\big)^2$. Let $z_\gamma \in [0,T)$ be the length of the initial germ of the pretemplate on which $f_0' = \gamma$. Then $s_b \ge e^{-z_\gamma}$, and for every admitted C*

$$\frac{R_e}{R} = s_b\tfrac{\hat\xi_i^2}{2}\,e^T\lambda^{-60}e^{Y_{\mathrm{end}}}, \qquad e_e = \frac{H_e}{\sqrt{2R_e}} = P_*s_b^{1/10}F_T(\lambda)\,e^{-T/2}\lambda^{30+60\lambda}e^{-(\frac12+\lambda)Y_{\mathrm{end}}}. \tag{1.6.47}$$

In particular, with

$$r_e := e^{-z_\gamma}\tfrac{\hat\xi_i^2}{2}\,e^T\lambda^{-60}e^{Y_{\mathrm{end}}}, \qquad \underline{e}_e := P_*e^{-z_\gamma/10}F_T(\lambda)\,e^{-T/2}\lambda^{30+60\lambda}e^{-(\frac12+\lambda)Y_{\mathrm{end}}},$$

which are fixed after Y_0 and before C, we have $R_e \ge r_eR$ and $e_e \ge \underline{e}_e$ for every admitted C; any admitted threshold may serve as C_0. (The symbol $\underline{e}_e$ is distinct from the collar width ε_e of Lemma 1.6.38.) With the normalization $\hat\xi_{s,b} = \hat\xi_{\mathrm{ref}}$ of the backward branch, $s_b = 1$ and both quantities in (1.6.47) are independent of C.

Proof. Normalization. By (B1) of Hypothesis 1.5.5 (the temporary pair of Theorem 1.8.10 is the prefix (S3), Remark 1.8.11), $E = P_*f(\beta)\big(\hat\xi/\hat\xi_{\mathrm{ref}}\big)^{1/5}$ on $[\frac{\hat\xi_{\mathrm{match}}^2}{2}, \frac{\hat\xi_{\mathrm{ref}}^2}{2}]$, so $\log H$ has slope exactly $\gamma = \frac35$ in $\log\frac{\hat\xi^2}{2}$ there. By (S3) of Lemma 1.8.8, $H = K_bf(\beta)(\hat\xi_{s,b}/\sqrt2)^{-2\lambda}F_\lambda(z)$ with $z = 2\log(\hat\xi/\hat\xi_{s,b})$, and $(\log F_\lambda)' = \gamma$ exactly for $z < z_\gamma$, while $(\log F_\lambda)' = f_0' < \gamma$ at points arbitrarily close to z_γ from above ($f_1' = 0$ there). Hence $2\log(\hat\xi_{\mathrm{ref}}/\hat\xi_{s,b}) \le z_\gamma$, that is $s_b \ge e^{-z_\gamma}$. Comparison at $\frac{\hat\xi_{\mathrm{match}}^2}{2}$, where $z = -5 - \log s_b < 0$, gives $K_b\big(\frac{\hat\xi_{s,b}^2}{2}\big)^{-\lambda-1/2}/\sqrt2 = P_*s_b^{1/10}$.

Radius. $\frac{\hat\xi_{p,b}^2}{2} = \frac{\hat\xi_{s,b}^2}{2}e^T\lambda^{-60}$ and $R_e = \frac{\hat\xi_{p,b}^2}{2}e^{Y_{\mathrm{end}}}$ by (1.15.32). With $\frac{\hat\xi_{s,b}^2}{2} = s_b\frac{\hat\xi_i^2}{2}R$ this is the first formula. The pulse length $Y_{\mathrm{end}} = Y_0 + \rho_e - T + 60\log\lambda$ is fixed by Y_0 and the outlet geometry; it does not depend on C.

Amplitude. By Lemma 1.8.7, $H(R_e,\beta) = H_ef(\beta)$ with $H_e = K_bF_\lambda(y_w)e^{\lambda y_w}R_e^{-\lambda}$, and on the wait $F_\lambda(y_w)e^{\lambda y_w} = F_T(\lambda)e^{\lambda T}$. Hence $e_e = K_b\big(\frac{\hat\xi_{s,b}^2}{2}\big)^{-\lambda-1/2}F_T(\lambda)e^{\lambda T}(R_e/\frac{\hat\xi_{s,b}^2}{2})^{-\frac12-\lambda}/\sqrt2$, and $\log(R_e/\frac{\hat\xi_{s,b}^2}{2}) = T + 60\log(1/\lambda) + Y_{\mathrm{end}}$ gives the second formula.

No finite-scale error. Both formulas are exact. The core and the core-side corrections lie in $[0, \frac{\hat\xi_{\mathrm{match}}^2}{2}]$. The edits (ii)–(v) of Lemma 1.8.8 that change H have compact support before $\frac{\hat\xi_{p,b}^2}{2}$, and

the pulse and its returns change only U. A compact edit of the field H does not change H after its support; the finite-scale errors of the construction live in the histories, not in the values R_e and $H(R_e,\cdot)$. The scalars $P_*, \lambda, T, F_T(\lambda), z_\gamma$ are fixed before Y_0 (Section 1.5.2), and Y_{end} is fixed with Y_0. $\frac{\hat\xi_i^2}{2} = B_{\mathrm{r1}} = eB_{\mathrm{r0}} \geq 271$ is the constant of Definition 1.20.22. It is fixed in step 4, after Y_0 and before Λ and C. So r_e and $\underline{e}_e$ are fixed in step 4, before C. The only C-dependence of the backward prefix is the common factor $(CP_*)^{10}$ of $\frac{\hat\xi_{\mathrm{ref}}^2}{2}$ and R, under which H scales like $R^{1/2}$ and E is invariant; in particular $K_b = \sqrt{2}P_* s_b^{1/10}\big(\frac{\hat\xi_{s,b}^2}{2}\big)^{1/2+\lambda}$ grows with C, but e_e does not. The factor λ^{-60} in R_e/R and the factor $\lambda^{30+60\lambda}e^{-(\frac12+\lambda)Y_{\mathrm{end}}}$ in e_e are extreme but fixed before C. □

Lemma 1.6.21 (The heat-coefficient factor)**.** *The common heat coefficient has the form* $c = c_B = K_B R^{\frac12+h} e^{-(\lambda-h)(Y_{\mathrm{end}}+L_o)}$ *of* (1.6.21)*, with*

$$K_B = \sqrt{2}\, a_A k_A^h J\, e_e \Big(\frac{R_e}{R}\Big)^{\frac12+h} e^{(\lambda-h)Y_{\mathrm{end}}}.$$

The transfer factors are independent of C*: with* $T_f = T_0/\lambda$ *and* $W = 30\log(1/\lambda)$*,*

$$k_A = e^{T_f+W}, \qquad e^{-\frac32\lambda(T_f+W)} \leq a_A \leq e^{-\frac12\lambda(T_f+W)}, \qquad J = \frac{\exp[-\int_0^\delta(\kappa-h)\,\mathrm{d}t]}{1-\rho} > 0.$$

By Lemma 1.6.20, $K_B \geq K_- := \sqrt{2}\, e^{-\frac32\lambda(T_f+W)} k_A^h J\, \underline{e}_e\, r_e^{\frac12+h} e^{(\lambda-h)Y_{\mathrm{end}}} > 0$ *for every admitted* C*. More precisely,* (1.6.47) *gives the exact value*

$$K_B = \sqrt{2}\, a_A k_A^h J\, P_* F_T(\lambda)\, \big(\tfrac{\hat\xi_i^2}{2}\big)^{\frac12+h}\, s_b^{\frac{1}{10}+(\frac12+h)}\, e^{hT}\lambda^{60(\lambda-h)},$$

in which Y_{end} *cancels. With* $s_b = 1$*,* K_B *is independent of* C*,* Y_0 *and* L_o*. For every admissible* s_b *the same holds for* $K_- = \sqrt{2}\, e^{-\frac32\lambda(T_f+W)} k_A^h J\, P_* F_T(\lambda) \big(\frac{\hat\xi_i^2}{2}\big)^{\frac12+h} e^{-z_\gamma(\frac{1}{10}+(\frac12+h))} e^{hT}\lambda^{60(\lambda-h)}$*.*

Proof. The transfer chain before Lemma 1.15.23 gives $c = H_A^b (R_A^b)^h J e^{-(\lambda-h)L_o}$ with $H_A^b = a_A H_e$ and $R_A^b = k_A R_e$, and $H_e R_e^h = \sqrt{2}\, e_e R_e^{\frac12+h}$. Comparison with (1.6.21) gives the formula for K_B. The transfer runs through the flattening interval of length T_f in $y = \log\frac{\hat\xi^2}{2}$ and the uniform λ-power wait of length W. On the first, Lemma 1.15.4 gives $-\frac32\lambda \leq \partial_y \log H \leq -\frac12\lambda$; on the second the slope is exactly $-\lambda$. The A11 edits leave the outlet germ unchanged (Lemma 1.15.23). Integration in y gives k_A and the bounds for a_A. The lengths T_f and W, and the template data κ, δ, ρ of J, are fixed before C. The lower bound for K_B follows. □

The amplitude identity for e_p. The following statements prove the exact identity for e_p used below, its limit as $C \to \infty$, and the uniform two-sided bounds. The coefficient chain gives $e_p(C, Y_0) = \Theta(Y_0)/\kappa((k_h e^B R)^{-1/5})$, in which every power of the large scale cancels (Proposition 1.6.27); the post-hold stop map has a coefficient κ that is a C^∞ positive function on a closed interval $[0, \varepsilon_*]$ (Lemma 1.6.26). The convergence is from below, the rate $R^{-1/5}$ is sharp, and the relative error bound is uniform in Y_0 (Theorem 1.6.29). Every use below needs only the uniform two-sided bounds of Theorem 1.6.29(iv). The statements labelled Hypotheses 1.6.22–1.6.25 are not additional standing hypotheses: H1.6.22, H1.6.24 and H1.6.25 restate the cited constructions, H1.6.23(2) is Lemmas 1.6.20 and 1.6.21, and H1.6.23(1) follows from the normalization $\frac{\hat\xi_{s,b}^2}{2} = \frac{\hat\xi_{\mathrm{ref}}^2}{2} = \frac{\hat\xi_i^2}{2}R$ of the backward branch (see the normalization in Lemma 1.8.20) and from the fact that R_g is $\frac{\hat\xi_{s,b}^2}{2}$

times a factor fixed before C (the moving graph $\frac{\hat\xi_s^2}{2} = \frac{\hat\xi_{s,b}^2}{2} e^s$ of Section 1.6.3.6); in the $G = 0$ sector $R_g = \frac{\hat\xi_{s,b}^2}{2} = \frac{\hat\xi_i^2}{2} R$.

Uses of the amplitude bounds.

U1 $m_- = c_{\mathrm{P}}\,\Theta_-(Y_0)^2/k_+^2$, the threshold-free choice made in the completion of the proof of Lemma 1.6.19 (after Corollary 1.6.30), in Lemma 1.6.19. It satisfies $m_- \le c_{\mathrm{P}} e_p^2 \le m_R$ for every admitted C, because $e_p \ge \Theta_-(Y_0)/k_+$. The alternative $(c_{\mathrm{P}}/4) e_{p,\infty}^2$ of Corollary 1.6.30(c) needs the threshold of Theorem 1.6.29(v) and the exact C-independence of K_B; it is not used. The interval $0 < m_- \le m_R \le m_+$ is used at Section 1.6.4 and proof of Lemma 1.6.36. There the pressure tolerance ε_p is fixed relative to m_- *before* Λ and the last choice of C, so m_- must not depend on C.

U2 The C-uniform positive normalized swirl scale e_g on the protected central hold (Section 1.26; Section 1.6.3). It enters the stress ceiling $\mathcal{T}_{\theta,\mathrm{old}} \gtrsim h\, e_g C^5$ and the denominators e_g at proof of Lemma 1.27.1, (1.27.6), (1.30.28).

U3 The scale-uniform correction amplitude e_* (Section 1.6.4) and the two-sided bounds of E on the positive-growth sectors (proof of Lemma 1.6.36). Both are proportional to e_p through the fixed prefix factor B_c of (1.6.49).

Definitions and inputs. Throughout, $0 < h < 10^{-2}$, $\nu = \nu_c \in (0, h/10)$ is the central exponent on the flat central band $\chi = 0$ (so $\omega \equiv 1$, $\nu \equiv \nu_c$ there; (1.6.25), Lemma 1.15.26), and $B > 0$ is the fixed hold length (1.6.19). We write $a := 1 - h$ and $r_{\mathrm{ref}} := (1-\nu)^{-1}$.

Pulse amplitude. On the flat central band the selected component is the scalar power $H_c(\frac{\hat\xi^2}{2}) = A_c(\hat\xi/\sqrt{2})^{-2\nu}$. The pulse entry $\frac{\hat\xi_p^2}{2} = R_g e^{T_b + W}$, with $W = 60\log(1/\nu)$, is scalar, and

$$H_p = A_c(\hat\xi_p/\sqrt{2})^{-2\nu}, \qquad e_p := \frac{H_p}{\hat\xi_p} = \frac{A_c}{\sqrt{2}} \big(\tfrac{\hat\xi_p^2}{2}\big)^{-\nu-1/2}. \tag{1.6.48}$$

The prefix factor $B_c = e_a/e_p = e^{T_b/2 + (1/2+\nu)W}/F_b$ (1.6.42) is fixed before Y_0:

$$e_a = B_c\, e_p. \tag{1.6.49}$$

Hypothesis 1.6.22 (Central coefficient chain). ((1.6.19), (1.6.20), proof of Lemma 1.6.19, (1.15.27).) The hold inlet is at R_h with amplitude $G_h = A_c R_h^{-\nu}$. The hold maps $(R_h, G_h, r) \mapsto (R_h e^B, G_h e^{-\nu B}, r')$ (1.6.19). The heat coefficient of the central component is

$$c = G_h R_h^h e^{(h-\nu)B}\, K_{\mathrm{old}}(R_h e^B, r'), \tag{1.6.50}$$

where, for an afterhold state at radius R with amplitude G, $K_{\mathrm{old}}(R, r') := c/(GR^h)$ is defined by the post-hold stop map and exact shot of Hypothesis 1.6.25. The memory return $I = i_s + \delta I\, \zeta(\hat\xi^2/(2R_m))$ changes the scalar field H only on $[R_m, 2R_m]$, with $2R_m < R_h$ (proof of Lemma 1.6.19). The primitive ratio equals r_{ref} on $2R_m \le \hat\xi^2/2 \le R_h$. The ν-hold preserves the equilibrium ratio (1.6.19), so

$$r' = r_{\mathrm{ref}} = (1-\nu)^{-1} \quad \text{exactly, independently of } C, Y_0. \tag{1.6.51}$$

The central and outer components share the same regular heat coefficient c (Section 1.6.3, Section 1.15, Proposition 1.15.25).

Hypothesis 1.6.23 (Scale structure). Let $R := (CP_*)^{10}$ be the model scale (Section 1.6.3; the backward template uses $\frac{\hat\xi^2_{\rm ref}}{2} = k_R(CP_*)^{10}$, proof of Lemma 1.6.38, and $E^0 = P_* f(\beta) e^{y/10}$ with $y = 2\log(\hat\xi/\hat\xi_{\rm ref})$).

1. $R_g = x_g R$, $\frac{\hat\xi^2_p}{2} = x_p R$, $R_h = k_h R$, with $x_g, x_p, k_h > 0$ not depending on C. Each of them equals $\frac{\hat\xi^2_i}{2}$ times a quantity that depends only on Y_0 and on data fixed before Y_0. Indeed $\frac{\hat\xi^2_p}{2} = R_g e^{T_b}\nu^{-60}$ (1.6.23); $R_h = a_h^{\rm hold} a_m^{\rm mem} \max_\eta R_o$ with $R_o = R_g e^{Y_0+\rho(\eta)}$ (Section 1.6.3); k_h is "fixed after the future geometry and Y_0, before C". The scale identities follow from the normalization $\hat\xi_{s,b} = \hat\xi_{\rm ref}$ (see the normalization in Lemma 1.8.20) and from the fact that R_g is $\frac{\hat\xi^2_{s,b}}{2}$ times a factor fixed before C (the moving graph $\frac{\hat\xi^2_s}{2} = \frac{\hat\xi^2_{s,b}}{2} e^s$ with s fixed before C, Section 1.6.3.6); in the $G = 0$ sector $R_g = \frac{\hat\xi^2_{s,b}}{2}$, so that $x_g = \frac{\hat\xi^2_i}{2}$. The constant $\frac{\hat\xi^2_i}{2} = B_{\rm r1}$ is fixed in step 4 of Section 1.5.2 (Definition 1.20.22), after Y_0. Every quantity used before step 4 is invariant under $\frac{\hat\xi^2_i}{2}$, in particular $\Theta(Y_0)$, m_- and the selection of Y_0. The powers of $\frac{\hat\xi^2_i}{2}$ cancel as in (1.6.61).

2. The common heat coefficient has the form (1.6.21)

$$c = c_B = K_B R^{\frac12+h} e^{-(\lambda-h)(Y_{\rm end}+L_o)},$$

with $K_B > 0$ independent of C. Support: $c = H_A^b (R_A^b)^h J e^{-(\lambda-h)L_o}$ with fixed transfers a_A, k_A, J (Section 1.15). $H_e/\sqrt{R_e}$ is a template amplitude of the backward model with the fixed normalization $E^0 = P_* f(\beta) e^{y/10}$ (proof of Lemma 1.6.38). "The central heat-coefficient calibration does not rescale the included endpoint P_*". The heat collar, rank-one primitive correction and three-E compensation keep c and the inlet germs (Section 1.15, Section 1.6.3).

Weaker form, sufficient for every use. The C-independence of K_B in (2) is stronger than needed. The uses U1–U3 need only a C-uniform bound $0 < K_- \le K_B \le K_+$, with $K_\pm$ independent of C. Then (1.6.61) holds with a C-dependent Θ between the values $\Theta_\mp$ obtained from $K_\mp$, Theorem 1.6.29(iv) and Corollary 1.6.30 hold with Θ_- in the lower and Θ_+ in the upper bounds (with the threshold-free choice $m_- = c_{\rm P}\Theta_-^2/k_+^2$), and only the limit statements (i)–(iii) and (v) of Theorem 1.6.29 use the exact C-independence. In this construction both forms hold: Lemma 1.6.20 gives R_e/R and e_e exactly, and Lemma 1.6.21 gives the C-uniform lower bound K_- and the exact value $K_B = \sqrt{2}\, a_A k_A^h J P_* F_T(\lambda) \big(\frac{\hat\xi^2_i}{2}\big)^{\frac12+h} e^{hT} \lambda^{60(\lambda-h)}$ for $\hat\xi_{s,b} = \hat\xi_{\rm ref}$.

Hypothesis 1.6.24 (Normalized deficit equation). For a scalar decreasing H with $\frac{I_{\hat\xi}}{\hat\xi} = H$ and logarithmic slope $\kappa = -\frac12 \hat\xi H_{\hat\xi}/H$, the deficit $w_d = \frac{\hat\xi^2}{2}\big(\frac{1}{1-h} - \frac{I}{\frac{\hat\xi^2}{2}H}\big)$ satisfies ((1.13.25), (1.13.26))

$$(\hat\xi^{-1}\partial_{\hat\xi}(w_d)) = \kappa\, w_d/\tfrac{\hat\xi^2}{2} + (h-\kappa)/(1-h).$$

In the normalized variables $x = \frac{\hat\xi^2}{2}/R$, $W = w_d/R$ this reads

$$W_x = \kappa(x)\, W/x + (h - \kappa(x))/a, \qquad a = 1-h, \tag{1.6.52}$$

and $\log(H/G)$ satisfies $\frac{d}{dx}\log(H/G) = -\kappa(x)/x$.

Hypothesis 1.6.25 (Exact shot). (Lemma 1.13.4; proof of Lemma 1.15.6.) If the drive ends on an open h-power germ $H_b = G_b(\frac{\hat\xi^2}{2}/R_b)^{-h}$ at a radius $R_b \ge R_*$ with positive deficit $C_b = G_b w_d(R_b) \asymp hG_bR_b^{4/5}$, then there is a nonnegative source τ_s whose solution ends on the exact heat pair with regular coefficient

$$c = c_{\mathrm{bank}} = G_bR_b^h. \tag{1.6.53}$$

The coefficient is realized *exactly* by the choice of λ_s in (1.13.45). The shot does not perturb c (Section 1.6.3).

Stop-map templates (proof of Lemma 1.15.6). We fix, before Y_0 and C:

- $\delta_{\mathrm{st}} \in (0, 0.45]$ and $\kappa_{\mathrm{st}} \in C^\infty([1,\infty))$ with $\kappa_{\mathrm{st}}(1) = \nu$ (flat), $\kappa_{\mathrm{st}} \equiv 2h$ on $[1+\delta_{\mathrm{st}}, \infty)$, $\nu \le \kappa_{\mathrm{st}} \le 2h$;
- $\kappa_1 \in C^\infty([0,1])$ with $\kappa_1 = 2h$ near 0, $\kappa_1 = h$ near 1, $h \le \kappa_1 \le 2h$;
- $c_t > 0$ and $c_w > 0$ with

$$Z_1 := c_t - \frac{c_w}{a}\int_0^1 (\kappa_1(z) - h)\, dz > 0. \tag{1.6.54}$$

For the afterhold radius R we put $\varepsilon := R^{-1/5}$ (proof of Lemma 1.15.6). The drive is the following, in $x = \frac{\hat\xi^2}{2}/R$. (a) Slope κ_{st} on $[1, x_{\mathrm{hit}}]$, where x_{hit} is the first point with $W = c_t\varepsilon$. (b) Slope $\kappa_1((x - x_{\mathrm{hit}})/(c_w\varepsilon))$ on $[x_{\mathrm{hit}}, x_{\mathrm{hit}} + c_w\varepsilon]$. (c) The h-power bank from $x_b := x_{\mathrm{hit}} + c_w\varepsilon$ on, followed by the exact shot of H1.6.25. The initial value is $W(1) = a^{-1} - r'$. By (1.6.51),

$$W(1) = W_1 := \frac{1}{1-h} - \frac{1}{1-\nu} = \frac{h-\nu}{(1-h)(1-\nu)} > 0. \tag{1.6.55}$$

The stop map is smooth down to $\varepsilon = 0$.

Lemma 1.6.26 (Regularity of the stop coefficient). *Define $\Phi_0(x) := -\int_1^x \kappa_{\mathrm{st}}(s)\, s^{-1} ds$. There are $\varepsilon_* > 0$ and C^∞ functions $x_{\mathrm{hit}}, x_b, g_b : [0,\varepsilon_*] \to (0,\infty)$ such that, for $0 < \varepsilon \le \varepsilon_*$, the drive (a)–(c) is well defined, its deficit stays positive, and the bank radius and amplitude are $R_b = Rx_b(\varepsilon)$, $G_b = G\, g_b(\varepsilon)$. Consequently, whenever the shot H1.6.25 applies,*

$$K_{\mathrm{old}}(R, r_{\mathrm{ref}}) = \kappa(R^{-1/5}), \qquad \kappa(\varepsilon) := g_b(\varepsilon)\, x_b(\varepsilon)^h, \tag{1.6.56}$$

with $\kappa \in C^\infty([0,\varepsilon_*])$, and

$$0 < k_- := \min_{[0,\varepsilon_*]} \kappa \le \kappa \le k_+ := \max_{[0,\varepsilon_*]} \kappa, \qquad L := \max_{[0,\varepsilon_*]} |\kappa'| < \infty. \tag{1.6.57}$$

Moreover, with x_z the zero of (1.6.59) below,

$$\kappa(0) = e^{\Phi_0(x_z)} x_z^h, \qquad \frac{d}{d\varepsilon}\log\kappa\Big|_{\varepsilon=0} = \frac{a\, Z_1}{x_z} > 0. \tag{1.6.58}$$

The data $\kappa_{\mathrm{st}}, \kappa_1, c_t, c_w, h, \nu, r_{\mathrm{ref}}$ do not depend on C or Y_0, so neither do $\kappa, k_\pm, L, \varepsilon_*$.

Proof. Step 1 (transition $[1, x_1]$, $x_1 = 1 + \delta_{\mathrm{st}}$). Let $x^\dagger = \sup\{x \le x_1 : W > 0 \text{ on } [1,x]\}$. On $[1, x^\dagger)$ we have $\kappa_{\mathrm{st}} W/x \ge 0$ and $h - \kappa_{\mathrm{st}} \ge -h$, so (1.6.52) gives $W_x \ge -h/a$. Hence $W(x) \ge W_1 - h\delta_{\mathrm{st}}/a$. For $\nu \le h/10$,

$$\frac{aW_1}{2h} = \frac{h-\nu}{2h(1-\nu)} \ge \frac{0.9}{2} = 0.45 \ge \delta_{\mathrm{st}},$$

so $W \geq W_1/2 > 0$ on $[1, x_1]$ and $x^\dagger = x_1$.

Step 2 (the $2h$ leg). On $[x_1, \infty)$, $\kappa_{\mathrm{st}} \equiv 2h$, and the solution of (1.6.52) is

$$W(x) = Ax^{2h} - \beta x, \qquad \beta = \frac{h}{a(1-2h)}, \qquad A = (W(x_1) + \beta x_1)x_1^{-2h} > 0. \tag{1.6.59}$$

The ratio $W/x = Ax^{2h-1} - \beta$ is strictly decreasing, since $2h < 1$. Hence W has exactly one zero $x_z = (A/\beta)^{1/(1-2h)} > x_1$ in (x_1, ∞), and $W > 0$ on $[1, x_z)$. At x_z, (1.6.52) gives $W_x(x_z) = -h/a < 0$. Since W is real-analytic on $[x_1, \infty)$, we can choose $\delta' \in (0, x_z - x_1)$ with $W_x \leq -h/(2a)$ on $J := [x_z - \delta', x_z + \delta']$. Put $m_0 := \min_{[1, x_z - \delta']} W > 0$ and

$$\varepsilon_1 := \min\{m_0,\ h\delta'/(2a)\}/(2c_t).$$

For $0 \leq \varepsilon \leq \varepsilon_1$ we have $c_t\varepsilon < m_0$, so the level $c_t\varepsilon$ is not attained on $[1, x_z - \delta']$. Since $W|_J$ is a strictly decreasing C^∞ diffeomorphism onto an interval containing $[0, h\delta'/(2a)]$, the first hitting point is

$$x_{\mathrm{hit}}(\varepsilon) = (W|_J)^{-1}(c_t\varepsilon),$$

which is C^∞ on $[0, \varepsilon_1]$ by the inverse function theorem. It has $x_{\mathrm{hit}}(0) = x_z$ and $x'_{\mathrm{hit}}(0) = c_t/W_x(x_z) = -ac_t/h$. For $0 < \varepsilon \leq \varepsilon_1$, $W \geq c_t\varepsilon > 0$ on $[1, x_{\mathrm{hit}}]$. In the coordinate $x = \frac{\hat{\xi}^2}{2}/R$, the amplitude obeys $\log(H(Rx)/G) = \Phi_0(x)$ on this interval. Its endpoint value $\Phi_0(x_{\mathrm{hit}}(\varepsilon))$ extends smoothly to $\varepsilon = 0$.

Step 3 (the slope change at width $c_w\varepsilon$). For $\varepsilon > 0$, substitute $W = \varepsilon Z$ and $x = x_{\mathrm{hit}}(\varepsilon) + c_w\varepsilon z$, $z \in [0, 1]$. Equation (1.6.52) and the amplitude equation become (proof of Lemma 1.15.6)

$$Z_z = c_w\Big[\frac{\kappa_1(z)\,\varepsilon Z}{x_{\mathrm{hit}}(\varepsilon) + c_w\varepsilon z} + \frac{h - \kappa_1(z)}{a}\Big], \quad \psi_z = -\frac{c_w\varepsilon\,\kappa_1(z)}{x_{\mathrm{hit}}(\varepsilon) + c_w\varepsilon z}, \quad Z(0) = c_t,\ \psi(0) = 0, \tag{1.6.60}$$

with $\psi = \log(H/H(Rx_{\mathrm{hit}}))$ in the physical radius. The range of $W|_J$ contains a neighborhood of zero since $W(x_z) = 0$ and $W_x(x_z) < 0$. Its local inverse therefore extends x_{hit} smoothly to negative ε near zero. Shrinking ε_1, we may assume $x_{\mathrm{hit}} \geq x_z/2$. Then the right side of (1.6.60) is C^∞ in $(z, Z, \psi, \varepsilon) \in [0, 1] \times \mathbb{R}^2 \times (-\varepsilon_2, \varepsilon_2)$, where $\varepsilon_2 := \min\{\varepsilon_1, x_z/(4c_w)\}$. Set

$$J(z, \varepsilon) = \int_0^z \frac{c_w\varepsilon\,\kappa_1(s)}{x_{\mathrm{hit}}(\varepsilon) + c_w\varepsilon s}\,\mathrm{d}s.$$

Direct integration gives $\psi = -J$ and

$$Z(z; \varepsilon) = e^{J(z,\varepsilon)}\left[c_t + \frac{c_w}{a}\int_0^z e^{-J(s,\varepsilon)}(h - \kappa_1(s))\,\mathrm{d}s\right].$$

The denominator is at least $x_z/4$ on the compact integration interval. Differentiation under the integral thus gives smooth dependence on ε through zero. At $\varepsilon = 0$,

$$Z(z; 0) = c_t - \frac{c_w}{a}\int_0^z (\kappa_1 - h) \geq Z_1 > 0, \qquad \psi(z; 0) = 0.$$

By continuity there is $\varepsilon_* \in (0, \varepsilon_2)$ with $Z(z; \varepsilon) \geq Z_1/2$ on $[0, 1] \times [0, \varepsilon_*]$. So the deficit $w_d = R\varepsilon Z$ is positive through the slope change, and at the bank $w_d(R_b) = R^{4/5}Z(1; \varepsilon) \asymp R^{4/5}$, as required by H1.6.25.

Step 4 (bank and coefficient). Put $x_b(\varepsilon) = x_{\mathrm{hit}}(\varepsilon) + c_w\varepsilon$ and $g_b(\varepsilon) = \exp\{\Phi_0(x_{\mathrm{hit}}(\varepsilon)) + \psi(1; \varepsilon)\}$. Both are C^∞ and positive on $[0, \varepsilon_*]$. After the bank begins, $H = Gg_b(\frac{\hat{\xi}^2}{2}/(Rx_b))^{-h}$, and by (1.6.53) $c = Gg_b(Rx_b)^h$. Hence $c/(GR^h) = g_b x_b^h = \kappa(\varepsilon)$, which is (1.6.56). Amplitude independence follows

from linearity in G. The bounds (1.6.57) hold because κ is continuous and positive on a compact interval and κ' is continuous.

Step 5 (first-order coefficient). We have $\Phi_0'(x_z) = -2h/x_z$, $x_{\mathrm{hit}}'(0) = -ac_t/h$, $x_b'(0) = -ac_t/h + c_w$, and $\partial_\varepsilon\psi(1;0) = -c_w\int_0^1 \kappa_1/x_z$. So

$$(\log\kappa)'(0) = \frac{2ac_t}{x_z} + \frac{h(-ac_t/h + c_w)}{x_z} - \frac{c_w\int_0^1\kappa_1}{x_z} = \frac{ac_t - c_w\int_0^1(\kappa_1 - h)}{x_z} = \frac{aZ_1}{x_z} > 0.$$

□

The stop parameters $\varepsilon = R^{-1/5}$ and $R_b^{-1/5}$ are smoothly equivalent at zero: $R_b^{-1/5} = \varepsilon x_b(\varepsilon)^{-1/5}$ has derivative $x_z^{-1/5} > 0$.

The exact amplitude identity.

Proposition 1.6.27 (Exact coefficient chain on the central band)**.** *Assume H1.6.22–H1.6.25. For every admitted (C, Y_0) with $k_h e^B R \ge R_\sharp := \max\{R_*/\min_{[0,\varepsilon_*]} x_b,\ \varepsilon_*^{-5}\}$ (so that the afterhold radius has $\varepsilon \le \varepsilon_*$ and the bank radius $R_b \ge R_*$),*

$$e_p(C, Y_0) = \frac{\Theta(Y_0)}{\kappa\big((k_h e^B R)^{-1/5}\big)}, \qquad \Theta(Y_0) := \frac{K_B\, e^{-(\lambda-h)(Y_{\mathrm{end}}+L_o)}\, k_h^{\nu-h}\, e^{-(h-\nu)B}\, x_p^{-\nu-1/2}}{\sqrt{2}}. \tag{1.6.61}$$

$\Theta(Y_0) > 0$ does not depend on C. Equivalently, $K_c = (R_o/R_h)^{h-\nu}e^{-(h-\nu)B}/\kappa((k_h e^B R)^{-1/5})$.

Proof. From (1.6.50), (1.6.51) and (1.6.56), $G_h = c\,R_h^{-h}e^{-(h-\nu)B}/\kappa((R_h e^B)^{-1/5})$ and $A_c = G_h R_h^\nu$. Substituting into (1.6.48) gives

$$e_p = \frac{c\,R_h^{\nu-h}e^{-(h-\nu)B}\big(\frac{\hat\xi_p^2}{2}\big)^{-\nu-1/2}}{\sqrt{2}\,\kappa}.$$

By H1.6.23, $c = K_B R^{\frac12+h}e^{-(\lambda-h)(Y_{\mathrm{end}}+L_o)}$, $R_h = k_h R$ and $\frac{\hat\xi_p^2}{2} = x_p R$. The total power of R is $(\frac12+h) + (\nu-h) - (\nu+\frac12) = 0$, which gives (1.6.61). The formula for $K_c = H_{\mathrm{out}}R_o^h/c$, with $H_{\mathrm{out}} = A_c R_o^{-\nu}$, follows in the same way. It agrees with (1.15.27). □

Remark 1.6.28 (Consistency with the e_p/e_{end} law). Let e_{end} be the endpoint ($\nu = \lambda$) pulse amplitude. With the same geometry map (1.6.48) and (1.6.23) at both angles, the ratio e_p/e_{end} equals the displayed product in the proof of Lemma 1.6.19 exactly. Thus (1.6.61) and that e_p/e_{end} law are the same identity. The only C-dependent factor in either is $1/K_{\mathrm{old}}$: $K_{w,\mathrm{end}} = A_w f(\beta_{\mathrm{end}})e^{(\lambda-h)L_o}$ (Lemma 1.15.23), and e_{end} is a template quantity under H1.6.23.

The limit, the rate, and uniform bounds.

Theorem 1.6.29 (Limit, rate and uniform bounds for e_p)**.** *Assume H1.6.22–H1.6.25, and fix $Y_0 \ge Y_{\min}$. Put $\varepsilon_C := (k_h(Y_0)e^B R)^{-1/5}$, with $R = (CP_*)^{10}$. Then:*

(i) (Limit) $e_p(C, Y_0) \to e_{p,\infty}(Y_0) := \Theta(Y_0)/\kappa(0) > 0$ as $C \to \infty$, and $K_c \to K_{c,\infty} = (R_o/R_h)^{h-\nu}e^{-(h-\nu)B}/\kappa(0) > 0$.

(ii) (Rate) For $k_h e^B R \ge R_\sharp$,

$$|e_p(C,Y_0) - e_{p,\infty}(Y_0)| \le \frac{L}{k_-}\, e_{p,\infty}(Y_0)\, \varepsilon_C = O_{Y_0}\big((k_h(Y_0)R)^{-1/5}\big) = O_{Y_0}(C^{-2}).$$

The constant L/k_- *in the* relative *error does not depend on* Y_0. *Since* $k_h(Y_0)$ *grows like* e^{Y_0}, *the relative convergence is uniform for* $Y_0 \ge Y_{\min}$.

(iii) (Sharpness and side) As $\varepsilon_C \to 0$,

$$e_p = e_{p,\infty}\Big[1 - \frac{(1-h)Z_1}{x_z}\,\varepsilon_C + O(\varepsilon_C^2)\Big].$$

The coefficient is strictly positive. So the rate $R^{-1/5}$ *cannot be improved, and* $e_p < e_{p,\infty}$ *for all sufficiently large* C.

(iv) (Uniform two-sided bounds) For $k_h e^B R \ge R_\sharp$,

$$\frac{\Theta(Y_0)}{k_+} \le e_p(C,Y_0) \le \frac{\Theta(Y_0)}{k_-}.$$

(v) (Threshold) If $\varepsilon_C \le k_-/(2L)$, *then* $e_p \ge e_{p,\infty}/2$. *This holds once* $R \ge (2L/k_-)^5/(k_h(Y_0)e^B)$, *a threshold that depends only on data fixed before* C.

Proof. (i) and (iv) follow from (1.6.61), the continuity of κ at 0, and (1.6.57); also $\kappa(0) \ge k_-$. For (ii),

$$|e_p - e_{p,\infty}| = \Theta\frac{|\kappa(\varepsilon_C) - \kappa(0)|}{\kappa(\varepsilon_C)\kappa(0)} \le \frac{\Theta}{\kappa(0)} \cdot \frac{L\varepsilon_C}{k_-}.$$

(iii) Taylor-expand $1/\kappa$ at 0 and use (1.6.58): $1/\kappa(\varepsilon) = \kappa(0)^{-1}[1 - (\log\kappa)'(0)\varepsilon + O(\varepsilon^2)]$, with $(\log\kappa)'(0) = aZ_1/x_z$ and $a = 1-h$. (v) follows from (ii). For C we have $\varepsilon_C \asymp C^{-2}$ because $R = (CP_*)^{10}$. □

Corollary 1.6.30 (Downstream quantities)**.** *Fix* Y_0 *and let* $R \ge R_\sharp/(k_h e^B)$.

(a) On the unedited hold $\frac{\hat\xi^2}{2} = R_h e^s$, $s \in [0,B]$, *the normalized swirl is*

$$e_g(s) = \frac{H}{\hat\xi} = e_p\Big(\frac{k_h e^s}{x_p}\Big)^{-1/2-\nu}.$$

Hence $e_g \to e_{g,\infty} > 0$ *at the same rate, and* $\Theta k_+^{-1}(k_h e^B/x_p)^{-1/2-\nu} \le e_g \le \Theta k_-^{-1}(k_h/x_p)^{-1/2-\nu}$, *uniformly in* C. *This is the* C*-uniform* e_g *used in the stress ceiling (Section 1.26) and at* (1.27.6) *and* (1.30.28).

(b) $e_a = B_c e_p$ (1.6.49) *and the correction amplitude* e_* *of Section 1.6.4 inherit the same two-sided bounds and limits.*

(c) With c_{P} *from the comparison* $c_{\mathrm{P}} e_p^2 \le m_R \le C_{\mathrm{P}} e_p^2$ (1.6.41), *either choice*

$$\begin{aligned} & m_- := \tfrac{c_{\mathrm{P}}}{4} e_{p,\infty}^2 && \text{(under the threshold of (v))},\\ \text{or}\quad & m_- := c_{\mathrm{P}}\,\Theta_-(Y_0)^2/k_+^2 && \text{(no threshold)}. \end{aligned}$$

(with Θ_- the value of Θ at $K_B = K_-$, Hypothesis 1.6.23(2), weaker form; the second choice is the one fixed in the completion of the proof of Lemma 1.6.19 and quoted in U1) is positive, does not depend on C, and satisfies $m_- \le c_{\mathrm{P}} e_p^2 \le m_R$ for every admitted C. The upper side $m_R \le C_{\mathrm{P}} e_p^2 \le C_{\mathrm{P}} \Theta^2 / k_-^2$ is the Y_0-selection (proof of Lemma 1.6.19), which uses only $K_{\mathrm{old}} \ge k_-$.

Proof. (a) On the unedited hold $H = A_c(\hat\xi/\sqrt{2})^{-2\nu}$ and $E = H/\hat\xi = e_p((\hat\xi/\hat\xi_p)^2)^{-1/2-\nu}$, with $(\hat\xi/\hat\xi_p)^2 = k_h e^s / x_p$ independent of C. The later spectral edit on the hold is compact and happens after e_p and $\mathcal{T}_{\theta,\mathrm{old}}$ are defined, so it does not enter. (b) is immediate. (c) uses Lemma 1.6.19 (1.6.41), whose constants do not depend on C and Y_0, together with Theorem 1.6.29(iv),(v). □

The bounds in Theorem 1.6.29(iv) control the amplitudes in U1–U3 uniformly in C before Λ and C are selected.

Completion of the proof of Lemma 1.6.19: the lower bound m_-. Only the lower bound $K_B \ge K_-$ is used (Hypothesis 1.6.23(2), weaker form). Lemma 1.6.21 proves it from Lemma 1.6.20, which concerns only the backward outlet. The backward outlet (R_e, H_e) is the exact output of the backward model with the fixed normalization $E^0 = P_* f(\beta) e^{y/10}$, $y = 2\log(\hat\xi/\hat\xi_{\mathrm{ref}})$, $\frac{\hat\xi_{\mathrm{ref}}^2}{2} = \frac{\hat\xi_i^2}{2}(CP_*)^{10}$, with $\frac{\hat\xi_i^2}{2} = B_{\mathrm{r1}}$ the entry-graph constant of the core (Definition 1.20.22, Remark 1.20.26) (backward chart, $b = 1$; Theorem 1.8.10). No finite-scale error enters R_e or H_e (proof of Lemma 1.6.20). Lemma 1.6.20 uses only the definitional part of (B1) and the proved (S2), (S3). Put $\varepsilon_C = (k_h(Y_0) e^B R)^{-1/5}$; this is the afterhold radius $R_h e^B$ to the power $-1/5$. Lemma 1.15.6 gives a smooth positive stop coefficient κ on a closed interval $[0, \varepsilon_*]$, with $K_{\mathrm{old}} = \kappa(\varepsilon_C)$. Lemma 1.6.26 proves the regularity of κ.

Let $k_- = \min \kappa$, $k_+ = \max \kappa$ and $L_\kappa = \max |\kappa'|$ on this interval. These numbers do not depend on C or Y_0. Let $\varepsilon_C \le \varepsilon_*$, and let the bank radius be at least the threshold R_* of Lemma 1.13.4. Then the coefficient chain gives the exact identity

$$e_p(C, Y_0) = \frac{\Theta(C, Y_0)}{\kappa(\varepsilon_C)}, \qquad \Theta(C, Y_0) = \frac{K_B\, e^{-(\lambda - h)(Y_{\mathrm{end}} + L_o)}\, k_h^{\nu - h}\, e^{-(h-\nu)B}\, x_p^{-\nu - 1/2}}{\sqrt{2}},$$

where $\frac{\hat\xi_p^2}{2} = x_p R$ and $R_h = k_h R$.

All powers of R cancel, because $(\frac12 + h) + (\nu - h) - (\nu + \frac12) = 0$. Thus Θ depends on C only through K_B, and by Lemma 1.6.21 (with $s_b = 1$) not at all. Θ is also independent of $\frac{\hat\xi_i^2}{2}$: $K_B \propto (\frac{\hat\xi_i^2}{2})^{\frac12 + h}$, while x_p and k_h are proportional to R_g/R, and $R_g = \frac{\hat\xi_{s,b}^2}{2} = \frac{\hat\xi_i^2}{2} R$ in the $G = 0$ sector (Lemma 1.6.20 with $s_b = 1$, and Hypothesis 1.6.23(1)), and the exponents again sum to $(\frac12 + h) + (\nu - h) - (\nu + \frac12) = 0$. So Θ and m_- depend only on data fixed up to Y_0, as the order requires. Let $\Theta_-(Y_0)$ be Θ with K_B replaced by K_- of Lemma 1.6.21. Then

$$e_p(C, Y_0) \ge \frac{\Theta_-(Y_0)}{k_+} > 0$$

for each admitted $C \ge C_0$. If K_B does not depend on C, then also $e_p \to \Theta/\kappa(0)$ with relative rate $(L_\kappa/k_-)\varepsilon_C$ (Theorem 1.6.29). We use only the lower bound.

The endpoint wait amplitude and coefficient factor have the same structure and unchanged open germs. With c_{P} from (1.6.41), we put

$$m_- := c_{\mathrm{P}}\, \Theta_-(Y_0)^2 / k_+^2 > 0.$$

Then $m_- \le m_R$ for each admitted C, and $m_+ = (\frac12 - h)/32$ gives the claimed interval. No scale threshold is necessary for m_-, so m_- is fixed before the core Λ and before the last choice of C. □

We set the central smoothing value to the actual $m_R = -\Pi_{\mathrm{ref}}(0)$ of Lemma 1.6.19. We do not use a central C^1 convergence of Π_{ref} in the scale. We use the uniform C^2 bound $\sup_{R\ge R_*}\|\Pi_{\mathrm{ref}}\|_{C^2([-1,1])} \le K_P$ of Proposition 1.18.4 and the central parity of Proposition 1.6.33 below.

In this subsection the *ideal reference* is the field whose canonical pressure is Π_{ref} in Proposition 1.18.4: the prefix, the wait, the pulse with its two returns, the central and outer futures with the central memory edit, the A10/A11 block, the heat replacement and its rank-one correction, the early heat correction with its partial fixed-λ extension, the two-row taper, the angular mixture and the inlet-germ connector. It does not contain the regular core, the core-to-reference five-moment correction, the pressure-class correction of Lemma 1.6.37, the activation, the capped loop and its restoration, or the spectral returns. These later operations are discussed in Remark 1.6.34.

Reflection symmetry. Axisymmetric Navier–Stokes is equivariant under $z \mapsto -z$ with $(u_r, u_\theta, u_z) \mapsto (u_r, u_\theta, -u_z)$. In the charts, $z \mapsto -z$ is $\eta \mapsto -\eta$ at fixed $(q, \frac{\hat\xi^2}{2})$. For profiles we put

$$(\mathcal{R}H)(\tfrac{\hat\xi^2}{2},\eta) = H(\tfrac{\hat\xi^2}{2},-\eta), \qquad (\mathcal{R}U)(\tfrac{\hat\xi^2}{2},\eta) = -U(\tfrac{\hat\xi^2}{2},-\eta), \qquad (\mathcal{R}P_{\mathrm{ax}})(\eta) = P_{\mathrm{ax}}(-\eta).$$

Lemma 1.6.31 (Reflection equivariance of the leading system)**.** *Let (H, U, P_{ax}) be smooth on $(0,\infty)\times[-1,1]$, and let the histories be (1.9.1) with $\mathfrak{M}_1 = \int_0^{\frac{\hat\xi^2}{2}} U$. Then the histories of $(\mathcal{R}H, \mathcal{R}U, \mathcal{R}P_{\mathrm{ax}})$ are $-\mathfrak{M}_1(\hat\xi,-\eta)$, $\mathfrak{M}_2(\hat\xi,-\eta)$, $-\mathfrak{M}_3(\hat\xi,-\eta)$, $\mathfrak{M}_4(\hat\xi,-\eta)$ and $P(\frac{\hat\xi^2}{2},-\eta)$, the radial velocity V of the leading system is mapped to $V(\frac{\hat\xi^2}{2},-\eta)$, and*

$$\widehat{\mathcal{T}}_{P,\theta}[\mathcal{R}\,\cdot\,](\tfrac{\hat\xi^2}{2},\eta) = \widehat{\mathcal{T}}_{P,\theta}[\,\cdot\,](\tfrac{\hat\xi^2}{2},-\eta), \qquad \widehat{\mathcal{T}}_{P,z}[\mathcal{R}\,\cdot\,](\tfrac{\hat\xi^2}{2},\eta) = -\widehat{\mathcal{T}}_{P,z}[\,\cdot\,](\tfrac{\hat\xi^2}{2},-\eta).$$

In particular $\mathcal{R}$ maps solutions of $\widehat{\mathcal{T}}_{P,\theta} = \widehat{\mathcal{T}}_{P,z} = 0$ to solutions, and if H is even in η then the canonical pressure $-\int_0^\infty H^2/(4\frac{\hat\xi^4}{4})\,\hat\xi\,\mathrm{d}\hat\xi$ is even.

Proof. The coefficients $d = 1-\eta^2$ and $L = 1-2h\eta^2$ are even. The parities of the histories follow from their definitions. In (1.9.2), the terms $\frac{H_{\hat\xi}}{\hat\xi} - H/\frac{\hat\xi^2}{2}$, $(\frac{\hat\xi^2}{2}+\mathcal{K})H$, $(1-h)\mathfrak{M}_2$, $(\frac12-h)\eta\mathfrak{M}_{2\eta}$, $d\mathfrak{M}_{3\eta}$ and $2(h-(\frac12-h))\eta\mathfrak{M}_3$ are even, because $\mathcal{K} = (1-2h)\eta\mathfrak{M}_1 + d\mathfrak{M}_{1\eta}$ is even. In (1.9.3), the terms $U_{\hat\xi}$, $(\frac{\hat\xi^2}{2}+\mathcal{K})U$, $(\frac12-h)(\mathfrak{M}_1 - \eta\mathfrak{M}_{1\eta})$, $4h\eta\mathfrak{M}_4$, $d\mathfrak{M}_{4\eta}$ and $\frac{\hat\xi^2}{2}((2+4h)\eta P - dP_\eta)$ are odd. The radial velocity $V = (2\eta\frac{\hat\xi^2}{2}U - (1-2h)\eta\mathfrak{M}_1 - d\mathfrak{M}_{1\eta})/L$ is even. The last claim is immediate. □

Lemma 1.6.32 (Central-band evenness of the ideal swirl)**.** *Let $\eta_c > 0$ be such that the flat angular mixture cutoff satisfies $\chi = 0$ on $|\eta| < \eta_c$. This η_c is fixed with the cutoff, before Y_0 and before the scale. Then for every admitted member, every $\hat\xi > 0$ and $|\eta| < \eta_c$, the swirl of the ideal reference satisfies*

$$H(\tfrac{\hat\xi^2}{2},-\eta) = H(\tfrac{\hat\xi^2}{2},\eta).$$

More precisely, on this band $H(\frac{\hat\xi^2}{2},\eta)$ is a function of $\frac{\hat\xi^2}{2}$ and η^2 only, built from scalar radial data and the even functions $d = 1-\eta^2$, ψ_o and $B_o(\eta) = B_o e^{k_o\eta^2}$. No parity of U, of the outlet graph ρ, or of any datum outside the band is used.

Proof. We go through the ideal reference in radial order on the band $|\eta| < \eta_c$.

Mixture weight and exponent. Since $\chi = 0$, the weight $\omega = (1-\chi)H_c/H_{\mathrm{out}}$ equals one, and (1.6.25) reads $\mathcal{F}(\nu,\eta) = \mathcal{F}(\nu_c,\eta)$. Since $\mathcal{F}_\nu > 0$, $\nu = \nu_c$ on the band. The outer component H_w has weight zero, so every operation that belongs to the outer component only is absent: the A10

transition and flattening, the A11 controls (Lemma 1.15.5), the heat replacement and its rank-one correction (Proposition 1.15.8, which is part of the outer component only by Proposition 1.15.22), the G-rise and the slow turnoff. These lie in the fixed-λ buffer beyond the ν transition, where $\chi = 1$ and $\nu = \lambda$ (Section 1.6.3: the mixture (1.6.25) and the fixed-λ buffer), and $G = 0$ on the central band (Remark 1.6.9, Lemma 1.6.13). (The bound $|\eta| \ge \eta_a$ alone would not suffice, since $\eta_a \le \eta_c/2$.) The early heat correction and its partial fixed-λ extension are zero on the open central band (Proposition 1.15.22 and the proof of Lemma 1.6.19). The two-row taper of Lemma 1.14.4 lies on the last flat-λ band, where $\nu = \lambda$; in any case its complete ΔC_p is zero.

Prefix, wait and pulse. By Lemma 1.6.13, the actual scalar prefix and wait give $H = A_c(\frac{\hat\xi^2}{2})^{-\nu_c}$ and $I = A_c(\frac{\hat\xi^2}{2})^{1-\nu_c}/(1-\nu_c) + K_c$ with scalar $A_c, K_c, \frac{\hat\xi_p^2}{2}, H_p, e_p, r_p, \sigma_p$, and $H_\eta = 0$ at fixed $\hat\xi$ on the pulse. The complete prefix pressure is the scalar $e_a^2 D_{\mathrm{pre}}$ of (1.6.43). The energy root A_p, the two returns and every axial amplitude change U only, not H (proof of Lemma 1.6.19). The outlet graph ρ enters only the comparison radius $R_o = R_g e^{Y_0+\rho}$ and the positions of the returns; the comparison outlet evaluates the same scalar physical field.

Inlet-germ connector. In Lemma 1.17.9, $\omega = 1$ and $\nu = \nu_c$ give $J_t/(R_o H_o) = e^{(1-\nu_c)t} - e^{(1-\nu_c)t} = 0$, and $J(0) = 0$. So $J \equiv 0$ and the connector is zero on the band.

Memory edit, hold, drive, stop and shot. The memory discrepancy $\delta I = (r_b - r_{\mathrm{ref}})\frac{\hat\xi_p^2}{2} H_p e^{-(1-\nu_c)W}$ of the proof of Lemma 1.6.19 is a scalar primitive constant, and its edit $\delta I\, \zeta(\frac{\hat\xi^2}{2}/R_m)$ has the scalar support $[R_m, 2R_m]$. The hold (1.6.19), the deficit drive, the narrow stop and the shot are scalar at fixed physical $\frac{\hat\xi^2}{2}$ (Proposition 1.15.22 and the proof of Proposition 1.18.3).

Lift, wing, blend and heat continuation. The lift is $H_L = d^{-h} g_*(\frac{\hat\xi^2}{2}/d)$, $\mathfrak{M}_{2L} = d^{1-h} i(\frac{\hat\xi^2}{2}/d)$ with scalar g_*, i (1.13.47). The wing (1.13.53) uses the even cutoff ψ_o, the even edge $B_o(\eta) = B_o e^{k_o \eta^2}$ (1.13.52) and scalar α_o, ℓ_b. The primitive blend (1.13.57) uses the radial cutoff χ_b and $\Delta = \mathfrak{M}_{2T} - \mathfrak{M}_{2b}$, which is even. The heat continuation is the lift of the same scalar trajectory, and for $x \ge M$ it is the common heat field of the two components.

Each piece is a function of $\frac{\hat\xi^2}{2}$ and η^2, so H is even on the band. □

Proposition 1.6.33 (Central parity of the reference pressure)**.** *For every admitted member,* $\Pi_{\mathrm{ref}}(-\eta) = \Pi_{\mathrm{ref}}(\eta)$ *for* $|\eta| < \eta_c$. *In particular* $\partial_\eta \Pi_{\mathrm{ref}}(0) = 0$ *for every member, and* $\sup_{R \ge R_*} |\partial_\eta \Pi_{\mathrm{ref}}(0)| = 0$.

Proof. $\Pi_{\mathrm{ref}} = -\int_0^\infty H^2/(4\frac{\hat\xi^4}{4})\,\hat\xi\, \mathrm{d}\hat\xi$ depends only on the swirl of the ideal reference. Lemma 1.6.32 gives the evenness on the band. Π_{ref} is C^1 by Proposition 1.18.4, so its derivative at 0 is zero. □

Remark 1.6.34 (Scope of central parity). Only the ideal central swirl and its canonical pressure are even. The axial pulse, drift offsets, core and velocity-dependent moment corrections need not be even. The core correction restores the edited reference's complete C_p; the pressure bank changes C_p by $\Pi_{\mathrm{ref}} - p_0$ and the axis datum by its negative; the loop and spectral returns have zero total C_p. Thus these operations can change partial pressures without changing the complete canonical pressure used in the central germ. No global parity on $[-1, 1]$ is required.

The same lemma supplies the local symmetry of the protected hold used in the spectral selection: on the band, $U = M = J = 0$ after the returns, H is even, and the restored histories are the outward canonical integrals of this even future.

Lemma 1.6.35 (Constantization on a narrow strip)**.** *Let* $\chi_2 \in G^{3/2}$ *be even, with* $0 \le \chi_2 \le 1$, $\chi_2 = 1$ *on* $[-1, 1]$, $\operatorname{supp}\chi_2 \subset [-2, 2]$, *and* $c_2 = \|\chi_2'\|_\infty$. *Set* $w = \min\{\frac{1}{4}, \varepsilon_p/(8K_P(2 + c_2))\}$. *For*

every member, with $\|f\|_{C^1} = \sup|f| + \sup|f'|$,

$$\|\chi_2(\cdot/w)(\Pi_{\mathrm{ref}} + m_R)\|_{C^1} \le 2K_P w(1 + c_2 + w) \le \varepsilon_p/4.$$

Proof. By Proposition 1.6.33, $q = \Pi_{\mathrm{ref}} + m_R$ satisfies $q(0) = q'(0) = 0$. The uniform C^2 bound gives $|q(\eta)| \le K_P\eta^2/2$ and $|q'(\eta)| \le K_P|\eta|$. On $|\eta| \le 2w$, therefore, $\|\chi_2 q\|_\infty \le 2K_P w^2$ and $\|(\chi_2(\cdot/w)q)'\|_\infty \le 2K_P w(c_2 + 1)$. Their sum is at most $\varepsilon_p(c_2 + 5/4)/(4(2 + c_2)) \le \varepsilon_p/4$. □

We put $\Pi^c = \Pi_{\mathrm{ref}} - \chi_2(\cdot/w)(\Pi_{\mathrm{ref}} + m_R)$. Then $\Pi^c \equiv -m_R$ on $|\eta| \le w$ and $\|\Pi^c - \Pi_{\mathrm{ref}}\|_{C^1} \le \varepsilon_p/4$, uniformly for $R \ge R_*$. This constantization does not supply the size bound for m_R. We select the approximation error less than a fixed fraction of m_- and keep the central constant germ.

The later three-E pressure correction has target $\Pi_{\mathrm{ref}} - p_0$, which is zero at the central plane. It keeps the physical pressure after its support, with the exact C_p offset stated above. The actual regular-core five-moment correction restores this edited reference. Later loop and spectral corrections have zero total C_p relative to it.

These corrections keep the selected central datum and its nonzero central-memory contribution. We solve the pulse normalization only one time. The canonical integral gives the pressure.

We fix the same pressure tolerance ε_p of Lemma 1.6.36 before the core coefficient ball. This tolerance includes the bounds for each pre-correction axial edit. We select fixed smoothing and cutoff scales and approximate the actual canonical datum by $p_0 \in G^{3/2}$ in C^1. We make p_0 equal to these analytic germs on endpoint neighborhoods and equal to the negative constant $-m_R$ on the central strip. Taylor's formula for the boundary-flat difference and the uniform C^2 bound make the endpoint cutoff error small in C^1.

Lemma 1.6.35 makes the central constantization cost at most $\varepsilon_p/4$ in C^1. We select the mollification scale $\epsilon \le w/8$ after w. It keeps the constant $-m_R$ on $|\eta| \le w/4$, because $\Pi^c \equiv -m_R$ on $|\eta| \le w$. On the remaining compact set a fixed Gevrey mollifier gives the approximation. By Lemma 1.6.19, not by smoothing alone, the actual m_R lies in the necessary interval. For a sufficiently small fixed approximation error relative to m_-, $p_0 < 0$ and

$$0 < m_- \le m_R \le m_+ < (\tfrac{1}{2} - h)/8.$$

The same smoothing scales give one Gevrey majorant for all large R. The full ideal future is complete, so this construction does not use a pressure fixed point. We permit the member-dependent $p_0(R)$ because the core constants are uniform in this bounded family.

Lemma 1.6.36 (Pressure-datum tolerance for the preceding axial corrections)**.** *There are constants $\varepsilon_p, \varepsilon_u > 0$, fixed before the core parameter Λ and the selection of C in step 4 of Section 1.5.2, with this property. We can select the pressure approximation with $\|p_0 - \Pi_{\mathrm{ref}}\|_{C^1} \le \varepsilon_p$ and one smoothing scale for the large-C family. The stated core and activation selections can reduce the axial mismatch of the construction to at most ε_u. After the step-4 selection of C (there is no later increase of C), all these operations keep one strict relaxed-cone margin. They are the pressure correction, the previous G_i-to-G interpolation, and the two U bumps of the five-history correction. Precisely, on the $G_i \to G$ annulus and on the supports of these corrections the corrected field satisfies $\frac{7}{10} \le a_s \le \frac{9}{10}$, $|b_s| \le B_0$, $|w| \le W_0 + 2$ and $p_1 \ge 3$, hence $v_s < 1$ and $P_c \ge \frac{18}{7}$, with B_0, W_0 as in the proof.*

Proof. We measure the axial mismatch in the normalized C^1_η coefficient norm. We keep the fixed radial templates and their first radial derivatives. The equivalent condition is smallness of the compact correction in $C^1_\eta C^1_x$ on each normalized support. This controls the first angular derivatives of M, J, S as well as the fields. We do not use pointwise smallness of the axial velocity alone.

These finite supports are fixed compact positive-growth sectors in the normalized variable $x = (\hat{\xi}/\hat{\xi}_*)^2$, with $\frac{\hat{\xi}_*^2}{2} = Rr_*(\eta)$ and $R \asymp C^{10}$. On these sectors the reference has $H \asymp C^{-1}(\hat{\xi}/\sqrt{2})^{6/5}$, so $E = H/\hat{\xi} \asymp C^{-1}R^{1/10}$ has positive lower and upper bounds that do not depend on large C. The finite factors and their required angular derivatives are those of the frozen normalized future geometry. We use the global scalar R and $\widehat{x} = \frac{\hat{\xi}^2}{2}/R$.

The normalized fields and histories are

$$H = R^{1/2}\widehat{H}, \quad E = \widehat{E}, \quad U = \widehat{U}, \quad M = R\widehat{M}, \quad I = R^{3/2}\widehat{I}, \quad J = R^{3/2}\widehat{J}, \quad S = R\widehat{S}, \quad C_p = \widehat{C}_p.$$

Thus each R cancels in the actual formulas for Q_s, N_s: their history ratios include $M/\frac{\hat{\xi}^2}{2}$, $I/(\frac{\hat{\xi}^2}{2}H)$, $J/(\frac{\hat{\xi}^2}{2}H)$ and $S/\frac{\hat{\xi}^2}{2}$. For example, the contribution from the pressure and energy history is $N_s^{S,P} = 4h\eta S/\frac{\hat{\xi}^2}{2} - d\partial_\eta(S/\frac{\hat{\xi}^2}{2}) + (2+4h)\eta P - dP_\eta$. The other axial terms use U, $M/\frac{\hat{\xi}^2}{2}$, $M_\eta/\frac{\hat{\xi}^2}{2}$ and $K/\frac{\hat{\xi}^2}{2}$, where $K = (1-2h)\eta M + dM_\eta$, and have the same scale cancellation.

Angular differentiation is at fixed $\widehat{x}$, because R is a scalar. The support coordinate $x = \widehat{x}/r_*(\eta)$ introduces only the fixed bounded derivatives of r_*. Thus the normalized history bounds hold for all large C, before we fix one member. The positive-growth source and its history formula give $Q_s \geq q_0 > 0$ there, with one positive constant for the same family.

The uniform pressure C^1 bound and normalized history bounds thus give $|w_{\mathrm{ref}}| \leq W_0$. We fix these constants for the axial interpolation and the two disjoint axial-correction supports together.

Before the pressure correction a datum change $\delta p = p_0 - \Pi_{\mathrm{ref}}$ does not change the fields or the swirl stress. Its effect on the axial numerator is

$$\delta N_s = 4(\tfrac{1}{2}+h)\eta\delta p - d\partial_\eta\delta p, \qquad \delta w = \frac{4(\frac{1}{2}+h)\eta\delta p - d\partial_\eta\delta p}{EQ_s}.$$

Thus

$\|\delta w\|_\infty \leq K_p\|\delta p\|_{C^1}$ with K_p independent of C on each one of these supports. This uniform normalized estimate lets us select the pressure tolerance before the core coefficient ball. Compactness for one selected C is not sufficient.

For an explicit cone margin we put $B_0 = \min\{1/5, 1/[10(W_0+2)]\}$. We select all normalized field and history perturbations so that

$$7/10 \leq a_s \leq 9/10, \quad |b_s| \leq B_0, \quad |w| \leq W_0 + 2,$$

and take the late radial scale so that $p_1 \geq 3$. On the supports of the additive E bumps of this correction and of the core five-moment correction ($E = e_*(x^{1/10} + v)$) we also require $|v| \leq \frac{1}{2}x^{1/10}$. This is one more upper bound on τ_b, fixed with τ_b. It gives $H \geq \frac{1}{2}H_{\mathrm{ref}} > 0$ there, which the definition of a_s presupposes (Lemma 1.20.50). Then

$$v_s = a_s + b_s^2/a_s \leq 9/10 + (1/25)/(7/10) < 1,$$

and

$$P_c = p_1\left(1 - \frac{b_s w}{a_s}\right) \geq 3\left(1 - \frac{1/10}{7/10}\right) = 18/7 > 2.$$

These are strict inequalities in the exact relaxed branch of the cone. We fix a normalized field/history tolerance $\tau_b > 0$ which implies these inequalities and also lies in the five-moment correction IFT neighborhood. This uses only the fixed normalized templates, their inverse matrix, $E \geq e_0$, $Q_s \geq q_0$, and W_0.

We first select ε_p so that $K_p\varepsilon_p < 1/2$. The normalized target of the three-E pressure correction must also be less than $\tau_b/10$. This condition includes its angular derivative and actual quadratic terms. The correction target divides δp by e_*^2, and $e_* \geq e_0$, so this is a C-independent selection.

We impose the previous negativity tolerance relative to m_- at the same time. For the fixed constant K_b in the normalized core-correction estimate that we use here, we select ε_u so that

$$K_b(\varepsilon_u/e_{\min} + \varepsilon_u^2/e_{\min}^2) < \tau_b/10.$$

The small axial datum and large Λ control the core part. The next memberwise activation and termination selections control the other error to the ε_u tolerance.

We then select C large so that

$$K_b(C^{-2}/e_{\min}^2 + C^{-10}/e_{\min} + C^{-16}/e_{\min}) < \tau_b/10$$

and $p_1 \geq 3$. Thus an increase of C controls only errors that tend to zero. It does not reduce a fixed pressure or axial mismatch.

The uniform C^2 pressure family and Proposition 1.6.33 give the constant central germ on $|\eta| \leq w/4$. Lemma 1.6.35 gives accuracy ε_p with one Gevrey smoothing scale. We then fix the related Gevrey majorant before Λ. After this, we select the central axial offset with $u_0 \leq (\frac{1}{2} - h)w/16$.

Then the drift root $\eta_0 = d_0u_0/(\frac{1}{2} - h) \leq w/16$ and its root neighborhood lie in the constant strip. We construct the core and its activation with this actual p_0. Thus their cone proof is not a perturbative comparison with Π_{ref}.

On the other pre-correction portions where $\frac{U_{\hat{\xi}}}{\hat{\xi}} = 0$, the previous $b_s = 0$ argument applies directly. On each axial interpolation and axial-correction support, we use the uniform estimate for the change in the axial numerator. The normalized C^1 coefficient bounds control the partial histories of all moment corrections. After the pressure correction M, I, J, S coincide with their reference values. The fifth row gives $C_{p,\mathrm{new}} - C_{p,\mathrm{ref}} = \Pi_{\mathrm{ref}} - p_0$, hence $p_0 + C_{p,\mathrm{new}} = \Pi_{\mathrm{ref}} + C_{p,\mathrm{ref}}$ by Lemma 1.6.37. □

Lemma 1.6.37 (Three-moment pressure correction)**.** *On a reserved positive-growth patch with radially constant $U = G(\eta)$, there is a compact E correction with*

$$(\Delta I, \Delta S, \Delta C_p) = (0, 0, \Pi_{\mathrm{ref}} - p_0).$$

It leaves M and J unchanged. After the patch M, I, J, S and the physical canonical pressure P equal their original values. C_p itself shifts by $\Pi_{\mathrm{ref}} - p_0$, compensated by the opposite change of axis datum. It keeps endpoint jets, though not necessarily open endpoint collars.

Proof. We normalize $\frac{\hat{\xi}^2}{2} = \frac{\hat{\xi}_*^2}{2}x$ and $E = e_*x^{1/10}$. For a sum v of three disjoint fixed smooth bumps, the actual increments are

$$\begin{aligned}
\Delta I &= \sqrt{2}\left(\tfrac{\hat{\xi}_*^2}{2}\right)^{3/2} e_* \int x^{1/2} v \, dx, \\
\Delta S &= -\tfrac{\hat{\xi}_*^2}{2} e_*^2 \left(\int x^{1/10} v \, dx + \tfrac{1}{2} \int v^2 dx \right), \\
\Delta C_p &= e_*^2 \left(\int x^{-9/10} v \, dx + \tfrac{1}{2} \int v^2/x \, dx \right).
\end{aligned}$$

The three powers $x^{1/2}, x^{1/10}, x^{-9/10}$ form a Chebyshev system on a positive compact interval. Narrow bumps around three distinct points give an invertible matrix. For sufficiently small fixed widths, its determinant stays nonzero.

The quantitative finite-dimensional IFT, with the displayed quadratic terms, solves the normalized small C^1 target. Because $U = G$ on the full support, $\Delta J = G\Delta I = 0$ and $\Delta M = 0$. We start the corrected reference with pressure p_0. After the correction, this gives

$$p_0 + C_{p,\mathrm{ref}} + \Delta C_p = \Pi_{\mathrm{ref}} + C_{p,\mathrm{ref}}.$$

Thus the future primitive maps and energy root stay unchanged.

The edited reference carries the offset $C_{p,1} = C_{p,0} + \Pi_{\mathrm{ref}} - p_0$. The earlier core five-moment correction targets this edited reference. Later loop and spectral corrections have $\Delta C_p = 0$ relative to that shifted baseline. Boundary-flat targets give boundary-flat coefficients by differentiation of the unique local solution.

This proves jet matching, not open collar equality. Before the correction only the axial pressure stress changes. On portions where $\frac{U_{\hat{\xi}}}{\hat{\xi}} = 0$, the $b_s = 0$, $a_s = .8$, $p_1 > 2$ relaxed-cone argument applies directly. The axial interpolation and the two axial-correction supports use the same C^1 pressure-datum tolerance proved in Lemma 1.6.36.

Inside this three-E correction $U = G$. Its normalized small coefficients keep $a_s < 2$ and positive Q. The patch is outside the protected inner Gevrey rectangle. Only the finite smoothness of the exterior construction is necessary for its coefficients. □

1.6.4.3 Core and five-history restoration

Lemma 1.6.38 (Quantitative endpoint complementary separation)**.** *For the selected backward reference and protected core-pressure family $p_0(R)$, there exist constants $\varepsilon_e, \delta_e > 0$ fixed before Λ and C. For these constants and all sufficiently large C in the later selected family,*

$$|Z_R(\eta)| \geq \delta_e \qquad (|\eta - \sigma| \leq \varepsilon_e, \quad \sigma = \pm 1).$$

Here $u = \lambda_{\mathrm{ch}}^{\frac{1}{2}+h}(4\beta + j_0)$, $\beta = \lambda_{\mathrm{ch}}^{\frac{1}{2}-h}\eta$ on the endpoint collars, $p_0(R) = \lambda_{\mathrm{ch}}^{1+2h}\Pi_0(\beta)$ there. These are the slice continuations (Lemma 1.6.8) of the backward values $4\beta + j_0$ and $\Pi_0(\beta)$, with weights $(\frac{1}{2} + h)$ and $2(\frac{1}{2} + h)$. We put

$$v = (\tfrac{1}{2} - h)\eta - du, \qquad Z_R = -vu' - (\tfrac{1}{2} + h)(1 + 2\eta u)u - 4(\tfrac{1}{2} + h)\eta p_0(R) + d\, p_0(R)'.$$

We can select the interior regularizer so that the alternative $\chi > .99$ or $|Z_R| \geq \delta$ holds with the same constants on the full core interval.

We keep the specified endpoint regularizer $s_0 = \sigma_* \lambda_{\mathrm{ch}}^{h-\frac{1}{2}}$ unchanged. No smaller σ_* is necessary.

Proof. The selected endpoint datum gives the lower bound. The fixed model selections above give $T_d = e^{M_d} + 10 > 10$, $P_* > e^{T_d} > e^{10} > 4$, and the unchanged temporary model inner power $E^0 = P_* f(\beta) e^{y/10}$ for $y \leq 0$, where $f(\beta) = (1 + \beta^2)^{-1}$. Thus the canonical pre-heat model datum satisfies

$$\Pi_0(\beta) = -\frac{1}{2}\int_{-\infty}^{\infty} E_{\mathrm{sched}}^2\, dy \leq -\frac{5}{2}P_*^2 f(\beta)^2, \qquad \Pi_0(\sigma) \leq -\frac{5}{8}P_*^2. \tag{1.6.62}$$

The main amplitude root changes U, not E.

The actual A11 controls have identically zero total C_p increment as functions of the angle. The complete heat/inverse edit and its real three-E compensation also have zero total C_p increment. On the protected terminal collars, where the angular cutoff χ_b of (1.14.16) equals one, the actual selected backward datum is thus this same Π_0. Where $\chi_b < 1$, the axis datum keeps the increment

$-(1-\chi_b)\Delta C_{p,f}$. The individual heat tail is not analytic. The central heat-coefficient calibration does not rescale the included endpoint P_*.

The pressure-class construction sets $p_0(R)$ equal to the displayed analytic datum in the chart on fixed protected core collars. This equality holds even when the complete exterior pressure has only matching endpoint jets.

The integral in (1.6.62) is the temporary model integral, not a claim that the regular core has that power law up to the axis. Integration only from a finite $\frac{\hat\xi_{\rm in}^2}{2}$ to $\frac{\hat\xi_{\rm ref}^2}{2}$ would give

$$-\frac{5}{2}P_*^2 f(\beta)^2[1-(\hat\xi_{\rm in}/\hat\xi_{\rm ref})^{2/5}].$$

The omitted positive amount is $\epsilon_C = (5/2)P_*^2 f^2(\hat\xi_{\rm in}/\hat\xi_{\rm ref})^{2/5} = O(C^{-2})$ for $\frac{\hat\xi_{\rm in}^2}{2}$ bounded independently of C after the core/reference selections and $\frac{\hat\xi_{\rm ref}^2}{2} = \frac{\hat\xi_i^2}{2}(CP_*)^{10}$. We must keep it in a truncated-prefix comparison.

Here the actual core five-moment correction restores the edited reference's full C_p, so its canonical datum is restored. For robustness, the remaining estimates also allow the weaker bound $p_0(R)(\sigma) \le -5P_*^2/8 + \epsilon_C$ with $0 \le \epsilon_C \le 1$. This tolerance does not represent a second physical compensation. If $\frac{\hat\xi_{\rm in}^2}{2}$ depends on the selected Λ, the other C threshold for $\epsilon_C \le 1$ is selected afterward. The collar width and numerator margin below do not depend on that threshold.

At the endpoints the exact chart gives

$$v(\sigma) = (\tfrac12 - h)\sigma, \quad u(\sigma) = 4\sigma + j_0, \quad u'(\sigma) = -\frac{2(\frac12+h)}{(\frac12-h)\sigma}u(\sigma) - 4.$$

Thus

$$\begin{aligned} Z_R(\sigma) &= -4(\tfrac12+h)\sigma[p_0(R)(\sigma) - p_{\rm req}(\sigma)], \\ p_{\rm req}(\sigma) &= \frac{u(\sigma)}{4\sigma} + \frac{(\frac12-h)}{(\frac12+h)} - \frac{u(\sigma)^2}{2} = -7 + \frac{(\frac12-h)}{(\frac12+h)} - \frac{15}{4}\sigma j_0 - \frac{j_0^2}{2} \ge -7. \end{aligned}$$

The last bound uses $h \le .01$, $j_0 \le .05$, and $(\frac12-h)/(\frac12+h) \ge 49/51$. Thus the exact model-datum version gives

$$|Z_R(\sigma)| \ge 2(5P_*^2/8 - 7) \ge 6, \qquad |Z_R(\sigma)| \ge 3P_*^2/8.$$

Even with $\epsilon_C \le 1$ it gives

$$|Z_R(\sigma)| \ge 2(5P_*^2/8 - 8) \ge 4, \qquad |Z_R(\sigma)| \ge P_*^2/4. \tag{1.6.63}$$

The two endpoints may have opposite signs. The core uses an absolute lower bound.

We next get one collar for all C in the full family. The same Gevrey majorant of $p_0(R)$ gives a uniform C^2 bound. The actual model also gives a direct endpoint bound. Without the zero-total-pressure controls, it has $E_{\rm sched} = c(y)f(\beta)^{\theta(y)}$, $0 \le \theta \le 1$.

The first unit turn has $\frac12\hat\xi\partial_{\hat\xi}\log H \le .6$. Each later selected model stage has $\frac12\hat\xi\partial_{\hat\xi}\log H \le 0$. The plateau has zero H slope. The A10 transition has slope between $-3\lambda/2$ and $-\lambda/2$.

The power, drive, and terminal model slopes are negative. Thus

$$|\Pi_0(\beta)| \le \tfrac12(5 + 2e^{.2})P_*^2 f(\beta)^2 < 4P_*^2 f(\beta)^2.$$

We fix T_0 for the fixed small real chart extension, and these statements hold on it. Differentiation of the separated integrand gives $|\partial_\beta E_{\rm sched}^2| \le 2E_{\rm sched}^2$ and $|\partial_\beta^2 E_{\rm sched}^2| \le 8E_{\rm sched}^2$.

The same integrable majorant thus proves $|\Pi_0'| \le 2|\Pi_0|$ and $|\Pi_0''| \le 8|\Pi_0|$. The fixed analytic chart yields a uniform collar bound $\|p_0(R)\|_{C^2} \le K_p P_*^2$, independent of the selected scale and uniform on the admitted normalized family. This bound is also independent of the length of an added decreasing-power interval.

For an explicit width, let B_u bound u, u', u'', B_p bound $p_0(R), p_0(R)', p_0(R)''$, and B_η, B_d bound $|\eta|, |d|$ on a fixed collar of width ε_0. We set

$$\begin{aligned} B_v &= (\tfrac{1}{2} - h)B_\eta + B_d B_u, \qquad B_{v,1} = (\tfrac{1}{2} - h) + 2B_\eta B_u + B_d B_u, \\ M_Z &= 1 + B_{v,1}B_u + B_v B_u + (\tfrac{1}{2} + h)[(1 + 4B_\eta B_u)B_u + 2B_u^2] \\ &\quad + [4(\tfrac{1}{2} + h) + (4(\tfrac{1}{2} + h) + 2)B_\eta + B_d]B_p. \end{aligned}$$

Exact differentiation gives

$$Z_R' = -v'u' - vu'' - (\tfrac{1}{2} + h)[(1 + 4\eta u)u' + 2u^2] - 4(\tfrac{1}{2} + h)p_0(R) - (4(\tfrac{1}{2} + h) + 2)\eta p_0(R)' + dp_0(R)'',$$

so $\sup_R \|Z_R'\| \le M_Z$. A uniform C^1 pressure bound alone would not justify this step.

We select

$$\varepsilon_e = \min(\varepsilon_0/2,\, 2/M_Z), \qquad \delta_e = 2. \tag{1.6.64}$$

The mean-value estimate and (1.6.63) prove the claimed collar bound. In the exact-datum version, one can also use $\min(\varepsilon_0/2, 3/M_Z)$ and $\delta_e = 3$.

We keep the specified s_0 on a smaller subcollar, and interpolate it to the freely small interior regularizer in the region where $|Z_R| \ge \delta_e$. On the complement of these collars and a fixed central root neighborhood, $|v|$ has a uniform positive minimum v_*. We take the interior $s_0 \le v_*/20$. This gives $\chi \ge 400/401 > .99$. Near the central root the established uniform nonzero-Z_R margin applies.

The minimum of the endpoint and central margins proves the global complementary alternative. We narrow only the inner core-germ collar: the outer G-rise, phase buffers, pulse supports and heat geometry do not move. The resulting fixed cutoff norms enter the next gauge and Λ selections, followed by C. They impose no retroactive smallness requirement on λ.

The actual curved-exit comparison is $w_Y = Z_R/(2Lb) + O(\Lambda^{-1})$, with one error constant for this datum family. We select Λ so the error is at most $\delta/(4 \sup Lb)$, together with the thresholds (Λ) of Theorem 1.20.28. Wherever $\chi \le .99$ this yields $|w_Y| \ge \delta/(4 \sup Lb) > 0$. The displayed p_2 formula in the core proof then gives the axial exit alternative by choosing C after the datum and Λ thresholds.

We then select the activation controls for that member. The other sector uses the Bessel $p_1 > 2 + c$ bound. This proves the quantitative endpoint inheritance necessary for that exit. □

The variable-scale Bessel core. Theorem 1.9.1 proves local axis existence. To reach the specified curved exit with these pressure data, we use the variable-scale Bessel core and curved-entry construction below. We give its estimates and parameter selections in full. We select a fixed positive radial scale $b(\eta)$ and gauges with $\psi' = Lb\, v/(v^2 + s_0^2)$, where $v = (\frac{1}{2} - h)\eta - du$, $L = 1 - 2h\eta^2$, and $s_0(\eta) > 0$ is the selected regularizer.

To match values and slopes, we first select u through the drift interpolation. We use same-sign Gevrey partitions on each side of its unique central root. We recover $u = ((\frac{1}{2} - h)\eta - v)/d$ away from the endpoints and keep the specified germs there. We select s_0 small away from a fixed root neighborhood so that $\chi > .99$ wherever $|Z|$ could be small.

This selection uses the quantitative endpoint margin proved in Lemma 1.6.38. We do not assume the alternative for the specified regularizer. On the collars, we set $b = \lambda_{\mathrm{ch}}$ and $s_0 = \sigma_* \lambda_{\mathrm{ch}}^{h - \frac{1}{2}}$. With

these values $Y = \Lambda b\frac{\hat\xi^2}{2} = \Lambda\frac{\hat\xi_b^2}{2}$ on the collars (Remark 1.6.7), and s_0 is the slice continuation of the backward constant σ_* for the weight $-(\frac12 - h)$. We start with an arbitrary positive Gevrey extension b_0.

Suppose that the integral of $b_0 Lv/(v^2+s_0^2)$ differs from the necessary endpoint value difference of ψ by Δ. We add $t\beta_+$ or $t\beta_-$ to b_0. The fixed nonnegative bumps β_+ and β_- have supports in $v>0$ and $v<0$, in that order. Their weighted integrals have opposite strict signs.

We select the relevant $t \ge 0$ to give Δ. The function b stays positive. We fix the additive constant of ψ on the left collar. Independently, we adjust a' by a compact bump to match its endpoint value difference. We keep $a' = (1+h)\lambda'_{\mathrm{ch}}/\lambda_{\mathrm{ch}}$ on collars.

These adjustments are independent of Λ. All extensions, partitions, bumps and interpolations of this paragraph are taken Gevrey-3/2 on $\mathcal{N}$. These are b_0, $\beta_\pm$, the a'-bump, the s_0 interpolation and the drift partitions, and also p_0 (construction following Lemma 1.6.35). The bumps are supported off the endpoint collars, where the explicit formulas above hold exactly. Gevrey-3/2 bumps with any prescribed compact support exist because $3/2 > 1$. We also take the coefficient radius ρ_0 below the Gevrey radius of these data. On the collars, $\log g$ is the slice continuation of the backward logarithm $\Lambda\psi_b(\eta_b) - \log C$, for the weight $1+h$ of F. In forward coordinates it is $\Lambda\psi_b(\eta_b) + (1+h)\log\lambda_{\mathrm{ch}} - \log C$. The central nonzero-$Z$ margin below and the off-root drift margin give the same support selections for the $p_0(R)$ family.

They also give one bound for its Gevrey data. We set

$$Y = \Lambda b\tfrac{\hat\xi^2}{2}, \quad \chi = v^2/(v^2+s_0^2), \quad g = C^{-1}e^{\Lambda\psi+a}, \quad F = g\Phi, \quad U = u + \Lambda^{-1}w.$$

The exact rescaled equations are

$$2(Y\Phi_{YY} + 2\Phi_Y) = -\chi\Phi + \Lambda^{-1}R_1, \qquad 2(Yw_{YY} + w_Y) = Z/(Lb) + \Lambda^{-1}R_2.$$

We work on a fixed buffered interval about $0 \le Y \le 4$ and a ball about the Bessel solution. The two radial inverses and $G^{3/2}$ coefficient algebra give uniform bounds and Lipschitz constants for J_2R_1, J_1R_2 on this ball. We do not assert that the raw differentiated remainders act boundedly on that same space. The fixed-data coefficient norm of g is at most one when we take C after Λ ((1.6.65) below).

Thus an increase of C does not change the contraction constants. We give the exact remainders and coefficient estimate for that statement. We write $\delta = \Lambda^{-1}$, $\alpha = b'/b$, $\mathcal{T} = \partial_\eta + \alpha D_Y$, $\mathcal{Q} = \int_0^Y g^2\Phi^2\,dY$, and let $\mathcal{A}_Y$ denote radial averaging. We put

$$k_0 = 2(\tfrac12 - h)\eta u + du', \quad k_1 = 2(\tfrac12 - h)\eta\mathcal{A}_Y w + d\mathcal{T}\mathcal{A}_Y w, \quad k = k_0 + \delta k_1, \quad v_U = v - \delta dw, \quad \zeta = \psi'.$$

Then $R_1 = B_1/L$, $R_2 = B_2/(Lb)$, where

$$\begin{aligned} B_1 &= b^{-1}\{dw\zeta\Phi - v_U(a'\Phi + \mathcal{T}\Phi) - (1+k)(D_Y\Phi + \Phi) - (h + 2h\eta U)\Phi\},\\ B_2 &= dwu' - v\mathcal{T}w + \delta dw\mathcal{T}w - (1+k)D_Y w - (\tfrac12 + h)w - 4(\tfrac12 + h)\eta uw - 2\delta(\tfrac12 + h)\eta w^2\\ &\quad - 4(\tfrac12 + h)\eta\mathcal{Q}/b - 2\eta Y g^2\Phi^2/b + (d/b)[\partial_\eta\mathcal{Q} + \alpha(D_Y\mathcal{Q} - \mathcal{Q})]. \end{aligned}$$

Let J_j invert $Y\partial_{YY} + j\partial_Y$ with zero axis value. The actual fixed point is

$$\Phi = (1 + J_2\chi/2)^{-1}[1 + \delta J_2(B_1/L)/2], \qquad w = YZ/(2Lb) + \delta J_1(B_2/(Lb))/2.$$

The coefficient norm. We fix $s = \frac32$, $R_0 \in (4.1, 10)$ (no argument uses the upper bound) and $Y_{\mathrm{buf}} \in (4, 4.1]$. Let K' be the compact angular interval of N8, with $[-1,1] \subset \operatorname{int} K'$ and $L > 0$ on K'. The data of the map below are the functions

$$\mathfrak{D} = \{\eta,\ d,\ v,\ \zeta,\ a',\ \alpha,\ u,\ u',\ 1+k_0,\ h + 2h\eta u,\ Z,\ \chi,\ b^{-1},\ L^{-1}\}$$

on K' (here $Z = Z_R = -vu' - (\frac{1}{2}+h)(1+2\eta u)u - 4(\frac{1}{2}+h)\eta p_0 + dp_0'$, as in Lemma 1.6.38), together with ψ and a through g.

(D) There are $\varrho_d \in (0,1]$ and $M_{\mathfrak{D}} \geq 1$ with $\|f\|_{\mathcal{G}_{\varrho_d}(K')} \leq M_{\mathfrak{D}}$ for every $f \in \mathfrak{D}$ (norm (1.11.2) on $K_\eta = K'$).

Lemma 1.6.39 (Condition (D) holds)**.** *There is one pair $(\varrho_d, M_{\mathfrak{D}})$ for which (D) holds for every member of the $p_0(R)$ family, both central offsets, every Λ and every C.*

Proof. One member. Every function in $\mathfrak{D}$ other than Z is built from u, s_0, b, d, v, L, η and a', which are $G^{3/2}$ on K': the collar formulas are real-analytic (N8), and the extensions and bump functions are chosen in $G^{3/2}$. Quotients by b, L and $v^2 + s_0^2 \geq s_0^2 > 0$ are $G^{3/2}$ with a loss of radius by Lemma 1.22.2(c), and exponentials by Lemma 1.22.2(a). This gives χ, ζ, α, b^{-1} and L^{-1}. The function Z contains p_0 and p_0'; p_0 is $G^{3/2}$ by its construction (the smoothing following Lemma 1.6.35), and p_0' costs one radius loss by Lemma 1.22.2(b).

The $p_0(R)$ family. On the collars $p_0(R)$ is the fixed germ $\lambda^{1+2h}\Pi_0(\beta)$, since Π_0 is fixed in step 4. On the central strip it is the constant $-m_R$ with $m_R \in [m_-, m_+]$. Elsewhere it is a mollification at a fixed scale ϵ of a function whose sup norm is bounded uniformly in R (the uniform C^2 bound on $\Pi_{\mathrm{ref}}(R)$). For a fixed $G^{3/2}$ mollifier ϕ_ϵ, $\|\partial^k(\phi_\epsilon * f)\|_\infty \leq \|f\|_\infty \|\partial^k \phi_\epsilon\|_{L^1} \leq \|f\|_\infty M_\phi (k!)^{3/2}(c\epsilon)^{-k}$. The cutoffs that glue the pieces are fixed $G^{3/2}$ functions. So the Gevrey norms of $p_0(R)$ and $p_0(R)'$ on K' are bounded uniformly in R, at a radius independent of R.

Parameters Λ, C. At fixed member R the explicit scale factors occur through g. Along the selected family Z_R also depends on $p_0(R)$, whose Gevrey bound and radius above are uniform in R. They therefore give one pair $(\varrho_d, M_{\mathfrak{D}})$ in (D) for all admitted Λ, C. □

The coefficient family $\mathfrak{D}$ is specified in step 4 of Section 1.5.2 before $(\varrho_d, M_{\mathfrak{D}})$, and $(\varrho_d, M_{\mathfrak{D}})$ is fixed before Λ. We put $\rho_0 := \varrho_d/2 \leq \frac{1}{2}$.

Definition 1.6.40 (Core coefficient norm)**.** For a formal series $G(Y,\eta) = \sum_{n\geq 0} G_n(\eta) Y^n$ with $G_n \in C^\infty(K')$ (one-sided derivatives at the ends) and for $\sigma \geq 0$ put

$$a_{n,k} = R_0^{-n}\rho_0^{-k}\frac{((n+k)!/n!)^s}{(n+1)^2(k+1)^2}, \qquad \|G\|_\sigma = \sup_{n,k\geq 0}\frac{\left\|\partial_\eta^k G_n\right\|_{L^\infty(K')}}{(n+1)^\sigma a_{n,k}}.$$

X_σ is the space of series with $\|G\|_\sigma < \infty$, and $\mathsf{X} = \mathsf{X}_0$, $\|G\| = \|G\|_0$. A function $f(\eta)$ is the series with $f_0 = f$; then $\|f\| = \sup_k \rho_0^k (k+1)^2 (k!)^{-s}\left\|\partial_\eta^k f\right\|_{L^\infty(K')}$.

This is the weighted supremum of [42, (B.4)], with Gevrey order s in place of 1 and R_0 in place of 20. Each X_σ is a Banach space: a Cauchy sequence converges uniformly in every coefficient and every derivative order, and the uniform limits of the derivatives are the derivatives of the limit. For $\sigma \leq \tau$, $\|G\|_\tau \leq \|G\|_\sigma$. If $\|f\|_{\mathcal{G}_{\varrho_d}} \leq M$, then $\left\|\partial_\eta^k f\right\|_{L^\infty} \leq M(k!)^s \varrho_d^{-k}$, so $\|f\| \leq M \sup_k (k+1)^2 2^{-k} = \frac{9}{4}M$. Thus $\|f\| \leq M_d := \frac{9}{4}M_{\mathfrak{D}}$ for $f \in \mathfrak{D}$. With $\left\|e^{\Lambda\psi + a}\right\|_{\mathcal{G}_{\varrho_d}} \leq \exp(\Lambda\|\psi\|_{\mathcal{G}_{\varrho_d}} + \|a\|_{\mathcal{G}_{\varrho_d}})$ (Lemma 1.22.2(a)) we get

$$\|g\| \leq 1 \qquad \text{whenever} \qquad C \geq C_{\mathrm{core}}(\Lambda) := \tfrac{9}{4}\exp(\Lambda\|\psi\|_{\mathcal{G}_{\varrho_d}} + \|a\|_{\mathcal{G}_{\varrho_d}}). \tag{1.6.65}$$

The functions ψ and a do not involve p_0; so $C_{\mathrm{core}}(\Lambda)$ is fixed with Λ, before C. They depend on the central offset through v; $C_{\mathrm{core}}(\Lambda)$ denotes the maximum over the two offsets.

On series we use D_Y (degree n times n), $\mathcal{A}_Y$ (degree n divided by $n+1$), multiplication by Y, $\mathcal{I}_Y = Y\mathcal{A}_Y = \int_0^Y$, and the transferred angular derivative $\mathsf{E} = Y\partial_\eta$, that is $(\mathsf{E}G)_{n+1} = \partial_\eta G_n$,

$(\mathsf{E}G)_0 = 0$. The inverses are $(J_jH)_{n+1} = H_n/((n+1)(n+j))$, $(J_jH)_0 = 0$, as in [42, (B.5)]. For K with $K_0 = 0$ put $(\widetilde{J}_jK)_m = K_m/(m(m+j-1))$, $m \geq 1$. Then

$$J_jH = \widetilde{J}_j(YH), \qquad Y(F\,\partial_\eta G) = F\,\mathsf{E}G, \qquad \partial_\eta \mathcal{Q} = \mathsf{E}\mathcal{A}_Y(g^2\Phi^2).$$

So an angular derivative is always paid for by the degree that the exterior inverse adds.

Lemma 1.6.41 (Algebra and radial operators)**.** *Let* $S := \sup_{N\geq 0}\sum_{i=0}^{N}(N+1)^2(i+1)^{-2}(N-i+1)^{-2}$, $c_P := S^2$ *and* $c_E := 4R_0/\rho_0$. *Then* $S \leq \pi^2/3 + 2 < 5.3$, *and for* $\sigma, \tau \geq 0$, $j \in \{1,2\}$*:*

(a) $\|FG\|_{\sigma+\tau} \leq c_P \|F\|_\sigma \|G\|_\tau$, *and* $\|fG\|_\sigma \leq S\,\|f\|\,\|G\|_\sigma$ *for a function* $f(\eta)$*;*

(b) $\|D_YG\|_{\sigma+1} \leq \|G\|_\sigma$, $\|\mathcal{A}_YG\|_\sigma \leq \|G\|_\sigma$, $\|D_Y\mathcal{A}_YG\|_\sigma \leq \|G\|_\sigma$, *and* $\|YG\|_\sigma, \|\mathcal{I}_YG\|_\sigma \leq 4R_0\,\|G\|_\sigma$*;*

(c) $\|\mathsf{E}G\|_{\sigma+s} \leq c_E\,\|G\|_\sigma$ *and* $\|\mathsf{E}\mathcal{A}_YG\|_{\sigma+s-1} \leq c_E\,\|G\|_\sigma$*;*

(d) $\|J_jH\| \leq 4R_0\,\|H\|_\sigma$ *if* $\sigma \leq 2$, *and* $\left\|\widetilde{J}_jK\right\| \leq 2^{3/2}\,\|K\|_\sigma$ *if* $\sigma \leq \frac{3}{2}$ *and* $K_0 = 0$*;*

(e) for a function $\chi(\eta)$ *put* $\mathsf{K}_\chi = J_2\chi/2$ *(multiplication first) and* $x = SR_0\,\|\chi\|/2$. *Then* $\left\|\mathsf{K}_\chi^m F\right\| \leq x^m(m+1)(m!)^{-2}\,\|F\|$. *Hence* $1+\mathsf{K}_\chi$ *is invertible on* X, *with* $\left\|(1+\mathsf{K}_\chi)^{-1}\right\| \leq \sum_{m\geq 0} x^m(m+1)/(m!)^2$, *and*

$$\Phi_0 := (1+\mathsf{K}_\chi)^{-1}1 = \sum_{n\geq 0}\frac{(-Y\chi/2)^n}{n!\,(n+1)!} = f_0(\chi Y) = \frac{2J_1(z)}{z}, \qquad z = \sqrt{2\chi Y}.$$

Proof. The constant S. Since $(N+1)/((i+1)(N-i+1)) \leq 1/(i+1) + 1/(N-i+1)$, the sum is at most $2\sum_{i\leq N}(i+1)^{-2} + 4H_{N+1}/(N+2) \leq \pi^2/3 + 2$, because $H_m \leq (m+1)/2$.

(a) $(FG)_n = \sum_{i+j=n} F_iG_j$, and $\partial_\eta^k(F_iG_j) = \sum_{l+m=k}\binom{k}{l}\partial_\eta^l F_i\,\partial_\eta^m G_j$. The powers of R_0, ρ_0 cancel in $a_{i,l}a_{j,m}/a_{n,k}$, and

$$\binom{k}{l}\frac{a_{i,l}a_{j,m}}{a_{n,k}} = \binom{k}{l}\Big[\binom{n}{i}\Big/\binom{n+k}{i+l}\Big]^s\frac{(n+1)^2(k+1)^2}{(i+1)^2(j+1)^2(l+1)^2(m+1)^2}.$$

By Vandermonde's identity $\binom{n+k}{i+l} \geq \binom{n}{i}\binom{k}{l}$, so the bracket factor is at most $\binom{k}{l}^{1-s} \leq 1$. Also $(i+1)^\sigma(j+1)^\tau \leq (n+1)^{\sigma+\tau}$. Summing the polynomial factor over i and over l gives at most $S\cdot S$. For a function f only $i = 0$ occurs, and the sum over l gives S.

(b) The first three are immediate. $(YG)_{n+1} = G_n$, and $a_{n,k}/a_{n+1,k} = R_0\big(\frac{n+1}{n+k+1}\big)^s\frac{(n+2)^2}{(n+1)^2} \leq 4R_0$; also $(n+1)^\sigma \leq (n+2)^\sigma$. Then $\mathcal{I}_Y = Y\mathcal{A}_Y$.

(c) $\partial_\eta^k(\mathsf{E}G)_{n+1} = \partial_\eta^{k+1}G_n$, and

$$\frac{a_{n,k+1}}{a_{n+1,k}} = \frac{R_0}{\rho_0}(n+1)^s\frac{(n+2)^2(k+1)^2}{(n+1)^2(k+2)^2} \leq \frac{4R_0}{\rho_0}(n+1)^s.$$

Since $(n+1)^{\sigma+s} \leq (n+2)^{\sigma+s}$, this gives the first bound. With $\mathcal{A}_Y$ the extra divisor $n+1$ lowers the power by one, and $s - 1 \geq 0$.

(d) $\left\|\partial_\eta^k(J_jH)_{n+1}\right\| \leq \|H\|_\sigma\,(n+1)^\sigma a_{n,k}/((n+1)(n+j))$. With (b), this is at most $4R_0(n+1)^{\sigma-2}\,\|H\|_\sigma\,a_{n+1,k} \leq 4R_0\,\|H\|_\sigma\,a_{n+1,k}$. For $\widetilde{J}_j$ the degree does not change, and $(m+1)^\sigma/(m(m+j-1)) \leq (m+1)^{3/2}/m^2 \leq 2^{3/2}$ for $m \geq 1$.

(e) $(\mathsf{K}_\chi^m F)_n = \chi^m F_{n-m}/(2^m \prod_{i=n-m}^{n-1}(i+1)(i+2))$. By (a) and (b) its norm factor is at most $\prod_{i=n-m}^{n-1} SR_0\,\|\chi\|\,(i+2)/(2(i+1)^3)$. The factor decreases in i, so the product is at most its value for $n=m$, which is $x^m(m+1)!/(m!)^3$. The Neumann series converges absolutely in operator norm and inverts $1+\mathsf{K}_\chi$ on both sides. Since $J_2 Y^n = Y^{n+1}/((n+1)(n+2))$, we get $(-\mathsf{K}_\chi)^m 1 = (-\chi Y/2)^m/(m!\,(m+1)!)$, which gives the displayed series; the Bessel form is the series $J_1(z) = \sum_n (-1)^n (z/2)^{2n+1}/(n!\,(n+1)!)$. □

The ball and the constants. Put $x_* = SR_0M_d/2$ and $N_\chi = \sum_{m\ge 0} x_*^m(m+1)/(m!)^2$. By Lemma 1.6.41(e), $\|(1+\mathsf{K}_\chi)^{-1}\| \le N_\chi$ and $\|\Phi_0\| \le N_\chi$; and $w_0 = Y Z L^{-1} b^{-1}/2$ has $\|w_0\| \le 2R_0 S^2 M_d^3$. Put

$$\mu = c_P \max\{1, M_d\}, \qquad M_B = 1 + \max\{N_\chi, 2R_0\mu^3\}, \qquad \Theta = 4R_0(4R_0 + c_E),$$
$$K_{\mathrm{core}} = 51\,\Theta\mu^8 M_B^2, \qquad \Lambda_{\mathrm{core}} = 7 N_\chi K_{\mathrm{core}}.$$

These depend only on s, R_0, ϱ_d and $M_{\mathfrak{D}}$. Let $\mathfrak{B} = \{(\Phi, w) \in \mathsf{X}^2 : \|\Phi - \Phi_0\| \le 1,\ \|w - w_0\| \le 1\}$, with the metric $\max\{\|\Phi - \Phi'\|, \|w - w'\|\}$. It is complete. The map is

$$\mathcal{M}(\Phi, w) = \Big(\Phi_0 + \frac{\delta}{2}(1+\mathsf{K}_\chi)^{-1} J_2 \frac{B_1}{L},\ \ w_0 + \frac{\delta}{2} J_1 \frac{B_2}{Lb}\Big), \qquad \delta = \Lambda^{-1},$$

which is the displayed fixed-point form: $(1+\mathsf{K}_\chi)\Phi = 1 + \frac{\delta}{2} J_2(B_1/L)$ is $\Phi = 1 + \frac{1}{2} J_2(-\chi\Phi + \delta B_1/L)$.

Proposition 1.6.42 (The core contraction)**.** *Assume (D). Let $\Lambda \ge \Lambda_{\mathrm{core}}$ and $C \ge C_{\mathrm{core}}(\Lambda)$. Then $\mathcal{M}$ maps $\mathfrak{B}$ into itself and is a contraction with constant at most $N_\chi K_{\mathrm{core}}/\Lambda \le \frac{1}{7}$. Its fixed point $(\Phi, w) = (\Phi_C, w_C)$ is real, and:*

(i) One has $\|\Phi - \Phi_0\| \le N_\chi K_{\mathrm{core}}/(2\Lambda)$ and also $\|w - w_0\| \le K_{\mathrm{core}}/(2\Lambda)$. In particular, for all n, k,

$$\big\|\partial_\eta^k \Phi_n\big\|_{L^\infty(K')} \le M_B a_{n,k}, \qquad \big\|\partial_\eta^k w_n\big\|_{L^\infty(K')} \le M_B a_{n,k}.$$

(ii) For each $\eta \in K'$ the series of Φ and w converge absolutely on $|Y| \le R_0$, so Φ, w are holomorphic in $|Y| < R_0$. For $0 < q < 1$ they are C^∞ on $[0, qR_0] \times K'$, with the bounds of Lemma 1.22.3 ($M = M_B$, and $M = N_\chi K_{\mathrm{core}}/(2\Lambda)$ for $\Phi - \Phi_0$, $w - w_0$). There they solve the exact rescaled equations as functions, with $\Phi(0,\cdot) = 1$ and $w(0,\cdot) = 0$.

(iii) The constants Λ_{core}, K_{core}, N_χ, M_B and the bounds in (i), (ii) do not depend on $\Lambda \ge \Lambda_{\mathrm{core}}$, on $C \ge C_{\mathrm{core}}(\Lambda)$, or on the member of the family covered by (D).

Proof. The monomials. Expand B_1 and B_2 with $v_U = v - \delta dw$, $U = u + \delta w$, $k = k_0 + \delta k_1$, $k_1 = 2(\frac{1}{2} - h)\eta \mathcal{A}_Y w + d\partial_\eta \mathcal{A}_Y w + d\alpha D_Y \mathcal{A}_Y w$ and $\mathcal{T} = \partial_\eta + \alpha D_Y$. Then B_1/L is a sum of 17 monomials:

$$dw\zeta\Phi,\ va'\Phi,\ \delta dwa'\Phi,\ v\partial_\eta\Phi,\ \delta dw\partial_\eta\Phi,\ v\alpha D_Y\Phi,\ \delta dw\alpha D_Y\Phi,\ (1+k_0)D_Y\Phi,\ (1+k_0)\Phi,$$
$$\delta\eta\mathcal{A}_Y w\,(D_Y\Phi, \Phi),\ \delta d\alpha D_Y\mathcal{A}_Y w\,(D_Y\Phi, \Phi),\ \delta d\,\partial_\eta\mathcal{A}_Y w\,(D_Y\Phi, \Phi),\ (h + 2h\eta u)\Phi,\ \delta\eta w\Phi,$$

each multiplied by $(bL)^{-1}$ and a constant of modulus at most 2; here $(D_Y\Phi, \Phi)$ stands for two monomials, one with each factor. Similarly $B_2/(Lb)$ is $(Lb)^{-1}$ times a sum of 17 monomials:

$$du'w,\ v\partial_\eta w,\ v\alpha D_Y w,\ \delta dw\partial_\eta w,\ \delta dw\alpha D_Y w,\ (1+k_0)D_Y w,$$
$$\delta\eta\mathcal{A}_Y w\,D_Y w,\ \delta d\alpha D_Y\mathcal{A}_Y w\,D_Y w,\ \delta d\,\partial_\eta\mathcal{A}_Y w\,D_Y w,\ w,\ \eta uw,\ \delta\eta w^2,$$
$$\eta b^{-1}\mathcal{Q},\ \eta b^{-1} Y g^2\Phi^2,\ db^{-1}\partial_\eta\mathcal{Q},\ db^{-1}\alpha Y g^2\Phi^2,\ db^{-1}\alpha\mathcal{Q},$$

with constants of modulus at most $4(\frac{1}{2}+h)<3$; here $D_Y\mathcal{Q}=Yg^2\Phi^2$ and $\mathcal{Q}=\mathcal{I}_Y(g^2\Phi^2)$. Each monomial contains at most seven data factors (counting g, with $\|g\|\le 1$ by (1.6.65)) and at most two factors that are linear in (Φ,w). These linear factors are $\Phi, w, \mathcal{A}_Y w, D_Y\mathcal{A}_Y w$ (in X), $D_Y\Phi, D_Y w$ (in X_1), and, after multiplication by Y, $\mathsf{E}\Phi, \mathsf{E}w$ (in X_s) and $\mathsf{E}\mathcal{A}_Y w$ (in X_{s-1}). The quadratic terms include the products of w or its averages with Φ and its derivatives, the products of two factors depending on w, and the terms from $g^2\Phi^2$. Any factors δ inside B_1, B_2 have modulus at most one. Both nonlinear terms in $\mathcal{M}$ carry the common exterior factor $\delta/2$.

Bounds. Let $(\Phi,w)\in\mathfrak{B}$, so $\|\Phi\|,\|w\|\le M_B$. A monomial without ∂_η lies in X_1 (it has at most one factor D_Y; $D_Y\mathcal{A}_Y w\in\mathsf{X}$), or in X_{s-1} for $db^{-1}\partial_\eta\mathcal{Q}=db^{-1}\mathsf{E}\mathcal{A}_Y(g^2\Phi^2)$. Lemma 1.6.41(a)–(d) bound J_j of it by $3\cdot 4R_0\max\{4R_0,c_E\}c_P^8\max\{1,M_d\}^7M_B^2\le 3\Theta\mu^8M_B^2$: at most eight products, at most one factor Y or $\mathsf{E}\mathcal{A}_Y$ inside, and the exterior J_j. A monomial with ∂_η is written as $J_j(H)=\widetilde{J}_j(YH)$, with the factor Y moved onto the differentiated factor. Then YH is a product with zero constant term in X_σ, $\sigma\le s$: the worst cases are $d\,(\mathsf{E}\mathcal{A}_Y w)D_Y\Phi$ and $d\,(\mathsf{E}\mathcal{A}_Y w)D_Y w$, in $\mathsf{X}_{(s-1)+1}=\mathsf{X}_s$, and $v\,\mathsf{E}\Phi$, $dw\,\mathsf{E}\Phi$, $v\,\mathsf{E}w$, $dw\,\mathsf{E}w$, also in X_s. Here radial averaging pays one power, which is the point of the two mixed products. Lemma 1.6.41(c),(d) bound $\widetilde{J}_j(YH)$ by $3\cdot 2^{3/2}c_E\mu^5M_B^2\le 3\Theta\mu^8M_B^2$. Summing over the 17 monomials,

$$\sup_{\mathfrak{B}}\Big\|J_2\frac{B_1}{L}\Big\|\le K_{\mathrm{core}},\qquad \sup_{\mathfrak{B}}\Big\|J_1\frac{B_2}{Lb}\Big\|\le K_{\mathrm{core}}.$$

Lipschitz constants. For two points of $\mathfrak{B}$, write the difference of a monomial by replacing its linear factors one at a time. Each replacement gives the same bound with one factor M_B replaced by the distance Δ. So both composites are Lipschitz on $\mathfrak{B}$ with constant $2K_{\mathrm{core}}/M_B\le 2K_{\mathrm{core}}$.

Contraction. By Lemma 1.6.41(e), $\|\mathcal{M}_1(\Phi,w)-\Phi_0\|\le\frac{\delta}{2}N_\chi K_{\mathrm{core}}\le\frac{1}{14}$ and $\|\mathcal{M}_2(\Phi,w)-w_0\|\le\frac{\delta}{2}K_{\mathrm{core}}\le\frac{1}{14}$. The two Lipschitz bounds give the contraction constant $\frac{\delta}{2}\max\{N_\chi,1\}2K_{\mathrm{core}}=N_\chi K_{\mathrm{core}}/\Lambda\le\frac{1}{7}$. The fixed point is the limit of the iterates from (Φ_0,w_0). The data are real, so the iterates and the limit are real. At the fixed point the first two bounds give (i). Then $\|\Phi\|,\|w\|\le M_B$ gives the coefficient bounds.

(ii) $|\Phi_n|\le M_BR_0^{-n}(n+1)^{-2}$ gives absolute convergence on $|Y|\le R_0$. Lemma 1.22.3 gives the bounds for every $\partial_Y^j\partial_\eta^k$ on $[0,qR_0]\times K'$. Its proof applies verbatim to every product, average, primitive and transferred derivative above, because these lie in some X_σ: the extra factor $(n+1)^\sigma$ only replaces c_j by $\sup_n(n+1)^{\sigma+j}(q/q_1)^n$. So on $[0,qR_0]\times K'$ the coefficient operations are the operations on functions: Cauchy products, termwise D_Y, $\mathcal{A}_Y$, $\mathcal{I}_Y$ and ∂_η. The fixed-point identity is, coefficient by coefficient,

$$\begin{aligned}&\Phi_0=1,\quad 2(n+1)(n+2)\Phi_{n+1}=-\chi\Phi_n+\delta[B_1/L]_n,\\ &w_0=0,\qquad\qquad 2(n+1)^2w_{n+1}=[Z/(Lb)]\mathbf{1}_{n=0}+\delta[B_2/(Lb)]_n,\end{aligned}$$

which is the coefficient form of the rescaled equations.

(iii) $\Lambda_{\mathrm{core}}, K_{\mathrm{core}}, N_\chi, M_B$ are built from $s, R_0, \rho_0=\varrho_d/2$ and $M_d=\frac{9}{4}M_{\mathfrak{D}}$. The parameter Λ enters only through $\delta\le 1$ and through g, and C only through g; the bound $\|g\|\le 1$ is all that is used. The data $\psi'=\zeta$, χ, b, s_0, u, a' do not depend on Λ or C (the adjustments of this paragraph are independent of Λ). □

Corollary 1.6.43 (Bounds of the core used later)**.** *Under Proposition 1.6.42, put* $q=4.1/R_0$, $q_1=(1+q)/2$, $\varrho_*=\rho_0(1-q_1^{1/s})^s$ *and* $\Gamma_{jk}=c_j4.1^{-j}(1-q_1^{1/s})^{-s}(k!)^s\varrho_*^{-k}$, *with* c_j *as in Lemma 1.22.3. On* $[0,4.1]\times K'$*:*

(a) $c_\Phi:=0.15\le\Phi\le\Phi_{\max}:=1.12$. *Hence* $F=g\Phi>0$.

(b) $|\partial_Y^j\partial_\eta^k\Phi| + |\partial_Y^j\partial_\eta^k w| \le 2M_B\Gamma_{jk}$ *and* $|\partial_Y^j\partial_\eta^k(\Phi-\Phi_0)| + |\partial_Y^j\partial_\eta^k(w-w_0)| \le N_\chi K_{\mathrm{core}}\Gamma_{jk}/\Lambda$. *In particular* $\|\Phi-\Phi_0\|_{C^1_Y} \le (\Gamma_{00}+\Gamma_{10})N_\chi K_{\mathrm{core}}/\Lambda$, *and* $|w|+|\partial_\eta w|+|w_Y| \le K_c$, $|\Phi_Y|+|\partial_\eta\Phi| \le K_c$ *with* $K_c = 2M_B(\Gamma_{00}+\Gamma_{01}+\Gamma_{10})$.

(c) $|R_1|+|R_2| \le K_R$, *where* K_R *depends only on* M_B, Γ_{jk} $(j,k\le 1)$, R_0, c_P *and the suprema of the data. Hence, as* $\partial_Y J_1 f = Y^{-1}\int_0^Y f$, $|w_Y - Z/(2Lb)| \le K_R/(2\Lambda)$.

(d) With $p_{1,0} := -2Y\Phi_{0,Y}/\Phi_0 = zJ_2(z)/J_1(z)$, $z=\sqrt{2\chi Y}$: $|p_{1,r}-p_{1,0}| \le K_{p1}/\Lambda$ *with* $K_{p1} = 8.2(\Gamma_{10}+\Gamma_{00})N_\chi K_{\mathrm{core}}/c_\Phi^2$.

All these constants are independent of $\Lambda \ge \Lambda_{\mathrm{core}}$ *and* $C \ge C_{\mathrm{core}}(\Lambda)$.

Proof. (a) $\Phi_0 = f_0(\chi Y) \in [f_0(4.1),1]$ for $0 \le \chi Y \le 4.1$, because the differentiated alternating series gives $f_0'(y) \le -1/4 + y/24 < 0$ on $[0,4.1]$. By (i), $|\Phi-\Phi_0| \le \|\Phi-\Phi_0\|\sum_n (n+1)^{-2} \le \frac{\pi^2}{6}\cdot\frac{N_\chi K_{\mathrm{core}}}{2\Lambda} \le 0.118$ for $\Lambda \ge \Lambda_{\mathrm{core}}$. For a rigorous numerical lower bound, the alternating series $f_0(y) = \sum_{n\ge0}(-y/2)^n/[n!(n+1)!]$ gives

$$f_0(41/10) \ge \sum_{n=0}^{5} \frac{(-41/20)^n}{n!(n+1)!} = \frac{74952160399}{276480000000} > 0.271.$$

The terms decrease in magnitude from $n=1$ onwards, so the omitted tail after the odd index 5 is nonnegative. Consequently $\Phi > 0.271 - 0.118 > 0.15$ and $\Phi \le 1.12$. (b) is Lemma 1.22.3 with $q = 4.1/R_0$ and (i). (c) $R_1 = B_1/L$ and $R_2 = B_2/(Lb)$ are the sums of the monomials above, evaluated pointwise. Their linear factors are Φ, w, their first Y- and η-derivatives, $\mathcal{A}_Y w$ and $\partial_\eta\mathcal{A}_Y w$ (bounded by the bounds of w, since $\mathcal{A}_Y$ does not increase $\|\cdot\|$), and $\mathcal{Q}$, $\partial_\eta\mathcal{Q}$, $Yg^2\Phi^2$ (with $\|\mathcal{Q}\| \le 4R_0c_P^3M_B^2$). Lemma 1.22.3 bounds each of them on $[0,4.1]\times K'$. For the last claim, the fixed point gives $w = YZ/(2Lb) + \frac{\delta}{2}J_1R_2$, and J_1 inverts $\partial_Y(Y\partial_Y)$ with zero axis value. (d) $|Y\Phi_Y/\Phi - Y\Phi_{0,Y}/\Phi_0| \le Y|\Phi_Y-\Phi_{0,Y}|/\Phi + Y|\Phi_{0,Y}||\Phi-\Phi_0|/(\Phi\Phi_0)$, with (a), (b), and $\Phi_0 \ge c_\Phi$. The alternating series for $-f_0'$ on $[0,41/10]$ yields $0 < -f_0'(y) \le 1/4$. The consecutive absolute terms have ratio $y/[2(n+1)(n+3)]$ for $n \ge 0$. Hence $|\Phi_{0,Y}| \le \chi/4$. □

Lemma 1.6.44 (Rational core margins)**.** *On* $0 \le x \le 41/10$, $f_0(x) > 271/1000$ *and* f_0 *is decreasing. The function* $p(x) = -2xf_0'(x)/f_0(x)$ *is strictly increasing there, and* $p(99/25) > 33/10$.

Proof. The alternating derivative series gives $-f_0'(x) \ge 1/4 - x/24 > 0$ on this interval. Together with the preceding rational lower bound at $41/10$, this proves the first claim. For $\phi(s) = f_0(xs)$, the equation $(s^2\phi')' + (x/2)s\phi = 0$ and its x derivative give

$$p'(x) = \frac{\int_0^1 s f_0(xs)^2\,\mathrm{d}s}{f_0(x)^2} > 0.$$

The regular axis value makes the integrated Wronskian vanish at zero. At $x = 99/25$, let F_6 be the series for $f_0(x)$ truncated after index six and N_6 the corresponding series for $-2xf_0'(x)$. Alternation gives $f_0(x) \le F_6$ and $-2xf_0'(x) \ge N_6$, and exact rational arithmetic gives

$$N_6 - \frac{33}{10}F_6 = \frac{52762664451387}{7000000000000000} > 0.$$

This proves the strict margin without rounded Bessel values. □

Order of the choices. s, R_0, Y_{buf} are absolute. $(\varrho_d, M_{\mathfrak{D}})$, hence ρ_0, N_χ, M_B, K_{core} and Λ_{core}, are fixed with the common Gevrey majorant in step 4 of Section 1.5.2, before Λ. The condition $\Lambda \ge \Lambda_{\mathrm{core}}$ is one of the Λ-thresholds of step 4, and $C \ge C_{\mathrm{core}}(\Lambda)$ is one of its C-thresholds. A later increase of C keeps $\|g\| \le 1$ and changes none of the constants above.

Proposition 1.6.42(i) and Corollary 1.6.43(a) give the $O(\Lambda^{-1})$ comparison and $F > 0$. The source floor

$$S_q \ge c + .9\Lambda L b \chi$$

is Lemma 1.20.24(a). Young's inequality absorbs the errors $O(\chi)+O(\sqrt{\chi})+O(\Lambda^{-1})$ near the unique drift root, and the positive χ term absorbs them away from it.

At $\frac{\hat\xi_a^2}{2} = 4/(\Lambda b)$, that is $Y = 4$, Corollary 1.6.43(d) and the values listed there give $p_1 \ge 3.326 - K_{p1}/\Lambda > 2 + c$ when $\chi > .99$ and $\Lambda \ge K_{p1}$; this threshold is contained in Λ_0 of Lemma 1.20.24(b), which is in the ledger. On the complementary sector, the uniform numerator margin bounds w_Y away from zero. This margin includes Lemma 1.6.38 on the specified collars. The formula $p_2^2 = 2bYw_Y^2/(\Lambda g^2 \Phi^2)$ then gives $p_1 + p_2^2/p_1 > 2 + c$ after an increase of C.

Reference first-strain constants. The reference quantities used by the activation equations are

$$p_{1,r} := -\frac{\hat\xi^2(\hat\xi^{-1}\partial_{\hat\xi}(F_r))}{F_r}, \qquad n_{s,r} := -2(\hat\xi^{-1}\partial_{\hat\xi}(U_r)).$$

For the actual core scaling $Y = \Lambda b\frac{\hat\xi^2}{2}$, $F_r = C^{-1}e^{\Lambda\psi+a}\Phi_C$ and $U_r = u + \Lambda^{-1}w_C$, they satisfy

$$p_{1,r} = -2Y\frac{(\Phi_C)_Y}{\Phi_C}, \qquad n_{s,r} = -2b(w_C)_Y.$$

The fixed coefficient ball, on its buffered positive interval, gives (Corollary 1.6.43(a),(b)) $\Phi_C \ge c_\Phi > 0$ and $|(\Phi_C)_Y| + |(w_C)_Y| \le K$ when the coefficient norm of $g = C^{-1}e^{\Lambda\psi+a}$ is at most one. Because b and the evaluation interval are fixed, there is a constant P_{ref}, independent of the later C, such that

$$|p_{1,r}| + \hat\xi|n_{s,r}| \le P_{\mathrm{ref}}.$$

Lemma 1.6.45 (Positivity of $p_{1,r}$, including the drift root)**.** *On $[0, Y_{\mathrm{buf}}] \times J$ let $c_\Phi \le \Phi_C \le \Phi_{\max}$ (coefficient ball), $K_1 = \sup|R_1|$ and $b_{\max} = \sup b$. These constants are uniform on the coefficient ball ($\|g\| \le 1$; B_1 contains no g), hence independent of C. Let η_0 be the unique root of $v = (\frac12 - h)\eta - du$, and let $N_0 = \{|\eta - \eta_0| \le r_N\}$ be its root neighbourhood. Assume $|u| + |u'| \le \frac38$ on N_0. This holds when $\|u - G\|_{C^1} \le \frac38$ on the central band, where $G = 0$; in particular under the drift selection $\|u - G\|_{C^1} \le \varepsilon_u/4 \le \frac14$ of Section 1.6.4.*

(a) Exactly, for $0 < Y \le Y_{\mathrm{buf}}$,

$$p_{1,r}(Y,\eta) = \frac{1}{Y\Phi_C(Y)}\int_0^Y s[\chi\Phi_C(s) - \Lambda^{-1}R_1(s)]\,\mathrm{d}s.$$

(b) If $\chi(\eta) \ge 2K_1/(c_\Phi\Lambda)$, then $p_{1,r} \ge c_\Phi\chi Y/(4\Phi_{\max})$.

(c) There is Λ_p, fixed with the core margins, such that for $\Lambda \ge \Lambda_p$ the set $\{\chi < 2K_1/(c_\Phi\Lambda)\}$ lies in N_0. On it, $-R_1 \ge c_\Phi/(2b_{\max})$ and $p_{1,r} \ge c_\Phi Y/(4\Lambda b_{\max}\Phi_{\max})$.

Hence $p_{1,r} > 0$ for $0 < Y \le Y_{\mathrm{buf}}$ on all angles. At the drift root, $\chi = 0$ and $p_{1,r} \asymp Y/\Lambda$.

Proof. (a) The equation $2(Y\Phi_{YY}+2\Phi_Y)=-\chi\Phi+\Lambda^{-1}R_1$ is $(Y^2\Phi_Y)_Y=\frac12 Y(-\chi\Phi+\Lambda^{-1}R_1)$. Since Φ is regular at $Y=0$, we get $Y^2\Phi_Y=\frac12\int_0^Y s(-\chi\Phi+\Lambda^{-1}R_1)\,\mathrm{d}s$, and $p_{1,r}=-2Y\Phi_Y/\Phi$. As a consequence, $|\Phi_Y|\le\frac14(\chi\Phi_{\max}+K_1/\Lambda)$. (b) Here the integrand is at least $s(\chi c_\Phi-K_1/\Lambda)\ge\frac12 s\chi c_\Phi$. (c) $\chi=v^2/(v^2+s_0^2)$ is continuous on the compact J, and it vanishes only at η_0. So $\chi_*=\min_{J\setminus N_0}\chi>0$, and $\Lambda\ge 2K_1/(c_\Phi\chi_*)$ puts the set in N_0. Put $\varepsilon=2K_1/(c_\Phi\Lambda)\le\frac12$. On the set, $|v|\le s_0\sqrt{2\varepsilon}$. Write $B_1=b^{-1}[-(1+k_0+h+2h\eta u)\Phi+\mathcal{E}]$ with

$$\mathcal{E}=dw\zeta\Phi-v_U(a'\Phi+\mathcal{T}\Phi)-(1+k_0)Y\Phi_Y-\Lambda^{-1}k_1(Y\Phi_Y+\Phi)-2h\Lambda^{-1}\eta w\Phi.$$

Then $|\zeta|\le Lb|v|/s_0^2$, $|v_U|\le|v|+\Lambda^{-1}d|w|$ and $|Y\Phi_Y|\le\frac14 Y_{\mathrm{buf}}(\varepsilon\Phi_{\max}+K_1/\Lambda)$. So $|\mathcal{E}|\le K_{\mathcal{E}}(\sqrt{\varepsilon}+\Lambda^{-1})$, where $K_{\mathcal{E}}$ depends only on the ball constants, $\min_{N_0}s_0$, b, a' and Y_{buf}. Since $(\frac12-h)+h=\frac12$, we have $1+k_0+h+2h\eta u=1+h+\eta u+du'\ge 1-|u|-|u'|\ge 1-\frac38=\frac58$. Take Λ_p such that also $K_{\mathcal{E}}(\sqrt{\varepsilon}+\Lambda^{-1})\le c_\Phi/8$. Then $-B_1\ge c_\Phi/(2b_{\max})$, and $-R_1=-B_1/L\ge -B_1$. Finally (a) with $\chi\Phi\ge 0$ gives $p_{1,r}\ge(Y\Phi_{\max})^{-1}\Lambda^{-1}\frac{c_\Phi}{2b_{\max}}\frac{Y^2}{2}$. □

The reference flattening multiplies these first derivatives by numbers in $[0,1]$. Thus the first-strain source estimate uses P_{ref}. The activation constants $V(C),K(C)$ can still depend on the selected member. In particular this does not bound the axial ratio $p_{2,r}^2/p_{1,r}$ with a bound independent of C.

Memberwise activation controls and their order. We write κ_{act} for the entry lemma's activation shear κ_0, t_{act} for its small activation width, and $\omega_{\mathrm{act},j}$ for the two last transition widths. None of these is physical time, and κ_{act} is unrelated to the later critical scalar-blend parameter. The order is displayed below. It does not assert a positive κ_{act} independent of C:

$$\text{uniform datum/gauge bounds, output radii, } \Lambda, T_s \text{ fixed} \longrightarrow C \text{ selected,}$$
$$\longrightarrow\ y_*(C),\ \Upsilon,\ y_1(\eta),\ \omega_0 \longrightarrow\ \kappa_{\mathrm{act}}(C) \longrightarrow\ t_{\mathrm{act}}(C) \longrightarrow\ \omega_2(C) \longrightarrow \text{ fix the actual higher jets.}$$

The next loop, spectral and completion parameters use that fixed member. On the axial alternative the reference has $p_{2,r}^2=2bYw_Y^2/(\Lambda g^2\Phi^2)\asymp C^2$, so $V(C):=\sup(p_{1,r}+p_{2,r}^2/p_{1,r})$ generally grows like C^2. If we fix $\kappa_{\mathrm{act}}>0$ before all sufficiently large C, then $\kappa_{\mathrm{act}}V(C)<1$ is impossible.

For a selected C the reference-entry estimates give finite constants $V(C)$, the fixed $P_{\mathrm{ref}}\ge\sup|p_{1,r}|$, and $K(C)$, uniform over the admitted reference-flattening widths. If the reference has reserve $v_r\ge 2+c_r$, their post-activation comparison up to the interpolation inlet reads

$$\big|P_c-[(1-\beta)p_1^0+\beta v^{00}(y)]\big|\le K(C)(2t_{\mathrm{act}}+\kappa_{\mathrm{act}}y_T),\qquad v_s\le 0.8+\kappa_{\mathrm{act}}V^0(C).$$

During interpolation the forward comparison includes the additional width ω_2 (Theorem 1.20.28(c)). On the backward side the scalar transport bound of Theorem 1.20.36(d) propagates the inlet margin. We select the positive scalar κ_{act} less than

$$\min\left\{\frac{1}{8(1+V(C))},\ \frac{.4}{1+P_{\mathrm{ref}}},\ \frac{\min(1,c_r)}{16(1+K(C))}\right\}.$$

We also put κ_{act} less than the finite source and axial-matching tolerances allocated to the activation shear itself.

More explicitly, let $\varepsilon_{\mathrm{late}}>0$ be the minimum of the specified late $O(\Lambda^{-1})$ and axial ε_u error budgets. We enlarge $K(C)$ to cover these comparisons and impose $K(C)\kappa_{\mathrm{act}}<\varepsilon_{\mathrm{late}}/8$. A later termination width cannot remove a previously fixed $O(\kappa_{\mathrm{act}})$ error. We then select t_{act} so that $K(C)t_{\mathrm{act}}<\min(1,c_r)/16$ and $K(C)t_{\mathrm{act}}<\varepsilon_{\mathrm{late}}/8$. We also keep it below the finitely many other flat-activation and endpoint tolerances for this κ_{act}.

We impose $t_{\mathrm{act}} \le \kappa_{\mathrm{act}}^2$ and the first-collar and termination budget of Remark 1.20.30(2). These upper bounds give strict $P_c > 2$ and $v_s < 1$ margins. We select the termination widths afterward to keep the reference $p_1 > 3$ slack, the late $O(\Lambda^{-1})$ source-error budget and the specified axial matching tolerance. These are finite positive upper tolerances for this member.

There is no uniform lower bound on the controls and no assertion that they can stay fixed when C increases. The inequalities above establish this order for each selected member.

The uniform output estimates necessary to select T_s and the matching budgets earlier do survive this order. In the moving coordinate y, the scalar cutoffs depend on y/t_{act} or $(y - y_1(\eta))/\omega_0$ and $(y - y_l - \omega_0)/\omega_2$. At fixed y, angular differentiation does not differentiate $\sigma(y/t_{\mathrm{act}})$ or the interpolation. It reaches the axial termination only through the fixed C-level template $y_1(\eta)$, which is chosen before κ_{act} (Definition 1.20.22). The first-radial equations use only their values:

$$U_y = -\kappa(y)\tfrac{\hat\xi^2}{2} n_{s,r}/2, \qquad (\log F)_y = -\kappa(y) p_{1,r}/2, \qquad 0 \le \kappa \le 1.$$

Axial termination multiplies the first expression by a scalar $0 \le \beta \le 1$. The output logarithmic slope is a convex combination of bounded slopes. No κ_y or β_y occurs in these first-radial prescriptions. On the fixed evaluation graph $\frac{\hat\xi^2}{2} = \frac{\hat\xi_i^2}{2}/b$, $\frac{\hat\xi_i^2}{2} = B_{\mathrm{r1}}$ (Definition 1.20.22), the moving coordinate is independent of the angle.

Integration thus gives the uniform fixed angular bounds for G_i and $\log(CE_i)$ even when we select the widths after C. We use these same bounds to select T_s, without fixed widths.

The placement of the cutoffs also controls derivatives of the histories. With $m(y,\eta) = M(\frac{\hat\xi_a^2}{2} e^y, \eta)$ and $s_a = (\log \frac{\hat\xi_a^2}{2})'$,

$$(\partial_\eta|_{\hat\xi})^2 M = m_{\eta\eta} - 2 s_a m_{y\eta} + s_a^2 m_{yy} - s_a' m_y, \qquad m_{yy} = \tfrac{\hat\xi^2}{2}(\rho + \rho_y),$$

where $\frac{M_{\hat\xi}}{\hat\xi} = \rho$. Thus the second angular derivative of a history uses only the first radial derivative of its density. The first derivative of the history-defined radial velocity uses this history derivative. Together with the moving-angular and first-radial field estimates this supplies the uniform first-physical-derivative/source budgets used before the selection of C.

No bounds on derivatives of the narrow cutoffs are necessary. One more radial derivative can introduce inverse widths. We assert only that the higher fixed-$\hat\xi$ jets and exterior Gevrey radii are finite for the selected member. Their constants can depend on C through the late controls. We fix them before the next loop frequencies, spectral response and integer selections, and completion thresholds.

We select the same scalar endpoint controls on the two sides. The endpoint coordinate y is one slice function. The quantities $\frac12 \hat\xi \partial_{\hat\xi} U$, n_s and $\frac{\hat\xi^2}{2} n_s$ are slice continuations with weights $(\frac12 + h)$, $(\frac12 + h) + 1$ and $(\frac12 + h)$. The chart factor in $\log F$ is radially constant. We select one C greater than the two amplitude thresholds.

We then take the minimum of the forward, backward, and two-endpoint tolerances for κ_{act}. Next, we take these minima for t_{act} at the selected shear, and then for the termination widths. The resulting cutoff profiles are the same on the two sides. They are single functions in slice variables. Thus they keep the equal slice jets of the equations and of all endpoint germs. The accepted endpoint numerator margin and specified-germ-zone selection precede this activation and are unchanged.

The curved-entry extension uses $y = 2\log(\hat\xi/\hat\xi_a)$, not fixed-$\hat\xi$ cutoffs. For each genuine history $m(y,\eta) = M(\frac{\hat\xi_a^2}{2} e^y, \eta)$,

$$\partial_\eta|_{\hat\xi} M = \partial_\eta|_y m - (\log \tfrac{\hat\xi_a^2}{2})' \partial_y m, \qquad \partial_y m = \tfrac12 \hat\xi M_{\hat\xi}.$$

Thus fixed-$\hat{\xi}$ first derivatives of histories do not differentiate a narrow cutoff. On $t_{\mathrm{act}} < y < 2t_{\mathrm{act}}$ we freeze the *values* of the reference first-strain constants $p_{1,r}, n_{s,r}$ at $\vartheta(y)$ (Definition 1.20.22(M0)). Multiplying them by a factor that can vanish would give $a_s = 0$ on the plateau. The comparison v^{00} above is the reserve of the frozen continuation (Theorem 1.20.28), not the activation-point value v_r.

Its source stays $\geq c_0 + .94\Lambda L b\chi$. With $B_{\mathrm{r}0} = \max\{100, 12 \max\sup b/\min\{\min c_0, s_\gamma\}\}$ and $B_{\mathrm{r}1} = eB_{\mathrm{r}0}$ (Definition 1.20.22), both common to the two members, the frozen continuation has $p_1 \geq c_0 \frac{\hat{\xi}^2}{2}/(4L) \geq 3$ on all of $\frac{\hat{\xi}^2}{2} \geq B_{\mathrm{r}0}/b$ (Lemma 1.20.25); in particular up to the evaluation graph $\frac{\hat{\xi}_i^2}{2}/b$, $\frac{\hat{\xi}_i^2}{2} = B_{\mathrm{r}1}$. We use the same normalized squared-flat Gevrey-3/2 step for the activation and its slice-continued cutoff data. We activate stress with $e = (1 - \kappa_{\mathrm{act}})\sigma(y/t_{\mathrm{act}})$ and shear $\partial_y U = -\kappa \frac{\hat{\xi}^2}{2} n_{s,r}/2$, $\partial_y \log F = -\kappa p_{1,r}/2$, $\kappa = 1 - e$.

The first collar has exact stress factorization $T_0 = eB_0^{\mathrm{field}}$ with a nonzero initial factor. An absolute error against flat stress does not justify it. Moving-coordinate comparisons give genuine-history errors $O(t_{\mathrm{act}} + \kappa_{\mathrm{act}})$. We end the axial shear at the angle-dependent level $y_1(\eta)$ of Definition 1.20.22(M1): early, at $y_e = y_*(C)/4$, where $|Z_R| \leq \delta_Z/2$, and at $y_l = \log(\Lambda B_{\mathrm{r}0}/4)$, where $|Z_R| \geq \delta_Z$. Only then do we interpolate the remaining shear to .8, at $y \geq y_l + \omega_0$. A transverse zero of Z_R off the drift root gives an obstruction to a single late termination under the hypotheses of Proposition 1.20.29.

On the output slab $\frac{1}{2}\hat{\xi}\partial_{\hat{\xi}} U = 0$, $\ell_r = .6$, and $p_1 > 2$ is invariant because at $p_1 = 2$ its radial derivative is $\frac{\hat{\xi}^2}{2} S_q/L - 1.2 > 0$. The evaluated output U and $\log(CE)$ have bounded fixed angular norms independent of the narrowing width and sufficiently large C. After we select C, we select the late widths for this member so that the extra $U - u$ errors are $O(1/\Lambda)$. Thus the large gauge gradient does not amplify an uncontrolled error.

On the endpoint collars $b = \lambda_{\mathrm{ch}}$, so the coordinate y is the backward reference coordinate written in slice variables. There $y_1 \equiv y_l$, and ω_0 and y_l are common to the two members, so the axial termination is the same function of y on both sides (Remark 1.20.30(3)). Thus the same flattening and activation cutoffs give equal slice jets of the germs. These estimates complete the curved-entry construction. The same Gevrey majorant and compact central pressure interval give uniform bounds for this $p_0(R)$ family.

Central root margin. With $v = (\frac{1}{2} - h)\eta - du$, the central constant-pressure numerator is $Z = -vu' - (\frac{1}{2} + h)(1 + 2\eta u)u + 4(\frac{1}{2} + h)\eta m_R$. At the drift root η_0, where $(\frac{1}{2} - h)\eta_0 = d_0 u_0$, it simplifies to

$$Z(\eta_0) = (\tfrac{1}{2} + h)u_0[-1 - 2\eta_0 u_0 + 4m_R d_0/(\tfrac{1}{2} - h)] \leq -(\tfrac{1}{2} + h)u_0/2.$$

For the selected small positive axial offset $u_0 \leq (\frac{1}{2} - h)w/16$, the root neighborhood of radius at most $w/8$ lies where $p_0 \equiv -m_R$. On this neighborhood, continuity gives a uniform nonzero lower bound. Away from that neighborhood the core lemma uses its separately selected small regularizer.

We do not assert that this simplified expression is equal to Z on the full sector. We use these uniform bounds to select the core parameter Λ, the matching radii, and the finite scalarization width. We then select a large C. We then select the activation and termination controls for this member. We do not fix them in the earlier selection. We match the actual core exit; it is not a pointwise approximation with reset histories.

Matching the growing profile and axial velocity. We next connect the curved core output to the specified growing profile. We match its amplitude before we correct the radial integrals. We extend its output power with $\frac{1}{2}\hat{\xi}\partial_{\hat{\xi}} U = 0$ and $\ell_r = .6$. At the curved entry graph $\frac{(\hat{\xi}_i(\eta))^2}{2}$ let

δ_l be the actual incoming logarithmic amplitude minus the desired growing-reference logarithmic amplitude. This is a finite angular function with the necessary endpoint germs.

With $y = 2\log(\hat{\xi}/\hat{\xi}_i)$, we replace the log amplitude by $\log F_{\text{target}} + (1 - \sigma(y/T_s))\delta_l$. We write $B = 1 + k$ for the actual axial-history coefficient and $v(U) = (\frac{1}{2} - h)\eta - dU$. The extra source term is

$$\frac{\sigma'(y/T_s)\delta_l}{T_s}[-B + v(U)(\log \tfrac{\hat{\xi}_i^2}{2})'].$$

The remaining terms are the convex combination of the endpoint sources under the same actual transport operator.

Their positive reserves survive the small core U error. All coefficients in the displayed error are fixed finite functions. We take a fixed sufficiently large T_s. This makes the error small and keeps the radial slope in, for example, $[.55, .65]$. The $p_1 = 2$ barrier persists after an increase of the fixed reference exit.

Throughout this interpolation $\frac{U_{\hat{\xi}}}{\hat{\xi}} = 0$, so $b_s = 0$ and the relaxed cone does not use a bounded axial ratio. We also use the same endpoint scalarization when we specify a nonzero endpoint control. The interior relative correction has zero endpoint jets.

At a large-scale positive-growth annulus the target swirl has fixed normalized minimum $e_{\min} > 0$. We replace the delivered radially constant G_i by G through a smooth interpolation that keeps the radial germs. This changes U on the interpolation annulus. The reference has $a_s = .8$, $b_s = 0$, positive Q, and a finite normalized axial ratio when the complete reference is fixed.

A sufficiently small $G_i - G$ controls the $b_s w$ and history errors there. After this edit the fields coincide with the ideal fields on an open outgoing collar, but their histories do not yet coincide. With $\frac{\hat{\xi}_*^2}{2} = Rr_*(\eta)$, $e_* = E_{\text{ref}}(\frac{\hat{\xi}_*^2}{2})$ and $H_* = \hat{\xi}_* e_*$, the actual normalized discrepancy is

$$\left(\frac{\Delta M}{\frac{\hat{\xi}_*^2}{2}e_*}, \frac{\Delta I}{\frac{\hat{\xi}_*^2}{2}H_*}, \frac{\Delta J - G\Delta I}{\frac{\hat{\xi}_*^2}{2}H_* e_*}, \frac{\Delta S - 2G\Delta M}{\frac{\hat{\xi}_*^2}{2}e_*^2}, \frac{\Delta C_p}{e_*^2}\right).$$

The next moment correction cancels this normalized vector on a region of positive stress. Absolute smallness at a flat stress edge would not suffice.

We select the drift interpolation close to the actual target G. The correct sign alone is insufficient. On the central band $G = 0$. On its fixed outer bridge $(\frac{1}{2} - h)\eta - dG$ has a strict same-sign margin. We select the tiny central and endpoint axial offsets first, and interpolate perturbations in this margin to make $\|u - G\|$ sufficiently small. The norm is the C^1_η norm of Lemma 1.6.36, and we take $\|u - G\|_{C^1([-1,1])} \le \varepsilon_u/4$ with $\varepsilon_u \le 1$. On the endpoint collars $u - G_e = \lambda_{\text{ch}}^{\frac{1}{2}+h} j_0$ exactly (paragraph 1.6.3.6), so this bound contains the endpoint offset. Therefore ε_u is selected before j_0. This is possible because ε_u depends only on τ_b, K_b, $e_{\min}$, K_H, s_γ and the constants of $j_\sharp$ (c_j, K_{geo}, K_{ax}, q_*, T_d, C_{ph}), all fixed before j_0. Then j_0 is selected with $K_{\text{ch}} j_0 \le \varepsilon_u/8$, where $K_{\text{ch}} := \sup(\lambda_{\text{ch}}^{\frac{1}{2}+h} + |(\lambda_{\text{ch}}^{\frac{1}{2}+h})'|)$ over the endpoint collars. The interpolated perturbations take the remaining $\varepsilon_u/8$. The complete activation error B_{act} of Remark 1.20.30(2) uses at most $\varepsilon_u/2$. We also take the strip width of Lemma 1.6.35 with $w < 4\eta_c$, so that the drift-root neighbourhood lies in the central band, where $G = 0$. These two upper bounds give (H_u) of Lemma 1.20.24, hence $p_{1,r} > 0$ at the drift root.

We select Λ to control the core part of the mismatch before C. After we select C, we decrease the activation and termination controls for this member. The resulting axial mismatch in the normalized C^1_η coefficient norm must be at most ϵ_u. The fixed radial templates keep their first radial derivatives.

We write $e_{\min} > 0$ for the fixed normalized swirl minimum. A constant times

$$\epsilon_u/e_{\min} + \epsilon_u^2/e_{\min}^2 + O(C^{-2}/e_{\min}^2 + C^{-10}/e_{\min} + C^{-16}/e_{\min}).$$

bounds the actual normalized correction error. We select ϵ_u against the finite correction and cone tolerances before C. Then we select C to control only the displayed decaying terms.

An increase of C does not reduce a fixed axial mismatch. This is the quantitative core-entry link necessary for the five-moment correction theorem.

We put the core-to-reference five-moment correction before the pressure correction of Lemma 1.6.37. We calculate its rank directly. Two U bumps have weights $1, x^{3/5}$. Three E bumps have weights $x^{1/2}, x^{1/10}, x^{-9/10}$.

We subtract $G\Delta I$ from ΔJ and $2G\Delta M$ from ΔS. This gives a block triangular derivative. The two Chebyshev determinants are nonzero. More explicitly, with disjoint U and E bump supports, we write $\delta U = e_* u(x)$, $\delta E = e_* v(x)$ and $\frac{\hat\xi^2}{2} = \frac{\hat\xi_*^2}{2} x$. The exact rows are

$$\begin{aligned}
\Delta M &= \tfrac{\hat\xi_*^2}{2} e_* \int u, \qquad \Delta I = \sqrt{2}\big(\tfrac{\hat\xi_*^2}{2}\big)^{3/2} e_* \int x^{1/2} v,\\
\Delta J - G\Delta I &= \sqrt{2}\big(\tfrac{\hat\xi_*^2}{2}\big)^{3/2} e_*^2 \int x^{3/5} u,\\
\Delta S - 2G\Delta M &= \tfrac{\hat\xi_*^2}{2} e_*^2 [\int u^2 - \int x^{1/10} v - \tfrac{1}{2}\int v^2],\\
\Delta C_p &= e_*^2 [\int x^{-9/10} v + \tfrac{1}{2}\int v^2/x].
\end{aligned}$$

Disjoint supports eliminate a mixed $\delta U \delta H$ term. The positive U-square energy stays in the calculation. We solve the two U rows, then the three E rows with that square contribution in the target. We fix the inverse and quadratic bounds after the displayed normalization, so the small-vector IFT gives a unique correction with its finite angular derivatives.

We include the specified endpoint corrections in the baseline before this solve, or we recover them by uniqueness of the identical endpoint map. A cutoff of a nonzero solution would destroy the equations. The IFT thus includes the quadratic S, C_p terms. The normalized core defects and their angular derivatives are small in the core-exit scaling.

The stated order gives this smallness: small axial data, large Λ, and then large C. These are relative estimates on the correction region, not absolute estimates at a flat stress edge. All supports lie in compact positive-stress sectors. The five-moment correction restores the exact corrected reference before the next profile and pressure correction. In particular the resulting complete core has datum p_0. After the pressure correction, the original actual future and its one energy root are unchanged.

1.6.5 Strict stress inequalities and the reserved radial layout

We now strengthen the relaxed stress inequalities to the strict cone conditions necessary for the packet construction. We keep the five specified radial integrals. We use the *capped* geometric loop of Lemma 1.19.2 and its slice-continued realization in Corollary 1.19.3. The cited lemma contains the full local loop construction. On the actively modified set where its variance cutoff is nonzero, its value bounds are $a_L < 5/2$ and $|b_L| < 5/4$.

Where that cutoff is zero, the loop keeps the original shear. We use the global first-strain bounds of that unchanged field. We assert no new cap there. We use the forward phase $N_{\mathrm{sh}}(\log \frac{\hat\xi^2}{2} + f(\eta))$.

Here f is smooth on $[-1,1]$, and $f = \log \lambda_{\mathrm{ch}}$ on the forward endpoint collars. There the phase equals the backward phase $N_{\mathrm{sh}} \log \frac{\hat{\xi}_b^2}{2}$ (Remark 1.6.7). In slice variables the joint phase on the collars is

$$N_{\mathrm{sh}}\big(\log \tfrac{\widetilde{\xi}^2}{2} + \tfrac{1}{(\frac{1}{2}-h)} \log |\eta_b(\widetilde{\eta})|\big), \tag{1.6.66}$$

which is one real-analytic function across $\widetilde{\eta} = 0$. For smoothness across $t = 0$, only the jets of f at ± 1 must agree with those of $\log \lambda_{\mathrm{ch}}$ (Lemma 1.6.8(c)).

Independent phases $N_{\mathrm{sh}} \log \frac{\hat{\xi}^2}{2}$ on the two sides would not have equal slice jets. The reason is $\log \frac{\hat{\xi}^2}{2} = \log \frac{\widetilde{\xi}^2}{2} + \frac{1}{(\frac{1}{2}-h)} \log |\eta|$, and $\log |\eta|$ has the $\widetilde{\eta}$-derivatives $\frac{1}{2}$ and $-\frac{1}{2}$ at 0 in the two tip charts. The integrated-history estimates below do not claim small raw angular derivatives of the oscillating fields. The modulation ends before the strict negative-power wait. We cancel the five-moment discrepancy introduced by the modulation with the earlier reserved compact correction.

The partial-history discrepancies are $O(N_{\mathrm{sh}}^{-2})$, with first angular derivatives $O(N_{\mathrm{sh}}^{-1})$. Complete exit jets have the stronger cancellations. We select one sufficiently large finite $N_{\mathrm{sh}}(C)$ and keep it fixed.

The selected support order is

$$\begin{aligned} &\text{loop and its moment correction} \longrightarrow \text{early positive-order and mean velocity corrections} \\ &\qquad \longrightarrow \text{pulse and actual returns} \longrightarrow \text{primitive-memory correction} \\ &\quad \longrightarrow \text{central gap} \longrightarrow \text{spectral five-moment correction} \longrightarrow \text{heat future}. \end{aligned} \tag{1.6.67}$$

We reserve the positive-order correction regions for completion coefficients. The leading profile stays unchanged there. The spectral correction and its moment restoration occur after these regions in the displayed radial order.

The five-history restoration and the slice-continued modulation keep the endpoint data of the leading family. Their comparison includes canonical outward pressure and the full heat tail, as recorded in Lemma 1.25.10. The remaining task for the leading data is spectral. Section 1.26 uses the reserved central interval and restores all five moments after its compact modification.

We first prove the conditional local radial estimates. The joint family uses their specified component results. It does not use a different global reference construction. We then verify its actual histories, pressure, and terminal corridors. We impose strict shear on this same family. The resulting pair supplies the leading datum for the slow and packet corrections.

1.7 The backward heat profile

Main result. Lemma 1.7.1 gives the positive heat factor for the same exterior profile. It proves the required derivative bounds and endpoint regularity directly. The argument uses only a convergent integral and differentiation.

The integral representation is the local backward heat formula in [42]. We prove its stated properties here.

Lemma 1.7.1 (The positive backward heat factor)**.** *For $h > 0$ and $z \geq 0$, we define*

$$\mathcal{H}_-(z) = \frac{1}{\Gamma(1+h)} \int_0^\infty e^{-v} v^h (1+zv)^{-h} \, \mathrm{d}v. \tag{1.7.1}$$

Here Γ *is the gamma function. The factor* $\mathcal{H}_-$ *is positive and smooth up to* $z = 0$ *from the right. It satisfies* $\mathcal{H}_-(0) = 1$ *and*

$$\mathcal{H}_-^{(k)}(z) = \frac{(-1)^k (h)_k}{\Gamma(1+h)} \int_0^\infty e^{-v} v^{h+k} (1+zv)^{-h-k}\, \mathrm{d}v, \qquad |\mathcal{H}_-^{(k)}(z)| \le (h)_k (1+h)_k. \tag{1.7.2}$$

The symbol $(b)_k$ *denotes the rising factorial, with* $(b)_0 = 1$*. For each fixed integer* $k \ge 1$ *and* $0 < h \le h_0 < 1/2$*, the derivative bound is at most* $C_{k,h_0} h$*.*

For $c > 0$*,* $r > 0$*, and* $t \le 0$*, we put* $s = r^2/2$*,* $\tau = -t$*, and*

$$K(r,t) = c s^{-\frac{1}{2}-h} \mathcal{H}_-(2\tau/s).$$

This field satisfies

$$\partial_t K = (\partial_{rr} + r^{-1}\partial_r - r^{-2})K, \qquad K_r < 0. \tag{1.7.3}$$

For $\hat\xi > 0$ *and* $|\eta| \le 1$*, the composition* $\mathcal{H}_-(2(1-\eta^2)/\frac{\hat\xi^2}{2})$ *is smooth up to the two angular endpoints. For fixed nonnegative integers* j, m*, it has the expansion*

$$(\tfrac{1}{2}\hat\xi\partial_{\hat\xi})^j \partial_\eta^m \left[\mathcal{H}_-(4d/\hat\xi^2) - 1 + \frac{2h(1+h)d}{\frac{\hat\xi^2}{2}} \right] = O_{j,m,h_0}\big(h(\tfrac{\hat\xi^2}{2})^{-2}\big), \qquad d = 1-\eta^2, \tag{1.7.4}$$

with one remainder constant for all $\frac{\hat\xi^2}{2} \ge 1$*,* $|\eta| \le 1$*, and* $0 < h \le h_0 < 1/2$*.*

Proof. The integrand in (1.7.1) is positive. Its kth derivative with respect to z has an integrable majorant on $z \ge 0$. We replace $(1+zv)^{-h-k}$ by 1 to get this majorant. Differentiation under the integral gives (1.7.2).

The gamma identity gives its bound and the value

$$\mathcal{H}_-^{(k)}(0) = (-1)^k (h)_k (1+h)_k.$$

For fixed $k \ge 1$, the product $(h)_k(1+h)_k$ has one factor h. Its other factors have bounds that depend only on k and h_0. This proves the stated uniform estimate.

We next derive the differential equation for the factor. For each $z \ge 0$, we define

$$F(v) = e^{-v} v^{1+h} (1+zv)^{-1-h}.$$

The function F vanishes at the two endpoints of $(0,\infty)$. Direct differentiation gives

$$F'(v) = e^{-v} v^h (1+zv)^{-h-2} (1+h-v-zv^2).$$

Thus, integration of $hF'/\Gamma(1+h)$ gives

$$z^2 \mathcal{H}_-'' + [1 + 2(1+h)z]\mathcal{H}_-' + h(1+h)\mathcal{H}_- = 0. \tag{1.7.5}$$

We set $z = 2\tau/s$ in the physical field. Its time derivative is

$$\partial_t K = -2c s^{-\frac{3}{2}-h} \mathcal{H}_-'(z).$$

Its radial operator is

$$(\partial_{rr} + r^{-1}\partial_r - r^{-2})K = 2c s^{-\frac{3}{2}-h} \left[z^2 \mathcal{H}_-'' + (2(\tfrac{1}{2}+h)+1) z \mathcal{H}_-' + ((\tfrac{1}{2}+h)^2 - \tfrac{1}{4})\mathcal{H}_- \right].$$

The identities $2(\frac{1}{2}+h)+1=2(1+h)$ and $(\frac{1}{2}+h)^2-1/4=h(1+h)$ reduce this expression to the same time derivative. This proves the equation in (1.7.3).

The ratio $-z\mathcal{H}_-'/\mathcal{H}_-$ is an average of $hzv/(1+zv)$ with a positive probability density. Thus,

$$0\le -\frac{z\mathcal{H}_-'(z)}{\mathcal{H}_-(z)}<h, \qquad \frac{rK_r}{2K}=-(\tfrac{1}{2}+h)-\frac{z\mathcal{H}_-'(z)}{\mathcal{H}_-(z)}<-\frac{1}{2}.$$

This gives $K_r<0$.

The endpoint composition uses only nonnegative arguments of $\mathcal{H}_-$. Each angular derivative contains powers of $(\frac{\hat\xi^2}{2})^{-1}$ and derivatives of $d=1-\eta^2$. No derivative divides by d. The derivative bounds thus give smooth limits at $\eta=\pm1$ for each fixed positive $\frac{\hat\xi^2}{2}$.

Taylor's formula gives the integral remainder

$$\mathcal{H}_-(z)-1+h(1+h)z=z^2\int_0^1(1-\theta)\mathcal{H}_-''(\theta z)\,\mathrm{d}\theta.$$

Each fixed derivative of the integral has a bound of order h on $0\le z\le 2$. We substitute $z=4d/\hat\xi^2$ and apply $(\frac{1}{2}\hat\xi\partial_{\hat\xi})^j\partial_\eta^m$. Each term keeps a factor $(\frac{\hat\xi^2}{2})^{-2}$ and a bounded polynomial in η. The derivative bounds give (1.7.4). □

1.8 The backward member and the class $\mathcal{O}^\flat$

Throughout this section we work in the backward chart $t=-\hat t(1-\beta^2)$, $z=\beta\hat t^{\frac12-h}$, $\hat\xi=r/\sqrt{\hat t}$, with $|\beta|\le1$ and $\varsigma=-1$. We write $L=1-2h\beta^2$, $d=1-\beta^2$, and $\kappa=1-e^{-3}$.

1.8.1 Edge weights

Lemma 1.8.1 (Squared-flat weights in a smooth edge variable)**.** *Let $s_0>0$, $a>0$ and $\varphi\in C^\infty([0,s_0])$ with $\varphi(0)=0$ and $\varphi'>0$. Put $w(s)=\exp(-a/\varphi(s)^2)$ for $s>0$ and $w(0)=0$. Then $w\in C^\infty([0,s_0])$ is flat at 0, and:*

(a) for every $B\in\mathbb{R}$ there is $s_B>0$ such that $s\mapsto s^{-B}w(s)$ is increasing on $(0,s_B]$;

(b) for every $M\ge0$ there are $s_M>0$ and C_M such that $\int_0^\delta s^{-M}w(s)\,\mathrm{d}s\le C_M\delta^{3-M}w(\delta)$ for $0<\delta\le s_M$;

(c) for every k there is C_k such that $|w^{(k)}(s)|\le C_k s^{-3k}w(s)$ on $(0,s_0]$;

(d) $w(s)^b s^{-N}\to0$ as $s\downarrow0$, for every $b>0$ and N.

For the weight ζ in (O2), (a)–(d) hold on each edge collar in its native logarithmic distance $s=d_a$ or $s=d_b$, with w replaced by ζ and possibly different constants.

Proof. Write $\varphi(s)=s\psi(s)$, where ψ is smooth and positive on $[0,s_0]$ and $\psi(0)=\varphi'(0)$. Put $g=a/\varphi^2=as^{-2}\psi^{-2}$. Since ψ^{-2} is smooth, the Leibniz rule gives $|g^{(j)}(s)|\le K_j s^{-2-j}$. Also $-g'(s)=s^{-3}\rho(s)$ with $\rho=2a\varphi'/\psi^3$, which is smooth and positive.

(a) We have $(s^{-B}w)'=s^{-B-3}w(\rho-Bs^2)$. This is positive when $s^2<\min\rho/|B|$.

(b) We have $w'=-g'w=s^{-3}\rho w$. Hence $s^{-M}w=s^{3-M}\rho^{-1}w'$. Integrate by parts on $[\epsilon,\delta]$ and let $\epsilon\to0$. The flatness of w removes the boundary term at 0, and

$$\int_0^\delta s^{-M}w=\delta^{3-M}\rho(\delta)^{-1}w(\delta)-\int_0^\delta(s^{3-M}\rho^{-1})'w.$$

Now $|(s^{3-M}\rho^{-1})'| \le K'_M s^{2-M} \le K'_M \delta^2 s^{-M}$ on $(0,\delta]$. For $\delta^2 \le 1/(2K'_M)$ this gives the claim with $C_M = 2/\min\rho$.

(c) Write $w^{(k)} = P_k w$. Then $P_0 = 1$ and $P_{k+1} = P'_k - g' P_k$. By induction, P_k is a finite sum of terms $s^{-p} r(s)$ with r smooth and $p \le 3k$: differentiation raises p by one, and multiplication by g' raises it by three. Hence $|P_k| \le C_k s^{-3k}$ on $(0, s_0]$.

(d) The statement is immediate from $w^b = e^{-ab/\varphi^2}$ and $\varphi(s) \le Cs$.

On a collar $\zeta = gw$ with g smooth and bounded above and below by positive constants. Thus (b) and (d) follow by comparison, (c) by Leibniz' rule, and (a) follows from $(\log(s^{-B}\zeta))' = s^{-3}\rho - B/s + g'/g > 0$ for s small. □

1.8.2 The outer collar of the backward member

We use the following facts of the construction.

(A1) For $\frac{\hat\xi^2}{2} \ge 2R_0$ the backward member is $U = M = J = 0$ and $H = H_0(1 - \rho\Psi(\frac{\hat\xi^2}{2}/B))$, where $H_0 = c(\hat\xi/\sqrt{2})^{-2h}\mathcal{H}_-(4d/\hat\xi^2)$ (the heat collar and wing defined before (1.15.10), with the backward chart convention of that subsection). Here $\Psi(v) = 1 - \sigma((v - e^{-3})/\kappa)$, with $\sigma(t) = f(t)/(f(t) + f(1-t))$ and $f(t) = e^{-1/t^2}$ for $t > 0$ (the terminal cutoff fixed before (1.15.1)). The edge $B > e^4 R_0$ is the edge of (1.15.2); it is scalar in the backward chart by (S2) of Lemma 1.8.7, whose proof does not use this clause. Moreover $0 < \rho < 1/4$ and $\rho \sup|v\Psi'(v)|/(1-\rho) < h/4$ (the choice of ρ at (1.15.1)). The rank-one bump of (1.15.10) is supported in $(\frac12\frac{\hat\xi_b^2}{2}, \frac34\frac{\hat\xi_b^2}{2})$, where there $\frac{\hat\xi_b^2}{2} = R_A e^{L_o}$ (not the outer edge); in particular at $\frac{\hat\xi^2}{2} < R_0$.

(A2) The $\varsigma = -1$ integrated stresses vanish for $\frac{\hat\xi^2}{2} \ge B$ (this is the zero-exterior-stress statement that clause (O1) requires). This follows from (A1), (A3) and Lemma 1.8.7, whose proof uses only (A1). For $\frac{\hat\xi^2}{2} \ge B$ we have $\Psi(\frac{\hat\xi^2}{2}/B) = 0$, so $H = H_0$ and $U = \mathfrak{M}_1 = \mathfrak{M}_3 = 0$; since $\mathfrak{M}_4(\infty) = 0$ and the pressure is canonical, $\mathfrak{M}_4 = \int_{(\frac{\hat\xi^2}{2})}^{\infty} H^2/(4s)\,\mathrm{d}s$ and $P = -\int_{(\frac{\hat\xi^2}{2})}^{\infty} H^2/(4s^2)\,\mathrm{d}s$. For $d > 0$ write $H_0 = d^{-h}G(\frac{\hat\xi^2}{2}/d)$ with $G(x) = cx^{-h}\mathcal{H}_-(2/x)$. The computation of (1.13.60) gives $4h\beta\mathfrak{M}_4 - d\mathfrak{M}_{4\beta} = \beta H^2/2 = -\frac{\hat\xi^2}{2}((2+4h)\beta P - dP_\beta)$, so the axial combination vanishes. The same identity holds at $d = 0$ by continuity. The differentiated heat bounds of Lemma 1.7.1 give integrable bounds for the two tails and their angular derivatives. With $\mathcal{K} = \mathfrak{M}_3 = 0$, the $\frac{\hat\xi^2}{2}$-derivative of $L\hat\xi^2\widehat{\mathcal{T}}_{P,\theta}$ is $L\hat\xi^2(\frac{H_{\hat\xi\hat\xi}}{\hat\xi^2} - \frac{H_{\hat\xi}}{\hat\xi^3}) - \frac12\hat\xi H_{\hat\xi} - hH - (\frac12 - h)\beta H_\beta$, which is (1.7.3) written in the backward chart ($(\frac12 - h) = 1 - (\frac12 + h)$); so $L\hat\xi^2\widehat{\mathcal{T}}_{P,\theta}$ is constant on $[B,\infty)$. As $\hat\xi \to \infty$ it tends to $(1-h)\iota_0 - (\frac12 - h)\beta\iota_0'$, where $\iota_0(\beta) = \int_0^\infty (H - c(\hat\xi/\sqrt{2})^{-2h})\,\hat\xi\,\mathrm{d}\hat\xi$, because $H - c(\hat\xi/\sqrt{2})^{-2h}$ and its β-derivative are $O((\frac{\hat\xi^2}{2})^{-h-1})$; and $\iota_0 = 0$ by Lemma 1.8.7.

(A3) The $\varsigma = -1$ stresses are

$$\widehat{\mathcal{T}}_{P,\theta} = \frac{H_{\hat\xi}}{\hat\xi} - \frac{2H}{\hat\xi^2} + \frac{(-\frac{\hat\xi^2}{2} + \mathcal{K})H + (1-h)\mathfrak{M}_2 - (\frac12 - h)\beta\mathfrak{M}_{2\beta} - d\mathfrak{M}_{3\beta} + 2(h - (\frac12 - h))\beta\mathfrak{M}_3}{L\hat\xi^2},$$

and, where $U = M = 0$, $\widehat{\mathcal{T}}_{P,z}$ is $(L\hat\xi)^{-1}$ times a linear combination, with constant coefficients bounded uniformly in $|\beta| \le 1$, of S, S_β, $\frac{\hat\xi^2}{2}P$ and $\frac{\hat\xi^2}{2}P_\beta$. The histories are normalized as in (1.9.1). For the axial stress compare (1.9.3). In the ς-version the side label multiplies only the U

and M terms. Indeed, for $t=\varsigma q d$, $z=\hat\zeta\hat t^{\frac12-h}$ (at fixed r) one has $\partial_z=(2\hat\zeta\hat t\partial_q+d\partial_{\hat\zeta})/(Lq^{\frac12-h})$, which does not depend on ς, and $\partial_t=\varsigma(\hat t\partial_q-(\frac12-h)\hat\zeta\partial_{\hat\zeta})/(Lq)$; only the terms generated by ∂_t change sign, and in (1.9.3) these are $\frac{\hat\xi^2}{2}U$ and $(\frac12-h)(\mathfrak M_1-\hat\zeta\mathfrak M_{1\hat\zeta})$ (Remark 1.8.14). The bound below uses only the structure of the stress, not any sign.

Lemma 1.8.2 (Outer collar of the backward member)**.** *Assume (A1)–(A3). Put $u=1-\frac{\hat\xi^2}{2}/B$. There are $u_0>0$ and constants such that for $0<u\le u_0$ and $|\beta|\le1$:*

(a) $c_0e^{-\kappa^2/u^2}\le\widehat{\mathcal T}_{P,\theta}\le C_0u^{-3}e^{-\kappa^2/u^2}$ *and* $|\widehat{\mathcal T}_{P,z}|\le C_0u^3e^{-\kappa^2/u^2}$*;*

(b) $|(\hat\xi^{-1}\partial_{\hat\xi})^j\partial_\beta^k(\widehat{\mathcal T}_{P,\theta},\widehat{\mathcal T}_{P,z})|\le C_{jk}u^{-3-3j}e^{-\kappa^2/u^2}$ *for all j,k;*

(c) $b_s=0$ *and* $a_s=v_s\ge2+h$*. Moreover* $\widehat{\mathcal T}_{P,\theta}=e^{-\kappa^2/u^2}u^{-3}b_\theta(u,\beta)$ *and* $\widehat{\mathcal T}_{P,z}=e^{-\kappa^2/u^2}u^3b_z(u,\beta)$ *with b_θ,b_z smooth on $[0,u_0]\times[-1,1]$ and $b_\theta(0,\cdot)>0$, so the unit direction $(b_\theta,u^6b_z)/|(b_\theta,u^6b_z)|$ extends smoothly to $\frac{\hat\xi^2}{2}=B$ with value $(1,0)$ (the analogue of [42, (4.32)]), and (1.5.1) holds on the collar with $\kappa'=1/2$;*

(d) clause (O2) holds at the outer edge with $\varphi_b(s)=(1-e^{-s})/\kappa$ and $a_b=1$, because $\kappa^2/u^2=1/\varphi_b(d_b)^2$; clause (O4) holds with $m=1-\rho\Psi(\frac{\hat\xi^2}{2}/B)$.

Proof. Step 0 (the cutoff). For $0<u\le\kappa/2$ put $t=1-u/\kappa\in[\frac12,1)$. Then $f(t)\in[e^{-4},e^{-1}]$ and $f(1-t)=e^{-\kappa^2/u^2}\le e^{-4}$. Hence

$$\frac{e^{-\kappa^2/u^2}}{e^{-1}+e^{-4}}\le\Psi(1-u)=\frac{f(1-t)}{f(t)+f(1-t)}\le e^4e^{-\kappa^2/u^2}.$$

The quotient formula and Lemma 1.8.1(c), applied with $\varphi(s)=s/\kappa$, give $|\Psi^{(k)}(1-u)|\le C_ku^{-3k}e^{-\kappa^2/u^2}$. For the lower bound on $|\Psi'|$: as $u\to0$,

$$-\Psi'(1-u)=\kappa^{-1}\sigma'(t)=\kappa^{-1}\frac{f'(1-t)f(t)+f(1-t)f'(t)}{(f(t)+f(1-t))^2},$$
$$f'(1-t)=2(\kappa/u)^3e^{-\kappa^2/u^2}.$$

So $|\Psi'(1-u)|\ge c\,u^{-3}e^{-\kappa^2/u^2}$ for small u.

Step 1 (the heat field has zero stress). Let $(H_0,\mathfrak M_{20},\mathfrak M_{40},P_0)$ be the heat profile and its histories, normalized so that they coincide with the actual histories for $\frac{\hat\xi^2}{2}\ge B$. Explicitly, $\mathfrak M_{20}(\hat\xi)=\mathfrak M_2(\sqrt{2B})-\int_{(\frac{\hat\xi^2}{2})}^{B}H_0$, $\mathfrak M_{40}(\hat\xi)=\int_{(\frac{\hat\xi^2}{2})}^{\infty}H_0^2/(4s)\,\mathrm ds$, $P_0(\frac{\hat\xi^2}{2})=-\int_{(\frac{\hat\xi^2}{2})}^{\infty}H_0^2/(4s^2)\,\mathrm ds$, with $\mathfrak M_1=\mathfrak M_3=0$. For fixed β, the map $\frac{\hat\xi^2}{2}\mapsto\mathcal H_-(4d/\hat\xi^2)$ is real-analytic on $\hat\xi>0$: if $d>0$ the integrand of (1.7.1) is analytic for $\operatorname{Re}z>0$, and if $d=0$ the map is constant. So the stresses of $(H_0,\mathfrak M_{20},\dots)$ are real-analytic in $\hat\xi>0$. By (A2) they vanish for $\frac{\hat\xi^2}{2}\ge B$, hence for all $\hat\xi>0$.

Step 2 (linearization). Put $V=\rho H_0\Psi(\frac{\hat\xi^2}{2}/B)\ge0$ and $E_w=\int_{(\frac{\hat\xi^2}{2})}^{B}V$. Then $H=H_0-V$ and $\mathfrak M_2=\mathfrak M_{20}+E_w$, because the primitives agree beyond B. The angular formula in (A3) is affine in $(H,\mathfrak M_2,\mathfrak M_{2\beta})$ when $\mathcal K=\mathfrak M_3=0$. Step 1 then gives

$$L\hat\xi^2\,\widehat{\mathcal T}_{P,\theta}=\tfrac{\hat\xi^2}{2}V+2LV-L\hat\xi^2\frac{V_{\hat\xi}}{\hat\xi}+(1-h)E_w-(\tfrac12-h)\beta E_{w,\beta}.$$

Similarly, $\widehat{\mathcal{T}}_{P,z}$ is the combination of (A3) evaluated at the deficits $\Delta\mathfrak{M}_4 = \int_{(\frac{\hat\xi^2}{2})}^{B} \frac{H^2-H_0^2}{4s}\,\mathrm{d}s$ and $\Delta P = -\int_{(\frac{\hat\xi^2}{2})}^{B} \frac{H^2-H_0^2}{4s^2}\,\mathrm{d}s$.

Step 3 (bounds). On $\frac{\hat\xi^2}{2} \in [B/2, B]$ the field H_0 is bounded above and below. By Lemma 1.7.1, $|\partial_\beta H_0| \le 8h(1+h)H_0/\frac{\hat\xi^2}{2}$ and $\frac12\hat\xi\partial_{\hat\xi}\log H_0 = -h - z\mathcal{H}_-'/\mathcal{H}_- \in [-h, 0)$ with $z = 4d/\hat\xi^2$. So $\frac{V_{\hat\xi}}{\hat\xi} = \rho[(\hat\xi^{-1}\partial_{\hat\xi}(H_0))\Psi + H_0\Psi'/B] \le 0$. Also $|E_{w,\beta}| \le \rho\int_{(\frac{\hat\xi^2}{2})}^{B} |\partial_\beta H_0|\Psi \le 8h(1+h)E_w/\frac{\hat\xi^2}{2}$, hence $|(\frac12 - h)\beta E_{w,\beta}| \le (1-h)E_w$ for $\frac{\hat\xi^2}{2} \ge 8$. Every term of $L\hat\xi^2\widehat{\mathcal{T}}_{P,\theta}$ other than the last is nonnegative, and the last is absorbed by the term $(1-h)E_w$. Hence $L\hat\xi^2\widehat{\mathcal{T}}_{P,\theta} \ge \frac{\hat\xi^2}{2}V$ and $\widehat{\mathcal{T}}_{P,\theta} \ge V/(2L) \ge c_0 e^{-\kappa^2/u^2}$ by Step 0. For the upper bound, Step 0 gives $|\frac{V_{\hat\xi}}{\hat\xi}| \le Cu^{-3}e^{-\kappa^2/u^2}$. Lemma 1.8.1(b) with $M = 0$ gives $E_w \le CBu^3e^{-\kappa^2/u^2}$. Also $|H^2 - H_0^2| \le 2\rho H_0^2\Psi$ and $|\partial_\beta(H^2 - H_0^2)| \le CH_0^2\Psi/\frac{\hat\xi^2}{2}$, since $\Psi(\frac{\hat\xi^2}{2}/B)$ does not depend on β. So $|\Delta\mathfrak{M}_4| + |\Delta\mathfrak{M}_{4\beta}| + \frac{\hat\xi^2}{2}|\Delta P| + \frac{\hat\xi^2}{2}|\Delta P_\beta| \le C\int_{(\frac{\hat\xi^2}{2})}^{B} \Psi(s/B)\,\mathrm{d}s \le Cu^3e^{-\kappa^2/u^2}$. This proves (a). For (b), each $\hat\xi^{-1}\partial_{\hat\xi}$ falls on Ψ, on H_0, or on a lower limit of integration, and Step 0 bounds each case; ∂_β falls only on H_0.

Step 4 (shear and cone). We have $b_s = 2\frac12\hat\xi\partial_{\hat\xi}U/E = 0$ and

$$\ell_r = \tfrac12\hat\xi\partial_{\hat\xi}\log H = \tfrac12\hat\xi\partial_{\hat\xi}\log H_0 + \frac{\rho(\frac{\hat\xi^2}{2}/B)|\Psi'(\frac{\hat\xi^2}{2}/B)|}{1-\rho\Psi} \le -h + \frac{4h(1+h)}{\frac{\hat\xi^2}{2}} + \frac{h}{4} \le -\frac{h}{2}$$

for $\frac{\hat\xi^2}{2} \ge 32(1+h)$. Hence $a_s = 2(1-\ell_r) \ge 2 + h$, and $v_s = a_s$. By (a), $\widehat{\mathcal{T}}_{P,z}/\widehat{\mathcal{T}}_{P,\theta} \le Cu^3 \to 0$. So $n_\theta \ge (1 + C^2u^6)^{-1/2}$ and $(v_s - 2)n_z^2 \le (2h+2)C^2u^6 \le \frac32 n_\theta^2$ for small u. This is (1.5.1) with $t_s = 0$ and $\kappa' = 1/2$.

Step 5 (weight and multiplier). Since $u = 1 - e^{-d_b}$, we have $\kappa^2/u^2 = 1/\varphi_b(d_b)^2$ with $\varphi_b(s) = (1-e^{-s})/\kappa$, which is smooth with $\varphi_b(0) = 0$ and $\varphi_b'(0) = 1/\kappa$. Put $\zeta_b = e^{-\kappa^2/u^2}$. Then (a) and (b) give (1.5.2) on the outer collar, because $u \ge c\delta$ there. Finally $E = H/\hat\xi = c_\infty(\hat\xi/\sqrt2)^{-1-2h}\mathcal{H}_-(4d/\hat\xi^2)(1 - \rho\Psi(\frac{\hat\xi^2}{2}/B))$ with $c_\infty = c/\sqrt2$, and $1 - m = \rho\Psi(\frac{\hat\xi^2}{2}/B)$ obeys the bounds of (O4) by Step 0.

Step 6 (factored forms). Since $1 - t = u/\kappa$, Step 0 gives $\Psi(1-u) = e^{-\kappa^2/u^2}q(u)$ with $q = (f(t) + f(1-t))^{-1}$. Here $f(t)$ is smooth and positive near $t = 1$, and $f(1-t) = e^{-\kappa^2/u^2}$ is smooth and flat at $u = 0$, so q is smooth on $[0, \kappa/2]$ and $q(0) = e$. Hence $V = e^{-\kappa^2/u^2}\rho H_0 q$, and, with $\hat\xi^{-1}\partial_{\hat\xi} = -B^{-1}\partial_u$,

$$\frac{V_{\hat\xi}}{\hat\xi} = -B^{-1}e^{-\kappa^2/u^2}u^{-3}\rho\big(2\kappa^2 H_0 q + u^3\partial_u(H_0 q)\big).$$

For the primitives we use the following fact: if $r(u,\beta)$ is smooth on $[0,u_0]\times[-1,1]$, then

$$\begin{aligned}\int_0^u e^{-\kappa^2/s^2}r(s,\beta)\,\mathrm{d}s &= e^{-\kappa^2/u^2}u^3\,\tilde r(u,\beta),\\ \tilde r(u,\beta) &= \frac{1}{2\kappa^2}\int_0^\infty e^{-\tau}(1+\tfrac{\tau u^2}{\kappa^2})^{-3/2}r\Big(\frac{u}{(1+\tau u^2/\kappa^2)^{1/2}},\beta\Big)\,\mathrm{d}\tau.\end{aligned} \tag{1.8.1}$$

and $\tilde r$ is smooth on $[0,u_0]\times[-1,1]$ with $\tilde r(0,\beta) = r(0,\beta)/(2\kappa^2)$. Indeed, the substitution $\kappa^2/s^2 = \kappa^2/u^2 + \tau$ gives the formula, and each (u,β)-derivative of the integrand is bounded by $C_k(1+\tau)^k e^{-\tau}$, so differentiation under the integral is allowed. Since $E_w = B\int_0^u V\,\mathrm{d}u'$, (1.8.1) gives $E_w = e^{-\kappa^2/u^2}u^3e_0$ and $E_{w,\beta} = e^{-\kappa^2/u^2}u^3e_1$ with e_0, e_1 smooth. By Step 2, $L\hat\xi^2\widehat{\mathcal{T}}_{P,\theta} = e^{-\kappa^2/u^2}u^{-3}\tilde b$, where

$\tilde b = L\hat\xi^2\rho(2\kappa^2 H_0 q + u^3\partial_u(H_0 q))/B + u^3(\frac{\hat\xi^2}{2}+2L)\rho H_0 q + u^6((1-h)e_0 - (\frac12 - h)\beta e_1)$ is smooth and $\tilde b(0,\beta) = 4L\kappa^2 e\rho H_0(B,\beta) > 0$. This gives $b_\theta = \tilde b/(L\hat\xi^2)$. For the axial stress, $H^2 - H_0^2 = -2H_0V + V^2 = e^{-\kappa^2/u^2} r$ with $r = \rho H_0 q(-2H_0 + e^{-\kappa^2/u^2}\rho H_0 q)$ smooth, and likewise for its β-derivative. So (1.8.1) gives $\Delta\mathfrak{M}_4, \Delta\mathfrak{M}_{4\beta}, \frac{\hat\xi^2}{2}\Delta P, \frac{\hat\xi^2}{2}\Delta P_\beta \in e^{-\kappa^2/u^2}u^3 C^\infty$, and (A3) gives the form of $\widehat{\mathcal{T}}_{P,z}$. □

Lemma 1.8.3 (The whole heat wing of the backward member)**.** *Assume (A1)–(A3). Let K_3 bound the sum of the absolute values of the coefficients in the expression of $\widehat{\mathcal{T}}_{P,z}$ in (A3). Put $\frac{\hat\xi_w^2}{2} = \max\{2R_0, 32(1+h)\}$, $H_0 = c(\hat\xi/\sqrt2)^{-2h}\mathcal{H}_-(4d/\hat\xi^2)$ and $E_0 = H_0/\hat\xi$. Assume*

$$(W)\qquad 9K_3 \sup\{E_0(\tfrac{\hat\xi^2}{2},\beta) : \tfrac{\hat\xi^2}{2} \ge \tfrac{\hat\xi_w^2}{2},\ |\beta|\le 1\} \le 1.$$

Then on $[\frac{\hat\xi_w^2}{2}, B)\times[-1,1]$: $b_s = 0$, $2+h \le a_s = v_s \le 2+2h$, $\widehat{\mathcal{T}}_{P,\theta} > 0$, $|\widehat{\mathcal{T}}_{P,z}| \le \widehat{\mathcal{T}}_{P,\theta}$, and (1.5.1) holds with $t_s = 0$ and with $\kappa' = \frac12$ in place of its κ (in this section $\kappa = 1 - e^{-3}$). With Lemma 1.8.2, (1.5.1) holds on $[\frac{\hat\xi_w^2}{2}, B]\times[-1,1]$ with a smooth unit direction up to $\frac{\hat\xi^2}{2} = B$, and F, a_s, $v_s - 2$ have positive lower bounds there.

Proof. Steps 1 and 2 of the proof of Lemma 1.8.2 use only (A1)–(A3) at the given point. They hold for every $\frac{\hat\xi^2}{2} \ge 2R_0$. So, with $V = \rho H_0\Psi(\frac{\hat\xi^2}{2}/B)$ and $E_w = \int_{(\frac{\hat\xi^2}{2})}^B V$,

$$L\hat\xi^2\widehat{\mathcal{T}}_{P,\theta} = \tfrac{\hat\xi^2}{2}V + 2LV - L\hat\xi^2\frac{V_{\hat\xi}}{\hat\xi} + (1-h)E_w - (\tfrac12 - h)\beta E_{w,\beta},$$

and $\widehat{\mathcal{T}}_{P,z}$ is the combination of (A3) evaluated at $\Delta\mathfrak{M}_4 = \int_{(\frac{\hat\xi^2}{2})}^B \frac{H^2-H_0^2}{4s}\,\mathrm{d}s$, $\Delta P = -\int_{(\frac{\hat\xi^2}{2})}^B \frac{H^2-H_0^2}{4s^2}\,\mathrm{d}s$ and their β-derivatives. For $\frac{\hat\xi^2}{2} < B$, $E_w > 0$.

Angular stress. Step 3 of that proof gives $\frac{V_{\hat\xi}}{\hat\xi} \le 0$ and $|E_{w,\beta}| \le 8h(1+h)E_w/\frac{\hat\xi^2}{2}$ for all $\frac{\hat\xi^2}{2} \ge 2R_0$. Since $(\frac12 - h) \le \frac12$ and $\frac{\hat\xi^2}{2} \ge 32(1+h)$, $|(\frac12 - h)\beta E_{w,\beta}| \le \frac12(1-h)E_w$. Hence $L\hat\xi^2\widehat{\mathcal{T}}_{P,\theta} \ge \frac{\hat\xi^2}{2}V + \frac12(1-h)E_w > 0$, and so $\widehat{\mathcal{T}}_{P,\theta} \ge (1-h)E_w/(4L\frac{\hat\xi^2}{2})$.

Axial stress. Since $0 \le V \le H_0$, $|H^2 - H_0^2| \le 2H_0V$. Since $\Psi(\frac{\hat\xi^2}{2}/B)$ and ρ do not depend on β, $\partial_\beta(H^2 - H_0^2) = 2H_0\partial_\beta H_0\,((1-\rho\Psi)^2 - 1)$. With $|\partial_\beta H_0| \le 8h(1+h)H_0/s$ (Lemma 1.7.1) this gives $|\partial_\beta(H^2 - H_0^2)| \le 32h(1+h)H_0V/s$. H_0 is positive and decreasing, since $\frac12\hat\xi\partial_{\hat\xi}\log H_0 \in [-h, 0)$, so $H_0(s)/s \le H_0(\frac{\hat\xi^2}{2})/\frac{\hat\xi^2}{2}$ for $s \ge \frac{\hat\xi^2}{2}$. Hence

$$|\Delta\mathfrak{M}_4| + \tfrac{\hat\xi^2}{2}|\Delta P| \le \frac{H_0(\frac{\hat\xi^2}{2})}{\frac{\hat\xi^2}{2}}E_w, \qquad |\Delta\mathfrak{M}_{4\beta}| + \tfrac{\hat\xi^2}{2}|\Delta P_\beta| \le \frac{16h(1+h)H_0(\frac{\hat\xi^2}{2})}{\frac{\hat\xi^4}{4}}E_w \le \frac{H_0(\frac{\hat\xi^2}{2})}{\frac{\hat\xi^2}{2}}E_w.$$

By (A3), $|\widehat{\mathcal{T}}_{P,z}| \le 2K_3H_0(\frac{\hat\xi^2}{2})E_w/(L\frac{\hat\xi^2}{2}\hat\xi)$. So $|\widehat{\mathcal{T}}_{P,z}|/\widehat{\mathcal{T}}_{P,\theta} \le 8K_3E_0/(1-h) \le 9K_3E_0 \le 1$.

Shear and cone. We have $U = 0$, so $b_s = t_s = 0$ and $v_s = a_s = 2(1-\ell_r)$, where $\ell_r = \frac12\hat\xi\partial_{\hat\xi}\log H_0 + \rho(\frac{\hat\xi^2}{2}/B)|\Psi'(\frac{\hat\xi^2}{2}/B)|/(1-\rho\Psi)$. The first term lies in $[-h, -h + 4h(1+h)/\frac{\hat\xi^2}{2}]$ and the second in $[0, h/4]$ by (A1). So $\ell_r \in [-h, -h/2]$ for $\frac{\hat\xi^2}{2} \ge 32(1+h)$. Then $n_\theta \ge 2^{-1/2}$ and $(v_s - 2)n_z^2 \le h < (2 - \frac12)n_\theta^2$. Also $F = H/(\hat\xi^2) \ge (1-\rho)H_0/(\hat\xi^2) > 0$ on the compact range. Lemma 1.8.2(c) covers the collar $0 < u \le u_0$ with the smooth direction. □

Lemma 1.8.4 (Condition (W) holds)**.** *In (A3), $K_3 \le 2+4h+4(\frac12+h) \le 4.08$. On the backward member, for $\hat\xi \ge \hat\xi_{p,b}$ (that is, after the wait),*

$$E \le 2P_* e^{T/10}\lambda^{30} \le 2e^{T/10}\lambda^{29.5},$$

with T the turn length of the prefix template. Hence $\sup_{\frac{\hat\xi^2}{2}\ge\frac{\hat\xi_w^2}{2}} E_0 \le 3e^{T/10}\lambda^{29.5} < 1/(9K_3)$ by (λ7), so (W) holds.

Proof. With $U=\mathfrak{M}_1=0$, the coefficients of $\mathfrak{M}_4, \mathfrak{M}_{4\beta}, \frac{\hat\xi^2}{2}P, \frac{\hat\xi^2}{2}P_\beta$ in $L\hat\xi\,\widehat{\mathcal{T}}_{P,z}$ are $4h\beta$, $-d$, $(2+4h)\beta$ and $-d$. Along the member $(\log E)' = \ell_r - \frac12$. On the pretemplate $[\frac{\hat\xi_{s,b}^2}{2}, \frac{\hat\xi_{s,b}^2}{2}e^T]$ we have $\ell_r = f_0' - \lambda f_1' \le \gamma = \frac35$, so $(\log E)' \le \frac{1}{10}$ there; it is $-\frac12-\lambda$ on the wait of length $60\log(1/\lambda)$, and negative afterwards. At $\frac{\hat\xi_{s,b}^2}{2}$, $E = P_* f \le P_*$. (The initial growth germ has length $z_\gamma \in [0,T)$, which is not bounded by 1 in general; so we keep the template factor $e^{T/10}$, which is fixed before λ.) The edits multiply E by at most 2. Also $E_0 \le E/(1-\rho)$ with $\rho < \frac14$, and $P_* < \lambda^{-1/2}$ by (1.6.18). □

1.8.3 An integrable majorant for the backward datum

Lemma 1.8.5 (Analyticity of the selected model datum)**.** *For the selected backward model in Lemma 1.8.6, the separated expression $E_{\mathrm{model}}(y,\beta) = c_0(y)(1+\beta^2)^{-\vartheta(y)}$ has a measurable integrable square majorant independent of β on a complex neighborhood of $[-1,1]$. Its canonical integral is analytic there. On $[-1,1]$ it satisfies $\beta\Pi_0'(\beta) > 0$ for $\beta \ne 0$ and $\Pi_0 \le -(5/2)P_*^2(1+\beta^2)^{-2}$.*

Proof. The amplitude and exponent are the actual finite smooth model templates. Thus they are measurable and bounded on each finite closed y interval. On $y \le 0$ the square is exactly $P_*^2(1+\beta^2)^{-2}e^{y/5}$. At the other end use the selected terminal *power model*, before its heat replacement: (1.15.2) gives

$$H(\tfrac{\hat\xi^2}{2}) = c(\hat\xi/\sqrt2)^{-2h}[1-\rho\Psi(\tfrac{\hat\xi^2}{2}/B)], \qquad c=\sqrt2\,c_\infty, \qquad E_{\mathrm{model}} = c_\infty(\hat\xi/\sqrt2)^{-1-2h}[1-\rho\Psi(\tfrac{\hat\xi^2}{2}/B)].$$

The bracket is bounded and these terminal parameters are scalar in β for the backward model, as recorded in the construction of Lemma 1.8.7. Therefore $c_0(y)^2 \le Ce^{-(1+2h)y}$ for all sufficiently large y. The finite intermediate templates and the two tails show $\int_{\mathbb{R}} c_0(y)^2\,dy < \infty$. This deduction uses the specified model; the bare separated form in (S1) alone would not imply integrability.

Choose a bounded simply connected complex neighborhood V of $[-1,1]$ with compact closure avoiding $\pm i$. The nonvanishing function $f(\zeta) = (1+\zeta^2)^{-1}$ has a holomorphic logarithm on V, chosen real on the real interval. On a smaller such neighborhood, $|\log f| \le K$. Uniformly for $0 \le \theta \le 1$,

$$|\exp(2\theta\log f(\zeta))| \le e^{2K}.$$

Thus $e^{2K}c_0^2$ dominates the complex integrand and is integrable. Dominated convergence gives continuity of its integral; Fubini and the vanishing contour integral of each holomorphic integrand give Morera's criterion. Hence $\Pi_0 = -\frac12\int c_0^2 f^{2\vartheta}\,dy$ is holomorphic. Equivalently, Cauchy estimates on a smaller neighborhood give integrable majorants for every fixed derivative.

For real β, evenness is immediate and differentiation gives

$$\beta\Pi_0'(\beta) = \frac{2\beta^2}{1+\beta^2}\int \vartheta c_0^2 f(\beta)^{2\vartheta}\,dy > 0 \quad (\beta \ne 0).$$

Strictness follows from $\vartheta = 1$ and $c_0 = P_* e^{y/10}$ on $y \le 0$, with $P_* > 0$. The same portion of the integral gives $\Pi_0 \le -(5/2)P_*^2 f^2$. Finally, at each β the restored core and loop pressure rows equal

their reference values and the A11 pressure increment is zero. The complete heat replacement and rank-one correction contribute $\Delta C_{p,f}(\beta)$, which the three-E bank cancels by (1.14.16) with $\chi_b = 1$ on the native band. Thus the actual and model pressure integrals agree after integration over all supports. □

1.8.4 Datum, exterior and reserved patches

Lemma 1.8.6 (The backward axis datum)**.** *Assume (S1).*

(S1) The model swirl of the backward member has the separated form $E_{\mathrm{model}} = c(y) f(\beta)^{\vartheta(y)}$, with $f = (1+\beta^2)^{-1}$, $y = 2\log(\hat{\xi}/\hat{\xi}_{\mathrm{ref}})$, $0 \le \vartheta \le 1$, and c, ϑ and all stage boundaries independent of β. On $y \le 0$ it equals $P_* f(\beta) e^{y/10}$. For each β the complete pressure increments of the selected edits sum to zero. The core restores the reference pressure row and the loop with its five returns restores that row. The A11 pressure row is zero. The heat replacement together with the rank-one correction has increment $\Delta C_{p,f}(\beta)$, and its three-E bank has increment $-\Delta C_{p,f}(\beta)$ on the whole native band ((1.14.16), Lemma 1.15.9). The pulse changes only U.

Then the canonical datum $\Pi_0(\beta) = -\int_0^\infty E^2/(\hat{\xi}^2)\,\hat{\xi}\,\mathrm{d}\hat{\xi}$ of the actual backward member equals $-\frac{1}{2}\int E_{\mathrm{model}}^2\,\mathrm{d}y$. It is analytic on one complex neighborhood of $[-1,1]$, it is even, and it satisfies $\beta\Pi_0'(\beta) > 0$ for $\beta \ne 0$ and $\Pi_0 \le -\frac{5}{2}P_*^2 f^2$. These are the properties that [42, Lemma 4.8(i)] states for its datum (there they are conclusions). They are the hypotheses on Π_0 used in [42, App. B.1] and in Theorem 1.8.10.

Proof. First compute the model integral. Lemma 1.8.5 constructs an integrable complex majorant from the finite templates and terminal power tail. This calculation supplies the analytic datum for the core construction. Once the core and banks have been selected, integration over their complete supports and the pressure balance in (S1) identify the model datum with the actual datum. For a cutoff inside an edit one keeps its partial pressure integral. With that majorant the analytic-datum argument is as follows. Choose a simply connected complex neighborhood of $[-1,1]$ that avoids $\pm i$. On it, $f^{2\vartheta} = \exp(2\vartheta \log f)$ is holomorphic and bounded uniformly in $\vartheta \in [0,1]$. The integrand is $O(e^{y/5})$ as $y \to -\infty$ and $O(e^{-(1+2h)y})$ as $y \to \infty$, so the integral is holomorphic. Evenness follows from $f(-\beta) = f(\beta)$. We have $\partial_\beta f^{2\vartheta} = -\frac{4\beta\vartheta}{1+\beta^2} f^{2\vartheta}$. Hence $\beta\Pi_0' = \frac{2\beta^2}{1+\beta^2}\int \vartheta c^2 f^{2\vartheta}\,\mathrm{d}y$, and this is positive because $\vartheta = 1$ on $y \le 0$. That piece alone contributes $-\frac{1}{2}\int_{-\infty}^0 P_*^2 f^2 e^{y/5}\,\mathrm{d}y = -\frac{5}{2}P_*^2 f^2$, and every other contribution is nonpositive. □

Lemma 1.8.7 (Heat exterior and moments of the backward member)**.** *Assume (A1). Then (S2) holds: in the backward chart the following do not depend on β: the A11 outlet (R_A, H_A), the value $\mathfrak{M}_2(R_A) = R_A H_A/(1-\lambda)$, the length L_o, the data δ and $p(\delta)$, the wing amplitude ρ of (1.15.1) (not the forward outlet graph of (1.6.23)), and the edge B. Then the moment and exterior assertions of (O3) hold for the backward member, with*

$$c_\infty = \frac{c}{\sqrt{2}}, \qquad c = H_A R_A^h J e^{-(\lambda-h)L_o}, \qquad J = \frac{p(\delta)e^{h\delta}}{1-\rho},$$

which is independent of β, and with heat factor $\mathcal{H} = \mathcal{H}_-$.

Proof. Proof of (S2). The numbers δ, $p(\delta)$, b, m_h and ρ are fixed once (the paragraph before Lemma 1.15.1 and (1.15.1)). The length L_o is the maximum of the scalar lower bounds (1.6.27) (which contains (1.15.5) and (1.15.28)) and the lower bound in the proof of Lemma 1.17.6; each one is a supremum or minimum over angles. In the backward chart $R_e = \frac{\hat{\xi}_{p,b}^2}{2} e^{Y_{\mathrm{end}}}$ is scalar (Subsection 1.15.7;

(1.15.32) and the sentence before it). On $[\frac{\hat\xi_{p,b}^2}{2}, R_e]$ the actual swirl is the model swirl: the pulse and its returns change only U (proof of Lemma 1.6.32; (I15) of Section 1.15.4.1), and the bumps of the loop returns, the restoration and the three-E bank have compact support before $\frac{\hat\xi_{p,b}^2}{2}$. By (S3) of Lemma 1.8.8 the model swirl there is $K_b(1+\beta^2)^{-1}F_\lambda(y_w)e^{\lambda y_w}(\hat\xi/\sqrt{2})^{-2\lambda}$. Hence $H(R_e,\beta) = H_e f(\beta)$ (Subsection 1.15.7), and the coefficient $H_e = K_b F_\lambda(y_w)e^{\lambda y_w}R_e^{-\lambda}$ is a scalar. The value $H(R_e,\beta)$ itself depends on β. The flattening (Lemma 1.15.4; proof of Lemma 1.17.4), with $J_0 = \log(1+\beta^2)$, equals $H_e/(1+\beta^2)$ at its inlet and $H_e e^{-\lambda y}/2$ wherever $s(y/T_f) = 1$. From there on the model does not depend on β (proof of Lemma 1.15.4). The two A11 edits $H \mapsto H(1+t_1(\beta)\psi_1 + t_2(\beta)\psi_2)$ have fixed relative supports that end before R_A (proofs of Lemmas 1.15.4 and 1.15.5). Hence $R_A = k_A R_e$ and $H_A = a_A H_e$, with the fixed transfers of Subsection 1.15.7, and row 1 gives $\mathfrak{M}_2(R_A) = R_A H_A/(1-\lambda)$ for every β. So $R_0 = R_A e^{L_o+\delta}$ and B are scalar ((1.15.2)). The remaining β-dependent edits are: the rank-one bump, on $(\frac{\hat\xi_b^2}{2}/2, \frac{3}{4}\frac{\hat\xi_b^2}{2}) \subset (R_A, R_0)$ since $L_o \ge \log 4$; the heat collar on $[R_0, 2R_0]$; and the heat factor $\mathcal{H}_-(4d/\hat\xi^2)$ for $\frac{\hat\xi^2}{2} \ge 2R_0$. They lie beyond R_A and change none of the listed data. This proves (S2).

The coefficient law is (1.15.3), and by (S2) every factor in it is scalar. For $\frac{\hat\xi^2}{2} \ge B$, (A1) gives $H = c(\hat\xi/\sqrt{2})^{-2h}\mathcal{H}_-(4d/\hat\xi^2)$. So $E = H/\hat\xi = c_\infty(\hat\xi/\sqrt{2})^{-1-2h}\mathcal{H}_-(4d/\hat\xi^2)$, with $U = V_0 = 0$. The function $\mathcal{H}_-$ of (1.7.1) is the function $\mathcal{H}$ of (1.7.1). Since $q^{-\frac12-h}(\hat\xi/\sqrt{2})^{-1-2h} = s^{-\frac12-h}$ and $2qd/s = 2\tau/s$, the physical swirl is $c_\infty s^{-\frac12-h}\mathcal{H}(2\tau/s)$. For the renormalized moment, Lemma 1.15.2 gives the primitive $c(\frac{\hat\xi^2}{2})^{1-h}/(1-h)$ beyond B for the power model. The rank-one correction of Proposition 1.15.8 cancels the full heat-edit discrepancy $D_I(\beta)$ for each β. So $\int_0^\infty (H - \sqrt{2}c_\infty(\hat\xi/\sqrt{2})^{-2h})\,\hat\xi\,\mathrm{d}\hat\xi = 0$. After the last pulse return $U = \mathfrak{M}_1 = \mathfrak{M}_3 = 0$ (Section 1.15), and $V_0 = 0$ by the divergence formula. So $M(\infty) = J(\infty) = 0$, and the point $\frac{\hat\xi_u^2}{2}$ may be taken after the last return. Finally, $S(\infty) = 0$ by the pulse root together with the three-E bank (Lemma 1.15.9). In the backward chart this bank solves its target for each β, because the construction is the same scalar construction for every β. □

Lemma 1.8.8 (Reserved power patches of the backward member)**.** *Put* $\frac{\hat\xi_{p,b}^2}{2} = \frac{\hat\xi_{s,b}^2}{2}e^T\lambda^{-60}$, *the backward pulse entry, and* $y_p = 2\log(\hat\xi/\hat\xi_{p,b})$.

(S3) For all $|\beta| \le 1$ *and* $\hat\xi \ge \hat\xi_{\mathrm{match}}$, *the backward model prefix is*

$$H = K_b(1+\beta^2)^{-1}(\hat\xi_{s,b}/\sqrt{2})^{-2\lambda}F_\lambda(2\log(\hat\xi/\hat\xi_{s,b})), \qquad U = G_b\,k(2\log(\hat\xi/\hat\xi_{s,b})),$$

with $G_b = 4\beta$ *and scalars* K_b *and* $\frac{\hat\xi_{s,b}^2}{2}$. *On the wait* $2\log(\hat\xi/\hat\xi_{s,b}) \ge T$ *we have* $k = 0$ *and* $F_\lambda(y) = F_\lambda(y_w)e^{-\lambda(y-y_w)}$. *This is the unedited reference extension. The actual fields on the two reserved slots follow from (S4).*

(S4) No edit of the backward member meets $I_{\mathrm{pos}} = \frac{\hat\xi_{p,b}^2}{2}e^{(-14,-9)}$ *or* $I_{\mathrm{mean}} = \frac{\hat\xi_{p,b}^2}{2}e^{(-8,-3)}$.

Both statements hold, and the reserve identity (1.5.4) *holds with* $c_{\mathrm{patch}} = K_b F_\lambda(y_w)e^{\lambda y_w}/\sqrt{2}$.

Proof. (S3) is the definition of the backward branch below (1.25.4). The wait clause is the continuation of the pretemplate beyond T, and $k = 0$ there (the pretemplate of Lemma 1.20.45).

(S4) The edits of the backward member, in the chart-covariant layout (O1)–(O8) before (1.23.5), are the following.

(i) The core of Theorem 1.8.10 on $[0, \frac{\hat\xi_{\mathrm{match}}^2}{2}]$ and the core-side corrections: the five-moment core correction, the pressure bank of Lemma 1.6.37, the activation, the termination and the $G_i \to G$ annulus. They lie before the growth arc, hence in $y_p < -W - T$.

(ii) The capped loop modulation, on $Y_{\mathrm{sh}} \subset \{y_p < -W+1\}$ (Lemma 1.20.49; the phase is $f = 0$ in this chart, Section 1.19).

(iii) The five restoration returns, in $C_c^\infty((-25,-20))$ (Lemma 1.13.7).

(iv) The three-E heat bank is supported in $-20 < y_p < -15$, after the five restoration bumps in $-25 < y_p < -20$ and before both power slots $(-14,-9)$ and $(-8,-3)$. This order leaves the heat-compensation rows in the incoming pulse data.

(v) The two-row I/C_p taper of Lemma 1.14.4 belongs to the forward chart. Its support on the native backward member is empty (Remark 1.8.9).

(vi) The pulse and its two returns, in $[0, Y-0.7)$; they change U only (proof of Lemma 1.6.32; Proposition 1.24.2).

(vii) The edits after $R_e = \frac{\hat\xi_{p,b}^2}{2} e^Y$: the A11 edits, the rank-one bump, the heat collar and the heat tail (Lemma 1.8.7).

Their coefficients depend on β, but their supports in y_p do not, because $\frac{\hat\xi_{p,b}^2}{2}$ is a scalar. None of them meets $[-14,-9] \cup [-8,-3]$. The positive-order bumps and the mean frame lie in the windows. They are finite-stage corrections, for which the reserve identity (1.5.4) reserves the windows, and they are not edits of the leading member.

Both windows lie in the exact wait $-W \le y_p \le 0$, that is, at $2\log(\hat\xi/\hat\xi_{s,b}) \in (T, T+W)$. There (S3) and (S4) give $U = 0$ and $H = K_b F_\lambda(y_w) e^{\lambda y_w}(1+\beta^2)^{-1}(\hat\xi/\sqrt{2})^{-2\lambda}$, so $E = c_{\mathrm{patch}}(1+\beta^2)^{-1}(\hat\xi/\sqrt{2})^{-1-2\lambda}$. The windows are fixed intervals in $\frac{\hat\xi^2}{2}$ with $\sup I_{\mathrm{pos}} < \inf I_{\mathrm{mean}}$. They lie after the activation collar and before $\frac{\hat\xi_w^2}{2}$, which follows the last pulse return. The factor e^T in $\frac{\hat\xi_{p,b}^2}{2}$ is necessary: without it the windows would sit at $y_p \in (-14-T, -9-T)$ and $(-8-T, -3-T)$, and could meet (iii) or (iv). □

Remark 1.8.9 (Dependence of the backward member). The central hold, its spectral edits and returns, and the variable exponent belong to the forward component. On its endpoint chart germ $|\hat\zeta| < 1$ implies $|\beta| > 1$, and spectral controls vanish near the endpoints, so these edits do not meet the backward domain $|\beta| \le 1$. The matching solves the central amplitude from c_B, leaving c_B fixed. Forward choices enter the backward member only through the lower bounds on L_o, C, Λ; Lemmas 1.8.2–1.8.8 hold for all admitted values.

1.8.5 The backward core and the interior cone

Theorem 1.8.10 (Axis connection for a general datum). *Fix M_d, $T_d = e^{M_d} + 10$, $P_* > e^{T_d}$, λ and $0 < h < \min\{1/100, \lambda, e^{-T_d}\}$. Let $I = [-\eta_I, \eta_I]$ with $1 < \eta_I \le 1.02$, and let Ω be a bounded simply connected complex neighbourhood of I. Let Π_0 be holomorphic on Ω, real and even on I, with $\Pi_0 \le -cP_*^2 f^2$ and $\eta\Pi_0'(\eta) > 0$ for $0 \ne \eta \in I$, for some $c > 0$ with $cP_*^2 \ge 1$. The temporary outer pair is $U_0 = 4\eta$, $E_0 = P_* f(\eta) x^{1/10}$, $x = (\hat\xi/\hat\xi_{\mathrm{ref}})^2$, with axis pressure Π_0; its five integrals from the axis are denoted $\mathbf{m}_0$ (computed by substitution in (1.1.2)). Let $\frac{\hat\xi_b^2}{2} = B_{\mathrm{r}0} \ge 100$ and $\frac{\hat\xi_i^2}{2} = B_{\mathrm{r}1} = eB_{\mathrm{r}0}$ (Definition 1.20.22, Remark 1.20.26) be fixed before Λ. Then one can choose, in this order, a matching tolerance ε_m, the offset $0 < j_0 \le .05$, the thresholds δ_* and σ_*, the scale Λ, the length T_{sh} and an amplitude threshold C_0, such that the following holds for every $C \ge C_0$. Put $\hat\xi_a = \hat\xi_0 = \sqrt{8/\Lambda}$, $\hat\xi_{\mathrm{ref}} = \hat\xi_i (CP_*)^5$, $\hat\xi_{\mathrm{match}} = e^{-5/2}\hat\xi_{\mathrm{ref}}$ and $f = (1+\eta^2)^{-1}$. After C, the activation controls $\kappa_0 = \kappa_{\mathrm{act}}$,*

$t_1 = t_{\mathrm{act}}$ and the widths of Definition 1.20.35 are chosen; every condition that the proof imposes on them is an upper bound that depends only on the choices made before the quantity it bounds. For all such choices, the profile (E, U, Π) on $[0, \frac{\hat\xi^2_{\mathrm{match}}}{2}] \times [-1, 1]$ constructed in the proof (paragraph 1.20.5), with $E = \hat\xi\phi/C$ and $\Pi = \Pi_0 + C_p$, has the following properties.

(i) $\phi > 0$, and ϕ, U, Π and $V_0/\frac{\hat\xi^2}{2}$ are smooth on $[0, \frac{\hat\xi^2_{\mathrm{match}}}{2}] \times [-1, 1]$, including $\hat\xi = 0$. There is $\frac{\hat\xi^2_{\mathrm{an}}}{2} \in (\frac{\hat\xi^2_a}{2}, \frac{\hat\xi^2_a}{2} e^{t_1}]$ such that these four functions and every fixed radial derivative of them are analytic in η on one complex neighbourhood of $[-1, 1]$, the same for all $\frac{\hat\xi^2}{2} \in [0, \frac{\hat\xi^2_{\mathrm{an}}}{2}]$, with finite bounds on every smaller compact neighbourhood. The profile solves (1.4.6) for $0 \le \hat\xi \le \hat\xi_a$, and $T_0 = 0$ there.

(ii) $a > 0$, $P_c > 2$ and $v_s < \mathcal{U}(P_c, J_c)$ on $(\frac{\hat\xi^2_a}{2}, \frac{\hat\xi^2_{\mathrm{match}}}{2}] \times [-1, 1]$. On the first collar $(\frac{\hat\xi^2_a}{2}, \frac{\hat\xi^2_{\mathrm{an}}}{2}]$ also $v_s > 2$. At the inner endpoint $a(\frac{\hat\xi^2_a}{2}, \eta) > 0$ and $v_s(\frac{\hat\xi^2_a}{2}, \eta) > 2 + c_{\mathrm{ex}}$, with $c_{\mathrm{ex}} = .2$. With $y_a = 2\log(\hat\xi/\hat\xi_a)$, the first collar has the factorization

$$T_0 = e^{-t_1^2/y_a^2} g_a(y_a) B_a(y_a, \eta), \qquad g_a(0) > 0, \qquad B_a(0, \eta) = F(\tfrac{\hat\xi^2_a}{2}, \eta) s(\tfrac{\hat\xi^2_a}{2}, \eta) \neq 0,$$

with g_a, B_a smooth through $y_a = 0$, and $|T_0| \ge c\, e^{-t_1^2/y_a^2}$, $|(\hat\xi^{-1}\partial_{\hat\xi})^{\alpha_1} \partial_\eta^{\alpha_2} T_0| \le C_\alpha e^{-t_1^2/y_a^2} y_a^{-N_\alpha}$ on $(\frac{\hat\xi^2_a}{2}, \frac{\hat\xi^2_{\mathrm{an}}}{2}] \times [-1, 1]$.

(iii) Near $\frac{\hat\xi^2_{\mathrm{match}}}{2}$ the fields equal (U_0, E_0), and $\mathbf{m}(\frac{\hat\xi^2_{\mathrm{match}}}{2}, \cdot) = \mathbf{m}_0(\frac{\hat\xi^2_{\mathrm{match}}}{2}, \cdot)$; both pressures have the axis value Π_0.

The choices of $\varepsilon_m, j_0, \delta_*, \sigma_*, \Lambda, T_{\mathrm{sh}}$ do not depend on C, and every condition on C is a lower bound; so $\frac{\hat\xi^2_{\mathrm{ref}}}{2}$ may exceed any prescribed bound. Statements (i)–(ii) remain true when $\frac{\hat\xi^2_{\mathrm{an}}}{2}$ is replaced by any smaller number in $(\frac{\hat\xi^2_a}{2}, \frac{\hat\xi^2_{\mathrm{an}}}{2}]$.

Theorem 1.8.10 is proved in paragraph 1.20.5: the actual core and frozen reference are Lemmas 1.20.33 and 1.20.34, the first collar is Lemma 1.20.40, the continuation to $\frac{\hat\xi_i^2}{2}$ is Proposition 1.20.38, and the transition and moment matching are Lemma 1.20.41. The following remark records the bounds needed for the continuation.

Remark 1.8.11 (Inputs for the backward core). The datum here differs from that of [42, Prop. 4.10]; Theorem 1.8.10 is therefore proved for the actual Π_0. The transport equations and moment estimates are Lemmas 1.4.1–1.4.3. The flat primitive is (1.4.10). The coefficient estimates used on the axis are proved in Lemma 1.20.32. The core estimates (B.13), (B.17)–(B.20) are established here in Lemma 1.20.33.

The continuation uses the following outputs, uniformly for $0 < t_1 \le \bar t$, proved in Lemma 1.20.34 unless indicated:

(F1) $p_{1,r} \ge 3.3$ on $\{\chi \ge .99\} \cap [\frac{\hat\xi^2_0}{2}, \frac{\hat\xi_i^2}{2}]$.

(F2) $\frac12 \hat\xi \partial_{\hat\xi} n_{s,r} + n_{s,r} = S_{n,r}/L$, $|S_{n,r} - Z_*| \le K_0\Lambda^{-1} + K\frac{\hat\xi^2}{2} C^{-2}$ and $|n_{s,r} - Z_*/L| \le K_0\Lambda^{-1} + K\frac{\hat\xi_i^2}{2} C^{-2}$; on $\{\chi \le .99\}$, $|n_{s,r}| \ge \delta_*/(2L)$ with the sign of Z_*.

(F3) On $0 < \frac{\hat\xi^2}{2} \le 4.1/\Lambda$, $n_s = -2\frac{U_{\hat\xi}}{\hat\xi} = Z_*/L + O(\Lambda^{-1})$; on the core, $p_1 = a = -2Y\Phi_Y/\Phi$, and $n_s = -2u_Y$ (Lemma 1.20.33).

(F4) $S_{q,r} \ge .94L\Lambda\chi + 2.4$, $l_r \le 1$, $p_{1,r} > 0$, $v_r \ge 3.2$ on $[\frac{\hat\xi_0^2}{2}, \frac{\hat\xi_i^2}{2}]$.

(F5) $p_{1,r} > 3$ for $3 \le \frac{\hat\xi^2}{2} \le \frac{\hat\xi_i^2}{2}$.

(F6) The fixed angular bounds M_k, N_k for $p_{1,r}, n_{s,r}$ are independent of large C and t_1.

(F7) $\phi_r = CF_r = CE_r/\hat\xi$ and ϕ_r^{-1} have uniform C_η^k bounds on $[0, \frac{\hat\xi_i^2}{2}]$; hence $E_r \le \hat\xi K_F/C$.

(F8) The first-collar cone is Theorem 1.20.36(a). Lemma 1.20.40 gives its factorization and analytic rectangle for every $0 < t_1 \le \bar t$, $0 < \kappa_0 < 1$.

Use the model integral of Lemma 1.8.6 as input to the core. Its real bounds give $c = 5/2$, $cP_*^2 \ge 1$ and $\beta\Pi_0'(\beta) > 0$ for $\beta \ne 0$. It is holomorphic on a simply connected neighborhood of $[-1,1]$ avoiding $\pm i$, and the parameter order gives $h < \lambda < e^{-2T_d}$. The temporary pair is (S3) of Lemma 1.8.8. The backward pressure bank has zero target and the core restores its unedited reference histories. Beyond $\frac{\hat\xi^2_{\mathrm{match}}}{2}$, Lemmas 1.8.17 and 1.8.18 compute the actual coefficients using the stated stress identities, Lemma 1.8.15, and the restored data. The factor $|\beta|$ in $|\Pi_\beta| \le C|\beta|E^2$ is retained: without it the wait estimate for $2\lambda w^2$ would grow like $K_{\mathrm{wt}}^2 \log^2(1/\lambda)$.

Remark 1.8.12 (Order of the joint choices). The joint order is

$$\begin{aligned} M_d, T_d, P_*, \lambda, h \;&\longrightarrow\; \tau_b, \varepsilon_u, \varepsilon_m, j_0, \delta_*, \sigma_* \\ &\longrightarrow\; \Lambda, T_s \;\longrightarrow\; C \;\longrightarrow\; y_*, \Upsilon, \Upsilon^b, \omega_0 \\ &\longrightarrow\; \kappa_{\mathrm{act}}, t_{\mathrm{act}}, \omega_{\mathrm{act},j} \;\longrightarrow\; N_{\mathrm{sh}}. \end{aligned}$$

(a) Step 1 selects λ, then h; all conditions on h are upper bounds.

(b) The backward datum is fixed by the model stage lengths before the core.

(c) Step 4 first chooses $\tau_b, \varepsilon_u, \varepsilon_m$, then $j_0 \le .05$ with $K_{\mathrm{geo}}K_{\mathrm{ax}}j_0 \le j_\sharp/2$ and $K_{\mathrm{ch}}j_0 \le \varepsilon_u/8$; the forward collar regularizer is $s_0 = \sigma_*\lambda_{\mathrm{ch}}^{h-\frac12}$ by Lemma 1.6.38. Choose $\Lambda, T_s = T_{\mathrm{sh}}$ and then C above both members' thresholds.

(d) Step 5 fixes $y_*(C), \Upsilon, \Upsilon^b, \omega_0$, then $\kappa_{\mathrm{act}} = \kappa_0$, $t_{\mathrm{act}} = t_1$, and $\omega_{\mathrm{act},j}$. Each late control is the minimum of the two sides' upper tolerances in Theorem 1.20.36 and Lemmas 1.20.37, 1.20.41. In particular $b_2 = t_1 + \kappa_0(1 + \omega_0^{-1})$ satisfies $K_{\mathrm{part}}b_2 \le 1$ for the uniform C^2 output family (Corollary 1.20.39); its stricter bounds are imposed after ω_0 is fixed. The core, reference and first-collar lemmas hold for every $0 < t_1 \le \bar t$, $0 < \kappa_0 < 1$, so these decreases preserve their conclusions.

(e) Step 6 selects the common loop frequency N_{sh} above all lower bounds, including that of Proposition 1.8.16.

Exact downstream history restoration prevents dependence of the earlier future choices on j_0.

The common radii are $\frac{\hat\xi_b^2}{2} = B_{\mathrm{r0}} \ge 100$, $\frac{\hat\xi_i^2}{2} = eB_{\mathrm{r0}}$, and $\frac{\hat\xi^2_{\mathrm{ref}}}{2} = \frac{\hat\xi_i^2}{2}(CP_*)^{10}$. The forward graph $\frac{\hat\xi_i^2}{2}/b$ is their slice continuation; its reference has $p_1 \ge 3$ for $\frac{\hat\xi^2}{2} \ge B_{\mathrm{r0}}/b$ (Lemma 1.20.25). Both output slabs have $\frac12\hat\xi\partial_{\hat\xi}U = 0$, $\ell_r = .6$ and $p_1 > 2$. The inlet-history symbol j_0 used in Section 1.13 is unrelated to the endpoint offset here.

Remark 1.8.13 (The selected backward profile). (a) The forward endpoint objects are the slice continuations of this backward pretemplate, pulse, returns, coefficient c_B, and core.

(b) Beyond $\frac{\hat\xi_p^2}{2}$ the schedule uses affine returns, flattening, A10/A11, the added λ leg, rank-one correction, drive and the wing $H_0(1-\rho\Psi(\frac{\hat\xi^2}{2}/B))$. This differs from [42, App. A] and fixes the actual datum of Lemma 1.8.6.

(c) The future edits must be compensated in the primitive and energy moments of (1.5.3).

(d) The pre-loop core has $v_s<1$ on part of $(\frac{\hat\xi_{\mathrm{an}}^2}{2},\frac{\hat\xi_{\mathrm{match}}^2}{2}]$ (Lemma 1.20.41); (B1) refers to this member, and the shared loop supplies the strict shear required by (B2).

Remark 1.8.14 (Parity of the stresses in the side label). In (1.9.2)–(1.9.3) with side label ς, the odd terms are $\varsigma\frac{\hat\xi^2}{2}H$, $-\varsigma(1-h)\mathfrak{M}_2$, $\varsigma(\frac12-h)\eta\mathfrak{M}_{2\eta}$, $\varsigma\frac{\hat\xi^2}{2}U$ and $-\varsigma(\frac12-h)(\mathfrak{M}_1-\eta\mathfrak{M}_{1\eta})$. The terms in $\mathcal{K}$, $\mathfrak{M}_3$, $\mathfrak{M}_4$, P and the radial-derivative parts are even.

(a) Where $U=\mathfrak{M}_1=\mathfrak{M}_3=0$, the same profile has $Q_f=1-(1-h)r+\dots$ and $Q_b=-1+(1-h)r-(\frac12-h)\eta\mathfrak{M}_{2\eta}/(\frac{\hat\xi^2}{2}H)$, with $r=\mathfrak{M}_2/(\frac{\hat\xi^2}{2}H)$. The forward central mechanisms therefore fail in the backward chart. For the hold $(\frac{\hat\xi^2}{2})^{-\nu_c}$ with $\nu_c=h/20$, $h=.005$, $Q_b=-0.00475$. For the growth arc $(\hat\xi/\sqrt{2})^{6/5}$ with $U=0$, $Q_b=-0.378$. Neither belongs to the backward member (Remark 1.8.9). Its growth stage has $U=4\beta$ and $Q_s(0)=(1.8-h)/1.6\approx1.12$ (Lemma 1.8.17(a), the value of [42, (A.25)]).

(b) On the endpoint collars the transported forward angular numerator equals the backward one at $d=0$, using $\lambda'_{\mathrm{ch}}(\pm1)=\mp2/(\frac12-h)$. The forward outer source $Q_{\mathrm{lin,f}}=(k-1)z$ with $k\ge2$ (Lemma 1.17.4) becomes $Q_b=z$, which is the case $k=2$.

(c) On the native backward pulse put $s=\lambda\log(X/X_{p,b})$, $X=\hat\xi^2/2$. Lemma 1.8.18 gives $w=(1-\lambda)R_b/(1/2-\lambda)-C_d\partial_sR_b+o(1)$. At $\beta=0$, $C_d=2/(1-h/\lambda)+O(\lambda)$, uniformly for $0<h<\lambda/6$. The backward cone estimate in Lemma 1.8.20 uses both terms.

Lemma 1.8.15 (Reflection parity of the backward member beyond $\frac{\hat\xi^2_{\mathrm{match}}}{2}$)**.** *Let $(E^\natural,U^\natural,\Pi^\natural)$ be the pre-loop backward member.*

(a) On $[\frac{\hat\xi^2_{\mathrm{match}}}{2},\frac{\hat\xi^2_p}{2}]$, $H^\natural$ is even and $U^\natural$ is odd in β. The histories $\mathfrak{M}_1,\mathfrak{M}_3$ are odd, $\mathfrak{M}_2,\mathfrak{M}_4,C_p$ are even, and $\Pi=\Pi_0+C_p$ is even.

(b) For $\frac{\hat\xi^2}{2}\in[\frac{\hat\xi^2_{\mathrm{match}}}{2},\frac{\hat\xi^2_p}{2}]$,

$$|\Pi_\beta|\le C|\beta|E^2,\qquad |\mathfrak{M}_{4\beta}|\le C|\beta|\tfrac{\hat\xi^2}{2}E^2(T_d+1+y),\qquad |\mathfrak{M}_1-\beta\mathfrak{M}_{1\beta}|\le\beta^2\sup|\mathfrak{M}_{1\beta\beta}|,$$

with constants independent of $\frac{\hat\xi^2_{\mathrm{ref}}}{2}$, h, L_o and Y_0, and uniform in $0<\lambda\le\lambda_0$ (see the paragraph "Uniformity" in the proof of (b)).

(c) The final member equals the pre-loop member, with all histories and Π, on $[Y_1,\infty)$. So (a)–(b) hold for it on $[Y_1,\frac{\hat\xi^2_p}{2}]$.

Parity of the core ($U_*=4\beta+j_0$), of the loop and of the pulse is not used.

Proof. (a) The histories are integrals from the axis of fields that are prescribed on $[\frac{\hat\xi^2_{\mathrm{match}}}{2},\frac{\hat\xi^2_p}{2}]$. By Theorem 1.8.10(iii), all five histories at $\frac{\hat\xi^2_{\mathrm{match}}}{2}$ equal those of the reference pair integrated from 0 ((1.1.2)): $\mathfrak{M}_{10}$ and $\mathfrak{M}_{30}$ are odd, and $\mathfrak{M}_{20}$, $\mathfrak{M}_{40}$, $C_{p,0}$ are even. Before the three-E correction, the

prefix on $[\frac{\hat\xi^2_{\mathrm{match}}}{2}, \frac{\hat\xi^2_p}{2}]$ consists of the reference pair, the growth turn, the turnoff $U = 4\beta k(y)$ with E a multiple of f, and the wait $U = 0$, $E = Kf(\beta)(\hat\xi/\sqrt{2})^{-1-2\lambda}$. The three-$E$ bank changes only the swirl on a compact part of the wait. The only non-local inputs are Π_0 and the targets of the three-E bank.

- Π_0 is even (Lemma 1.8.6). The pulse changes only U. The flattening cancels f exactly by (S1). A10/A11 are scalar relative edits with even targets. Hence E^2 is even on the whole future.
- The bank solves (1.14.16) with $\chi_b = 1$. Its Jacobian rows have coefficients in $f^{\pm1}$. Its targets ΔS_f, $\Delta C_{p,f}$ are changes of an even heat future: the inlet field is even by the previous item; H^{heat} depends on β through $d = 1-\beta^2$; H^b, H^m and D_I of (1.15.10) are even; Ψ and ρ are scalar. Uniqueness of the small solution gives $t_j(-\beta) = t_j(\beta)$.
- The pre-pulse two-row taper (Lemma 1.14.4) is a forward-chart angular device between the inner and the charted endpoint templates. It is absent on the backward member $|\beta| \le 1$ (Remark 1.8.9).

Lemma 1.6.31 gives the parities of the histories.

(b) *Uniformity.* Write $E^m = c(y)f(\beta)^{\vartheta(y)}$ for the separated model of (S1) and $\Pi^m(\frac{\hat\xi^2}{2}) = -\int_{(\frac{\hat\xi^2}{2})}^{\infty}(E^m)^2\,\mathrm{d}x/(2x)$. The bounds $1/2 \le f \le 1$ and $0 \le \vartheta \le 1$ give $|\partial_\beta^j (E^m)^2| \le C(E^m)^2$ for $j = 1, 2$ on the closed native band. Uniformly in $\hat\xi_{\mathrm{match}} \le \hat\xi \le \hat\xi_p$,

$$\int_{(\frac{\hat\xi^2}{2})}^{\infty}(E^m(x,\beta))^2\,\frac{\mathrm{d}x}{2x} \le C(E^m(\tfrac{\hat\xi^2}{2},\beta))^2.$$

Indeed, from $\frac{\hat\xi^2_{\mathrm{match}}}{2} = \frac{\hat\xi^2_{\mathrm{ref}}}{2}e^{-5}$ to the beginning of the wait the logarithmic lengths and the bounds on the logarithmic slopes are fixed by the prefix templates, uniformly in λ. From the beginning of the wait onward $H^m(x) \le CH^m(\frac{\hat\xi^2}{2})$ for all $x \ge \frac{\hat\xi^2}{2}$. The powers, flattening and drive have nonpositive slope and the terminal wing factor lies between $1-\rho$ and 1. Hence $(E^m(x))^2 \le C(E^m(\frac{\hat\xi^2}{2}))^2\frac{\hat\xi^2}{2}/x$ there. These bounds also dominate the first two angular derivatives under the integral.

For $\hat\xi_{\mathrm{match}} \le \hat\xi \le \hat\xi_p$, let $B(\frac{\hat\xi^2}{2},\beta)$ denote the pressure increment accumulated from the three-E bank up to $\frac{\hat\xi^2}{2}$. The actual core has restored the pressure row at $\frac{\hat\xi^2_{\mathrm{match}}}{2}$. The complete A11 pressure increment vanishes for every β by the second equation of Lemma 1.15.5, and the complete heat and rank-one increment is canceled by the full bank row in (1.14.16) since $\chi_b = 1$. Thus the actual and model axis data agree by Lemma 1.8.6. Integrating the pressure density forward gives the exact identity

$$\Pi(\tfrac{\hat\xi^2}{2},\beta) = \Pi^m(\tfrac{\hat\xi^2}{2},\beta) + B(\tfrac{\hat\xi^2}{2},\beta), \qquad B(\tfrac{\hat\xi^2}{2},\beta) = \int_{\frac{\hat\xi^2_{\mathrm{match}}}{2}}^{\frac{\hat\xi^2}{2}} \frac{E(x,\beta)^2 - E^m(x,\beta)^2}{2x}\,\mathrm{d}x.$$

In particular $B = 0$ before the bank, and after it $B = -\Delta C_{p,f}(\beta)$ up to $\frac{\hat\xi^2_p}{2}$. Inside the bank the integral runs only up to the evaluation radius $\frac{\hat\xi^2}{2}$. All angular derivatives below hold $\frac{\hat\xi^2}{2}$ fixed.

Take $k = 2$ in (1.14.15) and Lemma 1.14.5. After fixing the earlier parameters, increase the final scale so the relative edit $q = E/E^m - 1$ on the bank satisfies $\|q\|_{C^2_\beta} \le \varepsilon \le 1/2$ uniformly in x. Then $|\partial_\beta^j((E^m)^2(2q+q^2))| \le C\varepsilon(E^m)^2$ for $0 \le j \le 2$. On the native band $\frac{\hat\xi^2_p}{2}$ is scalar, and the

support lies in $\frac{\hat\xi_p^2}{2}e^{-20} \le x \le \frac{\hat\xi_p^2}{2}e^{-15}$. Whenever this integral meets the support, $1 \le \frac{\hat\xi^2}{2}/x \le e^{20}$ for contributing x, and $E^m(x)/E^m(\frac{\hat\xi^2}{2}) = (\frac{\hat\xi^2}{2}/x)^{1/2+\lambda}$. Thus $|\partial_\beta^j B(\frac{\hat\xi^2}{2},\beta)| \le C\varepsilon(E^m(\frac{\hat\xi^2}{2},\beta))^2$ for every partial or complete bank integral. The constant uses only the fixed logarithmic support and λ_0. Since Π is even and $(E^m(\frac{\hat\xi^2}{2},s))^2 \le 4(E^m(\frac{\hat\xi^2}{2},\beta))^2 \le 16E(\frac{\hat\xi^2}{2},\beta)^2$ for all s,β on the band, integration of $\Pi_{\beta\beta}$ from 0 to β gives $|\Pi_\beta| \le C|\beta|E(\frac{\hat\xi^2}{2},\beta)^2$. This constant is independent of $h,\lambda,L_o,Y_0,\frac{\hat\xi^2_{\mathrm{ref}}}{2}$ in the selected parameter order. For $\mathfrak{M}_4$ first use the unedited prefix. On the initial power arc, direct integration of $U^2-(E^m)^2/2$ gives $|\partial_\beta^j S| \le C\xi^2(E^m)^2$ at its exit for $j \le 2$. On the subsequent fixed interval of logarithmic length T, the ratios of radii are bounded, U and its first two angular derivatives are bounded and E^m is bounded away from zero with $|\partial_\beta^j E^m| \le CE^m$. Integration of the same differentiated density gives $|\partial_\beta^j S| \le C\xi^2(E^m)^2$ throughout this interval, uniformly over the allowed small h,λ. On the wait $U=0$. For $y = 2\log(\hat\xi/\hat\xi_w)$ measured from its inlet, (λ1) gives $\int_{\frac{\hat\xi_w^2}{2}}^{\frac{\hat\xi^2}{2}}(E^m)^2\,\mathrm{d}x \le ye^{2\lambda y}\frac{\hat\xi^2}{2}(E^m(\frac{\hat\xi^2}{2}))^2 \le 2y\frac{\hat\xi^2}{2}(E^m(\frac{\hat\xi^2}{2}))^2$ and $\frac{\hat\xi_w^2}{2}(E^m(\frac{\hat\xi_w^2}{2}))^2 \le 2\frac{\hat\xi^2}{2}(E^m(\frac{\hat\xi^2}{2}))^2$. This gives the factor T_d+1+y uniformly in λ. In the third bound, $\sup|\mathfrak{M}_{1\beta\beta}|$ is taken over $[\frac{\hat\xi^2_{\mathrm{match}}}{2},\frac{\hat\xi_p^2}{2}]$, where $U=0$ on the wait, so it is a template constant. On the bank the change of its density is $-\frac12(E^m)^2(2q+q^2)$ and has the same two-derivative bound just proved. Its partial integral is $O(\varepsilon\frac{\hat\xi^2}{2}E^2)$ by the fixed radius ratio. Thus $|\mathfrak{M}_{4\beta\beta}| \le C\frac{\hat\xi^2}{2}E^2(T_d+1+y)$ for the actual prefix. Evenness and integration from 0 to β give the stated factor $|\beta|$. Warning: the tail representation $\mathfrak{M}_4 = -\int_{(\frac{\hat\xi^2}{2})}^{\infty}(U^2-E^2/2)$ yields only $|\mathfrak{M}_{4\beta}|/\frac{\hat\xi^2}{2} \le C|\beta|E^2/\lambda$. That bound must not be inserted into the form $N_s = 4h\eta\mathfrak{M}_4/\frac{\hat\xi^2}{2} - d\partial_\eta(\mathfrak{M}_4/\frac{\hat\xi^2}{2}) + (2+4h)\eta P - dP_\eta$, because it would give $2\lambda w^2 \sim K_{\mathrm{wt}}^2/\lambda$. Lemma 1.8.17 uses the source S_n of (1.4.1)–(1.4.2), which contains Π, Π_β, E^2 and the geometric terms only.

(c) The loop modulation is supported in $(\frac{(\hat\xi_-^{\mathrm{loop}})^2}{2},\frac{\hat\xi_+^2}{2})$. Its returns restore all five histories and the field germs at Y_1 (Proposition 1.8.16). □

Proposition 1.8.16 (Strict cone from the inner edge through the first reserved patch)**.** *Take the pre-loop core and prefix in (B1), using Theorem 1.8.10 with the datum of Lemma 1.8.6. Let* $\frac{(\hat\xi_-^{\mathrm{loop}})^2}{2} < \frac{\hat\xi_+^2}{2} < Y_0 < Y_1$, *with* $\frac{(\hat\xi_-^{\mathrm{loop}})^2}{2}$ *in the first collar* $(\frac{\hat\xi_a^2}{2},\frac{\hat\xi_{\mathrm{an}}^2}{2})$ *of Theorem 1.8.10(i)–(ii) and* $(Y_0,Y_1) \subset \frac{\hat\xi_{p,b}^2}{2}e^{(-25,-20)}$. *Assume:*

(L1) The pre-loop member satisfies the relaxed cone on $[\frac{\hat\xi^2_{\mathrm{match}}}{2},\frac{\hat\xi_+^2}{2}]\times[-1,1]$, *with positive minima of* a, P_c-2 *and* $\mathcal{U}(P_c,J_c)-v_s$, *where* $\mathcal{U}$ *is the bound of* (1.4.8). *It satisfies the admissible cone on* $[\frac{\hat\xi_+^2}{2}e^{-\epsilon},Y_1]\times[-1,1]$ *for some* $\epsilon>0$, *with a positive minimum* μ_R *of the four gaps. On* (Y_0,Y_1) *it has* $U^\natural=0$ *and* $E^\natural = K(\beta)(\hat\xi/\sqrt{2})^{-1-2\lambda}$. *(This is Lemma 1.8.17(d). The outer strict collar of the loop lies in* $\{-W+\frac12 \le y_p \le -W+1\}$, *inside the wait, by Lemma 1.20.49.)*

(L2) The backward loop is a smooth period-one family $(a_L,-b_L)(\frac{\hat\xi^2}{2},\beta,\phi)$ *on* $I_b = [\frac{(\hat\xi_-^{\mathrm{loop}})^2}{2},\frac{\hat\xi_+^2}{2}]$ *with mean* $(a_s,-b_s)$, *equal to* $(a_s,-b_s)$ *near* ∂I_b, *and with a positive minimum* μ_L *of the four gaps* (1.19.4), *evaluated with the pre-loop vector* $\mathbf{p}$. *It is the loop of Lemma 1.19.2 with the data shared with the forward loop, (J1)–(J2) of Lemma 1.19.4. Independently chosen constants would not give the slice continuation of the forward loop (Remark 1.19.5). It is realized by*

(1.19.5) *with* $f = 0$ *and* $N = N_{\mathrm{sh}}$*, which has the form of [42, (4.38)]. Its returns are the five bumps of Step 3 of the proof, on* (Y_0, Y_1)*.*

Then there is N_* *such that for* $N_{\mathrm{sh}} \ge N_*$ *the final member satisfies* (1.5.1) *on* $[\frac{\hat\xi_a^2}{2}, Y_1] \times [-1,1]$*, and* F*,* a_s*,* $v_s - 2$ *have positive lower bounds there. The final member equals the pre-loop member on* $[0, \frac{(\hat\xi_-^{\mathrm{loop}})^2}{2}]$ *and on* $[Y_1, \infty)$*, with its histories and stress.*

Proof. The construction uses three local facts.

- Theorem 1.8.10(i)–(ii) supplies the regular core and its stress factorization on the first collar.
- Lemma 1.8.17(d), which supplies (L1).
- Lemmas 1.4.2 and 1.4.3 give the cone test and the five-moment correction.

We write $\Psi = (\Psi_1, \dots, \Psi_4)$ for the four gaps (1.19.4) as a function of $(a, b, \mathbf{p})$ on $\{a > 0\}$, where it is smooth; it is the map Ψ of [42, (4.35)]. For a rectangle $R = [\frac{\hat\xi_1^2}{2}, \frac{\hat\xi_2^2}{2}] \times [-1,1]$ and $k \ge 0$ we write $\|g\|_k = \max_{j \le k} \sup_R |\partial_\beta^j g|$.

Step 0: the pre-loop member on I_b*.* The pre-loop member $(U^\natural, E^\natural)$ has $E^\natural > 0$ and smooth fields, five histories $\mathbf{m} = (\mathfrak{M}_1, \mathfrak{M}_2, \mathfrak{M}_3, \mathfrak{M}_4, C_p)$ and pressure $P = \Pi_0 + C_p$ on $I_b \times [-1,1]$. This interval lies in the matched core and the template prefix preceding the heat bank, by (B1) and (L1). On $(\frac{\hat\xi_a^2}{2}, \frac{\hat\xi_{\mathrm{match}}^2}{2}]$, Theorem 1.8.10(ii) gives $a_s > 0$, $P_c > 2$ and $v_s < \mathcal{U}(P_c, J_c)$, and $v_s > 2$ on the first collar $(\frac{\hat\xi_a^2}{2}, \frac{(\hat\xi_{\mathrm{an}}{}')^2}{2}]$, where $\hat\xi_{\mathrm{an}}{}' > \hat\xi_-^{\mathrm{loop}}$ is the radius $\frac{\hat\xi_{\mathrm{an}}^2}{2}$ of Theorem 1.8.10(i)–(ii). With (L1), the relaxed cone holds on $I_b \times [-1,1]$, and $v_s > 2$ near both ends of I_b. Where $v_s > 2$, the relaxed cone is equivalent to $\Psi_3, \Psi_4 > 0$ (Lemma 1.4.2, first assertion; Lemma 1.19.1(i)). So (H0)–(H2) of Lemma 1.19.2 hold on I_b. Put

$$\mu_R = \min_{[\frac{\hat\xi_+^2}{2}, Y_1] \times [-1,1]} \ \min_i \Psi_i(a_s, b_s, \mathbf{p}) > 0,$$

which is positive by (L1).

Step 1: the modulation. Let $\mathcal{A}, \mathcal{B}$ be the zero-mean periodic primitives with $\partial_\phi \mathcal{A} = -\frac12(a_L - a_s)$ and $\partial_\phi \mathcal{B} = \frac12 E^\natural(b_L - b_s)$. They vanish near ∂I_b and are extended by zero. By (1.19.5) with $f = 0$,

$$E_N = E^\natural \exp(\mathcal{A}(\tfrac{\hat\xi^2}{2}, \beta, N \log \tfrac{\hat\xi^2}{2})/N), \qquad U_N = U^\natural + \mathcal{B}(\tfrac{\hat\xi^2}{2}, \beta, N \log \tfrac{\hat\xi^2}{2})/N,$$

and by (1.19.6), that is, the chain rule with $\frac12 \hat\xi \partial_{\hat\xi}(N \log \frac{\hat\xi^2}{2}) = N$,

$$a_N = a_L - \frac{2\frac12 \hat\xi \partial_{\hat\xi} \mathcal{A}}{N}, \qquad b_N = e^{-\mathcal{A}/N}\Big(b_L + \frac{2\frac12 \hat\xi \partial_{\hat\xi} \mathcal{B}}{N E^\natural}\Big).$$

Here $\frac12 \hat\xi \partial_{\hat\xi}$ acts with ϕ fixed, and all loop functions are evaluated at $\phi = N \log \frac{\hat\xi^2}{2}$. The phase does not depend on β, so $\partial_\beta^j[\mathcal{A}(\frac{\hat\xi^2}{2}, \beta, N \log \frac{\hat\xi^2}{2})] = (\partial_\beta^j \mathcal{A})(\frac{\hat\xi^2}{2}, \beta, N \log \frac{\hat\xi^2}{2})$ is bounded independently of N, and the same holds for $\mathcal{B}$, a_L, b_L. Hence, on $J = [\frac{(\hat\xi_-^{\mathrm{loop}})^2}{2}, Y_1]$, for each k there are constants independent of N with

$$\big\|U_N - U^\natural, E_N - E^\natural\big\|_k \le A_k/N, \qquad \|a_N - a_L, b_N - b_L\|_k \le B_k/N \ \text{ on } I_b, \tag{1.8.2}$$

and $(U_N, E_N) = (U^\natural, E^\natural)$ off I_b. The history increments $\Delta\mathbf{m}_N = \mathbf{m}_N - \mathbf{m}$ are integrals over $[\frac{(\hat\xi_-^{\mathrm{loop}})^2}{2}, \frac{\hat\xi^2}{2}]$ of the differences of the five densities U, H, UH, $U^2 - H^2/(4x)$, $H^2/(4x^2)$. Since $x \ge \frac{(\hat\xi_-^{\mathrm{loop}})^2}{2} > 0$, (1.8.2) gives $\|\Delta\mathbf{m}_N\|_k \le D_k/N$ on J.

In the backward chart $\mathbf{p} = (N_\theta, N_z)/F$, where (N_θ, N_z) is the $\varsigma = -1$ form of (1.19.2) (Remark 1.8.14 lists the terms that change sign). It is a polynomial in $H, U, F^{-1}, (\frac{\hat\xi^2}{2})^{-1}, L^{-1}, \beta$, the five histories (with P) and their first β-derivatives; it contains no radial derivative. On J we have $\hat\xi \ge \hat\xi_-^{\mathrm{loop}} > 0$, $L \ge 1 - 2h$, and $F_N \ge \frac12 \min_J F^\natural$ for N large. The product rule therefore gives

$$\|\mathbf{p}_N - \mathbf{p}\|_0 \le C\Big(\Big\|U_N - U^\natural, E_N - E^\natural\Big\|_1 + \|\Delta\mathbf{m}_N\|_1\Big) \le P_0/N \quad \text{on } J, \tag{1.8.3}$$

with C depending only on J, h, $\min_J F^\natural$, the C^1 norm of Π_0 and N-independent bounds of the inputs. (This is (1.4.7) with $k = 0$.) The same bound holds for any two profiles on a subinterval of J with the same axis pressure and N-independent bounds.

Step 2: the cone after modulation. Let $\mathcal{K} \subset \{a > 0\}$ be a compact neighbourhood of the closure of the values of $(a_L, b_L, \mathbf{p})$ on $I_b \times [-1,1] \times \mathbb{T}$ and of $(a_s, b_s, \mathbf{p})$ on $[\frac{\hat\xi_+^2}{2}, Y_1] \times [-1,1]$, and let C_Ψ bound the Lipschitz constant of Ψ on $\mathcal{K}$. By (1.8.2) and (1.8.3), for N large the modulated triples lie in $\mathcal{K}$, and

$$\begin{aligned} &\Psi_i(a_N, b_N, \mathbf{p}_N) \ge \mu_L - C_\Psi(B_0 + P_0)/N \ge \mu_L/2 && \text{on } I_b, \\ &\Psi_i(a_N, b_N, \mathbf{p}_N) \ge \mu_R - C_\Psi P_0/N \ge \mu_R/2 && \text{on } [\tfrac{\hat\xi_+^2}{2}, Y_1]. \end{aligned}$$

On I_b we used that μ_L is a minimum over all phases. On $[\frac{\hat\xi_+^2}{2}, Y_1]$ the shear is unchanged and only $\mathbf{p}$ moves.

Step 3: restoration of the five histories. On (Y_0, Y_1), (L1) gives $U^\natural = U_N = 0$ and $E^\natural = E_N = K(\beta)(\hat\xi/\sqrt{2})^{-1-2\lambda}$, with $K > 0$ smooth. Take $\beta_i(\frac{\hat\xi^2}{2}) = b_i^U(2\log(\hat\xi/\hat\xi_{p,b}))$ and $\gamma_j(\frac{\hat\xi^2}{2}) = (\hat\xi^2)^{-1/2} b_j^H(2\log(\hat\xi/\hat\xi_{p,b}))$, with the forward templates of (1.13.84). Their supports are chosen jointly inside $\log((Y_0, Y_1)/\frac{\hat\xi_{p,b}^2}{2}) \subset (-25, -20)$ (these are the five restoration returns of Lemma 1.8.8(S4)(iii); (J3) of Lemma 1.19.4). They are nonnegative, not identically zero, in $C_c^\infty((Y_0, Y_1))$, with ordered disjoint supports in each family. Put $u_c = \sum_i \alpha_i(\beta)\beta_i(\frac{\hat\xi^2}{2})$, $e_c = \sum_j \xi_j(\beta)\gamma_j(\frac{\hat\xi^2}{2})$, $c = (\alpha_1, \alpha_2, \xi_1, \xi_2, \xi_3)$, $U_f = U_N + u_c$ and $E_f = E_N + e_c$. The changes of $(\mathfrak{M}_1, \mathfrak{M}_3, \mathfrak{M}_2, \mathfrak{M}_4, C_p)$ at Y_1 are

$$\Big(\int u_c,\ \int (H^\natural u_c + \hat\xi u_c e_c),\ \int \hat\xi e_c,\ \int (u_c^2 - E^\natural e_c - \tfrac12 e_c^2),\ \int \frac{E^\natural e_c + e_c^2/2}{\frac{\hat\xi^2}{2}}\Big) = \mathsf{B}(\beta)c + \mathsf{Q}_\beta(c,c),$$

with all integrals over (Y_0, Y_1). The linear part is block diagonal. Its U-block has the rows $\int \beta_i$ and $\sqrt{2}K\int(\hat\xi/\sqrt{2})^{-2\lambda}\beta_i$; its E-block has the rows $\sqrt{2}\int(\frac{\hat\xi^2}{2})^{1/2}\gamma_j$, $-K\int(\hat\xi/\sqrt{2})^{-1-2\lambda}\gamma_j$ and $K\int(\frac{\hat\xi^2}{2})^{-3/2-\lambda}\gamma_j$. After division of the rows by the smooth nonzero factors $\sqrt{2}K$, $\sqrt{2}$, $-K$, K, these are matrices $\int x^{\alpha_i}\beta_j$ as in Lemma 1.4.3, with the distinct exponents $(0, -\lambda)$ and $(\frac12, -\frac12 - \lambda, -\frac32 - \lambda)$, since $\lambda > 0$ (equivalently Lemma 1.25.7 after $x = e^y$). So $\mathsf{B}(\beta)$ is smooth and invertible on $[-1,1]$, and Q is a smooth bilinear map. The datum $d_N = -\Delta\mathbf{m}_N(Y_1)$, in the same row order, satisfies $\|d_N\|_{C^j} \le D_j/N$. By the second assertion of Lemma 1.4.3 with $k = 1$, for $N \ge 8\max_{j=0,1}\nu_j^2 q_j D_j$ the equation $\mathsf{B}c + \mathsf{Q}(c,c) = d_N$ has a smooth solution with $\|c\|_{C^1} \le 2\nu_1 D_1/N$. Then $\mathbf{m}_f(Y_1) = \mathbf{m}(Y_1)$.

Since the bump shapes are fixed, $\left\|(\hat\xi^{-1}\partial_{\hat\xi})^r(u_c,e_c)\right\|_1 \le C/N$ for $r\le 1$. For N large, $E_f \ge \frac12 \min E^\natural$ on $[Y_0,Y_1]$, and the partial histories satisfy $\|\mathbf{m}_f-\mathbf{m}_N\|_1 \le C/N$ there. Also $a_f-a_N = -2\frac12\hat\xi\partial_{\hat\xi}\log(1+e_c/E_N)$ and $b_f-b_N = 2\frac12\hat\xi\partial_{\hat\xi}u_c/E_f$ are $O(1/N)$, and (1.8.3) for (U_f,E_f) against (U_N,E_N) on $[Y_0,Y_1]$ gives $\|\mathbf{p}_f-\mathbf{p}_N\|_0 = O(1/N)$. So the triples change by at most $C_{\rm rep}/N$ on $[Y_0,Y_1]$, with $C_{\rm rep}$ independent of N, and for $N \ge 4C_\Psi C_{\rm rep}/\mu_R$

$$\Psi_i(a_f,b_f,\mathbf{p}_f) \ge \mu_R/2 - C_\Psi C_{\rm rep}/N \ge \mu_R/4 \quad \text{on } [Y_0,Y_1].$$

For $\frac{\hat\xi^2}{2} \le Y_0$ the restoration changes nothing, so Step 2 gives $\Psi_i \ge \mu_L/2$ on I_b and $\Psi_i \ge \mu_R/2$ on $[\frac{\hat\xi_+^2}{2}, Y_0]$.

Step 4: agreement. All changes of the profiles are supported in $(\frac{(\hat\xi_-^{\rm loop})^2}{2}, Y_1)$. For $\hat\xi \le \hat\xi_-^{\rm loop}$ the fields, their histories from the axis and the axis pressure Π_0 are unchanged, hence so are P, V, $\mathbf{p}$, the shear and the stress. For $\frac{\hat\xi^2}{2} \ge Y_1$ the fields are unchanged and $\mathbf{m}_f(Y_1) = \mathbf{m}(Y_1)$. The history integrands agree beyond Y_1, so $\mathbf{m}_f = \mathbf{m}$ there, and all derived quantities agree (this is Lemma 1.4.1). This proves the last assertion. The finitely many lower bounds on N above depend only on data fixed before $N_{\rm sh}$, and N_* is their maximum (Remark 1.8.12(e)).

Step 5: the cone on $[\frac{\hat\xi_a^2}{2}, Y_1]$. The backward chart satisfies the defining equation for q in (1.6.2). Thus (1.19.3) with $\varsigma=-1$ gives $T_0 = F(\mathbf{p}-s)$, where $s=(a_s,-b_s)=a_s(1,t_s)$. Hence

$$T_\theta + t_s T_z = F(P_c - v_s), \qquad T_z - t_s T_\theta = F J_c.$$

Where all $\Psi_i>0$, we have $T_0\neq 0$, and $n = T_0/|T_0|$ satisfies

$$A_n := n_\theta + t_s n_z = \frac{P_c - v_s}{|\mathbf{p}-s|} > 0, \qquad B_n := n_z - t_s n_\theta = \frac{J_c}{|\mathbf{p}-s|},$$
$$G_n := 2 - (v_s-2)\frac{B_n^2}{A_n^2} = 2 - (v_s-2)\frac{J_c^2}{(P_c-v_s)^2} > 0.$$

On $[\frac{(\hat\xi_-^{\rm loop})^2}{2}, Y_1]$, Steps 2–3 give $\Psi_i \ge \min\{\mu_L/2, \mu_R/4\}$ for the final member. On $(\frac{\hat\xi_a^2}{2}, \frac{(\hat\xi_-^{\rm loop})^2}{2}]$ the final member is the pre-loop member, which satisfies the relaxed cone and $v_s>2$ there (Step 0, $\hat\xi_-^{\rm loop} < \hat\xi_{\rm an}{}'$); by Lemma 1.4.2 all $\Psi_i>0$ there. Near $\frac{\hat\xi_a^2}{2}$, the factorization of Theorem 1.8.10(ii) gives $T_0 = e^{-t_1^2/y_a^2} g_a(y_a) B_a(y_a,\beta)$, with g_a, B_a smooth through $y_a=0$, $g_a(0)>0$ and $B_a(0,\beta) = F(\frac{\hat\xi_a^2}{2},\beta)s(\frac{\hat\xi_a^2}{2},\beta) \neq 0$. On a collar $[\frac{\hat\xi_a^2}{2}, \frac{\hat\xi_a^2}{2}e^{\epsilon_1}]$ where $g_a>0$ and $B_a\neq 0$, $n = B_a/|B_a|$ extends smoothly to $\frac{\hat\xi_a^2}{2}$, with $n(\frac{\hat\xi_a^2}{2},\beta) = (1,t_s)/\sqrt{1+t_s^2}$, because $s = a_s(1,t_s)$ and $a_s(\frac{\hat\xi_a^2}{2},\beta)>0$. There $A_n = \sqrt{1+t_s^2}$, $B_n = 0$ and $G_n = 2$. Hence A_n and G_n are continuous and positive on the compact rectangle $[\frac{\hat\xi_a^2}{2}, Y_1]\times[-1,1]$, and $\kappa = \min\{1, \min A_n, \min G_n\} > 0$ gives (1.5.1): $A_n \ge \kappa$ and $(v_s-2)B_n^2 = (2-G_n)A_n^2 \le (2-\kappa)A_n^2$. Finally, F, a_s and v_s-2 are positive on $[\frac{\hat\xi_a^2}{2}, Y_1]\times[-1,1]$: on $[\frac{(\hat\xi_-^{\rm loop})^2}{2}, Y_1]$ by Steps 2–3, on $(\frac{\hat\xi_a^2}{2}, \frac{(\hat\xi_-^{\rm loop})^2}{2}]$ by Step 0, and at $\frac{\hat\xi_a^2}{2}$ by Theorem 1.8.10(ii) ($a(\frac{\hat\xi_a^2}{2},\beta)>0$, $v_s(\frac{\hat\xi_a^2}{2},\beta) > 2 + c_{\rm ex}$; $F>0$ since $\phi>0$). They are continuous on this compact rectangle, so they have positive lower bounds. □

Turnoff, wait and pulse coefficients of the backward member. The next two lemmas compute the backward pulse and turnoff coefficients using Lemmas 1.4.1 and 1.4.2. Write $z = 2\log(\hat\xi/\hat\xi_{s,b})$ with $\hat\xi_{s,b} = \hat\xi_{\rm ref}$, $\gamma = \frac35$, $f = (1+\beta^2)^{-1} = e^{-J_0}$, $J_0' = 2\beta/(1+\beta^2)$, $c_\beta = (\frac12 - h)\beta J_0' = (1-$

$2h)\beta^2/(1+\beta^2) \geq 0.49\beta^2$, and recall $d = 1-\beta^2$, $L = 1-2h\beta^2 \in [.98, 1]$. With $K_b = \sqrt{2}P_*(\frac{\hat\xi_{\rm ref}^2}{2})^{1/2+\lambda}$, the prefix (S3) reads

$$E = P_* f(\beta)F(z;\lambda)e^{-z/2}, \qquad U = 4\beta k(z), \qquad l = \tfrac12\hat\xi\partial_{\hat\xi}\log H = \partial_z \log F,$$

with $F = e^{\gamma z}$ ($z \leq 0$), $F = e^{f_0 - \lambda f_1}$ on $[0,T]$, and $F = F_T e^{-\lambda(z-T)}$ on the wait $z \geq T$. On $z \leq 0$ this is $E = P_* f x^{1/10}$. We use the following structure of the pretemplate (the subsection before Lemma 1.14.1, and (1.6.17)). There are $0 \leq z_1 \leq z_T$ and $z_T + T_d \leq z_2 \leq T$ such that:

(T1) on $[0, z_1]$ (growth turn), $f_1' = 0$, $0 \leq f_0' \leq \gamma$ and $k = 1$; on $[z_1, z_2]$ (plateau), $f_0' = f_1' = 0$ and $k(z) = k_{\rm off}(z - z_T)$, where $k_{\rm off}$ is the cutoff (1.6.17) extended by one to negative arguments; on $[z_2, T]$ (negative turn), $f_0' = 0$, $0 \leq f_1' \leq 1$ and $k = 0$;

(T2) the lengths z_1, $z_T - z_1$, $z_2 - z_T - T_d$, $T - z_2$ and the restrictions $f_0|_{[0,z_1]}$, $f_1|_{[z_2,T]}$ do not depend on M_d; only the turnoff stage has the length $T_d = e^{M_d} + 10$.

(T1) restates the definition: f_0' decreases to zero before the plateau and stays zero, $f_1' = 0$ through the plateau and through $\operatorname{supp} k'$, the turnoff lies inside the plateau, and k vanishes on a neighbourhood of the negative turn. (T2) is part of the definition of the pretemplate (the subsection before Lemma 1.14.1); it is the convention of [42, (A.6)–(A.9)], in which M_d is chosen first. It is used only to make e_d small against the constants K_ν, c_P of Step 4 below. In particular k is nonincreasing, $0 \leq k \leq 1$, $|k'| \leq e_d/(1 + (z - z_T))$ on $[z_T, z_T + T_d]$ and $k' = 0$ elsewhere, and $l = f_0' - \lambda f_1'$ on $[0, T]$.

Lemma 1.8.17 (Turnoff and wait coefficients of the backward member)**.** *Let $(E^\natural, U^\natural, \Pi^\natural)$ be the pre-loop backward member. For the coefficient calculation omit the three-E bank on the wait and retain the prescribed axis pressure. When the bank is restored, its relative field correction is at most $K_{\rm sc,2}(Y_0)/R_{\rm master}$, and every partial or completed pressure change up to the pulse is bounded by $C_{\rm geom}K_{\rm sc,2}(Y_0)E^2/R_{\rm master}$ by Lemma 1.8.15(b). This fixed-geometry error is absorbed at the final scale in Lemma 1.8.19. Let C_Π, C_p be the constants of Step 0 below. There are constants $q_0, c_P, K_\nu, c_w, C_w > 0$ and $\lambda_A > 0$, determined by γ, f_0, f_1, T_d, P_*, the lengths in (T2), C_Π and C_p, and bounded uniformly in $\lambda \leq \lambda_A$ and $h < \lambda/6$. They do not depend on $\frac{\hat\xi_{\rm ref}^2}{2}$, C, L_o or Y_0. Moreover c_P and K_ν do not depend on M_d. For $\lambda \leq \lambda_A$ the following hold for the coefficients Q_s, N_s of (1.4.1)–(1.4.2).*

(a) Reference arc $-5 \leq z \leq 0$: $Q_s = Q_{\rm ref} := [\gamma(4L-1) - h(1-8\beta^2) + ((\frac12 - h) + 4d)\beta J_0'](1+\gamma) \geq 1.08$, $b_s = 0$, $a = 0.8$. *(This is the value of [42, (A.25)].)*

(b) Pretemplate $0 \leq z \leq T$: $Q_s \geq q_1 := e^{-1.6 z_1}$ *on* $[0, z_1]$, *and* $Q_s \geq c_P(\beta^2 + e^{-(z-z_1)})$ *on* $[z_1, T]$; $Q_s(T) \geq q_0$. *Moreover* $\nu := N_s/E^2$ *satisfies* $|\nu| \leq K_\nu|\beta|(1 + (z - z_T)_+)$ *on* $[-5, T]$. *(These are the backward forms of [42, (A.26)] and of the bound* $|N_s|/E^2 \leq C|\eta|(1+y)$ *after it.)*

(c) Wait $y := z - T \in [0, 60\log(1/\lambda)]$: *with* $a_\beta := (\lambda - h + c_\beta)/(1-\lambda)$,

$$Q_s \geq c_w(\beta^2 + \lambda + e^{-(1-\lambda)y}), \qquad |Q_s - a_\beta| \leq K_Q e^{-(1-\lambda)y}, \qquad |N_s/E| \leq C_w|\beta|(1+y)e^{-(1/2-\lambda)y},$$

with $K_Q = \sup Q_s(T) + 5$. *(These are the backward forms of [42, (A.27)].)*

(d) Cone. *After M_d is increased (so that e_d is small against K_ν/c_P; this is the choice of M_d in Section 1.6.3) and for C above a threshold, the relaxed cone holds on $[\frac{\hat\xi_{\rm match}^2}{2}, \frac{\hat\xi_s^2}{2}e^T] \times [-1, 1]$, and the admissible cone holds wherever $f_1' > 0$ and on the whole wait. In particular (L1) of Proposition 1.8.16 holds, since $\frac{\hat\xi_+^2}{2}e^{-\epsilon}$ lies in the wait (Lemma 1.20.49). The positive minima in (L1) follow by compactness.*

Proof. Step 0 (sources). By Theorem 1.8.10(iii), at X_{match} the five histories equal those of $(4\beta, P_* f x^{1/10})$ integrated from the axis, with the same datum Π_0. Continue these data by (S3) up to the pulse inlet, omitting the three-E bank as above. The density identities and Lemma 1.4.1 give the same Π, Q_s, N_s on $[X_{\mathrm{match}}, X_{p,b}]$ for the matched core followed by this continuation and for the ideal-axis reference followed by the same continuation. They agree with the actual pre-loop quantities up to the bank. For the actual member through and after the bank one includes the corresponding partial integrals, as in Lemma 1.8.15(b). Its axial history is $\mathfrak{M}_1 = 4\beta\frac{\hat\xi^2}{2}\bar k$, where $\bar k(\frac{\hat\xi^2}{2}) = (\frac{\hat\xi^2}{2})^{-1}(\frac{\hat\xi^2_{\mathrm{ref}}}{2} + \int_{\frac{\hat\xi^2_{\mathrm{ref}}}{2}}^{\frac{\hat\xi^2}{2}} k) \in [0,1]$ does not depend on β. Since k is nonincreasing, $\bar k \ge k$, and $\partial_z \bar k = k - \bar k \le 0$. Hence $\mathcal{K} := (1-2h)\beta\mathfrak{M}_1 + d\mathfrak{M}_{1\beta} = 4L\frac{\hat\xi^2}{2}\bar k$ and $W = 1 - 4L\bar k$ (Lemma 1.4.1). Also $(\log E)_\beta = -J_0'$ and $H_c = (\frac12 - h)\beta + 4d\beta k$. So (1.4.1)–(1.4.2) gives

$$S_q = -l(1-4L\bar k) - h(1-8\beta^2 k) + ((\tfrac12 - h) + 4dk)\beta J_0', \tag{$\star$}$$

$$\begin{aligned} S_n &= \beta g + \beta E^2 + 4(\tfrac12 + h)\beta\Pi - d\Pi_\beta, \\ g &= -4k'(1-4L\bar k) - 4(\tfrac12 + h)(1-8\beta^2 k)k - 4((\tfrac12 - h) + 4dk)k, \end{aligned} \tag{$\star\star$}$$

using $\frac12\hat\xi\partial_{\hat\xi}U = 4\beta k'$, $U_\beta = 4k$ and $\frac12\hat\xi\partial_{\hat\xi}\Pi = E^2/2$. Here $|g| \le 12|k'| + 33 \le 45$, and $g = 0$ where $k = k' = 0$. *Pressure.* Since $\partial_z\Pi = E^2/2$, we have $\Pi(z) = \Pi(z_p) - \frac12\int_z^{z_p} E^2$, where $z_p = 2\log(\hat\xi_p/\hat\xi_{\mathrm{ref}})$, and $\partial_\beta E^2 = -2J_0' E^2$ on $[\frac{\hat\xi^2_{\mathrm{match}}}{2}, \frac{\hat\xi^2_p}{2}]$. Since $\partial_z \log E^2 = 2l - 1$, E^2 decreases at rate at least 1 on $[z_1, z_p]$ and changes at rate in $[-1, 0.2]$ on $[-5, z_1]$. Hence $\int_z^{z_p} E^2 \le K_E E^2(z)$ with $K_E = (z_1+6)e^{0.2(z_1+5)}$. At $\frac{\hat\xi^2_p}{2}$, Lemma 1.8.15(b) and the paragraph "Uniformity" of its proof give $|\Pi| + |\Pi_\beta|/|\beta| \le C_p E_p^2$, with C_p uniform in λ. On $[-5, T]$ we have $E \ge c_E E_T$, with $c_E > 0$ fixed by the template, and $E_p = E_T\lambda^{30+60\lambda}$; so $C_p E_p^2 \le E^2(z)$ there for λ small. On the wait we only have $E_p \le E(z)$. Hence $|\Pi| \le C_\Pi E^2$ and $|\Pi_\beta| \le C_\Pi|\beta|E^2$ on $[\frac{\hat\xi^2_{\mathrm{match}}}{2}, \frac{\hat\xi^2_s}{2}e^T]$ with $C_\Pi := 2K_E + 1$, which does not depend on M_d; and on the wait the same holds with $C_\Pi^{\mathrm{w}} := 2K_E + C_p$. Thus the pressure part of S_n is at most $C_3|\beta|E^2$ on $[\frac{\hat\xi^2_{\mathrm{match}}}{2}, \frac{\hat\xi^2_s}{2}e^T]$ and $C_3^{\mathrm{w}}|\beta|E^2$ on the wait, with $C_3 := 1 + 3.1C_\Pi$ and $C_3^{\mathrm{w}} := 1 + 3.1C_\Pi^{\mathrm{w}}$.

Step 1: (a) and the Q-bounds of (b). On the arc $l = \gamma$, $k = \bar k = 1$, and the profile is the pure power pair from the axis. So the regular primitives of Lemma 1.4.1 gives $Q_s = S_q/(1+\gamma)$, and $(\star)$ gives the formula in (a). Then $4L - 1 \ge 2.92$ and $h \le 10^{-2}$ give $Q_{\mathrm{ref}} \ge 1.742/1.6 \ge 1.08$. Also $b_s = \hat\xi^2\hat\xi^{-1}\partial_{\hat\xi}U/E = 0$ and $a = 2 - 2l = 0.8$ ((1.4.4)). On $[0, z_1]$: $k = \bar k = 1$ and $l \in [0, \gamma]$, so $S_q \ge l(4L-1) - h \ge -h$ and $\partial_z Q_s \ge -(1+\gamma)Q_s - h$. Hence $Q_s \ge 1.08e^{-1.6z_1} - hz_1 \ge q_1$ for h small. On $[z_1, T]$: $l \le 0$, so $(1+l)Q_s \le Q_s$ while $Q_s \ge 0$. On the plateau $(\star)$ gives $S_q \ge c_\beta - h$. On the negative turn $k = 0$, $|1 - 4L\bar k| \le 3$ and $|l| \le \lambda$, so $S_q \ge c_\beta - h - 3\lambda$. Hence $\partial_z Q_s + Q_s \ge c_\beta - 4\lambda$, and

$$Q_s(z) \ge q_1 e^{-(z-z_1)} + c_\beta(1 - e^{-(z-z_1)}) - 4\lambda \ge \tfrac12 q_1 e^{-(z-z_1)} + c_\beta(1 - e^{-(z-z_1)})$$

once $8\lambda \le q_1 e^{-(T-z_1)}$; in particular $Q_s > 0$, which justifies the comparison. With $c_\beta \ge .49\beta^2$ this gives the bound of (b) with $c_P := \min\{q_1/8, .245\}$, and $Q_s(T) \ge q_0 := \frac12 q_1 e^{-(T-z_1)}$.

Step 2: the N-bound of (b). Since $\partial_z \log E^2 = 2l - 1$, (1.4.1)–(1.4.2) gives $\partial_z\nu + 2l\nu = S_n/E^2$. On $[-5, z_2]$ we have $l \ge 0$, and on $[z_2, T]$ we have $l \ge -\lambda$ with $e^{2\lambda T} \le 2$ ((λ1) of (1.6.18)). Hence

$$|\nu(z)| \le 2\Big(|\nu(-5)| + |\beta|\int_{-5}^{z}(45E^{-2} + C_3)\Big).$$

We have $E^2 \ge P_*^2 f^2 e^{-1-z_1}$ on $[-5, z_1]$ and $E^2 \ge \frac12 P_*^2 f^2 e^{2f_0(z_1)-z}$ on $[z_1, T]$. With $P_* > e^{T_d}$ and $T = z_T + T_d + c_T$, where c_T does not depend on M_d by (T2), we get $\int_{-5}^{T} 45E^{-2} \le K_g :=$

$180[(z_1+5)e^{1+z_1}+2e^{z_T+c_T}]$. At $\frac{\hat\xi^2_{\rm match}}{2}$, N_s is the value of the reference pair from the axis: $N_s(\frac{\hat\xi^2_{\rm match}}{2}) = (\frac{\hat\xi^2_{\rm match}}{2})^{-1}\int_0^{\frac{\hat\xi^2_{\rm match}}{2}} S_n^{\rm ref}$, with $k=\bar k=1$, $k'=0$, $E^2=P_*^2f^2x^{1/5}$ and $\Pi^{\rm ref}=\Pi_0+\frac52P_*^2f^2x^{1/5}$. Since Π_0 is even, $|\Pi_0'|\le 8m_*|\beta|$ and $|\Pi_0|\le m_*$, where $m_*=|\Pi_0(0)|$ (proof of Lemma 1.20.42). Summing the geometric part ($\le 33|\beta|$) and the pressure part ($\le|\beta|(16.1P_*^2+10.1m_*)$), and using $E^2(\frac{\hat\xi^2_{\rm match}}{2})\ge P_*^2e^{-1}/4$, we get $|\nu(-5)|\le n_h|\beta|$ with $n_h:=4e(50+11m_*/P_*^2)$. Here m_*/P_*^2 is bounded independently of M_d: the model swirl is P_* times a profile that does not depend on M_d up to z_1, and it decays at rate at least 1 after z_1. Writing $z+5\le(z_T+5)(1+(z-z_T)_+)$, we obtain (b) with $K_\nu:=2(n_h+K_g+C_3(z_T+5))$.

Step 3: (c). On the wait $l=-\lambda$, $k=0$ and $\bar k=\bar k_Te^{-y}$ with $\bar k_T\le1$. So ($\star$) reads $S_q=(1-\lambda)a_\beta-4\lambda L\bar k_Te^{-y}$, and the exact solution of $\partial_yQ+(1-\lambda)Q=S_q$ is

$$Q_s=a_\beta+(Q_s(T)-a_\beta)e^{-(1-\lambda)y}-4L\bar k_T(1-e^{-\lambda y})e^{-(1-\lambda)y}.$$

This gives the bound for $|Q_s-a_\beta|$, since $a_\beta\le1$. For the lower bound, $1-e^{-\lambda y}\le 60\lambda\log(1/\lambda)\le q_0/8$ for λ small. So with $\epsilon:=e^{-(1-\lambda)y}$ we get $Q_s\ge a_\beta(1-\epsilon)+\frac{q_0}{2}\epsilon\ge\frac12\min\{1,\frac{q_0}{2}\}(a_\beta+\epsilon)$. Since $h<\lambda/6$, $a_\beta\ge\frac56\lambda+c_\beta\ge.49(\lambda+\beta^2)$. This gives the lower bound with $c_w:=.24\min\{1,q_0/2\}$, which does not depend on h. For N_s: $g=0$ on the wait, so $|S_n|\le C_3^{\rm w}|\beta|E^2$ and $\partial_y\nu-2\lambda\nu=S_n/E^2$. Hence $|\nu(y)|\le e^{2\lambda y}|\beta|(n_0+C_3^{\rm w}y)$, with $n_0:=K_\nu(1+T-z_T)$ from (b). Also $E=e_Tf(\beta)e^{-(1/2+\lambda)y}$ with $e_T=P_*F_T(\lambda)e^{-T/2}$, so

$$|N_s/E|=|\nu|E\le e_T|\beta|(n_0+C_3^{\rm w}y)e^{-(1/2-\lambda)y}\le C_w|\beta|(1+y)e^{-(1/2-\lambda)y},\qquad C_w:=e_T(n_0+C_3^{\rm w}).$$

$F_T(\lambda)$ is bounded uniformly in $\lambda\le\lambda_0$ (Lemma 1.14.1). So c_w and C_w are uniform in $\lambda\le\lambda_A$, and $K_{\rm wt}=C_w/c_w$ is as required in (1.6.18).

Step 4: (d). We use the test of Lemma 1.4.2. For fixed parameters the triples (a,b_s,w), $w=N_s/(EQ_s)$, range over a compact set, because $Q_s>0$ and all fields are continuous on the compact rectangle. Moreover $p_{s,1}=\frac{\hat\xi^2}{2}Q_s/L\ge\frac{\hat\xi^2_{\rm match}}{2}\min\{q_1,c_Pe^{-(T-z_1)},c_w\lambda\}$, which exceeds any fixed threshold once C (hence $\frac{\hat\xi^2_{\rm ref}}{2}$ and $\frac{\hat\xi^2_{\rm match}}{2}=\frac{\hat\xi^2_{\rm ref}}{2}e^{-5}$) is large. We also use the identity, valid for $P_c>2$,

$$\mathcal U(P_c,J_c)-2=\frac{(P_c-2)^2}{P_c-2+J_c^2/4+|J_c|\sqrt{(P_c-2)/2+J_c^2/16}}>0,$$

which follows from (1.4.8). So where $b_s=0$ and $a\le2$, the relaxed cone is equivalent to $a>0$ and $P_c=p_{s,1}>2$.

- On the arc and on $[0,z_1]$: $b_s=0$, $a=2-2l\in[0.8,2]$ and $P_c=p_{s,1}>2$, so the cone is relaxed.
- On the plateau: $a=2$ and $b_s=8\beta k'/E$. By (b), $|b_sw|=8|\beta||k'||\nu|/Q_s\le8K_\nu|k'|(1+\zeta)/c_P\le8K_\nu e_d/c_P$, where $\zeta=z-z_T$. Also, on the plateau $F=e^{f_0(z_1)}\ge1$ and $f\ge\frac12$, so $E\ge\frac12P_*e^{-(z_T+T_d)/2}$ on the turnoff, and $|b_s|\le8e_d/E\le16e^{z_T/2}e^{-T_d/2}$ since $P_*>e^{T_d}$ and $e_d\le1$. For M_d large, $|b_sw|\le\frac14$ and $b_s^2\le\frac14$. Then $a-b_sw>0$ and $2b_sw+b_s^2/a<2$, and Lemma 1.4.2 gives the relaxed cone, and the admissible cone where $v_s>2$.
- On the negative turn: $b_s=0$ and $a=2+2\lambda f_1'\in[2,2+2\lambda]$. By (b), $|w|=|\nu|E/Q_s\le K_w:=K_\nu(1+T)P_*e^{\gamma z_1}e^T/c_P$, a constant fixed before λ, so $(a-2)w^2\le2\lambda K_w^2<2$ for λ small. Lemma 1.4.2 gives the relaxed cone, and the admissible cone where $f_1'>0$, since there $v_s=a>2$.

- On the wait: $b_s = 0$, $a = 2 + 2\lambda$, and $2\lambda w^2 \le \frac{1}{2}$ by (c), as in the first paragraph of the proof of Lemma 1.8.19. Lemma 1.4.2 gives the admissible cone.

Finally, λ_A collects the finitely many upper bounds on λ used above ($h \le \lambda$ small against q_1; $8\lambda \le q_1 e^{-(T-z_1)}$; $60\lambda \log(1/\lambda) \le q_0/8$; $C_p E_p^2 \le E^2$ on $[-5, T]$; $2\lambda K_w^2 < 2$). Their constants are fixed before λ. □

Amplitude and ordinary angular derivatives on the backward pulse. Work first with the pre-heat model in the native variable $|\beta| \le 1$. Its pulse inlet $\frac{\hat\xi_p^2}{2}$ and length $Y = Y_{\mathrm{end}}$ are scalar by Lemma 1.8.7. Write $A_b = \mathrm{Amp}_b$, $K_{\mathrm{pulse}} = \int e^{-2\xi} R_0(\xi)^2 \, \mathrm{d}\xi$, and put $\tau = \tau_f^{\mathrm{en}}$ for the complete normalized model future. The wait has $W = 60 \log(1/\lambda)$ and $\sigma_p^0 = e^{2\lambda W}\sigma_b - (e^{2\lambda W} - 1)/(4\lambda)$. For the disjoint main and return supports, (1.6.26) becomes

$$K_{\mathrm{pulse}} A_b^2 + \lambda \sum_j K_j c_j^2 = B, \qquad B = \tfrac{1}{4} - \lambda\sigma_p^0 + e^{-2\lambda Y}(2\lambda\tau - \tfrac{1}{4}), \qquad K_j = \int_0^Y e^{-2\lambda y}\psi_j(y)^2 \, \mathrm{d}y.$$

Condition ($\lambda 3$) and (1.6.30) bound the two errors in B by $1/200$ each, so $0.24 \le B \le 0.26$. The pulse shape from [42, App. A.2–A.3] is

$$R_0(\xi) = (1 - \sigma(\xi - 10)) \int_0^\xi \sigma(v/0.02) \, \mathrm{d}v \quad (\xi \ge 0).$$

Since the step is nondecreasing from zero to one, $0 \le R_0(\xi) \le \xi$, $R_0'(\xi) \le 1$, and $R_0(\xi) \ge \xi - 0.02$ on $[0.02, 9]$. With $u = 9 - 0.02$,

$$\tfrac{1}{4} \ge K_{\mathrm{pulse}} \ge \int_{0.02}^{9} e^{-2\xi}(\xi - 0.02)^2 \, \mathrm{d}\xi = \tfrac{1}{4}e^{-0.04} - e^{-18}(u^2/2 + u/2 + 1/4) > 0.24019.$$

Consequently any positive root satisfies $A_b \le \sqrt{0.26/0.24019} < 1.041$.

To control the angular derivative, write $s_1 = 1/2 - \lambda$, $s_2 = 1/2 - 2\lambda$, $u_1 = m(0) = \mathfrak{M}_1/(\frac{\hat\xi_p^2}{2}E_p)$ and $u_2 = \mathfrak{M}_3/(\frac{\hat\xi_p^2}{2}H_pE_p)$ at the inlet, with $E_p = E(\frac{\hat\xi_p^2}{2}, \beta)$ here. The normalized end-of-turn moments and σ_b have bounded ordinary C^1_β norms: in (1.14.10)–(1.14.11) the β dependence is through 4β and $f = (1+\beta^2)^{-1}$. The quiet wait multiplies each incoming moment by $e^{-s_i W}$. Thus $\|u_i\|_{C^1_\beta} \le C_{\mathrm{pre}} e^{-s_i W}$. At fixed $\hat\xi$, both y and the translates $\psi_j(y) = \psi(y - Y + d_j)$ are independent of β.

Divide row i of (1.16.15) by $e^{s_i Y}$ and use the physical template R_0. Then $c = A_b b + g$ with

$$\widehat{A}_{ij} = e^{-s_i d_j} \int e^{s_i z}\psi(z) \, \mathrm{d}z, \qquad (\widehat{A}g)_i = -e^{-s_i Y} u_i,$$
$$(\widehat{A}b)_i = -\int_0^{\xi_m/\lambda} e^{-s_i(Y-v)} R_0(\lambda v) \, \mathrm{d}v.$$

The positive bump integrals are bounded above and below, and the two distinct offsets give $|\det \widehat{A}| \ge c_0\lambda$ by the mean value theorem applied to $e^{\lambda d_2} - e^{\lambda d_1}$. The matrix and b are independent of β. Hence

$$|b| + \|g\|_{C^1_\beta} \le C_{\mathrm{pre}} \lambda^{-1} e^{-s_2(Y - \xi_m/\lambda)} = O(e^{-c/\lambda})$$

by (1.6.30). In particular, this bounds the derivative of the affine term from the nonzero inlet data.

The energy polynomial has positive quadratic coefficient and constant term $\lambda \sum K_j g_j^2 - B < 0$ for small λ. Its unique positive root exceeds $1/2$, since at $1/2$ the polynomial is at most

$1/16 + O(e^{-c/\lambda}) - 0.24$. The amplitude derivative at the root, $2K_{\mathrm{pulse}}A_b + 2\lambda\sum K_j c_j b_j$, is bounded below by a positive template constant. Differentiating the full identity in β gives

$$(2K_{\mathrm{pulse}}A_b + 2\lambda\sum_j K_j c_j b_j)\,\partial_\beta A_b = -\lambda e^{2\lambda W}\partial_\beta\sigma_b + 2\lambda e^{-2\lambda Y}\partial_\beta\tau - 2\lambda\sum_j K_j c_j\,\partial_\beta g_j.$$

Here K_j are bounded and independent of β. Since $e^{2\lambda W}$ is bounded and $e^{-2\lambda Y}\|\partial_\beta\tau\|_\infty \le 1$, this proves, together with $\partial_\beta c = b\,\partial_\beta A_b + \partial_\beta g$,

$$0 < A_b < 1.041, \qquad \|\partial_\beta A_b\|_\infty \le C_{\mathrm{pre}}\lambda, \qquad \max_j \|c_j\|_{C^1([-1,1])} \le C_{\mathrm{pre}}e^{-c/\lambda}. \tag{1.8.4}$$

All derivatives here are ordinary derivatives, including at $\beta = 0$. On the native interval the three-E correction has the full target by Lemma 1.8.15. It preserves the inlet M, J and their normalizations. The paired heat and prefix changes satisfy $\delta\sigma_p = 2e^{-2\lambda Y}\delta\tau$ by Lemma 1.16.5, so they cancel identically in B and its derivative. The same positive root and affine returns therefore give (1.8.4) for the final member.

Lemma 1.8.18 (Pulse coefficients of the backward member)**.** *Assume (P1) and (P2) of Lemma 1.8.20 and $\lambda \le \lambda_A$. On the pulse write $\xi = \lambda y$, $y = 2\log(\hat\xi/\hat\xi_p)$, and $R_b = U/E = \mathrm{Amp}_b R_0(\xi) + \sum_j c_j\psi_j(y)$, where R_0 is the fixed pulse shape: smooth, zero for $\xi \le 0$, with bounded derivatives. Put $\beta_0 = \frac12 - \lambda$, $m = \mathfrak{M}_1/(\frac{\hat\xi^2}{2}E)$ and $a_\beta = (\lambda - h + c_\beta)/(1-\lambda)$. Then, uniformly in $|\beta| \le 1$, $h < \lambda/6$ and the pulse,*

$$\begin{aligned} m &= \frac{R_b}{\beta_0} - \frac{\lambda\partial_\xi R_b}{\beta_0^2} + m(0)e^{-\beta_0 y} + O(\lambda^2), \qquad |m(0)| + |\partial_\beta m(0)| \le K\lambda^{29},\\ |\partial_\beta m| &\le K\lambda(1+\log(1/\lambda)) + K\lambda^{29}, \qquad Q_s = a_\beta + O(\lambda^{29}),\\ \frac{N_s}{E} &= -R_b + ((\tfrac12 - h) + c_\beta)m - (\tfrac12 - h)\beta\partial_\beta m + O(\lambda^{28}), \end{aligned}$$

and, with $a = 2 + 2\lambda$ and $C_d = \lambda((\frac12 - h) + c_\beta)(1-\lambda)/(\beta_0^2(\lambda - h + c_\beta))$,

$$b_s = -(1+2\lambda)R_b + 2\lambda\partial_\xi R_b, \qquad w = \frac{N_s}{EQ_s} = \frac{(1-\lambda)R_b}{\beta_0} - C_d\partial_\xi R_b + o(1) \quad (\lambda \to 0).$$

These are [42, (A.28)–(A.30)] and the two formulas after (A.30), for the backward member. With the three-E bank, Q_s at the inlet changes by $O(1/R_{\mathrm{master}})$ (proof of Lemma 1.8.19), which is $O(\lambda^{30})$ for R_{master} large.

Proof. On the pulse $l = -\lambda$, the swirl is the wait power, so $\frac12\hat\xi\partial_{\hat\xi}\log E = -\frac12 - \lambda$ and $(\log E)_\beta = -J_0'$, and $U = ER_b$. m. From $\frac12\hat\xi\partial_{\hat\xi}(\mathfrak{M}_1/\frac{\hat\xi^2}{2}) = U - \mathfrak{M}_1/\frac{\hat\xi^2}{2}$ we get exactly $\partial_y m + \beta_0 m = R_b$. So $m = m(0)e^{-\beta_0 y} + \int_0^\infty e^{-\beta_0 v}R_b(y-v)\,\mathrm{d}v$, where the pulse part of R_b is extended by zero to $y < 0$. For the main part, Taylor's formula $R(\xi - \lambda v) = R(\xi) - \lambda v R'(\xi) + O(\lambda^2 v^2\|R''\|_\infty)$ gives $R/\beta_0 - \lambda R'/\beta_0^2 + O(\lambda^2)$. By (1.8.4) the return terms and their y derivatives are $O(e^{-c/\lambda})$. At fixed $\hat\xi$, differentiation under the convolution gives

$$|\partial_\beta m(y)| \le e^{-\beta_0 y}|\partial_\beta m(0)| + \beta_0^{-1}\Big(\|R_0\|_\infty|\partial_\beta A_b| + \sum_j \|\psi_j\|_\infty|\partial_\beta c_j|\Big).$$

This uses the integrable exponential kernel and the ordinary C^1_β bounds of (1.8.4) on the entire closed angular interval. At the inlet, $U = 0$ on the wait, so $\mathfrak{M}_1(\hat\xi_p)/\frac{\hat\xi_p^2}{2} = 4\beta\bar k_T\lambda^{60}$, while $E_p = e_T f\lambda^{30+60\lambda}$.

This gives the bound on $m(0)$ and $\partial_\beta m(0)$ with K depending on e_T^{-1}. Q_s. By Lemma 1.4.1, $W = 1-(1-2h)\beta Em - d(Em)_\beta$, and $|E_\beta| \le 2|\beta|E$. So (1.4.1)–(1.4.2) gives $S_q = \lambda W - h(1-2\beta U)+((\frac12-h)\beta+dU)J_0' = (1-\lambda)a_\beta+\varepsilon_q$ with $|\varepsilon_q| \le K_q E \le K_q E_p$. Variation of constants from the inlet, with $|Q_s(\frac{\hat\xi_p^2}{2})-a_\beta| \le K_Q\lambda^{60(1-\lambda)}$ by Lemma 1.8.17(c), gives $|Q_s-a_\beta| \le K_Q\lambda^{59}+2K_q e_T\lambda^{30}$. N_s. (1.4.3) gives $N_s/E = -WR_b+(\frac12-h)(Em-\beta(Em)_\beta)/E+(4h\beta\mathfrak{M}_4-d\mathfrak{M}_{4\beta})/(\frac{\hat\xi^2}{2}E)+((2+4h)\beta\Pi-d\Pi_\beta)/E$. Here $(Em)_\beta/E = \partial_\beta m - J_0'm$, so the second term is $((\frac12-h)+c_\beta)m-(\frac12-h)\beta\partial_\beta m$. Also $-WR_b = -R_b+O(E)$. By (P2) the last two terms are $O(E_p/\lambda)+O(E) = O(\lambda^{29})$, since $E \le E_p = e_T f\lambda^{30+60\lambda}$. *Shear.* $b_s = \hat\xi^2\hat\xi^{-1}\partial_{\hat\xi}U/E = 2[R_b\frac12\hat\xi\partial_{\hat\xi}\log E+\partial_y R_b] = -(1+2\lambda)R_b+2\lambda\partial_\xi R_b$ exactly, and $a = 2-2l = 2+2\lambda$. Insert m into N_s/E, and use $(\frac12-h)+c_\beta-\beta_0 = \lambda-h+c_\beta = (1-\lambda)a_\beta$ and $Q_s = a_\beta(1+O(\lambda^{28}))$, since $a_\beta \ge \frac56\lambda$. This gives

$$w = \frac{(1-\lambda)R_b}{\beta_0} - C_d\partial_\xi R_b + \frac{((\frac12-h)+c_\beta)(m(0)e^{-\beta_0 y}+O(\lambda^2))-(\frac12-h)\beta\partial_\beta m+O(\lambda^{28})}{Q_s}+O(\lambda^{27}).$$

The quotient is $O(\lambda)+O(\lambda^{28})$, apart from $|\beta\partial_\beta m|/Q_s$. That term is at most $K|\beta|\lambda(1+\log(1/\lambda))/(.49(\lambda+\beta^2)) \le K'\sqrt{\lambda}(1+\log(1/\lambda)) = o(1)$. □

Lemma 1.8.19 (Strict cone on the rest of the wait)**.** *Let c_w, C_w be the constants of Lemma 1.8.17(c) (the backward form of [42, (A.27)]):*

$$Q_s \ge c_w(\beta^2+\lambda+e^{-(1-\lambda)y}), \qquad |N_s/E| \le C_w|\beta|(1+y)e^{-(1/2-\lambda)y}$$

on the wait $y \in [0, 60\log(1/\lambda)]$. The factor $|\beta|$ comes from Lemma 1.8.15, and c_w is free of h because $\lambda-h \ge \frac56\lambda$. Put $K_{\rm wt} = C_w/c_w$. By Lemma 1.8.15(b) and the explicit factor λ in the lower bound for Q_s, it is bounded uniformly for $0<\lambda\le\lambda_0$. Assume $K_{\rm wt}^2\lambda(3+\log(1/\lambda))^2 \le \frac12$, as in (1.6.18). Then, for C above a threshold depending on Y_0 and λ (part of the step-4 choice of C, Section 1.5.2), (1.5.1) holds on $[Y_1, \frac{\hat\xi_p^2}{2}]\times[-1,1]$ for the final member, with $b_s = 0$, $a_s = v_s \ge 2+\lambda$ and $F>0$.

Proof. First take the member without the bank. With $U=0$, $b_s=0$ and $a = 2+2\lambda$. For $c = \lambda+e^{-(1-\lambda)y} > 0$, the maximum of $|\beta|/(\beta^2+c)$ on $[-1,1]$ is $1/(2\sqrt{c})$ if $c\le 1$ and $1/(1+c)$ if $c>1$. Both are bounded by $1/(2\sqrt{c})$, so

$$2\lambda w^2 \le \tfrac12 K_{\rm wt}^2(1+y)^2\min\{e^{-(1-2\lambda)y}, \lambda e^{\lambda y}\} \le K_{\rm wt}^2\lambda(3+\log(1/\lambda))^2 \le \tfrac12.$$

The second inequality follows by splitting at $y = \log(1/\lambda)$. For $K_{\rm wt} = 100$ and $\lambda = e^{-20}$ the maximum of the displayed minimum multiplied by $\frac12 K_{\rm wt}^2(1+y)^2$ is about $4.5\cdot10^{-3}$, near $y = \log(1/\lambda)$. Without the factor $|\beta|$ it would be about $K_{\rm wt}^2\log^2(1/\lambda)/2$. The test (1.4.9) has $a-b_s w = a > 2$ and $2-(a-2)w^2 \ge \frac32$. Also $p_{s,1} = \frac{\hat\xi^2}{2}Q_s/L \ge c_w\lambda\frac{\hat\xi^2}{2}$ is large, so Lemma 1.4.2 applies. Now add the bank. Lemma 1.14.5 with $k=2$ bounds its relative fixed-$\hat\xi$ angular jets through order two and its logarithmic radial jet by $O(K_{{\rm sc},2}(Y_0)/R_{\rm master})$ on $\frac{\hat\xi_{p,b}^2}{2}e^{(-20,-15)}$. Its coefficients are even (Lemma 1.8.15), and $U=0$. The partial histories and angular pressure term satisfy the bounds in the proof of Lemma 1.8.15(b). At fixed earlier parameters the changes in $\ell_r, Q_s, N_s/E$ are $O(R_{\rm master}^{-1})$ on the wait and the axial numerator retains its factor $|\beta|$. For $R_{\rm master}$ large both gaps stay above 1, $a-2 \ge \lambda$ and $Q_s \ge c_w\lambda/2$. Finally, on $[Y_1, \frac{\hat\xi_p^2}{2}]$ the final member equals the pre-loop member (Lemma 1.8.15(c)). □

Lemma 1.8.20 (Strict cone from the pulse inlet to the heat wing)**.** *Use (A1), the native prefix (S3) of Lemma 1.8.8, the A11 outlet (S2) of Lemma 1.8.7, Lemmas 1.8.15 and 1.8.19, and the following.*

(P1) On the pulse, $U/E = R_b := A_p\Phi(\lambda y) + \sum_j c_j\psi_j$, with $A_p\Phi = \mathrm{Amp}_b R_0$ and $\ell_r = -\lambda$. The actual coefficients satisfy (1.8.4), as proved above using the complete energy equation and the two affine moment equations.

(P2) Beyond the pulse inlet, on $[\frac{\hat\xi_p^2}{2}, \frac{\hat\xi_w^2}{2}]$, $|\Pi| + |\Pi_\beta| \le CE^2$ and $(|\mathfrak{M}_4| + |\mathfrak{M}_{4\beta}|)/\frac{\hat\xi^2}{2} \le CE\,E_p/\lambda$, where $E_p = \sup_{[\frac{\hat\xi_p^2}{2}, \frac{\hat\xi^2}{2}]} E$ is the pulse-inlet amplitude (E is nonincreasing beyond $\frac{\hat\xi_p^2}{2}$). The constant C is independent of h once $L_o \ge L_S$ of (1.15.5). A pointwise bound by CE^2/λ is not claimed: near R_0 and on the collar S/H^2 is of order $K_S \sim 1/h$. Source. *On the pulse and the adjoining unedited wait the swirl is the λ-power, with $|H_\beta| \le \|J_0'\|_\infty H$. Its outward energy and pressure contributions on this power are bounded by $H^2/(8\lambda)$ and $H^2/(4(1+2\lambda)\frac{\hat\xi_p^2}{2})$, respectively. For the axial contribution on $\frac{\hat\xi_p^2}{2} \le \frac{\hat\xi^2}{2} \le R_e$, (1.8.4) and the fixed pulse and return shapes give $|R_b| + |\partial_\beta R_b| \le C$. Since $U = ER_b$ and $|E_\beta| \le \|J_0'\|_\infty E$,*

$$\int_{(\frac{\hat\xi^2}{2})}^{R_e} (U^2 + |\partial_\beta(U^2)|)\,\mathrm{d}x \le C\int_{(\frac{\hat\xi^2}{2})}^{R_e} E^2\,\mathrm{d}x = C\,\frac{H(\frac{\hat\xi^2}{2})^2}{4\lambda}[1 - (\tfrac{\hat\xi^2}{2}/R_e)^{2\lambda}].$$

The endpoints are independent of β on the native band. Dividing by $\frac{\hat\xi^2}{2}$ and using $H^2 = \hat\xi^2 E^2$ gives $CE(\frac{\hat\xi^2}{2})E_p/\lambda$. Beyond R_e the axial field vanishes. The flattening, with its A11 bumps and its complete outward energy integral up to the added leg, is Lemma 1.15.4. On the added leg, the weighted bound (1.15.8), $E(y)S/H^2 \le E(0)/(4\lambda)$ with $E(0) \le E_p$, gives $S/\frac{\hat\xi^2}{2} = 2E^2S/H^2 \le E\,E_p/(2\lambda)$. Beyond the leg, on the transition, terminal power and collar up to $\frac{\hat\xi_w^2}{2} = 2R_0$ (a bounded radius ratio), we have $S \le H_{\mathrm{end}}^2 K_S$ with $H_{\mathrm{end}} = H_A e^{-\lambda L_o}$, $E \ge cE_{\mathrm{end}}$ and $E_{\mathrm{end}} = E(0)e^{-(1/2+\lambda)L_o}$. So $S/(\frac{\hat\xi^2}{2}E) \le CE(0)e^{-(1/2+\lambda)L_o}K_S \le CE(0)e^{-2\lambda L_o}K_S \le CE_p/(8\lambda)$, by (1.15.5) and $\frac12 + \lambda \ge 2\lambda$. The same holds for $\mathfrak{M}_{4\beta}$, by the β-derivative bounds of these lemmas. The pressure has no $1/h$ loss ((1.15.7); its density is x^{-2-2h}). For the heat and rank-one terms the absolute values of the differentiated energy and pressure densities have integrable envelopes, as in Proposition 1.15.8. Their partial outward integrals through the wing have the same bounds in the respective H_A^2 and H_A^2/R_A units as in (P3). Write $X = \hat\xi^2/2$ and $X_p = \hat\xi_p^2/2$. On the affected finite interval $R_A \le X \le 2R_0$ the ratios X/R_A and H/H_A are bounded above and below at fixed geometry. For $X_p \le X \le R_A$ the outward correction is the complete increment, and $H_A \le CH(X)$, $E(X) \le E_p$ give $H_A^2 \le 2C^2XE(X)E_p$ and $H_A^2/R_A \le 2C^2E(X)^2$. Thus increasing the last scale absorbs these normalized errors in the displayed bounds. These bounds are collected in Section 1.5.2 (paragraph after (λ1)–(λ7)).

(P3) After the last return, $U = \mathfrak{M}_1 = \mathfrak{M}_3 = 0$. The A11 edits are $O(\lambda^{30(1-\lambda)})$, and the relative field errors on the rank-one support and heat collar are $O(1/R_o)$. Source. *The pulse template and the two return bumps have compact support in y. The return coefficients solve the $\mathfrak{M}_1, \mathfrak{M}_3$ return equations (1.13.15), with the native affine coefficients just computed in (1.8.4). So $U = \mathfrak{M}_1 = \mathfrak{M}_3 = 0$ after the last return (as used in the proof of Lemma 1.8.7). The later edits change H only. The A11 target is $u_{\mathrm{model}} + u_{\mathrm{mem}}$, with $\|u_{\mathrm{model}}\|_{C^1} \le C\lambda^{30(1-\lambda)}$ and $\|u_{\mathrm{mem}}\|_{C^1} \le C\|\delta_{\mathrm{mem}}\|_{C^1}$ (Step 6 of the proof of Lemma 1.6.10). By Lemma 1.15.5 the edits are $O(\|u\|_{C^1})$. The memory part is at most λ^{30} once $Y_0 \ge Y_{\min}$, by Lemma 1.15.19(4) with $r_1 = \lambda^{30}$, a Y_0-threshold imposed after λ. The complete energy change divided by H_A^2 and*

the complete pressure change divided by H_A^2/R_A are $O(R_A^{-1})$, with their first native angular derivatives, by (R3) of Lemma 1.6.10. On the backward chart differentiation of the positive Laplace factor in (1.7.1) gives the native counterpart of (1.15.9). Substitution in the quadratic densities of Proposition 1.15.8 proves these bounds also for the absolute integrals needed in (P2).

Let $0 < h < \lambda/6$, and take the scale large. Then (1.5.1) holds on $[\frac{\hat\xi_p^2}{2}, \frac{\hat\xi_w^2}{2}] \times [-1,1]$ for the $\varsigma = -1$ stresses, with $F > 0$, $a_s \ge 2$ and $v_s - 2 \ge \min\{2\lambda, h\}$. The actual primitive satisfies

$$\frac{(1-h)\mathfrak{M}_2 - \frac{\hat\xi^2}{2}H - (\frac12 - h)\beta\,\mathfrak{M}_{2\beta}}{\frac{\hat\xi^2}{2}H} \ge \frac{5\lambda}{12(1-\lambda)}e^{-(1-h)\delta} \qquad (\tfrac{\hat\xi_p^2}{2} \le \tfrac{\hat\xi^2}{2} \le \tfrac{\hat\xi_w^2}{2},\ |\beta| \le 1).$$

Proof. Pulse. Put $\beta_0 = \frac12 - \lambda$ and $c = 2(\frac12 - h)\beta^2/(1+\beta^2) \in [0, (\frac12 - h)]$. By Lemma 1.8.18 (which uses (P1)–(P2) and Lemma 1.8.17(c) at the inlet), we have $Q_s = (\lambda - h + c)/(1-\lambda) + O(\lambda^{27})$ and $w = (1-\lambda)R_b/\beta_0 - C_d\partial_\xi R_b + o(1)$, $b_s = -(1+2\lambda)R_b + 2\lambda\partial_\xi R_b$, $a = 2 + 2\lambda$, where

$$C_d = \frac{\lambda((\frac12 - h) + c)(1-\lambda)}{\beta_0^2(\lambda - h + c)} \le \frac{2(1+O(\lambda))}{1 - h/\lambda} \le 2.4(1 + O(\lambda)).$$

The coefficient C_d decreases in c. On the main support $R_b = A_bR_0 \ge 0$ and $\partial_\xi R_b = A_bR_0' \le 1.041$. On the disjoint returns $|R_b| + \lambda|\partial_\xi R_b| = O(e^{-c/\lambda})$. Thus throughout the pulse $\partial_\xi R_b \le 1.05$ for small λ, and the negative part of R_b is exponentially small. The fixed C^1 norm of R_0 and the uniform expansion of w bound $|w|$ by a template constant. It follows that

- $b_s w \le \sup_{R\ge0}(-2R^2 + 2.52R) + o(1) \le 0.794 + o(1)$;
- $2b_s w + b_s^2/a \le \sup_{R\ge0}(-3.5R^2 + 5.04R) + o(1) = 1.8144 + o(1)$;
- $(a-2)w^2 = 2\lambda w^2 = o(1)$.

The first gap in (1.4.9) is at least $2 - 0.794 - o(1)$ and the second is at least $2 - 1.8144 - o(1)$. Both exceed 0.15 for sufficiently small λ in the stated parameter order. Since $p_{s,1} \ge \frac56\lambda\frac{\hat\xi_p^2}{2}$, Lemma 1.4.2 gives the admissible cone, with $v_s \ge a > 2$.

The actual primitive up to the A11 outlet. Write $\alpha = 1 - h$, $y = 2\log(\hat\xi/\hat\xi_p)$ and $\ell_r = \partial_y \log H$. Throughout this proof angular derivatives are taken at fixed $\hat\xi$. Define

$$z = \frac{\alpha\mathfrak{M}_2 - \frac{\hat\xi^2}{2}H - (\frac12 - h)\beta\mathfrak{M}_{2\beta}}{\frac{\hat\xi^2}{2}H}, \qquad z_\lambda = \frac{\lambda - h}{1-\lambda}, \qquad \zeta_\lambda = \frac{2\lambda}{3(1-\lambda)}.$$

Differentiating the actual primitive $\frac{\mathfrak{M}_{2\hat\xi}}{\hat\xi} = H$ gives

$$z_y + (1 + \ell_r)z = -h - \ell_r - (\tfrac12 - h)\beta\,\partial_\beta \log H. \tag{1.8.5}$$

This identity also holds while U and its histories are active.

At $\frac{\hat\xi_p^2}{2}$ the primitive agrees with that of the separated reference prefix. Indeed, the core restores the five reference histories at $\frac{\hat\xi_{\mathrm{match}}^2}{2}$ (Theorem 1.8.10), the loop and its restoration have zero combined increment (Lemma 1.8.15), and the three-E bank has $\Delta I = 0$ by (1.14.16). The backward pressure

bank has zero target. Thus $\mathfrak{M}_{2\beta} = -J_0'\mathfrak{M}_2$ there, and (1.6.22) gives $r_p = \mathfrak{M}_2/(\frac{\hat\xi_p^2}{2}H)$ from the positive finite-template ratio $r_b(\lambda)$. With $r_\lambda = (1-\lambda)^{-1}$ and $c_\beta = (\frac12 - h)\beta J_0' \ge 0$ we have

$$r_p = r_\lambda + (r_b - r_\lambda)\lambda^{60(1-\lambda)} \ge r_\lambda(1-\lambda^{60(1-\lambda)}), \qquad z(\tfrac{\hat\xi_p^2}{2}) = (\alpha + c_\beta)r_p - 1 \ge \zeta_\lambda.$$

For the last inequality use $\alpha + c_\beta \le 2$, $h < \lambda/6$ and $2\lambda^{60(1-\lambda)} \le \lambda/6$ for $\lambda \le 1/20$.

On the pulse the unedited swirl has $\ell_r = -\lambda$ and $\partial_\beta \log H = -J_0'$. On the flattening, with $v = \log(\frac{\hat\xi^2}{2}/R_e)$ and $\theta = 1 - s(v/T_f)$,

$$\log H^0 = \log H_e - \lambda v - \theta J_0 - (1-\theta)\log 2.$$

Here $\theta' \le 0$, $J_0 \le \log 2$ and $0 \le \theta \le 1$. Consequently $\partial_y \log H^0 \le -\lambda$ and $-(\frac12 - h)\beta\,\partial_\beta \log H^0 = \theta c_\beta \ge 0$. The following unedited wait and the A11 base power satisfy the same inequalities. For these fields the right side of (1.8.5) minus $(1+\ell_r)\zeta_\lambda$ is at least $\lambda - h - (1-\lambda)\zeta_\lambda > \lambda/6$.

For the actual A11 field put $g = \log(1 + t_1\psi_1 + t_2\psi_2)$, extended by zero off its supports. The uniform inverse in Lemma 1.15.5, the fixed translates and (P3) give

$$(1+\zeta_\lambda)|g_y| + (\tfrac12 - h)|\beta g_\beta| \le K_{11}\lambda^{28} + K_{\mathrm{mem}}\|\delta_{\mathrm{mem}}\|_{C^1} \le \lambda/12. \tag{1.8.6}$$

The first summand is made at most $\lambda/24$ at stage (λ5). The second is made at most $\lambda/24$ at stage $Y_{\min}$ in Step 6 of Lemma 1.6.10. This bound controls the loss in the differential inequality for the constant ζ_λ. The positive integrating factor for (1.8.5) now gives $z \ge \zeta_\lambda$ on $[\frac{\hat\xi_p^2}{2}, R_A]$ for every β.

The added leg, drive and heat collar. At the A11 outlet, R_A, H_A are scalar and the first row gives $\mathfrak{M}_2(R_A,\beta) = R_A H_A/(1-\lambda)$ identically in β by (S2) of Lemma 1.8.7. In particular $\mathfrak{M}_{2\beta}(R_A,\beta) = 0$. Start the scalar power model H^m there with this same primitive $\mathfrak{M}_2{}^m$, and define z^m by the formula for z. Then $z^m = z_\lambda$ on the leg $[R_A, \frac{\hat\xi_b^2}{2}]$, $\frac{\hat\xi_b^2}{2} = R_A e^{L_o}$. On the drive, with $t = 2\log(\hat\xi/\hat\xi_b)$,

$$(z^m)_t + (1-\kappa)z^m = \kappa - h, \qquad h \le \kappa \le \lambda.$$

Thus $z^m \ge z_\lambda e^{-\alpha t}$ up to $R_0 = \frac{\hat\xi_b^2}{2}e^\delta$. On $[R_0, 2R_0]$ the model is a pure $(\hat\xi/\sqrt{2})^{-2h}$ power since $2R_0 < Be^{-3}$, so $z^m(\frac{\hat\xi^2}{2}) = z^m(R_0)(\frac{\hat\xi^2}{2}/R_0)^{-\alpha}$. In particular, on the entire interval $[R_A, 2R_0]$,

$$z^m \ge m := z_\lambda e^{-\alpha\delta}2^{-\alpha} > \underline{z} := \frac{5\lambda}{12(1-\lambda)}e^{-\alpha\delta}.$$

Strictness follows from $\lambda - h > 5\lambda/6$ and $2^{-\alpha} > 1/2$.

For the actual field write $\epsilon = H/H^m - 1$ and $\Delta I(\frac{\hat\xi^2}{2}) = \int_{R_A}^{\frac{\hat\xi^2}{2}}(H - H^m)\,\mathrm{d}x$. The exact difference is

$$z - z^m = \frac{(\alpha\Delta I - (\frac12 - h)\beta\,\partial_\beta\Delta I)/(\frac{\hat\xi^2}{2}H^m) - (1+z^m)\epsilon}{1+\epsilon}. \tag{1.8.7}$$

Both perturbations vanish before $\frac{\hat\xi_b^2}{2}/2$. On $[\frac{\hat\xi_b^2}{2}/2, 2R_0]$ the rank-one formula (1.15.10), Proposition 1.15.8 and the collar estimate (1.15.9) give $|\epsilon| + |\epsilon_y| + |\epsilon_\beta| \le K/R_e$. Indeed the bump has size $\|D_I\|_{C^1}/(\frac{\hat\xi_b^2}{2}H^m(\frac{\hat\xi_b^2}{2})) = O((\frac{\hat\xi_b^2}{2})^{-1})$ and a fixed relative support. The collar has relative error $O(R_0^{-1})$, also after one logarithmic radial or angular derivative. Here all radius ratios are fixed before the final scale. On this interval $(\hat\xi/\hat\xi_b)^2 \in [1/2, 2e^\delta]$ and $H^m/H^m(\frac{\hat\xi_b^2}{2})$ is bounded above and below. Integrating $H^m\epsilon$ and $H^m\epsilon_\beta$ therefore gives

$$\frac{|\Delta I| + |\partial_\beta\Delta I|}{\frac{\hat\xi^2}{2}H^m} \le K'/R_e.$$

This includes the full primitive increment $-D_I(\beta)$ between the bump and the collar. Lemma 1.15.1 bounds r^m on the drive, and the power formulas bound z^m on the two adjoining pieces. Equation (1.8.7) gives $|z - z^m| \le K''/R_e$ uniformly in $\frac{\hat\xi^2}{2}, \beta$. At fixed $h, \lambda, \delta, L_o, Y_0$, increase the final scale C until this last bound is at most $(m - \underline{z})/2$ and $|\partial_y \log(1+\epsilon)| \le h/2$. Since $\zeta_\lambda > \underline{z}$ and $\frac{\hat\xi_w^2}{2} = 2R_0$ at this scale (Lemma 1.8.3), the actual z is at least $\underline{z}$ throughout $[\frac{\hat\xi_p^2}{2}, \frac{\hat\xi_w^2}{2}]$.

Cone after the last return. Here $U = \mathfrak{M}_1 = \mathfrak{M}_3 = 0$, so $b_s = 0$, $p_1 = \frac{\hat\xi^2}{2} z/L$, and (A3) gives $L\hat\xi^2 \widehat{\mathcal{T}}_{P,\theta} = H[\frac{\hat\xi^2}{2} z - 2L(1-\ell_r)]$. Equations (1.8.6) and (1.15.9) and the preceding scale choice give $\ell_r \le -h/2$. Also $|\ell_r| \le C_0\lambda$ by the flattening slope bound of Lemma 1.15.4, the drive range and the same edit estimates. Increasing C once more gives $\widehat{\mathcal{T}}_{P,\theta} \ge Hz/(4L)$ since $\frac{\hat\xi_p^2}{2}\underline{z}$ grows with the scale. Now (A3), (P2) and Lemma 1.8.4 imply

$$|\widehat{\mathcal{T}}_{P,z}|/\widehat{\mathcal{T}}_{P,\theta} \le C_1 E_p/(\lambda z) \le C_2 e^{T/10}\lambda^{27.5}.$$

The constant C_2 uses the fixed drive length δ through $\lambda/\underline{z} \le (12/5)e^\delta$ and the uniform bounds in (P2). The smallness condition at stage ($\lambda 7$) gives $2\widehat{\mathcal{T}}_{P,\theta}^2 > (a_s - 2)\widehat{\mathcal{T}}_{P,z}^2$ and $v_s - 2 = a_s - 2 = -2\ell_r \ge h$. Together with the pulse estimate this proves the claim. □

1.9 The forward leading system and a convergent axis construction

Main result. Theorem 1.9.1 constructs a regular solution near the axis from fixed Gevrey axis data. The solution is analytic in $\hat\xi^2$, with the axis parity required for a smooth Cartesian field. The theorem states the axial regularity, uniqueness class, and dependence of the constants.

1.9.1 Actual histories and the integrated equations

We write $F = \widehat{\Lambda}_P$, $U = \widehat{\mathcal{U}}_{P,z}$, $P = \widehat{\mathcal{P}}_P$, and $H = \hat\xi \widehat{\mathcal{U}}_{P,\theta} = \hat\xi^2 F$. In addition to $\mathfrak{M}_1$, we introduce the histories

$$\begin{aligned}
\mathfrak{M}_2 &= \int_0^{\hat\xi} \rho^2 \widehat{\mathcal{U}}_{P,\theta}(\rho, \hat\zeta)\, \mathrm{d}\rho,\\
\mathfrak{M}_3 &= \int_0^{\hat\xi} \rho^2 (\widehat{\mathcal{U}}_{P,z}\widehat{\mathcal{U}}_{P,\theta})(\rho, \hat\zeta)\, \mathrm{d}\rho,\\
\mathfrak{M}_4 &= \int_0^{\hat\xi} \rho (\widehat{\mathcal{U}}_{P,z}^2 - \tfrac{1}{2}\widehat{\mathcal{U}}_{P,\theta}^2)(\rho, \hat\zeta)\, \mathrm{d}\rho,\\
P &= P_{\mathrm{ax}}(\hat\zeta) + \int_0^{\hat\xi} \frac{\widehat{\mathcal{U}}_{P,\theta}(\rho, \hat\zeta)^2}{\rho}\, \mathrm{d}\rho.
\end{aligned} \tag{1.9.1}$$

The four integral histories vanish at $\hat\xi = 0$. The pressure has the specified axis value P_{ax}. We define

$$\mathcal{K} = (1-2h)\hat\zeta \mathfrak{M}_1 + d\mathfrak{M}_{1\hat\zeta}, \qquad \mathcal{C} = dU - (\tfrac{1}{2} - h)\hat\zeta, \qquad \mathcal{B} = 1 + \frac{2\mathcal{K}}{\hat\xi^2}.$$

All radial quotients in this section have their regular axis extensions. The integrated leading

stresses are

$$\widehat{\mathcal{T}}_{P,\theta} = \partial_{\hat\xi}\widehat{\mathcal{U}}_{P,\theta} - \frac{\widehat{\mathcal{U}}_{P,\theta}}{\hat\xi} + \frac{1}{L\hat\xi^2}\Big[(\tfrac12\hat\xi^2+\mathcal{K})H - (1-h)\mathfrak{M}_2 + (\tfrac12-h)\hat\zeta\mathfrak{M}_{2\hat\zeta} - d\mathfrak{M}_{3\hat\zeta} + (4h-1)\hat\zeta\mathfrak{M}_3\Big], \tag{1.9.2}$$

$$\widehat{\mathcal{T}}_{P,z} = \partial_{\hat\xi}\widehat{\mathcal{U}}_{P,z} + \frac{1}{L\hat\xi}\Big[(\tfrac12\hat\xi^2+\mathcal{K})U - (\tfrac12-h)(\mathfrak{M}_1 - \hat\zeta\mathfrak{M}_{1\hat\zeta}) + 4h\hat\zeta\mathfrak{M}_4 - d\mathfrak{M}_{4\hat\zeta} + \tfrac12\hat\xi^2((2+4h)\hat\zeta P - dP_{\hat\zeta})\Big]. \tag{1.9.3}$$

We do not add independent constants to these expressions.

Differentiation of $L\hat\xi^2\widehat{\mathcal{T}}_{P,\theta}$ and $L\hat\xi\widehat{\mathcal{T}}_{P,z}$, with (1.9.1), shows that $\widehat{\mathcal{T}}_{P,\theta} = \widehat{\mathcal{T}}_{P,z} = 0$ is equivalent, with the regular-axis constants fixed, to

$$L\left(F_{\hat\xi\hat\xi\hat\xi} + \frac{3}{\hat\xi}F_{\hat\xi}\right) = (dU - (\tfrac12-h)\hat\zeta)F_{\hat\zeta} - \mathcal{B}(\tfrac12\hat\xi F_{\hat\xi} + F) - h(1+2\hat\zeta U)F, \tag{1.9.4}$$

$$L\left(U_{\hat\xi\hat\xi\hat\xi} + \frac{1}{\hat\xi}U_{\hat\xi}\right) = (dU - (\tfrac12-h)\hat\zeta)U_{\hat\zeta} - \tfrac12\mathcal{B}\hat\xi U_{\hat\xi} - (\tfrac12+h)(1+2\hat\zeta U)U - (2+4h)\hat\zeta P - \hat\zeta\hat\xi^2F^2 + dP_{\hat\zeta}, \tag{1.9.5}$$

$$P_{\hat\xi} = \hat\xi F^2. \tag{1.9.6}$$

For the angular equation, the differentiated form is explicitly

$$L\left(H_{\hat\xi\hat\xi\hat\xi} - \frac{H_{\hat\xi}}{\hat\xi}\right) + \left(\frac{\hat\xi}{2} + \frac{\mathcal{K}}{\hat\xi}\right)H_{\hat\xi} + h(1+2\hat\zeta U)H - (dU - (\tfrac12-h)\hat\zeta)H_{\hat\zeta} = 0.$$

In the axial differentiation the two terms with $\frac12\hat\xi^2 F F_{\hat\zeta}$ cancel. Conversely, integration of the differentiated equations recovers (1.9.2)–(1.9.3): the axis limits of $L\hat\xi^2\widehat{\mathcal{T}}_{P,\theta}$ and $L\hat\xi\widehat{\mathcal{T}}_{P,z}$ are zero.

The signs of the drift $-(\frac12-h)\hat\zeta$ and the pressure terms in (1.9.5) agree with (1.6.7). Equations (1.9.4)–(1.9.6) describe the stress-free leading system. They do not set the lower-order radial inertia or the full axial diffusion of the physical Navier–Stokes equations to zero. In fact the tangential time derivative, radial diffusion and transport all have scale $\hat t^{-3/2-h}$. Axial diffusion has scale $\hat t^{-3/2+h}$, smaller by $\hat t^{2h}$.

In the radial equation, centrifugal acceleration and radial pressure have scale $\hat t^{-3/2-2h}$, but radial inertia and radial diffusion have scale $\hat t^{-3/2}$, again smaller by $\hat t^{2h}$. These are the terms the later slow expansion must restore.

1.9.2 The axis theorem

Theorem 1.9.1 (Regular-axis core)**.** *We let $K_{\hat\zeta}$ be a compact interval with $L > 0$. Suppose $F_{\mathrm{ax}}, U_{\mathrm{ax}}, P_{\mathrm{ax}}$ are real Gevrey-3/2 functions on a neighborhood of $K_{\hat\zeta}$. Then (1.9.4)–(1.9.6) have a solution with these axis values on $[0,\sqrt{2r_{\mathrm{ax}}}]\times K_{\hat\zeta}$, for some $r_{\mathrm{ax}} > 0$. The solution is analytic as a function of $\hat\xi^2$ in one complex disk and, on a smaller closed disk, satisfies*

$$\left\|(\hat\xi^{-1}\partial_{\hat\xi})^\ell\partial_{\hat\zeta}^k(F,U,P)\right\|_\infty \le CB_0(8\Lambda_{\mathrm{rad}})^\ell\ell!\,(2^{3/2}\Lambda_{\hat\zeta})^k(k!)^{3/2} \quad (\ell,k\ge0). \tag{1.9.7}$$

Here the finite constants depend on the fixed axis data, h, and $K_{\hat\zeta}$.

The solution is unique among solutions analytic in $\hat\xi^2$ on one radial neighborhood with smooth coefficient functions. If $F_{\mathrm{ax}} > 0$ and $P_{\mathrm{ax}} < 0$, we can reduce the radius so that $F > 0$ and $P < 0$.

Proof. We use power series in the squared radius, with the coefficient normalization

$$F = \sum_{n\ge 0} f_n \left(\frac{\hat\xi^2}{2}\right)^n, \qquad U = \sum_{n\ge 0} u_n \left(\frac{\hat\xi^2}{2}\right)^n, \qquad P = \sum_{n\ge 0} p_n \left(\frac{\hat\xi^2}{2}\right)^n.$$

We set

$$b_n = \delta_{n0} + \frac{2(\frac12 - h)\hat\zeta u_n + d u_n'}{n+1}.$$

The symbol b_n in this proof is local to the coefficient recursion. The exact recursion is

$$2L(n+1)(n+2) f_{n+1} = d \sum_{i+j=n} u_i f_j' - (\tfrac12 - h)\hat\zeta f_n' - \sum_{i+j=n} b_i (j+1) f_j - h f_n - 2h\hat\zeta \sum_{i+j=n} u_i f_j, \tag{1.9.8}$$

$$\begin{aligned} 2L(n+1)^2 u_{n+1} = {} & d \sum_{i+j=n} u_i u_j' - (\tfrac12 - h)\hat\zeta u_n' - \sum_{i+j=n} b_i j u_j - (\tfrac12 + h) u_n \\ & - 2(\tfrac12 + h)\hat\zeta \sum_{i+j=n} u_i u_j - 4(\tfrac12 + h)\hat\zeta p_n - 2\hat\zeta \sum_{i+j=n-1} f_i f_j + d p_n', \end{aligned} \tag{1.9.9}$$

$$p_{n+1} = \frac{1}{n+1} \sum_{i+j=n} f_i f_j. \tag{1.9.10}$$

An empty sum is zero.

The right sides use only coefficients from the previous recursion steps. In particular there is no division by $\mathcal{C}$. At the first step,

$$U_{\hat\xi\hat\xi}(0,\hat\zeta) = \frac{(dU_{\mathrm{ax}} - (\frac12 - h)\hat\zeta) U_{\mathrm{ax}}' - (\frac12 + h)(1 + 2\hat\zeta U_{\mathrm{ax}}) U_{\mathrm{ax}} - (2 + 4h)\hat\zeta P_{\mathrm{ax}} + d P_{\mathrm{ax}}'}{2L}. \tag{1.9.11}$$

The last term is necessary even though it vanishes at $\hat\zeta = \pm 1$.

We prove convergence with a joint radial and axial majorant. We put $s = 3/2$ and

$$w_{n,k} = \frac{(n+k)!^s}{n!^s (n+1)^2}, \qquad \|v\|_{\Lambda_{\mathrm{rad}},\Lambda_{\hat\zeta}} = \sup_{n,k\ge 0} \frac{\left\| \partial_{\hat\zeta}^k v_n \right\|_\infty}{\Lambda_{\mathrm{rad}}^n \Lambda_{\hat\zeta}^k w_{n,k}}. \tag{1.9.12}$$

We select $\Lambda_{\hat\zeta} \ge 1$ large enough for the axis data and the fixed analytic coefficients. After this, we select $\Lambda_{\mathrm{rad}} \ge 1$. The space of formal series with finite norm is complete.

A norm-Cauchy sequence converges coefficientwise in each C^k norm. These limit derivatives are compatible.

The bounds

$$\sup_k \sum_{\ell=0}^{k} \binom{k}{\ell}^{-1/2} \le 5, \qquad \sup_n \sum_{i+j=n} \frac{(n+2)^2}{(i+1)^2 (j+1)^2} \le 16 \tag{1.9.13}$$

have these proofs. Separation of the endpoint binomial coefficients gives the first bound. A split of the radial sum at $i = n/2$ gives the second bound. Vandermonde's inequality $\binom{n+k}{i+\ell} \ge \binom{n}{i}\binom{k}{\ell}$ then gives the algebra bound with constant $K_* = 80$.

We let $\mathscr{A}v = \int_0^1 v(t\frac{\hat\xi^2}{2},\hat\zeta)\,\mathrm{d}t$, $\mathscr{E} = \frac12\hat\xi\partial_{\hat\xi}$, and define

$$\mathscr{R}_j v = \sum_{n\ge0} \frac{v_n\big(\frac{\hat\xi^2}{2}\big)^{n+1}}{(n+1)(n+j)} \quad (j=1,2), \qquad \mathscr{I}v = \sum_{n\ge0} \frac{v_n\big(\frac{\hat\xi^2}{2}\big)^{n+1}}{n+1}.$$

Thus $(\frac{\hat\xi^2}{2}(\hat\xi^{-1}\partial_{\hat\xi})^2 + j\hat\xi^{-1}\partial_{\hat\xi})\mathscr{R}_j v = v$. Weight ratios give

$$\|\mathscr{A}v\| \le \|v\|, \qquad \left\|\tfrac{\hat\xi^2}{2}v\right\|, \|\mathscr{I}v\|, \|\mathscr{R}_j v\|, \|\mathscr{R}_j\mathscr{E}v\| \le 4\Lambda_{\mathrm{rad}}^{-1}\|v\|, \qquad \left\|\mathscr{R}_j\partial_{\hat\zeta}v\right\| \le 4\Lambda_{\hat\zeta}\Lambda_{\mathrm{rad}}^{-1}\|v\|.$$

All norms here are (1.9.12). We must estimate differentiated products before we estimate their factors independently.

The most restrictive term is $\mathscr{R}_j[(\mathscr{A}\partial_{\hat\zeta}v)\mathscr{E}w]$. For $i+j'=n$, the exact weight ratio is

$$\frac{w_{i,\ell+1}w_{j',k-\ell}}{w_{n+1,k}} = (i+1)^s\left[\frac{\binom{n+1}{i+1}}{\binom{n+k+1}{i+\ell+1}}\right]^s \frac{(n+2)^2}{(i+1)^2(j'+1)^2}.$$

After we include the Leibniz coefficient and the inverse denominator, the averaging and Euler operators leave

$$\frac{j'(i+1)^{s-1}}{(n+1)^2} \le 1.$$

The remaining sums are (1.9.13). Thus

$$\left\|\mathscr{R}_j[(\mathscr{A}\partial_{\hat\zeta}v)\mathscr{E}w]\right\| \le K_*\frac{\Lambda_{\hat\zeta}}{\Lambda_{\mathrm{rad}}}\|v\|\,\|w\|. \tag{1.9.14}$$

If the actual equation omits the average, Euler operator, or axial derivative, we omit that factor in the estimate. This gives

$$\|\mathscr{R}_j(vw)\|,\ \|\mathscr{R}_j[(\mathscr{A}v)w]\|,\ \|\mathscr{R}_j[v\mathscr{E}w]\|,\ \|\mathscr{R}_j[(\mathscr{A}v)\mathscr{E}w]\| \le K_*\Lambda_{\mathrm{rad}}^{-1}\|v\|\,\|w\|,$$
$$\left\|\mathscr{R}_j[(\partial_{\hat\zeta}v)w]\right\|,\ \left\|\mathscr{R}_j[(\mathscr{A}\partial_{\hat\zeta}v)w]\right\| \le K_*\Lambda_{\hat\zeta}\Lambda_{\mathrm{rad}}^{-1}\|v\|\,\|w\|.$$

For the second line the additional factor is $(i+1)^s/(n+1)^2$ or $(i+1)^{s-1}/(n+1)^2$, each at most one. Also

$$\left\|\mathscr{R}_j[\tfrac{\hat\xi^2}{2}(vw)]\right\| \le 16K_*\Lambda_{\mathrm{rad}}^{-2}\|v\|\,\|w\|, \qquad \|\mathscr{I}(vw)\| \le 4K_*\Lambda_{\mathrm{rad}}^{-1}\|v\|\,\|w\|.$$

We do not assert boundedness of $\partial_{\hat\zeta}$ or $\mathscr{E}$ alone on the coefficient space.

We replace the three differential left sides in (1.9.4)–(1.9.6) by $\mathscr{R}_2, \mathscr{R}_1, \mathscr{I}$ and add their axis values. In the new map Ψ, we expand $\mathcal{B} = 1 + 2(\frac12 - h)\hat\zeta\mathscr{A}U + d\mathscr{A}U_{\hat\zeta}$. We let $J_0 \ge 1$ bound the fixed Gevrey norms of the finitely many coefficient functions, with $1/(2L)$, and set

$$B_0 = \|(F_{\mathrm{ax}}, U_{\mathrm{ax}}, P_{\mathrm{ax}})\| + 1, \qquad C_* = 100K_*^2 J_0(1+\Lambda_{\hat\zeta}).$$

The displayed estimates and bilinear polarization give, on the unit ball around the axis data Y_{ax},

$$\|\Psi(Y) - Y_{\mathrm{ax}}\| \le \frac{C_*(1+B_0)^2}{\Lambda_{\mathrm{rad}}}, \qquad \left\|\Psi(Y) - \Psi(\widetilde Y)\right\| \le \frac{2C_*(1+B_0)}{\Lambda_{\mathrm{rad}}}\left\|Y - \widetilde Y\right\|.$$

We select $\Lambda_{\mathrm{rad}} \ge 4C_*(1+B_0)^2$. The map is a strict contraction.

Its fixed point obeys $|v_n| \le B_0\Lambda_{\mathrm{rad}}^n/(n+1)^2$, so the radial series converges for $|\hat\xi| < \sqrt{2/\Lambda_{\mathrm{rad}}}$. The inequality $(n+k)!/n! \le k!2^{n+k}$, with $2^{3/2}/4 < 1$, gives the axial Gevrey bound on $|\hat\xi| \le (2\Lambda_{\mathrm{rad}})^{-1/2}$. Cauchy's estimate on the smaller disk yields (1.9.7). All coefficient operations are thus legitimate on the new functions. Recursion (1.9.8)–(1.9.10) proves the stated uniqueness in the radial analytic class.

Positivity is a result of continuity after we reduce the radius. □

1.9.3 Divergence and Cartesian regularity

Formula (1.6.8) gives

$$\frac{V_{\hat\xi}}{\hat\xi} = \frac{(1+2h)\hat\zeta U + \hat\zeta\hat\xi U_{\hat\xi} - dU_{\hat\zeta}}{L}, \qquad \partial_z(q^{-1/2-h}U) = -q^{-1}\frac{V_{\hat\xi}}{\hat\xi}.$$

Because $r^{-1}\partial_r(ru_r^{\mathrm{lead}}) = q^{-1}V_{\hat\xi}/\hat\xi$, the divergence is zero. Also

$$\partial_r(q^{-1-2h}P) = rq^{-2-2h}F^2 = \frac{(u_\theta^{\mathrm{lead}})^2}{r}.$$

This is the leading centrifugal balance, not the full radial momentum equation.

The quotient $\overline{V} = 2V/\hat\xi^2$ is smooth and Gevrey on a slightly smaller axial radius, by (1.6.8) and (1.9.7). In Cartesian components the horizontal velocity is

$$u_1^{\mathrm{lead}} = \frac{\overline{V}}{2q}x_1 - q^{-1-h}Fx_2, \qquad u_2^{\mathrm{lead}} = \frac{\overline{V}}{2q}x_2 + q^{-1-h}Fx_1.$$

Their coefficients are smooth in r^2, z, t at each positive-time axis point. This proves the regular-axis interpretation used in (1.6.9).

1.10 A positive linear profile and one decreasing exit

Main result. Lemma 1.10.2 gives a positive scalar profile with one critical point. Lemma 1.10.1 transfers that profile to the fixed pressure background (1.10.1). These results do not treat the full variable pressure family.

Scope for the connection family. This section proves a scalar exit lemma for the fixed pressure background (1.10.1). The actual pressure family uses the paragraphs "The variable-scale Bessel core" and "Memberwise activation controls and their order". They have labels 1.6.4.3 and 1.6.4.3. Those arguments supply the variable Bessel construction, composite radial inverses, coefficient contraction, gauge-value matching, and quantitative core-to-correction bound for that family.

We fix (1.5.5). The zero-swirl background is

$$H = 0, \qquad U = \kappa\hat\zeta, \qquad P = -P_*(\hat\zeta), \qquad P_* = \frac{\kappa}{4(\frac12+h)} + \frac{\kappa^2}{2}\hat\zeta^2. \tag{1.10.1}$$

Substitution into the axial equation verifies the cancellation

$$\kappa(1-\kappa)\hat\zeta + 2(1+h)\kappa^2\hat\zeta^3 - 4(\tfrac12+h)\hat\zeta P_* + dP_*' = 0.$$

The linearized angular equation is

$$L\hat\xi^2\Big(\frac{H_{\hat\xi\hat\xi}}{\hat\xi^2} - \frac{H_{\hat\xi}}{\hat\xi^3}\Big) + (1+\kappa L)\tfrac12\hat\xi H_{\hat\xi} + h(1+2\kappa\hat\zeta^2)H + \hat\zeta\big((\tfrac12-h) - \kappa + \kappa\hat\zeta^2\big)H_{\hat\zeta} = 0. \tag{1.10.2}$$

We construct a positive product solution with no restriction on h/κ.

Lemma 1.10.1 (Analytic scale and amplitude)**.** *We set $\alpha = (\frac{1}{2} - h) - \kappa$ and $\beta = h/(1+\kappa)$. There are positive even analytic functions c, ϕ on a neighborhood of $[-1,1]$ such that*

$$(1+\kappa L) + \hat{\zeta}(\alpha + \kappa\hat{\zeta}^2)c_{\hat{\zeta}}/c = Lc, \tag{1.10.3}$$

$$h(1+2\kappa\hat{\zeta}^2) + \hat{\zeta}(\alpha+\kappa\hat{\zeta}^2)\phi_{\hat{\zeta}}/\phi = \beta Lc. \tag{1.10.4}$$

Their analytic neighborhood can depend on h, κ.

Proof. With the temporary variable $\zeta = \hat{\zeta}^2$, we solve

$$2\zeta(\alpha+\kappa\zeta)b_c' = (1+\kappa-2\kappa h\zeta)b_c - (1-2h\zeta).$$

The series $b_c = \sum_{n\geq 0} b_{c,n}\zeta^n$ gives

$$b_{c,0} = \frac{1}{1+\kappa}, \qquad [(n-1) - 2hn - (2n+1)\kappa]b_{c,n} = -2\kappa(n-1+h)b_{c,n-1} + 2h\,\mathbf{1}_{\{n=1\}}.$$

In particular

$$b_{c,1} = -\frac{2h}{(1+\kappa)(2h+3\kappa)}, \qquad m_c = b_{c,0} + b_{c,1} = \frac{3\kappa}{(1+\kappa)(2h+3\kappa)} > 0.$$

For $n \geq 2$, the denominator divided by $n-1$ is at least $1 - 4h - 5\kappa > .959995$. Thus the coefficients alternate and $|b_{c,n}/b_{c,n-1}| < 3\kappa$. We pair consecutive terms of the absolutely convergent tail. This gives

$$b_c(\zeta) \geq b_{c,0} + b_{c,1}\zeta \geq m_c \quad (0 \leq \zeta \leq 1).$$

On $|\zeta| \leq 2$, $|b_c'| < 2$.

The complex tube of radius $m_c/4$ about $[0,1]$ is convex and satisfies $|b_c| > m_c/2$. Thus $c(\hat{\zeta}) = 1/b_c(\hat{\zeta}^2)$ is analytic and positive. If $0 < \epsilon_{\hat{\zeta}} < \min(m_c/16, 1/16)$, the square map sends the complex $\epsilon_{\hat{\zeta}}$ tube about $[-1,1]$ to points at distance at most $2\epsilon_{\hat{\zeta}} + \epsilon_{\hat{\zeta}}^2 < m_c/4$ from $[0,1]$.

We define $\Phi(0) = 1$ by

$$\frac{\Phi'}{\Phi} = \frac{\beta(1-2h\zeta)/b_c(\zeta) - h(1+2\kappa\zeta)}{2\zeta(\alpha+\kappa\zeta)}.$$

The numerator vanishes at zero, so that singularity is removable. The other denominator stays away from zero on the tube. Integration and exponentiation give a positive analytic Φ on the real segment. We set $\phi(\hat{\zeta}) = \Phi(\hat{\zeta}^2)$.

The equations that define the functions give (1.10.3) and (1.10.4). □

Lemma 1.10.2 (The regular scalar mode)**.** *For $0 < \beta < 1$, we define*

$$g_\beta(\xi) = \frac{\xi}{2^{1+\beta}\Gamma(1+\beta)} \int_0^1 e^{-\xi s/2} s^\beta (1-s)^{-\beta}\, \mathrm{d}s. \tag{1.10.5}$$

Then $g_\beta > 0$ on $(0,\infty)$, $g_\beta'(0) > 0$, and

$$2\xi g_\beta'' + \xi g_\beta' + \beta g_\beta = 0.$$

We can differentiate its large-ξ expansion to each fixed derivative order. In particular

$$g_\beta(\xi) = \xi^{-\beta}(1 + O(\xi^{-1})), \qquad g_\beta'(\xi) = -\beta\xi^{-\beta-1} + O(\xi^{-\beta-2}).$$

The derivative has a unique zero on $(0,\infty)$.

Proof. The integral converges absolutely, and positivity is immediate. For $a(s) = s^{\beta}(1-s)^{-\beta}$, differentiation under the integral shows that the differential expression is the positive prefactor $\xi/[2^{1+\beta}\Gamma(1+\beta)]$ times the integral of

$$\partial_s\big[e^{-\xi s/2}s^{1+\beta}(1-s)^{1-\beta}\big].$$

The two boundary values vanish. For the asymptotics, we split the integral at $1/2$. The second part and each fixed ξ-derivative are exponentially small.

On the first part, we expand $(1-s)^{-\beta} = 1 + O(s)$ and rescale s by ξ. The leading gamma integral gives the coefficient one. The same integrable powers of s control successive derivatives. The derivative is initially positive and eventually negative. At a positive critical point the equation gives $g_\beta'' = -\beta g_\beta/(2\xi) < 0$.

Each zero of the derivative thus strictly crosses from positive to negative, so there can be only one. □

By (1.10.3)–(1.10.4),

$$H_{\mathrm{lin}}(\tfrac{\hat\xi^2}{2},\hat\zeta) = \phi(\hat\zeta)g_\beta(c(\hat\zeta)\tfrac{\hat\xi^2}{2}) \tag{1.10.6}$$

solves (1.10.2). It is positive for $\hat\xi > 0$. The positive minimum of c gives a finite same exit $\frac{\hat\xi_{\mathrm{e}}^2}{2}$ beyond the maximum of each member of the family:

$$\tfrac{\hat\xi_{\mathrm{e}}^2}{2} \ge 20, \qquad c_{\mathrm{e}} := \min_{\hat\zeta\in[-1,1]}\Big[-\phi(\hat\zeta)c(\hat\zeta)g_\beta'\Big(c(\hat\zeta)\hat\xi_{\mathrm{e}}^2/2\Big)\Big] > 0. \tag{1.10.7}$$

After we slightly reduce the enlarged interval $K_{\hat\zeta}$, this strict inequality holds on one radial neighborhood and throughout $K_{\hat\zeta}$. The differentiated asymptotics also give

$$\Big\|\partial_{\hat\zeta}^k(\tfrac12\hat\xi\partial_{\hat\xi})^j H_{\mathrm{lin}}(\tfrac{\hat\xi^2}{2},\cdot)\Big\|_\infty \le C_{j,k}(\tfrac{\hat\xi^2}{2})^{-\beta} \quad \text{for large } \tfrac{\hat\xi^2}{2}. \tag{1.10.8}$$

We do not assert uniformity of the constants in h,κ.

We use the free analytic axis data

$$F_{\mathrm{ax}} = \frac{\varepsilon}{2}\phi c\, g_\beta'(0), \qquad U_{\mathrm{ax}} = \kappa\hat\zeta, \qquad P_{\mathrm{ax}} = -P_*. \tag{1.10.9}$$

They determine the nonlinear core uniquely near the axis. Section 1.11 shows that the core reaches any fixed finite radius when ε is sufficiently small.

1.11 Nonlinear continuation on a fixed radial interval

Main result. Theorem 1.11.1 continues the specified small axis data across a fixed finite radial interval. For each fixed radial derivative order, it gives one positive axial Gevrey radius. The radius can depend on the interval and the fixed parameters.

Theorem 1.11.1 (Finite-interval core)**.** *We fix h,κ as in (1.5.5) and $0 < \hat\xi_* < \infty$. For all sufficiently small $\varepsilon > 0$, the axis data (1.10.9) generate a stress-free leading core (H_c, U_c, P_c) on $[0, \frac{\hat\xi_*^2}{2}] \times K_{\hat\zeta}$, after we fix a slightly enlarged $K_{\hat\zeta}$. It has the genuine histories (1.9.1), and*

$$H_c = \varepsilon H_{\mathrm{lin}} + O(\varepsilon^2), \qquad U_c = \kappa\hat\zeta + O(\varepsilon^2), \qquad P_c = -P_* + O(\varepsilon^2). \tag{1.11.1}$$

One $\varrho_* > 0$ works for each fixed $j \ge 0$. The errors in (1.11.1) and their j-th radial derivatives are $O_j(\varepsilon^2)$ in $\mathcal{G}_{\varrho_*}$, defined in this section.

The radius and constants can depend on $\frac{\hat\xi_*^2}{2}, h, \kappa$. For small ε, $H_c > 0$ for $\hat\xi > 0$, $F_c = H_c/(\hat\xi^2) > 0$, and $P_c < 0$. If $\hat\xi_* > \hat\xi_{\mathrm{e}}$, then $\frac{H_{c,\hat\xi}}{\hat\xi} < 0$ on one neighborhood of the exit (1.10.7).

1.11.1 The norm and the actual difference equations

For $0 < \varrho \le 1$, we put

$$\|v\|_{\mathcal{G}_\varrho} = \sum_{k\ge 0} \frac{\varrho^k}{(k!)^{3/2}} \left\|\partial_{\hat\zeta}^k v\right\|_{L^\infty(K_{\hat\zeta})}. \tag{1.11.2}$$

Vectors use the sum norm and matrices its induced operator norm. Leibniz's rule gives an algebra norm, because the residual binomial factor is $\binom{k}{j}^{-1/2} \le 1$. A change of index in the sum gives, for $0 < \varrho < \widehat\varrho \le 1$,

$$\left\|\partial_{\hat\zeta} v\right\|_{\mathcal{G}_\varrho} \le 8(\widehat\varrho - \varrho)^{-3/2} \|v\|_{\mathcal{G}_{\widehat\varrho}}. \tag{1.11.3}$$

The coefficient ratio is $\widehat\varrho^{-1}(k+1)^{3/2}(\varrho/\widehat\varrho)^k$, which has the stated bound.

The comparison background is

$$H_b = \varepsilon H_{\mathrm{lin}}, \qquad U_b = \kappa\hat\zeta, \qquad P_b = -P_* + \int_0^{\frac{\hat\xi^2}{2}} \frac{H_b(s,\hat\zeta)^2}{4s^2}\,\mathrm{d}s.$$

We integrate all its histories from zero. Linearity of the angular equation at fixed U_b gives $\mathcal{T}_{\theta,b} = 0$. The axial stress is $O(\varepsilon^2)$ on each fixed positive radial rectangle, because only the quadratic histories $\mathfrak{M}_{4b}, P_b$ differ from (1.10.1).

For a positive radius r_0 inside the same axis disk, we set

$$y = \log(\tfrac{\hat\xi^2}{2}/r_0), \qquad Y = \log(\tfrac{\hat\xi_*^2}{2}/r_0),$$
$$\mathbf{w} = (v,w) = (H - H_b, U - U_b), \qquad \mathbf{z} = (m,i,j,s,\pi) = \Delta(\mathfrak{M}_1,\mathfrak{M}_2,\mathfrak{M}_3,\mathfrak{M}_4,P).$$

Here s is a component of $\mathbf{z}$, used only in the next local formulas. The Gevrey exponent stays $3/2$. The exact history densities are

$$\begin{aligned} m_y &= \tfrac{\hat\xi^2}{2} w, & i_y &= \tfrac{\hat\xi^2}{2} v, & j_y &= \tfrac{\hat\xi^2}{2}(U_b v + H_b w + vw),\\ s_y &= \tfrac{\hat\xi^2}{2}(2U_b w + w^2) - (2H_b v + v^2)/4, & \pi_y &= (2H_b v + v^2)/(4\tfrac{\hat\xi^2}{2}). \end{aligned} \tag{1.11.4}$$

We write this polynomial vector as $G(y,\mathbf{w})$. It satisfies $G(y,0) = 0$.

We solve (1.9.2)–(1.9.3) for H_y, U_y and subtract the background. This gives

$$\begin{aligned} v_y = {} & -\tfrac{\hat\xi^2}{2}\mathcal{T}_{\theta,b} + \left(1 - \frac{\frac{\hat\xi^2}{2} + \mathcal{K}_b}{2L}\right) v - \frac{H(2(\frac12 - h)\hat\zeta m + d m_{\hat\zeta})}{2L}\\ & + \frac{(1-h)i - (\frac12 - h)\hat\zeta i_{\hat\zeta} + d j_{\hat\zeta} - 2(h - (\frac12 - h))\hat\zeta j}{2L},\\ w_y = {} & -\sqrt{\tfrac{\hat\xi^2}{2}/2}\,\mathcal{T}_{z,b} - \frac{\frac{\hat\xi^2}{2} + \mathcal{K}_b}{2L} w - \frac{U(2(\frac12 - h)\hat\zeta m + d m_{\hat\zeta})}{2L}\\ & + \frac{(\frac12 - h)(m - \hat\zeta m_{\hat\zeta}) - 4h\hat\zeta s + d s_{\hat\zeta} - \frac{\hat\xi^2}{2}((2+4h)\hat\zeta\pi - d\pi_{\hat\zeta})}{2L}. \end{aligned} \tag{1.11.5}$$

Thus

$$\mathbf{w}_y = \mathbf{F}_\varepsilon + A_0\mathbf{w} + B(y,\mathbf{w})\mathbf{z} + C(y,\mathbf{w})\mathbf{z}_{\hat\zeta}, \qquad \mathbf{z} = \mathbf{z}_0 + \int_0^y G(t,\mathbf{w}(t))\,\mathrm{d}t. \tag{1.11.6}$$

The matrices B, C are affine in $\mathbf{w}$. We read their entries directly from (1.11.5). All coefficients and their explicit $\hat\zeta$-derivatives have fixed Gevrey bounds on this finite rectangle.

In particular there is one axial derivative, behind two radial integrations in the integrated equation.

1.11.2 Initial data on an amplitude-independent disk

We select the contraction in Theorem 1.9.1 with one upper bound for the axis norms. The same contraction bound applies to complex ε in one small disk. Its polynomial iterates converge in the supremum norm on that disk. Thus their limit depends holomorphically on ε. At $\varepsilon = 0$ the solution is (1.10.1).

The first variation is H_{lin} in the swirl component and zero in the axial and pressure components, by the coefficient recursion. The first variations of the five histories coincide with those of the comparison background.

In particular, $\partial_\varepsilon \mathfrak{M}_2|_0 = \int_0^{\frac{\hat\xi^2}{2}} H_{\mathrm{lin}}$ and $\partial_\varepsilon \mathfrak{M}_3|_0 = \kappa\hat\zeta \int_0^{\frac{\hat\xi^2}{2}} H_{\mathrm{lin}}$. These two variations are generally nonzero. It is their differences from the background variations that vanish.

We select $0 < r_0 < \frac{\hat\xi_*^2}{2}$ strictly inside this uniform disk, before we reduce ε. We get

$$\mathbf{w}(0) = \mathbf{w}_0 = O(\varepsilon^2), \qquad \mathbf{z}(0) = \mathbf{z}_0 = O(\varepsilon^2) \tag{1.11.7}$$

at one positive Gevrey radius, with a reserve for $\partial_{\hat\zeta}\mathbf{z}_0$. We do not use the possibly smaller radius used to prove positivity of a particular axis solution to define r_0 or Y.

1.11.3 A contraction with two derivative placements

We select ϱ_0 less than the available data and coefficient radii, and $\nu > 0$ with $\nu Y \le \varrho_0/2$. We put

$$\varrho(y) = \varrho_0 - \nu y, \qquad \|\mathbf{w}\|_\lambda = \sup_{0\le y\le Y} e^{-\lambda y}\, \|\mathbf{w}(y)\|_{\mathcal{G}_{\varrho(y)}}.$$

We use functions continuous in each strictly smaller radius, with finite displayed norm. This is a complete space: a norm-Cauchy sequence is Cauchy in the supremum norm in each smaller-radius space, and the limit derivatives are compatible. We use its closed ball of radius δ, with $\delta e^{\lambda Y} \le 1$. All undamped values then lie in the unit ball.

We integrate (1.11.6) and substitute the history integral. The local term contributes at most C/λ to the Lipschitz constant. For undifferentiated histories, a difference in the inner variable gives C/λ^2. A difference in the outer coefficient gives CY/λ.

We estimate the term

$$\int_0^y C(u, \mathbf{w}(u)) \int_0^u \partial_{\hat\zeta} G(t, \mathbf{w}(t))\, \mathrm{d}t\, \mathrm{d}u.$$

We use the output radius $\varrho(y)$, not $\varrho(u)$, for this estimate. If the difference falls in the inner variable, (1.11.3) and the Bielecki weight give the kernel

$$\int_0^y (y-t)^{1-s_G} e^{-\lambda(y-t)}\, \mathrm{d}t \le \Gamma(2-s_G)\lambda^{s_G-2}, \qquad s_G = \frac{3}{2}. \tag{1.11.8}$$

If it falls in the outer coefficient, we attach the exponential weight to u. In that case

$$\begin{aligned}\int_0^y e^{-\lambda(y-u)} \int_0^u (y-t)^{-s_G}\, \mathrm{d}t\, \mathrm{d}u \\ = \frac{1}{s_G-1}\int_0^y e^{-\lambda v}(v^{1-s_G} - y^{1-s_G})\, \mathrm{d}v \le \frac{\Gamma(2-s_G)}{s_G-1}\lambda^{s_G-2}.\end{aligned} \tag{1.11.9}$$

The algebra estimates for G and its differences introduce only a finite coefficient constant and the factor ν^{-s_G}. The two kernels decay as $\lambda^{-1/2}$.

These estimates also establish the existence of the double integral in the output Gevrey space. On $u \le y - \epsilon_1$ it has a positive radius reserve. The integrable kernel in (1.11.9) controls the remaining endpoint portion. We do not assert that $\mathbf{z}_{\hat{\zeta}}(u)$ stays bounded in $\mathcal{G}_{\varrho(u)}$ for an arbitrary trial function. The crude single integral with kernel $(u-t)^{-3/2}$ would diverge.

We conclude that the integrated map has

$$\operatorname{Lip}\Psi \le C_0(\lambda^{-1} + \lambda^{-2} + \nu^{-3/2}\lambda^{-1/2}). \tag{1.11.10}$$

The map includes the actual terms $\mathbf{z}_0, \partial_{\hat{\zeta}}\mathbf{z}_0$. Their source contribution is $O(\varepsilon^2)$. Their affine difference contribution is $O(\varepsilon^2/\lambda)$. The same source bound holds for $\mathbf{w}_0, \mathbf{F}_\varepsilon$.

We fix λ so that (1.11.10) is at most $1/2$, then set $\delta = 2C_1\varepsilon^2$ and reduce ε until

$$2C_1\varepsilon^2 e^{\lambda Y} \le 1.$$

The map is a contraction and maps the closed ball into itself. This gives an actual solution on the fixed interval, with $\sup_y \|\mathbf{w}(y)\|_{\mathcal{G}_{\varrho(y)}} = O(\varepsilon^2)$. All constants fixed before this last choice are independent of ε.

1.11.4 Same radius, identification, and signs

We let $\varrho_{\min} = \inf_y \varrho(y) > 0$ and select

$$\varrho_* = \frac{1}{2}\varrho_{\min}, \qquad \varrho_j = \varrho_* + \frac{\varrho_{\min} - \varrho_*}{j+1}.$$

The equations (1.11.6) give inductively

$$\sup_y \left(\left\| \partial_y^j \mathbf{w} \right\|_{\mathcal{G}_{\varrho_j}} + \left\| \partial_y^j \mathbf{z} \right\|_{\mathcal{G}_{\varrho_j}} \right) \le C_j \varepsilon^2.$$

At each step, only one additional axial derivative of a previously controlled history is necessary. The necessary bound is a result of $\varrho_j - \varrho_{j+1} > 0$ through (1.11.3). Coefficients and sources have each fixed radial derivative at a same larger axial radius.

Restriction to ϱ_* proves the claimed same-radius statement. Constants can grow with j. Away from zero, $\hat{\xi}^{-1}\partial_{\hat{\xi}} = \left(\frac{\hat{\xi}^2}{2}\right)^{-1}\partial_y$. Near zero use (1.9.7) and reduce ϱ_* once.

The axis solution and the new solution have the same values and the same five histories at r_0. On a short overlap interval their difference satisfies the same integrated equation, with contraction constant bounded by $C(Y_1 + Y_1^2 + Y_1^{1/2})$ after a fixed radius reduction. They thus agree. This argument does not assume that the constructed axis solution belongs to the large-interval Bielecki ball. It proves the smooth matching and Theorem 1.11.1.

For completeness, near the axis the positive first variation is $H_{\mathrm{lin}}/(\hat{\xi}^2)$. It controls F_c. On compact positive radial intervals positivity is a result of $H_{\mathrm{lin}} > 0$ and (1.11.1). The pressure increment is $O(\varepsilon^2)$, but $\min P_* = \kappa/(4(\frac{1}{2} + h)) > 0$. Finally the negative derivative margin in (1.10.7) dominates the $O(\varepsilon^2)$ derivative error. Parity is a result of uniqueness: H_c, P_c are even in $\hat{\zeta}$, and U_c is odd.

1.12 An active protected collar and delayed angular insertion

Main result. Proposition 1.12.2 gives an active collar with strict cone inequalities and one axial Gevrey radius. Under its stated smallness conditions, Proposition 1.12.3 inserts the angular shape and restores all five histories. The corrections do not change the specified protected field.

The construction in this section uses the core only on a fixed finite interval. It ends with a growing reference and matched histories. Section 1.13 constructs the heat exterior.

1.12.1 Shear and admissibility

Where $F > 0$, we define

$$\mathfrak{a} = -\frac{\hat{\xi} F_{\hat{\xi}}}{F} = 2 - \frac{\hat{\xi} H_{\hat{\xi}}}{H}, \quad \mathfrak{b} = \frac{U_{\hat{\xi}}}{F}, \quad \mathfrak{v} = \mathfrak{a} + \frac{\mathfrak{b}^2}{\mathfrak{a}}, \quad \mathfrak{t} = -\frac{\mathfrak{b}}{\mathfrak{a}}. \tag{1.12.1}$$

We use the last two quantities only when $\mathfrak{a} > 0$. On $\mathfrak{v} > 2$, the strict directional cone is

$$\ell_{\pm}(\mathcal{T}) = \sqrt{2}(\widehat{\mathcal{T}}_{P,\theta} + \mathfrak{t}\widehat{\mathcal{T}}_{P,z}) \pm \sqrt{\mathfrak{v} - 2}(\widehat{\mathcal{T}}_{P,z} - \mathfrak{t}\widehat{\mathcal{T}}_{P,\theta}) > 0. \tag{1.12.2}$$

On $\mathfrak{v} \le 2$, the relaxed condition is

$$\widehat{\mathcal{T}}_{P,\theta} - \frac{\mathfrak{b}}{\mathfrak{a}}\widehat{\mathcal{T}}_{P,z} - (2 - \mathfrak{v})F > 0. \tag{1.12.3}$$

A relaxed interval alone is not admissible for the wave inverse, which assumes $\mathfrak{v} > 2$.

The analytic shape aligned with the axis pressure is

$$g(\eta) = \sqrt{1 + 2(\tfrac{1}{2} + h)\kappa\eta^2}, \qquad P_* = \frac{\kappa}{4(\frac{1}{2} + h)}g^2, \qquad \gamma = \frac{3}{5}. \tag{1.12.4}$$

On $[-1, 1]$, $g \ge 1$, $\|g\|_{C^1} \le 2$, and $\eta g_\eta \ge 0$.

1.12.2 Flat activation with actual histories

The additive activation of this subsection is the scalar reference example. The selected member uses the curved activation (1.23.1); after its first collar it continues by the modified activation (M0)+(M1) of Definition 1.20.22, and the backward member by Definition 1.20.35. Proposition 1.20.29 gives the obstruction for a single late termination under its transverse-zero hypothesis.

We select a nondecreasing smooth ψ, zero on $y \le 0$, one on $y \ge 1$, and equal to e^{-1/y^2} for sufficiently small positive y. After we fix $\frac{\hat{\xi}_e^2}{2}$, we select a small $c_a > 0$ and, on $\frac{\hat{\xi}_e^2}{2} \le \frac{\hat{\xi}^2}{2} \le B$, we put

$$H_+ = \varepsilon c_a \big(\tfrac{\hat{\xi}^2}{2}\big)^{\gamma} \psi(2\log(\hat{\xi}/\hat{\xi}_e)) g, \qquad H = H_c + H_+, \qquad U = U_c. \tag{1.12.5}$$

The core does not change at radii less than $\frac{\hat{\xi}_e^2}{2}$. We compute each history from (1.9.1), with the same axis pressure.

Lemma 1.12.1 (Factored activation estimates)**.** *After we fix c_a, then a finite $B > e\frac{\hat{\xi}_e^2}{2}$, and then reduce ε, the activated field satisfies*

$$\widehat{\mathcal{T}}_{P,\theta} \ge (\hat{\xi}^{-1}\partial_{\hat{\xi}}(H_+)) + .1H_+ > 0, \qquad |\widehat{\mathcal{T}}_{P,z}| \le C_B \varepsilon H_+, \qquad |\widehat{\mathcal{T}}_{P,z}|/\widehat{\mathcal{T}}_{P,\theta} \le C_B\varepsilon \tag{1.12.6}$$

on $\frac{\hat{\xi}_e^2}{2} < \frac{\hat{\xi}^2}{2} \le B$. Its shear has a finite upper bound and a positive lower bound for $\mathfrak{a}$, with $\mathfrak{b} = O_B(\varepsilon)$. It satisfies the applicable strict or relaxed condition (1.12.2) or (1.12.3).

Proof. First, we take $U = \kappa\eta$. Monotonicity gives $\mathfrak{M}_{2+} = \int_{\frac{\hat\xi_e^2}{2}}^{\frac{\hat\xi^2}{2}} H_+ \le \frac{\hat\xi^2}{2} H_+/(1+\gamma)$. The added angular numerator, before division by $L\hat\xi^2$, is

$$(1+\kappa L)\tfrac{\hat\xi^2}{2} H_+ + \left[-1 + h - \kappa + 4\kappa h\eta^2 + ((\tfrac12 - h) - \kappa d)\frac{\eta g_\eta}{g}\right]\mathfrak{M}_{2+}.$$

If the bracket is nonnegative this is at least $\frac{\hat\xi^2}{2} H_+$. If the bracket is negative, its ratio to $\frac{\hat\xi^2}{2} H_+$ is at least $1-(1+\kappa)/(1+\gamma) > .374$. Because $\frac{\hat\xi^2}{2} \ge 20$, the added stress is at least $(\hat\xi^{-1}\partial_{\hat\xi}(H_+)) + .13 H_+$. For the actual core, $U_c - \kappa\eta = O_B(\varepsilon^2)$. For a coefficient b on the fixed interval, monotonicity of H_+ and $|\partial_\eta H_+| \le C H_+$ give the pointwise bound

$$\left|\int_{\frac{\hat\xi_e^2}{2}}^{\frac{\hat\xi^2}{2}} b H_+ \,\mathrm{d}s\right| + \left|\partial_\eta \int_{\frac{\hat\xi_e^2}{2}}^{\frac{\hat\xi^2}{2}} b H_+ \,\mathrm{d}s\right| \le C_B \sup_{s,\eta}(|b| + |b_\eta|)\, H_+(\tfrac{\hat\xi^2}{2}, \eta).$$

The same bound applies with b/s or b/s^2, because $\hat\xi_e > 0$. The related history errors, with $\int (U_c - \kappa\eta) H_+$, keep the same flat factor and contribute $O_B(\varepsilon^2 H_+)$.

The only axial changes are

$$\Delta\mathfrak{M}_4 = -\int_{\frac{\hat\xi_e^2}{2}}^{\frac{\hat\xi^2}{2}} \frac{2H_c H_+ + H_+^2}{4s}\,\mathrm{d}s, \qquad \Delta P = \int_{\frac{\hat\xi_e^2}{2}}^{\frac{\hat\xi^2}{2}} \frac{2H_c H_+ + H_+^2}{4s^2}\,\mathrm{d}s.$$

These and their first axial derivatives have a bound by $C_B\varepsilon H_+$. Substitution into (1.9.3) proves (1.12.6). This is a factored bound at the flat edge, not an unweighted error divided by a flat function.

On the fixed first ramp, $H_{\mathrm{lin}} - \frac{\hat\xi^2}{2}(\hat\xi^{-1}\partial_{\hat\xi}(H_{\mathrm{lin}}))$ has a positive minimum. We select c_{a} so that

$$c_{\mathrm{a}}\left(\tfrac{\hat\xi^2}{2}\right)^{\gamma}[(1-\gamma)\psi - \psi']g$$

removes at most a quarter of that minimum. Then $\mathfrak{a} > 0$, with finite bounds. Beyond the ramp the added power has shear $4/5$, while $\frac{H_{c,\hat\xi}}{\hat\xi} < 0$. Because $\frac{U_{c,\hat\xi}}{\hat\xi} = O_B(\varepsilon^2)$, $\mathfrak{b} = O_B(\varepsilon)$.

We divide (1.12.2) by $\widehat{\mathcal{T}}_{P,\theta} > 0$ and use (1.12.6) to prove the strict branch. For the other branch, $(2-\mathfrak{a})F = \frac{H_{\hat\xi}}{\hat\xi}$. The left side of (1.12.3) is at least

$$-\frac{H_{c,\hat\xi}}{\hat\xi} + .1 H_+ - C_B\varepsilon^2 H_+ > 0.$$

□

Proposition 1.12.2 (A genuinely active protected collar)**.** *There is $\ell > 0$, fixed before $\varepsilon, \mathcal{R}$, such that $\frac{\hat\xi_e^2}{2} + 8\ell < \min(e\frac{\hat\xi_e^2}{2}, B)$. The activated field has $\frac{H_{\hat\xi}}{\hat\xi} < 0$, $\mathfrak{v} > 2$, strictly positive cone faces, and nonzero stress on $(\frac{\hat\xi_e^2}{2}, \frac{\hat\xi_e^2}{2} + 8\ell]$. On*

$$\mathcal{D}_{\mathrm{in}} = [0, \tfrac{\hat\xi_e^2}{2} + 4\ell] \times K_\eta$$

the leading coefficients and each fixed radial derivative have one positive axial Gevrey-3/2 radius.

Proof. By (1.10.6) and (1.10.7), $\hat{\xi}^{-1}\partial_{\hat{\xi}}H_{\mathrm{lin}} \le -c_{\mathrm{e}}$ at $\hat{\xi} = \hat{\xi}_{\mathrm{e}}$, uniformly in η on $[-1,1]$. On a slightly enlarged K_η the same bound holds after decreasing $c_{\mathrm{e}} > 0$. Flatness of ψ gives a collar where the derivative of

$$H_{\mathrm{lin}} + c_{\mathrm{a}}\big(\tfrac{\hat{\xi}^2}{2}\big)^{\gamma}\psi(2\log(\hat{\xi}/\hat{\xi}_{\mathrm{e}}))g$$

is at most $-c_{\mathrm{e}}/2$.

The $O_B(\varepsilon^2)$ nonlinear error gives $\frac{H_{\hat{\xi}}}{\hat{\xi}} \le -\varepsilon c_{\mathrm{e}}/4$. Thus $\mathfrak{a} > 2$ with a fixed margin, and the lemma gives strict admissibility. For small $y = 2\log(\hat{\xi}/\hat{\xi}_{\mathrm{e}}) > 0$,

$$\widehat{\mathcal{T}}_{P,\theta} \ge c\varepsilon y^{-3}e^{-1/y^2} > 0.$$

The rectangle includes positive stress. Theorem 1.11.1 supplies its core radius.

The added shape g is analytic. Radial derivatives of the cutoff are scalar multipliers independent of η. The histories and V use only finitely many axial derivatives, which one fixed radius reduction controls. The new radius is same to all fixed radial orders, with order-dependent constants. □

We select the inner coefficient cutoff to be one through $\frac{\hat{\xi}_{\mathrm{e}}^2}{2} + \ell$ and zero beyond $\frac{\hat{\xi}_{\mathrm{e}}^2}{2} + 3\ell$. The next shear modulation begins only after $\frac{\hat{\xi}_{\mathrm{e}}^2}{2} + 5\ell$, with an unchanged boundary neighborhood. These ordered radii leave the whole protected rectangle and its actual axis prefixes unchanged.

1.12.3 Remove the core before we insert the calibrated shape

For a fixed small tolerance δ_B, we select B so large that

$$\|H_{\mathrm{lin}}\|_{C^1_\eta} + \Big\|\tfrac{\hat{\xi}^2}{2}\big(\hat{\xi}^{-1}\partial_{\hat{\xi}}(H_{\mathrm{lin}})\big)\Big\|_{C^1_\eta} \le \delta_B c_{\mathrm{a}} B^{\gamma} \qquad (B \le \tfrac{\hat{\xi}^2}{2} \le 2B), \tag{1.12.7}$$

$$\int_0^{2B} \|H_{\mathrm{lin}}(s,\cdot)\|_{C^1_\eta}\,\mathrm{d}s + c_{\mathrm{a}}\int_0^{e\frac{\hat{\xi}_{\mathrm{e}}^2}{2}} s^{\gamma}[1-\psi(\log(s/\tfrac{\hat{\xi}_{\mathrm{e}}^2}{2}))]\,\mathrm{d}s \le \delta_B c_{\mathrm{a}} B^{1+\gamma}. \tag{1.12.8}$$

The first integral grows as $O(B^{1-\beta})$, by (1.10.8). We fix the omitted activation integral. We take a fixed smooth cutoff $\tau(\frac{\hat{\xi}^2}{2}/B)$, one near B and zero near $2B$, and set

$$H = \varepsilon c_{\mathrm{a}}\big(\tfrac{\hat{\xi}^2}{2}\big)^{\gamma} g + \tau H_c, \qquad U = \kappa\eta + \tau(U_c - \kappa\eta). \tag{1.12.9}$$

We include the bounds for the fixed logarithmic derivatives of τ in the choice of δ_B.

We compare the actual angular stress with the full-axis power. Then (1.12.7)–(1.12.8) bound the errors in $H, \frac{1}{2}\hat{\xi}H_{\hat{\xi}}, \mathfrak{M}_2/\frac{\hat{\xi}^2}{2}$ by $C\delta_B\varepsilon c_{\mathrm{a}}\big(\frac{\hat{\xi}^2}{2}\big)^{\gamma} + O_B(\varepsilon^2)$. The errors in $U, \mathfrak{M}_1$ are $O_B(\varepsilon^2)$, and $\mathfrak{M}_3 - \kappa\eta\mathfrak{M}_2 = O_B(\varepsilon^3)$. Thus $\widehat{\mathcal{T}}_{P,\theta} - \frac{H_{\hat{\xi}}}{\hat{\xi}}$ keeps a positive multiple of the power, while $\mathfrak{a} = 4/5 + O(\delta_B) + O_B(\varepsilon)$ and $\mathfrak{b} = O_B(\varepsilon)$. The exact zero-swirl cancellation makes $\widehat{\mathcal{T}}_{P,z} = O_B(\varepsilon^2)$ on this fixed interval, so $(\mathfrak{b}/\mathfrak{a})\widehat{\mathcal{T}}_{P,z} = O_B(\varepsilon^3)$. First small δ_B, then small ε, ensure $\mathfrak{v} < 1.2$ and the relaxed condition.

Beyond $2B$ put $a_{\mathrm{p}} = \varepsilon c_{\mathrm{a}}$. For the exact velocities $H = a_{\mathrm{p}}\big(\frac{\hat{\xi}^2}{2}\big)^{\gamma} g$, $U = \kappa\eta$, the histories have constants m, i_g, j:

$$\mathfrak{M}_1 = \kappa\eta\tfrac{\hat{\xi}^2}{2} + m, \quad \mathfrak{M}_2 = \frac{a_{\mathrm{p}}\big(\frac{\hat{\xi}^2}{2}\big)^{1+\gamma} g}{1+\gamma} + i_g, \quad \mathfrak{M}_3 = \kappa\eta\mathfrak{M}_2 + j.$$

The last constant is the actual integral of $(U-\kappa\eta)H$. The choice of the domination tolerance and amplitude as stated gives, with $\nu_0 = 10^{-3}$,

$$\frac{\|k_0\|_\infty}{2B} \le \nu_0, \quad \frac{\|i_g\|_{C^1}}{a_{\mathrm{p}}(2B)^{1+\gamma}} \le \nu_0, \quad \frac{\|j\|_{C^1}}{a_{\mathrm{p}}(2B)^{1+\gamma}} \le \nu_0, \quad k_0 = 2(\tfrac{1}{2}-h)\eta m + d m_\eta. \tag{1.12.10}$$

Here $\|v\|_{C^1} = \max(\|v\|_\infty, \|v_\eta\|_\infty)$ on $[-1,1]$.

1.12.4 The delayed shape and its positive margin

We fix $\chi_0 \in C^\infty$, zero near $[0,2]$, one near $[4,\infty)$, with $0 \le \chi_0 \le 1$, and let $L_\chi = \sup|s\chi_0'(s)|$.

Proposition 1.12.3 (Delayed insertion and exact restoration)**.** *Assume* (1.12.10) *and a smooth shape φ on a neighborhood of $[-1,1]$ with*

$$\delta_\varphi = \|\varphi - g\|_{C^1} \le \min\left(10^{-3}, [20\max(1, L_\chi)]^{-1}\right). \tag{1.12.11}$$

We keep the full field at radii less than $2B$, and set

$$H = a_{\mathrm{p}}\left(\tfrac{\hat\xi^2}{2}\right)^\gamma [g + \chi_0(\tfrac{\hat\xi^2}{2}/B)(\varphi - g)], \quad U = \kappa\eta \quad (2B \le \tfrac{\hat\xi^2}{2} \le 4B). \tag{1.12.12}$$

We continue with $H = a_{\mathrm{p}}\left(\frac{\hat\xi^2}{2}\right)^\gamma \varphi$ afterwards. The transition has $H > 0$, $3/5 \le \mathfrak{a} \le 1$, $\mathfrak{b} = 0$, and $\widehat{\mathcal{T}}_{P,\theta} - \frac{H_{\hat\xi}}{\hat\xi} \ge .14 a_{\mathrm{p}}\left(\frac{\hat\xi^2}{2}\right)^\gamma g$. The unpatched power leg has $\widehat{\mathcal{T}}_{P,\theta} - \frac{H_{\hat\xi}}{\hat\xi} \ge .15 a_{\mathrm{p}}\left(\frac{\hat\xi^2}{2}\right)^\gamma \varphi$.

We fix $\sigma > 0$ with finite $\|P_*/\sigma^2\|_{C^1}$ and set

$$a_{\mathrm{p}} = \sigma\mathcal{R}^{-1/10}, \qquad \varepsilon = \sigma/(c_{\mathrm{a}}\mathcal{R}^{1/10}). \tag{1.12.13}$$

For sufficiently large $\mathcal{R}$, a correction supported in $(\mathcal{R}/4096, \mathcal{R}/2048)$ restores all five histories to the full-axis φ-power reference with pressure constant $-P_*$. It keeps the velocity germs unchanged, $H > 0$, and the relaxed cone. Its scaled C^1_η size tends to zero. Higher smooth norms are finite for each fixed φ. We do not infer a uniform bound on them from (1.12.11).

Proof. We let $\mathscr{Q} = \widehat{\mathcal{T}}_{P,\theta} - \frac{H_{\hat\xi}}{\hat\xi}$. The constants m, j stay unchanged when $U = \kappa\eta$. Formula (1.9.2) gives

$$\mathscr{Q} = -\frac{2H}{\hat\xi^2} + \frac{[(1+\kappa L)\frac{\hat\xi^2}{2} + k_0]H + A_I\mathfrak{M}_2 + B_I\mathfrak{M}_{2\eta} + E_j}{L\hat\xi^2}, \tag{1.12.14}$$

where

$$A_I = -1 + h - \kappa + 4\kappa h\eta^2, \quad B_I = ((\tfrac{1}{2}-h) - \kappa d)\eta, \quad E_j = -d j_\eta + 2(h - (\tfrac{1}{2}-h))\eta j.$$

Their bounds are $|A_I| \le 1.001$, $|B_I| \le .5$, $|E_j| \le 2\|j\|_{C^1}$. For $H_g = a_{\mathrm{p}}\left(\frac{\hat\xi^2}{2}\right)^\gamma g$ with zero offsets,

$$\frac{\mathscr{Q}_{\mathrm{ref},g}}{H_g} = -\tfrac{2}{\hat\xi^2} + \frac{1 + \kappa L + (A_I + B_I g_\eta/g)/(1+\gamma)}{2L} \ge -\tfrac{2}{\hat\xi^2} + \frac{1 - (1+\kappa)/(1+\gamma)}{2} \ge .16249$$

on $\frac{\hat\xi^2}{2} \ge 2B \ge 40$.

The offsets cost less than $2.30\nu_0$, so $\mathscr{Q}_g \ge .16 H_g$. On the transition,

$$\|\Delta H\|_{C^1} \le \delta_\varphi a_{\mathrm{p}}\left(\tfrac{\hat\xi^2}{2}\right)^\gamma, \qquad \|\Delta\mathfrak{M}_2\|_{C^1} \le \delta_\varphi a_{\mathrm{p}}\left(\tfrac{\hat\xi^2}{2}\right)^{1+\gamma}/(1+\gamma).$$

Subtraction of (1.12.14) gives

$$\frac{|\Delta\mathscr{Q}|}{H_g} \le \delta_\varphi\left[\frac{1}{40}+\frac{1+\kappa+\nu_0}{1.96}+\frac{1.501}{1.96(1+\gamma)}\right] < 1.1\delta_\varphi.$$

This proves the .14 margin. Radial cutoff derivatives cancel in $\mathscr{Q}$, but we must include them in

$$\mathfrak{a} = \frac{4}{5} - \frac{2(\frac{\hat\xi^2}{2}/B)\chi_0'(\frac{\hat\xi^2}{2}/B)(\varphi-g)}{g+\chi_0(\frac{\hat\xi^2}{2}/B)(\varphi-g)}, \qquad \mathfrak{b}=0.$$

The deviation from $4/5$ is at most $4L_\chi\delta_\varphi \le 1/5$.

We must measure the outlet offset against the new full-axis reference. With $\Delta=\varphi-g$,

$$i_\varphi = i_g - \frac{a_{\mathrm{p}}(2B)^{1+\gamma}}{1+\gamma}\Delta + a_{\mathrm{p}}\int_{2B}^{4B} s^\gamma[\chi_0(s/B)-1]\Delta\,\mathrm{d}s. \tag{1.12.15}$$

It obeys $\|i_\varphi\|_{C^1}/[a_{\mathrm{p}}(4B)^{1+\gamma}] \le \nu_0+\delta_\varphi/(1+\gamma)$. Also $|\varphi_\eta/\varphi - g_\eta/g| \le 4\delta_\varphi$. The new reference bound is $.16249-.64\delta_\varphi$, and the offsets cost less than $2.31\nu_0+.49\delta_\varphi$.

These leave the .15 margin. All offset ratios continue to decrease along the power leg.

The other history changes are

$$\Delta\mathfrak{M}_1=0, \qquad \Delta\mathfrak{M}_3=\kappa\eta\Delta\mathfrak{M}_2,$$
$$\Delta\mathfrak{M}_4 = -\int_{2B}^{\frac{\hat\xi^2}{2}} \frac{2H_g\Delta H+(\Delta H)^2}{4s}\,\mathrm{d}s, \qquad \Delta P = \int_{2B}^{\frac{\hat\xi^2}{2}} \frac{2H_g\Delta H+(\Delta H)^2}{4s^2}\,\mathrm{d}s. \tag{1.12.16}$$

For completeness let s_g, p_g be the constant offsets of the hypothetical g-continuation and put $\frac{\hat\xi_*^2}{2}=4B$. Then

$$s_\varphi = s_g - \frac{a_{\mathrm{p}}^2}{4}\int_{2B}^{\frac{\hat\xi_*^2}{2}} s^{2\gamma-1}[2g\chi_0(s/B)\Delta+\chi_0(s/B)^2\Delta^2]\,\mathrm{d}s + \frac{a_{\mathrm{p}}^2(\varphi^2-g^2)(\frac{\hat\xi_*^2}{2})^{2\gamma}}{8\gamma},$$
$$p_\varphi = p_g + \frac{a_{\mathrm{p}}^2}{4}\int_{2B}^{\frac{\hat\xi_*^2}{2}} s^{2\gamma-2}[2g\chi_0(s/B)\Delta+\chi_0(s/B)^2\Delta^2]\,\mathrm{d}s - \frac{a_{\mathrm{p}}^2(\varphi^2-g^2)(\frac{\hat\xi_*^2}{2})^{2\gamma-1}}{4(2\gamma-1)}.$$

The pressure subtraction is integrable at zero because $2\gamma-2=-4/5>-1$. The new full-reference offsets satisfy

$$\Delta\mathfrak{M}_1=O_B(\varepsilon^2),\quad \Delta\mathfrak{M}_2=O_B(\varepsilon),\quad \Delta\mathfrak{M}_3=\kappa\eta\Delta\mathfrak{M}_2+O_B(\varepsilon^3),\quad \Delta\mathfrak{M}_4,\Delta P=O_B(\varepsilon^2) \tag{1.12.17}$$

in C^1_η. The reference pressure keeps $-P_*$.

On $\frac{\hat\xi^2}{2}=\mathcal{R}s$, $1/4096<s<1/2048$, we write the correction as

$$H=\sigma\sqrt{\mathcal{R}}(h_0+z), \qquad U=\sigma(w_0+v), \qquad h_0=\varphi s^\gamma, \quad w_0=\kappa\eta/\sigma.$$

We select z from three fixed interior bumps and v from two. After division by

$$(\sigma\mathcal{R},\ \sigma\mathcal{R}^{3/2},\ \sigma^2\mathcal{R}^{3/2},\ \sigma^2\mathcal{R},\ \sigma^2),$$

the five history increments are

$$\left(\int v,\ \int z,\ \int(w_0z+h_0v+zv),\ \int\left(2w_0v+v^2-\frac{h_0z}{2s}-\frac{z^2}{4s}\right),\ \int\left(\frac{h_0z}{2s^2}+\frac{z^2}{4s^2}\right)\right). \tag{1.12.18}$$

Each integral is over the fixed scaled interval. We apply row operations to the zero Jacobian. This gives the two weight systems $(1, s^{-2/5}, s^{-7/5})$ and $(1, s^{3/5})$, multiplied by nonzero powers of φ.

At distinct ordered evaluation points the power matrices are invertible. For three powers, we divide by the smallest power and apply Rolle's theorem. Three positive zeros would imply two positive zeros of a nontrivial combination of two distinct powers. A nontrivial combination of two distinct powers has at most one positive zero. The determinants stay nonzero for narrow fixed bumps.

The bounds $1-\delta_\varphi \le \varphi \le 2+\delta_\varphi$ and $\|\varphi\|_{C^1} \le 3$ give uniform inverse-Jacobian and first-derivative bounds. We write the finite map as $L_\eta c + Q_\eta(c,c)$. For small target d_*, iteration $c = L_\eta^{-1}[d_* - Q_\eta(c,c)]$ contracts on a fixed ball. Differentiation of the equation gives $\|c\|_{C^1} \le C\,\|d_*\|_{C^1}$. Smooth inputs give smooth coefficients.

By (1.12.17) and (1.12.13), the normalized negative offsets tend to zero when $\mathcal{R} \to \infty$. The pressure target is $O_B(\mathcal{R}^{-1/5}/c_{\mathrm{a}}^2)$. We select $\mathcal{R}/4096 > 4B$. The corrected outlet histories then equal the reference.

Last, we include the partial histories in the cone estimate. We write $H = \sigma\sqrt{\mathcal{R}}\,\widehat{H}$, $U = \sigma\widehat{U}$, and denote by $\overline{M}, \overline{I}, \overline{J}, \overline{S}, \overline{P}$ the five histories divided by the five stated scales. We set $\overline{K} = 2(\frac{1}{2}-h)\eta\overline{M} + d\overline{M}_\eta$. The normalized stresses $\widehat{T}_\theta = \widehat{\mathcal{T}}_{P,\theta}/(\sigma\sqrt{\mathcal{R}})$ and $\widehat{T}_z = \widehat{\mathcal{T}}_{P,z}/(\sigma\sqrt{\mathcal{R}})$ are

$$\begin{aligned}
\widehat{T}_\theta &= \frac{\widehat{H}_s - \widehat{H}/s}{\mathcal{R}} + \frac{(s+\sigma\overline{K})\widehat{H} - (1-h)\overline{I} + (\frac{1}{2}-h)\eta\overline{I}_\eta - \sigma d\overline{J}_\eta + 2\sigma(h-(\frac{1}{2}-h))\eta\overline{J}}{2Ls},\\
\widehat{T}_z &= \frac{\sqrt{2s}\widehat{U}_s}{\mathcal{R}} + \frac{(s+\sigma\overline{K})\widehat{U} - (\frac{1}{2}-h)(\overline{M}-\eta\overline{M}_\eta) + \sigma(4h\eta\overline{S} - d\overline{S}_\eta) + \sigma s(4(\frac{1}{2}+h)\eta\overline{P} - d\overline{P}_\eta)}{L\sqrt{2s}}.
\end{aligned} \tag{1.12.19}$$

Also

$$\mathfrak{a} = 2 - \frac{2s\widehat{H}_s}{\widehat{H}}, \qquad \mathfrak{b} = \frac{2\sqrt{2}\,s^{3/2}\widehat{U}_s}{\widehat{H}}.$$

There is no positive power of $\mathcal{R}$. The pressure contains the fixed bounded function $-P_*/\sigma^2$. For $\mathcal{R} \ge 1$, fixed σ, and $\widehat{H}, \mathfrak{a}$ bounded away from zero, these formulas give the uniform bound

$$\|\mathfrak{G}_{\mathrm{patch}} - \mathfrak{G}_{\mathrm{base}}\|_\infty \le C\,\|d_*\|_{C^1}, \qquad \mathfrak{G} = \widehat{T}_\theta - \frac{\mathfrak{b}}{\mathfrak{a}}\widehat{T}_z - \frac{(2-\mathfrak{v})\widehat{H}}{2\mathcal{R}s}. \tag{1.12.20}$$

The constant includes the fixed bump derivative norms and the normalized partial-history bounds. The base field has $\mathfrak{a} = \mathfrak{v} = 4/5$, $\mathfrak{b} = 0$, and $\mathfrak{G}_{\mathrm{base}} \ge .15h_0$.

After we impose the finite value thresholds which keep $\widehat{H} > 0$, $\mathfrak{a} > 0$ and $\mathfrak{v} < 2$, we also impose $\|d_*\|_{C^1} \le .075 \min h_0/C$. Then (1.12.20) proves a strictly positive relaxed margin on the full correction support. □

1.12.5 The outlet interface

The profile keeps the axis core, activates genuine stress in the protected rectangle, and first introduces φ after $2B$. At the matching exit the velocity germs and all five histories equal those of the calibrated reference. The same downstream velocities give identical history densities. Integration thus keeps the equality. We correct the transition's pressure and energy costs. We do not omit them.

For example the growing reference contributes

$$\int_0^{\sqrt{2\mathcal{R}}} \frac{(\sigma\mathcal{R}^{-1/10}(\hat{\xi}/\sqrt{2})^{6/5}\varphi)^2}{4\frac{\hat{\xi}^4}{4}}\,\hat{\xi}\,\mathrm{d}\hat{\xi} = \frac{5}{4}\sigma^2\varphi^2.$$

The axis constant stays $-P_*$, rather than a newly selected constant proportional to φ^2. The outer calibration must supply (1.12.11) for its actual root. The later shear modulation must start beyond $\frac{\hat{\xi}_e^2}{2}+5\ell$ and restore those same calibrated histories. Under these explicit outer inputs, each operation does not change the active protected rectangle or its same Gevrey radius.

1.13 The actual outer connection and its heat exterior

Main result. Proposition 1.13.1 gives a scalar outer extension with exact radial moment conditions. Corollary 1.13.6 identifies its heat exterior and endpoint derivatives. These are local components of the selected joint construction.

Role in the selected connection. This section constructs scalar outer components and their actual heat/primitive estimates. Its scalar pressure-root realization is a local component, not the selected global relative pressure calibration. For that calibration use the complete actual E field, the three-row pressure-class repair, and the core five-moment correction of the selected leading construction. On the native backward domain $|\beta|\le 1$, the full target in (1.14.16) preserves the canonical datum $\Pi_0(\beta)$ of Lemma 1.8.6. Its protected forward chart collars inherit the same datum. On the intermediate forward buffer the cutoff satisfies $0<\chi_b<1$ and the change of the canonical axis pressure is $-(1-\chi_b)\Delta C_{p,f}$. We fix the two-sided heat convention by $C_{\mathrm{tr}}=2^{\frac12+h}c_{\mathrm{old}}=2^h c_{\mathrm{bank}}$, thus $c_{\mathrm{bank}}=\sqrt{2}c_{\mathrm{old}}$. The full radial jet and pressure constant proof is Lemma 1.25.10. We do not infer Gevrey–3/2 regularity of a generic complete heat pressure here.

We now supply the outer input to Proposition 1.12.3. We select the pressure shape φ by an explicit quadratic equation with the complete future. We then select the axial pulse to supply that future's energy. The two calibrations keep the histories (1.9.1) with their original axis values. We fix h as in (1.6.1) throughout this section.

Constants can depend on h and on fixed smooth templates. We state each dependence on a parameter that we select later.

Proposition 1.13.1 (Outer connection)**.** *We can select the parameters in Proposition 1.12.3 so that its actual outlet reference has a smooth extension. The profiles $H>0$ and U on $(0,\infty)\times[-1,1]$ have the next properties. A bounded axial pulse returns $\mathfrak{M}_1,\mathfrak{M}_3$ to zero. Beyond that return, $U=\mathfrak{M}_1=\mathfrak{M}_3=0$, and at a finite radius the profile is the exact heat pair*

$$\begin{aligned} H &= d^{-h}\{c_{\mathrm{bank}}g_h(\tfrac{\hat{\xi}^2}{2}/d)+k_f g_f(\tfrac{\hat{\xi}^2}{2}/d)\},\\ \mathfrak{M}_2 &= d^{1-h}\{c_{\mathrm{bank}}i_h(\tfrac{\hat{\xi}^2}{2}/d)+k_f i_f(\tfrac{\hat{\xi}^2}{2}/d)\},\\ & c_{\mathrm{bank}},k_f>0. \end{aligned} \tag{1.13.1}$$

The functions on the right have their smooth limits at $d=0$.

On the same exterior the actual remaining histories are

$$\mathfrak{M}_4=\int_{(\frac{\hat{\xi}^2}{2})}^{\infty}\frac{H(s,\eta)^2}{4s}\,\mathrm{d}s,\qquad P=-\int_{(\frac{\hat{\xi}^2}{2})}^{\infty}\frac{H(s,\eta)^2}{4s^2}\,\mathrm{d}s. \tag{1.13.2}$$

Thus, as identities of smooth functions of η,

$$\begin{gathered} \int_0^\infty U=0,\qquad \int_0^\infty UH=0,\qquad \int_0^\infty (H-c_{\mathrm{bank}}(\hat{\xi}/\sqrt{2})^{-2h})=0,\\ \int_0^\infty\left(U^2-\frac{H^2}{4\frac{\hat{\xi}^2}{2}}\right)=0,\qquad \int_0^\infty\frac{H^2}{4\frac{\hat{\xi}^4}{4}}=P_*. \end{gathered} \tag{1.13.3}$$

Unmarked integrals in this display are with respect to $\frac{\hat\xi^2}{2}$. *The growing reference, its finite axial turnoff, and the initial part of the short slope transition belong to a compact relaxed segment. Once the logarithmic slope is negative, the slow ray, pulse, and heat connection satisfy the strict faces wherever their stress is nonzero.*

The exact heat exterior has zero stress. For this scalar component proposition, the active protected rectangle of Proposition 1.12.2 does not change. In the selected connection the related assertion applies to the actual variable-core curved protected domain and its finite solved cover in paragraph 1.22. The scalar proposition is not its core or activation construction.

After this, the shear-loop construction treats the compact relaxed segment. At the end of this section we prove the restoration statement which makes that operation compatible with (1.13.3). The proposition itself does not identify the leading field with a solution of the full equations.

1.13.1 A finite reference with the actual axis pressure

We write $\gamma = 3/5$, as in Section 1.12, and recall

$$P_* = P_0 g^2, \qquad P_0 = \frac{\kappa}{4(\frac12 + h)}, \qquad g = (1 + 2(\tfrac12 + h)\kappa\eta^2)^{1/2}.$$

For the moment let φ be a smooth positive shape close to g in C^1. We determine its actual value in the pressure calibration. We take a smooth nondecreasing $\chi_{\mathrm o}$, zero through $1/4$ and one from $3/4$ onwards, with bounded derivative. We put

$$w = (\tfrac{\hat\xi^2}{2}/\mathcal R)^{1/5}, \quad k(\tfrac{\hat\xi^2}{2}) = \kappa[1 - \chi_{\mathrm o}(w)], \quad H = H_0(\tfrac{\hat\xi^2}{2})\varphi, \quad U = \eta k(\tfrac{\hat\xi^2}{2}), \quad H_0 = \sigma\mathcal R^{-1/10}(\hat\xi/\sqrt2)^{6/5}. \tag{1.13.4}$$

We use this full-axis reference only to specify the matching histories. The core supplies the actual axis before this step. Its five integrals converge at zero. The early correction of Proposition 1.12.3 lies before the turnoff and restores the next histories:

$$m_0(\tfrac{\hat\xi^2}{2}) = \int_0^{\frac{\hat\xi^2}{2}} k(s)\,\mathrm ds, \qquad e_0(\tfrac{\hat\xi^2}{2}) = \int_0^{\frac{\hat\xi^2}{2}} k(s)^2\,\mathrm ds, \qquad j_0(\tfrac{\hat\xi^2}{2}) = \int_0^{\frac{\hat\xi^2}{2}} k(s)H_0(s)\,\mathrm ds,$$

$$\mathfrak M_1 = \eta m_0, \qquad \mathfrak M_2 = \frac{\frac{\hat\xi^2}{2}H_0\varphi}{1+\gamma}, \qquad \mathfrak M_3 = \eta\varphi j_0,$$

$$\mathfrak M_4 = \eta^2 e_0 - \frac{H_0^2\varphi^2}{8\gamma}, \qquad P = -P_* + \frac54\sigma^2 w\varphi^2, \qquad \mathcal K = Lm_0. \tag{1.13.5}$$

In particular the pressure constant is $-P_*$, independently of φ.

We let n_θ, n_z denote the nondiffusive parts of (1.9.2)–(1.9.3). We set $r_0 = m_0/\frac{\hat\xi^2}{2}$, $s_0 = j_0/(\frac{\hat\xi^2}{2}H_0)$, and $z_0 = \eta\varphi_\eta/\varphi$. Substitution gives

$$\frac{2Ln_\theta}{H} = 1 + Lr_0 - \frac{1-h}{1+\gamma} + \frac{(\frac12 - h)z_0}{1+\gamma} + s_0(-1 + 4h\eta^2 - dz_0). \tag{1.13.6}$$

Here $r_0 \ge 0$ and $0 \le s_0 \le \kappa/(1+\gamma)$. For $\varphi = g$, the terms with z_0 have a nonnegative combined coefficient.

For the calibrated nearby shape, their loss is $O(\|\varphi - g\|_{C^1})$. Thus, for the small neighborhood used in this proof, $n_\theta \ge .18H$ throughout turnoff.

The normalization $\sigma^2 \asymp \kappa$ is a result of (1.13.69). On $w \geq 1/4$, direct use of (1.13.5), with the term $-P_*$, yields

$$\mathfrak{a} = \frac{4}{5}, \qquad |\mathfrak{b}| \leq C\frac{\kappa}{\sigma}, \qquad \frac{|n_z|}{H} \leq C\left(\frac{\kappa}{\sigma} + \sigma + \frac{\|P_*\|_{C^1}}{\sigma}\right) \leq C\sqrt{\kappa}. \tag{1.13.7}$$

To check that no unscaled pressure term hides here, we divide the axial numerator by $\frac{\hat{\xi}^2}{2}$: its terms have sizes $O(\kappa)$, $O(\kappa^2)$, $O(\sigma^2 w)$, and $O(\|P_*\|_{C^1})$. Also $H = \sigma\sqrt{w\frac{\hat{\xi}^2}{2}}\varphi$. The derivative bound is a result of $|\frac{1}{2}\hat{\xi}k_{\hat{\xi}}| \leq C\kappa w$.

The constants are uniform on this fixed scaled annulus for φ in the selected C^1 neighborhood. For small κ, $\mathfrak{v} < 1$. The relaxed test is

$$n_\theta - (\mathfrak{b}/\mathfrak{a})n_z > H/\tfrac{\hat{\xi}^2}{2};$$

the diffusive terms have previously canceled in this expression. Equations (1.13.6)–(1.13.7) leave a reserve $.1H$ once $\frac{\hat{\xi}^2}{2} \geq 20$.

The velocity U is identically zero on a terminal collar. We define

$$A_0 = \int_0^1 k(\mathcal{R}s)\,\mathrm{d}s, \quad A_1 = \int_0^1 k(\mathcal{R}s)s^{3/5}\,\mathrm{d}s, \quad A_2 = \int_0^1 k(\mathcal{R}s)^2\,\mathrm{d}s.$$

At $\frac{\hat{\xi}^2}{2} = \mathcal{R}$ the exact data are

$$\begin{aligned} &\mathfrak{M}_1 = \eta\mathcal{R}A_0, && \mathfrak{M}_2 = \tfrac{5}{8}\sigma\mathcal{R}^{3/2}\varphi, && \mathfrak{M}_3 = \eta\sigma\mathcal{R}^{3/2}\varphi A_1, \\ &\mathfrak{M}_4 = \mathcal{R}[\eta^2 A_2 - \tfrac{5}{24}\sigma^2\varphi^2], && P = -P_* + \tfrac{5}{4}\sigma^2\varphi^2. \end{aligned} \tag{1.13.8}$$

In particular, we keep $\mathfrak{M}_{1\eta}$ and $\mathfrak{M}_{3\eta}$ after U vanishes.

1.13.2 The slow entrance and its finite wait

We select $0 < \mu \leq h/10$. In the logarithmic variable $y = \log(\frac{\hat{\xi}^2}{2}/\mathcal{R})$, we fix a smooth slope $p(y)$. It equals $3/5$ near zero, reaches $-\mu$ after a short fixed interval, and stays between these values. We let

$$\mathfrak{h}(y) = \exp\left(\int_0^y p(v)\,\mathrm{d}v\right), \qquad H = \sigma\sqrt{\mathcal{R}}\,\mathfrak{h}(y)\varphi, \qquad U = 0.$$

We write $\frac{\hat{\xi}_s^2}{2}$ for the start of the exact $-\mu$ segment.

Its short transition keeps $\mathfrak{M}_2/(\frac{\hat{\xi}^2}{2}H) < .7$, by continuity of the scalar ratio equation. On the exact slow segment,

$$r_i = \frac{\mathfrak{M}_2}{\frac{\hat{\xi}^2}{2}H}, \qquad (r_i)_y = 1 - (1-\mu)r_i, \qquad r_i \leq \frac{1}{1-\mu}. \tag{1.13.9}$$

The ratio is independent of η. The fixed histories in (1.13.8) and (1.9.2) give

$$\frac{\widehat{\mathcal{T}}_{P,\theta}}{H} \geq c(h-\mu) - C(\kappa + \|\varphi - g\|_{C^1}) - C/\tfrac{\hat{\xi}^2}{2}. \tag{1.13.10}$$

We will impose $\|\varphi - g\|_{C^1} \ll \mu$ and $\kappa \ll h$.

All pressure estimates in this subsection are for its actual canonical value, given by the pressure equation in this subsection. The constructed future satisfies $\|P\|_{C^1} \le CH^2/\frac{\hat\xi^2}{2}$ on this interval. We integrate the decreasing separated power up to the pulse exit. The remaining integral has the stated normalized future bound. We multiply its contribution at an earlier point by $(\frac{\hat\xi^2}{2}/a_*)^{1+2\mu} \le 1$.

The energy history, before the pulse, has the exact form

$$\mathfrak{M}_4 = \eta^2 \mathcal{R} A_2 - \varphi^2 D_0(\tfrac{\hat\xi^2}{2}),$$

where D_0 is a positive scalar integral. With y measured from $\frac{\hat\xi_s^2}{2}$,

$$D_0(\tfrac{\hat\xi^2}{2})/\tfrac{\hat\xi^2}{2} \le C\kappa(1+y)e^{-y}.$$

This is a result of $1 - e^{-2\mu y} \le 2\mu y$. A saturated $1/\mu$ bound does not suffice near the entrance. The term $\mathfrak{M}_1 - \eta\mathfrak{M}_{1\eta}$ vanishes, and substitution in (1.9.3) now gives

$$|\widehat{\mathcal{T}}_{P,z}|/H \le C\sqrt{\kappa}. \tag{1.13.11}$$

The constant includes the fixed future pressure bound. The same estimate holds on the short slope transition. Its angular reserve stays bounded away from zero there. On the slow ray use $\sqrt{2\mu}C\sqrt{\kappa} \ll h$ and (1.13.10). Thus the strict faces hold when $\mathfrak{a} > 2$, and the relaxed condition holds during the earlier part of the slope change.

We fix a small tolerance ϵ_c and take

$$T_w = 4\log\frac{C}{\epsilon_c h}, \qquad \tfrac{\hat\xi_p^2}{2} = \tfrac{\hat\xi_s^2}{2}e^{T_w}, \qquad E = \frac{H}{\hat\xi}. \tag{1.13.12}$$

This is a finite choice before κ, not a wait that grows when κ tends to zero. We set $\widehat{m} = \mathfrak{M}_1/(\frac{\hat\xi^2}{2}E)$, $\widehat{j} = \mathfrak{M}_3/(\frac{\hat\xi^2}{2}HE)$, and let the subscript p indicate evaluation at $\frac{\hat\xi_p^2}{2}$. The actual inlet bounds are

$$\begin{aligned}
\|\widehat{m}_p\|_{C^1} &\le C\sqrt{\kappa}e^{-(1/2-\mu)T_w}, & \left\|\widehat{j}_p\right\|_{C^1} &\le C\sqrt{\kappa}e^{-(1/2-2\mu)T_w},\\
\left|r_i(\tfrac{\hat\xi_p^2}{2}) - \frac{1}{1-\mu}\right| &\le Ce^{-(1-\mu)T_w}, & \mu\frac{|\mathfrak{M}_{4p}|}{\frac{\hat\xi_p^2}{2}E_p^2} &\le C\mu(1+T_w)e^{2\mu T_w} + C\mu\kappa,\\
\left\|\partial_\eta \frac{\mathfrak{M}_{4p}}{\frac{\hat\xi_p^2}{2}E_p^2}\right\|_\infty &\le C\kappa e^{2\mu T_w}.
\end{aligned} \tag{1.13.13}$$

For the last line, the term $-\varphi^2 D_0/H_p^2$ is scalar. Only the normalized axial energy contributes an angular derivative. Thus we introduce no $1/\mu$ angular loss at the inlet.

1.13.3 A bounded pulse with two exact returns

We let $x = 2\log(\hat\xi/\hat\xi_p)$, $L_p = 13/\mu$, and $a_* = \frac{\hat\xi_p^2}{2}e^{L_p}$. We select a nonnegative smooth function Φ compactly supported in $(1,2)$, normalized by $\int_0^{13} e^{-2\xi}\Phi(\xi)^2\,\mathrm{d}\xi = 1/4$. We take translates γ_1, γ_2 of a fixed smooth unit-integral bump, whose supports lie in the intervals of radius $1/4$ about $L_p - 3, L_p - 1$. Throughout the pulse prescribe

$$H = H_p e^{-\mu x}, \qquad U = E\,\mathfrak{p}(x,\eta), \qquad \mathfrak{p} = Q_p(\eta)\Phi(\mu x) + c_1(\eta)\gamma_1(x) + c_2(\eta)\gamma_2(x). \tag{1.13.14}$$

The energy equation determines the amplitude Q_p only after we select the pressure shape.

First regard $Q_p \in [.9, 1.2]$ as an independent scalar parameter, and solve

$$\int_0^{L_p} e^{(1/2-\mu)x}\mathfrak{p}\,\mathrm{d}x = -\frac{\mathfrak{M}_{1p}}{\frac{\hat\xi_p^2}{2}E_p},$$
$$\int_0^{L_p} e^{(1/2-2\mu)x}\mathfrak{p}\,\mathrm{d}x = -\frac{\mathfrak{M}_{3p}}{\frac{\hat\xi_p^2}{2}H_pE_p}. \tag{1.13.15}$$

These are the actual $\mathfrak{M}_1, \mathfrak{M}_3$ return equations. We normalize row i by the exponential at L_p. The two locations differ by 2, and the two exponents differ by μ. Thus the determinant is comparable to μ, with a fixed nonzero bump-integral factor.

The main source ends at $2/\mu$, but the return sites are near $13/\mu$. Thus, the unique coefficients are affine in Q_p and satisfy

$$\sup_{.9\le Q_p\le 1.2}\left(\|c_j(Q_p,\cdot)\|_{C^1_\eta} + \|\partial_{Q_p}c_j(Q_p,\cdot)\|_{C^1_\eta}\right) \le C\mu^{-K}e^{-c/\mu}. \tag{1.13.16}$$

The derivatives in this display hold the scalar parameter fixed. After composition with the energy root $Q_p(\eta)$, the chain rule adds the factor $1+\left\|Q_p'\right\|_\infty$, which the energy-root estimate controls. Each fixed number of x or $\xi = \mu x$ derivatives has the same form with a different finite K.

We do not set an inlet history to zero. On an open collar after the second bump, $U = \mathfrak{M}_1 = \mathfrak{M}_3 = 0$.

We let the desired true energy at a_* be $\mathfrak{M}_{4a_*} = H_{a_*}^2\tau_S(\eta)$, and set $K_j = \int_0^{L_p} e^{-2\mu x}\gamma_j(x)^2\,\mathrm{d}x$. The disjoint supports in (1.13.14) give the exact equation

$$\frac{Q_p^2}{4} + \mu\sum_{j=1}^{2} K_j c_j(Q_p,\eta)^2 = \frac{1-e^{-26}}{4} - \mu\frac{\mathfrak{M}_{4p}}{\frac{\hat\xi_p^2}{2}E_p^2} + 2\mu e^{-26}\tau_S. \tag{1.13.17}$$

The last coefficient is 2 because $H_{a_*}^2 = \hat\xi_p^2E_p^2e^{-26}$. We keep the quadratic return energies. If the right side is sufficiently close to $1/4$, the left side has a unique root in $[.9, 1.2]$.

Its derivative has a positive lower bound, for example .4. Differentiation of the same equation, with no independent choice of amplitude, gives

$$\|(Q_p)_\eta\|_\infty \le C\mu\kappa e^{2\mu T_w} + C\mu e^{-26}\|(\tau_S)_\eta\|_\infty + C\mu^{-K}e^{-c/\mu}. \tag{1.13.18}$$

We compute the true τ_S in (1.13.78). In particular we do not fix it to the diagnostic value $1/(8h)$.

Lemma 1.13.2 (The full pulse cone)**.** *For the actual histories in* (1.13.14)*, suppose* $\|\varphi - g\|_{C^1} \ll \mu$*, the inlet errors in* (1.13.13) *are at most* $\epsilon_c h$*, and*

$$\|\mathfrak{M}_4\|_{C^1} \le C_S\tfrac{\hat\xi^2}{2}E^2/\mu, \qquad \|P\|_{C^1} \le C_PE^2.$$

The two strict faces hold throughout the pulse and the two return bumps if the quantities

$$\mu/h, \quad \epsilon_c, \quad \|\eta(Q_p)_\eta\|_\infty/h, \quad \sup E_p/(\mu h), \quad 1/(\tfrac{\hat\xi_p^2}{2}h)$$

are sufficiently small after the fixed template bounds.

Proof. We write $\zeta = \varphi_\eta/\varphi$, $c_\eta = (\frac{1}{2} - h)\eta\zeta$, and $q_0 = h - \mu + c_\eta$. The nearflat bounds give $q_0 \geq ch$ and $(\frac{1}{2} - h) - c_\eta > 0$, also when $\eta\varphi_\eta$ is slightly negative. The normalized histories satisfy

$$(\widehat{m})_x + (1/2 - \mu)\widehat{m} = \mathfrak{p}, \quad (\widehat{j})_x + (1/2 - 2\mu)\widehat{j} = \mathfrak{p}, \quad (r_i)_x + (1 - \mu)r_i = 1. \tag{1.13.19}$$

With $\beta_p = 1/2 - \mu$, two integrations of the positive exponential kernel give

$$\widehat{m} = \frac{\mathfrak{p}}{\beta_p} - \frac{\mu\mathfrak{p}_\xi}{\beta_p^2} + O(\mu^2) + \widehat{m}_p e^{-\beta_p x}.$$

There are no boundary source terms at zero because the pulse is zero on its inlet germ. The same expansion holds after one eta derivative. The return derivatives satisfy (1.13.16).

We divide each nondiffusive stress by $H/(2L)$. The principal angular term is $q_0/(1-\mu) + O(\epsilon_c h)$. Its remaining history contribution is

$$E[2(\tfrac{1}{2} - h)\eta\widehat{m} + d(\widehat{m}_\eta + \zeta\widehat{m}) - d(\widehat{j}_\eta + 2\zeta\widehat{j}) + 2(h - (\tfrac{1}{2} - h))\eta\widehat{j}].$$

The linear axial term is $\mathfrak{p} - ((\frac{1}{2} - h) - c_\eta)\widehat{m} + (\frac{1}{2} - h)\eta\widehat{m}_\eta$. The nonlinear remainder is

$$\frac{\mathcal{K}U + 4h\eta\mathfrak{M}_4 - d\mathfrak{M}_{4\eta} + \frac{\hat{\xi}^2}{2}((2 + 4h)\eta P - dP_\eta)}{\frac{\hat{\xi}^2}{2}E}.$$

It has size $O(E/\mu)$. The formulas include the full energy and pressure derivatives. Radial diffusion contributes $O(1/\frac{\hat{\xi}^2}{2})$ in these units. Thus, for $z = \widehat{\mathcal{T}}_{P,z}/\widehat{\mathcal{T}}_{P,\theta}$,

$$\begin{aligned} z &= \frac{1 - \mu}{\beta_p}\mathfrak{p} + K_\eta\mathfrak{p}_\xi + \mathcal{E}, \\ K_\eta &= \frac{\mu((\frac{1}{2} - h) - c_\eta)(1 - \mu)}{\beta_p^2 q_0}, \qquad 0 \leq K_\eta \leq C\mu/h, \\ \|\mathcal{E}\|_\infty &\leq C\left(\epsilon_c + \frac{\mu^2}{h} + \frac{\|\eta(Q_p)_\eta\|_\infty}{h} + \frac{\sup E_p}{\mu h} + \frac{1}{\frac{\hat{\xi}_p^2}{2}h}\right). \end{aligned} \tag{1.13.20}$$

The angular denominator stays positive.

Its perturbation is less than a fixed fraction of q_0 under the same conditions. The exact shears are $\mathfrak{a} = 2 + 2\mu$ and $\mathfrak{b} = 2\mu\mathfrak{p}_\xi - (1 + 2\mu)\mathfrak{p}$. For $\widehat{\mathcal{T}}_{P,\theta} > 0$, the two faces are equivalent to

$$\mathfrak{a} - \mathfrak{b}z > 0, \qquad 2\mathfrak{b}z + \mathfrak{b}^2/\mathfrak{a} + (\mathfrak{a} - 2)z^2 < 2.$$

When the displayed small quantities decrease, the first left side tends to $2 + 2\mathfrak{p}^2$. The second left side tends to $-7\mathfrak{p}^2/2$.

The convergence bounds apply to the full pulse. The template and its derivatives stay bounded, so the two tests keep a fixed favorable margin, also where $\mathfrak{p} = 0$.

□

We now verify the hypotheses on $\mathfrak{M}_4, P$. Integration of the pulse densities and (1.13.13) gives $\|\mathfrak{M}_4\|_{C^1} \leq C\frac{\hat{\xi}_p^2}{2}E_p^2/\mu \leq Ce^{26}\frac{\hat{\xi}^2}{2}E^2/\mu$, The pressure bound is a result of the same future that enters its root equation. We include the fixed factor e^{26} before we select κ.

1.13.4 Scalarization of the velocity and its primitive

At a_*, we write $H = G_0\varphi$, $\mathfrak{M}_2 = \varphi i_a$, and $r_a = i_a/(a_*G_0)$. The ratio equation approaches its equilibrium through smaller values, so

$$\frac{1}{1-\mu} - \epsilon_r h \le r_a \le \frac{1}{1-\mu}. \tag{1.13.21}$$

This ratio and G_0 depend on the specified radial template, not on Q_p. We return $U, \mathfrak{M}_1, \mathfrak{M}_3$ to zero. On $[a_*, 2a_*]$, we let $H_{\mathrm{sc}}(\frac{\hat\xi^2}{2}) = G_0(\frac{\hat\xi^2}{2}/a_*)^{-\mu}$.

We select smooth functions $\chi_{\mathrm{sc}}, \beta_{\mathrm{sc}}$ of $\frac{\hat\xi^2}{2}/a_*$, with $\chi_{\mathrm{sc}} = 0$ near 1, $\chi_{\mathrm{sc}} = 1$ near 2, and a nonzero nonnegative bump β_{sc} supported in $(1,2)$. We define

$$D_{\mathrm{sc}} = \frac{i_a + \int_{\sqrt{2a_*}}^{2\sqrt{a_*}} H_{\mathrm{sc}}(1-\chi_{\mathrm{sc}})\,\hat\xi\,\mathrm{d}\hat\xi}{\int_{\sqrt{2a_*}}^{2\sqrt{a_*}} H_{\mathrm{sc}}\beta_{\mathrm{sc}}\,\hat\xi\,\mathrm{d}\hat\xi}, \qquad \psi_{\mathrm{sc}} = 1 - \chi_{\mathrm{sc}} - D_{\mathrm{sc}}\beta_{\mathrm{sc}}, \tag{1.13.22}$$

$$i(\tfrac{\hat\xi^2}{2}) = i_a + \int_{a_*}^{\frac{\hat\xi^2}{2}} H_{\mathrm{sc}}(s)\,\mathrm{d}s, \qquad j(\tfrac{\hat\xi^2}{2}) = i_a + \int_{a_*}^{\frac{\hat\xi^2}{2}} H_{\mathrm{sc}}(s)\psi_{\mathrm{sc}}(s)\,\mathrm{d}s,$$
$$H = H_{\mathrm{sc}}[1 + (\varphi-1)\psi_{\mathrm{sc}}], \qquad \mathfrak{M}_2 = i + (\varphi-1)j. \tag{1.13.23}$$

The coefficient and each fixed scaled derivative of ψ_{sc} have one bound for all ratios in (1.13.21). Its weighted integral is $\int H_{\mathrm{sc}}\psi_{\mathrm{sc}} = -i_a$. Thus $j = \psi_{\mathrm{sc}} = 0$ on an open outlet germ: H and $\mathfrak{M}_2$, with all jets, have become scalar.

On the inlet germ the pair is $(\varphi H_{\mathrm{sc}}, \varphi i)$. In particular $\frac{\mathfrak{M}_{2\hat\xi}}{\hat\xi} = H$ everywhere, with its actual inlet value.

We put $\delta_0 = \|\varphi - 1\|_{C^1}$. If $\delta_0 \ll \mu$, the logarithmic decay rate of H is $\mu + O(\delta_0) > 0$. The scalar ratio satisfies $i/(\frac{\hat\xi^2}{2}H_{\mathrm{sc}}) \le 1/(1-\mu)$, so

$$\tfrac{\hat\xi^2}{2}H_{\mathrm{sc}} - (1-h)i \ge \frac{h-\mu}{1-\mu}\tfrac{\hat\xi^2}{2}H_{\mathrm{sc}}.$$

The angular terms in (1.13.23) cost at most $C\delta_0\frac{\hat\xi^2}{2}H_{\mathrm{sc}}$. For large a_*,

$$\widehat{\mathcal{T}}_{P,\theta} \ge chH, \qquad \mathfrak{a} - 2 \asymp \mu. \tag{1.13.24}$$

The future constructed in this section has canonical estimates $\|\mathfrak{M}_4\|_{C^1} \le C_*G_0^2/h$ and $\|P\|_{C^1} \le C_*G_0^2/a_*$ here. Thus

$$|\widehat{\mathcal{T}}_{P,z}| \le C_*G_0^2/(h\sqrt{a_*}).$$

The strict faces hold if $C_*(G_0/\sqrt{a_*})\sqrt{\mu}/h^2$ is sufficiently small. This is an amplitude requirement, independent of the last radial limit. We verify the future estimates before we use this conclusion.

1.13.5 A scalar power segment with a controlled primitive deficit

For a scalar decreasing H with $\frac{\mathfrak{M}_{2\hat\xi}}{\hat\xi} = H$, we put $\lambda = -\frac{1}{2}\hat\xi H_{\hat\xi}/H$ and

$$w_d = \tfrac{\hat\xi^2}{2}\left(\frac{1}{1-h} - \frac{\mathfrak{M}_2}{\frac{\hat\xi^2}{2}H}\right). \tag{1.13.25}$$

On $\frac{\hat\xi^2}{2} \ge 2a_*$, differentiation and (1.9.2) give

$$(\hat\xi^{-1}\partial_{\hat\xi}(w_d)) = \lambda w_d/\tfrac{\hat\xi^2}{2} + \frac{h-\lambda}{1-h}, \qquad \widehat{\mathcal{T}}_{P,\theta} = \frac{2H}{\hat\xi^2}\left[\frac{(1-h)w_d}{2L} - (1+\lambda)\right]. \tag{1.13.26}$$

The full-eta stress includes the factor L. At $2a_*$, $w_d \asymp ha_*$, by (1.13.21). We increase λ smoothly from μ to $2h$ on a sufficiently short fixed fractional interval.

Then $0 < w_d/\frac{\hat\xi^2}{2} \le 2h$ still holds. On the $2h$ leg,

$$-1.011h \le (\hat\xi^{-1}\partial_{\hat\xi}(w_d)) = 2hw_d/\tfrac{\hat\xi^2}{2} - h/(1-h) \le -.96h.$$

The deficit reaches $4h(2a_*)^{4/5}$ at a radius bounded by a fixed multiple of a_*. There change λ smoothly from $2h$ to h over length $\epsilon_t(2a_*)^{4/5}$, with fixed small $\epsilon_t > 0$. Equation (1.13.26) keeps w_d between fixed positive multiples of $ha_*^{4/5}$.

End on an open h-power germ at radius R_b, with amplitude G. Then

$$H_b(\tfrac{\hat\xi^2}{2}) = G(\tfrac{\hat\xi^2}{2}/R_b)^{-h}, \quad \mathfrak{M}_{2b}(\hat\xi) = \frac{\frac{\hat\xi^2}{2}H_b(\frac{\hat\xi^2}{2})}{1-h} - C_b, \quad C_b = Gw_d(R_b) \asymp hGR_b^{4/5}. \tag{1.13.27}$$

The comparisons

$$2a_* \le R_b \le C_h a_*, \qquad c_h G_0 \le G \le C_h G_0 \tag{1.13.28}$$

are uniform for $0 < \mu \le h/10$ and the inlet ratio range. The amplitude bounds are a result of integration of the bounded logarithmic slope over this bounded radius ratio. We do not select a downstream power-segment parameter independently of this actual drive.

The axial estimate on the late drive must use its shrinking reserve. We continue the scalar drive by its exact h-power and denote its canonical tails by $\mathfrak{M}_{4\mathrm{ref}}, P_{\mathrm{ref}}$. Integration by parts gives

$$h\mathfrak{M}_{4\mathrm{ref}} + (\tfrac12 + h)\tfrac{\hat\xi^2}{2}P_{\mathrm{ref}} = -\frac14\int_{(\frac{\hat\xi^2}{2})}^{\infty}(\lambda(s)-h)H(s)^2\frac{s-\frac{\hat\xi^2}{2}}{s^2}\,\mathrm{d}s. \tag{1.13.29}$$

Indeed,

$$\frac{\mathrm{d}}{\mathrm{d}s}\left[H^2\frac{s-\frac{\hat\xi^2}{2}}{s}\right] = -2H^2\left(\frac{h}{s} - \frac{(\frac12+h)\frac{\hat\xi^2}{2}}{s^2}\right) - 2(\lambda-h)H^2\frac{s-\frac{\hat\xi^2}{2}}{s^2},$$

and the two boundary terms vanish. After the initial slope transition, $0 \le \lambda - h \le h$ and $R_b - \frac{\hat\xi^2}{2} \le Cw_d(\frac{\hat\xi^2}{2})/h$.

Thus

$$|h\mathfrak{M}_{4\mathrm{ref}} + (\tfrac12+h)\tfrac{\hat\xi^2}{2}P_{\mathrm{ref}}| \le CH(\tfrac{\hat\xi^2}{2})^2 w_d(\tfrac{\hat\xi^2}{2})^2/(h\tfrac{\hat\xi^4}{4}) \le CH(\tfrac{\hat\xi^2}{2})^2 w_d(\tfrac{\hat\xi^2}{2})/\tfrac{\hat\xi^2}{2}.$$

On the initial transition $w_d \asymp h\frac{\hat\xi^2}{2}$, and the direct bound ChH^2 gives the same conclusion. This gives

$$|\mathcal{T}_{z,\mathrm{ref}}|/\widehat{\mathcal{T}}_{P,\theta} \le CH/(\hat\xi/\sqrt{2}). \tag{1.13.30}$$

Suppose the true outer future satisfies, relative to the h-power tails,

$$\|\Delta\mathfrak{M}_{4b}\|_{C^1} \le C_* GC_b/R_b, \qquad \|\Delta P_b\|_{C^1} \le C_* GC_b/R_b^2. \tag{1.13.31}$$

On the drive these are the same functions of η, constant in radius.

Their exact extra axial numerator is

$$4h\eta\Delta\mathfrak{M}_{4b} - d(\Delta\mathfrak{M}_{4b})_\eta + \tfrac{\hat\xi^2}{2}[(2+4h)\eta\Delta P_b - d(\Delta P_b)_\eta].$$

Because the smallest angular reserve is cC_b/R_b, their stress ratio is at most $C_*G/\sqrt{R_b}$. Together with (1.13.30) this proves the drive cone when the actual future supplies (1.13.31).

1.13.6 The regular and fast heat modes

The scalar heat system, with its actual primitive, is

$$i' = g_*, \qquad g_*' = -(1/2 - 1/x)g_* + (1-h)i/(2x). \tag{1.13.32}$$

Here g_* is a temporary scalar velocity, distinct from the analytic angular shape g. It solves $2xg_*'' + xg_*' + hg_* = 0$.

Lemma 1.13.3 (Heat basis and differentiated asymptotics)**.** *There are positive velocities g_h, g_f, with canonical primitives $i_h > 0$, $i_f < 0$, that solve (1.13.32). They satisfy*

$$\begin{aligned} g_h(x) &= x^{-h}[1 + 2h(1+h)/x + O_h(x^{-2})], \\ i_h(x) &= x^{1-h}/(1-h) - 2(1+h)x^{-h} + O_h(x^{-h-1}), \end{aligned} \tag{1.13.33}$$

$$g_f(x) = 2x^h e^{-x/2}[1 + O_h(x^{-1})], \qquad i_f/g_f = -2 + O_h(x^{-1}), \qquad g_f'/g_f = -1/2 + O_h(x^{-1}). \tag{1.13.34}$$

We can differentiate the expansions to each fixed order. More, for each N and j,

$$g_h = x^{-h}\sum_{n=0}^{N} a_n x^{-n} + r_N, \quad a_n = \frac{2^n (h)_n (h+1)_n}{n!}, \quad |r_N^{(j)}(x)| \le C_{N,j,h} x^{-h-N-1-j}. \tag{1.13.35}$$

Proof. The explicit formulas are

$$\begin{aligned} g_h(x) &= \frac{x}{2^{1+h}\Gamma(1+h)} \int_0^1 e^{-xt/2} t^h (1-t)^{-h}\, \mathrm{d}t, & i_h(x) &= \int_0^x g_h(t)\, \mathrm{d}t, \\ g_f(x) &= g_h(x) \int_x^\infty \frac{e^{-t/2}}{g_h(t)^2}\, \mathrm{d}t, & i_f(x) &= -\int_x^\infty g_f(t)\, \mathrm{d}t. \end{aligned} \tag{1.13.36}$$

The first integral is positive and converges because $0 < h < 1$. Differentiation and integration by parts verify the second-order equation. For any solution of that equation,

$$\left[\frac{2xg_*' + (x-2)g_*}{1-h}\right]' = g_*.$$

For g_h this bracket tends to zero at the axis, and for g_f it tends to zero at infinity. It thus equals the related primitive in (1.13.36).

The fast formula is reduction of order for $g_*'' + g_*'/2 + hg_*/(2x) = 0$.

To prove (1.13.35), split the first integral with a smooth cutoff supported near t=0. Away from zero all x derivatives are exponentially small, with the integrable endpoint t=1. Near zero, Taylor's formula for $(1-t)^{-h}$, with remainder of order t^{N+1}, gives the coefficients after integration against $e^{-xt/2}t^h$. Each x derivative adds the related power of t and improves the remainder by one power of x. Differentiation of the prefactor gives the same bound.

The primitive expansion is a result of its exact bracket formula. Integration by parts in the fast integral then proves (1.13.34) and its derivative bounds. The primitive signs are a direct result of (1.13.36). □

The Wronskian in these conventions satisfies

$$W_+ = i_h g_f - i_f g_h > 0, \qquad W_+' = (1/x - 1/2)W_+. \tag{1.13.37}$$

Its sign is a result of the four signs in the lemma.

1.13.7 Positive shooting to the exact regular coefficient

The power segment (1.13.27) supplies an actual open inlet germ. In this subsection the functions are scalar. We take the full angular lift after shooting. We put $c_{\mathrm{bank}} = GR_b^h$, $\ell_b = R_b^{4/5}$, $W_s = \epsilon_s R_b$, and $b_s = R_b + W_s$, where $\epsilon_s > 0$ is a fixed small fraction. The scalar power-segment stress is

$$\tau_b(x) = \frac{(1-h)C_b}{2x} - \frac{(1+h)H_b(x)}{x} > 0 \quad (R_b \le x \le b_s)$$

for large R_b.

With $\vartheta(u) = e^{-1/u^2}$ for $u > 0$, zero for nonpositive arguments, we select the specific scalar templates

$$\chi_s(s) = \frac{\vartheta(1/2 - s)}{\vartheta(1/2 - s) + \vartheta(s - 1/4)}, \qquad \psi_s(s) = c_s \vartheta(s - 1/4)\vartheta(3/4 - s), \qquad \int_0^1 \psi_s = 1. \quad (1.13.38)$$

Thus $\chi_s = 1$ through $1/4$, positive until $1/2$, and zero thereafter, while $\psi_s > 0$ on $(1/4, 3/4)$. The second template is decreasing for $s > 1/2$. This additional choice will be useful for the outward weighted tails in the slow expansion.

Lemma 1.13.4 (Actual scalar shot)**.** *For sufficiently small ϵ_s and then sufficiently large R_b, there is a nonnegative source τ_s. It equals τ_b on the inlet germ and zero on an outlet germ. Its actual solution of*

$$i' = g_*, \qquad g_*' = -(1/2 - 1/x)g_* + (1-h)i/(2x) + \tau_s \quad (1.13.39)$$

starts from $(H_b, \mathfrak{M}_{2b})$ and ends in $(c_{\mathrm{bank}} g_h + k_f g_f, c_{\mathrm{bank}} i_h + k_f i_f)$, with $k_f > 0$. On the source interval,

$$|g_* - H_b| \le CC_b/W_s, \qquad |g_*' - H_b'| \le CC_b/W_s^2, \qquad -g_*' \asymp hG/R_b. \quad (1.13.40)$$

On $s = (x - R_b)/W_s \in [1/2, 3/5]$,

$$i - \mathfrak{M}_{2b} \ge cC_b, \qquad \tau_s \ge cC_b/W_s. \quad (1.13.41)$$

The selected fast exposure at b_s satisfies

$$F_b := k_f g_f(b_s) \le C\left[\frac{C_b}{R_b} e^{-W_s/3} + \frac{C_b}{W_s} e^{-W_s/12}\right]. \quad (1.13.42)$$

All endpoint matching holds on open germs.

Proof. We decompose the actual inlet pair in the heat basis at R_b, with coefficients c_0, k_0. The mode expansions give

$$\begin{aligned} D_c := c_{\mathrm{bank}} - c_0 &= (1-h)C_b R_b^{h-1}[1 + O_h(G/C_b + R_b^{-1})] > 0, \\ k_0 W_+(R_b) &= g_h(R_b)[C_b - 2(1+h)G/(1-h) + O_h(G/R_b)] > 0. \end{aligned} \quad (1.13.43)$$

Also $D_c/c_{\mathrm{bank}} = O(C_b/(GR_b)) = o(1)$, so $c_0 > 0$. Variation of constants gives

$$\begin{aligned} &c' = w_s \tau_s, \quad k' = v_s \tau_s, \qquad w_s = -i_f/W_+ > 0, \quad v_s = i_h/W_+ > 0, \\ &w_s = 2(1-h)x^{h-1}[1 + O_h(x^{-1})]. \end{aligned} \quad (1.13.44)$$

We prescribe

$$\tau_s(x) = \chi_s(s)\tau_b(x) + \lambda_s(C_b/W_s)\psi_s(s).$$

We set

$$B_0 = \int_{R_b}^{b_s} w_s \chi_s \tau_b \, \mathrm{d}x, \qquad B_1 = \frac{C_b}{W_s} \int_{R_b}^{b_s} w_s \psi_s \, \mathrm{d}x.$$

The exact choice

$$\lambda_s = (D_c - B_0)/B_1 = \tfrac{1}{2} + O_h(\epsilon_s + G/C_b + R_b^{-1}) \tag{1.13.45}$$

lies in $[1/4, 3/4]$ after the stated choices. Indeed, $B_0/D_c = O(W_s/R_b)$ and $B_1 = 2(1-h)C_b R_b^{h-1}[1 + O_h(\epsilon_s + R_b^{-1})] > 0$. Thus, $c(b_s) = c_{\mathrm{bank}}$ and $k(b_s) \geq k_0 > 0$.

The two modal coefficients stay positive, so $g_* > 0$.

The derivative estimate uses the actual source width. We set $y = g_* - H_b$, $z = i - \mathfrak{M}_{2b}$, $q_s = \tau_s - \tau_b$, $a_s = 1/2 - 1/x$, and $\beta_s = (1-h)/(2x)$. These are temporary ODE coefficients, not the shear variables. Then

$$y' = -a_s y + \beta_s z + q_s, \qquad z' = y, \qquad y(R_b) = z(R_b) = 0. \tag{1.13.46}$$

We have $a_s \geq 1/3$, $\|q_s\|_\infty \leq C C_b/W_s$, and $\|q_s'\|_\infty \leq C C_b/W_s^2$.

Stable convolution gives

$$\|y\|_\infty \leq 3[\|q_s\|_\infty + C(W_s/R_b)\,\|y\|_\infty].$$

For fixed small ϵ_s, we absorb this term and get $\|y\|_\infty \leq C C_b/W_s$, $\|z\|_\infty \leq C C_b$. The differentiated equation for $p_s = y'$ is

$$p_s' = -a_s p_s + (\beta_s - a_s')y + \beta_s' z + q_s', \qquad p_s(R_b) = 0.$$

A second convolution bounds its supremum by $C[C_b/(R_b W_s) + C_b/R_b^2 + C_b/W_s^2]$. This proves (1.13.40).

The error relative to hG/R_b is $O(\epsilon_s^{-2} R_b^{-1/5})$.

Integration of (1.13.46) gives

$$z(x) = 2\int_{R_b}^{x} \tau_s - 2\int_{R_b}^{x} \tau_b - 2y(x) + 2\int_{R_b}^{x} \frac{y(t)}{t}\,\mathrm{d}t + (1-h)\int_{R_b}^{x} \frac{z(t)}{t}\,\mathrm{d}t.$$

Thus

$$z(R_b + sW_s) = 2\lambda_s C_b \int_0^s \psi_s + O(C_b \epsilon_s + C_b/W_s).$$

The positive lower bounds for the bump and its accumulated integral on the plateau yield (1.13.41). The formula includes the power segment-source subtraction.

At large x, $v_s \leq C/g_f$ and $g_f(b_s)/g_f(x) \leq C e^{-(b_s - x)/3}$. The initial fast exposure is $O(C_b/R_b)$, and the source ends by $R_b + 3W_s/4$. Integration of (1.13.44) yields (1.13.42). On the remaining open interval the solution is homogeneous. Uniqueness gives all matching jets.

Its future stays decreasing by the regular slope and the exponentially suppressed fast slope. □

1.13.8 The full angular lift and a positive primitive bridge

For the actual trajectory of Lemma 1.13.4, we put

$$\mathfrak{M}_{2L}(\hat{\xi}, \eta) = d^{1-h} i(\tfrac{\hat{\xi}^2}{2}/d), \qquad H_L(\tfrac{\hat{\xi}^2}{2}, \eta) = d^{-h} g_*(\tfrac{\hat{\xi}^2}{2}/d), \qquad \tfrac{\hat{\xi}^2}{2} \geq R_b. \tag{1.13.47}$$

The endpoint argument in this proof justifies the interpretation at d=0. In the zero-$U, \mathfrak{M}_1, \mathfrak{M}_3$ region the exact primitive operator is

$$\mathcal{A}I = (\frac{I_{\hat{\xi}\hat{\xi}}}{\hat{\xi}^2} - \frac{I_{\hat{\xi}}}{\hat{\xi}^3}) + (1/(2L) - 1/\frac{\hat{\xi}^2}{2})\frac{I_{\hat{\xi}}}{\hat{\xi}} - (1-h)I/(L\hat{\xi}^2) + (\tfrac{1}{2} - h)\eta I_\eta/(L\hat{\xi}^2). \tag{1.13.48}$$

Substitution, without replacement of the trajectory by its terminal heat formula, gives

$$\mathcal{T}_{\theta,L} = \mathcal{A}\mathfrak{M}_{2L} = d^{-h-1}\tau_s(\tfrac{\hat{\xi}^2}{2}/d) \geq 0. \tag{1.13.49}$$

Also $N_s = xg_* - (1-h)i$ satisfies

$$N_s' = (1+h)g_* - N_s/2 + x\tau_s, \qquad N_s(R_b) = (1-h)C_b > 0.$$

Thus $i(x)/x^{1-h}$ is increasing. Its exact limit is $c_{\mathrm{bank}}/(1-h)$, so

$$i(\tfrac{\hat{\xi}^2}{2}) \leq \mathfrak{M}_{2L}(\hat{\xi}, \eta) \leq c_{\mathrm{bank}}(\tfrac{\hat{\xi}^2}{2})^{1-h}/(1-h), \qquad (\mathfrak{M}_{2L})_\eta = 2\eta d^{-h} N_s(\tfrac{\hat{\xi}^2}{2}/d). \tag{1.13.50}$$

On $\frac{\hat{\xi}^2}{2} \asymp R_b$, the source estimates and heat estimates yield

$$|H_L - H_b| \leq CC_b/R_b, \quad |(\hat{\xi}^{-1}\partial_{\hat{\xi}}(H_L)) - H_b'| \leq CC_b/R_b^2, \quad |(\mathfrak{M}_{2L})_\eta| \leq CC_b. \tag{1.13.51}$$

For the non-heat part, $\frac{\hat{\xi}^2}{2}/d \leq b_s$ forces $d \geq R_b/b_s$. For the other part, apply the regular asymptotics and the fast exposure (1.13.42).

This split is important: we never extrapolate the outlet fast mode backwards through the scalar source.

We select $\eta_0 > 0$ with $\eta_0^2 \leq \epsilon_s/1000$. The interval

$$J \Subset R_b + [.52, .54]W_s$$

can be fixed with length $c_J\epsilon_s R_b$ so that, for $|\eta| \leq 2\eta_0$, its sampled scalar argument lies in the plateau (1.13.41). We let ψ_o be smooth and even, zero for $|\eta| \leq \eta_0$, one for $|\eta| \geq 2\eta_0$, and increasing with $|\eta|$. We define

$$k_o = ((\tfrac{1}{2} - h)\eta_0^2)^{-1}, \qquad \mathcal{B}_o(\eta) = B_o e^{k_o\eta^2}, \quad B_o \geq b_s, \qquad \mathcal{B}_{\max} = \max_{[-1,1]} \mathcal{B}_o. \tag{1.13.52}$$

Here B_o/R_b is fixed.

Thus $\mathcal{B}_{\max}/R_b$, though possibly very large, is a fixed geometric constant. On the support of ψ_o, $(\frac{1}{2} - h)\eta\mathcal{B}_o' \geq 2\mathcal{B}_o$.

We take the smooth convex primitive

$$\mathcal{F}(y) = \begin{cases} \int_0^y e^{-1/v^2}\,\mathrm{d}v, & y > 0, \\ 0, & y \leq 0, \end{cases} \qquad \alpha_o = \epsilon_o hG/R_b,$$

where we select $\epsilon_o > 0$ after the geometry. We put

$$E_o = \alpha_o\ell_b^2\mathcal{F}((\mathcal{B}_o - \tfrac{\hat{\xi}^2}{2})/\ell_b), \quad \mathfrak{M}_{2T} = \mathfrak{M}_{2L} + \psi_o E_o, \quad H_T = H_L - \psi_o\alpha_o\ell_b\mathcal{F}'. \tag{1.13.53}$$

All arguments of $\mathcal{F}$ in this subsection are $(\mathcal{B}_o - \frac{\hat{\xi}^2}{2})/\ell_b$. The elementary inequalities $\mathcal{F}'' \geq 0$, $\mathcal{F} \leq y\mathcal{F}'$, and the edge inequality give, directly from (1.13.48),

$$\begin{aligned} \mathcal{A}E_o &= \alpha_o \mathcal{F}'' + \frac{\alpha_o \ell_b}{\frac{\hat{\xi}^2}{2}} \mathcal{F}' + \frac{\alpha_o \ell_b}{L\hat{\xi}^2}[((\tfrac{1}{2} - h)\eta \mathcal{B}_o' - \tfrac{\hat{\xi}^2}{2})\mathcal{F}' - (1-h)\ell_b \mathcal{F}] \\ &\geq \alpha_o \ell_b \mathcal{F}'/(2L). \end{aligned} \tag{1.13.54}$$

In addition,

$$\mathcal{T}_{\theta,T} = \mathcal{T}_{\theta,L} + \psi_o \mathcal{A}E_o + (\tfrac{1}{2} - h)\eta \psi_o' E_o/(L\hat{\xi}^2).$$

Each added term is nonnegative. The scalar source gives the bound at central angles on J. The wing gives the bound on $|\eta| \geq 2\eta_0$. Thus

$$\mathcal{T}_{\theta,T} \geq c\epsilon_o C_b/R_b \quad \text{on } J \times [-1,1]. \tag{1.13.55}$$

In the wing part, y is large on J for large R_b, so $\mathcal{F}'$ has a positive lower bound there.

We let $\Delta = \mathfrak{M}_{2T} - \mathfrak{M}_{2b}$. On J,

$$cC_b \leq \Delta \leq CC_b, \qquad |\frac{\Delta_{\hat{\xi}}}{\hat{\xi}}| \leq CC_b/R_b, \qquad |\Delta_\eta| \leq CC_b. \tag{1.13.56}$$

The lower bound uses (1.13.41) and (1.13.50). For the upper bound, $\mathfrak{M}_{2L} - \mathfrak{M}_{2b} \leq C_b$ and $E_o \leq \alpha_o \ell_b \mathcal{B}_o \leq C\epsilon_o C_b$. The derivative bounds are a result of (1.13.51) and the fixed edge geometry.

We select an increasing radial cutoff χ_b on J, constant near its endpoints, and define

$$\mathfrak{M}_2 = (1-\chi_b)\mathfrak{M}_{2b} + \chi_b \mathfrak{M}_{2T}, \qquad H = (1-\chi_b)H_b + \chi_b H_T + \chi_b' \Delta. \tag{1.13.57}$$

We use the power segment before J and the target after J. The primitive is actual, and the two endpoint germs match. The full product rule is

$$\widehat{\mathcal{T}}_{P,\theta} = (1-\chi_b)\mathcal{T}_{\theta,b} + \chi_b \mathcal{T}_{\theta,T} + 2\chi_b' \frac{\Delta_{\hat{\xi}}}{\hat{\xi}} + [\chi_b'' + (1/(2L) - 1/\tfrac{\hat{\xi}^2}{2})\chi_b']\Delta. \tag{1.13.58}$$

The term $\chi_b' \Delta/(2L)$ is favorable.

All adverse terms are $O(C_b/R_b^2)$. The two base stresses have reserve $c\epsilon_o C_b/R_b$. Thus the lower bound holds on the full join interval. The exact slope is

$$\frac{H_{\hat{\xi}}}{\hat{\xi}} = (1-\chi_b)H_b' + \chi_b H_T' + 2\chi_b' \frac{\Delta_{\hat{\xi}}}{\hat{\xi}} + \chi_b'' \Delta.$$

Its cutoff error relative to hG/R_b is $O(R_b^{-1/5})$.

We select ϵ_o so that $\epsilon_o \sup \mathcal{F}''$ is small relative to $(\mathcal{B}_{\max}/R_b)^{-1-h}$. This controls the positive slope correction in H_T'. Then, we enlarge R_b. We get

$$H > 0, \qquad 2 + c_h \leq \mathfrak{a} \leq 2 + C_h, \qquad \mathfrak{b} = 0 \tag{1.13.59}$$

through the bridge and target, with $c_h > 0$. The wing amplitude relative to H_L is small by the same choices.

1.13.9 Endpoint regularity and the full canonical tail estimates

We now prove (1.13.31) for the field just constructed. First, the canonical tails of the actual lifted scalar trajectory satisfy

$$\mathfrak{M}_{4L} = d^{-2h} S_s(\tfrac{\hat\xi^2}{2}/d), \qquad P_L = d^{-2h-1} P_s(\tfrac{\hat\xi^2}{2}/d),$$

where $S_s = \int_x^\infty g_*^2/(4s)$ and $P_s = -\int_x^\infty g_*^2/(4s^2)$. Their derivatives give the exact cancellation

$$4h\eta\mathfrak{M}_{4L} - d(\mathfrak{M}_{4L})_\eta = \eta H_L^2/2, \qquad (2+4h)\eta\tfrac{\hat\xi^2}{2} P_L - d\tfrac{\hat\xi^2}{2}(P_L)_\eta = -\eta H_L^2/2. \tag{1.13.60}$$

Thus $\mathcal{T}_{z,L} = 0$ throughout the lift, with its forced part.

Lemma 1.13.5 (Whole-future tails)**.** *The actual future from* (1.13.57)*, followed by* (1.13.53) *and its selected heat pair, satisfies*

$$\int_{\sqrt{2R_b}}^\infty |H - H_b|\,\hat\xi\,\mathrm{d}\hat\xi + \int_{\sqrt{2R_b}}^\infty |H_\eta|\,\hat\xi\,\mathrm{d}\hat\xi \le CC_b, \qquad 0 < H \le CG, \tag{1.13.61}$$

$$\left\| \mathfrak{M}_4(R_b) - \frac{G^2}{8h} \right\|_{C^1} \le C_* G C_b/R_b,$$

$$\left\| P(R_b) + \frac{G^2}{4(1+2h)R_b} \right\|_{C^1} \le C_* G C_b/R_b^2. \tag{1.13.62}$$

Here $\mathfrak{M}_4, P$ mean its canonical integrals. The constants are independent of R_b, G. All fixed-order eta derivatives of the canonical integrals exist continuously at the endpoints. Their higher-order constants are finite for the fixed construction.

A scale-uniform higher-order estimate is not part of the assertion.

Proof. We put $e_s(x) = g_*(x) - c_{\mathrm{bank}} x^{-h}$. On $[R_b, b_s]$,

$$|e_s| \le CC_b/W_s, \qquad |e_s'| \le CC_b/W_s^2.$$

For $x \ge b_s$, split into regular remainder and fast mode. The regular part obeys

$$|e_{\mathrm{reg}}| + |he_{\mathrm{reg}} + xe_{\mathrm{reg}}'| \le C_h c_{\mathrm{bank}} x^{-h-1},$$

and the fast part has exposure (1.13.42).

We change variables before we estimate d:

$$\int_{(\frac{\hat\xi^2}{2})}^\infty |H_L - H_b|\,\mathrm{d}t = d^{1-h}\int_{\frac{\hat\xi^2}{2}/d}^\infty |e_s(x)|\,\mathrm{d}x,$$

$$\int_{(\frac{\hat\xi^2}{2})}^\infty |(H_L - H_b)_\eta|\,\mathrm{d}t = 2|\eta| d^{-h}\int_{\frac{\hat\xi^2}{2}/d}^\infty |he_s + xe_s'|\,\mathrm{d}x. \tag{1.13.63}$$

For the non-heat part $d \ge \frac{\hat\xi^2}{2}/b_s \ge R_b/b_s$. The contribution to the first estimate is at most CC_b. The contribution to the second estimate is at most $C[hC_b + b_s C_b/W_s]$. The fixed ϵ_s is allowed in this constant. For a regular tail with inlet at $z = \frac{\hat\xi^2}{2}/d \ge b_s$, the second integral is at most $C_h c_{\mathrm{bank}} z^{-h}$, and

$$d^{-h} c_{\mathrm{bank}} (\tfrac{\hat\xi^2}{2}/d)^{-h} = c_{\mathrm{bank}} (\hat\xi/\sqrt{2})^{-2h} \le G.$$

If $\frac{\hat\xi^2}{2}/d < b_s$, d has a positive lower bound and the same bound applies with z replaced by b_s. Thus the regular contributions are $O_h(G)$. We absorb them because $C_b/G \to \infty$.

For the fast part, we let $z = \max(b_s, \frac{\hat\xi^2}{2}/d)$. Exponential decay gives $\int_z^\infty |hg_f + xg_f'| \le Czg_f(z)$. When $z = \frac{\hat\xi^2}{2}/d$, the decreasing exponential absorbs polynomial factors $(z/\frac{\hat\xi^2}{2})^h z$, with a remainder at most Cb_sF_b. When $z = b_s$, d has a positive lower bound and gives the same bound. The source-free buffer makes b_sF_b exponentially small compared with C_b.

The undifferentiated fast integral is easier. This proves the two L^1 estimates for the lift.

For the wing velocity $v_o = \psi_o\alpha_o\ell_b\mathcal{F}'$, direct integration gives, at $\frac{\hat\xi^2}{2} < \mathcal{B}_o$,

$$\int_{(\frac{\hat\xi^2}{2})}^\infty |v_o|\,\mathrm{d}t = |\psi_o|\alpha_o\ell_b^2\mathcal{F},$$
$$\int_{(\frac{\hat\xi^2}{2})}^\infty |(v_o)_\eta|\,\mathrm{d}t \le \alpha_o\ell_b^2|\psi_o'|\mathcal{F} + \alpha_o\ell_b|\psi_o\mathcal{B}_o'|\mathcal{F}'.$$

Flatness removes the moving-boundary term. With $\mathcal{F} \le y\mathcal{F}'$, $\mathcal{F}' \le 1$, and the fixed bounds for $\mathcal{B}_o/R_b, \mathcal{B}_o'/R_b$, their sum is at most $C\alpha_o\ell_bR_b \le CC_b$. The overshoot $\chi_b'\Delta$ and its eta derivative have L^1 norm at most CC_b, because $\chi_b' \ge 0$ and $\int_J \chi_b' = 1$. This proves (1.13.61).

The exact identities

$$\mathfrak{M}_4 - \mathfrak{M}_{4b} = \int_{R_b}^\infty \frac{(H-H_b)(H+H_b)}{4t}\,\mathrm{d}t, \qquad \mathfrak{M}_{4\eta} = \int_{R_b}^\infty \frac{HH_\eta}{2t}\,\mathrm{d}t$$

and their pressure counterparts with $-t^{-2}$ in place of t^{-1} prove (1.13.62) from (1.13.61). In particular, we keep all quadratic terms.

Uniform L^1 norms alone do not justify differentiation under these improper integrals. For $t \ge b_s$, the mode estimates give the same pointwise bound

$$|(H_L)_\eta| \le C_hc_{\mathrm{bank}}t^{-h-1} + C_hk_ft^{h+1}e^{-t/2}.$$

For the fast term, we write $x = t/d$ and absorb the additional powers of x/t by exponential monotonicity for $x \ge t$. On the finite modified region add a constant times its indicator. This is an integrable dominator independent of eta.

For completeness, (1.13.35), with N larger than the number of derivatives, gives on each positive compact radial interval

$$d^{-h}g_h(\tfrac{\hat\xi^2}{2}/d) = (\hat\xi/\sqrt{2})^{-2h}\sum_{n=0}^N a_n(d/\tfrac{\hat\xi^2}{2})^n + \mathcal{R}_N(\tfrac{\hat\xi^2}{2}, d), \quad |(\hat\xi^{-1}\partial_{\hat\xi})^j\partial_d^m\mathcal{R}_N| \le C_{N,j,m}d^{N+1-m}. \tag{1.13.64}$$

The primitive has the related expansion, with first term $(\frac{\hat\xi^2}{2})^{1-h}/(1-h) - 2(1+h)d(\hat\xi/\sqrt{2})^{-2h}$.

Each fixed derivative of the fast lift is a polynomially weighted exponential $O(d^{-K}e^{-\frac{\hat\xi^2}{2}/(2d)})$, thus is flat at d=0. These estimates prove actual smoothness at the two endpoints. For each fixed positive derivative order m they also give one tail dominator

$$M_m\mathbf{1}_{[R_b,\mathcal{B}_{\max}]} + C_mc_{\mathrm{bank}}t^{-h-1}\mathbf{1}_{[b_s,\infty)} + C_mk_ft^{q_m}e^{-t/2}\mathbf{1}_{[b_s,\infty)},$$

with finite M_m, q_m.

The same majorants also dominate products from derivatives of H^2. Dominated convergence proves the stated all-order smoothness of the canonical integrals. We do not use convergence of the infinite asymptotic series. □

The lemma supplies the future hypothesis (1.13.31). It also supplies the bounds used in (1.13.24). The finite scalar drive has bounded radial and amplitude ratios (1.13.28). Its energy integral is $O_h(G_0^2)$. Its pressure integral is $O_h(G_0^2/a_*)$. The reference tails of the power segment and the actual deviations then give $O_h(G_0^2/h)$ and $O_h(G_0^2/a_*)$, with their first eta derivatives.

1.13.10 The full cone at the wing and the outer support

On the power segment and bridge, the h-power reference has zero axial stress. Equation (1.13.62) thus gives

$$|\widehat{\mathcal{T}}_{P,z}| \le CGC_b/R_b^{3/2}, \qquad |\widehat{\mathcal{T}}_{P,z}|/\widehat{\mathcal{T}}_{P,\theta} \le CG/(\epsilon_o\sqrt{R_b}).$$

After J, compare the target with the actual lift, whose axial stress vanishes by (1.13.60). We put

$$Z_o = \psi_o\alpha_o\ell_b\mathcal{F}' + \eta\psi_o'\alpha_o\ell_b^2\mathcal{F}/\tfrac{\hat\xi^2}{2} \ge 0. \tag{1.13.65}$$

The angular calculation previously gives $\mathcal{T}_{\theta,T} \ge \mathcal{T}_{\theta,L} + cZ_o$. We verify the related axial bound without division by a flat angular cutoff.

We set $Q_o = H_T^2 - H_L^2 = -2H_Lv_o + v_o^2$. The complete difference of the canonical axial numerators is

$$\mathcal{N}_o = \eta\int_{(\frac{\hat\xi^2}{2})}^{\mathcal{B}_o} Q_o(s)\frac{hs - (\frac12+h)\frac{\hat\xi^2}{2}}{s^2}\,\mathrm{d}s - \frac{d}{4}\int_{(\frac{\hat\xi^2}{2})}^{\mathcal{B}_o}(Q_o)_\eta(s)\frac{s-\frac{\hat\xi^2}{2}}{s^2}\,\mathrm{d}s. \tag{1.13.66}$$

This includes the v_o^2 term. The previous source and mode estimates give $|(H_L)_\eta| \le CH_L$, $H_L(s) \le H_L(\frac{\hat\xi^2}{2})$ for $s \ge \frac{\hat\xi^2}{2}$, and $v_o \le H_L/2$. Thus

$$|Q_o| \le CH_L(\tfrac{\hat\xi^2}{2})v_o, \qquad |(Q_o)_\eta| \le CH_L(\tfrac{\hat\xi^2}{2})(v_o + |(v_o)_\eta|), \quad (v_o)_\eta = \alpha_o\ell_b\psi_o'\mathcal{F}' + \alpha_o\psi_o\mathcal{B}_o'\mathcal{F}''.$$

The terms without differentiated cutoffs in (1.13.66) have a bound by $CH_L(\frac{\hat\xi^2}{2})v_o(\frac{\hat\xi^2}{2})$, with the fixed bound for $\mathcal{B}_o/\frac{\hat\xi^2}{2}$. The ψ_o' term has a bound by

$$CH_L(\tfrac{\hat\xi^2}{2})\alpha_o\ell_b^2|\psi_o'|\mathcal{F}/\tfrac{\hat\xi^2}{2},$$

because $\int_{(\frac{\hat\xi^2}{2})}^{\mathcal{B}_o}\mathcal{F}'\,\mathrm{d}s = \ell_b\mathcal{F}$. The second term of Z_o controls it, because $|\eta| \ge \eta_0$ on the support of ψ_o'. The moving-edge term uses $\int_{(\frac{\hat\xi^2}{2})}^{\mathcal{B}_o}\mathcal{F}''\,\mathrm{d}s = \ell_b\mathcal{F}'$ and has a bound by $CH_L(\frac{\hat\xi^2}{2})v_o(\frac{\hat\xi^2}{2})|\mathcal{B}_o'|/\frac{\hat\xi^2}{2}$. Thus

$$|\mathcal{T}_{z,T}| \le C\frac{H_L(\frac{\hat\xi^2}{2})}{(\hat\xi/\sqrt{2})}Z_o, \qquad \mathcal{T}_{\theta,T} \ge \mathcal{T}_{\theta,L} + cZ_o. \tag{1.13.67}$$

The ratio is small for sufficiently small $G/\sqrt{R_b}$. Together with (1.13.59), this proves the strict faces throughout the target and bridge, with a positive normalized margin on their nonzero stress set.

We can select all cutoffs with the squared-flat function $\vartheta(s) = e^{-1/s^2}$ for $s > 0$, zero for nonpositive arguments. For example,

$$\psi_o(\eta) = \frac{\vartheta(\eta^2-\eta_0^2)}{\vartheta(\eta^2-\eta_0^2) + \vartheta(4\eta_0^2-\eta^2)}.$$

The outer stress support is the finite union of the lifted scalar source, the wing $\psi_o > 0$, $\frac{\hat\xi^2}{2} < \mathcal{B}_o(\eta)$, and the favorable $\eta\psi_o'$ contribution. At $|\eta| = \eta_0$ there can be an angular flat edge at a larger radius than the scalar source edge. We thus use the sum $\mathcal{T}_{\theta,L} + Z_o$ as its positive control.

We do not assert a single smooth radial support graph. Each fixed derivative has the bounds supplied by these explicit flat factors and the mode estimates.

Corollary 1.13.6 (The exact outer heat region)**.** *For $\frac{\hat\xi^2}{2} \ge \mathcal{B}_{\max}$, the pre-modulation calibrated field is (1.13.1) with $c_{\mathrm{bank}} = GR_b^h > 0$, $k_f > 0$, and $U = \mathfrak{M}_1 = \mathfrak{M}_3 = 0$. Its canonical stresses vanish. Its profiles and all fixed mixed $\frac{\hat\xi^2}{2}, \eta$ derivatives extend smoothly to $\eta = \pm 1$. The expansion (1.13.64) and the flat fast remainder describe their endpoint jets. In particular $H(\frac{\hat\xi^2}{2}, \pm 1) = c_{\mathrm{bank}}(\hat\xi/\sqrt{2})^{-2h}$.*

In physical variables its exterior angular velocity is

$$u_\theta^{\mathrm{lead}} = \frac{t^{-h}}{r}\left[c_{\mathrm{bank}} g_h\left(\frac{r^2}{2t}\right) + k_f g_f\left(\frac{r^2}{2t}\right)\right]. \tag{1.13.68}$$

Proof. For such radii the wing is zero, and $\frac{\hat\xi^2}{2}/d \ge b_s$, so the scalar trajectory is the selected homogeneous pair. Equations (1.13.49) and (1.13.60) give zero stress. The previous lemma proves the endpoint statements. Finally $t = qd$ and $\frac{\hat\xi^2}{2}/d = r^2/(2t)$ give (1.13.68) from (1.6.9). □

1.13.11 The pressure root is solved before the energy root

We now identify all histories with the actual prefix and remove the future hypotheses used earlier. This order of exposition constructs the future from scalar data first. It does not prescribe a pressure or an energy constant at a join radius.

We let $y_a = \log(a_*/\mathcal{R})$ and $\mathfrak{h}_a = \mathfrak{h}(y_a)$. We fixed the radial template from the turnoff to the pulse exit before this step, independently of φ, Q_p. We define

$$\begin{aligned} G_0 &= \sigma\sqrt{\mathcal{R}}\,\mathfrak{h}_a, \qquad \rho_a = \mathfrak{h}_a^2 e^{-y_a}, \\ \mathsf{A}_{\mathrm{pre}} &= \frac{5}{4} + \frac{1}{4}\int_0^{y_a} \mathfrak{h}(y)^2 e^{-y}\,\mathrm{d}y, \\ \mathsf{D} &= \mathsf{A}_{\mathrm{pre}} + \frac{\rho_a}{4(1+2h)}, \qquad \sigma^2 = P_0/\mathsf{D}. \end{aligned} \tag{1.13.69}$$

The term $5/4$ is the actual growing-reference integral in Section 1.12. The normalization uses a diagnostic scalar number only to fix a convenient positive σ.

It does not set the last exterior history. The short slope transition and positive slow decay give fixed positive lower and upper bounds for D. They apply to the full permitted μ range. In particular $\sigma^2 \asymp \kappa$, in agreement with the previous normalization.

After scalarization, the actual H and $\mathfrak{M}_2$ are independent of φ. We construct that drive, shot, blend and wing at the given scale and amplitude, and compute their actual integrals

$$p_{\mathrm{out}}(\eta) = \frac{a_*}{G_0^2}\int_{2\sqrt{a_*}}^{\infty} \frac{H^2}{4\frac{\hat\xi^4}{4}}\,\hat\xi\,\mathrm{d}\hat\xi, \qquad e_{\mathrm{out}}(\eta) = \frac{1}{G_0^2}\int_{2\sqrt{a_*}}^{\infty} \frac{H^2}{4\frac{\hat\xi^2}{2}}\,\hat\xi\,\mathrm{d}\hat\xi. \tag{1.13.70}$$

There is no U in this future. We let $p_{\mathrm{dr}}, e_{\mathrm{dr}}$ be the same normalized integrals restricted to the scalar

drive $[2a_*, R_b]$. With the deviations of Lemma 1.13.5,

$$p_{\mathrm{out}} = p_{\mathrm{dr}} + \frac{a_* G^2}{4(1+2h)R_b G_0^2} - \frac{a_*}{G_0^2}\Delta P_b,$$
$$e_{\mathrm{out}} = e_{\mathrm{dr}} + \frac{G^2}{8hG_0^2} + \frac{\Delta \mathfrak{M}_{4b}}{G_0^2}. \tag{1.13.71}$$

The pressure correction has a minus sign. The comparisons (1.13.28) and (1.13.62) give

$$\|p_{\mathrm{out}}\|_\infty \le C_{\mathrm{o}}, \quad \|e_{\mathrm{out}}\|_\infty \le C_{\mathrm{o}}/h, \quad \|(p_{\mathrm{out}})_\eta\|_\infty + \|(e_{\mathrm{out}})_\eta\|_\infty \le C_{\mathrm{o}} h a_*^{-1/5}. \tag{1.13.72}$$

The scalar drive itself contributes no eta derivative. The constant C_{o} depends on h and the fixed outer templates. We can fix one value for all $0 < \mu \le h/10$, before we select μ.

The bounds for D_{sc}, the drive ratios, and the power-segment deficit have this uniformity. All profiles and integrals are homogeneous with the stated powers of the amplitude, so their normalization has no hidden σ dependence.

In the scalarization region use $s = \frac{\hat{\xi}^2}{2}/a_*$, and regard ψ_{sc} as a function of s. Its exact pressure coefficients are

$$\mathsf{p}_2 = \frac{1}{4}\int_1^2 s^{-2\mu-2}\psi_{\mathrm{sc}}^2\,\mathrm{d}s, \quad \mathsf{p}_1 = \frac{1}{2}\int_1^2 s^{-2\mu-2}\psi_{\mathrm{sc}}(1-\psi_{\mathrm{sc}})\,\mathrm{d}s, \quad \mathsf{p}_0 = \frac{1}{4}\int_1^2 s^{-2\mu-2}(1-\psi_{\mathrm{sc}})^2\,\mathrm{d}s. \tag{1.13.73}$$

In particular, we do not assume positivity of p_1. The full actual pressure moment is equivalent to

$$(\mathsf{A}_{\mathrm{pre}} + \rho_a \mathsf{p}_2)\varphi^2 + \rho_a \mathsf{p}_1 \varphi + \rho_a(\mathsf{p}_0 + p_{\mathrm{out}}) = \mathsf{D} g^2. \tag{1.13.74}$$

Each future segment appears either in these local coefficients or in (1.13.70).

We write $A_2^\circ = \mathsf{A}_{\mathrm{pre}} + \rho_a \mathsf{p}_2 \ge 5/4$ and $B_1^\circ = \rho_a \mathsf{p}_1$. The desired root is

$$\varphi = \frac{-B_1^\circ + \sqrt{(B_1^\circ)^2 + 4A_2^\circ[\mathsf{D} g^2 - \rho_a(\mathsf{p}_0 + p_{\mathrm{out}})]}}{2A_2^\circ}. \tag{1.13.75}$$

For $C_{\mathrm{o}}\rho_a$ small, the bracket is positive, the root is positive, and its derivative denominator $2A_2^\circ\varphi + B_1^\circ$ has a positive lower bound. Evaluation of (1.13.74) at g and differentiation give

$$\|\varphi - g\|_{C^1} \le C_{\mathrm{o}}\rho_a, \qquad \|\varphi_\eta\|_\infty \le C\kappa + C_{\mathrm{o}}\rho_a h a_*^{-1/5}. \tag{1.13.76}$$

The future integral contributions are smooth at the two endpoints by the all-order part of Lemma 1.13.5.

Thus the root is smooth there. We can extend it smoothly to a neighborhood of the closed interval. No Gevrey assertion about this extension is necessary in the protected rectangle. There we kept the analytic shape g.

For energy, we define the same three coefficients with one fewer power of s in the denominator:

$$\mathsf{e}_2 = \frac{1}{4}\int_1^2 s^{-2\mu-1}\psi_{\mathrm{sc}}^2\,\mathrm{d}s, \quad \mathsf{e}_1 = \frac{1}{2}\int_1^2 s^{-2\mu-1}\psi_{\mathrm{sc}}(1-\psi_{\mathrm{sc}})\,\mathrm{d}s, \quad \mathsf{e}_0 = \frac{1}{4}\int_1^2 s^{-2\mu-1}(1-\psi_{\mathrm{sc}})^2\,\mathrm{d}s. \tag{1.13.77}$$

The actual target for the pulse is

$$\mathfrak{M}_{4a_*} = G_0^2[\mathsf{e}_2\varphi^2 + \mathsf{e}_1\varphi + \mathsf{e}_0 + e_{\mathrm{out}}], \qquad \tau_S = \mathsf{e}_2 + \frac{\mathsf{e}_1}{\varphi} + \frac{\mathsf{e}_0 + e_{\mathrm{out}}}{\varphi^2}. \tag{1.13.78}$$

It is the integral of the positive future swirl density. Equations (1.13.72) and (1.13.76) give

$$|\tau_S| \le C_{\mathrm{o}}/h, \qquad |(\tau_S)_\eta| \le C_{\mathrm{o}} \left(\frac{\kappa}{h} + \rho_a a_*^{-1/5} + h a_*^{-1/5} \right). \tag{1.13.79}$$

We substitute this function in (1.13.17).

Its value contribution is at most $C_{\mathrm{o}}(\mu/h)e^{-26}$. The contribution to the weighted derivative necessary by Lemma 1.13.2 is at most

$$C_{\mathrm{o}} e^{-26} \left[\frac{\mu\kappa}{h^2} + \frac{\mu}{h} \rho_a a_*^{-1/5} + \mu a_*^{-1/5} \right]. \tag{1.13.80}$$

Once these quantities and the inlet errors are small, the root $Q_p \in [.9, 1.2]$ exists with the stated derivative control. This solve includes the two exact returns (1.13.15). The energy equation includes their signed coefficients.

This order resolves the calibrations: first construct the future, then solve (1.13.75) for φ, and only then solve (1.13.17) for Q_p. A change of Q_p changes U alone. It does not change the pressure integral, the scalarization, or the two future integral contributions. A change of φ in scalarization leaves outlet H and $\mathfrak{M}_2$ unchanged. Thus no compatible-family fixed point is necessary.

1.13.12 Fixed-h parameter choices and identification of all histories

We give the choices in an order which also applies when φ depends on the last matching radius. First, we fix h, the scalar source templates, a small ϵ_s, the central overlap η_0, the edge geometry, and a sufficiently small ϵ_o. We fix constants in (1.13.72), the cone estimates, and the scalar entrance that apply to all $0 < \mu \le h/10$. We freeze $\epsilon_{\mathrm{cone}} > 0$ so that smaller sums of normalized errors in Lemma 1.13.2 keep the two strict faces. We allocate one tenth to each energy-derivative contribution and to each remaining cone input.

We select the inlet tolerances and the finite wait (1.13.12). With $\mu = \theta h$, decrease $\theta > 0$ so that

$$C \left(\frac{\mu}{h-\mu} + \frac{\mu^2}{h} + \mu(1+T_w)e^{2\mu T_w} \right) \ll 1, \quad C_{\mathrm{o}}(\mu/h)e^{-26} \ll 1, \quad C_{\mathrm{o}}\rho_a \ll \min(\mu, \delta_{\mathrm{del}}). \tag{1.13.81}$$

Here δ_{del} is the fixed tolerance in (1.12.11). We also impose $C\mu^{-K}e^{-c/\mu}/h < \min(\frac{1}{2}, \epsilon_{\mathrm{cone}}/10)$ (used in Lemma 1.13.2 through the energy derivative) and $\mu(1+T_w)e^{2\mu T_w} \le \varepsilon_c h$ (all inlet errors at most $\varepsilon_c h$), with $\varepsilon_c < \epsilon_{\mathrm{cone}}/10$. We also make each other normalized small term less than its $\epsilon_{\mathrm{cone}}/10$ bound.

All these conditions hold for small θ. These are attainable at each fixed h:

$$\frac{\mu}{h-\mu} \le \frac{\theta}{1-\theta}, \quad \frac{\mu^2}{h} = \theta^2 h, \quad \rho_a \le Ce^{-13/\mu}.$$

The relative-radius suppression in the last inequality comes from the long pulse. An increase in $\mathcal{R}$ would not decrease it.

Next, we select $\kappa > 0$, at most 10^{-6}, sufficiently small that $\kappa \ll \mu$, all finite-reference and wait cone errors satisfy their bounds, and

$$\frac{\sup E_p}{\mu h} \ll 1, \qquad C_{\mathrm{o}} \frac{G_0}{\sqrt{a_*}} \frac{\sqrt{\mu}}{h^2} \ll 1, \qquad C_{\mathrm{o}} \frac{G}{\sqrt{R_b}} \ll 1, \qquad C_{\mathrm{o}} e^{-26} \frac{\mu\kappa}{h^2} \ll 1.$$

The normalized amplitudes here are fixed multiples of $\sigma \asymp \sqrt{\kappa}$. A finite last radius suffices for these conditions. We fix the core parameters $\frac{\hat{\xi}_{\mathrm{e}}^2}{2}, c_{\mathrm{a}}, B, \ell$ as in Section 1.12. Their constants are allowed to depend on this fixed h and κ.

Last, we enlarge $\mathcal{R}$, with $\varepsilon = \sigma/(c_{\mathrm{a}}\mathcal{R}^{1/10})$, to satisfy the core amplitude threshold, the early five-history correction bound, and all radial requirements, with

$$\frac{1}{\frac{\hat{\xi}_p^2}{2}h} \ll 1, \qquad \epsilon_s^{-2}R_b^{-1/5} \ll 1, \qquad C_b/G \gg 1, \qquad C_{\mathrm{o}}e^{-26}[(\mu/h)\rho_a + \mu]a_*^{-1/5} \ll 1. \tag{1.13.82}$$

We construct the actual outer field at this radius and compute its integrals. Equation (1.13.76) supplies the hypothesis of Proposition 1.12.3 with the same bound for all such radii. We apply its early correction to the full-axis φ-reference (1.13.5). At its exit the velocities and all five histories agree with that reference.

Their densities agree after this radius, so integration proves the same equality through turnoff and the full pulse. We thus correct the early transition's pressure and energy costs. We do not omit them from (1.13.74).

The pressure equation gives the full-axis identity $\int_0^\infty H^2/(4\frac{\hat{\xi}^4}{4}) = P_*$. Thus the actual pressure is its negative canonical tail at each positive radius. The energy equation gives the actual value $\mathfrak{M}_4(a_*)$ equal to the future integral in (1.13.78). Because U vanishes thereafter, the actual $\mathfrak{M}_4$ is its canonical tail for all $\frac{\hat{\xi}^2}{2} \geq a_*$. Likewise the exact linear returns give $\mathfrak{M}_1 = \mathfrak{M}_3 = 0$ there.

The identity $\frac{\mathfrak{M}_{2\hat{\xi}}}{\hat{\xi}} = H$ holds through scalarization, the drive, the scalar shot and the primitive blend. On the heat exterior its selected primitive obeys

$$\mathfrak{M}_2 - \frac{c_{\mathrm{bank}}\big(\frac{\hat{\xi}^2}{2}\big)^{1-h}}{1-h} \longrightarrow 0.$$

Because $h < 1$ at zero and $h > 0$ at infinity, the renormalized primitive integral converges and equals zero. These facts prove all five identities (1.13.3).

The cone estimates used earlier now have their actual inputs. The future lemma supplies the scalarization and drive tails. The exact pressure root supplies the wait and pulse pressure. The energy root and actual density integration supply the pulse energy estimate. The proofs give each bound for the same future field.

This completes the proof of Proposition 1.13.1, with the pre-modulation calibrated field fixed. Later finite constants can depend on its higher smooth seminorms.

1.13.13 A late restoration which leaves the calibrated future unchanged

For the selected relative member, "late restoration" is late only relative to the capped modulation. We select its quiet power reserve after the loop and finish all five history corrections in the pre-pulse logarithmic window $-25 < 2\log(\hat{\xi}/\hat{\xi}_p) < -20$. The heat compensation (the three-E bank of Lemma 1.14.5) has its supports in $(-20, -15)$. The later positive-order correction interval is the first displayed interval. The mean correction interval is the second:

$$[-14, -9], \qquad [-8, -3]. \tag{1.13.83}$$

We do not move the later pulse returns.

On the restoration reserve $U = 0$ and $H = c_p\varphi(\eta)\big(\frac{\hat{\xi}^2}{2}\big)^{-\mu(\eta)}$, where $c_p\varphi > 0$ and $0 < \mu_{\min} \leq \mu(\eta) \leq \mu_{\max} < 1$. We keep the inlet cumulative M, J and do not reset them.

Lemma 1.13.7 (Restoration to the calibrated field)**.** *We fix the selected pre-modulation relative field and this strictly admissible quiet power reserve. Suppose that a modification has support before*

the reserve and outside the actual protected curved domain. Suppose that its complete five-history discrepancy is $O_k(\varepsilon)$ in each necessary fixed angular norm. Suppose also that its partial histories keep the cone up to the reserve. We fix nonnegative bumps $b_1^U, b_2^U, b_1^H, b_2^H, b_3^H \in C_c^\infty((-25,-20))$, not identically zero, with ordered disjoint supports in each family. Then there are coefficients α_j, β_j such that the correction

$$\delta U = \sum_{j=1}^{2} \alpha_j(\eta)\, b_j^U(y), \qquad \delta H = \sum_{j=1}^{3} \beta_j(\eta)\, b_j^H(y), \qquad y = 2\log(\hat{\xi}/\hat{\xi}_p(\eta)), \tag{1.13.84}$$

restores all five histories to the pre-modulation field.

Its coefficients and each fixed radial/angular norm are $O_k(\varepsilon)$. For sufficiently small ε the correction interval is strictly admissible. All fields and histories after its exit do not change. These include the early reserved patches, the later pulse and the canonical heat future. For the slice-continued capped loop, $\varepsilon = N_{\mathrm{sh}}^{-2}$. We do not assume smallness of pointwise angular oscillatory derivatives.

Proof. The target is the actual integrated discrepancy, with its original axis constants. We prove the partial-history hypothesis for the loop by Corollary 1.19.3. This correction result uses only the stated complete discrepancy.

We order the target histories as $(\mathfrak{M}_1, \mathfrak{M}_3; \mathfrak{M}_2, \mathfrak{M}_4, P)$. At zero correction the moment derivative is block diagonal. Its U weights are $(1, H)$. Its H weights are

$$(1, -H/(\hat{\xi}^2), H/(2\tfrac{\hat{\xi}^4}{4})).$$

On the reserve $H = c_p\varphi(\hat{\xi}/\sqrt{2})^{-2\mu}$, and with $\frac{\hat{\xi}^2}{2} = \frac{\hat{\xi}_p^2}{2}e^y$,

$$\int_0^\infty (\tfrac{\hat{\xi}^2}{2})^p b(y)\, \hat{\xi}\, \mathrm{d}\hat{\xi} = (\tfrac{\hat{\xi}_p^2}{2})^{p+1} \int e^{(p+1)y} b(y)\, \mathrm{d}y.$$

The U rows have $p+1 \in \{1, 1-\mu\}$, and the H rows have $p+1 \in \{1, -\mu, -1-\mu\}$.

These exponents are distinct, with one lower bound for their gaps for all $\mu(\eta)$ in its fixed compact range. A nontrivial sum of k exponentials with distinct real exponents has at most $k-1$ real zeros (Rolle's theorem and induction). Thus the determinant of each exponential matrix, integrated against the ordered nonnegative bumps, is nonzero. The factors $(\frac{\hat{\xi}_p^2}{2})^{p+1}$ and $c_p\varphi$ are smooth and positive.

Thus the two matrices have uniform smooth inverses on the compact η interval, also at $\eta = \pm 1$.

The exact map is this linear map plus quadratic terms, with the cross term in UH. A contraction, or the finite-dimensional implicit function theorem, gives smooth coefficients for the negative actual discrepancy. Differentiation of its equation in eta gives $O_k(\varepsilon)$ for each fixed k. The fixed bump templates have finite radial norms. We decrease ε after we fix this member.

Then the actual partial histories keep the strict reserve. The loop and its correction precede the pulse, so no propagation of an unrepaid loop discrepancy through the pulse or spectral sector is necessary.

The restored target uses (1.13.78) and the actual nonseparated pressure integral. The correction vanishes on radial endpoint neighborhoods of its correction interval. Its angular endpoint coefficients need not be zero.

The variable $y = 2\log(\widetilde{\xi}/\widetilde{\xi}_p)$ is one slice function (Lemma 1.6.8). The coefficients solve the same nonsingular system on the two sides, with the same templates (Step 3 of the proof of

Proposition 1.8.16) and targets of equal slice jets (Lemma 1.19.4). Thus the coefficients and the correction have equal slice jets. A bump that is fixed in $\frac{\hat\xi^2}{2}$ or in $\mathfrak{r}$ would not have this property.

After its exit the two fields have the same H,U and the same five initial history values.

The five density equations imply exact equality for each larger radii. Differentiation of these smooth identities proves equality of all eta jets as well. □

This lemma supplies the restoration step for the later spatial shear modulation. The algebraic loop lemma proves its existence and strictness on the previous relaxed interval. We freeze the selected leading field only after that modulation and this restoration. Prefix locality leaves the actual protected curved domain and its solved cover of paragraph 1.22 unchanged. Thus the member keeps one inner Gevrey radius. We use the outer calibrated shape only where smoothness is necessary.

1.14 Actual prefix data and the true affine pulse inlet

Main result. Lemmas 1.14.1–1.14.3 give the actual pulse inputs from the finite prefix. Lemmas 1.14.4 and 1.14.5 control the later moment corrections. The early estimates do not use the next heat correction.

This section supplies inlet data for the pulse calculation from the selected finite prefix and its actual moment corrections. It uses the same template as the actual inlet construction of Lemma 1.15.26, not an independently selected backward member. The heat edit is the same-heat/rank-one construction of the actual future construction of Proposition 1.15.8. We do not assign a new history at a pulse entry. Lemmas 1.14.1, 1.14.2, and 1.14.3 are a direct result of the finite-template integrals in this section, independently of the future heat edit.

Only the later heat-target and three-row correction construction use Proposition 1.15.8. Thus the early prefix bounds can first supply Lemma 1.15.26 and Proposition 1.15.20, before we use the actual heat correction and its last-scale estimates.

We write $\dot f = (\frac12 - h)\eta\partial_\eta f|_{\hat\xi}$, $a = 1-\nu$, $\alpha = 1/2+\nu$, $\beta = 1/2-\nu$, $\beta_2 = 1/2-2\nu$. We fix a small numerical $\lambda_0 < 1/20$. The histories are the actual primitives $\frac{M_{\hat\xi}}{\hat\xi} = U$, $\frac{I_{\hat\xi}}{\hat\xi} = H$, $\frac{J_{\hat\xi}}{\hat\xi} = UH$, $\frac{S_{\hat\xi}}{\hat\xi} = U^2 - H^2/(4\frac{\hat\xi^2}{2})$ and $\frac{P_{\hat\xi}}{\hat\xi} = H^2/(4\frac{\hat\xi^4}{4})$, with the specified origin histories and canonical outward pressure. On the pulse power interval use

$$y = 2\log(\hat\xi/\hat\xi_p), \quad Y = \log(R_o/\tfrac{\hat\xi_p^2}{2}), \quad H = H_o e^{\nu(Y-y)}, \quad E = H/\hat\xi,$$
$$u = \dot\nu, \quad v_p = \log \tfrac{\dot{\hat\xi}_p}{\hat\xi_p}, \quad w_o = \log \dot R_o.$$

We write $c = \log \dot H$, $q = h-\nu+c$ and $q_o = h-\nu+\log \dot H_o + \nu w_o$.

Thus $q = q_o + u(Y-y)$. A dot on $H_o, \frac{\hat\xi_p^2}{2}, R_o$ means the ordinary angular derivative of that displayed trace, multiplied by $(\frac12 - h)\eta$. With $r = I/(\frac{\hat\xi^2}{2}H)$, $m = M/(\frac{\hat\xi^2}{2}E)$ and $j = J/(\frac{\hat\xi^2}{2}HE)$, the exact full coefficient used here is

$$Q = 1 + \dot r + (q-a)r + E\{(2(\tfrac12 - h)\eta + b_\eta c)m + b_\eta \dot m - b_\eta \dot j + [2(h-(\tfrac12 - h))\eta - 2b_\eta c]j\}, \qquad b_\eta = (1-\eta^2)/((\tfrac12 - h)\eta).$$

This is the integrated angular stress identity. On the noncentral charts $|\eta| \ge \eta_a > 0$ its coefficients stay bounded.

On a $G = 0$ sector the axial template $U = Gk$ gives zero reference M, J from the ideal axis. The forward core correction restores these rows at its outlet, the pressure correction preserves them by

Lemma 1.6.37, and Lemma 1.13.7 cancels the combined discrepancy of the loop and its five returns. From that completed outlet to the pulse inlet the remaining swirl edits have $U = 0$, so $M_X = U$ and $J_X = UH$ keep $M = J = 0$ on this quiet interval. There the first three terms give the scalar expression for Q. Inside the pulse $U = EA_p\Phi(\nu y)$. Both histories must be evolved from the inlet by (1.16.2) and retained in Q through the two returns. Their complete increments cancel after the second return. On the open zero-history region beyond it the scalar expression applies again. The central pulse is treated in ordinary angular derivatives in Lemma 1.16.9. Constants K_{pre} depend only on the fixed charts, cutoffs, finite turnoff templates, and their selected finite derivatives. They also depend on T_d and the fixed large plateau bound P_*. They are uniform for $0 \le \nu \le \lambda \le \lambda_0$, $0 \le h \le \lambda_0$, and do not depend on ν_c, L_o, Y_0, or the last physical scale. Constants denoted $K_{\mathrm{sc}}(Y_0)$ can depend on all previously selected future data, with $h^{-1}, \nu_c^{-1}, L_o, Y_0$. The inverse last scale always multiplies them.

We never use them to select λ.

1.14.1 One explicit finite pretemplate, with its parameter endpoint

We use the shared smooth functions selected previously f_0, f_1 on $[0,T]$. We normalize $f_0(0) = f_1(0) = 0$. On the initial open germ, $f_0' = \gamma = 3/5$, $f_1' = 0$. Before the fixed axial-turnoff plateau, f_0' decreases in $[0,\gamma]$ to zero and stays zero. We keep $0 \le f_1' \le 1$ and $f_1' = 0$ through that plateau and through the support of the shared axial cutoff derivative k'. Equation (1.6.17) defines this shared axial cutoff.

We then raise f_1' smoothly from zero to one, so that it equals one on an open germ before T. All these operations have fixed lengths and fixed cutoffs. (T2) These lengths, and f_0 on the growth turn and f_1 on the negative turn, do not depend on M_d: only the turnoff stage, of length $T_d = e^{M_d} + 10$, does. The turnoff stage starts after the growth turn, on the plateau (as in [42, (A.6)–(A.9)]). This is used in Lemma 1.8.17. We put

$$F(z;\nu) = e^{f_0(z) - \nu f_1(z)}, \quad 0 \le z \le T, \qquad F(z;\nu) = e^{\gamma z} \quad (z \le 0),$$

and continue beyond T by $F_T(\nu)e^{-\nu(z-T)}$. The same endpoint is $T_b = T$. The same k equals one on the initial growth germ and vanishes on a neighborhood of the negative turn and all later moment corrections.

At $\nu = \lambda$ this is the jointly selected backward pretemplate.

Lemma 1.14.1 (The finite-template data have actual uniform parameter bounds)**.** *We define*

$$r_b(\nu) = \frac{\int_{-\infty}^{T} e^z F(z;\nu)\,\mathrm{d}z}{e^T F_T(\nu)}, \qquad \sigma_b^0(\nu) = -\frac{\int_{-\infty}^{T} F(z;\nu)^2\,\mathrm{d}z}{2F_T(\nu)^2}.$$

For each specified finite j, we consider their ν derivatives through order j. We also include $F_T^{\pm 1}$ and its derivatives through that order. The bound $K_{\mathrm{pre},j}$ applies to all these quantities on the closed interval $0 \le \nu \le \lambda_0$. For the $G = 0$ reference template these are the ratios $I/(XH)$ and $2S/H^2$ at the end of the finite turn, $X = \hat{\xi}^2/2$. Their transport to the pulse inlet gives the physical values on the genuine exponent transition by the completed returns described above.

Also

$$0 < r_b(\nu) < (1-\nu)^{-1}. \tag{1.14.1}$$

Proof. On $[0,T]$, we put $B_i = \|f_i\|_\infty$.

Explicitly

$$e^{-B_0 - \lambda_0 B_1} \le F \le e^{B_0 + \lambda_0 B_1}, \quad \partial_\nu^j F = (-f_1)^j F, \quad \partial_\nu^j F^2 = (-2f_1)^j F^2.$$

Integration of these bounds on the fixed interval proves the claims there. The earlier two integrals are $(1+\gamma)^{-1}$ and $(2\gamma)^{-1}$. Their parameter derivatives vanish. Differentiation of the positive denominator proves the ratio bounds.

Thus explicit functions and dominated integrals give the extension to $\nu = 0$. Compactness of $0 < \nu \le \lambda_0$ does not give this extension. The history equations $\frac{I_{\hat\xi}}{\hat\xi} = H$, $\frac{S_{\hat\xi}}{\hat\xi} = -H^2/(4\frac{\hat\xi^2}{2})$ prove the stated identification. In particular, we keep $\sigma_a = -1/(4\gamma)$. For the last assertion, the actual slope $\ell = f_0' - \nu f_1' \ge -\nu$, and $r_y = 1 - (1+\ell)r$. The positive constant $(1-\nu)^{-1}$ is a supersolution, but the true initial value $(1+\gamma)^{-1}$ is strictly less than it.

The scalar variation-of-constants formula keeps the strict inequality through the finite interval. This supplies the sign of the actual central memory, as well as its magnitude. □

1.14.2 The $G = 0$ wait and its fixed-physical-coordinate data

At $\frac{\hat\xi_b^2}{2} = R_g e^T$ write $H_b = H_a F_T$. We put $W = 60\log(1/\nu)$, $\frac{\hat\xi_p^2}{2} = \frac{\hat\xi_b^2}{2}e^W$, and $H_p = H_b e^{-\nu W}$. We set $\delta_b = r_b - a^{-1}$ and $\theta_\nu = e^{-aW} = \nu^{60(1-\nu)}$.

Lemma 1.14.2 (Actual variable-exponent inlet values and jets)**.** *On the genuine $G = 0$ transition, before any pulse,*

$$M_p = J_p = 0, \qquad \dot M_p = \dot J_p = 0, \tag{1.14.2}$$

$$r_p = a^{-1} + \delta_b \theta_\nu, \tag{1.14.3}$$

$$\sigma_p^0 = e^{2\nu W}\sigma_b^0 - \frac{e^{2\nu W} - 1}{4\nu}. \tag{1.14.4}$$

For $u = \dot\nu$ the fixed-$\hat\xi$ jet of r, evaluated at $\frac{\hat\xi_p^2}{2}$, is

$$(\dot r)_p = \frac{u}{a^2} + u\theta_\nu[\delta_b' - 60\delta_b\log\nu]. \tag{1.14.5}$$

Thus, with $q_p = q_o + uY$,

$$Q_p = \frac{q_p}{a} + \frac{u}{a^2} + \theta_\nu[(q_p - a)\delta_b + u\delta_b' - 60u\delta_b\log\nu]. \tag{1.14.6}$$

This is the full coefficient because $M = J = 0$. For the selected $u \ge 0$, $q_o > 0$, and $Y \ge 4W$, it gives

$$\frac{|Q_p - q_p/a - u/a^2|}{q_p} \le K_{\mathrm{pre}}\theta_\nu(1 + q_o^{-1}).$$

Also, once $\lambda\log(1/\lambda)$ is small,

$$|\sigma_p^0| + |\sigma_p^0 + \nu\partial_\nu\sigma_p^0| \le K_{\mathrm{pre}}[1 + T_d + \log(1/\nu)]. \tag{1.14.7}$$

Proof. For the reference we integrate $r_y + ar = 1$ and $\sigma_y = 2\nu\sigma - 1/2$ along the power wait. On the genuine exponent transition the core correction restores M, I, J, S, the pressure correction preserves these rows, and the loop with its returns has zero complete discrepancy. The two-row taper and three-swirl heat compensation are absent on this sector. Thus the transported values equal the actual ones at the pulse inlet. The zero M, J on an open quiet interval before the pulse give their zero fixed-radius angular jets there and at the inlet by smoothness. Here $v_p = \log\frac{\hat\xi^2}{2} = -60u/\nu$. The jet of a trace is

$$(\dot r)_p = u\partial_\nu r_p - v_p(1 - ar_p).$$

The $60au\delta_b\theta_\nu/\nu$ term from differentiation of θ_ν cancels the moving-entry term. This proves (1.14.5). Substitution of $Q = 1 + \dot r + (q-a)r$ proves (1.14.6). In its normalized error $u/q_p \le 1/Y$ and $60u|\log\nu|/q_p \le W/Y \le 1/4$.

For (1.14.7), we let $b = 2\nu W$ and use $e^b - 1 = b\int_0^1 e^{tb}\,\mathrm{d}t$. For all permitted positive exponents, b is small and $\nu b' = 120\nu[\log(1/\nu) - 1]$ has one bound. Thus the apparent $1/\nu$ term is $W/2$ times a smooth factor with one bound for all permitted positive exponents. Its logarithmic parameter derivative is $O(1+W)$. We apply Lemma 1.14.1 to the other term.

No future integral contribution enters these estimates. □

For completeness, the first fixed-$\hat\xi$ energy jet at the moving entry is also explicitly supplied. At a fixed physical wait time $t = 2\log(\hat\xi/\hat\xi_b)$ write

$$\sigma(t,\nu) = e^{2\nu t}\sigma_b^0 - \frac{1}{2}\int_0^t e^{2\nu(t-s)}\,\mathrm{d}s.$$

Then

$$(\dot\sigma)_p = u\left[e^{2\nu W}(\sigma_b^{0\prime} + 2W\sigma_b^0) - \int_0^W (W-s)e^{2\nu(W-s)}\,\mathrm{d}s\right], \tag{1.14.8}$$

so $|(\dot\sigma)_p| \le K_{\mathrm{pre}}|u|(1+W)^2$. The W' terms in the trace derivative cancel its moving-entry correction. One must not use $u\partial_\nu\sigma_p^0$ as the fixed-$\hat\xi$ jet.

Also, we put

$$R_1 = a^{-2} + \theta_\nu(\delta_b' + W\delta_b), \quad R_2 = 2a^{-3} + \theta_\nu(\delta_b'' + 2W\delta_b' + W^2\delta_b).$$

The actual fixed-$\hat\xi$ second jet of r is $\ddot r_p = \dot u R_1 + u^2 R_2$. Thus the first jet of Q is

$$(\dot Q)_p = \dot u R_1 + u^2 R_2 + (\dot q_p + u)r_p + (q_p - a)uR_1, \quad \dot q_p = \dot q_o + \dot u Y + u w_o. \tag{1.14.9}$$

Here $\dot q_p$ is the fixed-$\hat\xi$ jet evaluated at the moving pulse entry, not the derivative of the trace $q_o + uY$. That trace derivative is $\dot q_o + \dot u Y + u\dot Y$, and $\dot Y = w_o - v_p$ accounts for the difference.

All coefficients r_p, R_1, R_2 have K_{pre} bounds. The displayed $u, \dot u, q, \dot q$ are actual geometry/source quantities, not hidden inverse-ν_c constants. We never use their finite later bounds for an early choice of λ.

1.14.3 Actual fixed-λ turnoff data and affine memories

We use the unmodulated bridge reference fields in their actual moving coordinate $z = 2\log(\hat\xi/\hat\xi_s(\eta))$:

$$H = H_s(\eta)F(z;\lambda), \qquad U = G(\eta)k(z), \qquad e_s = H_s/\hat\xi_s.$$

The fixed bridge construction gives bounded finite jets of G, $\log\frac{\hat\xi_s^2}{2}$, $\log H_s$, and $e_s^{\pm1}$, with $e_s \asymp P_*$ up to fixed turn/chart factors. We evaluate this last statement just after the fixed growth-slope transition, before the long axial turnoff. It does not renormalize the distant wait inlet. The fixed phase spread and the explicitly specified G- and phase-cutoffs give these bounds directly. The radial scale cancels in e_s.

We put

$$\mu_0 = \int_{-\infty}^T e^z k(z)\,\mathrm{d}z, \quad \mu_1(\lambda) = \int_{-\infty}^T e^z k(z)F(z;\lambda)\,\mathrm{d}z, \quad \mu_2 = \int_{-\infty}^T e^z k(z)^2\,\mathrm{d}z,$$

and $E_b = e_s F_T e^{-T/2}$, $\frac{\hat\xi_b^2}{2} = \frac{\hat\xi_s^2}{2}e^T$.

Lemma 1.14.3 (The bridge supplies the real nonzero inlet data)**.** *At* $\frac{\hat{\xi}_b^2}{2}$ *the exact normalized reference traces are*

$$r_b = \frac{\int_{-\infty}^{T} e^z F \,\mathrm{d}z}{e^T F_T},$$

$$m_b := \frac{M_b}{\frac{\hat{\xi}_b^2}{2} E_b} = \frac{G\mu_0}{e^T E_b}, \qquad j_b := \frac{J_b}{\frac{\hat{\xi}_b^2}{2} H_b E_b} = \frac{G\mu_1}{e^T F_T E_b}, \tag{1.14.10}$$

$$\sigma_b := \frac{2S_b}{H_b^2} = \frac{G^2\mu_2}{e_s^2 F_T^2} - \frac{1}{2F_T^2}\int_{-\infty}^{T} F^2 \,\mathrm{d}z. \tag{1.14.11}$$

Their trace derivatives of each selected finite order have a bound by K_{pre}*. Their first fixed-*$\hat{\xi}$ *jets at* $\frac{\hat{\xi}_b^2}{2}$ *obey the same bound. After the true wait* $W = 60\log(1/\lambda)$*, before the moment corrections,*

$$|m_p| + |j_p| + |(\dot{m})_p| + |(\dot{j})_p| \le K_{\mathrm{pre}}\lambda^{30-120\lambda}, \qquad e_p \le K_{\mathrm{pre}}\lambda^{30}. \tag{1.14.12}$$

The ideal inlet σ_p^0 *and its first angular derivative satisfy*

$$|\sigma_p^0| + |\dot{\sigma}_p^0| \le K_{\mathrm{pre}}[1 + T_d + \log(1/\lambda)].$$

The full Q_p *differs from* q/a *by* $O_{C^1}(K_{\mathrm{pre}}\lambda^{60(1-\lambda)})$*. In particular the fixed chart floor* $q \ge q_* > 0$ *gives* $Q_p \ge q_*/2$ *for the single early choice of sufficiently small* λ*.*

Proof. The four trace formulas are direct changes of variable in the actual integrals from the ideal origin. The early exact powers are integrable and their integrals are explicit. On the remaining finite interval the previous exponential formulas bound each selected derivative.

This proves the bounds without an estimate of an unknown history by a newly assigned constant.

For a normalized trace f_b at the moving outlet, $(\dot{f})_b = \dot{f}_b - v_b f_y|_b$, where $v_b = \log \frac{\hat{\phi}}{\hat{\xi}^2}$. Because the outlet has $U = 0$ and exact slope $-\lambda$,

$$r_y = 1 - ar, \quad m_y = -\beta m, \quad j_y = -\beta_2 j, \quad \sigma_y = 2\lambda\sigma - 1/2.$$

This explicitly supplies the moving-boundary terms. The wait length is angularly constant on this sector. Thus

$$m_p = e^{-\beta W} m_b, \quad j_p = e^{-\beta_2 W} j_b, \quad (\dot{m})_p = e^{-\beta W}(\dot{m})_b, \quad (\dot{j})_p = e^{-\beta_2 W}(\dot{j})_b.$$

The two wait endpoints have the same logarithmic angular derivative, so we lose no extra trace term. This proves (1.14.12). The energy equation gives (1.14.4) with the actual (1.14.11). Because $\lambda W \ll 1$, it and its angular derivative have the stated bound.

For Q, $r_p - a^{-1} = O(\lambda^{60a})$ and the fixed-$\hat{\xi}$ jet of this remainder has the same bound. In the full nonlinear M, J correction, $E_p m_p = O(\lambda^{60})$ and $E_p j_p = O(\lambda^{60a})$, with the necessary derivatives. These identities use $\alpha + \beta = 1$ and $\alpha + \beta_2 = a$. All angular logarithmic coefficients on this flat-λ chart have fixed early bounds. Substitution into the exact Q formula proves the conclusion.

For its first jet use one additional fixed angular derivative of the explicitly smooth bridge templates. This introduces no future constant. □

1.14.4 Moving primitive corrections and their actual small targets

The two pre-pulse I/C_p bumps are the fixed width-0.3 translates at logarithmic positions $-2, -1$ relative to $\frac{\hat{\xi}_p^2}{2}$. They lie after the three-E reserve, outside the genuine variable-ν region. Write $a = 1 - \lambda$, $r_* = a^{-1}$, $D = r_b(\lambda) - r_*$, and $X_p = \hat{\xi}_p^2/2$. On the outer-active chart put

$$r_{w,\mathrm{tar}} = r_* + D\left[(1-\tau)(e^T R_{g,b}/R_o)^a + \tau(e^T R_{g,b}/R_e)^a\right].$$

The weights are constant on the two open ends of the phase interpolation. The input to the outer future is $I_w(R_o) = R_o H_w(R_o) r_{w,\mathrm{tar}}$. On the genuine exponent transition $\tau = 0$ and the existing equation (1.6.24) gives the primitive identity after multiplication by $R_o H_{\mathrm{out}}$, using $\omega = (1-\chi)H_c/H_{\mathrm{out}}$. On the phase bridge $\chi = 1, \nu = \lambda$. Impose the actual pre-pulse change $p = R_o H_{\mathrm{out}} r_{w,\mathrm{tar}} - I_{\mathrm{raw}}(R_o)$ there, and take $p = 0$ on the scalar and native backward pieces.

For the raw reference, its exact growth power from the ideal axis gives $I/(R_g H_a) = 1/(1+\gamma)$. The regular-axis insertion restores the reference I at its matching graph (Theorem 1.8.10, the five-row return of the forward core). Downstream the pressure bank has $\Delta I = 0$ by Lemma 1.6.37. The loop with its restoration has zero total first-primitive discrepancy, and the full or cut three-swirl heat bank has first row zero. These insertions are all completed before the test radius R_o; axial pulse and axial returns have fixed H. Thus the raw primitive at R_o is obtained by integrating the ideal H up to that radius, including its finite turn. In particular the substitution uses no claim about a primitive inside an uncompleted bank. Lemmas 1.14.1 and 1.14.3 and $r_y + (1-\lambda)r = 1$ on the power interval give

$$I_{\mathrm{raw}}(R_o)/(R_o H_{\mathrm{out}}) = r_* + D(e^T R_g/R_o)^a.$$

Here I_{raw} omits precisely the present two bumps. These identities may equivalently be used to select the reference before inserting the core and loop, since both later operations restore the indicated rows. As $R_o H_{\mathrm{out}}/(X_p H_p) = (R_o/X_p)^a$,

$$\frac{p}{X_p H_p} = D\lambda^{60a}\left[(1-\tau)(R_{g,b}/R_g)^a + \tau(R_{g,b}/(\ell R_g))^a - 1\right]. \tag{Taper}$$

The bracket and all its fixed angular derivatives are bounded by the fixed phase geometry. It is identically zero on both open ends. In particular

$$\|p/(X_p H_p)\|_{C^k_\eta} \le K_{\mathrm{pre},k}\lambda^{60(1-\lambda)}. \tag{1.14.13}$$

The first row below adds exactly p. Together with the scalar-sector inverse this yields

$$I_{\mathrm{pulse}}(R_o) = (1-\chi)I_c(R_o) + \chi I_w(R_o). \tag{Inlet}$$

The same convex identity for the velocity gives both zero inlet conditions of the connector. The small solution has zero coefficients wherever $p = 0$. Its energy on the interior bridge is retained in (1.14.14).

Lemma 1.14.4 (Quantitative actual two-row solve, with partial histories)**.** *On these supports put* $H_{\mathrm{new}} = H(1 + t_1\psi_1 + t_2\psi_2)$. *The exact* I/C_p *equations are*

$$\sum A_j t_j = p/(\tfrac{\hat{\xi}_p^2}{2} H_p), \qquad 2\sum B_j t_j + \sum C_j t_j^2 = 0,$$

where

$$A_j = \int e^{(1-\lambda)z}\psi_j \,\mathrm{d}z, \quad B_j = \int e^{-(1+2\lambda)z}\psi_j \,\mathrm{d}z, \quad C_j = \int e^{-(1+2\lambda)z}\psi_j^2 \,\mathrm{d}z.$$

They have a unique small solution that satisfies $\|t\|_{C^k} \le K_{\mathrm{pre},k}\lambda^{60(1-\lambda)}$. *The same bound controls the relative field error and the normalized partial* I, S, C_p *errors, with fixed-*$\hat{\xi}$ *jets. It applies on the two bump supports and the interval between them.*

At the exit $\Delta I = p$, $\Delta C_p = 0$, *and* M, J *and all velocity germs do not change. Its nonzero energy increment is*

$$\delta\sigma_p^{\mathrm{tap}} = -\frac{1}{2}\sum_j \int e^{-2\lambda z}(2t_j\psi_j + t_j^2\psi_j^2)\,\mathrm{d}z. \tag{1.14.14}$$

Proof. The distinct translate ratios of the two Jacobian rows differ by the exponent gap $2+\lambda$. The explicit coefficients extend smoothly to $\lambda = 0$, and their determinant there is nonzero. On the fixed closed small interval a constant fixed before we select λ thus bounds the inverse norm.

The remaining map is the displayed quadratic polynomial, with a fixed quadratic norm. The contraction $t = J^{-1}(d - \mathcal{Q}(t))$ on $|t| \le 2\left\|J^{-1}\right\||d|$ is valid whenever $4\left\|J^{-1}\right\|^2\|\mathcal{Q}\||d| < 1/2$. The same argument in C^k gives the asserted jets.

Partial integrals have a bound by the same finite-support densities. We do not set them to zero between supports. At fixed $\hat{\xi}$, $\dot{z} = -v_p$ contributes the real terms $-v_p\psi_j'$. Here v_p and all necessary jets are fixed early chart data. The energy formula is a result of $\frac{S_{\hat{\xi}}}{\hat{\xi}} = -H^2/(4\frac{\hat{\xi}^2}{2})$, and M, J do not change because $U = 0$ throughout these supports. □

The central memory correction occurs after the pulse and before the protected hold. Its actual discrepancy is $\delta I = (r_b - a^{-1})\frac{\hat{\xi}_p^2}{2}H_p e^{-aW}$. Normalized at R_o it is $(r_b - a^{-1})e^{-a(Y+W)}$. The explicit edit $I \mapsto I + \delta I\zeta(\frac{\hat{\xi}^2}{2}/R_m)$ has $\delta H = \delta I\zeta'/R_m$. Differentiation keeps $-\log\dot{R}_m(\frac{\hat{\xi}^2}{2}/R_m)\zeta''$ as well as $\dot{\delta I}$.

For the fixed normalized moving moment correction its first normalized jet is $K_{\mathrm{mem}}(1 + Y_0)^N e^{-(1-\lambda)Y_0}$. The constants can depend on the previously selected cutoff and ν_c. We make this term small with Y_0, not by λ. Because the moment correction is after the pulse, it changes none of the inlet M, I, J, S histories. Its genuine future energy and pressure integrals enter the pulse root and canonical pressure once.

The parameterized A11 moment correction also lies after the returns. Its input is the true transported primitive, never a reset.

1.14.5 The actual heat correction: late-scale bounds and exact bookkeeping

We let ΔS_f denote the signed change of the S history under the last postpulse same heat edit and rank-one correction. We denote its pressure-moment change by $\Delta C_{p,f}$. The rank-one correction makes their total primitive change zero. We first select all normalized geometry and Y_0. The rescaled stop ODE and explicit heat basis in Proposition 1.15.8 then give

$$\|\delta H\|_{C^k_\eta} \le C_k c\left(\tfrac{\hat{\xi}^2}{2}\right)^{-h-1}$$

on the heat collar and tail.

The compact rank-one bump has the related relative $O(R_{\mathrm{master}}^{-1})$ bound. Integration of $2H\delta H + \delta H^2$, with weights $\left(\frac{\hat{\xi}^2}{2}\right)^{-1}$ and $\left(\frac{\hat{\xi}^2}{2}\right)^{-2}$, thus gives the actual early-correction normalized target bound

$$\|d_{\mathrm{heat}}\|_{C^k} \le K_{\mathrm{sc},k}(Y_0)R_{\mathrm{master}}^{-1}. \tag{1.14.15}$$

The two far-tail envelopes are $c^2\left(\frac{\hat{\xi}^2}{2}\right)^{-2h-2}$ and $c^2\left(\frac{\hat{\xi}^2}{2}\right)^{-2h-3}$. Their integrals are finite for fixed $h > 0$. The formulas include moving-endpoint terms.

At the heat-splice inlet the difference vanishes on an open germ. This establishes the estimate at inverse scale zero by actual envelopes, not an assumed compact family of finite-scale fields.

On the fixed-λ extension, we use the previously specified angular cutoff χ_b. It is zero on the inner overlap and one on the protected terminal collars. We solve the actual three-row moment correction for

$$(\Delta I_b, \Delta S_b, \Delta C_{p,b}) = (0, -\chi_b \Delta S_f, -\chi_b \Delta C_{p,f}). \tag{1.14.16}$$

The cutoff acts on the target, not on coefficients of a nonlinear moment correction solution. At the protected collar this is the full backward history restoration. Elsewhere we keep its partial history restoration.

Lemma 1.14.5 (Real normalized three-row inverse and its first jets)**.** *We fix three nonnegative bumps on the actual second-power reserve. Their relative radii lie away from the two-row taper. They solve* (1.14.16) *for all sufficiently large last scales. The relative correction and its selected finite fixed-$\hat{\xi}$ jets are $O(K_{\mathrm{sc}}(Y_0)/R_{\mathrm{master}})$. At its exit I, M, J and the velocity germs equal their pre-edit values.*

The actual S, C_p changes are the last two target rows.

Proof. In $x = (\hat{\xi}/\hat{\xi}_*)^2$ write $E^0 = e_* f x^{-1/2-\lambda}$ and $\delta E = e_* v$, $v = \sum t_j b_j(x)$. We normalize the three rows by $(\frac{\hat{\xi}_*^2}{2})^{3/2} e_*$, $\frac{\hat{\xi}_*^2}{2} e_*^2$, and e_*^2. The exact map is

$$\sqrt{2} \int x^{1/2} v \, \mathrm{d}x, \quad -f \int x^{-1/2-\lambda} v \, \mathrm{d}x - \tfrac{1}{2} \int v^2 \, \mathrm{d}x, \quad f \int x^{-3/2-\lambda} v \, \mathrm{d}x + \tfrac{1}{2} \int v^2 \frac{\mathrm{d}x}{x}.$$

Its linear rows are three distinct powers.

Their Wronskian has one nonzero sign for $x > 0$. Integration of the related three-point determinant against the ordered positive bumps keeps that sign. The explicit coefficients, $f^{\pm 1}$, and all selected angular derivatives are bounded on the fixed closed template domain, with $\lambda = 0$. We denote the inverse norm by B_k and the quadratic norm by Q_k in C^k. The explicit condition $8B_k^2 Q_k \|d\|_{C^k} < 1$ gives a unique small branch and $\|t\|_{C^k} \le 2B_k \|d\|_{C^k}$.

Equation (1.14.15) supplies this condition by a later radius, with no new choice of λ.

Differentiation of the actual equation gives $(J + \mathcal{Q}'(t))\partial_\eta t = \partial_\eta d - (\partial_\eta J)t - (\partial_\eta \mathcal{Q})(t)$, with inverse norm at most $2B_0$. This proves the first jet bound directly. Higher fixed jets are a result of the same finite induction. Moving support derivatives introduce the fixed logarithmic graph derivatives, previously included in $K_{\mathrm{sc}}(Y_0)$. Actual partial history errors are a result of integration of these densities, with the quadratic terms.

Finally $U = 0$ gives exact M, J preservation, and the first row gives exact I preservation at the exit. □

Thus the actual pulse input is, with each moment-correction contribution,

$$\sigma_p = \sigma_p^0 + \delta\sigma_p^{\mathrm{tap}} - 2\chi_b \Delta S_f / H_p^2. \tag{1.14.17}$$

The three-row moment correction does not change the inlet Q. Its outlet I, M, J and velocity germs agree as smooth functions. Thus their angular derivatives also agree. The two-row taper changes Q by $O_{C^1}(K_{\mathrm{pre}} \lambda^{60a})$ as stated.

We must still calculate the canonical pressure from the same complete future. If $\Delta C_{p,f}$ is the future change, the pressure at the pulse inlet changes by $-\Delta C_{p,f}$, regardless of χ_b. The canonical axis datum in the intermediate bridge changes by $-(1 - \chi_b)\Delta C_{p,f}$. Addition of the moment correction's $-\chi_b \Delta C_{p,f}$ yields the same inlet pressure. The forward matching collar has $\chi_b = 1$ and hence zero residual, as does the whole native backward interval.

A zero total pressure change under the moment correction does not reset physical pressure.

Proposition 1.14.6 (The heat root cancellation and the actual bridge residual)**.** *We let* $\tau_S = S(R_o)/H_o^2$ *be the positive canonical future integral contribution. For this heat edit* $\delta\tau_S = -\Delta S_f/H_o^2$ *and* $H_o^2 = H_p^2 e^{-2\lambda Y}$*. Its exact contribution to the energy-root right-hand side is*

$$\delta[-\lambda\sigma_p + 2\lambda e^{-2\lambda Y}\tau_S] = -2\lambda(1-\chi_b)\Delta S_f/H_p^2. \tag{1.14.18}$$

It vanishes identically on the protected full-history restoration collars, with each differentiated identity. In the rest of the fixed-λ *bridge it has a genuine* $O_{C^1}(K_{\mathrm{sc}}(Y_0)/R_{\mathrm{master}})$ *bound and becomes small with the last radius.*

We do not assign the unchanged model pulse root to the full bridge.

Proof. The future signed S increment is the negative of its change in positive outward swirl-energy integral. We substitute this and (1.14.17). The displayed amplitude identity cancels the exponential. Differentiation of the identity keeps $\dot\chi_b$ and the moving-amplitude terms.

The normalized heat bound and the fixed finite bridge geometry prove the residual estimate. □

For an actual bridge root, keep (1.14.18) in the quadratic energy equation. Its model positive root has a fixed nonzero amplitude derivative. The previous small residual thus changes the root and its first jet by $O(K_{\mathrm{sc}}(Y_0)/R_{\mathrm{master}})$. This error must be less than each previously specified pulse tolerance, for example λ^2. This is one more lower bound on C, with constants fixed before C (L_o, Y_0, λ). It is part of the step-4 choice of C (Section 1.5.2).

It is not a term $K_f\lambda^{30}$. It does not impose early uniformity on K_f.

1.14.6 The actual affine return data

We write the two return equations as $A(\lambda, Y)c = -A_pP - (m_p, j_p)^T$ and set $c = A_pb + g$. After row factorization,

$$A = \mathrm{diag}(e^{\beta Y}, e^{\beta_2 Y})\widehat{A}, \quad \widehat{A}_{1j} = e^{-\beta d_j}L(\beta), \quad \widehat{A}_{2j} = e^{-\beta_2 d_j}L(\beta_2),$$

where $L(t) = \int e^{tz}\psi(z)\,\mathrm{d}z > 0$. The two distinct fixed offsets give $|\det\widehat{A}| \geq c\lambda$. Thus the actual affine term is

$$g = -\widehat{A}^{-1}(e^{-\beta Y}m_p, e^{-\beta_2 Y}j_p)^T, \tag{1.14.19}$$

and, with the trace derivatives of the true inlet data,

$$|g| + |\dot g| \leq K_{\mathrm{pre}}\lambda^{29-120\lambda}(1 + |\dot Y| + |v_p|)e^{-(1/2-2\lambda)Y}.$$

The λ^{-1} determinant cost is explicit.

We do not hide it in a constant that we then multiply by λ. The exponential makes this term small under the next Y_0 choice. On the genuine variable-exponent sector $g = 0$. The two-row and three-row swirl corrections keep m_p, j_p and the entry germ unchanged, so they do not add a missing affine datum. The full Gram energy equation keeps the $A_pb\cdot g$ and g^2 terms.

1.14.7 Outputs and other source estimates

Explicit integrals and finite nonlinear equations give all the necessary data. These include the actual finite-prefix ratios, their uniform parameter bounds, the fixed-coordinate bridge histories, and all inlet first jets. They also include the two-row primitive taper, the late heat-correction errors, and the affine return data. Earlier core/loop operations that have previously restored all five histories transmit these data.

The order is: fix the bridge/template data. We select λ. Select h, ν_c, the actual future geometry and L_o. We select the actual inverse/cutoff and Y_0. Last, we select one physical scale for the heat-correction and root residual tolerances.

We do not use an early power of λ to absorb a constant selected later. This section supplies the prefix inputs. We prove the native terminal source and whole primitive-mixture corridor in Lemmas 1.17.5, 1.17.8, and 1.17.9. They are not consequences of the prefix estimates alone.

1.15 Actual future realization and inlet order

Main result. Proposition 1.15.8 constructs the future profile and keeps its inlet data unchanged. Proposition 1.15.25 proves the order of the actual inlet coefficients. Other proofs establish the source-cone and pulse-response results.

This section constructs the future of the joint model before we select its pulse root and heat realization. We insert the scalar logarithmic length L_o *after* the model A11 outlet, where $U = M = J = 0$ and $I = \frac{\hat{\xi}^2}{2} H/(1-\lambda)$. It precedes a fixed transition from slope $-\lambda$ to slope $-h$. That transition and its wing are the selected terminal power model. All these choices precede the completion of the member.

Throughout, $0 < h < \lambda/6$, $0 < \lambda < 1/20$, and $a = 1 - h$. We fix these parameters before L_o. We also fix the chart, its compact comparison band, and the central hold length before L_o. We never use a bound that depends on these data to select λ retrospectively.

1.15.1 Exact terminal power model and its actual histories

We select once a smooth nondecreasing function $s : [0,1] \to [0,1]$, constant near the two endpoints, and a fixed $\delta > 0$. We put

$$\kappa(t) = \lambda - (\lambda - h)s(t/\delta), \qquad p(t) = \exp\left(-\int_0^t \kappa(v)\,\mathrm{d}v\right), \quad 0 \le t \le \delta.$$

The inlet ratio is $r_\lambda = (1-\lambda)^{-1}$. We let $r' + (1-\kappa)r = 1$, $r(0) = r_\lambda$, and set $b = r(\delta) - a^{-1}$.

Lemma 1.15.1 (A positive excess independent of the added length)**.** *This construction gives*

$$0 < b, \qquad b \ge \frac{\lambda - h}{(1-\lambda)(1-h)} e^{-a\delta}, \qquad r(t) \le r_\lambda.$$

The quantities b and p are independent of L_o, the inlet amplitude, and the absolute radius.

Proof. For $v = r - a^{-1}$ the exact equation is

$$v' + (1-\kappa)v = (\kappa - h)/a \ge 0, \qquad v(0) = \frac{\lambda - h}{(1-\lambda)a} > 0.$$

Variation of constants gives the lower bound, because $1 - \kappa \le a$. The constant r_λ is a supersolution because $1 - (1-\kappa)r_\lambda = (\kappa - \lambda)/(1-\lambda) \le 0$.

All equations are in logarithmic relative coordinates. □

To specify the terminal model without a new choice of primitive, take the next jointly selected smooth terminal cutoff:

$$\vartheta(t) = e^{-1/t^2}\ (t > 0), \quad \vartheta(t) = 0\ (t \le 0), \quad \sigma(t) = \frac{\vartheta(t)}{\vartheta(t) + \vartheta(1-t)}, \quad \Psi(v) = 1 - \sigma\left(\frac{v - e^{-3}}{1 - e^{-3}}\right).$$

Thus $\Psi:[0,\infty)\to[0,1]$ is nonincreasing. It equals one on $[0,e^{-3}]$ and zero on $[1,\infty)$, and all its positive-order derivatives vanish at both transition endpoints. We set

$$m_h=\int_0^1 v^{-h}\Psi(v)\,\mathrm{d}v>0.$$

We select $0<\rho<1/4$, after h,λ,δ, small enough that

$$\frac{b(1-\rho)}{\rho m_h}>e^{4a}. \tag{1.15.1}$$

For example, we can use each positive ρ less than the explicit threshold that this inequality gives.

The selected terminal slope restriction $\rho\sup|v\Psi'(v)|/(1-\rho)<h/4$ holds after we decrease ρ at this same stage. No parameter in this paragraph depends on L_o.

At the A11 outlet let the radius and swirl be $R_A,H_A>0$. On $0\le y=\log(\frac{\hat\xi^2}{2}/R_A)\le L_o$ prescribe

$$H=H_Ae^{-\lambda y},\qquad I=\frac{\frac{\hat\xi^2}{2}H}{1-\lambda},\qquad U=M=J=0.$$

We continue with $H=H_Ae^{-\lambda L_o}p(t)$ on $\frac{\hat\xi^2}{2}=R_Ae^{L_o+t}$, $0\le t\le\delta$, and integrate $\frac{I_{\hat\xi}}{\hat\xi}=H$. We write $R_0=R_Ae^{L_o+\delta}$ and $H_0=H_Ae^{-\lambda L_o}p(\delta)$. We define

$$\begin{aligned}&C=H_0R_0^h,\quad c=\frac{C}{1-\rho},\quad B=R_0\left(\frac{b(1-\rho)}{\rho m_h}\right)^{1/a},\\&H=c(\hat\xi/\sqrt{2})^{-2h}\left[1-\rho\Psi\left(\frac{\hat\xi^2}{2B}\right)\right]\qquad(\hat\xi\ge\sqrt{2R_0}).\end{aligned} \tag{1.15.2}$$

Lemma 1.15.2 (Exact primitive match and coefficient law)**.** *The fields in* (1.15.2) *join the previous h-power germ with each radial jet. With the actual inlet value of I, their primitive equals $c(\frac{\hat\xi^2}{2})^{1-h}/(1-h)$ beyond B. The regular power coefficient is*

$$c=H_AR_A^hJe^{-(\lambda-h)L_o},\qquad J=\frac{p(\delta)e^{h\delta}}{1-\rho}>0. \tag{1.15.3}$$

The number J is independent of L_o,R_A,H_A.

Proof. The separation in (1.15.1) gives $B>e^4R_0$, so the terminal formula equals $C(\hat\xi/\sqrt{2})^{-2h}$ on an open neighborhood of R_0.

Also $B>e^4R_0>e^3(2R_0)$ because $e>2$. At that point its actual primitive is $I(R_0)=H_0R_0(a^{-1}+b)=CR_0^a/a+bCR_0^a$. For the terminal formula,

$$I(R_0)-\frac{cR_0^a}{a}+\int_{\sqrt{2R_0}}^{\infty}(H-c(\hat\xi/\sqrt{2})^{-2h})\,\hat\xi\,\mathrm{d}\hat\xi=bCR_0^a-\rho cB^am_h=0.$$

Here the term over $[0,R_0]$ used to combine the integrals is legitimate because $\Psi=1$ there after the scale change, and $h<1$. The last equality is the definition of B.

It is an identity for the integrated primitive, not a reset at R_0. Formula (1.15.3) is a result of substitution. □

1.15.2 The complete heat-tail integral and the added leg

We let $\mathcal{H}(x)$ be the model with inlet at the transition inlet, normalized by its inlet amplitude, with $x = \frac{\hat{\xi}^2}{2}/(R_A e^{L_o})$. The previous construction gives one fixed function $\mathcal{H}$, independent of L_o, R_A, H_A, equal to a positive multiple of x^{-h} for large x. We define its *complete* integrals

$$K_S = \frac{1}{4}\int_1^\infty \mathcal{H}(x)^2 \frac{\mathrm{d}x}{x}, \qquad K_P = \frac{1}{4}\int_1^\infty \mathcal{H}(x)^2 \frac{\mathrm{d}x}{x^2}. \tag{1.15.4}$$

They include the full terminal power tail. In particular the pure tail beyond its last edge contributes its actual squared edge amplitude divided by $8h$ to K_S.

Lemma 1.15.3 (A scalar length controls the tail without a subsequent choice of λ)**.** *The numbers K_S, K_P are finite. For each fixed K_S select*

$$L_o \geq L_S := \frac{1}{2\lambda}\log^+(8\lambda K_S). \tag{1.15.5}$$

Then the complete canonical future from R_A obeys

$$S(R_A) = H_A^2\left[\frac{1-e^{-2\lambda L_o}}{8\lambda} + e^{-2\lambda L_o}K_S\right] \leq \frac{H_A^2}{4\lambda}, \tag{1.15.6}$$

$$-P(R_A) = \frac{H_A^2}{R_A}\left[\frac{1-e^{-(1+2\lambda)L_o}}{4(1+2\lambda)} + e^{-(1+2\lambda)L_o}K_P\right]. \tag{1.15.7}$$

Also, for each $0 \leq y \leq L_o$ and $E(y) = H_A(2R_A)^{-1/2}e^{-(1/2+\lambda)y}$,

$$E(y)\frac{S(R_A e^y)}{H(R_A e^y)^2} \leq \frac{E(0)}{4\lambda}. \tag{1.15.8}$$

These bounds continue to hold when L_o increases.

We do not impose a bound on the unattenuated K_S that is uniform when $h \to 0$.

Proof. The tail integrands are constant multiples of x^{-1-2h} and x^{-2-2h}. Their integrals are finite because we fixed $h > 0$. Integration of the added power leg gives the exact formulas. Condition (1.15.5) implies $e^{-2\lambda L_o}K_S \leq (8\lambda)^{-1}$.

At an intermediate point,

$$\frac{S}{H^2} = \frac{1-e^{-2\lambda(L_o-y)}}{8\lambda} + e^{-2\lambda(L_o-y)}K_S.$$

Multiplication by $E(y)$ leaves the tail term bounded by $E(0)e^{-2\lambda L_o}K_S e^{-(1/2-\lambda)y}$, which proves (1.15.8). This also explains why a bound on S/H^2 at each intermediate point is not necessary for this weighted estimate. □

Lemma 1.15.4 (The rebuilt flattening interval has uniform local integral bounds)**.** *We fix a compact angular interval on which a smooth J_0 and its first derivative are bounded. We select T_0 independently of λ, h so that, for $T_f = T_0/\lambda$,*

$$H(y,\beta) = H_e e^{-\lambda y}\exp[-\theta(y)J_0(\beta) - (1-\theta(y))\log 2], \qquad \theta = 1 - s(y/T_f),$$

has $-3\lambda/2 \leq \partial_y \log H \leq -\lambda/2$. The integral of H^2 and the integral of $|HH_\beta|$ over the flattening interval are at most CH_e^2/λ, with C independent of h, λ, T_f. Suppose the later uniform power wait and the added leg enter this model and satisfy (1.15.5). The same bound holds for their complete outward energy integral from the flattening inlet.

The normalized pressure integral and its first angular derivative have bounds independent of T_f.

Proof. We select T_0 so $\|s'\|_\infty \sup|\log 2 - J_0|/T_0 \le 1/2$. Then $H^2 \le CH_e^2 e^{-\lambda y}$ and $|H_\beta| \le \|J_0'\|_\infty H$. The first claims are a result of integration. The next wait has slope $-\lambda$.

Its own energy has a bound by its inlet amplitude squared divided by 8λ, and its transmitted downstream integral contribution has the exact attenuation factor. We apply (1.15.6) and keep this factor. The late model is independent of β in backward coordinates. For pressure the density contains the extra factor e^{-y}, so its integral has no $1/h$ or T_f loss. The two A11 bumps have fixed relative supports and bounded coefficients.

We must add their actual quadratic integrals. These satisfy the same bounds when the coefficients and their first derivatives stay bounded. □

Lemma 1.15.5 (The A11 small target stays uniform under the rebuilt flattening)**.** *Suppose the actual normalized ratio and its first angular derivative at the flattening inlet are bounded. On that interval let $r = I/(\frac{\xi^2}{2}H)$. Then r and r_β stay bounded independently of $T_f = T_0/\lambda$. After an unedited uniform λ-power wait of length $W = 30\log(1/\lambda)$,*

$$\|r - r_\lambda\|_{C^1_\beta} \le C\lambda^{30(1-\lambda)}.$$

The normalized moment Jacobian of the two nonnegative A11 translates has one inverse bound for all permitted λ, also at $\lambda = 0$.

Proof. We write $\ell = \partial_y \log H$. The exact equations are

$$r_y + (1+\ell)r = 1, \qquad (r_\beta)_y + (1+\ell)r_\beta = -\ell_\beta r.$$

Here $1 + \ell \ge 1 - 3\lambda/2 > 9/10$ and $|\ell_\beta| \le C\lambda$. Stable convolution proves the first assertion, without the integral of a constant error over T_f. On the wait, $r - r_\lambda$ and r_β decay at rate $1 - \lambda$.

For relative edits $H \mapsto H(1 + t_1\psi_1 + t_2\psi_2)$ on disjoint equal translates, the normalized equations are

$$A_1 t_1 + A_2 t_2 = u, \qquad 2B_1 t_1 + 2B_2 t_2 + C_1 t_1^2 + C_2 t_2^2 = 0,$$

where u is the normalized target-minus-current primitive discrepancy, $A_j = \int e^{(1-\lambda)z}\psi_j \,\mathrm{d}z$, $B_j = \int e^{-(1+2\lambda)z}\psi_j \,\mathrm{d}z$, $C_j = \int e^{-(1+2\lambda)z}\psi_j^2 \,\mathrm{d}z$. If the translate distance is $d_* > 0$, then $A_2/A_1 = e^{(1-\lambda)d_*}$ and $B_2/B_1 = e^{-(1+2\lambda)d_*}$. Their difference has a fixed positive magnitude on $0 \le \lambda \le 1/20$. Thus the determinant of the two-row Jacobian is bounded away from zero, and the quadratic implicit function theorem has a fixed small-data ball. Its solution and its first angular derivative are $O(\|u\|_{C^1})$.

The moment equations keep the actual target and total pressure increment unchanged. They do not assert zero energy change. □

1.15.3 The actual scalar coefficient map and the same fast mode

Lemma 1.15.6 (Post-hold stop map with a uniform positive coefficient)**.** *We fix $0 < \nu_c < h/10$ and the scalar post-hold normalized drive. There exist $R_*, k_-, k_+ > 0$ that depend only on these fixed data. The actual deficit drive and exact positive heat shot from any radius $R \ge R_*$ satisfy*

$$c = GR^h K_{\mathrm{old}}(R), \qquad 0 < k_- \le K_{\mathrm{old}}(R) \le k_+.$$

The map is independent of the amplitude G. Each fixed order of its logarithmic scale derivatives stays bounded.

Thus the same lower bound holds with $R = R_h e^{B_h}$ for each fixed $B_h \ge 0$ and all sufficiently large R_h.

Proof. Lemma 1.6.26 gives the complete argument, with the templates $\kappa_{\mathrm{st}}, \kappa_1$, the bound $\delta_{\mathrm{st}} \le 0.45$, the condition (1.6.54), the first hitting point and the regular extension through $\varepsilon = 0$; we summarize it. We use $x = \frac{\hat{\xi}^2}{2}/R$, $W = w_d/R$, $a = 1 - h$, and initially $W(1) = a^{-1} - (1 - \nu_c)^{-1} > 0$. We select a sufficiently short fixed smooth transition of the slope from ν_c to $2h$. The exact equation is

$$W_x = \kappa(x)W/x + (h - \kappa(x))/a.$$

By continuity this transition leaves $W > 0$.

We continue with $\kappa = 2h$. Its explicit solution is a multiple of x^{2h} minus $hx/[a(1 - 2h)]$, and has a finite first zero x_z. At that zero $W_x = -h/a \neq 0$. We stop at $W = c_t\epsilon$, where $\epsilon = R^{-1/5}$ and $c_t > 0$ is fixed. The implicit-function theorem gives a smooth $x_{\mathrm{hit}}(\epsilon)$ down to $\epsilon = 0$.

We change the slope to h over a width $c_w\epsilon$ in x, with fixed sufficiently small $c_w > 0$. The substitutions $W = \epsilon Z$ and $x = x_{\mathrm{hit}} + c_w\epsilon z$ give

$$Z_z = c_w \left[\frac{\kappa(z)\epsilon Z}{x_{\mathrm{hit}} + c_w\epsilon z} + \frac{h - \kappa(z)}{a} \right].$$

Thus $Z(1)$ stays positive after we fix c_w. The amplitude equation in this same coordinate is

$$(H/G)_z = -\frac{c_w\epsilon\kappa(z)}{x_{\mathrm{hit}} + c_w\epsilon z}(H/G).$$

It has a smooth positive limit.

Thus the power-segment radius and amplitude are $R_b = Rx_b(\epsilon)$ and $G_b = Gg_b(\epsilon)$, with x_b, g_b smooth and strictly positive down to zero. The power-segment deficit satisfies $C_b \asymp hG_bR_b^{4/5}$.

The exact scalar shot targets $c = G_bR_b^h$. The forced system (1.13.39), variation formula (1.13.44), and coefficient identity (1.13.45) give

$$\lambda_s = (D_c - B_0)/B_1, \quad D_c = (1 - h)C_bR_b^{h-1}[1 + O_h(G_b/C_b + R_b^{-1})],$$

$$B_1 = 2(1 - h)C_bR_b^{h-1}[1 + O_h(\epsilon_s + R_b^{-1})], \qquad B_0/D_c = O(\epsilon_s).$$

We select the fixed source fraction ϵ_s small and then R_* large. This gives $B_1 > 0$ and $\lambda_s \in [1/4, 3/4]$. The specified nonnegative source thus realizes the coefficient.

Thus $K_{\mathrm{old}} = g_bx_b^h$. The smooth maps on $0 \le \epsilon \le \epsilon_*$ give positivity, bounds, and logarithmic scale derivatives, not compactness of an open inverse-radius interval. Linearity of the scalar equations and the proportional deficit give amplitude independence. □

Lemma 1.15.7 (The outer heat correction uses the actual same fast mode)**.** *We let b_s be the scalar shot's source-free outlet and let c, k_f be its actual outlet heat coefficients. Suppose all central geometry has been fixed and $b_s \le M_cR_o$ on the comparison band. We increase the outer length L_o before we select the last scale. We make sure that the first outer heat-correction radius obeys $R_0 \ge 4M_cR_o$. Then its same heat field*

$$H^{\mathrm{heat}}(\tfrac{\hat{\xi}^2}{2}, \eta) = d^{-h}[cg_h(\tfrac{\hat{\xi}^2}{2}/d) + k_fg_f(\tfrac{\hat{\xi}^2}{2}/d)], \qquad d = 1 - \eta^2,$$

has, for each necessary fixed finite derivative order, the normalized power comparison

$$\left|(\tfrac{1}{2}\hat{\xi}\partial_{\hat{\xi}})^j\partial_\eta^m(H^{\mathrm{heat}} - c(\hat{\xi}/\sqrt{2})^{-2h})\right| \le C_{j,m}c(\tfrac{\hat{\xi}^2}{2})^{-h-1} \quad (\tfrac{\hat{\xi}^2}{2} \ge R_0). \tag{1.15.9}$$

Constants are uniform in the sufficiently large same radius, for the fixed normalized geometry.

They can depend on h, L_o. We do not use a small bound on the unexposed coefficient k_f.

Proof. The actual scalar shot gives

$$k_f g_f(b_s) \le C\left[\frac{C_b}{R_b}e^{-W_s/3}+\frac{C_b}{W_s}e^{-W_s/12}\right], \quad W_s=\epsilon_s R_b,$$

and $c=G_bR_b^h$. Its right side divided by cb_s^{-h} is a fixed polynomial in R_b times $e^{-c_*R_b}$. The exact fast-mode formula gives, for large $x\ge b_s$, $g_f(x)/g_f(b_s)\le Ce^{-(x-b_s)/3}$ with polynomial factors after any fixed number of derivatives.

Because $\frac{\hat\xi^2}{2}/d \ge \frac{\hat\xi^2}{2} \ge 4b_s$, this exponential absorbs all powers of $\frac{\hat\xi^2}{2}/d$ and d^{-1} generated by angular derivatives, with one bound when $d\downarrow 0$. The regular expansion $d^{-h}g_h(\frac{\hat\xi^2}{2}/d) = (\hat\xi/\sqrt{2})^{-2h}[1+O_h(d/\frac{\hat\xi^2}{2})]$, with its differentiated finite expansions, gives (1.15.9). These are the basis formulas (1.13.36) and (1.13.35) and the source-free exposure estimate (1.13.42). The ratio k_f/c does not change by one amplitude rescaling. Thus a smaller c from the new outer length does not introduce a new fast-mode normalization.

□

1.15.4 A rank-one actual primitive correction, with all inlet germs fixed

Chart convention. Lemma 1.15.7 is a forward formula on $|\eta_f|\le 1$ and is never evaluated at negative d_f. For the backward member use its positive Laplace heat factor

$$\mathcal{H}_-(z)=\frac{1}{\Gamma(1+h)}\int_0^\infty e^{-v}v^h(1+zv)^{-h}\,\mathrm{d}v, \qquad z\ge 0,$$

with $H_b=c(\hat\xi_b/\sqrt{2})^{-2h}\mathcal{H}_-(2d_b/\frac{\hat\xi_b^2}{2})$ in the same power segment coefficient convention. Differentiation under this positive integral gives its finite expansions, whose coefficients alternate in sign. The forward regular coefficients are $2^n(h)_n(1+h)_n/n!$ in $d_f/\frac{\hat\xi_f^2}{2}$. In slice variables $d/\frac{\hat\xi^2}{2}=\widetilde\eta/\frac{\widetilde\xi^2}{2}$ on the forward side and $d/\frac{\hat\xi^2}{2}=-\widetilde\eta/\frac{\widetilde\xi^2}{2}$ on the backward side. Thus the two expansions give the same one-sided slice jets of the heat exterior to each fixed order.

The fast term has zero continuation on the backward side and is flat at the seam on the forward side. This does not evaluate the Laplace integral at negative argument.

We use the same normalized collar cutoffs, terminal cutoff and rank-one bump on the two charts. Each support radius converts like $\frac{\hat\xi^2}{2}$, so each cutoff is a function of $(\hat\xi/\hat\xi_{\mathrm{supp}})^2=(\widetilde\xi/\widetilde\xi_{\mathrm{supp}})^2$ and is one slice function. The discrepancy D_I has weight $h-1$. Thus the bump $-D_I/\frac{\hat\xi_{\mathrm{bump}}^2}{2}\,\psi((\hat\xi/\hat\xi_{\mathrm{bump}})^2)$ has the weight h of H. Complete finite-order moment derivatives pass through the integrals: the discrepancy tail has a bound by $C(\frac{\hat\xi^2}{2})^{-h-1}$, and the quadratic tails decay faster. Thus these operations keep equal slice jets, not only equal field values.

Lemma 1.7.1 gives the positive backward heat factor and its finite derivative bounds. The expansion is (1.7.4). The forward expansion is (1.13.35).

The rank-one construction keeps $\frac{\hat\xi_b^2}{2}$, H_b, c, and the specified terminal edge fixed together. These quantities are not independent parameters: the previous power coefficient and c constrain the inlet amplitude. The correction thus keeps the inlet unchanged and restores the complete primitive.

We let $\frac{\hat\xi_b^2}{2}=R_Ae^{L_o}$, $R_0=e^\delta\frac{\hat\xi_b^2}{2}$, and B be the fixed model edge from (1.15.2). We increase L_o to at least $\log 4$. We take a fixed radial cutoff $\zeta(x)$ equal to zero near $x\le 1$ and one near $x\ge 2$. In the heat collar define

$$H^b(\tfrac{\hat\xi^2}{2})=(1-\zeta(\tfrac{\hat\xi^2}{2}/R_0))C(\hat\xi/\sqrt{2})^{-2h}+\zeta(\tfrac{\hat\xi^2}{2}/R_0)(1-\rho)H^{\mathrm{heat}}(\tfrac{\hat\xi^2}{2}), \quad R_0\le\tfrac{\hat\xi^2}{2}\le 2R_0.$$

We use the model up to R_0, and set $H^b = H^{\mathrm{heat}}(1 - \rho\Psi(\frac{\hat\xi^2}{2}/B))$ for $\frac{\hat\xi^2}{2} \ge 2R_0$.

These formulas agree on open germs because $B > e^4 R_0$. We let H^m be the whole power model with its same inlet fields. We select a fixed nonnegative $\psi \in C_c^\infty((1/2, 3/4))$ with $\int \psi = 1$ and put

$$D_I(\eta) = \int_{\sqrt{2R_0}}^{\infty} (H^b - H^m)(\tfrac{\hat\xi^2}{2}, \eta)\, \hat\xi \, \mathrm{d}\hat\xi, \qquad H^a = H^b - \frac{D_I(\eta)}{\frac{\hat\xi_b^2}{2}} \psi((\hat\xi/\hat\xi_b)^2). \tag{1.15.10}$$

Proposition 1.15.8 (Actual heat future with exact primitive and unchanged inlet)**.** *For each fixed normalized construction in this section, a sufficiently large same radius makes H^a positive. It keeps the original inlet H germ, the same regular and fast coefficients c, k_f, and the specified terminal edge and cutoff. Its full primitive increment relative to the model is zero:*

$$\int_0^\infty (H^a - H^m)\, \hat\xi \, \mathrm{d}\hat\xi = 0.$$

We integrate from the original inlet to get the actual primitive. It agrees with the same heat primitive after the terminal edge. There is no new integration constant at the drive inlet.

All fixed scaled derivatives of the correction are $O(R_o^{-1})$ in the appropriate model-amplitude units on its compact supports. The normalized complete energy and pressure increments are also $O(R_o^{-1})$, also for one angular derivative.

Proof. On the heat collar and terminal sector, (1.15.9) and the fixed cutoff bounds give

$$|\partial_\eta^m (H^b - H^m)| \le C_m c (\tfrac{\hat\xi^2}{2})^{-h-1}.$$

All endpoints and their logarithmic derivatives have fixed normalized bounds. The moving-boundary term under differentiation of D_I vanishes at R_0, because the difference is identically zero on its inlet germ.

Thus

$$\|D_I\|_{C^1} \le C_h c R_0^{-h}.$$

The integral of the second term of (1.15.10) is $-D_I$. Its support lies in the new power leg and has positive distance from the two endpoint germs. On this support H^m is comparable to $H_A e^{-\lambda L_o}$, and cR_0^{-h}/H^m is a fixed positive ratio. Thus the relative correction and its fixed scaled derivatives are $O((\frac{\hat\xi_b^2}{2})^{-1})$.

For the fixed selected L_o this is $O(R_o^{-1})$. Positivity holds when we increase the same radius sufficiently.

The model has the canonical renormalized primitive, and the actual heat primitive differs from $c(\frac{\hat\xi^2}{2})^{1-h}/a$ by $O(c(\hat\xi/\sqrt{2})^{-2h})$ at infinity. Thus zero total primitive difference proves equality with that actual heat primitive on the full terminal heat region. Backward integration from that region gives the actual primitive on the terminal wing and drive. We keep its small shift at the drive inlet. We do not replace it by the model equilibrium.

For energy and pressure use the exact increments

$$\Delta S = -\frac{1}{4} \int \frac{2H^m \delta H + \delta H^2}{\frac{\hat\xi^2}{2}}\, \hat\xi \, \mathrm{d}\hat\xi, \qquad \Delta C_p = \frac{1}{4} \int \frac{2H^m \delta H + \delta H^2}{\frac{\hat\xi^4}{4}}\, \hat\xi \, \mathrm{d}\hat\xi.$$

The compact bump and collar obey the previous relative bounds. Constant multiples of $c^2(\frac{\hat\xi^2}{2})^{-2h-2}$ and $c^2(\frac{\hat\xi^2}{2})^{-2h-3}$ dominate the far densities. These are integrable, also after one angular derivative.

Thus, measured at R_A, H_A,

$$\frac{\|D_I\|_{C^1}}{R_A H_A} \le \frac{C}{R_A} e^{-\lambda L_o}, \quad \frac{\|\Delta S\|_{C^1}}{H_A^2} \le \frac{C}{R_A} e^{-(1+2\lambda)L_o}, \quad \frac{\|\Delta C_p\|_{C^1}}{H_A^2/R_A} \le \frac{C}{R_A} e^{-(2+2\lambda)L_o}.$$

The harmless factors e^{δ}, J, ρ are in the fixed C. For the bump these exponents are a result of its mass bound and its radius comparable to $\frac{\hat{\xi}_b^2}{2}$. For the heat part they are a direct result of (1.15.3). The inequalities keep all quadratic terms. □

Lemma 1.15.9 (A single early history restoration, with no duplicated primitive row)**.** *Consider the backward member and its protected chart collars. Suppose the model pulse root gives $S(\infty) = 0$ and the model pressure uses its canonical axis datum. We apply the actual heat future and rank-one stated correction. The three swirl bumps with disjoint supports on the protected pre-pulse power reserve have the single target*

$$(\Delta I_{\text{bank}}, \Delta S_{\text{bank}}, \Delta C_{p,\text{bank}}) = (0, -\Delta S, -\Delta C_p).$$

For each fixed L_o, Y_0, a sufficiently large scale selected last admits a unique small solution.

It leaves the outlet inlet velocity germs, the same heat pair, and the selected model axial pulse unchanged. The actual A11 canonical primitive target is still its model target, because the complete downstream primitive discrepancy was previously canceled by (1.15.10).

Proof. On the reserve $U = 0$, so all swirl edits keep M, J unchanged. We write the three normalized edit coefficients as t_j. Then their moment Jacobian has rows with powers $1/2, -1/2 - \lambda, -3/2 - \lambda$ of the normalized radius. For three disjoint ordered nonnegative bumps, the determinant is nonzero.

The determinant of these powers at three ordered points has one sign. Multilinear integration against the positive bumps keeps that sign. The actual moment map has only quadratic remaining terms. We fix its inverse norm and quadratic norm after L_o, Y_0 and before the last radius. Proposition 1.15.8, rescaled to these actual early correction coordinates, makes its target $O_{L_o,Y_0}(R_{\text{master}}^{-1})$.

The quantitative finite-dimensional inverse-function theorem then gives the unique small branch.

Its first row is *zero*. Thus it does not correct the rank-one primitive correction a second time and does not alter the primitive at the A11 outlet. Its second row cancels the complete new swirl-energy integral. The unchanged model axial pulse thus stays the same root of the total energy equation. In the root notation this cancellation is explicit.

The actual early moment correction changes $\sigma_p = 2S_p/H_p^2$ by $-2\Delta S_f/H_p^2$, and the positive future integral contribution changes by $\delta\tau_S = -\Delta S_f/H_{\text{out}}^2$. Because $H_{\text{out}}^2 = H_p^2 e^{-2\nu Y}$,

$$-\nu\,\delta\sigma_p + 2\nu e^{-2\nu Y}\delta\tau_S = \frac{2\nu\Delta S_f}{H_p^2} - \frac{2\nu e^{-2\nu Y}\Delta S_f}{H_{\text{out}}^2} = 0.$$

All angular derivatives of this identity also cancel. The unedited finite-template formula for σ_p must thus include its actual moment correction increment when used for the edited member. Its third row restores the original total pressure moment, thus the same analytic axis pressure.

The radial integrals include all partial pressure and energy changes inside the moment corrections. On an intermediate fixed-λ buffer, we do not assert full cancellation of the future change by this moment correction. If we multiply its target by χ_b, the actual root keeps the remainder $-2\nu(1-\chi_b)\Delta S_f/H_p^2$ and its derivatives. It is $O_{L_o,Y_0}(R_{\text{master}}^{-1})$ and becomes small for the step-4 choice of C (Section 1.5.2), whose threshold uses only L_o and Y_0. The full-target identity preserves the model root on the protected forward collars and throughout the native backward chart.

Smallness on the fixed compact reserve keeps its strict model margin at sufficiently large radius. □

1.15.4.1 Conventions and inputs of the future ledger

Throughout, $0 < h < 10^{-2}$, $d = 1 - \eta^2$, and the parameter order (Section 1.5.2, and (1.6.18)) is

$$\text{templates} \;\to\; \lambda \;\to\; h < \lambda/6 \;\to\; \nu_c < h/10 \;\to\; B_h \;\to\; L_o \;\to\; \chi \;\to\; K_f \;\to\; Y_{\min} \;\to\; Y_0 \;\to\; C. \tag{1.15.11}$$

In particular $\nu_c < \lambda/60$ (Section 1.6.3). "Uniform" means independent of $Y_0 \geq Y_{\min}$ and of the master scale C (equivalently of the large radii, which grow like $(CP_*)^{10}$ at fixed Y_0, Section 1.6.3). Unless stated otherwise, constants may depend on everything to the left of K_f in (1.15.11).

Normalized future and its integrals. Let $R_o(\eta)$ be the comparison graph (inlet of the future), $R_o = R_g e^{Y_0 + \rho(\eta)}$ (Section 1.6.3, Section 1.15), and put $G(\eta) = H_{\text{out}}(\eta) = H(R_o(\eta), \eta)$. For $x \geq 1$ set

$$f(x,\eta) = \frac{H(R_o(\eta)x, \eta)}{G(\eta)}, \qquad \tau_S(\eta) = \frac{1}{4}\int_1^\infty f^2 \frac{\mathrm{d}x}{x}, \qquad \tau_P(\eta) = \frac{1}{4}\int_1^\infty f^2 \frac{\mathrm{d}x}{x^2}. \tag{1.15.12}$$

With the canonical outward normalization $S(\infty) = P(\infty) = 0$ (Lemma 1.15.9) we have $S(\frac{\hat\xi^2}{2}) = \frac{1}{4}\int_{(\frac{\hat\xi^2}{2})}^\infty H^2 s^{-1}\,\mathrm{d}s$ and $P(\frac{\hat\xi^2}{2}) = -\frac{1}{4}\int_{(\frac{\hat\xi^2}{2})}^\infty H^2 s^{-2}\,\mathrm{d}s$, hence $S(R_o) = G^2\tau_S$ and $-P(R_o) = G^2\tau_P/R_o$. Here $\partial_\eta f$ always denotes the derivative at fixed x.

Inputs. The proofs of this subsection, of Lemma 1.6.10 and of Proposition 1.15.27 use only the following definitions and results.

Tag	Content	Source
(I1)	Normalized geometry: all non-heat pieces of both components end before a fixed normalized $x = M$; physical radii vary with Y_0, C but the ratios do not. $R_m = a_m \max R_o$, $R_h = a_h R_m$; R_o/R_h lies in a fixed compact interval $[r_-, r_+]$.	proof of Lemma 1.6.19
(I2)	Stop/shot map: $x_b(\epsilon), g_b(\epsilon)$ smooth and positive on $0 \leq \epsilon \leq \epsilon_*$; prescribed slopes $\kappa \in [\nu_c, 2h]$ on the drive; $K_{\text{old}} = g_b x_b^h \in [k_-, k_+]$; amplitude independence.	Lemma 1.15.6
(I3)	Normalized shot response $Y, Y_\xi, Z = O(R_b^{-1/5})$, with bounded logarithmic-scale derivatives; $2 + c_h \leq a_s = 2 - \hat\xi H_{\hat\xi}/H \leq 2 + C_h$ on bridge and target.	proof of Proposition 1.15.22
(I4)	Heat comparison (1.15.13): $\lvert(\frac{1}{2}\hat\xi\partial_{\hat\xi})^j\partial_\eta^m(H^{\text{heat}} - c(\hat\xi/\sqrt{2})^{-2h})\rvert \leq C_{j,m}c(\frac{\hat\xi^2}{2})^{-h-1}$ for $\frac{\hat\xi^2}{2} \geq R_0$; backward chart through the positive Laplace factor.	Lemma 1.15.7, Section 1.15, (1.7.1), (1.7.2), (1.7.3), (1.7.4)
(I5)	A11: r, r_β bounded; two-row Jacobian invertible on $0 \leq \lambda \leq 1/20$; root and first β-derivative $O(\lVert u\rVert_{C^1})$.	Lemma 1.15.5
(I6)	Flattening: $-\frac{3}{2}\lambda \leq \partial_y \log H \leq -\frac{1}{2}\lambda$, $\lvert H_\beta\rvert \leq \lVert J_0'\rVert_\infty H$.	Lemma 1.15.4
(I7)	Actual heat future: $\lvert\partial_\eta^m(H^b - H^m)\rvert \leq C_m c(\frac{\hat\xi^2}{2})^{-h-1}$; $\lVert D_I\rVert_{C^1} \leq C_h c R_0^{-h}$; relative bump size $O((\frac{\hat\xi_b^2}{2})^{-1})$; zero primitive increment.	Proposition 1.15.8

(I8)	Central memory return $I = i_s + p\zeta(\frac{\hat\xi^2}{2}/R_m)$, $H = H_s + (p/R_m)\zeta'(\frac{\hat\xi^2}{2}/R_m)$; $\epsilon_I \le K_I(1+Y_0)^N e^{-(1-\nu_c)Y_0}$.	proof of Proposition 1.15.22
(I9)	Bridge and wing: $\Delta = I_T - I_b \asymp C_b$, χ_b on the shot's fixed plateau (adverse terms $O(C_b/R_b^2)$); $\ell_b = R_b^{4/5}$, $\alpha_o = \epsilon_o h G_b/R_b$, $B_o(\eta) = B_o e^{k_o\eta^2}$; lifted target $H_L = d^{-h} g(\frac{\hat\xi^2}{2}/d)$, regular at $d=0$.	proof of Proposition 1.15.22
(I10)	Coefficients: $H_c = cR_o^{-h}K_c$, $H_w = cR_o^{-h}K_w$, $0 < m_K \le K_c, K_w \le M_K$, $\lvert\dot{\log}(K_c/K_w)\rvert \le B$; K_c formula (1.6.28); $K_w = A_w f(\beta) e^{(\lambda-h)L_o}$, $f = f_0/(1+\beta^2)$, $\beta = \ell^{\frac12-h}\eta$.	Section 1.6.3, Lemma 1.15.23
(I11)	Ordering: L_o condition (1.6.29), $K_c \le K_w/2$ on the chart band, preserved by all corrections.	(1.15.28), Proposition 1.15.25
(I12)	Flat logit cutoff χ, fixed before Y_0, zero off the chart band and identically one on open endpoint collars and on the phase transition of R_g. Here $\omega = (1-\chi)H_c/H_{\mathrm{out}}$.	Section 1.6.3, Lemma 1.15.26
(I13)	Inverse for ν: $\mathcal{F}(\nu,\eta) = \frac{1}{1-\nu} + (r_b(\nu) - \frac{1}{1-\nu})e^{-(1-\nu)(Y_0+\rho-T)}$; r_b with uniform derivative bounds on $0 \le \nu \le \lambda_0$; Jensen bound (1.15.37).	(1.6.24), Lemma 1.15.26
(I14)	Inlet-germ connector $\zeta_g(t/\epsilon_g)J$, $J = I_{\mathrm{pow}} - I_\chi$, explicit $J_t/(R_oH_o)$.	Lemma 1.17.9
(I15)	$X_p = R_g e^{T_b(\nu)}\nu^{-60}$, $Y = \log(R_o/X_p)$, $H_p = H_{\mathrm{out}}e^{\nu Y}$, $H_a = H_p e^{\nu W}/F_b$, $W = 60\log(1/\nu)$. R_g is scalar on the exponent transition and charted on the fixed-λ phase bridge. $T_b = T$. The axial pulse preserves H.	(1.6.23), growth-radius convention
(I16)	Mixing identity (1.15.33) and the definitions q_i, c_{mix}, $v_o = w_o = \dot{\log} R_o$.	(1.15.29), (1.16.1)
(I17)	Lemmas used by (c): Lemma 1.15.6, Proposition 1.15.22, Lemma 1.15.7, Proposition 1.15.8, Lemma 1.15.5, Lemma 1.15.9, Lemma 1.15.2, Lemma 1.15.3, Lemma 1.15.23, Lemma 1.15.24, Proposition 1.15.25, Lemma 1.15.26.	Lemma 1.15.2, Lemma 1.15.4

Admitted parameter domain. Following Remark 1.6.9 the independent parameters are $\pi = (\mathfrak{m}, \epsilon) \in \mathcal{P} := \mathfrak{M}_{r_0} \times (0, \epsilon_0]$. Here ϵ is the inverse finite scale, and $\mathfrak{m}$ is the normalized incoming memory datum: the central $\hat p = p/(R_m H_s(R_m))$ of (I8) and the A11 target u of (I5), both in C^1 of the angular variable. The set $\mathfrak{M}_{r_0}$ is the ball of radius r_0 in C^1 on which (I5) and (I8) hold. The physical family (Y_0, C) enters only through a point of $\mathcal{P}$ and through the exponent field $\nu(\eta)$ of (I13). In the future $x \ge 1$ this field enters only through the inlet-germ connector on $1 \le x \le e^{\epsilon_g}$, and Lemmas 1.15.18 and 1.15.19 bound that dependence uniformly on the admitted family.

Structural hypotheses. We record the structure of the actual future in the form needed below. Each item is a direct restatement of the cited construction.

Hypothesis 1.15.10 (Structure of the actual future). For every $\pi \in \mathcal{P}$:

(A1) (Mixture, Section 1.6.3, Section 1.15, proof of Lemma 1.17.9.) For $\frac{\hat\xi^2}{2} \ge R_o$, $H = (1-\chi)H_c + \chi H_w + \delta H_{\mathrm{conn}}$, where $\chi = \chi(\eta) \in C^1$, $0 \le \chi \le 1$, $\chi = 0$ off the outer chart band, and

$\delta H_{\mathrm{conn}} = \hat\xi^{-1}\partial_{\hat\xi}[\zeta_g(t/\epsilon_g)J]$, $t = \log(\frac{\hat\xi^2}{2}/R_o)$, is the connector of (I14).

(A2) (Coefficients, (I10).) $G_i := H_i(R_o,\eta) = cR_o^{-h}K_i$, with $m_K \le K_i \le M_K$, $|K_i'| \le M_K$, and $|(\log R_o)'| + |\rho'| + |(\log R_g)'| \le M_K$ after enlarging the fixed geometric bound. The identity is $(\log R_o)' = \rho' + (\log R_g)'$.

(A3) (Geometry, (I1).) There is $M \ge 4$ such that every piece of H_c, H_w other than the exact heat field, and the connector, is supported in $x \le M$. For $x \ge M$, $H_c = H_w = H^{\mathrm{heat}}$, where H^{heat} is the common heat field with pair (c, k_f). Also $R_0 \le MR_o$.

(A4) (Heat comparison, (I4).) For $\frac{\hat\xi^2}{2} \ge R_0$ and $(j,m) \in \{(0,0),(1,0),(0,1)\}$,

$$\big|(\tfrac12\hat\xi\partial_{\hat\xi})^j\partial_\eta^m(H^{\mathrm{heat}} - c(\hat\xi/\sqrt{2})^{-2h})\big| \le C_{\mathrm{heat}}\, c\big(\tfrac{\hat\xi^2}{2}\big)^{-h-1}. \tag{1.15.13}$$

(A5) (Inner pieces.) On $[1,M]$ each normalized component $f_i = H_i(R_o x,\eta)/G_i$ has at most N_p pieces. They are of type (P) of Definition 1.15.11 with a common K_P, except that the heat regime of C6 uses the same first-derivative bounds directly. Lemma 1.15.17 verifies these estimates uniformly on $\mathcal{P}$.

(A6) (Regularity at fixed parameters.) For fixed π the field H is C^1 in $(\frac{\hat\xi^2}{2},\eta)$ on $\frac{\hat\xi^2}{2} \ge R_o$; this holds because every piece of the construction is smooth.

Definition 1.15.11 (Pieces of type (P))**.** A function $\varphi(x,\eta)$ on $[1,M]\times\Sigma$ is of type (P) with constant K if

$$\varphi(x,\eta) = b(\eta)\,\Phi(a(\eta)x,\eta),$$

where $a,b \in C^1(\Sigma)$ satisfy $a(\eta) \in [K^{-1},K]$, $|a'/a| \le K$ and $|b| + |b'| \le K$, and Φ is C^1 on $[K^{-1},KM]\times\Sigma$ with

$$|\Phi| + |\xi\partial_\xi\Phi| + |\partial_\eta\Phi| \le K.$$

The bound on $\xi\partial_\xi\Phi$ also bounds the first radial derivative since $\xi \ge K^{-1}$. Higher radial derivatives may grow on narrow layers. This holds for a scalar profile with bounded logarithmic slope, however fast the slope changes. It also holds for a moving layer whose amplitude is proportional to its width.

Lemma 1.15.12 (Pointwise first derivatives of type (P))**.** *If φ is of type (P) with constant K, then on $[1,M]\times\Sigma$*

$$|\varphi| \le K^2, \qquad |\partial_\eta\varphi| \le K^2 + K^3 + K^2 \le 3K^3.$$

Proof. With $\xi = a(\eta)x$, the chain rule at fixed x gives $\partial_\eta\varphi = b'\Phi + b\,[(a'/a)\,\xi\partial_\xi\Phi + \partial_\eta\Phi]$. Insert the bounds of Definition 1.15.11. We used $K \ge 1$. □

The abstract ledger estimate.

Lemma 1.15.13 (Ledger estimate)**.** *Let f be C^1 in η for each $x \ge 1$. Suppose that*

$$|f| + |\partial_\eta f| \le K_0 \qquad \text{on } [1,M]\times\Sigma, \tag{1.15.14}$$

$$|f| + |\partial_\eta f| \le K_\infty x^{-h} \qquad \text{on } [M,\infty)\times\Sigma. \tag{1.15.15}$$

Then $\tau_S,\tau_P \in C^1(\Sigma)$, with $\tau_S' = \frac12\int_1^\infty f\partial_\eta f\, x^{-1}\,\mathrm{d}x$ and similarly for τ_P, and

$$\int_1^\infty (f^2 + |f\partial_\eta f|)\Big(\frac1x + \frac{1}{x^2}\Big)\,\mathrm{d}x \le \Lambda := 2K_0^2(1+\log M) + 2K_\infty^2\Big(\frac{1}{2h}+1\Big). \tag{1.15.16}$$

In particular $\|\tau_S\|_{C^1} + \|\tau_P\|_{C^1} \le \Lambda$.

Proof. On $[1,M]$, $f^2+|f\partial_\eta f|\le 2K_0^2$, and $\int_1^M(x^{-1}+x^{-2})\,\mathrm{d}x\le\log M+1$. On $[M,\infty)$, $f^2+|f\partial_\eta f|\le 2K_\infty^2x^{-2h}$, and $\int_M^\infty x^{-2h}(x^{-1}+x^{-2})\,\mathrm{d}x=\frac{M^{-2h}}{2h}+\frac{M^{-1-2h}}{1+2h}\le\frac{1}{2h}+1$. This proves (1.15.16). The function $g(x):=\max(K_0^2\mathbf{1}_{[1,M]},K_\infty^2x^{-2h}\mathbf{1}_{[M,\infty)})(x^{-1}+x^{-2})$ dominates $|\partial_\eta(f^2)|(x^{-1}+x^{-2})/2$ uniformly in η and is integrable. Hence the mean value theorem bounds the difference quotients by g. Dominated convergence then gives the derivative formulas and their continuity. The C^1 bound follows because $\frac14\le\frac12\le1$. □

Remark 1.15.14. The exponent $h>0$ enters only through $1/(2h)$ from the heat tail. This is why K_f is selected after h. Lemma 1.15.15 proves (1.15.15) with no logarithmic factor; an envelope $K(1+\log x)x^{-h}$ would be weaker.

The heat tail.

Lemma 1.15.15 (Tail bound)**.** *Assume (A1)–(A4). Put* $K_{\mathrm{mix}}=(1-\chi)K_c+\chi K_w$ *and* $B_{\mathrm{mix}}:=2M_K(1+\|\chi'\|_\infty)/m_K$. *Then for* $x\ge M$,

$$|f|+|\partial_\eta f|\le K_\infty x^{-h},\qquad K_\infty:=\frac{1}{m_K}\Big[(1+C_{\mathrm{heat}})(1+B_{\mathrm{mix}}+2hM_K)+C_{\mathrm{heat}}+M_KC_{\mathrm{heat}}\Big].$$

Proof. By (A1), (A3), $H=H^{\mathrm{heat}}$ for $x\ge M$, and $G=(1-\chi)G_c+\chi G_w=cR_o^{-h}K_{\mathrm{mix}}$. The connector vanishes at $x=1$ (see Lemma 1.15.18), so it does not change G. Clearly $K_{\mathrm{mix}}\ge m_K$, and $|K_{\mathrm{mix}}'|\le|\chi'||K_w-K_c|+|K_c'|+|K_w'|\le 2M_K(1+\|\chi'\|_\infty)$, so $|(\log K_{\mathrm{mix}})'|\le B_{\mathrm{mix}}$. With $\frac{\hat\xi^2}{2}=R_ox\ge MR_o\ge R_0\ge1$, (1.15.13) with $j=m=0$ gives $|H^{\mathrm{heat}}|\le(1+C_{\mathrm{heat}})c(\hat\xi/\sqrt2)^{-2h}$, hence $|f|\le(1+C_{\mathrm{heat}})x^{-h}/m_K$. At fixed x,

$$\partial_\eta f=\frac{(\partial_\eta H^{\mathrm{heat}})(\frac{\hat\xi^2}{2},\eta)+(\log R_o)'\,(\frac12\hat\xi\partial_{\hat\xi}H^{\mathrm{heat}})(\sqrt{2(\frac{\hat\xi^2}{2})},\eta)}{G}-f\,[(\log K_{\mathrm{mix}})'-h(\log R_o)'].$$

By (1.15.13),

$$|\partial_\eta H^{\mathrm{heat}}|\le C_{\mathrm{heat}}c(\hat\xi/\sqrt2)^{-2h-2}\le C_{\mathrm{heat}}c(\hat\xi/\sqrt2)^{-2h}$$

and $|\frac12\hat\xi\partial_{\hat\xi}H^{\mathrm{heat}}|\le(h+C_{\mathrm{heat}})c(\hat\xi/\sqrt2)^{-2h}$. Divide by $G=cR_o^{-h}K_{\mathrm{mix}}$ and use $(\hat\xi/\sqrt2)^{-2h}R_o^h=x^{-h}$. Collecting terms gives the bound. The constant is crude but explicit. □

Lemma 1.15.16 (Heat comparison in the lifted heat regime)**.** *Let* $b_s\le M_cR_o$ *be the central shot outlet (Lemma 1.15.7), and let* $\mathcal{R}:=\{\frac{\hat\xi^2}{2}\ge R_o,\ \frac{\hat\xi^2}{2}/d\ge4b_s\}$. *Then* (1.15.13) *holds on* $\mathcal{R}$ *for the lifted central heat field* $H_L=d^{-h}[cg_h+k_fg_f](\frac{\hat\xi^2}{2}/d)$, *with a constant* C'_{heat} *uniform on* $\mathcal{P}$ *and in* $d\in(0,1]$.

Proof. The proof of Lemma 1.15.7 uses $\frac{\hat\xi^2}{2}\ge R_0$ only through $\xi:=\frac{\hat\xi^2}{2}/d\ge4b_s$ and $\frac{\hat\xi^2}{2}\ge1$. Under these conditions the fast-mode factor $g_f(\xi)/g_f(b_s)\le Ce^{-(\xi-b_s)/3}$, times polynomial factors, absorbs every power of ξ and of $d^{-1}=\xi/\frac{\hat\xi^2}{2}\le\xi$ that is produced by the derivatives in (1.15.13). The exposure $k_fg_f(b_s)/(cb_s^{-h})=\mathrm{poly}(R_b)e^{-c_*R_b}$ of (1.13.42) then gives a contribution $\le Cc(\frac{\hat\xi^2}{2})^{-h-1}$. For the regular part write $d^{-h}g_h(\frac{\hat\xi^2}{2}/d)=(\hat\xi/\sqrt2)^{-2h}\Gamma(d/\frac{\hat\xi^2}{2})$, with $\Gamma(z)=z^{-h}g_h(1/z)$. The regular expansion (1.13.35) gives $\Gamma(0)=1$ and $|\Gamma'|\le C$ on $[0,1/(4b_s)]$. Then $(\hat\xi/\sqrt2)^{-2h}|\Gamma-1|\le C(\frac{\hat\xi^2}{2})^{-h-1}d\le C(\frac{\hat\xi^2}{2})^{-h-1}$, $|\partial_\eta((\hat\xi/\sqrt2)^{-2h}\Gamma(d/\frac{\hat\xi^2}{2}))|=(\frac{\hat\xi^2}{2})^{-h-1}|\Gamma'||d'|\le2C(\frac{\hat\xi^2}{2})^{-h-1}$, and $\frac12\hat\xi\partial_{\hat\xi}((\hat\xi/\sqrt2)^{-2h}\Gamma)=-h(\hat\xi/\sqrt2)^{-2h}\Gamma-(\hat\xi/\sqrt2)^{-2h}(d/\frac{\hat\xi^2}{2})\Gamma'$, which gives the $j=1$ bound. For the backward member the same holds with the positive Laplace factor $\mathcal{H}_-$ (Section 1.15): $\mathcal{H}_-(0)=1$ and $|\mathcal{H}_-'(z)|\le h(1+h)$ by differentiation under the integral. □

The inner interval: identification of the pieces.

Lemma 1.15.17 (Uniform first derivatives on the inner interval)**.** *Under the construction in (I1)–(I9), (I14), the two normalized components f_i on $[1, M]$ have the finite decompositions in (A5). Their bounds depend only on the fixed templates, $h, \nu_c, \lambda, B_h, L_o, \epsilon_g$, and the memory radius r_0. The table gives the type (P) representations and the direct bounds in the heat regime of C6. Here R_{ref} denotes a fixed-ratio reference radius (R_h for central pieces, R_b for shot, bridge and wing pieces, and R_e for outer pieces in the backward chart), so $a = R_o/R_{\mathrm{ref}}$ ranges over a fixed compact set by (I1).*

Piece	Representation and the bounds of Definition 1.15.11	Source
Central component (full chart $-1 \le \eta \le 1$, scalar before the lift, Section 1.6.3)		
C1 inlet ν_c power, hold	$\Phi = \xi^{-\nu_c}$, $b = (G_{\mathrm{ref}}/G_c)$; $\xi\Phi_\xi = -\nu_c\Phi$, $\Phi_\eta = 0$.	(I1), (1.6.19) (1.6.19)
C2 memory return	$\Phi = \hat{p}(\eta)\,\zeta'(\xi R_h/R_m)\,H_s(R_m)/G_{\mathrm{ref}}$; $\lvert\hat{p}\rvert_{C^1} \le r_0$; $\xi\Phi_\xi$ involves ζ'', which is bounded.	(I8)
C3 drive and stop	$\Phi = H/G_{\mathrm{ref}}$ scalar, $\xi\Phi_\xi = -\kappa\Phi$ with $\kappa \in [\nu_c, 2h]$ *including* the transitions of width $c_w\epsilon$; $\Phi_\eta = 0$; $0 < \Phi \le 1$. Uniform in $\epsilon \to 0$ because only κ, not κ_x, enters.	(I2), proof of Lemma 1.15.6
C4 shot	Φ the normalized scalar shot profile; $\lvert\Phi\rvert + \lvert\xi\Phi_\xi\rvert \le K$ from the normalized response bounds and $G_b = Gg_b(\epsilon)$.	(I2), (I3)
C5 bridge blend	$(1-\chi_b)H_b$ as C4; $\chi_b H_T$ as C6; $\chi_b'\Delta$: $\Phi = \hat{\chi}_b'(\xi)\Delta/(R_bG_{\mathrm{ref}})$, with $\lvert\Delta\rvert + \lvert\frac{\hat{\xi}^2}{2}\frac{\Delta_{\hat{\xi}}}{\hat{\xi}}\rvert + \lvert\Delta_\eta\rvert \le KR_bG_b$ since I_b, I_T are primitives of pieces of type (P).	(I9), proof of Proposition 1.15.22
C6 lifted target $H_L = d^{-h}g(\frac{\hat{\xi}^2}{2}/d)$	If $d \ge d_* := R_b'/(4b_s)$, where R_b' is the inner edge of the bridge plateau (a fixed ratio to b_s): $a = R_o/(dR_b) \in [K^{-1}, K]$, $b = d^{-h}G_b/G_c$, $\Phi = g/G_b$; $\lvert d'/d\rvert \le 2/d_*$. If $d < d_*$: $\frac{\hat{\xi}^2}{2}/d \ge 4b_s$ on the target, so Lemma 1.15.16 applies, and the computation of Lemma 1.15.15 gives a pointwise bound for φ and $\partial_\eta\varphi$.	(I9), Lemma 1.15.16
C7 wing	$a = R_o/R_b$, $b = G_b/G_c$, $\varepsilon_t = R_b^{-1/5}$, $\beta_o = B_o(\eta)/R_b$, $s = (\beta_o - \xi)/\varepsilon_t$. Then $\Phi = -\epsilon_o h\psi_o\varepsilon_t F'(s)$, $\xi\Phi_\xi = \epsilon_o h\psi_o\xi F''(s)$, and $\Phi_\eta = -\epsilon_o h[\psi_o'\varepsilon_t F'(s) + \psi_o\beta_o' F''(s)]$. The scalar R_b is fixed in η, and F', F'' are bounded.	(I9), (A2), Proposition 1.15.22
Outer component on the chart band, with its actual A11 and heat corrections		
W1 post-pulse power, flattening	$f_w = \Phi(x, \beta(\eta))$, $a = 1$, with $\xi\partial_\xi \log\Phi = \partial_y \log H \in [-\frac{3}{2}\lambda, -\frac{1}{2}\lambda]$ and $\lvert\partial_\beta \log\Phi\rvert \le 2\lVert J_0'\rVert_\infty$; $\lvert\beta'\rvert$ is bounded on the band.	(I6), Section 1.15

W2 A11 wait and bumps	$H(1+t_1\psi_1+t_2\psi_2)$ with $\|t_j\|_{C^1} \le C\|u\|_{C^1} \le Cr_0$ and fixed ψ_j.	(I5)
W3 added leg, $\lambda \to h$ transition	pure λ-power; then $p(t)$ fixed, $t \in [0,\delta]$.	(1.15.2)
W4 heat collar, terminal cutoff	$(1-\zeta)C(\hat\xi/\sqrt{2})^{-2h} + \zeta(1-\rho)H^{\mathrm{heat}}$ and $H^{\mathrm{heat}}(1-\rho\Psi(\frac{\hat\xi^2}{2}/B))$: fixed cutoffs times fields controlled by (1.15.13).	Section 1.15, (I4)
W5 rank-one bump	$-(D_I/\frac{\hat\xi_b^2}{2})\psi((\hat\xi/\hat\xi_b)^2)$, $\|D_I\|_{C^1} \le C_h c R_0^{-h}$, so its relative size is $O((\frac{\hat\xi_b^2}{2})^{-1})$.	(I7), proof of Proposition 1.15.8

Proof. For each row we check the first-derivative bounds in (A5). The table records them, and we add the points that need comment.

(i) *Scalar pieces (C1–C4).* A field $H(\frac{\hat\xi^2}{2})$ that is independent of η has normalized form $f = \Phi(a(\eta)x)/\Phi(a(\eta))$, with $\Phi = H/G_{\mathrm{ref}}$ and $a = R_o/R_{\mathrm{ref}}$. Its fixed-x derivative is $\partial_\eta f = (\log a)'[\kappa(R_o) - \kappa(\frac{\hat\xi^2}{2})]f$, where $\kappa = -\frac12\hat\xi H_{\hat\xi}/H$. Only the logarithmic slope enters. This is why the narrow slope transition of width $c_w\epsilon$ in the stop (proof of Lemma 1.15.6) causes no loss as $\epsilon \to 0$, although $\frac{\kappa_{\hat\xi}}{\hat\xi} = O(\epsilon^{-1})$ there. On C1–C3, $1/\Phi(a)$ is bounded because a ranges over a compact set in the pure ν_c-power region. In general, $b = G_{\mathrm{ref}}/G_c$ is bounded by (A2), since G_{ref} is a fixed-ratio amplitude of the same component.

(ii) *Wing (C7).* The amplitude $\alpha_o\ell_b = \epsilon_o h G_b \varepsilon_t$ is proportional to the normalized width $\varepsilon_t = \ell_b/R_b = R_b^{-1/5}$. Differentiating the argument $(\beta_o - \xi)/\varepsilon_t$ produces ε_t^{-1}, which cancels this factor. So ∂_η and $\xi\partial_\xi$ produce the bounded kernel $F''(s) = 2s^{-3}e^{-1/s^2}$ for $s > 0$, extended by zero for $s \le 0$. The remaining first derivatives of ψ_o and $b = G_b/G_c$ multiply $\varepsilon_t F'$. The moving-kernel contribution has radial L^1 norm $O(\varepsilon_t)$ since $\int_0^\infty F'' = 1$.

(iii) *Lifted target (C6).* The central component is defined on the full chart (Proposition 1.15.22). Where $d \ge d_*$ the lift is of type (P) with $|(\log a)'| \le |(\log R_o)'| + 2/d_*$. Where $d < d_*$, every point $\frac{\hat\xi^2}{2}$ of the lifted target satisfies $\frac{\hat\xi^2}{2} \ge R_b'$ (bridge start) and $\frac{\hat\xi^2}{2}/d \ge R_b'/d_* \ge 4b_s$, where b_s/R_b' is a fixed ratio. So we are in the heat regime of Lemma 1.15.16. Its bounds on H, $X\partial_X H$ and $\partial_\eta H$, combined with the fixed-x chain rule of Lemma 1.15.15, directly give $|\varphi| + |x\partial_x\varphi| + |\partial_\eta\varphi| \le K$ on this part of $[1, M]$. The two estimates apply to the same lifted field at $d = d_*$.

(iv) *Bridge (C5).* The blend cutoff χ_b lives on the shot's fixed positive plateau, so $\chi_b' = R_b^{-1}\hat\chi_b'(\frac{\hat\xi^2}{2}/R_b)$. The adverse terms in proof of Proposition 1.15.22 are $O(C_b/R_b^2)$, which forces this normalized width. Since $\Delta \asymp C_b \asymp hG_bR_b^{4/5}$, the piece $\chi_b'\Delta$ is in fact $O(hR_b^{-1/5})$ relative to G_b. Its η-derivative involves Δ_η and $(\log R_o)'\frac{\hat\xi^2}{2}\frac{\Delta_{\hat\xi}}{\hat\xi}$, both $O(R_bG_b)$, so $\partial_\eta(\chi_b'\Delta) = O(G_b)$.

(v) *Outer pieces (W1–W5).* Use $x = X/R_o$, $y = \log x$. The graph $R_o = R_e/\ell$ on the forward band makes the relative radii of W1–W5 fixed. In W1 the normalized reference shape is the explicit flattening of Lemma 1.15.4 at $\beta = \ell^{1/2-h}\eta$. Its angular derivative is bounded since J_0, J_0' and β' are bounded there. The normalized powers and fixed transition p give the same bounds for W3.

For W2 take the actual outer inlet ratio $r_{w,\mathrm{tar}}$ in (Inlet). Set $a = 1-\lambda$, $r_* = a^{-1}$ and $D = r_b(\lambda) - r_*$. The transported reference has ratio $r_{\mathrm{tr}} = r_* + D(e^TR_{g,b}/R_e)^a$. The formula preceding (Taper) and $R_e = \ell R_o$ give

$$r_{w,\mathrm{tar}} - r_{\mathrm{tr}} = D(e^TR_{g,b}/R_e)^a(1-\tau)(\ell^a - 1).$$

Thus the discrepancy and its first angular derivative are bounded uniformly by $C(e^TR_{g,b}/R_e)^a$, since τ, ℓ have bounded first derivatives and $R_{g,b}, R_e$ are scalar. Transport to the A11 supports uses

$r_y + (1+\ell_r)r = 1$. Differentiating at fixed y gives the same stable equation with forcing $-(\partial_\eta \ell_r)r$. Here $1+\ell_r \ge 1 - 3\lambda/2$ and $|\partial_\eta \ell_r| \le C\lambda$. On the succeeding power wait the deviation from r_λ and its derivative decay by $e^{-(1-\lambda)W}$. Conversion to the bump units uses fixed relative radii. This yields the small target u of Lemma 1.15.5, with the admitted bound $\|u\|_{C^1} \le r_0$. In the fixed normalized coordinate its two-row map has constant coefficients. At the small solution its Jacobian and derivative equation are

$$D(t) = \begin{pmatrix} A_1 & A_2 \\ 2B_1 + 2C_1 t_1 & 2B_2 + 2C_2 t_2 \end{pmatrix}, \qquad D(t)t' = (u', 0)^{\mathsf{T}}.$$

The separated translates bound $D(t)^{-1}$ uniformly on this ball. Hence $|t| + |t'| \le C\|u\|_{C^1}$, and differentiating the actual profile times $1 + \sum t_j \psi_j$ bounds W2, including the interiors of its bumps.

For W4 evaluate the forward regular and fast modes on $d = 1 - \eta^2 \ge 0$, using Lemma 1.15.7. On the native backward side use (1.7.1) at its nonnegative argument. For $X = R_o x$ the angular derivative adds $(\log R_o)' X \partial_X$ to the fixed-X derivative. Both derivatives of the heat discrepancy have size $O(cX^{-h-1})$, and the cutoff radii have bounded logarithmic derivatives. For W5 the discrepancy in (1.15.10) vanishes on the moving inlet germ. Integration of this same majorant hence bounds $|D_I| + |D_I'|$ by $C_h c R_0^{-h}$. On the bump, division by its radius and the model amplitude gives $O(R_o^{-1})$ also after one angular or logarithmic radial derivative. Finally $G_w = cR_o^{-h} K_w$ has bounded logarithmic angular derivative by (A2). These estimates prove the required bounds in forward variables throughout the band. Equality of the two sets of physical slice jets for the heat field and A11 at the joining slice is proved in the paragraph on p. 306.

(vi) *Uniformity.* The pieces depend on (Y_0, C) only through $\pi \in \mathcal{P}$: the memory $\hat{p}, u \in \mathfrak{M}_{r_0}$, and the scale ϵ through the maps x_b, g_b, which are smooth down to $\epsilon = 0$, and through the factors $R_b^{-1/5}$, $\mathrm{poly}(R_b)e^{-c_* R_b}$, which are bounded by their values at ϵ_0. The number of pieces is fixed. □

Lemma 1.15.18 (Connector)**.** *Let $\nu(\eta)$ be the exponent of (I13), $a = 1-\nu$, $a_c = 1-\nu_c$, $a_w = 1-\lambda$, and $j(t,\eta) := J/(R_o H_o)$. On the fixed component power germ $0 \le t \le \epsilon_g$, the explicit formula of proof of Lemma 1.17.9 gives*

$$j_t = e^{at} - \omega e^{a_c t} - (1-\omega)e^{a_w t}, \qquad j(0,\cdot) = j_t(0,\cdot) = 0.$$

The normalized connector $\delta f = x^{-1}\partial_t[\zeta_g(t/\epsilon_g)j]$ ($t = \log x$) satisfies, for $\epsilon_g \le 1$,

$$|\delta f| \le (\tfrac{3}{2}\|\zeta_g'\|_\infty + 3)e\,\epsilon_g, \qquad |\partial_\eta \delta f| \le (|\nu'| + \lambda|\omega'|)(\tfrac{1}{2}\|\zeta_g'\|_\infty + 1)e\,\epsilon_g,$$

and $\delta f(1,\cdot) = 0$. With Lemma 1.15.19, both bounds are uniform on $\mathcal{P}$.

Proof. $|j_{tt}| = |ae^{at} - \omega a_c e^{a_c t} - (1-\omega)a_w e^{a_w t}| \le 3e^t$, so $|j_t| \le 3te^t$ and $|j| \le \frac{3}{2}t^2 e^t$. At fixed t, $\partial_\eta j_t = -\nu' t e^{at} - \omega'(e^{a_c t} - e^{a_w t})$, and $|e^{a_c t} - e^{a_w t}| \le (\lambda - \nu_c)te^t$. Hence $|\partial_\eta j_t| \le (|\nu'| + \lambda|\omega'|)te^t$ and $|\partial_\eta j| \le \frac{1}{2}(|\nu'| + \lambda|\omega'|)t^2 e^t$. Next, $\partial_t[\zeta_g j] = \epsilon_g^{-1}\zeta_g' j + \zeta_g j_t$, the support is $t \le \epsilon_g$, and fixed x means fixed t. Insert the bounds. At $t = 0$, $\zeta_g = 1$, so $\delta f = j_t(0) = 0$. (At fixed $\hat{\xi}$ one has $t_\eta = -(\log R_o)_\eta$. In the normalized variable, t is η-independent.) □

Lemma 1.15.19 (Uniform bounds for ν', ω' and the matched memory)**.** *Let $Y_* := \|\rho\|_\infty + T$ and $C_r := \sup_{0\le\nu\le\lambda_0}(|r_b - \frac{1}{1-\nu}| + |r_b' - \frac{1}{(1-\nu)^2}|) < \infty$ (Section 1.15). Put*

$$\varepsilon_\delta(Y_0) := C_r(1 + \|\rho'\|_\infty)(2 + Y_0 + Y_*)\, e^{-(1-\lambda)(Y_0 - Y_*)}.$$

1. *$|\omega'| \le C_\omega := 3M_K^2(1 + \|\chi'\|_\infty)/m_K^2$, independently of Y_0.*

2. *If* $\varepsilon_\delta(Y_0) \le \frac{1}{4}$, *then* $|\nu'| \le \frac{4}{3}\big[2\lambda C_\omega + 2(1+C_\omega)\varepsilon_\delta(Y_0)\big]$.

3. *The matched-memory datum* $\delta_{\mathrm{mem}}(\eta) = \delta(\nu(\eta),\eta)$, *with* $\delta(\nu,\eta) = (r_b(\nu) - \frac{1}{1-\nu})e^{-(1-\nu)(Y_0+\rho-T)}$, *satisfies* $\|\delta_{\mathrm{mem}}\|_{C^1} \le \varepsilon_\delta(Y_0)(2+|\nu'|_\infty)$. *On the fixed-*$\lambda$ *phase bridge this formula describes the raw memory. For the corrected outer inlet multiply* $\delta(\lambda,\eta)$ *by* $(1-\tau)(R_{g,b}/R_g)^{1-\lambda} + \tau(R_{g,b}/(\ell R_g))^{1-\lambda}$ *as in* (Taper). *The multiplier has bounded fixed derivatives on the selected chart; the corrected datum therefore satisfies the same smallness estimate with a fixed geometric constant. On the endpoint collars its product with the raw memory is constant.*

4. *The function* ε_δ *is decreasing for* $Y_0 \ge Y_*$. *Hence for every* $r_1 > 0$ *there is* $Y_{\min}(r_1)$ *such that* $\|\delta_{\mathrm{mem}}\|_{C^1} \le r_1$ *for all* $Y_0 \ge Y_{\min}$.

Proof. (1) $\omega = (1-\chi)K_c/K_{\mathrm{mix}}$, so $\omega' = [-\chi' K_c + (1-\chi)K_c']/K_{\mathrm{mix}} - (1-\chi)K_c K_{\mathrm{mix}}'/K_{\mathrm{mix}}{}^2$. Use (A2) and $|K_{\mathrm{mix}}'| \le 2M_K(1+|\chi'|)$. In (1.6.28), the factor $K_{\mathrm{old}}(R_h e^{B_h})^{-1}$ may vary with Y_0, but it is scalar in η and lies in $[1/k_+, 1/k_-]$. The ratio R_o/R_h and its logarithmic angular derivative are uniformly bounded by (I1) and (A2). Thus the coefficient bounds in (A2) are uniform in Y_0, and the fixed cutoff χ gives the stated uniform bound on ω'.

(2) Write $\Theta = Y_0 + \rho - T \in [Y_0 - Y_*, Y_0 + Y_*]$. Directly, $|\delta| \le C_r e^{-(1-\lambda)\Theta}$, $|\delta_\eta| \le |\rho'||\delta|$ and $|\delta_\nu| \le C_r(1+\Theta)e^{-(1-\lambda)\Theta}$, all at most ε_δ. Differentiating $\mathcal{F}(\nu,\eta) = \omega\mathcal{F}(\nu_c,\eta) + (1-\omega)\mathcal{F}(\lambda,\eta)$ gives

$$\mathcal{F}_\nu(\nu)\,\nu' = \omega'[\mathcal{F}(\nu_c) - \mathcal{F}(\lambda)] + \omega\delta_\eta(\nu_c) + (1-\omega)\delta_\eta(\lambda) - \delta_\eta(\nu).$$

Here $\mathcal{F}_\nu = (1-\nu)^{-2} + \delta_\nu \ge 1 - \varepsilon_\delta \ge \frac{3}{4}$, and $|\mathcal{F}(\nu_c) - \mathcal{F}(\lambda)| \le (\lambda - \nu_c)(1-\lambda)^{-2} + 2\varepsilon_\delta \le 2\lambda + 2\varepsilon_\delta$ for $\lambda \le 1/20$. The three δ_η terms contribute at most $2\varepsilon_\delta$ in total. Hence $|\nu'| \le \frac{4}{3}[C_\omega(2\lambda + 2\varepsilon_\delta) + 2\varepsilon_\delta]$, which is (2).

(3) $\partial_\eta \delta_{\mathrm{mem}} = \delta_\nu \nu' + \delta_\eta$.

(4) $\frac{\mathrm{d}}{\mathrm{d}Y}[(2+Y+Y_*)e^{-(1-\lambda)Y}] = e^{-(1-\lambda)Y}[1 - (1-\lambda)(2+Y+Y_*)] < 0$ for $Y \ge 0$. □

The proposition.

Proposition 1.15.20 (Uniform first-angular future integral contributions before Y_0)**.** *Fix all data to the left of* K_f *in* (1.15.11), *including* L_o, *the cutoff* χ, *the connector width* ϵ_g, *and a memory radius* r_0 *for which (I5), (I8) hold. Under Hypothesis 1.15.10, which the construction satisfies (each item restates it):*

1. *For every* $\pi \in \mathcal{P}$ *the complete normalized integrals* τ_S, τ_P *of the actual future are* C^1 *in* η, *and*

$$\int_1^\infty (f^2 + |f\partial_\eta f|)\Big(\frac{1}{x} + \frac{1}{x^2}\Big)\,\mathrm{d}x + \sup|w_o| \le K_f, \tag{1.15.17}$$

with $K_f = 2K_0^2(1+\log M) + 2K_\infty^2((2h)^{-1}+1) + (1/2-h)\|(\log R_o)'\|_\infty$. *Here* K_∞ *is as in Lemma 1.15.15,* $K_0 := 2N_pK_1(1+C_\omega) + 2C_{\mathrm{conn}}$, $K_1 := 3K_P^3$ *bounds* $|\varphi|$ *and* $|\partial_\eta\varphi|$ *for every inner piece (Lemma 1.15.12, and directly for the heat-regime part of row C6), and* C_{conn} *is the larger of the two bounds of Lemma 1.15.18. In particular* $|\tau_S| + |\dot\tau_S| + |\tau_P| + |\dot\tau_P| + |w_o| \le K_f$, *which is the input* (1.16.25) *at* (1.16.24).

2. K_f *is independent of* Y_0, *of* C, *and of* $\epsilon \in (0,\epsilon_0]$. *It may depend on* $h, \nu_c, \lambda, B_h, L_o, \chi, \epsilon_g, r_0$ *and the fixed templates.*

3. *There is* $Y_{\min}$ *such that for every* $Y_0 \ge Y_{\min}$ *the actual matched memory of the physical family lies in* $\mathfrak{M}_{r_0}$. *So (1) applies along the whole physical* (Y_0, C) *family, with the same* K_f.

4. (Inlet derivatives.) With $a = (\log G)'$ *and* $r = (\log R_o)'$,

$$S_\eta|_{\frac{\hat\xi^2}{2}=R_o} = G^2\big(2a\tau_S + \tau_S' + \tfrac{r}{4}\big), \qquad (-P)_\eta|_{\frac{\hat\xi^2}{2}=R_o} = \frac{G^2}{R_o}\big[(2a-r)\tau_P + \tau_P' + \tfrac{r}{4}\big].$$

For each subsequently fixed Y_0*, the early moment correction is admitted at a finite master-scale threshold* $C_0(Y_0, L_o)$ *by Lemma 1.15.9. No uniform bound for this threshold is asserted or needed.*

Proof. (1) By (A1) and the mixture algebra, $f = \omega f_c + (1-\omega) f_w + \delta f$, with $\omega = (1-\chi)K_c/K_{\mathrm{mix}} \in [0,1]$. On $[1, M]$: $|f| \le \max_i |f_i| + |\delta f|$ and

$$|\partial_\eta f| \le |\omega'|(|f_c| + |f_w|) + \omega|\partial_\eta f_c| + (1-\omega)|\partial_\eta f_w| + |\partial_\eta \delta f|.$$

Where $\omega \equiv 0$ (respectively $\omega \equiv 1$) on an open set, the corresponding product and its derivative vanish there, so f_c is needed only on $\overline{\{\chi < 1\}}$ and f_w only on the chart band, where they are defined. By Lemmas 1.15.17, 1.15.12, 1.15.18 and 1.15.19(1)–(2): $|f| \le N_p K_1 + C_{\mathrm{conn}}$ and $|\partial_\eta f| \le 2C_\omega N_p K_1 + N_p K_1 + C_{\mathrm{conn}}$, so (1.15.14) holds with K_0 as stated. By Lemma 1.15.15, (1.15.15) holds. Lemma 1.15.13 gives the integral bound. Finally By the definition of the physical outlet, $w_o = (1/2 - h)\eta(\log R_o)' = (1/2-h)\eta(\rho' + (\log R_g)')$. Hence $|w_o| \le (1/2-h)\|(\log R_o)'\|_\infty$. Also $|\dot\tau| = (\frac12 - h)|\eta||\tau'| \le |\tau'|$.

(2) Every constant entering K_0, K_∞ was shown to be uniform on $\mathcal{P}$ in Lemmas 1.15.17–1.15.19. The only h-dependence beyond the templates is $1/(2h)$.

(3) On the scalar/exponent sector use the raw matched memory δ_{mem}; on the phase bridge the actual outer memory contains the bounded multiplier in Lemma 1.15.19. At a fixed angle the normalized central memory return is linear in its inlet discrepancy. The transported ratio ODE is affine in its inlet value with bounded derivative of its transfer factor. Thus the contribution of the inlet memory to the A11 target is $O(\|\delta_{\mathrm{mem}}\|_{C^1})$ including the fixed multiplier, with a geometric constant. Add the Y_0-independent model term $O(\lambda^{30(1-\lambda)})$, which is inside the A11 ball by the choice of λ ((λ5) after (1.6.18)). Here the A11 ball is the small-data ball of Lemma 1.15.5, whose radius is a template constant uniform on $0 \le \lambda \le 1/20$; we fix the A11 part of r_0 with the templates, before λ, and take λ so small that the model part is at most half of it. Apply Lemma 1.15.19(4) with $r_1 = r_0/(2\|\mathrm{maps}\|)$, that is, $r_0/2$ divided by the norms of these linear maps; with the model part $\le r_0/2$ the total stays $\le r_0$.

(4) $S(R_o(\eta), \eta) = G^2\tau_S$. Differentiate in η and use $\frac{S_{\hat\xi}}{\hat\xi} = -H^2/(4\frac{\hat\xi^2}{2})$, so that $(\frac{S_{\hat\xi}}{\hat\xi})(\sqrt{2(R_o)})R_o' = -G^2 r/4$. Similarly $-P(R_o) = G^2\tau_P/R_o$ and $(\hat\xi^{-1}\partial_{\hat\xi}(-P)) = -H^2/(4\frac{\hat\xi^4}{4})$. □

Remark 1.15.21 (What is and is not used). (i) No pointwise bound on second or higher angular derivatives inside a narrow layer is used. Only first derivatives occur, and they are bounded pointwise because each narrow layer is either scalar (only κ enters) or has amplitude proportional to its width. (ii) If $|\varphi| \le K$ and $\int_1^M |\partial_\eta\varphi|\,\mathrm{d}x \le K$ uniformly, then $\int_1^M |f\partial_\eta\varphi| x^{-1}\,\mathrm{d}x \le K \sup|f|$. For the corresponding C^1 conclusion one may also assume joint C^1 regularity on the compact inner region for each fixed member, as in (A6). Continuity of the differentiated integral then follows on that region by compactness for the fixed member, and on the tail by the integrable majorant of Lemma 1.15.13. The displayed L^1 bound controls the derivative uniformly over the family. (iii) In row C7 the moving-boundary term in Φ_η is $-\epsilon_o h\psi_o\beta_o' F''((\beta_o - \xi)/\varepsilon_t)$. It has bounded height and $O(\varepsilon_t)$ radial L^1 norm by the change of variable $s = (\beta_o - \xi)/\varepsilon_t$. (iv) Item (1) includes $|w_o|$ in K_f, as required at (1.16.24); it is a pure geometry bound.

1.15.5 The actual central memory, hold, and scalar source

Proposition 1.15.22 (Central source supplied by the selected scalar future)**.** *We use the scalar equilibrium reference $r_c = (1-\nu_c)^{-1}$ and the post-hold drive and shot of Lemma 1.15.6. We put the actual primitive-memory return on a scalar interval $[R_m, 2R_m]$, after all axial returns and before $R_h > 2R_m$. The new outer rank-one correction is part of the outer component only. The pre-pulse heat-history restoration extension is zero on the open central band. Thus each edit does not change this central future after the memory return. (The later spectral implant on the first part of the hold, Section 1.26, is a separate edit and is not part of the component considered here.)*

Fix h, ν_c, the hold length B_h, the stop templates of Lemma 1.6.26, the shot, bridge and wing templates of Section 1.13, and the central geometry ratios of (I1). There are numbers $C_I, K_{\mathrm{tot}}, C_h', B_c, \varepsilon_c > 0$, depending only on these data and not on L_o, Y_0, the amplitude or the radius, with the following property. (The constant B_c here is not the constant of (1.6.49).) Impose

(L) $L_o \geq (\lambda - h)^{-1} \log^+(B_c E_{A,\max}/\varepsilon_c)$ (we select a finite enlargement of L_o before Y_0);

(Y) $C_I \epsilon_I \leq \nu_c/8$, with ϵ_I from (1.15.22); by (I8) this is a lower bound on Y_0;

(R) a last lower bound on the same radius (a lower bound on C at fixed L_o, Y_0).

Then on the full physical chart $-1 \leq \eta \leq 1$, for $\frac{\hat\xi^2}{2} \geq R_o(\eta)$, with $E_c = H/\hat\xi$:

(i) $H > 0$ and $T_\theta \geq 0$. On the compact preterminal path $R_o(\eta) \leq \frac{\hat\xi^2}{2} \leq \sup J$, with J the blend interval of (1.13.57), $T_\theta > 0$ with the explicit floors (1.15.25).

(ii) (Memory interval and hold.) For $R_o(\eta) \leq \frac{\hat\xi^2}{2} \leq R := R_h e^{B_h}$,

$$T_\theta \geq \tfrac{3}{10} h H_s, \qquad \nu_c \leq a_s - 2 \leq 3\nu_c, \qquad \frac{|T_z|}{T_\theta} \leq K_{\mathrm{hold}} E_c, \quad K_{\mathrm{hold}} = 11\Lambda_c,$$

where $\Lambda_c = B_h + \log(x_b^{\max}/r_-)$ is fixed by (1.15.23). In particular $|T_z|/T_\theta \leq K_{\mathrm{hold}} E_c/h$.

(iii) Wherever $T_\theta > 0$ we have $2 < a_s \leq 2 + C_h'$ and $|T_z| \leq K_{\mathrm{tot}} \left(\sup_{\frac{\rho^2}{2} \geq R_o} E_c\right) T_\theta$. Wherever $T_\theta = 0$, also $T_z = 0$.

(iv) $\sup_{\frac{\hat\xi^2}{2} \geq R_o} E_c \leq B_c E_{A,\max} e^{-(\lambda-h)L_o}$. Hence, under (L), this central component has nonnegative angular stress and satisfies the strict zero-axial-velocity source cone wherever its stress is nonzero. At its flat source boundaries this is a result of the relative estimate in (iii), not of a uniform positive stress bound.

(v) $I = i_s$ on $2R_m \leq \hat\xi^2/2 \leq R_h e^{B_h}$, so the hold and the coefficient map of Lemma 1.15.6 are evaluated at the reference ratio r_c, and $k_- \leq K_{\mathrm{old}} \leq k_+$.

The three conditions (L), (Y), (R) are monotone, so later enlargements of L_o, Y_0 or the radius keep them. We do not get the statement by division of an ordinary derivative by η.

Proof. Here $a = 1-h$, $d = 1-\eta^2$, and $L = 1 - 2h\eta^2 \in [1-2h, 1]$. Since $h < \lambda/6 \leq 1/120$, $L \geq 0.98$ and $1/(2L) \leq 0.52$. On the whole central future $U = M = J = 0$, and the canonical outward

histories are $S(\frac{\hat\xi^2}{2},\eta)=\int_{(\frac{\hat\xi^2}{2})}^{\infty} H^2/(4s)\,\mathrm{d}s$ and $P(\frac{\hat\xi^2}{2},\eta)=-\int_{(\frac{\hat\xi^2}{2})}^{\infty} H^2/(4s^2)\,\mathrm{d}s$. The exact formulas are

$$\mathcal{A}I=(\frac{I_{\hat\xi\hat\xi}}{\hat\xi^2}-\frac{I_{\hat\xi}}{\hat\xi^3})+(1/(2L)-1/\tfrac{\hat\xi^2}{2})\frac{I_{\hat\xi}}{\hat\xi}-aI/(L\hat\xi^2)+(\tfrac12-h)\eta I_\eta/(L\hat\xi^2),\tag{1.15.18}$$

$$T_\theta=\mathcal{A}I,\qquad T_z=\frac{4h\eta S-dS_\eta+\frac{\hat\xi^2}{2}((2+4h)\eta P-dP_\eta)}{L\hat\xi}.\tag{1.15.19}$$

The single actual energy root and the pressure identities supply their constants. We do not select these constants at the hold.

Step 0 (an exact formula for the axial numerator). Put $N:=L\hat\xi\,T_z$ and

$$\mathcal{D}(s,\eta):=\eta\,(s\partial_s+h)H(s,\eta)-\tfrac{d}{2}\,\partial_\eta H(s,\eta).$$

Then

$$N(\tfrac{\hat\xi^2}{2},\eta)=\int_{(\frac{\hat\xi^2}{2})}^{\infty} H\,\mathcal{D}\,\frac{s-\frac{\hat\xi^2}{2}}{s^2}\,\mathrm{d}s.\tag{1.15.20}$$

Indeed, $\frac{\mathrm{d}}{\mathrm{d}s}[H^2(s-\frac{\hat\xi^2}{2})/s]=2HH_s(s-\frac{\hat\xi^2}{2})/s+H^2\frac{\hat\xi^2}{2}/s^2$, and $H^2(s-\frac{\hat\xi^2}{2})/s\to0$ as $s\to\infty$ (the heat tail is $O(s^{-2h})$), so $\int_{(\frac{\hat\xi^2}{2})}^{\infty} HH_s(s-\frac{\hat\xi^2}{2})/s\,\mathrm{d}s=-\frac{X}{2}\int_{(\frac{\hat\xi^2}{2})}^{\infty} H^2/s^2\,\mathrm{d}s$. Hence

$$\int_{(\frac{\hat\xi^2}{2})}^{\infty} H(sH_s+hH)\frac{s-\frac{\hat\xi^2}{2}}{s^2}\,\mathrm{d}s=h\int_{(\frac{\hat\xi^2}{2})}^{\infty}\frac{H^2}{s}\,\mathrm{d}s-(\tfrac12+h)\tfrac{\hat\xi^2}{2}\int_{(\frac{\hat\xi^2}{2})}^{\infty}\frac{H^2}{s^2}\,\mathrm{d}s=4(hS+(\tfrac12+h)\tfrac{\hat\xi^2}{2}P).$$

Also $S_\eta+\frac{\hat\xi^2}{2}P_\eta=\frac12\int_{(\frac{\hat\xi^2}{2})}^{\infty} HH_\eta(s-\frac{\hat\xi^2}{2})s^{-2}\,\mathrm{d}s$; differentiation under the integral is justified by the integrable dominators in the proof of Lemma 1.13.5. Combining the two gives (1.15.20). Two cases are used below. (a) For a lifted field $H=d^{-h}g(\frac{\hat\xi^2}{2}/d)$ we have $\frac{d}{2}\partial_\eta H=\eta(s\partial_s+h)H$, so $\mathcal{D}\equiv0$. This is (1.13.60). (b) For a field that is scalar at fixed physical $\frac{\hat\xi^2}{2}$, with $\kappa=-sH_s/H$, we have $\mathcal{D}=\eta(h-\kappa)H$. With an h-power continuation this is (1.13.29). Finally, let $H^\sharp$ equal H on $[\frac{\hat\xi^2}{2},R_b]$ and the power germ $H_b=G_b(s/R_b)^{-h}$ on $[R_b,\infty)$. Then $S^\sharp(R_b)=G_b^2/(8h)$, $P^\sharp(R_b)=-G_b^2/[4(1+2h)R_b]$, and $\mathcal{D}^\sharp=0$ on $[R_b,\infty)$. For $\frac{\hat\xi^2}{2}\le R_b$ we get

$$N=\int_{(\frac{\hat\xi^2}{2})}^{R_b} H\mathcal{D}\frac{s-\frac{\hat\xi^2}{2}}{s^2}\,\mathrm{d}s+N_{\mathrm{tail}},\qquad N_{\mathrm{tail}}=4h\eta\Delta S_b-d\,\partial_\eta\Delta S_b+\tfrac{\hat\xi^2}{2}((2+4h)\eta\Delta P_b-d\,\partial_\eta\Delta P_b),$$
$$\Delta S_b(\eta)=S(R_b,\eta)-\frac{G_b^2}{8h},\qquad \Delta P_b(\eta)=P(R_b,\eta)+\frac{G_b^2}{4(1+2h)R_b}.\tag{1.15.21}$$

Step 1 (the data and the constants). Before the drive we write $H_s=A_c(\frac{\hat\xi^2}{2})^{-\nu_c}$ and $i_s=\frac{\hat\xi^2}{2}H_s/(1-\nu_c)$. We return the actual inlet memory $p(\eta)$ by

$$I=i_s+p\zeta(\tfrac{\hat\xi^2}{2}/R_m),\qquad H=H_s+\delta H,\quad \delta H=(p/R_m)\zeta'(\tfrac{\hat\xi^2}{2}/R_m),$$

where ζ is a fixed smooth cutoff, $\zeta=1$ on $[0,1]$ and $\zeta=0$ on $[2,\infty)$. So the power before this support keeps its actual constant p. On the compact normalized memory family (I8),

$$\epsilon_I:=\frac{\|p\|_{C^1}}{R_mH_s(R_m)}\le K_I(1+Y_0)^Ne^{-(1-\nu_c)Y_0}.\tag{1.15.22}$$

The pair equals the scalar reference (H_s, i_s) on $2R_m \le \hat\xi^2/2 \le R = R_h e^{B_h}$. There the drive of Lemma 1.6.26 starts, in $x = \frac{\hat\xi^2}{2}/R$ and $W = w_d/R$, with $\varepsilon = R^{-1/5}$. The drive has slope $\kappa_{\rm st} \in [\nu_c, 2h]$ on $[1, x_{\rm hit}]$, slope $\kappa_1 \in [h, 2h]$ on $[x_{\rm hit}, x_b]$, and the h-power germ from $R_b = Rx_b(\varepsilon)$. Its amplitude is $G_b = H(R_b)$ and its deficit is $C_b = G_b w_d(R_b) = G_b R^{4/5} Z(1;\varepsilon)$. From the proof of Lemma 1.6.26 we use the following data: $m_0 = \min_{[1,x_z-\delta']} W > 0$; $W_x \le -h/(2a)$ on $[x_z - \delta', x_z + \delta'] \ni x_{\rm hit}$; $W = \varepsilon Z \ge \varepsilon Z_1/2$ on $[x_{\rm hit}, x_b]$, with Z_1 from (1.6.54); $x_b^{\max} = \max_{[0,\varepsilon_*]} x_b$; and $Z_{\max} = \max Z$ on $[0,1] \times [0, \varepsilon_*]$. After R_b come the actual scalar shot (Lemma 1.13.4), the lift (1.13.47), the wing (1.13.53), the blend (1.13.57) on the interval $J \Subset R_b + [.52, .54]W_s$, and the exact heat pair. We select the original even ψ_o and edge $\mathcal{B}_o(\eta) = B_o e^{k_o \eta^2}$ with $(\frac12 - h)\eta\mathcal{B}_o' \ge 2\mathcal{B}_o$ on its support. We put $\ell_b = R_b^{4/5}$ and $\alpha_o = \epsilon_o h G_b/R_b$, and choose ϵ_o and then R_b as in Section 1.13. These results of Section 1.13 use the drive only through the open h-power germ (H_b, I_b), $I_b = \frac{\hat\xi^2}{2} H_b/a - C_b$, and through $C_b/G_b \to \infty$ and $C_b/(G_b R_b) \to 0$ at the rates $R_b^{\pm 1/5}$. Here $C_b \asymp G_b R_b^{4/5}$ with constants fixed by h and the stop templates; the extra fixed factor h in (1.13.27) only changes constants. Thus the following hold for this central future with constants fixed by the templates: (1.13.40), (1.13.49), (1.13.54), (1.13.55), (1.13.56), (1.13.58), (1.13.59), (1.13.61) (with $0 < H \le C_L G_b$ beyond R_b), (1.13.62) (with constant C_*), and (1.13.67) (with constants $C_{\rm wg}, c_{\rm wg}$). These are the inputs (I3) and (I9). By (I1), $R_o/R_h \in [r_-, r_+]$ and $R_m = R_h/a_h$. Put

$$\begin{aligned} \rho_m &:= \frac{1}{a_h r_-} \ge \sup \frac{R_m}{R_o}, \quad e^{\Lambda_c} := \frac{x_b^{\max} e^{B_h}}{r_-} \ge \sup \frac{R_b}{R_o}, \\ Z_\zeta &:= \|\zeta'\|_\infty + \|\zeta''\|_\infty, \qquad C_I := 1.1(Z_\zeta + \rho_m), \end{aligned} \tag{1.15.23}$$

and $c_1 := \min(c_t, Z_1/2)$. The radius condition (R) collects the following: $R_o \ge 22/h$; $R_m \ge 100$; $R \ge R_*$ and $\varepsilon \le \varepsilon_*$ (Lemma 1.15.6); $c_1 R^{4/5} \ge 5$ and $m_0 R \ge c_1 R^{4/5}$; $6C_* Z_{\max} R^{-1/5} \le h\Lambda_c$; and the large-$R_b$ thresholds of the results of Section 1.13 cited above.

Step 2 (memory interval and hold, $R_o \le \frac{\hat\xi^2}{2} \le R$). (a) Field. All of δH, $\frac{\hat\xi^2}{2}\delta\frac{H_{\hat\xi}}{\hat\xi} = (\frac{\hat\xi^2}{2}/R_m)(p/R_m)\zeta''$ and $\partial_\eta \delta H = (p'/R_m)\zeta'$ vanish outside $[R_m, 2R_m]$. They are bounded by $2\|\zeta^{(j)}\|_\infty \epsilon_I H_s(R_m)$, and $H_s(R_m) \le 2^{\nu_c} H_s(\frac{\hat\xi^2}{2}) \le 1.1 H_s(\frac{\hat\xi^2}{2})$ for $\frac{\hat\xi^2}{2} \le 2R_m$. So each is at most $2.2 Z_\zeta \epsilon_I H_s(\frac{\hat\xi^2}{2}) \le 2C_I \epsilon_I H_s(\frac{\hat\xi^2}{2}) \le \frac{\nu_c}{4} H_s(\frac{\hat\xi^2}{2})$ by (Y). Hence $(1 - \nu_c/4)H_s \le H \le (1 + \nu_c/4)H_s$, and

$$a_s - 2 = -\frac{\hat\xi H_{\hat\xi}}{H} = \frac{2(\nu_c H_s - \frac{\hat\xi^2}{2}\delta\frac{H_{\hat\xi}}{\hat\xi})}{H} \in \Big[\frac{1.5\nu_c}{1 + \nu_c/4}, \frac{2.5\nu_c}{1 - \nu_c/4}\Big] \subset [\nu_c, 3\nu_c].$$

So the logarithmic decay rate stays between $\nu_c/2$ and $2\nu_c$.

(b) Source. $T_\theta = \mathcal{A} i_s + \mathcal{A}(p\zeta)$, with $(\hat\xi^{-1}\partial_{\hat\xi}(i_s)) = H_s$, $((\hat\xi^{-1}\partial_{\hat\xi})^2(i_s)) = -\nu_c H_s/\frac{\hat\xi^2}{2}$ and $a i_s = (1-h)\frac{\hat\xi^2}{2} H_s/(1-\nu_c)$. Therefore

$$\begin{aligned} T_{\theta,s} :&= \mathcal{A} i_s = \frac{h - \nu_c}{2L(1-\nu_c)} H_s - \frac{2(1+\nu_c)}{\hat\xi^2} H_s, \\ \mathcal{A}(p\zeta) &= \frac{p}{R_m^2}\zeta'' + \Big(\frac{1}{2L} - \frac{2}{\hat\xi^2}\Big)\frac{p}{R_m}\zeta' + \frac{-ap + (\frac12 - h)\eta p_\eta}{L\hat\xi^2}\zeta. \end{aligned}$$

Since $L \le 1$ and $\nu_c < h/10$, the first coefficient is at least $(h - \nu_c)/2 \ge 0.45h$, and $(1+\nu_c)/\frac{\hat\xi^2}{2} \le 0.05h$ for $\frac{\hat\xi^2}{2} \ge 22/h$. So $T_{\theta,s} \ge 0.4 h H_s$. We have $|p| + |p_\eta| \le \epsilon_I R_m H_s(R_m)$, $a + (\frac12 - h) \le 3/2$, $\frac{\hat\xi^2}{2} \ge R_o$

and $R_m \ge 100$. On the support of ζ, also $R_m/\frac{\hat\xi^2}{2} \le \rho_m$ and $H_s(R_m) \le 1.1 H_s(\frac{\hat\xi^2}{2})$. Hence

$$\begin{aligned}|\mathcal{A}(p\zeta)| &\le 1.1\,\epsilon_I H_s(\tfrac{\hat\xi^2}{2})[0.01\|\zeta''\|_\infty + 0.53\|\zeta'\|_\infty + 0.77\rho_m] \\ &\le C_I\epsilon_I H_s(\tfrac{\hat\xi^2}{2}) \le \tfrac{\nu_c}{8} H_s(\tfrac{\hat\xi^2}{2}) \le 0.0125\, h H_s(\tfrac{\hat\xi^2}{2}).\end{aligned}$$

Thus $T_\theta \ge 0.38\, hH_s \ge \frac{3}{10} hH_s$.

(c) Axial ratio. We use (1.15.21). Outside $[R_m, 2R_m]$ the field on $[\frac{\hat\xi^2}{2}, R_b]$ is scalar with slope $\kappa \in [\nu_c, 2h]$: it is ν_c on the hold and buffer, and $\kappa_{\rm st}$ or κ_1 on the drive. So by Step 0(b), $|H\mathcal{D}| \le hH^2$ there. On $[R_m, 2R_m]$, $\mathcal{D} = \eta[(h-\nu_c)H_s + h\,\delta H + s\,\delta H_s] - \frac{d}{2}\partial_\eta \delta H$. By (a), $|\mathcal{D}| \le (h - \nu_c + \frac{(h+3/2)\nu_c}{4}) H_s \le hH_s$, and so $|H\mathcal{D}| \le 2hH_s^2$. The field decreases outside the memory support, so $H_s(s) \le H_s(\frac{\hat\xi^2}{2})$ on the hold and $H(s) \le H(R) = H_s(R) \le H_s(\frac{\hat\xi^2}{2})$ on the drive. With $(s - \frac{\hat\xi^2}{2})/s^2 \le 1/s$ and $R_b/\frac{\hat\xi^2}{2} \le e^{\Lambda_c}$, this gives

$$\Big|\int_{(\frac{\hat\xi^2}{2})}^{R_b} H\mathcal{D}\frac{s - \frac{\hat\xi^2}{2}}{s^2}\,\mathrm{d}s\Big| \le 2hH_s(\tfrac{\hat\xi^2}{2})^2 \log\frac{R_b}{\frac{\hat\xi^2}{2}} \le 2h\Lambda_c H_s(\tfrac{\hat\xi^2}{2})^2.$$

By (1.13.62), $|\Delta S_b|$ and $|\partial_\eta \Delta S_b|$ are at most $C_* G_b C_b/R_b$, and $|\Delta P_b|$ and $|\partial_\eta \Delta P_b|$ are at most $C_* G_b C_b/R_b^2$. Since $\frac{\hat\xi^2}{2} \le R_b$ and $4h + 1 + (2+4h) + 1 \le 6$, $|N_{\rm tail}| \le 6C_* G_b C_b/R_b$. Also $C_b \le Z_{\max} G_b R^{4/5}$, $R \le R_b$ and $G_b \le H_s(R) \le H_s(\frac{\hat\xi^2}{2})$. So by (R), $|N_{\rm tail}| \le 6C_* Z_{\max} R^{-1/5} H_s(\frac{\hat\xi^2}{2})^2 \le h\Lambda_c H_s(\frac{\hat\xi^2}{2})^2$. Hence $|N| \le 3h\Lambda_c H_s(\frac{\hat\xi^2}{2})^2$. With (b), $L \ge 0.98$ and $H_s \le (1-\nu_c/4)^{-1} H$,

$$\frac{|T_z|}{T_\theta} = \frac{|N|}{L\hat\xi\, T_\theta} \le \frac{3h\Lambda_c H_s^2}{0.98\cdot 0.3\, hH_s\hat\xi} \le 10.3\,\Lambda_c \frac{H_s}{\hat\xi} \le 11\Lambda_c E_c.$$

This proves (ii) with $K_{\rm hold} = 11\Lambda_c$. The explicit factor h cancels. The remaining constant depends on B_h, $x_b^{\max}$ and r_- in (1.15.23), which are fixed after h, ν_c. Since $h < 1$ this also gives $|T_z|/T_\theta \le K_{\rm hold} E_c/h$. The memory changes the canonical histories only for $\frac{\hat\xi^2}{2} \le 2R_m$, by $\Delta S_m = \int_{\max(\frac{\hat\xi^2}{2}, R_m)}^{2R_m} (2H_s\delta H + \delta H^2)\frac{\mathrm{d}s}{4s}$ and the analogous ΔP_m with weight $-1/(4s^2)$. These satisfy $|\Delta S_m| + |\partial_\eta \Delta S_m| + \frac{\hat\xi^2}{2}(|\Delta P_m| + |\partial_\eta \Delta P_m|) \le 2Z_\zeta(\epsilon_I + Z_\zeta \epsilon_I^2) H_s(R_m)^2$. The bound above includes them, because it uses the total field. Equation (1.15.19) includes them.

Step 3 (the drive, $R \le \frac{\hat\xi^2}{2} \le R_b$). Here I is scalar, with $\frac{I_{\hat\xi}}{\hat\xi} = H$. Put $w = \frac{\hat\xi^2}{2}(a^{-1} - I/(\frac{\hat\xi^2}{2}H))$ and $\kappa = -\frac{1}{2}\hat\xi H_{\hat\xi}/H$. Then $\frac{w_{\hat\xi}}{\hat\xi} = 1/a - 1 - \kappa I/(\frac{\hat\xi^2}{2}H)$ and $aI = \frac{\hat\xi^2}{2}H - awH$. Direct differentiation gives

$$\frac{w_{\hat\xi}}{\hat\xi} = \kappa w/\tfrac{\hat\xi^2}{2} + (h-\kappa)/a, \qquad T_\theta = \frac{2H}{\hat\xi^2}\left[\frac{aw}{2L} - (1+\kappa)\right]. \tag{1.15.24}$$

At $\frac{\hat\xi^2}{2} = R$, $w = R(a^{-1} - r_c) = RW_1$ by (v), since $W_1 = (h-\nu_c)/[a(1-\nu_c)]$, so $w \asymp h\frac{\hat\xi^2}{2}$ initially. The data of Step 1 give $W \ge \min(m_0, c_t\varepsilon, \varepsilon Z_1/2)$ on $[1, x_b]$, so by (R), $w \ge c_1 R^{4/5} \ge 5$ on the whole drive, including its late part where w shrinks to order $R_b^{4/5}$. Then $aw/(4L) \ge 1.2 \ge 1 + \kappa$, and

$$T_\theta \ge \frac{awH}{4L\frac{\hat\xi^2}{2}} > 0, \qquad a_s - 2 = 2\kappa \in [2\nu_c, 4h].$$

Thus a sufficiently large radius controls the viscous subtraction even at this shrinking normalized reserve. For the axial numerator, $|\int_{(\frac{\hat\xi^2}{2})}^{R_b} H\mathcal{D}(s-\frac{\hat\xi^2}{2})s^{-2}\,\mathrm{d}s| \le hH(\frac{\hat\xi^2}{2})^2(R_b-\frac{\hat\xi^2}{2})^2/(2\frac{\hat\xi^4}{4})$, because $|h-\kappa|\le h$, $H(s)\le H(\frac{\hat\xi^2}{2})$ and $(s-\frac{\hat\xi^2}{2})/s^2 \le (s-\frac{\hat\xi^2}{2})/\frac{\hat\xi^4}{4}$. We claim

$$h(R_b-\tfrac{\hat\xi^2}{2})^2 \le K_{\mathrm{dr}}\,\tfrac{\hat\xi^2}{2}\,w(\tfrac{\hat\xi^2}{2}), \qquad K_{\mathrm{dr}} := \max\Big\{\frac{h(x_b^{\max})^2}{m_0},\ \Big(2a+\frac{hc_w}{c_t}\Big)x_b^{\max},\ \frac{2hc_w^2}{Z_1}\Big\}.$$

In normalized variables we must show $h(x_b-x)^2 \le K_{\mathrm{dr}}xW$. On $[1, x_z-\delta']$ we have $W\ge m_0$ and $x\ge 1$. On $[x_z-\delta', x_{\mathrm{hit}}]$ we have $W(x)\ge c_t\varepsilon+\frac{h}{2a}(x_{\mathrm{hit}}-x)$. So $x_b-x=(x_{\mathrm{hit}}-x)+c_w\varepsilon \le (2a/h+c_w/c_t)W$, and $x_b-x\le x_b^{\max}\le x_b^{\max}x$. On $[x_{\mathrm{hit}}, x_b]$ we have $(x_b-x)^2\le c_w^2\varepsilon^2\le (2c_w^2/Z_1)\varepsilon W$, and $\varepsilon\le 1\le x$. Hence

$$\frac{|\int_{(\frac{\hat\xi^2}{2})}^{R_b} H\mathcal{D}(s-\frac{\hat\xi^2}{2})s^{-2}\,\mathrm{d}s|}{L\hat\xi\,T_\theta} \le \frac{hH^2(R_b-\frac{\hat\xi^2}{2})^2}{2\frac{\hat\xi^4}{4}}\cdot\frac{4\frac{\hat\xi^2}{2}}{a\hat\xi\,wH} \le \frac{2K_{\mathrm{dr}}}{a}E_c(\tfrac{\hat\xi^2}{2}).$$

For the tail part, $|N_{\mathrm{tail}}|\le 6C_*Z_{\max}G_b^2R^{4/5}/R_b$. Also

$$L\hat\xi T_\theta \ge \frac{awH}{2\hat\xi} \ge \frac{ac_1R^{4/5}G_b}{2\sqrt{2R_b}},$$

because $H\ge G_b$ and $\frac{\hat\xi^2}{2}\le R_b$. So the tail ratio is at most $K_{\mathrm{tl}}E_c(R_b)$, with $K_{\mathrm{tl}}=24C_*Z_{\max}/(ac_1)$ and $E_c(R_b)=G_b/\sqrt{2R_b}$. On the drive therefore $|T_z|/T_\theta\le(2K_{\mathrm{dr}}/a+K_{\mathrm{tl}})\sup E_c$.

Step 4 (power segment, $R_b\le\frac{\hat\xi^2}{2}\le\inf J$). Here $H=H_b$ and $I=I_b=\frac{\hat\xi^2}{2}H_b/a-C_b$, so $T_\theta = aC_b/(L\hat\xi^2)-(1+h)H_b/\frac{\hat\xi^2}{2}\ge aC_b/(4L\frac{\hat\xi^2}{2})$, because $C_b/G_b=w(R_b)\ge 5$ and $H_b\le G_b$. Also $a_s=2+2h$. On $[R_b,\inf J]$ the field is the h-power, so $\mathcal{D}=0$ there, and $S-S_b$, $P-P_b$ are the constants $\Delta S_b, \Delta P_b$ of (1.15.21). Hence $N=N_{\mathrm{tail}}$ also for $R_b\le\frac{\hat\xi^2}{2}\le\inf J$. Here $\frac{\hat\xi^2}{2}\le\inf J\le R_b+W_s=(1+\epsilon_s)R_b$. With $8h+4\epsilon_s\le 1$ (fixed small ϵ_s), the coefficient $4h+1+(\frac{\hat\xi^2}{2}/R_b)((2+4h)+1)$ is at most 6. So $|N|\le 6C_*G_bC_b/R_b$ and, using $(\hat\xi/\sqrt{2})\le\sqrt{2R_b}$, $|T_z|/T_\theta\le 6C_*G_bC_b/R_b\cdot 4\frac{\hat\xi^2}{2}/(a\hat\xi C_b)\le K_{\mathrm{ps}}E_c(R_b)$, with $K_{\mathrm{ps}}=34C_*/a$.

Step 5 (bridge J, target, heat region). On J the original radial primitive bridge on the shot's fixed positive plateau has the exact stress (1.13.58),

$$(1-\chi_b)T_{\theta,b}+\chi_bT_{\theta,T}+2\chi_b'\frac{\Delta_{\hat\xi}}{\hat\xi}+[\chi_b''+(1/(2L)-1/\tfrac{\hat\xi^2}{2})\chi_b']\Delta, \qquad \Delta=I_T-I_b\asymp C_b.$$

By (1.13.56) its adverse terms are $O(C_b/R_b^2)$. By Step 4 and (1.13.55) its base reserve is at least $c\epsilon_oC_b/R_b$. So by (R), $T_\theta\ge\frac{c}{2}\epsilon_oC_b/R_b$ on J. For $\frac{\hat\xi^2}{2}\in J$ the canonical tails satisfy $S-S_b=\int_{(\frac{\hat\xi^2}{2})}^{\infty}(H-H_b)(H+H_b)\frac{\mathrm{d}t}{4t}$ and $\partial_\eta S=\int_{(\frac{\hat\xi^2}{2})}^{\infty}HH_\eta\frac{\mathrm{d}t}{2t}$, and the pressure analogues with $-t^{-2}$. By (1.13.61) and $0<H,H_b\le C_LG_b$ they are bounded by CG_bC_b/R_b, respectively CG_bC_b/R_b^2, together with their η-derivatives. The h-power reference has $\mathcal{D}_b=0$. So $|N|\le C_JG_bC_b/R_b$, and $|T_z|/T_\theta\le K_JE_c(R_b)$ with $K_J=2C_J/(0.98\,c\,\epsilon_o)$, a template constant.

After J the field is the target $(H_T,I_T)=(H_L-\psi_o\alpha_o\ell_b\mathcal{F}', I_L+\psi_oE_o)$. By (1.13.49), (1.13.54) and $\eta\psi_o'\ge 0$,

$$T_{\theta,T}=d^{-h-1}\tau_s(\tfrac{\hat\xi^2}{2}/d)+\psi_o\mathcal{A}E_o+\frac{(\frac12-h)\eta\psi_o'E_o}{L\hat\xi^2}\ge T_{\theta,L}+c_{\mathrm{wg}}Z_o\ge 0,$$

$$Z_o=\psi_o\alpha_o\ell_b\mathcal{F}'+\eta\psi_o'\alpha_o\ell_b^2\mathcal{F}/\tfrac{\hat\xi^2}{2}.$$

By Step 0(a), $T_{z,L}=0$. So $T_{z,T}$ is the quadratic difference (1.13.66), and (1.13.67) gives $|T_{z,T}|\le C_{\mathrm{wg}}(H_L/(\hat\xi/\sqrt{2}))Z_o$. Since $v_o\le H_L/2$ we have $H_L\le 2H_T$. Hence $|T_z|/T_\theta\le(2\sqrt{2}C_{\mathrm{wg}}/c_{\mathrm{wg}})E_c$ wherever $T_\theta>0$. Where $T_\theta=0$, both $T_{\theta,L}=0$ and $Z_o=0$, so $T_z=0$. On bridge and target $2+c_h\le a_s\le 2+C_h$ by (1.13.59), and $H>0$ there. In the exact heat region (Corollary 1.13.6) both stresses vanish. All fixed endpoint derivatives come from the regular heat expansion and the flat fast remainder (proof of Lemma 1.13.5).

Step 6 (positivity, item (i)). $H>0$ follows from Step 2(a), from $H=H(R)\exp(-\int\kappa/x)$ on the drive, and from Step 5. By Steps 2–5,

$$T_\theta\ge\begin{cases}\frac{3}{10}hH_s, & R_o\le\frac{\hat\xi^2}{2}\le R,\\ \frac{awH}{4L\frac{\hat\xi^2}{2}}\ge\frac{ac_1R^{4/5}H}{4\frac{\hat\xi^2}{2}}, & R\le\frac{\hat\xi^2}{2}\le R_b,\\ \frac{aC_b}{4L\frac{\hat\xi^2}{2}}, & R_b\le\frac{\hat\xi^2}{2}\le\inf J,\\ \frac{c}{2}\epsilon_o\frac{C_b}{R_b}, & \frac{\hat\xi^2}{2}\in J,\end{cases}\qquad T_\theta\ge T_{\theta,L}+c_{\mathrm{wg}}Z_o\ge 0\quad\text{after } J. \tag{1.15.25}$$

The preterminal path $\{R_o(\eta)\le\frac{\hat\xi^2}{2}\le\sup J,\ |\eta|\le 1\}$ is compact and T_θ is continuous and positive on it. So for each admitted member its minimum m_c is positive.

Step 7 (the cone, items (iii) and (iv)). Put

$$K_{\mathrm{tot}}:=\max\Big\{K_{\mathrm{hold}},\ \frac{2K_{\mathrm{dr}}}{a}+K_{\mathrm{tl}},\ K_{\mathrm{ps}},\ K_J,\ \frac{2\sqrt{2}C_{\mathrm{wg}}}{c_{\mathrm{wg}}}\Big\},$$
$$C_h':=\max(C_h,4h)+1,\qquad \varepsilon_c:=\frac{1}{K_{\mathrm{tot}}\sqrt{C_h'}}.$$

Steps 2–5 give (iii), with $2<a_s\le 2+C_h'$ wherever $T_\theta>0$. Since $U=0$, the shear parameter $b_s=0$, so $s_v=a_s$ and $s_t=0$. Then (1.12.2) reads $\sqrt{2}T_\theta\pm\sqrt{a_s-2}\,T_z>0$, that is, $T_\theta>0$ and $(a_s-2)(T_z/T_\theta)^2<2$. If $\sup E_c\le\varepsilon_c$, then $(a_s-2)T_z^2\le C_h'K_{\mathrm{tot}}^2\varepsilon_c^2T_\theta^2=T_\theta^2<2T_\theta^2$ wherever $T_\theta>0$. This margin is relative, so it holds up to the flat edges of the wing and of the lifted source. Where the stress vanishes, nothing is required.

It remains to bound the amplitude. On $[R_o,R]$ we have $H\le(1+\nu_c/4)H_s(\frac{\hat\xi^2}{2})\le 1.001H(R_o)$, since $H(R_o)=H_s(R_o)$ because $R_o<R_m$. The drive decreases H. Beyond R_b, $H\le C_LG_b\le C_LH(R_o)$. So with $K_H:=\max(2,C_L)$ we get $E_c(\frac{\hat\xi^2}{2})\le K_HH(R_o)/\sqrt{2R_o}=K_HE_{c,o}$. By (1.6.28), $H_c(R_o)=K_ccR_o^{-h}$. By the outer coefficient law (1.15.3), $c=H_A^f(R_A^f)^hJe^{-(\lambda-h)L_o}$. Hence the exact same-coefficient law at the comparison inlet is

$$E_{c,o}=K_cJ(R_A^f/R_o)^{h+1/2}E_A^fe^{-(\lambda-h)L_o},\qquad E_A^f=\frac{H_A^f}{\sqrt{2R_A^f}}.$$

Here $K_c\le K_c^+$ by (1.6.29). J is independent of L_o (Lemma 1.15.2). The ratio R_A^f/R_o is the fixed chart-transfer ratio of Section 1.15 (k_A in the backward chart, Step 4 of the proof of Lemma 1.6.10). All of these are uniform in Y_0 and the admitted scale, and independent of L_o. Here $E_{A,\max}$ is uniform for all $Y_0\ge Y_{\min}$ and all admitted large scales. It is a result of the unchanged outer prepulse bound $E_p\le C_{\mathrm{pre}}\lambda^{30}$ (1.15.36). The postpulse power, flattening and fixed waits decrease E. With $B_c:=K_HK_c^+J\sup(R_A^f/R_o)^{h+1/2}$, which depends only on fixed geometry and central templates,

$$\sup_{\frac{\hat\xi^2}{2}\ge R_o}E_c\le B_cE_{A,\max}e^{-(\lambda-h)L_o}.$$

This is (iv). Under (L) the right side is at most ε_c, which completes the cone.

Order and monotonicity; item (v). The central normalized future (memory support, hold, drive, stop, shot, bridge, wing) has the same shape for every L_o; L_o enters only through the amplitude c. So C_I, K_{hold}, K_{tot}, C_h', ε_c and B_c are fixed before L_o. The ratios T_z/T_θ are homogeneous of degree one in the amplitude, which E_c accounts for, so these constants are also independent of the amplitude and of the radius. Condition (L) is a finite enlargement of L_o, imposed before Y_0. Condition (Y) is a lower bound on Y_0 by (1.15.22). Condition (R) comes last. Each is monotone, and all earlier length conditions continue to hold. We do not use the last radius alone to reduce a fixed normalized velocity: the radius enters only through the explicit thresholds listed in (R). For (v), $\zeta = 0$ on $[2,\infty)$ gives $I = i_s$ and $I/((\hat{\xi}^2/2)H) = r_c$ on $2R_m \le \hat{\xi}^2/2 \le R_h$. The hold map (1.6.19) preserves this ratio up to $R = R_h e^{B_h}$, the initial radius of the drive in Lemma 1.15.6. □

1.15.6 Scope and remaining source interfaces

The added length, actual scalar coefficient map, same fast exposure, actual heat collar, rank-one primitive correction, and single early history restoration have explicit formulas. They keep the actual inlet germ unchanged, with its radius, field, heat coefficient, and terminal edge fixed together. The rank-one support is a strict compact subinterval of the added power leg. At the last radius, that interval's positive model margin controls the actual field and history errors. We do not apply a compact-perturbation argument across a zero-stress terminal face. There we keep the exact selected heat field times the jointly fixed terminal cutoff, with its canonical outward histories.

We prove the positive outer terminal-face estimate and the angular primitive-mixture corridor in Lemmas 1.17.5, 1.17.8, and 1.17.9. The energy and pressure upper stated bounds supply none of their positive lower bounds. We prove the variable-exponent and central pulse responses in Lemmas 1.16.8 and 1.16.9. The global source-cone conclusion combines those results with the local constructions of this section.

We fix $0 < \nu_c < h/10$ and $h < \lambda/6$, the central hold length B_h, and its downstream scalar deficit/shot templates. In particular the central K_{old} in this section starts *after* the hold. It is not the coefficient map from the start of an earlier long pulse. The outer length L_o belongs to the equilibrium power extension just defined. This extension follows the model A11 moment correction and precedes the fixed λ-to-h transition.

1.15.7 An exact model ordering calculation

We select the full outer-active comparison band inside one fixed near-endpoint interval with lower endpoint at least η_a on the positive side, and use its reflection on the negative side. On that whole band we take the graph $R_o = R_e/\lambda_{\mathrm{ch}}$. In slice variables this is the backward outlet: $\widetilde{R}_o = R_e|\eta_b(\widetilde{\eta})|^{-1/(\frac{1}{2}-h)}$, one real-analytic graph on $\widetilde{\eta} < c_h$. We need $\widetilde{\eta} < c_h$ on the band, so that η_b is defined (Lemma 1.6.3).

We extend the graph smoothly into the central region before we select the angular cutoff. We make the extension where the outer cutoff is zero. Implicit differentiation of the chart equation (Remark 1.6.7) gives the exact speed

$$k = -(\tfrac{1}{2}-h)\eta\lambda_{\mathrm{ch}}'/\lambda_{\mathrm{ch}} = \frac{(\frac{1}{2}-h)(1+\lambda_{\mathrm{ch}})}{(\frac{1}{2}-h)-h\lambda_{\mathrm{ch}}(1-\eta^2)} = \frac{(\frac{1}{2}-h)(1+\lambda_{\mathrm{ch}})}{\frac{1}{2}-h\eta_b^2}, \qquad \eta_b = \lambda_{\mathrm{ch}}^{\frac{1}{2}-h}\eta. \quad (1.15.26)$$

The denominator is positive exactly for $\eta_b^2 < 1/(2h)$, that is, where the backward chart is a coordinate ($\widetilde{\eta} < c_h$).

We fix one sufficiently short physical interior band for all $0 < h \le 1/100$. The chart equation at $\eta = 1$, $\lambda_{\mathrm{ch}} = 1$ has derivative $2(\frac{1}{2} - h) \ge 49/50$ in λ_{ch}, uniformly for $0 \le h \le 1/100$. By the implicit function theorem and compactness of this h interval, the band can be chosen with $1 \le \lambda_{\mathrm{ch}} \le 2$ and with positive denominator in (1.15.26). In its interior $\lambda_{\mathrm{ch}} > 1$. For $\eta < 1$ also $\eta_b > 1$, so the denominator is less than $\frac{1}{2} - h = (\frac{1}{2} - h)$, and $1 + \lambda_{\mathrm{ch}} > 2$. Thus $k > 2$ for $\eta < 1$ and $k = 2$ at the endpoint.

Each outer model radius, with $R_A, \frac{\hat{\xi}_b^2}{2}, R_0, B$, is a scalar multiple of $\lambda_{\mathrm{ch}}^{-1}$, so it has this same speed. The same c and the terminal amplitude are scalar constants. This is an explicit source geometry on the whole outer-active band, not an inference from the speed at one endpoint.

We let the returned-pulse comparison graph be $R_o = R_e/\lambda_{\mathrm{ch}}(\eta)$ on its fixed chart band. We write $\beta = \lambda_{\mathrm{ch}}^{\frac{1}{2}-h}\eta = \eta_b$ and let $f(\beta) = f_0/(1+\beta^2) > 0$, $f_0 > 0$ fixed, be its actual angular profile. The backward model inlet is $H_e f(\beta)$. Its charted forward value is $H_w(R_o) = \lambda_{\mathrm{ch}}^h H_e f(\beta)$.

In backward scalar coordinates write $R_A^b = k_A R_e$ and $H_A^b = a_A H_e$, where $k_A, a_A > 0$ are the fixed transfers through flattening and the A11 wait interval.

The two transfer factors are independent of L_o and Y_0. The A11 edit leaves the outlet field germ unchanged. Their forward values are $R_A^f = R_A^b/\lambda_{\mathrm{ch}}$ and $H_A^f = \lambda_{\mathrm{ch}}^h H_A^b$. We put

$$J = \frac{\exp[-\int_0^\delta (\kappa - h)\,\mathrm{d}t]}{1-\rho}, \qquad A_w = (a_A k_A^h J)^{-1} > 0.$$

The same regular coefficient specified by the outer model is

$$c = H_A^b (R_A^b)^h J e^{-(\lambda - h)L_o}.$$

Lemma 1.15.23 (Outer inlet coefficient under a genuine power extension)**.** *For the previous actual model fields,*

$$K_w := \frac{H_w(R_o) R_o^h}{c} = A_w f(\beta) e^{(\lambda - h)L_o}.$$

The η-derivative of $\log K_w$ is independent of L_o. The graph derivative $(\frac{1}{2} - h)\eta\partial_\eta \log R_o$ does not change.

Proof. The factors λ_{ch}^h and $\lambda_{\mathrm{ch}}^{-h}$ cancel. We substitute $H_A^b = a_A H_e$ and $R_A^b = k_A R_e$.

The new length is scalar. We insert it strictly after R_o, so it does not change that graph or the angular function f. It also leaves the model ratio at the fixed later transition equal to $(1-\lambda)^{-1}$. Also $\dot{\log}\beta = (\frac{1}{2} - h)(1-k)$, so the actual outer power coefficient gives

$$q_w = (k-1)\left[\lambda - h + \frac{2(\frac{1}{2} - h)\beta^2}{1+\beta^2}\right] \ge q_* > 0.$$

The fixed chart band has positive distance from $\eta = 0$, and $k \ge 2$. Thus we select one q_* for all sufficiently small h, λ, before L_o and the later pulse length.

□

For the central component, we use the same specified c and solve its linear amplitude equation. We select the scalar hold inlet R_h as a fixed multiple of $\max R_o$:

$$G_h = \frac{c}{R_h^h e^{(h-\nu_c)B_h} K_{\mathrm{old}}(R_h e^{B_h}, (1-\nu_c)^{-1})}.$$

Its actual inlet coefficient is

$$K_c = \frac{(R_o/R_h)^{h-\nu_c} e^{-(h-\nu_c)B_h}}{K_{\mathrm{old}}(R_h e^{B_h}, (1-\nu_c)^{-1})}. \tag{1.15.27}$$

Thus a change of c changes its amplitude but cancels out of K_c.

Lemma 1.15.24 (Quantitative model ordering with fixed central geometry)**.** *Suppose the selected scalar stop/shot map has the verified scale bound $K_{\mathrm{old}} \ge k_- > 0$ for all sufficiently large R_h. We set*

$$K_c^+ = \frac{\sup_\eta (R_o/R_h)^{h-\nu_c} e^{-(h-\nu_c)B_h}}{k_-}, \qquad f_- := \min f(\beta) > 0.$$

The scalar choice

$$L_o \ge \frac{1}{\lambda - h} \log^+ \frac{2K_c^+}{A_w f_-} \tag{1.15.28}$$

gives $K_c \le K_w/2$ on the full fixed chart band for all admitted absolute scales. An increase in L_o improves this inequality. We fix B_h before L_o. Thus this choice does not use a uniform estimate in B_h.

Proof. We use (1.15.27) and Lemma 1.15.23. The lower bound for K_{old} is independent of the later outer parameter L_o: its scalar equations and normalized inlet ratio do not contain that parameter. We rescale its amplitude input linearly, and the coefficient map is amplitude independent. □

1.15.8 The mixing identity and a uniform cutoff under the actual order condition

We let a dot denote $(\frac{1}{2} - h)\eta\partial_\eta$ on a positive chart band. We write $H_o = (1-\chi)H_c + \chi H_w$, $\omega = (1-\chi)H_c/H_o$, $v_o = \dot{\log} R_o$, and $c_{\mathrm{mix}} = \dot{\log} H_o + \nu v_o$. The component powers have exponents ν_c, λ and sources $q_i = h - \nu_i + \dot{\log} H_i(R_o) + \nu_i v_o$. Then direct differentiation gives

$$h - \nu + c_{\mathrm{mix}} = \omega q_c + (1-\omega) q_w + \frac{\dot\chi (H_w - H_c)}{H_o} + (\nu - \bar\nu)(v_o - 1), \quad \bar\nu = \omega\nu_c + (1-\omega)\lambda. \tag{1.15.29}$$

An actual extension with $H_c \le H_w$ makes the third term nonnegative for any increasing cutoff. The bound on $\partial_\eta \log(K_c/K_w)$ does not by itself establish this sign.

The outer length does not enlarge that logarithmic derivative: the factor $e^{(\lambda-h)L_o}$ is scalar. Thus we can select the fixed logit construction after L_o, with its flat endpoint germs, without a change to R_o. The quantity v_o is independent of L_o.

1.15.9 Actual transfer by the rank-one primitive construction

We use the actual scalar stop and positive heat shot in Lemmas 1.15.6 and 1.15.7. These prove the k_- previously used and supply the actual same fast coefficient. We take L_o large enough for (1.15.28), the complete tail inequality $e^{-2\lambda L_o} K_S \le (8\lambda)^{-1}$, the separation of the outer heat-correction region from the central shot, and $L_o \ge \log 4$. All four are finite lower bounds after we fix h and the normalized component templates. The selected length is the maximum of these finite lower thresholds and the central amplitude threshold in Proposition 1.15.22.

We also include the geometric and primitive-gap thresholds in Lemma 1.17.3. All these thresholds use component data fixed before the angular mixture cutoff. The next mixed-cone amplitude conditions hold by Y_0. We freeze this single L_o before we select χ, K_f, Y_0, and the last scale. After those choices, we do not increase a length, and we keep a future integral contribution or root from the previous length.

We apply the explicit heat collar and the single compact primitive bump of Proposition 1.15.8. Its mass is the negative of the complete actual heat-edit primitive discrepancy. It is supported strictly inside the new leg, while all inlet velocity germs, c, k_f, and the specified terminal edge stay fixed. Its complete primitive increment is zero. The early three-row moment correction thus has first target zero and corrects only the actual energy and pressure discrepancies.

It does not perform a second primitive history restoration. Lemma 1.15.9 proves the small solution for each fixed L_o, Y_0 at a sufficiently large last radius.

Proposition 1.15.25 (Actual inlet order for the rebuilt family)**.** *The previous finite construction produces actual central and outer inlet fields with the same exact heat pair and*

$$H_c(R_o, \eta) \le \tfrac{1}{2} H_w(R_o, \eta).$$

Their actual coefficients are (1.15.27) *and Lemma 1.15.23, not only limits when the radius tends to infinity. The inequality is uniform on the fixed chart band for each sufficiently large admitted radius. It holds under the central primitive-memory correction and outer A11 parameter solve. Those operations keep each inlet H germ and the same heat pair unchanged.*

Proof. The scalar amplitude equation fixes the central coefficient to the specified c. The actual shot does not change that equation or the inlet scalar power. All later central corrections have support strictly after R_o and keep its value there unchanged. The actual outer heat collar and rank-one bump also leave the outer inlet field unchanged and use the specified c. Their complete primitive correction is zero, so the actual target at the A11 model outlet equals its model target.

We do not impose an artificial equilibrium on a different future. The early moment correction's zero first row leaves that target unchanged. Its other two rows restore the same model energy root and analytic axis pressure on the protected backward collars. A partially extended moment correction in the intermediate fixed-λ buffer keeps its actual small root change. We do not assert that it equals that model root.

Thus the coefficient calculation of Lemma 1.15.23 is exact for the new actual fields. We apply Lemma 1.15.24. For an admitted inlet-memory parameter, A11 solves its real target-minus-current equation on compact supports and does not change either inlet velocity or the postbank velocity. The central correction $I \mapsto I + \delta I \zeta$ has ζ constant on its inlet germ and zero before the hold, so it too leaves the stated values unchanged. □

1.15.10 The actual inverse, flat endpoints, and source floor

We can select the same scalar pretemplate with a constant terminal time $T_b = T$. We select fixed smooth f_0, f_1 as follows. We impose $f_0' = \gamma$ on the initial growth germ and $f_0' = 0$ before the fixed axial-turnoff plateau. We also impose $f_1' = 0$ through that plateau and $f_1' = 1$ near T. We set $F(y;\nu) = \exp(f_0(y) - \nu f_1(y))$.

At $\nu = \lambda$, we select this jointly as the backward pretemplate. We do not identify it with an independently frozen template. Its finite interval integrals and $F(T;\nu)^{-1}$ have one derivative bound for each specified finite order for all $0 \le \nu \le \lambda_0$. We fix these constants before the last choice of $\lambda \le \lambda_0$. In particular the reference integral $r_b(\nu)$ in the prefix integral formula has those bounds. We set

$$\mathcal{F}(\nu, \eta) = \frac{1}{1-\nu} + \left(r_b(\nu) - \frac{1}{1-\nu} \right) e^{-(1-\nu)(Y_0 + \rho(\eta) - T)}.$$

Here $\rho = \log(R_o/R_g) - Y_0$ is the specified graph function. It is unrelated to the terminal cutoff amplitude previously used. We use this inverse on the genuine $G = 0$ exponent transition. Its r_b is the explicit unedited finite-template integral of Lemma 1.14.1. The two-swirl primitive taper lies in the fixed-λ band. Lemma 1.14.4 gives its bounds.

We do not substitute its edited data into this exponent inverse.

Lemma 1.15.26 (A flat monotone inverse with the necessary weighted errors)**.** *We select a flat increasing cutoff on the fixed positive angular band whose logit derivative* $\mathfrak{l}$ *satisfies*

$$\mathfrak{l} := \dot{\log}(\chi/(1-\chi)) \geq B_* + 1, \qquad |\dot{\log}(K_c/K_w)| \leq B_*.$$

We take it to be a normalized squared-flat step in $|\eta|$*, nondecreasing in* $|\eta|$*, so that* $\dot{\chi} \geq 0$ *and* χ *has log-jets (Definition 1.23.6). We fix one such cutoff before* Y_0 *and the last radius. For all sufficiently large* Y_0 *the actual equation*

$$\mathcal{F}(\nu,\eta) = \omega\mathcal{F}(\nu_c,\eta) + (1-\omega)\mathcal{F}(\lambda,\eta)$$

has a unique solution $\nu_c \leq \nu \leq \lambda$*, constant on the flat collars, with* $\dot{\nu} \geq 0$*. It also satisfies*

$$|\nu - \bar{\nu}| \leq C(\lambda - \nu_c)^2\omega(1-\omega). \tag{1.15.30}$$

Here C *is uniform for small* λ*, independent of the next outer length and the absolute radius. Derivatives of the actual cutoff and of* ν *are finite after we select it.*

We do not assert that these bounds are uniform when L_o *varies.*

Proof. The remainder of $\mathcal{F}$ and its necessary ν derivatives and fixed-ν angular derivatives have a bound by $C(1+Y_0)^N e^{-(1-\lambda)Y_0}$. Write $\mathcal{F} = (1-\nu)^{-1} + \delta$ and increase the later threshold $Y_{\min}$ so that, uniformly on the admitted domain,

$$|\partial_\nu \delta| \leq \tfrac{1}{2}, \qquad |\partial_\nu^2 \delta| \leq 1.$$

The threshold may depend on the parameters already selected, but the following numerical bounds do not:

$$\mathcal{F}_\nu \geq \tfrac{1}{2}, \qquad |\mathcal{F}_{\nu\nu}| \leq 5 \quad (0 \leq \nu \leq \lambda \leq 1/20).$$

The interpolation remainder at $\bar{\nu}$ and the mean value theorem therefore prove the quantitative form

$$|\nu - \bar{\nu}| \leq 5(\lambda - \nu_c)^2\omega(1-\omega). \tag{1.15.31}$$

These value bounds use neither angular derivatives of the cutoff nor a lower bound on ν_c; no early parameter is reselected.

For monotonicity put $x = \mathcal{F}(\nu,\eta)$ and $g(x) = \dot{\mathcal{F}}(\nu(x),\eta)$, where we take the dot in the last expression at fixed ν. Two x derivatives of g have a bound by the same exponentially small remainder. The exact differentiated equation is

$$\mathcal{F}_\nu \dot{\nu} = \omega(1-\omega)(\mathfrak{l} - b_*)\Delta\mathcal{F} + \mathcal{D},$$

$$b_* = \dot{\log}(K_c/K_w), \quad \Delta\mathcal{F} = \mathcal{F}(\lambda) - \mathcal{F}(\nu_c), \quad |\mathcal{D}| \leq \tfrac{1}{2}\left\|g''\right\|_\infty \omega(1-\omega)(\Delta\mathcal{F})^2.$$

We select Y_0 to make the last bound smaller than half the first positive term. The same bounds apply where the cutoff is flat, because the two estimates have the same factor.

The bounds on b_* are independent of L_o: its added factor in K_w is scalar, and the scalar K_{old} has no angular dependence. The standard flat logit on a fixed positive band has a strictly positive lower bound for its logit derivative after multiplication by one fixed gain. Its endpoint extension is smooth. □

Proposition 1.15.27 (The source and amplitude outputs used by the pulse lemma)**.** *On the fixed chart band, we let $q_c = h - \nu_c$ and $q_w \geq q_* > 0$. Before we select L_o, we fix one chart bound q_* and one bound for $|v_o - 1|$ for all sufficiently small h, λ. We select λ once against those fixed bounds. After this, we pick Y_0. Then the actual source in (1.15.29) satisfies*

$$q_{\mathrm{out}} \geq ch\omega + \tfrac{1}{2}q_*(1-\omega), \qquad \frac{\nu}{q_{\mathrm{out}}} \leq C(\nu_c/h + \lambda).$$

For $\nu \geq \lambda/2$ it has a fixed positive lower bound independent of h, L_o.

The true pulse amplitude obeys

$$e_p \leq K_{\mathrm{env}} e_{\mathrm{end}} e^{-(\lambda-\nu)Y_{\mathrm{end}}}, \qquad e_{\mathrm{end}} \leq C_{\mathrm{pre}}\lambda^{30},$$

with e_{end} and Y_{end} as in (1.15.32), and with these prefactors independent of the next outer length, Y_0 and C; on the chart band, and everywhere if K_c^+ in (1.6.29) is defined with the supremum over the whole graph, they are also independent of h. In particular $\nu \leq \lambda/2$ gives the actual suppression $e_p \leq K_{\mathrm{env}} e_{\mathrm{end}} e^{-\lambda Y_{\mathrm{end}}/2}$, with K_{env} from Proposition 1.15.32. Off the band and without the choice M2, K_{env} depends on k_- and thus on h, ν_c, so it is not a constant of type K_{pre}.

Proof. The source floor and the quotient bound are Lemma 1.15.34 below (with $c = \frac{9}{10}$), and $\nu \geq \lambda/2$ gives $q_{\mathrm{out}} \geq \frac{29}{240}q_*$. The envelope and the bound for e_{end} are Proposition 1.15.32 and (1.15.36); its prefactor is K_{env}. The high-exponent branch $\nu \geq \lambda/2$ involves only points of the chart band (Lemma 1.15.34), where $K_{\mathrm{env}} = \Gamma_\rho \Gamma_g$ does not depend on h. □

Tags (I1)–(I17) below refer to the inputs of Section 1.15.4.1. Here K_c^+ is the constant of (1.6.29); the choice M2 means that the supremum in K_c^+ is taken over the whole comparison graph, not only the chart band. It raises the L_o threshold by a finite amount and is not needed for any use (remark after Proposition 1.15.32).

Definitions. For each η the pulse entry and amplitude are (I15)

$$\frac{\big(\hat\xi_p(\eta)\big)^2}{2} = R_g(\eta) e^{T_b(\nu)} \nu^{-60}, \qquad H_p = H(\tfrac{\hat\xi_p^2}{2}, \eta), \qquad e_p(\eta) = \frac{H_p}{\hat\xi_p}, \qquad \nu = \nu(\eta).$$

We define the *endpoint amplitude* and *endpoint pulse length* by

$$e_{\mathrm{end}} := e_p(1), \qquad Y_{\mathrm{end}} := \log \frac{R_o(1)}{\frac{\big(\hat\xi_p(1)\big)^2}{2}} = Y_0 + \rho(1) - T_b(\lambda) + 60\log\lambda. \tag{1.15.32}$$

This agrees with (1.6.21) . The symbol e_{out} is reserved for the normalized future energy $e_{\mathrm{out}}(\eta)$ of (1.13.70).

Hypothesis 1.15.28.

(B1) (Power interval; Section 1.16.1, (1.6.23), proof of Lemma 1.6.19.) On $[\frac{\big(\hat\xi_p(\eta)\big)^2}{2}, R_o(\eta)]$, $H(\frac{\hat\xi^2}{2}, \eta) = H_{\mathrm{out}}(\eta)(R_o/\frac{\hat\xi^2}{2})^{\nu(\eta)}$. Pulse, returns and moment corrections change U, M, J but not H there.

(B2) (Same coefficient; Section 1.6.3.) $H_{\mathrm{out}} = cR_o^{-h}K_{\mathrm{mix}}$, $K_{\mathrm{mix}} = (1-\chi)K_c + \chi K_w$, with one scalar c.

(B3) (Endpoint; I12, I13.) $\chi(1) = 1$ and $\nu(1) = \lambda$.

(B4) (Coefficients; (1.15.27), Lemma 1.15.23, Lemma 1.15.6.) $K_c = (R_o/R_h)^{h-\nu_c} e^{-(h-\nu_c)B_h}/K_{\text{old}}$ with $K_{\text{old}} \geq k_-$; on the chart band $K_w = A_w f(\beta) e^{(\lambda-h)L_o}$, $f = f_0/(1+\beta^2)$, $\beta = \ell^{\frac{1}{2}-h}\eta$, where ℓ solves $\ell(1-\eta^2) + 1 - \ell^{1-2h}\eta^2 = 0$ (Section 1.15); and $K_c \leq K_w/2$ on the band (I11).

Each item of Hypothesis 1.15.28 restates a property proved at the cited place ((B1): (1.6.23) and (I15); (B2): Section 1.6.3; (B3): (I12), (I13); (B4): (1.15.27), Lemma 1.15.23, Proposition 1.15.25 and (I11)). So the construction satisfies Hypothesis 1.15.28; it is not an additional assumption.

With $q_i = h - \nu_i + \dot{\log} H_i(R_o) + \nu_i v_o$, $c_{\text{mix}} = \dot{\log} H_o + \nu v_o$, $\omega = (1-\chi)H_c/H_o$ and $\bar{\nu} = \omega\nu_c + (1-\omega)\lambda$, the mixing identity (1.15.29) reads

$$h - \nu + c_{\text{mix}} = \omega q_c + (1-\omega) q_w + \frac{\dot{\chi}(H_w - H_c)}{H_o} + (\nu - \bar{\nu})(v_o - 1). \tag{1.15.33}$$

It is an exact algebraic identity for arbitrary C^1 functions χ, H_c, H_w, R_o, ν.

The exact identity.

Lemma 1.15.29 (Same-coefficient amplitude identity)**.** *Under (B1)–(B3), for every η,*

$$\frac{e_p(\eta)}{e_{\text{end}}} = \frac{K_{\text{mix}}(\eta)}{K_w(1)} \Big(\frac{\nu}{\lambda}\Big)^{60(\frac{1}{2}+\nu)} e^{-(\lambda-\nu)Y_{\text{end}}} e^{(\frac{1}{2}+\nu)(T_b(\lambda)-T_b(\nu))} e^{(\nu-h)(\rho(\eta)-\rho(1))} \Big(\frac{R_g(\eta)}{R_g(1)}\Big)^{-\frac{1}{2}-h}. \tag{1.15.34}$$

Equivalently, the product of the second and third factors equals

$$\nu^{60(\frac{1}{2}+\nu)} \lambda^{-60(\frac{1}{2}+\lambda)} e^{-(\lambda-\nu)(Y_{\text{end}} + 60\log(1/\lambda))}$$

when $T_b \equiv T$. This is the form "$e^{-(\lambda-\nu)(Y_{\text{end}}+W(\lambda))}$" of Section 1.6.3. With R_g scalar the last factor is 1, and (1.15.34) is exactly the display at proof of Lemma 1.6.19.

Proof. By (B1), $H_p = H_{\text{out}}(R_o/\frac{\hat{\xi}_p^2}{2})^\nu$. By (B2) and $R_o = R_g e^{Y_0+\rho}$,

$$e_p = \frac{c\,K_{\text{mix}}}{\sqrt{2}} R_o^{\nu-h} \Big(\frac{\hat{\xi}_p^2}{2}\Big)^{-\nu-\frac{1}{2}} = \frac{c\,K_{\text{mix}}}{\sqrt{2}} R_g^{-\frac{1}{2}-h} e^{(\nu-h)(Y_0+\rho)} e^{-(\frac{1}{2}+\nu)T_b(\nu)} \nu^{60(\frac{1}{2}+\nu)}.$$

At $\eta = 1$, $K_{\text{mix}} = K_w(1)$ and $\nu = \lambda$ by (B3). Divide and regroup the exponents using (1.15.32). □

The envelope.

Lemma 1.15.30 (Wait-factor ratio)**.** *The map $\nu \mapsto \nu^{60(\frac{1}{2}+\nu)}$ is strictly increasing on $(0,1)$. Hence $\nu^{60(\frac{1}{2}+\nu)}/\lambda^{60(\frac{1}{2}+\lambda)} \leq 1$ and $(\nu/\lambda)^{60(\frac{1}{2}+\nu)} \leq 1$ for $0 < \nu \leq \lambda$.*

Proof. $\frac{\mathrm{d}}{\mathrm{d}\nu} 60(\frac{1}{2}+\nu)\log\nu = 60\big(\log\nu + 1 + \frac{1}{2\nu}\big)$. The function $\log\nu + \frac{1}{2\nu}$ has its minimum at $\nu = \frac{1}{2}$, with value $1 - \log 2 > 0$. The second claim is trivial. □

Lemma 1.15.31 (Coefficient ratio)**.** *On the chart band, $\beta^2 = 1 + \ell(1-\eta^2) \geq 1$, hence $K_w(\eta) \leq K_w(1)$, and $K_{\text{mix}} \leq \max(K_c, K_w) \leq K_w(1)$. Off the band, $\chi = 0$, and*

$$\frac{K_{\text{mix}}}{K_w(1)} = \frac{K_c}{K_w(1)} \leq \frac{2K_c^{++}}{A_w f_0}, \qquad K_c^{++} := \frac{1}{k_-}.$$

If K_c^+ in (1.6.29) is defined with the supremum over the whole *graph (the choice M2), then $K_c \leq K_w(1)/2$ everywhere, and $K_{\text{mix}}/K_w(1) \leq 1$ for all η.*

Proof. The chart equation reads $\ell^{1-2h}\eta^2 = 1+\ell(1-\eta^2)$, and $\beta^2 = \ell^{1-2h}\eta^2$. Since f decreases in $|\beta|$ and $\beta(1)=1$, we get $f(\beta)\le f(1)$, so $K_w \le K_w(1)$ by (B4). With $K_c \le K_w/2$ on the band, $K_{\mathrm{mix}} \le K_w \le K_w(1)$. Off the band: $R_o < R_m < R_h$ (since $R_h = a_h a_m \max R_o$ with $a_m > 1$, $a_h > 2$) and $h-\nu_c > 0$, so $(R_o/R_h)^{h-\nu_c} \le 1$; also $e^{-(h-\nu_c)B_h} \le 1$ and $K_{\mathrm{old}} \ge k_-$; and $K_w(1) = A_w \frac{f_0}{2} e^{(\lambda-h)L_o} \ge A_w f_0/2$. Under the choice M2, (1.6.29) gives $K_w(1) \ge A_w f_- e^{(\lambda-h)L_o} \ge 2K_c^+ \ge 2\sup_\eta K_c$. □

Proposition 1.15.32 (Pulse-amplitude envelope)**.** *Assume Hypothesis 1.15.28 and $T_b \equiv T$ (Section 1.15). Let $\Gamma_\rho := e^{\lambda \operatorname{osc}\rho}$, where $\operatorname{osc}\rho = \sup\rho - \inf\rho$, and $\Gamma_g := \sup_\eta (R_g(\eta)/R_g(1))^{-\frac12 - h}$, which equals 1 in the backward chart. Then for every η*

$$e_p(\eta) \le K_{\mathrm{env}}\, e_{\mathrm{end}} \left(\frac{\nu}{\lambda}\right)^{60(\frac12+\nu)} e^{-(\lambda-\nu)Y_{\mathrm{end}}} \le K_{\mathrm{env}}\, e_{\mathrm{end}}\, e^{-(\lambda-\nu)Y_{\mathrm{end}}}, \tag{1.15.35}$$

where

$$K_{\mathrm{env}} = \Gamma_\rho \Gamma_g \cdot \begin{cases} 1 & \text{on the chart band, or everywhere under the choice M2,} \\ \max\{1, 2/(k_- A_w f_0)\} & \text{everywhere, without M2.} \end{cases}$$

In all cases K_{env} is independent of L_o, Y_0, C. On the band, and everywhere under the choice M2, it is also independent of h and ν_c; on the band one may replace Γ_ρ by $e^{\lambda \sup_{\mathrm{band}} |\log \ell|}$, which does not depend on the extension of the graph into the central region. For $\nu \le \lambda/2$ and $Y_{\mathrm{end}} \ge 0$, $e_p \le K_{\mathrm{env}} e_{\mathrm{end}} e^{-\lambda Y_{\mathrm{end}}/2}$. Moreover

$$e_{\mathrm{end}} = e_a(1) F_b(\lambda) e^{-T/2} \lambda^{60(\frac12+\lambda)} \le C_{\mathrm{pre}} \lambda^{30}, \qquad C_{\mathrm{pre}} := e_a(1)\, e^{-T/2} \sup_{0\le\lambda\le\lambda_0} F(T;\lambda), \tag{1.15.36}$$

where $e_a(1) = H_a(1)/\sqrt{2R_g(1)}$ is the endpoint growth-arc amplitude (proof of Lemma 1.6.19). It is fixed by the pre-pulse templates and is unchanged by every post-pulse construction.

Proof. Use (1.15.34). Bound $(\nu/\lambda)^{60(\frac12+\nu)} \le 1$ by Lemma 1.15.30, and $K_{\mathrm{mix}}/K_w(1)$ by Lemma 1.15.31. The T_b factor is 1. Since $\nu - h \in (-h, \lambda)$, we have $|\nu - h| \le \lambda$, so $e^{(\nu-h)(\rho-\rho(1))} \le \Gamma_\rho$. On the charted band $\rho - \rho(1) = -(1-\tau)\log\ell$ and $R_g/R_g(1) = \ell^{-\tau}$. Since $1 \le \ell \le 2$, the two graph factors together are bounded by $2^{\lambda+1/2+h}$. This bound is independent of the later length and radius selections. For (1.15.36), by (I15), $H_p = H_a F_b \nu^{60\nu}$ and $\frac{\hat\xi_p^2}{2} = R_g e^T \nu^{-60}$, so $e_p = e_a F_b e^{-T/2} \nu^{60(\frac12+\nu)}$. At $\eta = 1$ this is (1.15.36), and $\lambda^{60(\frac12+\lambda)} \le \lambda^{30}$. Here $F_b(\lambda) = \exp(f_0(T) - \lambda f_1(T))$ is bounded on $[0, \lambda_0]$ (Section 1.15). The post-pulse leg, heat correction, A11, memory return and three-bump restoration have supports disjoint from $\{\frac{\hat\xi^2}{2} \le \frac{(\hat\xi_p(1))^2}{2}\}$ or leave H unchanged outside compact pre-pulse bumps. So H_a and H_p at the endpoint are those of the pre-pulse model. □

Remark 1.15.33 (Which form is needed downstream). Every use of the envelope selects Y_0 after h, ν_c, L_o and K_f: Section 1.6.3, proof of Lemma 1.6.12, proof of Lemma 1.6.13, (1.16.24), proof of Lemma 1.16.9. So h- or ν_c-dependence of K_{env} is harmless there, and the non-M2 version suffices. The high-exponent branch $\nu \ge \lambda/2 \Rightarrow e_p \le K_p \lambda^{30}$ (1.16.24) needs an h-independent constant, because λ is chosen before h. It only involves points with $1-\omega \ge 29/120$ (Lemma 1.15.34), hence $\chi > 0$, hence the chart band. There $K_{\mathrm{env}} = \Gamma_\rho\Gamma_g$ with no h-dependence. Thus M2 is needed only to make the literal claim "prefactors independent of h" (Proposition 1.15.27) true off the band.

Lemma 1.15.34 (Source floor and quotient)**.** *Let* $q_{\mathrm{out}} := h - \nu + c_{\mathrm{mix}}$. *Assume the Jensen bound*

$$|\nu - \bar{\nu}| \le C_J(\lambda - \nu_c)^2\omega(1-\omega), \qquad \bar{\nu} = \omega\nu_c + (1-\omega)\lambda, \tag{1.15.37}$$

of Lemma 1.15.26, the band bounds $q_w \ge q_*$ *and* $|v_o - 1| \le V$, *and choose* λ *so small that* $C_J V\lambda^2 \le q_*/2$ *and* $C_J\lambda \le 1$. *Then*

$$q_{\mathrm{out}} \ge \tfrac{9}{10}h\,\omega + \tfrac{1}{2}q_*(1-\omega), \qquad \frac{\nu}{q_{\mathrm{out}}} \le \max\Big(\frac{10\nu_c}{9h}, \frac{4\lambda}{q_*}\Big),$$

and $\nu \ge \lambda/2$ *implies* $1-\omega \ge 29/120$ *and* $q_{\mathrm{out}} \ge \frac{29}{240}q_*$.

Proof. By the exact identity (1.15.33), $q_{\mathrm{out}} = \omega q_c + (1-\omega)q_w + \dot{\chi}(H_w - H_c)/H_o + (\nu - \bar{\nu})(v_o - 1)$. Here $q_c = h - \nu_c$ exactly, so $q_c \ge \frac{9}{10}h$. The third term is ≥ 0, because $\dot{\chi} = (\frac{1}{2} - h)\eta\chi' \ge 0$ and $H_w \ge 2H_c$ on the band, and it is 0 off the band. The last term is at least $-C_J V\lambda^2\omega(1-\omega) \ge -\frac{1}{2}q_*(1-\omega)$. Next, $\nu \le \bar{\nu} + C_J\lambda^2\omega(1-\omega) \le \omega\nu_c + 2(1-\omega)\lambda$, and the mediant inequality gives the quotient bound. If $\nu \ge \lambda/2$, then $\lambda/2 \le \lambda/60 + 2(1-\omega)\lambda$, using $\nu_c < \lambda/60$ (Section 1.6.3), so $1-\omega \ge \frac{1}{2}(\frac{1}{2} - \frac{1}{60}) = \frac{29}{120}$. □

1.15.11 Scope

This section proves the actual local inlet ordering and its source and amplitude consequences for the joint finite family. Inlet order alone does not prove the whole primitive-mixture corridor. Lemmas 1.17.8 and 1.17.9 prove that result. We prove the pulse responses in Lemmas 1.16.8 and 1.16.9, with the inputs established here.

1.16 Pulse response for the selected member

Main result. Lemma 1.16.8 proves the pulse estimates away from the central angular value for the selected member. Lemma 1.16.9 treats the center with ordinary angular derivatives. The conditional response estimates keep their explicit input assumptions.

1.16.1 The fixed-coordinate pulse identities and their response

We write $d = 1 - \eta^2$, and $\dot{f} = (\frac{1}{2} - h)\eta\partial_\eta f|_{\hat{\xi}}$. In this subsection $|\eta| \ge \eta_a > 0$. On an actual power interval put

$$y = 2\log(\hat{\xi}/\hat{\xi}_p(\eta)), \quad Y = \log(R_o/\tfrac{\hat{\xi}_p^2}{2}),$$
$$H = H_o e^{\nu(Y-y)}, \quad E = H/\hat{\xi}, \quad U = ER.$$

where $\nu = \nu(\eta)$ and all histories keep their actual inlet values. We set

$$a = 1-\nu, \quad \beta = 1/2 - \nu, \quad \beta_2 = 1/2 - 2\nu, \quad u = \dot{\nu}, \quad v = \log\tfrac{\hat{\xi}^2}{2}, \quad w_o = \log R_o,$$
$$c = \log H, \quad q = h - \nu + c, \quad q_o = h - \nu + \log H_o + \nu w_o.$$

We thus take derivatives of a function displayed in (y,η) with $\dot{} = (\frac{1}{2} - h)\eta\partial_\eta|_y - v\partial_y$. In particular

$$q = q_o + u(Y-y), \quad q_y = -u, \quad \dot{U} = E(\dot{R} + cR), \quad (\dot{Y - y}) = w_o. \tag{1.16.1}$$

We must not omit the term cR from the derivative of U.

Lemma 1.16.1 (Exact pulse and history identities)**.** *We put* $r = I/(\frac{\hat\xi^2}{2}H)$, $m = M/(\frac{\hat\xi^2}{2}E)$, $j = J/(\frac{\hat\xi^2}{2}HE)$, $s = S/H^2$, *and* $p = P/E^2$. *On the power interval the actual histories obey*

$$r_y + ar = 1, \qquad m_y + \beta m = R, \qquad j_y + \beta_2 j = R, \tag{1.16.2}$$

$$(\dot m)_y + \beta \dot m = \dot R + um, \qquad (\dot j)_y + \beta_2 \dot j = \dot R + 2uj. \tag{1.16.3}$$

The linear angular coefficient and its evolution are

$$Q_{\mathrm{lin}} = 1 + \dot r + (q-a)r, \qquad (Q_{\mathrm{lin}})_y + aQ_{\mathrm{lin}} = q. \tag{1.16.4}$$

We let $b_\eta = d/((\frac12 - h)\eta)$. *The full angular coefficient is*

$$Q = Q_{\mathrm{lin}} + E\{(2(\tfrac12 - h)\eta + b_\eta c)m + b_\eta \dot m - b_\eta \dot j + [2(h - (\tfrac12 - h))\eta - 2b_\eta c]j\}. \tag{1.16.5}$$

The full nondiffusive axial numerator, in the normalization used by $w = N/(EQ)$, *satisfies*

$$N/E = R + (q-\beta)m + \dot m + \mathcal{N}, \tag{1.16.6}$$

$$\mathcal{N} = E\{[2(\tfrac12 - h)\eta m + b_\eta(\dot m + cm)]R + 8h\eta s - 2b_\eta(\dot s + 2cs) + 4(\tfrac12 + h)\eta p - b_\eta(\dot p + 2cp)\}.$$

These formulas keep all M, J, S, P *terms.*

Proof. We use $\frac{M_{\hat\xi}}{\hat\xi} = U$, $\frac{I_{\hat\xi}}{\hat\xi} = H$, $\frac{J_{\hat\xi}}{\hat\xi} = UH$, $\frac{S_{\hat\xi}}{\hat\xi} = U^2 - E^2/2$, and $\frac{P_{\hat\xi}}{\hat\xi} = E^2/(\hat\xi^2)$. Because $E_y = -(1/2+\nu)E$, division by the displayed normalizations gives (1.16.2). The operators $\dot{}$ and ∂_y commute. Differentiation of the equations gives (1.16.3).

Substitution of $I = \frac{\hat\xi^2}{2}Hr$ into $1 - (1-h)I/(\frac{\hat\xi^2}{2}H) + \dot I/(\frac{\hat\xi^2}{2}H)$ gives (1.16.4). Its evolution is a result of $q_y = -u$, $\dot a = -u$ and the equation for r. Last, we substitute $M = \frac{\hat\xi^2}{2}Em$, $J = \frac{\hat\xi^2}{2}HEj$, $S = H^2 s$, $P = E^2 p$ into the actual integrated stress formulas. This gives (1.16.5) and (1.16.6) directly. □

For nonzero inlet memories, their differentiated data are not reset:

$$(\dot m)(0) = (\tfrac12 - h)\eta m_0' - v(R(0) - \beta m_0), \qquad (\dot j)(0) = (\tfrac12 - h)\eta j_0' - v(R(0) - \beta_2 j_0).$$

In the $G = 0$ variable-exponent sector memories and these data are zero. The affine formulas hold in the fixed-λ sector.

Lemma 1.16.2 (Actual canonical future integrals)**.** *Suppose* $R(Y) = 0$, *and write the actual outlet integral contributions as* $S(R_o) = H_o^2\tau_S$, $P(R_o) = -H_o^2\tau_P/R_o$. *We set* $\Delta = Y - y$, $b = 1 + 2\nu$, *and* $F(\nu,\Delta) = (1 - e^{-2\nu\Delta})/(8\nu)$. *Then*

$$s = F(\nu,\Delta) - \frac12\int_0^\Delta e^{-2\nu z}R(y+z,\eta)^2\,dz + e^{-2\nu\Delta}\tau_S, \tag{1.16.7}$$

$$p = -\frac{1}{2b} + e^{-b\Delta}\left(\frac{1}{2b} - 2\tau_P\right). \tag{1.16.8}$$

Their fixed-$\hat\xi$ *angular derivatives are*

$$\dot s = uF_\nu + \frac14 w_o e^{-2\nu\Delta} + u\int_0^\Delta z e^{-2\nu z}R^2\,dz - \int_0^\Delta e^{-2\nu z}R\dot R\,dz + e^{-2\nu\Delta}[\dot\tau_S - 2(u\Delta + \nu w_o)\tau_S], \tag{1.16.9}$$

$$\dot p = \frac{u}{b^2} + e^{-b\Delta}\left[-\frac{u}{b^2} - 2\dot\tau_P - (2u\Delta + bw_o)\left(\frac{1}{2b} - 2\tau_P\right)\right]. \tag{1.16.10}$$

In (1.16.9), *we evaluate* $R, \dot R$ *inside the integral at the physical radius* $\frac{\hat\xi^2}{2}e^z$.

Thus the derivative is genuinely at fixed physical $\frac{\hat\xi^2}{2}$, *with no deleted moving-inlet term.*

Proof. We integrate the two exact history equations from $\frac{\hat\xi^2}{2}$ to R_o. The change of variable $\frac{\rho^2}{2} = \frac{\hat\xi^2}{2}e^z$ gives the formulas. At fixed $\hat\xi$, the upper limit derivative is $\dot\Delta = w_o$, while the integrand derivative is $\dot R$ at $\frac{\hat\xi^2}{2}e^z$. Its upper boundary term vanishes because $R(Y) = 0$.

The power and future-integral boundary terms do not vanish and are the displayed terms. Finally $\dot S/H^2 = \dot s + 2cs$ and $\dot P/E^2 = \dot p + 2cp$. □

The exact unnormalized axial evolution, valid also off a power leg, is

$$\begin{aligned} N_y + N &= \mathcal{B}U_y + (\tfrac12 + h)U + \dot U + 2(\tfrac12 + h)\eta U^2 - dUU_\eta \\ &\quad + \eta E^2 + 4(\tfrac12 + h)\eta P - dP_\eta, \\ \mathcal{B} &= 1 + ((1-2h)\eta M + dM_\eta)/\tfrac{\hat\xi^2}{2}. \end{aligned} \tag{1.16.11}$$

It is a result of differentiation of the actual numerator, with the five history equations. The EE_η terms cancel. In particular its quiet version keeps the actual nonzero M, J memories through the initial value of N.

Lemma 1.16.3 (A response estimate proved after the denominator)**.** *We fix $0 < h \le \lambda < 1/8$, $0 < \nu_c \le \nu \le \lambda$, $u \ge 0$, $q_o > 0$, and a main window $0 \le y \le y_m \le Y/4$ and $0 \le \epsilon_a \le 1$. Suppose the specified pulse, independently of N or w, has $m_0 = j_0 = R(0) = 0$ and*

$$|R| \le C_0, \quad |R_y| \le C_0\nu, \quad |\dot R| \le C_0\epsilon_a q(y), \qquad \left|Q_{\rm lin}(0) - \frac{q(0)}{a} - \frac{u}{a^2}\right| \le \epsilon_I q(0).$$

Assume the actual canonical integrals and late returns, as explicitly given in Lemma 1.16.2, have the bound

$$\frac{(1+q)(|s|+|p|) + |\dot s| + |\dot p|}{q} \le C_1\nu^{-1}(1 + q_o^{-1}) + \epsilon_f. \tag{1.16.12}$$

Here this is an input estimate on the specified fields, not a bound on the response. We let $e_p = E(0)$ and $\epsilon_n = e_p[\nu^{-1}(1+q_o^{-1}) + \epsilon_f]$.

If $\epsilon_I + Y^{-1} + e_p(1+q_o^{-1})(1+\epsilon_a)$ is sufficiently small, then first

$$Q \ge \tfrac14 q > 0 \quad \text{on } [0, y_m]. \tag{1.16.13}$$

After we establish this lower bound,

$$|w - 2R| \le C\left[\nu + \frac{\nu}{q_o} + \epsilon_a + Y^{-1} + \epsilon_I + \epsilon_n\right]. \tag{1.16.14}$$

The constant depends only on C_0, C_1, η_a and fixed geometric bounds, not on Y, h^{-1}, or ν_c^{-1} except through the explicit quantities on the right.

Proof. Because $q(y) = q_o + u(Y - y)$ and $y_m \le Y/4$, on this window $u/q \le 4/(3Y)$ and $q(s)/q(y) \le 4/3$ for $0 \le s \le y$. The exact solution of (1.16.4) is

$$Q_{\rm lin}(y) = q(y)/a + u/a^2 + e^{-ay}[Q_{\rm lin}(0) - q(0)/a - u/a^2].$$

Thus $Q_{\rm lin} = q/a + O(q(\epsilon_I + Y^{-1}))$. The stable equations and zero data give $|m| + |j| \le C$ and $|\dot m| + |\dot j| \le Cq(\epsilon_a + Y^{-1})$. Because $c = q + \nu - h$, (1.16.5) yields

$$|Q - Q_{\rm lin}|/q \le Ce_p(1 + q_o^{-1})(1 + \epsilon_a + Y^{-1}).$$

This proves (1.16.13) from only the specified pulse and its histories. We do not divide by Q or estimate w at this step.

Next integrate by parts in the stable formula for m. Because $R(0) = 0$,

$$m - R/\beta = -\beta^{-1} \int_0^y e^{-\beta(y-s)} R_y(s)\, ds, \qquad |m - R/\beta| \le C\nu.$$

Thus $R + (q-\beta)m + \dot{m} = qR/\beta + O((1+q)\nu + q\epsilon_a + q/Y)$. The term $\mathcal{N}$ in (1.16.6) has a bound by $Cq\epsilon_n$ with (1.16.12). We divide only now by the proved lower bound for Q.

The replacement of q/Q by a costs $C(\epsilon_I + Y^{-1} + \epsilon_n)$, and $a/\beta = 2 + \nu/\beta$. This proves (1.16.14). □

Root and return maps. We let $\phi(y) = \Phi(\nu y)$ and $\psi_j(y) = \psi(y - Y + d_j)$, and write $R = A_p\phi + \sum_j c_j\psi_j$. The two actual moment equations are

$$\begin{aligned} \sum_j c_j \int_0^Y e^{\beta y}\psi_j(y)\, dy &= -m_0 - A_p \int_0^Y e^{\beta y}\phi(y)\, dy, \\ \sum_j c_j \int_0^Y e^{\beta_2 y}\psi_j(y)\, dy &= -j_0 - A_p \int_0^Y e^{\beta_2 y}\phi(y)\, dy. \end{aligned} \tag{1.16.15}$$

Thus $c = A_p b + g$, with the actual affine data g included. The energy equation is the complete quadratic form

$$\nu\left[A_p^2 G_{00} + 2A_p \sum_j c_j G_{0j} + \sum_{i,j} c_i c_j G_{ij}\right] = \frac{1 - e^{-2\nu Y}}{4} - \nu\sigma_p + 2\nu e^{-2\nu Y}\tau_S, \tag{1.16.16}$$

where $G_{ij} = \int_0^Y e^{-2\nu y}\phi_i\phi_j\, dy$, $\phi_0 = \phi$, $\phi_j = \psi_j$, and $\sigma_p = 2S(\frac{\hat{\xi}_p^2}{2})/H_p^2$. We can remove off-diagonal entries only after we check actual disjoint supports.

For the reserved disjoint main and return slots, $G_{00} = 1/(4\nu)$ and $G_{0j} = G_{12} = 0$. For each return

$$[c_j\psi(y - \dot{Y} + d_j)] = \dot{c}_j\psi - c_j w_o \psi', \tag{1.16.17}$$

and

$$[A_p\dot{\Phi}(\nu y)] = \dot{A}_p\Phi + A_p\Phi'(uy - \nu v), \qquad v = (T_b'(\nu) - 60/\nu)u \tag{1.16.18}$$

on the $G = 0$ same-R_g sector. These are fixed-$\hat{\xi}$ identities.

Lemma 1.16.4 (The actual variable-exponent root and return derivatives)**.** *We fix the main template Φ, smooth, supported in $0 < \xi < \xi_m$, and normalized by $\int e^{-2\xi}\Phi(\xi)^2\, d\xi = 1/4$. We use two fixed return bumps with disjoint supports and distinct offsets d_1, d_2. On the genuine variable-exponent $G = 0$ sector the heat-compensation moment correction and primitive taper are absent. The actual prefix has $m_0 = j_0 = 0$ and $\sigma_p = \sigma_p^0(\nu)$, with*

$$|\nu\sigma_p| \le \epsilon_p, \qquad |\sigma_p + \nu\sigma_p'| \le K_p[T_d + 1 + \log(1/\nu)]. \tag{1.16.19}$$

Assume its complete actual future integral contributions satisfy $|\tau_S| + |\dot{\tau}_S| \le K_f$, and $|u| + |\dot{Y}| + |w_o|$ have a fixed bound before we increase Y_0.

We select $Y(\eta) = Y_0 + \widehat{Y}(\eta; Y_0)$ with one bound $\sup \widehat{Y} - \inf \widehat{Y} \le C_Y$ for all admitted Y_0, so $Y_{\max} \le Y_{\min} + C_Y$. We fix C_Y after ν_c and the templates. We select $Y_{\min} \ge \max\{4(\xi_m+2)/\nu_c,\, 240\log(1/\nu_c)\}$

plus the fixed support separations. The second bound gives the condition $Y \ge 4W$ of Lemma 1.14.2 and (1.16.23), because $W = 60\log(1/\nu) \le 60\log(1/\nu_c)$. The second bound is in fact implied by the first: $4(\xi_m+2)/\nu_c \ge 8/\nu_c \ge 240\log(1/\nu_c)$ whenever $\nu_c\log(1/\nu_c) \le 1/30$, and this holds because $\nu_c < h/10 < 10^{-3}$. We keep it for explicitness. For small enough ϵ_p and large enough Y_0, the actual energy equation has one positive root A_p in a fixed compact interval about one. For a fixed polynomial $\mathcal{P}$ and fixed $c_r > 0$,

$$|b_j| + |\dot b_j| \le \mathcal{P}(Y_{\max})e^{-c_r Y_{\min}}, \tag{1.16.20}$$

$$|\dot A_p| \le CK_p|u|[T_d + 1 + \log(1/\nu)] + (1+K_f)\mathcal{P}(Y_{\max})e^{-c_r\nu_c Y_{\min}}. \tag{1.16.21}$$

Here $c_j = A_p b_j$. Constants in the first, nonattenuated term of (1.16.21) do not depend on future derivative bounds. These estimates do not use a response bound.

Proof. Factor the return matrix's two rows by $e^{\beta Y}$ and $e^{\beta_2 Y}$. The remaining entries are $e^{-\beta d_j}L(\beta)$ and $e^{-\beta_2 d_j}L(\beta_2)$, where $L(t) = \int e^{tz}\psi(z)\,dz > 0$.

Its determinant is, up to fixed positive factors, $e^{\nu d_2} - e^{\nu d_1}$, thus its absolute value is at least $c\nu$. The main right sides after the same row factorization have a bound by $C\nu^{-1}e^{-\beta_2(Y-\xi_m/\nu)}$. We differentiate this explicit two-by-two inverse, with the two exponents, $\dot\nu$, and $\dot Y$. Each derivative costs only a fixed polynomial in $Y_{\max}$ and the fixed ν_c^{-1}. We keep the exponential factor.

This proves (1.16.20).

Disjointness of the actual slots reduces (1.16.16) to

$$A_p^2 D_p = B_p, \qquad D_p = \frac14 + \nu\sum_j G_{jj}b_j^2 \ge \frac14, \quad B_p = \frac14 - \nu\sigma_p + e^{-2\nu Y}(2\nu\tau_S - \tfrac14).$$

The last exponential and the return correction are small after we select Y_0. Thus B_p has fixed positive upper and lower bounds and $A_p = \sqrt{B_p/D_p}$ is the unique positive root. The exact differentiated numerator is

$$\begin{aligned}\dot B_p = {} & -u(\sigma_p + \nu\sigma_p') \\ & + e^{-2\nu Y}\{2u\tau_S + 2\nu\dot\tau_S - 2(uY + \nu\dot Y)(2\nu\tau_S - \tfrac14)\}.\end{aligned}$$

The differentiated D_p is exponentially small by the return matrix calculation.

Differentiation of $A_p^2 D_p = B_p$ now proves the claim. □

Lemma 1.16.5 (Exact preservation of the root by the paired actual edit)**.** *We let ΔS_f be the complete downstream radial S increment of the heat collar and rank-one primitive correction, with their quadratic terms. On the protected full-history restoration collars, the early $U = 0$ three-row moment correction has the single target $(0, -\Delta S_f, -\Delta C_{p,f})$. It keeps I, M, J unchanged on its outlet germ and thus at the pulse inlet. In the normalizations of (1.16.16), the actual changes are*

$$\delta\sigma_p = -2\Delta S_f/H_p^2, \qquad \delta\tau_S = -\Delta S_f/H_o^2, \qquad \delta\sigma_p = 2e^{-2\nu Y}\delta\tau_S.$$

Thus, on those collars, the full energy numerator, its angular derivatives, and the selected positive root do not change.

The same assertion holds with affine inlet M, J and the full Gram polynomial.

Proof. The moment correction's zero first row and $U = 0$ give the first claim. The entry S_p changes by $-\Delta S_f$ while the canonical outlet value $S_o = -\int_{\sqrt{2R_o}}^{\infty}(U^2 - H^2/(4\frac{\hat\xi^2}{2}))\,\hat\xi\,d\hat\xi$ changes by the same quantity. Because $H_o/H_p = e^{-\nu Y}$,

$$-\nu\delta\sigma_p + 2\nu e^{-2\nu Y}\delta\tau_S = 0.$$

This is an identity of smooth functions of the member parameters, so its full differentiated identity includes the derivatives of ν, Y, H_p, H_o and still vanishes.

The main and return velocity profiles and their moment matrix do not change. Thus their full quadratic Gram polynomial does not change as well. Root uniqueness proves the assertion without a second normalization solve. □

Verification of the model prefix input from its actual finite template. The actual unbanked $G = 0$ template has a bounded finite-turn ratio $\sigma_b(\nu)$ and the actual wait $W = 60\log(1/\nu)$. Direct integration gives

$$\sigma_p = e^{2\nu W}\sigma_b - (e^{2\nu W} - 1)/(4\nu).$$

The finite-template integral that defines σ_b and its ν derivative have a bound by a constant K_p fixed with that template. Because $\nu W \ll 1$, differentiation of this displayed formula gives (1.16.19), with $\epsilon_p \le CK_p\lambda[T_d + 1 + \log(1/\lambda)]$. The proof uses the actual wait, not an imposed equilibrium history.

The fixed-λ bridge can have a heat correction whose S history differs from its target at this point. We use full cancellation in Lemma 1.16.5 only on the protected full-history restoration collars. The next estimates include the bridge residual. The canonical stress formulas always use the actual edited S, P.

The same wait proves the necessary angular-memory estimate. We put $\Xi = Q_{\mathrm{lin}}(-W)$. The exact formula is

$$Q_{\mathrm{lin}}(0) - q(0)/a - u/a^2 = e^{-aW}[\Xi - (q(0) + uW)/a - u/a^2]. \tag{1.16.22}$$

The source on the whole wait is $q(y) = q(0) - uy$. At its actual finite-template inlet, we write $r_b = r_b(\nu)$ and $v_b = \log \frac{\phi}{\hat{\phi}^2} = T_b'(\nu)u$.

Formula (1.16.4) gives directly

$$\Xi = 1 + ur_b' - v_b(1 - ar_b) + (q(0) + uW - a)r_b.$$

The finite-turn integral for r_b gives bounded r_b, r_b', T_b'. If $Y \ge 4W$, this proves

$$\epsilon_I \le CK_p\nu^{60(1-\nu)}(1 + q_o^{-1}). \tag{1.16.23}$$

In particular the inlet-source estimate $\nu/q_o \le C(\nu_c/h + \lambda)$ makes this small for all admitted inlet parameters. This calculation does not use the desired pulse response or the sign of the provisional finite-turn Ξ.

Lemma 1.16.6 (Admission of the actual $G = 0$ pulse from inlet/future outputs)**.** *We keep the actual same-R_g prefix, root, and disjoint returns just defined. Suppose the independently constructed inlet and future supply*

$$q_o > 0, \quad u = \dot\nu \ge 0, \quad \nu/q_o \le C_g(\nu_c/h + \lambda), \tag{1.16.24}$$

$$|\tau_S| + |\dot\tau_S| + |\tau_P| + |\dot\tau_P| + |w_o| \le K_f, \tag{1.16.25}$$

$$\nu \ge \lambda/2 \implies q_o \ge \tfrac{29}{240}q_* > 0, \quad e_p \le K_p\lambda^{30}, \tag{1.16.26}$$

$$\nu \le \lambda/2 \implies e_p \le K_e e_{\mathrm{end}} e^{-\lambda Y_{\mathrm{end}}/2}. \tag{1.16.27}$$

Here K_p, q_*, C_g are the stated nonattenuated prefix/geometry constants, without hidden inverse powers of the later selected h, ν_c or later future integral contributions. We fix the constants K_f, K_e, h, ν_c

before we increase Y_0, and $Y_{\max} - Y_{\min} \le C_Y$ as stated. Then the actual main pulse satisfies (1.16.13) *and* (1.16.14).

Its error tends to zero when we select λ, then ν_c/h, then Y_0 in that order, subject to these explicit inlet/future outputs. The leading construction must supply these outputs. This lemma does not assume or prove them by a response argument.

Proof. We let $y_m = (\xi_m + 2)/\nu$. The actual root and phase formulas give

$$\frac{|\dot{R}|}{q(y)} \le CK_p \frac{T_d + 1 + \log(1/\nu_c) + \xi_m/\nu_c + 60}{Y_{\min}} + (1 + K_f)\mathcal{P}(Y_{\max})e^{-c\nu_c Y_{\min}}/q_{\text{floor}},$$

where $q_{\text{floor}} = \min q_o > 0$ for the fixed member.

This uses $u/q(y) \le 4/(3Y)$ and keeps $-\nu v = -(\nu T_b' - 60)u$. Thus ϵ_a is small after Y_0, without division by u. The main-template bound gives $|R_y| \le C\nu$. Equation (1.16.23) supplies the angular memory.

Here is the necessary estimate of the canonical terms rather than an assumption about them. In (1.16.7)–(1.16.9), the main-support integrals satisfy

$$\int_0^\infty e^{-2\nu z}\,dz = (2\nu)^{-1}, \qquad \int_0^\infty z e^{-2\nu z}\,dz = (4\nu^2)^{-1}, \qquad |F_\nu| \le C\nu^{-2}.$$

For the next main point, $q(y + z) \le q(y)$, so its $R\dot{R}$ term has a bound by $C\epsilon_a q(y)/\nu$. Also $u/[q(y)\nu^2] \le C/(Y\nu^2) \le C/\nu$. All return-square and differentiated-return terms are exponentially small by (1.16.20).

The actual future terms have $\Delta \ge 3Y/4$ and so have a bound by $(1 + K_f)\mathcal{P}(Y_{\max})e^{-c\nu_c Y_{\min}}$. The explicit pressure formulas give the same conclusion with the stronger exponent $b \ge 1$. Thus (1.16.12) holds with C_1 that depends only on local geometry/templates and with $\epsilon_f = (1 + K_f)\mathcal{P}(Y_{\max})e^{-c\nu_c Y_{\min}}/q_{\text{floor}}$. We do not use λ^{30} to absorb an unattenuated K_f.

For $\nu \ge \lambda/2$, the nonlinear term is at most $CK_p\lambda^{29}$ plus the attenuated future error, by (1.16.26). For $\nu \le \lambda/2$, we use (1.16.27) after we fix the finite h^{-1}, ν_c^{-1} and future constants. It controls e_p/ν and $e_p/(\nu q_o)$. The linear term ν/q_o is small by (1.16.24). The explicit prefix/root/return formulas and the listed upstream outputs verify all hypotheses of Lemma 1.16.3.

We apply that lemma, in its order: denominator first, response second. □

Lemma 1.16.7 (Continuation through the full actual quiet and return region)**.** *Under the verified prefix/root/return formulas and the explicitly listed upstream outputs of Lemma 1.16.6, the denominator bound extends to $0 \le y \le Y$:*

$$Q(y) \ge c[q_o + u(Y - y)] > 0.$$

We let ϵ_m denote the main response error at $y_m = (\xi_m + 2)/\nu$, where $R = 0$. On the early quiet interval, $t = y - y_m \ge 0$, $y \le Y/2$,

$$|w(y)| \le C\epsilon_m e^{-\beta t} + CE(y_m)(1 + q_o^{-1})te^{-\beta t} + (1 + K_f)\mathcal{P}(Y_{\max})e^{-cY_{\min}}. \tag{1.16.28}$$

On the late quiet part and each actual return support,

$$|w| + |b_s| \le (1 + K_f)\mathcal{P}(Y_{\max})e^{-c_1 Y_{\min}}, \qquad b_s = 2R_y - (1 + 2\nu)R, \tag{1.16.29}$$

where the polynomial can contain the fixed q_{floor}^{-1} and ν_c^{-1}. All these portions have strict relaxed-cone margins after the same choices, followed by the physical large-radius choice.

Proof. We first establish Q without an estimate for w. Its linear part has the exact formula used in Lemma 1.16.3. Up to $Y/2$, $q(0)/q(y) \le 2$. After $Y/2$ its inlet-memory error divided by $q(y)$ has a bound by a fixed polynomial times $e^{-aY/2}$. Thus $Q_{\mathrm{lin}} \ge cq$ on the full interval.

Before the first return, the previously specified main pulse ends, and its actual stable histories satisfy

$$m(y) = e^{-\beta(y-y_m)}m(y_m), \qquad \dot m(y) = e^{-\beta(y-y_m)}[\dot m(y_m) + u(y-y_m)m(y_m)].$$

The same formulas hold for j, with β_2 and $2u$. These are solutions with actual nonzero outlet memories, not history resets. Substitution of them in (1.16.5) controls the early-half error by the same actual amplitude as on the main pulse. In the late half $E = e_p e^{-(1/2+\nu)y}$ and the stable histories are exponentially small.

On each return support, (1.16.20) and (1.16.17) give the same bounds by finite-interval stable convolution. This proves $Q \ge cq$ independently of N.

On a quiet interval, (1.16.11) gives, with $n = N/E$,

$$n_y + \beta n = E\mathcal{L}, \qquad \mathcal{L} = \eta + 4(\tfrac12 + h)\eta p - b_\eta(\dot p + 2cp).$$

The exact pressure identities imply

$$|\mathcal{L}| \le C(1+q+u) + (1+K_f)\mathcal{P}(Y_{\max})e^{-(1+2\nu)(Y-y)}.$$

On the early half, $u \le 2q/Y$ and the ratio of earlier to current q is at most two. Duhamel, divided only by the proved denominator, uses

$$\int_{y_m}^{y} e^{-\beta(y-s)}E(s)\,ds = E(y_m)e^{-\beta t}\frac{1-e^{-2\nu t}}{2\nu} \le E(y_m)te^{-\beta t}.$$

The future term has the exact convolution

$$\int_{y_m}^{y} e^{-\beta(y-s)}E(s)e^{-b(Y-s)}\,ds = E(y)e^{-b(Y-y)}(1-e^{-t}), \qquad b = 1+2\nu.$$

These prove (1.16.28). If $y \ge Y/2$, then $t \ge Y_{\min}/4$. The homogeneous term and local forcing are exponentially small after division by the fixed q_{floor}. The last exact convolution is also exponentially small because $E(y) \le e_p e^{-(1/2+\nu)Y/2}$.

Here $\dot m(y_m)$ and $\dot j(y_m)$ denote the fixed-$\hat\xi$ jets evaluated on the moving section $y = y_m$, not total derivatives of those traces.

On a return use the full algebraic identity (1.16.6), not a quiet equation with its nonzero U terms omitted. The return amplitudes, their fixed-$\hat\xi$ derivatives, and the inlet stable histories are exponentially small. The actual S, P and their derivatives, with the future integral contributions, have finite polynomial bounds from (1.16.7)–(1.16.10). We multiply their contribution by the exponentially small E. This proves (1.16.29).

After the second return, $M = J = 0$ identically, so their full parameter derivatives vanish too. Equation (1.16.16) includes their energy. Finally $a_s = 2 + 2\nu$ on the power pieces. The main pulse is close to $(a_s, b_s, w) = (2, -R, 2R)$ and the quiet/returns to $(2+2\nu, 0, 0)$. The large-p_1 cone inequalities have strict margins on these compact sets.

The finite physical radius controls the radial viscous and finite-p_1 errors after we fix the member's positive q_{floor}. □

The fixed-λ affine sector: explicit extra inputs and their use. Here $u = 0$, $c = \log \dot{K}$ and $q = h - \lambda + c \geq q_* > 0$ are independent of y. The same exact formulas hold, with m_0, j_0 and their true fixed-$\hat{\xi}$ derivatives. Suppose K_p bounds the inlet finite-prefix data and their angular derivatives. The actual wait gives

$$|m_0| + |\dot{m}(0)| + |j_0| + |\dot{j}(0)| \leq CK_p\lambda^{30-120\lambda},$$

because the stable rates are $1/2 - \lambda$ and $1/2 - 2\lambda$. The I-memory and its derivative gain $\lambda^{60(1-\lambda)}$. Thus one adds only these explicit exponentially propagated inlet terms to the proof of Lemma 1.16.3.

The return coefficients are genuinely affine, $c = A_p b + g$, with g determined by the actual inlet m_0, j_0 in (1.16.15). g and its derivative are $\mathcal{P}(Y)e^{-cY}$ times the displayed inlet bound. Equation (1.16.16) is then a quadratic polynomial $D_pA_p^2 + 2E_pA_p + F_p - B_p = 0$, with $D_p \geq 1/4$, and E_p, F_p exponentially small. Its derivative at the positive root has a positive lower bound. If $|\sigma_p^0| + |\dot{\sigma}_p^0| \leq K_p[T_d + 1 + \log(1/\lambda)]$, with the early two-row taper energy, then

$$|\dot{A}_p| \leq CK_p\lambda[T_d + 1 + \log(1/\lambda)] + C\epsilon_{\text{heat}} + (1 + K_f)\mathcal{P}(Y)e^{-cY}.$$

Here $\epsilon_{\text{heat}} = K_{\text{sc}}(Y_0)/R_{\text{master}}$ is the actual late-scale bridge residual of Proposition 1.14.6. The fixed-$\hat{\xi}$ phase derivative is now $-\lambda v\Phi'$, where the actual endpoint chart gives a fixed bound for $v = \log \frac{\rho}{2}$. We do not set it to zero. Thus the response and the full quiet/return argument extend with the additional error

$$C_{\text{pre}}\{\lambda[T_d + 1 + \log(1/\lambda)] + \lambda^{30-120\lambda}\} + C\epsilon_{\text{heat}} + (1 + K_f)\mathcal{P}(Y)e^{-cY},$$

in addition to the true nonlinear amplitude term Ce_p/λ. For the actual cutoff target

$$(0, -\chi_b\Delta S_f, -\chi_b\Delta C_{p,f}),$$

the exact residual in the energy numerator is $-2\lambda(1 - \chi_b)\Delta S_f/H_p^2$.

It and its first jet are $O(\epsilon_{\text{heat}})$. The positive root is transverse, so the same bound holds for its change and first jet. Only where $\chi_b = 1$ does Lemma 1.16.5 give exact root preservation. The compact estimate also applies to stress errors from partial moment correction. This is an implication from bounded actual affine inlet data.

The exact finite-prefix template and each included moment correction must supply those data. We cannot derive these data if we set M_p, J_p to zero.

Lemma 1.16.8 (Actual admission of the two away-from-zero pulse sectors)**.** *We use the jointly rebuilt family of Sections 1.15 and 1.14. Then one admissible parameter sequence gives the next bounds for the actual variable-exponent and fixed-λ affine pulses:*

$$Q \geq c[q_o + \dot{\nu}(Y - y)] > 0 \quad (0 \leq y \leq Y), \qquad |w - 2R| \leq \varepsilon_{\text{main}}.$$

The denominator bound holds throughout the pulse. The response bound holds on the main window for any specified sufficiently small $\varepsilon_{\text{main}}$. The quiet and return stated estimates also hold. We prove the denominator bound before we divide the axial numerator by it.

All five histories, their moving-coordinate first jets, and the nonzero inlet affine data are those of this actual member. The protected endpoint collars keep the selected backward root and all its finite parameter jets by exact history restoration and uniqueness. This statement applies to $|\eta| \geq \eta_a > 0$. The ordinary-angular central-plane proof is the distinct central pulse argument.

Proof. The actual prefix estimates, Lemma 1.14.1 and Lemma 1.14.2, prove the parameter-uniform r_b, σ_b and wait estimates, with $T_b = T$ and the fixed-$\hat{\xi}$ inlet jet.

On the genuine $G = 0$ sector its moment corrections are absent. The actual inlet estimate in Proposition 1.15.25, Lemma 1.15.26 and Proposition 1.15.27 gives (1.16.24)–(1.16.26) and the low-exponent amplitude suppression. These conclusions are a result of the actual coefficient order and its transverse inverse. None uses w or the desired pulse response. We construct the complete actual future by Proposition 1.15.8, with the real A11, central memory/shot and inlet-germ estimates.

Proposition 1.15.20 gives their uniform first-derivative integral bounds before Y_0 and thus supplies (1.16.25). This K_f is distinct from the next moment correction constant $K_{\mathrm{sc}}(Y_0)$ made small by the last scale. Late constants occur only with their displayed long-pulse attenuation.

Thus first fix the finite templates, then select the single early λ against K_{pre} and the desired main tolerance. We select $h < \lambda/6$ and then ν_c/h small. We select the actual future, its finite L_o thresholds, and the angular inverse/cutoff. We increase Y_0 to satisfy the slot separation, all root/return exponential estimates, and the explicit angular error bound in Lemma 1.16.6. The high-exponent nonlinear term is $O(K_{\mathrm{pre}}\lambda^{29})$.

The low-exponent term becomes small with Y_0 after we fix its constants. Thus the hypotheses of Lemma 1.16.3 hold for the actual field. Its denominator-first proof and Lemma 1.16.7 give the claimed whole pulse estimates.

On the fixed-λ bridge, Lemma 1.14.3 supplies the real m_0, j_0 and their fixed-$\hat{\xi}$ derivatives. Lemma 1.14.4 supplies the actual primitive taper and its nonzero energy integral. We fix their constants before λ. The actual affine return formula (1.14.19) keeps its explicit λ^{-1} determinant loss. Its factor $e^{-(1/2-2\lambda)Y}$ makes this contribution small when we increase Y_0. The full Gram equation keeps the mixed affine term and its square.

The only later bridge correction is Proposition 1.14.6. We select the last radius to make ϵ_{heat} smaller than the fixed main and cone tolerances. On the protected collars it is identically zero and Lemma 1.16.5 identifies the actual root with the selected backward root. Its differentiated identity and the uniqueness of the two-return linear solve identify all finite jets there. We do not select a second root independently.

Last, we use the same last radius for the radial viscous and finite cone thresholds. The main inequalities have strict margins near $(a_s, b_s, w) = (2, -R, 2R)$. The quiet and return margins are a result of the previously proved small bounds near $(2 + 2\nu, 0, 0)$. We do not assume independent freedom to select the physical amplitude. □

1.16.2 The flat central pulse with ordinary angular derivatives

Lemma 1.16.9 (Central pulse, quiet, and returns through $\eta = 0$)**.** *We consider the selected unlifted central component on an open band $\chi = 0$. Its scalar primitive precedes the next blend in (1.13.57). It has its actual scalar prefix and the admitted complete future of Proposition 1.15.20. After the parameter choices in this proof, the pulse, quiet intervals, and actual returns have uniform strict relaxed-cone margins. All angular estimates use ordinary ∂_η and cover $\eta = 0$. This is not an extension of an estimate with $1/\eta_a$ to the central plane.*

Indeed $\eta = zq^{h-\frac{1}{2}}$ and $\eta_z = q^{h-\frac{1}{2}}(1-\eta^2)/(1-2h\eta^2)$, so $\eta = 0$ is the regular plane $z = 0$ at positive time, not the cylindrical axis. This axis is $r = 0$, equivalently $\hat{\xi} = 0$, and the core theorem with $H = \hat{\xi}^2 F$ supplies its Cartesian regularity.

Proof. The exact absolute-memory cancellation of the selected central layout is

$$H = A_c(\hat{\xi}/\sqrt{2})^{-2\nu}, \qquad I = \frac{A_c\big(\frac{\hat{\xi}^2}{2}\big)^{1-\nu}}{1-\nu} + K_c, \qquad \nu = \nu_c,$$

with scalar A_c, K_c and scalar $\frac{\hat{\xi}_p^2}{2}, H_p, e_p, r_p, \sigma_p$. The evaluated memory at $R_o = R_g e^{Y_0+\rho(\eta)}$ equals $A_c R_g^{1-\nu}(r_b - (1-\nu)^{-1})e^{(1-\nu)T_b}$, independent of η. A curved evaluation graph is not a physically angular power.

Thus $H_\eta = E_\eta = (\frac{\hat{\xi}_p^2}{2})_\eta = \nu_\eta = 0$ at fixed $\hat{\xi}$ on the pulse. The actual $M_p = J_p = 0$ and $r_p \le r_{\mathrm{eq}} = (1-\nu)^{-1}$ are a result of the shared prefix and its ratio barrier, with $|r_p - r_{\mathrm{eq}}| \le K\nu^{60(1-\nu)}$.

We keep the previously selected smooth outlet graph ρ with its original endpoint germs and bounded ordinary ρ_η. We do not reflect or change this graph, its returns, or its actual fields. The ordinary C^1 bounds for τ_S, τ_P are those of Proposition 1.15.20 on the admitted product domain. We do not assume that their derivatives vanish at $\eta = 0$. We keep the scalar prefix energy σ_p and do not specify a new value. This same-member argument does not use optional even graph choices at the initial data stage.

We write $y = 2\log(\hat{\xi}/\hat{\xi}_p)$ and

$$R = U/E = A_p(\eta)\Phi(\nu y) + \sum_j c_j(\eta)\psi(y - Y + d_j), \qquad c_j = A_p\beta_j.$$

The actual two-return matrix and its ordinary derivatives give

$$|\beta_j| + |\partial_\eta \beta_j| \le \mathcal{P}(Y_{\max})e^{-c(Y_{\min} - \xi_m/\nu)}.$$

Its absolute determinant factor is $|e^{\nu d_2} - e^{\nu d_1}| \ge c\nu$. We put $K_j = \int_0^Y e^{-2\nu y}\psi(y - Y + d_j)^2 dy$. The same actual energy root, with all real future integral contributions, is

$$D_r A_p^2 = Z, \qquad D_r = \frac{1}{4} + \nu\sum_j K_j\beta_j^2,$$

$$Z = \frac{1 - e^{-2\nu Y}}{4} - \nu\sigma_p + 2\nu e^{-2\nu Y}\tau_S.$$

Ordinary differentiation gives

$$(A_p)_\eta = \frac{Z_\eta - A_p^2(D_r)_\eta}{2D_r A_p},$$

$$Z_\eta = e^{-2\nu Y}[\nu Y_\eta/2 + 2\nu(\tau_S)_\eta - 4\nu^2 Y_\eta \tau_S],$$

$$(D_r)_\eta = \nu\sum_j [(K_j)_\eta\beta_j^2 + 2K_j\beta_j(\beta_j)_\eta], \qquad (K_j)_\eta = -2\nu Y_\eta K_j.$$

The scalar prefix has $\nu|\sigma_p| \le K\nu[T_d + 1 + \log(1/\nu)]$. Thus A_p lies near one and $|(A_p)_\eta| \le K_f\mathcal{P}(Y_{\max})e^{-c_\nu Y_{\min}}$. This bound keeps the actual $Y_\eta = \rho_\eta$. We do not infer $(A_p)_\eta(0) = 0$ or an $O(|\eta|)$ estimate.

We let $a = 1-\nu$, $\beta = 1/2 - \nu$, $\beta_2 = 1/2 - 2\nu > 0$, $q = h - \nu$. The actual linear angular coefficient is

$$Q_{\mathrm{lin}} = q/a + (1-h)(r_{\mathrm{eq}} - r_p)e^{-ay} \ge q/a \ge ch.$$

For $m = M/(\frac{\hat{\xi}^2}{2}E)$ and $j = J/(\frac{\hat{\xi}^2}{2}HE)$, the genuine equations are

$$m_y + \beta m = R, \quad j_y + \beta_2 j = R, \quad m(0) = j(0) = 0,$$

and their ordinary angular derivatives satisfy the same equations with right side R_η. There is no moving-inlet term because $\frac{\hat{\xi}_p^2}{2}$ is scalar. The exact nonlinear correction is

$$Q - Q_{\mathrm{lin}} = E[2(\tfrac{1}{2} - h)\eta m + dm_\eta - dj_\eta + 2(h - (\tfrac{1}{2} - h))\eta j]. \tag{1.16.30}$$

On the main support $m = A_p m_\Phi$, $j = A_p j_\Phi$. Their angular derivatives contain $(A_p)_\eta$, not $\dot{A}_p/\eta$. On returns the actual derivative is $(c_j)_\eta \psi - c_j Y_\eta \psi'$. The stable equations give bounded m, j, m_η, j_η throughout the pulse. Thus $|Q - Q_{\rm lin}| \le KE$.

The actual same-coefficient amplitude obeys

$$e_p \le K_{\rm env} e_{\rm end} e^{-(\lambda-\nu)Y_{\rm end}}, \qquad \nu = \nu_c < h/10 < \lambda/2.$$

We select Y after the fixed constants so $Ke_p \le q/(4a)$. Then $Q \ge 3q/(4a)$, established before we estimate N_s or w. We do not assume parity of U, M, J or of this correction. Its exact central-plane value is

$$Q\big|_{\eta=0} = Q_{\rm lin} + E(m_\eta - j_\eta)\big|_{\eta=0},$$

and the same bound already controls these ordinary derivative terms.

We put $\Delta = Y - y$ and $b = 1 + 2\nu$. The actual canonical identities and ordinary fixed-$\hat{\xi}$ derivatives are

$$\begin{aligned}
\frac{S}{H^2} &= \frac{1 - e^{-2\nu\Delta}}{8\nu} - \frac{1}{2}\int_y^Y e^{-2\nu(s-y)} R(s,\eta)^2 ds + e^{-2\nu\Delta}\tau_S,\\
\frac{S_\eta}{H^2} &= e^{-2\nu\Delta}[(1/4 - 2\nu\tau_S)Y_\eta + (\tau_S)_\eta] - \int_y^Y e^{-2\nu(s-y)} R R_\eta \, ds,\\
\frac{P}{E^2} &= -\frac{1}{2b} + e^{-b\Delta}[1/(2b) - 2\tau_P],\\
\frac{P_\eta}{E^2} &= e^{-b\Delta}[-bY_\eta(1/(2b) - 2\tau_P) - 2(\tau_P)_\eta].
\end{aligned}$$

Here $R(Y) = 0$ on the outlet germ, so the return-square boundary term vanishes, but the formulas include the displayed power and future boundary terms. In particular, we do not set S_η, P_η to zero because H is scalar on the pulse. The ordinary future bounds and the true root/return derivatives give

$$(|S| + |S_\eta|)/H^2 + (|P| + |P_\eta|)/E^2 \le K_{\rm cen},$$

Here $K_{\rm cen}$ can depend on $1/\nu$ and the fixed future constants.

It is uniform for sufficiently large Y. The kernel integrates to at most $1/(2\nu)$. We do not use away-from-zero angular cancellation.

The exact axial identity is

$$\begin{aligned}
N_s/E &= R - (\tfrac{1}{2} - h)m + (\tfrac{1}{2} - h)\eta m_\eta + N_{\rm err},\\
N_{\rm err} &= E\big[(2(\tfrac{1}{2} - h)\eta m + d m_\eta)R + 2(4h\eta S/H^2 - dS_\eta/H^2)\\
&\qquad + 4(\tfrac{1}{2} + h)\eta P/E^2 - dP_\eta/E^2\big].
\end{aligned}$$

Thus $|N_{\rm err}| \le K_{\rm cen} E$, entirely in ordinary derivatives. The main-template stable equation gives $|m - R/\beta| \le K_\Phi \nu$ and $|m_\eta| \le K_\Phi |(A_p)_\eta|$. With $\beta - (\frac{1}{2} - h) = q$ and the actual inlet memory,

$$|w - 2R| \le K_\Phi[\nu/h + |(A_p)_\eta|/h + |r_p - r_{\rm eq}|/h] + K_{\rm cen} e_p/h. \tag{1.16.31}$$

First, we select ν/h small after the original finite C^3 template and prefix constants.

The real wait makes its memory term small. Then, we select Y to control the ordinary root derivative and the actual amplitude term, with $e_p/(\nu h)$ if it occurs in $K_{\rm cen}$. We do not claim a $C \to \infty$ amplitude reduction. The exact shears $a_s = 2 + 2\nu$, $b_s = 2R_y - (1 + 2\nu)R$ differ from $(2, -R)$ by $O_\Phi(\nu)$ on the main template, with its fixed fast fall. Equation (1.16.31) gives strict relaxed-cone margins near $(a_s, b_s, w) = (2, -R, 2R)$ through the adjacent phase window $y_m = (\xi_m + 2)/\nu$.

At the central plane the full identity is

$$\frac{N_s}{E}\Big|_{\eta=0} = R - (\tfrac{1}{2} - h)m + E\left[m_\eta R - \frac{2S_\eta}{H^2} - \frac{P_\eta}{E^2}\right]\Big|_{\eta=0}.$$

All terms are finite ordinary quantities previously controlled. We do not assume that they vanish. Its response is near $2R$, not $w = 0$.

On quiet intervals the exact equation is $(N_s)_y + N_s = \eta E^2 + 4(\frac{1}{2} + h)\eta P - dP_\eta$. Because Q is comparable to h, ordinary convolution gives

$$|w(y)| \le K\epsilon_m e^{-\beta(y-y_m)} + \frac{K_{\mathrm{cen}}}{h} E(y_m)(y - y_m)e^{-\beta(y-y_m)}.$$

This covers early and late quiet before the first return. After a return restart it at that return's outlet small value. The two actual return neighborhoods obey, by their real matrix bounds and fixed-width stable convolution,

$$|b_s| + |w| \le K_{\mathrm{cen}}\mathcal{P}(Y_{\max})e^{-cY_{\min}} + K_{\mathrm{cen}}e_p/h.$$

We take $Y_{\min} \ge 4(\xi_m + 2)/\nu$ plus the fixed return offsets. The same parameter choices make the right sides small. They give $2\nu w^2 < 1$ on quiet intervals and strict relaxed-cone margins on returns. After the last return $M = J = 0$ with all angular derivatives. The equation for the same root includes their energy, and their pressure contribution is zero because they change U only.

All displayed formulas are smooth on an open neighborhood of zero, where $d > 0$. No division by η occurs. Higher same-member jets are finite but not deduced from a C^1 bound. On a flat central band $|\eta| < \eta_c$, the variable-sector proof can start at $|\eta| \ge \eta_c/2$, with an open overlap where $\chi = 0$ and $\dot\nu = 0$. The two constructions use identical fields, histories, the unique positive energy root and the unique two-return solution. We do not perform new angular gluing at that overlap.

Finally normalized cone faces alone do not give the full finite-p test. The quantity $L_{\mathrm{geom}} = 1 - 2h\eta^2$ has a fixed positive lower bound, so

$$\inf_{\text{pulse}} \tfrac{\hat\xi^2}{2} Q/L_{\mathrm{geom}} \ge ch\tfrac{\hat\xi_p^2}{2} \longrightarrow \infty$$

when the master scale grows for this fixed Y. We fix all finite w and control norms, then we select C for this actual threshold, viscosity, and each admission $C \ge C_0(Y)$ of Proposition 1.15.20. Member-dependent activation follows that choice. This proves the central local estimate under its actual inputs, not the admission of each physical member or the full connection theorem. □

1.17 Actual primitive and source corridors

Main result. Lemmas 1.17.5 and 1.17.8 prove the source estimates at the terminal edge and on the angular mixture. Lemma 1.17.9 matches the inlet on a fixed overlap. Primitive positivity and source positivity use different bounds.

1.17.1 Source and primitive reserves on the actual corridor

We write $d = 1 - \eta^2$, and $\dot f = (\frac{1}{2} - h)\eta\partial_\eta f|_{\hat\xi}$. The nondiffusive pulse denominator and the outer primitive gap are different quantities. The next identities keep that distinction. With $H = \frac{I_{\hat\xi}}{\hat\xi}$, we define the full angular primitive operator

$$\mathcal{A}I = (\frac{I_{\hat\xi\hat\xi}}{\hat\xi^2} - \frac{I_{\hat\xi}}{\hat\xi^3}) - \frac{I_{\hat\xi}}{\hat\xi}/\frac{\hat\xi^2}{2} + [\tfrac{1}{2}\hat\xi I_{\hat\xi} - (1-h)I + (\tfrac{1}{2} - h)\eta I_\eta]/(L\hat\xi^2), \qquad L = 1 - 2h\eta^2. \quad (1.17.1)$$

This is the actual angular stress when $U = M = J = 0$.

Lemma 1.17.1 (Two distinct mixing identities)**.** *For an angular cutoff $\chi = \chi(\eta)$ and actual primitives I_c, I_w,*

$$\mathcal{A}[(1-\chi)I_c + \chi I_w] = (1-\chi)\mathcal{A}I_c + \chi\mathcal{A}I_w + \dot{\chi}(I_w - I_c)/(L\hat{\xi}^2). \tag{1.17.2}$$

For a radial cutoff $z = z(\frac{\hat{\xi}^2}{2})$, $\Delta = I_w - I_c$,

$$\mathcal{A}[(1-z)I_c + zI_w] = (1-z)\mathcal{A}I_c + z\mathcal{A}I_w + 2z'\frac{\Delta_{\hat{\xi}}}{\hat{\xi}} + [z'' + (1/(2L) - 1/\tfrac{\hat{\xi}^2}{2})z']\Delta. \tag{1.17.3}$$

No identity in this lemma implies the sign of Δ from an inequality on the inlet values of H_c, H_w alone.

Proof. We apply the product rule in (1.17.1). The angular cutoff is independent of $\frac{\hat{\xi}^2}{2}$, and the radial cutoff is independent of η.

All displayed cross terms thus occur one time. □

Lemma 1.17.2 (A tube margin after the actual pulse estimate)**.** *On a fixed member's compact tube suppose the actual full coefficient Q satisfies $Q \geq q_* > 0$, $H \geq H_* > 0$ and $a_s \leq a_*$, where $a_s = -\hat{\xi}^2\hat{\xi}^{-1}\partial_{\hat{\xi}}(H/(\hat{\xi}^2))/(H/(\hat{\xi}^2))$. If $\frac{\hat{\xi}^2}{2} \geq 2L_{\max}a_*/q_*$ there, then*

$$T_\theta = \frac{H}{2}(Q/L - a_s/\tfrac{\hat{\xi}^2}{2}) \geq H_*q_*/(4L_{\max}) > 0.$$

We let $M_* = \|(\hat{\xi}^{-1}\partial_{\hat{\xi}}, \partial_\eta)T_\theta\|_\infty$ on a slightly larger source domain. The margin survives on each enlargement with distance less than $H_*q_*/[8L_{\max}(1+M_*)]$, subject also to the actual support buffers.

Proof. Insert the scale inequality in the exact stress identity.

The last claim is a result of the mean-value estimate after we prove the lower bound throughout the tube. □

1.17.1.1 The actual outer component: primitive and source proofs

We use the finite future of Section 1.15, with $a = 1-h$ and $0 < h < \lambda/6$. It has an equilibrium λ leg of length L_o, the fixed slope transition $\kappa \in [h, \lambda]$, and one rank-one heat correction. We integrate its primitive from zero. We do not introduce an integration constant at a join radius. We select all the outer-active comparison band inside the chart band of (1.15.26).

There

$$R_A(\eta) = R_{A,b}/\lambda_{\mathrm{ch}}(\eta), \qquad k := \log^{\cdot} R_A = -(\tfrac{1}{2} - h)\eta\lambda'_{\mathrm{ch}}/\lambda_{\mathrm{ch}} \geq 2.$$

The same coefficient c and terminal deficit amplitude ρ are scalar. The transition end R_0 and terminal edge B have this same angular speed. These are properties of the rebuilt family, not properties inferred from inlet ordering.

Lemma 1.17.3 (A quantitative primitive gap on the full compact corridor)**.** *We put*

$$\beta_0 = \frac{\lambda - h}{(1-\lambda)a}e^{-a\delta} > 0, \qquad 0 < \rho \leq \frac{a\beta_0}{2(1+a\beta_0)}.$$

We make this additional terminal-amplitude choice before L_o. A finite lower bound for L_o depends on the fixed central geometry. The bound applies when L_o is at least this threshold. The actual

primitives obey $I_w \ge 2I_c$ from the same return graph through each central deviation and the outer A11 outlet. Thereafter, up to a fixed open terminal overlap, they obey

$$(I_w - I_c)/\tfrac{\hat\xi^2}{2} \ge m_g \lambda H_w > 0$$

for some $m_g > 0$ fixed before the last radius.

On the exact terminal wing the stronger identity is

$$I_w - I_c = E_w := \rho \int_{(\frac{\hat\xi^2}{2})}^{B(\eta)} H_0(s,\eta)\Psi(s/B(\eta))\,ds > 0 \quad (\tfrac{\hat\xi^2}{2} < B), \tag{1.17.4}$$

where $I_c = I_0$ is the same actual heat primitive.

Proof. First, we take a fixed normalized radial hull from R_o through all central deviations and the outer A11 outlet. We fix this hull before L_o. The central amplitude equation is linear, and its normalized shape is independent of c. The A11 construction precedes the added leg.

On this hull the outer template and its true inlet primitive are independent of L_o in outer inlet units. They are strictly positive. Quantitatively the last unedited fixed-width power segment before R_o gives $I_w(R_o) \ge c_1 R_o H_w(R_o)$ by direct integration of its positive H. The two-row taper has the explicit total primitive p of (Taper); its zero-row partner is the C_p constraint. Positivity of the entire incoming swirl and the last unedited segment give the bound regardless of the sign of p. The heat and pressure compensation banks each have zero total I increment. Positivity of H_w propagates the inlet bound across the hull.

Lemma 1.15.6 gives a finite upper bound for the actual central coefficient $I_c/(cR_o^a)$ there. One bound applies to all sufficiently large radii of the same family. The exact coefficient law Lemma 1.15.23 multiplies $I_w/(cR_o^a)$ by $e^{(\lambda-h)L_o}$. Thus a finite L_o gives $I_w \ge 2I_c$ throughout the hull. We increase it also so the rank-one support $[\frac{\hat\xi_b^2}{2}/2, 3\frac{\hat\xi_b^2}{2}/4]$ lies beyond that hull. These lower bounds on L_o are compatible.

On the model transition, $r = I/(\frac{\hat\xi^2}{2}H)$ satisfies $r' + (1-\kappa)r = 1$ and $r(0) = (1-\lambda)^{-1}$. For $v = r - a^{-1}$,

$$v' + (1-\kappa)v = (\kappa - h)/a \ge 0, \qquad v(t) \ge \beta_0 \quad (0 \le t \le \delta).$$

The exact coefficient law gives

$$\frac{H}{c(\hat\xi/\sqrt{2})^{-2h}} = (1-\rho)\exp\left(\int_t^\delta (\kappa - h)\,ds\right) \ge 1 - \rho.$$

Thus

$$\frac{I}{c(\frac{\hat\xi^2}{2})^{a}} - \frac{1}{a} \ge (1-\rho)\beta_0 - \frac{\rho}{a} \ge \frac{\beta_0}{2}.$$

On the previous equilibrium leg the same inequality holds with $r = (1-\lambda)^{-1}$ and a still larger amplitude ratio.

Its actual compact rank-one perturbation has relative size $O(R_o^{-1})$ in H, I and their necessary scaled derivatives. Thus the same radius selected last keeps a fixed fraction of this gap. The heat collar has the same error size. This compares with the actual heat primitive, because $I_0 - c(\frac{\hat\xi^2}{2})^{a}/a = O(c(\hat\xi/\sqrt{2})^{-2h})$ on the full exposed outer region.

At the terminal wing the rank-one construction has zero complete primitive discrepancy, thus $I_w = I_0$ beyond B. We integrate $H_w - H_0 = -\rho H_0 \Psi(\frac{\hat\xi^2}{2}/B)$ backward from B to get (1.17.4). On any compact attachment overlap strictly inside B, its positive gap and H_w have positive normalized

lower bounds. These bounds, the finite earlier hull, and the previous estimates give a single $m_g > 0$. We do not extend this compact argument to the zero gap at B.

There we use the exact formula. □

Lemma 1.17.4 (Actual outer source reserve before the terminal face)**.** *For the same family, after the last radius is sufficiently large,*

$$\mathcal{A}I_w \geq m_s \lambda H_w > 0.$$

This bound holds on the full compact path from the returned-pulse graph through the flattening, A11, added leg, drive, and heat collar. The path ends in a fixed open terminal attachment overlap. Here $m_s > 0$ is fixed with the normalized member. We do not assert a uniform bound when h or ρ tends to zero.

Proof. On the added model leg and drive, the backward shape is independent of the backward angular variable. Its exact charted primitive gives

$$\dot{I} = k(aI - \tfrac{\hat{\xi}^2}{2}H), \qquad L\hat{\xi}^2\mathcal{A}I = \tfrac{\hat{\xi}^2}{2}H(k-1)(ar-1) - 2L(1+\kappa)H.$$

the moving entry and its full history occur in the first identity. The previous proof gives $ar - 1 \geq a\beta_0$, with the stronger $(\lambda - h)/(1-\lambda)$ on the equilibrium leg. Because $k \geq 2$, the nondiffusive term has a fixed positive multiple of $\lambda\frac{\hat{\xi}^2}{2}H$.

A sufficiently large radius controls the displayed radial viscosity term. The rank-one perturbation and heat collar have $O(H/R_o)$ errors in $\mathcal{A}I$. Their supports are compact, and the same strictly positive model reserve controls these errors.

We now calculate the source on the flattening interval. In backward variables $(\xi, \beta) = (\lambda_{\mathrm{ch}}\frac{\hat{\xi}^2}{2}, \lambda_{\mathrm{ch}}^{\frac{1}{2}-h}\eta)$ set

$$Z = aI_b - \xi H_b - (\tfrac{1}{2} - h)\beta(I_b)_\beta, \quad z = Z/(\xi H_b), \quad \ell_r = \partial_{\log\xi}\log H_b.$$

For the transported comparison field and its transported primitive, write $Q^{\mathrm{tr}}_{\mathrm{lin,f}}$ for the following coefficient. In this comparison the chart formula gives

$$Q^{\mathrm{tr}}_{\mathrm{lin,f}} = (k-1)z, \qquad z_y + (1+\ell_r)z = -h - \ell_r - (\tfrac{1}{2} - h)\beta\partial_\beta \log H_b.$$

The rebuilt flattening uses $H_b = H_e e^{-\lambda y} e^{-\theta J_0 - (1-\theta)\log 2}$, with $J_0 = \log(1+\beta^2)$ and $\theta = 1 - s(y/T_f)$. Its exact right side is

$$-h - \ell_r + 2(\tfrac{1}{2} - h)\beta^2\theta/(1+\beta^2) \geq \lambda/3, \qquad 1 + \ell_r \in [1 - 3\lambda/2, 1 - \lambda/2].$$

At $X = R_o$ the transported outer coefficient has the source floor $q_w \geq q_*$ of Lemma 1.15.23. The inlet formula of Lemma 1.17.9 gives $Q^{\mathrm{tr}}_{\mathrm{lin,f}} = q_w/(1-\lambda) + O(e^{-a(Y_0 - O(1))})$. Indeed the chart derivative of the transported primitive is

$$\dot{I}^{\mathrm{tr}} = \ell^{h-1}\{(1-h)kI_b - k\xi H_b + (\tfrac{1}{2} - h)(1-k)\beta(I_b)_\beta\}.$$

Until the first A11 bump the actual outer swirl coincides with the transported swirl. Its primitive differs by the X-independent constant $D_I(\eta) = R_o H_w(R_o)[r_{w,\mathrm{tar}} - r_* - D(e^T R_{g,b}/R_e)^a]$ with $D = r_b(\lambda) - r_*$. The target above and bounded logarithmic graph slopes give $(|D_I| + |\dot{D}_I|)/(R_o H_w(R_o)) \leq Ce^{-a(Y_0 - O(1))}$, with C fixed before Y_0. The exact change of the forward linear coefficient is

$$Q_{\mathrm{lin,f}} - Q^{\mathrm{tr}}_{\mathrm{lin,f}} = \frac{\dot{D}_I - (1-h)D_I}{XH_w}.$$

Since $\partial_{\log X}\log(XH_w) \geq 1 - 3\lambda/2 > 0$, this estimate holds on the whole flattening and wait. Choose Y_0 to spend less than half the smaller of their source reserve and the normalized primitive-gap reserve of Lemma 1.17.3; the geometric constants precede Y_0. The actual A11 solve then restores the prescribed outlet ratio. On its two supports its partial, differentiated integrals are those of Lemma 1.15.5, by integrating the fixed bumps only up to X. Thus the transported comparison implies the positive bound for the actual component. Stable convolution thus yields $z \geq c\lambda$ on the whole flattening and the next power wait. The A11 coefficients and first jets are $O(\lambda^{30(1-\lambda)} + \|\delta_{\mathrm{mem}}\|_{C^1})$ by Lemma 1.15.5 and Proposition 1.15.20(3); the memory part is small for large Y_0 by Lemma 1.15.19(4). Their complete primitive perturbation has this same normalized bound, so they keep that reserve when the original early λ is small and Y_0 is large. Their terminal primitive is the equilibrium value previously used.

This covers each earlier piece of the path. □

Lemma 1.17.5 (Factor-preserving source and cone at the exact terminal edge)**.** *On the exact wing put*

$$V = \rho H_0(\tfrac{\hat\xi^2}{2},\eta)\Psi(\tfrac{\hat\xi^2}{2}/B), \quad E_w = \int_{(\frac{\hat\xi^2}{2})}^{B} V(s,\eta)\,ds, \quad v_s = V + E_w/\tfrac{\hat\xi^2}{2}, \quad v_g = E_w/\tfrac{\hat\xi^2}{2}.$$

We select the same decreasing squared-flat cutoff explicitly by $\Psi(z) = 1 - \sigma((z-e^{-3})/(1-e^{-3}))$, *where* $\sigma(t) = f(t)/(f(t)+f(1-t))$, $f(t) = e^{-1/t^2}$ *for* $t > 0$ *and* $f(t) = 0$ *for* $t \leq 0$. *We use the endpoint constant extensions. We take* ρ *smaller if necessary so* $\rho\sup|z\Psi'(z)|/(1-\rho) < h/4$, *before we select* L_o. *Then the same constants apply through the zero-stress face:*

$$\mathcal{A}I_w \geq c_s v_s, \qquad I_w - I_0 = \tfrac{\hat\xi^2}{2}v_g, \qquad |T_{z,w}| \leq C\frac{H_0}{(\hat\xi/\sqrt{2})}v_s.$$

The last bound keeps the actual canonical pressure and energy. For the same sufficiently long pulse wait, the full nonzero wing satisfies the finite relaxed-cone criterion. Its stress vanishes on the same exterior heat region. We do not continue a positive plateau through that region.

Proof. The same physical heat primitive satisfies $\mathcal{A}I_0 = 0$.

Because $\dot B = kB$ and the cutoff vanishes at B, differentiation under the actual integral, followed by integration by parts, gives

$$\begin{aligned}\dot E_w &= k\tfrac{\hat\xi^2}{2}V + akE_w + \mathcal{R},\\ \mathcal{R} &= \rho\int_{(\frac{\hat\xi^2}{2})}^{B}[\dot H_0 + k(s(H_0)_s + hH_0)]\Psi(s/B)\,ds.\end{aligned}$$

The exposed actual heat estimates (1.15.9) give $|\mathcal{R}| \leq CE_w/\tfrac{\hat\xi^2}{2}$. Thus the exact operator reads

$$L\hat\xi^2\mathcal{A}E_w = L\hat\xi^2(-\frac{V_{\hat\xi}}{\hat\xi} + V/\tfrac{\hat\xi^2}{2}) + (k-1)(\tfrac{\hat\xi^2}{2}V + aE_w) + \mathcal{R}.$$

For sufficiently large $\frac{\hat\xi^2}{2}$, H_0 is decreasing and $\frac{V_{\hat\xi}}{\hat\xi} \leq 0$. Because $k - 1 \geq 1$, the aE_w term absorbs the error.

This proves the source lower bound without subtraction of an absolute error from a vanishing stress.

For the axial estimate set $W = 2H_0V - V^2 \geq 0$. Subtraction of the same heat histories gives

$$\delta S = -\frac{1}{4}\int_{(\frac{\hat{\xi}^2}{2})}^{B} W(s)\frac{ds}{s}, \qquad \delta P = \frac{1}{4}\int_{(\frac{\hat{\xi}^2}{2})}^{B} W(s)\frac{ds}{s^2}.$$

Their angular derivatives include the moving cutoff. Integration of the terms $s\Psi'(s/B)/B$ by parts produces the lower boundary $W(\frac{\hat{\xi}^2}{2})$ and integrals with densities bounded by CH_0V/s or CH_0V/s^2. We treat the terms with $\Psi\Psi'$ by the same identity for $(\Psi^2)'$.

We keep all these terms. The upper terms vanish. Monotonicity of H_0 and the inequality $s \geq \frac{\hat{\xi}^2}{2}$ give

$$|\delta S| + |\dot{\delta S}| + \tfrac{\hat{\xi}^2}{2}(|\delta P| + |\dot{\delta P}|) \leq CH_0(\tfrac{\hat{\xi}^2}{2})v_s.$$

The heat axial stress is zero. We substitute these differences into

$$T_z = \{4h\eta S - b_\eta \dot{S} + \tfrac{\hat{\xi}^2}{2}((2+4h)\eta P - b_\eta \dot{P})\}/(L\hat{\xi}), \qquad b_\eta = d/((\tfrac{1}{2}-h)\eta),$$

which is bounded on this chart band.

This proves the claimed bound.

Here $U = 0$ and $b_s = 0$. The small cutoff amplitude makes $2 < a_s = 2 - \hat{\xi}H_{\hat{\xi}}/H \leq 2 + 3h$ for sufficiently large radius. In this case the exact finite cone test is

$$T_\theta > 0, \qquad 2T_\theta^2 > (a_s - 2)T_z^2,$$

because $p_1 - a_s = \hat{\xi}^2 T_\theta/H$ and $p_1 w = \hat{\xi}^2 T_z/H$. The ratio just proved is at most $CH_0/(\hat{\xi}/\sqrt{2})$ with the same constant up to the terminal edge. For this same member, a fixed multiple of the pulse-outlet amplitude bounds this amplitude.

After its fixed early inlet, the pulse-outlet amplitude has the factor $e^{-(1/2+\lambda)Y_{\mathrm{end}}}$. An increase in Y_0 after the future constants thus makes the strict cone inequality hold. We do not rescale the amplitude independently or divide by the flat deficit. □

Lemma 1.17.6 (The compact pure-swirl cone uses the same parameter order)**.** *The actual outer compact corridor in Lemma 1.17.4 satisfies the strict relaxed cone after the next choices. We impose a finite lower bound on L_o, then increase Y_0 as previously permitted, and last select the physical radius. This does not treat the physical amplitude as a new free rescaling parameter.*

Proof. All these pieces have $U = M = J = 0$. Their fixed normalized velocity, primitive, canonical S, P and necessary angular derivatives have finite bounds once we fix h, λ, ρ and the drive shape.

We compute the next K_{drv} from that transition and its wing, independently of L_o and of the later angular mixture cutoff. It is not a bound on the next mixture. The exact integrated axial formula thus gives on the drive $|w| \leq K_{\mathrm{drv}}E/q_{\min}$ with $q_{\min} = a\beta_0 > 0$. There $a_s \leq 2 + 2\lambda$ and the actual entry amplitude is $E_{\mathrm{transition}} = E_A e^{-(1/2+\lambda)L_o}$. With the early fixed upper bound $E_A \leq E_{\mathrm{pre,max}}$, we impose also the finite lower bound

$$L_o \geq \frac{1}{1/2+\lambda}\log^+\left(\frac{4\sqrt{\lambda}\,K_{\mathrm{drv}}E_{\mathrm{pre,max}}}{q_{\min}}\right).$$

It gives $2\lambda w^2 < 1/4$ on the drive after we include fixed shape factors in K_{drv}. We select this bound after h. A new choice of λ is not necessary.

The flattening, A11, previous added leg, and heat collar form a fixed normalized compact family after L_o. Lemma 1.17.4 gives their positive source lower bounds. Their canonical history bounds are

finite, with the full downstream integrals and all moving coordinate derivatives. In the actual family their amplitudes have a bound by $C_{L_o} e_{\mathrm{end}} e^{-(1/2+\lambda)Y_{\mathrm{end}}}$. Thus a larger Y_0 controls any remaining finite bound on w there and gives strict large-p_1 cone inequalities.

On the model power leg, multiplication of the future tail integral by $E(y)$ gives the same result. Its exact attenuation is $E_A e^{-2\lambda L_o} e^{-(1/2-\lambda)y}$. Finally the physical radius controls the finite-p_1 error, the radial viscosity, and the actual compact heat and moment perturbations. These last errors are $O(R_o^{-1})$ for the fixed L_o, Y_0 and consume only a fixed fraction of the previously strict margins. □

Lemma 1.17.7 (The actual central source estimate and its memory edit)**.** *The central component in* (1.15.27) *uses its scalar primitive before the next blend in* (1.13.57)*. It has a nonnegative angular source and a strict pure-swirl cone on its nonzero source set. Its source path connects the hold, deficit drive, shot/blend, and terminal wing. These claims apply to its actual inlet primitive, not an imposed equilibrium at R_o. After the blend interval J the component is $(H_L - \psi_o \alpha_o \ell_b \mathcal{F}',\ \mathfrak{M}_{2L} + \psi_o E_o)$, unchanged by the memory edit. On the compact preterminal path $\{R_o(\eta) \le \frac{\hat\xi^2}{2} \le \sup J\}$ its source has a positive minimum m_c.*

Proof. The central component is the central future of Proposition 1.15.22, with memory datum $p = \delta I$. Here

$$\delta I = (r_b - (1-\nu_c)^{-1}) \tfrac{\hat\xi_p^2}{2} H_p e^{-(1-\nu_c)W}$$

is the difference between the true inlet primitive and the reference $i_s = \frac{\hat\xi^2}{2} H_s/(1-\nu_c)$, $H_s = A_c (\frac{\hat\xi^2}{2})^{-\nu_c}$ (proof of Lemma 1.6.19). On the flat central band δI is a constant in the physical scalar component, and its evaluation on the moving graph introduces no new angular dependence. In general only its C^1 norm enters:

$$\epsilon_I = \frac{\|\delta I\|_{C^1}}{R_m H_s(R_m)} \le K_I (1+Y_0)^N e^{-(1-\nu_c)Y_0}$$

by (I8) and (1.15.22). So on $[R_o, R_m]$ the primitive is the true one, $i_s + \delta I$. We do not impose the equilibrium at R_o. On $[R_m, 2R_m]$ the actual edit is $I_c = i_s + \delta I \zeta(\frac{\hat\xi^2}{2}/R_m)$, with $\zeta = 1$ on the inlet germ and $\zeta = 0$ on the outlet germ. We select Y_0 so that condition (Y) of Proposition 1.15.22 holds, $C_I \epsilon_I \le \nu_c/8$. We now verify each assertion from the proof of that proposition.

Scalar primitive before the blend. By Steps 1–4 of that proof, the primitive is $i_s + \delta I \zeta(\frac{\hat\xi^2}{2}/R_m)$ on $[R_o, R_h e^{B_h}]$. It satisfies $\frac{I_{\hat\xi}}{\hat\xi} = H$ on the drive, and it equals $I_b = \frac{\hat\xi^2}{2} H_b/(1-h) - C_b$ on the power segment. These are scalar at fixed physical $\frac{\hat\xi^2}{2}$, apart from the C^1 datum δI. The lifted primitive $\mathfrak{M}_{2L}$ and the wing enter only on J, through (1.13.57), whose H includes $\chi_b' \Delta$. The lift is not extended backward to the central pulse entrance.

The memory edit. The cutoff gives $I = i_s$ and $H = H_s$ from $2R_m$ to R_h. These equalities continue along the power hold up to $R_h e^{B_h}$, where (1.6.19) gives $r_c = (1-\nu_c)^{-1}$. By Proposition 1.15.22(v), the stop map of Lemma 1.15.6 is evaluated at the reference ratio. Hence the drive, stop, power germ, shot, lift, wing and heat pair (c, k_f) are those of the reference, and after J the component is $\mathfrak{M}_{2L} + \psi_o E_o$. The memory edit returns before the hold and leaves this full shot/heat pair unchanged. The edit changes the canonical histories only for $\frac{\hat\xi^2}{2} \le 2R_m$. The increments are the integrals of $2H_s \delta H + (\delta H)^2$ against $1/(4s)$ and $-1/(4s^2)$, with the bound $2Z_\zeta(\epsilon_I + Z_\zeta \epsilon_I^2) H_s(R_m)^2$ (Step 2(c) of that proof). The axial estimate of Step 2 uses the total field, so it includes them. The pulse energy equation includes them too.

Nonnegative source and connected path. By (1.15.25):

- on the memory interval and hold, $T_\theta \ge \frac{3}{10} h H_s$;

- on the deficit drive, (1.15.24) gives $\mathcal{T}_{\theta,c} = \frac{2H}{\hat{\xi}^2}[\frac{(1-h)w_d}{2L} - (1+\kappa)] \geq (1-h)w_d H/(4L\frac{\hat{\xi}^2}{2})$, with $w_d \geq c_1 R^{4/5}$ kept by the stop of Lemma 1.15.6;
- on the power segment, $T_\theta \geq (1-h)C_b/(4L\frac{\hat{\xi}^2}{2})$;
- on J, by the full identity (1.13.58) with its favorable primitive-gap term, $T_\theta \geq \frac{c}{2}\epsilon_o C_b/R_b$. Its adverse terms are $O(C_b/R_b^2)$ against the $c\epsilon_o C_b/R_b$ source reserve.

These are positive and continuous on the compact preterminal path, so they have a positive minimum m_c for each admitted member. The late reserve shrinks like $R_b^{-1/5}$ in units of H. Its axial companion is the exact cancellation (1.15.20), equivalently (1.13.29). It is not a uniform positive lower bound continued to the stop. After J, the scalar shot, physical lift and wing obey (1.13.49) and (1.13.54), so $T_\theta \geq T_{\theta,L} + c_{\mathrm{wg}} Z_o \geq 0$. The stress vanishes exactly where both controls vanish, and there $T_z = 0$. This proves the terminal claim where the scalar source is zero.

Strict cone. By Proposition 1.15.22(iii), wherever $T_\theta > 0$ we have $2 < a_s \leq 2 + C_h'$ and $|T_z| \leq K_{\mathrm{tot}}(\sup E_c)T_\theta$. The tail estimates (1.13.62) and (1.13.61) include all quadratic swirl edits. The complete terminal axial calculation (1.13.66) includes the square of the wing deficit and the moving-edge and angular-cutoff derivatives. Then (1.13.67) bounds the terminal axial stress by the same positive factor Z_o. By Proposition 1.15.22(iv), $\sup E_c \leq B_c E_{A,\max} e^{-(\lambda-h)L_o} \leq \varepsilon_c$ under the fifth entry of (1.6.27). This gives the strict pure-swirl cone on the whole nonzero source set, including the compact memory segment.

We select all fixed normalized constants in these central estimates (C_I, K_{hold}, K_{tot}, C_h', B_c, ε_c) before L_o and Y_0. The scalar pressure and energy are always the canonical outward integrals of this same actual component. □

Lemma 1.17.8 (The canonical cross terms of the actual angular mixture)**.** *We use the central component of Lemma 1.17.7, with its axial bound with the same factor at its own terminal face. Then the actual angular mixture has the same strict cone and the connected source factors previously supplied. We do not assume linearity of the canonical quadratic histories.*

Proof. On the pure-swirl future put $H_\chi = (1-\chi)H_c + \chi H_w$. For the actual outward histories the exact cross-term identities are

$$\begin{aligned} S_\chi &= (1-\chi)S_c + \chi S_w - \chi(1-\chi)D_S, \\ P_\chi &= (1-\chi)P_c + \chi P_w + \chi(1-\chi)D_P, \\ D_S &= \frac{1}{4}\int_{(\frac{\hat{\xi}^2}{2})}^{\infty}(H_w - H_c)^2\frac{ds}{s}, \qquad D_P = \frac{1}{4}\int_{(\frac{\hat{\xi}^2}{2})}^{\infty}(H_w - H_c)^2\frac{ds}{s^2}. \end{aligned}$$

These include the complete future. They hold because the component and mixed pressures use the same canonical outward normalization. On the compact corridor, the actual integral estimates (1.13.61) and Proposition 1.15.20, together with the exposed same heat tail, give the uniform bound

$$D_S + \tfrac{\hat{\xi}^2}{2}D_P + |\dot{D}_S| + \tfrac{\hat{\xi}^2}{2}|\dot{D}_P| + |S_w - S_c| + \tfrac{\hat{\xi}^2}{2}|P_w - P_c| \leq K H_w(\tfrac{\hat{\xi}^2}{2})^2.$$

We fix the constant K before Y_0 and the last radius. After normalization at R_o, the two components' weighted square and first-jet integrals have these uniform bounds.

The positive outer field on this fixed compact corridor has a uniform lower bound in the same inlet units. This also covers the actual small memory and compact heat corrections. Differentiation introduces $\dot{\chi}(1-2\chi)D_{S,P}$ and $\chi(1-\chi)\dot{D}_{S,P}$. The exact angular source controls χH_w by its outer

component reserve and controls $\dot\chi H_w$ by its primitive gap. These axial terms include $\dot\chi(S_w - S_c)$ and $\dot\chi(P_w - P_c)$.

After division by the actual positive angular stress, a fixed constant times the same postpulse amplitude bounds them. The central component terms use its source estimate and axial factor from Lemma 1.17.7. An increase in the same Y_0 makes this ratio as small as necessary. The radial logarithmic slope of H_χ is the convex combination of the component slopes with weights $(1-\chi)H_c/H_\chi$ and $\chi H_w/H_\chi$. Thus its a_s lies in a fixed positive bounded interval.

The finite radius controls the compact finite-p_1 threshold.

There is a direct factor proof at the outer terminal face, where $I_c = I_0$. The mixture is $I_\chi = I_0 + \chi E_w$ and $H_\chi = H_0 - \chi V$, so

$$T_{\theta,\chi} \ge c[\chi v_s + \dot\chi v_g].$$

Its canonical differences use the exact density $W_\chi = 2\chi H_0 V - \chi^2 V^2$. The terminal calculation applies again. Thus the $\dot\chi$ terms contain $\int_{(\frac{\hat\xi^2}{2})}^{B} H_0 V/s$ or $\int_{(\frac{\hat\xi^2}{2})}^{B} H_0 V/s^2$ and have a bound by $CH_0\dot\chi E_w/\frac{\hat\xi^2}{2}$. The remaining terms have χv_s.

Thus

$$|T_{z,\chi}| \le C(H_0/(\hat\xi/\sqrt{2}))[\chi v_s + \dot\chi v_g].$$

This proves the finite cone up to each flat angular and radial face by the same amplitude choice, with places where the two factors vanish. At their simultaneous zero the field is the exact same heat field. We do not assert a relative bound on a quotient $0/0$. □

Lemma 1.17.9 (Actual inlet germ correction on a fixed short overlap)**.** *We can join the power pulse and the primitive mixture with their actual I, H and all radial and angular jets. We fix the join width before Y_0 with uniform admitted-family bounds. It does not change the component heat pair or any endpoint collar. The pulse's actual future data keep its complete canonical energy and pressure integrals.*

Proof. We write $t = \log(\frac{\hat\xi^2}{2}/R_o(\eta))$.

On a fixed open component power germ set $I_\chi = (1-\chi)I_c + \chi I_w$, $I_o = I_\chi(R_o)$ and $H_o = (\hat\xi^{-1}\partial_{\hat\xi}(I_\chi))(\sqrt{2(R_o)})$. The actual inverse for ν has previously matched I_o to the pulse trace. We define its exact continuation

$$I_{\mathrm{pow}}(t) = I_o + \frac{R_o H_o}{1-\nu}(e^{(1-\nu)t} - 1), \qquad J = I_{\mathrm{pow}} - I_\chi.$$

Then $J(0) = J_t(0) = 0$ as identities in the angular parameter. The component power formula gives

$$\frac{J_{tt}(0)}{R_o H_o} = \bar\nu - \nu, \quad \bar\nu = \frac{(1-\chi)H_c\nu_c + \chi H_w\lambda}{H_o}.$$

On a fixed short germ, the actual parameter inverse has one bound for each finite jet for all sufficiently large Y_0. Its explicit exponentially small remainder and positive F_ν give these bounds. Thus Ct^2, Ct^2, Ct bound $J/(R_oH_o)$, its partial angular jet at fixed t, and its first t derivative in that order. Its second t derivative is bounded. We fix the constants after h, ν_c, L_o and the angular cutoff, before Y_0.

Only these angular constants can depend on the later angular cutoff. For the radial slope we retain the vanishing mixture factor. Put

$$\Delta = \lambda - \nu_c, \quad W_g = \Delta^2\omega(1-\omega), \quad \bar\nu = \omega\nu_c + (1-\omega)\lambda, \quad j(t) = \frac{J(t)}{R_oH_o}, \qquad \omega = \frac{(1-\chi)H_c(R_o)}{H_o}.$$

Here ω is fixed under t differentiation. The exact formula is

$$j_t = e^{(1-\nu)t} - \omega e^{(1-\nu_c)t} - (1-\omega)e^{(1-\lambda)t}.$$

By (1.15.31), $|\nu - \bar{\nu}| \le 5W_g$. For $0 \le t \le 1$ and $0 \le z \le 1/20$, the function $g_t(z) = (1-z)e^{(1-z)t}$ satisfies $|g_t'| \le 2e$ and $|g_t''| \le 3e$. The mean value theorem between ν and $\bar{\nu}$ and the interpolation remainder between ν_c and λ give $|j_{tt}| \le (10e+3e/2)W_g \le 12eW_g$. Since $j(0) = j_t(0) = 0$, integration gives

$$|j_{tt}| \le 12eW_g, \qquad |j_t| \le 12eW_g t, \qquad |j| \le 6eW_g t^2. \tag{1.17.5}$$

These constants are independent of all later parameters and of $\nu_c > 0$. Fixed-$\frac{\hat{\xi}^2}{2}$ differentiation keeps $\dot{t} = -\log R_o$.

With the shape ζ_g already selected with the early radial templates, choose $0 < \epsilon_g \le 1$ below and set

$$I_{\text{new}} = I_\chi + \zeta_g(t/\epsilon_g)J.$$

It equals I_{pow} on an open inlet germ and the exact mixture past $t = \epsilon_g$. Because J and J_t vanish at zero, product differentiation gives the uniform bounds

$$|\delta H| \le C_{\text{germ}} W_g \epsilon_g H_o, \quad \tfrac{\hat{\xi}^2}{2}|\delta \frac{H_{\hat{\xi}}}{\hat{\xi}}| \le C_{\text{germ}} W_g H_o, \quad |\dot{\delta I}| \le C\epsilon_g R_o H_o, \quad |\mathcal{A}\delta I| \le C(\epsilon_g + R_o^{-1})H_o.$$

For the radial bounds, put $k_g(t) = \zeta_g(t/\epsilon_g)j(t)$. Then exactly

$$\delta H = H_o e^{-t}(k_g)_t, \qquad \tfrac{\hat{\xi}^2}{2}\delta \frac{H_{\hat{\xi}}}{\hat{\xi}} = H_o e^{-t}((k_g)_{tt} - (k_g)_t).$$

On $0 \le t \le \epsilon_g \le 1$, the product rule gives

$$|(k_g)_t| \le 12eW_g\epsilon_g(1 + Z_{g,1}/2), \qquad |(k_g)_{tt}| \le 12eW_g(1 + 2Z_{g,1} + Z_{g,2}/2),$$

which proves the displayed radial bounds by the definition of C_{germ}. There is no $1/\epsilon_g$ loss in the source estimate. The two powers of t in J compensate for the two differentiated cutoff factors. The moving t term keeps one power of t after one differentiation.

The unedited mixture has a uniform positive inlet source floor from its two actual component power sources and the nonnegative primitive-gap term. In fact on this germ the exact formulas are

$$I_i = \frac{\frac{\hat{\xi}^2}{2}H_i}{1-\nu_i} + \kappa_i(\eta), \qquad Q_i = \frac{q_i}{1-\nu_i} + \frac{\dot{\kappa}_i - (1-h)\kappa_i}{\frac{\hat{\xi}^2}{2}H_i}, \quad q_c = h - \nu_c, \quad q_w \ge q_* > 0.$$

The actual prefix and wait estimates give one small bound for that remainder on the admitted $Y_0 \ge Y_{\min}$ domain. These identities use $M = J = 0$ after the actual return solve and do not involve its response or cone. Thus this floor is available before we apply the pulse response lemma.

In addition, the actual matching of I_o, H_o matches their fixed-$\hat{\xi}$ angular primitive jet, consistently with the independently proved last-return denominator. The normalized family has bounded source derivatives on this germ. First, we select ϵ_g smaller than its fixed power-buffer width and than a fixed fraction of this source floor divided by C. This choice precedes Y_0 and the last radius. Then the physical radius controls the R_o^{-1} term.

We now verify strict shear with the weighted radial error. On this germ,

$$H_\chi = H_o[\omega e^{-\nu_c t} + (1-\omega)e^{-\lambda t}], \qquad -\tfrac{\hat{\xi}^2}{2}\frac{H_{\chi,\hat{\xi}}}{\hat{\xi}} = H_o[\omega\nu_c e^{-\nu_c t} + (1-\omega)\lambda e^{-\lambda t}].$$

Thus $e^{-1}H_o \le H_\chi \le H_o$ and $-\frac{\hat\xi^2}{2}\frac{H_{\chi,\hat\xi}}{\hat\xi} \ge e^{-1}H_o\bar\nu$ on $0 \le t \le \epsilon_g \le 1$. Since

$$W_g \le \lambda^2\omega(1-\omega) \le \lambda\bar\nu, \qquad W_g \le \lambda^2,$$

the early condition ($\lambda 9$) implies

$$\frac{H_o}{2e} \le H_{\mathrm{new}} \le 2H_o, \qquad -\frac{\hat\xi^2}{2}\frac{H_{\mathrm{new},\hat\xi}}{\hat\xi} \ge \frac{H_o\bar\nu}{2e}.$$

Consequently this pure-swirl connector satisfies

$$b_s = 0, \qquad v_s - 2 = a_s - 2 = -\frac{\hat\xi^2\frac{H_{\mathrm{new},\hat\xi}}{\hat\xi}}{H_{\mathrm{new}}} \ge \frac{\bar\nu}{2e} \ge \frac{\nu_c}{2e} > 0.$$

The same formulas give a fixed upper bound for a_s. Its canonical S, P and jets have fixed finite normalized bounds. The proved positive source floor and the same postpulse amplitude smallness therefore give the pure-swirl directional cone. Neither a decrease in ϵ_g alone nor amplitude smallness is used to establish strict shear.

The correction has zero total primitive increment and compact radial support. Its energy and pressure changes are the exact integrals of $2H_\chi\delta H + (\delta H)^2$, with their appropriate radial weights. We include these in the definition of the actual future before the pulse root. We do not set them to zero. On a flat angular collar $\chi = 0$ or 1, ν equals the related component exponent.

Its component is an exact power on this germ. Thus $J = 0$ identically. The full germ edit and all its parameter jets then vanish there, which keeps the exact endpoint identification unchanged. □

Native factors and assembly with the actual pulse estimate. For the explicit squared-flat cutoff all fixed jets of V and $E_w/\frac{\hat\xi^2}{2}$ have a bound by the same factor times a finite power of $1 + |\log\Psi|$. Near B, Ψ is a positive smooth multiple of $e^{-c/(1-\frac{\hat\xi^2}{2}/B)^2}$. Its derivatives cost inverse powers of $1 - \frac{\hat\xi^2}{2}/B$. Integration once gives $E_w/\frac{\hat\xi^2}{2}$ comparable to $V(1-\frac{\hat\xi^2}{2}/B)^3$ with fixed positive constants. These statements are a result of one integration by parts, with the remainder absorbed on a short terminal collar.

On its complement the factors are positive smooth functions on a compact interval. Thus v_s and v_g have the necessary logarithmic jet bounds. They have these bounds for each function. We never use the false inequality $V \le CE_w/\frac{\hat\xi^2}{2}$.

The native mixture now uses the actual positive gap from Lemma 1.17.3, the outer source from Lemma 1.17.4, and the exact terminal formulas. The angular identity (1.17.2) gives its nonnegative favorable term $\dot\chi(I_w - I_c)/(L\hat\xi^2)$. The actual central memory, hold, drive and shot estimate is Lemma 1.17.7. We treat the nonlinear canonical mixture in Lemma 1.17.8, and its real inlet power matching in Lemma 1.17.9. We first establish actual pulse admission and its prefix estimate.

The two tube estimates, compact positive corridors, and terminal factors then give a connected path from the protected correction interval to each source edge. The decreasing channel splices and weighted primitive argument in the proof of Lemma 1.24.3 then apply to these actual paths. We do not extend a path across a zero-stress heat interval.

1.18 Uniform finite-order pressure bounds

Main result. Proposition 1.18.4 bounds the complete pressure through two angular derivatives after we fix the wait parameter. The bound is uniform in the next scale. It does not assert uniformity in all wait parameters.

This section proves finite-order integral bounds. It does not assert uniform pointwise second-angular derivatives of the narrow central wing. All derivatives in this section are ordinary angular derivatives. We estimate the normalized future before Y_0. For the complete prefix pressure, we then fix Y_0 and the bound is uniform in the next large scale. These are different quantifiers.

Lemma 1.18.1 (The integrated second derivative of the central wing)**.** *In the actual scalar power-segment coordinate $x = \frac{\hat{\xi}^2}{2}/R_b$, we put $\varepsilon = R_b^{-1/5}$, $\beta(\eta) = B_o(\eta)/R_b$, and $\phi(y) = e^{-1/y^2}$ for $y > 0$, zero for nonpositive arguments. The normalized central wing velocity is, with $\mathcal{F}(y) = \int_0^y \phi(s)\,\mathrm{d}s$,*

$$v(x,\eta) = a_o \varepsilon \psi_o(\eta)\phi((\beta(\eta) - x)/\varepsilon), \qquad a_o = \epsilon_o h.$$

Here R_b, ε are scalar in η, and the fixed functions β, ψ_o have bounded derivatives through order two. On the fixed normalized interaction hull $1 \le x \le M$,

$$\|v\|_\infty + \|v_\eta\|_{L^1_x} \le C\varepsilon, \quad \|v_\eta\|_\infty \le C, \quad \|v_\eta\|^2_{L^2_x} \le C\varepsilon, \quad \|v_{\eta\eta}\|_{L^1_x} \le C.$$

The constants are independent of the sufficiently large power-segment scale.

The same bounds hold with the fixed weights x^{-1}, x^{-2}.

Proof. The substitution $y = (\beta - x)/\varepsilon$ gives

$$v_\eta = a_o \varepsilon \psi_o' \phi + a_o \psi_o \beta' \phi',$$

$$v_{\eta\eta} = a_o \varepsilon \psi_o'' \phi + a_o(2\psi_o'\beta' + \psi_o\beta'')\phi' + a_o\psi_o(\beta')^2\varepsilon^{-1}\phi''.$$

The actual functions satisfy

$$\int_0^\infty |\phi'|\,\mathrm{d}y = 1, \qquad \int_0^\infty (|\phi''| + |\phi'|^2)\,\mathrm{d}y < \infty, \qquad \|\phi'\|_\infty < \infty.$$

Indeed $\phi' = 2y^{-3}e^{-1/y^2}$ and $\phi'' = (4y^{-6} - 6y^{-4})e^{-1/y^2}$ on $y > 0$. A change of variables gives the claims.

The largest second derivative has height $O(\varepsilon^{-1})$ but width $O(\varepsilon)$. We bound its integral, but we do not declare $O(\varepsilon)$. The flat extension at $y = 0$ produces no moving-boundary jump. □

Lemma 1.18.2 (Second derivatives of the actual scalar shot and lift)**.** *We fix the shot fraction $\epsilon_s > 0$ and the scalar templates. For $R = R_b$, $y = g - H_b$, $z = i - I_b$, and $\epsilon_b = C_b/(G_b R)$, the actual shot has*

$$|y^{(j)}| \le CC_b/R^{j+1} \quad (0 \le j \le 2), \qquad |z| \le CC_b.$$

We use $\xi = \frac{\hat{\xi}^2}{2}/R$ with normalized field error $Y = y/G_b$ and primitive error $Z = z/(G_bR)$. They and their necessary mixed ξ and logarithmic scale derivatives through total order two have a uniform bound by $C\epsilon_b$. On fixed finite hulls, the actual lift and its heat continuation have one bound for all normalized angular derivatives through order two.

They have integrable quadratic tail majorants.

Proof. Subtract the exact reference power and its primitive from the shot system. With $a = 1 - h$ the difference satisfies

$$y' + Ay = Bz + q, \quad z' = y, \qquad A = \tfrac{1}{2} - \left(\tfrac{\hat{\xi}^2}{2}\right)^{-1}, \quad B = a/(\hat{\xi}^2), \quad q = \tau_s - \tau_b.$$

The source templates equal the power-segment source on an open inlet germ. Thus q and the solution differences vanish on that germ.

Its fixed fractional width and exact coefficient quotient give $|q^{(j)}| \le CC_b/R^{j+1}$ for $j \le 2$. For the scale derivatives, divide the numerator and denominator of the shot quotient by C_bR^{h-1} and integrate on the fixed source coordinate. The denominator has a positive lower bound. Differentiated regular heat asymptotics and the smooth stop maps in $R^{-1/5}$ bound each necessary normalized derivative. We do not differentiate the unexposed fast coefficient.

The stated stable estimates give $|y| \le CC_b/R$, $|z| \le CC_b$ and $|y'| \le CC_b/R^2$. We put $p = y'$ and $r = y''$. Exact differentiation gives

$$p' + Ap = (B - A')y + B'z + q',$$

$$r' + Ar = (B - 2A')p + (2B' - A'')y + B''z + q''.$$

The last right-hand side is $O(C_b/R^3)$ and r has zero inlet value. Because $A \ge 1/3$, its stable kernel proves the second-derivative bound without an initial boundary layer.

In the normalized coordinate set $Q = q/G_b$ and $T = R\partial_R$. The equations and their exact scale derivative are

$$Y_\xi + (R/2 - 1/\xi)Y - aRZ/(2\xi) = RQ, \quad Z_\xi = Y,$$

$$(TY)_\xi + (R/2 - 1/\xi)TY - aR(TZ)/(2\xi) = RTQ + Y_\xi - Y/\xi, \quad (TZ)_\xi = TY.$$

The kernel has integral $O(R^{-1})$. We absorb the Z coupling on the fixed sufficiently short fraction ϵ_s. Differentiation of this same system gives the mixed and second scale bounds.

Equivalently each scale derivative under the kernel adds a polynomial in $R(\xi - s)$ with the same integrable exponential. This adds no positive power of R to these normalized estimates.

For $H_L = d^{-h}g(\frac{\hat\xi^2}{2}/d)$, the non-heat part forces $d \ge R/b_s = (1 + \epsilon_s)^{-1}$. Two angular derivatives then use only g, $\frac{\hat\xi^2}{2}g'$, $\frac{\hat\xi^4}{4}g''$, which have just been bounded. On the source-free part use the regular expansion through at least two angular orders with its differentiated remainder and the actual exposed fast mode. Its exponential and the fixed source-free buffer absorb each inverse power of d from this fast mode. The two descriptions match on an open germ.

On the tail the new products $H_{L,\eta}^2$ and $H_LH_{L,\eta\eta}$ have the same integrable x^{-1} and x^{-2} weighted majorants as the normalized heat field. □

Proposition 1.18.3 (Actual normalized future has a uniform C^2 integral bound)**.** *We fix the normalized leading templates, h, ν_c, L_o, the angular mixture cutoff and the fixed-width inlet-germ connector. On the actual matched-memory family for all $Y_0 \ge Y_{\min}$ and all sufficiently large independent normalized scales, we define*

$$\tau_S(\eta) = \frac{1}{H_o(\eta)^2}\int_{\sqrt{2R_o(\eta)}}^{\infty} \frac{H(\frac{\hat\xi^2}{2},\eta)^2}{4\frac{\hat\xi^2}{2}}\,\hat\xi\,\mathrm{d}\hat\xi, \qquad \tau_P(\eta) = \frac{R_o(\eta)}{H_o(\eta)^2}\int_{\sqrt{2R_o(\eta)}}^{\infty} \frac{H(\frac{\hat\xi^2}{2},\eta)^2}{4\frac{\hat\xi^4}{4}}\,\hat\xi\,\mathrm{d}\hat\xi.$$

Then $\|\tau_S\|_{C^2} + \|\tau_P\|_{C^2} \le K_2$ with a finite K_2 fixed before Y_0. It can depend on the previously fixed parameters and connector width. It is not uniform when $h \downarrow 0$.

Proof. The true memories and their first two angular derivatives have a bound by $K(1+Y_0)^N e^{-(1-\lambda)Y_0}$ on the independent inverse-scale domain. The explicit exponent inverse has one bound for its mixed jets. Its exponentially small remainder has this same bound, and its ν derivative stays positive. Two implicit differentiations thus give one bound for $\nu, \nu_\eta, \nu_{\eta\eta}$ for all $Y_0 \ge Y_{\min}$. No future energy or pressure bound is an input to this inverse. The trace ratios $H_i(R_o)/H_o$ and the logarithmic derivatives of R_o, H_o through order two have fixed bounds.

In particular the scalar same coefficient has no angular derivative.

The central pre-lift hold, deficit drive and narrow stop are scalar at fixed physical $\frac{\hat{\xi}^2}{2}$ after the real memory return. Their moving stop width thus creates no angular derivative there. The memory edit $p(\eta)\zeta(\frac{\hat{\xi}^2}{2}/R_m)$ has fixed scalar support and the previous uniform C^2 small datum. Its field and quadratic integrals have uniform bounds. The previous proof gives one bound for the normalized value and scale maps of the scalar stop and shot.

The necessary second-radial bound for the fixed-fraction shot, and thus for its angular lift, is Lemma 1.18.2. The non-heat lift has $d = 1 - \eta^2$ bounded away from zero. Its normalized first and second angular derivatives are bounded on that fixed hull.

On the regular heat region all fixed differentiated asymptotic expansions are uniform, and the actual fast exposure is exponentially small after its fixed source-free buffer. Thus the normalized heat field and its first two angular derivatives have integrable quadratic majorants on the tail. This is a direct heat estimate at the selected scale, not a bound on an unexposed fast coefficient.

For the central wing, Lemma 1.18.1 is the necessary replacement for pointwise C^2 compactness. If f_L is the bounded normalized lift and $f = f_L - v$, then

$$\partial_\eta^2(f^2) = 2f_\eta^2 + 2ff_{\eta\eta}.$$

That lemma and $\|f\|_\infty$ control the $v_{\eta\eta}$ term in L^1. The v_η^2 term uses its L^2 bound. All cross terms obey the same bounds.

The radial primitive bridge is on a fixed fractional power interval. Its cutoff is scalar and its field is $(1-\chi_b)H_b + \chi_b H_T + \chi_b'\Delta$. Because $\Delta = I_T - I_b$, the integrals just estimated and the lifted primitive formula control its two angular derivatives. More explicitly its wing primitive divided by G_bR_b is $a_o\varepsilon^2\psi_o\mathcal{F}(y)$, and its second angular derivative is

$$a_o[\varepsilon^2\psi_o''\mathcal{F} + \varepsilon(2\psi_o'\beta' + \psi_o\beta'')\phi + \psi_o(\beta')^2\phi'].$$

It has one bound on the full hull, because $\mathcal{F}(y) \le y$ and $y \le C/\varepsilon$ there.

After division by the power-segment radius, the added field has uniform integrated second-angular bounds. The bridge stays in a fixed normalized hull. We do not discard a second derivative of its shrinking zero face.

All outer model pieces have fixed normalized shapes once L_o is chosen. Write their two moment equations as $M(t,\eta) = u(\eta)$. The partial inlet integrals include the explicit memory return of (Inlet). Its two angular derivatives are bounded on the fixed bump supports. The matched outlet and the power model have bounded normalized C^2 data. With $D = M_t$ at the small root,

$$t' = D^{-1}(u' - M_\eta), \qquad t'' = D^{-1}\{u'' - M_{\eta\eta} - 2M_{\eta t}t' - M_{tt}[t',t']\}.$$

The normalized bump shapes and the fixed inverse bound control every factor. This also bounds partial energy integrals inside either bump by twice differentiating on its fixed normalized interval. Higher-order equality of endpoint jets is established separately in the paragraph on p. 306.

The actual heat discrepancy and its two angular derivatives satisfy $Cc(\frac{\hat{\xi}^2}{2})^{-h-1}$. Differentiation of its full primitive integral twice is legitimate. The two moving lower-boundary terms vanish because the splice difference is zero on an open inlet germ. Thus $\|D_I\|_{C^2} \le CcR_0^{-h}$ in the fixed geometric units. This gives the actual rank-one bump and collar as $O(R_o^{-1})$ with their two normalized angular derivatives.

The complete quadratic energy and pressure increments are $O(R_o^{-1})$ in units H_A^2 and H_A^2/R_A, respectively, through the same two angular derivatives. The fixed terminal cutoff has bounded normalized derivatives. The previous majorants control the actual heat tail.

For the full angular mixture, differentiate $H_\chi = (1-\chi)H_c + \chi H_w$ twice. Its new terms are $2\chi'(H_{w,\eta} - H_{c,\eta}) + \chi''(H_w - H_c)$, in addition to the weighted component second derivatives. The finite cutoff derivatives and the previous L^∞, L^2 and L^1 bounds control each term in $\partial_\eta^2(H_\chi^2)$, with the cross products. The inlet-germ connector uses $\delta I = \zeta_g(t/\epsilon_g)J$, $t = \log(\frac{\hat\xi^2}{2}/R_o)$, $J = I_{\mathrm{pow}} - I_\chi$, $J(0) = J_t(0) = 0$. Its fixed-t jets through two angular derivatives and three t derivatives have a uniform bound by the explicit power formulas.

We fixed $\epsilon_g > 0$ before Y_0. The product rule with $t_\eta = -(\log R_o)_\eta$ gives a finite uniform bound for the complete quadratic integrals through two angular derivatives. The bound can depend on ϵ_g^{-1}. We do not use it to reselect that width.

Last, we apply the moving-lower-limit formula before rescaling. For $F = H^2/(4\frac{\hat\xi^4}{4})$,

$$\partial_\eta^2 \int_{\sqrt{2R_o}}^\infty F\,\hat\xi\,\mathrm{d}\hat\xi = \int_{\sqrt{2R_o}}^\infty F_{\eta\eta}\,\hat\xi\,\mathrm{d}\hat\xi - (\frac{F_{\hat\xi}}{\hat\xi})(\sqrt{2(R_o)})(R_o')^2 - 2F_\eta(R_o)R_o' - F(R_o)R_o''.$$

All boundary fields lie on the exact smooth inlet power germ, where $\frac{H_{\hat\xi}}{\hat\xi} = O(H_o/R_o)$ and $H_\eta = O(H_o)$. Each term has size $O(H_o^2/R_o)$, with two angular derivatives of the prefactor R_o/H_o^2. Replacement of $(\frac{\hat\xi^2}{2})^{-2}$ by $(\frac{\hat\xi^2}{2})^{-1}$ proves the energy bound.

We first compute the scalar drive integral in physical $\frac{\hat\xi^2}{2}$. We do not assume a uniform pointwise second derivative for the narrow moving stop in a moving normalized coordinate. This proves the claimed normalized C^2 bounds on the actual family. □

Proposition 1.18.4 (Complete ideal pressure before the last scale)**.** *We fix $Y_0 \ge Y_{\min}$ after the previous future and source choices. There exist $R_*(Y_0)$ and $K_P(Y_0) < \infty$ with the next property. The complete actual ideal pressure $\Pi_{\mathrm{ref}} = -\int_0^\infty H^2/(4\frac{\hat\xi^4}{4})\,\hat\xi\,\mathrm{d}\hat\xi$ includes the actual early heat correction and the partial fixed-λ extension. It satisfies*

$$\sup_{R_{\mathrm{master}} \ge R_*(Y_0)} \|\Pi_{\mathrm{ref}}\|_{C^2([-1,1])} \le K_P(Y_0).$$

We fix the two constants before the next core and last scale choices.

The conclusion has one bound for all admitted scales. Smoothness of each individual member alone does not give this bound. We do not assert uniformity in all Y_0 for the complete prefix pressure.

Proof. Before the future inlet, we use the explicit pretemplate and power coordinates. For this fixed Y_0 their log-lengths, parameter ranges, positive normalized radii and all cutoff widths range in fixed compact sets independent of the next scale. The uniform exponent inverse and the coefficient-map bounds give the same property for the actual inlet amplitudes and their first two angular derivatives.

The growing prefix has pressure density $O((\frac{\hat\xi^2}{2})^{-4/5})$ after its same radial normalization. Its angular derivatives have the same integrable power. On each remaining fixed piece, differentiation of the actual quadratic density and its moving endpoints gives a scale-independent finite bound. On power intervals, the integrals are explicit. We include the long fixed pulse and do not replace it by its endpoint value. Axial amplitudes and returns do not enter the pressure functional $\int H^2/(4\frac{\hat\xi^4}{4})$.

We fix the pulse swirl first as $H = H_o e^{\nu(Y-y)}$. The next energy root changes U/E, not H. Thus this argument uses no second-angular estimate for an axial root whose proof depends on these same future integral contributions.

We include the actual two-row primitive taper as well. Its target comes from the explicit finite-prefix primitives. Lemma 1.14.4 gives its normalized C^k solution and partial histories for each selected finite k. We take $k = 2$. Its complete ΔC_p is zero, with its quadratic contribution.

We can remove only that complete pressure integral from the sum. The local fields and the next energy equation include its nonzero partial pressures and energy integral.

The actual heat correction supplies C^2 targets $(0, -\chi_b \Delta S_f, -\chi_b \Delta C_{p,f})$ in the early moment correction's own units of size $K(Y_0)/R_{\mathrm{master}}$. The three distinct power rows have an invertible normalized value matrix independent of the large scale, and the full nonlinear map is quadratic. For large enough R_{master} its Jacobian has a fixed bounded inverse. We differentiate this same equation once and twice. That inverse multiplies the highest coefficient derivative.

Each other term is a product of bounded template derivatives and lower target or solution derivatives. Thus the actual moment-correction coefficients and their first two derivatives are $O(K(Y_0)/R_{\mathrm{master}})$. Integration keeps their cross and square terms with the same bound. We apply partial angular history restoration to the nonlinear target, so we include its cutoff derivatives. This does not use a fictitious reset of σ_p or the pressure constant.

The actual future contribution has the stronger scale-uniform bound of Proposition 1.18.3, multiplied by H_o^2/R_o and its bounded trace derivatives. This estimate includes the central primitive-memory correction and inlet-germ connector. Addition of the prefix, actual early moment correction and complete future proves the result. This is a fixed-Y_0 uniform bound. This argument does not prove C^2 convergence. The central constant germ comes from Proposition 1.6.33 and Lemma 1.6.35, not from a convergence in the scale. □

For the pressure-class correction, the same fixed-Y_0 coefficient bounds give a positive uniform lower bound for its local velocity scale e_*. Its reference power and finite-template factors are positive. Also, ν lies in $[\nu_c, \lambda]$, and K_{old} has positive upper and lower bounds. This lower bound can depend on Y_0. We can thus select the single C^1 approximation tolerance relative to e_*^2 and the actual central pressure interval before the last scale.

The C^2 bound supplies the uniform smoothing scale. With Proposition 1.6.33, it also supplies the central constant germ on a strip of width fixed by ε_p/K_P (Lemma 1.6.35). These are distinct uses. These two uses do not assume C^2 smallness of the central oscillation.

1.19 Strict shear with the specified histories

Main result. Proposition 1.19.6 gives strict shear where the stress is nonzero and keeps the specified histories unchanged. Its inputs are the relaxed cone and strict boundary collars in Lemma 1.19.2. It does not assume the later slow completion or packet atlas.

We fix the joint leading fields and their five actual histories from the axis, with the calibrated physical heat exterior. At this stage the inputs are the relaxed cone and strict boundary collars stated in (H0)–(H2) in this section. We use the scalar tools of Section 1.13 only for their specified component conclusions. The strict shear and exact returned histories are the leading data required for completion.

Strictification leaves the exterior and the protected curved domain unchanged. The resulting stress margin is available when the slow and packet corrections are made.

Throughout this section we fix all leading parameters, with $\mathcal{R}, \varphi, \mu$. Constants can depend on their actual values and smooth seminorms. We write

$$\mathfrak{r} = \hat{\xi}, \qquad E = H/\mathfrak{r} = \mathfrak{r}F.$$

The temporary radius $\mathfrak{r}$ is a profile variable. The physical radius stays $r = \sqrt{q}\,\mathfrak{r}$.

The pressure used to choose the loop. Write $X = \hat{\xi}^2/2$ and

$$C[H](X,\eta) = \int_0^X \frac{H(s,\eta)^2}{4s^2}\,\mathrm{d}s, \qquad b_{\mathrm{heat}}(\eta) = \chi_b(\eta)\Delta C_{p,f}(\eta).$$

Let $(H^{\mathrm{pre}}, U^{\mathrm{pre}})$ denote the actual field just before the shear loop. It contains the downstream heat splice and its rank-one primitive correction, the three-swirl heat compensation of (1.14.16), the pressure-class correction and the regular core with its five-row correction. The pulse uses its selected positive root. The heat target is determined by the downstream swirl and its rank-one correction, independently of the axial amplitude and of the loop frequency. The pressure-class correction sets the axis value p_0 using this complete reference (Proposition 1.18.4 and Lemma 1.6.37). The core correction returns its full pressure moment. Hence

$$p_0 = -C[H^{\mathrm{pre}}](\infty), \qquad P^{\mathrm{pre}} = p_0 + C[H^{\mathrm{pre}}].$$

Suppress only the three-swirl heat compensation, holding all other selections fixed, to obtain (H°, U°). This smooth comparison carries the *prescribed* pressure $P^\circ = p_0 + C[H^\circ]$. Its pressure normalized separately at infinity is $P^{\circ,\infty}(X) = C[H^\circ](X) - C[H^\circ](\infty)$. Put $D_C(X) = C[H^{\mathrm{pre}}](X) - C[H^\circ](X)$. The exact third row of (1.14.16), including its quadratic term, gives

$$D_C(\infty) = -b_{\mathrm{heat}}, \qquad P^\circ = P^{\circ,\infty} + b_{\mathrm{heat}}, \qquad P^{\mathrm{pre}} = P^\circ + D_C(X). \tag{1.19.1}$$

Below the heat bank $D_C = 0$. Above it $D_C = -b_{\mathrm{heat}}$. Inside it D_C is the partial integral of the difference of the two densities. The signs follow by integrating from the axis and hold with all smooth angular derivatives. In particular the prescribed pressure agrees identically with the physical pressure through the loop and its five returns. An angular derivative of b_{heat} can survive at the matching slice. The radial order is the loop, its five returns in $(-25,-20)$, the heat bank in $(-20,-15)$, and finally the two-row taper and the pulse. Fixing the heat target first is consistent with this radial order. The loop and its returns have zero combined change in every complete row, including C_p, by Lemma 1.13.7. They therefore preserve the selected axis normalization and the inlet data used for every subsequent operation.

1.19.1 Strictifying the shear while keeping the actual histories

We write the derivative-free terms in (1.9.2)–(1.9.3):

$$\begin{aligned} N_\theta &= \frac{(\frac{\hat{\xi}^2}{2} + \mathcal{K})H - (1-h)\mathfrak{M}_2 + (\frac{1}{2}-h)\hat{\zeta}\mathfrak{M}_{2\hat{\zeta}} - d\mathfrak{M}_{3\hat{\zeta}} + 2(h-(\frac{1}{2}-h))\hat{\zeta}\mathfrak{M}_3}{L\hat{\xi}^2}, \\ N_z &= \frac{(\frac{\hat{\xi}^2}{2} + \mathcal{K})U - (\frac{1}{2}-h)(\mathfrak{M}_1 - \hat{\zeta}\mathfrak{M}_{1\hat{\zeta}}) + 4h\hat{\zeta}\mathfrak{M}_4 - d\mathfrak{M}_{4\hat{\zeta}} + \frac{\hat{\xi}^2}{2}((2+4h)\hat{\zeta}P - dP_{\hat{\zeta}})}{L\hat{\xi}}. \end{aligned} \tag{1.19.2}$$

We set $\mathbf{p} = (N_\theta, N_z)/F$. The actual forward stresses obey

$$(\widehat{\mathcal{T}}_{P,\theta}, \widehat{\mathcal{T}}_{P,z}) = F(\mathbf{p} - (\mathfrak{a}, -\mathfrak{b})). \tag{1.19.3}$$

In particular, $\mathbf{p}$ uses profile values, their first axial derivatives, and the five histories, but no radial profile derivative. This permits an order-one change of shear with only a small change of $\mathbf{p}$.

For a candidate shear define

$$\mathcal{P} = p_1 + \mathfrak{t}p_2, \qquad \mathcal{J} = p_2 - \mathfrak{t}p_1, \qquad \mathfrak{t} = -\mathfrak{b}/\mathfrak{a}.$$

The strict cone is equivalent to positivity of the four gaps

$$\mathfrak{a}, \qquad \mathfrak{v}-2, \qquad \mathcal{P}-\mathfrak{v}, \qquad 2(\mathcal{P}-\mathfrak{v})^2-(\mathfrak{v}-2)\mathcal{J}^2. \tag{1.19.4}$$

On the relaxed branch $\mathfrak{v}\le 2$, condition (1.12.3) is $\mathcal{P}>2$. These are pointwise statements about the actual forward integrated vector in (1.19.2).

For the selected source, the loop domain has two boundary collars: its actual curved strict-entry collar and its strict prepulse power collar. The domain contains each relaxed point that we modify. The two boundary collars lie strictly inside the actual strict regions. We straighten this fixed fiber domain in one shared smooth radial coordinate. We then apply the geometric loop lemma.

The actual four-gap bounds supply its hypotheses. The physical profiles include the joint phase defined in this section; it is one slice function (1.6.66) and all fixed-$\hat\xi$ derivatives. In particular the physical phase stays $N(\log\frac{\hat\xi^2}{2}+f(\hat\zeta))$, with $\frac12\hat\xi\partial_{\hat\xi}(\log\frac{\hat\xi^2}{2}+f)=1$. The coordinate change does not replace this radial derivative or discard moving-angular history terms. For the scalar example only, we can write this domain as a fixed interval I_{sh} with left boundary after $\frac{\hat\xi_e^2}{2}+5\ell$, as in Proposition 1.12.2.

The selected pulse and its returns previously satisfy the strict cone and no oscillatory change is necessary.

We use the geometric loop lemma, Lemma 1.19.2 (proved in Subsection 1.19.2). The previous estimates verify its hypotheses (H0)–(H2) for this field. It contains no time derivative. The next modulation and history calculation use the forward equations, and Corollary 1.19.3 states which loop properties they use.

We let A_L, B_L be the zero-mean periodic primitives

$$\partial_\phi A_L=-\tfrac12(a_L-\mathfrak{a}), \qquad \partial_\phi B_L=\tfrac12 E(b_L-\mathfrak{b}).$$

They vanish on the boundary collars and extend by zero radially. We select one smooth f equal to $\log\lambda_{\mathrm{ch}}$ on the forward endpoint collars, and $f=0$ in the backward chart. The phase is then the slice function (1.6.66). For one shared integer $N=N_{\mathrm{sh}}$, we put

$$H_N=H\exp(A_L(\tfrac{\hat\xi^2}{2},\hat\zeta,N(\log\tfrac{\hat\xi^2}{2}+f(\hat\zeta)))/N), \qquad U_N=U+B_L(\tfrac{\hat\xi^2}{2},\hat\zeta,N(\log\tfrac{\hat\xi^2}{2}+f(\hat\zeta)))/N. \tag{1.19.5}$$

We let $\frac12\hat\xi\partial_{\hat\xi}$ act on the first variable with ϕ fixed.

Direct differentiation gives

$$a_N=a_L-\frac{2\frac12\hat\xi\partial_{\hat\xi}A_L}{N}, \qquad b_N=e^{-A_L/N}\left(b_L+\frac{2\frac12\hat\xi\partial_{\hat\xi}B_L}{NE}\right). \tag{1.19.6}$$

Profile-value changes are $O(N^{-1})$. We do not assert small radial or ordinary angular derivatives of the oscillatory values. Differentiation of the joint phase costs $Nf'(\hat\zeta)$. We keep $p_0=-C[H^{\mathrm{pre}}](\infty)$ from (1.19.1) and integrate the five actual densities

$$U_N, \quad H_N, \quad U_NH_N, \quad U_N^2-H_N^2/(4\tfrac{\hat\xi^2}{2}), \quad H_N^2/(4\tfrac{\hat\xi^4}{4}).$$

The zero phase means in the linear terms give partial-history changes $O(N^{-2})$, with first ordinary angular derivatives $O(N^{-1})$. The complete exit discrepancies are $O_k(N^{-2})$ for each fixed k.

These are the integration-by-parts estimates proved in Corollary 1.19.3, not pointwise angular estimates. Thus the actual integrated vector changes by $O(N^{-1})$. Equations (1.19.4) and (1.19.6)

give the strict cone on the loop patch. On its untouched collars the original strict reserve absorbs the small history change.

We use the nonlinear two-axial/three-angular history correction of Lemma 1.13.7 on a disjoint quiet power patch. This patch follows the loop and precedes the next pulse returns. The five restoration returns lie in the prepulse wait between offsets -25 and -20; the capped loop lies earlier, in $y_p < -W + 1$ (Section 1.20.5). They precede the heat compensation and the early positive-order and mean correction intervals. The word "late" here means late relative to the loop.

The complete exit discrepancies and the finite-dimensional implicit function theorem give correction coefficients $O_k(N^{-2})$. A sufficiently large N keeps this correction interval's fixed strict margin. We restore all five densities, with the actual energy and pressure density, once against the selected baseline.

At its endpoint the velocity germs and all five histories agree with the physical pre-loop field. At each larger radius both constructions use the same downstream edits and inlet rows, so their fields and all five histories agree there, including on the reserved patches and in the heat exterior. The late correction restores the last calibrated histories. It does not restore an earlier provisional pressure or energy bound.

1.19.2 The geometric loop lemma

We write $y = (\frac{\hat{\xi}^2}{2}, \hat{\zeta}) \in Y = I_{\mathrm{sh}} \times [-1, 1]$. The data are the smooth functions $\mathfrak{a}, \mathfrak{b}$ and $\mathbf{p} = (p_1, p_2)$ of the pre-modulation field on Y, smooth up to ∂Y.

Hypotheses.

(H0) $F > 0$ and $\mathfrak{a} > 0$ on Y.

(H1) At each $y \in Y$ either all four gaps (1.19.4) are positive (*strict point*), or $\mathfrak{v} \le 2$ and $\mathcal{P} > 2$ (*relaxed point*). By (1.12.3) and (1.19.3), this is (1.12.3).

(H2) There are closed radial collars $Y_{\mathrm{col}} = (I_{\mathrm{sh}} \setminus I^{\circ}_{\mathrm{sh},1}) \times [-1, 1]$, $I_{\mathrm{sh},1} \Subset I_{\mathrm{sh}}$, that consist of strict points.

Conditions (H0)–(H2) express the strict relaxed cone everywhere and the strict cone on radial boundary collars.

The relaxed condition includes $\mathfrak{a} > 0$ by definition (1.12.1). The selected collars are the actual curved-entry strict collar and the actual strict decreasing power. The scalar component results Proposition 1.12.2 and Section 1.13 apply only to that component example. We do not use its small axial-ratio slope-transition estimates as the selected source's cone estimate.

Ray coordinates. On $\{a > 0\}$ use the coordinates of Lemma 1.27.3,

$$a = \frac{v}{1 + t^2}, \qquad b = -\frac{vt}{1 + t^2}; \qquad t = -\frac{b}{a}, \quad v = a + \frac{b^2}{a}, \tag{1.19.7}$$

a diffeomorphism $\{a > 0\} \to (0, \infty)_v \times \mathbb{R}_t$. For fixed $\mathbf{p}$ put

$$\mathcal{P}(t) = p_1 + tp_2, \qquad \mathcal{J}(t) = p_2 - tp_1, \qquad \mathcal{Q}(t) = \mathcal{P}(t) - 2, \qquad T_+(\mathbf{p}) = \{t : \mathcal{Q}(t) > 0\}.$$

T_+ is an open half-line, all of $\mathbb{R}$, or empty. The point (a, b) with coordinates (v, t) has $\mathcal{P}, \mathcal{J}$ equal to $\mathcal{P}(t), \mathcal{J}(t)$. These quantities are constant along rays from the origin. The coordinate v varies along the ray.

Lemma 1.19.1 (Ray structure of the cone)**.** *We fix* $\mathbf{p}$ *and let* $a > 0$.

(i) The four gaps are positive iff $t \in T_+$ *and* $2 < v < w_*(t)$,

$$w_* = 2 + \frac{4\mathcal{Q}^2}{4\mathcal{Q} + \mathcal{J}^2 + |\mathcal{J}|\sqrt{\mathcal{J}^2 + 8\mathcal{Q}}} \in (2, \mathcal{P}].$$

(ii) The relaxed condition holds iff $t \in T_+$ *and* $v \le 2$. *Thus the admissible set* $\mathcal{A}(\mathbf{p}) = G(\mathbf{p}) \cup R(\mathbf{p})$ *(strict* $\cup$ *relaxed) equals* $\{t \in T_+,\ 0 < v < w_*(t)\}$, *an open set.*

(iii) For $\delta > 0$,

$$W_\delta = 2 + \frac{4\mathcal{Q}^2}{4\mathcal{Q} + \mathcal{J}^2 + \sqrt{\mathcal{J}^2(\mathcal{J}^2 + 8\mathcal{Q}) + \delta^2}}$$

is smooth in $(\mathbf{p}, t)$ *on* $\{\mathcal{Q} > 0\}$, *and* $w_* - \delta/4 \le W_\delta < w_*$.

(iv) On $G(\mathbf{p})$, $a^2 + b^2 < ap_1 - bp_2$. *In particular* $a^2 + b^2 < |\mathbf{p}|^2$.

Proof. Because $\mathfrak{t}b = -b^2/a$ and $\mathfrak{t}a = -b$, $\mathcal{P} - \mathfrak{v} = p_1 + \mathfrak{t}p_2 - a - b^2/a$ and, by (1.19.3), $\widehat{\mathcal{T}}_{P,\theta} + \mathfrak{t}\widehat{\mathcal{T}}_{P,z} = F(\mathcal{P} - \mathfrak{v})$, $\widehat{\mathcal{T}}_{P,z} - \mathfrak{t}\widehat{\mathcal{T}}_{P,\theta} = F\mathcal{J}$. If $\mathcal{Q} \le 0$ then $v > 2$ forces $v > \mathcal{P}$, so some gap fails. We let $\mathcal{Q} > 0$ and $s = v - 2$.

The fourth gap is $q(s) = 2(\mathcal{Q} - s)^2 - s\mathcal{J}^2 = 2s^2 - (4\mathcal{Q} + \mathcal{J}^2)s + 2\mathcal{Q}^2$, convex, with $q(0) = 2\mathcal{Q}^2 > 0$ and $q(\mathcal{Q}) = -\mathcal{Q}\mathcal{J}^2 \le 0$. Its roots are $\frac{1}{4}[(4\mathcal{Q} + \mathcal{J}^2) \pm |\mathcal{J}|\sqrt{\mathcal{J}^2 + 8\mathcal{Q}}]$, with product $\mathcal{Q}^2$, so the smaller is $s_* = w_* - 2 \in (0, \mathcal{Q}]$ as displayed. On $(0, s_*)$ $q > 0$ and $s < \mathcal{Q}$. For $s \ge s_*$ either $q \le 0$ or $s \ge \mathcal{Q}$. This is (i).

The relaxed condition is $\mathcal{P} > 2$ by (1.19.4)–(1.12.3), which is (ii). Openness is a result of continuity of w_* on $\{\mathcal{Q} > 0\}$. For (iii), $\sqrt{x + \delta^2} > \sqrt{x}$ gives $W_\delta < w_*$. The two denominators are at least $4\mathcal{Q}$ and differ by at most δ, so $w_* - W_\delta \le 4\mathcal{Q}^2\delta/(4\mathcal{Q})^2 = \delta/4$. For (iv), $\mathcal{P} > \mathfrak{v}$ multiplied by $a > 0$ is $ap_1 - bp_2 > a^2 + b^2$, and Cauchy–Schwarz gives $a^2 + b^2 < |(a, b)|\,|\mathbf{p}|$.

□

Lemma 1.19.2 (Capped geometric loop)**.** *Under (H0)–(H2), there is a smooth periodic loop* (a_L, b_L) *with exact mean* $(\mathfrak{a}, \mathfrak{b})$. *It equals the original shear on smaller strict radial collars and has fixed positive four-gap margins. On its active set*

$$0 < a_L < 5/2, \qquad |b_L| < 5/4.$$

Off that set it is the old shear. We do not claim a cap there.

Proof. We put $t_s = -\mathfrak{b}/\mathfrak{a}$, $v_s = \mathfrak{a}(1 + t_s^2)$, $P(t) = p_1 + p_2 t$, $J(t) = p_2 - p_1 t$. We select $0 < d_0 < \frac{1}{2}\min(P(t_s) - 2)$ and set

$$M(z) = \frac{1}{2\pi}\int_0^{2\pi} e^{z\sin\theta}\,\mathrm{d}\theta, \qquad t(\theta; \mu) = t_s + d_0 \frac{e^{\mu p_2 \sin\theta}/M(\mu p_2) - 1}{p_2}.$$

Since $M(0) = 1$ and $M'(0) = 0$, the quotient extends smoothly to $\mu\sin\theta$ at $p_2 = 0$. Thus $t = t_s + d_0\mu\sin\theta$ there. For every p_2 the mean of t is t_s and $P(t) \ge P(t_s) - d_0 > 2$. Write $p = p_2$ and $g = \log M$. For $p \ne 0$ the variance of t is

$$V(\mu, p) = \frac{d_0^2}{p^2}(e^{g(2\mu p) - 2g(\mu p)} - 1).$$

The exponent has derivative $2p[g'(2\mu p) - g'(\mu p)] > 0$ for $\mu > 0$, since g'' is the strictly positive variance of $\sin\theta$ under the tilted circle measure. At $p = 0$, $V(\mu, 0) = d_0^2\mu^2/2$, also strictly increasing for $\mu > 0$.

Also $M(z) \asymp e^{|z|}/\sqrt{|z|}$ for $|z| \geq 1$, so $V \to \infty$. We select one finite $\mu_{\max}$ with $V > 3/\min \mathfrak{a}$ on the compact parameter family. Its admissible upper ray bound exceeds 2 by one positive amount on the full compact family. We select $0 < \delta_L < 1$ so that this bound is more than $2 + \delta_L$. We also keep δ_L less than the strict boundary-collar reserve. We select a nonnegative cutoff ζ equal to one for $v_s \leq 2 + \delta_L/8$ and zero for $v_s \geq 2 + \delta_L/4$, and put

$$v_* = 2 + \delta_L/2, \quad r_L = \zeta(v_s)^2(v_* - v_s), \quad v = v_s + r_L, \qquad V(\mu, p_2) = r_L/\mathfrak{a}.$$

The square-root inverse is smooth at $r_L = 0$, because $V = d_0^2\mu^2/2 + O(\mu^4 p_2^2)$ and $\sqrt{r_L}$ is smooth. We reparametrize by $\mathrm{d}\phi/\,\mathrm{d}\theta = \mathfrak{a}(1 + t^2)/(2\pi v)$ and set $(a_L, -b_L) = v(1, t)/(1 + t^2)$. Because $\mathfrak{a}\langle 1 + t^2\rangle = v$, the signed pair $(a_L, -b_L)$ has period one and mean $(\mathfrak{a}, -\mathfrak{b})$. Where active, $2 < v \leq v_* < 5/2$, which gives the two displayed caps. Elsewhere the loop does not change.

The ray inequalities and compactness give the strict gaps. The lemma is applied twice, to the forward physical pre-loop member $(H^{\mathrm{pre}}, U^{\mathrm{pre}}, P^{\mathrm{pre}})$ on Y_{sh} and to the backward pre-loop member on I_b (Proposition 1.8.16, (L2)). We select all constants, cutoffs and circle origins once, as in (J1)–(J2) of Lemma 1.19.4, for the forward and the backward families. □

Corollary 1.19.3 (Relative phase and actual history estimates)**.** *With the joint phase in* (1.19.5)*, values change by $O(N^{-1})$. Partial histories change by $O(N^{-2})$, and their first angular derivatives change by $O(N^{-1})$. Complete exit moments change by $O_k(N^{-2})$ in each fixed angular norm. We do not assume small pointwise angular profile derivatives. A sufficiently large finite same N keeps the strict gaps, and the genuine nonlinear five-row history restoration restores all outlet histories.*

Proof. Each density difference has the form $N^{-1}g(\frac{\hat\xi^2}{2}, \hat\zeta, \phi) + N^{-2}r_N(\frac{\hat\xi^2}{2}, \hat\zeta, \phi)$, with g periodic of mean zero and smooth compact radial support. For its zero-mean primitive G,

$$g(\tfrac{\hat\xi^2}{2}, \hat\zeta, N(\log\tfrac{\hat\xi^2}{2} + f)) = \frac{\frac{\hat\xi^2}{2}}{N}\hat\xi^{-1}\partial_{\hat\xi}G(\tfrac{\hat\xi^2}{2}, \hat\zeta, N(\log\tfrac{\hat\xi^2}{2} + f)) - \frac{\frac{\hat\xi^2}{2}}{N}(\partial_1 G)(\hat\xi^2/2, \hat\zeta, N(\log(\hat\xi^2/2) + f)).$$

Here $\partial_1 G$ differentiates the squared-radius argument with the phase fixed. Integration by parts gives the partial N^{-2} bound. One angular derivative of its endpoint term costs Nf', which gives N^{-1}. For complete moments the boundary terms vanish.

Arbitrarily many integrations by parts control each fixed angular derivative, while the quadratic mean stays $O_k(N^{-2})$. The actual integrated stress uses these first-history derivatives. The exact radial shear identities (1.19.6) hold because $\frac{1}{2}\hat\xi\partial_{\hat\xi}(\log\frac{\hat\xi^2}{2} + f) = 1$. Thus its gaps change by $O(N^{-1})$. The two-U/three-E moment correction includes the quadratic U and E terms and has a nonzero normalized Jacobian.

Its unique small solution restores the actual five discrepancies. The shared phase is $N\log\frac{\hat\xi_b^2}{2}$ on the endpoint collars, which is the slice function (1.6.66). Thus these operations keep equal slice jets. We select the frequency after the actual member and correction tolerances. Higher profile derivatives are frozen only afterward. □

Lemma 1.19.4 (The backward capped loop is the slice continuation of the forward one)**.** *Let $W_f = Y_{\mathrm{sh}}$ be the forward loop domain (Section 1.19, Lemma 1.20.49) and $I_b = [\frac{(\hat\xi_-^{\mathrm{loop}})^2}{2}, \frac{\hat\xi_+^2}{2}]$ the*

backward one (Proposition 1.8.16). At $|\hat\zeta| = 1$ we have $\widetilde{\xi} = \hat\xi$ in both charts (Lemma 1.6.2). Let $W_f(\pm1)$ be the closed $\frac{\hat\xi^2}{2}$-interval of W_f at $\hat\zeta = \pm1$, and put

$$K_\Delta^{\pm} = (W_f(\pm1) \cup I_b) \setminus (\operatorname{int} W_f(\pm1) \cap \operatorname{int} I_b).$$

Assume the following.

(P) On endpoint neighbourhoods of $\hat\zeta = \pm1$, and for $\frac{\widetilde{\xi}^2}{2}$ near the slice images of W_f, I_b and the restoration reserve, the two physical pre-loop members, each with its actual heat compensation, have equal slice jets, including their five histories and their axis pressures.

(J1) Both loops are the loop of Lemma 1.19.2 with one set of data. These are one d_0, below half the minimum of $P(t_s) - 2$ over both windows; one $\mu_{\max}$; one δ_L, below the upper ray bounds and the strict collar reserves of both windows and subject to (J2); one cutoff ζ; $v_* = 2 + \delta_L/2$; and the origin $\phi = 0$ at $\theta = 0$. Both sides use one integer N_{sh} and the phase of (1.19.5), with $f = 0$ in the backward chart and $f = \log\lambda_{\mathrm{ch}}$ on the forward endpoint collars.

(J2) $v_s(\frac{\hat\xi^2}{2}, \pm1) > 2 + \delta_L/4$ for $\frac{\hat\xi^2}{2} \in K_\Delta^{\pm}$.

(J3) The backward restoration bumps of Step 3 of the proof of Proposition 1.8.16 are $\beta_i(\frac{\hat\xi^2}{2}) = b_i^U(y_p)$ and $\gamma_j(\frac{\hat\xi^2}{2}) = (\hat\xi^2)^{-1/2} b_j^H(y_p)$, with $y_p = 2\log(\hat\xi/\hat\xi_{p,b})$ and the templates of (1.13.84).

Condition (J2) can be met. Every point of $K_\Delta^{\pm}$ is strict for both members, so $\min_{K_\Delta^{\pm}}(v_s - 2) > 0$, and (J2) is one more upper bound on δ_L. This bound depends only on the two pre-loop members and the two windows, which are fixed before δ_L. If the windows have the same endpoints at $\hat\zeta = \pm1$, then (J2) follows from the collar reserve in (J1). Then the following hold.

(a) The pre-loop quantities $\mathfrak{a}$, $\mathfrak{b}$ and $\mathbf{p}$ of the two sides have equal slice jets, with weight 0.

(b) The loop shears (a_L, b_L) and the primitives A_L (weight 0) and B_L (weight $(\frac12 + h)$) have equal slice jets, as profiles with the auxiliary variable ϕ. So do the modulated fields H_N, U_N and their five histories.

(c) The restoration coefficients (weights $(\frac12 + h)$ for δU and h for δH), the restored fields and their histories have equal slice jets. Beyond the reserve both sides equal their pre-loop members.

Proof. (a). On each side the integrated stresses (1.9.2)–(1.9.3), with the side label ς of Remark 1.8.14, satisfy

$$\hat\xi^{-1}\partial_{\hat\xi}(L\hat\xi^2\widehat{\mathcal{T}}_{P,\theta}) = -Lq^{1+h}\, r\mathcal{R}_\theta, \qquad \hat\xi^{-1}\partial_{\hat\xi}(L\hat\xi\,\widehat{\mathcal{T}}_{P,z}) = -Lq^{\frac32+h}\mathcal{R}_z.$$

Here $\mathcal{R}_\theta, \mathcal{R}_z$ are the tangential momentum residuals of the physical leading field, with radial viscosity kept and axial viscosity removed. This follows by substitution of $\partial_t q = \varsigma/L$, $\partial_t\hat\zeta = -\varsigma(\frac12 - h)\hat\zeta/(qL)$, $\partial_z q = 2\hat\zeta\hat t^{\frac12+h}/L$ and $\partial_z\hat\zeta = d/(Lq^{\frac12-h})$ (from $t = \varsigma\hat t(1-\hat\zeta^2)$, $z = \hat\zeta\hat t^{\frac12-h}$), of $u_r = V/r$ and of $\Gamma = ru_\theta = \hat t^{-h}H$. Both sides vanish at the axis. So, with $\hat\xi\,\mathrm{d}\hat\xi = r\,\mathrm{d}r/\hat t$,

$$(\widehat{\mathcal{T}}_{P,\theta}, \widehat{\mathcal{T}}_{P,z}) = \hat t^{1+h}(K_\theta, K_z), \qquad K_\theta = -r^{-2}\int_0^r s^2\mathcal{R}_\theta\,\mathrm{d}s, \quad K_z = -r^{-1}\int_0^r s\mathcal{R}_z\,\mathrm{d}s,$$

in both charts. The physical primitive is taken at fixed (z,t) in either chart. Inserting $r = \sqrt{\hat t}\,\hat\xi$ gives the same weight $1+h$ on both sides, with the respective time sign in the transport terms of (1.19.3). So T_0 is a profile of weight $1 + h = (\frac12 + h) + \frac12$ of one physical pair. It is built from the

physical fields and the axis pressure by derivatives, products and radial primitives at fixed (z,t). Integration of the conservative form from the regular axis writes K_θ, K_z as local expressions in the physical fields, the physical radial histories (the slice forms of $\mathfrak{M}_1,\mathfrak{M}_2,\mathfrak{M}_3,\mathfrak{M}_4,P$) and their ∂_t,∂_z derivatives at the same point. So (P), which includes the five histories near the windows, and the Leibniz rule give equal slice jets of the two sides of T_0; no jets on the rest of $[0,\frac{\hat\xi^2}{2}]$ are needed. Also $\partial_r u_\theta - u_\theta/r = -\hat t^{-1-h}F\mathfrak{a}$ and $\partial_r u_z = \hat t^{-1-h}F\mathfrak{b}$ ((1.4.4); (T6)(i)). So $\mathfrak{a}$, $\mathfrak{b}$ and T_0/F have weight 0, and so does $\mathbf{p} = T_0/F + (\mathfrak{a},-\mathfrak{b})$. Here $F>0$ on both windows by (H0).

Feasibility of (J2). At $|\hat\zeta|=1$ slice profiles equal profiles, so by (a) the two members have the same $(\mathfrak{a},\mathfrak{b},\mathbf{p})$ at $(\frac{\hat\xi^2}{2},\pm1)$. Strictness and relaxedness are therefore common there. At $\hat\zeta=\pm1$ we have $\hat\xi_a(\pm1) = \hat\xi_a^0 < \hat\xi_-^{\mathrm{loop}}$ and $\hat\xi_p(\pm1) = \hat\xi_{p,b}$. So $W_f(\pm1)\subset\{y_a>0,\ y_p\le -W+1\}$, and $I_b\subset\{y_a>0\}$ lies below Y_1, hence in $\mathscr{P}$. The backward member is strict on the whole wait up to Y_1 (Lemma 1.8.17(d)). Each point of $W_f(\pm1)\cup I_b$ is admissible for its own member by (H1), hence for both. A relaxed point lies in $\operatorname{int} W_f(\pm1)$, because Y_{sh} contains every relaxed point of $\mathscr{P}$ in its interior (Lemma 1.20.49, (H2)). It also lies in $\operatorname{int} I_b$, because the backward member is strict on $(\frac{\hat\xi_a^2}{2},\frac{(\hat\xi_-^{\mathrm{loop}})^2}{2}]$, near ∂I_b and on $[\frac{\hat\xi_+^2}{2},Y_1]$ (Step 0 and (L1) of Proposition 1.8.16). Hence $K_\Delta^\pm$ is a compact set of strict points, and v_s-2 has a positive minimum on it.

(b). Write L for the map defined in the proof of Lemma 1.19.2, with the data (J1). It takes $(\mathfrak{a},\mathfrak{b},\mathbf{p})$ at one point and ϕ to (a_L,b_L). The map consists of $t(\theta;\mu)$, the root μ of $V(\mu,p_2)=r_L/\mathfrak{a}$ (smooth by N7 of Section 1.25.1), $v=\mathfrak{v}+r_L$, the inverse of the circle map with $\phi(0)=0$, and $(a_L,-b_L)=v(1,t)/(1+t^2)$. It is smooth, and it is the identity where $\zeta(\mathfrak{v})=0$. On its window each loop is L applied to the pre-loop values. Off the window the shear is unchanged. Fix $\widetilde\xi_0>0$ and compare the one-sided $\widetilde\eta$-jets at $(\frac{\widetilde\xi_0^2}{2},0)$. The window endpoints are continuous in $\hat\zeta$.

- If $\frac{\widetilde\xi_0^2}{2}\in\operatorname{int} W_f(\pm1)\cap\operatorname{int} I_b$, then short segments $\{\frac{\widetilde\xi_0^2}{2}\}\times[0,\epsilon)$ and $\{\frac{\widetilde\xi_0^2}{2}\}\times(-\epsilon,0]$ lie in the two windows. There both shears are L of inputs with equal jets, so the chain rule gives equal jets.
- If $\frac{\widetilde\xi_0^2}{2}$ lies in neither window, both shears are $(\mathfrak{a},\mathfrak{b})$ near the point, and (a) applies.
- Otherwise $\frac{\widetilde\xi_0^2}{2}\in K_\Delta^\pm$. By (J2) and continuity, $\mathfrak{v}>2+\delta_L/4$ on both segments for small ϵ. So $\zeta(\mathfrak{v})=0$ there, and both shears equal $(\mathfrak{a},\mathfrak{b})$ whether or not the segment lies in the window.

Thus (a_L,b_L) have equal slice jets, jointly smooth in ϕ. The zero-mean primitives A_L and B_L of $-\frac12(a_L-\mathfrak{a})$ and $\frac12 E(b_L-\mathfrak{b})$ are pointwise in $(\frac{\hat\xi^2}{2},\hat\zeta)$, with weights 0 and $(\frac12+h)$. By (J1) the phase is $N_{\mathrm{sh}}\log\frac{\hat\xi_b^2}{2}$ on the collars. This is the real-analytic slice function (1.6.66). The chain rule in $(\widetilde\eta,\phi)$ then gives equal jets for $A_L(\cdot,\cdot,\Theta)$ and $B_L(\cdot,\cdot,\Theta)$. Hence $H_N = H\exp(A_L/N)$ and $U_N = U + B_L/N$ have equal slice jets. Their five histories are radial primitives from the axis of densities that differ from the pre-loop ones on a compact radial set, so (1.6.4) applies.

(c). The complete exit discrepancy $\mathbf{d}=\mathbf{m}_N-\mathbf{m}$ is constant in $\frac{\hat\xi^2}{2}$ between the loop and the reserve, and it has equal slice jets by (b). By (J3), both corrections have the form (1.13.84) with the same templates in the slice function $y_p = 2\log(\widetilde\xi/\widetilde\xi_p)$. On the backward side $\delta H = \hat\xi e_c = \sum_j \xi_j b_j^H(y_p)$. The coefficient equation says that the exact five-history increment at the reserve exit equals $-\mathbf{d}$. In slice variables both sides use one integral formula, whose integrands are the pre-loop reserve fields (equal jets by (P)) times the common templates. Its Jacobian is invertible on both sides, also at $\hat\zeta=\pm1$ (Lemma 1.13.7; Step 3 of the proof of Proposition 1.8.16). Differentiation of the equation in $\widetilde\eta$ at 0 gives the same recursion for the one-sided jets of the unique small solutions. So the coefficients, and with them the restored fields and partial histories, have equal slice jets. After

the reserve both members equal their pre-loop members (Lemma 1.13.7; Step 4 of the proof of Proposition 1.8.16), and (P) applies. □

Remark 1.19.5 (Compatibility of the loop data). The loop may be active at $\hat{\zeta} = \pm 1$, so its slice jets require the common constants, phase and circle origin in (J1). Condition (J2) makes it inactive on the symmetric difference of the two windows; (J3) identifies the restoration maps whose unique small solutions are compared. Equal outlet moments alone would not identify the fields inside different restoration templates.

Proposition 1.19.6 (The strict leading field)**.** *We fix a sufficiently large finite N_{sh}, with $N_{\mathrm{sh}} \geq N_2$ (the transit threshold in the proof of Proposition 1.20.59), and apply the late stated correction. The leading field then has strictly admissible shear wherever its stress is nonzero. Its shear and normalized cone margins have fixed positive lower bounds. It agrees with the previous construction on the actual protected curved domain of paragraph 1.22 and on the two reserved patches. It also agrees in the canonical heat exterior.*

These agreements include the actual histories. In particular, these operations keep the same inner Gevrey radius, zero total axial flux, and canonical compensated angular primitive unchanged.

Proof. We prove uniformity on this one selected member. Put $d_c = \mathcal{P} - \mathfrak{v}$, $j_c = \mathcal{J}$, $t_s = -\mathfrak{b}/\mathfrak{a}$. On the live set, the two direction bounds follow from

$$A = \frac{F d_c}{|T_0|} = \frac{\sqrt{1+t_s^2}}{\sqrt{1+(j_c/d_c)^2}}, \qquad G = 2 - (\mathfrak{v}-2)(j_c/d_c)^2.$$

Thus if $\mathfrak{v} - 2 \geq s_* > 0$, $G \geq g_* > 0$, $d_c > 0$, then $A \geq [1 + (2-g_*)/s_*]^{-1/2}$. The unnormalized fourth gap is $d_c^2 G$. We check its quotient also at the faces of the active set.

Entry and modulation. On $0 < y_a \leq y_s$, Corollary 1.20.51 gives $\mathfrak{v} - 2 \geq \delta_0/2$, $d_c \geq e v_r/2$, and the fourth gap is at least $e^2 v_r^2/4$. The smooth factorization $T_0 = e\mathcal{B}$ gives $d_c/e \leq C$ on a smaller closed collar, using $F > 0$ and bounded t_s. Hence its normalized fourth gap has a positive lower bound. Choose $0 < y_{\mathrm{col}} < y_s$ and $\delta_L < 2\delta_0$ also below the backward strict reserve. The loop switch is zero there. The four-gap map is smooth and Lipschitz on the bounded set of shear and integrated-vector inputs with a_s bounded away from zero. Before modulation Theorem 1.20.58 supplies the actual admissible cover. On the relaxed portion Lemma 1.19.2 gives all four gaps a strictly positive minimum μ for the new shear and the old vector. Corollary 1.19.3 changes these inputs by at most K/N_{sh}. On the compact strict transit from the outlet of Y_{sh} to the reserve, and on the five restoration supports including the gaps between them, the change of the integrated inputs and their first angular jets is $O(N_{\mathrm{sh}}^{-2})$. These are the complete exit error and the partial integrals of the fixed restoration bumps. Choose one N_{sh} so both errors cost less than half their respective four-gap minima. After restoration all five rows return. On the three-swirl heat bank the relative partial-history and slope bounds of Proposition 1.20.56 tend to zero with the inverse master radius for fixed preceding scales. They spend half the strict quiet-power reserve. No lower bound for the absolute stress at a moving zero face enters these choices.

Pre-pulse, pulse and inlet. On the quiet power $a_s = 2 + 2\nu$, $b_s = 0$. The two pre-pulse bumps are confined to the fixed-λ sector, have relative C^1 size $O(\lambda^{60(1-\lambda)})$ by (Taper), and preserve a positive fraction of $a_s - 2 = 2\lambda$. Lemma 1.14.4 controls the partial histories between and inside the supports. The quiet-power source and finite-p_1 estimates then apply with these perturbations; after the bumps their energy correction is precisely (1.14.14). Through the main pulse, the quiet intervals and both axial returns, the swirl is the power template and $\mathfrak{v} - 2 \geq 2\nu_c$. Use Lemmas 1.16.8 and 1.16.9 in their respective angular regions. In the finite-p_1 test of Lemma 1.20.6 increase the master radius

after the positive lower bounds for Λ_1, Φ, Q on this compact family are fixed. This includes the interval up to $y_p = Y$. At $X = R_o$ identity (Inlet) applies. Lemma 1.17.9 supplies the positive slope and directional bounds on the following connector, up to its exact mixture germ.

Future and terminal faces. On the central hold $a_s - 2 \geq \nu_c$; on its drive $a_s - 2 = 2\kappa \geq 2\nu_c$, and its power piece has $a_s - 2 = 2h$ (Proposition 1.15.22). Use the slope bound (1.13.59) on the bridge and the differentiated heat slope $-\partial_{\log X} \log H_0 = h + O(X^{-1})$ on a passive heat component. On the outer flattening and wait one has $-\partial_{\log X} \log H \geq \lambda/2$ before the small A11 correction; its fixed-width relative bump derivatives are $O(\lambda^{30(1-\lambda)} + \|\delta_{\mathrm{mem}}\|_{C^1})$. The outer drive has $\kappa \geq h$. On its wing the slope perturbation is at most $h/4$ by the choice of ρ in Lemma 1.17.5. The slope of the mixture is the average with weights $(1-\chi)H_c/H, \chi H_w/H$. On compact pure-swirl pieces Lemmas 1.17.6–1.17.8 provide $T_\theta > 0$ and an upper bound for $|T_z|/T_\theta$ from the actual square histories. At a flat edge their bounds have the form $T_\theta \geq cw$, $|T_z| \leq KEw$ with the same w, also for the cutoff derivative term. On the final outer collar $w = \chi v_s + \dot{\chi} v_g$; on a central terminal component use its own positive shot and wing factors. The fixed upper slope and the small post-pulse amplitude make $(a_s - 2)(T_z/T_\theta)^2 \leq 2 - g_*$ for some $g_* > 0$. These bounds apply wherever the corresponding factor is positive.

Spectral edit and return hull. On the full compact central power hold the unedited radial slope has margin $2\nu_c$. The leading term in $(\delta H)_x$ is nonpositive and the fixed returns cost $O_C(d\Delta)$. The source admission in Section 1.26 gives $T_\theta \geq T_* > 0$ and $(a_s - 2)T_z^2 \leq T_*^2/4$ throughout the main edit and its returns. Thus the normalized fourth margin there is at least $7/4$, while $A = (1+(T_z/T_\theta)^2)^{-1/2}$ has its own positive floor. On the additional axial and curvature controls apply the four-gap map to the entire hull, including points between supports. The pre-control data range in a bounded set for fixed C, Δ, with the preceding uniform margins before the final width is chosen. The first-radial, first-angular and partial-history errors of (1.27.7) and (1.30.23) can be made smaller than half those margins divided by the Lipschitz constant, by the choice of the cutoff width followed by the width-bracket threshold. The exact five-row return restores the comparison field beyond the last support. Taking the minimum of the resulting bounds and the native backward margins supplies the joint constant. In the stress-free core and the exact heat exterior the stated direction bounds are only required on the live set. □

We denote this selected leading field by (F_0, U_0, V_0, P_0), with $H_0 = \hat{\xi}^2 F_0$, $E_0 = \mathfrak{r} F_0$, and stress $T_0 = (\widehat{\mathcal{T}}_{P,\theta}, \widehat{\mathcal{T}}_{P,z})$. We fix the frequency N_{sh} before we select any coefficient or wave frequency.

1.20 The admissible cover and the positivity of the leading stress

This section proves that the final leading stress is nonzero along every radial fiber, from the inner activation collar to the terminal faces. This is the input of the aggregate weight of Definition 1.23.6. The proof reduces to the algebraic identity $\widehat{\mathcal{T}}_{P,\theta} + \mathfrak{t}\widehat{\mathcal{T}}_{P,z} = F(\mathcal{P} - \mathfrak{v})$ (Lemma 1.20.1), so every strict or relaxed point has nonzero stress, and to a covering and compactness argument on the prefix (Proposition 1.20.59). The covering statement (Hypothesis 1.20.4, the standing Hypothesis 1.5.1) is reduced in Theorem 1.20.54. On the outer corridor and at the terminal faces positivity follows from the exact angular mixture identity (Proposition 1.20.62), and Corollary 1.20.63 gives radial connectivity of the stress support. We use the radial variables y_a, y_p and the radial order (1.23.5).

1.20.1 Inputs

The proofs of this section and of Proposition 1.23.8 use the following statements of the construction.

(J1) *Shear variables and stress–shear identity.* Where $F>0$: $\mathfrak{a}=-\hat\xi F_{\hat\xi}/F$, $\mathfrak{b}=U_{\hat\xi}/F$, $\mathfrak{v}=\mathfrak{a}+\mathfrak{b}^2/\mathfrak{a}$, $\mathfrak{t}=-\mathfrak{b}/\mathfrak{a}$ [(1.12.1)]. With $\mathbf{p}=(N_\theta,N_z)/F$ from [(1.19.2)],

$$(\widehat{\mathcal{T}}_{P,\theta},\widehat{\mathcal{T}}_{P,z})=F(\mathbf{p}-(\mathfrak{a},-\mathfrak{b}))\quad[(1.19.3)],\qquad \mathcal{P}=p_1+\mathfrak{t}p_2,\quad \mathcal{J}=p_2-\mathfrak{t}p_1.$$

A *strict point* has the four gaps $\mathfrak{a}$, $\mathfrak{v}-2$, $\mathcal{P}-\mathfrak{v}$, $2(\mathcal{P}-\mathfrak{v})^2-(\mathfrak{v}-2)\mathcal{J}^2$ positive [(1.19.4)]. A *relaxed point* has $\mathfrak{a}>0$, $\mathfrak{v}\le 2$, $\mathcal{P}>2$ [Section 1.19, (1.12.3), Section 1.19.2].

(J2) *Inner contract* (Lemma 1.21.1, eqs. (1.23.1)–(1.23.3) [(1.23.1), (1.23.2), (1.23.3)]). $e=(1-\kappa_{\mathrm{act}})\sigma(y_a/t_{\mathrm{act}})$ with σ the normalized squared-flat step. On $0<y_a\le y_{\mathrm{col}}$: $T_0=e\mathcal{B}$, $\mathcal{B}_\theta\ge b_*>0$, $|\mathcal{B}|\le b^*$; and $|D^jT_0|\le C_jw_{\mathrm{in}}(1+\log(1/w_{\mathrm{in}}))^{N_j}$ with $w_{\mathrm{in}}=c_{\mathrm{in}}e$.

(J3) *Integrated stresses* [(1.9.1), (1.9.2)]: $\widehat{\mathcal{T}}_{P,\theta}=H_{\hat\xi}/\hat\xi-2H/\hat\xi^2+N_\theta$, $\widehat{\mathcal{T}}_{P,z}=U_{\hat\xi}+N_z$ with

$$N_\theta=\frac{(\frac{\hat\xi^2}{2}+\mathcal{K})H-(1-h)\mathfrak{M}_2+(\frac12-h)\eta\mathfrak{M}_{2\eta}-d\mathfrak{M}_{3\eta}+2(h-(\frac12-h))\eta\mathfrak{M}_3}{L\hat\xi^2},$$
$$N_z=\frac{(\frac{\hat\xi^2}{2}+\mathcal{K})U-(\frac12-h)(\mathfrak{M}_1-\eta\mathfrak{M}_{1\eta})+4h\eta\mathfrak{M}_4-d\mathfrak{M}_{4\eta}+\frac{\hat\xi^2}{2}((2+4h)\eta P-dP_\eta)}{L\hat\xi}.$$

$\mathcal{K}=2(\frac12-h)\eta\mathfrak{M}_1+d\mathfrak{M}_{1\eta}$, and the histories are axis integrals [(1.9.1)].

(J4) *Capped loop and modulation*: Lemma 1.19.2, Corollary 1.19.3, Proposition 1.19.6, with hypotheses (H0)–(H2) [Section 1.19.2] verified for the selected field [Section 1.19].

(J5) *Restoration and heat compensation*: Lemma 1.13.7 (coefficients $O_k(\varepsilon)$, $\varepsilon=N_{\mathrm{sh}}^{-2}$, "strictly admissible for sufficiently small ε"); Lemma 1.15.9 ("smallness on the fixed compact reserve keeps its strict model margin").

(J6) *Saturation tube*: Proposition 1.24.2, $\widehat{\mathcal{T}}_{P,\theta}\ge cH>0$ on $K_0=\{\frac{\hat\xi_p^2}{2}e^{-14.5}\le\frac{\hat\xi^2}{2}\le R_oe^{-0.5}\}$ (all η) and on K_{ext} ($\eta\in K_1$, $\frac{\hat\xi^2}{2}\le R_+$). Lemma 1.17.2 gives an open buffer.

(J7) *Pure-swirl component identities*: before spectral implantation $U=\mathfrak{M}_1=\mathfrak{M}_3=0$ after the last pulse return [proof of Lemma 1.6.13], so $\widehat{\mathcal{T}}_{P,\theta}=\mathcal{A}\mathfrak{M}_2$ with $\mathcal{A}$ from [(1.17.1)]. For the final field use these component formulas outside the closed radial hull of the spectral edits and their returns; on that hull use the full integrated source as in Proposition 1.20.62. The angular and radial mixing identities hold [(1.17.2), (1.17.3)]. Component sources: $\mathcal{A}\mathfrak{M}_{2w}\ge m_s\lambda H_w$ on the full compact outer path [Lemma 1.17.4]; $\Delta/\frac{\hat\xi^2}{2}\ge m_g\lambda H_w$, $\Delta=\mathfrak{M}_{2w}-\mathfrak{M}_{2c}$ [Lemma 1.17.3]; the central component has a nonnegative angular source along hold, drive, shot/blend [Lemma 1.17.7, (1.15.24)].

(J8) *Scalar shot, lift, wing* [Lemma 1.13.4]. $\tau_s(x)=\chi_s(s)\tau_b+\lambda_s(C_b/W_s)\psi_s(s)$, $s=(x-R_b)/W_s$, $\chi_s=0$ for $s\ge\frac12$ [Section 1.13, proof of Lemma 1.13.4]. $\psi_s(s)=c_s\vartheta(s-\frac14)\vartheta(\frac34-s)$, $\tau_s\ge cC_b/W_s$ on $s\in[\frac12,\frac35]$ [(1.13.41)]. Lift source $\mathcal{A}\mathfrak{M}_{2L}=d^{-h-1}\tau_s(\frac{\hat\xi^2}{2}/d)$ [(1.13.49)]. Wing $E_o=\alpha_o\ell_b^2\mathcal{F}(y_o)$, $y_o=(\mathcal{B}_o(\eta)-\frac{\hat\xi^2}{2})/\ell_b$ [(1.13.53)], with ψ_o even, increasing in $|\eta|$, zero for $|\eta|\le\eta_0$ [Section 1.13], $(\frac12-h)\eta\mathcal{B}_o'\ge2\mathcal{B}_o$ on $\operatorname{supp}\psi_o$ [Section 1.13]. Common reserve on $J\times[-1,1]$ [(1.13.55)].

(J9) *Terminal face* (Lemma 1.17.5, Lemma 1.17.8). $V=\rho H_0\Psi(\frac{\hat\xi^2}{2}/B)$, $E_w=\int_{(\frac{\hat\xi^2}{2})}^{B}V$, $v_s=V+E_w/\frac{\hat\xi^2}{2}$, $v_g=E_w/\frac{\hat\xi^2}{2}$; $\frac{V_{\hat\xi}}{\hat\xi}\le0$ for large $\frac{\hat\xi^2}{2}$ [proof of Lemma 1.17.5]. At the outer face

($\mathfrak{M}_{2c} = \mathfrak{M}_{20}$): $\widehat{\mathcal{T}}_{P,\theta} \geq c[\chi v_s + \dot{\chi} v_g]$, $|\widehat{\mathcal{T}}_{P,z}| \leq C(H_0/(\hat{\xi}/\sqrt{2}))[\chi v_s + \dot{\chi} v_g]$ [proof of Lemma 1.17.8]. Here $\dot{f} = (\frac{1}{2} - h)\eta\partial_\eta f$ [Section 1.17.1].

1.20.2 The algebraic core

Lemma 1.20.1 (Admissible points have nonzero stress)**.** *Let $F > 0$, $\mathfrak{a} > 0$ and $(\widehat{\mathcal{T}}_{P,\theta}, \widehat{\mathcal{T}}_{P,z}) = F(\mathbf{p} - (\mathfrak{a}, -\mathfrak{b}))$. Then*

$$\widehat{\mathcal{T}}_{P,\theta} + \mathfrak{t}\widehat{\mathcal{T}}_{P,z} = F(\mathcal{P} - \mathfrak{v}), \qquad \widehat{\mathcal{T}}_{P,z} - \mathfrak{t}\widehat{\mathcal{T}}_{P,\theta} = F\mathcal{J}, \tag{1.20.1}$$

$$(1 + \mathfrak{t}^2)\,|T|^2 = F^2[(\mathcal{P} - \mathfrak{v})^2 + \mathcal{J}^2]. \tag{1.20.2}$$

At a strict point $\mathcal{P} - \mathfrak{v} > 0$. At a relaxed point $\mathcal{P} - \mathfrak{v} \geq \mathcal{P} - 2 > 0$. Hence at every admissible (strict or relaxed) point

$$|T| \;\geq\; \frac{F(\mathcal{P} - \mathfrak{v})}{\sqrt{1 + \mathfrak{t}^2}} \;>\; 0, \qquad \widehat{\mathcal{T}}_{P,\theta} + \mathfrak{t}\widehat{\mathcal{T}}_{P,z} > 0. \tag{1.20.3}$$

Moreover the two strict faces [(1.12.2)] *satisfy $\ell_+ + \ell_- = 2\sqrt{2}(\widehat{\mathcal{T}}_{P,\theta} + \mathfrak{t}\widehat{\mathcal{T}}_{P,z})$. The relaxed expression* [(1.12.3)] *equals $F(\mathcal{P} - 2)$.*

Proof. Write $\widehat{\mathcal{T}}_{P,\theta} = F(p_1 - \mathfrak{a})$, $\widehat{\mathcal{T}}_{P,z} = F(p_2 + \mathfrak{b})$. Then $\widehat{\mathcal{T}}_{P,\theta} + \mathfrak{t}\widehat{\mathcal{T}}_{P,z} = F(p_1 + \mathfrak{t}p_2 - \mathfrak{a} + \mathfrak{t}\mathfrak{b})$ and $\mathfrak{t}\mathfrak{b} = -\mathfrak{b}^2/\mathfrak{a}$, so $-\mathfrak{a} + \mathfrak{t}\mathfrak{b} = -\mathfrak{v}$. The second identity is similar. For (1.20.2), the map $(x, y) \mapsto (x + \mathfrak{t}y,\, y - \mathfrak{t}x)$ is $\sqrt{1 + \mathfrak{t}^2}$ times a rotation. The third gap is $\mathcal{P} - \mathfrak{v}$. On the relaxed branch $\mathfrak{v} \leq 2 < \mathcal{P}$. The face and relaxed identities are direct substitution. □

Remark 1.20.2. Lemma 1.20.1 is what the phrase "strictly admissible shear wherever its stress is nonzero" of Proposition 1.19.6 actually needs. Read alone, that phrase is circular. The lemma shows that the set of strict points is *contained in* $\{T \neq 0\}$. So the issue is only whether every point of the prefix is admissible. That is a covering statement, settled next.

1.20.3 Constant history shifts

Lemma 1.20.3 (Downstream effect of a completed modification)**.** *Let K be a compact subset of $\{\frac{\hat{\xi}^2}{2} \geq \frac{\hat{\xi}_0^2}{2} > 0\} \times [-1, 1]$. Suppose two smooth fields have the same (H, U) on K (with all $\frac{\hat{\xi}^2}{2}$- and η-derivatives), and their histories differ there by functions of η only: $(\delta\mathfrak{M}_1, \delta\mathfrak{M}_2, \delta\mathfrak{M}_3, \delta\mathfrak{M}_4, \delta P)(\eta)$. Put $\epsilon = \|(\delta\mathfrak{M}_1, \delta\mathfrak{M}_2, \delta\mathfrak{M}_3, \delta\mathfrak{M}_4, \delta P)\|_{C^1_\eta}$. Then on K*

$$|\delta\widehat{\mathcal{T}}_{P,\theta}| + |\delta\widehat{\mathcal{T}}_{P,z}| \leq C_K\,\epsilon, \qquad C_K = C\,\frac{1 + \sup_K(|H| + |U|) + \sup_K \frac{\hat{\xi}^2}{2}}{L_{\min}\min(\frac{\hat{\xi}_0^2}{2}, \sqrt{\frac{\hat{\xi}_0^2}{2}})}.$$

Proof. By (J3), $\widehat{\mathcal{T}}_{P,\theta}, \widehat{\mathcal{T}}_{P,z}$ are affine in the histories and their first η-derivatives. The coefficients are $H/(L\hat{\xi}^2)$, $U/(L\hat{\xi})$, $1/(L\hat{\xi}^2)$, $1/(L\hat{\xi})$ and $\frac{\hat{\xi}^2}{2}/(L\hat{\xi})$, times polynomials in η bounded on $[-1, 1]$. The terms $\frac{H_{\hat{\xi}}}{\hat{\xi}} - H/\frac{\hat{\xi}^2}{2}$ and $U_{\hat{\xi}}$ do not change. Explicitly, $\delta\widehat{\mathcal{T}}_{P,\theta} = [\delta\mathcal{K}\,H - (1 - h)\delta\mathfrak{M}_2 + (\frac{1}{2} - h)\eta\delta\mathfrak{M}_{2\eta} - d\delta\mathfrak{M}_{3\eta} + 2(h - (\frac{1}{2} - h))\eta\delta\mathfrak{M}_3]/(L\hat{\xi}^2)$, with $\delta\mathcal{K} = (1 - 2h)\eta\delta\mathfrak{M}_1 + d\delta\mathfrak{M}_{1\eta}$. The analogous formula holds for $\delta\widehat{\mathcal{T}}_{P,z}$. □

When a modification has compact radial support and has ended, the histories after its exit differ from the unmodified ones exactly by the complete exit discrepancy, a function of η alone. This holds because all five densities coincide there and the histories are axis integrals [(1.9.1)].

1.20.4 The prefix

Fix $y_{\mathrm{col}} > 0$ as in (J2) and put

$$\mathscr{P} = \{(\tfrac{\hat\xi^2}{2}, \eta) : \ \eta \in [-1,1],\ y_a > 0,\ y_p \le -14.5\}, \qquad \mathscr{P}_{\mathrm{c}} = \mathscr{P} \cap \{y_a \ge y_{\mathrm{col}}\}.$$

$\mathscr{P}_{\mathrm{c}}$ is compact, since $\frac{\hat\xi_a^2}{2}, \frac{\hat\xi_p^2}{2}$ are continuous and positive and (1.23.5) holds.

Hypothesis 1.20.4 (Admissible cover; collected from the construction). Use the smooth comparison $(H^\circ, U^\circ, P^\circ)$ of (1.19.1), with the delayed insertion, outer connection, bridge and the selected axis datum. In (Cov1) all inward histories are computed from (H°, U°) and the pressure is P°. The physical member used for the loop is $(H^{\mathrm{pre}}, U^{\mathrm{pre}}, P^{\mathrm{pre}})$.

(Cov1) $F^\circ > 0$ on $\mathscr{P}$ (input (R1) of Theorem 1.20.54). Every point of $\mathscr{P}_{\mathrm{c}}$ is a strict or relaxed point of (H°, U°). Every relaxed point lies in the interior of the loop domain Y_{sh}, and $Y_{\mathrm{sh}} \subset \{y_p < -25\}$. *Sources:* active collar strict [Proposition 1.12.2]; relaxed segment [Section 1.12, Proposition 1.12.3, Proposition 1.13.1]; (H0)–(H2) on Y_{sh} with strict boundary collars [Section 1.19, Section 1.19.2]; strict quiet power reserve and pre-pulse wait [Section 1.13, Lemma 1.13.7, Section 1.19.2]; the loop precedes its reserve [Section 1.19].

(Cov2) Between the collar and $y_p = -14.5$ the final leading field differs from (H°, U°) only by the following three edits and their partial and complete history increments. In comparing pressures the axis value is always p_0. (i) the modulation (1.19.5) on Y_{sh} ; (ii) the five restoration bumps in the reserve [Lemma 1.13.7]; (iii) the three heat-compensation swirl bumps [Lemma 1.15.9]. The spectral edits lie in $K_{\mathrm{spec}} \subset K_{\mathrm{ext}}$, beyond $y_p = -14.5$ [Proposition 1.24.2]. Positive-order slow coefficients do not change T_0.

1.20.5 Verification of the admissible cover for the selected member

Throughout this subsubsection we work with the *forward* selected member and its forward integrated vector (1.19.2); the backward cone is part of Hypothesis 1.5.5. We write $F = H/(\hat\xi^2)$, $E = H/\hat\xi$, $L = 1 - 2h\eta^2$, $d = 1 - \eta^2$, $\dot f = (\frac12 - h)\eta\,\partial_\eta f|_{\hat\xi}$, and, where $H > 0$,

$$\ell_r = \tfrac12 \hat\xi \partial_{\hat\xi} \log H, \qquad \mathfrak{a} = 2(1 - \ell_r), \qquad r = \frac{\mathfrak{M}_2}{\frac{\hat\xi^2}{2} H}.$$

We use the *full angular coefficient*

$$\begin{aligned} Q :&= \frac{L\, p_1}{\frac{\hat\xi^2}{2}} \\ &= \frac{(\frac{\hat\xi^2}{2} + \mathcal{K})H - (1-h)\mathfrak{M}_2 + (\frac12 - h)\eta\mathfrak{M}_{2\eta} - d\mathfrak{M}_{3\eta} + 2(h - (\frac12 - h))\eta\mathfrak{M}_3}{\frac{\hat\xi^2}{2} H}, \qquad (1.20.4) \\ \mathcal{K} &= 2(\tfrac12 - h)\eta\mathfrak{M}_1 + d\mathfrak{M}_{1\eta}, \end{aligned}$$

(the quantity Q of [Section 1.14, (1.16.5)] and Q_s of [Section 1.6.1]), and the axial numerator

$$N_s := \frac{(\frac{\hat\xi^2}{2} + \mathcal{K})U - (\frac12 - h)(\mathfrak{M}_1 - \eta\mathfrak{M}_{1\eta}) + 4h\eta\mathfrak{M}_4 - d\mathfrak{M}_{4\eta}}{\frac{\hat\xi^2}{2}} + (2 + 4h)\eta P - dP_\eta, \qquad (1.20.5)$$

so that $p_2 = \frac{\hat\xi^2}{2} N_s/(LE)$ and, where $Q \neq 0$, $w := p_2/p_1 = N_s/(EQ)$. All η-derivatives are at fixed $\hat\xi$.

Normalized gaps.

Lemma 1.20.5 (Normalized four-gap form)**.** *At a point with $F > 0$, $\mathfrak{a} > 0$ and $p_1 \neq 0$ put $w = p_2/p_1$,*

$$\Lambda_1 = 1 - \frac{\mathfrak{b} w}{\mathfrak{a}}, \qquad \Lambda_2 = w + \frac{\mathfrak{b}}{\mathfrak{a}}, \qquad \Phi = 2\Lambda_1^2 - (\mathfrak{v} - 2)\Lambda_2^2.$$

Then $\mathcal{P} = p_1\Lambda_1$, $\mathcal{J} = p_1\Lambda_2$, $\mathfrak{v} = \mathfrak{a} + \mathfrak{b}^2/\mathfrak{a}$, and the four gaps (1.19.4) are

$$\mathfrak{a}, \qquad \mathfrak{v} - 2, \qquad p_1\Lambda_1 - \mathfrak{v}, \qquad 2(p_1\Lambda_1 - \mathfrak{v})^2 - (\mathfrak{v} - 2)p_1^2\Lambda_2^2.$$

The point is relaxed iff $\mathfrak{v} \leq 2$ and $p_1\Lambda_1 > 2$. Moreover

$$\mathfrak{a}^2\Phi = (\mathfrak{a}^2 + \mathfrak{b}^2)\big[2 - 2\mathfrak{b}w - \mathfrak{b}^2/\mathfrak{a} - (\mathfrak{a} - 2)w^2\big]. \tag{1.20.6}$$

In particular the two "large-p_1 sufficient tests" of [Section 1.6.1], *$\mathfrak{a} - \mathfrak{b}w > 0$ and $2\mathfrak{b}w + \mathfrak{b}^2/\mathfrak{a} + (\mathfrak{a} - 2)w^2 < 2$, are exactly $\Lambda_1 > 0$ and $\Phi > 0$.*

Proof. $\mathfrak{t} = -\mathfrak{b}/\mathfrak{a}$ and $p_2 = wp_1$ give $\mathcal{P} = p_1 + \mathfrak{t}p_2 = p_1\Lambda_1$ and $\mathcal{J} = p_2 - \mathfrak{t}p_1 = p_1\Lambda_2$. Both sides of (1.20.6) are quadratic polynomials in w; the coefficients of w^2, w, 1 are, on both sides, $-\mathfrak{a}^3 + 2\mathfrak{a}^2 - \mathfrak{a}\mathfrak{b}^2 + 2\mathfrak{b}^2$, $-2\mathfrak{b}(\mathfrak{a}^2 + \mathfrak{b}^2)$ and $2\mathfrak{a}^2 - \mathfrak{a}\mathfrak{b}^2 + 2\mathfrak{b}^2 - \mathfrak{b}^4/\mathfrak{a}$. □

Lemma 1.20.6 (Finite-p_1 threshold)**.** *(a) If $\mathfrak{v} > 2$, $\Lambda_1 \geq \alpha > 0$, $\Phi \geq \phi > 0$ and $p_1 \geq \mathfrak{v}\max(2/\alpha, 8\Lambda_1/\phi)$, then $\mathcal{P} - \mathfrak{v} \geq p_1\Lambda_1/2$ and $2(\mathcal{P} - \mathfrak{v})^2 - (\mathfrak{v} - 2)\mathcal{J}^2 \geq p_1^2\phi/2$. (b) If $\mathfrak{v} \leq 2$, $\Lambda_1 \geq \alpha > 0$ and $p_1 \geq 4/\alpha$, then $\mathcal{P} - 2 \geq p_1\alpha/2$.*

Proof. (a) With $\rho = \mathfrak{v}/p_1 \leq \min(\alpha/2, \phi/(8\Lambda_1))$: $(\mathcal{P} - \mathfrak{v})/p_1 = \Lambda_1 - \rho \geq \Lambda_1/2$ and the fourth gap divided by p_1^2 is $\Phi - 4\Lambda_1\rho + 2\rho^2 \geq \phi/2$. (b) $p_1\Lambda_1 - 2 \geq p_1\alpha - p_1\alpha/2$. □

Transport of the angular coefficient.

Lemma 1.20.7 (Exact transport identity)**.** *Let $H > 0$ and U be smooth on a fiber interval, and let the histories satisfy $\frac{\mathfrak{M}_{1\hat\xi}}{\hat\xi} = U$, $\frac{\mathfrak{M}_{2\hat\xi}}{\hat\xi} = H$, $\frac{\mathfrak{M}_{3\hat\xi}}{\hat\xi} = UH$ with arbitrary (η-dependent) integration constants. With $D_y = \frac{1}{2}\hat\xi\partial_{\hat\xi}$,*

$$D_yQ + (1 + \ell_r)Q = S_q := \ell_r + h + \big((\tfrac{1}{2} - h)\eta - dU\big)\,\partial_\eta \log H|_{\hat\xi} + 2h\eta U + \ell_r \frac{\mathcal{K}}{\frac{\hat\xi^2}{2}}, \tag{1.20.7}$$

and $D_yp_1 = \frac{\hat\xi^2}{2}S_q/L - \ell_r p_1$.

Proof. Write $Q = 1 + \mathcal{K}/\frac{\hat\xi^2}{2} - (1 - h)r + (\frac{1}{2} - h)\eta\mathfrak{M}_{2\eta}/(\frac{\hat\xi^2}{2}H) + j$ with $j = (-d\mathfrak{M}_{3\eta} + 2(h - (\frac{1}{2} - h))\eta\mathfrak{M}_3)/(\frac{\hat\xi^2}{2}H)$. Since $D_y(\frac{\hat\xi^2}{2}H)^{-1} = -(1 + \ell_r)(\frac{\hat\xi^2}{2}H)^{-1}$, $\frac{\mathcal{K}_{\hat\xi}}{\hat\xi} = (1 - 2h)\eta U + dU_\eta$, $(\hat\xi^{-1}\partial_{\hat\xi}(\mathfrak{M}_{2\eta})) = H_\eta$ and $(\hat\xi^{-1}\partial_{\hat\xi}(\mathfrak{M}_{3\eta})) = U_\eta H + UH_\eta$: $D_yr = 1 - (1 + \ell_r)r$, $D_y(\mathcal{K}/\frac{\hat\xi^2}{2}) = (1 - 2h)\eta U + dU_\eta - \mathcal{K}/\frac{\hat\xi^2}{2}$, $D_y(\mathfrak{M}_{2\eta}/(\frac{\hat\xi^2}{2}H)) = H_\eta/H - (1 + \ell_r)\mathfrak{M}_{2\eta}/(\frac{\hat\xi^2}{2}H)$, $D_yj = -dU_\eta - dUH_\eta/H + 2(h - (\frac{1}{2} - h))\eta U - (1 + \ell_r)j$. Adding $(1 + \ell_r)Q$ gives (1.20.7). The second identity follows from $p_1 = \frac{\hat\xi^2}{2}Q/L$ and $D_y\frac{\hat\xi^2}{2} = \frac{\hat\xi^2}{2}$. □

Remark 1.20.8. $\frac{U_{\hat\xi}}{\hat\xi}$ does not occur in (1.20.7). The identity contains, as special cases, the negative-turn source (1.6.33) ($U = 0$, $H = K(\hat\xi_s/\sqrt{2})^{-2\lambda}F_\lambda$), the endpoint growth source [Section 1.6.3] ($U = G$, $\ell_r = \gamma$, $\mathfrak{M}_1 = G\frac{\hat\xi^2}{2}$), the turnoff equation (1.6.38) ($\ell_r = 0$, $\partial_\eta \log H|_{\hat\xi} = (\log f)'$), the wait source $S_{q,w}$ [Section 1.6.3] and the $p_1 = 2$ barrier $\frac{\hat\xi^2}{2}S_q/L - 1.2$ of [Section 1.6.4] ($\ell_r = 0.6$).

Lemma 1.20.9 (Barrier)**.** *On a fiber interval $y_0 \le y \le y_1$ ($y = \log \frac{\hat\xi^2}{2}$) let $1+\ell_r > 0$ and $\Lambda(y) = \int_{y_0}^{y}(1+\ell_r)$. Then*

$$Q(y) \ge e^{-\Lambda(y)}Q(y_0) + (1-e^{-\Lambda(y)}) \inf_{[y_0,y]} \frac{S_q}{1+\ell_r} \;\ge\; \min\Big\{Q(y_0), \inf_{[y_0,y]} \frac{S_q}{1+\ell_r}\Big\}.$$

If $S_q \ge 0$ on $[y_0,y]$, also $Q(y) \ge e^{-\Lambda(y)}Q(y_0)$.

Proof. Variation of constants in (1.20.7): $Q(y) = e^{-\Lambda(y)}Q(y_0) + \int_{y_0}^{y} e^{-(\Lambda(y)-\Lambda(s))}S_q(s)\,\mathrm{d}s$, and $S_q \ge m(1+\ell_r)$ with m the infimum. □

Quiet power regions.

Proposition 1.20.10 (Four gaps on $U \equiv 0$)**.** *Let $U \equiv 0$ on a fiber interval and $Q > 0$ there. Then $\mathfrak{b} = \mathfrak{t} = 0$, $\mathfrak{v} = \mathfrak{a} = 2(1-\ell_r)$, $\mathcal{P} = p_1 = \frac{\hat\xi^2}{2}Q/L$, $\mathcal{J} = p_2 = \frac{\hat\xi^2}{2}Qw/L$, and:*

(a) if $0 \le \ell_r < 1$, the point is relaxed iff $\frac{\hat\xi^2}{2}Q > 2L$;

(b) if $\ell_r < 0$, the point is strict iff $\frac{\hat\xi^2}{2}Q > 2L(1-\ell_r)$ and $-\ell_r w^2 < \theta^2$, where $\theta = 1-2L(1-\ell_r)/(\frac{\hat\xi^2}{2}Q)$; indeed the fourth gap equals $2p_1^2(\theta^2+\ell_r w^2)$;

(c) if $-\nu_1 \le \ell_r \le -\nu_0 < 0$ with $\nu_1 \le \frac14$, $\frac{\hat\xi^2}{2}Q \ge 4L(1+\nu_1)$ and $\nu_1 w^2 \le \frac18$, then $\mathfrak{a} \ge 2+2\nu_0$, $\mathfrak{v}-2 \ge 2\nu_0$, $\mathcal{P}-\mathfrak{v} \ge \frac{\hat\xi^2}{2}Q/(2L)$, the fourth gap is $\ge (\frac{\hat\xi^2}{2}Q/L)^2/4$, and $\widehat{\mathcal{T}}_{P,\theta} = \frac{H}{2}(\frac{Q}{L} - \frac{\mathfrak{a}}{\frac{\hat\xi^2}{2}}) \ge \frac{HQ}{4L}$.

Proof. Lemma 1.20.5 with $\mathfrak{b}=0$: $\Lambda_1 = 1$, $\Lambda_2 = w$, $\mathfrak{v}-2 = -2\ell_r$, $\mathcal{P}-\mathfrak{v} = p_1\theta$; the fourth gap is $2p_1^2\theta^2 + 2\ell_r p_1^2 w^2$. In (c), $\theta \ge \frac12$ and $-\ell_r w^2 \le \frac18$. Finally $\widehat{\mathcal{T}}_{P,\theta} = F(\mathcal{P}-\mathfrak{v})$ by Lemma 1.20.1 with $\mathfrak{t}=0$. □

Remark 1.20.11 (The deficit form of the third gap). If $U \equiv 0$ and $\ell_r = -\nu$ on the interval, put $q = h - \nu + \log\dot H$. Then

$$Q = \big[1-(1-\nu)r\big] + q\,r + \dot r + \frac{\mathcal{K}}{\frac{\hat\xi^2}{2}} + \frac{-d\mathfrak{M}_{3\eta} + 2(h-(\frac12-h))\eta\mathfrak{M}_3}{\frac{\hat\xi^2}{2}H},$$

the first bracket being the primitive deficit, ≥ 0 iff $r \le (1-\nu)^{-1}$. So the third gap is the deficit condition $\frac{\hat\xi^2}{2}\{[1-(1-\nu)r] + qr + \dot r\} + \mathcal{K} + (-d\mathfrak{M}_{3\eta} + 2(h-(\frac12-h))\eta\mathfrak{M}_3)/H > 2L(1+\nu)$. On $U\equiv 0$, $\mathfrak{M}_1, \mathfrak{M}_3$ (hence $\mathcal{K}$) are constant in $\frac{\hat\xi^2}{2}$, the $\mathfrak{M}_3$-term solves the homogeneous equation and enters only through the inlet value, and $S_q = q + \ell_r\mathcal{K}/\frac{\hat\xi^2}{2}$.

Lemma 1.20.12 (Fourth gap on an exact quiet wait)**.** *Let $0 < \nu \le \frac14$, $a = 1-\nu$, $\beta = \frac12 - \nu$. On $s = y - y_0 \in [0,S]$ let $U \equiv 0$, $\ell_r \equiv -\nu$, $S_q \ge q > 0$, $Q(0) = Q_0 > 0$, so that $E(s) = E_0 e^{-(1/2+\nu)s}$. Suppose*

$$|N_s| \le E\big[n_1 e^{-\beta s} + E(k_1 + k_2 s) + EQ(k_3 + k_4 s)\big] \tag{1.20.8}$$

with nonnegative constants. Then $Q \ge Q_0 e^{-as} + \frac{q}{a}(1-e^{-as})$ and, on $[0,S]$,

$$|w| \le \Psi + E_0\Big(k_3 + \frac{2k_4}{e}\Big), \qquad \Psi = \max\Big\{\frac{e\,(n_1 + E_0(k_1+k_2))}{Q_0},\; \frac{2n_1}{q} + \frac{E_0(k_1+k_2S)}{\sqrt{2Q_0 q}}\Big\}.$$

Hence $\nu w^2 \le \frac18$ on $[0,S]$ whenever

$$\nu\Big(\Psi + E_0\big(k_3 + 2k_4/e\big)\Big)^2 \le \frac18. \tag{F*}$$

Proof. The lower bound for Q is Lemma 1.20.9 with $S_q \ge q$. For $s \le 1$: $Q \ge Q_0 e^{-a} \ge Q_0/e$ and the first two terms of (1.20.8) divided by E are $\le n_1 + E_0(k_1+k_2)$. For $s \ge 1$: $1-e^{-as} \ge 1-e^{-3/4} \ge \frac12$, so $Q \ge Q_0 e^{-as} + q/(2a) \ge q/2$ and, by the arithmetic–geometric inequality, $Q \ge \sqrt{2Q_0 q/a}\, e^{-as/2}$. Thus $n_1 e^{-\beta s}/Q \le 2n_1/q$ and $E(k_1+k_2 s)/Q \le E_0(k_1+k_2 S)e^{-(1/2+\nu-a/2)s}/\sqrt{2Q_0 q/a} \le E_0(k_1+k_2 S)/\sqrt{2Q_0 q}$, since $\frac12+\nu-\frac{a}{2} = \frac{3\nu}{2} \ge 0$ and $a \le 1$. After division by EQ, the last term contributes at most $E(k_3+k_4 s) \le E_0(k_3 + 2k_4/e)$. Adding this to the preceding two contributions gives the stated bound for $|w|$.

□

Remark 1.20.13 (An S-independent form of (F*)). Under the hypotheses of Lemma 1.20.12 put $q' := \min\{Q_0, q/a\}$. The first assertion of that lemma gives $Q \ge q'$ on $[0,S]$. Also $E \le E_0 e^{-s/2}$ and $\sup_{s\ge 0} s e^{-s/2} = 2/e$. Dividing (1.20.8) by EQ gives, on $[0,S]$,

$$|w| \le \Psi' + E_0\Big(k_3 + \frac{2k_4}{e}\Big), \qquad \Psi' := \frac{n_1 + E_0(k_1 + 2k_2/e)}{q'}.$$

Hence $\nu w^2 \le \frac18$ on $[0,S]$ also whenever

$$\nu\Big(\Psi' + E_0(k_3 + 2k_4/e)\Big)^2 \le \frac18. \tag{F$^{*\prime}$}$$

This condition does not contain the wait length S (on the $G=0$ wait $S = W = 60\log(1/\nu)$). The constants k_i themselves may depend on other parameters, for example on Y_0; see Lemma 1.20.45 for how this is handled. Either (F*) or (F$^{*\prime}$) may be used wherever (F*) is quoted.

Lemma 1.20.14 (Pressure on the comparison wait)**.** *Fix an angle in the $G=0$ sector or the turnoff buffer. Set $X_1 = \hat\xi_1^2/2$, $X_p = \hat\xi_p^2/2$, with $X_1 \le X_p$, and let R_o be the pulse comparison outlet. On $[X_1, R_o]$ use the underlying power template H for the wait and pulse. Its axial returns do not enter the pressure integral. Omit the two-row taper when integrating the template. This convention gives P° at every prefix radius, since the taper lies beyond $y_p = -14.5$ and has zero complete C_p for every angle. At a radius inside the taper one adds its partial C_p from Lemma 1.14.4. Assume $\ell_r \le 0$, $|\partial_\eta \log H|_\rho| \le \kappa_0 + \kappa_1 \log(\rho^2/\hat\xi_1^2)$, $|(\log R_o)'| \le \rho_1$ and $|\ell_r(R_o)| = \nu \le 1/2$. Use the actual normalized future pressure τ_P of Proposition 1.18.3, with $\|\tau_P\|_{C^1} \le K_2$. Put*

$$\tau_P^* = \tau_P - \frac{R_o}{H_o^2} b_{\mathrm{heat}}, \qquad K = K_2 + 1, \qquad Y_* = \inf_\eta \log(R_o/X_p), \qquad \varepsilon_0 = (1+Y_*)e^{-Y_*}.$$

At the master scale chosen below, $\|\tau_P^*\|_{C^1} \le K$. For $X_1 \le X \le X_p$ and $s = \log(X/X_1)$, the comparison pressure on the template satisfies

$$|P^\circ| \le E^2(\tfrac12 + 2K\varepsilon_0),$$
$$|P^\circ_\eta| \le E^2[\kappa_0 + \kappa_1(s+1)] + E^2\varepsilon_0[\tfrac12\rho_1 + 2K + 4K(\kappa_0 + \kappa_1(s+1) + \rho_1)].$$

Once $Y_* \ge Y_P(K, \rho_1)$ these imply

$$|P^\circ| + |P^\circ_\eta| \le E^2[\tfrac32 + 2\kappa_0 + 2\kappa_1(s+1)].$$

(b) If $|\partial_\eta \log H|_\rho| \le \bar\kappa$ from X to R_o, then $|P^\circ| \le E^2$ and $|P^\circ_\eta| \le E^2(\frac12 + 2\bar\kappa)$ there at the evaluation radius, with the same taper convention.

Proof. At a prefix radius, (1.19.1) and the zero complete row of the taper give the exact outward formula

$$P^{\circ}(X) = -\int_{\hat{\xi}}^{\sqrt{2R_o}} E^2\,\frac{\mathrm{d}\rho}{\rho} - 2E_o^2\tau_P^*, \qquad 2E_o^2 = \frac{H_o^2}{R_o}. \tag{1.20.9}$$

The integral uses the power template on this interval. The actual downstream swirl beyond R_o is identical with and without the early heat bank.

To bound the outlet coefficient, the third normalized target in (1.14.15) and Lemma 1.14.5 give $\|b_{\mathrm{heat}}/e_*^2\|_{C^1} \le K_{\mathrm{sc}}(Y_0)/R_{\mathrm{master}}$. On the support of the heat target, $\nu = \lambda$ and $E = e_* f x^{-1/2-\lambda}$ on the bank power template, with $x = X/X_*$ and $X_* = \hat{\xi}_*^2/2$. At X_p the same power gives $e_*^2/E_p^2 = f^{-2}(X_p/X_*)^{1+2\lambda}$. The ratio X_p/X_* is fixed in the translated template or has bounded logarithmic first jet there. Along the pulse $E_p^2/E_o^2 = \exp((1+2\lambda)Y)$, $Y = \log(R_o/X_p)$. For fixed Y_0 the graph and amplitude bounds of Propositions 1.18.3 and 1.18.4 bound these two ratios and their first derivatives independently of R_{master}. The cutoff is already included in the differentiated target. Therefore

$$\left\| \frac{b_{\mathrm{heat}}}{2E_o^2} \right\|_{C^1} \le \frac{K'(Y_0)}{R_{\mathrm{master}}}.$$

First allow $K = K_2 + 1$ in the choice of Y_P and hence Y_0. Then impose $R_{\mathrm{master}} \ge K'(Y_0)$ at its usual selection. This proves the asserted C^1 outlet bound and retains the order of parameter choices.

Since $\frac{1}{2}\rho\partial_\rho \log E^2 = 2\ell_r - 1 \le -1$, the integral in (1.20.9) is at most $E^2/2$ and $E_o^2 \le E^2 e^{-r_o}$ with $r_o = \log(R_o/X) \ge Y_*$. At fixed $\hat{\xi}$ differentiation gives

$$P_\eta^{\circ} = -2\int_{\hat{\xi}}^{\sqrt{2R_o}} E^2\,\partial_\eta \log H|_\rho\,\frac{\mathrm{d}\rho}{\rho} - \tfrac{1}{2}E_o^2(\log R_o)' - 2\partial_\eta(E_o^2\tau_P^*).$$

Here $\partial_\eta E_o^2 = 2E_o^2[\partial_\eta \log H|_{\sqrt{2R_o}} + (\ell_r(R_o) - \frac{1}{2})(\log R_o)']$, with the partial derivative in the bracket taken before evaluating the trace. Changing variables to $r = \log(\rho^2/\hat{\xi}^2)$ bounds the integral term by $E^2\int_0^\infty e^{-r}(\kappa_0 + \kappa_1(s+r))\,\mathrm{d}r$. For $r_o \ge Y_* \ge 1$, $e^{-r_o}(\kappa_0 + \kappa_1(s+r_o)) \le \varepsilon_0(\kappa_0 + \kappa_1(s+1))$. This proves the first two estimates. Choose Y_P such that $\varepsilon_0(\rho_1/2 + 2K + 4K\rho_1) \le 1/2$, $4K\varepsilon_0 \le 1$ and $2K\varepsilon_0 \le 1/2$. For (b) use the constant $\bar{\kappa}$ in the differentiated integral. At a radius inside the two-row taper, both normalizations pick up its partial integral and its derivative. The bound for that correction is $O_{C^1}(K_{\mathrm{pre}}\lambda^{60a})$ in the units of Lemma 1.14.4. The partial change due to the three-row bank in the physical field is $D_C(X)$ in (1.19.1). □

The strict entry.

Lemma 1.20.15 (Strict-entry collar)**.** *On $0 < y_a \le y_1$ let the shear be prescribed by $(\mathfrak{a}, -\mathfrak{b}) = \kappa\,\mathbf{p}_r$ with $\kappa = 1 - e(y_a)$, where $\mathbf{p}_r = (p_{1,r}, p_{2,r})$ is the reference (protected) vector, $p_{1,r} \ge 2 + \delta_0$, $|\mathbf{p}_r| \le K$, and let $|\mathbf{p} - \mathbf{p}_r| \le \varepsilon(y_a)\,e(y_a)$ with $\varepsilon(y) \to 0$ as $y \downarrow 0$, uniformly in η. Put $\bar{t} = \sup|p_{2,r}|/p_{1,r}$. Every point at which*

$$e \le \frac{\delta_0}{2(2+\delta_0)}, \qquad \varepsilon(1+\bar{t}) \le \frac{p_{1,r}}{4}, \qquad \frac{K^2}{p_{1,r}}\varepsilon^2(1+\bar{t})^2 \le \frac{p_{1,r}^2}{4}$$

is strict, with $\mathfrak{v} - 2 \ge \delta_0/2$, $\mathcal{P} - \mathfrak{v} \ge \frac{3}{4}e\,p_{1,r}$ and fourth gap $\ge \frac{7}{8}e^2p_{1,r}^2$. In particular there is $y_s > 0$ such that every point of $\{0 < y_a \le y_s\}$ is strict.

Proof. $\mathfrak{t} = -\mathfrak{b}/\mathfrak{a} = p_{2,r}/p_{1,r}$ and $\mathfrak{v} = \kappa|\mathbf{p}_r|^2/p_{1,r} \ge \kappa(2+\delta_0) \ge 2 + \delta_0/2$. With $\delta\mathbf{p} = \mathbf{p} - \mathbf{p}_r$: $\mathcal{P} - \mathfrak{v} = e|\mathbf{p}_r|^2/p_{1,r} + \delta p_1 + \mathfrak{t}\delta p_2 \ge e(|\mathbf{p}_r|^2/p_{1,r} - \varepsilon(1+\bar{t})) \ge \frac{3}{4}e|\mathbf{p}_r|^2/p_{1,r}$, and $\mathcal{J} = \delta p_2 - \mathfrak{t}\delta p_1$, $|\mathcal{J}| \le \varepsilon e(1+\bar{t})$. Then $2(\mathcal{P}-\mathfrak{v})^2 - (\mathfrak{v}-2)\mathcal{J}^2 \ge \frac{9}{8}e^2p_{1,r}^2 - \frac{K^2}{p_{1,r}}\varepsilon^2e^2(1+\bar{t})^2 \ge \frac{7}{8}e^2p_{1,r}^2$. Since $e, \varepsilon \to 0$ as $y_a \downarrow 0$ uniformly on the compact angular interval, y_s exists.

□

Remark 1.20.16. For the selected member the prescription is $\partial_y \log F = -\kappa p_{1,r}/2$, $\partial_y U = -\kappa \frac{\hat\xi^2}{2} n_{s,r}/2$ [Section 1.6.4], equivalently $T_0 = e\mathcal{B}$ with $\mathcal{B}(0,\eta) = F_a \mathbf{p}_r$ (Lemma 1.21.1). The value differences $\mathbf{p} - \mathbf{p}_r$ are history and log-amplitude integrals of fields of size e with zero incoming values (proof of Lemma 1.21.1). Write $I(s) = \int_0^s \sigma(t)\,\mathrm{d}t$ for the squared-flat step from the flat-step definition in Section 1.4. For $0 < s \le 1/2$ put $z = (1-s)/s \ge 1$. Then

$$s^{-2} - (1-s)^{-2} = (z - z^{-1})(z + 2 + z^{-1}) \ge 8 \log z.$$

Consequently $\sigma/(1-\sigma) \le z^{-3}$, and $(\log\sigma)' = 2(1-\sigma)s^{-3}(1+z^{-3}) \ge 2s^{-3}$. Integration gives $I(s) \le s^3\sigma(s)/2$.

For $1/2 \le s < 1$, symmetry gives $I(s) = s - 1/2 + I(1-s)$. Put $A(s) = (s-1/2)/s^3$ and $x(s) = (1-s)^{-2} - s^{-2}$. On $[l,r] \subset [1/2,1]$ let $M = A(\min\{r, 3/4\})$ if $l \le 3/4$. The preceding bound on $I(1-s)$, the monotonicity of x, and the maximum of A at $3/4$ give

$$\frac{I(s)}{s^3\sigma(s)} \le M + \frac{M + \frac{1}{2}((1-l)/l)^3}{\sum_{j=0}^{12} x(l)^j/j!}.$$

For clarity, taking consecutive endpoints $(500, 505, 510, 520, 530, 550, 580, 620, 670, 700, 1000)/1000$ gives the following upper bounds for this rational expression, rounded upward in units of 10^{-5}.

$$57765,\ 54087,\ 56744,\ 51449,\ 54739,\ 54368,\ 55028,\ 57425,\ 58372,\ 59268.$$

Continuity covers $s = 1$. Thus $\int_0^y e \le 0.593\, e(y) y^3/t_{\mathrm{act}}^2$ for $y \le t_{\mathrm{act}}$, giving $\varepsilon(y) = Cy^3/t_{\mathrm{act}}^2$ for these integral errors. The selected collar below uses $\int_0^y e \le y e(y)$, valid for every y by monotonicity. The prescription $U_y = -\kappa\frac{\hat\xi^2}{2} n_{s,r}/2$ is divided by the actual E, so $-\mathfrak{b} = \kappa\rho p_{2,r}$ with $\rho = E_r/E = \exp(-\int_0^y e\, p_{1,r}/2) \in (0,1]$, not $\kappa p_{2,r}$; the term $(1-\rho)p_{2,r}$ in $\mathcal{J}$ is at most $\frac{1}{2}P_{\mathrm{ref}}P_2\, y\, e$. For the selected member, Lemma 1.20.20 therefore replaces Lemma 1.20.15; it needs no smallness of e and covers both branches. The core and the activation use the same forward axis pressure $p_0(R)$ and the same fields up to the inlet. Lemma 1.20.19 with $\mu = e$ gives $\varepsilon(y) = K_1(C)y$ for the comparison with the stress-free core. The formula for ρ gives $\varrho = P_{\mathrm{ref}} y/2$. Lemma 1.20.15 does not apply to the selected member as stated, for two reasons. The first is the one above: its shear form takes $\rho = 1$. The second is its hypothesis $p_{1,r} \ge 2 + \delta_0$, which fails on the axial sector. At the face $Y = 4$ the Bessel value is $p_{1,0} = zJ_2(z)/J_1(z) = 2 - zJ_0(z)/J_1(z)$ for $z = \sqrt{8\chi}$, $0 < \chi \le 1$, by the Bessel recurrence. Here $J_1(z) > 0$ throughout $0 < z \le \sqrt{8}$. Thus $p_{1,0} < 2$ precisely for $0 < \chi < j_{0,1}^2/8$, where $j_{0,1}^2/8 \simeq 0.72289825$ and $j_{0,1}$ is the first positive zero of J_0. At $\chi = 1/2$ the value is about 1.22358, and $p_{1,0} \to 0$ as $\chi \downarrow 0$. The face estimates used here are $v_r \ge 2 + c_r$ and $p_{1,r} > 0$ from (I2). The bound $p_{1,r} > 3$ in Section 1.6.4 applies on the termination region $B_0/b \le \frac{\hat\xi^2}{2} \le B_1/b$. Corollary 1.20.51 obtains the required strict collar $\{0 < y_a \le y_s\}$ from Lemma 1.20.20.

The zones with nonzero axial shear. Theorem 1.20.54(R3) concerns three zones with $\mathfrak{b} \ne 0$: (Z1) the core activation, its plateau and the axial termination [Section 1.6.4]; (Z2) the $G_i \to G$ annulus [Section 1.6.4]; (Z3) the two U bumps of the core five-moment correction [Section 1.6.4]. We write $\mathcal{N}_\theta = L\hat\xi^2 N_\theta$, $\mathcal{N}_z = L\hat\xi N_z$ for the numerators in (1.19.2), so $p_1 = \mathcal{N}_\theta/(L\hat\xi^2 F)$ and $p_2 = \mathcal{N}_z/(L\hat\xi F)$.

Proposition 1.20.17 ((Z2), (Z3) are closed)**.** *On the $G_i \to G$ annulus and on the two U-bump supports, Lemma 1.6.36 gives $\mathfrak{a} \in [\frac{7}{10}, \frac{9}{10}]$, $|\mathfrak{b}| \le B_0 = \min\{\frac{1}{5}, \frac{1}{10(W_0+2)}\}$, $|w| \le W_0 + 2$ and $p_1 \ge 3$. Hence $|\mathfrak{b}w|/\mathfrak{a} \le \frac{1}{7}$, $\mathfrak{v} < 1$ and $\mathcal{P} \ge \frac{18}{7}$. An explicit admissible τ_b: since $\mathfrak{b} = 2x\partial_x(\delta U)/E$, it suffices that the normalized $C_\eta^0 C_x^1$ size of the axial correction be $\le e_0 B_0/(2\sup_{\mathrm{supp}} x)$, that $|\delta Q_s| \le q_0/2$, and that $|\delta(N_s/E)| + W_0|\delta Q_s| \le q_0$. Then $|w - w_{\mathrm{ref}}| \le 2$.*

Lemma 1.20.18 (Radial derivatives of the numerators)**.** *For smooth $H>0$ and U, and histories with $\frac{\mathfrak{M}_{1\hat\xi}}{\hat\xi}=U$, $\frac{\mathfrak{M}_{2\hat\xi}}{\hat\xi}=H$, $\frac{\mathfrak{M}_{3\hat\xi}}{\hat\xi}=UH$, $\frac{\mathfrak{M}_{4\hat\xi}}{\hat\xi}=U^2-H^2/(4\frac{\hat\xi^2}{2})$, $\frac{P_{\hat\xi}}{\hat\xi}=H^2/(4\frac{\hat\xi^4}{4})$ and arbitrary η-dependent incoming values:*

$$\hat\xi^{-1}\partial_{\hat\xi}\mathcal{N}_\theta = h(1+2\eta U)H + (\tfrac{\hat\xi^2}{2}+\mathcal{K})\frac{H_{\hat\xi}}{\hat\xi} - (dU-(\tfrac12-h)\eta)H_\eta,$$

$$\hat\xi^{-1}\partial_{\hat\xi}\mathcal{N}_z = (\tfrac12+h)U(1+2\eta U) - (dU-(\tfrac12-h)\eta)U_\eta + (\tfrac{\hat\xi^2}{2}+\mathcal{K})\frac{U_{\hat\xi}}{\hat\xi} + \frac{\eta H^2}{\hat\xi^2} + (2+4h)\eta P - dP_\eta.$$

For a stress-free field $\mathcal{N}_z=-L\hat\xi^2\frac{U_{\hat\xi}}{\hat\xi}$.

Proof. Differentiate (1.19.2) using $\frac{\mathcal{K}_{\hat\xi}}{\hat\xi}=(1-2h)\eta U+dU_\eta$, $1-(\frac12-h)=(\frac12+h)$, $(1-2h)+4h=(1+2h)$ and $(\frac12+h)-h=\frac12$. The UU_η and HH_η terms cancel in pairs. □

Lemma 1.20.19 (Deviation of the integrated vector)**.** *Let $\mathcal{Z}=\{(y,\eta):0\le y\le y_T,\ \eta\in I\}$ with $\frac{\hat\xi^2}{2}=\frac{\left(\hat\xi_a(\eta)\right)^2}{2}e^y$ and I compact. Let (H^0,U^0) and (H,U) have positive swirl for $\hat\xi>0$ and coincide, together with the five incoming histories $\mathfrak{M}_1,\mathfrak{M}_2,\mathfrak{M}_3,\mathfrak{M}_4,C_p$, on $\{\frac{\hat\xi^2}{2}\le\frac{\left(\hat\xi_a(\eta)\right)^2}{2}\}$. Assume that they have the same axis pressure $P_{\mathrm{ax}}(\eta)$ on I, so their full pressures $P=P_{\mathrm{ax}}+C_p$ agree there. The fields are smooth on $\mathcal{Z}$, or continuous and piecewise smooth across finitely many fixed y-levels with the indicated bounds on each piece. Put $m_H=\partial_y\log(H/H^0)$ and $m_U=\partial_y(U-U^0)$, and suppose $|m_H|+|m_U|+|\partial_\eta|_y m_H|+|\partial_\eta|_y m_U|\le G\mu(y)$, where $0\le\mu\le1$ depends on y alone and $G\int_0^{y_T}\mu\le\frac12$. Then on $\mathcal{Z}$*

$$|p_i-p_i^0|\le K_Z\int_0^y\mu\qquad(i=1,2).$$

At each η, K_Z depends on y_T, on G and on the size of the data of (H^0,U^0) at that η: $(\frac{\hat\xi^2}{2})^{\pm1}$, L^{-1}, $(\frac{\hat\xi^2}{2}H^0)^{-1}$, $(E^0)^{-1}$, the reference fields, their fixed-y first angular derivatives, the histories and full pressure with their fixed-$\hat\xi$ first angular derivatives, and $|(\frac{\hat\xi_a^2}{2})'/\frac{\hat\xi_a^2}{2}|$. It does not depend on any cutoff width entering μ once the displayed bounds are fixed.

Proof. Write δ for actual minus reference and $\mathcal{I}(y)=\int_0^y\mu(s)\,\mathrm{d}s$. Integrating m_U,m_H and their fixed-y angular derivatives bounds $\delta U,\log(H/H^0)$ and their fixed-y angular derivatives by $G\mathcal{I}$. Since $G\mathcal{I}\le1/2$, this also bounds δH and its fixed-y angular derivative by $C\mathcal{I}$ on the reference range. For each history density ρ, the product rule gives the same bound for $\delta\rho$ and $\partial_\eta|_y\delta\rho$. Equality at the inlet gives

$$\delta m(y,\eta)=\int_0^y\frac{\left(\hat\xi_a(\eta)\right)^2}{2}e^s\,\delta\rho(s,\eta)\,\mathrm{d}s,\qquad \partial_\eta|_{\hat\xi}\delta m=\partial_\eta|_y\delta m-(\log\tfrac{\hat\xi_a^2}{2})'\tfrac{\hat\xi^2}{2}\delta\rho.$$

Hence $|\delta m|+|\partial_\eta|_{\hat\xi}\delta m|\le C(1+y)\mathcal{I}(y)$. With piecewise smooth data one splits the integral at the fixed y-levels. The common axis datum gives $\delta P=\delta C_p$ and $\partial_\eta|_{\hat\xi}\delta P=\partial_\eta|_{\hat\xi}\delta C_p$. In particular the pressure part $\frac{\hat\xi^2}{2}((2+4h)\eta\,\delta P-d\,\partial_\eta|_{\hat\xi}\delta P)$ of the axial numerator is controlled by the same estimate. Formula (1.19.2) and the positive lower bound on H/H^0 now give the two bounds for $\mathbf{p}$. □

Lemma 1.20.20 (Activation collar, v_r form)**.** *At a point let $p_{1,r}>0$, $v_r:=p_{1,r}+p_{2,r}^2/p_{1,r}\ge2+\delta_0$ with $0<\delta_0\le1$, $|p_{2,r}|\le P_2$, $|p_{2,r}|/p_{1,r}\le\bar t$ and $v_r\le V$. Suppose*

$$(\mathfrak{a},-\mathfrak{b})=\kappa(p_{1,r},\rho p_{2,r}),\quad 0<\kappa\le1,\ e=1-\kappa,\quad \rho\in(0,1],\ 1-\rho\le\varrho e,\ \varrho\le\tfrac14,\quad |p_i-p_{i,r}|\le\varepsilon e.$$

Assume (C1) $\varrho V+\varepsilon(1+\bar t)\le\delta_0/2$ *and (C2)* $V(\varrho P_2+\varepsilon(1+\bar t))^2\le 1$. *If* $\mathfrak v>2$ *and* $e>0$, *the point is strict, with* $\mathcal P-\mathfrak v\ge\frac12 ev_r$ *and fourth gap* $\ge\frac14 e^2v_r^2$. *If* $\mathfrak v\le 2$, *the point is relaxed, with* $\mathcal P-2\ge\delta_0/2$.

Proof. Exactly, $\mathcal P-\mathfrak v=ep_{1,r}+(\rho-\kappa\rho^2)p_{2,r}^2/p_{1,r}+\delta p_1+\mathfrak t\delta p_2$ and $\mathcal J=(1-\rho)p_{2,r}+\delta p_2-\mathfrak t\delta p_1$, with $\mathfrak t=\rho p_{2,r}/p_{1,r}$ and $\mathfrak v=\kappa(p_{1,r}+\rho^2p_{2,r}^2/p_{1,r})\le V$. Since $\rho-\kappa\rho^2\ge\rho e$ and $\rho\ge\frac34$: $\mathcal P-\mathfrak v\ge e(\frac34 v_r-\varepsilon(1+\bar t))\ge\frac12 ev_r$. Also $\mathcal P\ge v_r-\varrho V-\varepsilon(1+\bar t)$, and the fourth gap is $\ge\frac12 e^2v_r^2-Ve^2(\varrho P_2+\varepsilon(1+\bar t))^2\ge\frac14 e^2v_r^2$. □

Lemma 1.20.21 (Shear reductions are convex in the cone quantity)**.** *At a point with* $\mathfrak a>0$ *and* $\mathfrak v\le 2$, *suppose* $-\mathfrak b/\mathfrak a=\theta t$ *with* $\theta\in[0,1]$. *Suppose also* $|\mathbf p-\mathbf p^0|_\infty\le\delta$, $|t-t^{00}|\le\delta_t$, $v^{00}:=p_1^0+t^{00}p_2^0\ge 2+c_r$, *and* $p_1^0\ge 2+c_r$ *whenever* $\theta<1$. *Then*

$$\mathcal P-2\ge c_r-\delta(1+|t^{00}|)-\delta_t(|p_2^0|+\delta),\qquad |\mathcal P-[(1-\theta)p_1^0+\theta v^{00}]|\le\delta(1+|t^{00}|)+\delta_t(|p_2^0|+\delta).$$

Proof. $\mathcal P=(1-\theta)p_1+\theta(p_1+tp_2)$, with $|p_1-p_1^0|\le\delta$ and $|p_1+tp_2-v^{00}|\le\delta(1+|t^{00}|)+\delta_t(|p_2^0|+\delta)$. □

Quoted inputs. The following statements of the text are used. Items (I1) and (I3) are proved: (I1) is Proposition 1.6.42(ii) on $[0,Y_{\mathrm{buf}}]$, $Y_{\mathrm{buf}}\le 4.1$; in (I3), K_c and K_R are given by Corollary 1.6.43(b),(c), and $K_{wY}=K_R/2$ (Corollary 1.6.43(c), Lemma 1.20.24(c)); all three are independent of $\Lambda\ge\Lambda_{\mathrm{core}}$ and of $C\ge C_{\mathrm{core}}(\Lambda)$. The positivity clause and the bound $p_{1,r}\ge 3$ of (I2), and (I4), (I5), are proved in Lemmas 1.6.45 and 1.20.24. The clause $v_r\ge 2+c_r$ of (I2) and item (I6) are quoted from the places indicated. Here $Y_{\mathrm{buf}}>4$ is the end of the buffered core interval, and $y_{\mathrm{buf}}=\log(Y_{\mathrm{buf}}/4)$.

(I1) The core $F_r=C^{-1}e^{\Lambda\psi+a}\Phi_C$, $U_r=u+\Lambda^{-1}w_C$ is an exact solution of the stress-free leading system for $0\le Y\le Y_{\mathrm{buf}}$ (the contraction of the variable-scale Bessel core in Section 1.6.4.3, with its exact rescaled equations; Theorem 1.11.1 is the small-amplitude axis core with $U_c=\kappa\eta+O(\varepsilon^2)$ and is not the source).

(I2) For $4\le Y\le Y_{\mathrm{buf}}$: $v_r\ge 2+c_r$ on all angles, and $p_{1,r}\ge 3$ on $\{\chi\ge 400/401\}$ for sufficiently large Λ. Indeed $\chi Y\ge 1600/401>99/25$, so Lemma 1.6.44 gives $p_{1,0}>33/10$ and Corollary 1.6.43(d) controls its difference from $p_{1,r}$. The clause $p_{1,r}>0$ on all angles, including the drift root, is proved in Lemma 1.6.45 for $\Lambda\ge\Lambda_p$, with $p_{1,r}\ge c_\Phi Y/(4\Lambda b_{\max}\Phi_{\max})$ near the root.

(I3) For $4\le Y\le Y_{\mathrm{buf}}$: $|w_Y-Z_R/(2Lb)|\le K_{wY}/\Lambda$, $|R_2|\le K_R$, and $|w|+|\partial_\eta w|+|w_Y|\le K_c$ (the curved-exit comparison and the coefficient ball).

(I4) $|F|\le K_F/C$ and $|(\log F_a)'|\le K_\psi\Lambda$ on the activation zone.

(I5) The frozen continuation has $S_q^0\ge c_0+.94\Lambda Lb\chi$ with $c_0>0$ ("its source stays").

(I6) $|Z_R|\ge\delta_Z$ on the endpoint collars and on the root neighbourhood, where $\delta_Z:=\min\{\delta_e,\delta_{\mathrm{root}},\delta_*\}$ and δ_* is the margin of the backward axis alternative of Lemma 1.20.33(a) (common to both members, Definition 1.20.35); and $\chi\ge 400/401$ on the rest. Hence $\{|Z_R|<\delta_Z\}\subset\{\chi\ge 400/401\}$.

Here $Z_R=-vu'-(\frac12+h)(1+2\eta u)u-4(\frac12+h)\eta p_0+dp_0'$, and Λ-independent. It depends on the member through $p_0(R)$ and u_0.

Definition 1.20.22 (Modified activation (M0)+(M1))**.** Let ζ_3 be a Gevrey-3/2 step with $\zeta_3 = 0$ on $(-\infty, \frac{1}{4}]$ and $\zeta_3 = 1$ on $[1, \infty)$, and let σ be the shared squared-flat step. Put

$$B_{\mathrm{r0}} := \max\Big\{100,\ 12 \max_{\pm} \sup b^{\pm} / \min\{\min_{\pm} c_0^{\pm},\ s_\gamma\}\Big\}, \qquad \tfrac{\hat\xi_i^2}{2} := B_{\mathrm{r1}} := e\, B_{\mathrm{r0}},$$
$$y_l := \log(\Lambda B_{\mathrm{r0}}/4), \qquad y_T := y_l + 1,$$

where $\pm$ ranges over the forward and the backward member, and $s_\gamma > 0$ is the floor of the growth source of the forward reference future on its growth arc (Proposition 1.20.53). The constant s_γ is fixed in steps 1–3 of Section 1.5.2, so B_{r0} is still fixed with the core margins, before Λ. Only lower bounds on B_{r0} are used anywhere, so enlarging it changes no other argument.

(M0) *Freeze the values; do not kill them.* With $\vartheta(y) = t_{\mathrm{act}}\, g(y/t_{\mathrm{act}})$ and $g(s) = \int_0^s (1 - \sigma(s' - 1))\, \mathrm{d}s'$, the prescriptions use the values $p_1^\flat = p_{1,r}(\vartheta(y), \eta)$ and $n^\flat = n_{s,r}(\vartheta(y), \eta)$:

$$(\log F)_y = -\tfrac{1}{2}\big[(1 - \lambda)\kappa p_1^\flat + 0.8\lambda\big], \qquad U_y = -\tfrac{1}{2}\kappa\beta\tfrac{\hat\xi^2}{2} n^\flat.$$

(M1) *Angle-dependent axial termination.* Put $\Upsilon = \zeta_3(Z_R^2/\delta_Z^2)$ and $y_1 = y_e + (y_l - y_e)\Upsilon$, with $y_e = \omega_0 = \frac{1}{4} y_*(C)$. Here $y_*(C)$ is the minimum over both members of

$$\min\Big\{\tfrac{1}{2G},\ y_{\mathrm{buf}},\ \tfrac{1}{2P_{\mathrm{ref}}},\ \frac{\delta_0}{2(P_{\mathrm{ref}} V + K_1'(1 + \bar t + P_2))},\ \frac{1}{\sqrt{V}(P_{\mathrm{ref}} P_2/2 + K_1'(1 + \bar t))},\ \frac{1}{5K_1'}\Big\},$$

Here the constants for the early comparison are taken on the two natural stress-free cores, up to a common $y_{\mathrm{buf}} > 0$ within both buffers. Denote their fields by a subscript c and their inlet values ($y = 0$) by a subscript a. Put $g_c = n_{s,c}/p_{1,c}$, $R_a = \frac{\hat\xi_a^2}{2}/E_a$ (with $\hat\xi_a = \hat\xi_0$ on the backward side), and set

$$B = (1 + P_{\mathrm{ref}})/2, \quad M_R = e^{B y_{\mathrm{buf}}} \sup R_a,$$
$$T_e = M_R \sup |g_c|, \qquad K_t = M_R(\sup |\partial_y g_c| + B \sup |g_c|).$$

All suprema here include both compact core collars. Take P_{ref} to bound $p_{1,c}$ there. Positivity of E_a and $p_{1,c}$, and the core derivative estimates, make these constants finite at fixed C. On early angles ($y_1 = y_e$, $\partial_\eta y_1 = 0$), before interpolation, take G also to bound the two slope differences against the natural core and their fixed-y angular derivatives in Lemma 1.20.19 with $\mu = 1$. The core slopes involve only $p_{1,c}$, $\frac{\hat\xi^2}{2} n_{s,c}$; the actual slopes use their samples at ϑ, multiplied by bounded cutoffs, with $\partial_\eta|_y \beta = 0$ at these angles. These bounds are independent of all late widths. Use the pointwise-in-angle proof of that lemma on $0 \le y \le \min(y_{\mathrm{buf}}, 1/(2G))$. Its constant plus $\sup |\partial_y \mathbf{p}_c|$ gives a common K_p^a with $|p_i(y) - p_{i,a}| \le K_p^a y$ on this range before interpolation. Choose

$$K_1' \ge 1 + K_1 + K_p^a(1 + T_e) + K_t \sup |p_{2,a}|.$$

Thus G, K_1' are fixed before $y_*(C)$. When choosing the plateau bound V^0, include $P_{\mathrm{ref}}(1 + T_e^2)$ in its maximum. The termination is $\beta = 1 - \sigma((y - y_1(\eta))/\omega_0)$. The interpolation is $\lambda = \sigma((y - y_l - \omega_0)/\omega_2)$. It is angle-independent and starts after the termination has ended on every fiber.

Order. δ_Z and B_{r0} come with the core margins, before Λ. Next come the Λ-thresholds of Theorem 1.20.28 (with the error choice for w_Y) and the C-thresholds (with ledger step 4). Then, at the C-level, come $y_*(C)$, Υ, y_1 and ω_0, common to both members. After that κ_{act}, $t_{\mathrm{act}} \le \min\{y_*(C)/8, \kappa_{\mathrm{act}}^2\}$

and ω_2 are chosen (ledger step 5), and last the higher jets. The spectral controls c_{cut} (step 4 of Section 1.30.3) and d (step 6) come later and see the template only through the fixed member's higher jets.

Lemma 1.20.23 (Axial term on the frozen plateau)**.** *Let* $\frac{\hat\xi_f^2}{2}=\frac{\hat\xi_a^2}{2}e^{\vartheta_\infty}$. *Let* (H^0,U^0) *be the reference for* $\hat\xi\le\hat\xi_f$, *with* $F^0\equiv F_a:=F_r(\frac{\hat\xi_f^2}{2})$ *and* $U^0\equiv U_a:=U_r(\frac{\hat\xi_f^2}{2})$ *for* $\hat\xi\ge\hat\xi_f$. *Compute its pressure with the core datum* $p_0(R)$, *integrating* $\frac{P_{\hat\xi}{}^0}{\hat\xi}=(F^0)^2$ *forward from the incoming core pressure.*

(a) Exactly, for $\hat\xi\ge\hat\xi_f$, $\mathcal N_z^0(\frac{\hat\xi^2}{2})=-2L\frac{\hat\xi_f^2}{2}(\frac{U_{r,\hat\xi}}{\hat\xi})(\sqrt{2(\frac{\hat\xi^2}{2})})+c_1(\frac{\hat\xi^2}{2}-\frac{\hat\xi_f^2}{2})+\frac12\sigma_P(\frac{\hat\xi^2}{2}-\frac{\hat\xi_f^2}{2})^2$, *where* $\sigma_P=F_a^2[2\eta(1+2(\frac12+h))-2d(\log F_a)']$ *and, the reference being stress-free,*

$$\begin{aligned}c_1&=\Big[\hat\xi^{-1}\partial_{\hat\xi}\mathcal N_{z,r}(\hat\xi^2/2)\Big]_{\hat\xi=\hat\xi_f}\\&\quad-(\tfrac{\hat\xi_f^2}{2}+\mathcal K)\frac{U_{r,\hat\xi}}{\hat\xi}-(dU-(\tfrac12-h)\eta)\frac{U_{r,\hat\xi}}{\hat\xi}(\tfrac{\hat\xi_f^2}{2})'\\&=-Z_R-\frac{LbR_2}{\Lambda}-(\tfrac{\hat\xi_f^2}{2}+\mathcal K+(dU-(\tfrac12-h)\eta)(\tfrac{\hat\xi_f^2}{2})')bw_Y.\end{aligned}$$

(b) Hence $|c_1+Z_R|\le\varepsilon_1:=(LbK_R+K_U)/\Lambda+K_F^2C^{-2}(1+K_\psi)$. *Here* K_U *bounds* $(\frac{\hat\xi_f^2}{2}+|\mathcal K|+|dU-(\frac12-h)\eta||(\frac{\hat\xi_f^2}{2})'|)bK_c\Lambda$, *which is* $O(1)$ *because* $\frac{\hat\xi_f^2}{2}=O(\Lambda^{-1})$. *(c) Suppose* $|Z_R|\ge\zeta$, $K_{wY}/\Lambda\le\zeta/(4Lb)$ *and* $\varepsilon_1+2LbK_{wY}/\Lambda+\frac12|\sigma_P|\frac{\hat\xi_T^2}{2}\le\zeta/2$. *Then on* $[\frac{\hat\xi_f^2}{2},\frac{\hat\xi_T^2}{2}]$ *we have* $\operatorname{sgn}\mathcal N_z^0=-\operatorname{sgn}Z_R$, $|\mathcal N_z^0|\ge\frac12\zeta\frac{\hat\xi^2}{2}$, *and* $t^{00}p_2^\flat=-bw_Y\mathcal N_z^0/(LF_a^2p_1^\flat)\ge\zeta^2C^2\frac{\hat\xi^2}{2}/(8L^2K_F^2P_{\mathrm{ref}})$.

Proof. (a) For the frozen field $\frac{U_{\hat\xi}}{\hat\xi}=0$, $\frac{P_{\hat\xi}}{\hat\xi}=F_a^2$, and $P_\eta^0|_{\hat\xi}=P_\eta(\frac{\hat\xi_f^2}{2})+(F_a^2)'(\frac{\hat\xi^2}{2}-\frac{\hat\xi_f^2}{2})$. So by Lemma 1.20.18, $\hat\xi^{-1}\partial_{\hat\xi}\mathcal N_z^0$ is affine with slope σ_P. At $\frac{\hat\xi_f^2}{2}$ the values and histories are the reference's, $U_\eta^0=U_{r,\eta}+\frac{U_{r,\hat\xi}}{\hat\xi}(\frac{\hat\xi_f^2}{2})'$, and $\hat\xi^{-1}\partial_{\hat\xi}\mathcal N_{z,r}=-2L(\hat\xi^{-1}\partial_{\hat\xi}(\frac{\hat\xi^2}{2}\frac{U_{r,\hat\xi}}{\hat\xi}))=-2Lb(Yw_Y)_Y$ with $2(Yw_Y)_Y=Z_R/(Lb)+R_2/\Lambda$. (b) Follows from (a) and (I3), (I4). (c) We have $-2L\frac{\hat\xi_f^2}{2}\frac{U_{r,\hat\xi}}{\hat\xi}=-2Lb\frac{\hat\xi_f^2}{2}w_Y=-\frac{\hat\xi_f^2}{2}Z_R+O(LbK_{wY}\frac{\hat\xi_f^2}{2}/\Lambda)$; next, w_Y has the sign of Z_R and $|w_Y|\ge|Z_R|/(4Lb)$; finally $t^{00}=\frac{\hat\xi^2}{2}n^\flat/(E^0p_1^\flat)$ with $n^\flat=-2bw_Y$. □

Lemma 1.20.24 (Proof of (I4), (I5), of the positivity clause of (I2), and the constant in (I3))**.** *Use the coefficient-ball bounds of the core (Proposition 1.6.42, Corollary 1.6.43) on* $0\le Y\le Y_{\mathrm{buf}}$, *with* $4<Y_{\mathrm{buf}}\le4.1<j_{1,1}^2/2=7.341$ ($j_{1,1}=3.8317$ *the first zero of* J_1)*:* $\Phi\ge c_\Phi>0$, $|\Phi_Y|+|\partial_\eta|_Y\Phi|\le K$, $\|\Phi-\Phi_0\|_{C^1_Y}\le K/\Lambda$ *with* $\Phi_0=2J_1(z)/z$, $z=\sqrt{2\chi Y}$; *the bounds (I3) on* $w=w_C$; $|a'|+|b'/b|+|u'|\le K$; $\|g\|\le1$; *and* $s_0\ge s_{\min}>0$. *Let* N_0 *be the root neighbourhood of paragraph 1.6.4.3,* $\chi_N:=\min_{[-1,1]\setminus N_0}\chi>0$, *and assume*

$$(H_u)\qquad 1+h+\eta u+du'\ge2c_1>0\qquad\text{on } N_0.$$

(H_u) holds in the construction with $c_1=\frac38$. *Indeed,* $N_0\subset\{|\eta|\le w/4\}$ *(paragraph 1.6.4.3:* $\eta_0\le w/16$ *and radius* $\le w/8$*). The strip width is taken with* $w<4\eta_c$ *(only upper bounds on* w *are used), so* N_0 *lies in the central band, where* $G=0$. *The drift is selected with* $\|u-G\|_{C^1([-1,1])}\le\varepsilon_u/4\le\frac14$*: this is the drift part of the axial-mismatch budget, measured in the* C^1_η *norm of Lemma 1.6.36;*

see the drift selection in Section 1.6.4, after Lemma 1.6.37. Hence $|u|+|u'|\le\frac14$ *on* N_0*, and* $1+h+\eta u+du'\ge 1-|u|-|u'|\ge\frac34$*. The choice is compatible with central parity, since* Π_{ref} *does not contain the core (Proposition 1.6.33). It is also compatible with the five-moment correction, whose target is the core mismatch. It keeps the drift root unique and transversal, since* $v'=(\frac12-h)+2\eta u-du'\ge(\frac12-h)-|u|/8-|u'|\ge(\frac12-h)-\frac14>0$ *on* N_0*, because* $|\eta|\le\frac{1}{16}$ *there. Then there is* Λ_0*, depending only on these constants,* c_1 *and* χ_N*, such that for* $\Lambda\ge\Lambda_0$*:*

(a) the core source satisfies $S_q^r\ge c_1+.9\Lambda Lb\chi$ *on* $0<Y\le Y_{\mathrm{buf}}$*, and* $p_{1,r}>0$ *there on all angles;*

(b) $p_{1,r}\ge 3$ *on* $\{\chi\ge 400/401\}\times[4,Y_{\mathrm{buf}}]$*;*

(c) in (I3) one may take $K_{wY}=K_R/2$*;*

(d) (I4) holds with $K_F=\sup e^{\Lambda\psi+a}\sup\Phi$ *(independent of* C*) and* $K_\psi=\sup Lb/(2s_{\min})+K/\Lambda$*;*

(e) (I5) holds with $c_0=c_1$*, for every* $\vartheta_\infty\in[0,y_*/4]$ *and every* $\hat\xi\ge\hat\xi_f$*.*

Without (H_u)*, (a) and the core floor* $S_q\ge c+.9\Lambda Lb\chi$ *of the core construction can fail at the drift root* η_0*. There* $S_q^r=1+h+\eta_0u_0+d_0u'(\eta_0)+O(\Lambda^{-1})$*, and* $p_{1,r}=Y\big(1+h+\eta_0u_0+d_0u'(\eta_0)\big)/(2\Lambda Lb)+O(\Lambda^{-2})$*, so* $p_{1,r}<0$ *at* η_0 *if* $d_0u'(\eta_0)<-(1+h+\eta_0u_0)$*.*

Proof. Write $\delta=\Lambda^{-1}$. On the core $H=\hat\xi^2F$, so $\partial_\eta\log H|_{\hat\xi}=\Lambda\psi'+a'+\partial_\eta|_{\hat\xi}\log\Phi$, and $\partial_\eta|_{\hat\xi}\log\Phi=\partial_\eta|_Y\log\Phi+(b'/b)Y\Phi_Y/\Phi$ is bounded by K. Also $\ell_r=1-p_{1,r}/2$. From $\mathfrak M_1=\int_0^{\frac{\hat\xi^2}{2}}U=u\frac{\hat\xi^2}{2}+\delta\int_0^{\frac{\hat\xi^2}{2}}w$ we get $\partial_\eta|_{\hat\xi}\mathfrak M_1=u'\frac{\hat\xi^2}{2}+\delta\int_0^{\frac{\hat\xi^2}{2}}\partial_\eta|_\rho w$, hence $\mathcal K/\frac{\hat\xi^2}{2}=k_0+O(\delta)$ with $k_0=2(\frac12-h)\eta u+du'$. With $(\frac12-h)\eta-dU=v-\delta dw$, $\Lambda\psi'v=\Lambda Lb\chi$ and $2((\frac12-h)+h)=1$, (1.20.7) gives

$$S_q^r=\Lambda Lb\chi+\big[1+h+\eta u+du'\big]-\tfrac{p_{1,r}}{2}(1+k_0)-dw\psi'+O(|v|+\delta).$$

Here $|\psi'|=Lb|v|/(v^2+s_0^2)\le Lb\sqrt\chi/s_{\min}$ and $|v|\le K\sqrt\chi$. Moreover $|p_{1,r}|\le K(\chi+\delta)$: indeed $\Phi_{0,Y}=-J_2(z)/Y$, and $|J_2(z)|\le z^2/8=\chi Y/4$. So $S_q^r\ge\Lambda Lb\chi+[1+h+\eta u+du']-K_1(\sqrt\chi+\chi+\delta)$, with K_1 depending only on the listed constants. On N_0, $(\mathrm H_u)$ and $K_1\sqrt\chi\le\frac{c_1}{2}+K_1^2\chi/(2c_1)$ give $S_q^r\ge\frac32c_1-K_1\delta+(\Lambda Lb-K_1-K_1^2/(2c_1))\chi\ge c_1+.9\Lambda Lb\chi$ for Λ large. Off N_0, $\chi\ge\chi_N$ and the bracket is $\ge-K_2$, so $.1\Lambda Lb\chi_N\ge c_1+K_2+3K_1$ suffices.

Positivity. $Q_r=Lp_{1,r}/\frac{\hat\xi^2}{2}=-2L\Lambda b\,\Phi_Y/\Phi$ is continuous on $[0,Y_{\mathrm{buf}}]$. As $Y\downarrow0$, $\ell_r\to1$ and $D_yQ_r=Y\partial_YQ_r\to0$, so (1.20.7) gives $Q_r(0)=S_q^r(0)/2>0$. Let y_1 be the first value of $y=\log\frac{\hat\xi^2}{2}$ with $Q_r(y_1)=0$. Then $D_yQ_r(y_1)\le0$, while (1.20.7) gives $D_yQ_r(y_1)=S_q^r(y_1)>0$. So $Q_r>0$ and $p_{1,r}=\frac{\hat\xi^2}{2}Q_r/L>0$.

(b) $d(J_1(z)/z)/dz=-J_2(z)/z$ gives $-2Y\Phi_{0,Y}/\Phi_0=zJ_2(z)/J_1(z)=p(\chi Y)$. For $\chi\ge400/401$ and $4\le Y\le Y_{\mathrm{buf}}$, $99/25<1600/401\le\chi Y\le41/10$. Lemma 1.6.44 therefore gives $p(\chi Y)>33/10$ and $\Phi_0>271/1000$. The uniform $O(\Lambda^{-1})$ comparison then gives $p_{1,r}\ge3$ for Λ large.

(c) J_1 inverts $\partial_Y(Y\partial_Y)$ with zero axis value, so $\partial_YJ_1f=Y^{-1}\int_0^Yf$. The fixed point $w=YZ/(2Lb)+\delta J_1(R_2)/2$ gives $w_Y-Z_R/(2Lb)=(2\Lambda Y)^{-1}\int_0^YR_2$, hence $|w_Y-Z_R/(2Lb)|\le K_R/(2\Lambda)$.

(d) $F_r=C^{-1}e^{\Lambda\psi+a}\Phi\le K_F/C$. On the activation zone $(\log F)_y=-\frac12[(1-\lambda)\kappa p_1^\flat+0.8\lambda]\le0$, by (a) applied to $p_1^\flat=p_{1,r}(\vartheta,\eta)$, so $0<F\le F_r(\frac{\hat\xi_a^2}{2})\le K_F/C$. Since $Y_f=\Lambda b\frac{\hat\xi_f^2}{2}=4e^{\vartheta_\infty}$ does not depend on η, $\log F_a=-\log C+\Lambda\psi+a+\log\Phi(Y_f,\eta)$. So $(\log F_a)'=\Lambda\psi'+a'+\partial_\eta|_Y\log\Phi(Y_f,\eta)$ and $|\psi'|\le Lb/(2s_0)$.

(e) For $\hat\xi\ge\hat\xi_f$, $F^0=F_a(\eta)$ and $U^0=U_a=u+\delta w_a$ with $w_a=w(Y_f,\eta)$. Hence $\ell_r=1$, $\partial_\eta\log H^0|_{\hat\xi}=(\log F_a)'$, and $\mathfrak M_1{}^0=\mathfrak M_{1r}(\hat\xi_f)+U_a(\frac{\hat\xi^2}{2}-\frac{\hat\xi_f^2}{2})$. The terms $\pm U_a(\frac{\hat\xi_f^2}{2})'$ cancel because

$(\frac{\mathfrak{M}_{1r,\hat\xi}}{\hat\xi})(\sqrt{2(\frac{\hat\xi_f^2}{2})}) = U_a$, so $\partial_\eta|_{\hat\xi}\mathfrak{M}_1{}^0 = \partial_\eta|_{\hat\xi}\mathfrak{M}_{1r}(\hat\xi_f) + U_a'(\frac{\hat\xi^2}{2} - \frac{\hat\xi_f^2}{2})$ and $\mathcal{K}^0/\frac{\hat\xi^2}{2} = k_0 + O(\delta)$ uniformly in $\hat\xi \ge \hat\xi_f$. Thus S_q^0 is the expression in (a) with $p_{1,r}$ replaced by 0, and with w, Φ evaluated at $Y_f \in [4, Y_{\rm buf}]$. The same two cases, with .94 in place of .9, give $S_q^0 \ge c_1 + .94\Lambda L b\chi$. Under the sufficient condition for (H_u), $c_1 = \frac{3}{8}$ is absolute. So $B_{\rm r0}$ of Definition 1.20.22 is fixed before Λ, as that definition requires. □

Lemma 1.20.25 (The frozen reference far from the activation)**.** *Let $\frac{\hat\xi_f^2}{2}, F_a, U_a$ be as in Lemma 1.20.23, and let S_q^0, p_1^0 be the source and first strain of the frozen continuation ($\ell_r = 1$, $U \equiv U_a$, $H = \hat\xi^2 F_a$ for $\hat\xi \ge \hat\xi_f$).*

(a) With $k_a = 2(\frac12 - h)\eta U_a + dU_a'$ and $S_q^0(\infty) = 1 + h + ((\frac12 - h)\eta - dU_a)(\log F_a)' + 2h\eta U_a + k_a$, one has exactly

$$S_q^0(\tfrac{\hat\xi^2}{2}) = S_q^0(\infty) + \frac{\frac{\hat\xi_f^2}{2}}{\frac{\hat\xi^2}{2}}(S_q^0(\tfrac{\hat\xi_f^2}{2}) - S_q^0(\infty)) \qquad (\tfrac{\hat\xi^2}{2} \ge \tfrac{\hat\xi_f^2}{2}).$$

So S_q^0 on $[\frac{\hat\xi_f^2}{2}, \infty)$ is a convex combination of its two end values, and $|S_q^0(\frac{\hat\xi_f^2}{2}) - S_q^0(\infty)| \le K_k/\Lambda$, with $K_k = 2K_c(2(\frac12 - h) + d(1 + |b'/b|Y_{\rm buf}))$ and K_c the coefficient-ball bound of $|w| + |\partial_\eta w| + |w_Y|$ on $[0, Y_{\rm buf}]$. Hence the bound (I5) of the frozen continuation, at $\frac{\hat\xi_f^2}{2}$ and at $\hat\xi = \infty$, holds on all of $[\frac{\hat\xi_f^2}{2}, \infty)$.

(b) Assume (I5) on $[\frac{\hat\xi_f^2}{2}, \infty)$. Then $p_1^0(\frac{\hat\xi^2}{2}) \ge c_0\frac{\hat\xi^2}{2}/(4L)$ for all $\frac{\hat\xi^2}{2} \ge \sqrt{2}\frac{\hat\xi_f^2}{2}$, and $p_1^0 \ge 3$ for all $\frac{\hat\xi^2}{2} \ge B_{\rm r0}/b$. There is no upper limit: the bound holds up to the evaluation graph $\frac{\hat\xi_i^2}{2}/b$ for every fixed $\hat\xi_i$.

Proof. (a) For $\hat\xi > \hat\xi_f$, $F^0 = F_a$ and $U^0 = U_a$ are independent of $\frac{\hat\xi^2}{2}$. Since $H^0 = \hat\xi^2 F_a$, only $\mathcal{K}^0/\frac{\hat\xi^2}{2}$ depends on $\frac{\hat\xi^2}{2}$ in the source in (1.20.7). Moreover $\hat\xi^{-1}\partial_{\hat\xi}\mathcal{K}^0 = k_a$, so $\mathcal{K}^0(\frac{\hat\xi^2}{2}) = \mathcal{K}(\frac{\hat\xi_f^2}{2}) + k_a(\frac{\hat\xi^2}{2} - \frac{\hat\xi_f^2}{2})$. This gives the identity, with $S_q^0(\frac{\hat\xi_f^2}{2}) - S_q^0(\infty) = \mathcal{K}(\frac{\hat\xi_f^2}{2})/\frac{\hat\xi_f^2}{2} - k_a$. Here $\mathcal{K}(\frac{\hat\xi_f^2}{2})/\frac{\hat\xi_f^2}{2}$ is the mean over $[0, \frac{\hat\xi_f^2}{2}]$ of $(1 - 2h)\eta U_r + dU_{r,\eta}|_{\hat\xi} = k_0 + \Lambda^{-1}[(1 - 2h)\eta w + d(w_\eta + (b'/b)Y w_Y)]$, with $k_0 = (1 - 2h)\eta u + du'$. Next, $Y_f = \Lambda b\frac{\hat\xi_f^2}{2} = 4e^{\vartheta\infty}$ does not depend on η, so $U_a' = u' + \Lambda^{-1}w_\eta(Y_f, \eta)$ and $k_a = k_0 + \Lambda^{-1}[2(\frac12 - h)\eta w + dw_\eta](Y_f)$. The difference is at most K_k/Λ. (b) By Lemma 1.20.7 with $\ell_r = 1$, $(e^y p_1^0)_y \ge c_0\frac{\hat\xi_f^2}{2}e^{2y}/L$ for $y = 2\log(\hat\xi/\hat\xi_f)$. Moreover $p_1^0(\frac{\hat\xi_f^2}{2}) = p_{1,r}(Y_f) \ge 0$ by Lemma 1.6.45. So $p_1^0 \ge (c_0\frac{\hat\xi_f^2}{2}/L)\sinh y \ge c_0\frac{\hat\xi^2}{2}/(4L)$ for $y \ge \frac12\log 2$. For $\frac{\hat\xi^2}{2} \ge B_{\rm r0}/b$, Definition 1.20.22 gives $c_0\frac{\hat\xi^2}{2}/(4L) \ge 12\sup b\, c_0/(4bL\min c_0) \ge 3$, since $L \le 1$.

□

Remark 1.20.26 (One $\frac{\hat\xi_i^2}{2}$ for both sides). *Forward.* The termination lies in $[B_{\rm r0}/b, e^{\omega_0}B_{\rm r0}/b]$ on the late angles. The interpolation window is $[y_l + \omega_0, y_l + \omega_0 + \omega_2]$, and $\omega_0 + \omega_2 \le \frac{1}{24} + \frac{1}{12} < 1$, because $y_* \le 1/(2P_{\rm ref}) \le \frac16$ and $K_I \ge 3$. So the output slab starts before $B_{\rm r1}/b$, with $p_1 \ge \frac94$ (Theorem 1.20.28(d)), and keeps $p_1 > 2$ by (R4). Hence the forward side accepts every $\frac{\hat\xi_i^2}{2} \ge B_{\rm r1}$. For the actual field only $p_1 \ge \frac94$ is claimed on the window, and only $p_1 > 2$ is needed after it. The bound $p_1 \ge 3$ is a property of the frozen reference (Lemma 1.20.25). It is the forward counterpart

of "$p_{1,r} > 3$ for $\hat\xi_b \le \hat\xi \le \hat\xi_i$" in [42, Lemma B.4]. *Backward.* [42, Lemma B.4, Props. B.5, B.7] use $(\frac{\hat\xi_b^2}{2}, \frac{\hat\xi_i^2}{2}) = (100, 110)$ explicitly in four places. This text does not read them with another pair; it proves the corresponding statements for $(\frac{\hat\xi_b^2}{2}, \frac{\hat\xi_i^2}{2}) = (B_{\mathrm{r0}}, B_{\mathrm{r1}})$:

(i) $p_{1,r} > 3$ on $[\frac{\hat\xi_b^2}{2}, \frac{\hat\xi_i^2}{2}]$: Lemma 1.20.34(c) gives $\frac{\hat\xi^2}{2} p_{1,r} \ge \frac{\hat\xi_0^2}{2} p_{1,r}(\frac{\hat\xi_0^2}{2}) + 1.2(\frac{\hat\xi^4}{4} - \frac{\hat\xi_0^4}{4})$, hence $p_{1,r} > 3$ for all $\frac{\hat\xi^2}{2} \ge 3$. Lemma 1.20.34(a),(b) gives $S_{q,r} \ge .94L\Lambda\chi + 2.4$ from ξ_0 onward. After ξ_f the source is a convex combination of its value at ξ_f and its limiting value $S_\infty \ge .94L\Lambda\chi + 2.6$. The latter bound follows from the axis expansion (1.20.11) and the frozen identity in that lemma.

(ii) "Both transitions fit strictly before $\frac{\hat\xi_i^2}{2}$": Lemma 1.20.37(a), since $2\log(\hat\xi_i/\hat\xi_b) = 1 > \omega_0 + \omega_2$. The output slab up to $\frac{\hat\xi_i^2}{2}$ is Lemma 1.20.37(c).

(iii) The constants $L_0 = 2\log(\hat\xi_i/\hat\xi_0)$ and $\frac{\hat\xi_i^2}{2} N_k \kappa_0$ of [42, Lemma B.7]: (B.32) for this design is Lemma 1.20.37(b), with constants fixed before C and κ_0.

(iv) $\frac{\hat\xi_{\mathrm{ref}}^2}{2} = \frac{\hat\xi_i^2}{2}(CP_*)^{10}$, $\frac{\hat\xi_{\mathrm{sep}}^2}{2} = \frac{\hat\xi_i^2}{2} e^{T_{\mathrm{sh}}}$ and the amplitude threshold $(R_*/\frac{\hat\xi_i^2}{2})^{1/10}/P_*$ ([42, §4.6, Step 1], Section 1.14) are definitions; in $x = (\hat\xi/\hat\xi_{\mathrm{ref}})^2$ the moment matching of Lemma 1.20.41 does not contain $\frac{\hat\xi_i^2}{2}$ (remark after Lemma 1.20.37).

So the choice $(\frac{\hat\xi_b^2}{2}, \frac{\hat\xi_i^2}{2}) = (B_{\mathrm{r0}}, B_{\mathrm{r1}})$ adds no step outside the proof of Theorem 1.8.10. *Common choice.* On the endpoint collars $b = \lambda_{\mathrm{ch}}$ and $y_1 \equiv y_l = \log(\Lambda B_{\mathrm{r0}}/4)$ is common to the two members. So the backward termination radius is forced to be $\frac{\hat\xi_b^2}{2} = \frac{\hat\xi_0^2}{2} e^{y_l} = B_{\mathrm{r0}}$, with $\frac{\hat\xi_0^2}{2} = 4/\Lambda$. Definition 1.20.22 takes $B_{\mathrm{r0}} \ge 100$ and $\frac{\hat\xi_i^2}{2} = B_{\mathrm{r1}} = eB_{\mathrm{r0}} \ge 271 > 110$. The forward evaluation graph $\frac{\hat\xi^2}{2} = \frac{\hat\xi_i^2}{2}/b$ is then the slice continuation of the backward $\hat\xi = \hat\xi_i$, and (B.34) forces the same $k_R = \frac{\hat\xi_i^2}{2}$ in $\frac{\hat\xi_{\mathrm{ref}}^2}{2} = \frac{\hat\xi_i^2}{2}(CP_*)^{10}$ on both sides. B_{r0} and $\frac{\hat\xi_i^2}{2}$ are fixed with the core margins, before Λ.

Lemma 1.20.27 (Source deviation on the plateau; bounds uniform in C)**.** *Let (H, U) be the actual field of Definition 1.20.22 and let (H^0, U^0) be the frozen continuation of Lemma 1.20.23, on one fiber. Fix $y \in [2t_{\mathrm{act}},\ y_l + \omega_0]$, so that $\hat\xi \ge \hat\xi_f$, $\ell_r^0 = 1$ and $\lambda = 0$. Put*

$$\mathcal{I}_{\mathrm{act}} := 2t_{\mathrm{act}} + \kappa_{\mathrm{act}} y_T, \qquad c_\ell := 1 + \mathcal{K}/\tfrac{\hat\xi^2}{2} - ((\tfrac12 - h)\eta - dU)(\log \tfrac{\hat\xi_a^2}{2})',$$

so that $S_q = \ell_r c_\ell + h + ((\frac12 - h)\eta - dU)\,\partial_\eta|_y \log H + 2h\eta U$ (Lemma 1.20.7 with $\partial_\eta|_{\hat\xi} = \partial_\eta|_y - (\log \frac{\hat\xi_a^2}{2})'\partial_y$). Then

$$|S_q - S_q^0 - (\ell_r - 1)c_\ell| \le K_S(\Lambda)\,\mathcal{I}_{\mathrm{act}},$$

$$K_S(\Lambda) := G_0(2(\tfrac12 - h) + 2d\,|b'/b| + d\,(|b'/b| + K_\psi\Lambda) + 2h) + d\,(1 + y_T)\,G_1 + \sup|(\tfrac12 - h)\eta - dU|\,K_p,$$

where

- $G_0 := B_{\mathrm{r1}} K_c + P_{\mathrm{ref}}$;
- $G_1 := B_{\mathrm{r1}} K_c'(1 + (2 + y_T)\|y_1'\|_\infty)$;
- $K_p := \sup_{Y \le Y_{\mathrm{buf}}} |\partial_\eta p_{1,r}|$;
- *K_c, K_c' bound $|w|, |\partial_\eta w|, |w_Y|, |Y w_{YY}|, |\partial_\eta w_Y|$ and $|\partial_\eta(\frac{\hat\xi^2}{2} n_{s,r})|$ on the coefficient ball.*

These bounds are uniform in $C \geq C_0(\Lambda)$ (Remark 1.20.26 and (I3)), and $\|y_1'\|_\infty \leq (y_l - y_e)\|\zeta_3'\| \, 2\sup|Z_R Z_R'|/\delta_Z^2$ (Remark 1.20.30(2)). Hence K_S depends on Λ (through $K_\psi\Lambda$ and $y_T = \log(\Lambda B_{\mathrm{r}0}/4) + 1$) and on data fixed before Λ. It is bounded uniformly in $C \geq C_0(\Lambda)$ and does not depend on κ_{act}, t_{act}, ω_0 or ω_2. Moreover $|(\ell_r - 1)c_\ell| \leq \frac{1}{2}\kappa_{\mathrm{act}} P_{\mathrm{ref}} K_\ell$ with $K_\ell := \sup|c_\ell^0| + 1$, taken over the frozen field (so independent of κ_{act}), which is bounded uniformly in Λ and C; the actual c_ℓ differs from c_ℓ^0 by $O(\mathcal{I}_{\mathrm{act}})$, absorbed by the $+1$ once the late widths are small.

Proof. C enters the field in two ways. As the scalar factor C^{-1} in H it does not affect S_q or S_q^0, which depend on H only through ℓ_r and $\partial_\eta \log H$. It also changes the profile shape: through Φ_C, w_C (the fixed point containing $g = C^{-1}e^{\Lambda\psi+a}$), the offset u_0 chosen after C, $p_0(R)$ with $\frac{\hat\xi_{\mathrm{ref}}^2}{2} = \frac{\hat\xi_i^2}{2}(CP_*)^{10}$ (hence Z_R, Υ and y_1), and $y_*(C)$. Every such input enters the estimates below only through the coefficient-ball bounds, the C^2 bound on $p_0(R)$, the bound on $\|y_1'\|_\infty$, and the two offsets, all of which are uniform in $C \geq C_0(\Lambda)$. Write $\delta U = U - U^0$, $\Delta_H = \log(H/H^0)$, $\delta\mathcal{K} = \mathcal{K} - \mathcal{K}^0$. Since $\ell_r^0 = 1$,

$$S_q - S_q^0 - (\ell_r - 1)c_\ell = (c_\ell - c_\ell^0) + ((\tfrac{1}{2} - h)\eta - dU)\partial_\eta|_y \Delta_H - d\,\delta U\,\partial_\eta|_y \log H^0 + 2h\eta\,\delta U,$$

with $c_\ell - c_\ell^0 = \delta\mathcal{K}/\frac{\hat\xi^2}{2} + d\,\delta U(\log\frac{\hat\xi_a^2}{2})'$ and $(\log\frac{\hat\xi_a^2}{2})' = -b'/b$. The slope differences m_U and m_H against the frozen field are bounded as follows:

- On $[0, 2t_{\mathrm{act}}]$, the actual axial slope and the core slope before freezing give $|m_U| \leq \frac{1}{2}X(|n^\flat| + \mathbf{1}_{\{y\leq\vartheta_\infty\}}|n_{s,r}(y)|) \leq B_{\mathrm{r}1}K_c$, using $X = \hat\xi^2/2$ and taking the uniform core constant K_c to bound both slope contributions. Also $|m_H| \leq P_{\mathrm{ref}}$.
- After $2t_{\mathrm{act}}$, $m_U = -\frac{1}{2}\kappa_{\mathrm{act}}\beta\frac{\hat\xi^2}{2}n^\flat$ and $m_H = -\frac{1}{2}\kappa_{\mathrm{act}}p_1^\flat$.

Hence $|\delta U| \leq G_0\mathcal{I}_{\mathrm{act}}$ and $|\partial_\eta|_y\Delta_H| \leq K_p\mathcal{I}_{\mathrm{act}}$; the cutoff $\sigma(\cdot/t_{\mathrm{act}})$ depends on y only. In $\partial_\eta|_y\delta U = \int_0^y \partial_\eta m_U$, the angle-dependent factor $\partial_\eta\beta = -y_1'\partial_s\beta$ is integrated by parts against $\frac{\hat\xi^2}{2}n^\flat$, which is smooth in s there:

$$\Big|\int_0^y \partial_\eta\beta\,\tfrac{\hat\xi^2}{2}n^\flat\,\mathrm{d}s\Big| \leq \|y_1'\|_\infty\Big(2\sup|\tfrac{\hat\xi^2}{2}n^\flat| + \int_0^y|\partial_s(\tfrac{\hat\xi^2}{2}n^\flat)|\,\mathrm{d}s\Big).$$

No factor $1/\omega_0$ occurs, and with the factor κ_{act} this gives $|\partial_\eta|_y\delta U| \leq G_1\mathcal{I}_{\mathrm{act}}$. Then $|\delta\mathcal{K}|/\frac{\hat\xi^2}{2} \leq (1-2h)|\delta\mathfrak{M}_1|/\frac{\hat\xi^2}{2} + d|\partial_\eta|_{\hat\xi}\delta\mathfrak{M}_1|/\frac{\hat\xi^2}{2}$. Here $|\delta\mathfrak{M}_1| \leq \frac{\hat\xi^2}{2}\sup|\delta U|$ and $\partial_\eta|_{\hat\xi}\delta\mathfrak{M}_1 = \partial_\eta|_y\delta m - (\log\frac{\hat\xi_a^2}{2})'\frac{\hat\xi^2}{2}\delta U$, as in the proof of Lemma 1.20.19. Finally $\partial_\eta|_y \log H^0 = (\log\frac{\hat\xi_a^2}{2})' + (\log F_a)'$, and $|(\log F_a)'| \leq K_\psi\Lambda$ by (I4). This is the only Λ-growing factor, and it multiplies $\delta U = O(\mathcal{I}_{\mathrm{act}})$. □

Theorem 1.20.28 ((V) and the four gaps on the activation zone)**.** *Assume (I1)–(I6) and Definition 1.20.22, together with the following thresholds.*

(Λ) $K_{wY}/\Lambda \leq \delta_Z/(8\sup Lb)$ *and* $(\sup LbK_R + K_U + 2\sup LbK_{wY})/\Lambda \leq \delta_Z/8$.

(C) $K_F^2C^{-2}(1 + K_\psi + (6 + 2K_\psi\Lambda)B_{\mathrm{r}1}/b_{\min}) \leq \delta_Z/8$ *and* $C^2 \geq 24\Lambda\max\{\sup(bL^2), 1\}K_F^2P_{\mathrm{ref}}/\delta_Z^2$.

(late) $\kappa_{\mathrm{act}} \leq \min\{$*Section 1.6.4*, $1/(8(1 + V^0))\}$ *and* $t_{\mathrm{act}} \leq \min\{y_*(C)/8, \kappa_{\mathrm{act}}^2\}$. *Put* $\varepsilon_{\mathrm{act}} = K_Z(C)(\mathcal{I}_{\mathrm{act}} + \omega_2)$. *Require* $\varepsilon_{\mathrm{act}}(1 + T^{00} + P_2^0) + \varepsilon_{\mathrm{act}}^2 \leq \frac{1}{4}$ *and* $\frac{B_{\mathrm{r}1}}{b_{\min}L_{\min}}[\frac{1}{2}\kappa_{\mathrm{act}}P_{\mathrm{ref}}K_\ell + K_S(\Lambda)\mathcal{I}_{\mathrm{act}}] \leq \frac{1}{4}$, *with* $\mathcal{I}_{\mathrm{act}} = 2t_{\mathrm{act}} + \kappa_{\mathrm{act}}y_T$. *All coefficients in these two bounds are fixed before $\kappa_{\mathrm{act}}, t_{\mathrm{act}}, \omega_2$. The coefficients of the source bound are already fixed with Λ by Lemma 1.20.27. Choose $\kappa_{\mathrm{act}}, t_{\mathrm{act}}$ small enough to leave strict slack in the first bound at $\omega_2 = 0$, then choose $\omega_2 > 0$ small enough to keep it. Finally $K_I(C)\,\omega_2 \leq \frac{1}{4}$.*

In these thresholds:

- V^0, T^{00}, P_2^0 *bound the corresponding suprema over the frozen plateau and over* $\vartheta_\infty \in [0, y_*/4]$, *with the additional early-collar bound on* V^0 *in Definition 1.20.22.*
- $K_Z(C)$ *bounds the deviation in Lemma 1.20.19 and that of* t^{full} *from* t^{00} *in part (c), uniformly over the frozen family through the end of interpolation. On transition angles it includes* $(y_l - y_e)\|\Upsilon'\|\|\sigma'\|/\omega_0$.
- $K_S(\Lambda)$ *and* K_ℓ *are the constants of Lemma 1.20.27.* K_S *bounds* $|S_q - S_q^0 - (\ell_r - 1)c_\ell|/\mathcal{I}_{\mathrm{act}}$, *where* $c_\ell = 1 + \mathcal{K}/\frac{\hat\xi^2}{2} - ((\frac12 - h)\eta - dU)(\log\frac{\hat\xi_a^2}{2})'$ *is the* ℓ_r*-coefficient of* S_q. K_S *is* $O(\Lambda)$, *through* $d\,\delta U\,\partial_\eta \log H^0$ *with* $|\partial_\eta \log H^0| \le |b'/b| + K_\psi\Lambda$, *and it does not depend on* C. *The deviation enters only through* $\mathcal{I}_{\mathrm{act}}$; *it is not a fixed* $O(\Lambda^{-1})$ *quantity.*
- $K_I(C)$ *is* 3 *plus a uniform upper bound for* $|\frac{\hat\xi^2}{2}S_q/L|$ *on the interpolation windows of widths* $0 < \omega_2 \le 1/2$ *lying in* $y \le y_T$. *Such a bound follows from the source formula in the proof of Lemma 1.20.27. The interpolation enters* $(\log F)_y$ *through the bounded value of the angle-independent step. Fixed-y angular differentiation of its radial integral introduces no derivative of that step. The other inputs* $U, \mathfrak{M}_1, \mathcal{K}$ *have already been fixed there, since axial termination is complete.*

Under these assumptions every point of the activation zone, from the face to the end of the interpolation, is strict or relaxed:

(a) For $0 < y \le t_{\mathrm{act}}$, *on all angles: strict points have* $\mathcal{P} - \mathfrak{v} \ge \frac12 e v_r$ *and fourth gap* $\ge \frac14 e^2 v_r^2$. *Relaxed points have* $\mathcal{P} - 2 \ge \delta_0/2$, *where* $\delta_0 = \min(c_r, 1)$.

(b) On $\{|Z_R| \le \delta_Z/2\}$ *(early termination,* $\chi \ge 400/401$*):* $\mathcal{P} - 2 \ge \delta_0/2$ *for* $t_{\mathrm{act}} \le y \le y_e + \omega_0$. *After that* $\mathfrak{b} = 0$, $\mathfrak{a} \le 0.4$, *and* $p_1 \ge \frac52$ *until the interpolation starts.*

(c) On $\{|Z_R| \ge \delta_Z/2\}$*:* $v^{00} \ge 3$ *on* $[t_{\mathrm{act}}, y_T]$, $p_1^0 \ge 3$ *wherever* $\beta < 1$, *and* $\mathcal{P} - 2 \ge \frac12$. *This is (V). Once the termination has started, the comparison is* $|\mathcal{P} - [(1-\beta)p_1^0 + \beta v^{00}]| \le \frac14$.

(d) On the interpolation window $[y_l + \omega_0, y_l + \omega_0 + \omega_2]$ *(where* $\mathfrak{b} = 0$ *and* $\mathfrak{a} \in (0, 0.8]$*):* $p_1 \ge \frac94$. *This value is also the inlet of the output slab, where (R4) applies.*

Proof. (a) The actual forward activation, the stress-free core and its frozen continuation all use the selected $p_0(R)$ of Section 1.6.4. They share the whole core up to $\frac{\hat\xi_a^2}{2}$, hence the full inlet pressure and the five incoming histories as functions of η. This verifies the pressure hypothesis of Lemma 1.20.19 for both forward comparisons. On $0 < y \le t_{\mathrm{act}}$, $\beta = 1$ and $\vartheta = y$. Apply Lemma 1.20.20 with $\varepsilon = K_1 y$, $\varrho = P_{\mathrm{ref}} y/2$ and $y \le y_*$.

(b) Here $\Upsilon = \Upsilon' = 0$, including at the cutoff level $|Z_R| = \delta_Z/2$ by smoothness. Thus β has zero fixed-y angular derivative on this set. For $t_{\mathrm{act}} \le y \le y_e + \omega_0 \le y_*/2$ we have $\kappa = \kappa_{\mathrm{act}}$ and $\lambda = 0$. Write $R(y) = \frac{\hat\xi^2}{2}(y)/E(y)$ on this fiber. Since $E = \hat\xi F$,

$$(\log R)_y = (1 + \kappa p_{1,c}(\vartheta))/2, \qquad t^{\mathrm{full}} = R(y) g_c(\vartheta(y)), \qquad t_a = R_a g_c(0) = p_{2,a}/p_{1,a}.$$

These identities hold from the inlet until interpolation. Hence $R \le M_R$ on the early collar and $|R(y) - R_a| \le B M_R y$. Since $0 \le \vartheta(y) \le y$, we have $|t^{\mathrm{full}}| \le T_e$ and $|t^{\mathrm{full}} - t_a| \le K_t y$. This accounts

for the radial factor at the evaluation point. In particular $\mathfrak{v} = \kappa_{\mathrm{act}} p_1^\flat (1 + \beta^2 (t^{\mathrm{full}})^2) \le \kappa_{\mathrm{act}} V^0 < 1$ for $y \ge t_{\mathrm{act}}$ on this collar. The choice of K_1' and the inlet comparison in Definition 1.20.22 give

$$|p_1 - p_{1,a}| \le K_1' y, \qquad |p_1 + t^{\mathrm{full}} p_2 - v_a| \le K_1' y, \qquad v_a = p_{1,a} + t_a p_{2,a}.$$

Indeed the second error is at most $(1 + T_e) K_p^a y + |p_{2,a}| K_t y$. Here $\mathcal{P} = (1 - \beta) p_1 + \beta (p_1 + t^{\mathrm{full}} p_2)$. The fourth and last entries in the definition of y_* give $K_1' y \le \min(\delta_0/4, 1/10)$ for $y \le y_*/2$. At the inlet $p_{1,a} \ge 3$ and $v_a \ge 2 + c_r$ by (I2). Thus $\mathcal{P} \ge 2 + \delta_0/2$ and $p_1 \ge 5/2$ throughout the early termination. After the termination, $\mathfrak{b} = 0$, $\mathfrak{a} = \kappa_{\mathrm{act}} p_1^\flat \le 0.4$ and $\ell_r \in [0.8, 1]$. The transport law is $D_y p_1 = \frac{\hat\xi^2}{2} S_q / L - \ell_r p_1$ (Lemma 1.20.7). By Lemma 1.20.27, $|S_q - S_q^0| \le \frac{1}{2} \kappa_{\mathrm{act}} P_{\mathrm{ref}} K_\ell + K_S(\Lambda) \mathcal{I}_{\mathrm{act}}$. So (I5) and (late), with $\frac{\hat\xi^2}{2} \le B_{\mathrm{r1}}/b_{\min}$, give $\frac{\hat\xi^2}{2} S_q / L \ge .94 \cdot 4 \cdot \frac{400}{401} - \frac{1}{4} \ge 3.5$. The barrier then gives $p_1 \ge \frac{5}{2}$.

(c) At the evaluation point y take the frozen continuation with $\vartheta_\infty = \vartheta(y)$. This level is held fixed in the comparison up to y. Since $\vartheta(y) \le y$ and $\vartheta(y) \le 2 t_{\mathrm{act}} \le y_*/4$, we have $\hat\xi_f \le \hat\xi$ and the uniform frozen bounds apply. Use Lemma 1.20.23(c) with $\zeta = \delta_Z/2$ and thresholds (Λ) and (C). Since $\frac{\hat\xi^2}{2} \ge 4/(\Lambda b)$, $t^{00} p_2^0 \ge \delta_Z^2 C^2 / (8 \Lambda b L^2 K_F^2 P_{\mathrm{ref}}) \ge 3$. Also $p_1^0 \ge 0$, by Lemma 1.20.9 with $S_q^0 > 0$ and $p_1^0(\frac{\hat\xi_f^2}{2}) = p_{1,r}(Y_f) > 0$ (Lemma 1.6.45). Where $\beta < 1$, one of two cases holds. If $y_1 = y_l$, Lemma 1.20.25(b) gives $p_1^0 \ge c_0 \frac{\hat\xi^2}{2} / (4L) \ge 3$ for $\frac{\hat\xi^2}{2} \ge B_{\mathrm{r0}}/b$. Otherwise $\Upsilon < 1$, so $\chi \ge \frac{400}{401}$ and $p_1^0 \ge \min\{p_{1,r}, 3.75\} \ge 3$. Apply Lemma 1.20.19 with $\mu = 1$ on $[0, 2t_{\mathrm{act}}]$ and on the interpolation window, and $\mu = \kappa_{\mathrm{act}}$ between them. The slope bounds of (M0)–(M1) and their fixed-y angular derivatives hold on each side of the freezing level, with the transition factor recorded in $K_Z(C)$. During interpolation $\lambda(y)$ is bounded and angle-independent, so the fixed-y angular slope bounds there are uniform in ω_2. The integral of μ is at most $\mathcal{I}_{\mathrm{act}} + \omega_2$. Also $t^{\mathrm{full}} = t^{00} E^0 / E$ at the evaluation point. The log-amplitude bound in the same proof gives $|E^0/E - 1| \le C(\mathcal{I}_{\mathrm{act}} + \omega_2)$. Since $|t^{00}| \le T^{00}$ on the fixed frozen family, the choice of $K_Z(C)$ gives $\delta, \delta_t \le \varepsilon_{\mathrm{act}}$. Thus Lemma 1.20.21 bounds the error in the convex combination by

$$\delta(1 + |t^{00}|) + \delta_t(|p_2^0| + \delta) \le \varepsilon_{\mathrm{act}}(1 + T^{00} + P_2^0) + \varepsilon_{\mathrm{act}}^2 \le \tfrac{1}{4}.$$

Here $\mathfrak{v} \le 0.8 + \kappa_{\mathrm{act}} V^0 < 1$. On the interpolation window $\beta = 0$ and $\mathcal{P} = p_1$, so the same comparison controls $|p_1 - p_1^0|$ there.

(d) At the interpolation inlet $p_1 \ge 5/2$ by (b), or $p_1 \ge 3 - 1/4$ by (c) with $\beta = 0$. Suppose p_1 reaches $9/4$ in the window. Between its last crossing of $5/2$ before that time and its first subsequent crossing of $9/4$, the equation $D_y p_1 = \frac{\hat\xi^2}{2} S_q / L - \ell_r p_1$ and $\ell_r \le 1$ give $D_y p_1 \ge -(K_I - 3) - 5/2 > -K_I$. Integrating over this interval would give $1/4 < K_I \omega_2$, contrary to the width condition. □

Proposition 1.20.29 (A single late termination near a transverse zero)**.** *Suppose the forward core datum has an interior zero η_* of Z_R with $Z_R'(\eta_*) \ne 0$ and $v(\eta_*) \ne 0$. Consider the frozen plateau of Lemma 1.20.23, with the axial shear kept on until $\frac{\hat\xi^2}{2} \ge B_{\mathrm{r0}}/b$. For sufficiently large Λ and then sufficiently large C, $v^{00} < 0$ at a radius before termination, on an interval of angles near η_*. For these fixed scales the actual unmodified plateau has $\mathcal{P} < 2$ there for sufficiently small late activation controls. The thresholds are for the given transverse zero. For varying data the same thresholds apply if the zeros stay in a compact interior interval with uniform positive lower bounds for $|Z_R'(\eta_*)|$ and $|v(\eta_*)|$ and the standing uniform core data bounds.*

Proof. Write $\gamma = Z_R/(Lb)$, $z = \Lambda \gamma(\eta)$ and $k_* = v(\eta_*)\gamma'(\eta_*)/(2L(\eta_*)b(\eta_*)) \ne 0$. In a neighbourhood of η_*, bounded z gives $|\eta - \eta_*| = O(\Lambda^{-1})$ by the inverse function theorem. At fixed Λ, $g = C^{-1} e^{\Lambda\psi + a}$ and its first derivative are $O_\Lambda(C^{-1})$. Increase C so that the terms involving g^2, $\mathcal{Q}$ and $\partial_\eta \mathcal{Q}$ in B_2

are $O(\Lambda^{-1})$ uniformly on the core buffer. By Corollary 1.6.43(b), $w = Y\gamma/2 + O(\Lambda^{-1})$ with its first derivatives. In B_2 the term $-v\mathcal{T}w$ contributes $-vY\gamma'/2 + O(\Lambda^{-1})$; all the remaining terms are $O(\Lambda^{-1})$. Thus $R_2 = -k_*Y + O(\Lambda^{-1})$ for bounded z and $0 \le Y \le Y_{\mathrm{buf}}$.

At the freezing level $Y_f = 4e^{\vartheta_\infty}$, integrate $2(Yw_Y)_Y = \gamma + R_2/\Lambda$ from the regular axis to obtain

$$w_Y(Y_f) = \frac{z - k_*Y_f/2}{2\Lambda} + O(\Lambda^{-2}), \qquad (Yw_Y)_Y(Y_f) = \frac{z - k_*Y_f}{2\Lambda} + O(\Lambda^{-2}).$$

Take the closed interval $5/8 \le z/(k_*Y_f) \le 7/8$. Writing $q = z/(k_*Y_f)$, we have $(q - 1/2)(q - 1) \le -3/64$ there for either sign of k_*. It corresponds to an angular interval of positive length for all sufficiently large Λ; (I6) gives $\chi \ge 400/401$ there. Since $\frac{\hat\xi_f^2}{2}, \mathcal{K}(\frac{\hat\xi_f^2}{2}), (\frac{\hat\xi_f^2}{2})' = O(\Lambda^{-1})$, Lemma 1.20.23(a) gives, uniformly on this smaller interval,

$$-bw_Yc_1 = 2Lb^2w_Y(Yw_Y)_Y + O(\Lambda^{-3}) \le -c_*/\Lambda^2$$

with $c_* > 0$. The estimate is uniform for the allowed Y_f in the core buffer.

Fix $\frac{\hat\xi_\dagger^2}{2} = B_{\mathrm{r0}}/(2\sup b)$ and let $D_\dagger = \frac{\hat\xi_\dagger^2}{2} - \frac{\hat\xi_f^2}{2} \ge \frac{\hat\xi_\dagger^2}{2}/2$ for large Λ. This radius is before the single late termination. Multiplying the exact frozen numerator by $-bw_Y$ gives

$$-bw_Y\mathcal{N}_z^0(\tfrac{\hat\xi_\dagger^2}{2}) = 2Lb^2\tfrac{\hat\xi_f^2}{2}w_Y^2 - bw_Yc_1D_\dagger - \tfrac12 bw_Y\sigma_PD_\dagger^2 \le O(\Lambda^{-3}) - c_*D_\dagger/\Lambda^2 + O_\Lambda(C^{-2}).$$

Here $|\sigma_P| = O_\Lambda(C^{-2})$ by (I4). The frozen transport law, with $\ell_r = 1$ beyond $\frac{\hat\xi_f^2}{2}$, gives $(\hat\xi^{-1}\partial_{\hat\xi}(\frac{\hat\xi^2}{2}p_1^0)) = \frac{\hat\xi^2}{2}S_q^0/L$ there. Lemma 1.20.25(a) and the core bounds therefore give $|p_1^0(\frac{\hat\xi_\dagger^2}{2})| = O_\Lambda(1)$ uniformly in C and Y_f. Since $p_1^\flat > 0$ and $F_a \le K_F/C$, it follows that

$$LF_a^2p_1^\flat v^{00}(\tfrac{\hat\xi_\dagger^2}{2}) = LF_a^2p_1^\flat p_1^0(\tfrac{\hat\xi_\dagger^2}{2}) - bw_Y\mathcal{N}_z^0(\tfrac{\hat\xi_\dagger^2}{2}) < 0$$

after first fixing Λ large enough and then taking C large enough. For fixed Λ, C, the comparison of Theorem 1.20.28(c) up to $\frac{\hat\xi_\dagger^2}{2}$ uses only the value and history estimates of Lemma 1.20.19 and $t^{\mathrm{full}} = t^{00}E^0/E$. With $\beta = 1$, $\lambda = 0$ throughout this plateau, it gives $|\mathcal{P} - v^{00}| \le K(C)(2t_{\mathrm{act}} + \kappa_{\mathrm{act}}y_T)$ independently of the sign of v^{00}. Taking this error below one proves the claim. Transversality is an additional hypothesis for this obstruction; the modified construction uses (I6). □

Remark 1.20.30 (Compatibility of (M0)+(M1)). (1) *Reference pressure.* The ideal reference of Proposition 1.6.33 excludes the regular core, the activation and the five-moment correction (Section 1.6.4). So Π_{ref} is unchanged and Υ need not be even. In the activation zone H is fixed by the $\mathfrak{a}$-prescription, and β does not enter it. Downstream, the five-moment correction solves its three E rows with the U-square contribution in the target (Section 1.6.4). The normalized E-bump amplitudes and hence H there change by $O(B_{\mathrm{act}})$, with the complete axial budget in (2). The complete C_p is unchanged because that row is exact. The change is absorbed by the control decrease at Section 1.6.4. (M0) changes the activation H relative to v5. This is a per-member recomputation. (2) *Five-moment rows.* Write $t = t_{\mathrm{act}}$, $k = \kappa_{\mathrm{act}}$, $X(s) = X_ae^s$ and $n(s) = n_{s,r}(s,\eta)$. The symmetry of the step gives $\vartheta_\infty = 3t/2$, so $X_f = X(3t/2)$. For $y \ge 2t$, integrating (M0) from X_a and the core slope from X_a to X_f gives exactly

$$U(y) - U_r(X_f) = -\frac{k}{2}\int_0^y \beta(s)X(s)n^\flat(s)\,\mathrm{d}s + D_{\mathrm{col}},$$
$$D_{\mathrm{col}} = \frac12\int_0^{3t/2} X(s)n(s)\,\mathrm{d}s - \frac12\int_0^t (\kappa(s) - k)X(s)n(s)\,\mathrm{d}s.$$

Here $\beta = 1$, $n^\flat = n$ on $[0,t]$. Since $X_a = 4/(\Lambda b)$, the buffered core bounds in Lemma 1.20.27 give $\|D_{\mathrm{col}}\|_{C^1_\eta} \le K_{\mathrm{col}} t/\Lambda$. For $0 \le y \le y_T$ the same identity holds with the second integral in D_{col} stopped at $\min(y,t)$. In the integral multiplying k, differentiating β at fixed s costs at most $\|y_1'\|_\infty \|\sigma'\|_{L^1} \sup|Xn^\flat|$ after integration, also for a partial upper limit. The remaining terms are bounded by the core estimates and $y \le y_T$. Thus

$$\|U(y) - U_r(X_f)\|_{C^1_\eta|_y} \le B_{\mathrm{act}} := kK_\beta(C) + K_{\mathrm{col}} t/\Lambda.$$

The constants are fixed before k, t. In particular $\|y_1'\|_\infty \le (y_l - y_e)\|\zeta_3'\|_\infty \, 2\sup|Z_R Z_R'|/\delta_Z^2$, uniformly in C at fixed Λ. For the completed termination integral, further angular derivatives of its translated cutoff can be moved onto the smooth radial factor by integration by parts on its transition. Choose k, then $t \le \min\{y_*/8, k^2\}$ so that $B_{\mathrm{act}} \le \varepsilon_u/2$ and the late source bounds below hold. The factorization $T_0 = eB$ and the weight w_{in} live inside $\{y < y_e\}$, where $\beta \equiv 1$. The slow-solve cutoff $(R_{\mathrm{need}}, R_{\mathrm{cut}})$ of Lemma 1.21.1 is unchanged. (3) *Collars, covariance, two members.* On the collars $\Upsilon \equiv 1$ by (I6), so $y_1 = y_l$. The quantities ω_0, B_{r0} and y_l are common to both members, so β there is the same function of $y = 2\log(\hat\xi/\hat\xi_a)$ on both sides, with $b = \lambda_{\mathrm{ch}}$. The slice identity of Section 1.6.4 holds. The backward member uses Υ^b built from Z_* (Definition 1.20.35); Proposition 1.20.43 gives one activation on the collars. The pulse bumps (in y_p) are not touched. (4) *Gevrey class.* $Z_R \in G^{3/2}$. So $y_1 \in G^{3/2}(J)$, and it is constant near ± 1. $\beta = 1 - \sigma(\log(\frac{\hat\xi^2}{2}/(\frac{\hat\xi_a^2}{2}e^{y_1}))/\omega_0)$ is closure (g) of Lemma 1.25.5, the class of the shared cutoff (Proposition 1.22.4). (M0) is $\phi(\vartheta(y),\eta)$, also closure (g). (5) *E8 and E9.* E8: see the replacement of the comparison display at Section 1.6.4. E9: (M0).

The backward member. We use the chart of Remark 1.8.14 with $\varsigma = -1$, $\frac{\hat\xi_0^2}{2} = 4/\Lambda$, $y = 2\log(\hat\xi/\hat\xi_0)$, the core of Lemma 1.20.33 below, and its flattened reference (ϕ_r, U_r) of (1.20.13), with integrated coefficients $p_{s,r} = (p_{1,r}, p_{2,r})$ and $n_{s,r}$.

Lemma 1.20.31 (Transport laws with the side label)**.** *For smooth $H > 0$, U and histories as in Lemma 1.20.18, put $Q^{(\varsigma)} = [\varsigma\frac{\hat\xi^2}{2}H + \mathcal{K}H - \varsigma(1-h)\mathfrak{M}_2 + \varsigma(\frac12 - h)\eta\mathfrak{M}_{2\eta} - d\mathfrak{M}_{3\eta} + 2(h - (\frac12 - h))\eta\mathfrak{M}_3]/(\frac{\hat\xi^2}{2}H)$ and $\mathcal{N}_z^{(\varsigma)} = \varsigma\frac{\hat\xi^2}{2}U + \mathcal{K}U - \varsigma(\frac12 - h)(\mathfrak{M}_1 - \eta\mathfrak{M}_{1\eta}) + 4h\eta\mathfrak{M}_4 - d\mathfrak{M}_{4\eta} + \frac{\hat\xi^2}{2}((2 + 4h)\eta P - dP_\eta)$. Then*

$$D_y Q^{(\varsigma)} + (1+\ell_r)Q^{(\varsigma)} = S_q^{(\varsigma)} := \varsigma(\ell_r + h) + (\varsigma(\tfrac12 - h)\eta - dU)\partial_\eta \log H + 2h\eta U + \ell_r \frac{\mathcal{K}}{\frac{\hat\xi^2}{2}},$$

$$\hat\xi^{-1}\partial_{\hat\xi}\mathcal{N}_z^{(\varsigma)} = \varsigma((\tfrac12 + h)U + (\tfrac12 - h)\eta U_\eta + \tfrac12\hat\xi U_{\hat\xi}) + (1+2h)\eta U^2 - dUU_\eta + \mathcal{K}\frac{U_{\hat\xi}}{\hat\xi} + \frac{\eta H^2}{\hat\xi^2} + (2+4h)\eta P - dP_\eta.$$

For the frozen field ($\frac{U_{\hat\xi}}{\hat\xi} = 0$, F constant beyond $\frac{\hat\xi_f^2}{2}$), $(\hat\xi^{-1}\partial_{\hat\xi})^2\mathcal{N}_z^{(\varsigma)} = \sigma_P$ is the same for both labels.

Proof. The proof of Lemma 1.20.7 applies term by term. The constant ς term gives $\varsigma(1+\ell_r)$, and the $\varsigma(1-h)r$ term gives $-\varsigma(1-h)$. The ς-odd numerator terms $\varsigma\frac{\hat\xi^2}{2}U - \varsigma(\frac12 - h)(\mathfrak{M}_1 - \eta\mathfrak{M}_{1\eta})$ have $\frac{\hat\xi^2}{2}$-derivative $\varsigma((\frac12 + h)U + \frac12\hat\xi U_{\hat\xi} + (\frac12 - h)\eta U_\eta)$. The terms carrying σ_P are even. □

The backward core for a general datum. Let Π_0, $I = [-\eta_I, \eta_I]$, Ω and c be as in Theorem 1.8.10. For $0 < j_0 \le .05$ and $\sigma_* > 0$ define

$$U_* = 4\eta + j_0, \quad H_* = (\tfrac12 - h)\eta + dU_*, \quad W_* = 1 - dU_*' - 2(\tfrac12 - h)\eta U_*,$$

$$Z_* = -(\tfrac12+h)(1-2\eta U_*)U_* - H_*U_*' - d\Pi_0' + 4(\tfrac12+h)\eta\Pi_0,$$

$$\chi = \frac{H_*^2}{H_*^2+\sigma_*^2}, \qquad \zeta_* = -\frac{LH_*}{H_*^2+\sigma_*^2}, \qquad \xi_0 = \Lambda\zeta_*, \qquad \phi_* = \exp\Big(\Lambda\int_0^\eta \zeta_*\Big),$$

the radial variable $Y = \Lambda\frac{\hat\xi^2}{2}$, $\frac{\hat\xi_0^2}{2} = 4/\Lambda$, and $f_0(z) = \sum_{\alpha\ge0}(-z/2)^\alpha/(\alpha!(\alpha+1)!)$, so that $f_0(z) = 2J_1(s)/s$ with $s=\sqrt{2z}$. The coefficient space $\mathcal{B}_\rho$ consists of sequences $F=(F_\alpha)_{\alpha\ge0}$ of smooth functions on I, standing for $\sum_\alpha F_\alpha(\eta)Y^\alpha$, with the norm $\|F\|_\rho = \sup_{\alpha,\beta}\sup_I|\partial_\eta^\beta F_\alpha|/a_{\alpha\beta}$, where $a_{\alpha\beta} = 20^{-\alpha}\rho^{-\beta}\beta!\binom{\alpha+\beta}{\beta}(\alpha+1)^{-2}(\beta+1)^{-2}$. The operators J_ν (inverse of $Y\partial_Y^2+\nu\partial_Y$ with zero axis value), $\mathcal{I}F = \int_0^Y F$, $\mathcal{A}_{\rm rad} = Y^{-1}\mathcal{I}$ and $Y\partial_Y$ act coefficientwise. $\mathcal{B}_\rho$ is complete: for a Cauchy sequence each $\partial_\eta^\beta F_\alpha$ converges uniformly on I, the limits are the derivatives of the limit coefficients, and the weighted bounds pass to the limit.

Lemma 1.20.32 (Coefficient estimates at the axis)**.** *The space $\mathcal{B}_\rho$ is an algebra. The operators J_ν ($\nu=1,2$), $\mathcal{A}_{\rm rad}$, multiplication by Y, $\mathcal{I}$ and $\partial_\eta\mathcal{I}$ are bounded on it. Moreover,*

$$\|J_\nu[(\partial_\eta F)(Y\partial_Y G)]\|_\rho \le C_\rho\|F\|_\rho\|G\|_\rho.$$

This estimate also holds with either derivative omitted and with any fixed number of additional undifferentiated factors, multiplying the right-hand side by their norms and changing the constant.

Proof. Write $w_j=(j+1)^{-2}$. Splitting the sum at $n/2$ gives $\sum_{i=0}^n w_iw_{n-i}\le Cw_n$ with $C=8\sum_{j\ge0}w_j$. In the Leibniz rule at radial degree n and derivative order l, the factorials cancel against $\binom{l}{k}$. The remaining factor

$$\frac{\binom{i+k}{k}\binom{n-i+l-k}{l-k}}{\binom{n+l}{l}} \le 1$$

counts a subset of all choices of l elements from $n+l$. The convolution estimate in each index now gives the product bound C^2. At degree $i+1$ the coefficients of $\mathcal{I}F$ and $J_\nu F$ are $F_i/(i+1)$ and $F_i/((i+1)(i+\nu))$ respectively, by integration and by differentiating Y^{i+1}. Both constant coefficients vanish. Averaging divides degree i by $i+1$. The two weight comparisons

$$\frac{a_{i,k}}{a_{i+1,k}} \le 80, \qquad \frac{a_{i,k+1}}{a_{i+1,k}} = \frac{20(i+1)}{\rho}\frac{(i+2)^2}{(i+1)^2}\frac{(k+1)^2}{(k+2)^2} \le \frac{80(i+1)}{\rho}$$

give all the single-operator bounds, including the parameter derivative after integration. For the mixed estimate, assign the degree gained from J_ν to the differentiated coefficient F_i. Bound its $(k+1)$st derivative by $80(i+1)a_{i+1,k}\|F\|_\rho/\rho$. If G has degree j, its radial derivative contributes j. At output degree N one has $(i+1)j\le N(N-1+\nu)$, the divisor in J_ν. What remains is precisely the product convolution at degree N. For an omitted derivative use $a_{i,k}\le 80a_{i+1,k}$ or replace j by 1. Extra undifferentiated factors enter the same convolution without changing the divisor bound. □

Lemma 1.20.33 (The backward core for a general datum)**.**

(a) On I, $L\ge.97$ and $-W_*\ge2.85$. H_* has exactly one zero η_0 in I; it satisfies $-j_0/4\le\eta_0<0$ and $Z_*(\eta_0)>0$. Hence one can choose $\delta_*>0$ and then $\sigma_*>0$ such that $\chi>.99$ on $\{\eta\in I:|Z_*(\eta)|\le\delta_*\}$; every smaller σ_* has the same property.

(b) There are $r_1>0$, $\Lambda_0\ge1$, for each $\Lambda\ge\Lambda_0$ a threshold $C_0(\Lambda)\ge\sup_{\Omega_1}|\phi_*|$, where $\Omega_1=\{\eta\in\mathbb{C}:\operatorname{dist}(\eta,I)<r_1\}$, and a complex neighbourhood $\mathcal{N}$ of $[0,4.1]\times I$, independent of Λ and C,

with the following property. For $\Lambda \ge \Lambda_0$ and $C \ge C_0(\Lambda)$ there are Φ, u, holomorphic on $\mathcal{N}$ and real on $[0,4.1]\times I$, with $\Phi(0,\cdot)=1$ and $u(0,\cdot)=0$, such that

$$\phi = \phi_*\Phi, \qquad U = U_* + \Lambda^{-1}u, \qquad \Pi = \Pi_0 + \Lambda^{-1}\mathcal{I}(g^2\Phi^2), \qquad g = \phi_*/C, \tag{1.20.10}$$

solve (1.4.6) with $\frac{\Pi_{\hat\xi}}{\hat\xi} = \phi^2/C^2$ ((1.1.3)) on $0 \le Y \le 4.1$, and for all $r,s \ge 0$

$$\sup_{[0,4.1]\times I} \Big|\partial_Y^r \partial_\eta^s \Big(\Phi - f_0(Y\chi),\ u + \frac{YZ_*}{2L}\Big)\Big| \le \frac{C_{r,s}}{\Lambda}, \tag{1.20.11}$$

with $C_{r,s}$ independent of $\Lambda \ge \Lambda_0$ and $C \ge C_0(\Lambda)$.

(c) After increasing Λ_0, and then $C_0(\Lambda)$, the following hold on $[0,4.1]\times I$, that is, for $0 \le \frac{\hat\xi^2}{2} \le 4.1/\Lambda$, with constants K_0, c_1, C_1 independent of $\Lambda \ge \Lambda_0$ and $C \ge C_0(\Lambda)$.

(c1) $\Phi \ge c_0 := .26$ and $\phi > 0$. The leading residual stress vanishes, $T_0 = 0$, and $p_1 = a = -2Y\Phi_Y/\Phi$, $n_s = -2u_Y$, $p_2 = -b_s$.

(c2) $|Y\Phi_Y/\Phi| + |H_*\partial_\eta \log\Phi| \le K_0(\chi + \Lambda^{-1})$.

(c3) $S_q \ge 2.5 + .95\Lambda L\chi$.

(c4) $p_1(0,\eta) = 0$, $0 < p_1 \le C_1$ for $\hat\xi > 0$, and $p_1/\frac{\hat\xi^2}{2} \ge c_1$, with its continuous extension at $\hat\xi = 0$ understood. Also $|n_s - Z_*/L| \le K_0\Lambda^{-1}$.

(c5) At $\frac{\hat\xi_0^2}{2}$: $p_1 \ge 3.3$ on $\{\chi \ge .99\}$, and $v := p_1 + p_2^2/p_1 > 2.2$ on I.

(c6) For each k and r, the C^k_η norms of ∂_Y^r of $\Phi^{\pm1}$, $\log\Phi$, u, p_1 and n_s are bounded independently of $\Lambda \ge \Lambda_0$ and $C \ge C_0(\Lambda)$.

These are the conclusions of [42, Props. B.2, B.3] for the datum Π_0. In this text (B.13) denotes (1.20.11), and (B.20), (B.17), (B.18), (B.19) denote (c2), (c3), (c4), (c5).

Proof. (a) On I we have $|\eta| \le 1.02$ and $h \le .01$, so $L \ge 1 - 2h(1.02)^2 \ge .97$; since $U_*' = 4$, $-W_* = 3 - 8h\eta^2 + (1-2h)j_0\eta \ge 3 - .084 - .051 \ge 2.85$. For $|\eta| < 1$ the function $H_*/d = (\frac12 - h)\eta/d + 4\eta + j_0$ increases strictly from $-\infty$ to $+\infty$, so it has exactly one zero η_0, and $\eta_0((\frac12 - h) + 4d_0) = -d_0 j_0$ with $d_0 = 1 - \eta_0^2$ gives $-j_0/4 \le \eta_0 < 0$. For $1 \le |\eta| \le 1.02$ we have $|(1-\eta^2)(4\eta + j_0)| \le .0404 \cdot 4.13 < .17 < (\frac12 - h)|\eta|$, so $H_* \ne 0$ there. At η_0: $U_*(\eta_0) = -(\frac12 - h)\eta_0/d_0$, so $|U_*(\eta_0)| \le .51|\eta_0|$ and $|1 - 2\eta_0 U_*(\eta_0)| \le 1.01$; the term H_*U_*' vanishes; $-d_0\Pi_0'(\eta_0) \ge 0$, because $\eta_0 < 0$ and $\eta\Pi_0' > 0$; and $4(\frac12 + h)\eta_0\Pi_0(\eta_0) \ge 4(\frac12 + h)|\eta_0| cP_*^2 f(\eta_0)^2 \ge 1.99\, cP_*^2|\eta_0|$. Hence $Z_*(\eta_0) \ge |\eta_0|(1.99\, cP_*^2 - .27) > 0$, as $cP_*^2 \ge 1$. By continuity $Z_* > Z_*(\eta_0)/2$ on a neighbourhood N_0 of η_0 in I. Take $0 < \delta_* < Z_*(\eta_0)/2$. Then $\{|Z_*| \le \delta_*\} \subset I \setminus N_0$, where $|H_*| \ge h_0$ for some $h_0 > 0$, and every $\sigma_* \le h_0/10$ gives $\chi \ge 100/101 > .99$ there.

(b) *Step 1: the equations.* Choose $r_1 > 0$ with $\overline{\Omega_1} \subset \Omega$ such that L and $H_*^2 + \sigma_*^2$ have no zero on $\overline{\Omega_1}$; this is possible, as $L \ge .97$ and $H_*^2 + \sigma_*^2 \ge \sigma_*^2$ on I. Ω_1 is convex, so ζ_*, ϕ_* and the functions below are holomorphic on it, and $\phi_* > 0$ on I. If $C \ge \sup_{\Omega_1}|\phi_*|$, then $|g| \le 1$ on Ω_1. Insert (1.20.10) into (1.4.1)–(1.4.2). Since $E = \hat\xi\phi_*\Phi/C$ and $H = \hat\xi^2\phi_*\Phi/C$, we have $l = 1 + (Y\partial_Y)\log\Phi$ and $(\log E)_\eta = \xi_0 + \partial_\eta\log\Phi$. Also $H_c = H_* + \Lambda^{-1}du$, and, as $\mathcal{A}_{\rm rad}(U_*) = U_*$, $W = W_* + \Lambda^{-1}B$ with $B = -(1-2h)\eta\mathcal{A}_{\rm rad}(u) - d\partial_\eta\mathcal{A}_{\rm rad}(u)$. In the variable $\frac{\hat\xi^2}{2}$, $\frac{\Pi_{\hat\xi}}{\hat\xi} = \phi^2/C^2 = g^2\Phi^2$; so $\Pi = \Pi_0 + \Lambda^{-1}p$ with $p = \mathcal{I}(g^2\Phi^2)$, and $(Y\partial_Y)\Pi = \Lambda^{-1}(Y\partial_Y)p$, $(Y\partial_Y)p = Yg^2\Phi^2$. Since $H_*\xi_0 = -\Lambda L\chi$, the sources of (1.4.1)–(1.4.2) are, exactly,

$$S_q = \Lambda L\chi - \frac{LR_1}{\Phi}, \qquad S_n = Z_* - \Lambda^{-1}LR_2,$$

$$LR_1 = [W + h(1-2\eta U) + du\zeta_*]\Phi + W(Y\partial_Y)\Phi + H_c\partial_\eta\Phi,$$
$$LR_2 = [(\tfrac12 + h)(1-4\eta U_*) + dU_*']u - (1+2h)\eta\Lambda^{-1}u^2 + W(Y\partial_Y)u$$
$$+ H_*\partial_\eta u + d\Lambda^{-1}u\partial_\eta u - (2+4h)\eta p + d\partial_\eta p - 2\eta(Y\partial_Y)p.$$

(For S_n expand $-(\frac12+h)(1-2\eta U)U$, $-H_cU_\eta$ and $-d\Pi_\eta + (2+4h)\eta\Pi$ in powers of Λ^{-1}; the terms of order zero add up to Z_*.) Moreover $\frac{\hat\xi^2}{2}(\frac{\phi_{\hat\xi\hat\xi}}{\hat\xi^2} - \frac{\phi_{\hat\xi}}{\hat\xi^3}) + 2\frac{\phi_{\hat\xi}}{\hat\xi} = \Lambda\phi_*(Y\Phi_{YY} + 2\Phi_Y)$ and $\frac{\hat\xi^2}{2}(\frac{U_{\hat\xi\hat\xi}}{\hat\xi^2} - \frac{U_{\hat\xi}}{\hat\xi^3}) + \frac{U_{\hat\xi}}{\hat\xi} = Yu_{YY} + u_Y$. So, where $\Phi \neq 0$, (1.4.6) is equivalent to

$$2(Y\Phi_{YY} + 2\Phi_Y) = -\chi\Phi + \Lambda^{-1}R_1, \qquad 2(Yu_{YY} + u_Y) = -Z_*/L + \Lambda^{-1}R_2. \tag{1.20.12}$$

Step 2: the fixed coefficients. Fix $\rho = r_1/4$. A function m of η alone, holomorphic on Ω_1 with $|m| \le M$ there, is an element of $\mathcal{B}_\rho$ with only $\alpha = 0$. Cauchy's inequality on discs of radius $r_1/2$ gives $|m^{(\beta)}| \le M\beta!(2/r_1)^\beta$ on I, hence $\|m\|_\rho \le MK_\rho$ with $K_\rho = \sup_\beta 2^{-\beta}(\beta+1)^2 < \infty$. This applies to χ, ζ_*, U_*, W_*, H_*, Z_*/L, $1/L$, d, η and $(\frac12+h)(1-4\eta U_*) + dU_*'$, with bounds independent of Λ and C; and to g, with $\|g\|_\rho \le K_\rho$ for every Λ and every $C \ge \sup_{\Omega_1}|\phi_*|$.

Step 3: the angular term. By Lemma 1.20.32, $(J_2F)_{\alpha+1} = F_\alpha/((\alpha+1)(\alpha+2))$, and $a_{\alpha\beta}/a_{\alpha+1,\beta} = 20\frac{(\alpha+2)^2}{(\alpha+1)^2}\frac{\alpha+1}{\alpha+\beta+1} \le 80$. So if $F_\alpha = 0$ for $\alpha < b$, then $\|J_2F\|_\rho \le \frac{80}{(b+1)(b+2)}\|F\|_\rho$ and $(J_2F)_\alpha = 0$ for $\alpha < b+1$. Let M_χ be the norm of multiplication by χ on $\mathcal{B}_\rho$ from Lemma 1.20.32; it preserves the vanishing of the coefficients below a given degree, since χ does not depend on Y. For $T = J_2\chi/2$ (multiplication first) we get $\|T^k\| \le (40M_\chi)^k/(k!(k+1)!)$, so $(1+T)^{-1} = \sum_k (-T)^k$ converges in operator norm. Since $(Y\partial_Y^2 + 2\partial_Y)Y^n = n(n+1)Y^{n-1}$, $\Phi_0 := f_0(Y\chi)$ satisfies $2(Y\Phi_{0,YY} + 2\Phi_{0,Y}) = -\chi\Phi_0$ and $\Phi_0(0) = 1$, that is, $\Phi_0 = 1 - T\Phi_0 = (1+T)^{-1}1$. Also $u_0 := -YZ_*/(2L) = J_1(-Z_*/(2L))$.

Step 4: contraction. R_1 and R_2 are finite sums of products of the following factors: fixed functions of Step 2 and powers of $\Lambda^{-1} \le 1$; at most two of Φ, u, $\mathcal{A}_{\rm rad}(u)$; at most one of $\partial_\eta\Phi$, $\partial_\eta u$, $\partial_\eta\mathcal{A}_{\rm rad}(u)$; at most one of $(Y\partial_Y)\Phi$, $(Y\partial_Y)u$; and p, $\partial_\eta p = \partial_\eta\mathcal{I}(g^2\Phi^2)$, $(Y\partial_Y)p = Yg^2\Phi^2$. Applying Lemma 1.20.32 term by term, the maps $(\Phi,u) \mapsto J_2R_1$ and $(\Phi,u) \mapsto J_1R_2$ are bounded and Lipschitz on the ball $\mathbb{B} = \{\|\Phi - \Phi_0\|_\rho \le 1,\ \|u - u_0\|_\rho \le 1\}$ of $\mathcal{B}_\rho^2$. For the Lipschitz bound, change one factor of each product at a time. The constant K_N depends on ρ, the bounds of Step 2 and $\|\Phi_0\|_\rho, \|u_0\|_\rho$, but not on $\Lambda \ge 1$ or on $C \ge \sup_{\Omega_1}|\phi_*|$. Put

$$\mathcal{S}(\Phi,u) = \Big(\Phi_0 + \frac{(1+T)^{-1}J_2R_1}{2\Lambda},\ u_0 + \frac{J_1R_2}{2\Lambda}\Big).$$

For $\Lambda \ge \Lambda_0 := 2K_N(1 + \|(1+T)^{-1}\|)$, $\mathcal{S}$ maps $\mathbb{B}$ into itself and is a contraction with constant $\le \frac12$. Its fixed point satisfies $\|\Phi - \Phi_0\|_\rho + \|u - u_0\|_\rho \le K_N'/\Lambda$. The data are real on I, so $\mathcal{S}$ preserves the closed set of real coefficient sequences, and the fixed point is real. Applying $1+T$, the fixed point satisfies $\Phi = 1 + J_2(-\chi\Phi + \Lambda^{-1}R_1)/2$ and $u = J_1(-Z_*/L + \Lambda^{-1}R_2)/2$; so, coefficientwise, (1.20.12) holds with $\Phi(0) = 1$, $u(0) = 0$.

Step 5: analyticity and (B.13). For $F \in \mathcal{B}_\rho$, $|\partial_\eta^\beta F_\alpha| \le \|F\|_\rho a_{\alpha\beta}$ on I. Hence the Taylor series of F_α at each $\eta_r \in I$ converges to F_α on $|\eta - \eta_r| < \rho$ (the remainder of order N is at most $\|F\|_\rho 20^{-\alpha}\binom{\alpha+N}{N}(|\eta-\eta_r|/\rho)^N \to 0$), so F_α extends holomorphically to $\{\mathrm{dist}(\eta,I) < \rho\}$. On $\mathrm{dist}(\eta,I) \le q\rho$, $q = \frac38$, the identity $\sum_\beta \binom{\alpha+\beta}{\beta}q^\beta = (1-q)^{-\alpha-1}$ gives $|F_\alpha| \le \|F\|_\rho 20^{-\alpha}(1-q)^{-\alpha-1}$. So for $|Y| \le 5$, $\sum_\alpha |F_\alpha||Y|^\alpha \le \|F\|_\rho\frac85\sum_\alpha(.4)^\alpha = \frac83\|F\|_\rho$. Put $\mathcal{N} = \{|Y| < 5\} \times \{\mathrm{dist}(\eta,I) < 3\rho/8\}$. Then $F = \sum_\alpha F_\alpha Y^\alpha$ is holomorphic on $\mathcal{N}$, with $\sup_{\mathcal{N}}|F| \le \frac83\|F\|_\rho$. The products and operators of Step 4 correspond to the same operations on these functions, so (1.20.12) holds on $\mathcal{N}$. Cauchy's inequality on polydiscs of radii $(\frac12, \frac{\rho}{8})$ centred on $[0,4.1] \times I$, which lie in $\mathcal{N}$, gives $\sup_{[0,4.1]\times I}|\partial_Y^r\partial_\eta^s F| \le r!\,s!\,2^r(8/\rho)^s\frac83\|F\|_\rho$. Applied to $F = \Phi - \Phi_0$ and $F = u - u_0$, this is (1.20.11).

By (c1) below, $\Phi > 0$ on the real rectangle. So, by Step 1, (1.20.10) solves (1.4.6) there. It is analytic in $\frac{\hat\xi^2}{2} = Y/\Lambda$, so ϕ, U, Π are smooth at the axis.

(c) (c1): $f_0(z) = 2J_1(s)/s$ is decreasing on $[0, 4.1]$, by the differentiated series estimate $f_0'(z) \le -1/4 + z/24 < 0$; and $f_0(4.1) > .271$ by the rational alternating-series lower bound in the proof of Corollary 1.6.43. Since $0 \le Y\chi \le 4.1$ on the real rectangle, (1.20.11) gives $\Phi \ge .271 - C_{0,0}/\Lambda \ge .26$ for Λ large, and $\phi = \phi_*\Phi > 0$. The regular solution of each equation of (1.4.1)–(1.4.2) is unique, because the homogeneous solutions $C_Q/(\frac{\hat\xi^2}{2}H)$ and $C_N/\frac{\hat\xi^2}{2}$ are singular at $\hat\xi = 0$ (the regular primitives of Lemma 1.4.1). The function $\widetilde Q = -2L\frac{\phi_{\hat\xi}}{\hat\xi}/\phi$ is smooth at $\hat\xi = 0$, and $(Y\partial_Y)\widetilde Q + (1+l)\widetilde Q = -2L(\frac{\hat\xi^2}{2}(\frac{\phi_{\hat\xi\hat\xi\hat\xi}}{\hat\xi^2} - \frac{\phi_{\hat\xi}}{\hat\xi^3}) + 2\frac{\phi_{\hat\xi}}{\hat\xi})/\phi = S_q$ by (1.4.6); hence $Q_s = \widetilde Q$. Likewise $\widetilde N = -2L\frac{U_{\hat\xi}}{\hat\xi}$ is regular and $(Y\partial_Y)\widetilde N + \widetilde N = -2L(\frac{\hat\xi^2}{2}(\frac{U_{\hat\xi\hat\xi}}{\hat\xi^2} - \frac{U_{\hat\xi}}{\hat\xi^3}) + \frac{U_{\hat\xi}}{\hat\xi}) = S_n$, so $N_s = \widetilde N$. Thus $p_1 = \frac{\hat\xi^2}{2}Q_s/L = -2(Y\partial_Y)\log\phi = 2 - 2l = a$, $n_s = N_s/L = -2\frac{U_{\hat\xi}}{\hat\xi} = -2u_Y$, and $p_2 = \frac{\hat\xi^2}{2}n_s/E = -2(Y\partial_Y)U/E = -b_s$. So $p_s = s$, $T_0 = F(p_s - s) = 0$ ((1.4.4)), and $a = -2Y\Phi_Y/\Phi$.

(c2): $Y\partial_Y\Phi_0 = Y\chi f_0'(Y\chi)$ and $H_*\partial_\eta\Phi_0 = YH_*\chi' f_0'(Y\chi)$, with $|H_*\chi'| = 2H_*^2\sigma_*^2|H_*'|/(H_*^2+\sigma_*^2)^2 \le 2|H_*'|\chi$. With (1.20.11) and $\Phi \ge c_0$ this gives (c2).

(c3): By Step 1, $S_q = -Wl - h(1-2\eta U) - H_c(\log E)_\eta$ with $l = 1 + Y\Phi_Y/\Phi$. The bounds of Step 4 give $|u| + |\partial_\eta u| + |B| \le K_0$ on the real rectangle, so $|U| \le 4.2$ for Λ large. Hence: $-Wl = -W_* - W_*Y\Phi_Y/\Phi - \Lambda^{-1}Bl \ge 2.85 - K_0(\chi + \Lambda^{-1})$ by (a) and (c2); $-h(1-2\eta U) \ge -9.6h \ge -.096$; $-H_c(\log E)_\eta = \Lambda L\chi - du\zeta_* - H_*\partial_\eta\log\Phi - \Lambda^{-1}du\partial_\eta\log\Phi \ge \Lambda L\chi - K_0L\sqrt{\chi}/\sigma_* - K_0(\chi+\Lambda^{-1})$, since $|\zeta_*| \le L|H_*|/(H_*^2+\sigma_*^2) \le L\sqrt{\chi}/\sigma_*$. So $S_q \ge 2.75 + \Lambda L\chi - K_0\chi - K_0L\sqrt{\chi}/\sigma_* - K_0/\Lambda$. Young's inequality gives $K_0L\sqrt{\chi}/\sigma_* \le .025\Lambda L\chi + 10K_0^2L/(\Lambda\sigma_*^2)$, and $K_0\chi \le .025\Lambda L\chi$ for $\Lambda \ge 42K_0$. Since σ_* is fixed before Λ, $S_q \ge 2.5 + .95\Lambda L\chi$ for Λ large.

(c4) At fixed η, write the regular primitive of Lemma 1.4.1 in the scaled variable $Y = \Lambda\xi^2/2$. For $Y > 0$ it gives

$$Q_s(Y) = \frac{\int_0^Y y\Phi(y)S_q(y)\,\mathrm{d}y}{Y^2\Phi(Y)} \ge \frac{2.5c_0}{2\sup\Phi}.$$

The bound extends to $Y = 0$ by continuity. Thus $p_1/\frac{\hat\xi^2}{2} = Q_s/L \ge c_1 := 1.25c_0/\sup\Phi$. The bound $p_1 \le C_1$ follows from $p_1 = -2Y\Phi_Y/\Phi$, and $n_s = -2u_Y = Z_*/L + O(\Lambda^{-1})$ from (1.20.11).

(c5): At $Y = 4$, $Y\Phi_Y = Y\chi f_0'(Y\chi) + O(\Lambda^{-1})$, so $p_1 = -2zf_0'(z)/f_0(z) + O(\Lambda^{-1})$ with $z = 4\chi$. From $f_0 = 2J_1(s)/s$ we get $-2zf_0'/f_0 = sJ_2(s)/J_1(s)$, which is strictly larger than $33/10$ for $z \ge 99/25$, with a fixed positive margin by Lemma 1.6.44. So $p_1 \ge 3.3$ on $\{\chi \ge .99\}$ for Λ large, and there $v \ge p_1 > 2.2$. On $\{\chi < .99\}$, (a) gives $|Z_*| > \delta_*$, so $|n_s| \ge \delta_*/2$ for Λ large, by (c4) and $L \le 1$. At $\frac{\hat\xi_0^2}{2} = 4/\Lambda$, $|p_2| = \frac{\hat\xi_0^2}{2}|n_s|/E = C\sqrt{2/\Lambda}\,|n_s|/(\phi_*\Phi) \ge C\sqrt{2/\Lambda}\,\delta_*/(2\sup_I\phi_*\sup\Phi)$. With $p_1 \le C_1$, $p_2^2/p_1 > 2.2$ once $C \ge C_0(\Lambda)$ for a suitable $C_0(\Lambda)$.

(c6): This follows from the $\mathcal{B}_\rho$ bounds of Steps 4–5, from (c1) and from the identities in (c1). □

The backward reference on $[\frac{\hat\xi_0^2}{2}, \frac{\hat\xi_i^2}{2}]$. Put $\xi_0^2/2 = 4/\Lambda$, $y = 2\log(\xi/\xi_0)$ and $Y = \Lambda\xi^2/2$. Fix $\bar t > 0$ with $4e^{2\bar t} < 4.1$ and choose $0 < t_1 \le \bar t$. Let $(\phi_{\mathrm{nat}}, U_{\mathrm{nat}})$ be the axis solution in Lemma 1.20.33. Its flattened reference agrees with it on $y \le t_1$. With those inlet values prescribe

$$\partial_y(\log\phi_r, U_r) = \big[1 - \sigma((y-t_1)/t_1)\big]\,\partial_y(\log\phi_{\mathrm{nat}}, U_{\mathrm{nat}}) \qquad (t_1 < y < 2t_1), \tag{1.20.13}$$

and extend both functions constantly in y for $y \ge 2t_1$. Compute pressure and the two integrated coefficients from the axis using Lemma 1.4.1 with the same Π_0. Thus $p_{1,r} = \xi^2Q_{s,r}/(2L)$ and $n_{s,r} = N_{s,r}/L$. Here $\xi_f^2/2 = (\xi_0^2/2)e^{2t_1} \le 4.1/\Lambda$. K_0 denotes constants independent of $\Lambda \ge \Lambda_0$, $C \ge C_0(\Lambda)$ and $t_1 \in (0, \bar t]$. K, K_k denote constants that may depend on Λ but not on C or t_1.

Lemma 1.20.34 (The backward reference on $[\frac{\hat\xi_0^2}{2},\frac{\hat\xi_i^2}{2}]$)**.** *Let $\frac{\hat\xi_i^2}{2}\ge 110$ be fixed before Λ. After increasing Λ_0 and then $C_0(\Lambda)$, (a)–(g) hold for every $t_1\in(0,\bar t]$. So the lemma imposes no condition on t_1 (Remark 1.8.12(d)).*

(a) Frozen identity. *On $[\frac{\hat\xi_f^2}{2},\infty)$, $\phi_r=\phi_a:=\phi_r(\frac{\hat\xi_f^2}{2},\cdot)$, $U_r=U_a:=U_r(\frac{\hat\xi_f^2}{2},\cdot)$ and $l_r=1$. With $k_a=(1-2h)\eta U_a+dU_a'$ and $S_\infty:=-(1-k_a)-h(1-2\eta U_a)-((\frac12-h)\eta+dU_a)(\log\phi_a)'$,*

$$S_{q,r}(\tfrac{\hat\xi^2}{2})=S_\infty+\frac{\frac{\hat\xi_f^2}{2}}{\frac{\hat\xi^2}{2}}(S_{q,r}(\tfrac{\hat\xi_f^2}{2})-S_\infty)\qquad(\tfrac{\hat\xi^2}{2}\ge\tfrac{\hat\xi_f^2}{2}).$$

(b) $S_\infty\ge .94L\Lambda\chi+2.6$. Hence $S_{q,r}\ge .94L\Lambda\chi+2.4$ and $l_r\le 1$ on $[\frac{\hat\xi_0^2}{2},\infty)$.

(c) $p_{1,r}>0$ and $p_{1,r}(\frac{\hat\xi^2}{2})\ge p_{1,r}(\frac{\hat\xi_0^2}{2})(\hat\xi_0/\hat\xi)^2+1.2(\frac{\hat\xi^2}{2}-\frac{\hat\xi_0^4}{4}/\frac{\hat\xi^2}{2})$ on $[\frac{\hat\xi_0^2}{2},\infty)$. So $p_{1,r}>3$ for $\frac{\hat\xi^2}{2}\ge 3$. Moreover $v_r=p_{1,r}+p_{2,r}^2/p_{1,r}\ge 3.2$ on $[\frac{\hat\xi_0^2}{2},\frac{\hat\xi_i^2}{2}]$. We put $c:=1$, so that $v_r>2+c$.

(d) On the core, $p_1=a=-2Y\Phi_Y/\Phi$ and $n_s=-2u_Y$. Moreover $p_{1,r}\ge 3.3$ on $\{\chi\ge .99\}\times[\frac{\hat\xi_0^2}{2},\infty)$.

(e) For each k, $\|\phi_r^{\pm1}\|_{C_\eta^k}\le K_k$ on $[0,\infty)$; so $E_r=\hat\xi\phi_r/C\le\hat\xi K_F/C$ with $K_F:=\sup\phi_r$. Also $\|\Pi_r-\Pi_0\|_{C_\eta^k}\le K_k\frac{\hat\xi^2}{2}C^{-2}$.

(f) $|S_{n,r}-Z_*|\le K_0\Lambda^{-1}+K\frac{\hat\xi^2}{2}C^{-2}$ on $[\frac{\hat\xi_0^2}{2},\infty)$, and $|n_{s,r}-Z_*/L|\le K_0\Lambda^{-1}+K\frac{\hat\xi_i^2}{2}C^{-2}$ on $[\frac{\hat\xi_0^2}{2},\frac{\hat\xi_i^2}{2}]$. In particular, on $\{\chi\le .99\}$ the function $n_{s,r}$ has the sign of Z_* and $|n_{s,r}|\ge\delta_*/(2L)$.

(g) For each k, the C_η^k norms of $p_{1,r}$ and $n_{s,r}$ on $[\frac{\hat\xi_0^2}{2},\frac{\hat\xi_i^2}{2}]$ are bounded by constants M_k,N_k independent of C and t_1.

Proof. (a) For $y\ge 2t_1$, (1.20.13) gives $\partial_y\log\phi_r=\partial_yU_r=0$. Since $H=\hat\xi^2\phi/C$, $l_r=1+\frac12\hat\xi\partial_{\hat\xi}\log\phi_r=1$. Also $(\log E_r)_\eta=(\log\phi_a)'$ at fixed $\hat\xi$, because $\frac{\hat\xi_0^2}{2}$ does not depend on η, and $\mathfrak M_{1r}(\hat\xi)=\mathfrak M_{1r}(\hat\xi_f)+U_a(\frac{\hat\xi^2}{2}-\frac{\hat\xi_f^2}{2})$. With $\mathcal K=(1-2h)\eta\mathfrak M_1+d\mathfrak M_{1\eta}$ we have $W=1-\mathcal K/\frac{\hat\xi^2}{2}$ (Lemma 1.4.1, $\mathcal A_{\rm rad}(U)=\mathfrak M_1/\frac{\hat\xi^2}{2}$). So $W_r=1-k_a-(\mathcal K_r(\frac{\hat\xi_f^2}{2})-k_a\frac{\hat\xi_f^2}{2})/\frac{\hat\xi^2}{2}$, and the source $S_q=-Wl-h(1-2\eta U)-H_c(\log E)_\eta$ of (1.4.1)–(1.4.2) becomes $S_{q,r}=S_\infty+(\mathcal K_r(\frac{\hat\xi_f^2}{2})-k_a\frac{\hat\xi_f^2}{2})/\frac{\hat\xi^2}{2}$. Evaluating at $\frac{\hat\xi_f^2}{2}$ gives the identity. (This is Lemma 1.20.25(a) for $\varsigma=-1$.)

(b) On $y\le t_1$ the reference is the axis profile; on $[t_1,2t_1]$ (1.20.13) integrates $\frac12\hat\xi\partial_{\hat\xi}U_{\rm nat}=\Lambda^{-1}Y\partial_Yu$ and $\frac12\hat\xi\partial_{\hat\xi}\log\phi_{\rm nat}=Y\partial_Y\log\Phi$. Hence, with $Y_1=4e^{t_1}$ and $s(y)=1-\sigma((y-t_1)/t_1)$,

$$U_a=U_*+\Lambda^{-1}u_a,\qquad u_a=u(Y_1,\cdot)+\int_{t_1}^{2t_1}s\,(Y\partial_Yu)(4e^y,\cdot)\,\mathrm dy,$$
$$\log\phi_a=\log\phi_*+\ell_a,\qquad \ell_a=\log\Phi(Y_1,\cdot)+\int_{t_1}^{2t_1}s\,(Y\partial_Y\log\Phi)(4e^y,\cdot)\,\mathrm dy.$$

All arguments lie in $[0,4.1]$. By (B.13) with $r,s\le 2$ and $\Phi\ge c_0$ (Lemma 1.20.33(c1)): $|u_a|+|u_a'|+|\ell_a'|\le K_0$. Moreover $|H_*\ell_a'|\le K_0(\chi+\Lambda^{-1})$. Indeed, (B.13) gives $\partial_\eta\Phi=Y\chi'f_0'(Y\chi)+O(\Lambda^{-1})$ and $\partial_\eta(Y\Phi_Y)=Y\chi'[f_0'+Y\chi f_0'']Y\chi)+O(\Lambda^{-1})$, and $|H_*\chi'|=2H_*^2\sigma_*^2|H_*'|/(H_*^2+\sigma_*^2)^2\le 2|H_*'|\chi$. Now we estimate the three parts of S_∞.

- By (B.1), $-(1-k_a) = -W_* + 2(\frac12 - h)\eta(U_a - U_*) + d(U_a - U_*)' \ge -W_* - 3K_0/\Lambda$, and $-W_* = 3 - 8h\eta^2 + (1-2h)j_0\eta \ge 2.87$, since $h \le 10^{-2}$ and $j_0 \le .05$.
- Next, $-h(1-2\eta U_a) \ge -9.2h \ge -.093$, since $|U_a| \le 4.1$.
- By (B.3), $-H_*\Lambda\zeta_* = \Lambda L\chi$. So $-((\frac12 - h)\eta + dU_a)(\log\phi_a)' = -(H_* + \Lambda^{-1}du_a)(\Lambda\zeta_* + \ell_a') = \Lambda L\chi - du_a\zeta_* - H_*\ell_a' - \Lambda^{-1}du_a\ell_a'$. Here $|du_a\zeta_*| \le K_0L|H_*|/(H_*^2+\sigma_*^2) \le K_0L\sqrt{\chi}/\sigma_*$.

Hence $S_\infty \ge 2.77 + \Lambda L\chi - K_0L\sqrt{\chi}/\sigma_* - K_0\chi - K_0/\Lambda$. Young's inequality gives $K_0L\sqrt{\chi}/\sigma_* \le .03\Lambda L\chi + K_0^2L/(.12\Lambda\sigma_*^2)$, and $K_0\chi \le .03\Lambda L\chi$ for $\Lambda \ge 35K_0$. Since σ_* is fixed before Λ (B.40), $S_\infty \ge .94\Lambda L\chi + 2.6$ for Λ large. On $[\frac{\hat\xi_0^2}{2}, \frac{\hat\xi_0^2}{2}e^{t_1}]$ the reference is the core: there $S_{q,r} \ge 2.5 + .95L\Lambda\chi$ by (B.17), and $l_r = 1 - p_1/2 \le 1$ by Lemma 1.20.33(c1),(c4). On $[\frac{\hat\xi_0^2}{2}e^{t_1}, \frac{\hat\xi_f^2}{2}]$, that is, $t_1 \le y \le 2t_1$, (1.20.13) gives $U_r = U_* + \Lambda^{-1}u^\flat$ and $\log\phi_r = \log\phi_* + \ell^\flat$, where $u^\flat(y)$ and $\ell^\flat(y)$ are the expressions for u_a and ℓ_a with the upper limit $2t_1$ replaced by y, and $l_r = 1 + s(y)(Y\partial_Y\log\Phi)(4e^y,\cdot)$. Since $s \ge 0$ and $Y\partial_Y\log\Phi = -p_1/2 < 0$, $l_r \le 1$, and $|l_r - 1| \le K_0(\chi + \Lambda^{-1})$ by (B.20). The bounds $|u^\flat| + |u^{\flat\prime}| + |\ell^{\flat\prime}| \le K_0$ and $|H_*\ell^{\flat\prime}| \le K_0(\chi+\Lambda^{-1})$ hold as for u_a, ℓ_a. Moreover $W_r = 1 - \mathcal{K}_r/\frac{\hat\xi^2}{2}$, where $\mathcal{K}_r/\frac{\hat\xi^2}{2}$ is the mean over $[0, \frac{\hat\xi^2}{2}]$ of $(1-2h)\eta U_r + dU_r'$; so $|W_r - W_*| \le K_0/\Lambda$. Write $-W_rl_r = -W_r - W_r(l_r - 1)$. Then the three estimates above apply at each such $\frac{\hat\xi^2}{2}$, with one more error term $|W_r(l_r-1)| \le K_0(\chi+\Lambda^{-1})$, which is absorbed in the same way. So $S_{q,r} \ge .94\Lambda L\chi + 2.4$ on $[\frac{\hat\xi_0^2}{2}, \frac{\hat\xi_f^2}{2}]$ as well. On $[\frac{\hat\xi_f^2}{2}, \infty)$, $S_{q,r}$ is a convex combination of $S_{q,r}(\frac{\hat\xi_f^2}{2})$ and S_∞ by (a), and $l_r = 1$.

(c) From (1.4.1)–(1.4.2) and $p_1 = \frac{\hat\xi^2}{2}Q_s/L$, $\frac12\hat\xi\partial_{\hat\xi}p_{1,r} = \frac{\hat\xi^2}{2}S_{q,r}/L - l_rp_{1,r}$, since L does not depend on $\frac{\hat\xi^2}{2}$. We have $p_{1,r}(\frac{\hat\xi_0^2}{2}) > 0$ by Lemma 1.20.33(c4). At a first zero $\rho > \hat\xi_0$ we would have $\frac12\hat\xi\partial_{\hat\xi}p_{1,r} = \frac{\rho^2}{2}S_{q,r}/L > 0$, which is impossible. So $p_{1,r} > 0$. With $l_r \le 1$ and $L \le 1$, $\hat\xi^{-1}\partial_{\hat\xi}(\frac{\hat\xi^2}{2}p_{1,r}) \ge \frac{\hat\xi^2}{2}S_{q,r}/L \ge 2.4\frac{\hat\xi^2}{2}$, and integration from $\frac{\hat\xi_0^2}{2}$ gives the comparison. For $\frac{\hat\xi^2}{2} \ge 3$ and $\frac{\hat\xi_0^2}{2} \le 1$ it gives $p_{1,r} \ge 1.2(3 - \frac13) > 3$. The bound $v_r \ge 3.2$ is proved after (g).

(d) For $y \le t_1$ the reference is the axis profile, whose leading residual stress vanishes (Lemma 1.20.33(c1)). By (1.4.4), $T_0 = F(p_s - s) = 0$ gives $p_1 = a = 2 - 2l = -\hat\xi^2\hat\xi^{-1}\partial_{\hat\xi}\log\phi = -2Y\Phi_Y/\Phi$ and $p_2 = -b_s$, that is, $n_s = -2\frac{U_{\hat\xi}}{\hat\xi} = -2u_Y$. By (B.13), with $f_0 \ge .27$ on $[0, 4.1]$ and $\Phi \ge c_0$ (Lemma 1.20.33(c1)), at $Y = 4$:

$$p_{1,r}(\tfrac{\hat\xi_0^2}{2}) = \Big[-\frac{2zf_0'(z)}{f_0(z)}\Big]_{z=4\chi} + O(\Lambda^{-1}) = \Big[\frac{sJ_2(s)}{J_1(s)}\Big]_{s=\sqrt{8\chi}} + O(\Lambda^{-1}).$$

Here $f_0(z) = 2J_1(s)/s$ with $s = \sqrt{2z}$ (the series defining f_0). Lemma 1.6.44 gives a fixed strict margin above $33/10$ when $z \ge 99/25$. So $p_{1,r}(\frac{\hat\xi_0^2}{2}) \ge 3.3$ on $\{\chi \ge .99\}$ for Λ large. For $y \ge 0$, $l_r \le 1$ and $p_{1,r} > 0$ give $\partial_y p_{1,r} + p_{1,r} \ge \frac{\hat\xi^2}{2}S_{q,r}/L \ge .94\Lambda\chi\frac{\hat\xi^2}{2} \ge 3.72e^y$. Hence $p_{1,r} \ge (p_{1,r}(0) - 1.86)e^{-y} + 1.86e^y \ge \min\{p_{1,r}(0), 3.72\} \ge 3.3$.

(e) On $[0, \frac{\hat\xi_0^2}{2}e^{t_1}]$, $\phi_r = \phi_*\Phi$; on $[\frac{\hat\xi_0^2}{2}e^{t_1}, \frac{\hat\xi_f^2}{2}]$, $\log\phi_r = \log\phi_* + \ell(y,\cdot)$ with ℓ as in (b) up to y; and $\phi_r = \phi_a$ afterwards. Now $\|\log\phi_*\|_{C^k} \le \Lambda\|\int_0^\eta \zeta_*\|_{C^k}$, and (B.13) and $\Phi \ge c_0$ bound ℓ. This gives K_k. The pressure follows from $\frac{\Pi_{\hat\xi}}{\hat\xi} = E^2/(\hat\xi^2) = \phi^2/C^2$ ((1.1.3)).

(f) Insert U_r, Π_r in the source $S_n = -W\frac12\hat\xi\partial_{\hat\xi}U - (\frac12 + h)(1-2\eta U)U - H_cU_\eta - d\Pi_\eta + (2 + 4h)\eta\Pi + 2\eta\frac12\hat\xi\partial_{\hat\xi}\Pi$ of (1.4.1)–(1.4.2). If U_r is replaced by U_* and Π_r by Π_0, this is exactly Z_* of

(B.1). The errors are as follows: $|U_r - U_*| + |\partial_\eta(U_r - U_*)| + |\frac12\hat\xi\partial_{\hat\xi}U_r| \le K_0/\Lambda$ (by (B.13) and (b)); $|W_r| \le K_0$; $\|\Pi_r - \Pi_0\|_{C^1} \le K\frac{\hat\xi^2}{2}C^{-2}$ by (e); and $2\eta\frac12\hat\xi\partial_{\hat\xi}\Pi_r = \eta E_r^2 = 2\eta\frac{\hat\xi^2}{2}\phi_r^2/C^2$. Then $n = N/L$ solves $\partial_y n + n = S_{n,r}/L$ with $n(\frac{\hat\xi_0^2}{2}) = Z_*/L + O(\Lambda^{-1})$ (Lemma 1.20.33(c4)). Variation of constants gives the bound on $[\frac{\hat\xi_0^2}{2}, \frac{\hat\xi_i^2}{2}]$. On $\{\chi \le .99\}$, (B.2) gives $|Z_*| > \delta_*$, and the sign follows for Λ, then C, large.

(g) On $[\frac{\hat\xi_0^2}{2}, \frac{\hat\xi_f^2}{2}]$, $p_{1,r}$ and $n_{s,r}$ solve $\frac12\hat\xi\partial_{\hat\xi}p_{1,r} = \frac{\hat\xi^2}{2}S_{q,r}/L - l_r p_{1,r}$ and $\frac12\hat\xi\partial_{\hat\xi}n_{s,r} + n_{s,r} = S_{n,r}/L$ ((1.4.1)–(1.4.2)), with initial values at $\frac{\hat\xi_0^2}{2}$ bounded in C^k_η by Lemma 1.20.33(c6), over a y-interval of length $2t_1 \le 2\bar t$. The coefficients $S_{q,r}$, l_r, $S_{n,r}$ are bounded in C^k_η by the expressions in (b) and (f), (B.13) and (e), with constants depending on Λ only. Gronwall's inequality gives the bounds there. On $[\frac{\hat\xi_f^2}{2}, \frac{\hat\xi_i^2}{2}]$, (a) and (c) give $\frac{\hat\xi^2}{2}p_{1,r} = \frac{\hat\xi_f^2}{2}p_{1,r}(\frac{\hat\xi_f^2}{2}) + L^{-1}[S_\infty(\frac{\hat\xi^4}{4} - \frac{\hat\xi_f^4}{4})/2 + (S_{q,r}(\frac{\hat\xi_f^2}{2}) - S_\infty)\frac{\hat\xi_f^2}{2}(\frac{\hat\xi^2}{2} - \frac{\hat\xi_f^2}{2})]$. Here S_∞ and $S_{q,r}(\frac{\hat\xi_f^2}{2}) - S_\infty = \mathcal{K}_r(\frac{\hat\xi_f^2}{2})/\frac{\hat\xi_f^2}{2} - k_a$ are explicit in U_a, ϕ_a and in averages of U_r over $[0, \frac{\hat\xi_f^2}{2}]$; (b), (e) and (B.13) bound them in C^k_η. Similarly, $n_{s,r}(\frac{\hat\xi^2}{2}) = ((\hat\xi_f/\hat\xi)^2)n_{s,r}(\frac{\hat\xi_f^2}{2}) + (L\frac{\hat\xi^2}{2})^{-1}\int_{\frac{\hat\xi_f^2}{2}}^{\frac{\hat\xi^2}{2}} S_{n,r}$, with $S_{n,r}$ bounded in C^k_η by (e), (f). (By contrast $p_{2,r} = \frac{\hat\xi^2}{2}n_{s,r}/E_r = C\sqrt{\frac{\hat\xi^2}{2}/2}\,n_{s,r}/\phi_r$ grows linearly in C, as in [42].)

Proof of $v_r \ge 3.2$ in (c). On $\{\chi \ge .99\}$, $v_r \ge p_{1,r} \ge 3.3$ by (d). On $\{\chi < .99\}$, (f) gives $|n_{s,r}| \ge \delta_*/(2L)$, so $p_{2,r}^2 = \frac{\hat\xi^4}{4}n_{s,r}^2/E_r^2 = C^2\frac{\hat\xi^2}{2}n_{s,r}^2/(2\phi_r^2) \ge C^2\frac{\hat\xi_0^2}{2}\delta_*^2/(8K_F^2)$, using $L \le 1$ and (e); with $p_{1,r} \le M_0$ from (g), $v_r \ge p_{2,r}^2/p_{1,r} \ge C^2\frac{\hat\xi_0^2}{2}\delta_*^2/(8K_F^2M_0) \ge 3.2$ after increasing $C_0(\Lambda)$. Here $\frac{\hat\xi_0^2}{2}$, K_F and M_0 do not depend on C or t_1. □

Definition 1.20.35 (Backward activation (M0)+(M1))**.** Set $\kappa_0 = \kappa_{\rm act}$ and $t_1 = t_{\rm act}$. Starting from the core values at $y = 0$, define the first collar by

$$\kappa(y) = 1 - (1-\kappa_0)\sigma(y/t_1), \qquad \partial_y \log\phi = -\tfrac12\kappa(y)p_{1,r}, \qquad \partial_y U = -\tfrac14\kappa(y)\xi^2 n_{s,r} \quad (0 < y \le t_1). \tag{1.20.14}$$

For $y > t_1$ it uses Definition 1.20.22 with the same σ, ζ_3, ϑ, ω_0, y_e, $B_{\rm r0}$, y_l and ω_2. The frozen values are $p^\flat = p_s^{\rm core}(\frac{\hat\xi_0^2}{2}e^{\vartheta(y)})$ and $n^\flat = n_s^{\rm core}(\frac{\hat\xi_0^2}{2}e^{\vartheta(y)})$, taken from the stress-free core. This is legitimate because $4e^{2t_1} < 4.1$ and the core exists on $Y \le 4.1$ (Lemma 1.20.33). On $\vartheta \le t_1$ these values equal $p_{s,r}$, $n_{s,r}$. The termination level is $y_1^b = y_e + (y_l - y_e)\Upsilon^b$, with $\Upsilon^b = \zeta_3(Z_*^2/\delta_Z^2)$ and $\delta_Z \le \delta_*$. Here Z_* and δ_* are the axial numerator and the margin of the axis alternative of Lemma 1.20.33(a): $\{\chi \le .99\} \subset \{|Z_*| > \delta_*\}$ (Lemma 1.20.33(a)). Hence $\{|Z_*| < \delta_Z\} \subset \{\chi > .99\}$, since $\delta_Z \le \delta_*$. The radius $\frac{\hat\xi_b^2}{2}$ of [42, Prop. B.5] is replaced by $B_{\rm r0} \ge 100$, and $\frac{\hat\xi_i^2}{2} \ge B_{\rm r1}$.

Theorem 1.20.36 (Backward analogue of Theorem 1.20.28)**.** *Assume the hypotheses of Theorem 1.8.10 on Π_0, the choices of Lemma 1.20.33, and Definition 1.20.35. The facts (F1)–(F7) of Remark 1.8.11 are then Lemma 1.20.34. Assume the thresholds (Λ), (C) and (late) of Theorem 1.20.28, with Z_R replaced by Z_* and (I5) replaced by (F4). Write $y_{\rm in} = y_l + \omega_0$ for the interpolation inlet. Use the backward comparison only up to $y_{\rm in}$, with $\varepsilon_b = K_Z(2t_1 + \kappa_0 y_T)$. Choose κ_0, then t_1, so that $\varepsilon_b(1+T^{00})(1+P_2^0) + \varepsilon_b^2 \le 1/10$. Also require $G(2t_1 + \kappa_0 y_T) \le 1/2$ for the slope bound G of the backward plateau comparison. Once ω_0 is fixed, G, K_Z can be chosen uniformly in t_1, κ_0 by the estimates in part (c). Take K_I to cover the backward source as well, uniformly for $0 < \omega_2 \le 1/2$ on windows in $y \le y_T$. Finally choose ω_2 to satisfy the forward width conditions and $K_I\omega_2 \le 1/20$. Then for the $\varsigma = -1$ stresses every point of $(\frac{\hat\xi_0^2}{2}, \frac{\hat\xi_i^2}{2}]$, up to the end of the interpolation,*

is strict or relaxed. In the relaxed case $a > 0$, $v_s \le 2$ and $P_c > 2$; since $\mathcal{U}(P_c, J_c) > 2$ whenever $P_c > 2$ (the identity in Step 4 of the proof of Lemma 1.8.17), this is (1.4.8). More precisely:

(a) On $0 < y \le t_1$ the conclusion of Theorem 1.20.28(a) holds, with $\delta_0 = \min(c, 1)$: strict points have $P_c - v_s \ge \frac{1}{2} e v_r$ and fourth gap $\ge \frac{1}{4} e^2 v_r^2$, and relaxed points have $v_s \le 2$ and $P_c - 2 \ge \delta_0/2$. Since $v_s \to v_r > 2 + c$ as $y \downarrow 0$, the admissible cone holds on a first collar, with $v_s > 2 + c/2$.

(b) On $\{|Z_*| \le \delta_Z/2\}$ (early termination; $\chi > .99$, so $p_{1,r} > 2.3$ by (F1)): $P_c - 2 \ge \min\{0.2, c/2\}$ up to $y_e + \omega_0$, where we take $c = 0.2$ in the reference bound $v_r > 2 + c$ of Lemma 1.20.34(c). After that $b_s = 0$, $a \le 0.4$, and $p_1 \ge 2.2$ until interpolation begins.

(c) On $\{|Z_*| \ge \delta_Z/2\}$:

$$v^{00} = p_{1,r} + t^{00} p_{2,r} \;\ge\; p_{1,r} + \frac{\delta_Z^2 C^2 \frac{\hat\xi^2}{2}}{32 L^2 K_F^2 P_{\mathrm{ref}}} \;\ge 3,$$

with $p_{1,r} \ge 2.3$ wherever $\beta < 1$ and $\Upsilon^b < 1$, and $p_{1,r} > 3$ for $\frac{\hat\xi^2}{2} \ge B_{\mathrm{r}0}$. Hence $P_c - 2 \ge 0.1$. This is (V) for $\varsigma = -1$.

(d) On the interpolation window, $p_1 \ge 2.15$.

Proof. The cone algebra (Lemma 1.20.20, Lemma 1.20.21) involves only a, b_s and p_s, so it is independent of ς. For $\varsigma = -1$ the same difference estimate follows from the signed numerator formulas of Remark 1.8.14. The actual activation and the backward reference of Lemma 1.20.34 coincide with the constructed core up to $\frac{\hat\xi_0^2}{2}$. Both use its prescribed axis function $\Pi_0(\beta)$ and integrate $\frac{P_{\hat\xi}}{\hat\xi} = E^2/(\hat\xi^2)$ from that datum, including on the frozen continuation. Thus $\delta P = \delta C_p$ with equal incoming values and angular derivatives, exactly as required by Lemma 1.20.19. This comparison holds for each prescribed datum in Theorem 1.8.10. For the selected member the subsequent complete moment identities in Lemma 1.8.6 identify it with the canonical datum. The side label enters only the transport laws, Lemma 1.20.31, and these are what (1.4.2) uses. (For $\varsigma = -1$, $Q^{(-1)}$, $S_q^{(-1)}$ and $\mathcal{N}_z^{(-1)}/\frac{\hat\xi^2}{2}$ give Q_s of (1.4.3), $-Wl - h(1 - 2\eta U) - H_c(\log E)_\eta$ and N_s.)

(a) On $0 < y \le t_1$ the design is (1.20.14): $a = \kappa p_{1,r}$, $\frac{1}{2}\hat\xi \partial_{\hat\xi} U = -\kappa \frac{\hat\xi^2}{2} n_{s,r}/2$, $\partial_y \log \phi = -\kappa p_{1,r}/2$ with $\kappa = 1 - e$, $e = (1 - \kappa_0)\sigma(y/t_1)$. This is (M0) with $\vartheta(y) = y$, $\lambda = 0$, $\beta = 1$ (Remark 1.22.8). Hence $(a, -b_s) = \kappa(p_{1,r}, \rho p_{2,r})$ with $\rho = E_r/E$, since $b_s = \hat\xi^2 \hat\xi^{-1} \partial_{\hat\xi} U/E$ and $p_{2,r} = \frac{\hat\xi^2}{2} n_{s,r}/E_r$. Exactly, $\log(E/E_r) = \int_0^y e\, p_{1,r}/2 \in [0, \frac{1}{2} P_{\mathrm{ref}} y e]$, so $\rho \le 1$ and $1 - \rho \le \varrho e$ with $\varrho = P_{\mathrm{ref}} y/2$. Here P_{ref} bounds $p_{1,r}$ on the core. The slope differences against the reference are $m_H = e\, p_{1,r}/2$ and $m_U = e \frac{\hat\xi^2}{2} n_{s,r}/2$. They are bounded by $Ge(y)$ together with their fixed-y η-derivatives, with G from Lemma 1.20.33(c6). Lemma 1.20.19 with $\hat\xi_a = \hat\xi_0$ and $\mu = e$ (nondecreasing, ≤ 1) gives $|p_i - p_{i,r}| \le K_Z \int_0^y e \le K_Z y\, e$. Lemma 1.20.20 with $\varepsilon = K_Z y$, $\varrho = P_{\mathrm{ref}} y/2$, $\delta_0 = \min(c, 1)$, $v_r > 2 + c$ (Lemma 1.20.34(c)), and P_2, $\bar t$, V the bounds of $|p_{2,r}|$, $|p_{2,r}|/p_{1,r}$, v_r on the first collar (finite once C is fixed), then gives (a) for t_1 small; t_1 is chosen after C in Remark 1.8.12. This replaces [42, (B.27)–(B.29)]. The factorization of the stress on this collar is Lemma 1.20.40(a); it is not used here.

(b) On the early angles $y_1^b = y_e$ and $\partial_\eta y_1^b = 0$. The core sampled in Definition 1.20.35 is the natural core of Lemma 1.20.33; at $\frac{\hat\xi_0^2}{2}$ its values agree with those of the backward reference. Thus (F1) and (F4) give $p_{1,a} \ge 3.3$ and $v_a \ge 2 + c$ at that inlet. On $[t_1, y_e + \omega_0]$ the radial factor $\frac{\hat\xi^2}{2}/E$ and the sampled quotient $n_{s,c}/p_{1,c}$ obey the same two identities as in Theorem 1.20.28(b). The signed version of Lemma 1.20.19 applies with the common axis pressure and $\mu = 1$. The common K_1' therefore gives

$|p_1 - p_{1,a}| \le K_1' y$ and $|p_1 + t^{\mathrm{full}} p_2 - v_a| \le K_1' y$. Since $y \le y_*/2$, the error is at most $\min(\delta_0/4, 1/10)$, with $\delta_0 = \min(c, 1)$. The same convex combination gives $P_c \ge 2 + \min\{0.2, c/2\}$, $p_1 \ge 2.2$ and $v_s \le \kappa_0 V^0 < 1$. After termination, $\frac{1}{2}\hat\xi \partial_{\hat\xi} p_1 = \frac{\hat\xi^2}{2} S_q/L - \ell_r p_1$ with $|S_q - S_{q,r}| \le \frac{1}{4}$ by Lemma 1.20.27 and (late), and (F4) (the proof of Lemma 1.20.27 applies verbatim to $S_q^{(-1)}$ of Lemma 1.20.31, with $c_\ell^{(-1)} = -1 + \mathcal{K}/\frac{\hat\xi^2}{2} - (-(\frac{1}{2} - h)\eta - dU)(\log \frac{\hat\xi_a^2}{2})'$ and the comparison field (1.20.13), which has $\ell_r = 1$ for $y \ge 2t_1$) gives $S_{q,r} \ge .94 L\Lambda\chi + 2.4$. So $\frac{\hat\xi^2}{2} S_q/L \ge (\frac{\hat\xi^2}{2}/L)(.94 L\Lambda\chi + 2.15) \ge .94 \cdot 4 \cdot .99 > 3.7$, and the barrier keeps $p_1 \ge \min\{2.3 - 0.1, 3.7\} = 2.2$.

(c) By (F2), $\frac{1}{2}\hat\xi \partial_{\hat\xi} n_{s,r} + n_{s,r} = S_{n,r}/L$ with $S_{n,r} = Z_* + O(\Lambda^{-1}) + o_{t_1}(1) + O(C^{-2})$, and $n_{s,r}(\frac{\hat\xi_0^2}{2}) = Z_*/L + O(\Lambda^{-1})$ by (F3). ([42] states the sign claim only on $\chi \le .99$, [42, proof of Lemma B.4]; the extension to $|Z_*| \ge \delta_Z/2$ is the following line.) Where $|Z_*| \ge \delta_Z/2$ and the remainders are $\le \delta_Z/4$, the explicit solution $n_{s,r} = e^{-y} n_{s,r}(\frac{\hat\xi_0^2}{2}) + \int_0^y e^{-(y-s)} S_{n,r}/L$ keeps the sign of Z_* and satisfies $|n_{s,r}| \ge \delta_Z/(4L)$; the same holds for $n^\flat$. Then $t^{00} p_{2,r} = \frac{\hat\xi^4}{4} n^\flat n_{s,r}/(E_r^2 p_1^\flat) \ge \frac{\hat\xi^4}{4}(\delta_Z/4L)^2/(\hat\xi^2 K_F^2 C^{-2} P_{\mathrm{ref}})$, with $E_r = \hat\xi \phi_r/C \le \hat\xi K_F/C$ (F7). This gives the display. By (C) and $\frac{\hat\xi^2}{2} \ge \frac{\hat\xi_0^2}{2} = 4/\Lambda$, the right side is $\ge 4 \cdot 24/32 = 3$. (F1), (F5) give $p_{1,r} > 0$, $p_{1,r} > 2.3$ on $\chi > .99$, and $p_{1,r} > 3$ for $\frac{\hat\xi^2}{2} \ge B_{\mathrm{r}0}$. For $t_1 \le y \le y_{\mathrm{in}}$, compare with the flattened reference of Lemma 1.20.34. Take $\mu = 1$ up to $2t_1$ and $\mu = \kappa_0$ afterwards in the signed deviation estimate. The reference slopes are bounded with their fixed-y angular derivatives on the first interval by the core formulas in Lemma 1.20.34(b); afterwards F_r, U_r are constant in $\frac{\hat\xi^2}{2}$. The angular derivative of β costs at most $\|\sigma'\|_\infty \|(y_1^b)'\|_\infty/\omega_0$, fixed with C. Since $\lambda = 0$ through y_{in}, the slope bounds give $\int_0^y \mu \le 2t_1 + \kappa_0 y_T$. Hence the value and history errors satisfy $\delta \le \varepsilon_b$, and $t^{\mathrm{full}} = t^{00} E_r/E$ gives $\delta_t \le \varepsilon_b$ upon including the fixed bound for t^{00} in K_Z. Lemma 1.20.21 gives a total error at most $\varepsilon_b(1 + T^{00} + P_2^0) + \varepsilon_b^2 \le 1/10$, with $c_r = 0.3$ on the transition angles and $c_r = 1$ elsewhere. Also $v_s \le 0.8 + \kappa_0 V^0 < 1$.

(d) At the inlet $\beta = 0$. Part (b) gives $p_1 \ge 2.2$ on the early angles. On the other angles part (c) gives $p_1 \ge p_{1,r} - 1/10 \ge 2.2$ by (F1) on the transition angles and (F5) at the late termination. Throughout $[y_{\mathrm{in}}, y_{\mathrm{in}} + \omega_2]$ one has $\beta = 0$, $P_c = p_1$ and $0 < a \le .8$. Here $\ell_r = 1 - a/2 \le 1$. The signed source contains ℓ_r, $\partial_\eta|_{\hat\xi} \log H$, U and $\mathcal{K}/\frac{\hat\xi^2}{2}$. The interpolation enters ℓ_r by its bounded value and enters $\partial_\eta \log H$ through a radial integral with $\partial_\eta|_y \lambda = 0$ and $\hat\xi_a = \hat\xi_0$ constant. The axial field is constant in $\frac{\hat\xi^2}{2}$ on this window and the history averages stay bounded. This gives $|\frac{\hat\xi^2}{2} S_q^{(-1)}/L| \le K_I - 3$ uniformly in its width. The term $-.4\lambda$ in $(\log F)_y$ contributes exactly $-.4\omega_2 \int_0^1 \sigma(s)\,\mathrm{d}s = -\omega_2/5$ across the window, by the symmetry of the step (Remark 1.20.16). The comparison using ε_b stops at y_{in}, and we use the scalar transport equation from there. On any crossing from 2.2 down to 2.15, restrict to the interval from the last upper crossing to the first lower crossing. There $D_y p_1 \ge -(K_I - 3) - 2.2 > -K_I$. Integration would give $1/20 < K_I \omega_2$, contrary to the choice of width. Thus $P_c = p_1 \ge 2.15$ on the closed window, which also gives the margin asserted in (c) there. □

Lemma 1.20.37 (Backward interpolation and outlet bounds)**.** *For the backward design of Definition 1.20.35, with* $\frac{\hat\xi_b^2}{2} = B_{\mathrm{r}0}$, $\frac{\hat\xi_i^2}{2} = B_{\mathrm{r}1} = eB_{\mathrm{r}0}$ *and* $y_T = y_l + 1 = 2\log(\hat\xi_i/\hat\xi_0)$, *the following hold.*

(a) The termination and the interpolation end before $\frac{\hat\xi_i^2}{2}$*:* $y_1^b + \omega_0 \le y_l + \omega_0 < y_l + \omega_0 + \omega_2 < y_T$.

(b) Exit values. *Put* $\ell_i = \log(CE(\frac{\hat\xi_i^2}{2}, \cdot))$, $G_i = U(\frac{\hat\xi_i^2}{2}, \cdot)$, $L_0 = 2\log(\hat\xi_i/\hat\xi_0)$, *and let* M_k^c, N_k^c *bound*

p_1, n_s of the core in C^k_η (Lemma 1.20.33(c6)). Then

$$\|\ell_i\|_{C^k} \le B_k := \|\log\phi_* + \log\Phi(4,\cdot)\|_{C^k} + \tfrac12(M^c_k + .8)L_0 + \tfrac12\log(\hat\xi_i^2),$$

$$\|G_i - U_*\|_{C^k} \le \frac{C^{\mathrm{nat}}_k}{\Lambda} + C^{\mathrm{join}}_k(\Lambda)(t_1+\kappa_0), \qquad C^{\mathrm{join}}_k(\Lambda) := c_k\tfrac{\hat\xi_i^2}{2}N^c_k\big[1+(1+y_l)(1+\|\Upsilon^b\|_{C^k})\big]^k.$$

Here C^{nat}_k comes from (B.13), and c_k is a combinatorial constant. B_k and C^{join}_k do not depend on C, t_1, κ_0, ω_0 or ω_2.

(c) Output slab. *On $[\frac{\hat\xi_0^2}{2}e^{y_s}, \frac{\hat\xi_i^2}{2}]$, $y_s = y_l + \omega_0 + \omega_2$, we have $a = .8$, $\frac12\hat\xi\partial_{\hat\xi}U = 0$, $b_s = 0$, $S_q \ge .9$ and $p_1 > 2$. So the relaxed cone holds there, and at $\frac{\hat\xi_i^2}{2}$: $a = .8$, $\frac12\hat\xi\partial_{\hat\xi}U = 0$, $p_1 > 2$.*

Proof. (a) $y^\flat_1 \le y_l$, and $\omega_0 + \omega_2 < 1$ (Remark 1.20.26, forward part; the backward member uses the same widths). (b) On $(0,t_1]$ the slope of $\log\phi$ is $-\kappa p_{1,r}/2$ with $\kappa \le 1$, and $p_{1,r}$ is the core value there. After t_1 it is $-\frac12[(1-\lambda)\kappa_0 p^\flat_1 + .8\lambda]$ with the core values $p^\flat_1$, and λ does not depend on η. Integrating over $[0,L_0]$ and adding $\frac12\log(\hat\xi_i^2)$ gives B_k, since $\log\phi(\frac{\hat\xi_0^2}{2}) = \log\phi_* + \log\Phi(4,\cdot)$. For G_i: $U(\frac{\hat\xi_0^2}{2}) = U_* + \Lambda^{-1}u(4,\cdot)$; on $(0,t_1]$, $\partial_y U = -\kappa\frac{\hat\xi^2}{2}n_{s,r}/2$ contributes at most $\frac12\frac{\hat\xi_0^2}{2}e^{\bar t}N^c_k t_1$; after t_1, $\partial_y U = -\frac12\kappa_0\beta\frac{\hat\xi^2}{2}n^\flat$. The angle-dependent factor $\beta(y - y^b_1(\eta))$ is handled as in (R5) of Proposition 1.20.38: each ∂_η of β is $-y^{b\prime}_1\partial_y\beta$, which is integrated by parts against $\frac{\hat\xi^2}{2}n^\flat$. The function $n^\flat$ does not depend on y on $\operatorname{supp}\beta'$, because $y_e > 2t_1$. So no power of ω_0^{-1} occurs, and $\int_0^{y_T}\frac{\hat\xi^2}{2}\,dy \le \frac{\hat\xi_i^2}{2}$. (c) On the slab $\lambda = 1$ and the termination has ended, so $\partial_y\log\phi = -.4$, $l = .6$, $a = 2 - 2l = .8$, $\frac12\hat\xi\partial_{\hat\xi}U = 0$ and $b_s = 0$. Compare with the reference (1.20.13), which has $l_r = 1$ there. As in the proof of Theorem 1.20.36(b), $S_q - S_{q,r} = (l-1)c_\ell + \Delta$ with $c_\ell = -W$ (here $(\log\frac{\hat\xi_a^2}{2})' = 0$). Here Δ is the quantity bounded in Lemma 1.20.27. That proof uses the slopes only through m_U and the fixed-y derivatives $\partial_\eta m_U$, $\partial_\eta m_H$. On the interpolation window and the slab $m_U = 0$ and $\partial_\eta m_H = -\frac12(1-\lambda)\kappa_0\partial_\eta p^\flat_1$. So the bound $|\Delta| \le K_S(\Lambda)\mathcal{I}_{\mathrm{act}} \le \frac14$ of (late) holds up to y_T. Moreover $\mathcal{K}/\frac{\hat\xi^2}{2}$ is the mean of $(1-2h)\eta U + dU_\eta$, and $U - U_* = O(\Lambda^{-1}) + O(\mathcal{I}_{\mathrm{act}})$ in C^1_η. So $-W \le -W_* + .05 \le 3.1$ after decreasing $\kappa_{\mathrm{act}}, t_{\mathrm{act}}$, which the order (late) allows. Hence, by Lemma 1.20.34(b), $S_q \ge S_{q,r} - .4\cdot 3.1 - \frac14 \ge 2.4 - 1.49 > .9$. At the inlet of the slab $p_1 \ge 2.15$ (Theorem 1.20.36(d)). At a first point with $p_1 = 2$, $\frac12\hat\xi\partial_{\hat\xi}p_1 = \frac{\hat\xi^2}{2}S_q/L - .6p_1 \ge .9\frac{\hat\xi^2}{2} - 1.2 > 0$, since $\frac{\hat\xi^2}{2} \ge B_{\mathrm{r0}} \ge 100$. So $p_1 > 2$ on the slab. Since $v_s = a = .8 < 2 < \mathcal{U}(P_c,J_c)$ and $P_c = p_1 > 2$, the cone is relaxed. □

[42, Prop. B.8] and [42, (B.33)–(B.39)] involve $\frac{\hat\xi_i^2}{2}$ only through $\frac{\hat\xi^2_{\mathrm{ref}}}{2} = \frac{\hat\xi_i^2}{2}(CP_*)^{10}$, $\frac{\hat\xi^2_{\mathrm{sep}}}{2} = \frac{\hat\xi_i^2}{2}e^{T_{\mathrm{sh}}}$ and (B.32). In the normalized variable $x = (\hat\xi/\hat\xi_{\mathrm{ref}})^2$, $x_{\mathrm{sep}} = e^{T_{\mathrm{sh}}}/(CP_*)^{10}$ does not contain $\frac{\hat\xi_i^2}{2}$. These steps are proved in Lemma 1.20.41; the change of $\frac{\hat\xi_i^2}{2}$ adds nothing to them.

Proposition 1.20.38 (The continuation to $\frac{\hat\xi_i^2}{2}$)**.** *Assume the hypotheses of Theorem 1.8.10, the choices of Lemma 1.20.33, and the thresholds of Theorem 1.20.36 and Lemma 1.20.37. Let the backward member on $[0,\frac{\hat\xi_i^2}{2}]$ be the core of Lemma 1.20.33 on $[0,\frac{\hat\xi_0^2}{2}]$, the first collar (1.20.14) on $0 < y \le t_1$ (Lemma 1.20.40), and the design of Definition 1.20.35 for $y > t_1$. Then:*

(a) on $(\frac{\hat\xi_0^2}{2},\frac{\hat\xi_i^2}{2}]\times[-1,1]$, $a > 0$, $P_c > 2$ and $v_s < \mathcal{U}(P_c,J_c)$;

(b) there is $y_c \in (0, t_1]$ such that $v_s > 2$, and hence the admissible cone holds, on $(\frac{\hat\xi_0^2}{2}, \frac{\hat\xi_0^2}{2} e^{y_c}] \times [-1, 1]$;

(c) at $\frac{\hat\xi_i^2}{2}$, $a = .8$, $\frac{1}{2}\hat\xi \partial_{\hat\xi} U = 0$ and $p_1 > 2$;

(d) For each $k \geq 0$ there are constants B_k', C_k^{nat} and $C_k^{\mathrm{part}}(\Lambda)$, independent of C, t_1, κ_0 and the widths, such that

$$\sup_{0 \leq \frac{\hat\xi^2}{2} \leq \frac{\hat\xi_i^2}{2}} \| \log \phi(\tfrac{\hat\xi^2}{2}, \cdot) \|_{C_\eta^k} \leq B_k', \tag{1.20.15}$$

$$\sup_{0 \leq \frac{\hat\xi^2}{2} \leq \frac{\hat\xi_i^2}{2}} \| U(\tfrac{\hat\xi^2}{2}, \cdot) - U_* \|_{C_\eta^k} \leq \frac{C_k^{\mathrm{nat}}}{\Lambda} + C_k^{\mathrm{part}}(\Lambda)\big[t_1 + \kappa_0(1 + \omega_0^{-(k-1)_+})\big]. \tag{1.20.16}$$

Here $(k-1)_+ = \max\{k-1, 0\}$ and $0 < \omega_0 < 1$. At $\hat\xi = \hat\xi_i$ the sharper estimate of Lemma 1.20.37(b) holds without the inverse-width factor. All angular derivatives of the selected member are finite; uniformity over the late widths at partial radii is asserted only with the factor in (1.20.16).

Proof. (a) By Theorem 1.20.36, every point of $(\frac{\hat\xi_0^2}{2}, \frac{\hat\xi_i^2}{2}]$ up to the end of the interpolation is strict or relaxed, and by Lemma 1.20.37(c) the points of the output slab up to $\frac{\hat\xi_i^2}{2}$ are relaxed. A strict point satisfies the admissible cone, which contains (1.4.8). A relaxed point has $a > 0$, $v_s \leq 2$ and $P_c > 2$, and

$$\mathcal{U}(P_c, J_c) - 2 = \frac{(P_c - 2)^2}{P_c - 2 + J_c^2/4 + |J_c|\sqrt{(P_c-2)/2 + J_c^2/16}} > 0$$

(multiply $\mathcal{U} - 2 = (P_c - 2) + J_c^2/4 - |J_c|\sqrt{(P_c-2)/2 + J_c^2/16}$ by the conjugate expression); so $v_s \leq 2 < \mathcal{U}(P_c, J_c)$. At strict points $a > 0$ as well: on $0 < y \leq t_1$, $a = \kappa p_{1,r}$ with $\kappa \geq \kappa_0 > 0$ and $p_{1,r} > 0$ (Lemma 1.20.33(c4)); for $y > t_1$, $a = (1-\lambda)\kappa_0 p_1^\flat + .8\lambda > 0$, with the core values $p_1^\flat > 0$. (b) is Theorem 1.20.36(a). (c) is Lemma 1.20.37(c). (d) On $[0, \frac{\hat\xi_0^2}{2}]$, the estimates follow from Lemma 1.20.33(c6) and (1.20.11). For $\hat\xi \geq \hat\xi_0$ put $y = 2\log(\hat\xi/\hat\xi_0)$ and $a(\eta) = y_1^b(\eta)$. The cutoffs in the equation for $\log\phi$ are independent of η, and the angular derivatives of the sampled core values $p_1^\flat$ are bounded uniformly in C and t_1. Integrating that equation up to any $y \leq y_T$ proves (1.20.15), as in Lemma 1.20.37(b).

For U, the interval $0 \leq y \leq t_1$ contributes at most $K_k(\Lambda)t_1$ in C_η^k. On the remaining interval its increment is

$$-\frac{\kappa_0}{2}\int_{t_1}^{y} \beta(s,\eta) g(s,\eta)\, \mathrm{d}s, \qquad \beta(s,\eta) = 1 - \sigma\Big(\frac{s - a(\eta)}{\omega_0}\Big), \quad g(s,\eta) = \tfrac{\hat\xi_0^2}{2} e^s n^\flat(s,\eta),$$

with the integral omitted when $y \leq t_1$. The angular derivatives of g through order k are bounded by $\frac{\hat\xi_i^2}{2} N_k^c$, up to a fixed norm constant: the freezing map depends on s alone and takes its values in the buffered core interval. Moreover

$$a = \omega_0 + (y_l - \omega_0)\Upsilon^b, \qquad \|a\|_{C_\eta^k} \leq (1 + y_l)(1 + \|\Upsilon^b\|_{C_\eta^k}).$$

The right-hand side is fixed before C. For $j \geq 1$, Faà di Bruno expresses $\partial_\eta^j \beta$ as a sum of terms

$$\omega_0^{-m} \sigma^{(m)}\Big(\frac{s - a(\eta)}{\omega_0}\Big) P_{j,m}(a', \dots, a^{(j)}), \qquad 1 \leq m \leq j,$$

where $P_{j,m}$ is a fixed polynomial. Each term is supported in $a(\eta) \le s \le a(\eta) + \omega_0$. Consequently

$$\sup_{\eta} \int_{t_1}^{y_T} |\partial_\eta^j \beta(s,\eta)| \, \mathrm{d}s \le K_j(\Lambda)\omega_0^{1-j}, \qquad \int_{t_1}^{y_T} |\beta(s,\eta)| \, \mathrm{d}s \le y_T.$$

Leibniz' rule gives the same bound for every partial upper limit $y \le y_T$, and proves (1.20.16). At the completed endpoint y_T, a term containing $\partial_s^m \beta$ is integrated by parts $m-1$ times. Every boundary term contains a positive-order derivative of β and vanishes, and the remaining factor satisfies $\int |\partial_s \beta| \, \mathrm{d}s = 1$. On its support $n^\flat$ is constant in s, so the transferred s-derivatives fall on e^s. This recovers the sharper endpoint estimate of Lemma 1.20.37(b). □

Corollary 1.20.39 (The finite angular budget for the outer join)**.** *Put* $K_{\mathrm{part}} = C_2^{\mathrm{part}}(\Lambda)$*, increasing it to at least one if necessary, and set*

$$b_2 := t_1 + \kappa_0(1 + \omega_0^{-1}), \qquad \delta_U := \frac{C_2^{\mathrm{mat}}}{\Lambda} + K_{\mathrm{part}} b_2.$$

On the family of late controls satisfying

$$K_{\mathrm{part}} b_2 \le 1, \tag{1.20.17}$$

the fields on $[0, \frac{\hat\xi_i^2}{2}]$ *obey*

$$\sup_{\hat\xi} \|U(\tfrac{\hat\xi^2}{2}, \cdot)\|_{C^2_\eta} \le K(\Lambda), \qquad \sup_{\hat\xi} \|\phi(\tfrac{\hat\xi^2}{2}, \cdot)\|_{C^2_\eta} \le K(\Lambda),$$

with constants independent of C *and of the late widths. They also satisfy*

$$\sup_{\hat\xi} \|U(\tfrac{\hat\xi^2}{2}, \cdot) - U_*\|_{C^2_\eta} \le \delta_U, \qquad \|G_i - 4\eta\|_{C^2_\eta} \le j_0 + \delta_U.$$

For every fixed Λ *and every selected* C*, condition* (1.20.17)*, and any prescribed stricter upper bound on* b_2*, can be imposed in step 5 of Section 1.5.2:* $\omega_0 > 0$ *is fixed first, then* κ_0*, then* t_1*.*

Proof. Use (1.20.16) with $k = 2$ and (1.20.15). The C^2 bound on ϕ follows by differentiating its exponential. For a prescribed bound $b_2 \le \varepsilon$, first choose $\kappa_0 \le \varepsilon/[2(1 + \omega_0^{-1})]$, then choose $t_1 \le \varepsilon/2$, intersecting these conditions with the previous upper bounds. These choices preserve positivity of both parameters and require no increase of C. □

Comparison with [42]. In [42, App. B] the continuation after t_1 is the one in the proof of [42, Prop. B.5]. The following steps there use the current-value activation (1.20.14) essentially; for the design of Definition 1.20.35 they are replaced by new proofs.

(R1) In the proof of Prop. B.5, after t_1: "Formula (B.29) now gives $P_c > 2 + c/2$ and $v_s < 1$". With the frozen ratio, $P_c = p_{1,r} + t^{00} p_{2,r} \ne v_r$. It is replaced by Theorem 1.20.36(b),(c).

(R2) The β-step at $\frac{\hat\xi_b^2}{2}$: "$P_c = p_{1,r} + \beta p_{2,r}^2/p_{1,r} + o(1) > 2$". It is replaced by Lemma 1.20.21 inside Theorem 1.20.36(c), now at the angle-dependent level y_1^b, with $\frac{\hat\xi_b^2}{2} := B_{\mathrm{r0}}$.

(R3) "κ_0 small compared to $V_{\max}$". It is replaced by $v_s \le .8 + \kappa_0 V^0 < 1$ (the plateau supremum V^0).

(R4) The inlet of the $a \to .8$ interpolation, "$P_c = p_1 > 2$ by continuity from the margin at $\frac{\hat\xi_b^2}{2}$". It is replaced by Theorem 1.20.36(b),(d).

(R5) The proof of Lemma B.7, which assumes angle-independent cutoffs ("only integrals of bounded cutoff values"). At the completed endpoint $\frac{\hat\xi_i^2}{2}$, for each j, $\int \partial_\eta^j \beta(y - y_1^b(\eta))\, g\, \mathrm{d}y$ is integrated by parts. Here $n^\flat$ is constant in y on $\operatorname{supp}\beta'$, since $y_e > 2t_1$, so no inverse power of ω_0 occurs. By Faà di Bruno the constant is polynomial in $\|y_1^b\|_{C^k}$: $C_k^{\mathrm{join}}(\Lambda)$ is replaced by $C_k^{\mathrm{join}}(\Lambda)(1 + \|y_1^b\|_{C^k})^k$, with $\|y_1^b\|_{C^k} \le y_l \|\Upsilon^b\|_{C^k}$. This depends on Λ and Z_*, not on C, and it multiplies κ_0. The endpoint U-increment is $O(\kappa_0)$ uniformly in ω_0; at partial radii the angular derivatives obey (1.20.16). The outer moment matching uses only the finite C^2 budget of Corollary 1.20.39.

The other steps of [42, App. B] are proved in this text for the datum Π_0: Props. B.2–B.3 in Lemma 1.20.33; Lemma B.4, on all of $[\frac{\hat\xi_0^2}{2}, \frac{\hat\xi_i^2}{2}]$, in Lemma 1.20.34; the cone on the first collar in Theorem 1.20.36(a); the factorization of Prop. B.5 and Cor. B.6 in Lemma 1.20.40; the final $a = .8$ slab and (B.32) in Lemma 1.20.37; and (B.33)–(B.39) with Prop. B.8 in Lemma 1.20.41. In the order Remark 1.8.12, $y_*(C), \Upsilon^b, \omega_0$ are inserted between C, $\frac{\hat\xi_{\mathrm{ref}}^2}{2}$ and κ_0, with $\delta_Z \le \delta_*$ fixed with δ_*.

Proof of Theorem 1.8.10. Two lemmas remain: the first collar, and the part between $\frac{\hat\xi_i^2}{2}$ and $\frac{\hat\xi_{\mathrm{match}}^2}{2}$.

Lemma 1.20.40 (The first collar: factorization and analytic rectangle)**.** *Let $\Lambda \ge \Lambda_0$ and $C \ge C_0(\Lambda)$ be as in Lemma 1.20.33, and let $0 < t_1 \le \bar t$ and $0 < \kappa_0 < 1$. Let the member be the core on $[0, \frac{\hat\xi_0^2}{2}]$, and on $0 < y = 2\log(\hat\xi/\hat\xi_0) \le t_1$ let it be given by (1.20.14): with $e_a = (1 - \kappa_0)\sigma(y/t_1)$ and $\kappa = 1 - e_a$,*

$$\partial_y \log\phi = -\kappa p_{1,c}/2, \qquad \partial_y U = -\kappa \tfrac{\hat\xi^2}{2} n_{s,c}/2, \qquad \Pi = \Pi_0 + C_p,$$

where $p_{1,c}$ and $n_{s,c}$ are the values of the core at the same $\frac{\hat\xi^2}{2}$; they are defined, since $\Lambda \frac{\hat\xi_0^2}{2} e^{t_1} \le 4e^{\bar t} < 4.1$.

(a) Factorization. *$e_a = e^{-t_1^2/y^2} g_a(y)$, with $g_a(y) = (1 - \kappa_0)(e^{-t_1^2/y^2} + e^{-t_1^2/(t_1-y)^2})^{-1}$ smooth and positive on $[0, t_1)$ and $g_a(0) = (1 - \kappa_0)e$. On $[0, t_1/2] \times [-1, 1]$, $T_0 = e_a B_0$, where B_0 is smooth in (y, η), equivalently in $(\frac{\hat\xi^2}{2}, \eta)$, and $B_0(0, \eta) = F(\frac{\hat\xi_0^2}{2}, \eta) p_{s,c}(\frac{\hat\xi_0^2}{2}, \eta) = F(\frac{\hat\xi_0^2}{2}, \eta) s(\frac{\hat\xi_0^2}{2}, \eta) \ne 0$. Consequently there is $y_B \in (0, t_1/2]$ such that $|T_0| \ge c\, e^{-t_1^2/y^2}$ and $|(\hat\xi^{-1}\partial_{\hat\xi})^{\alpha_1} \partial_\eta^{\alpha_2} T_0| \le C_\alpha e^{-t_1^2/y^2} y^{-3|\alpha|}$ on $(0, y_B] \times [-1, 1]$.*

(b) Analytic rectangle. *There is a complex neighbourhood $\mathcal{N}_1$ of $[-1, 1]$, not depending on $\frac{\hat\xi^2}{2}$, such that for every $r \ge 0$ the functions $(\hat\xi^{-1}\partial_{\hat\xi})^r F$, $(\hat\xi^{-1}\partial_{\hat\xi})^r U$, $(\hat\xi^{-1}\partial_{\hat\xi})^r (V_0/\frac{\hat\xi^2}{2})$ and $(\hat\xi^{-1}\partial_{\hat\xi})^r \Pi$ ($F = \phi/C$) extend from $[0, \frac{\hat\xi_0^2}{2} e^{t_1}] \times [-1, 1]$ to continuous functions on $[0, \frac{\hat\xi_0^2}{2} e^{t_1}] \times \mathcal{N}_1$ that are holomorphic in η. In particular they are bounded on $[0, \frac{\hat\xi_0^2}{2} e^{t_1}] \times \mathcal{N}_1'$ for every compact $\mathcal{N}_1' \subset \mathcal{N}_1$. They are smooth in $(\frac{\hat\xi^2}{2}, \eta)$ on $[0, \frac{\hat\xi_0^2}{2} e^{t_1}] \times [-1, 1]$, including $\hat\xi = 0$.*

(a) and (b) hold for every $t_1 \in (0, \bar t]$ and every $\kappa_0 \in (0, 1)$.

Proof. (a) By the definition of the flat step in Section 1.4, $\sigma(y/t_1) = e^{-t_1^2/y^2}/(e^{-t_1^2/y^2} + e^{-t_1^2/(t_1-y)^2})$ for $0 < y < t_1$, which gives the form of e_a; the denominator tends to e^{-1} as $y \downarrow 0$, and all its derivatives extend smoothly to $y = 0$. Put $\delta_0 = t_1/2$ and $K = [-1, 1]$. For $k \ge 0$ let $\mathcal{E}_k$ be the set of

functions $e_a y^k b$ with $b \in C^\infty([0,\delta_0]\times K)$. They are smooth on $[0,\delta_0]\times K$ and vanish to infinite order at $y=0$. $\mathcal{E}_k$ is closed under sums, under products with smooth functions and with each other, and under ∂_η; $\mathcal{E}_3 \subset \mathcal{E}_0$; and $e^w - 1 = w\int_0^1 e^{\theta w}\,\mathrm{d}\theta \in \mathcal{E}_k$ if $w \in \mathcal{E}_k$.

(1) If $w \in \mathcal{E}_0$ and m is smooth, then $\int_0^y w\,m\,\mathrm{d}y' \in \mathcal{E}_3$. Indeed $wm = e^{-t_1^2/u^2}\widetilde{b}(u,\eta)$ with $\widetilde{b}$ smooth, and (1.4.10), with $c = t_1^2$ and $j=0$, gives $\int_0^y = \frac12 e^{-t_1^2/y^2} y^3 B = e_a y^3 B/(2g_a)$ with B smooth on $[0,\delta_0]\times K$.

(2) The core is stress-free (Lemma 1.20.33(c1)), so $\partial_y \log\phi_c = -p_{1,c}/2$ and $\partial_y U_c = -\frac{\hat\xi^2}{2} n_{s,c}/2$. With (1.20.14) and agreement at $y=0$, $\log(\phi/\phi_c) = \frac12\int_0^y e_a p_{1,c}$ and $U - U_c = \frac12\int_0^y e_a \frac{\hat\xi^2}{2} n_{s,c}$. Both lie in $\mathcal{E}_3$ by (1). Hence $E/E_c - 1 = \phi/\phi_c - 1 \in \mathcal{E}_3$, and $H - H_c$, $E^2 - E_c^2$, $UH - U_cH_c$, $U^2 - U_c^2$ lie in $\mathcal{E}_3$.

(3) The two profiles agree for $\hat\xi \le \hat\xi_0$. So each difference of the five integrals of (1.1.2) is $\int_0^y (\cdots)\frac{\hat\xi_0^2}{2} e^{y'}\,\mathrm{d}y'$ of a function in $\mathcal{E}_3$, hence lies in $\mathcal{E}_3$ by (1); so do its η-derivatives. The pressures differ by $\Delta C_p \in \mathcal{E}_3$.

(4) By Lemma 1.4.1, (1.4.3) holds for both profiles. So $Q_s - Q_{s,c}$ and $N_s - N_{s,c}$ are sums of products of smooth functions with differences from (2)–(3); use $\Delta(1/H) = -\Delta H/(HH_c)$. Hence they lie in $\mathcal{E}_3$, and so does $p_s - p_{s,c}$ ((1.4.4); $1/E - 1/E_c = (E_c/E - 1)/E_c$).

(5) By (1.20.14), $s = (a, -b_s) = \kappa\,(p_{1,c}, \frac{\hat\xi^2}{2} n_{s,c}/E)$, and the stress-free core has $s_c = p_{s,c} = (p_{1,c}, \frac{\hat\xi^2}{2} n_{s,c}/E_c)$. Writing $E_c/E = 1 + w$ with $w \in \mathcal{E}_3$, we get $\kappa E_c/E - 1 = -e_a + (1-e_a)w$. So $s - p_{s,c} = -e_a p_{s,c} + \mathcal{E}_3$.

Hence $T_0 = F(p_s - s) = F[(p_s - p_{s,c}) + e_a p_{s,c}] + \mathcal{E}_3 = e_a(Fp_{s,c} + y^3 b)$ for a smooth b. Put $B_0 = Fp_{s,c} + y^3 b$. Then $B_0(0,\eta) = F(\frac{\hat\xi_0^2}{2},\eta) p_{s,c}(\frac{\hat\xi_0^2}{2},\eta)$, which is nonzero because $F > 0$ and $p_{1,c}(\frac{\hat\xi_0^2}{2}) > 0$; and $s(\frac{\hat\xi_0^2}{2}) = p_{s,c}(\frac{\hat\xi_0^2}{2})$, since $\kappa = 1$ at $y=0$. By continuity and compactness $|B_0|$ and g_a are bounded below on $[0,y_B]\times K$ for some $y_B \in (0,\delta_0]$, which gives the lower bound. Every derivative of $e^{-t_1^2/y^2}$ of order m is $e^{-t_1^2/y^2}$ times a polynomial in $1/y$ of degree $3m$, and $y = 2\log(\hat\xi/\hat\xi_0)$ with $\hat\xi \ge \hat\xi_0 > 0$; this gives the upper bounds.

(b) By Lemma 1.20.33(b),(c1), Φ and u are holomorphic on $\mathcal{N}$, and $\Phi \ge .26$ on $[0,4.1]\times I$. By uniform continuity, there is $\epsilon_1 \in (0,1)$ such that $\mathcal{N}_1 := \{\mathrm{dist}(\eta,[-1,1]) < \epsilon_1\}$ satisfies $[0,4.1]\times\mathcal{N}_1 \subset \mathcal{N}$, $\mathcal{N}_1 \subset \Omega_1$, and $|\Phi| \ge .1$ on $[0,4.1]\times\mathcal{N}_1$. On $[0,\frac{\hat\xi_0^2}{2}]$, $F = \phi_*\Phi/C$, $U = U_* + \Lambda^{-1}u$ and $\Pi = \Pi_0 + \Lambda^{-1}\mathcal{I}(g^2\Phi^2)$ are holomorphic in (Y,η). On $[\frac{\hat\xi_0^2}{2}, \frac{\hat\xi_0^2}{2}e^{t_1}]$,

$$\phi = \phi_*\Phi\exp\Big(\frac12\int_0^y e_a\,p_{1,c}\Big), \qquad U = U_* + \Lambda^{-1}u + \frac12\int_0^y e_a\,\frac{\rho^2}{2} n_{s,c}\,\mathrm{d}y',$$

with $p_{1,c} = -2Y\Phi_Y/\Phi$ and $n_{s,c} = -2u_Y$, which are holomorphic in $\eta \in \mathcal{N}_1$ and continuous in $Y \le 4e^{t_1} < 4.1$. Integrals in y of such functions are holomorphic in η, and ∂_y of them are the integrands; e_a is smooth in y. Hence each $(\hat\xi^{-1}\partial_{\hat\xi})^r\phi$ and $(\hat\xi^{-1}\partial_{\hat\xi})^r U$ has the asserted extension. So do $(\hat\xi^{-1}\partial_{\hat\xi})^r\Pi$, because $\Pi = \Pi_0 + \int_0^{\frac{\hat\xi^2}{2}} F^2$ and Π_0 is holomorphic on $\Omega \supset \mathcal{N}_1$, and $(\hat\xi^{-1}\partial_{\hat\xi})^r(V_0/\frac{\hat\xi^2}{2})$, because (1.1.3) gives $V_0/\frac{\hat\xi^2}{2} = L^{-1}(2\eta U - (1-2h)\eta\int_0^1 U(\theta\frac{\hat\xi^2}{2},\cdot)\,\mathrm{d}\theta - d\int_0^1 \partial_\eta U(\theta\frac{\hat\xi^2}{2},\cdot)\,\mathrm{d}\theta)$. Joint smoothness in $(\frac{\hat\xi^2}{2},\eta)$ follows from the same formulas. Neither (a) nor (b) used a lower bound on t_1 or κ_0. □

Lemma 1.20.41 (From $\frac{\hat\xi_i^2}{2}$ to $\frac{\hat\xi_{\mathrm{match}}^2}{2}$: transition and moment matching)**.** *Assume the conclusions of Proposition 1.20.38, with late controls satisfying (1.20.17). Let $\ell_i=\log(CE(\frac{\hat\xi_i^2}{2},\cdot))$ and $G_i=U(\frac{\hat\xi_i^2}{2},\cdot)$. Let B_0 be the bound of $\|\ell_i\|_{C^0}$ in Lemma 1.20.37(b), and fix*

$$T_{\mathrm{sh}}\ge 20\|\sigma'\|_\infty(B_0+\log 2). \tag{1.20.18}$$

Fix nonnegative, nonzero smooth functions β_1,β_2 and β_3,β_4,β_5 on $(0,\infty)$; within each of the two groups they are supported in the interiors of ordered disjoint compact subintervals of (e^{-6},e^{-5}). With $y_i=2\log(\hat\xi/\hat\xi_i)$ and $x=(\hat\xi/\hat\xi_{\mathrm{ref}})^2$, continue the member beyond $\frac{\hat\xi_i^2}{2}$ as follows, with $\Pi=\Pi_0+C_p$:

(I) for $\frac{\hat\xi_i^2}{2}\le\frac{\hat\xi^2}{2}\le\frac{\hat\xi_{\mathrm{ref}}^2}{2}e^{-8}$: $U=G_i$ and $\log E=-\log C+\frac{y_i}{10}+(1-\sigma(\frac{y_i}{T_{\mathrm{sh}}}))\ell_i+\sigma(\frac{y_i}{T_{\mathrm{sh}}})\log f$ (the formula [42, (B.34)]); for $y_i\ge T_{\mathrm{sh}}$ this is $E=E_0$, because $C^{-1}(\hat\xi/\hat\xi_i)^{1/5}=P_*x^{1/10}$;

(II) for $e^{-8}\le x\le e^{-6}$: $E=E_0$ and $U=4\eta+(1-\sigma(\log x+8))(G_i-4\eta)$;

(III) for $e^{-6}\le x\le e^{-5}$: $U=4\eta+c_1\beta_1+c_2\beta_2$ and $E=E_0+c_3\beta_3+c_4\beta_4+c_5\beta_5$, with $c=(c_1,\dots,c_5)\in C^\infty([-1,1];\mathbb{R}^5)$ chosen in (b); and $(U,E)=(U_0,E_0)$ near $x=e^{-5}$.

There is $\varepsilon_m\in(0,1]$, depending only on P_*, h, Π_0 and the bumps, with the following property. Let $j_0\le\varepsilon_m/4$, let Λ be larger and then C larger than thresholds depending on the earlier choices, and let t_1 and κ_0 be smaller than thresholds depending on the earlier choices; the conditions are listed in the proof. Then:

(a) On $[\frac{\hat\xi_i^2}{2},\frac{\hat\xi_{\mathrm{ref}}^2}{2}e^{-8}]$: $l\in[.55,.65]$, $a\in[.7,.9]$, $b_s=0$, $S_q>1$ and $p_1>2$. Hence $v_s=a<1$ and the relaxed cone holds there.

(b) There is c with $\|c\|_{C^1}\le 1$ such that the member is smooth on $[0,\frac{\hat\xi_{\mathrm{match}}^2}{2}]\times[-1,1]$, $E>0$ for $\hat\xi>0$, $E(0,\eta)=0$ with positive limiting $E/\hat\xi$, it equals (U_0,E_0) near $\frac{\hat\xi_{\mathrm{match}}^2}{2}=\frac{\hat\xi_{\mathrm{ref}}^2}{2}e^{-5}$, and $\mathbf{m}(\frac{\hat\xi_{\mathrm{match}}^2}{2},\cdot)=\mathbf{m}_0(\frac{\hat\xi_{\mathrm{match}}^2}{2},\cdot)$. On $e^{-8}\le x\le e^{-5}$ it satisfies

$$Q_s\ge Q_{\min}/2,\quad E\ge e_{\mathrm{m}}/2,\quad |a-.8|\le .1,\quad |N_s/(EQ_s)|\le w_*,\quad |b_s|\le .1/(1+w_*), \tag{1.20.19}$$

with the constants of Step 2 of the proof. Hence $v_s<1$, $P_c>2$, and the relaxed cone holds there.

Proof. Norms $\|\cdot\|_{C^k}$ are in $\eta\in[-1,1]$. We restrict the late controls to the nonempty family (1.20.17). Constants denoted by K may depend on Λ, $\frac{\hat\xi_i^2}{2}$ and T_{sh}, but are uniform in C and in this family. Put

$$b_2=t_1+\kappa_0(1+\omega_0^{-1}),\qquad \delta_U=C_2^{\mathrm{nat}}/\Lambda+K_{\mathrm{part}}b_2.$$

By Corollary 1.20.39,

$$\|U(\tfrac{\hat\xi^2}{2},\cdot)-U_*\|_{C^2}\le\delta_U\quad(0\le\tfrac{\hat\xi^2}{2}\le\tfrac{\hat\xi_i^2}{2}),\qquad \|G_i-4\eta\|_{C^2}\le j_0+\delta_U. \tag{1.20.20}$$

(a) Put $H=\hat\xi E$. On (I), $l=\frac12\hat\xi\partial_{\hat\xi}\log H=\frac12+\frac12\hat\xi\partial_{\hat\xi}\log E=.6+T_{\mathrm{sh}}^{-1}\sigma'(y_i/T_{\mathrm{sh}})(\log f-\ell_i)$. Since $|\log f-\ell_i|\le\log 2+B_0$, (1.20.18) gives $|l-.6|\le.05$. So $a=2-2l\in[.7,.9]$; and $\frac12\hat\xi\partial_{\hat\xi}U=0$, so $b_s=0$. For the source of (1.4.1)–(1.4.2): $\mathcal{A}_{\mathrm{rad}}(U)=\mathfrak{M}_1/\frac{\hat\xi^2}{2}$ is an average of U over $[0,\frac{\hat\xi^2}{2}]$, and $U=G_i$ on $[\frac{\hat\xi_i^2}{2},\frac{\hat\xi^2}{2}]$. So (1.20.20) gives $|W-W_*|\le2\delta_U$ on $[-1,1]$, and $-W\ge2.8$ if $\delta_U\le.02$, by

Lemma 1.20.33(a). Also $|G_i| \le 4.1$, so $-h(1-2\eta U) \ge -9.2h \ge -.092$. For the gradient term, $(\log E)_\eta = (1-\sigma)\ell_i' + \sigma(\log f)'$ and $H_c = (\frac12 - h)\eta + dG_i = H_* + d(G_i - U_*)$. On $0 < y \le t_1$, $\partial_y \log\phi = -\kappa p_{1,c}/2$; for $y > t_1$, $\partial_y \log\phi = -\frac12[(1-\lambda)\kappa_0 p_1^\flat + .8\lambda]$ (Definition 1.20.35). Here κ and λ do not depend on η, and $p_{1,c}$, $p_1^\flat$ are core values. Since $\ell_i = \frac12\log(\hat\xi_i^2) + \log\phi_* + \log\Phi(4,\cdot) + \int_0^{L_0}\partial_y\log\phi\,dy$ with $L_0 = 2\log(\hat\xi_i/\hat\xi_0)$, we get

$$\ell_i' = \xi_0 + \partial_\eta \log\Phi(4,\cdot) + e_1, \qquad |e_1| \le \tfrac12(t_1 + \kappa_0 L_0)M_1^c =: \varepsilon_\ell,$$

where M_1^c bounds p_1 of the core in C^1 (Lemma 1.20.33(c6)). By $H_*\xi_0 = -\Lambda L\chi$, $|\xi_0| \le \Lambda L\sqrt{\chi}/\sigma_*$, (c2) and $|H_*| \le 4.6$,

$$-H_c\ell_i' \ge \Lambda L\chi - K_0(\chi + \Lambda^{-1}) - 4.6\varepsilon_\ell - \delta_U\Lambda L\sqrt{\chi}/\sigma_* - \delta_U(K_0 + \varepsilon_\ell).$$

By Young's inequality $\delta_U\Lambda L\sqrt{\chi}/\sigma_* \le .05\Lambda L\chi + 5\delta_U^2\Lambda/\sigma_*^2$. For $\Lambda \ge 2K_0$ and $\varepsilon_\ell \le 1$ this gives $-H_c\ell_i' \ge -e_2$, with $e_2 := K_0/\Lambda + 4.6\varepsilon_\ell + 5\delta_U^2\Lambda/\sigma_*^2 + \delta_U(K_0+1)$. Also $2\eta H_* = 2((\frac12 - h) + 4d)\eta^2 + 2dj_0\eta \ge -d^2 j_0^2/(2((\frac12 - h) + 4d)) \ge -j_0^2/8$, so $-H_c(\log f)' = 2\eta H_c/(1+\eta^2) \ge -j_0^2/8 - \delta_U$. Hence

$$S_q = -Wl - h(1-2\eta U) - H_c(\log E)_\eta \ge .55\cdot 2.8 - .092 - e_2 - .0004 - \delta_U > 1.4$$

whenever $e_2 + \delta_U \le .04$. Since

$$\delta_U^2\Lambda \le \frac{2(C_2^{\mathrm{nat}})^2}{\Lambda} + 2\Lambda K_{\mathrm{part}}^2 b_2^2,$$

this condition holds for Λ larger than a threshold depending on K_0, σ_* and C_2^{nat}, and then for b_2 and $t_1 + \kappa_0 L_0$ below positive thresholds depending on Λ. The latter two bounds are imposed after C, by decreasing κ_0 and then t_1. By (1.4.1)–(1.4.2), $\frac12\hat\xi\partial_{\hat\xi}p_1 = \frac{\hat\xi^2}{2}S_q/L - lp_1$, since L does not depend on $\frac{\hat\xi^2}{2}$. We have $p_1(\frac{\hat\xi_i^2}{2}) > 2$ (Proposition 1.20.38(c)). At a first point $\rho > \hat\xi_i$ with $p_1 = 2$ we would have $\frac12\hat\xi\partial_{\hat\xi}p_1 \ge \frac{\rho^2}{2} - 1.3 > 0$, since $\frac{\rho^2}{2} \ge \frac{\hat\xi_i^2}{2} \ge 271$; this is impossible. So $p_1 > 2$. As $b_s = 0$: $t_s = 0$, $v_s = a < 1$, $P_c = p_1 > 2$, and $\mathcal{U}(P_c, J_c) > 2 > v_s$ by the identity in the proof of Proposition 1.20.38.

(b) *Step 1: normalized formulas.* Rescale by $\rho = \frac{\hat\xi_{\mathrm{ref}}^2}{2}$ as in the change of scale in Lemma 1.4.3: $\widehat U(x) = U(\frac{\hat\xi_{\mathrm{ref}}^2}{2}x)$, $\widehat E(x) = E(\frac{\hat\xi_{\mathrm{ref}}^2}{2}x)$. Then $\widehat H = \sqrt{2x}\widehat E$, and the five functions $\widehat{\mathbf m}$ of the change of scale in Lemma 1.4.3 are the integrals (1.1.2) of $(\widehat U, \widehat E)$ in x. Since $I/(\frac{\hat\xi^2}{2}H) = \widehat I/(x\widehat H)$, $M/\frac{\hat\xi^2}{2} = \widehat M/x$, $S/\frac{\hat\xi^2}{2} = \widehat S/x$ and $C_p = \widehat C_p$, formula (1.4.3) holds with $(\frac{\hat\xi^2}{2}, H, \mathbf m)$ replaced by $(x, \widehat H, \widehat{\mathbf m})$ and the same Π_0 (this is (1.4.3)). So on $R = [e^{-8}, e^{-5}] \times [-1, 1]$, the quantities Q_s, N_s, a, b_s are those of the hatted pair, and $\frac{\hat\xi_{\mathrm{ref}}^2}{2}$ enters only through $p_1 = \frac{\hat\xi_{\mathrm{ref}}^2}{2}xQ_s/L$ and $p_2 = \frac{\hat\xi_{\mathrm{ref}}^2}{2}xN_s/(L\widehat E)$.

Step 2: the reference. For (U_0, E_0), (1.1.2) gives $\widehat M_0 = 4\eta x$, $\widehat J_0 = 4\eta\widehat I_0$, $\widehat I_0/(x\widehat H_0) = \frac58$ and $\partial_\eta\widehat I_0 = -2\eta f\widehat I_0$; so $W = -3 + 8h\eta^2$, and (1.4.3) gives

$$Q_{s,0} = 3 - 8h\eta^2 + \tfrac58[1 - h - 4d + 8(h - (\tfrac12 - h))\eta^2 + 2((\tfrac12 - h) + 4d)\eta^2 f],$$

independent of x. At $h = 0$ this is $\frac98 + \frac58\eta^2(9 - 8\eta^2)f \ge \frac98$, and its h-derivative is $2\eta^2 - \frac54\eta^2 f - \frac58 \ge -\frac58$; so $Q_{s,0} \ge 1.11$ on $[-1,1]$. Put $Q_{\min} = \min_R Q_{s,0} \ge 1.11$, $e_{\mathrm m} = \min_R E_0 = P_* e^{-.8}/2$, and $w_* = 1 + \max_R |N_{s,0}/(E_0 Q_{s,0})| < \infty$. These depend only on P_*, h and Π_0.

Step 3: the tolerance. Let C_L be the constant of (1.4.7) for $k = 0$, $\frac{\hat\xi_0^2}{2} = e^{-8}$, $\frac{\hat\xi_1^2}{2} = e^{-5}$, $e_{\min} = e_{\mathrm m}/2$, and the common bound $1 + \max_R \|(U_0, E_0, \widehat{\mathbf m}_0)\|_1$. We apply it to the hatted pairs of

the reference and of the member, the latter continued by (U_0, E_0) beyond $x = e^{-5}$. For the member put

$$\Delta := \|\Delta(\widehat{U}, \widehat{E})\|_1 + \|\Delta\widehat{\mathbf{m}}\|_1 + \sup_R(|D_x\Delta\widehat{U}| + |D_x\Delta\widehat{E}|),$$

where Δ denotes the difference with the reference and $\|\cdot\|_1$ is the norm of (1.4.7) on R. There is $\varepsilon_1 \in (0,1]$, depending on $Q_{\min}$, e_{m}, w_*, C_L and $\sup_R|D_xE_0|$, such that $\Delta \le \varepsilon_1$ implies (1.20.19) on R. Indeed, $|\Delta Q_s| + |\Delta N_s| \le C_L\Delta$ by (1.4.7); $E \ge E_0 - \Delta$; $a - .8 = -2D_x\log(\widehat{E}/E_0)$ and $b_s = 2D_x\widehat{U}/\widehat{E}$, with $D_xU_0 = 0$, are $O(\Delta)$; and so is $N_s/(EQ_s) - N_{s,0}/(E_0Q_{s,0})$. (1.20.19) gives $v_s = a + b_s^2/a \le .9 + .01/.7 < 1$. With $G := Q_s - b_sN_s/(aE)$ we have $|b_sN_s/(aEQ_s)| \le \frac{1}{7}$, so $G \ge \frac{6}{7}Q_s \ge \frac{3}{7}Q_{\min}$, and $P_c = \frac{\hat\xi^2}{2}G/L \ge \frac{\hat\xi^2_{\mathrm{ref}}}{2}e^{-8}\cdot\frac{3}{7}Q_{\min} > 2$ if $\frac{\hat\xi^2_{\mathrm{ref}}}{2} \ge 5e^8$, a lower bound on C. So the relaxed cone holds on R, as in (a).

Step 4: the discrepancy before the correction. Let $x_{\mathrm{sep}} = e^{T_{\mathrm{sh}}}(CP_*)^{-10}$ and require $x_{\mathrm{sep}} < e^{-8}$. On $[0, \frac{\hat\xi_i^2}{2}]$, Corollary 1.20.39 gives $\|U\|_{C^2} \le K$ and $\|CE\|_{C^2} = \|\hat\xi\hat\phi\|_{C^2} \le K(\hat\xi/\sqrt{2})$. On $[\frac{\hat\xi_i^2}{2}, \frac{\hat\xi_i^2}{2}e^{T_{\mathrm{sh}}}]$, formula (I) and Lemma 1.20.37(b) give $\|U\|_{C^2} + \|CE\|_{C^2} \le K$. These constants are uniform over the family (1.20.17); in particular they can be fixed before C is selected. Integrating (1.1.2) and using the change of scale in Lemma 1.4.3,

$$\|\widehat{M}\|_{C^2} + \|\widehat{S}\|_{C^2} \le Kx_{\mathrm{sep}}, \qquad \|\widehat{I}\|_{C^2} + \|\widehat{J}\|_{C^2} \le KC^{-1}x_{\mathrm{sep}}^{3/2}, \qquad \|\widehat{C}_p\|_{C^2} \le KC^{-2} \qquad (x = x_{\mathrm{sep}});$$

for $\widehat{C}_p$ write $E^2/(\hat\xi^2) = C^{-2}(CE)^2/(\hat\xi^2)$. By (1.1.2), $\|\widehat{\mathbf{m}}_0(x_{\mathrm{sep}})\|_{C^2} \le K(x_{\mathrm{sep}} + x_{\mathrm{sep}}^{1/5})$. Hence

$$\|\Delta\widehat{\mathbf{m}}(x_{\mathrm{sep}})\|_{C^2} \le \omega(C) := K(x_{\mathrm{sep}}^{1/5} + C^{-1}) \longrightarrow 0 \qquad (C \to \infty),$$

with K independent of C, t_1, κ_0 and the widths. On $[x_{\mathrm{sep}}, e^{-6}]$ we have $\widehat{E} = E_0$ and $\widehat{U} - 4\eta = \theta(x)\Delta_G$, with $\Delta_G := G_i - 4\eta$, $\theta = 1$ on (I) and $\theta = 1 - \sigma(\log x + 8)$ on (II). The integrands of the five differences are $(\theta\Delta_G,\ 0,\ \theta\Delta_G\widehat{H}_0,\ \theta\Delta_G(\theta\Delta_G + 8\eta),\ 0)$. So, if $\|\Delta_G\|_{C^2} \le 1$, then $\|\Delta\widehat{\mathbf{m}}(x) - \Delta\widehat{\mathbf{m}}(x_{\mathrm{sep}})\|_{C^2} \le K_1\|\Delta_G\|_{C^2}$ for $x \le e^{-6}$, with K_1 depending only on P_*. Also $|D_x\Delta\widehat{U}| \le \|\sigma'\|_\infty|\Delta_G|$. So on $[e^{-8}, e^{-6}]$,

$$\Delta \le K_3(\|\Delta_G\|_{C^2} + \omega(C)), \qquad K_3 := 2 + K_1 + \|\sigma'\|_\infty.$$

Step 5: the correction. On $[e^{-7}, e^{-6}]$ the member equals (U_0, E_0), and on (III) it is (U_0, E_0) plus the five bumps. Lemma 1.4.3 applies with $u_c = 4\eta$, $E_0 = P_*f(\eta)x^\alpha$ and $\alpha = \frac{1}{10} \notin \{-\frac{1}{2}, \frac{1}{2}, \frac{3}{2}\}$, and with the bumps of Lemma 1.4.3. After the row operations $J \mapsto J - 4\eta I$, $S \mapsto S - 8\eta M$ and division by the fixed normalizing factors, which together form an invertible matrix $\mathcal{T}(\eta)$ smooth in η, the change of the normalized moments across (III) is $F_\eta(c) = B(\eta)c + Q_\eta(c,c)$. Here B and the bilinear Q are smooth, and $B(\eta)$ is invertible for every $\eta \in [-1,1]$. By continuity and compactness the norms β_0, β_2 of B^{-1} (pointwise, and as multiplication on C^2) and κ_0', κ_2' of Q (pointwise, and on C^2) are finite. Since the reference has no correction, $\widehat{\mathbf{m}}(e^{-5}) = \widehat{\mathbf{m}}_0(e^{-5})$ is equivalent to

$$F_\eta(c) = d(\eta) := -\mathcal{T}(\eta)\Delta\widehat{\mathbf{m}}(e^{-6}, \eta).$$

By Lemma 1.4.3, if $8\beta_0^2\kappa_0'\|d\|_{C^0} \le 1$ and $8\beta_2^2\kappa_2'\|d\|_{C^2} \le 1$, this has a smooth solution with $\|c\|_{C^2} \le 2\beta_2\|d\|_{C^2}$. On (III), $\Delta\widehat{U}$, $\Delta\widehat{E}$, their D_x-derivatives and $\Delta\widehat{\mathbf{m}}(x) - \Delta\widehat{\mathbf{m}}(e^{-6})$ are bounded in $\|\cdot\|_1$ by $K_\beta\|c\|_{C^1}$ when $\|c\|_{C^1} \le 1$, with K_β depending on P_* and the bumps. Hence on (III), $\Delta \le K_3(\|\Delta_G\|_{C^2} + \omega(C)) + 3K_\beta\|c\|_{C^1}$.

Choice of ε_m. Let $\tau := c_2\|\mathcal{T}\|_{C^2}K_3$, where $c_2 \le 4$ is the product constant of the C^2 norm ($\|fg\|_{C^2} \le c_2\|f\|_{C^2}\|g\|_{C^2}$). Choose $\varepsilon_m \in (0,1]$ such that $2K_3\varepsilon_m + 12K_\beta\beta_2\tau\varepsilon_m \le \varepsilon_1$, $16\beta_0^2\kappa_0'\tau\varepsilon_m \le 1$, $16\beta_2^2\kappa_2'\tau\varepsilon_m \le 1$ and $4\beta_2\tau\varepsilon_m \le 1$. It depends only on P_*, h, Π_0 and the bumps. Suppose $\|\Delta_G\|_{C^2} \le \varepsilon_m$ and $\omega(C) \le \varepsilon_m$. Then $\|d\|_{C^2} \le 2\tau\varepsilon_m$, Lemma A.2 applies, $\|c\|_{C^2} \le 4\beta_2\tau\varepsilon_m \le 1$,

and $\Delta \le \varepsilon_1$ on all of R. By (1.20.20), $\|\Delta_G\|_{C^2} \le \varepsilon_m$ holds if $j_0 \le \varepsilon_m/4$, $C_2^{\mathrm{nat}}/\Lambda \le \varepsilon_m/4$ and $K_{\mathrm{part}} b_2 \le \varepsilon_m/2$. The conditions on Λ and C are lower bounds. The conditions on b_2 and $t_1 + \kappa_0 L_0$ are late upper bounds, compatible with (1.20.17) and with the selection of κ_0 before t_1.

Step 6: conclusion. With this c, Step 3 gives (1.20.19) and the relaxed cone on R, and $E \ge e_{\mathrm{m}}/2 > 0$ there; on (I), $E > 0$ by its formula. The member is smooth: σ is flat at 0 and 1; at $\frac{\hat\xi_i^2}{2}$ it continues the output slab, on which $\frac12 \hat\xi \partial_{\hat\xi} \log E = .1$ and $\frac12 \hat\xi \partial_{\hat\xi} U = 0$ (Lemma 1.20.37(c)); (I) ends in its ideal part, because $x_{\mathrm{sep}} < e^{-8}$; and the bumps have compact support in (e^{-6}, e^{-5}). Near $x = e^{-5}$ the member equals (U_0, E_0), and $\widehat{\mathbf{m}}(e^{-5}) = \widehat{\mathbf{m}}_0(e^{-5})$, that is, $\mathbf{m}(\frac{\hat\xi^2_{\mathrm{match}}}{2}, \cdot) = \mathbf{m}_0(\frac{\hat\xi^2_{\mathrm{match}}}{2}, \cdot)$ by the change of scale in Lemma 1.4.3. Both pressures are $\Pi_0 + C_p$. □

Proof of Theorem 1.8.10. Order of choices. (1) Let ε_m be given by Lemma 1.20.41. (2) Choose $0 < j_0 \le \min\{.05, \varepsilon_m/4\}$, together with the other upper bounds of Remark 1.8.12(c). (3) Choose δ_* and then σ_* by Lemma 1.20.33(a). (4) Choose $\Lambda \ge \Lambda_0$ of Lemma 1.20.33, above the thresholds of Lemma 1.20.34, Theorem 1.20.36, Lemma 1.20.37 and Lemma 1.20.41. (5) Choose T_{sh} by (1.20.18); B_0 depends on Λ and $\frac{\hat\xi_i^2}{2}$, not on C. (6) Choose $C_0 \ge C_0(\Lambda)$ of Lemma 1.20.33, above the thresholds of Lemma 1.20.34, Theorem 1.20.36 and Lemma 1.20.41 (in particular $\omega(C) \le \varepsilon_m$, $\frac{\hat\xi^2_{\mathrm{ref}}}{2} \ge 5e^8$, $x_{\mathrm{sep}} < e^{-8}$), and let $C \ge C_0$. (7) Fix $y_*(C)$, Υ^b and ω_0 (Definition 1.20.35), and then choose κ_0, t_1 and the widths below the upper bounds of Theorem 1.20.36, Lemma 1.20.37 and Lemma 1.20.41. Lemmas 1.20.33, 1.20.34 and 1.20.40 impose no condition on κ_0 or t_1.

The constant in the discrepancy bound $\omega(C)$ is fixed using the uniform family (1.20.17). Thus step (6) does not depend on the eventual values of the late controls. After C fixes $\omega_0 > 0$, step (7) imposes $K_{\mathrm{part}} b_2 \le 1$, the stricter b_2 bounds in Lemma 1.20.41, and its bound on $t_1 + \kappa_0 L_0$. Their intersection is nonempty by Corollary 1.20.39. Higher angular derivatives are then bounded for this fixed member by (1.20.16); they are not used to select C.

The profile. On $[0, \frac{\hat\xi^2_{\mathrm{match}}}{2}]$ the member is the core of Lemma 1.20.33 on $[0, \frac{\hat\xi_0^2}{2}]$, the first collar (1.20.14) on $0 < y \le t_1$, the design of Definition 1.20.35 up to $\frac{\hat\xi_i^2}{2}$ (Proposition 1.20.38), and (I)–(III) of Lemma 1.20.41 up to $\frac{\hat\xi^2_{\mathrm{match}}}{2}$, with $\Pi = \Pi_0 + C_p$.

(i) Smoothness on $[0, \frac{\hat\xi^2_{\mathrm{match}}}{2}]$ and $\phi > 0$: Proposition 1.20.38 and Lemma 1.20.41(b). Put $\frac{\hat\xi^2_{\mathrm{an}}}{2} = \frac{\hat\xi_a^2}{2} e^{\min\{y_c, y_B\}}$, with y_c from Proposition 1.20.38(b) and y_B from Lemma 1.20.40(a). Then the analytic rectangle on $[0, \frac{\hat\xi^2_{\mathrm{an}}}{2}]$ is Lemma 1.20.40(b). The equations (1.4.6) on $[0, \frac{\hat\xi_a^2}{2}]$ and $T_0 = 0$ there are Lemma 1.20.33(b),(c1).

(ii) The relaxed cone holds on $(\frac{\hat\xi_a^2}{2}, \frac{\hat\xi_i^2}{2}]$ by Proposition 1.20.38(a), and on $[\frac{\hat\xi_i^2}{2}, \frac{\hat\xi^2_{\mathrm{match}}}{2}]$ by Lemma 1.20.41(a),(b). On $(\frac{\hat\xi_a^2}{2}, \frac{\hat\xi^2_{\mathrm{an}}}{2}]$, $v_s > 2$ by Proposition 1.20.38(b). At $\hat\xi_a = \hat\xi_0$ the member is the stress-free core, so $s = p_s$; hence $a = p_1 > 0$, $t_s = p_2/p_1$ and $v_s = p_1 + p_2^2/p_1 > 2.2$ (Lemma 1.20.33(c1),(c4),(c5)). The asserted stress factorization and its bounds on $(\frac{\hat\xi_a^2}{2}, \frac{\hat\xi^2_{\mathrm{an}}}{2}]$ are Lemma 1.20.40(a), with $g_a(y_a)$ and $B_a = B_0$.

(iii) Lemma 1.20.41(b).

Steps (1)–(5) do not involve C, and the conditions on C in (6) are lower bounds; so $\frac{\hat\xi^2_{\mathrm{ref}}}{2} = \frac{\hat\xi_i^2}{2}(CP_*)^{10}$ may be taken as large as required. Every condition in (7) is an upper bound depending only on earlier choices. Decreasing $\frac{\hat\xi^2_{\mathrm{an}}}{2}$ keeps (i) and (ii). □

Lemma 1.20.42 (Z_* on the endpoint collars)**.** *Let* $m_* = |\Pi_0(0)| \ge \frac52 P_*^2$. *At* $\eta = \pm 1$, $Z_*(\pm1) = -(\frac12 + h)(1 \mp 2U_*)U_* \mp 4(\frac12 - h) \pm 4(\frac12 + h)\Pi_0(\pm1)$ *with* $U_* = \pm 4 + j_0$, *so* $\operatorname{sgn} Z_*(\pm1) = \mp 1$ *and*

$|Z_*(\pm1)| \geq (\frac{1}{2}+h)m_* - 21$. *On* $1-|\eta| \leq \epsilon_c := \min\{\epsilon_e, (\frac{1}{2}+h)/76\}$ *we have* $|Z_*| \geq \frac{3}{4}(\frac{1}{2}+h)m_* - 22 \geq \delta_e$.

Proof. By Lemma 1.8.6, $\Pi_0 = -\frac{1}{2}\int c^2 f^{2\vartheta}\,\mathrm{d}y$ with $0 \leq \vartheta \leq 1$. Since $f^{2\vartheta} \geq f^2$ and $f(\pm1) = \frac{1}{2}$, we get $|\Pi_0(\pm1)| \geq m_*/4$. Also $|\partial_\eta f^{2\vartheta}| \leq 2f^{2\vartheta}$ and $|\partial_\eta^2 f^{2\vartheta}| \leq 8f^{2\vartheta}$, so $|\Pi_0'| \leq 2m_*$ and $|\Pi_0''| \leq 8m_*$. At $d=0$ the non-pressure part of Z_* is at most $(\frac{1}{2}+h)\cdot 7.1\cdot 4.05 + 4(\frac{1}{2}-h) \leq 17 \leq 21$ (with $j_0 \leq .05$), and $4(\frac{1}{2}+h)|\Pi_0(\pm1)| \geq (\frac{1}{2}+h)m_*$; the sign is that of $\pm4(\frac{1}{2}+h)\Pi_0(\pm1) < 0$ for $+$. On $[-1,1]$, with $U_* = 4\eta + j_0$, the non-pressure part of Z_*' is at most $33.3 + 18.6 + 2 + 32.4 + 16 \leq 105$, and the pressure part at most $(4 + 8 + 4(\frac{1}{2}+h) + 8(\frac{1}{2}+h))m_* \leq 19m_*$; so $|Z_*'| \leq 105 + 19m_*$. The mean-value theorem on the collar gives $|Z_*| \geq (\frac{1}{2}+h)m_* - 21 - \epsilon_c(105+19m_*) \geq \frac{3}{4}(\frac{1}{2}+h)m_* - 22$, and this is $\geq 2 = \delta_e$ since $m_* \geq \frac{5}{2}P_*^2$ and $P_* > e^{T_d}$. □

Proposition 1.20.43 (One activation on the endpoint collars)**.** *With Definitions 1.20.22 and 1.20.35, the forward leading data on endpoint neighbourhoods of* $\eta = \pm1$ *are the transports of the backward data on the whole activation collar, through the termination and the interpolation.*

Proof. On the collars $\Upsilon = \Upsilon^b \equiv 1$, because $|Z_R| \geq \delta_e \geq \delta_Z$ there by (I6), and $|Z_*| \geq \delta_e \geq \delta_Z$ by Lemma 1.20.42 (the collar width is $\leq \epsilon_c$). So $y_1 = y_1^\flat = y_l$, and β and λ are the same functions of y. The frozen values are compositions of the core with the common $\vartheta(y)$, and the forward core on the collars is the transported backward core. The prescriptions $(\log F)_y = -\frac{1}{2}[(1-\lambda)\kappa p_1^\flat + .8\lambda]$ and $U_y = -\frac{1}{2}\kappa\beta\frac{\hat\xi^2}{2}n^\flat$ are covariant under the chart change. So both members solve the same transported ODE in y with the same data at $y=0$. Lemma 1.22.10 writes the transported strains and the shared termination and interpolation explicitly, and proves this assertion on the whole two transition intervals. □

For the wait estimates in (R5)–(R6), which are used on $\mathscr{P}$ only, extend (H°, U°) along the power template to X_p by suppressing the two-row taper in $-2.15 < y_p < -0.85$. In this calculation alone all five inward histories are integrated on that extension with the same axis value p_0. They agree with the comparison histories, with all angular derivatives, for $y_p \leq -14.5$ because the suppressed supports are farther out. The complete taper pressure row is zero, so the outlet formula remains (1.20.9). At X_p the velocity and its local derivatives, hence the source datum $q_p = h - \nu + \log\dot H|_{X_p}$, agree. The actual pulse instead uses the full signed primitive increment of (Taper) and the actual energy in (1.14.17). Both inlet moments are calculated with the taper present.

The $G=0$ sector.

Proposition 1.20.44 (Cover on the $G=0$ sector)**.** *Fix* η *in the* $G=0$ *sector (central band and variable-*ν *band). Assume:*

(G0-i) from the exit $\frac{(\hat\xi_g(\eta))^2}{2}$ *of the last core/pressure correction on the growth arc to the pulse entry* $\frac{\hat\xi_p^2}{2}$*:* $U \equiv 0$, $\mathfrak{M}_1 = \mathfrak{M}_3 = 0$, $H = H_a(\eta)\mathsf{F}(\log(\frac{\hat\xi^2}{2}/R_g);\nu(\eta))$, *with* R_g *independent of* η, $\mathsf{F} = e^{\gamma z}$ $(z \leq 0)$, $e^{f_0 - \nu f_1}$ $(0 \leq z \leq T)$, $\mathsf{F}_T e^{-\nu(z-T)}$ $(T \leq z \leq T+W)$, $f_0' \in [0,\gamma]$, $f_1' \in [0,1]$, $f_1(0) = 0$, $\frac{\hat\xi_p^2}{2} = R_g e^{T+W}$ [Section 1.14];

(G0-ii) $\mathfrak{M}_2 = \frac{\hat\xi^2}{2}H/(1+\gamma)$ *at* $\frac{\hat\xi_g^2}{2}$ *(restored reference histories)* [proof of Lemma 1.6.14, Section 1.6.4];

(G0-iii) $u = \dot\nu \geq 0$ *and* $q_p := h - \nu + \log\dot H(\frac{\hat\xi_p^2}{2}) \geq q_o > 0$ (1.16.24).

Then on $[\frac{\hat\xi_q^2}{2},\frac{\hat\xi_p^2}{2}]$*: (a)* $S_q\ge q_o$*; on the growth arc* $Q=S_q/(1+\gamma)\ge\gamma/(1+\gamma)=\frac38$*; (b)* $Q\ge q_\flat:=\min\{\frac38,q_o/(1+\gamma)\}$*, and* $Q\ge\frac38e^{-(1+\gamma)z}$ *for* $0\le z\le T$*; (c) every point with* $\ell_r\ge0$ *is relaxed if* $\frac{\hat\xi_2^2}{2}q_\flat>2L$*; (d) every point with* $\ell_r<0$ *is strict if* $\frac{\hat\xi_2^2}{2}q_\flat\ge4L(1+\nu)$ *and* $\nu w^2\le\frac18$*; (e) on the exact wait the condition* $\nu w^2\le\frac18$ *holds under* (1.20.8) *with* $n_1=0$ *and* (F*) *for* $Q_0=\frac38e^{-(1+\gamma)T}$*,* $q=q_o$*,* $S=W$*.*

Proof. By (G0-i), $\ell_r=\gamma$ $(z<0)$, $f_0'-\nu f_1'$ $(0\le z\le T)$, $-\nu$ $(z\ge T)$; so $\ell_r\ge-\nu$ and $1+\ell_r\in[1-\nu,1+\gamma]$. Since $\partial_\eta\log\mathsf F=-\nu_\eta f_1(z)$ $(z\le T)$ resp. $-\nu_\eta(f_1(T)+z-T)$ and $u\ge0$, $f_1'\ge0$, the function $c(z)=\log\dot H$ is nonincreasing in z, hence $c\ge c(\frac{\hat\xi_p^2}{2})=q_p-h+\nu$. With $U=\mathfrak M_1=0$, (1.20.7) gives $S_q=\ell_r+h+c\ge-\nu+h+c(\frac{\hat\xi_p^2}{2})=q_p\ge q_o$, and on the growth arc $S_q=\gamma+h+c\ge\gamma+\nu+q_p\ge\gamma$. On the arc, (G0-ii) and $(\hat\xi^{-1}\partial_{\hat\xi}(\frac{\hat\xi_2^2}{2}H/(1+\gamma)))=H$ give $r\equiv(1+\gamma)^{-1}$, $\dot r=0$, so $Q=1+(c-1+h)r=S_q/(1+\gamma)$: this is (a). Lemma 1.20.9 gives (b). (c), (d) are Proposition 1.20.10(a),(b) (with $\theta\ge\frac12$, $-\ell_r\le\nu$). (e) is Lemma 1.20.12 with the inlet value from (b) at $z=T$. □

Lemma 1.20.45 ((R6) on the $G=0$ sector)**.** *Fix* η *in the* $G=0$ *sector and assume (G0-i)–(G0-iii). Let* $z=\log(\frac{\hat\xi_2^2}{2}/R_g)$*, which at fixed* $\hat\xi$ *does not depend on* η*, and let* $z_1\in[0,T]$ *be the point after which* $f_0'=0$*. Since* $f_1'=0$ *wherever* $f_0'>0$ [Section 1.14]*,* $\ell_r\ge0$ *for* $z<z_1$ *and* $\ell_r=-\nu f_1'\in[-\nu,0]$ *for* $z\ge z_1$*. Put* $q=h-\nu+\log\dot H$*,* $s=z-z_1$*,* $\sigma=\mathfrak M_4/(\frac{\hat\xi_2^2}{2}E^2)$*,* $E_1=E(z_1)$*,* $\nu'=|\nu_\eta|$ *at this* η *(it does not depend on* $\frac{\hat\xi_2^2}{2}$*), and* $Y_*=\inf_\eta\log(R_o/\frac{\hat\xi_p^2}{2})$*. Let* $K_\sigma\ge|\sigma(z_1)|+|\partial_\nu\sigma(z_1)|$ *be the template bound (on the sector* σ *depends only on the shape* $F(\cdot;\nu)$*; Lemma 1.14.1). Assume* $2\lambda(T+60\log(1/\lambda))\le\log2$*, so* $e^{2\nu(T+W)}\le2$*, and* $Y_*\ge\max\{1,Y_P\}$ *(Lemma 1.20.14). Here we use the selected flat central band of Lemma 1.6.13, the pulse envelope of Proposition 1.15.27 and the two lower bounds on* q_o *of Lemma 1.15.34. To include* $\eta=0$*, define the coefficient*

$$b_\eta=\begin{cases}0, & |\eta|<\eta_c,\\ ((\frac12-h)|\eta|)^{-1}, & |\eta|\ge\eta_c.\end{cases}$$

On the inner band both $\partial_\eta\log H|_{\hat\xi}$ *and* ν_η *vanish on the intervals in (a).*

(a) From the growth arc to R_o*,* $q\ge q_o$*,* q *is nonincreasing in* z*, and* $|\partial_\eta\log H|_{\hat\xi}\le b_\eta(q+h+\nu)$*. From the growth arc to* $\frac{\hat\xi_p^2}{2}$ *(where* $U\equiv0$*),* $Q\ge q/(1+\gamma)$ *and* $|\nu_\eta|\le b_\eta q/Y_*$*.*

(b) On $z_1\le z\le T+W$*,*

$$|w|\le E_1W_1,$$
$$W_1=(1+\gamma)\left[\frac{2K_\sigma+3.5+8hK_\sigma+8h/e}{q_o}+b_\eta\frac{2K_\sigma+16K_\sigma/e+32/e^2}{Y_*}\right]$$
$$+(1+\gamma)b_\eta(1+(h+\nu)/q_o)(4K_\sigma+6+4/e).$$

Once q_o *has a uniform positive lower bound,* $Y_*\ge1$*,* $b_\eta\le((\frac12-h)\eta_c)^{-1}$ *and* $\nu\le\lambda$ *bound* W_1 *independently of* Y_0 *and the wait length* W*.*

(c) $\nu w^2\le\frac18$ *on* $\{\ell_r<0\}$ *in both regimes of Proposition 1.15.27:*

(i) where $\nu \ge \lambda/2$: there $|\eta| \ge \eta_c$ (since $\nu = \nu_c < \lambda/60$ on the central band) and $q_o \ge q_{\rm hi}$. So $W_1 \le W_{\rm hi} := \sup\{W_1|_{q_o=q_{\rm hi},\,\eta=\eta_c,\,Y_*=1} :\ 0<h\le 10^{-2},\ 0\le\nu\le\lambda_0\}$. This supremum is finite, because W_1 is increasing in h and ν and $(\frac12 - h) \ge 0.49$. So $W_{\rm hi}$ depends only on data fixed before λ, and the condition is $\lambda\,(2^{32}e^T K_{\rm pre}C_{\rm pre})^2 W_{\rm hi}^2 \le \frac18$;

(ii) where $\nu \le \lambda/2$, once Y_0 is large: see the proof.

The constants in (i) are $K_{\rm pre}, C_{\rm pre}, T, K_\sigma$ (prefix and template), $q_{\rm hi} := \frac{29}{240}q_*$ (the floor of Lemma 1.15.34 for $\nu \ge \lambda/2$, where q_* is the chart floor, fixed before λ in Proposition 1.15.27) and η_c. Here η_c is the inner edge of the positive angular band of the flat logit. Lemma 1.15.26 asks only for a flat cutoff on a fixed positive band, and the text selects the cutoff after h (before Y_0). We take the band itself among the angular supports of step 1 of Section 1.5.2, with $\eta_c \ge 2\eta_a$. The band lies in the $G = 0$ region, inside the fixed chart band, and before the fixed-λ buffer (where $\chi = 1$, $\nu = \lambda$ and the G-rise begins). The logit profile and its gain are still selected after h, as in the text. This is a design choice. With it, and with $W_{\rm hi}$ the supremum above, (i) is an upper bound on λ by constants fixed before λ. It is condition (λ2) after (1.6.18). With (d) of Proposition 1.20.44, this lemma replaces hypothesis (e) of that proposition.

Proof. (a) The first two claims are in the proof of Proposition 1.20.44: $c = \log \dot H$ is nonincreasing, and $q \ge q_p \ge q_o$. On the pulse power interval $q = q_o + u(Y - y) \ge q_o$. On the growth arc $Q = (\gamma+\nu+q)/(1+\gamma)$. Afterwards, up to $\frac{\hat\xi_p^2}{2}$ (where $U \equiv 0$ and (1.20.7) reads $D_y Q + (1+\ell_r)Q = q+\nu+\ell_r$), $\phi = Q - q/(1+\gamma)$ satisfies $\phi_z = -(1+\ell_r)\phi + q(1 - \frac{1+\ell_r}{1+\gamma}) + (\nu+\ell_r) - \frac{q_z}{1+\gamma}$. Every term after the first is ≥ 0, because $\ell_r \le \gamma$, $\ell_r \ge -\nu$ and $q_z \le 0$. So $\phi \ge 0$ persists (this is the barrier of the main text, [Section 1.6.3]). On $|\eta| < \eta_c$ the rate is the constant ν_c and R_g, H_a are scalar by (1.6.42). The growth field is $H_a e^{\gamma z}$, and on the finite turn it is $H_a F(z;\nu_c)$. On the subsequent wait and pulse it is $A_c(\frac{\hat\xi^2}{2})^{-\nu_c}$ by Lemma 1.6.13. Thus both angular derivatives in (a) vanish there, including at the axis. On $|\eta| \ge \eta_c$, $(\frac12 - h)\eta\,\partial_\eta \log H|_{\hat\xi} = q - h + \nu$ up to R_o, since the pulse changes only U. Also $q \ge q_p \ge uY \ge uY_*$ up to $\frac{\hat\xi_p^2}{2}$ by (1.14.6), where $u = (\frac12 - h)\eta\nu_\eta \ge 0$. Taking absolute values gives the two bounds in (a).

(b) On the sector $U = \mathfrak M_1 = \mathfrak M_3 = 0$, so $N_s = (4h\eta\mathfrak M_4 - d\mathfrak M_{4\eta})/\frac{\hat\xi^2}{2} + (2+4h)\eta P - dP_\eta$. Also $\sigma_z = -\frac12 - 2\ell_r\sigma$, and $(\partial_\eta\sigma)_z = -2\ell_r\partial_\eta\sigma - 2(\partial_\eta\ell_r)\sigma$ at fixed z (that is, fixed $\hat\xi$), with $|\partial_\eta\ell_r| = |\nu_\eta f_1'| \le \nu'$ and $|\partial_\eta\sigma(z_1)| \le \nu' K_\sigma$. Gronwall with $e^{2\nu(T+W)} \le 2$ gives $|\sigma| \le 2K_\sigma + s$ and $|\partial_\eta\sigma| \le \nu'(2K_\sigma + 8K_\sigma s + 2s^2)$. Put $\kappa = b_\eta(q+h+\nu)$. Since q is nonincreasing, κ bounds $|\partial_\eta \log H|$ at fixed radius on all of $[\frac{\hat\xi^2}{2}, R_o]$. Lemma 1.20.14(b) gives $|P| \le E^2$ and $|P_\eta| \le E^2(\frac12 + 2\kappa)$. Hence

$$|N_s| \le E^2\big[4h(2K_\sigma + s) + 2K_\sigma + 3.5 + \nu'(2K_\sigma + 8K_\sigma s + 2s^2)\big] + E^2\kappa\big[2(2K_\sigma + s) + 6\big].$$

Divide by EQ and use (a) to obtain $1/Q \le (1+\gamma)/q_o$, $\nu'/Q \le (1+\gamma)b_\eta/Y_*$ and $\kappa/Q \le (1+\gamma)b_\eta(1 + (h+\nu)/q_o)$. Then $E \le E_1 e^{-s/2}$, $\sup s e^{-s/2} = 2/e$ and $\sup s^2 e^{-s/2} = 16/e^2$ give (b). The terms of size $\nu_\eta Y_0$ in $(\log H_a)'$ (from $H_a = H_p e^{\nu W}/F_b$, $H_p = H_{\rm out}e^{\nu Y}$, (1.6.23)) are inside κ, and they are absorbed by $Q \gtrsim q \ge uY$. This is the mechanism of $S_{q,w} = q_o + \dot\nu(Y_0 + \tau_f - y) + \dots$ [Section 1.6.3].

(c) $E_1 \le e^T E_b$ and $e_p = E_b \nu^{60(1/2+\nu)}$, with $e_p \le K_{\rm env}C_{\rm pre}\lambda^{30}e^{-(\lambda-\nu)Y_{\rm end}}$ (Proposition 1.15.27). In regime (i) ($\nu \ge \lambda/2$) only points of the chart band occur (Lemma 1.15.34); there $K_{\rm env} = \Gamma_\rho\Gamma_g$ does not depend on h or ν_c, and Γ_ρ may be replaced by $e^{\lambda \sup_{\rm band}|\log\ell|} \le 2^{\lambda_0}$ (Proposition 1.15.32 and the remark after it). This is a constant of type $K_{\rm pre}$, and in regime (i) we absorb it into $K_{\rm pre}$. In regime (i), $\nu^{-30-60\nu} \le 2^{30}\lambda^{-30}e^{60\lambda\log(2/\lambda)}$, so $E_b \le 2^{32}K_{\rm pre}C_{\rm pre}$, and $\nu \le \lambda$. In regime (ii), $q_o \ge \min(ch, q_*/2)$, hence W_1^2 is uniformly bounded once h, λ, ν_c are fixed and $Y_* \ge 1$. Write

$$\Delta_e = T_b(\lambda) - \rho(1) + 60\log(1/\lambda), \qquad Y_{\rm end} = Y_0 - \Delta_e.$$

This is the endpoint length in (1.6.23) and (1.15.32). The offset is fixed before Y_0. Take Y_0 large enough that $Y_{\mathrm{end}} \geq 0$. Since $2(\lambda-\nu) \geq \lambda$, the squared envelope contributes at most $e^{-\lambda Y_{\mathrm{end}}} = e^{\lambda\Delta_e} e^{-\lambda Y_0}$. Using $\nu\lambda^{60} \leq \lambda^{61}$ and $\nu^{-60-120\nu} \leq e^2 \nu_c^{-60}$ gives

$$\nu E_1^2 \leq e^{2T+2} (K_{\mathrm{env}} C_{\mathrm{pre}})^2 \lambda^{61} \nu_c^{-60} e^{\lambda\Delta_e} e^{-\lambda Y_0}.$$

Multiplication by the bound for W_1^2 proves $\nu w^2 \leq 1/8$ for large Y_0. Where $\ell_r < 0$, $-\ell_r w^2 \leq \nu w^2 \leq 1/8$, which is the hypothesis of Proposition 1.20.44(d). Since $\mathfrak{M}_4$ is integrated forward from the template, no tail representation and no $1/\lambda$ factor enter (compare Lemma 1.8.15(b)). □

Remark 1.20.46 (Inlet positivity on the wait). The barrier "$Q \geq cq$" on the wait [Section 1.6.3] requires $Q \geq cq$ at the wait inlet, which is not shown; (1.16.22) gives Q only at $y_p = 0$. Proposition 1.20.44(b) supplies the inlet: $Q(\frac{\hat\xi_b^2}{2}) \geq \frac{3}{8} e^{-(1+\gamma)T}$, a constant fixed with the template, before λ, h, ν_c and the scale.

The $G \neq 0$ sector.

Proposition 1.20.47 (Cover on the $G \neq 0$ sector)**.** *Fix η in the near-endpoint buffer where $G \neq 0$. Assume: (i) Lemma 1.6.14 (growth arc and turnoff are relaxed or strict, $Q \geq q_{\min} > 0$ through the turnoff, and its two large-p_1 tests with margin 1 [(1.6.39)]); (ii) from the end of the turnoff to $\frac{\hat\xi_p^2}{2}$: $U \equiv 0$ and $S_q \geq s_* > 0$, where by Lemma 1.20.7 and (1.6.33) $S_q = \ell_r + h + \log\dot{K} - (\lambda+\ell_r)\dot{s} + \ell_r \mathcal{K}/\frac{\hat\xi^2}{2}$ (chart reserve [(1.6.33)]; on the flat-λ wait $S_q \geq q_* - \lambda|\mathcal{K}|/\frac{\hat\xi^2}{2}$ with $|\mathcal{K}|/\frac{\hat\xi^2}{2} \leq K_{\mathrm{pre}}$ by (1.14.10)); (iii) (1.20.8) on the negative turn and the wait, with n_1 the decaying $\mathfrak{M}_1$-term (1.14.12), and (F*). Then, for $\frac{\hat\xi^2}{2} q_\sharp \geq 4L(1+\lambda)$ with $q_\sharp = \min\{q_{\min}, s_*/(1+\gamma)\}$, every point from the growth arc to $\frac{\hat\xi_p^2}{2}$ is relaxed or strict, and every point with $\ell_r < 0$ is strict. On the turnoff, Lemma 1.20.5 shows that points with $\frac{U_{\hat\xi}}{\hat\xi} \neq 0$ have $\mathfrak{v} = 2 + \mathfrak{b}^2/2 > 2$ and must be (and, by (i) and Lemma 1.20.6, are) strict.*

Proof. Lemma 1.20.9 from the end of the turnoff gives $Q \geq q_\sharp$. Then Proposition 1.20.10 and Lemma 1.20.12; on the turnoff Lemma 1.20.6(a) with $\alpha = \phi = 1$ and $p_1 = \frac{\hat\xi^2}{2} Q/L \geq \frac{\hat\xi^2}{2} q_{\min}/L$. □

Lemma 1.20.48 (Inputs (ii)–(iii) of Proposition 1.20.47)**.** *Work on I_{off}^+ of Definition 1.6.15, where $\eta \geq \eta_a$ (the other end by reflection) with the bridge fields $H = K(\hat\xi_s/\sqrt{2})^{-2\lambda} F_\lambda(z)$, $z = 2\log(\hat\xi/\hat\xi_s(\eta))$, $\frac{\hat\xi_s^2}{2} = \frac{\hat\xi_{s,b}^2}{2} e^{s(\eta)}$, of (1.6.33) and Lemma 1.6.14. Use the data stated there: $(\log f)' = K'/K - \lambda s' \geq c_f > 0$, $|\dot{s}| \leq S_{\mathrm{ph}}$, and, from the end z_e of the turnoff to $\frac{\hat\xi_p^2}{2}$, $U \equiv 0$, $-\lambda \leq \ell_r \leq 0$ with $\ell_r = F_\lambda'/F_\lambda$ a function of z alone, and $|K_M|/\frac{\hat\xi^2}{2} \leq K_M^*$, $K_M = (1-2h)\eta\mathfrak{M}_1 + d\mathfrak{M}_{1\eta}$.*

(a) Exactly, $S_q = h + (\frac{1}{2} - h)\eta(\log f)' + \ell_r(1 - \dot{s} + K_M/\frac{\hat\xi^2}{2})$. Hence $S_q \geq s_* := \frac{1}{2}(\frac{1}{2} - h)\eta_a c_f$ from z_e to $\frac{\hat\xi_p^2}{2}$ whenever $\lambda(1 + S_{\mathrm{ph}} + K_M^*) \leq \frac{1}{2}(\frac{1}{2} - h)\eta_a c_f$. On the flat-$\lambda$ wait this reads $S_q = q - \lambda K_M/\frac{\hat\xi^2}{2}$ with $q = h - \lambda + \log\dot{K}$.

(b) Let (P) $|P| + |P_\eta| \leq K_P E^2$ hold there. From z_e on, $-\lambda \leq \ell_r \leq 0$ (plateau, negative turn, wait) and $|\partial_\eta \log H|_{\hat\xi}| \leq \kappa_1$, with κ_1 defined next. So Lemma 1.20.14, with (κ_0, κ_1) replaced by $(\kappa_1, 0)$, gives (P) with $K_P = \frac{3}{2} + 2\kappa_1$ once Y_0 is large. Let the trace $\sigma = \mathfrak{M}_4/(\frac{\hat\xi^2}{2} E^2)$ at z_e satisfy $|\sigma_e| + |\partial_\eta \sigma_e| \leq K_\sigma$. Put $\kappa_1 = \sup|(\log K)'| + 2\lambda \sup|s'|$ and $s = z - z_e$, and suppose

$e^{2\lambda(z_p-z_e)} \le 2$ *and* $2\lambda(2K_\sigma + z_p - z_e) \le \frac12$. *Then* (1.20.8) *holds on* $[z_e, z_p]$ *with* $k_3 = k_4 = 0$ *and*

$$n_1 = \sup_\eta \frac{(\frac12 - h)(|\mathfrak{M}_{1\infty}| + |\mathfrak{M}_{1\infty}'|)}{\frac{\hat\xi_e^2}{2} E_e}, \qquad k_2 = 4h + 2\kappa_1,$$
$$k_1 = (8h + 4\kappa_1 + 2)K_\sigma + \sup|s'| + (4(\tfrac12 + h) + 1)K_P,$$

where $\mathfrak{M}_{1\infty}(\eta)$ *is the constant value of* $\mathfrak{M}_1$ *after the turnoff.*

(c) With $q_\sharp' := \min\{q_{\min}, s_*/2\}$ *one has* $Q \ge q_\sharp'$ *from* z_e *to* $\frac{\hat\xi_p^2}{2}$, *and* $|w| \le W_\sharp := [n_1 + E_e^*(k_1 + 2k_2/e)]/q_\sharp'$, $E_e^* = \sup E_e$. *Hence* $\lambda w^2 \le \frac18$ *on the negative turn and on the wait if* $\lambda W_\sharp^2 \le \frac18$. *Then every point there with* $\ell_r < 0$ *and* $\frac{\hat\xi^2}{2} Q \ge 4L(1+\lambda)$ *is strict (Proposition 1.20.10(b),(c)).*

All constants are fixed with the bridge template before λ, *so the conditions on* λ *are upper bounds of the type* (1.6.18) *(*$W_\sharp$ *is of size* $P_*(1+T_d)$, *as in its first condition). This replaces the quoted inputs (ii)–(iii) of Proposition 1.20.47 and the negative-turn bound of (R6) on the buffer. The bound (P) is Lemma 1.20.14, applied for* Y_0 *large after* λ. *The constant* K_P *involves only* κ_1, *which is fixed before* λ, *so the order is respected.*

Proof. (a) $\dot s = (\frac12 - h)\eta s'$ and $\dot{\log K} = (\frac12 - h)\eta K'/K = (\frac12 - h)\eta(\log f)' + \lambda\dot s$. Substituting in (1.6.33), $S_q = \ell_r + h + (\frac12 - h)\eta(\log f)' + \lambda\dot s - (\lambda + \ell_r)\dot s + \ell_r K_M/\frac{\hat\xi^2}{2}$, which is the identity. Then $(\frac12 - h)\eta(\log f)' \ge (\frac12 - h)\eta_a c_f$ and $|\ell_r(1 - \dot s + K_M/\frac{\hat\xi^2}{2})| \le \lambda(1 + S_{\rm ph} + K_M^*)$. With $\ell_r = -\lambda$, $q = h - \lambda + (\frac12 - h)\eta(\log f)' + \lambda\dot s$.

(b) Since $U \equiv 0$, $\mathfrak{M}_1 = \mathfrak{M}_{1\infty}(\eta)$ does not depend on $\frac{\hat\xi^2}{2}$, $\mathfrak{M}_{1\eta} = \mathfrak{M}_{1\infty}'$, and $(\frac{\hat\xi^2}{2} + \mathcal{K})U = 0$ in (1.20.5). As $E = H/\hat\xi$, $\partial_z \log E = \ell_r - \frac12 \in [-\frac12 - \lambda, -\frac12]$, so $E_e e^{-(1/2+\lambda)s} \le E \le E_e e^{-s/2}$ and $(\frac{\hat\xi^2}{2})^{-1} = e^{-s}/\frac{\hat\xi_e^2}{2} \le E e^{-\beta s}/(\frac{\hat\xi_e^2}{2} E_e)$ with $\beta = \frac12 - \lambda$. This bounds the $\mathfrak{M}_1$-term by $E n_1 e^{-\beta s}$. From $\frac{\mathfrak{M}_{4\hat\xi}}{\hat\xi} = -E^2/2$ and $\mathfrak{M}_4 = \frac{\hat\xi^2}{2}E^2\sigma$ one gets $\sigma_z = -\frac12 - 2\ell_r\sigma$, and, since ℓ_r depends on z only, $(\partial_\eta|_z\sigma)_z = -2\ell_r\,\partial_\eta|_z\sigma$. Gronwall gives $|\sigma| \le e^{2\lambda s}(|\sigma_e| + s/2) \le 2K_\sigma + s$, $|\partial_\eta|_z\sigma| \le 2K_\sigma$ and $|\sigma_z| \le \frac12 + 2\lambda|\sigma| \le 1$. At fixed $\hat\xi$, $\partial_\eta|_{\hat\xi}\sigma = \partial_\eta|_z\sigma - s'\sigma_z$ and $\partial_\eta|_{\hat\xi}\log E = \partial_\eta|_{\hat\xi}\log H = (\log K)' - (\lambda + \ell_r)s'$, so $|\partial_\eta|_{\hat\xi}\log E| \le \kappa_1$. Hence, with $\mathfrak{M}_4/\frac{\hat\xi^2}{2} = E^2\sigma$ and $\mathfrak{M}_{4\eta}/\frac{\hat\xi^2}{2} = 2E^2\sigma\,\partial_\eta|_{\hat\xi}\log E + E^2\partial_\eta|_{\hat\xi}\sigma$,

$$|4h\eta\mathfrak{M}_4/\tfrac{\hat\xi^2}{2}| + |d\mathfrak{M}_{4\eta}/\tfrac{\hat\xi^2}{2}| \le E^2[(4h + 2\kappa_1)(2K_\sigma + s) + 2K_\sigma + \sup|s'|].$$

The pressure part is $\le (4(\frac12 + h) + 1)K_P E^2$ by (P). Adding the three parts gives (1.20.8) with the stated constants.

(c) At z_e, $Q \ge q_{\min}$ (Lemma 1.6.14); from z_e on, $1+\ell_r \in [1-\lambda, 1+\lambda]$ and $S_q \ge s_*$, so $S_q/(1+\ell_r) \ge s_*/2$ and Lemma 1.20.9 gives $Q \ge q_\sharp'$. Then $|w| = |N_s|/(EQ) \le [n_1 e^{-\beta s} + E(k_1 + k_2 s)]/q_\sharp' \le W_\sharp$, using $E(k_1 + k_2 s) \le E_e(k_1 + 2k_2/e)$ (Remark 1.20.13). Where $\ell_r < 0$, $-\ell_r w^2 \le \lambda w^2 \le \frac18 < \theta^2$ for $\theta \ge \frac12$. □

Layout and the reduction.

Lemma 1.20.49 (Radial layout)**.** *On every fiber the power template underlying the comparison has wait* $\{-W \le y_p \le 0\}$ *with* $W = 60\log(1/\nu) \ge 60\log 20 > 179$. *Every relaxed point of the comparison in* $\mathscr{P}$ *has* $y_p < -W$. *Hence* $Y_{\rm sh}$ *can be chosen in* $\{y_p < -W + 1\} \subset \{y_p < -178\}$ *with its outer strict collar in* $\{-W + \frac12 \le y_p \le -W + 1\}$, *where* $\ell_r \equiv -\nu$; *the transit, the restoration reserve* $(-25, -20)$ *and the support assigned to the physical heat compensation (ending before* -15*) all lie in this wait.*

Proof. $\nu \le \lambda \le \lambda_0 < \frac{1}{20}$ [Section 1.14]. On the comparison prefix $-W \le y_p \le -14.5$ we have $\ell_r = -\nu < 0$, $U = 0$; by Propositions 1.20.44, 1.20.47 they are strict. □

The inputs (R1), (R2), (R4).

Lemma 1.20.50 ((R1): positivity of H° on $\mathscr{P}$)**.** *On each fiber, every piece of (H°, U°) that meets $\mathscr{P}$ has one of the following five forms.*

(i) On the activation zone and the output slab (Definition 1.20.22; $\lambda \equiv 1$ on the slab), and in the backward chart on the endpoint collars (Proposition 1.20.43), the exponential form $H = \hat\xi^2 F_r(\frac{\hat\xi_a^2}{2}, \eta)\exp(-\frac{1}{2}\int_0^y[(1-\lambda)\kappa p_1^\flat + 0.8\lambda])$. Here $F_r(\frac{\hat\xi_a^2}{2}, \eta) = C^{-1}e^{\Lambda\psi+a}\Phi(4,\eta)$ and $\Phi \ge c_\Phi > 0$.

(ii) On the amplitude matching, $H = H_{\mathrm{tgt}}\exp((1-\sigma(y/T_s))\delta_l)$.

(iii) Power or exponential-template forms with positive amplitude, on the following pieces:

- *the matched growing profile, $c_{\mathrm{ref}}(\eta)(\frac{\hat\xi^2}{2})^\gamma$;*
- *the growth arc, turnoff, negative turn and wait of the $G = 0$ sector, $H_a\mathsf{F}(z;\nu)$ with $\mathsf{F} = e^{\gamma z}, e^{f_0-\nu f_1}, \mathsf{F}_T e^{-\nu(z-T)}$;*
- *the buffer, $K(\hat\xi_s/\sqrt{2})^{-2\lambda}F_\lambda$ with $K > 0$ and $F_\lambda = \exp\int \ell_r$;*
- *the restoration reserve, $c_p\varphi(\hat\xi/\sqrt{2})^{-2\mu}$.*

Where the scalar insertion of Proposition 1.12.3 is used, its form is the convex combination $a_{\mathrm{p}}(\frac{\hat\xi^2}{2})^\gamma[(1-\chi_0)g + \chi_0\varphi]$ with $g, \varphi > 0$.

(iv) The $G_i \to G$ annulus and the U bumps, which do not change H.

(v) The additive compact E bumps $E = e_*(x^{1/10} + v(x))$, $\frac{\hat\xi^2}{2} = \frac{\hat\xi_*^2}{2}x$: three in the core five-moment correction and three in the pressure bank (Lemma 1.6.37).

No other piece of H° meets $\mathscr{P}$. The loop modulation, the restoration bumps and the heat-compensation bumps are (i)–(iii) of (Cov2), and they are not part of H°. The two-row taper lies in $y_p \in (-2.15, -0.85)$ and the pulse in $y_p \ge 0$. On (i)–(iv), $H^\circ > 0$ is immediate. On (v), $H^\circ > 0$ holds if and only if $v > -x^{1/10}$. This is not *implied by the form of the piece. It holds under the tolerance $|v| \le \frac{1}{2}x^{1/10}$ of Lemma 1.6.36, and then $H^\circ \ge \frac{1}{2}H_{\mathrm{ref}}$. τ_b forces $\mathfrak{a} \in [0.7, 0.9]$ on the support, and $H = H_{\mathrm{ref}} > 0$ at the support edge. So $\log H$ has a bounded $\log\frac{\hat\xi^2}{2}$-derivative there, and by continuity H cannot reach 0.*

Proof. In (i)–(iii) every factor is positive. These factors are $\hat\xi > 0$, exponentials, $\Phi(4,\eta) \ge c_\Phi$, and the amplitudes H_{tgt}, c_{ref}, H_a, K, $c_p\varphi$ and a_{p}. In (v), $H = \sqrt{\hat\xi_*^2 x}\, e_*(x^{1/10} + v) \ge \frac{1}{2}\hat\xi e_* x^{1/10} = \frac{1}{2}H_{\mathrm{ref}}$. The coefficients of these bumps solve a small-vector IFT whose target is $\le \tau_b/10$ in normalized norm. So the tolerance $|v| \le \frac{1}{2}\min_{\mathrm{supp}} x^{1/10}$ is an upper bound on τ_b in terms of the fixed templates. It is fixed before ε_u, as τ_b is. □

Corollary 1.20.51 (Strict entry collar)**.** *Assume the hypotheses of Theorem 1.20.28(a), with V and $\delta_0 = \min(c_r, 1)$ as there, and put*

$$y_s := t_{\mathrm{act}}\,\sigma^{-1}\Big(\frac{\delta_0}{3V(1-\kappa_{\mathrm{act}})}\Big) \in (0, t_{\mathrm{act}}).$$

Then every point of $\{0 < y_a \le y_s\}$*, on all angles, is strict, with* $\mathfrak{v} - 2 \ge \delta_0/2$*,* $\mathcal{P} - \mathfrak{v} \ge \frac{1}{2}ev_r$ *and fourth gap* $\ge \frac{1}{4}e^2v_r^2$*.*

Proof. Since $V \ge 2 + \delta_0$ and $\kappa_{\mathrm{act}} \le \frac{1}{8}$, the argument of σ^{-1} lies in $(0,1)$, so y_s is defined and $y_s < t_{\mathrm{act}}$. On $0 < y \le y_s$ we have $e = (1-\kappa_{\mathrm{act}})\sigma(y/t_{\mathrm{act}}) \le \delta_0/(3V)$. In Lemma 1.20.20, $\mathfrak{v} = \kappa(v_r - (1-\rho^2)p_{2,r}^2/p_{1,r})$, $1-\rho^2 \le 2\varrho e \le \frac{e}{2}$ and $p_{2,r}^2/p_{1,r} \le V$. Hence $\mathfrak{v} \ge (1-e)(v_r - \frac{1}{2}eV) \ge v_r - \frac{3}{2}eV \ge 2 + \frac{\delta_0}{2}$. So the strict branch of Lemma 1.20.20 applies. □

Lemma 1.20.52 (Source floor on the output slab)**.** *Assume the hypotheses of Lemma 1.20.24, with* (H_u) *and its constant* c_1*, and Definition 1.20.22. Fix a fiber and put* $c_s := \frac{3}{5}c_1$*. Consider the field after the interpolation window, continued with* $\lambda \equiv 1$ *and* $\beta \equiv 0$ *to all* $\frac{\hat\xi^2}{2} \ge \frac{\hat\xi_a^2}{2}e^{y_l+\omega_0+\omega_2}$*. On this range* $\ell_r \equiv \frac{3}{5}$*,* $U \equiv G_i(\eta)$*, and the histories are integrated from the axis. Put* $\delta_U := K_c/\Lambda + B_{\mathrm{act}}$*, with* B_{act} *from Remark 1.20.30(2). For the output* G_i *this bounds* $\|G_i - u\|_{C^1_\eta}$ *by (I3). Let* $K_a = \sup|a'| + \sup|\partial_\eta|_Y \log\Phi(4,\cdot)| + \frac{2}{5}\sup|b'/b|$*,* $K_p = \frac{1}{2}\sup_{4\le Y\le Y_{\mathrm{buf}}}|\partial_\eta|_Y p_{1,r}|$ *and* $|v| \le K_v\sqrt{\chi}$*, and put*

$$\varepsilon_s := B_{\mathrm{act}}(3 + 3K_a + \Lambda K_\psi) + K_p(2t_{\mathrm{act}} + \kappa_{\mathrm{act}}y_T)(1+K_v).$$

Then, with $k_0 = 2(\frac{1}{2} - h)\eta u + du'$*,* $K_{s1} = K_aK_v + K_c\sup Lb/s_{\min}$ *and* $K_{s2} = 3K_c(1+K_a)$*,*

$$S_q \ge \Lambda Lb\chi + \Big[\tfrac{3}{5}(1+k_0) + h + 2h\eta u\Big] - K_{s1}\sqrt{\chi} - \frac{K_{s2}}{\Lambda} - \varepsilon_s.$$

The bracket equals $\frac{3}{5}[1 + h + \eta u + du'] + \frac{2}{5}h(1+2\eta u)$*, so it is* $\ge \frac{6}{5}c_1 = 2c_s$ *on* N_0*. There is* Λ_s*, depending only on the constants of Lemma 1.20.24, on* c_1 *and on* χ_N*, such that, if* $\Lambda \ge \Lambda_s$ *and* $\varepsilon_s \le c_s/4$*, then*

$$S_q \ge c_s + .9\Lambda Lb\chi \qquad \text{for all } \tfrac{\hat\xi^2}{2} \ge \tfrac{\hat\xi_a^2}{2}e^{y_l+\omega_0+\omega_2}.$$

Proof. (1) *The angular log-derivative.* On this range $\log F = \log F_r(\frac{\hat\xi_a^2}{2},\eta) - \frac{1}{2}\int_0^y[(1-\lambda)\kappa p_1^\flat + 0.8\lambda]\,dy'$ with $y = 2\log(\hat\xi/\hat\xi_a)$, and $\partial_y \log F = -\frac{2}{5}$. We use $\partial_\eta|_{\hat\xi} = \partial_\eta|_y - (\log\frac{\hat\xi_a^2}{2})'\partial_y$, $(\log\frac{\hat\xi_a^2}{2})' = -b'/b$, and the fact that $Y = \Lambda b\frac{\hat\xi_a^2}{2} = 4$ is fixed. They give $\partial_\eta \log H|_{\hat\xi} = \Lambda\psi' + r_1$ with $r_1 = a' + \partial_\eta|_Y\log\Phi(4,\eta) - \frac{2}{5}b'/b - \frac{1}{2}\int_0^y(1-\lambda)\kappa\,\partial_\eta|_Y p_{1,r}(4e^\vartheta,\eta)\,dy'$. Here λ,κ,ϑ do not depend on the angle, $\kappa \le 1$ on $[0,2t_{\mathrm{act}}]$, $\kappa = \kappa_{\mathrm{act}}$ afterwards, and $1-\lambda = 0$ after the window. Hence $|r_1| \le K_a + K_p(2t_{\mathrm{act}} + \kappa_{\mathrm{act}}y_T)$. (2) *The history term.* After the end $\frac{(\hat\xi_1(\eta))^2}{2}$ of the termination $U \equiv G_i$. At fixed $\hat\xi$ this gives $\mathcal{K}(\frac{\hat\xi^2}{2}) = \mathcal{K}(\frac{\hat\xi_1^2}{2}) + k_{G_i}(\frac{\hat\xi^2}{2} - \frac{\hat\xi_1^2}{2})$, where $k_{G_i} = (1-2h)\eta G_i + dG_i'$; the terms $\pm G_i(\frac{\hat\xi_1^2}{2})'$ cancel. So $\mathcal{K}/\frac{\hat\xi^2}{2}$ is a convex combination of two quantities. The first is $\mathcal{K}(\frac{\hat\xi_1^2}{2})/\frac{\hat\xi_1^2}{2}$, the mean of $(1-2h)\eta U + d\partial_\eta|_{\hat\xi}U$ over $[0,\frac{\hat\xi_1^2}{2}]$. The second is k_{G_i}. For the first mean, Remark 1.20.30(2) also bounds partial upper limits at fixed y. At fixed X, $\partial_\eta U = \partial_\eta|_y U - (\log X_a)'U_y$. On $0 \le y \le 2t_{\mathrm{act}}$ the extra term is $O(\Lambda^{-1})$ because $X = O(\Lambda^{-1})$ there, and afterwards it is $O(\kappa_{\mathrm{act}})$ by (M0) until it vanishes at termination. On the core, $U - u = \Lambda^{-1}w_C(\Lambda bX,\eta)$ and its first fixed-X angular derivative are $O(\Lambda^{-1})$. Use the uniform core constants in K_c before choosing Λ, and include the post-collar constant in K_β before choosing κ_{act}. Both entries in the convex combination then differ from k_0 by at most $2\delta_U$. (3) *Assembly.* By (1.20.7), $S_q = \frac{3}{5}(1 + \mathcal{K}/\frac{\hat\xi^2}{2}) + h + (v - d(G_i - u))(\Lambda\psi' + r_1) + 2h\eta G_i$, where $v = (\frac{1}{2} - h)\eta - du$ and $v\Lambda\psi' = \Lambda Lb\chi$. Write $G_i - u = \Lambda^{-1}w_f + \Delta U$, where $w_f = w_C(4e^{\vartheta_\infty},\eta)$ and $\Delta U = G_i - U_r(X_f)$. Then $|dw_f\psi'| \le K_cLb\sqrt{\chi}/s_{\min}$, $|d\Delta U\Lambda\psi'| \le B_{\mathrm{act}}\Lambda K_\psi$ and $|vr_1| \le K_vK_a\sqrt{\chi} + K_vK_p(2t_{\mathrm{act}} + \kappa_{\mathrm{act}}y_T)$. For the remaining error terms, $|d(G_i-u)r_1| + \frac{3}{5}|\mathcal{K}/\frac{\hat\xi^2}{2} - k_0| + 2h|G_i - u| \le \delta_U(\frac{3}{2} + K_a) + K_p(2t_{\mathrm{act}} + \kappa_{\mathrm{act}}y_T)$. This gives the displayed bound. The bracket

identity uses $2((\frac{1}{2}-h)+h)=1$, so that $1+k_0+h+2h\eta u = 1+h+\eta u+du'$. On N_0, (H_u) and $|\eta u|\le \frac{1}{64}$ give the bracket $\ge \frac{6}{5}c_1$. (4) *The two cases* are those of Lemma 1.20.24(a). On N_0, $K_{s1}\sqrt{\chi}\le \frac{c_s}{2}+K_{s1}^2\chi/(2c_s)$, so $S_q\ge \frac{3}{2}c_s - K_{s2}/\Lambda - \varepsilon_s + (\Lambda L b - K_{s1}^2/(2c_s))\chi \ge c_s + .9\Lambda L b\chi$ once $K_{s2}/\Lambda \le c_s/4$ and $.1\Lambda L_{\min}b_{\min}\ge K_{s1}^2/(2c_s)$. Off N_0, $\chi\ge\chi_N$ and the bracket is $\ge -K_{s3}$, with K_{s3} the supremum of its modulus. There $.1\Lambda L_{\min}b_{\min}\chi_N \ge 2c_s + K_{s3}+K_{s1}+K_{s2}$ suffices. □

Proposition 1.20.53 ((R4): the zones with $\mathfrak{b}=0$ before the growth arc)**.** *Take the forward member and a fixed η. Let $S^{\mathrm{ref}}_{q,\gamma}=\gamma(1+k_G)+h+v(G)\partial_\eta \log H_{\mathrm{ref}}|_{\hat\xi}+2h\eta G$, with $k_G=(1-2h)\eta G+dG'$, be the growth source of the reference future* [Section 1.6.3, proof of Lemma 1.6.14]. *Put $s_\gamma:=\inf S^{\mathrm{ref}}_{q,\gamma}$ over its growth arc. Then $s_\gamma\ge\gamma$ on the $G=0$ sector (proof of Proposition 1.20.44(a)), and $s_\gamma\ge(1+\gamma)q_{\min}$ on the buffer ((G1-i)); see step (0) of the proof for why these floors apply to k_G. Let $K_H=\sup|\partial_\eta\log H_{\mathrm{ref}}|_{\hat\xi}|$ on the growth arc. This is independent of $\frac{\hat\xi^2}{2}$ there, and it may contain $\nu_\eta Y_0$. Both s_γ and K_H are fixed in steps 1–3. Let $K_m=\sup(1+|\mathcal{K}/\frac{\hat\xi^2}{2}|+|v(G_i)||b'/b|)$, let $|\delta_l|\le K_\delta(\Lambda)$ with K_δ as in step (0) of the proof (independent of C and of the late widths), and put $m_4:=\min\{c_s,s_\gamma/2\}$. Assume Lemma 1.20.52, Theorem 1.20.28(d), Lemma 1.6.36, B_{r0} as in Definition 1.20.22, and*

(a) $\varepsilon_u(K_H+\frac{1}{2})\le s_\gamma/4$ and $\frac{6}{5}\delta_U\le s_\gamma/4$;

(b) $T_s\ge 20\sup|\sigma'|\,K_\delta(\Lambda)\max\{1,K_m/m_4\}$.

Then the following hold.

(i) Output slab $y_a\in[y_l+\omega_0+\omega_2,y_T]$. *Here $\mathfrak{b}=0$, $\mathfrak{a}=\frac{4}{5}$, $\frac{\hat\xi^2}{2}S_q/L\ge\frac{36}{5}>2\ell_r$ and $p_1\ge\frac{9}{4}$. Every point is relaxed with $\mathcal{P}-2\ge\frac{1}{4}$.*

(ii) Amplitude matching and the matched profile, *from $\frac{\hat\xi_i^2}{2}/b$ to the $G_i\to G$ annulus. Here $\mathfrak{b}=0$, $\mathfrak{a}\in[0.7,0.9]$, $S_q\ge\frac{3}{4}m_4$, $\frac{\hat\xi^2}{2}S_q/L>12>2\ell_r$ and $p_1\ge\frac{9}{4}$. Every point is relaxed with $\mathcal{P}-2\ge\frac{1}{4}$.*

(iii) From the annulus to $\frac{\hat\xi_g^2}{2}$, off the supports of (R3). *This includes the E bumps of the five-moment correction and the pressure bank. Here $\mathfrak{b}=0$, $\mathfrak{a}\in[0.7,0.9]$, $Q\ge q_0/2$ and $p_1\ge 3$ (Lemma 1.6.36, with C above its threshold). Every point is relaxed with $\mathcal{P}-2\ge 1$, provided $H>0$ on the E supports (Lemma 1.20.50). No barrier is needed here.*

So (R4) holds in the following corrected form. The inlet condition is $p_1\ge\frac{9}{4}$ at the slab inlet; $Q>0$ there would not suffice for the barrier. The barrier condition $\frac{\hat\xi^2}{2}S_q>2L\ell_r$ holds on (i) and (ii).

Proof. With $\mathfrak{b}=0$, Lemma 1.20.5 gives $\Lambda_1=1$ and $\mathfrak{v}=\mathfrak{a}=2(1-\ell_r)$. So for $0\le\ell_r<1$ a point is relaxed iff $p_1>2$, and then $\mathcal{P}-2=p_1-2$. By Lemma 1.20.7, $D_yp_1=\frac{\hat\xi^2}{2}S_q/L-\ell_rp_1$. Where $\ell_r>0$, variation of constants (as in Lemma 1.20.9) gives

$$p_1(y)\ge\min\Big\{p_1(y_0),\ \inf_{[y_0,y]}\frac{\frac{\hat\xi^2}{2}S_q}{L\ell_r}\Big\}.$$

(0) *Three facts about the reference.* (a) The histories in $S^{\mathrm{ref}}_{q,\gamma}$. On the reference growth arc the actual histories are $\mathfrak{M}_1=G\frac{\hat\xi^2}{2}$, $\mathfrak{M}_2=\frac{\hat\xi^2}{2}H/(1+\gamma)$ and $\mathfrak{M}_3=G\mathfrak{M}_2$ [proof of Lemma 1.6.14]. So $\partial_\eta|_{\hat\xi}\mathfrak{M}_1=G'\frac{\hat\xi^2}{2}$ and $\mathcal{K}/\frac{\hat\xi^2}{2}=k_G$ *exactly*; the idealized k_G is the actual history term. Moreover

$\partial_\eta \log H_{\mathrm{ref}}|_{\hat\xi}$ does not depend on $\frac{\hat\xi^2}{2}$ on the arc. On the $G=0$ sector it equals $(\log H_a)'$, because R_g does not depend on η ((G0-i)). On the buffer it equals $(\log K)' - (\lambda+\gamma)s'$ (the γ-power part of F_λ). Hence $S^{\mathrm{ref}}_{q,\gamma}$ is constant in $\frac{\hat\xi^2}{2}$ along the arc. The floors of Proposition 1.20.44(a) and of (G1-i) are proved for $\hat\xi \ge \hat\xi_g$. There the five-moment correction and the bank have restored the reference histories ((G0-ii); Lemma 1.6.37), so they bound this same constant. Hence they hold on the whole arc, down to $\frac{\hat\xi_i^2}{2}/b$. (b) $c_{\mathrm{ref}} = H_a R_g^{-\gamma}$ (on the buffer, $c_{\mathrm{ref}} = K(\frac{\hat\xi_s^2}{2})^{-\lambda-\gamma}$). From the end of the matching to $\frac{\hat\xi_g^2}{2}$ the field has $\ell_r = \gamma$, except on the compact E supports. The $G_i \to G$ annulus and the U bumps do not change H. After the annulus the fields coincide with the ideal fields (Section 1.6.4, paragraph "Matching the growing profile and axial velocity"), and after the last E support $H = H_a(\frac{\hat\xi^2}{2}/R_g)^\gamma$ by (G0-i). The E bumps are compact, and outside their supports the field is the γ-power continuation of the target. Comparing the two γ-powers outside the supports gives $c_{\mathrm{ref}}(\frac{\hat\xi^2}{2})^\gamma = H_a(\frac{\hat\xi^2}{2}/R_g)^\gamma$. So $\partial_\eta \log H_{\mathrm{tgt}}|_{\hat\xi} = \partial_\eta \log H_{\mathrm{ref}}|_{\hat\xi}$. (c) K_δ. We have $\delta_l = \log(CE_i) - \log(CE_{\mathrm{ref}}(\frac{\hat\xi_i^2}{2}/b))$. On the reference CH_{ref} is the frozen normalized future geometry, independent of C (Lemma 1.6.36: $H \asymp C^{-1}(\hat\xi/\sqrt{2})^{6/5}$). Also $\log(CF_i) = \Lambda\psi + a + \log\Phi(4,\eta) - \frac12\int_0^{y_T}[(1-\lambda)\kappa p_1^\flat + 0.8\lambda]$, with $0 \le p_1^\flat \le P_{\mathrm{ref}}$ from the core coefficient ball. That ball is uniform over the $p_0(R)$ family (paragraph 1.6.4.3: "the same Gevrey majorant and compact central pressure interval give uniform bounds for this $p_0(R)$ family"). Hence $K_\delta(\Lambda) \le \Lambda \sup|\psi| + \sup|a| + \sup|\log\Phi(4,\cdot)| + \frac12 y_T(P_{\mathrm{ref}}+1) + \sup|\log(CH_{\mathrm{ref}}(\frac{\hat\xi_i^2}{2}/b))| + \log(\hat\xi_i^2/b_{\min})$. This depends on Λ, B_{r0} and the core and reference constants, and not on C or the late widths. This is the uniform bound "for G_i and $\log(CE_i)$" of paragraph 1.6.4.3, which the text uses to select T_s.

(i) After the window $\lambda \equiv 1$ and $\beta \equiv 0$, so $(\log F)_y = -\frac25$, $\ell_r = \frac35$ and $\frac{U_{\hat\xi}}{\hat\xi} = 0$. By Lemma 1.20.52, $S_q \ge c_s$. Also $\frac{\hat\xi^2}{2} \ge \frac{\hat\xi_a^2}{2}e^{y_l} = B_{\mathrm{r0}}/b$, $L \le 1$ and $c_s \ge \frac35 \min c_0$, so $\frac{\hat\xi^2}{2}S_q/L \ge 12\cdot\frac35 = \frac{36}{5}$. The inlet value is $p_1 \ge \frac94$ (Theorem 1.20.28(d)). So $p_1 \ge \min\{\frac94, 12\}$.

(ii) With $y = \log(b(\hat\xi/\hat\xi_i)^2)$ and $\log H = \log H_{\mathrm{tgt}} + (1-\sigma(y/T_s))\delta_l$, one has $\ell_r = \frac35 - \sigma'(y/T_s)\delta_l/T_s \in [0.55, 0.65]$ by (b). The incoming slab and the target both have $\ell_r = \frac35$, so $\log H_{\mathrm{in}} - \log H_{\mathrm{tgt}} = \delta_l(\eta)$. Hence, exactly,

$$S_q = \sigma S_{\mathrm{tgt}} + (1-\sigma)S_{\mathrm{in}} + \frac{\sigma'(y/T_s)\delta_l}{T_s}\big[-(1+\mathcal{K}/\tfrac{\hat\xi^2}{2}) + v(G_i)(\log(\tfrac{\hat\xi_i^2}{2}/b))'\big]$$

. Here S_{in} is the continued slab source, with $S_{\mathrm{in}} \ge c_s$ by Lemma 1.20.52. S_{tgt} is the source of H_{tgt} with $U = G_i$ and the actual histories. Step (2) of that lemma gives $|\mathcal{K}/\frac{\hat\xi^2}{2} - k_G| \le 2\delta_U + \varepsilon_u/2$. The axial mismatch gives $\|G_i - G\|_{C^1} \le \varepsilon_u$, and $\partial_\eta \log H_{\mathrm{tgt}}|_{\hat\xi} = \partial_\eta \log H_{\mathrm{ref}}|_{\hat\xi}$. So $|S_{\mathrm{tgt}} - S^{\mathrm{ref}}_{q,\gamma}| \le \frac65\delta_U + \varepsilon_u(K_H + \frac25) \le \frac{s_\gamma}{2}$ by (a). The last term is $\le m_4/4$ by (b), so $S_q \ge \frac34 m_4$. Beyond the matching, $S_q = S_{\mathrm{tgt}} \ge s_\gamma/2$. Since $\frac{\hat\xi^2}{2} \ge \frac{\hat\xi_i^2}{2}/b = eB_{\mathrm{r0}}/b$ and $m_4 \ge \frac12\min\{\min c_0, s_\gamma\}$, we get $\frac{\hat\xi^2}{2}S_q/L \ge e\cdot 12\cdot\frac34\cdot\frac12 > 12$. So $p_1 \ge \min\{\frac94, 12/0.65\} = \frac94$.

(iii) These are the normalized estimates of Lemma 1.6.36 on the fixed compact x-range of the R-scale corrections: $|\delta Q_s| \le q_0/2$, $\mathfrak{a} \in [0.7, 0.9]$, and $p_1 = \frac{\hat\xi^2}{2}Q/L \ge c_g C^{10} q_0/2 \ge 3$.

Order. s_γ and K_H are fixed in steps 1–3. B_{r0} and the upper bound (a) on ε_u come in step 4, before Λ; ε_u has only upper bounds. $\Lambda \ge \Lambda_s$ and $K_c/\Lambda \le s_\gamma/10$ come with the other Λ-thresholds. T_s in (b) comes after Λ and before C (step 4), as the text requires. In ε_s the first collar contributes at most $K_{\mathrm{col}}t_{\mathrm{act}}(3+3K_a+\Lambda K_\psi)/\Lambda$. At fixed Λ, C, choose κ_{act} so that $\varepsilon_s < c_s/4$ and $B_{\mathrm{act}} < \min(s_\gamma/10, \varepsilon_u/2)$ at $t_{\mathrm{act}} = 0$, using only the displayed upper bounds at zero. Then take $0 < t_{\mathrm{act}} \le \min\{y_*/8, \kappa_{\mathrm{act}}^2\}$ so that both strict inequalities persist. This is the order of step 5. □

Theorem 1.20.54 (Reduction of (Cov1))**.** *For the forward selected member, (Cov1) holds provided the following hold for the comparison $(H^\circ, U^\circ, P^\circ)$ with the prescribed pressure of (1.19.1):*

(R1) $H^\circ > 0$ *on* $\mathscr{P}$*. This is direct from the exponential and power forms of the pieces, except on the additive E bumps of the five-moment correction and of the pressure bank, where it needs the tolerance $|\delta E| \le \frac{1}{2}E_{\mathrm{ref}}$ (Lemma 1.20.50).*

(R2) The hypotheses of Lemma 1.20.20 on $0 < y_a \le t_{\mathrm{act}}$. They replace the entry hypotheses of Lemma 1.20.15, which fail for the selected member (Remark 1.20.16). They hold by Theorem 1.20.28(a), under (I1), (I2) and $t_{\mathrm{act}} \le y_*(C)/8$. The strict collar $\{0 < y_a \le y_s\}$ is Corollary 1.20.51.

(R3) On the zones with $\mathfrak{b} \neq 0$: Proposition 1.20.17 covers the $G_i \to G$ annulus and the U bumps. Theorem 1.20.28 covers the activation, the plateau, the axial termination and the interpolation, under the quoted inputs (I1)–(I6) and with the design of Definition 1.20.22. The obstruction for a single late termination in Proposition 1.20.29 assumes a transverse zero off the drift root.

(R4) The zones with $\mathfrak{b} = 0$ before the growth arc: the output slab ($\ell_r = 0.6$), the amplitude matching and matched profile, and the $\mathfrak{b} = 0$ part of the R-scale corrections, including the pressure bank [Section 1.6.4, proof of Lemma 1.6.37]*. On the first two the input is $p_1 \ge \frac{9}{4}$ at the slab inlet together with $\frac{\hat{\xi}^2}{2}S_q > 2L\ell_r$; $Q > 0$ at the inlet would not suffice. On the third it is $p_1 \ge 3$ directly. Proposition 1.20.53 proves these under its conditions (a), (b), Lemma 1.20.52 and $B_{\mathrm{r0}} \ge 12 \sup b/s_\gamma$.*

(R5) (G0-i)–(G0-iii) of Proposition 1.20.44 and (i)–(iii) of Proposition 1.20.47 on the power extension of the comparison wait. Their conclusions are restricted to $\mathscr{P}$.

(R6) On the same extension use (1.20.8) and (F) on each sector and the fourth-gap bound $\nu \sup(|N_s|/(EQ))^2 \le \frac{1}{8}$ on the finite negative turn.*

(R7) Scale: $\frac{\hat{\xi}^2}{2}q_\flat \ge 4L(1+\lambda)$ and $\frac{\hat{\xi}^2}{2}q_\sharp \ge 4L(1+\lambda)$ on $\mathscr{P} \cap \{y_a \ge y_{\mathrm{col}}\}$ beyond the growth-arc entry; $\frac{\hat{\xi}^2}{2}Q > 2L$ on (R4).

Under (R1)–(R7) every point of $\mathscr{P}_{\mathrm{c}}$ is strict or relaxed, every relaxed point lies in the interior of a loop domain $Y_{\mathrm{sh}} \subset \{y_p < -25\}$ whose two radial collars are strict, and every point of $\mathscr{P}_{\mathrm{c}} \cap \{y_p \ge -W\}$ is strict with the quantitative margins of Proposition 1.20.10(c).

Proof. (R1) is Lemma 1.20.50. The entry collar is Theorem 1.20.28(a) with Corollary 1.20.51; this is (R2). The rest follows from (R3), Proposition 1.20.53 (this is (R4), with Lemma 1.20.5 and the p_1-barrier of Lemma 1.20.7), Propositions 1.20.44 and 1.20.47, and Lemma 1.20.49. □

Remark 1.20.55 (Input (R7) is a choice of C). The margins $q_\flat$ (Proposition 1.20.44, through q_o: Proposition 1.15.27) and $q_\sharp$ (Proposition 1.20.47, through $q_{\min}$ and s_* of Lemma 1.20.48) are fixed in steps 1–3 of Section 1.5.2, before C (step 4). On every fiber the growth arc follows the core five-moment correction and the pressure bank [Section 1.6.4], whose supports are $\frac{\hat{\xi}^2}{2} = Rr_*(\eta)x$ with x in a fixed compact subset of $(0,\infty)$, r_* bounded below, and $R \asymp C^{10}$ (proof of Lemma 1.6.36). So $\frac{\hat{\xi}^2}{2} \ge c_g C^{10}$ on $\mathscr{P}$ beyond the growth-arc entry, with $c_g > 0$ from the frozen normalized geometry. Since $L \le 1$ and $\lambda < \frac{1}{20}$, the first two conditions of (R7) hold once $C^{10} \ge 4.2/(c_g \min\{q_\flat, q_\sharp\})$. This is a threshold of the same kind as the finite-p threshold for C in the proof of the central pulse

estimate. The third condition, $\frac{\hat{\xi}^2}{2}Q > 2L$ on the (R4) zones, is $p_1 > 2$. It is not a scale condition: it is the barrier of (R4) ($p_1 > 2$ is invariant where $\frac{\hat{\xi}^2}{2}S_q > 2L\ell_r$) with the inlet value $p_1 \geq \frac{9}{4}$ of Theorem 1.20.28(d).

(Cov2) and the parameter order.

Proposition 1.20.56 ((Cov2) and normalized persistence)**.** *Use $(H^\circ, U^\circ, P^\circ)$ and the physical pre-loop field of (1.19.1). Up to $y_p = -14.5$ the changes from the comparison to the final field are exactly (i)–(iii) in (Cov2) with their inward history increments. Through the entrance of the heat bank the two pre-loop triples and all their inward histories agree. From the end of the five returns to $y_p = -14.5$ the final field and its histories equal the physical pre-loop ones. On this interval $\mathscr{P}_4$, $U = 0$ and ℓ_r, Q, w of the physical field differ from the comparison by $O(K_{\mathrm{sc}}(Y_0)/R_{\mathrm{master}})$, allowing a larger fixed-Y_0 constant. The strict margins of Proposition 1.20.10(b) persist at every sufficiently large master scale.*

Proof. The five returns lie in $(-25, -20)$ and the three heat bumps lie in $(-20, -15)$. The two-row I/C_p taper lies in $(-2.15, -0.85)$. The central memory edit, A11, the germ connector and the spectral corrections are outside the prefix (Section 1.14, Lemma 1.17.9 and (1.6.67)). The reserved patches carry only positive-order corrections. Below the heat bank the pre-loop velocity densities coincide from the axis, and (1.19.1) identifies the pressures. The loop and its returns have zero complete difference in each row relative to the physical baseline by Lemma 1.13.7. Thus beyond the reserve all partial histories, including those inside the heat bank, are exactly the physical pre-loop histories.

For the comparison on $\mathscr{P}_4$, take δ to mean physical pre-loop minus comparison. The heat bank changes H only where $U = 0$, hence $\delta M = \delta J = 0$ and $\delta P = D_C$. Put $\epsilon = K_{\mathrm{sc}}(Y_0)/R_{\mathrm{master}}$, with the constants below allowed to depend on fixed geometry. In bank coordinates, Lemma 1.14.5 bounds the relative field and its first jets by $O(\epsilon)$. Integrate its three displayed densities up to the running radius, retaining the cross and square terms. With H°, E° in the denominators this gives

$$|\delta\ell_r| + \sum_{j=0}^{1}\left(\frac{|\partial_\eta^j \delta I|}{XH^\circ} + \frac{|\partial_\eta^j \delta S|}{X(E^\circ)^2} + \frac{|\partial_\eta^j D_C|}{(E^\circ)^2}\right) \leq C\epsilon.$$

The derivatives are at fixed X. The moving bump coordinates have bounded logarithmic graph derivatives. From the bank through $y_p = -14.5$, X/X_* and the relative power amplitude range in fixed compact subsets of $(0, \infty)$ on its angular support. This also bounds the *complete* offsets $\delta S = -\chi_b \Delta S_f$ and $D_C = -b_{\mathrm{heat}}$ remaining after the last bump. Where the heat target vanishes on an open sector the fields agree there, with the bounds extending to its boundary.

In (1.20.4), multiply by H before subtracting the two formulas. Since M, J are unchanged the surviving terms are bounded by the relative H error, the normalized I error and its first angular derivative. The coefficient $1 + \mathcal{K}/X$ is bounded by the inlet estimates, and Q° is bounded by its transport equation on the fixed wait. Thus $|\delta Q| \leq C\epsilon$. In (1.20.5), $U = 0$ on both fields and the M terms cancel, giving $|\delta N_s| \leq C\epsilon(E^\circ)^2$. The comparison has $Q^\circ \geq \min(q_\flat, q_\sharp) > 0$ and $|w^\circ|$ bounded by (R6), with $\nu \geq \nu_c > 0$. The normalized wait amplitudes E° are bounded there by the selected pulse and template bounds (Proposition 1.15.27 and the fixed log-distance to the pulse). Subtracting $w = N_s/(EQ)$ gives $|\delta w| \leq C\epsilon$. For the comparison, $\ell_r^\circ = -\nu$, $\theta^\circ \geq 1/2$ and $-\ell_r^\circ (w^\circ)^2 \leq 1/8$ by Proposition 1.20.10(c). Since Q° has a uniform positive floor, the change of $2L(1-\ell_r)/(XQ)$ is $O(\epsilon)$ using (R7). Choose the master scale to keep $\ell_r < 0$, $\theta > 0$ and $\theta^2 + \ell_r w^2 > 0$, using the initial slack of at least $1/8$ in the last inequality. This proves the strict inequalities in Proposition 1.20.10(b). □

Remark 1.20.57 (Dependencies of the cover). (1) The selected-source clauses (A4)–(A5) use the cover, not conversely. (2) Inputs (R1)–(R7) use the constructed templates, inlet data, turnoff and restoration estimates; positivity of F° is (R1). (3) Theorem 1.20.54 supplies the selected-member cover, including the regions not covered by the scalar-component example. (4) Lemma 1.14.5 gives relative field and partial-history jets $O(K_{\mathrm{sc}}(Y_0)/R_{\mathrm{master}})$. Its normalized rows are $\sqrt{2}\int x^{1/2}v$, $-f\int x^{-1/2-\lambda}v-\frac{1}{2}\int v^2$, and $f\int x^{-3/2-\lambda}v+\frac{1}{2}\int v^2/x$. The Chebyshev determinant and the small-target inverse bounds are uniform on $0\le\lambda\le\lambda_0$. After the bank $\delta I=0$ and $\delta S,\delta C_p$ are constant. Below the bank, separately imposing zero pressure at infinity on the omitted-bank field would give $P^{\circ,\infty}=P^{\mathrm{pre}}-b_{\mathrm{heat}}$. With the prescribed axis value we have $P^\circ=P^{\mathrm{pre}}$ exactly there by (1.19.1). These are the estimates used in Proposition 1.20.56. (5) The loop lies in $y_p<-W+1$ and its five returns in $-25<y_p<-20$. (6) The correction annuli use Lemma 1.6.36; activation uses Theorem 1.20.28 with Definition 1.20.22.

Theorem 1.20.58 (The admissible cover)**.** *The comparison with prescribed axis pressure and the physical field constructed in the order of Section 1.5.2 satisfy (Cov1)–(Cov2) of Hypothesis 1.20.4, hence Hypothesis 1.5.1.*

Proof. Theorem 1.20.54 reduces (Cov1) to (R1)–(R7). Table 1.5 records the estimates just proved, and Table 1.6 identifies the core inputs to the activation theorem. All thresholds are those of the cited statements, imposed in the order of Section 1.5.2.

Table 1.5: Estimates for the cover.

Input	Estimate and choices
(R1)	Lemma 1.20.50: the core lower bound and positive multiplicative pieces; choose the additive bump tolerance so $\lvert v\rvert\le x^{1/10}/2$ and the pressure-bank target below $\tau_b/10$.
(R2)	Theorem 1.20.28(a), Corollary 1.20.51: choose $y_*(C)$, then $\kappa_{\mathrm{act}}\le 1/8$ and $t_{\mathrm{act}}\le y_*(C)/8$.
(R3)	Proposition 1.20.17 and Theorem 1.20.28(b)–(d): the pressure/axial tolerance, core thresholds, and (M0)–(M1), followed by the stated late bounds and $K_I\omega_2\le 1/4$.
(R4)	Proposition 1.20.53, Lemma 1.20.52: the inlet $p_1\ge 9/4$, the stated bounds on ε_u, $\delta_U=K_c/\Lambda+B_{\mathrm{act}}$, and T_s; $B_{\mathrm{r0}}\ge 12\sup b/s_\gamma$, $\Lambda\ge\Lambda_s$, $\varepsilon_s\le c_s/4$.
(R5)	The common geometry and exact histories of Section 1.14, Lemmas 1.14.1, 1.6.14, 1.6.37; monotonicity from Lemma 1.15.26, the actual inlet bounds of Proposition 1.15.27, and Lemma 1.20.48. Use (λ4), (λ8), $K_{\mathrm{geo}}K_{\mathrm{ax}}j_0\le j_\sharp/2$ and choose Y_0 with the outlet allowance K_2+1 in Lemma 1.20.14.
(R6)	Lemma 1.20.45 and Lemma 1.20.48(b),(c), with (λ1), (λ2), (λ8), $\eta_c\ge 2\eta_a$, and large Y_0. The comparison pressure uses Lemma 1.20.14(b) with τ_P^*. Lemma 1.15.34 gives the high-exponent floor.
(R7)	Remark 1.20.55: $C^{10}\ge 4.2/(c_g\min(q_\flat,q_\sharp))$ and (λ5); the remaining condition is the (R4) barrier.
(Cov2)	Proposition 1.20.56, using the support order and the relative jets of Lemma 1.14.5; see Remark 1.20.57(4).

Table 1.6: Core inputs to the activation estimate.

Input	Established bound
(I1)	Proposition 1.6.42 in the norm of Definition 1.6.40, with Λ large and then $\|C^{-1}e^{\Lambda\psi+a}\| \le 1$.
(I2)	The Bessel and axial alternatives of paragraph 1.6.4.3 and Lemma 1.6.38; Lemmas 1.20.24(b), 1.6.45 give the additional lower bounds.
(I3)	Lemma 1.20.24(c), with $K_{wY} = K_R/2$, and the core-ball remainder bounds.
(I4)	Lemma 1.20.24(d).
(I5)	Lemmas 1.20.24(e), 1.20.25(a); (H_u) follows from $\|u - G\|_{C^1} \le \varepsilon_u/4 \le 1/4$ and $w < 4\eta_c$.
(I6)	The endpoint margin of Lemma 1.6.38, the central root margin of paragraph 1.6.4.3, and the choice $s_0 \le v_*/20$ off that neighbourhood; the backward thresholds are those of Definition 1.20.35.

The axial alternative in (I2) holds throughout $4 \le Y \le Y_{\mathrm{buf}}$: $w_Y = Z_R/(2Lb) + O(\Lambda^{-1})$, $p_{1,r} \le P_{\mathrm{ref}}$, and $p_{2,r}^2 = 2bYw_Y^2/(\Lambda g^2\Phi^2)$ has the required lower bound at large C. On the complementary sector the Bessel ratio $zJ_2(z)/J_1(z)$ increases for $z < j_{1,1}$. For (R5) on the buffer, apply Lemma 1.20.14 with (κ_0, κ_1) replaced by $(\kappa_1, 0)$ and with the outlet in (1.20.9).

Finally Lemma 1.20.49 places the loop in $\{y_p < -W + 1\}$, with outer strict collar $-W + 1/2 \le y_p \le -W + 1$ and inner strict collar $0 < y_a \le y_s$. Every relaxed point has $y_p < -W$ and $y_a > y_s$, hence lies inside the loop window. This proves (Cov1); (Cov2) is the cited persistence estimate. The inputs precede the loop and the aggregate weight, so the argument uses neither selected-source clauses (A4)–(A5) nor the later inverse or backward-completion hypotheses. □

Proposition 1.20.59 (Prefix positivity)**.** *Assume Hypothesis 1.20.4, (J2), (J4), (J5), and let* N_{sh} *be as large as* [proof of Corollary 1.19.3, Proposition 1.19.6] *allow and the heat-compensation scale as large as* [Lemma 1.15.9] *allows. Then the final leading stress satisfies* $T_0 \neq 0$ *on* $\mathscr{P}$*. Moreover there is* $c_{\mathscr{P}} > 0$ *with*

$$|T_0(\tfrac{\hat\xi^2}{2}, \eta)| \;\ge\; c_{\mathscr{P}}\, e(y_a) \qquad \text{on } \mathscr{P}. \tag{1.20.21}$$

Combined with (J6), $|T_0| \ge c\, e(y_a)$ *also holds on* $\mathscr{P} \cup K_0 \cup \{Y - \frac{1}{2} \le y_p \le Y - \frac{1}{2} + \epsilon_0\}$ *for some* $\epsilon_0 > 0$.

Proof. Collar. The regular core and activation were solved with the physical datum p_0. Below the heat bank (1.19.1) gives $P^{\mathrm{pre}} = P^\circ$ exactly. The loop is inactive on the protected entry collar and the later returns preserve the complete pressure row. Thus the actual stress has the factor $e(y_a)$ of the collar construction (Section 1.12). By (J2), on $0 < y_a \le y_{\mathrm{col}}$, $|T_0| \ge \widehat{\mathcal{T}}_{P,\theta} \ge e\,\mathcal{B}_\theta \ge b_* e$.

Decomposition of $\mathscr{P}_{\mathrm{c}}$. By (Cov1)–(Cov2), $\mathscr{P}_{\mathrm{c}}$ is the union of four compact pieces (closures of radial intervals between the listed supports, at each η; their endpoints are continuous in η):

(i) $\mathscr{P}_1 = \mathscr{P}_{\mathrm{c}} \cap \{\frac{\hat\xi^2}{2} \le (\frac{\hat\xi^2_{\mathrm{sh}}}{2})^+(\eta)\}$, where $(\frac{\hat\xi^2_{\mathrm{sh}}}{2})^+$ is the outer end of Y_{sh}. It contains the collar overlap and Y_{sh}.

(ii) $\mathscr{P}_2$, the transit from $(\frac{\hat\xi^2_{\mathrm{sh}}}{2})^+$ to the start of the restoration reserve.

(iii) $\mathscr{P}_3$, the restoration reserve.

(iv) $\mathscr{P}_4$, from the end of the reserve to $y_p = -14.5$. It contains the heat-compensation bumps.

(i). On $\mathscr{P}_1$ the two pre-loop triples coincide, including $\mathbf{p}^{\mathrm{pre}} = \mathbf{p}^{\circ}$ from their common pressure and histories. Prior to the loop the final field is the physical pre-loop field. On Y_{sh}, Lemma 1.19.2 supplies a loop with fixed positive four-gap margins against $\mathbf{p}^{\mathrm{pre}}$ and strict radial collars. Equation (1.19.6) gives $a_N - a_L, b_N - b_L = O(N^{-1})$ by smoothness of the periodic primitives on the compact window. Corollary 1.19.3 gives $\mathbf{p}_N - \mathbf{p}^{\mathrm{pre}} = O(N^{-1})$ with this same axis datum. Continuity of the gaps for $\mathfrak{a} \geq \min a_L/2$ leaves a positive margin for $N \geq N_1$. Lemma 1.20.1 gives $T_0 \neq 0$.

(ii). On the transit $\mathscr{P}_2$, (Cov1) and the location of its relaxed points give $m_2 = \min |T^{\mathrm{pre}}| > 0$ by compactness. The velocities equal the physical pre-loop velocities. The complete loop exit error is $O_k(N^{-2})$ in C^k_η, and it is the entire change in each inward history. The pressure difference equals the C_p row of this error because the axis value is the same. By Lemma 1.20.3, $|T_0 - T^{\mathrm{pre}}| \leq C_{\mathscr{P}_2} N^{-2} < m_2/2$ for $N \geq N_2$.

(iii). The physical pre-loop field on $\mathscr{P}_3$ is the strict quiet power with $U = 0$ and $H = c_p \varphi X^{-\mu(\eta)}$ and has $m_3 = \min |T^{\mathrm{pre}}| > 0$ for the fixed member. To the $O_k(N^{-2})$ incoming shift add the five return bumps and their partial histories, each $O_k(N^{-2})$ by Lemma 1.13.7. The stress formulas are smooth in the values, first radial derivatives, inward histories and their first angular derivatives on this compact reserve. Hence $|T_0 - T^{\mathrm{pre}}| < m_3/2$ for $N \geq N_3$. At the exit the five differences vanish exactly.

(iv). On $\mathscr{P}_4$ the final field and its five histories are the physical pre-loop ones. Proposition 1.20.56 applies the strict quiet-power test with their actual heat-bank partial integrals and complete offsets. Thus $T_0 \neq 0$ for the selected large master scale. The heat target and this scale precede the choice of N_{sh}. Taking $N_{\mathrm{sh}} \geq \max(N_1, N_2, N_3)$ gives $T_0 \neq 0$ on $\mathscr{P}_{\mathrm{c}}$. By continuity and compactness $m := \min_{\mathscr{P}_{\mathrm{c}}} |T_0| > 0$. Since $e \leq 1$, (1.20.21) holds with $c_{\mathscr{P}} = \min(b_*, m)$. The last assertion is (J6) together with the open-buffer statement of Lemma 1.17.2. The overlap of $\mathscr{P}$ and K_0 is $y_p = -14.5$. □

Remark 1.20.60 (Parameter order). The thresholds N_1, N_2, N_3 depend only on quantities fixed with the member before N_{sh}: the loop margins, m_2, m_3, and the compact sets. Proposition 1.19.6 fixes N_{sh} after the actual member and correction tolerances. So this proof needs no reordering. Only the requirement $N_{\mathrm{sh}} \geq N_2$ is new. It is of the same kind as the bound on the complete exit discrepancy in Corollary 1.19.3, and it is included in Proposition 1.19.6.

1.20.6 The outer corridor and the terminal faces

Lemma 1.20.61 (Exact mixture and wing identities)**.** *With* $\mathcal{A}\mathfrak{M}_2 = (\frac{\mathfrak{M}_{2\hat{\xi}\hat{\xi}}}{\hat{\xi}^2} - \frac{\mathfrak{M}_{2\hat{\xi}}}{\hat{\xi}^3}) - \frac{\mathfrak{M}_{2\hat{\xi}}}{\hat{\xi}}/\frac{\hat{\xi}^2}{2} + [\frac{\hat{\xi}^2}{2}\frac{\mathfrak{M}_{2\hat{\xi}}}{\hat{\xi}} - (1-h)\mathfrak{M}_2 + (\frac{1}{2} - h)\eta\mathfrak{M}_{2\eta}]/(L\hat{\xi}^2)$ [(1.17.1)]*:*

(a) $\mathcal{A}[(1-\chi)\mathfrak{M}_{2c} + \chi\mathfrak{M}_{2w}] = (1-\chi)\mathcal{A}\mathfrak{M}_{2c} + \chi\mathcal{A}\mathfrak{M}_{2w} + \dot{\chi}(\mathfrak{M}_{2w} - \mathfrak{M}_{2c})/(L\hat{\xi}^2)$*, where* $\dot{\chi} = (\frac{1}{2} - h)\eta\chi_\eta$.

(b) For $E_o = \alpha_o \ell_b^2 \mathcal{F}((\mathcal{B}_o(\eta) - \frac{\hat{\xi}^2}{2})/\ell_b)$,

$$\mathcal{A}E_o - \frac{\alpha_o \ell_b \mathcal{F}'}{2L} = \alpha_o \mathcal{F}'' + \frac{\alpha_o \ell_b}{\frac{\hat{\xi}^2}{2}}\mathcal{F}' + \frac{\alpha_o \ell_b}{L\hat{\xi}^2}\Big[((\tfrac{1}{2} - h)\eta\mathcal{B}_o' - 2\mathcal{B}_o)\mathcal{F}' + \ell_b(2y\mathcal{F}' - (1-h)\mathcal{F})\Big].$$

If $(\frac{1}{2} - h)\eta\mathcal{B}_o' \geq 2\mathcal{B}_o$*, then every term is* ≥ 0*, because* $\mathcal{F}'' \geq 0$ *and* $\mathcal{F} \leq y\mathcal{F}'$*. This proves* (1.13.54) *with room to spare.*

(c) $\mathcal{A}[\mathfrak{M}_{2L} + \psi_o E_o] = \mathcal{A}\mathfrak{M}_{2L} + \psi_o \mathcal{A}E_o + (\frac{1}{2} - h)\eta\psi_o' E_o/(L\hat{\xi}^2)$ [Section 1.13].

Proof. Product rule. □

Proposition 1.20.62 (Positivity on the outer corridor and terminal collars)**.** *Assume (J7)–(J9) and the actual spectral source estimates on the protected hold of Section 1.26. Let χ be nondecreasing in $|\eta|$, so $\dot\chi \ge 0$. On the pure-swirl mixture after the connector has reached its exact mixture germ, outside the radial hull of the spectral perturbations and their returns,*

$$\widehat{\mathcal{T}}_{P,\theta} = (1-\chi)\widehat{\mathcal{T}}_{P,\theta,c} + \chi\,\mathcal{A}\mathfrak{M}_{2w} + \dot\chi\,\frac{\Delta}{L\hat\xi^2} \;\ge\; 0, \tag{1.20.22}$$

and each summand is ≥ 0. Specifically:

(a) on the compact preterminal corridor outside that hull,

$$\begin{aligned}\widehat{\mathcal{T}}_{P,\theta} &\ge (1-\chi)m_c + \chi m_s \lambda \min H_w \\ &\ge \min(m_c, m_s\lambda \min H_w) > 0,\end{aligned}$$

where $m_c > 0$ is the central source floor on its compact path [(1.15.24), proof of Lemma 1.17.7]. *On the portion of the corridor changed by spectral edits the final field satisfies $T_{0,\theta} \ge cH > 0$ on the full compact interval through the last spectral return;*

(b) after the central blend J,

$$\widehat{\mathcal{T}}_{P,\theta,c} \ge \tfrac{(\frac12 - h)}{2}\,(w_L + w_1 + w_2),$$

with

$$w_L = d^{-h-1}\tau_s(\tfrac{\hat\xi^2}{2}/d), \qquad w_1 = \psi_o\alpha_o\ell_b f_o(y_o),$$
$$w_2 = \eta\psi_o'\alpha_o\ell_b^2\mathcal{F}(y_o)/\tfrac{\hat\xi^2}{2}.$$

See (1.23.4);

(c) at the outer terminal face, $\widehat{\mathcal{T}}_{P,\theta} \ge c[\chi v_s + \dot\chi v_g]$ (J9).

Proof. (1.20.22) is Lemma 1.20.61(a) with $\widehat{\mathcal{T}}_{P,\theta} = \mathcal{A}\mathfrak{M}_2$ on $U = \mathfrak{M}_1 = \mathfrak{M}_3 = 0$ (J7). $\widehat{\mathcal{T}}_{P,\theta,c} \ge 0$ by the nonnegative central source (J7). $\mathcal{A}\mathfrak{M}_{2w} > 0$ by [Lemma 1.17.4]. $\Delta \ge 0$ by $\Delta/\frac{\hat\xi^2}{2} \ge m_g\lambda H_w$ [Lemma 1.17.3]. $\dot\chi \ge 0$ by Definition 1.23.6. For (a), use $(1-\chi)+\chi = 1$. For (b), after J the central component is $\mathfrak{M}_{2L} + \psi_o E_o$, unchanged by the memory edit [proof of Lemma 1.17.7]. By Lemma 1.20.61(b),(c) and $L \le 1$: $\widehat{\mathcal{T}}_{P,\theta,c} \ge w_L + \psi_o\alpha_o\ell_b\mathcal{F}'/(2L) + (\frac12 - h)w_2/(2L) \ge w_L + \frac12 w_1 + \frac{(\frac12-h)}{2}w_2$. Note $\eta\psi_o' \ge 0$ because ψ_o increases in $|\eta|$. (c) is quoted. For the final field on the edited angular support take the entire radial interval from the first spectral bump through the last return, including the gaps. The principal edit has signed radial slope; the full angular-stress formula on the hold gives $T_\theta \ge T_* > 0$ after choosing C and then the spectral width (Remark 1.27.2(a)). For the axial and curvature controls the actual source budget (1.27.7) and the partial, upper-limit-uniform bounds (1.30.23) keep a strict fraction of this margin. These estimates use the full integrated M, J, I, S, P, including their angular derivatives. The bound for the principal first-angular history uses L_ζ before m is chosen. Since H has a finite positive maximum on the selected compact hull, this gives the stated lower bound relative to H. On the fixed slow cutoff beyond the main envelope, the lower controls start from the old compact hold margin. Their first radial changes are $O_C(|t_6|)$ by the templates in Section 1.30.5.1. Their field and first-angular changes at fixed X are $O_C(d|t_6|)$ since x/d is independent of η there. The same bound for partial moments and fixed-shape returns follows by integrating their density differences and differentiating the uniform five-row inverse. The selected $|t_6|$ is exponentially small up to a polynomial in d^{-1}, so this margin persists across the slow

cutoff. Outside the union of the edited angular supports the old field applies. Before the first radial edit the axis histories and the pressure offset agree, and after the last return all five histories agree exactly. This recovers (1.20.22) there for the final member and proves the corridor assertion used below. □

Corollary 1.20.63 (Radial connectivity of the stress support)**.** *Under the hypotheses of Propositions 1.20.59 and 1.20.62, for each η the set $Z_\eta = \{\frac{\hat\xi^2}{2} : T_0(\frac{\hat\xi^2}{2}, \eta) \neq 0\}$ is the single open interval $(\frac{(\hat\xi_a(\eta))^2}{2}, \frac{(\hat\xi_{\mathrm{end}}(\eta))^2}{2})$. Here $\frac{(\hat\xi_{\mathrm{end}}(\eta))^2}{2}$ is the supremum of the values of $X = \hat\xi^2/2$ at which one of the factors $(1-\chi)w_L$, $(1-\chi)w_1$, $(1-\chi)w_2$, χv_s, $\dot\chi v_g$ (and, on K_2, the hold) is positive.*

Proof. Proposition 1.20.59 covers the interval up to $y_p = Y - \frac{1}{2} + \epsilon_0$. From this level through Y apply the quiet and return bounds of Lemmas 1.16.8 and 1.16.9. Lemma 1.17.9 starts on the same power germ and reaches the pure mixture with positive angular stress. Proposition 1.20.62 covers the subsequent compact corridor and edited hull. At each terminal face, the positive factors in (b),(c) are positive on initial radial intervals up to their respective cutoffs. Their union meets the preceding corridor. Beyond their last active edge the field is the exact heat pair, whose two stresses vanish. This proves the asserted fiber interval. □

Remark 1.20.64 (Role of radial connectivity). A moment-subtracted primitive can persist between its source and its correction support. The connected positive channels in Corollary 1.20.63 keep that entire path inside the stress support, as required by Lemma 1.24.3.

1.21 The selected curved inner weight and protected domain

Lemma 1.21.1 (Inner weight and protected completion domain)**.** *For the selected member, we put $y = 2\log(\hat\xi/\hat\xi_a(\hat\zeta))$ and keep the activation $e = (1-\kappa_{\mathrm{act}})\sigma(y/t_{\mathrm{act}})$. On a sufficiently small positive collar the leading stress is $T_0 = e\mathcal{B}$, where*

$$\mathcal{B}(0,\hat\zeta) = F_a(\hat\zeta)(p_{1,r}, p_{2,r}), \qquad \mathcal{B}_\theta \geq b_* > 0, \qquad |\mathcal{B}| \leq b^*.$$

The inner edge weight is $w_{\mathrm{in}} = c_{\mathrm{in}} e$ for $y > 0$ and zero for $y \leq 0$, with a fixed sufficiently small memberwise constant. For each fixed mixed profile derivative D^j,

$$cw_{\mathrm{in}} \leq T_{0,\theta} \leq Cw_{\mathrm{in}}, \qquad |T_{0,z}| \leq Cw_{\mathrm{in}},$$
$$|D^j w_{\mathrm{in}}| + |D^j T_0| \leq C_j w_{\mathrm{in}}(1 + \log(1/w_{\mathrm{in}}))^{N_j}.$$

Its positive fractional powers have flat extensions through the activation face, and the normalized stress direction has logarithmic jet bounds. We continue the edge as a connected positive channel to the protected mean correction region. We solve the slow equation on a finite union of protected rectangles. The full support of its shared Gevrey-3/2 termination cutoff lies inside that solved union. These selections are slice continuations of the backward selections, so their mixed jets agree in slice variables (Lemma 1.6.8).

Proof. The shear prescription in the curved-entry construction gives the stated factorization. We select the squared-flat step with the other data. The assertion does not apply to an arbitrary prescribed smooth activation step. On its flat edge, $e = c\exp(-t_{\mathrm{act}}^2/y^2)$ up to a smooth positive factor with bounded jets.

The exact differences from the reference are integrals of $e\frac{\hat\xi^2}{2}n_{s,r}/2$ and $ep_{1,r}/2$. The radial-primitive differences for these fields have zero incoming values. Thus e times a finite inverse power of y bounds each fixed derivative. The identity $\partial_{\hat\zeta}|_{\hat\xi} = \partial_{\hat\zeta}|_y - (\log\frac{\hat\xi_a^2}{2})'\partial_y$ keeps this class.

The bound $y^{-1} \le C(1+\log(1/e))^{1/2}$ gives the displayed estimates. The positive theta limit supplies the lower bound needed for quotient differentiation. In general $T_{0,z}/T_{0,\theta} \to p_{2,r}/p_{1,r}$, not zero. The strict direction margin is the curved-entry cone margin.

Equations (1.23.2)–(1.23.3) and their derivative and primitive estimates establish these bounds. The connected continuation of the weight, not an isolated compact bump, is the input to Lemma 1.24.3.

We solve the slow equation before we cut off its coefficients. We select the needed and buffer levels $0 < y_{\mathrm{need}} < y_{\mathrm{buf}}$ of $y_a = 2\log(\hat\xi/\hat\xi_a(\hat\zeta))$, that is, the constant levels $\Xi_{\mathrm{need}} = e^{y_{\mathrm{need}}} < \Xi_{\mathrm{buf}}$ of the scaled radius $\varpi = (\hat\xi/\hat\xi_a(\hat\zeta))^2$. We select the termination transition at positive levels of y_a in the strict entry collar, away from its zero-stress face. The weight has a positive minimum on that compact derivative support.

We solve the arbitrary-coefficient regular-axis Volterra equation in $(\varpi,\hat\zeta)$ on one rectangle $[0,\Xi]\times U$, with $\Xi_{\mathrm{cut}} = e^{\epsilon}\Xi_{\mathrm{need}} < \Xi < \Xi_{\mathrm{buf}}$ for the protected domain of Hypothesis 1.22.1. No angular cover and no overlap identification are needed. At each finite coefficient order the convergent iteration allows a smaller positive angular radius.

The termination cutoff equals one through Ξ_{need} and is zero from Ξ_{cut}. It is a fixed Gevrey-3/2 step of $(y_a - y_{\mathrm{need}})/\epsilon$, so it is a function of ϖ alone. Thus each fixed ϖ-derivative of the cut coefficients keeps one positive angular Gevrey radius at fixed ϖ. This is the construction of paragraph 1.22.

The shared logarithmic coordinate and the graphs are slice functions, so the full cutoff jets agree in slice variables. All constants are for the fixed member. We do not assert one positive radius for all shrinking activation widths or all large C. □

1.21.1 The joint cutoff gauge and the same finite algorithms

Lemma 1.21.2 (Joint cutoff)**.** *Let $L_{\mathrm{cut}}(\hat\zeta) > 0$ be smooth on $[-1,1]$, and put $\widetilde q = \hat t_b$ for $t \le 0$ and $\widetilde q = \hat t_f/L_{\mathrm{cut}}(\hat\zeta_f)$ for $t \ge 0$.*

(a) The function $\widetilde q/\widetilde Q$ is C^∞ across $\widetilde\eta = 0$ if and only if L_{cut} and λ_{ch} have equal jets at $\hat\zeta = \pm1$.

(b) If this holds, each stage cutoff $\chi(\widetilde q/\delta_n)$ is one C^∞ function across $t = 0$ for $z \ne 0$. On $t \le 0$ it is the backward cutoff $\chi(\hat t_b/\delta_n)$. On $t \ge 0$ it is $\chi(\hat t_f/(L_{\mathrm{cut}}(\hat\zeta)\delta_n))$.

We apply these cutoffs to potentials and mean fluxes before differentiation. They keep the equal slice jets of the completed physical fields.

Proof. On $t \le 0$, $\widetilde q/\widetilde Q = |\hat\zeta_b|^{-1/(\frac12-h)} =: \gamma(\widetilde\eta)$ by Lemma 1.6.2. The function γ is real-analytic on $\widetilde\eta < c_h$ by Lemma 1.6.3. On $t \ge 0$, $\widetilde q/\widetilde Q = |\hat\zeta_f|^{-1/(\frac12-h)}/L_{\mathrm{cut}}(\hat\zeta_f)$, and $\gamma = |\hat\zeta_f|^{-1/(\frac12-h)}/\lambda_{\mathrm{ch}}(\hat\zeta_f)$ by (1.6.16). The map $\hat\zeta_f \mapsto \widetilde\eta$ is a diffeomorphism at ±1.

Thus the two one-sided jets agree if and only if L_{cut} and λ_{ch} have equal jets at ±1. This proves (a). For (b), multiply the smooth glued function $\widetilde q/\widetilde Q$ of (a) by $\widetilde Q/\delta_n$ and compose with χ. The two one-sided cutoff formulas therefore have equal jets. Products with fields that have equal slice jets keep equal slice jets.

This includes the jets that differentiation of the potentials gives.

We use $L_{\mathrm{cut}} = \lambda_{\mathrm{ch}}$ on the endpoint collars. We extend $\log \lambda_{\mathrm{ch}}$ with fixed smooth cutoffs and then exponentiate this extension, so L_{cut} is positive. The alternative $\chi(\lambda_{\mathrm{ch}} \hat{t}_f/\delta_n)$ is not smooth across $t = 0$. In slice variables its argument is $\widetilde{Q}\lambda_{\mathrm{ch}}|\hat{\zeta}_f|^{-1/(\frac{1}{2}-h)}/\delta_n$.

At $\widetilde{\eta} = 0$ the $\widetilde{\eta}$-derivative of $\lambda_{\mathrm{ch}}|\hat{\zeta}_f|^{-1/(\frac{1}{2}-h)}$ is $3/(2(\frac{1}{2}-h))$, but the derivative of γ is $-1/(2(\frac{1}{2}-h))$. The reciprocal factor is thus required. A cutoff of the differentiated fields does not include the derivative terms of the potential construction. □

1.22 The protected leading core and its angular regularity

Selected curved domain. The selected core-entry theorem supplies a protected Gevrey–3/2 core in its shared Gevrey–3/2 geometry. We use the scaled radius $\varpi = \big(\hat{\xi}/\hat{\xi}_a(\hat{\zeta})\big)^2 = e^{y_a}$ of the protected core. We select constant levels $\Xi_{\mathrm{need}} < \Xi_{\mathrm{cut}} = e^{\epsilon}\Xi_{\mathrm{need}} < \Xi < \Xi_{\mathrm{buf}}$ of ϖ, and put $R_*(\hat{\zeta}) = \frac{\big(\hat{\xi}_a(\hat{\zeta})\big)^2}{2}\Xi_*$ for the corresponding graphs. We select the full possible cutoff-transition region $[\Xi_{\mathrm{need}}, \Xi_{\mathrm{cut}}]$ compactly inside the actual first strict positive collar, at positive distance from its zero edge $\varpi = 1$.

Thus the actual weight has a positive minimum on the cutoff derivative support. This support never meets a flat zero face. We do not claim uniformity when the activation widths decrease.

Hypothesis 1.22.1 (Forward leading data in the scaled-radius class). Let U be a compact neighborhood of the angular range, with ± 1 in its interior (N8). For the forward leading data $G \in \{F_0, U_0, w_0\}$ and each $j \geq 0$, there is $\varrho_1 > 0$ such that $\sup_{0 \leq \varpi \leq \Xi} \big\| \partial_\varpi^j G^\natural(\varpi, \cdot) \big\|_{\mathcal{G}_{\varrho_1}} < \infty$ on U, where $G^\natural(\varpi, \eta) = G(\xi_a(\eta)\sqrt{\varpi}, \eta)$.

The core is built in $Y = \Lambda b \frac{\hat{\xi}^2}{2} = 4\varpi$, and the curved activation in $y_a = \log \varpi$. Proposition 1.22.4 below derives this regularity from the core contraction. For the backward member the corresponding statement holds with the interval U_b of the backward analytic core in place of U. This follows from Theorem 1.8.10(i) on the analytic rectangle before the loop (Theorem 1.8.10(i) and Lemma 1.20.40(b); a finite $\mathcal{G}^1$ norm bounds the Gevrey-3/2 norm), because $\frac{\hat{\xi}_{a,b}^2}{2}$ is constant there. The backward inner solves use U_b.

We put $y_{\mathrm{need}} = \log \Xi_{\mathrm{need}}$, and select a normalized squared-flat Gevrey–3/2 scalar step in $(y_a - y_{\mathrm{need}})/\epsilon$. It equals one through Ξ_{need} and has full support in $\varpi < \Xi_{\mathrm{cut}}$. We place its derivative support in the reserved compact strict-positive collar. It is a function of ϖ alone, so products with it keep a positive angular Gevrey–3/2 radius at fixed ϖ for each fixed ϖ-derivative.

Order of selection. The levels are shared by the two sides (paragraph below) and are selected after the backward member is fixed, hence after the radius $\frac{\hat{\xi}_{\mathrm{an}}^2}{2}$ of the analytic rectangle of the backward member (Theorem 1.8.10(i) on the analytic rectangle before the loop, from Theorem 1.8.10(i), with $\frac{\hat{\xi}_{\mathrm{an}}^2}{2}$ before the loop interval, as (B1) requires). With $\frac{\big(\hat{\xi}_a^0\big)^2}{2} = 4/\Lambda$ we require

$$1 < \Xi_{\mathrm{need}} < \Xi_{\mathrm{cut}} < \Xi < \min\left\{ \frac{\Lambda(\hat{\xi}_{\mathrm{an}}^2/2)}{4},\ e^{t_{\mathrm{act}}},\ e^{y_s},\ \frac{(\hat{\xi}_-^{\mathrm{loop}})^2}{(\hat{\xi}_a^0)^2} \right\}, \qquad (\hat{\xi}_a^0)^2 \Xi/2 < \inf I_{\mathrm{pos}}. \quad (1.22.1)$$

Here $y_* > 0$ is the end level of the forward strict entry collar, and I_{pos} is the reserved patch of (B5), which lies after the activation collar by (S4). Nothing earlier in the construction bounds y_{need} from below. The only requirements on the transition are that it lie at positive levels of y_a in the strict entry collar, away from the zero-stress face, with a positive weight minimum on its derivative support (the selection of the termination transition after the proof of Lemma 1.21.1, and

the paragraph above). The graphs $R_{\mathrm{need}}, R_{\mathrm{buf}}$ are used nowhere else except through these levels. So (1.22.1) is feasible. All upper levels exceed one and are fixed before $\Xi_{\mathrm{need}}, \Xi_{\mathrm{cut}}, \Xi$. On the entire positive portion of the protected rectangle the strict entry bound $\mathfrak{v} - 2 \ge \delta_0/2 > \delta_L/4$ turns off the forward loop. The backward radius inequality keeps the rectangle before the backward loop. On $(1, e^{t_{\mathrm{act}}}]$ the activation factor $e = (1-\kappa_{\mathrm{act}})\sigma(y_a/t_{\mathrm{act}})$ is positive, so the weight still has a positive minimum on the cutoff derivative support. On $\varpi \le e^{t_{\mathrm{act}}}$ the two members are built by the same formulas (Proposition 1.22.7), and there the reference values are taken only at $Y \le 4e^{t_{\mathrm{act}}} < 4.1$ (Proposition 1.22.4). On the backward side we use a radius $\frac{\hat\xi_-^2}{2} \in (\frac{(\hat\xi_a^0)^2}{2}, \frac{(\hat\xi_a^0)^2}{2}\Xi_{\mathrm{need}})$ and the inner rectangle $[0, \frac{(\hat\xi_a^0)^2}{2}\Xi]$, with $\frac{(\hat\xi_a^0)^2}{2}\Xi \le \frac{\hat\xi_{\mathrm{an}}^2}{2}$. We also require $\frac{(\hat\xi_a^0)^2}{2}\Xi < \frac{(\hat\xi_-^{\mathrm{loop}})^2}{2}$, where $\hat\xi_-^{\mathrm{loop}} > \hat\xi_a$ is the radius of (B1) up to which the final backward member equals the pre-loop member (the inner end of the loop of Proposition 1.8.16). This is possible because the backward member, and with it $\frac{(\hat\xi_-^{\mathrm{loop}})^2}{2}$, is fixed before the levels. It places the whole inner rectangle $[0, \frac{(\hat\xi_a^0)^2}{2}\Xi]$ where the final backward member is the analytic member of Theorem 1.8.10(i) with the activation (1.20.14), as in Lemma 1.20.40(b) and Proposition 1.22.7. The radius $\frac{\hat\xi_-^2}{2}$ chosen in this paragraph is a different, smaller radius; $\frac{\hat\xi_-^2}{2}$ denotes it in the backward core and its slow pressure extension.

Lemma 1.22.2 (Operations in $\mathcal{G}_\varrho$). *Let $s \ge 1$ and $0 < \varrho \le 1$, and let $\|\cdot\|_{\mathcal{G}_\varrho}$ be the norm (1.11.2) on a compact interval $K_{\hat\zeta} = U$, with $(k!)^{3/2}$ replaced by $(k!)^s$.*

(a) $\|fg\|_{\mathcal{G}_\varrho} \le \|f\|_{\mathcal{G}_\varrho}\|g\|_{\mathcal{G}_\varrho}$, $\|1\|_{\mathcal{G}_\varrho} = 1$ *and* $\left\|e^f\right\|_{\mathcal{G}_\varrho} \le e^{\|f\|_{\mathcal{G}_\varrho}}$.

(b) For $0 < \varrho' < \varrho$: $\|f\|_{\mathcal{G}_{\varrho'}} \le \|f\|_{L^\infty} + (\varrho'/\varrho)\|f\|_{\mathcal{G}_\varrho}$ *and* $\left\|\partial_{\hat\zeta} f\right\|_{\mathcal{G}_{\varrho'}} \le C_s(\varrho-\varrho')^{-s}\|f\|_{\mathcal{G}_\varrho}$.

(c) If f is real, $f \ge m > 0$ on U and $\|f\|_{\mathcal{G}_\varrho} \le M$, then $\|1/f\|_{\mathcal{G}_{\varrho'}} \le 2/m$ for $\varrho' = \varrho m/(4M)$.

(d) Let $g(\sigma, \hat\zeta)$ be such that each $\partial_{\hat\zeta}^k g$ is continuous on $[\sigma_0, \sigma_1] \times U$, and let $\|g(\sigma,\cdot)\|_{\mathcal{G}_\varrho} \le M$ for all σ. Then $\left\|\int_{\sigma_0}^{\sigma_1} g(\sigma,\cdot)\,\mathrm{d}\sigma\right\|_{\mathcal{G}_\varrho} \le M(\sigma_1 - \sigma_0)$.

Proof. (a) This is Leibniz's rule with $\binom{k}{j}^{1-s} \le 1$, as after (1.11.2). The exponential series converges in this Banach algebra. (b) The terms with $k \ge 1$ carry the factor $(\varrho'/\varrho)^k \le \varrho'/\varrho$. For the derivative, shift the index and use $\sup_k (k+1)^s x^k \le C_s(1-x)^{-s}$ with $x = \varrho'/\varrho$. Then use $\varrho \le 1 \le s$. (c) We have $m \le f \le \|f\|_{L^\infty} \le M$. Put $h = 1 - f/M$. Then $0 \le h \le 1 - m/M$ and $\|h\|_{\mathcal{G}_\varrho} \le 2$. By (b), $\|h\|_{\mathcal{G}_{\varrho'}} \le 1 - m/(2M)$. So $1/f = M^{-1}\sum_{n\ge 0} h^n$ converges in $\mathcal{G}_{\varrho'}$, with norm at most $2/m$. (d) Differentiate under the integral and apply Tonelli's theorem to $\sum_k \varrho^k (k!)^{-s} \int \left\|\partial_{\hat\zeta}^k g(\sigma,\cdot)\right\|_{L^\infty} \mathrm{d}\sigma$. □

Lemma 1.22.3 (From the core coefficient norm to fixed Y). *Let $s \ge 1$, $R_0 > 0$ and $0 < \rho_0 \le 1$, and let $a_{n,k}$ be the weights of paragraph 1.6.4.3. Let $G(Y, \hat\zeta) = \sum_{n\ge 0} G_n(\hat\zeta) Y^n$, with $\left\|\partial_{\hat\zeta}^k G_n\right\|_{L^\infty(K)} \le M\, a_{n,k}$ for all $n, k \ge 0$. Let $0 < q < 1$, and put $q_1 = (1+q)/2$, $\varrho_* = \rho_0(1 - q_1^{1/s})^s$ and $c_j = \sup_{n\ge 0} n^j (q/q_1)^n$. Then for $j \ge 0$, $0 \le Y \le qR_0$, $\hat\zeta \in K$ and $k \ge 0$,*

$$|\partial_Y^j \partial_{\hat\zeta}^k G(Y, \hat\zeta)| \le M\, c_j\, (qR_0)^{-j} (1 - q_1^{1/s})^{-s}\, (k!)^s \varrho_*^{-k}. \tag{1.22.2}$$

Hence $\sup_{0\le Y\le qR_0} \left\|\partial_Y^j G(Y,\cdot)\right\|_{\mathcal{G}_\varrho} < \infty$ for every j and every $\varrho < \varrho_*$.

Proof. We have $a_{n,k} \le R_0^{-n}\rho_0^{-k}(k!)^s\binom{n+k}{k}^s$. The series may be differentiated termwise, so $|\partial_Y^j\partial_{\hat\zeta}^k G| \le \sum_{n\ge j} n^j|\partial_{\hat\zeta}^k G_n|(qR_0)^{n-j} \le M(qR_0)^{-j}\rho_0^{-k}(k!)^s\sum_n n^j q^n\binom{n+k}{k}^s$. Next, $n^jq^n \le c_j q_1^n$. Since $\sum a_n^s \le (\sum a_n)^s$ for $a_n \ge 0$ and $s \ge 1$, $\sum_n\binom{n+k}{k}^s x^n \le \big(\sum_n\binom{n+k}{k}x^{n/s}\big)^s = (1-x^{1/s})^{-s(k+1)}$ for $0 \le x < 1$. This gives (1.22.2). Summing it against $\varrho^k(k!)^{-s}$ gives the last claim. □

Proposition 1.22.4 (Hypothesis 1.22.1 holds)**.** *Let the forward core (Φ, w) be the fixed point of paragraph 1.6.4.3 on the angular interval K' of N8, with $U \subset \operatorname{int} K'$. Use the Gevrey-3/2 data chosen in that paragraph and assume (1.22.1). Then there is $\varrho_1 > 0$ such that $\big(\frac{\hat\xi_a^2}{2}\big)^{\pm1} \in \mathcal{G}_{\varrho_1}$ and, for every $j \ge 0$,*

$$\sup_{0\le\varpi\le\Xi}\big\|\partial_\varpi^j G^\natural(\varpi,\cdot)\big\|_{\mathcal{G}_{\varrho_1}} < \infty \qquad (G = F_0, U_0, w_0, P_0).$$

In particular Hypothesis 1.22.1 holds, with one radius for all j.

Proof. The coefficient norm of paragraph 1.6.4.3 is the weighted supremum of Definition 1.6.40, the analogue of [42, (B.4)]. Its fixed point satisfies $\big\|\partial_{\hat\zeta}^k\Phi_n\big\|_{L^\infty(K')}, \big\|\partial_{\hat\zeta}^k w_n\big\|_{L^\infty(K')} \le M_B a_{n,k}$ for all n, k (Proposition 1.6.42(i), with $\Lambda \ge \Lambda_{\mathrm{core}}$ and $C \ge C_{\mathrm{core}}(\Lambda)$). So Lemma 1.22.3 applies to Φ and w with $M = M_B$, and we take $q = 4.1/R_0 < 1$.

Data. By the Gevrey choices of the core construction and N8, the functions b, s_0, u, a', ψ', p_0 and L are Gevrey-3/2 on $\mathcal{N}$, and $b, s_0, L > 0$. By Lemma 1.22.2(a)–(c), the functions $b^{\pm1}$, $\big(\frac{\hat\xi_a^2}{2}\big)^{\pm1} = (\Lambda b/4)^{\mp1}$, $\nu = -b'/b$, L^{-1}, u, p_0 and $g = C^{-1}e^{\Lambda\psi+a}$ lie in $\mathcal{G}_\varrho(U)$ for some $\varrho > 0$.

The radius. Since $\frac{\hat\xi_a^2}{2} = 4/(\Lambda b)$, we have $Y = \Lambda b\frac{\hat\xi^2}{2} = 4\varpi$ on the whole rectangle. Let $y = \log\varpi \le \log\Xi \le t_{\mathrm{act}}$ by (1.22.1). Here $t_{\mathrm{act}} = t_1 \le \bar t$, with $4e^{2\bar t} < 4.1$ (the choice of $\bar t$ in the paragraph before Lemma 1.20.34), by Remark 1.8.12(d). So every value of Φ, w used below is taken at $Y \le 4e^{t_{\mathrm{act}}} < 4.1 = qR_0$. There $\Phi \ge c_\Phi = 0.15$ (Corollary 1.6.43(a)). By Lemma 1.22.3 and Lemma 1.22.2(c), the functions $\partial_Y^j\Phi$, $\partial_Y^j w$ and $\partial_Y^j(1/\Phi)$ are bounded in $\mathcal{G}_\varrho$ uniformly for $Y \le 4.1$, for every j and one $\varrho > 0$.

Core, $\varpi \le 1$. Here the activation factor e vanishes, and the leading data are the core: $F_0^\natural = g\,\Phi(4\varpi,\hat\zeta)$ and $U_0^\natural = u + \Lambda^{-1}w(4\varpi,\hat\zeta)$. Also $\partial_\varpi^j = 4^j\partial_Y^j$.

First collar, $1 \le \varpi \le \Xi$. For $0 \le y \le t_{\mathrm{act}}$, Definition 1.20.22 gives $\vartheta(y) = y$ (because $g(s) = s$ for $s \le 1$). It also gives $\beta = 1$ (because $y_1 \ge y_e = y_*/4 \ge 2t_{\mathrm{act}}$) and interpolation 0 (because $y_l + \omega_0 > t_{\mathrm{act}}$). So the prescriptions are $(\log F)_y = -\frac12\kappa p_{1,r}$ and $U_y = -\frac12\kappa\frac{\hat\xi^2}{2}n_{s,r}$, with $\kappa(y) = 1 - (1-\kappa_{\mathrm{act}})\sigma(y/t_{\mathrm{act}})$ and the reference values at $Y = 4e^y$. We have $p_{1,r} = -2Y\Phi_Y/\Phi$, and $\frac{\hat\xi^2}{2}n_{s,r} = -\hat\xi_a^2 be^y w_Y = -(8/\Lambda)e^y w_Y$. Hence

$$F_0^\natural = g\,\Phi(4,\hat\zeta)\exp\int_0^y \kappa(s)\frac{4e^s\Phi_Y}{\Phi}(4e^s,\hat\zeta)\,\mathrm{d}s, \qquad U_0^\natural = u + \frac{w(4,\hat\zeta)}{\Lambda} + \frac{4}{\Lambda}\int_0^y \kappa(s)e^s w_Y(4e^s,\hat\zeta)\,\mathrm{d}s.$$

By Lemma 1.22.2(a),(d), both lie in $\mathcal{G}_\varrho$ uniformly in $\varpi \in [1,\Xi]$. We have $\partial_\varpi = e^{-y}\partial_y$, so each ∂_ϖ^j of these expressions is a finite sum of products of the following factors: derivatives of κ (bounded functions of y alone, for the fixed member); powers of $e^{\pm y}$; and Y-derivatives of Φ, w, $1/\Phi$ at $Y = 4e^y$, together with the exponential factor. The same bounds apply. Since $\kappa - 1$ is flat at $y = 0$, and the prescriptions with $\kappa = 1$ reproduce the core, the two representations agree to infinite order at $\varpi = 1$.

w_0 and P_0. Here $V_0 = (2\hat\zeta\frac{\hat\xi^2}{2}U_0 - (1-2h)\hat\zeta\mathfrak{M}_1 - d\mathfrak{M}_{1\hat\zeta})/L$ with $\mathfrak{M}_1 = \int_0^{\frac{\hat\xi^2}{2}} U_0$. At fixed ξ, $\partial_\eta|_\xi = \partial_\eta|_\varpi - 2(\xi_a'/\xi_a)\varpi\partial_\varpi$. Substituting $s = \varpi u$ in the radial average gives

$$w_0^\natural = (V_0/\tfrac{\hat\xi^2}{2})^\natural = L^{-1}\big[2\hat\zeta U_0^\natural - (1-2h)\hat\zeta\mathscr{A}^\natural U_0^\natural - d\big(\mathscr{A}^\natural\partial_{\hat\zeta}U_0^\natural - \nu(U_0^\natural - \mathscr{A}^\natural U_0^\natural)\big)\big],$$

and $P_0^\natural = p_0 + \frac{\hat\xi_a^2}{2}\mathscr{P}^\natural((F_0^\natural)^2)$, because $H^2/(4\frac{\hat\xi^4}{4}) = F^2$. We have $\partial_\varpi^j \mathscr{A}^\natural G = \int_0^1 t^j(\partial_\varpi^j G)(t\varpi,\cdot)\,\mathrm{d}t$ and $\partial_\varpi \mathscr{P}^\natural G = G$. Lemma 1.22.2(a),(b), with one radius loss for $\partial_{\hat\zeta}$, gives the bounds at a smaller radius ϱ_1.

Finally, $\{\varpi \le \Xi\}$ ends in the buffered activation collar by (1.22.1) and Lemma 1.21.1. The loop starts beyond ξ_{an}, the five-moment and pressure corrections are in their reserved slots (Lemma 1.20.49), and the spectral interval comes after the returned pulse (Section 1.32). Their supports are disjoint from this rectangle. □

Remark 1.22.5. For a larger rectangle, $e^{t_{\mathrm{act}}} < \Xi < \Xi_{\mathrm{buf}}$, the same proof applies. It uses ϑ and the interpolation (functions of y alone) and the termination $\beta = 1 - \sigma((y - y_1(\hat\zeta))/\omega_0)$. The last needs Gevrey composition with $y_1 \in G^{3/2}$ (Remark 1.20.30(4)). Proposition 1.22.7 needs $\Xi \le e^{t_{\mathrm{act}}}$.

1.22.1 Order-zero compatibility on the collars

Lemma 1.22.6 (The forward core is the transported backward core on the collars)**.** *Assume (B1). Then for* $0 \le Y = \Lambda\frac{\hat\xi_b^2}{2} \le 4.1$ *the backward core is the profile* $\phi = \phi_*\Phi_b$, $U = U_* + \Lambda^{-1}u_b$, $\Pi = \Pi_0 + \int_0^{\frac{\hat\xi^2}{2}} \phi^2/C^2$ *of Lemma 1.20.33. It has* $\Phi_b(0,\cdot) = 1$ *and* $u_b(0,\cdot) = 0$*, and it is analytic in* $(Y,\hat\zeta)$ *on a common complex neighbourhood of* $[0,4.1]\times I$*, for an interval* $I \supset [-1,1]$*. Both facts are part of Lemma 1.20.33(b); no bound of the backward core uniform in* Λ *is used. Let the forward core data on the endpoint collars be the slice continuations of paragraph 1.6.4.3 and Lemma 1.6.38:*

$$b = \lambda_{\mathrm{ch}},\quad s_0 = \sigma_*\lambda_{\mathrm{ch}}^{h-\frac12},\quad u = \lambda_{\mathrm{ch}}^{\frac12+h}U_*\circ\varphi,\quad p_0 = \lambda_{\mathrm{ch}}^{1+2h}\,\Pi_0\circ\varphi,\quad g = \lambda_{\mathrm{ch}}^{1+h}\,(\phi_*/C)\circ\varphi,$$

with $\varphi = \lambda_{\mathrm{ch}}^{\frac12-h}\hat\zeta$*. Fix* $\epsilon' > 0$ *so small that* $K_+ = [1, 1+\epsilon']$ *lies in the collar and* $\varphi(K_+) \subset [-1,1]$*, and define* K_- *at* -1 *in the same way. Then there is* Λ_J*, independent of* C*, such that for* $\Lambda \ge \Lambda_J$ *and* $C \ge C_{\mathrm{core}}(\Lambda)$

$$\Phi(Y,\hat\zeta) = \Phi_b(Y,\varphi(\hat\zeta)),\qquad w(Y,\hat\zeta) = \lambda_{\mathrm{ch}}(\hat\zeta)^{\frac12+h}\,u_b(Y,\varphi(\hat\zeta))\qquad (0\le Y\le 4.1,\ \hat\zeta\in K_\pm).$$

Proof. We treat K_+. *Step 1: covariance.* The backward core (F_b,U_b,P_b) solves the $\varsigma=-1$ stress-free leading system on $\{\Lambda\frac{\hat\xi_b^2}{2}\le 4.1\}$, with axis pressure Π_0. Its slice continuation, with the weights $1+h$, $(\frac12+h)$ and $2(\frac12+h)$ of F, U and P, is $\tau(F_b,U_b,P_b) = (\lambda_{\mathrm{ch}}^{1+h}F_b, \lambda_{\mathrm{ch}}^{\frac12+h}U_b, \lambda_{\mathrm{ch}}^{1+2h}P_b)\circ\Phi$, with Φ the chart change in (1.6.16). It solves the $\varsigma=+1$ system on $\{\Lambda\lambda_{\mathrm{ch}}\frac{\hat\xi^2}{2}\le 4.1,\ \hat\zeta\in K_+\}$ by covariance of the physical equation. The truncated physical fields coincide, so their residuals coincide. The coefficients of the distinct q-powers then correspond, and the leading rows are the coefficients of the lowest power. The radial primitive in P transports because $\frac{\hat\xi_b^2}{2} = \lambda_{\mathrm{ch}}\frac{\hat\xi^2}{2}$ at fixed $\hat\zeta$, and $(1+2h) = 1+2h$.

Step 2: the fixed-point form. On the collar, $Y = \Lambda b\frac{\hat\xi^2}{2} = \Lambda\frac{\hat\xi_b^2}{2}$. By the data identities, $\tau F_b = g\,\Phi^{\mathrm{tr}}$, $\tau U_b = u + \Lambda^{-1}w^{\mathrm{tr}}$ and $\tau P_b(0,\cdot) = p_0$, where $\Phi^{\mathrm{tr}} = \Phi_b(Y,\varphi(\hat\zeta))$ and $w^{\mathrm{tr}} = \lambda_{\mathrm{ch}}^{\frac12+h}u_b(Y,\varphi(\hat\zeta))$. The rescaled equations of paragraph 1.6.4.3 are an exact rewriting of the leading system in these variables. So $(\Phi^{\mathrm{tr}},w^{\mathrm{tr}})$ solves them, with $\Phi^{\mathrm{tr}}(0,\cdot)=1$ and $w^{\mathrm{tr}}(0,\cdot)=0$. These functions are analytic in Y. Among such functions with zero axis value, J_ν is the only inverse of $Y\partial_{YY} + \nu\partial_Y$: the other homogeneous solutions are constants, $\log Y$ or $Y^{1-\nu}$. Hence $(\Phi^{\mathrm{tr}},w^{\mathrm{tr}})$ is a fixed point of the forward map $\mathcal{T}_+$, which is the map of paragraph 1.6.4.3 with all angular norms taken over K_+. This map is local in $\hat\zeta$: it is built from products, $\partial_{\hat\zeta}$, $\mathcal{A}_Y$, J_ν and $\int_0^Y$.

Step 3: uniqueness of the Taylor coefficients. For each $\hat\zeta \in K_+$ both pairs are analytic in Y near $[0, 4.1]$. The forward fixed point is analytic on $|Y| < R_0$, $R_0 > 4.1$, because its coefficient norm is finite. The transported pair is analytic because the backward core is analytic on a common complex neighbourhood of $[0, 4.1] \times I$ (Lemma 1.20.33(b)) and $\varphi(K_+) \subset [-1, 1]$. Expand $\Phi = \sum_n \Phi_n Y^n$ and $w = \sum_n w_n Y^n$, with coefficients smooth in $\hat\zeta \in K_+$, and do the same for $(\Phi^{\mathrm{tr}}, w^{\mathrm{tr}})$. On coefficients, the operations in B_1, B_2 act as follows: products are convolutions, $\partial_{\hat\zeta}$ and $\mathcal{T}$ act coefficientwise (with D_Y inside $\mathcal{T}$), D_Y multiplies the degree-n coefficient by n, $\mathcal{A}_Y$ divides it by $n+1$, and $\mathcal{Q} = \int_0^Y g^2\Phi^2$ and $Yg^2\Phi^2$ raise the degree by one. So the degree-n coefficients $[B_1]_n$, $[B_2]_n$ depend only on Φ_m, w_m with $m \le n$, their $\hat\zeta$-derivatives and the data. The rescaled equations of paragraph 1.6.4.3, taken coefficient by coefficient, are

$$2(n+1)(n+2)\Phi_{n+1} = -\chi\Phi_n + \delta[B_1/L]_n, \qquad 2(n+1)^2 w_{n+1} = [Z/(Lb)]\,\mathbf{1}_{n=0} + \delta[B_2/(Lb)]_n,$$

with $\Phi_0 = 1$ and $w_0 = 0$. Both pairs satisfy them (Step 2). By induction on n they have the same coefficients, so they agree near $Y = 0$, and by analyticity on all of $[0, 4.1]$. This step uses only the analyticity of the backward core (Lemma 1.20.33(b)). It does not use the coefficient ball of that proof, nor any bound of the backward core that is uniform in Λ. So $\Lambda_J := \Lambda_{\mathrm{core}}$, the threshold of the forward contraction (Proposition 1.6.42, which also needs $C \ge C_{\mathrm{core}}(\Lambda)$ and gives C-independent constants), and the bound $R_0 < 10$ is not needed. □

Proposition 1.22.7 (Order-zero slice jets on the inner rectangle)**.** *Assume (B1) and (1.22.1) (in particular $\Xi \le e^{t_{\mathrm{act}}}$), $4 < Y_{\mathrm{buf}} \le 4.1 < R_0 < 10$, $\Lambda \ge \Lambda_J$ and $C \ge C_{\mathrm{core}}(\Lambda)$ (both needed by Lemma 1.22.6). Assume also that the two members use the step σ from the flat-step definition in Section 1.4, with $\kappa_{\mathrm{act}} = \kappa_0$ and $t_{\mathrm{act}} = t_1$ (Remark 1.8.12(d)). Then on $\{\frac{\hat\xi_b^2}{2} \le \frac{(\hat\xi_a^0)^2}{2}\Xi\}$, for $\hat\zeta \in K_\pm$, the forward leading data (F_0, U_0, w_0, P_0) are the slice continuations of the backward ones. These are the order-zero slice jets on the common protected rectangle.*

Proof. We treat K_+. The variable $y_a = \log\varpi$ is one slice function, because $\varpi_f = \varpi_b$ by (1.6.16) and the transported activation radius. On $\varpi \le 1$ the claim for F_0 and U_0 is Lemma 1.22.6. On $1 \le \varpi \le \Xi \le e^{t_1}$ the forward data are given by the first-collar formulas in the proof of Proposition 1.22.4. By (B1), the backward data there are given by (1.20.14). On $0 < y < t_1$ the reference is the analytic axis profile by (1.20.13), and

$$e_a = (1-\kappa_0)\sigma(y/t_1), \quad \kappa = 1 - e_a, \quad \partial_y \log\phi = -\kappa p_{1,r}/2, \quad \tfrac12\hat\xi\partial_{\hat\xi}U = -\kappa\tfrac{\hat\xi^2}{2}n_{s,r}/2.$$

For this stress-free reference, $p_{1,r} = -\hat\xi^2\hat\xi^{-1}\partial_{\hat\xi}\log\phi$ and $n_{s,r} = -2\hat\xi^{-1}\partial_{\hat\xi}U$. So the two sides use the same formulas with the same $\kappa(y)$. Their reference coefficients $p_{1,r}$ and $\frac{\hat\xi^2}{2}n_{s,r}$ transport with weights 0 and $(\frac12 + h)$, by Lemma 1.22.6. The chart factors $\lambda_{\mathrm{ch}}^{1+h}$ of F and $\lambda_{\mathrm{ch}}^{\frac12+h}$ of U do not depend on y. Hence the forward fields and the transported backward fields solve the same linear ODE in y, with the same value at $y = 0$, and so they coincide. The leading radial velocity V_0 is defined by the divergence formula on an open angular set, and this formula is covariant: V_0 has weight 0, and the change of radial variable in (1.6.4) transports its axis integral. So $w_0 = V_0/\frac{\hat\xi^2}{2}$ transports with weight 1. For the pressure, $P_0 = p_0 + \int_0^{\frac{\hat\xi^2}{2}} F_0^2$, with $p_0 = \lambda_{\mathrm{ch}}^{1+2h}\Pi_0 \circ \varphi$ on the collar, and $\int_0^{\frac{\hat\xi^2}{2}} \lambda_{\mathrm{ch}}^{2+2h} F_{0,b}(\lambda_{\mathrm{ch}}x, \varphi)^2\,\mathrm{d}x = \lambda_{\mathrm{ch}}^{1+2h}\int_0^{\frac{\hat\xi_b^2}{2}} F_{0,b}^2$. Thus $\ell_f = \tau\ell_b$ on $\{\varpi \le \Xi\} \times K_+$, which is the backward side $t \le 0$ of the slice. The forward data are C^∞ across $\hat\zeta = 1$ (Proposition 1.22.4 and N8). So in slice variables $\widetilde g_f$ is smooth near $\widetilde\eta = 0$ and equals $\widetilde g_b$ for $\widetilde\eta \le 0$. Their one-sided $\widetilde\eta$-derivatives at 0 therefore agree, which is Definition 1.6.5. □

Remark 1.22.8 (The shared activation design). The backward member uses Definition 1.20.35: the analytic core and the first collar $0 \le y_a \le t_1$ agree with the forward design by Proposition 1.22.7, and after t_1 both sides use the transported frozen strains and shared termination controls. Theorem 1.20.36, Proposition 1.20.38 and Lemma 1.20.41 supply the backward cone and continuation bounds for this choice. Proposition 1.20.43 gives the endpoint compatibility stated below. The analytic rectangle of the backward core lies in $y_a \le t_1$ and is unaffected by the later continuation.

Hypothesis 1.22.9 (One activation design on the endpoint collars). On endpoint neighbourhoods of $\hat\zeta = \pm 1$, the forward leading data on the activation collar $y_a \ge t_{\mathrm{act}}$ (through the termination and interpolation) have equal slice jets with the backward ones.

1.22.2 Termination and interpolation on the endpoint collars

Lemma 1.22.10 (Covariance through the two transitions)**.** *The activations of Definitions 1.20.22 and 1.20.35 have matching slice jets through termination and interpolation.*

Proof. Write $\ell = \lambda_{\mathrm{ch}}(\hat\zeta_f)$ and $\beta = \varphi(\hat\zeta_f)$ for the chart change. On the endpoint collars $\frac{\hat\xi_b^2}{2} = \ell\frac{\hat\xi_f^2}{2}$ and $\frac{\hat\xi_{a,b}^2}{2} = \ell\frac{\hat\xi_{a,f}^2}{2}$, so $y = 2\log(\hat\xi_f/\hat\xi_{a,f}) = 2\log(\hat\xi_b/\hat\xi_{a,b})$ is invariant. The identities of Lemma 1.22.6 give $F_f = \ell^{1+h}F_b$ and $U_f = \ell^{\frac12+h}U_b$ in these coordinates. Since ℓ is independent of y, the reference strains $p_1 = -2\partial_y \log F$ and $n_s = -2\hat\xi^{-1}\partial_{\hat\xi}U$ transform with weights 0 and $(\frac12 + h) + 1$. Evaluation at the shared frozen coordinate $\vartheta(y)$ preserves these identities. In particular, at the current radius, $\frac{\hat\xi_f^2}{2}n_f^\flat = \ell^{\frac12+h}\frac{\hat\xi_b^2}{2}n_b^\flat$.

On endpoint neighborhoods, $|Z_R|, |Z_*| \ge \delta_e \ge \delta_Z$ by (I6) and Lemma 1.20.42. Thus $\Upsilon = \Upsilon^b = 1$ there and the common termination function is

$$b(y) = 1 - \sigma((y - y_l)/\omega_0),$$

and both interpolation functions are exactly $a(y) = \sigma((y - y_l - \omega_0)/\omega_2)$. The parameters y_l, ω_0, ω_2, the freeze ϑ and κ are shared by the two definitions. Thus both sides satisfy throughout both transitions

$$(\log F)_y = -\tfrac12[(1-a)\kappa p_1^\flat + 0.8a], \qquad U_y = -\tfrac12\kappa b\tfrac{\hat\xi^2}{2}n^\flat.$$

The first equation preserves the factor ℓ^{1+h}, and the second preserves $\ell^{\frac12+h}$. Integration from the already matched core inlet proves equality of the transported solutions through the entire interval, including where $b = 0$ and where $a = 1$. Differentiation in the angular parameter gives all endpoint jets. The axis-normalized primitives and pressure are then transported by the radial integral formulas in slice variables. □

1.23 The actual aggregate weight

We next specify a weight on the actual stress support. It is a sum of finitely many component weights, not a distance to an enclosing shell. At the selected inner edge use the actual shear activation, not the additive scalar example (1.12.5). For the fixed member put

$$y = 2\log(\hat\xi/\hat\xi_a(\hat\zeta)), \quad e = (1 - \kappa_{\mathrm{act}})\sigma(y/t_{\mathrm{act}}), \quad \kappa = 1 - e.$$

Here σ is the shared squared-flat step selected jointly for this existential construction. It does not replace an arbitrary previously fixed activation profile. Near zero, scaling gives a positive smooth

factor times $\exp(-t_{\mathrm{act}}^2/y^2)$. The actual prescriptions and factored stress are

$$\begin{aligned} U_y &= -\kappa \tfrac{\hat{\xi}^2}{2} n_{s,r}/2, \qquad (\log F)_y = -\kappa p_{1,r}/2, \\ T_0 &= eB, \qquad B(0,\hat{\zeta}) = F_a(\hat{\zeta}) p_r(0,\hat{\zeta}), \quad B_\theta(0,\hat{\zeta}) > 0. \end{aligned} \tag{1.23.1}$$

The last factorization and its continuous nonzero edge value are those of the selected curved-entry theorem. On the first collar $0 < y \le t_{\mathrm{act}}$ these are the prescriptions of Definition 1.20.22: there $\vartheta(y) = y$, $\beta = 1$ and the interpolation vanishes. After the collar the activation continues by (M0)+(M1) of that definition.

On a sufficiently small collar set

$$w_{\mathrm{in}} = c_{\mathrm{in}} e(y) \quad (y > 0), \qquad w_{\mathrm{in}} = 0 \quad (y \le 0). \tag{1.23.2}$$

We select c_{in} small. For memberwise positive constants,

$$c w_{\mathrm{in}} \le T_{0,\theta} \le C w_{\mathrm{in}}, \qquad |T_{0,z}| \le C w_{\mathrm{in}}, \qquad |T_0| \ge c w_{\mathrm{in}}. \tag{1.23.3}$$

In general $T_{0,z}/T_{0,\theta} \to p_{2,r}/p_{1,r}$, not zero.

We do not claim quadratic axial suppression or extra y^3 factor.

To verify all specified jets rather than only smoothness, the exact prescribed differences on this collar are

$$U - U_r = \int_0^y e(s) \tfrac{\hat{\xi}^2}{2}(s) n_{s,r}(s)/2 \, \mathrm{d}s, \qquad \log F - \log F_r = \int_0^y e(s) p_{1,r}(s)/2 \, \mathrm{d}s.$$

$C_j e y^{-N_j}$ bounds each fixed derivative of e. Because e increases, $\int_0^y e \le y e(y)$. We differentiate these identities, exponentiate, and integrate the genuine history densities.

These operations give the same e times inverse-power bounds for all fixed mixed difference jets. For fixed $\hat{\xi}$, we use $\partial_{\hat{\zeta}}|_{\hat{\xi}} = \partial_{\hat{\zeta}}|_y - (\log \frac{\hat{\xi}^2}{2})' \partial_y$. The integrated stress is a finite algebraic expression in these quantities, with nonzero denominators on the collar. We subtract the zero core stress to get

$$|D^j w_{\mathrm{in}}| + |D^j T_0| \le C_j w_{\mathrm{in}} [1 + \log(1/w_{\mathrm{in}})]^{N_j}.$$

Here $y^{-1} \le C[1 + \log(1/e)]^{1/2}$. Constants may depend on the fixed activation width. Division by e gives conormal bounds for B. The actual factorization gives its bounded value and positive limit.

The rough derivative estimate does not give these conclusions. Thus direction jets are logarithmically bounded and each positive fractional power has flat zero-extension jets on this smooth curved edge. The true strict collar gives the normalized cone margins. A small-axial-direction test does not replace these margins.

For the outer part use the explicit scalar lift and wing of the heat construction. We denote its fixed width by ℓ_b, its positive amplitude by α_o, its radial boundary by $\mathcal{B}_o(\hat{\zeta})$, and its angular cutoff by ψ_o. We write

$$y_o = \frac{\mathcal{B}_o(\hat{\zeta}) - \frac{\hat{\xi}^2}{2}}{\ell_b}, \qquad f_o(y) = e^{-1/y^2} \ (y > 0), \qquad \mathcal{F}(y) = \int_0^y f_o(s) \, \mathrm{d}s,$$

with zero extensions. Here $\mathcal{F}$ is only a scalar wing primitive, distinct from the coefficient F_0.

If τ_s is the nonnegative compact scalar shooting source, the local edge factors are

$$w_L = d^{-h-1} \tau_s(\tfrac{\hat{\xi}^2}{2}/d), \qquad w_1 = \psi_o \alpha_o \ell_b f_o(y_o), \qquad w_2 = \hat{\zeta} \psi_o' \alpha_o \ell_b^2 \mathcal{F}(y_o)/\tfrac{\hat{\xi}^2}{2}. \tag{1.23.4}$$

For the scalar source choices, we take $\vartheta(s) = e^{-1/s^2}$ for $s > 0$, zero in all other cases, and

$$\psi_s(s) = c_s \vartheta(s - 1/4)\vartheta(3/4 - s), \qquad \int \psi_s = 1.$$

We select χ_s by the normalized squared-flat step decreasing from one to zero on $(1/4, 1/2)$.

These choices satisfy the shooting construction and make ψ_s decreasing for $s > 1/2$. The lift source is identically zero near $\hat{\zeta} = \pm 1$ on this fixed outer hull, so its written powers of d cause no endpoint singularity. Beyond the bridge the component lower estimate gives $T_{\theta,c} \geq c(w_L + w_1 + w_2)$. The mixed derivatives of both stresses for the selected mixture are estimated in Lemma 1.23.8a.

The aggregate weight. On the forward chart use Definition 1.23.6. Every channel has the common rising factor $e(y_a)$, an angular multiplier and a nonincreasing radial factor. Its comparison with the actual stress uses Propositions 1.20.59 and 1.20.62 and Corollary 1.20.63. The inputs (J1)–(J9) are listed in Section 1.20.1. Throughout $d = 1 - \eta^2$, $L = 1 - 2h\eta^2$ and $0 < h < 10^{-2}$. Constants may depend on the selected member. In either native chart write

$$y_a = \log \frac{\frac{\hat{\xi}^2}{2}}{\frac{\left(\hat{\xi}_a(\hat{\zeta})\right)^2}{2}}, \qquad y_p = \log \frac{\frac{\hat{\xi}^2}{2}}{\frac{\left(\hat{\xi}_p(\hat{\zeta})\right)^2}{2}}.$$

The activation and pulse-entry graphs are smooth and positive on each native interval. Their change of coordinates, hence equality of the logarithmic arguments under pullback, holds on the endpoint collars (Lemma 1.21.1 and (1.6.16)). The forward center has its own geometry. The backward construction in Section 1.24.3 uses its native pulse outlet, one pressure rectangle and a scalar weight.

Radial order on a forward fiber. For each forward η, in increasing $X = \xi^2/2$,

(O1) the protected core, where $T_0 \equiv 0$ ($y_a \leq 0$);

(O2) the activation collar $0 < y_a \leq y_{\mathrm{col}}$, with $T_0 = e\mathcal{B}$ (J2) of Section 1.20.1;

(O3) the loop domain Y_{sh}, containing every relaxed point [Section 1.19];

(O4) the restoration reserve inside $-25 < y_p < -20$ [Section 1.13, Section 1.19];

(O5) the heat-compensation (three-E) bumps, ending before $y_p = -15$ [Section 1.13, Lemma 1.15.9];

(O6) the start of the saturation tube K_0 at $y_p = -14.5$; the positive-velocity slot $(-14, -9)$; the protected mean slot $\Sigma := \{-8 \leq y_p \leq -3\}$ [(1.13.83), Proposition 1.24.2];

(O7) the pulse ($y_p = 0$), its returns ending before $y_p = Y(\hat{\zeta}) - 0.7$, and the end $R_o e^{-0.5}$ of K_0 ($y_p = Y - 0.5$) [Proposition 1.24.2];

(O8) the outer future of the returned pulse, with the pure-swirl formula off the final spectral edit hull: central hold (with the spectral support inside K_{ext}, outlet R_+), deficit drive, shot/blend J, lift and wing, and the outer (wing) component with its terminal edge B [Lemma 1.17.4, Lemma 1.17.5, Lemma 1.17.6, Lemma 1.13.4].

Here $Y(\hat{\zeta}) = \log(R_o / \frac{\left(\hat{\xi}_p(\hat{\zeta})\right)^2}{2})$ by (1.25.5). The activation collar precedes Y_{sh} (scalar example: collar to $\frac{\hat{\xi}_e^2}{2} + 8\ell$, loop after $\frac{\hat{\xi}_e^2}{2} + 5\ell$, [Proposition 1.12.2, Section 1.12, Section 1.19]). In particular

$$\frac{\left(\hat{\xi}_a(\hat{\zeta})\right)^2}{2} e^{t_{\mathrm{act}}} < \frac{\left(\hat{\xi}_p(\hat{\zeta})\right)^2}{2} e^{-25} \qquad (\hat{\zeta} \in [-1, 1]). \tag{1.23.5}$$

The inner estimate is used up to y_{col}, and the rising factor is constant from t_{act} onwards. On a compact middle interval with $y_a \geq y_{\mathrm{col}} > 0$, one has $e(y_a) \geq e(y_{\mathrm{col}}) > 0$.

Logarithmic calculus. Write $\phi_N(u) = u(1+\log(1/u))^N$ and, for any positive function w, $L_w = 1+\log_+(1/w) = 1+\max\{0, \log(1/w)\}$. For $w \leq 1$ this is $1+\log(1/w)$. In general $L_w \geq 1$, and the proofs below use only this. (For a sum of several channels, which can exceed 1, the unmodified $1+\log(1/w)$ can be negative.)

Lemma 1.23.1. *Let $N \geq 0$ and $C \geq 1$. Write $K_N^* = \sup_{v\geq 0} e^{-v}(1+v)^N$, so $K_N^* = 1$ for $0 \leq N \leq 1$ and $K_N^* = N^N e^{1-N}$ for $N > 1$.*

(a) If $0 < w \leq e^{-2}$ and $0 < u \leq \min(Cw, e^{-2})$, then $\phi_N(u) \leq \max(C, K_N^*)\phi_N(w)$.

(b) If $0 < w_i \leq \mathsf{W}$, then $w_i L_{w_i}^N \leq K_N^* \, \mathsf{W} L_{\mathsf{W}}^N$, where $L_{\mathsf{W}} = 1+\log_+(1/\mathsf{W})$.

(c) If $f_1, \dots, f_k \in (0,1]$ satisfy $|D^j f_\ell| \leq C_j f_\ell L_{f_\ell}^{N_j}$, then $f = \prod f_\ell$ and $g = \sum f_\ell$ satisfy the same type of bound with L_f resp. L_g, with new constants.

(d) If $w \geq 0$ is continuous and smooth on its positivity set and satisfies $|D^j w| \leq C_j w L_w^{N_j}$ $(j \leq k)$, then $|D^j \log w| \leq C_j' L_w^{N_j'}$ and, for $\beta > 0$, w^β extends by zero to a C^k function, flat at $\{w = 0\}$.

Proof. (a) Write $u = we^{-\delta}$ with $\delta \geq -\log C$. Then $\phi_N(u) = we^{-\delta}(L_w+\delta)^N$. If $\delta < 0$, this is $\leq C\,\phi_N(w)$. If $\delta \geq 0$, $e^{-\delta}(L_w+\delta)^N \leq L_w^N \sup_{\delta\geq 0} e^{-\delta}(1+\delta)^N = L_w^N K_N^*$, using $L_w \geq 1$. Differentiation of $e^{-v}(1+v)^N$ gives the displayed value of K_N^*. (b) For $w_i = \mathsf{W}e^{-v}$, $v \geq 0$, one has $L_{w_i} \leq L_{\mathsf{W}} + v$. Thus $w_i L_{w_i}^N \leq \mathsf{W} L_{\mathsf{W}}^N e^{-v}(1+v)^N$, since $L_{\mathsf{W}} \geq 1$. (c) For products: $L_{f_\ell} \leq L_f$ because $f \leq f_\ell \leq 1$, and Leibniz. For sums: $f_\ell \leq g$ and $f_\ell L_{f_\ell}^N \leq C_N g L_g^N$ by (b). (d) Faà di Bruno for log. For w^β: every derivative is w^β times a polynomial in derivatives of $\log w$, hence $\leq Cw^\beta L_w^N \to 0$ at $\{w = 0\}$. Difference quotients give the flat extension, as in the proof of Lemma 1.23.8. □

Lemma 1.23.2 (Explicit factors)**.** *The following functions satisfy log-jet bounds on their positivity sets and have the stated monotonicity. Here $\sigma(t) = f(t)/(f(t)+f(1-t))$ and $f(t) = e^{-1/t^2}\mathbf{1}_{t>0}$* [Lemma 1.17.5].

(a) σ is nondecreasing, $\sigma' > 0$ on $(0,1)$; σ, $1-\sigma$ and σ' have log-jets. So $e(y_a)$ is nondecreasing in $\frac{\hat\xi^2}{2}$, equals $e_\infty := 1-\kappa_{\mathrm{act}}$ for $y_a \geq t_{\mathrm{act}}$, and has log-jets (also in $\hat\zeta$ at fixed $\hat\xi$, by $\partial_{\hat\zeta}|_{\hat\xi} = \partial_{\hat\zeta}|_{y_a} - (\log \frac{\hat\xi_a^2}{2})'\partial_{y_a}$).

(b) $\psi_s(s) = c_s f(s-\frac14) f(\frac34 - s)$ has $(\log\psi_s)' = \dfrac{2}{(s-1/4)^3} - \dfrac{2}{(3/4-s)^3}$, which is < 0 for $s \in (\frac12, \frac34)$. So $w_L(\cdot, \hat\zeta)$ is decreasing on $\frac{\hat\xi^2}{2}/d \in (R_b + \frac12 W_s, R_b + \frac34 W_s)$ and zero afterwards ($\chi_s = 0$ for $s \geq \frac12$).

(c) w_1 and w_2 are nonincreasing in $\frac{\hat\xi^2}{2}$ on $\frac{\hat\xi^2}{2} \leq \mathcal{B}_o(\hat\zeta)$ and vanish after, since $f_o = \mathcal{F}'$ and $\mathcal{F}$ increase in y_o and $1/\frac{\hat\xi^2}{2}$ decreases. Also $\hat\zeta\psi_o' \geq 0$.

(d) Ψ is nonincreasing. Where $\frac{V_{\hat\xi}}{\hat\xi} \leq 0$ [proof of Lemma 1.17.5]*, V, E_w, $v_g = E_w/\frac{\hat\xi^2}{2}$ and $v_s = V + E_w/\frac{\hat\xi^2}{2}$ are nonincreasing in $\frac{\hat\xi^2}{2}$.*

(e) $c\,y^3 f(y) \le \mathcal{F}(y) \le \min(yf(y),\, Cy^3 f(y))$ *for* $0 < y \le y_1$, *and* $\mathcal{F} \le yf$ *for all* $y > 0$. *So* $\mathcal{F}(y_o)$ *has log-jets.*

Proof. (a) Direct differentiation gives

$$\sigma' = 2(t^{-3} + (1-t)^{-3})\frac{e^g}{(1+e^g)^2}, \qquad g = t^{-2} - (1-t)^{-2}.$$

Near 0, $\sigma \asymp e^{-1/t^2}$ and every derivative divided by σ has at most a fixed inverse power of t; since $L_\sigma \asymp t^{-2}$, this gives the log-jet bounds. The other endpoint and $1-\sigma, \sigma'$ are treated identically, using $L_w = 1 + \log_+(1/w)$.

(b) The derivative of the displayed logarithmic slope is $-6(s-\frac{1}{4})^{-4} - 6(\frac{3}{4}-s)^{-4} < 0$, and the slope vanishes at $s = 1/2$. This proves the claimed sign. Parts (c)–(d) follow from the stated monotonicities and $V \ge 0$.

(e) Monotonicity gives $\mathcal{F}(y) \le yf(y)$. Since $f' = 2y^{-3}f$, l'Hopital's rule gives $\mathcal{F}(y)/(y^3 f(y)) \to 1/2$ at zero. The two-sided bound follows near zero and then on each fixed compact positive interval. Differentiating $\mathcal{F}' = f$ gives its log-jets. □

Channel data and the definition of W.

Definition 1.23.3 (Channel datum)**.** A *channel* is a pair (α, ρ) with:

(Ch1) $\alpha : [-1,1] \to [0,1]$ smooth, with log-jets on $\{\alpha > 0\}$, and independent of $\frac{\hat\xi^2}{2}$;

(Ch2) $\rho : (0,\infty) \times [-1,1] \to [0,1]$ smooth, with log-jets on $\{\rho > 0\}$; $\rho = 1$ on $\{y_p \le -3\}$; $\frac{\hat\xi^2}{2} \mapsto \rho(\frac{\hat\xi^2}{2}, \hat\zeta)$ nonincreasing for every $\hat\zeta$; $\rho = 0$ for $\hat\xi \ge \hat\xi_W$ (a fixed finite radius);

(Ch3) (*lower compatibility*) $c_{\mathrm{ch}}\,\alpha\rho \le |T_0|$ on $\{y_a \ge y_{\mathrm{col}}\}$ for some $c_{\mathrm{ch}} > 0$.

Lemma 1.23.4 (Monotone splice)**.** *Let* $u > 0$ *be a constant. Let* $v \ge 0$ *be smooth with log-jets on* $\{v > 0\}$ *and nonincreasing in* $\frac{\hat\xi^2}{2}$ *on* $\hat\xi \ge \hat\xi_1(\hat\zeta)$. *Assume that* $v(\frac{\hat\xi^2}{2}, \hat\zeta) = 0$ *for* $\hat\xi \ge \hat\xi_W$, *with one finite* $\frac{\hat\xi_W^2}{2}$ *independent of* $\hat\zeta$ *and larger than* $\sup_{\hat\zeta} \frac{\left(\hat\xi_2(\hat\zeta)\right)^2}{2}$. *Let* $\hat\xi_1 < \hat\xi_2$ *be smooth in* $\hat\zeta$ *with* $\frac{\left(\hat\xi_1(\hat\zeta)\right)^2}{2} > \frac{\left(\hat\xi_p(\hat\zeta)\right)^2}{2} e^{-3}$. *Set* $z = \sigma((\frac{\hat\xi^2}{2} - \frac{\hat\xi_1^2}{2})/(\frac{\hat\xi_2^2}{2} - \frac{\hat\xi_1^2}{2}))$ *and* $0 < \epsilon \le u / \sup_{\frac{\hat\xi_1^2}{2} \le \frac{\hat\xi^2}{2} \le \frac{\hat\xi_2^2}{2}} v$. *Then*

$$\rho := u^{-1}\big[(1-z)u + z\epsilon v\big]$$

satisfies (Ch2), and

$$\hat\xi^{-1}\partial_{\hat\xi}\rho = u^{-1}\big[z\epsilon\frac{v_{\hat\xi}}{\hat\xi} + \frac{z_{\hat\xi}}{\hat\xi}(\epsilon v - u)\big] \le 0.$$

Moreover $\rho = 1$ *for* $\hat\xi \le \hat\xi_1$, $\rho = \epsilon v/u$ *for* $\hat\xi \ge \hat\xi_2$, *and* $\min(1, \epsilon v/u) \le \rho \le 1$.

Proof. The derivative formula is C10. $\frac{z_{\hat\xi}}{\hat\xi} \ge 0$ and $\epsilon v \le u$ on $[\frac{\hat\xi_1^2}{2}, \frac{\hat\xi_2^2}{2}]$; $\frac{v_{\hat\xi}}{\hat\xi} \le 0$ on $\hat\xi \ge \hat\xi_1$. Log-jets: $(1-z)$ and z have log-jets by Lemma 1.23.2(a); use Lemma 1.23.1(c). This holds even where v vanishes on $[\frac{\hat\xi_1^2}{2}, \frac{\hat\xi_2^2}{2}]$ (e.g. $w_1 + w_2 = 0$ for $|\hat\zeta| \le \hat\zeta_0$), since then $\rho = 1 - z$ there. □

Remark 1.23.5. In the splice $W_j = (1-z)u + z\epsilon_j v_j$ of Lemma 1.23.4 the corridor factor u is a constant. So the sign of $(\hat\xi^{-1}\partial_{\hat\xi}(W_j))$ is immediate and nothing else is needed.

Definition 1.23.6 (The aggregate weight)**.** Let $e_\infty = 1 - \kappa_{\mathrm{act}}$. On the forward side define

$$\mathsf{W}(\tfrac{\hat\xi^2}{2},\hat\zeta) = e(y_a)\sum_{i\in\mathcal{C}_*} c_i\,\alpha_i(\hat\zeta)\,\rho_i(\tfrac{\hat\xi^2}{2},\hat\zeta), \qquad w_i := c_i e(y_a)\alpha_i\rho_i, \tag{1.23.6}$$

with the following channels.

(i) *Main channel* m: $\alpha_m \equiv 1$, $\rho_m = R_0 := 1 - \sigma((y_p - Y(\hat\zeta) + \frac12)/\epsilon_0)$. This single channel takes the place of the native inner edge w_{in} of (1.23.3) and of any separate base channel on the strict prefix.

(ii) *Extension* e: $\alpha_e = a(\hat\zeta)$ (squared-flat, $= 1$ on K_1, supported in K_2), $\rho_e = R_1(\frac{\hat\xi^2}{2})$ (squared-flat, falling in the outlet buffer after R_+). Its rising factor is the common factor $e(y_a)$. A separate rising factor $L(y)$, $w_e = c_e a(\hat\zeta)L(y)R_1(\frac{\hat\xi^2}{2})$, is also admissible: its rising edge lies in $\mathscr{P}$, where Proposition 1.20.59 applies.

(iii) *Central channels* ($\alpha = 1 - \chi$). These are two splices from Lemma 1.23.4 on one fixed, $\hat\zeta$-independent interval $[\frac{\hat\xi^2_{1,c}}{2}, \frac{\hat\xi^2_{2,c}}{2}] \Subset J$: ρ_{cL} with $v = w_L$, and ρ_{cW} with $v = w_1 + w_2$. Use the same splice cutoff for both. Equivalently, this is one splice of $v = w_L + w_1 + w_2$. The hypotheses of Lemma 1.23.4 hold for every $\hat\zeta$. First, $\frac{\hat\xi^2_{1,c}}{2} > R_b$, and R_b lies in the pure-swirl future (O8), beyond $\frac{(\hat\xi_p(\hat\zeta))^2}{2}e^{-3}$. Second, for $\hat\xi \ge \hat\xi_{1,c}$ the shot argument satisfies $s = (\frac{\hat\xi^2}{2}/d - R_b)/W_s \ge (\frac{\hat\xi^2}{2} - R_b)/W_s \ge 0.52$, because $d \le 1$. There $\chi_s = 0$ and ψ_s is decreasing (Lemma 1.23.2(b)), so w_L is nonincreasing. Third, $w_1 + w_2$ is nonincreasing by Lemma 1.23.2(c). Together, $W_c := e(y_a)[c_{cL}\rho_{cL} + c_{cW}\rho_{cW}]$ is the "central hold channel".

(iv) *Outer wing channel* s: $\alpha_s = \chi$, ρ_s the splice of v_s on a compact attachment overlap $[\frac{\hat\xi^2_{1,s}}{2}, \frac{\hat\xi^2_{2,s}}{2}]$ in the pure-swirl corridor. Here $\frac{\hat\xi^2_{1,s}}{2}$ lies beyond the radius after which $\frac{V_{\hat\xi}}{\hat\xi} \le 0$ [proof of Lemma 1.17.5], so $\frac{V_{\hat\xi}}{\hat\xi} \le 0$ on all of $[\frac{\hat\xi^2_{1,s}}{2}, \infty)$, as (Ch2) requires. This is possible because the terminal lower bound $\widehat{\mathcal{T}}_{P,\theta} \ge c\,\chi v_s$ of (J9) holds, with $v_s > 0$, on that large-$\frac{\hat\xi^2}{2}$ range before B. One can take $X_{i,s} = (1 - \epsilon_i)B(\eta)$ with $0 < \epsilon_2 < \epsilon_1$ sufficiently small on $\operatorname{supp}\chi$. This compact overlap lies in the exact terminal model after the central deviations and has $\min v_s > 0$, by Lemmas 1.17.3 and 1.17.5.

(v) *Gap channel* g: put $K_g = \max\{1, \|\dot\chi\|_\infty\}$ and $\alpha_g = \dot\chi/K_g$. Take ρ_g to be the splice of v_g on the same overlap. For a coefficient $\widehat{c}_g$ of $\dot\chi\rho_g$, set $c_g = K_g\widehat{c}_g$, so the summand in (1.23.6) is $e\widehat{c}_g\dot\chi\rho_g$.

(vi) No further channel is required for the selected forward mixture. Its two components and their gap are precisely (iii)–(v).

The angular cutoffs χ of the outer mixture, ψ_o and a are normalized squared-flat steps in $|\hat\zeta|$, with χ and ψ_o nondecreasing in $|\hat\zeta|$; then $\dot\chi \ge 0$ and $\hat\zeta\psi_o' \ge 0$, and all angular factors have log-jets. The constants $c_i > 0$ are chosen last, small enough that $\mathsf{W} \le e^{-2}$. We put

$$\mathsf{W} \le e^{-2}, \qquad \mathcal{L}_W = 1 + \log(1/\mathsf{W}) \quad (\mathsf{W} > 0). \tag{1.23.7}$$

Remark 1.23.7 (The central splice lies in J). $J \Subset R_b + [0.52, 0.54]W_s$ is a set of physical $\frac{\hat\xi^2}{2}$. At $\frac{\hat\xi^2}{2} \in J$ the scalar argument of w_L is $s = (\frac{\hat\xi^2}{2}/d - R_b)/W_s \geq 0.52$ for every $\hat\zeta$, because $d \leq 1$. For $|\hat\zeta| \leq 2\hat\zeta_0$ it lies in the plateau $[\frac{1}{2}, \frac{3}{5}]$ [Section 1.13]; for larger $|\hat\zeta|$ it is larger, and w_L is decreasing or zero there. So one splice of $v = w_L + w_1 + w_2$ at J is monotone for every $\hat\zeta$. (Ch3) holds on the splice interval by the common reserve $\widehat{\mathcal{T}}_{P,\theta} \geq c\epsilon_o C_b/R_b$ on $J \times [-1, 1]$ [(1.13.55)], and after J by Proposition 1.20.62(b).

Properties.

Proposition 1.23.8 (Properties of the forward weight)**.** *For the selected forward member under Propositions 1.20.59 and 1.20.62, the weight of Definition 1.23.6 satisfies*

(W1) Exact one-sided monotonicity. *For every i and $\hat\zeta$, $w_i(\cdot, \hat\zeta)$ is nondecreasing on $(0, \frac{(\hat\xi_p(\hat\zeta))^2}{2} e^{-3}]$ and nonincreasing on $[\frac{(\hat\xi_a(\hat\zeta))^2}{2} e^{t_{\rm act}}, \infty)$. In particular, for every i,*

$$w_i(s, \hat\zeta) \leq w_i(\tfrac{\hat\xi^2}{2}, \hat\zeta) \quad (s \leq \tfrac{\hat\xi^2}{2} \leq \tfrac{\hat\xi_p^2}{2} e^{-3}), \qquad w_i(s, \hat\zeta) \leq w_i(\tfrac{\hat\xi^2}{2}, \hat\zeta) \quad (\tfrac{\hat\xi_a^2}{2} e^{t_{\rm act}} \leq \tfrac{\hat\xi^2}{2} \leq s).$$

With constant 1 this is the bound $w_i(s) \leq C w_i(\mathsf{R})$ for the one-sided radial integrals. It rests on the monotonicity of W_c, $(1-\chi)W_c$ and of the inner connector.

(W2) Plateau on the protected slot. $\mathsf{W} \geq c_m e_\infty$ *on* $\{y_a \geq t_{\rm act},\ y_p \leq Y(\hat\zeta) - \frac{1}{2}\}$, *in particular on* $\Sigma(\hat\zeta) = \{-8 \leq y_p \leq -3\}$ *for every* $\hat\zeta \in [-1, 1]$.

(W3) Two-sided stress comparison. $|T_0| \geq c\mathsf{W}$ *on* $\{\mathsf{W} > 0\}$. $T_0 = 0$ *on* $\{\mathsf{W} = 0\}$. $|D^j T_0| + |D^j \mathsf{W}| \leq C_j \mathsf{W} \mathcal{L}_W{}^{N_j}$.

(W4) Regularity. $\mathsf{W} \in C^\infty$. *For* $\beta > 0$, W^β *extends flatly by zero.* $\operatorname{supp} \mathsf{W} \subset \{\frac{\hat\xi^2}{2} \leq \frac{\hat\xi_W^2}{2}\}$.

(W5) Positive floor on higher supports. *If $n \geq 2$ and T_n vanishes on $\{y_a \leq \delta_n\}$ and is supported in $\mathscr{P} \cup K_0 \cup K_{\rm ext}$* [proof of Proposition 1.24.2], *then* $\mathsf{W} \geq c_n > 0$ *on* $\operatorname{supp} T_n$.

Lemma 1.23.8a (Mixed terminal derivatives of the stress and the velocity deficit)**.** *Write $X = \xi^2/2$, $D = (\partial_X, \partial_\eta|_X)$, $X_{\rm mid} = \min_i X_{1,i}$ over the terminal splices in Definition 1.23.6, and put*

$$V_* = (1-\chi)(\rho_{cL} + \rho_{cW}) + \chi\rho_s + \dot\chi\rho_g.$$

Let $H_{\rm heat}$ be the numerator of the homogeneous heat swirl matched at the outlet of the scalar shooting construction. On $X \geq X_{\rm mid}$ every word of length j satisfies

$$|D^j T_0| + |D^j(H - H_{\rm heat})| \leq C_j V_* (1 + \log_+(1/V_*))^{N_j}. \tag{U}$$

The right side is zero at $V_* = 0$. The constants are for the fixed selected member; they are uniform in X, η on the indicated domain.

Proof. Fix a compact radial interval containing the terminal overlaps and all departures from the common heat pair to their right. Its lower endpoint is positive. All comparisons below with wL_w^N mean the same comparison for every fixed mixed derivative, with exponent and constant allowed to depend on its order. Fixed positive multipliers do not affect this class, by Lemma 1.23.1. Use the *same* heat field and primitive (H_0, I_0) obtained at the end of the actual shot, including its fast mode.

Thus $H_0 = H_{\mathrm{heat}}$ throughout this proof. On this compact interval their mixed jets are bounded. Indeed the scalar solutions are smooth for $x = X/d > 0$; at $d = 0$ the regular heat asymptotics and the exponential fast tail give their smooth one-sided lifts (the heat pair in (1.13.1)). The following estimates need no uniform backward continuation in a free scale parameter.

For the scalar lift compare (i, g_*) with the matched homogeneous pair (i_0, g_0) at $x_* = R_b + 3W_s/4$. They agree there, as the forcing vanishes past x_* and their outlet data coincide. For $R_b + W_s/2 \le x \le x_*$ the difference is

$$-\int_x^{x_*} G(x,s)(0,\tau_s(s))^{\mathsf{T}}\,\mathrm{d}s,$$

where G is the fundamental matrix of (1.13.39). On this fixed compact interval its derivatives are bounded. The forcing is nonnegative and nonincreasing there, so the integral is $O(\tau_s(x))$. Differentiating the system bounds every higher derivative by the forcing and finitely many of its derivatives. Formula (1.13.38) gives $|\partial_x^k \tau_s| \le C_k \tau_s L_{\tau_s}^{N_k}$ there. Above x_* the difference is zero. Where this difference is nonzero on the post-blend terminal interval, $d \ge X/x_* > 0$. Consequently all mixed derivatives of $I_L - I_0, H_L - H_0$ there are bounded by $C_j w_L L_{w_L}^{N_j}$, including the moving edge.

The remaining central differences in (1.13.53) are $\psi_o \alpha_o \ell_b^2 \mathcal{F}(y_o)$ and $-\psi_o \alpha_o \ell_b f_o(y_o)$. On the fixed hull $\mathcal{F}(y) \le y f_o(y)$ for $y > 0$; its positive-order derivatives are derivatives of f_o. The smooth edge graph, the squared-flat factors and the product rule therefore bound these differences and their jets by $C_j w_1 L_{w_1}^{N_j}$. On the blend J the sum of the two central splice factors has a positive minimum. Indeed the shot forcing has a positive floor when $|\eta| \le 2\eta_0$ by (1.13.41), and for the remaining angles $\psi_o = 1$ and $\mathcal{B}_o > \sup J$ by (1.13.52). The common splice is a convex interpolation between positive constants and positive multiples of $w_L + w_1 + w_2$ with fixed coefficients. Before its splice the sum equals two. Thus on the entire terminal hull the two central differences, including the actual smooth blend and its cutoff derivative, are controlled by the class of $\rho_{cL} + \rho_{cW}$.

On the exact outer collar $I_w - I_0 = E_w$, $H_w - H_0 = -V$. For $u = 1 - X/B(\eta) > 0$ close to zero write $V = A(u,\eta)\exp(-\kappa^2/u^2)$, $\kappa = 1 - e^{-3}$. The explicit cutoff and the positive heat factor make A smooth and bounded above and below there, on the closed angular support of this component. All assertions about the outer field are restricted to its chart. Its products with the squared-flat cutoff extend by zero on the inactive central region, since the one-sided jets are bounded up to the start of the angular transition. Then $E_w = B(\eta)\int_0^u A(v,\eta) e^{-\kappa^2/v^2}\,\mathrm{d}v$. Differentiation at fixed X costs only finite powers of u^{-1} and bounded derivatives of the edge graph. The zeroth-order integral is at most $Cue^{-\kappa^2/u^2}$; angular derivatives at fixed u satisfy the same bound, and an upper-limit derivative gives the integrand. Since $v_s = V + E_w/X \asymp e^{-\kappa^2/u^2}$, every such loss is a power of L_{v_s}. Both differences are zero beyond the edge. On the compact outer splice v_s has a positive minimum and to its left $\rho_s = 1$. Smoothness there and the preceding explicit collar estimate prove the corresponding bounds with weight ρ_s.

The angular multipliers have log-jet bounds. Multiplying the preceding estimates by $1 - \chi$ and χ and applying the product and sum inequalities of Lemma 1.23.1 bounds the mixed differences $I - I_0$ and $D_H = H - H_0$ and their jets by $C_j V_* L_{V_*}^{N_j}$. This argument also covers simultaneous radial and angular zero faces. The splices lie after the central spectral return wherever it was active, so $U = M = J = 0$ here. With the canonical outward normalization the exact remaining differences are

$$S - S_0 = \int_X^\infty \frac{2H_0 D_H + D_H^2}{4s}\,\mathrm{d}s, \qquad P - P_0 = -\int_X^\infty \frac{2H_0 D_H + D_H^2}{4s^2}\,\mathrm{d}s.$$

In particular the square contains all mixed-component terms. Every angular derivative of either integrand satisfies the same class bound. The integrands vanish beyond a fixed finite radius. By the monotone splice formula $V_*(s,\eta) \le V_*(X,\eta)$ for $s \ge X \ge X_{\mathrm{mid}}$ (each radial factor is constant before

its own splice). Lemma 1.23.1(b) therefore bounds the integrals of all these angular derivatives by the class at X. Radial derivatives evaluate derivatives of the integrand at the lower limit. This proves the mixed bounds for both histories. For the heat comparison $\mathcal{A}I_0 = 0$ by the homogeneous scalar equation. Also $H_0 = d^{-h} g_0(X/d)$ obeys $\eta(X\partial_X + h)H_0 - (d/2)\partial_\eta H_0 = 0$, including $d = 0$ by continuity. Formula (1.15.20) therefore gives zero axial heat stress with these very outward histories. Subtract this pair in (1.15.18)–(1.15.19). The coefficients are smooth and bounded with their derivatives on this hull, since $X > 0$ and $L \geq 1 - 2h$. The resulting estimates hold for both stress components. Outside the hull the heat identities give zero identically. □

Proof of Proposition 1.23.8. (W1). By (Ch2), $\rho_i = 1$ on $y_p \leq -3$ for every channel. For channels (iii)–(vi) this holds because $\frac{\hat\xi_{1,i}^2}{2} > \frac{\hat\xi_p^2}{2} e^{-3}$. For R_0 it holds because $Y - \frac{1}{2} > 0$. For R_1 it holds because R_+ lies beyond $\frac{\hat\xi_p^2}{2}$. So on $(0, \frac{\hat\xi_p^2}{2} e^{-3}]$, $w_i = c_i \alpha_i(\hat\zeta) e(y_a)$, which is nondecreasing in $\frac{\hat\xi^2}{2}$ (Lemma 1.23.2(a)). On $[\frac{\hat\xi_a^2}{2} e^{t_{\mathrm{act}}}, \infty)$, $e = e_\infty$ and $w_i = e_\infty c_i \alpha_i \rho_i$, which is nonincreasing. The two intervals overlap by (1.23.5).

(W2). $\mathsf{W} \geq w_m = c_m e(y_a) R_0 = c_m e_\infty$ there.

(W3), lower bound. Since $e \leq 1$, (Ch3) for each channel gives $\mathsf{W} \leq \sum_i c_i \alpha_i \rho_i \leq (\sum_i c_i c_{\mathrm{ch},i}^{-1}) |T_0|$ on $\{y_a \geq y_{\mathrm{col}}\}$. On the collar $\mathsf{W} \leq (\sum c_i) e \leq C|T_0|$ by (J2). It remains to verify (Ch3) channel by channel. (i): Proposition 1.20.59 with its last assertion: $R_0 > 0$ only on $y_p < Y - \frac{1}{2} + \epsilon_0$, where $|T_0| \geq c$ away from the collar. (ii): $|T_0| \geq c$ on $\{y_a \geq y_{\mathrm{col}},\ \hat\zeta \in K_2,\ \frac{\hat\xi^2}{2} \leq R_+ + \text{buffer}\}$, by K_0, K_{ext} (J6) and central hold positivity on $K_2 \setminus K_1 \subset \{\chi = 0\}$, where no spectral edit occurs [proof of Proposition 1.24.2]. (iii): before $\frac{\hat\xi_{2,cL}^2}{2}$ resp. $\frac{\hat\xi_{2,cW}^2}{2}$, Proposition 1.20.59, (J6), Proposition 1.20.62(a) and the common reserve $\widehat{\mathcal{T}}_{P,\theta} \geq c\epsilon_o C_b / R_b$ on $J \times [-1, 1]$ [(1.13.55)] give $|T_0| \geq c$. The same reserve covers the part of J after $\frac{\hat\xi_{2,cW}^2}{2}$. After J, (b) gives $\widehat{\mathcal{T}}_{P,\theta} \geq (1 - \chi)\frac{(\frac{1}{2} - h)}{2}(w_L + w_1 + w_2)$ plus nonnegative terms. (iv)–(v) On the compact outer chart from the end of J to $X_{2,s} = (1 - \epsilon_2)B(\eta)$, both $\mathcal{A}I_w$ and $(I_w - I_c)/(2LX)$ have positive minima. This follows on the earlier compact path from Lemmas 1.17.3 and 1.17.4, and on the exact wing from $I_w - I_c = \rho \int_X^B H_0(s)\Psi(s/B)\, ds$, the source estimate of Lemma 1.17.5, and separation from B. Thus (1.20.22) gives $T_\theta \geq c(\chi + \dot\chi)$, including approach to the angular zero face. This pays for $\chi\rho_s + \dot\chi\rho_g$ before and through the compact splice. Beyond the splice use (c) with v_s, v_g. The separate spectral hull has its own floor. Combining with the central channel in (iii) proves (Ch3).

(W3), zero set. The main cutoff ends at $X = R_o e^{-1/2+\epsilon_0} < R_o$. Its successors have a positive total angular coefficient $(1 - \chi) + \chi = 1$ and their splices are after the inlet. On $K_2 \Subset \{\chi = 0\}$, R_+ lies within the scalar hold outlet, before the drive and the shot interval J. Choose the extension width inside this open buffer with its end before $\inf J$, where the central splices are still one. The main and extension cutoffs therefore introduce no additional terminal radius. The remaining channel edges are the live central and outer edges in Corollary 1.20.63. Below activation and after their last edge the core or exact heat field has zero stress. Conversely each live channel bounds $|T_0|$ from below by (Ch3). Hence $\{\mathsf{W} > 0\} = \{T_0 \neq 0\}$.

(W3), upper bounds. W: Lemma 1.23.1(c) with Lemmas 1.23.2, 1.23.4. T_0: split $\{\mathsf{W} > 0\}$ into three parts. (1) The collar $0 < y_a < y_{\mathrm{col}}$: by (J2), $|D^j T_0| \leq C\phi_{N_j}(c_{\mathrm{in}} e)$. Since $\mathsf{W} \geq c_m e$ there ($R_0 = 1$), Lemma 1.23.1(a) with $u = c_{\mathrm{in}} e \leq (c_{\mathrm{in}}/c_m)\mathsf{W}$ gives $\leq C\mathsf{W}\mathcal{L}_W{}^{N_j}$. (2) The compact middle $\{y_a \geq y_{\mathrm{col}},\ \frac{\hat\xi^2}{2} \leq \frac{\hat\xi_{\mathrm{mid}}^2}{2}\}$: here $\mathsf{W} \geq c_{\mathrm{mid}} > 0$. This holds because $(1 - \chi)c_{cL} e_\infty + \chi c_s e_\infty \geq e_\infty \min(c_{cL}, c_s)$ on the falling edge of R_0, and the same two splices remain one up to X_{mid}. Before this falling edge the main channel gives $\mathsf{W} \geq c_m e(y_{\mathrm{col}}) > 0$ by monotonicity. T_0 is smooth on this compact set, so $|D^j T_0| \leq C_j \leq C_j' \mathsf{W}$. (3) $X \geq X_{\mathrm{mid}}$: Lemma 1.23.8a, $V_* \leq [e_\infty \min\{\min_{i \neq g} c_i, c_g/K_g\}]^{-1}\mathsf{W}$.

For each fixed N, Lemma 1.23.1(a) therefore bounds $V_*(1+\log_+(1/V_*))^N$ by $C_N \mathsf{W}\mathcal{L}_W^N$ on the positive set, with zero extension at its boundary. Apply this to both terms in (U). This proves (W3) and the forward velocity estimate stated on p. 6.

(W4). Products and sums of smooth functions; Lemma 1.23.1(d). The radius $\frac{\hat\xi_W^2}{2}$ is the largest of the edges R_0-end, R_1-end, $d(R_b+\frac34 W_s)$, $\mathcal{B}_{\max}$, B.

(W5). On $\{y_a \ge \delta_n\} \cap (\mathscr{P} \cup K_0)$, $\mathsf{W} \ge c_m \min(e(\delta_n), e_\infty)$. On K_{ext}, $\mathsf{W} \ge c_e e_\infty$ ($a=1$ on K_1, $R_1 = 1$ up to R_+). □

Lemma 1.23.9 (Aggregate jets and direction)**.** *Assume Hypothesis 1.5.1. For each fixed profile multi-index j,*

$$|D^j \mathsf{W}| + |D^j T_0| \le C_j \mathsf{W}\mathcal{L}_W^{N_j}, \qquad |T_0| \ge c\mathsf{W}. \tag{1.23.8}$$

Powers of $\mathcal{L}_W$ bound all fixed derivatives of $T_0/|T_0|$ on the positive set. We fix $\beta > 0$. The function W^β extends smoothly and flatly by zero across the full zero set. The same conclusion holds for each function whose jets satisfy the bound $C_j \mathsf{W}^\beta \mathcal{L}_W^{N_j}$. On the backward side the same conclusions follow from Lemma 1.24.4 and the same differentiation argument.

Proof. The jet bounds and $|T_0| \ge c\mathsf{W}$ are (W3) of Proposition 1.23.8; $\mathsf{W} \in C^\infty$ and the flat zero extension of W^β are (W4) and Lemma 1.23.1(d). Finite differentiation of a norm and reciprocal proves the direction bounds: on the positive set each derivative of $T_0/|T_0|$ is a polynomial in the quotients $D^j T_0/|T_0|$, which are bounded by powers of $\mathcal{L}_W$ by (W3). The same chain rule proves the estimates for W^β and for each function whose jets satisfy the bound $C_j \mathsf{W}^\beta \mathcal{L}_W^{N_j}$. Each such jet tends to zero at the zero set. Difference quotients along coordinate segments establish the successive zero-extension derivatives.

We assume no smooth limit of the unit direction at a corner or regularity of the union boundary. □

The moment-subtracted radial inverse.

Proposition 1.23.10 (Moment-subtracted radial inverse)**.** *Let $\beta_0 = \big(\frac{\hat\xi^2}{2}\big)^{-1} b(y_p)$ with $b \ge 0$, $\int b = 1$, $\operatorname{supp} b \Subset (-8,-3)$, and $\chi_m = \int_{(\frac{\hat\xi^2}{2})}^\infty \beta_0$ [(1.24.1)]. Let g be smooth, supported in $\hat\xi \le \hat\xi_{\text{hull}}$, with $|D^j g| \le C_j \mathsf{W}\mathcal{L}_W{}^{N_j}$ for $|j| \le k$, $D \in \{\hat\xi^{-1}\partial_{\hat\xi}, \partial_{\hat\zeta}|_{\hat\xi}\}$. Then*

$$\mathcal{I}_{\chi_m} g = \int_{(\frac{\hat\xi^2}{2})}^\infty g \,\mathrm{d}s - \chi_m \int_0^\infty g \,\mathrm{d}s$$

satisfies $|D^j \mathcal{I}_{\chi_m} g| \le C_j' \mathsf{W}\mathcal{L}_W{}^{N_j'}$ for $|j| \le k$. The same holds for $Jg = \int_0^\infty g$ times any smooth function supported in Σ.

Proof. Reduction to sup bounds. We have

$$\hat\xi^{-1}\partial_{\hat\xi}\mathcal{I}_{\chi_m} g = -g + \beta_0\, Jg,$$
$$\partial_{\hat\zeta}^\ell \mathcal{I}_{\chi_m} g = \mathcal{I}_{\chi_m}\partial_{\hat\zeta}^\ell g - \sum_{0<r\le\ell} \binom{\ell}{r} (\partial_{\hat\zeta}^r \chi_m) J \partial_{\hat\zeta}^{\ell-r} g.$$

Integration is from 0 or to ∞ at fixed $\hat\xi$, so there are no moving-boundary terms; g is flatly zero-extended. β_0 and $\partial_{\hat\zeta}^r \chi_m$ ($r \ge 1$) are supported in Σ, where $\mathsf{W} \ge c_m e_\infty$ (W2), and $|Jh| \le \frac{\hat\xi_{\text{hull}}^2}{2} \sup|h|$.

So all derivatives reduce to: (a) the class bound for $D^j g$ itself, (b) bounded terms supported in Σ, (c) sup bounds of $\mathcal{I}_{\chi_m} h$ for $h = \partial_{\hat\zeta}^{\ell} g$, which is again in the class.

Sup bound. Let $|h| \le C\mathsf{W}\mathcal{L}_W{}^N = C\phi_N(\mathsf{W})$. We use two one-sided comparisons of W itself. Both follow from the product form (1.23.6), with $\alpha_i, \rho_i \le 1$ by (Ch1)–(Ch2):

(W1′) $\mathsf{W}(s,\hat\zeta) \le C_1 \mathsf{W}(\frac{\hat\xi^2}{2},\hat\zeta)$ for $s \le \frac{\hat\xi^2}{2} \le \frac{\hat\xi_p^2}{2} e^{-3}$, with $C_1 = \sum_i c_i/c_m$. Indeed $\mathsf{W}(s) \le e(y_a(s)) \sum_i c_i \le e(y_a(\frac{\hat\xi^2}{2})) \sum_i c_i$, since e is nondecreasing. Also $\mathsf{W}(\frac{\hat\xi^2}{2}) \ge w_m(\frac{\hat\xi^2}{2}) = c_m e(y_a(\frac{\hat\xi^2}{2}))$, since $R_0 = 1$ on $y_p \le -3$.

(W1″) $\mathsf{W}(s,\hat\zeta) \le \mathsf{W}(\frac{\hat\xi^2}{2},\hat\zeta)$ for $\frac{\hat\xi_a^2}{2} e^{t_{\mathrm{act}}} \le \frac{\hat\xi^2}{2} \le s$. There $e = e_\infty$, and each ρ_i is nonincreasing in $\frac{\hat\xi^2}{2}$ by (Ch2).

(W1) implies both, but neither needs monotonicity of the individual channels on $(0, \frac{\hat\xi_p^2}{2} e^{-3}]$, a decomposition into channels, or a lower bound for the stress. If $y_p \le -8$, then $\chi_m = 1$ and $\mathcal{I}_{\chi_m} h = -\int_0^{\frac{\hat\xi^2}{2}} h$. By (W1′) and Lemma 1.23.1(a) with $C = C_1$,

$$\Big|\int_0^{\frac{\hat\xi^2}{2}} h\Big| \le C \int_0^{\frac{\hat\xi^2}{2}} \phi_N(\mathsf{W}(s,\hat\zeta))\,\mathrm{d}s \le C \tfrac{\hat\xi_{\mathrm{hull}}^2}{2} K_N \phi_N(\mathsf{W}(\tfrac{\hat\xi^2}{2},\hat\zeta)), \qquad K_N = \max(C_1, N^N e^{1-N}).$$

If $y_p \ge -3$, then $\chi_m = 0$ and $\mathcal{I}_{\chi_m} h = \int_{(\frac{\hat\xi^2}{2})}^{\infty} h$. The same bound holds by (W1″), since $\frac{\hat\xi^2}{2} \ge \frac{\hat\xi_p^2}{2} e^{-3} > \frac{\hat\xi_a^2}{2} e^{t_{\mathrm{act}}}$ by (1.23.5). On Σ, $|\mathcal{I}_{\chi_m} h| \le 2\frac{\hat\xi_{\mathrm{hull}}^2}{2} \sup|h| \le C \le C(c_m e_\infty)^{-1}\mathsf{W}$.

Constants. The reduction step and the sup bound give $C_j' \le K_j' \max_{j'\le j} C_{j'}$ and $N_j' = \max_{j'\le j} N_{j'}$, so there is no logarithmic loss. Here K_j' depends only on j, the $N_{j'}$, b, $\frac{\hat\xi_p^2}{2}$, $\frac{\hat\xi_{\mathrm{hull}}^2}{2}$, $c_m e_\infty$ and C_1, and not on g. So the bound is linear in the source constants. □

Remark 1.23.11 (Inputs and powers of the radial weight). (1) *Inputs.* Only (W1′), (W1″) and (W2) enter. They follow from Definition 1.23.6, (Ch1)–(Ch2) and (1.23.5). Hypothesis 1.20.4 and the terminal estimate of Lemma 1.23.8a enter only (W3), that is, whether the actual sources and stresses belong to the class. The mapping property does not depend on them.

(2) *Powers.* For $\beta > 0$, W^β satisfies (W1′) with C_1^β, satisfies (W1″), and is at least $(c_m e_\infty)^\beta$ on Σ. Also $\min(1,\beta)\mathcal{L}_W \le 1 + \beta\log(1/\mathsf{W}) \le \max(1,\beta)\mathcal{L}_W$. Hence the proposition holds with W replaced by W^β, in particular for the $\sqrt{\mathsf{W}}$ classes. For $\beta < 1$, $\mathsf{W}^\beta \le e^{-2\beta}$ may exceed e^{-2}; for example $\sqrt{\mathsf{W}} \le e^{-1}$. This is harmless, because the proof of Lemma 1.23.1(a) uses only $L_w \ge 1$.

1.24 One-sided regularity of the leading fields

Lemma 1.24.1 (One-sided regularity supplied by the leading construction)**.** *We fix an admitted finite choice in the actual leading construction. This choice includes the regular-axis Gevrey data, buffered activation, and explicit prefix and future fields. It also includes the finite memory and moment corrections on their selected nonsingular branches and the transverse positive pulse root. The root and matrix margins here are the outputs of those finite constructions, not conclusions of endpoint matching.*

We consider either physical side independently on any finite radial hull. Its fields, potentials, five histories, and physical pressure are C^∞ through the closed angular endpoints. Its noncompact history

and pressure integrals admit each fixed endpoint derivative. This assertion uses no positive-order slow coefficient, packet stage, completed force, or equality of two previously assumed jets.

Proof. The finite prefix is the same fixed template with its positive scales. The exponent inverse has $F_\nu > 0$. Finite implicit differentiation gives smooth field and moving support maps. The central stop is smooth in the actual $R^{-1/5}$ variable.

The shot coefficient is its explicit positive scalar ratio. Section 1.15 gives the exact formulas for the outer heat collar and rank-one bump. These statements apply to the maps on each side independently. They do not use a comparison between the sides.

We do not claim a bound uniform when the width decreases or across all derivative orders.

Each compact moment target is an integral of the fields specified before this step and their full quadratic densities. It is smooth in the parameters, with moving endpoints. If $\mathcal{B}(c,p)=0$ is one of its selected moment equations, the finite construction selects an invertible value matrix $\mathcal{B}_c$. Differentiation gives

$$\mathcal{B}_c\partial_{\hat\zeta}^k c = -\mathcal{B}_p\partial_{\hat\zeta}^k p + \mathcal{R}_k(c,p,\dots,\partial_{\hat\zeta}^{k-1}c,\partial_{\hat\zeta}^{k-1}p).$$

All fixed derivatives thus exist on that same branch. The affine axial returns are ordinary matrix inverses. The positive energy root has its established nonzero derivative. This proves their smoothness without a comparison of either solution to the other side.

The order used for these statements is concrete. We specify the model swirl and its future. We compute the actual heat discrepancies and cancel the total primitive discrepancy by the rank-one correction. We solve the early correction equations with first target zero and their actual S, C_p targets.

Then integrate the actual prefix histories and solve the axial returns and actual positive energy equation. On a full-compensation protected collar, exact cancellation makes the model root the actual root. On a partial extension, we keep the true residual. This order does not reset the pressure datum or any primitive constant.

The swirl and its canonical integral determine smoothness of the full pressure. This does not assume a desired axial-root equality.

At the axis, check the two signs directly in the recursion. We write $\varsigma=+1$ for the forward chart and $\varsigma=-1$ for the backward chart, and $F=\sum f_n\big(\frac{\hat\xi^2}{2}\big)^n$, $U=\sum u_n\big(\frac{\hat\xi^2}{2}\big)^n$, $P=\sum p_n\big(\frac{\hat\xi^2}{2}\big)^n$. We set

$$b_n^{(\varsigma)} = \varsigma\delta_{n0} + \frac{2(\frac12-h)\hat\zeta u_n + du_n'}{n+1}.$$

The distinct physical chart equations give

$$\begin{aligned}
2L(n+1)(n+2)f_{n+1} &= d\sum_{i+j=n} u_i f_j' - \varsigma(\tfrac12-h)\hat\zeta f_n' \\
&\quad - \sum_{i+j=n} b_i^{(\varsigma)}(j+1)f_j - \varsigma h f_n - 2h\hat\zeta\sum_{i+j=n} u_i f_j,\\
2L(n+1)^2u_{n+1} &= d\sum_{i+j=n} u_i u_j' - \varsigma(\tfrac12-h)\hat\zeta u_n' \\
&\quad - \sum_{i+j=n} b_i^{(\varsigma)} j u_j - \varsigma(\tfrac12+h)u_n - 2(\tfrac12+h)\hat\zeta\sum_{i+j=n} u_i u_j \\
&\quad - 4(\tfrac12+h)\hat\zeta p_n - 2\hat\zeta\sum_{i+j=n-1} f_i f_j + dp_n',\\
p_{n+1} &= \frac{1}{n+1}\sum_{i+j=n} f_i f_j.
\end{aligned}$$

For $\varsigma = +1$ these are (1.9.8)–(1.9.10). For $\varsigma = -1$ the coefficients are $\mathcal{B} = -1 + \mathcal{K}/\frac{\hat{\xi}^2}{2}$ and $\mathcal{C} = dU + (\frac{1}{2} - h)\hat{\zeta}$. The radial diffusion and pressure-integral signs do not change. Thus the radial denominators equal $2L(n+1)(n+2)$, $2L(n+1)^2$, and $n+1$, with $L > 0$ on the fixed angular interval.

Each convolution term has the same absolute majorant (1.9.12). The factors ς have absolute value one. We take the larger fixed coefficient constants. The proof of Theorem 1.9.1 then gives the one-sided Gevrey/analytic solution on each side.

This construction uses the axis data on each side. It does not use endpoint equality to construct a solution. The selected smooth activation and its finite radial ODE keep smooth parameter dependence on the buffered hull. We fix the value margins before this application.

A finite collection of closed annular pieces suffices for this one member. The capped loop of Lemma 1.19.2 also gives a smooth one-sided map. We invert $V(\mu, p_2) = d_0^2\mu^2/2 + O(\mu^4 p_2^2)$ in $\sqrt{r_L}$. The function $\sqrt{r_L}$ equals the selected smooth nonnegative cutoff times a strictly positive smooth factor.

The circle reparametrization has a positive derivative. We fix the finite shared N_{sh} as previously specified. Composition with its joint phase (1.6.66), the complete quadratic histories, and the nonsingular five-moment solve remain smooth by Corollary 1.19.3. No bound uniform in N_{sh} is necessary here.

Its compact spectral controls after this stage are smooth and vanish on endpoint neighborhoods. Their five-history returns keep the outgoing constants fixed before this step. They do not supply the axis solution.

On the heat tail, the distinct forward basis and backward positive Laplace integral give the stated bounds for each fixed k. These bounds are (1.25.6) and their backward counterparts. The differentiated renormalized primitive, energy, and pressure densities satisfy the bounds $C_k(\frac{\hat{\xi}^2}{2})^{-h-1}$, $C_k(\frac{\hat{\xi}^2}{2})^{-1-2h}$ and $C_k(\frac{\hat{\xi}^2}{2})^{-2-2h}$. The fast forward term is flat at its endpoint and has an integrable exponential dominator.

It is zero on the backward continuation. Near the regular axis the actual densities are integrable because $H = O(\frac{\hat{\xi}^2}{2})$ and $U = O(1)$. Dominated differentiation, with the actual moving-boundary terms, proves the history assertion. This uses only one-sided majorants, not equality of their integrals. □

Scope of the regularity result. The lemma is a regularity consequence of the admitted finite leading maps just listed. Their source-cone, core and spectral admission remain the obligations of the leading construction. It is not an inference from selected admissibility or from the completed-field theorem. The next theorem proves endpoint equality from these one-sided jets. The packet equality proof must use this same atlas first.

1.24.1 The actual late pressure corridor

Proposition 1.24.2 (Two-tube pressure saturation)**.** *We put* $y = 2\log(\hat{\xi}/\hat{\xi}_p(\hat{\zeta}))$. *The positive velocity slots lie in* $(-14, -9)$ *and mean slots in* $(-8, -3)$. *The loop compensation is in* $(-25, -20)$, *heat compensation ends before* -15, *and the last pulse return ends before* $Y - .7$. *The late pressure saturation is contained in*

$$K_0 = \{\tfrac{\hat{\xi}_p^2}{2} e^{-14.5} \le \tfrac{\hat{\xi}^2}{2} \le R_o e^{-.5}\}, \qquad K_{\mathrm{ext}} = \{\hat{\zeta} \in K_1,\ \tfrac{\hat{\xi}_p^2}{2} e^{-14.5} \le \tfrac{\hat{\xi}^2}{2} \le R_+\}.$$

Here $K_1 \Subset K_2 \Subset \{\chi = 0\}$ *contains the full central spectral support, and* R_+ *lies in the scalar hold outlet buffer after all spectral returns. On these sets* $T_\theta \ge cH > 0$ *for the selected member. We do not claim an all-angle rectangle to* R_+.

Proof. Lemma 1.16.8 supplies the actual denominator first on the variable-exponent and fixed-λ affine sectors, with the full quiet intervals and the two true returns. Its actual prefix estimates are Lemmas 1.14.2, 1.14.3, and 1.14.4. The protected root cancellation and the kept bridge residual are Proposition 1.14.6. No return memory is reset.

Lemma 1.16.9 supplies the distinct ordinary-angular positive denominator through $\hat{\zeta} = 0$. This does not extend a $1/\eta_a$ estimate to the central plane. The true central memory correction and scalar hold are Proposition 1.15.22 and Lemma 1.17.7.

The exact stress is $T_\theta = (H/2)(Q/L - a_s/\frac{\hat{\xi}^2}{2})$. After we impose the radial-scale threshold, Lemma 1.17.2 gives a positive stress floor for the selected member. The actual first stress derivatives give its open tube extension. We impose these finite thresholds on the same selected member before its source and spectral controls are fixed. The actual small spectral partial-history and source bound keeps the reserved fraction on K_{ext}.

No spectral modification occurs in $K_2 \setminus K_{\mathrm{spec}}$. Thus the full pressure row puts P1/P2 in these two actual tubes, without a claim of an all-angle rectangle to R_+. Native activation and terminal weights remain outside the tubes. □

1.24.2 Weights on the two tubes and generic radial primitives

Lemma 1.24.3 (Actual component-weighted radial inverse)**.** *Assume Hypothesis 1.5.1. The selected member has a finite component weight* $\mathsf{W} \le e^{-2}$ *with the native activation and terminal zero faces. This weight covers the full pressure saturation in Proposition 1.24.2. It satisfies* (1.23.8)*. We take a source in* $\mathsf{W}(1+\log(1/\mathsf{W}))^N$ *with its fixed mixed jets.*

The source may meet a new angular or radial taper. Its moment-subtracted radial primitive belongs to the same class, with a possibly larger finite logarithmic exponent.

We impose no scalar all-angle outer-middle interval.

Proof. Use Definition 1.23.6. Proposition 1.23.8(W2)–(W5) gives the stress comparison, log-jets, native zero faces and a positive floor on the pressure-saturation supports. The protected subtraction uses

$$\begin{gathered}\beta_0(\tfrac{\hat{\xi}^2}{2},\hat{\zeta}) = (\tfrac{\hat{\xi}^2}{2})^{-1} b(2\log(\hat{\xi}/\hat{\xi}_p(\hat{\zeta}))), \qquad b = b_0, \quad \int b = 1, \quad \operatorname{supp} b \Subset (-8,-3),\\ \chi_m(\tfrac{\hat{\xi}^2}{2},\hat{\zeta}) = \int_{(\frac{\hat{\xi}^2}{2})}^{\infty} \beta_0(s,\hat{\zeta})\,\mathrm{d}s.\end{gathered} \tag{1.24.1}$$

Thus

$$\mathcal{I}_{\chi_m} g = \int_{(\frac{\hat{\xi}^2}{2})}^{\infty} g - \chi_m \mathcal{J} g$$

is an outward tail after the slot and minus an inward tail before it. Proposition 1.23.10 bounds it in the same weighted class, including sources meeting a taper.

If Z commutes with the raw integral, then

$$[Z, \mathcal{I}_{\chi_m}] g = -(Z\chi_m)\mathcal{J} g. \tag{1.24.2}$$

This term is supported in the protected slot and is coefficient-flat when the full moment is. The correction moments $c_\beta = \int \frac{\hat{\xi}^2}{2}\beta_0\,\hat{\xi}\,\mathrm{d}\hat{\xi}$ and $c_\theta = \int \hat{\xi}\beta_0\,\hat{\xi}\,\mathrm{d}\hat{\xi}$ are differentiated as functions of $\hat{\zeta}$.

The logarithmic argument $y_p = 2\log(\hat{\xi}/\hat{\xi}_p)$ is a common slice function on the endpoint overlaps. Accordingly $\beta_0, \chi_m, c_\beta, c_\theta$ have weights $1, 0, -1, -\frac{1}{2}$ by the change of chart (1.6.16). Hence $\omega_z = \beta_0/\bar{q}$, $\omega_\theta = \beta_0/(\bar{q}^{3/2} c_\theta)$ and $\bar{q} c_\beta$ are the same physical functions under this collar identification. Each

native chart defines its own continuation away from the overlaps. The physical derivative of the full flux $\bar{q}c_\beta M_D$ keeps all these moment derivatives and their slice jets.

The compensator acts on the individual moments. Late P_1, P_2 or spectral pieces may have nonzero moments; their compensated primitives use the same $\mathcal{I}_{\chi_m}$ and remain on the two saturation tubes and early positive middle. The weight introduces no change of field or pressure normalization. □

1.24.3 The backward side: one saturation rectangle and the weight $c_b\zeta$

Proposition 1.24.2 and Lemma 1.24.3 are statements about the forward member. Their proofs use the forward pulse lemmas, the central spectral component and the forward native channels, and none of these exists on the backward member (Remark 1.8.9). This subsection proves the backward statements that the joint finite stages use on $t < 0$. The backward stress is positive on the whole open annulus, so no tube structure is needed.

Throughout we work in the backward chart of Section 1.8, with $\varsigma = -1$, $\hat{\zeta} = \beta$, and the backward member of Hypothesis 1.5.5. Write $X = \xi^2/2$, $X_a = \xi_{a,-}^2/2$, $X_p = \xi_{p,b}^2/2$, $B = \xi_{b,-}^2/2$, $d_a = \log(X/X_a)$, $d_b = \log(B/X)$ and $\delta = \min(1, d_a, d_b)$ in the active annulus. The radii are scalars on the native backward chart. We write $R_e = \frac{\hat{\xi}_{p,b}^2}{2} e^{Y_{\mathrm{end}}}$ for the backward outlet, as in (1.15.32), and

$$\frac{\hat{\xi}_{\mathrm{ret}}^2}{2} = \frac{\hat{\xi}_{p,b}^2}{2} e^{Y_{\mathrm{end}} - 0.7} = R_e e^{-0.7}.$$

By (S4)(vi) of Lemma 1.8.8, the pulse and its two returns lie in $\hat{\xi} < \hat{\xi}_{\mathrm{ret}}$. (In the reserve identity (1.5.4) and in the proof of Lemma 1.8.8 the symbol $\frac{\hat{\xi}_v^2}{2}$ denotes the end of the leading meridional support.)

Let $\mathscr{P}_b = \{d_a > 0,\ \log(X/X_p) \le -14.5\}$ and

$$K_b = [X_p e^{-14.5},\ R_e e^{-0.5}] \times [-1, 1].$$

The closed rectangle covers the two slots, pulse and last meridional return. On its wait and pulse segments the proofs of Lemmas 1.8.19 and 1.8.20 give $Q_s \ge c\lambda$ and bounded a_s, hence $T_\theta/H = Q_s/(2L) - a_s/(2X) \ge c' > 0$ after the same finite scale choice. On the last quiet segment the latter proof gives $T_\theta/H \ge z/(4L)$ with z bounded below. The native geometry gives $X_a e^{t_{\mathrm{act}}} < X_p e^{-8} < X_p < R_e < B$.

To realize the weight in (B3), take $R_e < X_1 < X_2 < B$ and put $z(X) = \sigma_{\mathrm{step}}((X - X_1)/(X_2 - X_1))$, $u = 1 - X/B$, $q(u) = \exp(-\kappa^2/u^2)$ for $u > 0$, zero for $u \le 0$. Set

$$\omega_b(X) = 1 - z(X) + z(X)q(u), \qquad \zeta(X) = e(d_a)\omega_b(X)/e_\infty, \qquad \mathsf{W}_b = c_b\zeta, \quad 0 < c_b \le e^{-2}.$$

Use the constant zero extension through the inner face. Write $\mathcal{L}_b = 1 + \log(1/\mathsf{W}_b)$ on the positivity set. Near the inner edge the factor is $\sigma_{\mathrm{step}}(d_a/t_{\mathrm{act}})$; the denominator of the step is smooth and bounded away from zero. Thus $a_a = t_{\mathrm{act}}^2$, $\varphi_a(s) = s$ in (O2). At the outer edge $a_b = 1$ and $\varphi_b(s) = (1 - e^{-s})/\kappa$. The common activation of the native entry construction (Section 1.8 and Lemma 1.21.1) gives (1.23.3) here. This factorization and the two actual stress factors of Lemma 1.8.2 give (1.5.2) on these collars with this very ζ. Between them the stress is nonzero by (B2) on a compact set and $\zeta > 0$; smoothness gives the upper estimates there for all fixed derivatives. This selects a witness to (B3) and changes no leading field.

Lemma 1.24.4 (The backward weight)**.** *Use the native member of (B2), (B5), its edge factorizations and the preceding choice in (B3).*

(a) There are $0 < c \le C$ *with* $c\delta^{-2} \le \mathcal{L}_b \le C\delta^{-2}$ *on* $(\frac{\hat\xi_a^2}{2}, \frac{\hat\xi_b^2}{2})$. *For all* k, $|(\hat\xi^{-1}\partial_{\hat\xi})^k \mathsf{W}_b| \le C_k \mathsf{W}_b \mathcal{L}_b^{3k/2}$. *The leading stress satisfies* $|T_0| \ge c\mathsf{W}_b$ *and* $|\partial^\alpha T_0| \le C_\alpha \mathsf{W}_b \mathcal{L}_b^{N_\alpha}$ *on* $(\frac{\hat\xi_a^2}{2}, \frac{\hat\xi_b^2}{2})\times[-1,1]$. *Thus* (1.23.8) *holds with* $\mathsf{W} = \mathsf{W}_b$, *and* W_b *does not depend on* $\hat\zeta$.

(b) Let $\hat\xi_a < \hat\xi_1 \le \hat\xi_2 < \hat\xi_b$ *and* $N \ge 0$. *There is* C *such that*

$$\mathsf{W}_b(s)\mathcal{L}_b(s)^N \le C\,\mathsf{W}_b(\tfrac{\hat\xi_1^2}{2})\mathcal{L}_b(\tfrac{\hat\xi_2^2}{2})^N \quad \text{whenever } s \le \tfrac{\hat\xi_2^2}{2} \le \tfrac{\hat\xi_2^2}{2} \quad \text{or} \quad \tfrac{\hat\xi_1^2}{2} \le \tfrac{\hat\xi_2^2}{2} \le s,$$

with the conventions $\mathsf{W}_b = 0$ *and* $\mathsf{W}_b\mathcal{L}_b^N = 0$ *off* $(\frac{\hat\xi_a^2}{2}, \frac{\hat\xi_b^2}{2})$.

(c) The correction region $I_{\mathrm{mean}} = \frac{\hat\xi_{p,b}^2}{2} e^{(-8,-3)}$ *has compact closure in* $(\frac{\hat\xi_a^2}{2}, \frac{\hat\xi_b^2}{2})$, *and* $\frac{\hat\xi_{p,b}^2}{2}$ *is a constant.*

(d) The native analogues of (W1)–(W5) *hold with the single channel* $w_b = \mathsf{W}_b$, *the slot* I_{mean}, *the prefix* $\mathscr{P}_b$ *and the rectangle* K_b. *In* (W5) *the hypothesis is* $\operatorname{supp} T_n \subset (\mathscr{P}_b \cup K_b) \cap \{d_a \ge \delta_n\}$ *for some* $\delta_n > 0$.

Proof. (a) By (B3), $\varphi_a = \mathrm{id}$ and $\varphi_b(s) = (1 - e^{-s})/\kappa$. On the inner collar $\log(1/\zeta) = a_a d_a^{-2} - \log g_a$, and on the outer collar $\log(1/\zeta) = a_b \varphi_b(d_b)^{-2} - \log g_b$ with $\varphi_b(s) \asymp s$. Both g_a and g_b are bounded above and below. On the rest of $(\frac{\hat\xi_a^2}{2}, \frac{\hat\xi_b^2}{2})$, ζ and δ lie between positive constants. This gives the comparison $\mathcal{L}_b \asymp \delta^{-2}$. Lemma 1.8.1(c), the chain rule in $d_a = 2\log(\hat\xi/\hat\xi_a)$ and $d_b = 2\log(\hat\xi_b/\hat\xi)$, and the bounds on g_a, g_b give $|(\hat\xi^{-1}\partial_{\hat\xi})^k \zeta| \le C_k \zeta \delta^{-3k}$. By (1.5.2), which (B2)–(B3) supply, $|T_0| \ge c\zeta$ and $|\partial^\alpha T_0| \le C_\alpha \zeta \delta^{-m_\alpha}$. Now use $\delta^{-1} \le C\mathcal{L}_b^{1/2}$.

(b) For the stated interior radii, ω_b is nonincreasing and e is nondecreasing, with disjoint transition intervals and a plateau between them. Consequently $\mathsf{W}_b(s) \le C\,\mathsf{W}_b(X)$ on either indicated segment. In the inward case the constant is one up to X_1, and beyond X_1 the possible evaluation points belong to the compact interval $[X_1, \xi_2^2/2] \Subset (X_a, B)$ if it is nonempty. In the outward case the constant is one from $X_a e^{t_{\mathrm{act}}}$ onwards; the remaining evaluation points lie in $[\xi_1^2/2, X_a e^{t_{\mathrm{act}}}] \Subset (X_a, B)$ if nonempty. The zero extensions satisfy the same comparison on the stated segments. Apply Lemma 1.23.1(a) to include L^N.

(c) By Lemma 1.8.8, $\frac{\hat\xi_{p,b}^2}{2} = \frac{\hat\xi_{s,b}^2}{2} e^T \lambda^{-60}$ is a scalar and both windows lie in the exact wait, after the activation collar. The wait ends at $\frac{\hat\xi_{p,b}^2}{2} < \frac{\hat\xi_{\mathrm{ret}}^2}{2} < R_e < \frac{\hat\xi_b^2}{2}$ (Lemma 1.8.7 and (A1) of Lemma 1.8.2: $R_e < R_A < R_0 < B$). (d) For $X \le X_p e^{-3}$, $\omega_b = 1$ and the single channel is nondecreasing. For $X \ge X_a e^{t_{\mathrm{act}}}$, $e = e_\infty$ and $\omega_b' = z'(q-1) + z\,\partial_X q \le 0$. This is the constant-one form of (W1). The channel equals c_b throughout $[X_a e^{t_{\mathrm{act}}}, R_e]$, giving (W2) with the native outlet. Part (a), the two explicit smooth flat edges and Lemma 1.23.1(d) give (W3)–(W4), including all positive powers and the exact zero set. For (W5), $\omega_b = 1$ on $\mathscr{P}_b \cup K_b$ and $\mathsf{W}_b \ge c_b e(\delta_n)/e_\infty$ wherever $d_a \ge \delta_n$. Placement of any higher-order source in that set is a hypothesis of (W5). □

The proof of Proposition 1.23.10 now applies in the backward coordinate X with this same prescribed subtraction bump. Before the slot the compensated integral is the negative inward integral, after it the ordinary outward integral, and on the slot the plateau gives the bound. Differentiation in X gives $-g + \beta_0 \int g$; angular differentiation commutes with the native scalar bank. The constants are linear in the source seminorms with exactly the fixed-bank dependence of (iv).

If a native backward post-return trial map is used, place its five ordered nonnegative bumps in $Y_{\mathrm{end}} - .65 < \log(X/X_p) < Y_{\mathrm{end}} - .55$, after the two returns and before flattening. Here $U = 0$ and $H = c(\beta)X^{-\lambda}$ with $\min c > 0$, by (S4) of Lemma 1.8.8 and (P1) of Lemma 1.8.20. Lemma 1.27.5 on the closed native angular interval gives its uniform Jacobian bound. The selected backward amplitudes for this additional trial bank are zero.

1.25 Endpoint geometry and parameter maps

Conventions for the endpoint analysis. We fix $0 < h < 10^{-2}$, $d(\hat\zeta) = 1-\hat\zeta^2$ and $L(\hat\zeta) = 1-2h\hat\zeta^2$. The forward chart is $q - z^2q^{2h} = t$, $\hat\xi = r/\sqrt{q}$, $\hat\zeta = z\hat t^{h-\frac12}$, so $t = q\,d(\hat\zeta)$. The backward chart is $t = -q\,d(\hat\zeta)$. We write $\mathfrak{r} = \hat\xi$, $E = H/\mathfrak{r}$ and $y = 2\log(\hat\xi/\hat\xi_p(\hat\zeta))$, where $\frac{\hat\xi_p^2}{2}$ is the pulse-entry graph.

1.25.1 The endpoint geometry and one-sided calculus

Lemma 1.25.1 (Chart facts)**.**

(a) (1.6.7) $\hat t_t = L^{-1}$, $\hat t_z = 2\hat\zeta\hat t^{\frac12+h}/L$, $\hat\zeta_t = -(\frac12-h)\hat\zeta/(qL)$, $\hat\zeta_z = dq^{h-\frac12}/L$. *The map* $(\hat t,\hat\zeta)\mapsto(z,t) = (\hat\zeta\hat t^{\frac12-h}, dq)$ *has Jacobian* $-Lq^{\frac12-h}$. *This Jacobian is nonzero on* $\{\hat t > 0,\ L > 0\}$, *which contains a neighbourhood of* $\hat\zeta = \pm1$.

(b) Near $(z_0,0)$ *with* $z_0 \neq 0$, *the map* $(z,t)\mapsto(\hat t,\hat\zeta)$ *is a real-analytic diffeomorphism. It maps* $\{t \geq 0\}$ *onto* $\{\mathrm{sgn}(z_0)\hat\zeta \leq 1\}$. *Thus one-sided smoothness of a profile in* $\hat\zeta$ *at* $\hat\zeta = \pm1$ *is equivalent to one-sided smoothness in* t *of the corresponding physical field at* $t = 0$.

(c) (Chart change, (1.6.16).) *Put* $G(\ell,\hat\zeta) = \ell^{1-2h}\hat\zeta^2 + \ell\hat\zeta^2 - \ell - 1$. *The relations* $\hat t_b = \hat t_f/\ell$, $\hat\zeta_b = \ell^{\frac12-h}\hat\zeta_f$, $\frac{\hat\xi_b^2}{2} = \ell\frac{\hat\xi_f^2}{2}$ *describe the same physical point exactly when* $G(\ell,\hat\zeta_f) = 0$. *At* $\hat\zeta = \pm1$ *we have* $G(1,\pm1) = 0$ *and* $G_\ell(1,\pm1) = (1-2h) \neq 0$. *Hence* $\ell = \lambda_{\mathrm{ch}}(\hat\zeta)$ *is real-analytic on a neighbourhood of each endpoint, with* $\ell(\pm1) = 1$ *and* $\ell'(\pm1) = \mp2/(\frac12-h)$. *For* $\hat\zeta_f < 1$ *near* 1 *we have* $\hat\zeta_b > 1$.

Proof. Part (a) is (1.6.7); its nonzero Jacobian and the analytic inverse function theorem give (b), since $t = q(1-\eta^2)$ and $q > 0$. Eliminating t from the two chart formulas gives $G = 0$. At $(\ell,\hat\zeta) = (1,\pm1)$, $G_\ell = 2(\frac12-h)$ and $G_{\hat\zeta} = \pm4$, so the analytic implicit function theorem gives (c) and $\ell'(\pm1) = \mp2/(\frac12-h)$. Finally $(\ell^{\frac12-h}\hat\zeta)' = -1$ at $\hat\zeta = 1$, which gives $\hat\zeta_b > 1$ for $\hat\zeta_f < 1$ sufficiently close to 1. □

Remark 1.25.2. Near either endpoint, the transport map of Lemma 1.25.1(c) evaluates the backward profile at $\frac{\hat\xi_b^2}{2} = \lambda_{\mathrm{ch}}(\hat\zeta_f)\frac{\hat\xi_f^2}{2}$ and $\hat\zeta_b = \lambda_{\mathrm{ch}}(\hat\zeta_f)^{\frac12-h}\hat\zeta_f$. On the interior side $|\hat\zeta_f| < 1$, this uses the backward angular extension at $|\hat\zeta_b| > 1$. Composition of the jointly smooth extended profile with this map gives a smooth transported germ at fixed $\hat\xi_f$. Here $\frac{\hat\xi_b^2}{2}$ varies with $\hat\zeta_f$ and may cross the flat activation edge of Lemma 1.20.40. On the protected inner rectangle, Proposition 1.22.7 gives the order-zero slice jets. The angular Gevrey-3/2 estimates are at fixed $\varpi = (\hat\xi/\hat\xi_a(\hat\zeta))^2$, as in Proposition 1.22.4. The one-sided heat-exterior estimates are given in (1.13.35) and Lemma 1.7.1.

One-sided calculus on closed angular domains.

Definition 1.25.3 (Class $\mathcal{S}$)**.** Let $J = [-1,1]$ and let $a,b\colon J\to[0,\infty)$ be continuous with $a \leq b$. Put $\Omega = \{(\frac{\hat\xi^2}{2},\hat\zeta) : \hat\zeta\in J,\ a(\hat\zeta) \leq \frac{\hat\xi^2}{2} \leq b(\hat\zeta)\}$. A function $f\colon\Omega\to\mathbb{R}^N$ belongs to $\mathcal{S}(\Omega)$ if near each point it is the restriction of a smooth function in the profile coordinates. On a full-dimensional closed rectangle it suffices that f be smooth on the interior and its derivatives, including f itself, extend continuously to the boundary, by the following lemma. Restrictions of the buffered smooth charts used below give the local extensions on variable strips, including at a collapsed fiber. Near $\hat\zeta = \pm1$ the distinguished one-sided coordinate is $p = 1\mp\hat\zeta$. At $\hat\xi = 0$ it is the regular-axis smoothness of Section 1.9.

Lemma 1.25.4 (Smooth extension across the faces of a rectangle)**.** *Let a function on a closed rectangle of positive side lengths be smooth in the interior. If all its partial derivatives extend continuously to the rectangle, with order zero equal to the given function, then it extends smoothly to a neighborhood of the rectangle.*

Proof. We use Seeley's reflection formula [44]. Use a coordinate $s \geq 0$ normal to one face and write y for the remaining coordinates. Set $b_j = -2^j$. For $0 \leq j \leq N$ put

$$c_{j,N} = \prod_{\substack{0 \leq l \leq N \\ l \neq j}} \frac{1 - b_l}{b_j - b_l}.$$

For fixed j this product converges as $N \to \infty$, since each factor with $l > j$ is $1 + O_j(2^{-l})$. Furthermore $|c_{j,N}| \leq C 2^{-j(j+1)/2}$ uniformly in N. Indeed the factors with $l < j$ supply $\prod_{l<j} 2^{l-j}$, and the remaining products are bounded by $\prod_{l \geq 0}(1 + 2^{-l}) \prod_{l \geq 1}(1 - 2^{-l})^{-2}$. Polynomial interpolation at 1 gives $\sum_{j=0}^{N} c_{j,N} b_j^m = 1$ for $N \geq m$. The bound permits passage to the limit, giving $\sum_{j \geq 0} c_j b_j^m = 1$ for every $m \geq 0$.

Choose a smooth ϕ equal to one near zero with support inside the normal coordinate interval. For $s < 0$ set

$$Ef(s, y) = \sum_{j \geq 0} c_j (\phi f)(b_j s, y), \qquad Ef(s, y) = f(s, y) \quad (s \geq 0),$$

where ϕf is extended by zero beyond its support on the positive half-line. After m normal derivatives, the series converges uniformly with any fixed number of tangential derivatives because $\sum_j |c_j| 2^{jm} < \infty$. Its trace at zero is the corresponding derivative of f by the moment identity. This gives a smooth extension across one face, including one-sided tangential derivatives at the remaining faces. Apply the construction at the two ends of each coordinate in succession to obtain a neighborhood of every corner. □

Lemma 1.25.5 (Closure)**.** *$\mathcal{S}$ is closed under smooth composition, fixed finite sums, radial integrals with smooth limits or integrable majorants for every derivative, a smooth locally finite partition of unity, and multiplication by a fixed smooth cutoff followed by zero extension when the cutoff is supported in the domain. These facts follow by the chain rule, the Leibniz rule and differentiation under the integral sign. It is also closed under the following operations.*

(f) ***Implicit functions.*** *Let $\mathcal{O} \subset \mathbb{R}^N$ be open, $F \in \mathcal{S}(\mathcal{O} \times J)$ (one-sided in $\hat{\zeta}$ only), and $c\colon J \to \mathcal{O}$ continuous, with $F(c(\hat{\zeta}), \hat{\zeta}) = 0$ and $\det D_c F(c(\hat{\zeta}), \hat{\zeta}) \neq 0$ for* every *$\hat{\zeta} \in J$, including $\hat{\zeta} = \pm 1$. Then $c \in C^\infty(J)$ (one-sided at ± 1), and $D_c F\, \partial_{\hat{\zeta}}^k c = -\partial_{\hat{\zeta}}^k F + \mathcal{R}_k(\partial_{\hat{\zeta}}^{<k} c)$. Moreover $\inf_J |\det D_c F(c(\hat{\zeta}), \hat{\zeta})| > 0$ and $\sup_J |\partial_{\hat{\zeta}}^k c| < \infty$ for each k.*

(g) ***Moving logarithmic coordinates.*** *Let $\frac{\hat{\xi}_*^2}{2} \in \mathcal{S}(J)$ with $\hat{\xi}_* > 0$, and let $\phi \in C^\infty(\mathbb{R} \times J)$. Then $\phi(2 \log(\hat{\xi}/\hat{\xi}_*(\hat{\zeta})), \hat{\zeta}) \in \mathcal{S}(\{\frac{\hat{\xi}^2}{2} > 0\} \times J)$ and $\partial_{\hat{\zeta}}|_{\hat{\xi}} = \partial_{\hat{\zeta}}|_y - (\log \frac{\hat{\xi}_*^2}{2})' \partial_y$.*

(h) ***Finite linear algebra.*** *If $M \in \mathcal{S}$ is a square-matrix function with $\det M \neq 0$ on the compact domain, then $M^{-1} \in \mathcal{S}$ and $\sup |M^{-1}| < \infty$.*

(i) ***Integrals with smooth limits.*** *Let $g \in \mathcal{S}(\Omega)$, and let $\alpha, \beta \in \mathcal{S}(J)$ have values in $[a, b]$. Then $\int_{\alpha(\hat{\zeta})}^{\beta(\hat{\zeta})} g(s, \hat{\zeta})\, \mathrm{d}s \in \mathcal{S}(J)$. The $\hat{\zeta}$-derivatives include the boundary terms $\beta' g(\beta, \hat{\zeta}) - \alpha' g(\alpha, \hat{\zeta})$. Noncompact integrals are covered by (b) when the dominators are $\hat{\zeta}$-independent.*

Proof. For (f), extend F smoothly across each endpoint in the distinguished angular variable, using the extension described above and localizing in c. The ordinary implicit function theorem applies at $(c(\pm1),\pm1)$; continuity of c and local uniqueness identify the restriction of that smooth branch with the given solution. Differentiate $F(c(\hat\zeta),\hat\zeta)=0$ to obtain the stated recursion. The determinant has a positive minimum on compact J, so induction bounds every derivative. Parts (g), (h), (i) follow from the chain rule, Cramer's rule and Leibniz's rule, respectively; the latter retains both moving-endpoint terms. For improper integrals use the stated derivative dominators. □

Remark 1.25.6 (Uniformity is automatic for one member). Every "uniform in $\hat\zeta$" assertion for the selected data is a statement about one fixed member on the compact interval J. By Lemma 1.25.5(f), it reduces to *pointwise* nondegeneracy at every $\hat\zeta\in J$, including ±1, together with continuity up to ±1. The parameter order does not require uniformity in the large parameters (C, Y_0, N_{sh}, widths) here. We do not claim it. What must be checked is therefore exactly the list of nondegeneracies in Section 1.25.2, *at the endpoints.*

Lemma 1.25.7 (Ordered exponential determinants)**.** *Let $a_1<\cdots<a_n$ be real. Let $\phi_1,\dots,\phi_n\ge0$ be integrable and not a.e. zero, with* $\operatorname{supp}\phi_j\subset[s_j,t_j]$ *and $t_j<s_{j+1}$. Assume $\int e^{a_iy}\phi_j(y)\,\mathrm{d}y<\infty$ for all i,j. Then*

$$\Delta(a;\phi):=\det\Big[\int e^{a_iy}\phi_j(y)\,\mathrm{d}y\Big]_{i,j=1}^{n}>0.$$

The same holds with e^{a_iy} replaced by x^{a_i} on $x>0$ and ordered supports in x.

Proof. The ordered exponential functions form a Chebyshev system: their initial Wronskians are positive Vandermonde determinants times positive exponentials. Continuity on the connected ordered node chamber and coalescence at a common node give $\det[e^{a_iy_j}]>0$ on the ordered support product. Multilinearity and Fubini integrate this determinant against $\prod_j\phi_j(y_j)$; the product is positive on a set of positive measure. The stated integrability justifies Fubini term by term. The power version follows by $x=e^y$. □

Remark 1.25.8. The identity $W(u^{\alpha_1},\dots,u^{\alpha_k})=\prod_{i<j}(\alpha_j-\alpha_i)\,u^{\sum\alpha_i-k(k-1)/2}$ gives the sign of every power Wronskian for ordered exponents on $u>0$.

1.25.2 Nondegeneracy on the closed angular interval

Each item lists the construction, its pointwise nondegeneracy, and why that nondegeneracy holds at $\hat\zeta=\pm1$.

N1. Exponent inverse (Lemma 1.15.26). The exponent $\nu(\hat\zeta)\in[\nu_c,\lambda]$ solves $\mathcal{F}(\nu,\hat\zeta)=\omega\mathcal{F}(\nu_c,\hat\zeta)+(1-\omega)\mathcal{F}(\lambda,\hat\zeta)$, with $\mathcal{F}_\nu\ge c>0$ uniformly (proof of Lemma 1.15.26). The cutoff ω is flat on collars, and ν is constant there. Thus near $\hat\zeta=\pm1$, ν is a constant, trivially in $\mathcal{S}$. Away from the collars, Lemma 1.25.5(f) applies with $N=1$. Hence $\nu\in C^\infty(J)$, and $\mu(\hat\zeta):=\nu(\hat\zeta)\in[\nu_c,\lambda]$.

N2. Two-return matrix. After the row factorization by $e^{\beta Y}$ and $e^{\beta_2 Y}$, with $\beta=\frac12-\nu$ and $\beta_2=\frac12-2\nu$, the matrix is $[e^{-\beta d_j}\mathcal{L}(\beta);\ e^{-\beta_2 d_j}\mathcal{L}(\beta_2)]$, with $\mathcal{L}(t)=\int e^{tz}\psi(z)\,\mathrm{d}z>0$. Its determinant is exactly

$$\mathcal{L}(\beta)\mathcal{L}(\beta_2)\,e^{-\beta(d_1+d_2)}\big(e^{\nu d_2}-e^{\nu d_1}\big),\qquad |e^{\nu d_2}-e^{\nu d_1}|\ge\nu|d_2-d_1|e^{-\nu\max_j|d_j|}\ge\nu_c|d_2-d_1|e^{-\lambda\max_j|d_j|},$$

and all factors are continuous in $\nu\in[\nu_c,\lambda]$, so the bound is uniform on J. The return coefficients b_j (and g_j in the affine sector) are therefore $\mathcal{S}$ functions by Lemma 1.25.5(h), and $c_j=A_pb_j+g_j$ once $A_p\in\mathcal{S}$ (N3).

N3. Transversality of the positive energy root.

Lemma 1.25.9. *Let $D_p, E_p, F_p, B_p \in \mathcal{S}(J)$ satisfy, at every $\hat\zeta \in J$,*

$$D_p \ge \tfrac14, \qquad B_p - F_p \ge b_0 > 0. \tag{1.25.1}$$

Then $\mathcal{P}(A) = D_pA^2 + 2E_pA + F_p - B_p$ has exactly one positive root, namely $A_p = (-E_p + \sqrt{E_p^2 + D_p(B_p - F_p)})/D_p$. We have $A_p \in \mathcal{S}(J)$ and

$$\mathcal{P}'(A_p) = 2\sqrt{E_p^2 + D_p(B_p - F_p)} \;\ge\; \sqrt{b_0} \qquad \text{on } J.$$

Proof. The product of the roots is $(F_p - B_p)/D_p < 0$, so the roots are real and of opposite signs. The displayed A_p is the positive root. Direct substitution gives the identity for $\mathcal{P}'(A_p)$. Then $2\sqrt{E_p^2 + D_p(B_p - F_p)} \ge 2\sqrt{b_0/4}$. Smoothness follows from Lemma 1.25.5(a), since the radicand is at least $b_0/4 > 0$. □

Verification of (1.25.1) for the selected member.

- In the variable-exponent sector ($G = 0$; proof of Lemma 1.16.4), $E_p = F_p = 0$ and $D_p = \frac14 + \nu\sum_j G_{jj}b_j^2 \ge \frac14$. Moreover $B_p = \frac14 - \nu\sigma_p + e^{-2\nu Y}(2\nu\tau_S - \frac14) \ge \frac14 - \epsilon_p - e^{-2\nu_c Y_{\min}}(\frac14 + 2\lambda K_f)$. This uses (1.16.19) ($|\nu\sigma_p| \le \epsilon_p$) and $|\tau_S| \le K_f$ (1.16.24).
- In the fixed-λ affine sector (Section 1.16.1), which contains the endpoint collars because $\nu \equiv \lambda$ there (N1), the same bound holds for B_p with $\nu = \lambda$. Also $D_p \ge \frac14$, and E_p, F_p are $O(\mathcal{P}(Y)e^{-cY})$ times the inlet bound $CK_p\lambda^{30-120\lambda}$ (Section 1.16.1).
- In the central sector (Lemma 1.16.9), $\nu = \nu_c$ is constant and the energy identity is the same disjoint-slot identity.

After the choices (ϵ_p small through λ, then Y_0 large; Lemma 1.16.4, proof of Lemma 1.16.8), (1.25.1) holds with $b_0 = \frac18$ at every $\hat\zeta \in J$. Since ν is constant near ±1 and all integrals have compact y-support or the dominators (1.25.6), the coefficients belong to $\mathcal{S}$, and Lemma 1.25.9 gives $\mathcal{P}'(A_p) \ge 2^{-3/2}$. This proves the transversality of the positive energy root on the *closed* interval. It uses only the finiteness of K_f before Y_0 (the ledger, G8), not its value.

N4. A11 two-row map (Lemma 1.15.5). At $t = 0$, the Jacobian of $(t_1, t_2) \mapsto (A_1t_1 + A_2t_2,\ 2B_1t_1 + 2B_2t_2 + C_1t_1^2 + C_2t_2^2)$ has determinant

$$2(A_1B_2 - A_2B_1) = 2A_1B_1(e^{-(1+2\lambda)d_*} - e^{(1-\lambda)d_*}),$$

where $A_1, B_1 > 0$ and $d_* > 0$. Its modulus is at least $2A_1B_1(e^{19d_*/20} - e^{-d_*}) > 0$ for $0 \le \lambda \le 1/20$. The quadratic implicit function theorem on a fixed small-data ball gives the solution. Its $\hat\zeta$-dependence enters only through the normalized target $u(\hat\zeta) \in \mathcal{S}$, so Lemma 1.25.5(f) applies at every $\hat\zeta \in J$.

N5. Stop and shot maps (Lemma 1.15.6). The slope-$2h$ solution of $W_x = \kappa W/x + (h - \kappa)/a$ is $Kx^{2h} - hx/(a(1 - 2h))$. At its first zero, $W_x = -h/a \ne 0$. Hence the hit point $x_{\mathrm{hit}}(\epsilon)$ of $W = c_t\epsilon$ is C^∞ on $[0, \epsilon_0]$ by Lemma 1.25.5(f), with ϵ as the one-sided parameter. The rescaled transition gives $x_b(\epsilon), g_b(\epsilon)$, smooth and positive down to $\epsilon = 0$, by smooth dependence of ODE solutions (closure (c)). The angle enters only through $\epsilon = R(\hat\zeta)^{-1/5}$ with $R \ge R_*$ smooth, and through the shot coefficient $c = GR^hK_{\mathrm{old}}(R)$. Here $K_{\mathrm{old}} \in [k_-, k_+]$ is a smooth function of $\log R$ with bounded logarithmic derivatives (Lemma 1.15.6). The compositions belong to $\mathcal{S}(J)$.

N6. Five-row determinants. *(a) Positive-order slow solve with the moving bumps.* Changing variables $\mathfrak{r} = \hat{\xi}_p e^{y/2}$ in the five moment rows of (1.1.2) and factoring the nonzero row constants gives

$$\begin{aligned} \det B_U &= \tfrac{1}{4}(\hat{\xi}_p^2)^{(p_1+p_2+2)/2}\Delta((1, 1-\mu); b^U), \\ \det B_E &= \tfrac{1}{8}(\hat{\xi}_p^2)^{(s_1+s_2+s_3+3)/2}\Delta((\tfrac{3}{2}, -\tfrac{1}{2}-\mu, \tfrac{1}{2}-\mu); b^E). \end{aligned} \tag{1.25.2}$$

where $(p_1, p_2) = (1, 1-2\mu)$, $(s_1, s_2, s_3) = (2, -2-2\mu, -2\mu)$ and Δ is the moment determinant with rows in the displayed order. Lemma 1.25.7 gives a fixed nonzero sign after row reordering. For the E block the exponent gaps remain at least one for $\mu \in [0, \lambda]$, so compactness gives a positive minimum. For the U block,

$$\Delta_U = \iint b_1^U(y_1) b_2^U(y_2) e^{y_1+y_2}(e^{-\mu y_2} - e^{-\mu y_1})\, \mathrm{d}y_1\, \mathrm{d}y_2.$$

The fixed support gap $y_2 - y_1 \geq g > 0$ gives $|\Delta_U| \geq c\mu \geq c\nu_c$. Since $\hat{\xi}_p > 0$ and $\mu \in [\nu_c, \lambda]$ are smooth on compact J, the prefactors are bounded away from zero and both inverses lie in $\mathcal{S}(J)$. This proves the determinant bounds in part (vi).

(b) Five-history inverses (Lemma 1.27.5; Lemma 1.13.7). At $U = 0$ the linearizations of $\int U, \int H, \int UH, \int (U^2 - H^2/4\frac{\hat{\xi}^2}{2}), \int H^2/4\frac{\hat{\xi}^4}{4}$ are δU, δH, $H\delta U$, $-H\delta H/(\hat{\xi}^2)$ and $H\delta H/(2\frac{\hat{\xi}^4}{4})$. Hence the Jacobian is block diagonal, with weights $(1, H)$ on U columns and $(1, -H/2\frac{\hat{\xi}^2}{2}, H/2\frac{\hat{\xi}^4}{4})$ on H columns. With $H = c\varphi(\hat{\xi}/\sqrt{2})^{-2\mu}$ these are the powers $(0, -\mu)$ and $(0, -1-\mu, -2-\mu)$ times row factors $1, c\varphi$ and $1, -c\varphi/2, c\varphi/2$, which are nonzero because $\min\varphi > 0$. Lemma 1.25.7 (power form) gives nonzero determinants for nonnegative ordered bumps of any width, with $|\det| \geq c\mu_{\min}$ for the U block. The finite-dimensional implicit function theorem, Lemma 1.25.5(f), then gives coefficients in $\mathcal{S}(J)$ on the closed interval. On the early nonlinear restoration reserve the selected perturbation is $O(N_{\mathrm{sh}}^{-2})$ by Lemma 1.13.7. On the compact angular interval continuity of the Jacobian, or the bound on $D_z Q_\eta$ in Lemma 1.27.5, gives the same positive lower bound up to a fixed fraction after increasing N_{sh}. For the late forward bank away from the central power germ, Lemma 1.27.5a computes the determinant of the same uncut columns on the actual mixture. The selected spectral coefficients have compact central angular support (Proposition 1.24.2, Section 1.26, proof of Lemma 1.25.10) and vanish identically near $\hat{\zeta} = \pm 1$.

N7. Capped loop (Lemma 1.19.2). Put $M = I_0$ and $z = \mu p_2$. The variance of $t(\theta; \mu)$ is exactly

$$V(\mu, p_2) = d_0^2 \frac{M(2z)/M(z)^2 - 1}{p_2^2} = d_0^2 \mu^2\, \mathcal{G}(\mu^2 p_2^2), \qquad \mathcal{G}(s) = \tfrac{1}{2} - \tfrac{3}{32}s + \tfrac{11}{576}s^2 - \dots,$$

with $\mathcal{G}$ real analytic and positive on $[0, \infty)$. The singularity at $s = 0$ is removable by the displayed series; at every positive real s, $I_0(\sqrt{s}) > 0$. For strict monotonicity, $\partial_z \log I_0(z)$ is the expectation of $\cos\theta$ under the positive density proportional to $e^{z\cos\theta}$, and its derivative is the strictly positive variance of $\cos\theta$. Thus $\partial_z \log(M(2z)/M(z)^2) > 0$ for $z > 0$. The elementary bounds $ce^z/\sqrt{z} \leq M(z) \leq Ce^z/\sqrt{z}$ for $z \geq 1$ give $M(2z)/M(z)^2 \geq c\sqrt{z} \to \infty$. For the lower bound, integrate the defining average of $e^{z\cos\theta}$ over $|\theta| \leq z^{-1/2}$; for the upper bound use $1 - \cos\theta \geq 2\theta^2/\pi^2$ on $[-\pi, \pi]$. Thus for $s = \mu^2$ the normalized variance $V/d_0^2 = s\mathcal{G}(sp_2^2)$ is unbounded when $p_2 \neq 0$ and equals $s/2$ when $p_2 = 0$. The variance of t at $p_2 = 0$ is $d_0^2 s/2$. No entire extension in complex s is asserted. Hence $s \mapsto s\mathcal{G}(sp_2^2)$ is a smooth increasing bijection of $[0, \infty)$ onto itself, with derivative $\frac{1}{2}$ at $s = 0$. Write $\rho = r_L/(a_s d_0^2)$. Then $\mu^2 = \rho\,\sigma(\rho, p_2)$ with σ smooth and positive.

Since $\sqrt{r_L} = \zeta(v_s)\sqrt{v_* - v_s}$ and $v_* - v_s \geq \delta_L/4$ on $\operatorname{supp}\zeta$, we get $\mu = \sqrt{\rho}\,\sigma^{1/2} \in \mathcal{S}$. The circle reparametrization has $\partial_\theta\phi = a_s(1+t^2)/(2\pi v) > 0$. Its inverse is smooth by Lemma 1.25.5(f). The loop data on $Y = I_{\mathrm{sh}} \times [-1,1]$ are smooth up to ∂Y (Section 1.19.2). The phase is $N_{\mathrm{sh}}(\log \frac{\hat\xi^2}{2} + f(\hat\zeta))$ with $f = \log\lambda_{\mathrm{ch}}$ on the endpoint collars (Section 1.6.5), which is analytic there.

N8. Protected core and rectangle cover. On the endpoint collars the core inputs satisfy

$$b = \lambda_{\mathrm{ch}}, \quad s_0 = \sigma_*\lambda_{\mathrm{ch}}^{h-\frac12}, \quad a' = (1+h)\lambda'_{\mathrm{ch}}/\lambda_{\mathrm{ch}}, \quad u = \lambda_{\mathrm{ch}}^{\frac12+h}(4\beta + j_0), \qquad \beta = \lambda_{\mathrm{ch}}^{\frac12-h}\hat\zeta.$$

They are analytic there by Lemma 1.25.1(c), and the intervening extensions are Gevrey–3/2. The formula $u = ((\frac12 - h)\hat\zeta - v)/d$ is used only away from the endpoints. Thus the inputs, including $\frac{\hat\xi_a^2}{2} = 4/(\Lambda b)$ and the quotients with positive denominators s_0, L, are Gevrey on a neighbourhood $\mathcal{N} \supset J$. Choose $J \subset \operatorname{int} K' \subset \mathcal{N}$ with $L > 0$. The core contraction and Proposition 1.22.4 give the required fixed-ϖ bounds there. The coefficients $d\partial_{\hat\zeta}$ and L^{-1} extend across the two endpoints on $[0,\Xi] \times U$, with $J \subset \operatorname{int} U \subset K'$ and (1.22.1). Thus the protected leading rectangle has both angular endpoints in its interior.

1.25.3 The actual leading endpoint jets along the full radial path

We compare the two sides in the slice chart of Subsection 1.6.2. Each field and history has the weight of (1.6.4), and the axis pressure p_{ax} has weight $2(\frac12 + h)$. Two tip-chart profiles of the same physical quantity have the same slice profile (Definition 1.6.4). The radial primitives from the axis have the same form in slice variables, because $\hat t\,\hat\xi\,\mathrm{d}\hat\xi = \widetilde Q\,\widetilde\xi\,\mathrm{d}\widetilde\xi$:

$$\begin{gathered}\widetilde M = \int_0^{\widetilde\xi} \rho\,\widetilde U\,\mathrm{d}\rho, \quad \widetilde I = \int_0^{\widetilde\xi} \rho\,\widetilde H\,\mathrm{d}\rho,\\ \widetilde J = \int_0^{\widetilde\xi} \rho\,\widetilde U\widetilde H\,\mathrm{d}\rho, \quad \widetilde S = \int_0^{\widetilde\xi} \rho(\widetilde U^2 - \tfrac12\widetilde E^2)\,\mathrm{d}\rho,\\ \widetilde C_p = \int_0^{\widetilde\xi} \frac{\widetilde E^2}{\rho}\,\mathrm{d}\rho,\end{gathered} \tag{1.25.3}$$

where the integrands are pulled back to radius ρ at fixed slice angular coordinate, and $\widetilde H = \widetilde\xi\,\widetilde E$.

These are statements about actual primitives, not choices of new constants. In particular $\widetilde P = \widetilde p_{\mathrm{ax}} + \widetilde C_p$ includes the two summands with the same weight $2(\frac12 + h)$. For explicit formulas on the forward collars we use the chart change λ_{ch} of Remark 1.6.7.

The selected backward model first fixes its extended pulse root and analytic datum $\Pi_0 = -\int_0^\infty E^2_{\mathrm{model}}/(\hat\xi^2)\,\hat\xi\,\mathrm{d}\hat\xi$. It includes the same equilibrium λ leg of length L_o and the jointly selected terminal shape as the forward future. The actual heat replacement keeps its inlet field, same heat coefficient and terminal edge fixed. Its rank-one correction (1.15.10) cancels the complete primitive discrepancy, with zero remainder.

The later pre-pulse three-E correction has targets $(0, -\Delta S_f, -\Delta C_{p,f})$, with $U = 0$ there, as in Lemma 1.15.9. The first target is zero. This correction does not change the primitive a second time. Thus the heat replacement together with its pre-pulse repayment has zero complete S and C_p increments on the full-compensation collars. The A11 target is determined separately by its incoming primitive, and its energy contribution enters both pulse equations.

For clarity, the endpoint field identification is explicit. On the flat-λ bridge we put $\beta = \lambda_{\mathrm{ch}}^{\frac{1}{2}-h}\hat{\zeta}$ and

$$K = K_b \frac{\lambda_{\mathrm{ch}}^{h-\lambda}}{1+\beta^2}, \quad \frac{\hat{\xi}_s^2}{2} = \frac{\hat{\xi}_{s,b}^2}{2} e^{-\rho_s \log \lambda_{\mathrm{ch}}}, \quad H = K(\hat{\xi}_s/\sqrt{2})^{-2\lambda} F_\lambda(2\log(\hat{\xi}/\hat{\xi}_s)), \quad U = Gk(2\log(\hat{\xi}/\hat{\xi}_s)). \tag{1.25.4}$$

Here F_λ, k are the same scalar pre-template and cutoff as on the backward branch. On the endpoint overlap $\rho_s = 1$ and G is the charted value. *Definition of the backward branch.* For every $|\beta| \le 1$ and $\hat{\xi} \ge \hat{\xi}_{\mathrm{match}}$, the backward model prefix is (1.25.4) at $\lambda_{\mathrm{ch}} = 1$: $H = K_b(1+\beta^2)^{-1}(\hat{\xi}_{s,b}/\sqrt{2})^{-2\lambda} F_\lambda(2\log(\hat{\xi}/\hat{\xi}_{s,b}))$ and $U = G_b\, k(2\log(\hat{\xi}/\hat{\xi}_{s,b}))$, with $G_b = 4\beta$ and scalars K_b and $\frac{\hat{\xi}_{s,b}^2}{2}$. On $[0, \hat{\xi}_{\mathrm{match}}^2/2]$ the pre-loop member is the profile of Theorem 1.8.10. Its actual continuation through the compensation bank, pulse and heat wing is specified by (B1)–(B6). The scalars are normalized by the reference pair of (B1): the reference arc $F_\lambda = e^{\gamma z}$, $z \le 0$, ends at $\hat{\xi}_{s,b} = \hat{\xi}_{\mathrm{ref}}$, where the growth turn of the pretemplate begins, as in [42, (A.7)] (the growth turn starts at $x = 1$; Lemma 1.8.4 bounds its growth by the template factor $e^{T/10}$). Thus $\hat{\xi}_{s,b} = \hat{\xi}_{\mathrm{ref}}$ and $K_b = \sqrt{2}\, P_*\big(\frac{\hat{\xi}_{\mathrm{ref}}^2}{2}\big)^{1/2+\lambda}$. Lemma 1.6.20 needs only $\frac{\hat{\xi}_{s,b}^2}{2} \ge e^{-z_\gamma}\frac{\hat{\xi}_{\mathrm{ref}}^2}{2}$, which (B1) forces. The edits of Lemma 1.8.8 act on this model. The model has the factor $f_b(\beta)^\vartheta$ of the proof of Lemma 1.6.14, with $\vartheta = 1$ up to the backward outlet R_e and ϑ equal to the flattening θ after R_e.

There K has weight $h-\lambda$, $\frac{\hat{\xi}_s^2}{2}$ converts like $\frac{\hat{\xi}^2}{2}$, and F_λ, k are functions of $2\log(\hat{\xi}/\hat{\xi}_s) = 2\log(\widetilde{\xi}/\widetilde{\xi}_s)$. On the endpoint collars the entire reference template in (1.25.4) is the slice continuation of the backward reference template (Lemma 1.6.8). The pretemplate ends at $\frac{\hat{\xi}_s^2}{2}e^T$ (Lemma 1.14.3), and the actual $60\log(1/\lambda)$ wait then gives $\frac{\hat{\xi}_p^2}{2} = \frac{\hat{\xi}_s^2}{2}e^T\lambda^{-60}$, as in (1.6.23). On the endpoint collars the backward outlet R_e and the backward pulse entry $\frac{\hat{\xi}_{p,b}^2}{2} = \frac{\hat{\xi}_{s,b}^2}{2}e^T\lambda^{-60}$ are constants.

On the forward collars $R_o = R_e/\lambda_{\mathrm{ch}}$ and $\frac{\hat{\xi}_p^2}{2} = \frac{\hat{\xi}_{p,b}^2}{2}/\lambda_{\mathrm{ch}}$. Thus on the two collars the pulse length $Y = \log(R_o/\frac{\hat{\xi}_p^2}{2})$ is the constant

$$Y_{\mathrm{end}} = \log \frac{R_e}{\frac{\hat{\xi}_{p,b}^2}{2}} = \log \frac{R_e \lambda^{60} e^{-T}}{\frac{\hat{\xi}_{s,b}^2}{2}}. \tag{1.25.5}$$

In slice variables $Y = \log(\widetilde{R}_o/\frac{\widetilde{\xi}_p^2}{2})$, and this ratio does not depend on the chart. The fixed-coordinate turnoff keeps $U_{\hat{\zeta}} = G'k - Gk's'$.

It does not suppress any moving-graph derivative. The pure outer future begins before actual A.10 and keeps actual A.11, the drive, wing and their canonical primitive. The full reference also includes its pre-pulse heat compensation. These choices first determine the E-field and all E-correction targets.

The pressure follows from the chosen swirl. Compute the actual prefix histories and the two affine axial returns using that swirl. The paragraph on p. 306 differentiates the two A11 equations at their common inlet and tracks their nonzero energy increment in both pulse equations. It then identifies the unique positive axial root. The later heat changes cancel against their pre-pulse compensation on the full-compensation endpoint germ. On the partial extension retain the residual of Lemma 1.15.9.

Exact cancellation holds only on the protected full-compensation endpoint germ. In the pulse normalization

$$K_{\mathrm{pulse}} = \int e^{-2\xi} R_0(\xi)^2 \, \mathrm{d}\xi, \quad \Phi = \frac{R_0}{2\sqrt{K_{\mathrm{pulse}}}}, \quad A_{\mathrm{amp}} = 2\sqrt{K_{\mathrm{pulse}}}\,\mathrm{Amp}_b,$$

the products $A_{\mathrm{amp}}\Phi$ and $\mathrm{Amp}_b R_0$ are equal. The root uniqueness assertion applies to this physical field, not identical names for differently normalized amplitudes.

For each fixed mixed derivative order, the actual heat estimates of Section 1.13 give on one tail

$$|\partial_{\hat\zeta}^{a}(\hat\xi^{-1}\partial_{\hat\xi})^{b}H| \le C_k\big(\tfrac{\hat\xi^2}{2}\big)^{-h-b}, \qquad |\partial_{\hat\zeta}^{a}(\hat\xi^{-1}\partial_{\hat\xi})^{b}(H - c_H(\hat\xi/\sqrt{2})^{-2h})| \le C_k\big(\tfrac{\hat\xi^2}{2}\big)^{-h-1-b}, \qquad a+b\le k. \tag{1.25.6}$$

The fast lift has polynomial-times-exponential bounds and zero endpoint jets. The negative-time branch uses the nonnegative-argument Laplace integral

$$H_-(Z) = \frac{1}{\Gamma(1+h)}\int_0^\infty e^{-v}v^h(1+Zv)^{-h}\,\mathrm{d}v, \qquad Z\ge 0.$$

Its nth derivative at zero is $(-1)^n(h)_n(1+h)_n$.

In slice variables $d/\frac{\hat\xi^2}{2} = \widetilde\eta/\frac{\widetilde\xi^2}{2}$ on the forward side and $d/\frac{\hat\xi^2}{2} = -\widetilde\eta/\frac{\widetilde\xi^2}{2}$ on the backward side (Lemma 1.6.2). Also $\hat t^{-h}(\hat\xi/\sqrt{2})^{-2h} = \widetilde Q^{-h}(\widetilde\xi/\sqrt{2})^{-2h}$. Thus the backward regular branch has the slice profile $c_H(\widetilde\xi/\sqrt{2})^{-2h}H_-(-2\widetilde\eta/\frac{\widetilde\xi^2}{2})$ for $\widetilde\eta\le 0$, with c_H in the forward coefficient convention. Its one-sided jet at $\widetilde\eta = 0$ is

$$\partial_{\widetilde\eta}^{n}\widetilde H\big(\tfrac{\widetilde\xi^2}{2},0\big) = c_H\,2^n(h)_n(1+h)_n\,\big(\tfrac{\widetilde\xi^2}{2}\big)^{-h-n} \qquad (n\ge 0). \tag{1.25.7}$$

The forward regular branch has the coefficients $2^n(h)_n(1+h)_n/n!$ in $d/\frac{\hat\xi^2}{2}$, so its one-sided jet is the same.

The sign of the Laplace derivatives cancels the sign of $\widetilde\eta$. If the same trace is $C_{\mathrm{tr}}r^{-1-2h}$, the two sides have the physical jets

$$\partial_t^n u_\theta(r,0) = C_{\mathrm{tr}}4^n(h)_n(1+h)_n r^{-1-2h-2n}.$$

In the backward and forward normalizations, $C_{\mathrm{tr}} = 2^{\frac12+h}c_{\mathrm{old}} = 2^h c_{\mathrm{bank}}$, so $c_H = c_{\mathrm{bank}} = \sqrt{2}c_{\mathrm{old}}$. This statement applies to one-sided jets.

It does not evaluate the Laplace integral at a negative argument.

The differentiated I_{ren}, S, C_p densities have, in the stated order, the bounds $C_k\big(\frac{\hat\xi^2}{2}\big)^{-h-1}$, $C_k\big(\frac{\hat\xi^2}{2}\big)^{-1-2h}$ and $C_k\big(\frac{\hat\xi^2}{2}\big)^{-2-2h}$. M and J have no exterior density. These are integrable. On the compact prefix, we use one enclosing hull.

At the regular axis $E = O((\hat\xi/\sqrt{2}))$, $H = O(\frac{\hat\xi^2}{2})$, $U = O(1)$. For the temporary model $E = O(\big(\frac{\hat\xi^2}{2}\big)^{.1})$ the pressure density is $O(\big(\frac{\hat\xi^2}{2}\big)^{-.8})$. Thus all fixed derivatives pass through the complete history and pressure integrals. Moving endpoints contribute their actual density terms.

These one-sided dominators justify the integral differentiations used in the next comparison. Equality of the full reference pressure jets also uses a match of the compact prefix and its actual correction constants. A shared heat velocity coefficient alone does not prove it.

Lemma 1.25.10 (Full-path identification of the leading jets)**.** *The selected backward and forward fields, pressures and five radial histories have the same physical slice jets along their full radial paths, with the common exterior normalization and integrable differentiated tails above.*

Proof. We use three facts.

(i) The slice profile of an object does not depend on the tip chart (Definition 1.6.4).

(ii) Each side is one-sided smooth (Lemma 1.24.1).

(iii) The design objects of the two sides are slice continuations of the backward objects (Lemma 1.6.8).

Each object below comes from a finite sequence of products, radial primitives from the axis, nonsingular finite solves and dominated full-path integrals. Each of these operations keeps equal slice jets. For products this is the Leibniz rule. For radial primitives it is (1.25.3).

For full-path integrals we use the dominators (1.25.6) and differentiate under the integral. Let $\mathcal{F}(c,p)=0$ be a solve with invertible $\mathcal{F}_c$. Differentiation in $\widetilde{\eta}$ at $\widetilde{\eta}=0$ gives the jets of c from the jets of p. The recursion is the same on the two sides.

Reference swirl, partial histories and the pulse root. Use the ring of one-sided slice jets at fixed $\widetilde{X}=\widetilde{\xi}^2/2$ and either sign of z. All cross-side comparisons of the actual heat and correction fields below are equalities in this ring. The template identities are evaluated on the endpoint collars where $\tau=1$. No continuation of the negative-time heat integral to a negative argument is required. Write $\ell=\lambda_{\mathrm{ch}}$, $X_b=\ell X$, $\beta=\ell^{1/2-h}\eta$. On the endpoint collars (1.25.4) gives the same reference template with $H_+=\ell^h H_-(X_b,\beta)$ and $U_+=\ell^{1/2+h}U_-(X_b,\beta)$ up to the pulse. The axial taper, translated slots and their limits in $y=\log(X/X_p)$ have the same germs because $X_{p,b}=\ell X_p$. The reference primitive starts at the ideal power, and the five-row insertion restores it at the matching graph as in the derivation of (Taper). The pressure and heat banks have zero complete I row. On the endpoint collars the pre-pulse taper in (Taper) is zero. The axial returns never change the swirl. Thus the actual $I/(R_oH_o)$ at the start of flattening is exactly $r_*+(r_b(\lambda)-r_*)(e^TR_{g,b}/R_e)^{1-\lambda}$, on both sides in native dimensionless units.

On the flattening and subsequent power wait $r=I/(XH)$ solves $r_y+(1+\partial_y\log H)r=1$ with this same initial datum and the transported coefficients. Subtract the two equations and use the integrating factor. The difference and each successive slice jet are zero. At the entrance to A11 the incoming ratio and the required outlet $r_\lambda=1/(1-\lambda)$ therefore agree between sides. The normalized target u in Lemma 1.15.5 has identical jets, although it can vary with β. Its coefficients A_j,B_j,C_j are the integrals of the same translated bumps in y. Subtract their two implicit systems and differentiate successively. The invertible Jacobian identifies both small coefficient jets. Inside either support the respective moment integrals have the same integrands and the same normalized upper limit. In particular A11's quadratic swirl-energy increment is included on both sides.

Compute the two actual future heat corrections before choosing the axial amplitude. In common slice units the heat collar cutoffs have the same relative supports and the regular and fast contributions have the jets in (1.25.7). Differentiation under the full discrepancy integral is justified by the three tail dominators above. The rank-one primitive correction therefore has the same target and scalar denominator in common units. At the pre-pulse heat bank $\chi_b=1$; the three targets are $0,-\Delta S_f,-\Delta C_{p,f}$ in their respective weights. Its invertible actual quadratic moment map gives the same small coefficients. This also identifies the partial integrals through the three bumps.

For the axial pulse put $A=\mathrm{Amp}_b$ in the common R_0 normalization, $c_j=Ab_j+g_j$. Dividing M,J by $X_pE_p, X_pH_pE_p$ gives identical inlet rows and the same two-by-two return matrix on both sides. Therefore all b_j,g_j agree in the jet ring. In these units the complete energy equation is

$$K_{\mathrm{pulse}}A^2+\lambda\sum_j K_j(Ab_j+g_j)^2=\tfrac14-\lambda\sigma_p+e^{-2\lambda Y}(2\lambda\tau_S-\tfrac14).$$

Here $\sigma_p=2S_p/H_p^2$ and τ_S includes the two A11 bumps. Under $X_b=\ell X$, S and H_p^2 both have weight $2h$. The normalized full-compensation heat contribution vanishes by (1.14.18). This cancellation leaves the generally nonzero A11 energy in both equations. The coefficients now agree, and the unique

positive root has a nonzero amplitude derivative by (N3). Successive differentiation gives the same physical amplitude and all axial-return coefficients. In the forward notation $A_{\mathrm{amp}} = 2\sqrt{K_{\mathrm{pulse}}}\,A$ and $A_{\mathrm{amp}}\Phi = AR_0$.

For any partially traversed reference bank the weight of its integrated row follows from $dX_b = \ell\,dX$. For M, I, J, S, C_p the resulting weights are $h - \frac{1}{2}, h - 1, 2h - \frac{1}{2}, 2h, 1 + 2h$, respectively. In particular $\partial_X[I_+ - \ell^{h-1}I_-(\ell X, \beta)] = H_+ - \ell^h H_-(\ell X, \beta)$. The common reference values at each inlet and the common partial integrands identify the jets at every intermediate radius. The remaining construction inserts the actual pressure class, regular core and loop as follows.

Pressure class. The pressure-class correction solves $\Delta I = \Delta S = 0$, $\Delta C_p = \Pi_{\mathrm{ref}} - p_0$, $\Delta M = \Delta J = 0$. On the full-compensation collars ($\chi_b = 1$), Π_{ref} has the slice jets of the analytic model Π_0 by (1.6.40). The Gevrey datum p_0 equals the analytic Π_0 germ in slice variables on smaller endpoint neighborhoods. Thus the target $\Pi_{\mathrm{ref}} - p_0$ has zero slice jets.

The three distinct power rows give an invertible Jacobian. Differentiation of the unique small nonlinear solution shows that all its endpoint derivatives vanish. This is jet equality, not open-collar equality. Downstream physical P does not change, and C_p has the stated offset.

Core. The variable-scale core has the specified slice-continued velocity, pressure and swirl-gauge germs (Lemma 1.6.38). The two-sign gauge-bump construction matches gauge values and slopes. On $\varpi \le e^{t_{\mathrm{act}}}$ the forward core and activation are the slice continuations of the backward ones (Lemma 1.22.6 and Proposition 1.22.7). This replaces the appeal to a regular radial uniqueness of the core. For $y_a \ge t_{\mathrm{act}}$ we use Hypothesis 1.22.9 (Remark 1.22.8). The activation datum in Hypothesis 1.22.9 is supplied by Proposition 1.20.43 and Lemma 1.22.10; this uses the selected joint termination, before the loop. Its earlier two-U/three-E correction targets the pressure-edited reference.

Its equations include $\Delta J - G\Delta I$, $\Delta S - 2G\Delta M$ and the two quadratic bump terms. The targets and the slice-continued templates thus have equal slice jets. The invertible nonlinear Jacobian identifies the correction jets. The absolute core-correction coefficients can be nonzero.

Only the difference of their slice jets is zero. This construction does not cut off a nonzero coefficient.

Loop, restoration and spectral controls.

Apply Lemma 1.19.4 to the *physical* pre-loop members of (1.19.1) and (B1) of the backward construction. On the full-compensation collars, (1.6.40), the pressure-class prescription and the preceding core return give, in the ring of slice jets,

$$p_{0,+} = \ell^{1+2h}\Pi_0(\beta), \qquad P_+^{\mathrm{pre}}(X, \eta) = \ell^{1+2h}P_-^{\mathrm{pre}}(\ell X, \beta).$$

Indeed the first equality identifies the axis value. For the second integrate the matching physical swirl densities from that axis, using $X_b = \ell X$ and the C_p weight $1 + 2h$. The same change of variables in the other four rows gives the weights computed above. It identifies all five inward histories on the two windows and their common restoration reserve. The equality incorporates the two actual heat-bank targets and all intermediate upper limits. There is no requirement that the jet of the individual heat correction vanish. This discharges (P), including the pressure contribution to the axial component of $\mathbf{p}$.

The joint choices of Lemma 1.19.2 and Proposition 1.8.16 give (J1)–(J3). The loop is a smooth function of the common shears and integrated vector with one circle origin. Its phase (1.6.66) is $N_{\mathrm{sh}} \log(\ell X)$ in the forward endpoint chart and $N_{\mathrm{sh}} \log X_b$ on the backward side. The strict collar cutoff makes the loop inactive on the difference of the windows. Lemma 1.19.4 therefore identifies the modulated fields and their complete exit discrepancies in slice jets. The five return equations use those discrepancies with the opposite sign and the common templates of (J3). The invertible return

Jacobian identifies the unique small coefficients to every order. At the reserve exit this restores the physical pre-loop histories on each side. Their complete pressure integrals are unchanged by the joint modulation and return. The common heat-pressure normalization thus persists all the way to the exterior. The spectral modification, centerings and all its compensation controls have compact central angular support. Thus they vanish on endpoint neighborhoods at each radius. Their complete C_p return keeps the edited pressure constant.

□

1.26 The protected hold and the selected spectrum

The physical resolvent estimates are first proved conditionally. We verify their hypotheses for the selected leading field before defining the shift on its selected pair of angular bands. Theorem 1.30.1 and Proposition 1.31.4 select one leading member with an unstable frozen eigenvalue. They also give the spectral gaps, quadratic phase deficit, and profile bounds for the propagation argument. The input is the family from Section 1.6, with its strict stress margins, same heat tail, and reserved central hold.

We modify this same family on compact supports and restore all five radial moments. First, we prove that a simple eigenvalue branch exists on the true radial domain. We then use its physical response rank to center the maximum and set the curvature. These arguments use no estimates for the completed background.

1.26.1 The protected hold and its quantitative margins

The spectral construction uses five properties:

- a gap between the scalar power and the heat exponent,
- a positive stress ceiling,
- a nonzero local angular-velocity slope,
- global first-strain and product bounds,
- exact restoration of five moments outside the spectral interval.

The protected hold supplies $U = M = J = 0$, $H = G(\frac{\hat{\xi}^2}{2}/R)^{-\nu_c}$ and

$$\Omega_c = H/(\hat{\xi}^2), \qquad S_0 = -2(1+\nu_c)\Omega_c \neq 0.$$

The local symmetry on this protected hold is a property of the full leading future before spectral implantation, not of the previous pulse. On the central band $\chi = 0$, the outer A10/A11 field is absent for each $\frac{\hat{\xi}^2}{2}$. The mixture inlet-germ correction is zero there because the power and actual primitive germs agree.

We also keep the real scalar δI memory correction. Its scalar cutoff lies in $[R_m, 2R_m]$, after $\max R_o$ and before $R_h > 2R_m$. It restores the same future before the hold, without a change to ρ.

For that restored future the actual lift formulas are $I_L = d^{1-h} i(\frac{\hat{\xi}^2}{2}/d)$ and $H_L = d^{-h} g_*(\frac{\hat{\xi}^2}{2}/d)$ with scalar shot functions. The central-wing cutoff is even and its edge is $B_o(\eta) = B_o \exp(k_o \eta^2)$, with scalar amplitude and width. The primitive blend uses radial-only χ_b and includes the actual $\chi_b' \Delta$ correction. The two primitives and Δ are even.

The same scalar heat coefficients and their even d-lift complete this full radial future. Earlier pressure and core corrections restore the edited reference before it. These actual support and field formulas, not the scalar value of H on the hold alone, make its canonical outward integrals S, P even. The same energy root and exact returns identify the retained histories with those outward integrals.

Together with $U = M = J = 0$, the integrated source then gives $T_z(\frac{\hat{\xi}^2}{2}, 0) = 0$. The normalized chart factor satisfies $Q(Z) - Z^2 Q(Z)^{2h} = 1$, so Q is even and $\eta(Z)$ is odd. $\Omega = Q^{-1-h} F(R^2/(2Q), \eta(Z))$ is even locally on this hold. This argument does not assert parity after spectral implantation, its moment corrections, or completion. The source formulas are equations (1.13.47), (1.13.52), (1.13.53) and (1.13.57).

The stress ceiling on the protected central hold is comparable to $e_g C^5$. Here e_g denotes the positive normalized swirl scale on this hold. On the unedited hold $\frac{\hat{\xi}^2}{2} = R_h e^s$, $0 \le s \le B$, we have $e_g(s) = e_p(k_h e^s / x_p)^{-1/2-\nu}$. The two-sided bounds for e_p in the proof of Lemma 1.6.19 thus give two-sided bounds for e_g that do not depend on C.

We first fix the finite geometry and pulse parameters. This positive lower bound can be very small. The source estimates in Lemma 1.27.1 ("Piecewise first-radial and true-return admission") and the source selections in Section 1.30.2 give this ceiling.

After the capped-loop modulation the leading data satisfy the global bounds

$$\Omega_{\max} \le K/C, \qquad B_{\mathrm{rest}} \le K, \qquad P_{\mathrm{rest}} \le K/C, \tag{1.26.1}$$

with the retained-source constants fixed before the late spectral integer. The compact spectral modification contributes to the actual bound $P_{\mathrm{actual}} \le K(1+\Delta)/C$. The bound P_{rest} does not include this contribution. We select $\Delta = C^\sigma$, $0 < \sigma < 5$. The ceiling then dominates Δ, and the unwanted products and pre-existing strain are small relative to it.

1.26.2 The selected physical frozen spectrum

The spectral argument is Theorem 1.30.1 in Section 1.30, with Proposition 1.31.4. At the moving radial center $r_c(Z) = \sqrt{\hat{\xi}_c^2 Q(Z)}$, we put

$$\beta_n(Z,k) = n\Omega_c(Z) + kW_c(Z), \qquad \mu_D = \Lambda + i\beta_n, \qquad D_{\mathrm{sp}} = \mu_D + in(\Omega - \Omega_c) + ik(W - W_c).$$

Here Λ is the physical resolvent parameter.

We translate only its denominator: $B = 2\Omega + r\Omega_r$ and each numerator keep the true profile. A contour Γ in μ_D represents the physical contour $\Gamma - i\beta_n$. This is not a rotating-frame change of the time-dependent operator.

For the leading data above, Lemma 1.6.20 holds and the local parity on the protected hold is Lemma 1.6.32. Theorem 1.30.1 and Proposition 1.31.4 then give the following. The leading data admit one finite C, with $\Delta = C^\sigma$ and $0 < \sigma < 5$. They admit one integer $m \ge 30$, a width d_m, and compact controls with exact five-history returns. The operator is the frozen inviscid velocity generator with the physical Leray projection. Only the labels $\pm m$ attain its maximal spectral real part over all $n \in \mathbb{Z}$ and $(Z,k) \in \mathbb{R}^2$. The positive-label physical eigenvalue has the unique maximizing phase $(Z,k) = (0,0)$. It is algebraically simple and satisfies $\Re\lambda_0 = \lambda_c > g > 0$. Its radial complement lies in $\Re z \le g$. The other angular labels have a gap of at least $c_C \Delta d_m^2$ from the maximal spectral real part (see (1.31.9)). Near the pole, the same branch has a quadratic deficit, not a uniform gap.

We record four outputs of the selection at the pole $(Z,k) = (0,0)$ of the positive label. They are established in the proof of Theorem 1.30.1 and Proposition 1.32.1, not in Sections 1.27–1.29:

(a) the centering $\lambda_Z = \lambda_k = \lambda_{Zk} = 0$, from the six-real centering map of Lemma 1.30.36 with the exact jet relations (1.30.15); (b) $\Re\lambda_{kk} < 0$, from the pole comparison $-C_A\Delta \le a_m^2\Re\lambda_{kk}/h^2 \le -c_A\Delta$ before (1.30.25); (c) the exact complex curvature identity (1.32.2) with the real constant $C_q > 0$, equivalently the complex Riccati identity with real $q = a_m^2 C_q/\Delta$; (d) the Gaussian reserve (1.32.1), with the margin 1/16 of (1.30.25). On the selected branch $X > b_d$, put $\eta_q = X - b_d/2 - \sqrt{X^2 - b_d X}$, where $b_d = \frac{1}{2}(1 + (1-2h)/h) = \frac{1}{2}(h^{-1} - 1) > 1/4$. Then $\eta_q < 1/8 \iff X > (b_d + \frac{1}{4})^2$, and $\eta_q \le 1/16 \iff X \ge 2(b_d + \frac{1}{8})^2$. Sections 1.28–1.29 supply only the regularity of these jets (Proposition 1.28.8(vi), Proposition 1.29.13; chart-wide in Lemma 1.30.34), the normalization $\ell e = 1$, and the conjugate-pair symmetry (Proposition 1.29.13(iv)). The physical contour, true adjoint, and pressure reconstruction satisfy the finite weighted ladders of the proof of Theorem 1.30.1. The actual all-Z coefficient bounds and small-viscosity inputs hold for this same fixed source.

In this spectral argument d denotes the narrow implant width, not the earlier angular factor $1 - \eta^2$. With $\alpha = |n|d$, $b = kr_0 d$, and $A_{\mathrm{sc}} = (\alpha^2 + b^2)^{1/2}$, the normalized two-layer model is

$$\mu_D^2 = \Delta^2 t(y)^2 \frac{\alpha^2}{A_{\mathrm{sc}}^2}\left[\frac{e^{-4A_{\mathrm{sc}}}}{4} - (A_{\mathrm{sc}} - \tfrac{1}{2})^2\right].$$

This ideal model omits the pre-existing power slope. Its positive root has a strictly concave maximum at $(\alpha, b, y) = (\alpha_{\mathrm{m}}, 0, 0)$, where $1 - 2\alpha_{\mathrm{m}} = e^{-4\alpha_{\mathrm{m}}}$.

For the signed pre-existing power slope $s_{\mathrm{old}} = -2(1+\nu_c)\Omega_g < 0$, the implant changes the slope by $-\Delta t(y)$. The retained two-interface comparison model thus has inner-slope magnitude $S_t = \Delta t - s_{\mathrm{old}} > 0$ and exact dispersion

$$\mu_D^2 = \frac{\alpha^2}{A_{\mathrm{sc}}^2}\left\{\frac{\Delta^2 t^2 e^{-4A_{\mathrm{sc}}}}{4} - \left[(\Delta t - s_{\mathrm{old}})A_{\mathrm{sc}} - \Delta t/2\right]^2\right\}. \tag{1.26.2}$$

In particular S_t is not $\Delta t + s_{\mathrm{old}}$. Equations (1.30.6)–(1.30.8) prove its exact determinant and quantitative persistent perturbation bounds.

For completeness, the global coefficient input uses the exact identities

$$\Omega = Q^{-1-h}F, \quad W = Q^{-\frac{1}{2}-h}U, \quad V_r = Q^{-1/2}V/\hat{\xi}, \quad r\,dr = Q\,\hat{\xi}\,\mathrm{d}\hat{\xi},$$

$$Z\partial_Z \log Q = \frac{2\eta^2}{1-2h\eta^2}, \qquad Z\partial_Z \eta = \frac{\eta(1-\eta^2)}{1-2h\eta^2}.$$

They give the global weighted pointwise and radial L^2 bounds from the actual normalized fields and differentiated closed-end heat tails. We keep the regular-axis Cartesian germs. Compactness of a physical Z chart does not give these global bounds.

The spectral modification and its later moment corrections have zero total increments in the five histories of this same member. The correction supports avoid the core, spectral interval and endpoint germs. Thus the canonical pressure and pulse inputs agree before their full radial hull, while the full histories and same heat field agree after its exit. Inside that hull the equations keep the partial-history changes and the pressure between individual supports. The stress-cone estimates control these changes.

We do not assert that they vanish outside the individual correction supports. We fix the physical leading fields with the spectral controls and all five returns. The same completion uses this same member with its endpoint jets and stress margins. It does not select the spectrum again or change the leading fields.

1.27 The source family and its quantitative bounds

Main result. Lemmas 1.27.1 and 1.27.4 give source and form bounds before spectral selection. They apply to the actual leading family with its stated parameter order and exact histories.

Lemma 1.27.5 gives the local inverse that corrects five terminal histories. These results do not assume a spectral pair of maximal growth.

The forward construction uses a leading profile with the stated cone, history, edge, and coefficient conditions. This section gives its dependence on the next spectral choices.

We verify these bounds before we apply the spectral comparison. Section 1.32 then selects and fixes one member for the forward completion.

1.27.1 A radius-independent product bound

In the leading source variables, we write

$$p = (N_\theta, N_z)/F, \qquad a = 2 - \hat{\xi} H_{\hat{\xi}}/H, \qquad b = U_{\hat{\xi}}/F \ (= \mathfrak{b} \text{ of } (1.12.1)),$$

on the active set, with the conventions of Section 1.13 and (1.19.3). The relaxed cone used in the source construction contains

$$a^2 + b^2 \le a p_1 - b p_2. \tag{1.27.1}$$

All inequalities in this section apply to the actual profile and its complete radial histories, with its pressure constants.

We write R_{match} for the next matching radius to distinguish it from the similarity radius R in the forward construction.

1.27.2 Source bounds on all columns before spectral selection

Lemma 1.27.1 (Piecewise first-radial and true-return admission)**.** *We fix the normalized prefix and future geometry, actual variable pulse length, return templates, the same heat construction, and pressure/core-data family before C. We impose $C \ge C_0(Y)$ for the endpoint compensation.*

We then set $\Delta = C^\sigma$, $0 < \sigma < 5$. The actual preloop profile satisfies

$$\sup_{\hat{\xi},\eta}(|F| + |\hat{\xi} F_{\hat{\xi}}|) \le K/C, \qquad \sup_{\hat{\xi},\eta} \hat{\xi} \Big|\frac{U_{\hat{\xi}}}{\hat{\xi}}\Big| \le K. \tag{1.27.2}$$

Apply the capped loop, its true correction, the main perturbation, and the allowed controls with their true returns, with the late width obeying $K d\Delta \le C^{-1}$ (as imposed in the proof). Then, with one bound for all frozen Z,

$$\|\Omega\|_\infty \le K/C, \quad \|r\Omega_r\|_\infty + \|W_r\|_\infty \le K(1+\Delta), \quad \sup(2|\Omega B| + |\Omega W_r|) \le K(1+\Delta)/C. \tag{1.27.3}$$

We subtract the explicit second-derivative layers.

The residual weighted radial second-derivative constant J_C is finite. It is independent of the late pair (m, d_m) along the width bracket. This independence is required because N_0, and with it the bound $J_C/(|n|g)$, is fixed before m. We do not assume uniformity in C.

Proof. The next piecewise calculations prove (1.27.2). Positivity alone does not imply this estimate.

(i) On the fixed core, activation and reference entry, $F = C^{-1}$ times a core factor with one bound. The activation laws are $\partial_y \log F = -\kappa(y)p_{1,r}/2$ and $\partial_y U = -\kappa(y)\frac{\hat{\xi}^2}{2}n_{s,r}/2$, where

$$\kappa(y) = 1 - (1 - \kappa_{\mathrm{act}})\sigma(y/t_{\mathrm{act}}), \qquad \kappa_{\mathrm{act}} \le \kappa(y) \le 1.$$

Here the reference quantities are explicitly

$$p_{1,r} = -\hat{\xi}^2(\hat{\xi}^{-1}\partial_{\hat{\xi}}(F_r))/F_r = -2Y(\Phi_C)_Y/\Phi_C,$$
$$n_{s,r} = -2(\hat{\xi}^{-1}\partial_{\hat{\xi}}(U_r)) = -2b(w_C)_Y, \quad Y = \Lambda b\tfrac{\hat{\xi}^2}{2}.$$

The fixed core coefficient ball gives $\Phi_C \ge c > 0$. Its first Y derivatives have one bound when $\|C^{-1}e^{\Lambda\psi+a}\| \le 1$.

Thus $|p_{1,r}| + \hat{\xi}|n_{s,r}| \le P_{\mathrm{ref}}$ with P_{ref} independent of the last C. This does not assert a uniform bound for the different axial ratio $p_{2,r}^2/p_{1,r}$.

Thus the first-radial identities are $\hat{\xi}F_{\hat{\xi}} = -\kappa(y)p_{1,r}F$ and $\frac{U_{\hat{\xi}}}{\hat{\xi}} = -\kappa(y)n_{s,r}/2$. The controlled reference bounds and $0 \le \kappa(y) \le 1$ give $|F| + |\hat{\xi}F_{\hat{\xi}}| \le K/C$ and $\hat{\xi}|\frac{U_{\hat{\xi}}}{\hat{\xi}}| \le K$ throughout the actual activation, even when its selected widths depend on C.

Reference flattening also multiplies the actual derivative by a number in $[0, 1]$. No derivative of κ or of an arbitrarily narrow interpolating cutoff enters these first-radial identities.

Derivatives of the narrow cutoffs first enter field derivatives of total order at least two. These include mixed $(\frac{\hat{\xi}^2}{2}, \eta)$ derivatives and the related fixed-r Z jets. Thus, with $y = 2\log(\hat{\xi}/\hat{\xi}_a(\eta))$,

$$\partial_\eta|_{\hat{\xi}} = \partial_\eta|_y - (\log \tfrac{\hat{\xi}^2}{\hat{\xi}_a^2})'\partial_y,$$

so one derivative of $\frac{U_{\hat{\xi}}}{\hat{\xi}} = -\kappa(y)n_{s,r}/2$ in η includes $\kappa_y(y)(\log \frac{\hat{\xi}^2}{\hat{\xi}_a^2})'n_{s,r}/2$.

By contrast, one angular derivative of the integrated equations for U and $\log F$ differentiates the upper endpoint and the reference coefficients. It uses only the values of κ.

For the fixed selected member, all necessary cutoff derivatives are finite.

The radial second-derivative terms contribute to J_C. The mixed terms contribute to the related ordinary source-jet constants.

We do not assign width-independent higher-jet bounds to these terms.

(ii) On the Full intermediate scalarization/growth interval,

$$F = C^{-1}\big(\tfrac{\hat{\xi}^2}{2}\big)^{-2/5}e^{l(\frac{\hat{\xi}^2}{2})}/\sqrt{2}, \qquad |l| + |\tfrac{1}{2}\hat{\xi}l_{\hat{\xi}}| \le K, \quad \hat{\xi} \ge \hat{\xi}_i > 0.$$

Differentiation gives the same first-radial bounds.

Here U is radially constant except for its actual fixed-log flattening. This calculation covers the interval, not only its entrance and exit.

(iii) At the actual core five-correction and pressure-class three-E correction, write $\frac{\hat{\xi}^2}{2} = C^{10}x$, $E = e_*f(x)$, $U = e_*u(x)$. Their fixed normalized bump maps have bounded coefficients and derivatives.

The pressure-class three-row derivative has independent weights $x^{1/2}, x^{1/10}, x^{-9/10}$. Thus $|E| + |\frac{1}{2}\hat{\xi}E_{\hat{\xi}}| + |U| + |\frac{1}{2}\hat{\xi}U_{\hat{\xi}}| \le K$, and

$$|F| + |\hat{\xi}F_{\hat{\xi}}| + \hat{\xi}|\frac{U_{\hat{\xi}}}{\hat{\xi}}| \le KC^{-5}.$$

The pressure-class correction changes its axis constant with the compensating sign.

It does not keep all five histories.

(iv) The outer two-E correction, retained pre-A.10/A.11 block, and actual heat compensation use their actual I/C_p or $I/S/C_p$ targets.

The A.11 determinant gap is $2+\lambda$. Their small normalized branches have fixed relative bumps and the same bound as in (iii).

In particular the model-first heat compensation has normalized coefficients $O(R^{-1})$ only AFTER its admission $C \ge C_0(Y)$. No partial-history change is set to zero before the actual correction exit.

(v) Slope turns, the actual U turnoff, negative wait, main pulse and translated returns have fixed finite logarithmic/phase templates. Their exact quadratic energy equation gives bounded $A = 1 + o(1)$ and bounded return coefficients.

The equation includes the complete energy of the future and returns. Their values and first radial derivatives thus satisfy (iii), with constants that depend on the fixed Y, ν_c, λ.

(vi) On the actual scalar shot, $|g'_* - H'_b| \le KC_b/W_s^2$. We use the source-free buffer to expose the fast mode before we use its tail estimates. In the whole ordered future, the angular cutoff has no radial derivative.

Thus the radial derivative of the blend is the convex blend of the component derivatives.

(vii) On the narrow central wing,

$$\delta H = -\psi\alpha\ell f((B - \tfrac{\hat{\xi}^2}{2})/\ell), \quad \delta\frac{H_{\hat{\xi}}}{\hat{\xi}} = \psi\alpha f'((B - \tfrac{\hat{\xi}^2}{2})/\ell), \quad \alpha = \epsilon hG/R.$$

Thus $\frac{\hat{\xi}^2}{2}|\delta\frac{H_{\hat{\xi}}}{\hat{\xi}}| \le KG$ because the amplitude compensates for the first width derivative.

The potentially large second derivative contributes to J_C.

We do not claim a uniform higher-order bound.

(viii) The same heat tail uses its actual exposed fast contribution and differentiated regular heat estimates on the closed angular range.

The endpoint charts are the actual matched charts. No large unexposed fast coefficient is continued through a backward chart.

These calculations apply to the fixed jointly constructed leading family and its actual normalized corrections. They do not apply to arbitrary relaxed profiles.

They establish (1.27.2) before any spectral count.

For $Q - Z^2Q^{2h} = 1$, $\eta = ZQ^{h-\frac{1}{2}}$ and $\hat{\xi} = r/\sqrt{Q}$, Q, η are independent of r and $Q \geq 1$. The EXACT identities are

$$\begin{aligned} \Omega &= Q^{-1-h}F, \\ r\Omega_r &= Q^{-1-h}\hat{\xi}F_{\hat{\xi}}, \\ W_r &= Q^{-1-h}U_{\hat{\xi}}, \end{aligned} \tag{1.27.4}$$

$$\begin{aligned} r^2\Omega_{rr} &= Q^{-1-h}(4\tfrac{\hat{\xi}^4}{4}(\frac{F_{\hat{\xi}\hat{\xi}}}{\hat{\xi}^2} - \frac{F_{\hat{\xi}}}{\hat{\xi}^3}) + \hat{\xi}F_{\hat{\xi}}), \\ rW_{rr} &= Q^{-1-h}\hat{\xi}(\frac{U_{\hat{\xi}}}{\hat{\xi}} + \hat{\xi}^2(\frac{U_{\hat{\xi}\hat{\xi}}}{\hat{\xi}^2} - \frac{U_{\hat{\xi}}}{\hat{\xi}^3})). \end{aligned} \tag{1.27.5}$$

Thus the preloop product is $O(C^{-1})$ on Each Z column.

Actual compact normalized transitions plus regular axis and differentiated heat tail give finite weighted second-radial constants after we fix C. Rapid angular derivatives do not enter these radial identities.

We use the actual capped selector on its modified set, with $a_L < 5/2$ and $|b_L| < 5/4$. We keep the old shear elsewhere.

Its direct strain/product identities give

$$B_{\mathrm{mod}} \leq 7|\Omega_{\mathrm{ref}}|, \qquad P_{\mathrm{mod}} \leq 9|\Omega_{\mathrm{ref}}|^2.$$

We select a finite actual loop frequency $N(C)$. Its exact nonlinear five-return correction must have physical first-radial error $e \leq cC^{-2}$.

The product expansion is

$$B_{\mathrm{bank,new}} \leq B_{\mathrm{bank}} + 3e, \qquad P_{\mathrm{bank,new}} \leq P_{\mathrm{bank}} + 11B_{\mathrm{bank}}e + 7e^2.$$

Outside the modulation and correction, the actual field and its radial first derivatives remain unchanged. The partial histories can still change there. These estimates keep the preloop bounds.

Its now fixed second derivatives, with any finite size in $N(C)$, enter J_C.

Put $x = \log(\hat{\xi}/\hat{\xi}_c) = \log(r/r_c(\eta))$, $y = \eta/\ell_m$, and take the nonnegative radial cutoff χ_m equal to one on the two rounded corners and the interval between them. The physical edit and its native lift are

$$\delta\Omega = -d\Delta\, t(y)\kappa_\sigma(x/d)\chi_m(x), \qquad \delta F = Q^{1+h}\delta\Omega, \qquad \delta H = \hat{\xi}^2\delta F.$$

Thus $\|\delta\Omega\|_\infty \leq Kd\Delta$ and $\|r\delta\Omega_r\|_\infty \leq K\Delta$. The η-support of the main edit is $|\eta| \leq \ell_m Y_*$, with $\ell_m = r_0 L_\zeta/m$. On the compact power hold, $(H_{\mathrm{old}})_x = -2\nu_c H_{\mathrm{old}}$ with $\min H_{\mathrm{old}} > 0$. At fixed η,

$$(\delta H)_x = -\hat{\xi}^2 Q^{1+h}\Delta\, t(y)\kappa'_\sigma(x/d)\chi_m(x) + O_C(d\Delta).$$

The leading term is nonpositive since $t \geq 0$ and $\kappa'_\sigma \geq 0$. The fixed return bumps change H and H_x by $O_C(d\Delta)$ by (1.30.23). Thus $H > 0$ and $a_s - 2 = -H_x/H > 0$ everywhere on the hull for every sufficiently late width, also when the main edit is multiplied by any number in $[0, 1]$ and its returns are solved anew. The main edit changes only H. Three H returns solve the I, S, P equations by the invertible three-column block of Lemma 1.27.5. They preserve the M, J rows since $U = 0$ on the hold. Uniqueness of the small five-coefficient solution therefore gives zero for both U returns. Hence $U = M = 0$ and $b_s = 0$ throughout this hull, and the fourth cone gap is $2\mathcal{T}_\theta^2 > (a_s - 2)\mathcal{T}_z^2$. We use these explicit conditions on the support Σ of the edit and its return corrections:

(a) $\mathcal{T}_\theta \geq T_* > 0$ after the edit;

(b) $a_s - 2 \leq A_*$;

(c) $\mathcal{T}_{z,\mathrm{old}}$ is odd in η and $|\partial_\eta \mathcal{T}_{z,\mathrm{old}}| \leq K_z$, so $|\mathcal{T}_{z,\mathrm{old}}| \leq K_z|\eta|$;

(d) $|\mathcal{T}_z - \mathcal{T}_{z,\mathrm{old}}| \leq \varepsilon_h(d,m)$, with $\varepsilon_h \leq T_*/(4\sqrt{A_*})$ for every late m, by the choice of L_ζ before m (Remark 1.27.2(d)). The width is not free after m: $d = d_m$ with $md_m = \alpha_{d_m} \in [\alpha_\sigma - \delta\alpha, \alpha_\sigma + \delta\alpha]$.

The numbers T_*, A_*, K_z depend on C, Δ, h, e_g, ν_c and the old field, but not on m or d. Remark 1.27.2 below gives their orders: $T_* \asymp h\, e_g C^5$, $A_* \asymp C^{5+\sigma}/e_g$ and $K_z \asymp e_g^2 C^5/\nu_c$. The support condition of the main edit is

$$\ell_m Y_* \leq \eta_{\mathrm{G10}} := \frac{T_*}{4K_z\sqrt{A_*}} \asymp h\,\nu_c\, e_g^{-1/2} C^{-(5+\sigma)/2}, \qquad \varepsilon_h \leq \frac{T_*}{4\sqrt{A_*}}.$$

Under these conditions $(a_s - 2)\mathcal{T}_z^2 \leq A_*(K_z\ell_m Y_* + \varepsilon_h)^2 \leq T_*^2/4$. Thus $2\mathcal{T}_\theta^2 - (a_s - 2)\mathcal{T}_z^2 \geq \frac{7}{4}T_*^2 > 0$ wherever $a_s > 2$. A sufficiently large m gives both conditions. For the first, $\ell_m Y_* = r_0 L_\zeta Y_*/m$. The second holds for every late m, by the choice of L_ζ before m in Remark 1.27.2(d).

Remark 1.27.2 (Orders of the constants of the support condition). The support condition above uses the constants T_*, A_*, K_z of (a)–(d). *Inputs.* The native lift $\delta F = Q^{1+h}\delta\Omega$ above satisfies $\|\delta\Omega\|_\infty \leq Kd\Delta$, $\|r\delta\Omega_r\|_\infty \leq K\Delta$ (proof of Lemma 1.27.1); its η-support is $|\eta| \leq \ell_m Y_*$ (proof of Theorem 1.30.1, Section 1.30.18). At the post-return gap $U = M = J = 0$ and S, P are even. On the fixed normalized hold and its return hull Proposition 1.15.22 gives $T_{\theta,\mathrm{old}} \geq (3/10)hH_s$. Since the hold is a positive fixed power on a compact normalized interval, $\inf H_s \geq c_H e_g C^5$ with $c_H > 0$ fixed by that normalized geometry. Put $c_{\mathrm{hold}} = 3c_H/10$. Then $T_{\theta,\mathrm{old}} \geq c_{\mathrm{hold}} h e_g C^5$ and $\Delta/T_\theta = O(C^{\sigma-5})$ (Section 1.26, proof of Theorem 1.30.1). Scales $A_g \asymp C^{10}$, $B_g \asymp e_g C^5$ (proof of Lemma 1.27.1). Order: C, L_ζ, then late m, with $d = d_m \in [(\alpha_\sigma - \delta\alpha)/m, (\alpha_\sigma + \delta\alpha)/m]$ given by the intermediate value theorem; thus $d \to 0$ only along $m \to \infty$, and $d/\ell_m = md/(r_0 L_\zeta)$ stays of order $\alpha_\sigma/(r_0 L_\zeta)$ (proof of Theorem 1.30.1, Section 1.30.18). On the edit support $b_s = 0$ (since $U = 0$), so $t_s = 0$, $\mathcal{P} = p_1$, $\mathcal{J} = p_2$, $v_s = a_s$, and the fourth gap is $2(\mathcal{P} - v_s)^2 - (v_s - 2)\mathcal{J}^2 = F^{-2}[2T_\theta^2 - (a_s - 2)T_z^2]$.

Values of the constants. (a) On the pure-swirl hold, (1.15.18) and $H = \hat{\xi}^2 F$ give the exact increment

$$\delta T_\theta = \hat{\xi}\,\partial_{\hat{\xi}}\delta F + \frac{\delta H}{2L} - \frac{(1-h)\delta I}{L\hat{\xi}^2} + \frac{(\frac{1}{2} - h)\eta\,\partial_\eta \delta I}{L\hat{\xi}^2}.$$

The first term is $O(\Delta)$. On the fixed radial hull, the partial-integral estimates of (1.30.23) give $|\delta H| + |\delta I| + \ell_m|\partial_\eta \delta I| = O_C(d\Delta)$ for the main edit and its returns. Since $|\eta| \leq \ell_m Y_*$ and the hull is separated from the axis, the last three terms are $O_C(d\Delta)$. Choose C large using $\Delta/C^5 = C^{\sigma-5}$, then m large using $d \leq a_+/m$. This gives $T_\theta \geq T_* = \frac{1}{2}c_{\mathrm{hold}} h e_g C^5$. (b) The exact logarithmic-slope increment is $\delta\ell_r = (\hat{\xi}\,\partial_{\hat{\xi}}\delta H/2 - \ell_{r,\mathrm{old}}\delta H)/H$, where H is the edited value. Here $|\partial_{\hat{\xi}}\delta H/\hat{\xi}| = |2\delta F + \hat{\xi}\,\partial_{\hat{\xi}}\delta F| \lesssim \Delta$, $H \asymp e_g C^5$ and $\hat{\xi}^2/2 \asymp C^{10}$. Thus $A_* = K_a C^{5+\sigma}/e_g$ bounds $a_s - 2 = -2\ell_r$, including the old value $2\nu_c$ and the $O_C(d\Delta)$ return errors. (c) With $U = M = 0$, $T_z = N_z = [4h\eta S - dS_\eta + \frac{\hat{\xi}^2}{2}((2+4h)\eta P - dP_\eta)]/(L\hat{\xi})$. This is odd by evenness of S, P. The C_η^2 history bounds $|S| + |S_{\eta\eta}| \lesssim H^2/\nu_c$ and $|P| + |P_{\eta\eta}| \lesssim E^2$ give $K_z = K\, e_g^2 C^5/\nu_c$. (d) The main edit has the rounded-clamp plateau out to a fixed physical cutoff (Hypothesis 1.30.12(b)). The lift factor $Q^{1+h} = (1-\eta^2)^{-1-h}$ and its first derivative are bounded on the central collar. Its partial-history

changes are therefore $O_C(d\Delta)$, and one η-derivative costs $\ell_m^{-1} = m/(r_0 L_\zeta)$. The width is tied to the integer ($md_m = \alpha_{d_m} \le 2\alpha_\sigma$), so this gives

$$\varepsilon_h \le K(C)\frac{d\Delta}{\ell_m} \le \frac{2\alpha_\sigma K(C)\Delta}{r_0 L_\zeta}.$$

This bound does NOT vanish as $m \to \infty$. We therefore fix L_ζ, before m, so large that $2\alpha_\sigma K(C)\Delta/(r_0 L_\zeta) \le T_*/(8\sqrt{A_*})$; this is the condition stated in Section 1.30.2 (the "nonvanishing first-η/history bound"). Then $\varepsilon_h \le T_*/(4\sqrt{A_*})$ for every late m. Substituting,

$$\eta_{\mathrm{G10}} = \frac{T_*}{4K_z\sqrt{A_*}} = c\,h\,\nu_c\,e_g^{-1/2}C^{-(5+\sigma)/2}.$$

Hypotheses (a)–(d) restate bounds of the text; (c) needs the C_η^2 history bound on the hold, which is an input (Proposition 1.18.4 for P, and ac-fa:future-C2 (Proposition 1.18.3) for the energy). K_z and A_* are given as orders, not with explicit constants.

Satisfiability and order. T_*, A_*, K_z depend on C, Δ, h, e_g, ν_c, the old field and the fixed profiles t, w_0. They do not depend on m or d. Hence m large enough that $r_0 L_\zeta Y_*/m \le \eta_{\mathrm{G10}}$, with $d = d_m$ in its bracket and L_ζ fixed before m as in (d), satisfies the support condition $\ell_m Y_* \le \eta_{\mathrm{G10}}$, $\varepsilon_h \le T_*/(4\sqrt{A_*})$. All other late-$m$ requirements are also upper bounds on ℓ_m or exponential-smallness requirements ((1.30.22), proof of Lemma 1.27.1), so they are compatible.

We use $A_g \asymp C^{10}$, $B_g \asymp e_g C^5$. The exact five-moment correction map has row normalization

$$\mathrm{diag}(B_g\sqrt{A_g}, A_gB_g, B_g^2\sqrt{A_g}, B_g^2, B_g^2/A_g)$$

and normalized densities

$$\int u, \quad \int h, \quad \int uh, \quad \int (u^2 - h^2/(4x)), \quad \int h^2/(4x^2).$$

Its fixed separated-template derivative is invertible, and its quadratic part has a bound. $KC^5 d\Delta/e_g$ plus their square bounds the main discrepancies.

The actual small-branch coefficients tend to zero with d, and for fixed C their conversion to physical radial C^1 and C^2 norms stays bounded. We impose a total first-radial error after the returns of at most C^{-2} and $Kd\Delta \le C^{-1}$.

Expansion of $4\Omega^2 + 2|\Omega r \Omega_r| + |\Omega W_r|$ then gives (1.27.3). In particular, the term $d\Delta^2$ satisfies the necessary bound because $d\Delta \le C^{-1}$.

We use no distance gain in this global estimate.

The away-center shapes lie on the actual old power germ outside the main corners. Their affine formulas are Taylor limits only.

We first compute their actual inverse response matrix. We define V_q to include that inverse applied to the physical target minus the base, and set $\Theta = K_{\mathrm{shape}} V_q c_{\mathrm{cut}}^2/\Delta$.

Select

$$\Theta \le 1, \qquad K_{\mathrm{form}}\Theta/g \le \eta_*/32, \qquad K_{\mathrm{form}}\Delta\Theta/g^2 \le \eta_*/32, \tag{1.27.6}$$

$$\frac{K_{\mathrm{source}} V_q c_{\mathrm{cut}}}{e_g\Delta} \le \epsilon_C, \qquad \epsilon_C = cC^{-(\sigma+5)/2-2}. \tag{1.27.7}$$

We also make the source bound (1.27.7) smaller than the actual compact source/cone and partial-history tolerance. We also require $K_{\mathrm{ctrl}}(\Theta/g + \Delta\Theta/g^2) \le \varpi_{\mathrm{bulk}}/4$, with the Rouché margin of Lemma 1.29.9. These inequalities have no positive lower constraint on c_{cut}.

For $\delta\Omega = d\theta w(\xi)$ and $\delta W = d\varepsilon w(\xi)$,

$$\int \frac{|n\delta\Omega_{rr}|}{\sqrt{n^2/r^2+k^2}}\,\mathrm{d}r \le K\Theta, \qquad \int \frac{|k\delta W_{rr}|}{\sqrt{n^2/r^2+k^2}}\,\mathrm{d}r \le K_C|\varepsilon|.$$

These are absolute total variations. The products with one radial derivative remain in (1.27.3).

The pole/first/mixed centerings have scaled coefficients $p_C(m)e^{-c_C m}$, with the polynomial raw axial inverse retained. Their actual quadratic returns remain in the same five-correction map. Sufficiently large m makes their total radial, angular, and history errors smaller than the prescribed tolerances.

The fixed-physical returns of the curvature control have an additional d factor. Equation (1.27.7) controls their first-angular error.

Last, we subtract the explicit second-derivative densities before we set

$$J_C = \sup_{r,Z}\{r^2|\Omega_{rr,\mathrm{res}}| + 7r|\Omega_r| + 8|\Omega| + r|W_{rr,\mathrm{res}}| + 3|W_r|\} < \infty.$$

For example, if we subtract $\theta w''/(r^2 d)$, we get $-\theta w'/r^2$. The main affine geometric remainder is $O(\Delta)$. At fixed Z the physical cutoffs and return shapes have uniform radial C^2 bounds.

The full actual second derivatives may grow like $1/d$. We select C so that $K(1+\Delta)/(Cg^2) < \eta_*/8$.

We next select the actual cutoff for (1.27.6). We then select finite N_0 so that $J_C/(|n|g)+3/(4n^2) < \eta_*/8$.

The same late width satisfies each remaining tolerance. This proves the claimed source admission without the assumption of a winner, corridor theorem, or propagator.

□

Lemma 1.27.3 (Actual capped source bounds)**.** *Fix the normalized actual future/core geometry, pulse length and correction supports. For sufficiently large C, put $\Delta = C^\sigma$, $0 < \sigma < 5$.*

The actual returned source before the perturbation has, with one bound for all Z,

$$\|\Omega\|_\infty \le K/C, \qquad \|r\Omega_r\|_\infty + \|W_r\|_\infty \le K, \qquad 2|\Omega B| + |\Omega W_r| \le K/C.$$

The capped loop of Lemma 1.19.2 uses $a < 5/2$, $|b| < 5/4$ on its modified set. Outside that set we keep the old field. Its actual five-history correction has physical first-derivative error at most C^{-2}.

After main and allowed rank controls, $d\Delta \le C^{-1}$ and the same correction allowance give $2|\Omega B| + |\Omega W_r| \le K(1+\Delta)/C$.

Proof. Lemma 1.27.1 establishes the actual piecewise radial bounds, normalized correction inverse and capped-loop products.

These calculations precede any spectral count. In the normalized chart $\Omega = Q^{-1-h}F$, $r\Omega_r = Q^{-1-h}\hat{\xi}F_{\hat{\xi}}$ and $W_r = Q^{-1-h}U_{\hat{\xi}}$, so $Q \ge 1$ keeps each bound for each Z.

The loop's first derivative parameters satisfy the stated cap. We select its frequency finitely before the residual higher-derivative constant J_C and the late integer.

□

Lemma 1.27.4 (Global form and local observation bounds)**.** *Let $g = c_g\Delta$. Subtract all explicit main and signed extra $1/d$ layer densities from the actual second derivatives.*

The residual constant J_C is finite and independent of sufficiently late d. Uniformly in all Z, k, all Λ with $\Re\Lambda \ge g$ (so that $|D| \ge g$), and $|n| \ge N_0$,

$$\eta_{\mathrm{sm}} \le \frac{K(1+\Delta)}{Cg^2} + \frac{J_C}{|n|g} + \frac{3}{4n^2}. \tag{1.27.8}$$

The signed layers have total variation Θ *and obey*

$$\eta_{\text{noncorner}} \le \eta_{\text{sm}} + K\Theta/g + K\Delta\Theta/g^2 + K_C p(m) e^{-c_C m} < \eta_*. \tag{1.27.9}$$

Fixed physical returns are included in J_C *and the actual product bound, not in a global exponential remainder.*

At the pole the global $H^{-1} \to H^1$ *inverse difference is* $O(d/c_g)$*, with the explicit constant of Lemma 1.30.2. Only an explicitly localized source–observation Green response has the remote bound* $K_C d^{-N} e^{-c_C/d}$*.*

Proof. We use the exact denominators $D = \Lambda + in\Omega + ikW$, $|D| \ge g$, and the actual products $2\Omega B$ and ΩW_r. Sections 1.30.3, 1.30.6 and 1.30.7 compute the radial remainder, layer total variations and the distinct unweighted-global and exponentially weighted-local resolvent identities.

We select C for the product term and the rank-dependent cutoff for the layer bounds. We next select N_0 for $J_C/(|n|g)$.

Last, we select m for the finite-label overlap and local errors. The main, trial, and return supports remain in the actual protected power interval before the heat drive.

The corrections restore all five histories. □

1.27.3 The large derivative and the five histories

At the post-return gap described in Section 1.13, $U = M = J = 0$, H is a positive power germ. The canonical pressure and stress histories are even in η.

This local parity is not imposed on remote pulses. The five radial densities whose terminal values must remain fixed are

$$U, \quad H, \quad UH, \quad U^2 - \frac{H^2}{4\frac{\hat\xi^2}{2}}, \quad \frac{H^2}{4\frac{\hat\xi^4}{4}}. \tag{1.27.10}$$

We keep their full partial integrals during the perturbation.

Terminal equalities alone do not keep the intermediate cone.

Lemma 1.27.5 (Post-return moment inverse)**.** *Let* P *be a compact subinterval of that post-return gap with* $U = 0$ *and* $H = c\phi(\eta)(\hat\xi/\sqrt{2})^{-2\mu}$*. We fix* $\mu > 0$ *here. The function* ϕ *has a positive minimum on the closed* η*-interval.*

Select two disjoint U*-control supports and three disjoint* H*-control supports in* P*, ordered in the radial variable. For sufficiently narrow smooth bumps, their five coefficients map to the outgoing discrepancies in (1.27.10).*

This map has a smooth local inverse, uniform in η *and through one* η *derivative. When its input discrepancy is small, the same discrepancy norm controls the coefficient and first-*η *bounds.*

All five outgoing histories then agree with the original histories.

Proof. At zero control the derivative is block triangular.

Subtract U times the H row. The two U columns have weights $(1, H)$, while the three H columns have weights $(1, -H/(\hat\xi^2), H/(2\frac{\hat\xi^4}{4}))$. On P these are, in this order, the distinct powers $(1, X^{-\mu})$ and $(1, X^{-1-\mu}, X^{-2-\mu})$, where $X = \xi^2/2$, up to nonzero row factors (including the minus sign of the energy row). For ordered nonnegative nonzero bumps, multilinearity integrates the point-evaluation determinant over their ordered supports. A nonzero combination of n distinct powers has at most $n-1$ distinct positive zeros, by dividing by the first power and applying Rolle's theorem inductively in $\log X$. Thus the integrand has one strict sign on the product of the supports.

Compactness of the closed η-interval and $\min \phi > 0$ give a finite uniform inverse.

The exact discrepancy is $L_\eta c + Q_\eta(c, c)$, where one constant bounds the quadratic term and its first η derivative on a fixed coefficient ball. A contraction for $c = L_\eta^{-1}(d - Q_\eta(c, c))$ thus gives the smooth inverse.

Differentiate this fixed-point equation and absorb the small quadratic derivative. This gives the stated first-η bound. Beyond P, identical terminal values and identical densities propagate identical complete histories.

□

Lemma 1.27.5a (The selected late return on the full angular interval)**.** *On the fixed forward return slots chosen in the hold, use the same two U and three H trial columns for every $\eta \in [-1, 1]$. Their outlet Jacobian at the selected amplitudes has absolute determinant bounded below by a positive constant on that interval. The selected amplitudes vanish off the central spectral support.*

Proof. Put $X = \xi^2/2$ and first use the actual field before spectral implantation. The slots lie above $R_h > 2R_m > \max R_o$, after all meridional returns. Here $U = 0$ and $H = (1 - \chi)H_c + \chi H_w$. On the central component the power hold has $H_c > 0$ and $(H_c)_X < 0$ by Proposition 1.15.22(ii),(v). On $\operatorname{supp} \chi$ the choice of L_o in Lemma 1.17.3 puts the entire central hull before the outer rank-one support and hence before the end of the added power leg; see also (1.15.10). Here is a direct slope check on all possible pieces of that leg and its inlet. In flattening, $\partial_{\log X} \log H_w \le -\lambda/2$ by the computation in Lemma 1.17.4. On the adjoining waits and added leg the slope is $-\lambda$. On A11 the multiplier is $1 + \sum t_i \psi_i(\log X - \text{const})$, with fixed smooth shapes; the logarithmic derivative changes by at most $C \max_i |t_i|$. Lemma 1.15.5 and the A11 bound in Lemma 1.17.4 give $\max_i |t_i| \le C(\lambda^{30(1-\lambda)} + \|\delta_{\text{mem}}\|_{C^1})$. In the stated order of choices take λ small for the first term and Y_0 large at fixed λ for the second, making the slope error $< \lambda/2$. The chart pullback rescales X and H by positive factors constant on each radial fiber, so it preserves the logarithmic slope. These cases prove $H > 0$, $H_X < 0$ on and between the slots at every angle before implantation.

At zero amplitude the two blocks, up to row order, are the integrals against the respective bumps of $(1, H)$ and $(1, -H/(2X), H/(2X^2))$. For the first block the point determinant is $H(X_2) - H(X_1) < 0$. For the second block multiply column i by $X_i^2/H(X_i) > 0$. The resulting rows are $F_i, -X_i/2, 1/2$, with $F_i = X_i^2/H(X_i)$. For every triple from the three supports,

$$\frac{F_3 - F_2}{X_3 - X_2} \ge F_2 \frac{X_3 + X_2}{X_2^2} > \frac{F_2}{X_2 - X_1} > \frac{F_2 - F_1}{X_2 - X_1}.$$

The middle inequality uses $X_2 > 2X_1$ and $X_3 > X_2$. The two secant slopes therefore give a fixed nonzero determinant sign. Integrating these point determinants against the ordered products of bumps proves that both block determinants are nonzero. The columns and the unedited field are smooth up to both angular endpoints. Compactness gives a positive minimum for the absolute five-row determinant once the old member and its bank are fixed.

The main and trial edits are disjoint from the return columns. On these columns the exact discrepancy map is $z \mapsto L_\eta z + Q_\eta(z, z)$ plus a term independent of z, with Q_η uniformly bounded. Thus a single ball about zero has $\|L_\eta^{-1}(D_z Q_\eta(z, z))\| < 1/2$ at every angle. On every bounded $y = \eta/\ell_m$ chart, (1.30.23) bounds the actual solution and its mixed derivatives by $O_C(d_m \Delta)$. On the rest of the fixed slow cutoff the lower controls can still be present. There their values are $O_C(d_m r_T)$ on a fixed radial hull. Every change in a moment density contains an edited factor, so the uniform inverse just proved gives $|z| = O_C(d_m \Delta)$ there as well. Outside the supports of all edits the discrepancy and its small solution are zero. The uncut columns keep the same Jacobian there. □

At the center $X_c = \hat{\xi}_c^2/2$, $\eta = 0$, the strict cone requires $a > 2$, $\mathcal{T}_\theta > 0$ and $2\mathcal{T}_\theta^2 - (a-2)\mathcal{T}_z^2 > 0$. The rounded odd clamp vanishes at $x = 0$ and has derivative one there. Consequently the main edit has $\delta H(X_c, 0) = 0$ and $\delta\Omega_x(X_c, 0) = -\Delta$. Its inward partial moment $\delta I(X_c, 0) = \int_0^{X_c} \delta H(X, 0)\, \mathrm{d}X$ is positive because the clamp is negative on the inner part of its nonnegative cutoff, and all return slots lie farther out. Since $Q = L = 1$ at $\eta = 0$, the exact stress increment in Remark 1.27.2(a) gives

$$\delta\mathcal{T}_\theta(X_c, 0) = -\Delta - (1-h)\delta I(X_c, 0)/\hat{\xi}_c^2.$$

Choose a strict ceiling with reserve,

$$\Delta < \rho_{\mathrm{ceil}}\, \mathcal{T}_{\theta,\mathrm{old}}(X_c, 0), \qquad 0 < \rho_{\mathrm{ceil}} < 1. \tag{1.27.11}$$

If $t \in [0, 1]$ multiplies the main edit, its partial moment at X_c is $t\,\delta I(X_c, 0)$ even when the outgoing returns are solved anew. Thus

$$\mathcal{T}_\theta(t; X_c, 0) = \mathcal{T}_{\theta,\mathrm{old}}(X_c, 0) - t\big[\Delta + (1-h)\delta I(X_c, 0)/\hat{\xi}_c^2\big].$$

At fixed C the partial-moment contribution is $O_C(d\Delta)$. Take the width bracket late enough to make it less than $(1-\rho_{\mathrm{ceil}})\mathcal{T}_{\theta,\mathrm{old}}(X_c, 0)/2$. On the main hull the full stress and the first angular derivative of its histories satisfy Remark 1.27.2(a)–(d) uniformly in t, with L_ζ chosen before m. Consequently $\mathcal{T}_\theta \geq T_*$ and the fourth gap in physical stress units is at least $7T_*^2/4$ there. Lemma 1.27.5 restores the five outgoing moments. Choose $\varepsilon_{\mathrm{src}} > 0$ below the resulting compact cone and return-inverse margins.

We divide this tolerance among all later controls.

For a local U correction $dc\, w((x - x_0)/d)$, the two U-history errors are $O(d^2|c|)$. On new zero-U supports, the energy error is quadratic, $O(d^3|c|^2)$, with the fixed-return squares.

New mixed-jet controls use fresh supports for this reason. An H-only perturbation leaves the M, J histories unchanged. Thus its three H returns correct only I, S, P.

1.27.4 A noncircular choice of the spectral source parameters

Theorem 1.30.1, together with Section 1.30.19, establishes the uniform preselection estimates used here. Lemma 1.31.3 gives the strict model and exterior margins, Lemma 1.31.1 gives the differentiated local resolvent, and Lemma 1.31.2 gives the real response inverse.

Section 1.32 verifies their source hypotheses in parameter order before selection of the late integer.

Lemma 1.27.6 (Finite weighted Leray and scalar pressure bounds)**.** *On the fixed cylindrical angular sector m, set*

$$\|f\|_{H^s_w}^2 = \sum_{|\alpha| \leq s} \|\langle y\rangle^w \partial_y^\alpha f\|_2^2.$$

For nonnegative integers s, j, $w \geq 0$, and $|m| > s + \lceil w\rceil + j + 2$, with one bound for real k,

$$\|\partial_k^j P_k f\|_{H^s_w} \leq C\|f\|_{H^s_{w+j}}.$$

Only nonnegative weights are asserted.

If the sector margin permits one more derivative, then, for $0 < \vartheta < 1$,

$$\|(\partial_k^j P_k - \partial_k^j P_{k'})f\|_{H^s_w} \leq C|k - k'|^\vartheta \|f\|_{H^s_{w+j+\vartheta}}.$$

The scalar Fourier/decaying pressure representative $S_k = \Delta_k^{-1}\,\mathrm{div}_k$ instead satisfies

$$\|\partial_k^j S_k f\|_{H^s_w} \leq C\|f\|_{H^s_{w+j+1}}$$

with sufficient positive-weight margin $|m| > s + \lceil w\rceil + j + 3$.

Proof. Put $n = |m| - 1$; by (1.28.2) the sector lies in $\mathcal{A}_n$. The first estimate is Corollary 1.28.5(a) with $\ell = 0$; its margin $\lceil w \rceil + j \le n$ follows from $|m| > s + \lceil w \rceil + j + 2$. The pressure estimate is Corollary 1.28.5(c); its margin $\lceil w \rceil + j + 1 \le n$ follows from $|m| > s + \lceil w \rceil + j + 3$. For the Hölder estimate the extra margin is $\lceil w \rceil + j + 1 \le n$. If $|k - k'| \le 1$, the estimate is Corollary 1.28.5(b). If $|k-k'| > 1$, the first estimate at k and at k' gives the bound $2C \|f\|_{H^s_{w+j}} \le 2C|k-k'|^{\vartheta} \|f\|_{H^s_{w+j+\vartheta}}$. All constants are uniform in $k \in \mathbb{R}$ by Corollary 1.28.5. The margins actually used are $\lceil w \rceil + j + 1 \le |m|$, with one more for the pressure, and they do not depend on s. For integer w the first margin cannot be lowered (Remark 1.28.4). □

Finite derivative and moment bounds. For $m \ge 30$, the leading ladder $s = 6, w = 7 - j, j \le 5$, its sixth k derivative at $w = 1$, and the first-corrector ladder $s = 4, w = 6 - j, j \le 4$ satisfy the necessary strict inequalities. The scalar pressure estimate uses its additional input moment.

A tail estimate keeps the *remaining* weight w. It does not keep seven moments after differentiation.

This lemma does not assert the sharp real-weight range for each $w < m$, and does not construct eigenprofiles or supply their different contour resolvent assumptions.

1.28 The positive moment ladder and the weighted profile bootstrap

The Fourier–Bessel and angular Hardy estimates below give the positive moment ladder in Corollary 1.28.5. Proposition 1.28.8 then gives the weighted profile bounds of Section 1.30.12. The angular margin that we need is weaker than the sufficient margins $m > s + \lceil w \rceil + j + 2$ used in the text, and it does not depend on the Sobolev order s.

1.28.1 Notation

We write $x \in \mathbb{R}^2$ for the horizontal variable, $R = |x|$, $\langle x \rangle = (1 + |x|^2)^{1/2}$, and $\hat{f}(\xi) = \int e^{-ix\cdot\xi} f(x)\,\mathrm{d}x$, so that $\left\|\hat{f}\right\|_2 = 2\pi \|f\|_2$ and $\widehat{x^\alpha f} = (i\partial_\xi)^\alpha \hat{f}$. For an integer $s \ge 0$ and a real $w \ge 0$,

$$\|u\|^2_{H^s_w} = \sum_{|\beta| \le s} \left\| \langle x \rangle^w D^\beta u \right\|_2^2, \qquad L^2_w = H^0_w,$$

on scalar or $\mathbb{C}^d$-valued functions; $D = \partial_x$ are Cartesian derivatives. On a fixed angular sector the squared Cartesian norm differs from the radial $L^2(R\,\mathrm{d}R)$ normalization by the factor 2π. For an integer $W \ge 0$,

$$c_W \left\| \langle x \rangle^W f \right\|_2 \le \sum_{|\alpha| \le W} \left\| \partial^\alpha_\xi \hat{f} \right\|_2 \le C_W \left\| \langle x \rangle^W f \right\|_2, \qquad \left\| \nabla^q_\xi \hat{f} \right\|_2 = 2\pi \left\| |x|^q f \right\|_2, \tag{1.28.1}$$

where $|\nabla^q g|^2 = \sum_{i_1,\dots,i_q} |\partial_{i_1} \cdots \partial_{i_q} g|^2$.

Angular classes. A scalar $g \in L^2(\mathbb{R}^2)$ has the expansion $g = \sum_{\ell \in \mathbb{Z}} g_\ell(R) e^{i\ell\theta}$. For an integer $n \ge 0$, $\mathcal{A}_n$ is the closed subspace of the g with $g_\ell = 0$ for $|\ell| < n$; a vector-valued function is in $\mathcal{A}_n$ when each Cartesian component is. The orthogonal projection Π_n onto $\mathcal{A}_n$ acts circle by circle; it commutes with multiplication by radial functions and is a contraction on every $L^2(\omega(|x|)\,\mathrm{d}x)$.

(A1) The Fourier transform commutes with rotations, so it maps $\mathcal{A}_n$ onto $\mathcal{A}_n$.

(A2) With $\partial_\pm = \partial_1 \pm i\partial_2$ one has $\partial_\pm(g \circ \mathsf{R}_\alpha) = e^{\mp i\alpha}(\partial_\pm g) \circ \mathsf{R}_\alpha$ for the counterclockwise rotation R_α. Thus $\partial_\pm$ maps the ℓ-th mode to the $(\ell \pm 1)$-st, and $\partial_i(\mathcal{A}_n \cap H^1) \subset \mathcal{A}_{n-1}$ for $n \geq 1$, since $\partial_1 = \frac{1}{2}(\partial_+ + \partial_-)$, $\partial_2 = \frac{1}{2i}(\partial_+ - \partial_-)$.

(A3) A smooth $g \in \mathcal{A}_\nu$ satisfies $g(\xi) = O(|\xi|^\nu)$ at 0: its Taylor polynomial of degree $< \nu$ contains only angular modes $|\ell| < \nu$, and these modes of g vanish, so the Taylor polynomial vanishes. Combined with (A2), $|\partial^\alpha g(\xi)| \leq C|\xi|^{\nu-|\alpha|}$ near 0 for $|\alpha| \leq \nu$.

Sectors. Let $\mathcal{R}_\alpha$ rotate the first two components of a vector in $\mathbb{C}^3$. For $\mu \in \mathbb{Z}$ the sector $\mathcal{H}_\mu$ is the set of $u \in L^2(\mathbb{R}^2;\mathbb{C}^3)$ with $u(\mathsf{R}_\alpha x) = e^{i\mu\alpha}\mathcal{R}_\alpha u(x)$ for all α. This is the fixed cylindrical angular sector of the text: in cylindrical components $u = e^{i\mu\theta}(u_R, u_\theta, u_z)(R)$. Since $(\mathcal{R}_\alpha u)_1 \pm i(\mathcal{R}_\alpha u)_2 = e^{\pm i\alpha}(u_1 \pm iu_2)$, the functions $u_1 \pm iu_2$ have the single modes $\mu \pm 1$ and u_3 has the mode μ. Hence

$$\mathcal{H}_\mu \subset \mathcal{A}_{\max\{|\mu|-1,0\}}, \qquad \mathcal{H}_\mu \oplus \mathcal{H}_{-\mu} \subset \mathcal{A}_{\max\{|\mu|-1,0\}}. \tag{1.28.2}$$

A matrix function M is *equivariant* if $M(\mathsf{R}_\alpha x) = \mathcal{R}_\alpha M(x)\mathcal{R}_\alpha^{-1}$; then multiplication by M maps $\mathcal{H}_\mu$ into itself. A Fourier multiplier with an equivariant symbol maps $\mathcal{H}_\mu$ into itself. Radial functions and Fourier multipliers with radial scalar symbols (for example $(1+\epsilon(1-\Delta))^{-1}$ and radial mollifiers) also preserve each $\mathcal{H}_\mu$ and each $\mathcal{A}_n$.

Symbols. For integers $j \geq 0$, $W \geq 0$ and $M_0 > 0$, let $\mathsf{S}^{-j}_W(M_0)$ be the set of matrix functions $a \in C^W(\mathbb{R}^2 \setminus \{0\})$ with

$$|\partial_\xi^\alpha a(\xi)| \leq M_0|\xi|^{-j-|\alpha|}, \qquad |\alpha| \leq W,\ \xi \neq 0.$$

For $f \in \mathcal{A}_n$ with $j \leq n$ and $\langle x\rangle^j f \in L^2$, Lemma 1.28.1 below gives $a\hat{f} \in L^2$, and we put $a(D)f = \mathcal{F}^{-1}(a\hat{f})$.

1.28.2 Angular Hardy inequality and the multiplier ladder

Lemma 1.28.1 (Angular Hardy inequality)**.** *Let $1 \leq q \leq n$ be integers and $g \in \mathcal{A}_n \cap H^q(\mathbb{R}^2)$. Then*

$$\big\||\xi|^{-q}g\big\|_2 \leq \frac{(n-q)!}{n!}\,\|\nabla^q g\|_2\,.$$

More generally, if $\nu \geq 1$, $b \in \mathbb{R}$ and $h \in \mathcal{A}_\nu \cap H^1_{\mathrm{loc}}$, then $\int |h|^2|\xi|^{-2b} \leq \nu^{-2}\int |\nabla h|^2|\xi|^{2-2b}$ (both sides may be infinite).

Proof. In polar coordinates $\xi = \varrho(\cos\phi, \sin\phi)$, for almost every ϱ the restriction $h(\varrho,\cdot)$ lies in $H^1(S^1)$ and $\partial_\phi h = \xi_1\partial_2 h - \xi_2\partial_1 h$, so $|\partial_\phi h| \leq \varrho|\nabla h|$. Its Fourier coefficients vanish for $|\ell| < \nu$; Parseval on the circle gives $\int_0^{2\pi}|h|^2\,\mathrm{d}\phi \leq \nu^{-2}\int_0^{2\pi}|\partial_\phi h|^2\,\mathrm{d}\phi \leq \nu^{-2}\varrho^2\int_0^{2\pi}|\nabla h|^2\,\mathrm{d}\phi$. Multiply by ϱ^{1-2b} and integrate. For the first claim apply the second with $h = \partial_{i_1}\cdots\partial_{i_r}g \in \mathcal{A}_{n-r}$ (by (A2)), $\nu = n-r \geq n-q+1 \geq 1$ and $b = q-r$, for $r = 0, 1, \ldots, q-1$, and sum over the indices. □

Lemma 1.28.2 (Density)**.** *Let $s \geq 0$ and $0 \leq W \leq n$ be integers. The set $\mathcal{D}_n = \{f \in \mathcal{A}_n : \hat{f} \in C_c^\infty(\mathbb{R}^2 \setminus \{0\})\}$ is dense in $\mathcal{A}_n \cap H^s_W$. If the functions are $\mathbb{C}^3$-valued, the same holds inside each sector $\mathcal{H}_\mu$ with $|\mu| - 1 \geq W$.*

Proof. All operations below commute with rotations, so they preserve $\mathcal{A}_n$ and the sectors. (i) For a radial cutoff $\chi \in C_c^\infty$, $\chi(x/L)f \to f$ in H^s_W as $L \to \infty$: the terms with derivatives on the cutoff are $O(L^{-1})$ and the rest tends to zero by dominated convergence. (ii) For f supported in a fixed ball,

convolution with a radial mollifier converges in H^s, hence in H^s_W. (iii) Now $f \in C_c^\infty \cap \mathcal{A}_n$, so $\hat f$ is a Schwartz function in $\mathcal{A}_n$. By (A3), each $\xi^\beta \hat f$ satisfies $|\partial^\alpha(\xi^\beta \hat f)| \le C|\xi|^{n-|\alpha|}$ for $|\xi| \le 1$, $|\alpha| \le n$. Let $\chi_\epsilon = \chi(\xi/\epsilon)$ with $\chi = 1$ near 0. For $|\alpha| \le W \le n$, $|\partial^\alpha(\chi_\epsilon \xi^\beta \hat f)| \le C \sum_{i \le |\alpha|} \epsilon^{-i}|\xi|^{n-|\alpha|+i} 1_{|\xi|\le 2\epsilon} \le C 1_{|\xi|\le 2\epsilon}$, whose L^2 norm tends to zero. By (1.28.1) (applied to $D^\beta f$), $\mathcal{F}^{-1}((1-\chi_\epsilon)\hat f) \to f$ in H^s_W. A further cutoff $\chi(\epsilon\xi)$ at high frequency costs $o(1)$ because $\hat f$ is a Schwartz function. □

Proposition 1.28.3 (Weighted multiplier ladder)**.** *Let $s \ge 0$, $j \ge 0$ and $n \ge 0$ be integers and $w \ge 0$ real, with*

$$\lceil w \rceil + j \le n. \tag{1.28.3}$$

Let $a \in \mathsf{S}^{-j}_{\lceil w \rceil}(M_0)$. Then for every $f \in \mathcal{A}_n \cap H^s_{w+j}$ and $|\beta| \le s$,

$$\left\| \langle x \rangle^w D^\beta a(D) f \right\|_2 \le C M_0 \left(\left\| \langle x \rangle^{w+j} f \right\|_2 + \left\| \langle x \rangle^w D^\beta f \right\|_2 \right), \tag{1.28.4}$$

and in particular $\|a(D)f\|_{H^s_w} \le C M_0 \|f\|_{H^s_{w+j}}$, with $C = C(s,w,j,n)$.

Moreover, let $a_\epsilon \in \mathsf{S}^{-j}_{\lceil w \rceil}(M_0)$ for $0 \le \epsilon \le 1$, and let $\partial^\alpha a_\epsilon \to \partial^\alpha a_0$ pointwise on $\mathbb{R}^2 \setminus \{0\}$ for $|\alpha| \le \lceil w \rceil$. Then $a_\epsilon(D)f \to a_0(D)f$ in H^s_w for every $f \in \mathcal{A}_n \cap H^s_{w+j}$.

Proof. Fix $\chi \in C_c^\infty(B_2)$, radial, with $\chi = 1$ on B_1, and write

$$D^\beta a(D) f = T^\beta_{\mathrm{low}} f + T_{\mathrm{high}} D^\beta f, \qquad T^\beta_{\mathrm{low}} = ((i\xi)^\beta a \chi)(D), \quad T_{\mathrm{high}} = (a(1-\chi))(D).$$

This is an identity between L^2 functions on the Fourier side.

Step 1: integer weight W and $f \in \mathcal{D}_n$, $W + j \le n$. High part. On $|\xi| \ge 1$ we have $|\partial^\alpha a| \le M_0$, so $|\partial^\alpha(a(1-\chi))| \le C M_0$ for $|\alpha| \le W$. By (1.28.1) and the Leibniz rule, $\left\| \langle x \rangle^W T_{\mathrm{high}} g \right\|_2 \le C M_0 \left\| \langle x \rangle^W g \right\|_2$ for every $g \in L^2_W$; no angular condition is used. *Low part.* By (1.28.1), $\left\| \langle x \rangle^W T^\beta_{\mathrm{low}} f \right\|_2 \le C \sum_{|\alpha| \le W} \left\| \partial^\alpha (\xi^\beta a \chi \hat f) \right\|_2$. Leibniz gives terms $\partial^{\alpha-\gamma}(\xi^\beta a \chi)\, \partial^\gamma \hat f$, $\gamma \le \alpha$. Since $|\partial^\mu \xi^\beta| \le C|\xi|^{|\beta|-|\mu|}$, $|\partial^\nu a| \le M_0 |\xi|^{-j-|\nu|}$ and $|\partial^\kappa \chi| \le C|\xi|^{-|\kappa|} 1_{B_2}$, we get

$$|\partial^{\alpha-\gamma}(\xi^\beta a \chi)| \le C M_0 |\xi|^{-q} 1_{B_2}, \qquad q = j + |\alpha| - |\gamma| - |\beta|.$$

If $q \le 0$ the term is bounded by $C M_0 \left\| \partial^\gamma \hat f \right\|_2 \le C M_0 \left\| |x|^{|\gamma|} f \right\|_2$. If $q \ge 1$ we apply Lemma 1.28.1 to $g = \partial^\gamma \hat f$, which lies in $\mathcal{A}_{n-|\gamma|}$ by (A1)–(A2); the condition $q \le n - |\gamma|$ is $j + |\alpha| - |\beta| \le n$, which holds by $|\alpha| \le W$ and $W + j \le n$. The term is bounded by $C M_0 \left\| \nabla^q \partial^\gamma \hat f \right\|_2 \le C M_0 \left\| |x|^{q+|\gamma|} f \right\|_2$, and $q + |\gamma| \le j + W$. Thus

$$\left\| \langle x \rangle^W T^\beta_{\mathrm{low}} f \right\|_2 \le C M_0 \left\| \langle x \rangle^{W+j} f \right\|_2. \tag{1.28.5}$$

Step 2: all $f \in \mathcal{A}_n \cap L^2_{W+j}$. Lemma 1.28.1 with $q = j - |\beta|$ (or no Hardy if $q \le 0$) shows that $T^\beta_{\mathrm{low}} f \in L^2$ and that $f \mapsto T^\beta_{\mathrm{low}} f$ is continuous from $\mathcal{A}_n \cap L^2_{W+j}$ to L^2. By Lemma 1.28.2 (with $s = 0$, weight $W + j \le n$), (1.28.5) extends to this space.

Step 3: real w. Let $W_0 = \lfloor w \rfloor$, $W_1 = \lceil w \rceil$; then $W_1 + j \le n$. The operator $T^\beta_{\mathrm{low}} \Pi_n$ is bounded from $L^2(\langle x \rangle^{2(W_i+j)}\, dx)$ to $L^2(\langle x \rangle^{2W_i}\, dx)$, $i = 0, 1$, because Π_n is a contraction on these spaces. We give the weighted interpolation argument used here and below. Write $v(x) = \langle x \rangle$ and $L^2_a = L^2(v^{2a}\, dx)$. Suppose $T : L^2_{a_i} \to L^2_{b_i}$ has norm at most $M_i > 0$ for $i = 0, 1$. Let $a(z) = (1-z)a_0 + z a_1$ and define $b(z)$ in the same way. For compactly supported unit vectors $f, g \in L^2$, the function

$$H(z) = M_0^{z-1} M_1^{-z} \langle T(v^{-a(z)} f), v^{b(\bar z)} g \rangle$$

is bounded and continuous on $0 \le \Re z \le 1$ and holomorphic inside, using the pairing linear in its first entry. Compact support bounds all weight powers in the input and test vector, and each endpoint estimate gives $|H| \le 1$ on its vertical boundary. For $\epsilon > 0$, apply the maximum modulus principle to $e^{\epsilon(z^2-1)}H(z)$ on the strip truncated at heights $\pm L$. Its horizontal boundary values tend uniformly to zero as $L \to \infty$. Sending $\epsilon \downarrow 0$ gives $|H(\vartheta)| \le 1$ for $0 \le \vartheta \le 1$. Duality and density give

$$\|T\|_{L^2_{a(\vartheta)} \to L^2_{b(\vartheta)}} \le M_0^{1-\vartheta} M_1^{\vartheta}. \tag{1.28.6}$$

Applying this estimate with $a_i = W_i + j$, $b_i = W_i$ gives $\left\| \langle x \rangle^w T^{\beta}_{\mathrm{low}} f \right\|_2 \le C M_0 \left\| \langle x \rangle^{w+j} f \right\|_2$. The same interpolation applies to T_{high} on $L^2_{W_i}$. Summing the two parts gives (1.28.4); summing over $|\beta| \le s$ gives the H^s_w bound, since both norms on the right of (1.28.4) are bounded by $\|f\|_{H^s_{w+j}}$.

Step 4: strong convergence. The operators $a_\epsilon(D)$ are uniformly bounded from $\mathcal{A}_n \cap H^s_{w+j}$ to H^s_w by (1.28.4). The set $\mathcal{D}_n$ is dense in $\mathcal{A}_n \cap H^s_{W_1+j}$ (Lemma 1.28.2), which is dense in $\mathcal{A}_n \cap H^s_{w+j}$ by step (i) of that proof. For $f \in \mathcal{D}_n$ the functions $\partial^\alpha(\xi^\beta(a_\epsilon - a_0)\hat{f})$ are supported in the fixed compact set $\operatorname{supp} \hat{f} \subset \mathbb{R}^2 \setminus \{0\}$, are uniformly bounded there, and tend to zero pointwise. Dominated convergence and (1.28.1) give $a_\epsilon(D)f \to a_0(D)f$ in $H^s_{W_1} \subset H^s_w$. A uniformly bounded family that converges on a dense set converges strongly. □

Remark 1.28.4 (Sharpness of the margin). For integer w the margin (1.28.3) cannot be lowered. For $f = R^n e^{-R^2/2} e^{in\theta} \in \mathcal{A}_n$ and $a(\xi) = (\xi_1 + i\xi_2)/|\xi|^2 \in \mathsf{S}^{-1}_W$, the function $u = a(D)f$ is $u = c\, R^{n+1}\, {}_1F_1(n+1; n+2; -R^2/2)\, e^{i(n+1)\theta}$, which decays exactly like R^{-n-1}. Hence $\langle x \rangle^w u \in L^2$ if and only if $w < n$, although $\langle x \rangle^{w+1} f \in L^2$ for all w.

1.28.3 The Leray ladder

Let $p = (\xi, k) \in \mathbb{R}^3$ and $\mathsf{P}(\xi, k) = I - p \otimes p/|p|^2$, the 3×3 symbol of the Leray projector P_k at vertical frequency k. Let $\mathsf{S}(\xi, k) = -ip^{\mathsf{T}}/|p|^2$ be the symbol of the scalar pressure representative $S_k = \Delta_k^{-1} \operatorname{div}_k$, and $G = \nabla_h \Delta_h^{-1}$ the horizontal divergence primitive of Corollary 1.28.5(c), with symbol $-i\xi/|\xi|^2$.

Corollary 1.28.5 (Positive moment ladder). *Let $s, j, \ell \ge 0$ be integers, $w \ge 0$ real, and $n = |\mu| - 1$ for a sector $\mathcal{H}_\mu$ (or $\mathcal{H}_\mu \oplus \mathcal{H}_{-\mu}$). Let $a \in C^\ell(I)$ be positive on a compact interval I. All constants below are uniform in $k \in \mathbb{R}$ and $T \in I$.*

(a) If $\lceil w \rceil + j \le n$, i.e. $|\mu| \ge \lceil w \rceil + j + 1$, then for $f \in \mathcal{H}_\mu \cap H^s_{w+j}$

$$\left\| \partial_k^j \partial_T^\ell [P_{a(T)k}] f \right\|_{H^s_w} \le C \|f\|_{H^s_{w+j}}.$$

For $\ell = 0$, $a \equiv 1$ this gives the first estimate of Lemma 1.27.6 with the weaker margin $|\mu| \ge \lceil w \rceil + j + 1$ in place of $|\mu| > s + \lceil w \rceil + j + 2$.

(b) Under the margin of (a), $k \mapsto \partial_k^j P_k f$ is continuous in H^s_w for $f \in \mathcal{H}_\mu \cap H^s_{w+j}$. If moreover $\lceil w \rceil + j + 1 \le n$, it is differentiable in H^s_w for $f \in \mathcal{H}_\mu \cap H^s_{w+j+1}$, with derivative $\partial_k^{j+1} P_k f$, and for $0 \le \vartheta \le 1$, $|k - k'| \le 1$,

$$\left\| (\partial_k^j P_k - \partial_k^j P_{k'}) f \right\|_{H^s_w} \le C |k - k'|^\vartheta \|f\|_{H^s_{w+j+\vartheta}}.$$

(c) If $\lceil w \rceil + j + 1 \le n$, then $\left\| \partial_k^j S_k f \right\|_{H^s_w} \le C \|f\|_{H^s_{w+j+1}}$ for $f \in \mathcal{H}_\mu$; and if $\lceil w \rceil + 1 \le |\mu|$, then $\|G\phi\|_{H^s_w} \le C \|\phi\|_{H^s_{w+1}}$ for scalars ϕ of the single mode μ.

(d) Let N_c be an equivariant matrix function with $\operatorname{supp} N_c \subset B_L$ *and* $\|N_c\|_{C^s} < \infty$. *If* $\lceil w \rceil \le n$, *then for* $u \in \mathcal{H}_\mu \cap H^s$

$$\|P_k N_c P_k u\|_{H^s_w} \le C\langle 2L\rangle^w \|N_c\|_{C^s} \|u\|_{H^s}.$$

(e) All statements hold for functions with values in a Hilbert space Y (for example H^{10}_Y), since the multipliers act pointwise in Y.

Proof. (a) The function P is smooth on $\mathbb{R}^3 \setminus \{0\}$ and homogeneous of degree 0. By the chain rule, $\partial_T^\ell[\mathsf{P}(\xi, a(T)k)]$ is a finite sum of terms $c(T)\, h(\xi, a(T)k)$ with c a polynomial in $a^{-1}, a', \dots, a^{(\ell)}$ and $h(\xi,\kappa) = \kappa^b \partial_\kappa^b \mathsf{P}(\xi,\kappa)$, $b \le \ell$, which is again smooth on $\mathbb{R}^3 \setminus \{0\}$ and homogeneous of degree 0. Then $\partial_\xi^\alpha \partial_k^j$ of such a term is $c(T)a(T)^j$ times a function homogeneous of degree $-j-|\alpha|$, evaluated at $(\xi, a(T)k)$; it is bounded by $C|(\xi, a(T)k)|^{-j-|\alpha|} \le C|\xi|^{-j-|\alpha|}$. Thus the symbol lies in $\mathsf{S}^{-j}_W(C)$ for every W, uniformly in k, T. By (1.28.2) we may apply Proposition 1.28.3.

(b) Continuity: apply the last part of Proposition 1.28.3 to $a_\epsilon = \partial_k^j \mathsf{P}(\cdot, k+\epsilon)$. Differentiability: the difference quotient has symbol $\int_0^1 \partial_k^{j+1}\mathsf{P}(\cdot, k+t\epsilon)\,\mathrm{d}t$, which is uniformly in S^{-j-1} and converges pointwise with its ξ-derivatives. For the Hölder bound let $b = \partial_k^j \mathsf{P}(\cdot,k) - \partial_k^j \mathsf{P}(\cdot,k') = \int_{k'}^k \partial_\kappa^{j+1}\mathsf{P}\,\mathrm{d}\kappa$; then $b \in \mathsf{S}^{-j-1}(C|k-k'|)$ and $b \in \mathsf{S}^{-j}(C)$. In the splitting of the proof of Proposition 1.28.3, the low part maps $L^2_{w+j+1} \to L^2_w$ with norm $C|k-k'|$ and $L^2_{w+j} \to L^2_w$ with norm C. Applying (1.28.6) to its composition with Π_n gives $L^2_{w+j+\vartheta} \to L^2_w$ with norm $C|k-k'|^\vartheta$. The high part has $|\partial^\alpha(b(1-\chi))| \le C|k-k'|$, so it maps $L^2_w \to L^2_w$ with norm $C|k-k'| \le C|k-k'|^\vartheta$.

(c) The symbols S and $-i\xi/|\xi|^2$ are homogeneous of degree -1 and smooth away from the origin, so the argument of (a) puts $\partial_k^j \mathsf{S}$ in S^{-j-1}; apply Proposition 1.28.3 with $j+1$. A scalar of the single mode μ lies in $\mathcal{A}_{|\mu|}$.

(d) P_k is an L^2 contraction commuting with D^β, so $\|P_k u\|_{H^s} \le \|u\|_{H^s}$. The field $N_c P_k u$ lies in $\mathcal{H}_\mu$, is supported in B_L, and $\|N_c P_k u\|_{H^s_w} \le C\langle L\rangle^w \|N_c\|_{C^s}\|u\|_{H^s}$. Apply (a) with $j=0$.

(e) Apply the scalar statements to $\langle f, y\rangle_Y$ for an orthonormal basis (y_i) of Y and sum, or repeat the proof verbatim with Y-valued Plancherel. □

Remark 1.28.6 (Norm continuity of the decaying sandwich). Let N be an equivariant matrix function with $\langle x\rangle N \in L^\infty$ and $|\mu| \ge 2$. Then on $\mathcal{H}_\mu \cap L^2$, $\|P_k N P_k - P_{k'} N P_{k'}\|_{L^2\to L^2} \le C|k-k'|\ \|\langle x\rangle N\|_\infty$. Indeed $P_k N P_k - P_{k'} N P_{k'} = (P_k - P_{k'})N P_k + P_{k'} N (P_k - P_{k'})$. For the first term use (a), (b) with $j=0$, $\vartheta = 1$, $w=0$ and the input $NP_k u$, whose L^2_1 norm is at most $\|\langle x\rangle N\|_\infty \|u\|_2$. For the second term use duality inside $\mathcal{H}_\mu$: $\|N(P_k - P_{k'})u\|_2 = \sup_v |\langle u, (P_k - P_{k'})N^* v\rangle|$ over unit $v \in \mathcal{H}_\mu$, and $N^* v \in \mathcal{H}_\mu$. This is the norm continuity behind the uniform contours in the text; together with the uniform L^2 resolvent bound at one parameter it gives (B3) of Definition 1.28.7 on a smaller chart.

1.28.4 The weighted profile bootstrap

We state the bootstrap of Section 1.30.12 and Lemma 1.35.2 as an abstract proposition. Its hypotheses are exactly the inputs that the text proves elsewhere.

Definition 1.28.7 (Setting of the bootstrap)**.**

(B1) $\mathcal{X}$ is one sector $\mathcal{H}_{\mu_0}$ or a pair $\mathcal{H}_{\mu_0} \oplus \mathcal{H}_{-\mu_0}$, with $|\mu_0| \ge 2$, and $n_0 = |\mu_0| - 1$. We write $\mathcal{X}^s_w = \mathcal{X} \cap H^s_w$.

(B2) $\Lambda = I_Z \times I_k$ is a compact rectangle and $N(Z,k) = N_0(Z) + kN_1(Z)$, where $N_0(Z), N_1(Z)$ are equivariant matrix functions on $\mathbb{R}^2$. For integers $s_0 \ge 2$ and $l_0 \ge 0$, the maps $Z \mapsto N_i(Z)$ are C^{l_0} from I_Z into the Banach space $C^{s_0}_0(\mathbb{R}^2)$ of C^{s_0} functions whose derivatives of order $\le s_0$ are bounded and tend to zero at infinity. We put $A(Z,k) = -P_k N(Z,k) P_k$ on $\mathcal{X}$.

(B3) $\Gamma \subset \mathbb{C}\setminus\{0\}$ is a finite union of rectifiable closed curves, $c_0 = \min_\Gamma |z| > 0$, Γ lies in the resolvent set of $A(Z,k)$ on $\mathcal{X}_0^0$ for every $(Z,k) \in \Lambda$, and $K_0 = \sup_{\Lambda\times\Gamma} \|(z - A(Z,k))^{-1}\|_{\mathcal{X}_0^0 \to \mathcal{X}_0^0} < \infty$.

For the selected member: (B1) holds with $\mu_0 = m \geq 30$, so $n_0 \geq 29$. (B2) holds for every finite s_0 and for $l_0 = 17$: the multiplication form of N on the sector is the matrix of (1.29.1) (on $\mathcal{H}_{\pm m}$: transport $\pm im\Omega + \Omega\mathcal{J}$ from $\Omega\partial_\theta$ acting on Cartesian components, rotational stretching $\Omega\mathcal{J}$, so $2\Omega\mathcal{J}$ in all, $r\Omega_r\, e_\theta \otimes e_r = (\Omega_r/r)\, x^\perp \otimes x$, $W_r\, e_z \otimes e_r$, axial ikW; in the pair case N acts on each summand separately), and Lemma 1.32.2 gives $|\partial_Z^l \partial_r^j \Omega| \leq C\langle r\rangle^{-2-2h-j}$ for $l \leq 18$, while W and the controls have a common radial support bound on the compact axial chart. One more bounded and decaying Z-derivative than l_0 gives the C^{l_0} property into $C_0^{s_0}$. Cartesian smoothness at the axis is the regular-axis property of the source. For (B3), the simple branch has an isolating circle in $\{\Re z > 0\}$ by Sections 1.30.11–1.30.12. At the pole the complement lies in $\{\Re z \leq g\}$ by (P3). Choose $g < g' < \Re\lambda_0$ and a compact contour in the resolvent set enclosing the complement to the left of g' and excluding the pole. Boundedness of the frozen operator controls the exterior of a sufficiently large disk. Norm continuity and the resolvent identity keep the compact contour in the resolvent set of every operator on a smaller phase rectangle, with a uniform bound. Finitely many rectangles give the local chart bounds.

Proposition 1.28.8 (Weighted profile bootstrap)**.** *Work in the setting of Definition 1.28.7. Let $R(z) = R(z;Z,k) = (z - A(Z,k))^{-1}$. All constants are uniform in $(Z,k) \in \Lambda$ and $z \in \Gamma$.*

(i) Unweighted regularity. *For $0 \leq s \leq s_0$, $R(z)$ maps $\mathcal{X}_0^s$ into itself with a uniform bound.*

(ii) Weights. *For $0 \leq s \leq s_0$ and real $w \geq 0$ with $\lceil w\rceil \leq n_0$, $R(z)$ maps $\mathcal{X}_w^s$ into itself with a uniform bound; on $\mathcal{X}_w^s$ it is the restriction of the L^2 resolvent.*

(iii) Parameter jets. *Let $j \geq 0$, $l \leq l_0$, and $\lceil w\rceil + j \leq n_0$. Then $(Z,k) \mapsto R(z;Z,k)f$ has all mixed derivatives $\partial_Z^{l'}\partial_k^{j'}$, $l' \leq l$, $j' \leq j$, in $\mathcal{X}_w^s$ for $f \in \mathcal{X}_{w+j}^s$, taken in any order and continuous in (Z,k,z). They satisfy*

$$\partial_Z^l \partial_k^j R = \sum c\, R\, A_{(a_1,b_1)} R \cdots A_{(a_r,b_r)} R, \qquad A_{(a,b)} = \partial_Z^a \partial_k^b A. \tag{1.28.7}$$

For $l + j > 0$ the sum runs over $r \geq 1$ and $(a_i,b_i) \neq (0,0)$ with $\sum a_i = l$, $\sum b_i = j$, with universal coefficients c. For $l = j = 0$ the sole term is R with coefficient one. Each $A_{(a,b)}$ maps $\mathcal{X}_{v+b}^s$ to $\mathcal{X}_v^s$ for $\lceil v\rceil + b \leq n_0$, and $\big\|\partial_Z^l\partial_k^j R\big\|_{\mathcal{X}_{w+j}^s \to \mathcal{X}_w^s} \leq C$. A Z derivative costs no moment; a k derivative costs one.

(iv) Contour integrals. *Let $g(z;Z,k)$ be continuous on $\Gamma' \times \Lambda$, with $\Gamma' \subset \Gamma$ a union of components. Assume all mixed derivatives $\partial_Z^a\partial_k^b g$, $0 \leq a \leq l$, $0 \leq b \leq j$, exist in any order, are jointly continuous in (z,Z,k), and are uniformly bounded there. Then $\mathcal{I} = \frac{1}{2\pi i}\int_{\Gamma'} g(z;\cdot)R(z;\cdot)\,\mathrm{d}z$ has the mapping properties of (iii). This applies to the Riesz projection ($g = 1$) and, on rectangles where (vi) gives these mixed derivatives of λ, to the reduced resolvent $(A-\lambda)^{-1}Q = \frac{1}{2\pi i}\oint \frac{R(z)}{\lambda - z}\,\mathrm{d}z$ on a positively oriented isolating circle. It also applies to $e^{t(A-\lambda)}Q = \frac{1}{2\pi i}\oint_\Gamma e^{t(z-\lambda)}R(z)\,\mathrm{d}z$ with Γ around the complementary spectrum. In the last case*

$$\big\|\partial_Z^l\partial_k^j[e^{t(A-\lambda)}Q]\big\|_{\mathcal{X}_{w+j}^s \to \mathcal{X}_w^s} \leq C(1+t)^{l+j}e^{-t\,\delta_\Gamma}, \qquad \delta_\Gamma = \inf_\Lambda \Re\lambda - \max_\Gamma \Re z.$$

(v) Adjoint. *The same statements hold for $A(Z,k)^* = -P_k N(Z,k)^* P_k$ on the conjugate curves $\overline{\Gamma}$.*

(vi) Profiles. *Let $\gamma \subset \Gamma$ enclose exactly one eigenvalue $\lambda(Z,k)$ of $A(Z,k)$ on $\mathcal{X}_0^0$ for every $(Z,k) \in \Lambda$, algebraically simple, with Riesz projection $\Pi(Z,k)$. Let $W \geq 0$, $\lceil W \rceil \leq n_0$, $s \leq s_0$. Fix $(Z_*,k_*) \in \Lambda$, choose $\phi \in \mathcal{X}_W^s$ (for example $\Pi(Z_*,k_*)$ applied to a compactly supported smooth field) and $\psi \in \mathcal{X}_0^0$ with $\langle \Pi(Z_*,k_*)\phi,\psi\rangle \neq 0$. On a smaller rectangle $\Lambda' \ni (Z_*,k_*)$ the normalized profile $e = \Pi\phi/\langle \Pi\phi,\psi\rangle$ and $\lambda = \langle Ae,\psi\rangle$ satisfy*

$$\left\|\partial_Z^l \partial_k^j e\right\|_{H^s_{W-j}} \leq C, \qquad |\partial_Z^l \partial_k^j \lambda| \leq C, \qquad l \leq l_0,\ j \leq W.$$

All the displayed mixed derivatives exist in either order and are jointly continuous in (Z,k), in the indicated weighted space for e. The adjoint profile has the same bounds by (v). Any other normalization that differs by a scalar factor with these $C^{l_0,\lfloor W\rfloor}$ bounds keeps them.

(vii) Pressure. *The primitive pressure of e, $\pi = S_k(Ne)$ up to the sign convention, satisfies $\left\|\partial_Z^l \partial_k^j \pi\right\|_{H^s_{W-j-1}} \leq C$ for $j \leq W-1$, provided $\lceil W \rceil \leq n_0$.*

Proof. We write $\|v\|_{(\sigma)}^2 = \int (1+|\xi|^2)^\sigma |\hat v|^2$, equivalent to the H^σ norm for integers σ. The operators $L = 1-\Delta_h$, $J_\epsilon = (1+\epsilon L)^{-1}$ and $L_\epsilon = LJ_\epsilon$ ($\epsilon > 0$) are radial multipliers; they preserve $\mathcal{X}$ and commute with P_k, and P_k is a contraction in every $\|\cdot\|_{(\sigma)}$. Multiplication by M satisfies $\|Mv\|_{H^s_w} \leq C\,\|M\|_{C^s}\,\|v\|_{H^s_w}$.

(i). Let $\sigma \geq 0$ be an integer with $\sigma+2 \leq s_0$ and suppose $\|R(z)\|_{(\sigma)} \leq K_\sigma$ on $\mathcal{X}$. Let $f \in \mathcal{X}_0^{\sigma+2}$ and $u = R(z)f \in \mathcal{X}_0^\sigma$. One has the exact identities

$$[L_\epsilon, N] = J_\epsilon [L,N] J_\epsilon, \qquad (z-A)L_\epsilon u = L_\epsilon f - P_k J_\epsilon [L,N] J_\epsilon P_k u,$$

the first because $[J_\epsilon, N] = -\epsilon J_\epsilon [L,N] J_\epsilon$ and $L_\epsilon = \epsilon^{-1}(1-J_\epsilon)$. Here $[L,N]v = -(\Delta N)v - 2\sum_i (\partial_i N)\partial_i v$, so $\|[L,N]v\|_{(\sigma)} \leq C_N \|v\|_{(\sigma+1)}$ with $C_N \leq C\,\|N\|_{C^{\sigma+2}}$. By Cauchy–Schwarz on the Fourier side, $\|J_\epsilon v\|_{(\sigma+1)}^2 \leq \|L_\epsilon v\|_{(\sigma)}\,\|J_\epsilon v\|_{(\sigma)}$. With $X_\epsilon = \|L_\epsilon u\|_{(\sigma)} < \infty$ we obtain

$$X_\epsilon \leq K_\sigma \|f\|_{(\sigma+2)} + K_\sigma C_N X_\epsilon^{1/2} \|u\|_{(\sigma)}^{1/2}, \quad \text{so} \quad X_\epsilon \leq 2K_\sigma \|f\|_{(\sigma+2)} + K_\sigma^2 C_N^2 K_\sigma \|f\|_{(\sigma)}.$$

The bound is uniform in ϵ, and $X_\epsilon \uparrow \|Lu\|_{(\sigma)}$ by monotone convergence. Hence $u \in \mathcal{X}_0^{\sigma+2}$ with $\|u\|_{(\sigma+2)} \leq C\,\|f\|_{(\sigma+2)}$. Starting from $\sigma = 0$ (B3) this gives $\sigma = 2$. The rotation average $u \mapsto \frac{1}{2\pi}\int_0^{2\pi} e^{-i\mu_0\alpha} \mathcal{R}_\alpha^{-1} u(\mathsf{R}_\alpha \cdot)\,d\alpha$ (summed over $\pm\mu_0$ in the pair case) is a bounded projection onto $\mathcal{X}$ in each H^σ commuting with L; complex interpolation of $R(z)$ composed with it gives $\sigma = 1$. Induction in steps of two from $\sigma = 0, 1$ gives all $s \leq s_0$.

(ii). By Corollary 1.28.5(a) with $j = 0$, $\|P_k\|_{\mathcal{X}_v^s \to \mathcal{X}_v^s} \leq C_P$ for $0 \leq v \leq w$ (uniformly, by the interpolation in the proof of Proposition 1.28.3). Let $\chi \in C_c^\infty(B_2)$ be radial, $\chi = 1$ on B_1, and split $N = N_c + N_t$ with $N_c = \chi(x/L)N$. Since all derivatives of order $\leq s$ of N tend to zero at infinity uniformly on Λ, we can fix L with $c_0^{-1} C_P^2 C\,\|N_t\|_{C^s} \leq \frac{1}{2}$. Then $T = z^{-1} P_k N_t P_k$ has norm $\leq \frac{1}{2}$ on $\mathcal{X}_w^s$ and on $\mathcal{X}_0^s$. For $f \in \mathcal{X}_w^s$ and $u = R(z)f \in \mathcal{X}_0^s$ (by (i)), the equation $(z-A)u = f$ reads

$$u + Tu = g, \qquad g = z^{-1}(f - P_k N_c P_k u).$$

By Corollary 1.28.5(d), $g \in \mathcal{X}_w^s$ with $\|g\|_{H^s_w} \leq c_0^{-1}(\|f\|_{H^s_w} + C\langle 2L\rangle^w \|u\|_{H^s})$. The Neumann series for $(I+T)^{-1}g$ converges in $\mathcal{X}_w^s$ and in $\mathcal{X}_0^s \supset \mathcal{X}_w^s$ to the same limit, and $I+T$ is injective on $\mathcal{X}_0^s$; hence $u = (I+T)^{-1}g \in \mathcal{X}_w^s$ and $\|u\|_{H^s_w} \leq 2\,\|g\|_{H^s_w} \leq C\,\|f\|_{H^s_w}$.

(iii). We use two elementary facts. (F1) If $B(h) \in \mathcal{B}(Y,Y')$ are uniformly bounded and $B(h) \to B(0)$ strongly, and $y(h) \to y(0)$ in Y, then $B(h)y(h) \to B(0)y(0)$ in Y'. (F2) Products of

strongly differentiable, uniformly bounded families obey the product rule. By Corollary 1.28.5(a)–(b), $k \mapsto P_k^{(b)}$ is strongly continuous from $\mathcal{X}^s_{v+b}$ to $\mathcal{X}^s_v$ and strongly differentiable from $\mathcal{X}^s_{v+b+1}$ to $\mathcal{X}^s_v$, with derivative $P_k^{(b+1)}$, whenever the margins hold. By (B2), $Z \mapsto N(Z,k)$ is C^{l_0} in multiplier norm on every $\mathcal{X}^s_v$, and N is affine in k. Hence

$$A_{(a,b)} = - \sum_{b_1+b_2+b_3=b,\ b_2\le 1} \frac{b!}{b_1!b_2!b_3!}\, P_k^{(b_1)} (\partial_Z^a \partial_k^{b_2} N) P_k^{(b_3)}$$

maps $\mathcal{X}^s_{v+b} \to \mathcal{X}^s_v$, $\lceil v \rceil + b \le n_0$, and has the corresponding strong continuity and differentiability. The resolvent identity $R(z;k+\epsilon) - R(z;k) = R(z;k+\epsilon)\big(A(k+\epsilon) - A(k)\big)R(z;k)$, the uniform bounds of (ii) and (F1) show strong continuity of R on each $\mathcal{X}^s_v$, and

$$\epsilon^{-1}\big(R(k+\epsilon) - R(k)\big) f = R(k+\epsilon)\big[\epsilon^{-1}(A(k+\epsilon) - A(k))R(k)f\big] \longrightarrow R\, A_{(0,1)} R\, f$$

in $\mathcal{X}^s_v$ for $f \in \mathcal{X}^s_{v+1}$, since $R(k)f \in \mathcal{X}^s_{v+1}$. The Z derivative is the same with norm convergence and no loss of weight. Induction on $l + j$ with (F2), applied to the words in (1.28.7), proves (iii); the weights decrease along each word from $w + j$ to w by $\sum b_i = j$, and the resolvent factors are bounded on each intermediate weight by (ii). The resolvent is norm continuous in z on each $\mathcal{X}^s_v$.

(iv). For $f \in \mathcal{X}^s_{w+j}$ the mixed derivative of the integrand is

$$\sum_{a=0}^{l} \sum_{b=0}^{j} \binom{l}{a} \binom{j}{b} (\partial_Z^a \partial_k^b g)(\partial_Z^{l-a} \partial_k^{j-b} R) f.$$

Every term is continuous in $\mathcal{X}^s_w$ on the compact parameter set and contour by (iii), since the resolvent factor costs at most j moments. Uniform bounds of the same kind at all lower orders dominate the strong difference quotients on the finite-length contour, by integrating the next derivative on each parameter segment. Dominated convergence gives the asserted mixed derivatives of the Bochner integral. First apply this argument with $g = 1$. Once (vi) has been obtained from this case, $|\lambda - z|$ has a positive minimum on the isolating circle times the smaller closed rectangle, so $(\lambda - z)^{-1}$ has the required mixed derivatives. For $t \ge 0$, the chain rule on the same rectangle gives $|\partial_Z^a \partial_k^b e^{t(z-\lambda)}| \le C(1+t)^{a+b} e^{t(\Re z - \Re \lambda)}$ for $a \le l$, $b \le j$, which yields the stated semigroup estimate.

(v). N^* is equivariant and satisfies (B2); $\|(\bar z - A^*)^{-1}\|_{L^2} = \|(z - A)^{-1}\|_{L^2}$, so (B3) holds on $\overline{\Gamma}$. Apply (i)–(iv) to A^*. We do not dualize a weighted bound.

(vi). Apply (iv) with $g = 1$ to $\Pi\phi$. Every mixed derivative of order (a,b), $a \le l_0$, $b \le \lfloor W \rfloor$, is continuous in $H^s_{W-b} \subset L^2$. Pairing with ψ gives the same scalar mixed derivatives of the denominator, which stays bounded away from zero on a smaller closed rectangle containing (Z_*, k_*). The quotient rule gives the claimed derivatives of e in H^s_{W-b}. The projection has rank one and $\langle e, \psi\rangle = 1$, hence $\lambda = \langle Ae, \psi\rangle$. In the Leibniz expansion of $\partial_Z^a \partial_k^b (Ae)$, a factor $A_{(a',b')}$ acts on a profile derivative in $H^s_{W-b+b'}$ and maps it into H^s_{W-b} by (iii). These products are strongly continuous there. Pairing with ψ yields all the indicated mixed derivatives of λ on the same rectangle.

(vii). By Corollary 1.28.5(c) applied to the jets of $Ne \in \mathcal{X}^s_{W-j'}$: the term $(\partial_k^a S_k)\partial^{j-a}(Ne)$ needs the margin $\lceil W - j - 1 \rceil + a + 1 \le n_0$, which follows from $\lceil W \rceil \le n_0$. □

Corollary 1.28.9 (The weighted profile data of Section 1.30.12)**.** *For the selected member, with $m \ge 30$, Proposition 1.28.8 gives:*

(a) the leading right and adjoint profiles in H^6_{7-j}, $0 \le j \le 6$ (the sixth k derivative at weight one), with $l \le 17$ ordinary Z derivatives: $s = 6$, $W = 7$, margin $7 \le 29$, $l_0 = 17$ (estimate (1.35.3));

(b) the upgrade (1.35.4): $s = 18$, $W = 9$, $j \le 2$;

(c) the scalar pressure with $s \le 18$ and weight $8-j$, margin $9 \le 29$;

(d) the Riesz projection, the eigenvalue with its mixed jets, and the reduced Laurent coefficient $S = (A-\lambda)^{-1}Q$ on the same ladder;

(e) the first correctors $E_1 = -SR_1$ and v_1 in H^4_{6-j}, $0 \le j \le 4$, with sixteen Z derivatives, provided *the residual R_1 has the form displayed after (1.35.5), with $\partial_Z \mathcal{B}_0 \in C^5_b$, $\langle x\rangle^{-1} R_h \in L^\infty$ and $D^\beta R_h \in L^\infty$ for $1 \le |\beta| \le 5$. To verify the three coefficient bounds, write W for the axial leading profile and $\mathcal{B}_0 = (\Omega y^\perp, W)$. Solenoidality and regularity at the axis give*

$$R_h(y,Z) = -y \int_0^1 \theta\, \partial_Z W(\theta y, Z)\, \mathrm{d}\theta.$$

On a fixed Z-chart the integrand has support at $|\theta y| \le R_W$. Each differentiated term containing the factor y is bounded by $R_W \|\partial_Z W\|_{C^{|\beta|}}$ by the substitution $r = \theta|y|$. The remaining terms are bounded by $|\beta| \|\partial_Z W\|_{C^{|\beta|-1}}$. The same formula at order zero bounds R_h. The differentiated swirl tail of Lemma 1.32.2, together with regularity at the axis and compact radial support of W, gives $\partial_Z \mathcal{B}_0 \in C^5_b$. For e with the ladder (a) and $i \le j+1 \le 5$: $\Delta_h \partial_k^i e \in H^4_{7-i}$; $\frac{1}{2} y \cdot \nabla_h \partial_k^i e \in H^5_{6-i}$; $R_h \cdot \nabla_h \partial_k^i e \in H^5_{6-i}$; $G \partial_Z \partial_k^i e_z \in H^6_{6-i}$ by Corollary 1.28.5(c) (G acts on the mode-m scalar e_z, and $(G\phi, 0) \in \mathcal{H}_m$); F_0 is a bounded multiplication on the sector; the terms with e_k use $\partial_k^{j+1} e \in H^6_{6-j}$; the pressure term uses (c). Leibniz in k with Corollary 1.28.5(a) for $P_k^{(a)}$ then gives $\partial_k^j R_1 \in H^4_{6-j}$, and (iii)–(iv) give $\partial_k^j E_1 \in H^4_{6-j}$. The count even allows $j \le 5$;

(f) the following estimate for the frozen complement at $Z = 0$. For a stress $\mathsf{S}(k)$ with two bounded k derivatives in H^9_6 on the compact interaction hull, write $Q = I - \Pi$ for the complementary projection and $F = P_k \operatorname{div}_k \mathsf{S}$. For $j \le 2$, $q \le 4$ and $t \ge 0$,

$$\Big\| \langle R\rangle D_R^q\, \partial_k^j \big[e^{t(A(k)-\lambda(k))} Q(k) F(k) \big]_{k=0} \Big\|_2 \le C(1+t)^2 e^{-ct} \sum_{i \le j} \|\partial_k^i \mathsf{S}\|_{H^9_6}.$$

Indeed, Corollary 1.28.5(a) bounds $\partial_k^j F$ in H^8_{6-j}. Leibniz's rule in (1.28.7) bounds the resolvent response in the same space for $j \le 2$. Proposition 1.28.8(iv) gives the time factor, and $D_R^q u = \hat{x}^{\otimes q} : \nabla^q u$ gives the stated radial bound. For a rescaled frequency $a(T)k$ the associated projector derivatives are covered by Corollary 1.28.5(a).

The largest margin used is $\lceil w \rceil + j + 1 \le 10$ (pressure on the macro ladder), far below $m - 1 \ge 29$. The sufficient conditions $m > s + \lceil w \rceil + j + 2$ of the text are not needed but are implied.

1.29 Conditional physical resolvent estimates

Main result. Lemma 1.29.2 converts a scalar inverse bound into a physical velocity resolvent bound under its stated form and layer hypotheses. Propositions 1.29.13 and 1.29.18 give simplicity and viscous persistence under their stated spectral hypotheses.

The high-frequency lemmas give the other conditional resolvent estimates. Theorem 1.30.1 verifies these hypotheses for the selected member.

Throughout this section Λ is the physical spectral parameter. At the radial center that depends on the parameter put

$$\beta_n = n\Omega_c(Z) + kW_c(Z), \qquad \mu_D = \Lambda + i\beta_n.$$

The scalar denominator is $D = \mu_D + in(\Omega - \Omega_c) + ik(W - W_c)$, but all rotation and strain numerators keep the true Ω and $B = 2\Omega + r\Omega_r$.

We translate centered contours back by $-i\beta_n$. This is not a rotating-frame conjugation of the evolution.

The lemmas below are conditional tools for a fixed smooth source. Theorem 1.30.1 verifies their stated scalar, form, and spectral hypotheses for the selected member.

We defer the nonautonomous propagation argument to Section 1.34.

1.29.1 From the scalar pencil to a true velocity resolvent

We now freeze this one source, a real axial frequency k, and a nonzero angular label n.

We must retain the pressure and the constraint when we promote the scalar Green estimate to physical L^2. Write $a = n/r$, $Q = a^2 + k^2$, $q = Q^{1/2}$, $D = \Lambda + in\Omega + ikW$, $B = 2\Omega + r\Omega_r$ and $C = aB + kW_r$.

We write the inhomogeneous resolvent equations as

$$\begin{aligned} Du - 2\Omega v + p_r &= f_r, & Dv + Bu + iap &= f_\theta, \\ Dw + W_r u + ikp &= f_z, & u_r + u/r + iav + ikw &= 0. \end{aligned} \tag{1.29.1}$$

We first interpret them on smooth compactly supported forcing terms, then by density. The elimination does not assume divergence-free forcing. The projected resolvent remains restricted to the physical solenoidal subspace.

Lemma 1.29.1 (Physical exclusion for each fixed finite set of angular labels)**.** *For every control in the admitted ball, the low-frequency strip and the high-axial-frequency range overlap uniformly on the late width bracket.*

They give spectral exclusion on the prescribed half-plane $\Re z \geq g$. They also bound the physical resolvent for each real axial frequency and angular label $|n| < N_0$.

This argument does not extend the $|n| \geq 2$ Liouville/Hardy reduction to zero.

Proof. We fix the old source data and perturbation strength Δ, with old first-strain bound K_0.

Throughout the late width bracket the actual frozen column obeys

$$|\Omega| + |r\Omega_r| + |W_r| \leq K_{\mathrm{geom}}(K_0 + \Delta).$$

Large rounded-corner Ω_{rr} does not enter this bound. We select the high-k metric as follows.

It equals $d_* = K_0/\Delta$ on a fixed annulus that contains all perturbation and curvature supports. It equals one near the axis and infinity.

The transitions occur where the old strain bound applies. Then

$$A_\delta \leq K_{\mathrm{geom}}|n|/r_0, \quad J_\delta \leq K_{\mathrm{geom}}/r_0^2, \quad L \leq K_{\mathrm{geom}}(K_0 + \Delta).$$

Choose K_0 with a fixed slack $\epsilon_0 = K_0 - \|\partial_r W_{\mathrm{bg}}\|_\infty > 0$ in the old strain bound. The main angular edit and the curvature template change only Ω. On the supports of the axial trial templates, $r \geq r_{\min} > 0$ uniformly on the bracket. At fixed axial parameter, $\partial_r \xi = (rd)^{-1}$, hence

$$\partial_r W_{\mathrm{ctl}} = \frac{\chi(\eta)}{r} \sum_j (\mathsf{b}_j + \eta c_j) w'_{U,j}(\xi), \qquad \|\partial_r W_{\mathrm{ctl}}\|_\infty \leq K_{\mathrm{tpl}} r_T.$$

Here K_{tpl} depends on the fixed templates, the cutoff and $r_{\min}$. Choose the trial radius after these data so that $K_{\mathrm{tpl}} r_T \leq \epsilon_0/3$. The coefficients of the return bumps are $O_C(d\Delta)$ uniformly on this

ball by (1.30.23). For the zeroth-order bound on the entire central support, the edited fields have amplitude $O_C(d\Delta)$ on a fixed radial hull, and each difference of moment densities contains an edited factor. The uniformly bounded inverse of the five-moment map on that collar gives the same bound for the return coefficients. Their shapes are fixed in x on a compact annulus, so their physical radial derivatives have the same bound. The remaining exponentially small corrections contribute $O_C(d^{-N}e^{-c_C/d})$ there by Hypothesis 1.30.12(f). The edits vanish outside the central axial support. With C fixed, take the upper endpoint of the width bracket small enough that these last two bounds together are at most $2\epsilon_0/3$. Thus $|W_r| \le K_0$ throughout the annulus for every trial. The metric growth rate satisfies $\gamma_\delta \le K_{\mathrm{geom}}\sqrt{K_0\Delta} + K_0/2$.

The early choice of C, with $\Delta = C^\sigma$, gives $\gamma_\delta/g = O(\Delta^{-1/2}) < 1/2$. We select $\gamma_\delta < \gamma < g$ with $\gamma - \gamma_\delta \ge c\Delta$.

The exact metric energy identity then yields a physical resolvent bound for $|k| \ge K_n$, where

$$K_n \ge \frac{2A_\delta L}{d_*(\gamma - \gamma_\delta)}, \qquad K_n^2 \ge \frac{J_\delta}{2d_*}.$$

One sufficient threshold has $r_0K_n \le K'_{\mathrm{geom}}(|n|\Delta/K_0 + \sqrt{\Delta/K_0} + 1)$, independent of width d. For $n = 0$ the pressure error A_δ vanishes.

The low-strip energy estimate (proof of Theorem 1.30.1: the strain bound $K + K\Delta\sqrt{A_{\mathrm{lo}}} < g$, with the separately bounded background, lower controls and returns of Section 1.30.5.1) covers $d(1 + |n| + |k|r_0) \le A_{\mathrm{lo}}$. We select $d(1 + N_0 + \max_{|n|<N_0} r_0K_n) < A_{\mathrm{lo}}$, so these ranges overlap.

This proves exclusion for all real k on $\Re z \ge g$. It also gives physical resolvent bounds for $|n| < N_0$.

We hide no threshold that involves Δ/d. This is a frozen-column statement, not a completed-wave gradient bound.

□

Lemma 1.29.2 (Forced scalar-to-velocity estimate)**.** *Fix $|n| \ge 2$ and a parameter set $\mathcal{S}$ on which $\Re\Lambda \ge g > 0$. Retain the two main rounded signed corner layers as V_{main} and all late curvature/centering layers as V_{extra}.*

Let $E : H^1(\mathbb{R}) \to H^{-1}(\mathbb{R})$ denote the remaining exact transformed scalar bulk form, after those layers have been removed. Suppose, with one bound on $\mathcal{S}$, that

$$|\langle Eu, v\rangle| \le \eta\|u\|_{H^1}\|v\|_{H^1}, \qquad u, v \in H^1(\mathbb{R}), \qquad 0 \le \eta < 1,$$

where $\|u\|_{H^1}^2 = \|u'\|_2^2 + \|u\|_2^2$ and H^{-1} carries the dual norm. Each layer is assigned to one and only one of E, V_{main} and V_{extra}.

Suppose the two-main-layer inverse satisfies $\|(-\partial_z^2 + 1 + E + V_{\mathrm{main}})^{-1}\|_{H^{-1}\to H^1} \le M_*$ with one bound on $\mathcal{S}$, and $\|V_{\mathrm{extra}}\|_{H^1\to H^{-1}} \le \varepsilon$ with $M_*\varepsilon < 1$. On compact scaled frequency the first bound follows from a two-interface determinant margin $|\det N| \ge \delta > 0$ and sufficiently small fixed rounding.

At high scaled frequency it follows from the different signed-layer Schur bound of Lemma 1.31.3. Suppose also that $\|\Omega\|_\infty$, $\|r\Omega_r\|_\infty$, $\|W_r\|_\infty$, and $\|(B, W_r)\|_\infty$ are finite.

Then the true frozen Leray-projected inviscid velocity generator $A_{0,n,k}$ obeys

$$\sup_{(\Lambda,k)\in\mathcal{S}} \|(\Lambda - A_{0,n,k})^{-1}\|_{L^2_\sigma(r\,\mathrm{d}r)\to L^2_\sigma(r\,\mathrm{d}r)} \le C(g, \eta, \delta, n, \Delta, \textit{source jets})\left(1 + \frac{M_*}{1 - M_*\varepsilon}\right). \tag{1.29.2}$$

The bound is independent of k and $\Im\Lambda$ on $\mathcal{S}$. For a family, the scalar inverse factor $M_*/(1 - M_*\varepsilon)$ and the indicated source bounds must be uniform. The reconstruction uses the actual axis and exterior.

Proof. Eliminate v, w and pressure from (1.29.1). With $F_t = af_\theta + kf_z$, the forcing in the second-order radial equation simplifies distributionally to

$$F = -Qf_r/D - \frac{i}{D}[F_t' - (Q'/Q)F_t] + \frac{2\Omega k(af_z - kf_\theta)}{D^2}. \tag{1.29.3}$$

The derivatives of D cancel in this expression.

The proof uses no derivative of the force in L^2.

Put $z = \int^r q(\varrho)\,\mathrm{d}\varrho$ and $c(r) = (q/r)^{1/2}$, and write $u = c\psi$. Then

$$\int_0^\infty |u|^2 r\,\mathrm{d}r = \int_{\mathbb{R}} |\psi|^2\,\mathrm{d}z, \qquad \|Q^{-1/2}(\partial_r + 1/r)u\|_{L^2(r\,\mathrm{d}r)} = \|\psi_z + b_{\mathrm{geo}}\psi\|_{L^2_z}, \tag{1.29.4}$$

where $b_{\mathrm{geo}} = (1 - f_0)/(2rq)$, $f_0 = n^2/(n^2 + k^2r^2)$, and $\|b_{\mathrm{geo}}\|_\infty \le 1/(2|n|)$.

These are exact identities. They give the necessary physical inf–sup control of the radial derivative.

The transformed forcing $h = -F/(q^2c)$ has the form

$$h = f_r/(Dc) - H_{\mathrm{rot}} + \partial_z J - b_{\mathrm{forcing}}J, \quad J = \frac{iF_t}{Dqc}, \quad H_{\mathrm{rot}} = \frac{2\Omega k(af_z - kf_\theta)}{D^2q^2c}, \quad b_{\mathrm{forcing}} = b_{\mathrm{geo}} - \frac{D'}{qD}. \tag{1.29.5}$$

The D'/D term is the derivative of the exact density and must be retained. Since $|D| \ge g$ and $|D'|/q \le \|r\Omega_r\|_\infty + \|W_r\|_\infty$, (1.29.4) gives

$$\|h\|_{H_z^{-1}} \le C_F\|f\|_{L^2(r\,\mathrm{d}r)}, \quad C_F = \frac{2 + b_*}{g} + \frac{2\|\Omega\|_\infty}{g^2}, \quad b_* = \frac{1}{2|n|} + \frac{\|r\Omega_r\|_\infty + \|W_r\|_\infty}{g}.$$

The actual scalar equation is $L_b\psi + V_{\mathrm{main}}\psi + V_{\mathrm{extra}}\psi = h$, where $L_b = L_0 + E$ and $L_0 = -\partial_z^2 + 1$. The map $L_0 : H^1 \to H^{-1}$ is an isometric isomorphism for the stated norms.

Thus $\|L_0^{-1}E\|_{H^1\to H^1} \le \eta < 1$, and

$$L_b^{-1} = (I + L_0^{-1}E)^{-1}L_0^{-1}, \qquad \|L_b^{-1}\|_{H^{-1}\to H^1} \le b_0 = (1 - \eta)^{-1}.$$

This Neumann argument applies to the complex, non-selfadjoint bulk form. We apply Cauchy–Schwarz and the H^1 point-trace inequality to the absolute coefficient and layer bounds in (1.27.8)–(1.27.9).

This gives the stated bilinear form bounds. The main and extra layers stay in their assigned terms.

We use no L^∞ bound on a narrow layer. For clarity, the compact-A point-layer limit is $V_{\mathrm{main}} = \sum_{j=1}^2 \gamma_j\delta_{z_j}$, $|\gamma_j| \le \Delta/g$. Point evaluation on $H^1(\mathbb{R})$ has norm $1/\sqrt{2}$.

With $G_j = L_b^{-1}\delta_{z_j}$ and $\psi_0 = L_b^{-1}h$, its two trace values solve

$$Nt = (\psi_0(z_1), \psi_0(z_2)), \qquad N_{ij} = \delta_{ij} + \gamma_j G_j(z_i), \qquad \psi = \psi_0 - \sum_j \gamma_j t_j G_j.$$

If $M = 1 + \Delta b_0/(2g)$, $|\det N| \ge \delta$ gives $\|N^{-1}\| \le 2M/\delta$ and thus a point-layer $H^{-1} \to H^1$ bound. On a compact A interval, fixed-width smooth corner layers converge to these point forms at rate $O(\sqrt{\sigma})$ by the one-dimensional H^1 trace inequality.

The resolvent identity transfers the bound to the rounded main layers. At high A this comparison is not uniform, and the different single-sign diagonal and exponentially small cross-layer Schur argument of Lemma 1.31.3 supplies M_*.

The late layers satisfy $\|V_{\mathrm{extra}}\|_{H^1\to H^{-1}} \le Cc_{\mathrm{cut}}^2/(\Delta g)+Cm^N e^{-cm}$ by (1.27.9). They may overlap the main layers and have either sign.

Apply the resolvent identity to their form action. This gives the actual scalar estimate

$$\|\psi\|_{H^1_z} \le C_S\|h\|_{H^{-1}_z}, \qquad C_S = \frac{M_*}{1-M_*\varepsilon}. \tag{1.29.6}$$

For tangential reconstruction put $t=(v,w)$, $\mathbf{b}=(a,k)$, $\mathbf{c}=(B,W_r)$ and $\Pi_\perp = I-\mathbf{b}\otimes\mathbf{b}/Q$. Direct substitution in (1.29.1) gives

$$p = \frac{-D(\partial_r+1/r)u+iCu-iF_t}{Q}, \qquad t = \frac{\Pi_\perp(f_t-\mathbf{c}u)}{D}+\frac{i\mathbf{b}(\partial_r+1/r)u}{Q}. \tag{1.29.7}$$

The second term enforces divergence.

Equations (1.29.4), (1.29.6) and (1.29.7) yield a bound of the form

$$\|(u,v,w)\|_{L^2(r\,\mathrm{d}r)} \le \left[g^{-1}+(2+(2|n|)^{-1}+\|\mathbf{c}\|_\infty/g)C_SC_F\right]\|f\|_{L^2(r\,\mathrm{d}r)}.$$

For fixed parameters qp is in L^2 by (1.29.7). The radial equation gives p_r in L^2.

Thus the physical pressure gradient is an admissible gradient distribution and the Leray projector annihilates it. The form solution has the true regular-axis and decaying-exterior behavior.

A homogeneous physical L^2 solution has $\psi\in H^1$ by divergence and (1.29.4). Scalar uniqueness then forces $\psi=0$ and (1.29.7) forces its tangential part to vanish.

Density extends the construction to all L^2 forcing. This proves the true projected resolvent estimate. □

Lemma 1.29.3 (Positive spectrum and a local complement)**.** *For one fixed angular label, extend the physical generator to the fixed full-vector angular Hilbert space by $A_0=-P_kN_kP_k$. Under the regular-axis and decaying-exterior source bounds, it is a compact perturbation of the bounded skew-adjoint transport $-iP_k(n\Omega+kW)P_k$.*

Thus all spectrum in $\Re z>0$ consists of isolated eigenvalues with finite algebraic multiplicity. Suppose the main-layer Fredholm determinant d of Definition 1.29.7 has one and only one zero, of order one, in the half-disk Ω_+ of (1.29.10).

Then, under (I1)–(I3), the physical generator has one and only one eigenvalue in $\{\Re z>g\}$ (Lemma 1.29.12). Proposition 1.29.13 proves that this eigenvalue is algebraically simple.

On a smaller fixed (Z,k) chart its Riesz complement has a uniform forward bound Ce^{a_2t} for any $a_2>g$ below that band.

Proof. Each stretching term contains a radial input or output.

On a compact annulus away from the axis, solenoidality expresses the radial derivative through the tangential components. Localized radial extraction is bounded into one-dimensional H^1 and compact into L^2: approximation by cell averages on a mesh of width δ has finite rank and L^2 error at most $C\delta\|u'\|_2$ by the fundamental theorem of calculus. The radial weight is comparable to one on this annulus.

At infinity, source strain tends to zero and truncation is small in norm. At the axis, subtract the rigid-rotation matrix $2\Omega(0)J_h$.

The residual is $O(r)$ or $O(r^2)$ by the smooth axis germ. The identity $P_0J_hP_0=0$ makes the remaining localized rigid rotation a compact commutator $[P_0,\chi]J_hP_0$.

Truncate its weakly singular kernel near the diagonal. Then use Hilbert–Schmidt compactness off the diagonal. For $k\neq 0$, low-horizontal-frequency Hilbert–Schmidt truncation and high-frequency symbol decay show that $(P_k-P_0)\chi$ is compact.

Thus the strain sandwich is compact.

The source multiplier has $L^2 \cap L^\infty$ coefficients. For $|k - k'| \le 1$, the Leray symbol obeys $\|P_k(\xi_h) - P_{k'}(\xi_h)\| \le C \min(1, |k - k'|/|\xi_h|)$.

Split output horizontal frequency at q_0. The low-frequency composition with a fixed source multiplier is Hilbert–Schmidt of size $Cq_0\|N\|_2$.

The high part costs $C|k - k'|q_0^{-1}\|N\|_\infty$. We set $q_0 = |k - k'|^{1/2}$ and use adjoints for the right projection.

This proves joint norm continuity of $A_0(Z, k)$ on a compact parameter chart, including $k = 0$ (for $|n| \ge 2$, Remark 1.28.6 even gives a Lipschitz bound). This does *not* assert norm continuity of the bare P_k.

For $\Re z > 0$ factor the physical resolvent equation as its invertible transport part times $I + K(z)$ with $K(z)$ compact. Approximate $K(z_0)$ in norm by a finite-rank F; locally $I + K(z) - F$ is invertible by a Neumann series. Invertibility of $I + K(z)$ then reduces to that of the finite matrix on the range of F for $I + F(I + K(z) - F)^{-1}$, by block elimination. Thus failure of invertibility is equivalent to a nontrivial kernel, and the forced scalar reduction and its axis/exterior correspondence identify the positive physical spectrum. Sections 1.30.3–1.30.7 prove the actual source admission and the pole global $O(d/c_g)$ comparison (Lemma 1.30.2). These sections also prove the trace-class main layers, the centered Rouché count and the nonzero-b local comparison.

At the pole the correct model is

$$D_0(\Lambda) = \frac{\mu_D^2 - \lambda_*^2}{\mu_D^2 + \alpha^2 S^2}, \qquad \lambda_*^2 = \Delta^2 e^{-4\alpha}/4 - (S\alpha - \Delta/2)^2 > 0.$$

Thus its positive centered root corresponds to a generally complex physical pole $\lambda_* - im\Omega_c(0)$. Actual OLD and return terms cost algebraically in GLOBAL inverse norm.

Only localized response estimates use exponential support separation. We exclude large $|\mu_D|$ on the main supports, but we control the remote bulk by $|D| \ge g$, not by a false global $1/|\mu_D|$ estimate.

The true-domain determinant has one simple zero on its translated physical region. Forced reconstruction and the residue argument below transfer it to a rank-one algebraically simple physical pole.

Norm continuity keeps one fixed contour and a slightly relaxed complement line on a smaller (Z, k) chart. Bounded-operator contour calculus then gives $\|e^{tA_0}(I - P)\| \le Ce^{a_2 t}$.

The extra kernel of the full-space Leray extension lies at zero and does not affect the positive count. □

Remark 1.29.4 (The low labels $n = 0, \pm 1$). The proved physical energy/resolvent Lemma 1.29.1 at the start of this section supplies the low-label input. Its high-k threshold depends on the first strain, not on the rounded-corner second derivative, and does not depend on the late width.

It thus overlaps the low-strip bound. We do not invoke the $|n| \ge 2$ scalar reduction for these labels.

1.29.2 Algebraic simplicity of the selected band

Throughout this subsection we fix the source, the integer $n = m \ge 30$ and the width $d = d_m$. We write $A = A_{0,m,k}(Z)$ for the inviscid frozen generator restricted to the solenoidal sector $L^2_\sigma = L^2_\sigma(r\,\mathrm{d}r)$, with angular label m and axial frequency k. It is a bounded operator.

Contour projections. For a bounded operator and a contour enclosing a separated part of its spectrum, let $R(z) = (z - A)^{-1}$ and $P = (2\pi i)^{-1} \int_\Gamma R(z)\,\mathrm{d}z$. The resolvent identity $R(z)R(w) = (R(w) - R(z))/(z - w)$, integrated on nested copies of Γ, gives $P^2 = P$ and $PR(w) = R(w)P$. For w inside the contour, $(2\pi i)^{-1} \int_\Gamma R(z)/(z - w)\,\mathrm{d}z$ is an inverse for $w - A$ on $\ker P$: multiplication on either side gives $I - P$ there. For w outside, the negative of the same integral is an inverse on $\operatorname{Ran} P$, since multiplication gives P on that space. Thus a contour surrounding an isolated spectral point has nonzero projection. On a one-dimensional range the restriction of A equals that point times the identity, and the complementary inverse expands in a Neumann series. The same contour identities apply to a closed operator with nonempty resolvent: the integrals take values in its graph domain since $AR(z) = zR(z) - I$. Finally if P, Q are projections and $\|P - Q\| < 1$, $Q|_{\operatorname{Ran} P}$ and $P|_{\operatorname{Ran} Q}$ are injective, which preserves rank whenever either range is finite-dimensional.

The full-space extension $-P_k N_k P_k$ of Lemma 1.29.3 equals $A \oplus 0$ with respect to $L^2 = L^2_\sigma \oplus (I - P_k)L^2$, so its spectral data in $\{\Re z > 0\}$ coincide with those of A. An eigenvalue λ_0 of a bounded operator is *algebraically simple* if it satisfies two conditions.

It is isolated in the spectrum, and its Riesz projection $P = (2\pi i)^{-1} \oint (z - A)^{-1}\,\mathrm{d}z$ has rank one.

Then $P = e \otimes \ell$ with $Ae = \lambda_0 e$, $\ell A = \lambda_0 \ell$, $\ell e = 1$, and

$$(z - A)^{-1} = \frac{P}{z - \lambda_0} - \sum_{j \ge 0} (z - \lambda_0)^j S^{j+1}, \qquad S = \big((A - \lambda_0)|_{\operatorname{Ran}(I-P)}\big)^{-1}(I - P),$$

by the contour calculation above. The complementary Laurent series has the minus sign displayed above for this definition of S.

When the isolated eigenvalue has finite algebraic multiplicity and geometric multiplicity one, a nontrivial Jordan chain forces $\ell e = 0$ for its left and right eigenvectors. Under this qualification, the normalization $\ell e = 1$ in (1.35.7) is equivalent to algebraic simplicity.

The rank-one argument below supplies the geometric multiplicity-one property. Neither conclusion follows from a simple zero of a scalar function alone without that passage.

Imported facts. We use the next statements, each of which is proved, or stated as a hypothesis that has been verified, in the indicated place. The spectral parameter is Λ.

$D = \Lambda + in\Omega + ikW$ and $D' = in\Omega_r + ikW_r$, so that D' does *not* depend on Λ, and $|D| \ge \Re\Lambda$.

(I1) *Elimination* (proof of Lemma 1.29.2, (1.29.3)–(1.29.7)). For $\Re\Lambda > 0$ there are operators

$$\mathcal{L}(\Lambda)\colon H^1(\mathbb{R}) \to H^{-1}(\mathbb{R}), \quad \mathfrak{h}(\Lambda)\colon L^2_\sigma \to H^{-1}(\mathbb{R}), \quad \mathfrak{J}(\Lambda)\colon H^1(\mathbb{R}) \to L^2_\sigma, \quad \mathfrak{T}(\Lambda)\colon L^2_\sigma \to L^2_\sigma.$$

These are the scalar operator $L_b + V_{\text{main}} + V_{\text{extra}}$, the forcing map $f \mapsto h$ of (1.29.5), the reconstruction $\psi \mapsto (c\psi,\ -\Pi_\perp \mathbf{c}\, c\psi/D + i\mathbf{b}(\partial_r + 1/r)(c\psi)/Q)$, and $f \mapsto (0, \Pi_\perp f_t/D)$.

They have this property: if $\mathcal{L}(\Lambda)$ is invertible, then $\Lambda \in \rho(A)$ and

$$(\Lambda - A)^{-1} = \mathfrak{J}(\Lambda)\mathcal{L}(\Lambda)^{-1}\mathfrak{h}(\Lambda) + \mathfrak{T}(\Lambda). \tag{1.29.8}$$

Thus, the proof of Lemma 1.29.2 constructs this solution for smooth compactly supported f, bounds it in L^2, proves uniqueness, and extends by density.

We use the quantitative constant M_* only for uniformity, not for (1.29.8).

(I2) *Holomorphy.* In all four operators Λ enters only through the bounded multipliers D^{-1} and D^{-2} (inspect (1.29.3), (1.29.5), (1.29.7).

The coefficient $b_{\text{forcing}} = b_{\text{geo}} - D'/(qD)$ is of this form because D' is Λ-independent). Since $\Lambda \mapsto D^{-j}$ is holomorphic with values in L^∞ on $\{\Re\Lambda > 0\}$, all four operator families are holomorphic there in the respective operator norms.

(I3) *Main layers* (proof of Lemma 1.31.3, two-layer equation). In the scaled radial coordinate ξ of Lemma 1.31.3 at the pole $(Z,k)=(0,0)$, $\mathcal{L}(\Lambda)=\mathcal{L}_0(\Lambda)+\mathcal{V}(\Lambda)$, where $\mathcal{V}$ consists of the two rounded main layers.

They act as multiplication by $c_j(\cdot,\Lambda)=is_jh_j/D(\cdot,\Lambda)$, $j=\pm$, with $h_j\ge 0$ supported in $[z_j-\sigma_j,z_j+\sigma_j]$ and $\int h_j\le C\Delta$.

And $\mathcal{L}_0$ (coercive bulk, OLD smooth terms, remote returns, late layers V_{extra}) is holomorphic on a neighborhood of the closed region $\overline{\Omega_+}$ of (1.29.10). It is also boundedly invertible there. Invertibility of $\mathcal{L}_0$ is the coercivity bound $\left\|L_b^{-1}\right\|\le(1-\eta)^{-1}$ of Lemma 1.29.2 plus the actual global form allowance of (1.27.9).

At the pole, after we remove the explicit main layers, the residual $B_\xi=d(2\Omega_x+\Omega_{xx})$ gives an unweighted global $O(d/c_g)$ comparison, explicit in Lemma 1.30.2. Their TOTAL VARIATION and actual amplitude bound signed extra layers.

We include fixed physical returns in the residual J_C and product bound. Their global norm is not exponentially small.

Section 1.30.7 supplies the precise Neumann and trace-norm estimates. The unused form reserve is positive.

(I4) *Model* (Lemma 1.31.3, (1.31.6)). The model operator is $\mathcal{L}_{\mathrm{mod}}=\mathcal{L}_{0,\mathrm{mod}}+\mathcal{V}_{\mathrm{mod}}$, $\mathcal{L}_{0,\mathrm{mod}}=-\partial_\xi^2+\alpha^2$, $\mathcal{V}_{\mathrm{mod}}=\sum_{j=\pm}\gamma_j(\Lambda)\,\delta_{\xi_j}\otimes\delta_{\xi_j}$, $\xi_\pm=\pm1$, $\gamma_\mp=j_\mp$ the jump strengths of Lemma 1.31.3 with $S=\Delta-s_0$, and $\lambda_*^2>0$.

We use on $H^1(\mathbb{R})$ the norm $\|v'\|_2^2+\alpha^2\|v\|_2^2$ and on H^{-1} its dual norm. Then $(-\partial^2+\alpha^2)^{-1}$ has kernel $e^{-\alpha|x-y|}/(2\alpha)$, and for point evaluations

$$\|\delta_s\|_{H^{-1}}^2=\frac{1}{2\alpha},\qquad \|\delta_s-\delta_t\|_{H^{-1}}^2=\frac{1-e^{-\alpha|s-t|}}{\alpha}\le|s-t|\,. \tag{1.29.9}$$

The affine change from the scaled coordinate ξ to the Liouville coordinate z conjugates all operators below by one fixed isomorphism.

This keeps ranks, invertibility, and Fredholm determinants. Fix

$$\Omega_+=\{\Lambda:\ \Re\Lambda>g,\ |\Lambda+i\beta_n|<R_0\},\qquad R_0>1+\sup_{(Z,k)\in\mathcal{C}_0}\|A_{0,m,k}(Z)+i\beta_nI\|\,, \tag{1.29.10}$$

Here g is the positive separating line actually admitted in Theorem 1.30.1.

No unproved enlargement down to $\lambda_*/4$ is made.

The set $\mathcal{C}_0$ is the compact phase chart of Lemma 1.29.3. Since $\|A+i\beta_nI\|<R_0$, no physical spectrum lies outside this centered disk.

On a small phase chart use a fixed translated contour with a strict buffer, or the equivalent continuous translated contour family.

1.29.2.1 The main-layer determinant

Lemma 1.29.5 (Determinants of trace-class perturbations)**.** *On a complex Hilbert space put $D(K)=\det(I+K)$ for trace-class K. This is entire in trace norm, is multiplicative on products of the operators $I+K$, and is nonzero exactly when $I+K$ is invertible. Moreover*

$$|D(K)|\le e^{\|K\|_1},\qquad |D(K)-D(L)|\le\|K-L\|_1e^{\max(\|K\|_1,\|L\|_1)}.$$

At invertible points $|D(K)|\|(I+K)^{-1}\| \le e^{\|K\|_1}$. *For* $A : \mathbb{C}^m \to H$, $B : H \to \mathbb{C}^m$, *one has* $D(AB) = \det_{\mathbb{C}^m}(I+BA)$. *More generally, if* $A : H_2 \to H_1$ *and* $B : H_1 \to H_2$ *are Hilbert–Schmidt, then* $\det_{H_1}(I+AB) = \det_{H_2}(I+BA)$.

Proof. For finite-rank K, compute the ordinary determinant on a finite-dimensional space containing its range. Enlargement leaves it unchanged by triangularity. For finite-rank factors the last identity follows by eliminating either off-diagonal block in $\left(\begin{smallmatrix} I & A \\ -B & I \end{smallmatrix}\right)$. Write $K = \sum_i s_i u_i \otimes v_i^*$ in singular vectors of unit norm, with $\sum_i s_i = \|K\|_1$. The identity just proved expresses the homogeneous term of degree q as a sum over q distinct indices of the product of their s_i times the corresponding minor of $(\langle u_j, v_i\rangle)_{ij}$. Such a minor is the inner product of two exterior products of unit vectors and has modulus at most one. The same argument works for any sum of unit rank-one operators with scalar coefficients. In particular, the degree-q term is bounded by $\|K\|_1^q/q!$. On replacing K by $K+tE$ and adjoining a singular-vector expansion of E, the terms linear in t are bounded at degree q by $\|E\|_1\|K\|_1^{q-1}/(q-1)!$. Summation and integration along the segment from K to L give both displayed bounds.

Truncating singular-vector expansions approximates every trace-class operator in trace norm. The bounds therefore give a unique continuous extension, equal to the sum of the homogeneous polynomials just constructed. Indeed the degree-q bounds and their difference bounds extend each polynomial by continuity (or by polarization), and the series converges uniformly on trace-norm balls. This proves holomorphy. Multiplicativity passes from finite rank by $\|XY\|_1 \le \|X\|\|Y\|_1$, which follows by expanding Y in unit rank-one operators. If $I+K$ is invertible, $(I+K)^{-1} = I-(I+K)^{-1}K$ and multiplicativity gives $D(K) \neq 0$. Conversely write $K = F+E$ with F finite rank and $\|E\| < 1$. The factorization $I+K = (I+E)(I+(I+E)^{-1}F)$ reduces the converse to finite-dimensional invertibility. For the two-space identity approximate A, B by finite-rank maps in Hilbert–Schmidt norm. Their products converge in trace norm in both orders: expanding $AB = \sum_j Ae_j \otimes (B^*e_j)^*$ in an orthonormal basis of H_2 gives $\|AB\|_1 \le \|A\|_2\|B\|_2$ by Cauchy–Schwarz. The finite-dimensional block identity therefore passes to the limit. Finally for unit vectors u, v, multiplicativity applied to $I+K+tu\otimes v^*$ gives the derivative $D(K)\langle (I+K)^{-1}u, v\rangle$. Its bound above proves the inverse estimate. □

Lemma 1.29.6 (Trace-class layers)**.** *Let* $I \subset \mathbb{R}$ *be a bounded interval. Restriction* $\varrho\colon H^1(\mathbb{R}) \to L^2(I)$ *and its adjoint* $\varrho^*\colon L^2(I) \to H^{-1}(\mathbb{R})$ *are Hilbert–Schmidt.*

Thus, if $c(\cdot,\Lambda) \in L^\infty(I)$ *depends holomorphically on* Λ *in* L^∞, *multiplication* $M_c = \varrho^* c\, \varrho$ *is a holomorphic family in the trace ideal* $\mathfrak{S}_1(H^1, H^{-1})$. *Also, if* $\operatorname{supp} c \subset [z_0-\sigma, z_0+\sigma]$ *and* $\gamma = \int c$, *then*

$$\|M_c - \gamma\, \delta_{z_0} \otimes \delta_{z_0}\|_{\mathfrak{S}_1} \le \sqrt{2/\alpha}\, \sqrt{\sigma} \int |c|\,. \tag{1.29.11}$$

Proof. $\|\cdot\|_{H^1(\mathbb{R})}$ dominates $\|\cdot\|_{H^1(I)}$ (with the same weights), so it suffices to treat $H^1(I) \hookrightarrow L^2(I)$.

The Neumann cosines ϕ_j, $j \ge 0$, are orthogonal in $L^2(I)$ and $H^1(I)$, with $\|\phi_j\|_{H^1}^2 / \|\phi_j\|_{L^2}^2 = \alpha^2 + (\pi j/|I|)^2$. The singular values of the embedding are thus $(\alpha^2 + (\pi j/|I|)^2)^{-1/2}$, which are square summable.

The adjoint statement follows by duality. A product of two Hilbert–Schmidt operators with a bounded middle factor satisfies $\|ABC\|_1 \le \|A\|_2\|B\|\|C\|_2$: expand $ABC = \sum_j Ae_j \otimes (C^*B^*e_j)^*$ for an orthonormal basis of the intermediate space and apply Cauchy–Schwarz. Holomorphy in $\mathfrak{S}_1$ follows from holomorphy of $\Lambda \mapsto c(\cdot,\Lambda)$ in $B(L^2(I))$.

By (1.29.9), $s \mapsto \delta_s \otimes \delta_s$ is trace-norm continuous and has trace norm $(2\alpha)^{-1}$. For a measurable representative of c, the product $c(s)\,\delta_s \otimes \delta_s$ is strongly measurable, with integrable trace norm

$|c(s)|/(2\alpha)$ on I. Testing its Bochner integral against two H^1 functions gives $M_c = \int_I c(s)\,\delta_s \otimes \delta_s\,\mathrm{d}s$. Thus $M_c - \gamma\delta_{z_0} \otimes \delta_{z_0} = \int c(s)(\delta_s \otimes \delta_s - \delta_{z_0} \otimes \delta_{z_0})\,\mathrm{d}s$.

A rank-one operator $x \otimes y$ has trace norm $\|x\|\,\|y\|$, and $\delta_s \otimes \delta_s - \delta_{z_0} \otimes \delta_{z_0} = (\delta_s - \delta_{z_0}) \otimes \delta_s + \delta_{z_0} \otimes (\delta_s - \delta_{z_0})$. By (1.29.9) its trace norm is at most $2(2\alpha)^{-1/2}\,|s - z_0|^{1/2} \le \sqrt{2/\alpha}\sqrt{\sigma}$ on the support. □

The positive magnitude $S = \Delta - s_0$ of the inner slope determines the two Doppler values. Only the implanted jump Δ contributes a corner mass. Here $s_0 < 0$ is the signed OLD derivative, and the unrounded retained local limit model has centered profile $s_0\xi - \Delta\,\mathrm{clamp}(\xi, -1, 1)$.

Its inner derivative is $s_0 - \Delta = -S$. The persistent errors satisfy (1.30.8).

We impose these bounds before we round and before the late-width limit. Thus, in (1.31.3), $B_\xi = 2d\Omega_x + (\Omega_x)_\xi$.

The first term and the fixed OLD contribution to B_ξ stay $O(d)$ locally (we keep the signed OLD slope itself in D). The two limit jumps of Ω_x have masses $-\Delta, +\Delta$.

With the left/right convention of Lemma 1.31.3, the limit values of V_d are $S, -S$, in this order. Thus

$$\gamma_- = -\frac{i\alpha\Delta}{\mu_D + i\alpha S}, \qquad \gamma_+ = \frac{i\alpha\Delta}{\mu_D - i\alpha S}.$$

On $\overline{\Omega_+}$, $\Re\Lambda \ge g > 0$.

Across a layer of width σ, the variation of D^{-1} is at most $C\sigma/g^2$, with constants that depend on the fixed source. Its integrated coefficient thus differs from γ_j by $O(\sigma) + o_d(1)$.

Lemma 1.29.6 then gives trace-norm convergence of each layer to its point form. The source selection fixes a sufficiently small σ against the ideal contour margin before the choice of d small.

This comparison changes no axis or exterior boundary condition.

Definition 1.29.7. On a neighborhood of $\overline{\Omega_+}$ put $K(\Lambda) = \mathcal{L}_0(\Lambda)^{-1}\mathcal{V}(\Lambda) \in \mathfrak{S}_1(H^1)$ and

$$d(\Lambda) = \det(I + K(\Lambda)),$$

the Fredholm determinant on $H^1(\mathbb{R})$. Analogously $d_{\mathrm{mod}}(\Lambda) = \det(I + \mathcal{L}_{0,\mathrm{mod}}^{-1}\mathcal{V}_{\mathrm{mod}})$.

By Lemma 1.29.6 and (I3), K is holomorphic in $\mathfrak{S}_1$, so d is holomorphic by Lemma 1.29.5. Also $d(\Lambda) \ne 0$ if and only if $I + K(\Lambda)$ is invertible by the same lemma, that is, if and only if $\mathcal{L}(\Lambda) = \mathcal{L}_0(\Lambda)(I + K(\Lambda))$ is invertible.

For the model, $\mathcal{V}_{\mathrm{mod}}$ has rank two. The Sylvester identity $\det(I + \sum_j a_j \otimes b_j) = \det[\delta_{ij} + b_i(a_j)]$ of Lemma 1.29.5 gives

$$d_{\mathrm{mod}}(\Lambda) = \det\left[\delta_{ij} + \gamma_j\,G(\xi_i, \xi_j)\right] = \frac{\mu_D^2 - \lambda_*^2}{\mu_D^2 + \alpha^2 S^2} = D_0(\Lambda),$$

where $G(x, y) = e^{-\alpha|x-y|}/(2\alpha)$ and the strengths are the retained-slope coefficients computed above.

We expand the rank-two determinant and get its numerator $\mu_D^2 + (S\alpha - \Delta/2)^2 - \Delta^2 e^{-4\alpha}/4$.

Thus D_0 in the proof of Lemma 1.29.3 is d_{mod}. On $\overline{\Omega_+}$ it is holomorphic, its only zero is $\Lambda_* = \lambda_* - i\beta_n$, where $\lambda_* > 0$ is the centered root.

It is simple because $D_0'(\Lambda_*) = 2\lambda_*/(\lambda_*^2 + \alpha^2 S^2) \ne 0$.

Lemma 1.29.8 (Hypotheses for Rouché's theorem)**.** *Put $\delta_0 = \min_{\partial\Omega_+} |D_0| > 0$. Suppose that, with one bound for $\Lambda \in \partial\Omega_+$,*

$$\epsilon_{\mathrm{bulk}} = \left\|\mathcal{L}_0^{-1} - \mathcal{L}_{0,\mathrm{mod}}^{-1}\right\|_{H^{-1}\to H^1}, \qquad \epsilon_{\mathrm{lay}} = \sum_{j=\pm}\left(\sqrt{\sigma_j}\int|c_j| + \left|\int c_j - \gamma_j\right|\right) \tag{1.29.12}$$

satisfy $(\epsilon_{\mathrm{bulk}}\,\|\mathcal{V}\|_{\mathfrak{S}_1} + C_\alpha \left\|\mathcal{L}_{0,\mathrm{mod}}^{-1}\right\| \epsilon_{\mathrm{lay}}) e^{1+\|K\|_{\mathfrak{S}_1}+\|K_{\mathrm{mod}}\|_{\mathfrak{S}_1}} < \delta_0$, *with* $C_\alpha = \sqrt{2/\alpha} + (2\alpha)^{-1}$.

Then

$$|d(\Lambda) - D_0(\Lambda)| < |D_0(\Lambda)| \qquad (\Lambda \in \partial\Omega_+), \tag{1.29.13}$$

and d has one and only one zero in Ω_+, of order one.

Proof. By Lemma 1.29.5, $|\det(I+X) - \det(I+Y)| \le \|X-Y\|_{\mathfrak{S}_1} \exp(1 + \|X\|_{\mathfrak{S}_1} + \|Y\|_{\mathfrak{S}_1})$.

Write $K - K_{\mathrm{mod}} = (\mathcal{L}_0^{-1} - \mathcal{L}_{0,\mathrm{mod}}^{-1})\mathcal{V} + \mathcal{L}_{0,\mathrm{mod}}^{-1}(\mathcal{V} - \mathcal{V}_{\mathrm{mod}})$ and use the ideal property and (1.29.11), together with $\|\delta_z \otimes \delta_z\|_{\mathfrak{S}_1} = (2\alpha)^{-1}$ for the difference of the strengths. This gives (1.29.13).

For $0 \le t \le 1$, $f_t = D_0 + t(d - D_0)$ is nonzero on the boundary. The integer $(2\pi i)^{-1} \oint f_t'/f_t$ is its number of interior zeros with multiplicity: remove small disks about the zeros and integrate $(\log f_t)'$ locally, using the residue of a zero of order j, which equals j. This integral is continuous in t, hence constant, proving the claimed count. □

Lemma 1.29.9 (Factorised Rouché margin)**.** *Let $\mathcal{K}_0$ be the compact chart on which Lemma 1.29.8 is applied: $\alpha \in [\alpha_-, \alpha_+] \subset (0,\infty)$ and $s = S/\Delta \in [1, 1+q_0]$. We require $g < \lambda_*(\alpha, s) < R_0$ on $\mathcal{K}_0$, where $\lambda_*^2 = \Delta^2 e^{-4\alpha}/4 - (S\alpha - \Delta/2)^2$. Then $D_0 \neq 0$ on $\partial\Omega_+$ throughout the chart. At $s = 1$ the lower inequality is exactly $F_c(\alpha) > 0$, where $c = g/\Delta$ and $F_c = e^{-4\alpha}/4 - (\alpha - 1/2)^2 - c^2$. For $c = 0.05, 0.10, 0.15$ the respective pairs of roots are approximately $(0.05379, 0.63209)$, $(0.11790, 0.60899)$ and $(0.20111, 0.56225)$. The admissible open interval for the lower inequality has the exact roots as endpoints. Indeed $F_c'(0) = 0$, $F_c'' = 4e^{-4\alpha} - 2$ changes sign once on the positive axis, and $F_c(0) < 0 < F_c(0.4)$ with $F_c(\alpha) \to -\infty$. The late bracket $\alpha_\sigma \pm \delta\alpha$ about $\alpha_{\mathrm{m}} = 0.3984$ can be chosen strictly inside all three intervals. The upper inequality uses the separate choice of R_0. Write the two layer points as $\xi_1 = -1$, $\xi_2 = 1$, the strengths as $\gamma_1 = \gamma_-$, $\gamma_2 = \gamma_+$, and put*

$$M(\Lambda) := \left[\delta_{ij} + \gamma_j G(\xi_i, \xi_j)\right]_{i,j=1}^{2}, \qquad G(x,y) = \frac{e^{-\alpha|x-y|}}{2\alpha},$$

so that $\det M = D_0$ by the Sylvester identity above. Put

$$\kappa_R := \sup_{\mathcal{K}_0}\sup_{\partial\Omega_+} \frac{|\gamma_+| + |\gamma_-|}{2\alpha}, \qquad \rho_R := 1 + \sup_{\mathcal{K}_0}\sup_{\partial\Omega_+} \frac{(|\gamma_+|^2 + |\gamma_-|^2)^{1/2}}{\sqrt{2}\,\alpha} \left\|M^{-1}\right\|_{\mathbb{C}^2\to\mathbb{C}^2}, \qquad \varpi := \frac{1}{5\rho_R}.$$

These numbers are finite, because $D_0 \neq 0$ on $\partial\Omega_+$ and $\mathcal{K}_0 \times \partial\Omega_+$ is compact. They depend only on the normalized model and the contour. Suppose that, uniformly on $\partial\Omega_+$,

$$C_\alpha \epsilon_{\mathrm{lay}} \le \min\{1, \varpi/2\}, \qquad \epsilon_{\mathrm{bulk}} \le \varpi_{\mathrm{bulk}} := \frac{\varpi}{2(\kappa_R + 1)}.$$

Then $|d(\Lambda) - D_0(\Lambda)| \le \frac{1}{5} e^{6/5} |D_0(\Lambda)| < |D_0(\Lambda)|$ on $\partial\Omega_+$. Thus d has exactly one zero in Ω_+, and this zero is simple.

Proof. We use the norm $\|v\|_N^2 = \|v'\|^2 + \alpha^2\|v\|^2$ on $H^1(\mathbb{R})$. In this norm $\mathcal{L}_{0,\mathrm{mod}}^{-1} : H^{-1} \to H^1$ is the Riesz isometry, $\|\delta_z\|_{H^{-1}}^2 = (2\alpha)^{-1}$, and $\sup|v|^2 \le \|v\|\|v'\| \le \|v\|_N^2/(2\alpha)$. A rank-one operator $x \otimes \phi$ has trace norm $\|x\|\|\phi\|$. Thus $\|K_{\mathrm{mod}}\|_{\mathfrak{S}_1} \le \kappa_R$ and $\|\mathcal{V}_{\mathrm{mod}}\|_{\mathfrak{S}_1} \le \kappa_R$.

Step 1: the perturbation. Then $\|\mathcal{V}\|_{\mathfrak{S}_1} \le \kappa_R + C_\alpha\epsilon_{\mathrm{lay}} \le \kappa_R + 1$. The decomposition in the proof of Lemma 1.29.8 gives

$$\|K - K_{\mathrm{mod}}\|_{\mathfrak{S}_1} \le \epsilon_{\mathrm{bulk}}(\kappa_R + 1) + C_\alpha\epsilon_{\mathrm{lay}} \le \tfrac{1}{2}\varpi + \tfrac{1}{2}\varpi = \varpi.$$

Step 2: the inverse of the rank-two model. Define $\mathsf{A} : \mathbb{C}^2 \to H^1$ by $\mathsf{A}e_j = \gamma_j \mathcal{L}_{0,\mathrm{mod}}^{-1}\delta_{\xi_j}$ and $\mathsf{B}^* : H^1 \to \mathbb{C}^2$ by $\mathsf{B}^* v = (v(\xi_1), v(\xi_2))$. Then $K_{\mathrm{mod}} = \mathsf{A}\mathsf{B}^*$ and $I_2 + \mathsf{B}^*\mathsf{A} = M$. Also $\|\mathsf{A}\| \le$

$(|\gamma_+|^2+|\gamma_-|^2)^{1/2}(2\alpha)^{-1/2}$ and $\|\mathsf{B}^*\| \le \alpha^{-1/2}$. On $\partial\Omega_+$ the matrix M is invertible, and the Woodbury identity gives

$$(I+K_{\mathrm{mod}})^{-1} = I - \mathsf{A}M^{-1}\mathsf{B}^*, \qquad \left\|(I+K_{\mathrm{mod}})^{-1}\right\|_{H^1\to H^1} \le \rho_R.$$

Step 3: factorisation. Put $Y = (I+K_{\mathrm{mod}})^{-1}(K-K_{\mathrm{mod}}) \in \mathfrak{S}_1$. Then $I+K = (I+K_{\mathrm{mod}})(I+Y)$ and $\|Y\|_{\mathfrak{S}_1} \le \rho_R\varpi = \frac{1}{5}$. The Fredholm determinant is multiplicative by Lemma 1.29.5, so $d = D_0\det(I+Y)$. Its difference estimate with the second operator equal to zero gives $|\det(I+Y)-1| \le \|Y\|_{\mathfrak{S}_1}e^{1+\|Y\|_{\mathfrak{S}_1}} \le \frac{1}{5}e^{6/5} < 0.67$. Hence $|d-D_0| < |D_0|$ on $\partial\Omega_+$. The scalar Rouché theorem counts zeros with multiplicity, and D_0 has exactly one zero in Ω_+, which is simple. □

Remark 1.29.10 (Size of the margin). The factorization uses the finite inverse norm of the rank-two model, instead of the exponentially small sufficient tolerance obtained by applying determinant continuity directly to K and K_{mod}. Only positivity of the uniform margin on $\mathcal{K}_0$ is used below.

Section 1.30.7 gives the two quantities in (1.29.12). The global pole inverse comparison is given explicitly by Lemma 1.30.2 and includes the actual old field.

The rounded, centered Doppler mass estimate gives the main-layer trace difference. At nonzero b use the compact-observation true-domain comparison, not global convergence of changing operator domains.

Lemmas 1.30.8 and 1.30.33 give the typed local inverse and trace-class comparison on fixed spaces. We do not compare either persistent comparison error against the d^2 integer gap.

1.29.2.2 A simple zero gives a simple pole of rank one

Lemma 1.29.11 (Simple zero of the determinant)**.** *Let H be a Hilbert space, $U \ni \lambda_0$ open, $K\colon U \to \mathfrak{S}_1(H)$ holomorphic, and $d = \det(I+K)$. If $d(\lambda_0) = 0 \ne d'(\lambda_0)$, then on a punctured disk about λ_0*

$$(I+K(\Lambda))^{-1} = \frac{R_0}{\Lambda-\lambda_0} + \mathcal{H}(\Lambda), \qquad \operatorname{rank} R_0 = 1,$$

with $\mathcal{H}$ holomorphic, and $\dim\ker(I+K(\lambda_0)) = 1$.

The same holds for $\mathcal{L}^{-1} = (I+K)^{-1}\mathcal{L}_0^{-1}$ whenever $\mathcal{L} = \mathcal{L}_0(I+K)$ with $\mathcal{L}_0$ holomorphic and invertible.

Proof. Let Π_N be orthogonal projections of rank N that increase strongly to I.

Since $K(\lambda_0)^*$ is compact, $\|K(\lambda_0)(I-\Pi_N)\| = \|(I-\Pi_N)K(\lambda_0)^*\| \to 0$. Fix N and $r>0$ with $\|K(\Lambda)(I-\Pi_N)\| \le \frac{1}{2}$ for $|\Lambda-\lambda_0| \le r$.

Put $G = K(I-\Pi_N)$ and $F = K\Pi_N$. Then $I+G$ is invertible with holomorphic inverse, $\det(I+G) \ne 0$, and

$$I+K = (I+G)(I+\widetilde{F}), \qquad \widetilde{F} = (I+G)^{-1}K\Pi_N = \sum_{j=1}^{N} a_j \otimes e_j^*, \quad a_j = (I+G)^{-1}Ke_j,$$

where (e_j) is an orthonormal basis of $\operatorname{Ran}\Pi_N$.

Write $e_i^*(x) = \langle x, e_i\rangle$ for the linear coordinate. With $M(\Lambda) = [\delta_{ij} + e_i^*(a_j(\Lambda))]_{i,j\le N}$, multiplicativity and the Sylvester identity give $d = \det(I+G)\det M$, so $\det M$ has a simple zero at λ_0. Applying the coordinates to $(I+\widetilde{F})x = y$ gives $M\xi = (e_i^*(y))_i$, $\xi_i = e_i^*(x)$, hence

$$(I+\widetilde{F})^{-1} = I - \sum_{j,l} a_j\,(M^{-1})_{jl}\,e_l^*. \tag{1.29.14}$$

Write $\det M = (\Lambda - \lambda_0)\mu(\Lambda)$, $\mu(\lambda_0) \neq 0$, and $M^{-1} = \operatorname{adj} M / \det M$.

Then

$$M^{-1} = \frac{\operatorname{adj} M(\lambda_0)}{(\Lambda - \lambda_0)\mu(\lambda_0)} + \text{holomorphic}.$$

Jacobi's formula gives

$$(\det M)'(\lambda_0) = \operatorname{tr}\big(\operatorname{adj} M(\lambda_0) M'(\lambda_0)\big) \neq 0.$$

Thus $\operatorname{adj} M(\lambda_0) \neq 0$. This gives $\operatorname{rank} M(\lambda_0) = N - 1$, $\ker M(\lambda_0)$ is a line, and $\operatorname{adj} M(\lambda_0)$, whose columns lie in $\ker M(\lambda_0)$ because $M \operatorname{adj} M = \det M\, I$, has rank one.

We insert this identity in (1.29.14) and multiply on the right by the holomorphic invertible $(I+G)^{-1}$. Thus $(I+K)^{-1}$ has at most a simple pole, with residue of rank at most one.

The residue is nonzero. If it were zero, $(I+K)^{-1}$ would stay bounded near λ_0 and $I + K(\lambda_0)$ would be invertible. This contradicts $d(\lambda_0) = 0$. Last, $x \in \ker(I + \widetilde{F}(\lambda_0))$ iff $x = -\sum_j a_j \xi_j$ with $\xi \in \ker M(\lambda_0)$, so the kernel is a line.

Right multiplication by $\mathcal{L}_0^{-1}$, holomorphic and invertible, keeps all these statements.

□

1.29.2.3 Transfer to the physical generator

Lemma 1.29.12 (Physical rank of the band)**.** *At the pole $(Z,k) = (0,0)$ assume (I1)–(I3), and that d has in Ω_+ one and only one zero λ_0, of order one. Then $\sigma(A) \cap \{\Re\Lambda > g\} = \{\lambda_0\}$ and λ_0 is an algebraically simple eigenvalue of A.*

If $\mathcal{L}^{-1}$ has residue $R_0 = \varphi \otimes \chi$ at λ_0, then

$$P = \mathfrak{J}(\lambda_0) R_0\, \mathfrak{h}(\lambda_0), \qquad e \in \operatorname{span}\{\mathfrak{J}(\lambda_0)\varphi\}, \qquad \ell \in \operatorname{span}\{\chi \circ \mathfrak{h}(\lambda_0)\}. \tag{1.29.15}$$

Proof. Location. For $\Lambda \in \Omega_+ \setminus \{\lambda_0\}$, $d(\Lambda) \neq 0$, so $\mathcal{L}(\Lambda)$ is invertible and $\Lambda \in \rho(A)$ by (I1). Points with $|\Lambda + i\beta_n| \geq R_0$ are resolvent points by (1.29.10).

λ_0 is an eigenvalue. Let $0 \neq \varphi \in \ker \mathcal{L}(\lambda_0)$ and $U = \mathfrak{J}(\lambda_0)\varphi$. Given $u = c\varphi$, the θ, z and divergence equations of (1.29.1) with $f = 0$ form a linear system for (v, w, p) with matrix $\left(\begin{smallmatrix} D & 0 & ia \\ 0 & D & ik \\ ia & ik & 0 \end{smallmatrix}\right)$, whose determinant is $DQ \neq 0$.

Its unique solution is (1.29.7). The radial equation is the scalar equation $\mathcal{L}(\lambda_0)\varphi = 0$, from which it was derived. By (1.29.4), $\|u\|_{L^2(r\,\mathrm{d}r)} = \|\varphi\|_2 \neq 0$ and $\left\| Q^{-1/2}(\partial_r + 1/r)u \right\| \leq \|\varphi\|_{H^1}\,(1 + \frac{1}{2|n|})$, so $(v, w) \in L^2$, because $|\mathbf{b}|\, Q^{-1/2} = 1$ and $\|\Pi_\perp \mathbf{c}\, u/D\| \leq \|\mathbf{c}\|_\infty \|u\| / g$.

The pressure is an admissible gradient as in the proof of Lemma 1.29.2. Thus $0 \neq U \in \ker(\lambda_0 - A)$.

Rank. By Lemma 1.29.11, $\mathcal{L}^{-1} = R_0/(\Lambda - \lambda_0) + \mathcal{H}$ near λ_0, $\operatorname{rank} R_0 = 1$. Insert this in (1.29.8).

By (I2), $\mathfrak{J}(\Lambda) = \mathfrak{J}(\lambda_0) + O(\Lambda - \lambda_0)$ and similarly for $\mathfrak{h}$, while $\mathfrak{T}$ and $\mathfrak{J}\mathcal{H}\mathfrak{h}$ are holomorphic. Integration over a small circle gives (1.29.15) for the Riesz projection, so $\operatorname{rank} P \leq 1$.

Since λ_0 is an isolated point of $\sigma(A)$, $P \neq 0$ by the contour identities above. Thus $\operatorname{rank} P = 1$, and the formulas for e, ℓ follow from $P = e \otimes \ell$.

□

Proposition 1.29.13 (Simple band on a phase chart)**.** *Assume the hypotheses of Lemma 1.29.12 and, at the pole, the boundary margin $\delta_\Gamma := \min_\Gamma |d| > 0$ on $\Gamma = \partial\Omega_+$, including its segment on $\Re z = g$. Then there is a compact neighborhood $\mathcal{C} \subset \mathcal{C}_0$ of $(0,0)$ such that for each $(Z,k) \in \mathcal{C}$ the following hold.*

(i) $A_{0,m,k}(Z)$ has one and only one eigenvalue $\lambda(Z,k)$ in $\{\Re z > g\}$. It is algebraically simple, and its Riesz projection $P(Z,k)$ has rank one.

(ii) with e_0, ℓ_0 the pole eigenvectors, $\ell_0 e_0 = 1$,

$$e = Pe_0, \qquad \ell = \frac{\ell_0 P}{\ell_0 P e_0}, \qquad \lambda = \frac{\ell_0 A P e_0}{\ell_0 P e_0}, \qquad \ell e = 1, \qquad |\ell_0 P e_0 - 1| \le \tfrac{1}{2}; \tag{1.29.16}$$

(iii) P, e, ℓ, λ are jointly continuous in operator norm, and C^{18} in Z in operator norm at fixed k. Each additional regularity of $z \mapsto (z - A(Z,k))^{-1}$ on a fixed contour (in particular the weighted k-differentiability of Lemma 1.35.2) passes to P, e, ℓ, λ through (1.29.16).

(iv) for the conjugate sector, with C the real-field conjugation, $A_{0,-m,-k}(Z) = \mathsf{C} A_{0,m,k}(Z) \mathsf{C}$. Thus $P_{-m}(Z,-k) = \mathsf{C} P_m(Z,k) \mathsf{C}$ has rank one with eigenvalue $\overline{\lambda(Z,k)}$.

Proof. The boundary margin gives $\Gamma \subset \rho(A(0,0))$ by (I1) and the invertible bulk in (I3). For the counted member, Lemma 1.29.9 supplies $\delta_\Gamma \ge (1 - e^{6/5}/5) \min_\Gamma |D_0| > 0$.

Together with (1.29.10) and Lemma 1.29.12, $\sup_\Gamma \|(z - A(0,0))^{-1}\| =: M_\Gamma < \infty$. The proof of Lemma 1.29.3 gives joint norm continuity of $(Z,k) \mapsto A(Z,k)$ on $\mathcal{C}_0$, including $k = 0$.

We select $\mathcal{C}$ such that the three inequalities hold there:

$$\begin{aligned} &\|A(Z,k) - A(0,0)\| \le (2M_\Gamma)^{-1}, \\ &\|P(Z,k) - P(0,0)\| < \min\{1, (2\,\|\ell_0\|\,\|e_0\|)^{-1}\}, \\ &|\beta_n(Z,k) - \beta_n(0,0)| < 1. \end{aligned}$$

The second resolvent identity and a Neumann series give $(z - A(Z,k))^{-1}$ on Γ.

Its continuity in (Z,k) has one modulus for all $z \in \Gamma$. The contour formula $P(Z,k) = (2\pi i)^{-1} \oint_\Gamma (z - A(Z,k))^{-1}\,\mathrm{d}z$ thus permits the second bound.

Whether β_n in (1.29.10) is read at (Z,k) or at the pole, the bound $\|A(Z,k) + i\beta_n I\| < R_0 - 1$ on $\mathcal{C}_0$ and the third inequality place the spectrum of $A(Z,k)$ in $\{|z + i\beta_n(0,0)| < R_0\}$. Hence $\sigma(A(Z,k)) \cap \{\Re z > g\}$ lies inside Γ, and $P(Z,k)$ is its Riesz projection.

The injection argument for projections at distance < 1 gives (i). Then $|\ell_0 P e_0 - 1| = |\ell_0 (P - P_0) e_0| \le \frac{1}{2}$. Since $P = e \otimes \ell$ is rank one with $APe_0 = \lambda P e_0$, we get the formulas (1.29.16) directly.

For (iii), P_k does not depend on Z. The coefficients of N_k have eighteen ordinary Z derivatives that are bounded, continuous in (x, Z) and uniformly decaying as $r \to \infty$ on the compact chart (Lemma 1.32.2; the core, the axial velocity and the controls are smooth, the last two with compact radial support). Uniform continuity on bounded radial sets and the uniform decay make $Z \mapsto \partial_Z^l N_k$ continuous into L^∞ for $l \le 18$.

Thus $Z \mapsto A$ is C^{18} in $B(L^2)$. Differentiate $R = (z - A)^{-1}$ by $\partial R = R(\partial A)R$ under the contour integral, and use (1.29.16), in which the only denominator $\ell_0 P e_0$ stays in $[\frac{1}{2}, \frac{3}{2}]$ in modulus.

Item (iv) is the identity $\overline{e^{i(m\theta + kz)}} = e^{i(-m\theta - kz)}$ for the real coefficients of the source. □

Proposition 1.29.14 (Viscous persistence of simplicity)**.** *Let T_ν, $K = K_{Z,k}$ and the convergences (1.29.20) be as in the proof of Proposition 1.29.18, with one convergence modulus on $\mathcal{C} \times \Gamma$. Then for $0 \le \nu \le \nu_0$ the viscous Riesz projection $P_\nu(Z,k) = (2\pi i)^{-1} \oint_\Gamma (z - A_{\nu,Z,k})^{-1}\,\mathrm{d}z$ satisfies $\sup_{\mathcal{C}} \|P_\nu - P_0\| \to 0$.*

In particular it has rank one, the viscous band is algebraically simple, and $e^{tA_\nu} P_\nu = e^{t\lambda_\nu} P_\nu$.

Proof. Write $R_\nu = (z - T_\nu)^{-1}$.

$\|R_\nu\| \le (\Re z)^{-1}$ on Γ. From $z - A_\nu = (z - T_\nu)(I - R_\nu K)$,

$$(z - A_\nu)^{-1} = (I - R_\nu K)^{-1} R_\nu = R_\nu + (I - R_\nu K)^{-1} R_\nu K R_\nu.$$

Since T_ν is maximal dissipative, R_ν is holomorphic in $\{\Re z > 0\} \supset \overline{\Omega_+}$, so $\oint_\Gamma R_\nu \, dz = 0$ and $P_\nu = (2\pi i)^{-1} \oint_\Gamma (I - R_\nu K)^{-1} R_\nu K R_\nu \, dz$.

By (1.29.20), $R_\nu K \to R_0 K$ and $K R_\nu \to K R_0$ in norm. Thus $(I - R_\nu K)^{-1} \to (I - R_0 K)^{-1}$ in norm ($I - R_0 K = R_0(z - A_0)$ is invertible on Γ), and

$$\|R_\nu K R_\nu - R_0 K R_0\| \le \|R_\nu K - R_0 K\| \, \|R_\nu\| + \|R_0\| \, \|K R_\nu - K R_0\| \to 0.$$

All limits are uniform on $\mathcal{C} \times \Gamma$, so $\|P_\nu - P_0\| < 1$ for $\nu \le \nu_0$, and restriction of each projection to the other's range is injective, so the rank is one.

On the invariant line $\operatorname{Ran} P_\nu$, A_ν acts as multiplication by λ_ν. □

Remark 1.29.15 (Where simplicity is used. Inviscid versus viscous). (1) The scalar band calculus of Section 1.35 uses the *inviscid* frozen operator. By (1.35.6), $L_0 = A(Z,k) + i(\frac{1}{2} - h)Zk$ with $A = -P_k N P_k$ undilated and inviscid.

Viscosity enters only through F_1 at order ρ. The normalization $\ell e = 1$, the splitting $Q = I - e\ell$, the reduced resolvent R_Q and the compatibility (1.35.11) all use Proposition 1.29.13.

With a Jordan block one would have $\ell e = 0$ and (1.35.12) would be ill posed. (2) Proposition 1.29.18 uses only the viscous Riesz projection: the shift $S_\nu = d_0 \chi P_\nu$ lowers the whole spectral subspace whatever its rank. We need simplicity of the viscous band only where we write the frozen semigroup on the band as $e^{t\lambda} P$ (Corollary 1.34.15).

With a Jordan block a factor $1 + t\,\|N\|$ would appear. Proposition 1.29.14 supplies this for $0 \le \nu \le \nu_0$, and Proposition 1.29.13 for $\nu = 0$.

(3) Inputs: the convergences (1.29.12) as $d, \sigma \to 0$ at the pole, and the compact-sandwich convergence (1.29.20). We assert them in the proofs of Lemmas 1.29.3 and Proposition 1.29.18.

The present subsection makes precise that operator-norm closeness of the bulk inverses and convergence of the two complex layer integrals suffice.

1.29.3 High axial frequency and the viscosity bridge

The complement estimate from a compact phase chart does not control $|k| \to \infty$, and viscosity is not a norm-small bounded perturbation of Euler. We handle the two obstructions in physical velocity space.

Lemma 1.29.16 (Uniform high-$|k|$ velocity energy)**.** *Fix a smooth source column and an angular label n. Let $\delta(r)$ equal one near the axis and outside a compact annulus, with $0 < d_* \le \delta \le 1$, and put in Cartesian components*

$$M = I + (\delta - 1) e_\theta \otimes e_\theta, \quad A_\delta = \|(1-\delta) n / r\|_\infty, \quad J_\delta = \|\Delta_h M\|_\infty,$$

$$\gamma_\delta = \sup_r \left(\frac{|2\Omega - \delta B|}{2\sqrt{\delta}} + \frac{|W_r|}{2} \right), \qquad L = \|\nabla U\|_\infty.$$

For the true solenoidal viscous generator $A_{\nu,n,k}$ and its homogeneous evolution, $E = \langle v, Mv \rangle$ satisfies

$$\tfrac{1}{2} E' \le \left(\gamma_\delta + \frac{2 A_\delta L}{|k| d_*} \right) E - \nu \int (\nabla_h v)^* M \nabla_h v - \nu \left(k^2 - \frac{J_\delta}{2 d_*} \right) E. \tag{1.29.17}$$

If $\gamma_\delta < \gamma < g$, a finite K selected so that $K \ge 2A_\delta L / [d_*(\gamma - \gamma_\delta)]$ and $K^2 \ge J_\delta / (2 d_*)$ gives, with one bound for all $|k| \ge K$ and $\nu \ge 0$,

$$\|e^{t A_{\nu,n,k}}\| \le d_*^{-1/2} e^{\gamma t}, \qquad \|(z - A_{\nu,n,k})^{-1}\| \le \frac{d_*^{-1/2}}{\Re z - \gamma} \quad (\Re z > \gamma).$$

Proof. The scalar transport $i(n\Omega + kW)$ contributes no real energy.

The non-skew stretching terms contribute $\Re[(2\Omega - \delta B)\bar{u}v_\theta - W_r\bar{w}u]$. Cauchy–Schwarz in $(u, \sqrt{\delta}v_\theta, w)$ bounds this by $\gamma_\delta E$.

For solenoidal v, the divergence of the unprojected equation gives $\Delta_k p = -2\,\mathrm{div}_k[(v\cdot\nabla)U]$. Since $|k| > 0$, the whole-space multiplier bound yields $\|p\|_2 \le 2L\|v\|_2/|k|$.

The metric modifies only the angular component, so $\mathrm{div}_k(Mv) = (\delta - 1)inv_\theta/r$. There is no δ' term.

Integration of the pressure pairing by parts thus costs at most $2A_\delta LE/(|k|d_*)$. In Cartesian coordinates the exact viscous identity is

$$\Re\langle Mv, \nu\Delta_k v\rangle = -\nu\int(\nabla_h v)^* M\nabla_h v - \nu k^2 E + \tfrac{\nu}{2}\int v^*(\Delta_h M)v.$$

The last term is bounded by $\nu J_\delta E/(2d_*)$.

This proves (1.29.17). Gronwall and $d_*\|v\|_2^2 \le E \le \|v\|_2^2$ give the semigroup estimate, and its Laplace integral gives the resolvent estimate.

Density justifies the calculation on the Stokes domain. □

Remark 1.29.17 (The energy computation in Lemma 1.29.16). In cylindrical components $v = (u, v_\theta, w)$, the frozen operator acts by $Nv = i\phi v + (-2\Omega v_\theta,\ Bu,\ W_r u)$ with $\phi = n\Omega + kW$ and $B = 2\Omega + r\Omega_r$, and $\partial_t v = -P_k(Nv) + \nu\Delta_k v$ for solenoidal v. Since $M = \mathrm{diag}(1, \delta, 1)$ in these components and $i\phi$ is scalar, $\Re\langle Mv, -i\phi v\rangle = 0$, and $-\Re\langle Mv, (-2\Omega v_\theta, Bu, W_r u)\rangle = \Re\int[(2\Omega - \delta B)\bar{u}v_\theta - W_r\bar{w}u]$. Pointwise, $|2\Omega - \delta B||u||v_\theta| \le \frac{|2\Omega-\delta B|}{2\sqrt{\delta}}(|u|^2 + \delta|v_\theta|^2)$ and $|W_r||w||u| \le \frac{|W_r|}{2}(|u|^2 + |w|^2)$, which gives $\gamma_\delta E$. With the physical pressure p used above, $-P_k Nv = -Nv - \nabla_k p$ and $\Delta_k p = -\,\mathrm{div}_k(Nv) = -2\,\mathrm{div}_k[(v\cdot\nabla)U]$, because $\mathrm{div}[(U\cdot\nabla)v] = \mathrm{div}[(v\cdot\nabla)U] = \mathrm{tr}(\nabla U\nabla v)$ for solenoidal U, v, and $\mathrm{div}_k\,\Delta_k v = 0$. The symbol of $\Delta_k^{-1}\,\mathrm{div}_k$ has norm $|(\xi, k)|^{-1} \le |k|^{-1}$, and $|(v\cdot\nabla)U| \le L|v|$; so $\|p\|_2 \le 2L\,\|v\|_2/|k|$. Since $\langle v, \nabla_k p\rangle = 0$, $|\langle Mv, \nabla_k p\rangle| = |\langle \mathrm{div}_k((M - I)v), p\rangle| \le A_\delta\,\|v_\theta\|\,\|p\| \le 2A_\delta L\,\|v\|^2/|k| \le 2A_\delta LE/(|k|d_*)$. The viscous identity follows from $\Re\int v^*(\partial_i M)\partial_i v = -\frac{1}{2}\int v^*(\Delta_h M)v$ (M is real symmetric and smooth, because $\delta = 1$ near the axis). For $\nu > 0$ the semigroup is analytic, so E is differentiable for $t > 0$ and Gronwall applies; for $\nu = 0$ the generator is bounded.

The source bounds quantify $\gamma_\delta < g$. We use these hypotheses, with a bound C for the old field:

(i) $|\Omega| \le C$ and $|W_r| \le C$ on the whole line, including the perturbation annulus;

(ii) $|B| \le C + \Delta$ everywhere, and the region $|B| > C$ lies in a compact annulus;

(iii) $\Delta \ge C$.

Lemma 1.29.1 gives the bound $|W_r| \le K_0$ on the annulus uniformly over the admitted trial ball and late widths. Put $d_* = C/\Delta$ and make $\delta = d_*$ on that annulus, with transitions where $|B| \le C$.

Then direct substitution gives

$$\gamma_\delta \le 2\sqrt{C\Delta} + C/2. \tag{1.29.18}$$

For a target line $g = c_g\Delta$, selection of the source ratio Δ/C large makes a strict margin. The main edit changes Ω by at most $Kd\Delta$ on the annulus. If we include this change in (i), the right side of (1.29.18) increases by at most $Kd\Delta^{3/2}C^{-1/2}$. This term tends to zero as $d \to 0$.

We fix the cutoff before K and $\nu \downarrow 0$. Its derivative norm J_δ may be large but finite.

It affects only the next finite threshold K.

Proposition 1.29.18 (Frozen viscous transfer)**.** *Fix the selected source of Proposition 1.31.4 and a positive line g above the strict large-$|Z|$ and large-$|k|$ energy rates of Lemma 1.27.3 and Lemma 1.29.16. Take a compact rectangle containing the remaining phases and the supports of the shifts. For $n = \pm m$ let $0 \le \chi \le 1$ have compact support in the simple-band patch of Lemma 1.30.34, and put $S_\nu = d_0 \chi P_\nu$ there, extending it by zero off the support. For the other labels $n \in F$ put $S_\nu = 0$.*

Assume a uniform inviscid separation on the rectangle: for some $\epsilon > 0$, the complementary spectrum on the support, and the full spectrum wherever the shift is zero, have real part at most $g - \epsilon$. On each shifted band require also

$$\Re\lambda_0(Z,k) - d_0\chi(Z,k) \le g - \epsilon.$$

Section 1.33 verifies these inequalities for the selected line g_f and the two physical cutoffs.

Then, for some $\nu_0 > 0$ and all $0 \le \nu \le \nu_0$, the band and Riesz projection persist on the support of χ and

$$\sup_{Z,k,\Re z \ge g,\, 0 \le \nu \le \nu_0} \|(z - A_{\nu,Z,k} + S_\nu)^{-1}\| < \infty. \tag{1.29.19}$$

For each $g_1 > g$, one bound $C_{g_1} e^{g_1 t}$ holds for the frozen shifted semigroup, for all these parameters.

Proof. On the fixed extended angular Hilbert space decompose

$$A_{\nu,Z,k} = T_{\nu,Z,k} + K_{Z,k}, \quad T_\nu = \nu(\Delta_h - k^2) - iP_k(n\Omega + kW)P_k,$$

where the strain sandwich K is compact by Lemma 1.29.3. Here the Fourier heat multiplier generates contractions. Adding the bounded skew-adjoint compression to its generator gives an evolution by iteration of the integral equation against the heat semigroup: the jth iterated integral on $[0,t]$ has norm at most $(t\|P_k(n\Omega + kW)P_k\|)^j/j!$. The resulting semigroup has generator T_ν on the heat domain. Indeed its Laplace transform for large positive z is the Neumann series for $(z - T_\nu)^{-1}$ there. On that dense domain differentiation of the squared norm gives $2\Re\langle T_\nu u, u\rangle \le 0$, so the semigroup is a contraction. Its Laplace integral exists for every $\Re z > 0$ and gives the inverse on that half-plane by integration by parts, first on the generator domain and then by closure. This proves maximal dissipativity.

For $\Re z > 0$, $\|(z - T_\nu)^{-1}\| \le (\Re z)^{-1}$. The heat semigroup converges strongly to the identity as $\nu \to 0$ on each bounded time interval, and so do the adjoints.

Bounded skew transport keeps this convergence through Duhamel. On a compact (Z,k,z) set it is uniform on compact vector sets by finite norm nets for the coefficients.

The norm-compact family of compact $K_{Z,k}$ thus gives the two sandwich limits

$$(R_{T_\nu} - R_{T_0})K \longrightarrow 0, \qquad K(R_{T_\nu} - R_{T_0}) \longrightarrow 0 \tag{1.29.20}$$

in operator norm, with one convergence modulus on that set. The second uses adjoint strong convergence.

This compact-sandwich convergence uses strong convergence and compactness. It makes no operator-norm smallness assertion for the unbounded perturbation $\nu\Delta_h$.

Cover the compact shift support by finitely many neighborhoods with fixed contours in $\Re z > 0$ isolating the inviscid band. On each contour the two limits in (1.29.20) give $\|P_\nu - P_0\| \to 0$ uniformly by the contour argument of Proposition 1.29.14. This step uses only the unshifted contours. The projections have rank one for small ν and agree on overlaps by spectral isolation (shrink the neighborhoods if necessary). Consequently $S_\nu \to S_0$ in norm uniformly on the rectangle. The zero extension of S_0 is norm continuous and compact-valued.

Write $R_\nu = (z - T_\nu)^{-1}$. On a compact set of z with $\Re z \geq g$, the shifted Fredholm factors satisfy, uniformly on the rectangle,

$$I - R_\nu(K - S_\nu) \longrightarrow I - R_0(K - S_0) \quad \text{in operator norm.}$$

Indeed the variation of S_ν costs at most $g^{-1}\|S_\nu - S_0\|$, and strong convergence of R_ν is uniform on the images of the unit ball under the norm-compact family of compact operators $K - S_0$. The inviscid projection commutes with A_0. The shift subtracts $d_0\chi$ on its range and preserves the complementary restriction. The two separation inequalities therefore put $\Re z \geq g$ in $\rho(A_0 - S_0)$. The limiting Fredholm factors are norm continuous there by the same compactness argument, and their inverses are uniformly bounded on the compact parameter set. Neumann inversion gives the same bound for the perturbed factors. Multiplication on the right by R_ν gives the required shifted resolvent.

On the rectangle, T_ν has imaginary numerical range bounded by $\sup|n\Omega + kW|$ uniformly in ν. Thus $\|R_\nu\|$ tends to zero uniformly as $|\Im z| \to \infty$ in $\Re z \geq g$, and also as $\Re z \to \infty$. Since $K - S_\nu$ is uniformly bounded, a Neumann series handles these two tails. Outside the rectangle the shift is zero and the two strict exterior energy bounds give the resolvent bound by Laplace transformation. Taking the minimum viscosity threshold over the finite labels proves (1.29.19).

The crude physical energy bound is uniform in ν. The Hilbert-space Plancherel resolvent-to-semigroup lemma gives the stated evolution bound after a small relaxation from g to g_1.

□

Imported inputs. Section 1.33 defines the finite angular set F and pair shift used in the selected application. The next estimate is conditional on the inputs listed here.

Fix $n \in F$ and $(Z, k) \in \mathbb{R}^2$. Let $H_{n,k}$ be the solenoidal L^2 fields of angular label n and axial wavenumber k.

Let $A_\nu(Z, k)$ be the frozen leading generator with viscosity $\nu \geq 0$. $S_\nu(Z, k) = d_0\chi_\pm P_{\nu,\pm m}$ for $n = \pm m$, $S_\nu = 0$ for the other angular labels ((1.33.1)).

(I1) *Structure* (Lemma 1.29.3): $A_\nu = T_\nu + K$ on $H_{n,k}$. Here T_ν is maximal dissipative with numerical range in $\{\Re w \leq 0,\ |\Im w| \leq \Phi\}$, where $\Phi = \sup|n\Omega + kW|$.

The operator $K = K(Z, k)$ is compact. The map $(Z, k) \mapsto K$ is norm continuous on compact sets, with $k = 0$.

The operators T_ν have the same core. On the fixed extended angular space of Proposition 1.29.18, the resolvents and their adjoints converge strongly to their inviscid limits as $\nu \downarrow 0$, uniformly on compact subsets of $\{(z, Z, k) : \Re z > 0\}$ on each fixed vector, as proved before (1.29.20). At $\nu = 0$ the resolvents and their adjoints are strongly continuous in (Z, k): the bounded multipliers $n\Omega + kW$ vary continuously and P_k is strongly continuous, including at $k = 0$.

(I2) *Spectral exclusion at* $\nu = 0$. This input is the normal-mode exclusion of Lemma 1.31.3, Proposition 1.31.4 and its extension to $n = 0, \pm 1$ in Remark 1.29.4. For (Z, k) in a compact rectangle $\mathcal{R} = [-Z_1, Z_1] \times [-K_1, K_1]$, $\sigma(A_0 - S_0) \cap \{\Re z \geq g_1\} = \varnothing$.

(I3) *Exteriors*: for $|Z| \geq Z_1$ the symmetric strain is below $g_1 - \delta$ (Lemma 1.27.3 and the choice of Δ).

For $|k| \geq K_1$ the metric energy of Lemma 1.29.16 gives $\|e^{tA_\nu}\| \leq C_H e^{(g_1 - \delta)t}$, with one bound for all $\nu \geq 0$.

$S_\nu = 0$ on the two exteriors.

(I4) The continuity and convergence clauses of (F2) in Section 1.34 hold, namely $\sup_{\mathcal{R}} \|S_\nu - S_0\| \to 0$ as $\nu \to 0$, and S_0 is norm continuous on $\mathcal{R}$.

Lemma 1.29.19 (Uniform frozen shifted semigroup)**.** *There are $\nu_0 > 0$, C_F and $g_1' < \lambda_c$ such that, for each $n \in F$, $(Z,k) \in \mathbb{R}^2$ and $0 \le \nu \le \nu_0$,*

$$\|e^{t(A_\nu - S_\nu)(Z,k)}\|_{H_{n,k} \to H_{n,k}} \le C_F e^{g_1' t}, \qquad t \ge 0.$$

Proof. On the exteriors (I3) gives the claim with $g_1' = g_1 - \delta$ (energy identity, resp. the metric), since $S_\nu = 0$ there. Fix $(Z,k) \in \mathcal{R}$ and write $A_s = A_\nu - S_\nu$, $K_s = K - S_\nu$ (compact, $\|K_s\| \le C_K$ on $\mathcal{R}$).

Step 1 (far resolvent region). The numerical range of A_s lies in $\Theta = \{\Re w \le C_K,\ |\Im w| \le \Phi + C_K\}$. The operator A_s is a bounded perturbation of a maximal dissipative operator.

Thus each z with $\operatorname{dist}(z,\Theta) > 0$ in the unbounded component of $\mathbb{C} \setminus \overline{\Theta}$ is in the resolvent set and $\|(z - A_s)^{-1}\| \le \operatorname{dist}(z,\Theta)^{-1}$. Indeed $\|(z - A_s)u\| \ge \operatorname{dist}(z,\Theta)\|u\|$ by pairing with u. Large positive z are resolvent points by Neumann inversion against $z - T_\nu$. The resolvent set is both open and relatively closed in this component: near each of its points inversion persists on a disk of radius $\operatorname{dist}(z,\Theta)$ by the displayed bound. Hence the whole component is in the resolvent set. Put $Y = 2(\Phi_{\mathcal{R}} + C_K) + 1$, $X = C_K + 1$, where $\Phi_{\mathcal{R}} = \sup_{(Z,k)\in\mathcal{R}} \|n\Omega(\cdot, Z) + kW(\cdot, Z)\|_\infty < \infty$.

Then $\|(z - A_s)^{-1}\| \le 1$ on $\{\Re z \ge X\} \cup \{\Re z \ge g_1,\ |\Im z| \ge Y\}$.

Step 2 (compact region). Let $\Gamma = \{g_1 \le \Re z \le X,\ |\Im z| \le Y\}$. For $\Re z > 0$, $z \in \rho(T_\nu)$ with $\|(z - T_\nu)^{-1}\| \le (\Re z)^{-1}$, and

$$z - A_s = (I - F_\nu(z))(z - T_\nu), \qquad F_\nu(z) = K_s(z - T_\nu)^{-1}.$$

At $\nu = 0$, $F_0(z)$ is compact, and by (I2) $z - A_s$ is invertible, thus so is $I - F_0(z)$.

Write $R_\nu = (z - T_\nu)^{-1}$ and use the common extended angular space of Proposition 1.29.18. On $\Gamma \times \mathcal{R}$,

$$F_\nu - F_0 = (K - S_0)(R_\nu - R_0) + (S_0 - S_\nu)R_\nu.$$

The first term converges to zero uniformly in norm by the adjoint resolvent convergence in (1.29.20): the family $(K - S_0)^*$ is norm compact and consists of compact operators. The second is bounded by $g_1^{-1} \sup_{\mathcal{R}} \|S_\nu - S_0\|$, which tends to zero by (I4).

At $\nu = 0$, the same compact-operator argument and strong continuity of R_0^* in the phase parameters give norm continuity of F_0. The resolvent identity gives continuity in z. By (I2) and compactness, $M_0 = \sup_{\Gamma\times\mathcal{R}} \|(I - F_0)^{-1}\| < \infty$. Choose ν_0 so that $\sup_{\Gamma\times\mathcal{R}} \|F_\nu - F_0\| \le (2M_0)^{-1}$ for every $0 \le \nu \le \nu_0$. Neumann inversion gives $\|(I - F_\nu)^{-1}\| \le 2M_0$ and hence $\|(z - A_s)^{-1}\| \le 2M_0/g_1$ throughout the rectangle.

Step 3 (semigroup). Steps 1–2 give $\sup_{\Re z \ge g_1} \|(z - A_s)^{-1}\| \le M'$ with one bound for all $(Z,k,\nu) \in \mathcal{R} \times [0,\nu_0]$. Also A_s generates a semigroup with $\|e^{tA_s}\| \le e^{C_K t}$: iterate the integral equation against the contraction e^{tT_ν}, bounding its jth term by $(C_K t)^j/j!$. The explicit estimate of Lemma 1.34.7 gives $\|e^{tA_s}\| \le C(M', C_K, g_1, g_1')e^{g_1' t}$ for any $g_1' \in (g_1, \lambda_c)$.

The constants depend only on M', C_K, g_1, g_1', thus are uniform. The maximum over the finitely many $n \in F$ and the two exteriors proves the lemma.

□

Remarks. (1) The lemma is purely qualitative-compact: C_F is finite but not explicit. Proposition 1.34.8 uses only this property. We fix this constant before L, and L before the ancient threshold. (2) Inputs (I1)–(I2) are Lemma 1.29.3 and the finite-label paragraph.

The present lemma converts that *spectral* information into a *uniform semigroup* bound. (3) For fixed (n,k), compactness of K places the essential spectrum of the frozen inviscid operator on $i\mathbb{R}$.

Lemma 1.29.3 proves the compactness in (I1).

This is consistent with the WKB analysis at fixed (n,k) (radial short waves have $\xi \parallel e_r$ and zero local growth). Lemma 1.29.3 gives its proof, and we do not re-derive it here.

1.29.4 The far-angular physical space

We cannot simply send the fixed finite-angle argument below through $|n| \to \infty$. Here is the physical norm behind the far-angular frozen estimate.

On $H = L^2((0,\infty), r\,\mathrm{d}r)$ define

$$q^2 = n^2/r^2 + k^2, \quad P = -\partial_r^2 - r^{-1}\partial_r + q^2, \quad R = q^{-1}(\partial_r + 1/r), \quad V = \operatorname{Dom} R.$$

Here R has its maximal distributional domain $\{u \in H : Ru \in H\}$. The natural poloidal closed form is $H_{\mathrm{pol}} = I + R^*R$. If $p = (av_\theta + kw)/q$ and $s = (kv_\theta - aw)/q$, solenoidality gives $Ru = -ip$.

With $x = -H_{\mathrm{pol}}u$ and $y = is$,

$$\|x\|_{V^*}^2 = \langle u, H_{\mathrm{pol}}u\rangle = \|u\|_2^2 + \|p\|_2^2. \tag{1.29.21}$$

Thus $(x,y) \in V^* \times H$ is the physical velocity space under an equivalent fixed anisotropic norm. A derivative of an arbitrary L^2 forcing is a bounded V^* functional, not an H forcing.

Lemma 1.29.20 (Uniform far-angular frozen resolvent)**.** *Suppose the fixed source has, uniformly in Z, finite norms $\|\Omega\|_\infty$, $\|W\|_\infty$, $\|B\|_\infty$, $\|W_r\|_\infty$, $\|r\Omega_r\|_\infty$ and $J := \sup_{r,Z}(|B|+r|B_r|+|W_r|+r|W_{rr}|)$; these are its stated weighted radial jets. Suppose also that it has the strict small-product margin $\sqrt{2C_s\|\Omega\|_\infty(\|B\|_\infty + \|W_r\|_\infty)} < g$, where C_s is the scalar derivative-resolvent constant below.*

There is a finite N_{far} with the next property. For $|n| \ge N_{\mathrm{far}}$, all real k, Z, all $\nu \ge 0$, and $\Re z \ge g$, the true physical velocity resolvent has one bound.

Proof. Set $\phi = n\Omega + kW$, $D = z + i\phi + \nu P$ and $\beta_0 = \|\phi'/q\|_\infty$. The scalar real-part identity and the commutator with multiplication by ϕ give $\|D^{-1}\|_{H\to H} \le g^{-1}$ and

$$\|\nu P D^{-1}\|_{H\to H} \le (1 + \beta_0/g)^{1/2}.$$

For $|n| \ge 3$, integration by parts in the Bessel operator yields

$$\|u''\| + \|qu'\| + \|q^2u\| \le C\|Pu\|. \tag{1.29.22}$$

$(4/n^2)\|q^2u\|^2$ bounds the only negative term in the squared expansion.

Differentiation of $R = q^{-1}(\partial_r + 1/r)$ with (1.29.22) gives $\|[R,P]u\| \le C|n|^{-1}\|Pu\|$.

The commuted equation $D(Ru) = RF - i(\phi'/q)u - \nu[R,P]u$ thus gives $\|D^{-1}\|_{V\to V} \le C_s/g$ and $\|\nu P D^{-1}\|_{V\to V} \le C_s$, with $C_s = C(1+\beta_0/g)^2$ independent of n, k, ν. The same calculation holds for D^*, since a change of the imaginary signs does not affect the estimates.

Duality with the pivot H thus gives the correctly ordered bounds $\|D^{-1}\|_{V^*\to V^*} \le C_s/g$ and $\|D^{-1}\nu P\|_{V^*\to V^*} \le C_s$. The second operator is the adjoint of $\nu P(D^*)^{-1} : V \to V$.

The four entries and their weak-space estimate are explicit below. Put $a = n/r$, $\zeta = a^2/q^2$, $\vartheta = ak/q^2$ and $c = 2\vartheta/(rq)$.

The exact cylindrical vector-Laplacian reduction, with x, y as in (1.29.21), gives

$$G_{xx} = -\frac{2\zeta}{r}\partial_r + \frac{-4\zeta^2 + 6\zeta - 1}{r^2}, \qquad G_{xy} = c\left[-\partial_r^2 + \frac{3 - 4\zeta}{r}\partial_r + q^2 + \frac{-3 + 8\zeta - 5\zeta^2}{r^2}\right],$$
$$G_{yx} = cq^2, \qquad G_{yy} = \frac{\zeta^2 - 1}{r^2}.$$

These are the viscous terms that remain after we remove the diagonal νP from the two scalar equations. G_{xy} keeps the second derivative. Since $rq \geq |n|$, $|\vartheta| \leq 1/2$ and $|r^j \partial_r^j \zeta| \leq C_j$, $|r^j \partial_r^j c| \leq C_j/|n|$ for each of the finitely many derivatives below, with one bound for all k.

Let $P_\epsilon = P + \epsilon$, $\epsilon > 0$, and first work on the same smooth radial core. Positivity of P and (1.29.22) give

$$\|u''\| + \|qu'\| + \|q^2 u\| \leq C\|P_\epsilon u\|, \qquad u = P_\epsilon^{-1} h, \tag{1.29.23}$$

with C independent of n, k, ϵ.

The formal adjoint G_{xy}^* has second-, first- and zeroth-order coefficients bounded, in this order, by $C/|n|$, $C/(|n|r)$ and $Cq^2/|n|$. Thus $\|G_{xy}^* P_\epsilon^{-1}\|_{H\to H} \leq C/|n|$, and duality yields $\|P_\epsilon^{-1} G_{xy}\|_{H\to V^*} \leq C/|n|$.

For $G_{yx} = cq^2$, the necessary adjoint map is $cq^2 P_\epsilon^{-1} : H \to V$. Its H bound follows from (1.29.23).

Application of $R = q^{-1}(\partial_r + 1/r)$ gives

$$\|R(cq^2 u)\| \leq \frac{C}{|n|}\|qu'\| + \frac{C}{n^2}\|q^2 u\|, \qquad u = P_\epsilon^{-1} h.$$

Thus this block is $O(|n|^{-1})$ from V^* to H. The yy block has $|G_{yy}| \leq Cq^2/n^2$, so $\|P_\epsilon^{-1} G_{yy}\|_{H\to H} \leq C/n^2$ by the same adjoint argument.

For the V^* diagonal block set $A_0 = G_{xx}^*$. Its first- and zeroth-order coefficients are $O(r^{-1})$ and $O(r^{-2})$. This gives $\|A_0 P_\epsilon^{-1}\|_{H\to H} \leq C/|n|$.

On the smooth core the exact commutator identity is

$$RA_0 P_\epsilon^{-1} = A_0 P_\epsilon^{-1} R + [R, A_0] P_\epsilon^{-1} - A_0 P_\epsilon^{-1} [R, P] P_\epsilon^{-1}.$$

The coefficients of $[R, A_0]$ have the bound $C/(|n|r)$ at first order and $C/(|n|r^2)$ at zeroth order. Estimate (1.29.23) bounds its composition with P_ϵ^{-1} by C/n^2.

(1.29.22) and the previous $[R, P]$ bound give the same bound for the last term. Thus $A_0 P_\epsilon^{-1} : V \to V$ costs $C/|n|$.

Duality proves $P_\epsilon^{-1} G_{xx} : V^* \to V^*$ with that norm. The core estimates extend by density to the four stated bounded compositions.

They do not require a uniform bound for the bare P_ϵ^{-1} at $k = 0$.

With the anisotropic y weight $\alpha_0 > 0$, these four blocks give

$$\sup_{\epsilon>0} \|(P + \epsilon)^{-1} G\|_{V^*\times H \to V^*\times H} \leq C_G(1 + \alpha_0 + \alpha_0^{-1})/|n|$$

with one bound for all k, ϵ. On the same core, factor $D^{-1}\nu G = [D^{-1}\nu P + \nu\epsilon D^{-1}](P + \epsilon)^{-1} G$ with the ordered V^* and H bounds above.

For each fixed ν, let $\epsilon \downarrow 0$ in the uniform norm inequality. We assert no convergence of $(P+\epsilon)^{-1} G$. This makes the viscous coupling $O(C_s(1 + \alpha_0 + \alpha_0^{-1})/|n|)$, with one bound for all ν.

The smooth inviscid diagonal coupling is $O(C_s J/(|n|g))$ for a fixed source constant J. The two off-diagonal couplings have bounds $2\|\Omega\|_\infty$ and $\|B\|_\infty + \|W_r\|_\infty$ in the isometry (1.29.21).

Selection of $\alpha_0^2 = 2C_s\|\Omega\|_\infty/(\|B\|_\infty + \|W_r\|_\infty)$ balances them when the two factors are positive. If one factor vanishes, select any sufficiently small or large fixed positive α_0 to control the remaining one-way coupling.

In the nondegenerate case this perturbation norm is

$$\frac{C_s J}{|n|g} + \frac{\sqrt{2C_s\|\Omega\|_\infty(\|B\|_\infty + \|W_r\|_\infty)}}{g} + \frac{C_s C_G(1+\alpha_0+\alpha_0^{-1})}{|n|}.$$

The strict source margin makes the middle term smaller than one. Select N_{far} to absorb the two $|n|^{-1}$ terms.

Neumann inversion on $V^* \times H$, followed by the exact inverse of (1.29.21), gives the physical L^2 estimate for arbitrary solenoidal L^2 forcing. To identify the inverse with the physical generator rather than a formal weak pencil, start on compact smooth solenoidal poloidal fields.

The exact cylindrical momentum and divergence identities give the preconditioned equation there, with the four G blocks and the V^* forcing. For $\nu > 0$ these fields are a graph core of the fixed-fiber Stokes operator with bounded smooth source coefficients.

For $\nu = 0$ the fixed-fiber inviscid operator is bounded on physical L^2. The bounded maps just proved extend the identity to the physical generator domain.

At sufficiently large real z the standard physical resolvent exists and agrees with the Neumann candidate on that core. The two candidates are analytic and locally bounded on the stated half-plane.

The resolvent identity then extends their equality and the left/right inverse properties throughout $\Re z \geq g$ (with analyticity on its open interior). This supplies the claimed physical resolvent, not only a solution of the transformed equations.

□

Remark 1.29.21 (Complete computations for Lemma 1.29.20). We give the identities and estimates used above. Fix $|n| \geq 3$, $k \in \mathbb{R}$, Z, $\nu \geq 0$ and $\Re z \geq g$. Constants C are absolute unless a dependence is shown. Put $\alpha = a/q$, $\kappa = k/q$ (so $\alpha^2+\kappa^2 = 1$), $T = \partial_r + 1/r$, $L = -\partial_r^2 - r^{-1}\partial_r$, so $P = L + q^2$ and $R = q^{-1}T$. In $H = L^2(r\,\mathrm{d}r)$ one has $R^*v = -(v/q)'$. We use $q \geq |n|/r$, $q \geq |k|$ and $q^2 \geq 2|nk|/r$.

Step 1: the transformed equations. Let $v = (u, v_\theta, w)$ be a smooth compactly supported solenoidal field of the sector (n,k) (smooth in Cartesian variables). Put $E = (z + N_{n,k} - \nu\Delta)v$; then $(z - A_{\nu,n,k})v = E + \nabla_{n,k}\pi$ with $\pi = -S_k(N_{n,k}v)$. Let $E_p = (aE_\theta + kE_z)/q$, $E_s = (kE_\theta - aE_z)/q$, $p = (av_\theta + kw)/q = iRu$, $s = (kv_\theta - aw)/q$, $x = -(I + R^*R)u$ and $y = is$. The gradient $(\pi', ia\pi, ik\pi)$ has p component $iq\pi$ and s component 0, and $\pi' - iR^*(iq\pi) = 0$. For a solenoidal field f, $f_p = iRf_r$, so $f_r - iR^*f_p = (I + R^*R)f_r$. Thus the isometry $\Phi\colon v \mapsto (x,y)$ of (1.29.21) satisfies

$$\Phi(z - A_{\nu,n,k})v = \big(-(E_r - iR^*E_p),\ iE_s\big).$$

With $\phi = n\Omega + kW$ and $C = aB + kW_r$ one has the identity

$$C = \phi' + 2a\Omega.$$

Direct substitution of $v_\theta = \alpha p + \kappa s$, $w = \kappa p - \alpha s$ and of the cylindrical vector Laplacian gives, exactly,

$$\begin{aligned} -(E_r - iR^*E_p) &= (z + i\phi + \nu P)x - \nu(G_{xx}x + G_{xy}y) - im_0u - 2i\Omega\kappa\, y, \\ iE_s &= (z + i\phi + \nu P)y - \nu(G_{yx}x + G_{yy}y) + i(\kappa B - \alpha W_r)u, \end{aligned}$$

where $u = -(I + R^*R)^{-1}x$, the blocks G are those displayed in the proof, and

$$m_0 = (C/q^2)' - C/(rq^2).$$

In the first component $-E_r + iR^*E_p$, the commutator with $i\phi$, the radial Coriolis term and the projected stretching give

$$i(\phi'/q)Ru + 2i\Omega\alpha Ru + iR^*(Cu/q) = i\,\frac{C}{q^2}(u' + u/r) - i(Cu/q^2)' = -im_0 u.$$

Here $C = \phi' + 2a\Omega$ gives the cancellation of u'. The pressure has dropped out of both lines. Since $|a|/q^2 \le r/|n|$, $|k|/q^2 \le r/(2|n|)$, $|(a/q^2)'| \le 1/|n|$ and $|(k/q^2)'| \le 1/|n|$,

$$\|m_0\|_\infty \le 2J/|n|, \qquad |2\Omega\kappa| \le 2\,\|\Omega\|_\infty, \qquad |\kappa B - \alpha W_r| \le \|B\|_\infty + \|W_r\|_\infty.$$

Step 2: the scalar operator $D = z + i\phi + \nu P$. (a) First take $\nu > 0$. The set $C_c^\infty(0,\infty)$ is a core for P, since $n^2 \ge 1$. For $u \in \operatorname{Dom} P$, $\Re\langle Du, u\rangle \ge g\|u\|^2$. Maximal accretivity of $\nu P + i\phi$ gives $\|D^{-1}\|_{H\to H} \le g^{-1}$. For $\nu = 0$, D is multiplication by $z + i\phi$ on H, with the same inverse bound. In that case νP denotes the zero operator on H. (b) For $u \in \operatorname{Dom} P$, $\langle \phi u, Pu\rangle = \int(\phi|u'|^2 + \phi q^2|u|^2 + \phi' u\bar{u}')r\,\mathrm{d}r$ and $|\int \phi' u\bar{u}' r\,\mathrm{d}r| \le \beta_0\,\|qu\|\,\|u'\| \le \frac{\beta_0}{2}\langle Pu, u\rangle$. Thus, with $F = Du$, $\nu^2\,\|Pu\|^2 \le \|F\|\,\nu\,\|Pu\| + \frac{\beta_0}{2}\nu\langle Pu, u\rangle$ and $\nu\langle Pu, u\rangle \le \|F\|\,\|u\| - g\,\|u\|^2 \le \|F\|^2/(4g)$. Solving the quadratic inequality gives $\|\nu P D^{-1}\|_{H\to H} \le \frac{1}{2}(1 + (1 + \beta_0/(2g))^{1/2}) \le (1 + \beta_0/g)^{1/2}$. (c) For $f \in \operatorname{Dom} P$, integration by parts on the core gives

$$\|Pf\|^2 = \|Lf\|^2 + 2\,\|qf'\|^2 + \left\|q^2 f\right\|^2 - 4\int \frac{n^2}{r^4}|f|^2 r\,\mathrm{d}r \ge \|Lf\|^2 + 2\,\|qf'\|^2 + \left(1 - \frac{4}{n^2}\right)\left\|q^2 f\right\|^2,$$

since $n^2/r^4 \le q^4/n^2$. With $\|f''\| \le \|Lf\| + \|qf'\|/|n|$ this is (1.29.22) for $|n| \ge 3$. Also $\|(P + \epsilon)f\| \ge \|Pf\|$ for $\epsilon > 0$, which gives (1.29.23). (d) The commutator is

$$[R, P]f = q^{-1}\Big(-\frac{f'}{r^2} + \frac{(1 - 2n^2)f}{r^3}\Big) + \Big((q^{-1})'' + \frac{(q^{-1})'}{r}\Big)Tf + 2(q^{-1})'(Tf)'.$$

Here $0 \le (q^{-1})' = n^2/(r^3q^3) \le 1/(rq) \le 1/|n|$ and $|(q^{-1})''| \le 6/(r^2 q)$. Each term is bounded by $C|n|^{-1}(|f''| + |qf'| + |q^2 f|)$, so (c) gives $\|[R, P]f\| \le C|n|^{-1}\,\|Pf\|$. (e) Write q_k, R_k, P_k, D_k, V_k for the operators and space at axial frequency k, and fix $\nu > 0$. If $k \ne 0$, $F \in V_k$ and $u = D_k^{-1}F$, then $u \in \operatorname{Dom} P_k$. The form identity $\langle P_k u, u\rangle = \|u'\|^2 + \|q_k u\|^2$, together with $q_k \ge |n|/r$ and $q_k^{-1} \le |k|^{-1}$, gives $R_k u \in H$. Testing on $C_c^\infty(0,\infty)$ now gives

$$D_k(R_k u) = G_k, \qquad G_k = R_k F - i(\phi_k'/q_k)u - \nu[R_k, P_k]u$$

in distributions. The right side belongs to H by (d). Since the test functions form a core for D_k^*, $\langle R_k u, D_k^*\varphi\rangle = \langle G_k, \varphi\rangle$ extends to $\varphi \in \operatorname{Dom} D_k^*$. Thus $R_k u \in \operatorname{Dom} D_k$ and $D_k R_k u = G_k$. Writing $\beta_k = \|\phi_k'/q_k\|_\infty$ (the constant denoted by β_0 in the lemma), (a), (b) and (d) give

$$\|R_k u\| \le g^{-1}L_k, \qquad \|\nu P_k R_k u\| \le (1 + \beta_k/g)^{1/2}L_k,$$
$$L_k = \|R_k F\| + \left[\frac{\beta_k}{g} + \frac{C}{|n|}(1 + \beta_k/g)^{1/2}\right]\|F\|.$$

At $k = 0$, take $F \in V_0$ and $u_k = D_k^{-1}F$. Since $R_k F = (q_0/q_k)R_0 F$, the preceding bound applies with $\|R_k F\| \le \|R_0 F\|$ and $\beta_k \le \|r\Omega'\|_\infty + \|W'\|_\infty$. On the common domain $\operatorname{Dom} P_0$, $P_k = P_0 + k^2$ and $D_k - D_0 = ikW + \nu k^2$. The resolvent identity yields

$$\|u_k - u_0\| \le g^{-2}(|k|\|W\|_\infty + \nu k^2)\|F\|.$$

Along a sequence $k \to 0$ a subsequence of $R_k u_k$ converges weakly in H. For every compactly supported smooth φ, $R_k^*\varphi = -(\varphi/q_k)' \to R_0^*\varphi$ in H, so the weak limit is the distribution $R_0 u_0$. This puts u_0 in V_0: under the unitary map $u(r) \mapsto e^s u(e^s)$, $s = \log r$, R_0 becomes $|n|^{-1}\partial_s$ with domain $H^1(\mathbb{R})$. The same core argument now gives $D_0(R_0 u_0) = G_0$ in H, and the two displayed bounds hold at $k = 0$ with β_k evaluated there.

Finally $R_k(\nu P_k u) = \nu P_k R_k u + \nu[R_k, P_k]u$ in distributions, with both terms on the right in H. This proves the stated V_k bounds for D_k^{-1} and $\nu P_k D_k^{-1}$ with $C_s = C(1 + \beta_k/g)^2$. For $\nu = 0$, $u = F/(z + i\phi_k)$ directly gives $R_k u = (R_k F - i(\phi_k'/q_k)u)/(z + i\phi_k)$, and the viscous term is zero. Complex conjugation gives the same estimates for D_k^*. (f) With the pivot H, D^{-1} and $D^{-1}\nu P$ extend to V^* as the adjoints of $(D^*)^{-1}$ and $\nu P(D^*)^{-1}$ on V. Thus $\|D^{-1}\|_{V^*\to V^*} \le C_s/g$ and $\|D^{-1}\nu P\|_{V^*\to V^*} \le C_s$. On H, $\|D^{-1}\nu P\| = \|\nu P(D^*)^{-1}\| \le (1 + \beta_0/g)^{1/2} \le C_s$.

Step 3: the viscous blocks. Let $P_\epsilon = P + \epsilon$, $h \in H$ and $u = P_\epsilon^{-1}h$, so $\|u''\| + \|qu'\| + \|q^2 u\| \le C\|h\|$. The coefficients satisfy $|\zeta| \le 1$, $|\vartheta| \le \frac{1}{2}$, $|r^j \partial_r^j \zeta| \le C$ and $|r^j \partial_r^j c| \le C/|n|$ for $j \le 3$, uniformly in k; indeed $c = 2nkr/(n^2 + k^2 r^2)^{3/2}$ is $|n|^{-1}$ times a fixed function of kr/n.

- *yy*: $|G_{yy}| \le r^{-2} \le q^2/n^2$, so $\|P_\epsilon^{-1} G_{yy}\|_{H\to H} = \|G_{yy} P_\epsilon^{-1}\|_{H\to H} \le C/n^2$.
- *xy*: the formal adjoint G_{xy}^* in H has second-, first- and zeroth-order coefficients bounded by $C/|n|$, $C/(|n|r)$ and $C(q^2 + r^{-2})/|n|$. Hence $\left\|G_{xy}^* u\right\| \le C|n|^{-1}(\|u''\| + \|qu'\| + \|q^2 u\|) \le C|n|^{-1}\|h\|$. We define $P_\epsilon^{-1} G_{xy} \colon H \to V^*$ by $\langle P_\epsilon^{-1} G_{xy} y, \varphi\rangle = \langle y, G_{xy}^* P_\epsilon^{-1}\varphi\rangle$; its norm is at most $C/|n|$.
- *yx*: $G_{yx} = cq^2$ is real and $|cq^2| = 2|\vartheta|q/r \le q^2/|n|$. Also $R(cq^2 u) = q^{-1}(cq^2)' u + cq(u' + u/r)$ with $|(cq^2)'|/q \le C/r^2 \le Cq^2/n^2$ and $|cq| \le 1/r \le q/|n|$. Thus $\|cq^2 P_\epsilon^{-1} h\|_V \le C|n|^{-1}\|h\|$, and its adjoint $P_\epsilon^{-1} G_{yx} \colon V^* \to H$ has norm at most $C/|n|$.
- *xx*: $A_0 = G_{xx}^* = (2\zeta/r)\partial_r + (2\zeta'/r + (-4\zeta^2 + 6\zeta - 1)/r^2)$ has first- and zeroth-order coefficients bounded by C/r and C/r^2. So $\|A_0 u\| \le C(\|qu'\|/|n| + \|q^2 u\|/n^2) \le C|n|^{-1}\|h\|$. For $h \in C_c^\infty(0,\infty)$, by the argument of Step 2(e), $RA_0 P_\epsilon^{-1} h = A_0 P_\epsilon^{-1} Rh + [R, A_0]P_\epsilon^{-1} h - A_0 P_\epsilon^{-1}[R, P]P_\epsilon^{-1} h$. The first-order operator $[R, A_0]$ has coefficients bounded by $C/(|n|r)$ and $C/(|n|r^2)$, so the second term is at most $Cn^{-2}\|h\|$. By (d) and $\|PP_\epsilon^{-1}\| \le 1$, the third term is at most $Cn^{-2}\|h\|$. Hence $\|A_0 P_\epsilon^{-1}\|_{V\to V} \le C/|n|$, and its adjoint $P_\epsilon^{-1} G_{xx} \colon V^* \to V^*$ has norm at most $C/|n|$.

In the norm $\|(x,y)\|_*^2 = \|x\|_{V^*}^2 + \alpha_0^2\|y\|^2$, the block operator $\mathcal{T}_\epsilon = P_\epsilon^{-1} G$ thus has norm at most $C_G(1 + \alpha_0 + \alpha_0^{-1})/|n|$, uniformly in ϵ and k.

Step 4: the a priori estimate. Let v be as in Step 1, $(x,y) = \Phi v$, and $\mathfrak{D} = \mathrm{diag}(D, D)$. Since $|n| \ge 3$, the components of v vanish at the axis like $r^{|n|-1}$, so $x, y \in \mathrm{Dom}\, P$ and $\mathfrak{D}^{-1}\mathfrak{D}(x,y) = (x,y)$. Step 1 gives $\mathfrak{D}^{-1}\Phi(z - A_{\nu,n,k})v = (x,y) + \mathcal{K}(x,y)$ with $\mathcal{K} = \mathfrak{D}^{-1}\mathcal{N} - \mathfrak{D}^{-1}\nu G$, where $\mathcal{N}$ collects the three inviscid couplings of Step 1. By Step 1 and Step 2(f), $\|\mathfrak{D}^{-1}\mathcal{N}_{xx}\| \le 2C_s J/(|n|g)$, $\|\mathfrak{D}^{-1}\mathcal{N}_{xy}\|_{H\to V^*} \le 2C_s\|\Omega\|_\infty/g$ and $\|\mathfrak{D}^{-1}\mathcal{N}_{yx}\|_{V^*\to H} \le (\|B\|_\infty + \|W_r\|_\infty)/g$. In the norm $\|\cdot\|_*$ an off-diagonal block operator with entries of norms b_1 ($H \to V^*$) and b_2 ($V^* \to H$) has norm $\max(b_1/\alpha_0, \alpha_0 b_2)$. With $\alpha_0^2 = 2C_s\|\Omega\|_\infty/(\|B\|_\infty + \|W_r\|_\infty)$ the off-diagonal part of $\mathfrak{D}^{-1}\mathcal{N}$ has norm at most $\theta_0 = \sqrt{2C_s\|\Omega\|_\infty(\|B\|_\infty + \|W_r\|_\infty)}/g < 1$. If one of the two factors vanishes, a fixed large or small α_0 makes this norm at most $\theta_0 := \frac{1}{2}$. For every $\epsilon > 0$, $\mathfrak{D}^{-1}\nu G(x,y) = \mathrm{diag}(D^{-1}\nu P_\epsilon)\mathcal{T}_\epsilon(x,y)$ with $\|D^{-1}\nu P_\epsilon\| \le C_s + \nu\epsilon C_s/g$ on V^* and on H. Letting $\epsilon \downarrow 0$ gives $\|\mathfrak{D}^{-1}\nu G(x,y)\|_* \le C_s C_G(1 + \alpha_0 + \alpha_0^{-1})|n|^{-1}\|(x,y)\|_*$ for all $\nu \ge 0$. Choose $N_{\mathrm{far}} \ge 3$ so that $C_s(2J/g + C_G(1 + \alpha_0 + \alpha_0^{-1}))/N_{\mathrm{far}} \le \frac{1}{2}(1 - \theta_0)$. For $|n| \ge N_{\mathrm{far}}$ these bounds give $\|\mathcal{K}(x,y)\|_* \le$

$\theta_1 \|(x,y)\|_*$ with $\theta_1 = \frac{1}{2}(1+\theta_0) < 1$. Hence

$$\|v\|_2 \le c_* \|(z - A_{\nu,n,k})v\|_2 , \qquad c_* = \frac{\max(1,\alpha_0)}{\min(1,\alpha_0)} \frac{C_s}{g(1-\theta_1)},$$

uniformly in $|n| \ge N_{\mathrm{far}}$, k, Z, $\nu \ge 0$ and $\Re z \ge g$.

Step 5: identification with the physical resolvent. For $\nu > 0$ the fields of Step 1 form a core of the fixed-fiber Stokes generator $A_{\nu,n,k}$; for $\nu = 0$ they are dense and $A_{0,n,k}$ is bounded. So the a priori estimate holds on $\mathrm{Dom}\, A_{\nu,n,k}$. Write $A_{\nu,n,k} = T_\nu + K$ as in Proposition 1.29.18, with T_ν maximal dissipative and K bounded; then $\{\Re z > \|K\|\} \subset \rho(A_{\nu,n,k})$. If $z \in \rho(A_{\nu,n,k})$ with $\Re z \ge g$, then $\|(z - A_{\nu,n,k})^{-1}\| \le c_*$, so the disk of radius c_*^{-1} about z lies in the resolvent set. Hence $\rho(A_{\nu,n,k}) \cap \{\Re z \ge g\}$ is open and closed in the connected set $\{\Re z \ge g\}$ and is not empty. So it is the whole half-plane, with $\|(z - A_{\nu,n,k})^{-1}\| \le c_*$. This is the physical resolvent bound of the lemma.

1.30 Full-frequency spectral selection for one member

Main result. Theorem 1.30.1 selects one actual leading member with a unique conjugate pair of maximal growth and the necessary complex physical spectral data. Its proof includes each angular label and each real axial frequency.

The theorem applies to the frozen leading field. It does not assert nonautonomous propagation or nonlinear branching.

Theorem 1.30.1 (Actual frozen selection and viscous interface)**.** *Lemma 1.6.20 holds for the leading family; the local parity on the protected hold is Lemma 1.6.32. For the actual capped leading family with its return corrections in Section 1.27, one joint selection gives a unique conjugate pair of maximal growth $\pm m$. The same selection gives its physical complex simple pole, translated contours, true pressure and adjoint, and finite weighted profile data.*

It also gives the all-Z inputs (B1),(B2),(F1)–(F4) *stated in Section 1.34 and proved in Sections 1.30.14–1.30.17. This is a frozen spectral statement, not a conclusion about nonautonomous propagation or nonlinear branching.*

The parameter and source hypotheses are those of the proof below, not an assumed spectral winner.

Precisely, put $g = c_g\Delta$, $a_m = m/r_0$, and (only in this list) $b_d = \frac{1}{2}(1 + 2(\frac{1}{2} - h)/h)$. Let $\lambda(Z,k)$ be the physical eigenvalue of the positive-label band of the final selected source (after all centering and curvature controls and their return corrections), $\lambda_0 = \lambda(0,0)$, and let subscripts denote derivatives at $(Z,k) = (0,0)$. Then:

(S1) Items 1–3 of Section 1.30.1 hold: $\pm m$ is the unique conjugate pair of maximal growth over all labels and all real (Z,k), attained only at $(Z,k) = (0,0)$; $\Re\lambda_0 - g$ is a fixed positive multiple of Δ; λ_0 is algebraically simple with radial complement in $\Re z \le g$; neighboring labels optimized over phase lie below $\Re\lambda_0$ by at least $c_C\Delta d_m^2$; the deficit of the band near $(0,0)$ is quadratic. By Lemma 1.30.34, every (n,k,Z) whose frozen spectrum meets $\{\Re z \ge g\}$ lies in one compact chart $\mathcal{K}$ (uniformly in late m), on which the band is a single algebraically simple isolated eigenvalue with norm-continuous rank-one Riesz projection.

(S2) (Exact centering) $\lambda_Z = \lambda_k = \lambda_{Zk} = 0$.

(S3) (Axial-frequency curvature) there are fixed $0 < c_A < C_A$ with $|a_m^2\lambda_{kk}/h^2| \le C_A\Delta$ and $-C_A\Delta \le a_m^2\Re\lambda_{kk}/h^2 \le -c_A\Delta$; in particular $\Re\lambda_{kk} < 0$. These bounds are proved for the pre-centering branch with strict slack; the centering moves λ_{kk} by at most $K_C e_m$, which the late m keeps inside that slack. C_q is chosen with the same slack.

(S4) (Exact complex Riccati identity) the real *number* $q := a_m^2 C_q/\Delta > 0$ *satisfies, exactly and in* $\mathbb{C}$,

$$\frac{\lambda_{kk}}{h^2}q^2 + \Big(1 + \frac{2(\frac{1}{2}-h)}{h}\Big)q - \lambda_{ZZ} = 0, \tag{1.30.1}$$

which is (1.32.2) *multiplied by* a_m^2.

(S5) (Gaussian reserve) $X := -\Re(\lambda_{kk})\, q/(2h^2)$ *satisfies* $X > b_d$ *and* $\eta_q := X - b_d/2 - \sqrt{X^2 - b_d X} \le \frac{1}{16}$, *equivalently* $X \ge 2(b_d + \frac{1}{8})^2$. *In particular* $\eta_q < \frac{1}{8}$, *equivalently* $X > (b_d + \frac{1}{4})^2$. *Consequently* $\Re\lambda_{ZZ} = 2q(b_d - X) < 0$, *and the real Hessian of* $\Re\lambda$ *at* $(0,0)$ *is diagonal and negative definite.*

Item (S2) is Lemma 1.30.36 (applied in Section 1.30.10) and is not changed by the curvature control (paragraph 1.30.18); item (S3) is the pole comparison in Section 1.30.18; item (S4) is the target-minus-base solve of Section 1.30.10, exact by paragraph 1.30.18; item (S5) is (1.30.25) *with the choice of* C_q *there. The conjugate band at* $-m$ *has the conjugate data.*

Proof with explicit source and operator hypotheses. **1.30.1 Inputs and precise output**

The previous source construction supplies the actual leading family, its five exact histories, and its capped strictification. It also supplies the protected central power hold, fixed normalized return corrections, and the same heat tail.

The next argument uses their explicit field and return correction identities, not an assumed spectral winner. We fix the physical center and the two distinct operator norms below.

We use the elementary form, trace, and ODE arguments below. We also use the exact scalar-to-velocity elimination of Lemma 1.29.2 and the fixed-sector weighted Leray and pressure estimate of Lemma 1.27.6.

The other inputs are the explicit source and return identities. None assumes a last winner.

We reprove the weighted local Green comparison in Section 1.30.6 in its necessary positive-angular compact range. We use the high-k metric-energy identity with its actual first-strain hypotheses, not as a claim of all-frequency exclusion.

For one sufficiently large but finite C, we set $\Delta = C^\sigma$, with $0 < \sigma < 5$. We construct a finite integer $m \ge 30$, an actual width d_m, controls, and exact return corrections on the same leading source.

They have the next properties:

1. Its only global frozen angular labels of maximal growth are $\pm m$. The positive-label branch and its real conjugate have the unique phase (Z,k)=(0,0). The positive-label eigenvalue λ_0 is generally COMPLEX, with $\Re\lambda_0 > g > 0$.
2. The selected radial eigenvalue is algebraically simple. Its radial complement at the pole has spectrum in Re $z \le g$, while $\Re\lambda_0 - g$ is a fixed positive multiple of Δ.
   Neighboring angular labels, optimized over phase, lie below $\Re\lambda_0$ by at least $c_C\ \Delta\ d_m^2$. Distant regimes have a fixed gap.
   There is no uniform positive gap from λ_0 to the same branch at phases that tend to (0,0). There the deficit is quadratic.
3. The physical resolvent, translated isolating contours, rank-one Riesz projection, adjoint, genuine pressure and necessary finite weighted profile derivatives exist for this fixed member. Leading profiles have five k and seventeen ordinary Z derivatives on the stated weighted ladder. First correctors keep their separately graded four-k ladder. All constants may depend on the selected m and source, but not ancient time.

1.30.2 Source choices before any spectral conclusion

Freeze the actual normalized early/future geometry and pulse length, pressure approximation/core family and return correction supports. Select C large and $\Delta = C^{\sigma}$.

For the returned background before the main implant and its controls, the source bounds hold uniformly in frozen Z,

$$\begin{gathered}\|\Omega\|_\infty \le K/C, \quad \|\Omega\|_\infty + \|r\Omega_r\|_\infty + \|W_r\|_\infty \le K, \\ \sup\{2|\Omega(2\Omega + r\Omega_r)| + |\Omega W_r|\} \le K/C.\end{gathered} \tag{1.30.2}$$

On the modulated set the shear caps give the strain and product estimates of Lemma 1.27.3. Choose a finite $N(C)$ large enough that the dedicated five-history return correction has physical first-radial error at most $C^{-2}/4$. The product expansion for the returns then preserves (1.30.2), with the remaining error allowance available for the spectral returns.

The finite cap is part of this estimate. The central spectral hold is unedited, U=0, physically even in the central axial variable, and has a nonzero power slope.

Its stress ceiling is $\mathcal{T}_\theta \ge c\, e_g\, C^5$. Thus $\Delta/\mathcal{T}_\theta \to 0$ because $\sigma < 5$.

The five spectral return bumps are the fixed radial shapes of Lemma 1.27.5a, after all local trial supports and before the heat drive. In normalized variables their exact map is

$$\int u, \quad \int h, \quad \int uh, \quad \int (u^2 - h^2/(4x)), \quad \int h^2/(4x^2).$$

with an invertible fixed five-by-five derivative and bounded quadratic part. Main discrepancy $O(C^5\, d\Delta/e_g)$, and its actual quadratic correction, tend to zero with d. For fixed C, one constant bounds all these first/second radial return norms for sufficiently small d. We do not discard any return or replace it with a global exponential estimate.

We restore their full histories and pressure endpoints, so this keeps the heat tail and core pressure that we selected before.

Select a fixed rounded main shape and envelope t(y), t(0)=1, $0 \le t \le 1$, even, uniquely maximized at zero with $t''(0) < 0$. The pole profile does not depend on the axial envelope scale L_ζ.

The unrounded normalized pole model below thus gives a robust negative kk-curvature interval before we select L_ζ. Use this interval to select the finite Gaussian factor Cq.

We then select L_ζ large enough for the actual nonvanishing first-η/history bound. The rounded plateau has fixed physical width. The main edit and its five returns change each partial history by $O_C(d\Delta)$. The same estimate holds after one $y = \eta/\ell_m$ derivative by the moment calculation in (1.30.23), also with a fixed upper integration limit. For the changes in the partial histories and the coefficients of the main return correction, the first physical angular derivative is therefore bounded by

$$K(C)\frac{d\Delta}{\ell_m} \le \frac{a_+ K(C)\Delta}{r_0 L_\zeta} \qquad (d \in [a_-/m, a_+/m]).$$

Here $K(C)$ includes the fixed return shapes and the smooth conversion to physical fields on their support. Choose L_ζ so that this last bound is at most $\min\{T_*/(8\sqrt{A_*}), C^{-2}/4\}$, with T_*, A_* as in Remark 1.27.2. We also impose $\Delta/L_\zeta^2 \ll 1/\Delta$ for the physical-center curvature target.

The two conditions precede the choice of m.

We select all later local control supports strictly inside the actual open power hold. For any such fixed selected C there is a positive compact C^1/history cone tolerance $\epsilon_{\mathrm{src}}(C)$.

The form conditions below are different requirements. We impose the condition that the curvature cutoff's radial C^1 and normalized first-η/partial-history changes are smaller than this actual tolerance.

This includes the trial support outside the main corners. No argument infers this tolerance from form positivity.

Pole-U and other exponentially small controls meet it by late m. Choose the fixed slow cutoff of the lower controls inside the central even collar, equal to one near zero. Its support can be taken in the old strict hold margin by compactness of the radial hull and continuity from $\eta = 0$. The shrinking main and curvature supports lie in this collar for all sufficiently late m.

1.30.3 Centered parameter and all-Z global form budget

At the source center that depends on the parameter $r_c(Z) = \sqrt{\hat{\xi}_c^2 Q(Z)}$, put

$$\beta_n(Z,k) = n\Omega_c(Z) + kW_c(Z), \quad \mu_D = \Lambda + i\beta_n,$$
$$D = \mu_D + in(\Omega - \Omega_c) + ik(W - W_c).$$

We rewrite only D: $B = 2\Omega + r\Omega_r$ and each rotation/axial numerator use the true Ω. $\Re D = \Re\mu_D = \Re\Lambda$.

The physical contour related to Γ in μ_D is $\Gamma - i\beta_n$. This is an exact spectral-parameter translation, not a Z-dependent rotating transformation of the PDE.

Remove the two main rounded-corner second-derivative densities and all explicitly listed compact scaled extra-control densities. The residual radial coefficients have a finite bound J_C independent of late d, with each actual old, heat, loop and fixed-return correction term.

In particular for $\delta\Omega = d\theta w(\xi)$, the subtracted term is $\theta w''/(r^2 d)$. The geometric remainder $-\theta w'/r^2$ stays in J_C.

We do NOT assert that one constant bounds the full actual Ω_{rr} for all d.

We require $d\Delta \le C^{-1}$ and the total physical C^1 return correction error $\le C^{-2}$. Then the product bound is

$$P_{\text{actual}} \le K(1+\Delta)/C. \tag{1.30.3}$$

For $|n| \ge N_0$ the true Liouville scalar bulk has principal part $-\partial_z^2 + 1$ and smooth relative form bound

$$\eta_{\text{sm}} \le \frac{K(1+\Delta)}{Cg^2} + \frac{J_C}{|n|g} + \frac{3}{4n^2}, \qquad g = c_g\Delta. \tag{1.30.4}$$

For the geometric term put $p = (rQ)^{-1}$, $w = r^{-1}$, $x = \log r$, $z_r = \sqrt{w/p}$, $A = (n^2 + k^2r^2)^{1/2}$, $\theta = k^2r^2/A^2$, and $\sigma = (pw)^{1/4} = A^{-1/2}$. For $u = \sigma\varphi$, the term $-(p\varphi')' + w\varphi$, multiplied by σ/w, is $-u_{zz} + (1 + \sigma_{zz}/\sigma)u$. Since $z_x = A$, $A_x/A = \theta$, $\theta_x = 2\theta(1-\theta)$,

$$\frac{\sigma_{zz}}{\sigma} = \frac{-\theta + 7\theta^2/4}{A^2}, \qquad \left|\frac{\sigma_{zz}}{\sigma}\right| \le \frac{3}{4n^2}.$$

Indeed the numerator ranges from $-1/7$ to $3/4$ for $0 \le \theta \le 1$, and $A^2 \ge n^2 > 0$. This also gives the relative quadratic-form bound in (1.30.4). The two exact full-W bounds that give (1.30.4) are

$$\left|\frac{k[W'' - W'/r - (Q'/Q)W']}{DQ}\right| \le \frac{r|W''| + 3|W'|}{2|n|g},$$
$$\left|\frac{2\Omega k(kB - nW'/r)}{QD^2}\right| \le \frac{2|\Omega B| + |\Omega W'|}{g^2}, \qquad Q = n^2/r^2 + k^2.$$

The actual $Q(Z) \geq 1$ normalization decreases each radial quantity in (1.30.2)–(1.30.4). Fixed-Z radial differentiation does not differentiate η.

This proves the all-Z scope, not only a pole estimate.

A compact scaled angular extra $\delta\Omega = d\theta w$ has absolute Liouville layer mass

$$\int \frac{|n\delta\Omega_{rr}|}{\sqrt{Q}}\, \mathrm{d}r \leq K|\theta|.$$

an axial extra $\delta W = d\epsilon w$ has mass $\leq K_C|\epsilon|$ by $|k|/\sqrt{Q} \leq 1$. These are TOTAL VARIATION bounds.

Select the curvature cutoff after its actual rank/target constants so its mass Θ obeys $K\Theta/g$ and $K\Delta\Theta/g^2$ below their fixed allowances. Fresh centerings have mass $p_C(m)e^{-c_C m}$.

Their smallness is due to amplitude, not distance. We count fixed physical returns in J_C and (1.30.3).

Explicit bulk bound at the pole. At the pole the scalar problem is the pencil (1.31.3) on $H^1(\mathbb{R})$ in the variable $\xi = (\log r - x_0)/d$. In $x = \log r$ the planar Rayleigh operator has no curvature term, so this pencil is exact. Its coefficient is $B_\xi = d\,\zeta_x$ with $\zeta = 2\Omega + \Omega_x$. We split $B_\xi = B_{\mathrm{lay}} + B_{\mathrm{bulk}}$. Here B_{lay} is the sum of the two main rounded-corner densities and the listed control densities that we removed above. The remainder B_{bulk} is real. Write $I_\sigma = [-1-\sigma_{\mathrm{r}}, 1+\sigma_{\mathrm{r}}]$ for the implant interval with its rounding width $\sigma_{\mathrm{r}} \leq 1$, and $\|v\|_N^2 = \|v'\|^2 + \alpha^2\|v\|^2$.

Lemma 1.30.2 (Explicit pole bulk bound)**.** *Let $\Re\mu_D \geq g = c_g\Delta$ and $\alpha > 0$. Suppose that $|B_{\mathrm{bulk}}| \leq \Delta\beta_{\mathrm{in}}$ on I_σ and $|B_{\mathrm{bulk}}| \leq \Delta\beta_{\mathrm{out}}$ on $\mathbb{R}\setminus I_\sigma$. Put $W = i\alpha B_{\mathrm{bulk}}/(\mu_D + i\alpha V_d)$, $\mathcal{L}_0 = -\partial_\xi^2 + \alpha^2 + W$ and $\mathcal{L}_{0,\mathrm{mod}} = -\partial_\xi^2 + \alpha^2$.*

(i) For $u, v \in H^1(\mathbb{R})$,

$$\Big|\int_{\mathbb{R}} Wu\bar{v}\, \mathrm{d}\xi\Big| \leq \eta_{\mathrm{pole}}\|u\|_N\|v\|_N, \qquad \eta_{\mathrm{pole}} := \frac{1}{c_g}\Big[(1+\sigma_{\mathrm{r}})\beta_{\mathrm{in}} + \frac{\beta_{\mathrm{out}}}{\alpha}\Big].$$

(ii) If $\eta_{\mathrm{pole}} < 1$, then $\mathcal{L}_0 : H^1 \to H^{-1}$ is invertible and

$$\epsilon_{\mathrm{bulk}} = \Big\|\mathcal{L}_0^{-1} - \mathcal{L}_{0,\mathrm{mod}}^{-1}\Big\|_{H^{-1}\to H^1} \leq \frac{\eta_{\mathrm{pole}}}{1-\eta_{\mathrm{pole}}}.$$

(iii) For the actual pole profile, let Ω_{sm} collect the old field, the fixed physical returns and the remaining smooth corrections after removing the implant and the listed angular controls. Set

$$J_{\mathrm{tot}} := \|2\partial_x\Omega_{\mathrm{sm}} + \partial_x^2\Omega_{\mathrm{sm}}\|_\infty + 2\sum_j |\theta_j|\,\|w_j'\|_\infty, \qquad H_\chi := \|2\chi_m' + \chi_m''\|_\infty,$$

where the controls are $\delta\Omega = d\theta_j w_j(\xi)$ and χ_m is the fixed physical cutoff, equal to one on $|x| \leq a$. If $d(1+\sigma_{\mathrm{r}}) \leq a$, one may take

$$\beta_{\mathrm{in}} = 2d + \frac{dJ_{\mathrm{tot}}}{\Delta}, \qquad \beta_{\mathrm{out}} = \frac{dJ_{\mathrm{tot}}}{\Delta} + d^2H_\chi.$$

Consequently

$$\eta_{\mathrm{pole}} \leq \frac{d}{c_g}\left[2(1+\sigma_{\mathrm{r}}) + \left(1+\sigma_{\mathrm{r}}+\frac{1}{\alpha}\right)\frac{J_{\mathrm{tot}}}{\Delta} + \frac{dH_\chi}{\alpha}\right].$$

Proof. (i) On $\mathbb{R}$ we have $|v(\xi)|^2 \le \|v\|\|v'\| \le \|v\|_N^2/(2\alpha)$. Also $|\mu_D + i\alpha V_d| \ge \Re\mu_D \ge g$, because V_d is real. On I_σ we get $|W| \le \alpha\Delta\beta_{\mathrm{in}}/g$, and so

$$\int_{I_\sigma} |W||u||v| \le \frac{\alpha\Delta\beta_{\mathrm{in}}}{g}\,(2+2\sigma_{\mathrm{r}})\sup|u|\sup|v| \le \frac{(1+\sigma_{\mathrm{r}})\beta_{\mathrm{in}}}{c_g}\|u\|_N\|v\|_N.$$

Off I_σ we get $|W| \le \alpha\Delta\beta_{\mathrm{out}}/g$ and $\|u\|\|v\| \le \|u\|_N\|v\|_N/\alpha^2$.

(ii) In the norm $\|\cdot\|_N$ the operator $\mathcal{L}_{0,\mathrm{mod}} : H^1 \to H^{-1}$ is the Riesz isometry. By (i), $T = \mathcal{L}_{0,\mathrm{mod}}^{-1}W$ has $\|T\|_{H^1\to H^1} \le \eta_{\mathrm{pole}} < 1$. Then $\mathcal{L}_0 = \mathcal{L}_{0,\mathrm{mod}}(I+T)$ and $\mathcal{L}_0^{-1} - \mathcal{L}_{0,\mathrm{mod}}^{-1} = ((I+T)^{-1} - I)\mathcal{L}_{0,\mathrm{mod}}^{-1}$, whose norm is at most $\eta_{\mathrm{pole}}/(1-\eta_{\mathrm{pole}})$.

(iii) Write $x = \log(r/r_c)$ at the pole, so that $\xi = x/d$. For $\Omega_{\mathrm{main}} = -d\Delta\mathfrak{t}\,\kappa_\sigma(\xi)\chi_m(x)$, subtracting the corner density gives

$$d(2\partial_x + \partial_x^2)\Omega_{\mathrm{main}} + \Delta\mathfrak{t}\,\kappa_\sigma''\chi_m = -2d\Delta\mathfrak{t}\,\kappa_\sigma'\chi_m - d^2\Delta\mathfrak{t}\,\kappa_\sigma(2\chi_m' + \chi_m'').$$

Indeed $\chi_m' = 0$ on the support of κ_σ', so the mixed product vanishes. The first term is supported in I_σ and has modulus at most $2d\Delta$. The second is supported outside I_σ and has modulus at most $d^2\Delta H_\chi$. Each control leaves $2d\theta_j w_j'$ after its layer $\theta_j w_j''$ is removed. Adding $d(2\partial_x + \partial_x^2)\Omega_{\mathrm{sm}}$ gives the stated bounds. □

The fixed background, the radial bounds for the returns and the bounded trial amplitudes give a common upper bound J_{pole} for J_{tot} on all late width brackets. Since H_χ is fixed, $\eta_{\mathrm{pole}} = O(d)$ uniformly on the pole bracket $\alpha \ge \alpha_- > 0$.

Remark 1.30.3 (Moderate widths). The sufficient condition $\eta_{\mathrm{pole}} < 1$ is imposed only at late width. No conclusion at moderate width is used in the selection.

The bulk form allowance on the compact chart. Lemma 1.30.2 treats the pole $b = 0$. The local Green comparison of Section 1.30.19.2 needs the same allowance on its whole compact chart, with $b \neq 0$ and with the controls. We use the exact scalar operator of Proposition 1.30.10: $m_d = A_d^2 + P_d - c_d$ with P_d from (1.30.33) and the main-layer coefficient c_d from (1.30.34), and the retained operator m_{ret} of Definition 1.30.11. In Hypothesis 1.30.12 write the curvature edit as $\delta\Omega = d\sum_{j=1}^2 \tau_j w_{e,j}(\xi)$. Here $w_{e,j}$ are the two angular response templates with the normalization of Section 1.30.3. We allow a fixed column amplitude $|\tau| \le \Theta_e$. The selected column takes $\tau = \theta(\eta)$, with $\sup|\theta| = O(c_{\mathrm{cut}}^2)$. Let K_w bound the C^2 norms of the template vectors w_Ω, w_U, w_e as maps from their finite-dimensional amplitude spaces, K_ϕ the C^2 norms of the return shapes, and $K_\chi = \|\chi_m'\|_\infty + \|\chi_m''\|_\infty$. The six lower controls range in the ball $|t_6| \le r_T$. On the chart, $\alpha \in [\alpha_*, \alpha^*]$, $|b| \le b^*$, $|y| \le y^*$, $\eta = \ell y$, and $\Re\mu \ge g_1 = c_g\Delta$.

Lemma 1.30.4 (Bulk form allowance on the compact chart)**.** *There are constants Ψ_1, Ψ_2, Ψ_3, depending only on $c_g, \alpha_*, \alpha^*, b^*, y^*, |I|, \inf r_c, \sigma_{\mathrm{r}}$ and the constants above, and not on d, ℓ, r_T or Θ_e, such that for $d\Delta \le C^{-1}$, $d(1+\sigma_{\mathrm{r}}) \le a$ and all u, v,*

$$\Big|\int (m_d - A_d^2)u\bar v\Big| \le \eta_0\|u\|_{E_d}\|v\|_{E_d}, \qquad \Big|\int (m_{\mathrm{ret}} - A_0^2)u\bar v\Big| \le \eta_0\|u\|_{E_0}\|v\|_{E_0},$$

$$\eta_0 := \frac{2d(1+\sigma_{\mathrm{r}})}{c_g} + d\,\Psi_1 + (\ell + r_T + \Theta_e)\Psi_2 + \frac{\Psi_3}{C} + \Psi_1 d^{-N_E}e^{-c_E/d}.$$

In particular Hypothesis 1.30.15 holds with $\eta_0 \le \frac12$ once C is large, r_T, Θ_e are small and then d is small. In the order of Section 1.30.3, the trial radius for τ is fixed before c_{cut} is chosen to put

θ inside that ball. Finally $\ell = \ell_m \le (r_0 L_\zeta/\alpha_*)d$. The rotation constant Ψ_3 is uniform in $C \ge 1$. The control constant Ψ_2 may depend on the fixed C, the selected template norms K_w and the chart lower bound $\inf r_c$. After fixing these, take r_T and Θ_e small and then take ℓ_m small at the late width. Thus each contribution multiplying Ψ_2 meets its assigned form allowance. For the rotation allowance Ψ_3/C, use the post-implant product bound (1.27.3) divided by g_1^2, and use (1.30.2) for the retained background. Neither step uses a second derivative of the background. Ψ_1 contains the background constant K_S, also through K', K'' in the θ_d term. By Lemma 1.30.13, K_S may depend on C and N_{sh}, and it is fixed before L_ζ, c_{cut} and d. This is harmless, because Ψ_1 multiplies only d and $d^{-N_E}e^{-c_E/d}$, and d is selected last. The selected six lower controls have size $\mathrm{poly}(d^{-1})e^{-c_C/d}$ by Lemma 1.30.36, so $|t_6| \le r_T$ at late widths.

Proof. We use three elementary bounds for $u, v \in E_d$. Since $A_d \ge \alpha \ge \alpha_*$, we have $\|u\| \le \|u\|_{E_d}/\alpha$ and $\sup|u|^2 \le \|u\|\|u'\| \le \|u\|_{E_d}^2/(2\alpha)$. Hence, for a measurable q,

(a) if $\operatorname{supp} q \subset I$, then $|\int q u\bar v| \le \frac{|I|}{2\alpha}\sup|q|\,\|u\|_{E_d}\|v\|_{E_d}$;

(b) $|\int q u\bar v| \le \alpha^{-2}\sup|q|\,\|u\|_{E_d}\|v\|_{E_d}$;

(c) $|\int q A_d^2 u\bar v| \le \sup|q|\,\|u\|_{E_d}\|v\|_{E_d}$.

Also $|D| \ge \Re\mu \ge g_1$. By (1.30.33)–(1.30.34),

$$m_d - A_d^2 = V_{\mathrm{geo}} + \frac{i}{D}(\alpha B_\xi^{\mathrm{bulk}} + \tfrac{b}{r_c}dW_{xx}) - \frac{2id\theta_d}{D}F + \frac{2\Omega\, be^{d\xi}(be^{d\xi}B - \alpha W_r)}{D^2},$$

with $F = \alpha B + bW_x/r_c$ and $B_\xi^{\mathrm{bulk}} = B_\xi + \Delta\mathfrak{t}\kappa_\sigma''\chi_m$; the added term is exactly the density removed in c_d. We bound the terms in turn.

Geometry. $|V_{\mathrm{geo}}| \le d^2$, so (b) gives d^2/α_*^2.

Main implant. With $\Omega_{\mathrm{main}} = -d\Delta\mathfrak{t}\kappa_\sigma(x/d)\chi_m(x)$ and $\partial_x = d^{-1}\partial_\xi$,

$$d(2\partial_x + \partial_x^2)\Omega_{\mathrm{main}} + \Delta\mathfrak{t}\kappa_\sigma''\chi_m = -2d\Delta\mathfrak{t}\kappa_\sigma'\chi_m - 2d\Delta\mathfrak{t}\kappa_\sigma'\chi_m' - d^2\Delta\mathfrak{t}\kappa_\sigma(2\chi_m' + \chi_m'').$$

The middle term vanishes, because κ_σ' is supported in I_σ, where $\chi_m = 1$. The first term is supported in I_σ with $|\kappa_\sigma'| \le 1$, so (a) gives $\frac{\alpha\cdot 2d\Delta}{g_1}\cdot\frac{2(1+\sigma_{\mathrm{r}})}{2\alpha} = \frac{2d(1+\sigma_{\mathrm{r}})}{c_g}$. The last term is bounded by $3K_\chi d^2\Delta$, so (b) gives $3K_\chi d^2/(\alpha_* c_g)$.

Background, returns and exponentially small parts. These contribute $d(2\partial_x + \partial_x^2)\Omega$ with $|\cdot| \le 3d(K_S + K_z K_\phi + K_E d^{-N_E}e^{-c_E/d})$, and (b) gives at most $3\alpha^* d(K_S + K_z K_\phi + K_E d^{-N_E}e^{-c_E/d})/(\alpha_*^2 g_1)$.

Angular controls. For $\delta\Omega = d\,\eta\chi(\eta)a_j w_{\Omega,j}(\xi)$ we get $d(2\partial_x + \partial_x^2)\delta\Omega = \eta\chi a_j(2dw_{\Omega,j}' + w_{\Omega,j}'')$, supported in I and bounded by $3\ell y^* r_T K_w$. The extra control gives the same with Θ_e in place of $\ell y^* r_T$. By (a) the two give at most $\frac{3|I|K_w}{2g_1}(\ell y^* r_T + \Theta_e)$, after the factor α in the numerator cancels against (a).

Axial terms. For the axial controls $dW_{xx} = \chi\sum_j(\mathsf{b}_j + \eta c_j)w_{U,j}''$, supported in I and bounded by $(1 + \ell y^*)r_T K_w$. By (a) with $\alpha \ge \alpha_*$ this gives $\frac{b^*|I|(1+\ell y^*)K_w}{2\alpha_*\inf r_c\, g_1}\,r_T$. The background and returns give $d(K_S + K_z K_\phi)$, and (b) applies.

The θ_d term. $|\theta_d| \le 1$, $|B| \le 2\|\Omega\|_\infty + \|\Omega_x\|_\infty \le \Delta + K'$ and $|W_x| \le K''$, with K', K'' depending on K_S, K_z, K_ϕ, K_w for $C \ge 1$ and $r_T \le 1$. By (b) the term gives at most $2d(\alpha^*(\Delta + K') + b^* K''/\inf r_c)/(\alpha_*^2 g_1)$. At fixed C and $g_1 = c_g\Delta$ this is absorbed in $d\Psi_1$.

Rotation. Since $b^2 e^{2d\xi} \le A_d^2$ and $2\alpha|b|e^{d\xi} \le A_d^2$, (c) gives at most $(2\|\Omega B\|_\infty + \|\Omega W_r\|_\infty)/g_1^2$. For the actual coefficients, (1.27.3) gives the numerator bound $K(1+\Delta)/C$, enlarging K by a fixed numerical factor for the separate suprema. Since $g_1 = c_g\Delta$ and $\Delta \ge 1$, its quotient by g_1^2 is at most

$2K/(c_g^2 C)$. For the retained coefficients, (1.30.2) gives $|\Omega_\natural| \le K/C$ and the main slope is at most Δ. The explicit templates bound the remaining control slopes by $K_{\mathrm{tpl}}(r_T + \Theta_e)$ on the compact chart. After division by g_1^2 their contribution is absorbed in $\Psi_2(r_T + \Theta_e)$, and the background and main contributions in Ψ_3/C, with Ψ_3 independent of C.

Adding the bounds gives the first estimate. For m_{ret}, Definition 1.30.11 contains only the control terms and the rotation term $2\Omega_\natural b(bB_{\mathrm{ret}} - \alpha\mathcal{W}'/r_c)/D_{\mathrm{ret}}^2$. The same bounds, with $A_0^2 = \alpha^2 + b^2$ in (a)–(c), give the second estimate without the terms that contain d. □

Corollary 1.30.5 (Retained determinant on separated parameter sets)**.** *Let $\mathcal{E}$ be a set of pairs (p, μ) in the chart with $\Re\mu \ge g_1$ on which the point determinant D_0 of (1.30.35) satisfies $\inf_{\mathcal{E}} |D_0| = \delta_{\mathcal{E}} > 0$. Use $A_0 = (\alpha^2 + b^2)^{1/2}$ in the Green kernel, the energy norm and C_{A_0} of Lemma 1.29.9. Take the suprema defining κ_R, ρ_R over $\mathcal{E}$, and assume they are finite. With $\varpi = (5\rho_R)^{-1}$ and $\varpi_{\mathrm{bulk}} = \varpi/[2(\kappa_R + 1)]$, impose, uniformly in the test pairs and the controls,*

$$C_{A_0}\epsilon_{\mathrm{lay}} \le \min(1, \varpi/2), \qquad (\ell + r_T + \Theta_e)\Psi_2 + \Psi_3/C \le \tfrac{1}{2}\varpi_{\mathrm{bulk}}.$$

Then $|f_{\mathrm{ret}} - D_0| \le 0.67|D_0|$ and $|f_{\mathrm{ret}}| \ge 0.33\,\delta_{\mathcal{E}}$ there. If $\{p\} \times \Gamma \subset \mathcal{E}$ and the point model has one simple zero and no other zeros inside Γ, the rounded retained determinant also has one zero there, counted with multiplicity.

Proof. The retained form bound of Lemma 1.30.4 gives $\eta_{\mathrm{ret}} \le \varpi_{\mathrm{bulk}}/2$. Since $\mathcal{L}_0 = -\partial_\xi^2 + A_0^2$ is the Riesz isometry on E_0, its inverse and the retained inverse differ by at most $\eta_{\mathrm{ret}}/(1 - \eta_{\mathrm{ret}}) \le \varpi_{\mathrm{bulk}}$ in $B(E_0^*, E_0)$. Write K_{mod} for the point-layer operator and $K = \mathcal{L}_{\mathrm{ret}}^{-1}\mathcal{V}_{\mathrm{ret}}$ on E_0. The trace estimate and the rank-two inverse in Lemma 1.29.9 give, at each test point,

$$\|(I + K_{\mathrm{mod}})^{-1}(K - K_{\mathrm{mod}})\|_{\mathfrak{S}_1} \le \rho_R\big[(\kappa_R + 1)\epsilon_{\mathrm{bulk}} + C_{A_0}\epsilon_{\mathrm{lay}}\big] \le \tfrac{1}{5}.$$

The determinant factorization in that lemma yields the stated relative bound. The identity $\det(I + \mathcal{A}\mathcal{B}) = \det(I + \mathcal{B}\mathcal{A})$ of Lemma 1.30.28 identifies $\det(I + K)$ with f_{ret}. On each counting contour Rouché's theorem gives the assertion about multiplicity. □

The bulk form allowance (H2) holds on the full chart. Lemma 1.30.34 specifies the sets on which this corollary gives a root count or a zero-free region.

Select a normalized allowance $\eta_* > 0$ below coercivity and high-A Schur margins. Fix also the Rouché margin $\varpi_{\mathrm{bulk}} = \varpi/(2(\kappa_R + 1))$ of Lemma 1.29.9. It depends only on the normalized model and the contour. By (1.30.10), the pole comparison of Lemma 1.30.2 and the control allowances (1.27.6), the persistent allowances in ϵ_{bulk} satisfy

$$\epsilon_{\mathrm{bulk}} \le K_{\mathrm{cmp}}\big[\epsilon_{\mathrm{old}} + \eta_{\mathrm{fixed}} + \sqrt{\sigma_{\mathrm{round}}}\big] + K_{\mathrm{ctrl}}\big[\Theta/g + \Delta\Theta/g^2 + p_C(m)e^{-c_C m}\big] + \omega_{\mathrm{tot}}(d).$$

Here K_{cmp} is the constant of (1.30.10), K_{ctrl} is the constant of the control allowances, and $\omega_{\mathrm{tot}}(d) = K\omega_C(d) + 2\eta_{\mathrm{pole}}(d)$, valid when $\eta_{\mathrm{pole}} \le \frac{1}{2}$. For $d \le 1$ and $\alpha \ge \alpha_-$, Lemma 1.30.2(iii) gives

$$2\eta_{\mathrm{pole}} \le 2dB_{\mathrm{pole}}/c_g, \qquad B_{\mathrm{pole}} := 2(1 + \sigma_{\mathrm{r}}) + (1 + \sigma_{\mathrm{r}} + \alpha_-^{-1})J_{\mathrm{pole}}/\Delta + H_\chi/\alpha_-.$$

Thus $\omega_{\mathrm{tot}}(d) \to 0$ as $d \to 0$. We fix these allowances in this order:

1. Select C so that the first term of (1.30.4), $O(C^{-1-\sigma})$, is $< \eta_*/8$, and so that $K_{\mathrm{cmp}}(\epsilon_{\mathrm{old}} + \eta_{\mathrm{fixed}}) \le \varpi_{\mathrm{bulk}}/4$.

2. Fix the rounding so that $K_{\mathrm{cmp}}\sqrt{\sigma_{\mathrm{round}}} \le \varpi_{\mathrm{bulk}}/8$.

3. After all fixed controls are selected, select finite N0 so that the remaining smooth terms are $< \eta_*/8$.

4. Select the extra controls so that $\eta_{\mathrm{extra}} < \eta_*/8$ and $K_{\mathrm{ctrl}}(\Theta/g + \Delta\Theta/g^2) \le \varpi_{\mathrm{bulk}}/4$; the late layers have $\Theta \propto c_{\mathrm{cut}}^2$, and c_{cut} has no positive lower bound.

5. Select the centerings so that $K_{\mathrm{ctrl}} p_C(m) e^{-c_C m} \le \varpi_{\mathrm{bulk}}/8$.

6. Take $d = d_m$ (that is, m large: d is not free after m, since $m d_m = \alpha_{d_m}$ by Section 1.30.9; every condition below constrains only d, or $\ell_m \le (r_0 L_\varsigma / a_-)d$) so small that $\omega_{\mathrm{tot}}(d) \le \varpi_{\mathrm{bulk}}/8$ and $C_\alpha \epsilon_{\mathrm{lay}} \le \min\{1, \varpi/2\}$. For the pole part it suffices that $K\omega_C(d) \le \varpi_{\mathrm{bulk}}/16$ and

$$d \le \min\left\{1, \frac{a}{1+\sigma_{\mathrm{r}}}, \frac{c_g\, \varpi_{\mathrm{bulk}}}{32 B_{\mathrm{pole}}}\right\},$$

because then $\eta_{\mathrm{pole}} \le \varpi_{\mathrm{bulk}}/32 \le \frac{1}{2}$ and $2\eta_{\mathrm{pole}} \le \varpi_{\mathrm{bulk}}/16$. With the factorised margin of Lemma 1.29.9 this is a mild late-width condition.

Thus $\eta_{\mathrm{total}} < \eta_*/2$ and $\epsilon_{\mathrm{bulk}} \le \varpi_{\mathrm{bulk}}$, with unused strict reserve. There is NO global d^{-N} exp(-c/d) term.

The related bulk inverse is bounded $H_z^{-1} \to H_z^1$ by $(1 - \eta_{\mathrm{total}})^{-1}$, on the true axis/exterior domain.

The reserved Θ and C^{-2} allowances bound the next controls. We first prove the comparison without these controls and compute its rank.

We then add controls under the same bounds. We select the persistent product/rounding allowances against fixed model margins.

We never compare them with Δd^2.

1.30.4 The model and its strict normalized margins

Let $\alpha = |n|d$, b=kr0d, $A = \sqrt{\alpha^2 + b^2}$, $y = (m/r_0)\eta/L_\varsigma$. Subtract the central imaginary Doppler value. The ideal two-interface equation is

$$\mu_D^2 = \Delta^2 t(y)^2 \frac{\alpha^2}{A^2} D_0(A), \qquad D_0(A) = e^{-4A}/4 - (A - 1/2)^2. \tag{1.30.5}$$

Its positive root has unique global maximum $c_*\Delta$ at $(\alpha_{\mathrm{m}}, 0, 0)$, where $1 - 2\alpha_{\mathrm{m}} = e^{-4\alpha_{\mathrm{m}}}$, $D_0(\alpha_{\mathrm{m}}) > 0$. Thus $D_0' = 1 - 2A - e^{-4A}$ first increases and then decreases through one positive zero.

At the maximum the real Hessian is diagonal with entries

$$\frac{\Delta D_0''}{2\sqrt{D_0}}, \qquad -\frac{\Delta\sqrt{D_0}}{\alpha_{\mathrm{m}}^2}, \qquad \Delta t''(0)\sqrt{D_0}.$$

all strictly negative. Select a small convex box K around this point where the Hessian stays $\le -c\Delta$ I.

We select $g = c_g\Delta$ below and sufficiently close to the maximum. The whole ideal superlevel near g then lies inside K.

The determinant has a strict separation on the complement of a slightly smaller box. We fix all these NORMALIZED constants before C and d.

The retained old affine slope s0 changes (1.30.5) to

$$\frac{\alpha^2}{A^2}\{\Delta^2 t^2 e^{-4A}/4 - [(\Delta t - s_0)A - \Delta t/2]^2\}.$$

Signed-slope convention and persistent margin budget. The symbol $s_0 = -2(1+\nu_c)\Omega_g < 0$ denotes the signed old power derivative, not its positive magnitude. The centered unrounded profile is

$$V(\xi) = s_0\xi - \Delta t\ \mathrm{clamp}(\xi, -1, 1), \qquad V(-1) = S_t, \quad V(1) = -S_t, \quad S_t = -(s_0 - \Delta t) > 0.$$

The inner signed slope is $-S_t$.

A center Doppler translation cannot remove s_0 from these endpoint differences. In particular, we must not change the signed s_0 in the rank kernels below. For $J = \Delta t$, the two point strengths and their exact determinant are

$$\begin{aligned} \gamma_- &= \frac{-i\alpha J}{\mu_D + i\alpha S_t}, \qquad \gamma_+ = \frac{i\alpha J}{\mu_D - i\alpha S_t}, \\ D_{\mathrm{ret}}(\mu_D) &= \frac{\mu_D^2 - M_{\mathrm{ret}}}{\mu_D^2 + \alpha^2 S_t^2}, \qquad M_{\mathrm{ret}} = \frac{\alpha^2}{A^2}\left\{\frac{J^2 e^{-4A}}{4} - (S_t A - J/2)^2\right\}. \end{aligned} \tag{1.30.6}$$

The sum of the strengths is $-2\alpha^2 J S_t/(\mu_D^2 + \alpha^2 S_t^2)$. Their product is $\alpha^2 J^2/(\mu_D^2 + \alpha^2 S_t^2)$.

We insert the free Green kernel $e^{-A|\xi-\zeta|}/(2A)$ to prove the displayed determinant. Put $q = s_0/\Delta$. (In this subsection only. This $q < 0$ is unrelated to the Gaussian curvature $q > 0$ of item (S4) of Theorem 1.30.1.)

The exact normalized radicand is

$$\frac{M_{\mathrm{ret}}}{\Delta^2} = \frac{\alpha^2}{A^2}\left\{t^2 D_0(A) + 2qtA(A - 1/2) - q^2A^2\right\}. \tag{1.30.7}$$

The cross term has a plus sign. It persists as $d \to 0$.

Here are quantitative choices of its allowance. Fix the compact comparison set K_0, with $0 < A_{\mathrm{lo}} \le A \le A_{\mathrm{hi}}$, and the box of the maximum K used above.

Let $r > 0$ be a lower bound for the ideal normalized positive root on K. Let $H > 0$ be its negative Hessian margin there.

Let $\delta_{\mathrm{det}}, \delta_{\mathrm{sep}} > 0$ be the fixed normalized contour and exterior-superlevel separation margins. For $\epsilon = \|q\|_{C^2(K_0)}$, the product rule applied to (1.30.7) gives

$$\|M_{\mathrm{ret}}/\Delta^2 - M_{\mathrm{ideal}}/\Delta^2\|_{C^2(K_0)} \le K_2(\epsilon + \epsilon^2).$$

Here K_2 is a finite sum of the absolute product-rule coefficients and the $C^2(K_0)$ norms of $(\alpha^2/A^2)tA(A - 1/2)$ and α^2.

On radicands at least $r^2/2$, the square-root map has a finite C^2 Lipschitz constant K_{root}: differentiate to get $f'/(2\sqrt{f})$ and $f''/(2\sqrt{f}) - (f')^2/(4f^{3/2})$. Require

$$\begin{aligned} K_2(\epsilon + \epsilon^2) < \min(r^2/2, 1), \qquad K_{\mathrm{root}}K_2(\epsilon + \epsilon^2) < H/8, \\ K_{\mathrm{det}}\epsilon < \delta_{\mathrm{det}}/8, \qquad K_{\mathrm{sep}}\epsilon < \delta_{\mathrm{sep}}/8. \end{aligned} \tag{1.30.8}$$

To define the last two finite constants, write $z = \mu_D/\Delta$ in (1.30.6).

Its denominator $z^2 + \alpha^2(t - q)^2$ has a strictly positive modulus minimum on the fixed compact contour at $q = 0$, because $\Re z \ge c_g > 0$. We first restrict ϵ to keep half that minimum.

We then select derivative bounds $K_{\mathrm{det}}, K_{\mathrm{sep}}$ for this rational function on the contour and compact exterior comparison set. This also handles zero radicands, where we must not use a square-root derivative. The independent low-frequency, small-angular-fraction and high-frequency exclusions outside K_0 use absolute slopes and total layer mass.

Use $|S_t| \le \Delta + |s_0|$, not $|S_t| \le \Delta$.

On the actual unedited power germ, $|s_0| = 2(1+\nu_c)|\Omega_g| \le K/C$, so its normalized value is $O(C^{-1-\sigma})$. Add the finite threshold (1.30.8) to the early choice of C.

After we fix C, L_ζ, we evaluate the old germ at $\eta = (r_0 L_\zeta/m)y$. Its first two normalized y derivatives satisfy the same allocated bound for sufficiently late m.

The limit background has no α, b derivatives. Finite-d geometric errors remain in the different local finite-jet comparison.

Rounding, bulk $O(d)$ comparison and the later controls consume different fractions of the unused strict margins. No persistent term is charged against Δd^2.

The retained maximum differs from the ideal one by $O(\epsilon)$, by the negative second derivative and the mean value theorem. All later choices use this retained branch.

Its rounded maximum gives the width bracket. Its actual negative kk interval gives C_q, and its actual trial responses give the rank inverse.

The ordered construction selects the member subject to these finite inequalities. Section 1.30.18 gives the actual protected-germ derivative bounds, the whole-width-bracket comparison, and the corrected response/source margins for this selection.

1.30.5 Exhaustive frequency exclusion, with $\alpha \to 0$

These estimates are for resolvents, not only formal eigenfunctions.

1.30.5.1 4a. Outside the main axial support

For $|y| = |\eta|/\ell_m > Y_*$ the main envelope vanishes. The physical curvature cutoff also vanishes there since $\zeta = a_m \eta = L_\zeta y$ and we take $c_{\mathrm{cut}} \sup\{|s| : \chi(s) \ne 0\} < L_\zeta Y_*$ for that cutoff. The lower controls use a fixed slow cutoff $\chi(\eta)$, which can still be active. On this collar their first radial strains are

$$r\partial_r \delta\Omega = \eta\chi(\eta) \sum_j a_j w'_{\Omega,j}(\xi), \qquad \partial_r \delta W = \frac{\chi(\eta)}{r} \sum_j (\mathsf{b}_j + \eta c_j) w'_{U,j}(\xi).$$

Their nonzero radial derivatives lie in $r \ge r_{\min} > 0$, so the energy contribution is bounded by $K_{\mathrm{tpl}} r_T$ on the trial ball. The fixed-shape returns contribute $O_C(d\Delta)$ on the whole slow cutoff by the uniform five-row inverse, as in the proof of Lemma 1.29.1. The remaining exponentially small pieces contribute $O_C(d^{-N} e^{-c_C/d})$. Outside the union of the edit supports only the background contributes. Let $K_0 < g$ bound the old energy growth uniformly in Z. After fixing the templates impose $K_{\mathrm{tpl}} r_T \le (g - K_0)/4$ (also ≤ 1), and at fixed C take the whole width bracket late enough for the two return and remainder bounds together to be at most $\min\{1, (g-K_0)/4\}$. Thus on $|y| > Y_*$ the numerical range lies in $\Re z \le (K_0 + g)/2$ for all trials. The same coercive estimate for the adjoint gives the physical inverse throughout $\Re z \ge g$.

1.30.5.2 4b. Low total scaled frequency

The true divergence constraint on the fixed-relative perturbation annulus gives the radial trace bound

$$\int_{\mathrm{main}} |u_r|^2 r \, \mathrm{d}r \le K d (1 + |n| + |k| r_0) \|u\|^2.$$

The large strain is a radial/azimuthal cross term. Cauchy–Schwarz bounds its energy by $K\Delta \sqrt{d + \alpha + |b|}\|u\|^2$.

The bounded part consists of the background, the cutoff remainders of the main edit, the lower and curvature controls and their returns. As in (4a), their increments have a fixed unit allowance after decreasing the trial radii and taking the bracket late. Include these allowances in the background energy constant K. With $g \geq c_g\Delta$, take $\Delta = C^\sigma$ sufficiently large that $K \leq c_g\Delta/4$ and choose $A_{\mathrm{lo}} > 0$ such that $K\sqrt{A_{\mathrm{lo}}} \leq c_g/4$. Then $K + K\Delta\sqrt{A_{\mathrm{lo}}} \leq c_g\Delta/2 < g$. Both choices precede the late width.

Then we exclude $d + \alpha + |b| \leq A_{lo}$, also for n=k=0. The number A_{lo} depends only on K, Δ and c_g, and the trace constant comes from one fixed relative cutoff. Both are fixed before m and do not depend on $d = d_m$. The same forced estimate gives a physical resolvent.

1.30.5.3 Each finite label $|n| < N_0$

The exact metric identity of Lemma 1.29.16 is valid for ANY fixed n. Let $\delta = K_0/\Delta$ on a fixed-relative annulus that contains all main/trial supports, $\delta = 1$ near axis/infinity, with transitions in old-bounded regions. Here K0 is a fixed first-strain bound.

We include the extra curvature's C^1 allowance. The actual estimates are

$$\gamma_\delta \leq K_{\mathrm{geom}}\sqrt{K_0\Delta} + K_0/2, \quad A_\delta \leq K_{\mathrm{geom}}|n|/r_0,$$
$$J_\delta \leq K_{\mathrm{geom}}/r_0^2, \quad L \leq K_{\mathrm{geom}}(K_0 + \Delta).$$

Select the early C so $\gamma_\delta \leq g/2$ and put $\gamma = 3g/4$. The physical forced energy estimate applies for

$$|k| \geq K_n, \quad K_n \geq \frac{2A_\delta L}{\delta_{\min}(\gamma - \gamma_\delta)}, \quad K_n^2 \geq J_\delta/(2\delta_{\min}).$$

These finite K_n are independent of d. After we fix N0, we let $K_{\mathrm{fin}} = \max_{|n|<N_0} K_n$ and select $d(1 + N_0 + r_0K_{\mathrm{fin}}) < A_{\mathrm{lo}}$, which holds for late m because $d = d_m \leq 2\alpha_\sigma/m$. Then the high-k and low-strip ranges overlap for all these labels.

This gives the finite-label extension of Lemma 1.29.1. It does not divide a scalar formula by n=0.

1.30.5.4 Small angular fraction for $|n| \geq N_0$

On either main layer r/r0 stays in a fixed compact interval that tends to one as $d \to 0$. With $h_j = |n\Omega_{rr,j}|/Q$ in Liouville coordinates,

$$M_j = \int h_j \, \mathrm{d}z = \int \frac{|n\Omega_{rr,j}|}{\sqrt{Q}} \, \mathrm{d}r \leq K\Delta\alpha/A. \tag{1.30.9}$$

The bulk inverse in Section 1.30.3 is on H^1_z with principal norm $\|v'\|^2 + \|v\|^2$. Point evaluation has one norm bound.

Thus the absolute main-layer Birman–Schwinger norm is at most K $\sum_j M_j/g$. Select a fixed $\epsilon_{\mathrm{ang}} > 0$ so $K\Delta\ \epsilon_{\mathrm{ang}}/g < 1/2$.

Neumann inversion excludes all modes with $\alpha/A \leq \epsilon_{\mathrm{ang}}$. This includes $\alpha \to 0$ with nonzero b and is independent of any lower bound on α.

The old terms, actual returns, b-dependent W terms, and signed extra layers enter the bulk bound (1.30.4). That bound has one positive coercivity constant. This step omits none of them.

After 4b–4d, in any remaining compact A range one has $A \geq c\ A_{lo}$ and $\alpha \geq \epsilon_{\mathrm{ang}}$ c $A_{lo} > 0$, a FIXED normalized lower bound. Thus the next E_α weighted comparison never approaches its degenerate endpoint.

There is no hidden C-dependent shrinking α contour constant.

1.30.5.5 4e. High A

Use the actual two smooth sign-definite main layers, not a point-layer approximation. In Liouville z the exact row-sign equation is

$$Dg_j + is_j \sum_l \sqrt{h_j} G_{\text{base}} \sqrt{h_l} g_l = 0.$$

The real principal inverse G_{real} is self-adjoint. Thus each diagonal D+i $s_j \sqrt{h_j} G_{\text{real}} \sqrt{h_j}$ has real part $\geq g$ and inverse norm $\leq g^{-1}$.

The two estimates are

$$\|\sqrt{h_+} G_{\text{real}} \sqrt{h_-}\| \leq K\Delta e^{-cA},$$
$$\|\sqrt{h_i}(G_{\text{base}} - G_{\text{real}})\sqrt{h_j}\| \leq K\Delta\eta_{\text{total}}.$$

The second follows from the global form resolvent identity, not a remote exponential estimate. Select η_* so $K\Delta\eta_* < g/8$, and A_{hi} so $K\Delta e^{-cA_{\text{hi}}} < g/8$.

Signed extra-layer blocks cost $K\Theta/g$ and $K\Delta\Theta/g^2$. Section 1.30.3 bounds these terms by the stated margins. The block Schur inverse is thus uniform for $A \geq A_{hi}$.

This covers arbitrarily high n and k without a delta approximation beyond its range.

The remaining parameters satisfy $cA_{\text{lo}} \leq A \leq A_{\text{hi}}$ and $\alpha \geq \alpha_{\min} > 0$, with bounded b and $|y| \leq Y_*$ by Section 1.30.5.1. These estimates cover every angular label, real k and frozen Z.

1.30.6 True-domain compact comparison and large centered imaginary parameter

On the remaining compact range the exact radial principal form in ξ is

$$-\partial_\xi^2 + A_d(\xi)^2, \quad A_d^2 = \alpha^2 + b^2 e^{2d\xi},$$
$$E_{d,b} = \{v \in H^1 : be^{d\xi} v \in L^2\}.$$

We do not replace its domain by a fixed unweighted H^1 perturbation. Conjugate its closed form by a weak exponential weight $e^{\beta\langle\xi\rangle}$ with β^2 below a fixed fraction of $(1-\eta_*)\alpha_{\min}^2$.

Cauchy–Schwarz absorbs the first-derivative cross term. This gives weighted bulk inverses on the true line/axis/exterior. The exact pullback from z has $|A_d'/A_d| \leq d$.

This geometric term is form-small with one bound.

For parameter derivatives use a finite descending ladder $\beta_0 > \cdots > \beta_N > 0$ with gaps greater than Kd. Multipliers $e^{Kd|\xi|}(1+|\xi|)^p$ are bounded from each stronger weight to the next weaker one.

Centered D has local expression

$$D = \mu_D + i\alpha V_d + \frac{ibW}{r_0 d}, \qquad |V_d| + |W|/d \leq K_C(1+|\xi|).$$

On the protected hold the background W vanishes, and the axial templates contribute bounded multiples of r_T to W/d. Any exponentially small remainder divided by d is uniformly bounded at late widths. The angular bound follows from the first radial derivative on the hold.

Two derivatives in (α, b, y) thus has a finite stronger-to-weaker bound. We do not silently treat any uncontrolled d^{-1} as uniform.

Actual remote sources at a fixed physical log-distance lie at $|\xi| \geq c/d$. Their local response and finite derivatives are $\leq K_C\ d^{-N}\ e^{-c_C/d}$.

Their global norm does not have this exponential bound.

Split comparisons at $|\xi| \le M$. On that interval, the actual Taylor expansion of the smooth power hold and fixed scaled templates gives convergence with derivatives.

The limit is the retained-old rounded local pencil. The remaining local-gap part is small in descending weights as $M \to \infty$.

The remote part has the previous exponential estimate. First $d \to 0$, then $M \to \infty$ proves local Green convergence and two parameter derivatives on this compact positive-α range.

The nonvanishing old rotation/product terms have their explicit small normalized allowance. We do not call them $o_d(1)$.

Rounding adds $O(\sqrt{\sigma_{\text{round}}})$ by the H^1 point-trace inequality. Thus the fixed-contour comparison is

$$K[\epsilon_{\text{old}} + \eta_{\text{fixed}} + \sqrt{\sigma_{\text{round}}} + \omega_C(d)], \quad \omega_C(d) \longrightarrow 0. \tag{1.30.10}$$

The precise local norm is $H^{-1}(I) \to H^1(I)$. Lemmas 1.30.7 and 1.30.8 prove weighted inverse derivatives, with the mixed phase/control jets.

The same local C^2 comparison applies near the simple root. On local main supports, derivatives in y hit only the fixed taper and scaled shapes.

Derivatives of remote old data bring finite fixed-C constants and exponential distance gain. Its small Ω_g/Δ ratio controls the local old product and its finite derivatives.

Thus the C^2 allowance near the maximum is genuinely small, not inferred from a value-only global form bound.

For $|\mu_D|$ large, K_C bounds the residual Doppler on main supports on the compact phase set. Thus the main-layer norm is $O(\Delta/(|\mu_D| - K_C))$.

The inequality $|D| \ge g$ gives one bound for the bulk inverse, even if remote Doppler values resonate with $\Im\mu_D$. Thus Neumann inversion excludes sufficiently large centered $|\mu_D|$.

We do not assume global $1/|\mu_D|$ decay, and a large physical $|\Lambda|$ alone would be the wrong criterion.

1.30.7 Centered Fredholm count and the pre-control simple branch

At b=0 the exact pole pencil is

$$-v'' + \alpha^2 v + i\alpha B_\xi v/D = 0, \qquad B = 2\Omega + \Omega_x.$$

We remove the two main layers. Then actual old/smooth/fixed-return terms have $B_\xi = d(2\Omega_x + \Omega_{xx})$. Thus the global unweighted form difference from $-\partial_\xi^2 + \alpha^2$ is $O(K_C\ \mathrm{d/g})$.

Fresh centerings, when added later, have their own small amplitude. The Neumann inverse difference is $\le 2K_C\ \mathrm{d/g}$ once the form norm is less than $1/2$.

The quadratic η curvature edit vanishes at the pole.

For a compact layer c supported at distance at most σ from ξ_j, the rank-one trace estimate is

$$\|M_c - (\int c)\delta_j \otimes \delta_j\|_{\mathfrak{S}_1} \le \sqrt{2/\alpha}\sqrt{\sigma}\int |c|.$$

The true limit strengths are

$$\gamma_- = \frac{-i\alpha\Delta}{\mu_D + i\alpha S}, \quad \gamma_+ = \frac{i\alpha\Delta}{\mu_D - i\alpha S}, \quad S = \Delta - s_0.$$

Write $K = \mathcal{L}_0^{-1}\mathcal{V}$ for the trace-class layer operator and K_{mod} for its point-layer model. Then

$$\|K - K_{\mathrm{mod}}\|_{\mathfrak{S}_1} \le \epsilon_{\mathrm{bulk}}\|\mathcal{V}\|_{\mathfrak{S}_1} + C_\alpha \epsilon_{\mathrm{lay}}$$

in the energy norm of Lemma 1.29.9. On its separated contour the hypotheses $\epsilon_{\mathrm{bulk}} \le \varpi_{\mathrm{bulk}}$ and $C_\alpha \epsilon_{\mathrm{lay}} \le \min\{1, \varpi/2\}$ give $\|Y\|_{\mathfrak{S}_1} \le 1/5$, where $Y = (I + K_{\mathrm{mod}})^{-1}(K - K_{\mathrm{mod}})$. Factor $I + K = (I + K_{\mathrm{mod}})(I + Y)$. With $D_0 = \det(I + K_{\mathrm{mod}})$ this gives $|\det(I + K) - D_0| \le (e^{6/5}/5)|D_0| < |D_0|$ on the boundary. Rouché therefore preserves the root count on this fixed contour.

At compact nonzero b, use the local Green/layer comparison in Section 1.30.6 rather than a false global operator-domain convergence. Restriction to the compact layer supports and the same finite trace-factorization give the related compact determinant comparison.

Lemma 1.30.33 gives the two Hilbert–Schmidt factors and the fixed-space rounding comparison.

The ideal/retained-old determinant has one and only one positive root in K and a uniform nonzero bound on the remaining positive half-disk. Sections 1.30.5–1.30.6 thus give one simple local branch $\mu_d(\alpha, b, y)$ for the actual source before rank and centering controls.

It has small normalized C^2 error and a strictly negative real Hessian on a smaller K. There is no other spectrum on $\Re\Lambda \ge g$ outside that branch.

A simple determinant zero gives a rank-one scalar Laurent pole by the finite-matrix reduction in Lemma 1.29.11. This is the first point where simplicity is concluded. It was not a hypothesis in selection of the source.

1.30.8 Actual away-center rank, with the real old power slope

We select scaled open intervals outside the two main rounded corners, for example inside a plateau region $\xi > 1 + \sigma_{\mathrm{round}}$. These intervals come before the fixed-physical radial cutoff and the later return corrections by a strict margin.

Arrange the main profile to contain such a fixed interval. Late d places it inside the actual protected power hold.

It misses $\xi = 0$. On this region the limit eigenfunction is the decaying free solution $v = C_e\, e^{-\alpha\xi}$, while the retained old power contributes a nonzero affine slope $s_0 = -2(1 + \nu_c)\Omega_g$.

The actual power is not literally affine. Section 1.30.6 covers its Taylor error of O(d) in the necessary local jets.

Write $D_0 = \mu + i\alpha(V_{\mathrm{offset}} + s_0\, \xi)$. An angular trial d $w(\xi)$ has response proportional to

$$\begin{aligned} &\int \frac{v^2 i\alpha w''}{D_0}, \qquad K_\Omega = i\alpha(v^2/D_0)'' \\ &= C_e^2 e^{-2\alpha\xi}\alpha^3 \left[\frac{4i}{D_0} - \frac{4s_0}{D_0^2} - \frac{2is_0^2}{D_0^3}\right]. \end{aligned} \tag{1.30.11}$$

There is one nonreal pole, with nonzero third-order coefficient because $s_0 \neq 0$. If all real-interval values lay on one complex line, multiplication by a fixed phase and analytic reflection would force a conjugate pole as well, impossible.

Thus select two points with noncollinear values and then two narrow real smooth bumps in that actual interval. The response determinant is nonzero.

For the axial trial the actual normalized kernel (given by differentiation of the rotation–axial terms of the same scalar pencil in Lemma 1.30.35) is

$$K_U = C_e^2 e^{-2\alpha\xi}\alpha^2 \left[\frac{4i}{D_0} - \frac{4(s_0 + \Omega_0)}{D_0^2} - \frac{2is_0(s_0 + 2\Omega_0)}{D_0^3}\right]. \tag{1.30.12}$$

Here Ω_0 is the local old power value and $s_0 = -2(1+\nu_c)\Omega_0$, so $s_0(s_0+2\Omega_0) = 4\nu_c(1+\nu_c)\Omega_0^2 \neq 0$. Its third-order pole cannot cancel, and the same reflection argument supplies two noncollinear real trial responses on any such open interval.

Choose these bumps at the maximizer α_σ of the retained rounded pole branch. Let $M_j(\alpha)$ be the retained normalized real response matrices for these fixed bumps on that branch at $b = y = 0$ (including the angular response in the curvature normalization), and put $R_0 = \max_j \|M_j(\alpha_\sigma)^{-1}\|$. The axial matrices here have had the physical factor d divided out. The simple-root contour gives continuity in α of the root and of its derivatives with respect to the bump amplitudes. The decaying pole solution can be normalized by its exterior coefficient $C_e = 1$ locally: vanishing of C_e would give zero Cauchy data beyond the corners. The kernel integrals over the fixed bumps, including the nonzero simple-root response factors, are consequently continuous in α.

Choose $\delta\alpha > 0$ with $[\alpha_\sigma - \delta\alpha, \alpha_\sigma + \delta\alpha]$ inside the strict concavity interval and

$$\max_j \sup_{|\alpha-\alpha_\sigma|\le\delta\alpha} \|M_j(\alpha) - M_j(\alpha_\sigma)\| < \frac{1}{8R_0}. \tag{1.30.13}$$

There are only finitely many matrices. Fix this interval and the bump shapes before the late integer m. The finite-width comparison at the *same* $\alpha = md$ and the distant return estimates are uniform on this interval, as detailed in Section 1.30.18. The resulting normalized inverse bound may depend on C and ν_c. Restoring the axial factor d costs d^{-1} in that block. Use these bounds and the fixed C^1/total variation norms of the shapes when choosing c_{cut}.

Recompute all constants after the envelope choice. We do not reuse any old response inverse. We explicitly include the local compact source C^1/history tolerance from Section 1.30.2 in c_{cut} inequalities.

Smallness of a layer form alone does not ensure the power-germ cone survives.

1.30.9 Actual width IVT and discrete angular gap

On the pre-centering pole branch $f_d(\alpha) = \Re\mu_d(\alpha, 0, 0)$, local C^2 comparison gives a unique maximizer α_d in J and $f_d'' \le -c\Delta$. Let α_σ be the maximum of the retained-old rounded limit branch.

With the fixed $\delta\alpha$ of (1.30.13), set

$$d_\pm = (\alpha_\sigma \pm \delta\alpha)/m.$$

For all sufficiently late m, $|\alpha_d - \alpha_\sigma| < \delta\alpha/2$ throughout this bracket. Continuity of the actual source/return correction maps and local simple root makes $md - \alpha_d$ continuous and of opposite signs at $d_\pm$.

The IVT supplies d_m with $md_m = \alpha_{d_m}$. We do not assume a width derivative or an implicit-function theorem in d.

Taylor's integral identity at this actual maximum yields

$$f_{d_m}(md_m) - f_{d_m}(nd_m) \ge c\Delta(n-m)^2 d_m^2. \tag{1.30.14}$$

for neighboring labels in J. Outside the smaller J the fixed contour/model margin gives a fixed deficit. Thus we never subtract an O(d) model error from the d^2 neighbor gap.

That would be invalid.

1.30.10 Physical complex centering and quadratic curvature without losing the winner

Local evenness and W=0 give zero limit first/mixed phase jets. Each nonlocal odd source is at fixed physical log-distance, so Section 1.30.6 gives defects $e_m = p_C(m)e^{-c_C m}$ in the normalized finite jets.

The two-real-direction controls from Section 1.30.8 cancel selected complex λ_k, λ_Z and λ_{Zk} by triangular small solves, with exact return corrections. p_C absorbs a raw U inverse's polynomial d^{-1}.

They perturb pole values and finite phase derivatives by at most $K_C\ e_m$. We do not assert that any neighbor is centered.

The physical and centered jets obey EXACTLY

$$\begin{aligned} \lambda_Z &= \mu_{D,Z} - in\Omega_c' - ikW_c', \quad \lambda_k = \mu_{D,k} - iW_c, \\ \lambda_{ZZ} &= \mu_{D,ZZ} - in\Omega_c'' - ikW_c'', \quad \lambda_{Zk} = \mu_{D,Zk} - iW_c', \quad \lambda_{kk} = \mu_{D,kk}. \end{aligned} \tag{1.30.15}$$

Lemmas 1.30.35 and 1.30.36 derive the physical response kernel and the actual six-real centering map, with the differentiated return correction.

Away-center trial supports and later return corrections leave center germs unchanged. $W_c = 0$ and $\Omega_c'(0) = 0$, but Ω_c'' is generally nonzero. For the last quadratic control use the actual post-centering λ_{kk} and target

$$\begin{aligned} \frac{\lambda_{ZZ,\mathrm{target}}}{a_m^2} &= \frac{a_m^2\lambda_{kk}}{h^2}(C_q/\Delta)^2 + (1 + 2(\tfrac{1}{2} - h)/h)C_q/\Delta, \\ \mu_{D,ZZ,\mathrm{target}} &= \lambda_{ZZ,\mathrm{target}} + im\Omega_c'', \qquad a_m = m/r_0. \end{aligned}$$

The exact center calculation gives $|m\Omega_c''/a_m^2| \le K_{\mathrm{bg}}(C)/m + K_{\mathrm{env}}\Delta/L_\zeta^2 + K_{\mathrm{geo}}\Delta r_0^2/m^2$. Section 1.30.2 makes the middle term small before the choice of m.

The target-minus-current-base inverse thus gives $|v_m| \le V_q(C)/\Delta$, where Vq includes the actual rank inverse. We must not multiply it by that inverse again.

Set $\theta = (\widehat{\zeta}^2/2)\chi(\widehat{\zeta}/c_{\mathrm{cut}})v_m$, $\widehat{\zeta} = a_m\eta$. Select c_{cut} so its total variation, source C^1/history errors and global form slots satisfy Sections 1.30.2–1.30.3.

The real linear response is negative with one strict margin on a smaller (α, b, y) chart. Analytic eigenvalue expansion in the control amplitude, with its exact cutoff factor, gives

$$\Re(\lambda_{\mathrm{final}} - \lambda_{\mathrm{pre}}) \le -\frac{c_C\widehat{\zeta}^2\chi(\widehat{\zeta}/c_{\mathrm{cut}})}{\Delta} \le 0. \tag{1.30.16}$$

Thus the remainder is $O((\widehat{\zeta}^2\chi)^2)$. If we reduce c_{cut}, the remainder is at most half the negative linear term even at the flat edge. We use no absolute-C^k perturbation argument there.

The quadratic control leaves each pole value and first phase jet unchanged. The intermediate phase/angle annulus and broad exterior have fixed deficits. The cutoff's amplitude/form bound makes its effect smaller than these deficits.

Before this quadratic edit, strict phase concavity bounds a neighbor's optimized gain over its pole value by $K_C\ e_m^2/c_{ph}$. Here $c_{ph} > 0$ is the actual finite normalized phase Hessian margin.

(It may depend on L_ζ). Select the same late m so

$$K_C(e_m + e_m^2/c_{\mathrm{ph}}) < c\Delta d_-^2/4. \tag{1.30.17}$$

Then (1.30.14), (1.30.16) and (1.30.17) give the unique positive-angular winner m after optimization over phase. Reality of the coefficients gives $\lambda_{-m}(Z,k) = \overline{\lambda_m(Z,-k)}$ on the reflected chart.

The selected physical Hessian has negative real diagonal entries and mixed jet zero. We include the exact physical Gaussian target. We do not replace it by a real-only curvature statement.

1.30.11 Physical pressure, full resolvent exclusion and adjoint

The scalar zero/pole calculation of Sections 1.30.4–1.30.10 is not itself the selected spectral definition. The spectral objects are those of the physical frozen generator. This subsection states the physical conclusions and proves them from the conditional lemmas of Section 1.29. Throughout, $A = A_{0,n,k}(Z) = -P_k N_k P_k$ is the inviscid frozen generator on $L^2_\sigma = L^2_\sigma(r\,\mathrm{d}r)$ of label n and real axial frequency k; $a = n/r$, $Q = a^2 + k^2$, $q = Q^{1/2}$, $D = \Lambda + in\Omega + ikW$, $B = 2\Omega + r\Omega_r$, $C = aB + kW_r$ and $F_t = af_\theta + kf_z$; and $\mathcal{L}(\Lambda)$, $\mathfrak{h}(\Lambda)$, $\mathfrak{J}(\Lambda)$, $\mathfrak{T}(\Lambda)$ are the operators of (I1).

Proposition 1.30.6 (Physical pressure, exclusion, simple pole and adjoint)**.** *For the selected member, every late width of the bracket and every control of the admitted ball:*

(P1) (Pressure and resolvent.) *Let $|n| \geq 2$, $k \in \mathbb{R}$, $\Re\Lambda > 0$, and let $\mathcal{L}(\Lambda)\colon H^1(\mathbb{R}) \to H^{-1}(\mathbb{R})$ be invertible. Then $\Lambda \in \rho(A)$ and (1.29.8) holds. For $f \in L^2_\sigma$ let $(u, v, w) = (\Lambda - A)^{-1} f$ and*

$$p = \frac{-D(\partial_r + 1/r)u + iCu - iF_t}{Q}.$$

Then (u, v, w, p) solves the unprojected system (1.29.1), $qp \in L^2(r\,\mathrm{d}r)$, $p_r \in L^2(r\,\mathrm{d}r)$, and $\nabla_{n,k} p = (p_r, iap, ikp)$ is orthogonal to L^2_σ, so P_k annihilates it. On a parameter set where the hypotheses of Lemma 1.29.2 hold, the bound (1.29.2) holds.

(P2) (Exclusion.) *If the frozen spectrum at (n, k, Z) meets $\{\Re z \geq g\}$, then $p = (|n|d, kr_c d, y) \in \mathcal{K}$ of Lemma 1.30.34, and $|n| \geq 2$. Each exclusion of Sections 1.30.5–1.30.7 excludes the whole physical spectrum, not only smooth normal modes.*

(P3) (Simple pole.) *For $p \in \mathcal{K}$ the spectrum of A in $\{\Re z > g_\Gamma\}$ is one eigenvalue λ. It is algebraically simple, its Riesz projection is $P = e \otimes \ell$ with $Ae = \lambda e$, $\ell A = \lambda \ell$ and $\ell e = 1$, the Laurent expansion of Section 1.29.2 holds with $S = ((A - \lambda)|_{\mathrm{Ran}(I-P)})^{-1}(I - P)$, and the radial component of e is not zero. At the pole $(Z, k) = (0, 0)$ of the label m, $\lambda_0 = \mu_0 - im\Omega_c(0)$ with μ_0 the centered root, and $\sigma(A) \setminus \{\lambda_0\} \subset \{\Re z \leq g\}$.*

(P4) (Adjoint.) *For $z \in \rho(A)$ one has $\bar z \in \rho(A^*)$, $A^* = -P_k N_k^* P_k$, and $(\bar z - A^*)^{-1} = ((z - A)^{-1})^*$ with the same norm, so every contour bound for A holds for A^* on the conjugate contour. In (P3) write $\ell = \langle \cdot, e^\sharp \rangle$. Then the Riesz projection of A^* at $\bar\lambda$ is $P^* = \langle \cdot, e \rangle e^\sharp$, $A^* e^\sharp = \bar\lambda e^\sharp$, $\langle e, e^\sharp \rangle = 1$, and ℓ is a multiple of $\chi \circ \mathfrak{h}(\lambda)$, where $\varphi \otimes \chi$ is the residue of $\mathcal{L}^{-1}$ in (1.29.15). The adjoint primitive pressure $\pi^\sharp = S_k(N_k^* e^\sharp)$, $S_k = \Delta_k^{-1} \operatorname{div}_k$, satisfies $-N_k^* e^\sharp + \nabla_k \pi^\sharp = \bar\lambda e^\sharp$. The left data are those of this non-selfadjoint operator, not of an orthogonal substitute.*

(P5) (Contours.) *Let (Z_*, k_*) be a phase of the label m with $p_* \in \mathcal{K}$. There are a compact rectangle Λ_*, which is a neighborhood of (Z_*, k_*), and a fixed closed curve $\Gamma_* \subset \{\Re z \geq g_\Gamma\}$ such that for all $(Z, k) \in \Lambda_*$: $\Gamma_* \subset \rho(A(Z, k))$, $\sup_{\Lambda_* \times \Gamma_*} \|(z - A(Z, k))^{-1}\| < \infty$, and Γ_* encloses exactly one eigenvalue of $A(Z, k)$, which is algebraically simple; it is the band eigenvalue $\lambda(Z, k)$ when $p(Z, k) \in \mathcal{K}$. Finitely many such rectangles cover the compact set of phases of the label m with $p \in \mathcal{K}$.*

Proof. For (P1), the forced elimination of Lemma 1.29.2 gives $U = \mathfrak{J}\mathcal{L}^{-1}\mathfrak{h} f + \mathfrak{T} f$ and the displayed pressure, first for smooth solenoidal f. The bounds (I1)–(I2) give $U \in L^2_\sigma$. Indeed $u = c\psi$, $\psi \in H^1$,

and (1.29.4) controls u and $Q^{-1/2}(\partial_r + 1/r)u$. Since $|C|/q \le \|B\|_\infty + \|W_r\|_\infty$ and $|F_t|/q \le |(f_\theta, f_z)|$, the pressure formula gives $qp \in L^2$; the radial equation gives $p_r = f_r - Du + 2\Omega v \in L^2$. Thus $\nabla_{n,k} p \in L^2$ is orthogonal to L^2_σ by integration by parts and density, and projection gives $(\Lambda - A)U = f$. All these maps are bounded in f, so density extends the right inverse.

For injectivity, a solenoidal L^2 kernel vector satisfies $(\partial_r + 1/r)u = -i(av + kw)$, hence $\psi = u/c \in H^1$. Its tangential equations and divergence constraint have determinant $DQ \neq 0$; they give the same pressure and reconstruction with $f = 0$. The radial equation is $\mathcal{L}\psi = 0$ in H^{-1}, so $\psi = u = v = w = 0$. This proves the sandwich formula and the resolvent estimate, with the true axis/exterior conditions.

For (P2), Lemma 1.30.34(ii),(iii) puts every dangerous phase in $\mathcal{K}$. Its scalar exclusions are physical by (P1); the remaining fixed low labels, including $0, \pm 1$, are excluded by Lemma 1.29.1. On $\mathcal{K}$, $|n| = \alpha/d \ge 2$ for late m.

For (P3), the chart-wide simple root and the large-$|\mu|$ exclusion in the strip $g_\Gamma \le \Re\mu < g$ give a single pole in $\Re z > g_\Gamma$. The physical transfer and Laurent expansion are Lemma 1.29.12 and Section 1.29.2, applied to $\Omega_\Gamma - i\beta_n$. The rank-one Riesz projection has no nilpotent part. Its radial component is $c\varphi \neq 0$ by (1.29.15) and (1.29.4). At the selected pole the translation is $\lambda_0 = \mu_0 - im\Omega_c(0)$, and the exclusion on $\Re z > g$ gives the stated radial complement.

For (P4), take Hilbert adjoints in the resolvent and contour identities. This gives P^* and its normalized eigenvector, while (1.29.15) identifies ℓ with the forced scalar row. The adjoint pressure follows from $(I - P_k)g = \nabla_k S_k g$; its positive weighted bounds are obtained by applying Proposition 1.28.8 to A^*, not by dualizing a positive-weight bound for A.

Finally fix a phase in $\mathcal{K}$ and translate its contour to Γ_*. The frozen generator is norm continuous, including at $k = 0$ (Lemma 1.29.3). If its variation on a rectangle is at most $(2M_*)^{-1}$, where $M_* = \sup_{\Gamma_*} \|(z - A(Z_*, k_*))^{-1}\|$, the Neumann series bounds all resolvents there by $2M_*$. Shrinking the rectangle keeps its Riesz projection within distance one of the original rank-one projection, hence of rank one. The chart-wide exclusion identifies this pole with the band eigenvalue. Compactness gives a finite cover, proving (P5). □

Thus each exclusion of Sections 1.30.5–1.30.7 excludes the whole physical spectrum. The physical pole is the one of (P3), with its true pressure and adjoint. On the full phase family, the direct-integral real-growth statements are those of Section 1.30.1. Near the maximum the same branch has the quadratic phase deficit of Section 1.30.10; it has no uniform positive gap there.

1.30.12 Required finite weighted spectral data for this same member

The finite weighted data of the selected member are given by Proposition 1.28.8 and Corollary 1.28.9. We verify their hypotheses for this member and list the outputs. These are consequences of the actual selected source and of Proposition 1.30.6; they are not properties inferred from spectral simplicity, and they are selected after the member is frozen.

(B1). $\mathcal{X} = \mathcal{H}_m$, or $\mathcal{H}_m \oplus \mathcal{H}_{-m}$ treated as a direct sum (the operator preserves each summand, and the conjugate summand is given by Proposition 1.29.13(iv)); $m \ge 30$, so $n_0 = m - 1 \ge 29$.

(B2). On $\mathcal{H}_{\pm m}$ the operator $N(Z, k) = N_0(Z) + kN_1(Z)$ is multiplication by equivariant matrix functions: $N_1 = iW$, and N_0 collects the transport $\pm im\Omega + \Omega\mathcal{J}$ ($\Omega\partial_\theta$ acting on Cartesian components), the rotational stretching $\Omega\mathcal{J}$, the term $r\Omega_r\, e_\theta \otimes e_r = (\Omega_r/r)\, x^\perp \otimes x$ and $W_r\, e_z \otimes e_r$. The angular velocity has the heat tail $\Omega = O(R^{-2-2h})$, with each radial derivative gaining one power. On the compact axial chart the axial velocity, the controls and the return corrections have a common radial support bound (Lemma 1.32.2). At the axis the coefficients are smooth Cartesian functions by the regular-axis property. Hence, for every finite s_0, the maps $Z \mapsto N_i(Z)$ have eighteen

Z derivatives bounded in C^{s_0} and decaying at infinity, uniformly on compact Z intervals. Thus they are C^{17} into $C_0^{s_0}$, that is, $l_0 = 17$.

(B3). Proposition 1.30.6(P5) gives, around each phase of the band chart, a rectangle Λ_* and a fixed isolating curve Γ_* with $\min_{\Gamma_*} |z| \geq g_\Gamma > 0$ and a uniform resolvent bound; finitely many rectangles cover the chart. The adjoint statement is (P4). For a complementary semigroup, (P3) puts the complement at the pole in $\{\Re z \leq g\}$, and A is bounded. Thus for $g < g' < \Re\lambda_0$ a fixed closed curve in $\{\Re z \leq g'\} \cup \{|z| > \|A\| + 1\}$ that encloses $\sigma(A) \setminus \{\lambda_0\}$ and avoids 0 lies in the resolvent set with a uniform bound on a small rectangle, by the same Neumann argument. This is argued at the pole; on the other rectangles of the chart the same argument applies with g_Γ in place of g, by (P3) and (P5).

With (B1)–(B3) verified, Proposition 1.28.8 and Corollary 1.28.9 supply the profile, pressure, corrector and complementary-semigroup table on each rectangle. In particular the leading profiles have H^6_{7-j} bounds for $j \leq 6$ (weight one at $j = 6$), the first correctors have H^4_{6-j} bounds for $j \leq 4$, and the leading upgrade is H^{18}_{9-j} for $j \leq 2$. There are seventeen ordinary Z derivatives of the leading profiles and sixteen of the correctors. A k derivative spends one moment; the scalar pressure spends one additional moment. The adjoint uses the same argument applied directly to A^*.

The normalization of (1.29.16) differs from that of Proposition 1.28.8(vi) by a scalar factor with the same jets. The largest multiplier margin used is $\lceil w \rceil + j + 1 \leq 10 \leq m - 1$; even the conservative Sobolev-dependent margin for the leading upgrade is $18 + 9 + 2 = 29 < 30 \leq m$. The physical corrector equations and their signs are fixed in Lemma 1.35.2. The compact-hull H^{14} estimate for the later full-curl construction is separate from the selection of the leading field.

1.30.13 One parameter order, replacements, and exact scope

The full order is:

- actual normalized source/pulse/future/core data and return corrections
- C large, $\Delta = C^\sigma$, actual capped loop plus its true return correction
- normalized model margins and robust pole-k target interval
- fixed rounding, Gaussian factor, envelope L_ζ
- pre-control true-domain form/Green/count and simple branch
- away-center rank shapes/inverse, physical target and c_{cut}
- residual J_C, finite N0/high-k thresholds
- one large m for the full width bracket, actual d_m by IVT
- exact first/mixed centering, target-minus-base curvature, true returns
- freeze THIS source, then finite weighted/profile/completion thresholds.

Whenever a requirement depends on a previously fixed finite constant, we include it in the late m threshold before the IVT. We do not silently replace any selected m after completion.

The normalized source and cutoff slots ensure that the controls, once added, do not invalidate the pre-control form/exterior comparison. The small source C^1 allowance and the global scalar-form allowance are different inequalities.

We impose the two inequalities.

The actual statements in the source-choice, preselection and physical resolvent sections use the distinct global and local norms above. We keep the complex physical eigenvalue, signed Laurent coefficient and dilation symbol $\lambda + i(\frac{1}{2} - h)Zk$ at each downstream call site.

Global comparisons use the stated algebraic norm. We use remote exponential decay only for separated local responses.

This proof closes the frozen full-frequency selection and necessary fixed-member spectral data on the explicitly admitted actual leading-source construction. It does not by itself prove joint endpoint packet-atlas admission, positive pressure-saturated completion weights, nonautonomous prepared propagation, an exact completed-base mode, or NS nonuniqueness.

If any actual piece/return correction input in Section 1.30.2 is not realized, the theorem cannot be applied to a generic only compatible profile.

1.30.14 Actual all-Z B1/B2, not a compact-chart substitution

This section and Sections 1.30.15–1.30.17 extend the conclusion to the frozen small-viscosity inputs.

The exact leading profiles are (1.6.11). Write $F = H/(\hat{\xi}^2)$.

Then

$$\Omega = Q^{-1-h}F(\tfrac{\hat{\xi}^2}{2},\eta),\quad W = Q^{-\frac{1}{2}-h}U(\tfrac{\hat{\xi}^2}{2},\eta),$$
$$V_{\mathrm{phys}} = Q^{-1/2}\frac{V(\frac{\hat{\xi}^2}{2},\eta)}{\hat{\xi}},\quad \hat{\xi} = r/\sqrt{Q},$$
$$Q - Z^2Q^{2h} = 1,\quad \eta = ZQ^{h-\frac{1}{2}}.$$

The actual source is smooth at $\hat{\xi} = 0$, with F and $2V/\hat{\xi}^2$ regular. It has U=V=0 beyond one fixed normalized radius.

It also has differentiated $H = O((\hat{\xi}/\sqrt{2})^{-2h})$ on its heat exterior. All fixed $(\frac{1}{2}\hat{\xi}\partial_{\hat{\xi}},\partial_\eta)$ jets on the intervening closed normalized hull are finite, with one bound for $-1 \le \eta \le 1$.

These statements hold after the actual main/rank/return edits: those edits are compact and lie strictly inside the hull. Their finite constants can grow with selected m, which is now fixed. The endpoint heat expansion and matching, not compactness of a physical-Z chart, supplies the closed-η tail bounds.

In particular F and each necessary $\frac{1}{2}\hat{\xi}\partial_{\hat{\xi}}/\eta$ jet are $O((1+\frac{\hat{\xi}^2}{2})^{-1-h})$.

Direct differentiation gives

$$Z\partial_Z \log Q = \frac{2\eta^2}{1-2h\eta^2},\quad Z\partial_Z\eta = \frac{\eta(1-\eta^2)}{1-2h\eta^2},$$
$$\partial_Z \log Q, \partial_Z\eta = O(Q^{h-\frac{1}{2}}),\quad \partial_Z^2 \log Q, \partial_Z^2\eta = O(Q^{2h-1}). \tag{1.30.18}$$

The apparent quotients by Z are removable at zero. Each ordinary Z derivative of a normalized profile is thus a finite combination of $\frac{1}{2}\hat{\xi}\partial_{\hat{\xi}}$ and ∂_η derivatives.

The related nonpositive Q power bounds its coefficients. Cartesian horizontal differentiation contributes the factor $Q^{-1/2}$.

At r=0 use the regular vector germs, not singular cylindrical component bounds.

This proves the B1 derivatives of $\mathcal{U}_0 = r\Omega\, e_\theta + W$ ez through total order two, and Vphys er through total order one. One bound applies for all Z.

For the remaining B1 statements use $r\,\mathrm{d}r = Q\hat{\xi}\,\mathrm{d}\hat{\xi}$. For example $\|W\|^2_{L^2_h}$ is a fixed multiple of $Q^{-2h}\int |U|^2\,\hat{\xi}\,\mathrm{d}\hat{\xi} = Q^{-2h}$ times a bounded normalized integral.

Likewise $\|\Omega\|^2$ and $\|\nabla_h\mathcal{U}_0\|^2$ carry nonpositive Q powers. The actual Ω heat tail is square integrable because $h > 0$.

Pointwise,

$$r^2|\nabla_h U_0| \le KQ^{-h},\quad r|W| \le KQ^{-h},\quad r|\Omega| \le K,$$
$$r|\partial_Z\Omega| \le KQ^{-1}.$$

For large radii use the differentiated heat decay. For bounded radii use the regular germs and compact hull.

Thus the exact weighted B1 norms are finite. Formula (1.30.18) also bounds $Z\partial_Z$ of $\Omega, W, \nabla_h \mathcal{U}_0$. $r\partial_r = \hat{\xi}^2 \hat{\xi}^{-1} \partial_{\hat{\xi}}$ proves their horizontal dilation bounds. This is B2.

Also the first-strain norms have uniform convergence to zero as $|Z| \to \infty$ (their prefactors contain Q^{-1-h}). $\Omega, W, \nabla_h \mathcal{U}_0$ tend to zero as $|(r, Z)| \to \infty$.

Thus a large-Z exterior with strain below any fixed positive g_{far} is available after the selected member is frozen. We do not assert or need a rate uniform over different m.

1.30.15 Far angular labels: actual F4 and its parameter order

Take a fixed $g_{\text{far}} = c_{\text{far}}\,\Delta$ below the model exclusion line, with $c_{\text{far}} > 0$. The selected source satisfies

$$\begin{gathered} \beta_0 = \left\| \frac{n\Omega_r + kW_r}{\sqrt{n^2/r^2 + k^2}} \right\|_\infty \le \|r\Omega_r\|_\infty + \|W_r\|_\infty \le K(1+\Delta), \\ C_s = K_{\text{ell}}(1 + \beta_0/g_{\text{far}})^2 \le K_{\text{fixed}}, \\ \frac{2C_s\|\Omega\|_\infty(\|B\|_\infty + \|W_r\|_\infty)}{g_{\text{far}}^2} \le \frac{K_{\text{fixed}}(1+\Delta)}{C\Delta^2} < 1/16. \end{gathered} \tag{1.30.19}$$

The last inequality is an early C condition, uniform over the width bracket and the allowed controls. The capped-loop/source first bounds and the explicit control/return allowances prove it.

Cs does not contain the large second derivatives of the rounded layer. Those enter only a finite last-source constant J below.

In particular the choice of late N_{far} is not an extra constraint $m > N_{\text{far}}$.

For clarity the usable analytic lemma is the actual weak-space calculation in Lemma 1.29.20. The next argument gives its norm statement and proof dependencies.

On $H = L^2(r\ \mathrm{dr})$, $q^2 = n^2/r^2 + k^2$, $P = -\partial_r^2 - r^{-1}\partial_r + q^2$, $R = q^{-1}(\partial_r + 1/r)$, V=DomR. Solenoidality gives the exact isometry from velocity to (x,y) in $V^* \times H$ with $x = -(I + R^*R)u$, $y = i(kv_\theta - (n/r)w)/q$.

In particular $\|x\|_{V^*}^2 = \|u\|^2 + \|q^{-1}((n/r)v_\theta + kw)\|^2$. One must not treat the differentiated radial forcing as an H forcing.

For $D = z + i(n\Omega + kW) + \nu P$ and Re $z \ge g_{\text{far}}$, real-part energy, its commutator and the adjoint equation give

$$\begin{aligned} \|D^{-1}\|_H \le g_{\text{far}}^{-1}, \quad \|\nu P D^{-1}\|_H \le (1 + \beta_0/g_{\text{far}})^{1/2}, \\ \|D^{-1}\|_V \le C_s/g_{\text{far}}, \quad \|\nu P D^{-1}\|_V \le C_s, \\ \|D^{-1}\|_{V^*} \le C_s/g_{\text{far}}, \quad \|D^{-1}\nu P\|_{V^*} \le C_s. \end{aligned}$$

The last composition order is essential. We commute R and use $\|[R,P]u\| \le K|n|^{-1}\|Pu\|$ and the Bessel estimate $\|u''\| + \|qu'\| + \|q^2 u\| \le K\|Pu\|$ for $|n| \ge 3$ to get the estimates.

$4/n^2$ absorbs its only adverse square term. For finitely large n necessary to absorb the commutator enlarge N_{far}.

Constants depend on β_0/g_{far}, not on n,k or ν.

The exact four cylindrical viscous residual blocks G are those displayed in the proof of Lemma 1.29.20. Their regularized compositions satisfy, with any fixed anisotropic y weight $a_0 > 0$,

$$\sup_{\epsilon > 0} \|(P+\epsilon)^{-1} G\|_{V^* \times H \to V^* \times H} \le \frac{K_G(1 + a_0 + a_0^{-1})}{|n|}.$$

This follows from the absolute coefficient bounds $|r^j\partial_r^j(a^2/q^2)| \le K_j$, $|r^j\partial_r^j(2ak/(rq^3))| \le K_j/|n|$ and the previous elliptic estimate. For the V* diagonal use its adjoint on V and commute R.

For the off-diagonal second-order block use the adjoint composed with $(P+\epsilon)^{-1}$. Thus we use no unbounded bare P^{-1} at k=0. Factor $D^{-1}\nu G$ through $D^{-1}\nu P + \nu\epsilon D^{-1}$, then let $\epsilon \to 0$ in the norm inequality for each fixed ν.

This gives a uniform $O(C_s(1+a_0+a_0^{-1})/|n|)$ perturbation, with all $\nu \ge 0$.

The smooth inviscid diagonal error is Cs $J/(|n|g_{\mathrm{far}})$, with J finite for the selected source. Balance the two physical off-diagonal bounds $2\|\Omega\|$ and $\|B\| + \|W_r\|$ by $a_0^2 = 2C_s\|\Omega\|/(\|B\| + \|W_r\|)$.

Its contribution is the square root of (1.30.19). Thus take

$$N_{\mathrm{far}} > \max(m,3), \quad \frac{C_s J}{N_{\mathrm{far}} g_{\mathrm{far}}} + \frac{C_s K_G(1+a_0+a_0^{-1})}{N_{\mathrm{far}}} < 1/4.$$

Neumann inversion now holds in the exact physical space with one bound for all Z,k, $|n| \ge N_{\mathrm{far}}$, $\nu \ge 0$, Re $z \ge g_{\mathrm{far}}$. We first identify this inverse with the physical operator on its compact smooth solenoidal graph core.

Density and the resolvent identity from large positive real z extend that identification. This proves F4, not only a formal pencil inverse.

It covers unbounded imaginary physical z directly.

No centered bounded contour is necessary in this regime.

1.30.16 Compact strain, small viscosity, true shifts and F1/F2

Fix now the finite set $F = \{|n| < N_{\mathrm{far}}\}$. We remove the selected pair near its maximum.

The inviscid result of Sections 1.30.5–1.30.11 then gives these sectors a positive spectral separation over all phase. Let $\delta > 0$ satisfy $16\delta < \min(\delta_{\mathrm{ang}}, \Re\lambda_0 - g, \Re\lambda_0 - g_{\mathrm{far}}, \Re\lambda_0/2)$.

Select a compact physical phase mask $\chi_\pm$ equal to one wherever the selected band exceeds $\Re\lambda_0 - 7\delta$, and taper only where it lies strictly below $\Re\lambda_0 - 6\delta$.

Use the pole rectangle and the choice of δ in Section 1.33. On the positive sector take supp $\chi_+ \subset \{\Re\lambda > \Re\lambda_0 - 8\delta\}$ inside that rectangle and put $\chi_-(Z,k) = \chi_+(Z,-k)$.

Put $S_{0,\pm m} = d_0\chi_\pm P_{0,\pm m}$, $d_0 \ge 8\delta$, and zero elsewhere. These are the actual oblique Riesz projections, not orthogonal eigenvector projectors.

Compactness here means compact radial operators over compact phase support, NOT finite rank in the full axial variable.

For each fixed n the extended generator splits as

$$A_\nu = T_\nu + K, \quad T_\nu = \nu(\Delta_h - k^2) - iP_k(n\Omega + kW)P_k.$$

T_ν is maximal dissipative. The stretching sandwich K is compact: on an annulus the radial input is H^1 by divergence, thus compact in L^2. Indeed, on a finite radial interval the projection onto averages on cells of length δ has finite rank and incurs L^2 error at most $\delta\|\partial_r v_r\|_2$ by integration and Cauchy–Schwarz. The measure $r\,\mathrm{d}r$ is equivalent to $\mathrm{d}r$ on that annulus.

The adjoint handles radial output. At infinity the actual strain has uniform convergence to zero.

At the axis subtract rigid rotation $2\Omega(0)J_h$. The remainder is O(r) or $O(r^2)$, and P0JhP0=0 makes the localized rigid term a compact commutator.

For $k \ne 0$, $(P_k - P_0)$ times a compact spatial cutoff is compact by low-frequency Hilbert–Schmidt truncation and high-frequency symbol decay. This works also for $n = 0, \pm 1$.

No false low-label Hardy estimate is invoked.

On a compact parameter rectangle K is a norm-continuous norm-compact family. We split horizontal frequency at q0 and use $\|P_k - P_{k'}\| \le K \min(1, |k-k'|/|\xi_h|)$; this gives source-sandwiched norm difference $O(q_0\|N\|_2 + |k-k'|q_0^{-1}\|N\|_\infty)$, thus Hölder 1/2.

We prove the source L^2 and L^∞ assumptions in Section 1.30.14. This does not assert bare Pk norm continuity at k=0.

Ordinary Z dependence is smooth by the actual bounded derivatives.

As $\nu \to 0$, $R_{T_\nu}(z)$ and their adjoints have strong convergence with one convergence modulus on compact vector/parameter sets in $\Re z > 0$. This follows from strong heat-semigroup convergence and bounded skew Duhamel.

Compactness gives the two

$$(R_{T_\nu} - R_{T_0})K \longrightarrow 0, \qquad K(R_{T_\nu} - R_{T_0}) \longrightarrow 0.$$

in norm. On each actual translated physical contour from Section 1.30.11, Fredholm inversion is thus uniform for small ν.

The Riesz projection converges in norm: its free T_ν contour integral is zero, while the remaining resolvent term has compact sandwiches on the two sides. Finite covers of the fixed band support give one fixed $\nu_0 > 0$ and continuous rank-one P_ν.

Define $S_\nu = d_0 \chi P_\nu$ on the phase chart and extend it by zero. The cutoff χ is independent of ν, so every S_ν is supported in the same compact set $\operatorname{supp}\chi$. The uniform norm convergence of the projections there gives $\sup\|S_\nu - S_0\| \to 0$ and a common norm bound for $0 \le \nu \le \nu_0$, after decreasing ν_0 if necessary. Also $S_\nu = P_k S_\nu P_k$.

This proves F2. We can use the family of physical contours patchwise.

Its dependence on β_n stays harmless on the fixed compact phase set, and we never drop it.

Here is the full half-plane argument, rather than convergence only on one circle. The actual small strain in Section 1.30.14 controls large $|Z|$, all $\nu \ge 0$.

For each of the finitely many n, the high-k metric estimate of Section 1.30.5c gives a uniform small-growth exterior, all $\nu \ge 0$. Take the finite maximum threshold.

Select the shift support inside the remaining compact rectangle. There the transport norm is finite, say Φ, and $\|K - S_\nu\| \le C_K$.

The numerical range lies in $\{z : \Re z \le C_K,\ |\Im z| \le \Phi + C_K\}$. Outside a larger rectangle one constant bounds the resolvent, with $\nu \to 0$.

On the remaining compact half-plane rectangle above $g_f = \Re\lambda_0 - 6\delta$, the inviscid shifted inverse exists by the actual winner and mask layout. Factor

$$z - A_\nu + S_\nu = [I - (K - S_\nu)R_{T_\nu}(z)](z - T_\nu).$$

The compact factor has uniform norm convergence by the adjoint strong sandwich and F2. A finite cover yields a uniform inverse for $0 \le \nu \le \nu_0$.

Thus one constant bounds the full shifted physical resolvent for all phase and Re $z \ge g_f$. The crude physical semigroup energy bound is uniform in ν.

The Hilbert-space Plancherel resolvent-to-semigroup argument (Lemma 1.34.7, used with its explicit finite constants) gives

$$\begin{gathered} \|e^{t(A_{\nu,n} - S_{\nu,n})}\| \le C_F e^{g_1 t}, \\ g_f < g_1 < \Re\lambda_0, \quad n \in F, \quad Z, k \in \mathbb{R}, \quad 0 \le \nu \le \nu_0. \end{gathered} \tag{1.30.20}$$

A small rate relaxation is necessary. No claim at the boundary rate follows for free. This proves F1 independently of the nonautonomous leading propagation.

We select all constants and ν_0 after we fix this single selected source. We make no $\nu \to 0$ operator-norm claim for $\nu\Delta$.

1.30.17 Last spectral and leading-field hypotheses and their scope

Sections 1.30.14–1.30.16 give (B1), (B2), (F1), (F2) and (F4) as stated in Section 1.34. F3 is the same single all-Z metric $\delta(r)$ of Section 1.30.5c and Lemma 1.27.1.

We impose its $\gamma_\delta/g = O(\Delta^{-1/2})$ condition at early C and it remains valid after the allowed source edits. The order is: source and real winner $\to$ actual gap $\delta \to N_{\mathrm{far}}$ and finite-label exteriors $\to \nu_0/C_F \to$ block length and ancient-time threshold.

We select the last two quantities only after the previous quantities.

The late N_{far} depends on selected m. We impose no circular $m > N_{\mathrm{far}}$.

The finite spectral data include leading profiles with five k and seventeen ordinary Z derivatives. First correctors have four k and sixteen Z derivatives.

The data also include the finite extra eigenvalue and pressure derivatives in Section 1.30.12. Eighteen source Z jets suffice for the displayed first-symbol products.

The smooth actual source permits these without selection of a new member. The fixed-member weighted upgrade for the macro H^9 domain remains as in Section 1.30.12.

The proof of B1/B2 uses no finite weighted bootstrap: we derive them directly from the leading source, and this avoids that possible cycle.

This proves the frozen spectral and small-viscosity hypotheses for the independent fixed-block packet comparison. It does not itself prove that comparison, its nonautonomous S1/S2 estimates, the completed-wave clock, or the nonlinear theorem.

In particular the later propagation argument is not used to justify (1.30.20). The joint gauge gives $Q_\gamma \geq c_L Q$.

□

1.30.18 Actual-member admission of the retained model

The argument uses the actual scalar hold and the five-polynomial return correction of Lemma 1.27.5. It also uses the source-form bound of Lemma 1.27.1 and the true-domain weighted resolvent identity of Section 1.30.6.

It does not use an old retained-slope dispersion or a full-frequency theorem as an input.

The protected old chart. Select a closed radial interval strictly inside the unedited scalar power hold and a central collar $|\eta| \leq \eta_0 < 1$. There $U = 0$ and $F(\frac{\hat\xi^2}{2}) = F_g((\hat\xi/\hat\xi_c)^2)^{-1-\nu_c}$ is independent of η.

Since $Q - Z^2Q^{2h} = 1$ and $\eta = ZQ^{h-\frac12}$, one has $Q = (1-\eta^2)^{-1}$. With $r_c(\eta) = \sqrt{\hat\xi_c^2 Q}$ and $r_0 = \hat\xi_c$, the actual old component then satisfies

$$\begin{aligned} \Omega_{\mathrm{old}}(r_c(\eta)e^{d\xi}, \eta) &= \Omega_g(1-\eta^2)^{1+h}e^{-2(1+\nu_c)d\xi}, \\ s_0(\eta) &= -2(1+\nu_c)\Omega_g(1-\eta^2)^{1+h}. \end{aligned} \tag{1.30.21}$$

We define s_0 as a derivative with respect to physical log-radius. This derivative does not run along the center that depends on the parameter.

Fix $\eta_1 < \eta_0$ and $a > 0$ so that $|\eta| \leq \eta_1$, $|\log(r/r_c)| \leq a$ stays in this hold. For $s_g = -2(1+\nu_c)\Omega_g$, admissible bounds on $|s_0|, |s_0'|, |s_0''|$ are, in this order,

$$M_0 = |s_g|, \quad M_1 = 2(1+h)|s_g|\eta_1, \quad M_2 = 2(1+h)|s_g|\{1 + 2h\eta_1^2(1-\eta_1^2)^{h-1}\}.$$

The old radial cutoff and the five return bumps of Lemma 1.27.5a lie outside a smaller such rectangle. The trial columns are defined at all angles in the native radial coordinate. The amplitudes solved for here are central.

We add the main perturbation to this old component. We do not replace the old component. Fresh rank supports avoid $\xi = 0$.

Their fields and their returns vanish near the center that depends on the parameter for each η. Thus these bounds and the old center germ remain unchanged by controls.

We keep the main-envelope contribution to the center separately below. For $|y| \le Y_*$ put $\ell_m = r_0 L_\zeta / m$ and impose $\ell_m Y_* \le \min\{\eta_1/2, \eta_{\mathrm{G10}}\}$, with η_{G10} of the main-edit support condition.

Then

$$\|s_0(\ell_m y)/\Delta\|_{C^2_y} \le \frac{M_0}{\Delta} + \frac{\ell_m M_1}{\Delta} + \frac{\ell_m^2 M_2}{\Delta}. \tag{1.30.22}$$

The value term is $O(C^{-1-\sigma})$. The early choice of C makes it small. After L_ζ, we select m large enough to make the derivative terms small.

The limit model has no α, b dependence in s_0, since we fix its center and old source. We do not omit finite-width pullback derivatives. They enter the next modulus.

One comparison on the full width bracket. Select the retained contour and positive-α compact phase chart by (1.30.8), then fix the rounding. Use $J_d = [a_-/m, a_+/m]$ with $a_\pm = \alpha_\sigma \pm \delta\alpha$ from (1.30.13). Its image under $d \mapsto md$ contains the rounded maximum.

On $|\xi| \le M$, Taylor's formula in (1.30.21) gives

$$\left| \frac{\Omega_{\mathrm{old}}(r_c e^{d\xi}) - \Omega_{\mathrm{old}}(r_c)}{d} - s_0(\eta)\xi \right| \le K_C d M^2 e^{K_C d M}.$$

After two α, b, y derivatives the same estimate holds with a larger fixed polynomial in M. $\Re D \ge g$ controls reciprocal Doppler denominators.

The rounded perturbation is one fixed smooth scaled template. The nonvanishing old rotation/product terms keep their different normalized amplitude and form allowances: we do not put them in a vanishing modulus.

Let u denote the trial controls t, together with the curvature amplitude when it is held fixed. Write $\mathfrak{d}_d(y, u)$ for the five outgoing moment discrepancies before the return bumps are added, with $\eta = \ell_m y$. On the fixed radial hull of the edits, $x = \frac{1}{2} 2\log(\hat\xi/\hat\xi_c)$ is independent of η. Thus at fixed $\hat\xi$ the main template $\kappa_\sigma(x/d)\chi_m(x)$ is bounded and every y derivative of its envelope acts on $\mathfrak{t}(y)$. The trial templates depend on x/d and their slow angular factors are evaluated at $\ell_m y$. Conversion between (Ω, W) and (H, U) uses smooth bounded factors on this hull, which is separated from $\hat\xi = 0$. It follows that the edits $(\delta H, \delta U)$ and their mixed (y, u) derivatives through order four are $O_C(d\Delta)$ on a fixed trial ball, uniformly for $\ell_m \le \ell_0$.

Each difference of the five densities (1.27.10) contains at least one edited factor. The unedited factors and the moment weights have bounded derivatives on the hull. Integration over its fixed $\hat\xi$ interval therefore gives $\|\mathfrak{d}_d\|_{C^4_{y,u}} \le K_C d\Delta$, uniformly on any fixed y interval containing both the phase chart and $[-Y_*, Y_*]$, once m is large enough that $|\ell_m y| \le \eta_1$ there. The same estimate holds for each partial integral, uniformly in its upper limit. With a_+/m sufficiently small, the outgoing discrepancies lie in the inverse ball of Lemma 1.27.5. On the disjoint return supports the equation is exactly

$$L_{\ell_m y} z + Q_{\ell_m y}(z, z) = -\mathfrak{d}_d(y, u).$$

Its linear and quadratic coefficients are integrals of fixed shapes and smooth background factors, so their first four y derivatives are uniformly bounded. The inverse of $L_{\ell_m y}$ is uniform there. The

small solution has $|z| \le K_C d\Delta$, and the derivative of the left side in z has a uniformly bounded inverse on a smaller fixed ball. After differentiation in (y,u), each term other than this derivative times the highest derivative of z contains a derivative of $\mathfrak{d}_d$ or a lower derivative of z, including z itself. Induction gives

$$\max_{j+|\gamma|\le 4} \sup_{y,u} \left|\partial_y^j \partial_u^\gamma [z(\ell_m y, u, d)]\right| \le K_{\mathrm{bank}}(C) d\Delta, \qquad d \in [a_-/m, a_+/m]. \tag{1.30.23}$$

With the templates and trial ball fixed, the constants are independent of m, d, L_ζ for $\ell_m \le \ell_0$. The moments are independent of the spectral variables α, b. Substitution into the five densities gives the same bound for partial history changes through the return supports. For j physical angular derivatives of z at fixed u, the right side is multiplied by ℓ_m^{-j}. In particular $d/\ell_m \le a_+/(r_0 L_\zeta)$ in the source-cone estimate.

A derivative in the frozen curvature amplitude a differentiates a trial supported on a radial interval of length $O_C(d)$. Thus $\partial_a \mathfrak{d}_d = O_C(d^2)$ and $\partial_a z = O_C(d^2)$. Inserting the selected $\theta(\eta)$ contributes $O_C(d^2\|\theta'\|_\infty)$ to the first angular derivative of the returns, which tends to zero since $\|\theta'\|_\infty = O_C(m)$ for the fixed cutoff. For each fixed m, the moment integrands and their (y,u) derivatives are continuous in $d > 0$ and dominated on the fixed hull throughout the bracket. The implicit equation gives the same continuity for z and these derivatives.

Reserve a descending exponential-weight ladder in the true-domain resolvent identity before selection of d. The principal pullback obeys $|A_d'/A_d| \le d$.

Each of the two parameter derivatives consumes one fixed weight gap. The old and return multipliers have at most polynomial growth times $e^{Kd|\xi|}$.

A cutoff at $|\xi| = M$ thus bounds the local Green comparison and its first two phase derivatives by

$$\Phi_C(m, M) = K_C \left\{ \frac{a_+}{m} P(M) e^{K_C a_+ M/m} + e^{-\beta M} + \sup_{0<d\le a_+/m} d^{-N} e^{-c_C/d} \right\}. \tag{1.30.24}$$

We also include the stated persistent and rounding terms. Here P is a fixed polynomial, $N < \infty$, and $\beta, c_C > 0$.

The last term includes the true distant returns in (1.30.23) and all fixed old pieces.

Their global contribution is only form-small.

Only this weighted local response is exponential. Axis and exterior conditions remain those of the true-domain inverse.

First select M for the middle term. Then select one lower integer threshold for the other two, with one bound for each $d \in J_d$ and each later m. The supremum tends to zero.

Formula (1.30.22) bounds the remaining variation of the retained model over the phase chart.

The rounded layer-to-point estimate is $O(\sqrt{\sigma_{\mathrm{round}}})$. Its differentiated L^1 bounds follow from the fixed smooth template and the reciprocal-Doppler derivative bounds.

Differentiated resolvent identities and contour Cauchy integrals transfer the same estimates to the simple root and its two phase derivatives. The contour minimum is that of the determinant, fixed after (1.30.8).

Thus the actual source root is continuous in d and C^2-close with one comparison modulus on the full bracket. This establishes the width-comparison input for the retained determinant.

Rank and the shared source margins. At $b = y = 0$ the limit rounded pole pencil is free outside the corners. Its exterior solution is $C_e e^{-\alpha\xi}$, and $D = \mu_D + i\alpha(V_{\mathrm{offset}} + s_g\xi)$.

The kernels (1.30.11) and (1.30.12) are thus its actual limit responses. Use the fixed bumps and R_0 of (1.30.13), and write $r_C = R_0^{-1}$. Their scaled support radii times d are smaller than a

for late m. Let $M_{j,d}^{\mathrm{pre}}$ denote the normalized pre-centering response at $\alpha = md$. The local Green comparison at fixed rounding and pole response, (1.30.23)–(1.30.24), and the exponentially small local contribution of the differentiated returns give

$$\max_j \sup_{d\in J_d} \|M_{j,d}^{\mathrm{pre}} - M_j(md)\| < \frac{1}{8R_0}$$

for all sufficiently large m. For the axial response the comparison is taken in b before restoring the factor $r_0 d$ from ∂_k, as in Lemma 1.30.36. The retained comparison already contains the fixed rounding and old slope. Together with (1.30.13) this gives a distance less than $1/(4R_0)$ from $M_j(\alpha_\sigma)$, uniformly on J_d. The Neumann series gives an inverse norm at most $4R_0/3$.

On a nonzero clipped-ramp plateau, the actual Ω_0 includes a constant $O(d\Delta)$ main offset. It is not Ω_g: $s_g(s_g + 2\Omega_g) = 4\nu_c(1+\nu_c)\Omega_g^2$ is the LIMITING identity only.

Impose in addition $(a_+/m)\Delta \le \epsilon_{\mathrm{rank}}\nu_c|\Omega_g|$ and the analogous old Taylor-variation bound on the selected finite support, with ϵ_{rank} fixed small after the kernel constants and R_0. We include these finite-width errors in (1.30.24).

Include their sum with the return errors in the preceding $1/(8R_0)$ finite-width budget. The threshold is finite because we fix ν_c, Ω_g before m.

The raw axial inverse still costs d^{-1}.

The pole comparison first gives fixed $0 < c_A < C_A$ with

$$|a_m^2\lambda_{kk}/h^2| \le C_A\Delta, \qquad -C_A\Delta \le a_m^2\Re\lambda_{kk}/h^2 \le -c_A\Delta$$

on the late bracket. The complex bound uses the full complex local C^2 comparison, not only its real part.

Physical $\lambda_{kk} = \mu_{D,kk}$. Select one C_q for this full interval.

More explicitly, put $B = 1 + 2(\frac{1}{2} - h)/h$, $b = B/2$ and $X = -\frac{1}{2}(a_m^2\Re\lambda_{kk}/h^2)C_q/\Delta$. Select C_q so $X > b$ and

$$X - b/2 - \sqrt{X^2 - bX} = \frac{b^2}{4(X - b/2 + \sqrt{X^2 - bX})} \le 1/16. \tag{1.30.25}$$

This leaves half the necessary $1/8$ reserve.

Also require $\delta_q = c_A C_q^2 - |B|C_q > 0$. Reserve $|\Re(\mu_{D,ZZ,\mathrm{base}}/a_m^2)| \le \delta_q/(4\Delta)$ by the envelope and late-coordinate bounds below.

More precisely, $\ell_m = L_\zeta/a_m$, $y = \eta/\ell_m$, and $\eta_Z(0) = 1$, $\eta_{ZZ}(0) = 0$. For the retained pre-edit source root at fixed $\alpha = md$ one has

$$a_m^{-2}\Re\lambda_{ZZ}^{\mathrm{pre}}(0,0) = L_\zeta^{-2}\partial_y^2\Re\mu_d^{\mathrm{pre}}(\alpha,0,0).$$

The center Doppler term is imaginary. Use the compact retained-branch C^2 bound in the normalized variable y, including the previously fixed rounding error. Denote its bound on the closed α bracket by $M\Delta$, chosen before L_ζ; include the lower centerings by enlarging to $(M+1)\Delta$ for large m. Require $L_\zeta^2 \ge 4(M+1)\Delta^2/\delta_q$. This gives the displayed real base reserve in the same units as the prescribed curvature. The real target-minus-base increment is then at most $-3\delta_q/(4\Delta)$. We next select L_ζ for the first-angular and history bounds and require $K_{\mathrm{env}}\Delta/L_\zeta^2 \le \epsilon_J/(3\Delta)$.

The exact center calculation, with the main-envelope value, gives

$$|m\Omega_c''/a_m^2| \le \frac{K_{\mathrm{bg}}(C)}{m} + \frac{K_{\mathrm{env}}\Delta}{L_\zeta^2} + \frac{K_{\mathrm{geo}}\Delta r_0^2}{m^2}. \tag{1.30.26}$$

For old, $\Omega_c''(0) = -2(1+h)\Omega_g$. The main center value is $O(d\Delta)$, its envelope derivative is $O(d\Delta a_m^2/L_\zeta^2)$, and slow geometry costs $O_C(d\Delta)$.

Since $md \in [a_-, a_+]$, these give the displayed uniform bound. Away-center controls and returns do not change it.

Impose

$$m_0 \geq 3K_{\mathrm{bg}}(C)\Delta/\epsilon_J, \qquad m_0^2 \geq 3K_{\mathrm{geo}}\Delta^2 r_0^2/\epsilon_J.$$

Together with the slow-coordinate threshold, these bound the center term by ϵ_J/Δ throughout the bracket.

The same local C^2 comparison and envelope scaling give $|\mu_{D,ZZ,\mathrm{base}}/a_m^2| \leq K_{\mathrm{base}}/\Delta$ after lower centerings. The choice of L_ζ bounds the base envelope term.

The factors m^{-1}, m^{-2} bound the old and geometric terms. The applied centerings are polynomial-times-exponentially small.

Set

$$K_q = C_A C_q^2 + |B| C_q, \qquad V_q = K_{\mathrm{norm}}(2R_0)(K_q + \epsilon_J + K_{\mathrm{base}}).$$

Use the actual λ_{kk} and the exact imaginary center term in the target-minus-base solve. The coefficient then obeys $|v_m| \leq V_q/\Delta$.

We count the rank inverse once. Select ϵ_J and the base-envelope allowance below the strict real negative-target reserve.

The finite-dimensional nonlinear remainder is uniform on a fixed amplitude ball by the same contour and polynomial return correction derivative bounds.

For precision, use the same normalized local trial-amplitude vector a in the return correction, response and actual-pencil form estimates. The angular quadratic channel is $a = \theta$ up to a fixed norm-equivalence factor.

We include the polynomial d^{-1} conversion in the raw axial channel when we measure the earlier centering vector in these coordinates. Let $r_B > 0$ be a trial-input radius for the polynomial return correction, with half its discrepancy domain reserved for the pre-control $O_C(d\Delta)$ error.

Let M_Γ bound the pre-control inverse on its compact contour in the actual form spaces, with $E_{d,b}$ at nonzero b. Let K_Γ bound the trial-plus-return correction pencil's Lipschitz variation in those same spaces.

The normalized finite trial map and the whole-bracket comparison give one set of these bounds for all late widths. Select

$$r_\Gamma \leq (4M_\Gamma K_\Gamma)^{-1}.$$

If $K_\Gamma = 0$ this restriction is unnecessary.

The resolvent identity then keeps the contour inverse throughout this amplitude ball.

Let $r_R > 0$ be a ball for the bounded first two response derivatives. If K_R bounds variation of the normalized response matrix, set $r_{\mathrm{rank}} \leq (8R_0K_R)^{-1}$, and drop this restriction when $K_R = 0$.

Here the base matrix is the actual one after the lower centerings. The pre-centering matrix is within $1/(4R_0)$ of its retained value at α_σ by the two preceding $1/(8R_0)$ bounds. Increase the late-integer threshold until the change from the lower centerings, including the polynomial raw-axial conversion, is less than $1/(4R_0)$ uniformly on J_d. The post-centering distance is then below $1/(2R_0)$, giving base inverse norm at most $2R_0$.

Continuation in this amplitude ball is at most $4R_0$. The target solve above uses the base inverse in V_q, not this continuation bound a second time.

Reserve a radius $r_{\mathrm{form}} > 0$ for the independent frozen angular amplitude. In Lemma 1.30.4 and Corollary 1.30.5 take $\Theta_e = r_{\mathrm{form}}$: first leave strict room in both bulk allowances at $\Theta_e = 0$, then

choose $\Psi_2 r_{\mathrm{form}}$ smaller than the room on both comparison sets. The common constants in these bounds are fixed before the late width. Put

$$r_* = \min(r_B, r_\Gamma, r_R, r_{\mathrm{rank}}, r_{\mathrm{form}}) > 0, \qquad K_\chi = \tfrac{1}{2} \sup_z |z^2 \chi(z)|, \tag{1.30.27}$$

with K_χ enlarged by the fixed finite-channel norm conversion. This is an amplitude ball, not a requirement that the possibly large second-jet coefficient v_m be small.

Section 1.30.2 gives the actual strict cone and partial-history tolerance $\epsilon_{\mathrm{src}}(C) > 0$. It applies on the unedited hold, the selected trial intervals, and the full return hull.

We do not infer it from spectral coercivity. Select $c_{\mathrm{cut}} > 0$ so

$$\begin{aligned} K_{\mathrm{hist}} \frac{c_{\mathrm{cut}} V_q}{e_g \Delta} < \epsilon_{\mathrm{src}}(C)/8, \qquad K_{\mathrm{rad}} \frac{c_{\mathrm{cut}}^2 V_q}{\Delta} < \epsilon_{\mathrm{src}}(C)/8, \\ K_{\mathrm{form}} \frac{c_{\mathrm{cut}}^2 V_q}{\Delta} < \eta_{\mathrm{extra}}/8, \qquad K_\chi \frac{c_{\mathrm{cut}}^2 V_q}{\Delta} < r_*/4. \end{aligned} \tag{1.30.28}$$

For the compactly supported curvature cutoff also impose $c_{\mathrm{cut}} \sup\{|s| : \chi(s) \neq 0\} < L_\zeta Y_*$. Then its support lies in the main axial envelope range. We keep its maximum amplitude small enough for the quadratic remainder bound below.

We keep the same flat cutoff factor. There is no lower bound on c_{cut}. Explicitly: let K_R bound the variation of the normalized response matrix on the phase chart. The real linear increment is then at most $-\frac{\delta_q}{2\Delta} \frac{1}{2} \widehat{\zeta}^2 \chi$ on the smaller chart of radius $\rho_{\mathrm{sm}} = \min\{\rho_{\mathrm{chart}}, \delta_q/(4V_q K_R)\}$. Let $\delta_{\mathrm{int}} > 0$ be the fixed deficit of $\Re\lambda$ below $\Re\lambda_0$ outside this smaller chart, given by the strict Hessian and the global exclusion, and let K_{lip} bound the Lipschitz dependence of the simple root on the control amplitude (Theorem 1.30.30). We also require $K_{\mathrm{lip}} K_\chi c_{\mathrm{cut}}^2 V_q/\Delta < \delta_{\mathrm{int}}/2$.

We use no high derivative of the next selected field in this choice. Thus $\sup|\theta| \leq K_\chi c_{\mathrm{cut}}^2 V_q/\Delta$.

Enlarge the same late-integer threshold. The previous centering vector, with its raw-axial polynomial conversion, must then have norm less than $r_*/4$ throughout the width bracket. We also impose that the pre-control return correction discrepancy uses less than its reserved half-domain.

The total control amplitude is then below $r_*/2$, and the full segment used for Taylor's theorem lies in each ball above.

The source/history/form inequalities remain different conditions. Neither they nor the analytic-ball condition alone implies the others.

All are finitely many upper bounds on c_{cut} and late lower bounds on m. At the center, with derivatives taken in $\widehat{\zeta}$, $\theta = \theta' = 0$ while $\theta'' = v_m$.

Exactness of the centering and curvature identities. Freeze the selected label and write $\Lambda(\eta, k, a)$ for the physical eigenvalue of the band when the curvature-control amplitude vector is frozen at the constant value a, with all lower controls in place and with the return coefficients $z(\eta, t, a, d)$ of the same five-equation system. For each fixed m, d, Theorem 1.30.30, applied below with $y = \eta/\ell_m$, gives a C^2 function Λ near $(0, 0, 0)$. The final band is $\lambda(\eta, k) = \Lambda(\eta, k, \theta(\eta))$, and $\theta(0) = \theta_\eta(0) = 0$, $\theta_{\eta\eta}(0) = a_m^2 v_m$. The chain rule therefore gives, exactly,

$$\lambda(0, k) = \Lambda(0, k, 0), \qquad \lambda_\eta = \Lambda_\eta, \qquad \lambda_{\eta k} = \Lambda_{\eta k}, \qquad \lambda_{\eta\eta} = \Lambda_{\eta\eta} + a_m^2 \, \Lambda_a \cdot v_m,$$

all at the origin with $a = 0$. Hence the curvature control does not change λ_k, λ_{kk} (which depend only on $\lambda(0, \cdot)$), nor the zeros $\lambda_Z = \lambda_{Zk} = 0$ produced by Lemma 1.30.36; and λ_{ZZ} is an *affine* function of v_m. Since $\eta = ZQ^{h-\frac{1}{2}}$ is odd in Z with $\partial_Z \eta(0) = 1$, Z- and η-jets at the center agree through order two. Its linear part Λ_a is the angular response matrix M_Ω with its return correction,

whose real 2×2 form has inverse at most $2R_0$. Thus (1.32.2) is a real 2×2 linear system for v_m with right side the target minus the post-centering base. Its unique solution makes the complex identity hold exactly with the real number $q = a_m^2 C_q/\Delta$ and with the actual post-centering λ_{kk}, which the control leaves unchanged. No nonlinear remainder enters this identity. The analytic expansion (1.30.16) is used only for $\eta \neq 0$.

The dependence of Λ on the curvature control is through the value $\theta(\eta)$ in the frozen column. The frozen operator (1.29.1) is columnar: it contains no Z-derivatives of the source. The five-moment return inverse of Lemma 1.27.5 is pointwise in η, so its coefficients are $z(\eta, t, \theta(\eta), d)$.

In Definition 1.30.11 the independent amplitude τ is the variable a of $\Lambda(\eta, k, a)$. Both pencils contain the same angular profile $\sum_j \tau_j w_{e,j}$, including its first and second radial derivatives. Estimate (1.30.23) controls the mixed derivatives of the five return coefficients on this trial ball. The bulk allowance and the two retained determinant margins hold for every $|\tau| \le r_*$. Thus Lemmas 1.30.18 and 1.30.23 and Theorem 1.30.30 give a C^4 simple root in the joint variables before setting $\tau = \theta(\eta)$. At fixed m, d, $y = \eta/\ell_m$ and $b = kr_c(\eta)d$ are smooth, and the Doppler translation of (1.30.15) gives the physical root used above.

No absolute C^2-smallness claim replaces the factor-preserving negative-increment proof.

Last take one integer above a list of thresholds. The list is support containment, (1.30.22), (1.30.23), (1.30.24), rank convergence, finite-label overlap, actual errors in the return correction source, and

$$K_C\{p_C(m)e^{-c_C m} + p_C(m)^2 e^{-2c_C m}/c_{\mathrm{phase}}\} < c\Delta(a_-/m)^2/4.$$

We fix all constants before this selected integer. The corrected continuous width IVT selects one actual member.

The previous choices make the persistent old errors smaller than their stated margins. We compare only genuinely exponential defects with its neighbor gap.

Later pressure, adjoint and weighted profile constants belong to this finite source. This admission uses the leading source constructed above.

1.30.19 Typed local Green, determinant and physical control interfaces

Main result. Lemma 1.30.33 transfers the typed local Green estimate to the actual determinant. Lemma 1.30.36 then gives the actual six-real control map, with all return corrections.

For the two results, assume the admitted source and correction family from the construction.

All constants below refer to one source after we fix its finite future geometry, with the added length L_o. The construction supplies the actual source and the admissible return correction. We do not infer it from a spectral model.

We fix the rounded main templates and a compact parameter set $p = (\alpha, b, y)$ with $\alpha \ge \alpha_* > 0$. We also fix a translated complex contour with a positive buffer in $\Re\mu \ge g$.

In the local Green and determinant estimates below write $t = (t_6, \tau)$, where $t_6 = (a, \mathsf{b}, c) \in \mathbb{R}^6$ denotes the six lower controls and $\tau \in \mathbb{R}^2$ is the independent frozen curvature amplitude. Use a fixed compact product $\mathcal{T} = \mathcal{T}_6 \times \overline{B}(0, r_*)$, with $\mathcal{T}_6$ inside the admitted lower-control ball and the product inside the joint return domain. The radii may be decreased before the cutoff choice in (1.30.28).

Widths range over $J_d = [a_-/m, a_+/m]$. No derivative with respect to d is necessary. The definition of a bulk inverse excludes the main layers. The exact scalar operator and the retained rounded model are displayed in Propositions 1.30.9, 1.30.10 and Definition 1.30.11.

1.30.19.1 The true-domain inverse and the local norm

Let $w(\xi) = \langle \xi \rangle$ and

$$H^1_\beta = \{u : e^{\beta w} u \in H^1(\mathbb{R})\}, \qquad H^{-1}_\beta = \{f : e^{\beta w} f \in H^{-1}(\mathbb{R})\}.$$

The second definition uses multiplication of distributions, with the related pullback norm. For the actual principal coefficient $A_d^2 = \alpha^2 + b^2 e^{2d\xi}$ use the true form domain

$$E_{d,\beta} = \{u \in H^1_\beta : be^{d\xi} e^{\beta w} u \in L^2\}.$$

In particular, the domain is not declared independent of b or d.

The lower-order bulk terms satisfy the actual relative form allowance, strictly below one, after the main layers have been removed. In the original Liouville form these terms are multiplication forms and the small geometric first-order term. This first-order term has coefficient $|A_d'/A_d| \le d$.

Lemma 1.30.7 (Weighted bulk inverse and its typed derivatives)**.** *For sufficiently small fixed $\beta_0 > 0$ and all sufficiently late d, the actual bulk inverse $R_d = \mathcal{L}_d^{-1}$ satisfies*

$$R_d : H^{-1}_\beta \longrightarrow E_{d,\beta}, \qquad \|R_d f\|_{H^1_\beta} + \|be^{d\xi} e^{\beta w} R_d f\|_2 \le K_C \|f\|_{H^{-1}_\beta} \quad (0 \le \beta \le \beta_0).$$

For the retained inverse the corresponding target is $e^{-\beta w} E_0$ with $E_0 = H^1$ equipped with its A_0-norm. The adjoints satisfy the respective bounds. Select a finite ladder $\beta_0 > \beta_1 > \cdots > \beta_N > 0$, with $N \ge 12$, before d. (Theorem 1.30.24 uses the explicit ladder $\beta_0 = \frac{1}{2}\alpha_* \sqrt{1-\eta_0}$ with gaps $\beta_0/10$ on $[-\beta_0, \beta_0]$, and $d \le \beta_0/(20K_e)$.)

We take parameter derivatives in the fixed weighted Sobolev spaces of Lemma 1.30.23. For any phase or control parameters u, v,

$$(R_d)_u = -R_d (\mathcal{L}_d)_u R_d, \tag{1.30.29}$$

$$(R_d)_{uv} = R_d (\mathcal{L}_d)_v R_d (\mathcal{L}_d)_u R_d + R_d (\mathcal{L}_d)_u R_d (\mathcal{L}_d)_v R_d - R_d (\mathcal{L}_d)_{uv} R_d. \tag{1.30.30}$$

Each displayed product uses successive ladder levels.

It is not a bounded-perturbation identity on one unweighted operator domain. The same finite construction supplies derivatives with at most two phase derivatives and at most two control derivatives.

Proof. Use the exact Liouville operator of Proposition 1.30.10. The actual source satisfies Hypothesis 1.30.12 by its displayed source/return formulas and Lemma 1.30.13; Lemma 1.30.4 verifies the uniform form allowance of Hypothesis 1.30.15. For $\ell = \ell_m$ and $d \in J_d$, (1.30.23) gives the uniform mixed (y,t) bounds in Hypothesis 1.30.12(d). The physical k derivative is converted using $\partial_k = r_0 d\, \partial_b$ (or $r_c(\eta) d\, \partial_b$ in Section 1.30.19.2), so this conversion introduces no d^{-1} loss. Lemma 1.30.20 then gives the weighted inverse on the true $E_{d,\beta}$ domain, including $b = 0$. The adjoint has the same form allowance. Its exponential-weight argument is unchanged.

Lemma 1.30.18 bounds every required coefficient derivative by $K_C(1+|\xi|)^P e^{K_C d|\xi|}$, with at most a fixed d^{-N} on remote supports; it includes the derivatives of the actual return equations. The multiplication and cross-domain lemmas 1.30.21–1.30.22 put each coefficient between successive weight levels. The difference-quotient proof of Lemma 1.30.23 gives (1.30.29)–(1.30.30) and the mixed list through two phase and two control derivatives. Choose the finite gaps first and then d so that each absorbs $e^{K_C d|\xi|}$. No common unweighted form domain or derivative in d is required. □

We fix a bounded interval I that contains the two main layers and each local trial support, with a strict support buffer. Let $r_I : H^1(\mathbb{R}) \to H^1(I)$ be restriction and let r_I^* be its distributional transpose from $H^{-1}(I) = (H^1(I))^*$ to $H^{-1}(\mathbb{R})$.

Define the actual localized Green operator by

$$G_{d,I} = r_I R_d r_I^* : H^{-1}(I) \longrightarrow H^1(I).$$

Equivalently one may insert smooth cutoffs equal to one on I and use a slightly larger interval. All constants then include those fixed cutoffs.

Pointwise Green-kernel convergence does not replace this operator norm.

Lemma 1.30.8 (One local comparison on the full late width bracket)**.** *Let $G_{\mathrm{ret,I}}$ be the retained rounded bulk Green operator, retaining all nonvanishing old terms. On the compact contour, phase and control set, for each necessary derivative $\partial_p^\gamma \partial_t^\zeta$, $|\gamma| \le 2$, $|\zeta| \le 2$, one has*

$$\|\partial_p^\gamma \partial_t^\zeta (G_{d,I} - G_{\mathrm{ret,I}})\|_{H^{-1}(I)\to H^1(I)} \le K_C\{dP(M)e^{K_C dM} + e^{-\beta M} + d^{-N}e^{-c_C/d}\}.$$

Here N, P are finite, the derivative list and all weight gaps are fixed first, and $d \in J_d$.

We add separately allocated persistent model allowances only when we compare the retained operator to the simpler ideal model. We do not include them in a quantity claimed to vanish.

Proof. Hypothesis 1.30.12 describes the source of the construction (inputs (I4)–(I9) below), and Hypothesis 1.30.15 is Lemma 1.30.4. Theorem 1.30.24 below then bounds every mixed derivative of order at most four in $s = (p, t)$, in particular every $\partial_p^\gamma \partial_t^\zeta$ with $|\gamma| \le 2$, $|\zeta| \le 2$, by $C_A\omega(d)$ for $0 < d \le d_1$, uniformly on the compact contour, phase and control sets. Corollary 1.30.25 turns this into the displayed three-term bound, with N replaced by $N' = N + P$ and $c_C = \min(c_E, \gamma a/2)$, for every $M \ge 1$; take m so large that $J_d \subset (0, d_1]$. The coefficient discrepancy is $O(d)$ times a polynomial-exponential weight on the whole power hold $|\xi| \le a/d$, so the splitting at $|\xi| = M$ is not needed. The persistent model allowances between the retained and the ideal model are Proposition 1.30.32. □

Tags (I1)–(I12) refer to the inputs listed below.

Inputs. We use the conventions of the text: $0 < h < 10^{-2}$; $Q = (1 - \eta^2)^{-1}$ on the central chart (Section 1.30.18); $\Delta = C^\sigma$. Inputs with their line numbers:

(I1) Velocity resolvent system, (1.29.1): $Du - 2\Omega v + p_r = f_r$, $Dv + Bu + iap = f_\theta$, $Dw + W_r u + ikp = f_z$, $u_r + u/r + iav + ikw = 0$; $a = n/r$, $Q = a^2 + k^2$, $D = \Lambda + in\Omega + ikW$, $B = 2\Omega + r\Omega_r$, $C = aB + kW_r$.

(I2) Centered spectral parameter, proof of Theorem 1.30.1 and Section 1.29: $\mu_D = \Lambda + i\beta_n$, $\beta_n = n\Omega_c + kW_c$, $D = \mu_D + in(\Omega - \Omega_c) + ik(W - W_c)$, $\Re D = \Re\mu_D$.

(I3) Scaled variables, proof of Theorem 1.30.1, Section 1.30.19: $\alpha = |n|d$, $b = kr_0 d$ (we use $b = kr_c(\eta)d$; see Remark 1.30.17), $A_d^2 = \alpha^2 + b^2 e^{2d\xi}$, $y = (m/r_0)\eta/L_\zeta$, i.e. $\eta = \ell y$ with $\ell = \ell_m = r_0 L_\zeta/m$ (Section 1.30.18).

(I4) Protected power hold, (1.30.21): $\Omega_{\mathrm{old}}(r_c(\eta)e^{d\xi}, \eta) = \Omega_g(1 - \eta^2)^{1+h}e^{-2(1+\nu_c)d\xi}$, $U = 0$ (hence $W = 0$) on $|\eta| \le \eta_1$, $|\log(r/r_c)| \le a$. The old radial cutoff and the five return bumps lie outside this rectangle (Section 1.30.18). Fresh supports avoid $\xi = 0$.

(I5) Main rounded perturbation and envelope, proof of Theorem 1.30.1: centered profile $V = s_0\xi - \Delta\mathfrak{t}(y)\,\mathrm{clamp}(\xi,-1,1)$, rounded at fixed width σ_{round}, clipped at a physical radius.

(I6) Controls, Section 1.30.3. In a frozen column write

$$\mathcal{V} = \eta\chi(\eta)\sum_j a_j w_{\Omega,j} + \sum_j \tau_j w_{e,j}, \qquad \mathcal{W} = \chi(\eta)\sum_j (\mathsf{b}_j + \eta c_j) w_{U,j}.$$

Then $\delta\Omega = d\mathcal{V}$, $\delta W = d\mathcal{W}$. Derivatives in y here hold τ fixed. The selected field is obtained by evaluation at $\tau = \theta(\ell y)$.

(I7) Return corrections, Lemma 1.27.5 and (1.30.23). The five coefficients multiply fixed physical radial shapes at a positive log-distance from the center. Their mixed (y,t) derivatives through order four are $O_C(d\Delta)$ on the width bracket.

(I8) The pre-implant bounds are (1.30.2). After the main edit, controls and returns, (1.27.3) gives $\|\Omega\|_\infty \le K/C$, $\|r\Omega_r\|_\infty + \|W_r\|_\infty \le K(1+\Delta)$ and $\sup(2|\Omega B| + |\Omega W_r|) \le K(1+\Delta)/C$. At the pole $r\partial_r(\Omega_{\mathrm{bg}} + \Omega_{\mathrm{main}}) = s_g - \Delta$. After subtracting the explicit layers the residual second derivatives have the width-independent bound J_C of Lemma 1.27.1.

(I9) Exponentially small corrections (fresh centerings, pre-control correction vector): mass $p_C(m)e^{-c_C m}$ (proof of Theorem 1.30.1) and size $\mathrm{poly}(d^{-1})e^{-c_C/d}$ (Lemma 1.30.36). These previously selected corrections are held fixed in τ. The full change in the five return coefficients when τ varies is included in (I7).

(I10) Bulk form allowance, (1.27.8), (1.27.9), Section 1.30.19.

(I11) Retained determinant, contour and margins, proof of Theorem 1.30.1, proof of Lemma 1.29.3.

(I12) Local Green operator, Section 1.30.19: $G_{d,I} = r_I R_d r_I^*$, $H^{-1}(I) = (H^1(I))^*$; determinant $K_{d,I} = M_{c_d} j G_{d,I} j^*$ (Lemma 1.30.33).

1.30.19.2 The exact scalar operator and the retained model

Proposition 1.30.9 (Exact elimination)**.** *Let (u,v,w,p) solve (I1) with $f=0$ on an interval where $D \neq 0$, and put $\varphi = ru$. Then $v = -(Bu + iap)/D$, $w = -(W_r u + ikp)/D$, $p = Q^{-1}(-D\varphi'/r + iC\varphi/r)$, and the radial equation equals $D\,\mathcal{E}_r[\varphi]$, where*

$$\mathcal{E}_r[\varphi] = -\Big(\frac{\varphi'}{rQ}\Big)' + \frac{\varphi}{r} + \frac{i}{D}\Big(\frac{C}{rQ}\Big)'\varphi + \frac{2\Omega k(kB - nW_r/r)}{rQD^2}\varphi. \tag{1.30.31}$$

In particular the D' terms cancel exactly. Moreover $rQ\,(C/(rQ))' = C' - C/r - CQ'/Q$, which is the potential of the text (Section 1.30.19).

Proof. The tangential equations give v, w. Substituting them in the divergence equation gives $\varphi'/r - iCu/D + Qp/D = 0$, which is the stated p (equivalently (1.29.7)). In $-D^{-1}\times$(radial equation), the coefficient of φ' is $(1/(rQ))' + (rQD)^{-1}(D' - iC + 2i\Omega n/r)$. Since $D' = in\Omega_r + ikW_r$ and $C = nB/r + kW_r$, the bracket is $in\Omega_r - in(2\Omega + r\Omega_r)/r + 2i\Omega n/r = 0$. The rotation terms combine as $\frac{2\Omega}{rD^2}(-B + \frac{nC}{rQ}) = -\frac{2\Omega k(kB - nW_r/r)}{rQD^2}$, since $Q = (n/r)^2 + k^2$ and $C = (n/r)B + kW_r$. □

We derive the scalar pencil for the positive angular label. Fix η and put $r = r_c(\eta)e^{d\xi}$, $n = \alpha/d > 0$, $k = b/(r_c d)$, so that $kr = be^{d\xi}/d$ and $r^2 Q\,d^2 = A_d^2 := \alpha^2 + b^2 e^{2d\xi}$. Write $x = d\xi = \log(r/r_c)$ and $\theta_d := b^2 e^{2d\xi}/A_d^2 \in [0,1)$.

Proposition 1.30.10 (Log-radial Liouville form)**.** *With* $\varphi = A_d\psi$,

$$A_d\, r\, \mathcal{E}_r[A_d\psi] = -\psi'' + A_d^2\psi + P_d\psi, \tag{1.30.32}$$

$$P_d = V_{\mathrm{geo}} + \frac{iA_d^2}{D}\,\partial_\xi\Big[\frac{\alpha B + be^{d\xi}W_r}{A_d^2}\Big] + \frac{2\Omega\, be^{d\xi}\,(be^{d\xi}B - \alpha W_r)}{D^2}, \qquad V_{\mathrm{geo}} = d^2(3\theta_d^2 - 2\theta_d). \tag{1.30.33}$$

Here $' = \partial_\xi$, $be^{d\xi}W_r = bW_x/r_c$ *and* $\partial_\xi(be^{d\xi}W_r) = bdW_{xx}/r_c$, $B_\xi = d(2\Omega_x + \Omega_{xx})$, *and* $\frac{iA_d^2}{D}\partial_\xi[F/A_d^2] = \frac{i}{D}(F_\xi - 2d\theta_d F)$ *for* $F = \alpha B + bW_x/r_c$.

Proof. One has $d/dr = (rd)^{-1}\partial_\xi$ and $1/(rQ) = rd^2/A_d^2$. Hence $\varphi'/(rQ) = d\,\varphi_\xi/A_d^2$ and $r\,(\varphi'/(rQ))' = \partial_\xi(A_d^{-2}\varphi_\xi)$, so that $r\mathcal{E}_r[\varphi] = -\partial_\xi(A_d^{-2}\varphi_\xi) + \varphi + (\text{potential})\varphi$, with potential $\frac{i}{D}\partial_\xi[(\alpha B + be^{d\xi}W_r)/A_d^2] + \frac{2\Omega be^{d\xi}(be^{d\xi}B - \alpha W_r)}{A_d^2 D^2}$. For $\varphi = A\psi$ one has $A\,\partial_\xi(A^{-2}(A\psi)') = \psi'' + A(A'/A^2)'\psi$. Since $A'/A = d\theta_d$ and $\theta_d' = 2d\theta_d(1-\theta_d)$, this gives $-A(A'/A^2)' = 2(A'/A)^2 - A''/A = d^2(3\theta_d^2 - 2\theta_d)$. □

At $b = 0$, (1.30.32) reduces to the pole pencil $-\psi'' + \alpha^2\psi + i\alpha B_\xi\psi/D$ (proof of Theorem 1.30.1, Section 1.30.19). For general b, (1.30.33) is the explicit form of "the true Liouville scalar bulk" . Here $|V_{\mathrm{geo}}| \le d^2$ replaces the first-order geometric term with $|A_d'/A_d| \le d$ (proof of Theorem 1.30.1, Section 1.30.19).

Main layers and bulk. Write $\Omega_{\mathrm{main}} = -d\Delta\mathfrak{t}(y)\kappa_\sigma(\xi)\chi_m(x)$ (Hypothesis 1.30.12(b)). In $B_\xi = d(2\partial_x + \partial_x^2)\Omega$, the term in which both x derivatives hit $\kappa_\sigma(x/d)$ is $-\Delta\mathfrak{t}(y)\kappa_\sigma''(\xi)\chi_m(x)$. Thus the main-layer coefficient and the remaining bulk are

$$c_d := \frac{-i\alpha\Delta\mathfrak{t}(y)\kappa_\sigma''(\xi)\chi_m(d\xi)}{D}, \qquad m_d := A_d^2 + P_d - c_d, \qquad \mathcal{L}_d := -\partial_\xi^2 + m_d. \tag{1.30.34}$$

The full pencil is $\mathcal{L}_d + c_d$.

The retained rounded model and the ideal model. Let $c_\nu = 2(1+\nu_c)$, $\Omega_\natural(\eta) = \Omega_g(1-\eta^2)^{1+h}$, $s_0(\eta) = -c_\nu\Omega_\natural(\eta)$ (1.30.21), $A_0^2 = \alpha^2 + b^2$.

Definition 1.30.11 (Retained rounded bulk)**.** With $\mathcal{V}, \mathcal{W}$ as in (I6), $\eta = \ell y$, and primes denoting ξ derivatives, put

$$V_{\mathrm{ret}} = s_0(\eta)\xi - \Delta\mathfrak{t}(y)\kappa_\sigma + \mathcal{V}, \qquad D_{\mathrm{ret}} = \mu + i\alpha V_{\mathrm{ret}} + ib\,\mathcal{W}/r_c,$$
$$B_{\mathrm{ret}} = 2\Omega_\natural + V_{\mathrm{ret}}'.$$

The bulk and corner coefficients are

$$P_{\mathrm{ret}} = \frac{i}{D_{\mathrm{ret}}}\left(\alpha\mathcal{V}'' + \frac{b}{r_c}\mathcal{W}''\right) + \frac{2\Omega_\natural b}{D_{\mathrm{ret}}^2}\left(bB_{\mathrm{ret}} - \frac{\alpha}{r_c}\mathcal{W}'\right),$$
$$m_{\mathrm{ret}} = A_0^2 + P_{\mathrm{ret}}, \qquad c_{\mathrm{ret}} = \frac{-i\alpha\Delta\mathfrak{t}(y)\kappa_\sigma''}{D_{\mathrm{ret}}}, \qquad \mathcal{L}_{\mathrm{ret}} = -\partial_\xi^2 + m_{\mathrm{ret}}.$$

This is the pointwise limit $d \to 0$ of (m_d, c_d) at fixed (ξ, μ, p, t, ℓ). It keeps all nonvanishing old terms: the slope s_0 in D and the rotation/product term $2\Omega_\natural b^2 B_{\mathrm{ret}}/D_{\mathrm{ret}}^2$, which is the persistent allowance of proof of Theorem 1.30.1. For the constructed source the retained coefficients are evaluated at $\ell = \ell_m$ for every $d \in [a_-/m, a_+/m]$. Both models in the comparison use this same value of ℓ. The *ideal* bulk is $\mathcal{L}_0 = -\partial_\xi^2 + A_0^2$, with kernel $e^{-A_0|\xi-\zeta|}/(2A_0)$. With point layers $\gamma_\pm\delta_{\pm1}$ its determinant is (1.30.6):

$$\det\begin{pmatrix} 1 + \frac{\gamma_-}{2A} & \frac{\gamma_+ e^{-2A}}{2A} \\ \frac{\gamma_- e^{-2A}}{2A} & 1 + \frac{\gamma_+}{2A} \end{pmatrix} = \frac{\mu^2 - M_{\mathrm{ret}}}{\mu^2 + \alpha^2 S_t^2}, \quad M_{\mathrm{ret}} = \frac{\alpha^2}{A^2}\Big\{\frac{J^2 e^{-4A}}{4} - \Big(S_t A - \frac{J}{2}\Big)^2\Big\} \tag{1.30.35}$$

Hypotheses and coefficient bounds. Fix compact sets $\mathcal{P} = \{(\alpha, b, y) : \alpha_* \le \alpha \le \alpha^*,\ |b| \le b^*,\ |y| \le y^*\}$, with $\ell_0 y^* \le \eta_1/2$, and the compact product $\mathcal{T}$ of lower controls and frozen amplitudes specified in Section 1.30.19. Put $\mathcal{S} = \mathcal{P} \times \mathcal{T}$, $s = (p, t)$, $t = (t_6, \tau)$. The estimates below hold on any family $\mathcal{D}$ of pairs (d, ℓ) with $d > 0$, $0 < \ell \le \ell_0$ on which the hypotheses hold with common constants. In the application, $\mathcal{D}$ consists of $\ell = \ell_m$, $d \in [a_-/m, a_+/m]$ for all sufficiently large integers m. Let Γ be the translated contour with region Ω_Γ. Fix $\rho > 0$ and an open set $U \supset N_\rho := \{z : \operatorname{dist}(z, \overline{\Omega_\Gamma}) \le \rho\}$ with $\Re z \ge g_1 > 0$ on U (Section 1.30.19).

Hypothesis 1.30.12 (Source structure; (I4)–(I9)). In the coordinates (x, η), $x = \log(r/r_c(\eta))$, the frozen fields decompose as

$$\tilde\Omega = \Omega_{\mathrm{bg}} + \Omega_{\mathrm{main}} + \Omega_{\mathrm{ctl}} + \Omega_{\mathrm{rtn}} + \Omega_{\mathrm{exp}}, \qquad \tilde W = W_{\mathrm{bg}} + W_{\mathrm{ctl}} + W_{\mathrm{rtn}} + W_{\mathrm{exp}},$$

where:

(a) (hold, (1.30.21)) for $|x| \le a$, $|\eta| \le \eta_1$: $\Omega_{\mathrm{bg}} = \Omega_\natural(\eta) e^{-c_\nu x}$, $W_{\mathrm{bg}} = 0$ and $\Omega_{\mathrm{rtn}} = W_{\mathrm{rtn}} = 0$;

(b) (main) $\Omega_{\mathrm{main}} = -d\Delta\mathfrak{t}(y)\kappa_\sigma(x/d)\chi_m(x)$, where $\kappa_\sigma = \mathrm{clamp}(\cdot, -1, 1) * \varrho_\sigma$ with a compactly supported even mollifier; $\chi_m \in C_c^\infty$ is fixed in x as the widths vary, with $\chi_m = 1$ on $|x| \le a$, and $\mathfrak{t} \in C^\infty$;

(c) (controls) Ω_{ctl}, W_{ctl} as in (I6), with smooth templates supported in fixed compact subsets of I that avoid $\xi = 0$ and $\operatorname{supp}\kappa_\sigma''$;

(d) (returns) $\Omega_{\mathrm{rtn}} = \sum_i z_i(\eta, t, d)\phi_i(x)$ and similarly for W_{rtn}, with $\phi_i \in C_c^\infty(\{|x| > a\})$. For each $(d, \ell) \in \mathcal{D}$ the coefficients of that member satisfy

$$\max_{j+|\gamma|\le 4} \sup_{|y|\le y^*,\, t\in\mathcal{T}} \left|\partial_y^j \partial_t^\gamma [z_i(\ell y, t, d)]\right| \le K_z.$$

(e) (background) $\sum_{j\le 2,\, l\le 4} \sup_{x\in\mathbb{R}, |\eta|\le\eta_1} (|\partial_x^j \partial_\eta^l \Omega_{\mathrm{bg}}| + |\partial_x^j \partial_\eta^l W_{\mathrm{bg}}|) \le K_S$. Here $\Omega_{\mathrm{bg}} = Q^{-1-h} F_{\mathrm{bg}}$ and $W_{\mathrm{bg}} = Q^{-\frac12-h} U_{\mathrm{bg}}$ are the fields of the leading member before the spectral layers (b)–(d),(f). This item is Lemma 1.30.13: K_S is fixed in step 6 of Section 1.5.2 right after N_{sh}, before L_ζ, c_{cut}, m and d; it may depend on C;

(f) (exponentially small) $\sum_{j\le 2, |\kappa|\le 4} \sup |\partial_x^j \partial_{(\eta,t)}^\kappa (\Omega_{\mathrm{exp}}, W_{\mathrm{exp}})| \le K_E d^{-N_E} e^{-c_E/d}$.

For each fixed (d, ℓ) all fields are C^4 in (η, t), jointly continuous with their derivatives in (x, η, t). The center values are $\Omega_c = \tilde\Omega(0, \eta)$ and $W_c = \tilde W(0, \eta)$.

Lemma 1.30.13 (Background jets before the spectral layers)**.** *Let $(H_{\mathrm{bg}}, U_{\mathrm{bg}})$, $F_{\mathrm{bg}} = H_{\mathrm{bg}}/(\hat\xi^2)$, be the leading profiles (1.6.11) of the leading member as it stands right after the capped-loop frequency N_{sh} is fixed (step 6 of Section 1.5.2). This member consists of the regular-axis core, the activation and termination, the prefix, the pulse and its returns, the stop, shot and A11 maps, the capped loop with its dedicated return correction, the restorations, the future with its rank-one correction and heat collar, and the heat field. It does* not *contain the main layer, the controls (including the curvature control), the five spectral return bumps or the exponentially small corrections of Hypothesis 1.30.12(b)–(d),(f). As in Section 1.30.14 put*

$$\Omega_{\mathrm{bg}} = Q^{-1-h} F_{\mathrm{bg}}(\tfrac{\hat\xi^2}{2}, \eta), \qquad W_{\mathrm{bg}} = Q^{-\frac12-h} U_{\mathrm{bg}}(\tfrac{\hat\xi^2}{2}, \eta), \qquad Q = (1-\eta^2)^{-1}, \quad \tfrac{\hat\xi^2}{2} = \frac{r^2}{2Q}.$$

(i) In the chart $x = \log(r/r_c(\eta))$ of Hypothesis 1.30.12 one has exactly $\frac{\hat\xi^2}{2} = \frac{\hat\xi_c^2}{2}e^{2x}$, so

$$\Omega_{\rm bg}(x,\eta) = (1-\eta^2)^{1+h} F_{\rm bg}(\tfrac{\hat\xi_c^2}{2}e^{2x},\eta), \qquad W_{\rm bg}(x,\eta) = (1-\eta^2)^{\frac12+h} U_{\rm bg}(\tfrac{\hat\xi_c^2}{2}e^{2x},\eta),$$

and $\partial_x = \hat\xi^2\hat\xi^{-1}\partial_{\hat\xi}$ at fixed η, $\partial_\eta|_x = \partial_\eta|_{\hat\xi}$.

(ii) For every $0 < \eta_* < 1$,

$$K_S(\eta_*) := \sum_{j\le 2,\, l\le 4} \sup_{x\in\mathbb{R},\,|\eta|\le\eta_*} (|\partial_x^j\partial_\eta^l \Omega_{\rm bg}| + |\partial_x^j\partial_\eta^l W_{\rm bg}|) \le C_1(1+\tfrac{\hat\xi_{\rm heat}^2}{2})^2\mathcal{N}_h + C_2\mathcal{K}_{\rm heat} < \infty,$$

where $\frac{\hat\xi_{\rm heat}^2}{2}$, $\mathcal{N}_h$ and $\mathcal{K}_{\rm heat}$ are defined in the proof, C_1 depends only on η_* and h, and C_2 only on η_*. Hypothesis 1.30.12(e) holds with $K_S := K_S(\eta_*)$ for every $\eta_1 \le \eta_*$; one may take for η_* the central collar of the protected hold (Section 1.30.18).

(iii) K_S is determined by the data of steps 1–5 of Section 1.5.2 and by $N_{\rm sh}$. It does not depend on the pole interval, the rounding, L_ζ, $c_{\rm cut}$, the control vector t, the curvature amplitude, m, $d = d_m$ or ℓ_m. It may depend on C, $\Delta = C^\sigma$, $N_{\rm sh}$ and the step-5 widths, as step 5 of Section 1.5.2 allows for the higher leading-data jets. In particular the bound of Hypothesis 1.30.12(e) is uniform in d.

Proof. (i) $r_c(\eta)^2 = \hat\xi_c^2 Q(\eta)$ (Section 1.30.18) and $\hat\xi = r/\sqrt{Q}$ give $\frac{\hat\xi^2}{2} = \frac{\hat\xi_c^2}{2}(r/r_c)^2 = \frac{\hat\xi_c^2}{2}e^{2x}$, and $Q^{-1-h} = (1-\eta^2)^{1+h}$, $Q^{-\frac12-h} = (1-\eta^2)^{\frac12+h}$. Since x is a function of $\frac{\hat\xi^2}{2}$ alone, $\partial_x = \hat\xi^2\hat\xi^{-1}\partial_{\hat\xi}$ at fixed η and ∂_η at fixed x is ∂_η at fixed $\hat\xi$. No derivative of r_c occurs in this chart. On the hold, $F_{\rm bg} = F_g((\hat\xi/\hat\xi_c)^2)^{-1-\nu_c}$ gives $\Omega_{\rm bg} = \Omega_g(1-\eta^2)^{1+h}e^{-c_\nu x}$, which is (1.30.21) and Hypothesis 1.30.12(a).

Inputs. All three concern only the pieces listed in the statement.

(L1) *Finite hull and axis.* For every $\hat\xi_1 < \infty$, $H_{\rm bg}, U_{\rm bg} \in C^\infty([0,\frac{\hat\xi_1^2}{2}]\times[-1,1])$. This is Lemma 1.24.1 for the admitted finite choice of the leading construction (its proof uses no slow coefficient, packet stage, completed field or spectral input), together with item N7 of Section 1.25.2 for the capped loop. Near the axis the member is the protected core, whose (F,U,P) are analytic in $\frac{\hat\xi^2}{2}$ with the mixed bounds (1.9.7) (Theorem 1.9.1, item N8 of Section 1.25.2). The loop agrees with the previous construction on the protected curved domain (Proposition 1.19.6). Hence also $F_{\rm bg} \in C^\infty([0,\frac{\hat\xi_1^2}{2}]\times[-1,1])$: near the axis it is the core F, and away from it $F_{\rm bg} = H_{\rm bg}/(\hat\xi^2)$ with $\frac{\hat\xi^2}{2}$ bounded below.

(L2) *Heat exterior.* There is $\hat\xi_{\rm heat} < \infty$ such that $U_{\rm bg} = 0$ and $H_{\rm bg} = (1-\eta^2)^{-h} g_*(\frac{\hat\xi^2}{2}/(1-\eta^2))$, $g_* = c_{\rm bank}g_h + k_f g_f$, for $\hat\xi \ge \hat\xi_{\rm heat}$. For the pre-modulation calibrated field this holds with $\frac{\hat\xi_{\rm heat}^2}{2} = \mathcal{B}_{\max}$ (Corollary 1.13.6, (1.13.52)). For the member of the statement it holds with $\hat\xi_{\rm heat} = \hat\xi_{\rm lead}^+$ defined by

$$\frac{(\hat\xi_{\rm lead}^+)^2}{2} = \max\{M \max_{[-1,1]} R_o, \mathcal{B}_{\max}, \sup_{\hat\zeta} B_{\rm f}(\hat\zeta)\}.$$

Here M is the normalized support bound in Hypothesis 1.15.10(A3) and $B_{\rm f}$ is the terminal edge of (1.15.2) in the forward chart. The pulse and core edits, the loop and its restoration end before R_o by Lemma 1.20.49. The future edits end in the terminal wings and the central heat bank ends at (1.13.52). Above the displayed maximum only the heat pair remains.

(L3) *Heat-mode jets.* By (1.13.35) with $N = 0$, $|y^i g_h^{(i)}(y)| \le C_i y^{-h}$ for $y \ge b_s$. The fast mode solves $2yg'' + yg' + hg = 0$, so $g_f^{(i)} = p_i g_f + q_i g_f'$ with polynomials p_i, q_i in y^{-1}. By (1.13.34), $|g_f| + |g_f'| \le C y^h e^{-y/2}$. Hence $|y^i g_f^{(i)}| \le C_i y^{-h}$ on $y \ge b_s$, and therefore $|(y\partial_y)^k g_*(y)| \le C_k y^{-h}$ for $y \ge b_s$ and $k \le 7$.

(ii) *The hull* $x \le x_h := \frac{1}{2} 2\log(\hat\xi_{\rm heat}/\hat\xi_c)$. Let $R_h = [0, \frac{\hat\xi_{\rm heat}^2}{2}] \times [-\eta_*, \eta_*]$ and

$$\mathcal{N}_h = \sum_{b\le 2,\, l\le 4} \|(\hat\xi^{-1}\partial_{\hat\xi})^b \partial_\eta^l (F_{\rm bg}, U_{\rm bg})\|_{L^\infty(R_h)},$$

which is finite by (L1). For $j \ge 1$, $(\frac{1}{2}\hat\xi\partial_{\hat\xi})^j = \sum_{b=1}^j S(j,b) (\frac{\hat\xi^2}{2})^b (\hat\xi^{-1}\partial_{\hat\xi})^b$ with $S(1,1) = S(2,1) = S(2,2) = 1$. By (i) and the Leibniz rule in η,

$$|\partial_x^j \partial_\eta^l \Omega_{\rm bg}| \le 2^j \sum_{l'\le l} \binom{l}{l'} \|\partial_\eta^{l-l'}(1-\eta^2)^{1+h}\|_{L^\infty[-\eta_*,\eta_*]} \sum_{b\le j} (\tfrac{\hat\xi_{\rm heat}^2}{2})^b \|(\hat\xi^{-1}\partial_{\hat\xi})^b \partial_\eta^{l'} F_{\rm bg}\|_{L^\infty(R_h)},$$

and the same with $(1-\eta^2)^{\frac12+h}$ and $U_{\rm bg}$ for $W_{\rm bg}$. Summing over $j \le 2$, $l \le 4$ gives at most $C_1(1 + \frac{\hat\xi_{\rm heat}^2}{2})^2 \mathcal{N}_h$.

The heat exterior $x \ge x_h$. Here $W_{\rm bg} = 0$, and by (L2) $Q^{-1-h} F_{\rm bg} = Q^{-1-h} Q^h g_*(\frac{\hat\xi^2}{2} Q)/(\hat\xi^2)$, that is

$$\Omega_{\rm bg} = \varphi(y) := \frac{g_*(y)}{2y}, \qquad y = \tfrac{\hat\xi^2}{2} Q = e^s, \quad s = 2x + \lambda(\eta), \quad \lambda(\eta) = \log \tfrac{\hat\xi_c^2}{2} - \log(1-\eta^2).$$

Since $Q \ge 1$, $y \ge \frac{\hat\xi_{\rm heat}^2}{2} \ge \mathcal{B}_{\max} \ge b_s$. Put $\Phi(s) = \varphi(e^s)$. Then $\Phi^{(i)}(s) = ((y\partial_y)^i \varphi)(y) = (2y)^{-1}((y\partial_y - 1)^i g_*)(y)$, so by (L3) $|\Phi^{(i)}| \le C_i y^{-1-h} \le C_i (\frac{\hat\xi_{\rm heat}^2}{2})^{-1-h}$ for $i \le 6$. Let $\mathcal{K}_{\rm heat} := \max_{i\le 6} \sup_{y \ge \frac{\hat\xi_{\rm heat}^2}{2}} |\Phi^{(i)}| < \infty$. By Faà di Bruno's formula,

$$\partial_x^j \partial_\eta^l \Phi(s) = 2^j \sum_{k=1}^{l} \Phi^{(j+k)}(s)\, B_{l,k}(\lambda', \dots, \lambda^{(l-k+1)})$$

for $l \ge 1$, and $\partial_x^j \Phi(s) = 2^j \Phi^{(j)}(s)$. Since λ is smooth on $|\eta| \le \eta_* < 1$, the sum over $j \le 2$, $l \le 4$ is at most $C_2 \mathcal{K}_{\rm heat}$. The two regions cover $x \in \mathbb{R}$, and this proves (ii). For $\eta_1 \le \eta_*$ the supremum in Hypothesis 1.30.12(e) is taken over a smaller set.

(iii) The functions $F_{\rm bg}, U_{\rm bg}$ and the radius $\hat\xi_{\rm heat} = \hat\xi_{\rm lead}^+$ are fixed by the pieces listed in the statement; $\frac{(\hat\xi_{\rm lead}^+)^2}{2}$ is fixed at step 4 by (L2). Each of these pieces is fixed in steps 1–5 of Section 1.5.2, or is the loop of frequency $N_{\rm sh}$, which is the first choice of step 6. Thus (L1)–(L3) are available before the spectral selection. None of the later choices enters $F_{\rm bg}, U_{\rm bg}$: they only add the layers (b)–(d),(f) of Hypothesis 1.30.12. The dependence on C comes through the step-5 widths and $N_{\rm sh}$; Remark 1.25.6 records that no uniformity in these parameters is claimed. □

Remark 1.30.14 (Relation to (M3), and where K_S enters). Lemma 1.32.2 gives tail and jet bounds of the same kind for the *selected* member, in (r, Z). That member contains the main, control and return layers, so those constants depend on the selected m, and they are proved after the selection. Lemma 1.30.13 applies the same three ingredients (axis regularity, the finite hull, the heat tail) to the background, which is fixed before the selection. It uses the profile chart, in which $x = \frac{1}{2} 2\log(\hat\xi/\hat\xi_c)$.

K_S enters Lemma 1.30.4 only through Ψ_1, which multiplies d and $d^{-N_E}e^{-c_E/d}$. It enters Lemma 1.30.18 through K_1, and through it $\omega(d)$, $\omega'(d)$ and the constants of Theorem 1.30.30, whose smallness conditions are met by taking d small. The retained margin (Corollary 1.30.5) does not contain K_S. Since d is selected after C and N_{sh}, a C-dependent K_S is harmless.

This K_S is not the postdrive energy constant K_S of Section 1.15, and it is not $K_S(\Lambda)$ of Lemma 1.20.27.

Hypothesis 1.30.15 (Form allowance; (I10)). There are $\eta_0 < 1$ and $d_0 > 0$ such that for all $(d,\ell) \in \mathcal{D}$ with $d \le d_0$ and all $(\mu, s) \in U \times \mathcal{S}$ one has

$$\Big|\int (m_d - A_d^2)u\bar v\Big| \le \eta_0 \|u\|_{E_d}\|v\|_{E_d}, \qquad \Big|\int (m_{\mathrm{ret}} - A_0^2)u\bar v\Big| \le \eta_0 \|u\|_{E_0}\|v\|_{E_0},$$

with $\|u\|_{E_d}^2 = \|u'\|^2 + \|A_d u\|^2$ and $\|u\|_{E_0}^2 = \|u'\|^2 + A_0^2\|u\|^2$.

Hypothesis 1.30.16 (Retained determinant margin on the counting set). Let $\mathcal{S}_\Gamma \subset \mathcal{S}$ be compact and let $f_{\mathrm{ret}}(z,s) = \det(I + K_{\mathrm{ret},I}(z,s))$ as in Section 1.30.19.4. For each $s \in \mathcal{S}_\Gamma$, $|f_{\mathrm{ret}}| \ge \delta_\Gamma > 0$ on Γ and $f_{\mathrm{ret}}(\cdot, s)$ has exactly one zero in Ω_Γ, counted with multiplicity.

Remark 1.30.17 (Normalization of b). Elsewhere the text writes $b = kr_0 d$, and we write $b = kr_c(\eta)d$. Since $r_c = r_0(1-\eta^2)^{-1/2}$ is smooth on $|\eta| \le \eta_1$, the two choices differ by a smooth y-dependent reparametrization of $\mathcal{P}$. C^4 bounds transfer, with constants depending on η_1.

Let $K_e := 4 + 5c_\nu$, $P := 6$, $N := 4 + N_E$.

Lemma 1.30.18 (Coefficient bounds). *Assume Hypothesis 1.30.12. There is K_1, depending only on the constants in Hypothesis 1.30.12, on $\mathcal{P}, \mathcal{T}, g_1, \sigma$, the templates and Δ, such that the following estimates hold for $|\kappa| \le 4$, $j \le 1$, $(\mu, s) \in U \times \mathcal{S}$ and $(d,\ell) \in \mathcal{D}$ with $d \le d_0$.*

(C1) $|\partial_s^\kappa \partial_\mu^j m_d(\xi)| \le K_1 d^{-N}(1+|\xi|)^P e^{K_e d|\xi|}$ *for all* $\xi \in \mathbb{R}$;

(C2) the same bound without d^{-N} *for* $|\xi| \le a/d$;

(C3) $|\partial_s^\kappa \partial_\mu^j (m_d - m_{\mathrm{ret}})(\xi)| \le K_1(d + d^{-N}e^{-c_E/d})(1+|\xi|)^P e^{K_e d|\xi|}$ *for* $|\xi| \le a/d$;

(C4) $|\partial_s^\kappa \partial_\mu^j m_{\mathrm{ret}}(\xi)| \le K_1(1+|\xi|)^P$ *for all* ξ;

(C5) on I: $|\partial_s^\kappa \partial_\mu^j c_d| + |\partial_s^\kappa \partial_\mu^j c_{\mathrm{ret}}| \le K_1$ *and* $|\partial_s^\kappa \partial_\mu^j (c_d - c_{\mathrm{ret}})| \le K_1(d + d^{-N}e^{-c_E/d})$, *provided* $d(1+\sigma) \le a$.

Proof. Every term of m_d is a product of: (i) the smooth functions A_d^2, θ_d, $b^2e^{2d\xi}$, r_c^{-1}; (ii) field quantities $\tilde\Omega$, $\tilde\Omega_x$, B_ξ – (main density), W_x, dW_{xx}; (iii) D^{-1} and D^{-2}. Here $|D| \ge \Re\mu \ge g_1$, and $\partial_\mu^q D^{-l}$ is bounded by $(l+q)!/(l! g_1^{l+q})$. For (i), for $0 \le q \le 4$, $|\partial_b^q A_d^2| + |\partial_b^q \theta_d| + |\partial_b^q (b^2 e^{2d\xi})| \le K e^{4d|\xi|}$, with $\alpha \ge \alpha_*$. Indeed write $\theta_d = f(be^{d\xi}/\alpha)$, $f(t) = t^2/(1+t^2)$; each fixed derivative of f is bounded on the real line, and a b derivative costs $e^{d\xi}/\alpha$. The same bound holds for the required mixed α derivatives, since α ranges in a fixed compact subset of $(0,\infty)$. The choice $K_e = 4 + 5c_\nu$ includes this corrected envelope; it changes only the subsequent small-d thresholds.

Global bound (C1). At fixed x, the return derivatives in s differentiate $z_i(\ell y, t, d)$ directly. By Hypothesis 1.30.12(d), the resulting field derivatives, including up to two x derivatives, are bounded by $K_z \sum_i \|\phi_i\|_{C^2}$. For the background, each y derivative supplies a factor ℓ in (e). Items (b), (c) and (f) bound the corresponding (y,t) derivatives of the other fields. Hence the derivatives of $(\tilde\Omega - \Omega_c)/d$ and $(\tilde W - W_c)/(r_c d)$ through order four are $O(d^{-1})$. Since $|D| \ge g_1$, at most four such factors occur upon differentiating a reciprocal Doppler denominator. This gives the factor d^{-4} in (C1). For the

field factors in (ii), $B_\xi = d(2\partial_x + \partial_x^2)\tilde{\Omega}$. After subtraction of its corner density the main contribution is the sum of the two bounded terms computed in Lemma 1.30.2(iii). Their (y,t) derivatives are bounded since only $\mathfrak{t}(y)$ varies. The controls contribute bounded multiples of the fixed template derivatives, and the terms from (f) are $O(d^{-N_E-1}e^{-c_E/d})$.

Hold bounds (C2), (C3). For $|\xi| \le a/d$, Hypothesis 1.30.12(a)–(c) give exactly

$$\begin{aligned} V_d &= \Omega_\natural \frac{e^{-c_\nu d\xi} - 1}{d} - \Delta\mathfrak{t}\kappa_\sigma(\xi) \\ &\quad + \mathcal{V}(\xi) + \frac{\Omega_{\exp} - \Omega_{\exp}(0)}{d}, \\ \frac{\tilde{W} - W_c}{d} &= \mathcal{W}(\xi) + \frac{W_{\exp} - W_{\exp}(0)}{d}. \end{aligned}$$

Hence $|V_d| \le K(1+|\xi|)e^{c_\nu d|\xi|}$, up to an exponentially small term, and each D-derivative costs a polynomial factor (C2). By Taylor's formula, $|(e^{-c_\nu d\xi} - 1)/d + c_\nu\xi| \le \frac{1}{2}c_\nu^2 d\xi^2 e^{c_\nu d|\xi|}$. Hence

$$|D - D_{\mathrm{ret}}| \le \tfrac{1}{2}\alpha\Omega_\natural c_\nu^2 d\xi^2 e^{c_\nu d|\xi|} + Kd^{-N_E-1}e^{-c_E/d}.$$

The remaining differences on the hold are as follows.

- $A_d^2 - A_0^2 = b^2(e^{2d\xi} - 1)$.
- $V_{\mathrm{geo}} = O(d^2)$, and $-2d\theta_d F/D = O(d(1+|\xi|)e^{c_\nu d|\xi|})$.
- Modulo the terms of Hypothesis 1.30.12(f), $B - B_{\mathrm{ret}} = 2(\tilde{\Omega} - \Omega_\natural) + \Omega_\natural c_\nu(1 - e^{-c_\nu d\xi})$, where $\tilde{\Omega} - \Omega_\natural = \Omega_\natural(e^{-c_\nu d\xi} - 1) + d(-\Delta\mathfrak{t}\kappa_\sigma + \mathcal{V})$.
- After subtracting the main density, B_ξ equals $2d\tilde{\Omega}_x + d\,\partial_x^2\Omega_{\mathrm{bg}} + \mathcal{V}''$ up to (f). Its retained counterpart is $\mathcal{V}''$.
- $bW_x/r_c = b\mathcal{W}'/r_c$ and $bdW_{xx}/r_c = b\mathcal{W}''/r_c$ up to (f).
- $2\Omega b^2 e^{2d\xi}B - 2\Omega_\natural b^2 B_{\mathrm{ret}} = O(d(1+|\xi|)e^{K_e d|\xi|})$.
- $D^{-q} - D_{\mathrm{ret}}^{-q} = O(|D - D_{\mathrm{ret}}|)$.

On the hold, fix (p, t_6) and put $E = \partial_{\tau_j}\Omega_{\exp}$, $H = \partial_{\tau_j}W_{\exp}$, evaluated at $x = d\xi$. Write E_c, H_c for their values at $x = 0$ in the same column. The returns vanish throughout the hold. With $w = w_{e,j}$,

$$\begin{aligned} \partial_{\tau_j}V_d &= w + (E - E_c)/d, \\ \partial_{\tau_j}B &= w' + 2dw + 2E + E_x, \\ \partial_{\tau_j}B_\xi &= w'' + 2dw' + d(2E_x + E_{xx}), \\ \partial_{\tau_j}(D - D_{\mathrm{ret}}) &= \frac{i}{d}\left[\alpha(E - E_c) + \frac{b}{r_c}(H - H_c)\right]. \end{aligned}$$

The retained field derivatives in the first three rows are w, w', w''. By Hypothesis 1.30.12(f), the last row and its further mixed s-derivatives of order at most three are $O(Kd^{-N_E-1}e^{-c_E/d})$, as are the terms involving E in the first three rows for $d \le 1$. Here $\eta = \ell y$, and r_c^{-1} has bounded derivatives on the chart. In the selected family (I9) fixes the exponential corrections in τ, so $E = H = 0$ and the last row vanishes exactly. In both cases the order-one term $i\alpha w''/D_{\mathrm{ret}}$ is present in the retained variation.

For the reciprocal differences, factor $D^{-q} - D_{\mathrm{ret}}^{-q} = (D_{\mathrm{ret}} - D)\sum_{j=0}^{q-1} D^{-j-1} D_{\mathrm{ret}}^{-(q-j)}$. The product rule leaves one coefficient difference, or a derivative of one, in every term. The hold identities bound each such difference by d times its polynomial-exponential envelope plus (f). A y derivative acts on the same background, envelope and slow control factors in both pencils, with τ fixed. Derivatives of the curvature templates are uniformly bounded on their fixed support. This proves (C3) also for mixed derivatives containing ∂_τ through the stated order. (C4) follows from Definition 1.30.11, since $|V_{\mathrm{ret}}| \le K(1+|\xi|)$ and the templates are bounded. For (C5), $c_d - c_{\mathrm{ret}} = -i\alpha\Delta\mathfrak{t}\kappa''_\sigma(D^{-1} - D_{\mathrm{ret}}^{-1})$ on $\operatorname{supp}\kappa''_\sigma \subset \{|\xi| \le 1+\sigma\}$, where $\chi_m(d\xi) = 1$. □

Remark 1.30.19. If the main and control templates are centered at the fixed radius r_0 instead of $r_c(\eta)$, then in ξ they are shifted by $-\frac{1}{2}\log(1-\eta^2)/d = O(\ell^2/d)$. On $J_d = [a_-/m, a_+/m]$ one has $\ell_m = r_0 L_\zeta/m \le (r_0 L_\zeta/a_-)d$, so the shift is $O(d)$ and (C3) persists.

1.30.19.3 Weighted inverses and the local comparison

Let $w = \langle\xi\rangle$, $\|u\|_{H^1}^2 = \|u'\|^2 + \alpha_*^2\|u\|^2$, and $H^{-1} = (H^1)^*$. Note $\|u\|_{H^1} \le \|u\|_{E_d}$ and $\|f\|_{H^{-1}} \le \alpha_*^{-1}\|f\|_{L^2}$. For $\beta \in \mathbb{R}$ set $H_\beta^{\pm 1} = e^{-\beta w}H^{\pm 1}$ and $E_{d,\beta} = e^{-\beta w}E_d$ (Section 1.30.19). Put

$$\beta_0 := \tfrac{1}{2}\alpha_*\sqrt{1-\eta_0}, \qquad M_0 := \frac{2}{1-\eta_0}, \qquad a_d(u,v) = \int u'\bar{v}' + m_d u\bar{v}.$$

Lemma 1.30.20 (Weighted bulk inverse)**.** *Assume Hypothesis 1.30.15. For $|\beta| \le \beta_0$ and $f \in H_\beta^{-1}$ there is a unique $u \in E_{d,\beta}$ with $a_d(u,\phi) = \langle f, \phi\rangle$ for all $\phi \in C_c^\infty$. Moreover $\|e^{\beta w}u\|_{E_d} \le M_0\|e^{\beta w}f\|_{H^{-1}}$. Extensions for different β agree on intersections. The same holds for $\mathcal{L}_{\mathrm{ret}}$ with E_0.*

Proof. Put $v = e^{\beta w}u$ and $a_\beta(v, v_2) := a_d(e^{-\beta w}v, e^{\beta w}v_2)$. Then

$$a_\beta(v, v_2) = \int v'\bar{v}_2' + m_d v\bar{v}_2 + \beta w'(v'\bar{v}_2 - v\bar{v}_2') - \beta^2 w'^2 v\bar{v}_2.$$

On the diagonal $v'\bar{v} - v\bar{v}' = 2i\Im(v'\bar{v})$, so the first-order term has zero real part. Since $|w'| \le 1$,

$$\Re a_\beta(v,v) \ge (1-\eta_0)\|v\|_{E_d}^2 - \beta^2\|v\|^2 \ge (1 - \eta_0 - \beta^2/\alpha_*^2)\|v\|_{E_d}^2 \ge \tfrac{1-\eta_0}{2}\|v\|_{E_d}^2,$$

and $|a_\beta(v,v_2)| \le (1+\eta_0+2|\beta|/\alpha_* + \beta^2/\alpha_*^2)\|v\|_{E_d}\|v_2\|_{E_d}$. Represent the bounded form on the Hilbert space E_d by $a_\beta(v,\phi) = (Tv,\phi)_{E_d}$. The lower bound on its real part gives $\|Tv\| \ge (1-\eta_0)\|v\|/2$, and the same inequality holds for T^*. Thus T has closed range with orthogonal complement $\ker T^* = 0$. Inverting it on the Riesz representative of the source gives $a_\beta(v,\phi) = \langle e^{\beta w}f, \phi\rangle$ and the stated bound. Then $u = e^{-\beta w}v$ solves the original problem, because $\{e^{\beta w}\phi : \phi \in C_c^\infty\} = C_c^\infty$ is dense in E_d. Uniqueness holds because $a_\beta(v,\phi) = 0$ for all ϕ forces $a_\beta(v,v) = 0$, hence $v = 0$. Consistency of the extensions follows from uniqueness in $E_{d,\min(\beta_1,\beta_2)}$. □

The inverse estimate in Lemma 1.30.7 follows; its parameter-derivative assertions are proved below in Lemma 1.30.23. The real part of the weight commutator vanishes, so no $d\beta$ loss occurs.

For a measurable m and $\gamma > 0$ put $\mathsf{M}_\gamma(m) = \sup_\xi |m(\xi)|e^{-\gamma w(\xi)}$.

Lemma 1.30.21 (Multiplication)**.** $\|e^{(\beta-\gamma)w}mu\|_{H^{-1}} \le \alpha_*^{-2}\mathsf{M}_\gamma(m)\|e^{\beta w}u\|_{H^1}$ *for every real β. If $|m| \le K(1+|\xi|)^P e^{K_e d|\xi|}$ and $K_e d \le \gamma/2$, then $\mathsf{M}_\gamma(m) \le KC_{P,\gamma}$ with*

$$C_{P,\gamma} = \sup_{u\ge 0}(1+u)^P e^{-\gamma u/2} = \begin{cases} 1, & \gamma \ge 2P, \\ (2P/\gamma)^P e^{\gamma/2 - P}, & 0 < \gamma < 2P. \end{cases}$$

Indeed the logarithmic derivative is $P/(1+u) - \gamma/2$, so the maximum for $P \ge 0$ occurs at $u = \max\{0, 2P/\gamma - 1\}$. If in addition $X \ge 2P/\gamma$, then $\sup_{|\xi|\ge X}|m|e^{-\gamma w} \le K(1+X)^P e^{-\gamma X/2}$.

Lemma 1.30.22 (Resolvent identity across form domains)**.** *Let $0 < \gamma$, $\beta - \gamma \geq -\beta_0$, $\beta \leq \beta_0$, and $K_e d \leq \gamma/2$. For $f \in H^{-1}_{\beta}$ one has $R_{\mathrm{ret}} f \in E_{d,\beta-\gamma}$ and*

$$R_d f - R_{\mathrm{ret}} f = -R_d\big[(m_d - m_{\mathrm{ret}}) R_{\mathrm{ret}} f\big] \quad \text{in } E_{d,\beta-\gamma}.$$

The same identity holds with the retained inverse replaced by an actual inverse at (μ', s', d') when $K_e \max(d, d') \leq \gamma/2$.

Proof. Put $u_r = R_{\mathrm{ret}} f$, so that $e^{\beta w} u_r \in H^1$. Since $|b e^{d\xi}| e^{(\beta-\gamma)w} \leq b^* e^{\beta w} e^{(d-\gamma)w}$ and $d < \gamma$, one has $u_r \in E_{d,\beta-\gamma}$. By (C1) and (C4), $\mathsf{M}_\gamma(m_d - m_{\mathrm{ret}}) < \infty$, so $g := (m_d - m_{\mathrm{ret}}) u_r \in H^{-1}_{\beta-\gamma}$ by Lemma 1.30.21. Let $z = R_d f - u_r + R_d g$. For $\phi \in C_c^\infty$, $a_d(z, \phi) = \langle f, \phi \rangle - a_{\mathrm{ret}}(u_r, \phi) - \int (m_d - m_{\mathrm{ret}}) u_r \bar{\phi} + \langle g, \phi \rangle = 0$. Uniqueness in Lemma 1.30.20 gives $z = 0$. □

Lemma 1.30.23 (Differentiability and the word formula)**.** *Assume Hypotheses 1.30.12–1.30.15. Let $\gamma_1 = \beta_0/10$ and $d \leq \gamma_1/(2K_e)$. Then The map $s \mapsto R_d(\mu, s)$ is C^4 into the fixed space $B(H^{-1}_{\beta_0}, H^1_{-\beta_0})$, including at $b = 0$, and is holomorphic there in $\mu \in U$. For each multiset κ of $k \leq 4$ derivative labels,*

$$\partial_s^\kappa R = \sum_{(B_1,\dots,B_l)} (-1)^l \, R\, m_{B_1} R\, m_{B_2} \cdots m_{B_l} R, \qquad m_B := \partial_s^B m, \tag{1.30.36}$$

where the sum runs over ordered *set partitions of the k label positions (75 words for $k = 4$). At each fixed s, each word also maps H^{-1}_{β} to the actual form domain $E_{d,\beta-l\gamma}$ for every γ with $K_e d \leq \gamma/2$ and $-\beta_0 \leq \beta - l\gamma \leq \beta \leq \beta_0$, with norm $\leq M_0^{l+1} \prod_i \alpha_*^{-2} \mathsf{M}_\gamma(m_{B_i})$. The same holds for R_{ret}.*

Proof. Write $\delta = \gamma_1$. At fixed d, (C1) and $K_e d \leq \delta/2$ bound the tails of $e^{-\delta w} \partial_s^\kappa m_d$ by $K_1 d^{-N}(1 + |\xi|)^P e^{-\delta|\xi|/2}$ for $|\kappa| \leq 4$. Together with joint continuity on bounded intervals this gives continuity in M_δ up to order four. By Lemma 1.30.21, multiplication by m_B is therefore $C^{4-|B|}$ with values in $B(H^1_\beta, H^{-1}_{\beta-\delta})$. Use weights in $[-\beta_0, \beta_0]$ throughout. The inclusion $E_{d,\beta} \hookrightarrow H^1_\beta$ has norm at most one for every b. In these fixed spaces the cross-domain identity, with coefficients m_h, m at two nearby parameters and inverses R_h, R, gives

$$\|R_h - R\|_{H^{-1}_\beta \to H^1_{\beta-\delta}} \leq M_0^2 \alpha_*^{-2} \mathsf{M}_\delta(m_h - m).$$

In a coordinate direction the identity

$$\frac{R(s + he_i) - R(s)}{h} + R m_i R = -R(s + he_i)\Big[\frac{m(s + he_i) - m(s)}{h} - m_i\Big] R - (R(s + he_i) - R(s)) m_i R$$

gives $\partial_i R = -R m_i R$ in $B(H^{-1}_\beta, H^1_{\beta-2\delta})$. Indeed the multiplier difference quotient in the first term converges in M_δ, and in the second term m_i and $R_h - R$ each use one gap. Differentiate the products inductively. In a word with l multipliers each multiplier uses one gap and each undifferentiated inverse is continuous with one gap. Differentiating one inverse uses two gaps for that factor, hence at most $(2l + 2)\delta$ in total. For the fourth derivative $l \leq 3$, and continuity of the resulting words costs at most $9\delta < 2\beta_0$. The product rule gives exactly the ordered partitions in (1.30.36). Complex difference quotients give holomorphy in μ by the same identity. For a mixed word of order at most four one further differentiated inverse costs at most 10δ, still within the ladder. The coefficient multipliers are holomorphic at the weaker weight by (C1) and the local Cauchy formula. Finally, at fixed s the leftmost inverse takes values in $E_{d,\beta-l\gamma}$ by Lemma 1.30.20. Applying Lemma 1.30.21 to the l multipliers gives the stated form-norm bound. □

The local comparison. Let $I \supset [-1-\sigma, 1+\sigma] \cup \operatorname{supp}(\text{templates})$ be a fixed bounded interval, and $w_I = \max_I \langle \xi \rangle$. For $|\beta| \le \beta_0$ put $c_I(\beta) = e^{|\beta| w_I}(1 + |\beta|/\alpha_*)$. Then $\|r_I^* f\|_{H_\beta^{-1}} \le c_I(\beta)\|f\|_{H^{-1}(I)}$ and $\|r_I u\|_{H^1(I)} \le c_I(\beta)\|e^{\beta w} u\|_{H^1}$. This follows from $\|\phi v\|_{H^1(I)} \le (\|\phi\|_\infty + \|\phi'\|_\infty/\alpha_*)\|v\|_{H^1(I)}$ and $\|r_I^*\| \le 1$.

Theorem 1.30.24 (Local $C^{2,2}$ Green comparison)**.** *Assume Hypotheses 1.30.12–1.30.15. Put* $\gamma = \beta_0/5$,

$$\omega(d) := K_1 C_{P,\gamma}(d + d^{-N} e^{-c_E/d}) + 2K_1 d^{-N}(1 + a/d)^P e^{-\gamma a/(2d)}, \qquad K_\gamma := 2\alpha_*^{-2} K_1 C_{P,\gamma},$$

and let $d_1 \le d_0$ *satisfy* $d_1 \le \beta_0/(20K_e)$, $a/d_1 \ge 2P/\gamma$, *and* $K_1 d^{-N}(1+a/d)^P e^{-\gamma a/(2d)} \le K_1 C_{P,\gamma}$ *for* $d \le d_1$. *Then for every* $(d,\ell) \in \mathcal{D}$ *with* $d \le d_1$, *every multi-index* κ *in* $s = (p,t)$ *with* $|\kappa| \le 4$ *(in particular every* $\partial_p^{\gamma'}\partial_t^{\zeta}$ *with* $|\gamma'| \le 2$, $|\zeta| \le 2$*), and all* $(\mu, s) \in U \times \mathcal{S}$, *one has*

$$\|\partial_s^\kappa (G_{d,I} - G_{\mathrm{ret},I})\|_{H^{-1}(I)\to H^1(I)} \le C_A\, \omega(d), \qquad C_A = 675\, c_I(\beta_0)^2 M_0^6 \max(1, K_\gamma)^4 \alpha_*^{-2}. \quad (1.30.37)$$

In particular $\le 2C_A K_1 C_{P,\gamma}\, d$ *once the exponential terms are below* $C_{P,\gamma} d$. *Moreover* $\|\partial_s^\kappa G_{\bullet,I}\| \le C_A' := 75\, c_I(\beta_0)^2 M_0^5 \max(1,K_\gamma)^4$ *uniformly for* $\bullet \in \{d, \mathrm{ret}\}$. *Since* $\mu \mapsto \partial_s^\kappa(G_{d,I} - G_{\mathrm{ret},I})$ *is holomorphic on* $U \supset N_\rho$ *(Lemma 1.30.23), Cauchy's estimate gives* $\|\partial_\mu^j \partial_s^\kappa (G_{d,I} - G_{\mathrm{ret},I})\| \le j!(2/\rho)^j C_A \omega(d)$ *on* $\{\operatorname{dist}(\mu, \overline{\Omega_\Gamma}) \le \rho/2\}$ *(Cauchy circles of radius* $\rho/2$*).*

Proof. By Lemma 1.30.23, $\partial^\kappa G_{\bullet,I} = r_I(\partial^\kappa R_\bullet) r_I^*$ is a signed sum of $r_I W_\bullet(\pi) r_I^*$ over at most 75 ordered partitions $\pi = (B_1, \dots, B_l)$, $l \le 4$. Telescoping gives

$$W_d - W_{\mathrm{ret}} = \sum_i X_1^d \cdots X_{i-1}^d (X_i^d - X_i^{\mathrm{ret}}) X_{i+1}^{\mathrm{ret}} \cdots,$$

a sum of at most $2l+1 \le 9$ terms. If $X_i = R$, Lemma 1.30.22 gives $R_d - R_{\mathrm{ret}} = -R_d(m_d - m_{\mathrm{ret}})R_{\mathrm{ret}}$. If $X_i = m_B$, the factor is $\partial^B(m_d - m_{\mathrm{ret}})$. Each resulting word thus has at most 6 inverses and at most 5 multiplications, exactly one of which is a difference. Use weights $\beta_0, \beta_0 - \gamma, \dots, \beta_0 - 5\gamma = 0$. By (C2), (C4) and Lemma 1.30.21, the non-difference factors obey $\alpha_*^{-2}\mathsf{M}_\gamma(\partial^B m_\bullet) \le K_\gamma$. On $|\xi| \le a/d$ this uses (C2); on $|\xi| > a/d$, (C1) and the tail estimate give at most $K_1 C_{P,\gamma}$. The difference factors obey $\mathsf{M}_\gamma \le \omega(d)$: (C3) on the hold, and (C1)+(C4) with the tail estimate outside. Combining with $c_I(\beta_0)c_I(0) \le c_I(\beta_0)^2$ and $75 \times 9 = 675$ gives (1.30.37). The bound C_A' is the same count without telescoping. μ-derivatives are *not* expanded into words: that would need one more weight gap per ∂_μ. They follow from holomorphy and Cauchy's estimate. □

Corollary 1.30.25 (The three-term form)**.** *Under the same hypotheses,* $C_A\omega(d) \le K_C\{d + d^{-N'}e^{-c_C/d}\}$ *with* $K_C = 2C_A K_1(C_{P,\gamma} + (1+a)^P)$, $N' = N + P$ *and* $c_C = \min(c_E, \gamma a/2)$. *Hence, for every* $M \ge 1$, *every polynomial* $P(M) \ge 1$ *and every* $\beta > 0$, *the left side of (1.30.37) is at most* $K_C\{dP(M)e^{K_C dM} + e^{-\beta M} + d^{-N'}e^{-c_C/d}\}$, *because* $d \le dP(M)e^{K_C dM}$. *This is the inequality of Lemma 1.30.8, and also the modulus (1.30.24) uniformly on* J_d.

Corollary 1.30.26 (Continuity in the width)**.** *Fix* ℓ *and an interval of widths* $d \le d_1$ *with* $(d,\ell) \in \mathcal{D}$. *If the returns and the fields in Hypothesis 1.30.12(f), evaluated at* $\eta = \ell y$, *are continuous in* d *with their indicated derivatives, then* $d \mapsto \partial_s^\kappa G_{d,I}$ *is continuous in operator norm on this interval. This follows from Lemma 1.30.22 with* (d', s) *in place of ret and dominated convergence in* M_γ. *For the width selection in Theorem 1.30.1 one fixes* m *and takes the entire bracket* J_d *with* $\ell = \ell_m$.

Remark 1.30.27 (Change of radial coordinate). All derivatives of the localized Green operator and of its Fredholm determinant are taken on the fixed interval I in ξ. To identify the physical pencil at a fixed phase, let $z(0)=0$, $dz = A_d\,d\xi$, and $(Tu)(z(\xi)) = \sqrt{A_d(\xi)}u(\xi)$. Then

$$\|Tu\|^2_{H^1_z} = \|A_d u\|_2^2 + \|u' + (A_d'/2A_d)u\|_2^2.$$

Since $A_d \geq \alpha_*$ and $|A_d'/A_d| \leq d$, $T : E_d \to H^1_z$ and its inverse have uniform bounds. The inverse is $v \mapsto A_d^{-1/2} v\circ z$. The scalar normalization for velocity is $\psi_{\mathrm{ms}} = \sqrt{d}\,T\psi$ by (1.29.4) and $\varphi = ru = A_d\psi$. Changing variables in the form and its forcing identifies the kernels and inverses at this fixed phase. In particular, the bulk inverse composed with the layer form transforms by similarity, since the dual change on the forcing cancels between the two factors. Its determinant after adding the identity is invariant. We obtain the phase derivatives of the centered root from this scalar determinant in ξ, with the exact Doppler translation for the physical root.

1.30.19.4 Determinant, Rouché, and the root with its derivatives

Let $j : H^1(I) \to L^2(I)$ be the embedding, with the norm $\|u'\|^2 + \alpha_*^2\|u\|^2$ on $H^1(I)$. Its singular values are $(\alpha_*^2 + (\pi l/|I|)^2)^{-1/2}$, $l \geq 0$ (Neumann cosines), so

$$\|j\|^2_{\mathfrak{S}_2} = \|j^*\|^2_{\mathfrak{S}_2} = \frac{|I|}{2\alpha_*}\coth(\alpha_*|I|) + \frac{1}{2\alpha_*^2} \tag{1.30.38}$$

Put $K_{\bullet,I} = M_{c_\bullet} j G_{\bullet,I} j^*$ on $L^2(I)$ and $f_\bullet(z,s) = \det(I + K_{\bullet,I}(z,s))$.

Lemma 1.30.28 (Factorization and trace bounds). *(a) $\mathcal{L}_d + c_d$ is invertible $E_d \to E_d^*$ if and only if $f_d \neq 0$. (b) $z \mapsto K_{\bullet,I}$ is holomorphic into $\mathfrak{S}_1$, $s \mapsto K_{\bullet,I}$ is C^4 into $\mathfrak{S}_1$, and*

$$\begin{aligned}\|\partial^\kappa(K_d - K_{\mathrm{ret}})\|_{\mathfrak{S}_1} \leq \|j\|^2_{\mathfrak{S}_2} \sum_{\kappa' \leq \kappa} \binom{\kappa}{\kappa'} \\ \times \Big(\|\partial^{\kappa'} c_d\|_{L^\infty(I)} \|\partial^{\kappa-\kappa'}(G_d - G_{\mathrm{ret}})\| \\ + \|\partial^{\kappa'}(c_d - c_{\mathrm{ret}})\|_{L^\infty(I)} \|\partial^{\kappa-\kappa'} G_{\mathrm{ret}}\| \Big).\end{aligned}$$

By (C5) and Theorem 1.30.24, the right side is at most $C_K\omega'(d)$, with $\omega'(d) = \omega(d) + K_1(d + d^{-N}e^{-c_E/d})$, and $\sup \|\partial^\kappa K_\bullet\|_{\mathfrak{S}_1} \leq B_K$.

Proof. (a) Since c_d is supported in I, the layer form is $\langle M_{c_d}u, v\rangle = \int_I c_d\,u\bar v$, i.e. $M_{c_d} = r_I^* j^* M_{c_d} j r_I$ as a map $E_d \to E_d^*$. Hence $R_d M_{c_d} = \mathcal{A}\mathcal{B}$ with $\mathcal{A} = R_d r_I^* j^* : L^2(I) \to E_d$ and $\mathcal{B} = M_{c_d} j r_I : E_d \to L^2(I)$. Moreover $\mathcal{B}\mathcal{A} = K_{d,I}$, and $\mathcal{L}_d + c_d = \mathcal{L}_d(I + \mathcal{A}\mathcal{B})$ with $\mathcal{L}_d$ invertible. Now $I + \mathcal{A}\mathcal{B}$ is invertible if and only if $I + \mathcal{B}\mathcal{A}$ is, since $(I+\mathcal{A}\mathcal{B})^{-1} = I - \mathcal{A}(I+\mathcal{B}\mathcal{A})^{-1}\mathcal{B}$ and the converse follows on interchanging the two factors, and $I + K_{d,I}$ is invertible if and only if $f_d \neq 0$. (b) Use $\|ABC\|_{\mathfrak{S}_1} \leq \|A\|_{\mathfrak{S}_2}\|B\|\|C\|_{\mathfrak{S}_2}$ and the Leibniz rule, which is legitimate because each factor is C^4 in its operator norm (Lemma 1.30.23 and Hypothesis 1.30.12). □

Lemma 1.30.29 (Calculus of Fredholm determinants). *Let $\Phi(X) = \det(I + X)$ on $\mathfrak{S}_1$. Then $|D^j\Phi(X)[H_1,\dots,H_j]| \leq e^{\|X\|_1 + j}\prod_i \|H_i\|_1$ and $|(D^j\Phi(X) - D^j\Phi(Y))[H]| \leq e^{\max(\|X\|_1,\|Y\|_1)+j+1}\|X - Y\|_1 \prod \|H_i\|_1$. For C^k families $K_1(s), K_2(s)$ with $\|\partial^{\kappa'} K_i\|_1 \leq B_K$ and $\|\partial^{\kappa'}(K_1 - K_2)\|_1 \leq \varepsilon_K$ for $|\kappa'| \leq k$,*

$$|\partial^\kappa(\Phi(K_1) - \Phi(K_2))| \leq \mathrm{Bell}_k(k+1)e^{B_K + k + 1}(1 + B_K)^k\,\varepsilon_K, \qquad |\kappa| = k$$

($\mathrm{Bell}_4 = 15$).

Proof. Φ is entire on $\mathfrak{S}_1$ and $|\Phi(X)| \le e^{\|X\|_1}$ by Lemma 1.29.5. Apply Cauchy's estimate to $(z_i) \mapsto \Phi(X + \sum z_i H_i)$ on the polycircle $|z_i| = \|H_i\|_1^{-1}$. The Lipschitz bound follows from $D^j\Phi(X) - D^j\Phi(Y) = \int_0^1 D^{j+1}\Phi(Y + \tau(X-Y))[X-Y, \cdot]\,\mathrm{d}\tau$. The chain rule is the multivariate Faà di Bruno formula over unordered set partitions, $\partial^\kappa \Phi(K) = \sum_\pi D^{|\pi|}\Phi(K)[\partial^{B_1}K, \dots]$. Telescope each term. □

Theorem 1.30.30 (Root transfer). *Assume Hypotheses 1.30.12, 1.30.15 and 1.30.16. Let F bound $|\partial_s^\kappa f_\bullet|$ on $N_\rho \times \mathcal{S}$ for $|\kappa| \le 4$. By Lemma 1.30.29, $F \le \mathrm{Bell}_4\, e^{B_K+4}(1+B_K)^4$. Put $\varepsilon(d) = 15 \cdot 5\, e^{B_K+5}(1+B_K)^4 C_K \omega'(d)$. If $\varepsilon(d) \le \delta_\Gamma/2$, then:*

(i) for every $s \in \mathcal{S}_\Gamma$, $f_d(\cdot, s)$ has exactly one zero $\mu_d(s)$ in Ω_Γ, and it is simple;

(ii) on $\mathcal{S}_\Gamma$, the contour formula $\mu_\bullet(s) = \frac{1}{2\pi i}\oint_\Gamma z\,\partial_z f_\bullet / f_\bullet\,\mathrm{d}z$ defines a locally C^4 root, and for $|\kappa| \le 4$

$$|\partial_s^\kappa(\mu_d - \mu_{\mathrm{ret}})| \le C_\mu\,\varepsilon(d), \qquad C_\mu = \frac{|\Gamma|\sup_\Gamma|z|}{2\pi}\,2^{k+1}\,\mathrm{Fub}_k\Big(\frac{2}{\delta_\Gamma}\Big)^{k+2}(1+F)^{k+1}\Big(1+\frac{1}{\rho}\Big)^{k+1},$$

with $\mathrm{Fub}_4 = 75$;

(iii) for $n = \alpha/d > 0$ the physical root is $\Lambda_d = \mu_d - i\beta_n$, where $\beta_n = (\alpha/d)\Omega_c + [b/(r_c d)]W_c$. Its real part equals $\Re\mu_d$, and its complex jets follow by differentiating this translation. For $n < 0$ use conjugation as in Lemma 1.30.34.

Proof. (i) On Γ, $|f_d - f_{\mathrm{ret}}| \le \varepsilon(d) < \delta_\Gamma \le |f_{\mathrm{ret}}|$, so Rouché's theorem gives the same number of zeros, namely one; hence the zero is simple. (ii) On Γ, $|f_\bullet| \ge \delta_\Gamma/2$. By Cauchy's estimate on discs of radius ρ, $|\partial_z\partial^\kappa(f_d - f_{\mathrm{ret}})| \le \varepsilon/\rho$ and $|\partial_z\partial^\kappa f_\bullet| \le F/\rho$ on Γ. Continuity on the ambient chart preserves the nonzero contour and its count in a relative neighbourhood of each point of $\mathcal{S}_\Gamma$. We may therefore differentiate there under the integral, also at the boundary of the counting set. Write $h_\bullet = \partial_z f_\bullet \cdot (1/f_\bullet)$. By Faà di Bruno, $\partial^\kappa(1/f)$ is a sum over set partitions with $|\pi|!\, f^{-|\pi|-1}\prod \partial^B f$, so its size is at most $\mathrm{Fub}_k(2/\delta_\Gamma)^{k+1}(1+F)^k$. Its d-versus-ret difference is at most that bound times $(2/\delta_\Gamma)(k+1)\varepsilon$. Leibniz for $h_d - h_{\mathrm{ret}}$ gives the stated C_μ. (iii) The translation is exact (proof of Theorem 1.30.1). □

Remark 1.30.31 (Persistent allowances). The smallness required in Theorem 1.30.30 is $O(d)$ and is met by late m. The separate Rouché margin of the retained model (Lemma 1.29.9) concerns the *persistent* allowances between the retained and the ideal model. That is Proposition 1.30.32, not this theorem.

Retained versus ideal model (persistent allowance).

Proposition 1.30.32. *With $R_0 = \mathcal{L}_0^{-1}$, which is isometric $E_0^* \to E_0$: $\|R_{\mathrm{ret}} - R_0\|_{E_0^*\to E_0} \le \eta_0/(1-\eta_0)$, by $R_{\mathrm{ret}} - R_0 = -R_{\mathrm{ret}}P_{\mathrm{ret}}R_0$. Here η_0 is the form bound of P_{ret}, which is controlled by $|2\Omega_\natural b^2 B_{\mathrm{ret}}|/g_1^2$ and by the control and template masses (proof of Theorem 1.30.1, (1.30.3)). This error does* not *vanish as $d \to 0$. It is charged to the fixed model margins (1.30.8), as stated there (Lemma 1.30.8).*

Rotation contribution to the phase Hessian. Before adding the trial controls, put $z = \mu/\Delta$ and $p = (\alpha, b, y)$. On the fixed compact phase box about the model maximum and a bounded normalized contour buffer with $\Re z \ge g_1/\Delta > 0$, write

$$D_* := D_{\mathrm{ret}}/\Delta = z + i\alpha[(s_0/\Delta)\xi - \mathfrak{t}(y)\kappa_\sigma(\xi)], \qquad B_{\mathrm{ret}} = 2\Omega_\natural + s_0 - \Delta\mathfrak{t}(y)\kappa_\sigma'.$$

Here $\alpha \ge \alpha_* > 0$, $|\kappa_\sigma|, |\kappa_\sigma'| \le 1$, and $|\ell y| \le \eta_1/2 < 1$. The formula for $\Omega_\natural$ in Definition 1.30.11 gives $|\partial_y^j s_0| \le K|s_0|$ and $|\partial_y^j \Omega_\natural| \le K/C$ for $j \le 2$, uniformly in $\ell \le \ell_0$. Solving the displayed formula for $(s_0/\Delta)\xi$ gives $|(s_0/\Delta)\xi| \le K(1 + |D_*|)$. Hence every phase derivative of D_* of order one or two is bounded by $K|D_*|$, even as $|\xi| \to \infty$. The product rule now gives

$$\max_{|\gamma|\le 2} \left\| \partial_p^\gamma \left(\frac{2\Omega_\natural b^2 B_{\mathrm{ret}}}{\Delta^2 D_*^2} \right) \right\|_\infty \le \frac{K}{C\Delta}.$$

The retained and free domains are both $H^1(\mathbb{R})$, with uniformly equivalent norms on this box. Differentiating their inverse identities through order two gives bounded inverse derivatives since $A_0^2 = \alpha^2 + b^2$ has bounded derivatives there. Each derivative of $R_{\mathrm{ret}} - R_0 = -R_{\mathrm{ret}} P_{\mathrm{ret}} R_0$ therefore costs at most $K/(C\Delta)$ from H^{-1} to H^1. The corner form and its first two phase derivatives have uniformly bounded trace norm from H^1 to H^{-1}: integrate the rank-one form $\delta_\xi \otimes \delta_\xi$ against the corresponding derivative of c_{ret}, using $\|\kappa_\sigma''\|_1 \le 2$ and the bounds for D_*. Lemma 1.30.29 gives the same $K/(C\Delta)$ bound for the determinant difference and its two phase derivatives. Cauchy's formula on the buffer controls its z derivative. On the simple-root contour the logarithmic derivative formula of Theorem 1.30.30 then bounds the rotation contribution to the normalized root in C^2 by $K/(C\Delta)$. All constants here are independent of the rounding width. Choose C at the early slope selection so that this contribution fits the reserved normalized Hessian and contour margins.

1.30.19.5 Fixed-support trace norm and the simple root

Lemma 1.30.33 (The local determinant factorization)**.** *Let $j : H^1(I) \to L^2(I)$ be the embedding and let c_d be the sum of the rounded main-layer coefficients on I. We fix the rounding and put*

$$K_{d,I} = M_{c_d}\, j G_{d,I} j^* \quad \text{on } L^2(I).$$

This is trace class and holomorphic in the spectral parameter.

Its Fredholm determinant has the same zeros and algebraic multiplicities as the true-domain main-layer pencil. Also

$$\begin{aligned}\|K_{d,I} - K_{\mathrm{ret},I}\|_{\mathfrak{S}_1} \le \|j\|_{\mathfrak{S}_2}^2 \big(&\|c_d\|_\infty \|G_{d,I} - G_{\mathrm{ret},I}\|_{H^{-1}\to H^1} \\ &+ \|c_d - c_{\mathrm{ret}}\|_\infty \|G_{\mathrm{ret},I}\|_{H^{-1}\to H^1}\big).\end{aligned}$$

The same bound, with the finite Leibniz sum, holds for the necessary phase/control derivatives.

Constants may depend on the fixed rounding.

Proof. Lemma 1.30.28 gives the factorization on the fixed interval. Explicitly, $j : H^1(I) \to L^2(I)$ has square-summable singular values comparable to $(\alpha_*^2 + (\pi l/|I|)^2)^{-1/2}$, so $\|jGj^*\|_{\mathfrak{S}_1} \le \|j\|_{\mathfrak{S}_2}^2 \|G\|$. Expand $M_{c_d} j G_{d,I} j^* - M_{c_{\mathrm{ret}}} j G_{\mathrm{ret},I} j^*$ and apply this inequality and Leibniz to obtain the displayed estimates. The true-domain perturbation factors as AB with $A = R_d r_I^* j^*$ and $B = M_{c_d} j r_I$, whereas $BA = K_{d,I}$. Both factors are Hilbert–Schmidt because j and j^* are Hilbert–Schmidt and the restriction, multiplier and bulk inverse are bounded. The two determinants agree as analytic functions by Lemma 1.29.5, so their zero multiplicities agree. Only the fixed-space product BA is compared between widths. □

For passage from fixed rounding to point layers, use the global trace estimate for the norm $\|u'\|_2^2 + \alpha_*^2 \|u\|_2^2$

$$\|M_c - (\int c)\delta_{\xi_j} \otimes \delta_{\xi_j}\|_{\mathfrak{S}_1(H^1(\mathbb{R}), H^{-1}(\mathbb{R}))} \le \sqrt{2/\alpha_*}\sqrt{\sigma} \int |c|.$$

This trace ideal is between the displayed global Sobolev spaces. It is not the trace ideal on $L^2(I)$ used for $K_{d,I}$.

For this rounding step, we use the retained determinant on the fixed $H^1(\mathbb{R})$ space. The bounded retained inverse maps the layer form into the trace-class operator $R_{\mathrm{ret}} M_c$.

This operator converges to $R_{\mathrm{ret}}\gamma\delta_{\xi_j} \otimes \delta_{\xi_j}$. If the retained bulk also varies with rounding, add its different $H^{-1} \to H^1$ inverse difference times the bounded layer trace norm.

The determinant is continuous in this global trace norm. For each fixed positive rounding the AB/BA identity equates this retained determinant to its $L^2(I)$ determinant.

We do not assert a $\sigma \downarrow 0$ trace-norm limit of $M_c j G_I j^*$ on $L^2(I)$: $\|M_c\|_\infty$ can diverge in that limit. The same inequality applies to each parameter derivative of c, because we fix the scaled centers $\xi_j = \pm 1$. This uses differentiated L^1 masses, not a rounding-uniform L^∞ bound.

Fix rounding against the retained contour margin before selection of the late width. The determinant difference inequality and the previous trace bound then give Rouché on that contour.

Near its unique simple zero,

$$\mu(p,t) = \frac{1}{2\pi i} \int_\Gamma z \, \frac{\partial_z \det(I + K_I(z,p,t))}{\det(I + K_I(z,p,t))} \, dz$$

recovers the centered root. The contour denominator stays bounded away from zero, so differentiation of this formula gives the same finite phase/control comparison.

Cauchy's formula on the contour buffer bounds the spectral derivative. For $n > 0$ the physical root is $\Lambda = \mu_d - i[n\Omega_c(Z) + kW_c(Z)]$. The conjugation formula below recovers the band at $n < 0$.

Physical algebraic simplicity is then the proved factorization (1.29.8) and Lemma 1.29.12, not a new assumption.

Lemma 1.30.34 (Chart-wide simple band)**.** *Fix normalized constants $0 < c_\Gamma < c_g$ and $\rho_\Gamma \in (0, c_\Gamma/2)$ BEFORE C, together with the other normalized model constants of Section 1.30.4. Put $g_\Gamma = c_\Gamma \Delta$, $\epsilon_\Gamma = \frac{1}{2}(g - g_\Gamma)$ and $\rho = \rho_\Gamma \Delta$. Set $g_1 = g_\Gamma - 2\rho > 0$. The large-$|\mu_D|$ estimate in Section 1.30.6 holds with this lower bound on $\Re\mu_D$. Choose its radius R_Γ also larger by at least Δ than the largest positive point root on $\mathcal{P}$. Put*

$$\Omega_\Gamma = \{\mu : \Re\mu > g_\Gamma, \ |\mu| < R_\Gamma\}, \qquad \Gamma = \partial\Omega_\Gamma.$$

The open $3\rho/2$-neighbourhood of $\overline{\Omega_\Gamma}$ contains N_ρ and lies in $\Re\mu > g_1$. In Lemma 1.30.4 we use $g_1/\Delta = c_\Gamma - 2\rho_\Gamma$ for the normalized lower line. Let $\lambda_{*,\mathrm{ret}}(p) \geq 0$ be the positive root of the retained determinant (1.30.6) (0 if $M_{\mathrm{ret}} \leq 0$), and put $\mathcal{K} = \{p = (\alpha, b, y) \in \mathcal{P} : \lambda_{*,\mathrm{ret}}(p) \geq g - \epsilon_\Gamma\}$. Here $\mathcal{P}$ is the compact chart of Section 1.30.19.2, chosen to contain the superlevel set $\{\lambda_{*,\mathrm{ret}} \geq g - 2\epsilon_\Gamma\}$ in its interior. The set $\mathcal{K}$ depends on m only through $s_0(\ell_m y)/\Delta$; it is compact, and contained in a fixed compact subset of $\mathcal{P}$ uniformly in late m. We do NOT claim that $\mathcal{K}$ lies in the concavity box of Section 1.30.4, and we do not use concavity on $\mathcal{K}$. Then, for every sufficiently late selected width $d = d_m$, every control in the admitted ball, every integer n, real k and frozen Z, put $p = (|n|d, kr_c d, y)$. Write $\mu_{+,d}(\alpha, b, y)$ for the centered root of the positive-label pencil on $\mathcal{K}$, with the controls suppressed. Define

$$\mu_{-,d}(\alpha, b, y) = \overline{\mu_{+,d}(\alpha, -b, y)}.$$

(i) If $p \in \mathcal{K}$, then $n \neq 0$. The pencil for this signed label has exactly one zero in Ω_Γ, namely $\mu_{\operatorname{sgn} n,d}(p)$, and it is simple. The number $\Lambda = \mu_{\operatorname{sgn} n,d}(p) - i\beta_n$ is an algebraically simple isolated eigenvalue of the physical frozen operator. Its Riesz projection $P = (2\pi i)^{-1} \oint_{\Gamma - i\beta_n} (z - A)^{-1} \, \mathrm{d}z$ has rank one. The resolvent is bounded on $\Gamma - i\beta_n$ uniformly on $\mathcal{K}$, and P and Λ are norm-continuous on $\mathcal{K}$;

(ii) if $p \notin \mathcal{K}$, the physical frozen operator has no spectrum in $\{\Re z \ge g\}$;

(iii) hence every (n, k, Z) whose spectrum meets $\{\Re z \ge g\}$ has $p \in \mathcal{K}$. For such a point, the spectrum in $\{\Re z > g_\Gamma\}$ is the single simple eigenvalue of (i).

The chart estimates are uniform in p, $d \in J_d$ and the joint trial set $\mathcal{T}$. The value τ can be frozen independently on the chart. In the exterior the curvature edit carries its prescribed cutoff $\theta(\eta)$, while the lower controls still range over their full ball. Section 1.30.5.1 includes their first strains and their returns wherever $|y| > Y_*$.

Proof. Two comparison sets. First let $n > 0$. Put

$$\mathcal{E}_{\mathrm{in}} = \mathcal{K} \times \Gamma,$$
$$\mathcal{E}_{\mathrm{out}} = \{(p, \mu) : p \in \mathcal{P},\ \lambda_{*,\mathrm{ret}}(p) \le g - \epsilon_\Gamma,\ \Re\mu \ge g,\ |\mu| \le R_\Gamma\}.$$

The second set uses the closed sublevel. Write $D_0 = (\mu^2 - M_{\mathrm{ret}})/(\mu^2 + \alpha^2 S_t^2)$ as in (1.30.35). Its denominator has no zero for $\Re\mu > 0$. On $\mathcal{K}$ the positive root is at least $g_\Gamma + \epsilon_\Gamma$ and is at distance at least Δ from the circular boundary in the radial direction. On $\mathcal{E}_{\mathrm{out}}$ every point root has real part at most $g - \epsilon_\Gamma$, including the purely imaginary roots when $M_{\mathrm{ret}} < 0$. Thus D_0 has a positive modulus minimum on each nonempty comparison set.

These minima have common positive lower bounds $\delta_{\mathrm{in}}, \delta_{\mathrm{out}}$ for all admitted widths. Indeed, divide μ, S_t by Δ and M_{ret} by Δ^2. The parameters $\alpha, b, \mathfrak{t}(y), s_0(\ell_m y)/\Delta$ range in fixed compact intervals by Section 1.30.4. Allow all values in those intervals satisfying the respective closed separation inequalities, with the same normalized gaps. On bounded normalized spectral sets the rational function is continuous and nonzero there. At infinity it tends to one uniformly. The entries of the point matrix in Lemma 1.29.9 are bounded there as well, since $A_0 \ge \alpha_*$ and $|\gamma_\pm| \le \alpha^*\Delta/g_1$. Its inverse is uniformly bounded by the two-by-two adjugate formula. This fixes common κ_R, ρ_R for $\mathcal{E}_{\mathrm{in}} \cup \mathcal{E}_{\mathrm{out}}$ before C.

From point layers to rounded retained layers. On the support of either rounded corner, the control templates vanish. The signed mollifier at that corner has unit mass in absolute value and width σ_{round}. The unrounded clamp is Lipschitz, so the retained Doppler value there differs from its point value at $\xi = \pm 1$ by $O(\Delta\sigma_{\mathrm{round}})$, uniformly in the two comparison sets. Both denominators have modulus at least g_1. Consequently $\int |c_j| = O(1)$ and $|\int c_j - \gamma_j| = O(\sigma_{\mathrm{round}})$ in (1.29.12). The trace error $C_{A_0}\epsilon_{\mathrm{lay}}$ is $O(\sqrt{\sigma_{\mathrm{round}}})$. Impose the two inequalities of Corollary 1.30.5 using the common κ_R, ρ_R. The order in Section 1.30.3 allows the Ψ_3/C allowance first, the rounding and control amplitudes next, and the ℓ_m allowance by late m. The corollary gives

$$\inf_{\mathcal{E}_{\mathrm{in}} \times \mathcal{T}} |f_{\mathrm{ret}}| \ge 0.33\,\delta_{\mathrm{in}}, \qquad \inf_{\mathcal{E}_{\mathrm{out}} \times \mathcal{T}} |f_{\mathrm{ret}}| \ge 0.33\,\delta_{\mathrm{out}}.$$

On $\mathcal{K}$ the point determinant has exactly one zero inside Γ, so the rounded retained determinant has the same count.

From rounded retained layers to the actual pencil. With rounding fixed, Lemmas 1.30.28 and 1.30.29 give $\sup |f_d - f_{\mathrm{ret}}| \le C_{\mathrm{det}}\omega'(d)$ on both sets, uniformly on the control ball. Here $\omega'(d) \to 0$ by Lemma 1.30.28. Take m large enough that this bound is below $0.33 \min(\delta_{\mathrm{in}}, \delta_{\mathrm{out}})/2$ throughout J_d, omitting the bound for an empty set. Theorem 1.30.30 now applies with $\mathcal{S}_\Gamma = \mathcal{K} \times \mathcal{T}$ and $\delta_\Gamma = 0.33\delta_{\mathrm{in}}$. On $\mathcal{E}_{\mathrm{out}}$ the triangle inequality gives $|f_d| \ge 0.33\delta_{\mathrm{out}}/2$. This excludes the closed half-plane up to R_Γ for $p \in \mathcal{P} \setminus \mathcal{K}$. Outside $\mathcal{P}$ we use the exclusions of Section 1.30.5 (4a–4e) and the separation of Section 1.30.4, which hold at the line g. For $|\mu| \ge R_\Gamma$ we use the large-$|\mu|$ argument above. This proves (ii), and also excludes large $|\mu|$ in $g_\Gamma \le \Re\mu < g$, which the second clause of (iii) needs.

Physical statement. (I1) and (I2) hold at every (n, Z, k) with $\Re\Lambda > 0$ and $|n| \geq 2$, since the elimination of Lemma 1.29.2 holds for all $|n| \geq 2$ and real k. Every $p \in \mathcal{K}$ has $|n| = \alpha/d \geq \alpha_* m/(2\alpha_\sigma) \geq 2$ for late m, and the labels $|n| < 2$ are excluded in physical space by Lemma 1.29.1. (I3) is replaced by the factorization of Lemma 1.30.28(a), $\mathcal{L}_d + c_d = \mathcal{L}_d(I + \mathcal{A}\mathcal{B})$ with $\mathcal{B}\mathcal{A} = K_{d,I}$, where the weighted bulk of Lemma 1.30.20 is invertible. Lemma 1.29.11 applies to f_d, and $(I + \mathcal{A}\mathcal{B})^{-1} = I - \mathcal{A}(I + \mathcal{B}\mathcal{A})^{-1}\mathcal{B}$ keeps a rank-one residue. The proof of Lemma 1.29.12 therefore applies verbatim at each $p \in \mathcal{K}$, with Ω_+ replaced by $\Omega_\Gamma - i\beta_n$.

Resolvent bound and continuity. On Γ one has $|f_d| \geq \delta_\Gamma/2$. The Fredholm bound $\|(I+K)^{-1}\| \leq e^{\|K\|_{\mathfrak{S}_1}+1}/|\det(I+K)|$ of Lemma 1.29.5 and $\sup \|K_{d,I}\|_{\mathfrak{S}_1} \leq B_K$ bound $(I + K_{d,I})^{-1}$ on Γ. In the factorization of Lemma 1.30.28, the restriction $E_d \to H^1(I)$, the multiplier c_d on I, and the bulk inverse $E_d^* \to E_d$ have uniform bounds by (C5) and (H2). Thus the full scalar inverse is uniformly bounded $E_d^* \to E_d$. Remark 1.30.27 transfers this bound to $H_z^{-1} \to H_z^1$ by the form change. The forcing estimate (1.29.5) and the reconstruction (1.29.7) are uniform here since $|D| \geq g_1$, $|D'|/q \leq \|r\Omega_r\|_\infty + \|W_r\|_\infty$, and $|C|/q \leq \|B\|_\infty + \|W_r\|_\infty$. The physical sandwich (1.29.8) gives the asserted uniform contour bound. Norm continuity follows from the norm continuity of $(Z, k) \mapsto A$ (proof of Lemma 1.29.3), the Neumann argument of Proposition 1.29.13 at each point, and a finite cover of the compact set $\mathcal{K}$ for each label.

For $n > 0$ let $\mathcal{J}$ denote componentwise complex conjugation from the $(n, -k)$ sector onto the $(-n, k)$ sector. The real frozen coefficients and the divergence constraint in (1.29.1) give

$$A_{-n,k} = \mathcal{J} A_{n,-k} \mathcal{J}^{-1}, \qquad \beta_{-n}(Z, k) = -\beta_n(Z, -k).$$

The point radicand is even in b, so $\mathcal{K}$ is invariant under $b \mapsto -b$. The centered half-disk is invariant under conjugation. Conjugating the physical resolvent at $\bar{z}$ therefore gives the resolvent at z for the reflected label, with identical norm. In particular,

$$\Lambda_{-n}(Z, k) = \overline{\Lambda_n(Z, -k)}, \qquad P_{-n}(Z, k) = \mathcal{J} P_n(Z, -k) \mathcal{J}^{-1}.$$

For each available mixed jet, $\partial_Z^i \partial_k^j \Lambda_{-n}(Z, k) = (-1)^j \overline{\partial_Z^i \partial_k^j \Lambda_n(Z, -k)}$; the same reflection rule holds for projection derivatives under $\mathcal{J}$. This proves (i) and (ii) for negative labels. Lemma 1.29.1 covers $n = 0$ for every trial. Part (iii) follows.

The lowered line is one convenient choice. The region Ω_+ of (1.29.10) cannot carry a uniform count up to the level set $\{\Re\lambda = g\}$, where the root touches its boundary. A family of translated small disk contours around the root would also work. □

Consequently Proposition 1.29.14 holds with $\mathcal{C}$ replaced by $\mathcal{K}$ (in the (Z, k) variables of the labels $\pm m$) and Γ by $\Gamma - i\beta_{\pm m}$. The compact-sandwich modulus is uniform on $\mathcal{K} \times \Gamma$ by a finite cover.

1.30.19.6 Physical control kernels and the six-real map

We take the next variation in the physical spectral parameter. Controls vanish near the center that depends on the parameter, so their variations of $n\Omega_c + kW_c$ are zero.

Write $a = n/r$, $Q = a^2 + k^2$, $B = 2\Omega + r\Omega_r$, and $C = aB + kW_r$. Elimination from the physical velocity-pressure system gives the scalar rotation/axial potential terms

$$\frac{i}{D}\{C' - C/r - CQ'/Q\} + \frac{2\Omega k(kB - aW_r)}{D^2}.$$

At $k = 0$ its logarithmic radial reduction, with $n = \alpha/d$, is the actual pole pencil

$$-v_{\xi\xi} + \alpha^2 v + \frac{i\alpha B_\xi}{D} v = 0.$$

At the base of the response calculation all independent amplitudes vanish. On a fixed trial interval separated from the rounded main corners, the retained pole solution is $v = C_e e^{-\alpha\xi}$ and

$$D_0 = \mu + i\alpha(V_{\text{off}} + s_0\xi), \qquad s_0 = -2(1+\nu_c)\Omega_g \neq 0.$$

The interval lies inside the actual old power hold before the distant return corrections.

We keep finite-width old Taylor and plateau offsets as errors, and we do not replace them with an exact affine old field.

Lemma 1.30.35 (Derivation of the two physical response kernels)**.** *Select real compactly supported trials $\delta\Omega = d\,w(\xi)$ and $\delta W = d\,w(\xi)$ on that interval. The leading angular response and axial k-derivative response equal the same nonzero root factors times these respective quantities:*

$$\int K_\Omega w\,d\xi, \qquad d\int K_U w\,d\xi,$$

where

$$\begin{aligned} K_\Omega &= i\alpha(v^2/D_0)'', \\ K_U &= i(v^2/D_0)'' + 2\Omega_g\alpha(v^2/D_0^2)' \\ &= C_e^2 e^{-2\alpha\xi}\alpha^2\left[\frac{4i}{D_0} - \frac{4(s_0+\Omega_g)}{D_0^2} - \frac{2is_0(s_0+2\Omega_g)}{D_0^3}\right]. \end{aligned}$$

Each kernel has two real compactly supported trial functions whose responses are linearly independent over $\mathbb{R}$.

Proof. At the pole the scalar pencil is symmetric for the complex bilinear pairing $\int uv$, so differentiation at its simple root gives

$$\delta\mu = -\frac{\int v\,\delta\mathcal{L}\,v\,d\xi}{\int v\,\partial_\mu\mathcal{L}\,v\,d\xi}.$$

The denominator is nonzero. A zero denominator makes the first-order solvability condition give a generalized scalar root. This contradicts the proved simple determinant zero. It is a fixed nonzero complex factor and thus keeps real rank.

For the angular trial, $\delta B = w' + 2dw$, so $\delta B_\xi = w'' + 2dw'$. We multiply the variation of D^{-1} by the old $B_\xi = O(d)$ on this interval.

Thus the normalized limit is $i\alpha w''/D_0$. Two integrations by parts give K_Ω.

For the axial trial,

$$\delta W_r = w'/r, \qquad \delta W_{rr} + \delta W_r/r = w''/(dr^2).$$

Multiply the radial scalar equation by d^2r^2 and differentiate in the physical k at zero. The two displayed potential terms give the leading expression

$$\delta(\partial_k\mathcal{L}) = d\{iw''/D_0 - 2\Omega_g\alpha w'/D_0^2\} + O_C(d^2)$$

on the fixed trial support.

Derivatives of Q at $k = 0$ vanish. The denominator variation on the remaining old pole potential has an additional $B_\xi = O(d)$, thus is in the stated error.

The bounds for the old Taylor error and $d\Delta$ plateau offset control the difference between the true Ω and Ω_g there. Centering deletes no rotation term.

Two integrations by parts in the first term and one in the second give the displayed K_U. The identities $D_0' = i\alpha s_0$ and $(v^2)' = -2\alpha v^2$ give its expanded formula.

The expanded angular kernel has cubic coefficient $-2iC_e^2e^{-2\alpha\xi}\alpha^3s_0^2/D_0^3$. The axial cubic coefficient is nonzero because

$$s_0(s_0+2\Omega_g)=4\nu_c(1+\nu_c)\Omega_g^2\neq 0.$$

This identity is for the retained old germ, not the finite-width plateau value.

Each meromorphic kernel has one nonreal pole. Its conjugate is not another pole, since $\Re\mu>0$ and s_0 is real and nonzero.

Suppose its values on an open real interval lie on one real line in $\mathbb{C}$. Rotation by a constant phase and analytic reflection then force a pole at the conjugate point.

This is impossible. Select two points with noncollinear values, then two sufficiently narrow smooth real bumps about those points.

Their integrals still have nonzero two-real determinant.

□

For the six-real centering map restrict the joint control family to $\tau=0$ and write $t=t_6$ in the rest of this calculation. Select two bumps $w_{\Omega,j}$ and two $w_{U,j}$ as above and fix an angular cutoff supported in the fixed central even collar and equal to one near $Z=0$, as in Section 1.30.2. Use the actual controls

$$\delta\Omega=d\,\eta\chi(\eta)\sum_{j=1}^{2}a_jw_{\Omega,j},\qquad \delta W=d\,\chi(\eta)\sum_{j=1}^{2}b_jw_{U,j}+d\,\eta\chi(\eta)\sum_{j=1}^{2}c_jw_{U,j}.$$

All supports avoid the center germ.

For each control vector $t=(a,b,c)$, we solve the actual five-equation return system on its admitted implicit ball. Define the physical six-real map

$$\mathcal{F}_d(t)=(\Re\Lambda_Z,\Im\Lambda_Z,\Re\Lambda_k,\Im\Lambda_k,\Re\Lambda_{Zk},\Im\Lambda_{Zk})(0,0;t).$$

We know the coordinate factor $\partial_Z\eta(0)$, and it is nonzero (it is one for $\eta=ZQ^{h-\frac12}$ at the center). The map uses the PHYSICAL jets of Λ, so its zero gives $\lambda_Z=\lambda_k=\lambda_{Zk}=0$ exactly at the phase used for the centered Gaussian. By (1.30.15) the centered jets then equal $\mu_{D,Z}=im\Omega_c'(0)$, $\mu_{D,k}=iW_c(0)$ and $\mu_{D,Zk}=iW_c'(0)$. These vanish in the protected local model, because the old germ is even in η, $\kappa_\sigma(0)=0$, the controls avoid the center, and $W=0$ there. If the exponentially small distant pieces of Hypothesis 1.30.12(f) reach the center value, the centered jets are at most $K_Cd^{-N}e^{-c_C/d}$. The centered Gaussian uses these physical jets.

Lemma 1.30.36 (The actual control Jacobian, with all returns)**.** *We fix the normalized response bumps. Then the actual derivative $D\mathcal{F}_d(0)$ is invertible for each sufficiently late width in the whole bracket. Its inverse costs at most a fixed polynomial in d^{-1}.*

The derivative includes the actual return corrections. The small pre-control defect has a unique local correcting control vector of size $\mathrm{poly}(d^{-1})e^{-c_C/d}$.

We use this same vector in the source, its histories, and its selected spectral branch.

Proof. We first omit the distant return corrections and take the retained local limit. At $k=0$ the horizontal eigenvalue is independent of the axial field W.

We solve the horizontal pencil first and then reconstruct vertical velocity. Controls with a factor η vanish at $Z=0$.

Thus, in the row order $(\Lambda_Z,\Lambda_k,\Lambda_{Zk})$ and column order (a,b,c), the two-real block matrix is lower triangular. Its diagonal blocks are

$$(\partial_Z\eta)M_\Omega,\qquad dM_U,\qquad d(\partial_Z\eta)M_U,$$

up to the same nonzero simple-root factors computed above.

The last row may depend on the first two groups. We do not assume diagonal structure.

To evaluate a diagonal entry for a trial $\eta\chi(\eta)w$, first freeze the coefficient of w at an independent scalar amplitude v. Estimate (1.30.23) and the local Green comparison apply with v among the controls, since it multiplies one fixed template. In the frozen column the derivative with respect to the original trial coefficient at zero is $\eta\chi(\eta)\,\partial_v\Lambda|_{v=0}$. At $Z=0$ its Z derivative differentiates the explicit angular factor, with coefficient $\partial_Z\eta(0)$. The same identity after one physical k derivative retains the factor $r_0 d$ from $b=r_0 dk$.

Thus normalized diagonal convergence uses the pole local response and its b derivative, not a generic $O(d)$ error divided by ℓ_m. Other mixed entries may have polynomial inverse-width costs, and we keep them in the lower blocks.

Equation (1.30.13) and the same-phase comparison give uniformly invertible normalized diagonal blocks for $md\in[a_-,a_+]$. Hence the local triangular matrix is invertible. The two axial blocks explain the possible d^{-1} losses.

All off-diagonal entries have the finite polynomial bounds supplied by the typed mixed derivatives.

Finite-width Taylor and rounded-Green comparison keep these normalized blocks by Lemmas 1.30.8 and 1.30.33. Fix the actual retained rank margin first.

In addition require the plateau offset $d\Delta$ and the old Taylor variation to be below its allocated tolerance relative to $\nu_c|\Omega_g|$. These are late-width conditions.

They do not require a rank margin uniform in C or ν_c.

For the actual returns, (1.30.23) bounds the mixed (y,t) derivatives. A physical angular derivative of a return coefficient costs $\ell_m^{-1}\le a_+/(r_0L_\varsigma d)$ on J_d. Each return multiplier is supported at $|\xi|\ge a/d$, while the trial interval I is fixed. In the weighted resolvent identity each term containing such a multiplier gains the tail factor of Lemma 1.30.21. Thus the local contribution of each differentiated return is bounded by $K_C d^{-N}e^{-c_C/d}$ for some finite N, including the physical derivative conversions.

We multiply by the polynomial inverse of the triangular local matrix and the result still tends to zero. Thus the actual Jacobian is an invertible small perturbation.

We do not assert it to be triangular.

In the protected local model, the old germ and main envelope are even in Z, and $W=0$. Thus the local pole pencil is even in k.

The three pre-control jets vanish there. The distant pieces give their actual nonzero values, and the same mixed weighted comparison bounds these values by $K_C d^{-N}e^{-c_C/d}$.

The finite second control derivatives of $\mathcal{F}_d$ have at most polynomial inverse-width bounds, again with the differentiated return correction.

Select a radius $r_d=c_C d^N$ small enough that the Jacobian varies by at most half its inverse margin on that radius. The exponentially small defect is eventually smaller than a fixed fraction of $r_d/\|D\mathcal{F}_d(0)^{-1}\|$.

The contraction map

$$t\longmapsto t-D\mathcal{F}_d(0)^{-1}\mathcal{F}_d(t)$$

then maps the ball into itself and has Lipschitz constant below one. It gives the claimed correction and its size.

Uniqueness is local on this ball. We make no assertion about large controls.

These field/history changes must still obey the previously allocated actual source-cone and form tolerances. Their polynomial norms times this exponential size allow one late-width threshold to satisfy those finite tolerances on the same member.

□

1.30.19.7 Three short exclusion estimates and the last covering order

These estimates use the actual first-strain, layer-mass and form allowances of the selected source. They do not create those inputs.

On a fixed relative radial annulus put $x = \log r$ and $F = ru_r$. The physical divergence equation gives

$$F_x = -inru_\theta - ikr^2 u_z.$$

After a fixed relative cutoff, $\|F\|_2 \le C\|u\|_{L^2(rdr)}$ and $\|F_x\|_2 \le C(1 + |n| + |k|r_0)\|u\|_{L^2(rdr)}$.

The one-dimensional trace inequality thus bounds the radial energy on a width-d main layer by

$$\int_{\text{main}} |u_r|^2 r dr \le Cd(1 + |n| + |k|r_0)\|u\|_2^2.$$

Cauchy–Schwarz gives its strain cross term at most $C\Delta\sqrt{d + |n|d + |k|r_0 d}\|u\|_2^2$. Adding the background and the bounded control and return strains as in Section 1.30.5.2 gives the low-strip energy margin.

The forced and adjoint estimates give its resolvent. Viscosity contributes a nonnegative dissipative term.

At high total scaled frequency use the real Green kernel $G_0(z, z') = e^{-|z-z'|}/2$. The two positive layer magnitudes have masses $M_j \le C\Delta$ and separation at least cA.

Thus

$$\|\sqrt{h_i} G_0 \sqrt{h_j}\| \le \tfrac{1}{2} e^{-cA}\sqrt{M_i M_j} \le C\Delta e^{-cA} \quad (i \ne j).$$

The trace map $J_j : H^1 \to L^2$, $J_j u = \sqrt{h_j} u$, has norm at most $C\sqrt{M_j}$. A residual form of norm $\eta_* < 1$ changes this block by at most $C\Delta\eta_*/(1 - \eta_*)$ by the $H^{-1} \to H^1$ resolvent identity.

Each single-sign diagonal $D + is_j J_j G_0 J_j^*$ has real part at least g, thus inverse norm at most g^{-1}. We first bound the form term by the choice of η_*.

We then bound the cross-layer term by the choice of A_{hi}. This is the signed-layer Schur estimate, with its actual order of choices.

For fixed angular/axial labels, the radial extraction is compact on a finite annulus by divergence and the cell-average approximation of Lemma 1.29.3. Its adjoint handles radial output.

Actual strain decay makes the exterior cutoff error tend to zero. At the axis subtract the constant rotation $2\Omega(0)J_h$; the remaining coefficients vanish at the axis.

For $k = 0$, $P_0 J_h P_0 = 0$, so a localized rotation is a Leray commutator. Its near-diagonal kernel satisfies the bound $C|x - y|^{-1}$ in two dimensions.

We remove a distance-ϵ diagonal, which has Schur error $O(\epsilon)$, and the remaining localized kernel is Hilbert–Schmidt. For fixed $k \ne 0$, the localized difference $P_k - P_0$ is Hilbert–Schmidt at low horizontal frequency and has arbitrarily small high-frequency norm.

This proves the compact-strain assertion for each fixed sector, not a statement uniform over all angular labels.

For $|y| > Y_*$ use the physical energy exclusion of Section 1.30.5.1, including the collar where lower controls and their returns persist after the main envelope ends.

The low strip overlaps the finite set of low angular labels after the choice of their finite high-k maximum and then a small d. For the remaining labels, layer-mass Neumann inversion covers small α/A, and the signed Schur argument covers large A.

The remaining compact positive-α chart is the domain of the local determinant comparison above. Actual branch Taylor estimates, the late width choice and the same actual controls give the integer-label and phase deficits.

We use the far-angular physical lemma after we fix the selected source and selected m. We select its N_{far} after, not before, that m.

For the remaining finitely many sectors, compact-sandwich convergence and the shifted resolvent use only $\Re\Lambda_\nu \le \lambda_c + o_\nu(1)$, or an arbitrary fixed ϵ relaxation. We assert no monotonicity of nonnormal spectra under addition of viscosity.

After the controls, continuity gives a convex pole neighborhood on which the real Hessian stays negative definite. Section 1.33 chooses the shift margin and mask inside the weighted contour rectangle using this neighborhood, the pole pairing and the global spectral exclusion.

This late chart and shift choice changes no early source, C_q, return correction, width, or selected integer. It establishes the local-to-global chart implication, but it does not infer a whole-chart maximum from a Hessian at one point alone.

1.31 Consequences of the spectral selection theorem

Main result. Proposition 1.31.4 identifies the angular pair of maximal growth and the full complex phase curvature for the leading member of Theorem 1.30.1. The previous lemmas state the local Green bounds, response rank, and frequency exclusion used in that selection.

Their proofs use Theorem 1.30.1 and Section 1.30.19.

1.31.1 Frozen comparison and signed layers

We record the comparison norms and layer signs used in the determinant argument. With $\epsilon_{\mathrm{old}} = (|s_0| + |\Omega_c|)/\Delta$, allocated bulk remainder η_{bulk}, rounding width σ_{round}, and a local comparison modulus $\omega_C(d) \to 0$, the comparison on fixed separating contours is

$$\| \det_{\text{actual}} - \det_{\text{ideal}} \| \le K(\epsilon_{\mathrm{old}} + \eta_{\mathrm{bulk}} + \sqrt{\sigma_{\mathrm{round}}} + \omega_C(d)).$$

The local C^2 branch estimate has the same structure.

An increase in m does not remove the retained nonzero old slope or rotation. We select C first, then the rounding width, then d.

An alternative comparison uses the limit pencil with the old terms retained. It does not use the pencil with zero old terms.

These errors must be smaller than the fixed contour and Hessian margins. We do not compare them with Δ/m^2.

The width selection uses the *actual* maximizer:

$$\Re\mu_d(md) - \Re\mu_d(nd) \ge c\Delta(n-m)^2 d^2.$$

Only the next exponentially small nonlocal centering errors must be smaller than this adjacent-label gap.

For the high-frequency two-layer equation with $f_j = \sqrt{h_j}\psi/D$ and $s_j = \operatorname{sign}\Omega_j''$, the exact equation is

$$Df_j + i\sum_l s_l\sqrt{h_j}G_{\mathrm{base}}\sqrt{h_l}f_l = 0.$$

The equation with row signs holds for $g_j = s_j f_j$, which is a diagonal unitary conjugation. This conjugation keeps the cross-block norms and diagonal accretivity.

The model determinant and its exclusion at large imaginary parts use $\mu_D = \Lambda + i(n\Omega_c + kW_c)$. The physical contours differ by the translation $-i(n\Omega_c + kW_c)$.

If we use the crude bound, we select a centered radius greater than $\|A + i(n\Omega_c + kW_c)I\|$ after m. The global pole comparison is $O(d)$.

Only localized Green responses decay exponentially with the distance. Sections 1.30.5–1.30.7 prove the complete frequency coverage and distinguish these norms.

We set $x = \log r$, $\xi = (x - x_0)/d$ and

$$\alpha = |n|d, \quad b = kr_0 d, \quad A_d^2 = \alpha^2 + b^2 e^{2d\xi}, \quad \mu_D = \Lambda + i(n\Omega_c + kW_c). \tag{1.31.1}$$

The physical spectral parameter is Λ.

Centering only rewrites $D = \mu_D + in(\Omega - \Omega_c) + ik(W - W_c)$. It does not replace the true $B = 2\Omega + r\Omega_r$ or any rotation–axial numerator.

Lemma 1.31.1 (Joint-phase local Green regularity)**.** *We use a compact centered contour in the positive half-plane and a compact scaled phase range, with $\alpha \geq \alpha_{\min} > 0$. The bulk inverse on its true domain has bounds on a finite descending scale of exponential weights.*

Its two local phase derivatives satisfy these bounds. Remote source–observation responses at physical log-distance bounded below cost $K_C d^{-N} e^{-c_C/d}$.

The global unweighted inverse difference is only $O(d/c_g)$ at the pole (Lemma 1.30.2).

Proof. Sections 1.30.5–1.30.7 first remove the small-angular-fraction regime and then prove the weighted true-domain estimate with $E_{d,b} = \{v \in H^1 : be^{d\xi} v \in L^2\}$.

The necessary principal bound is

$$\|L_b^{-1}\|_{H^{-1} \to H^1} \leq (1 - \eta_{\text{total}})^{-1}. \tag{1.31.2}$$

At the pole the exact equation is

$$-v'' + \alpha^2 v + \frac{i\alpha B_\xi}{\mu_D + i\alpha V_d} v = 0. \tag{1.31.3}$$

This local comparison, with retained OLD terms, is

$$\|\mu_d - \mu_{\text{model}}\|_{C^2(\text{local})} \leq K\Delta(\epsilon_{\text{old}} + \eta_{\text{fixed}} + \sqrt{\sigma_{\text{round}}} + \omega_C(d)). \tag{1.31.4}$$

These errors must be smaller than the fixed contour and Hessian margins. We do not compare them with the integer gap.

□

Lemma 1.31.2 (Two real source directions)**.** *The actual old power interval permits two angular and two axial trial shapes, all disjoint from the center. Their real response matrices are nondegenerate.*

The normalized matrices remain invertible after the exact correction of five histories. The raw axial inverse can have size d^{-1}.

Proof. We compute the physical angular and axial kernels in Section 1.30.8 and Lemma 1.30.35. Their nonremovable third-order poles give the real rank.

Lemma 1.30.36 treats the actual return correction and the normalized system of six real equations. These results keep the nonzero power slope and distinguish the exponentially small local return response from its algebraic global form bound.

□

Lemma 1.31.3 (Rounded model and complete phase exclusion)**.** *The actual source has a unique simple branch near the normalized model maximum and no positive spectrum above the selected line outside that branch. This includes all finite labels, small angular fraction, compact phase, large total frequency and the exterior axial region.*

Proof. The centered ideal determinant gives

$$\mu_D^2 = \Delta^2 t(y)^2 \frac{\alpha^2}{A^2} D_0(A), \quad D_0(A) = e^{-4A}/4 - (A - 1/2)^2, \quad A^2 = \alpha^2 + b^2. \tag{1.31.5}$$

With the retained nonzero old slope this becomes

$$\mu_D^2 = \frac{\alpha^2}{A^2}\{\Delta^2 t(y)^2 e^{-4A}/4 - [(\Delta t(y) - s_0)A - \Delta t(y)/2]^2\}. \tag{1.31.6}$$

Here $s_0 < 0$ is the signed old derivative. Thus the positive inner-slope magnitude is $\Delta t - s_0$.

Equations (1.30.6)–(1.30.8) give the exact determinant and the different bounds for persistent C^2 and contour errors. They imply that its normalized maximum is nondegenerate.

The exact low-frequency estimate is

$$\int_{\text{main}} |u_r|^2 r \, \mathrm{d}r \le K d(1 + |n| + |k| r_0)\|u\|_2^2, \tag{1.31.7}$$

$$\Re\langle Au, u\rangle \le [K + K\Delta\sqrt{d + \alpha + |b|}]\|u\|_2^2. \tag{1.31.8}$$

Sections 1.30.4–1.30.7 prove the low-strip estimate, the high-frequency form estimate and the compact positive-real-part comparison. Section 1.30.19 gives the order of the cover over all phases.

Together they establish the pre-control simple branch, before we use the response rank to select the controls. □

Proposition 1.31.4 (Actual integer winner and physical phase center)**.** *For the leading member selected in Theorem 1.30.1 (and identified in Proposition 1.32.1), the unique positive angular label of maximal growth is m, at $(Z, k) = (0, 0)$. The negative label is its real conjugate.*

The physical pole λ_0 is generally complex. It has the prescribed full complex physical Hessian and a true real-growth gap between neighbor labels. Precisely, at $(Z, k) = (0, 0)$ the positive-label band satisfies items (S2)–(S5) of Theorem 1.30.1: $\lambda_Z = \lambda_k = \lambda_{Zk} = 0$, $\Re\lambda_{kk} < 0$, the exact complex identity (1.30.1) with the real $q = a_m^2 C_q/\Delta > 0$, and the Gaussian reserve $X > (b_d + \frac{1}{4})^2$ (in fact $\eta_q \le 1/16$); hence $\Re\lambda_{ZZ} = 2q(b_d - X) < 0$.

Proof. We denote the maximizer of the actual pole branch by α_d. The intermediate value theorem on the width interval gives $md_m = \alpha_{d_m}$.

Integral Taylor concavity gives

$$\Re\mu_{d_m}(md_m, 0, 0) - \Re\mu_{d_m}(nd_m, 0, 0) \ge c\Delta(n - m)^2 d_m^2 \tag{1.31.9}$$

nearby, with fixed deficits elsewhere, by Sections 1.30.9–1.30.11. Those sections also prove that the exact returns and the full flat quadratic cutoff keep the branch and this gap.

We use the physical identities

$$\lambda_{ZZ} = \mu_{D,ZZ} - im\Omega_c'', \quad \lambda_{Zk} = \mu_{D,Zk} - iW_c', \quad \lambda_{kk} = \mu_{D,kk}$$

at the selected phase, not a real-only curvature target. The centering is Lemma 1.30.36; the curvature identity is exact by paragraph 1.30.18, and the reserve is (1.30.25). Sections 1.30.9–1.30.11 prove the gap, complex Gaussian target, whole physical resolvent exclusion and rank-one projection. □

1.32 Selection of the same leading member

Main result. Proposition 1.32.1 selects one leading member with the necessary source histories, endpoint data, heat tail, and spectral pair of maximal growth. Lemma 1.32.2 gives its radial decay and finite axial derivatives.

The selection precedes the completion and its later analytic thresholds.

1.32.1 Radial placement and the pressure-class correction

Subsection 1.5.2 fixes the parameter order. Proposition 1.32.1 below verifies the spectral selection for the same leading member.

The radial placement below differs from the parameter order.

The selected radial order is

$$\begin{aligned}\text{loop modulation and return correction} &\longrightarrow \text{early positive-order and mean-velocity corrections}\\ &\longrightarrow \text{main pulse, true returns and primitive correction}\\ &\longrightarrow \text{central spectral perturbation and its return correction}\\ &\longrightarrow \text{heat drive, blend and tail.}\end{aligned}$$

The spectral correction follows the perturbation and precedes the future heat profile. It does not precede the early correction of positive-order moments.

At the outlet of the spectral edit and its compensating return, all five histories recover their incoming reference values at that radius. This preserves the calibrated energy root, pressure, and heat coefficient.

After we fix the selected leading source, the early affine targets for positive-order moments include *all* later meridional contributions. Only the positive-order velocities vanish early.

The pressure hull retained for these corrections is specified in assertion (iii) of the main theorem.

The pressure-class correction. The pressure-class correction has $(\Delta I, \Delta S, \Delta C_p) = (0, 0, \Pi_{\mathrm{ref}} - p_0)$ and $\Delta M = \Delta J = 0$. Thus it keeps M, I, J, S and physical pressure P, but not C_p itself.

The axis datum changes by the opposite amount:

$$p_0 + C_{p,\mathrm{ref}} + \Delta C_p = \Pi_{\mathrm{ref}} + C_{p,\mathrm{ref}}.$$

The earlier core correction matches the edited reference. This pressure-class correction does not change the loop and spectral corrections of five histories.

Those corrections have net ΔC_p equal to zero. The pressure-class correction does not leave all five histories unchanged.

Proposition 1.32.1 (One actual jointly selected member)**.** *The actual leading construction and its normalized corrections give the same finite member as Theorem 1.30.1.*

This member keeps its cone, protected endpoint germs and heat tail. Each spectral edit together with its return restores all five reference histories at its outlet. The separate pressure-class bank has the offset just computed. Its physical frozen pair of maximal growth is the conjugate pair $\pm m$. For this member, with $a_m = m/r_0$, $q = a_m^2 C_q/\Delta > 0$ and $b_d = \frac{1}{2}(1 + 2(\frac{1}{2} - h)/h)$, the positive-label band satisfies at $(Z, k) = (0, 0)$: $\lambda_Z = \lambda_k = \lambda_{Zk} = 0$; $\Re\lambda_{kk} < 0$; the exact complex identity (1.32.2), equivalently (1.30.1); and the reserve (1.32.1), equivalently $X > (b_d + \frac{1}{4})^2$ (items (S2)–(S5) of Theorem 1.30.1). The annular inverse and the centered Gaussian use these same jets. The six-real centering is obtained by Lemma 1.30.36 in the proof of Theorem 1.30.1.

Proof. We use the order in Sections 1.30.2, 1.30.8–1.30.10 and 1.30.13. We first select the normalized geometry and core family, then C.

For this C, we select the same activation shear $\kappa_{\mathrm{act}}(C)$. We next select the activation width $t_{\mathrm{act}}(C)$, then the termination widths $\omega_{\mathrm{act},j}(C)$.

We then fix the actual higher source jets.

With $\Delta = C^{\sigma}$, we next select the capped loop and exact correction. This choice includes the persistent signed-slope thresholds in (1.30.8).

Here $s_0 < 0$ and the inner slope magnitude is $S_t = \Delta t - s_0$, not $\Delta t + s_0$. The Green estimates and spectral count give the simple branch before we use its inverse response matrix.

We fix C_q from the retained branch's pole-k curvature interval. We then select L_ζ to make Δ/L_ζ^2 sufficiently small before we select the integer.

On the branch $X > b_d$ selected in item (S5) of Theorem 1.30.1, the Gaussian reserve is

$$X - b_d/2 - \sqrt{X^2 - b_d X} < 1/8, \quad X = -\tfrac{1}{2}\Re(a_m^2\lambda_{kk}/h^2)C_q/\Delta > b_d, \quad b_d = \tfrac{1}{2}(1 + 2(\tfrac{1}{2} - h)/h). \tag{1.32.1}$$

The actual nonzero power slope gives the response rank away from the center. We select its cutoff to satisfy the form bound on total variation and the source and partial-history tolerances.

Last, we select one m for the full width interval and apply the intermediate value theorem to the actual maximizer. We then correct the exact histories of the controls.

The curvature condition uses the PHYSICAL complex eigenvalue:

$$\frac{\lambda_{ZZ}}{a_m^2} = \frac{a_m^2\lambda_{kk}}{h^2}(C_q/\Delta)^2 + (1 + 2(\tfrac{1}{2} - h)/h)C_q/\Delta, \qquad \mu_{D,ZZ} = \lambda_{ZZ} + im\Omega_c''. \tag{1.32.2}$$

This system solves for the target minus the base and includes the nonzero imaginary curvature at the center. The quadratic control keeps its whole flat cutoff factor.

The actual neighbor gap follows from the selected branch's concavity, not by subtraction of an $O(d)$ comparison error from d^2. No late analytic or completion threshold changes this source.

□

Lemma 1.32.2 (Selected radial tail and finite axial jets)**.** *For the one leading source selected in Proposition 1.32.1, write its swirl velocity as $r\Omega(r, Z)$. For each finite pair of orders $j, l \geq 0$, uniformly for $r \geq 0$ and $Z \in \mathbb{R}$,*

$$|\partial_Z^l \partial_r^j \Omega(r, Z)| \leq C_{j,l}\langle r\rangle^{-2-2h-j}.$$

The axial velocity $\mathcal{U}(r, Z)$ vanishes when $r^2 \geq 2\frac{\hat{\xi}_U^2}{2}\mathcal{Q}(Z)$. On each compact axial interval the axial velocity and the centering controls therefore have a common finite radial support bound.

For the physical swirl speed the corresponding bound is $|\partial_Z^l \partial_r^j (r\Omega)| \leq C_{j,l}\langle r\rangle^{-1-2h-j}$. In the fixed angular sectors the transport and strain multipliers involve Ω and $r\partial_r\Omega$; both have the faster decay in the display above. These bounds include the eighteen ordinary axial derivatives used by the contour and profile bootstrap.

Proof. Use the chart at $t = 1$, regular-axis analyticity and the finite-hull bounds of Lemma 1.24.1. The differentiated heat estimates are (1.13.35) and (1.13.34). The chart and heat estimates bound the derivatives of Ω uniformly in Z, with regularity at the axis supplying the bound for $r \leq 1$. For the support assertion use $\hat{\xi} = r/\sqrt{\mathcal{Q}(Z)}$: the axial profile vanishes for $\hat{\xi} \geq \hat{\xi}_U$, and the centering controls are placed in fixed bounded $\frac{\hat{\xi}^2}{2}$-intervals. Taking the supremum of $\mathcal{Q}$ on a compact axial interval gives the stated radial bound there.

□

1.33 The selected physical two-band shift

Main result. Proposition 1.31.4 and the four frequency regimes give the physical shift in (1.33.1) for the selected source. The construction also gives the frozen inputs for Section 1.34.

These conclusions apply to the leading member, before completion.

For the last fixed d_m, the exclusion over all phases and Proposition 1.31.4 give $\delta_{\mathrm{ang}} \geq c\Delta d_m^2 > 0$. This number separates the conjugate pair $\{m, -m\}$ from all other frozen modes.

The large-$|Z|$ old-strain energy, Lemma 1.29.16, and Lemma 1.29.20 reduce the remainder to finitely many labels $F = \{n : |n| < N_{\mathrm{far}}\}$ on one compact (Z, k) rectangle. This family includes $n = 0, \pm 1$.

The compact-strain proof of Lemma 1.29.3 applies to each fixed low label: neither radial compactness on an annulus nor the rigid-axis subtraction requires $|n| \geq 2$. Thus the normal-mode exclusion, combined with compact Fredholm theory, controls the full positive physical spectrum of these sectors.

Let $g_{\mathrm{coarse}} = g = c_g\Delta$ be the exclusion line of Theorem 1.30.1. Fix the source and write the pole projection as $P_{0,m}(0,0) = e_0\ell_0$ with $\ell_0 e_0 = 1$. Continuity of $P_{0,m}$ and of the Hessian gives an open rectangle U about the pole, symmetric in k, with closure inside the weighted rectangle of Proposition 1.28.8. On $\overline{U}$ we have $|\ell_0 P_{0,m}(Z,k)e_0 - 1| \leq 1/2$ and $D^2\Re\lambda < 0$. Fix a smaller symmetric open rectangle $0 \in U' \Subset U$. The compact phase reduction above and Lemma 1.30.34 confine every selected band value above g_{coarse} to a compact set on which the band is continuous. Its unique maximum in sector m is at the pole. Hence there is $\eta_* > 0$ such that every band value in that sector outside U' has real part at most $\lambda_c - \eta_*$ wherever it exceeds g_{coarse}.

Choose $\delta > 0$ with $8\delta < \eta_*$ and $16\delta < \min\{\delta_{\mathrm{ang}}, \lambda_c - g_{\mathrm{coarse}}, \lambda_c - g_{\mathrm{far}}, \lambda_c/2\}$. Set $g_f = \lambda_c - 6\delta$, $g_1 = \lambda_c - 4\delta$, $g_2 = \lambda_c - 2\delta$. The closed set $\{\Re\lambda \geq \lambda_c - 7\delta\}$ is compactly contained in $\{\Re\lambda > \lambda_c - 8\delta\} \subset U'$. Choose $0 \leq \chi_+ \leq 1$ smooth, equal to one on the closed set and supported in the open set. Set $\chi_-(Z,k) = \chi_+(Z,-k)$. Both supports thus have positive distance to the boundary of U.

With $d_0 \geq 8\delta$, we define

$$S_{\nu,\pm m} = d_0\chi_\pm P_{\nu,\pm m}, \qquad S_{\nu,n} = 0 \quad (n \notin \{m, -m\}). \tag{1.33.1}$$

Each $P_{\nu,\pm m}$ is the true physical Riesz projection. It is rank one and norm-continuous on all of $\operatorname{supp}\chi_\pm \subset \mathcal{K}$, by Lemma 1.30.34 and Proposition 1.29.14 with local isolating contours on $\mathcal{K}$. For joint dependence on viscosity and phase, work on the fixed extended angular space of Proposition 1.29.18. For $\nu > 0$ its generator is $\nu\Delta_h + A_0(Z,k) - \nu k^2 I$ on the common domain $H^2 \cap \mathsf{H}_n$. Lemma 1.29.3 gives norm continuity of $A_0(Z,k)$. Thus the generator is jointly continuous as a map from this domain, with its H^2 norm, to H_n. At each point of a local isolating contour the resolvent maps H_n boundedly to the domain by the closed graph theorem. The resolvent identity and a Neumann series give joint norm continuity of the resolvent locally, uniformly along the compact contour. Integration gives joint norm continuity of $P_{\nu,\pm m}$ at positive viscosity. At $\nu = 0$ use the uniform convergence of Proposition 1.29.14 and the continuity of $P_{0,\pm m}$. Multiplication by $\chi_\pm$ and extension by zero give a jointly strongly Borel measurable family on the whole phase space.

Where $\chi_\pm = 1$ the shifted inviscid rate is at most $\lambda_c - 8\delta$. Elsewhere on these bands it is at most $\lambda_c - 7\delta$. The other spectrum of the selected labels lies at or below g_{coarse} by Lemma 1.30.34, and the remaining labels have inviscid rate at most $\lambda_c - \delta_{\mathrm{ang}}$. Both bounds are below $\lambda_c - 7\delta$. Together with the exterior energy estimates above, this verifies Proposition 1.29.18 at $g = g_f$, with inviscid margin δ on the rectangle. The two symbols form a norm-compact family of compact radial operators on their fixed phase supports.

We quantize the auxiliary shift by the *definition* $\mathcal{S}_\epsilon = P_\epsilon T_\epsilon^* S_{\nu,n}(Z,k) T_\epsilon P_\epsilon$, where T_ϵ is the Gaussian axial FBI transform. The conjugate masks and real Gaussian windows make this operator real on the $\pm m$ pair.

It is not globally finite-rank in the axial variable.

Hypotheses for the selected member before packet comparison. The assumptions (B1),(B2),(F1)–(F4) displayed in Section 1.34 are conclusions of Sections 1.30.14–1.30.17 for the selected source. The order is last m, then $N_{\mathrm{far}} > m$, finite exteriors, actual viscosity threshold, and only then the block length.

1.34 Leading propagation from frozen physical estimates

Main result. Proposition 1.34.14 gives leading auxiliary propagation on all angular sectors from the frozen hypotheses stated below. Corollary 1.34.15 gives the related unshifted leading bound.

These results use the frozen leading field independently of the completion.

This section proves the two fixed-block estimates used in Proposition 1.34.14 and Corollary 1.34.15. We first state the evolution and all its inputs.

Proposition 1.34.8 then proves a general low-axial-frequency packet comparison and derives each error term. We combine these estimates to prove the two block lemmas.

The actual leading equation. By (1.6.9), (1.6.10) and (1.6.11), the leading velocity is self-similar. Set $y = x_h/t^{1/2}$, $Z = z/t^{\frac{1}{2}-h}$, $\rho = t^h$.

Then

$$u^{\mathrm{lead}}(x,t) = t^{-\frac{1}{2}-h}\mathfrak{B}(y,Z;\rho), \qquad \mathfrak{B} = \mathcal{U}_0 + \rho\mathcal{U}_1, \quad \mathcal{U}_0 = r\Omega(r,Z)e_\theta + W(r,Z)e_z, \quad \mathcal{U}_1 = \mathcal{V}(r,Z)e_r. \tag{1.34.1}$$

Here $r = |y|$, $r\Omega = \mathcal{H}$, $W = \mathcal{U}$, and $\mathcal{V}$ is the radial profile of (1.6.11) (the factor ρ comes from $u_r^{\mathrm{lead}} = t^{-1/2}\mathcal{V}$).

With $\nabla_\rho = (\nabla_y, \rho\partial_Z)$ one has $\operatorname{div}_\rho \mathfrak{B} = 0$. The *actual leading equation* is the linearization of the Navier–Stokes equations about u^{lead}, $v_t + \mathbb{P}(u^{\mathrm{lead}}\cdot\nabla v + v\cdot\nabla u^{\mathrm{lead}}) = \Delta v$, $\operatorname{div} v = 0$, written for $V(y,Z,s)$, $v = t^{-\frac{1}{2}-h}V(x_h/t^{1/2}, z/t^{\frac{1}{2}-h})$, in canonical time s.

Its primitive symbols are (1.35.5).

We write $U_{\mathrm{lead}}(s,\sigma)$ for its propagator on $L^2_\sigma(\,\mathrm{d}y\,\mathrm{d}Z)$ and $U^\sharp_{\mathrm{lead}}$ for the propagator of the shifted equation $V_s = (\cdots) - \mathcal{S}(s)V$. Here $\mathcal{S}(s) = P_\rho T_\rho^* S_{\rho,n}(Z,k) T_\rho P_\rho$, $\rho = \rho(s)$, on the sectors $\pm m$ and $\mathcal{S}(s) = 0$ on all others.

The definition after (1.33.1) applies (isotropic Gaussian window, $\hbar = \rho$, viscosity label $\nu = \rho$). We can use a different fixed amplitude normalization t^{-c} of V, or add a bounded generator term of norm $O(\rho)$.

On a block of length L, either change multiplies the propagator bound by $1 + O(\rho L e^{CL})$. This does not change any statement below.

Since u^{lead} is axisymmetric, the *vector angular sectors*

$$\mathsf{H}_n = \{f \in L^2(\mathbb{R}^2;\mathbb{C}^3) : f(R_\varphi y) = e^{in\varphi}\widehat{R}_\varphi f(y)\ \forall\varphi\}, \qquad n \in \mathbb{Z},$$

give an orthogonal decomposition of $L^2(\mathbb{R}^2;\mathbb{C}^3)$. Here $\widehat{R}_\varphi$ rotates the horizontal components.

The leading generator, the shift, and each horizontal Fourier multiplier that commutes with rotations keep this decomposition. This includes all Leray projectors.

On H_n one has,

$$r\Omega e_\theta \cdot \nabla_y = \Omega(r, Z)\,(in + J), \tag{1.34.2}$$

where J is the constant generator of $\widehat{R}_\varphi$ (differentiate the covariance relation at $\varphi = 0$). For $f \in \mathsf{H}_n$ the Cartesian components $f_1 \pm i f_2$ and f_3 are scalar angular modes $n \pm 1$ and n.

Thus, for $|n| \geq 2$, we have

$$\|f/r\|_{L^2(\mathbb{R}^2)} \leq (|n| - 1)^{-1} \|\nabla_y f\|_{L^2(\mathbb{R}^2)}. \tag{1.34.3}$$

Thus, $\|\nabla g\|^2 = \|\partial_r g\|^2 + j^2 \|g/r\|^2$ for a scalar mode j and $\|f/r\|^2 = \frac{1}{2}\|(f_1 + i f_2)/r\|^2 + \frac{1}{2}\|(f_1 - i f_2)/r\|^2 + \|f_3/r\|^2$.

Inputs. All constants below may depend on the frozen source and on m. We use the next hypotheses.

Remark 1.34.13 gives the source of each bound and the order of choices.

(B1) Profile bounds. There is $C_{\mathfrak{B}}$ such that, with one bound for all $Z \in \mathbb{R}$ (Cartesian components, $r = |y|$): (a) $|\nabla_y^i \partial_Z^j \mathcal{U}_0| + |\partial_Z^j \Omega| \leq C_{\mathfrak{B}}$ for $i + j \leq 2$, and $|\mathcal{U}_1| + |\nabla_y \mathcal{U}_1| + |\partial_Z \mathcal{U}_1| \leq C_{\mathfrak{B}}$. (b) $\|\Omega(\cdot, Z)\|_{L^2(\mathbb{R}^2)} + \|W(\cdot, Z)\|_{L^2(\mathbb{R}^2)} + \|\nabla_y \mathcal{U}_0(\cdot, Z)\|_{L^2(\mathbb{R}^2)} \leq C_{\mathfrak{B}}$, and $\langle r\rangle^2 |\nabla_y \mathcal{U}_0| + r|\Omega| + r|W| + r|\partial_Z \Omega| \leq C_{\mathfrak{B}}$.

(B2) Dilation jets. $|y \cdot \nabla_y f| + |Z \partial_Z f| \leq C_{\mathfrak{B}}$ for $f \in \{\Omega,\, W,\, \nabla_y \mathcal{U}_0\}$.

(F1) Low-label frozen bound. For $(z, k) \in \mathbb{R}^2$ and $0 \leq \nu \leq \nu_0$ let $A_{\nu,n}(z, k)$ be the frozen physical generator on $X_k = P_k \mathsf{H}_n$ of Lemma 1.29.3 and Proposition 1.29.18 (coefficients $\mathcal{U}_0(\cdot, z)$, viscosity $\nu(\Delta_y - k^2)$). For each $n \in F$ there are C_F and the rate $g_1 < \lambda_c$ of (1.33.1) such that $\|e^{t(A_{\nu,n}(z,k) - S_{\nu,n}(z,k))}\|_{X_k \to X_k} \leq C_F e^{g_1 t}$ for all $t \geq 0$, $(z, k) \in \mathbb{R}^2$, $\nu \in [0, \nu_0]$.

(F2) Shift symbol. For $n = \pm m$ and $0 \leq \nu \leq \nu_0$, assume $\operatorname{supp} S_{\nu,n} \subset W_S$ for one compact set $W_S \subset \mathbb{R} \times [-K_S, K_S]$, with $\sup_{\nu,n,w} \|S_{\nu,n}(w)\| \leq M_S$. For each $v \in \mathsf{H}_n$, assume $(\nu, w) \mapsto S_{\nu,n}(w)v$ is Borel measurable with values in H_n, using the common extended angular space. The inviscid symbol $S_{0,n}$ is norm continuous and has rank at most one. For every ν in this range, $S_{\nu,n} = P_k S_{\nu,n} P_k$, and $\delta_S(\nu) := \sup_w \|S_{\nu,n}(w) - S_{0,n}(w)\| \to 0$ as $\nu \downarrow 0$.

(F3) High-axial metric. There are a smooth radial $\delta(r) \in [d_*, 1]$, equal to one near $r = 0$ and outside a compact annulus, and $\gamma \in (\gamma_\delta, g_1)$, where $\gamma_\delta := \sup_{r,Z}\big(|2\Omega - \delta B|/(2\sqrt{\delta}) + |\partial_r W|/2\big)$, $B = 2\Omega + r\partial_r \Omega$. The supremum is over *all* $Z \in \mathbb{R}$.

Here is the common choice of metric and the axial jet calculation. At frozen time one write $Q - Z^2 Q^{2h} = 1$, $d_0 = 1/2 - h$, $\xi = R/\sqrt{Q}$, $\eta = Z Q^{-d_0}$, $L = 1 - 2h\eta^2$. Direct differentiation gives

$$\partial_Z(Q^{-w} f) = \frac{Q^{-w-d_0}}{L}[-2w\eta f - \eta\xi f_\xi + (1 - \eta^2) f_\eta], \qquad \partial_R(Q^{-w} f) = Q^{-w-1/2} f_\xi.$$

Since $Q \geq 1$, $L \geq 1 - 2h$, these identities iterate on the bounded native hull. At the axis use the regular Cartesian representatives. In the exterior each Euler derivative of the heat expansion preserves its stated decay. For example $Q^{-1-h-j/2}\langle R/\sqrt{Q}\rangle^{-2-2h-j} = (Q + R^2)^{-1-h-j/2}$. This gives uniform fixed Cartesian jets at all Z.

The large part of $R\Omega_R$ is supported in $\xi_- \leq \xi \leq \xi_+$, $|\eta| \leq \eta_* < 1$, including the returned controls. Since $Q = (1 - \eta^2)^{-1}$, its radial projection lies in $[\xi_-, \xi_+/\sqrt{1 - \eta_*^2}]$. Enlarge this annulus inside the old-strain region and take $\delta = K_0/\Delta$ throughout it, with smooth transitions to one in the old region. The first-strain bounds of Lemma 1.29.1 and Remark 1.29.17 bound $|W_R|$ and $|\Omega|$ by K_0 and the large strain by $C\Delta$. On the complement use the old bound on $R\Omega_R$. Substitution gives $\gamma_\delta \leq C\sqrt{K_0 \Delta} + C K_0$; the parameter choice in the finite-label exclusion puts this below the reserved

rate. The function δ is independent of Z. **(F4) Far-angular frozen resolvent.** There are N_{far}, $g_{\mathrm{far}} < g_1$ and M_{far} such that $\|(\zeta - A_{\nu,n}(z,k))^{-1}\| \le M_{\mathrm{far}}$ for $\mathrm{Re}\,\zeta \ge g_{\mathrm{far}}$, $|n| \ge N_{\mathrm{far}}$, $(z,k) \in \mathbb{R}^2$, $\nu \in [0,\nu_0]$ (Lemma 1.29.20). We take $N_{\mathrm{far}} > \max(m,2)$, so $F = \{|n| < N_{\mathrm{far}}\} \ni \pm m$ and the shift vanishes for $|n| \ge N_{\mathrm{far}}$.

On X_k the frozen generator is, with $\nabla_k = (\nabla_y, ik)$, $\Delta_k = \Delta_y - k^2$ and $\mathfrak{M}_0(z)f = (f_h \cdot \nabla_y)\mathcal{U}_0(\cdot,z)$,

$$A_{\nu,n}(z,k) = \widetilde{A}_0(w) + \nu\Delta_k, \qquad \widetilde{A}_0(w) = -\mathcal{U}_0(z)\cdot\nabla_k - (2P_k - I)\mathfrak{M}_0(z), \qquad w = (z,k). \quad (1.34.4)$$

Thus, for $f \in X_k$ and $\mathrm{div}_y \mathcal{U}_{0,h} = 0$, $\mathrm{div}_k(\mathcal{U}_0 \cdot \nabla_k f) = \mathrm{div}_k(\mathfrak{M}_0 f)$ (the expansion of the two sides has the same $ik(\nabla_y W)\cdot f_h$ terms), so $(I-P_k)(\mathcal{U}_0\cdot\nabla_k f) = (I-P_k)\mathfrak{M}_0 f$ and $-P_k(\mathcal{U}_0\cdot\nabla_k + \mathfrak{M}_0)f$ equals the displayed expression. The scalar axial dilation $i(\frac12 - h)zk$ of (1.35.6) is unimodular in the frozen semigroup and is not part of $A_{\nu,n}$.

1.34.1 Block coordinates

Lemma 1.34.1 (Exact block reduction)**.** *Fix s_0, $L > 0$ with $\kappa L \le \frac12$, $\kappa = \rho(s_0)$, $t_0 = t(s_0)$. For $s \in [s_0, s_0 + L]$ put $\lambda = t_0/t(s)$ and $(\mathcal{J}_s V)(y,Z) = \lambda^{\frac12+h} V(\lambda^{1/2}y, \lambda^{\frac12-h}Z)$.*

Then:

(i) $1 - \kappa L \le \lambda \le 1$, *and* $\|\mathcal{J}_s\|, \|\mathcal{J}_s^{-1}\| \le (1-\kappa L)^{-C_h}$.

(ii) $\widetilde{V}(s) = \mathcal{J}_s V(s)$ *solves, on the* fixed *space* $X_\kappa = \{\mathrm{div}_\kappa \widetilde{V} = 0\}$,

$$\partial_s \widetilde{V} = \gamma(s)\, P_\kappa\big[-\mathcal{U}_s\cdot\nabla_\kappa\widetilde{V} - (\widetilde{V}\cdot\nabla_\kappa)\mathcal{U}_s + \kappa\Delta_\kappa\widetilde{V}\big] - \widetilde{\mathcal{S}}(s)\widetilde{V}, \quad (1.34.5)$$

with $\gamma = \lambda^{-1-h}$, $\mathcal{U}_s(y,Z) = \lambda^{\frac12+h}\mathfrak{B}(\lambda^{1/2}y, \lambda^{\frac12-h}Z; \rho(s))$, $\Delta_\kappa = \Delta_y + \kappa^2\partial_Z^2$, P_κ the Leray projector for ∇_κ, and $\widetilde{\mathcal{S}}(s) = \mathcal{J}_s\mathcal{S}(s)\mathcal{J}_s^{-1}$.

(iii) Under (B1)–(B2), with $\delta\mathcal{U}(s) = \mathcal{U}_s - \mathcal{U}_{s_0}$,

$$\sup_s\big(\|\delta\Omega\|_\infty + \|\delta W\|_\infty + \|\nabla_\kappa\delta\mathcal{U}\|_\infty + \|\delta\mathcal{U}_r\|_\infty\big) \le C\kappa(1+L),$$

The radial term here is unweighted: (B1)–(B2) provide $O(\kappa(1+L))$, not $O(\kappa^2(1+L))$. We do not impose an additional dilation-jet assumption on U_1. The downstream packet time-variation estimate uses only this bound.

Here $\delta\Omega$ is the variation of the angular velocity of $\mathcal{U}_s$ and $\delta\mathcal{U}_r$ that of its radial component.

(iv) Under (F2), on shifted blocks with $\rho(s_0+L) \le \nu_0$, $\sup_s \|\gamma(s)^{-1}\widetilde{\mathcal{S}}(s) - \mathcal{S}(s_0)\| \le \varepsilon_{\mathcal{S}}(\kappa, L)$ with $\varepsilon_{\mathcal{S}}(\kappa,L) \to 0$ as $\kappa \downarrow 0$ for fixed L.

Proof. (i) $t^{-h} = -hs$ gives $\lambda = (1 - h\kappa(s-s_0))^{1/h}$, and Bernoulli's inequality $(1/h \ge 1)$ gives $\lambda \ge 1 - \kappa L$. A change of variables gives $\|\mathcal{J}_s V\| = \lambda^{-\frac14 + \frac32 h}\|V\|$.

(ii) $\widetilde{V}(y_0, Z_0, s) = t_0^{\frac12+h} v(t_0^{1/2}y_0, t_0^{\frac12-h}Z_0, t)$. Since $t_0^{h-\frac12} = t_0^{-1/2}\kappa$, the physical gradient is $t_0^{-1/2}\nabla_\kappa$ and the physical Laplacian is $t_0^{-1-h}\kappa\Delta_\kappa$.

The physical Leray projector is thus P_κ, independent of s. Also $t_0^{\frac12+h}u^{\mathrm{lead}}(t_0^{1/2}y_0, t_0^{\frac12-h}Z_0, t) = \mathcal{U}_s(y_0,Z_0)$ and $\partial_s = t^{1+h}\partial_t$.

Inserting these in the physical linearized equation gives (1.34.5).

(iii) $\delta\mathcal{U}$ is the difference of $\lambda^{\frac12+h}\mathfrak{B}(\lambda^{1/2}y, \lambda^{\frac12-h}Z; \rho(s))$ and $\mathfrak{B}(y,Z;\kappa)$. The mean value theorem along $\theta \mapsto (\theta^{1/2}y, \theta^{\frac12-h}Z)$, $\theta \in [\lambda,1]$, together with (B2) and $|\rho(s) - \kappa| \le C\kappa^2 L$, bounds the $\mathcal{U}_0$-part by $C(1-\lambda)$ (the θ-derivative of $\theta^{\frac12+h}f(\theta^{1/2}y, \theta^{\frac12-h}Z)$ is $\theta^{h-\frac12}((\frac12+h)f + \frac12 y\cdot\nabla_y f + (\frac12 - h)Z\partial_Z f)$).

This argument also applies to Ω and $\nabla_y \mathcal{U}_0$. The $\kappa\partial_Z$ components of $\nabla_\kappa \delta\mathcal{U}$ are $O(\kappa)$ by (B1)(a), and the $\rho\mathcal{U}_1$ part is $O(\kappa)$ with $O(\kappa)$ gradient by (B1)(a).

Use (i).

(iv) On a shifted block take $\rho(s_0 + L) \le \nu_0$. Let

$$\varphi^{a,\hbar}_{z,k}(Z) = (a/\pi\hbar)^{1/4} e^{ik(Z-z)/\hbar - a(Z-z)^2/(2\hbar)}.$$

For the unitary dilation $(\mathcal{D}_\mu f)(Z) = \mu^{1/2} f(\mu Z)$ one checks directly $\mathcal{D}_\mu \varphi^{a,\hbar}_{z,k} = \varphi^{a\mu^2,\hbar}_{z/\mu,\mu k}$, and $\varphi^{a,\hbar}_{z,k} = \varphi^{a\kappa/\hbar,\kappa}_{z,k\kappa/\hbar}$ with $(2\pi\hbar)^{-1}\,\mathrm{d}z\,\mathrm{d}k = (2\pi\kappa)^{-1}\,\mathrm{d}z\,\mathrm{d}k'$. Thus the axial part of $\mathcal{J}_s \mathcal{S}(s) \mathcal{J}_s^{-1}$ is the anti-Wick quantization at $\hbar = \kappa$ with window parameter $a(s) = \lambda^{1-h}$ of the symbol $S_{\rho(s),n} \circ \Phi_s$.

Indeed $\rho(s) = \kappa\lambda^{-h}$, so an old packet centre (z_0, k_0) becomes $(\lambda^{h-\frac12} z_0, \lambda^{\frac12} k_0)$. Thus the symbol is evaluated at $\Phi_s(z,k) = (\lambda^{\frac12 - h} z, \lambda^{-\frac12} k) = (\lambda^{\frac12 - h} z, \lambda^{-1/2} k)$. Its axial support lies in $|k| \le \lambda^{1/2} K_S$, and $a(s) = \lambda^{1-h} \le 1$. We conjugate this quantization on H_n by the unitary radial dilation of ratio $\lambda^{1/2}$.

The projector is P_κ by (ii). For any window g, Plancherel in k/κ followed by integration in the centre z gives

$$(2\pi\kappa)^{-1} \int |\langle f, e^{ik(\cdot - z)/\kappa} g(\cdot - z)\rangle|^2 \,\mathrm{d}z\,\mathrm{d}k = \int |f(Z)|^2 |g(Z-z)|^2 \,\mathrm{d}Z\,\mathrm{d}z = \|f\|_2^2 \|g\|_2^2.$$

(1) Applying this identity to the difference of the windows gives $\|T_a - T_1\| = \|\varphi^a_{0,0} - \varphi^1_{0,0}\|_2$. The value $\langle \varphi^a_{0,0}, \varphi^1_{0,0}\rangle = (2\sqrt{a}/(1+a))^{1/2}$ then gives $\|T_a - T_1\| \le \sqrt{2}|a-1| \le C\kappa L$.

(2) The supports of $S_{0,n} \circ \Phi_s$ and $S_{0,n}$ lie in a fixed compact set for $\lambda \ge 1/2$. There $|\Phi_s(w) - w| \le C\kappa L$, so uniform continuity gives $\|S_{0,n} \circ \Phi_s - S_{0,n}\|_\infty \le \omega(C\kappa L)$. (3) Replacing the viscous symbols by $S_{0,n}$ costs at most $\delta_S(\rho(s)) + \delta_S(\kappa)$, uniformly small by (F2) since $\kappa \le \rho(s) \le 2^h \kappa$.

(4) the unitary radial dilations converge strongly to the identity, so their conjugation has uniform norm convergence on the norm-compact set $\{S_{0,n}(w)\}$ of compact operators. (5) $|\gamma^{-1} - 1| \le C\kappa L$.

Summing gives (iv). □

We reparametrize time by $\sigma = \int_{s_0}^s \gamma$, so $\sigma \in [0, \sigma_L]$, $L \le \sigma_L \le L(1 - \kappa L)^{-1-h}$, and (1.34.5) becomes $\partial_\sigma \widetilde{V} = \mathcal{L}(\sigma)\widetilde{V}$ with

$$\mathcal{L}(\sigma)u = -\mathcal{U}_\sigma \cdot \nabla_\kappa u - (2P_\kappa - I)\big((u \cdot \nabla_\kappa)\mathcal{U}_\sigma\big) + \kappa\Delta_\kappa u - \mathcal{S}_\sigma u, \qquad u \in X_\kappa, \tag{1.34.6}$$

$\mathcal{S}_\sigma = \gamma^{-1}\widetilde{\mathcal{S}}$. The identity $P_\kappa[-\mathcal{U}\cdot\nabla_\kappa u - (u\cdot\nabla_\kappa)\mathcal{U}] = -\mathcal{U}\cdot\nabla_\kappa u - (2P_\kappa - I)(u\cdot\nabla_\kappa)\mathcal{U}$ on X_κ is the one used for (1.34.4), now with $\mathrm{div}_\kappa \mathcal{U}_\sigma = 0$.

By (F2) the transformed operator-valued multiplier is strongly measurable on each vector in (σ, z, k). The time reparametrization and the packet-centre map are continuous, as are the radial dilations on each vector and the Gaussian analysis windows in L^2. Applying the uniform multiplier bound and Fubini to the packet pairing gives measurability of $\langle \mathcal{S}_\sigma u, v\rangle$ for fixed u, v. The other form coefficients are continuous in time. On the solenoidal H^1 form domain the positive diffusion coefficient κ supplies coercivity after adding a constant multiple of the L^2 form. Set $\mathcal{H}_n = L^2(\mathbb{R}_Z; \mathsf{H}_n) \cap X_\kappa$.

Here is a construction on each such block. Let V be its solenoidal H^1 space and $H = \mathcal{H}_n$. The form $a_\sigma(u,v) = -\langle \mathcal{L}(\sigma)u, v\rangle$ obeys $|a_\sigma(u,v)| \le C\|u\|_V \|v\|_V$ and $\Re a_\sigma(u,u) \ge c_\kappa \|u\|_V^2 - C\|u\|_H^2$. Here $c_\kappa > 0$ is needed only for existence at fixed κ. Choose an H-orthonormal sequence in V whose increasing finite spans are dense in V, by applying Gram–Schmidt to a countable dense set. In each span solve the matrix equation for the form with projected initial data and with a source $f \in L^2(V')$

if desired. Measurable bounded coefficients suffice: iteration of the integral equation on a finite interval bounds the jth homogeneous integral by $(CT)^j/j!$. Testing with the solution and using the two form bounds gives $\sup\|u_N\|_H^2+\int\|u_N\|_V^2\le C_{\kappa,T}(\|u(\tau)\|_H^2+\int\|f\|_{V'}^2)$. Take a weak limit in $L^2(V)$ and integrate against smooth time multiples of the finite-span vectors. The resulting weak equation extends by density to $u'=\mathcal{L}u+f\in L^2(V')$ and includes the initial pairing at τ.

For completeness, such u has a continuous H representative and $\|u(t)\|^2-\|u(r)\|^2=2\Re\int_r^t\langle u',u\rangle$. Indeed $u\in H^1(V')$ has traces in V'; reflect at the endpoints and mollify in time. The smooth approximants converge in $L^2(V)$ and their derivatives in $L^2(V')$. For a smooth difference w, $\sup_t\|w(t)\|_H^2\le T^{-1}\int\|w\|_H^2+2\|w'\|_{L^2(V')}\|w\|_{L^2(V)}$, by integrating its derivative from a point below the mean. This gives convergence in $C(H)$ and the identity on taking limits. It gives uniqueness by the form bound. The resulting homogeneous operators $\widetilde{U}(\sigma,\tau)$ obey the evolution law by uniqueness. Solving the time-reversed adjoint form from $y\in H$ and applying the polarized identity proves

$$\langle u(\sigma),y\rangle=\langle u(\tau),\widetilde{U}(\sigma,\tau)^*y\rangle+\int_\tau^\sigma\langle f(t),\widetilde{U}(\sigma,t)^*y\rangle\,\mathrm{d}t.$$

Here the identification of the backward solution with the adjoint follows by testing first against a homogeneous forward solution started at t. For an H-valued source in $L^1(H)$ the same formula follows by truncation, using the homogeneous energy bound.

By Lemma 1.34.1,

$$U^\sharp_{\mathrm{lead},n}(s_0+L,s_0)=\mathcal{J}_{s_0+L}^{-1}\,\widetilde{U}(\sigma_L,0)\,\mathcal{J}_{s_0}. \tag{1.34.7}$$

Crude bounds. Transport is skew ($\mathrm{div}_\kappa\mathcal{U}_\sigma=0$) and $\|2P_\kappa-I\|=1$, so for $v(\sigma)=\widetilde{U}(\sigma,0)v_0$

$$\tfrac12\tfrac{\mathrm{d}}{\mathrm{d}\sigma}\|v\|^2+\kappa\|\nabla_\kappa v\|^2\le C_*\|v\|^2,\qquad\|v(\sigma)\|\le e^{C_*\sigma}\|v_0\|,\qquad\int_0^{\sigma_L}\|\nabla_\kappa v\|\,\mathrm{d}\sigma\le C_L\kappa^{-1/2}\|v_0\|, \tag{1.34.8}$$

with $C_*=2C_{\mathfrak{B}}+\sup\|S\|$ independent of n, s_0.

1.34.2 Phase-space toolkit

Fix $\kappa\in(0,1]$ and a window parameter $a>0$. Put $\varphi_w=\varphi^{a,\kappa}_{z,k}$, $w=(z,k)$, and

$$\ell=(\kappa/a)^{1/2},\qquad d=(a\kappa)^{1/2},\qquad \ell d=\kappa.$$

Let $\mathcal{P}=L^2(\mathbb{R}^2,\,\mathrm{d}w/(2\pi\kappa);\mathsf{H}_n)$ and

$$(Tf)(w)=\langle f,\varphi_w\rangle_{L^2_Z},\qquad T^*G=(2\pi\kappa)^{-1}\int G(w)\varphi_w\,\mathrm{d}w,$$

with T acting fibrewise in y.

By the preceding window identity and polarization $T^*T=I$, $\|T\|=\|T^*\|=1$, and $\Pi=TT^*$ is the orthogonal projection onto $\operatorname{Ran}T$. With $\widehat{f}(\zeta)=\int e^{-iZ\zeta}f(Z)\,\mathrm{d}Z$ one computes

$$\widehat{\varphi_w}(\zeta)=c_a e^{-iz\zeta}e^{-(\kappa\zeta-k)^2/(2a\kappa)},\quad c_a^2=2(\pi\kappa/a)^{1/2},\qquad\kappa\partial_Z\varphi_w=(ik-a(Z-z))\varphi_w, \tag{1.34.9}$$

$$|\langle\varphi_{w'},\varphi_w\rangle|=\exp\Big(-\frac{(z-z')^2}{4\ell^2}-\frac{(k-k')^2}{4d^2}\Big). \tag{1.34.10}$$

Lemma 1.34.2 (Two Schur bounds)**.** *Let $\beta\ge0$ be measurable, $X\sim N(0,d^2/2)$, $Y\sim N(0,\ell^2/2)$.*

(a) If $B(\zeta,k)\in\mathcal{L}(\mathsf{H}_n)$ is strongly measurable with $\|B(\zeta,k)\|\le\beta(\kappa\zeta-k)$, the operator $\widehat{(\mathsf{S}_BG)}(\zeta)=(2\pi\kappa)^{-1}\int\widehat{\varphi_w}(\zeta)B(\zeta,k)G(w)\,\mathrm{d}w$ satisfies $\|\mathsf{S}_B\|_{\mathcal{P}\to L^2}\le(\mathbb{E}\beta(X)^2)^{1/2}$.

(b) Suppose $(Z,z)\mapsto B(Z,z)u$ is jointly measurable for every $u\in\mathsf{H}_n$, with $B(Z,z)\in\mathcal{L}(\mathsf{H}_n)$ and $\|B(Z,z)\|\le\beta(Z-z)$, the operator

$$T_B^*G(Z)=(2\pi\kappa)^{-1}\int B(Z,z)\varphi_w(Z)G(w)\,\mathrm{d}w$$

satisfies $\|T_B^*\|\le(\mathbb{E}\beta(Y)^2)^{1/2}$. In particular $\|T_B^*\|\le\ell\|\beta(u)/u\|_\infty/\sqrt{2}$.

Proof. (a) Put $\widehat{G}(\zeta,k)=\int e^{-iz\zeta}G(z,k)\,\mathrm{d}z$. By (1.34.9) and Cauchy–Schwarz in k, $\|\widehat{\mathsf{S}_BG}(\zeta)\|^2\le(2\pi\kappa)^{-2}c_a^2\int e^{-x^2/(a\kappa)}\beta(x)^2\,\mathrm{d}x\int\|\widehat{G}(\zeta,k)\|^2\,\mathrm{d}k$.

Integrate in ζ, use Plancherel twice and $c_a^2(2\pi\kappa)^{-1}=(\pi a\kappa)^{-1/2}$. Note $(\pi a\kappa)^{-1/2}e^{-x^2/(a\kappa)}$ is the density of X.

(b) $\int\varphi_{z,k}(Z)G(z,k)\,\mathrm{d}k=(a/\pi\kappa)^{1/4}e^{-a(Z-z)^2/(2\kappa)}g_z(Z-z)$ with $g_z(u)=\int e^{iku/\kappa}G(z,k)\,\mathrm{d}k$ and $\int\|g_z\|^2\,\mathrm{d}u=2\pi\kappa\int\|G(z,k)\|^2\,\mathrm{d}k$. First take bounded simple G of bounded support. Joint strong measurability on vectors makes the product under the integral measurable. Cauchy–Schwarz in z gives

$$\|T_B^*G(Z)\|^2\le(2\pi\kappa)^{-2}(a/\pi\kappa)^{1/2}\int\beta(Z-z)^2e^{-a(Z-z)^2/\kappa}\,\mathrm{d}z\int\|g_z(Z-z)\|^2\,\mathrm{d}z;$$

integration in Z and density then give the bounded extension whenever $\mathbb{E}\beta(Y)^2<\infty$.

The density of Y is $(a/\pi\kappa)^{1/2}e^{-au^2/\kappa}$. □

Lemma 1.34.3 (Bargmann commutators and packet tails)**.** *(a) If $S:\mathbb{R}^2\to\mathcal{L}(\mathsf{H}_n)$ is bounded with $\|S(w)-S(w')\|\le\omega(|w-w'|)$, we get $\|[S,\Pi]\|_{\mathcal{P}\to\mathcal{P}}\le2\,\mathbb{E}\,\omega(|\Xi|)$, $\Xi=(\Xi_1,\Xi_2)$ independent, $\Xi_1\sim N(0,2\ell^2)$, $\Xi_2\sim N(0,2d^2)$. The same bound holds for $[\Pi,F]$ when $F(w)$ depends only on k, with $\|(F(k)-F(k'))x\|\le\omega(|k-k'|)$ on a fixed vector x. We apply this bound to $x\,c(w)$, with c scalar.*

(b) Let $\Sigma\subset\mathbb{R}$ be closed, let $|\chi|\le1$ be supported in Σ, and put $\Sigma_r=\{k:\operatorname{dist}(k,\Sigma)\ge r\}$. For $j=0$ and every $r>0$, or for $j=1,2$ and $r\ge d$,

$$\|\mathbf{1}_{\Sigma_r}(1+|k|)^jT\chi(\kappa D_Z)\|\le C_j(1+\sup_{\xi\in\Sigma}|\xi|+r)^je^{-r^2/(4d^2)}.$$

For $j=0$ the prefactor is the absolute constant $C_0=2^{1/4}$.

Proof. (a) Π has kernel $(2\pi\kappa)^{-1}\langle\varphi_{w'},\varphi_w\rangle$ with respect to $\mathrm{d}w'$. $[S,\Pi]$ has kernel $(2\pi\kappa)^{-1}(S(w)-S(w'))\langle\varphi_{w'},\varphi_w\rangle$.

Schur's test with (1.34.10), the substitution $w'-w=(x,y)$ and $(2\pi\kappa)^{-1}4\pi\ell d=2$ give the claim. For $[\Pi,F]$ the kernel is $(2\pi\kappa)^{-1}\langle\varphi_{w'},\varphi_w\rangle(F(k')-F(k))x$, and it acts on scalar functions.

(b) By (1.34.9), $\int|Tf(z,k)|^2\,\mathrm{d}z=c_a^2(2\pi)^{-1}\int e^{-(\kappa\zeta-k)^2/(a\kappa)}|\widehat{f}(\zeta)|^2\,\mathrm{d}\zeta$, and $c_a^2(2\pi\kappa)^{-1}e^{-x^2/(a\kappa)}$ is the density of $N(0,d^2/2)$. For $\kappa\zeta\in\Sigma$ and $k\in\Sigma_r$, $|k-\kappa\zeta|\ge r$ and $1+|k|\le1+|\kappa\zeta|+|k-\kappa\zeta|$.

For $j=0$, splitting the Gaussian exponent gives, for every $r>0$,

$$\int_{|u|\ge r}\frac{e^{-u^2/d^2}}{\sqrt{\pi}\,d}\,\mathrm{d}u\le\sqrt{2}\,e^{-r^2/(2d^2)}.$$

Taking a square root gives the unweighted bound. For $j=1,2$, the same split leaves the $2j$-th moment of a Gaussian with standard deviation d, bounded by $C_j(1+|\kappa\zeta|+d)^{2j}$ after adding $1+|\kappa\zeta|$ to $|u|$. Use $d\le r$ and take a square root. □

Lemma 1.34.4 (Leray differences)**.** *Let $P(\xi_h,k)=I-\xi\xi^{\mathsf{T}}/|\xi|^2$, $\xi=(\xi_h,k)$. Then $\|\partial_kP\|\le|\xi|^{-1}$, thus $\|P(\xi_h,k')-P(\xi_h,k)\|\le\min(2,|k'-k|/|\xi_h|)$.*

Thus, with $S_P:=P_\kappa T^*-T^*P_k:\mathcal{P}\to L^2(\mathbb{R}_Z;\mathsf{H}_n)$ and $\Pi_q=\mathbf{1}_{|D_y|\le q}$:

(a) (all n) $\|S_P(1-\Pi_q)\| + \|(1-\Pi_q)S_P\| \le \sqrt{2}\,d/q$ *and, for a matrix field* V, $\|\Pi_q V\|_{L^2\to L^2} \le (q/2\sqrt{\pi})\|V\|_{L^2(\mathbb{R}^2)}$.

(b) ($|n|\ge 2$) on H_n, $\|(P_{k'}-P_k)r^{-1}\| + \|r^{-1}(P_{k'}-P_k)\| \le 2|k'-k|/(|n|-1)$, *and* $\|S_P r^{-1}\| + \|r^{-1}S_P\| \le \sqrt{2}\,d/(|n|-1)$.

(c) $S_P(2P_k - I) = (I-2P_\kappa)S_P$ *and* $\kappa\partial_Z S_P = S_P(ik) + P_\kappa R_1 - R_1 P_k$, *where* $R_1 = T^*_{-a(Z-z)}$ *has* $\|R_1\| \le d/\sqrt{2}$.

Proof. Write $P = I - \hat\xi\hat\xi^{\mathsf T}$. Then $\partial_k P = -(u\hat\xi^{\mathsf T} + \hat\xi u^{\mathsf T})$ with $u = \partial_k\hat\xi \perp \hat\xi$, $|u| = (1-\hat\xi_3^2)^{1/2}/|\xi|$, and the norm of $u\hat\xi^{\mathsf T} + \hat\xi u^{\mathsf T}$ is $|u|$.

(a) S_P is S_B of Lemma 1.34.2(a) with $B(\zeta,k) = P(D_y,\kappa\zeta) - P(D_y,k)$. On $\mathrm{Ran}(1-\Pi_q)$ its norm is at most $|\kappa\zeta - k|/q$, and $\mathbb{E}X^2 = d^2/2$.

Π_q commutes with T, P_κ, P_k. The Hilbert–Schmidt norm of $\Pi_q V$ is $\|\check{\mathbf{1}}_{|\xi|\le q}\|_2\|V\|_2 = (q/2\sqrt{\pi})\|V\|_2$.

(b) $P_{k'} - P_k = m(D_y)|D_y|^{-1}$ with $\|m\| \le |k'-k|$, m rotation covariant. For $g\in\mathsf{H}_n$ with $\widehat{g}$ vanishing near 0, (1.34.3) gives $\|r^{-1}|D_y|^{-1}g\| \le (|n|-1)^{-1}\|g\|$.

By duality and density $\||D_y|^{-1}r^{-1}\|_{\mathsf{H}_n} \le (|n|-1)^{-1}$. Adjoints give the second operator.

The S_P bounds follow as in (a) with $\beta(x) = |x|/(|n|-1)$ (r^{-1} commutes with T, T^*. We first define the operators on $r\mathsf{H}_n \cap \mathsf{H}_n$ and then extend them).

(c) Expand the two sides. The second identity follows from (1.34.9): $\kappa\partial_Z T^*G = T^*(ikG) + R_1 G$. □

Lemma 1.34.5 (Axial cutoff commutators)**.** *Let* $b(Z)\in\mathcal{L}(\mathsf{H}_n)$ *with* $\|\partial_Z b\|_\infty < \infty$ *and* $\chi\in C_c^\infty(\mathbb{R})$. *Then* $\|[b,\chi(\kappa D_Z/K)]\| \le (\kappa/K)\|\partial_Z b\|_\infty\|u\check\chi\|_{L^1}$ *and* $\|[b,\chi(\kappa D_Z/K)]\kappa\partial_Z\| \le C_\chi\kappa\|\partial_Z b\|_\infty$, *with* C_χ *independent of* K.

Also $\|[\chi(\kappa D_Z/K), T^*ST]\| \le C_\chi \sup\|S\|\, d/K$ *for each bounded phase-space multiplier* $S(w)$.

Proof. $\chi(\kappa D_Z/K)$ is convolution with $(K/\kappa)\check\chi(K\cdot/\kappa)$, so the commutator has kernel $(K/\kappa)\check\chi(K(Z-Z')/\kappa)(b(Z)-b(Z'))$. Schur's test gives the first bound.

For the second bound, $[b,\chi]\kappa\partial_Z = [b,\widetilde\chi] - \chi[b,\kappa\partial_Z]$ with $\widetilde\chi(k) = ik\chi(k/K) = iK\psi(k/K)$, $\psi(x) = x\chi(x)$, and $[b,\kappa\partial_Z] = -\kappa\partial_Z b$. For the last, $\chi(\kappa D_Z/K)T^* - T^*\chi(k/K)$ is S_B with $\|B\| \le \|\chi'\|_\infty|\kappa\zeta-k|/K$, its adjoint likewise, and $\chi(k/K)$ commutes with $S(w)$.

□

Lemma 1.34.6 (Frozen smoothing, uniform in n)**.** *Under (B1)(a), for each* n, w, $\kappa\in(0,1]$ *and* $0<\tau\le L$,

$$\|e^{\tau(\widetilde A_0(w)+\kappa\Delta_k)}\|_{X_k} \le e^{m_1\tau}, \qquad \|\nabla_k e^{\tau(\widetilde A_0(w)+\kappa\Delta_k)}\|_{X_k} \le C_L(\kappa\tau)^{-1/2},$$

Here $m_1 = C_{\mathfrak B}$, *and* C_L *depends only on* L *and* $C_{\mathfrak B}$. *The same holds for the shifted generator (with* $m_1 + \sup\|S\|$*), and for the gradient part* $e^{\tau\kappa\Delta_k}(I-P_k)$.

Proof. Let $f' = (\widetilde A_0 + \kappa\Delta_k)f$, $f(0)\in X_k$ smooth. Transport is skew and $\|2P_k - I\| = 1$, so $\frac12(\|f\|^2)' + \kappa\|\nabla_k f\|^2 \le m_1\|f\|^2$.

∇_k commutes with P_k and Δ_k. Derivatives fall only on the coefficients' y-dependence. This gives $\frac12(\|\nabla_k f\|^2)' \le 2m_1\|\nabla_k f\|^2 + m_2\|f\|\|\nabla_k f\|$, $m_2 = \sup|\nabla_y^2\mathcal{U}_0|$, where we omit the nonpositive viscous term $-\kappa\|\nabla_k\nabla_k f\|^2$. Thus $(\tau\|\nabla_k f\|^2)' \le (1 + (4m_1+m_2)\tau)\|\nabla_k f\|^2 + m_2\tau\|f\|^2$.

Integrate and use $\kappa\int_0^\tau\|\nabla_k f\|^2 \le e^{2m_1\tau}\|f(0)\|^2$.

For the shifted generator use Duhamel with the bounded shift. None of the constants involves n: all computations are in Cartesian components.

□

Lemma 1.34.7 (Resolvent to semigroup with explicit constant)**.** *Let A generate a C_0-semigroup on a separable Hilbert space with $\|e^{tA}\| \le e^{\omega t}$, and let $\sup_{\mathrm{Re}\,\zeta \ge g} \|(\zeta - A)^{-1}\| \le M$, $g \le \omega$. Then $\|e^{tA}\| \le C(\omega - g, M) e^{gt}$ for all $t \ge 0$, with $C = \max(e^{3(\omega-g)}, 4M^2 e^{2(\omega-g)})$.*

Proof. Fix $\chi \in C^\infty$, $\chi = 0$ near 0, $\chi = 1$ on $[1, \infty)$, $0 \le \chi' \le 2$. For $x \in H$ put $u(t) = \chi(t) e^{tA} x$ and $v = \chi' e^{tA} x$.

Then $u = \int_0^t e^{(t-s)A} v(s)\, \mathrm{d}s$, so $\widehat{u}(\zeta) = (\zeta - A)^{-1} \widehat{v}(\zeta)$ for $\mathrm{Re}\,\zeta > \omega$, where $\widehat{\ }$ is the Laplace transform. v is supported in $[0,1]$, so $\widehat{v}$ is holomorphic on the full complex plane and $\int \|\widehat{v}(c + i\xi)\|^2 \, \mathrm{d}\xi = 2\pi \int_0^1 e^{-2ct} \|v\|^2 \le 8\pi e^{2(\omega - g)_+} \|x\|^2$ for $c \ge g$.

First let $x \in D(A^2)$. Then $v = \chi' e^{tA} x$ has two continuous derivatives and compact support in $(0,1)$. Two integrations by parts give $\|\widehat{v}(c + i\xi)\| = O_x((1 + |\xi|)^{-2})$, uniformly for $g \le c \le \omega + 1$. Invert the Laplace transform on $c = \omega + 1$ by Fourier inversion. Cauchy's integral formula on rectangles moves the line of inversion to $c = g$: the two horizontal integrals vanish by this decay and the uniform resolvent bound. Thus Plancherel on the new line gives

$$\int_0^\infty e^{-2gt} \|u(t)\|^2 \, \mathrm{d}t \le (2\pi)^{-1} M^2 \int \|\widehat{v}(g + i\xi)\|^2 \, \mathrm{d}\xi \le 4M^2 e^{2(\omega - g)} \|x\|^2.$$

$D(A^2)$ is dense: smooth positive-time averages $\int \varphi_\epsilon(t) e^{tA} x \, \mathrm{d}t$ approximate x and are in every generator domain power by integration by parts. Approximation and Fatou give the bound for all x.

The same holds for A^*.

For $t \ge 3$ and $s \in [1, t-1]$, $\langle e^{tA} x, y \rangle = \langle e^{sA} x, e^{(t-s)A^*} y \rangle$. Integration over s and the Cauchy–Schwarz inequality give $(t-2) e^{-gt} |\langle e^{tA} x, y \rangle| \le 4M^2 e^{2(\omega - g)} \|x\| \|y\|$.

For $t \le 3$ use $e^{\omega t}$. □

1.34.3 Low axial frequencies: the packet comparison

Fix a sector n, the window parameter $a \ge 1$, a cutoff level $K_1 \ge 1$ and $\chi \in C_c^\infty$, $\chi = 1$ on $[-1,1]$, $\mathrm{supp}\,\chi \subset [-2,2]$, $0 \le \chi \le 1$. Put $\chi_{\mathrm{low}} = \chi(\kappa D_Z / K_1)$.

The frozen symbol of (1.34.6) at $\sigma = 0$ is $\widetilde{A}_0(w) + \kappa\Delta_k - S(w)$, $S = S_{\kappa,n}$, and we use its extension

$$\widehat{E}_\tau(w) = e^{\tau(\widetilde{A}_0(w) + \kappa\Delta_k - S(w))} P_k + e^{\tau\kappa\Delta_k} (I - P_k) \tag{1.34.11}$$

to all of H_n, and the synthesis

$$Q(\tau) = P_\kappa T^* \widehat{E}_\tau T : \ \mathcal{H}_n \to X_\kappa, \qquad Q(0)u = u \quad (u \in X_\kappa). \tag{1.34.12}$$

The actual shift at $\sigma = 0$ is $\mathcal{S}_0 = P_\kappa T_1^* S T_1 P_\kappa$ (window $a = 1$).

Proposition 1.34.8 (Low-frequency packet comparison)**.** *Assume (B1)–(B2). On shifted sectors assume (F2) and $\rho(s_0 + L) \le \nu_0$. Let C_E, g be such that $\|e^{\tau(\widetilde{A}_0(w) + \kappa\Delta_k - S(w))}\|_{X_k} \le C_E e^{g\tau}$ for $|k| \le 3K_1$, $z \in \mathbb{R}$, $\tau \ge 0$. Then for $\sigma \le \sigma_L$ and $v_0 \in X_\kappa$,*

$$\|\widetilde{U}(\sigma, 0) \chi_{\mathrm{low}} v_0\| \le \big[(C_E + 1) e^{g\sigma} + e^{C_* \sigma_L} \mathcal{E}\big] \|v_0\|, \tag{1.34.13}$$

Here C depends only on L, C_E, $C_{\mathfrak{B}}$, χ and $\sup \|S\|$; it does not depend on n, s_0:

(i) if $a = 1$ (any n) and $q \in (0,1]$,

$$\mathcal{E} \le C(1 + |n| + K_1)\big[\kappa^{1/2} + q + \kappa^{1/2} q^{-1} + \kappa L\big] + \mathcal{E}_S(\kappa) + \mathsf{t};$$

(ii) if $S \equiv 0$, $|n| \geq 2$ *and* $a = |n|$,

$$\mathcal{E} \leq C\big[(|n| + K_1)\ell + (1 + K_1/|n|)d + \kappa^{1/2} + \kappa d K_1 + (|n| + K_1)\kappa L\big] + \mathsf{t};$$

where $\mathsf{t} = C(1 + K_1)^2 e^{-K_1^2/(4d^2)}$ *(packet tails).*

Here $\mathcal{E}_S \equiv 0$ *if* $S \equiv 0$, *and in general* $\mathcal{E}_S(\kappa) \to 0$ *as* $\kappa \downarrow 0$ *under (F2).*

Proof. Step 0: Duhamel. By linearity we take $\|v_0\| = 1$. Set $f = \chi_{\mathrm{low}} v_0$, $G(\tau) = \widehat{E}_\tau T f$, $G_\sigma = P_k G$, $G_g = (I - P_k)G$. By Lemma 1.34.6, its L^2-in-time form $\kappa \int_0^{\sigma_L} \|\nabla_k \widehat{E}_\tau(w) f\|^2 \, \mathrm{d}\tau \leq C\|f\|^2$, Plancherel in w and $\kappa \partial_Z T^* = T^* i k + R_1$, the function $Q(\cdot)\chi_{\mathrm{low}} v_0$ lies in $C([0, \sigma_L]; X_\kappa) \cap L^2(0, \sigma_L; H^1)$ with time derivative in $L^2(0, \sigma_L; H^{-1})$.

Let $D(\tau) = \partial_\tau Q \chi_{\mathrm{low}} v_0 - \mathcal{L}(\tau) Q \chi_{\mathrm{low}} v_0 \in H^{-1}$. We show that $D(\tau) \in L^2$ and

$$\int_0^{\sigma_L} \|D(\tau)\| \, \mathrm{d}\tau \leq \mathcal{E}\|v_0\|. \tag{1.34.14}$$

The difference $Q\chi_{\mathrm{low}} v_0 - \widetilde{U}(\cdot, 0)\chi_{\mathrm{low}} v_0$ is the variational solution with zero datum and source D. Apply the forward–backward pairing proved after (1.34.6) to this difference and to arbitrary terminal data. This gives $\widetilde{U}(\sigma, 0)\chi_{\mathrm{low}} v_0 = Q(\sigma)\chi_{\mathrm{low}} v_0 - \int_0^\sigma \widetilde{U}(\sigma, \tau) D(\tau) \, \mathrm{d}\tau$.

The frozen bound applies on X_k for $|k| \leq 3K_1$, and the heat semigroup is contractive on $X_k^\perp$. Here $g \geq 0$: at $k = 0$ choose a fixed z outside the shift support and take unit vertical fields $c_R e^{in\theta}\psi(r/R)e_z$ with $\psi \in C_c^\infty((1, 2))$. They are solenoidal, their Laplacians are $O_n(R^{-2})$ in L^2, and their angular transport tends to zero by (B1)(b). Stretching vanishes on these fields. Thus zero belongs to the approximate spectrum of this fiber, which excludes exponential decay. Consequently $\|\widehat{E}_\tau(w)\| \leq (C_E + 1)e^{g\tau}$ on the inner band. On all fibers Lemma 1.34.6 gives $\|\widehat{E}_\tau(w)\| \leq e^{C_* \tau}$. Use the $j = 0$ bound of Lemma 1.34.3(b) with $\Sigma = [-2K_1, 2K_1]$ and $r = K_1$ to obtain $\|Q(\sigma)\chi_{\mathrm{low}}\| \leq (C_E + 1)e^{g\sigma} + 2^{1/4} e^{C_* \sigma} e^{-K_1^2/(4d^2)}$ for every $d > 0$. Together with (1.34.8) and the integrated defect estimate below, this yields (1.34.13).

For the defect we need the full second moment. In the Fourier marginal of (1.34.9), k is integrated against a Gaussian of mean $\kappa\zeta$ and variance $d^2/2$. Plancherel gives

$$\|kTf\|_{\mathcal{P}}^2 = \|\kappa D_Z f\|_2^2 + \tfrac{1}{2} d^2 \|f\|_2^2 \leq (4K_1^2 + d^2/2)\|f\|_2^2.$$

Since k commutes with the fiber evolution, $\|G(\tau)\| \leq C_L$ and

$$\|kG(\tau)\| \leq C_L(K_1 + d) \quad (0 \leq \tau \leq \sigma_L), \qquad \|\nabla_k G(\tau)\| \leq C_L(\kappa\tau)^{-1/2} \quad (0 < \tau \leq \sigma_L). \tag{1.34.15}$$

Step 1: exact defect formula. On H_n, by (1.34.2), $\mathcal{U}_0(Z) \cdot \nabla_\kappa = \Omega(Z)(in + J) + W(Z)\kappa\partial_Z$ and $\mathcal{U}_0(z) \cdot \nabla_k = \Omega(z)(in + J) + ikW(z)$. Split $\mathcal{L}(\tau) = \mathcal{L}_{00} + \kappa\mathcal{L}_{01} + \kappa\Delta_\kappa - \mathcal{S}_\tau + \delta\mathcal{L}(\tau)$, where $\mathcal{L}_{00} = -\mathcal{U}_0 \cdot \nabla_\kappa - (2P_\kappa - I)\mathfrak{M}_0$ with the actual Z-dependent $\mathcal{U}_0$ at $\sigma = 0$.

The term $\kappa\mathcal{L}_{01}$ collects the terms with $\kappa\mathcal{U}_1$ or $u_z \kappa \partial_Z \mathcal{U}_0$ (all bounded, except $-\kappa\mathcal{V}\partial_r$). The term $\delta\mathcal{L}(\tau)$ contains the terms with $\mathcal{U}_\tau - \mathcal{U}_0$.

Define R_v by $\Delta_\kappa T^* = T^* \Delta_k + R_v$. We have $\partial_\tau Q\chi_{\mathrm{low}} v_0 = P_\kappa T^*[(\widetilde{A}_0 + \kappa\Delta_k - S)G_\sigma + \kappa\Delta_k G_g]$ and $Q\chi_{\mathrm{low}} v_0 = P_\kappa T^* G = T^* G_\sigma + S_P G$.

Since Δ_κ commutes with P_κ and Δ_k with P_k,

$$\Delta_\kappa(T^* G_\sigma + S_P G) = \Delta_\kappa P_\kappa T^* G = P_\kappa(T^* \Delta_k G + R_v G),$$

so the viscous contributions combine to $\kappa P_\kappa T^* \Delta_k G - \kappa P_\kappa(T^* \Delta_k G + R_v G) = -\kappa P_\kappa R_v G$. (Here we use the free heat on the gradient part of (1.34.11).) With $P_\kappa T^* \widetilde{A}_0 G_\sigma = T^* \widetilde{A}_0 G_\sigma + S_P \widetilde{A}_0 G_\sigma$

(because $P_k\widetilde{A}_0P_k=\widetilde{A}_0P_k$) we get the exact identity

$$\begin{aligned}D&=[T^*\widetilde{A}_0-\mathcal{L}_{00}T^*]G_\sigma+S_P\widetilde{A}_0G_\sigma-\mathcal{L}_{00}S_PG-\kappa P_\kappa R_vG-\kappa\mathcal{L}_{01}P_\kappa T^*G\\&\quad+[\mathcal{S}_0P_\kappa T^*G-P_\kappa T^*SG_\sigma]+(\mathcal{S}_\tau-\mathcal{S}_0)P_\kappa T^*G-\delta\mathcal{L}(\tau)P_\kappa T^*G.\end{aligned}\tag{1.34.16}$$

By (1.34.9) and $\kappa\partial_Z[-a(Z-z)\varphi_w]=[-a\kappa-a(Z-z)(ik-a(Z-z))]\varphi_w$,

$$R_vG=2T^*_{-a(Z-z)}(ikG)-a\kappa T^*G+T^*_{a^2(Z-z)^2}G,\qquad\|R_vG\|\le\sqrt{2}d\|kG\|+2d^2\|G\|,$$

by Lemma 1.34.2(b) ($a\ell=d$, $a\kappa=d^2$, $\mathbb{E}Y^4=3\ell^4/4$).

We bound the terms of (1.34.16) in order.

(1) Coefficient variation. Using $\kappa\partial_ZT^*G=T^*(ikG)+R_1G$, $R_1=T^*_{-a(Z-z)}$,

$$[\mathcal{L}_{00}T^*-T^*\widetilde{A}_0]G_\sigma=-T^*_{B_1}G_\sigma-T^*_{B_2}(ikG_\sigma)-W(Z)R_1G_\sigma-(2P_\kappa-I)T^*_{B_3}G_\sigma-2S_P\mathfrak{M}_0(z)G_\sigma,$$

with $B_1=(\Omega(Z)-\Omega(z))(in+J)$, $B_2=W(Z)-W(z)$, $B_3=\mathfrak{M}_0(Z)-\mathfrak{M}_0(z)$ (the last term arises from $2P_\kappa T^*-2T^*P_k=2S_P$). By (B1)(a) and Lemma 1.34.2(b) the sum of the norms of the first four terms is at most

$$C\big[((|n|+1)\ell+d+\ell)\|G\|+\ell\|kG\|\big].$$

Equation (1.34.15) bounds this by $C_L[(|n|+K_1)\ell+d]$, since $\ell d=\kappa\le d$ and $K_1\ge1$.

(2) Projection defects. By (1) and Lemma 1.34.4(c), the terms of (1.34.16) containing S_P are

$$\Big\{2S_P\mathfrak{M}_0(z)-S_P\Omega(z)(in+J)-S_PW(z)\,ik-(I-2P_\kappa)S_P\mathfrak{M}_0(z)\Big\}G_\sigma$$

and

$$\Omega(Z)(in+J)S_PG+W(Z)S_P(ikG)+W(Z)(P_\kappa R_1-R_1P_k)G+(2P_\kappa-I)\mathfrak{M}_0(Z)S_PG.$$

Thus each is S_P composed with a coefficient $V\in\{\Omega(in+J),W,\mathfrak{M}_0\}$ on its right or on its left, applied to G or kG. A right coefficient is frozen at z and is a multiplication on $\mathcal{P}$. A left coefficient is frozen at Z. The exception is $W(Z)(P_\kappa R_1-R_1P_k)G$, which is $\le2\|W\|_\infty d\|G\|/\sqrt{2}$.

In case (i) insert $I=\Pi_q+(1-\Pi_q)$ next to V. Π_q commutes with T,T^*,P_κ,P_k.

By Lemma 1.34.4(a) and (B1)(b), $\|S_PV\|+\|VS_P\|\le C(\|V\|_\infty d/q+q\sup_Z\|V(\cdot,Z)\|_{L^2})$. Only the coefficient $\Omega(in+J)$ costs $|n|+1$, and only W multiplies kG. Since $d=\sqrt{\kappa}\le1$, the total is at most $C_L(|n|+1+K_1)(q+d/q)$.

In case (ii) write $V=r^{-1}(rV)$ (resp. $(rV)r^{-1}$ on the left). By Lemma 1.34.4(b) and (B1)(b), $\|S_PV\|+\|VS_P\|\le Cd(|n|+1)/(|n|-1)\le3Cd$ for $V=\Omega(in+J)$ and $\le Cd/|n|$ for $V\in\{W,\mathfrak{M}_0\}$.

Equation (1.34.15) thus bounds the total by $C_Ld[1+(K_1+d)/|n|]\le C_Ld(1+K_1/|n|)$ after enlarging C_L, since $d^2/|n|=\kappa\le d$.

The factor $(|n|-1)^{-1}$ from (1.34.3) controls $|n|$ in the coefficient $n\Omega$. Small frequency width d alone does not give this bound.

(3) Viscous and κ-terms. By the bound for R_v and (1.34.15), $\kappa\|R_vG\|\le C_L\kappa(dK_1+d^2)$. In case (ii), $\sigma_L\le2^{1+h}L$ and $d^2=\kappa|n|$, so the integrated κd^2 term is bounded by $C_L\kappa L|n|$. Also $\|\kappa\mathcal{L}_{01}P_\kappa T^*G\|\le C\kappa(\|\nabla_yG\|+\|G\|)\le C_L\kappa^{1/2}\tau^{-1/2}+C_L\kappa$, because ∇_y commutes with P_κ and T^* and $|\mathcal{V}|\le C_{\mathfrak{B}}$.

(4) Shift (only $n=\pm m$, $a=1$, $\ell=d=\kappa^{1/2}$). By $TP_\kappa T^*=T(T^*P_k+S_P)=\Pi P_k+TS_P$, $T^*\Pi=T^*$ and $SP_k=S$,

$$\mathcal{S}_0P_\kappa T^*G-P_\kappa T^*SG_\sigma=P_\kappa T^*S(\Pi-I)P_kG+P_\kappa T^*S\,TS_PG=P_\kappa T^*[S,\Pi]P_kG+P_\kappa T^*S\,TS_PG.$$

Write $S = S_0 + (S - S_0)$ with $\|S - S_0\| \le \delta_S(\kappa)$ by (F2), and let ω_S be a modulus of continuity of the compactly supported continuous S_0.

By Lemma 1.34.3(a), $\|[S_0, \Pi]\| \le 2\mathbb{E}\,\omega_S(|\Xi|)$. For the second term, $\|S_0 T S_P\| = \|S_P^* T^* S_0^*\|$ and $S_P^* T^* S_0^* = (TP_\kappa - P_k T)T^* S_0^* = T S_P S_0^* + [\Pi, P_k] S_0^*$.

Write $S_0(w) = e(w) \otimes \ell_0(w)^*$ (rank one. e, ℓ_0 may be selected continuous on the compact W_S, vanishing outside it, after multiplying by the scalar cutoff), so $S_0^* G = \ell_0\, c$ with $c(w) = \langle G(w), e(w)\rangle$, $|c| \le C\|G\|$.

Given $\eta > 0$, select finitely many vectors ℓ_j and continuous scalar a_j on W_S with $\sup_w \|\ell_0(w) - \sum_j a_j(w)\ell_j\| \le \eta$. For this, use a partition of unity subordinate to a cover on which ℓ_0 oscillates by less than η. For each fixed ℓ_j, $k \mapsto P_k \ell_j$ is continuous. The reason is dominated convergence in the horizontal Fourier variable, since $P(\xi_h, k)$ is continuous in k for $\xi_h \neq 0$. Thus $\omega_j(x) = \sup\{\|(P_{k'} - P_k)\ell_j\| : |k| \le K_S, |k' - k| \le x\} \to 0$ as $x \to 0$, and $\omega_j \le 2\|\ell_j\|$.

Lemma 1.34.2(a) with $B(\zeta, k) = (P(D_y, \kappa\zeta) - P(D_y, k))\ell_j$, $\beta = \omega_j$, and Lemma 1.34.3(a) with $F = P_k$, $x = \ell_j$, give $\|S_0 T S_P\| \le C\eta + C\sum_j \|a_j\|_\infty (\mathbb{E}\,\omega_j(|X|)^2)^{1/2} + C\sum_j \|a_j\|_\infty \mathbb{E}\,\omega_j(|\Xi|)$. Together with Lemma 1.34.1(iv) for $\mathcal{S}_\tau - \mathcal{S}_0$, the shift terms are bounded by

$$\mathcal{E}_S(\kappa) = C\Big[\delta_S(\kappa) + \mathbb{E}\,\omega_S(|\Xi|) + \inf_{\eta > 0}\Big(\eta + \sum_j \|a_j\|_\infty \big((\mathbb{E}\omega_j(|X|)^2)^{1/2} + \mathbb{E}\,\omega_j(|\Xi|)\big)\Big) + \varepsilon_{\mathcal{S}}(\kappa, L)\Big].$$

This tends to zero as $\kappa \downarrow 0$.

For fixed η, the finitely many expectations tend to zero by dominated convergence.

The Gaussian variables have variances $O(\kappa)$, and the moduli stay bounded.

(5) Time variation. By Lemma 1.34.1(iii), (1.34.2), (1.34.15) and $\kappa\partial_Z P_\kappa T^* G = P_\kappa(T^* ikG + R_1 G)$, the coefficient and radial transport contributions give

$$\|\delta\mathcal{L}(\tau) P_\kappa T^* G\| \le C_L\kappa(1 + |n| + K_1 + d) + C_L\kappa\|\nabla_y G\|.$$

In case (i), $d \le 1$, and in case (ii), $d \le |n|$. Integration of the first term therefore costs at most $C_L\kappa L(1 + |n| + K_1)$.

We integrate (1)–(5) over $[0, \sigma_L]$. The only singular factor is $\tau^{-1/2}$.

This gives (1.34.14) with the stated $\mathcal{E}$. In case (i) $\ell = d = \kappa^{1/2}$.

□

1.34.4 High axial frequencies and very far angular labels

Lemma 1.34.9 (High axial output)**.** *Assume (B1) and (F3). On shifted sectors assume also (F2) and $\rho(s_0 + L) \le \nu_0$. Put $K_S = 0$ on unshifted sectors. Let $\alpha_\delta = \|(1-\delta)/r\|_\infty$ and $K_1 \ge \max\{1, 8K_S\}$, and suppose*

$$\gamma' := \gamma_\delta + \frac{8\alpha_\delta |n| C_{\mathfrak{B}}}{K_1 d_*} + \frac{C_0'\kappa(1 + L)}{d_*} \le \gamma, \tag{1.34.17}$$

where C_0' depends only on $C_{\mathfrak{B}}$ and δ. Put $\chi_{\mathrm{out}} = \chi(4\kappa D_Z/K_1)$, $\epsilon_c = \kappa^{1/2} + \kappa|n|/K_1 + e^{-K_1^2/(256\kappa)}$.

For $v_0 \in X_\kappa$ and $v(\sigma) = \widetilde{U}(\sigma, 0)(1 - \chi_{\mathrm{low}})v_0$, $0 \le \sigma \le \sigma_L$,

$$\|\chi_{\mathrm{out}} v(\sigma)\| \le C_L\epsilon_c\|v_0\|, \qquad \|(1 - \chi_{\mathrm{out}})v(\sigma)\| \le d_*^{-1/2} e^{\gamma\sigma}\|v_0\| + C_L\epsilon_c\|v_0\|,$$

with C_L independent of n and s_0.

Proof. Commutators. Let $X \in \{\chi_{\mathrm{out}}, 1 - \chi_{\mathrm{out}}\}$. X commutes with P_κ, Δ_κ and with each function of y alone.

By Lemma 1.34.5 (with $K = K_1/4$), (B1)(a) and (1.34.2): $\|[X,\Omega](in+J)\| \le C\kappa(|n|+1)/K_1$. $\|[X,W]\kappa\partial_Z\| \le C\kappa$.

$\|(2P_\kappa - I)[X,\mathfrak{M}]\| \le C(\kappa/K_1 + \kappa)$ (the $\rho\mathcal{U}_1$ part of $\mathfrak{M}$ is $O(\kappa)$ and (B1) gives no $\partial_Z\nabla_y\mathcal{U}_1$ bound, so its commutator is only $O(\kappa)$; the $h_z\kappa\partial_Z\mathcal{U}_0$ part commutes at $O(\kappa^2/K_1)$ by (B1)(a); the extra $C\kappa$ is below $\kappa^{1/2}$ in ϵ_c).

$\|\kappa[X,\mathcal{V}]\partial_r u\| \le C\kappa^2 K_1^{-1}\|\nabla_y u\|$. At $s = s(\tau)$ the shift has window $a_s = \lambda^{1-h}$ and momentum width $d_s = (\kappa a_s)^{1/2}$. Since X commutes with P_κ and the radial dilation, Lemma 1.34.5 gives $\|[X,\mathcal{S}_\tau]\| \le CM_S d_s/K_1 \le CM_S\sqrt{\kappa}/K_1$ on shifted sectors. Here $\gamma(s)^{-1} \le 1$.

Thus, with (1.34.8), $\int_0^{\sigma_L}\|[X,\mathcal{L}(\tau)]v(\tau)\|\,\mathrm{d}\tau \le C_L(\kappa^{1/2} + \kappa|n|/K_1)\|v_0\|$.

Low output. $\chi_{\mathrm{out}}(1-\chi_{\mathrm{low}}) = 0$ because $\chi(4k/K_1) = 0$ for $|k| \ge K_1/2$ and $1-\chi(k/K_1) = 0$ for $|k| \le K_1$. Thus $\chi_{\mathrm{out}}v(\sigma) = \int_0^\sigma \widetilde{U}(\sigma,\tau)[\chi_{\mathrm{out}},\mathcal{L}(\tau)]v(\tau)\,\mathrm{d}\tau$.

Use (1.34.8).

High output. $h = (1-\chi_{\mathrm{out}})v \in X_\kappa$ has axial frequencies $|k| \ge K_1/4$ and solves $h' = \mathcal{L}h + f$ with $f = [I-\chi_{\mathrm{out}},\mathcal{L}]v = -[\chi_{\mathrm{out}},\mathcal{L}]v$. Let $M = I + (\delta(r)-1)e_\theta\otimes e_\theta$ (a smooth Cartesian matrix field, $M = I$ near the axis) and $E = \langle h, Mh\rangle$, so $d_*\|h\|^2 \le E \le \|h\|^2$.

We use $\mathcal{L}h = -\mathcal{U}_\tau\cdot\nabla_\kappa h - \mathfrak{M}h + 2(I-P_\kappa)\mathfrak{M}h + \kappa\Delta_\kappa h - \mathcal{S}_\tau h$, $\mathfrak{M}h = (h\cdot\nabla_\kappa)\mathcal{U}_\tau$. (a) Since $\mathrm{div}_\kappa\mathcal{U}_\tau = 0$ and M does not depend on Z, $\mathrm{Re}\langle Mh, -\mathcal{U}_\tau\cdot\nabla_\kappa h\rangle = \frac12\int h^*(\mathcal{U}_{\tau,h}\cdot\nabla_y M)h$.

With $\partial_\theta(e_\theta\otimes e_\theta) = -(e_r\otimes e_\theta + e_\theta\otimes e_r)$ and the frame form $(h\cdot\nabla)(r\Omega e_\theta + We_z) = -\Omega h_\theta e_r + (r\Omega)'h_r e_\theta + \partial_r W h_r e_z + O(\kappa)$, one finds for the swirl/axial part

$$\tfrac12 h^*(\Omega\partial_\theta M)h - \mathrm{Re}\,h^*M(h_h\cdot\nabla_y)\mathcal{U}_0 = \mathrm{Re}\big[(2\Omega - \delta B)\bar h_r h_\theta - \partial_r W\,\bar h_z h_r\big] \le \gamma_\delta\, h^*Mh$$

pointwise, by Cauchy–Schwarz in $(h_r, \sqrt{\delta}h_\theta, h_z)$. For the dilated coefficients $\mathcal{U}_\tau$ we evaluate the same expression with $\delta(\lambda^{-1/2}r)$ in place of $\delta(r)$ after we substitute $r \mapsto \lambda^{1/2}r$.

$r\delta'$ is bounded and $1-\lambda \le \kappa L$ holds, so this changes γ_δ by at most $C\kappa L/d_*^{3/2}$. The radial-velocity terms $\kappa\mathcal{V}\partial_r M$, $\kappa(h\cdot\nabla)\mathcal{U}_1$ and $h_z\kappa\partial_Z\mathcal{U}_0$ contribute at most $C\kappa|h|^2$.

(b) Pressure: $2\,\mathrm{Re}\langle Mh, (I-P_\kappa)\mathfrak{M}h\rangle = 2\,\mathrm{Re}\langle (I-P_\kappa)(M-I)h, \mathfrak{M}h\rangle$ because $(I-P_\kappa)$ is self-adjoint and $(I-P_\kappa)h = 0$. Since $\mathrm{div}_\kappa((\delta-1)h_\theta e_\theta) = (\delta-1)r^{-1}\partial_\theta h_\theta = (\delta-1)(in/r)h_\theta$ ($h_\theta = h\cdot e_\theta$ is a scalar mode n) and this function has axial frequencies $\ge K_1/4$, $\|(I-P_\kappa)(M-I)h\| = \|\nabla_\kappa\Delta_\kappa^{-1}[(\delta-1)(in/r)h_\theta]\| \le 4\alpha_\delta|n|\|h\|/K_1$.

Thus the pressure term is at most $8\alpha_\delta|n|C_{\mathfrak{B}}\|h\|^2/K_1$. (c) $\mathrm{Re}\langle Mh, \kappa\Delta_\kappa h\rangle = -\kappa\int(\nabla_\kappa h)^* M\nabla_\kappa h + \frac{\kappa}{2}\int h^*(\Delta_y M)h \le \frac{\kappa}{2}\|\Delta_y M\|_\infty\|h\|^2$.

(d) On a shifted sector fix τ and let $J_s = [-\lambda^{1/2}K_S, \lambda^{1/2}K_S]$. By (F2) and the change of packet centres in Lemma 1.34.1(iv), the transported symbol vanishes for $k \notin J_s$. The radial dilation preserves its norm, $P_\kappa h = h$, and the synthesis map is a contraction. Therefore $\|\mathcal{S}_\tau h\| \le M_S\|\mathbf{1}_{J_s}(k)T_{a_s}h\|_{\mathcal{P}}$. Plancherel in the centre z, with (1.34.9), gives

$$\|\mathbf{1}_{J_s}(k)T_{a_s}h\|_{\mathcal{P}}^2 = \frac{1}{2\pi}\int_{\mathbb{R}}\|\widehat{h}(\zeta)\|_{\mathsf{H}_n}^2\left(\int_{J_s}\frac{e^{-(k-\kappa\zeta)^2/d_s^2}}{\sqrt{\pi}\,d_s}\,\mathrm{d}k\right)\mathrm{d}\zeta.$$

On the Fourier support of h, $|\kappa\zeta| \ge K_1/4$. Hence for $k \in J_s$ we have $|k-\kappa\zeta| \ge K_1/8$. Splitting the Gaussian exponent in half bounds the inner integral by $\sqrt{2}\exp[-K_1^2/(128d_s^2)]$. Taking a square root and using $d_s^2 = \kappa\lambda^{1-h} \le \kappa$ yields

$$\|\mathcal{S}_\tau h\| \le 2^{1/4}M_S e^{-K_1^2/(256d_s^2)}\|h\| \le 2^{1/4}M_S e^{-K_1^2/(256\kappa)}\|h\|.$$

On every other sector the shift vanishes.

By $\|h\|^2 \le E/d_*$, (a)–(d) give $\frac12 E' \le \gamma' E + |\langle Mh, f - \mathcal{S}_\tau h\rangle|$, thus $(\sqrt{E})' \le \gamma'\sqrt{E} + d_*^{-1/2}(\|f\| + \|\mathcal{S}_\tau h\|)$ and $\|h(\sigma)\| \le d_*^{-1/2}e^{\gamma'\sigma}\|v_0\| + d_*^{-1}\int_0^\sigma e^{\gamma'(\sigma-\tau)}(\|f\| + \|\mathcal{S}_\tau h\|)\,\mathrm{d}\tau$. Use $\gamma' \le \gamma$, the commutator bound and (1.34.8).

□

Lemma 1.34.10 (Very far angular labels)**.** *Assume (B1). There is C_U (it depends only on $C_{\mathfrak{B}}$ and N_{far}) such that for $|n| \geq N_\kappa := 1 + (C_U/\kappa)^{1/2}$, each block with $\kappa L \leq \frac{1}{2}$ and $0 \leq \sigma \leq \sigma_L$, $\|\widetilde{U}(\sigma,0)\|_{\mathcal{H}_n \to \mathcal{H}_n} \leq e^{C_U \kappa \sigma}$.*

Proof. On X_κ the pressure term is orthogonal to v and transport is skew, so $\frac{1}{2}(\|v\|^2)' \leq \int |\nabla_\kappa \mathcal{U}_\sigma||v|^2 - \kappa\|\nabla_y v\|^2$, $|\cdot|$ the matrix norm. By (B1)(b) and $\lambda \geq \frac{1}{2}$, $|\nabla_y \mathcal{U}_{0,\sigma}| \leq C\langle \lambda^{1/2} r\rangle^{-2} \leq C_U r^{-2}$, and by (B1)(a) the remaining entries of $\nabla_\kappa \mathcal{U}_\sigma$ are $\leq C_U \kappa$.

By (1.34.3), $C_U \int r^{-2}|v|^2 \leq C_U(|n|-1)^{-2}\|\nabla_y v\|^2 \leq \kappa \|\nabla_y v\|^2$. The shift vanishes for $|n| \geq N_{\mathrm{far}}$, and we may take C_U so large that $N_\kappa \geq N_{\mathrm{far}}$ for $\kappa \leq 1$.

□

1.34.5 The two block lemmas

Lemma 1.34.11 (Low-label physical FBI block)**.** *Assume (B1)–(B2) and (F1)–(F3). Put $C_0 = C_F + 1 + d_*^{-1/2}$.*

For each $L > 0$ there are $\kappa_1(L) > 0$ and $\varepsilon_F(L,\kappa)$ with $\varepsilon_F(L,\kappa) \to 0$ as $\kappa \downarrow 0$ such that for all $n \in F$ (with $0, \pm 1$) and all s_0 with $\rho(s_0) \leq \kappa_1(L)$,

$$\|U^\sharp_{\mathrm{lead},n}(s_0 + L, s_0)\| \leq C_0 e^{g_1 L} + \varepsilon_F(L, \rho(s_0)).$$

C_0 is independent of L and of s_0.

Proof. Fix $K_1 \geq \max\{1, 8K_S\}$ so large that $8\alpha_\delta N_{\mathrm{far}} C_{\mathfrak{B}}/(K_1 d_*) \leq \frac{1}{2}(\gamma - \gamma_\delta)$. K_1 does not depend on L.

Then (1.34.17) holds for $|n| < N_{\mathrm{far}}$ once $\kappa \leq \kappa_1(L)$, with $\kappa_1(L)$ also so small that $\kappa L \leq \frac{1}{2}$ and $2^h \kappa \leq \nu_0$, which keeps $\rho(s) \leq \nu_0$ throughout the block. By (F1) (with $\nu = \kappa$), the hypothesis of Proposition 1.34.8 holds with $C_E = C_F$, $g = g_1$.

For $v_0 \in X_\kappa$ write $v_0 = \chi_{\mathrm{low}} v_0 + (1 - \chi_{\mathrm{low}})v_0$. Proposition 1.34.8(i) with $q = \kappa^{1/4}$ and Lemma 1.34.9 give

$$\|\widetilde{U}(\sigma_L, 0)\| \leq (C_F + 1)e^{g_1 \sigma_L} + d_*^{-1/2} e^{\gamma \sigma_L} + e^{C_* \sigma_L}\big[C(1 + N_{\mathrm{far}} + K_1)(\kappa^{1/4} + \kappa L) + \mathcal{E}_S(\kappa) + \mathfrak{t}\big] + C_L \kappa^{1/2}.$$

Conjugate by (1.34.7), use Lemma 1.34.1(i), $\sigma_L \leq L(1 - \kappa L)^{-1-h}$ and $\gamma < g_1$.

Collect each term other than $C_0 e^{g_1 L}$ into ε_F. □

Lemma 1.34.12 (Squeezed far-angular blocks)**.** *Assume (B1)–(B2), (F3) and (F4). There are C_1 and, for each L, C_L such that for $|n| \geq N_{\mathrm{far}}$, each sufficiently small $\kappa = \rho(s_0)$ and each s_0,*

$$\|U_{\mathrm{lead},n}(s_0 + L, s_0)\| \leq C_1 e^{g_1 L} + C_L \kappa^{1/4}.$$

C_1 and C_L are independent of n.

Proof. The modifications relative to the previous proof are the next.

(1) *Frozen bound.* (F4), Lemma 1.34.6 (crude rate $m_1 = C_{\mathfrak{B}}$, uniform in n) and Lemma 1.34.7 give $\|e^{\tau A_{\kappa,n}(w)}\| \leq C_{\mathrm{far}} e^{g_{\mathrm{far}}\tau}$ with $C_{\mathrm{far}} = C(m_1 - g_{\mathrm{far}}, M_{\mathrm{far}})$ independent of n, w, κ.

(2) *Very far labels.* For $|n| \geq N_\kappa$, Lemma 1.34.10 gives $\|\widetilde{U}(\sigma_L, 0)\| \leq 1 + C_L \kappa$, with one bound on these labels.

(3) *Squeezed windows.* For $N_{\mathrm{far}} \le |n| < N_\kappa$ take $a = |n|$, so $\ell = (\kappa/|n|)^{1/2}$, $d = (\kappa|n|)^{1/2}$, and take $K_1 = B|n|$ with B fixed by (1.34.17): $8\alpha_\delta C_{\mathfrak{B}}/(Bd_*) < \frac{1}{2}(\gamma - \gamma_\delta)$. Since $\kappa|n|^2 \le 4C_U$ in this range,

$$|n|\ell = d = (\kappa|n|)^{1/2} \le (4C_U)^{1/4}\kappa^{1/4}, \qquad (|n| + K_1)\kappa L \le C(1+B)L\kappa^{1/2}, \qquad \frac{K_1^2}{d^2} = \frac{B^2|n|}{\kappa}.$$

Here $K_1 \ge d$ as soon as $\kappa \le B^2$, so (1.34.15) gives $\|kG\| \le C_L K_1$ for unit input on these blocks. Proposition 1.34.8(ii) thus gives $\mathcal{E} \le C(1+B)(\kappa^{1/4} + L\kappa^{1/2}) + Ce^{-B^2/(8\kappa)}$, with one bound for all n (the term $\kappa d K_1 = B\kappa^{3/2}|n|^{3/2}$ is $\le CB\kappa^{3/4}$, and $(1+B|n|)^2 e^{-B^2|n|/(4\kappa)} \le C_B e^{-B^2/(8\kappa)}$).

This estimate is uniform in n by item (2) in the proof of Proposition 1.34.8. The coefficient variation contributes $|n|\ell$.

For the Leray-projection defect, we write $n\Omega$ as $r^{-1} \cdot (nr\Omega)$. Lemma 1.34.4(b) gives the factor $(|n| - 1)^{-1}$, so this defect contributes d.

An isotropic window ($a = 1$) would give $|n|\ell = |n|\kappa^{1/2}$, which is not small for $|n| \sim \kappa^{-1/2}$.

(4) *High axial input.* Lemma 1.34.9 with $K_1 = B|n|$ has commutator error $C_L(\kappa^{1/2} + \kappa/B)$ and rate γ. We use no second-derivative semigroup bound.

The combination of (1)–(4), as in the previous proof, gives the claim with $C_1 = C_{\mathrm{far}} + 1 + d_*^{-1/2}$. □

Remark 1.34.13 (Frozen estimates and parameter order). (a) *Frozen family.* The comparison uses only these frozen-operator bounds. It uses the uniform semigroup bound (F1) on $|k| \le 3K_1$. For the far-angular range, it uses (F4) and Lemma 1.34.7.

It uses the uniform H^1 smoothing of Lemma 1.34.6, proved here with one bound for all n. For the shift it also uses (F2), including the common compact support of the viscous symbols.

We use no Lipschitz or C^2 dependence of $A_{\nu,n}(z,k)$ on (z,k), no C_k^2 Leray bound, and no second-derivative semigroup bound. For the (z,k)-dependence, we use the source coefficients and their bounded Z-derivatives (B1)(a). We also use their $L^2(\mathbb{R}_y^2)$ or r^{-1} decay (B1)(b) and the exact Leray identities of Lemma 1.34.4.

(b) *Actual sources of the inputs.* Sections 1.30.14–1.30.17 prove these hypotheses for this last selected source. B1 and B2 follow directly from the all-Z Q-chart, regular vector-axis germs and differentiated heat tail.

Physical supports may grow like $\sqrt{Q}$. F4 uses the actual small product and the $V^* \times H$ viscous weak inverse.

F1 follows from compact strain, the two strong/adjoint-strong sandwich limits, the whole half-plane Fredholm cover and a strict rate relaxation. For (F2), (1.33.1) and the local contour argument following it give joint strong measurability. The physical viscous Riesz projections converge uniformly on the fixed cutoff support, and the cutoff gives the same compact support bound at every viscosity.

F3 is the same all-Z radial metric in Lemma 1.29.1. These are frozen inputs proved before this nonautonomous packet comparison.

Completed-background propagation is not an antecedent of any of them. (c) *Parameter order.* We first fix the source, m, δ, γ, and g_1.

We then select $N_{\mathrm{far}} > \max(m, 2)$. Next, (1.34.17) gives K_1 for finite labels and B for far labels.

We then select the block length L. Only after these choices do we select the ancient threshold, so $\kappa = \rho(s_0)$ is small.

C_0, C_1 do not depend on L, K_1 or B. This is the order used in Proposition 1.34.14.

Proposition 1.34.14 (All-angular leading auxiliary evolution)**.** *We fix the one frozen source and the real two-band physical shift* (1.33.1)*. Then fixed $g_2 < \lambda_c$, C and T_0 exist such that*

$$\|U_{\mathrm{lead}}^\sharp(s,\sigma)\|_{L^2 \to L^2} \le Ce^{g_2(s-\sigma)}, \qquad \sigma \le s \le -T_0.$$

On the angular sum that excludes $\pm m$, this is an estimate for the unshifted leading equation.

Proof. The shift moves the selected simple bands below g_f where their cutoffs equal one.

On each transition the unshifted growth is below g_f. All other finite labels have the strict global winner gap.

Fix one block length L_b so the constant $(C_0 + C_1)e^{g_1 L_b}$ is absorbed into $e^{g_2 L_b}$ with strict reserve. Only after this choice, make the ancient threshold large enough for each fixed-block $o(1)$ error and each $C_{L_b}\kappa^{1/4}$ error, with $\kappa = \rho(s_0)$. These are the errors ε_F and $C_L\kappa^{1/4}$ of Lemmas 1.34.11 and 1.34.12.

Iterate the block bounds from Lemmas 1.34.11 and 1.34.12. A last partial block contributes only one output-time constant.

The leading source is axisymmetric, so the angular sectors are invariant and orthogonal. If U_m denotes the propagator on sector m, then $\|(\bigoplus_m U_m)f\|_2^2 = \sum_m \|U_m f_m\|_2^2$ and $\|\bigoplus_m U_m\| = \sup_m \|U_m\|$. The uniform sector bounds therefore give the claimed norm on the full space. The pair shift is zero on each other label by (1.33.1).

□

Corollary 1.34.15 (Unshifted leading upper growth)**.** *For each fixed $\epsilon_g > 0$ there are $C_{\epsilon_g}, T_{\epsilon_g} < \infty$ such that the unshifted axisymmetric leading propagator satisfies*

$$\|U_{\mathrm{lead}}(s,\sigma)\|_{L^2\to L^2} \le C_{\epsilon_g} e^{(\lambda_c+\epsilon_g)(s-\sigma)}, \qquad \sigma \le s \le -T_{\epsilon_g}.$$

The constant is uniform over all ancient initial times and all angular labels.

Proof. Repeat the finite-label Gaussian block construction with $S = 0$.

The unshifted frozen bound follows from the shifted one. On the shift chart, $S_\nu = d_0\chi P_\nu$ commutes with A_ν, and P_ν is the rank-one Riesz projection of the simple band λ_ν (Propositions 1.29.13 and 1.29.14).

Thus

$$e^{tA_\nu} = e^{t(A_\nu - S_\nu)} + \big(e^{t\lambda_\nu} - e^{t(\lambda_\nu - d_0\chi)}\big)P_\nu,$$

and Lemma 1.29.19 gives $\|e^{tA_\nu}\| \le C_F e^{g_1' t} + 2\sup\|P_\nu\|\, e^{t\Re\lambda_\nu}$. On the chart $\Re\lambda_0(Z,k) \le \lambda_c$, because the centered band has negative definite real Hessian at its maximum λ_c (Proposition 1.32.1 and (1.30.1)).

Also, $\Re\lambda_\nu \le \lambda_c + o_\nu(1)$, $\sup\|P_\nu\| \le C$ by Propositions 1.29.18 and 1.29.14. Off the chart, and for all labels other than $\pm m$, $S_\nu = 0$ and Lemma 1.29.19 applies directly.

This gives the frozen bound $Ce^{(\lambda_c+\epsilon_g/4)t}$ for $\nu \le \nu_0$.

Removing the compact pair shift does not change the far-angular physical estimate. Apply Proposition 1.34.8 and Lemmas 1.34.9 and 1.34.10 with $S \equiv 0$. Use the unshifted frozen bound in place of (F1).

For each fixed block length L_b, these results give the actual block bound $C_0 e^{(\lambda_c+\epsilon_g/2)L_b} + o_{L_b}(1)$. The bound is uniform in the ancient initial time of the block.

Select L_b so $C_0 \le e^{\epsilon_g L_b/4}$, then make the ancient threshold large enough that the error fits the remaining $\epsilon_g L_b/4$ reserve. Iteration and one last partial block give the stated estimate.

This is a semigroup bound.

It does not assert a numerical-range inequality in the standard physical L^2 inner product. □

The proposition applies to the axisymmetric leading generator. The completed base is generally nonaxisymmetric and may couple all angular labels, with $+m$ and $-m$.

The completed-field argument subsequently combines this estimate with the packet bounds before removing the shift and constructing the causal inverse. Leading angular invariance is not passed to that completed operator.

1.35 Finite physical reference profiles and kernel calculus

Main result. The leading profile bounds control the finite physical kernels and the right and adjoint first correctors.

The global row keeps its stated graph domain and is not a smoothing operator. We fix the selected source and angular pair from the previous sections.

We write $T = -s = t^{-h}/h$, $\rho = (hT)^{-1} = t^h$, and $k = -i\rho\partial_Z$. We use $S \asymp (1 + |\log\rho|)^{6/5}$.

$P(S)$ denotes a fixed-degree polynomial. The scalar shift mask C_s has symbol χ_+ in sector m and χ_- in sector $-m$, as in (1.33.1). Both symbols equal one near the pole.

We fix this mask before we select the shrinking preparation radius. These reference results use only the selected source and its true-velocity spectral pair.

The pair is the PHYSICAL pair of Theorem 1.30.1. Its eigenvalue λ is generally complex.

All resolvents below are those of the undilated physical generator A, on its translated physical contours. We use the centering variable $\mu_D = \Lambda + i(n\Omega_c + kW_c)$ only in the frozen scalar determinant.

We never substitute it for λ in the evolution or the primitive pressures.

For a scalar symbol a we use left quantization

$$\mathrm{Op}_\rho(a)f(Z) = \int_{\mathbb{R}} \widehat{a}(Z,u)f(Z-\rho u)\,\mathrm{d}u. \tag{1.35.1}$$

Lemma 1.35.1 (Finite left-kernel composition)**.** *Suppose a, b have compact k support in one fixed chart. Suppose $\partial_k^j a$ for $0 \le j \le 3$ have the weighted radial-symbol bounds used for (1.35.1), and put $\mathcal{C}_a = \sup_{Z,k}\sum_{j\le 3}\|\partial_k^j a(Z,k)\|$ (operator norm on the fixed weighted radial space; a has k-support in one fixed compact set).*

Also suppose b, b_Z have the same radial-symbol bounds for ∂_k^j, $j \le 2$, and b_Z is $1/2$-Hölder in Z uniformly in these k-derivatives; put $\mathcal{C}_b = \sup_{Z,k}\sum_{j\le 2}(\|\partial_k^j b\| + \|\partial_k^j b_Z\|) + \sup_k \sum_{j\le 2}[\partial_k^j b_Z]_{C_Z^{1/2}}$. (This gives $\int \sup_Z |\widehat{b}(Z,v)| + [\partial_Z\widehat{b}(\cdot,v)]_{C^{1/2}}\,\mathrm{d}v \le C\mathcal{C}_b$, which the Schur test uses.) The factor $P(S)$ for finite products below comes from the seminorms $\mathcal{C}_a, \mathcal{C}_b$ of the factors (coefficients, masks and cutoffs), each of which is at most $P(S)$. Then, as bounded L^2_Z operators,

$$\mathrm{Op}_\rho(a)\,\mathrm{Op}_\rho(b) = \mathrm{Op}_\rho(ab) + \frac{\rho}{i}\,\mathrm{Op}_\rho(a_k b_Z) + \mathcal{R}_\rho, \qquad \|\mathcal{R}_\rho\|_{2\to 2} \le C\rho^{3/2}\mathcal{C}_a\mathcal{C}_b. \tag{1.35.2}$$

The constant is uniform for the fixed finite profile and mask family.

For a finite product of such factors the same expansion holds with the sum of the ordered first brackets and a $C\rho^{3/2}P(S)$ remainder.

Proof. Three integrations by parts in the Fourier variable give $|\widehat{a}(Z,u)| \le C\mathcal{C}_a(1+|u|)^{-3}$.

In particular $\int |u|^{3/2}|\widehat{a}(Z,u)|\,\mathrm{d}u \le C\mathcal{C}_a$. The exact kernel of the product contains $\widehat{b}(Z-\rho u, v)$.

Taylor expansion at Z gives its value, the first term $-\rho u\partial_Z\widehat{b}(Z,v)$, and a remainder bounded by $C\rho^{3/2}|u|^{3/2}$ times the Hölder seminorm. The Fourier moment of u gives a_k/i with the stated left-ordering convention.

Schur's test on these kernels proves (1.35.2). A telescoping expansion handles each additional factor.

We fix word length and mask-family size. The finitely many ordinary coefficient and cutoff derivatives increase the bound only by $P(S)$. A mere $C^{2,1/2}$ bound in k would not give the necessary absolute $3/2$ moment.

This estimate uses the actual five-derivative profile bounds. □

Lemma 1.35.2 (Finite weighted profile bootstrap)**.** *For the selected leading source of Theorem 1.30.1, fix the selected angular integer $m \geq 30$ and a compact (Z,k) chart about its simple true-velocity eigenvalue. The unweighted full physical contour resolvent and its adjoint have uniform bounds on one contour $\Gamma \subset \{\Re z > 0\}$ that isolates it.*

On this compact chart the axial field and controls have bounded radial support. Outside that support, the coefficients of the fixed-sector multiplier N are combinations of Ω and $r\partial_r\Omega$, with $O(\langle r\rangle^{-2-2h})$ decay and one additional power for each radial derivative, by Lemma 1.32.2. They have bounded ordinary Z derivatives through order eighteen.

We can select the leading right and adjoint profiles with, for $0 \leq j \leq 5$, $0 \leq l \leq 17$,

$$\|\partial_Z^l \partial_k^j e\|_{H^6_{7-j}} + \|\partial_Z^l \partial_k^j v\|_{H^6_{7-j}} \leq C_{l,j}. \tag{1.35.3}$$

The scalar eigenvalue and its fixed-chart extension also have the six mixed phase derivatives used by the scalar Weyl calculus. The same contour argument gives one more k derivative with output radial weight H^6_1 and the selected $m \geq 30$.

The first physical right and adjoint homological correctors E_1, v_1 include their pressure and divergence terms. They have H^4_{6-j} bounds for $0 \leq j \leq 4$ and ordinary Z derivatives through order sixteen.

All constants may depend on this fixed source, m, the chart and the derivative order, but are independent of ρ. The same physical contour bootstrap also supplies

$$\|\partial_Z^l \partial_k^j e\|_{H^{18}_{9-j}} + \|\partial_Z^l \partial_k^j v\|_{H^{18}_{9-j}} \leq C_{l,j}, \qquad j \leq 2, \tag{1.35.4}$$

for the fixed ordinary axial orders used below.

In the subsequent low-profile construction the two graded corrector losses leave the embedding $H^{16}_5 \subset H^{14}_5$. Interacting compact radial tensors have weight six.

This stronger radial assertion does not add a fifth k derivative to the first corrector.

Proof. The actual hypotheses of Proposition 1.28.8 were verified in Section 1.30.12: the source has the differentiated heat tail and compact axial/control hull of Lemma 1.32.2, eighteen ordinary Z jets, and the physical isolating contours of Proposition 1.30.6. The argument applies separately to A and A^* and precedes completion and propagation. Corollary 1.28.9 therefore gives (1.35.3) and (1.35.4), including the sixth k derivative at weight one. A k derivative spends one moment and a Z derivative spends only coefficient jets. The conservative largest margin is $18 + (9-j) + j + 2 = 29 < m$, with the stated extra pressure moment on its own ladder; no later increase of m is needed.

The first corrector costs at most two radial derivatives and one moment. For the compact stress the longest path uses one low-profile derivative, one principal curl, two viscous derivatives, one first-corrector curl, and nine stress derivatives, totaling fourteen. These Sobolev orders are separate from the ordinary coefficient and ρ-power counts. Compact interaction multipliers supply the stress weight six without removing the global pressure tails. It remains to identify the physical right and left first residuals; this calculation fixes their signs and the scalar connection.

For the right and left correctors, fix one complex angular sector and write $v = (v_h, v_z)$. Write $\mathcal{B}_0 = (U_h, W)$ for its leading horizontal/axial field, and $(R_h, 0)$ for its radial correction.

With $\nabla_k = (\nabla_h, ik)$, the primitive symbols on this chart are

$$\begin{aligned} F_0(Z,k)v &= -U_h \cdot \nabla_h v - ikWv - v_h \cdot \nabla_h \mathcal{B}_0 + i(\tfrac{1}{2} - h)Zk\, v, \\ F_1(Z,k)v &= (\Delta_h - k^2 + (\tfrac{1}{2} + h) + \tfrac{1}{2} y \cdot \nabla_h)v - R_h \cdot \nabla_h v - v_h \cdot \nabla_h (R_h, 0) - v_z \partial_Z \mathcal{B}_0. \end{aligned} \tag{1.35.5}$$

Thus $F_\rho = F_0 + \rho F_1 + O(\rho^2)$, and on physical solenoidal radial vectors

$$L_0 = P_k F_0 P_k = A(Z,k) + i(\tfrac{1}{2} - h)Zk\, I, \qquad \mu(Z,k) = \lambda(Z,k) + i(\tfrac{1}{2} - h)Zk. \tag{1.35.6}$$

In this subsection $\mu = b_{\mathrm{pr}} = \lambda + i(\frac{1}{2} - h)Zk$ denotes the principal DILATION symbol, not the frozen Doppler coordinate μ_D. The exact physical jets at the selected phase obey $\lambda_{ZZ} = \mu_{D,ZZ} - im\Omega_c''$, $\lambda_{Zk} = \mu_{D,Zk} - iW_c'$ and $\lambda_{kk} = \mu_{D,kk}$.

We install the full complex target in (1.32.2).

Here $A = -P_k N P_k$ is the *undilated* frozen operator of the previous contour argument, with eigenvalue λ. The principal axial dilation $i(\frac{1}{2} - h)Zk$ occurs in F_0 and μ once.

In particular $(F_0)_k$ and μ_Z below include its left-composition derivatives. The $\frac{1}{2} y \cdot \nabla_h$ in F_1 is the remaining *radial* dilation.

F_1 does not contain another $i(\frac{1}{2} - h)Zk$. The scalar band operator $B = \mathrm{Op}_\rho(\mu + \rho c_1)$ keeps the same principal axial term on its full extension.

Explicitly, $(F_0)_k = i((\frac{1}{2} - h)Z - W)I$ and $\mu_Z = \lambda_Z + i(\frac{1}{2} - h)k$ on primitive vectors. Thus the order-ρ product terms in the two residuals include the axial drift without a second copy in F_1.

On the fixed sectors $\pm m$, write $G = \nabla_h \Delta_m^{-1}$ for the horizontal divergence primitive in Corollary 1.28.5(c). For the right corrector, the exact first primitive residual is

$$R_1 = P_k\big[F_1 e - (F_0 - \mu)(G\partial_Z e_z, 0) - i(F_0)_k e_Z + i e_k \mu_Z - hke_k - e_3 \pi_Z\big].$$

Here $e_3 = (0,0,1)$ is the axial unit vector, e_z is the vertical component of e, π_Z differentiates the full primitive pressure, and F_1 includes the radial viscosity, radial dilation and axial $-k^2$ term.

The pressure estimate uses one radial moment, G one, and the dilation one. Viscosity uses two horizontal derivatives.

Thus the profile and coefficient bounds put R_1 in H^4_{6-j} for $j \le 4$, with the necessary ordinary Z jets. The reduced contour resolvent gives $E_1 = -(L_0 - \mu)^{-1}(I - e\ell)R_1 = -(A - \lambda)^{-1}(I - e\ell)R_1$ on the spectral complement in the same graded class.

We give the left calculation, with its solvability condition. We first work on one complex member of the real conjugate pair, with the primitive and band conventions (1.35.5)–(1.35.6).

Let ℓ be the actual left eigenrow (not generally e^*). $v = \ell^*$, $\ell e = 1$, and $P_k F_0^* v = \bar\mu v$.

The primitive adjoint pressure is fixed by

$$F_0^* v - \bar\mu v = \nabla_k p_v. \tag{1.35.7}$$

The star is the radial Hilbert adjoint with its cylindrical measure. In particular $(y\cdot\nabla_h)^* = -y\cdot\nabla_h - 2$.

We set $C_e = (G\partial_Z e_z, 0)$ and $C_v = (G\partial_Z v_z, 0)$. The first right residual displayed above fixes the band connection $c_1 = \ell R_1$, and the complement equation gives $E_1 = -R_Q Q R_1$, where $Q = I - e\ell$ and $R_Q = (L_0 - \mu)^{-1} Q$.

The physical right column $J_{\mathrm{corr}} = \mathrm{Op}_\rho(e) - \rho\,\mathrm{Op}_\rho(C_e) + \rho\,\mathrm{Op}_\rho(E_1)$, with its exact divergence restoration, thus has a right defect $R = LJ_{\mathrm{corr}} - (J_{\mathrm{corr}})_s - J_{\mathrm{corr}}\,\mathrm{Op}_\rho(\mu + \rho c_1)$ of size $O(\rho^{3/2}P(S))$ after a fixed inner phase cutoff. To see the effect of the physical projection, first remove the principal pressure using $\nabla_\rho\,\mathrm{Op}_\rho(p) = \mathrm{Op}_\rho(\nabla_k p) + \rho e_3\,\mathrm{Op}_\rho(p_Z)$. The equations for c_1, E_1 imply $P_k r_1 = 0$ for the remaining unprojected first coefficient r_1. Put $p_1 = \Delta_k^{-1}\,\mathrm{div}_k\, r_1$, so $r_1 = \nabla_k p_1$. With a smooth symbol cutoff χ supported in this chart and equal to one on a neighbourhood of the working cutoff, one has exactly

$$\rho P_\rho\,\mathrm{Op}_\rho(\chi r_1) = -\rho^2 P_\rho e_3\,\mathrm{Op}_\rho(\partial_Z(\chi p_1)).$$

The pressure bound of Corollary 1.28.5(c) spends one of the moments in H^4_{6-j}. The resulting symbol and its first two k-derivatives are uniformly bounded on the larger chart, so its kernel has integrable

axial decay. The right side is $O(\rho^2 P(S))$. For symbols supported away from the working cutoff the zeroth and first products vanish, and (1.35.2) bounds the localized remainder by $O(\rho^{3/2}P(S))$. The same gradient identity applies to the adjoint coefficient after its complement equation is solved.

For any physical adjoint column H and $K_{\mathrm{raw}} = H^*$, the exact left defect $T_{\mathrm{raw}} = (K_{\mathrm{raw}}L + (K_{\mathrm{raw}})_s - BK_{\mathrm{raw}})P$ satisfies on the same smooth core

$$T^*_{\mathrm{raw}} = P(F^*_\rho H + H_s - HB^*), \qquad B = \mathrm{Op}_\rho(\mu + \rho c_1). \tag{1.35.8}$$

Thus $PL^*H = PF^*_\rho H$ and $PP_sP = 0$. In particular the time sign is plus.

For left quantization $a\#b = ab - i\rho a_k b_Z + O(\rho^{3/2})$, the actual adjoint symbols are

$$F^*_\rho = F^*_0 + \rho(F^*_1 - i\partial_Z\partial_k F^*_0) + O(\rho^{3/2}), \qquad B^* = \bar\mu + \rho(\bar c_1 - i\partial_Z\partial_k\bar\mu) + O(\rho^{3/2}).$$

Here $\partial_s \mathrm{Op}_\rho(v)$ contributes $h\rho k v_k$ at first order. We apply (1.35.8) to $H_0 = \mathrm{Op}_\rho(v) - \rho\,\mathrm{Op}_\rho(C_v)$.

For a scalar left symbol p, the axial derivative $\rho\partial_Z$ acts on both the oscillatory kernel and p. Thus $\nabla_\rho \mathrm{Op}_\rho(p) = \mathrm{Op}_\rho(\nabla_k p) + \rho e_3 \mathrm{Op}_\rho(\partial_Z p)$, where $e_3 = (0,0,1)$. Applying this identity to the pressure in (1.35.7) gives the following coefficient of ρ:

$$\begin{aligned} r_v = P_k\big[&(F^*_1 - i(F^*_0)_{kZ})v - (F^*_0 - \bar\mu)C_v - i(F^*_0)_k v_Z + iv_k\bar\mu_Z + hkv_k \\ &- e_3(p_v)_Z - v\bar c_1 + iv\bar\mu_{kZ}\big]. \end{aligned} \tag{1.35.9}$$

The F^*_1 term includes the radial viscosity, radial dilation adjoint, axial diffusion and lower-order source terms.

We cannot replace the two adjoint-quantization terms and total pressure derivative in (1.35.9) by a coefficientwise complex conjugate of the right residual.

The selected component of (1.35.9) vanishes for a reason independent of the weighted estimate. Let $S_0 = H^*_0 J_{\mathrm{corr}}$ and $\widetilde T$ be the left defect of H^*_0.

Direct finite-kernel composition gives

$$S_0 = I + \rho\,\mathrm{Op}_\rho(s_1) + O(\rho^{3/2}P(S)), \quad s_1 = \ell(E_1 - C_e) - C^*_v e - i\ell_{kZ}e - i\ell_k e_Z.$$

Exact differentiation, with no assumed scalar connection, yields

$$\widetilde T J_{\mathrm{corr}} = H^*_0 R + (S_0)_s + S_0 B - BS_0. \tag{1.35.10}$$

The first term is $O(\rho^{3/2}P(S))$ locally. At fixed input Fourier frequency ζ a column symbol is evaluated at $k = \rho\zeta$. Hence $\rho_s = h\rho^2$ gives

$$\partial_s\Big(\rho^p\,\mathrm{Op}_\rho(a)\Big) = h\rho^{p+1}\,\mathrm{Op}_\rho(pa + k\partial_k a).$$

Differentiate the two finite columns in $H^*_0 J_{\mathrm{corr}}$ on the smooth core. Every positive-degree term contributes $O(\rho^2 P(S))$. In the two degree-zero terms, taking the adjoint and composing at principal order costs $O(\rho P(S))$ inside the prefactor $h\rho$, by (1.35.2). Their sum has principal symbol $k\partial_k(v^*e)$, which vanishes where $v^*e = 1$. Fixed cutoffs with a buffer inside this plateau give $(S_0)_s = O(\rho^2 P(S))$ there. The differentiated symbols use at most four leading k-jets, within (1.35.3).

For the axial dilation $D = Z\partial_Z$ the exact commutator on the core is $[D, \mathrm{Op}_\rho(a)] = \mathrm{Op}_\rho((Z\partial_Z - k\partial_k)a)$. Since $D^* = -D - I$, the leading commutator of S_0 with D differentiates the same constant pairing. Its contribution with the factor ρ is $O(\rho^2 P(S))$ on the plateau. For the remaining scalar part of B, the order-ρ commutator is $[s_1, \lambda] = 0$ on each branch. Comparing the first-order coefficients in (1.35.10) gives

$$e^* r_v = 0. \tag{1.35.11}$$

Equivalently, the real two-column matrix has zero selected projection.

This is the Fredholm compatibility condition, not a consequence of $KJ = I$ alone.

The adjoint reduced resolvent keeps the positive weighted spaces by the different A^* core/tail and commutator argument above. Define

$$v_1 = -R_Q^* r_v, \qquad e^* v_1 = 0, \qquad (L_0^* - \bar{\mu}) v_1 + r_v = 0. \tag{1.35.12}$$

Formula (1.35.9) uses one radial moment in C_v and pressure, one in dilation, and two horizontal derivatives in viscosity.

The kZ symbol derivatives use coefficient jets without an additional radial moment. Thus, for $0 \le j \le 4$ and each necessary $l \le 16$,

$$\|\partial_Z^l \partial_k^j r_v\|_{H^4_{6-j}} + \|\partial_Z^l \partial_k^j v_1\|_{H^4_{6-j}} \le C_{l,j}.$$

Difference quotients justify differentiation of the reduced resolvent on the same finite weight ladder.

The selected source provides the eighteen ordinary coefficient jets, and (1.35.3) provides the extra leading seventeenth Z derivative for the explicit v_Z term. This proves the claimed first-corrector bounds for the actual adjoint, with pressure and divergence.

□

1.36 The Gram metric of the leading field

1.36.1 A viscosity-uniform finite-time metric

Fix a physical reference time Q and set $\rho = Q^h$, $t = Q + Q^{1+h}\theta$, $y = x/\sqrt{Q}$. If B_0 is the leading field in these coordinates, the physical solenoidal linearization is

$$\partial_\theta v = \rho \Delta_y v - \mathbb{P}\big[(B_0 \cdot \nabla_y) v + (v \cdot \nabla_y) B_0\big]. \tag{1.36.1}$$

Here Q is constant on the block.

Thus $\mathbb{P}$ is the ordinary Cartesian Leray projector and the viscosity is the scalar ρ. We do not introduce an anisotropic ellipticity ratio. For block length $L = o(\log(1/\rho))$, $\rho L \to 0$ and $t/Q = 1 + O(\rho L)$.

The finite leading jets on this comparable-time interval are uniform in Q. The canonical-to-isotropic coordinate map is unitary after its Jacobian factor, and its amplitude ratio at two endpoints is $1 + O(\rho L)$.

Also $\mathrm{d}s/\,\mathrm{d}\theta = 1 + O(\rho L)$.

Write $P = \mathbb{P}$, $Q_\perp = I - P$, and $(G_0)_{ij} = \partial_j B_0^i$, and extend (1.36.1) to the whole vector space by

$$A_{\mathrm{ext}} = -B_0 \cdot \nabla - G_0 + 2 Q_\perp G_0 P + (G_0 - G_0^\top) Q_\perp + \rho \Delta - S_{\mathrm{app}}. \tag{1.36.2}$$

On PL^2, this is the shifted leading physical generator. A_{ext} keeps the physical and gradient blocks.

We select the approximation $S_{\mathrm{app}} = P\,\mathrm{Op}_{AW}(T_{\mathrm{app}})P$ once from the compact family of leading shifts on the fixed phase chart. Approximate the compact radial values by finitely many smooth compactly supported profiles and the continuous parameter dependence by a smooth finite partition.

The anti-Wick analysis and synthesis maps are contractions. Thus the operator-norm error is at most the uniform symbol error plus the controlled viscous and quantization comparison.

Select this fixed error inside the leading gap. We never use it as a small low-return error multiplied by a subpower reverse constant.

The smooth compact-frequency symbol gives

$$\|S_{\mathrm{app}}\|_{H^{-m}\to H^m} \le C_m \tag{1.36.3}$$

for each necessary fixed m.

In particular the shift is a smoothing high-input term in the metric argument.

Transport of the shift to the physical box. Set $s = -t^{-h}/h$, $t = Q+Q^{1+h}\theta$, $\kappa = Q^h$, $\lambda = Q/t$. Write $a_Q = \sup|1-\lambda|$ on $|\theta| \le L_{\mathrm{box}}(Q) + L_G$; then $a_Q = O(\kappa(L_{\mathrm{box}} + L_G)) = o(1)$. We have $ds/d\theta = (Q/t)^{1+h} = 1 + O(a_Q)$. The ratio of the canonical-to-physical L^2 normalization at the two endpoints is $(t_2/t_1)^{1/4-3h/2}$; either direction costs at most $\exp(C\kappa r)$ at separation r. Thus the exact transported shift $S_{\mathrm{tr}}(\theta)$, including $ds/d\theta$, has solenoidal evolution bound $C_P e^{(g_2+o(1))r}$, $g_2 = \lambda_c - 2\delta_{\mathrm{sp}}$, where δ_{sp} denotes the fixed spectral gap parameter δ of Section 1.33.

Fix $\epsilon_0 > 0$. The compact continuous family of rank-one inviscid symbols is uniformly approximable to ϵ_0 by a single smooth finite sum of smooth compactly supported radial range and test vectors with smooth compactly supported phase coefficients. Use a finite cover and partition of unity, approximating each of the finitely many range and test vectors in L^2. Supports and symmetries can be chosen on the fixed two-sector chart. Use this symbol to define S_{app} with the packet window at reference time Q. In the variables $y_h = x_h/\sqrt{Q}$, $Z_0 = z/Q^{1/2-h}$, Lemma 1.34.1(ii),(iv) conjugates the projector exactly to P_κ, the window parameter to λ^{1-h}, and the phase center to $(\lambda^{1/2-h}Z, \lambda^{-1/2}k)$ in the symbol. These algebraic formulas also hold for $\lambda > 1$ on the negative part of the box. For $1/2 \le \lambda \le 2$, the window difference has analysis norm $O(a_Q)$ by the Plancherel identity in that lemma. The symbol change is at most its uniform continuity modulus at Ca_Q. Radial dilation changes the inviscid compact operator family by $o(1)$ in norm, by finite-rank approximation; the viscous replacement costs $\sup_{\nu\le 2\kappa}\delta_S(\nu) = o(1)$. The additional time factor differs from one by $O(a_Q)$. These estimates, and contraction of analysis, synthesis and projection, give

$$\sup_\theta \|P(S_{\mathrm{tr}}(\theta) - S_{\mathrm{app}})P\| \le \epsilon_0 + o(1)$$

in physical box coordinates. All $o(1)$ terms tend to zero for the prescribed length family.

For the uniform smoothing bound, the physical axial coordinate is $y_3 = Z_0/\kappa$. Thus its derivative is $\kappa\partial_{Z_0}$. On synthesis, it multiplies the modulated packet by ik or differentiates its normalized Gaussian window with L^2 cost $O(\sqrt{\kappa})$. Iteration gives sums of bounded multipliers on the fixed compact k-support and normalized differentiated windows. Their synthesis norms are bounded by the same Plancherel identity. Horizontal derivatives act on the finitely many smooth radial output vectors. The adjoint analysis uses the corresponding input vectors. Splitting the smooth finite-rank symbol into these analysis and synthesis factors therefore gives $\|S_{\mathrm{app}}\|_{H^{-m}\to H^m} \le C_{m,\epsilon_0}$ for each fixed m, uniformly in Q. The physical Leray projector commutes with derivatives.

Duhamel and Gronwall now give the rate $g_2 + o(1) + C_P(\epsilon_0 + o(1))$. Choose $C_P\epsilon_0 < \delta_{\mathrm{sp}}/4$, then take Q small so that the rate is at most $g_0 = \lambda_c - 3\delta_{\mathrm{sp}}/2$. The smoothing constants are fixed before this last choice. For the unshifted estimate use both shifts zero.

Lemma 1.36.1 (Finite-time Gram and tame commutators)**.** *Let $C_P e^{g_0 r}$ bound the restriction to the solenoidal subspace of the propagator for (1.36.2), where $g_0 < g_G$, and choose a fixed L_0 with $C_P^2 e^{-2(g_G-g_0)L_0} \le 1/2$. We need this bound for $0 \le r \le L_0$, uniformly in the starting time and viscosity. Assume the leading fields have bounded finite jets on $[s, s+L_0]$. Assume the volume-preserving flow maps on this time horizon are uniformly bi-Lipschitz and that all positive-order derivatives of the maps and their inverses needed below are uniformly bounded. For bounded velocity the displacement over a time $r \le L_0$ is at most r times its supremum norm. In the shifted application*

choose $g_G = \lambda_c - \delta_{\mathrm{sp}}$; then $g_0 < g_G < \lambda_c$. Also assume that the fixed smooth shift obeys (1.36.3). There is a positive self-adjoint metric $M(s)$ that commutes with P, $I \le M \le CI$, and a fixed C such that

$$\langle u, (M_s + A_{\mathrm{ext}}^* M + M A_{\mathrm{ext}})u\rangle \le 2g_G\langle u, Mu\rangle + C\,\|Q_\perp u\|_2^2 - 2\rho\,\|\nabla u\|_2^2 . \tag{1.36.4}$$

For each fixed m, $M = \mathrm{Op}(m_0) + R_M$, where m_0 lies in a bounded $S^0_{1,0}$ set and $R_M : H^{-m} \to H^m$ has a fixed bound.

Thus, for every bounded real Lipschitz vector field W and bounded Lipschitz scalar b,

$$\|[M, W\cdot\nabla]\|_{2\to 2} \le C(\|W\|_\infty + \|\nabla W\|_\infty), \tag{1.36.5}$$

$$\|[b, M]\|_{2\to H^1} \le C(\|b\|_\infty + \|\nabla b\|_\infty). \tag{1.36.6}$$

All constants are independent of $0 \le \rho \le 1$ and of higher derivatives of W and b.

Proof. Let $U(s+r, s)$ be the evolution of (1.36.2) for $0 \le r \le L_0$, where L_0 is fixed, independent of the longer partition block length used later. Take

$$M(s) = I + c\int_0^{L_0} e^{-2g_G r} U(s+r, s)^* U(s+r, s)\,\mathrm{d}r.$$

The physical and gradient subspaces are invariant, so M commutes with P.

Fixed-interval energy bounds give $I \le M \le CI$. We differentiate $\langle u, Mu\rangle$ along $u_s = A_{\mathrm{ext}}u$, with the upper and lower endpoints of the future integral.

Writing $U_L = U(s + L_0, s)$, the evolution law gives the exact form identity

$$\begin{aligned}&\langle u, (M_s + A_{\mathrm{ext}}^* M + M A_{\mathrm{ext}} - 2g_G M)u\rangle\\ &\quad = 2\,\mathrm{Re}\langle u, A_{\mathrm{ext}}u\rangle - 2g_G\,\|u\|_2^2 + c(e^{-2g_G L_0}\,\|U_L u\|_2^2 - \|u\|_2^2).\end{aligned}$$

The real transport form vanishes because $\operatorname{div} B_0 = 0$. All zeroth-order terms in (1.36.2) are bounded on L^2. Thus the first two terms on the right are at most $C_0\,\|u\|_2^2 - 2\rho\,\|\nabla u\|_2^2$, with C_0 independent of ρ. By the choice of L_0, the squared, weighted physical endpoint norm is at most $\frac{1}{2}\,\|Pu\|_2^2$. The two invariant output blocks are orthogonal, so the expression in parentheses is at most $-\frac{1}{2}\,\|Pu\|_2^2 + C_{L_0}\,\|Q_\perp u\|_2^2$ by the fixed-interval bound on the gradient block. Taking $c \ge 2\max\{C_0, 1\}$ absorbs the physical zeroth-order term. This proves (1.36.4) with its full diffusion coefficient, also at $\rho = 0$.

We next prove the uniform symbol assertion. Factor the unitary volume-preserving scalar transport $F(t, s)$ from U.

We record the finite symbol calculation used here. If p, q have orders m_1, m_2, the left symbol of their product, through terms of order $m_1 + m_2 - N + 1$, is

$$\sum_{|\beta|<N} \frac{1}{i^{|\beta|}\beta!}(\partial_\xi^\beta p)(\partial_x^\beta q).$$

Indeed composition of the two Fourier kernels gives the oscillatory integral of $e^{-iy\cdot\eta}p(x, \xi+\eta)q(x+y, \xi)$ with measure $(2\pi)^{-d}\,\mathrm{d}y\,\mathrm{d}\eta$. Taylor expansion of the last factor in y and integration by parts in η give the sum. In the integral remainder the N powers of y move to N frequency derivatives of p. To bound the resulting integral, use $(1-\Delta_y)^L$ and $(1-\Delta_\eta)^L$ on the exponent, dividing by $\langle\eta\rangle^{2L}$ and $\langle y\rangle^{2L}$ respectively. The remaining derivatives of $p(x, \xi+\eta)$ are bounded using $\langle\xi+\eta\rangle^a \le C_a\langle\xi\rangle^a\langle\eta\rangle^{|a|}$; extra frequency derivatives can be estimated at the original order when only integrability is needed.

Choose $2L > d + |m_1 - N| + 1$ for an undifferentiated bound and increase it for the finitely many specified derivatives. This makes both integrals absolutely convergent, bounds the remainder at order $m_1 + m_2 - N$, and justifies the identities by smooth truncation. The same Taylor expansion at $y = x$ converts a two-point amplitude $p(x, y, \xi)$ on a fixed neighborhood of the diagonal into a left symbol to any required finite order. After N integrations by parts in ξ its remainder amplitude has order $m_1 - N$. For $N > m_1 + 2m + d + 2$ its kernel and the finitely many derivatives up to $\lceil m \rceil$ in each spatial variable are bounded on that neighborhood by absolute frequency integration. Schur's bound, applied to those derivatives, gives $H^{-m} \to H^m$. In particular this calculation applies to the adjoint kernel.

For a volume-preserving change of variables Φ with uniformly bounded derivatives and inverse derivatives, the transformed phase is $(\Phi(x) - \Phi(y)) \cdot \xi = (x - y) \cdot J(x, y)^T \xi$, where J is the average of $D\Phi$ on the segment. In a fixed neighborhood of the diagonal J and J^{-1} are uniformly bounded with their required derivatives, by the lower bound on $D\Phi$ and its continuity modulus there. The substitution $\eta = J^T \xi$ therefore gives an amplitude of the same order, to which the preceding computation applies. Away from this neighborhood $|\Phi(x) - \Phi(y)| \geq c|x - y|$; integration by parts in ξ gives an integrable kernel with as many integrable spatial derivatives as required. These facts prove the coordinate change, composition and adjoint bounds used in the metric construction.

Then $F^* \Delta F$ is a scalar divergence-form operator with symbol $-q_2 + q_1$. It is elliptic with one positive lower bound $q_2 \geq c|\xi|^2$, and q_1 has order one. The bounded zero-order matrix term becomes a Ψ^0 operator under this smooth coordinate change.

We split the Leray symbol at a smooth compact low-frequency cutoff. This gives a standard smooth symbol at high frequency and a remainder that maps $H^{-m} \to H^m$ for each fixed m.

We take no derivative of the Leray symbol at $\xi = 0$. Duhamel treats this remainder and S_{app} with fixed Sobolev bounds.

For the smooth-symbol part, set $J(t, s) = \int_s^t \rho(r)\, \mathrm{d}r$ and solve the matrix ODE $G_t = (-\rho q_2 + c_0)G$, $G(s, s) = I$. Because q_2 is scalar, differentiation gives, for each necessary fixed multi-index,

$$|\partial_x^\mu \partial_\xi^\nu G| \leq C_{\mu,\nu} \langle \xi \rangle^{-|\nu|} (1 + J|\xi|^2)^K e^{-cJ|\xi|^2}$$

outside a fixed low-frequency ball.

Recursively construct symbols $a_j \in S^{-j}$, $a_0 = G$, $a_j(s) = 0$ for $j \geq 1$. In the finite Kohn–Nirenberg product expansion, a β derivative of the quadratic symbol $-\rho q_2$ applied to $a_{j-|\beta|}$ has net order $2 - |\beta| - (j - |\beta|)$ before time integration.

Integration of $\rho e^{-c|\xi|^2 J}$ contributes $|\xi|^{-2}$. A term from ρq_1 has one lower order.

A derivative of c_0 contributes its ordinary $|\xi|^{-|\beta|}$ gain. Induction gives $a_j \in S^{-j}$ with one bound even when ρ vanishes on a subinterval.

More explicitly, to determine a_j keep the terms $(\partial_\xi^\beta q_2)\partial_x^\beta a_l$ with $l + |\beta| = j$, $|\beta| \geq 1$, the q_1 terms with $l + |\beta| + 1 = j$, and the c_0 terms with $l + |\beta| = j$, $|\beta| \geq 1$. Include their viscosity multipliers, signs and the composition coefficients displayed above. Integrate their sum against $G(t, \tau)$ from s to t. The factors $e^{-c|\xi|^2 J(t,\tau)}$ and $e^{-c|\xi|^2 J(\tau,s)}$ combine, consuming fixed polynomials in $|\xi|^2 J(t, s)$ at a slightly smaller c. Thus the same induction works with the differentiated Gaussian bounds. Truncation at $j = N$ leaves a residual of order at most $1 - N$ (the worst term is the uncancelled second-order symbol with one frequency derivative). For $H^{-m} \to H^m$ choose $N > 2\lceil m \rceil + d + 4$, and take the ordinary product expansion to at least this order plus three. The residual and its spatial kernel derivatives through the required orders are then integrable by dyadic frequency integration, with constants independent of ρ. In particular $m = 1$ gives the bound needed for the commutators. For clarity, the bounds just obtained for the finite parametrix do give an operator bound for the true remainder, uniformly as the viscosity tends to zero. For the exact pulled-back

evolution on a fixed interval, commute up to m spatial derivatives with its scalar uniformly elliptic divergence-form diffusion. After one integration by parts the commutators contribute at most $\frac{1}{2}c\rho\|\nabla u\|_{H^m}^2 + C_m\rho\|u\|_{H^m}^2$; derivatives of the bounded order-zero symbols act boundedly on H^m. Gronwall gives $\|U(t,s)\|_{H^m\to H^m} \le C_{m,L_0}$, also at $\rho = 0$. The same calculation for the adjoint in reversed elapsed time gives the dual H^{-m} propagation bound. The transport pullback and its inverse have bounded Sobolev norms on this fixed interval. Thus the residual of the order-N parametrix, uniformly $H^{-m} \to H^m$ as above, integrated against the exact evolution for a time at most L_0, has the same uniform bound. A smoothing part of the original generator is treated by the same Duhamel identity using the two Sobolev bounds and (1.36.3). The leading parametrix has the identity as its initial value. Consequently $U = F(\mathrm{Op}(a) + R)$ with $R : H^{-m} \to H^m$ uniformly, for each of the finitely many required m.

Composition and integration of U^*U give the stated representation of M.

For its Ψ^0 part T, the identity

$$[T, W_j\partial_j] = [T\partial_j, W_j] - T(\partial_j W_j) + W_j[T, \partial_j]$$

reduces the estimate to commutators of order-one operators with a Lipschitz multiplier.

We give the endpoint estimate used here. If $P = p(x, D)$ is a matrix operator of order one with bounded $S^1_{1,0}$ seminorms and b is a bounded scalar Lipschitz function, then

$$\|[P, b]\|_{2\to 2} \le C_p(\|b\|_\infty + \|\nabla b\|_\infty).$$

First reduce to a Fourier multiplier. Split the output into unit cubes and cut the input to a fixed enlargement of each cube. The separated kernel is integrable in both variables uniformly: on a dyadic frequency shell $|\xi| \asymp 2^j$ its size is bounded by $C_N 2^{j(d+1)}(1 + 2^j|x - y|)^{-N}$, by frequency integration by parts in dimension d. Sum over $j \ge 0$ where $|x - y| \ge 1$. For the near part multiply the symbol in x by a fixed translated cutoff equal to one on the output cube, and expand it in Fourier series on a larger fixed cube. Each coefficient is an order-one multiplier with its required seminorms bounded by $C_N(1 + |\ell|)^{-N}$ by integration by parts in x. The modulation commutes with b, the coefficients sum in ℓ, and the enlarged input cubes have bounded overlap.

For a multiplier P let u_j, b_j be the smooth inhomogeneous Fourier pieces at $|\xi| \asymp 2^j$ ($j = 0$ includes the low ball). Use smooth radial cutoffs obtained by differencing successive dilates of one cutoff equal to one on the unit ball. Plancherel gives $\sum_j \|u_j\|_2^2 \le C\|u\|_2^2$ by finite overlap. Write $u_{<j-c} = \sum_{k<j-c} u_k$ with c a fixed large integer, and set $B = \|b\|_\infty + \|\nabla b\|_\infty$. We use

$$\|b_j\|_\infty \le C2^{-j}B, \qquad \sum_{j\ge 0} \|(2^j b_j)u_{<j+C_0}\|_2^2 \le C_{C_0}B^2\|u\|_2^2 \tag{$*$}$$

for every fixed integer C_0. To check this, for $j > 0$ write $2^j b_j$ as a sum of annular Schwartz convolutions of the components of ∇b, by inserting $\sum_\ell \xi_\ell^2/|\xi|^2 = 1$ on the shell. Their kernels are dilates with uniformly bounded L^1 norm. For every dyadic cube Q of side 2^{-m}, $m \ge 0$, $\sum_{j\ge m}\int_Q |2^j b_j|^2 \le CB^2|Q|$. Indeed split each component into its restriction to $3Q$ and its complement. The first sum is bounded by Plancherel and finite frequency overlap. For the second the integrable kernel tails beyond distance 2^{-m} give $C2^{m-j}B$ on Q. The term at $j = 0$ uses $\|b\|_\infty$. On a cube of side 2^{-j}, $\sup_Q |u_{<j+C_0}| \le C \inf_Q \mathcal{M}u$, where $\mathcal{M}$ is the centered ball maximal average of $|u|$; this follows by summing the Schwartz convolution kernel on concentric annuli. For each level t sum the preceding cube bound over the maximal dyadic subcubes of side at most one in $\{\mathcal{M}u > t\}$ and integrate against $2t\,\mathrm{d}t$. This proves (*) since $\|\mathcal{M}u\|_2 \le C\|u\|_2$. For this last inequality choose disjoint balls with averages exceeding t whose fivefold enlargements cover the level set (choose

successively by decreasing dyadic radius); truncating $|u|$ at $t/2$ gives $|\{\mathcal{M}u > t\}| \le Ct^{-1}\int_{|u|>t/2}|u|$. Layer integration proves the square bound.

Expand $[P,b]u$ over the pairs of input frequencies. For $b_{<j-c}u_j$, both outputs have frequency $\asymp 2^j$. Localize P to a slightly larger shell. The first absolute moment of this kernel is at most C, by the shell bound above, and $\|\nabla b_{<j-c}\|_\infty \le CB$. The difference $b_{<j-c}(y) - b_{<j-c}(x)$ bounds each commutator by $CB\|u_j\|_2$, and finite overlap sums the squares. For $b_j u_{<j-c}$ the outputs are also annular. The norms of $P(b_j u_{<j-c})$ square-sum by (*) and the shell bound $\|P\| \le C2^j$ there. For $b_j P u_{<j-c}$ use $CB\sum_{k<j-c}2^{k-j}\|u_k\|_2$, whose squares sum by convolution with the summable sequence 2^{-l}, $l \ge 0$.

For $|j-k| \le c$ pair with a test vector v. Only $v_{<j+C_0}$ contributes for a fixed sufficiently large C_0 by frequency support. For the term $P(b_j u_k)$ move P^* onto this low cutoff and use $\|b_j P^* v_{<j+C_0}\|_2 \le CB\sum_{l<j+C_0}2^{l-j}\|v_l\|_2$. For $b_j P u_k$ apply Cauchy–Schwarz to $\|2^{-j}Pu_k\|_2\|(2^j b_j)v_{<j+C_0}\|_2$ and use (*). The finitely many low blocks satisfy the same estimates. These bounds prove the commutator inequality, first on frequency truncations and then by pairing with smooth test vectors and passage to the limit. They apply to $P = T\partial_j$ and $P = \partial_j T$ with the uniform seminorms of the symbol constructed above. The other terms in the displayed commutator identity have order zero. For clarity their L^2 boundedness follows from the same cube Fourier expansion: the multiplier bound is now $\sup_\xi |p(\xi)|$ and the separated kernel is integrable.

For the smoothing part use $W\cdot\nabla f = \operatorname{div}(Wf) - (\operatorname{div} W)f$. The map $R_M : H^{-1} \to H^1$ bounds $\|R_M(W\cdot\nabla f)\|_2$ by $C(\|W\|_\infty + \|\operatorname{div} W\|_\infty)\|f\|_2$, while $\|W\cdot\nabla R_M f\|_2 \le C\|W\|_\infty\|f\|_2$. Last $\partial_j[b,T] = (\partial_j b)T - [\partial_j T, b]$ and the same order-one commutator bound prove the second estimate.

We handle the smoothing remainder by multiplication in H^1. □

1.37 Proof of the main statement

Proof of Theorem 1. We assemble the leading and frozen suppliers, in their order of selection. Section 1.5.2 first fixes the geometric supports and correction templates, then λ, h, ν_c, then the normalized complete radial futures. The simultaneous geometry, heat-coefficient and positive-energy equations in Section 1.6.3 determine their common targets. The pressure-class bank fixes the actual axis datum before the variable-scale core is solved. Proposition 1.6.42 and Theorem 1.8.10 supply the forward and backward regular cores. Their axis reconstruction is exactly (1.1.2)–(1.1.3).

The selected C precedes its activation and termination widths. Theorem 1.20.58 and Proposition 1.20.56 give the cover for the physical pre-loop member. Equations (1.19.1) and (1.20.9) identify its pressure through the five returns and retain the heat correction in the comparison wait. Lemma 1.19.2 and Corollary 1.19.3 then supply the finite capped strictification and its five-history return. On the backward side the component suppliers assembled in Remark 1.5.6 give the matched core and finite pre-loop prefix of (B1), the native strict cone and weight of (B2)–(B3), and the compensated heat exterior, reserved power patches and terminal multiplier of (B4)–(B6). Item (B7) concerns the subsequent finite completion.

The protected core estimate is Proposition 1.22.4; its backward leading counterpart follows from the analytic core and first collar of Theorem 1.8.10 on the rectangle of (1.22.1). For the entry radius, $\xi_a^2/2 = 4/(\Lambda b)$ with $b = \lambda_{\mathrm{ch}}$ on the forward collars and $b = 1$ on the backward core (Lemma 1.22.6). For the pulse radius, the prefix (1.25.4) has $\xi_{s,+}^2 = \xi_{s,-}^2/\lambda_{\mathrm{ch}}$ on the same collars and $\xi_p^2 = \xi_s^2 e^T \lambda^{-60}$ on both sides. These formulas give the two graph identities in (iii). Only these leading-data assertions are used. The moving correction maps have nonzero Jacobians by (N1)–(N8) in Section 1.25.2. For the late forward bank, Lemma 1.27.5a proves the lower bound on the whole closed angular interval at the selected amplitudes. Lemma 1.21.1 supplies the actual activation factor

and protected cutoff domain. The two pressure tubes are Proposition 1.24.2. Proposition 1.23.8 and Lemma 1.24.3, with the native backward weight and primitive estimates of Lemma 1.24.4 and the ensuing primitive estimate, give (iv). For the forward terminal deficit, Lemma 1.23.8a estimates the mixed jets relative to the matched heat field. The terminal splices lie beyond the spectral returns on their active angular support. The comparison of V_* with W in (W3) therefore gives the stated estimate for this same selected member. Equation (1.2.6) is precisely Proposition 1.23.10 after the substitution $s = \rho^2/2$. In particular it keeps the complete moment subtraction and all partial histories.

For this fixed leading family, the source admission and retained slope allowances are proved before any spectral count. Theorem 1.30.1 then chooses one finite m and its width, solves the exact physical centering and complex curvature controls, and restores their actual five histories. Proposition 1.32.1 identifies this member with the previously calibrated source. Its admitted controls preserve the cone, protected core and heat coefficient. It supplies the spectral maximum, the neighbor gap and (1.2.8); the negative definite real Hessian gives the displayed local quadratic deficit by Taylor's theorem. Lemma 1.32.2 proves the all-order leading tails independently of completion. Proposition 1.28.8 and Corollary 1.28.9 provide the stated leading contour and profile estimates.

After this final m is fixed, Sections 1.30.14–1.30.17 and Section 1.33 choose N_{far}, the viscosity threshold and physical shifts. These give precisely (B1)–(B2) and (F1)–(F4) of Section 1.34, hence (v)–(vi), without a completed-field or nonautonomous estimate.

Proposition 1.22.7 gives the protected order-zero identity. Lemma 1.25.10 identifies the full native slice jets, including the matched pressure offsets and the complete outward histories. The spectral amplitudes vanish near both angular endpoints. Lemma 1.6.6 then yields the smooth physical joining in (ii) with the weights in (1.6.4). Lemmas 1.8.7 and 1.7.1 and the forward heat-tail estimates give the common heat coefficient and differentiated exterior bounds. Lemma 1.21.2 supplies the single physical gauge.

Proposition 1.34.14 and Corollary 1.34.15 prove (vii) directly from these frozen inputs. Their fixed-block comparisons precede every completed-field estimate. On each future interval in (vii) one has $\sup_{0\le r\le L_G} |t(\theta+r)/Q - 1| \le Q^h(L_{\mathrm{box}}(Q) + L_G) = o(1)$. The coordinate calculation of the paragraph on p. 432 supplies the finite-box solenoidal rate and jet bounds. The first-order flow ODE gives bounded derivatives of the flow and its inverse for a fixed horizon. Choose L_G by $C_P^2 e^{-2(g_G - g_0)L_G} \le 1/2$, then take Q small enough on the enlarged box. Lemma 1.36.1 gives (1.2.11) and its commutators. The unshifted argument uses the starting rate $\lambda_c + \epsilon/2$ and Gram rate $\lambda_c + \epsilon$. The fixed-interval estimates use the leading jets with t/Q in a fixed neighborhood of one and the same L_G. These bounds, the constant c and the commutator constant C_M can therefore be fixed before L_{box}. The displayed $o(1)$ determines how small Q must be for a given family to enter that neighborhood.

Finally the floor in (viii) puts $c_i S_\ell$ between two fixed positive constants. Since $6/5 > 1$, the negative term $-c\ell^{6/5}$ dominates every fixed multiple of ℓ in the logarithm of the tail bound. This fixes the band schedule using only h and T_g. □

Chapter 2

Craik–Criminale perturbations and a smooth Navier–Stokes force

Fix the leading pair of Theorem 1 on the two sides of the blow-up time $t = 0$. Its stress prescribes a covariance that the velocity correction must realize. We add transverse oscillatory packets, localized by exact curls, and correct their mean interaction. The two time sides use one choice of cutoffs. The ordinary residual of the completed velocity B and pressure p_B gives one smooth force f with fixed compact spatial support. Part 3 uses this same background and its singular strong L^2 trace $B(0)$ for every continuation. A common cutoff switches the background on and off at regular times. The resulting family on $[-T_{\mathrm{in}}, T_{\mathrm{out}}]$ starts from rest at $-T_{\mathrm{in}}$ under one smooth force of compact space-time support.

The leading pair supplied by Theorem 1

The supplying statement is Theorem 1 in Chapter 1. The only result used from Part 1 is its main theorem. We record its data here so that all subsequent references to Theorem 1 refer to the following eight assertions for a single pair of fields. There are parameters

$$0 < h < \lambda/6 < 1/120, \qquad C > 1, \quad 0 < \sigma < 5, \quad \Delta = C^{\sigma}, \quad c_{\mathrm{heat}} > 0, \quad m \in \mathbb{N},\ m \geq 30.$$

Write $x = (x_1, x_2, z)$, $r = (x_1^2 + x_2^2)^{1/2}$ and denote the cylindrical unit vectors by e_r, e_θ, e_z. For $\varepsilon = \pm 1$ and $\varepsilon t > 0$, let $q = q_\varepsilon(t, z)$ be the unique root $q > |z|^{2/(1-2h)}$ of $q - z^2 q^{2h} = \varepsilon t$. Put $\xi = r/\sqrt{q}$, $\eta = z q^{h-1/2}$, $d = 1 - \eta^2$ and $L = 1 - 2h\eta^2$. The profiles E, U, V, P on each side belong to $C^\infty(\mathcal{D})$, $\mathcal{D} = [0, \infty) \times [-1, 1]$, with all derivatives continuous up to its faces locally in ξ.

(i) *Fields, stress and moments.* The physical fields are

$$B_\varepsilon^0 = q^{-1/2}(V/\xi)e_r + q^{-1/2-h}(Ee_\theta + Ue_z), \qquad p_\varepsilon^0 = q^{-1-2h}P.$$

At fixed η define the histories componentwise by

$$(M, I, J, S, C_p) = \int_0^\xi (\rho U,\ \rho^2 E,\ \rho^2 UE,\ \rho(U^2 - E^2/2),\ E^2/\rho)(\rho, \eta)\ \mathrm{d}\rho.$$

Then $P = C_p - C_p(\infty, \eta)$ and $V = [\eta\xi^2 U - (1-2h)\eta M - dM_\eta]/L$. Put $B = B_\varepsilon^0$, $p = p_\varepsilon^0$, $D_B = \partial_t + B_r\partial_r + B_z\partial_z$ and $\Delta_r = \partial_r^2 + r^{-1}\partial_r$. The normalized integrated stress $T_0 = (T_{0,\theta}, T_{0,z})$

is the regular radial primitive from the axis in

$$\begin{aligned} r^{-1}\partial_r(rB_r) + \partial_z B_z = 0, \qquad & \partial_r p = B_\theta^2/r, \\ D_B B_\theta + B_r B_\theta/r - (\Delta_r - r^{-2})B_\theta = -r^{-2}\partial_r(r^2 q^{-1-h} T_{0,\theta}), & \\ D_B B_z + \partial_z p - \Delta_r B_z = -r^{-1}\partial_r(r q^{-1-h} T_{0,z}). & \end{aligned}$$

The four profiles $E/\xi, U, V/\xi^2, P$ are smooth in (ξ^2, η) at the axis, and $E > 0$ for $\xi > 0$. At every (z,t) on either side,

$$\int_0^\infty r B_z \, \mathrm{d}r = 0, \qquad \int_0^\infty r^2 (B_\theta - c_{\mathrm{heat}} r^{-1-2h}) \, \mathrm{d}r = 0.$$

Both integrals converge. Each loop or spectral modification together with its five-history restoration has zero net change in the five histories at the completed outlet of Table 2.6. For the pressure bank alone the outlet change is $(0,0,0,0,\Pi_{\mathrm{ref}} - p_0)$ when the axis pressure changes from Π_{ref} to p_0. Hence $p_0 + C_{p,\mathrm{new}} = \Pi_{\mathrm{ref}} + C_{p,\mathrm{ref}}$ at that outlet. Inside each bank the five histories use the actual radial integrands up to the observation radius.

(ii) *Common exterior and joining data.* Above a fixed ξ_{heat}, $U = V = 0$ and the physical swirl $K_\varepsilon(r,t)$ solves $\partial_t K_\varepsilon = (\Delta_r - r^{-2})K_\varepsilon$. Both sides have the same leading tail $E = c_{\mathrm{heat}}\xi^{-1-2h}(1 + O(\xi^{-2}))$ and the differentiated expansions of Lemma 2.3.20. For $z \neq 0$ use $\widetilde{Q} = |z|^{2/(1-2h)}$, $\widetilde{\xi} = r/\sqrt{\widetilde{Q}}$, $\widetilde{\eta} = t/\widetilde{Q}$. If a physical scalar is $q^{-w}g$, its slice profile is $\widetilde{g} = |\eta|^{2w/(1-2h)}g$. The two slice profiles have equal $\widetilde{\eta}$-derivatives of every order at $\widetilde{\eta} = 0$ for every $\widetilde{\xi} \geq 0$. This holds for $(V/\xi, E, U, M, I, J, S, C_p, P)$ with respective weights $(\frac{1}{2}, \frac{1}{2}+h, \frac{1}{2}+h, h-\frac{1}{2}, h-1, 2h-\frac{1}{2}, 2h, 1+2h, 1+2h)$. The positive physical cutoff gauge $\widetilde{q}$ is smooth away from $(z,t) = (0,0)$ and equals q_- on $t \leq 0$, $q_+/L_{\mathrm{cut}}(\eta_+)$ on $t \geq 0$. Near $\eta_+ = \pm 1$, $L_{\mathrm{cut}} = \lambda_{\mathrm{ch}}$ is the positive branch with endpoint value one in $\eta_+^2 \lambda_{\mathrm{ch}}^{1-2h} = 1 + \lambda_{\mathrm{ch}}(1 - \eta_+^2)$.

(iii) *Protected core, correction domains and finite-dimensional solves.* Each side has smooth positive graphs $\xi_a(\eta), \xi_p(\eta)$. On an open collar of each endpoint let $l = \lambda_{\mathrm{ch}}(\eta)$ and $\eta_b = l^{1/2-h}\eta$. With the backward radii continued as constants,

$$\xi_{j,-}(\eta_b)^2 = l\, \xi_{j,+}(\eta)^2, \qquad j \in \{a, p\}.$$

On $0 \leq \varpi = (\xi/\xi_a)^2 \leq \Xi$ and on a fixed angular neighborhood of $[-1,1]$, the pullbacks G of $E/\xi, U, V/\xi^2, P$ satisfy $|\partial_\varpi^j \partial_\eta^k G| \leq C_j r_G^{-k}(k!)^{3/2}$ with a common $r_G > 0$. The shared Gevrey-3/2 cutoff is one below Ξ_{need} and zero above Ξ_{cut}, where $1 < \Xi_{\mathrm{need}} < \Xi_{\mathrm{cut}} < \Xi$; its derivative support lies in a strict entry collar with weight bounded away from zero, as in (2.3.1). On the backward side the entry graph is constant and the core through the first collar satisfies $C_j r_b^{-k} k!$ angular bounds before the first loop. On both sides the intervals I_{pos} and I_{mean} are respectively $-14 < y_p < -9$ and $-8 < y_p < -3$ for $y_p = 2\log(\xi/\xi_p(\eta))$. There $H = \xi E = c(\eta)\xi^{-2\mu(\eta)}$, $c > 0$, $0 < \nu_c \leq \mu \leq \lambda$; U is radially constant and is zero on I_{pos}. For nonnegative nonzero bumps b_j with strictly ordered disjoint compact supports inside either interval, the matrices $(\int_0^\infty \xi^{s_i} b_j(y_p) \, \mathrm{d}\xi)_{ij}$ have uniformly bounded inverses for $s = (1, 1-2\mu)$ and $s = (2, -2-2\mu, -2\mu)$. At each selected five-history return the Jacobian with respect to two axial and three swirl amplitudes is uniformly invertible. The six-real spectral control map, including its returns, has invertible Jacobian at the selected parameters.

For reference, the leading parameter properties used below on the closed angular interval are the transverse exponent inverse (N1), the invertible two-return moment matrix (N2), the positive

energy root A_p with $\mathcal{P}'(A_p) \geq 2^{-3/2}$ for the outgoing energy defect $\mathcal{P}$ (N3), the invertible two-row correction Jacobian at the selected small-data branch (N4), the transverse stop and smooth shot (N5), the moving axial and swirl moment inverses and the five-history Jacobians just described (N6(a),(b)), the smooth orientation-preserving circle reparametrization of the loop (N7), and the protected angular extension with $L > 0$ (N8). The selected pulse, return, stop, shot and loop parameters are smooth through both angular endpoints.

The late forward pressure hull is contained in the two tubes K_0, K_{ext} defined in Proposition 2.3.2. On both $T_{0,\theta} \geq cH > 0$; the extended tube is restricted to the central angular set containing the spectral returns. For the backward data (B1)–(B6), (B1) supplies the pre-loop regular core, the analytic collar retained by the final member, and the matching arc of Lemma 2.3.3, with its five incoming histories. Conditions (B2) and (B3) give the strict cone of (iv) and the weight of Lemma 2.3.11. Condition (B4) gives the compensated moments and the actual heat exterior of Lemma 2.3.5, (B5) the two untouched power slots, and (B6) the terminal multiplier and stress jets of Lemma 2.3.4. The support order for this same member is recorded in Table 2.6.

Its step numbers have the following meaning. Step 1 fixes the chart geometry and exponents, step 2 the normalized outer and central profiles, and step 3 the pulse lengths and pressure target. Step 4 fixes the core parameters, then the scale C and the physical radii. Step 5 fixes the activation and joining parameters. Step 6 fixes the loop before selecting the angular mode m and its spectral controls. Step 7 selects the completion cutoffs after the leading fields are fixed.

(iv) *Strict stress margins, weights and radial inverse.* Let $F = E/\xi$, $\mathbf{S} = (\xi\partial_\xi F, \partial_\xi U)$, $a = -\xi F_\xi/F$, $b = U_\xi/F$, $v = a + b^2/a$, $t_s = -b/a$. On $\mathcal{A}_\varepsilon = \{T_0 \neq 0\}$ put $n = T_0/|T_0|$. There are uniform $c_s > 0$ and $0 < \delta_c < 2$ such that

$$F, a, v - 2 \geq c_s, \qquad n_\theta + t_s n_z \geq \delta_c, \qquad (v-2)(n_z - t_s n_\theta)^2 \leq (2-\delta_c)(n_\theta + t_s n_z)^2.$$

There $-|\mathbf{S}|^2 < 2FS_\theta < 0$, $n \cdot \mathbf{S} < 0$ and $(n \cdot \mathbf{S})^2 > |\mathbf{S}|^2 + 2FS_\theta$. Each side has a smooth $0 \leq \mathsf{W} \leq e^{-2}$, positive precisely on $\mathcal{A}_\varepsilon$, which lies between $\xi_a(\eta)$ and a finite terminal radius. The weight is positive on the pressure tubes and bounded below on I_{mean}. All its positive powers extend flatly by zero. For every word D^j of length j in $\xi^{-1}\partial_\xi, \partial_\eta|_\xi$, with $\mathcal{L}_W = 1 + \log(1/\mathsf{W})$, one has on the active set

$$c\mathsf{W} \leq |T_0|, \qquad |D^j T_0| + |D^j \mathsf{W}| \leq C_j \mathsf{W} \mathcal{L}_W^{N_j}.$$

On the forward side set $X = \xi^2/2$. Let X_{mid} be the least starting radius $X_{1,i}$ of the terminal radial splices of the weight, in the X coordinate. Let H_{heat} denote the numerator of the matched homogeneous heat swirl, including its fast component, in the same chart as $H_+ = \xi E_+$. For $X \geq X_{\mathrm{mid}}$ and every word D^j as above there are constants C_j, N_j for this member such that

$$\left|D^j(H_+ - H_{\mathrm{heat}})\right| \leq C_j\, \mathsf{W}\, \mathcal{L}_W^{N_j}.$$

The right side is extended by zero at $\mathsf{W} = 0$, including points where a radial and an angular terminal face meet. On the compact middle region $y_a = 2\log(\xi/\xi_a) \geq y_{\mathrm{col}}$, $X \leq X_{\mathrm{mid}}$, for a fixed inner collar width $y_{\mathrm{col}} > 0$, the forward weight has a positive lower bound.

The entry stress and the backward terminal stress have the factorizations (2.3.3) and Lemma 2.3.4, respectively. For every g supported in the fixed radial hull, zero where $\mathsf{W} = 0$

and obeying these weighted upper bounds through order k, the moment-subtracted primitive

$$\mathcal{I}_m g = \int_\xi^\infty g(\rho,\eta)\rho\,\mathrm{d}\rho - \chi_m(\xi,\eta)\int_0^\infty g(\rho,\eta)\rho\,\mathrm{d}\rho$$

obeys bounds of the same form through order k, with constants linear in the finite family of input seminorms. Here χ_m is the normalized moving mean cutoff in (2.3.10). Its commutator and the estimates for mean-bump multiples of the full integral are (2.3.8) and Proposition 2.3.12.

(v) *The physical frozen instability of this same forward member.* For $y \in \mathbb{R}^2$, $Z \in \mathbb{R}$, let $\mathcal{Q} = q_+(1,Z)$, $R = |y|$ and $\langle R\rangle = (1+R^2)^{1/2}$. Define

$$\mathcal{U}_0(y,Z) = R\Omega(R,Z)e_\theta + W(R,Z)e_z, \qquad R\Omega = \mathcal{Q}^{-1/2-h}E_+(R/\sqrt{\mathcal{Q}}, Z\mathcal{Q}^{-1/2+h}),$$

with $W = \mathcal{Q}^{-1/2-h}U_+(\xi,\eta)$ and $\mathcal{U}_1 = \mathcal{Q}^{-1/2}(V_+(\xi,\eta)/\xi)e_r$, where $(\xi,\eta) = (R/\sqrt{\mathcal{Q}}, Z\mathcal{Q}^{-1/2+h})$. Values on the axis are taken by smooth extension. Below the spatial L^2 norms at fixed Z use Lebesgue measure on $\mathbb{R}^2_y$. For every $j,l \ge 0$,

$$|\partial_Z^l \partial_R^j \Omega(R,Z)| \le C_{j,l}\langle R\rangle^{-2-2h-j}.$$

The axial profile is zero for $R \ge \xi_U\sqrt{\mathcal{Q}(Z)}$, for a finite ξ_U. There is one all-Z constant $C_{\mathfrak{B}}$ for the following profile and dilation bounds:

$$\begin{gathered}
|\nabla_y^i \partial_Z^j \mathcal{U}_0| + |\partial_Z^j \Omega| \le C_{\mathfrak{B}} \quad (i+j \le 2),\\
|\mathcal{U}_1| + |\nabla_y \mathcal{U}_1| + |\partial_Z \mathcal{U}_1| \le C_{\mathfrak{B}},\\
\langle R\rangle^2 |\nabla_y \mathcal{U}_0| + R(|\Omega| + |W| + |\partial_Z \Omega|) \le C_{\mathfrak{B}},\\
\|\Omega(\cdot,Z)\|_2 + \|W(\cdot,Z)\|_2 + \|\nabla_y \mathcal{U}_0(\cdot,Z)\|_2 \le C_{\mathfrak{B}},\\
|y\cdot\nabla_y f| + |Z\partial_Z f| \le C_{\mathfrak{B}} \quad (f = \Omega, W, \nabla_y \mathcal{U}_0).
\end{gathered}$$

For $n \in \mathbb{Z}$ and $k \in \mathbb{R}$ let

$$\begin{aligned}
\mathsf{H}_n &= \{v \in L^2(\mathbb{R}^2_y;\mathbb{C}^3) : v(R_\varphi y) = e^{in\varphi}\widehat{R}_\varphi v(y) \text{ in } L^2 \text{ for every } \varphi\},\\
X_{n,k} &= \{v \in \mathsf{H}_n : \nabla_y \cdot v_h + ikv_3 = 0 \text{ in distributions}\}.
\end{aligned}$$

Here $v_h = (v_1, v_2)$, R_φ is planar rotation, and $\widehat{R}_\varphi = \mathrm{diag}(R_\varphi, 1)$. P_k is the horizontal Fourier multiplier with symbol $I - \zeta\otimes\zeta/|\zeta|^2$, $\zeta = (\zeta_h, k) \ne 0$; its restriction to H_n is the orthogonal projection onto $X_{n,k}$. For $\nu \ge 0$ the frozen generator on $X_{n,k}$ is

$$A_{\nu,n}(Z,k)v = -P_k[(\mathcal{U}_0\cdot\nabla_k)v + (v_h\cdot\nabla_y)\mathcal{U}_0] + \nu(\Delta_y - k^2)v, \qquad \nabla_k = (\nabla_y, ik).$$

Its domain is $X_{n,k}\cap H^2$ for $\nu > 0$ and all of $X_{n,k}$ for $\nu = 0$. Write $s(A) = \sup\{\Re z : z \in \operatorname{spec} A\}$. The supremum of $s(A_{0,n}(Z,k))$ over $(n,Z,k) \in \mathbb{Z}\times\mathbb{R}^2$ is a number $\lambda_c > 0$ attained precisely at $(m,0,0)$ and $(-m,0,0)$. On a neighborhood of $(0,0)$ the m sector has an algebraically simple eigenvalue $\lambda(Z,k)$, with $\lambda_0 = \lambda(0,0)$ and $\Re\lambda_0 = \lambda_c$. Its $-m$ counterpart is $\overline{\lambda(Z,-k)}$. For some $c_g, c, c_C, c_*, C_* > 0$ and $g = c_g\Delta$,

$$\lambda_c - g \ge c\Delta, \qquad \sup_{z\in\operatorname{spec} A_{0,m}(0,0)\setminus\{\lambda_0\}} \Re z \le g, \qquad \sup_{\substack{n\ne\pm m\\(Z,k)\in\mathbb{R}^2}} s(A_{0,n}(Z,k)) \le \lambda_c - \delta_{\mathrm{ang}},$$

where $\delta_{\mathrm{ang}} \geq c_C \Delta d_m^2 > 0$. Here d_m is the positive relative width of the selected radial spectral layer. On that neighborhood,

$$c_*(Z^2 + k^2) \leq \lambda_c - \Re\lambda(Z,k) \leq C_*(Z^2 + k^2).$$

Let $r_0 > 0$ be the center radius of the spectral layer at $Z = 0$. There exist $0 < c_A \leq C_A$ and $C_q > 0$ with the following properties. The physical complex derivatives, evaluated at the pole, obey

$$\begin{gathered}
\lambda_Z = \lambda_k = \lambda_{Zk} = 0, \qquad a_m = m/r_0, \\
-C_A\Delta \leq a_m^2 \Re\lambda_{kk}/h^2 \leq -c_A\Delta, \quad |a_m^2\lambda_{kk}/h^2| \leq C_A\Delta, \\
q_G = a_m^2 C_q/\Delta > 0, \qquad \frac{\lambda_{kk}}{h^2} q_G^2 + \left(\frac{1}{h} - 1\right) q_G - \lambda_{ZZ} = 0, \\
b_d = \frac{1}{2h} - \frac{1}{2}, \qquad X_G = -\frac{\Re\lambda_{kk}}{2h^2} q_G > b_d, \qquad X_G - \frac{b_d}{2} - \sqrt{X_G^2 - b_d X_G} \leq \frac{1}{16}.
\end{gathered}$$

The displayed Riccati identity is an equality in $\mathbb{C}$. The conjugate label has the conjugate data.

On a fixed pole chart, right and adjoint eigenvectors can be normalized by $\langle e, e^\sharp \rangle = 1$ so that

$$\|\partial_Z^l \partial_k^j e\|_{H^6_{7-j}} + \|\partial_Z^l \partial_k^j e^\sharp\|_{H^6_{7-j}} \leq C \qquad (0 \leq j \leq 6,\ 0 \leq l \leq 17).$$

Here H^s_w consists of the distributions with finite norm $\sum_{|\alpha| \leq s} \|\langle y \rangle^w \partial_y^\alpha f\|_2$, and $\langle e, e^\sharp \rangle$ is the $L^2(\mathbb{R}^2; \mathbb{C}^3)$ pairing. For $0 \leq j \leq 2$ the same profile bound holds in H^{18}_{9-j}, and the corresponding scalar pressure profiles obey the H^s_{8-j} bound for $0 \leq s \leq 18$ on this range. For parameter derivatives on a fixed space, extend $A_{0,n}$ by zero on $(I - P_k)\mathsf{H}_n$. On a compact phase rectangle about the origin there are positively oriented contours, uniform on that rectangle, isolating the selected eigenvalue and the complementary spectrum. They are finite unions of closed rectifiable curves in the common resolvent set at positive distance from zero. For z on those contours the resolvent and its adjoint satisfy

$$\|\partial_Z^l \partial_k^j (z - A_{0,\pm m})^{-1}\|_{H^s_{w+j} \cap \mathsf{H}_{\pm m} \to H^s_w \cap \mathsf{H}_{\pm m}} \leq C \quad (l \leq 17,\ \lceil w \rceil + j \leq m - 1)$$

for every fixed integer $s \geq 0$, real $w \geq 0$ and integers $j, l \geq 0$ in the displayed ranges; the constant may depend on s, w, j, l and the rectangle. At the limiting weight the derivatives are taken strongly on each datum. The physical Leray multiplier on each selected sector satisfies $\|\partial_k^j P_k f\|_{H^s_w} \leq C\|f\|_{H^s_{w+j}}$ for $\lceil w \rceil + j \leq m - 1$. Integration of $(2\pi i)^{-1}(z - A)^{-1}\,\mathrm{d}z$ around the simple eigenvalue defines its Riesz projection. That projection and the resolvent on its complementary invariant subspace obey the same bounds.

(vi) *Uniform frozen data for later evolution.* There are $\nu_0 > 0$, $N_{\mathrm{far}} > \max(m, 2)$, $g_{\mathrm{far}} < g_1 < \lambda_c$, $C_F, M_{\mathrm{far}} < \infty$, and compactly phase-supported shifts $S_{\nu,\pm m} = d_0 \chi_\pm P_{\nu,\pm m}$, zero on the other angular sectors. Here $d_0 > 0$; $0 \leq \chi_\pm \leq 1$ are smooth compactly supported functions on the simple-eigenvalue charts, equal to one near $(0,0)$ and satisfying $\chi_-(Z,k) = \chi_+(Z,-k)$. Both supports are compactly contained in one open rectangle U about the pole, symmetric in k, whose closure lies in the weighted contour rectangle of (v). On $\overline{U}$ the Hessian of $\Re\lambda$ is negative definite and $|\ell_0 P_{0,m}(Z,k)e_0 - 1| \leq 1/2$, where $P_{0,m}(0,0) = e_0\ell_0$ and $\ell_0 e_0 = 1$. On each support $P_{\nu,\pm m}$ is the Riesz projection onto the continuation of that simple eigenvalue at viscosity ν. The following norms are operator norms on $X_{n,k}$:

$$\begin{aligned}
\|e^{\tau(A_{\nu,n}(Z,k) - S_{\nu,n}(Z,k))}\| &\leq C_F e^{g_1 \tau} \quad (|n| < N_{\mathrm{far}},\ \tau \geq 0), \\
\|(z - A_{\nu,n}(Z,k))^{-1}\| &\leq M_{\mathrm{far}} \qquad (|n| \geq N_{\mathrm{far}},\ \Re z \geq g_{\mathrm{far}}),
\end{aligned}$$

uniformly in $(Z,k)\in\mathbb{R}^2$ and $0\le\nu\le\nu_0$. Extend the shifts by zero on $(I-P_k)\mathsf{H}_n$, so $S_{\nu,n}=P_kS_{\nu,n}P_k$. On the common space H_n they have uniformly bounded norms, are strongly Borel measurable in (ν,Z,k), are norm continuous at $\nu=0$, and satisfy $\sup_{Z,k}\|S_{\nu,n}-S_{0,n}\|\to0$ as $\nu\downarrow0$. There are also $0<d_*\le1$ and a smooth function $\delta(R)\in[d_*,1]$, equal to one near the axis and outside an annulus, and $\gamma<g_1$ such that

$$\sup_{R,Z}\left\{\frac{|2\Omega-\delta(2\Omega+R\Omega_R)|}{2\sqrt{\delta}}+\frac{|W_R|}{2}\right\}<\gamma.$$

These are the all-phase frozen estimates; the subsequent leading and completed evolution estimates use this same source.

(vii) *Independent leading evolution and its Gram metric.* For $t>0$, put $s=-t^{-h}/h$, $\rho=t^h$, $y=x_h/\sqrt{t}$, $Z=z/t^{1/2-h}$ and let P_ρ be the orthogonal projection onto $X_\rho=\{v\in L^2(\mathbb{R}^2_y\times\mathbb{R}_Z;\mathbb{C}^3):\operatorname{div}_y v_h+\rho\partial_Z v_3=0\}$. The unshifted operator $U_{\mathrm{lead}}(s,\sigma):X_{\rho(\sigma)}\to X_{\rho(s)}$ maps the initial value of v at σ to its value at s, where $w(x,t)=t^{-1/2-h}v(y,Z,s)$ solves

$$\partial_t w-\Delta w+\mathbb{P}\big[(B_+^0\cdot\nabla)w+(w\cdot\nabla)B_+^0\big]=0,\qquad \operatorname{div}w=0.$$

$\mathbb{P}$ is the orthogonal projection onto divergence-free fields in physical $L^2(\mathbb{R}^3;\mathbb{C}^3)$. To define the shifted evolution $U^\sharp_{\mathrm{lead}}$, subtract $P_\rho T_\rho^*S_{\rho,n}T_\rho P_\rho v$ from the right-hand side of the equation for $\partial_s v$ in sector n. Here $S_{\rho,n}$ acts by multiplication in (Z,k), and the axial Gaussian transform with phase measure $\mathrm{d}Z\,\mathrm{d}k/(2\pi\rho)$ is

$$(T_\rho v)(y,Z,k)=(\pi\rho)^{-1/4}\int_{\mathbb{R}}e^{-(z'-Z)^2/(2\rho)-ik(z'-Z)/\rho}v(y,z')\,\mathrm{d}z'.$$

There are $g_2<\lambda_c$, $C,T_0<\infty$ such that

$$\|U^\sharp_{\mathrm{lead}}(s,\sigma)\|_{2\to2}\le Ce^{g_2(s-\sigma)}\qquad(\sigma\le s\le-T_0).$$

For every $\epsilon>0$ there are $C_\epsilon,T_\epsilon<\infty$ with

$$\|U_{\mathrm{lead}}(s,\sigma)\|_{2\to2}\le C_\epsilon e^{(\lambda_c+\epsilon)(s-\sigma)}\qquad(\sigma\le s\le-T_\epsilon).$$

Both estimates are uniform over all angular sectors and all ancient initial times.

The leading field also supplies the fixed finite-time Gram constants. For the fixed horizon L_G below, prescribe a family $L_{\mathrm{box}}(Q)\ge0$ such that $L_{\mathrm{box}}(Q)+L_G=o(\log(1/Q^h))$ as $Q\downarrow0$. The starting times satisfy $|\theta|\le L_{\mathrm{box}}(Q)$ and the coefficients are taken on $[\theta,\theta+L_G]$. In the isotropic coordinates $t=Q+Q^{1+h}\theta$, $y=x/\sqrt{Q}\in\mathbb{R}^3$, $\rho=Q^h$, put $B_0(y,\theta)=Q^{1/2+h}B_+^0(\sqrt{Q}y,Q+Q^{1+h}\theta)$, $P=\mathbb{P}$, $Q_\perp=I-P$ and $(G_0)_{ij}=\partial_{y_j}(B_0)_i$. One may fix a smooth physical approximation S_{app} of the two-band shift, of the form $P\operatorname{Op}_{\mathrm{AW}}(S_{\mathrm{sm}})P$, where $\operatorname{Op}_{\mathrm{AW}}(S_{\mathrm{sm}})$ is the Gaussian analysis, multiplication by S_{sm} and synthesis just defined, transferred to the box coordinates. The smooth finite-rank radial symbol S_{sm} has compact phase support, with $\|S_{\mathrm{app}}\|_{H^{-j}\to H^j}\le C_j$ at each required finite order. For the whole-space extension

$$A_{\mathrm{ext}}=-B_0\cdot\nabla-G_0+2Q_\perp G_0P+(G_0-G_0^\top)Q_\perp+\rho\Delta-S_{\mathrm{app}},$$

there are a fixed rate $g_G<\lambda_c$, a finite horizon L_G, and a positive self-adjoint operator $M(\theta)$ on $L^2(\mathbb{R}^3;\mathbb{C}^3)$ commuting with P. In terms of the propagator U_{ext} generated by A_{ext} in box time,

$$M(\theta)=I+c\int_0^{L_G}e^{-2g_Gr}U_{\mathrm{ext}}(\theta+r,\theta)^*U_{\mathrm{ext}}(\theta+r,\theta)\,\mathrm{d}r\quad(c>0).$$

It satisfies $I \le M \le C_M I$ and, as a quadratic-form inequality on $H^1(\mathbb{R}^3;\mathbb{C}^3)$ at interior box times,

$$\langle u, (\partial_\theta M + A_{\mathrm{ext}}^* M + M A_{\mathrm{ext}})u\rangle \le 2g_G\langle u, Mu\rangle + C_M\|Q_\perp u\|_2^2 - 2\rho\|\nabla u\|_2^2.$$

For every bounded real Lipschitz vector field $W:\mathbb{R}^3\to\mathbb{R}^3$ and every bounded real Lipschitz function $b:\mathbb{R}^3\to\mathbb{R}$,

$$\|[M, W\cdot\nabla]\|_{2\to 2} \le C_M(\|W\|_\infty + \|\nabla W\|_\infty),$$
$$\|[b, M]\|_{2\to H^1} \le C_M(\|b\|_\infty + \|\nabla b\|_\infty).$$

The constants g_G, L_G, c, C_M are fixed before the box-length family. For each such family they apply at every stated start once Q is below a threshold that may depend on the family. The same C_M applies to every such W and b. For the unshifted leading equation the same construction, with $S_{\mathrm{app}} = 0$, gives the Gram inequality at any fixed rate $\lambda_c + \epsilon$. The horizon and constants are chosen from the leading propagator and leading jets before the completed clock is estimated.

(viii) *The schedule reserved for completion.* With $T_g = 4+\sqrt{2}$ (the larger eigenvalue of $\left(\begin{smallmatrix}3&1\\1&5\end{smallmatrix}\right)$), use the common physical gauge in (ii) and fix, for all sufficiently large band indices ℓ,

$$Q_\ell = 2^{-\ell}, \quad \rho_\ell = Q_\ell^h, \quad S_\ell = \ell^{6/5}, \qquad i(\ell) = \left\lfloor \frac{(1+h)\ell\log 2 - (6/5)\log\ell}{\log T_g} \right\rfloor.$$

Then $c_i = T_g^{i(\ell)} Q_\ell^{1+h} \asymp S_\ell^{-1}$, $|i(\ell+1) - i(\ell)| \le C$, and for every fixed $B, N, M, c > 0$,

$$Q_\ell^{-B} S_\ell^N e^{-cS_\ell} = O(Q_\ell^M).$$

2.1 The local packet ansatz

The separated packets have a *Craik–Criminale type* form because a transverse polarization multiplies a rapidly oscillating phase transported by the local background, with its actual transport defect retained. The envelope and exact curl localize this wave to one packet.

Let u_{B} denote the divergence-free slow velocity obtained from the slow Borel construction of Proposition 2.10.1. On a band $Q = 2^{-\ell}$ write its cylindrical components in the variables

$$\rho = Q^h, \quad S = \ell^{6/5}, \quad (\mathsf{R},\mathsf{Z},\mathsf{T}) = (r/\sqrt{Q}, z/Q^{1/2-h}, t/Q), \qquad Q^{1/2+h}u_{\mathrm{B}} = (b, \mathsf{R}F_b, G_b).$$

The auxiliary sampling is $Y_{\mathrm{phys}} = v_r r^{d_r} + v_t t \pmod{\mathbb{Z}^2}$, with $v_r = (1, 1-\sqrt{2})$ and $v_t = (\sqrt{2}-1, 1)$. Here $d_r > 1$ is the radial exponent in (2.13.7). The level-i cover is $\pi_i(Y) = J_g^i Y \pmod{\mathbb{Z}^2}$, with $J_g = \left(\begin{smallmatrix}3&1\\1&5\end{smallmatrix}\right)$ and $c_i = (4+\sqrt{2})^i Q^{1+h} \asymp S^{-1}$. For a signed label γ of color $\mu(\gamma)$, let $c_{\mu(\gamma)}$ be the center of its torus rectangle from Lemma 2.13.1. On a lift of that rectangle write $\pi_i(Y) - c_{\mu(\gamma)} = \xi_{\mathrm{aux}} v_r + \zeta v_t$ and $v = (\zeta + r_0)/c_i$, so $L_p = 2r_0/c_i \asymp S$. The evaluated pulse derivative is $t_* = \rho\partial_{\mathsf{T}} + \partial_v$. The phase and its normal are

$$\Phi = p\theta + p_z\mathsf{Z}/\rho + x_0\mathsf{R} - v(pF_b + p_z G_b), \qquad n = \sqrt{Q}\nabla_x\Phi, \qquad k = \lceil \rho^{-1/2}\rceil. \tag{2.1.1}$$

The coefficients p, p_z, x_0 in (2.13.15) fix the angular, axial and radial parts of the initial phase on the box. The angular coefficient is rounded so that kp is a nonzero integer, as required by periodicity in

θ. The gradient is taken after physical sampling. The phase satisfies $(\partial_t + u_{\mathrm{B}} \cdot \nabla_x)\Phi = Q^{-1-h}\mathcal{E}_\Phi$ with $\mathcal{E}_\Phi = O(\rho S^C)$; its explicit defect is kept in the linear residual (2.13.37).

For a signed label $\gamma = (\beta, \varsigma)$, the real homogeneous pulse polarization $t^h_\varsigma(v)$ satisfies $n \cdot t^h_\varsigma = 0$. It is the frame lift of the homogeneous solution specified in Lemma 2.13.2 and (2.13.25). Use the slow partition coefficient η_β of (2.13.11), the transverse and temporal cutoffs χ_g, ψ of (2.13.39), and the aggregate cutoff ϑ_q of (2.13.10). Define

$$a_\gamma = \vartheta_q \sqrt{\rho}\, \eta_\beta a_{\beta,\varsigma} \chi_g(\xi_{\mathrm{aux}}) \psi(v) t^h_\varsigma, \qquad d_\gamma = \frac{n \times a_\gamma}{k|n|^2}.$$

The physical packet is the *exact* curl

$$w_\gamma = \nabla_x \times [-Q^{-h} d_\gamma \sin(k\Phi)] = Q^{-1/2-h}[a_\gamma \cos(k\Phi) - b_\gamma \sin(k\Phi)], \qquad b_\gamma = \mathrm{curl}_*\, d_\gamma. \tag{2.1.2}$$

Here curl_* is the coefficient curl with evaluated radial and axial derivatives and the cylindrical connection, as in (2.13.30). All coefficients are sampled at Y_{phys}; thus every cutoff derivative remains in b_γ and $\operatorname{div} w_\gamma = 0$ exactly.

The positive numbers $a^2_{\beta,\varsigma}$ solve the two-column covariance system of Proposition 2.13.5. For their sum, wherever the squared partition is complete, the principal Haar radial-cross pair before the aggregate cutoff is $q_\varepsilon^{-1-h}\mathcal{T}_0 = \widetilde{q}^{-1-h}\widetilde{T}_0$, where $\widetilde{T}_0 = (\widetilde{q}/q_\varepsilon)^{1+h}\mathcal{T}_0$. The cutoff multiplies this pair by ϑ_q^2. The actual angular covariance of one packet is $\frac{1}{2}Q^{-1-2h}(a_\gamma \otimes a_\gamma + b_\gamma \otimes b_\gamma)$. The mean equations keep this full sampled tensor, including all six entries, rather than substituting its auxiliary Haar average. Higher packet and mean corrections successively improve the residual. After the common diagonal choice and spatial localization, the ordinary residual of the completed velocity and pressure gives the force in the following theorem.

2.2 Main statement

Write $x = (x_1, x_2, z)$, $r = (x_1^2 + x_2^2)^{1/2}$, and let e_r, e_θ, e_z be the cylindrical unit vectors for $r > 0$. Fix the leading profiles, pressure normalization, common cutoff gauge $\widetilde{q}$ and spectral data of Theorem 1. For $t \neq 0$, put $\varepsilon = \operatorname{sgn} t$, let $q > |z|^{2/(1-2h)}$ satisfy $q - z^2 q^{2h} = |t|$, and set $\xi = r/\sqrt{q}$, $\eta = z q^{-1/2+h}$. The leading velocity is

$$B_0(x,t) = q^{-1/2}\frac{V_\varepsilon(\xi,\eta)}{\xi} e_r + q^{-1/2-h}(E_\varepsilon(\xi,\eta)e_\theta + U_\varepsilon(\xi,\eta)e_z),$$

with its smooth Cartesian extension at $r = 0$. The intermediate velocity u_{B} and pressure p_s obey the stress estimate (2.6.33) with tangential stress K_B. The velocity B below includes the packet and mean corrections to u_{B}.

All spatial norms without a domain are over $\mathbb{R}^3$, in the space variable displayed. For a vector v and scalar π put

$$\mathscr{N}(v,\pi) = \partial_t v - \Delta v + \operatorname{div}(v \otimes v) + \nabla\pi, \qquad [\operatorname{div}(v \otimes v)]_i = \sum_{j=1}^{3} \partial_{x_j}(v_i v_j).$$

Write $L^2_\sigma = \{v \in L^2(\mathbb{R}^3;\mathbb{R}^3) : \operatorname{div} v = 0 \text{ in } \mathcal{D}'\}$ and $H^1_\sigma = H^1(\mathbb{R}^3;\mathbb{R}^3) \cap L^2_\sigma$.

Theorem 2 (Completion on both sides of the singular time)**.** *For this leading pair there exist $T_-, T_b, R_* > 0$ and a velocity, pressure and force (B, p, f) solving the forced Navier–Stokes equations with viscosity one on $\mathbb{R}^3 \times I$, $I = (-T_-, T_b)$. The force is smooth, B and f have spatial support in $\overline{B_{R_*}(0)}$ at every time, and B has a common strong L^2 trace u_0 at zero that is essentially unbounded in every neighborhood of the origin. The same choice of fields has all the following properties.*

(i) *Construction of the completed field.* Use the band parameters

$$Q_\ell = 2^{-\ell}, \quad \rho_\ell = Q_\ell^h, \quad S_\ell = \ell^{6/5}, \quad \varkappa = 10^{-5}$$

for all sufficiently large integers ℓ. The band partition (2.13.11) uses the common physical gauge $\widetilde{q}$. On an active band $1/2 \le \widetilde{q}/Q_\ell \le 2$, and $Q_\ell \asymp \widetilde{q} \asymp q$ throughout its fixed enlargement. There is one choice of the cover, rounded levels, phases and frames in Theorem 2.10.2 and of the finite states in Proposition 2.15.2 on both time sides. Denote their uncut velocities and pressures by $(u^{[n]}, p^{[n]})$, $n \ge 0$. They consist of the angular mean $u_M^{[n]}$, the packet sum $w^{[n]}$ of zero angular mean, and the pressure $p^{[n]}$, including the slow part. The waves have the curl form (2.1.2) and its finite-harmonic corrections. There is a common sequence $\delta_n > 0$, $\delta_{n+1} \le \delta_n/4$. With $\chi_n = \chi(\widetilde{q}/\delta_n)$ as in (2.18.5), form the cut increments of (2.18.6) from consecutive finite states. In particular the cut wave increment is $\nabla \times (\chi_n \mathcal{A}_n)$, where $\nabla \times \mathcal{A}_n = w^{[n+1]} - w^{[n]}$, and the cut pressure increment is $\chi_n(p^{[n+1]} - p^{[n]})$. The radial mean increment includes the flux correction in (2.18.6). Let (u_∞, p_∞) be their locally finite sum (2.18.12) starting from the initialized state at $n = 0$. For $t \ne 0$ the physical fields are

$$B = \chi_{\mathrm{loc}} u_\infty - \mathcal{B}_{\mathrm{div}}(\nabla \chi_{\mathrm{loc}} \cdot u_\infty), \qquad p = \chi_{\mathrm{loc}} p_\infty.$$

Here $\chi_{\mathrm{loc}} \in C_c^\infty(B_{R_*}(0))$ equals one near the origin and $\mathcal{B}_{\mathrm{div}}$ is the fixed annular right inverse of the divergence in (2.18.23). The cutoff and the inverse are the same at every time. The force off the joining time is

$$f(x,t) = \mathscr{N}(B,p)(x,t) \qquad (t \ne 0). \tag{2.2.1}$$

(ii) *Physical equation and solution class.* We have $B \in C(I; L^2_\sigma) \cap L^2_{\mathrm{loc}}(I; H^1_\sigma)$, $f \in C^\infty(\mathbb{R}^3 \times I; \mathbb{R}^3)$, and B, p are smooth on $(\mathbb{R}^3 \times I) \setminus \{(0,0)\}$. For every $t \in I$ the spatial pressure distribution is

$$p(t) = -\frac{1}{4\pi|\cdot|} * \Big(\operatorname{div} f(t) - \sum_{i,j=1}^{3} \partial_{x_i} \partial_{x_j} (B_i(t) B_j(t)) \Big),$$

where $*$ is spatial convolution. For every $\psi \in C_c^\infty(\mathbb{R}^3)$, $t \mapsto \langle p(t), \psi \rangle$ is continuous on I. In spacetime distributions,

$$\partial_t B - \Delta B + \operatorname{div}(B \otimes B) + \nabla p = f, \qquad \operatorname{div} B = 0. \tag{2.2.2}$$

The momentum identity holds against every vector test function in $C_c^\infty(\mathbb{R}^3 \times I; \mathbb{R}^3)$.

(iii) *Trace, dissipation and past blowup.* The value $u_0 = B(0) \in L^2_\sigma$ is smooth on $\mathbb{R}^3 \setminus \{0\}$, has support in $\overline{B_{R_*}(0)}$, and $\lim_{t \to 0^-} \|B(t) - u_0\|_2 = \lim_{t \to 0^+} \|B(t) - u_0\|_2 = 0$. Set $\mathfrak{d}(x) = r^2 + |z|^{1/(1/2-h)}$. On some punctured spatial neighborhood of zero, $|B(x,t)| \le C \mathfrak{d}(x)^{-1/2-h}$ for all $t \in I \setminus \{0\}$. There are $C, \epsilon_0 > 0$ such that

$$\sup_{t \in I} \int_{\{\mathfrak{d} < \epsilon\}} |B(x,t)|^2 \, \mathrm{d}x \le C \epsilon^{1/2-3h} \qquad (0 < \epsilon < \epsilon_0). \tag{2.2.3}$$

Write $c_{\mathrm{bank}} = 2^{-h} c_{\mathrm{heat}} > 0$, where c_{heat} is the common physical swirl coefficient of Theorem 1(ii). Thus c_{bank} multiplies the regular heat mode in (2.18.18). There exist $c_{\mathrm{cusp}}, r_{\mathrm{cusp}} > 0$ such that

$$u_0(x) \cdot e_\theta = c_{\mathrm{bank}} 2^h r^{-1-2h} \quad \text{for } 0 < r < r_{\mathrm{cusp}}, \quad 0 < |z| < c_{\mathrm{cusp}} r^{1-2h}. \tag{2.2.4}$$

In particular $\operatorname{ess\,sup}_{|x|<a} |u_0(x)| = \infty$ for every $a > 0$, and $\lim_{t \uparrow 0} \|B(t)\|_\infty = \infty$. Each $B(t_-)$, $-T_- < t_- < 0$, is a smooth compactly supported solenoidal datum. For all $s, t \in I$ with $s \le t$,

$$\frac{1}{2}\|B(t)\|_2^2 + \int_s^t \|\nabla B(\sigma)\|_2^2 \, \mathrm{d}\sigma = \frac{1}{2}\|B(s)\|_2^2 + \int_s^t \int_{\mathbb{R}^3} f(x,\sigma) \cdot B(x,\sigma) \, \mathrm{d}x \, \mathrm{d}\sigma. \tag{2.2.5}$$

(iv) *Forward estimates and the spectrum of the leading field.* On both time sides, for $x \neq 0$ near the joining tip, $|B(x,t)| \le C\mathfrak{d}(x)^{-1/2-h}$. For any m, L_0, on the tip hull on each side the ordinary residual relative to the smooth slow force satisfies $|\partial_{x,t}^{\le m}\mathscr{E}_\infty| \le C_{m,L_0} q_\pm^{L_0}$. The constants apply to the same completed sum. For each $j \in \mathbb{N}$, $j \ge 1$, and each $\epsilon > 0$ there are constants $C, C_{j,\epsilon}$ such that for $x \in \mathbb{R}^3$ and $0 < t < T_b$,

$$\begin{aligned} |B(x,t)| &\le C(t+\mathfrak{d}(x))^{-1/2-h}, \\ |\nabla_x^j B(x,t)| &\le C_{j,\epsilon}(t+\mathfrak{d}(x))^{-1/2-h-(1+h)j/2-\epsilon}. \end{aligned} \tag{2.2.6}$$

In particular,

$$\|B(t)\|_\infty \le Ct^{-1/2-h}, \qquad \|\nabla_x^j B(t)\|_\infty \le C_j t^{-1/2-h-j} \quad (j \ge 1). \tag{2.2.7}$$

On the inner localization ball $|\nabla_x^j B_0(x,t)| \le C_j(t+\mathfrak{d}(x))^{-1/2-h-j/2}$ for $j \ge 0$. The leading component in (i) is B_+^0 for $t > 0$ and B_-^0 for $t < 0$. Thus its endpoint jets and differentiated heat tails are those of Theorem 1(i)–(iii), with the forward radial and axial estimates in (2.18.28) and Proposition 2.18.5(M3). Its frozen operators, their isolating contours, eigenvectors, reduced resolvents, projections, shifts and Gram metrics are precisely the objects of Theorem 1(v)–(vii), with all the bounds there. In particular the physical shift retains the same $d_0, \chi_\pm$ and rectangle U. The Gram estimates retain the box lengths, starting times and small-Q threshold dependence of clause (vii) of that theorem. Let $\lambda(Z,k)$ be the simple eigenvalue for angular sector m in that theorem, where $Z = z/t^{1/2-h}$ and k is the symbol of $-it^h\partial_Z$ at the frozen time $t > 0$. Put $\lambda_0 = \lambda(0,0)$ and $\lambda_c = \Re\lambda_0 > 0$. At $(Z,k) = (0,0)$,

$$\lambda_Z = \lambda_k = \lambda_{Zk} = 0, \qquad \frac{\lambda_{kk}}{h^2} q_G^2 + (h^{-1}-1)q_G - \lambda_{ZZ} = 0$$

for the same $q_G > 0$ as in that theorem. With $b_d = (h^{-1}-1)/2$ and $X_G = -q_G\Re\lambda_{kk}/(2h^2)$, the selected curvature satisfies

$$X_G > b_d, \qquad X_G - b_d/2 - \sqrt{X_G^2 - b_d X_G} \le 1/16.$$

The branch on sector $-m$ is $\overline{\lambda(Z,-k)}$. If U_{lead} and $U_{\mathrm{lead}}^\sharp$ denote the unshifted and two-band shifted evolutions of B_+^0 in the canonical time $s = -t^{-h}/h$ defined in Theorem 1(vii), there are $g_2 < \lambda_c$ and $C, T_0 > 0$ such that $\|U_{\mathrm{lead}}^\sharp(s,s')\|_{2\to 2} \le Ce^{g_2(s-s')}$ for $s' \le s \le -T_0$. For every $\epsilon > 0$ there are $C_\epsilon, T_\epsilon > 0$ such that $\|U_{\mathrm{lead}}(s,s')\|_{2\to 2} \le C_\epsilon e^{(\lambda_c+\epsilon)(s-s')}$ for $s' \le s \le -T_\epsilon$.

(v) *The correction and its clock.* Let $W = B - B_0$ on $t > 0$. For a fixed reference time $Q > 0$, use

$$t = Q + Q^{1+h}\theta, \qquad y = x/\sqrt{Q}, \qquad \rho = Q^h, \qquad S = (1+\log(1/\rho))^{6/5}.$$

For $F = B, W$ write $F_Q(y,t) = Q^{1/2+h}F(\sqrt{Q}\,y, t)$. A block has $|\theta| \le L(Q)$ with $0 \le L(Q) = o(\log(1/\rho))$ as $Q \downarrow 0$. All suprema below are over $y \in \mathbb{R}^3$ and all indicated times on that block. Each $o(1)$ is uniform there as $Q \downarrow 0$. A factor $P(S)$ denotes a polynomial bound independent of Q and the number of active stages, with constants allowed to depend on the fixed member, the requested derivative orders, η and K when present.

There is a nonnegative physical function E on positive time, given by the sum (2.22.3) of the principal pulse envelopes (2.22.2). At most 32 signed labels have nonzero slow cutoff at

any point. Put $E_Q(y,t) = E(\sqrt{Q}\,y,t)$. For every $0 < \eta < 1/2 - 3\varkappa$ and all sufficiently small $Q > 0$,

$$\|W_Q\|_\infty \le \rho^{1/2} P(S), \qquad |\nabla_y W_Q| \le (Q/t)^{1+h} E_Q + C\rho^\eta \le 2E_Q + C\rho^\eta, \tag{2.2.8}$$
$$\|E_Q\|_\infty \le CS^{1/4}, \qquad \|\nabla_y E_Q\|_\infty \le \rho^{-\varkappa} P(S).$$

For every fixed $K > 0$ let $a = -K\sum_\gamma \Phi_\gamma^\sharp$ be the real clock of (2.22.5): on each label Φ_γ is the slow cutoff times the normalized zero-Haar primitive of its Gaussian envelope in the temporal torus direction, and $\sharp$ evaluates at Y_{phys} on its level cover. In particular a vanishes outside the slow supports. With $a_Q(y,t) = a(\sqrt{Q}\,y,t)$ and $\partial_s = t^{1+h}\partial_t$ at fixed Q, y, one has

$$\partial_s a_Q = -KE_Q + r_Q, \qquad \|r_Q\|_\infty = o(1), \tag{2.2.9}$$

$$\|a_Q\|_\infty \le C_K S^{3/4}(1 + \log S), \quad \|\nabla_y a_Q\|_\infty \le \rho^{-\varkappa} P(S), \tag{2.2.10}$$
$$\|B_Q \cdot \nabla_y a_Q\|_\infty + \rho(\|\Delta_y a_Q\|_\infty + \|\nabla_y a_Q\|_\infty^2) = o(1).$$

In particular, uniformly on these blocks,

$$\frac{\sup_t(\sup_y a_Q(y,t) - \inf_y a_Q(y,t))}{\log(1/\rho)} \longrightarrow 0 \quad (Q \downarrow 0), \qquad \exp(\operatorname{osc}_y a_Q) = \rho^{-o(1)}. \tag{2.2.11}$$

(vi) *Finite coefficients, joining and the physical remainder.* For each positive slow order n, the pressure P_n is determined by the radial recursion (2.6.5) and $P_n(0,\eta) = 0$, with the signed backward equations of Section 2.7.1 on $t < 0$. The late positive-order pressure terms, including their support beyond the positive-order velocities, obey the two-tube inclusion of Proposition 2.3.2 on $t > 0$ and Proposition 2.7.2 on $t < 0$. The sampled means retain the pressure moments in the state integrals (2.14.42) and the complete-moment subtraction in (2.13.67). The leading stress vanishes on the heat gaps. For the slow, packet, mean and pressure fields in Lemma 2.20.2, all corresponding one-sided physical derivatives agree at $t = 0$, $x \neq 0$, on their common construction domain. The one-sided smoothness and tip estimates hold independently on each side as in Lemma 2.20.3.

More precisely, take any finite stage n, ordinary depth $J \ge 0$ and finite-state coefficient c in the recursion of Proposition 2.12.3. Write a for its power of ρ_ℓ in that recursion, w for its weight W, $\sqrt{\mathsf{W}}$ or 1, and e for its envelope 1 or the function $P(v)$ in (2.13.23). Here W is the native weight in (2.13.3). Let $x_{\mathrm{sl}} = (\mathsf{R}, \mathsf{Z}, \mathsf{T})$ and $Y \in \mathbb{T}^2 = \mathbb{R}^2/\mathbb{Z}^2$ be the slow and auxiliary variables of its chart. For $I \in \mathbb{N}_0^3$, $|I| \le J$, and $\alpha \in \mathbb{N}_0^2$, there are constants independent of I, α, ℓ and the label, with

$$|\partial_{x_{\mathrm{sl}}}^I \partial_Y^\alpha c| \le C_{n,J} \rho_\ell^a S_\ell^{b_{n,J}} w \mathcal{L}_W^{N_{n,J}} e\,(K_{n,J} S_\ell^{B_{n,J}})^{|\alpha|}(|\alpha|!)^2. \tag{2.2.12}$$

Here $\mathcal{L}_W = 1 + \log(1/\mathsf{W})$ on $\mathsf{W} > 0$, with the logarithmic factor omitted on unweighted charts. Weighted coefficients have their smooth zero extensions at the support boundaries. The auxiliary multipliers P^{-1} and $e^{\pm K\Phi}$ have the corresponding relative derivative estimate with $a = 0$, $w = 1$ and e equal to the multiplier itself, by Lemma 2.12.7 and Corollary 2.12.11(c). The single sequence (δ_n) satisfies (2.18.11) simultaneously on the two sides through ordinary order $\max(n, 80)$ at stage n. In particular the same sequence covers the 72 derivatives used in the finite linear preparation.

For every $N, j \in \mathbb{N}_0$ there are $C_{N,j}, q_{N,j} > 0$ such that on either side in the construction ball, for $0 < q < q_{N,j}$,

$$\max_{|\mu|\le j} |\partial^{\mu}_{x,t}(u_\infty - u^{[N]})| \le C_{N,j} q^{h\beta_N - (1/2+h) - 3j}, \qquad \beta_N = 1 - 4\varkappa + N/5. \tag{2.2.13}$$

Here $\mu \in \mathbb{N}_0^4$ is an ordinary Cartesian spacetime multi-index. For the same (u_∞, p_∞), every $j, M \in \mathbb{N}_0$ admits $C_{j,M}, q_{j,M} > 0$ such that on this domain, for $0 < q < q_{j,M}$,

$$\max_{|\mu|\le j} |\partial^{\mu}_{x,t}(\mathscr{N}(u_\infty, p_\infty) - \mathbf{f}_s)| \le C_{j,M} q^M.$$

For $t \neq 0$ the slow reference force is

$$\mathbf{f}_s = \mathscr{N}(u_{\mathrm{B}}, p_s) + (\partial_r + 2/r)(K_B)_\theta e_\theta + (\partial_r + 1/r)(K_B)_z e_z.$$

The radial expression has its regular Cartesian extension at the axis. The force has a smooth extension across $t = 0$ on the construction domain, as in (2.11.2).

(vii) *Packet inverses and mean corrections.* On every sufficiently small source band the finite states in (i) use the cover of Lemma 2.13.1. For its active labels Φ, n are given by (2.1.1), $n_{\tan} = (n \cdot e_\theta)e_\theta + (n \cdot e_z)e_z$, and $|n| \ge |n_{\tan}| \ge c > 0$. Every fixed coefficient derivative I of the normalized phase transport defect $Q_\ell^{1+h}(\partial_t + u_{\mathrm{B}} \cdot \nabla_x)\Phi$ is bounded by $C_I \rho_\ell S_\ell^{B_I}$. On its pulse interval $[0, L_p]$, $L_p \asymp S_\ell$, the homogeneous propagator in the frame (2.13.20) satisfies the Gaussian estimates of Lemma 2.13.2, with envelope (2.13.23).

The classes $\mathcal{M}^a, \mathcal{W}^a$ are defined by (2.13.4)–(2.13.5) on the same cover. For each finite set of nonzero harmonic indices m' and $f_{m'} \in \mathcal{W}^a$, the zero-initial-data solution of (2.13.26) has transverse amplitude $t_{m'} \in \mathcal{W}^a$ with $n \cdot t_{m'} = 0$, and pressure $\pi_{m'} \in \mathcal{W}^{a+1/2}$. The finite signed harmonics satisfy the product identity (2.13.52). For $\mu = u_M - u_{\mathrm{B}}$, the θ, z components of $Q_\ell^{1/2+h}\mu$ belong to $\mathcal{M}^{1-\varkappa}$ and its radial component belongs to $\mathcal{M}^2$, as in (2.13.51). The auxiliary solenoidal correction satisfies (2.14.33). For every $g \in \mathcal{M}^a$ supported in the fixed radial hull and having zero Haar mean $\int_{\mathbb{T}^2} g \, \mathrm{d}Y = 0$ at each slow point (unit Haar mass), let Ig, Jg be the shifted radial tail and complete integral (2.13.66). For the inner cutoff χ of Lemma 2.13.9, $Ig - \chi Jg \in \mathcal{M}^{a+\varkappa}$; for each fixed $j, N \ge 0$, with the observation radius in the closed annulus (2.13.1), $\|\partial^{\le j} Jg\|_\infty \le C_{j,N} \rho_\ell^{a+N} S_\ell^{B_{j,N}}$. Haar averaging, directional inversion and radial primitives obey the finite derivative estimates of Corollary 2.12.18.

On a fixed enlarged band annulus $0 < \mathsf{R}_- \le \mathsf{R} \le \mathsf{R}_+$, fix the band during differentiation and assume the local labels have comparable scales as in Lemma 2.17.1. For each fixed integer $j \ge 0$, real $d_0 \ge 0$, and band field g of physical prefactor $Q_\ell^{-d_0}$, its sampled derivatives satisfy $|\partial_{x,t}^{\le j} g| \le C_{j,d_0} Q_\ell^{-d_0-3j} \mathcal{N}_j(g)$, where $\mathcal{N}_j$ is the sum of the weighted harmonic coefficient seminorms defined in Lemma 2.17.1, under the domain conditions of Lemma 2.18.2. The corresponding normalized physical velocity correction satisfies (2.18.27) with the envelope E in (v).

In canonical positive-time coordinates $R = r/\sqrt{t}$, $Z = z/t^{1/2-h}$, $\rho = t^h$, let $V_s = t^{1/2+h}(u_{\mathrm{B}} - B_0)$ at the same physical point. For every fixed spatial derivative order the global suprema of its azimuthal and axial vector components are $O(\rho^2)$, and that of its radial vector component is $O(\rho^3)$. Component derivatives at the axis mean derivatives of their regular Cartesian representatives. The calculation at Proposition 2.6.15, the paragraph on p. 485, also records the stronger decay before localization. On each enlarged band chart the slow velocity has

components $Q^{1/2+h}u_{\mathrm{B}} = (b, \mathsf{R}F_b, G_b)$, with $b = O(\rho_Q)$ and $F_b - F_{\mathrm{lead}}, G_b - G_{\mathrm{lead}} = O(\rho_Q^2)$ for every fixed ordinary coefficient derivative. The active waves lie in a fixed annulus $0 < \mathsf{R}_- \le \mathsf{R} \le \mathsf{R}_+ < \infty$. For some fixed mesh exponent K_{mesh}, a compact band meets $O(S_\ell^{3K_{\mathrm{mesh}}})$ labels, a radial line meets $O(S_\ell^{K_{\mathrm{mesh}}})$, and the slow supports have bounded pointwise overlap. Overlapping bands, including those on a radial line, have one common torus cover at the lowest active level. The differences of levels are uniformly bounded and the covering maps preserve normalized Haar measure. Distinct labels with intersecting slow supports have disjoint enlarged auxiliary preimages, also for each fixed derivative of their extended fields.

Before physical localization, each cutoff finite prefix consists of the slow field, the physical carrier-free mean $u_M - u_{\mathrm{B}}$, and a finite sum on each band of label-supported exact curls. Each signed wave on label α has carrier $e^{ijk_\ell\Phi_\alpha}$, $j \in \mathbb{Z} \setminus \{0\}$, with angle-independent coefficient and $k_\ell = \lceil \rho_Q^{-1/2} \rceil$. Coefficient derivatives hold the representative data and rounded constants fixed. Its angular integer $n_\alpha = k_\ell p_\alpha$ satisfies $|n_\alpha| \ge 2m + 1$ for the selected background mode m. The principal amplitudes of the primary curls have class $\mathcal{W}^{1/2}$; all higher curls have principal amplitudes in $\mathcal{W}^{1-3\varkappa}$. For a principal amplitude of order a, its tangential and radial curl remainders belong to $\mathcal{W}^{a+1/2-\varkappa}$ and $\mathcal{W}^{a+3/2}$, respectively. Distinct-label wave products vanish; on one label the relative indices add, with exact cancellation of the full phase at total index zero. The pulse inverse preserves label support. The mean iteration applies its Haar, directional and shifted radial operators to carrier-free coefficients.

2.3 Notation and hypotheses for the completion

2.3.1 Slow coefficients, mean and oscillations

Symbol	Definition
$\rho, \mathscr{L}, \varkappa$	Physical q^h, logarithmic factor, and iteration loss 10^{-5}, distinct from κ.
$\alpha_n, \beta_n, \delta_n$	Stage orders and cutoff scales in Section 2.4.
Q, ρ_Q, S_ℓ	Frozen band scale $2^{-\ell}$, Q^h, and $\ell^{6/5}$. ρ in band calculations means ρ_Q. We hold a band scale fixed under differentiation.
$\mathsf{R}, \mathsf{Z}, \mathsf{T}$	Band coordinates $r/Q^{1/2}, z/Q^{\frac{1}{2}-h}, t/Q$, distinct from R, Z in the theorem.
$F_n, U_n, V_n, P_n, \lambda_n$	Slow coefficients and order $\lambda_n = 2nh$. $F_0 = F$, $U_0 = U$, $V_0 = V$.
$\mathsf{W}, \mathcal{L}_W$	Positive aggregate support weight and $1 + \log(1/\mathsf{W})$. W is not a wave velocity.
$\mathcal{M}^a, \mathcal{W}^a$	Weighted mean and wave coefficient classes, (2.13.4)–(2.13.5). The superscript distinguishes $\mathcal{M}^a$ from the history $\mathfrak{M}_1$.
y, Π	Auxiliary torus point and normalized Haar projection, $\langle\cdot\rangle_\theta$ is the physical cylindrical angular mean.
J_g, v_r, v_t, d_r	Fixed integer covering matrix, its radial and temporal directions, and radial exponent $d_r > 1$.
$\Phi, k, m, P(v)$	Carrier phase, carrier integer, harmonic index, and Gaussian pulse envelope. The pulse variable v is local.
ϑ_q	Single aggregate edge cutoff. We keep its derivatives and missing principal covariance.
$u_s, \pi_s, K_{\mathrm{B}}, \mathbf{f}_s$	Slow reference velocity, pressure, two-component stress and smooth two-row residual.
Q_s	Symmetric cross target $\mathcal{Q}_\times(K_{\mathrm{B}})$, whose full divergence has the additional radial row in (2.14.2).
$\mathsf{S}, \mathsf{C}_0, \mathsf{D}_0, g_s$	Normalized slow cross, full initial canonical tensor, its cross-target difference, and the radial source (2.15.9).

Symbol	Definition
$P_C, \delta_C, P_s^{\mathrm{add}}, \epsilon_s$	Full initial pressure/root and their additional order-two parts (2.15.11)–(2.15.15).
u_M, w, p_w	Actual angle-independent mean, oscillatory wave field, and wave pressure, before we take their sum.
$B_{\mathrm{H}}, V_{\mathrm{H}}, G_{\mathrm{H}}$	Haar radial, swirl and axial coefficients. In particular V_{H} is not the leading radial profile V.
$\mathcal{Q}_\times(a), A_*, d_*$	Symmetric pure-cross tensor, canonical residual cross, and the explicit cutoff reserve.
$\mathsf{C}^{\mathrm{act}}, \mathsf{C}^{\mathrm{can}}$	Actual full covariance and its canonical tensor, related by (2.15.3).
K_d, Φ_θ, Φ_z	Three radial state integrals (2.14.42), with full covariance and pressure flux.
a, p, c_*, s_*, b_*	Temporary finite-step orders in (2.15.21). Here $p = a + 1/2$ is an order, but $p(x,t)$ denotes physical pressure.
$\mathbf{f}_{\mathrm{ref}}, G_{\mathrm{flat}}, \mathsf{B}_{\mathrm{flat}}$	Fixed initialized reference force, flat vector remainder and flat tensor remainder in the ordinary finite-state equation.

$\mathcal{S}$ consists of the functions smooth on the interior of the stated radial–angular domain whose partial derivatives of every order extend continuously to its boundary. We use $1 \mp \hat{\zeta}$ at the angular endpoints and $\hat{\xi}^2/2$ at the axis. We write $\mathcal{G}_J(m, e; L)$ for the mixed weighted Gevrey–2 class of Definition 2.12.4, with torus variable y; in Section 2.12.1 the radicand of a protected root is written $\mathfrak{X}$, while $S = S_\ell$ and $P(v)$ (the Gaussian envelope) keep their meaning from Section 2.13. $G_f \simeq_\kappa G_b$ is the endpoint jet equality of Definition 2.6.10.

2.3.2 Leading coefficients used in the completion

We specialize Theorem 1 to the coordinates and coefficient norms of the finite construction. In the formulas below a one-dimensional radial integral with variable s uses the measure $\xi\, d\xi$ under $s = \xi^2/2$.

Protected core and cutoffs. With $\varpi = (\hat{\xi}/\hat{\xi}_a(\hat{\zeta}))^2$, the cutoff is one for $\varpi \le \Xi_{\mathrm{need}}$ and vanishes for $\varpi \ge \Xi_{\mathrm{cut}}$. The selected levels obey

$$1 < \Xi_{\mathrm{need}} < \Xi_{\mathrm{cut}} < \Xi \le \min\Big\{\frac{\Lambda^{\frac{\hat{\xi}_{\mathrm{an}}^2}{2}}}{4},\ e^{t_{\mathrm{act}}}\Big\}, \qquad \Xi_{\mathrm{cut}} < e^{y_*}, \qquad \frac{\big(\hat{\xi}_a^0\big)^2}{2}\,\Xi < \inf I_{\mathrm{pos}}. \tag{2.3.1}$$

The transition lies in the strictly positive entry collar. On $0 \le \varpi \le \Xi$, every fixed radial derivative of $F_0, U_0, V_0/\hat{\xi}^2, P_0$ satisfies a common Gevrey–3/2 angular bound. On the backward side the corresponding components are angularly analytic on a fixed neighborhood of the interval, through the first collar and before the loop. The forward and backward order-zero components have equal slice jets on this rectangle. For a compact angular interval $K_{\hat{\zeta}}$ the norm used here is

$$\|v\|_{\mathcal{G}_\varrho} = \sum_{k\ge 0} \frac{\varrho^k}{(k!)^{3/2}} \left\|\partial_{\hat{\zeta}}^k v\right\|_{L^\infty(K_{\hat{\zeta}})}. \tag{2.3.2}$$

Lemma 2.3.1 (Joint cutoff). *Let $L_{\mathrm{cut}}(\hat{\zeta}) > 0$ be smooth on $[-1,1]$, and put $\widetilde{q} = \hat{t}_b$ for $t \le 0$ and $\widetilde{q} = \hat{t}_f/L_{\mathrm{cut}}(\hat{\zeta}_f)$ for $t \ge 0$.*

(a) The function $\widetilde{q}/\widetilde{Q}$ is C^∞ across $\widetilde{\eta} = 0$ if and only if L_{cut} and λ_{ch} have equal jets at $\hat{\zeta} = \pm 1$.

(b) If this holds, each stage cutoff $\chi(\widetilde{q}/\delta_n)$ is one C^∞ function across $t=0$ for $z\neq 0$. On $t\le 0$ it is the backward cutoff $\chi(\hat{t}_b/\delta_n)$. On $t\ge 0$ it is $\chi(\hat{t}_f/(L_{\mathrm{cut}}(\hat{\zeta})\delta_n))$.

We apply these cutoffs to potentials and mean fluxes before differentiation. They keep the equal slice jets of the completed physical fields.

Pressure tubes and reserved patches. Theorem 1(ii)–(iv) gives the following tube bounds, backward slots and outer collar for this same member.

Proposition 2.3.2 (Two-tube pressure saturation)**.** *We put $y=2\log(\hat{\xi}/\hat{\xi}_p(\hat{\zeta}))$. The positive velocity slots lie in $(-14,-9)$ and mean slots in $(-8,-3)$. The loop compensation is in $(-25,-20)$, heat compensation ends before -15, and the last pulse return ends before $Y-.7$. The late pressure saturation is contained in*

$$K_0=\{\tfrac{\hat{\xi}_p^2}{2}e^{-14.5}\le\tfrac{\hat{\xi}^2}{2}\le R_o e^{-.5}\},\qquad K_{\mathrm{ext}}=\{\hat{\zeta}\in K_1,\ \tfrac{\hat{\xi}_p^2}{2}e^{-14.5}\le\tfrac{\hat{\xi}^2}{2}\le R_+\}.$$

Here $K_1\Subset K_2\Subset\{\chi=0\}$ contains the full central spectral support, and R_+ lies in the scalar hold outlet buffer after all spectral returns. On these sets $T_\theta\ge cH>0$ for the selected member. We do not claim an all-angle rectangle to R_+.

Lemma 2.3.3 (Reserved power patches of the backward member)**.** *Put $\frac{\hat{\xi}_{p,b}^2}{2}=\frac{\hat{\xi}_{s,b}^2}{2}e^T\lambda^{-60}$, the backward pulse entry, and $y_p=2\log(\hat{\xi}/\hat{\xi}_{p,b})$.*

(S3) Write $X=\hat{\xi}^2/2$ and $X_j=\hat{\xi}_j^2/2$. For $|\beta|\le 1$ and $\hat{\xi}\ge\hat{\xi}_{\mathrm{match}}$ the backward comparison template is

$$H=K_b(1+\beta^2)^{-1}(\hat{\xi}_{s,b}/\sqrt{2})^{-2\lambda}F_\lambda(2\log(\hat{\xi}/\hat{\xi}_{s,b})),\qquad U=G_b\,k(2\log(\hat{\xi}/\hat{\xi}_{s,b})),$$

with $G_b=4\beta$ and scalars K_b and $\frac{\hat{\xi}_{s,b}^2}{2}$. On the wait $2\log(\hat{\xi}/\hat{\xi}_{s,b})\ge T$ we have $k=0$ and $F_\lambda(y)=F_\lambda(y_w)e^{-\lambda(y-y_w)}$. At X_{match} the actual pre-loop member has the five histories of the reference pair integrated from the axis with its prescribed axis pressure. Its velocities agree with (S3) on $[X_{\mathrm{match}},X_{p,b}]\setminus X_{p,b}e^{(-20,-15)}$. The three-swirl bank in the omitted interval contributes its actual partial histories, including its outgoing energy and pressure increments. The later pulse, its returns and the heat wing enter at their own radii. On the exterior (B4) gives the backward heat profile of Lemma 2.3.5.

(S4) The leading edits miss both $I_{\mathrm{pos}}=X_{p,b}e^{(-14,-9)}$ and $I_{\mathrm{mean}}=X_{p,b}e^{(-8,-3)}$. The native axial pulse and its two returns have support in $0\le y_p<Y_{\mathrm{end}}-0.7$, with $R_e=X_{p,b}e^{Y_{\mathrm{end}}}$, by the backward support layout of Theorem 1(iii).

On both reserved intervals the actual backward velocities therefore satisfy

$$U=0,\qquad E=\frac{c_{\mathrm{patch}}}{1+\beta^2}(\hat{\xi}/\sqrt{2})^{-1-2\lambda},\qquad c_{\mathrm{patch}}=K_bF_\lambda(y_w)e^{\lambda y_w}/\sqrt{2}.$$

Put $l=\lambda_{\mathrm{ch}}(\eta_f)$ near either endpoint. The coordinate y_p identifies these intervals under $X_b=lX_f$, $X_{p,b}=lX_{p,f}$. In the forward chart the endpoint jets of the swirl on these intervals are those of

$$c_{\mathrm{patch}}\frac{l^{h-\lambda}}{1+(l^{1/2-h}\eta_f)^2}(\xi_f/\sqrt{2})^{-1-2\lambda}.$$

Indeed E has weight $1/2+h$ and $\xi_b=l^{1/2}\xi_f$. In the interior of the forward angular interval the power patches have the coefficient and exponent of (iii).

Lemma 2.3.4 (Outer collar of the backward member)**.** *For the selected backward wing of Theorem 1(iii)–(iv), put $u = 1 - \frac{\hat\xi^2}{2}/B$. There are $u_0 > 0$ and constants such that for $0 < u \le u_0$ and $|\beta| \le 1$:*

(a) $c_0 e^{-\kappa^2/u^2} \le \widehat{\mathcal{T}}_{P,\theta} \le C_0 u^{-3} e^{-\kappa^2/u^2}$ *and* $|\widehat{\mathcal{T}}_{P,z}| \le C_0 u^3 e^{-\kappa^2/u^2}$*;*

(b) $|(\hat\xi^{-1}\partial_{\hat\xi})^j \partial_\beta^k (\widehat{\mathcal{T}}_{P,\theta}, \widehat{\mathcal{T}}_{P,z})| \le C_{jk} u^{-3-3j} e^{-\kappa^2/u^2}$ *for all j, k;*

(c) $b_s = 0$ *and* $a_s = v_s \ge 2 + h$*. Moreover* $\widehat{\mathcal{T}}_{P,\theta} = e^{-\kappa^2/u^2} u^{-3} b_\theta(u,\beta)$ *and* $\widehat{\mathcal{T}}_{P,z} = e^{-\kappa^2/u^2} u^3 b_z(u,\beta)$ *with b_θ, b_z smooth on $[0,u_0]\times[-1,1]$ and $b_\theta(0,\cdot) > 0$, so the unit direction $(b_\theta, u^6 b_z)/|(b_\theta, u^6 b_z)|$ extends smoothly to $\frac{\hat\xi^2}{2} = B$ with value $(1,0)$. On a sufficiently short collar $n_\theta \ge 1/2$ and $(v_s - 2)n_z^2 \le (3/2)n_\theta^2$ for this unit direction n, since v_s is bounded there and $n_z = O(u^6)$ uniformly in β;*

(d) clause (O2) holds at the outer edge with $\varphi_b(s) = (1 - e^{-s})/\kappa$ and $a_b = 1$, because $\kappa^2/u^2 = 1/\varphi_b(d_b)^2$; clause (O4) holds with $m = 1 - \rho\Psi(\frac{\hat\xi^2}{2}/B)$.

Lemma 2.3.5 (Heat exterior and moments of the backward member)**.** *For the selected backward heat exterior, (S2) reads as follows: in the backward chart the following do not depend on β: the A11 outlet (R_A, H_A), the value $\mathfrak{M}_2(R_A) = R_A H_A/(1-\lambda)$, the length L_o, the data δ and $p(\delta)$, the wing amplitude ρ, and the edge B. For $\hat\xi^2/2 \ge B$ the backward profile is*

$$U = V = 0, \qquad E = c_\infty (\hat\xi/\sqrt{2})^{-1-2h}\, \mathcal{H}_-(4d/\hat\xi^2), \qquad c_\infty = \frac{H_A R_A^h J e^{-(\lambda-h)L_o}}{\sqrt{2}}, \qquad J = \frac{p(\delta)e^{h\delta}}{1-\rho}.$$

Thus c_∞ is independent of β. In the notation of the five histories, $M(\infty) = J(\infty) = S(\infty) = 0$, and

$$\int_0^\infty [H - \sqrt{2}\, c_\infty (\hat\xi/\sqrt{2})^{-2h}] \hat\xi \, \mathrm{d}\hat\xi = 0.$$

The last meridional return gives $U = V = 0$ from its exit through the exterior. These are the exterior and moment data of Theorem 1(i)–(iv) in the backward normalization.

Activation, logarithmic weights and moment subtraction. On the selected entry collar let $y = 2\log(\hat\xi/\hat\xi_a)$ and $e(y) = (1 - \kappa_{\mathrm{act}})\sigma(y/t_{\mathrm{act}})$, with σ the shared squared-flat step. The first collar and the subsequent termination and interpolation have matching leading slice jets at both endpoints by Theorem 1(ii)–(iii). The radial core data, the boundary coefficients $n_{s,r}, p_{1,r}$ and the stress direction p_r give the following identities there.

$$\begin{aligned} U_y = -\kappa \tfrac{\hat\xi^2}{2} n_{s,r}/2, \qquad (\log F)_y = -\kappa p_{1,r}/2, \\ T_0 = eB, \qquad B(0,\hat\zeta) = F_a(\hat\zeta) p_r(0,\hat\zeta), \quad B_\theta(0,\hat\zeta) > 0. \end{aligned} \tag{2.3.3}$$

With $w_{\mathrm{in}} = c_{\mathrm{in}} e$ for $y > 0$ and zero for $y \le 0$, shrinking the collar if necessary gives

$$c w_{\mathrm{in}} \le T_{0,\theta} \le C w_{\mathrm{in}}, \qquad |T_{0,z}| \le C w_{\mathrm{in}}, \qquad |T_0| \ge c w_{\mathrm{in}}. \tag{2.3.4}$$

The entry precedes the first restoration slot by the strict inequality

$$\frac{\big(\hat\xi_a(\hat\zeta)\big)^2}{2} e^{t_{\mathrm{act}}} < \frac{\big(\hat\xi_p(\hat\zeta)\big)^2}{2} e^{-25} \qquad (\hat\zeta \in [-1,1]). \tag{2.3.5}$$

Definition 2.3.6 (Component weight of the selected field)**.** On the forward member the finite component set $\mathcal{C}_*$ consists of the main channel, the outlet extension, and the retained central, wing and mixture channels. Each angular multiplier α_i is independent of $\hat{\xi}$. The radial multipliers ρ_i equal one up to $y_p = -3$ and are nonincreasing after activation. The coefficients $c_i > 0$ are chosen once so that

$$\mathsf{W}(\tfrac{\hat{\xi}^2}{2}, \hat{\zeta}) = e(y_a) \sum_{i \in \mathcal{C}_*} c_i \, \alpha_i(\hat{\zeta}) \, \rho_i(\tfrac{\hat{\xi}^2}{2}, \hat{\zeta}), \qquad w_i := c_i e(y_a) \alpha_i \rho_i, \tag{2.3.6}$$

$$\mathsf{W} \le e^{-2}, \qquad \mathcal{L}_W = 1 + \log(1/\mathsf{W}) \quad (\mathsf{W} > 0). \tag{2.3.7}$$

For a differentiating operator Z commuting with the raw radial integral, the protected subtraction gives

$$[Z, \mathcal{I}_{\chi_m}] g = -(Z\chi_m) \mathcal{J} g. \tag{2.3.8}$$

where $\mathcal{J} g = \int_0^\infty g \, \xi \, d\xi$ in the radial variable, and the support of $Z\chi_m$ lies in the mean slot.

Lemma 2.3.7 (Squared-flat weights in a smooth edge variable)**.** *Let $s_0 > 0$, $a > 0$ and $\varphi \in C^\infty([0, s_0])$ with $\varphi(0) = 0$ and $\varphi' > 0$. Put $w(s) = \exp(-a/\varphi(s)^2)$ for $s > 0$ and $w(0) = 0$. Then $w \in C^\infty([0, s_0])$ is flat at 0, and:*

(a) for every $B \in \mathbb{R}$ there is $s_B > 0$ such that $s \mapsto s^{-B} w(s)$ is increasing on $(0, s_B]$;

(b) for every $M \ge 0$ there are $s_M > 0$ and C_M such that $\int_0^\delta s^{-M} w(s) \, \mathrm{d}s \le C_M \delta^{3-M} w(\delta)$ for $0 < \delta \le s_M$;

(c) for every k there is C_k such that $|w^{(k)}(s)| \le C_k s^{-3k} w(s)$ on $(0, s_0]$;

(d) $w(s)^b s^{-N} \to 0$ as $s \downarrow 0$, for every $b > 0$ and N.

Proof. Write $\varphi(s) = s\psi(s)$ with ψ smooth and positive. Then $(\log w)' = 2a\varphi'/\varphi^3 \asymp s^{-3}$ near zero, which gives (a). For s sufficiently small, $(s^{3-M} w)' \ge c s^{-M} w$, giving (b) by integration. Differentiating $w = \exp(-a/\varphi^2)$ gives (c), since the jth derivative of a/φ^2 is $O(s^{-2-j})$. Exponential decay gives (d) and flatness at zero. □

Lemma 2.3.8. *Put $L_w = 1 + \log_+(1/w)$, $\phi_N(u) = u(1 + \log(1/u))^N$ for $0 < u \le 1$, and $K_N^* = \sup_{v \ge 0} e^{-v}(1+v)^N$. Thus $K_N^* = 1$ for $0 \le N \le 1$ and $K_N^* = N^N e^{1-N}$ for $N > 1$. Fix $N \ge 0$, $C \ge 1$.*

(a) If $0 < w \le e^{-2}$ and $0 < u \le \min(Cw, e^{-2})$, then $\phi_N(u) \le \max(C, K_N^*) \phi_N(w)$.

(b) If $0 < w_i \le \mathsf{W}$, then $w_i L_{w_i}^N \le K_N^* \mathsf{W} L_{\mathsf{W}}^N$.

(c) If $f_1, \dots, f_k \in (0, 1]$ satisfy $|D^j f_\ell| \le C_j f_\ell L_{f_\ell}^{N_j}$, then $f = \prod f_\ell$ and $g = \sum f_\ell$ satisfy the same type of bound with L_f resp. L_g, with new constants.

(d) Suppose $w \ge 0$ is continuous, is C^k on $\{w > 0\}$, and $|D^j w| \le C_j w L_w^{N_j}$ there for $1 \le j \le k$. Then $|D^j \log w| \le C_j' L_w^{N_j'}$ there for $1 \le j \le k$. For each $\beta > 0$, extension of w^β by zero is C^k, with all derivatives through order k zero on $\{w = 0\}$.

Proof. Write $u = we^{-v}$. For $v \geq 0$ use $e^{-v}(L_w + v)^N \leq K_N^* L_w^N$; for $-\log C \leq v < 0$ use $e^{-v} \leq C$. The same positive-v inequality with $w = \mathsf{W}$ proves (b), since $L_{w_i} \leq L_{\mathsf{W}} + v$. Leibniz' rule, $L_{f_i} \leq L_f$, and (b) give (c). For (d) the chain rule gives $|D^j w^\beta| \leq C w^\beta L_w^{M_j}$, which tends to zero on approach to the zero set by continuity. Along any coordinate segment starting at a zero, bound the difference on the terminal component of $\{w > 0\}$ by the length of the segment times the supremum of the next derivative. This supremum tends to zero as the segment shrinks. Inducting on $j < k$ shows that the continuous zero extensions are the actual derivatives. □

Native weights and radial primitives. For D any fixed word in $\hat{\xi}^{-1}\partial_{\hat{\xi}}$ and $\partial_{\hat{\zeta}}|_{\hat{\xi}}$, put $\mathcal{L}_W = 1 + \log(1/\mathsf{W})$ on the positive set. For the aggregate weight of the selected member the following are the five bounds in Theorem 1(iv).

Proposition 2.3.9 (Properties of W)**.**

(W1) Exact one-sided monotonicity. *For every i and $\hat{\zeta}$, $w_i(\cdot, \hat{\zeta})$ is nondecreasing on $(0, \frac{(\hat{\xi}_p(\hat{\zeta}))^2}{2} e^{-3}]$ and nonincreasing on $[\frac{(\hat{\xi}_a(\hat{\zeta}))^2}{2} e^{t_{\mathrm{act}}}, \infty)$. In particular, for every i,*

$$w_i(s, \hat{\zeta}) \leq w_i(\tfrac{\hat{\xi}^2}{2}, \hat{\zeta}) \ \ (s \leq \tfrac{\hat{\xi}^2}{2} \leq \tfrac{\hat{\xi}_p^2}{2} e^{-3}), \qquad w_i(s, \hat{\zeta}) \leq w_i(\tfrac{\hat{\xi}^2}{2}, \hat{\zeta}) \ \ (\tfrac{\hat{\xi}_a^2}{2} e^{t_{\mathrm{act}}} \leq \tfrac{\hat{\xi}^2}{2} \leq s).$$

With constant 1 this is the bound $w_i(s) \leq C w_i(\mathsf{R})$ for the one-sided radial integrals. It rests on the monotonicity of W_c, $(1-\chi)W_c$ and of the inner connector.

(W2) Plateau on the protected slot. $\mathsf{W} \geq c_m e_\infty$ *on* $\{y_a \geq t_{\mathrm{act}},\ y_p \leq Y(\hat{\zeta}) - \frac{1}{2}\}$, *in particular on* $\Sigma(\hat{\zeta}) = \{-8 \leq y_p \leq -3\}$ *for every* $\hat{\zeta} \in [-1, 1]$.

(W3) Two-sided stress comparison. $|T_0| \geq c\mathsf{W}$ *on* $\{\mathsf{W} > 0\}$. $T_0 = 0$ *on* $\{\mathsf{W} = 0\}$. $|D^j T_0| + |D^j \mathsf{W}| \leq C_j \mathsf{W} \mathcal{L}_W{}^{N_j}$.

(W4) Regularity. $\mathsf{W} \in C^\infty$. *For $\beta > 0$, W^β extends flatly by zero.* $\operatorname{supp} \mathsf{W} \subset \{\frac{\hat{\xi}^2}{2} \leq \frac{\hat{\xi}_W^2}{2}\}$.

(W5) Positive floor on higher supports. *If $n \geq 2$ and T_n vanishes on $\{y_a \leq \delta_n\}$ and is supported in $\mathscr{P} \cup K_0 \cup K_{\mathrm{ext}}$* [Proposition 2.3.2]*, then $\mathsf{W} \geq c_n > 0$ on* $\operatorname{supp} T_n$.

Lemma 2.3.10 (Aggregate jets and direction)**.** *Use the cover of Theorem 1(iv). For each fixed profile multi-index j,*

$$|D^j \mathsf{W}| + |D^j T_0| \leq C_j \mathsf{W} \mathcal{L}_W^{N_j}, \qquad |T_0| \geq c\mathsf{W}. \tag{2.3.9}$$

Powers of $\mathcal{L}_W$ bound all fixed derivatives of $T_0/|T_0|$ on the positive set. We fix $\beta > 0$. The function W^β extends smoothly and flatly by zero across the full zero set. The same conclusion holds for each function whose jets satisfy the bound $C_j \mathsf{W}^\beta \mathcal{L}_W^{N_j}$.

Lemma 2.3.11 (The backward weight)**.** *Assume (B2), (B3) and (B5).*

(a) There are $0 < c \leq C$ with $c\,\delta^{-2} \leq \mathcal{L}_b \leq C\delta^{-2}$ on $(\frac{\hat{\xi}_a^2}{2}, \frac{\hat{\xi}_b^2}{2})$. For all k, $|(\hat{\xi}^{-1}\partial_{\hat{\xi}})^k \mathsf{W}_b| \leq C_k \mathsf{W}_b \mathcal{L}_b^{3k/2}$. The leading stress satisfies $|T_0| \geq c\mathsf{W}_b$ and $|\partial^\alpha T_0| \leq C_\alpha \mathsf{W}_b \mathcal{L}_b^{N_\alpha}$ on $(\frac{\hat{\xi}_a^2}{2}, \frac{\hat{\xi}_b^2}{2}) \times [-1, 1]$. Thus (2.3.9) holds with $\mathsf{W} = \mathsf{W}_b$, and W_b does not depend on $\hat{\zeta}$.

(b) Let $\hat\xi_a < \hat\xi_1 \le \hat\xi_2 < \hat\xi_b$ *and* $N \ge 0$. *There is* C *such that*

$$\mathsf{W}_b(s)\mathcal{L}_b(s)^N \le C\,\mathsf{W}_b(\tfrac{\hat\xi^2}{2})\mathcal{L}_b(\tfrac{\hat\xi^2}{2})^N \quad \text{whenever } s \le \tfrac{\hat\xi^2}{2} \le \tfrac{\hat\xi_2^2}{2} \quad \text{or} \quad \tfrac{\hat\xi_1^2}{2} \le \tfrac{\hat\xi^2}{2} \le s,$$

with the conventions $\mathsf{W}_b = 0$ *and* $\mathsf{W}_b\mathcal{L}_b^N = 0$ *off* $(\frac{\hat\xi_a^2}{2}, \frac{\hat\xi_b^2}{2})$.

(c) The correction region $I_{\mathrm{mean}} = \frac{\hat\xi_{p,b}^2}{2}e^{(-8,-3)}$ *has compact closure in* $(\frac{\hat\xi_a^2}{2}, \frac{\hat\xi_b^2}{2})$, *and* $\frac{\hat\xi_{p,b}^2}{2}$ *is a constant.*

The subtraction bank is supported in the protected slot and has total mass one:

$$\beta_0(\tfrac{\hat\xi^2}{2}, \hat\zeta) = (\tfrac{\hat\xi^2}{2})^{-1} b(2\log(\hat\xi/\hat\xi_p(\hat\zeta))), \qquad \int b = 1, \quad \operatorname{supp} b \Subset (-8,-3),$$
$$\chi_m(\tfrac{\hat\xi^2}{2}, \hat\zeta) = \int_{(\frac{\hat\xi^2}{2})}^{\infty} \beta_0(s, \hat\zeta)\,\mathrm{d}s. \tag{2.3.10}$$

Proposition 2.3.12 (Moment-subtracted radial inverse)**.** *Let* $\beta_0 = (\frac{\hat\xi^2}{2})^{-1} b(y_p)$ *with* $b \ge 0$, $\int b = 1$, $\operatorname{supp} b \Subset (-8,-3)$, *and* $\chi_m = \int_{(\frac{\hat\xi^2}{2})}^{\infty} \beta_0$ [(2.3.10)]. *Let* g *be smooth, supported in* $\hat\xi \le \hat\xi_{\mathrm{hull}}$, *with* $|D^j g| \le C_j \mathsf{W}{\mathcal{L}_W}^{N_j}$ *for* $|j| \le k$, $D \in \{\hat\xi^{-1}\partial_{\hat\xi}, \partial_{\hat\zeta}|_{\hat\xi}\}$. *Then*

$$\mathcal{I}_{\chi_m} g = \int_{(\frac{\hat\xi^2}{2})}^{\infty} g\,\mathrm{d}s - \chi_m \int_0^{\infty} g\,\mathrm{d}s$$

satisfies $|D^j \mathcal{I}_{\chi_m} g| \le C_j' \mathsf{W}{\mathcal{L}_W}^{N_j'}$ *for* $|j| \le k$. *The same holds for* $Jg = \int_0^\infty g$ *times any smooth function supported in* Σ.

Lemma 2.3.13 (Actual component-weighted radial inverse)**.** *Use the cover of Theorem 1(iv). The selected member has a finite component weight* $\mathsf{W} \le e^{-2}$ *with the native activation and terminal zero faces. This weight covers the full pressure saturation in Proposition 2.3.2. It satisfies* (2.3.9). *We take a source in* $\mathsf{W}(1+\log(1/\mathsf{W}))^N$ *with its fixed mixed jets.*

The source may meet a new angular or radial taper. Its moment-subtracted radial primitive belongs to the same class, with a possibly larger finite logarithmic exponent.

We impose no scalar all-angle outer-middle interval.

Remark 2.3.14 (Scope of the radial estimate). (1) The radial estimate uses the inward and outward comparisons of the weight and the positive floor on the subtraction bank. (2) It also holds with any positive power W^β, with $1+\log(1/\mathsf{W}^\beta)$ comparable to $\mathcal{L}_W$. (3) At fixed slow axial coordinate and band time, $\hat\zeta$ and $\bar q$ are fixed and $\hat\xi = \mathsf{R}/\sqrt{\bar q}$. On the bounded hull the same comparisons hold for the scaled radial primitive. If Z commutes with radial integration, its commutator with the moment subtraction is $-(Z\chi_m)\int g\,\xi\,d\xi$. (4) On a prescribed ordinary derivative list the weighted bounds apply to each auxiliary derivative. Haar averaging, the shifted integrals and their finite Gevrey losses are specified in Corollary 2.12.18.

2.3.3 Tip coordinates, slice jets, and the heat exterior

Let $q = \hat t$, $\eta = \hat\zeta$, $d = 1-\eta^2$ and $L = 1 - 2h\eta^2$. On the side $\varsigma = \operatorname{sgn} t$ the member of Theorem 1 is reconstructed in the chart

$$q - z^2 q^{2h} = \varsigma t, \qquad \hat\xi = r/\sqrt{q}, \qquad \eta = z q^{-1/2+h}, \qquad z = \eta q^{1/2-h}, \quad t = \varsigma q d. \tag{2.3.11}$$

At a fixed physical point the positive root is uniquely determined by $q > |z|^{2/(1-2h)}$. Implicit differentiation gives the following positive-time formulas. On the negative-time side the time derivatives acquire a factor -1.

$$\begin{aligned} \hat{t}_t &= L^{-1}, & \hat{t}_z &= 2\hat{\zeta}\hat{t}^{1/2+h}/L, \\ \hat{\xi}_t &= -\hat{\xi}/(2\hat{t}L), & \hat{\xi}_z &= -\hat{\zeta}\hat{\xi}\hat{t}^{-1/2+h}/L, \\ \hat{\zeta}_t &= -(\tfrac{1}{2}-h)\hat{\zeta}/(\hat{t}L), & \hat{\zeta}_z &= d\hat{t}^{-1/2+h}/L. \end{aligned} \tag{2.3.12}$$

For the scale $t > 0$ with $r = \sqrt{t}\,R$, $z = t^{1/2-h}Z$, write $q = t\mathcal{Q}$. Then

$$\mathcal{Q} - Z^2\mathcal{Q}^{2h} = 1, \qquad \hat{\zeta} = Z\mathcal{Q}^{-1/2+h}, \qquad \hat{\xi} = \frac{R}{\sqrt{\mathcal{Q}}}. \tag{2.3.13}$$

The radial, angular and axial components in physical variables, and their normalized coefficients, are

$$u_\theta^{\mathrm{lead}} = \hat{t}^{-1/2-h}\widehat{\mathcal{U}}_{P,\theta}, \qquad u_z^{\mathrm{lead}} = \hat{t}^{-1/2-h}\widehat{\mathcal{U}}_{P,z}, \qquad u_r^{\mathrm{lead}} = \hat{t}^{-1/2}\widehat{\mathcal{U}}_{P,r} = \frac{V}{r}. \tag{2.3.14}$$

$$\mathcal{H}(R,Z) = \mathcal{Q}^{-1/2-h}\frac{H(\hat{\xi}^2/2,\hat{\zeta})}{\hat{\xi}}, \quad \mathcal{U}(R,Z) = \mathcal{Q}^{-1/2-h}U(\hat{\xi}^2/2,\hat{\zeta}), \quad \mathcal{V}(R,Z) = \mathcal{Q}^{-1/2}\frac{V(\hat{\xi}^2/2,\hat{\zeta})}{\hat{\xi}}. \tag{2.3.15}$$

Radial integration and the two stress entries. Write $E = \widehat{\mathcal{U}}_{P,\theta}$, $F = E/\hat{\xi}$, $H = \hat{\xi}E$ and $U = \widehat{\mathcal{U}}_{P,z}$. The zero constant of integration at the axis gives

$$\mathfrak{M}_1[\widehat{\mathcal{U}}_P](\hat{\xi},\hat{\zeta}) = \int_0^{\hat{\xi}} \rho U(\rho^2/2,\hat{\zeta})\,\mathrm{d}\rho, \qquad V = \frac{\hat{\zeta}\hat{\xi}^2 U - (1-2h)\hat{\zeta}\mathfrak{M}_1 - d\mathfrak{M}_{1\hat{\zeta}}}{L}. \tag{2.3.16}$$

$$\begin{aligned} \mathfrak{M}_2 &= \int_0^{\hat{\xi}} \rho^2 \widehat{\mathcal{U}}_{P,\theta}(\rho,\hat{\zeta})\,\mathrm{d}\rho, \\ \mathfrak{M}_3 &= \int_0^{\hat{\xi}} \rho^2 (\widehat{\mathcal{U}}_{P,z}\widehat{\mathcal{U}}_{P,\theta})(\rho,\hat{\zeta})\,\mathrm{d}\rho, \\ \mathfrak{M}_4 &= \int_0^{\hat{\xi}} \rho (\widehat{\mathcal{U}}_{P,z}^2 - \tfrac{1}{2}\widehat{\mathcal{U}}_{P,\theta}^2)(\rho,\hat{\zeta})\,\mathrm{d}\rho, \\ P &= P_{\mathrm{ax}}(\hat{\zeta}) + \int_0^{\hat{\xi}} \frac{\widehat{\mathcal{U}}_{P,\theta}(\rho,\hat{\zeta})^2}{\rho}\,\mathrm{d}\rho. \end{aligned} \tag{2.3.17}$$

Here $\mathcal{K} = (1-2h)\eta\mathfrak{M}_1 + d\mathfrak{M}_{1\eta}$. In the positive chart the angular and axial integrated equations have the form

$$\widehat{\mathcal{T}}_{P,\theta} = \partial_{\hat\xi}\widehat{\mathcal{U}}_{P,\theta} - \frac{\widehat{\mathcal{U}}_{P,\theta}}{\hat\xi} + \frac{1}{L\hat\xi^{2}}\Big[(\tfrac12\hat\xi^{2}+\mathcal{K})H - (1-h)\mathfrak{M}_{2} + (\tfrac12-h)\hat\zeta\mathfrak{M}_{2_{\hat\zeta}} - d\mathfrak{M}_{3_{\hat\zeta}} + (4h-1)\hat\zeta\mathfrak{M}_{3}\Big], \tag{2.3.18}$$

$$\widehat{\mathcal{T}}_{P,z} = \partial_{\hat\xi}\widehat{\mathcal{U}}_{P,z} + \frac{1}{L\hat\xi}\Big[(\tfrac12\hat\xi^{2}+\mathcal{K})U - (\tfrac12-h)(\mathfrak{M}_{1} - \hat\zeta\mathfrak{M}_{1_{\hat\zeta}}) + 4h\hat\zeta\mathfrak{M}_{4} - d\mathfrak{M}_{4_{\hat\zeta}} + \tfrac12\hat\xi^{2}\big((2+4h)\hat\zeta P - dP_{\hat\zeta}\big)\Big]. \tag{2.3.19}$$

Where their denominators are nonzero the corresponding shear quantities are

$$\mathfrak{a} = -\frac{\hat\xi F_{\hat\xi}}{F} = 2 - \frac{\hat\xi H_{\hat\xi}}{H}, \quad \mathfrak{b} = \frac{U_{\hat\xi}}{F}, \quad \mathfrak{v} = \mathfrak{a} + \frac{\mathfrak{b}^{2}}{\mathfrak{a}}, \quad \mathfrak{t} = -\frac{\mathfrak{b}}{\mathfrak{a}}. \tag{2.3.20}$$

Removing the displayed radial derivative terms from the two stresses gives (N_θ, N_z), and $\mathbf{p} = (N_\theta, N_z)/F$ obeys

$$(\widehat{\mathcal{T}}_{P,\theta}, \widehat{\mathcal{T}}_{P,z}) = F\big(\mathbf{p} - (\mathfrak{a}, -\mathfrak{b})\big). \tag{2.3.21}$$

The regularity required below at the axis is smoothness of F, U, P in $(\hat\xi^{2}, \eta)$, part (i) of Theorem 1. For the angular Gevrey norm one also has

$$\big\|\partial_{\hat\zeta} v\big\|_{\mathcal{G}_\varrho} \le 8(\widehat\varrho - \varrho)^{-3/2}\,\|v\|_{\mathcal{G}_{\widehat\varrho}}. \tag{2.3.22}$$

for $0 < \varrho < \widehat\varrho \le 1$, by bounding $\widehat\varrho^{-1}(k+1)^{3/2}(\varrho/\widehat\varrho)^{k}$ in the defining series.

2.3.3.1 Change of chart at the joining slice

For $z \neq 0$ the coordinates on the joining slice are

$$\widetilde{Q} = |z|^{2/(1-2h)}, \qquad \widetilde\xi = \frac{r}{\sqrt{\widetilde Q}}, \qquad \widetilde\eta = \frac{t}{\widetilde Q}. \tag{2.3.23}$$

Lemma 2.3.15 (Tip and slice coordinates)**.** *On the physical side of sign σ, the two charts are related by*

$$\widetilde{Q} = \hat t|\hat\zeta|^{2/(1-2h)}, \qquad \widetilde\xi = \hat\xi|\hat\zeta|^{-1/(1-2h)}, \qquad \widetilde\eta = \sigma(1-\hat\zeta^{2})|\hat\zeta|^{-2/(1-2h)}. \tag{2.3.24}$$

At $\eta = \pm1$ the derivative of $\widetilde\eta$ with respect to η is $-2\sigma\eta$. The extended backward chart thus overlaps the forward chart for $0 \le \widetilde\eta < c_h$, where $c_h = ((2h)^{-1} - 1)(2h)^{1/(1-2h)}$.

Proof. Substitute $z = \eta q^{1/2-h}$ and $t = \sigma q d$. For $a = |\eta|$ the derivative of $(1-a^{2})a^{-2/(1-2h)}$ is $-2a^{-1-2/(1-2h)}(1-2ha^{2})/(1-2h)$, giving both assertions. □

Definition 2.3.16 (Weight and equal slice jets)**.** For a physical scalar $q^{-w}g$, write its slice representative as $\widetilde{Q}^{-w}\widetilde g$, where

$$\widetilde g(\tilde\xi^{2}/2, \widetilde\eta) = |\hat\zeta|^{2w/(1-2h)} g(\hat\xi^{2}/2, \hat\zeta), \tag{2.3.25}$$

The backward and forward representatives have equal slice jets if their one-sided derivatives satisfy

$$\partial_{\widetilde{\eta}}^{k}\widetilde{g}_b(\,\cdot\,,0)=\partial_{\widetilde{\eta}}^{k}\widetilde{g}_f(\,\cdot\,,0)\qquad(k\ge 0)\tag{2.3.26}$$

at each fixed value of the remaining slice variables. For the leading profiles and histories the weights are

g	E	U	H	M	I	J	S	C_p	P
w	$\frac{1}{2}+h$	$\frac{1}{2}+h$	h	$h-\frac{1}{2}$	$h-1$	$2h-\frac{1}{2}$	$2h$	$1+2h$	$1+2h$

(2.3.27)

Lemma 2.3.17 (Joining equal slice jets)**.** *One-sided smooth physical fields on $z\neq 0$ join smoothly at $t=0$ if and only if their slice jets agree there.*

Proof. Away from $z=0$, the slice map is a smooth coordinate chart. At fixed spatial point the kth physical time derivative is $\widetilde{Q}^{-w-k}\partial_{\widetilde{\eta}}^{k}\widetilde{g}$. Tangential derivatives follow by differentiating the identical smooth traces. Gluing the resulting derivatives successively gives the assertion. □

Remark 2.3.18 (The two native charts). On this overlap the explicit coordinate change is

$$\hat{t}_b=\hat{t}_f/\lambda_{\mathrm{ch}},\quad \hat{\xi}_b=\lambda_{\mathrm{ch}}^{1/2}\hat{\xi}_f,\quad \hat{\zeta}_b=\lambda_{\mathrm{ch}}^{1/2-h}\hat{\zeta}_f,\qquad \lambda_{\mathrm{ch}}=(\hat{\zeta}_b/\hat{\zeta}_f)^{2/(1-2h)}.\tag{2.3.28}$$

The scale factor solves $\eta_f^2\lambda_{\mathrm{ch}}^{1-2h}=1+\lambda_{\mathrm{ch}}(1-\eta_f^2)$ and $\lambda_{\mathrm{ch}}(\pm1)=1$, $\lambda_{\mathrm{ch}}'(\pm1)=\mp4/(1-2h)$.

Lemma 2.3.19 (Design objects as one slice function)**.** *Let g_b be a backward object of weight w. Suppose that $\widetilde{g}_b$ is the restriction to $\widetilde{\eta}\le 0$ of a function $\widetilde{g}$ that is C^∞ on $\{|\widetilde{\eta}|<\epsilon\}$, with $0<\epsilon<c_h$. The forward profile $g_f=|\hat{\zeta}|^{-2w/(1-2h)}\widetilde{g}$ near $\hat{\zeta}=\pm1$ is the* slice continuation *associated with the chosen extension $\widetilde{g}$.*

(a) The objects g_b and g_f have equal slice jets, and $\widetilde{Q}^{-w}\widetilde{g}$ is C^∞ across $t=0$ for $z\neq 0$.

(b) Suppose that g_b is a formula in $(\hat{t}_b,\hat{\xi}_b,\hat{\zeta}_b)$ that is defined and smooth for $|\hat{\zeta}_b|$ near 1 on the two sides of 1. Choose $\widetilde{g}$ to be this formula expressed in slice variables on the two-sided collar. Then $g_f(\hat{\xi}^2/2,\hat{\zeta})=\lambda_{\mathrm{ch}}^{w}g_b(\lambda_{\mathrm{ch}}\hat{\xi}^2/2,\lambda_{\mathrm{ch}}^{1/2-h}\hat{\zeta})$ there.

(c) A one-sided smooth forward profile g_f' has equal slice jets with g_b if and only if $g_f'-g_f$ has zero $\hat{\zeta}$-jets at $\hat{\zeta}=\pm1$.

Proof. The two representatives describe one scalar $\widetilde{Q}^{-w}\widetilde{g}$ on the collar. Substitution of the preceding scale change gives (b). The endpoint Jacobian in Lemma 2.3.15 is nonzero and the weight factor is smooth and positive, which gives (c). □

2.3.3.2 Heat formulas on the fixed exterior

Write $X=\hat{\xi}^2/2$. The central wing has terminal graph $\mathcal{B}_o(\hat{\zeta})$ and uniform bound $\mathcal{B}_{\max}=\max_{[-1,1]}\mathcal{B}_o$. We use $X_{\mathrm{lead}}^{+}=(\hat{\xi}_{\mathrm{lead}}^{+})^2/2$ for the forward leading heat threshold in (2.18.3) and $X_{\mathrm{all}}=\hat{\xi}_{\mathrm{all}}^2/2$ for the enclosing bound of the two-sided completion in (2.18.2).

Lemma 2.3.20 (Exterior fields and differentiated tails)**.** *The two heat exteriors in Theorem 1(ii) have the following normalizations. On the negative side put $s=r^2/2$, $\tau=-t$. Up to its fixed positive coefficient the azimuthal component is $s^{-1/2-h}\mathcal{H}_-(2\tau/s)$, with*

$$\mathcal{H}_-(z)=\frac{1}{\Gamma(1+h)}\int_0^\infty e^{-v}v^h(1+zv)^{-h}\,\mathrm{d}v. \tag{2.3.29}$$

$$\mathcal{H}_-^{(k)}(z)=\frac{(-1)^k(h)_k}{\Gamma(1+h)}\int_0^\infty e^{-v}v^{h+k}(1+zv)^{-h-k}\,\mathrm{d}v,\qquad |\mathcal{H}_-^{(k)}(z)|\le (h)_k(1+h)_k. \tag{2.3.30}$$

In particular $\mathcal{H}_-(0)=1$ *and the positive exterior component* K *satisfies*

$$\partial_t K=(\partial_{rr}+r^{-1}\partial_r-r^{-2})K,\qquad K_r<0. \tag{2.3.31}$$

For $\hat\xi^2/2\ge\mathcal{B}_{\max}$ *the pre-modulation forward field has* $U=M=J=0$ *and vanishing canonical stresses. Its homogeneous pair, with* $c_{\mathrm{bank}}=GR_b^h>0$*, and its physical swirl are*

$$\begin{aligned} H&=d^{-h}\{c_{\mathrm{bank}}g_h(\tfrac{\hat\xi^2}{2}/d)+k_f g_f(\tfrac{\hat\xi^2}{2}/d)\},\\ \mathfrak{M}_2&=d^{1-h}\{c_{\mathrm{bank}}i_h(\tfrac{\hat\xi^2}{2}/d)+k_f i_f(\tfrac{\hat\xi^2}{2}/d)\},\\ &\quad c_{\mathrm{bank}},k_f>0. \end{aligned} \tag{2.3.32}$$

$$u_\theta^{\mathrm{lead}}=\frac{t^{-h}}{r}\left[c_{\mathrm{bank}}g_h\left(\frac{r^2}{2t}\right)+k_f g_f\left(\frac{r^2}{2t}\right)\right]. \tag{2.3.33}$$

Here the two basis profiles and their primitives are

$$\begin{aligned} g_h(x)&=\frac{x}{2^{1+h}\Gamma(1+h)}\int_0^1 e^{-xt/2}t^h(1-t)^{-h}\,\mathrm{d}t, & i_h(x)&=\int_0^x g_h(t)\,\mathrm{d}t,\\ g_f(x)&=g_h(x)\int_x^\infty\frac{e^{-t/2}}{g_h(t)^2}\,\mathrm{d}t, & i_f(x)&=-\int_x^\infty g_f(t)\,\mathrm{d}t. \end{aligned} \tag{2.3.34}$$

At large x *they obey*

$$\begin{aligned} &g_h(x)=x^{-h}[1+2h(1+h)/x+O_h(x^{-2})],\\ &i_h(x)=x^{1-h}/(1-h)-2(1+h)x^{-h}+O_h(x^{-h-1}), \end{aligned} \tag{2.3.35}$$

$$g_f(x)=2x^he^{-x/2}[1+O_h(x^{-1})],\qquad i_f/g_f=-2+O_h(x^{-1}),\qquad g_f'/g_f=-1/2+O_h(x^{-1}). \tag{2.3.36}$$

$$g_h=x^{-h}\sum_{n=0}^N a_nx^{-n}+r_N,\quad a_n=\frac{2^n(h)_n(h+1)_n}{n!},\quad |r_N^{(j)}(x)|\le C_{N,j,h}x^{-h-N-1-j}. \tag{2.3.37}$$

The fast expansion may be differentiated to each fixed order. On compact positive radial intervals substitution of $x=\hat\xi^2/(2d)$ *gives*

$$d^{-h}g_h(\tfrac{\hat\xi^2}{2}/d)=(\hat\xi/\sqrt{2})^{-2h}\sum_{n=0}^N a_n(d/\tfrac{\hat\xi^2}{2})^n+\mathcal{R}_N(\tfrac{\hat\xi^2}{2},d),\quad |(\hat\xi^{-1}\partial_{\hat\xi})^j\partial_d^m\mathcal{R}_N|\le C_{N,j,m}d^{N+1-m}. \tag{2.3.38}$$

for each fixed differentiation order with $N > j + m$. The lifted fast mode and all its fixed derivatives are flat at $d = 0$.

In particular, with c_H the common leading heat amplitude and k fixed, the exterior tails obey

$$|\partial_{\hat\zeta}^{a}(\hat\xi^{-1}\partial_{\hat\xi})^{b}H| \le C_k(\tfrac{\hat\xi^2}{2})^{-h-b}, \qquad |\partial_{\hat\zeta}^{a}(\hat\xi^{-1}\partial_{\hat\xi})^{b}(H - c_H(\hat\xi/\sqrt{2})^{-2h})| \le C_k(\tfrac{\hat\xi^2}{2})^{-h-1-b}, \qquad a+b \le k. \tag{2.3.39}$$

Proof. For the backward factor differentiate under the positive Laplace integral. The bound displayed above follows from the gamma integral. Its differential equation, obtained by integration by parts, gives the swirl heat equation. For the forward factor, expand $(1-t)^{-h}$ at 0 in the integral for g_h, splitting at $t = 1/2$. The second part and all fixed x derivatives are exponentially small. The resulting gamma integrals on the first part give a_n and the stated differentiated remainders. Reduction of order gives g_f, and integration by parts in its tail gives the fast expansion. □

2.3.4 Finite-stage estimates and the backward completion

Hypothesis 2.3.21 (Gevrey inventory). At each finite stage, the inventory Hypothesis 2.12.22 holds.

The clock and packet operations are listed in Table 2.5. For the mean iteration and initialization, Proposition 2.16.1 takes (I1), (I2) and the packet inventory (I3). Theorem 2.16.2 assembles them. Its backward application here uses the ordinary induction on p. 494. Input (I1) is Lemma 2.12.31, on both sides and with one constant v_*. Its construction inputs are the positivity of the leading swirl on a closed neighbourhood of $\operatorname{supp} b$ inside the slot (the F_{lead} lower bound on $t > 0$; $E_0 > 0$ on I_{mean}, Lemma 2.3.3, on $t < 0$) and the positive ledger orders. The tail lemma of (I2) is Proposition 2.3.12, with Remark 2.3.14. It uses the product form of the weight. The shifted-primitive, complete-moment and T_0^{-1} statements of (I2) are Lemma 2.13.9, (2.14.13) and (2.14.31), with Gevrey forms Corollary 2.12.18(ii), (iv).

The backward leading data are those of Theorem 1(i)–(iv). For use in the finite stages we state the additional backward completion property, retaining its designation (B7).

(B7) *Backward estimates for the joint packet, mean and return stages.* The joint construction runs one algorithm on the two sides of $t = 0$. On $t < 0$ its native weight is $\mathsf{W}_b = c_b\zeta$, where ζ is the weight of (B3) (Lemma 2.20.6). For this member, the packet, mean and return stages of Sections 2.12–2.14, restricted to $t < 0$, have the following properties.

- (i) At every finite stage they satisfy the order classes and the finite seminorm bounds that Lemma 2.20.3 lists. The classes are (2.13.4), (2.13.5) and (2.14.4), with $\mathsf{W} = \mathsf{W}_b$, the value margins and the q_b-thresholds (proved: Theorem 2.7.5(b), (c)).
- (ii) The backward sources that the forward text places in the two tubes of Proposition 2.3.2 lie in the class (2.14.4) with $\mathsf{W} = \mathsf{W}_b$. Their radial primitives obey the bounds of Lemma 2.3.13. Those two results are forward statements.
- (iii) The bound $\frac{\hat\xi_{\mathrm{all}}^2}{2}$ of (2.18.2) exceeds the backward hulls and the backward heat onset. On $t < 0$ every finite correction vanishes for $\hat\xi \ge \hat\xi_{\mathrm{all}}$. (This item is proved in Lemma 2.8.9, for the choice of $\frac{\hat\xi_{\mathrm{all}}^2}{2}$ in (2.18.2), which includes the backward outer edge B.)
- (iv) Proposition 2.8.6 holds on $U_- = U \cap \{t \le 0\}$, with q_b and H_- in place of q_f and the forward heat profile. (Given (i) and (iii), this item is Proposition 2.8.10.)

The slow sum for $t < 0$ is constructed in Lemma 2.20.7. Remark 2.20.8 gives the final diagonal choice and localization. For the finite slow coefficients this is not assumed either: it

is Lemma 2.6.4. Their endpoint identification with the forward side is Proposition 2.6.5, using the Gevrey bound of Theorem 1(iii) on the forward leading data; it is not an assumption on the forward algorithm.

For (B7)(i), Theorem 2.7.5 transfers the finite operations using the inputs of Remark 2.7.4 and Table 2.2. The weight is $\mathsf{W}_b = c_b\zeta$ (Lemma 2.20.6); the slow reference is Lemma 2.20.7. Item (ii) is Section 2.7.1, item (iii) is Lemma 2.8.9 with $\frac{\hat{\xi}_{\mathrm{all}}^2}{2} > B$, and item (iv) is Proposition 2.8.10. The last diagonal and localization are then Remark 2.20.8 and Lemma 2.20.3.

The slow coefficients require a separate comparison: Lemma 2.6.4 constructs the backward analytic solution, and Proposition 2.6.5 compares it in the invariant radius $\varpi = \big(\hat{\xi}/\hat{\xi}_a(\eta)\big)^2$. Its leading-data and order-zero inputs are the core bounds of Theorem 1(ii)–(iii), with $4e^{2t_{\mathrm{act}}} < 4.1 < R_0 < 10$, $\Xi \le e^{t_{\mathrm{act}}}$ and the stated lower bounds on Λ. Beyond the inner rectangle the common activation has the same endpoint jets on both sides by that theorem. Theorem 2.7.1 and Proposition 2.10.1 supply the slow reference jets; only then is finite-stage jet transfer applied. Residual flatness follows from (2.18.16), and the exterior heat field from (B7)(iii) and Section 2.3.3.2.

2.4 From the leading stress to a smooth force

The completion adds slow terms, a tangential mean, localized waves and the necessary divergence corrections. On the backward side these operations adapt [42, Secs. 5–10]. The forward side and the gluing in slice variables are new.

One set of coordinates controls the endpoint derivatives. The construction uses one finite initialization and one diagonal selection after the finite stages.

We define the force from the completed background and its pressure:

$$f = \partial_t B - \Delta B + \operatorname{div}(B \otimes B) + \nabla p_B.$$

The completion makes this force smooth through zero, with fixed compact spatial support. The background has one strong L^2 trace and finite dissipation. We do not require a divergence-free force. We do not require bounded background derivatives at the singular point.

The remaining reductions have distinct analytical roles. The slow expansion removes the inner residual to all orders. We make the Borel choice on divergence potentials. Oscillatory exact curls realize the leading positive stress, and the next signed corrections use that same positive leading amplitude. The mean equations keep each component of the actual covariance. The slow reference has only a two-row stress divergence. At initialization, a compact pressure and a protected swirl root cancel the radial divergence of the full covariance. The actual state and force include its pressure moment and axial gradient. Compact radial primitives and three state moments then give finite improvements of the residual. Last, cutoffs applied to potentials and an exact mean-flux repair produce a locally finite diagonal sum.

Sections 2.14–2.18 prove the two quantitative limit inputs that we state here. For small q, we write $\rho = q^h$, $\mathscr{L}(q) = 1 + \log^{6/5}(1/q)$. We fix the iteration loss $\varkappa = 10^{-5}$, which differs from the core strain κ. The finite-stage orders are

$$\alpha_n = 1 - 3\varkappa + \frac{n}{5}, \qquad \beta_n = \alpha_n - \varkappa.$$

For each fixed physical derivative order m, the necessary comparison with a fixed finite state is

$$\left|\partial^{\le m}\big(\mathscr{N}(u,p) - \mathscr{N}(u^N,p^N)\big)\right| \le C_{N,m} q^{h\beta_N - (8+2h+3m)}, \qquad \mathscr{N}(v,\pi) = \partial_t v - \Delta v + \operatorname{div}(v\otimes v) + \nabla\pi. \tag{2.4.1}$$

The loss is independent of N. We fix N before q tends to zero. This is what permits all-order flatness of the ordinary residual. It is not sufficient to prove flatness of an augmented equation without control of its stress divergence.

2.4.1 Weights, cutoffs and the common trace

Main result. We construct one background on the two sides of zero from the selected leading fields. Its Navier–Stokes residual defines one smooth external force with fixed compact spatial support. The background has one strong L^2 trace and finite dissipation. Subsection 2.4.2 proves these results.

The completion first adds the slow terms, tangential mean, principal and higher waves, curl corrections, and summation remainder. It then applies a fixed spatial localization with its divergence correction. The two time directions use one selection of radial data, endpoint jets, finite operations, and summation parameters. These results are about the background alone.

The slow and mean construction of Section 2.6 uses different velocity and pressure support graphs (paragraph "Positive-order support and the full pressure hull" and Lemma 2.20.1). Beyond the early positive velocity graph $\frac{\hat{\xi}_v^2}{2}$ the positive-order velocities vanish, while the first two pressure coefficients can stay nonzero up to $\frac{\hat{\xi}_P^2}{2}$, which lies beyond the full support of the later leading meridional and spectral returns. Theorem 2.7.1 gives the full radial endpoint data of the two sides, before any atlas or packet/mean locality statement. We then select the independent joint slow Borel realization of Proposition 2.10.1, and only then the one physical atlas of Theorem 2.10.2, in the gauge $\widetilde{q}$ of (2.10.1); on each band $Q_\ell = 2^{-\ell}$ and $\mathcal{S}_\ell = \ell^{6/5}$ are computed from this gauge. The finite-stage estimates are Proposition 2.12.3; its proof (Section 2.12.1) uses the pointwise weighted Gevrey–2 classes of Theorem 2.12.23, under Hypothesis 2.3.21, and not a Fourier algebra (Remark 2.12.25). After one uncut finite initialization, (2.15.18)–(2.15.20), we use one pressure-inclusive physical diagonal.

2.4.2 The single smooth force and the same strong trace

We use one fixed spatial localization and its annular divergence correction on the two sides of zero. This section and Lemma 2.3.1 prove equal slice jets of the full finite algorithms on the two sides. All radial history paths and tails enter that comparison. Away from the spatial tip, Lemma 2.3.17 turns this equality into C^∞ joining.

We fix one joint all-order diagonal one time. It includes the two full cutoff sequences and their velocity and pressure states. For each derivative order and flatness power, we compare the same completed pair with a sufficiently long finite prefix on a smaller neighborhood. The velocity and pressure tail estimates, together with the finite-residual identity, prove that this residual is flat to each order. All these estimates hold for the same completed pair, as proved in Lemmas 2.20.2 and 2.20.3 and Proposition 2.20.4.

The two Navier–Stokes residuals thus define one smooth external force across zero, supported in the fixed spatial localization region (Lemma 2.18.1(e)). This result does not assume the symmetry $f(t) = f(-t)$.

For clarity, the physical tail estimate used here is

$$|\partial^j_{\mathrm{phys}}(B_\infty - B^{[N]})| \le C\hat{t}^{h\beta_N - (\frac{1}{2}+h)-3j}, \qquad \beta_N = 1 - 4\varkappa + N/5.$$

For each specified finite jet we select a sufficient N. To bound the energy-level first derivative one can take $N \ge \lceil 15/h \rceil$. We estimate the field at order zero without the loss for its first derivative.

The finite-wave axial carrier costs $\hat{t}^{-1/2}$, not $\hat{t}^{h-\frac{1}{2}}$. These bounds are

$$|B| \lesssim \hat{t}^{-\frac{1}{2}-h} \log^b(1/\hat{t}), \qquad |\nabla B| \lesssim \hat{t}^{-1-h} \log^b(1/\hat{t}). \tag{2.4.2}$$

Cartesian axis regularity and the outer heat estimates $|B| \le Cr^{-1-2h}$, $|\nabla B| \le Cr^{-2-2h}$ complete these bounds outside the chart hull. The radial boundary of this hull is comparable to $\sqrt{\hat{t}}$. Integration first in r, θ gives

$$\int |B|^2 r \, dr d\theta \le Cq^{-2h} \log^b(1/\hat{t}), \qquad \int |\nabla B|^2 r \, dr d\theta \le Cq^{-1-2h} \log^b(1/\hat{t}).$$

Because $\hat{t} \asymp |t| + |z|^{1/(\frac{1}{2}-h)}$, the mass in $r^2 + |z|^{1/(\frac{1}{2}-h)} < s$ is at most $Cs^{\frac{1}{2}-3h} \log^b(1/s) = Cs^{1/2-3h} \log^b(1/s)$, which tends to zero. Also

$$\|\nabla B(t)\|_2^2 \le C|t|^{-1/2-3h} \log^b(1/|t|), \tag{2.4.3}$$

which is integrable. Together with fixed annular localization, these estimates give global tightness and one strong L^2 trace, not only local weak convergence.

We have thus fixed a single spatially localized background on the two sides of zero, one smooth external force, and one strong L^2 trace. All later linear and nonlinear estimates hold for this completed field. We use longer finite prefixes only to estimate it. They do not define new backgrounds or forces.

2.5 The selected relative source interface

Main result. Definition 2.5.1 states the six conditions for the leading source and its completion data. Lemma 2.18.3 verifies them for the selected member. The definition alone does not prove those conditions.

The construction is a map of one jointly selected two-sided leading source and one fixed angular integer. It does not identify that source with the scalar reference outside an arbitrary compact modification. The scalar exterior enters through the heat pair of Theorem 1(ii). The background input used throughout this chapter is Theorem 1. Specifically, (i) fixes the velocity, pressure and all five histories in the native chart. Part (ii) fixes the common heat exterior, the transition to the physical slice chart and the differentiated endpoint data. Parts (iii)–(iv) fix the protected core, the moving correction intervals, the admissible cone, the terminal multiplier and the weights for the moment-subtracted radial inverse. Parts (v)–(viii) identify the selected forward member, its spectral estimates and the band schedule. References below to particular leading formulas identify the normalization or the component estimate for this member. The new conditions on the positive-order coefficients, the packet cover and the finite mean corrections are established in the following sections.

Definition 2.5.1 (Selected relative admissibility)**.** The source consists of the actual physical fields, axis pressure and five histories integrated from the axis. Its data satisfy:

(A1) A regular protected Gevrey–3/2 core with its actual curved activation, and the factored terminal heat/wing germs.

The inner coefficient solve and termination use the finite protected-rectangle cover and shared Gevrey cutoff of paragraph 2.3.2. The full support of this cutoff lies inside the solved union. The positive-stress and mean correction intervals are the untouched moving power patches of this source.

(A2) Smooth Cartesian fields at the radial axis, smooth one-sided endpoint profiles, and positive swirl on $\hat{\xi} > 0$.

(A3) The canonical pressure and compensated angular primitive use all actual moment corrections and all radial integration constants.

Positive-order velocities end at $\frac{\hat{\xi}_v^2}{2}$. Their pressure can extend to $\frac{\hat{\xi}_P^2}{2}$ after the last leading meridional return. We do not impose the ordering $\frac{\hat{\xi}_U^2}{2} < I_{\mathrm{pos}}$.

(A4) The actual capped-loop strictification and the compact spectral edits after it keep the four normalized cone margins on each selected buffered patch. They also keep the strict packet shear and frame margins of Section 2.13.

(A5) The full pressure-saturation hull is the two-tube set of Proposition 2.3.2. The weights are the actual connected native-plus-tube components constructed in Lemma 2.3.13, with its generic inward/outward and moment-subtracted weighted radial mappings. The conditions include native inner and terminal factors and all logarithmic derivative bounds. The selected inner factor is $w_{\mathrm{in}} = c_{\mathrm{in}} e$ from (2.3.3)–(2.3.4). The two stress components are of order e, with no assumed axial y^3 gain.

Positivity and logarithmic jets of an arbitrary aggregate weight alone are not this condition.

(A6) The leading and finite slow data of the two sides have the full radial endpoint jets proved in Theorem 2.7.1. Proposition 2.10.1 supplies their same slow Borel background. We select packet and mean controls jointly in the physical atlas of Theorem 2.10.2.

The inner inverse uses (A1)–(A2).

The affine five-row solve uses the actual moving correction intervals in (A1), and its pressure row uses the complete hull in (A3). The edge inverses use the native factors of (A5), not positivity of an arbitrary aggregate weight. The live mean matrix uses velocity, while its initialization uses the actual pressure, with P_1, P_2. The same labels and finite algorithms use (A6). We select each fixed derivative order after we fix this member.

These conditions supply no spectral theorem.

Actual pressure and choice order. The pressure-class correction solves $\Delta I = \Delta S = 0$, $\Delta C_p = \Pi_{\mathrm{ref}} - p_0$. Thus M, I, J, S and downstream physical P do not change, and $C_{p,\mathrm{new}} = C_{p,\mathrm{ref}} + \Pi_{\mathrm{ref}} - p_0$. The earlier core five-moment correction targets this edited reference. All later loop and spectral history corrections restore its actual five histories. We select core data and gauges before C.

We select activation tolerances $\kappa_{\mathrm{act}}(C), t_{\mathrm{act}}(C), \omega_{\mathrm{act}}(C)$ for that member with the same two-sided minima. We then freeze their higher jets. They are distinct from the later analytic κ_{crit}. The finite loop frequency precedes the spectral implant. Positive-stress and mean correction intervals stay in the pre-pulse wait. The independently constructed slow Borel background precedes the packet atlas.

We then construct one packet/mean diagonal.

Physical diagonal. Each stage cutoff is $\chi(\widetilde{q}/\delta_n)$ with the joint gauge (2.10.1), which is one smooth function across $t = 0$ (Lemma 2.3.1). We cut potentials and exact mean fluxes before differentiation, and we keep all new brackets.

2.6 Slow completion and its edge weights

Main result. Proposition 2.6.15 gives a divergence-free slow reference with a flat augmented residual and the stated weighted stress bounds. The construction assumes the strictly admissible leading member and its five radial histories. Lemmas 2.6.1, 2.3.10, and 2.6.9 give the inverse and weight estimates.

We fix the strictly admissible leading member of Theorem 1, including its five radial histories. We fix all its parameters, with $\mathcal{R}, \varphi, \mu$. Constants may depend on their actual smooth seminorms. We use $\mathfrak{r} = \hat{\xi}$ and $E = H/\mathfrak{r} = \mathfrak{r}F$.

The physical radius is $r = \sqrt{q}\,\mathfrak{r}$. We construct each finite slow coefficient and keep its full pressure support. We then realize the coefficients by a divergence-preserving Borel sum. This supplies the slow part of the endpoint data before we select the same atlas and packet completion.

2.6.1 Positive-order support and the full pressure hull

We select a smooth graph $\frac{\left(\hat{\xi}_v(\hat{\zeta})\right)^2}{2}$ after the positive velocity correction region and before the mean correction region. For each $n \geq 1$, the cutoff and the *full* five moment equations give

$$F_n = U_n = M_n = V_n = 0 \quad (\tfrac{\hat{\xi}^2}{2} \geq \frac{\left(\hat{\xi}_v(\hat{\zeta})\right)^2}{2}).$$

The first moment gives $M_n = 0$. The divergence formula then gives $V_n = 0$.

The leading U_0, M_0, V_0 can be nonzero there. We substitute these identities into the actual radial recursion. We keep its leading axial viscosity term. On this open region, the result is

$$\Omega_0 = \Omega_{\mathrm{lead}}, \qquad \Omega_1 = -\mathsf{Z}_0^{[2]} V_0, \qquad \Omega_k = 0 \ (k \geq 2),$$

$$\hat{\xi}^{-1}\partial_{\hat{\xi}} P_1 = -\frac{\Omega_0}{\hat{\xi}^2}, \qquad \hat{\xi}^{-1}\partial_{\hat{\xi}} P_2 = \frac{\mathsf{Z}_0^{[2]} V_0}{\hat{\xi}^2}, \qquad \hat{\xi}^{-1}\partial_{\hat{\xi}} P_n = 0 \ (n \geq 3).$$

The third moment includes the full known radial numerator integral, not its truncation at the early correction region. Together with $P_n(0) = 0$, this moment fixes the exterior constant. If $\frac{\hat{\xi}_P^2}{2}$ encloses the true last leading meridional return, with any spectral edit, then

$$P_n = 0 \ (\tfrac{\hat{\xi}^2}{2} \geq \tfrac{\hat{\xi}_P^2}{2}, n \geq 1), \qquad P_n = 0 \ (\tfrac{\hat{\xi}^2}{2} \geq \tfrac{\hat{\xi}_v^2}{2}, n \geq 3).$$

Only P_1, P_2 may continue across the meridional region after this support.

Their additional axial residuals are $\mathsf{Z}_{-2(\frac{1}{2}+h)+2h} P_1 - \mathsf{Z}^{[2]}_{-(\frac{1}{2}+h)} U_0$ and $\mathsf{Z}_{-2(\frac{1}{2}+h)+4h} P_2$, in this order, with the operators of (2.6.1). The two positive corridors of Proposition 2.3.2 contain their full radial saturation. These corridors are the all-angle pulse corridor and its central extension through the spectral returns. We select the enclosing graph inside these corridors.

We do not prove an all-angle rectangular extension to the spectral radius. Their fixed buffers separate the pressure support from the two zero faces. These buffers give the stated weighted inverse bounds without a new flat face.

The compact-support statements after this step use $\frac{\hat{\xi}_P^2}{2}$ for pressure and $\frac{\hat{\xi}_v^2}{2}$ for positive velocities. The mean patch keeps leading *velocity*, not leading pressure. Its current matrix uses velocity only. Its root identity uses the full actual slow pressure and does not assume equality to P_0.

Section 2.18 uses the enclosing hull $\frac{\hat{\xi}_P^2}{2}$. These support statements do not move the correction region past the pulse. They do not assume that the leading velocity vanishes in the early correction region.

Weighted primitive estimate. We do not replace the pressure support by a scalar all-angle middle. Lemma 2.3.13 constructs the actual w_0, w_e two-tube components and connected native channels and proves the generic weighted radial mapping, with angular/radial tapers. The moment subtraction uses the actual moving protected density and keeps its derivatives. The same proved mapping covers the compact late P_1, P_2 residuals and each generic mean or packet primitive after this step. Endpoint positivity or full moments alone do not imply these assertions.

2.6.2 The exact forward coefficient equations

We set $\lambda_n = 2nh$, $b = -(\frac{1}{2}+h) - \frac{1}{2}$, and $c = -(\frac{1}{2}+h)$. For a profile f define

$$\mathsf{T}_\gamma f = L^{-1}(-\gamma f + (\tfrac{1}{2}-h)\hat\zeta f_{\hat\zeta} + \tfrac{1}{2}\hat\xi f_{\hat\xi}), \qquad \mathsf{Z}_\gamma f = L^{-1}(2\gamma\hat\zeta f + d f_{\hat\zeta} - 2\hat\zeta\tfrac{1}{2}\hat\xi f_{\hat\xi}), \qquad \mathsf{Z}_\gamma^{[2]} = \mathsf{Z}_{\gamma-(\frac{1}{2}-h)}\mathsf{Z}_\gamma. \tag{2.6.1}$$

The forward chart gives $\partial_t(\hat t^\gamma f) = -\hat t^{\gamma-1}\mathsf{T}_\gamma f$ and $\partial_z(\hat t^\gamma f) = \hat t^{\gamma-(\frac{1}{2}-h)}\mathsf{Z}_\gamma f$. We keep the minus sign in the time identity throughout.

At order n seek the physical fields

$$u_n = \hat t^{\lambda_n}\frac{V_n}{r}e_r + \hat t^{-\frac{1}{2}-h+\lambda_n}(E_n e_\theta + U_n e_z), \qquad p_n = \hat t^{-1-2h+\lambda_n}P_n, \qquad E_n = \mathfrak{r}F_n. \tag{2.6.2}$$

For $n \ge 1$ their axis values F_n, U_n, P_n are zero. We define

$$M_n = \int_0^{\frac{\hat\xi^2}{2}} U_n \,\mathrm{d}x, \qquad V_n = L^{-1}\big(2\hat\zeta\tfrac{\hat\xi^2}{2}U_n - 2((\tfrac{1}{2}-h)+\lambda_n)\hat\zeta M_n - dM_{n,\hat\zeta}\big). \tag{2.6.3}$$

This gives $\frac{V_{n,\hat\xi}}{\hat\xi} = -\mathsf{Z}_{c+\lambda_n}U_n$, the exact coefficient divergence equation.

Negative-index coefficients are zero. The radial inertia numerator is

$$\mathfrak{R}_k = -\mathsf{T}_{\lambda_k}V_k + \sum_{i+j=k}\left[V_i\left(\frac{V_{j,\hat\xi}}{\hat\xi} - \frac{V_j}{\hat\xi^2}\right) + U_i\mathsf{Z}_{\lambda_j}V_j\right] - \hat\xi^2\big(\frac{V_{k,\hat\xi\hat\xi}}{\hat\xi^2} - \frac{V_{k,\hat\xi}}{\hat\xi^3}\big) - \mathsf{Z}^{[2]}_{\lambda_{k-1}}V_{k-1}. \tag{2.6.4}$$

We omit the last term for $k = 0$. The exact pressure recursion is

$$\frac{P_{n,\hat\xi}}{\hat\xi} = \sum_{i+j=n}F_iF_j - \frac{\mathfrak{R}_{n-1}}{\hat\xi^2}, \qquad P_n(0,\hat\zeta) = 0 \quad (n \ge 1). \tag{2.6.5}$$

The tangential residual profiles at order n are

$$\begin{aligned} r_{\theta,n}/\mathfrak{r} = {} & -\mathsf{T}_{b+\lambda_n}F_n + \sum_{i+j=n}\left[V_i\big(\frac{F_{j,\hat\xi}}{\hat\xi} + F_j/\frac{\hat\xi^2}{2}\big) + U_i\mathsf{Z}_{b+\lambda_j}F_j\right] \\ & - 2\big(\tfrac{\hat\xi^2}{2}\big(\frac{F_{n,\hat\xi\hat\xi}}{\hat\xi^2} - \frac{F_{n,\hat\xi}}{\hat\xi^3}\big) + 2\frac{F_{n,\hat\xi}}{\hat\xi}\big) - \mathsf{Z}^{[2]}_{b+\lambda_{n-1}}F_{n-1}, \\ r_{z,n} = {} & -\mathsf{T}_{c+\lambda_n}U_n + \sum_{i+j=n}\left[V_i\frac{U_{j,\hat\xi}}{\hat\xi} + U_i\mathsf{Z}_{c+\lambda_j}U_j\right] \\ & + \mathsf{Z}_{-2(\frac{1}{2}+h)+\lambda_n}P_n - 2\big(\tfrac{\hat\xi^2}{2}\big(\frac{U_{n,\hat\xi\hat\xi}}{\hat\xi^2} - \frac{U_{n,\hat\xi}}{\hat\xi^3}\big) + \frac{U_{n,\hat\xi}}{\hat\xi}\big) - \mathsf{Z}^{[2]}_{c+\lambda_{n-1}}U_{n-1}. \end{aligned} \tag{2.6.6}$$

Their physical factor is $\hat{t}^{-\frac{3}{2}-h+\lambda_n}$. Substitution of (2.6.2) into the cylindrical equations gives these formulas. For $u_\theta = r\Phi$, we divide the angular equation by r.

Its radial diffusion is $\Phi_{rr} + 3r^{-1}\Phi_r$, and its radial transport is $u_r\Phi_r + 2u_r\Phi/r$. These terms give the two angular operators in (2.6.6). We multiply the radial equation by r to get $\hat{\xi}^2 \frac{P_{n,\hat{\xi}}}{\hat{\xi}} - \hat{\xi}^2 \sum F_i F_j + \mathfrak{R}_{n-1}$. The index shift uses $2(\frac{1}{2}+h) - 1 = 2h$.

2.6.3 A full-rectangle inner inverse

We use Lemma 2.6.2 on the single rectangle $[0,\Xi] \times U$, with a slightly larger angular neighborhood for its radius reserve. Its k-fold Volterra estimate is

$$C^k (k/\delta)^{sk} (2\Xi)^k/(2k)!, \qquad s = 3/2 < 2,$$

and its kth root tends to zero. The same iteration proves uniqueness in the class $\mathcal{U}^\natural$. We do not use an angular partition of PDE solutions, and no overlap identification is needed. Radial differentiation uses one additional radius, smaller than the previous radius, for all fixed radial orders.

Finite ordinary jets alone would not suffice for this recursive claim. The shared logarithmic choice $y_a = 2\log(\hat{\xi}/\hat{\xi}_a(\hat{\zeta}))$ is one slice function, because $\frac{\hat{\xi}^2_{a,b}}{2} = \lambda_{\mathrm{ch}} \frac{\hat{\xi}^2_{a,f}}{2}$ on the collars gives $y_a = 2\log(\widetilde{\xi}/\widetilde{\xi}_a)$. We do not use the same additive $\frac{\hat{\xi}^2}{2}$-offset in the two charts.

We apply the next linear inverse on each rectangle with the stated specifications.

For the next local inverse write $\mathcal{D}_{\mathrm{in}} = [0, R_j] \times U_j$ for the current rectangle. This notation does not denote a global selected rectangle. We prove the linear inverse used here. We fix a real λ.

Let (f, u, p) denote the current angular, axial and pressure coefficients, with zero axis data. We write

$$M = \int_0^{\frac{\hat{\xi}^2}{2}} u \,\mathrm{d}x, \quad v = L^{-1}(2\hat{\zeta}\tfrac{\hat{\xi}^2}{2}u - 2((\tfrac{1}{2}-h)+\lambda)\hat{\zeta}M - dM_{\hat{\zeta}}), \quad p = \int_0^{\frac{\hat{\xi}^2}{2}} (2F_0 f + g_p)\,\mathrm{d}x.$$

After completion of the lower orders, we solve these equations on $\mathcal{D}_{\mathrm{in}}$:

$$\begin{aligned}
2(\tfrac{\hat{\xi}^2}{2}(\frac{f_{\hat{\xi}\hat{\xi}}}{\hat{\xi}^2} - \frac{f_{\hat{\xi}}}{\hat{\xi}^3}) + 2\frac{f_{\hat{\xi}}}{\hat{\xi}}) &= -\mathsf{T}_{b+\lambda} f + V_0(\frac{f_{\hat{\xi}}}{\hat{\xi}} + f/\tfrac{\hat{\xi}^2}{2}) + v(\frac{F_{0,\hat{\xi}}}{\hat{\xi}} + F_0/\tfrac{\hat{\xi}^2}{2}) + U_0 \mathsf{Z}_{b+\lambda} f + u\mathsf{Z}_b F_0 + g_\theta,\\
2(\tfrac{\hat{\xi}^2}{2}(\frac{u_{\hat{\xi}\hat{\xi}}}{\hat{\xi}^2} - \frac{u_{\hat{\xi}}}{\hat{\xi}^3}) + \frac{u_{\hat{\xi}}}{\hat{\xi}}) &= -\mathsf{T}_{c+\lambda} u + V_0 \frac{u_{\hat{\xi}}}{\hat{\xi}} + v\frac{U_{0,\hat{\xi}}}{\hat{\xi}} + U_0 \mathsf{Z}_{c+\lambda} u + u\mathsf{Z}_c U_0 + \mathsf{Z}_{-2(\frac{1}{2}+h)+\lambda} p + g_z.
\end{aligned} \tag{2.6.7}$$

For $\lambda = \lambda_n$, the known sources are

$$\begin{aligned}
g_p &= \sum_{\substack{i+j=n\\ i,j\geq 1}} F_i F_j - \mathfrak{R}_{n-1}/(\hat{\xi}^2),\\
g_\theta &= \sum_{\substack{i+j=n\\ i,j\geq 1}} [V_i(\frac{F_{j,\hat{\xi}}}{\hat{\xi}} + F_j/\tfrac{\hat{\xi}^2}{2}) + U_i \mathsf{Z}_{b+\lambda_j} F_j] - \mathsf{Z}^{[2]}_{b+\lambda_{n-1}} F_{n-1},\\
g_z &= \sum_{\substack{i+j=n\\ i,j\geq 1}} [V_i \frac{U_{j,\hat{\xi}}}{\hat{\xi}} + U_i \mathsf{Z}_{c+\lambda_j} U_j] - \mathsf{Z}^{[2]}_{c+\lambda_{n-1}} U_{n-1}.
\end{aligned} \tag{2.6.8}$$

In particular the two shifted viscosity sources carry minus signs, also at $n = 1$, when the positive-positive sums are empty.

Lemma 2.6.1 (Inner Gevrey inverse)**.** *We consider the leading coefficients and g_θ, g_z, g_p on a fixed finite rectangle. Assume $1 \le s < 2$ and that all radial derivatives of these data are bounded at one common positive axial Gevrey-s radius. The bound may depend on the radial order. Theorem 1(iii) supplies this common radius for the leading data. Then (2.6.7) has a unique regular-axis solution with the stated zero axis values and a positive axial Gevrey radius shared by the solution components. All fixed radial derivatives of $f, u, p, M/\frac{\hat\xi^2}{2}, v/\frac{\hat\xi^2}{2}$ are bounded at one smaller positive radius. We impose no radial smallness, shear sign, or radial analyticity.*

Proof. Let $V_0 = \frac{\hat\xi^2}{2} w_0$ and introduce the radial average $\mathscr{A}u = \int_0^1 u(t\frac{\hat\xi^2}{2}, \hat\zeta)\,\mathrm{d}t$. Then $v = \frac{\hat\xi^2}{2}\mathscr{Q}[u]$, where

$$\mathscr{Q}[u] = L^{-1}\big(2\hat\zeta u - 2((\tfrac12 - h) + \lambda)\hat\zeta \mathscr{A}u - d\mathscr{A}u_{\hat\zeta}\big).$$

Thus $v(\frac{F_{0,\hat\xi}}{\hat\xi} + F_0/\frac{\hat\xi^2}{2}) = (\frac{\hat\xi^2}{2}\frac{F_{0,\hat\xi}}{\hat\xi} + F_0)\mathscr{Q}[u]$ is regular at zero. We set

$$a_0 = \frac{-1 - 2\hat\zeta U_0}{2L} + \frac{w_0}{2}, \quad \beta_0 = \frac{-(\frac12 - h)\hat\zeta + dU_0}{L}, \quad \alpha_\gamma = \frac{\gamma(1 + 2\hat\zeta U_0)}{L}.$$

We move the complete current radial derivative to the left to get

$$\begin{aligned}
2(\tfrac{\hat\xi^2}{2}(\frac{f_{\hat\xi\hat\xi}}{\hat\xi^2} - \frac{f_{\hat\xi}}{\hat\xi^3}) + 2\frac{f_{\hat\xi}}{\hat\xi}) - \hat\xi^2 a_0 \frac{f_{\hat\xi}}{\hat\xi} &= \beta_0 f_{\hat\zeta} + (\alpha_{b+\lambda} + w_0)f + (\tfrac{\hat\xi^2}{2}\frac{F_{0,\hat\xi}}{\hat\xi} + F_0)\mathscr{Q}[u] + (\mathsf{Z}_b F_0)u + g_\theta,\\
2(\tfrac{\hat\xi^2}{2}(\frac{u_{\hat\xi\hat\xi}}{\hat\xi^2} - \frac{u_{\hat\xi}}{\hat\xi^3}) + \frac{u_{\hat\xi}}{\hat\xi}) - \hat\xi^2 a_0 \frac{u_{\hat\xi}}{\hat\xi} &= \beta_0 u_{\hat\zeta} + \alpha_{c+\lambda}u + \tfrac{\hat\xi^2}{2}\frac{U_{0,\hat\xi}}{\hat\xi}\mathscr{Q}[u] + (\mathsf{Z}_c U_0)u + \mathsf{Z}_{-2(\frac12+h)+\lambda}p + g_z.
\end{aligned} \tag{2.6.9}$$

The same a_0 occurs in the two equations. We split $p = \int_0^{\hat\xi^2/2} 2F_0 f + \int_0^{\frac{\hat\xi^2}{2}} g_p$. Its unknown part contributes

$$\frac{1}{L}\left[2(-(1+2h)+\lambda)\hat\zeta\int_0^{\hat\xi^2/2} 2F_0 f + d\int_0^{\frac{\hat\xi^2}{2}}(2F_{0,\hat\zeta}f + 2F_0 f_{\hat\zeta}) - 4\hat\zeta\tfrac{\hat\xi^2}{2}F_0 f\right].$$

Each unknown axial derivative is now visible and occurs only once. The known pressure part uses one derivative of g_p. A preliminary fixed radius reduction controls this derivative and all explicit coefficient derivatives. We denote this radius by $\varrho_0 \le 1$.

In the variable $\mathfrak{r} = \hat\xi$, the left operators are

$$\partial_{\mathfrak{r}\mathfrak{r}} + \left(\frac{m}{\mathfrak{r}} - \mathfrak{r}a_0\right)\partial_{\mathfrak{r}}, \qquad m = 3 \text{ or } 1.$$

We put $\mathcal{A}_0(\mathfrak{r}) = \int_0^{\mathfrak{r}} t a_0(t^2/2)\,\mathrm{d}t$. Their regular zero-axis inverses are

$$\mathscr{R}_m G(\mathfrak{r}) = \int_0^{\mathfrak{r}} t^{-m} e^{\mathcal{A}_0(t)} \int_0^t z^m e^{-\mathcal{A}_0(z)} G(z)\,\mathrm{d}z\,\mathrm{d}t. \tag{2.6.10}$$

The discarded homogeneous derivative is a multiple of $\mathfrak{r}^{-m}e^{\mathcal{A}_0}$, which is incompatible with axis regularity.

Because $(z/t)^m \le 1$, the norm of the inverse is bounded by a fixed constant times the two-integration operator

$$J^2 g(\mathfrak{r}) = \int_0^{\mathfrak{r}} (\mathfrak{r} - z) g(z)\,\mathrm{d}z.$$

The exponential factors are bounded in the Gevrey norm algebra on the fixed rectangle. No sign condition on a_0 is necessary.

Let $\mathscr{K}$ be the unknown part of the right side of (2.6.9) followed by these inverses. For $0 < \varrho < \widehat{\varrho} \le \varrho_0$, the algebra and radius-loss estimates give

$$\sup_{z\le\mathfrak{r}} \|\mathscr{K}(f,u)(z)\|_{\mathcal{G}_\varrho} \le C(1+(\widehat{\varrho}-\varrho)^{-s})J^2\left(\sup_{z\le\cdot}\|(f,u)(z)\|_{\mathcal{G}_{\widehat{\varrho}}}\right)(\mathfrak{r}). \tag{2.6.11}$$

An average or primitive at an intermediate radius has a bound from the supremum up to that radius. Its replacement by the supremum at the last endpoint before iteration would lose the next gain.

Let $\mathbf{G}$ be the known source after the inverses and let R_* be the fixed upper endpoint of $\mathfrak{r}$. With $\delta = \varrho_0 - \varrho$, we divide the radius loss into k equal pieces in the estimate for $\mathscr{K}^k\mathbf{G}$. The identity $J^{2k}1 = \mathfrak{r}^{2k}/(2k)!$ gives

$$\sup_{\mathfrak{r}\le R_*}\left\|\mathscr{K}^k\mathbf{G}\right\|_{\mathcal{G}_\varrho} \le \|\mathbf{G}\|_{\mathcal{G}_{\varrho_0};\infty}\frac{[C(k/\delta)^s]^k R_*^{2k}}{(2k)!}. \tag{2.6.12}$$

The k-th root tends to zero like k^{s-2}. Thus the Neumann series converges on the full prescribed finite rectangle. To pass $\mathscr{K}$ through the sum, we use convergence at an intermediate radius and then (2.6.11). For a homogeneous difference, iteration of $\mathbf{z} = \mathscr{K}^k\mathbf{z}$ with the same estimate proves uniqueness in the stated Gevrey class.

Differentiating (2.6.10) in the upper limit and putting $z = t\hat{\xi}$ in its inner integral gives

$$\frac{1}{\hat{\xi}}\partial_{\hat{\xi}}(\mathscr{R}_m G)(\hat{\xi}) = e^{\mathcal{A}_0(\hat{\xi})}\int_0^1 t^m e^{-\mathcal{A}_0(t\hat{\xi})}G(t\hat{\xi})\,\mathrm{d}t. \tag{2.6.13}$$

Its value at the axis is $G(0)/(m+1)$. The arguments of the profiles under the integral are $t^2\hat{\xi}^2/2$. A derivative in $\hat{\xi}^2/2$ there costs the bounded factor t^2. By induction the derivative of order $j+1$ on the left therefore requires at most order j of the unknowns on the right and one further angular derivative. Take the successive angular radius losses to be $2^{-j-2}\varrho$ for $j \ge 0$, starting at a solution radius ϱ below the common data radius. Their sum is $\varrho/2$, so every fixed radial order is bounded at $\varrho/2$. The constants may grow with j. Integration gives the same conclusion for the pressure and the average, and one further fixed loss handles the angular derivative in $v/(\hat{\xi}^2/2)$. □

The scaled radius. Let $\hat{\xi}_a(\hat{\zeta}) > 0$ be the activation graph, and put

$$\varpi = \left(\hat{\xi}/\hat{\xi}_a(\hat{\zeta})\right)^2 = e^{y_a}, \qquad \mathfrak{s} = \sqrt{2\varpi}, \qquad \nu = 2\hat{\xi}_a'/\hat{\xi}_a, \qquad g^\natural(\varpi,\hat{\zeta}) = g(\hat{\xi}_a(\hat{\zeta})\sqrt{\varpi},\hat{\zeta}).$$

At fixed $\hat{\zeta}$ the variables $\frac{\hat{\xi}^2}{2}$ and ϖ are proportional. Hence

$$\begin{gathered}
(\tfrac{1}{2}\hat{\xi}\partial_{\hat{\xi}}g)^\natural = \varpi\partial_\varpi g^\natural, \qquad (\partial_{\hat{\zeta}}g|_{\hat{\xi}})^\natural = (\partial_{\hat{\zeta}} - \nu\varpi\partial_\varpi)g^\natural,\\
2(\tfrac{\hat{\xi}^2}{2}(\frac{f_{\hat{\xi}\hat{\xi}}}{\hat{\xi}^2} - \frac{f_{\hat{\xi}}}{\hat{\xi}^3}) + 2\frac{f_{\hat{\xi}}}{\hat{\xi}})^\natural = \tfrac{2}{\frac{\hat{\xi}_a^2}{2}}(\varpi f^\natural_{\varpi\varpi} + 2f^\natural_\varpi), \qquad 2(\tfrac{\hat{\xi}^2}{2}(\frac{u_{\hat{\xi}\hat{\xi}}}{\hat{\xi}^2} - \frac{u_{\hat{\xi}}}{\hat{\xi}^3}) + \frac{u_{\hat{\xi}}}{\hat{\xi}})^\natural = \tfrac{2}{\frac{\hat{\xi}_a^2}{2}}(\varpi u^\natural_{\varpi\varpi} + u^\natural_\varpi),\\
(\mathscr{A}u)^\natural = \mathscr{A}^\natural u^\natural := \int_0^1 u^\natural(t\varpi,\hat{\zeta})\,\mathrm{d}t, \qquad \Big(\int_0^{\frac{\hat{\xi}^2}{2}} g\,\mathrm{d}x\Big)^\natural = \tfrac{\hat{\xi}^2}{\hat{\xi}_a^2}\mathscr{P}^\natural g^\natural := \tfrac{\hat{\xi}^2}{\hat{\xi}_a^2}\int_0^\varpi g^\natural(\sigma,\hat{\zeta})\,\mathrm{d}\sigma.
\end{gathered} \tag{2.6.14}$$

In particular $M/\frac{\hat\xi^2}{2} = \mathscr{A}u$ identically, and

$$\big((\mathscr{A}u)_{\hat\zeta}|_{\hat\xi}\big)^\natural = \mathscr{A}^\natural(\partial_{\hat\zeta}u^\natural) - \nu(u^\natural - \mathscr{A}^\natural u^\natural), \tag{2.6.15}$$

$$\Big(\partial_{\hat\zeta}\Big|_{\hat\xi}\int_0^{\frac{\hat\xi^2}{2}} g\,\mathrm{d}x\Big)^\natural = \big(\tfrac{\hat\xi_a^2}{2}\big)'\,\mathscr{P}^\natural g^\natural + \tfrac{\hat\xi_a^2}{2}\,\mathscr{P}^\natural(\partial_{\hat\zeta}g^\natural) - \big(\tfrac{\hat\xi_a^2}{2}\big)'\varpi g^\natural. \tag{2.6.16}$$

The first identity uses $\varpi\partial_\varpi\mathscr{A}^\natural u^\natural = u^\natural - \mathscr{A}^\natural u^\natural$. The second follows from the first line of (2.6.14) and one integration by parts in σ.

Lemma 2.6.2 (Inner Gevrey inverse in the scaled radius)**.** *Let $1 \le s < 2$, let U be a compact interval on which $L > 0$, and let $\|\cdot\|_{\mathcal{G}_\varrho}$ be the norm (2.3.2) on $K_{\hat\zeta} = U$ with $(k!)^{3/2}$ replaced by $(k!)^s$. Suppose $\frac{\hat\xi_a^2}{2}$ and $1/\frac{\hat\xi_a^2}{2}$ have finite $\mathcal{G}_{\varrho_1}$ norm for some $\varrho_1 > 0$. Fix $\Xi > 0$ and suppose that, for each $j \ge 0$,*

$$\sup_{0\le\varpi\le\Xi}\big\|\partial_\varpi^j G^\natural(\varpi,\cdot)\big\|_{\mathcal{G}_{\varrho_1}} < \infty \qquad (G = F_0, U_0, w_0, g_\theta, g_z, g_p).$$

Then:

(i) (2.6.7) has exactly one solution (f,u,p) on $\{\frac{\hat\xi^2}{2} \le \frac{(\hat\xi_a(\hat\zeta))^2}{2}\Xi,\ \hat\zeta \in U\}$ with zero axis values in the class $\mathcal{U}^\natural$ of pairs (f,u) that are bounded, continuous up to $\varpi = 0$, C^2 in ϖ for $\varpi > 0$, and satisfy $\sup_{\varpi\le\Xi}\big\|(f^\natural,u^\natural)(\varpi,\cdot)\big\|_{\mathcal{G}_\varrho} < \infty$ for some $\varrho > 0$.

(ii) There is $\varrho' > 0$ such that, for each j, ∂_ϖ^j of $f^\natural, u^\natural, p^\natural, (M/\frac{\hat\xi^2}{2})^\natural = \mathscr{A}^\natural u^\natural$ and $(v/\frac{\hat\xi^2}{2})^\natural$ is bounded in $\mathcal{G}_{\varrho'}$ uniformly in $\varpi \le \Xi$.

(iii) If $\frac{\hat\xi_a^2}{2}$ is constant on U, then $\mathcal{U}^\natural$ is the class of Lemma 2.6.1 on $[0, \frac{\hat\xi_a^2}{2}\Xi] \times U$, and the two lemmas give the same solution.

Proof. We write the regularized system (2.6.9) in $(\varpi,\hat\zeta)$ by (2.6.14)–(2.6.16). The total coefficient of the unknown $f_{\hat\zeta}|_{\hat\xi}$ in the angular row, and of $u_{\hat\zeta}|_{\hat\xi}$ in the axial row, is β_0. By (2.6.14) it produces $\beta_0\partial_{\hat\zeta}f^\natural - \nu\beta_0\varpi\partial_\varpi f^\natural$, and the same for u. We move the second term to the left and multiply by $\frac{\hat\xi_a^2}{2}$. In the variable $\mathfrak{s}$ the left operators become

$$\partial_{\mathfrak{s}\mathfrak{s}} + \Big(\frac{m}{\mathfrak{s}} - \mathfrak{s}\widehat{a}_0\Big)\partial_{\mathfrak{s}}, \qquad \widehat{a}_0 = \tfrac{\hat\xi_a^2}{2}\Big(a_0^\natural - \frac{\nu\beta_0^\natural}{2}\Big), \qquad m = 3 \text{ or } 1,$$

because $2(\varpi g_{\varpi\varpi\varpi} + 2g_{\varpi\varpi}) = g_{\mathfrak{s}\mathfrak{s}} + 3g_{\mathfrak{s}}/\mathfrak{s}$, $2(\varpi g_{\varpi\varpi\varpi} + g_{\varpi\varpi}) = g_{\mathfrak{s}\mathfrak{s}} + g_{\mathfrak{s}}/\mathfrak{s}$ and $2\varpi g_{\varpi\varpi} = \mathfrak{s}g_{\mathfrak{s}}$. The drift $\widehat{a}_0$ is the same in the two rows, as a_0 is in the original. The right sides are $\frac{\hat\xi_a^2}{2}$ times the right sides of (2.6.9), rewritten as follows.

- $\mathscr{Q}[u]$ becomes $\mathscr{Q}^\natural[u] = L^{-1}(2\hat\zeta u^\natural - 2((\frac12 - h) + \lambda)\hat\zeta\mathscr{A}^\natural u^\natural - d\mathscr{A}^\natural(\partial_{\hat\zeta}u^\natural) + d\nu(u^\natural - \mathscr{A}^\natural u^\natural))$, by (2.6.15).
- The unknown pressure part $\int_0^{\hat\xi^2/2} 2F_0 f$ enters through $\mathsf{Z}_{-(1+2h)+\lambda}$. By (2.6.14) and (2.6.16) its contribution is

$$\begin{aligned}\frac{1}{L}\Big[&2(-(1+2h)+\lambda)\hat\zeta\tfrac{\hat\xi_a^2}{2}\mathscr{P}^\natural(2F_0^\natural f^\natural)\\ &+ d\big((\tfrac{\hat\xi_a^2}{2})'\mathscr{P}^\natural(2F_0^\natural f^\natural) + \tfrac{\hat\xi_a^2}{2}\mathscr{P}^\natural\partial_{\hat\zeta}(2F_0^\natural f^\natural)\\ &- (\tfrac{\hat\xi_a^2}{2})'\varpi\,2F_0^\natural f^\natural\big) - 4\hat\zeta\tfrac{\hat\xi_a^2}{2}\varpi F_0^\natural f^\natural\Big].\end{aligned}$$

- All other unknown terms are of order zero, with coefficients built from $F_0^\natural, U_0^\natural, w_0^\natural$, ∂_ϖ of them, $(\partial_{\hat\zeta} - \nu\varpi\partial_\varpi)$ of them, $(\frac{\hat\xi_a^2}{2})^{\pm 1}$, ν, $\hat\zeta$, d and L^{-1}.

Thus the three structural facts used in the proof of Lemma 2.6.1 hold in $(\mathfrak{s}, \hat\zeta)$: one common drift on the left; each unknown angular derivative occurs once, either explicitly with coefficient $\frac{\hat\xi_a^2}{2}\beta_0^\natural$ or inside $\mathscr{A}^\natural$ or $\mathscr{P}^\natural$; all remaining unknown terms are of order zero. The coefficients, after a finite number of $\hat\zeta$-derivatives, are bounded in $\mathcal{G}_{\varrho_0}$ uniformly in ϖ for some $0 < \varrho_0 \le \varrho_1$, by the algebra property and (2.3.22). The average $\mathscr{A}^\natural$ and primitive $\mathscr{P}^\natural$ at radius $\mathfrak{s}$ are bounded by the supremum up to $\mathfrak{s}$. The inverse (2.6.10) with $\mathcal{A}_0(\mathfrak{s}) = \int_0^{\mathfrak{s}} t\widehat{a}_0(t^2/2, \hat\zeta)\,dt$ is bounded by a constant times J^2, because $(z/t)^m \le 1$ and the exponential factors lie in the Gevrey algebra. Hence (2.6.11) and (2.6.12) hold with $\mathfrak{s}$ for $\mathfrak{r}$, and the existence, uniqueness and axis-regularity parts of the proof of Lemma 2.6.1 apply word for word. For uniqueness: a bounded C^2 solution with zero axis value of $g'' + (m/\mathfrak{s} - \mathfrak{s}\widehat{a}_0)g' = G$, with bounded G, equals $\mathscr{R}_m G$, because the other homogeneous solutions are unbounded or nonzero at the axis. So a solution in $\mathcal{U}^\natural$ satisfies the integral equation $\mathbf{z} = \mathscr{K}\mathbf{z} + \mathbf{G}$, and the homogeneous difference satisfies $\mathbf{z} = \mathscr{K}^k\mathbf{z} \to 0$. Part (ii) follows from (2.6.13) with $\mathfrak{s}$ and $\mathcal{A}_0$ as above, as in Lemma 2.6.1. For (iii), $\nu = 0$ and $\hat\xi^2/2 = (\hat\xi_a^2/2)\varpi$ is a fixed rescaling of the squared radius. □

For application at order n, divisibility of each source is important. If $V_j = \frac{\hat\xi^2}{2}w_j$, then

$$V_i\Big(\frac{V_{j,\hat\xi}}{\hat\xi} - V_j/(\hat\xi^2)\Big) = \frac{\hat\xi^2}{2}w_i\Big(w_j/2 + \frac{\hat\xi^2}{2}\frac{w_{j,\hat\xi}}{\hat\xi}\Big).$$

T and Z keep divisibility by $\frac{\hat\xi^2}{2}$. Thus each term of $\mathfrak{R}_k$ is divisible by $\frac{\hat\xi^2}{2}$, with the shifted viscosity, and $\mathfrak{R}_k/\frac{\hat\xi^2}{2}$ is smooth at the axis.

The sources (2.6.8) use only finitely many derivatives of finalized lower orders. For example the pressure source can use four axial derivatives of a lower axial profile, after inclusion of the last pressure derivative. A finite radius reduction controls these derivatives. Lemma 2.6.2 thus solves each finite coefficient order on the protected rectangle $[0, \Xi] \times U$ of paragraph 2.3.2, in the class $\mathcal{U}^\natural$ (Gevrey in $\hat\zeta$ at fixed ϖ).

Its positive radius may decrease with n. At each fixed n, all fixed ϖ-derivatives share one smaller radius.

Remark 2.6.3 (Why the scaled radius). On the endpoint collars $\frac{\hat\xi_{a,b}^2}{2} = \lambda_{\mathrm{ch}}\frac{\hat\xi_{a,f}^2}{2}$ (paragraph 2.3.2), and $\frac{\hat\xi_{a,b}^2}{2} = \frac{(\hat\xi_a^0)^2}{2} = 4/\Lambda$ is constant. With $\Phi(\frac{\hat\xi^2}{2}, \hat\zeta) = (\lambda_{\mathrm{ch}}(\hat\zeta)\frac{\hat\xi^2}{2}, \varphi(\hat\zeta))$, $\varphi = \lambda_{\mathrm{ch}}^{\frac12 - h}\hat\zeta$, we get $\varpi_f = (\hat\xi_f/\hat\xi_{a,f})^2 = \lambda_{\mathrm{ch}}(\hat\xi_f/\hat\xi_a^0)^2 = \varpi_b$. So the chart change is $(\varpi, \hat\zeta) \mapsto (\varpi, \varphi(\hat\zeta))$: it does not mix the radius into the angle. In the fixed-$\hat\xi$ variables, $\partial_{\hat\zeta_f}|_{\hat\xi_f}$ applied to $g_b \circ \Phi$ contains $\lambda'_{\mathrm{ch}}\frac{\hat\xi_f^2}{2}\hat\xi_b^{-1}\partial_{\hat\xi_b}g_b$. Iterating this derivative introduces radial derivatives up to the angular order. Bounds for each fixed radial order alone give no angular Gevrey bound for that composition. At fixed ϖ only angular derivatives enter.

Lemma 2.6.4 (The backward slow coefficients)**.** *Assume (B1), the backward graph and slot data (S3)–(S4) of Lemma 2.3.3, and (2.3.1). Here $\frac{\hat\xi_{\mathrm{an}}^2}{2}$ is the endpoint of the analytic rectangle of the backward member: $\hat\xi_{\mathrm{an}} < \hat\xi_-^{\mathrm{loop}}$, as (B1) requires, and we take it in $(\frac{(\hat\xi_a^0)^2}{2}, \frac{(\hat\xi_a^0)^2}{2}e^{t_c}]$, where $\frac{(\hat\xi_a^0)^2}{2}e^{t_c} \le \frac{(\hat\xi_a^0)^2}{2}e^{t_1}$ is the end of the supplied analytic core rectangle. Then the backward graphs are constants: $\hat\xi_{a,b} = \hat\xi_a^0$ (that is, $b \equiv 1$ in $\frac{\hat\xi_a^2}{2} = 4/(\Lambda b)$ on the backward side, as (B1) requires) and $\frac{\hat\xi_{p,b}^2}{2} = \frac{\hat\xi_{s,b}^2}{2}e^T\lambda^{-60}$ (by*

(S3) and Lemma 2.3.3). The backward termination cutoff χ_{term} *of paragraph 2.3.2 is a step in* $y_a = 2\log(\hat\xi/\hat\xi_a^0)$*, hence a function of* $\frac{\hat\xi^2}{2}$ *alone; it equals one on* $[0, \frac{\hat\xi^2_{\mathrm{keep}}}{2}]$*,* $\frac{\hat\xi^2_{\mathrm{keep}}}{2} = \frac{(\hat\xi_a^0)^2}{2}\Xi_{\mathrm{need}}$*, and zero for* $\frac{\hat\xi^2}{2} \ge \frac{\hat\xi^2_{\mathrm{cut}}}{2} = \frac{(\hat\xi_a^0)^2}{2}\Xi_{\mathrm{cut}}$*. Put* $R_{\mathrm{in}} = \frac{(\hat\xi_a^0)^2}{2}\Xi$*. By (2.3.1),* $\frac{\hat\xi^2_{\mathrm{cut}}}{2} < R_{\mathrm{in}} \le \frac{\hat\xi^2_{\mathrm{an}}}{2}$ *and* $R_{\mathrm{in}} < \inf I_{\mathrm{pos}}$*. Fix* $\frac{\hat\xi^2_-}{2} \in (\frac{(\hat\xi_a^0)^2}{2}, \frac{\hat\xi^2_{\mathrm{keep}}}{2})$*. (This radius is used in Proposition 2.7.2. It is smaller than the radius* $\frac{(\hat\xi_-^{\mathrm{loop}})^2}{2}$ *of (B1), the inner end of the selected loop.) For a compact interval* K *and* $\varrho > 0$ *let* $\|\cdot\|_{\mathcal{G}^1_\varrho(K)}$ *be the norm (2.3.2) on* $K_{\hat\zeta} = K$*, with* $(k!)^{3/2}$ *replaced by* $k!$*. There is a compact interval* U_b *with* $[-1,1] \subset \operatorname{int} U_b$ *and* $L > 0$ *on* U_b *such that the following hold.*

(a) Leading data. *The backward leading data* $G \in \{F_0, U_0, w_0 = V_0/\frac{\hat\xi^2}{2}, P_0\}$ *extend analytically in* $\hat\zeta$ *to* $[0, \frac{\hat\xi^2_{\mathrm{an}}}{2}] \times U_b$*, and there is* $\varrho_0 > 0$ *with* $\sup_{0 \le \frac{\hat\xi^2}{2} \le \frac{\hat\xi^2_{\mathrm{an}}}{2}} \big\|(\hat\xi^{-1}\partial_{\hat\xi})^j G(\frac{\hat\xi^2}{2}, \cdot)\big\|_{\mathcal{G}^1_{\varrho_0}(U_b)} < \infty$ *for every* j*.*

(b) Inner solutions. *For every* $n \ge 1$ *the* $\varsigma = -1$ *inner system (2.6.7), with the sources (2.6.8) built from the orders below* n *as in (c), has on* $[0, R_{\mathrm{in}}] \times U_b$ *exactly one regular-axis solution with zero axis values and a positive* $\mathcal{G}^1$ *radius. There is* $\varrho_n > 0$ *such that every fixed radial derivative of* $f, u, p, M/\frac{\hat\xi^2}{2}, v/\frac{\hat\xi^2}{2}$ *is bounded in* $\mathcal{G}^1_{\varrho_n}(U_b)$*, uniformly in* $\frac{\hat\xi^2}{2} \le R_{\mathrm{in}}$*. Hence each of them extends holomorphically in* $\hat\zeta$ *to* $\mathcal{N}_n = \{\hat\zeta \in \mathbb{C} : \operatorname{dist}(\hat\zeta, U_b) < \varrho_n\}$*, with modulus bounded uniformly in* $\frac{\hat\xi^2}{2} \le R_{\mathrm{in}}$*. On* U_b *this solution solves the* $\varsigma = -1$ *system with the continued leading data and the continued lower-order sources. Its restriction to* $[-1,1]$ *is the backward inner solution* $(F_n^{\mathrm{in}}, U_n^{\mathrm{in}}, P_n^{\mathrm{in}}, \dots)$ *of Section 2.6.*

(c) Coefficients. *The backward coefficients* F_n, U_n, M_n, V_n, P_n *of Section 2.6 (the cutoff* χ_{term}*, the bumps (2.6.19) in* $y = 2\log(\hat\xi/\hat\xi_{p,b})$ *supported in* I_{pos}*, and the solve (2.6.20) with* $\mu = \lambda$*) are* C^∞ *on* $[0,\infty) \times [-1,1]$*, including one-sided* $\hat\zeta$*-derivatives at* ± 1*. The quotients* $M_n/\frac{\hat\xi^2}{2}, V_n/\frac{\hat\xi^2}{2}$ *extend smoothly to* $\hat\xi = 0$*. The swirl amplitude is* $E_n = \hat\xi F_n$*. The normalized quotient* F_n *and the Cartesian velocity are smooth at the axis by Lemma 2.11.1. On* $[0, R_{\mathrm{in}}]$ *one has* $F_n = \chi_{\mathrm{term}} F_n^{\mathrm{in}}$ *and* $U_n = \chi_{\mathrm{term}} U_n^{\mathrm{in}}$*, and* M_n, V_n, P_n *are the axis integrals (2.6.3), (2.6.5) of these. On* $[0, \frac{\hat\xi^2_{\mathrm{keep}}}{2}]$ *all of them equal the inner solution.*

The backward analytic rectangle and its fixed radial derivative bounds are leading data in Theorem 1(iii).

Proof. Two facts on $\mathcal{G}^1$*.* (i) If g is holomorphic on $\{\operatorname{dist}(\hat\zeta, K) < 2\varrho\}$ with $|g| \le M$, Cauchy's estimate on circles of radius 2ϱ gives $\big\|\partial_{\hat\zeta}^k g\big\|_{L^\infty(K)} \le M k! (2\varrho)^{-k}$, so $\|g\|_{\mathcal{G}^1_\varrho(K)} \le 2M$. (ii) Conversely, let $\|g\|_{\mathcal{G}^1_\varrho(K)} \le M$. For $\hat\zeta_0 \in K$ the Taylor series of g at $\hat\zeta_0$ is bounded by M on the disc $|\hat\zeta - \hat\zeta_0| < \varrho$, and it equals g at the real points of that disc, because the Taylor remainder of order k is at most $M(|\hat\zeta - \hat\zeta_0|/\varrho)^{k+1}$. Two such discs meet in a connected set that meets $\mathbb{R}$, so the local sums define one holomorphic extension of g to $\{\operatorname{dist}(\hat\zeta, K) < \varrho\}$, bounded by M. Since $k! \le (k!)^{3/2}$, a finite $\mathcal{G}^1_\varrho$ norm also bounds the norm (2.3.2) at the same radius.

Proof of (a). The analytic rectangle supplied by Theorem 1(iii) contains the core and the first collar through $\hat\xi_{\mathrm{an}}$. On this rectangle F_0, U_0, w_0, P_0 are analytic in $\hat\zeta$ on a common complex neighbourhood $\mathcal{N}$ of $[-1,1]$. Every fixed radial derivative is bounded on a smaller common neighbourhood $\mathcal{N}'$. Choose $\varrho_0 \in (0,1]$ with $\{\operatorname{dist}(\hat\zeta, [-1,1]) < 4\varrho_0\} \subset \mathcal{N}'$ and $(1+\varrho_0)^2 < 1/(2h)$,

and put $U_b = [-1-\varrho_0, 1+\varrho_0]$. Then $L = 1 - 2h\hat\zeta^2 > 0$ on U_b, and $\{\operatorname{dist}(\hat\zeta, U_b) < 2\varrho_0\} \subset \mathcal{N}'$. Fact (i) with $K = U_b$ gives (a).

Proof of (b) and (c). We induct on $n \geq 1$ and assume (b) and (c) below n. On $[0, R_{\mathrm{in}}]$ the bumps vanish, since $R_{\mathrm{in}} < \inf I_{\mathrm{pos}}$. So for $1 \leq j < n$, $F_j = \chi_{\mathrm{term}} F_j^{\mathrm{in}}$ and $U_j = \chi_{\mathrm{term}} U_j^{\mathrm{in}}$ there, and M_j, V_j, P_j are the axis integrals (2.6.3), (2.6.5) of these. We use the same formulas on $[0, R_{\mathrm{in}}] \times U_b$, with the continued inner solutions of (b). The sources (2.6.8) at order n are finite sums of products of these lower-order fields, of the leading data, of finitely many of their $\frac{\hat\xi^2}{2}$- and $\hat\zeta$-derivatives, of radial averages and primitives from the axis, and of the regular quotients $\mathfrak{R}_{n-1}/\frac{\hat\xi^2}{2}$ (divisibility by $\frac{\hat\xi^2}{2}$, see the axis argument following (2.6.8)). The step χ_{term} depends on $\frac{\hat\xi^2}{2}$ only. The analytic norm is an algebra by the Leibniz rule. Cauchy estimates on a smaller neighbourhood bound each additional angular derivative, and bounded radial averages preserve these estimates. Thus (a) and the induction hypothesis imply that every fixed radial derivative of F_0, U_0, w_0 and of g_θ, g_z, g_p is bounded in $\mathcal{G}^1_\varrho(U_b)$, uniformly in $\frac{\hat\xi^2}{2} \leq R_{\mathrm{in}}$, for some $\varrho > 0$. Lemma 2.6.1 applies on $[0, R_{\mathrm{in}}] \times U_b$ with $s = 1$. It holds for the $\varsigma = -1$ system, because ς enters only the coefficients a_0, β_0 and α_γ (through the sign of the time operator T), and the lemma uses no sign of any coefficient (Remark 2.7.4). It gives the unique regular-axis solution with a positive $\mathcal{G}^1$ radius, and a radius $\varrho_n > 0$ at which every fixed radial derivative of $f, u, p, M/\frac{\hat\xi^2}{2}, v/\frac{\hat\xi^2}{2}$ is bounded uniformly in $\frac{\hat\xi^2}{2} \leq R_{\mathrm{in}}$. Fact (ii) gives the holomorphic extension to $\mathcal{N}_n$. By construction this solution solves the system on U_b with the continued data. Its restriction to $[-1, 1]$ solves the system there with the restricted data, which by the induction hypothesis are the backward data of Section 2.6, and its norm (2.3.2) on $K_{\hat\zeta} = [-1, 1]$ is finite. The uniqueness in Lemma 2.6.1, whose proof uses no angular boundary data (equivalently Lemma 2.6.2(iii), since $\frac{\hat\xi^2_{a,b}}{2}$ is constant), shows that this restriction is the backward inner solution of Section 2.6. This proves (b) at order n.

For (c) at order n: the construction of Section 2.6 multiplies the inner F_n, U_n by χ_{term}, adds the bumps (2.6.19), which are functions of $\frac{\hat\xi^2}{2}$ alone because $\frac{\hat\xi^2_{p,b}}{2}$ is constant, with coefficients from (2.6.20), and reconstructs M_n, V_n, P_n from the axis. In the backward chart B_U and B_E are constant invertible matrices (Lemma 2.6.12, with $\mu = \lambda$ by (T4) of Remark 2.7.4), and $e_*\varphi$ is a positive multiple of $(1+\beta^2)^{-1}$ (Lemma 2.3.3). The uncorrected moments are integrals of finitely many products with compact radial support: each product contains a positive-order factor, or a factor U_0 or V_0, and these vanish after the last pulse return (Lemma 2.3.5). The leading data are C^∞ on each finite radial hull up to $\hat\zeta = \pm 1$ (Theorem 1(ii)), and so are the lower orders by (c). Hence the uncorrected moments and the bump coefficients are smooth up to $\hat\zeta = \pm 1$. With the inner solution of (b), which is holomorphic near $[-1, 1]$, this gives (c). On $[0, \frac{\hat\xi^2_{\mathrm{keep}}}{2}]$ the cutoff is one and the bumps vanish, so the coefficients equal the inner solution there. □

Proposition 2.6.5 (Endpoint jets of the positive-order inner solutions)**.** *Assume the hypotheses of Lemma 2.6.4, and let the forward inner solves use Lemma 2.6.2 on $[0, \Xi] \times U$, with (2.3.1). Fix the endpoint $\hat\zeta = 1$ (the case -1 is the same) and $\epsilon > 0$ small. Assume the Gevrey bound of Theorem 1(iii), and*

(J0) the forward leading data $\ell_f = (F_0, U_0, w_0, P_0)_f$ and the backward leading data have equal slice jets at $\hat\zeta = \pm 1$ for $\frac{\hat\xi^2}{2} \leq \frac{(\hat\xi^0_a)^2}{2}\Xi$. Theorem 1(ii)–(iii) supplies both (J0) and the Gevrey bound.

Then for every $n \geq 1$ the forward and backward inner solutions $F_n^{\mathrm{in}}, U_n^{\mathrm{in}}$, and P_n^{in}, $M_n^{\mathrm{in}}/\frac{\hat\xi^2}{2}$, $V_n^{\mathrm{in}}/\frac{\hat\xi^2}{2}$, have equal slice jets (Definition 2.3.16) on $\frac{\hat\xi^2}{2} \leq \frac{(\hat\xi^0_a)^2}{2}\Xi$. With Theorem 2.6.13 this gives equal slice

jets on the full radial path for F_n, U_n, M_n, V_n, P_n in $X = \xi^2/2$ and for $E_n = \xi F_n$ in ξ.

Proof. We induct on n. Assume that all coefficients of orders below n have equal slice jets (for $n = 1$ this is (J0)). Write $\tau_w g = \lambda_{\mathrm{ch}}^w \, g \circ \Phi$ with Φ as in Remark 2.6.3; by Lemma 2.3.19(c), equal slice jets of g_f and g_b means that $g_f - \tau_w g_b$ is flat at $\hat\zeta_f = 1$, for any smooth extension of g_b across $\hat\zeta_b = 1$. We have $\varphi(1) = 1$ and $\varphi'(1) = (\frac12 - h)\lambda'_{\mathrm{ch}}(1) + 1 = -1$, so φ maps $[1-\epsilon, 1]$ onto an interval $[1, 1+\epsilon']$ of the extended backward chart (Lemma 2.3.15).

Step 1: continuation of the backward solution. By Lemma 2.6.4(b), $x_b = (F_n^{\mathrm{in}}, U_n^{\mathrm{in}})_b$ is the restriction to $[-1,1]$ of the solution on $[0, \frac{(\hat\xi_a^0)^2}{2}\Xi] \times U_b$, which is holomorphic in $\hat\zeta$ on the complex neighbourhood $\mathcal{N}_n$ of U_b, with bounds uniform in $\frac{\hat\xi^2}{2} \le \frac{(\hat\xi_a^0)^2}{2}\Xi$. Take ϵ so small that $[1, 1+\epsilon'] \subset U_b$. So the continuation of x_b to $\hat\zeta_b \in [1, 1+\epsilon']$ solves the $\varsigma = -1$ system there, with the continued leading data ℓ_b and the continued lower-order sources S_b (Lemma 2.6.4(b)). No extension of a one-sided profile is needed.

Step 2: covariance. Let $\mathcal{L}_\varsigma[\ell]$ be the order-n linear inner operator of the ς-chart with leading data ℓ, and $\mathcal{S}_\varsigma[G]$ the source built from lower-order data G by (2.6.8). On the overlap of the forward chart with the extended backward chart, $q_b = q_f/\lambda_{\mathrm{ch}}(\hat\zeta)$ (Remark 2.3.18). For backward profiles $G_0, \dots, G_n$ and their transports τG_j (weights (2.7.1)), the two truncated physical fields are equal. Hence their physical residuals are equal. The residual is a finite sum $\sum_k q^{\gamma_k} r_k(\frac{\hat\xi^2}{2}, \hat\zeta)$ with distinct exponents γ_k (they differ by multiples of $2h$), and at fixed $(\frac{\hat\xi^2}{2}, \hat\zeta)$ the powers q^{γ_k} are linearly independent functions of $q > 0$. So the coefficients correspond: $r_k^f[\tau G] = \lambda_{\mathrm{ch}}^{\kappa_k} r_k^b[G] \circ \Phi$ for a weight κ_k. The order-n rows are these coefficients up to the factor $\mathfrak{r}$ ((2.6.6)), which is positive for $\hat\xi > 0$ and transports by $\lambda_{\mathrm{ch}}^{1/2}$; the identities extend to $\hat\xi = 0$ by continuity. Thus

$$\mathcal{L}_+[\tau\ell_b](\tau x) - \mathcal{S}_+[\tau G] = \lambda_{\mathrm{ch}}^{\kappa}\big(\mathcal{L}_-[\ell_b]x - \mathcal{S}_-[G]\big) \circ \Phi. \tag{2.6.17}$$

The sign change of the time operator with ς is part of this identity. The radial averages and primitives are covariant because $\frac{\hat\xi_b^2}{2} = \lambda_{\mathrm{ch}} \frac{\hat\xi_f^2}{2}$ at fixed $\hat\zeta$ (Lemma 2.6.11(b)). By Step 1, $x^{\mathrm{tr}} := \tau x_b$ solves $\mathcal{L}_+[\tau\ell_b]x^{\mathrm{tr}} = \mathcal{S}_+[\tau G_b]$ on $\varpi \le \Xi$, $\hat\zeta \in [1-\epsilon, 1]$, with zero axis values; it is smooth in $(\frac{\hat\xi^2}{2}, \hat\zeta)$ up to the axis because $\frac{\hat\xi_b^2}{2} = \lambda_{\mathrm{ch}} \frac{\hat\xi_f^2}{2}$.

Step 3: the transported solution is in the class. Remark 2.6.3 gives

$$(x^{\mathrm{tr}})^\natural(\varpi, \hat\zeta) = \lambda_{\mathrm{ch}}(\hat\zeta)^w \, x_b\left(\frac{(\hat\xi_a^0)^2}{2}\,\varpi, \varphi(\hat\zeta)\right).$$

For ϵ small, φ maps a complex neighborhood W of $[1-\epsilon, 1]$ into $\mathcal{N}_n$, and λ_{ch}^w is holomorphic and bounded on W. Since the bounds of Lemma 2.6.4(b) are uniform for $\frac{\hat\xi^2}{2} \le \frac{(\hat\xi_a^0)^2}{2}\Xi$, $(x^{\mathrm{tr}})^\natural(\varpi, \cdot)$ is holomorphic on W with a bound uniform in $\varpi \le \Xi$. Cauchy's estimate, as in the proof of Lemma 2.6.4, gives $x^{\mathrm{tr}} \in \mathcal{U}^\natural$ on $[0, \Xi] \times [1-\epsilon, 1]$.

Step 4: a flat residual. The forward solution x_f solves $\mathcal{L}_+[\ell_f]x_f = \mathcal{S}_+[G_f]$ and lies in $\mathcal{U}^\natural$ by the Gevrey bound of Theorem 1(iii) and Lemma 2.6.2. Put $z = x_f - x^{\mathrm{tr}}$. Then $z \in \mathcal{U}^\natural$, z has zero axis values, and

$$\mathcal{L}_+[\ell_f]z = -r, \qquad r = \mathcal{S}_+[\tau G_b] - \mathcal{S}_+[G_f] + (\mathcal{L}_+[\ell_f] - \mathcal{L}_+[\tau\ell_b])x^{\mathrm{tr}}.$$

The operator $\mathcal{L}_+[\ell]$ is affine in ℓ, and $\mathcal{S}_+$ is a finite sum of products, chart operators and radial primitives of lower-order data. By (J0), the induction hypothesis and Lemma 2.6.11(a),(b), r is smooth and flat at $\hat\zeta = 1$: all $\partial_\varpi^j \partial_{\hat\zeta}^k r(\varpi, 1)$ vanish.

Step 5: flatness of z. In the integral form of Lemma 2.6.2, $z = \mathscr{K} z + \mathbf{G}$, where $\mathbf{G}$ is the inverse applied to $-r$. Hence $z = \sum_{k<N} \mathscr{K}^k \mathbf{G} + \mathscr{K}^N z$ for every N. Each term $\mathscr{K}^k \mathbf{G}$ is flat at $\hat\zeta = 1$: $\mathscr{K}$ consists of multiplication by coefficients smooth up to $\hat\zeta = 1$, one $\hat\zeta$-derivative, $\mathscr{A}^\natural$, $\mathscr{P}^\natural$ and the inverse (2.6.10) at fixed $\hat\zeta$, and each of these keeps flatness, by differentiation under integrals over compact ranges. By (2.6.12) applied to z, $\sup_\varpi \left\| \mathscr{K}^N z \right\|_{\mathcal{G}_\varrho} \to 0$ for some $\varrho > 0$, and this norm bounds $\varrho^k (k!)^{-s} \sup_\varpi |\partial_{\hat\zeta}^k \mathscr{K}^N z(\varpi, 1)|$. So $\partial_{\hat\zeta}^k z(\varpi, 1) = 0$ for all k and ϖ. By Lemma 2.6.2(ii) for x_f and Step 1 for x^{tr}, z is C^∞ in $(\varpi, \hat\zeta)$; differentiation of these identities in ϖ shows that z is flat at $\hat\zeta = 1$. The map $(\frac{\hat\xi^2}{2}, \hat\zeta) \mapsto (\varpi, \hat\zeta)$ fixes $\{\hat\zeta = 1\}$, so z is flat in $(\frac{\hat\xi^2}{2}, \hat\zeta)$, and Lemma 2.3.19(c) gives equal slice jets of $F_n^{\mathrm{in}}, U_n^{\mathrm{in}}$. The pressure, $M/\frac{\hat\xi^2}{2} = \mathscr{A} u$ and $v/\frac{\hat\xi^2}{2}$ follow by Lemma 2.6.11(a),(b) and (2.6.17).

Step 6: the remaining coefficients. This is input (I3) of Theorem 2.6.13. That theorem transports the cutoff (a function of $y_a = \log \varpi$), the bumps in y and the moment solve, and gives the claim on the full radial path. □

Remark 2.6.6 (Formal jets at $t = 0$ do not replace Step 3). At $\hat\zeta = \pm 1$ one has $d = 0$ and $\beta_0(\pm 1) = \mp \varsigma(\frac{1}{2} - h)/L(1) \neq 0$. In (2.6.9) the other angular derivatives of the unknowns carry the factor d (in $\mathscr{Q}[u]$ and in the pressure part). Differentiating the system k times in $\hat\zeta$ at $\hat\zeta = \pm 1$ therefore expresses $\partial_{\hat\zeta}^{k+1}(f, u)(\cdot, \pm 1)$ through $\partial_{\hat\zeta}^{j}(f, u)(\cdot, \pm 1)$, $j \le k$, their radial derivatives and primitives, and the data jets. So the endpoint jets are determined by the endpoint traces $(f, u)(\cdot, \pm 1)$, which are the $t = 0$ values. Equality of slice jets is thus equivalent to equality of the two traces, given equal data jets. The traces are not determined by local data. Within one chart they are fixed by the Neumann series, as in Step 5, but the two charts have different Neumann operators (the drift a_0 contains ς). So a formal-jet argument at $t = 0$ still needs the class statement of Step 3.

Corollary 2.6.7 (Two-sided prefixes; the step $A^+ \in \mathcal{M}^{c_*}$)**.** *Let $f \in \mathcal{M}^{c_*}$ (weighted class with weight W) and let the two full moments $\int \mathsf{R}^2 f_\theta$, $\int \mathsf{R} f_z$ vanish. Then $A_\theta^+ = -\mathsf{R}^{-2} \int_0^{\mathsf{R}} x^2 f_\theta = \mathsf{R}^{-2} \int_{\mathsf{R}}^\infty x^2 f_\theta$ and the analogous A_z^+ belong to $\mathcal{M}^{c_*}$. One uses the inward form for $\frac{\hat\xi^2}{2} \le \frac{\hat\xi_p^2}{2} e^{-3}$ and the outward form for $\frac{\hat\xi^2}{2} \ge \frac{\hat\xi_a^2}{2} e^{t_{\mathrm{act}}}$. These ranges overlap by (2.3.5), and (W1) applies on each. The subtracted density $\omega \propto \beta_0$* [proof of Lemma 2.14.2] *is supported in Σ, where $\mathsf{W} \ge c$. On the support, R is bounded above and below on the radial hull* (2.13.1) .

Corollary 2.6.8 (The protected slot)**.** *On every radial line (fixed (Z, T), hence fixed $\hat\zeta$) the interval $\Sigma(\hat\zeta) = \{-8 \le y_p \le -3\}$ is a protected radial slot with $\mathsf{W} \ge c_m e_\infty$. The radial-mixing cutoff χ of* [Lemma 2.13.9] *and the moving correction function of* [Section 2.14] *may be taken with derivative support in Σ. This is the choice $\chi = \chi_m$ already made in* (2.14.12) *. Then "ordinary bounded estimates suffice there"* [proof of Lemma 2.13.9] *is justified by (W2).*

Lemma 2.6.9 (Weighted radial primitives)**.** *The component aggregate* (2.3.7) *of the selected member keeps its $\mathsf{W}\mathcal{L}^N_W$ mixed-jet class under the actual moment-subtracted radial inverse. This conclusion includes sources that meet the new angular and radial tapers. We permit fixed radial Jacobian factors on the annular hull. The protected subtraction uses the actual moving density* (2.3.10)*. The mapping property follows from the product form of W and its protected bank floor, as in Remark 2.3.14(1).*

Proof. This is Proposition 2.3.12: its density β_0 and cutoff χ_m are those of (2.3.10), and its hypothesis is only the class bound of the source, so sources that meet the new angular and radial tapers are included. Fixed smooth radial Jacobian factors on the annular hull keep the class (Lemma 2.3.8(c) and the Leibniz rule). The moving-density identity keeps all derivatives of the

correction density in (2.3.8). This supplies the actual mapping used in (2.14.13). The mapping property itself is proved in Proposition 2.3.12. That proof uses only the two one-sided comparisons (W1′), (W1″) and the slot plateau (W2) of the product-form weight of Definition 2.3.6, not a lower bound for the stress. Remark 2.3.14 covers the slow chart $(\mathsf{R},\mathsf{Z},\mathsf{T})$, the powers W^{β} and the Gevrey classes of Section 2.12.1. □

2.6.4 Five linear moments and compact positive-order profiles

We use the shared curved Gevrey cutoff of paragraph 2.3.2. It equals one through R_{need}. Its full support lies at radii less than R_{cut} inside the solved union. We multiply the current inner F_n, U_n by this cutoff.

On the positive-order patch I_{pos}, we add two fixed ordered bumps to U_n and three to $E_n = \mathfrak{r}F_n$. The bumps are functions of $y = 2\log(\hat{\xi}/\hat{\xi}_p(\hat{\zeta}))$; see (2.6.19). We have fixed all lower coefficients. We reconstruct M_n, V_n, P_n from (2.6.3) and (2.6.5), with their actual axis values.

The five constraints, integrated with respect to $\mathfrak{r}$, are

$$\begin{aligned} m_{n,1} &= \int_0^\infty \mathfrak{r}U_n \,\mathrm{d}\mathfrak{r} = 0, & m_{n,2} &= \int_0^\infty \mathfrak{r}^2 E_n \,\mathrm{d}\mathfrak{r} = 0,\\ m_{n,3} &= \int_0^\infty \partial_{\mathfrak{r}} P_n \,\mathrm{d}\mathfrak{r} = 0, & m_{n,4} &= \int_0^\infty \mathfrak{r}^2 \sum_{i+j=n} U_i E_j \,\mathrm{d}\mathfrak{r} = 0,\\ m_{n,5} &= \int_0^\infty \left[\mathfrak{r}\sum_{i+j=n} U_i U_j - \frac{\mathfrak{r}^2}{2}\partial_{\mathfrak{r}} P_n\right] \mathrm{d}\mathfrak{r} = 0. \end{aligned} \tag{2.6.18}$$

We use the derivative form of the last moment before removal of the pressure plateau. It avoids the integral of a tentative nonzero constant pressure to infinity.

On this patch the leading profile is $U_0 = 0$, $E_0 = e_*\varphi(\hat{\zeta})\mathfrak{r}^{-1-2\mu}$. The bumps are functions of the moving logarithmic variable $y = 2\log(\hat{\xi}/\hat{\xi}_p(\hat{\zeta}))$. Here $\frac{\hat{\xi}_p^2}{2}$ is the pulse-entry graph of Proposition 2.3.2, not the exterior hull $\frac{\hat{\xi}_P^2}{2}$. We fix nonnegative, not identically zero $b_1^U, b_2^U, b_1^E, b_2^E, b_3^E \in C_c^\infty((-14,-9))$, with ordered disjoint supports in each family.

We set

$$U_n = \chi U_n^{\mathrm{in}} + \sum_j \alpha_j(\hat{\zeta}) b_j^U(y), \qquad E_n = \chi E_n^{\mathrm{in}} + \sum_j \beta_j(\hat{\zeta}) b_j^E(y). \tag{2.6.19}$$

We write the bump coefficients as $\boldsymbol{\alpha}$ for U_n and $\boldsymbol{\beta}$ for E_n. The moments are affine in these coefficients. There is no current-order quadratic term because $n \ge 1$.

The exact equations are

$$B_U\boldsymbol{\alpha} = -\begin{pmatrix} m_{n,1}^0 \\ m_{n,4}^0/(e_*\varphi)\end{pmatrix}, \qquad B_E\boldsymbol{\beta} = -\begin{pmatrix} m_{n,2}^0 \\ m_{n,3}^0/(2e_*\varphi) \\ -m_{n,5}^0/(e_*\varphi)\end{pmatrix}, \tag{2.6.20}$$

where the superscript denotes the uncorrected moments, and

$$\begin{aligned} (B_U)_{ij}(\hat{\zeta}) &= \int_0^\infty \mathfrak{r}^{p_i} b_j^U\left(\log(\mathfrak{r}^2/((\hat{\xi}_p(\hat{\zeta}))^2))\right)\mathrm{d}\mathfrak{r}\\ &= \tfrac{1}{2}((\hat{\xi}_p(\hat{\zeta}))^2)^{(p_i+1)/2}\int e^{(p_i+1)y/2} b_j^U(y)\,\mathrm{d}y, \qquad (p_1,p_2) = (1, 1-2\mu). \end{aligned}$$

$$(B_E)_{ij}(\hat{\zeta}) = \tfrac{1}{2}((\hat{\xi}_p(\hat{\zeta}))^2)^{(s_i+1)/2}\int e^{(s_i+1)y/2} b_j^E(y)\,\mathrm{d}y, \quad (s_1,s_2,s_3) = (2, -2-2\mu, -2\mu).$$

For example, $\partial_{\mathfrak{r}} P_n = 2E_0E_n/\mathfrak{r} + (\sum_{i,j\ge1} E_iE_j - \mathfrak{R}_{n-1})/\mathfrak{r}$. This verifies the pressure row and the minus sign in the fifth row of (2.6.20).

Thus $B_U(\hat\zeta) = \frac12 \operatorname{diag}((\hat\xi_p^2)^{(p_i+1)/2})\widehat B_U$ with a matrix $\widehat B_U$ that depends on $\hat\zeta$ only through the patch exponent $\mu(\hat\zeta)$ (it is constant when μ is), and in the same way for B_E. The exponents $(p_i+1)/2 \in \{1, 1-\mu\}$ and $(s_i+1)/2 \in \{\frac32, -\frac12-\mu, \frac12-\mu\}$ are distinct because $\mu > 0$. A nontrivial sum of k exponentials with distinct real exponents has at most $k-1$ real zeros (Rolle's theorem and induction). Thus $\det[e^{a_iy_j}]$ has one strict sign on the ordered set $y_1 < \cdots < y_k$.

Its integral against the product of the ordered nonnegative bumps is nonzero. The two matrices are invertible for every $\hat\zeta$. Because $\frac{\hat\xi_p^2}{2}$ and φ are smooth and φ is bounded away from zero, (2.6.20) gives smooth coefficients of arbitrary finite size. We use no global Gevrey bound on these discrepancies or on φ.

The variable $y = 2\log(\widetilde\xi/\widetilde\xi_p)$ is one slice function (Lemma 2.3.19). A bump that is fixed in $\mathfrak{r}$ is not: its backward and forward first slice jets differ by $\mathfrak{r}b'(\mathfrak{r})/(2(\frac12-h))$ (Subsection 2.3.3). The bumps lie outside the inverse rectangle and the cutoff transition region, so their axis prefixes cannot change its equations or regularity.

For the selected early-correction construction, we select $\frac{(\hat\xi_v(\hat\zeta))^2}{2}$ after the positive velocity correction region and before the mean correction region. The first moment and coefficient divergence identity give $F_n = U_n = M_n = V_n = 0$ there for $n \ge 1$, but do not set the leading meridional field to zero. The recursion at the start of this section keeps $\mathfrak{R}_1 = -\mathsf{Z}_0^{[2]}V_0$, thus the explicit P_1, P_2 continuations through the leading support after this region. We select an enclosing $\frac{\hat\xi_P^2}{2}$ after the true last leading meridional return.

We keep this uppercase exterior-support notation throughout. It differs from the pulse-entry graph $\frac{(\hat\xi_p(\hat\zeta))^2}{2}$ in Lemma 2.3.13 and Section 2.14. The full third moment, not its truncation at the early correction region, makes the last pressure constant zero. Thus the support assertion is

$$\begin{aligned} (E_n, U_n, V_n, M_n) &= 0 \quad (\tfrac{\hat\xi^2}{2} \ge \tfrac{(\hat\xi_v(\hat\zeta))^2}{2},\ n \ge 1), \\ P_n &= 0 \quad (\tfrac{\hat\xi^2}{2} \ge \tfrac{\hat\xi_P^2}{2},\ n \ge 1), \\ P_n &= 0 \quad (\tfrac{\hat\xi^2}{2} \ge \tfrac{(\hat\xi_v(\hat\zeta))^2}{2},\ n \ge 3). \end{aligned} \tag{2.6.21}$$

The mean patch keeps the leading velocity, with the actual positive pressure corrections kept in its initialization.

We do not assume $\frac{\hat\xi_P^2}{2}$ to precede the early mean correction region. The two extra pressures' full radial saturation lies in the actual positive middle corridor.

Slow jet equality with covariant bumps. We write $\mathfrak{r} = \hat\xi$ and $E = \mathfrak{r}F$. The moment bumps of (2.6.19) are functions of $y = 2\log(\hat\xi/\hat\xi_p(\hat\zeta))$; this makes the slow coefficients transport across $t = 0$ with equal endpoint jets.

Inputs.

(I1) Endpoint germ l: $\hat\zeta^2 l^{1-2h} = 1 + l(1-\hat\zeta^2)$, $l(\pm1) = 1$; $q_b = q_f/l$, $\frac{\hat\xi_b^2}{2} = l\frac{\hat\xi_f^2}{2}$, $\hat\zeta_b = l^{\frac12-h}\hat\zeta_f$ (Section 2.7). Implicit differentiation gives $l'(\pm1) = \mp 2/(\frac12-h)$. We write $\Phi(\frac{\hat\xi^2}{2}, \hat\zeta) = (l(\hat\zeta)\frac{\hat\xi^2}{2}, l(\hat\zeta)^{\frac12-h}\hat\zeta)$, so that $\Phi(\frac{\hat\xi^2}{2}, \pm1) = (\frac{\hat\xi^2}{2}, \pm1)$.

(I2) For the physical coefficients of (2.6.2) and (2.6.3), backward-to-forward transport multiplies the pullbacks of E_n, U_n, F_n, P_n, V_n by $l^{1/2+h-\lambda_n}, l^{1/2+h-\lambda_n}, l^{1+h-\lambda_n}, l^{1+2h-\lambda_n}, l^{-\lambda_n}$, respectively, where $\lambda_n = 2nh$ as in (2.7.1).

(I3) Inner inverse and its jet identification: Lemmas 2.6.1 and 2.6.2, and Steps 1–5 of the proof of Proposition 2.6.5, under the hypotheses of Proposition 2.6.5. At order n these steps give equal slice jets of the inner solutions from equal slice jets of all coefficients of orders below n; regular-axis uniqueness alone does not give them (Remark 2.6.6). Theorem 2.6.13 and Proposition 2.6.5 are therefore one induction on n, with base case the leading identification.

(I4) The entry-graph identity of Theorem 1(iii) and (I1) give $\varpi_b = \varpi_f$ on the open collars. Thus the inner cutoff in $y_a = \log \varpi$ is covariant.

(I5) The pulse-graph identity of the same clause gives $\hat{\xi}_{p,b}(l^{1/2-h}\hat{\zeta})^2 = l\,\hat{\xi}_{p,f}(\hat{\zeta})^2$ there. Thus $y = 2\log(\hat{\xi}/\hat{\xi}_p)$ agrees on the two sides, both in the positive-velocity slot $(-14,-9)$ and in the mean slot $(-8,-3)$ (Proposition 2.3.2).

(I6) The leading profile is the untouched power patch $U_0 = 0$, $E_0 = e_*\varphi(\hat{\zeta})\mathfrak{r}^{-1-2\mu}$, $\mu > 0$, $\min\varphi > 0$ on the positive-velocity slot of Theorem 1(iii). The ordered moment blocks on this patch are invertible by Lemma 2.6.12. The slots lie outside the inner inverse rectangles and the cutoff transition region (Section 2.6; Definition 2.5.1 "untouched moving power patches").

(I7) The five moments (2.6.18), the pressure row identity $\partial_{\mathfrak{r}}P_n = 2E_0E_n/\mathfrak{r} + (\cdots)$ (Section 2.6) and the hull/dominator statement proof of Theorem 2.7.1.

Definition 2.6.10. Write $X = \xi^2/2$ and $X_{\mathrm{hull}} = \xi_{\mathrm{hull}}^2/2$. Let G_f, G_b be smooth in (X,η) up to the faces of their own closed rectangles $[0, X_{\mathrm{hull}}] \times \{1-\epsilon \le |\eta| \le 1\}$, and let $\kappa \in \mathbb{R}$. We write $G_f \simeq_\kappa G_b$ if, for all $a, k \ge 0$ and $0 \le X \le X_{\mathrm{hull}}$,

$$\partial_X^a \partial_\eta^k [G_f - l^\kappa \widetilde{G}_b \circ \Phi](X, \pm 1) = 0,$$

where $\widetilde{G}_b$ is a smooth extension across the angular endpoint and, at $X = X_{\mathrm{hull}}$, across the outer radial face as well. Such a local extension is obtained by applying Lemma 2.8.2 successively in the two normal coordinates. The argument lX remains nonnegative at the axis. Because $\Phi(\frac{\hat{\xi}^2}{2}, \pm 1) = (\frac{\hat{\xi}^2}{2}, \pm 1)$ and Φ is analytic, the jet of $\widetilde{G}_b \circ \Phi$ at $\hat{\zeta} = \pm 1$ depends only on the one-sided jet of G_b (Faà di Bruno), so the definition is independent of the extension. For $\hat{\zeta}$-only functions the definition is the same with no $\frac{\hat{\xi}^2}{2}$.

For an odd radial amplitude $\xi F(X,\eta)$ we compare F by this definition and recover the amplitude in the variable ξ. These normalized relations are equivalent to the transported physical jets of Theorem 2.7.1 at $z \neq 0$, using (2.11.1) at the spatial axis.

Lemma 2.6.11 (Transport calculus)**.**

(a) If $G_f \simeq_\kappa G_b$ and $H_f \simeq_{\kappa'} H_b$ then $G_fH_f \simeq_{\kappa+\kappa'} G_bH_b$.

(b) If $G_f \simeq_\kappa G_b$ then $\int_0^{\frac{\hat{\xi}^2}{2}} G_f\,\mathrm{d}x \simeq_{\kappa-1} \int_0^{\frac{\hat{\xi}^2}{2}} G_b\,\mathrm{d}x$.

(c) If $G_f \simeq_\kappa G_b$, with supports in $\hat{\xi} \le \hat{\xi}_{\mathrm{hull}}$ for $|\hat{\zeta}| \ge 1-\epsilon$ and an integrable axis dominator for each derivative, then $\int_0^\infty \mathfrak{r}^s G_f\,\mathrm{d}\mathfrak{r} \simeq_{\kappa-(s+1)/2} \int_0^\infty \mathfrak{r}^s G_b\,\mathrm{d}\mathfrak{r}$ (as functions of $\hat{\zeta}$).

Proof. (a) Leibniz. (b) Substitute $x_b = lx$: $\int_0^{\hat\xi^2/2} G_f\,\mathrm{d}x - l^{\kappa-1}\int_0^{l\hat\xi^2/2} \widetilde G_b(x_b,\hat\zeta_b)\,\mathrm{d}x_b = \int_0^{\hat\xi^2/2}[G_f(x,\hat\zeta) - l^{\kappa}\widetilde G_b(lx,\hat\zeta_b)]\,\mathrm{d}x$. The integrand is flat at $\hat\zeta = \pm1$ uniformly on the compact interval, so every $(\hat\xi^{-1}\partial_{\hat\xi})^a\partial_{\hat\zeta}^k$ of the integral vanishes there. (c) Substitute $\mathfrak{r}_b = l^{1/2}\mathfrak{r}$ and use the compact hull and the axis dominators in (I7). For an integrand containing $E_n = \mathfrak{r}F_n$, absorb $\mathfrak{r}$ into the monomial weight before applying (c). □

Lemma 2.6.12 (Exponential Vandermonde)**.** *Let $a_1,\dots,a_k$ be distinct reals and let $b_1,\dots,b_k \ge 0$, $b_j \not\equiv 0$, be integrable with ordered supports* $\operatorname{supp} b_1 < \cdots < \operatorname{supp} b_k$*, and assume all displayed exponential moments are finite. Then* $\det\big[\int e^{a_i y} b_j(y)\,\mathrm{d}y\big] \neq 0$.

Proof. A nonzero linear combination of k exponentials with distinct real exponents has at most $k-1$ real zeros: divide by the exponential of the least exponent, differentiate, and apply Rolle's theorem inductively. Thus $\det[e^{a_i y_j}]$ has one strict sign on $y_1 < \cdots < y_k$. Multilinearity and Fubini express the asserted determinant as

$$\int \det[e^{a_i y_j}] \prod_j b_j(y_j)\,\mathrm{d}y_1\cdots\mathrm{d}y_k,$$

which is nonzero. When $a_1 < \cdots < a_k$, the sign is positive: at $y_j = jT$, the identity permutation uniquely maximizes $\sum_j j a_{\pi(j)}$ as $T\to\infty$, and continuity fixes the sign on the ordered set. All integrals used here have compact bump supports. □

Theorem 2.6.13 (Slow jet equality with covariant bumps)**.** *Define the positive-order corrections by (2.6.19), with bumps $b_j^U(y), b_j^E(y)$, $y = 2\log(\hat\xi/\hat\xi_p(\hat\zeta))$, supported in the positive-velocity slot $(-14,-9)$. Assume (I1)–(I7). Then for every $n\ge1$ the matrices $B_U(\hat\zeta), B_E(\hat\zeta)$ have smooth inverses. For the fields smooth in $X = \xi^2/2$ one has*

$$\begin{aligned} U_{n,f} &\simeq_{1/2+h-\lambda_n} U_{n,b}, \quad F_{n,f} \simeq_{1+h-\lambda_n} F_{n,b},\\ M_{n,f} &\simeq_{h-1/2-\lambda_n} M_{n,b}, \quad V_{n,f} \simeq_{-\lambda_n} V_{n,b}, \qquad P_{n,f} \simeq_{1+2h-\lambda_n} P_{n,b}. \end{aligned}$$

The azimuthal amplitude has the transported endpoint jets

$$\partial_\xi^a\partial_\eta^k\Big[E_{n,f}(\xi,\eta) - l^{1/2+h-\lambda_n}\widetilde E_{n,b}(\sqrt{l}\,\xi, l^{1/2-h}\eta)\Big]\Big|_{\eta=\pm1} = 0 \quad (a,k\ge0,\ 0\le\xi\le\xi_{\mathrm{hull}}), \tag{2.6.22}$$

where $\widetilde E_{n,b} = \xi_b \widetilde F_{n,b}$. The axis is included. For the actual positive orders choose the common hull strictly beyond the pressure and velocity supports in (2.6.21). All six coefficients are zero beyond this hull, including their one-sided endpoint jets.

Proof. The substitution $\mathfrak{r} = (\hat\xi_p^2 e^y)^{1/2}$ gives

$$(B_U)_{ij} = \tfrac12(\hat\xi_p^2)^{(p_i+1)/2}\int e^{(p_i+1)y/2} b_j^U(y)\,\mathrm{d}y,$$

and the analogous formula for B_E. The exponents are $\{1, 1-\mu\}$ and $\{\frac32, -\frac12-\mu, \frac12-\mu\}$, respectively. They are distinct, so Lemma 2.6.12 gives invertibility. Smooth positive $\frac{\hat\xi_p^2}{2}, \varphi$ and smooth $\mu>0$ give smooth inverses and coefficients.

Induct on n, starting from the leading identification. Input (I3), applied to the already matched lower orders, gives the inner-solution jets; it uses the transported uniqueness class of Proposition 2.6.5.

The cutoff preserves these jets because y_a is invariant. Similarly, (I5) gives $y_f = y_b \circ \Phi$, including all endpoint jets.

Transport both bump coefficient vectors by $(\alpha^{\mathrm{tr}}, \beta^{\mathrm{tr}}) = l^{1/2+h-\lambda_n}(\widetilde{\alpha}_b, \widetilde{\beta}_b)(l^{1/2-h}\eta)$ and form the trial fields

$$\widetilde{U}_n = \chi U^{\mathrm{in}}_{n,f} + \sum_j \alpha^{\mathrm{tr}}_j b^U_j(y_f), \qquad \widetilde{F}_n = \chi F^{\mathrm{in}}_{n,f} + \sum_j \beta^{\mathrm{tr}}_j b^E_j(y_f)/\xi.$$

The bump quotients vanish near the axis. Since $\xi_b = \sqrt{l}\,\xi$, these trial fields have the U_n and F_n transport weights above. Insert $(\widetilde{U}_n, \xi\widetilde{F}_n)$ into the five moments. Their endpoint jets vanish by Lemma 2.6.11(c), the lower-order induction and the row weights in Theorem 2.7.1. The full pressure and quadratic terms are included, and (I7) justifies differentiation over the common hull.

At the current order the rows are affine, and $U_0 = 0$ separates the U and E blocks. In the U block their coefficient matrix is $\mathrm{diag}(1, e_*\varphi_f)B_U$. Subtract its exact zero-row equation for α_f from the endpoint-flat equation for α^{tr}. The smooth inverse shows that $\alpha_f - \alpha^{\mathrm{tr}}$ is flat. Hence the corrected U_n has the required jets. The same argument applies to E_n, with the invertible matrix $\mathrm{diag}(1, 2e_*\varphi_f, -e_*\varphi_f)B_E$ for rows $(2, 3, 5)$.

Thus the corrected F_n has the same jets as $\widetilde{F}_n$, including at $X = 0$. Multiplying its transport difference by ξ gives exactly the bracket in (2.6.22), since $l^{1/2+h-\lambda_n}\xi_b = l^{1+h-\lambda_n}\xi$. The chain rule in ξ proves the assertion at every radial order. The formula $M_n = \int_0^X U_n$, Lemma 2.6.11, and the covariant velocity and pressure recursions give the remaining weights. For $G = M_n, V_n$ the smooth quotient $G/X = \int_0^1 (\partial_X G)(sX, \eta)\,\mathrm{d}s$ has transport weight $w(G) + 1$, also at $X = 0$. These quotients supply the radial Cartesian velocity and cutoff potential at the axis. This completes the joint induction with Proposition 2.6.5. □

Remark 2.6.14 (Support graph). With slots at $y \in (-14, -9)$ and mean slots at $(-8, -3)$, the graph $\frac{\left(\hat{\xi}_v(\hat{\zeta})\right)^2}{2} := \frac{\left(\hat{\xi}_p(\hat{\zeta})\right)^2}{2} e^{-17/2}$ is admissible in Section 2.6. It is chart-covariant. The support statement (2.6.21) is unchanged.

2.6.5 Conservation closes the stress primitives

We define the signed coefficient stresses by

$$T_{n,\theta} = -\mathfrak{r}^{-2} \int_0^{\mathfrak{r}} s^2 r_{\theta,n}(s)\,\mathrm{d}s, \qquad T_{n,z} = -\mathfrak{r}^{-1} \int_0^{\mathfrak{r}} s r_{z,n}(s)\,\mathrm{d}s. \tag{2.6.23}$$

They vanish on the kept inner solve collar. To close them at the outer boundary we must verify zero total residual moments. For any smooth axisymmetric solenoidal field, we set $\mathcal{R} = \mathscr{N}(u, p)$.

The exact conservative identities are

$$\begin{aligned} r^2\mathcal{R}_\theta &= \partial_t(r^2 u_\theta) + \partial_r(r^2 u_r u_\theta) + \partial_z(r^2 u_z u_\theta) - \partial_r(r^2\partial_r u_\theta - r u_\theta) - \partial_{zz}(r^2 u_\theta), \\ r\mathcal{R}_z &= \partial_t(r u_z) + \partial_r(r u_r u_z) + \partial_z[r(u_z^2 + p)] - \partial_r(r\partial_r u_z) - \partial_{zz}(r u_z). \end{aligned} \tag{2.6.24}$$

At positive order the radial boundary terms vanish by Cartesian axis regularity and compact support. The time and flux integrals are scalar powers of q times $m_{n,2}, m_{n,4}$ in the angular equation and $m_{n,1}, m_{n,5}$ in the axial equation. All vanish identically before physical differentiation.

The axial viscosity of positive orders uses the same lower-order zero moments. At order one, its axial component uses the zero leading total axial flux.

The remaining angular term uses the canonical leading primitive. Let $u_{\mathrm{pow}}(r)$ be the fixed, z-independent pure-power trace of the heat profile. Exact canonical matching gives

$$\int_0^\infty r^2[u_{\theta,0}(r, z, t) - u_{\mathrm{pow}}(r)]\,\mathrm{d}r = 0. \tag{2.6.25}$$

$\mathfrak{r}^2 E_0\,\mathrm{d}\mathfrak{r} = H_0\,\hat{\xi}\,\mathrm{d}\hat{\xi}$, so this equals the zero renormalized limit of the actual angular primitive, with its additive constant.

The integral converges at zero and infinity. Locally in (z,t), beyond a uniform finite physical radius the leading swirl is the genuine heat field, independent of z. Thus axial derivatives pass under the compensated integral. The subtracted pure power has zero axial derivative.

This proves the exceptional order-one angular moment.

We extract each finite coefficient from (2.6.24) to get

$$\int_0^\infty \mathfrak{r}^2 r_{\theta,n}\,\mathrm{d}\mathfrak{r} = 0, \qquad \int_0^\infty \mathfrak{r} r_{z,n}\,\mathrm{d}\mathfrak{r} = 0. \tag{2.6.26}$$

The forward time sign changes only a derivative of an identically zero moment. It does not change these cancellations. Equations (2.6.23) also have an exterior-integral form with a plus sign. We use this equality at the flat outer boundary. Smooth vanishing of the local source alone does not remove an exterior primitive constant.

2.6.6 The one exceptional outer viscosity coefficient

On $\hat{\xi} \ge \hat{\xi}_P$, equation (2.6.21) and $U_0 = V_0 = 0$ make each $\mathfrak{R}_k$ vanish. Thus there is no late positive-order pressure plateau or tail. The only residual that can reach the true outer edge is

$$r_{\theta,1} = -\mathfrak{r}\mathsf{Z}_b^{[2]} F_0, \qquad r_{z,1} = 0. \tag{2.6.27}$$

For $n \ge 2$ the swirl at that lower order has compact support, so $T_n = 0$ on $\hat{\xi} \ge \hat{\xi}_P$.

On a kept scalar component the outer numerator has the form

$$H_0 = d^{-h} g_*(\tfrac{\hat{\xi}^2}{2}/d) - \psi_o \alpha_o \ell_b f_o(y_o).$$

The physical scalar-lift swirl equals

$$q^{-\frac{1}{2}-h}\frac{d^{-h} g_*(\frac{\hat{\xi}^2}{2}/d)}{\hat{\xi}} = r^{-1} t^{-h} g_*(r^2/(2t)),$$

independent of physical z, even on the forced scalar shooting interval. Its contribution to (2.6.27) is thus zero. This identity avoids derivatives of crude bounds on apparently singular powers of d.

The wing coefficient is $-\psi_o \alpha_o \ell_b f_o(y_o)/(\hat{\xi}^2)$. The exact operator $\mathsf{Z}_b^{[2]}$ has order two with bounded coefficients and fixed jets on the outer annular hull, because its only coordinate denominator is L. The explicit squared-flat factors thus give

$$|D^j r_{\theta,1}| \le C_j w_1 [1 + \log(1/w_1)]^{N_j} \le C_j' \mathsf{W}\mathcal{L}_W^{N_j'}.$$

For the actual mixture $F_0 = (1-\chi)F_c + \chi F_w$ the axial derivative also acts on χ. On the forward terminal annulus use the velocity estimate in Theorem 1(iv), recorded on p. 440. Write $X = \mathfrak{r}^2/2$, $H_0 = 2XF_0$ and $F_{\mathrm{heat}} = H_{\mathrm{heat}}/(2X)$. In physical variables $q^b F_{\mathrm{heat}} = u_{\theta,\mathrm{heat}}/r$, with $b = -1-h$. At fixed r,t this quantity is independent of z. Applying the chart identity (2.6.1) twice gives $\mathsf{Z}_b^{[2]} F_{\mathrm{heat}} = 0$. The coefficients of $\mathsf{Z}_b^{[2]}$, the factor $\mathfrak{r}$ and $1/(2X)$ have bounded derivatives on the compact annular hull, where $X > 0$ and $L \ge 1 - 2h$. Hence for a word D^j of length j in $\partial_X, \partial_\eta|_X$, the product rule gives

$$\begin{aligned} |D^j r_{\theta,1}| &= |D^j\{\mathfrak{r}\mathsf{Z}_b^{[2]}[(H_0 - H_{\mathrm{heat}})/(2X)]\}| \\ &\le C_j \sum_{|I|\le j+2} |D^I(H_0 - H_{\mathrm{heat}})| \le C_j' \mathsf{W}\mathcal{L}_W^{N_j'}. \end{aligned}$$

This estimate is for the differentiated mixture, including derivatives of its angular cutoff at radial and angular terminal faces. The jets vanish on its terminal zero set. Outside the hull the field equals the heat field. On the intervening compact middle corridor the positive lower bound for W in (iv) and smoothness give the same estimate. Thus on the outer region the source has the input bound required by the radial inverse of Lemma 2.3.13.

The compact spectral modification gives a compact residual in the two-tube saturation. We do not claim that this residual independently has zero moment. The complete actual residual has its true zero moment. By (2.6.26), the stress is the exact tail

$$T_{1,\theta}(\mathfrak{r},\hat{\zeta}) = \mathfrak{r}^{-2}\int_{\mathfrak{r}}^{\infty} s^2 r_{\theta,1}(s,\hat{\zeta})\,\mathrm{d}s. \tag{2.6.28}$$

Lemma 2.6.9 proves the same weighted bound for all its fixed jets, also at angular faces and corners. The inner inverse makes each positive-order stress zero near the first edge. The actual two-tube/native aggregate covers the remaining compact part and keeps its full partial-pressure paths. We thus get

$$|D^j T_n| \le C_{n,j}\mathsf{W}\mathcal{L}_W^{N_{n,j}} \quad (n \ge 1), \tag{2.6.29}$$

with no logarithmic loss for $n \ge 2$, whose stresses have fixed compact interior support.

The argument uses the actual zero-meridional route. A construction with additional late axial controls must include another outer pressure and viscosity check.

2.6.7 Borel realization on divergence potentials

For a finite truncation let $u^{[N]} = \sum_{n=0}^{N} u_n$, $p^{[N]} = \sum_{n=0}^{N} p_n$, and

$$K^{[N]} = \sum_{n=0}^{N} q^{-1-h+\lambda_n} T_n.$$

For a two-component tangential stress define

$$\mathscr{D}_r(K) = (\partial_r + 2/r)K_\theta e_\theta + (\partial_r + 1/r)K_z e_z.$$

This notation specifies the two tangential forcing components. It does not discard the additional radial terms in the realization of a full covariance tensor after this step.

The recursions and stress primitives give on each fixed profile hull

$$|\partial^{\le m}[\mathscr{N}(u^{[N]},p^{[N]}) + \mathscr{D}_r(K^{[N]})]| \le C_{N,m} q^{2h(N+1)-2-m}. \tag{2.6.30}$$

All terms with order less than $N+1$ cancel algebraically. The radial base loss is $2(\frac{1}{2}+h)+\frac{1}{2} < 2$. The tangential loss is $(\frac{1}{2}+h)+1 < 2$.

Each fixed physical derivative costs at most one additional power of q^{-1} on the bounded hull. Powers of λ_n affect the constants, not the exponent loss. At the axis the Cartesian formulas and divisibility by $\frac{\hat{\xi}^2}{2}$ supply this estimate without a punctured-axis bound.

The meridional potential for the n-th coefficient is

$$\Psi_n = q^{\frac{1}{2}-h+\lambda_n} M_n(\tfrac{\hat{\xi}^2}{2},\hat{\zeta}), \qquad u_{r,n} = -r^{-1}\partial_z\Psi_n, \quad u_{z,n} = r^{-1}\partial_r\Psi_n.$$

We take $\chi(s) = 1 - \psi_1(s-1)$, where the explicit smooth step of Lemma 2.12.16 is zero on $(-\infty,0]$ and one on $[1,\infty)$. Thus $\chi = 1$ on $[0,1]$ and $\chi = 0$ on $[2,\infty)$. Let $\widetilde{q}$ be the physical gauge (2.10.1). With the same $c_n \uparrow \infty$, we sum $\chi(c_n\widetilde{q})\Psi_n$ before differentiation.

We use the same cutoffs for swirl, pressure and coefficient stresses. The actual radial component is

$$\chi(c_n\widetilde{q})q^{\lambda_n}r^{-1}V_n - r^{-1}\Psi_n c_n\chi'(c_n\widetilde{q})\partial_z\widetilde{q}. \tag{2.6.31}$$

This is the product rule for $-r^{-1}\partial_z$. The axial component is $\chi(c_n\widetilde{q})q^{-\frac{1}{2}-h+\lambda_n}U_n$, because $\partial_r\widetilde{q}=0$.

The two terms vanish after the positive velocity support. Pressure uses its larger hull $\frac{\hat{\xi}_P^2}{2}$. The potential is $O(r^2)$ at the axis and the field has zero divergence. We do not use the $-2\hat{\zeta}/L$ bracket with a modified gauge.

The displayed physical formula keeps each derivative of L_{cut}.

We now state the coefficient regularity for the diagonal selection. At order n each fixed seminorm is finite. We impose no growth bound in n. For each n, the choice of c_n uses the finite normalized profile seminorms of orders $j \le n$.

The list includes those of T_n/W for $n \ge 2$. We select the constant large enough that these seminorms satisfy

$$C_{n,j}\, q^{nh} \le 2^{-n} \qquad (0 < q \le 2L_{\max}/c_n, j \le n). \tag{2.6.32}$$

Here $L_{\max} \ge \sup(q/\widetilde{q})$ on the joint domain.

The factor q^{nh} uses only half of the actual positive-order power $q^{\lambda_n} = q^{2nh}$. The other half controls the tail. We enlarge the constants to include all cutoff derivatives used in those finite seminorms. Derivatives by $q\partial_q$ of $\chi(c_n\widetilde{q})$ have fixed bounded shapes.

Physical derivatives use only the fixed powers in (2.6.30). We may add any finite set of such budgets at order n, and select c_n so that it increases successively.

For fixed positive q the sum is locally finite. For a fixed jet order j, its tail has the bound $\sum_{n\ge j} 2^{-n}q^{nh}$. To compare with any fixed finite prefix and get a prescribed higher power of q, we first select a longer prefix N. The tail after this prefix has order at least $q^{h(N+1)}$ in each fixed normalized seminorm.

The cutoffs of the finite terms through N equal one for sufficiently small q. We select N after the desired physical derivative and remainder power. The previous bound and (2.6.30) prove flatness of the realized augmented residual. This comparison uses finite prefixes.

It does not interchange an uncontrolled infinite formal series with the equations.

Proposition 2.6.15 (The slow reference)**.** *There are smooth positive-time fields (u_B, p_B), with $\operatorname{div} u_B = 0$, and a tangential stress K_B, such that*

$$|\partial^j[\mathscr{N}(u_B,p_B) + \mathscr{D}_r(K_B)]| \le C_{j,M}q^M \qquad \text{for each fixed } j, M \tag{2.6.33}$$

near $q=0$ on the bounded profile hull. With $\rho = q^h$, on the annular stress hull each fixed jet made from $q\partial_q, \hat{\xi}^{-1}\partial_{\hat{\xi}}, \partial_{\hat{\zeta}}$ satisfies

$$\begin{aligned} q^{\frac{1}{2}+h}u_{\theta,B} - E_0 &= O(\rho^2), & q^{\frac{1}{2}+h}u_{z,B} - U_0 &= O(\rho^2),\\ q^{1/2}u_{r,B} - V_0/\hat{\xi} &= O(\rho^2), & q^{\frac{1}{2}+h}u_{r,B} &= O(\rho). \end{aligned} \tag{2.6.34}$$

On the mean patch all positive velocity coefficients, with the cutoff differentiation terms, vanish. In each fixed profile jet, we put $K_B = q^{-1-h}\widehat{T}$,

$$|D^j(\widehat{T} - T_0)| \le C_j\rho^2\mathsf{W}\mathcal{L}_W^{N_j}. \tag{2.6.35}$$

Proof. The construction and finite-prefix comparison prove the divergence and residual assertions. The first positive coefficient has order q^{2h}, and (2.6.31) has the same order. The tail bounds prove

(2.6.34). For (2.6.35), the exceptional first coefficient has the explicit logarithmic estimate proved before this step.

Each coefficient of order at least two has support where W has a positive lower bound. Thus its normalized weighted jets are ordinary finite seminorms in (2.6.32). The finite initial block and the geometric tail then share one finite logarithmic exponent at each fixed jet order. An arbitrary sequence whose logarithmic losses grow at one edge does not give this conclusion.

The proof uses compact support of the higher coefficients. □

Global slow velocity in canonical units. On the full bounded native velocity hull subtract the order-zero field before converting to canonical units. At fixed derivative order j retain $1 \le n \le N$ with $N \ge \max(j, 2)$. In the tangential normalization $q^{1/2+h}$ and the radial normalization $q^{1/2}$ each term is q^{2nh} times a bounded smooth profile. For the cutoff derivative in (2.6.31) use $\partial_z \widetilde{q} = O(q^{1/2+h})$. In radial units its absolute value is bounded by

$$Cq^{2nh}(c_n q)\,|\chi'(c_n\widetilde{q})|\,|M_n/\xi|.$$

Here $c_n q$ is bounded on the derivative support and $M_n = O(\xi^2)$ at the axis. Fixed normalized derivatives have the same bounds with their own profile constants. Budget (2.6.32) controls the rest by $\sum_{n>N} 2^{-n} q^{nh} = O(q^{2h})$ for small q. The positive velocity coefficients, including their full flux primitives, vanish beyond their support by the zero total flux. These assertions hold through the axis by the Cartesian regularity of the profiles.

On $t > 0$ write $Y = x'/\sqrt{t}$, $R = |Y|$, $Z = z/t^{d_0}$, $d_0 = 1/2 - h$, $\rho_t = t^h$. Set $\mathcal{Q} = q_f/t$, $\xi = R/\sqrt{\mathcal{Q}}$, $\eta = Z\mathcal{Q}^{-d_0}$. Then $\mathcal{Q} - Z^2\mathcal{Q}^{2h} = 1$ and $\mathcal{Q} \ge 1$. For a normalized profile $G(q_f, \xi, \eta)$, a horizontal derivative in Y costs $\mathcal{Q}^{-1/2}$ in native Cartesian coordinates, and

$$\partial_Z G = \frac{\mathcal{Q}^{-d_0}}{1 - 2h\eta^2}\,[\,2\eta q G_q - \eta\xi G_\xi + (1-\eta^2)G_\eta\,].$$

The denominator has a positive lower bound. Put $V_s = t^{1/2+h}(u_{\mathrm{B}} - B_0)$ and let D act in (Y, Z). For each fixed j the canonical estimates on the native construction are

$$\begin{aligned} |D^{\le j}(V_{s,\theta} e_\theta)| + |D^{\le j}(V_{s,z} e_z)| &\le C_j \rho_t^2 \mathcal{Q}^{-1/2+h}, \\ |D^{\le j}(V_{s,r} e_r)| &\le C_j \rho_t^3 \mathcal{Q}^{-1/2+2h}. \end{aligned} \tag{2.6.36}$$

The vectors are differentiated in Cartesian components through the axis using (2.11.1). Both powers of $\mathcal{Q}$ are negative. The unlocalized difference is zero beyond the native velocity hull. On the fixed localization annulus all physical jets of the slow field and the divergence repair are bounded by off-origin regularity. Beyond the localization the leading heat tail has bounded physical jets, and the leading profiles on the native hull obey the same bounds away from the origin. In canonical units these far-field contributions are $O_j(t^{1/2+h}) = O_j(\rho_t^3)$. Together the estimates give the global sup bounds.

On buffered dyadic charts q/Q stays in a fixed positive compact interval. Their coordinate transformations use only L in the denominator and have bounded fixed jets. On the annular hull the additional division by the normalized radius in the swirl coefficient is harmless. Thus (2.6.34) gives the chart background inputs: radial coefficient $O(\rho)$, and changes of the two tangential coefficients $O(\rho^2)$, in each fixed ordinary jet. Near a nonzero point of the initial slice the fields are one-sided smooth by Proposition 2.8.6(a). Equation (2.6.33) asserts flatness at the singular tip, not zero initial jets at each other spatial point.

2.6.8 The signed stress bound and one edge cutoff

The leading physical stress is $K_0 = q^{-1-h}T_0$. On a dyadic chart its normalized size is $Q^{1+2h}K_0$ of order $\rho\mathsf{W}$, because $2(\frac{1}{2}+h)-(\frac{1}{2}+h)-\frac{1}{2}=h$. The same calculation applied to (2.6.35) gives

$$Q^{1+2h}(K_B - K_0) \in \mathcal{M}^3. \tag{2.6.37}$$

Here $\mathcal{M}^a$ denotes the weighted slow source convention for the next argument: finite logarithmic factors times $C_j\rho^a\mathsf{W}$ bound each fixed normalized jet.

The present source is real and independent of the physical angle and auxiliary variables. Its order-three assertion permits either sign. The factor $\mathcal{L}_W^{N_j}$ is unbounded near the edge, so (2.6.35) does not imply a uniform positive cone for the total uncut stress. The waves will use the positive leading amplitude and treat (2.6.37) as a signed correction.

We fix the single cutoff for these edges. We set $S(q) = \log^{6/5}(1/\widetilde{q})$ and select a fixed $c_e > 0$. We take Θ equal to one on $(-\infty, 1]$ and zero on $[2,\infty)$. For this physical aggregate cutoff only, we use $\mathsf{W}_* = c_*|\widetilde{T}_0|$ from Theorem 2.10.2. We keep the native W in all component and primitive classes.

The two kept logarithmic classes are equivalent.

$$\vartheta_q = \Theta\Big(\frac{\log(1/\mathsf{W}_*)}{c_e S(q)}\Big) \quad (\mathsf{W}_* > 0), \qquad \vartheta_q = 0 \quad (\mathsf{W}_* = 0). \tag{2.6.38}$$

The physical potentials use this cutoff before curl. All later signed updates use the same one.

We define the amplitudes and inverses on the larger native buffer $\mathsf{W} > e^{-3c_eS}$. It contains the physical cutoff support for all sufficiently large S. Indeed, if $\mathsf{W}_* \ge e^{-2c_eS}$, then $\mathsf{W} \le e^{-3c_eS}$ would contradict $\mathsf{W}_* \le C\mathsf{W}\mathcal{L}_W^{N_0}$, since $e^{-3c_eS}(1+3c_eS)^{N_0} = o(e^{-2c_eS})$ and $w(1+\log(1/w))^{N_0}$ increases near $w = 0$.

On this buffer, Lemma 2.3.10 gives polynomial S bounds for all fixed coefficient and direction jets. The relative order-three slow correction has size at most $C\rho^2S^N = o(1)$ there, so it is small against the original positive leading covariance. Where $1-\vartheta_q \neq 0$, $c\mathsf{W} \le \mathsf{W}_* \le e^{-c_eS}$ with a fixed member-dependent $c > 0$. For $\alpha > 0$ and fixed N, this gives $\mathsf{W}^\alpha\mathcal{L}_W^N \le C_{\alpha,N}e^{-\alpha c_eS/2}$, also for the zero extension at $\mathsf{W} = 0$. This absorbs the finite powers of q^{-1} from each fixed physical differentiation.

This exponential absorption, rather than a kept-region bound on inverse edge distances, estimates the discarded region.

Derivatives of ϑ_q in exact curls and the induced covariance differences remain as physically flat errors. The same cutoff multiplies the principal cross target by ϑ_q^2. The radial primitive class keeps the weight W, not the artificial smaller weight $\vartheta_q^2\mathsf{W}$. This distinction keeps the conclusion of Lemma 2.6.9 valid at the artificial cutoff edge.

The wave construction takes the leading strict geometry, the ordinary background rates, and the signed order-three stress as inputs. The slow reference still satisfies an augmented equation. The next wave and mean corrections remove its stress.

2.7 The full radial endpoint data and the joint physical atlas

Main result. Theorem 2.7.1 identifies the full radial endpoint jets of the jointly selected leading data and finite slow coefficients. Theorem 2.10.2 gives one physical packet atlas. Lemma 2.20.2 proves equality after this step for finite packet and mean stages. The construction selects the member and its packet graph jointly.

Theorem 2.7.1 (Actual full radial endpoint jets)**.** *We consider the selected joint leading construction and its prescribed moment compensation. All actual fields, potentials, five histories and pressure constants of the two sides have equal slice jets (Definition 2.3.16) on the full radial path. The same holds at each finite positive slow order. By Lemma 2.3.17, the physical objects are C^∞ across $t = 0$ at points with $z \neq 0$. Lemma 2.20.2 proves the packet and mean statements after the construction of the physical atlas.*

Proof. For the order-zero terms, the full radial endpoint jets, including the canonical pressure and the five histories, are the supplied data of Theorem 1(i)–(ii). Their differentiated tail bounds permit integration at fixed endpoint coordinate. We verify the assertion at each positive slow order on this same pair. *Positive slow orders.* For the positive slow hierarchy the actual exponent is $\lambda_n = 2nh$. The physical coefficients have the weights

$$w(E_n) = w(U_n) = (\tfrac{1}{2} + h) - \lambda_n, \quad w(F_n) = 1 + h - \lambda_n, \quad w(P_n) = 2(\tfrac{1}{2} + h) - \lambda_n, \quad w(V_n) = -\lambda_n. \tag{2.7.1}$$

The last weight holds because $\hat{t}^{\lambda_n} V_n/r$ is the physical quantity. The positive-order inner solutions have equal slice jets by Proposition 2.6.5. It uses the backward analyticity of Lemma 2.6.4, the scaled-radius class of Lemma 2.6.2, and the Gevrey bound of Theorem 1(iii). We do not compare the two Neumann series term by term. They are not conjugate term by term: the drift contains the side label ς, and in fixed-$\hat{\xi}$ variables $\partial_{\hat{\zeta}_f}$ contains a radial derivative. Termwise evaluation is used only inside one chart (Step 5 of that proof).

This is not a locality assertion for an arbitrary smooth PDE.

The five affine moments are (2.6.18), with all lower-order quadratic data kept. Their weights are

$$(\tfrac{1}{2} + h) - \lambda_n - 1, \quad (\tfrac{1}{2} + h) - \lambda_n - \tfrac{3}{2}, \quad 2(\tfrac{1}{2} + h) - \lambda_n, \quad 2(\tfrac{1}{2} + h) - \lambda_n - \tfrac{3}{2}, \quad 2(\tfrac{1}{2} + h) - \lambda_n - 1.$$

The correction bumps (2.6.19) are functions of $y = 2\log(\hat{\xi}/\hat{\xi}_p(\hat{\zeta}))$, and $y = 2\log(\widetilde{\xi}/\widetilde{\xi}_p)$ is one slice function. We insert the slice-continued backward coefficients into the forward affine moment map.

The moments that we get and the backward moments, which are zero, have equal slice jets. Subtraction from the exact forward solve and smooth invertibility of $B_U(\hat{\zeta}), B_E(\hat{\zeta})$ up to $\hat{\zeta} = \pm 1$ show that the coefficient differences have zero slice jets. Thus the corrected F_n, U_n and their reconstructed M_n, V_n, P_n have equal slice jets in X, and $E_n = \xi F_n$ has the ξ-jets of (2.6.22). The exponent rows $(1, 1 - 2\mu)$ and $(2, -2 - 2\mu, -2\mu)$ give nonzero exponential Vandermonde determinants.

The third row integrates through the full leading meridional hull after this region. After the early velocity correction, $\mathfrak{R}_1 = -\mathsf{Z}_0^{[2]} V_0$ may leave P_1, P_2. Only the full third row makes their last constant zero.

These integrands have a compact same hull that ends at $\frac{\hat{\xi}_P^2}{2}$ and regular axis bounds. For the exceptional leading angular subtraction use the integrable differentiated heat tails of Theorem 1(ii). Thus each differentiated moment is legitimate.

This completes the leading and finite slow comparison. It gives the input jets for the atlas and the finite packet and mean algorithm that follow. It assumes no regularity or matching conclusion for that next algorithm. □

2.7.1 Backward pressure saturation and finite transfer

Proposition 2.7.2 (Backward pressure saturation)**.** *Assume (B1)–(B5), the backward slot assertions (S3)–(S4) and (2.3.1), so that Lemma 2.6.4 applies. We also use the proved Lemmas 2.3.4(d) (the terminal multiplier of the selected backward wing), 2.3.5 and 2.3.3. All three are leading data of*

Theorem 1(iii)–(iv). Let $\frac{\hat\xi_-^2}{2}$ *be the radius chosen in Lemma 2.6.4. In the backward chart the following hold.*

(a) $\frac{\hat\xi_a^2}{2} < \frac{\hat\xi_-^2}{2} < \inf I_{\mathrm{pos}} < \sup I_{\mathrm{mean}} < \frac{\hat\xi_{\mathrm{ret}}^2}{2} < R_e < \frac{\hat\xi_b^2}{2}$. *Also* $U_0 = M_0 = V_0 = 0$ *for* $\hat\xi \ge \hat\xi_{\mathrm{ret}}$.

(b) For $n \ge 1$: $E_n = U_n = F_n = M_n = V_n = 0$ *for* $\frac{\hat\xi^2}{2} \ge \frac{\hat\xi_{p,b}^2}{2} e^{-9}$, *and* $P_n = 0$ *for* $\hat\xi \ge \hat\xi_{\mathrm{ret}}$. *For* $n \ge 3$, $P_n = 0$ *already for* $\frac{\hat\xi^2}{2} \ge \frac{\hat\xi_{p,b}^2}{2} e^{-9}$. *On* $\frac{\hat\xi^2}{2} \ge \frac{\hat\xi_{p,b}^2}{2} e^{-9}$,

$$\hat\xi^{-1}\partial_{\hat\xi} P_1 = -\frac{\mathfrak{R}_0}{\hat\xi^2}, \qquad \hat\xi^{-1}\partial_{\hat\xi} P_2 = \frac{\mathsf{Z}_0^{[2]} V_0}{\hat\xi^2},$$

with the $\varsigma = -1$ *operators.*

(c) For $n \ge 1$, $T_n = 0$ *on* $\hat\xi \le \hat\xi_-$. *For* $n \ge 2$, $\operatorname{supp}_{\hat\xi} T_n \subset [\hat\xi_-, \hat\xi_{\mathrm{ret}}]$, *and* $\operatorname{supp}_{\hat\xi} T_1 \subset [\hat\xi_-, \hat\xi_b]$. *On* $\hat\xi \ge \hat\xi_{\mathrm{ret}}$ *the order-one residual is* $r_{\theta,1} = -\mathfrak{r}\mathsf{Z}_b^{[2]} F_0$, $r_{z,1} = 0$.

(d) For every $n \ge 1$ *and every fixed profile derivative,*

$$|\partial^I T_n| \le C_{n,I}\, \zeta\, \delta^{-N_{n,I}} \le C'_{n,I}\, \mathsf{W}_b \mathcal{L}_b^{N'_{n,I}} \qquad (\tfrac{\hat\xi_a^2}{2} < \tfrac{\hat\xi^2}{2} < \tfrac{\hat\xi_b^2}{2},\ |\hat\zeta| \le 1),$$

with $N_{n,I} = 0$ *for* $n \ge 2$. *Thus (2.6.29) holds with* $\mathsf{W} = \mathsf{W}_b$.

(e) The late pressure saturation is contained in the compact all-angle rectangle

$$K_b = [\tfrac{\hat\xi_{p,b}^2}{2} e^{-9}, \tfrac{\hat\xi_{\mathrm{ret}}^2}{2}] \times [-1, 1], \qquad \min_{K_b} \mathsf{W}_b > 0.$$

This means the set where P_1 *or* P_2 *is nonzero beyond the positive-order velocity support, together with the supports there of the axial residuals* $\mathsf{Z}_{-2(\frac12+h)+2h} P_1 - \mathsf{Z}^{[2]}_{-(\frac12+h)} U_0$ *and* $\mathsf{Z}_{-2(\frac12+h)+4h} P_2$. *Every smooth function supported in* K_b *lies in the* W_b*-classes (2.13.4) and (2.14.4) with* $N_I = 0$, *once its powers of* ρ *and* S *are given.*

Proof. (a) Lemma 2.6.4 takes $\frac{\hat\xi_-^2}{2} < \frac{(\hat\xi_a^0)^2}{2}\Xi_{\mathrm{need}} < \inf I_{\mathrm{pos}}$. The windows lie in the exact wait (Lemma 2.3.3). The pulse starts at $y_p = 0$, and the pulse and its two returns end before $y_p = Y_{\mathrm{end}} - 0.7$ by the native pulse support in Lemma 2.3.3(S4). Then Lemma 2.3.11(c) gives the chain. After the last pulse return $U = M = J = 0$, and $V_0 = 0$ by the divergence formula. The edits after R_e change H only (Lemma 2.3.5, and the terminal multiplier of Lemma 2.3.4(d)).

(b) These are the coefficients of Section 2.6 in the backward chart (Lemma 2.6.4(c)). The inner cutoff ends at $\frac{\hat\xi_{\mathrm{cut}}^2}{2} < \inf I_{\mathrm{pos}}$, and the bumps lie in $I_{\mathrm{pos}} = \frac{\hat\xi_{p,b}^2}{2} e^{(-14,-9)}$. So $U_n = E_n = 0$ for $\frac{\hat\xi^2}{2} \ge \frac{\hat\xi_{p,b}^2}{2} e^{-9}$. The first moment gives $M_n = m_{n,1} = 0$ there, and (2.6.3) gives $V_n = 0$. Every term of $\mathfrak{R}_k$ in (2.6.4) contains a factor V_j or a derivative of one, and the side label changes only the sign of T. Beyond $\frac{\hat\xi_{p,b}^2}{2} e^{-9}$, the term $\sum F_i F_j$ of (2.6.5) vanishes for $n \ge 1$, and $\mathfrak{R}_k = -\mathsf{Z}^{[2]}_{\lambda_{k-1}} V_{k-1}$ for $k \ge 1$. This gives the two displayed derivatives and $\hat\xi^{-1}\partial_{\hat\xi} P_n = 0$ for $n \ge 3$. Beyond $\frac{\hat\xi_{\mathrm{ret}}^2}{2}$, also $\mathfrak{R}_0 = \mathfrak{R}_1 = 0$ by (a). Since $P_n(0) = 0$ and the third moment $m_{n,3} = 0$ of (2.6.18) holds, P_n vanishes wherever $\hat\xi^{-1}\partial_{\hat\xi} P_n$ vanishes on the whole exterior. Indeed $P_n(\frac{\hat\xi^2}{2}) = m_{n,3} - \int_{\hat\xi}^{\infty} \partial_\rho P_n \, \mathrm{d}\rho$ with $m_{n,3} = 0$.

(c) On $[0, \frac{\hat\xi_{\mathrm{keep}}^2}{2}] \supset [0, \frac{\hat\xi_-^2}{2}]$ every coefficient of order at most n equals its inner solution (Lemma 2.6.4(c)), and the inner system is the vanishing of the order-n residual rows. So

$r_{\theta,n} = r_{z,n} = 0$ there, and (2.6.23) gives $T_n = 0$ on $[0, \frac{\hat\xi_-^2}{2}]$. The zero total residual moments (2.6.26) hold for $\varsigma = -1$, because the time sign multiplies only a derivative of an identically zero moment. Their order-one angular row uses the compensated moment (2.6.25), whose backward inputs are (B4) (Lemma 2.3.5: $\int_0^\infty (H - \sqrt{2}c_\infty(\hat\xi/\sqrt{2})^{-2h})\,\hat\xi\,\mathrm{d}\hat\xi = 0$, and a z-independent heat swirl for $\frac{\hat\xi^2}{2} \ge B$). So T_n also has the exterior form, with a plus sign. For $n \ge 2$ and $\hat\xi \ge \hat\xi_{\mathrm{ret}}$, each term of (2.6.6) contains a positive-order coefficient that vanishes by (b), or one of U_0, V_0, which vanish by (a), or $\mathsf{Z}^{[2]}$ applied to a coefficient of order $n-1 \ge 1$. So $r_{\theta,n} = r_{z,n} = 0$ there, and the exterior form gives $T_n = 0$. For $n = 1$ the same count leaves $-\mathfrak{r}\mathsf{Z}_b^{[2]} F_0$ in the angular row, and the axial row vanishes, since $P_1 = 0$ and $U_0 = 0$ there. For $\hat\xi \ge \hat\xi_b$ the leading swirl is the z-independent heat field (Lemma 2.3.5). So $r_{\theta,1} = 0$ there and $T_1 = 0$.

(d) For $n \ge 2$, T_n is smooth with support in $[\frac{\hat\xi_-^2}{2}, \frac{\hat\xi_{\mathrm{ret}}^2}{2}] \times [-1,1]$, where ζ has a positive lower bound. Hence $|\partial^I T_n| \le C\zeta$. For $n = 1$ the same holds on $[\frac{\hat\xi_-^2}{2}, \frac{\hat\xi_b^2}{2}e^{-s_0}]$. Take the outer collar $d_b \le s_0$, with $\frac{\hat\xi_b^2}{2}e^{-s_0} > \frac{\hat\xi_{\mathrm{ret}}^2}{2}$ after shrinking s_0. By (O4), which for the backward member is Lemma 2.3.4(d) with $m = 1 - \rho\Psi(\frac{\hat\xi^2}{2}/B)$, $u_{\theta,0} = K(r,t)\,m(\frac{\hat\xi^2}{2})$, where K is the physical heat field. It is independent of z (Lemma 2.3.5), and m depends on $\frac{\hat\xi^2}{2}$ only. Since K does not depend on z, $\partial_{zz}(Km) = K\partial_{zz}m$. The ∂_z identity of (2.6.1), obtained on both sides by differentiating $q - z^2q^{2h} = |t|$ at fixed t, applied with the exponents 0 and $-(\frac12 - h)$, gives $\partial_z m = \hat t^{\,h-\frac12}\mathsf{Z}_0 m = \hat t^{\,h-\frac12} a_z \partial_y m$ and

$$\partial_{zz} m = \hat t^{\,2h-1}\mathsf{Z}_{-(\frac12-h)}(a_z\partial_y m) = \hat t^{\,2h-1}(a_z^2\partial_{yy}m + b_z\partial_y m),$$
$$a_z = -\frac{2\hat\zeta}{L}, \quad b_z = \frac{-2(\frac12 - h)\hat\zeta a_z + d\partial_{\hat\zeta}a_z}{L},$$

with $y = \log\frac{\hat\xi^2}{2}$, so that $\frac12\hat\xi\partial_{\hat\xi} = \partial_y$ and m depends on y only. So $\partial_{zz}(Km) = Kq^{2h-1}(a_z^2\partial_{yy}m + b_z\partial_y m)$, and a_z, b_z have bounded $\hat\zeta$-jets. By Lemma 2.3.4(d), $|(\hat\xi^{-1}\partial_{\hat\xi})^j(1-m)| \le C_j w_b(d_b)\delta^{-N_j}$, with $w_b(s) = e^{-a_b/\varphi_b(s)^2}$. Hence $|\partial^I r_{\theta,1}| \le C_I w_b(d_b)\delta^{-N_I}$. Write $T_{1,\theta} = \mathfrak{r}^{-2}\int_{\mathfrak{r}}^\infty \varrho^2 r_{\theta,1}\,\mathrm{d}\varrho$. The integral runs over $[\frac{\hat\xi^2}{2}, \frac{\hat\xi_b^2}{2}]$, since $m = 1$ beyond $\frac{\hat\xi_b^2}{2}$. In the variable d_b the Jacobian is bounded. Lemma 2.3.7(b), with $\varphi = \varphi_b$, gives $|T_{1,\theta}| \le C\delta^{3-N} w_b(\delta)$. An $\hat\zeta$-derivative falls on the integrand. A radial derivative falls on $\mathfrak{r}^{-2}$ or on the lower limit, and the lower-limit term is the integrand at $\frac{\hat\xi^2}{2}$. So $|\partial^I T_{1,\theta}| \le C_I w_b(d_b)\delta^{-N_I'}$. Also $T_{1,z} = 0$ there, by (c). Finally $\zeta = g_b w_b(d_b)$ with $g_b \ge c$ on the collar, and Lemma 2.3.11(a) converts δ^{-N} into $\mathcal{L}_b^{N/2}$.

(e) This follows from (a), (b) and Lemma 2.3.11(c): K_b is a compact subset of $(\frac{\hat\xi_a^2}{2}, \frac{\hat\xi_b^2}{2}) \times [-1,1]$, and ζ is continuous and positive there. □

Remark 2.7.3 (The backward slow stress). The proof of (2.6.35) uses two inputs: the explicit estimate for the first coefficient, and the fact that each coefficient of order at least two is supported where W has a positive lower bound. On $t < 0$ both are Proposition 2.7.2(c)–(d), with $\mathsf{W} = \mathsf{W}_b$. So on $t \le 0$ the sentence "Higher stresses use the positive saturation" in the proof of Proposition 2.10.1 holds with Proposition 2.7.2 in place of Proposition 2.3.2. The same increasing c_n then give (2.6.35) and (2.6.37) on $t < 0$ with W_b.

Remark 2.7.4 (Side-specific inputs of the finite stages on $t < 0$). The proofs in Sections 2.12–2.14 use the following inputs that are stated, or proved, only for the forward member. For each one we give the backward replacement.

(T1) *The aggregate weight*, through Lemma 2.3.10 and (2.13.3). These enter the classes (2.13.4), (2.13.5) and (2.14.4), the amplitude bounds (2.13.41), the aggregate cutoff (2.13.10), and the first-exit argument of Lemma 2.13.1. Backward replacement: Lemma 2.3.11(a). The first-exit argument needs only $|\partial \log \mathsf{W}| \le C S_\ell^{p_0}$ on $\{\mathsf{W}_* \ge e^{-CS_\ell}\}$, and there $\mathcal{L}_b \le C S_\ell$. On $t < 0$ the kept set is the compact sub-annulus $\{\mathsf{W}_* \ge e^{-CS_\ell}\} \subset \{\delta \ge c S_\ell^{-1/2}\}$, and the active set has no zero-stress gaps. (Indeed $\mathsf{W}_* \ge e^{-CS_\ell}$ and $|T_0| \le C \mathsf{W}_b \mathcal{L}_b^{N_0}$ give $\mathsf{W}_b \ge c\, e^{-C' S_\ell}$, so $\mathcal{L}_b \le C'' S_\ell$ and $\delta \ge c S_\ell^{-1/2}$ by Lemma 2.3.11(a).) A slow box of the joint mesh can meet both sides of $t = 0$. In the first-exit argument we then use $\log \mathsf{W}_*$, $\mathsf{W}_* = c_* |\widetilde{T}_0|$. On each closed side $|\partial \log \mathsf{W}_*| \le C \mathcal{L}^N \le C S_\ell^N$ on the kept buffer, by (2.13.3) on that side. Across $t = 0$ the order-zero slice jets of $\widetilde{T}_0$ agree (Theorem 1(ii), including the activation collar), so W_* is continuous there. Even a jump of the native weights, $\mathsf{W}_b / \mathsf{W}_f \in [c\mathcal{L}^{-N}, C\mathcal{L}^N]$ at the slice, changes $\log \mathsf{W}$ by $O(\log S_\ell)$, which is $o(S_\ell)$. So the contradiction in the proof of Lemma 2.13.1 persists.

(T2) *Saturation and the two tubes*, Proposition 2.3.2. It is used in the proof of Proposition 2.10.1, in (A5), in Lemma 2.20.1, at (2.18.2), and for the radial saturation in the proof of Proposition 2.15.2. Backward replacement: Proposition 2.7.2. The backward pressure hull is $\frac{\hat\xi_{\mathrm{ret}}^2}{2}$.

(T3) *Weighted primitives*, Lemma 2.3.13 and Lemma 2.6.9. They are used in Lemma 2.13.9, (2.14.13), Lemma 2.15.1 (for P_s^{add}) and the radial responses P_D, P_C. Backward replacement: Lemma 2.13.10.

(T4) *The profile on the protected patches.* The forward moment bumps in (2.6.19) use $U_0 = 0$ on I_{pos}. On I_{mean} the state map of Lemma 2.14.3 uses the radially constant axial velocity G_*. On both patches $H = K(\hat\zeta)\big(\frac{\hat\xi^2}{2}\big)^{-\nu(\hat\zeta)}$ with $\nu_c \le \nu \le \lambda$ in the moving pulse coordinate. Backward replacement: (S3)–(S4) of Lemma 2.3.3. These give $U = 0$, so $G_* = 0$, and $H = K_b F_\lambda(y_w) e^{\lambda y_w} (1+\beta^2)^{-1} (\hat\xi/\sqrt{2})^{-2\lambda}$ on both windows, with $\frac{\hat\xi_{p,b}^2}{2}$ a scalar. Thus $\mu \equiv \lambda > 0$, and the exponential Vandermonde blocks (2.14.50) have distinct exponents.

(T5) *Swirl lower bound on the protected region.* By (2.14.11), $k = (\mathsf{R}/\bar q) X^{-1} b(y_p)$ on the band annulus. Its fiberwise support is $\{y_p \in \operatorname{supp} b\}$, compactly contained in $-8 < y_p < -3$. The positive-order velocities and fluxes vanish throughout this slot by (2.6.21) on the forward side and Proposition 2.7.2(b) on the backward side. The differentiated potential cutoff in (2.6.31) vanishes there as well. Thus $V_s = V_{\mathrm{lead}}$ on both sides. For the backward power law of Lemma 2.3.3, $\bar q_b = q_b/Q \in (1/4, 4)$ on an enlarged band gives

$$V_s \;\ge\; v_{*,b}^{\mathrm{o}} := \tfrac{1}{8}\, c_{\mathrm{patch}} \big(\tfrac{\hat\xi_{p,b}^2}{2} e^{-3}\big)^{-1/2-\lambda} > 0 \qquad \text{on } \operatorname{supp} k,$$

independently of the band. The positive forward leading swirl also has a uniform lower bound on the closed subslot of Lemma 2.12.31.

(T5′) *Value margins of the inventory.* On both sides $V_s = V_{\mathrm{lead}} \ge 4 v_*$ on Ω_k with the constant of Lemma 2.12.31. The threshold for $V_M \ge 2 v_*$ controls the initialization root δ_C and the subsequent positive-order mean increments at the current stage. Lemma 2.12.30 applies verbatim: it uses only $\sup_{0<w\le e^{-2}} w(1+\log(1/w))^N < \infty$ and a positive weight plateau on a slow neighbourhood Ω_k of $\operatorname{supp} k$. On $t < 0$ this plateau is $\min_{\overline{I_{\mathrm{mean}}}} \mathsf{W}_b > 0$, by Lemma 2.3.11(c). Hence (I1) holds on $t < 0$, with the single constant v_* of Lemma 2.12.31.

That constant is one quarter of the minimum of the leading swirl over $\overline{\Omega_k}$ on both sides, and the lemma proves the bound on both sides. The single threshold is the smaller of the two sides' thresholds, which in ℓ means the larger. The five-row (velocity-only) matrix uses $\mu \equiv \lambda > 0$ by (T4).

(T6) *Cone and frame.* The inputs are (2.13.2) and the lower bounds for $F_{\mathrm{lead}}, \mathfrak{a}, \mathfrak{v} - 2$, used in (2.13.14) and in Proposition 2.13.5. The strict leading field of Theorem 1(iv), fixed at the start of Section 2.13, is the forward source of these inputs: strict shear where the stress is nonzero, uniform margins, and agreement on the protected domain, the patches and the heat exterior. Backward replacement: (B2) for the strict cone and the margins, (B4) for the heat exterior, and (S4) of Lemma 2.3.3 for the patches. In more detail, the content of Theorem 1(iv) for the final backward member is the following.

- The stress is nonzero on the open annulus and the shear is strict there by (B2)–(B3).
- The normalized margins of (B2) hold on the closed annulus. The stress direction extends smoothly to the inner edge and to the outer edge B, where Lemma 2.3.4(c) gives its value.
- The protected interval through $\hat{\xi}_-^{\mathrm{loop}}$ carries the leading backward core, with the analytic bounds used in Lemma 2.6.4(a).
- Agreement on the windows: (S4).
- The backward heat exterior and the flux and compensated angular moment identities follow from Lemma 2.3.5.

Normalizations in the backward chart.

(i) Since $E = \hat{\xi} F$, the shears in (2.3.20) are $a = 1 - \hat{\xi} E_{\hat{\xi}}/E = -\hat{\xi} F_{\hat{\xi}}/F = \mathfrak{a}$ and $b_s = U_{\hat{\xi}}/F = \mathfrak{b}$. Thus $t_s = -b_s/a = \mathfrak{t}$ and $v_s = a(1 + t_s^2) = \mathfrak{v}$.

(ii) Write $\mathcal{R}_\theta, \mathcal{R}_z$ for the leading tangential residuals with axial viscosity removed. Integrating the two radial divergences in (2.6.23) gives

$$K_\theta = -r^{-2} \int_0^r s^2 \mathcal{R}_\theta \, \mathrm{d}s, \qquad K_z = -r^{-1} \int_0^r s \mathcal{R}_z \, \mathrm{d}s.$$

Regularity at the axis fixes both constants. Hence the leading physical stress $q_b^{-1-h} T_{0,b}$ is the stress of the backward field in Theorem 1(i), whose shear form is (2.3.21) with $\varsigma = -1$.

(iii) For $T_{0,b} \neq 0$ multiply the two normalized inequalities of (B2) by $|T_{0,b}|$ and $|T_{0,b}|^2$, respectively. This gives both lines of (2.13.2) for any $0 < \delta_c \leq \kappa$. At the two stress edges the same inequalities follow by continuity.

The joint δ_c is the minimum of the two sides' constants. The lower bounds for $F, \mathfrak{a}, \mathfrak{v} - 2$ in Section 2.13 are those of (B2), by (i). No sign of $\mathfrak{b}$, and hence of U, is used. In $g_0 = F_0(-\mathfrak{a}, \mathfrak{b})$ only $\mathfrak{a} > 0$ enters $N_\theta < 0$, and $\lambda_0^2 = 2\mathfrak{a} F_0^2 (1 - 2/\mathfrak{v})$ uses only $\mathfrak{a} > 0$ and $\mathfrak{v} > 2$.

(T7) *The slow-time sign.* It appears in "the slow-time sign is positive" after (2.13.12), in (2.13.17), and in t_*. On $t < 0$ the formulas are the same in the physical T. Only terms $\rho_Q \partial_{\mathsf{T}}$ carry the sign. They enter with a positive power of ρ_Q, in absolute seminorms, and no step inverts ∂_{T} (proof of Lemma 2.20.3). The pulse variable v increases with physical time on both sides, because $Y_{\mathrm{phys}} = v_r r^{d_r} + v_t t$. So Lemma 2.13.2 applies unchanged.

(T8) *The slow background*, (2.6.34) and (2.6.37). Backward replacement: the Borel argument of Proposition 2.6.15, which does not depend on the side, with Remark 2.7.3 for the stress.

(T9) *Clock, schedule and auxiliary orders*: Lemmas 2.12.1, 2.12.2 and Proposition 2.12.3. These are statements about the one joint schedule, the torus and the operation graph. They use the slow source only through its supremum and support. In Lemma 2.12.1, "$\hat{t} \gg t$" reads "$\hat{t} \gg |t|$" on $t < 0$, since there $\hat{t}_b - z^2 \hat{t}_b^{2h} = |t|$. Hypothesis 2.3.21 is a reading of the algorithm. Its verification in Proposition 2.16.1 uses three inputs.

- The side-specific inputs to (S4)–(S10) and the order of their use are listed in the proof of Theorem 2.16.2.
- For (I1), (T5′) gives the leading $4v_*$ floor. The finite-stage margin follows once the preceding increments are small at ordinary order zero, as proved for the current inputs on p. 494.
- Input (I2). Its tail lemma is Lemma 2.13.10 on $t < 0$.

The negative-time induction is given on p. 494.

(T10) *Initial-slice regularity.* After (2.6.34) and after (2.13.29), one-sided smoothness at a point of the initial slice with $z \neq 0$ is cited from Proposition 2.8.6(a). This is a regularity statement, not one of the finite estimates. On $t < 0$ it is (B7)(iv), which Proposition 2.8.10 derives from (B7)(i) and (B7)(iii).

(T11) *The compensated angular moment* (2.6.25), which gives the order-one angular row of (2.6.26). It uses canonical matching and the z-independence of the leading swirl beyond a finite physical radius. On $t < 0$ both are (B4): Lemma 2.3.5 gives $\int_0^\infty (H - \sqrt{2} c_\infty (\hat{\xi}/\sqrt{2})^{-2h})\, \hat{\xi}\, \mathrm{d}\hat{\xi} = 0$, and $E = c_\infty (\hat{\xi}/\sqrt{2})^{-1-2h} \mathcal{H}_-(4d/\hat{\xi}^2)$ for $\frac{\hat{\xi}^2}{2} \geq B$, whose physical swirl $c_\infty s^{-\frac{1}{2}-h} \mathcal{H}(2\tau/s)$ does not depend on z.

The preceding list supplies the side-specific inputs for the finite transfer in Theorem 2.7.5. The remaining operations concern the joint atlas and torus, real-coefficient inner inverses, the physical pulse clock, or finite algebraic solves on the stated value domains. The mean, return and limit stages also require an enclosure beyond $\frac{\hat{\xi}^2_{\mathrm{ret}}}{2}$ and the backward heat onset; Lemma 2.8.9 supplies it with $\frac{\hat{\xi}^2_{\mathrm{all}}}{2} > B$, and Proposition 2.8.10 gives the one-sided regularity. Slow endpoint comparison remains the separate argument of Proposition 2.6.5.

Theorem 2.7.5 (Item (B7)(i) holds)**.** *Use the selected backward data (B1)–(B6) of Theorem 1(i)–(iv), let (2.3.1) hold, and fix the joint data of the parameter ordering of Theorem 1(iii). Then on $t < 0$, at every finite stage n, the packet, mean and return stages of Sections 2.12–2.14 have the following properties.*

(a) Every coefficient lies in its class (2.13.4), (2.13.5) or (2.14.4) with $\mathsf{W} = \mathsf{W}_b$, with the order of the finite-order ledger (the same order as on $t > 0$), and satisfies the finite seminorm bounds that Lemma 2.20.3 lists, including the pure-auxiliary Gevrey bounds (2.12.3).

(b) The value margins hold: $V_s \geq 2v_*$ and $V_M \geq 2v_*$ on $\Omega_k \times \mathbb{T}^2$, with the constant v_* of Lemma 2.12.31.

(c) The $\hat{t}_b$-thresholds of stage n are finitely many conditions $C_i \rho_Q^{a_i} S_\ell^{B_i} \leq c_i$ with $a_i > 0$, each holding for $\ell \geq \ell_i$.

These assertions furnish part (i) of condition (B7).

Proof. Transfer and inputs. Each finite proof step is either side-neutral or uses one of (T1)–(T11) of Remark 2.7.4. The side-neutral operations are the joint atlas and torus calculus, real-coefficient inner inverses, the physical pulse clock, algebraic solves on admitted value domains, and the finite identities of the algorithm. In particular no mean or return step inverts an evolution in physical time.

The table below records the side-specific uses and their backward replacements. The only forward-only objects are the aggregate weight and its primitive bounds, saturation/late pressure, the moving power patches and correction moments, protected swirl margins, slow background and one-sided initial-slice regularity. These are precisely the inputs listed in the table. Joint cutoff and diagonal formulas are definitions; they introduce no further side estimate. The auxiliary-order row uses Theorem 2.16.2, whose backward suppliers are the weight, primitive and protected-margin bounds rather than (B7).

The table. For each result, the column "(S)-steps" lists the inputs among (T1)–(T11) that its proof uses; the last column gives the backward replacement and the check of its hypotheses.

Table 2.2: Transfer of the finite stages to $t < 0$.

result (forward proof)	(S)-steps	backward replacement; its hypotheses
Lemmas 2.12.1, 2.12.2	(T9)	$\hat{t}_b - z^2\hat{t}_b^{2h} = \lvert t\rvert$, so "$\hat{t} \gg t$" reads "$\hat{t} \gg \lvert t\rvert$"; the schedule is joint
Section 2.13.1: (2.13.1), (2.13.2), (2.13.3), classes	(T1), (T6)	Lemma 2.3.11(a) and Lemma 2.20.6(b); the cone input and the lower bounds of $F, \mathfrak{a}, \mathfrak{v} - 2$ from (B2) by (T6)(i)–(iii); the radial hull: $\hat{\xi}_a \le \hat{\xi} \le \hat{\xi}_b$ with $\bar{q}_b \in (\frac{1}{4}, 4)$
Section 2.13.2, (2.13.10), Lemma 2.13.1	(T1)	the first-exit argument of (T1): $\mathcal{L}_b \le CS_\ell$ on the kept set (Lemma 2.3.11(a)); across $t = 0$, continuity of W_* by Theorem 2.7.1 with the activation jets of Theorem 1(ii)
Section 2.13.3: (2.13.13)–(2.13.22)	(T6), (T7)	(B2) for $F_0 > 0$, $\mathfrak{a} > 0$, $\mathfrak{v} > 2$ (so $\lambda_0^2 > 0$, $c_0 \neq 0$); the forward defect (2.13.17) is written in the physical clock (T7)
Lemma 2.13.2	(T7)	the pulse variable increases with physical time on both sides ($Y_{\mathrm{phys}} = v_r r^{d_r} + v_t t$); no other input
Proposition 2.13.3, (2.13.28), (2.13.29)	(T7), (T10)	(T7) as above; (T10) is a regularity remark after (2.13.29), not used for any estimate of (a)–(c)
Lemma 2.13.4, (2.13.37)	(T7)	the terms $\pm\rho_Q \partial_{\mathsf{T}}$ carry a positive power of ρ_Q in absolute seminorms (proof of Lemma 2.20.3)
Proposition 2.13.5	(T6), (T1)	the cone input from (B2) ((T6)(iii), joint δ_c); $\lvert T_0\rvert \ge c\mathsf{W}_b$ and the log-jets from Lemma 2.3.11(a)
Proposition 2.13.6	(T1), (T8)	Lemma 2.3.11(a); (2.6.37) on $t < 0$ from Lemma 2.20.7(c) and Remark 2.7.3 (hypotheses of Proposition 2.7.2)
Proposition 2.13.7	(T1)	classes only: Lemma 2.3.11(a)
Lemma 2.13.9	(T3), (T1)	Lemma 2.13.10(a), (b): inward and outward comparisons from Lemma 2.3.11(b) with $\frac{\hat{\xi}_1^2}{2} = \frac{\hat{\xi}_{p,b}^2}{2} e^{-8}$, $\frac{\hat{\xi}_2^2}{2} = \frac{\hat{\xi}_{p,b}^2}{2} e^{-3}$
Section 2.14, (2.14.1)	(T8)	the slow reference on $t < 0$: Lemma 2.20.7(b), (c)
Shifted primitives, (2.14.11)–(2.14.12); Lemma 2.14.1	(T3), (T4)	Lemma 2.13.10(a)–(c): $\frac{\hat{\xi}_{p,b}^2}{2}$ constant, c_β, c_θ constants, the $\Big(\frac{\big(\hat{\xi}_p(\hat{\zeta})\big)^2}{2}\Big)'$ terms vanish
Lemma 2.14.2	(T3), (T4), (T5)	Lemma 2.13.10; (T4); the margin $V_M \ge 2v_*$ by (T5′)
State integrals and five rows; Lemma 2.14.3	(T4), (T8)	(T4): $U = 0$, $G_* = 0$, $H = K_b F_\lambda(y_w) e^{\lambda y_w} (1+\beta^2)^{-1} (\hat{\xi}/\sqrt{2})^{-2\lambda}$ on both windows ((S3)–(S4) of Lemma 2.3.3), so $\mu \equiv \lambda > 0$ and the Vandermonde blocks (2.14.50) are nonsingular; Lemma 2.20.7
Canonical tensor, (2.15.1)–(2.15.5)	(T1)	ϑ_q and the classes as in the atlas row
Initialization (2.15.17)–(2.15.20); Lemma 2.15.1	(T2), (T3), (T5), (T8)	late P_1, P_2 in the compact rectangle K_b with $\min_{K_b} \mathsf{W}_b > 0$ (Proposition 2.7.2(b), (e)), used in place of Proposition 2.3.2 in Lemma 2.20.1; P_s^{add} by Lemma 2.13.10; $V_s = \bar{q}_b^{-\frac{1}{2}-h} E_0 \ge 4v_*$ on Ω_k with no threshold (T5′); Lemma 2.20.7(c)

result	(S)-steps	backward replacement
Paired step, (2.15.21)–(2.15.51)	(T1), (T5)	Lemma 2.3.11(a); the margins of Lemma 2.12.30 with the plateau $\min_{\overline{I_{\mathrm{mean}}}} \mathsf{W}_b > 0$ (Lemma 2.3.11(c))
Proposition 2.15.2	(T2), (T4)	the radial saturation in K_b (Proposition 2.7.2(e)); (T4)
Proposition 2.12.3, Section 2.12.1	(T9), (T1), (T3), (T5′)	Apply last, after the ordinary value margins, derivative bounds, packet inventory and mean inventory on both sides. Theorem 2.16.2 then gives the factorial bounds.

The slow coefficients and the slow Borel stage, which precede these rows, are Lemma 2.6.4 and Lemma 2.20.7; the compensated moment (T11) enters only there, through Proposition 2.7.2(c) and (B4).

Ordinary induction on the negative-time chart. Work on a fixed band Q, with $\rho = Q^h$. In this paragraph order u means the full ordinary class $\mathcal{M}^u$ or $\mathcal{W}^u$, with W_b or its square root as in (2.14.4). Integrated scalars have its unweighted seminorms. The constants and finite input derivative orders may depend on the stage. The slow input from Lemma 2.20.7 and Proposition 2.7.2 is available before the packet iteration.

Operators and value domains. Use physical $\mathsf{T} = t/Q$. With $T_b = -\mathsf{T}$ the time operator is $-\rho\partial_{T_b} + c\, v_t \cdot \partial_Y$. Applied to the pulse variable it still equals one. In particular the zero-data normal ODE and its damping in Proposition 2.13.7 use the same forward pulse parameter. The operator T_0^{-1} in Lemma 2.14.2 acts on Y. Its estimate (2.14.31) spends finitely many ordinary derivatives and a polynomial in S. On the compact band $\partial_{\mathsf{T}}\bar{q} = -(1-2h\eta^2)^{-1}$, and all fixed jets of $\bar{q}, \eta$ are bounded. The signed slow derivative of every mean coefficient thus retains the factor ρ. Lemma 2.13.10 controls the subtracted shifted primitives, grants the extra $\varkappa$ for zero Haar mean, and gives coefficient-flat zero-Haar full moments. Its moving-subtraction terms are retained. A flat full moment multiplied by a protected bump belongs to every required weighted order because the bump lies on a fixed positive plateau. The unprotected endpoint and deletion errors keep their explicit exponential or weight factor in the ordinary residual.

Here is the matrix estimate used at each call of the state map. In the normalized frame (2.14.47) the last three rows are linear in the current Haar velocities V_H, G_H or independent of them. For the leading matrix L_0, the constant axial value and the exponent $\mu = \lambda > 0$ on the backward patch give the two power blocks (2.14.50). Their ordered bump determinants have a fixed positive absolute minimum by the integral determinant formula in Lemma 2.14.3. Bounded positive band factors preserve this minimum. On the compact bump hull,

$$\|L - L_0\| \le C(\|V_H - V_{\mathrm{lead}}\|_\infty + \|G_H - G_{\mathrm{lead}}\|_\infty).$$

The same inequality for any fixed jet holds with a finite sum of lower jets on the right, by differentiation under the bump integral. The slow velocity here equals its leading value by Proposition 2.7.2(b). Immediately before a solve the difference on the right is a finite sum of the *already constructed* increments below, each of positive order. Thus one value threshold gives $\|L_0^{-1}(L - L_0)\| \le 1/2$. Inverse differentiation uses this same threshold. For a swirl solve the leading value on $\operatorname{supp} k$ is at least $4v_*$. At each occurrence keep the preceding velocity increments smaller in sup norm than v_* in total, and the incoming $|\mathsf{R}kM| \le v_*^2/2$. Use the rationalized expression $\mathsf{R}kM/(\sqrt{V^2 + \mathsf{R}kM} + V)$ on an open plateau containing $\operatorname{supp} k$, and its smooth zero extension beyond that plateau. These inequalities will use only inputs of the current operation.

R19–R22 and the uncut initialization R22′. The cross tensor in (2.15.3) cancels its negative in the ordinary equation and has both zero tangential divergence moments. The leading signed target and the slow correction have normalized orders one and three by Lemma 2.20.7(c) and Proposition 2.7.2.

Apply the positive and signed packet maps with the original leading amplitudes and the backward cone and weight from (T1), (T6). The exact cosine–sine quadrature in Proposition 2.13.6 gives D_0 of order one with Haar radial crosses of order $3-\varkappa$. The other entries use the ordinary order one. In (2.14.14), division by R is bounded on this annulus. Hence f_D, M_D have order one, and $g_s = \rho\,\partial_{\mathsf{Z}}\mathsf{S}_z, M_s = \mathcal{J} g_s$ have order two. Integration is on the full backward pressure hull, including P_1, P_2. Lemma 2.13.10 supplies both endpoint weights of P_s^{add}. These estimates give the two root margins above before forming δ_C. Rationalization in (2.15.15) makes ϵ_s order two. The pressure and both additional swirl state integrals consequently have order two. The carrier derivative of a principal packet costs $\rho^{-1/2}$. Its product with ϵ_s and the order-1/2 packet has order two.

Write $s_0 = 1-\varkappa$ for the mean fluctuation order in this paragraph. The Haar projection of (2.15.12) kills the fast radial derivative. Its force has order two. The complementary force has order s_0. Lemma 2.14.2 at $\nu = s_0$ gives tangential order s_0, radial order two, Haar force of order at least two and complementary force of order $2-3\varkappa$. It preserves zero full axial flux. Integrating the actual stresses and velocities gives three states of order one. Every quadratic fluctuation product has order $2s_0 > 1$. This supplies the perturbation of the *first* matrix. Lemma 2.14.3 gives states of order two and moments of order three. Apply the auxiliary map to the complement at $\nu = 2-3\varkappa$. Its new state contribution has order $3-4\varkappa$. The second matrix now acts on states of order at least $2-3\varkappa$. Its output states and moments have orders $4-6\varkappa$ and $5-6\varkappa$. The remaining Haar force has order two. Subtract its two actual moments and apply the backward primitive to obtain a compact cross of order two. Its $\rho\partial_{\mathsf{Z}}$ radial return has order three, controlling both the pressure and the protected swirl change. This gives states of order three, Haar force of order four, complementary force of order $3-5\varkappa$, and zero radial row, as in (2.15.20). The first and second harmonic source orders are $a_0 = 1-3\varkappa$ and $1-\varkappa$ by the ordinary packet bounds. These dominate every entry of (2.15.22) at $a = a_0$.

R23–R26. Assume (2.15.22) at the start of one uncut stage $a \ge a_0$. Use $p = a + 1/2$, $c_* = a+1-3\varkappa$, $s_* = p-\varkappa$, $b_* = p+1-3\varkappa$. The signed update uses only the original strictly positive leading amplitude. In (2.15.29) the two cutoff factors sum to one and cancel the order-p Haar cross. The remaining crossed terms have orders $2a$, $p+2-\varkappa$, $a+a_0$, $2a$, all at least c_*. The tensor thus has order p and its two Haar radial crosses have order c_*. This proves the input order of the next radial root. Its change of the three states has order p from (2.15.36). By (2.15.34), the Haar and complementary forces have orders c_* and s_*, respectively. The latter uses the one fast radial derivative loss $\varkappa$.

At $\nu = s_*$ the auxiliary map adds tangential order s_*, radial order $p+1$, and pressure order p. The new complementary force has order b_*. The Haar state contributions of the fluctuations have order at least $s_* + s_0 > p$. This supplies the current five state targets in (2.14.48) and the positive-order velocity perturbation in the matrix estimate above. The Haar state map now gives order $d_H = \min(2p, p+2)$ to the states and $d_H + 1$ to their two force moments. Its added Haar and complementary forces have orders $p+1$ and at least $p+2-2\varkappa$ by (2.14.46). Therefore the remaining pointwise Haar force is of order c_*. Subtract its actual moments using the normalized protected bumps and apply Lemma 2.13.10 to (2.15.40). Both full moments of the subtracted terms are zero, so these two ordinary prefixes are compact and have order c_*. In particular, the incoming quantities satisfy

$$A_z^+ \in \mathcal{M}^{c_*}, \qquad g_{\mathrm{rad}} = \rho\partial_{\mathsf{Z}} A_z^+ \in \mathcal{M}^{c_*+1}, \qquad \left|\partial^I N_{\mathrm{rad}}\right| \le C_{n,I}\rho^{c_*+1} S^{B_{n,I}}, \quad N_{\mathrm{rad}} = \int g_{\mathrm{rad}}\,\mathrm{d}\mathsf{R}.$$

The last inequality follows by integration on a uniformly bounded band annulus. The native weight times each fixed log power is bounded. This supplies the value margin before (2.15.42). Its root difference from the Haar-base root gains s_0 since the derivative of $V \mapsto \sqrt{V^2 + x} - V$ is $O(|x|)$ on

the protected branch. This proves the Haar and perpendicular orders $c_* + 1$, $c_* + 1 + s_0$ for that root. Squaring cancels the radial row. In (2.15.43) the output force orders are $c_* + 2$ and b_*. The state order is $c_* + 1$ since $2p - (c_* + 1) = a - a_0 \geq 0$ and $p + 2 > c_* + 1$. The full flux remains zero.

Against a wave of principal order at least $1/2$, the differentiated carrier in (2.15.49) costs $\rho^{-1/2}$ and is multiplied by the new tangential mean of order s_*. Their product has order at least $s_* + 1/2 - 1/2 = s_*$. The radial mean has order $p + 1$, and the evaluated radial derivative of an amplitude costs at most $\varkappa$, as in (2.15.50). The wave source after the harmonic solve and signed update therefore has order $a + 1/2 - 3\varkappa$. With $a' = a + 1/5$ the wave, new cross stress and weaker tangential force each beat their required orders $a', a' + 1/2, a' + 1$ by $3/10 - 3\varkappa > 0$. The three state orders beat $a' + 1/2$ by $13/10 - 3\varkappa$. The Haar force is stronger and the radial equation holds identically. Both mean increments and new wave corrections retain the starting classes. This proves the induction in ordinary seminorms.

For each fixed stage, the root and matrix estimates use bounds from earlier steps of the construction. Taking the maximum of their band thresholds is legitimate since $\rho^{\alpha} S^{B} \to 0$ for every fixed $\alpha > 0, B$. Higher derivative estimates use those value margins, the weighted primitive bounds, and product and inverse differentiation. With these ordinary stage bounds established, apply Theorem 2.16.2 to its inventory on both sides and then Proposition 2.12.3. The common diagonal and the initial-slice argument follow in the order stated after Table 2.4. □

Theorem 2.7.6 (The backward member at all finite stages)**.** *The backward leading member satisfies the leading conditions (B1)–(B6) of Theorem 1 and the completion condition (B7).*

Proof. Conditions (B1)–(B6) are the backward leading data of Theorem 1(i)–(iv). For condition (B7) we verify the four finite-stage requirements as follows. (ii): Proposition 2.7.2 and Lemma 2.13.10, under (B1)–(B5), (S3)–(S4) and (2.3.1). (iii): Lemma 2.8.9, for the choice (2.18.2) of $\frac{\hat{\xi}_{\mathrm{all}}^2}{2}$ (step 7). (i): Theorem 2.7.5, which uses (B1)–(B6) and (ii). (iv): Proposition 2.8.10, from (i) and (iii). □

2.8 One-sided regularity at the initial slice away from the tip

Throughout this subsection, the leading source satisfies Definition 2.5.1. For the field supplied by Theorem 1, the six conditions of this definition are verified in Lemma 2.18.3. We write $\mathbb{H} = \mathbb{R}^3 \times [0, \infty)$. For an open $U \subset \mathbb{R}^4$ put $U_+ = U \cap \mathbb{H}$ and $U_+^{\circ} = U \cap \{t > 0\}$.

Definition 2.8.1 (One-sided smooth functions)**.** Let $\mathcal{P} \subset \mathbb{R}^k$ be open and distinguish one coordinate p_k of $\mathcal{P}$. We put $\mathcal{P}_+ = \mathcal{P} \cap \{p_k \geq 0\}$. Let K be a finite product of compact intervals and tori. A function $f : \mathcal{P}_+ \times K \to \mathbb{C}^N$ belongs to $C^{\infty}(\mathcal{P}_+ \times K)$ if it is C^{∞} on $\{p_k > 0\} \times K^{\circ}$ and each partial derivative extends continuously to $\mathcal{P}_+ \times K$. For $\mathcal{P} = U \subset \mathbb{R}^4$ the distinguished coordinate is t.

Lemma 2.8.2 (Smooth extension in one normal coordinate)**.** *If $f \in C^{\infty}(\mathcal{P}_+ \times K)$ and $\psi \in C_c^{\infty}(\mathcal{P})$, then $g = \psi f$ extends smoothly to $\mathbb{R}^k \times K$. After zero extension outside $\mathcal{P}$ in the positive half-space, the extension is linear in g, bounded in each C^m norm, and preserves any fixed support restriction in the tangential variables.*

Proof. Write $p = (p', s)$. For $0 \leq i \leq N$ set

$$a_{i,N} = \prod_{\substack{0 \leq j \leq N \\ j \neq i}} \frac{1 + 2^j}{2^j - 2^i}.$$

Interpolating the monomial x^n at the nodes -2^j and evaluating at $x=1$ gives $\sum_{i=0}^{N} a_{i,N}(-2^i)^n = 1$ for $0 \le n \le N$. For $j < i$ extract 2^{j-i} from the absolute value of each factor. The remaining product is at most $\prod_{j\ge 0}(1+2^{-j})\prod_{j\ge 1}(1-2^{-j})^{-2} < \infty$. Hence $|a_{i,N}| \le C2^{-i(i+1)/2}$. For fixed i the factors with $j > i$ are $1 + O_i(2^{-j})$, so $a_i = \lim_{N\to\infty} a_{i,N}$ exists. Dominated convergence gives $\sum_{i\ge 0} a_i(-2^i)^n = 1$ for every n.

Choose a smooth compactly supported cutoff ϕ equal to one near zero. Keep $Eg = g$ on $s \ge 0$ and, for $s < 0$, put

$$Eg(p', s, \kappa) = \sum_{i\ge 0} a_i (\phi g)(p', -2^i s, \kappa),$$

where ϕ acts in the normal coordinate. A derivative of order at most m costs at most 2^{im} in each summand, and $\sum_i |a_i| 2^{im} < \infty$. The differentiated series therefore converge uniformly up to the boundary, with C^m norm at most $C_m \|g\|_{C^m}$. The moment identities match every normal derivative there, also after tangential differentiation. The fundamental theorem of calculus in s, applied successively to these derivatives, proves smoothness across zero. The formula leaves (p', κ) fixed, which proves the support assertion. □

Lemma 2.8.3 (The chart at the initial slice)**.** *Let $z_0 \ne 0$ and $\hat t_0 = |z_0|^{1/(\frac12 - h)}$. There is a neighbourhood N of $(z_0, 0)$ in $\mathbb{R}^2$ where $\hat t, \hat\zeta, d$ extend real-analytically, with $\hat t \in [\hat t_0/2, 2\hat t_0]$. The map $(z, t) \mapsto (\hat t, \hat\zeta)$ is a real-analytic diffeomorphism from N onto a neighbourhood of $(\hat t_0, \operatorname{sgn} z_0)$. It maps $N \cap \{t \ge 0\}$ onto $\{\operatorname{sgn}(z_0)\hat\zeta \le 1\}$.*

Also, $d = t/\hat t$. Thus $d \ge 0$ if and only if $t \ge 0$. On a band with $Q/\hat t \in [1/4, 4]$, the coordinates $(\mathsf{R}, \mathsf{Z}, \mathsf{T}) = (r/\sqrt{Q}, z/Q^{\frac12 - h}, t/Q)$ are linear in (r, z, t). The map $(\bar q, \hat\zeta) \mapsto (\mathsf{Z}, \mathsf{T})$ has signed Jacobian $-L\bar q^{\frac12 - h}$ in this forward-chart ordering. Its absolute Jacobian $L\bar q^{\frac12 - h}$ is bounded away from zero.

Proof. We put $\Phi(\hat t, z, t) = \hat t - z^2 \hat t^{2h} - t$. At $(\hat t_0, z_0, 0)$, $\partial_q \Phi = 1 - 2hz_0^2 \hat t_0^{2h-1} = 1 - 2h > 0$, because $z_0^2 = \hat t_0^{1-2h}$ and $2(\frac12 - h) + 2h - 1 = 0$. The analytic implicit function theorem gives an analytic $\hat t(z, t)$ near $(z_0, 0)$, for t of the two signs, which coincides with (2.3.11) for $t > 0$. Then $\hat\zeta = z\hat t^{h - \frac12}$ and $d = 1 - \hat\zeta^2 = t/\hat t$ are analytic.

The determinant of $(\hat t, \hat\zeta) \mapsto (z, t) = (\hat\zeta \hat t^{\frac12 - h}, dq)$ is $-Lq^{\frac12 - h} \ne 0$ ((2.3.12) and the line after it), so the inverse function theorem applies. Because $\hat t > 0$, $t \ge 0 \iff d \ge 0 \iff |\hat\zeta| \le 1$. The band statements are those of Section 2.13.1 (Section 2.13). □

In slice variables the lemma is explicit. Near $(z_0, 0)$ the forward chart is $\hat\zeta = \hat\zeta_f(\widetilde\eta)$ and $\hat t = \widetilde Q |\hat\zeta_f(\widetilde\eta)|^{-1/(\frac12 - h)}$, where $\hat\zeta_f$ is the real-analytic inverse of the forward conversion (Lemma 2.3.15). The condition $t \ge 0$ is $\widetilde\eta \ge 0$.

Lemma 2.8.4 (Endpoint regularity of the leading data)**.** *Let the leading source be the selected member of Theorem 1, with its slow and packet data, and $\hat\xi_1 < \infty$. We consider H, U, V, the five histories (2.3.17), P, and the stresses $\mathcal{T}_0 = (\widehat{\mathcal{T}}_{P,\theta}, \widehat{\mathcal{T}}_{P,z})$. We include the aggregate weight W from (2.3.7) and ϑ_q at each fixed $q > 0$. Also include the slow coefficients $F_n, U_n, V_n, M_n, P_n, T_n$ $(n \ge 1)$.*

All these functions belong to $C^\infty([0, \frac{\hat\xi_1^2}{2}] \times [-1, 1])$. Here, $\hat\zeta$ is the distinguished coordinate at each endpoint $\hat\zeta = \pm 1$. More precisely:

(i) on the selected protected domain the core, activation, termination and shared-cutoff data and the inner-solve coefficients are C^∞ on the finite union of rectangles and its curved protected subdomain constructed in paragraph 2.3.2;

(ii) the middle parameter maps, the pulse and returns, and the stop, shot, A11, loop and restoration maps are one-sided smooth on $[-1, 1]$, respectively on $[0, \frac{\hat\xi_1^2}{2}] \times [-1, 1]$;

(iii) the heat lift $H_L = d^{-h} g_*(\frac{\hat\xi^2}{2}/d)$ *and* $\mathfrak{M}_{2L} = d^{1-h} i(\frac{\hat\xi^2}{2}/d)$ *are* C^∞ *in* $(\frac{\hat\xi^2}{2}, d)$ *on* $[(\frac{\hat\xi_1^2}{2})', \frac{\hat\xi_1^2}{2}] \times [0, d_1]$ *for each* $\hat\xi_1 > 0$*, with the remainder bounds (2.3.38);*

(iv) H, U, V*, the five histories,* P *and* $\mathcal{T}_0$ *belong to* $C^\infty([0, \frac{\hat\xi_1^2}{2}] \times [-1, 1])$*;*

(v) W *and, at each fixed* $q > 0$*,* ϑ_q *belong to* $C^\infty([0, \frac{\hat\xi_1^2}{2}] \times [-1, 1])$*;*

(vi) the slow coefficients $F_n, U_n, V_n, M_n, P_n, T_n$ $(n \ge 1)$ *belong to* $C^\infty([0, \frac{\hat\xi_1^2}{2}] \times [-1, 1])$*;*

(vii) on the heat exterior the physical leading velocity and pressure are C^∞ *on* $\{(x, t) : r > 0,\ t \ge 0,\ \frac{\hat\xi^2}{2} > X^+_{\mathrm{lead}}\}$*, up to* $t = 0$*.*

Proof. Parts (i), (ii), (v) and (vi) are Theorem 2.9.1 below, applied with the same $\frac{\hat\xi_1^2}{2}$: (i) the selected protected domain, (ii) the middle parameter maps, (v) the weight W and the cutoff ϑ_q of (2.6.38), (vi) the slow coefficients. Theorem 2.9.1(ii) and (v) use part (iii), which is proved here.

(iii) *Heat lift.* For $\frac{\hat\xi^2}{2} \ge R_b$, $H_L = d^{-h} g_*(\frac{\hat\xi^2}{2}/d)$. Where the scalar argument lies in the forced interval, $\frac{\hat\xi^2}{2}/d \le b_s$ forces $d \ge R_b/b_s$. There H_L is a smooth function of $(\frac{\hat\xi^2}{2}, \hat\zeta)$. For $\frac{\hat\xi^2}{2}/d \ge b_s$, $g_* = c_{\mathrm{bank}} g_h + k_f g_f$.

We fix N and $x = \frac{\hat\xi^2}{2}/d$. By induction,

$$(\hat\xi^{-1}\partial_{\hat\xi})^j \partial_d^m [d^{-h}\phi(\tfrac{\hat\xi^2}{2}/d)] = d^{-h-m-j} \sum_{k \le m} c_{mkj} \left(x^k \phi^{(k)}\right)^{(j)}(x).$$

Applied to the remainder $\phi = r_N$ of (2.3.37), for which $|r_N^{(l)}(x)| \le C x^{-h-N-1-l}$, this gives

$$|(\hat\xi^{-1}\partial_{\hat\xi})^j \partial_d^m \mathcal{R}_N| \le C(\tfrac{\hat\xi^2}{2})^{-h-N-1-j} d^{N+1-m}.$$

This is (2.3.38).

The main part is the polynomial $c_{\mathrm{bank}} \sum_{n \le N} a_n (\frac{\hat\xi^2}{2})^{-h-n} d^n$. For the fast part, $|g_f^{(l)}(x)| \le C_l x^h e^{-x/2}$ by (2.3.36) and (2.3.34), so each $(\frac{\hat\xi^2}{2}, d)$ derivative of $d^{-h} g_f(\frac{\hat\xi^2}{2}/d)$ is $O(d^{-K} e^{-\frac{\hat\xi^2}{2}/(2d)})$. Because N is arbitrary, $H_L \in C^\infty([(\frac{\hat\xi_1^2}{2})', \frac{\hat\xi_1^2}{2}] \times [0, d_1])$ in $(\frac{\hat\xi^2}{2}, d)$, $\hat\xi_1 > 0$, and $d = 1 - \hat\zeta^2$ is a polynomial in $\hat\zeta$. The same applies to $\mathfrak{M}_{2L} = d^{1-h} i(\frac{\hat\xi^2}{2}/d)$.

(iv) *Histories, pressure, stress.* The histories and P are the axis integrals (2.3.17) over $[0, \frac{\hat\xi^2}{2}] \subset [0, \frac{\hat\xi_1^2}{2}]$ of one-sided smooth integrands. No improper integral is necessary for $\hat\xi \le \hat\xi_1$. The stresses (2.3.18)–(2.3.19) are polynomial in these quantities, their first $\hat\zeta$-derivatives, L^{-1}, and the regular axis quotients by $\frac{\hat\xi^2}{2}$. No denominator d occurs: all denominators are L, $\frac{\hat\xi^2}{2}$ (regular at the axis) and $\hat\xi$.

(vii) *Physical heat field.* By (2.3.33), $u_\theta^{\mathrm{lead}} = r^{-1} t^{-h} g_*(r^2/(2t))$ on the exterior. For $r \ge r_1 > 0$, we set $y = r^2/(2t)$. Part (iii) gives

$$t^{-h} g_h(y) = (r^2/2)^{-h} \sum_{n \le N} a_n (2t/r^2)^n + t^{-h} r_N(y), \quad |\partial_t^k \partial_r^j (t^{-h} r_N(y))| \le C_{N,j,k} t^{N+1-k},$$

and the fast mode is flat at $t = 0$. Thus u^{lead} is C^∞ up to $t = 0$ for $r > 0$. Its pressure $-\int_r^\infty (u_\theta^{\mathrm{lead}})^2 s^{-1}\, \mathrm{d}s$ inherits this by the differentiated slow and fast tail bounds in Lemma 2.3.20. $\square$

Lemma 2.8.5 (Operations that keep one-sided smoothness)**.** *We use the notation of Definition 2.8.1. These operations keep the class $C^\infty(\mathcal{P}_+ \times K)$.*

(a) Sums and products keep the class. Composition with a smooth function also keeps it if an open set that contains the range closure is in that function's domain. Composition with a diffeomorphism of $\mathcal{P}$ that keeps $\{p_k \geq 0\}$ has the same property.

(b) We consider integration in a variable of K or in an internal radial variable. Let the integration limits depend smoothly on the other variables. Assume compact support in the integration variable, or an integrable parameter-independent dominator for each derivative of the integrand. This operation keeps the class.

(c) We consider the linear ODE in the internal variable $v \in [0, L]$, $\partial_v z = A(p, \kappa, v)z + g(p, \kappa, v)$, $z|_{v=0} = z_0(p, \kappa)$. If its coefficients belong to the class, its solution map keeps the class.

(d) We consider a Fourier multiplier in a torus variable y, independent of p. If it satisfies $\|Tf\|_{C^j_{\mathsf{y}}} \leq C_j \|f\|_{C^{j+M}_{\mathsf{y}}}$, it keeps the class.

(e) Suppose $w \in C^\infty(\mathcal{P}_+ \times K)$, $w \geq 0$, $\Omega = \{w > 0\}$, and $f \in C^\infty(\Omega)$. Assume $|\partial^\alpha f| \leq C_\alpha w^\beta (1 + \log(1/w))^{N_\alpha}$ on Ω for some $\beta > 0$. Then the zero extension of f belongs to the class.

Proof. (a) We use the chain rule. (b) The compact support or dominators justify differentiation under the integral. Dominated convergence gives continuity of these integrals up to $p_k = 0$. (c) Adjoin a constant component to z so that the affine equation has coefficient matrix $B = \left(\begin{smallmatrix} A & g \\ 0 & 0 \end{smallmatrix}\right)$ and initial vector $(z_0, 1)$. Iterating its integral equation gives the ordered integrals of $B(v_1) \cdots B(v_n)(z_0, 1)$ over $0 < v_n < \cdots < v_1 < v$. On any compact parameter box, derivatives of order at most m in (p, κ) of the nth integral are bounded by $(n+1)^m C_m^{n+1} L^n / n!$ by the product rule and the simplex volume. Every differentiated series converges uniformly up to $p_k = 0$. The sum solves the integral equation and is unique, since iterating the difference equation bounds a difference by $(C_0 L)^n / n!$ times its supremum for every n. Derivatives in v follow from the equation. (d) T commutes with ∂_p^α, and $p \mapsto \partial_p^\alpha f(p, \cdot)$ is continuous into C^{j+M}_{y} up to $p_k = 0$. Thus $p \mapsto \partial_p^\alpha Tf$ is continuous into C^j_{y}. (e) Each derivative of f tends to zero at points of $\{w = 0\}$, because w is continuous and $s^\beta (1 + \log(1/s))^N \to 0$.

The parameter domain is locally convex (a half-ball times intervals or torus charts). Let p_* satisfy $w(p_*) = 0$. We select a coordinate direction e such that $p_* + \sigma e$ lies in the domain. We consider the last component of Ω that the segment $[p_*, p_* + \sigma e]$ meets.

It starts at a point of $\{w = 0\}$ where $\partial^\alpha f = 0$. The mean value theorem on that component gives $|\partial^\alpha f(p_* + \sigma e)| \leq |\sigma| \sup |\nabla \partial^\alpha f|$ over the segment, which is $o(|\sigma|)$. Thus all one-sided derivatives exist at p_*, vanish, and are continuous. This is the argument of Lemma 2.3.10, written on the closed parameter set. □

Proposition 2.8.6 (One-sided smoothness at the initial slice)**.** *Fix the leading source of Theorem 1, with the slow and packet data of Lemma 2.18.3. Let $x_0 = (x_0', z_0) \in B_{R_*}$, $z_0 \neq 0$. There is a neighbourhood U of $(x_0, 0)$ in $\mathbb{R}^4$ such that:*

(a) The slow reference $(u_s, \pi_s, K_{\mathrm{B}})$ and its residual $\mathbf{f}_s$ are smooth on the closed neighborhood. This includes $\mathbf{f}_{\mathrm{ref}} = \mathbf{f}_s$, by (2.15.19). The initialized state $(u^{[0]}, p^{[0]})$ and each zero-extended cut increment of (2.18.6) have the same property. It also holds for u_∞, p_∞ and the localized $(u, p, \mathbf{f})$ of (2.18.23). All these objects belong to $C^\infty(U_+)$.

(b) If $r_0^2 > 2X_{\mathrm{all}} q_0$, we can select U such that (u_∞, p_∞) is the exact heat field on U_+. Then $\mathbf{f}_\infty = 0$ there.

The same conclusion (b) holds at each $(x_0, 0)$ with $z_0 = 0$, $r_0 > 0$. Independently, each fixed uncut finite state and its $A_*^n, d_*^n, G_{\mathrm{flat},n}, \mathsf{B}_{\mathrm{flat},n}$ are smooth up to $t = 0$ at points strictly inside that state's admitted q domain. The neighborhood for this last assertion may depend on n. We do not claim one positive domain for all uncut stages.

Proof. We select $U = B_\epsilon(x_0) \times (-\epsilon, \epsilon)$ with ϵ so small that Lemma 2.8.3 applies on the (z, t) projection, $q \in [q_0/2, 2q_0]$, and r and $\frac{\hat{\xi}^2}{2}$ vary in compact sets. The fixed construction ball and time interval lie in the admitted domain $q < q_{\mathrm{base}}$ of the initialized state by (2.18.19). For any other uncut finite state considered independently, we restrict to a point strictly inside its own admitted domain. Its finitely many value margins are uniform for $\hat{\zeta} \in [-1, 1]$ and hold up to $t = 0$. We do not select q_0 less than all the infinitely many stage thresholds.

Step 1: local finiteness. On U_+, only finitely many of these functions or labels are nonzero, or different from one:

- the band functions $\beta(\log_2 \widetilde{q} + \ell)$, with support in $Q \in (\widetilde{q}/2, 2\widetilde{q})$, by (2.13.11),
- the slow boxes of mesh $S_\ell^{-K_{\mathrm{mesh}}}$ that meet the bounded set of band coordinates,
- the graph labels, with boundedly many slow supports through a point, by Lemma 2.13.1,
- the Borel cutoffs $\chi(c_n \widetilde{q})$, because $c_n \uparrow \infty$, by Section 2.6,
- the single last stage family $\chi_n = \chi(\widetilde{q}/\delta_n)$, with $\delta_n \downarrow 0$, from Section 2.18.

More explicitly, $\widetilde{q} \geq q_0/(2C_L)$ on this neighborhood, so a nonzero stage cutoff must satisfy $2\delta_n \geq q_0/(2C_L)$. There are only finitely many such indices. Each active cut term lies inside its own admitted domain by (2.18.10). At its outer domain boundary it is identically zero on a neighborhood.

Each fixed finite state has finitely many relative harmonics per label. Thus the completed objects in (a) are finite local sums of admitted terms. The remaining cut increments vanish identically there. The next finite-operation argument applies to each active term, to the initialized state and, independently, to any fixed uncut state on its own admitted domain.

Step 2: the variables. Each term depends on (x, t) only through these variables:

- $q, \hat{\zeta}, \frac{\hat{\xi}^2}{2}$ for the slow and mean coefficients,
- the band coordinates $(\mathsf{R}, \mathsf{Z}, \mathsf{T})$ of finitely many bands with $Q \asymp q_0$,
- the angle θ,
- the sampled torus point $\mathsf{y} = J_g^{i_0} Y_{\mathrm{phys}}$, where $Y_{\mathrm{phys}} = v_r r^{d_r} + v_t t$.

By Lemma 2.8.3 these are analytic in (x, t) on U away from the axis. Waves and mean increments are supported in $\mathsf{R} \geq \mathsf{R}_- > 0$ ((2.13.1) and the protected hull), where r^{d_r} and the cylindrical frame are smooth. Near the axis only the actual selected regular core and its slow coefficients are present on the protected domain. The variable-core construction supplies the regular-axis fields, and paragraph 2.3.2 supplies their finite-cover slow inverse with zero regular-axis data and the full-support Gevrey cutoff.

Since the radial and angular velocity components are r times smooth functions of r^2, conversion to Cartesian components replaces re_r, re_θ by $(x_1, x_2, 0), (-x_2, x_1, 0)$. The axial component and

pressure are smooth in r^2. We combine these identities with the matched leading and slow data from Theorem 2.7.1. We use also the finite packet and mean jets from Lemma 2.20.2 and the local finiteness in Step 1.

These results give Cartesian smoothness on the stated non-tip neighborhood. This includes the two signs of t where the neighborhood meets the joining slice. $J_g^i Y_{\mathrm{phys}}$ has v_t component $T_g^i t$. The pulse variable $v = (\zeta + r_0)/c_i$ is affine in t, with the band-constant rate $T_g^i/c_i = Q^{-1-h}$. Its v_r component does not depend on t. Thus the "fast" pulse time is a nondegenerate affine function of t whose rate is frozen by the q-selected band.

These operations do not use the similarity clock t^{-h}. Band selection uses the physical gauge, not t alone.

Step 3: the leading and slow data. We consider a term $q^\gamma f(\frac{\hat\xi^2}{2}, \hat\zeta)$ with f from Lemma 2.8.4. We multiply it by smooth cutoffs in q. Lemmas 2.8.4 and 2.8.5(a) place the result in $C^\infty(U_+)$. The physical derivatives of such terms are again of this form: $\partial_t(q^\gamma f) = -q^{\gamma-1}\mathsf{T}_\gamma f$, $\partial_z(q^\gamma f) = q^{\gamma-(\frac12-h)}\mathsf{Z}_\gamma f$ ((2.6.1)), whose only denominator is L. This gives (a) for $u_s, \pi_s, K_{\mathrm{B}}, \mathbf{f}_s$.

Step 4: packets. The phase (2.13.16), normal, frame (2.13.20) and projected matrix (2.13.21) come from band-frozen constants and background coefficients by (a). The principal inverse (Proposition 2.13.3) and the homogeneous pulse (Lemma 2.13.2) solve linear ODEs in v with $(\mathsf{R}, \mathsf{Z}, \mathsf{T}, \xi)$ fixed. We use (c). The value hypotheses of Lemma 2.13.2 are uniform on the closed band atlas $\bar q \in [1/2, 2]$, $|\hat\zeta| \le 1$ (Section 2.13), so they hold at $\mathsf{T} = 0$. For the positivity in (2.13.25), $z_\pm$ is the solution of the linear system with data $(P(0), 0)$.

The Riccati equation only proves its sign. The amplitudes (2.13.40) use a matrix inverse and square roots of $y \ge c\sqrt{S}\mathsf{W}$. The signed quotients (2.13.47) have $\sqrt{\mathsf{W}}$-weighted jets. We use (a) on $\{\mathsf{W} > 0\}$ and (e) across $\{\mathsf{W} = 0\}$. The Haar projection Π and the covariances are torus integrals: (b). Curls, the temporal cutoff $\psi(v)$, the aggregate cutoff and sampling are (a).

Step 5: mean maps. The shifted primitives (2.14.8) integrate in the radial variable with (Z, T) fixed and radial support in the hull: (b). The inverse T_0^{-1} in Lemma 2.14.2 is a torus multiplier with $M = 4$: (d). The roots (2.14.16), (2.14.35), (2.14.54), (2.15.11), (2.15.42) are smooth functions of radicands at least $V_M^2/2$: (a). The five-row solve (2.14.48) inverts a matrix of radial integrals at fixed (z, t) with a uniform margin (Section 2.14): (b) and (a).

The states (2.14.42) are radial integrals of compactly supported differences: (b). There is no integral in z or t anywhere in Sections 2.6–2.18 (Section 2.14). The only T- and Z-operations are derivatives.

Step 6: cutoffs, pressures and the force. We apply (a) and (b) to the cutoffs $\chi_n(\widetilde q)$ and their zero extensions, justified by (2.18.10). They also apply to the divergence-preserving prefix in (2.18.6), a radial integral at fixed (z, t). The localization χ_{loc} and $b_{\mathrm{loc}} = \mathcal{B}_{\mathrm{div}} g_{\mathrm{loc}}$ are finite sums of integrals over fixed bounded boxes. Thus (a) and (b) apply to them as well.

See Section 2.18. Each pressure in the construction is local in (z, t). The leading and slow pressures are the axis integrals (2.6.5). The packet pressures are the coefficients (2.13.27).

The mean pressures are radial primitives with zero endpoints. This construction uses no elliptic or Leray solve. Thus $u, p \in C^\infty(U_+)$, and so is $\mathbf{f} = \mathscr{N}(u, p)$, a differential polynomial in (u, p).

(b) If $r_0^2 > 2X_{\mathrm{all}} q_0$, then $X > X_{\mathrm{all}}$ on a neighbourhood. There $\mathsf{W} = 0$, because $\hat\xi_{\mathrm{all}} \ge \hat\xi_W$, the support radius of W (Proposition 2.3.9(W4); $\frac{\hat\xi_{\mathrm{all}}^2}{2}$ exceeds the outer terminal edge B and the extension buffer), so all packets vanish. The condition $\hat\xi \ge \hat\xi_P$ of (2.6.21), makes all positive slow orders vanish. Also, $T_{1,\theta} = 0$ by (2.6.28).

By Lemma 2.18.1(d), every finite correction (packets, mean increments with their pressures and roots, cut increments) vanishes there. The remaining field is the exact heat field from Lemma 2.3.20, by Lemma 2.18.1(a). It solves (2.2.2) with zero force.

It is z-independent, satisfies $u_r = u_z = 0$, and has g_* that solves the heat ODE. For $z_0 = 0$, $r_0 > 0$: $q \le |z|^{1/(\frac12 - h)} + t/(1-2h) \to 0$ at $(x_0, 0)$, so $\frac{\hat\xi^2}{2} = r^2/(2q) \to \infty$ and the same holds on a neighbourhood. □

Corollary 2.8.7 (The force on the closed half-space)**.** $\mathbf{f} \in C^\infty(\mathbb{R}^3 \times [0,T])$ *in the sense of Definition 2.8.1, it vanishes to infinite order at* $(0,0)$*, and*

$$|\partial_{x,t}^{\le m} \mathbf{f}_\infty(x,t)| \le C_{m,M}(t + |z|^{1/(\frac12 - h)})^M \qquad \text{on } B_{R_*} \times [0,T] \tag{2.8.1}$$

for each m, M*. Lemma 2.8.2, with a time cutoff equal to one near zero, gives a smooth extension of* $\mathbf{f}$ *across* $t = 0$ *with the same compact spatial support.*

Proof. Away from $(0,0)$, each point of $\mathbb{R}^3 \times \{0\}$ has $z \ne 0$, or $z = 0, r > 0$, or lies outside the localization ball. Proposition 2.8.6 and the explicit annular formulas give one-sided smoothness. For (2.8.1): where $\frac{\hat\xi^2}{2} > X_{\mathrm{all}}$, $\mathbf{f}_\infty = 0$ by Proposition 2.8.6(b). On the bounded profile hull $q \le |z|^{1/(\frac12 - h)} + t/(1-2h)$, and (2.18.17), (2.6.33), (2.15.19) give $C_{m,M} q^M$ for $t > 0$, with bounds independent of $\hat\zeta \in [-1,1]$.

By the continuity in (a), the same bound holds at $t = 0$, $z \ne 0$. Because $t + |z|^{1/(\frac12 - h)} \le C|(x,t)|$ near the origin, each derivative of $\mathbf{f}$ tends to zero at $(0,0)$. One-sided difference quotients in the directions $\pm e_i$ and $+e_t$ then show that the zero extension at $(0,0)$ has all derivatives equal to zero and continuous. □

Remark 2.8.8. The endpoint formulas have this denominator structure. No object divides by d, by $\sqrt{d}$, or by t: the chart Jacobian is $-Lq^{\frac12 - h}$, and $\mathsf{T}_\gamma, \mathsf{Z}_\gamma$ have only L in their denominators. The only negative powers of d are $d^{-h} g_*(\frac{\hat\xi^2}{2}/d)$, $d^{1-h} i(\frac{\hat\xi^2}{2}/d)$ and $d^{-h-1}\tau_s(\frac{\hat\xi^2}{2}/d)$. The first two are one-sided smooth by Lemma 2.8.4(iii), and the third vanishes identically near $d = 0$.

No operation evaluates a coefficient at $\mathsf{T} < 0$ to produce a value at $\mathsf{T} \ge 0$. The extensions mentioned in Section 2.13 are never used for physical values. The initial jets at $z \ne 0$ are in general nonzero. In the wing near $\hat\zeta = \pm 1$, $\mathsf{W} > 0$ and the q_0-band carries waves at $\mathsf{T} = 0$.

We do not assert vanishing there.

The backward side. The rest of this subsection proves items (iii) and (iv) of condition (B7). We work on $t < 0$ in the backward chart (2.3.11), with $\varsigma = -1$, $\tau = -t$, $\hat\xi = r/\sqrt{q_b}$, the weight W_b of Lemma 2.3.11 and the radius $\frac{\hat\xi^2_{\mathrm{ret}}}{2}$ of Section 2.7.1.

Lemma 2.8.9 (The backward exterior and the bound $\frac{\hat\xi^2_{\mathrm{all}}}{2}$)**.** *Assume the hypotheses of Proposition 2.7.2. Let* $B = \frac{\hat\xi^2_b}{2}$ *be the outer edge of Lemma 2.3.4.*

(a) $\frac{\hat\xi^2_{\mathrm{ret}}}{2} < B$*. On* $\{\frac{\hat\xi^2}{2} \ge B\}$ *we have* $T_0 = 0$, $\mathsf{W}_b = \mathsf{W}_* = 0$ *and* $\vartheta_q = 0$*, and every positive-order slow coefficient* $E_n, U_n, F_n, M_n, V_n, P_n, T_n$ $(n \ge 1)$ *vanishes. There the slow reference* $(u_s, \pi_s, K_{\mathrm{B}})$ *is the leading field, with* $K_{\mathrm{B}} = 0$*: the swirl* $c_\infty s^{-\frac12 - h}\mathcal{H}_-(2\tau/s)$*,* $s = r^2/2$*, of Lemma 2.3.5,* $u_r = u_z = 0$*, and the outward pressure* $-\int_r^\infty u_\theta^2 \varrho^{-1}\,\mathrm{d}\varrho$*. It solves the Navier–Stokes equations with zero force, so* $\mathbf{f}_s = 0$ *there.*

(b) Every finite correction of the joint algorithm on $t < 0$ *vanishes on* $\{\frac{\hat\xi^2}{2} \ge B\}$*. This covers the packets with their potentials and oscillatory pressures, the initialization, every mean increment with its pressure and roots, the reservoir* d_**, the flat remainders* $G_{\mathrm{flat}}, \mathsf{B}_{\mathrm{flat}}$*, and the cut increments* (2.18.6)*.*

Hence, for the choice (2.18.2), $\frac{\hat\xi_{\rm all}^2}{2}$ *exceeds the backward hulls and the backward heat onset, and on* $t<0$ *every finite correction vanishes for* $\hat\xi\ge\hat\xi_{\rm all}$. *This is (B7)(iii). On* $\{\frac{\hat\xi^2}{2}\ge\frac{\hat\xi_{\rm all}^2}{2}\}\cap\{t<0\}$, (u_∞,p_∞) *is the field of (a) and* $\mathbf{f}_\infty=0$. *(The forward counterpart and the list of all supports are Lemma 2.18.1.)*

Proof. (a) By Proposition 2.7.2(a), $\frac{\hat\xi_{\rm ret}^2}{2}<R_e<\frac{\hat\xi_b^2}{2}=B$. For $\frac{\hat\xi^2}{2}\ge B$, the exact heat exterior in Lemma 2.3.5 gives $T_0=0$. So $\mathsf{W}_*=c_*|T_0|=0$, and $\vartheta_q=0$ by (2.13.10). Also $\mathsf{W}_b=0$ off $(\frac{\hat\xi_a^2}{2},\frac{\hat\xi_b^2}{2})$ by the convention of Lemma 2.3.11. By Proposition 2.7.2(b), $E_n=U_n=F_n=M_n=V_n=0$ for $\frac{\hat\xi^2}{2}\ge\frac{\hat\xi_{p,b}^2}{2}e^{-9}$ and $P_n=0$ for $\hat\xi\ge\hat\xi_{\rm ret}$. By Proposition 2.7.2(c), $T_n=0$ for $\hat\xi\ge\hat\xi_b$; for $n\ge2$ this already holds beyond $\frac{\hat\xi_{\rm ret}^2}{2}$. So every cut slow term $\chi(c_n\widetilde q)(\cdots)$, including the radial cutoff term built from M_n, vanishes there. The slow stress is $K_{\rm B}=0$ there, since its order-zero part is T_0. The terminal departure $-\rho H_0\Psi(\frac{\hat\xi^2}{2}/B)$ vanishes to every order for $\frac{\hat\xi^2}{2}\ge B$, since Ψ is smooth and zero on $[1,\infty)$. Lemma 2.3.5 gives $H=c(\hat\xi/\sqrt2)^{-2h}\mathcal{H}_-(4d/\hat\xi^2)$ and $U=M=J=V_0=0$, and the physical swirl $c_\infty s^{-\frac12-h}\mathcal{H}_-(2\tau/s)$. The histories are normalized at infinity as in Lemma 2.3.5, so the pressure is the outward centrifugal integral. The swirl is independent of z and solves the swirl heat equation (2.3.31). A z-independent pure swirl whose pressure balances the centrifugal force solves the Navier–Stokes equations exactly. Hence $\mathbf{f}_s=0$ on $\{\frac{\hat\xi^2}{2}\ge B\}$.

(b) We induct on the finite stage. Each object of a stage is built from three kinds of input: the slow stress $K_{\rm B}$ and the slow fields, the cutoff ϑ_q, and objects of earlier stages. Each operation below preserves vanishing on $\{\frac{\hat\xi^2}{2}\ge B\}$.

- Packets. Every wave potential and oscillatory pressure carries its factor ϑ_q^j with $j\ge1$ (Section 2.14, before (2.15.3)). The principal wave is $\vartheta_q a_\gamma\cos-\widetilde b_\gamma\sin$, where $\widetilde b_\gamma$ is the curl remainder of $\vartheta_q d_\gamma$. The signed and harmonic responses are solved from sources supported in earlier supports. The pulse equations and the torus inverse act at a fixed slow point. So all packet fields and their Gaussian endpoint terms vanish where $\vartheta_q=0$, in particular on $\{\frac{\hat\xi^2}{2}\ge B\}$.

- Tensors. Covariances of these waves vanish there. The slow cross target $\mathcal{Q}_\times(K_{\rm B})$ vanishes there by (a), and so does $d_*=(1-\vartheta^2)(S_0+K_s+\cdots)$, since S_0 and K_s are parts of $K_{\rm B}$ and the added K are built from earlier supports. So $\mathsf{B}_{\rm flat}=-\mathcal{Q}_\times(d_*)$ vanishes there. The term $(1-\vartheta^j)F_m$ in $G_{\rm flat}$ vanishes with the source F_m.

- Mean maps. In (2.14.11), $\chi=0$ for $\frac{\hat\xi^2}{2}\ge\frac{\hat\xi_{p,b}^2}{2}e^{-3}$, so $\mathcal{I}_\chi f=\mathcal{I}f=\int_{\mathsf R}^\infty f$ there, and it vanishes beyond $\operatorname{supp}f$. This covers (2.14.14), (2.15.11) (with $g_s=\rho\partial_{\mathsf Z}\mathsf S_z$, which vanishes on $\{\frac{\hat\xi^2}{2}\ge B\}$ by (a)) and the P of (2.14.35) and (2.14.54). In (2.15.42), $P_{\rm rad}=\int_{\mathsf R}^\infty g_{\rm rad}-\chi N_{\rm rad}$, with the same conclusion. Full moments enter only through the bumps k,ω_θ,ω_z and through χ, and these are supported in $\frac{\hat\xi^2}{2}\le\frac{\hat\xi_{p,b}^2}{2}e^{-3}<B$ (Lemma 2.3.11(c)). The roots (2.14.16), (2.14.35), (2.14.54), (2.15.11) and (2.15.42) vanish off $\operatorname{supp}k$, by their rationalized forms. The auxiliary seed (2.14.33) uses T_0^{-1} at a fixed slow point and moments times bumps. Its radial prefix is compact at the outer end, by the exact zero axial moment. The state seeds of Lemma 2.14.3 are templates in $I_{\rm mean}$. Their prefix (2.14.51) is compact by $F=0$, and p_0 is supported in $\operatorname{supp}v$. The reconstruction (2.15.40) has zero outer endpoints, so A^+ vanishes beyond $\operatorname{supp}h^2\cup\operatorname{supp}\omega$.

- Last diagonal. χ_n multiplies each increment, and the radial prefix in (2.18.6) vanishes beyond the hull by (2.18.4).

The base of the induction is the slow reference and ϑ_q, which are covered by (a). This proves (b). The final assertions follow from (a), (b) and $\frac{\hat\xi_{\mathrm{all}}^2}{2} > B$. Note that B is fixed with the leading member, before $\frac{\hat\xi_{\mathrm{all}}^2}{2}$ is chosen. □

Proposition 2.8.10 (Backward one-sided smoothness at the initial slice)**.** *Assume the leading properties (B1)–(B5) of Theorem 1 and item (i) of condition (B7), together with the inputs of Proposition 2.7.2, and choose* $\frac{\hat\xi_{\mathrm{all}}^2}{2}$ *as in* (2.18.2)*. Let* $x_0 = (x_0', z_0) \in B_{R_*}$ *and* $U = B_\epsilon(x_0) \times (-\epsilon, \epsilon)$*, and put* $U_- = U \cap \{t \le 0\}$*. In Definition 2.8.1 take* $\tau = -t$ *as the distinguished coordinate.*

(a) Let $z_0 \neq 0$*. For small* ϵ*, the restrictions to* $t \le 0$ *of the objects listed in Proposition 2.8.6(a) belong to* $C^\infty(U_-)$*. These objects are the slow reference and* $\mathbf{f}_s$*, the initialized state, each zero-extended cut increment,* u_∞, p_∞*, and the localized* $(u, p, \mathbf{f})$*.*

(b) Suppose $r_0^2 > \hat\xi_{\mathrm{all}}^2 |z_0|^{1/(\frac12 - h)}$*, or* $z_0 = 0$ *and* $r_0 > 0$*. Then, for small* ϵ*,* (u_∞, p_∞) *on* $U_- \setminus \{t = 0, z = 0, r = 0\}$ *is the backward heat field of Lemma 2.8.9(a). This field belongs to* $C^\infty(U_-)$*, and* $\mathbf{f}_\infty = 0$ *there.*

Each fixed uncut finite state is also smooth up to $t = 0$ *from below at points strictly inside its own admitted* q_b*-domain. Thus (B7)(iv) holds. Its input (B7)(i), including the value margins, is Theorem 2.7.5.*

Proof. Chart. q_b is the root $q > |z|^{1/(\frac12 - h)}$ of $q - z^2 q^{2h} = \tau$. The proof of Lemma 2.8.3, with t replaced by τ, applies verbatim, because $\partial_q(q - z^2 q^{2h}) = 1 - 2h$ at (q_0, z_0). So $(z, t) \mapsto (q_b, \hat\zeta_b)$ is a real-analytic diffeomorphism near $(z_0, 0)$. It maps $N \cap \{t \le 0\}$ onto $\{\mathrm{sgn}(z_0)\hat\zeta_b \le 1\}$, and $d_b = 1 - \hat\zeta_b^2 = \tau/q_b \ge 0$ if and only if $t \le 0$. The band Jacobian has the opposite sign, $+L\bar q^{\frac12 - h}$, and the same absolute value. The time identity of (2.6.1) becomes $\partial_t(q_b^\gamma f) = +q_b^{\gamma-1}\mathsf{T}_\gamma f$, while the ∂_z identity is unchanged. The only denominator is still L.

Leading data, weight and slow data. This step replaces Lemma 2.8.4, which is a forward statement.

- Theorem 1(ii) treats either physical side. It gives H, U, V, the five histories, P and $\mathcal{T}_0$ in $C^\infty([0, \frac{\hat\xi_1^2}{2}] \times [-1, 1])$, with $\hat\zeta_b$ distinguished at ± 1. On the heat tail it uses the positive Laplace integral of Lemma 2.3.20.

- W_b does not depend on $\hat\zeta_b$. It is smooth on $(\frac{\hat\xi_a^2}{2}, \frac{\hat\xi_b^2}{2})$, and its zero extension is flat (Lemma 2.3.7(d), Lemma 2.3.11(a)), so $\mathsf{W}_b \in C^\infty([0, \frac{\hat\xi_1^2}{2}] \times [-1, 1])$. By (B3), $\mathsf{W}_* = c_*|T_0| \ge c\mathsf{W}_b > 0$ on $(\frac{\hat\xi_a^2}{2}, \frac{\hat\xi_b^2}{2}) \times [-1, 1]$, with $|\partial^\alpha T_0| \le C_\alpha \mathsf{W}_b \mathcal{L}_b^{N_\alpha}$. Hence ϑ_q is smooth at each fixed $q_b > 0$, and it is flat on $\{\mathsf{W}_* = 0\}$ by Lemma 2.8.5(e).

- The positive-order coefficients are those of Lemma 2.6.4(c). They are C^∞ on $[0, \infty) \times [-1, 1]$ up to $\hat\zeta_b = \pm 1$; on the inner rectangle they are holomorphic in $\hat\zeta$ on a neighbourhood of $[-1, 1]$, with bounds uniform in $\frac{\hat\xi_2^2}{2}$. Their stresses obey Proposition 2.7.2(c)–(d).

- The slow reference is that of Lemma 2.20.7. Its item (d) is exactly the continuity of every fixed physical derivative up to $\hat\zeta_b = \pm 1$, that is, up to $t = 0$, on compact sets with $q_b > 0$.

This gives Step 3 of the proof of Proposition 2.8.6 on U_-, for $u_s, \pi_s, K_{\mathrm{B}}, \mathbf{f}_s$.

Local finiteness, variables, cutoffs. Steps 1, 2 and 6 of that proof apply verbatim. They use only the following:

- the joint gauge $\widetilde{q} = q_b$ of (2.10.1);
- the joint atlas of Theorem 2.10.2, made once on the union of the two sides;
- the Borel cutoffs $\chi(c_n\widetilde{q})$ and the stage cutoffs χ_n, which are locally finite at $q_b \geq q_0/2$;
- the sampled point $J_g^i Y_{\mathrm{phys}}$, $Y_{\mathrm{phys}} = v_r r^{d_r} + v_t t$, whose pulse variable is affine in t with the same positive rate Q^{-1-h} on the two sides;
- the fixed localization, which is independent of t.

None of these uses the sign of t.

Packets and means. Steps 4–5 of that proof use the operations (a)–(e) of Lemma 2.8.5. Each acts at fixed (z,t) (Lemma 2.20.5). So no value at $t \leq 0$ is computed from values at $t > 0$. The value hypotheses are part of the value margins of (B7)(i). They are the hypotheses of Lemma 2.13.2 on the closed backward band atlas $\bar{q}_b \in [\frac{1}{2}, 2]$, $|\hat{\zeta}_b| \leq 1$, the radicand bounds $\geq V_M^2/2$, and the five-row margin. Their backward sources are the following.

- On I_{mean} the leading swirl is $E_0 = c_{\mathrm{patch}}(1+\beta^2)^{-1}(\hat{\xi}/\sqrt{2})^{-1-2\lambda} > 0$ (Lemma 2.3.3), and the positive slow velocities vanish there (Proposition 2.7.2(b)). So $V_s \geq v_* > 0$ uniformly in $|\hat{\zeta}_b| \leq 1$.
- $\frac{\hat{\xi}_{p,b}^2}{2}$ is constant and $\mu = \lambda$ (Remark 2.7.4, (T4)). So the blocks (2.14.50) have the exponents $(2, -2-2\lambda, -2\lambda)$ and $(1, 1-2\lambda)$. The normalized leading determinant is then a nonzero constant times positive smooth row and column factors in $\hat{\zeta}_b$, up to $\hat{\zeta}_b = \pm 1$.
- The amplitude roots of $y \geq c\sqrt{S}\mathsf{W}_b$ are smooth wherever $\mathsf{W}_b > 0$. That set includes $\hat{\zeta}_b = \pm 1$ inside the annulus, and Lemma 2.8.5(e) applies at $\frac{\hat{\xi}_a^2}{2}$ and $\frac{\hat{\xi}_b^2}{2}$.
- The weighted primitives are those of Lemma 2.13.10, with smooth zero extension at $\frac{\hat{\xi}_a^2}{2}$ and $\frac{\hat{\xi}_b^2}{2}$.

This proves (a). The assertion for uncut states follows as in the forward proof.

(b) If $r_0^2 > \hat{\xi}_{\mathrm{all}}^2 |z_0|^{1/(\frac{1}{2}-h)}$, then $\frac{\hat{\xi}^2}{2} = r^2/(2q_b) > \frac{\hat{\xi}_{\mathrm{all}}^2}{2}$ on a neighbourhood, because $q_b(z_0,0) = |z_0|^{1/(\frac{1}{2}-h)}$. If $z_0 = 0$ and $r_0 > 0$, then $q_b \leq |z|^{1/(\frac{1}{2}-h)} + \tau/(1-2h) \to 0$, which is (2.18.19) with τ in place of t. So again $\hat{\xi} > \hat{\xi}_{\mathrm{all}}$ near $(x_0, 0)$. By Lemma 2.8.9, the fields there are the swirl $K = c_\infty s^{-\frac{1}{2}-h}\mathcal{H}_-(2\tau/s)$ with its outward pressure, and $\mathbf{f}_\infty = 0$. $\mathcal{H}_-$ is smooth on $[0,\infty)$ up to 0 (Lemma 2.3.20), and $2\tau/s \geq 0$ is smooth on $\{r > 0\}$. So $K \in C^\infty(U_-)$ by Lemma 2.8.5(a), using Lemma 2.8.2 near the zero argument of $\mathcal{H}_-$. Each derivative $\partial_t^k \partial_r^j K$ is bounded by $C_{jk} s^{-\frac{1}{2}-h-k} r^{-j}$, by (2.3.30). So the pressure integral admits an integrable dominator on $[r,\infty)$, and Lemma 2.8.5(b) applies. The Cartesian frame is smooth for $r > 0$. □

2.9 Endpoint regularity of the selected data

Theorem 2.9.1 (Endpoint regularity of the selected leading and slow data)**.** *Let the selected member be that of Theorem 1. Let $\hat{\xi}_1 < \infty$. Then:*

(i) The protected core data, curved activation, termination and shared Gevrey cutoff, and the inner-solve coefficients at every finite slow order, belong to $\mathcal{S}$ on the protected domain. The protected domain is bounded by graphs in $\mathcal{S}(J)$. These functions, written in $(\varpi,\hat\zeta)$ with $\varpi=(\hat\xi/\hat\xi_a(\hat\zeta))^2$, are restrictions of functions that are Gevrey-3/2 in $\hat\zeta$ at fixed ϖ on a neighbourhood of J (for the core data this is the Gevrey bound of Theorem 1(iii)).

(ii) The middle parameter maps $\nu,\frac{\hat\xi_p^2}{2},Y,A_p,b_j,g_j,c_j$, the pulse and returns $A_p\Phi(\nu y)+\sum_j c_j\psi(y-Y+d_j)$, and the stop, shot, A11, loop and restoration maps belong to $\mathcal{S}(J)$ or $\mathcal{S}([0,\frac{\hat\xi_1^2}{2}]\times J)$. The positive energy root satisfies $\mathcal{P}'(A_p)\ge 2^{-3/2}$ on J.

(v) $\mathsf{W}\in\mathcal{S}([0,\frac{\hat\xi_1^2}{2}]\times J)$. At each fixed $q>0$, ϑ_q of (2.6.38) belongs to $\mathcal{S}([0,\frac{\hat\xi_1^2}{2}]\times J)$ and vanishes identically on a neighbourhood of $\{\mathsf{W}_*=0\}$; by (W3) of Proposition 2.3.9 this set equals $\{\mathsf{W}=0\}$.

(vi) For each $n\ge 1$, the functions F_n,U_n,V_n,M_n,P_n,T_n belong to $\mathcal{S}([0,\frac{\hat\xi_1^2}{2}]\times J)$. The five-row matrices satisfy $\inf_J|\det B_U|\ge c\nu_c>0$ and $\inf_J|\det B_E|>0$.

Proof. **(i)** N8 supplies an open angular neighbourhood of J with $L>0$. Theorem 1(iii) verifies the leading-data bounds there in $\varpi=(\hat\xi/\hat\xi_a)^2$, and Lemma 2.6.2 solves each finite slow order on $[0,\Xi]\times U$. The recursive sources contain finitely many derivatives of finalized lower orders; divisibility of $\mathfrak{R}_{n-1}$ by $\frac{\hat\xi^2}{2}$ removes the axis quotient. The shared cutoff depends on ϖ alone and is supported inside this rectangle. The smooth coordinate change back to $(\frac{\hat\xi^2}{2},\hat\zeta)$ proves membership in $\mathcal{S}$. The activation is flat at $\varpi=1$, and $T_0=eB$ with the smooth positive collar factor of (2.3.3); later edits avoid this protected domain.

(ii) N1–N7 verify the actual nondegeneracies on the closed interval: the exponent inverse, two-return matrix, positive energy root, A11 map, stop/shot map, five-history inverses and loop reparametrization. The implicit function theorem at each endpoint gives their one-sided smooth parameter dependence, after smoothly extending the coefficient maps to an open neighbourhood. Their targets are compact radial integrals of earlier smooth fields or future integrals with the differentiated exterior bounds (2.3.39); the heat endpoint estimate is part (iii) of Lemma 2.8.4. For a moving pulse term the chain rule is

$$\partial_{\hat\zeta}[c_j\psi(y-Y+d_j)]=c_j'\psi-c_j[(\log\tfrac{\hat\xi_p^2}{2})'+Y']\psi',\qquad y=2\log(\hat\xi/\hat\xi_p).$$

The templates have fixed smooth compact supports, so the moving support faces are flat. N3 gives $\mathcal{P}'(A_p)\ge 2^{-3/2}$.

(v) Definition 2.3.6 expresses W as a finite sum of products of smooth angular factors, the flat activation, monotone splices and terminal deficit factors. Moving endpoint integrals defining E_w preserve $\mathcal{S}$. The only apparent singularity is $w_L=d^{-h-1}\tau_s(\frac{\hat\xi^2}{2}/d)$: on its fixed hull $\frac{\hat\xi^2}{2}\ge R_b$, compact support of τ_s makes it zero when $d<R_b/b_s$; on the remaining support d is bounded below. Thus w_L and W lie in $\mathcal{S}$.

At fixed $q>0$, the cutoff $\vartheta_q=\Theta(\log(1/\mathsf{W}_*)/(c_eS(q)))$ is identically zero where $\mathsf{W}_*<e^{-2c_eS(q)}$. Where it can be nonzero, $|\widetilde{T_0}|$ is smooth and positive, so composition proves smoothness. On the selected member (W3) identifies $\{\mathsf{W}_*=0\}$ with $\{\mathsf{W}=0\}$.

(vi) Induct on n. Part (i) treats the cut inner solution. The moving bumps are smooth; N6(a) gives smooth inverse moment matrices, and their full-hull targets are integrals of smooth lower-order expressions. Hence their coefficients and corrected F_n,U_n lie in $\mathcal{S}$. The axis primitives reconstruct

M_n, V_n, P_n without d^{-1}; divisibility removes the $\left(\frac{\hat\xi^2}{2}\right)^{-1}$ terms. The two late pressures are retained explicitly:

$$(\hat\xi^{-1}\partial_{\hat\xi}(P_1)) = -\mathfrak{R}_0/(\hat\xi^2), \qquad (\hat\xi^{-1}\partial_{\hat\xi}(P_2)) = \mathsf{Z}_0^{[2]}V_0/(\hat\xi^2) \quad (\tfrac{\hat\xi_v^2}{2} \le \tfrac{\hat\xi^2}{2} \le \tfrac{\hat\xi_P^2}{2}).$$

The residual expressions and their radial primitives then give $T_n \in \mathcal{S}$. For $n \ge 2$ they have compact interior support. For the exceptional T_1 use (2.6.28): its heat contribution vanishes because the physical heat swirl is z-independent, including endpoint derivatives by continuity; the remaining wing and mixture terms have compact smooth support. The determinant bounds are those of N6(a). □

Remark 2.9.2 (Support and covariance of the moving bumps). The bumps in (2.6.19) are fixed in $y = 2\log(\hat\xi/\hat\xi_p)$, so their supports stay inside $-14 < y < -9$ for each angle. The coordinate y is preserved by the endpoint chart change. By (2.7.1) the forward vectors of bump coefficients have the endpoint jets of $\ell^{1/2+h-\lambda_n}(\widetilde\alpha_b, \widetilde\beta_b)(\ell^{1/2-h}\eta_f)$. Theorem 2.6.13 proves this by the two invertible moment blocks and gives (2.6.22) for the reconstructed swirl.

Remark 2.9.3 (Selected angular functions). Every selected angular function and graph is the restriction to $J = [-1, 1]$ of a C^∞ function on $K_{\hat\zeta}$: b, s_0, u, a, ψ, $\frac{\hat\xi_a^2}{2}$, $\frac{\hat\xi_p^2}{2}$, R_o, Y, $\mathcal{B}_o$, $\mathcal{B}_w$, R_{need}, R_{buf}, the cutoffs $\omega, \chi, \psi_o, a(\hat\zeta)$, the shapes $\varphi, K, e_*\varphi$, and f in the loop phase. The core inputs are Gevrey-3/2. On the endpoint collars each is given by its chart-transported formula through λ_{ch}, which is real-analytic near ±1 by the analytic implicit function theorem applied to the scale equation in Remark 2.3.18, whose λ derivative is $1 - 2h$ at each endpoint. This only makes explicit that the profiles are extended to $K_{\hat\zeta}$ (Section 2.19); smooth extension of a function given on J is always possible (Lemma 2.8.2), and the collar formulas are explicit.

Remark 2.9.4 (Covariance of the late restoration). On the restoration interval $-25 < y < -20$, where $y = 2\log(\hat\xi/\hat\xi_p)$, write the two corrections as

$$\delta U = \sum_{i=1}^{2} \alpha_i b_i^U(y), \qquad \delta H = \hat\xi\,\delta E = \sum_{j=1}^{3} \beta_j b_j^H(y).$$

Both sides use the same nonnegative smooth templates with compact, ordered, disjoint supports within each family. The five-history map on this reserve has a uniformly invertible Jacobian by Theorem 1(iii).

Here is the covariance of their exact coefficient equations. Put $\ell = \lambda_{\mathrm{ch}}$, $\hat\zeta_b = \ell^{\frac12-h}\hat\zeta_f$, and let Φ map $c = (\alpha_1, \alpha_2, \beta_1, \beta_2, \beta_3)$ to the increments of (M, J, I, S, P), with the axis datum fixed. Define

$$C_\ell = \mathrm{diag}(\ell^{\frac12+h} I_2, \ell^h I_3), \qquad R_\ell = \mathrm{diag}(\ell^{h-\frac12}, \ell^{2h-\frac12}, \ell^{h-1}, \ell^{2h}, \ell^{1+2h}).$$

For transported reserve fields, $\frac{\hat\xi_b^2}{2} = \ell\frac{\hat\xi_f^2}{2}$ and $\frac{\hat\xi_{p,b}^2}{2} = \ell\frac{\hat\xi_{p,f}^2}{2}$ give

$$\Phi_f(\hat\zeta_f, C_\ell c) = R_\ell \Phi_b(\hat\zeta_b, c).$$

Indeed $y_b = y_f$, $\hat\xi_f\,\mathrm{d}\hat\xi_f = \ell^{-1}\hat\xi_b\,\mathrm{d}\hat\xi_b$, and the five histories in (2.3.27) have the indicated weights. This includes the quadratic terms: $\delta U\delta H$ has weight $(\frac12 + h) + h$, while δU^2 and $(\delta H)^2/(4\frac{\hat\xi^2}{2})$ both have weight $(1 + 2h)$ since $(1 + 2h) = 1 + 2h$.

When the two pre-modulation members, their five histories and axis pressures have equal slice jets on the loop and restoration reserve, the map and its target therefore satisfy this identity to

every endpoint order. Differentiating the coefficient equation, its invertible Jacobian determines each next coefficient jet from the preceding ones. The unique small branches therefore have equal slice jets, with weights $(\frac{1}{2}+h)$ and h; the same change of variables proves this for partial histories. This gives the restoration step in Theorem 2.7.1. The spectral controls have compact central angular support, so their endpoint jets vanish.

2.9.1 Finite algorithms in the common cutoff gauge

We use the same finite algebraic selections, slice-continued endpoint controls, physical labels and thresholds on the two sides. The same diagonal schedule is $S_\ell = \ell^{6/5}$. At each positive $\hat{t}$ the construction is locally finite. Equality of the full radial input jets, exact histories, and differentiated tail dominators propagates through each finite algorithm, and then through the locally finite sum.

Equality of slice jets (Definition 2.3.16), not open-collar equality of each exterior edit, is the assertion used here. Lemma 2.3.1 gives the required cutoff prescription. We select the finite thresholds only after we fix the source constants and all moment-correction inverses. We reserve ordinary source depth $J_{\mathrm{src}} = 80$ and prepared depth $J_{\mathrm{prep}} = 72$ in that same joint diagonal (paragraph 2.18.4).

The longest path uses $59+8+2=69$ levels for one output derivative; the additional output derivative and two source-band connections bring it to $59+8+3+2=72=J_{\mathrm{prep}}$, with zero margin, and the source export keeps eight more levels. This reserves the required regularity. The $128\varkappa$ loss accounts for the operations performed, not for the higher jets that these operations do not use. We keep also the auxiliary pure Gevrey estimates where that proof uses them, the radial mean's ρ^2 factor, and the global physical tails.

The completion uses these quantitative estimates. Finite smoothness alone does not replace them.

2.10 The same gauge and finite construction

We select one fixed positive smooth L_{cut} on $[-1,1]$ equal to λ_{ch} near the two endpoints. We define on the actual joined physical domain

$$\widetilde{q} = \hat{t}_b \quad (t \le 0), \qquad \widetilde{q} = \hat{t}_f / L_{\mathrm{cut}}(\hat{\zeta}_f) \quad (t \ge 0). \tag{2.10.1}$$

Near a joining point with $z \neq 0$, $\widetilde{q} = \widetilde{Q}\gamma(\widetilde{\eta})$ with $\gamma(\widetilde{\eta}) = |\hat{\zeta}_b(\widetilde{\eta})|^{-1/(\frac{1}{2}-h)}$. This holds for $t \le 0$ by Lemma 2.3.15 and for $t \ge 0$ by (2.3.28).

Thus $\widetilde{q}$ is one real-analytic function of $(\widetilde{Q}, \widetilde{\eta})$ there, and it does not depend on the radial coordinate. Only the jets of L_{cut} at ± 1 matter for smoothness across $t=0$ (Lemma 2.3.1). We impose no positive smooth extension through the singular tip.

Proposition 2.10.1 (Independent same slow Borel)**.** *The positive slow coefficients admit one potential-level Borel choice before the packet atlas. Its endpoint jets agree and its kept weighted derivative bounds supply the background for the next construction.*

Proof. At order n, we select c_n after the two sides' finitely many new seminorms, with the weighted stress and all potential brackets. We use $\chi(c_n\widetilde{q})$ before differentiation, as in (2.6.31). The current finite norms do not use a packet construction. Positive powers of $\hat{t}$ allow all finite demands, with one increasing c_n.

The exceptional first stress uses the native factored edge bound. On $t \ge 0$ higher stresses use the positive saturation just proved. On $t \le 0$ the requirements are the budgets (2.6.32) for the backward

coefficients, whose seminorms are finite (Proposition 2.7.2, Lemma 2.6.4(c)). Each budget is upward closed in c_n, so the same increasing c_n meets them (Lemma 2.20.7(a)). This gives $b = O(\rho)$ and $F_b - F_0, G_b - G_0 = O(\rho^2)$ in each prescribed kept derivative norm. At $\hat{t}_0 > 0$ only finitely many terms survive locally. Lemma 2.11.2, with the common physical gauge, passes Theorem 2.7.1 to the actual sum, including every potential cutoff bracket and the stress primitives. □

Theorem 2.10.2 (One physical packet atlas)**.** *The two sides admit one joint labelled graph, integer choices, enlarged-preimage separation and spare torus slot. Their restriction uses the same finite controls, whose endpoint jets agree. Lemma 2.20.2 independently proves equality of these finite packet fields.*

Proof. The actual strict leading estimate gives the packet-direction margin of Section 2.13. An arbitrary positive weight does not give this margin. We put $t = -b/a$, $v = a(1 + t^2)$, $P = p_1 + tp_2$, $J = p_2 - tp_1$. Then

$$T_\theta + tT_z = F(P - v), \qquad T_z - tT_\theta = FJ, \qquad P - v > 0, \quad 2(P - v)^2 - (v - 2)J^2 > 0.$$

On each closed active interior piece the positive minima of $F, a, v - 2$ and of

$$\frac{P - v}{\sqrt{(p_1 - a)^2 + (p_2 + b)^2}}, \qquad \frac{2(P - v)^2 - (v - 2)J^2}{(P - v)^2}$$

supply the frame margin.

The inner formula $T_0 = eB_0$ and the factor-preserving terminal formulas give the normalized limits at flat faces. We do not minimize unnormalized stress there. The capped-loop partial-history bounds keep these ratios, and the spectral source controls satisfy their allocated compact source budgets. These are the specified strict-source inputs, not a consequence of the spectral eigenvalue alone.

We use the labels and scales of Section 2.13 with band coordinate $\tilde{q}/Q$, not independently selected $\hat{t}_f/Q$. On a physical band the native chart $\hat{t}$ and $\tilde{q}$ are comparable by fixed constants. All normalized coordinate derivatives have the same finite bounds. Mesh the union physical domain once.

Enlarged bands satisfy $|\log_2 \tilde{q} + \ell| < 2$, so intersections have $|\ell - \ell'| < 4$. The level difference and mesh ratios are thus bounded independently of the band. The first-exit log-weight estimate in Lemma 2.13.1 keeps the larger buffer and direction margin. Finite degree gives finitely many colors.

We select rational centers that avoid the finitely many equations $c_\mu = J_g^d c_{\mu'}$ for the allowed level differences. We exclude the identical color at $d = 0$. We exclude self differences only for $d > 0$. We shrink the auxiliary radius to less than the minimum finite separation. A point outside all these finite preimages has an open ball that avoids them.

We fix the finite list of relative configurations before reducing the radius to obtain a spare slot for each.

The shared stress norm gauge is $c_*|\widetilde{T}_0|$, with $\widetilde{T}_0 = (\tilde{q}/\hat{t})^{1+h} T_0$ on the two sides, that is, $\widetilde{T}_{0,f} = L_{\mathrm{cut}}^{-1-h} T_{0,f}$ and $\widetilde{T}_{0,b} = T_{0,b}$. Because T_0 has weight $1 + h$, $\widetilde{T}_0$ is γ^{1+h} times the slice profile of T_0. The actual native weight satisfies $cW \le |T_0| \le CW \log^N(1/W)$ with its differentiated bounds, so this mesh gauge gives equivalent kept logarithmic classes. Native component weights and protected-root cutoffs remain in the component algorithm. On a nonzero face use the smooth positive root and frame inverse.

On a zero face the actual factored bounds $|D^j W| \le C_j W \log^{N_j}(1/W)$ give derivative bounds by $W^b \log^N(1/W)$, $b > 0$, thus zero jets after zero extension. This proves square-root compatibility

for these factors. It gives no such conclusion for arbitrary nonnegative smooth functions. Signed amplitudes divide only by the original uncut positive root.

We select each label representative, rounded carrier, phase, sign, frame and initial pulse data once in the joint physical chart. A radial line has one finite band set because $\partial_r \widetilde{q} = 0$. On level i the clock is $\rho\partial_{\mathsf{T}} + c_i v_t \cdot \partial_{y_i}$. On one cover i_0 it is $\rho\partial_{\mathsf{T}} + T_g^{i_0} Q^{1+h} v_t \cdot \partial_y$.

Pullback by $J_g^{i-i_0}$ recovers c_i. Thus this operation introduces no covering-degree factor and does not change the pulse length. The controls just constructed have matching endpoint jets on the whole physical radial path. Lemma 2.20.2 uses them only after we fix this atlas.

The same potential/flux cutoff uses the gauge (2.10.1). Lemma 2.20.3 and Proposition 2.20.4 give its finite algorithms and the one two-sided diagonal. Thus atlas construction does not presume a completed packet field.

□

2.11 Axis regularity and the slow force at the joining time

Fix $0 < h < \frac{1}{2}$ and $\lambda_n = 2nh$. On either open time side, $\hat{t}$ is the native positive root of $\hat{t} - z^2\hat{t}^{2h} = |t|$, $\hat{\xi} = r/\sqrt{\hat{t}}$ and $\hat{\zeta} = z\hat{t}^{h-1/2}$. The construction uses one physical gauge $\widetilde{q}$, smooth through $t = 0$ when $z \neq 0$, with $\widetilde{q} = \hat{t}/L_{\mathrm{cut}}(\hat{\zeta})$ on the forward side and $\widetilde{q} = \hat{t}$ on the backward side. The positive function L_{cut} is bounded above and below as in (2.10.1).

2.11.1 Axis regularity in Cartesian coordinates

Lemma 2.11.1 (Normalized profiles and Cartesian velocities)**.** *Suppose F_n, U_n, P_n are smooth functions of $\hat{\xi}^2$ up to $\hat{\xi} = 0$ and up to the angular endpoints. Define, as in (2.6.3),*

$$M_n(\tfrac{\hat{\xi}^2}{2}, \hat{\zeta}) = \int_0^{\frac{\hat{\xi}^2}{2}} U_n(s, \hat{\zeta})\, \mathrm{d}s, \qquad V_n = \frac{2\hat{\zeta}\frac{\hat{\xi}^2}{2} U_n - 2((\frac{1}{2} - h) + \lambda_n)\hat{\zeta} M_n - (1 - \hat{\zeta}^2)\partial_{\hat{\zeta}} M_n}{1 - 2h\hat{\zeta}^2}.$$

Then $2M_n/\hat{\xi}^2$ and $2V_n/\hat{\xi}^2$, defined at zero by continuity, are smooth functions of $\hat{\xi}^2$. The physical coefficient of (2.6.2) is, in Cartesian coordinates $x' = (x_1, x_2)$,

$$u_n = q^{\lambda_n - 1}\frac{V_n}{\hat{\xi}^2}(x', 0) + q^{-1-h+\lambda_n} F_n(x'^{\perp}, 0) + q^{-\frac{1}{2}-h+\lambda_n} U_n e_z, \qquad x'^{\perp} = (-x_2, x_1). \tag{2.11.1}$$

It is smooth at the spatial axis wherever $q > 0$. The same is true after cutting the meridional potential $\Psi_n = q^{\frac{1}{2}-h+\lambda_n} M_n$ by a smooth function of $\widetilde{q}$ and then differentiating it to recover the velocity.

Proof. The identity

$$\frac{M_n(\frac{\hat{\xi}^2}{2}, \hat{\zeta})}{\frac{\hat{\xi}^2}{2}} = \int_0^1 U_n(s\tfrac{\hat{\xi}^2}{2}, \hat{\zeta})\, \mathrm{d}s$$

and differentiation on the compact interval $[0, 1]$ give the first quotient. Dividing the displayed formula for V_n by $\hat{\xi}^2/2$ gives the second, since $1 - 2h\hat{\zeta}^2 \geq 1 - 2h > 0$. Substitution of $e_r = (x', 0)/r$, $e_\theta = (x'^{\perp}, 0)/r$ and $E_n = \hat{\xi} F_n$ gives (2.11.1). A smooth one-sided function of $\hat{\xi}^2$ composed with $\hat{\xi}^2 = |x'|^2/q$ is smooth in x': the chain rule off the axis gives continuous derivatives of all orders at the axis. For completeness, to identify these derivatives, translate a line segment by arbitrarily small vectors in the two-dimensional x'-plane so that it misses the axis; apply the fundamental

theorem of calculus on the translated segment and pass to the limit. Induction gives the assertion at every order. Finally

$$\Psi_n = \frac{r^2}{2} q^{-\frac{1}{2}-h+\lambda_n} \frac{M_n}{\frac{\hat{\xi}^2}{2}}.$$

Its cut version is $r^2 a(t, r^2, z)$ with a smooth. Its meridional velocity is $(-r\partial_z a)e_r + (2a + r\partial_r a)e_z$, which has smooth Cartesian components. This also accounts for the derivative of the cutoff. □

The swirl amplitude $E_n = \xi F_n$ is smooth in ξ and its quotient is smooth in $X = \xi^2/2$. For the actual first correction the zero axis data and (2.6.7)–(2.6.8) give, with $b = -1 - h$, $d_0 = 1/2 - h$,

$$4(F_1)_X(0, \pm 1) = -\mathsf{Z}_b^{[2]} F_0(0, \pm 1) = -\frac{4b(b - d_0)}{(1 - 2h)^2} F_0(0, \pm 1) \neq 0.$$

Here V_1/X vanishes at the axis by the radial average formula, and the selected core in (B1) has $F_0(0, \pm 1) > 0$, with the same leading endpoint values on the two sides. Hence E_1 has a nonzero $X^{3/2}$ term. The relation (2.6.22) and the Cartesian formula above are the endpoint comparisons through the axis.

2.11.2 Cutoffs preserve the actual endpoint jets

Lemma 2.11.2 (Joining a locally finite cut sum)**.** *Let $H_n^{\pm}$ have equal physical jets on a smooth joining hypersurface, and let g be a common positive smooth function near a point of that hypersurface. If $c_n \to \infty$ and $\chi \in C^\infty(\mathbb{R})$ vanishes on $[2, \infty)$, then*

$$\sum_n \chi(c_n g) H_n^+ \quad \text{and} \quad \sum_n \chi(c_n g) H_n^-$$

have equal jets there. This assertion remains true after any fixed smooth differential operator, in particular the operator recovering meridional velocity from its potential.

Proof. Shrink the neighborhood so that $g \geq \epsilon > 0$. For all sufficiently large n, $c_n \epsilon > 2$, so the corresponding summand and all its derivatives vanish on this neighborhood. Only a fixed finite set of indices remains. For any multi-index α, the difference of the jets of a surviving product is

$$\sum_{\beta \leq \alpha} \binom{\alpha}{\beta} \partial^\beta [\chi(c_n g)] \left(\partial^{\alpha-\beta} H_n^+ - \partial^{\alpha-\beta} H_n^-\right) = 0.$$

The chain rule includes every derivative of g; it is not replaced by a formula using the native q on both sides. Applying a differential operator uses finitely many of these identities at higher order. □

Application to the slow stress. Theorem 2.7.1 supplies the jets of every finite velocity, pressure and potential coefficient. The stress coefficients have the same property: their defining sources are the coefficients of the physical residual of finite truncations, and hence finite differential polynomials in these fields. The identification is made in slice variables, with the physical powers restored, so that it includes the change of sign of the native time operator. At a fixed slow order the same extraction of a scaling power is used on both sides. The stress primitives (2.6.23) can equivalently be taken in the physical radial variable:

$$K_{n,\theta}(r) = -r^{-2} \int_0^r s^2 R_{n,\theta}(s)\, \mathrm{d}s, \qquad K_{n,z}(r) = -r^{-1} \int_0^r s R_{n,z}(s)\, \mathrm{d}s.$$

Here $R_{n,\theta}, R_{n,z}$ denote the physical residual contributions at that scaling order, including their q powers. Changing variables $s = q^{1/2}\mathfrak{s}$ gives exactly the displayed normalized primitives in (2.6.23). Differentiation under these finite integrals preserves the matching jets. Near the axis the stresses vanish on the protected core (proved below), so the factors r^{-1}, r^{-2} cause no problem. Apply Lemma 2.11.2 with $g = \widetilde{q}$, the smooth Borel cutoff and the common c_n of Proposition 2.10.1. It proves the matching jets of the actual u_s, p_s, K_B, including the potential cutoff brackets.

2.11.3 Extension of the slow force through the origin

Lemma 2.11.3 (Removal of a flat puncture)**.** *Let F be smooth on a punctured neighborhood of 0 in $\mathbb{R}^d$. Suppose that for every multi-index α and every integer $M \geq 0$ there are a neighborhood and a finite constant such that $|\partial^\alpha F(y)| \leq C_{\alpha,M}|y|^M$ there. Then $F(0) = 0$ defines a smooth extension, and every derivative at zero is zero.*

Proof. Extend each $\partial^\alpha F$ by zero, calling the extension G_α. The bound with $M = 1$ gives continuity. The bound with $M = 2$ gives $|G_\alpha(v) - G_\alpha(0)|/|v| \to 0$, so G_α is differentiable at zero with derivative zero. Away from zero its derivatives are $G_{\alpha+e_i}$, which are continuous everywhere. Thus G_α is C^1 and has these derivatives. Induction proves the claim. □

Proposition 2.11.4 (The same smooth slow force)**.** *Use the following results for the same coefficient construction and Borel sequence.*

(i) the flat augmented residual estimates (2.6.33) and Lemma 2.20.7(b) on the forward and backward sides, respectively;

(ii) the finite endpoint-jet theorem and common gauge used to apply Lemma 2.11.2;

(iii) the slow reference of Lemma 2.18.1(d), which equals the exact heat exterior beyond one fixed $\hat{\xi}_{\mathrm{all}}$, with $K_B = 0$ and zero force.

On the common construction domain the force

$$f_s = \mathscr{N}(u_s, p_s) + \mathscr{D}_r K_B \qquad (t \neq 0) \tag{2.11.2}$$

extends to one smooth force across the entire joining slice, and its full space-time jet at $(t, x) = (0, 0)$ is zero. Its values away from that point are the actual residual values and their common traces.

Proof. First consider a slice point with $z \neq 0$. The common gauge is positive there. Lemma 2.11.2, its stress application, and the Cartesian axis formula give smooth joining of u_s, p_s, K_B. The operator $\mathscr{D}_r$ is smooth for $r > 0$; on the protected axis neighborhood $K_B = 0$. Thus (2.11.2) is smooth across this portion of the slice. At $z = 0, r > 0$, continuity of $\hat{t}$ to zero and positivity of r give an open physical neighborhood on which $r^2 > \hat{\xi}_{\mathrm{all}}^2 \hat{t}$. By (iii) the force vanishes throughout that neighborhood on both time sides, so it extends as zero there. This proves smoothness on a punctured neighborhood of the origin.

It remains to verify a bound at the origin, not merely endpoint jets at positive $\hat{t}$. Set $a = |z|^{1/(\frac{1}{2}-h)}$. The function $Q \mapsto Q - z^2 Q^{2h}$ vanishes at a, and on $Q \geq a$ its derivative lies in $[1 - 2h, 1]$. The mean value theorem therefore gives on either side

$$a + |t| \leq \hat{t} \leq a + \frac{|t|}{1 - 2h}. \tag{2.11.3}$$

Since $1/(\frac{1}{2} - h) > 1$, this implies $\hat{t} \leq C|(t, x)|$ near the origin. Choose a bounded profile hull strictly containing $[0, \frac{\hat{\xi}_{\mathrm{all}}^2}{2}]$. On it, (i) bounds every physical derivative of f_s by $C_{\alpha,M}\hat{t}^M$; outside it

the derivative is zero by (iii). The constants are uniform over the angular interval, including its endpoints. Thus

$$|\partial^{\alpha} f_s(t,x)| \le C'_{\alpha,M} |(t,x)|^{M} \qquad (t \neq 0).$$

The already established punctured joining passes the same inequalities to $t = 0, x \neq 0$ by continuity. Lemma 2.11.3 now gives the claimed smooth extension and its zero jet.

The extra radial component of the covariance divergence in (2.14.2) is handled in the initialization. □

2.12 The pulse clock and the choice of schedule

Main result. Lemma 2.12.1 bounds the torus clock inverse under its stated pulse-scale assumption. Lemma 2.12.2 gives a compatible schedule. Proposition 2.12.3 controls all auxiliary orders at each finite stage for that schedule.

The next anisotropic Fourier calculation gives the subpower loss of the clock primitive. On one pulse let

$$v_r = (1, 1-\sqrt{2}), \qquad v_t = (\sqrt{2}-1, 1), \qquad y = c_\mu + \xi v_r + \zeta v_t.$$

We write $Q = 2^{-\ell}$, $S = S_\ell$, and $c_i = T_g^i Q^{1+h}$. The pulse endpoint relation is $v/L_p = 1/2 + \zeta/(2r_0)$, so we can use a fixed smooth endpoint cutoff with a buffer in the nonnegative strain majorant

$$E(y) = A_{\mathrm{slow}} S^{1/4} \chi_+(\xi) \psi_+\left(\frac{1}{2} + \frac{\zeta}{2r_0}\right) \exp\left(-\frac{c'\zeta^2}{c_i^2 S}\right). \tag{2.12.1}$$

The scalar A_{slow} has one value bound for the full parameter family and has the actual slow support. The cutoff transitions in (2.12.1) are Gaussian tails.

Lemma 2.12.1 (Anisotropic clock inverse)**.** *Suppose $c_i S$ stays in a fixed positive compact interval and E is (2.12.1). There is a unique zero-Haar smooth periodic solution to*

$$c_i D_{v_t} \Phi = E - \Pi E,$$

and

$$\|\Phi\|_\infty \le C |A_{\mathrm{slow}}| S^{3/4} (1 + \log S).$$

Suppose the completed source has bounded pointwise overlap of slow labels. Then the sum of these primitives satisfies the same bound with the largest active scale S_t. This conclusion also covers active labels with $q \gg t$.

Proof. We set $\epsilon = S^{-1/2}$ and $g_S(u) = \psi_+(1/2 + \epsilon u/(2r_0)) e^{-c' u^2/(c_i S)^2}$. The family g_S has Schwartz seminorm bounds independent of the family index, and $E = A_{\mathrm{slow}} S^{1/4} \chi_+(\xi) g_S(\zeta/\epsilon)$. Let $a_n = n \cdot v_r$, $b_n = n \cdot v_t$, and $D = |\det(v_r, v_t)|$. The exact change of variables gives

$$\widehat{E}(n) = D A_{\mathrm{slow}} S^{-1/4} e^{-2\pi i n \cdot c_\mu} \widehat{\chi}_+(a_n) \widehat{g}_S(\epsilon b_n),$$

and thus, for each fixed M,

$$|\widehat{E}(n)| \le C_M |A_{\mathrm{slow}}| S^{-1/4} (1 + |a_n|)^{-M} (1 + \epsilon |b_n|)^{-M}.$$

The divisor is $2\pi i c_i b_n$, because $D_{v_t} = \partial_\zeta$, rather than a_n. The quadratic-irrational direction has $|b_n| \ge c/(1+|n|)$ for $n \neq 0$.

We claim that for $M > 3$,

$$\sum_{n\neq 0} \frac{(1+|a_n|)^{-M}(1+\epsilon|b_n|)^{-M}}{|b_n|} \leq C_M(1+\log(1/\epsilon)). \tag{2.12.2}$$

The image of $\mathbb{Z}^2$ under $n \mapsto (a_n, b_n)$ is a fixed full-rank lattice with one bound for the point count in each unit square. On $|b_n| < 1$, invertibility gives $|n| \leq C(1+|a_n|)$. The Diophantine bound absorbs the divisor into one extra power of $1+|a_n|$.

This unit-cell sum converges. On $|b_n| \geq 1$, count unit cells with horizontal index j and vertical index $k \geq 1$. A constant times

$$\sum_j (1+|j|)^{-M} \sum_{k\geq 1} \frac{(1+\epsilon k)^{-M}}{k}.$$

bounds the sum. The second sum is logarithmic for $k \leq \epsilon^{-1}$ and has one bound on its full tail.

This proves (2.12.2). We divide the nonzero Fourier coefficients by $2\pi i c_i b_n$ and sum their absolute values. The estimate $c_i^{-1} \leq CS$ then proves the stated $S^{3/4}$ bound. Arbitrarily large fixed M gives smoothness.

An integer torus cover pulls back the source and its primitive together. Its chain rule gives the specified power of T_g. Normalized Haar measure and the supremum norm do not change. The slow factor remains outside the torus inverse, so its support does not enlarge.

At each physical point only boundedly many slow labels overlap, and their scales satisfy $S_j \leq CS_t$. The sum over these active labels gives the last assertion. A sum over all labels on a saturated radial line does not give a valid estimate. □

Lemma 2.12.2 (Schedule compatibility)**.** *For $1 < p < 4/3$, we select*

$$S_\ell = \ell^p, \qquad i(\ell) = \left\lfloor \frac{(1+h)\ell \log 2 - p \log \ell}{\log T_g} \right\rfloor.$$

Then $c_i = T_g^{i(\ell)} Q^{1+h} \asymp S_\ell^{-1}$, adjacent indices differ by a bounded integer, and the clock-weight contrast is $\rho_Q^{-o(1)}$. For each fixed $B, N, M, c > 0$, $Q^{-B} S_\ell^N e^{-cS_\ell} = O(Q^M)$. In particular all these conclusions hold for $p = 6/5$.

Proof. The floor changes $T_g^{i(\ell)}$ by only a fixed factor. The difference between consecutive floor arguments stays bounded. This proves the second assertion. Lemma 2.12.1 gives

$$\log \mathfrak{P}(\rho_Q) \leq C\ell^{3p/4}(1+\log \ell) = o(\ell) = o(\log(1/\rho_Q))$$

because $p < 4/3$.

Logarithms give the flatness assertion: $(B+M)\ell \log 2 + Np \log \ell - c\ell^p \to -\infty$ because $p > 1$. For $p = 6/5$ the clock exponent is $3p/4 = 9/10$. The remaining source inequalities compare fixed powers of S_ℓ with positive powers of ρ_Q. The finite mesh choice does not change.

Thus the strict positive-power margins remain. We construct the pulse level, mesh, labels, and same cutoff with this one schedule. We do not take them from a completed $p = 2$ source. □

2.12.1 All auxiliary orders for the actual schedule

The next proposition gives one auxiliary radius at each finite stage and finite ordinary derivative depth.

Proposition 2.12.3 (Finite-stage factorial radius recursion)**.** *Assume Hypothesis 2.3.21. We use $S_\ell = \ell^{6/5}$, the rounded levels in (2.13.7), and Gevrey–2 transverse and temporal auxiliary cutoffs. For each finite stage n and ordinary slow derivative depth J, there are constants $C_{n,J}, r_{n,J} > 0$ and finite exponents $B_{n,J}, b_{n,J}$. They are independent of the auxiliary multiindex and the band. All finite-state coefficient functions have length radius $r_{n,J} S^{-B_{n,J}}$, their original amplitude order, and polynomial-S norm bounds. Precisely, every such coefficient f at stage n satisfies, for all $|I| \le J$ and all $\alpha \in \mathbb{N}^2$,*

$$|\partial_x^I \partial_{\mathsf{y}}^\alpha f| \le C_{n,J}\, \rho^a S^{b_{n,J}}\, \mathfrak{w}\, \mathcal{L}_W{}^{N_{n,J}}\, e\, L_{n,J}^{|\alpha|}(|\alpha|!)^2, \qquad L_{n,J} \le K_{n,J} S^{B_{n,J}}. \tag{2.12.3}$$

Here the order a, the slow weight $\mathfrak{w} \in \{\mathsf{W}, \mathsf{W}^{1/2}, 1\}$ and the envelope $e \in \{1, P\}$ are those of the finite-order ledger for f, the constants are independent of α, ℓ and the label, and the length radius is $r_{n,J} S^{-B_{n,J}} = 1/L_{n,J}$. For the auxiliary multipliers P^{-1} and $e^{\pm K\Phi}$, (2.12.3) holds with $a = 0$, $\mathfrak{w} = 1$ and $e = |f|$. The one last diagonal can satisfy these bounds together with the ordinary source, support, and moment conditions.

The proof uses the pointwise mixed classes of Definition 2.12.4, which retain the slow weight and Gaussian envelope in (2.12.3). Products, analytic compositions under the available value margins, pulse ODEs and commuting linear operations preserve these classes. Theorem 2.12.23 combines their finite depth and radius losses; the operation inventory verifies that its hypotheses cover the actual construction.

2.12.1.1 Data and conventions

Data used. The proof uses the following data of the construction.

(S1) Bands $Q = 2^{-\ell}$, $\rho = \rho_Q = Q^h$, $S = S_\ell = \ell^{6/5}$; slow variables $x = (\mathsf{R}, \mathsf{Z}, \mathsf{T})$ on enlarged band boxes; torus variable $\mathsf{y} \in \mathbb{T}^2 = \mathbb{R}^2/\mathbb{Z}^2$ (Section 2.13.1, proof of Lemma 2.13.1).

(S2) Torus geometry: $J_g = \left(\begin{smallmatrix} 3 & 1 \\ 1 & 5 \end{smallmatrix}\right)$, $T_g = 4 + \sqrt{2}$, $\Lambda_g = 4 - \sqrt{2}$, $v_r = (1, 1 - \sqrt{2})$, $v_t = (\sqrt{2} - 1, 1)$ (2.13.6). Scales $c_i = T_g^i Q^{1+h}$ with $T_g^{-1} S^{-1} < c_i \le S^{-1}$, and $m_i = \Lambda_g^i Q^{d_r/2}$ (2.13.9).

(S3) Separated graph, finite coloring, rectangles $c_\mu + \xi v_r + \zeta v_t$, $|\xi|, |\zeta| < 2r_0$, with disjoint enlarged auxiliary preimages for meeting labels. Bounded level differences $0 \le \Delta \le \Delta_{\max}$, and lifts $f_i(J_g^{i-i_0}\mathsf{y})$ (Lemma 2.13.1).

(S4) Pulse coordinate $v = (\zeta + r_0)/c_i \in [0, L_p]$, $L_p = 2r_0/c_i \asymp S$ (Section 2.13.2). Evaluated operators $D_{\mathsf{R}} = \partial_{\mathsf{R}} + \lambda a_r(\mathsf{R}) v_r \cdot \partial_{\mathsf{y}}$, $D_z = \rho \partial_{\mathsf{Z}}$, $t_* = \rho \partial_{\mathsf{T}} + \partial_v$ (2.13.12).

(S5) Phase and normal $n = (x_0 - v(H_\Phi)_{\mathsf{R}}, p/\mathsf{R}, p_z - \rho v (H_\Phi)_{\mathsf{Z}})$, affine in v (2.13.16). Bounds $|n - B_p(s, K)| + |\partial_v n| \le C/S$, $|n|, |n_{\tan}| \ge c$, and polynomial-S bounds for every fixed ordinary derivative (2.13.19). Frame U_f, M_f, B_f, B_f^ℓ (2.13.20), matrices K_b, A_Φ (2.13.21), value gate (2.13.22).

(S6) Envelope $P(v) = \exp \int_{L_p/2}^v (\lambda - d_{\mathrm{ref}})$ and the propagator bound $\|V_m(v, w)\| \le C_0 P(v)/P(w)$ with $C_0 \le e^{C_E L_p/S}$, uniform over the finite harmonic set (Lemma 2.13.2).

(S7) Principal inverse and pressure (Proposition 2.13.3), temporal cutoff and endpoint error ((2.13.28), (2.13.29)), exact curl (Lemma 2.13.4), positive covariance (Proposition 2.13.5), signed update and harmonic step (Proposition 2.13.6, Proposition 2.13.7).

(S8) Classes $\mathcal{M}^a$, $\mathcal{W}^a$ ((2.13.4), (2.13.5)), slow weight $\mathsf{W} \le e^{-2}$, $\mathcal{L}_W = 1 + \log(1/\mathsf{W})$ (2.13.3) and the finite-sum rule (Section 2.13.1).

(S9) Directional inverse $\|D_v^{-1} f\|_{C^m} \le C_m \|f\|_{C^{m+4}}$ and Diophantine bound ((2.13.64), (2.13.65)). Shifted radial mixing (Lemma 2.13.9, (2.14.13)), T_0^{-1} ((2.14.31), proof of Lemma 2.14.2).

(S10) Protected roots of torus-dependent arguments: δ_D ((2.14.16), (2.14.19)), δ ((2.14.35), (2.14.54)), δ_C ((2.15.11), (2.15.15)), δ_{rad} (2.15.42). Slow amplitude roots $a_{\beta,\varsigma} = \sqrt{y}$, $\delta a_\pm$ ((2.13.40), (2.13.41), (2.15.26)). Current matrix inverse (proof of Lemma 2.14.3).

Conventions. Throughout, $L \ge 1$. Enlarging L preserves every bound of the form (2.12.3), so radii can only be decreased. Multi-indices $I \in \mathbb{N}^3$ are slow and $\alpha \in \mathbb{N}^2$ are auxiliary. $|A|_1$ denotes the maximal column absolute sum of a matrix A, and $I! = \prod I_k!$.

2.12.1.2 Classes and elementary inequalities

Definition 2.12.4 (Mixed weighted Gevrey–2 class)**.** Let $\Omega \subset \mathbb{R}^3$ be a slow domain, $U \subset \mathbb{T}^2$ open, $J \in \mathbb{N}$, $L \ge 1$. Let $m = (m_I)_{|I| \le J}$ be nonnegative functions on Ω with $m_{I'} \le m_I$ whenever $|I'| \le |I|$; replace m_I by $\max_{|I'| \le |I|} m_{I'}$ if needed. Let $e > 0$ be a function on U. Then $f \in \mathcal{G}_J(m, e; L)$ on $\Omega \times U$ means $f \in C^\infty$ and

$$|\partial_x^I \partial_{\mathsf{y}}^\alpha f(x, \mathsf{y})| \le m_I(x)\, e(\mathsf{y})\, L^{|\alpha|} (|\alpha|!)^2 \qquad (|I| \le J,\ \alpha \in \mathbb{N}^2,\ (x, \mathsf{y}) \in \Omega \times U).$$

The bound depends on α only through $|\alpha|$. If f vanishes outside $\Omega \times K$ with $K \subset U$ compact, its zero extension lies in $\mathcal{G}_J(m, \tilde{e}; L)$ on $\Omega \times \mathbb{T}^2$ for every positive $\tilde{e}$ with $\tilde{e} = e$ on K. This is how label coefficients supported in their enlarged rectangles (S3) become torus functions.

Lemma 2.12.5 (Elementary inequalities)**.** *For all integers $p, q, j, k, l \ge 0$:*

(E1) $a_q := \sum_{j=0}^{q} \binom{q}{j}^{-1} \le 8/3$, *with equality exactly at* $q = 3, 4$;

(E2) $\binom{p}{j} j! \, ((l + p - j)!)^2 \le ((l + p)!)^2$ *for* $0 \le j \le p$;

(E3) $((p + k)!)^2 \le 4^{p+k} (p!)^2 (k!)^2$;

(E4) for $\alpha \in \mathbb{N}^2$, $\sum_{\beta \le \alpha, |\beta| = j} \binom{\alpha}{\beta} = \binom{|\alpha|}{j}$ *(Vandermonde);*

(E5) for $t \ge 1$, $\inf_{p \ge 0} (p!)^2 t^{-p} \le e^4 (1 + \sqrt{t}) e^{-2\sqrt{t}}$.

Proof. (E1) For $q \ge 1$ separate the $j = 0$ term and use $\binom{q}{j}^{-1} = (j/q) \binom{q-1}{j-1}^{-1}$. Pairing j and $q + 1 - j$ in the remaining sum gives $a_q = 1 + \frac{q+1}{2q} a_{q-1}$. Then $a_0, \dots, a_4 = 1, 2, \frac{5}{2}, \frac{8}{3}, \frac{8}{3}$. For $q \ge 5$, $\frac{q+1}{2q} \le \frac{3}{5}$, so $a_q \le 1 + \frac{3}{5} \cdot \frac{8}{3} < \frac{8}{3}$ by induction. (E2) $\binom{p}{j} j! = p(p-1) \cdots (p-j+1) \le (l+p) \cdots (l+p-j+1) = \frac{(l+p)!}{(l+p-j)!}$. Hence the left side is at most $(l + p)! \, (l + p - j)! \le ((l + p)!)^2$. (E3) $\binom{p+k}{k} \le 2^{p+k}$. (E4) Compare the coefficients of x^j in $(1 + x)^{\alpha_1} (1 + x)^{\alpha_2} = (1 + x)^{|\alpha|}$. (E5) Concavity of $\log x$ bounds the trapezoidal sum on $[1, p]$ by its integral. This gives $\log(p!) - \frac{1}{2} \log p \le p \log p - p + 1$ for integers $p \ge 1$. Take $p = \lfloor \sqrt{t} \rfloor$. Then $(p!)^2 t^{-p} \le e^2 p \, (p^2/t)^p e^{-2p}$, with $(p^2/t)^p \le 1$, $p \le \sqrt{t}$ and $e^{-2p} \le e^2 e^{-2\sqrt{t}}$. □

Definition 2.12.6 (Compatible envelopes)**.** Fix a label with pulse interval $[0,L_p]$. A positive function E on $[0,L_p]$ is *δ-compatible with constant C_E* if it extends holomorphically to $\Sigma_\delta=\{v\in\mathbb{C}:\operatorname{dist}(v,[0,L_p])\le\delta\}$ and $|E(v+\omega)|\le C_E E(v)$ for $v\in[0,L_p]$, $|\omega|\le\delta$.

Lemma 2.12.7 (Envelopes)**.** *Let $S\ge S_0$. The functions P, $1/P$ and the Gaussian factor $G(v)=\exp(-c'(v-L_p/2)^2/S)$ are 1-compatible, with constants independent of ℓ and the label. Products of compatible envelopes are compatible. If E is δ-compatible, then, as a function of ζ on the pulse rectangle, $|\partial_\xi^l\partial_\zeta^j E|=0$ for $l>0$ and $|\partial_\zeta^j E|\le C_E j!(c_i\delta)^{-j}E$.*

Proof. Write $y=s(v)=\varsigma(u_p/2+u_pv/L_p)$ and $a=\lambda-d_{\mathrm{ref}}=\lambda_0[(1+y^2)^{-1/2}-(1+y^2)(1+u_p^2)^{-3/2}]$ (proof of Lemma 2.13.2). For $\operatorname{dist}(v,[0,L_p])\le 2$ one has $|\operatorname{Im}y|\le 2u_p/L_p$ and $\operatorname{Re}(1+y^2)\ge 1/2$ once $L_p\ge 4u_p$. Hence a is holomorphic there, with $|a|\le C_a$, where C_a depends only on the compact ranges of λ_0,u_p. For $|\omega|\le 1$, $|P(v+\omega)|/P(v)=\exp\operatorname{Re}\int_v^{v+\omega}a\in[e^{-C_a},e^{C_a}]$. This proves the claims for P and $1/P$. For G, $|G(v+\omega)|/G(v)=\exp(-c'\operatorname{Re}(2(v-L_p/2)\omega+\omega^2)/S)\le e^{c'(L_p+1)/S}\le C$, because $L_p\asymp S$. Products are immediate. Finally, Cauchy's estimate on the disc of radius δ gives $|\partial_v^j E(v)|\le j!\delta^{-j}C_E E(v)$. Since v depends only on ζ and $\partial_\zeta=c_i^{-1}\partial_v$, the last claim follows. □

2.12.1.3 The pointwise jet algebra; products and analytic composition

Lemma 2.12.8 (Pointwise jet algebra)**.** *Fix $P_0=(x_0,\mathsf{y}_0)$, J, $L\ge 1$ and $\mu>0$. For a smooth g let $\sigma(g)=(\partial_x^I\partial_{\mathsf{y}}^\alpha g(P_0))_{|I|\le J,\alpha\in\mathbb{N}^2}$, and put*

$$\mathcal{N}(g)=\frac{8}{3}\sum_{|I|\le J}\frac{\mu^{|I|}}{I!}\sup_{\alpha}\frac{|\partial_x^I\partial_{\mathsf{y}}^\alpha g(P_0)|}{L^{|\alpha|}(|\alpha|!)^2}.$$

Then $\mathcal{N}(gh)\le\mathcal{N}(g)\mathcal{N}(h)$.

Proof. Let $s_K(g)=\sup_\beta|\partial_x^K\partial_{\mathsf{y}}^\beta g(P_0)|/(L^{|\beta|}(|\beta|!)^2)$. By Leibniz, (E4) and (E1),

$$\begin{aligned}|\partial_x^I\partial_{\mathsf{y}}^\alpha(gh)(P_0)|&\le\sum_{K\le I}\binom{I}{K}s_K(g)s_{I-K}(h)\\&\quad\times L^{|\alpha|}\sum_j\binom{|\alpha|}{j}(j!)^2((|\alpha|-j)!)^2\\&\le\frac{8}{3}(|\alpha|!)^2L^{|\alpha|}\sum_{K\le I}\binom{I}{K}s_K(g)s_{I-K}(h).\end{aligned}$$

Multiplying by $\frac{8}{3}\mu^{|I|}/I!$ and summing over $|I|\le J$ gives

$$\begin{aligned}\mathcal{N}(gh)&\le(\tfrac{8}{3})^2\sum_{|I|\le J}\sum_{K\le I}\frac{\mu^{|K|}s_K(g)}{K!}\frac{\mu^{|I-K|}s_{I-K}(h)}{(I-K)!}\\&\le\mathcal{N}(g)\mathcal{N}(h).\end{aligned}$$

□

Lemma 2.12.9 (Products; type P)**.** *If $f\in\mathcal{G}_J(m^f,e^f;L_f)$ and $g\in\mathcal{G}_J(m^g,e^g;L_g)$, then $fg\in\mathcal{G}_J(m^{fg},e^fe^g;\max(L_f,L_g))$ with $m_I^{fg}=\frac{8}{3}\sum_{K\le I}\binom{I}{K}m_K^fm_{I-K}^g\le\frac{8}{3}2^{|I|}m_I^fm_I^g$.*

Proof. This is the first display of the proof of Lemma 2.12.8, with $L=\max(L_f,L_g)$ and the pointwise majorants inserted. □

Orders add and weights multiply, exactly as in the finite-order product rule (Section 2.13.1). Since $P \le 1$ and $\mathsf{W} \le e^{-2}$, one may use $P^2 \le P$ and $\mathsf{W}^2 \le \mathsf{W}$ where the ledger does so.

Lemma 2.12.10 (Analytic composition with a value margin; type C)**.** *Let $u = (u_1, \dots, u_k)$ be smooth on $\Omega \times U$. Assume:*

(i) for $(I, \alpha) \neq (0, 0)$, $|I| \le J$: $|\partial_x^I \partial_y^\alpha u_i| \le M L_u^{|\alpha|} (|\alpha|!)^2$;

(ii) F is holomorphic on a neighbourhood of every closed polydisc $\overline{D}(u(P_0), r)$, $P_0 \in \Omega \times U$, and $B(P_0) := \sup_{\overline{D}(u(P_0),r)} |F| < \infty$.

Put $L = L_u \max(1, 32M/(3r))$ and $\mu^{-1} = 3(1 + 32M/(3r))$ (three slow variables). Then, at every P_0, for $|I| \le J$ and all α,

$$|\partial_x^I \partial_y^\alpha F(u)(P_0)| \le \tfrac{3}{8}(2^k + \tfrac{5}{3}) B(P_0)\, I!\, \mu^{-|I|}\, L^{|\alpha|} (|\alpha|!)^2.$$

Proof. Put $w_0 = u(P_0)$ and use $\mathcal{N}$ of Lemma 2.12.8 at P_0 with these L, μ. Since $u_i - w_{0,i}$ vanishes at P_0, hypothesis (i) gives $\mathcal{N}(u_i - w_{0,i}) \le \frac{8}{3}[ML_u/L + M(e^{3\mu} - 1)]$. The choice of L gives $ML_u/L \le 3r/32$. The choice of μ and $\log(1 + x) \ge x/(1 + x)$ give $e^{3\mu} - 1 \le 3r/(32M)$. Hence $\mathcal{N}(u_i - w_{0,i}) \le r/2$.

Write $F(w) = \sum_\beta c_\beta (w - w_0)^\beta$ on $\overline{D}(w_0, r)$. Cauchy gives $|c_\beta| \le B(P_0) r^{-|\beta|}$. Fix (I, α) and let $q = |I| + |\alpha|$. Taylor's formula with holomorphic remainder writes $F(w) = \sum_{|\beta| \le q} c_\beta (w - w_0)^\beta + \sum_{|\beta| = q+1} (w - w_0)^\beta G_\beta(w)$. In the remainder, each term contains $q + 1$ factors vanishing at P_0, so its (I, α)-derivative at P_0 vanishes. For $|\beta| > q$, the (I, α)-component of $\sigma((u - w_0)^\beta)$ vanishes for the same reason. Hence, componentwise, $\sigma(F(u)) = \sum_\beta c_\beta\, \sigma((u - w_0)^\beta)$, with finitely many nonzero terms in each component. The constant term has $\mathcal{N}(c_0) = \frac{8}{3}|c_0| \le \frac{8}{3} B(P_0)$, and Lemma 2.12.8 bounds the other terms, so

$$\mathcal{N}(F(u)) \le \frac{8}{3} B(P_0) + \sum_{\beta \neq 0} B(P_0) r^{-|\beta|} \prod_i \mathcal{N}(u_i - w_{0,i})^{\beta_i} \le B(P_0) \Big(\frac{8}{3} + \sum_{\beta \neq 0} 2^{-|\beta|} \Big) = \Big(2^k + \frac{5}{3} \Big) B(P_0).$$

Reading off the (I, α)-component of $\mathcal{N}$ gives the claim. □

Corollary 2.12.11 (Protected roots, divisions and exponentials)**.**

(a) Rationalized root. *Let $V, \mathfrak{X}$ be real, with $v_* \le V \le V^*$ and $|\mathfrak{X}| \le V^2/4$ (value margin; Lemma 2.12.30 with $\theta \le \frac{1}{4}$ under input (I1) of Proposition 2.16.1; Lemma 2.14.1 states only $|\mathfrak{X}| \le V^2/2$, and proof of Lemma 2.15.1 only positivity). Assume $V, \mathfrak{X}$ satisfy (i) of Lemma 2.12.10 with constants M, L_u. Then*

$$\sqrt{V^2 + \mathfrak{X}} - V = \mathfrak{X} \cdot H(V, \mathfrak{X}), \qquad H = \frac{1}{\sqrt{V^2 + \mathfrak{X}} + V} \in \mathcal{G}_J(m^H, 1; L_u \max(1, 32M/(3r))),$$

with $r = \min(v_*/8, v_*^2/8)$ and $m_I^H = \frac{3}{8}(4 + \frac{5}{3}) \cdot \frac{8}{7} v_*^{-1} I! \mu^{-|I|}$. So the root keeps the amplitude order, weight and envelope of $\mathfrak{X}$ (Lemma 2.12.9). The same holds for the difference of two roots in (2.15.15), whose denominator is a sum of two such square roots.

(b) Division by a positive amplitude. *If $c \le w \le C$ and w satisfies (i), then $1/w \in \mathcal{G}_J$ with $r = c/2$ and $B \le 2/c$. In particular this applies to z_+/P for the positive homogeneous pulse ((2.13.25), Lemma 2.13.2), using Lemmas 2.12.7 and 2.12.19.*

(c) Exponentials (relative form). *If u satisfies (i), then*

$$|\partial_x^I \partial_{\mathsf{y}}^\alpha e^u| \le \frac{3}{8}(2+\frac{5}{3}) e^r e^{\operatorname{Re} u(P_0)} I!\mu^{-|I|} L^{|\alpha|}(|\alpha|!)^2$$

for every $r>0$. The envelope $e^{\operatorname{Re} u}$ is kept and only derivatives of u enter L. For example, clock weights $e^{\pm K\Phi}$ keep the value contrast of Lemma 2.12.1; the polynomial-S derivative constants of Φ enter only the radius.

Proof. (a) Let $|V'-V|\le r$ and $|\mathfrak{X}'-\mathfrak{X}|\le r$. Then $\operatorname{Re}(V'^2+\mathfrak{X}') \ge V^2-2Vr-r^2-V^2/4-r \ge \frac{23}{64}V^2>0$, using $r\le V/8$ and $r\le V^2/8$. Thus the principal root is holomorphic, has positive real part, and $|H|\le 1/(\operatorname{Re} V')\le 1/(V-r)\le \frac{8}{7v_*}$. Apply Lemma 2.12.10 with $k=2$. (b) and (c) are Lemma 2.12.10 with $F(w)=1/w$ on $\overline{D}(w_0,c/2)$ and with $F=\exp$, for which $\sup_{\overline{D}(w_0,r)}|F| = e^{\operatorname{Re} w_0+r}$. □

Matrix inverses whose entries are slow (the current matrix, $\mathcal{H}_\beta$, radial moment matrices; proof of Proposition 2.13.5, proof of Lemma 2.14.3) and the slow amplitude roots $\sqrt{y_{\beta,\varsigma}}$, $\delta a_\pm$ are y-independent. They are covered by Lemma 2.12.29 at their ordinary jet bounds. Multiplication by these coefficients preserves the input radius by Corollary 2.12.18(v).

2.12.1.4 Coefficients analytic in the pulse variable; evaluated derivatives; linear changes; cutoffs

Lemma 2.12.12 (Analytic-in-v coefficients; leaf type A)**.** *Let $c(x,v)$ be holomorphic in $v\in\Sigma_\delta$ for each x, with $\sup_{\Sigma_\delta}|\partial_x^I c|\le K_c$ for $|I|\le J$. Then, on the pulse rectangle in the coordinates (ξ,ζ), $|\partial_x^I\partial_\xi^l\partial_\zeta^j c|=0$ for $l>0$ and $|\partial_x^I\partial_\zeta^j c|\le K_c j!(c_i\delta)^{-j}$. In torus coordinates, $c\in\mathcal{G}_J(K_c,1;|A^{-1}|_1/(c_i\delta))$ with $A=[v_r\ v_t]$, $|A^{-1}|_1=(1+\sqrt{2})/2=1.2071\ldots$. For $\delta=1$ this gives $L\le 1.21\,T_gS$.*

Proof. The first two claims follow from Cauchy's estimate in v and $\partial_\zeta = c_i^{-1}\partial_v$. The last claim follows from Lemma 2.12.14, because $(\xi,\zeta)=A^{-1}(\mathsf{y}-c_\mu-k)$. □

Lemma 2.12.13 (Strip holomorphy of the pulse coefficients)**.** *There are S_0, K_0 and, for each J, constants K_J, b_J, all independent of ℓ and the label, with the following property. For $S\ge S_0$, each of*

$$n,\ \partial_v n,\ (n\cdot n)^{-1},\ |n_{\tan}|^{\pm1},\ s,\ s_a,\ \sqrt{1+s^2}^{\pm1},\ U_f,\ M_f^{\pm1},\ B_f,\ B_f^\ell,\ \mathsf{P}_n,\ A_\Phi,\ E_f,\ \lambda,\ d_p,\ A_m,\ \mathcal{E}_\Phi,$$

as well as the coefficients of D_Φ, D_0 in the evaluated derivatives $\mathcal{D},\mathcal{Z}$ of (2.13.35) and the coefficient $i/(k_\ell m\, n\cdot n)$ of the pressure formula (2.13.27), extends holomorphically to Σ_1 with $\sup_{\Sigma_1}|\partial_x^I(\cdot)|\le K_J S^{b_J}$ for $|I|\le J$. The listed phase, frame and principal ODE entries are bounded by K_0 at order zero. The differentiated coefficient $\mathcal{D}n_r + n_r/\mathsf{R} + \mathcal{Z}n_z$ in D_Φ can grow polynomially in S: it contains $-v(H_\Phi)_{\mathsf{RR}}$. Every fixed slow derivative of $\mathcal{E}_\Phi$ is $O(\rho S^{B_J})$ by (2.13.17). Here $|n|^2$ and $|n_{\tan}|$ are continued as $n\cdot n$ and $(n_\theta^2+n_z^2)^{1/2}$ (principal branch). Hence Lemma 2.12.12 applies with $\delta=1$.

Proof. n is affine in v, with slope $\partial_v n = -((H_\Phi)_{\mathsf{R}},0,\rho(H_\Phi)_{\mathsf{Z}})$ independent of v and $|\partial_v n|\le C/S$ (S5). For real $v\in[-2,L_p+2]$, $n(v)$ differs from n at the nearest point of $[0,L_p]$ by at most $2C/S$. So $|n|,|n_{\tan}|\ge c/2$ there for $S\ge S_0$. For $v+iw$ with $|w|\le 1$,

$$n\cdot n = |n(v)|^2 - w^2|\partial_v n|^2 + 2iw\, n(v)\cdot\partial_v n, \qquad \operatorname{Re}\ge c^2/4 - C^2/S^2 \ge c^2/8,$$

and likewise for $n_\theta^2+n_z^2$. Thus $(n\cdot n)^{-1}$ and the principal $(n_\theta^2+n_z^2)^{\pm1/2}$ are holomorphic and bounded. The function s is affine with $|\operatorname{Im} s|\le u_p/L_p$. The function $s_a = n_r/|n_{\tan}|$ has real values bounded on $[0,L_p]$ (S5) and imaginary part $O(1/S)$ on the strip. Therefore $\operatorname{Re}(1+s^2), \operatorname{Re}(1+s_a^2)\ge 1/2$.

Also $\det M_f = -2c_0\sqrt{1+s^2}$ with $|c_0| = \sqrt{(\sigma_v-2)/2} \ge c > 0$ (Section 2.13.1, (2.13.14)). Every listed object is a polynomial in these holomorphic quantities, in K_b, F_b, G_b, b, ρ, $k_\ell^2\rho$ and their slow derivatives, divided by powers of the bounded-below denominators. This gives holomorphy. The value bounds follow from the real bounds (S5) plus $O(1/S)$ on the strip. A slow derivative falls on the v-independent coefficients $x_0, p/\mathsf{R}, (H_\Phi)_\mathsf{R}, (H_\Phi)_\mathsf{Z}, K_b$, whose fixed derivatives are $O(S^{B_I})$ (Section 2.13.1, Section 2.13.3), times at most $|v|^{|I|} \le (L_p+3)^{|I|}$. Faà di Bruno then gives $K_J S^{b_J}$. The harmonic set is finite and enters only the constants through $m^2 d_p$. □

Lemma 2.12.14 (Linear changes, lifts and covers; type V)**.** *Let $g(\mathsf{y}) = h(A\mathsf{y}+c)$ with a real 2×2 matrix A. If $h \in \mathcal{G}_J(m,e;L)$, then $g \in \mathcal{G}_J(m, e\circ(A\cdot+c); |A|_1 L)$. Translations are isometries. The relevant constants are $|J_g^\Delta|_1 \le 6^\Delta$ ($\Delta \le \Delta_{\max}$; the values are $1,6,34,188,1028$ for $\Delta = 0,\dots,4$), $|A|_1 = \sqrt{2}$ and $|A^{-1}|_1 = (1+\sqrt{2})/2 < 1.21$.*

Proof. $\partial_{\mathsf{y}_k} g = \sum_j A_{jk}(\partial_j h)(A\mathsf{y}+c)$. Iterating, $|\partial^\alpha g| \le \prod_{i=1}^{|\alpha|}(\sum_j |A_{jk_i}|)\max_{|\beta|=|\alpha|}|\partial^\beta h| \le |A|_1^{|\alpha|} m\, e\, L^{|\alpha|}(|\alpha|!)^2$. □

Lemma 2.12.15 (Evaluated derivatives; type E)**.** *Let $f \in \mathcal{G}_{J+1}(m,e;L)$, let $c(x)$ be slow with $|\partial^K c| \le c_K$, and let $w \in \mathbb{R}^2$. Then $\partial_{x_j} f \in \mathcal{G}_J(m_{\cdot+e_j}, e; L)$, and $c\, w\cdot\partial_{\mathsf{y}} f \in \mathcal{G}_J(m'', e; 4L)$ with $m''_I = 4L|w|_1 \sum_{K\le I}\binom{I}{K} c_K m_{I-K}$. Consequently $D_\mathsf{R}, D_z, t_*, \mathcal{D}, \mathcal{Z}$ and $(\mathcal{D}+\mathsf{R}^{-1})$ (S4, Section 2.13) map $\mathcal{G}_{J+1}(m,e;L)$ into $\mathcal{G}_J(\cdot,e;4L)$. The amplitude factors are those of the finite-order ledger: $|\lambda| \asymp \rho^{-\varkappa} S^{-\rho_g}$ for the auxiliary part of D_R, the factor ρ for D_z, $c_{\mathrm{aux}} = c_{i_0}$ for t_*. There is an extra polynomial factor $4L$.*

Proof. Use Leibniz in x and $|w\cdot\partial_{\mathsf{y}}\partial^\alpha f| \le |w|_1 m\, e\, L^{|\alpha|+1}((|\alpha|+1)!)^2 \le |w|_1 m\, e\,(4L)^{|\alpha|+1}(|\alpha|!)^2$, by (E3) with $k=1$. □

The angular derivative $\mathsf{R}^{-1}\partial_\theta$ acts only on the phase $e^{ik_\ell m\Phi}$. It produces the multiplier $ik_\ell mp/\mathsf{R}$ (2.13.16), a slow coefficient. Phases never enter coefficients: products of different labels vanish identically by separation (S3; proof of Proposition 2.13.5), and same-label phases combine exactly.

Lemma 2.12.16 (Gevrey–2 cutoffs; leaf type K)**.** *Let $\phi(s) = e^{-1/s}$ for $s>0$ and $\phi = 0$ otherwise. Then $|\phi^{(p)}| \le 3^p (p!)^2$ for all p. The step $\psi_1(s) = \phi(s)/(\phi(s)+\phi(1-s))$ equals 0 on $(-\infty,0]$ and 1 on $[1,\infty)$, and satisfies $|\psi_1^{(p)}| \le C_1 K_1^p (p!)^2$ with absolute C_1, K_1. Consequently, for each fixed support and plateau there are cutoffs $\chi_g(\xi)$ and $\psi_0(\cdot)$ with $|\partial^p\chi| \le C_\chi K_\chi^p (p!)^2$. The temporal cutoff $\psi(v) = \psi_0(\frac12 + \frac{\zeta}{2r_0})$ then lies in $\mathcal{G}(C_\chi, 1; 1.21 K_\chi/(2r_0))$, independently of S.*

Proof. For $s>0$, the disc $|w-s| \le s/2$ is mapped by $w\mapsto 1/w$ onto the disc with real diameter $[\frac{2}{3s}, \frac{2}{s}]$, so $\mathrm{Re}(1/w) \ge \frac{2}{3s}$. Cauchy gives $|\phi^{(p)}(s)| \le p!(2/s)^p e^{-2/(3s)} \le p!\, 2^p (3p/(2e))^p \le 3^p (p!)^2$, using $p^p e^{-p} \le p!$. At $s \le 0$ all derivatives vanish. The denominator satisfies $\phi(s)+\phi(1-s) \ge 2e^{-2}$ everywhere and has derivatives $\le 2\cdot 3^p (p!)^2$. So Lemma 2.12.10 (with $F = 1/w$, $r = e^{-2}$) and Lemma 2.12.9 give ψ_1. Products, dilations and translations of ψ_1 give the cutoffs; the last claim then follows from Lemma 2.12.14. □

2.12.1.5 The transfer principle for ∂_{y}-commuting linear operations

Lemma 2.12.17 (Transfer principle; type T)**.** *Let $\mathcal{T}$ be a linear operator on smooth functions on $\Omega\times U$ such that:*

(T-a) $\partial_{\mathsf{y}}^\alpha \mathcal{T} f = \mathcal{T}\partial_{\mathsf{y}}^\alpha f$ for all admissible f and all α;

(T-b) (finite-order estimate) there are $J' \ge J$, $k \in \mathbb{N}$, $C_{\mathcal{T}}$, an output majorant m' and an envelope e' such that, if $|\partial_x^{I'}\partial_{\mathsf{y}}^{\beta} g| \le m_{I'} e$ for $|I'| \le J'$, $|\beta| \le k$, then $|\partial_x^I \mathcal{T} g| \le C_{\mathcal{T}} m'_I e'$ for $|I| \le J$.

Then $f \in \mathcal{G}_{J'}(m, e; L)$ implies $\mathcal{T} f \in \mathcal{G}_J\big(C_{\mathcal{T}}(4L)^k (k!)^2 m', e'; 4L\big)$.

Proof. Fix α and let $g_\alpha = \partial_{\mathsf{y}}^{\alpha} f$. For $|\beta| \le k$, (E3) and $L \ge 1$ give $|\partial_x^{I'}\partial_{\mathsf{y}}^{\beta} g_\alpha| \le m_{I'} e\, L^{|\alpha|+|\beta|}((|\alpha|+|\beta|)!)^2 \le \lambda_\alpha m_{I'} e$, with $\lambda_\alpha = (4L)^{|\alpha|}(|\alpha|!)^2 (4L)^k (k!)^2$. Apply (T-b) to g_α/λ_α; by linearity, $|\partial_x^I \mathcal{T} g_\alpha| \le \lambda_\alpha C_{\mathcal{T}} m'_I e'$. By (T-a), $\partial_x^I \partial_{\mathsf{y}}^{\alpha} \mathcal{T} f = \partial_x^I \mathcal{T} g_\alpha$. If $k = 0$, take $\lambda_\alpha = L^{|\alpha|}(|\alpha|!)^2$ instead; then $\mathcal{T} f \in \mathcal{G}_J(C_{\mathcal{T}} m', e'; L)$, with no radius loss. □

The point of Lemma 2.12.17 is that one *fixed* finite-order estimate of $\mathcal{T}$ suffices for *all* auxiliary orders. No auxiliary-order-dependent integration by parts or Fourier bookkeeping is needed.

Corollary 2.12.18 (Operations of type T in the construction)**.** *The following satisfy (T-a) and (T-b). The values of k and e' are listed; the output majorant m' is the finite-order class map of the text.*

(i) Haar average Π*: $k = 0$, $e' = 1$, provided $e \le 1$ (true for $e \in \{1, P\}$). For $\alpha \ne 0$, $\partial^\alpha \Pi f = 0 = \Pi \partial^\alpha f$.*

(ii) Directional torus inverse D_v^{-1}, $v \in \{v_r, v_t\}$*, on zero-Haar functions: $k = 4$, and $e' = 1$ provided $e \le 1$. It is a Fourier multiplier, and*

$$\|D_v^{-1} g\|_\infty \le \sum_{n \ne 0} \frac{|\hat g(n)|}{2\pi |v \cdot n|} \le \frac{4 \sum_{n \ne 0} |n|^{-3}}{(2\pi)^5 c_D} \max_k \|\partial_{\mathsf{y}_k}^4 g\|_\infty =: C_{\mathrm{inv}} \max_k \|\partial_{\mathsf{y}_k}^4 g\|_\infty.$$

Here $|v \cdot n| \ge c_D/|n|$ with $c_D = (4 + 2\sqrt{2})^{-1/2} = 0.382683\ldots$ (sharp), and

$$\sum_{n \ne 0} |n|^{-3} = 4\zeta(3/2)\beta(3/2) = 9.03362\ldots, \qquad C_{\mathrm{inv}} \le 0.00965.$$

We also used $|\hat g(n)| \le 4 \max_k \|\partial_k^4 g\|_\infty / (2\pi|n|)^4$ (choose k with $|n_k| = |n|_\infty \ge |n|/\sqrt{2}$). This replaces (2.13.65); no Fourier-algebra inverse is used (Remark 2.12.25). With the band constant c^{-1} of (vii) it gives the torus inverse $T_0^{-1} = c^{-1} D_{v_t}^{-1}$ of (2.14.31). There $c = c_{\mathrm{aux}} = T_g^{i_0} Q^{1+h}$ (2.13.12), and $i_0 \ge i(\ell) - \Delta_{\max}$ (S3) with (S2) gives $c^{-1} \le T_g^{1+\Delta_{\max}} S$.

(iii) Clock inverse $c_i^{-1} D_{v_t}^{-1}(E - \Pi E)$ *(Lemma 2.12.1, Lemma 2.23.1): (i)+(ii), with $c_i^{-1} \le T_g S$. The sharp value bound $\|\Phi\|_\infty \le C|A_{\mathrm{slow}}| S^{3/4}(1 + \log S)$ of Lemma 2.12.1 is used for $\alpha = 0$ and is not replaced.*

(iv) Shifted radial primitives I, J, I_χ *((2.13.66)) and $\mathcal{B} = a_r^{-1}(v_r \cdot \partial_{\mathsf{y}})^{-1}$, $\mathcal{A} = \partial_{\mathsf{R}} \mathcal{B}$ (Section 2.14): the shift $\lambda(s^{d_r} - \mathsf{R}^{d_r}) v_r$ is y-independent, so (T-a) holds by differentiation under the integral (compact radial hull). (T-b) is Lemma 2.13.9 at depth J, with the two-sided radial weight for I_χ, the corresponding one-sided weight for a raw tail, and the unweighted complete-moment estimate for Jf. If $Jf = 0$, then $I = I_\chi$ on this source and the inward tail is $-I_\chi$. The proof uses $K \ge J + 2$ integrations by parts with $\mathcal{B}$ ($K \ge J + \lceil N/\varkappa \rceil + 2$ for a complete moment with gain N), each costing four auxiliary derivatives by (ii); in the s-form each output ∂_{R} costs at most one more. Thus $k \le 4K + J$ and one may take slow input depth $J' = J + K$, since each $\mathcal{A}$ differentiates once in the slow radial variable. Here $e' = 1$ for $e \le 1$. For a complete moment this transfer uses the input inverse length at depth J'. The estimate (2.12.5) below uses only the inverse length at depth J for every gain N. The operators $\mathcal{B}$ and $\mathcal{A}$ use (ii) with (v), and type E for the slow derivative in $\mathcal{A}$.*

(v) Multiplication by slow functions *(slow cutoffs $\eta_{\ell,a}$, ϑ_q, weights, background, slow amplitudes $a_{\beta,\varsigma}$, Haar matrices, the current matrix inverse, radial moment inverses): $k=0$, $e'=e$.*

(vi) Slow integral and Volterra operators acting at fixed y *(radial moments, $-\mathsf{R}^{-1}\int_0^{\mathsf{R}} x\,f\,dx$ (2.15.40), the radial primitives P_s^{add} (2.15.14), slow moment inverses): $k=0$, and $e'=e$ because e depends only on y. (T-b) is the corresponding finite-order lemma of the text.*

(vii) Finite linear combinations and band normalization constants.

2.12.1.6 The pulse ODE; type O

Lemma 2.12.19 (Gevrey–2 zero-data and homogeneous pulse inverse)**.** *On one label rectangle, with (ξ,ζ) coordinates and $v=(\zeta+r_0)/c_i\in[0,L_p]$, let z solve*

$$c_i\partial_\zeta z = A(x,\zeta)z + g(x,\xi,\zeta), \qquad z|_{v=0}=z^0,$$

where A is a ξ-independent 2×2 matrix and z^0 is a constant vector. Assume:

(O1) (S6) the fundamental matrix satisfies $\|V(x;v,w)\|\le C_0P(v)/P(w)$ for $0\le w\le v\le L_p$, uniformly in x;

(O2) $|\partial_x^I\partial_\zeta^j A|\le K_A H_\zeta^j\, j!$ for $|I|\le J$ and all j;

(O3) $|\partial_x^I\partial_\xi^l\partial_\zeta^p g|\le m_I(x)L^{l+p}((l+p)!)^2P(v)$ for $|I|\le J$ and all l,p, with m_I nondecreasing in $|I|$;

(O4) $|z^0|\le M_0P(0)$.

Let $\beta=\max(1,C_0L_p)$ and $\gamma=2^JK_A$, and put

$$D_J(x)=(C_0M_0+\beta m_J(x))\,(\beta(1+\gamma))^J, \qquad \Lambda=\max\Big(L,\ 2H_\zeta,\ c_i^{-1}(\beta^{-1}+2^{J+1}K_A)\Big).$$

Then, for $|I|\le J$ and all l,p,

$$|\partial_x^I\partial_\xi^l\partial_\zeta^p z|\le D_J(x)\,\Lambda^{l+p}((l+p)!)^2P(v).$$

Proof. In v the equation reads $\partial_v z=Az+g$. The differentiated integral series in the proof of Lemma 2.8.5(c) converges on each compact parameter box and finite v interval. This justifies the parameter derivatives below.

Step 1 (no ζ-derivatives). Let $Z_{I,l}=\partial_x^I\partial_\xi^l z$. Since $\partial_\xi A=0$ and z^0 is constant, $Z_{I,l}$ solves $\partial_v Z_{I,l}=AZ_{I,l}+G_{I,l}$ with $G_{I,l}=\partial_x^I\partial_\xi^l g+\sum_{0<K\le I}\binom{I}{K}(\partial_x^K A)Z_{I-K,l}$. The initial value is z^0 for $(I,l)=0$ and 0 otherwise. Duhamel and (O1) give $|Z_{I,l}(v)|\le C_0P(v)\big[\delta_{I,l,0}M_0+L_p\sup_w|G_{I,l}(w)|/P(w)\big]$. Let $E_{k,l}=\max_{|I|=k}\sup|Z_{I,l}|/P$. Since $\sum_{0<K\le I}\binom{I}{K}<2^{|I|}$,

$$E_{k,l}\le C_0\delta_{k,l,0}M_0+\beta\big[m_kL^l(l!)^2+2^kK_A\max_{i<k}E_{i,l}\big].$$

By induction, $E_{k,l}\le D_kL^l(l!)^2$ with $D_k=(C_0M_0+\beta m_k)(\beta(1+\gamma))^k$: the step uses $1+\gamma\beta^k(1+\gamma)^{k-1}\le\beta^k(1+\gamma)^k$.

Step 2 (induction on p). Assume the claim for all orders $\le p$ in ζ, all $|I|\le J$ and all l. Step 1 is the case $p=0$, since $L\le\Lambda$. Differentiating the equation,

$$\partial_\zeta^{p+1}\partial_x^I\partial_\xi^l z=c_i^{-1}\Big[\partial_x^I\partial_\xi^l\partial_\zeta^p g+\sum_{K\le I}\sum_{j\le p}\binom{I}{K}\binom{p}{j}(\partial_x^K\partial_\zeta^j A)\,\partial_x^{I-K}\partial_\xi^l\partial_\zeta^{p-j}z\Big].$$

No term on the right has order $p+1$ in ζ. By (O2), (O3), the induction hypothesis and (E2),

$$\begin{aligned}|\cdot| &\le c_i^{-1}\Big[m_J L^{l+p}((l+p)!)^2 + 2^J K_A D_J \sum_{j\le p}\binom{p}{j} j! H_\zeta^j \Lambda^{l+p-j}((l+p-j)!)^2\Big]P\\ &\le c_i^{-1}[m_J + 2^{J+1}K_A D_J]\Lambda^{l+p}((l+p)!)^2 P,\end{aligned}$$

using $\Lambda \ge 2H_\zeta$, so that $\sum_j (H_\zeta/\Lambda)^j \le 2$. Since $m_J \le D_J/\beta$ and $\Lambda \ge c_i^{-1}(\beta^{-1} + 2^{J+1}K_A)$, this is $\le D_J \Lambda^{l+p+1}((l+p+1)!)^2 P$. □

Corollary 2.12.20 (Principal inverse, homogeneous pulse, cut and curled fields)**.** *Let $f_m \in \mathcal{G}_J(m, P; L)$ for a finite harmonic set. Then the following hold:*

1. *the zero-data amplitude $t_m = B_f z_m$, $z'_m = A_m z_m - B_f^\ell \mathsf{P}_n f_m$ (proof of Proposition 2.13.3), lies in $\mathcal{G}_J(m^t, P; L_t)$;*
2. *the pressure (2.13.27) lies in $\mathcal{G}_J(k_\ell^{-1} m^\pi, P; L_t)$;*
3. *ψt_m and the potential C_m in (2.13.31) obey the same depth-J estimates, with the factor k_ℓ^{-1} for C_m. For the curl remainder r_m, take $f_m \in \mathcal{G}_{J+1}(m, P; L)$. Put $L_+ = L_t(J+1)$ and let M_+ bound the normalized depth-$(J+1)$ majorants of $k_\ell C_m$ on the annulus. At depth J and radius $4L_+$, the majorants for r_m and its radial component are, respectively,*

$$C_J k_\ell^{-1} M_+(1 + |\lambda| L_+), \qquad C_J k_\ell^{-1} \rho_Q M_+.$$

   These give the orders in (2.13.33).
4. *the homogeneous pulse $(z_+, z_-) = V_1(\cdot, 0)(P(0), 0)$ ((2.13.25), proof of Lemma 2.13.2) lies in $\mathcal{G}_J(m^h, P; L_h)$;*
5. *$z_+/P \in \mathcal{G}_J(m^h, 1; L'_h)$.*

Here b_J is a finite exponent chosen at the fixed slow depth J to cover the coefficient and product bounds below, and $m_I^h = C_J S^{|I|(1+b_J)}$. In particular the value estimate has a band-independent constant, while slow derivatives can cost powers of S. The constants satisfy $L_t, L_h \le C_J S^{1+b_J} \max(L, 1)$, with m^t, m^π equal to m times $C_J S^{1+J(1+b_J)}$. In particular the source power ρ^a, the slow weight and the envelope P are kept, as in Lemma 2.13.2.

Proof. Put $D = -B_f^\ell \mathsf{P}_n$. On the strip of Lemma 2.12.13, D has a uniform value bound. Its slow derivatives through any fixed depth J have a bound $C_J S^{u_J}$, with $u_0 = 0$. This follows by Leibniz's rule for its two factors. The coefficient is independent of ξ. Cauchy's estimate in v and $c_i^{-1} \le T_g S$ bound $\partial_x^K \partial_\zeta^j D$ by $C_J S^{u_J}(T_g S)^j j!$. By Lemma 2.12.14 the radius for f_m in (ξ, ζ) is at most $\sqrt{2}L$. Choose $L_g = 2\max\{1, \sqrt{2}L, T_g S\}$. For $0 \le j \le p$,

$$\binom{p}{j} j!((l+p-j)!)^2 \le ((l+p)!)^2.$$

Use this inequality in the differentiated product Df_m, summing the geometric factors $(T_g S/L_g)^j$ and the finitely many slow splittings. Thus (O3) holds with L_g and majorant $C_J S^{u_J} m_I$ at depth $|I| \le J$, for the nondecreasing input majorants. The uniform value bound supplies $u_0 = 0$ when applying this argument at depth zero.

For (O2), take $H_\zeta = c_i^{-1}$ and $K_A = C_J S^{v_J}$ from the same strip bound, with $v_0 = 0$ for the principal ODE coefficients. By (S6), $C_0 \le e^{C_E L_p/S} = O(1)$, so $\beta = \max(1, C_0 L_p) \le CS$. For zero initial data Lemma 2.12.19 now gives the depth-J amplitude factor and radius

$$C_J S^{1+u_J+J(1+v_J)}, \qquad \Lambda \le \max\{L_g, 2T_g S, C_J S^{1+v_J}\}.$$

The slow majorant in this formula is the maximum of the input majorants through the chosen depth. Apply the same calculation through $|I|$ for an individual jet. Returning to y costs a factor at most 1.21 in the radius. Multiplying by B_f to obtain t_m costs a fixed polynomial in S at positive slow depth and a uniform value factor at depth zero. This follows from the same Cauchy and product estimates. For (2) and (3), use the explicit formulas (2.13.27) and (2.13.31). Apply the product, strip, evaluated-derivative and cutoff estimates in Lemmas 2.12.9, 2.12.13, 2.12.15 and 2.12.16. After extracting k_ℓ^{-1}, the pressure multipliers in (2.13.27) have uniformly bounded strip values and polynomial bounds at every fixed slow depth. The frame and the uncut potential multiplier have the same strip estimates. Lemma 2.12.16 gives the Gevrey–2 estimate for the fixed compact cutoff with a band-independent radius, and the product rule combines the two estimates. For $J \ge 1$ enlarge b_J to absorb $u_J + Jv_J$ and the finitely many additional product exponents into Jb_J, with b_J also large enough for the displayed radius. At $J = 0$ the forced amplitude and pressure cost CS and the homogeneous amplitude costs C. This proves the stated exponents for the principal quantities and the ODE row of Table 2.3. Each term of r_m uses at most one slow derivative of C_m. Indeed $\mathcal{D} = \partial_{\mathsf{R}} + \lambda a_r D_{v_r}$ costs one slow derivative and at most $C_J|\lambda|L_+$ for the auxiliary derivative by Lemma 2.12.15. The coefficient a_r and its prescribed derivatives are bounded on the fixed annulus. The connection R^{-1} is bounded there. The radial component of r_m is $-\rho_Q \partial_{\mathsf{Z}} C_{m,\theta}$, which explains its better majorant. The evaluated-derivative row of Table 2.3 retains these factors. For (4), use Lemma 2.12.19 at depth $|I|$ with $g = 0$ and $M_0 = 1$. Its factor $D_{|I|} = C_0[\beta(1 + 2^{|I|}K_A)]^{|I|}$ gives the displayed m_I^h. The initial value $P(0)$ is independent of x because (2.13.23) uses frozen box constants. For (5), multiply by $1/P$ using Lemma 2.12.7. This factor also has zero slow derivatives. The lower bound in (2.13.25) permits division by z_+/P using Corollary 2.12.11(b). □

2.12.1.7 One finite stage: the operation graph and the composite bound

Definition 2.12.21 (Finite-stage operation graph)**.** For a stage n (including the finite initialization, Section 2.4.1), $\mathfrak{G}_n$ is a finite directed acyclic graph. A vertex t is a *label-indexed family* $\{f_{t,\gamma}\}$ of scalar coefficient components produced by one operation applied uniformly over labels. It carries a type $\tau(t) \in \{\mathrm{P}, \mathrm{C}, \mathrm{E}, \mathrm{O}, \mathrm{T}, \mathrm{V}, \Sigma\}$, or is a leaf of type S (slow, y-independent), A (Lemma 2.12.13), K (Lemma 2.12.16) or Env (Lemma 2.12.7). Type Σ is a label sum with pointwise overlap $\le N_{\mathrm{ov}}$ in the slow supports, or a sum over lifts (S3). Its closure rule is trivial: the majorant is multiplied by N_{ov} and L is the maximum over the summands. The finite-order ledger assigns to t an order a_t, a weight $\mathfrak{w}_t \in \{\mathsf{W}, \mathsf{W}^{1/2}, 1\}$ and an envelope $e_t \in \{1, P\}$. The normalized pulse z_+/P is one output of the pulse estimate. Its proof multiplies the envelope P of z_+ by P^{-1}, whose relative derivative estimate is given in Lemma 2.12.7. Indeed (2.13.24) gives $P(0)^{-1} \ge e^{cL_p/4}$. The clock exponentials are used only as weights in the evolution estimate and have the separate relative bound in Corollary 2.12.11(c).

Hypothesis 2.12.22 (Inventory). Every coefficient produced at stage n is a vertex of $\mathfrak{G}_n$. Each ledger assertion at t is obtained by applying the amplitude rule of $\tau(t)$ to the ledger entries of the parents of t. Where the ledger uses an exact cancellation or a structural gain, the vertex is the post-cancellation or split expression of Definition 2.12.32, and gains of type T are applied on the ∂_{y}-invariant subspaces of Lemma 2.12.28.

This is a reading of the finite stage (Sections 2.13–2.18 and the initialization), not a new assumption on the construction; it is the standing Hypothesis 2.3.21, and Proposition 2.16.1 in Section 2.16 verifies it for the mean–wave stage with the closure lemmas of Section 2.12.1.8.

type / lemma	p_t	radius factor κ_t; S-power β_t	extra depth / amplitude factor
P product 2.12.9	1	1; 0	0; $\frac{8}{3}2^J$ (orders add)
C composition 2.12.10, 2.12.11	1	$\max(1, 32M_0/(3r))$; roots: $r = r_\theta$, $\theta \le \frac{1}{2}$, $k \le 3$; b_M	0; $\frac{3}{8}(2^k + \frac{5}{3})B\,J!\mu^{-J}$
E eval. derivative 2.12.15	1	4; 0	1; $4L\lvert w\rvert_1 2^J \lVert c\rVert_{C^J}$ (incl. $\rho^{-\varkappa}$, ρ)
O pulse ODE 2.12.19, 2.12.20	1	C_J; $1 + b_J$	0; $C_J S^{1+J(1+b_J)}$
T ∂_y-commuting 2.12.17, 2.12.18	1	4; 0	$J' - J$; $C_{\mathcal{T}}(4L)^k(k!)^2$
V linear change 2.12.14	1	$\le 6^{\Delta_{\max}}$; 0	0; 1
Σ label sum Def. 2.12.21	1	1; 0	0; N_{ov}
leaf S / A / K / Env –, 2.12.12, 2.12.16, 2.12.7	–	1 / $1.21T_g$ / $1.21K_\chi/2r_0$ / $1.21T_g$; 0 / 1 / 0 / 1	–

Table 2.3: Closure data for the inverse length $L_t \le \kappa_t S^{\beta_t} \max(L_*, 1)$, with L_* the maximum over the parents. For composition take $M \le M_0 S^{b_M}$, $b_M \ge 0$, so $\max(1, 32M/(3r)) \le \kappa_t S^{b_M}$.

Theorem 2.12.23 (All-auxiliary-order bound at one finite stage)**.** *Assume Hypothesis 2.12.22 and the inputs (S1)–(S10). Fix n and J. Then there are an input depth $J_0 < \infty$ and, for every vertex t of $\mathfrak{G}_n$, constants C_t, b_t, N_t, K_t, B_t, independent of α, of $\ell \ge \ell_0$ and of the label, such that every $f_{t,\gamma}$ satisfies*

$$f_{t,\gamma} \in \mathcal{G}_J\big(C_t \rho^{a_t} S^{b_t} \mathfrak{w}_t \mathcal{L}_W{}^{N_t},\, e_t;\, K_t S^{B_t}\big).$$

Take $\beta_t \ge 0$ and $\kappa_t \ge 1$ in Table 2.3, including the leaf data. Let $\mathscr{P}_n$ be all directed paths from a leaf to any vertex, including single leaves. In (2.12.3) one may take

$$B_{n,J} = \max_{\pi \in \mathscr{P}_n} \sum_{t \in \pi} \beta_t, \qquad K_{n,J} = \max_{\pi \in \mathscr{P}_n} \prod_{t \in \pi} \kappa_t.$$

The two maxima can occur on different paths.

Proof. Order $\mathfrak{G}_n$ topologically. Starting with output depth J, assign to each parent the depth of its child plus the extra depth in Table 2.3; take the maximum if a parent has several children. Finiteness gives one input depth J_0. The slow leaves have every required finite ordinary jet, and the other leaves satisfy Lemmas 2.12.13, 2.12.16 and 2.12.7.

Apply the closure lemma for each vertex at its assigned depth. It gives

$$L_t \le \kappa_t S^{\beta_t} \max(L_*, 1), \qquad B_t = B_* + \beta_t, \quad K_t = \kappa_t K_*,$$

where B_* and K_* are the separate maxima over the parents (respectively 0 and 1 at a leaf). Induction gives the maximum path sum and maximum path product among paths ending at t. The amplitude

rules are unchanged: products add orders; a protected root is $\mathfrak{X}$ times an order-zero factor; evaluated derivatives carry their recorded slow coefficient; the pulse inverse preserves both the weight and P; and type T uses the finite-order map on its specified invariant subspace. Hypothesis 2.12.22 requires the post-cancellation expressions at every structural gain. Linear changes and bounded-overlap sums preserve the same classes.

The extra factors from these rules are powers of L_*, S, the fixed value margins and the finite-depth constants. Since $L_* \le K_* S^{B_*}$, they enlarge only C_t, b_t, N_t, not the ledger order a_t, weight $\mathfrak{w}_t$ or envelope e_t. Each constant depends on the fixed graph, coefficient bounds, value margins, finite harmonic set, torus geometry and overlap bound. It is independent of α, band and label. Taking the two maxima over the vertices gives the stated bounds. □

Corollary 2.12.24 (Gevrey flatness of the Gaussian endpoint errors)**.** *For each fixed ordinary order and all α, the endpoint residual $(1-\psi)f_m + \psi' t_m$ of (2.13.28) satisfies $|\partial_x^I \partial_{\mathsf{y}}^{\alpha}(\cdot)| \le C\rho^a S^b e^{-c_* S} L^{|\alpha|}(|\alpha|!)^2$, with $L \le K S^B$ and $c_* > 0$. This is the all-auxiliary-order form of (2.13.29).*

Proof. On $\operatorname{supp}(1-\psi) \cup \operatorname{supp}\psi'$ one has $|v - L_p/2| \ge L_p/5$. Hence $P \le e^{-c(L_p/5)^2/L_p}$ by (2.13.24). Apply Theorem 2.12.23 together with Lemmas 2.12.9 and 2.12.16. □

Remark 2.12.25 (Relation to the Fourier algebra). For $e = 1$, (E5) gives $|\hat f(j)| \le e^4 M(1+\sqrt{t})e^{-2\sqrt{t}}$, $t = \sqrt{2}\pi|j|/L$, and therefore $\|f\|_R \le CM(1+L)^2$ at $R = \pi/(2\sqrt{2}L)$. Conversely, maximizing $t^{2p}e^{-(1-\sqrt{\theta})t}$ with $t = \sqrt{R|j|}$ and using $(2p)! \le 4^p (p!)^2$ gives $\|D^\alpha f\|_\infty \le (K_\theta/R)^{|\alpha|}(|\alpha|!)^2 \|f\|_R$. Thus the two descriptions agree without an envelope. The pointwise class is used here to retain P: dropping it from a zero-data source introduces the factor $\int_0^v P(w)^{-1}\,\mathrm{d}w$, which can be exponentially large in S.

The last diagonal. For fixed (n, J), the quantities $C_{n,J}, b_{n,J}, N_{n,J}, K_{n,J}, B_{n,J}$ are finite and are fixed before δ_n. The conditions $\rho^\gamma \ll L_{n,J}^{-1} = K_{n,J}^{-1} S^{-B_{n,J}}$ and $C_{n,J}\rho^\epsilon S^{b_{n,J}} \le 2^{-n}$ are finitely many conditions of the form $\rho^\epsilon S^B \to 0$. They are met on one decreasing threshold together with (2.18.11). The flatness $Q^{-B}S^N e^{-cS} = o(Q^M)$ is Lemma 2.12.2. No uniform-in-n radius is asserted or needed (Section 2.4.1).

2.12.1.8 Closure lemmas for the mean–wave stage

The inventory of the mean–wave stage (the mean equations, the finite initialization and the paired step; Proposition 2.16.1) uses four facts that the closure lemmas above do not state in the needed form: the protected roots there have the relative margin $|\mathfrak{X}| \le V^2/2$ (Lemma 2.14.1), not $V^2/4$; several ledger assertions are *structural gains* for perpendicular parts of roots ((2.14.17), (2.14.38), (2.14.56), Section 2.14); several gains of type T hold only on the zero-Haar (or zero-moment) subspace ((2.14.13), proof of Lemma 2.14.2, (2.13.68)); and many vertices are y-independent. Lemmas 2.12.26–2.12.30 supply these facts.

Lemma 2.12.26 (Protected roots with a relative margin $\theta < 1$)**.** *Fix $0 \le \theta < 1$ and $v_* > 0$, and put $r_\theta = (1-\theta)\min(v_*, v_*^2)/8$.*

(a) Let $V, \mathfrak{X}$ be real, $V \ge v_*$, $|\mathfrak{X}| \le \theta V^2$. If $|V' - V| \le r_\theta$ and $|\mathfrak{X}' - \mathfrak{X}| \le r_\theta$ ($V', \mathfrak{X}' \in \mathbb{C}$), then $\operatorname{Re}(V'^2 + \mathfrak{X}') \ge \frac{39}{64}(1-\theta)V^2$ and $\operatorname{Re} V' \ge \frac{7}{8}v_*$.

(b) If, in addition, $V, \mathfrak{X}$ satisfy (i) of Lemma 2.12.10 with constants M, L_u, then

$$\sqrt{V^2+\mathfrak{X}} - V = \mathfrak{X}\, H(V,\mathfrak{X}), \qquad H = \frac{1}{\sqrt{V^2+\mathfrak{X}}+V},$$
$$H \in \mathcal{G}_J\Big(\tfrac{3}{8}(4+\tfrac{5}{3})\tfrac{8}{7v_*}\, I!\, \mu^{-|I|},\, 1;\, L\Big),$$

with $L = L_u \max(1, 32M/(3r_\theta))$ and $\mu^{-1} = 3(1+32M/(3r_\theta))$.

(c) If $V \ge v_*$, $|\mathfrak{X}_1|, |\mathfrak{X}_2| \le \theta V^2$ and $V, \mathfrak{X}_1, \mathfrak{X}_2$ satisfy (i), then

$$H_2(V,\mathfrak{X}_1,\mathfrak{X}_2) = \big(\sqrt{V^2+\mathfrak{X}_1} + \sqrt{V^2+\mathfrak{X}_2}\big)^{-1}$$

satisfies $\sup|H_2| \le B_2 := 4/(\sqrt{39(1-\theta)}\, v_*)$ and $H_2 \in \mathcal{G}_J(\frac{3}{8}(8+\frac{5}{3})B_2\, I!\, \mu^{-|I|}, 1; L)$, with L, μ as in (b), and $\sqrt{V^2+\mathfrak{X}_1} - \sqrt{V^2+\mathfrak{X}_2} = (\mathfrak{X}_1 - \mathfrak{X}_2)H_2$.

For $\theta \le \frac{1}{4}$ one may instead use the radius $\min(v_*, v_*^2)/8$ of Corollary 2.12.11(a).

Proof. (a) Write $V' = V + d$. Then $\operatorname{Re} V'^2 \ge V^2 - 2V|d| - |d|^2$ and $\operatorname{Re}\mathfrak{X}' \ge -\theta V^2 - r_\theta$. Since $V \ge v_*$, one has $r_\theta \le (1-\theta)V/8$ and $r_\theta \le (1-\theta)V^2/8$. Hence $2Vr_\theta \le \frac{16}{64}(1-\theta)V^2$, $r_\theta^2 \le \frac{1}{64}(1-\theta)V^2$ and $r_\theta \le \frac{8}{64}(1-\theta)V^2$, so $\operatorname{Re}(V'^2 + \mathfrak{X}') \ge (1-\theta)V^2(1-\frac{25}{64})$. Also $\operatorname{Re} V' \ge V - r_\theta \ge \frac{7}{8}v_*$. (b) By (a), the principal root $R' = \sqrt{V'^2+\mathfrak{X}'}$ is holomorphic on the polydisc and $\operatorname{Re} R' > 0$. Thus $|R'+V'| \ge \operatorname{Re} V' \ge \frac{7}{8}v_*$, so $B(P_0) \le \frac{8}{7v_*}$. Apply Lemma 2.12.10 with $k=2$ and $r = r_\theta$, with the corrected constant $\frac{3}{8}(2^k + \frac{5}{3})$. (c) For $\operatorname{Re} z \ge 0$ one has $\operatorname{Re}\sqrt{z} = \sqrt{(|z| + \operatorname{Re} z)/2} \ge \sqrt{\operatorname{Re} z}$. By (a), each root has real part at least $\sqrt{39(1-\theta)/64}\, v_*$, which gives B_2. Apply Lemma 2.12.10 with $k=3$. The identity is the rationalization. □

Lemma 2.12.27 (Mean-value split of a protected root)**.** *Let $F(W,Y) = \sqrt{W^2+Y} - W$. Let $W_0, W_1, \mathfrak{X}, \bar{\mathfrak{X}}$ be real, satisfy (i) of Lemma 2.12.10 with constants M, L_u, and assume*

$$W_0, W_1 \ge v_*, \qquad |\mathfrak{X}|, |\bar{\mathfrak{X}}| \le \theta v_*^2 \quad (0 \le \theta < 1).$$

Then, identically,

$$F(W_1,\mathfrak{X}) = F(W_0,\bar{\mathfrak{X}}) + (W_1 - W_0)\,\bar{\mathfrak{X}}\, G(W_0,W_1,\bar{\mathfrak{X}}) + (\mathfrak{X} - \bar{\mathfrak{X}})\, H_2(W_1,\mathfrak{X},\bar{\mathfrak{X}}), \tag{2.12.4}$$

where H_2 is as in Lemma 2.12.26(c) and

$$G(w_0,w_1,y) = -\int_0^1 \frac{d\tau}{R_\tau(R_\tau + w_\tau)}, \qquad w_\tau = w_0 + \tau(w_1 - w_0), \quad R_\tau = \sqrt{w_\tau^2 + y}.$$

Moreover $G \in \mathcal{G}_J(\frac{3}{8}(8+\frac{5}{3})B_G\, I!\mu^{-|I|}, 1; L)$ with L, μ as in Lemma 2.12.26(b) and $B_G = 64/(7\sqrt{39(1-\theta)}\, v_*^2)$. If W_0 and $\bar{\mathfrak{X}}$ are y*-independent, then $F(W_0,\bar{\mathfrak{X}})$ is* y*-independent and*

$$(I-\Pi)F(W_1,\mathfrak{X}) = (I-\Pi)\big[(W_1-W_0)\bar{\mathfrak{X}}\, G + (\mathfrak{X}-\bar{\mathfrak{X}})H_2\big].$$

Proof. The rationalization gives $F(W_1,\mathfrak{X}) - F(W_1,\bar{\mathfrak{X}}) = (\mathfrak{X}-\bar{\mathfrak{X}})H_2(W_1,\mathfrak{X},\bar{\mathfrak{X}})$. For fixed Y, $\partial_W F = W/R - 1 = -(R-W)/R = -Y/(R(R+W))$ with $R = \sqrt{W^2+Y}$. The fundamental theorem of calculus along w_τ gives $F(W_1,\bar{\mathfrak{X}}) - F(W_0,\bar{\mathfrak{X}}) = (W_1-W_0)\bar{\mathfrak{X}}\, G(W_0,W_1,\bar{\mathfrak{X}})$. This proves (2.12.4).

For the bound, let $|w_i' - W_i| \le r_\theta$ and $|y' - \bar{\mathfrak{X}}| \le r_\theta$. Then $|w_\tau' - w_\tau| \le r_\theta$, $w_\tau \ge v_*$ and $|\bar{\mathfrak{X}}| \le \theta v_*^2 \le \theta w_\tau^2$. Lemma 2.12.26(a) gives $|R_\tau'| \ge \operatorname{Re} R_\tau' \ge \sqrt{39(1-\theta)/64}\, v_*$ and $|R_\tau' + w_\tau'| \ge \operatorname{Re} w_\tau' \ge \frac{7}{8}v_*$. So the integrand is holomorphic in (w_0', w_1', y'), continuous in τ, and bounded by B_G. Hence G is holomorphic on the polydisc with $\sup|G| \le B_G$. Apply Lemma 2.12.10 with $k=3$. The last claim follows because $(I-\Pi)$ annihilates y-independent functions. □

Use. In the four ledger assertions listed below (Table 2.4, rows R7, R13, R18, R24) the parents are: W_0 the Haar swirl (V_{H} or $V_{\mathrm{H}}+v$ with slow v), W_1 the full swirl in the radicand, $\bar{\mathfrak{X}} = \mathsf{R}k\,\overline{M}$ with $\overline{M} = \int \Pi g\, d\mathsf{R}$ the slow full moment, and $\mathfrak{X} = \mathsf{R}kM$. The amplitude rule of type P then gives the ledger order of the perpendicular part: the order of $W_1 - W_0$ (namely s) plus the order of $\overline{M}$, and a coefficient-flat term from $\mathfrak{X} - \bar{\mathfrak{X}}$. The hypotheses $W_0, W_1 \geq v_*$ and $|\mathfrak{X}|, |\bar{\mathfrak{X}}| \leq \theta v_*^2$ of Lemma 2.12.27 are not stated elsewhere in this absolute form (Lemma 2.14.1 gives only $|\mathfrak{X}| \leq V_M^2/2$, and nothing for $\bar{\mathfrak{X}}$). In rows R7, R13, R18 and R24 they are supplied by Lemma 2.12.30, because $\mathfrak{X} = \mathsf{R}kM$ and $\bar{\mathfrak{X}} = \mathsf{R}k\overline{M}$ have positive ledger orders. This is the exact form of the "integral mean-value formula" (2.14.20). $F(W_0, \bar{\mathfrak{X}})$ is a slow vertex.

Lemma 2.12.28 (Transfer on a ∂_{y}-invariant subspace)**.** *Let $\mathcal{V}$ be a linear space of smooth functions on $\Omega \times U$ with $\partial_{\mathsf{y}}^{\alpha}\mathcal{V} \subset \mathcal{V}$ for all α. Let $\mathcal{T}$ be linear on $\mathcal{V}$, with (T-a) of Lemma 2.12.17 for $f \in \mathcal{V}$, and with (T-b) for all $g \in \mathcal{V}$. Then the conclusion of Lemma 2.12.17 holds for every $f \in \mathcal{V} \cap \mathcal{G}_{J'}(m, e; L)$. The following subspaces are ∂_{y}-invariant:*

(i) $\mathcal{V}_0 = \{f : \Pi f = 0\}$;

(ii) $\mathcal{V}_1 = \{f : \Pi f = 0,\ \mathcal{J}(\mathsf{R}f) = 0\}$ *and the integrand space* $\mathcal{V}_{\mathrm{int}} = \{h : \Pi h = 0,\ \mathcal{J}h = 0\}$. *Multiplication by* R *maps* $\mathcal{V}_1$ *into* $\mathcal{V}_{\mathrm{int}}$. *The same invariance holds for the constraint* $\mathcal{J}(\mathsf{R}^2 f) = 0$;

(iii) $\mathcal{V}_0$ *for functions of the slow variables with one slow variable held fixed (the subspaces are defined fibrewise).*

Proof. In the proof of Lemma 2.12.17, (T-b) is applied only to g_α/λ_α with $g_\alpha = \partial_{\mathsf{y}}^{\alpha} f$, and $g_\alpha \in \mathcal{V}$. For (i): $\Pi\partial_{\mathsf{y}}^{\alpha} f = 0$ for $\alpha \neq 0$ because the integral of a derivative of a periodic function vanishes, and $\Pi\partial^0 f = \Pi f$. For (ii), the translation in (2.14.8) commutes with every auxiliary derivative. Hence $\mathcal{J}(\mathsf{R}^j \partial_{\mathsf{y}}^{\alpha} f) = \partial_{\mathsf{y}}^{\alpha}\mathcal{J}(\mathsf{R}^j f)$ for $j = 0, 1, 2$. On $\mathcal{V}_{\mathrm{int}}$, $\mathcal{L}h = -\mathcal{I}_\chi h$ because $\mathcal{J} = \mathcal{I} + \mathcal{L}$ and $\mathcal{I}_\chi = \mathcal{I} - \chi\mathcal{J}$. □

Partial primitives. For $f \in \mathcal{M}^a \cap \mathcal{V}_0$, (2.13.67) gives $\mathcal{I}_\chi f \in \mathcal{M}^{a+\varkappa}$. On $\mathcal{V}_{\mathrm{int}}$ the same estimate holds for $\mathcal{L}$. In (2.14.33), $\gamma_{\mathsf{Z}} \in \mathcal{V}_1$ and $\mathsf{R}\gamma_{\mathsf{Z}} \in \mathcal{V}_{\mathrm{int}}$. Thus the prefix in $\beta = -\rho\mathsf{R}^{-1}\mathcal{L}(\mathsf{R}\gamma_{\mathsf{Z}})$ gains $\varkappa$ before the explicit factor ρ. Corollary 2.12.18(iv) transfers this bound at each fixed slow depth.

Complete moments. Let $f \in \mathcal{M}^a \cap \mathcal{V}_0$ have the mixed bound (2.12.3) with its $\mathcal{M}^a$ weight, envelope $e \leq 1$ and input inverse length $1 \leq L \leq K_J S^{B_J}$ at slow depth J. For every $N \geq 0$, on the observation annulus of (2.13.68) we have

$$\|\partial_x^I \partial_{\mathsf{y}}^{\alpha}\mathcal{J}f\|_\infty \leq C_{J,N}\rho^{a+N}S^{b_{J,N}}(4L)^{|\alpha|}(|\alpha|!)^2, \qquad |I| \leq J. \tag{2.12.5}$$

Here L is the same for every gain N. To see this, fix $g = \partial_x^I \mathcal{J}f$. Write $U = \mathsf{R}^{d_r}$ and $u = s^{d_r} - U$ as in Lemma 2.13.10(a). The complete integral ranges over $\mathbb{R}$ after zero extension. At fixed u its translation $\lambda u v_r$ is independent of the slow variables. Differentiating thus uses only slow derivatives of the source through J and bounded derivatives of the radial Jacobian on the fixed source hull. Since $\mathsf{W}\mathcal{L}_W^d$ is bounded for every fixed d and the envelope is at most one, this gives

$$\|\partial_{\mathsf{y}}^{\alpha} g\|_\infty \leq AL^{|\alpha|}(|\alpha|!)^2, \qquad A = C_J\rho^a S^{b_J}.$$

The ordinary estimate (2.13.68) gives separately $\|g\|_\infty \leq D_N = C'_{J,N}\rho^{a+4N}S^{d_{J,N}}$. Only this latter estimate uses ordinary source derivatives of depth increasing with N.

For $t = 2\pi|k|_\infty/L$, integrate by parts in a coordinate with $|k_i| = |k|_\infty$. By (E5) of Lemma 2.12.5, $|\widehat{g}(k)| \le CA(1+\sqrt{t})e^{-2\sqrt{t}}$, using the value bound A for $t < 1$. Interpolation with $|\widehat{g}(k)| \le D_N$ gives

$$|\widehat{g}(k)| \le CA^{3/4}D_N^{1/4}(1+\sqrt{t})^{3/4}e^{-3\sqrt{t}/2}.$$

For $j = |\alpha|$, $t^j e^{-\sqrt{t}} \le 4^j(j!)^2$, by maximizing $s^{2j}e^{-s}$ at $s = 2j$. Grouping k by integer intervals of $|k|_\infty/L$ gives $\sum_k (1+\sqrt{t})^{3/4}e^{-\sqrt{t}/2} \le C(1+L)^2$ in dimension two. Fourier summation therefore bounds $\|\partial_{\mathsf{y}}^\alpha g\|_\infty$ by $C(1+L)^2A^{3/4}D_N^{1/4}(4L)^j(j!)^2$. The first factors have order ρ^{a+N} with a polynomial in S, since L has a polynomial bound in S. This proves (2.12.5). In the finite operation graph it suffices to reserve the largest flatness gain used at each vertex.

Lemma 2.12.29 (y-independent vertices)**.** *If f is y-independent and $|\partial_x^I f| \le m_I$ for $|I| \le J$, then $f \in \mathcal{G}_J(m, 1; L)$ for every $L \ge 1$. In particular, for every vertex that is a Haar projection, a radial moment of a Haar projection, a state integral, a five-row datum or a slow-matrix inverse, Theorem 2.12.23 reduces to the finite-order ledger. Exact cancellations among such vertices ((2.14.37), (2.14.52), (2.14.57), (2.15.29)) need no post-cancellation vertex.*

Proof. $\partial_{\mathsf{y}}^\alpha f = 0$ for $\alpha \ne 0$. □

Lemma 2.12.30 (Value margins from positive orders)**.** *Let V be a vertex with $V \ge 2v_*$ on an open slow set $\Omega_k \times \mathbb{T}^2$, and let v, $\mathfrak{X}$ be vertices with ledger orders $a_v, a_{\mathfrak{X}} > 0$ and envelopes ≤ 1. Here v is the sum of all increments of the current stage that enter the base of the root (at (2.14.35), (2.14.54) and (2.15.42) the base is the updated swirl), and the ledger bound of $\mathfrak{X}$ may carry the weight $\mathfrak{w}$, $\sqrt{\mathfrak{w}}$, or no weight. Fix $\theta \in (0,1)$. Then there is ℓ_1, depending only on the ledger constants of $v, \mathfrak{X}$ at slow order 0, such that for $\ell \ge \ell_1$: $V + v \ge v_*$ and $|\mathfrak{X}| \le \theta v_*^2$ on $\Omega_k \times \mathbb{T}^2$.*

Proof. At $I = \alpha = 0$ the ledger gives $|v| \le C\rho^{a_v}S^b\,\mathfrak{w}\mathcal{L}_W{}^N \le CC_N\rho^{a_v}S^b$, because $\sup_{0<w\le e^{-2}} w(1+\log(1/w))^N =: C_N < \infty$ (and likewise with $\sqrt{w}$). The radicands $\mathsf{R}kM$ contain full radial moments, whose bounds are unweighted (Section 2.14); they are needed only on $\Omega_k \supset \operatorname{supp} k$, where the weight has a positive plateau, so the unweighted bound there is a weighted one up to a constant. Since $\rho^{a_v}S^b = 2^{-\ell h a_v}\ell^{6b/5} \to 0$, the claim follows for v, and likewise for $\mathfrak{X}$. □

This is the precise content of "a single sufficiently small threshold satisfies all these conditions" (proof of Proposition 2.15.2) for the five protected roots: the base swirls are V_M, $V_M + v$ or V_s, with $V_M \ge 2v_*$ on the protected regions (Section 2.14) and $V_s \ge 2v_*$ (proof of Lemma 2.15.1); the increments v, δ_C and the radicand perturbations $\mathsf{R}kM$ have positive orders. The roots are needed only on a slow neighbourhood Ω_k of $\operatorname{supp} k$ (Section 2.14, proof of Lemma 2.14.1); $\mathfrak{X}\,H$ vanishes on $(\Omega_k \setminus \operatorname{supp} k) \times \mathbb{T}^2$ and is extended by zero.

Lemma 2.12.31 (Uniform swirl margin on both sides; input (I1))**.** *Fix $-8 < a_- < a_+ < -3$ with $\operatorname{supp} b \subset (a_-, a_+)$; this is possible because $\operatorname{supp} b \Subset (-8,-3)$. On each side let $\Omega_k = \{a_- < y_p < a_+\}$, intersected with the enlarged band boxes. Here $y_p = 2\log(\hat{\xi}/\hat{\xi}_p(\eta))$ on $t > 0$ and $y_p = 2\log(\hat{\xi}/\hat{\xi}_{p,b})$ on $t < 0$, with $\frac{\hat{\xi}^2}{2} = \mathsf{R}^2/(2\bar{q})$. So Ω_k is an open slow neighbourhood of $\operatorname{supp} k$ with $\overline{\Omega_k} \subset \Sigma$.*

Let V_{lead} be the swirl entry of the normalized leading field: on $t > 0$, $\mathsf{R}F_{\mathrm{lead}}$ (after (2.13.1)); on $t < 0$, $\bar{q}_b^{-\frac{1}{2}-h}E_0$ with the backward patch swirl $E_0 = c_{\mathrm{patch}}(1+\beta^2)^{-1}(\hat{\xi}/\sqrt{2})^{-1-2\lambda}$ (Lemma 2.3.3). Put

$$v_* := \tfrac{1}{4}\min\Big\{\min_{\overline{\Omega_k},\,t>0} V_{\mathrm{lead}},\ \min_{\overline{\Omega_k},\,t<0} V_{\mathrm{lead}}\Big\}.$$

Then $v_* > 0$ is independent of n, ℓ and the label. On both sides $V_s = V_{\mathrm{lead}} \ge 4v_*$ on Ω_k. For each stage n there is ℓ_n such that $V_M \ge 2v_*$ there for $\ell \ge \ell_n$, uniformly in the auxiliary variables. This v_* is the constant of input (I1), of (T5′) and of the root radius $r_{1/2} = \min(v_*, v_*^2)/16$.

Proof. Positivity.

- On $t > 0$: $\overline{\Omega_k}$ lies in the closure of the actual active set, where F_{lead} has a positive uniform lower bound (after (2.13.1)). Also $\mathsf{R} \geq \mathsf{R}_- > 0$. So $V_{\mathrm{lead}} \geq \mathsf{R}_- \inf F_{\mathrm{lead}} > 0$. (Alternatively, $\overline{\Omega_k} \subset K_0$, where Proposition 2.3.2 gives $T_\theta \geq cH > 0$.)

- On $t < 0$: $\overline{\Omega_k} \subset I_{\mathrm{mean}} = \frac{\hat{\xi}_{p,b}^2}{2} e^{(-8,-3)}$, where $E_0 > 0$ (Lemma 2.3.3), and $\bar{q}_b \in (\frac{1}{4}, 4)$. So $V_{\mathrm{lead}} \geq \frac{1}{8} c_{\mathrm{patch}} (\frac{\hat{\xi}_{p,b}^2}{2} e^{a_+})^{-1/2-\lambda} > 0$.

The band normalization $\mathsf{R} = r/\sqrt{Q}$, $\mathsf{Z} = z/Q^{\frac{1}{2}-h}$, $\mathsf{T} = t/Q$ is the self-similar scaling of the leading field. So on each side V_{lead} is one continuous function of the slow variables, the same for all ℓ, on the compact set $\overline{\Omega_k}$. Hence $v_* > 0$, and it does not depend on ℓ, n or the label.

On this subslot every positive-order slow velocity and potential cutoff term vanishes by (2.6.21), (2.6.31) and Proposition 2.7.2(b). Thus $V_s = V_{\mathrm{lead}}$. The ledger expresses $V_M - V_s$ as a finite sum of positive-order vertices with envelopes bounded by one:

- the initialization roots of order at least one, including the order-two difference in (2.15.15);
- the tangential mean increments of the earlier stages, $(\Delta u_M)_{\tan} \in \mathcal{M}^{s_*}$ with $s_* \geq \frac{3}{2} - 4\varkappa$ (2.15.47);
- $V^\perp \in \mathcal{M}^s$ (2.14.6).

These lie in the W-classes on $t > 0$ and in the W_b-classes on $t < 0$. At order 0 each term is bounded by $C\rho_Q^a S_\ell^B \sup_{0<w\leq 1} w(1 + \log(1/w))^N$ (also with $\sqrt{w}$, or with no weight), and $a > 0$. So

$$|V_M - V_{\mathrm{lead}}| + |V_s - V_{\mathrm{lead}}| \leq C_n\, 2^{-\ell h a_n} \ell^{6B_n/5}, \qquad a_n > 0.$$

The right side tends to 0 and decreases for $\ell > 6B_n/(5ha_n \log 2)$. Hence it is $\leq 2v_*$ for $\ell \geq \ell_n$, the larger of the two sides' thresholds. Thus $V_M \geq 4v_* - 2v_* = 2v_*$.

No circularity. v_* is fixed by the two leading members, before any stage. The constants C_n, a_n, B_n come from the stage-n operations, which use v_* and the data of stage $n-1$, but not ℓ_n. Each stage imposes finitely many conditions of the form $C_i \rho_Q^{a_i} S_\ell^{B_i} \leq c_i$ with $a_i > 0$: those of Lemma 2.12.30 on both sides, where on $t < 0$ the plateau is $\min_{\overline{I_{\mathrm{mean}}}} \mathsf{W}_b > 0$ by Lemma 2.3.11(c), and the two above. Each holds on a tail $\ell \geq \ell_i$, so one threshold $\ell \geq \max_i \ell_i$ works. This is the single small-q threshold of the proof of Proposition 2.15.2. □

Definition 2.12.32 (Post-cancellation and split vertices)**.** A vertex may be given by an exact identity $f = \Phi(\text{parents})$, where Φ is a finite expression in operations of Table 2.3, provided the identity holds as an identity of functions of (x, y). Every bound on $\Phi(\text{parents})$ then holds for f, including all y-derivatives. The identities used in Lemma 2.13.1, Lemma 2.13.2, Proposition 2.13.3 are:

(X1) $n \cdot a_m = n \cdot r_m$ (proof of Lemma 2.13.4). It holds because $n \cdot B_f \equiv 0$ algebraically (Section 2.13.3: $n \cdot (e_r - s_a K_a) = n_r - s_a |n_{\tan}| = 0$ and $n \cdot N_a = 0$), so $n \cdot t_m \equiv 0$ and $n \cdot \psi t_m \equiv 0$.

(X2) the linear identity (2.13.37), a polynomial in vertices of types A, E, P, S;

(X3) the rationalized roots ((2.14.19) and its analogues), Lemma 2.12.26;

(X4) the mean-value splits (2.12.4) of δ_D, δ (auxiliary), δ (state map), δ_{rad}, and the slow-plus-flat split of δ_C ((2.14.20), (2.14.38), (2.14.56), proof of Lemma 2.15.1, Section 2.14);

(X5) the fast-time identities $T_0 v = -f_\theta + \omega_\theta \mathcal{J}(\mathsf{R}^2 f_\theta)$, $T_0 \gamma = -f_z + \omega_z \mathcal{J}(\mathsf{R} f_z)$ (2.14.34). They hold because $T_0 T_0^{-1} = I$ on $\mathcal{V}_0$ and T_0 commutes with $\mathcal{J}$;

(X6) the Haar splitting $(I-\Pi)(ab) = a_{\mathrm{H}} b^{\perp} + a^{\perp} b_{\mathrm{H}} + (I-\Pi)(a^{\perp} b^{\perp})$, $(I-\Pi) a_{\mathrm{H}} = 0$, used for the perpendicular sources and forces ((2.14.39), proof of Lemma 2.14.3, (2.15.35));

(X7) the moving-commutator identities $\rho P_{\mathsf{Z}} = \rho \mathcal{I}_\chi g_{\mathsf{Z}} - \rho \chi_{\mathsf{Z}} \mathcal{J} g$ and (2.14.23) ((2.14.12), Section 2.14);

(X8) the root cancellations $g + \mathcal{D} P = kM$ and $E_r = 0$ ((2.14.15), proof of Lemma 2.14.2, proof of Lemma 2.14.3, (2.15.13)). The output 0 is a trivial vertex, and the remaining rows are the explicit expressions ((2.15.12), (2.15.34), (2.15.43)).

(X9) the moment anchor (2.14.10), which gives $\mathcal{J}(\mathsf{R}^2 v) = \mathcal{J}(\mathsf{R}\gamma) = 0$ in (2.14.33). Since $\Pi\gamma = 0$ and $\mathcal{J}(\mathsf{R}\gamma_{\mathsf{Z}}) = \partial_{\mathsf{Z}} \mathcal{J}(\mathsf{R}\gamma) = 0$, the prefix acts on $\mathsf{R}\gamma_{\mathsf{Z}} \in \mathcal{V}_{\mathrm{int}}$;

(X10) $\Pi \circ \mathcal{J} = \int \circ \Pi$ (proof of Lemma 2.14.1), which defines $\overline{M} = \int \Pi f$.

Proof of Proposition 2.12.3. Hypothesis 2.3.21 is Hypothesis 2.12.22. Under it and the data (S1)–(S10), Theorem 2.12.23 gives (2.12.3) at every vertex of the finite operation graph, with the radius recursion of Table 2.3 ($p_t = 1$). The cancellations, structural gains and protected roots of the mean–wave stage are covered by Lemmas 2.12.26–2.12.30 and Definition 2.12.32. The last diagonal is fixed as in the paragraph "The last diagonal" above, and the flatness $Q^{-B} S^N e^{-cS} = o(Q^M)$ is Lemma 2.12.2. □

2.13 Separated packets, Gaussian inversion, and the actual covariance

Main result. Proposition 2.13.5 constructs the positive leading packet covariance under the stated strict-source assumptions. Propositions 2.13.6 and 2.13.7 give finite corrections on the same graph. Lemma 2.13.9 gives the weighted radial primitive bounds. The mean construction must still solve the full covariance and pressure equations.

We fix the selected relative leading field supplied by Theorem 1(iv) and Theorem 2.7.1 and its slow background from Proposition 2.6.15. We select the packet geometry once for this background. Corrections after this step change the coefficients on its labelled supports, but do not change its phases, covering levels, or positive leading amplitudes. The signed covariance inverse divides by a known positive leading amplitude. We do not assume positivity of the higher slow stress.

The construction has two different averages. The notation $\langle \cdot \rangle_\theta$ continues to mean the physical angular average in cylindrical components. We write Π for normalized Haar integration on the auxiliary torus. We sample a torus function physically after differentiation. In particular, an identity for ΠC does not identify the sampled covariance with its Haar average. The mean response in Section 2.14 uses the full sampled tensor.

2.13.1 The full half-space atlas and the coefficient classes

For a dyadic band put

$$Q = 2^{-\ell}, \qquad \rho_Q = Q^h, \qquad S_\ell = \ell^{6/5}, \qquad \mathsf{R} = r/\sqrt{Q}, \quad \mathsf{Z} = z/Q^{\frac{1}{2}-h}, \quad \mathsf{T} = t/Q.$$

We select the labels with the one physical gauge $\widetilde{q}$ of (2.10.1). In each half-chart $\bar{q}_b - \mathsf{Z}^2 \bar{q}_b^{2h} = -\mathsf{T}$ or $\bar{q}_f - \mathsf{Z}^2 \bar{q}_f^{2h} = \mathsf{T}$, where $\bar{q}_b = \hat{t}_b/Q$ and $\bar{q}_f = \hat{t}_f/Q$. The physical band coordinate is $\widetilde{q}/Q$.

Because $\hat{t}/\widetilde{q}$ lies in a fixed positive compact interval, the native normalized chart $\bar{q} = \hat{t}/Q$ also lies in such an interval on $1/2 \le \widetilde{q}/Q \le 2$. The absolute value of the native-to-physical Jacobian is $L\bar{q}^{\frac{1}{2}-h}$ and stays bounded away from zero. The atlas is the joint physical construction of Theorem 2.10.2. Its fields have matching full jets at the joining slice.

We do not claim equality on an open collar. There is no endpoint angular cutoff. We do not round levels or carriers independently with $\hat{t}_f$ on the second side. The active radial hull has

$$0 < \mathsf{R}_- \le \mathsf{R} \le \mathsf{R}_+ < \infty. \tag{2.13.1}$$

We fix its constants with the leading field.

The normalized fixed background is

$$Q^{\frac{1}{2}+h} u_{\mathrm{B}} = (b, \mathsf{R}F_b, G_b), \qquad b = O(\rho_Q), \qquad F_b - F_{\mathrm{lead}},\ G_b - G_{\mathrm{lead}} = O(\rho_Q^2).$$

These estimates hold for each fixed ordinary coefficient derivative on the enlarged band charts. The notation F_b is a band coefficient, not a new choice of the leading profile F. The leading shear quantities have positive uniform lower bounds for $F_{\mathrm{lead}}, \mathfrak{a}, \mathfrak{v} - 2$ on the closure of the actual active set and its selected strict buffers.

We use these bounds only on the selected buffered boxes. The full radial product hull can contain stress-free points. For a fixed $0 < \delta_c < 2$, made smaller if necessary, the leading target $\mathcal{T}_0 = (\widehat{\mathcal{T}}_{P,\theta}, \widehat{\mathcal{T}}_{P,z})$ satisfies

$$\begin{aligned} \widehat{\mathcal{T}}_{P,\theta} + \mathfrak{t}\widehat{\mathcal{T}}_{P,z} &\ge \delta_c |\mathcal{T}_0|, \\ (\mathfrak{v} - 2)(\widehat{\mathcal{T}}_{P,z} - \mathfrak{t}\widehat{\mathcal{T}}_{P,\theta})^2 &\le (2 - \delta_c)(\widehat{\mathcal{T}}_{P,\theta} + \mathfrak{t}\widehat{\mathcal{T}}_{P,z})^2. \end{aligned} \tag{2.13.2}$$

These are the strictified leading estimates, not estimates for an uncut sum of signed higher stresses.

We use the aggregate weight W of Lemma 2.3.10, normalized so that $\mathsf{W} \le e^{-2}$, and put $\mathcal{L}_W = 1 + \log(1/\mathsf{W})$ where it is positive. Thus

$$|\mathcal{T}_0| \ge c\mathsf{W}, \qquad |\partial^I \mathcal{T}_0| + |\partial^I \mathsf{W}| \le C_I \mathsf{W} \mathcal{L}_W^{N_I}. \tag{2.13.3}$$

In a fixed same torus chart, $f \in \mathcal{M}^a$ means

$$|\partial^I f| \le C_I \rho_Q^a S_\ell^{B_I} \mathsf{W} \mathcal{L}_W^{N_I} \tag{2.13.4}$$

for each fixed ordinary derivative in $(\mathsf{R}, \mathsf{Z}, \mathsf{T}, \mathsf{y})$. We use compatible representations and smooth zero extensions at the actual support boundaries. A labelled pulse coefficient belongs to $\mathcal{W}^a$ when its bound is

$$|\partial^I f| \le C_I \rho_Q^a S_\ell^{B_I} \sqrt{\mathsf{W}} \mathcal{L}_W^{N_I} P(v). \tag{2.13.5}$$

We define the envelope P in the next paragraph. Before temporal truncation this estimate holds on the whole pulse interval. After truncation the coefficient is smoothly zero outside a compact subinterval. The constants and the logarithmic powers depend on the derivative order. They also depend on a fixed finite harmonic set.

This statement applies to ordinary derivatives. For each fixed ordinary depth, Proposition 2.12.3 independently proves the all-auxiliary Gevrey–2 factorial majorant. The finite-order constants here do not imply it.

The next finite-sum property controls intersections of edges. If $\mathsf{W} = \sum_i w_i$, we write $w_i = \mathsf{W} e^{-u_i}$, $u_i \ge 0$. Then

$$\frac{w_i}{\mathsf{W}} [1 + \log(1/w_i)]^N = e^{-u_i} (\mathcal{L}_W + u_i)^N \le C_N \mathcal{L}_W^N.$$

Finite sums, products, and finite differentiation thus keep the stated logarithmic bounds.

Division by $|\mathcal{T}_0|$ in (2.13.3) gives polynomial $\mathcal{L}_W$ bounds for each fixed derivative of its unit direction. It does not assume that this direction has a limit at each corner of $\{\mathsf{W} > 0\}$. Each positive power W^{β}, with its logarithmic derivative losses, extends flatly by zero. These facts apply to the explicit squared-flat edge factors and their finite sum.

We assume no assertion about arbitrary smooth flat weights.

2.13.2 A fixed separated graph and compatible covering maps

The torus geometry uses the integer matrix

$$J_g = \begin{pmatrix} 3 & 1 \\ 1 & 5 \end{pmatrix}, \quad \Lambda_g = 4 - \sqrt{2}, \quad T_g = 4 + \sqrt{2}, \quad v_r = (1, 1 - \sqrt{2}), \quad v_t = (\sqrt{2} - 1, 1). \tag{2.13.6}$$

The vectors are orthogonal eigenvectors. We set

$$\rho_g = \frac{\log \Lambda_g}{\log T_g}, \qquad d_r = 2[(1+h)\rho_g - h\varkappa], \qquad i(\ell) = \left\lfloor \log_{T_g} \frac{Q^{-1-h}}{S_\ell} \right\rfloor. \tag{2.13.7}$$

We use only sufficiently large bands, with $i(\ell) \geq 0$.

Because $\Lambda_g^2 - T_g = 14 - 9\sqrt{2} > 0$,

$$d_r > 1 + h - 2h\varkappa > 1. \tag{2.13.8}$$

Physical sampling is

$$Y_{\mathrm{phys}} = v_r r^{d_r} + v_t t \pmod{\mathbb{Z}^2}, \qquad \pi_i(Y) = J_g^i Y \pmod{\mathbb{Z}^2}.$$

On a band the temporal and radial auxiliary scales are

$$c_i = T_g^i Q^{1+h} \asymp S_\ell^{-1}, \qquad m_i = \Lambda_g^i Q^{d_r/2} \asymp \rho_Q^{-\varkappa} S_\ell^{-\rho_g}. \tag{2.13.9}$$

For the kept mesh set put $\mathsf{W}_* = c_* |\widetilde{T}_0|$, normalized to less than e^{-2}, as in Theorem 2.10.2. Its logarithmic classes are equivalent to those of the native W. All later component estimates, roots, and signed divisions keep that native weight and the original uncut positive amplitude. There is one physical aggregate cutoff.

We select a fixed smooth function Θ, equal to one on $(-\infty, 1]$ and zero on $[2, \infty)$, and let

$$\vartheta_q = \Theta\left(\frac{\log(1/\mathsf{W}_*)}{c_e \log^{6/5}(1/\widetilde{q})} \right) \quad \text{on } \{\mathsf{W}_* > 0\}, \qquad \vartheta_q = 0 \quad \text{on } \{\mathsf{W}_* = 0\}. \tag{2.13.10}$$

Here $c_e > 0$ is the fixed constant of (2.6.38) for the aggregate weight. In each band, its support lies in a kept region $\mathsf{W} \geq e^{-CS_\ell}$.

We define the amplitudes in a larger region. This region has a strictly larger constant in the exponential. Fixed margins between these constants absorb the harmless comparison between $\log^{6/5}(1/\widetilde{q})$ and $(\log 2)^{6/5} S_\ell$ on overlapping bands.

We select a smooth squared partition on the line: if $b_*(s) = e^{-1/(1-s^2)}$ for $|s| < 1$, and zero in all other cases, we put

$$\beta(s) = \frac{b_*(s)}{(\sum_{j \in \mathbb{Z}} b_*(s-j)^2)^{1/2}}.$$

Its denominator is positive and smooth, and $\sum_j \beta(s-j)^2 = 1$. For a fixed integer K_{mesh}, we use the slow cutoffs

$$\eta_{\ell,a} = \beta(\log_2 \widetilde{q} + \ell) \prod_{j=1}^{3} \beta(S_\ell^{K_{\mathrm{mesh}}} x_j - a_j), \qquad x = (\mathsf{R}, \mathsf{Z}, \mathsf{T}). \tag{2.13.11}$$

We select the boxes that meet the kept set, with representatives in that set.

We include the two signs $\varsigma = \pm 1$ for each box. The signs share one slow cutoff. We count them only once in its squared partition. We select all boxes that contribute where $\vartheta_q \neq 0$. Their squared sum is then one there.

Lemma 2.13.1 (Buffered mesh and one covering geometry)**.** *We can fix the exponent K_{mesh}, the countable labelled graph, a finite coloring, and one auxiliary rectangle radius $r_0 > 0$. These choices precede the small-q amplitude threshold. Enlarged active slow boxes remain in the larger aggregate buffer. Distinct labels whose slow supports meet have disjoint enlarged auxiliary preimages.*

This holds also for each fixed derivative of smoothly extended label fields. A full radial line at fixed z, t, with $\partial_r \widetilde{q} = 0$, has a single permitted same cover, with one bound for the differences of band levels. The next operations keep this cover.

Proof. We consider the first derivatives of $\log \mathsf{W}$, the leading unit direction, and the specified background coefficients on the larger kept region. They satisfy bounds by the fixed powers $S_\ell^{p_0}, S_\ell^{p_1}, S_\ell^{p_2}$, in this order. We select

$$K_{\mathrm{mesh}} > \max(3, p_0 + 2, p_1 + 2, p_2 + 3).$$

If an enlarged box first left the larger buffer, the change in $\log \mathsf{W}$ up to the first exit would be at most $C S_\ell^{p_0 - K_{\mathrm{mesh}}}$.

A passage across the buffer must change the value by a quantity comparable to S_ℓ, a contradiction for large ℓ. The same diameter estimate keeps the fixed directional cone margin. This first-exit argument uses the buffered region where the logarithmic bounds hold.

We join labels whose enlarged slow boxes meet on the union of the two physical half-domains. We fix the set of active labels before choosing the coloring and radius. Intersections satisfy $|\ell - \ell'| < 4$ because the enlarged bands use $|\log_2 \widetilde{q} + \ell| < 2$. We bound their coordinate changes and adjacent mesh-width ratios.

Thus the graph has a finite degree that depends on K_{mesh} and is independent of ℓ. There are $O(S_\ell^{3K_{\mathrm{mesh}}})$ labels in a compact band and $O(S_\ell^{K_{\mathrm{mesh}}})$ along a radial line, but only boundedly many slow supports pass through one point. We bound the level difference on an edge because

$$i(\ell) = \left\lfloor \frac{(1+h)\ell \log 2 - \frac{6}{5} \log \ell}{\log T_g} \right\rfloor$$

and adjacent indices differ by a bounded integer.

Greedy coloring uses at most one more color than the degree. For its finitely many colors, we select rational centers $c_\mu \in \mathbb{T}^2$. We impose $c_\mu \neq J_g^\Delta c_\nu$ modulo $\mathbb{Z}^2$ for each nonnegative allowed level difference $0 \leq \Delta \leq \Delta_{\max}$, except the identical color at $\Delta = 0$. Each choice forbids only finitely many points: J_g^Δ and $J_g^\Delta - I$, for $\Delta > 0$, have nonzero determinant.

The minimum distance $d_* > 0$ of these finitely many differences from the integer lattice is positive. We select r_0 sufficiently small. Then the rectangles

$$c_\mu + \xi v_r + \zeta v_t, \qquad |\xi|, |\zeta| < 2r_0,$$

are injectively parametrized, and $2r_0(|v_r|+|v_t|)(1+\max_\Delta \|J_g^\Delta\|) < d_*/2$. If two adjacent preimages met, the higher covering map would contradict this inequality.

Derivatives have no larger supports, which proves the derivative-product assertion.

For finitely many active levels put $i_0 = \min i$ and $\mathsf{y} = J_g^{i_0} Y$. A level-i function becomes $f_i(J_g^{i-i_0}\mathsf{y})$. Its rectangle has 14^{i-i_0} distinct lifts. These are distinct copies. We do not identify or average them.

Cover changes have bounded linear derivative factors. The cover keeps normalized Haar measure: in the Fourier expansion the cover sends frequency n to $(J_g^\Delta)^\top n$, and only the zero frequency remains zero. There is no degree factor in Haar averages.

Because q is independent of r, radial saturation meets the same finite set of bands. Radial integration, torus translation, products, smooth functions on fixed positive value domains, and directional Fourier multipliers keep functions on this same cover. We solve the principal ODE on each whole translated pulse path. Uniqueness keeps the same compatibility. No stage after this point refines the covers. □

On one lift write $J_g^{i-i_0}\mathsf{y} - c_\mu - k = \xi v_r + \zeta v_t$, and set

$$v = (\zeta + r_0)/c_i, \qquad L_p = 2r_0/c_i \asymp S_\ell.$$

The evaluated coefficient derivatives are

$$D_{\mathsf{R}} = \partial_{\mathsf{R}} + \lambda a_r(\mathsf{R}) v_r \cdot \partial_{\mathsf{y}}, \quad D_z = \rho_Q \partial_{\mathsf{Z}}, \quad t_* = \rho_Q \partial_{\mathsf{T}} + c_{\mathrm{aux}} v_t \cdot \partial_{\mathsf{y}}, \tag{2.13.12}$$

where $a_r(\mathsf{R}) = d_r \mathsf{R}^{d_r-1}$, $\lambda = \Lambda_g^{i_0} Q^{d_r/2}$, and $c_{\mathrm{aux}} = T_g^{i_0} Q^{1+h}$. Thus $D_{\mathsf{R}} v = D_z v = 0$, $t_* v = 1$. In pulse coordinates $t_* = \rho_Q \partial_{\mathsf{T}} + \partial_v$. In particular the slow-time sign is positive. The pulse length remains $O(S_\ell)$, rather than $O(S_\ell^{K_{\mathrm{mesh}}})$, because slow mesh refinement does not change the levels.

2.13.3 Rounded phases and the moving normal plane

At a box representative freeze leading values $F_0 > 0$ and $g_0 = (\mathsf{R}\partial_{\mathsf{R}} F_{\mathrm{lead}}, \partial_{\mathsf{R}} G_{\mathrm{lead}})$. We put

$$\begin{aligned} &N = g_0/|g_0|, \qquad K = (-N_z, N_\theta), \\ &\lambda_0^2 = -2F_0 N_\theta (2F_0 N_\theta + |g_0|), \qquad c_0 = \lambda_0/(2F_0 N_\theta) < 0. \end{aligned} \tag{2.13.13}$$

$g_0 = F_0(-\mathfrak{a}, \mathfrak{b})$, and direct substitution gives

$$\lambda_0^2 = 2\mathfrak{a} F_0^2 (1 - 2/\mathfrak{v}) > 0, \qquad c_0^2 = (\mathfrak{v} - 2)/2. \tag{2.13.14}$$

All these value bounds are uniform on the selected active boxes.

Let $u_p = 2/\sqrt{\delta_c}$, $k_\ell = \lceil \rho_Q^{-1/2} \rceil$, and define

$$\begin{aligned} B_p^2 &= \frac{\lambda_0}{\rho_Q k_\ell^2 (1+u_p^2)^{3/2}}, \qquad s(v) = \varsigma(u_p/2 + u_p v/L_p), \\ (\widetilde{p}/\mathsf{R}_0, p_z) &= B_p \left(K - \frac{\varsigma u_p g_0}{L_p |g_0|^2} \right), \qquad x_0 = \varsigma B_p u_p/2. \end{aligned} \tag{2.13.15}$$

Let m be the angular integer of the selected member (Theorem 1). We fix it before the forward completion of Proposition 2.24.1. For the joint physical label, we select $k_\ell p$ once as an integer nearest to $k_\ell \widetilde{p}$ among the admissible integers.

An integer n is admissible if $|n| \geq 2m+1$. We use a fixed tie rule. Thus $|p - \widetilde{p}| \leq (2m+2)k_\ell^{-1}$, $|k_\ell p| \geq 2m+1$, and each nonzero relative harmonic has nonzero integer angular frequency. (The rounding loss after this is $O_m(S_\ell/k_\ell)$.

Constants may depend on the fixed m.) We hold all representative data and rounded constants fixed under coefficient derivatives.

We set

$$\begin{aligned} H_\Phi &= pF_b + p_z G_b, \qquad \Phi = p\theta + p_z \mathsf{Z}/\rho_Q + x_0 \mathsf{R} - vH_\Phi, \\ n &= \nabla_* \Phi = (x_0 - v(H_\Phi)_{\mathsf{R}},\ p/\mathsf{R},\ p_z - \rho_Q v(H_\Phi)_{\mathsf{Z}}). \end{aligned} \tag{2.13.16}$$

Here $\nabla_* = (D_{\mathsf{R}}, \mathsf{R}^{-1}\partial_\theta, D_z)$. The exact forward transport defect is

$$\mathcal{E}_\Phi = (t_* + bD_{\mathsf{R}} + F_b\partial_\theta + G_b D_z)\Phi = -\rho_Q v[(H_\Phi)_{\mathsf{T}} + G_b(H_\Phi)_{\mathsf{Z}}] + bn_r. \tag{2.13.17}$$

In the derivation of this formula, the two order-one terms $-H_\Phi$ and $pF_b + p_z G_b$ cancel. Reversing only the slow time derivative changes its contribution from $-\rho_Q v(H_\Phi)_{\mathsf{T}}$ to $+\rho_Q v(H_\Phi)_{\mathsf{T}}$, a change of $+2\rho_Q v(H_\Phi)_{\mathsf{T}}$. We use the displayed formula throughout this section.

The estimate for frozen coefficients applies to values, not only derivatives. The background changes by $O(S_\ell^{p_2 - K_{\mathrm{mesh}}} + \rho_Q^2)$ on an enlarged box. In the radial normal, we multiply this error by $v = O(S_\ell)$. The choice of mesh thus gives

$$S_\ell(S_\ell^{p_2 - K_{\mathrm{mesh}}} + \rho_Q^2) = O(S_\ell^{-2}) + o(S_\ell^{-1}). \tag{2.13.18}$$

Rounding and the axial part give an error $O_m(S_\ell/k_\ell + \rho_Q S_\ell)$, also $o(S_\ell^{-1})$. Thus, after one value threshold,

$$|n - B_p(s,K)| + |\partial_v n| \le C/S_\ell, \qquad |n|, |n_{\tan}| \ge c > 0. \tag{2.13.19}$$

Each fixed ordinary derivative of these quantities has polynomial S_ℓ bounds, and each fixed derivative of $\mathcal{E}_\Phi$ is $O(\rho_Q S_\ell^{B_I})$. A polynomial bound alone would not imply (2.13.19).

Let $K_a = n_{\tan}/|n_{\tan}|$, $N_a = ((K_a)_z, -(K_a)_\theta)$, and $s_a = n_r/|n_{\tan}|$. In cylindrical component space define

$$\begin{aligned} U_f &= [e_r - s_a K_a, N_a], \\ M_f &= \begin{pmatrix} 1 & 1 \\ c_0\sqrt{1+s^2} & -c_0\sqrt{1+s^2} \end{pmatrix}, \quad B_f = U_f M_f, \quad B_f^\ell = M_f^{-1}\begin{pmatrix} e_r^\top \\ N_a^\top \end{pmatrix}. \end{aligned} \tag{2.13.20}$$

The columns span $n^\perp$, $B_f^\ell B_f = I$, and all value norms stay bounded. Their fixed derivatives have losses given by polynomial powers of S_ℓ.

We write

$$K_b = \begin{pmatrix} 0 & -2F_b & 0 \\ 2F_b + \mathsf{R}(F_b)_{\mathsf{R}} & 0 & 0 \\ (G_b)_{\mathsf{R}} & 0 & 0 \end{pmatrix}, \qquad A_\Phi = -K_b + \frac{n[n^\top K_b - (\partial_v n)^\top]}{|n|^2}. \tag{2.13.21}$$

At the frozen reference, the projected $-K_b$ in the coordinates $(e_r - sK, N)$ is

$$\begin{pmatrix} 0 & 2F_0 N_\theta/(1+s^2) \\ -(2F_0 N_\theta + |g_0|) & 0 \end{pmatrix}.$$

Its eigenvectors are the columns of M_f, with eigenvalues $\pm\lambda_0/\sqrt{1+s^2}$. The normal and frame estimates now give

$$\begin{aligned} B_f^\ell(A_\Phi B_f - \partial_v B_f) &= \mathrm{diag}(\lambda, -\lambda) + E_f, \qquad \lambda = \lambda_0/\sqrt{1+s^2}, \\ \|E_f\| + |d_p - d_{\mathrm{ref}}| &\le C/S_\ell, \qquad d_p = \rho_Q k_\ell^2 |n|^2 \ge 0, \\ d_{\mathrm{ref}} &= \frac{\lambda_0(1+s^2)}{(1+u_p^2)^{3/2}}. \end{aligned} \tag{2.13.22}$$

On the real pulse interval the normal, the frame in (2.13.20) and the matrix in (2.13.21) are real, so (2.13.22) gives $E_f(v) \in \mathbb{R}^{2\times 2}$. The terms from the moving normal and $\partial_v B_f$ have size $O(S_\ell^{-1})$. The constant in this estimate may depend on the graph fixed before this step and r_0. We select the small-q threshold after those choices.

2.13.4 The Gaussian inverse and positive homogeneous pulse

Lemma 2.13.2 (Gaussian pulse inverse)**.** *Suppose $L_p \asymp S$, λ_0 ranges in a fixed positive compact interval, and $E(v) \in \mathbb{C}^{2\times 2}$, $d(v) \ge 0$ satisfy $\|E\| + |d - d_{\mathrm{ref}}| \le C_E/S$. Assume all fixed parameter and pulse derivatives of E, d are bounded by polynomial powers of S. The constants λ_0, L_p are fixed under parameter derivatives. We define*

$$P(v) = \exp\left(\int_{L_p/2}^{v} [\lambda(w) - d_{\mathrm{ref}}(w)]\, \mathrm{d}w \right). \tag{2.13.23}$$

For $A_m = \mathrm{diag}(\lambda, -\lambda) + E - m^2 d I$, its forward fundamental matrix satisfies, for each nonzero integer m,

$$\|V_m(v,w)\| \le C \frac{P(v)}{P(w)}, \qquad 0 \le w \le v \le L_p, \qquad e^{-C(v-L_p/2)^2/L_p} \le P(v) \le e^{-c(v-L_p/2)^2/L_p}. \tag{2.13.24}$$

The zero-data inverse keeps the source power ρ_Q^a, slow weight, and Gaussian envelope. It has finite additional polynomial losses for each fixed derivative and finite harmonic set. If $E(v) \in \mathbb{R}^{2\times 2}$ on $[0, L_p]$, then, for S above a threshold independent of those derivative orders, the solution with $m = 1$ and initial value $(P(0), 0)$ is real and obeys

$$z_+ \asymp P > 0, \qquad |z_-/z_+| \le C/S. \tag{2.13.25}$$

Proof. Let $y = u_p/2 + u_p v/L_p$. The net growth $a = \lambda_0[(1+y^2)^{-1/2} - (1+y^2)/(1+u_p^2)^{3/2}]$ vanishes at the midpoint and satisfies

$$a' = -\frac{u_p \lambda_0 y}{L_p}[(1+y^2)^{-3/2} + 2(1+u_p^2)^{-3/2}], \qquad -C/L_p \le a' \le -c/L_p.$$

Two integrations about the midpoint prove the two Gaussian bounds. We integrate from the midpoint on each side of it, so the bounds hold on all of $[0, L_p]$. Take a complex solution of the homogeneous first-harmonic equation. It satisfies

$$\tfrac{1}{2}\partial_v |z|^2 \le [a(v) + C_E/S]|z|^2.$$

Integration gives $\|V_1(v,w)\| \le e^{C_E L_p/S} P(v)/P(w)$. Scalar damping commutes with the whole matrix, so uniqueness gives

$$V_m(v,w) = e^{-(m^2-1)\int_w^v d(a)\,\mathrm{d}a}\, V_1(v,w).$$

The prefactor is at most one. This proves the value bound with one constant for all nonzero integers m.

For $z_m' = A_m z_m + g_m$, $z_m(0) = 0$, Duhamel gives

$$z_m(v) = \int_0^v V_m(v,w) g_m(w)\, \mathrm{d}w.$$

A source bound $|g_m(w)| \le C\rho_Q^a S^B \omega P(w)$, with ω fixed along the pulse, becomes $|z_m(v)| \le C\rho_Q^a S^{B+1}\omega P(v)$. For a parameter multi-index I, differentiation gives the same zero-data equation with source

$$\partial^I g_m + \sum_{0<J\le I} \binom{I}{J} (\partial^J A_m)\partial^{I-J} z_m.$$

Induction uses only finitely many lower derivatives and adds finite powers of S.

The equation gives the pulse derivatives. For a fixed finite harmonic set, the factors m^2 enter constants only. We use the bounds for differentiated sources directly. This avoids uncontrolled derivatives of their bounding weight.

For the positivity assertion take E real on $[0, L_p]$. Let $c_\lambda = \lambda_-/\sqrt{1+(3u_p/2)^2}$ and select $K_0 = 2(C_E+1)/c_\lambda$. The scalar equation

$$r' = E_{21} + (-2\lambda + E_{22} - E_{11})r - E_{12}r^2, \qquad r(0) = 0,$$

points strictly inward at $r = \pm K_0/S$ once S exceeds a fixed threshold. For example it suffices that $S \ge 2K_0$ and $(2C_E K_0 + C_E K_0^2)/S < c_\lambda K_0 - C_E$. The right side of the second inequality is positive.

We solve this scalar equation first, then set

$$z_+ = P(0)\exp\int_0^v (\lambda - d + E_{11} + E_{12}r)\,\mathrm{d}w, \qquad z_- = rz_+.$$

Substitution proves the original system without a prior assumption that z_+ has no zeros. Also, $|\partial_v \log(z_+/P)| \le C/S$. This proves (2.13.25).

The differentiated linear equation and Duhamel estimate control derivatives of this homogeneous solution. They use no additional smallness condition on a Riccati derivative. □

Proposition 2.13.3 (Principal inverse for finite complex harmonics)**.** *On the fixed graph and one sufficiently small band domain, let $f_m \in \mathcal{W}^a$ for a finite set of nonzero integers m. There is a unique pair: a zero-data amplitude t_m with constraint $n\cdot t_m = 0$ and a pressure coefficient π_m. They solve*

$$\partial_v t_m + K_b t_m + m^2 d_p t_m + ik_\ell mn\pi_m = -f_m. \tag{2.13.26}$$

They satisfy $t_m \in \mathcal{W}^a$ and $\pi_m \in \mathcal{W}^{a+1/2}$. The construction keeps all fixed slow and transverse supports, same-cover representations, and one-sided endpoint jets. Multiplication by the later fixed pulse cutoff restores temporal support.

Proof. With $\mathsf{P}_n = I - n\otimes n/|n|^2$, we solve

$$z_m' = [\mathrm{diag}(\lambda,-\lambda) + E_f - m^2 d_p I]z_m - B_f^\ell \mathsf{P}_n f_m, \qquad z_m(0) = 0, \quad t_m = B_f z_m.$$

Lemma 2.13.2 applies by (2.13.22). We differentiate $n\cdot B_f = 0$. This shows that $A_\Phi B_f - \partial_v B_f$ lies in $n^\perp$.

Thus the two-coordinate solution solves the full projected equation. Its normal row gives

$$\pi_m = \frac{i}{k_\ell m|n|^2}[n\cdot K_b t_m - (\partial_v n)\cdot t_m + n\cdot f_m]. \tag{2.13.27}$$

The factor $k_\ell^{-1} \le \rho_Q^{1/2}$ proves the pressure gain. It also proves uniqueness of the pressure, while the projected ODE proves uniqueness of the amplitude.

Translated same-cover paths solve the same equation, so uniqueness supplies compatibility without identification of distinct preimages. If a source vanishes along a whole slow/transverse path, its zero-data solution vanishes there. Smooth parameter dependence and the weighted derivative estimates give the claimed zero extensions and one-sided jets. □

Choose a fixed Gevrey–2 cutoff ψ_0 supported in $(1/6, 5/6)$ and equal to one on $[3/10, 7/10]$, with $|\partial^p \psi_0| \le C_\chi K_\chi^p (p!)^2$ by Lemma 2.12.16. Then $\psi(v) = \psi_0(v/L_p)$ is supported in $(L_p/6, 5L_p/6)$ and equals one on $[3L_p/10, 7L_p/10]$. Let hats denote multiplication by ψ,

$$\partial_v \widehat{t}_m + K_b \widehat{t}_m + m^2 d_p \widehat{t}_m + i k_\ell m n \widehat{\pi}_m + f_m = (1-\psi) f_m + \psi' t_m. \tag{2.13.28}$$

For this supported residual identity, assume that the source has a smooth zero extension at the pulse endpoints. The actual finite sources we use next satisfy this condition.

The inverse can fill the pulse interval. The displayed equation keeps this temporal support error. Each term on its right has $P \le e^{-cS_\ell}$. After any fixed physical derivative, with phase and frame derivatives, the bound is

$$C Q^{-B} S_\ell^N e^{-cS_\ell} = O(q^M) \quad \text{for each fixed } M. \tag{2.13.29}$$

Polynomial label counts do not change this conclusion. At an initial point with $z \neq 0$ these fields are one-sided smooth by Proposition 2.8.6(a). We keep their actual jets. We do not set them to zero. All-power flatness in (2.13.29) is the statement at the singular tip.

2.13.5 Exact curls and the physical linear remainder

For the remaining calculations abbreviate $\mathcal{D} = D_{\mathsf{R}}$, $\mathcal{Z} = \rho_Q \partial_{\mathsf{Z}}$. The normalized cylindrical operators, with their connections, are

$$\begin{aligned} \operatorname{curl}_* C &= (\mathsf{R}^{-1}\partial_\theta C_z - \mathcal{Z} C_\theta, \mathcal{Z} C_r - \mathcal{D} C_z, (\mathcal{D} + \mathsf{R}^{-1}) C_\theta - \mathsf{R}^{-1}\partial_\theta C_r), \\ \operatorname{div}_* a &= (\mathcal{D} + \mathsf{R}^{-1}) a_r + \mathsf{R}^{-1}\partial_\theta a_\theta + \mathcal{Z} a_z. \end{aligned} \tag{2.13.30}$$

The evaluated coordinate derivatives commute, and $\mathcal{D}(\mathsf{R}^{-1}) = -\mathsf{R}^{-2}$. Substitution in (2.13.30) cancels the six mixed derivatives. Thus the identity $\operatorname{div}_* \operatorname{curl}_* = 0$ holds.

Lemma 2.13.4 (Exact curl and its linear residual)**.** *Let $t_m \in \mathcal{W}^a$ be temporally cut, with $n \cdot t_m = 0$, and put*

$$\begin{aligned} C_m &= \frac{i n \times t_m}{k_\ell m |n|^2}, \\ r_m &= (-\mathcal{Z} C_{m,\theta},\ \mathcal{Z} C_{m,r} - \mathcal{D} C_{m,z},\ (\mathcal{D} + \mathsf{R}^{-1}) C_{m,\theta}), \qquad a_m = t_m + r_m. \end{aligned} \tag{2.13.31}$$

Then

$$\operatorname{curl}_*(C_m e^{i k_\ell m \Phi}) = a_m e^{i k_\ell m \Phi}, \qquad \operatorname{div}_*(a_m e^{i k_\ell m \Phi}) = 0, \tag{2.13.32}$$

with

$$C_m \in \mathcal{W}^{a+1/2}, \quad r_m \in \mathcal{W}^{a+1/2-\varkappa}, \quad r_{m,r} \in \mathcal{W}^{a+3/2}, \quad n \cdot a_m \in \mathcal{W}^{a+1/2-\varkappa}. \tag{2.13.33}$$

The physical potential and velocity for this coefficient have factors Q^{-h} and $Q^{-\frac{1}{2}-h}$, in this order. Suppose (t_m, π_m) solves the principal equation with source $-f_m$.

We consider its full physical linear residual about u_{B}, with pressure $Q^{-1-2h}\pi_m e^{i k_\ell m \Phi}$. This residual equals the source, the explicit temporal error, and a coefficient in $\mathcal{W}^{a+1/2-3\varkappa}$. All terms use force normalization $Q^{-\frac{3}{2}-2h}$.

Proof. The principal term of the curl is $ik_\ell mn \times C_m = t_m$, by the triple-product identity. The remaining coefficient curl equals r_m. Ordinary differentiation keeps the class exponent. The operator $\mathcal{D}$ loses at most $\varkappa$, while $\mathcal{Z}$ gains one.

Together with $k_\ell^{-1} \le \rho_Q^{1/2}$ these facts prove (2.13.33). The last assertion uses $n \cdot a_m = n \cdot r_m$, not false tangency of the full curl. Compatibility and smooth zero extension hold by the coefficient bounds and the fixed supports. The physical chain rule gives the stated normalization, and thus exact physical solenoidality.

The next full linear identity specifies the derivative loss. Let

$$J_\theta = \begin{pmatrix} 0 & -1 & 0 \\ 1 & 0 & 0 \\ 0 & 0 & 0 \end{pmatrix}, \qquad H_r = \operatorname{diag}(1,1,0),$$

and write the actual background matrix as

$$K_{\mathrm{full}} = \begin{pmatrix} b_{\mathsf{R}} & -2F_b & \mathcal{Z}b \\ 2F_b + \mathsf{R}(F_b)_{\mathsf{R}} & b/\mathsf{R} & \mathsf{R}\mathcal{Z}F_b \\ (G_b)_{\mathsf{R}} & 0 & \mathcal{Z}G_b \end{pmatrix}, \qquad K_{\mathrm{full}} - K_b = O(\rho_Q). \tag{2.13.34}$$

For a coefficient vector a, we define

$$\begin{aligned} D_\Phi a &= 2(n_r\mathcal{D} + n_z\mathcal{Z})a + (\mathcal{D}n_r + n_r/\mathsf{R} + \mathcal{Z}n_z)a + 2p\mathsf{R}^{-2}J_\theta a, \\ D_0 a &= (\mathcal{D}^2 + \mathsf{R}^{-1}\mathcal{D} + \mathcal{Z}^2)a - \mathsf{R}^{-2}H_r a. \end{aligned} \tag{2.13.35}$$

The exact vector Laplacian is

$$\Delta_*(a e^{ik_\ell m\Phi}) = e^{ik_\ell m\Phi}[-k_\ell^2 m^2 |n|^2 a + ik_\ell m D_\Phi a + D_0 a]. \tag{2.13.36}$$

The two vector connection terms are present. The principal ODE leaves the next coefficient:

$$\begin{aligned} \mathcal{E}_m^{\mathrm{lin}} = {} & (r_m)_v + (K_{\mathrm{full}} + m^2 d_p I) r_m + (K_{\mathrm{full}} - K_b) t_m \\ & + (\rho_Q \partial_{\mathsf{T}} + b\mathcal{D} + G_b\mathcal{Z}) a_m + ik_\ell m \mathcal{E}_\Phi a_m \\ & - i\rho_Q k_\ell m D_\Phi a_m - \rho_Q D_0 a_m + (\mathcal{D}\pi_m, 0, \mathcal{Z}\pi_m). \end{aligned} \tag{2.13.37}$$

The curl and pressure rows gain $1/2 - \varkappa$. The first viscous row gains the same amount, and two radial viscous derivatives gain $1 - 2\varkappa$.

The defect row gains $1/2$ because $\mathcal{E}_\Phi = O(\rho_Q S^B)$. Slow transport gains at least $1 - \varkappa$. Pulse derivatives keep the exponent. These bounds, with those on the curl remainder inside the viscous terms, imply the conservative gain $1/2 - 3\varkappa$ for each fixed coefficient jet.

Source and temporal terms keep their exact signs from (2.13.26) and (2.13.28). At the last step $Q^{-\frac{3}{2}-2h} = Q^{-\frac{3}{2}-2h}$, so pressure, viscosity, and nonlinear terms use the same force normalization. □

The small power gain in Lemma 2.13.4 is not flatness of the ordinary force. Only the identified Gaussian endpoint and aggregate-deletion errors satisfy (2.13.29). Each later finite correction keeps this distinction.

2.13.6 Positive leading amplitudes and all six covariance entries

The homogeneous pulse from Lemma 2.13.2 is $t_\varsigma^h = B_f(z_+, z_-)^\top$. Its radial component $x_\varsigma = z_+ + z_-$ is positive, comparable to P, and

$$\frac{t^h_{\varsigma,\tan}}{x_\varsigma} = c_0\sqrt{1+s^2}N - sK + O(S_\ell^{-1}). \tag{2.13.38}$$

A polynomial in S_ℓ times P bounds all fixed derivatives.

We select a nonzero, nonnegative transverse bump $\chi_g(\xi)$ of Gevrey class 2, $|\partial^p\chi_g| \le C_\chi K_\chi^p (p!)^2$ (Lemma 2.12.16), supported in $|\xi| < r_0$. For a slow box $\beta = (\ell, a)$, we define

$$\begin{aligned} M_{\beta,\varsigma} &= C_g c_i \int_0^{L_p} \psi(v)^2 t_\varsigma^h(v) \otimes t_\varsigma^h(v)\,\mathrm{d}v, \\ C_g &= \frac{|\det(v_r, v_t)|}{2}\int_{-r_0}^{r_0} \chi_g(\xi)^2\,\mathrm{d}\xi. \end{aligned} \tag{2.13.39}$$

Let $\mathcal{H}_\beta$ be the two-by-two matrix whose columns are the $(r\theta, rz)$ pairs of these matrices. The factor $1/2$ is the physical angular cosine-square average.

Proposition 2.13.5 (Leading positive covariance)**.** *On the side with native scale q_ε let $\widetilde{T}_0 = (\widetilde{q}/q_\varepsilon)^{1+h}\mathcal{T}_0$. For the normalized leading target*

$$T_\beta = (Q/q_\varepsilon)^{1+h}\mathcal{T}_0 = (Q/\widetilde{q})^{1+h}\widetilde{T}_0$$

the numbers

$$y_\beta = \mathcal{H}_\beta^{-1}T_\beta, \qquad a_{\beta,\varsigma} = \sqrt{y_{\beta,\varsigma}} \tag{2.13.40}$$

are well defined and positive on the buffered label domains. They obey

$$c\sqrt{S_\ell}\,\mathsf{W} \le y_{\beta,\varsigma}, \qquad y_{\beta,\varsigma} \le C\sqrt{S_\ell}|T_\beta|, \qquad |\partial^I a_{\beta,\varsigma}| \le C_I S_\ell^{B_I}\sqrt{\mathsf{W}}\mathcal{L}_W^{N_I}. \tag{2.13.41}$$

They produce a real exact-curl field of zero physical angular mean. Its full normalized angular covariance belongs to $\mathcal{M}^1$.

Before the same aggregate cutoff, its principal Haar radial-cross pair is the prescribed leading physical stress $q_\varepsilon^{-1-h}\mathcal{T}_0 = \widetilde{q}^{-1-h}\widetilde{T}_0$ wherever the squared partition is complete. After that cutoff, we multiply the principal pair by ϑ_q^2. The construction keeps all curl and cutoff covariance terms.

Proof. The cone (2.13.2) gives

$$-T_\beta\cdot N \ge c|T_\beta|, \qquad \left|c_0\frac{T_\beta\cdot K}{T_\beta\cdot N}\right| \le \sqrt{1-\delta_c/2} < \frac{u_p}{\sqrt{1+u_p^2}}.$$

The frozen coefficients on the buffered boxes keep a fixed intermediate margin. Let $A_\varsigma = C_g c_i\int\psi^2 x_\varsigma^2\,\mathrm{d}v$. The two-sided Gaussian bounds give $A_\varsigma \asymp S_\ell^{-1/2}$.

They also give

$$\int \psi^2 x_\varsigma^2 \frac{|v - L_p/2|}{L_p}\,\mathrm{d}v \le CS_\ell^{-1/2}\int\psi^2 x_\varsigma^2\,\mathrm{d}v.$$

Thus the ς-column of $\mathcal{H}_\beta$ is

$$A_\varsigma\{c_0\sqrt{1+u_p^2}N - \varsigma u_p K + O(S_\ell^{-1/2})\}.$$

For the limiting columns, we write $z_\varsigma = A_\varsigma y_\varsigma$. Their sum equals $(T_\beta \cdot N)/(c_0\sqrt{1+u_p^2}) > 0$, and the absolute difference divided by this sum is strictly less than one by the cone inequality.

Thus z_ς are comparable to $|T_\beta|$. The small column errors keep these bounds. So $y_\varsigma \asymp \sqrt{S_\ell}|T_\beta|$. So the physical packet coefficient $\sqrt{y_\varsigma}$ has height $S_\ell^{1/4}$ times the fixed stress amplitude. The clock uses this exact covariance normalization, together with $c_i \asymp S_\ell^{-1}$ and $L_p \asymp S_\ell$, in its calculation.

An arbitrary S_ℓ^B cannot replace it. This also yields a polynomial bound for $\mathcal{H}_\beta^{-1}$. We differentiate the inverse matrix and square root a fixed number of times. We use the lower bound in (2.13.41) and (2.13.3).

The remaining losses are finite powers of S_ℓ and $\mathcal{L}_W$.

For each signed label define the real coefficients

$$\begin{aligned} a_\gamma &= \sqrt{\rho_Q}\,\eta_\beta a_{\beta,\varsigma}\chi_g\psi\, t_\varsigma^h, \\ d_\gamma &= \frac{n \times a_\gamma}{k_\ell |n|^2}, \qquad b_\gamma = (-\mathcal{Z}d_{\gamma,\theta},\, \mathcal{Z}d_{\gamma,r} - \mathcal{D}d_{\gamma,z},\, (\mathcal{D}+\mathsf{R}^{-1})d_{\gamma,\theta}). \end{aligned} \tag{2.13.42}$$

On the actual kept field multiply a_γ, d_γ by ϑ_q before computation of the new b_γ. Each derivative acts on the full coefficient, with the slow, transverse, temporal, and aggregate cutoffs. The potential and its physical curl are

$$A_w = -\sum_\gamma Q_\gamma^{-h} d_\gamma \sin(k_\gamma \Phi_\gamma), \qquad w = \sum_\gamma Q_\gamma^{-\frac{1}{2}-h}[a_\gamma \cos(k_\gamma\Phi_\gamma) - b_\gamma \sin(k_\gamma\Phi_\gamma)]\big|_{Y=Y_{\mathrm{phys}}}. \tag{2.13.43}$$

We evaluate the potential in the first expression at Y_{phys} before its physical curl. The identity $-k_\ell n \times d_\gamma = a_\gamma$ proves the sign in (2.13.43). The angular frequency is a nonzero integer, so $\langle w\rangle_\theta = 0$. The sum is locally finite for $q > 0$, and Lemma 2.13.1 eliminates each cross-label product, with differentiated products.

For a single label put $j = -\mathcal{Z}d_\theta$, $k_c = \mathcal{Z}d_r - \mathcal{D}d_z$, and $l_c = (\mathcal{D}+\mathsf{R}^{-1})d_\theta$. The six entries of the actual angular covariance equal

$$\begin{aligned} C_\gamma = \tfrac{1}{2}(a_\gamma \otimes a_\gamma + b_\gamma \otimes b_\gamma), \quad & C_{rr} = (a_r^2 + j^2)/2, \quad C_{r\theta} = (a_r a_\theta + jk_c)/2, \quad C_{rz} = (a_r a_z + jl_c)/2, \\ & C_{\theta\theta} = (a_\theta^2 + k_c^2)/2, \quad C_{\theta z} = (a_\theta a_z + k_c l_c)/2, \quad C_{zz} = (a_z^2 + l_c^2)/2. \end{aligned} \tag{2.13.44}$$

The physical tensor is $\sum_\gamma Q_\gamma^{-1-2h} C_\gamma$ after sampling. The principal–curl cross terms vanish here because the amplitudes are real and the two quadratures are cosine and sine. We do not claim this cancellation for general complex corrections.

The coefficient bounds are

$$a_\gamma \in \mathcal{W}^{1/2}, \quad d_\gamma \in \mathcal{W}^1, \quad b_{\gamma,r} \in \mathcal{W}^2, \quad b_{\gamma,\theta}, b_{\gamma,z} \in \mathcal{W}^{1-\varkappa}. \tag{2.13.45}$$

Thus all six principal entries are in $\mathcal{M}^1$, while for $E_c = b_\gamma \otimes b_\gamma/2$,

$$(E_c)_{rr} \in \mathcal{M}^4, \qquad (E_c)_{r\theta}, (E_c)_{rz} \in \mathcal{M}^{3-\varkappa}, \qquad (E_c)_{\tan,\tan} \in \mathcal{M}^{2-2\varkappa}. \tag{2.13.46}$$

The same bounds hold on a adjacent reference band. We bound the normalization ratios and the same-cover changes.

Haar integration of the principal part of one box is $\rho_Q \eta_\beta^2 \sum_\varsigma y_{\beta,\varsigma} M_{\beta,\varsigma}$. Its radial-cross pair is $\rho_Q \eta_\beta^2 T_\beta$. The physical scaling is exact:

$$Q^{-1-2h}\rho_Q T_\beta = q_\varepsilon^{-1-h}\mathcal{T}_0 = \widetilde{q}^{-1-h}\widetilde{T}_0.$$

The squared partition sum gives the stated pair.

The four other Haar entries are the entries at those four positions in these same matrices. We do not select them freely or remove them. The Haar curl pair from (2.13.46) remains present as well. □

The smooth aggregate cutoff changes the completed curl by $\nabla\vartheta_q \times A_w$. This is more than multiplication of its velocity. On its deletion and transition set, $\mathsf{W} \le e^{-c\log^{6/5}(1/\widetilde{q})}$. For any fixed $\beta > 0$, $\mathsf{W}^{\beta}\mathcal{L}^N_W$ absorbs each finite logarithmic loss and then each fixed physical power of q^{-1}.

All cutoff-curl and deleted weighted terms are thus physically flat. We do not claim arbitrary smallness relative to $\vartheta_q^2\mathsf{W}$. No later inverse divides by ϑ_q.

2.13.7 Signed cross corrections using the original amplitude

Proposition 2.13.6 (One signed covariance update)**.** *Let $K(r,z,t)$ be a real two-component stress, independent of the auxiliary torus, whose coherent band representative $\Sigma_\beta = Q_\beta^{1+2h}K$ belongs to $\mathcal{M}^p$, $p > 1$. Let w_0 be the original real first-harmonic field and w_{sgn} the signed exact curl formed from its positive amplitudes in (2.13.40). The principal order of w_{sgn} is $\mathcal{W}^{p-1/2}$. The principal linear Haar radial-cross pair of $\mathsf{C}(w_0 + w_{\mathrm{sgn}}) - \mathsf{C}(w_0)$, where $\mathsf{C}(w) = \langle w \otimes w\rangle_\theta$, is K on a complete partition, or $\vartheta_q^2 K$ with the same cutoff. This full covariance increment has normalized order $\mathcal{M}^p$. After subtracting the linear target, its Haar radial-cross remainder is $\mathcal{M}^{\min(2p-1,p+2-\varkappa)}$, before explicitly flat cutoff terms. About w_0 and a mean satisfying (2.13.51), the added nonzero momentum has order $\mathcal{W}^{p-3\varkappa}$ apart from the retained Gaussian endpoint errors. For a current wave $w_0 + Y$, the covariance increment also contains $\mathrm{Cross}(Y, w_{\mathrm{sgn}})$. An earlier first harmonic of principal order a_j can contribute at normalized order $p - \frac{1}{2} + a_j$.*

Proof. With the original matrix $\mathcal{H}_\beta$ fixed, we define

$$\delta y_\beta = \mathcal{H}_\beta^{-1}(\Sigma_\beta/\rho_Q), \qquad s_{\beta,\varsigma} = \frac{\delta y_{\beta,\varsigma}}{2\sqrt{y_{\beta,\varsigma}}}. \tag{2.13.47}$$

Only the original positive y occurs in the denominator. The covariance normalization uses the factor ρ_Q^{-1}. Fixed differentiation and (2.13.41) give

$$|\partial^I \delta y| \le C_I \rho_Q^{p-1} S^B \mathsf{W}\mathcal{L}^N_W, \qquad |\partial^I s| \le C_I \rho_Q^{p-1} S^B \sqrt{\mathsf{W}}\mathcal{L}^N_W.$$

Thus these quotients have smooth zero extensions wherever we use their weighted uncut definitions. On buffered kept labels multiply them by ϑ_q before extension outside the buffer. The two exact scalar identities are

$$2\sqrt{y}\, s = \delta y, \qquad (\sqrt{y} + s)^2 = y + \delta y + s^2. \tag{2.13.48}$$

There is no nonlinear square root of the signed target here.

We replace $a_{\beta,\varsigma}$ in (2.13.42) by $s_{\beta,\varsigma}$. We keep each other original object fixed. We denote these real principal, potential, and curl coefficients by g, e, f. Their orders are

$$g \in \mathcal{W}^{p-1/2}, \qquad e \in \mathcal{W}^p, \qquad f_r \in \mathcal{W}^{p+1}, \quad f_\theta, f_z \in \mathcal{W}^{p-\varkappa}. \tag{2.13.49}$$

The multiplier is independent of the pulse variable because K is Haar independent. The same real homogeneous pulse and its inherited pressure thus solve the principal equation. The pressure has order $\mathcal{W}^p$, with its temporal cutoff source kept as in (2.13.28).

For a single label of w_0, with original coefficients a, b in (2.13.43), the normalized covariance difference between $w_0 + w_{\mathrm{sgn}}$ and w_0 is

$$\Delta C_\gamma = \tfrac{1}{2}\{a \otimes g + g \otimes a + g \otimes g + b \otimes f + f \otimes b + f \otimes f\}. \tag{2.13.50}$$

This single symmetric-tensor formula specifies all six entries and keeps the full zero-Haar part. Its principal linear part has Haar average $\rho_Q \eta_\beta^2 \sum_\varsigma \delta y_{\beta,\varsigma} M_{\beta,\varsigma}$. Its physical radial-cross pair equals $\eta_\beta^2 K$.

The four remaining entries of this linear tensor are generally of order $\mathcal{M}^p$. The quadratic principal part is $\mathcal{M}^{2p-1}$, the curl-linear tangential block is $\mathcal{M}^{p+1-2\varkappa}$, and its radial-cross pair is $\mathcal{M}^{p+2-\varkappa}$. The curl-quadratic terms are higher. This proves both estimates about w_0. For a current wave $w_0 + Y$, bilinearity adds the angular average of $Y \otimes w_{\mathrm{sgn}} + w_{\mathrm{sgn}} \otimes Y$. Only the relative harmonics $m = \pm 1$ of Y on the same label survive angular averaging. Multiplication by the principal coefficient of w_{sgn} gives order $a_j + p - \frac{1}{2}$, with higher orders from the coefficient curls by (2.13.49). An in-phase multiple of the original first harmonic can attain this order in a Haar radial cross. The finite return retains this tensor in (2.15.30) with the orders in (2.15.31).

For the momentum comparison let the current mean be $u_M = u_{\mathrm{B}} + \mu$, with a coherent full-torus lift that satisfies

$$(Q^{\frac{1}{2}+h}\mu)_\theta, (Q^{\frac{1}{2}+h}\mu)_z \in \mathcal{M}^{1-\varkappa}, \qquad (Q^{\frac{1}{2}+h}\mu)_r \in \mathcal{M}^2. \tag{2.13.51}$$

Lemma 2.13.4, with $a = p - 1/2$, gives the linear cost $\mathcal{W}^{p-3\varkappa}$. The precise bilinear identity (2.13.52) gives old–new cost $\mathcal{W}^{p-\varkappa}$ and new–new cost $\mathcal{W}^{2p-1-\varkappa}$. The mean interaction has order $\mathcal{W}^{p-\varkappa}$.

Thus the linear cost dominates. If other finite exact-curl harmonics of orders a_j are present, each additional mixed cost is $\mathcal{W}^{p-1/2+a_j-\varkappa}$, and we keep the full covariance. This is the form used in the finite stage.

Under the same cutoff, implement the signed quotient as $\vartheta_q s$, never as a division by $\vartheta_q \sqrt{y}$. The intended linear target becomes $\vartheta_q^2 K$. Expansion of the actual curls adds the terms with $\nabla\vartheta_q \times A_w$ and $\nabla\vartheta_q \times A_g$, all physically flat by the weighted estimates. For relative positivity on the kept set, $|\delta y|/y \le C\rho_Q^{p-1} S^B$ there, after absorption of the kept logarithmic losses. One more finite value threshold makes this ratio small. No derivative-dependent threshold is necessary. □

In particular the signed slow stress of (2.6.37) is eligible with $p = 3$. It produces principal order $\mathcal{W}^{5/2}$, radial curl order $\mathcal{W}^4$, and tangential curl order $\mathcal{W}^{3-\varkappa}$. Its covariance is $\mathcal{M}^3$, its unmatched Haar cross is $\mathcal{M}^{5-\varkappa}$, and its nonzero momentum cost is $\mathcal{W}^{3-3\varkappa}$. The leading real curl cross error remains $\mathcal{M}^{3-\varkappa}$. Thus this initialization uses positive leading amplitudes and a signed higher update. It never assumes positivity of the full uncut slow target.

2.13.8 Finite complex harmonics and their complete residual

For angle-independent coefficient vectors define

$$\begin{aligned} \mathcal{C}(X,Y) &= X_r \mathcal{D}Y + X_z \mathcal{Z}Y + (X_\theta/\mathsf{R}) J_\theta Y, \\ \mathcal{B}_m(X,Y) &= \mathcal{C}(X,Y) + ik_\ell m (X \cdot n) Y, \qquad E_m = e^{ik_\ell m \Phi}. \end{aligned} \tag{2.13.52}$$

Then the identity $((XE_l)\cdot\nabla_*)(YE_m) = \mathcal{B}_m(X,Y)E_{l+m}$ holds. The radial and angular connection terms in $\mathcal{C}$ are $-X_\theta Y_\theta/\mathsf{R}$ and $X_\theta Y_r/\mathsf{R}$, in this order. For exact-curl coefficients of principal orders α, β,

$$\mathcal{B}_m(X_l, Y_m) \in \mathcal{W}^{\alpha+\beta-\varkappa}. \tag{2.13.53}$$

$\mathcal{D}$ loses $\varkappa$. The bound $n \cdot X_l \in \mathcal{W}^{\alpha+1/2-\varkappa}$ controls the carrier cost k_ℓ. This holds for each signed complex harmonic. We use no real-parity cancellation.

Proposition 2.13.7 (Finite nonzero-harmonic correction)**.** *We keep the original graph, phase, inverse and positive amplitudes. Suppose the current mean satisfies* (2.13.51) *with a compatible lift. A finite nonzero-harmonic source in* $\mathcal{W}^a$ *has a source-controlled principal correction of order* $\mathcal{W}^a$*. Its curl is exact.*

The linear remainder has order $\mathcal{W}^{a+1/2-3\varkappa}$*, with the stated flat endpoint family. All new quadratic harmonics and the full covariance are the next finite sums. For the original principal wave, the first correction has source orders*

$$a_1 = 1 - 3\varkappa, \qquad a_2 = 1 - \varkappa, \tag{2.13.54}$$

and leaves nonzero residual orders

$\lvert m\rvert$	1	2	3	4
order	$3/2 - 6\varkappa$	$3/2 - 4\varkappa$	$3/2 - 2\varkappa$	$2 - 3\varkappa.$

(2.13.55)

Its covariance increment is $\mathcal{M}^{3/2-3\varkappa}$*. We must enter this increment in the mean response in full.*

Proof. We write the original real coefficient as $c = (a + ib)/2$, so the wave is $cE_1 + \bar{c}E_{-1}$. Exact divergence gives

$$k_\ell n \cdot b = (\mathcal{D} + \mathsf{R}^{-1})a_r + \mathcal{Z}a_z, \qquad (\mathcal{D} + \mathsf{R}^{-1})b_r + \mathcal{Z}b_z = 0. \tag{2.13.56}$$

In particular $n \cdot a = 0$, but in general $n \cdot c \neq 0$. The complete second-harmonic coefficient is

$$\begin{aligned} f_2 = \mathcal{B}_1(c,c) = \tfrac{1}{4}\{&\mathcal{C}(a,a) - \mathcal{C}(b,b) - k_\ell(n\cdot b)a \\ &+ i[\mathcal{C}(a,b) + \mathcal{C}(b,a) - k_\ell(n\cdot b)b]\}. \end{aligned} \tag{2.13.57}$$

The possible order-$\rho_Q^{1/2}$ term $k_\ell(n \cdot a)a$ equals zero. The zero harmonic is $[\mathcal{C}(a,a) + \mathcal{C}(b,b) + k_\ell(n \cdot b)a]/2$, which by (2.13.56) equals the cylindrical divergence of (2.13.44). For any symmetric coefficient tensor the three divergence rows are

$$\operatorname{Div}_* C = \begin{pmatrix} \mathcal{D}C_{rr} + \mathcal{Z}C_{rz} + (C_{rr} - C_{\theta\theta})/\mathsf{R} \\ \mathcal{D}C_{r\theta} + \mathcal{Z}C_{\theta z} + 2C_{r\theta}/\mathsf{R} \\ \mathcal{D}C_{rz} + \mathcal{Z}C_{zz} + C_{rz}/\mathsf{R} \end{pmatrix}. \tag{2.13.58}$$

Thus subtraction of the physical angular mean keeps all six entries, not only the radial-cross pair or its Haar average.

We take $t = a/2$, $r_c = ib/2$, and their actual first-harmonic pressure. The first-harmonic source, apart from the explicitly kept temporal term, is

$$f_1 = \mathcal{E}_1^{\mathrm{lin}} + \mathcal{I}_1(M,c), \qquad M = Q^{\frac{1}{2}+h}\mu, \qquad \mathcal{I}_m(M,U) = \mathcal{B}_m(M,U) + \mathcal{B}_0(U,M). \tag{2.13.59}$$

Here $\mathcal{E}_1^{\mathrm{lin}}$ equals (2.13.37), with its pressure gradient. The full-torus mean interaction is

$$\begin{aligned} \mathcal{I}_m(M,U) = {}& M_r\mathcal{D}U + M_z\mathcal{Z}U + (M_\theta/\mathsf{R})J_\theta U + ik_\ell m(M\cdot n)U \\ &+ U_r\mathcal{D}M + U_z\mathcal{Z}M + (U_\theta/\mathsf{R})J_\theta M. \end{aligned} \tag{2.13.60}$$

No auxiliary separation removes a term with M. The worst mean carrier has order $1 - \varkappa$. The other terms are higher. In (2.13.57), $\mathcal{C}(a,a)$ and $k_\ell(n\cdot b)a$ have that same order, while the remaining terms are higher.

Lemma 2.13.4 thus gives the source orders (2.13.54).

We apply Proposition 2.13.3 to each signed source $f_{\pm1}, f_{\pm2}$, then apply the same temporal cutoff and Lemma 2.13.4. We denote the full curled coefficients by U_j, with $U_{-j} = \bar{U}_j$. Their principal orders are a_j, and their pressures have order $a_j + 1/2$. Conjugacy holds by uniqueness of the real-coefficient ODE, with the factor i/m in its pressure and potential formulas.

The cut inverse remains inside the original enlarged separation rectangle even if its uncropped solution fills the pulse interval. A coherent mean on the full auxiliary torus restricts to each original label. It uses no larger wave supports.

For an arbitrary finite old harmonic family X_l and a finite correction family U_j, the exact added quadratic coefficient is

$$G_s = \sum_{l+j=s} [\mathcal{B}_j(X_l, U_j) + \mathcal{B}_l(U_j, X_l)] + \sum_{j+k=s} \mathcal{B}_k(U_j, U_k). \tag{2.13.61}$$

We keep the zero value of s for the mean. For the first step $X_{\pm1} = c, \bar{c}$, and the only new frequencies are $0, \pm1, \pm2, \pm3, \pm4$. The new nonzero residual, modulo its explicitly flat endpoint family, is

$$\mathbf{1}_{\{|s|=1,2\}}[\mathcal{E}_s^{\mathrm{lin}} + \mathcal{I}_s(M, U_s)] + G_s.$$

Equation (2.13.53) gives the first two minima:

$$\begin{aligned} |s| = 1 &: \min(a_1 + \tfrac{1}{2} - 3\varkappa, a_1 + \tfrac{1}{2} - \varkappa, \tfrac{1}{2} + a_2 - \varkappa, a_1 + a_2 - \varkappa) = \tfrac{3}{2} - 6\varkappa, \\ |s| = 2 &: \min(a_2 + \tfrac{1}{2} - 3\varkappa, a_2 + \tfrac{1}{2} - \varkappa, \tfrac{1}{2} + a_1 - \varkappa, 2a_1 - \varkappa) = \tfrac{3}{2} - 4\varkappa. \end{aligned}$$

The remaining two are $\min(\frac{1}{2} + a_2 - \varkappa, a_1 + a_2 - \varkappa)$ and $2a_2 - \varkappa$. This proves (2.13.55).

The full first-step covariance increment is

$$\Delta C_\gamma = 2\,\mathrm{Re}[c \otimes \bar{U}_1 + U_1 \otimes \bar{c} + U_1 \otimes \bar{U}_1 + U_2 \otimes \bar{U}_2]. \tag{2.13.62}$$

Mixed frequencies 1 and 2 do not survive the physical angular average. Each tensor product in (2.13.62) contains its full principal and curl coefficients. The smallest order is $1/2 + a_1 = 3/2 - 3\varkappa$.

The other terms are higher. For a general finite family the same rule is $\sum_m X_m \otimes X_{-m}$, with the two signs included. It supplies all six entries and does not assert real-quadrature cancellation for complex data. By exact solenoidality, its divergence equals the additional angular mean of the nonlinear term. □

The estimates in Proposition 2.13.7 have finite seminorm dependence. A source jet of order m uses at most $m+3$ potential derivatives, $m+1$ pressure derivatives, and $m+1$ mean derivatives. It also uses finitely many phase and background jets. The ODE inverse adds polynomial losses, and the exact curl uses one additional derivative. We can thus estimate a new residual with finitely many additional input jets. Harmonic counts may grow at later finite stages, but no such count changes the fixed graph or the value threshold of the principal inverse.

For the same cutoff, the nonflat representatives of the first-step source are $\vartheta_q f_1$ and $\vartheta_q^2 f_2$. The ODE holds the slow point fixed, so uniqueness gives correction potentials $\vartheta_q A_1$ and $\vartheta_q^2 A_2$, with pressures of the same powers. The discrepancy from the exact cut residual consists of explicit commutators. For example,

$$\begin{aligned} L_{u_{\mathrm{B}}}(\vartheta_q w) + \nabla(\vartheta_q p_w) = \vartheta_q[L_{u_{\mathrm{B}}} w + \nabla p_w] + (\partial_t \vartheta_q + u_{\mathrm{B}} \cdot \nabla \vartheta_q - \Delta \vartheta_q) w \\ - 2\sum_j (\partial_j \vartheta_q) \partial_j w + p_w \nabla \vartheta_q, \end{aligned} \tag{2.13.63}$$

with the additional linear operator applied to $\nabla \vartheta_q \times A_w$ when we use the actual curl.

Ordered products obey

$$(\vartheta_q^a X\cdot\nabla)(\vartheta_q^b Y)=\vartheta_q^{a+b}(X\cdot\nabla)Y+b\vartheta_q^{a+b-1}(X\cdot\nabla\vartheta_q)Y.$$

We keep each derivative-of-cutoff term and each curl commutator. These terms are physically flat. We use this identity to track the remaining powers at stages after this point. The harmonic index alone does not determine them.

The Haar linear cross has the explicit discrepancy $(1-\vartheta_q^2)K$. Section 2.14 keeps it as a pure-cross remainder without an inverse.

2.13.9 Weighted radial mixing on the same cover

The mean response uses radial primitives of the sampled zero-Haar tensor. Here the strict inequality $d_r>1$ from (2.13.8) gives, on the fixed hull, $a_r(\mathsf{R})=d_r\mathsf{R}^{d_r-1}\geq a_*>0$. The proof also specifies why the aggregate weight survives a compact primitive at angular edges.

For either $v=v_r$ or v_t, the quadratic irrationality in (2.13.6) gives

$$|v\cdot n|\geq\frac{c}{1+|n|},\qquad n\in\mathbb{Z}^2\setminus\{0\}.\tag{2.13.64}$$

For example $v_r\cdot n=(n_1+n_2)-\sqrt{2}n_2$. Its product with its conjugate is a nonzero integer, while that conjugate is $O(|n|)$. The zero-mean Fourier inverse thus satisfies

$$\|D_v^{-1}f\|_{C^m(\mathbb{T}^2)}\leq C_m\|f\|_{C^{m+4}(\mathbb{T}^2)},\qquad D_v=v\cdot\partial_{\mathsf{y}}.\tag{2.13.65}$$

We divide the Fourier coefficient by $2\pi iv\cdot n$ and integrate by parts $m+4$ times. The remainder has the summable majorant $(1+|n|)^{-3}$ in dimension two. The exact covering rule is $D_v^{-1}(f\circ\pi_i)=\lambda_v^{-i}(D_v^{-1}f)\circ\pi_i$.

Remark 2.13.8 (The radial inverse in slow and oscillatory coordinates). We apply the ordinary weighted radial inverse of Theorem 1(iv).

1. *Slow chart.* At fixed (Z,T) the quantities $\bar q$ and $\hat\zeta$ are fixed, and $\hat\xi=\mathsf{R}/\sqrt{\bar q}$ increases with R (see (2.14.11) and (2.14.12)). The radial integrals of the wave stage are $\int\cdot\,\mathrm{d}\mathsf{R}=\int\cdot\sqrt{\bar q}\,\mathrm{d}\hat\xi$, with a fixed smooth Jacobian on the hull (2.13.1). Derivatives $\partial_{\mathsf{Z}},\partial_{\mathsf{T}}$ commute with them up to (2.14.12), whose coefficients $\chi_{\mathsf{Z}},\chi_{\mathsf{T}}$ are supported in Σ. So the same one-sided integral estimates hold for derivatives in $(\mathsf{R},\mathsf{Z},\mathsf{T})$. For the shifted integrals, use the variables $U=\mathsf{R}^{d_r}$, $u=s^{d_r}-\mathsf{R}^{d_r}$ of the proof of Lemma 2.13.10. In these variables the shift λuv_r depends neither on U nor on (Z,T), so coefficient derivatives produce no factor λ.

2. *Gevrey classes (Section 2.12.1).* If the source does not depend on y, neither does the output, and Lemma 2.12.29 applies. For the unshifted operator at fixed y (Corollary 2.12.18(vi)), (T-a) holds by differentiation under the integral, since the support is compact in the hull. By linearity and the linear constants of the ordinary weighted inverse, (T-b) holds with $k=0$, $e'=e$ and output majorant $m'_I=\max_{I'\leq I}m_{I'}$ (with the same powers of $\mathcal{L}_W$), times $C_{\mathcal{T}}=\max_{|I|\leq J}K'_I$. So Lemma 2.12.17 maps $\mathcal{G}_J(m,e;L)$ into $\mathcal{G}_J(C_{\mathcal{T}}m',e;L)$. There is no radius loss, and $C_{\mathcal{T}}$ does not depend on α, on the band ℓ or on the label, because W, b, $\frac{\hat\xi_p^2}{2}$ and the band chart are ℓ-independent. For the shifted operators of Corollary 2.12.18(iv), use the outward weight on the outer side and the inward weight on the inner side. The difference $I_\chi=I-\chi J$ combines these bounds at both ends. The full moment is estimated without a radial weight. When it vanishes the compensated identity applies to each raw tail, with the sign determined by its orientation. The supremum may be taken at the shifted auxiliary point, and $e\leq1$ gives $e'=1$. The rest of (T-b) is Lemma 2.13.9.

Lemma 2.13.9 (Shifted radial mixing with aggregate weight)**.** *Let $f \in \mathcal{M}^a$ have $\Pi f = 0$, with support in the fixed radial hull. We use its same cover and define*

$$If(\mathsf{R},\mathsf{y}) = \int_{\mathsf{R}}^{\infty} f(s,\mathsf{y}+\lambda(s^{d_r}-\mathsf{R}^{d_r})v_r)\,\mathrm{d}s,$$
$$Jf(\mathsf{R},\mathsf{y}) = \int_{0}^{\infty} f(s,\mathsf{y}+\lambda(s^{d_r}-\mathsf{R}^{d_r})v_r)\,\mathrm{d}s. \tag{2.13.66}$$

We fix the slow parameters in the two integrals. We select a smooth radial cutoff χ that equals one at the inner edge and zero at the outer edge.

We place its transition in the protected region where $\mathsf{W} \geq c > 0$. Then

$$I_\chi f := If - \chi Jf \in \mathcal{M}^{a+\varkappa}. \tag{2.13.67}$$

For the complete moment, take ordinary coefficient derivatives at observation radii $\mathsf{R} \in [\mathsf{R}_-,\mathsf{R}_+]$ in (2.13.1). For all fixed m,N,

$$\|\partial^{\leq m} Jf\|_\infty \leq C_{m,N}\rho_Q^{a+N} S_\ell^{B_{m,N}}. \tag{2.13.68}$$

The assertions include signed sources and fixed smooth radial multipliers.

Each output seminorm uses only finitely many source seminorms, and the same cover is unchanged.

Proof. Let $B = a_r(\mathsf{R})^{-1}D_{v_r}^{-1}$ and $\mathcal{A}f = \partial_{\mathsf{R}}(Bf)$, with this derivative ordinary and at fixed y. The weight is independent of y, so (2.13.65) keeps the weighted derivative bounds. The positive radial denominator and finite differentiation show that $\mathcal{A}$ keeps them as well. Integration by parts in the shifted variable gives the identity

$$If = -\lambda^{-1}Bf - \lambda^{-1}I(\mathcal{A}f), \qquad Jf = -\lambda^{-1}J(\mathcal{A}f). \tag{2.13.69}$$

Boundary terms at the endpoints of the full support vanish by smooth flat extension. The partial integral has the displayed local boundary term. It is not an arbitrarily flat moment.

The radial tail bounds from Lemma 2.6.9 apply to all the differentiated integrands. To determine their role at angular zeros, on the outer region $\{y_p \geq -3\}$ we write $\mathsf{W} = \sum_i w_i$ and use the componentwise bound $w_i(s,\hat\zeta) \leq w_i(\mathsf{R},\hat\zeta)$ for $s \geq \mathsf{R}$, which is (W1) of Proposition 2.3.9; summing this inequality gives the comparison for the aggregate. On the inner region $\{y_p \leq -3\}$ the inward comparison gives $\mathsf{W}(s,\hat\zeta) \leq C_1\mathsf{W}(\mathsf{R},\hat\zeta)$ for $s \leq \mathsf{R}$. At fixed (Z,T), $\frac{\hat\xi^2}{\hat\zeta}$ increases with R (Remark 2.13.8(1)). On the bounded radial hull,

$$\sup_{0<u\leq C\mathsf{W}(\mathsf{R},\hat\zeta)} u[1+\log(1/u)]^N \leq C_N\mathsf{W}(\mathsf{R},\hat\zeta)\mathcal{L}_W(\mathsf{R},\hat\zeta)^N.$$

Thus outward tails keep the aggregate logarithmic class even when an angular factor vanishes.

At the inner edge the compact primitive uses the exact identity

$$If - Jf = -\int_0^{\mathsf{R}} f(s,\mathsf{y}+\lambda(s^{d_r}-\mathsf{R}^{d_r})v_r)\,\mathrm{d}s,$$

and thus the inward-tail estimate. Independent estimates of If and χJf at that edge would not prove the weighted assertion. The protected transition has $\mathsf{W} \geq c$, so ordinary bounded estimates suffice there. Parameter derivatives act on zero-extended integrands and have no moving-boundary contributions. In the variables $U = \mathsf{R}^{d_r}$, $u = s^{d_r} - \mathsf{R}^{d_r}$ the shift is $\lambda u v_r$. It depends neither on U nor on (Z,T) (Remark 2.13.8(1); proof of Lemma 2.13.10(a)). So an ordinary coefficient derivative

of If, Jf or $I_\chi f$ falls on the integrand, on the fixed Jacobian or on χ, with no factor λ. This gives $I_\chi f \in \mathcal{M}^a$ for every $f \in \mathcal{M}^a$, the first assertion of (2.14.13). The count of powers of λ below is only an upper bound.

We iterate (2.13.69) k times. After m ordinary output derivatives a crude remainder loses at most λ^m, from the shift. We select $k \geq m+2$. This leaves at least one inverse power of λ, also in the compact remainder.

In the inner region, we combine its two complete moments into the inward tail before the estimate. Each explicit boundary term also has an inverse power of λ. Because $\lambda^{-1} \asymp \rho_Q^{\varkappa} S_\ell^{\rho_g}$, this proves (2.13.67). For the complete moment there are no partial boundary terms.

The choice $k \geq m + \lceil N/\varkappa \rceil + 2$ proves (2.13.68). Extra radial multipliers have bounded fixed derivatives on the hull and enter the same argument. The finitely many additional torus and slow derivatives equal the finite seminorm dependence claimed in the statement. □

The same cover is necessary here. Radial integration fixes $q, \hat{\zeta}$, so it sees a bounded collection of band levels even when it crosses many radial boxes. The Fourier inverse, translation, and complete or partial shifted integrals are all operations on the same same torus. Higher derivative orders and higher finite stages change constants, not the permitted covering level or the radial nonstationarity exponent. In particular a pointwise sampled zero-Haar covariance has no assumed smallness beyond its $\mathcal{M}^a$ order. Only its complete radial moments have the arbitrary-power gain.

2.13.10 The finite-source radial primitives on both time sides

For a forward source with a moving radial or angular taper, use the weight and the moment-subtracted primitive in Theorem 1(iv). Replacing the auxiliary point by its prescribed translation leaves this weight fixed. The coefficient proof of Lemma 2.13.9 then applies to the shifted primitive: the zero-Haar partial primitive gains $\rho^{\varkappa}$ and the full moment is coefficient-flat. Angular and temporal derivatives of the moving subtraction leave the rank-one term $-(Z\chi_m)\mathcal{J}g$ on the protected slot; it is flat whenever the full moment is. For the native backward field the proof is as follows.

Lemma 2.13.10 (Backward weighted radial primitives)**.** *Assume (B2), (B3) and (B5). On $t<0$ take the classes (2.13.4) and (2.14.4) with $\mathsf{W} = \mathsf{W}_b$, and the band charts of Section 2.14 with $\bar{q} = q_b/Q$. Take β_0, χ, k and $\mathcal{I}_\chi$ as in (2.14.11), with $\hat{\xi}_p = \hat{\xi}_{p,b}$, and $\mathcal{I}, \mathcal{L}, \mathcal{J}$ as in (2.14.8). Let $f \in \mathcal{M}^a$, possibly multiplied by fixed smooth radial factors on the hull.*

(a) $\mathcal{I}_\chi f \in \mathcal{M}^a$. It vanishes for $\hat{\xi} \leq \hat{\xi}_a$ and for $\hat{\xi} \geq \hat{\xi}_b$, with smooth zero extension. The same conclusion holds for each fixed auxiliary translate $(\mathcal{I}_\chi f)(\mathsf{R}, \mathsf{y}+\theta)$ and when the source of $\mathcal{I}_\chi$ is multiplied by ϑ_q or by the Borel and flux cutoffs.

(b) If $\Pi f = 0$, then $\mathcal{I}_\chi f \in \mathcal{M}^{a+\varkappa}$, and $\mathcal{J} f$ is coefficient-flat.

(c) The commutators (2.14.12) and (2.3.8) lie in $\mathcal{M}^a$. They are coefficient-flat when $\Pi f = 0$, and they vanish when f is auxiliary-independent with $\int f \, \mathrm{d}\mathsf{R} = 0$. The moments c_β, c_θ of (2.3.8) are constants.

Thus Lemma 2.6.9, (2.14.13) and Lemma 2.13.9 hold on $t<0$ with $\mathsf{W} = \mathsf{W}_b$. Together with Proposition 2.7.2, the conclusions of Lemma 2.3.13 hold on $t<0$, with the single component W_b in place of the native-plus-tube aggregate.

Proof. Geometry. At fixed (Z, T), $\frac{\hat{\xi}^2}{2} = Q\mathsf{R}^2/(2\hat{t}_b)$ is a smooth increasing function of R, with bounded jets on the hull, because $\hat{t}_b/Q$ lies in a fixed compact interval. By Lemma 2.3.11(c), χ is a function

of $\frac{\hat\xi^2}{2}$ alone. It equals one for $\frac{\hat\xi^2}{2} \le \frac{\hat\xi^2_{p,b}}{2}e^{-8}$ and zero for $\frac{\hat\xi^2}{2} \ge \frac{\hat\xi^2_{p,b}}{2}e^{-3}$. Choose $\frac{\hat\xi^2_1}{2} = \frac{\hat\xi^2_{p,b}}{2}e^{-8}$ and $\frac{\hat\xi^2_2}{2} = \frac{\hat\xi^2_{p,b}}{2}e^{-3}$ in Lemma 2.3.11(b), and let $c_1 = \min\{\mathsf{W}_b(\frac{\hat\xi^2}{2}) : \frac{\hat\xi^2_1}{2} \le \frac{\hat\xi^2}{2} \le \frac{\hat\xi^2_2}{2}\} > 0$.

(a). Put $U = \mathsf{R}^{d_r}$ and $F(U,\mathsf{y}) = f(\mathsf{R},\mathsf{y})/(d_r\mathsf{R}^{d_r-1})$, extended by zero. The change of integration variable gives

$$\mathcal{I}f = A_+, \quad \mathcal{L}f = A_-, \quad A_\pm(U,\mathsf{y}) = \int_{\mathbb{R}_\pm} F(U+u,\mathsf{y}+\lambda u v_r)\,\mathrm{d}u, \qquad \mathcal{I}_\chi f = (1-\chi)A_+ - \chi A_-.$$

At fixed u the shift depends on neither U nor (Z,T). So a coefficient derivative falls on F or on χ only, with no factor λ. The zero extension produces no boundary terms. Write $x = \hat\xi^2/2$ and $x_i = \hat\xi_i^2/2$. The term χA_- can be nonzero only for $x \le x_2$. Every integration point in A_- then has radial coordinate at most $x \le x_2$, where the inward estimate of Lemma 2.3.11(b) applies. Likewise $(1-\chi)A_+$ can be nonzero only for $x \ge x_1$, so the outward estimate applies throughout its integration interval. These two comparisons and the bounded length of the hull give $|\partial^I \mathcal{I}_\chi f| \le C\rho^a S^{B_I}\mathsf{W}_b\mathcal{L}_b^{N_I}$. Terms with derivatives of χ are supported in $[x_1,x_2]$, where $\mathsf{W}_b \ge c_1$. This also covers the constant parts of the cutoff inside that interval. For $\hat\xi \le \hat\xi_a$, $A_- = 0$ and $\chi = 1$; for $\hat\xi \ge \hat\xi_b$, $A_+ = 0$ and $\chi = 0$. The bound $\mathsf{W}_b\mathcal{L}_b^N$ is flat at $\frac{\hat\xi_a^2}{2}, \frac{\hat\xi_b^2}{2}$ (Lemma 2.3.7(d)), which gives the smooth zero extension. Translating the compensated expression by a fixed θ in y preserves the estimates since W_b is independent of y. For the individual tails, $\mathcal{I}f = \mathcal{J}f$ below the source and $\mathcal{L}f = \mathcal{J}f$ above it. The compensation is what gives vanishing at both ends. For the cutoffs: ϑ_q is a smooth function of $\log(1/\mathsf{W}_*)/(c_e\log^{6/5}(1/\widetilde{q}))$, and $\mathsf{W}_* \asymp |T_0|$. By Lemma 2.3.11(a), each fixed derivative of $\log\mathsf{W}_*$ is bounded by a power of $\mathcal{L}_b$. The cutoffs $\chi(c_n\widetilde{q})$ and $\chi(\widetilde{q}/\delta_n)$ do not depend on R.

(b). The weight does not depend on y, so $\mathcal{B} = a_r^{-1}(v_r\cdot\partial_\mathsf{y})^{-1}$ and $\mathcal{A} = \partial_\mathsf{R}\mathcal{B}$ keep $\mathcal{M}^a$ by (2.13.65). The identities $\mathcal{I}f = -\lambda^{-1}\mathcal{B}f - \lambda^{-1}\mathcal{I}\mathcal{A}f$ and $\mathcal{J}f = -\lambda^{-1}\mathcal{J}\mathcal{A}f$ of (2.14.13) do not involve the weight. The boundary term $\lambda^{-1}\mathcal{B}f$ is evaluated at the observation point. The integrated terms are estimated by (a), with the inward representation where $\chi = 1$ and the outward one where $\chi = 0$. The iteration count of the proof of Lemma 2.13.9 and $\lambda^{-1} \asymp \rho^{\varkappa}S^{\rho_g}$ give the gain. The full moment has no boundary terms, so it has every power, unweighted.

(c). We have $\chi_\mathsf{Z}, \chi_\mathsf{T}$ supported where $\hat\xi_1 \le \hat\xi \le \hat\xi_2$, so $\mathsf{W}_b \ge c_1$ there. Also $|\partial^I\mathcal{J}f| \le C\rho^a S^{B_I}$. This gives the class. Coefficient-flatness follows from (b). If f does not depend on y, then $\mathcal{J}f = \int f\,\mathrm{d}\mathsf{R}$. Since $\frac{\hat\xi^2_{p,b}}{2}$ is constant, $c_\beta = \frac{\hat\xi^2_{p,b}}{2}\int e^y b(y)\,\mathrm{d}y$ and $c_\theta = \hat\xi_{p,b}\int e^{y/2}b(y)\,\mathrm{d}y$. The terms with $(\frac{(\hat\xi_p(\hat\zeta))^2}{2})'$ in (2.14.12) vanish.

The operations common to both native weights are the shifted integrals, the Diophantine integration by parts, the bank commutator and the slice-function property of $y = 2\log(\widetilde{\xi}/\widetilde{\xi}_p)$. The component construction of that proof (native channels, tubes, connectors and angular tapers) has no backward counterpart and is not needed. By Lemma 2.3.11(a) the single component W_b already satisfies (2.3.9). □

2.13.11 Output for the finite mean–wave stage

The positive leading construction and the signed $\mathcal{M}^3$ slow update give an actual six-entry covariance in $\mathcal{M}^1$, with unmatched Haar radial crosses of order $\mathcal{M}^{3-\varkappa}$. Each finite source correction keeps the original separated supports and same covers. Its new nonzero harmonics and complete covariance are the actual finite sums (2.13.61) and (2.13.62). The signed map realizes a given Haar-independent pair in its principal linear cross with the original wave. Equation (2.13.50) gives the full increment about that wave. The later return also includes the mixed tensor with the other current harmonics

in (2.15.30). Lemma 2.13.9 applies to the zero-Haar parts of the aggregate tensors and to their radial moments.

All these operations have all-fixed-order coefficient estimates and finite seminorm dependence. Only the positive-amplitude and kept value requirements impose smallness thresholds. Derivative orders and finite harmonic counts enlarge constants. The finite mean–wave stage must still use the actual mean response and support moments. This section supplies its wave and radial-mixing operators, without a replacement of those mean equations by a covariance average or principal-amplitude equation.

2.14 The mean equations and the finite iteration

Main result. Proposition 2.15.2 gives compatible actual fields at each finite stage, with the stated order improvement and one fixed reference force. It starts from the initialized state and keeps all six covariance entries, pressure terms, and flat remainders. This section does not take an infinite sum.

The wave construction leaves two different errors. The packet inverse corrects its nonzero angular modes. Its angular mean is the divergence of the full covariance of the exact curls. This covariance contains diagonal and tangential entries as well as the two prescribed radial crosses. We first construct compact mean responses to this full tensor. Three radial state integrals will replace the axial primitives that would lose control without this replacement at $\hat{\zeta} = \pm 1$.

The aggregate cutoff introduces one more distinction. The covariance of the cut waves is an actual covariance, but the square of that cutoff multiplies its principal cross. We keep this discrepancy in an explicit pure-cross tensor. The mean equation then has an exact canonical form, while the ordinary equation contains the flat tensor divergence for this canonical form. The limit argument uses the two equations.

2.14.1 The fixed reference and the coefficient conventions

We fix the leading profile, its slow realization, and the packet family constructed in the previous sections. We write (u_s, π_s) for the slow reference and K_{B} for its two-component signed stress. The identity supplied by Proposition 2.6.15 is

$$\mathscr{N}(u_s, \pi_s) + \mathscr{D}_r K_{\mathrm{B}} = \mathbf{f}_s, \qquad \mathscr{D}_r K = (\partial_r + 2/r) K_\theta e_\theta + (\partial_r + 1/r) K_z e_z. \tag{2.14.1}$$

Here $\mathscr{N}$ includes the pressure gradient, as in (2.4.1).

We define the symmetric cross target $\mathsf{Q}_s = \mathcal{Q}_\times(K_{\mathrm{B}})$ by (2.15.1). Its full divergence is

$$\operatorname{div} \mathsf{Q}_s = \mathscr{D}_r K_{\mathrm{B}} + (\partial_z K_{\mathrm{B},z}) e_r. \tag{2.14.2}$$

Thus Q_s is a covariance target, not a Reynolds stress for the unchanged slow field with residual $\mathbf{f}_s$. Its normalized leading part is of order $\rho\mathsf{W}$, and the higher slow stress is a signed $\mathcal{M}^3$ term.

The reference force equals the known smooth slow residual: $\mathbf{f}_{\mathrm{ref}} = \mathbf{f}_s$. We use no preliminary infinite mean sum or radial-force adjustment. The independent slow Borel realization precedes the packet atlas. The next mean initialization is finite.

We use Π for normalized Haar projection in the auxiliary torus. It differs from the physical angular mean $\langle\cdot\rangle_\theta$. We write u_M for the actual mean field. It is independent of the physical angle but may depend on the auxiliary variables before evaluation.

On a band $Q = 2^{-\ell}$ put $\rho = Q^h$ and use $(\mathsf{R}, \mathsf{Z}, \mathsf{T}) = (r/Q^{1/2}, z/Q^{\frac{1}{2}-h}, t/Q)$ for the band coordinates, with the physical labels selected from the same gauge of (2.10.1). Thus $Q \asymp q$ with

fixed constants. These differ from the t-similarity variables in (2.3.13). All band normalizations in this section use the constant Q.

We do not differentiate a moving choice of band. Velocities, pressures and forces have scales

$$Q^{-\frac{1}{2}-h}, \qquad Q^{-1-2h}, \qquad Q^{-\frac{3}{2}-2h}, \tag{2.14.3}$$

in this order. Statements about $\mathcal{M}^a$ or $\mathcal{W}^a$ refer to the normalized coefficients in those classes.

We recall that $\mathcal{M}^a$ means, for each fixed ordinary coefficient multi-index I,

$$|\partial^I f| \le C_I \rho^a S^{B_I} \mathsf{W}(1+\log(1/\mathsf{W}))^{N_I}, \qquad S = \ell^{6/5}. \tag{2.14.4}$$

The class includes smooth zero extension at the true support edges. The wave class $\mathcal{W}^a$ has $\sqrt{\mathsf{W}}$ in place of W and the packet Gaussian factor. A scalar full radial moment has the analogous unweighted bounds.

Each output seminorm may use finitely many higher input seminorms. The exponent a is independent of the ordinary derivative order. The constants and logarithmic powers can depend on that order. We write "coefficient-flat" for an unweighted bound of each ρ order on the absolute lift, with bounds independent of its auxiliary variables.

This alone does not imply each weighted order in (2.14.4).

We set

$$\varkappa = 10^{-5}, \qquad s = 1-\varkappa, \qquad a_0 = 1-3\varkappa. \tag{2.14.5}$$

The current mean will have the form

$$Q^{\frac{1}{2}+h} u_M = (b_M, V_M, G_M) = (\rho B_{\mathrm{H}} + b^\perp, V_{\mathrm{H}} + V^\perp, G_{\mathrm{H}} + G^\perp), \quad \begin{cases} b^\perp \in \mathcal{M}^{s+1+\varkappa}, \\ V^\perp, G^\perp \in \mathcal{M}^s, \end{cases} \tag{2.14.6}$$

where the perpendicular terms have zero Haar mean. The coefficients $B_{\mathrm{H}}, V_{\mathrm{H}}, G_{\mathrm{H}}$ have bounded fixed jets, with the allowed polynomial S factors. On the fixed protected repair regions, the full swirl V_M is positive with a lower bound independent of the auxiliary point.

The current five-row matrix is invertible. These value margins hold initially by the unchanged power patches. Each finite update will keep them after a smaller positive q threshold.

2.14.2 Shifted radial primitives and the complete radial response

We write y for the auxiliary torus coordinate. We keep Π for its Haar projection. On one cover the evaluated derivatives are

$$\mathcal{D} = \partial_{\mathsf{R}} + \lambda a_r(\mathsf{R}) v_r \cdot \partial_{\mathsf{y}}, \qquad \mathcal{T} = \rho \partial_{\mathsf{T}} + c\, v_t \cdot \partial_{\mathsf{y}}, \qquad \Delta_* = \mathcal{D}^2 + \mathsf{R}^{-1}\mathcal{D} + \rho^2 \partial_{\mathsf{Z}}^2. \tag{2.14.7}$$

Here $a_r(\mathsf{R}) = d_r \mathsf{R}^{d_r - 1}$, $\lambda \asymp \rho^{-\varkappa} S^{-\rho_g}$ and $c \asymp S^{-1}$, with the fixed constants and directions of the packet construction. The radial hull stays in a fixed compact subset of $(0,\infty)$, and a_r has a positive lower bound there. The operators in (2.14.7) commute with ∂_{Z}, and $\mathcal{D}$ commutes with $\mathcal{T}$.

For an auxiliary coefficient f, we define

$$\begin{aligned} \mathcal{I} f(\mathsf{R}, \mathsf{y}) &= \int_{\mathsf{R}}^{\infty} f(x, \mathsf{y} + \lambda(x^{d_r} - \mathsf{R}^{d_r}) v_r)\, \mathrm{d}x, \\ \mathcal{L} f(\mathsf{R}, \mathsf{y}) &= \int_{0}^{\mathsf{R}} f(x, \mathsf{y} + \lambda(x^{d_r} - \mathsf{R}^{d_r}) v_r)\, \mathrm{d}x, \qquad \mathcal{J} f = \mathcal{I} f + \mathcal{L} f. \end{aligned} \tag{2.14.8}$$

We hold the slow parameters fixed. At the physical auxiliary sample these are the actual radial integrals at fixed z, t. In particular

$$\mathcal{D}\mathcal{I}f = -f, \quad \mathcal{D}\mathcal{L}f = f, \quad \mathcal{D}\mathcal{J}f = 0, \qquad [\partial_{\mathsf{Z}}, \mathcal{I}] = [\mathcal{T}, \mathcal{I}] = 0, \tag{2.14.9}$$

and the same commutation holds for $\mathcal{L}, \mathcal{J}$.

A full moment is covariantly constant, rather than necessarily independent of the lifted R coordinate. Thus

$$\mathcal{J}f(x, \mathsf{y} + \lambda(x^{d_r} - \mathsf{R}^{d_r})v_r) = \mathcal{J}f(\mathsf{R}, \mathsf{y}). \tag{2.14.10}$$

We use this identity for each product of a full moment and a bump.

To evaluate the complete moment at any physical radius, fix an anchor $\mathsf{R}_c \in [\mathsf{R}_-, \mathsf{R}_+]$. On either time side its value at the physical sample is exactly

$$\mathcal{J}f(\mathsf{R}_c, \lambda \mathsf{R}_c^{d_r} v_r + T_g^{i_0} t v_t).$$

Indeed the shift in (2.14.10) cancels the full $\lambda \mathsf{R}^{d_r} v_r$ in the sample. Thus the sampled moment is constant along the physical radial line and extends to the axis with all radial derivatives zero. Its time and axial jets there are those of the anchored expression. At $t = 0, z \neq 0$ the common cover and the matched integrand jets give equality of these jets by differentiation on the compact integration interval. Ordinary radial derivatives at fixed auxiliary point in (2.13.68) use the annulus, where every derivative of R^{d_r} is bounded.

The protected correction region is a moving fiber interval. It is not one fixed interval in $\frac{\hat{\xi}^2}{2}$ for all angles. We put $y = 2\log(\hat{\xi}/\hat{\xi}_p(\hat{\zeta}))$ and select once a nonnegative $b \in C_c^\infty((-8, -3))$ with $\int b(y)\, \mathrm{d}y = 1$. On the actual source of Section 2.6 set

$$\begin{aligned} \beta_0(\tfrac{\hat{\xi}^2}{2}, \hat{\zeta}) &= (\tfrac{\hat{\xi}^2}{2})^{-1} b(y), \qquad \chi(\tfrac{\hat{\xi}^2}{2}, \hat{\zeta}) = \int_y^\infty b(v)\, \mathrm{d}v, \\ k &= -\mathcal{D}\chi = \mathsf{R}\beta_0(\tfrac{\hat{\xi}^2}{2}, \hat{\zeta})/\bar{q}, \quad \mathcal{I}_\chi = \mathcal{I} - \chi\mathcal{J}, \quad \bar{q} = q/Q. \end{aligned} \tag{2.14.11}$$

Thus $\int \beta_0\, \hat{\xi}\, \mathrm{d}\hat{\xi} = 1$ fiberwise.

The cutoff is one before this buffered correction region and zero after it. We fix the graph $\frac{\hat{\xi}_p^2}{2}$, all correction shapes, and the source member before the ancient threshold. On the closed angular interval, they and the specified fixed slow jets have finite bounds. The graph $\frac{\hat{\xi}_p^2}{2}$ has a finite upper bound and a positive lower bound. Constants may depend on this member.

We do not assume one correction region at fixed $\hat{\xi}$. The two-tube weighted primitive construction in Lemma 2.3.13 gives the actual full radial weight path. The pressure support between the tubes extends beyond the velocity correction region.

Only the raw integrals in (2.14.9) commute with slow derivatives. At fixed R, with all band parameters fixed as in (2.14.7), the exact additional identities are

$$[\partial_{\mathsf{Z}}, \mathcal{I}_\chi]g = -\chi_{\mathsf{Z}}\mathcal{J}g, \qquad [\mathcal{T}, \mathcal{I}_\chi]g = -\rho\chi_{\mathsf{T}}\mathcal{J}g. \tag{2.14.12}$$

χ has no auxiliary dependence. In particular

$$y_{\mathsf{Z}} = -\partial_{\mathsf{Z}} \log(\bar{q}\tfrac{(\hat{\xi}_p(\hat{\zeta}))^2}{2}), \qquad \chi_{\mathsf{Z}} = b(y)\partial_{\mathsf{Z}} \log(\bar{q}\tfrac{(\hat{\xi}_p(\hat{\zeta}))^2}{2}).$$

The same formula holds with T in place of Z. The band chart satisfies $\hat{\zeta} = \mathsf{Z}\bar{q}^{h-\frac{1}{2}}$ and $\bar{q} - \mathsf{Z}^2\bar{q}^{2h} = \pm\mathsf{T}$. Thus

$$\bar{q}_{\mathsf{T}} = \frac{\pm 1}{1 - 2h\hat{\zeta}^2}, \qquad \hat{\zeta}_{\mathsf{T}} = -(\tfrac{1}{2} - h)\hat{\zeta}\bar{q}_{\mathsf{T}}/\bar{q}.$$

The denominator is at least $1-2h>0$ and $\bar{q}\asymp 1$ on each actual band.

The same implicit equation bounds each specified fixed Z,T jet. Thus $\mathcal{T}\chi=\rho\chi_{\mathsf{T}}$ really has one positive ρ factor, with the $(\frac{(\hat{\xi}_p(\hat{\zeta}))^2}{2})'\hat{\zeta}_{\mathsf{T}}$ term. It is not an unscaled time derivative. Haar projection and auxiliary derivatives commute with multiplication by χ because it is auxiliary independent.

These are real supported coefficients, not flat errors. Higher commutators are the full finite Leibniz sums. Derivatives of the correction function have support in the protected slot and bounded fixed slow jets, so multiplication by them has order zero in ρ. On that slot the actual weight has a positive plateau.

For zero-Haar g, only the factor $\mathcal{J}g$ in these commutators is coefficient-flat.

The shifted inverse from Lemma 2.13.9 gives

$$\mathcal{I}_\chi:\mathcal{M}^a\longrightarrow\mathcal{M}^a,\qquad \Pi f=0\implies \mathcal{I}_\chi f\in\mathcal{M}^{a+\varkappa},\quad \mathcal{J}f \text{ coefficient-flat.} \tag{2.14.13}$$

For clarity, the gain in the second assertion is valid for each fixed ordinary derivative. We set $\mathcal{B}f=a_r^{-1}(v_r\cdot\partial_{\mathsf{y}})^{-1}f$ and $\mathcal{A}f=\partial_{\mathsf{R}}\mathcal{B}f$. Integration by parts gives

$$\mathcal{I}f=-\lambda^{-1}\mathcal{B}f-\lambda^{-1}\mathcal{I}\mathcal{A}f,\qquad \mathcal{J}f=-\lambda^{-1}\mathcal{J}\mathcal{A}f.$$

After m derivatives a crude shifted remainder costs at most $(1+\lambda)^m$. More than $m+1$ integrations by parts leave the gain λ^{-1}. Arbitrarily many give any specified power for a full moment. The inner representation of $\mathcal{I}_\chi$ is the inward tail by exact cancellation, and its outer representation is the outward tail.

The aggregate tail bounds thus keep W throughout. We fix the requested output order and gain, and this gives a finite number of extra derivatives.

Lemma 2.14.1 (Radial response to a symmetric tensor)**.** *Let* D *be the normalized coefficient of a smooth symmetric tensor supported in the true radial hull. We define*

$$f_D=\frac{\mathsf{D}_{rr}-\mathsf{D}_{\theta\theta}}{\mathsf{R}}+\rho\partial_{\mathsf{Z}}\mathsf{D}_{rz},\qquad M_D=\mathcal{J}f_D,\qquad P_D=-\mathsf{D}_{rr}+\mathcal{I}_\chi f_D. \tag{2.14.14}$$

Then P_D *has zero inner and outer endpoints and*

$$(\mathrm{Div}_*\,\mathsf{D})_r+\mathcal{D}P_D=kM_D. \tag{2.14.15}$$

If the current full swirl is positive on $\operatorname{supp}k$ *and* $|\mathsf{R}kM_D|\le V_M^2/2$*, the pure swirl*

$$\delta_D=\sqrt{V_M^2+\mathsf{R}kM_D}-V_M \tag{2.14.16}$$

cancels (2.14.15)*, with zero remainder.*

It does not change divergence or axial velocity. If $\mathsf{D}\in\mathcal{M}^p$*, then* $P_D\in\mathcal{M}^p$*. Also,*

$$(\delta_D)_H\in\mathcal{M}^p,\qquad (\delta_D)_\perp\in\mathcal{M}^{p+s} \tag{2.14.17}$$

for a mean that satisfies (2.14.6)*.*

Proof. The three complete tensor-divergence rows are

$$\mathrm{Div}_*\,\mathsf{D}=\begin{pmatrix}\mathcal{D}\mathsf{D}_{rr}+(\mathsf{D}_{rr}-\mathsf{D}_{\theta\theta})/\mathsf{R}+\rho\partial_{\mathsf{Z}}\mathsf{D}_{rz}\\(\mathcal{D}+2/\mathsf{R})\mathsf{D}_{r\theta}+\rho\partial_{\mathsf{Z}}\mathsf{D}_{z\theta}\\(\mathcal{D}+1/\mathsf{R})\mathsf{D}_{rz}+\rho\partial_{\mathsf{Z}}\mathsf{D}_{zz}\end{pmatrix}. \tag{2.14.18}$$

Equations (2.14.9) give (2.14.15). In particular the integral of the radial derivative of D_{rr} is exact. We keep the term $-\mathsf{D}_{rr}$ in the pressure.

The root changes the centrifugal force by

$$-\frac{(V_M+\delta_D)^2-V_M^2}{\mathsf{R}}=-kM_D.$$

Its rationalized form

$$\delta_D=\frac{\mathsf{R}kM_D}{\sqrt{V_M^2+\mathsf{R}kM_D}+V_M} \tag{2.14.19}$$

also proves smooth extension by zero at the bump boundary. We use only the positive branch on this protected neighborhood.

Haar projection commutes with the shifted integrals. Thus $M_D=\overline{M}_D+M_{D,\mathrm{flat}}$, where $\overline{M}_D=\int \Pi f_D\,\mathrm{d}\mathsf{R}$ has order p and the complement is coefficient-flat. The pressure bounds hold by (2.14.13). Its perpendicular part includes $-\mathsf{D}_{rr}^{\perp}$ and generally has no extra gain.

For $F(W,N)=\sqrt{W^2+\mathsf{R}kN}-W$,

$$F_W=-\frac{\mathsf{R}kN}{\sqrt{W^2+\mathsf{R}kN}\,[\sqrt{W^2+\mathsf{R}kN}+W]}. \tag{2.14.20}$$

Each fixed jet of this expression has the order of N. We compare $F(V_M,\overline{M}_D)$ with $F(V_{\mathrm{H}},\overline{M}_D)$. The integral mean-value formula gives order $p+s$.

The flat moment adds only a flat term. Projection proves (2.14.17). All denominator estimates use the stated value margin and finitely many input jets. □

The pressure endpoint affects the axial flux. With the actual angular moments

$$c_\beta(\hat\zeta)=\int \tfrac{\hat\xi^2}{2}\beta_0(\tfrac{\hat\xi^2}{2},\hat\zeta)\,\hat\xi\,\mathrm{d}\hat\xi=\frac{\big(\hat\xi_p(\hat\zeta)\big)^2}{2}B_1,\qquad B_1=\int e^y b(y)\,\mathrm{d}y,$$

Fubini gives the useful identity

$$\begin{aligned}\int \mathsf{R}(\Pi\mathsf{D}_{zz}+\Pi P_D)\,\mathrm{d}\mathsf{R}&=\int \mathsf{R}\left[\Pi\mathsf{D}_{zz}-\frac{\Pi\mathsf{D}_{rr}+\Pi\mathsf{D}_{\theta\theta}}{2}\right]\mathrm{d}\mathsf{R}\\&\quad+\frac{\rho}{2}\partial_{\mathsf{Z}}\int \mathsf{R}^2\Pi\mathsf{D}_{rz}\,\mathrm{d}\mathsf{R}-\bar q c_\beta\overline{M}_D.\end{aligned} \tag{2.14.21}$$

Thus the radial repair also changes the state that controls axial momentum. The fifth frame row includes this contribution.

Its axial force differentiates the full last product:

$$-\rho\partial_{\mathsf{Z}}(\bar q c_\beta\overline{M}_D)=-\rho(\bar q c_\beta)_{\mathsf{Z}}\overline{M}_D-\rho\bar q c_\beta\partial_{\mathsf{Z}}\overline{M}_D. \tag{2.14.22}$$

We do not hold c_β or $\bar q$ constant in this equation. Pointwise,

$$\rho(P_D)_{\mathsf{Z}}=-\rho(\mathsf{D}_{rr})_{\mathsf{Z}}+\rho\mathcal{I}_\chi(\partial_{\mathsf{Z}}f_D)-\rho\chi_{\mathsf{Z}}M_D. \tag{2.14.23}$$

This is the actual pressure contribution used in the axial force.

2.14.3 The current auxiliary response

We first give the actual cylindrical increment and then estimate it. For a normalized correction $n = (\beta, v, \gamma)$ to the mean (2.14.6), let $\mathcal{B}(n)$ denote its momentum increment without pressure. It is

$$\begin{aligned}
\mathcal{B}_r(n) &= \mathcal{T}\beta + b_M\mathcal{D}\beta + \rho G_M\beta_{\mathsf{Z}} + \beta\mathcal{D}b_M + \rho\gamma(b_M)_{\mathsf{Z}} - 2V_M v/\mathsf{R} \\
&\quad - \rho(\Delta_* - \mathsf{R}^{-2})\beta + \beta\mathcal{D}\beta + \rho\gamma\beta_{\mathsf{Z}} - v^2/\mathsf{R}, && (2.14.24)\\
\mathcal{B}_\theta(n) &= \mathcal{T}v + b_M\mathcal{D}v + \rho G_M v_{\mathsf{Z}} + b_M v/\mathsf{R} + \beta\mathcal{D}V_M + \rho\gamma(V_M)_{\mathsf{Z}} + V_M\beta/\mathsf{R} \\
&\quad - \rho(\Delta_* - \mathsf{R}^{-2})v + \beta\mathcal{D}v + \rho\gamma v_{\mathsf{Z}} + \beta v/\mathsf{R}, && (2.14.25)\\
\mathcal{B}_z(n) &= \mathcal{T}\gamma + b_M\mathcal{D}\gamma + \rho G_M\gamma_{\mathsf{Z}} + \beta\mathcal{D}G_M + \rho\gamma(G_M)_{\mathsf{Z}} - \rho\Delta_*\gamma \\
&\quad + \beta\mathcal{D}\gamma + \rho\gamma\gamma_{\mathsf{Z}}. && (2.14.26)
\end{aligned}$$

The pressure increment is $(\mathcal{D}P, 0, \rho P_{\mathsf{Z}})$, and exact solenoidality means

$$(\mathcal{D} + \mathsf{R}^{-1})\beta + \rho\gamma_{\mathsf{Z}} = 0. \tag{2.14.27}$$

In particular the centrifugal term has no factor ρ. The time and viscous terms in (2.14.24) are part of the radial source. A centrifugal-only correction does not solve that equation.

Lemma 2.14.2 (Auxiliary response on the current mean)**.** *Suppose* (2.14.6) *holds and let* $f = (0, f_\theta, f_z)$ *have zero Haar mean, with* $f_\theta, f_z \in \mathcal{M}^\nu$, $\nu \geq s$. *There are actual compact corrections* $m = (\beta, \xi, \gamma)$ *and* P *such that*

$$f + \mathcal{B}(m) + (\mathcal{D}P, 0, \rho P_{\mathsf{Z}}) = (0, \mathcal{R}_\theta, \mathcal{R}_z), \qquad \mathcal{J}(\mathsf{R}\gamma) = 0, \qquad \operatorname{div}_* m = 0. \tag{2.14.28}$$

We set $d_\nu = \nu + s$. *The bounds are*

$$\beta \in \mathcal{M}^{\nu+1+\varkappa}, \quad \xi, \gamma \in \mathcal{M}^\nu, \quad P \in \mathcal{M}^{\min(\nu+\varkappa, d_\nu)}, \tag{2.14.29}$$

$$\Pi\mathcal{R}_{\tan} \in \mathcal{M}^{d_\nu+1}, \qquad (1-\Pi)\mathcal{R}_{\tan} \in \mathcal{M}^{\min(\nu+1-2\varkappa, d_\nu+s)}. \tag{2.14.30}$$

The complete force moments have the Haar orders in (2.14.30) *plus coefficient-flat zero-Haar parts. A finite threshold restriction keeps the same current class and protected value margins. We add an old Haar force to* $\Pi\mathcal{R}_{\tan}$. *This map does not cancel it.*

Proof. Let $T_0 = c\, v_t \cdot \partial_{\mathsf{y}}$. The quadratic irrational directions give

$$\|T_0^{-1} f\|_{C^j_{\mathsf{y}}} \leq C_j c^{-1} \|f\|_{C^{j+4}_{\mathsf{y}}}, \qquad \Pi f = 0. \tag{2.14.31}$$

By (2.13.64) for v_t, the reciprocal Fourier multiplier $(2\pi i\, c\, v_t \cdot n)^{-1}$ grows at most linearly in the integer frequency. After j derivatives, the C^{j+4} bound leaves an absolutely summable cubic decay on $\mathbb{Z}^2$. This inverse keeps the slow support and has only a polynomial loss in S.

We normalize protected bumps by

$$\begin{aligned}
\omega_z &= \beta_0(\tfrac{\hat\xi^2}{2}, \hat\zeta)/\bar q, \qquad \omega_\theta = \frac{\beta_0(\frac{\hat\xi^2}{2}, \hat\zeta)}{\bar q^{3/2} c_\theta(\hat\zeta)}, \\
c_\theta(\hat\zeta) &= \int \hat\xi \beta_0(\tfrac{\hat\xi^2}{2}, \hat\zeta)\, \hat\xi \, \mathrm{d}\hat\xi = \hat\xi_p(\hat\zeta) B_{1/2}, \\
B_{1/2} &= \int e^{y/2} b(y)\, \mathrm{d}y.
\end{aligned}$$

They satisfy $\int \mathsf{R}\omega_z \,\mathrm{d}\mathsf{R} = \int \mathsf{R}^2\omega_\theta \,\mathrm{d}\mathsf{R} = 1$. These normalizations are exact at each slow point. For example

$$\begin{aligned}(\omega_z)_\mathsf{Z} &= \bar{q}^{-1}(\beta_0)_\mathsf{Z} - \omega_z\partial_\mathsf{Z}\log\bar{q},\\ (\omega_\theta)_\mathsf{Z} &= \frac{(\beta_0)_\mathsf{Z}}{\bar{q}^{3/2}c_\theta} - \omega_\theta\big(\tfrac{3}{2}\partial_\mathsf{Z}\log\bar{q} + \partial_\mathsf{Z}\log c_\theta\big),\\ \partial_\mathsf{Z}c_\beta &= c_\beta\partial_\mathsf{Z}\log\frac{\big(\hat{\xi}_p(\hat{\zeta})\big)^2}{2}, \qquad \partial_\mathsf{Z}c_\theta = \tfrac{1}{2}c_\theta\partial_\mathsf{Z}\log\frac{\big(\hat{\xi}_p(\hat{\zeta})\big)^2}{2}.\end{aligned} \tag{2.14.32}$$

Full Leibniz differentiation gives the T identities and higher jets. In the seed for this construction, γ_Z includes $-(\omega_z)_\mathsf{Z}\mathcal{J}(\mathsf{R}\gamma_0)$ and $-\omega_z\partial_\mathsf{Z}\mathcal{J}(\mathsf{R}\gamma_0)$.

The derivative of the exact zero flux is zero. Thus its radial prefix remains compact. The fast auxiliary operator T_0 does not differentiate the moving geometry. Its cancellation in the next argument does not change.

We set

$$\begin{aligned} v_0 &= -T_0^{-1}f_\theta, & \gamma_0 &= -T_0^{-1}f_z,\\ v &= v_0 - \omega_\theta\mathcal{J}(\mathsf{R}^2 v_0), & \gamma &= \gamma_0 - \omega_z\mathcal{J}(\mathsf{R}\gamma_0),\\ \beta &= -\rho\mathsf{R}^{-1}\mathcal{L}(\mathsf{R}\gamma_\mathsf{Z}). \end{aligned} \tag{2.14.33}$$

The anchor (2.14.10) and the two bump normalizations give $\mathcal{J}(\mathsf{R}^2 v) = \mathcal{J}(\mathsf{R}\gamma) = 0$. For example $\mathcal{J}(\mathsf{R}\omega_z\mathcal{J}(\mathsf{R}\gamma_0)) = (\int \mathsf{R}\omega_z \,\mathrm{d}\mathsf{R})\mathcal{J}(\mathsf{R}\gamma_0)$. All three seed components are zero-Haar. Equation (2.14.27) holds by (2.14.9), and the exact zero axial moment makes the prefix compact at its outer end.

Commutation with ∂_Z gives $\mathcal{J}(\mathsf{R}\gamma_\mathsf{Z}) = 0$, so the prefix is $-\mathcal{I}_\chi(\mathsf{R}\gamma_\mathsf{Z})$. Its zero-Haar integrand gains $\varkappa$ by (2.14.13). This proves the seed bounds in (2.14.29). The fast-time cancellation keeps the explicit errors

$$T_0 v = -f_\theta + \omega_\theta\mathcal{J}(\mathsf{R}^2 f_\theta), \qquad T_0\gamma = -f_z + \omega_z\mathcal{J}(\mathsf{R}f_z). \tag{2.14.34}$$

They are coefficient-flat, but exact compactness uses their subtraction.

We apply the full radial repair to $g = \mathcal{B}_r(\beta, v, \gamma)$:

$$M = \mathcal{J}g, \qquad P = \mathcal{I}_\chi g, \qquad \delta = \sqrt{(V_M + v)^2 + \mathsf{R}kM} - (V_M + v), \qquad \xi = v + \delta. \tag{2.14.35}$$

Then $g + \mathcal{D}P = kM$, and the root cancels this remaining radial term, with zero remainder. The pressure has the two zero endpoints. The full current swirl $V_M + v$, with its fluctuation, occurs in the root.

To estimate its moment, we introduce the actual correlations

$$\begin{aligned} A_{rr} &= 2\Pi(b^\perp\beta) + \Pi(\beta^2),\\ A_{rz} &= \Pi(G^\perp\beta + b^\perp\gamma + \beta\gamma),\\ A_{\theta\theta} &= 2\Pi(V^\perp v) + \Pi(v^2). \end{aligned} \tag{2.14.36}$$

Solenoidality of the two fields rewrites radial convection in conservative form and gives the identity

$$\Pi g = (\partial_\mathsf{R} + \mathsf{R}^{-1})A_{rr} + \rho\partial_\mathsf{Z}A_{rz} - A_{\theta\theta}/\mathsf{R}. \tag{2.14.37}$$

The averaged time and viscous seed terms vanish. The term $2\Pi(V^\perp v)$ is generally nonzero, so the correct Haar order is $d_\nu = \min(2\nu, \nu + s) = \nu + s$.

Integration of (2.14.37) gives

$$\overline{M} = \int \frac{A_{rr} - A_{\theta\theta}}{\mathsf{R}} \, \mathrm{d}\mathsf{R} + \rho \partial_{\mathsf{Z}} \int A_{rz} \, \mathrm{d}\mathsf{R}.$$

The complementary full moment is flat. Thus $\Pi P \in \mathcal{M}^{d_\nu}$ and $P^\perp \in \mathcal{M}^{\nu+\varkappa}$. We compare with $F(V_{\mathrm{H}}, \overline{M})$.

Equation (2.14.20) gives

$$\Pi\delta \in \mathcal{M}^{d_\nu}, \qquad \delta^\perp \in \mathcal{M}^{d_\nu + s}. \tag{2.14.38}$$

After (2.14.34), we estimate the seed force with these complete groups of terms in (2.14.25)–(2.14.26):

term group	order at least
$\rho\partial_{\mathsf{T}}(v,\gamma),\ \rho G_{\mathrm{H}}\partial_{\mathsf{Z}}(v,\gamma)$	$\nu+1$
$\rho B_{\mathrm{H}}\mathcal{D}(v,\gamma)$	$\nu+1-\varkappa$
$\rho\mathcal{D}^2(v,\gamma)$	$\nu+1-2\varkappa$
live-fluctuation interactions	$\nu+s+1$
quadratic seed interactions	$2\nu+1$
ρP_{Z}	$\min(\nu+1+\varkappa, d_\nu+1)$.

(2.14.39)

Connection terms have the indicated transport bounds. Axial viscosity has order $\nu+3$. In particular, we use the improved radial fluctuation bound in (2.14.6) for the current interaction row. The endpoint root changes the angular force by

$$\mathcal{T}\delta + (b_M+\beta)\mathcal{D}\delta + \rho(G_M+\gamma)\delta_{\mathsf{Z}} + (b_M+\beta)\delta/\mathsf{R} - \rho(\Delta_* - \mathsf{R}^{-2})\delta. \tag{2.14.40}$$

Its slow comparison has order $d_\nu+1$. Its perpendicular part has order $d_\nu+s$. The fast time derivative gives the lowest order. This proves the perpendicular assertion in (2.14.30).

For the stronger Haar assertion keep the conservative form. With $\overline{\delta} = \Pi\delta$, we define

$$\begin{aligned} C_{r\theta} &= \Pi(b^\perp\xi + \beta V^\perp + \beta\xi), & C_{z\theta} &= \Pi(G^\perp\xi + V^\perp\gamma + \gamma\xi), \\ C_{rz} &= \Pi(b^\perp\gamma + \beta G^\perp + \beta\gamma), & C_{zz} &= 2\Pi(G^\perp\gamma) + \Pi(\gamma^2). \end{aligned}$$

We set $L^0_\theta = \partial^2_{\mathsf{R}} + \mathsf{R}^{-1}\partial_{\mathsf{R}} - \mathsf{R}^{-2} + \rho^2\partial^2_{\mathsf{Z}}$. Then the exact new Haar forces are

$$\begin{aligned} h_\theta &= \rho\partial_{\mathsf{T}}\overline{\delta} - \rho L^0_\theta\overline{\delta} + (\partial_{\mathsf{R}} + 2/\mathsf{R})(\rho B_{\mathrm{H}}\overline{\delta} + C_{r\theta}) + \rho\partial_{\mathsf{Z}}(G_{\mathrm{H}}\overline{\delta} + C_{z\theta}), \\ h_z &= (\partial_{\mathsf{R}} + 1/\mathsf{R})C_{rz} + \rho\partial_{\mathsf{Z}}(C_{zz} + \Pi P). \end{aligned} \tag{2.14.41}$$

The radial correlations have order $d_\nu + 1 + \varkappa$, the transport term $\rho B_{\mathrm{H}}\overline{\delta}$ has order $d_\nu+1$, and the axial ones have order d_ν. After projection ∂_{R} is an ordinary derivative, so the two rows have order $d_\nu+1$. Integration of the conservative equations gives the same Haar order for the two force moments. Full zero-Haar moments are flat by (2.14.13).

At the last step $\Pi\beta = \Pi\gamma = 0$, $\nu \geq s$, and (2.14.38) keep (2.14.6). Only finitely many value restrictions keep the swirl and frame margins. □

2.14.4 Three actual state integrals and the five protected rows

This subsection uses physical units for the state identities. Let $\mathsf{C}^{\mathrm{act}} = \langle w \otimes w \rangle_\theta$ be the actual covariance of the current exact wave, interpreted on its canonical auxiliary lift. All differences from the slow reference have compact radial support.

We define

$$F_d = \int_0^\infty r\Pi(u_{M,z} - u_{s,z})\,\mathrm{d}r, \qquad K_d = \int_0^\infty r^2\Pi(u_{M,\theta} - u_{s,\theta})\,\mathrm{d}r,$$
$$\Phi_\theta = \int_0^\infty r^2\left[\Pi(u_{M,z}u_{M,\theta}) - u_{s,z}u_{s,\theta} + \Pi\mathsf{C}^{\mathrm{act}}_{z\theta}\right]\,\mathrm{d}r, \tag{2.14.42}$$
$$\Phi_z = \int_0^\infty r\left[\Pi(u^2_{M,z}) - u^2_{s,z} + \Pi\pi - \pi_s + \Pi\mathsf{C}^{\mathrm{act}}_{zz}\right]\,\mathrm{d}r.$$

Form the differences inside these integrals before integration. We do not integrate an individual nonintegrable background tail. In particular Φ_z includes pressure and diagonal covariance.

The cross target has zero $z\theta$ and zz entries, so we subtract no reference stress in these fluxes. For the mean residual relative to the two tangential equations in (2.14.1), the two tangential moments obey

$$J_\theta = (\partial_t - \partial_{zz})K_d + \partial_z\Phi_\theta, \qquad J_z = (\partial_t - \partial_{zz})F_d + \partial_z\Phi_z. \tag{2.14.43}$$

To verify the first identity, angular transport multiplied by r^2 is

$$\partial_r(r^2u_ru_\theta) + \partial_z(r^2u_zu_\theta),$$

and the radial viscous integral of a compact swirl difference is $[r^2\partial_r u_\theta - ru_\theta]_0^\infty = 0$. The radial stress term has endpoint $[r^2\mathsf{D}_{r\theta}]$.

The axial calculation uses the radial flux ru_ru_z, viscous endpoint $[r\partial_r u_z]$, and stress endpoint $[r\mathsf{D}_{rz}]$. Pressure contributes only $\partial_z\int r(\pi - \pi_s)\,\mathrm{d}r$. All these endpoints vanish for the differences under consideration. The slow stress contributes only the vanishing endpoints $[r^2K_{\mathrm{B},\theta}]_0^\infty$ and $[rK_{\mathrm{B},z}]_0^\infty$.

This calculation does not replace $\mathscr{D}_rK_{\mathrm{B}}$ by the full divergence in (2.14.2). Haar projection commutes with evaluated physical derivatives, so the same calculation proves (2.14.43) on the lift.

All mean increments constructed here have zero full axial flux. Initially the radial correction is pure swirl, and the auxiliary correction has the exact zero flux in (2.14.28). Thus $F_d = 0$ throughout. We keep K_d, in place of a possibly incompatible zero angular moment after the square-root correction.

Lemma 2.14.3 (Primitive-free state correction)**.** *Suppose the normalized states $(K_d, \Phi_\theta, \Phi_z)$ have all fixed jets of order $a > 0$, with row scales*

$$Q^{1-h}, \qquad Q^{\frac{1}{2}-2h}, \qquad Q^{-2h}, \tag{2.14.44}$$

in this order. There is a protected compact mean increment with zero axial flux and zero full radial momentum increment. The new three states have order

$$d_a = \min(2a, a+2). \tag{2.14.45}$$

Its normalized tangential velocity and pressure have order a.

Its radial velocity has order $a+1$. Its added pointwise Haar force has order $a+1$. Its added perpendicular tangential force has order at least

$$\min(a + s + 1 - \varkappa, d_a + s). \tag{2.14.46}$$

The two force moments have Haar order $d_a + 1$ and a coefficient-flat zero-Haar complement.

Proof. Let $V_{\mathrm{H}} = \Pi u_{M,\theta}$ and $G_{\mathrm{H}} = \Pi u_{M,z}$ in physical units for these frame equations. A Haar-independent seed (v, γ) has five linear rows

$$\begin{aligned} F &= \int r\gamma \,\mathrm{d}r, & K &= \int r^2 v \,\mathrm{d}r, & C_0 &= \int 2V_{\mathrm{H}} v/r \,\mathrm{d}r, \\ A_0 &= \int r^2 (G_{\mathrm{H}} v + V_{\mathrm{H}} \gamma) \,\mathrm{d}r, & B_0 &= \int r(2G_{\mathrm{H}}\gamma - V_{\mathrm{H}} v) \,\mathrm{d}r. \end{aligned} \tag{2.14.47}$$

The next construction uses the five smooth fiberwise protected variations. We then solve the linear system

$$(F, K, C_0, A_0, B_0) = (0, -K_d, 0, -\Phi_\theta, -\Phi_z). \tag{2.14.48}$$

This replaces the angular seed target. It does not add a sixth row.

The leading pressure of this seed is

$$p_0(r) = -\int_r^\infty 2V_{\mathrm{H}}(x) v(x)/x \,\mathrm{d}x, \qquad \int r p_0(r) \,\mathrm{d}r = -\int r V_{\mathrm{H}}(r) v(r) \,\mathrm{d}r. \tag{2.14.49}$$

The condition $C_0 = 0$ gives the two pressure endpoints. Thus B_0 is the pressure-inclusive linear axial flux.

We construct the frame on the actual moving mean correction interval. We select three ordered nonnegative swirl bumps and two ordered nonnegative axial bumps in fixed normalized subintervals $\xi = (\hat{\xi}/\hat{\xi}_p(\hat{\zeta}))^2 \in (e^{-8}, e^{-3})$. Their buffered closures are disjoint and lie inside the unchanged power patches. The leading axial velocity there is radially constant, say G_* in physical units.

The turnoff and loop restoration end before this wait. The main pulse starts at $y = 0$. Its exact profile here is $H = K(\hat{\zeta})(\frac{\hat{\xi}^2}{2})^{-\nu(\hat{\zeta})}$, with $\nu_c \le \nu(\hat{\zeta}) \le \lambda$. The heat compensation ends before $y = -15$ and the primitive corrections start after $y = -3$. We write $\mu(\hat{\zeta}) := \nu(\hat{\zeta})$ for its H-power exponent.

The physical swirl has power $r^{-1-2\mu(\hat{\zeta})}$. Thus $\mu(\hat{\zeta})$ lies in a fixed compact subset of $(0, \infty)$. This is the early-correction exponent. We do not replace it by the spectral hold exponent.

Let $H_*(\hat{\zeta}) = H(\frac{(\hat{\xi}_p(\hat{\zeta}))^2}{2}, \hat{\zeta}) > 0$ be the actual leading power coefficient evaluated at the pulse graph, and $E_* = H_*/\hat{\xi}_p$. We select the profile variations in (H, U) to be

$$a_j(\tfrac{\hat{\xi}^2}{2}, \hat{\zeta}) = H_*(\hat{\zeta}) A_j(\xi), \qquad b_j(\tfrac{\hat{\xi}^2}{2}, \hat{\zeta}) = E_*(\hat{\zeta}) B_j(\xi),$$

with three A_j and two B_j as just specified. We fix the normalization amplitudes as smooth positive functions, not unknowns in the current solve. The seed keeps all their derivatives, with graph derivatives.

First make the exact triangular row operations

$$A_0 \longmapsto A_0 - G_* K, \qquad B_0 \longmapsto B_0 - 2G_* F.$$

They remove the leading constant axial velocity. Their determinant is one, and they act on the targets and the matrix. The actual solve remains (2.14.48), not a changed physical target.

At each angle put $u = \sqrt{(\hat{\xi}/\hat{\xi}_p(\hat{\zeta}))^2}$. Up to invertible nonzero row factors and positive column factors the leading swirl and axial blocks have powers

$$(2, -2 - 2\mu(\hat{\zeta}), -2\mu(\hat{\zeta})), \qquad (1, 1 - 2\mu(\hat{\zeta})), \tag{2.14.50}$$

in this order. The first block consists of the K, C_0, B_0 rows. The second consists of F, A_0.

We include the swirl-template factor u^{-1} in the positive column density. We do not change the row exponent. Each determinant is the integral over the ordered supports of the generalized Vandermonde for those exponents. For each initial subfamily of k powers the Wronskian is

$$\prod_{1\le i<j\le k}(\alpha_j-\alpha_i)u^{\sum_{i=1}^{k}\alpha_i-k(k-1)/2},$$

which never vanishes on $u>0$. Thus these powers form an extended complete Chebyshev system.

Multilinearity and Fubini give the precise integral identity

$$\det\left[\int u^{\alpha_i}\phi_j(u)\,du\right]=\int\cdots\int\det[u_j^{\alpha_i}]\prod_j\phi_j(u_j)\,du_1\cdots du_n.$$

The nonnegative templates are nonzero on ordered disjoint supports. The ordered-point determinant has one nonzero sign, so cancellation is impossible. The exponent family stays compact and separated, and the normalized supports have fixed positive gaps.

Thus the absolute normalized determinant has a positive minimum over the closed angular interval. The actual scale and amplitude row/column factors, and their inverses, also stay bounded there for the fixed member. This proves a uniform-in-angle inverse, not only pointwise rank or a fixed-$\hat\xi$ spectral-gap argument.

In band units these same variations give $v_j=\bar q^{-\frac12-h}a_j(\frac{\hat\xi^2}{2},\hat\zeta)/\hat\xi$ and $\gamma_j=\bar q^{-\frac12-h}b_j(\frac{\hat\xi^2}{2},\hat\zeta)$. The actual row factors are

$$\operatorname{diag}(\bar q^{\frac12-h},\bar q^{1-h},\bar q^{-1-2h},\bar q^{\frac12-2h},\bar q^{-2h}).$$

They and their inverses are bounded. The actual Haar velocities are a perturbation with one positive-power bound on these moving patches.

We select the value threshold so that the normalized matrix perturbation is less than half the leading inverse margin. The current inverse and all its specified fixed jets then exist. We differentiate the inverse with $\partial M^{-1}=-M^{-1}(\partial M)M^{-1}$. We include each moving-template derivative.

This uses finite slow seminorms but no extra negative power of ρ. Exact downstream history restoration keeps these early patches. We claim no bound uniform in the member and no global Gevrey property of its angular coefficients.

We set the physical radial seed to

$$\beta=-r^{-1}\int_0^r x\partial_z\gamma(x,z,t)\,\mathrm{d}x. \tag{2.14.51}$$

The target $F=0$ gives compactness at the outer endpoint and exact divergence. The seed and p_0 are supported in the fixed member's moving protected hull, which may include the intervals between the bumps. The matrix solve and (2.14.44) give normalized orders a for v,γ,p_0 and $a+1$ for β.

We now use band units again. We write $\beta=\rho x$ and compute the complete radial source $g=\mathcal{B}_r(\beta,v,\gamma)$ from (2.14.24). Its Haar part splits as

$$\Pi g=g_0+g_1,\qquad g_0=-2V_{\mathrm H}v/\mathsf R,\qquad g_1=-v^2/\mathsf R+\rho^2A_r,\qquad \int g_0\,\mathrm{d}\mathsf R=0, \tag{2.14.52}$$

where

$$\begin{aligned}A_r&=x_{\mathsf T}+B_{\mathrm H}x_{\mathsf R}+G_{\mathrm H}x_{\mathsf Z}+xB_{\mathrm H,\mathsf R}+\gamma B_{\mathrm H,\mathsf Z}\\&\quad-(\partial_{\mathsf R}^2+\mathsf R^{-1}\partial_{\mathsf R}-\mathsf R^{-2}+\rho^2\partial_{\mathsf Z}^2)x+xx_{\mathsf R}+\gamma x_{\mathsf Z}.\end{aligned} \tag{2.14.53}$$

This keeps the actual radial inertia.

In particular, x_{T} contains γ_{ZT} through the prefix. Each fixed jet of g_1 has order d_a in (2.14.45). The perpendicular radial source has order $a+s$. Its leading term is $-2V^{\perp}v/\mathsf{R}$.

We define

$$M=\mathcal{J}g,\quad P=\mathcal{I}_{\chi}g,\quad \delta=\sqrt{(V_M+v)^2+\mathsf{R}kM}-(V_M+v). \tag{2.14.54}$$

Then the complete increment $(\beta, v+\delta, \gamma)$ cancels the full radial equation. The pressure decomposes as

$$P=p_0+p_1+P^{\perp},\qquad p_1\in\mathcal{M}^{d_a},\qquad P^{\perp}\in\mathcal{M}^{a+s+\varkappa},\qquad \Pi P^{\perp}=0. \tag{2.14.55}$$

Here $p_1=\mathcal{I}_{\chi}g_1$. The full radial moment has slow part $\int g_1\,\mathrm{d}\mathsf{R}$ of order d_a and a flat complement. A comparison of the root with $F(V_{\mathrm{H}}+v,\int g_1)$ gives

$$\Pi\delta\in\mathcal{M}^{d_a},\qquad \delta-\delta_{\mathrm{slow}}\in\mathcal{M}^{d_a+s}+\{\text{coefficient-flat terms}\}. \tag{2.14.56}$$

We return to physical units and expand the actual states after the increment. Equations (2.14.48) and (2.14.49) give the identity

$$\begin{aligned} K_d^{+}&=\int r^2\Pi\delta\,\mathrm{d}r,\\ \Phi_{\theta}^{+}&=\int r^2[\Pi(u_{M,z}\delta)+\gamma v+\gamma\Pi\delta]\,\mathrm{d}r,\\ \Phi_{z}^{+}&=\int r[\gamma^2+\Pi(P-p_0)]\,\mathrm{d}r. \end{aligned} \tag{2.14.57}$$

This mean step keeps the covariance fixed. The targets cancel its old state contribution. We do not delete this contribution. The term $\Pi(u_{M,z}\delta)$ includes its fluctuation correlation.

Each new row in (2.14.57) has normalized order d_a. Differentiation of (2.14.43) gives one ρ in the normalized moment equation. This gives order d_a+1. In particular the angular time derivative of $\int r^2\Pi\delta$ remains.

The next finite step cancels this known state. It does not solve an evolution equation for an unknown moment.

The Haar-independent seed contributes pointwise Haar force of order $a+1$ by (2.14.25)–(2.14.26). Its leading perpendicular interactions are $\beta\mathcal{D}(V^{\perp},G^{\perp})$ of order $a+s+1-\varkappa$. The perpendicular pressure has higher order. The fast-time derivative of the root complement in (2.14.56) has order d_a+s.

This proves (2.14.46). Shifted mixing makes the full moment complements flat. The construction does not invert the differential expression (2.14.53) with a finite-dimensional implicit function theorem. □

Moving corrections, force terms, and endpoint covariance. Each pressure derivative in (2.14.41), (2.15.12) and (2.15.43) is the derivative of the actual moving correction expression. In particular if $P=\mathcal{I}_{\chi}g$,

$$\rho P_{\mathsf{Z}}=\rho\mathcal{I}_{\chi}g_{\mathsf{Z}}-\rho\chi_{\mathsf{Z}}\mathcal{J}g.$$

For a Haar moment of order d the second term has order $d+1$, not coefficient-flat. The tensor repair has order $p+1$.

The auxiliary map has order $d_{\nu}+1$, and the state-map remainder has order d_a+1. Initialization has order three for M_s. The last cross correction has order c_*+2. The state-map leading p_0 and its full axial derivative have orders a and $a+1$.

The displayed force tables include these rows. Time derivatives of the root and moving templates also keep their actual ρ factor. Spatial viscosity and radial derivatives are the full product rules in (2.14.24)–(2.14.26). No such ordinary Haar contribution enters a flat remainder or a change of force.

The exact physical state identities differentiate the whole moving integrands. Moving support boundaries give zero terms because the bumps have smooth zero extensions and supports in one fixed compact set. Geometry is independent of the auxiliary torus variables. Thus it multiplies the finite-stage pure-auxiliary Gevrey bounds by fixed slow-jet constants. There is no loss in their ρ orders or a requirement of joint slow-variable Gevrey regularity.

On an endpoint chart $\frac{\hat\xi_b^2}{2} = \lambda_{\mathrm{ch}}\frac{\hat\xi_f^2}{2}$ and $\frac{\hat\xi_{p,b}^2}{2} = \lambda_{\mathrm{ch}}\frac{\hat\xi_{p,f}^2}{2}$, so $y = 2\log(\widetilde{\xi}/\widetilde{\xi}_p)$ is one slice function. Direct substitution and change of variables give

$$\begin{aligned} \beta_{0,f}(\tfrac{\hat\xi_f^2}{2}) &= \lambda_{\mathrm{ch}}\beta_{0,b}(\lambda_{\mathrm{ch}}\tfrac{\hat\xi_f^2}{2}), & \chi_f(\tfrac{\hat\xi_f^2}{2}) &= \chi_b(\lambda_{\mathrm{ch}}\tfrac{\hat\xi_f^2}{2}), \\ c_{\beta,f} &= \lambda_{\mathrm{ch}}^{-1}c_{\beta,b}, & c_{\theta,f} &= \lambda_{\mathrm{ch}}^{-1/2}c_{\theta,b}, \qquad \bar q_f = \lambda_{\mathrm{ch}}\bar q_b. \end{aligned} \tag{2.14.58}$$

Thus ω_z, ω_θ and $\bar q c_\beta$ are the same physical functions on the two sides, and so is $k = \mathsf{R}\beta_0/\bar q$. The raw shifted integrals use the same physical radial path and same band/auxiliary data.

They, the actual full moments, and the radicands thus have equal slice jets. The five templates a_j, b_j are slice continuations with weights h and $(\frac12 + h)$. The band velocities have weight $-(\frac12 + h) + h + \frac12 = 0$ in the swirl row and $-(\frac12 + h) + (\frac12 + h) = 0$ in the axial row, so they are slice functions. Thus the physical five matrices and their uniquely solved seed velocities have equal slice jets. This is equality of endpoint jets, not an assertion that the two-sided fields agree on an open collar.

2.15 The finite packet and mean corrections

2.15.1 The canonical tensor and its explicit flat remainder

For a physical two-vector $a = (a_\theta, a_z)$ define the symmetric pure-cross tensor

$$\mathcal{Q}_\times(a) = \begin{pmatrix} 0 & a_\theta & a_z \\ a_\theta & 0 & 0 \\ a_z & 0 & 0 \end{pmatrix} \quad \text{in the } (r,\theta,z) \text{ frame.} \tag{2.15.1}$$

Its two tangential divergence moments equal zero:

$$\int r^2(\operatorname{div}\mathcal{Q}_\times(a))_\theta \,\mathrm{d}r = 0, \qquad \int r(\operatorname{div}\mathcal{Q}_\times(a))_z \,\mathrm{d}r = 0 \tag{2.15.2}$$

for smooth, radially compact a regular at the axis. The radial component is $r^{-1}\partial_\theta a_\theta + \partial_z a_z$. For the angle-independent mean coefficients used here this reduces to $\partial_z a_z$, which the radial equation must cancel.

Let ϑ be the single aggregate cutoff used in the packet construction, (2.6.38). It equals one where $\mathsf{W}_* \ge \exp(-c_e S(q))$, and vanishes where $\mathsf{W}_* \le \exp(-2c_e S(q))$, with $S(q) = \log^{6/5}(1/\tilde q)$ and $\mathsf{W}_* = c_*|\widetilde{T}_0|$; by the equivalence of the logarithmic classes of W_* and W, its deletion set lies in $\{\mathsf{W} \le \exp(-cS(q))\}$ for a fixed $c > 0$. It is independent of the physical angle and auxiliary variables. Each potential and oscillatory pressure keeps its source-prescribed power ϑ^j.

The real homogeneous families use $j = 1$. We keep the inhomogeneous conventions that use $j = 2$. No inverse divides by ϑ.

We maintain an auxiliary-independent physical vector d_* and define

$$\mathsf{C}^{\mathrm{can}} = \mathsf{C}^{\mathrm{act}} + \mathcal{Q}_\times(d_*), \qquad \mathsf{B}_{\mathrm{flat}} = -\mathcal{Q}_\times(d_*). \tag{2.15.3}$$

The symbol d_* is a tensor coefficient and is unrelated to the coordinate function $d(\hat{\zeta}) = 1 - \hat{\zeta}^2$. We do not assume that $\mathsf{C}^{\mathrm{can}}$ is positive semidefinite. We call only $\mathsf{C}^{\mathrm{act}}$ a covariance.

For a distinct pure-cross stress A_*, the canonical mean residual is

$$E^{\mathrm{can}} = \mathscr{N}(u_M, \pi) + \operatorname{div} \mathsf{C}^{\mathrm{can}} + \operatorname{div} \mathcal{Q}_\times(A_*) - \mathbf{f}_{\mathrm{ref}}. \tag{2.15.4}$$

The exact ordinary equation has the form

$$\mathscr{N}(u_M + w, \pi + p_w) - \mathbf{f}_{\mathrm{ref}} = E^{\mathrm{can}} - \operatorname{div} \mathcal{Q}_\times(A_*) + \mathrm{Osc}(F) + G_{\mathrm{flat}} + \operatorname{div} \mathsf{B}_{\mathrm{flat}}. \tag{2.15.5}$$

Here F is the finite family of canonical nonzero-harmonic force coefficients. The term G_{flat} contains the explicitly kept Gaussian endpoint terms and missing-source cutoff terms.

It has zero physical angular mean, but may have a radial component. We will arrange $E^{\mathrm{can}}_r = 0$. This does not say that the actual ordinary radial residual vanishes. Equation (2.15.5) is a physical identity after auxiliary evaluation.

Each use of $\mathcal{M}^a$ or $\mathcal{W}^a$ in its estimate applies to the normalized lifted coefficients with the prefactors (2.14.3) restored.

The two state fluxes in (2.14.42) do not change if we replace $\mathsf{C}^{\mathrm{act}}$ by $\mathsf{C}^{\mathrm{can}}$. The added tensor has zero $z\theta$ and zz entries. Equation (2.15.2) also shows that the tangential moment identities (2.14.43) hold for (2.15.4). The states remain actual velocity, pressure and covariance integrals. They are not virtual states of an altered covariance.

On the derivative support of ϑ, the logarithmic weight bounds give polynomial-S ordinary jets of ϑ. Thus a cutoff derivative inside an exact curl has its usual finite coefficient order. We keep that order. For the real homogeneous principal and signed waves, the principal cosine and full coefficient sine remain in quadrature.

Thus their mixed angular averages vanish even when the derivative acts on ϑ. This keeps the improved cross-curl order of the signed construction. For a complex inhomogeneous response, we use all six product terms without this extra cancellation.

The explicitly missing canonical term at a harmonic solve is $(1 - \vartheta^j)F_m$. It has a positive $\sqrt{\mathsf{W}}$ factor and the support lies where $\mathsf{W} \le \exp(-cS(q))$. A finite q power times a polynomial in S times $\exp(-c'S)$ bounds each fixed lifted derivative. It is thus flat to each order on the lift and after physical differentiation.

The same argument with W in place of its square root applies to $(1 - \vartheta^2)K$ for a canonical mean source K. These are the flat terms for the next argument. An arbitrary unweighted-flat function would not justify division by W or $\sqrt{\mathsf{W}}$. We use no flat remainder from (2.15.5) as an inverse input.

2.15.2 Initialization on the actual slow reference

Let S_0 be the physical leading cross target and K_s the higher slow cross stress, so $K_{\mathrm{B}} = S_0 + K_s$ and $\mathsf{Q}_s = \mathcal{Q}_\times(K_{\mathrm{B}})$. Their normalized orders are 1 and 3. The positive principal amplitudes of Proposition 2.13.5 use S_0 only. Their actual cut principal Haar cross is $\vartheta^2 S_0$.

We set

$$d_{*,\mathrm{base}} = (1 - \vartheta^2)S_0. \tag{2.15.6}$$

The canonical principal cross then equals S_0 everywhere, also in the deleted region. There, (2.15.6) uses the globally supplied slow target in place of an uncut amplitude.

We apply Proposition 2.13.6 to the actual signed $\mathcal{M}^3$ target K_s, with the same original positive amplitudes. We add $(1 - \vartheta^2)K_s$ to d_* and keep all actual covariance and momentum terms of the signed wave. In the notation (g, f_r, f_θ, f_z) of (2.13.49), substitution of $p = 3$ gives

$$g \in \mathcal{W}^{5/2}, \qquad f_r \in \mathcal{W}^4, \qquad (f_\theta, f_z) \in \mathcal{W}^{3-\varkappa}. \tag{2.15.7}$$

The full added covariance is $\mathcal{M}^3$.

After its principal linear Haar cross cancels K_s, the new Haar cross error is $\mathcal{M}^{5-\varkappa}$. The homogeneous quadratic term has order 5, and the cross-curl term has order $5-\varkappa$. Its nonzero momentum residual is $\mathcal{W}^{3-3\varkappa}$. The original principal cross-curl error remains $\mathcal{M}^{3-\varkappa}$. Thus the actual constructed tensor

$$\mathsf{D}_0 = Q^{1+2h}(\mathsf{C}^{\mathrm{can}} - \mathsf{Q}_s) \in \mathcal{M}^1, \qquad \Pi(\mathsf{D}_0)_{r\theta}, \Pi(\mathsf{D}_0)_{rz} \in \mathcal{M}^{3-\varkappa}. \tag{2.15.8}$$

Its other four entries are the actual covariance entries minus the slow reference. Order one suffices for these entries.

The two-row reference uses the full canonical tensor in the radial initialization. We put

$$\mathsf{S} = Q^{1+2h}K_{\mathrm{B}}, \quad \mathsf{C}_0 = Q^{1+2h}\mathsf{C}^{\mathrm{can}} = \mathsf{D}_0 + \mathcal{Q}_\times(\mathsf{S}), \quad g_s = \rho\partial_{\mathsf{Z}}\mathsf{S}_z \in \mathcal{M}^2. \tag{2.15.9}$$

The source g_s is auxiliary-independent. Its fixed-jet bounds hold by (2.6.37) with one additional slow derivative, with the actual Borel cutoffs.

The exact initial normalized residual is

$$Q^{\frac{3}{2}+2h}[\mathscr{N}(u_s,\pi_s) + \operatorname{div}\mathsf{C}^{\mathrm{can}} - \mathbf{f}_s] = \operatorname{Div}_*\mathsf{D}_0 + g_s e_r. \tag{2.15.10}$$

Its radial row uses C_0. Its tangential rows use D_0. We do not assume that the canonical tensor is positive semidefinite.

Only its actual covariance part is positive semidefinite.

Lemma 2.15.1 (Full-covariance initialization)**.** *We write $(b_s, V_s, G_s) = Q^{\frac{1}{2}+h}u_s$. We define*

$$\begin{aligned} f_C &= \frac{(\mathsf{C}_0)_{rr} - (\mathsf{C}_0)_{\theta\theta}}{\mathsf{R}} + \rho\partial_{\mathsf{Z}}(\mathsf{C}_0)_{rz}, \qquad M_C = \mathcal{J}f_C, \\ P_C &= -(\mathsf{C}_0)_{rr} + \mathcal{I}_\chi f_C, \qquad \delta_C = \sqrt{V_s^2 + \mathsf{R}\,k\,\mathcal{J}f_C} - V_s. \end{aligned} \tag{2.15.11}$$

Here $k = -\mathcal{D}\chi$ is the radial cutoff derivative and $M_C = \mathcal{J}f_C$ is the genuine full shifted radial moment. Thus the radicand contains the product $\mathsf{R}\,k\,\mathcal{J}f_C$.

there is no operator denoted R_k. All integrals in this response use the full actual tensor/pressure hull, not just the early velocity correction support. In particular π_s includes the late P_1, P_2 of Section 2.6. We do not replace it by its leading part P_0.

For sufficiently small q, these are a compact pressure and a protected pure-swirl increment of normalized order one. The root is auxiliary-independent up to a protected coefficient-flat term. The exact normalized residual after this correction has rows

$$\begin{aligned} E_r^R &= 0, \\ E_\theta^R &= (\mathcal{D} + 2/\mathsf{R})(\mathsf{D}_0)_{r\theta} + \rho\partial_{\mathsf{Z}}(\mathsf{D}_0)_{z\theta} + \Theta_s\delta_C, \\ E_z^R &= (\mathcal{D} + 1/\mathsf{R})(\mathsf{D}_0)_{rz} + \rho\partial_{\mathsf{Z}}((\mathsf{D}_0)_{zz} + P_C), \end{aligned} \tag{2.15.12}$$

where

$$\Theta_s v = \mathcal{T}v + b_s\mathcal{D}v + \rho G_s v_{\mathsf{Z}} + b_s v/\mathsf{R} - \rho(\Delta_* - \mathsf{R}^{-2})v.$$

The Haar tangential force has order two and its complement has order $1-\varkappa$.

The two pressure endpoints vanish, and the axial velocity and its full flux are unchanged.

Proof. We apply the exact calculation of Lemma 2.14.1 to C_0 at the slow mean. The complete radial identity is

$$(\mathrm{Div}_*\,\mathsf{C}_0)_r + \mathcal{D}P_C - \frac{(V_s+\delta_C)^2 - V_s^2}{\mathsf{R}} = kM_C - kM_C = 0. \tag{2.15.13}$$

The increment has no radial or axial velocity. Its only radial momentum change is the displayed centrifugal term.

Its only tangential velocity-equation increment is $\Theta_s\delta_C$. The pressure adds $\rho\partial_{\mathsf{Z}}P_C$ to the axial equation. This proves all three rows in (2.15.12).

To isolate the additional correction, let $(f_D, M_D, P_D, \delta_D)$ be the response formulas (2.14.14)–(2.14.16) applied to D_0 at the same slow mean. Because the cross target has zero diagonal entries,

$$f_C = f_D + g_s, \quad M_s = \mathcal{J}g_s, \quad P_s^{\mathrm{add}} = \mathcal{I}_\chi g_s, \quad P_C = P_D + P_s^{\mathrm{add}}. \tag{2.15.14}$$

The source g_s is generally nonflat. Near the inner edge, $P_s^{\mathrm{add}} = -\int_0^{\mathsf{R}} g_s$.

Near the outer edge, $P_s^{\mathrm{add}} = \int_{\mathsf{R}}^{\infty} g_s$. Lemma 2.6.9, applied after each fixed differentiation, gives $P_s^{\mathrm{add}} \in \mathcal{M}^2$ on the actual full support, also at angular zero faces and corners. The cutoff transition lies where the weight has a positive lower bound. In particular $\rho\partial_{\mathsf{Z}}P_s^{\mathrm{add}} \in \mathcal{M}^3$, also for derivatives of χ and M_s.

This scalar correction is consistent between bands: in physical units it is

$$p_s^{\mathrm{add}}(r,z,t) = \int_r^{\infty} \partial_z K_{\mathrm{B},z}(x,z,t)\,\mathrm{d}x - \chi(\tfrac{\hat{\xi}^2}{2}) \int_0^{\infty} \partial_z K_{\mathrm{B},z}(x,z,t)\,\mathrm{d}x.$$

It normalizes to $Q^{-1-2h}P_s^{\mathrm{add}}$ on each constant band. The full canonical response uses the same lift and its covariantly constant moments. The added source introduces no new cover.

The difference of the roots is

$$\epsilon_s := \delta_C - \delta_D = \frac{\mathsf{R}kM_s}{\sqrt{V_s^2 + \mathsf{R}k(M_D+M_s)} + \sqrt{V_s^2 + \mathsf{R}kM_D}} \in \mathcal{M}^2. \tag{2.15.15}$$

On the protected subslot $V_s = V_{\mathrm{lead}} \geq 4v_*$ on both sides, by Lemma 2.12.31. This velocity bound uses the zero positive-order velocities and fluxes there. The late positive-order pressure enters the state defects separately.

For the actual pressure targets we retain its full value. Since M_D, M_s have orders one and two, one value threshold makes the two radicands positive. Rationalization gives smooth zero extension and all fixed-jet estimates at this same threshold. The zero-Haar full moment of f_D is coefficient-flat.

The quantities g_s and V_s have no auxiliary dependence. The two roots and their difference are thus slow up to protected coefficient-flat terms. With $b_s = \rho B_s$, each slow term in $\Theta_s\epsilon_s$ has order three. Finite fast derivatives of the flat complement remain flat.

This verifies the additional axial and angular force terms.

For the whole response, Haar projection removes the fast radial derivative in (2.15.12). The two Haar cross errors have order $3-\varkappa$. The other tensor, pressure and slow-root terms have order at least two. Before projection, the worst radial derivative loses $\varkappa$. This gives the asserted complementary order. We keep all six tensor entries. □

The extra pressure has the actual state contribution

$$\int \mathsf{R}P_s^{\mathrm{add}}\,\mathrm{d}\mathsf{R} = \frac{\rho}{2}\partial_{\mathsf{Z}} \int \mathsf{R}^2\mathsf{S}_z\,\mathrm{d}\mathsf{R} - \bar{q}c_\beta M_s. \tag{2.15.16}$$

Fubini gives this identity, as in (2.14.21). It has order two, as do $\int \mathsf{R}^2 \Pi \epsilon_s$ and $\int \mathsf{R}^2 G_s \Pi \epsilon_s$, the other two state changes relative to the D_0 response. We do not use the condition $M_s = 0$.

The new mean remains eligible for (2.13.51). Its repair-specific interaction with a packet of principal order a is at least $\mathcal{W}^{a+3/2}$. The largest term is the carrier factor of order $\rho^{-1/2}$ times ϵ_s times that packet. For the principal family this is order two. The slow sequence and the fixed Gaussian background are unchanged.

The initial auxiliary construction is the proof of Lemma 2.14.2 with a slow background up to a flat swirl term. This applies with $\nu = s = 1 - \varkappa$. Its nonlinear radial moment has order $2s$, its pressure order is $\min(s + \varkappa, 2s) = 1$, and its perpendicular force order is $2 - 3\varkappa$.

The actual output satisfies

$$\begin{gathered}(u_M - u_s)_{\tan} \in \mathcal{M}^s, \quad (u_M - u_s)_r \in \mathcal{M}^2, \quad E_H \in \mathcal{M}^2, \quad E_\perp \in \mathcal{M}^{2-3\varkappa}, \\ F_d = 0, \qquad (K_d, \Phi_\theta, \Phi_z) \text{ have order 1.}\end{gathered} \tag{2.15.17}$$

The last assertion holds directly by (2.14.42). The Haar velocity, pressure and covariance defects have order one. The fluctuation products have order $2s > 1$. We do not infer smallness of a state from smallness of its derivative.

We next apply the state map one time, without any cutoff or infinite summation. In Lemma 2.14.3 take the actual order-one states of (2.15.17), with the actual canonical covariance fixed. Its output orders are

$$(K_d, \Phi_\theta, \Phi_z) : 1 \longmapsto 2, \qquad \text{state moments} : 3, \qquad F_d = 0. \tag{2.15.18}$$

This is an actual compact mean increment with zero full axial flux.

The associated pressure and swirl response cancel its radial momentum change, with zero remainder. The initial canonical radial row equals zero by (2.15.13). Thus the canonical radial row remains zero. Its added Haar force has order two. Its perpendicular force has order at least $3 - 2\varkappa$, which gives the force bounds in (2.15.17).

Its radial velocity has order two, in particular it keeps the specified order-two current radial class.

There is no demand that these three states become coefficient-flat before the paired iteration. Their order two is stronger than the input order $2 - 3\varkappa$ used in the next finite cycle. We reduce the same small-q threshold once to keep all value margins for this finite operation. Fixed higher seminorms may grow.

The last diagonal then controls them. In particular

$$\mathbf{f}_{\mathrm{ref}} = \mathbf{f}_s, \qquad \mathbf{f}_{\mathrm{ref}} - \mathbf{f}_s \equiv 0. \tag{2.15.19}$$

Each exact finite equation keeps the finite flat vector and tensor remainders. The zero preliminary force adjustment does not discard these remainders.

One finite cycle now raises this uncut finite initialization to the paired input orders. We apply Lemma 2.14.2 at $\nu_0 = 2 - 3\varkappa$. Its new perpendicular force is $\mathcal{M}^{3-5\varkappa}$, and its new state contribution has order $\nu_0 + s = 3 - 4\varkappa$. The previous states have order two by (2.15.18), so their sum has at least the weaker order $2 - 3\varkappa$.

We apply Lemma 2.14.3 with the weaker input order $2 - 3\varkappa$. It gives state order $4 - 6\varkappa$ and moments of order $5 - 6\varkappa$. The remaining Haar pointwise force still has order two. We reconstruct its compact moment-subtracted cross stress by the formula (2.15.40).

This stress has order two. Its radial pressure and swirl correction have state order three and force order four. We find

$$\begin{gathered}A_* \in \mathcal{M}^2, \qquad E_H^{\mathrm{can}} \in \mathcal{M}^4, \qquad E_\perp^{\mathrm{can}} \in \mathcal{M}^{3-5\varkappa}, \qquad E_r^{\mathrm{can}} = 0, \\ (K_d, \Phi_\theta, \Phi_z) \text{ have order 3}, \qquad F_d = 0.\end{gathered} \tag{2.15.20}$$

At this actual mean, the nonzero source decomposition has first harmonic order $1-3\varkappa$. Its second harmonic order is $1-\varkappa$. The signed slow correction in (2.15.7) has only higher-order terms.

Thus the canonical oscillatory source belongs to $\mathcal{W}^{a_0}$. Initialization produces actual fields, not a prescribed list of unproved state bounds.

2.15.3 One paired wave–mean step

Let $a \ge a_0$ and abbreviate, in this step,

$$p = a + \tfrac{1}{2}, \qquad c_* = a + 1 - 3\varkappa, \qquad s_* = p - \varkappa, \qquad b_* = p + 1 - 3\varkappa, \qquad \gamma_* = \tfrac{1}{2} - 3\varkappa. \tag{2.15.21}$$

The letter p in (2.15.21) is only an order. We continue to write pressures as π, P, p_w. Suppose the current actual finite state has the mean class (2.14.6) and the wave $w = w_0 + v$.

Assume its structured exact-curl remainder has order a_0 and its equation is (2.15.5). Its canonical data obey

$$F \in \mathcal{W}^a, \quad A_* \in \mathcal{M}^p, \quad E_r^{\mathrm{can}} = 0, \quad E_{\tan}^{\mathrm{can}} \in \mathcal{M}^{a+1}, \quad (K_d, \Phi_\theta, \Phi_z) \text{ have order } p, \quad F_d = 0. \tag{2.15.22}$$

The wave uses finitely many relative harmonics on each original label, with one finite bound at this stage. Its old principal remainder has order a_0, its tangential coefficient curl has order $a_0 + 1/2 - \varkappa$, and its radial curl has order $a_0 + 3/2$.

The construction gives these coefficient decompositions. They are not estimates on an unspecified sampled divergence-free field.

The initialized state (2.15.20) satisfies all these conditions at $a = a_0$. We now construct the next state with the same leading amplitudes, graph, phases, and reference force.

2.15.3.1 The harmonic correction and the signed cross cancellation

We apply the finite-harmonic construction of Proposition 2.13.7 to the canonical source F. We call the actual exact curl z, its pressure p_z, and its normalized coefficient at relative harmonic m on label γ by $Z_{\gamma,m}$. If $X_{\gamma,m}$ is the current normalized wave coefficient, the complete physical covariance increment is

$$(\Delta \mathsf{C}_z)_{ij} = \sum_{\gamma} Q_\gamma^{-1-2h} \sum_{m \ne 0} \left(X_{\gamma,m,i} Z_{\gamma,-m,j} + Z_{\gamma,m,i} X_{\gamma,-m,j} + Z_{\gamma,m,i} Z_{\gamma,-m,j} \right). \tag{2.15.23}$$

This formula includes all six pairs $(i,j) \in \{rr, r\theta, rz, \theta\theta, \theta z, zz\}$.

Reality means $X_{\gamma,-m} = \overline{X_{\gamma,m}}$, and by the same method for $Z_{\gamma,m}$. Different labels have no product by the disjoint enlarged supports. The expression is the physical angular covariance on the auxiliary lift. After evaluation, it is the actual covariance, not a Haar surrogate.

The factors Q_γ^{-1-2h} enter before formation of a signed source or physical moment.

The new velocity has principal order a, tangential curl order $a + 1/2 - \varkappa$ and radial curl order $a + 3/2$. Thus

$$Q^{1+2h} \Delta \mathsf{C}_z \in \mathcal{M}^p, \qquad F \text{ after the harmonic step} \in \mathcal{W}^{a+\gamma_*}, \tag{2.15.24}$$

apart from the explicitly kept flat errors. The harmonic count remains finite. The old d_* is unchanged in this substep, so the canonical and actual tensor differences are the same.

We define the actual Haar-independent signed source

$$K = A_* - \Pi(\Delta \mathsf{C}_z)_{r\tan}, \qquad (\cdot)_{r\tan} = ((\cdot)_{r\theta}, (\cdot)_{rz}). \tag{2.15.25}$$

Its normalized coefficient $Q^{1+2h}K$ belongs to $\mathcal{M}^p$ on the full buffered source domain. The signed map of Proposition 2.13.6 uses, for each original slow label,

$$\delta y = H_\beta^{-1}(\Sigma_\beta/\rho), \qquad \delta a_\pm = \frac{\delta y_\pm}{2\sqrt{y_{\mathrm{lead},\pm}}}, \qquad \Sigma_\beta = Q^{1+2h}K. \tag{2.15.26}$$

The original squared amplitude obeys $y_{\mathrm{lead},\pm} \geq c\sqrt{S_\ell}\,\mathsf{W}$. The slow jets of $\delta y_\pm$ retain a factor W; the weighted division estimate (2.13.47) gives $\delta a_\pm$ of order $\rho^{p-1}\sqrt{\mathsf{W}}$ with logarithmic jets. The principal velocity of the actual curl h has order $p - 1/2 = a$.

We set $w^+ = w + z + h$ and update the explicit remainder by

$$d_*^+ = d_* + (1 - \vartheta^2)K. \tag{2.15.27}$$

After subtraction of the old A_*, the mean must correct the tensor

$$\begin{aligned} \mathsf{D}^{\mathrm{can}} &= \mathsf{C}^{\mathrm{can},+} - \mathsf{C}^{\mathrm{can}} - \mathcal{Q}_\times(A_*) \\ &= \mathsf{C}^{\mathrm{act},+} - \mathsf{C}^{\mathrm{act}} - \mathcal{Q}_\times(A_*) + \mathcal{Q}_\times((1-\vartheta^2)K). \end{aligned} \tag{2.15.28}$$

In particular the old d_* cancels with zero remainder. The actual principal linear Haar cross of h is $\vartheta^2 K$, and thus

$$\Pi(\Delta\mathsf{C}_z)_{r\tan} + \vartheta^2 K + (1-\vartheta^2)K - A_* = 0. \tag{2.15.29}$$

This is the exact cancellation at the artificial cutoff boundary.

The remaining covariance is the full tensor sum

$$\Delta\mathsf{C}_z + [\mathsf{C}(w_0 + h) - \mathsf{C}(w_0)] + \mathrm{Cross}(v + z, h) - \mathcal{Q}_\times(A_*) + \mathcal{Q}_\times((1-\vartheta^2)K), \tag{2.15.30}$$

where $\mathrm{Cross}(Y,h)_{ij} = \sum_m (Y_{m,i}H_{-m,j} + H_{m,i}Y_{-m,j})$. Here the coefficients in Cross are physical coefficients, and the sum includes the labels as in (2.15.23).

We keep all six entries of each term. We apply (2.15.29). Then the two Haar radial crosses have these possible orders:

$$\begin{array}{c|c} h\text{–}h & 2a \\ w_0\text{–}h \text{ coefficient curls} & p + 2 - \varkappa \\ v\text{–}h & a + a_0 = c_* \\ z\text{–}h & 2a. \end{array} \tag{2.15.31}$$

The improved cross-curl line uses the real sine–cosine quadrature. This quadrature also covers derivatives of ϑ.

Because $a \geq a_0$, all four orders are at least c_*. Thus, with the original normalization,

$$Q^{1+2h}\mathsf{D}^{\mathrm{can}} \in \mathcal{M}^p, \qquad Q^{1+2h}\Pi\mathsf{D}^{\mathrm{can}}_{r\tan} \in \mathcal{M}^{c_*}. \tag{2.15.32}$$

The other four entries are actual covariance differences and can have the weaker order p. The zero-Haar tensor is also actual, because the complementary term in (2.15.28) is Haar independent.

The signed map's linear nonzero residual has order $p - 3\varkappa = a + \gamma_*$. Its products with w_0, v and z have orders at least $p - \varkappa$, $a + a_0 - \varkappa$ and $2a - \varkappa$, in this order. All exceed or equal the specified $a + \gamma_*$ order. Thus (2.15.24) remains valid after h at the old mean. The source-prescribed ϑ^j potential/pressure factors contribute their exact $(1 - \vartheta^j)F_m$ terms to G_{flat}, as previously described.

2.15.3.2 The full radial, auxiliary and state corrections

Before the mean update, the canonical residual with no distinct old cross stress equals

$$E^{\mathrm{can}} + \operatorname{div} \mathsf{D}^{\mathrm{can}}. \tag{2.15.33}$$

We apply Lemma 2.14.1 to $\widehat{\mathsf{D}} = Q^{1+2h}\mathsf{D}^{\mathrm{can}}$ at the current mean. Its pressure is (2.14.14), with all diagonal and axial tensor terms, and its root uses the current V_M. The exact remaining normalized tangential rows are

$$\begin{aligned} e_\theta^{\mathrm{rad}} &= E_\theta^{\mathrm{can}} + (\mathcal{D} + 2/\mathsf{R})\widehat{\mathsf{D}}_{r\theta} + \rho\partial_{\mathsf{Z}}\widehat{\mathsf{D}}_{z\theta} + \Theta_{u_M}\delta_D, \\ e_z^{\mathrm{rad}} &= E_z^{\mathrm{can}} + (\mathcal{D} + 1/\mathsf{R})\widehat{\mathsf{D}}_{rz} + \rho\partial_{\mathsf{Z}}(\widehat{\mathsf{D}}_{zz} + P_D), \qquad e_r^{\mathrm{rad}} = 0, \end{aligned} \tag{2.15.34}$$

where E^{can} and P_D use the normalization in this display. The operator Θ_{u_M} is (2.14.40) without the seed β, γ.

After Haar projection the cross derivatives have order c_* by (2.15.32). Other tensor and slow-root terms have order $p+1$. The perpendicular radial derivative costs at most $\varkappa$. Thus

$$e_{H,\tan}^{\mathrm{rad}} \in \mathcal{M}^{c_*}, \qquad e_{\perp,\tan}^{\mathrm{rad}} \in \mathcal{M}^{s_*}. \tag{2.15.35}$$

We keep the state order p at this point. The covariance update changes Φ_θ, Φ_z by the actual integrals $\int r^2 \Pi \mathsf{D}_{z\theta}^{\mathrm{can}}\,\mathrm{d}r$ and $\int r \Pi \mathsf{D}_{zz}^{\mathrm{can}}\,\mathrm{d}r$, each of order p. On each label, we set $\delta_D^{\mathrm{ph}} = Q^{-\frac{1}{2}-h}\delta_D$ and $P_D^{\mathrm{ph}} = Q^{-1-2h}P_D$. The radial response changes the physical states by

$$\int r^2 \Pi \delta_D^{\mathrm{ph}}\,\mathrm{d}r, \qquad \int r^2 \Pi (u_{M,z}\delta_D^{\mathrm{ph}})\,\mathrm{d}r, \qquad \int r \Pi P_D^{\mathrm{ph}}\,\mathrm{d}r, \tag{2.15.36}$$

again of order p. The middle integral includes the current axial fluctuation. This establishes state control from the actual quantities, without an integral of a residual moment in z.

We apply Lemma 2.14.2 to $e_\perp^{\mathrm{rad}}$ at $\nu = s_* = p - \varkappa$. Its nonlinear Haar order is $d_A = s_* + s = p + 1 - 2\varkappa$. The outputs relevant here are

$$\begin{aligned} m_{A,\tan} \in \mathcal{M}^{s_*}, \quad m_{A,r} \in \mathcal{M}^{p+1}, \quad P_A \in \mathcal{M}^p, \\ e_{\perp,\tan} \in \mathcal{M}^{b_*}, \qquad \text{new Haar force} \in \mathcal{M}^{p+2-2\varkappa}. \end{aligned} \tag{2.15.37}$$

The old Haar force remains $\mathcal{M}^{c_*}$. The axial seed keeps zero Haar mean with zero full flux.

In the state formulas, the linear zero-Haar seed terms disappear after projection. The fluctuation correlations and root/pressure terms have order at least $d_A > p$. The current state is thus still of order p.

Now apply Lemma 2.14.3 at order p, on the actual post-auxiliary mean. We put $d_H = \min(2p, p+2)$ and $j_2 = d_H + 1$. It gives

$$\begin{aligned} (K_d, \Phi_\theta, \Phi_z) \text{ have order } d_H, \qquad \text{Haar force moments have order } j_2, \\ \text{added Haar force} \in \mathcal{M}^{p+1}, \qquad \text{added perpendicular force} \in \mathcal{M}^{p+2-2\varkappa}. \end{aligned} \tag{2.15.38}$$

In the last assertion $\min(p+s+1-\varkappa, d_H+s) = p+2-2\varkappa$ because $p \geq 3/2 - 3\varkappa$. Thus the actual residual at this point is $e^2 = (0, h^2 + r^2)$, with

$$h^2 \in \mathcal{M}^{c_*}, \qquad r^2 \in \mathcal{M}^{b_*}, \qquad \Pi r^2 = 0, \qquad m_\theta = \int \mathsf{R}^2 h_\theta^2\,\mathrm{d}\mathsf{R}, \quad m_z = \int \mathsf{R} h_z^2\,\mathrm{d}\mathsf{R} \tag{2.15.39}$$

of scalar order j_2.

All full zero-Haar moment complements remain coefficient-flat. The state map does not cancel the pointwise Haar force itself.

2.15.3.3 Compact Haar cross reconstruction and its radial correction

We subtract the actual moments in (2.15.39) and define the new distinct stress by ordinary Haar-independent prefixes:

$$\begin{aligned} f_{H,\theta} &= h_\theta^2 - \omega_\theta m_\theta, \quad A_\theta^+ = -\mathsf{R}^{-2}\int_0^{\mathsf{R}} x^2 f_{H,\theta}(x)\,\mathrm{d}x, \\ f_{H,z} &= h_z^2 - \omega_z m_z, \quad A_z^+ = -\mathsf{R}^{-1}\int_0^{\mathsf{R}} x f_{H,z}(x)\,\mathrm{d}x. \end{aligned} \tag{2.15.40}$$

The two moments of f_H equal zero. The two prefixes thus have zero outer as well as inner endpoints, and the two-sided weight estimates give $A^+ \in \mathcal{M}^{c_*}$. We reconstruct only the Haar force. Application of these prefixes to the uncanceled perpendicular force would generally leave an exterior tail. Its complete moments can be nonzero.

The divergence of this symmetric cross tensor is

$$\mathrm{Div}_*\,\mathcal{Q}_\times(A^+) = (g_{\mathrm{rad}}, -f_{H,\theta}, -f_{H,z}), \qquad g_{\mathrm{rad}} = \rho\partial_{\mathsf{Z}} A_z^+ \in \mathcal{M}^{c_*+1}. \tag{2.15.41}$$

Let $N_{\mathrm{rad}} = \int g_{\mathrm{rad}}\,\mathrm{d}\mathsf{R}$ and use the actual current swirl after the two previous mean maps to set

$$P_{\mathrm{rad}} = \int_{\mathsf{R}}^{\infty} g_{\mathrm{rad}}(x)\,\mathrm{d}x - \chi N_{\mathrm{rad}}, \qquad \delta_{\mathrm{rad}} = \sqrt{V_{M,\mathrm{current}}^2 + \mathsf{R}kN_{\mathrm{rad}}} - V_{M,\mathrm{current}}. \tag{2.15.42}$$

This cancels g_{rad} with zero remainder and has zero pressure endpoints. Its Haar swirl and pressure have order c_*+1, and its perpendicular swirl has order c_*+1+s. The new canonical residual equals

$$\begin{aligned} E_r^{\mathrm{can},+} &= 0, \\ E_\theta^{\mathrm{can},+} &= r_\theta^2 + \omega_\theta m_\theta + \Theta_{\mathrm{current}}\delta_{\mathrm{rad}}, \\ E_z^{\mathrm{can},+} &= r_z^2 + \omega_z m_z + \rho\partial_{\mathsf{Z}} P_{\mathrm{rad}}. \end{aligned} \tag{2.15.43}$$

The stress is $A_*^+ = A^+$, not $A_* + A^+$: the cancellation of the old stress occurs in (2.15.33).

The comparisons

$$j_2 \geq c_* + 2, \qquad c_* + 1 + s > b_* \tag{2.15.44}$$

give

$$E_H^{\mathrm{can},+} \in \mathcal{M}^{c_*+2}, \qquad E_\perp^{\mathrm{can},+} \in \mathcal{M}^{b_*}. \tag{2.15.45}$$

The last radial correction changes the actual states by $\int r^2\Pi\delta_{\mathrm{rad}}$, $\int r^2\Pi(u_{M,z}\delta_{\mathrm{rad}})$ and $\int r\Pi P_{\mathrm{rad}}$, all of order c_*+1. Addition of $\mathcal{Q}_\times(A^+)$ does not change their defining flux entries. Because

$$\min(d_H, c_*+1) = c_*+1, \tag{2.15.46}$$

the last states have order c_*+1. Their two source moments have Haar order c_*+2, with the full zero-Haar flat complements kept. The inequalities in (2.15.44) and (2.15.46) hold on the two branches of d_H: $2p-(c_*+1) = a - a_0 \geq 0$ and $p+2-(c_*+1) = 1/2 + 3\varkappa > 0$.

2.15.3.4 Feedback on each wave coefficient

Let Δu_M be the sum of the four actual mean increments: the covariance radial root, auxiliary response, state response, and last radial correction. We compute each increment on the updated current mean. Their nonlinear mean equations then telescope. Their combined normalized bounds are

$$(\Delta u_M)_{\tan} \in \mathcal{M}^{s_*}, \qquad (\Delta u_M)_r \in \mathcal{M}^{p+1}, \qquad \Delta\pi \in \mathcal{M}^p. \tag{2.15.47}$$

Each increment has zero full axial flux.

To include the mean change in the wave equation, we take coefficients X, Y on a fixed label and define

$$\begin{aligned} \mathcal{C}(X,Y) &= X_r \mathcal{D}Y + \rho X_z \partial_{\mathsf{Z}} Y + (X_\theta/\mathsf{R})\mathcal{J}_{\mathrm{rot}} Y, \qquad \mathcal{J}_{\mathrm{rot}} Y = (-Y_\theta, Y_r, 0), \\ \mathcal{B}_m(X,Y) &= \mathcal{C}(X,Y) + ikm(X\cdot n)Y. \end{aligned} \tag{2.15.48}$$

This is the full cylindrical coefficient formula for the ordered convective product, with the connection and carrier terms. At each coefficient Y_m of $w^+ = w + z + h$, the additional source equals

$$\mathcal{B}_m(\Delta u_M, Y_m) + \mathcal{B}_0(Y_m, \Delta u_M). \tag{2.15.49}$$

We assume no auxiliary support separation of the mean.

All current Y_m have principal order at least $1/2$. The largest term is $ikm((\Delta u_M)_{\tan}\cdot n_{\tan})Y_m$, of order s_*. The radial derivative, radial transport, connection and axial transport terms have respective lower bounds

$$s_* + \tfrac{1}{2} - \varkappa, \qquad p + \tfrac{3}{2} - \varkappa, \qquad s_* + \tfrac{1}{2}, \qquad s_* + \tfrac{3}{2}. \tag{2.15.50}$$

The radial carrier uses the stronger order $p+1$ of the radial mean increment.

Thus (2.15.49) belongs to $\mathcal{W}^{s_*}$, strictly higher than $a + \gamma_*$. It includes the leading wave, each old correction, the harmonic response and the signed response. The last nonzero canonical source then satisfies

$$F^+ \in \mathcal{W}^{a+\gamma_*}. \tag{2.15.51}$$

The finite harmonic set may increase, but the construction uses only finitely many products and convolutions.

2.15.4 Finite return and compatible actual states

Proposition 2.15.2 (Finite paired return)**.** *We start from the initialized actual state (2.15.20). For each finite integer $n \ge 0$, the previous construction gives actual fields*

$$(u_M^n, \pi^n, w^n, p_w^n, A_*^n, d_*^n)$$

on a sufficiently small positive q domain. Their physical parameter domain is the full interval $-1 \le \hat{\zeta} \le 1$. They have the same fixed graph and phase family and satisfy (2.15.5) with one fixed reference force.

At

$$\alpha_n = a_0 + n/5 \tag{2.15.52}$$

the invariant (2.15.22) holds with $a = \alpha_n$. Each state has exact divergence and zero full axial velocity defect. Each mean pressure increment has zero radial endpoints, and each wave increment is an actual curl of its supplied physical potential.

For a step from order a, the stronger outputs are

quantity	*normalized order*
F^+	$a + 1/2 - 3\varkappa$
A_*^+	$c_* = a + 1 - 3\varkappa$
$E_H^{\mathrm{can},+}$	$c_* + 2$
$E_\perp^{\mathrm{can},+}$	$b_* = a + 3/2 - 3\varkappa$
$(K_d^+, \Phi_\theta^+, \Phi_z^+)$	$c_* + 1$
full tangential force moments	$c_* + 2$ *in Haar + flat*
$(\Delta u_M)_{\tan}$, $(\Delta u_M)_r$	s_*, $p+1$
$\Delta\pi$	p.

(2.15.53)

The flat remainders in the ordinary equation have all fixed lifted and physical jets flat at the singular tip. Their constants can depend on the finite state. No infinite sum of these remainders is part of this proposition.

Proof. The previous construction gives the initialization. The one-step algebra is (2.15.28)–(2.15.51). It gives the table. To return at $a' = a + 1/5$, the limiting comparisons are

$$\begin{aligned} (a + \gamma_*) - a' &= 3/10 - 3\varkappa, \\ c_* - (a' + 1/2) &= 3/10 - 3\varkappa, \\ b_* - (a' + 1) &= 3/10 - 3\varkappa, \\ (c_* + 1) - (a' + 1/2) &= 13/10 - 3\varkappa > 0. \end{aligned} \tag{2.15.54}$$

The Haar force is stronger still. Because $s_* > s$ and $p + 1 > 2$, the mean increment keeps the low-order mean bounds. The distinct root and auxiliary estimates keep the sharper fluctuation bounds in (2.14.6). Because $a \geq a_0$, the two new wave corrections keep the old structured principal and curl orders.

This verifies each component of the invariant.

All inverses use the same actual coefficients on their source neighborhoods. The nonzero ODEs hold slow variables fixed, so on a half-box that meets $\mathsf{T} = 0$ they never leave the physical half-space. Radial integrals, the moment matrix and state targets keep z, t, thus $q, \hat{\zeta}$, fixed (see Lemma 2.8.5(c)). There is no axial segment integral in (2.14.48).

The fixed-cover construction of Lemma 2.13.1 thus applies on the complete radial saturation at each finite stage. Products, directional inverses, shifted primitives and the smooth root keep that cover. The canonical physical operations agree on overlaps. We do not join independently constructed band fields.

Each step uses only finitely many value restrictions. They apply to source domain eligibility, the packet inverse value hypotheses, positivity of the four current roots, and the current matrix margin. Their errors are positive powers of ρ times finite logarithmic factors. A single sufficiently small threshold satisfies all these conditions.

Once the denominators have a value margin, their derivatives use only finitely many higher input jets. They impose no new domain restriction for each derivative order. The harmonic bound and these constants may depend on the stage.

The updates to d_* and G_{flat} are finite sums of the explicit deletion and Gaussian-tail terms. Their positive weight factors give lifted flatness before sampling. The physical derivative bridge then gives their physical flatness. The accumulated old d_* cancels from (2.15.28). Only the explicitly factored $(1 - \vartheta^2)K$, at its stated $\mathcal{M}^p$ order, enters the mean response. No operation applies a weighted inverse to an unweighted-flat remainder.

At the last step, we restrict the same earlier states to the next admitted q domain. This constructs a compatible sequence of actual finite fields. The exact ordinary residual remains (2.15.5). We keep its cross-stress divergence and its flat tensor divergence. □

The output for the last diagonal is now concrete. For each finite n, we write its wave difference as $\operatorname{curl} B_n$ and its mean difference as m_n. The previous formulas give their actual potentials, pressures, and prefixes, and

$$\operatorname{div} m_n = 0, \qquad \int_0^\infty r(m_n)_z \, \mathrm{d}r = 0. \tag{2.15.55}$$

The second identity is what permits a q cutoff of the mean followed by a compact radial divergence repair. The diagonal construction in Section 2.18 selects finitely many seminorm bounds at each

stage and compares the field with one fixed genuine prefix at a time. It uses the flat terms of that prefix in (2.15.5), and uses no infinite sum of $\mathsf{B}^n_{\mathrm{flat}}$ or G^n_{flat}.

2.16 The inventory of the mean–wave stage

Table 2.4: Inventory of Section 2.14 and of the finite initialization. "S" marks y-independent vertices.

row	place in this text	vertex	type	closure hypotheses / remark
R0	(2.14.1)–(2.14.6)	$\mathsf{Q}_s = \mathcal{Q}_\times(K_{\mathrm{B}})$; $\rho B_{\mathrm{H}}, V_{\mathrm{H}}, G_{\mathrm{H}} = \Pi(Q^{\frac12+h}u_M)$; $b^\perp, V^\perp, G^\perp = (I-\Pi)(Q^{\frac12+h}u_M)$	S; T(i)	Haar split of the current mean, the parents of X4 and X6
R1	(2.14.7)	$\mathcal{D}, \mathcal{T}, \Delta_*$ applied to vertices	E	slow coeffs; $\lambda \asymp \rho^{-\varkappa} S^{-\rho_g}$, $c \asymp S^{-1}$
R2	(2.14.8)–(2.14.10); (2.14.11)	$\mathcal{I}, \mathcal{L}, \mathcal{J}, \mathcal{I}_\chi = \mathcal{I} - \chi\mathcal{J}$	T(iv),(v)	Auxiliary translations commute. Lemma 2.13.9 uses the two-sided weight for $\mathcal{I}_\chi$, one-sided tails and an unweighted full moment. On $\mathcal{V}_0$ the compensated primitive gains $\varkappa$ and the full moment satisfies (2.12.5). On $\mathcal{V}_{\mathrm{int}}$ the inward prefix equals $-\mathcal{I}_\chi$.
R3	(2.14.11)–(2.14.12) and the displays after it; bump normalization and (2.14.32) (proof of Lemma 2.14.2); (2.14.58) with the slice-jet paragraph	b, β_0, χ, k, y, $\bar q$, $\bar q_{\mathsf{T}}$, η_{T}, ω_z, ω_θ, c_β, c_θ	S; X7	$\frac{\xi^2}{2} \ge \frac{\hat\xi_p^2}{2} e^{-8}$ on $\operatorname{supp} b$; $\inf \frac{\hat\xi_p^2}{2} > 0$; $1 - 2h\eta^2 \ge 1 - 2h$; $B_{1/2} \ge e^{-4}$; $\lambda_{\mathrm{ch}}(\eta)$ has bounded fixed slow jets on the endpoint collars. The endpoint identities produce no vertex
R4	after (2.14.13)	$\mathcal{B} = a_r^{-1}(v_r \cdot \partial_y)^{-1}$, $\mathcal{A} = \partial_{\mathsf{R}}\mathcal{B}$	T(ii),(v), E	on $\mathcal{V}_0$; $a_r \ge a_* > 0$
R5	(2.14.14)	f_D, $M_D = \mathcal{J} f_D$, $P_D = -\mathsf{D}_{rr} + \mathcal{I}_\chi f_D$	P,E,S,T,Σ	$M_D = \overline{M}_D + \mathcal{J}(I-\Pi) f_D$ (flat, $\mathcal{V}_0$)
R6	(2.14.16), (2.14.19)	$\delta_D = \mathfrak{X} H(V_M, \mathfrak{X})$, $\mathfrak{X} = \mathsf{R}k M_D$	C (k=2), P	margin $\lvert\mathfrak{X}\rvert \le V_M^2/2$: $\theta = \frac12$, Lemma 2.12.26 (not Cor. 2.12.11(a))
R7	(2.14.17), (2.14.20)	$(\delta_D)_\perp$	X4: C (k=3), P, T(i)	Lemma 2.12.27, $W_0 = V_{\mathrm{H}}$, $W_1 = V_M$
R8	(2.14.21)–(2.14.23)	pressure flux, moving force	S; X7	slow / exact identities
R9	(2.14.24)–(2.14.26)	$\mathcal{B}_r, \mathcal{B}_\theta, \mathcal{B}_z$	P,E,S,Σ	polynomial in u_M, seed, $\mathcal{D}, \mathcal{T}, \Delta_*$
R10	(2.14.31); (2.14.33)	$T_0^{-1} = c^{-1} D_{v_t}^{-1}$, v_0, γ_0	T(ii),(vii)	on $\mathcal{V}_0$ (input zero-Haar by the hypothesis of Lemma 2.14.2); $k = 4$, $e' = 1$; factor $c^{-1} \le T_g^{1+\Delta_{\max}} S$ by (S2)–(S3)
R11	(2.14.33)	v, γ; $\beta = -\rho \mathsf{R}^{-1} \mathcal{L}(\mathsf{R}\gamma_{\mathsf{Z}})$	Σ,P,T,E	$\mathcal{J}(\mathsf{R}^2 v_0)$ flat on $\mathcal{V}_0$; $\gamma_{\mathsf{Z}} \in \mathcal{V}_1$, hence $\mathsf{R}\gamma_{\mathsf{Z}} \in \mathcal{V}_{\mathrm{int}}$ by X9. The prefix gains $\varkappa$ there
R12	(2.14.34), (2.14.35)	residual rows; g, M, P; $\delta = F(V_M + v, \mathsf{R}kM)$; $\xi = v + \delta$	X5; P,E,T; C	margin by Lemma 2.12.30 ($v \in \mathcal{M}^\nu$, $\nu \ge s$)
R13	(2.14.38) and the two lines before it	$P^\perp = \mathcal{I}_\chi(I-\Pi)g$; $\delta^\perp$	T on $\mathcal{V}_0$; X4	$W_0 = V_{\mathrm{H}}$, $W_1 = V_M + v$, $W_1 - W_0 = V^\perp + v$
R14	(2.14.36), (2.14.37), $\overline{M}$; (2.14.41)	A_{rr}, A_{rz}, $A_{\theta\theta}$, $C..$, $\bar\delta$, h_θ, h_z, $\overline{M}$	T(i)$\circ$P: S	Lemma 2.12.29
R15	(2.14.39), (2.14.40)	force groups; $\Theta\delta$	P,E; X6	$T_0\delta = T_0\delta^\perp$ via R13
R16	(2.14.42); (2.14.47)–(2.14.51); (2.14.57)	states, five rows, frame, matrix inverse, seeds v_j, γ_j, β, p_0	S	slow inverse with margin (proof of Lemma 2.14.3, before (2.14.51)); Lemma 2.12.29
R17	(2.14.52)–(2.14.55)	$g = \mathcal{B}_r(\beta, v, \gamma)$; M, P; p_1; $P^\perp$	P,E,T; X6	$g^\perp$ by X6 (leading $-2V^\perp v/\mathsf{R}$); $p_0 = \mathcal{I} g_0$ (slow)
R18	(2.14.54), (2.14.56)	δ (state map); $\delta - \delta_{\mathrm{slow}}$	C; X4	$W_0 = V_{\mathrm{H}} + v$, $W_1 = V_M + v$; $\bar{\mathfrak{X}} = \mathsf{R}k \int g_1$

row	place in this text	vertex	type	closure hypotheses / remark
R19	(2.15.1)–(2.15.5) and the flat-term paragraph after it	$\mathcal{Q}_\times$, ϑ, d_*, $\mathsf{C}^{\mathrm{can}}$, $\mathsf{B}_{\mathrm{flat}}$, E^{can}, $(1-\vartheta^j)F_m$	S,Σ,P	ϑ slow, polynomial-S jets
R20	(2.15.6)–(2.15.10)	$d_{*,\mathrm{base}}$, D_0, S, C_0, g_s; unpaid rows	S,Σ; E	signed update from Propositions 2.13.6 and 2.13.7
R21	(2.15.11)–(2.15.13) (Lemma 2.15.1)	f_C, M_C, P_C, δ_C; rows E^R; $\Theta_s\delta_C$	as R5, R6; E,P; X8	slow pressure with its late P_1, P_2 is S (Lemma 2.20.1); $V_s \geq v_*$ and positivity of the radicands: proof of Lemma 2.15.1, after (2.15.15); margin via Lemma 2.12.30
R22	(2.15.14)–(2.15.16) and the next paragraph	M_s, P_s^{add} (slow); $\epsilon_s = \mathsf{R}k M_s H_2$; state changes $\int \mathsf{R}P_s^{\mathrm{add}}$, $\int \mathsf{R}^2\Pi\epsilon_s$, $\int \mathsf{R}^2 G_s \Pi\epsilon_s$; feedback of ϵ_s on packets	S; C (k=3); T(i)∘P: S; as R25	Lemma 2.12.26(c); feedback into (2.13.51) as (2.15.49)
R22′	(2.15.17)–(2.15.20)	initial auxiliary map on the slow mean; one uncut state map (2.15.18); one auxiliary/state/cross cycle; $\mathbf{f}_{\mathrm{ref}} = \mathbf{f}_s$	as R10–R18, R24	no new operation; finitely many steps, no cutoff and no infinite sum; margins by Lemma 2.12.30
R23	(2.15.21)–(2.15.33)	harmonic correction $z, p_z, Z_{\gamma,m}$; $\Delta\mathsf{C}_z$, K, δy, $\delta a_\pm$, w^+, d_*^+, $\mathsf{D}^{\mathrm{can}}$, Cross; products of the signed residual with w_0, v, z	(I3); Σ,P; S	labels: overlap (S3); finite harmonics; y_{lead} lower bound (after (2.15.26)); harmonic step by Proposition 2.13.7; the extra Cross$(v+z,h)$ has the orders in (2.15.31)
R24	(2.15.34)–(2.15.46)	e^{rad}; aux/state maps; h^2, r^2; $f_H, A^+, g_{\mathrm{rad}}, N_{\mathrm{rad}}, P_{\mathrm{rad}}$; δ_{rad}; state changes of $\delta_{\mathrm{rad}}, P_{\mathrm{rad}}$	E,P,Σ; S; C; X4	δ_{rad}: $W_0 = V_{\mathrm{H,cur}}$, $W_1 = V_{M,\mathrm{cur}}$, $\mathfrak{X} = \bar{\mathfrak{X}}$ slow; last state changes T(i)∘P: S
R25	(2.15.47)–(2.15.51)	Δu_M; $\mathcal{C}$, $\mathcal{B}_m$; feedback; F^+	Σ; P,E,A,S	n type A; envelope P from Y_m
R26	Proposition 2.15.2, its proof and (2.15.55)	finite return; m_n, curl B_n	as R0–R25; Σ	no new operation

Proposition 2.16.1 (Inventory of the mean–wave stage)**.** *Assume the inputs (S1)–(S10) and, in addition:*

(I1) the value invariant $V_M \geq 2v_*$ on the protected regions (the paragraph after (2.14.6)) and $V_s \geq 2v_*$ (proof of Lemma 2.15.1, after (2.15.15)), and the single small-q threshold (proof of Proposition 2.15.2, "Each step uses only finitely many value restrictions"). The text states $V_M > 0$ with an unnamed lower bound and $V_s \geq v_*^{\circ}$ (written v_* there), with its own constant. Lemma 2.12.31 proves both bounds with one constant v_*, independent of the stage, of ℓ and of the label. The threshold statement is Lemma 2.12.30;

(I2) the finite-order statements, in finite-depth form, of the shifted primitives and complete moments (Lemma 2.13.9; (2.14.13) and the paragraph after it), of T_0^{-1} ((2.14.31)), and of the slow Volterra and tail lemmas (Lemma 2.6.9; proved as Proposition 2.3.12, with Remark 2.13.8(1)–(2) for the slow chart and the Gevrey classes; on $t < 0$, Lemma 2.13.10). Their Gevrey forms are Corollary 2.12.18(ii), (iv) and (vii);

(I3) the vertices of Section 2.13 (wave coefficients, principal inverse, exact curl, covariances and signed update) as given in Section 2.12.1.

Then every coefficient produced in Section 2.14 and in the finite initialization (2.15.17)–(2.15.20) is a vertex of $\mathfrak{G}_n$ of the type listed in Table 2.4, possibly through an identity of Definition 2.12.32.

The closure hypotheses of its type hold, with Lemmas 2.12.26–2.12.30 in addition to the lemmas of Table 2.3. Each ledger assertion is the amplitude rule of its type applied to the parents' ledger entries. Hence Hypothesis 2.12.22 holds for these operations, and Theorem 2.12.23 applies with $k \le 3$ *in type* C *and with the root radius* $r_{1/2} = \min(v_*, v_*^2)/16$.

Proof. The rows of Table 2.4 follow the text in order. (1) Every operator in the range commutes with ∂_{y}. The operator is either a multiplication by a y-independent function, Π, a Fourier multiplier $(T_0^{-1}, \mathcal{B})$, a superposition of y-translations by y-independent vectors $(\mathcal{I}, \mathcal{L}, \mathcal{J})$, a slow integral at fixed y, or an evaluated derivative with slow coefficients. No coefficient is evaluated at the physical sample inside the graph. (2) The slow geometric divisors have bounded inverses on their specified supports: $\mathsf{R}, a_r, \bar{q}, c_\theta$, X on $\operatorname{supp} b$, and $1 - 2h\eta^2$. The finite matrix solves use their stated inverse estimates and the scalar band constants carry their recorded powers. In R23 the signed update divides by $2\sqrt{y_{\mathrm{lead}}}$. By (2.13.41), $y_{\mathrm{lead}} \ge c\sqrt{S_\ell}\,\mathsf{W}$, while every fixed slow jet of δy carries W. Differentiating (2.13.47) leaves the factor $\sqrt{\mathsf{W}}$ with the allowed logarithmic powers. Both factors are independent of the auxiliary variable. The protected root denominators satisfy Lemmas 2.12.26–2.12.27. The logarithm and ϑ act only on slow data. (3) The five protected roots have the base and radicand of Lemma 2.12.26. Lemma 2.12.30 under (I1), with $\theta \le \frac{1}{4}$, gives the margin $|\mathfrak{X}| \le \theta v_*^2 \le V^2/4$ directly. Lemma 2.14.1 states the weaker $|\mathfrak{X}| \le V^2/2$, which Lemma 2.12.26 with $\theta = \frac{1}{2}$ also covers. (4) The structural gains are covered: perpendicular parts of roots by X4 and Lemma 2.12.27; zero-Haar and zero-moment gains of type T by Lemma 2.12.28; perpendicular sources by X6; residual rows by X5, X7, X8. (5) All Haar quantities, state integrals and matrix data are y-independent, so Lemma 2.12.29 applies to them. (6) The number of operations per stage is finite. The integration-by-parts counts are fixed by the slow order and the requested gain, never by α. The label and harmonic sums are of type Σ with the overlap of (S3). The finite initialization (row R22′; Section 2.4.1 states it in one sentence) introduces no operation beyond (2.15.17)–(2.15.20). The lines of Section 2.14 that no row lists are statements, ledger assertions or identities of Definition 2.12.32, and they produce no coefficient. □

The packet stage. Proposition 2.16.1 covers Section 2.14 and the finite initialization; its input (I3) is the packet stage, whose vertices are covered by the closure lemmas of Section 2.12.1. Table 2.5 lists them in the order of Section 2.13, with the clock of Section 2.12.

Table 2.5: Inventory of the clock and of the packet stage (Sections 2.12 and 2.13). "S" marks y-independent vertices.

row	place in this text	vertex	type	closure lemma / hypotheses
P0	Lemma 2.12.1	clock inverse $c_i^{-1} D_{v_t}^{-1}(E - \Pi E)$	T	Corollary 2.12.18(iii); the associated exponential weights satisfy the separate relative estimate of Corollary 2.12.11(c)
P1	Section 2.13.1; (2.13.10), (2.13.11)	background band coefficients b, F_b, G_b, the matrix K_b of (2.13.21) and $H_\Phi = pF_b + p_z G_b$ of (2.13.16); W, $\mathcal{L}_W$, W_*; ϑ_q; slow cutoffs $\eta_{\ell,a}$; band constants ρ_Q, $k_\ell = \lceil \rho_Q^{-1/2} \rceil$, c_i, λ	S	Lemma 2.12.29; finite-order bounds of the text
P2	Lemma 2.13.1	lifts $f_i(J_g^{i-i_0}\mathsf{y})$, translations	V	Lemma 2.12.14, $\Delta \le \Delta_{\max}$ by (S3)
P3	(2.13.12)	D_{R}, D_z, t_* applied to vertices	E	Lemma 2.12.15
P4	(2.13.13)–(2.13.22)	frozen constants F_0, g_0, N, K, λ_0, c_0, B_p, u_p, x_0, p, p_z, k_ℓ; and H_Φ, K_b (slow, from P1)	S	frozen at a representative; held fixed under derivatives

row	place	vertex	type	closure lemma / hypotheses
P5	(2.13.16)–(2.13.22)	n, $\partial_v n$, $(n\cdot n)^{-1}$, $\lvert n_{\tan}\rvert^{\pm1}$, s, s_a, $K_a = n_{\tan}/\lvert n_{\tan}\rvert$, N_a, U_f, $M_f^{\pm1}$, B_f, B_f^{ℓ}, P_n, A_Φ, E_f, λ, d_p, A_m, $\mathcal{E}_\Phi$	A	Lemma 2.12.13 (with Lemma 2.12.12, $\delta = 1$); $\lvert n\rvert, \lvert n_{\tan}\rvert \ge c$ and $\lvert c_0\rvert \ge c$ by (2.13.19), (2.13.14); the phase $e^{ik_\ell m\Phi}$ never enters a coefficient (paragraph after Lemma 2.12.15)
P6	(2.13.23)	P, Gaussian factor	Env	Lemma 2.12.7; the reciprocal envelope occurs inside the normalized pulse in P7
P7	Lemma 2.13.2	z_m (zero-data), $z_\pm$, z_+/P	O; C	Lemma 2.12.19, Corollary 2.12.20(1), (4), (5); Corollary 2.12.11(b) with $z_+ \asymp P$ by (2.13.25)
P8	Proposition 2.13.3, (2.13.27)	$t_m = B_f z_m$, π_m	O, P, A	Corollary 2.12.20(1), (2)
P9	(2.13.28), (2.13.29)	ψ, $\widehat{t}_m = \psi t_m$, residual $(1-\psi)f_m + \psi' t_m$	K, P	Lemma 2.12.16; Corollaries 2.12.20(3), 2.12.24
P10	Lemma 2.13.4, (2.13.31)–(2.13.37)	C_m, r_m; coefficients of D_Φ, D_0; linear remainder	E, P, A, S	Corollary 2.12.20(3); Lemma 2.12.13; identities (X1), (X2) of Definition 2.12.32
P11	(2.13.39), Proposition 2.13.5	$x_\varsigma = z_+ + z_-$ (sum of two O-vertices, type Σ); $M_{\beta,\varsigma}$, $\mathcal{H}_\beta^{\pm1}$, the target $T_\beta = (Q/\widetilde{q})^{1+h}\widetilde{T}_0$ (slow), y_β, $a_{\beta,\varsigma} = \sqrt{y_{\beta,\varsigma}}$ (integrals over the pulse at a slow point); χ_g; packet coefficients $a_\gamma, d_\gamma, b_\gamma$	S; K; P, A, E	Lemma 2.12.29 and the paragraph after Corollary 2.12.11 (slow roots and inverses, $y_\beta \ge c\sqrt{S}\mathsf{W} > 0$); Lemma 2.12.16; Lemmas 2.12.9, 2.12.13, 2.12.15
P12	(2.13.44), (2.13.46)	covariance entries of one label; label sums	P, Σ	Lemma 2.12.9; cross-label products vanish by (S3); overlap N_{ov}
P13	Proposition 2.13.6, (2.13.47)–(2.13.51)	$\delta a_\pm$, signed division by the positive leading amplitude, signed squares, full covariance	S; P, Σ	weighted division (2.13.47), $y_\beta \ge c\sqrt{S_\ell}\mathsf{W}$; Lemma 2.12.9
P14	Proposition 2.13.7, (2.13.52)–(2.13.63)	bilinear products, finite convolution, first and second sources, harmonic principal inverses, complex covariance, cut commutator	P, Σ, E, O, K	Lemmas 2.12.9, 2.12.15, 2.12.16; Corollary 2.12.20 for each harmonic of the finite set
P15	Lemma 2.13.9, (2.13.66)–(2.13.69)	I, J, I_χ, $\mathcal{B}, \mathcal{A}$	T	Corollary 2.12.18(ii), (iv); compensated gain on $\mathcal{V}_0$, prefix gain on $\mathcal{V}_{\mathrm{int}}$, and complete moments by (2.12.5)

Theorem 2.16.2 (Hypothesis 2.3.21 holds)**.** *Fix the jointly selected member of Theorem 1, including its backward core, strict cone, heat exterior, native weights and protected slots. These leading data are fixed before the finite-stage condition (B7). The backward ordinary estimates used here are proved on p. 494 before the factorial bound. At every finite stage n, and on each side of $t = 0$, every coefficient produced by the clock (Section 2.12), the packet stage (Section 2.13), the mean–wave stage and the finite initialization (Section 2.14) is a vertex of $\mathfrak{G}_n$ as Hypothesis 2.12.22 requires. Each cut increment in Section 2.18 appends finitely many vertices of the same types to its stage graph. Summation and spatial localization act on the sampled fields. Hence Hypothesis 2.3.21 holds, and Proposition 2.12.3 holds at every finite stage on both sides, with W on $t > 0$ and W_b on $t < 0$.*

Proof. Data on the two signs. (S1)–(S3) use the joint schedule and the finite torus cover. In (S4) the negative slow coordinate changes sign while the pulse derivative retains coefficient one. In (S5)–(S7) use the backward packet rows of the transfer table, specifically the strict shear and nonzero tangential normal, the oriented damped pulse inverse, the value gate, and the covariance cone. (S8) uses Lemmas 2.3.11 and 2.20.6 on $t < 0$. In (S9) the joint Diophantine multiplier is fixed; the shifted primitives use Lemma 2.13.10. In (S10) use the ordinary value margins and finite thresholds before differentiating a root or a matrix inverse. The sign identity and the budgets for the slow flux

derivative are recorded in Proposition 2.6.15 and Lemma 2.20.3. The accumulation of the ordinary margins is proved on p. 494.

Clock and packets. Table 2.5. Each row names the closure lemma, and the hypotheses of that lemma are the cited construction bounds: the value bounds (2.13.19) and $|c_0| \ge c$ for the strip lemma; (2.13.22) and (S6) for the pulse ODE; (2.13.25) for the division by z_+; the weighted lower bound $y_\beta \ge c\sqrt{S_\ell}\mathsf{W}$ and (2.13.47) for the slow roots and their signed updates. On $t < 0$ the inputs of these bounds are (B2) and Lemma 2.3.11(a), as listed in (T1), (T6) of Remark 2.7.4.

Mean–wave stage and initialization. Proposition 2.16.1, with its inputs checked as follows. (I1): Lemma 2.12.31 on both sides, with one v_*. On $t > 0$ its positivity input is the lower bound of F_{lead} on the closure of the active set (after (2.13.1)); on $t < 0$ it is $E_0 > 0$ on I_{mean} (Lemma 2.3.3) and the vanishing of the positive slow corrections there (Proposition 2.7.2(b)). The threshold part is Lemma 2.12.30, whose weight plateau is (W2) of Proposition 2.3.9 on $t > 0$, and $\min_{\overline{I_{\mathrm{mean}}}} \mathsf{W}_b > 0$ on $t < 0$ (Lemma 2.3.11(c)). (I2): Lemma 2.13.9, (2.14.13) and (2.14.31), with Gevrey forms Corollary 2.12.18(ii), (iv), (vii); the tail lemma is Proposition 2.3.12 on $t > 0$, which uses only the product form of the weight (Remark 2.3.14), and Lemma 2.13.10 on $t < 0$. (I3) follows from the preceding packet table on the chosen sign. For clarity, several operations in the last inventory rows can be checked before any factorial estimate. In R19 substitute $\mathsf{C}^{\mathrm{can}} = \mathsf{C}^{\mathrm{act}} + \mathcal{Q}_\times(d_*)$ and $\mathsf{B}_{\mathrm{flat}} = -\mathcal{Q}_\times(d_*)$ in (2.15.5). The two occurrences of $\mathrm{Div}\,\mathcal{Q}_\times(d_*)$ cancel identically on each time side. The two integrated tangential moments vanish by (2.15.2). Thus this change of representation introduces no new derivative loss or inverse.

In R21 the two radicands are $V_s^2 + \mathsf{R}kM_D$ and $V_s^2 + \mathsf{R}k(M_D + M_s)$. On the protected mean subslot on both sides $V_s = V_{\mathrm{lead}} \ge 4v_*$. The orders of M_D, M_s are one and two. Given their incoming ordinary bounds, $|\mathsf{R}k|(|M_D| + |M_s|) \le v_*^2/2$ after increasing the common band threshold. The rationalized root difference (2.15.15) therefore inherits the order of M_s by the product and chain rules. In R24 use the *current* value $V = V_{M,\mathrm{current}} \ge 2v_*$ and $N_{\mathrm{rad}} = \int \rho\partial_{\mathsf{Z}} A_z^+ \, d\mathsf{R}$ of order $c_* + 1$. The same calculation gives $\delta_{\mathrm{rad}} = \mathsf{R}kN_{\mathrm{rad}}/(\sqrt{V^2 + \mathsf{R}kN_{\mathrm{rad}}} + V)$ of that order. Squaring the equation cancels the radial row in (2.15.43). The extra s in its perpendicular component requires the current Haar split of R24. For a current state matrix $L = L_0 + E$ on the compact patch, $\|L_0^{-1}E\| \le 1/2$ likewise gives $\|L^{-1}\| \le 2\|L_0^{-1}\|$ before differentiation. The ordinary bounds for the incoming N_{rad}, the current perturbation E, and the R26 return are proved on p. 494.

The limit stage. In (2.18.6), multiplication by the slow cutoff χ_n and by its slow derivative is of type T(v). The physical radial prefix lifts to $\mathcal{L}(\mathsf{R}\gamma_n)$ in (2.14.8). On the axial Haar part it is the slow integral of type T(vi). On the zero-Haar seed it equals $-\mathcal{I}_\chi(\mathsf{R}\gamma_n^\perp)$ by the anchored flux identity. Type T(iv) on $\mathcal{V}_{\mathrm{int}}$ therefore gives the gain in (2.18.8), with the finite input depth of Corollary 2.12.18(iv). The additional cutoff curl in (2.18.7) is a slow multiplier applied to the potential. The slow jets of each cutoff factor are bounded independently of δ_n on its bands, as verified at (2.18.9). Localization acts on the physically sampled fields (u_∞, p_∞).

Every coefficient of stage n is therefore a vertex of the listed type, and each ledger assertion is the amplitude rule of its type applied to its parents. This is Hypothesis 2.12.22. Theorem 2.12.23 and the proof of Proposition 2.12.3 after Definition 2.12.32 give the factorial bounds. The constant v_* is fixed by the two leading members before any stage, and each stage adds finitely many thresholds $\ell \ge \ell_i$ (proof of Lemma 2.12.31), so these choices occur at step 7 of the parameter ordering in Theorem 1(iii). □

2.17 Derivative bounds on the whole profile hull

2.17.1 The bridge with an arbitrary physical prefactor

Lemma 2.17.1 (Bridge for velocity, stress and force). *On a fixed enlarged band annulus let*

$$g=\sum_{\gamma,m} Q_\gamma^{-e}E_\gamma f_{\gamma,m}(w,\mathsf{y}(w))e^{imk_\gamma\Phi_\gamma},\qquad w=(t/Q,x'/Q^{1/2},z/Q^{\frac12-h}),$$

where Q is fixed during differentiation, $Q_\gamma/Q\in[1/2,2]$, $e\ge0$ is fixed, and E_γ is a cylindrical unit vector, a tensor product of such vectors, or the scalar 1. Use the fixed atlas of Section 2.13.1, the evaluated operators (2.13.12), and the phase (2.13.16). The bounds used below are

$$\lambda=O(Q^{-h\varkappa}S^C),\quad c=O(S^C),\quad k_\gamma\le 2Q^{-h/2},\quad |\partial^j_{\mathrm{phys}}\Phi_\gamma|\le C_jQ^{-j(1+h)-h}S^{C_j}\quad(j\ge1).$$

Here $\varkappa=10^{-5}$, $S\le C(1+|\log Q|)^{6/5}$, and all the fixed jets of the evaluated operators obey the same stated bounds. In common band and torus coordinates put

$$\mathcal{N}_j(g)=\sum_{\gamma,m}(1+|m|)^j\max_{|I|\le j}\|\partial^I f_{\gamma,m}\|_\infty.$$

The sum ranges over the labels in the local band representation and their relative harmonics; it includes their count. Then

$$|\partial^{\le j}_{\mathrm{phys}}g|\le C_{j,e}Q^{-e-3j}\mathcal{N}_j(g),\tag{2.17.1}$$

with constants independent of the stage and its harmonic count. In particular it applies to $e=(\frac12+h),2(\frac12+h),2(\frac12+h)+\frac12$.

Proof. At order zero the unit frames and phases have modulus at most one, and $Q_\gamma^{-e}\le 2^eQ^{-e}$. The triangle inequality gives $|g|\le 2^eQ^{-e}\mathcal{N}_0(g)$ with no logarithmic loss. For $j\ge1$, a term differentiating the phase l times in the Faà di Bruno formula has positive orders $a_1+\cdots+a_l=j$. Its bound, before the coefficient seminorm, is

$$C_j(1+|m|)^jQ^{-j(1+h)-(3h/2)l}S^{C_j}\le C_j(1+|m|)^jQ^{-j(1+5h/2)}S^{C_j}.$$

On the annulus all frame jets cost at most $Q^{-j/2}$. The evaluated radial, axial and time operators are respectively

$$Q^{-1/2}(\partial_{\mathsf{R}}+\lambda a_r\cdot\nabla_{\mathsf{y}}),\quad Q^{h-\frac12}\partial_{\mathsf{Z}},\quad Q^{-1-h}(Q^h\partial_{\mathsf{T}}+cv_t\cdot\nabla_{\mathsf{y}}).$$

Repeated chain and product rules, with the fixed coefficient-jet bounds, give the same conservative exponent $j(1+5h/2)$ for the evaluated coefficient. Distributing j derivatives among the coefficient, phase and frame adds their orders to j, not to $3j$. Summing the resulting bounds therefore gives $C_{j,e}Q^{-e-j(1+5h/2)}S^{C_j}\mathcal{N}_j(g)$. Since $\delta_j=j(2-5h/2)>0$, $\sup_{0<Q\le1}Q^{\delta_j}(1+|\log Q|)^{6C_j/5}<\infty$. This proves (2.17.1), also for lower derivative orders. The only role of e was the fixed prefactor and 2^e; no derivative was taken of a point-dependent choice of band. □

2.17.2 Quantitative axis bounds for the slow sum

Lemma 2.17.2 (Cartesian power calculus). *Let $P(\sigma,\frac{\hat\xi^2}{2},\hat\zeta)$, $\sigma=\log\hat t$, have bounded normalized jets of every fixed order on $\sigma\le0$, $0\le\hat\xi\le\hat\xi_1$, $|\hat\zeta|\le1$. For $g=\hat t^{\,a}P(\log\hat t,\frac{\hat\xi^2}{2},\hat\zeta)x'^{\alpha}$ and $b=a+|\alpha|/2$, every order-m physical derivative satisfies*

$$|\partial^m_{\mathrm{phys}}g|\le C_m\|P\|_{C^m}\hat t^{\,b-m}\quad(\hat t\le1,\ \tfrac{\hat\xi^2}{2}\le\tfrac{\hat\xi_1^2}{2}),$$

including the axis. The constant may depend on $a,\alpha,m,h,\frac{\hat\xi_1^2}{2}$.

Proof. Set $w = (1 - 2h\hat{\zeta}^2)^{-1}$ and $d = 1 - \hat{\zeta}^2$. On the forward side,

$$\partial_t g = \hat{t}^{a-1} x'^{\alpha} w(aP + P_\sigma - \tfrac{1}{2}\hat{\xi} P_{\hat{\xi}} - (\tfrac{1}{2} - h)\hat{\zeta} P_{\hat{\zeta}}),$$
$$\partial_z g = \hat{t}^{a-(\frac{1}{2}-h)} x'^{\alpha} w(2\hat{\zeta}(aP + P_\sigma - \tfrac{1}{2}\hat{\xi} P_{\hat{\xi}}) + d P_{\hat{\zeta}}),$$
$$\partial_{x_i} g = \hat{t}^{a-1} x_i x'^{\alpha} \frac{P_{\hat{\xi}}}{\hat{\xi}} + \alpha_i q^a x'^{\alpha - e_i} P.$$

The time formula changes sign on the backward side; the other formulas do not. The effective powers $a + |\alpha|/2$ decrease by $1, (\frac{1}{2} - h), 1/2$, respectively. Coefficients belong to the algebra generated by $\frac{\hat{\xi}^2}{2}, \hat{\zeta}, w$, which is stable under differentiation and bounded on the fixed hull at every fixed order. Induction proves the formula as a finite sum of terms with effective power at least $b - m$. Use $|x'| \le (\hat{\xi}_1^2 \hat{t})^{1/2}$ and $\hat{t} \le 1$ to bound it. The continuous Cartesian derivatives at the axis are identified as in Lemma 2.11.1, so the same bounds hold there. □

Proposition 2.17.3 (A bound for the slow reference on the full hull)**.** *The Borel constants in* (2.6.32) *can be chosen by the prescribed diagonal so that on each time side, including the spatial axis,*

$$|\partial_{\mathrm{phys}}^{\le m} u_s| \le C_m \hat{t}^{-\frac{1}{2}-h-m} \qquad (\hat{t} \le 1,\ \tfrac{\hat{\xi}^2}{2} \le \tfrac{\hat{\xi}_1^2}{2}). \tag{2.17.2}$$

This uses no growth assumption on the uncut coefficients as $n \to \infty$.

Proof. Include in the finite budgets at order n the normalized jets through order n of $F_n, U_n, M_n/\frac{\hat{\xi}^2}{2}, V_n/\frac{\hat{\xi}^2}{2}$ multiplied by the two cutoff shapes $\chi(c_n q/L_{\mathrm{cut}})$ and $\widehat{\chi}(c_n q/L_{\mathrm{cut}})$, where $\widehat{\chi}(s) = s\chi'(s)$. These are finite by Lemma 2.11.1. Their uniform bounds can be chosen independently of c_n: derivatives in σ and $\hat{\zeta}$ of the cutoff are fixed bounded shapes in $c_n e^{\sigma}/L_{\mathrm{cut}}$. Taking a supremum over all $\sigma \in \mathbb{R}$ makes this independence literal; restriction to $\sigma \le 0$ only decreases the supremum. The additional bounds are included in (2.6.32). The thresholds $c_n \ge 2L_{\max}(2^n C_{n,j})^{1/(nh)}$ for $j \le n$ are finite, so they can be met on both sides with one increasing sequence.

For each fixed m and $n \ge \max(1, m)$, derivatives of $\hat{t}^{2nh}$ times a cut normalized profile are bounded on its support by $C_m(1+n)^m 2^{-n}\hat{t}^{nh}$. This is summable uniformly on $\hat{t} \le 1$. Finitely many smaller indices have finite bounds as well. Consequently the following four normalized sums have bounded jets of every fixed order:

$$P_1 = \sum_{n\ge 0} \chi_n \hat{t}^{\lambda_n} V_n/(\hat{\xi}^2), \qquad P_2 = \sum_{n\ge 0} \chi_n \hat{t}^{\lambda_n} F_n,$$
$$P_3 = \sum_{n\ge 0} \chi_n \hat{t}^{\lambda_n} U_n, \qquad P_4 = -\sum_{n\ge 1} \widehat{\chi}_n \hat{t}^{\lambda_n} a(\hat{\zeta}) M_n/(\hat{\xi}^2),$$

where $\chi_0 = 1$ in the uncut leading convention, and

$$a(\hat{\zeta}) = w\left(2\hat{\zeta} - d\frac{L'_{\mathrm{cut}}(\hat{\zeta})}{L_{\mathrm{cut}}(\hat{\zeta})}\right).$$

On the backward side take $L_{\mathrm{cut}} = 1$ in this formula. If the leading order is also cut, include its single cutoff bracket in P_4; it is a finite smooth term, and the same bounds apply. Since $\partial_z \log \widetilde{q} = \hat{t}^{h-\frac{1}{2}} a(\hat{\zeta})$, the actual potential-cut formula is

$$u_s = \hat{t}^{-1} P_1(x', 0) + \hat{t}^{-1-h} P_2(x'^{\perp}, 0) + \hat{t}^{-\frac{1}{2}-h} P_3 e_z + \hat{t}^{-1} P_4(x', 0).$$

The four effective powers are $-1/2, -(\frac{1}{2}+h), -(\frac{1}{2}+h), -(\frac{1}{2}+h) + h$, all at least $-(\frac{1}{2}+h)$. Lemma 2.17.2 proves (2.17.2). The sums are locally finite when $\hat{t} > 0$, so the termwise formulas and derivatives are the actual fields. □

2.17.3 Why the finite errors vanish near the axis

Lemma 2.17.4 (Protected core)**.** *There is $\hat{\xi}_\flat > 0$, independent of the finite stage, on which $K_B = 0$, $u^{[N]} = u_s$, and $p^{[N]} = p_s$. All three error terms $E_N, \mathcal{Q}_\times(A_N), \mathrm{Osc}(F_N)$ in (2.18.1) vanish there, on either time side.*

Proof. The leading stress is $T_0 = e\mathcal{B}$, where the selected edge factor e vanishes for $\hat{\xi} \le \hat{\xi}_a(\hat{\zeta})$ by (2.3.3) and Definition 2.3.6. Every channel of the weight has this factor. Positive-order residuals vanish on the kept regular inner solve, and their stress primitives are taken from the axis by (2.6.23). Hence $T_n = 0$ on that core for all $n \ge 1$. On the backward side the support also follows from Proposition 2.7.2(c), with $\hat{\xi}_a < \hat{\xi}_-$. Multiplication by the Borel cutoffs preserves this open zero set, so $K_B = 0$ there and $\mathscr{N}(u_s, p_s) = f_s$.

Let $c_Q q \le Q \le C_Q q$ be the fixed band comparison, and choose

$$\frac{\hat{\xi}_\flat^2}{2} = \min\left\{ \min_{|\hat{\zeta}|\le 1} \frac{\big(\hat{\xi}_a(\hat{\zeta})\big)^2}{2}, \tfrac{1}{2} c_Q \mathsf{R}_-^2 \right\} > 0.$$

If $\hat{\xi} < \hat{\xi}_\flat$ then $\mathsf{R}^2 = \hat{\xi}^2 q/Q < \mathsf{R}_-^2$ in every active band. Each wave, protected bump and seed velocity vanishes on the whole radial segment from the axis to that point. The initial tensor C_0 vanishes there since each physical covariance is a wave product and the initial reserves $(1-\vartheta^2)S_0$, $(1-\vartheta^2)(K_B - S_0)$ vanish there. In (2.15.11), $\chi = 1$ there, so $\mathcal{I}_\chi f_C = -\mathcal{L} f_C$ is minus the shifted integral from the axis. Its integrand vanishes on this segment; thus $P_C = 0$. The protected roots are extended by zero outside their subslot.

For the initialized state in (2.15.20), let h_j be the remaining pointwise Haar force and m_j its full moment after the auxiliary and state corrections. The corrected pressure and seed increments vanish on the same core by their inward integrals and annular supports. Thus h_j and the protected moment bumps ω_j vanish there. The actual initial cross stress of (2.15.40) is

$$A_{*,j}(\mathsf{R}) = -\mathsf{R}^{-d_j} \int_0^{\mathsf{R}} x^{d_j} (h_j - \omega_j m_j)(x)\, \mathrm{d}x = 0, \qquad d_\theta = 2, \quad d_z = 1.$$

At the next stage $K = A_* - \Pi(\Delta \mathsf{C}_z)_{r\tan} = 0$ on the core. Its reserve update $(1-\vartheta^2)K$ therefore vanishes. The new cross, pressure and velocities again vanish there by the same prefixes and support argument. This proves the induction for the reserve, canonical covariance and kept cross. Every nonzero-harmonic force contains a wave factor or its derivative, hence also vanishes there. The canonical residual (2.15.4) consequently reduces on this open set to $\mathscr{N}(u_s, p_s) - f_s = 0$. The canonical-to-actual identity identifies these as E_N, A_N, F_N. All their physical derivatives vanish on the same set. On its complement, every band has $\mathsf{R} \ge (\hat{\xi}_\flat^2/C_Q)^{1/2} > 0$, as required by the bridge. □

2.17.4 The finite-state and finite-residual estimates

Proposition 2.17.5 (Completion bounds including the axis)**.** *For fixed N, on the domain where all uncut stages below N are defined, one has*

$$|\partial_{\mathrm{phys}}^{\le m} u^{[N]}| \le C_{N,m} \hat{t}^{-\frac{1}{2}-h-3m}. \tag{2.17.3}$$

The finite residual satisfies

$$\Big|\partial_{\mathrm{phys}}^{\le m}\Big[\mathscr{N}(u^{[N]}, p^{[N]}) - f_s - G_{\mathrm{flat},N} - \operatorname{div} B_{\mathrm{flat},N}\Big]\Big| \le C_{N,m} \hat{t}^{h\alpha_N - K_m},$$
$$K_m = 2(\tfrac{1}{2} + h) + 3m + 4. \tag{2.17.4}$$

Both estimates include the spatial axis.

Proof. The input finite identity is $u^{[N]} = u_s + \mathfrak{b}^{[0]} + \sum_{n<N}(\Delta u_{M,n} + \Delta w_n)$ by (2.15.20) and the paired step of Section 2.14. For fixed N, m, the normalized carrier-aware seminorms of these increments are bounded by a finite sum of $C_{N,m}\rho_Q^a S^{B_{N,m}}$ with $a > 0$. The initialization estimates in Section 2.14 and the finite order bounds of Lemma 2.20.3 give the positive powers in the normalized coefficient classes. Their constants may depend on N, m. Since $\rho_Q = Q^h$, these seminorms are uniformly bounded as $Q \to 0$. Lemma 2.17.1 with $e = (\frac{1}{2} + h)$, the fixed comparison $Q \asymp \hat{t}$, and Proposition 2.17.3 prove (2.17.3).

For the residual use (2.18.1), where $E_N \in \mathcal{M}^{\alpha_N+1}$, $A_N \in \mathcal{M}^{\alpha_N+1/2}$, $F_N \in \mathcal{W}^{\alpha_N}$. For each fixed seminorm the edge factors are bounded, using $\sup_{0<w\le e^{-2}} w^{\epsilon}(1 + |\log w|)^k < \infty$, and the remaining loss is S^B for a finite B. Forces have physical prefactor $Q^{-\frac{3}{2}-2h}$ and stresses Q^{-1-2h} by (2.14.3). Thus the bridge gives, respectively,

$$|\partial^{\le m} E_N| \le C Q^{h\alpha_N + h - 2(\frac{1}{2}+h) - 1/2 - 3m} S^B,$$
$$|\partial^{\le m} \operatorname{div} \mathcal{Q}_\times(A_N)| \le C Q^{h\alpha_N + h/2 - 2(\frac{1}{2}+h) - 3m - 3} S^B,$$
$$|\partial^{\le m} \operatorname{Osc}(F_N)| \le C Q^{h\alpha_N - 2(\frac{1}{2}+h) - 1/2 - 3m} S^B.$$

Relative to the exponent $h\alpha_N - K_m$, the positive spare powers are $h + 7/2$, $1 + h/2$, and $7/2$. Each absorbs its fixed logarithmic factor. Lemma 2.17.4 supplies zero on the protected core and a uniform positive radial bound elsewhere, so this bridge argument covers the whole hull. □

2.18 The physical limit, the initial trace, and localization

Main result. Proposition 2.18.5 completes the selected member of Theorem 1 (admissible by Lemma 2.18.3) with the stated field, trace, force, and derivative bounds. The construction uses one last packet/mean diagonal and fixed spatial localization. Proposition 2.8.6 gives one-sided regularity away from the singular point. The constants depend on the selected source and finite choices.

The finite construction in Section 2.14 supplies actual velocity and pressure fields on successively smaller positive-$\hat{t}$ domains. We start with the fixed graph, phase family, and leading field. We now select the increment domains so that their sum is smooth at each positive time. Its ordinary Navier–Stokes residual then extends smoothly to the initial boundary.

2.18.1 Finite states and a derivative loss independent of the stage

We keep the orders introduced in Section 2.4,

$$\alpha_n = 1 - 3\varkappa + n/5, \qquad \beta_n = \alpha_n - \varkappa, \qquad \varkappa = 10^{-5}.$$

We write the finite states as $u^{[n]} = u_M^{[n]} + w^{[n]}$, with total pressure $p^{[n]}$. They use one fixed smooth reference force $\mathbf{f}_{\mathrm{ref}}$. The ordinary equation, with the two explicit flat remainders, has the form

$$\mathscr{N}(u^{[n]}, p^{[n]}) - \mathbf{f}_{\mathrm{ref}} = E_n - \operatorname{div} \mathcal{Q}_\times(A_n) + \operatorname{Osc}(F_n) + G_{\mathrm{flat},n} + \operatorname{div} B_{\mathrm{flat},n}. \tag{2.18.1}$$

Here E_n, A_n, F_n have orders $\mathcal{M}^{\alpha_n+1}$, $\mathcal{M}^{\alpha_n+1/2}$, and $\mathcal{W}^{\alpha_n}$, in this order, for their normalized coefficients. We evaluate (2.18.1) in physical coordinates with the prefactors specified by the physical scaling. The formula is the canonical-to-actual identity (2.15.5). In particular, we keep $B_{\mathrm{flat},n}$ in the physical equation.

Each fixed state has finitely many relative harmonics per label. Each fixed physical derivative of its two flat remainders is smaller than each power of $\hat{t}$. The initialized pressure includes the full P_C

of (2.15.11), and its radial cancellation is (2.15.13). The added pressure moment (2.15.16) enters the actual states before the finite return.

Thus (2.18.1) is the ordinary three-component equation. It has no uncanceled slow radial source. The fixed reference force equals the slow smooth residual $\mathbf{f}_s$: (2.15.19) records that the preliminary mean-force adjustment is identically zero. Initialization uses the one uncut state map (2.15.18) and one finite cycle, not an additional infinite diagonal. Lemma 2.17.4 proves that its three finite error terms vanish on a fixed open core around the axis. Proposition 2.11.4 supplies the smooth slow reference force.

We fix once and for all an enclosing profile bound

$$\begin{aligned} X_{\mathrm{all}} > \max\{&\tfrac{\hat\xi_P^2}{2},\ \text{all leading meridional and spectral returns,}\\ &\text{mean/packet hulls, } \tfrac{\left(\hat\xi^+_{\mathrm{lead}}\right)^2}{2},\ \tfrac{\hat\xi_W^2}{2},\ B\}. \end{aligned} \tag{2.18.2}$$

Here $\frac{\hat\xi_P^2}{2}$ is after the last leading return, $\frac{\left(\hat\xi^+_{\mathrm{lead}}\right)^2}{2}$ is the forward heat onset (2.18.3) and $\frac{\hat\xi_W^2}{2}$ is the support radius of the forward weight (Proposition 2.3.9(W4)); Lemma 2.18.1 lists the supports of all pieces. The last entry B is the outer edge of the backward member, also written $\frac{\hat\xi_b^2}{2}$ in Section 2.7.1 and Lemma 2.8.9. It is a scalar fixed with the leading member (statement (S2) of Lemma 2.3.5), so this choice of $\frac{\hat\xi_{\mathrm{all}}^2}{2}$ is still made once, before the finite iteration. On $t<0$, in the backward chart $\hat\xi = r/\sqrt{\hat t_b}$, B bounds the backward pressure hull $\frac{\hat\xi_{\mathrm{ret}}^2}{2}$, the backward packet and mean supports and the backward heat onset (Lemma 2.8.9). The full third slow moment makes the pressure constant zero only after that hull. Each mean pressure primitive uses the full path between the supports, even beyond the early velocity correction region. The genuine positive saturation is Proposition 2.3.2.

We insert no positive weight in an actual zero-stress heat gap. The central wing bound is fixed with the leading data. Equations (2.18.3) and (2.18.2) give $\mathcal{B}_o(\hat\zeta) \le \mathcal{B}_{\max} \le X^+_{\mathrm{lead}} < X_{\mathrm{all}}$. The enclosing bound X_{all} is independent of the finite iteration index. We impose no new pressure cutoff at the early correction region or same pre-heat separator on all angular fibers.

2.18.2 Heat-exterior radii and the spatial support of the background

Write $X = \hat\xi^2/2$. We record the radii used in Lemma 2.8.9 and Proposition 2.18.5. The leading radii are fixed in the order of Theorem 1(iii). We write $\hat\xi = r/\sqrt{\hat t_f}$ on $t>0$ and $\hat\xi = r/\sqrt{\hat t_b}$ on $t<0$, $d = 1-\hat\zeta^2$, and $y_p = 2\log(\hat\xi/\hat\xi_p(\hat\zeta))$ with the pulse-entry graph $\frac{\hat\xi_p^2}{2}$ ($\hat\xi_p = \hat\xi_{p,b}$, a scalar, in the backward chart; y_p is chart-covariant, see the paragraph before the radial order (O1)–(O8) preceding (2.3.5)). A leading member is *the exact heat exterior* on a set if there $U = \mathfrak{M}_1 = \mathfrak{M}_3 = 0$, the histories are canonical, $\mathfrak{M}_4 = \int_{(\frac{\hat\xi^2}{2})}^{\infty} H^2/(4s)\,\mathrm{d}s$ and $P = -\int_{(\frac{\hat\xi^2}{2})}^{\infty} H^2/(4s^2)\,\mathrm{d}s$, and

- on $t>0$: $H = d^{-h} g_*(\frac{\hat\xi^2}{2}/d)$ with $g_* = c_{\mathrm{bank}} g_h + k_f g_f$, the heat pair (2.3.32) (Lemma 2.3.20); both components of the forward member end in this same pair by Theorem 1(ii);
- on $t<0$: $H = c(\hat\xi/\sqrt{2})^{-2h}\mathcal{H}_-(4d/\hat\xi^2)$ with the scalar c of Lemma 2.3.5 and the positive Laplace factor (2.3.29).

The physical field of an exact heat exterior is the z-independent pure swirl with its outward centrifugal pressure; it solves the Navier–Stokes equations with zero force (proof of Proposition 2.8.6(b); proof of Lemma 2.8.9(a)).

Put

$$X^{+}_{\mathrm{lead}} := \max\Big\{M \max_{[-1,1]} R_o,\ \mathcal{B}_{\max},\ \sup_{\hat\zeta} B_{\mathrm{f}}(\hat\zeta)\Big\}. \tag{2.18.3}$$

Here R_o is the inlet graph of the future, $M \geq 4$ bounds its normalized radius, and $\mathcal{B}_{\max}$ bounds the central wing edge. The outer wing ends at $B_{\mathrm{f}}(\hat\zeta)$, a fixed multiple of $\lambda_{\mathrm{ch}}(\hat\zeta)^{-1}$ on the forward endpoint band. Its backward edge B is constant by (S2) of Lemma 2.3.5. These are the leading radii supplied by Theorem 1(iii).

Lemma 2.18.1 (Heat-exterior radii and spatial support)**.**

(a) Forward leading member. *At the end of step 6 of Theorem 1(iii), the departures from the exact heat exterior in rows F1–F13 of Table 2.6 have support in* $\{X \leq X^{+}_{\mathrm{lead}}\}$. *With or without the spectral layers of step 6, the forward member agrees with the exact heat exterior on* $X \geq X^{+}_{\mathrm{lead}}$, *with all jets agreeing at* $X = X^{+}_{\mathrm{lead}}$. *The ratio* $\frac{\left(\hat\xi^{+}_{\mathrm{lead}}\right)^2}{2}/\max R_o$ *is bounded by constants fixed in steps 1–3 (input (I1)), and* $\frac{\left(\hat\xi^{+}_{\mathrm{lead}}\right)^2}{2}$ *is fixed in step 4, with the master scale* C. *Steps 5 and 6 do not change it.*

(b) Backward leading member. *The departures from the exact heat exterior in rows B1–B10 have support in* $\{X \leq B\}$. *The backward member agrees with the exact heat exterior on* $X \geq B$, *with all jets agreeing at* $X = B$. *The ratio* B/R_e *is fixed in steps 2–3, the ratio* $R_e/(CP_*)^{10}$ *in step 4 before* C, *and* B *with* C *in step 4, before step 5.*

(c) Leading stress, weight and cutoff. *On* $t > 0$, $T_0 = 0$, $\mathsf{W} = 0$, $\mathsf{W}_* = 0$ *and* $\vartheta_q = 0$ *on* $\{\frac{\hat\xi^2}{2} \geq \frac{\hat\xi^2_W}{2}\}$, *where* $\frac{\hat\xi^2_W}{2}$ *is the support radius of Proposition 2.3.9(W4). By the proof of (W4),* $\frac{\hat\xi^2_W}{2}$ *is the largest of the edges* R_0*-end,* R_1*-end,* $d(R_b + \frac{3}{4}W_s)$, $\mathcal{B}_{\max}$ *and* B, *all radii of the leading member, so* $\frac{\hat\xi^2_W}{2}$ *is a step-4 radius, although the weight itself is built in step 7. On* $t < 0$ *the same holds on* $\{\frac{\hat\xi^2}{2} \geq B\}$, *with* W_b *in place of* W.

(d) Completion. *Let* $\frac{\hat\xi^2_{\mathrm{all}}}{2}$ *be the bound (2.18.2), fixed in step 7; it exceeds* $\frac{\left(\hat\xi^{+}_{\mathrm{lead}}\right)^2}{2}$, $\frac{\hat\xi^2_W}{2}$, $\frac{\hat\xi^2_P}{2}$ *and* B. *On each side of* $t = 0$, *on* $\{\frac{\hat\xi^2}{2} \geq \frac{\hat\xi^2_{\mathrm{all}}}{2}\}$*: every positive-order slow coefficient and stress vanishes; the slow reference* $(u_s, \pi_s, K_{\mathrm{B}})$ *is the leading exact heat exterior, with* $K_{\mathrm{B}} = 0$ *and* $\mathbf{f}_s = 0$*; every finite correction of the joint algorithm vanishes (the packets with their potentials and oscillatory pressures, the initialization, every mean increment with its pressure and roots, the reservoir* d_*, *the flat remainders* $G_{\mathrm{flat}}, \mathsf{B}_{\mathrm{flat}}$, *and the cut increments (2.18.6)); and* (u_∞, p_∞) *is the physical exact heat field, with* $\mathbf{f}_\infty = 0$. *In physical variables* $\{\frac{\hat\xi^2}{2} \geq \frac{\hat\xi^2_{\mathrm{all}}}{2}\}$ *is* $\{r^2 \geq 2\frac{\hat\xi^2_{\mathrm{all}}}{2}\hat t_f\}$ *on* $t > 0$ *and* $\{r^2 \geq 2\frac{\hat\xi^2_{\mathrm{all}}}{2}\hat t_b\}$ *on* $t < 0$.

(e) Spatial support of the completed background. *Let* $0 < a < b < R_*$, *the cutoff* χ_{loc} *and the connected annulus* $\mathcal{O} \Subset B_{R_*}\setminus\{0\}$ *be those of the localization (2.18.23), and put* $K := \overline{B_b} \cup \overline{\mathcal{O}}$, *a compact subset of* B_{R_*}. *The localized background* $(u, p, \mathbf{f})$ *satisfies* $\operatorname{supp} u(t), \operatorname{supp} p(t), \operatorname{supp} \mathbf{f}(t) \subset K$ *for every* $t \neq 0$ *of the construction interval, on* both *sides of* $t = 0$*; the trace* u_0 *is supported in* K*; and the extension of* $\mathbf{f}$ *through* $t = 0$ *keeps its support in* K. *The numbers* R_*, a, b, *the cutoff* χ_{loc} *and* $\mathcal{O}$ *are fixed once for both sides, in step 7, after* $\frac{\hat\xi^2_{\mathrm{all}}}{2}$ *and the sequence* δ_n *(Section 2.18); they do not depend on* n *or on the side.*

Table 2.6: Supports of the pieces of the two members and of the completion. "Step" is the step of the parameter ordering of Theorem 1(iii) at which shape and relative position are fixed; physical radii of rows F and B scale with $\frac{\hat{\xi}_p^2}{2}$ and R_o and are fixed with C in step 4.

row	piece	support	step	input
F1	core, five-moment core correction, pressure bank, activation and termination, $G_i \to G$ annulus	$y_p < 0$: before the growth arc and the exact wait $\{-W \le y_p \le 0\}$	4, 5	Theorem 1(iii), forward support layout
F2	capped loop	$Y_{\mathrm{sh}} \subset \{y_p < -W + 1\}$	6	
F3	five restoration returns	$-25 < y_p < -20$	6	
F4	three-E heat bank	$-20 < y_p < -15$	3–4	
F5	two-row I/C_p taper	$-2.15 < y_p < -0.85$	3	
F6	pulse and its returns (they change U only)	$0 \le y_p < Y(\hat{\zeta}) - 0.7$, $\frac{\hat{\xi}_p^2}{2} e^Y = R_o$	3	
F7	A10 transition, flattening, A11 edits	between R_o and the A11 outlet R_A; the A11 bumps have fixed relative supports ending before R_A	2	
F8	rank-one bump	$(\frac{1}{2}\frac{\hat{\xi}_b^2}{2}, \frac{3}{4}\frac{\hat{\xi}_b^2}{2})$, $\frac{\hat{\xi}_b^2}{2} = R_A e^{L_o} < R_0$	2	
F9	heat collar	$[R_0, 2R_0]$	2	
F10	outer wing correction $-\rho H^{\mathrm{heat}} \Psi(X/B_{\mathrm{f}})$	$[2R_0, B_{\mathrm{f}}]$	2	
F11	central future: memory return, hold, deficit drive, stop/shot, blend, lift, central wing	$[R_m, 2R_m]$, then $x \le M$. Wing support in $\{\psi_o > 0,\ X < \mathcal{B}_o(\hat{\zeta})\}$, $\mathcal{B}_o \le \mathcal{B}_{\max}$	2	
F12	inlet-germ connector	$1 \le x \le e^{\epsilon_g}$	3	
F13	spectral layers: main layer, controls (curvature control included), five spectral returns, exponentially small controls	inside the central hold, in the central even collar, before the deficit drive; hence $x \le M$	6	Theorem 1(iii),(v)
B1	core and core-side corrections, activation, termination, $G_i \to G$ annulus	$[0, \frac{\hat{\xi}^2_{\mathrm{match}}}{2}]$ and $y_p < -W - T$	4, 5	Theorem 1(iii), backward support layout
B2	capped loop	$y_p < -W + 1$	6	
B3	restoration returns	$-25 < y_p < -20$	6	
B4	three-E heat bank	$-20 < y_p < -15$	3–4	
B5	forward two-row taper (absent here)	$\varnothing$	—	
B6	pulse and its two returns (U only)	$0 \le y_p$, $\frac{\hat{\xi}^2}{2} < \frac{\hat{\xi}^2_{\mathrm{ret}}}{2} = R_e e^{-0.7}$	3	Lemma 2.3.3(S4)
B7	flattening and A11 edits	$[R_e, R_A)$	2	
B8	rank-one bump	$(\frac{1}{2}\frac{\hat{\xi}_b^2}{2}, \frac{3}{4}\frac{\hat{\xi}_b^2}{2}) \subset (R_A, R_0)$	2	
B9	heat collar	$[R_0, 2R_0]$	2	
B10	wing correction $-\rho H_0 \Psi(X/B)$	$[2R_0, B]$, $B > e^4 R_0$	2	Lemma 2.3.4(d)

row	piece	support	step	input
C1	positive-order slow coefficients	$t>0$: E_n,U_n,V_n,M_n in $\hat\xi<\hat\xi_v(\hat\zeta)$, P_n in $\hat\xi<\hat\xi_P$; $t<0$: $\frac{\hat\xi^2}{2}<\frac{\hat\xi_{p,b}^2}{2}e^{-9}$, P_n in $\hat\xi<\hat\xi_{\mathrm{ret}}$, T_1 in $[\frac{\hat\xi_-^2}{2},B]$	7	(2.6.21), (2.6.28); Proposition 2.7.2(b), (c)
C2	weight, cutoff ϑ_q, packets	$t>0$: $\hat\xi\le\hat\xi_W$; $t<0$: $X\le B$	7	Proposition 2.3.9(W3)–(W4), (2.13.10); Lemma 2.8.9(a)
C3	mean frame, bumps k, radial cutoff transition	$-8<y_p<-3$	7	(2.14.11)
C4	all finite corrections and cut increments	$\hat\xi<\hat\xi_{\mathrm{all}}$ (both sides)	7	part (d); Lemma 2.8.9(b)
C5	localized background $(u,p,\mathbf{f})$	$K=\overline{B_b}\cup\overline{\mathcal{O}}\subset B_{R_*}$	7	(2.18.23); part (e)

Proof. (a)–(b), leading exteriors and choice order. Table 2.6 records the supports and suppliers of the leading pieces. For the forward ideal future, the central component equals the selected heat pair beyond $\mathcal{B}_{\max}$, and the outer component equals it beyond B_{f} because $\Psi(\frac{\hat\xi^2}{2}/B_{\mathrm{f}})=0$. Their complete moment identities give the canonical $\mathfrak{M}_2,\mathfrak{M}_4,P$ there. The later core, loop, bank and restoration edits lie before $\frac{\hat\xi_p^2}{2}<R_o$ and restore their moments; the spectral edits and returns lie in the central hold, before MR_o. Consequently neither the fields nor their canonical constants change beyond $\frac{(\hat\xi_{\mathrm{lead}}^+)^2}{2}$.

The backward edits in rows B1–B6 end before $\frac{\hat\xi_{\mathrm{ret}}^2}{2}<R_e$, and rows B7–B9 end by $2R_0<B$. On the last wing $H-H_0=-\rho H_0\Psi(X/B)$. Since $H_0>0$ and $\Psi(1-u)>0$ for small $u>0$, its support contains $X=B$. All derivatives of this difference vanish there because Ψ is smooth and zero on $[1,\infty)$. Lemma 2.3.5 gives the heat field and canonical histories on $X\ge B$. On each time side the fields and histories are smooth at the radial edge, so their equality on the open exterior gives equality of all jets at the edge. For the choice order, M, $\mathcal{B}_{\max}/R_b$ and the normalized terminal ratios are fixed in steps 1–3, while R_o,R_b,R_A scale with $(CP_*)^{10}$. On the backward side,

$$R_A=k_AR_e,\qquad R_0=R_Ae^{L_o+\delta},\qquad B=R_0\Big(\frac{b(1-\rho)}{\rho m_h}\Big)^{1/(1-h)}.$$

The fixed transfers and Y_{end} determine these ratios before C. With $R=(CP_*)^{10}$ the outlet formula for the selected member gives

$$\frac{R_e}{R}=s_b\frac{\hat\xi_i^2}{2}e^T\lambda^{-60}e^{Y_{\mathrm{end}}},$$

whose right side is fixed in the parameter ordering of Theorem 1(iii). Thus both enclosure radii are fixed with C in step 4. Subsequent activation, loop and spectral changes remain inside them.

(c). Proposition 2.3.9(W3)–(W4) gives $T_0=\mathsf{W}=0$ beyond $\frac{\hat\xi_W^2}{2}$ and hence $\mathsf{W}_*=\vartheta_q=0$. Its listed edges are leading-member radii. The backward assertion is Lemma 2.8.9(a).

(d). On $\hat\xi\ge\hat\xi_{\mathrm{all}}$, parts (a)–(c) and (2.6.21) remove every positive-order slow field, including the late P_1,P_2. The stresses of order at least two vanish beyond $\frac{\hat\xi_P^2}{2}$; the exceptional stress (2.6.28) vanishes in the exact heat exterior by the z-independence of that field. Thus $K_{\mathrm{B}}=\mathbf{f}_s=0$ there.

The support induction of Lemma 2.8.9(b) applies on either side: every wave potential and oscillatory pressure carries a positive power of ϑ_q; the mean cutoff and bumps vanish beyond

$y_p = -3$; compensated pressure primitives have zero outer endpoints; rationalized roots vanish with their source. Finally, the zero full flux (2.18.4) makes the potential of each cut increment vanish outside the same hull. These operations therefore preserve exterior vanishing at every finite stage and in the final locally finite sum. The remaining field is the exact heat solution. The physical description follows from $\hat{\xi} = r/\sqrt{\hat{t}}$.

(e). Formula (2.18.23) gives $u = \chi_{\mathrm{loc}} u_\infty - b_{\mathrm{loc}}$ and $p = \chi_{\mathrm{loc}} p_\infty$. The cutoff is supported in B_b and the fixed divergence inverse has support in $\mathcal{O}$, so both fields and their local differential residual $\mathscr{N}(u,p)$ are supported in K. Their trace and time extension retain this spatial support. The same cutoff and inverse are selected once after $\frac{\hat{\xi}_{\mathrm{all}}^2}{2}$ and the diagonal support buffers; they do not depend on the stage or side. □

On a dyadic band $Q \asymp \hat{t}$, let $\rho_Q = Q^h$ and let $S \asymp 1 + \log^{6/5}(1/Q)$. Our coefficient seminorms include ordinary slow and same-torus derivatives and all radial prefixes used by the mean map. They also include the sum of absolute harmonic coefficients, with weight $(1+|m|)^j$ at order j. We convert the finitely many adjacent band normalizations to this Q.

Label counts along a fixed radial hull use only powers of S. All these seminorms are finite for a fixed state and a fixed j. Their constants can depend on the stage.

The weight estimates of Section 2.6 imply

$$\mathsf{W}^{\epsilon}\big(1+\log(1/\mathsf{W})\big)^{N} \le C_{\epsilon,N} \quad (\epsilon > 0,\ N < \infty).$$

Applied to the differentiated coefficients, this removes the edge weights with no change to their power of ρ_Q. We do not use derivatives of a distance to the union of zero faces. The Gaussian factor is at most one.

Lemma 2.18.2 (Physical derivative bridge)**.** *On the fixed closed enlarged band annulus $0 < \mathsf{R}_- \le \mathsf{R} \le \mathsf{R}_+$, for local labels on comparable bands, keep Q frozen while differentiating. At every fixed physical order j and $e \ge 0$, a band object with physical prefactor Q^{-e} satisfies*

$$|\partial_{\mathrm{phys}}^{\le j} g| \le C_{j,e} Q^{-e-3j} \mathcal{N}_j(g).$$

Here $\mathcal{N}_j$ is the carrier-aware coefficient seminorm defined in Lemma 2.17.1, including the sum over active labels and harmonics. The derivative loss is independent of the finite stage and its harmonic count. The relevant exponents are $e = (\frac{1}{2} + h)$ for velocity, $e = 2(\frac{1}{2} + h)$ for pressure and stress, and $e = 2(\frac{1}{2} + h) + \frac{1}{2}$ for force.

Proof. Lemma 2.17.1 proves the claim from the frozen evaluated operators and the original phase estimates. At order zero the triangle inequality has no logarithmic loss. At positive order the strict margin $3 - (1 + 5h/2) > 0$ absorbs the fixed logarithms. The band is frozen during differentiation. The annular restriction is supplied for the finite errors by Lemma 2.17.4; slow coefficients reaching the axis use Proposition 2.17.3 instead. □

2.18.3 Cutoffs which keep the exact divergence

The genuine increments are

$$\Delta u_{M,n} = u_M^{[n+1]} - u_M^{[n]}, \qquad \Delta w_n = w^{[n+1]} - w^{[n]} = \nabla \times \mathcal{A}_n, \qquad \Delta p_n = p^{[n+1]} - p^{[n]}.$$

The potential $\mathcal{A}_n$ includes all homogeneous and inhomogeneous packet corrections. Each mean increment satisfies

$$\operatorname{div} \Delta u_{M,n} = 0, \qquad \int_0^\infty r(\Delta u_{M,n})_z(r,z,t)\,\mathrm{d}r = 0. \tag{2.18.4}$$

The second identity is the full sampled moment, rather than only its auxiliary Haar projection. The auxiliary mean map enforces it by its complete-moment subtraction, the state map has an exact zero-flux row, and the radial feedback is pure swirl. Thus each component of the finite return keeps (2.18.4).

We fix $\chi \in C^\infty([0,\infty);[0,1])$ that equals one on $[0,1]$ and zero on $[2,\infty)$. We take the cutoff of (2.6.31), so that $\chi(s) = \chi_{\mathrm{O}}(s/2)$ (Remark 2.20.8). We set $\chi_n = \chi(\widetilde{q}/\delta_n)$. We use the same physical gauge from (2.10.1) on the two sides:

$$\widetilde{q} = q_b \quad (t<0), \qquad \widetilde{q} = q_f/L(\hat{\zeta}_f) \quad (t>0), \qquad L = L_{\mathrm{cut}} = \lambda_{\mathrm{ch}} \text{ on endpoint neighborhoods.} \tag{2.18.5}$$

Here $0 < L_- \le L \le L_+ < \infty$ is fixed, and $\widetilde{q}$ is independent of r, θ and the auxiliary variables.

By Lemma 2.3.1 each χ_n is one C^∞ function across $t = 0$ for $z \neq 0$, with all normal jets. The alternative $\chi(\lambda_{\mathrm{ch}} q_f/\delta_n)$ is not smooth there. This same gauge determines the physical dyadic labels, rounding, centers, and auxiliary covers before this step. They are not independently rounded again from q_f.

All the band estimates use $Q \asymp \widetilde{q} \asymp q$ with fixed comparison constants. We define

$$\begin{aligned}
(\widetilde{\Delta u}_{M,n})_{\theta,z} &= \chi_n (\Delta u_{M,n})_{\theta,z}, \\
(\widetilde{\Delta u}_{M,n})_r &= \chi_n (\Delta u_{M,n})_r - \frac{\partial_z \chi_n}{r} \int_0^r s (\Delta u_{M,n})_z(s,z,t)\, \mathrm{d}s, \\
\widetilde{\Delta w}_n &= \nabla \times (\chi_n \mathcal{A}_n), \qquad \widetilde{\Delta p}_n = \chi_n \Delta p_n.
\end{aligned} \tag{2.18.6}$$

Because $\widetilde{q}$ is independent of r, θ, the radial divergence of the added prefix is $-(\partial_z \chi_n)(\Delta u_{M,n})_z$. It cancels with zero remainder $\mathrm{div}(\chi_n \Delta u_{M,n})$.

The prefix vanishes before and after the same radial hull by (2.18.4). It thus creates no exterior radial tail. All fields extend smoothly by zero across their genuine support edges.

For the wave cutoff,

$$\widetilde{\Delta w}_n = \chi_n \Delta w_n + \nabla \chi_n \times \mathcal{A}_n. \tag{2.18.7}$$

Its extra normalized velocity coefficient has the factor $\rho_Q(\partial_{\mathsf{Z}} \chi_n)$ times a potential coefficient of order $\alpha_n + 1/2$. It has order $\alpha_n + 3/2$, zero axial component, and zero cylindrical angular mean. Thus we keep all cutoff curls, with their radial components.

The mean prefix in band coordinates is

$$-\rho_Q(\partial_{\mathsf{Z}} \chi_n) \mathsf{R}^{-1} \mathcal{L}(\mathsf{R}\gamma_n),$$

where γ_n is the normalized axial increment. The physical integral at fixed (z,t) samples its integrand at $\mathsf{y} + \lambda(s^{d_r} - \mathsf{R}^{d_r}) v_r$ in the lift (2.14.8). Set $p = \alpha_n + 1/2$ and split $\gamma_n = \gamma_{n,\mathrm{H}} + \gamma_n^\perp$ by Π. The Haar term is the axial seed of Lemma 2.14.3 at order p. Its first row (2.14.48) is $\int \mathsf{R}\gamma_{n,\mathrm{H}}\, \mathrm{d}\mathsf{R} = 0$. The fluctuating term is the zero-Haar axial seed of (2.14.33) at $s_* = p - \varkappa$, with $\mathcal{J}(\mathsf{R}\gamma_n^\perp) = 0$. The other two mean increments in (2.15.47) change only the swirl component of the velocity. On both time sides the zero-moment identities give

$$\mathcal{L}(\mathsf{R}\gamma_{n,\mathrm{H}}) \in \mathcal{M}^p, \qquad \mathcal{L}(\mathsf{R}\gamma_n^\perp) = -\mathcal{I}_\chi(\mathsf{R}\gamma_n^\perp) \in \mathcal{M}^{s_*+\varkappa} = \mathcal{M}^p. \tag{2.18.8}$$

For the first bound the shift acts trivially, so the inward and outward ordinary tails agree up to sign. The second is (2.14.13) on $\mathcal{V}_{\mathrm{int}}$. Since R^{-1} is bounded on the prefix hull, its prefactor ρ_Q gives the cut radial mean order $p + 1 = \alpha_n + 3/2$, the same as the term $\chi_n(\Delta u_{M,n})_r$ by (2.15.47).

All fixed ordinary coefficient derivatives of χ_n are uniform in Q, δ_n: on their support $Q/\delta_n = (\widetilde{q}/\delta_n)/(\widetilde{q}/Q)$ stays bounded, and the band atlas has bounded fixed jets. Thus the cut velocity and normalized pressure increments have seminorm bounds

$$C_{n,j}\rho_Q^{\alpha_n} S^{B_{n,j}}, \tag{2.18.9}$$

while the distinct radial mean bound keeps $\rho_Q^{\alpha_n+3/2}$. The constants include the fixed-order harmonic weights.

2.18.4 A locally finite sum

For each n, we select an admitted native-q threshold $a_n > 0$ for the two finite states in the n-th increment. It must also cover the increment's potential, pressure, radial prefixes, and all value margins. The finite construction provides these objects on $0 < q < a_n$, with the closed angular endpoints included. We do not claim a lower bound uniform in n.

Let $q_{\mathrm{base}} > 0$ be a fixed admitted threshold for the initialized state $(u^{[0]}, p^{[0]})$. We select δ_n successively, with $\delta_n \le \delta_{n-1}/4$, and impose the strict support buffer

$$2C_L\delta_n < a_n, \tag{2.18.10}$$

where C_L bounds $q/\widetilde{q}$ on the two sides. Thus evaluate each nonzero cutoff or cutoff derivative strictly in that increment's admitted domain. For $j \le \max(n, 80)$ impose on $\widetilde{q} \le 2\delta_n$

$$C_{n,j}\rho_Q^{\alpha_n} S^{B_{n,j}} \le 2^{-n-4}\rho_Q^{\beta_n}. \tag{2.18.11}$$

We enlarge these finite constants to include each specified coefficient, pressure, potential, full radial-prefix and weighted harmonic seminorm through order $\max(n, 80)$, on the two sides. We include in this same finite list the admitted finite-stage pure-auxiliary Gevrey radii/norms and all current value margins. We do not infer them from a fixed ordinary derivative count. These are constraints for each finite stage and finite prefix, not convergence in one Gevrey Banach space.

We impose also the radial budget

$$C^r_{n,j}\rho_Q^{\alpha_n+3/2} S^{B^r_{n,j}} \le 2^{-n-4}\rho_Q^2.$$

Its spare exponent is $\alpha_n - \frac{1}{2} \ge \frac{1}{2} - 3\varkappa > 0$. The velocity and pressure budget (2.18.11) has spare exponent $\alpha_n - \beta_n = \varkappa > 0$. For fixed $h > 0$, a positive power of q^h dominates each fixed logarithm as $q \downarrow 0$.

We can thus impose these finite conditions simultaneously for all smaller q. No bound uniform in n or in h is necessary. This is one last packet/mean diagonal. The independent slow Borel sum of Proposition 2.10.1 precedes the atlas. It is not a preliminary infinite mean iteration.

Derivative or flatness claims after this step use a finite prefix of this same completed sum. They do not select a new cutoff sequence or a different completed member.

The selected ordinary reservation. We fix $J_{\mathrm{src}} = 80$ ordinary coefficient levels for the source export and $J_{\mathrm{prep}} = 72$ for the finite preparation. At each stage the finite list just specified includes these eighty levels. For stages greater than eighty it continues to increase with the stage. The finite-stage construction supplies each prescribed finite list. Thus the same positive spare powers permit this choice before we fix the single sequence δ_n.

For a demanded physical output norm, we select a sufficiently long finite prefix in (2.18.13). This same diagonal controls the remaining tail in that norm. We use one completion and keep the

leading source, activation, and spectral selection unchanged. The preparation uses at most fifty-nine stress levels, eight return levels, and two output levels.

At most two more source-band connections give $69 + 2 \le 72$. The allocation with three intermediate derivatives and two output derivatives gives $59 + 8 + 3 + 2 = 72$. Eight ordinary levels remain between the prepared reservation and the source export. These spare regularity levels do not create extra $\rho^{-\varkappa}$ factors: the coefficient loss comes only from the operations performed. The pure-auxiliary Gevrey estimates and the weighted radial ladder are distinct inputs.

This ordinary derivative bound does not imply them.

We extend each cut increment by zero beyond its admitted domain. This is a genuine smooth extension, not an extension of the uncut finite states. $\hat{t}/\widetilde{q} \le C_L$ implies that χ_n and all its derivatives are identically zero whenever $\hat{t} > 2C_L\delta_n$. By (2.18.10), there is an open zero buffer before the boundary $\hat{t} = a_n$.

At the cutoff boundary $\widetilde{q} = 2\delta_n$, the smooth function χ and all its derivatives vanish. The uncut coefficients have a neighborhood as their domain. Radial prefixes keep $\hat{t}, \hat{\zeta}$ fixed, so the same buffer applies to the mean flux correction. The curl formula keeps all cutoff derivatives. The endpoint argument after this proves the stated one-sided smoothness at $t = 0$ on these admitted domains.

We select the fixed physical construction ball and T so that $\hat{t} < \hat{t}_{\mathrm{base}}$ there, and put

$$u_\infty = u^{[0]} + \sum_{n\ge 0}(\widetilde{\Delta u}_{M,n} + \widetilde{\Delta w}_n), \qquad p_\infty = p^{[0]} + \sum_{n\ge 0}\widetilde{\Delta p}_n. \tag{2.18.12}$$

On a neighborhood of each point with $\hat{t} > 0$, only finitely many terms are nonzero. The fields are smooth there. The identity $\operatorname{div} u_\infty = 0$ holds. Near the physical axis the corrections vanish, and the unchanged core supplies Cartesian smoothness.

At positive time this construction covers the whole physical $\hat{\zeta}$-interval. It uses no angular cutoff of the velocity.

For a fixed N, all χ_n, $n < N$, equal one at sufficiently small $\hat{t}$. Their sum then equals the finite state $(u^{[N]}, p^{[N]})$. If $N \ge j$, (2.18.11) gives the coefficient tail bound

$$\|\text{tail from } N\|_j \le 2^{-N-3}\rho_Q^{\beta_N}.$$

Lemma 2.18.2 gives, for each fixed m and sufficiently large fixed N,

$$\begin{aligned} |\partial_{\mathrm{phys}}^{\le m}(u_\infty - u^{[N]})| &\le C_{N,m}\hat{t}^{h\beta_N - (\frac{1}{2}+h) - 3m}, \\ |\partial_{\mathrm{phys}}^{\le m}(p_\infty - p^{[N]})| &\le C_{N,m}\hat{t}^{h\beta_N - 2(\frac{1}{2}+h) - 3m}. \end{aligned} \tag{2.18.13}$$

For a smaller fixed N, we consider the finitely many indices less than m. Their original estimates and the positive spare exponent $\varkappa$ give their bounds.

2.18.5 The ordinary residual and its smooth extension

Proposition 2.17.5 proves, on the support of the tail and including the spatial axis,

$$|\partial_{\mathrm{phys}}^{\le m} u^{[N]}| \le C_{N,m}\hat{t}^{-\frac{1}{2}-h-3m}.$$

Its force-scale bridge argument and (2.18.1) give

$$|\partial_{\mathrm{phys}}^{\le m}[\mathcal{N}(u^{[N]}, p^{[N]}) - \mathbf{f}_{\mathrm{ref}} - G_{\mathrm{flat},N} - \operatorname{div} B_{\mathrm{flat},N}]| \le C_{N,m}\hat{t}^{h\alpha_N - K_m}, \quad K_m = 2(\tfrac{1}{2}+h) + 3m + 4. \tag{2.18.14}$$

This loss includes the derivative of the kept cross stress.

We set $v_N = u_\infty - u^{[N]}$ and $\pi_N = p_\infty - p^{[N]}$. Exact subtraction gives

$$\mathscr{N}(u_\infty, p_\infty) - \mathscr{N}(u^{[N]}, p^{[N]}) = \partial_t v_N - \Delta v_N + (u^{[N]} \cdot \nabla) v_N + (v_N \cdot \nabla) u^{[N]} + (v_N \cdot \nabla) v_N + \nabla \pi_N. \tag{2.18.15}$$

It includes all interactions between different stages, all cutoff commutators and the full pressure-cutoff gradient. The Laplacian term has loss at most $(\frac{1}{2} + h) + 3m + 6$, mixed convection at most $2(\frac{1}{2} + h) + 3m + 3$, and the pressure term at most $2(\frac{1}{2} + h) + 3m + 3$.

The tail-square term has the additional nonnegative exponent $h\beta_N$. Thus

$$|\partial_{\mathrm{phys}}^{\le m}[\mathscr{N}(u_\infty, p_\infty) - \mathscr{N}(u^{[N]}, p^{[N]})]| \le C_{N,m} \hat{t}^{h\beta_N - H_m}, \qquad H_m = 2(\tfrac{1}{2} + h) + 3m + 7. \tag{2.18.16}$$

The loss H_m does not depend on N.

Given m and an integer L_0, first fix N so large that

$$h\beta_N - H_m > L_0, \qquad h\alpha_N - K_m > L_0.$$

Then restrict $\hat{t}$ to less than the finitely many thresholds for this prefix. Its two flat remainders satisfy each fixed physical power estimate. Equations (2.18.14) and (2.18.16) prove

$$|\partial_{\mathrm{phys}}^{\le m} \mathscr{E}_\infty| \le C_{m,L_0} \hat{t}^{L_0}, \qquad \mathscr{E}_\infty = \mathscr{N}(u_\infty, p_\infty) - \mathbf{f}_{\mathrm{ref}}. \tag{2.18.17}$$

This argument uses only the remainders of one fixed finite state. This argument uses no infinite sum of flat remainders.

We next check the actual boundary jets. If $z \neq 0$ at $t = 0$, Proposition 2.8.6 gives one-sided smooth velocity, pressure and residual on a neighbourhood of the point in the closed half-space. If $z = 0, r > 0$, the point lies in the exact heat exterior for all sufficiently small positive times. There the physical swirl includes the two heat modes:

$$u_\theta^{\mathrm{heat}} = \frac{t^{-h}}{r} \left[c_{\mathrm{bank}} g_h\left(\frac{r^2}{2t}\right) + k_f g_f\left(\frac{r^2}{2t}\right) \right], \tag{2.18.18}$$

where $k_f > 0$ is the fast coefficient produced by the shot.

The fast term and all its fixed physical derivatives are exponentially small as $t \downarrow 0$ on compact positive radial intervals. The heat-exterior estimates in Theorem 1(ii) give all one-sided jets on compact positive radial intervals. Its meridional components vanish. The pressure uses the exterior normalization, so its radial tail and all these jets also converge.

The finite pressure corrections vanish there. These local descriptions agree on their overlaps.

The defining equation for $\hat{t}$ gives

$$|z|^{1/(\frac{1}{2}-h)} + t \le \hat{t}(z,t) \le |z|^{1/(\frac{1}{2}-h)} + \frac{t}{1-2h}. \tag{2.18.19}$$

the derivative of $\hat{t} - z^2 \hat{t}^{2h}$, at arguments greater than its positive zero, lies between $1 - 2h$ and one. Near the spacetime origin, $\hat{t} \le C|(x,t)|$. By (2.18.17), each physical derivative of $\mathscr{E}_\infty$ thus extends continuously to zero there with zero jet. Together with the off-origin jets, Taylor's integral formula on the closed half-space verifies their compatibility at each finite order. Thus $\mathscr{E}_\infty$, and thus $\mathbf{f}_\infty = \mathbf{f}_{\mathrm{ref}} + \mathscr{E}_\infty$, is smooth up to $t = 0$.

For the selected two-sided member, Theorem 2.7.1 and Proposition 2.20.4 give the actual backward jets of this force. The matching traces give smoothness of the joined force across $t = 0$. For a one-sided construction, Lemma 2.8.2 gives a smooth extension after localization and bounds it at each finite C^k order.

At nonzero initial spatial points, we use the actual boundary jets. We do not claim that they vanish.

2.18.6 A strong local trace on a fixed physical ball

The full $\hat{\zeta}$-domain, together with (2.18.19), supplies the construction on $B_{R_*} \times (0,T]$ for sufficiently small fixed $R_*, T > 0$. We define $\mathfrak{d}(x) = r^2 + |z|^{1/(\frac{1}{2}-h)}$. $Cq^{-\frac{1}{2}-h}$ bounds the slow field on its bounded profile hull. Its radial component has the smaller prefactor $\hat{t}^{-1/2} = \hat{t}^h \hat{t}^{-\frac{1}{2}-h}$.

The principal wave and the finite initialization have positive normalized powers with fixed logarithms. Equation (2.18.11) provides a summable bound for the remaining increments. In particular the additional swirl $Q^{-\frac{1}{2}-h}\epsilon_s$ from (2.15.15) has size $\hat{t}^{-1/2+h}(1+|\log \hat{t}|)^N$ on a fixed profile annulus. We bound its squared initial mass where $\hat{t} \le \epsilon$ by

$$C\int_0^\epsilon \hat{t}^{h-\frac{1}{2}}(1+|\log\hat{t}|)^N \,\mathrm{d}\hat{t} = C\int_0^\epsilon \hat{t}^{-1/2+h}(1+|\log\hat{t}|)^N \,\mathrm{d}\hat{t}. \tag{2.18.20}$$

For $\hat{t} \ge 2t$, the same uniform bound uses $z = \pm\hat{t}^{\frac{1}{2}-h}\sqrt{1-t/\hat{t}}$. The region $t \le \hat{t} \le 2t$ has volume $O(t^{\frac{3}{2}-h})$ and squared mass $O(t^{1/2+h}(1+|\log t|)^N)$. Thus this new velocity term has its own strong L^2 trace and does not alter the leading cusp. Its pressure has size $\hat{t}^{-1}$ and its axial gradient has size $\hat{t}^{-3/2+h}$.

We do not assume smooth extension of these quantities at the tip. They remain in the actual pressure and mean force throughout the finite iteration, whose ordinary residual the previous argument estimates. We select the profile hull to contain $\{\frac{\hat{\xi}^2}{2} \le 2X_{\mathrm{all}}\} \times K_{\hat{\zeta}}$. On the profile hull $r^2 \le Cq$, so $\mathfrak{d}(x) \le C'\hat{t}$.

On its complement the exact heat formula and the scalar-mode bound give $|u_\theta^{\mathrm{heat}}| \le C(\hat{t}+r^2)^{-\frac{1}{2}-h}$. Thus

$$|u_\infty(x,t)| \le C\mathfrak{d}(x)^{-\frac{1}{2}-h}, \qquad x \ne 0, \quad 0 < t \le T. \tag{2.18.21}$$

This is a bound on the completed sum, not just on individual packet coefficients.

Cylindrical integration gives the exact sublevel volume

$$|\{\mathfrak{d} < s\}| = \frac{2\pi}{(\frac{1}{2}-h)+1} s^{\frac{3}{2}-h}.$$

Thus

$$\int_{\{\mathfrak{d}<\epsilon\}} \mathfrak{d}^{-1-2h}\,\mathrm{d}x = C_h \epsilon^{\frac{1}{2}-3h}, \qquad 1+(\tfrac{1}{2}-h)-2(\tfrac{1}{2}+h) = \frac{1}{2}-3h > 0. \tag{2.18.22}$$

The off-origin jets define a smooth pointwise trace $u_{\infty,0}$ on $B_{R_*} \setminus \{0\}$. Dominated convergence with (2.18.21) proves strong local L^2 convergence.

We pass to the limit in $\int u_\infty(t)\cdot\nabla\zeta = 0$. This proves that the trace is divergence-free as a distribution. We impose no condition on a selected value at the origin.

2.18.7 Compact spatial localization without an initial defect

We select $0 < a < b < R_*$ and a smooth physical cutoff χ_{loc}, equal to one on B_a, supported in B_b. The function

$$g_{\mathrm{loc}} = \nabla\chi_{\mathrm{loc}} \cdot u_\infty$$

is smooth through $t = 0$, supported on a fixed annulus, and has integral zero. At positive time this holds by the divergence theorem applied to $\chi_{\mathrm{loc}}u_\infty$. At time zero, continuity on the annulus gives the result.

We use a fixed compact divergence inverse on a slightly larger connected annulus $\mathcal{O} \Subset B_{R_*} \setminus \{0\}$. Here is an explicit construction, with its parameter regularity. We cover the fixed support of g_{loc} by finitely many boxes with closures in $\mathcal{O}$. We add boxes along paths to connect the intersection graph.

We fix a partition of unity and a spanning tree. At each non-root box, we subtract its current integral times a fixed unit-integral bump in its intersection with its parent. We add that bump to the parent's piece. We start at the leaves.

This gives box-supported pieces g_i with integral zero. The root has zero integral because the original sum does.

For such a piece g_i in $I_1 \times I_2 \times I_3$, we select unit-integral bumps $\zeta_j \in C_c^\infty(I_j)$. We put

$$G_1(x_2, x_3) = \int_{\mathbb{R}} g_i(s, x_2, x_3)\, \mathrm{d}s, \qquad G_2(x_3) = \int_{\mathbb{R}} G_1(s, x_3)\, \mathrm{d}s.$$

The vector

$$\begin{aligned} b_1(x) &= \int_{-\infty}^{x_1} [g_i(s, x_2, x_3) - \zeta_1(s) G_1(x_2, x_3)]\, \mathrm{d}s, \\ b_2(x) &= \zeta_1(x_1) \int_{-\infty}^{x_2} [G_1(s, x_3) - \zeta_2(s) G_2(x_3)]\, \mathrm{d}s, \\ b_3(x) &= \zeta_1(x_1)\zeta_2(x_2) \int_{-\infty}^{x_3} G_2(s)\, \mathrm{d}s \end{aligned}$$

has divergence g_i and compact support in the box. Each primitive vanishes at the two ends because its integrand has zero integral.

The sum of the box solutions gives a linear operator $\mathcal{B}_{\mathrm{div}}$ with fixed compact support in $\mathcal{O}$. Its operations are finite sums, multiplication by fixed smooth functions, and integration over bounded sets. It commutes with time differentiation and is continuous in each fixed smooth seminorm.

Let $b_{\mathrm{loc}} = \mathcal{B}_{\mathrm{div}} g_{\mathrm{loc}}$, and define

$$u = \chi_{\mathrm{loc}} u_\infty - b_{\mathrm{loc}}, \qquad p = \chi_{\mathrm{loc}} p_\infty, \qquad \mathbf{f} = \mathscr{N}(u, p). \tag{2.18.23}$$

We select the smooth off-origin pressure representative previously specified before application of the cutoff. These fields extend by zero outside B_{R_*}, u has zero divergence, and $(u, p, \mathbf{f}) = (u_\infty, p_\infty, \mathbf{f}_\infty)$ on a fixed ball about the origin. Where a cutoff or divergence correction acts, all velocity and pressure jets are smooth through the initial time.

Thus $\mathbf{f}$ is smooth up to $t = 0$ and has fixed compact spatial support. The same time-normal extension does not change spatial coordinates. It gives a smooth extension through $t = 0$ with the same support.

The annular correction converges smoothly, while $\chi_{\mathrm{loc}} u_\infty$ converges strongly in L^2. Thus

$$u_0 = \chi_{\mathrm{loc}} u_{\infty,0} - b_{\mathrm{loc}}(0), \qquad u \in C([0, T]; L^2(\mathbb{R}^3)).$$

The trace has compact support, is smooth off the origin and is distributionally divergence-free.

To keep the full equation through the initial slice, let $N(x) = -1/(4\pi|x|)$, so that $\Delta N = \delta_0$, and define the spatial distribution

$$p_{\mathrm{can}}(t) = N * \big(\operatorname{div} \mathbf{f}(t) - \partial_i \partial_j (u_i(t) u_j(t))\big). \tag{2.18.24}$$

The source supports lie in one fixed compact set and $u_i u_j \in C([0, T]; L^1)$, so this is a continuous family of distributions. At positive time it equals the compact smooth pressure p, because convolution with N inverts Δp for such a function. We integrate the classical equation from $s > 0$ against an arbitrary smooth compactly supported spacetime test.

Strong L^2 convergence controls the initial boundary term. Continuity in L^1 controls the quadratic term. We place Δ on the test function to pass to the limit in the viscous term. Equation (2.18.24) controls the pressure limit.

The full distributional equation thus holds with trace u_0, also for tests which are not divergence-free.

2.18.8 The singular cusp and the energy identity

Use the enclosing bound X_{all} from (2.18.2). For $X \geq X_{\mathrm{all}}$ the leading field is the exact heat field, and each velocity or pressure correction after this point vanishes (Lemma 2.18.1(a), (d)). This statement applies after the last meridional and spectral return. It does not apply at the exit of the early velocity correction region. Because $c_{\mathrm{bank}} > 0$, the asymptotic $g_h(\xi) \sim \xi^{-h}$ and exponential decay of g_f in (2.18.18) gives on the open cusp

$$0 < |z| < \left(\frac{r^2}{4X_{\mathrm{all}}} \right)^{\frac{1}{2}-h} \quad \Longrightarrow \quad (u_0)_\theta = c_{\mathrm{bank}} 2^h r^{-1-2h} \tag{2.18.25}$$

inside the unchanged localization ball.

$\frac{\hat{\xi}^2}{2}(r, z, 0) > 2X_{\mathrm{all}}$, so each such point remains strictly in the heat region for small positive time. Each neighborhood of the origin contains positive-measure subsets of this cusp with arbitrarily large displayed amplitude. Thus the trace is essentially unbounded. The selected leading tangential profile is also nonzero on a bounded similarity set of positive measure.

At the last step the smooth positive-time equation, same compact support and strong trace satisfy the hypotheses of Lemma 2.19.2. That lemma gives (2.19.1) and finite integrated H^1 dissipation. The compact positive-time pressure, with the initial radial correction, contributes zero work against the solenoidal velocity. The selected smooth force contains no singular pressure gradient. This completes the physical conclusion from the finite construction.

2.18.9 The output of the admissible-source construction

Lemma 2.18.3 (The selected six-clause source interface)**.** *Take the leading pair, with the strict cover of Theorem 1(iv), and assume Hypothesis 2.3.21 (through Proposition 2.12.3). We equip the jointly selected member of Theorem 1 with the same slow and packet data from the next construction. This member satisfies all six clauses of Definition 2.5.1. This statement does not identify it with an unmodified scalar reference field.*

Proof. This is Theorem 2.18.4 below. These results supply the source and finite-algorithm inputs for this member. The source and finite-algorithm conclusions are distinct from the frozen spectral conclusion of Theorem 1(v)–(vi). □

Theorem 2.18.4 (The six clauses for the selected member)**.** *Equip the leading pair of Theorem 1 with the slow and packet data constructed in this chapter. Under the finite-stage inventory of Hypothesis 2.3.21, this member satisfies (A1)–(A6) of Definition 2.5.1.*

Proof. **(A1)** Theorem 1(ii)–(iv) fixes the heat and terminal germs, the protected scaled rectangle, the strict cutoff collar and the unchanged power intervals $-14 < y_p < -9$ and $-8 < y_p < -3$. The loop restorations and the later spectral modification leave these intervals available for the two corrections. Lemma 2.6.2 supplies the slow inner inverse on this same rectangle.

(A2) The selected leading field is smooth in Cartesian coordinates on the axis, has positive swirl for $\hat{\xi} > 0$ and has the full one-sided endpoint jets of Theorem 1(i)–(iii). Theorem 2.9.1 and the heat endpoint estimate propagate this regularity to the slow coefficients.

(A3) The pressure-class bank imposes $\Delta I = \Delta S = \Delta M = \Delta J = 0$ and $\Delta C_p = \Pi_{\mathrm{ref}} - p_0$, and the core correction targets this edited reference. Loop and spectral restorations use the nonsingular five-history maps of N6(b). The first slow moment and divergence identity give the velocity support in (2.6.21); the full third row removes the pressure constant only after the last meridional return. Thus the two late pressures remain in the full hull (2.18.2), as required by Lemma 2.20.1.

(A4) The strict cone and frame margins of the final leading member, including its spectral modification and all the five-moment returns, are part of Theorem 1(iii)–(v). Use the closed active pieces inside those margins when fixing the packet atlas of Theorem 2.10.2.

(A5) Theorem 1(iii)–(iv) supplies the two actual pressure tubes, the native weights and their logarithmic derivative bounds, the protected mean slot and the moment-subtracted radial inverse. The endpoint regularity required after slow correction is Theorem 2.9.1(v).

(A6) Theorem 2.7.1 uses Proposition 2.6.5 and Theorem 2.6.13 for the inner solve and moving bumps, together with the transported core and loop/restoration templates. The finite solves have the isolated branches of N2–N8. Proposition 2.10.1 uses the common gauge; its sum is locally finite at $q_0 > 0$. The joint atlas and schedule are Theorem 2.10.2 and Lemma 2.12.2. Hypothesis 2.3.21 supplies the actual factorial bounds through Proposition 2.12.3. These are exactly the inputs of the common cutoff (2.18.5). □

For this source let $B_0(x,t) = u^{\mathrm{lead}}(x,t)$ be its leading field (2.3.14) on $\mathbb{R}^3 \times (0,\infty)$. Let $B_* = u$ and $p_* = p$, $\mathbf{f}_* = \mathbf{f}$, $u_{0,*}$ be the output of Sections 2.6–2.18, and $W = B_* - B_0$. We put

$$\mathfrak{d}(x) = r^2 + |z|^{1/(\frac{1}{2}-h)}, \qquad \rho = t^h, \qquad S = (1 + \log(1/\rho))^{6/5}.$$

For similarity variables let $\mathcal{Q}(Z) \geq 1$ solve (2.3.13), $\hat{\zeta}(Z) = Z\mathcal{Q}^{h-\frac{1}{2}} \in (-1,1)$, $\hat{\xi} = R/\sqrt{\mathcal{Q}}$, and

$$\Omega(R,Z) = \frac{\mathcal{H}(R,Z)}{R} = \mathcal{Q}^{-1-h} F(\tfrac{\hat{\xi}^2}{2}, \hat{\zeta}), \qquad \mathcal{U} = \mathcal{Q}^{-\frac{1}{2}-h} U(\tfrac{\hat{\xi}^2}{2}, \hat{\zeta}), \qquad \mathcal{V} = \frac{V(\frac{\hat{\xi}^2}{2}, \hat{\zeta})}{R},$$

This gives the identity $B_0 = t^{-\frac{1}{2}-h}(\mathcal{H}e_\theta + \mathcal{U}e_z) + t^{-1/2}\mathcal{V}e_r$.

Proposition 2.18.5 (The forward construction estimates)**.** *Fix the leading source of Theorem 1, with the slow and packet data of Lemma 2.18.3. The constructions of Sections 2.6–2.18, with the choices made in the parameter ordering of Theorem 1(iii) and the stage orders of Subsection 2.4, produce $(B_*, p_*, \mathbf{f}_*, u_{0,*})$ with these properties. All constants depend on the source and on these finite choices.*

(M0) The conclusions of Theorem 2.19.1, with the profiles (2.3.15) of this source.

(M1) Envelope and jets. *There is $t_* > 0$ such that for $0 < t \leq t_*$, $x \neq 0$, each $\epsilon > 0$ and each $j \geq 1$,*

$$|B_*(x,t)| \leq C(t + \mathfrak{d}(x))^{-\frac{1}{2}-h}, \qquad |\nabla_x^j B_*(x,t)| \leq C_{j,\epsilon}(t + \mathfrak{d}(x))^{-(\frac{1}{2}+h)-\frac{1+h}{2}j-\epsilon}, \tag{2.18.26}$$

and $|\nabla_x^j B_0(x,t)| \leq C_j(t + \mathfrak{d}(x))^{-\frac{1}{2}-h-j/2}$ on $|x| \leq 1$. In particular (2.24.1) holds with $N_0 = (\frac{1}{2}+h)$ and $N_j = (\frac{1}{2}+h) + j$ $(j \geq 1)$, (2.18.21) holds, and $\sup_x t^{\frac{1}{2}+h+j/2}|\nabla_x^j B_0(x,t)| \leq C_j$.

(M2) Completed-wave bounds. *For* $0 < t \le t_*$, *with* $W^\natural(y,t) = t^{\frac12+h} W(\sqrt{t}\,y, t)$,

$$\|W^\natural(t)\|_\infty \le \rho^{1/2} P(S), \quad \|\nabla_y W^\natural(t)\|_\infty \le P(S), \quad |\nabla_y W^\natural| \le C(E + \rho^{\eta_0}), \tag{2.18.27}$$

for a fixed polynomial P, *each fixed* $0 < \eta_0 < 1/2 - 5\varkappa$, *and the envelope* $E \ge 0$ *of Lemma 2.22.5, which satisfies* $\|E\|_\infty \le P(S)$ *and* $\|\nabla_y E\|_\infty \le \rho^{-\varkappa} P(S)$. *These are the source bounds (2.22.1). On a block with fixed reference time* Q, *write* $\rho = Q^h$, $t = Q + Q^{1+h}\theta$, $|\theta| \le L$ *and* $y = x/\sqrt{Q}$. *Since* $t/Q = 1 + \rho\theta$, *the value, gradient and space scales in the two normalizations differ by factors* $1 + O(\rho L)$ *when* $\rho L \to 0$.

(M3) Leading tails and axial jets. *For all* $j, l \ge 0$ *and all* $(R, Z) \in [0,\infty) \times \mathbb{R}$,

$$|\partial_Z^l \partial_R^j \Omega(R,Z)| \le C_{j,l} \langle R \rangle^{-2-2h-j}, \tag{2.18.28}$$

and for $R^2 \ge 2X^+_{\mathrm{lead}} \mathcal{Q}(Z)$, $\Omega = R^{-2} g_*(R^2/2)$ *is independent of* Z. *The fields* $\mathcal{U}, \mathcal{V}$ *vanish for* $R^2 \ge 2\frac{\hat\xi_U^2}{2} \mathcal{Q}(Z)$, *and* $|\partial_Z^l \partial_R^j \mathcal{U}| \le C_{j,l} \mathcal{Q}^{-(\frac12+h)-j/2-l(\frac12-h)}$, $|\partial_Z^l \partial_R^j \mathcal{V}| \le C_{j,l} \mathcal{Q}^{-1/2-j/2-l(\frac12-h)}$ *(here* $\mathcal{V} = \mathcal{Q}^{-1/2} V/\hat\xi$ *and* $V/\frac{\hat\xi^2}{2}$ *is regular at the axis). In particular these bounds are uniform in* Z *at every fixed finite axial derivative order.*

(M4) Initial slice. *The conclusions of Proposition 2.8.6 and Corollary 2.8.7.*

Proof. (M0), (M4). We use the six conditions in their actual order. The protected core and endpoint factors in (A1)–(A2) supply Lemma 2.6.1 and the native edge calculus. Clause (A3) supplies the full five-row targets and the pressure hull after this region. The radial pressure/root correction and the state equations keep these terms by Section 2.20.1.

We use the strict source margins in (A4) and the generic weighted primitive bound in (A5), Lemma 2.3.13. They give the packet inverse, radial mixing, and current mean operations. We do not replace that lemma by a scalar all-angle middle lower bound. Clause (A6) fixes the same slow background, one physical atlas and the 6/5 finite-stage factorial budgets before any last cutoff sequence.

We run the one uncut finite initialization (2.15.18) and the finite improvement cycle on its admitted domains. The ordinary finite equation is (2.18.1), with full pressure and the two flat remainders. The support buffers (2.18.10) then define smooth zero-extended increments. (2.18.12) is one last packet/mean diagonal. Its fixed-prefix estimates prove ordinary residual flatness. They do not just prove flatness of an augmented equation.

Proposition 2.8.6 uses only the fixed initialized state and locally finite cut terms. We use uncut states after this step only inside their own admitted domains. Corollary 2.8.7, localization, the strong trace argument and Lemma 2.19.2 thus give (M0) and (M4). These conclusions use the actual source in each of the cited finite algorithms.

Two comparisons. By (2.18.19), $q \asymp t + |z|^{1/(\frac12-h)}$. We fix $\frac{\hat\xi_1^2}{2} \ge X_{\mathrm{all}}$ that bounds the profile hull. On $\{\frac{\hat\xi^2}{2} \le \frac{\hat\xi_1^2}{2}\}$, $q \ge \max(t, |z|^{1/(\frac12-h)}, r^2/(\hat\xi_1^2))$, so $q \ge c(t+\mathfrak{d})$. Conversely $q \le C(t+\mathfrak{d})$, so $q \asymp t + \mathfrak{d}$ there. On $\{\frac{\hat\xi^2}{2} > X_{\mathrm{all}}\}$, $r^2 = \hat\xi^2 q \ge 2X_{\mathrm{all}} \max(t, |z|^{1/(\frac12-h)})$, thus $r^2 \ge c(t+\mathfrak{d})$.

(M1). Exterior. On $\{\frac{\hat\xi^2}{2} > X_{\mathrm{all}}\}$ inside the localization ball, B_* is the heat field (Proposition 2.8.6(b), Lemma 2.18.1(d)), $u_\theta = 2^h r^{-1-2h} G(r^2/(2t))$ with $G(y) = y^h g_*(y)$. (2.3.37) and (2.3.36) bound $y^k G^{(k)}$ on $y \ge b_s$ for each k. Because $\partial_r = (2y/r)\partial_y$ and the frame costs r^{-1}, $|\nabla_x^j u| \le C_j r^{-1-2h-j} \le C_j (t+\mathfrak{d})^{-\frac12-h-j/2}$.

Hull, finite state. We fix N. On $\{\frac{\hat\xi^2}{2} \le \frac{\hat\xi_1^2}{2}\}$ the field $u^{[N]}$ is a finite sum (Step 1 of Proposition 2.8.6) of these pieces. (1) Slow terms $q^\gamma f(\frac{\hat\xi^2}{2}, \hat\zeta)$ with $\gamma \ge -(\frac12+h)$. One radial derivative costs $q^{-1/2} \hat\xi \hat\xi^{-1} \partial_{\hat\xi}$,

one axial derivative costs $q^{h-\frac12}\mathsf{Z}_\gamma$, and near the axis one radial Cartesian derivative costs $q^{-1/2}$ from $r=\sqrt{q}\,\hat\xi$ and smoothness in $\hat\xi^2$ at the axis.

All profile jets are bounded on $[0,\frac{\hat\xi_1^2}{2}]\times[-1,1]$ by Lemma 2.8.4. Thus this piece is $O(q^{-\frac12-h-j/2})$, because $q^{h-\frac12}\le q^{-1/2}$ for $q\le 1$. (2) Waves on bands $Q\in(\widetilde q/2,2\widetilde q)$. Since $q=q_f=L_{\rm cut}(\eta_f)\widetilde q$ with $L_{\rm cut}$ bounded above and below by positive constants, $Q\asymp q$ uniformly. Their normalized coefficients lie in $\mathcal{W}^a$ with $a\ge 1/2$, so they are bounded by $\rho_Q^{1/2}S_\ell^B$ after $\mathsf{W}^\epsilon\mathcal{L}_W^N\le C$ (Section 2.18).

One physical derivative gives at most one of these factors. The carrier factor is $k_\ell|m||\nabla_x\Phi|=k_\ell|m|Q^{-1/2}|n|\le C|m|\rho_Q^{-1/2}Q^{-1/2}$, by (2.13.16), (2.13.19), $k_\ell\le 2\rho_Q^{-1/2}$, $\partial_z\Phi=Q^{h-\frac12}\rho_Q^{-1}n_z=Q^{-1/2}n_z$ and $r^{-1}\partial_\theta\Phi=Q^{-1/2}n_\theta$. A sampled radial coefficient derivative $Q^{-1/2}D_{\mathsf R}$ has size $\le Q^{-1/2}\rho_Q^{-\varkappa}S^C$ by (2.13.9). An axial coefficient derivative contributes $Q^{h-\frac12}$. A frame derivative contributes $r^{-1}\le Q^{-1/2}/\mathsf{R}_-$.

The pulse variable does not depend on x (Step 2). Because $\varkappa<1/2$, the carrier dominates, and the j-th derivative is $\le C_jQ^{-\frac12-h}\rho_Q^{1/2}(Q^{-1/2}\rho_Q^{-1/2})^jS^{C_j}$. Boundedly many labels overlap at a point (Lemma 2.13.1). (3) Mean increments and the initialization.

These are normalized classes $\mathcal{M}^a$, $a>0$, with sampled radial derivative cost $Q^{-1/2}\rho_Q^{-\varkappa}S^C$. The initial extra swirl has size $q^{-1/2+h}(1+|\log q|)^N\le Cq^{-\frac12-h}$ (Section 2.18). Altogether, for $j\ge1$, we get $|\nabla_x^ju^{[N]}|\le C_{N,j}q^{-(\frac12+h)-\frac{1+h}{2}j}(1+\log(1/q))^{C_j}$, and for $j=0$, we get $|u^{[N]}|\le C_Nq^{-\frac12-h}$, because $\rho^{1/2}S^B$ stays bounded.

Tail. By (2.18.13), $|\nabla_x^j(u_\infty-u^{[N]})|\le C_{N,j}q^{h\beta_N-(\frac12+h)-3j}$. We select $N=N(j)$ with $h\beta_N\ge 3j$. This changes no exponent.

Localization. $B_*=\chi_{\rm loc}u_\infty-b_{\rm loc}$. On the fixed annulus $\mathfrak{d}\ge c(a)>0$, so the bounds proved before this step bound the jets of u_∞ and of $g_{\rm loc}=\nabla\chi_{\rm loc}\cdot u_\infty$ with bounds independent of t. The operator $\mathcal{B}_{\rm div}$ is continuous in each fixed seminorm (Section 2.18). These terms are $O(1)$.

The two comparisons give (2.18.26). The factor $(t+\mathfrak{d})^{-\epsilon}$ absorbs the logarithms. Because $t+\mathfrak{d}\ge t$ and the exponents are negative, $\|\nabla^jB_*(t)\|_\infty\le C_jt^{-N_j}$ with $N_0=(\frac12+h)$ and with $N_j=(\frac12+h)+\frac{1+h}{2}j+\epsilon\le(\frac12+h)+j$ for $j\ge1$, with $\epsilon\le(1-h)/2$. For B_0 only piece (1) and the exterior occur. This gives the stated bound without carrier loss. For $|x|\ge1$, either $r\ge1/\sqrt2$ or $|z|\ge1/\sqrt2$, so $\mathfrak{d}(x)\ge c_h>0$. On the profile hull the first comparison gives $q\ge c$. The leading prefactors $q^{-1/2}$, $q^{-1/2-h}$ and the spatial derivative factors $q^{-1/2}$, $q^{h-1/2}$ are then bounded, as are all fixed profile jets. In the heat exterior the second comparison gives $r^2\ge c$, and the differentiated heat bound gives $|\nabla_x^jB_0|\le C_jr^{-1-2h-j}\le C_j'$. These regions cover $|x|\ge1$ uniformly as $t\downarrow0$.

(M2). We apply Lemma 2.22.5 to this source. At reference time $Q=t$ its value and gradient bounds give (2.18.27), with the same envelope E and its spatial derivative bound. The proof of that lemma uses the finite-state classes, the physical tail, and the localization directly. Its proof does not use this proposition or the later spectral selection. There, we include the slow difference $u_{\rm B}-B_0$ in W.

(M3). At $t=1$ the leading velocity is $\mathcal{H}e_\theta+\mathcal{U}e_z+\mathcal{V}e_r$ with $q=\mathcal{Q}(Z)$. The chart identities with $t=1$ give $\partial_Z(\mathcal{Q}^\gamma f)=\mathcal{Q}^{\gamma-(\frac12-h)}\mathsf{Z}_\gamma f$ and $\partial_Rf(\frac{\hat\xi^2}{2})=\mathcal{Q}^{-1/2}f_{\hat\xi}$. By induction, we get $\partial_Z^l\partial_R^j(\mathcal{Q}^{-1-h}F)=\mathcal{Q}^{-(\frac12+h)-1/2-j/2-l(\frac12-h)}G_{jl}(\frac{\hat\xi^2}{2},\hat\zeta)$, where G_{jl} combines a finite number of $(\frac{\hat\xi^2}{2},\hat\zeta)$-jets of F, of powers of $\hat\xi$, of $\hat\zeta$, d and L^{-1}. Here F is smooth in $X=\hat\xi^2/2$ and $\hat\zeta$ at the axis by Theorem 1(i). Since $\hat\xi^{-1}\partial_{\hat\xi}=\partial_X$, each fixed mixed jet in the displayed expression extends continuously to the axis. Thus $\hat\xi^a(\hat\xi^{-1}\partial_{\hat\xi})^bF$ is bounded there for $a\ge0$ and each fixed integer $b\ge0$.

Lemma 2.8.4 bounds G_{jl} on $[0,\frac{\hat\xi_1^2}{2}]\times[-1,1]$, with one bound when $|Z|\to\infty$ ($\hat\zeta\to\pm1$). On

$R^2 \le 2\frac{\hat\xi_1^2}{2}\mathcal{Q}$ and $R \ge 1$, $\mathcal{Q}^{-(\frac12+h)-1/2-j/2} \le CR^{-2-2h-j}$ because $(\frac12+h)+1/2 = 1+h$. For $R \le 1$ the bound is trivial because $\mathcal{Q} \ge 1$. On $R^2 \ge 2X^+_{\mathrm{lead}}\mathcal{Q}$ we have $\frac{\hat\xi^2}{2}/d = R^2/2 \ge X^+_{\mathrm{lead}} \ge \mathcal{B}_{\max} \ge b_s$, and by (2.3.33) at $t=1$, $\Omega = R^{-2}g_*(R^2/2)$.

This is Z-independent and, by (2.3.37) and (2.3.36), satisfies $|\partial_R^j\Omega| \le C_jR^{-2-2h-j}$. The two descriptions agree on the overlap, because they define one function. The statements for $\mathcal{U},\mathcal{V}$ hold by the same argument with $U = M = 0$ for $\hat\xi \ge \hat\xi_U$, which gives $V = 0$ by (2.3.16). □

Remark 2.18.6 (Inputs to the next arguments). Proposition 2.18.5 adds no new estimate to the forward analysis. It collects, with explicit exponents, the bounds (2.6.34), (2.6.30) (Section 2.6), the class bounds of Sections 2.13–2.14, Lemma 2.18.2, (2.18.13) and the heat asymptotics. Its correctness is conditional on those statements. The linear and nonlinear arguments use only finiteness of N_j for $j \le 4$.

With $N_j = (\frac12+h)+j$, the choice $K = 2$ satisfies $K > 1+h$, $K > 1$ and $K(j+1)/2 \ge N_j$ for $0 \le j \le 4$, since $j+1-N_j = 1-(\frac12+h) > 0$ and $2 > 1+h$. The estimate (2.18.28) for Ω is uniform in Z. The support radius for $\mathcal{U},\mathcal{V}$ is bounded by $(\hat\xi_U^2\mathcal{Q}(Z))^{1/2}$. The profile calculus uses its supremum on a compact axial chart.

The upstream inputs are the actual six clauses verified in Lemma 2.18.3. In particular (A5) consists of the native inner/terminal component calculus together with the two-tube aggregate and generic primitive theorem, Lemma 2.3.13. It is not a positive lower bound on an all-angle middle rectangle. Clause (A6) supplies the full endpoint and joint-atlas choices. The finite construction uses these precise weighted domains and controls together with the strict source margins in Theorem 1(iv).

2.19 The forward base

Main result. Theorem 2.19.1 restricts the completed background to $t \ge 0$. Its initial datum is the singular strong L^2 trace $u_0 = B(0)$. Lemma 2.19.2 derives the energy identity from the stated trace and support properties. The coordinates and normalized profiles are those of Theorem 1(i), (v).

Theorem 2.19.1 (Forward restriction of the completed background)**.** *Take the jointly selected exponent h and source parameters of Theorem 1. This choice gives $T > 0$, a compactly supported divergence-free $u_0 \in L^2(\mathbb{R}^3)$, and a solution $(u,p,\mathbf{f})$ of (2.2.2) on $\mathbb{R}^3 \times (0,T]$. They have the next properties.*

The datum u_0 is smooth off the origin and essentially unbounded in each neighborhood of the origin. The velocity satisfies

$$u \in C([0,T];L^2(\mathbb{R}^3)) \cap C^\infty(\mathbb{R}^3 \times (0,T]), \qquad u(0) = u_0,$$

and its spatial support lies in one fixed compact set on this time interval. The pressure is smooth for positive time. The force has compact spatial support, and it extends smoothly to a neighborhood of $\mathbb{R}^3 \times [0,T]$.

The selected leading profiles are nonzero on some bounded set. The equation holds distributionally with initial datum u_0. Also $u \in L^2(0,T;H^1(\mathbb{R}^3))$, and

$$\frac12\|u(t)\|_2^2 + \int_0^t \|\nabla u(s)\|_2^2\,\mathrm{d}s = \frac12\|u_0\|_2^2 + \int_0^t\int_{\mathbb{R}^3} \mathbf{f}(x,s)\cdot u(x,s)\,\mathrm{d}x\,\mathrm{d}s. \tag{2.19.1}$$

We select the source and exponents jointly, choosing the bridge exponent before its compatible h. The conditional analytic and completion estimates hold for every fixed h satisfying their stated

source hypotheses. The forward datum and force here are those of the same two-sided completion. The zero initial velocity of the full evolution in Part 3 occurs earlier, at $t = -T_{\mathrm{in}}$.

The proof uses the full construction. Section 2.18 gives its physical conclusion.

Proposition 2.18.5 states the quantitative bounds for linear analysis of the selected member. These bounds control jets, completed-wave size, and leading tails. On a similarity set the volume element is

$$\mathrm{d}x = t^{\frac{3}{2}-h} R \, \mathrm{d}R \, \mathrm{d}\theta \, \mathrm{d}Z, \tag{2.19.2}$$

so the leading tangential field has L^2 scale t^{ω}, $\omega = (1 - 6h)/4$.

Lemma 2.19.2 (Energy identity from the trace)**.** *Suppose the smooth velocity and pressure solve* (2.2.2) *at positive times with the stated force. Suppose the velocity has the strong L^2 trace in Theorem 2.19.1. Suppose the force has the smoothness stated in that theorem. Suppose one fixed compact set contains the velocity support for the full time interval. Then* (2.19.1) *and finite dissipation hold.*

Proof. For $0 < s < t$, the smooth equation and compact support give the energy identity on $[s, t]$.

Strong continuity gives one bound for $\|u(\tau)\|_2$ on $[0, T]$. We let K be one fixed compact set that contains the velocity support at each time.

Smoothness of the force gives one bound for $\|\mathbf{f}(\tau)\|_{L^2(K)}$ on this interval. Thus the work integral converges when $s \downarrow 0$. The initial energy converges strongly, while $\int_s^t \|\nabla u\|_2^2$ increases monotonically. The identity then gives a finite limit and (2.19.1). □

2.20 The joint physical completion

Main result. Proposition 2.20.4 gives matching physical jets away from the origin, one smooth spatially compact force, and one strong trace. It assumes the stated one-sided leading inputs, the same atlas, and the single last diagonal. The construction selects the two sides jointly and keeps the full canonical pressure. It does not continue an arbitrary previously completed backward solution.

Lemma 2.20.1 (Late pressure and the current early mean correction)**.** *The early mean/root supports may precede the last leading meridional and spectral return. The actual slow pressure, with its late P_1, P_2, is admissible input to the initialization and current state map of Section 2.14. We integrate all state and pressure primitives on the whole enclosing hull* (2.18.2)*.*

Proof. Beyond the positive-order velocity correction region, its zero axial-flux moment gives $U_n = V_n = M_n = 0$ for $n \geq 1$. It does not imply $V_0 = 0$. The exact radial recurrence (2.6.4)–(2.6.5) thus keeps

$$(\hat{\xi}^{-1}\partial_{\hat{\xi}}(P_1)) = -\frac{\mathfrak{R}_0}{\hat{\xi}^2}, \qquad (\hat{\xi}^{-1}\partial_{\hat{\xi}}(P_2)) = \frac{\mathsf{Z}_0^{[2]} V_0}{\hat{\xi}^2}.$$

Their derivatives vanish only after the last leading return.

The third row of (2.6.18), integrated over that full path, makes their last constants zero. For $n \geq 3$ the exterior recurrence vanishes after the positive velocity support. The affine targets include the known lower-order $\mathfrak{R}$ terms. The argument does not use the current unknown order to assume its own pressure compactness.

Proposition 2.3.2 supplies the positive radial paths, with the specified angular buffers. On $t < 0$ these are Proposition 2.7.2(b),(e) and Lemma 2.13.10: one compact all-angle rectangle, and no buffers are needed.

We use the actual moving fiber correction family of (2.14.11). Lemma 2.3.13 gives its generic weighted primitive domain. Its slow commutators are (2.14.12), not zero. The complete axial force includes (2.14.23) and the derivative of the full flux product (2.14.22).

These ordinary Haar terms have the stated positive orders. They do not enter a flat remainder. The state-map argument proves the moving five-template inverse. It includes the compact angular exponent family and the exact endpoint identities (2.14.58).

On the early mean patch $V_s = V_{\mathrm{lead}}$. On the closed subslot containing the protected supports its lower bound is uniform on both sides by Lemma 2.12.31. The two linear blocks in (2.14.50) depend on the current Haar velocities $V_{\mathrm{H}}, G_{\mathrm{H}}$. Integration of the induced seed pressure gives their fifth row, which includes pressure.

This row does not substitute the background pressure into a leading-only matrix. The actual slow pressure may differ from P_0 on this patch. It enters the state defects and all later targets as written.

In particular the initial tensor is the full C_0, not just the covariance cross defect D_0. With the genuine radial moment $M_C = \mathcal{J} f_C$ and $k = -\mathcal{D}\chi$, the exact row is

$$(\mathrm{Div}_*\, \mathsf{C}_0)_r + \mathcal{D} P_C - \frac{(V_s + \delta_C)^2 - V_s^2}{\mathsf{R}} = k\mathcal{J} f_C - k\mathcal{J} f_C = 0, \quad \delta_C = \sqrt{V_s^2 + \mathsf{R}\, k\, \mathcal{J} f_C} - V_s.$$

We include the nonflat $g_s = \rho \partial_{\mathsf{Z}} S_z$ in f_C. The complete-moment subtraction makes the pressure response compact.

Its support can include the space between the early and late supports. The square root is supported only where k is supported. One value condition $|\mathsf{R} k \mathcal{J} f_C| \le V_s^2/2$ fixes a smooth branch. Rationalization permits differentiation of the same branch to each fixed order.

It uses no new positivity threshold for all orders. The added pressure and its axial derivative stay in the equations. They do not enter a selected force.

The one uncut state map (2.15.18) raises order one to two. The next finite auxiliary/state/cross cycle gives (2.15.20). The incoming order two dominates $2 - 3\varkappa$. The next state order is $4 - 6\varkappa$, and the cross-pressure/swirl feedback has order three.

Each uncut canonical radial row has zero residual. The equations keep the explicit ordinary flat vector and tensor remainders. Thus no preliminary infinite mean sum or additional force adjustment is necessary. □

Lemma 2.20.2 (Jet transfer through the same finite physical algorithm)**.** *We take the actual one-sided leading inputs of Theorem 1(ii). We use their leading/slow endpoint identification in Theorem 2.7.1 and the same physical controls of Theorem 2.10.2. Each admitted finite packet/mean stage has one-sided smooth fields and equal slice jets (Definition 2.3.16). This conclusion includes pressure, potentials, full radial histories, and the actual residual. The claim includes all explicit endpoint and deletion remainders, not just their equivalence modulo flat functions of the ancient scale.*

Proof. We induct first on the finite construction stage. First form the actual finite expressions on each side. We solve the zero-data pulse ODEs, current finite matrices, and positive roots on their admitted value domains. Then compare jets.

Smooth parameter dependence gives one-sided jets. These existence domains depend on the given source and the previous stage. They do not use the equality conclusion of this proof.

For the comparison at a fixed stage use induction on normal derivative order k. At $k = 0$, the physical inputs in slice variables, selected labels, rounded integers, and frames agree. The whole pulse paths and zero initial data also agree. Matrix solutions use the same invertible matrix and

positive roots use the same positive branch. Thus their values coincide. Products and exact curls then keep the equality.

For $k \geq 1$, write the two expressions in slice variables and compare their one-sided $\widetilde{\eta}$-jets at $\widetilde{\eta} = 0$. A current implicit equation $\mathcal{F}(c, a) = 0$ gives

$$\mathcal{F}_c(\partial_n^k c_f - \partial_n^k c_b) = -\mathcal{F}_a(\partial_n^k a_f - \partial_n^k a_b) + \mathcal{R}_k(\text{previously matched lower jets}) = 0.$$

The value Jacobian is the same one and is invertible. For a pulse ODE $z' = A(v)z + f(v)$, the kth jet difference satisfies the same homogeneous ODE with zero initial data and zero forcing.

The coefficient and forcing jets are the current matched inputs. The lower solution jets agree by the previous induction. Uniqueness gives zero on the full pulse path.

Haar integration uses the same compact cover and normalized measure. The fixed torus inverse acts on the same zero-mean Fourier coefficients and commutes with these parameter derivatives. Each shifted radial primitive uses the complete same path, the actual constant, and the same shift $Y + [(r')^{d_r} - r^{d_r}]v_r$. Compact hulls or the one-sided heat dominators justify differentiation. The same argument applies to full moments, with pressure constants and quadratic lower-order data. A comparison at one radius does not replace this whole-path identity.

At the last step, the same potential/flux cutoff is $\chi(\widetilde{q}/\delta_n)$. Its argument is $\hat{t}_f/(L_{\mathrm{cut}}\delta_n)$ on the forward endpoint chart and $\hat{t}_b/\delta_n$ on the backward chart. In slice variables it is $\widetilde{Q}\gamma(\widetilde{\eta})/\delta_n$, one smooth function (Lemma 2.3.1). We apply it before differentiation and keep each curl or mean-prefix bracket. The cutoff and all its parameter jets thus agree on the two sides.

Thus the induction includes these terms and each actual Gaussian-endpoint or aggregate-deletion output. This completes the two finite inductions. □

Lemma 2.20.3 (Two-sided finite estimates precede the same diagonal)**.** *We fix the leading pair of Theorem 1 and the joint physical atlas. Each finite packet and mean estimate for the completion holds on each side before we compare its jets. We use the maximum of its constants, the union of its finite derivative lists, and the minimum of its native scale thresholds. This gives one diagonal and the backward residual and value bounds in the joining proposition. It does not solve a backward physical heat initial-value problem. For $t < 0$, Lemma 2.20.7 constructs the slow background. Theorem 2.7.5 proves the finite packet, mean and return bounds using Proposition 2.7.2 and Lemmas 2.13.10 and 2.20.6. The proof below identifies the time sign and the joint choice of constants in those estimates. The support statement (B7)(iii) is Lemma 2.8.9, and the backward one-sided smoothness (B7)(iv) is Proposition 2.8.10.*

Proof. The actual evaluated clock in (2.13.12) is

$$t_* = \rho\partial_T + c_i v_t \cdot \partial_{y_i} = \rho\partial_T + \partial_v, \qquad t_* v = 1.$$

Here $T_b^{\mathrm{slow}} = -T$ denotes only the local slow coordinate. The evaluated time derivative is $-\rho\partial_{T_b^{\mathrm{slow}}} + \partial_v$. For comparison, a native slow coefficient obeys the exact physical identity

$$\partial_t(q^p f(X, \eta)) = \frac{\operatorname{sgn}(t)\, q^{p-1}}{1 - 2h\eta^2}(pf - Xf_X - d_0\eta f_\eta), \qquad X = r^2/(2q), \quad d_0 = 1/2 - h.$$

This follows by differentiating $q - z^2 q^{2h} = |t|$ at fixed x. The pulse derivative keeps its orientation and the physical viscous damping $j^2 d_p \geq 0$ keeps its sign.

Frames and normal constraints come from the same physical operator, with its full pressure and cylindrical connections. The zero-data inverse acts along v, and the torus inverse acts in the auxiliary variable. Both inverses use the indicated pulse or auxiliary coordinate.

In the exact finite identities the remaining slow-time term is thus $\pm\rho\partial_T$. Its sign may change its coefficient, but not its positive power or the bound in an absolute finite seminorm. Products, full curls, current Haar matrices, radial moment inverses and protected square roots use the same algebraic formulas on each physical restriction. First impose a root or matrix margin at value level.

Differentiation then keeps that branch at all fixed orders. The kept source weights and their log-jet bounds are inputs on the two closed sides. Endpoint matching alone does not imply them. On $t<0$ they are Lemmas 2.3.11 and 2.13.10 and Proposition 2.7.2. Remark 2.7.4 lists the remaining side-specific inputs and their backward sources.

Induction on the finite stage keeps the actual order classes. Principal waves have order $1/2$, and finite higher waves start at $1-3\varkappa$. Tangential means start at $1-\varkappa$, and radial means start at two. The cut radial mean increment has order $\alpha_n+3/2$ by (2.18.8).

These are the exact gains of the finite construction. A change in the explicit slow sign does not change them. For each stage and each prescribed finite norm list, we apply the estimates on the two sides and take their maximum constants. We include the actual pure-auxiliary Gevrey radii and current value margins in this list.

A finite ordinary derivative bound does not imply these conditions.

We select the single δ_n only after we know these finite data and the two native admitted thresholds. Then impose the support condition (2.18.10) and the bounds (2.18.11) simultaneously on the two sides. Their strictly positive spare powers dominate each fixed logarithm for the fixed $h>0$. At $\hat t_0>0$ these sums are locally finite, so Lemma 2.20.2 passes their jets to the actual completed fields.

At the singular tip, we use the distinct finite-prefix comparison. For any fixed m,L_0, we select one finite N with

$$h\beta_N-(2(\tfrac12+h)+3m+7)>L_0,\qquad h\alpha_N-K_m>L_0.$$

The same completed sum then satisfies $|\partial_{\mathrm{phys}}^{\le m}\mathscr{E}_\infty|\le C_{m,L_0}\hat t_\pm^{L_0}$ on the two sides by (2.18.16). This selects a finite prefix for an estimate, not a new diagonal.

Each side's chart satisfies $\hat t_\pm-z^2\hat t_\pm^{2h}=|t|$. Thus $\hat t_\pm\asymp|t|+|z|^{1/(\frac12-h)}$. Thus arbitrary $\hat t$-flatness supplies zero physical residual jets at the tip. Off-tip equality alone would not imply this estimate.

For the trace bound, we consider the fixed profile hull $r^2\le Cq_\pm$. The slow field has size $Cq_\pm^{-\frac12-h}$ there, including the axis, by Proposition 2.17.3 with $m=0$. The finite wave and initialization terms have additional positive powers of ρ. The same diagonal gives a summable value tail.

Thus $|u_\infty|\le C\mathfrak{d}^{-\frac12-h}$ there, where $\mathfrak{d}=r^2+|z|^{1/(\frac12-h)}$. Outside that hull, the forward heat formula and the backward positive Laplace integral give the same value bound. The integrand gives $H_-(Z)\le C\min(1,Z^{-h})$ directly. This is the two-sided version of (2.18.21).

It is a value estimate, independent of the residual-jet argument. The fixed localization is on a smooth off-origin annulus and keeps the two conclusions with its full pressure gradient. □

Proposition 2.20.4 (One same completion and its actual joining force)**.** *Use the leading backward member of Theorem 1(i)–(iv). We use the actual one-sided leading construction from Theorem 1(ii) and the leading and slow endpoint identification from Theorem 2.7.1. We use the same finite controls and the single last diagonal from (2.18.5)–(2.18.11). The completed velocity and pressure have identical physical jets on the two sides of the joining slice away from the origin. After the same fixed spatial localization, the actual residuals define one smooth spatially compact force across that slice.*

The completed velocities have one strong L^2 trace. This conclusion uses the actual finite-stage estimates on the two sides.

Proof. Lemma 2.20.2 first gives the actual finite fields and their equal slice jets by stage and jet-order induction. Lemma 2.20.3 supplies the finite estimates on the two physical sides before we select the single diagonal. In particular its negative slow-time coefficient does not change the pulse orientation or the viscous sign. All finite pressure terms, whole shifted paths, cutoff brackets and explicit endpoint outputs remain in these statements.

At $z_0 \neq 0$, $\widetilde{q}_0 > 0$. Only finitely many slow Borel and last packet terms survive on a neighborhood, so their actual sums have matching jets. The joining slice is $\widetilde{\eta} = 0$, and $\partial_t \widetilde{\eta} = 1/\widetilde{Q} \neq 0$. Lemma 2.3.17 turns the equal slice jets into C^∞ joining. At $z = 0, r > 0$, $\hat{\xi} \to \infty$ when time approaches the joining slice.

The whole neighborhood lies beyond $\frac{\hat{\xi}_{\mathrm{all}}^2}{2}$ for sufficiently small times. The same regular heat coefficient and the time-flat fast mode give the jets there, with the canonical outward pressure and no residual constant. These two arguments are not statements that the complete fields coincide on an open collar.

At the spacetime origin, we apply (2.18.17) and its independent backward bound from Lemma 2.20.3. They give zero jets for the residual relative to the same slow reference force. Proposition 2.11.4 proves that this actual slow force is smooth across the slice and flat at the origin, using both one-sided flatness bounds and the heat exterior. An endpoint-jet argument at $\hat{t}_0 > 0$ alone would not prove this fact. Thus the joined actual residual is smooth across the full joining slice.

We use the same fixed spatial cutoff and the same fixed compact annular divergence inverse in (2.18.23). Their derivatives act only on a smooth off-origin annulus. Matching input jets imply matching correction and residual jets there. The same scalar cuts the pressure. We keep its full gradient.

This gives one spatially compact force.

At the last step the distinct value estimate in Lemma 2.20.3 bounds the two actual completed envelopes by $C\mathfrak{d}^{-\frac{1}{2}-h}$, $\mathfrak{d} = r^2 + |z|^{1/(\frac{1}{2}-h)}$. The exact sublevel volume gives

$$\int_{\{\mathfrak{d}<\epsilon\}} \mathfrak{d}^{-1-2h}\, dx = C_h \epsilon^{\frac{1}{2}-3h}, \qquad 1 + (\tfrac{1}{2} - h) - 2(\tfrac{1}{2} + h) = \tfrac{1}{2} - 3h > 0.$$

The off-origin traces just identified coincide. We apply dominated convergence first outside $\{\mathfrak{d} < \epsilon\}$.

Then let ϵ decrease to zero. This gives strong L^2 convergence to that same trace from each side. Localization keeps it and exact divergence. The pressure-distribution argument (2.18.24) gives the full distributional equation.

Tests against divergence-free fields alone do not suffice. □

2.20.1 Backward stage estimates and finite time locality

The slow Borel stage and the native backward weight are proved below. After that reference has been supplied, the two sides use one finite packet, mean and return algorithm with shared discrete choices.

Lemma 2.20.5 (Time locality after the slow reference)**.** *Fix the labels, centres, auxiliary radius, representatives, frames, rounded integers, schedule, cutoffs and diagonal scales of the joint construction, and regard the slow reference as an input. Every finite packet, mean, return and initialization step of Sections 2.13–2.14, every finite last-cut step, and the spatial localization of Section 2.18 acts at fixed physical time using only finitely many time derivatives of its inputs. Its restriction to either open time side therefore depends only on inputs on that side. For smooth inputs with matching slice jets and the uniform bounds and supports required by these operations, the output slice jets match as well.*

Proof. Products and physical derivatives have this property. Pulse equations are solved in the pulse variable with the slow point fixed; their smooth parameter dependence follows from the pulse estimates. Torus inverses and Haar projections act in the auxiliary variable. Radial primitives, shifted primitives and moments integrate at fixed (z,t); the support and derivative bounds allow differentiation under the integrals. Finite matrix solves and roots preserve smooth jets on their protected value domains. In (2.18.6) the cutoff multipliers have matching physical jets. Its mean prefix integrates the same matched axial increment over the same physical interval at fixed (z,t), and the cutoff curl differentiates the matched potential. Finally the box divergence inverse and the Bessel inverse act only in space, with their stated derivative bounds. A finite composition has finite time-derivative order, and differentiating it to any fixed order proves the jet assertion. No state identity is inverted in time. □

The lemma does not cover the infinite-series inner slow inverse. For that inverse the required transported uniqueness and slice-jet comparison are Proposition 2.6.5; the subsequent slow Borel sum is Proposition 2.10.1. Lemma 2.20.2 then applies to the finite operations covered above. Passing to a diagonal limit additionally uses the derivative budgets of Section 2.18.

Lemma 2.20.6 (The backward native weight)**.** *Assume (B3), and let ζ be the weight of clause (O2) for the backward member, extended by zero. Choose $c_b>0$ so that $\mathsf{W}_b=c_b\zeta\le e^{-2}$, and put $\mathcal{L}_b=1+\log(1/\mathsf{W}_b)$ on $(\frac{\hat\xi_a^2}{2},\frac{\hat\xi_b^2}{2})$. Put $\delta=\min\{1,2\log(\hat\xi/\hat\xi_a),2\log(\hat\xi_b/\hat\xi)\}$.*

(a) There are $0<c\le C$ with $c\,\delta^{-2}\le\mathcal{L}_b\le C\delta^{-2}$ on $(\frac{\hat\xi_a^2}{2},\frac{\hat\xi_b^2}{2})$.

(b) In each band chart the backward leading target satisfies (2.13.3) with $\mathsf{W}=\mathsf{W}_b$.

(c) Let f be a function on a band chart. The bounds $|\partial^I f|\le C_I\rho_Q^a S^{B_I}\mathsf{W}_b\mathcal{L}_b^{N_I}$ for all I hold if and only if, for all I, $|\partial^I f|\le C'_I\rho_Q^a S^{B_I}\zeta\delta^{-d_I}$ holds with suitable C'_I and d_I. The same holds with $\sqrt{\mathsf{W}_b}$ and $\sqrt{\zeta}$ in place of W_b and ζ, and with the factor $P(v)$.

Thus the classes (2.13.4) and (2.13.5) on the backward side use W_b and $\sqrt{\mathsf{W}_b}$, respectively, with $\rho_Q=Q^h$.

Proof. (a) Write $\varphi_a(s)=s\psi_a(s)$ with $\psi_a>0$ smooth, as in the proof of Lemma 2.3.7. On the inner collar $d_a\le s_0$ we have

$$\log(1/\zeta)=a_a\varphi_a(d_a)^{-2}-\log g_a(\tfrac{\hat\xi^2}{2})=a_a d_a^{-2}\psi_a(d_a)^{-2}+O(1).$$

Fix $s_1\le\min\{s_0,1\}$ so small that $\delta=d_a$ on $\{d_a\le s_1\}$; then $\mathcal{L}_b\asymp\delta^{-2}$ there, since $\mathcal{L}_b\ge 3$. The outer collar is the same with φ_b. On the rest of $(\frac{\hat\xi_a^2}{2},\frac{\hat\xi_b^2}{2})$, both ζ and δ lie between positive constants.

(b) By (O2), $|T_0|\ge c\zeta=(c/c_b)\mathsf{W}_b$, and $|\partial^\alpha T_0|\le C_\alpha\zeta\delta^{-m_\alpha}\le C\mathsf{W}_b\mathcal{L}_b^{m_\alpha/2}$ by (a). Lemma 2.3.7(c), the chain rule in $d_a=2\log(\hat\xi/\hat\xi_a)$ and $d_b=2\log(\hat\xi_b/\hat\xi)$, and the bounds on g_a,g_b give $|(\hat\xi^{-1}\partial_{\hat\xi})^k\zeta|\le C_k\zeta\delta^{-3k}$. On this backward band $q=q_b=\widetilde q$, so in its chart $\frac{\hat\xi^2}{2}=Q\mathsf{R}^2/(2q)$ with q/Q and R in fixed compact intervals. All fixed jets of the change of variables are bounded, and so is the factor $(Q/q)^{1+h}$ of the normalized target. The Faà di Bruno formula and (a) then give (2.13.3).

(c) By (a), $\delta^{-d}\le C\mathcal{L}_b^{d/2}$ and $\mathcal{L}_b^N\le C\delta^{-2N}$. Also $\sqrt{\mathsf{W}_b}=\sqrt{c_b}\sqrt{\zeta}$. □

Lemma 2.20.7 (The backward slow Borel stage)**.** *Assume the hypotheses of Proposition 2.7.2. Let (c_n) increase, with $c_n\ge 2c_{n-1}$, and satisfy (2.6.32) for the forward and for the backward coefficients; this is the choice of Proposition 2.10.1, and it exists by (a). Let (u_B,p_B,K_B) be the slow reference of Proposition 2.6.15, built with $\chi(c_n\widetilde q)$, and consider it on $t<0$, where $\widetilde q=q_b$ by (2.10.1).*

(a) For each n, the backward budgets of order n in (2.6.32) are finitely many inequalities $C_{n,j}q^{nh} \le 2^{-n}$ on $0 < q \le 2L_{\max}/c_n$, with constants $C_{n,j}$ that do not depend on c_n. Each holds for all c_n above a finite threshold.

(b) On $t < 0$, $\operatorname{div} u_B = 0$ and (2.6.33) holds on the bounded profile hull.

(c) On $t < 0$, (2.6.34) holds on the annular stress hull, and (2.6.35), (2.6.37) hold with $\mathsf{W} = \mathsf{W}_b$. On I_{mean} every positive-order velocity term, with its cutoff term, vanishes, so u_B equals the leading velocity there.

(d) Every fixed physical derivative of u_B, p_B, K_B and of the residual in (2.6.33) extends continuously to $\hat\zeta_b = \pm 1$, that is, to $t = 0$ from below, on compact sets with $q_b > 0$.

(e) For $t < 0$, $q_b(z,t)$ is the unique root $q > |z|^{1/(\frac12 - h)}$ of $q - z^2 q^{2h} = -t$.

Proof. (a) For $n \ge 1$ the backward coefficients $F_n, U_n, P_n, M_n/\frac{\hat\xi^2}{2}, V_n/\frac{\hat\xi^2}{2}$ are C^∞ on $[0,\infty)\times[-1,1]$ up to $\hat\zeta_b = \pm 1$ (Lemma 2.6.4(c)) and vanish for $\hat\xi \ge \hat\xi_{\mathrm{ret}}$ (Proposition 2.7.2(b)). So each fixed normalized seminorm on the compact hull is finite. For $n \ge 2$, T_n is supported in $[\frac{\hat\xi_-^2}{2}, \frac{\hat\xi_{\mathrm{ret}}^2}{2}]\times[-1,1]$ (Proposition 2.7.2(c)), where W_b has a positive minimum ($\mathsf{W}_b = c_b\zeta$ is continuous and positive on $(\frac{\hat\xi_a^2}{2}, \frac{\hat\xi_b^2}{2})$ by (O2), and $[\frac{\hat\xi_-^2}{2}, \frac{\hat\xi_{\mathrm{ret}}^2}{2}] \subset (\frac{\hat\xi_a^2}{2}, \frac{\hat\xi_b^2}{2})$ by Proposition 2.7.2(a)), so the seminorms of T_n/W_b are finite as well. The cutoff factors have $(q\partial_q)^j\chi(c_nq_b) = ((\sigma\partial_\sigma)^j\chi)(c_nq_b)$, which is bounded independently of n, and $\partial_r q_b = 0$; so the cutoff derivatives enter the constants $C_{n,j}$ independently of c_n. Thus $C_{n,j}q^{nh} \le 2^{-n}$ holds on $0 < q \le (2^nC_{n,j})^{-1/(nh)}$, that is, on $0 < q \le 2L_{\max}/c_n$ for every $c_n \ge 2L_{\max}(2^nC_{n,j})^{1/(nh)}$. A larger c_n shrinks the range of q, so each budget is upward closed. We choose c_n above the finitely many thresholds of both sides and above $2c_{n-1}$.

(b) Each term is $\chi(c_nq_b)$ times a swirl with θ-independent amplitude, plus the curl of $\chi(c_nq_b)\Psi_n r^{-1}e_\theta$ (2.6.31); so it is divergence-free, and the sum is locally finite on $q_b > 0$. Flatness is the finite-prefix comparison after (2.6.32). It uses only (2.6.30), the budgets of (a), and the uniform cutoff bounds of (a). On $t < 0$, (2.6.30) holds with the same proof: the recursions (2.6.4)–(2.6.6) are written with the $\varsigma = -1$ operators, the only change being the sign of T_γ in $\partial_t(q_b^\gamma f) = +q_b^{\gamma-1}\mathsf{T}_\gamma f$ (proof of Proposition 2.8.10, "Chart"). The cancellation of the orders up to N and the count of exponents do not use this sign, and the stress primitives (2.6.23) do not depend on the side. So the forward argument applies verbatim on $t < 0$.

(c) The rates follow from the tail bound $\sum_{n\ge j} 2^{-n}q^{nh}$ of the budgets and from the order q^{2h} of the first coefficient, as in the proof of Proposition 2.6.15. The weighted stress bound and (2.6.37) are Remark 2.7.3. By Proposition 2.7.2(b), $E_n = U_n = M_n = V_n = 0$ on $I_{\mathrm{mean}} \subset \{\frac{\hat\xi^2}{2} \ge \frac{\hat\xi_{p,b}^2}{2}e^{-9}\}$ for $n \ge 1$. So each cut term vanishes there, including the term $-r^{-1}\Psi_n c_n\chi'(c_nq_b)\partial_z q_b$ of (2.6.31), since $\Psi_n = q_b^{\frac12 - h + \lambda_n}M_n$.

(d) Let $\mathcal{C}$ be a compact set in $\{t \le 0\}$ with $q_b \ge \delta > 0$ on $\mathcal{C}$. Then $\chi(c_nq_b) = 0$ near $\mathcal{C}$ when $c_n\delta > 2$, so only finitely many terms survive there. Near points of $\mathcal{C}$ with $t = 0$ (hence $z \ne 0$), $(z,t) \mapsto (q_b, \hat\zeta_b)$ is a real-analytic diffeomorphism onto a one-sided neighbourhood (proof of Proposition 2.8.10, "Chart"); for $t < 0$ the map q_b is smooth. Each surviving term, and the leading term, is a finite combination of powers of q_b, of the cutoff $\chi(c_nq_b)$ and of the profiles $F_n, U_n, P_n, M_n/\frac{\hat\xi^2}{2}, V_n/\frac{\hat\xi^2}{2}, T_n$ $(n \ge 0)$ at $\hat\xi = r/\sqrt{q_b}$, $\hat\zeta_b = z/q_b^{\frac12 - h}$. Physical derivatives act through (2.6.1) in the backward chart, whose coefficients are polynomials in $\hat\zeta_b$, d, $\frac12\hat\xi\partial_{\hat\xi}$, $\partial_{\hat\zeta}$ divided by powers of $L \ge 1 - 2h$, and through $\hat\xi = r/\sqrt{q_b}$, with the smooth Cartesian representatives near $r = 0$ that axis regularity gives (Lemma 2.6.1, and the Cartesian form of the potentials, as for $t > 0$). All these

profiles are C^∞ on $[0,\infty)\times[-1,1]$ up to $\hat{\zeta}_b=\pm1$: the positive orders by Lemma 2.6.4(c), and the leading data by Theorem 1(ii). So every fixed physical derivative is, on $\mathcal{C}\cap\{t<0\}$, a finite sum of products of functions that are continuous up to $\hat{\zeta}_b=\pm1$.

(e) At $q=|z|^{1/(\frac12-h)}$ the left side is zero. Above this endpoint its derivative is $1-2hz^2q^{2h-1}\ge 1-2h>0$, and it tends to infinity with q. □

Remark 2.20.8 (The last diagonal and the localization). For a mean increment with zero full flux (2.18.4), set $\Psi=r^{-1}\int_0^r s(\Delta u_{M,n})_z\,\mathrm{d}s$. Since $\partial_r\widetilde{q}=0$, the radial and axial components of $\operatorname{curl}(\chi_n\Psi e_\theta)$ are respectively $\chi_n(\Delta u_{M,n})_r-(\partial_z\chi_n)\Psi$ and $\chi_n(\Delta u_{M,n})_z$. Thus the same potential cut (2.18.6) applies on both sides, with one sequence δ_n chosen by Lemma 2.20.3.

The localization (2.18.23) cuts the velocity and corrects its divergence by the spatial annular inverse $\mathcal{B}_{\mathrm{div}}$. Proposition 2.20.4 requires only the off-origin smoothness and matching slice jets of (u_∞,p_∞), the flat residual at the origin, and the value bound. On $t<0$ these follow from (B7), Lemma 2.20.3 and the diagonal estimates of Section 2.18.

Remark 2.20.9 (Backward stage suppliers). The slow coefficients and their jets are supplied by Lemma 2.6.4 and Proposition 2.6.5; the slow sum by Lemma 2.20.7 and Proposition 2.10.1. The atlas uses (B2), Lemma 2.20.6, and the common choices of Theorem 2.10.2. The packet, mean and return estimates are Theorem 2.7.5; their weighted inputs and supports are Section 2.7.1 and Lemma 2.8.9. The last cut and spatial localization use Remark 2.20.8. Finite-stage jet transfer is Lemma 2.20.2 after the slow reference jets have been supplied.

2.21 Energy and past blowup for the background

Corollary 2.21.1 (Blowup of the jointly reconstructed past and energy)**.** *The selected joined base has an essentially unbounded trace. It satisfies $\|u(t)\|_\infty\to\infty$ as $t\uparrow0$ through the negative side. Any fixed earlier slice is a smooth datum. On the joined constructed interval the base satisfies the ordinary global energy identity and has finite integrated H^1 dissipation.*

Proof. The cusp (2.18.25) uses the enclosing bound $\frac{\hat{\xi}_{\mathrm{all}}^2}{2}$ and $c_{\mathrm{bank}}>0$, inside the ball untouched by localization. It has positive three-dimensional measure, not just the plane $z=0$. Thus the same trace is essentially unbounded. Suppose a sequence of negative times increases to zero and has one bound for its L^∞ norm. Strong L^2 convergence gives an almost-everywhere convergent subsequence. The trace then has the same bound, which is a contradiction. The trace belongs to L^2 because $h<1/6$.

For times bounded away from zero, classical integration of the smooth physical equation gives the energy identity on each side. The compact pressure contributes zero work. The uniform L^2 bound and smooth compact force bound make its work integrable. Strong L^2 convergence permits an endpoint limit at zero.

This limit bounds and identifies the integrated dissipation on each side. The sum of the two identities cancels the identical energies at zero. This calculation uses physical forward time on the negative interval. It does not reverse the viscosity sign or use a backward energy inequality.

For all $s\le t$ in the constructed interval,

$$\tfrac12\|u(t)\|_2^2+\int_s^t\|\nabla u(\tau)\|_2^2\,d\tau=\tfrac12\|u(s)\|_2^2+\int_s^t\langle\mathbf{f}(\tau),u(\tau)\rangle\,d\tau.$$

□

2.22 The completed-source envelope

Main result. Lemma 2.22.5 gives value, gradient, overlap, and clock bounds for the completed field. It assumes a fixed admissible leading source and the stated completion schedule. The envelope includes the actual completed wave sum and its corrections. We fix an admissible leading source, a finite angular integer m, and its $p = 6/5$ forward completion.

We write $s = -t^{-h}/h$ and $\rho = t^h$. In the band and stage cutoffs of this section $q = \widetilde{q} = q_f/L_{\mathrm{cut}}(\eta_f)$. The fixed smooth L_{cut} has a positive lower bound and bounded normalized derivatives. Thus $\widetilde{q} \asymp q_f$ and $\widetilde{q} \geq ct$. The physical leading stress has the two exact representations

$$q_f^{-1-h}\mathcal{T}_0 = \widetilde{q}^{-1-h}\widetilde{T}_0, \qquad \widetilde{T}_0 = L_{\mathrm{cut}}^{-1-h}\mathcal{T}_0.$$

The time and gradient factors in Lemma 2.22.2 come from the physical band coordinates. The same cutoffs remain independent of r and of the auxiliary variables, so we keep their full radial-prefix divergence correction.

The forward construction supplies the exact leading field $B_0 = u^{\mathrm{lead}}$, the slow reference u_{B}, and the completed field B_*. In this section and in the completed-background estimates $W = B_* - B_0 = (u_{\mathrm{B}} - B_0) + (B_* - u_{\mathrm{B}})$. On a comparable-time block, we use the same letters for their isotropically rescaled versions. These are the source estimates used here.

For fixed $\varkappa > 0$, the leading coefficients have bounded jets at each specified fixed derivative order. The envelope E of Definition 2.22.1 satisfies

$$\|W\|_\infty \leq \rho^{1/2}P(S), \qquad |\nabla W| \leq C(E + \rho^\eta), \qquad \|E\|_\infty \leq P(S), \quad \|\nabla E\|_\infty \leq \rho^{-\varkappa}P(S), \tag{2.22.1}$$

Here P is a fixed polynomial, with $S = S_{\mathrm{mask}}(s) := (1 + \log(1/\rho(s)))^{6/5}$ on the ancient range $0 < \rho < 1$. We fix $\eta > 0$ in the next argument. On a source band $Q_\gamma = 2^{-\ell} \asymp \widetilde{q}$ the discrete pulse scale is $S_\gamma = \ell^{6/5}$. Since $Q_\gamma \gtrsim t$, $S_\gamma \leq C_h S_{\mathrm{mask}}(s)$. On the subfamily $Q_\gamma \asymp t$ the two scales are comparable. The full envelope also includes the labels with $Q_\gamma \gg t$.

These are estimates for the actual completed wave sum, with its return and localization terms. The support and derivative claims behind (2.22.1) belong to the source construction, not to the next energy argument.

Definition 2.22.1 (Label pulse envelopes)**.** Let $\gamma = (\beta, \varsigma)$, $\beta = (\ell, a)$, range over the signed labels of Proposition 2.13.5. We write $Q_\gamma = 2^{-\ell}$, $\rho_\gamma = Q_\gamma^h$, $S_\gamma = \ell^{6/5}$, $i_\gamma = i(\ell)$ as in (2.13.7), $c_\gamma = T_g^{i_\gamma} Q_\gamma^{1+h}$, $L_\gamma = 2r_0/c_\gamma$, and let $c_{\mu(\gamma)}$ be the colour centre of γ from Lemma 2.13.1. On the level-i_γ torus, $(\xi_\gamma, \zeta_\gamma)$ are the coordinates of the injectively parametrized rectangle $\mathcal{R}_\gamma = \{c_{\mu(\gamma)} + \xi v_r + \zeta v_t : \ |\xi|, |\zeta| < 2r_0\}$. Let $c_a > 0$ be the constant of the upper Gaussian bound in (2.13.24) and put $c_P = c_a/(2r_0 T_g)$.

We define the torus profile

$$e_\gamma(y) = S_\gamma^{1/4}\, \chi_g(\xi_\gamma)\, \psi_0\Big(\tfrac{1}{2} + \tfrac{\zeta_\gamma}{2r_0}\Big) \exp\Big(-\frac{c_P \zeta_\gamma^2}{c_\gamma^2 S_\gamma}\Big) \quad (y \in \mathcal{R}_\gamma), \qquad e_\gamma = 0 \text{ off } \mathcal{R}_\gamma, \tag{2.22.2}$$

where χ_g is the transverse bump of (2.13.39) (support in $|\xi| < r_0$). The temporal cutoff profile is ψ_0, with $\psi(v) = \psi_0(v/L_p)$ (support in $(1/6, 5/6)$, that is, $|\zeta| < 2r_0/3$). Thus e_γ is smooth on $\mathbb{T}^2$. With the slow cutoff η_β of (2.13.11) put $E_\gamma(x, y) = \eta_\beta(x) e_\gamma(y)$, $x = (\mathsf{R}, \mathsf{Z}, \mathsf{T})$ the band-ℓ coordinates, and denote by $F^\sharp(t, r, z) = F(x(t, r, z), J_g^{i_\gamma} Y_{\mathrm{phys}}(r, t))$ the physical sample of a lifted function. For a constant C_0 fixed in Lemma 2.22.3 and $\tau > 0$ set

$$E^{[\tau]} = C_0 \sum_\gamma \Big(\frac{\tau}{Q_\gamma}\Big)^{1+h} E_\gamma^\sharp, \qquad E := E^{[t]}. \tag{2.22.3}$$

E is the envelope in (2.22.1).

Lemma 2.22.2 (Pulse coordinates and the same normalization factor)**.** *We fix a label γ and a lift of $\mathcal{R}_\gamma$.*

(a) There are constants ξ^0, ζ^0 (which can depend on the lift) with $\xi_\gamma = \Lambda_g^{i_\gamma} r^{d_r} - \xi^0$ and $\zeta_\gamma = T_g^{i_\gamma} t - \zeta^0$ at the physical sample. In particular the pulse variable $v = (\zeta_\gamma + r_0)/c_\gamma$ satisfies $\nabla_x v = 0$ and $Q_\gamma^{1+h}\partial_t v = 1$. Also $v - L_\gamma/2 = \zeta_\gamma/c_\gamma$ and $v/L_\gamma = \frac{1}{2} + \zeta_\gamma/(2r_0)$.

(b) Let Q be the reference time of an isotropic block, $\rho = Q^h$, and $y = x/\sqrt{Q}$. The block time derivative is $Q^{1+h}\partial_t$. For a lifted scalar coefficient f,

$$\sqrt{Q}\,\partial_r f^\sharp = (Q/Q_\gamma)^{1/2}(D_{\mathsf{R}} f)^\sharp, \qquad \sqrt{Q}\,\partial_z f^\sharp = (Q/Q_\gamma)^{1/2}(\rho_\gamma \partial_{\mathsf{Z}} f)^\sharp,$$
$$Q^{1+h}\partial_t f^\sharp = (Q/Q_\gamma)^{1+h}(c_\gamma \partial_\zeta f + \rho_\gamma \partial_{\mathsf{T}} f)^\sharp, \qquad D_{\mathsf{R}} = \partial_{\mathsf{R}} + \Lambda_g^{i_\gamma} Q_\gamma^{d_r/2} a_r(\mathsf{R})\, v_r \cdot \partial_y,$$

where $\partial_\zeta = v_t \cdot \partial_y$.

(c) For a velocity $w = Q_\gamma^{-\frac{1}{2}-h} V^\sharp$, with V a lifted coefficient vector in cylindrical components, the block-normalized gradient $\nabla_y(Q^{\frac{1}{2}+h} w) = Q^{1+h}\nabla_x w$ obeys

$$|\nabla_y(Q^{\frac{1}{2}+h} w)| \le \Big(\frac{Q}{Q_\gamma}\Big)^{1+h} \big(|D_{\mathsf{R}} V| + |\mathsf{R}^{-1}\partial_\theta V| + |\rho_\gamma \partial_{\mathsf{Z}} V| + \mathsf{R}^{-1}|V|\big)^\sharp.$$

Because $(\frac{1}{2}+h) + \frac{1}{2} = 1 + h$, the spatial factor in (c) and the temporal factor in (b) are the same number $(Q/Q_\gamma)^{1+h}$.

Proof. (a) v_r, v_t are eigenvectors of J_g with eigenvalues Λ_g, T_g (direct check: $J_g v_r = (4-\sqrt{2}, 6-5\sqrt{2}) = \Lambda_g v_r$, $J_g v_t = (3\sqrt{2}-2, 4+\sqrt{2}) = T_g v_t$). Thus $J_g^i Y_{\mathrm{phys}} = \Lambda_g^i r^{d_r} v_r + T_g^i t\, v_t$. We subtract $c_\mu + k$ and expand in the orthogonal basis (v_r, v_t). This gives the formulas, with $\xi^0 = (c_\mu + k)\cdot v_r/|v_r|^2$, $\zeta^0 = (c_\mu + k)\cdot v_t/|v_t|^2$. The statements on v hold because $c_\gamma = T_g^i Q_\gamma^{1+h}$ and $L_\gamma = 2r_0/c_\gamma$.

(b) With $r = \sqrt{Q_\gamma}\mathsf{R}$, $z = Q_\gamma^{\frac{1}{2}-h}\mathsf{Z}$, $t = Q_\gamma \mathsf{T}$ and (a), the chain rule gives $\sqrt{Q_\gamma}\partial_r = \partial_{\mathsf{R}} + \sqrt{Q_\gamma} d_r r^{d_r - 1}\Lambda_g^i v_r \cdot \partial_y = D_{\mathsf{R}}$, $\sqrt{Q_\gamma}\partial_z = Q_\gamma^h \partial_{\mathsf{Z}} = \rho_\gamma \partial_{\mathsf{Z}}$, and $Q_\gamma^{1+h}\partial_t = \rho_\gamma \partial_{\mathsf{T}} + T_g^i Q_\gamma^{1+h} v_t \cdot \partial_y$. The q-band factor of η_β is a function of (Z, T) through the chart, so the formula includes it. Multiplication by $(Q/Q_\gamma)^{1/2}$ and $(Q/Q_\gamma)^{1+h}$, in this order, gives (b).

(c) In cylindrical components the Cartesian gradient of a vector field consists of ∂_r, $r^{-1}\partial_\theta$, ∂_z of the components plus the connection terms u_θ/r, u_r/r. We multiply by $Q^{1+h} = Q^{\frac{1}{2}+h}\sqrt{Q}$ and use (b) and $\sqrt{Q}/r = (Q/Q_\gamma)^{1/2}/\mathsf{R}$. The total factor is $(Q/Q_\gamma)^{\frac{1}{2}+h}(Q/Q_\gamma)^{1/2} = (Q/Q_\gamma)^{1+h}$. □

Lemma 2.22.3 (Principal pulse bound without loss in S)**.** *There are constants C_0, C, B that depend only on the fixed leading data, graph, r_0, χ_g, ψ_0, and u_p. They do not depend on ℓ, S_γ, or ρ_γ. There is also a threshold on q. Under this threshold, the cut principal wave of label γ,*

$$w_\gamma = Q_\gamma^{-\frac{1}{2}-h}\big[\vartheta_q a_\gamma \cos(k_\ell \Phi) - \widetilde{b}_\gamma \sin(k_\ell \Phi)\big]^\sharp,$$

with a_γ from (2.13.42) and $\widetilde{b}_\gamma$ the curl remainder of $\vartheta_q d_\gamma$, satisfies

$$|\nabla_y(Q^{\frac{1}{2}+h} w_\gamma)| \le \Big(\frac{Q}{Q_\gamma}\Big)^{1+h}\big[C_0 E_\gamma^\sharp + C\rho_\gamma^{1/2-2\varkappa} S_\gamma^B\big]. \tag{2.22.4}$$

Proof. By Lemma 2.22.2(c) it suffices to bound the evaluated derivatives of the coefficient vector $V = \vartheta_q a_\gamma \cos(k_\ell \Phi) - \widetilde{b}_\gamma \sin(k_\ell \Phi)$. We write $\nabla_* = (D_{\mathsf{R}}, \mathsf{R}^{-1}\partial_\theta, \rho_\gamma \partial_{\mathsf{Z}})$.

The phase gradient. Φ depends on the torus variable only through v, and $D_{\mathsf{R}} v = \partial_{\mathsf{Z}} v = 0$ by Lemma 2.22.2(a). Thus $\nabla_* \Phi = n$ as specified in (2.13.16). The term $-v H_\Phi$ contributes $-v \nabla_* H_\Phi$, and v grows up to $L_\gamma \asymp S_\gamma$. We bound its radial part: at the frozen representative, $(\widetilde{p}/\mathsf{R}_0, p_z) \cdot g_0 = B_p (K \cdot g_0 - \varsigma u_p / L_p) = -\varsigma B_p u_p / L_p$, because $K \perp N \parallel g_0$ by (2.13.13).

So the order-one part of $(H_\Phi)_{\mathsf{R}}$ vanishes identically and $x_0 - v (H_\Phi)_{\mathsf{R}}^{\mathrm{frz}} = B_p s(v)$. The deviation of $(H_\Phi)_{\mathsf{R}}$ from its frozen value is $O(k_\ell^{-1} + S_\gamma^{p_2 - K_{\mathrm{mesh}}} + \rho_\gamma^2)$, and after multiplication by $v \le C S_\gamma$, it is $o(1)$ because $K_{\mathrm{mesh}} > p_2 + 3$. The axial part $\rho_\gamma v (H_\Phi)_{\mathsf{Z}}$ is $O(\rho_\gamma S_\gamma)$. This is (2.13.18)–(2.13.19): $|n - B_p(s(v), K)| \le C / S_\gamma$.

Because $|s(v)| \le 3u_p/2$, $|K| = 1$, and $B_p^2 = \lambda_0 / (\rho_\gamma k_\ell^2 (1 + u_p^2)^{3/2}) \le \lambda_{\max}$ (as $\rho_\gamma k_\ell^2 \ge 1$),

$$|n| \le C_n := \lambda_{\max}^{1/2} (1 + 9u_p^2/4)^{1/2} + 1.$$

Thus the spatial gradient of the phase and the physical carrier wave vector $k_\ell Q_\gamma^{-1/2} n$ do not grow along the pulse.

The amplitude. By (2.13.41), $a_{\beta,\varsigma} = \sqrt{y_{\beta,\varsigma}} \le (C_y \sqrt{S_\gamma} |T_\beta|)^{1/2}$. Here the exact covariance normalization gives

$$|T_\beta| = (Q_\gamma / q_f)^{1+h} |\mathcal{T}_0| = (Q_\gamma / \widetilde{q})^{1+h} |\widetilde{T}_0| \le C\, \mathsf{W}\, \mathcal{L}_W^{N_0} \le C_T.$$

Indeed $\widetilde{q}/Q_\gamma \in (1/2, 2)$ where $\eta_\beta \neq 0$, $\widetilde{T}_0 = L_{\mathrm{cut}}^{-1-h} \mathcal{T}_0$, and (2.13.3) bounds the native stress. The function $u(1 + \log(1/u))^{N_0}$ is bounded on $(0, e^{-2}]$. The constant C_y comes from the inversion of the 2×2 matrix with columns $A_\varsigma \{c_0 \sqrt{1 + u_p^2} N - \varsigma u_p K + O(S^{-1/2})\}$, $A_\varsigma \asymp S^{-1/2}$. The cone margin gives one bound for the inverse of the limit. It is independent of S.

Next, $t_\varsigma^h = B_f (z_+, z_-)^\top$ with $\|B_f\| \le C_f$ and $|z_-| \le (C/S) z_+$. From the explicit formulas in the proof of Lemma 2.13.2,

$$\frac{z_+(v)}{P(v)} = \exp \int_0^v (d_{\mathrm{ref}} - d_p + E_{11} + E_{12} r)\, \mathrm{d}w \le \exp\Big(\frac{L_\gamma}{S_\gamma} (2C_E + C_E K_0) \Big) \le e^{C_1},$$

because $L_\gamma \le 2 r_0 T_g S_\gamma$. Thus $|t_\varsigma^h| \le C_h P(v)$. At the last step $k_\ell \rho_\gamma^{1/2} \le 1 + \rho_\gamma^{1/2} \le 2$ and $0 \le \vartheta_q \le 1$.

The Gaussian in the clock variable. By (2.13.24) and Lemma 2.22.2(a),

$$P(v) \le \exp\Big(-c_a \frac{(v - L_\gamma/2)^2}{L_\gamma} \Big) = \exp\Big(-\frac{c_a c_\gamma S_\gamma}{2 r_0} \frac{\zeta_\gamma^2}{c_\gamma^2 S_\gamma} \Big) \le \exp\Big(-\frac{c_P \zeta_\gamma^2}{c_\gamma^2 S_\gamma} \Big),$$

because $c_\gamma S_\gamma \in (T_g^{-1}, 1]$ by the floor in (2.13.7). Also $\psi(v) = \psi_0(\tfrac{1}{2} + \zeta_\gamma / (2 r_0))$.

The principal term. $\nabla_* V$ contains $-k_\ell \sin(k_\ell \Phi)\, \vartheta_q a_\gamma \otimes n$. We collect the factors to get

$$k_\ell |\vartheta_q a_\gamma| |n| \le 2 C_n C_h (C_y C_T)^{1/2}\, S_\gamma^{1/4} \eta_\beta \chi_g(\xi_\gamma) \psi(v) P(v) \le C_0 E_\gamma, \qquad C_0 := 2 C_n C_h (C_y C_T)^{1/2}.$$

The remaining terms. By (2.13.45), $a_\gamma \in \mathcal{W}^{1/2}$, $d_\gamma \in \mathcal{W}^1$, $b_\gamma \in \mathcal{W}^{1-\varkappa}$. The factor $\sqrt{\mathsf{W}} \mathcal{L}_W^N P(v)$ in (2.13.5) stays bounded. On the support of derivatives of ϑ_q, $\mathcal{L}_W \le C S_\gamma$, and (2.13.3) gives $|\partial^I \vartheta_q| \le C_I S_\gamma^{B_I}$ for ordinary derivatives. The torus part of D_{R} has coefficient $\Lambda_g^i Q_\gamma^{d_r/2} \asymp \rho_\gamma^{-\varkappa} S_\gamma^{-\rho_g}$ by (2.13.9).

Thus $|\cos(k_\ell \Phi) \nabla_* (\vartheta_q a_\gamma)| \le C \rho_\gamma^{1/2 - 2\varkappa} S_\gamma^B$. $\widetilde{b}_\gamma$ equals $\vartheta_q b_\gamma$ plus terms bilinear in first derivatives of ϑ_q and d_γ, so $|\widetilde{b}_\gamma| + |\nabla_* \widetilde{b}_\gamma| \le C \rho_\gamma^{1 - 2\varkappa} S_\gamma^B$. This gives $k_\ell |n| |\widetilde{b}_\gamma| \le C \rho_\gamma^{1/2 - 2\varkappa} S_\gamma^B$. The connection term $\mathsf{R}^{-1} |V| \le C \rho_\gamma^{1/2} S_\gamma^{1/4}$ on the radial hull.

Their sum gives (2.22.4). □

Lemma 2.22.4 (Order-to-gradient rule)**.** *On an isotropic block with reference Q, let γ be a label active at the point, so $Q_\gamma \ge c_L Q$ and $S_\gamma \le C_h S$.*

(a) If $X \in \mathcal{W}^a$ is a coefficient on γ at a relative harmonic m, $|m| \le m_*$, then

$$|\nabla_y (Q^{\frac12+h} Q_\gamma^{-\frac12-h} (X e^{ik_\ell m\Phi})^\sharp)| \le C (Q/Q_\gamma)^{1+h} \rho_\gamma^{a-1/2} S_\gamma^B.$$

(b) If $M \in \mathcal{M}^a$ is a normalized mean coefficient, then

$$|\nabla_y ((Q/Q_\gamma)^{1/2+h} M^\sharp)| \le C (Q/Q_\gamma)^{1+h} \rho_\gamma^{a-\varkappa} S_\gamma^B.$$

(c) For $0 \le \delta \le 1$, $(Q/Q_\gamma)^{1+h} \rho_\gamma^\delta S_\gamma^B \le C_L C_h^B \rho^\delta S^B$.

Proof. On the block, $t/Q \in [\frac12, 2]$ (as $\rho L \to 0$). Active labels satisfy $\widetilde{q}/Q_\gamma \in (1/2, 2)$. The native equation $q_f - z^2 q_f^{2h} = t$ and $\widetilde{q} = q_f/L_{\mathrm{cut}}$ give $Q_\gamma \gtrsim t \asymp Q$, whence $\ell \le \log_2(1/Q) + C_L$ and $S_\gamma \le C_h S$. (a) The carrier derivative gives $k_\ell |m||n||X| \le C m_* \rho_\gamma^{a-1/2} S^B$. The derivative $\nabla_* X$ has loss at most $\rho_\gamma^{-\varkappa} S^B$.

The connection term is $O(\rho_\gamma^a S^B)$. We use Lemma 2.22.2(c) and $\varkappa < \frac12$. (b) We apply the same argument without the carrier. (c) $(Q/Q_\gamma)^{1+h} \rho_\gamma^\delta = \rho^\delta (Q/Q_\gamma)^{1+h-h\delta} \le C_L \rho^\delta$. □

The preparation uses finite source estimates from this same completion, with the derivative bound in paragraph 2.18.4: ordinary coefficient jets through $J_{\mathrm{src}} = 80$. For each finite requested output list, we enlarge the finite prefix in (2.18.13) and decrease its admitted ancient threshold. The high-wave, mean, and pressure decomposition does not change after this. The extra derivative estimates apply to the finite coefficients and the simultaneous physical output tails. They do not assert that those tails are Gaussian inverse inputs. They also do not deduce the distinct pure-auxiliary Gevrey bounds from ordinary jets.

Lemma 2.22.5 (Quantitative strain of the completed $p = 6/5$ member)**.** *Let B_* be the forward completion of the selected member of Theorem 1 (admissible by Lemma 2.18.3, using the weight and core bounds of Theorem 1(iii)–(iv) and the slow inverse below), $W = B_* - B_0$, and fix $0 < \eta < \frac12 - 3\varkappa$. After a sufficiently late finite prefix and q threshold, the next hold on each sufficiently ancient isotropic block, with Q its reference time and $\rho = Q^h$.*

(i) $\|W\|_\infty \le \rho^{1/2} P(S)$.

(ii) $|\nabla_y W| \le E^{[Q]} + C\rho^\eta \le 2E + C\rho^\eta$, *where* $E^{[Q]} = (Q/t)^{1+h} E$.

(iii) $\|E\|_\infty \le C S^{1/4}$ *and* $\|\nabla_y E\|_\infty \le \rho^{-\varkappa} P(S)$.

(iv) At each physical point at most $N_0 = 32$ labels have $\eta_\beta \ne 0$.

(v) For each γ, $C_0 E_\gamma$ has the form of Lemma 2.23.1, with $A_{\mathrm{slow}} = C_0 \eta_\beta$ ($0 \le A_{\mathrm{slow}} \le C_0$), $\chi_+ = \chi_g$, $\psi_+ = \psi_0$, $c' = c_P$, $S = S_\gamma$, $c_i = c_\gamma$, and $c_\gamma S_\gamma \in (T_g^{-1}, 1]$. Also $\Pi E_\gamma \le C \eta_\beta S_\gamma^{-1/4}$.

(vi) Let φ_γ be the zero-Haar solution of $c_\gamma \partial_\zeta \varphi_\gamma = e_\gamma - \Pi e_\gamma$ and $\Phi_\gamma = C_0 \eta_\beta \varphi_\gamma$. Then, with $\partial_s = t^{1+h} \partial_t$,

$$\partial_s \sum_\gamma \Phi_\gamma^\sharp = E - r, \qquad r = \sum_\gamma \Big(\frac{t}{Q_\gamma}\Big)^{1+h} [C_0 \Pi E_\gamma - \rho_\gamma \partial_{\mathsf{T}} \Phi_\gamma]^\sharp, \tag{2.22.5}$$

with $\|r\|_\infty = O(S^{-1/4} + t^{(1+h)/2} + \rho P(S))$.

The envelope E in (ii) and in (2.22.5) is the same function.

Proof. Step 1: decomposition. We select the finite index N in (2.18.13) with $h\beta_N \geq (\frac{1}{2}+h)+3$. By (2.18.12),

$$B_* = u^{[0]} + \sum_{n<N} (\widetilde{\Delta u}_{M,n} + \widetilde{\Delta w}_n) + W_{\mathrm{tail}} + W_{\mathrm{loc}},$$

where W_{tail} is the sum over $n \geq N$, with support in $q \leq 2\delta_N$. The term W_{loc} collects the physical localization and compact off-origin flux correction from Section 2.18. By (2.15.22), (2.14.6), (2.15.17) and (2.15.53), the finite-state part equals

$$u_B + (u_M - u_B) + \sum_{\gamma} w_\gamma + v,$$

where $Q^{\frac{1}{2}+h}(u_M-u_B)_{\tan} \in \mathcal{M}^{1-\varkappa}$ and $Q^{\frac{1}{2}+h}(u_M-u_B)_r \in \mathcal{M}^2$. The stage-$n$ increments have orders $s_* \geq \frac{3}{2} - 4\varkappa$ and $p+1$.

The term v is a finite sum of exact curls over labels and relative harmonics. Its principal coefficient belongs to $\mathcal{W}^{a_0}$, with $a_0 = 1-3\varkappa$. Its tangential curl belongs to $\mathcal{W}^{a_0+1/2-\varkappa}$, and its radial curl belongs to $\mathcal{W}^{a_0+3/2}$. This includes the signed initialization ($\mathcal{W}^{5/2}$), and all stage-n harmonic corrections z and signed corrections h (principal order $\alpha_n \geq a_0$).

The cut increments obey (2.18.9). The cutoff factors χ_n have ordinary coefficient jets bounded independently of Q, δ_n. The two axial-prefix bounds in (2.18.8) preserve the radial mean order $p+1$, and (2.18.7) accounts for the derivative of the cutoff in each wave curl. Each label-indexed correction keeps the slow and transverse supports of its label (Proposition 2.13.3 and the proof of Proposition 2.13.7).

($\mathrm{H}_{\mathrm{slow}}$) Put $V_s = t^{1/2+h}(u_B - B_0)$ in the canonical variables $Y = x'/\sqrt{t}$, $Z = z/t^{1/2-h}$. On the full native velocity hull (2.6.36) gives canonical jets of size $O(t^{2h}\mathcal{Q}^{-1/2+h})$ for the azimuthal and axial vector components and $O(t^{3h}\mathcal{Q}^{-1/2+2h})$ for the radial vector component, where $\mathcal{Q} = q_f/t \geq 1$. For the isotropic block the exact conversion at fixed t is

$$\begin{aligned} Q^{1/2+h}(u_B - B_0) &= (Q/t)^{1/2+h} V_s, \\ Q^{1+h}\nabla_{x'}(u_B - B_0) &= (Q/t)^{1+h}\nabla_Y V_s, \\ Q^{1+h}\partial_z(u_B - B_0) &= (Q/t)^{1+h} t^h \partial_Z V_s. \end{aligned}$$

The ratio t/Q is bounded above and below. The unlocalized difference vanishes beyond its native velocity hull. Thus its normalized value and strain are $O(\rho^2)$ on the full block, including the regular axis and points with no active labels. In particular the strain is $O(\rho^\eta)$.

($\mathrm{H}_{\mathrm{far}}$) For each fixed $q_* > 0$ the region $\widetilde{q} \geq q_*$ stays away from the tip on ancient blocks. The off-origin regularity of Proposition 2.8.6 bounds the physical jets on compact portions, including the localization annulus and its flux correction. At large $|x|$ the localized field is zero. For the unlocalized leading field the native profiles and their derivatives stay bounded when q_f is bounded below on the profile hull, and the exterior heat gradient is $O(r^{-2-2h})$ where r is bounded below. These bounds give $O(Q^{1+h})$ for the normalized far-field gradient.

Step 2: principal waves. Lemma 2.22.3 and Lemma 2.22.4(c) with $\delta = \frac{1}{2} - 2\varkappa$ give

$$\Big|\nabla_y \sum_{\gamma} Q^{\frac{1}{2}+h} w_\gamma\Big| \leq C_0 \sum_{\gamma} (Q/Q_\gamma)^{1+h} E_\gamma^\sharp + C N_0 \rho^{1/2-2\varkappa} S^B = E^{[Q]} + C N_0 \rho^{1/2-2\varkappa} S^B,$$

because at most N_0 labels contribute at a point (Step 6).

Step 3: wave corrections. Lemma 2.22.4(a),(c) with $a = a_0$ give $|\nabla_y(Q^{\frac12+h}v)| \le C\rho^{1/2-3\varkappa}S^B$. The curl parts have orders $\ge a_0+\frac12-\varkappa$ and contribute $O(\rho^{1-4\varkappa}S^B)$. There are finitely many stages $n<N$ and finitely many harmonics, so the constants are finite, with fixed polynomial degrees. They must not grow with the number of active stages.

Step 4: means. Lemma 2.22.4(b),(c) give $|\nabla_y Q^{\frac12+h}(u_M-u_B)| \le C\rho^{1-2\varkappa}S^B$.

Step 5: tail and physical regions. On $\operatorname{supp} W_{\mathrm{tail}}$, we apply the diagonal bound (2.18.11) to the cut increments with their exact prefix corrections. This gives (2.18.13) with $m=1$ on the full tail support, with cutoff transitions. Thus $Q^{1+h}|\nabla_x W_{\mathrm{tail}}| \le CQ^{1+h}q^{h\beta_N-(\frac12+h)-3} \le CQ^{1+h}$, as $h\beta_N \ge (\frac12+h)+3$ and $q\le 1$. By ($\mathrm{H_{far}}$) and ($\mathrm{H_{slow}}$) the remaining parts are $O(Q^{1+h}+\rho^\eta)$.

Step 6: overlap. $\eta_\beta \ne 0$ requires $|\log_2 q+\ell|<1$, at most two values of ℓ, and $|S_\ell^{K_{\mathrm{mesh}}}x_j-a_j|<1$, at most two values of each a_j. With two signs ς this gives $N_0 \le 2\cdot 2^3\cdot 2$.

Step 7: conclusion of (i), (ii). Steps 2–5 give $|\nabla_y W| \le E^{[Q]} + C\rho^{1/2-3\varkappa}S^B + C\rho^\eta$. Because $S=(1+\log(1/\rho))^{6/5}$ and $\eta<\frac12-3\varkappa$, $\rho^{1/2-3\varkappa}S^B \le \rho^\eta$ for ρ less than a threshold that depends on B,η. On the block $t/Q = 1+O(\rho L)$ with $\rho L\to 0$, and $E^{[Q]} = (Q/t)^{1+h}E \le 2E$. The same decomposition at value level proves (i): $|a_\gamma| \le C\rho_\gamma^{1/2}S_\gamma^{1/4}$, all other pieces are smaller. For the principal value the band conversion is $(Q/Q_\gamma)^{\frac12+h}\rho_\gamma^{1/2} = \rho^{1/2}(Q/Q_\gamma)^{(1+h)/2} \le C_L\rho^{1/2}$, including labels with $Q_\gamma \gg Q$.

Step 8: (iii). $E_\gamma \le S_\gamma^{1/4} \le C_h^{1/4}S^{1/4}$, the weights $(t/Q_\gamma)^{1+h}$ are bounded by the fixed gauge and band comparison constants, and at most N_0 terms are nonzero. For the gradient, Lemma 2.22.2(b) and (a) show that ∇_x does not differentiate ζ_γ. The operator $D_{\mathsf R}$ differentiates $\chi_g(\xi_\gamma)$ with coefficient $\le C\rho_\gamma^{-\varkappa}$, and ordinary slow derivatives of η_β have loss $S_\gamma^{K_{\mathrm{mesh}}}$. Thus $|\nabla_y E| \le C\rho^{-\varkappa}S^{K_{\mathrm{mesh}}+1/4}$.

Step 9: (v). The form is (2.22.2) itself. For the Haar mean, $dy = |\det(v_r,v_t)|\,\mathrm{d}\xi\,\mathrm{d}\zeta$ and

$$\Pi e_\gamma \le |\det(v_r,v_t)|\,\|\chi_g\|_{L^1}S_\gamma^{1/4}\int_{\mathbb R} e^{-c_P\zeta^2/(c_\gamma^2 S_\gamma)}\,\mathrm{d}\zeta = |\det(v_r,v_t)|\,\|\chi_g\|_{L^1}\sqrt{\pi/c_P}\,c_\gamma S_\gamma^{3/4} \le CS_\gamma^{-1/4}.$$

Step 10: (vi). Lemma 2.23.1 gives φ_γ smooth with $\|\varphi_\gamma\|_\infty \le CS_\gamma^{3/4}(1+\log S_\gamma)$. By Lemma 2.22.2(b) with Q replaced by t, $t^{1+h}\partial_t\Phi_\gamma^\sharp = (t/Q_\gamma)^{1+h}[C_0(E_\gamma-\Pi E_\gamma)+\rho_\gamma\partial_{\mathsf T}\Phi_\gamma]^\sharp$. The sum over γ gives (2.22.5) with the same weights $(t/Q_\gamma)^{1+h}$ as in (2.22.3). For the bound on r: if $Q_\gamma \le \sqrt{t}$ then $S_\gamma \ge 2^{-6/5}S_t$ and the term is $O(S^{-1/4})$.

If $Q_\gamma \ge \sqrt{t}$ the weight is $\le t^{(1+h)/2}$. Also $|\rho_\gamma\partial_{\mathsf T}\Phi_\gamma| \le C\rho_\gamma S_\gamma^{K_{\mathrm{mesh}}+1}$, and Lemma 2.22.4(c) converts the weighted sum to $O(\rho P(S))$. At most N_0 terms are nonzero. □

Fixed constants for the actual clock and Gram. Only the original principal pulses enter E. All finite-prefix corrections after this step and the diagonal tail enter the ρ^η remainder, not an extra S^b in the principal height. The Gram metric of Theorem 1(vii) uses only the fixed leading field B_0 and its fixed smooth shift approximation. Its finite symbol constants do not involve derivatives of the completed W.

The single finite prefix in the previous proof supplies one fixed polynomial $P(S)$. The infinite tail satisfies the geometric bound (2.18.11). The fixed prefix and geometric tail do not let the number of active stages increase the Gram constants.

2.23 The clock of the completed packet field

2.23.1 The pulse clock and its contrast

In the pulse torus let $v_r = (1, 1-\sqrt{2})$ and $v_t = (\sqrt{2}-1, 1)$. These vectors are orthogonal.

For a band $Q = 2^{-\ell}$ the schedule sets $S_\ell = \ell^{6/5}$ and selects the auxiliary level $i(\ell)$ so that

$$c_i = T_g^{i(\ell)} Q^{1+h} \asymp S_\ell^{-1}, \qquad i(\ell) = \left\lfloor \frac{(1+h)\ell \log 2 - (6/5)\log \ell}{\log T_g} \right\rfloor. \tag{2.23.1}$$

The floor contributes only a fixed multiplicative factor. The Gaussian width in the temporal torus coordinate ζ is comparable to $\epsilon = S_\ell^{-1/2}$.

The endpoint cutoff is a fixed smooth function of the normalized pulse time $v/L_p = 1/2 + \zeta/(2r_0)$, since $L_p = 2r_0/c_i$.

Lemma 2.23.1 (Zero-Haar clock primitive)**.** *Suppose the primary strain envelope of one pulse is dominated by*

$$E(y) = A_{\mathrm{slow}} S^{1/4} \chi_+(\xi)\psi_+\left(\frac{1}{2} + \frac{\zeta}{2r_0}\right) \exp\left(-\frac{c'\zeta^2}{c_i^2 S}\right), \quad y = c_\mu + \xi v_r + \zeta v_t.$$

The displayed cutoffs are fixed smooth functions. The coefficient A_{slow} is independent of the torus variables and bounded in value.

The product $c_i S$ stays in a fixed compact subinterval of $(0, \infty)$.

Let Π denote Haar averaging on the torus. The periodic equation

$$c_i D_{v_t} \Phi = E - \Pi E, \qquad \Pi\Phi = 0, \tag{2.23.2}$$

has a smooth solution that satisfies

$$\|\Phi\|_\infty \le C|A_{\mathrm{slow}}| S^{3/4}(1 + \log S). \tag{2.23.3}$$

Suppose only boundedly many slow labels overlap at each physical point.

Their pulled-back primitives sum to at most $C S_t^{3/4}(1 + \log S_t)$, where $S_t = (1 + \log(1/t^h))^{6/5}$ bounds the active S_γ up to a fixed factor by Lemma 2.22.4. Thus the clock contrast $B_a = \exp(\operatorname{osc} a)$ for $a = -K\Phi_{\mathrm{all}}$ and fixed K is $\rho^{-o(1)}$.

Proof. Lemma 2.12.1 gives the solution, its smoothness and the bound (2.23.3), with unchanged slow support. The bounded-overlap summation is part of that lemma.

Thus

$$\log B_a \le CKS_t^{3/4}(1 + \log S_t) = O\big((\log(1/\rho))^{9/10} \log\log(e/\rho)\big) = o(\log(1/\rho)),$$

which gives the stated contrast. □

Remark 2.23.2 (Time profile and exponent margin). Fix a physical point (r, z) and apply Lemma 2.22.2(a). Each passage of the sampled torus line through $\mathcal{R}_\gamma$ produces this bump in block time θ:

$$\Big(\frac{Q}{Q_\gamma}\Big)^{1+h} C_0 \eta_\beta \chi_g(\xi_\gamma) S_\gamma^{1/4} \psi_0\Big(\frac{v}{L_\gamma}\Big) e^{-c_P(v - L_\gamma/2)^2/S_\gamma}, \qquad v = \Big(\frac{Q}{Q_\gamma}\Big)^{1+h}(\theta - \theta_k).$$

Its θ-integral is at most $C_0\sqrt{\pi/c_P}\, S_\gamma^{3/4}$.

This is independent of the band normalization. The height factor $(Q/Q_\gamma)^{1+h}$ cancels the dilation $\mathrm{d}v/\,\mathrm{d}\theta = (Q/Q_\gamma)^{1+h}$.

This dilation is the neighboring-band relation $t_* v = (Q_{\mathrm{ref}}/Q_\ell)^{1+h}$. If the principal height were $S^{1/4+b}$, the proof of Lemma 2.23.1 would give $\|\Phi\|_\infty \lesssim S^{3/4+b}(1 + \log S) = \ell^{\frac{6}{5}(\frac{3}{4}+b)}(1 + \log \ell)$, which is $o(\ell)$ iff $b < \frac{1}{12}$.

Lemma 2.22.3 gives $b = 0$: the constant C_0 contains no power of S.

Lemma 2.23.3 (Clock derivatives of the completed member)**.** *We include each actual source label, also those with $Q_j \gg t$. Select the axisymmetric physical cutoff inside the ball where the completed field equals the source field.*

The logarithmic clock $a = -K\Phi_{\mathrm{all}}$ satisfies, on the isotropic block,

$$a_s = -KE + r_{\mathrm{av}}, \qquad \|r_{\mathrm{av}}\|_\infty = o(1), \tag{2.23.4}$$

$$\|\nabla a\|_\infty \le \rho^{-\varkappa} P(S), \qquad \|B_* \cdot \nabla a\|_\infty + \rho(\|\Delta a\|_\infty + \|\nabla a\|_\infty^2) = o(1). \tag{2.23.5}$$

The bounds are global on each sufficiently ancient comparable-time block and use the one fixed $p = 6/5$ completion.

Proof. The first assertion is (2.22.5) of Lemma 2.22.5, with $\Phi_{\mathrm{all}} = \sum_\gamma \Phi_\gamma^\sharp$ and $r_{\mathrm{av}} = Kr$. The envelope there is the same function E that dominates $|\nabla W|$ in (2.22.1).

The weights $(t/Q_\gamma)^{1+h}$ in the two statements come from the single identity $(\frac{1}{2} + h) + \frac{1}{2} = 1 + h$ of Lemma 2.22.2. The bound $\|r\|_\infty = O(S^{-1/4} + t^{(1+h)/2} + \rho P(S)) = o(1)$ includes the trace labels $Q_\gamma \gg t$.

The sampled band derivatives obey $r\partial_r = R_j D_{R_j}$, $r\partial_z = \rho_j R_j \partial_{Z_j}$, with $D_{R_j} = \partial_{R_j} + m_i a_r(R_j) v_r \cdot \partial_Y$. The source hull has R_j in a fixed positive compact interval, $m_i \lesssim \rho_j^{-\varkappa} P(S_j)$, and $Q_j \gtrsim t$.

The fixed primitive jets thus give $\|\nabla a\|_\infty \le \rho_t^{-\varkappa} P(S_t)$. A second radial derivative, with the cylindrical connection, costs at most $\rho_j^{-2\varkappa}$, but axial derivatives gain ρ_j.

Thus $\rho\Delta a = O(\rho^{1-2\varkappa} P(S))$. The normalized radial background velocity has an extra ρ_j factor, and the primary wave value is $O(\rho_j^{1/2} P(S_j))$.

In block variables their products with the radial clock derivative are bounded by

$$C(Q/Q_j)^{1+h} \rho_j^{1/2-\varkappa} P(S_j).$$

The axial velocity has bounded band amplitude, while the axial clock derivative gains ρ_j, giving $C(Q/Q_j)^{1+h} \rho_j P(S_j)$. For either $d = 1/2 - \varkappa$ or $d = 1$, $(Q/Q_j)^{1+h} \rho_j^d = \rho^d (Q/Q_j)^{1+h-hd} \le C\rho^d$, since $Q_j \gtrsim t \asymp Q$. This gives the bound $O(\rho^{1/2-\varkappa} P(S))$ uniformly on the full block. Azimuthal transport vanishes by axisymmetry.

The fixed outer cutoff and flux repair act away from the singular tip, where their physical jets stay bounded and contribute $O(t^{1+h})$ after normalization. The factor $\rho^{1-2\varkappa} P(S)$ bounds the squared gradient.

This proves the second line. □

The lower bound $p > 1$ in the schedule is different: for each fixed $B, N, M > 0$, the endpoint deletion term $Q^{-B} S^N e^{-cS} = O(Q^M)$ because $S = \ell^p$ grows faster than ℓ. The upper bound $p < 4/3$ is what makes the clock exponent $3p/4$ sublinear in ℓ.

Thus $p = 6/5$ satisfies the two requirements. We normalize $a = -K\Phi_{\mathrm{all}}$ with its zero exterior, so $\min a \le 0 \le \max a$ and $e^{\max a}$ and $e^{-\min a}$ are at most B_a.

We do not introduce a time-dependent additive gauge.

2.24 Completion of the selected member

Main result. Proposition 2.24.1 completes the selected leading profile with one schedule, one last diagonal, and one fixed spatial localization. It gives a base, pressure, and one force. The velocity has a strong singular trace and finite dissipation.

Proposition 2.24.1 (One completed source)**.** *Fix the selected leading pair of Theorem 1 and use the finite slow construction of Section 2.6. We apply the source construction of Sections 2.6–2.18 to the one leading profile in Theorem 1, with the schedule of Lemma 2.12.2 at $p = 6/5$. We select one fixed family of covers, labels, and phases. We select one finite-state return sequence, Borel diagonal, and spatial localization. These fields $(B_*, p_*, f_*, u_{0,*})$ satisfy the conclusions of the forward theorem.*

They have positive-time smoothness, and B_* and f_* have fixed compact spatial support. The force f_* extends smoothly through zero. The velocity has a strong singular L^2 trace and finite dissipation. For each fixed finite spatial derivative order j, there are member-dependent C_j, N_j with

$$\|\nabla_x^j B_*(t)\|_\infty \le C_j t^{-N_j} \quad (0 < t < t_j). \tag{2.24.1}$$

In particular, we select the force and trace once and together.

Proof. Lemma 2.18.3 verifies the six conditions for this selected member. The construction keeps its protected core, actual endpoint germs, and early moving correction regions fixed. The spectral modification and all its returns occupy a distinct hull after those regions. We do not assume that they precede the positive-order correction region.

The full third slow moment and the current radial pressure correction keep P_1, P_2 through the last meridional return, as in Section 2.20.1. Lemma 2.3.13 gives the two-tube weight and generic primitive estimate. It supplies the actual radial-mixing and mean domains, with their angular tapers. Strict positivity alone does not imply those bounds.

The full endpoint theorem and the same slow Borel choice precede the single physical atlas. These are the inputs used in the actual algorithms of Sections 2.6–2.14.

We use S_ℓ and $i(\ell)$ from Lemma 2.12.2 in the packet construction. Its $L_p \asymp S_\ell$ Gaussian inverse has a bounded factor e^{CL_p/S_ℓ}. Its radial mixing and mean returns keep the positive ρ_Q exponents. All fixed powers of S_ℓ are subpower.

The only superalgebraic deletion input is $Q^{-B} S_\ell^N e^{-cS_\ell}$, supplied by that lemma. The slow, packet, and mean constructions use the same physical aggregate cutoff. Thus their finite-state estimates and the physical-limit argument apply with one consistent schedule.

After one uncut finite initialization, each finite five-row mean step solves the current pressure and covariance increments. The one last packet/mean diagonal uses the strict admitted-domain buffers of (2.18.10). Its zero-extended cut increments make the ordinary residual flat in each fixed physical jet. There is no preliminary infinite mean diagonal or reference-force adjustment.

Section 2.18 reconstructs the compact divergence correction in a fixed off-origin annulus and defines the actual unprojected force from that localized field. Its estimates give smooth extension through $t = 0$, not only smoothness for $t > 0$. The same section proves the strong singular L^2 trace. The energy lemma in Section 2.19 then gives finite dissipation.

Lemma 2.18.3 and Proposition 2.18.5(M1) give (2.24.1) with $N_0 = (\frac{1}{2} + h)$ and $N_j = (\frac{1}{2} + h) + j$ for $j \ge 1$.

We select all labels, cutoffs, and Borel data once after we fix the leading profile. Spectral and nonlinear arguments after this stage may enlarge a finite prefix or shorten the time interval, but cannot change these choices. □

2.25 Proof of the main statement

Proof of Theorem 2. The ordinary induction on p. 494 supplies the backward rows before Theorem 2.16.2 and Proposition 2.12.3 are applied. We invoke Theorem 1 once and keep its selected paired source and all its frozen data. In particular its full slice jets include the actual pressure

and its five histories after the shear loop and restoration. These are the jets used in the two-sided pressure reconstruction below.

Slow reference and finite construction. The transported inner solve and its endpoint jets give the joint slow Borel sum by Proposition 2.10.1; the joint packet and mean atlas is Theorem 2.10.2. The pressure saturation and weighted primitive results retain the whole late pressure hull, including the two late pressures and every integration constant. These inputs give the six-clause completion interface verified in Lemma 2.18.3; that lemma is used as a statement about this selected member, not as a new choice of member.

The finite inventory and Proposition 2.12.3 provide the distinct ordinary and pure-auxiliary estimates. The separated principal packets realize the positive leading covariance; Propositions 2.13.6 and 2.13.7 use that same protected leading amplitude for signed higher corrections. They do not require positivity of each higher slow stress. The exact curl construction retains divergence, and the mean equations retain the complete sampled covariance rather than replacing physical angular averaging by auxiliary Haar averaging. The radial pressure/root initialization keeps its new pressure moment and axial pressure gradient. The finite return cycle of Proposition 2.15.2 therefore applies to the actual initialized state with the full pressure.

One diagonal and its ordinary residual. Lemma 2.12.2 fixes the 6/5 schedule. At each finite stage all controls and all cutoffs are selected together on both time sides. Lemma 2.20.3 gives the estimates on each side before taking maximum constants, minimum thresholds and their one common cutoff sequence. The sign of the slow time coefficient on the negative side changes neither the pulse orientation nor viscous damping; no backward physical heat evolution is inverted. Cutting potentials and fluxes before differentiation keeps the full bracket terms in the ordinary finite equation (2.18.1).

The physical derivative bridge and last diagonal give (2.2.13). For every ordinary derivative depth m and every requested power L_0, choose one finite prefix with $h\beta_N - (8 + 2h + 3m) > L_0$, and enlarge it if needed for the finite residual order. The ordinary residual comparison (2.18.16) then gives a q^{L_0} bound for the actual residual relative to the slow force on both sides. This is a comparison with one already fixed completed sum. Proposition 2.11.4 supplies smoothness of the slow reference force at the tip. Thus the conclusion concerns the ordinary Navier–Stokes residual, including pressure, and not only an augmented stress equation. The simultaneous factorial budgets and the ordinary reservation give (2.2.12) and clause (vi).

Joining, localization and the full equation. Lemma 2.20.2 transfers all finite physical slice jets, including those of pressure, moments, shifted paths and cutoff brackets. At a nonzero point of the joining slice the actual Borel and last packet sums are locally finite; in the exterior the common regular heat coefficient and the time-flat fast mode give the same conclusion. These are equal slice jets, not equality on an open time collar. Proposition 2.20.4 combines this joining with the independent residual flatness at the spacetime tip. The fixed localization (2.18.23) acts only on a smooth off-origin annulus, preserves exact divergence and keeps the full pressure gradient. It therefore gives the smooth compactly supported force (2.2.1) and the stated support.

The same proposition gives the uniform value bound in clause (iv). Since $h < 1/6$, the exact sublevel integral

$$\int_{\{\mathfrak{d}<\epsilon\}} \mathfrak{d}^{-1-2h}\, dx = C_h \epsilon^{1/2-3h}$$

gives (2.2.3). Smooth joining away from the origin and this uniform integrability give the common strong L^2 trace. For completeness the global pressure representative is

$$p(t) = N * \big(\operatorname{div} f(t) - \partial_i \partial_j (B_i(t) B_j(t))\big), \qquad N(x) = -\frac{1}{4\pi|x|}.$$

It agrees with the compact smooth pressure for $t \neq 0$ and is continuous in spatial distributions because $B \otimes B$ is continuous in L^1. Passing to the joining slice in the classical equation, with strong L^2 convergence for its time boundary term, proves the full distributional equation without an impulse.

Trace singularity and energy. Beyond the complete late profile hull every correction vanishes. The common positive heat bank gives the explicit cusp (2.18.25), hence (2.2.4), in the unchanged localization ball. Its positive-volume subcusps show essential unboundedness. If a sequence of negative times approaching zero had bounded L^∞ norms, strong L^2 convergence would give an almost-everywhere convergent subsequence with bounded limit, a contradiction. Classical energy identities hold on each side away from zero. The bounded L^2 norm, smooth spatially compact force and strong trace permit their endpoint limits at zero, identify the finite dissipation, and cancel the identical trace energies. This is the argument of Corollary 2.21.1, and proves (2.2.5) in physical forward time on the entire interval.

Choose the endpoints strictly inside the constructed domains. Take T_b less than the positive completion and source-estimate horizons, and T_- less than the available backward horizon. The two-sided envelope and the arbitrarily high ordinary residual estimates follow on this single interval from Lemma 2.20.3 and Proposition 2.20.4; this is the trace and energy argument of clause (iii). *The forward propagation inputs.* Proposition 2.18.5 supplies (2.2.6), the unchanged leading tail bounds and all polynomial spatial jets. Lemma 2.22.5 applied to this same completion gives (2.2.8), including the overlap bound 32 and the sharp principal height $S^{1/4}$. Higher corrections and the diagonal tail remain in its small remainder. The zero-Haar primitive in Lemma 2.23.1, summed over these same labels, has size $CS^{3/4}(1 + \log S)$. Its exact physical derivative is the envelope in (2.2.8), up to the averaged remainder (2.22.5); this remainder includes the large-reference-scale labels and tends to zero. Lemma 2.23.3 gives the remaining normalized transport and derivative bounds in (2.2.9). Since $S^{3/4}(1 + \log S) = o(\log(1/\rho))$, the contrast is (2.2.11).

All finite leading Gram and frozen spectral constants are those already supplied by Theorem 1. None is selected using derivatives of W, an exact linearized mode, or a completed propagator. The separated cover and phase estimates in Lemma 2.13.1 and (2.13.19) are fixed before the first finite update. The Gaussian inverse, exact curl and finite product formulas preserve these representations through Proposition 2.15.2; the zero-Haar radial estimate retains the same cover. The physical derivative estimate and the geometric budget then apply to the same diagonal. This gives (vii). This proves the assertions for one fixed completed base. □

Chapter 3

Nonunique continuations from zero initial velocity

Theorem 3 constructs a real one-parameter family from rest under one smooth force of compact space-time support. The common negative-time evolution blows up at $t = 0$. The continuations separate at every positive time of a common interval. The residual estimates for the completed field are proved on pp. 697 and 705.

Input from the smooth completion

The supplying statement is Theorem 2 in Chapter 2. We use Theorem 2 of Part 2 in the following form. All seven clauses describe the same choice of fields, spectral data and packet family. Write $x = (x_h, z)$, $r = |x_h|$ and $\mathfrak{d}(x) = r^2 + |z|^{1/(1/2-h)}$. The selected exponent satisfies $0 < h < 1/100$. For $t \neq 0$, q is the unique solution of $q - z^2 q^{2h} = |t|$ with $q > |z|^{2/(1-2h)}$. Set $\xi = r/\sqrt{q}$ and $\eta = zq^{-1/2+h}$.

(i) *Fields and finite approximations.* There are $T_-, T_b, R_* > 0$, a real velocity B, pressure p_B and force f on $\mathbb{R}^3 \times I$, $I = (-T_-, T_b)$. The solenoidal leading field on each side is

$$B_0 = B_\pm^0 = q^{-1/2}(V_\pm/\xi)e_r + q^{-1/2-h}(E_\pm e_\theta + U_\pm e_z) \qquad (\pm t > 0),$$

where the profiles are evaluated at (ξ, η) and extended smoothly to the axis. On each sufficiently small dyadic source band let $Q = 2^{-\ell}$, $\rho = Q^h$, $S = \ell^{6/5}$ and $\varkappa = 10^{-5}$. In slow coordinates $(\mathsf{R}, \mathsf{Z}, \mathsf{T}) = (r/\sqrt{Q}, z/Q^{1/2-h}, t/Q)$ write $Q^{1/2+h}u_{\mathrm{B}} = (b, \mathsf{R}F_b, G_b)$ in the cylindrical frame, where u_{B} is the slow background including its positive-order terms. On the enlarged packet charts $b = O(\rho)$, and F_b, G_b differ from the corresponding leading angular-rate and axial profiles by $O(\rho^2)$ through each fixed ordinary coefficient order. The finite velocities $u^{[N]} = u_M^{[N]} + w^{[N]}$ consist of their angular mean and a sum of zero-angular-mean curl packets. Their pressures $p^{[N]}$ include the slow pressure and the full covariance. One decreasing sequence $\delta_{N+1} \leq \delta_N/4$ selects the finite increments on both sides. A smooth scalar cutoff at scale δ_N of the common physical gauge $\widetilde{q} \asymp q$ multiplies each pressure increment and each wave potential before its curl is taken. The band partition uses this same gauge, so $Q \asymp \widetilde{q} \asymp q$ on each enlarged source band. The radial mean is corrected to preserve flux. Denote the resulting sums by (u_∞, p_∞). They agree with (B, p_B) on a fixed inner ball. Outside it, a fixed spatial cutoff and an annular divergence correction localize B, and the same cutoff localizes p_∞.

(ii) *Equation and regularity.* $B \in C(I; L^2_\sigma) \cap L^2_{\mathrm{loc}}(I; H^1_\sigma)$ and $f \in C^\infty(\mathbb{R}^3 \times I)$. Both $B(t)$ and $f(t)$ are supported in $\overline{B_{R_*}(0)}$. The fields B, p_B are smooth off the spacetime origin and satisfy, in spacetime distributions,

$$\partial_t B - \Delta B + \operatorname{div}(B \otimes B) + \nabla p_B = f, \qquad \operatorname{div} B = 0.$$

The spatial pressure representative is weakly continuous in time and is normalized on each slice by

$$p_B = -\frac{1}{4\pi|\cdot|} * \left(\operatorname{div} f - \sum_{i,j} \partial_i \partial_j (B_i B_j) \right),$$

where convolution is in space.

(iii) *Trace and energy.* $u_0 = B(0)$ is the common strong L^2 trace, smooth away from the origin. For some $c_0, c_1, r_1 > 0$ its swirl equals $c_0 r^{-1-2h}$ on $0 < r < r_1$, $0 < |z| < c_1 r^{1-2h}$. In particular u_0 is essentially unbounded on every ball about zero. Each $B(t_-)$, $-T_- < t_- < 0$, is smooth and compactly supported, and $\|B(t)\|_\infty \to \infty$ as $t \uparrow 0$. The global energy identity (3.1.1) holds for B with $g = f$ on every compact subinterval of I, including across zero.

(iv) *Forward estimates and leading spectrum.* For $0 < t < T_b$ and every integer $j \geq 1$ and $\epsilon > 0$,

$$|B| \lesssim (t + \mathfrak{d})^{-1/2-h}, \qquad |\nabla_x^j B| \lesssim_{j,\epsilon} (t + \mathfrak{d})^{-1/2-h-(1+h)j/2-\epsilon}.$$

In particular $\|\nabla^j B(t)\|_\infty \lesssim_j t^{-1/2-h-j}$ for $j \geq 1$. In the inner ball $|\nabla_x^j B_0| \lesssim_j (t+\mathfrak{d})^{-1/2-h-j/2}$ for $j \geq 0$. In forward variables $y = x_h/\sqrt{t}$, $R = |y|$, $Z = z/t^{1/2-h}$ and $s = -t^{-h}/h$, the leading field has the form $t^{1/2+h} B^0_+ = \mathcal{U}_0 + t^h \mathcal{U}_1$, where $\mathcal{U}_0 = R\Omega(R, Z) e_\theta + W(R, Z) e_z$ and $\mathcal{U}_1$ is radial. For every $j, l \geq 0$, $|\partial_Z^l \partial_R^j \Omega| \lesssim_{j,l} \langle R \rangle^{-2-2h-j}$, and W has bounded radial support uniformly on compact Z intervals.

Let H_n consist of the $v \in L^2(\mathbb{R}^2_y; \mathbb{C}^3)$ satisfying $v(R_\varphi y) = e^{in\varphi} \operatorname{diag}(R_\varphi, 1) v(y)$ for every planar rotation R_φ. Write $\nabla_k = (\nabla_y, ik)$, $X_{n,k} = \mathsf{H}_n \cap \ker(\nabla_k \cdot)$, and let P_k be the orthogonal projection onto this kernel, with horizontal Fourier symbol $I - \zeta \otimes \zeta / |\zeta|^2$, $\zeta = (\zeta_h, k) \neq 0$. The frozen operator is

$$A_{\nu,n} v = -P_k \left[(\mathcal{U}_0 \cdot \nabla_k) v + (v_h \cdot \nabla_y) \mathcal{U}_0 \right] + \nu(\Delta_y - k^2) v,$$

with domain $H^2 \cap X_{n,k}$ for $\nu > 0$ and $X_{n,k}$ for $\nu = 0$. The largest spectral real part over all inviscid fibers is $\lambda_c = \Re \lambda_0 > 0$, attained only at $(n, Z, k) = (\pm m, 0, 0)$. Here $m \geq 30$ is fixed. Near $(0, 0)$ there is a simple eigenvalue $\lambda(Z, k)$ on sector m, with $\lambda(0, 0) = \lambda_0$ and $\lambda_c - \Re\lambda(Z, k) \asymp Z^2 + k^2$. The branch on sector $-m$ is $\overline{\lambda(Z, -k)}$. There is a strict spectral gap on the complement at the pole and a uniform gap on the other sectors. At the pole the complex derivatives satisfy

$$\lambda_Z = \lambda_k = \lambda_{Zk} = 0, \qquad (\lambda_{kk}/h^2) q_G^2 + (h^{-1} - 1) q_G - \lambda_{ZZ} = 0.$$

Writing $\Delta > 0$ for the chosen shear scale, r_0 for the layer radius, $a_m = m/r_0$, the selected $q_G = a_m^2 C_q / \Delta$ is positive, $-a_m^2 \Re\lambda_{kk}/h^2 \asymp \Delta$ and $|a_m^2 \lambda_{kk}/h^2| \lesssim \Delta$. With $b_d = (h^{-1} - 1)/2$ and $X_G = -q_G \Re\lambda_{kk}/(2h^2)$,

$$X_G > b_d, \qquad X_G - b_d/2 - \sqrt{X_G^2 - b_d X_G} \leq 1/16.$$

On a compact rectangle about the pole, there are uniform contours isolating the eigenvalue and its complementary spectrum. On the fixed angular space extend $A_{0,n}$ by zero on $I - P_k$. On these contours its resolvent, its adjoint, the reduced resolvent and the Riesz projection obey

$$\|\partial_Z^l \partial_k^j D\|_{H^a_{w+j}\cap \mathsf{H}_n \to H^a_w \cap \mathsf{H}_n} \lesssim_{a,w,j,l} 1, \quad n = \pm m, \quad 0 \le l \le 17, \quad w \ge 0, \quad \lceil w \rceil + j \le m - 1.$$

Here a, j, l are nonnegative integers and $\|v\|_{H^a_w} = \sum_{|\alpha|\le a} \|\langle y\rangle^w \partial_y^\alpha v\|_2$. At the limiting weight the parameter derivatives act strongly on each datum. On these sectors the physical Leray multiplier satisfies $\|\partial_k^j P_k f\|_{H^a_w} \le C\|f\|_{H^a_{w+j}}$ for $\lceil w \rceil + j \le m - 1$. The physical pressure estimates hold on the same contour chart. The right and adjoint eigenvectors admit the normalization and bounds in (3.6.3).

With $\rho = t^h$, the leading evolution U_{lead} is the solenoidal physical linearization about B_+^0 in canonical time, acting on $v = t^{1/2+h} w$. The shifted evolution subtracts the axial Gaussian quantization of $S_{\rho,\pm m} = d_0 \chi_\pm P_{\rho,\pm m}$ between the canonical solenoidal projections. Here $P_{\nu,\pm m}$ is the continued eigenvalue's Riesz projection, $d_0 > 0$ and the smooth phase cutoffs satisfy $\chi_-(Z,k) = \chi_+(Z,-k)$ and equal one near zero. Both supports are compactly contained in one fixed open rectangle U about the pole, symmetric in k, whose closure lies in the weighted contour rectangle. On $\overline{U}$ the Hessian of $\Re\lambda$ is negative definite and $|\ell_0 P_{0,m}(Z,k) e_0 - 1| \le 1/2$, where $P_{0,m}(0,0) = e_0 \ell_0$ and $\ell_0 e_0 = 1$. Extend $S_{\nu,n}$ by zero on $(I - P_k)\mathsf{H}_n$. In operator norm on the common angular space H_n, $\sup_{Z,k} \|S_{\nu,n} - S_{0,n}\| \to 0$ as $\nu \downarrow 0$. The other shifts vanish. Uniformly in phase and $0 \le \nu \le \nu_0$, for some $g_{\mathrm{far}} < g_1 < \lambda_c$ and $N_{\mathrm{far}} > m$, the shifted frozen semigroups have norm $\le Ce^{g_1 u}$ for $u \ge 0$ on $|n| < N_{\mathrm{far}}$. On $|n| \ge N_{\mathrm{far}}$ the resolvent is uniformly bounded on $\Re z \ge g_{\mathrm{far}}$. Uniformly in all angular sectors, for $s' \le s$ sufficiently negative,

$$\|U^\sharp_{\mathrm{lead}}(s,s')\| \le Ce^{g_2(s-s')}, \qquad \|U_{\mathrm{lead}}(s,s')\| \le C_\epsilon e^{(\lambda_c+\epsilon)(s-s')} \quad (g_2 < \lambda_c,\ \epsilon > 0).$$

In the isotropic boxes of (v) the leading evolution fixes the Gram rate, horizon L_G and metric bounds before the box-length family. For each prescribed family $L_{\mathrm{box}}(Q) \ge 0$ with $L_{\mathrm{box}}(Q) + L_G = o(\log(1/Q^h))$, the following Gram bounds are uniform at starts $|\theta| \le L_{\mathrm{box}}(Q)$ for all sufficiently small Q. The coefficients are taken on $[\theta, \theta + L_G]$ and the threshold for Q may depend on the family. The smoothed shift has bounded $H^{-j} \to H^j$ norm at every fixed order. The whole-space extension (3.4.2) has a positive Gram metric $I \le M \le CI$ commuting with the Leray projector and satisfying (3.4.3) and (3.4.4). Its rate is strictly below λ_c with the shift and is $\lambda_c + \epsilon$ without it.

(v) *Correction and clock.* Here write $W = B - B_0$. In a box of reference time $Q > 0$ let $t = Q + Q^{1+h}\theta$, $y = x/\sqrt{Q}$, $\rho = Q^h$ and $S = (1+\log(1/\rho))^{6/5}$. Put $F_Q(y,t) = Q^{1/2+h} F(\sqrt{Q}\, y, t)$ for velocities, and $E_Q = E(\sqrt{Q}\, y, t)$, $a_Q = a(\sqrt{Q}\, y, t)$ for scalars. The nonnegative E is the sum of the slow-cutoff principal pulse envelopes. For every fixed $K > 0$, a is the sum of $-K$ times their normalized, zero-Haar-mean temporal primitives, each multiplied by its slow cutoff and evaluated on its own cover. For $0 < \eta' < 1/2 - 3\varkappa$ the following hold uniformly on

$|\theta| \le L(Q) = o(\log(1/\rho))$ as $Q \downarrow 0$:

$$\begin{gathered}
\|W_Q\|_\infty \le \rho^{1/2} P(S), \qquad |\nabla_y W_Q| \le (Q/t)^{1+h} E_Q + C\rho^{\eta'}, \\
\|E_Q\|_\infty \le C S^{1/4}, \qquad \|\nabla_y E_Q\|_\infty + \|\nabla_y a_Q\|_\infty \le \rho^{-\varkappa} P(S), \\
\partial_s a_Q = -K E_Q + r_Q, \quad \|r_Q\|_\infty = o(1), \qquad \partial_s = t^{1+h}\partial_t \quad \text{at fixed } Q, y, \\
\|a_Q\|_\infty \le C_K S^{3/4}(1 + \log S), \qquad \exp(\operatorname{osc}_y a_Q) = \rho^{-o(1)}, \\
\|B_Q \cdot \nabla_y a_Q\|_\infty + \rho(\|\Delta_y a_Q\|_\infty + \|\nabla_y a_Q\|_\infty^2) = o(1).
\end{gathered}$$

Each $P(S)$ denotes a polynomial bound independent of Q and of the number of active stages.

(vi) *Finite coefficients and tail.* At every finite stage N and chosen ordinary depth J, a coefficient c of order ρ^a, weight $w \in \{1, \mathsf{W}, \sqrt{\mathsf{W}}\}$ and envelope $e \in \{1, P(v)\}$ satisfies

$$|\partial^I_{\mathsf{R},\mathsf{Z},\mathsf{T}} \partial^\alpha_Y c| \le C_{N,J} \rho^a S^{b_{N,J}} w\, \mathcal{L}_W^{D_{N,J}}\, e\, (K_{N,J} S^{B_{N,J}})^{|\alpha|} (|\alpha|!)^2 \qquad (|I| \le J,\ \alpha \in \mathbb{N}_0^2).$$

Here $Y \in \mathbb{T}^2$ is the auxiliary variable, $\mathcal{L}_W = 1 + \log(1/\mathsf{W})$ where $\mathsf{W} > 0$ and the logarithmic factor is omitted on unweighted charts. The constants are uniform over labels and bands. Weighted coefficients extend smoothly by zero. The relative derivative estimates apply also to the reciprocal Gaussian envelope and the exponentials of the single-label clock primitives. The same cutoff sequence in (i) reserves $\max(N, 80)$ ordinary derivatives at stage N, including the 72 used in the finite preparation. The one-sided finite coefficient jets match at $t = 0$ off the origin. For every finite N, j, inside the construction ball and for sufficiently small q,

$$\max_{|\mu| \le j} |\partial^\mu_{x,t}(u_\infty - u^{[N]})| \le C_{N,j} q^{h(1-4\varkappa+N/5)-(1/2+h)-3j}.$$

The unlocalized momentum residual relative to its smooth slow force is $O(q^M)$ through each fixed physical derivative order for every M.

(vii) *Packet geometry and inverses.* On a source band of (i) write $Q = 2^{-\ell}$ and $\rho = \rho_Q = Q^h$. The waves lie in a fixed closed annulus in $\mathsf{R} > 0$. A compact band meets $O(S^{3K_{\mathrm{mesh}}})$ labels and a radial line meets $O(S^{K_{\mathrm{mesh}}})$ for a fixed mesh exponent. At most 32 signed labels have nonzero slow cutoff at any point. Meeting bands have cover levels differing by a bounded integer. For distinct meeting signed labels the enlarged packet rectangles have disjoint preimages on the common lowest cover. The rounded angular winding of each active carrier satisfies $k_\ell p \in \mathbb{Z}$ and $|k_\ell p| \ge 2m+1$, where $k_\ell = \lceil \rho^{-1/2} \rceil$. All coefficient derivatives hold the representative data and rounded constants fixed. For its phase Φ and normal $n = \sqrt{Q}\nabla_x \Phi$, $|n| \ge |n_{\tan}| \ge c > 0$, where $n_{\tan}$ is the projection of n onto $\operatorname{span}(e_\theta, e_z)$. Every fixed coefficient derivative of $Q^{1+h}(\partial_t + u_{\mathrm{B}} \cdot \nabla_x)\Phi$ is $O(\rho P(S))$.

The precise coefficient operators and weights used here are given in the packet definitions below. On the pulse interval $[0, L_p]$, $L_p \asymp S$, the transverse homogeneous propagator on nonzero harmonic j satisfies $\|V_j(v, w)\| \le C P(v)/P(w)$ for $0 \le w \le v \le L_p$. The zero-initial-data inverse sends an input in $\mathcal{W}^a$ to a transverse velocity in $\mathcal{W}^a$ and pressure in $\mathcal{W}^{a+1/2}$. Products obey the exact signed harmonic product rule. The primary and higher principal curl amplitudes have orders $1/2$ and $1 - 3\varkappa$, respectively. For an amplitude of order a, the tangential and radial curl remainders have orders $a + 1/2 - \varkappa$ and $a + 3/2$ in the wave classes. Distinct-label wave products vanish, and on a single label opposite indices cancel the entire phase. For $\mu = u_M - u_{\mathrm{B}}$, the angular and axial components of $Q^{1/2+h}\mu$ lie in $\mathcal{M}^{1-\varkappa}$ and its radial component lies in $\mathcal{M}^2$. If $g \in \mathcal{M}^a$ is supported on the fixed radial hull with zero Haar

mean at each slow point, the shifted tail and complete integral obey $Ig - \chi Jg \in \mathcal{M}^{a+\varkappa}$ and $\|\partial^{\le j} Jg\|_\infty \le C_{j,N}\rho^{a+N}S^{B_{j,N}}$ on the hull for any fixed j, N. Haar averaging, the zero-mean directional primitive and the radial integrals preserve the finite derivative estimates specified in the packet definitions. The slow source in clause (vii) also provides the full-space estimate in the canonical variables $R = r/\sqrt{t},\ Z = z/t^{1/2-h}$. For $V_s = t^{1/2+h}(u_{\mathrm{B}} - B_0)$, its tangential and axial components are $O_j(\rho^2)$ and its radial component is $O_j(\rho^3)$ in every fixed ordinary spatial jet, using Cartesian vector components through the axis. This is the global slow estimate at Proposition 2.6.15 of Part 2. On a fixed enlarged band annulus hold Q fixed during differentiation and take $1/2 \le Q_\gamma/Q \le 2$ for the labels in its local representation. For physical prefactor Q_γ^{-d}, $d \ge 0$, sampled derivatives through order j are bounded by

$$C_{j,d}Q^{-d-3j}\sum_{\gamma,m'}(1+|m'|)^j \max_{|I|\le j}\|\partial^I f_{\gamma,m'}\|_\infty,$$

where $f_{\gamma,m'}$ are the harmonic coefficients in the common band and torus coordinates. The normalized velocity correction satisfies the envelope bounds in (v).

Coordinates and operators for the packet input. Write $Q = 2^{-\ell}$, $\rho_Q = Q^h$, $S_\ell = \ell^{6/5}$, and $(\mathsf{R}, \mathsf{Z}, \mathsf{T}) = (r/Q^{1/2}, z/Q^{1/2-h}, t/Q)$. On a physical band write the normalized slow field as $Q^{1/2+h}u_{\mathrm{B}} = (b, \mathsf{R}F_b, G_b)$. The torus $\mathbb{T}^2 = \mathbb{R}^2/\mathbb{Z}^2$ has normalized Haar measure. Set

$$J_g = \begin{pmatrix} 3 & 1 \\ 1 & 5 \end{pmatrix}, \quad \Lambda_g = 4 - \sqrt{2}, \quad T_g = 4 + \sqrt{2}, \quad v_r = (1, 1-\sqrt{2}), \quad v_t = (\sqrt{2}-1, 1), \quad \rho_g = \frac{\log \Lambda_g}{\log T_g}.$$

Put $d_r = 2[(1+h)\rho_g - h\varkappa] > 1$ and $i(\ell) = \lfloor \log_{T_g}(Q^{-1-h}/S_\ell)\rfloor$. The physical torus point is $r^{d_r}v_r + tv_t$ modulo $\mathbb{Z}^2$. For the finite active levels let i_0 be their minimum. On their common cover $Y = J_g^{i_0}(r^{d_r}v_r + tv_t)$ a level-i function is evaluated at $J_g^{i-i_0}Y$. With $\lambda_{\mathrm{aux}} = \Lambda_g^{i_0}Q^{d_r/2}$, $a(R) = \lambda_{\mathrm{aux}}R^{d_r}v_r$ and $c_{\mathrm{aux}} = T_g^{i_0}Q^{1+h}$, physical sampling induces

$$D_{\mathsf{R}} = \partial_{\mathsf{R}} + a'(\mathsf{R})\cdot\nabla_Y, \qquad D_z = \rho_Q\partial_{\mathsf{Z}}, \qquad t_* = \rho_Q\partial_{\mathsf{T}} + c_{\mathrm{aux}}v_t\cdot\nabla_Y, \qquad \nabla_* = (D_{\mathsf{R}}, \mathsf{R}^{-1}\partial_\theta, D_z).$$

On a lifted rectangle centered over $c_\mu \in \mathbb{T}^2$, write $J_g^{i-i_0}Y - c_\mu = \xi_{\mathrm{aux}}v_r + \zeta v_t$ modulo the lattice. With the fixed rectangle radius $r_0 > 0$, put $c_i = T_g^i Q^{1+h}$, $v = (\zeta + r_0)/c_i$ and $L_p = 2r_0/c_i$. Then $D_{\mathsf{R}}v = D_z v = 0$, $t_* v = 1$.

At a box representative freeze $F_0 = F_{\mathrm{lead}} > 0$ and $g_0 = (\mathsf{R}\partial_{\mathsf{R}}F_{\mathrm{lead}}, \partial_{\mathsf{R}}G_{\mathrm{lead}})$. Define $N = g_0/|g_0|$, $K = (-N_z, N_\theta)$, $\lambda_{\mathrm{box}} = \sqrt{-2F_0N_\theta(2F_0N_\theta + |g_0|)} > 0$, and $c_0 = \lambda_{\mathrm{box}}/(2F_0N_\theta)$. Let $\delta_c \in (0,2)$ denote the fixed strict cone margin, $u_p = 2/\sqrt{\delta_c}$, $k_\ell = \lceil \rho_Q^{-1/2}\rceil$, and $\varsigma = \pm 1$ the packet sign. For representative radius R_0,

$$s(v) = \varsigma u_p(1/2 + v/L_p), \qquad B_p^2 = \frac{\lambda_{\mathrm{box}}}{\rho_Q k_\ell^2(1+u_p^2)^{3/2}},$$

$$(\widetilde{p}/\mathsf{R}_0, p_z) = B_p\left(K - \frac{\varsigma u_p g_0}{L_p|g_0|^2}\right), \qquad x_0 = \varsigma B_p u_p/2,$$

where $B_p > 0$. Choose $k_\ell p$ nearest to $k_\ell\widetilde{p}$ among integers of modulus at least $2m+1$, with a fixed tie rule. For $H_\Phi = pF_b + p_z G_b$ the phase and its normalized normal are

$$\Phi = p\theta + p_z\mathsf{Z}/\rho_Q + x_0\mathsf{R} - vH_\Phi, \qquad n = \nabla_*\Phi = (x_0 - v\partial_{\mathsf{R}}H_\Phi,\ p/\mathsf{R},\ p_z - \rho_Q v\partial_{\mathsf{Z}}H_\Phi).$$

Put $K_a = n_{\tan}/|n_{\tan}|$, $N_a = ((K_a)_z, -(K_a)_\theta)$, $s_a = n_r/|n_{\tan}|$, viewing tangential vectors as vectors in the (e_θ, e_z)-plane. In cylindrical components set

$$M_f = \begin{pmatrix} 1 & 1 \\ c_0\sqrt{1+s^2} & -c_0\sqrt{1+s^2} \end{pmatrix}, \quad B_f = [e_r - s_a K_a, N_a] M_f, \qquad B_f^\ell = M_f^{-1} \begin{pmatrix} e_r^\top \\ N_a^\top \end{pmatrix},$$
$$K_b = \begin{pmatrix} 0 & -2F_b & 0 \\ 2F_b + \mathsf{R}\partial_{\mathsf{R}} F_b & 0 & 0 \\ \partial_{\mathsf{R}} G_b & 0 & 0 \end{pmatrix}, \quad A_\Phi = -K_b + \frac{n[n^\top K_b - (\partial_v n)^\top]}{|n|^2}.$$

The wave envelope and damping in these coordinates are

$$\lambda(v) = \frac{\lambda_{\mathrm{box}}}{\sqrt{1+s(v)^2}}, \qquad d_{\mathrm{ref}}(v) = \frac{\lambda_{\mathrm{box}}(1+s(v)^2)}{(1+u_p^2)^{3/2}}, \qquad d_p = \rho_Q k_\ell^2 |n|^2,$$
$$P(v) = \exp\left(\int_{L_p/2}^{v} (\lambda(w) - d_{\mathrm{ref}}(w))\, dw \right), \qquad E_f = B_f^\ell (A_\Phi B_f - \partial_v B_f) - \mathrm{diag}(\lambda, -\lambda).$$

For nonzero relative harmonic j, the frame generator is $\mathrm{diag}(\lambda, -\lambda) + E_f - j^2 d_p I$. For $E_j = e^{ijk_\ell \Phi}$, angle-independent coefficients satisfy

$$((XE_l)\cdot\nabla_*)(Y' E_j) = E_{l+j}\left[X_r D_{\mathsf{R}} Y' + X_z D_z Y' + \frac{X_\theta}{\mathsf{R}} J_\theta Y' + ijk_\ell (X\cdot n) Y' \right],$$
$$J_\theta(y_r, y_\theta, y_z) = (-y_\theta, y_r, 0).$$

For a carrier-free coefficient f, let $g_{R,Y}(x) = f(x, \mathsf{Z}, \mathsf{T}, Y + a(x) - a(R))$. At fixed slow parameters,

$$If(R,Y) = \int_R^\infty g_{R,Y}(x)\, dx, \qquad Jf(R,Y) = \int_0^\infty g_{R,Y}(x)\, dx, \qquad \mathcal{L}f(R,Y) = \int_0^R g_{R,Y}(x)\, dx.$$

Thus $D_{\mathsf{R}} If = -f$, $D_{\mathsf{R}} Jf = 0$, and $D_{\mathsf{R}} \mathcal{L} f = f$. Define $\Pi f = \int_{\mathbb{T}^2} f\, dY$. For $T_0 = c_{\mathrm{aux}} v_t \cdot \nabla_Y$, the zero-Haar inverse divides the Fourier coefficient of frequency $\nu \neq 0$ by $2\pi i c_{\mathrm{aux}}\, v_t \cdot \nu$ and sets the constant coefficient to zero. For $D_v = v \cdot \nabla_Y$ the corresponding multiplier is $(2\pi i\, v\cdot\nu)^{-1}$ on nonzero frequencies for each of the two fixed eigenvector directions above.

Weight, coefficient classes and radial cutoff. The native weight is a scalar function $0 \le \mathsf{W} \le e^{-2}$ of the slow variables of the selected leading field on each side. It is independent of Y. The following equivalent description determines its coefficient classes directly from B_0. At fixed (z,t), set $p_0(r) = -\int_r^\infty B_{0,\theta}(s)^2\, ds/s$, $D = \partial_t + B_{0,r}\partial_r + B_{0,z}\partial_z$, and $\Delta_r = \partial_r^2 + r^{-1}\partial_r$. Define the leading stress $\mathcal{T}_0 = (T_{0,\theta}, T_{0,z})$ by the regular radial primitives

$$\mathcal{R}_\theta = DB_{0,\theta} + r^{-1} B_{0,r} B_{0,\theta} - (\Delta_r - r^{-2}) B_{0,\theta}, \qquad q^{-1-h} T_{0,\theta} = -r^{-2} \int_0^r s^2 \mathcal{R}_\theta(s)\, ds,$$
$$\mathcal{R}_z = DB_{0,z} + \partial_z p_0 - \Delta_r B_{0,z}, \qquad q^{-1-h} T_{0,z} = -r^{-1} \int_0^r s \mathcal{R}_z(s)\, ds.$$

Choose a fixed $c_* > 0$ with $w_0 = c_* |\mathcal{T}_0| \le e^{-2}$. The native weight has the same zero set as w_0 and obeys $c\mathsf{W} \le w_0 \le C\mathsf{W}\mathcal{L}_W^N$ on the common positive set, with $\mathcal{L}_W = 1 + \log(1/\mathsf{W})$. All fixed slow derivatives of W and $\mathcal{T}_0$ are bounded by $C_I \mathsf{W} \mathcal{L}_W^{N_I}$. Thus $1 + \log(1/w_0) \asymp \mathcal{L}_W$; either W or w_0 gives exactly the classes below, after changing the allowed logarithmic exponent. The native weight is used with its one-sided values in the two charts.

For $a \in \mathbb{R}$ and every ordinary multi-index I in $(\mathsf{R}, \mathsf{Z}, \mathsf{T}, Y)$, membership means that some $C_I, B_I, N_I \geq 0$, uniform over bands and labels in a fixed finite stage and harmonic set, satisfy the corresponding estimate

$$f \in \mathcal{M}^a : \qquad |\partial^I f| \leq C_I \rho_Q^a S_\ell^{B_I} \mathsf{W} \mathcal{L}_W^{N_I},$$
$$f \in \mathcal{W}^a : \qquad |\partial^I f| \leq C_I \rho_Q^a S_\ell^{B_I} \sqrt{\mathsf{W}} \mathcal{L}_W^{N_I} P(v).$$

The second estimate is on the lifted rectangle and full pulse interval, with a smooth zero extension after temporal truncation. In both classes take compatible representatives on common covers and smooth zero extensions at support boundaries, interpreting $\mathsf{W}^\gamma \mathcal{L}_W^N$ as zero when $\mathsf{W} = 0$ and $\gamma > 0$.

Fix a closed annulus $[\mathsf{R}_-, \mathsf{R}_+] \Subset (0, \infty)$ containing the radial supports of the source coefficients on the band charts. For each angle η, the selected source has a positive pulse-entry radius $\xi_p(\eta)$; the protected slot $-8 \leq y_p = 2\log(\xi/\xi_p(\eta)) \leq -3$ lies inside this hull and $\mathsf{W} \geq c > 0$ there. With a fixed $b_{\mathrm{cut}} \in C_c^\infty((-8,-3))$, $b_{\mathrm{cut}} \geq 0$, $\int b_{\mathrm{cut}} = 1$, the subtraction cutoff is $\chi(\xi,\eta) = \int_{y_p}^\infty b_{\mathrm{cut}}(s)\, ds$. Hence $I - \chi J$ uses the inward primitive with negative sign before the slot and the outward primitive after it. Each fixed output seminorm of this operator uses finitely many input seminorms. Haar averaging costs no auxiliary derivatives, and for $v = v_r, v_t$ the zero-Haar primitive satisfies $\|D_v^{-1} g\|_{C_Y^j} \leq C_j \|g\|_{C_Y^{j+4}}$. For T_0^{-1} the bound has the additional factor $c_{\mathrm{aux}}^{-1} = O(S_\ell)$.

3.1 Energy solutions and the physical linearization

Fix the velocity B, pressure representative $p_B := p$, force f, and times $T_-, T_b > 0$ given by Theorem 2. They are defined on $I \times \mathbb{R}^3$, where $I = (-T_-, T_b)$. Write $u_0 = B(0)$ for the strong L^2 trace, $B_* = B|_{0<t<T_b}$, and $K = \{x \in \mathbb{R}^3 : |x| \leq R_*\}$, with R_* the support radius in that theorem. Thus $\operatorname{supp} B(t) \cup \operatorname{supp} f(t) \subset K$ for $t \in I$. We use time-first ordering (t, x) for spacetime fields in this chapter. All velocity traces use the strongly continuous L^2 representatives.

For $m \geq 0$ an integer, $H^m = H^m(\mathbb{R}^3; \mathbb{R}^3)$ has norm $\|v\|_{H^m}^2 = \sum_{|\alpha| \leq m} \|\partial_x^\alpha v\|_2^2$, where $\|\cdot\|_2$ is the spatial L^2 norm. Put $H_\sigma^m = \{v \in H^m : \operatorname{div} v = 0 \text{ in } \mathcal{D}'(\mathbb{R}^3)\}$ and $L_\sigma^2 = H_\sigma^0$. The subscript σ specifies the solenoidal subspace. For vector fields v, w and a tensor $\mathcal{Q}$ write $(v \otimes w)_{ij} = v_i w_j$ and $(\operatorname{div} \mathcal{Q})_i = \sum_{j=1}^3 \partial_{x_j} \mathcal{Q}_{ij}$.

Definition 3.1.1 (Distributional solution and global energy identity)**.** Let $J = [a, b)$ or $[a, b]$ be a time interval, let $u_{\mathrm{in}} \in L_\sigma^2$, and let g be a prescribed smooth force on a neighborhood of $J \times \mathbb{R}^3$ with fixed compact spatial support. A solution with these data is a pair (u, p) with real velocity

$$u \in C(J; L_\sigma^2) \cap L_{\mathrm{loc}}^2(J; H_\sigma^1), \qquad u(a) = u_{\mathrm{in}},$$

and real scalar pressure $p \in \mathcal{D}'((a,b) \times \mathbb{R}^3)$ satisfying

$$\partial_t u - \Delta u + \operatorname{div}(u \otimes u) + \nabla p = g \quad \text{in } \mathcal{D}'((a,b) \times \mathbb{R}^3; \mathbb{R}^3).$$

The equality is tested against all compactly supported smooth vector fields. Adding a spatial constant depending distributionally on time gives the same pressure gradient. A solution satisfies the global energy identity if, for every $s, t \in J$ with $s \leq t$,

$$\frac{1}{2}\|u(t)\|_2^2 + \int_s^t \|\nabla u(r)\|_2^2 \, \mathrm{d}r = \frac{1}{2}\|u(s)\|_2^2 + \int_s^t \int_{\mathbb{R}^3} g(r,x) \cdot u(r,x) \, \mathrm{d}x \, \mathrm{d}r. \tag{3.1.1}$$

Let $h > 0$ and $\lambda_0 \in \mathbb{C}$ be the anisotropy exponent and the selected frozen eigenvalue at $(Z, k) = (0, 0)$ in the positive angular sector m of Theorem 2. Put

$$\lambda_c = \operatorname{Re} \lambda_0 > 0, \qquad \Lambda_* = \lambda_c / h, \qquad \tau = t^{-h}, \qquad s = -\tau/h \quad (t > 0).$$

Let $\mathbb{P}$ be the spatial Fourier multiplier with matrix $I_3 - \zeta \otimes \zeta/|\zeta|^2$ for $\zeta \in \mathbb{R}^3 \setminus \{0\}$ and value I_3 at 0. Define the linearization on solenoidal fields by

$$\mathcal{L}_B z = \partial_t z - \Delta z + \mathbb{P}\,\mathrm{div}(B \otimes z + z \otimes B). \tag{3.1.2}$$

3.2 Main statement

Theorem 3 (Nonunique continuations from rest under one force)**.** *For the completed field (B, p_B, f) constructed in Theorem 2, there exist $T_{\mathrm{in}}, T_{\mathrm{out}} > 0$, one real force $F \in C_c^\infty((-T_{\mathrm{in}}, T_{\mathrm{out}}) \times \mathbb{R}^3; \mathbb{R}^3)$, and a family $(u^{(a)}, p^{(a)})$, $-1 \le a \le 1$, on $[-T_{\mathrm{in}}, T_{\mathrm{out}}] \times \mathbb{R}^3$.*

(i) Linear instability at the joining trace. *For some $0 < t_* < \min\{T_b, T_{\mathrm{out}}\}$ there is a real solenoidal field $V \in C([0, t_*]; L^2_\sigma) \cap L^2(0, t_*; H^1_\sigma)$. It has $V(0) = 0$, is smooth for $0 < t \le t_*$, and solves $\mathcal{L}_B V = 0$ there. There are $M, c_V, C_V > 0$ such that, for $0 < t \le t_*$ and $\tau = t^{-h}$,*

$$c_V \tau^{-M} e^{-1.1\Lambda_* \tau} \le \|V(t)\|_2, \qquad \|V(t)\|_{H^3} \le C_V \tau^M e^{-0.9\Lambda_* \tau}. \tag{3.2.1}$$

(ii) Common evolution from zero initial velocity. *Every pair is a solution of Definition 3.1.1 with datum $u^{(a)}(-T_{\mathrm{in}}) = 0$ and force $g = F$. Each real velocity belongs to $C([-T_{\mathrm{in}}, T_{\mathrm{out}}]; L^2_\sigma) \cap L^2(-T_{\mathrm{in}}, T_{\mathrm{out}}; H^1_\sigma)$ and satisfies (3.1.1) for every pair of times in $[-T_{\mathrm{in}}, T_{\mathrm{out}}]$. Each velocity and its pressure representative are jointly smooth at every $(x, t) \ne (0, 0)$, up to the temporal endpoints by restriction. The velocities coincide on $[-T_{\mathrm{in}}, 0]$ and vanish on an initial time interval. For all negative t sufficiently close to zero the common velocity equals $B(t)$ and $F(t) = f(t)$. Also $F(0) = f(0)$ by smoothness. In particular,*

$$\lim_{t \uparrow 0} \|u^{(0)}(t)\|_\infty = \infty, \qquad u^{(a)}(0) = u_0 = B(0), \qquad \operatorname*{ess\,sup}_{|x| < r} |u_0(x)| = \infty \quad (r > 0).$$

Here u_0 is the common strong L^2 trace from both sides, supported in K and smooth on $\mathbb{R}^3 \setminus \{0\}$. The support of $F(t)$ and that of the distinguished velocity $u^{(0)}(t)$ lie in K for all t.

(iii) Separation of the real family. *For every $a \ne b$ in $[-1, 1]$ and every $0 < t \le T_{\mathrm{out}}$, $\|u^{(a)}(t) - u^{(b)}(t)\|_2 > 0$. On $0 < t \le t_*$ the distinguished solution equals $B(t)$ and the force equals $f(t)$. On that interval, for constants $C_w > 0$, $L \ge 0$ common to the family,*

$$\|u^{(a)}(t) - B(t) - aV(t)\|_{H^3} \le C_w a^2 \tau^L e^{-3\Lambda_* \tau/2}.$$

With $Q_a = u^{(a)} - u^{(0)}$ and $\mathcal{Q}_a = u^{(0)} \otimes Q_a + Q_a \otimes u^{(0)} + Q_a \otimes Q_a$, the pressure correction at $t > 0$ is the $L^2(\mathbb{R}^3)$ representative

$$p^{(a)} - p^{(0)} = (-\Delta)^{-1} \sum_{i,j} \partial_i \partial_j (\mathcal{Q}_a)_{ij}.$$

The representatives agree throughout the common past.

Conclusion of the three parts. For the three-dimensional incompressible Navier–Stokes equations with viscosity one, there exist $T_{\mathrm{in}}, T_{\mathrm{out}} > 0$, a single force $F \in C_c^\infty((-T_{\mathrm{in}}, T_{\mathrm{out}}) \times \mathbb{R}^3; \mathbb{R}^3)$, and real distributional solutions $(u^{(a)}, p^{(a)})$, $a \in [-1, 1]$, on the common interval $[-T_{\mathrm{in}}, T_{\mathrm{out}}]$. Each velocity vanishes near $-T_{\mathrm{in}}$, belongs to the energy class of Definition 3.1.1, and satisfies the energy identity for F for every pair of time endpoints. The velocities agree on $[-T_{\mathrm{in}}, 0]$, and $\lim_{t \uparrow 0} \|u^{(0)}(t)\|_\infty = \infty$.

Their common two-sided strong L^2 trace at zero is smooth off the origin and essentially unbounded in every ball about it. The force and $u^{(0)}$ are supported in one fixed ball, including at $t = 0$. At each $0 < t \le T_{\mathrm{out}}$ the velocities are pairwise distinct in L^2. Each pair $(u^{(a)}, p^{(a)})$ is jointly smooth away from the single spacetime point $(0, 0)$.

Theorem 1 of Part 1 selects one leading pair satisfying its stated clauses. Part 2 completes that pair on both sides. The residual estimates on pp. 697 and 705 apply to that completion. Clauses (ii) and (iii) of Theorem 3 give the Main theorem in the front matter.

3.3 Linear inputs for this background

Proposition 3.3.1 (Exact mode and faster physical inverse)**.** *For the completed background fixed above there are $M, c_V, C_V > 0$, $t_0 \in (0, T_b)$ and a real solution V of $\mathcal{L}_B V = 0$ on $(0, t_0) \times \mathbb{R}^3$ which satisfies (3.2.1) for $0 < t \le t_0$. It is smooth for $0 < t < t_0$, and extends with $V(0) = 0$ to $C([0, t_0]; L^2_\sigma) \cap L^2(0, t_0; H^1_\sigma)$. Let $U_B(t, t')$ denote the solution operator from time $t' > 0$ to time $t \ge t'$ for the homogeneous equation (3.1.2) with initial datum in L^2_σ.*

For each fixed $0 < \epsilon < \Lambda_*/2$, the full physical evolution $U_B(t, t')$ satisfies, at sufficiently large τ,

$$\|U_B(t, t')\|_{L^2_\sigma \to L^2_\sigma} \le C_\epsilon \tau^\epsilon e^{(\Lambda_* + \epsilon)(\tau' - \tau)}, \qquad 0 < t' \le t, \quad \tau' = t'^{-h}. \tag{3.3.1}$$

In particular, set $\beta = 3\Lambda_*/2$ and define

$$\|F\|_{Y_\beta(T)} = \operatorname*{ess\,sup}_{\tau \ge T} e^{\beta\tau} \|F(t)\|_{H^2}, \qquad \|w\|_{X_{\beta,L}(T)} = \operatorname*{ess\,sup}_{\tau \ge T} e^{\beta\tau} \tau^{-L} \|w(t)\|_{H^3}.$$

For each norm take the space of strongly measurable functions $t \mapsto F(t) \in H^2_\sigma$ or $t \mapsto w(t) \in H^3_\sigma$ on $0 < t \le T^{-1/h}$ of finite norm, modulo equality almost everywhere. There are fixed $L \ge 0$, $C_G, T_0 > 0$ with $T_0^{-1/h} < T_b$ and bounded linear right inverses

$$G_T : Y_\beta(T; H^2_\sigma) \longrightarrow X_{\beta,L}(T; H^3_\sigma), \qquad \mathcal{L}_B G_T F = F, \qquad \|G_T\| \le C_G \quad (T \ge T_0). \tag{3.3.2}$$

The operators preserve real-valued data and are causal in the following sense. If two sources agree almost everywhere up to a time t, their images agree almost everywhere up to t.

Proof. The completion theorem fixes the selected $p = 6/5$ source and supplies its actual packet schedule, bounded overlap, and the completed-source and clock bounds of Theorem 2(v). Together with the unchanged frozen spectral and leading Gram data carried by that theorem, these are the inputs to Theorem 3.5.1. It applies without a shift and gives (3.3.1) for B. Its physical rate is $\Lambda_* = \lambda_c/h$ because $s = -t^{-h}/h$.

For the mode, the finite prepared construction (Lemma 3.7.7) and the critical inverse (Proposition 3.9.34) use this fixed source and its selected conjugate spectral pair. Lemma 3.10.2 places the residual of the paired Gaussian in the domain of that inverse. Proposition 3.10.4 subtracts its image and produces an exact real mode for $\mathcal{L}_B$. Its lower bound survives because the critical correction is smaller than the paired Gaussian. Returning to physical coordinates gives (3.2.1); positive-time smoothing gives its H^3 upper bound with a fixed polynomial loss. The exponential upper bound gives the zero strong trace and finite dissipation, as proved in that proposition.

Finally the global spatial jet bounds through order four of Theorem 2(iv) and (3.3.1) are the hypotheses of Proposition 3.11.3. It gives (3.3.2) for the same physical linearization, with constants uniform under increasing T. All finite preparations and threshold choices here take place after B is fixed. They do not select a new background or force. □

3.3.1 A sufficient criterion for branching

Theorem 3.3.2 uses a real mode and a bound for the full propagator of one completed background to produce a family on a common forward interval. Time zero in this criterion is the singular slice.

We work on $\mathbb{R}^3$ with unit viscosity and the unprojected physical force. For a divergence-free velocity u, the equation is

$$\partial_t u - \Delta u + \operatorname{div}(u \otimes u) + \nabla p = f, \qquad \operatorname{div} u = 0. \tag{3.3.3}$$

Where the letter f could denote a profile, we write $\mathbf{f}$ for the physical force; the scalar φ denotes the angular shape in the construction. The pressure and the difference of the velocities can have noncompact tails. For the positive-time restriction set $I_+ = (0, T_b)$. The data for the branching implication are exactly

$$(B_*, p_*, f_*) = (B, p_B, f)\big|_{I_+ \times \mathbb{R}^3}, \qquad u_{0,*} = B(0) = u_0. \tag{3.3.4}$$

Theorem 3.3.2 (Branching implication)**.** *Suppose (B_*, p_*) solves the unprojected equation with force f_* and strong trace $u_{0,*}$. Assume the forward energy and smoothness properties of Theorem 2(ii)–(iv), including the fixed compact spatial support of B_*, f_* and the Newtonian pressure representative in (ii). Suppose this same base also satisfies the jet bound (3.3.5) and the propagator bound (3.3.8). Suppose V is a real solenoidal solution of (3.3.6) with the mode bounds (3.3.7). There are $t_* \in (0, T_b)$, $L \geq 0$ and $C > 0$ such that for every $a \in [-1, 1]$ the fields*

$$u_a = B_* + q_a, \qquad q_a = aV + w_a, \qquad p_a = p_* + \pi_a$$

solve (3.3.3) on $[0, t_*]$ with the same force f_* and trace $u_{0,*}$. Each pair is a real solution in Definition 3.1.1, satisfies (3.1.1), and is smooth at positive times. The pressure correction $\pi_a(t) \in L^2$ is given by (3.12.8). At $a = 0$ the solution is the completed base. With $\beta = 3\Lambda_*/2$ and $\tau = t^{-h}$, for every $a, b \in [-1, 1]$ and every $0 < t \leq t_*$,

$$\begin{aligned} \|w_a(t)\|_{H^3} &\leq C a^2 \tau^L e^{-\beta\tau}, \\ \|w_a(t) - w_b(t)\|_{H^3} &\leq C|a-b|\tau^L e^{-\beta\tau}, \\ \|u_a(t) - u_b(t)\|_2 &\geq \tfrac{1}{2} c_V |a-b| \tau^{-M} e^{-1.1\Lambda_*\tau}. \end{aligned}$$

Here, for some fixed $N_j \geq 0$,

$$\|\nabla_x^j B_*(t)\|_{L^\infty} \leq C_j t^{-N_j}, \qquad 0 \leq j \leq 4. \tag{3.3.5}$$

The completed linearization and its exact mode satisfy

$$\mathcal{L}_{B_*} z = \partial_t z - \Delta z + \mathbb{P}\operatorname{div}(B_* \otimes z + z \otimes B_*), \qquad \mathcal{L}_{B_*} V = 0. \tag{3.3.6}$$

The mode has these bounds for fixed $M, C_V, c_V > 0$ and all sufficiently large $\tau = t^{-h}$:

$$\|V(t)\|_{H^3} \leq C_V \tau^M e^{-0.9\Lambda_*\tau}, \qquad \|V(t)\|_2 \geq c_V \tau^{-M} e^{-1.1\Lambda_*\tau}. \tag{3.3.7}$$

We denote the L^2_σ evolution of $\mathcal{L}_{B_*} z = 0$ by $U_*(t, t')$, $0 < t' \leq t$. The propagator bound is: for some fixed $0 < \epsilon < \Lambda_*/2$ there are C_ϵ, T_ϵ such that, with $\tau = t^{-h}$, $\tau' = t'^{-h}$,

$$\|U_*(t, t')\|_{L^2_\sigma \to L^2_\sigma} \leq C_\epsilon \, \tau^\epsilon \, e^{(\Lambda_* + \epsilon)(\tau' - \tau)}, \qquad 0 < t' \leq t, \ \tau \geq T_\epsilon. \tag{3.3.8}$$

This bound applies to all physical frequencies at a rate slightly more than the mode rate. It does not assume a spectral gap at rates less than Λ_*. (Theorem 3.5.1 gives it for each $\epsilon > 0$.) At $\beta = 3\Lambda_*/2$, we define

$$\|F\|_{Y_\beta(T)} = \operatorname*{ess\,sup}_{\tau \geq T} e^{\beta\tau}\|F(t)\|_{H^2},$$
$$\|z\|_{X_{\beta,L}(T)} = \operatorname*{ess\,sup}_{\tau \geq T} e^{\beta\tau}\tau^{-L}\|z(t)\|_{H^3}.$$

By Proposition 3.11.3, (3.3.5) and (3.3.8) give the full physical causal inverse

$$G_T : Y_\beta(T; H^2_\sigma) \longrightarrow X_{\beta,L}(T; H^3_\sigma), \qquad \mathcal{L}_{B_*} G_T F = F, \qquad \|G_T\| \leq C_G. \tag{3.3.9}$$

Here one finite L, one C_G, and one T_0 apply to each $T \geq T_0$.

Section 3.12 uses the exact real mode and one propagator rate $\Lambda_* + \epsilon < \beta$ to obtain the family. A leading-field eigenvalue, an auxiliary shifted propagator, or a selected-band Green function does not suffice. Section 3.9 constructs the mode. Section 3.11 derives the faster inverse. Theorem 3 applies this implication to the completed member.

Conventions. The source construction uses the bridge exponent λ_{br}, abbreviated locally to λ in its component formulas. The spectral branch uses $\lambda(Z, k)$. The physical exponential rate is Λ_*. The fast variables are

$$s = -\frac{t^{-h}}{h}, \qquad \tau = t^{-h}, \qquad \rho = t^h = \tau^{-1}. \tag{3.3.10}$$

If $\lambda_c = \operatorname{Re}\lambda_0 > 0$ is a canonical-time growth rate, its physical-time exponential rate is $\Lambda_* = \lambda_c/h$.

We use $\beta_c = 3\lambda_c/2$ and $\beta = \beta_c/h = 3\Lambda_*/2$. A source-band scale $Q = 2^{-\ell}$ uses $\rho_Q = Q^h$ and $S_\ell = \ell^{6/5}$. The quantities ρ_Q and S_ℓ are not the spectral radius of a mask that we fix after this. $\mathbb{P}$ denotes the whole-space Leray projector. For positive physical time, $R = r/t^{1/2}$ and $Z = z/t^{1/2-h}$ are physical similarity coordinates.

A local spectral chart defines its own (Z, k) with a different definition.

Symbol	Definition and point of selection
$h, \varkappa$	fixed anisotropy and iteration-loss exponents, $\varkappa = 10^{-5}$ in the source schedule
C, Δ	same source scale after normalized geometry and pressure/core data, $\Delta = C^\sigma$ before the late angular integer
m	one late finite angular winner, with conjugate sector $-m$
C_s	fixed physical auxiliary shift mask, frozen before the smaller cubic blend radius
B_*, p_*, f_*	one completed base, pressure and unprojected force after all source choices
V	exact real solution of the linearization about B_*
G_T	causal Duhamel inverse at the faster rate β (from (3.3.8))
a, w_a	real amplitude $a \in [-1, 1]$ and its quadratic correction on one common interval

3.3.2 Canonical coordinates and physical normalization

The tip variables $\hat{t}, \hat{\xi}, \hat{\zeta}$ describe the leading profiles; $\widehat{\Lambda}_P$ is their normalized angular velocity, not a spectral parameter or growth rate. The propagation coordinates R, Z use the positive physical time t, whereas Z, k in the frozen formulas denote the locally specified axial phase variables. In the propagation calculus the ordered axial operator is $-i\rho\partial_Z$. We write τ_b for the backward logarithmic clock (the backward chart also uses the physical duration $-t$) and τ_f for the forward fast clock,

denoted τ below. At a frozen phase μ_D translates the resolvent denominator only; it neither changes the time-dependent frame nor replaces the selected complex eigenvalue λ_0. The center gauge $g_\pm$ in the critical inverse is a separate time-dependent normalization.

$$(\hat\xi,\hat\zeta)=\left(\frac{r}{\hat t^{1/2}},\frac{z}{\hat t^{\frac12-h}}\right),\qquad (R,Z)=\left(\frac{r}{t^{1/2}},\frac{z}{t^{\frac12-h}}\right)\quad (t>0),$$
$$\tau_b=-\log(-t)\quad (t<0),\qquad \tau_f=t^{-h},\quad s=-\tau_f/h,\quad \rho=\tau_f^{-1}\quad (t>0),$$
$$\mu_D=\Lambda+i\big(n\Omega_c(Z)+kW_c(Z)\big),\qquad \lambda_0=\mu_0-im\Omega_c(0),$$
$$\lambda_c=\operatorname{Re}\lambda_0,\qquad \Lambda_*=\lambda_c/h.$$

Theorem 2(iv) carries the frozen spectral data, the leading evolution bounds and its Gram metric for this field. Clause (v) supplies the completed-source and clock estimates at the same normalization. We use them first for unshifted propagation and then for the prepared shift. The unshifted propagator uses no prepared system. The shifted and critical inverses use their own prepared and gauged domains, which we give at each use. We write $\rho=t^h$, $s=-t^{-h}/h$, and $\mathcal{S}\asymp\log(1/\rho)^{6/5}$. The notation $\mathcal{P}(\mathcal{S})$ denotes a fixed polynomial. The limit $t\downarrow 0$ corresponds to $s\to-\infty$, which also corresponds to $\tau=t^{-h}\to\infty$. An *ancient cutoff* restricts the estimates to sufficiently negative s. We select each fixed polynomial before this restriction.

3.4 Full-frequency propagation for the completed field

Main result. Lemma 3.4.4 gives full propagation from its leading, high-frequency, and filter bounds for the same completed source. The clock, Gram, and transported-filter lemmas establish its hypotheses.

For the shifted application, also assume the stated prepared-column bounds. The reverse bound remains independent of the block length.

Write $B_*=B_0+W$ for the decomposition fixed by Theorem 2. Its finite-prefix and tail estimates bound W in the physical boxes, and its clock uses the same principal pulse envelope that controls the completed gradient. We insert these bounds in the high-frequency and transported-filter estimates below. In the isotropic boxes of Theorem 2(v), write W for B_*-B_0 in the rescaled variables. For an admissible fixed $\eta>0$, the construction gives

$$\|W\|_\infty\le\rho^{1/2}P(S),\qquad |\nabla W|\le C(E+\rho^\eta),\qquad \|E\|_\infty\le P(S),\quad \|\nabla E\|_\infty\le\rho^{-\varkappa}P(S),\quad (3.4.1)$$

Here $\rho=Q^h$, $S=(1+\log(1/\rho))^{6/5}$, and E is the physical sample in the fixed coordinates $y=x/\sqrt{Q}$, $\theta=(t-Q)/Q^{1+h}$. All block generators, sources and filter derivatives below use θ. For $s=-t^{-h}/h$ the exact clock change is

$$j_Q:=\frac{\mathrm{d}s}{\mathrm{d}\theta}=(Q/t)^{1+h}=1+O(\rho L),\qquad \partial_\theta a=-KE+\widetilde r,\qquad \widetilde r=j_Qr_Q+K(1-j_Q)E=o(1).$$

The last bound follows from the clock identity in Theorem 2(v), $\|E\|_\infty\le P(S)$ and $L=o(\log(1/\rho))$. A canonical shift or source in the fixed spatial coordinates acquires the common scalar factor j_Q in the block equation. The principal diffusion coefficient in that equation is exactly ρ. For use with the leading metric supplied by Theorem 2(iv), let $P=\mathbb{P}$, $Q_\perp=I-P$, and $G_0=\nabla B_0$. The whole-space extension is

$$A_{\mathrm{ext}}=-B_0\cdot\nabla-G_0+2Q_\perp G_0P+(G_0-G_0^\top)Q_\perp+\rho\Delta-S_{\mathrm{app}}.\qquad (3.4.2)$$

Write $L_0 = L_G$ for the fixed horizon of the chosen Gram metric and g_1 for its form rate in the block estimates. In the shifted case any larger fixed rate below λ_c also gives the inequality, since $M \geq I$. The metric M commutes with P, obeys $I \leq M \leq CI$, and satisfies

$$\langle u, (\partial_\theta M + A_{\mathrm{ext}}^* M + M A_{\mathrm{ext}})u\rangle \leq 2g_1\langle u, Mu\rangle + C\,\|Q_\perp u\|_2^2 - 2\rho\,\|\nabla u\|_2^2\,. \tag{3.4.3}$$

Thus, for every bounded real Lipschitz vector field W and bounded Lipschitz scalar b,

$$\|[M, W\cdot\nabla]\|_{2\to 2} \leq C(\|W\|_\infty + \|\nabla W\|_\infty), \tag{3.4.4}$$

$$\|[b, M]\|_{2\to H^1} \leq C(\|b\|_\infty + \|\nabla b\|_\infty). \tag{3.4.5}$$

3.4.1 Weighted Hodge control and the high Gram estimate

Clause (v) of Theorem 2 supplies the gradient error for every exponent strictly below $c_{\mathrm{source}} := 1/2 - 3\varkappa$. Select fixed exponents

$$0 < \eta < \min\{c_{\mathrm{source}}, (1/2 - 2\varkappa)/3\}, \qquad 2\varkappa + \eta < \alpha < 1/2, \qquad N = \rho^{-\alpha}. \tag{3.4.6}$$

Take $\eta = 1/10$, $\alpha = 1/4$ and leakage order $M = 8$.

These satisfy the displayed inequalities and the differentiated-column requirement in Lemma 3.7.12. With $\varkappa = 10^{-5}$, $\mu := \alpha - 2\varkappa - \eta \geq 0.14998 > 1/8$ and $M\alpha - 2\varkappa - 2\eta \geq 1.79998 > 1$.

We select all finite source and metric jets, the fixed phase shift mask, and the constant clock multiplier K before the ancient threshold.

Lemma 3.4.1 (Smooth high-pass weighted Leray estimate)**.** *Let $P = \mathbb{P}$, $Q_\perp = I - P$, and $\chi_N = \chi(D/N)$, with $\chi = 0$ on $|\xi| \leq 1$ and $\chi = 1$ on $|\xi| \geq 2$. For real bounded Lipschitz a, normalized by $\inf a \leq 0 \leq \sup a$, let $L_a = \|\nabla a\|_\infty$, and $B_a = e^{\operatorname{osc} a}$, the three operators $T_N = P\chi_N, Q_\perp\chi_N, \chi_N$ obey*

$$\|e^a T_N e^{-a} - T_N\|_{2\to 2} \leq C B_a L_a/N. \tag{3.4.7}$$

If a solenoidal v has padded low leakage $\|\chi_{\mathrm{lo}}(D/(cN))v\|_2 \leq \zeta V_{\mathrm{tot}}$, then, for $u = e^a v$ and $d_H = CB_a^2 L_a/N$,

$$\|Q_\perp u\|_2 + \|u\|_{H^{-1}} \leq C(N^{-1} + d_H)\,\|u\|_2 + CB_a\zeta V_{\mathrm{tot}}. \tag{3.4.8}$$

The same right side, with a fixed metric constant, bounds the low-frequency leakage of Mu and $\|Q_\perp Mu\|_2$.

Proof. The high-pass factor makes the symbol of T_N smooth at $\xi = 0$. At unit scale, its inverse Fourier transform is a possible matrix multiple of δ_0 plus a principal-value kernel k.

This kernel satisfies $|k(z)| \leq C|z|^{-d}$ for $|z| \leq 1$ and has arbitrary rapid decay at infinity.

We split the order-zero symbol into dyadic annuli: the jth kernel satisfies the bound $C_M 2^{jd}(1 + 2^j|z|)^{-M}$, and summation gives these near and far bounds. The delta contribution cancels in the conjugation difference.

The remaining kernel is $k_N(x-y)(e^{a(x)-a(y)} - 1)$, absolutely integrable at the diagonal since the bracket is at most $B_a L_a|x-y|$. The two Schur integrals are bounded by $CB_aL_a\int |z||k_N(z)|\,\mathrm{d}z = CB_aL_a/N$.

We have not used a weighted sharp Fourier projection.

Choose a smooth high cutoff χ_H whose transition is at a fixed fraction of N and for which $1 - \chi_H$ is supported on the unit plateau of the given low cutoff. Put $T = P\chi_H(D)$. Since $Pv = v$, $\|(I - T)v\|_2 \leq C\zeta V_{\mathrm{tot}}$. The identity

$$u - Tu = e^a(I - T)v + (e^a T e^{-a} - T)u$$

and (3.4.7) bound its norm by $CB_a\zeta V_{\mathrm{tot}} + CB_aL_aN^{-1}\|u\|_2$. Now $Q_\perp Tu = 0$ and $\|Tu\|_{H^{-1}} \le CN^{-1}\|u\|_2$ by its Fourier support. This proves (3.4.8) and bounds the low leakage of u on any smaller separated pad.

Take $W = e_j$ in (3.4.4). Then $\|[M,\partial_j]\|_{2\to2} \le C$. For the translation $\tau_z f(x) = f(x+z)$, integration of $\tau_{tz}M\tau_{-tz}$ from $t=0$ to 1, first on smooth data, gives $\|[M,\tau_z]\|_{2\to2} \le C|z|$. Let $A_N = \psi(D/N)$ be a smooth compactly supported low cutoff, equal to one on the smaller pad and supported where $\chi_H = 0$. Its convolution kernel has absolute first moment $N^{-1}\int |z|\,|\check\psi(z)|\,\mathrm{d}z$, hence $\|[A_N,M]\|_{2\to2} \le C/N$. Since $A_NT = 0$, we obtain $\|A_NMu\|_2 \le CN^{-1}\|u\|_2 + C\|(I-T)u\|_2$. Finally $Q_\perp Mu = MQ_\perp u$, so (3.4.8) controls this term as well.

□

Lemma 3.4.2 (High Gram with the actual filtering source)**.** *We suppose a smooth solenoidal high-filtered field h obeys*

$$\partial_\theta h = \rho\Delta h - B_*\cdot\nabla h - (\nabla B_*)h - \nabla p - S_p h + F_h, \qquad \operatorname{div} F_h = 0, \tag{3.4.9}$$

where we keep F_h. We first calculate on smooth solenoidal H^1 fields with the stated padded high leakage. Energy approximation then extends the result.

Only $\nabla p \in L^2$, not $p \in L^2$, is necessary. Suppose its padded leakage is $\zeta \le C_M e^{c_M L}N^{-M}$ on a block of length L. Restrict here to a block family $L = o(\log(1/\rho))$.

The physical padded radius is that of (3.4.19)*.*

Select fixed $c_0, c_F > 0$, with the fixed cutoff nesting ratios, so that

$$n_L = c_0 e^{-c_F L}N, \qquad n_L \le c_L N/C_{\mathrm{pad}}, \qquad n_L^{-1} = c_0^{-1}e^{c_F L}\rho^{\alpha}. \tag{3.4.10}$$

We fix C_{pad} here. Use only blocks with $n_L \ge 1$. Each application of Lemma 3.4.1 below uses n_L in place of its generic frequency parameter N.

In particular its Hodge defect is $d_{H,L} = CB_a^2L_a/n_L$, and its H^{-1} gain and the fixed metric's low–high off-diagonal gain are n_L^{-1}. The same padded leakage ζ suffices, after a fixed cutoff enlargement.

No factor n_L^{-1} is charged to the low remainder. Under (3.4.1)*, the clock derivative bounds in Theorem 2(v), and Theorem 2(iv), a sufficiently large fixed K gives, with $u = e^a h$ and $Y^2 = \langle u, Mu\rangle$,*

$$\tfrac12\partial_\theta Y^2 + \tfrac{\rho}{2}\|\nabla u\|_2^2 \le (g_1 + o(1))Y^2 + \mathrm{Re}\langle Mu, e^aF_h\rangle + CB_a^6\rho^{-4\varkappa-4\eta}P(S)\zeta^2V_{\mathrm{tot}}^2. \tag{3.4.11}$$

Here $S_p = 0$, or S_p is a prepared shift that satisfies the high-input bound of Lemma 3.7.15.

The $o(1)$ is uniform after these finite choices along the block lengths of (3.4.23)*. Estimate* (3.4.12) *controls its cutoff-dependent part.*

In the zero-shift case no column assumption is necessary.

Proof. The divergence of (3.4.9), with $\operatorname{div} B_* = \operatorname{div} h = 0$ and the solenoidal shift and source, gives

$$\nabla p = -2Q_\perp((\nabla B_*)h), \qquad \|\nabla p\|_2 \le 2\,\|\nabla B_*\|_\infty\,\|h\|_2\,.$$

We only use the gradient. Since M commutes with P,

$$|\langle Mu, e^a\nabla p\rangle| = |\langle Q_\perp(e^aMu), \nabla p\rangle|.$$

Put $w = Mu$ and $r_{H,L} = C(n_L^{-1} + B_a^2L_a/n_L)$. Since $[M,P] = 0$, Lemma 3.4.1 at n_L and its metric low-leakage assertion give

$$\|Q_\perp w\|_2 + \|\chi_{\mathrm{lo}}(D/(cn_L))Pw\|_2 \le Cr_{H,L}\,\|u\|_2 + CB_a\zeta V_{\mathrm{tot}},$$

with a fixed nested cutoff ratio $c > 0$.

Decompose

$$Q_\perp(e^a w) = Q_\perp(e^a P w) + Q_\perp(e^a Q_\perp w).$$

For the first term, split the solenoidal Pw at the same padded radius n_L. Use the high-pass conjugation estimate on its high part, and estimate its low part directly.

Estimate the second term by $e^{\max a} \|Q_\perp w\|_2$.

Since $e^{\max a}, e^{-\min a} \le B_a$, this gives

$$\|Q_\perp(e^a M u)\|_2 \le C B_a r_{H,L} \|u\|_2 + C B_a^2 \zeta V_{\mathrm{tot}}.$$

We use the gradient bound $\|\nabla p\|_2 \le P(S) e^{-\min a} \|u\|_2$ in the pressure pairing. The pressure work is at most a fixed subpower factor times $n_L^{-1} \rho^{-\varkappa} \|u\|_2^2$, plus $C B_a^3 P(S) \zeta V_{\mathrm{tot}} \|u\|_2$.

The homogeneous coefficient tends to zero under (3.4.24). Comparing the unprojected leading terms in (3.4.9) with (3.4.2) also produces the forms of $2Q_\perp G_0 P$ and $(G_0 - G_0^\top) Q_\perp$. Since $[M, P] = 0$ and G_0 is bounded, their absolute values are at most $C \|Q_\perp u\|_2 \|u\|_2$. Estimate (3.4.8) thus gives $C r_{H,L} \|u\|_2^2 + C B_a \zeta V_{\mathrm{tot}} \|u\|_2$, with $r_{H,L} = o(1)$. The gradient block in (3.4.3) is controlled by the related Hodge defect squared. To keep the stated squared remainder, put $a_1 = 2\varkappa + 2\eta > 0$ and use

$$C B_a^3 P(S) \zeta V_{\mathrm{tot}} \|u\|_2 \le \rho^{a_1} \|u\|_2^2 + C B_a^6 \rho^{-a_1} P(S)^2 \zeta^2 V_{\mathrm{tot}}^2.$$

At a late threshold $P(S) \le \rho^{-a_1}$, so the last term is bounded by $C B_a^6 \rho^{-4\varkappa - 4\eta} P(S) \zeta^2 V_{\mathrm{tot}}^2$, the remainder below.

Thus we apply no inverse Laplacian to the low-frequency pressure potential.

When the shift is present, its block form is $S_p = j_Q d_0 J_* C_s K_*$, with the columns and row pulled back to the fixed coordinates and the *same* fixed phase mask C_s as the low reference. The actual cutoff row $C_s K_r$ maps H^{-1} to scalar L^2.

Its adjoint test column has bounded radial H^1 profiles and compact axial frequency on the fixed mask. This assertion does not apply to the uncut row.

Normalization differs by $O(\delta + \rho^\nu P(S))$ (Lemma 3.7.9), with $\nu = .99872$ and $\delta = \rho^{2/5}$. The prepared column has L^2 norm $P(S)$, so for the padded high input

$$\|e^a S_p h\|_2 \le C B_a P(S)(e^{c_F L} N^{-1} + \delta) \|u\|_2 + C B_a P(S) \zeta V_{\mathrm{tot}}.$$

This treats $S_p - S_{\mathrm{app}}$ as a small high-input work term.

For $S_p = 0$ this full shift contribution is zero. In the other case the fixed smooth S_{app} is itself $H^{-1} \to L^2$ bounded and thus costs $C \|u\|_{H^{-1}} \|u\|_2$, with the same n_L-scale Hodge bound.

The retained error δ has no flow factor. We do not assert that the global row K_* smooths arbitrary high frequencies.

For the wave transport form put $d = \rho^\eta$, $b = (E + d)^{1/2}$, $f = bu$, $Z = W/(E + d)$, and $R_b = [b, M] b^{-1}$. By (3.4.1) and (3.4.4),

$$\|Z\|_\infty \le \rho^{1/2 - \eta} P(S), \quad \|\nabla Z\|_\infty \le C + \rho^{1/2 - \varkappa - 2\eta} P(S), \quad \|R_b\|_{2 \to H^1} \le \rho^{-\varkappa - \eta} P(S).$$

Since $W = B_* - B_0$ is solenoidal,

$$\operatorname{div} Z = -\frac{W \cdot \nabla E}{(E + d)^2} = -2 Z \cdot \nabla \log b, \qquad \|\operatorname{div} Z\|_\infty \le \rho^{1/2 - \varkappa - 2\eta} P(S)$$

by (3.4.1). The exact factorization is

$$\operatorname{Re}\langle M u, W \cdot \nabla u \rangle = \operatorname{Re}\langle M f, Z \cdot \nabla f \rangle + \operatorname{Re}\langle R_b f, Z \cdot \nabla f \rangle - \operatorname{Re}\langle M f + R_b f, (Z \cdot \nabla \log b) f \rangle.$$

For $\mathcal{T}_Z = Z\cdot\nabla$, the adjoint is $\mathcal{T}_Z^* = -\mathcal{T}_Z - \operatorname{div} Z$. Hence

$$2\operatorname{Re}\langle Mf, \mathcal{T}_Z f\rangle = \operatorname{Re}\langle f, ([M,\mathcal{T}_Z] - (\operatorname{div} Z)M)f\rangle.$$

The first estimate of (3.4.4) applies to this Z. Integration by parts bounds the second term of the factorization by $\|R_b\|_{2\to H^1}(\|Z\|_\infty + \|\operatorname{div} Z\|_\infty)\|f\|_2^2$. The last term is bounded by $\frac{1}{2}(\|M\| + \|R_b\|_{2\to 2})\|\operatorname{div} Z\|_\infty\|f\|_2^2$. Thus the absolute value of the wave transport form is at most

$$C(1+\rho^{1/2-\varkappa-2\eta}P(S) + \rho^{1/2-2\varkappa-3\eta}P(S))\,\|f\|_2^2 \le C\int (E+d)|u|^2.$$

Here the strict choice of η in (3.4.6) makes the two displayed errors small. For stretching write $\nabla W = b^2 G_W$, $\|G_W\|_\infty \le C$.

Then

$$\langle Mu, (\nabla W)u\rangle = \langle Mbu + [b,M]u, G_W bu\rangle.$$

Since M is self-adjoint and b is real, duality upgrades $[b,M] : L^2 \to H^1$ to $[b,M] : H^{-1} \to L^2$. More explicitly, $\|[b,M]\|_{H^{-1}\to L^2} \le \rho^{-\varkappa-\eta/2}P(S)$, and the high part of u has H^{-1} norm at most $CB_a^2P(S)n_L^{-1}\rho^{-\varkappa}\|u\|$.

The bound $\|u\| \le \rho^{-\eta/2}\|bu\|$ then gives a relative form error

$$q_L \le \mathcal{E}_0(\rho)e^{c_F L}\rho^\mu, \qquad \mu = \alpha - 2\varkappa - \eta > 0, \qquad \log\mathcal{E}_0 = o(\log(1/\rho)), \tag{3.4.12}$$

plus the retained padded leakage. The envelope $\mathcal{E}_0$ contains only fixed powers of B_a and the finite source and metric bounds, taken on a fixed comparable-time hull.

It is independent of L. These estimates use only the stated first derivative bounds on the wave.

This is a proof for total-high fields. It does not import an angular-high localization theorem.

For the clock term, we must prove a lower form estimate. The second commutator bound in (3.4.4), the high H^{-1} gain in (3.4.8), and $\|u\|_2 \le d^{-1/2}\|bu\|_2$ give

$$\operatorname{Re}\langle Mu, Eu\rangle \ge (1 - Cq_L)\,\|bu\|_2^2 - Cd\,\|u\|_2^2$$

apart from the explicitly retained low-leakage term.

This follows also from the exact identity $\langle Mu, Eu\rangle = \langle Mbu, bu\rangle + \langle [b,M]u, bu\rangle - d\langle Mu, u\rangle$. The exponent in (3.4.12) is positive by (3.4.6).

We bound this diagonal form error before we use the high growth gap. It is not part of the large reverse coefficient.

Its limit is justified by (3.4.24). Fix K larger than the combined transport and stretching form constant.

Then $\partial_\theta a = -KE + \widetilde{r}$ absorbs those two wave forms. $\widetilde{r} = o(1)$ and $d = o(1)$ leave only $o(1)Y^2$.

Last scalar conjugation of diffusion contributes $-2\rho\nabla a\cdot\nabla u + \rho(|\nabla a|^2 - \Delta a)u$. In $\frac{1}{2}\partial_\theta Y^2$, (3.4.3) supplies $-\rho\,\|\nabla u\|_2^2$. The work of the first conjugation term satisfies

$$2\rho|\operatorname{Re}\langle Mu, \nabla a\cdot\nabla u\rangle| \le \tfrac{\rho}{2}\,\|\nabla u\|_2^2 + 2\rho\|M\|^2\,\|\nabla a\|_\infty^2\,\|u\|_2^2.$$

This leaves $-\frac{\rho}{2}\,\|\nabla u\|_2^2$ in the half-energy inequality. The last term on the right is $o(1)Y^2$ by the clock derivative bounds in Theorem 2(v) and $I \le M \le CI$. The same bounds apply to the work of $\rho(|\nabla a|^2 - \Delta a)$ and $B_*\cdot\nabla a$. Apply Young's inequality to each term linear in the padded leakage.

A same upper bound for their squared remainders is $CB_a^6\rho^{-4\varkappa-4\eta}P(S)\zeta^2V_{\mathrm{tot}}^2$. This yields (3.4.11).

The proof integrates this squared energy inequality before the square root. It never divides its leakage term by Y pointwise.

□

3.4.2 Transported total-frequency filters

Let $A_{\mathrm{ref}} = A_{\mathrm{lead}} - S_{\mathrm{ref}}$ be the physical leading reference, extended as in (3.4.2). Here $S_{\mathrm{ref}} = 0$ in the unshifted application.

In the prepared application it uses the same fixed C_s as S_p and has a smoothing finite-profile kernel. The exact fixed reference differs from the spectral reference by $o(1)$ on physical L^2.

Assume the selected reference has a fixed propagation rate g_{ref}. Only the shifted application requires $g_{\mathrm{ref}} < \lambda_c$.

Keep $D = S_p - S_{\mathrm{ref}}$ outside the leading commutator. All the filter identities and commutator bounds below hold with either choice.

When the two shifts vanish, $D = 0$.

Lemma 3.4.3 (Exact filtered equations and their bounds)**.** *On a block $0 \le \theta \le L$ with $\rho L \to 0$, let F_θ be the volume-preserving scalar flow generated by $-B_0 \cdot \nabla$. Fix a scalar cutoff $\chi \in C_c^\infty(\mathbb{R}^3)$ with $0 \le \chi \le 1$ and $\chi = 1$ near zero, and put*

$$C_\theta = F_\theta \chi(D/N) F_\theta^{-1}, \quad L_\theta = P C_\theta P, \quad H_\theta = P - L_\theta, \quad \Psi_\theta = \dot{L}_\theta + [L_\theta, A_{\mathrm{ref}}].$$

For the actual physical solution

$$v_\theta = (A_{\mathrm{lead}} + R - S_p)v + f = (A_{\mathrm{ref}} + R - D)v + f, \qquad Rv = -P\,\mathrm{div}(W \otimes v + v \otimes W),$$

define $l = L_\theta v$, $h = H_\theta v$.

Then $v = l + h$ and

$$l_\theta = A_{\mathrm{ref}} l + L_\theta(R - D)(l + h) + \Psi_\theta(l + h) + L_\theta f, \tag{3.4.13}$$

$$h_\theta = (A_{\mathrm{lead}} + R - S_p)h + H_\theta(R - D)l - L_\theta(R - D)h - \Psi_\theta(l + h) + H_\theta f. \tag{3.4.14}$$

No filtered range is claimed invariant. For each fixed finite list of derivatives, with constants that depend only on the frozen source,

$$\|\Psi_\theta\|_{2\to 2} \le C e^{cL}(N^{-1} + \rho N), \tag{3.4.15}$$

$$\|L_\theta P\,\mathrm{div}\, T\|_2 \le C e^{cL} N \|T\|_2, \tag{3.4.16}$$

$$\|L_\theta R\|_{2\to 2} \le C e^{cL} \rho^{1/2-\alpha} P(S), \tag{3.4.17}$$

$$\|Rl\|_2 \le C P(S) \|l\|_2 + C e^{cL} \rho^{1/2-\alpha} P(S) \|l\|_2 + C e^{cL} \rho^{1/2} P(S) \|v\|_2. \tag{3.4.18}$$

For each fixed finite M, a smooth physical low cutoff strictly inside the transported high region satisfies

$$\|\chi_{\mathrm{lo}}(D/(c_L N)) H_\theta\|_{2\to 2} \le \zeta, \qquad \zeta \le C_M e^{c_M L} N^{-M}, \quad c_L \ge c_0 e^{-C_0 L}. \tag{3.4.19}$$

Proof. The transport identity $\dot{C}_\theta + [C_\theta, -B_0 \cdot \nabla] = 0$ is exact.

Write $F_\theta g = g \circ \Phi$ and $\Psi = \Phi^{-1}$. Each positive-order spatial derivative of Φ, Ψ used here is bounded by $C_j e^{c_j L}$, by induction in the differentiated flow equation. Both maps preserve volume. These estimates use the leading field on the block. In box coordinates $y = x/\sqrt{Q}$, one has $\xi = |y_h|/\sqrt{q/Q}$, $\eta = Q^h y_3 (q/Q)^{h-1/2}$ and $q/Q \ge t/Q$, with t/Q bounded away from zero. The leading finite-jet and exterior bounds imported in Theorem 2(iv), with regular Cartesian representatives at the axis, give the required uniform velocity derivatives. We first verify the frequency separation estimate used for the low frequencies of the Leray projector.

Physical low frequencies. Choose $n = c_L N$ with $c_L = c/(1 + \sup_\theta \|D\Psi\|_\infty)$ and $c > 0$ small enough that all the affine pullbacks of the support of $\chi_{\mathrm{lo}}(D/n)$ lie strictly inside the plateau of $\chi(D/N)$. In particular $c_L \geq c_0 e^{-C_0 L}$ with fixed $c_0, C_0 > 0$. For $g = \chi_{\mathrm{lo}}(D/n)w$, we prove

$$\|(I - \chi(D/N))(g \circ \Psi)\|_2 \leq C_M e^{c_M L} N^{-M} \|w\|_2.$$

It is enough to use any positive integer M. Write $A_x(z) = \Psi(x) - D\Psi(x)z$ and $R_x(z) = \Psi(x - z) - A_x(z)$, so $|R_x(z)| \leq Ce^{cL}|z|^2$. For $j \leq M$ and q on the segment from $A_x(z)$ to $\Psi(x - z)$, the differentiated low kernel gives

$$|D^j g(q)| \leq C_j n^j (1 + N|z|)^5 (H_n * |w|)(\Psi(x)), \qquad H_n(y) = n^3(1 + n|y|)^{-5}.$$

Indeed $n|q - \Psi(x)| \leq n\|D\Psi\|_\infty |z| \leq CN|z|$. Expand $g(A_x + R_x)$ at A_x through order $M - 1$ in R_x. For each positive-order term replace R_x by its Taylor polynomial in z through degree $M + 1$. Every resulting term is a polynomial times $(D^j g)(A_x(z))$. Its Fourier support as a function of z is contained in the affine image of the low-frequency ball (its reflection obeys the same plateau bound). Thus integration against $N^3 \check{\chi}(Nz)$ evaluates that term at $z = 0$. The zero-order term gives $g(\Psi(x))$ and the others vanish there.

The Taylor remainder contributes at most $C_M e^{c_M L} n^M N^{-2M} (H_n * |w|)(\Psi(x))$. For $1 \leq j < M$, the error in replacing $R_x^{\otimes j}$ is bounded by $C_M e^{c_M L} |z|^{M+2+2(j-1)} (1+|z|)^{C_M}$, using the Taylor remainder for one factor and the quadratic vanishing of every other factor. Its integrated contribution is at most $C_M e^{c_M L} n^j N^{-M-2j} (H_n * |w|)(\Psi(x))$. These bounds follow from the Schwartz moments of $\check{\chi}$ and $N \geq 1$. Since $n \leq CN$, volume preservation and Young's inequality prove the displayed L^2 bound. Conjugating by F_θ bounds $(I - C_\theta)\chi_{\mathrm{lo}}(D/n)$, and adjunction gives the reverse order. The same argument applies to any smaller smooth padded low cutoff. The Leray multipliers on the outside commute with the physical low cutoff, giving (3.4.19).

Projected commutator. The extension (3.4.2) preserves solenoidal and gradient fields. For solenoidal v, $\operatorname{div}((B_0 \cdot \nabla)v) = \operatorname{div}(G_0 v)$ by $\operatorname{div} B_0 = 0$. For $v = \nabla\varphi$ the transport and matrix terms combine to $-\nabla(B_0 \cdot \nabla\varphi)$. The smoothing shift acts on the solenoidal subspace and vanishes on gradients. Hence on solenoidal data the filtered commutator is the compression of $\dot{C}_\theta + [C_\theta, A_{\mathrm{ext}}]$ with the indicated fixed reference shift. The transport terms cancel exactly.

The kernel of C_θ is $K_\theta(x, y) = N^3 \check{\chi}(N(\Phi(x) - \Phi(y)))$. The first kernel moment bounds $[C_\theta, G_0]$ by Ce^{cL}/N. To treat P split it by a smooth cutoff supported in the padded low ball. On its low part use the preceding estimate for $C_\theta - I$ on both sides of a slightly larger low cutoff. The residual multiplier is bounded on L^2. The high part has a kernel with absolute first moment at most C/n away from its possible delta term, by the dyadic estimate in Lemma 3.4.1. Also $(\nabla_x + \nabla_y)K_\theta$ has Schur norm at most Ce^{cL}. Indeed its derivative on $\check{\chi}$ is multiplied by $D\Phi(x) - D\Phi(y)$, bounded by $Ce^{cL}|x-y|$. Integrating this estimate on simultaneous translates of x, y gives $\|[C_\theta, T_z]\|_{2\to 2} \leq Ce^{cL}|z|$ for translation T_z. Integrating against the high kernel proves $\|[C_\theta, P]\| \leq Ce^{cL}/N$. The same bound holds for $I - P$.

The smoothing shift and its adjoint map L^2 to H^1. Conjugation by the flow and the estimate $\|(I - \chi(D/N))u\|_2 \leq CN^{-1}\|\nabla u\|_2$ bound the shift commutator by Ce^{cL}/N. Finally the kernel of $[\Delta, C_\theta]$ is $(\Delta_x - \Delta_y)K_\theta$. The coefficient of the second kernel derivatives contains $D\Phi(x)D\Phi(x)^\top - D\Phi(y)D\Phi(y)^\top = O(e^{cL}|x - y|)$, while the first derivative terms have coefficients bounded by Ce^{cL}. Changing variables by the volume-preserving map in both Schur integrals gives $Ce^{cL}N$. Together these estimates yield the first line of (3.4.15). Differentiate $l = L_\theta v$. We rearrange the commutator terms and get its first equation in (3.4.13).

Subtract it from the true equation to get the second. Their sum is the original equation, with F_h for Lemma 3.4.2.

The masks are self-adjoint contractions but are not projections.

For a tensor flux, duality puts one derivative on $PC_\theta P$. In transported coordinates the cutoff is supported at $|\xi| \lesssim N$.

The finite flow jets give $\|\nabla C_\theta\| \le Ce^{cL}N$. This yields the second line.

We apply this estimate to $W \otimes v + v \otimes W$ with $\|W\|_\infty \le \rho^{1/2}P(S)$ to get the third bound. For the reverse estimate write

$$Rl = -P\big[(W \cdot \nabla)l + (l \cdot \nabla)W\big].$$

The stretching term costs $P(S)\,\|l\|_2$, without a flow derivative.

For the transport term, write $v_\Phi = F_\theta^{-1}Pv$, $g = \chi(D/N)v_\Phi$, and $F_\theta g = g \circ \Phi$, so $l = P(g \circ \Phi)$. Choose a smooth compactly supported ψ equal to one on the unit ball and put $Q_\Lambda = \psi(D/\Lambda)$, where $\Lambda = c_\chi(1+\|D\Phi\|_\infty)N$ and $\operatorname{supp}\chi \subset \{|\xi| \le c_\chi\}$, $c_\chi \ge 1$. For fixed x, let $A_x(y) = \Phi(x)+D\Phi(x)(y-x)$. The Fourier support of $g \circ A_x$ lies in $\{|\xi| \le \Lambda\}$, and its derivative at x equals that of $g \circ \Phi$. Hence, with $\psi_\Lambda^\vee$ the convolution kernel of Q_Λ,

$$\nabla(I - Q_\Lambda)(g \circ \Phi)(x) = \int \nabla\psi_\Lambda^\vee(x-y)\big[g(A_x(y)) - g(\Phi(y))\big]\,dy.$$

Here $|A_x(y) - \Phi(y)| \le \frac{1}{2}\|D^2\Phi\|_\infty|x-y|^2$. Every point w of the segment joining these two arguments satisfies $N|w - \Phi(x)| \le \Lambda|x-y|$. For $H_N(z) = N^3(1+N|z|)^{-5}$, the kernel of $\nabla\chi(D/N)$ therefore gives

$$|\nabla g(w)| \le CN(1+\Lambda|x-y|)^5(H_N * |v_\Phi|)(\Phi(x)).$$

The integral of $|\nabla\psi_\Lambda^\vee(z)|\,|z|^2(1+\Lambda|z|)^5$ is $O(\Lambda^{-1})$. Volume preservation and $\|H_N\|_1 = O(1)$ give $\|\nabla(I-Q_\Lambda)(g\circ\Phi)\|_2 \le C(N/\Lambda)\|D^2\Phi\|_\infty\|v_\Phi\|_2$. Since P commutes with Q_Λ and Cartesian derivatives,

$$\|\nabla l\|_2 \le C\Lambda\|l\|_2 + C(N/\Lambda)\|D^2\Phi\|_\infty\|v\|_2 \le Ce^{cL}(N\|l\|_2 + \|v\|_2).$$

Multiplication by $\|W\|_\infty \le \rho^{1/2}P(S)$ gives the last two terms of (3.4.18) because $N = \rho^{-\alpha}$.

Thus the only potentially large reverse constant has no e^{cL} factor.

The physical low-frequency estimate at the start of the proof applies to $H_\theta = P(I - C_\theta)P$, completing the proof. □

3.4.3 Propagation transfer for the two applications

Lemma 3.4.4 (From two-band block estimates to a full propagator)**.** *In canonical time s, consider the completed equation $v_s = (A_{\mathrm{lead}} + R - S)v + f$ with a bounded shift S, possibly zero. Suppose its leading reference propagates at rate g_0, and the finite-time metric and high Gram estimate above hold at rate g_1.*

Assume the exact filtered equations satisfy (3.4.15)–(3.4.19) *and, when a shift is present, the two shift bounds* (3.7.39)*. The reverse coefficient is $M_0 \le B_a^C P(S)$ independently of the block length.*

A fixed subpower factor times the quantities in (3.4.22) *bounds each small coefficient. In the zero-shift case the shift terms in that list are absent.*

Then for each fixed $g > \max(g_0, g_1)$ an ancient threshold gives

$$\|U_S(s,r)\|_{2\to2} \le C_*(\rho(s))e^{g(s-r)}, \qquad r \le s, \qquad C_*(\rho) = \rho^{-o(1)}. \tag{3.4.20}$$

We fix the source, shift and physical solution during block restarts. We restart only the analysis filters.

Proof. On a positive-time compact interval the coefficients and bounded shift are smooth.

Galerkin approximation and the parabolic energy estimate construct the physical evolution. Select $\gamma > 0$ and g_* with $\max(g_0, g_1) < g_* - 2\gamma < g_* + 2\gamma < g$.

Fix η, α as in (3.4.6), and a finite M with

$$M\alpha > 2\varkappa + 2\eta + 1. \tag{3.4.21}$$

We fix the finite source, flow and shift jets before the ancient threshold. On one block of length L, let X and Y_* be the suprema of $e^{-g_*\theta}\|l(\theta)\|_2$ and the related weighted high Gram norm.

Set $F_* = \int_0^L e^{-g_*\theta}\|f(\theta)\|_2 \,\mathrm{d}\theta$. Truncate the integral at an earlier endpoint when necessary. Duhamel for the exact low equation (3.4.13) uses the full physical reference propagator.

The low-output wave estimate, the shift comparison when present, and the connection bound give

$$X \le CX_0 + \epsilon_L(X + B_aY_*) + CF_*.$$

We apply Lemma 3.4.2 to the exact high equation and keep each term of its F_h. We integrate the squared inequality before we take a square root.

The reverse stretching and bounded high-output shift column give M_0X, while the padded leakage gives a small term because of (3.4.21):

$$Y_* \le CY_0 + M_0X + \epsilon_H(X + Y_*) + CB_aF_*, \qquad M_0 = B_a^C P(S).$$

All fixed constants are independent of block length.

More explicitly, a fixed subpower factor times one of

$$e^{cL}\rho^{\alpha}, \quad e^{cL}\rho^{1-\alpha}, \quad e^{cL}\rho^{1/2-\alpha}, \quad \delta, \quad \rho^{\nu}, \quad e^{cL}\rho^{M\alpha-2\varkappa-2\eta}. \tag{3.4.22}$$

bounds each term in ϵ_L, ϵ_H. The first two come from Ψ_θ. The third bounds the low-output wave, the reverse transport $(W \cdot \nabla)l$ and the high-carrier shift output. In the reverse transport estimate, $v = l + h$ gives $e^{-g_*\theta}\|v(\theta)\|_2 \le X + B_aY_*$.

The next two come from the prepared retained part. The last comes from the square root of the soft-high leakage remainder.

After an increase of the fixed c, the first term also bounds the prepared row's physical high-input gain n_L^{-1}. Separately the diagonal high-energy calculation requires q_L of (3.4.12) to be small.

Its power μ is not bounded by the larger power α in this list.

This also includes the $O(\rho)$ reference normalization. Because B_a and M_0 are subpower, for any $L = o(\log(1/\rho))$ each product in (3.4.22) with their fixed powers tends to zero. First absorb ϵ_HY_*, then substitute into the low inequality.

The only nontrivial Schur factor is $\epsilon_LB_aM_0 = o(1)$. M_0 itself need not be small.

This gives a block estimate with a subpower prefactor.

For clarity, a finite block does not require a balanced metric whose condition number would be $\sqrt{M_0/\epsilon_L}$. The positive off-diagonal Volterra matrix is

$$J = \begin{pmatrix} 0 & \epsilon \\ M_0 & 0 \end{pmatrix}, \qquad \omega = \sqrt{\epsilon M_0}, \qquad e^{LJ} = \cosh(\omega L)I + \frac{\sinh(\omega L)}{\omega}J.$$

If $\omega L \le 1$, its operator norm does not exceed $C(1 + M_0L)$.

Time-dependent nonnegative coefficients bounded by these entries obey the same comparison through their iterated Duhamel series. The potentially large reverse term M_0 contains no e^{cL}, by the exact product-rule estimate in (3.4.18).

This is what makes the next choice noncircular.

Select a predetermined envelope

$$\mathfrak{P}(\rho) = \exp\Big(C(\log(e/\rho))^{9/10}\log\log(e^e/\rho)\Big)\,(1+\log(e/\rho))^C$$

large enough for the finite source constants, clock contrast, metric and coordinate comparisons, all bounded on a fixed comparable-time hull. In particular the envelopes for B_a and $M_0 = B_a^C P(S)$ are fixed before L.

The envelope is independent of proof blocks and has $\log\mathfrak{P} = o(\log(1/\rho))$. Take, with D a fixed large constant,

$$L(\rho) = D\big[1+\log\mathfrak{P}(\rho)+\log(2+M_0(\rho))+\log\log(e^e/\rho)\big]. \tag{3.4.23}$$

Then $L = o(\log(1/\rho))$, $\rho L \to 0$, $\omega L \to 0$, and each $e^{cL}\rho^a$ in (3.4.22) and (3.4.12) still tends to zero.

With $L_{\mathrm{box}}(Q) = L(Q^h)$ and the fixed L_G, this family satisfies the Gram condition in Theorem 2(iv). We take Q below the threshold for this family.

The next inequalities give one explicit threshold for all these estimates. Let $a_* = 1/8$, with the concrete exponents fixed above. Select a fixed finite $c_* \ge c_F$ that dominates all the flow exponents in the filter and leakage bounds.

Let $\mathcal{E}(\rho)$ be a fixed subpower envelope for all products of $\mathcal{E}_0, B_a, M_0, P(S)$ in the rate, Schur, and Volterra estimates. Include the extra factor $B_a M_0$ in the Schur test.

We first fix D. Then we decrease ρ_0 so that, for $\rho \le \rho_0$,

$$c_F L + \log(1/c_0) \le \tfrac{\alpha}{2}\log(1/\rho), \tag{3.4.24}$$

$$c_* L + \log\mathcal{E}(\rho) + 2\log(1+L) \le \tfrac{a_*}{2}\log(1/\rho). \tag{3.4.25}$$

These inequalities follow from $L = o(\log(1/\rho))$ and $\log\mathcal{E} = o(\log(1/\rho))$.

The first gives $n_L \ge \rho^{-\alpha/2} \ge 1$. The second bounds each listed flow-dependent error, with q_L, and its necessary Schur or Volterra product by $\rho^{a_*/2}$.

Thus $\epsilon_L B_a M_0 = o(1)$ and $\epsilon M_0 L^2 = o(1)$. The remaining clock and diffusion errors carry no flow factor. We make them smaller than the fixed rate reserve at the same late threshold.

We use only finite jets and one H^{-1} high-input gain. We do not absorb any e^{cL} into M_0. At a block endpoint, reconstruct the *same* physical $v = l + h$ and restart only the analysis filters.

All source labels, the column data, when present, and the bounded shift remain fixed. The spatial coordinate change with its amplitude ratio contributes $1 + O(\rho L)$ between block endpoints. For each subinterval $[\theta_1, \theta_2]$ the elapsed canonical time is $\int_{\theta_1}^{\theta_2} j_Q \,\mathrm{d}\theta = (\theta_2 - \theta_1)(1 + O(\rho L))$. Thus converting an exponential bound in either time changes its rate by $O(\rho L) = o(1)$, within the fixed rate reserve. This also applies on the fixed horizon used to construct the block Gram metric. We multiply the endpoint comparison by $C(1 + M_0 L)$ and divide its logarithm by L.

The result is at most $C'/D + o(1)$.

With γ fixed, choose D so that $C'/D < \gamma/2$. Then take T large enough that the $o(1)$ term costs at most $\gamma/2$ on $s \le -T$. This fixed rate absorbs the prefactors of all complete blocks.

Input-time factors (the first partial block and $B_a(\rho(r))$) are absorbed in the same way. Since $\log(1/\rho(r)) \le \log(1/\rho(s)) + \log(1 + h(s-r))$ and $\log C_*$ has $o(1)$ derivative in $\log(1/\rho)$, we get $C_*(\rho(r)) \le C_\epsilon C_*(\rho(s))(1 + h(s-r))^\epsilon$. This gives an arbitrarily small loss of rate. At the output time only the last partial block keeps one $C_*(\rho(s)) = \mathfrak{P}(\rho(s))^C = \rho(s)^{-o(1)}$ factor at the output time.

This proves (3.4.20) at the prescribed rate g. The reference block length L_0 used to build M stayed fixed. We did not replace it by (3.4.23).

□

Physical convention. The generator and Leray projector here are the unrotated physical operators. We use $\lambda_c = \Re\lambda_0$.

The frozen imaginary spectral translation is not a time-dependent coordinate change. All-angular uniformity comes from the far-label Hardy/window proof, not a fixed-label constant.

The actual completed clock inputs are those of Theorem 2(v).

3.5 The full propagator without a shift

Main result. Theorem 3.5.1 bounds the unshifted physical evolution at all angular and axial frequencies for the last completed source.

Its rate has an arbitrarily small positive excess over the selected growth rate. The proof uses no prepared column or critical inverse.

Theorem 3.5.1 (All-frequency propagator without shift)**.** *Fix the one selected $p = 6/5$ source of Theorem 2. Let $U_*(s,r)$ be the evolution of the completed physical equation $v_s = A_* v$ on all of $\mathcal{H}$.*

This includes all angular and axial frequencies, with $A_* = A_{\mathrm{lead}} + R$ as in (3.8.1) and no shift. For each $\epsilon > 0$ there is an ancient threshold T_ϵ such that

$$\|U_*(s,r)\|_{2\to 2} \le C_*(\rho(s))\, e^{(\lambda_c+\epsilon)(s-r)}, \qquad r \le s \le -T_\epsilon, \qquad C_*(\rho) = \rho^{-o(1)}. \tag{3.5.1}$$

In physical variables this is (3.3.1).

Proof. We apply Lemma 3.4.4 with $S = 0$. The leading evolution and its Gram bounds carried by Theorem 2(iv) supply respectively the rates $g_0 = \lambda_c + \epsilon/8$ and $g_1 = \lambda_c + \epsilon/4$ on each angular label. The source and clock bounds are those of Theorem 2(v). In the exact filtered equations $S_p = S_{\mathrm{ref}} = S_{\mathrm{app}} = 0$, so $D = 0$ and the prepared-column terms are absent.

The reverse stretching term $(l\cdot\nabla)W$ costs $P(S)\|l\|_2$ independently of block length. The reverse transport term has the small coefficients of (3.4.18), as in the transfer lemma.

The transfer lemma with $g = \lambda_c + \epsilon/2$ gives (3.5.1), and we enlarge its rate if necessary. This application uses no prepared column or critical inverse.

Physical form. With $a_0 = (\frac{1}{2}+h) - (1+(\frac{1}{2}-h))/2 = -\frac{1}{4} + \frac{3}{2}h < 0$, the canonical and physical L^2 norms satisfy $\|u_c(s)\| = t^{a_0}\|u(t)\|$. The coordinate change conjugates U_* to the physical evolution, as in the proof of Proposition 3.10.4.

Thus, for $t' \le t$,

$$\|U_*(t,t')\| \le (t/t')^{|a_0|} C_*(\rho(s)) e^{(\lambda_c+\epsilon)(\tau'-\tau)/h} = (\tau'/\tau)^{|a_0|/h}\, \tau^{o(1)}\, e^{(\Lambda_*+\epsilon/h)(\tau'-\tau)}.$$

Since $\tau'/\tau \le 1 + (\tau'-\tau)$ for $\tau \ge 1$, the polynomial factor is at most $C_{\epsilon'} e^{\epsilon'(\tau'-\tau)}$. We rename ϵ to get (3.3.1).

□

3.6 Physical reference columns for the selected spectral pair

3.6.1 Fixed-chart quantization and profile identities

Put $T = -s$, $\rho = (hT)^{-1}$, and $k = -i\rho\partial_Z$ on axial functions. Fix the selected positive angular sector and its conjugate, and take the projections and pressures of the undilated physical generator. On the conjugate pair let C_s be the scalar left quantization, sector by sector, of $\chi_{s,+} = \chi_+$ and $\chi_{s,-} = \chi_-$ from Theorem 2(iv). Its two symbol supports lie strictly inside the fixed rectangle U, and both symbols equal one near the pole.

For a scalar symbol a we use left quantization

$$\mathrm{Op}_\rho(a)f(Z)=\int_{\mathbb{R}}\widehat{a}(Z,u)f(Z-\rho u)\,\mathrm{d}u. \tag{3.6.1}$$

Lemma 3.6.1 (A finite composition estimate on the selected chart)**.** *Suppose a,b have compact k support in one fixed chart. Suppose $\partial_k^j a$ for $0\le j\le 3$ have the weighted radial-symbol bounds used for (3.6.1), and put $\mathcal{C}_a=\sup_{Z,k}\sum_{j\le 3}\|\partial_k^j a(Z,k)\|$ (operator norm on the fixed weighted radial space; a has k-support in one fixed compact set).*

Also suppose b,b_Z have the same radial-symbol bounds for ∂_k^j, $j\le 2$, and b_Z is $1/2$-Hölder in Z uniformly in these k-derivatives; put $\mathcal{C}_b=\sup_{Z,k}\sum_{j\le 2}(\|\partial_k^j b\|+\|\partial_k^j b_Z\|)+\sup_k\sum_{j\le 2}[\partial_k^j b_Z]_{C_Z^{1/2}}$. (This gives $\int\sup_Z|\widehat{b}(Z,v)|+[\partial_Z\widehat{b}(\cdot,v)]_{C^{1/2}}\,\mathrm{d}v\le C\mathcal{C}_b$, which the Schur test uses.) The factor $P(S)$ for finite products below comes from the seminorms $\mathcal{C}_a,\mathcal{C}_b$ of the factors (coefficients, masks and cutoffs), each of which is at most $P(S)$. Then, as bounded L^2_Z operators,

$$\mathrm{Op}_\rho(a)\,\mathrm{Op}_\rho(b)=\mathrm{Op}_\rho(ab)+\frac{\rho}{i}\,\mathrm{Op}_\rho(a_k b_Z)+\mathcal{R}_\rho,\qquad \|\mathcal{R}_\rho\|_{2\to 2}\le C\rho^{3/2}\mathcal{C}_a\mathcal{C}_b. \tag{3.6.2}$$

The constant is uniform for the fixed finite profile and mask family.

For a finite product of such factors the same expansion holds with the sum of the ordered first brackets and a $C\rho^{3/2}P(S)$ remainder.

Proof. Three integrations by parts in the Fourier variable give $|\widehat{a}(Z,u)|\le C\mathcal{C}_a(1+|u|)^{-3}$.

In particular $\int|u|^{3/2}|\widehat{a}(Z,u)|\,\mathrm{d}u\le C\mathcal{C}_a$. The exact kernel of the product contains $\widehat{b}(Z-\rho u,v)$.

Taylor expansion at Z gives its value, the first term $-\rho u\partial_Z\widehat{b}(Z,v)$, and a remainder bounded by $C\rho^{3/2}|u|^{3/2}$ times the Hölder seminorm. The Fourier moment of u gives a_k/i with the stated left-ordering convention.

Schur's test on these kernels proves (3.6.2). A telescoping expansion handles each additional factor.

We fix word length and mask-family size. The finitely many ordinary coefficient and cutoff derivatives increase the bound only by $P(S)$. A mere $C^{2,1/2}$ bound in k would not give the necessary absolute $3/2$ moment.

This estimate uses the actual five-derivative profile bounds. □

Lemma 3.6.2 (Weighted physical profiles on the selected chart)**.** *Let e be the right eigenprofile and v the adjoint eigenprofile in the normalization $\ell=v^*$, $\ell e=1$. The leading weighted estimates are*

$$\|\partial_Z^l\partial_k^j e\|_{H^6_{7-j}}+\|\partial_Z^l\partial_k^j v\|_{H^6_{7-j}}\le C_{l,j}. \tag{3.6.3}$$

for $0\le j\le 5$, $0\le l\le 17$. The compact-chart eigenvalue has the six phase derivatives used below. More precisely Proposition 1.28.8(vi) and Corollary 1.28.9(a),(d) of Part 1 give the same bound for $j=6$, $0\le l\le 17$, $m\ge 30$, with range H^6_1 for each profile. Only the leading ladder is extended to $j=6$. Also,

$$\|\partial_Z^l\partial_k^j e\|_{H^{18}_{9-j}}+\|\partial_Z^l\partial_k^j v\|_{H^{18}_{9-j}}\le C_{l,j},\qquad j\le 2, \tag{3.6.4}$$

for the fixed axial orders of the finite preparation. The first right and adjoint correctors have H^4_{6-j} bounds through $j=4$ frequency and sixteen axial derivatives.

Proof. Theorem 2(iv) gives the weighted contour and reduced-resolvent bounds for the selected physical pair, its pressure and its adjoint. In the finite profile estimates a k derivative spends one radial moment, and a Z derivative acts on an ordinary coefficient. These bounds give the two displayed estimates. We record the first-order calculation because the adjoint row enters the exact mode construction.

For the right and left correctors, fix one complex angular sector and write $v = (v_h, v_z)$. Write $\mathcal{B}_0 = (U_h, W)$ for its leading horizontal/axial field, and $(R_h, 0)$ for its radial correction.

With $\nabla_k = (\nabla_h, ik)$, the primitive symbols on this chart are

$$\begin{aligned} F_0(Z,k)v &= -U_h \cdot \nabla_h v - ikWv - v_h \cdot \nabla_h \mathcal{B}_0 + i(\tfrac{1}{2} - h)Zk\, v, \\ F_1(Z,k)v &= (\Delta_h - k^2 + (\tfrac{1}{2} + h) + \tfrac{1}{2} y \cdot \nabla_h)v - R_h \cdot \nabla_h v - v_h \cdot \nabla_h (R_h, 0) - v_z \partial_Z \mathcal{B}_0. \end{aligned} \tag{3.6.5}$$

Thus $F_\rho = F_0 + \rho F_1 + O(\rho^2)$, and on physical solenoidal radial vectors

$$L_0 = P_k F_0 P_k = A(Z,k) + i(\tfrac{1}{2} - h)Zk\, I, \qquad \mu(Z,k) = \lambda(Z,k) + i(\tfrac{1}{2} - h)Zk. \tag{3.6.6}$$

On the fixed sectors $\pm m$, write $G = \nabla_h \Delta_m^{-1}$ for the horizontal divergence primitive of (3.7.26). Write $F_0 e - \mu e = \nabla_k \pi$. After subtracting this principal pressure, the first right coefficient has frozen projection

$$R_1 = P_k \big[F_1 e - (F_0 - \mu)(G\partial_Z e_z, 0) - i(F_0)_k e_Z + i e_k \mu_Z - hke_k - e_3 \pi_Z \big].$$

Denote the vector inside the brackets by H_e, so $R_1 = P_k H_e$. Here $e_3 = (0,0,1)$ is the axial unit vector, e_z is the vertical component of e, π_Z differentiates the full primitive pressure, and F_1 includes the radial viscosity, radial dilation and axial $-k^2$ term.

The pressure estimate uses one radial moment, G one, and the dilation one. Viscosity uses two horizontal derivatives.

Thus $\partial_k^j H_e$ and $\partial_k^j R_1$ belong to H^4_{6-j} for $j \le 4$, with the stated ordinary Z jets. For the projected coefficient distribute the k derivatives over $P_k H_e$ and use the positive moment ladder in clause (iv). The reduced contour resolvent gives $E_1 = -(L_0 - \mu)^{-1}(I - e\ell)R_1 = -(A - \lambda)^{-1}(I - e\ell)R_1$ on the spectral complement in the same graded class.

Let ℓ be the actual left eigenrow (not generally e^*). $v = \ell^*$, $\ell e = 1$, and $P_k F_0^* v = \bar{\mu} v$.

The primitive adjoint pressure is fixed by

$$F_0^* v - \bar{\mu} v = \nabla_k p_v. \tag{3.6.7}$$

The star is the radial Hilbert adjoint with its cylindrical measure. In particular $(y \cdot \nabla_h)^* = -y \cdot \nabla_h - 2$.

We set $C_e = (G\partial_Z e_z, 0)$ and $C_v = (G\partial_Z v_z, 0)$. The first right residual displayed above fixes the band connection $c_1 = \ell R_1$, and the complement equation gives $E_1 = -R_Q Q R_1$, where $Q = I - e\ell$ and $R_Q = (L_0 - \mu)^{-1} Q$.

For the corrected right column $J_{\mathrm{corr}} = \mathrm{Op}_\rho(e) - \rho\, \mathrm{Op}_\rho(C_e) + \rho\, \mathrm{Op}_\rho(E_1)$ with its exact divergence restoration, the remaining first primitive coefficient is

$$r_e = H_e + (F_0 - \mu)E_1 - ec_1, \qquad P_k r_e = R_1 + (L_0 - \mu)E_1 - ec_1 = 0.$$

The second equality uses $P_k E_1 = E_1$ and the reduced equation. To transfer this cancellation to the physical projection P_ρ, let r be such a coefficient on the working plateau and set $p_1 = \Delta_k^{-1} \operatorname{div}_k r$. Then $r = \nabla_k p_1$. Choose a fixed smooth phase cutoff ζ supported in that chart and equal to one on a neighborhood of the inner mask. Left quantization gives, for any scalar symbol p,

$$\nabla_\rho\, \mathrm{Op}_\rho(p) = \mathrm{Op}_\rho(\nabla_k p) + \rho e_3\, \mathrm{Op}_\rho(\partial_Z p). \tag{3.6.8}$$

Since $\nabla_k(\zeta p_1) = \zeta r$ and $P_\rho \nabla_\rho = 0$,

$$\rho P_\rho \operatorname{Op}_\rho(\zeta r) = -\rho^2 P_\rho e_3 \operatorname{Op}_\rho(\partial_Z(\zeta p_1)). \tag{3.6.9}$$

For $r = r_e$ the unprojected coefficient has $\partial_Z^l \partial_k^j r_e \in H^4_{6-j}$ for $l \le 1$, $j \le 2$. Here $F_0 - \mu$ is order zero on the fixed angular sector. The scalar pressure ladder in clause (iv) spends one further moment, giving $\partial_Z^l \partial_k^j p_1 \in H^4_{5-j}$ in the same range: a derivative of order i of the pressure map spends $i+1$ moments on $\partial_k^{j-i} r_e$. Two integrations by parts in k now bound the last column in (3.6.9) from L^2_Z to $L^2_{y,Z}$ uniformly on the chart. The physical projection has norm one.

The primitive products use (3.6.2). Inserting the larger chart cutoff before the inner right mask costs $O(\rho^2 P(S))$ by fixed-support separation: the principal profiles supply four frequency jets at order two and the terms prefactored by ρ supply three at order one (Lemma 3.9.8 and Corollary 3.9.10). The principal physical pressure contributes $-e_3\pi_Z$ to H_e by (3.6.8). Equation (3.6.9) controls the remaining frozen gradient. Exact solenoidality makes $LJ_{\mathrm{corr}} - (J_{\mathrm{corr}})_s$ solenoidal, so the resulting right defect $R = LJ_{\mathrm{corr}} - (J_{\mathrm{corr}})_s - J_{\mathrm{corr}} \operatorname{Op}_\rho(\mu + \rho c_1)$, after the inner right cutoff, has norm $O(\rho^{3/2} P(S))$ from L^2_Z to $L^2_{y,Z}$.

For any physical adjoint column H and $K_{\mathrm{raw}} = H^*$, the exact left defect $T_{\mathrm{raw}} = (K_{\mathrm{raw}} L + (K_{\mathrm{raw}})_s - BK_{\mathrm{raw}})P$ satisfies on the same smooth core

$$T^*_{\mathrm{raw}} = P(F^*_\rho H + H_s - HB^*), \qquad B = \operatorname{Op}_\rho(\mu + \rho c_1). \tag{3.6.10}$$

Thus $PL^*H = PF^*_\rho H$ and $PP_sP = 0$.

For left quantization $a\#b = ab - i\rho a_k b_Z + O(\rho^{3/2})$, the actual adjoint symbols are

$$F^*_\rho = F^*_0 + \rho(F^*_1 - i\partial_Z \partial_k F^*_0) + O(\rho^{3/2}), \qquad B^* = \bar\mu + \rho(\bar c_1 - i\partial_Z \partial_k \bar\mu) + O(\rho^{3/2}).$$

Here $\partial_s \operatorname{Op}_\rho(v)$ contributes $h\rho k v_k$ at first order. We apply (3.6.10) to $H_0 = \operatorname{Op}_\rho(v) - \rho \operatorname{Op}_\rho(C_v)$.

Applying (3.6.8) to p_v in (3.6.7) gives the following frozen projection of the first adjoint coefficient. Denote the vector inside its brackets by H_v.

$$\begin{aligned} r_v = P_k\big[&(F^*_1 - i(F^*_0)_{kZ})v - (F^*_0 - \bar\mu)C_v - i(F^*_0)_k v_Z + iv_k\bar\mu_Z + hkv_k \\ &- e_3(p_v)_Z - v\bar c_1 + iv\bar\mu_{kZ}\big]. \end{aligned} \tag{3.6.11}$$

The F^*_1 term includes the radial viscosity, radial dilation adjoint, axial diffusion and lower-order source terms.

The selected component of (3.6.11) vanishes for a reason independent of the weighted estimate. Let $S_0 = H^*_0 J_{\mathrm{corr}}$ and $\widetilde T$ be the left defect of H^*_0.

Direct finite-kernel composition gives

$$S_0 = I + \rho \operatorname{Op}_\rho(s_1) + O(\rho^{3/2} P(S)), \quad s_1 = \ell(E_1 - C_e) - C_v^* e - i\ell_{kZ} e - i\ell_k e_Z.$$

Exact differentiation, with no assumed scalar connection, yields

$$\widetilde T J_{\mathrm{corr}} = H^*_0 R + (S_0)_s + S_0 B - BS_0. \tag{3.6.12}$$

The first term is $O(\rho^{3/2} P(S))$ locally. We compute $(S_0)_s$ from the two physical columns. In the ordinary axial Fourier representation of (3.6.1), the symbol on a fixed input is $a(Z, \rho\zeta)$ at frequency ζ. For a fixed symbol a, $\rho_s = h\rho^2$ therefore gives the exact identity

$$\partial_s(\rho^p \operatorname{Op}_\rho(a)) = h\rho^{p+1} \operatorname{Op}_\rho(pa + k\partial_k a). \tag{3.6.13}$$

For any two of the fixed finite columns $H = \sum_{p=0}^{2} \rho^p \operatorname{Op}_\rho(v_p)$ and $J = \sum_{p=0}^{2} \rho^p \operatorname{Op}_\rho(j_p)$ used here, differentiate H^*J on the smooth core. For a chart calculation extend its symbols by fixed cutoffs equal to one near the working plateau. The fixed Hilbert pairing gives $(H^*)_s = (H_s)^*$. Every term containing a positive-degree coefficient, including a divergence restoration, is $O_{2\to2}(\rho^2 P(S))$. The two remaining products, divided by $h\rho$, have principal symbols $(k\partial_k v_0)^* j_0$ and $v_0^*(k\partial_k j_0)$. Replacing each product by its principal symbol costs $O_{2\to2}(\rho P(S))$ by the order-one remainder in Lemma 3.9.8 and the adjoint kernel formula in Corollary 3.9.11. The constant horizontal parts act exactly. The compact parts use at most four leading k derivatives, including the displayed derivative, and three for the positive-degree terms. Thus

$$(H^*J)_s = h\rho \operatorname{Op}_\rho(k\partial_k(v_0^* j_0)) + O_{2\to2}(\rho^2 P(S)). \tag{3.6.14}$$

For $S_0 = H_0^* J_{\mathrm{corr}}$, the leading pairing is $\ell e = 1$ on the chart. After a fixed cutoff inside the chart the displayed principal term has size $O(\rho^2 P(S))$, by the same order-one product estimate.

The dilation in B is $(\frac{1}{2} - h)\rho D$, $D = Z\partial_Z$. On the core, $[D, \operatorname{Op}_\rho(a)] = \operatorname{Op}_\rho((Z\partial_Z - k\partial_k)a)$, also after taking adjoints since $D^* = -D - I$. Applying the product rule to H^*J, its leading commutator with D has symbol $(Z\partial_Z - k\partial_k)(v_0^* j_0)$. This vanishes on the same plateau, leaving a localized $O(\rho^2 P(S))$ contribution from ρD. For the remaining scalar part of B, the order-ρ commutator coefficient is $[s_1, \lambda] = 0$ on each conjugate branch, with the finite composition remainder from (3.6.2). Comparing the order-ρ coefficients in (3.6.12) gives

$$e^* r_v = 0. \tag{3.6.15}$$

Equivalently, the real two-column matrix has zero selected projection.

$$v_1 = -R_Q^* r_v, \qquad e^* v_1 = 0, \qquad (L_0^* - \bar{\mu})v_1 + r_v = 0. \tag{3.6.16}$$

Formula (3.6.11) uses one radial moment in C_v and pressure, one in dilation, and two horizontal derivatives in viscosity.

The kZ symbol derivatives use coefficient jets without an additional radial moment. The same first-order bounds apply before the frozen projection. Thus, for $0 \le j \le 4$ and $0 \le l \le 16$,

$$\|\partial_Z^l \partial_k^j H_v\|_{H^4_{6-j}} + \|\partial_Z^l \partial_k^j r_v\|_{H^4_{6-j}} + \|\partial_Z^l \partial_k^j v_1\|_{H^4_{6-j}} \le C_{l,j}.$$

For the corrected adjoint column the remaining primitive coefficient is $r_{\mathrm{adj}} = H_v + (F_0^* - \bar{\mu})v_1$. Equation (3.6.16) gives $P_k r_{\mathrm{adj}} = 0$. Its pressure $p_{1,\mathrm{adj}} = \Delta_k^{-1} \operatorname{div}_k r_{\mathrm{adj}}$ therefore satisfies the same H^4_{5-j} estimates for $l \le 1$, $j \le 2$ used in (3.6.9). Difference quotients justify differentiation of the reduced resolvent on the same finite weight ladder.

The first-order terms use at most two horizontal derivatives and one radial moment. The reduced contour bounds of Theorem 2(iv) therefore give the stated bounds on both correctors. □

Lemma 3.6.3 (Dynamic fixed-reference normalizer)**.** *Let E_1, v_1 be the current right and adjoint first radial correctors, with the physical divergence and pressure restorations, supplied by Lemma 3.6.2. Select one fixed phase cutoff ζ_d equal to one on each row, shift and parametrix support.*

Here $J_{\mathrm{alg}} = \operatorname{Op}_\rho(e) - \rho \operatorname{Op}_\rho(C_e)$ and $H_{\mathrm{alg}} = H_0 = \operatorname{Op}_\rho(v) - \rho \operatorname{Op}_\rho(C_v)$, with the fixed horizontal extensions of the leading profiles outside the phase chart used in the proof below. The fields C_e, C_v are the divergence corrections defined above.

With the same primitive G, define the physical columns

$$J_{\mathrm{ref}} = J_{\mathrm{alg}} + \rho \operatorname{Op}_\rho(\zeta_d E_1) - \rho^2 \operatorname{Op}_\rho(G\partial_Z(\zeta_d E_{1,z}), 0),$$
$$H_{\mathrm{ref}} = H_{\mathrm{alg}} + \rho \operatorname{Op}_\rho(\zeta_d v_1) - \rho^2 \operatorname{Op}_\rho(G\partial_Z(\zeta_d v_{1,z}), 0).$$

Set $K_{\mathrm{raw}} = H^*_{\mathrm{ref}}$, $M_{\mathrm{ref}} = K_{\mathrm{raw}} J_{\mathrm{ref}}$, *and* $K_{\mathrm{ref}} = M_{\mathrm{ref}}^{-1} K_{\mathrm{raw}}$. *The previous profile bootstrap gives leading* k *derivatives through five, first-corrector derivatives through four, and ordinary* Z *derivatives through sixteen.*

Thus $K_{\mathrm{ref}} J_{\mathrm{ref}} = I_2$, *and* $E_{\mathrm{ref}} := M_{\mathrm{ref}} - I = \rho \widetilde{E}_{\mathrm{ref}}$ *has finite compact-phase kernels that satisfy*

$$\|E_{\mathrm{ref}}\|_{H^{-2}_{\mathrm{ax},\rho} \to L^2} + \|E_{\mathrm{ref}}\|_{L^2 \to H^2_{\mathrm{ax},\rho}} \le C\rho. \tag{3.6.17}$$

The exact fixed-reference shift $d_0 J_{\mathrm{ref}} C_s K_{\mathrm{ref}}$ *is bounded* $H^{-1}_{\mathrm{iso}} \to H^1_{\mathrm{iso}}$. *The global unmasked* K_{ref} *is not claimed to be smoothing.*

Proof. Work in the positive angular sector. On U, Theorem 2(iv) gives $c = \ell_0 P_{0,m}(Z,k) e_0$ with $|c| \ge 1/2$. Use $e = P_{0,m} e_0 / c$ and $\ell = \ell_0 P_{0,m}$, so $\ell_0 e = \ell e = 1$. This fixes the gauge before the reference normalizer and the prepared columns are constructed. At $k = 0$ the horizontal equation is independent of the vertical velocity, and the vertical diagonal operator is multiplication by $-im\Omega$. Since $\Re \lambda_0 > 0$, its adjoint eigenvector equation gives $(\ell_0^*)_z = 0$. Thus $e_\infty = ((e_0)_h, 0)$ and ℓ_0^* are horizontally solenoidal and belong to $\operatorname{Ran} P_k$ for every k, with $\ell_0 e_\infty = 1$. Choose a real smooth phase cutoff χ supported in the pole chart and equal to one on a neighborhood of all working masks. Extend the right column and left row by

$$\widetilde{e} = \chi e + (1-\chi) e_\infty, \qquad \widetilde{\ell} = \ell_0 + \chi\big[\ell - (\ell \widetilde{e})\ell_0\big].$$

The terms multiplied by χ extend by zero off the chart. Since $\ell_0 \widetilde{e} = 1$, we have $\widetilde{\ell}\widetilde{e} = 1$ throughout the transition. On $\{\chi = 1\}$ the profiles coincide with e, ℓ, and off $\operatorname{supp} \chi$ they equal e_∞, ℓ_0. Both $\widetilde{e}$ and $\widetilde{\ell}^*$ belong to $\operatorname{Ran} P_k$. The fixed cutoff and scalar pairings preserve the finite weighted profile bounds by the product rule. Use the conjugate extension in the negative sector. The resulting pointwise pairing is I_2, so the identity part cancels in $M_{\mathrm{ref}} - I$.

In each remaining finite compact-phase kernel, the left composition formula of Lemma 3.6.1 produces an explicit $\rho u \partial_Z$ difference or one of the displayed ρ correctors. This gives $E_{\mathrm{ref}} = \rho \widetilde{E}_{\mathrm{ref}}$ with uniform fixed kernel moments.

The derivatives of ζ_d occur inside the divergence corrections. We use no cutoff of an uncorrected physical vector. Left multiplication by $\langle \rho D_Z \rangle^2$ inserts compact k^2 and terms $\rho k \partial_Z \widetilde{E}_{\mathrm{ref}}$ and $\rho^2 \partial_Z^2 \widetilde{E}_{\mathrm{ref}}$.

Right multiplication inserts $1 + k^2$ on the input symbol. The finite k and Z derivative bounds, with Schur's test, keep the explicit ρ factor.

Duality then proves (3.6.17).

The scalar mask maps $H^{-1}_{\mathrm{ax},\rho}$ into $H^1_{\mathrm{ax},\rho}$. With $M_{\mathrm{ref}} = I + E_{\mathrm{ref}}$, the exact identity $M_{\mathrm{ref}}^{-1} = I - E_{\mathrm{ref}} + E_{\mathrm{ref}} M_{\mathrm{ref}}^{-1} E_{\mathrm{ref}}$ uses its middle inverse only on L^2, where two bounds it.

The first-order versions of (3.6.17), the physical H^1 profile bounds and their duals thus give $J_{\mathrm{ref}} C_s K_{\mathrm{ref}} : H^{-1}_{\mathrm{iso}} \to H^1_{\mathrm{iso}}$. The physical endpoint columns encode the pressure constraint.

The adjoint first residual (3.6.11), its compatibility (3.6.15), and the solution (3.6.16) give the dynamic first-order cancellation. We prove its output-local operator bound in Lemma 3.6.5.

□

Lemma 3.6.4 (Reference normalizer commutators)**.** *For every fixed smooth phase mask* F *on the reference chart,*

$$\|[F, M_{\mathrm{ref}}^{-1}]\|_{L^2 \to L^2} + \|[F, M_{\mathrm{ref}}^{-1}]\|_{H^{-2}_{\mathrm{ax},\rho} \to L^2} \le C_F \rho^2.$$

Across nested fixed plateaux the off-plateau part of $M_{\mathrm{ref}}^{-1} - I$ *is* $O(\rho^3)$, *also with the localized axial graph placement.*

Proof. Expand the exact products in $M_{\mathrm{ref}} = H_{\mathrm{ref}}^{*} J_{\mathrm{ref}}$ through first order, using Lemma 3.9.8 and the adjoint conversion in Corollary 3.9.11. The pointwise leading pairing is I_2, including the horizontal extension. Thus

$$M_{\mathrm{ref}} = I + \rho\,\mathrm{Op}_{\rho}(s_1) + R_2, \qquad \|R_2\|_{H^{-2}_{\mathrm{ax},\rho}\to L^2} + \|R_2\|_{L^2\to H^{2}_{\mathrm{ax},\rho}} \le C\rho^2,$$

with the symbol s_1 computed before (3.6.12) and the fixed cutoff factors from the reference construction. The order-two leading remainder needs four k derivatives; terms with an explicit ρ need only the order-one remainder and three k derivatives. The two graph derivatives are ordinary Z derivatives. For the order-one commutator of $\mathrm{Op}_{\rho}(s_1)$, its explicit first leading derivative uses at most one further leading k jet. Hence all terms use at most five leading and four corrector k jets, within the stated ordinary Z ladders. The identity part of the extension is treated exactly; the other symbols have fixed compact support. It follows that $[F, M_{\mathrm{ref}}] = O(\rho^2)$ in the same graph placement.

Write $E = M_{\mathrm{ref}} - I$. The graph extension $M_{\mathrm{ref}}^{-1} = I - (M_{\mathrm{ref}}^{-1}|_{L^2})E$ follows by direct multiplication, since $E : H^{-2} \to L^2$ is $O(\rho)$. The exact inverse commutator now proves the displayed bound. For the separated assertion use the exact products defining E, with nested fixed masks at their radial Hilbert interfaces. The two leading profile factors use order-three separation and five k jets; terms containing a first corrector use order two and keep their ρ; terms with a ρ^2 divergence restoration need only order one. The subtracted identity has arbitrary-order smooth-mask separation. Thus a separated E is $O(\rho^3)$ in the indicated graph placement. Insert nested fixed masks in E^2 and use the exact finite identity

$$M_{\mathrm{ref}}^{-1} = I - E + E^2 - E^3 M_{\mathrm{ref}}^{-1}.$$

The first two nonidentity terms have a separated E factor; the last term is $O(\rho^3)$ by the norm of E and its graph endpoint bounds. All remainders are retained. This proves the fixed-gap inverse assertion without assigning a symbol class to the exact inverse. □

Lemma 3.6.5 (Output-local dynamic left row)**.** *Let L be the selected-source leading physical generator, B its current scalar band generator, and put*

$$T_{\mathrm{raw}} = K_{\mathrm{raw}} L + (K_{\mathrm{raw}})_s - B K_{\mathrm{raw}}, \qquad T_{\mathrm{ref}} = K_{\mathrm{ref}} L + (K_{\mathrm{ref}})_s - B K_{\mathrm{ref}}.$$

Extend the adjoint column by its fixed horizontal physical reference outside a larger phase chart. Keep the same unbounded axial dilation identically in L and B.

For a real fixed cutoff χ supported in the inner eigenbundle chart, write $C_\chi = \mathrm{Op}_{\rho}(\chi)^{*}$. On arbitrary solenoidal physical L^2 inputs, for any fixed $0 < \theta \le 1/2$,

$$\|C_\chi T_{\mathrm{raw}}\|_{2\to 2} + \|C_\chi T_{\mathrm{ref}}\|_{2\to 2} \le C_\chi \rho^{1+\theta} P(S). \tag{3.6.18}$$

For the annular conclusion choose χ equal to one on a fixed neighborhood of the supports of the full shift and all inner masks. Their closed union then has positive distance from $\operatorname{supp} d\chi$*. Choose a smooth annular symbol equal to one near* $\operatorname{supp} d\chi$*, compactly supported in the chart and still separated from that union. Write C_{ann} for its left quantization.*

For $K_\chi = C_\chi K_{\mathrm{ref}}$ one has

$$K_\chi L + (K_\chi)_s - B K_\chi = R_{\mathrm{int}} + \rho C_{\mathrm{ann}} A_{\mathrm{ann}}, \quad \|R_{\mathrm{int}}\|_{2\to 2} \le C\rho^{1+\theta} P(S), \quad \|A_{\mathrm{ann}}\|_{2\to 2} \le C P(S). \tag{3.6.19}$$

The assertion is output-localized. It does not assert a small uncut row or move a cutoff through the physical Leray projector.

Proof. Equation (3.6.16) constructs the corrected adjoint column with its $-\rho^2 G\partial_Z(v_1)_z$ divergence restoration. This column is physical.

Apply (3.6.10) on the smooth core. The principal gradient in (3.6.7) leaves $-\rho e_3 \operatorname{Op}_\rho((p_v)_Z)$ after physical projection. This contribution is included in H_v in (3.6.11). Compatibility (3.6.15) and the reduced equation (3.6.16) give $P_k r_{\mathrm{adj}} = 0$ on the chart. With a larger fixed cutoff equal to one near the right mask, (3.6.9) bounds its contribution by $C\rho^2 P(S)$ from L^2_Z to $L^2_{y,Z}$. The finite product remainders in Lemma 3.6.1 and the separated cutoff errors estimated there for the right column give the full $O(\rho^{3/2}P(S))$ bound after the fixed right cutoff on the adjoint column.

The Hilbert adjoint gives the first term of (3.6.18) on unweighted global physical input. The cutoff acts on the row's output.

The global extension does not require an uncut L^2 row bound. The same axial $i(\frac{1}{2}-h)Zk$ terms cancel before estimation.

The remaining uncut reference defect is a polynomial of degree at most two in k, with fixed weighted radial-profile coefficients. Right localization of its adjoint column uses

$$k\#\chi = k\chi - i\rho\chi_Z, \qquad k^2\#\chi = k^2\chi - 2i\rho k\chi_Z - \rho^2\chi_{ZZ}.$$

Its polynomial terms then become bounded compact-frequency symbols.

We put no derivative on the arbitrary input. Its global graph norm is $L^2_{\mathrm{phys}} \to H^{-2}_{\mathrm{ax},\rho}$ with a fixed $P(S)$ cost.

At the selected pole, the left eigenvector has zero vertical component because $k = 0$ decouples. Its fixed horizontal extension is thus P_k-solenoidal for each k and commutes with scalar dilation.

The compact corrections have the moments and jets in (3.6.3) and (3.6.16).

Exact normalization obeys

$$T_{\mathrm{ref}} = M_{\mathrm{ref}}^{-1}T_{\mathrm{raw}} + [(M_{\mathrm{ref}}^{-1})_s + M_{\mathrm{ref}}^{-1}B - BM_{\mathrm{ref}}^{-1}]K_{\mathrm{raw}}. \tag{3.6.20}$$

For the exact columns of Lemma 3.6.3, the extended leading pairing is I_2 everywhere, including the cutoff transition. Equation (3.6.14) therefore gives $\|(M_{\mathrm{ref}})_s\|_{2\to2} \le C\rho^2 P(S)$ globally. Differentiating $M_{\mathrm{ref}}^{-1}M_{\mathrm{ref}} = I$ and using $\|M_{\mathrm{ref}}^{-1}\|_{2\to2} \le 2$ gives

$$(M_{\mathrm{ref}}^{-1})_s = -M_{\mathrm{ref}}^{-1}(M_{\mathrm{ref}})_s M_{\mathrm{ref}}^{-1}, \qquad \|(M_{\mathrm{ref}}^{-1})_s\|_{2\to2} \le 4C\rho^2 P(S).$$

The fixed-column formula also bounds $K_{\mathrm{raw}} = H^*_{\mathrm{ref}}$ on physical L^2. For the commutator in (3.6.20), use $[M_{\mathrm{ref}}^{-1}, B] = -M_{\mathrm{ref}}^{-1}[M_{\mathrm{ref}}, B]M_{\mathrm{ref}}^{-1}$ on the core. The dilation calculation after (3.6.14) applies to the globally normalized pairing. On the inner plateau the remaining order-ρ coefficient is $[s_1, \lambda] = 0$ on each scalar branch. The first-order product formula leaves $O(\rho^{3/2}P(S))$ there.

We select a nested cutoff equal to one near $\operatorname{supp}\chi$. The raw bound applies there.

Across this fixed separation, the leading order-three estimate and the ρ order-two corrector estimate of (SC2) apply with the axial graph placement. The leading ladder supplies five k derivatives and five ordinary Z derivatives; the corrector supplies four k derivatives and four ordinary Z derivatives. The ρ^2 restoration is bounded directly in the right-masked output space. Lemma 3.6.4 handles the exact normalizer across the same fixed plateaux. These bounds are $O(\rho^2 P(S))$ or better, and do not spend extra radial moments on an arbitrary physical input.

The exact inverse $M_{\mathrm{ref}}^{-1} = I - E_{\mathrm{ref}} + E_{\mathrm{ref}}M_{\mathrm{ref}}^{-1}E_{\mathrm{ref}}$ and (3.6.17) control the remaining normalizer factors.

This proves the second term of (3.6.18) and does not treat an H^{-2} input as L^2.

Last, we differentiate $K_\chi = C_\chi K_{\mathrm{ref}}$:

$$K_\chi L + (K_\chi)_s - BK_\chi = C_\chi T_{\mathrm{ref}} + [(C_\chi)_s + C_\chi B - BC_\chi]K_{\mathrm{ref}}.$$

The order-ρ scalar bracket has symbol $c_{\mathrm{ann}} = hk\chi_k - i(\chi_k\mu_Z - \mu_k\chi_Z)$, supported where $d\chi \neq 0$. We select $A_{\mathrm{ann}} = \mathrm{Op}_\rho(c_{\mathrm{ann}}\ell)$ and multiply it by the larger cutoff C_{ann}.

Their zeroth and first product differences vanish because the annular cutoff is one on a fixed neighborhood of the symbol support. Lemma 3.6.1 gives an $O(\rho^{3/2}P(S))$ remainder and proves (3.6.19).

Section 3.9 estimates the completed-wave perturbation separately by its $O(\rho^{1/2}P(S))$ value. □

3.7 Finite prepared columns and their two-band bounds

Main result. Lemma 3.7.7 constructs a prepared column for the fixed completed source and its selected simple spectral pair. Lemmas 3.7.12 and 3.7.15 give its derivative and two-band bounds.

The proof fixes source derivatives and completion accuracy before it decreases the ancient threshold. Its ordinary derivative count remains different from its radial Sobolev requirements.

3.7.1 Actual radial and coefficient domains of the preparation

The norms below are for the one fixed selected member. Constants may depend on its finite radial jets, contour, integer m and masks, but not on ρ or on the active source-band index.

The contour and reduced inverses are those of the physical operator A, with physical complex pole λ_0. We make no rotating-coordinate change in the evolution.

Lemma 3.7.1 (Physical Taylor column with exact divergence and pressure)**.** *Use the physical eigenprofile in the normalization $\ell_0 e(Z,k) = 1$ of Lemma 3.7.9, and its full primitive pressure π, so that $F_0 e - (\lambda + i(\frac{1}{2} - h)Zk)e = \nabla_k \pi$. This normalization is fixed before forming the first corrector of Lemma 3.6.2: R_1, E_1, c_1 below are all computed in this same gauge. Here $e_3 = (0,0,1)$ denotes the axial unit vector, whereas e_z denotes the vertical component of e. Write $p_2 = T_2 e$, $\pi_2 = T_2\pi$ for total-degree-two Taylor polynomials at $(0,0)$, and let z_2 be the homogeneous degree-two part of $(p_2)_z$. Put $G_h f = (Gf, 0)$, $C_0 = G_h e_{Z,z}(0,0)$, $E = E_1(0,0)$, and*

$$c_0 = c_* := c_1(0,0) = \ell_0 R_1(0,0). \tag{3.7.1}$$

Here R_1, E_1, c_1 are the physical primitive residual, reduced corrector, and connection defined before (3.6.10); in particular

$$R_1(0) = P_0\big[F_1(0)e_0 - (F_0(0) - \lambda_0)C_0 - iF_{0,k}(0)e_Z(0) - e_3\pi_Z(0)\big], \qquad (A_0 - \lambda_0)E + R_1(0) - e_0 c_* = 0.$$

Set

$$J_{\mathrm{low}} = \mathrm{Op}_\rho(p_2 - ikG_h z_2 - \rho G_h \partial_Z (p_2)_z + \rho E - i\rho k G_h E_z). \tag{3.7.2}$$

This finite column has degree at most three and is exactly div_ρ*-free. Equivalently, with*

$$b_2 = T_2(e_h + ikGe_z, e_z), \qquad J_{\mathrm{low}} = \mathcal{T}_\rho \,\mathrm{Op}_\rho(b_2 + \rho E), \tag{3.7.3}$$

every coefficient inside $\mathcal{T}_\rho$ is horizontally solenoidal. Let

$$H = (F_0(0) - \lambda_0)E + F_1(0)e_0 - (F_0(0) - \lambda_0)C_0 - iF_{0,k}(0)e_Z(0) - e_3\pi_Z(0) - e_0 c_*.$$

Then $P_0 H = 0$. Define its regular-axis, decaying angular pressure $\pi_1 = \Delta_h^{-1}\,\mathrm{div}_h H_h$, and put

$$\Pi_{\mathrm{low}} = \mathrm{Op}_\rho(\pi_2) + \rho\pi_1, \qquad B_{\mathrm{quad}} = \lambda_0 + \tfrac{1}{2}\lambda_{ZZ}Z^2 + i(\tfrac{1}{2} - h)Zk + \tfrac{1}{2}\lambda_{kk}k^2 + \rho c_*. \tag{3.7.4}$$

For the leading primitive generator F_ρ and each admitted mask C_r, $\rho^{2/5} \le r \le r_{\mathrm{out}}$,

$$\left\|(F_\rho J_{\mathrm{low}} - (J_{\mathrm{low}})_s - J_{\mathrm{low}} B_{\mathrm{quad}} - \nabla_\rho \Pi_{\mathrm{low}}) C_r\right\|_{L^2_Z \to L^2_{y,Z}} \le C(r^3 + \rho r + \rho^2). \tag{3.7.5}$$

Here F_ρ is the leading primitive generator; defects from the completed source are treated by the subsequent finite cells. The constant depends only on the fixed leading profiles and mask shape, not on S. The native column coefficients have H^{16}_5 bounds; two physical observation derivatives leave H^{14}_3.

Proof. Taylor differentiation of $\mathrm{div}_h\, e_h + ike_z = 0$ gives $\mathrm{div}_h (p_2)_h + ik(p_2)_z = ikz_2$. For a left symbol p one has exactly

$$\mathrm{div}_\rho \,\mathrm{Op}_\rho(p) = \mathrm{Op}_\rho(\mathrm{div}_h\, p_h + ikp_z + \rho \partial_Z p_z).$$

Since $\mathrm{div}_h\, G = I$ and $P_0 E = E$, the three horizontal corrections in (3.7.2) cancel these terms exactly. Expanding (3.7.3) proves the equivalent formula. In particular $\mathcal{T}_\rho$ differentiates the complete scalar input; it is not applied directly to $T_2 e$.

The reduced corrector equation gives $P_0 H = 0$. At $k = 0$ the vertical block of P_0 is the identity, so $H_z = 0$ and $H_h = \nabla_h \pi_1$. The fixed-sector pressure estimate supplies this primitive, including its noncompact tail.

For the residual use the full primitive symbols (3.6.5), not a projected differential row. The equation $F_0 e - (\lambda + i(\frac{1}{2} - h)Zk)e = \nabla_k \pi$ cancels the principal Taylor terms of degrees zero, one, and two. The term $-ikG_h z_2$ has degree three. At constant order ρ, left composition contributes $-iF_{0,k}(0)e_Z(0)$, while the physical pressure gradient contributes $e_3 \pi_Z(0)$. The column correction is $E - C_0$ at this order. Also $\partial_s \,\mathrm{Op}_\rho(a) = h\rho\,\mathrm{Op}_\rho(k\partial_k a)$ for a fixed symbol; this has no constant phase term for p_2. The right scalar product has no constant first bracket because $\mu_Z(0,0) = 0$. Thus its remaining constant ρ coefficient is exactly $H - \nabla_h \pi_1 = 0$.

All other terms are cubic in phase, ρ times a positive phase degree, or of order ρ^2. This expansion is finite: F_0 is affine in k, F_1 is at most quadratic in k, the column has degree at most three, and B_{quad} is quadratic. The undisplayed leading primitive term has an explicit ρ^2 factor and radial differential order at most two, with a uniform weighted graph bound from H^{s+2}_{w+1} to H^s_w on the fixed chart. The coefficient bounds just recorded place every column coefficient in this graph domain. Taylor's formula in Z and $\|Z^a k^b C_r\| \le C_{a,b} r^{a+b}$, with $[k, Z] = -i\rho$ and $\rho \le r^2$, prove (3.7.5) before projection. The same proof applies to bounded families of mask shapes.

The polynomial p_2 uses only the $j \le 2$ part of (3.6.4). Its least remaining weight is seven, so $G_h z_2$ retains weight six. The pole formula for $R_1(0)$ costs at most two positive radial derivatives and one moment: viscosity has order two, dilation and the full pressure primitive use their stated moment, and C_0 uses one G. The contour inverse preserves the resulting finite weighted space. In particular $E \in H^{16}_6$, and $G_h E_z \in H^{16}_5$. The other coefficients have at least this regularity. The scalar pressure estimate also gives the required finite bounds for π_1; no compact pressure support is asserted. Two observation dilations each cost at most one derivative and one moment, leaving H^{14}_3. This uses no prepared propagator or critical inverse. □

Lemma 3.7.2 (Actual complete carrier-zero stress domain)**.** *Let $\mathcal{U} f(R, Y) = f(R, Y - \lambda_{\mathrm{aux}} R^{d_r} v_r)$. Expand the stress in its finite scalar right words as $\mathsf{S} = \sum_{p,q} \mathsf{S}_{pq} Z^p k^q$. For each tensor coefficient set*

$$\|\mathsf{S}_{pq}\|_{\mathcal{D}} = \sum_{\ell=0}^{2} \sum_{a=0}^{16} \sum_{|b| \le 10} \sup_{T,Z} \left\|\partial_Y^b \mathcal{U}^{-1} (\partial_T^\ell \partial_Z^a \mathsf{S}_{pq})\right\|_{L^2(\mathbb{T}^2_Y; H^9_R(\langle R\rangle^6))}, \qquad \|\mathsf{S}\|_{\mathcal{D}} = \sum_{p,q} \|\mathsf{S}_{pq}\|_{\mathcal{D}}.$$

The supremum is over the fixed observation chart and the torus carries normalized Haar measure. Ordinary derivatives act on the indicated coefficient with the right word fixed. The source-band shear

is independent of T, Z. The norm includes the two observation-time and sixteen ordinary axial derivatives used in the finite construction. The source gives $J_{\mathrm{src}} = 80$ ordinary derivatives.

Theorem 2(vi) reserves $J_{\mathrm{prep}} = 72$ for preparation. We count the actual coefficient loss in (3.7.31).

It is distinct from the radial order in (3.7.7). For the actual RAW construction, before global physical projection,

$$\mathsf{S} = \mathsf{S}_{\mathrm{mean}} + \mathsf{S}_{\mathrm{match}}, \qquad \mathsf{S}_{\mathrm{mean}} = M \otimes J_{\mathrm{low}} + J_{\mathrm{low}} \otimes M,$$
$$\mathsf{S}_{\mathrm{match}} = \sum_{\alpha, j \neq 0} (Z_{\alpha,j} \otimes Y_{\alpha,-j} + Y_{\alpha,-j} \otimes Z_{\alpha,j}), \quad M = u_M - u_B, \quad Z = X + H,$$

where Y is extracted from $J_{\mathrm{low}} + B_0 + B_1$, one has

$$\|\mathsf{S}\|_{\mathcal{D}} \leq C\rho^{1-128\varkappa} P(S).$$

The stress has a fixed compact radial interaction hull on the selected phase chart.

Its actual scalar pressure and complementary response need not be compact. Haar and non-Haar components, all finite source harmonics, and the full symmetric mean tensor are included.

Proof. We first prove stronger radial estimates.

An H^6 bound alone does not give an H^9 bound. For $A = -P_k N P_k$, we apply the physical contour inverse to $(1 - \Delta_h)(1 + \epsilon(1 - \Delta_h))^{-1} u$.

Since $[1 - \Delta_h, A] = -P_k[1 - \Delta_h, N]P_k$ is first order, interpolation absorbs the top norm and inductively gives each necessary finite unweighted Sobolev order. We apply the same argument to A^*.

We split $N = N_{\mathrm{core}} + N_{\mathrm{tail}}$. The first is compactly supported. The second, with its necessary derivatives, is small after an increase of a fixed radial core.

The weighted Leray estimate and a Neumann argument then give

$$e, v \in H^{18}_R(\langle R \rangle^9), \qquad \partial_k^j e, \partial_k^j v \in H^{18}_R(\langle R \rangle^{9-j}), \quad j \leq 2.$$

All prescribed ordinary Z derivatives have the same radial ladder. The largest sector requirement is $18 + (9 - j) + j + 2 = 29 < m$ for $m \geq 30$.

For pressure, we use $s \leq 17, w \leq 8 - j$. Thus $s + w + j + 3 \leq 28 < m$ and the input moment satisfies $w + j + 1 \leq 9$.

We use physical derivatives at a fixed radius. We first pull back radial spectral charts that depend on the parameter with their exact connection.

This is compatible with, and does not increase, the different five-k/seventeen-Z H^6 ladder and the four-k/sixteen-Z H^4 corrector ladder.

The native low formula, displayed in the construction below, is

$$J_{\mathrm{low}} = \mathcal{T}_\rho \operatorname{Op}_\rho(b_2 + \rho E), \qquad b_2 = T_2(e_h + ikGe_z, e_z), \quad E = E_1(0, 0).$$

This is the horizontal Taylor pullback of Lemma 3.7.1, with its complete primitive pressure. The only viscous profile response is the single ρE; no second viscosity is applied in forming this low column. Its primitive subprincipal row is F_1 of (3.6.5), whose greatest positive radial order is two (Δ_h); the physical projection is applied only in the defining equation for E.

Dilation and transport have order one. The full pressure and divergence primitives use their stated moments.

They do not require two additional positive radial derivatives. The first primitive response has a conservative H_6^{16} bound.

Thus the last exact divergence chart gives the native regularity

$$J_{\mathrm{low}}^{\mathrm{native}} \in H_5^{16}, \qquad \partial_T^{\ell} J_{\mathrm{low}}^{\mathrm{physical}} \in H_{5-\ell}^{16-\ell}, \quad \ell = 0, 1, 2. \tag{3.7.6}$$

The actual observation pullback is $U_T f(R) = a_0(T) f(a_1(T) R)$ on a compact positive T interval. Each T derivative contributes at most one $R\partial_R$ and bounded scalar factors.

The homogeneity of G permits this commutation with dilation, with another G term. It adds no positive radial operator.

Thus two derivatives leave H_3^{14}. We do not assert that they keep a global H_5^{14} norm.

This same argument keeps the actual low pressure pair on its admitted moment ladder. The finite pole Taylor words only acquire scalar T factors.

This operation does not introduce extra profile-k derivatives.

After we form this low column, the largest radial derivative count for the matched stress is

$$1 \text{ (initial RAW source)}, \quad 2 \ (B_0 \text{ curl}), \quad 4 \ (B_0 \text{ viscous residual}), \quad 5 \ (B_1 \text{ curl}), \quad 14 \text{ (final } H^9).$$

The two observation derivatives can fall on the spectral factor. The complete demand on the original leading profile is then

$$2 \ (S_0 e) + 2 \text{ (observation pullback)} + 1 + 1 + 2 + 1 + 9 = 18. \tag{3.7.7}$$

The actual H^{18} bounds suffice for this count.

An unused ρ exponent does not replace these bounds. A residual time/dilation term has order one.

It replaces its order-two viscous term in that branch of the calculation. It does not follow that term. If a time derivative lands on a smooth source or frame coefficient, the spectral demand is no larger.

Parameter differentiation of the finite cell ODE distributes this same order between coefficients and the forcing term, and it adds no new radial operator. We do not send $B_{2,\mathrm{high}}$ back into this initial macro input.

We multiply on the fixed compact interaction hull. The remaining weight three in (3.7.6) then permits any fixed compact weight, with stress weight six.

This is not compactness of the global low profile or its pressure. It supplies the two observation jets in the stress domain stated above.

For the frozen-k family in Lemma 3.7.4, we hold an actual right-word stress coefficient fixed as radial input. Those kernel parameter derivatives do not differentiate its finite pole Taylor coefficients again.

They do not require extra phase jets of the profile.

Finite source means and high velocities have their actual same compact hull, enlarged past the two velocity and pressure endpoints and all spectral returns. The cell ODE at fixed slow variables keeps RAW coefficient support.

Its potential curl is local. We multiply the noncompact J_{low} by compact M.

We apply the global Leray projector only after this support statement. We do not use it to infer compact pressure support.

The opposite phases cancel before differentiation: $D_R^q(e^{ijK\Phi} z\, e^{-ijK\Phi} y) = D_R^q(zy)$. We fix the remaining selected angular carrier. Each evaluated radial derivative then costs at most $\rho^{-\varkappa} P(S)$, not $\rho^{-1/2}$.

The primary odd symmetric tensor and its sign-independent B_1 rows vanish identically before divergence. Each remaining type starts at order at least $1 - 3\varkappa$.

The types are MJ_{low}, source-curl times B_0, and primary times the half-order cell correction. They also include higher source H times a principal cell, and X times the cell generated by H.

We remove high products from different labels only before any operation that extends auxiliary support. We do not remove mean and later macro interactions by this procedure.

The conservative coefficient count has sixteen levels for the finite raw/curl/cell/pressure calculation ($2 + 3 \cdot 3$ plus five). It also has nine radial, ten origin, and sixteen Z levels.

Two observation-time levels, two frozen-k levels, and four coordinate connections complete the count of fifty-nine. This $\rho^{1-62\varkappa}P(S)$ is stronger than the stated $\rho^{1-128\varkappa}P(S)$.

Ordinary origin derivatives actually cost only fixed powers of S. If an observation shear that depends on time has $a_T \neq 0$, H^{10}_Y after two time derivatives uses raw Y derivatives through twelve.

The time/connection allowance includes these derivatives. The fixed source-band shear has $a_T = 0$.

Compact radial support permits weight six. The divergence is in H^8.

For two phase derivatives the weighted Leray bound with $s = 8, w \leq 2, j \leq 2$ requires $m > 14$. Scalar pressure needs the additional input moment $w + j + 1 \leq 5$ and $m > 15$.

The tensor Cartesian shifts by at most two leave room below $m = 30$. Thus the macro response keeps the full physical pressure tail.

Multiplication by a high source localizes later re-excitation, not the pressure itself. The pole-to-physical pressure displacement remains $\rho^{\nu} r P(S)$ on a radius-r right mask, where $\nu = 1 - 128\varkappa$.

We do not declare it an $O(\rho^2)$ tail. □

Finite RAW plateau and the order of construction. In the canonical variable $Z = z/t^{1/2-h}$, choose $\zeta \in C^{\infty}_c(\mathbb{R}_Z)$ equal to one on a fixed neighborhood of the Z-projection of the larger reference mask. Multiply the raw forcing and potential coefficients by $\zeta(Z)$ before forming their curls and restoring divergence, retaining all derivatives of ζ. Input-frequency cutoffs act on the far right of each word, preserving polynomial dependence on k inside the word. The pole macro kernel acts in radial/auxiliary variables, not in an input-k family, and keeps this coefficient support.

Every derivative of the cutoff is supported a fixed positive Z-distance from the reference mask. The stronger frozen-parameter estimate of Lemma 3.7.4 gives the necessary finite mixed T, k and radial-moment bounds for these actual stress families.

It does not change the coefficientwise construction or create an input-k dependence of this macro inverse. We first prove Lemma 3.7.2.

We then construct its macro response and finite re-excitation. Next, we derive the coarse $L^2 \to H^2$ column bound.

Only after these steps do we estimate the omitted completed-source multiplier. This order does not use a full-column bound to prove its own macro input.

We prove the bounds for the genuine OUTPUT errors and their typed graph extension in Lemma 3.9.4. We do not return any of them to a Gaussian-weighted source inverse. All eigenvalues in this section are the actual unrotated physical complex eigenvalues. The physical band symbol is $b_{\mathrm{pr}} = \lambda + i(\frac{1}{2} - h)Zk$, never the Doppler-centered resolvent parameter μ_D.

Profiles, pressure and their derivatives use the same physical fixed-chart gauge as Section 3.6.

Lemma 3.7.3 (Selected-pole radial complementary clock)**.** *At the selected angular integer $m \geq 30$, let $A_0 = -P_0 N_0 P_0$ be the bounded inviscid physical radial generator at the pole $(Z, k) = (0, 0)$.*

It has simple eigenvalue λ_0, Riesz projection P_{band}, and $Q_0 = I - P_{\mathrm{band}}$.

Suppose S *is a compact interaction-hull stress with nine radial Sobolev derivatives and ten Hilbert auxiliary-origin derivatives. The eight derivatives evaluated at the origin are bounded by the ten* L^2 *derivatives: Fourier inversion in the two auxiliary variables and Cauchy–Schwarz use* $\int_{\mathbb{R}^2}\langle\xi\rangle^{-4}\,\mathrm{d}\xi<\infty$.

Then the causal complementary clock equation has a physical, pressure-compatible solution. For its frozen radial kernel $\mathcal{K}_T(r)$*, with one bound on a fixed compact positive observation-*T *interval,*

$$\|\partial_T^j\mathcal{K}_T(r)\|_{H^8\to H^8}\le C_j(1+r)^j e^{-cr},\quad j=0,1,2. \tag{3.7.8}$$

Its response has H^8 *and four weighted radial-derivative bounds by* $C\|\mathsf{S}\|_{H^9}$*. These bounds use the same fixed origin-derivative norms.*

The constants refer to this selected source and do not involve an arbitrary scalar input derivative.

Proof. Use the full right-half-plane count in Theorem 2(iv).

It places the full complementary L^2 spectrum to the left of a fixed $a_1<\Re\lambda_0$. A small isolating circle alone does not give this conclusion.

The current smooth Cartesian coefficient matrix and its first eight spatial derivatives stay bounded, so A_0 is bounded on H^8. With $L=1-\Delta_h$, the fixed-sector Leray projector commutes with L, and $[L,A_0]=-P_0[L,N_0]P_0$ is first order.

For $L_\epsilon=L(1+\epsilon L)^{-1}$, apply a separated L^2 resolvent to

$$(z-A_0)L_\epsilon u=L_\epsilon f+(1+\epsilon L)^{-1}[L,A_0](1+\epsilon L)^{-1}u.$$

Interpolate the first-order term between H^{2j-2} and H^{2j}, absorb its top norm, and induct for $j=1,\dots,4$. The limit $\epsilon\downarrow 0$ proves H^8 resolvent preservation on a separated contour.

The inverse identities hold on a dense core and thus on H^8. No new H^8 spectrum appears.

A rectangle around the full bounded complementary spectrum, with right edge between a_1 and $\Re\lambda_0$, gives the following bound. Indeed the integral of $e^{rz}(z-A_0)^{-1}$ divided by $2\pi i$ on a large circle is e^{rA_0}: expand the resolvent in powers of A_0/z and integrate term by term. Deform the circle to the complementary rectangle and the isolated simple pole. The pole contributes $e^{r\lambda_0}P_{\mathrm{band}}$. On the rectangle the resolvent is bounded and $\Re(z-\lambda_0)\le -c$, which proves

$$\|e^{r(A_0-\lambda_0)}Q_0\|_{H^8\to H^8}\le Ce^{-cr},\qquad r\ge 0. \tag{3.7.9}$$

We next show on the fixed phase chart that the sandwich $A(Z,k)=-P_kN(Z,k)P_k$ has two derivatives in the same-space operator norm. Write $L^2_v=L^2(\langle y\rangle^{2v}\,\mathrm{d}y)$ for all real v. Let D stand for $\partial_k^bP_k$ with $d=b$, or, for $0<|k-k'|\le 1$, for $(\partial_k^bP_k-\partial_k^bP_{k'})/|k-k'|^\vartheta$ with $d=b+\vartheta$, where $0<\vartheta<\min(1,2h)$ and $0\le b\le 2$. The positive moment ladder (Corollary 1.28.5(a),(b) of Part 1) bounds $D:L^2_{u+d}\to L^2_u$ for $u\ge 0$ at the finite indices below. The symbol of D is Hermitian, so duality in the unweighted pairing also gives $D:L^2_0\to L^2_{-d}$ from its bound $L^2_d\to L^2_0$. Interpolating these last two arrows in the weighted L^2 scale gives $D:L^2_v\to L^2_{v-d}$ for $0\le v\le d$. For $v\ge d$ this is the original positive ladder. The constants are uniform in k,k'.

Consider a product-rule term with a derivatives on the left projector and b on the right, $a+b\le 2$. Write $\delta_L=\delta_R=0$ for a derivative bound. In a difference of products assign ϑ to the projector being differenced, if any, and zero to the other. For $w=0,1,2$ the domain chain is

$$L^2_w\longrightarrow L^2_{w-b-\delta_R}\xrightarrow{\partial N}L^2_{w+a+\delta_L}\longrightarrow L^2_w.$$

Here ∂N denotes the coefficient with its assigned parameter and spatial derivatives, including order zero. The required increase of weight is $a+b+\delta_R+\delta_L\le 2+\vartheta<2+2h$. The differentiated

coefficients are $O(\langle y\rangle^{-2-2h})$, including all relevant ordinary Z derivatives, while W has bounded radial support on the chart. Differences on the middle coefficient obey the same estimate times the parameter increment, since one additional coefficient derivative is bounded with that decay. Cartesian derivatives commute with the projector multipliers. Apply the L^2 chain to every Leibniz term after at most eight Cartesian derivatives. Those derivatives shift the vector angular sector by at most eight, so $m \geq 30$ supplies the positive-ladder margins on both sides, also for a differenced projector. This gives the same chain in the H^8 estimates.

On smooth, rapidly decaying data of the selected angular sector the positive ladder gives strong differentiation through order two. The preceding bounds give operator-norm continuity of the candidate derivatives, with ϑ-Hölder second derivatives: telescope a difference of the three factors using the displayed chain. Integrating each derivative along a parameter segment on the dense class and extending the identity by continuity proves differentiability in operator norm. In particular, uniformly on a smaller compact chart,

$$(Z,k) \longmapsto A(Z,k) \quad \text{belongs to } C^{2,\vartheta}\big(\overline{U};\mathcal{L}(H^8_w \cap \mathsf{H}_m)\big), \qquad w=0,1,2, \tag{3.7.10}$$

where $\overline{U}$ denotes the compact chart under consideration. The proof applies separately to the conjugate sector. The resolvent identity on the fixed contour now gives the corresponding derivatives of the reduced kernel on the projected compact-stress data.

3.7.2 The raw pressure pair and its operator domains

The construction keeps the generator sign and the accumulated raw velocity-pressure pair. We write

$$\mathcal{R}(J,\Pi) = F_*J - J_s - J(\lambda_0 + B_2) - \nabla\Pi, \qquad P\mathcal{R} = E_0(J).$$

We split the exact raw residual as $\mathcal{R}(J_i,\Pi_i) = L_i + h_i + F_i^{\mathrm{out}}$.

Here h_i is the retained high input compatible with the Gaussian norm. The term F_i^{out} is the sum of physical output errors.

With $C_{\mathrm{gen}}(h) = C_{10}(-h)$, we keep velocity and pressure and write

$$\mathcal{R}(C_i,\pi_i) = -h_i + D_i^{\mathrm{ret}} + F^{\mathrm{out}}_{\mathrm{cell},i}, \qquad (J_{i+1},\Pi_{i+1}) = (J_i + C_i, \Pi_i + \pi_i),$$

$$h_{i+1} = H_{\mathrm{raw}} D_i^{\mathrm{ret}}, \qquad F^{\mathrm{out}}_{i+1} = F_i^{\mathrm{out}} + F^{\mathrm{out}}_{\mathrm{cell},i}.$$

The local extraction precedes global projection. We do not invert endpoint or deletion errors again in the Gaussian-weighted input norm.

Exponential smallness in physical space does not imply smallness in that norm. The gain $P(S)(r + \rho^{1/2-128\varkappa})$ applies only to retained inputs.

We estimate the flat outputs after a fixed number of physical derivatives. We estimate the completed localization tail simultaneously in physical L^2 and gradient column norms.

Projection does not keep compact label support. We do not reset any pressure lift.

Its gradient differentiates the scalar input and the coefficients. The retained mean tensor includes the full zero-carrier mean and each opposite-carrier matching tensor from higher prefixes.

It is not restricted to the Haar part. Tangential mean size $\rho^{1-\varkappa}$ is not a ρ^2 tail.

We recompute the scalar b_0 from these full sources.

For $w = 0,1,2$, equation (3.7.10) supplies the same-space $C^{2,\vartheta}$ bounds. The undifferentiated sandwich also maps H^8_0 into H^8_2: multiplication by N restores two moments between the unweighted inner and weighted outer projectors. Thus on a contour separated from zero, the known unweighted solution $u = (z-A)^{-1}f$ with $f \in H^8_w$ satisfies $u = z^{-1}(f + Au) \in H^8_w$, with the uniform resolvent

bound there. Lemma 3.7.4 proves the stronger compact-stress estimates through weight six, including two observation and two frozen-frequency derivatives and the longitudinal pressure. That argument uses only nonnegative weights. Its bare projector jets are strongly continuous on data at the limiting moment.

For $Uf(R,Y) = f(R, Y - a(R))$, we use the evaluated norm $\|U^{-1}b\|_{H^{10}_Y H^8_{R,2}}$. This map is not a Sobolev isometry at a fixed origin.

We conjugate the compact stress *before* projection and divergence. At $Y_{\mathrm{phys}} = a(R) + Y_t$, the shear cancels and H^{10}_Y provides eight pointwise origin jets by $H^2(\mathbb{T}^2) \hookrightarrow C^0$.

We include two additional auxiliary derivatives in the count. Lemma 3.7.2 proves the actual coefficient count of fifty-nine conservative $\varkappa$ levels.

This count is within the $128\varkappa$ allowance. The different radial depth is H^{18}_9 for the leading profile.

The native low column lies in H^{16}_5. After at most two physical observation-time derivatives, its available domain is H^{14}_3.

Equations (3.7.6)–(3.7.7) give these domains. These radial depths are different from the phase-derivative H^6/H^4 ladder.

Weight six on the compact stress gives the actual pressure moments. We keep ten conjugated auxiliary derivatives.

We keep raw origin derivatives through twelve when two observation-time connections act. The whole radial complement and all auxiliary Haar modes remain in the macro response.

The OUTPUT class has the simultaneous right-masked physical L^2/H^1 operator bounds of Lemma 3.9.4. That lemma also states its semiclassical graph domain.

Identity (O5) of Lemma 3.9.5 gives the exact normalizer extension. Neither result is an estimate in the Gaussian-weighted source norm.

We use the same spatial cutoff $\zeta(Z)$ before the macro and high-cell construction. We do not declare an arbitrary global projected profile compact.

The proof below uses these domains.

Pole projection versus actual physical projection. For the full matching/mean stress S, the coefficientwise finite construction uses $F_{\mathrm{mac},0} = -\operatorname{div}_h S$ and $f_{\mathrm{mac}} = P_0 F_{\mathrm{mac},0}$, with its pole pressure representative. It does not hide the exact arbitrary-input multiplier P_k in a finite polynomial.

The difference to $-P_\rho \operatorname{div}_\rho S$ remains in the full physical zero-carrier error, with bound $\rho^\nu(r+\rho)P(S)$ on the stated stress moment ladder. Fixed outer-plateau leakage and shrinking-mask annular estimates keep their different rescaled costs.

We keep these distinctions in the actual finite-kernel and critical-inverse proofs below.

For the undifferentiated frozen $k = 0$ response, the weighted output follows from the actual vorticity equation. For $v = e^{r(A_0-\lambda_0)}Q_0 f$ and $\omega = \operatorname{curl}_h v_h$,

$$\omega_r = -(\lambda_0 + im\Omega)\omega - v_h \cdot \nabla\zeta.$$

The source has $(1+R^2)D^j\nabla\zeta \in L^\infty$ for $j \le 4$.

Damped Duhamel, induction on j, and (3.7.9) bound $(1+R^2)D^j\omega$ through order four with a smaller exponential rate. For each angular sector generated by four Cartesian derivatives, $|n| \ge m - 4 > 1$.

In logarithmic radius the Biot–Savart equation is $[(\partial_x - 1)^2 - n^2]\Psi = F$, whose Fourier denominator has no real zero. Thus $\|R\nabla_h\psi\|_2 \le C_n\|R^2\omega\|_2$.

The exact vertical equation $(v_z)_r = -(\lambda_0 + im\Omega)v_z - W'v_R$ keeps the compact W' contribution. For $f = P_0 \operatorname{div}_h \mathsf{S}$, curl removes horizontal pressure and the vertical input stays compact.

Thus

$$\|v(r)\|_{H^8} + \sum_{|j|\le 4} \|RD^j v(r)\|_2 \le Ce^{-cr}\|\mathsf{S}\|_{H^9}. \tag{3.7.11}$$

The selected Riesz subtraction has the same finite weighted vorticity tail by its eigen-equation. Lemma 3.7.4 gives the mixed k derivatives with radial moments.

Their horizontal divergence is generally nonzero, so the curl-only calculation does not give them. They act on the admitted projected compact-stress family.

We do not assert that bare $\partial_k P_k$ on arbitrary unweighted inputs is bounded. The weighted sandwich argument in Section 3.7.2 and its full positive-ladder realization in that lemma keep longitudinal pressure and the full complementary contour.

For the observation band let $A_c(T) = c(T)U_T A_0 U_T^{-1}$, $\lambda_{\mathrm{obs}}(T) = c(T)\lambda_0$, $P_c(T) = U_T P_{\mathrm{band}} U_T^{-1}$, $Q_c = I - P_c$, where $c(T) = T^{-1-h}$ and U_T is the exact radial coordinate and amplitude map. Select a fixed $d > 0$ and set $B_T = A_c - \lambda_{\mathrm{obs}} - dP_c$.

The full e^{rB_T} decays. $\mathcal{K}_T(r) = e^{rB_T}Q_c$.

Radial dilation commutes with the $k = 0$ Leray projector and its commutators differentiate only smooth order-zero coefficients. Thus A_c', A_c'', P_c', P_c'' are bounded on H^8, although U_T' need not be.

The exact derivative includes the endpoint

$$\partial_T \mathcal{K}_T(r) = \int_0^r e^{(r-u)B_T} B_T' e^{uB_T} Q_c \, \mathrm{d}u - e^{rB_T} P_c'.$$

One more derivative and the full shifted semigroup prove (3.7.8).

The source-band translation $\mathcal{U}f(R,Y) = f(R, Y - \lambda_{\mathrm{aux}} R^{d_r} v_r)$ conjugates the evaluated radial derivative to ∂_R and commutes with $T_0 = c_{\mathrm{aux}} v_t \cdot \partial_Y$. Thus, coefficient by coefficient,

$$b(T) = \mathcal{U} \int_0^\infty \mathcal{K}_T(r) \mathcal{U}^{-1} f(T, Y - c_{\mathrm{aux}} r v_t) \, \mathrm{d}r$$

solves $(T_0 + \lambda_{\mathrm{obs}} - A_c^{\mathrm{lift}})b = Q_c^{\mathrm{lift}} f$ with each Haar mode retained. In the kernel the source origin is $Y + \lambda_{\mathrm{aux}}(R'^{d_r} - R^{d_r})v_r - c_{\mathrm{aux}} r v_t$.

At the physical sample, the output radial translation cancels. The original source origin stays the same.

Minkowski and (3.7.11) apply to the conjugated response in $H_Y^{10} H_R^8$, not to an asserted bounded shear on $C_Y^8 H_R^8$.

Translation in the torus is unitary in these Hilbert origin norms, and the radial kernel commutes with all origin derivatives. The two-dimensional H_Y^2 embedding gives eight pointwise-origin derivatives.

At physical evaluation $Y = a(R) + Y_t$, the shear cancels and evaluated radial derivatives are ordinary radial derivatives of the conjugated response at Y_t. We conjugate the projected source as the full operator $\mathcal{U} P \operatorname{div} \mathcal{U}^{-1}$.

We do not commute the shear through pressure. Ordinary derivatives of its compact input have the stated finite source losses.

Here the source-band shear $a(R)$ is fixed independently of observation T. In a chart that depends on time its $a_T \partial_Y$ connection must be retained. This uses two additional auxiliary derivative levels under the selected eighty-level ordinary source bound.

The prepared reservation is seventy-two, as fixed in Theorem 2(vi).

Last the undifferentiated pole vertical coefficient is compact on that hull. We assert no such compactness for its k derivatives.

For $G = \nabla_h \Delta_m^{-1}$, its exterior Poisson branch is $c_g R^{-m}$. Interior elliptic estimates give $\|Gg\|_{H^3} + \sum_{|j|\le 4} \|RD^j Gg\|_2 \le C\|g\|_{H^3}$.

Thus $\mathcal{T}_\rho b = (b_h - \rho G \partial_Z b_z, b_z)$ is physical. The scalar pressure from compact stress is $\Delta_h^{-1} \operatorname{div}_h^2 \mathsf{S}$.

The other term obeys $\|\Delta_h^{-1} \operatorname{div}_h (N_0 b)_h\|_2 \le C_m \|R(N_0 b)_h\|_2$, by the same fixed-sector radial estimate. These include noncompact pressure tails.

The unlifted original pole response b is horizontally solenoidal, and $\mathcal{T}_\rho b$ is physically divergence-free. The one-moment bound (3.7.26) also controls the mixed-family norms and pressure comparisons.

It does not assert that applying $\mathcal{T}_\rho$ independently to b_k or b_{kk} makes either one physically divergence-free. □

3.7.3 Mixed frozen-parameter and radial-moment macro domain

Main result. Lemma 3.7.4 gives the mixed parameter estimates on the full rectangular domain of Section 3.7.2. Its inputs are the actual selected source, its spectral gap, and compact stresses with the stated derivatives.

The proof gives the whole-complement contour, positive moment ladder, and longitudinal pressure terms. The macro kernel stays fixed coefficientwise at $k = 0$.

The family estimate permits the finite parameter and pressure comparisons. It does not make the kernel depend on the input frequency of a right word.

Lemma 3.7.4 (Mixed complementary macro estimate)**.** *Fix the actual selected angular integer $m \ge 30$ and source. Write H^s_w for the fixed-sector Cartesian radial Sobolev norm*

$$\|u\|^2_{H^s_w} = \sum_{|\beta| \le s} \|\langle R \rangle^w D_h^\beta u\|^2_{L^2(R\,\mathrm{d}R)}$$

on the full three-component vector space.

At the pole $Z = 0$ let

$$A(k) = -P_k N(k) P_k, \qquad N(k) = N_0 + ikWI,$$

with the actual physical eigenvalue $\lambda(k)$, selected Riesz projection $\Pi(k)$ and complement $Q(k) = I - \Pi(k)$. Take a stress $\mathsf{S}(k)$ on the compact interaction hull. It has two bounded k jets in H^9_6. Let $j \le 2$ and $q \le 4$. Then one has

$$\begin{aligned} &\Big\| \langle R \rangle D_R^q\, \partial_k^j \Big[e^{t(A(k) - \lambda(k))} Q(k) P_k \operatorname{div}_k \mathsf{S}(k) \Big] \Big|_{k=0} \Big\|_2 \\ &\qquad \le C(1+t)^2 e^{-ct} \sum_{i \le j} \|\partial_k^i \mathsf{S}\|_{H^9_6}, \qquad t \ge 0. \end{aligned} \tag{3.7.12}$$

The output before D_R^q lies in H^8_{6-j}.

The actual adjoint family has the related positive-weight estimate, proved on its own contour. On a compact positive observation T interval the physical conjugated family has, for $\ell, j \le 2$,

$$\begin{aligned} &\Big\| \partial_T^\ell \partial_k^j \Big[\mathcal{K}_T(t,k) P_{a(T)k} \operatorname{div}_{a(T)k} \mathsf{S}(T,k) \Big] \Big\|_{H^8_{6-j}} \\ &\qquad \le C(1+t)^{\ell+j} e^{-ct} \sum_{b \le \ell,\, i \le j} \|\partial_T^b \partial_k^i \mathsf{S}\|_{H^9_6}. \end{aligned} \tag{3.7.13}$$

Here $a(T) > 0$ is the exact radial-dilation frequency factor.

All coefficients, projections and pressures are the unrotated physical ones. The bounds also hold for H^{10}_Y-valued radial data.

Constants belong to this fixed source and compact chart, not to ancient time.

Proof.

Actual source and whole-complement gap. The differentiated heat-tail bounds in Theorem 2(iv) and the profile estimates in Lemma 3.6.2 give a compact radial core and

$$D_h^\beta N_0 = O(\langle R\rangle^{-2-2h-|\beta|})$$

for the necessary finite derivatives outside it.

W is compact on the relevant frozen hull. The constants may depend on the last m.

We shrink the real k chart. The full physical spectral count gives constants $a, c > 0$ such that

$$\sup \Re\sigma(A(k)|_{\operatorname{Ran} Q(k)}) \le a, \qquad \Re\lambda(k) \ge a + 4c. \tag{3.7.14}$$

The zero gradient branch of the full-vector extension is in the complement.

Take $a > 0$. Equation (3.7.10) with $w = 0$ gives norm continuity of $A(k)$ on the fixed-sector H^8 space.

The resolvent identity on a compact boundary thus keeps one separated complementary rectangle on a smaller k chart and keeps the simple selected Riesz rank. The operator norms have one bound. Select a large circle outside that bound.

We do not select unrelated contours at different k.

Full projector derivatives. For $p = (\xi_1, \xi_2, k)$, $P_k = I - p \otimes p/|p|^2$. At zero,

$$P_0' = -\frac{e_3 \otimes \xi_h + \xi_h \otimes e_3}{|\xi_h|^2}, \qquad P_0'' = -\frac{2e_3 \otimes e_3}{|\xi_h|^2} + \frac{2\xi_h \otimes \xi_h}{|\xi_h|^4}. \tag{3.7.15}$$

Thus the formula keeps horizontal gradients that the vertical component forces. We do not presume that the differentiated velocity is horizontally solenoidal.

For the physical Leray multiplier of Theorem 2(iv), the sector estimate with $\lceil w\rceil + j \le m - 1$ gives

$$\|\partial_k^j P_k f\|_{H^s_w} \le C\|f\|_{H^s_{w+j}}, \qquad j \le 2, \quad 0 \le w \le 6 - j, \quad s \le 8. \tag{3.7.16}$$

Each k derivative of the full multiplier costs one inverse $|\xi_h|$. For integer weights, multiplication by a Cartesian coordinate corresponds to differentiation in its horizontal Fourier variable.

For a pure nonzero angular mode v of order l, the pointwise inequality $|l||v|/|\xi_h| \le |\nabla_{\xi_h} v|$ follows by writing the angular derivative in polar coordinates. More generally $\||\xi_h|^{-a} v\|_2 \le |l|^{-1}\||\xi_h|^{1-a}\nabla v\|_2$. Iterate on the Cartesian derivatives, which split into the two orders $l \pm 1$, to control each integral inverse power by derivatives of the same order. The positive lower bound on the remaining angular order justifies all the divisions.

Interpolation between adjacent integer moment bounds gives the real weights. Even the sufficient condition $m > s + \lceil w\rceil + j + 2$ holds here since its right side is at most $16 < 30$. The nonnegative mass k^2 in the pressure Bessel inverse does not worsen the $k = 0$ bound.

This is a positive moment ladder, not boundedness of bare P_0' on arbitrary unweighted inputs. In particular, for a compact-core coefficient N_c,

$$P_k N_c P_k : H^8_0 \longrightarrow H^8_w, \qquad w \le 6.$$

The inner projector is unweighted bounded. Multiplication places its output in the fixed core.

The outer projector is bounded in the weighted norm.

This estimate includes its pressure tail and does not assert compact support.

Weighted inverse on the full contour. We select a rectangle Γ around the full bounded complementary spectrum. It excludes $\lambda(k)$ and has its right edge in $(a, a+c)$.

Its other edges lie beyond the relevant uniform operator bounds and

$$|z| \geq c_0 > 0, \qquad \Re(z - \lambda(k)) \leq -3c, \qquad z \in \Gamma. \tag{3.7.17}$$

The unweighted H^8 inverse is uniform there. The actual L^2 inverse and the regularized commutator $[1 - \Delta_h, A] = -P[1 - \Delta_h, N]P$ give this bound.

We use the previous four-step unweighted Sobolev bootstrap, through (3.7.9) and its localized sandwich argument. We use no mixed or weighted conclusion of Lemma 3.7.3 as an input here.

We enlarge only the left and horizontal edges beyond the direct operator norm bounds on the finitely many weighted spaces. We do not assume a weighted right spectral bound when we place the right edge.

Split $N = N_c + N_t$ by a fixed smooth radial cutoff. The equation $(z - A)u = f$ is

$$u = z^{-1} f - z^{-1} P_k N_c P_k u - z^{-1} P_k N_t P_k u. \tag{3.7.18}$$

Enlarge the core so that, simultaneously for $0 \leq w \leq 6$,

$$\|z^{-1} P_k N_t P_k\|_{H^8_w \to H^8_w} \leq \tfrac{1}{2}. \tag{3.7.19}$$

All coefficient derivatives through order eight decay, and the cutoff derivatives have the same tail decay.

Thus the multiplication norm on H^8_w tends to zero. The projector bounds on this finite ladder are uniform.

The denominator is $\min_\Gamma |z|$, not $\Re z$, so this argument includes the left and horizontal contour edges.

For $f \in H^8_w$ let $u \in H^8_0$ be the known unweighted solution. The compact-core term in (3.7.18) belongs to H^8_w, and $C\|u\|_{H^8_0}$ bounds this term.

We invert $I + z^{-1} P_k N_t P_k$ in H^8_w against this known right side and denote the solution by u_w. The same tail inverse exists in H^8_0.

Comparison of the two equations there gives $u_w = u$. This proves weighted membership before we use a weighted norm of u.

Thus

$$\sup_{k, z \in \Gamma} \|(z - A(k))^{-1}\|_{H^8_w \to H^8_w} < \infty, \qquad 0 \leq w \leq 6. \tag{3.7.20}$$

The inverse identities extend from a dense core. Weighted injectivity also follows from $H^8_w \subset H^8_0$.

The same argument applies at each nonzero unweighted resolvent point, with its own finite core. There is thus no additional weighted right-hand spectrum.

Behavior at $z = 0$ is inside the complementary contour, not on its boundary. This proves, rather than assumes, that the contour represents the full weighted complement.

Run the proof separately for $A(k)^* = -P_k N(k)^* P_k$ on the conjugate contour. Its coefficients have the same tails and its unweighted inverse is the actual Hilbert adjoint inverse.

This supplies positive-weight adjoint bounds. Dualizing a positive-weight right estimate alone would not do so.

Mixed resolvent jets and the actual input. The product rule, (3.7.16), and bounded multiplication by $N, N' = iWI$, with $N'' = 0$, give

$$A^{(j)}(k) : H^8_{w+j} \longrightarrow H^8_w, \qquad j \le 2.$$

We can select all intermediate weights between zero and six. For $R(z,k) = (z - A(k))^{-1}$, difference quotients on this ladder give

$$R_k = RA_kR, \qquad R_{kk} = RA_{kk}R + 2RA_kRA_kR. \tag{3.7.21}$$

These are bounded jet operators $H^8_{w+j} \to H^8_w$, and they have STRONG continuity on each admitted source family.

At this saturated moment ladder we do not infer any operator-norm continuity or norm-Hölder estimate for bare projector derivatives. We can first differentiate smooth compact data. Density and the uniform weighted bounds then give the result for the admitted data.

Strong difference quotients justify the contour integrals below. An extra positive moment, or the decay-restored full sandwich, would be necessary for a different norm-Hölder assertion.

That assertion is not necessary here. There is no horizontal divergence-free hypothesis on the differentiated unknown.

Set $F(k) = P_k \operatorname{div}_k \mathsf{S}(k)$, and keep the vertical ik term. Since divergence is first order and affine in k,

$$\|F^{(j)}(k)\|_{H^8_{6-j}} \le C \sum_{i \le j} \|\partial_k^i \mathsf{S}\|_{H^9_6}, \qquad j \le 2. \tag{3.7.22}$$

For derivatives of RF, the total moment loss of all factors is j.

It is not j for each factor. Thus

$$\|\partial_k^j (RF)\|_{H^8_{6-j}} \le C \sum_{i \le j} \|\partial_k^i \mathsf{S}\|_{H^9_6}, \qquad z \in \Gamma. \tag{3.7.23}$$

At $j = 2$ four moments remain.

The same argument on the physical selected-pole contour supplies the Riesz projection and its first two jets. The adjoint argument supplies the left jets.

They agree on the dense unweighted core with the physical projections. Thus their weighted restrictions do not change the physical graph, normalization, or left–right pairing.

The actual J_{low} and its finite derivatives stay on their previously established ladder. A compact tensor that contains these factors is admissible when it satisfies the actual H^9_6 bound.

Dunford and longitudinal pressure. In the full physical vector space,

$$e^{t(A(k)-\lambda(k))} Q(k) F(k) = \frac{1}{2\pi i} \int_\Gamma e^{t(z-\lambda(k))} R(z,k) F(k) \, \mathrm{d}z. \tag{3.7.24}$$

The gradient zero branch is inside Γ and decays after subtraction of $\lambda(k)$. At each real k the actual forcing is solenoidal.

Its differentiated family has the longitudinal components in (3.7.15). Up to two derivatives of this identity give at most $(1+t)^2$ from the scalar exponential.

We combine (3.7.17) and (3.7.23) to get the stronger H^8_{6-j} bound. This proves (3.7.12), with a spare positive decay rate.

This uses the full complementary contour, not a pole-only circle.

For $f_{\mathrm{raw}} = \operatorname{div}_k \mathsf{S}$ and $w = R(z,k)P_k f_{\mathrm{raw}}$, $z \neq 0$ implies $\operatorname{div}_k w = 0$. The actual pressure gradient is

$$\nabla_k \pi = (I - P_k)(f_{\mathrm{raw}} - N(k)w). \tag{3.7.25}$$

We differentiate the whole right side and keep P_k', P_k'' and all vertical components.

The total moment loss is at most j, so the horizontal gradient has the H^8_{6-j} bound. The angular identity $(im/R)\pi = (\nabla_h \pi)_\theta$, together with regular-axis Hardy, fixes the gauge and bounds the scalar pressure, for example in H^8_{5-j}.

There is no constant angular pressure mode. In particular

$$\partial_k^j (ik\pi) = ik\pi^{(j)} + ij\pi^{(j-1)}$$

keeps its second term.

Integration of (3.7.25) on the same contour gives the physical complementary pressure with the same decay. We do not artificially declare any pressure tail compact.

For completeness the horizontal Hodge part is explicit. At zero,

$$\operatorname{div}_h v_h^{(j)} = -ijv_z^{(j-1)}, \qquad (v_h^{(j)})_{\mathrm{long}} = \nabla_h \Delta_h^{-1}(-ijv_z^{(j-1)}), \quad j = 1, 2.$$

The fixed-sector order-minus-one Hardy estimate is

$$G = \nabla_h \Delta_m^{-1} : H^s_{w+1} \longrightarrow H^s_w. \tag{3.7.26}$$

To see the estimate, on an angular mode of absolute order $l > 0$ the fundamental solutions of the radial Laplace equation are $R^{\pm l}$. Matching the regular and decaying solutions at the source radius gives

$$\Delta_l^{-1} f(R) = -\frac{1}{2l} \int_0^\infty e^{-l|\log R - \log q|} f(q) q \, \mathrm{d}q.$$

Continuity and the jump $[R\partial_R] = 1$ verify the kernel with respect to $q\,\mathrm{d}q$. Either component of its gradient is bounded by $CR^{-1} \int e^{-l|\log R - \log q|} |f(q)| q \, \mathrm{d}q$. Multiply by $R\langle R\rangle^w$ and put $x = \log R$, $y = \log q$. Since $\langle R\rangle^w / \langle q\rangle^w \le e^{w|x-y|}$, Young's inequality with kernel $e^{-(l-w)|x-y|}$ gives the desired weighted $L^2(R\,\mathrm{d}R)$ estimate when $l > w$. Cartesian derivatives commute with the whole-plane inverse gradient on smooth sector data; their modes have absolute order at least $m - s$ (one further shift for vector components), still greater than w. Density gives the stated Sobolev estimate. Since $v^{(j-1)} \in H^8_{7-j}$, its longitudinal component has at least H^8_{6-j}. The transverse component is the remainder, not the whole derivative.

A later single divergence primitive uses one of the four remaining moments. It leaves weight three, which exceeds the H^3_1 physical cutoff requirement.

In the actual pole lift $T_\rho b = (b_h - \rho G \partial_Z b_z, b_z)$ the ordinary axial derivative is part of the input jet budget, not supplied by G. The original UNLIFTED pole response b is horizontally solenoidal, and $T_\rho b$ is physically divergence-free.

The same one-moment norm bound controls derivative and pressure comparisons. But we do not assert horizontal solenoidality of b_k, b_{kk} or physical solenoidality of independently formed $T_\rho b_k, T_\rho b_{kk}$.

The rectangular observation domain. To keep H^8 under two observation derivatives, we use a fixed physical radial chart. We do not differentiate the stress by a dilation.

The exact projector identity is

$$U_T P_k U_T^{-1} = P_{a(T)k}, \qquad A_T(k) = -c(T) P_{a(T)k} N_T(k) P_{a(T)k}.$$

Here $a(T) > 0$ is the actual frequency-scaling factor. The rescaled matrix N_T includes the true axial multiplier.

Two T derivatives apply $R\partial_R$ to SOURCE coefficients, not to the unknown or stress. Their multiplier bounds and $O(R^{-2-2h})$ tails remain uniform by the fixed source jets.

Projector differentiation produces $k^b\partial_k^b P$. After j additional k derivatives, $C|\xi_h|^{-j}$ bounds each term, because $|k|/(|\xi_h|^2 + k^2)^{1/2} \le 1$.

Thus

$$\partial_T^\ell \partial_k^j A_T : H^8_{w+j} \longrightarrow H^8_w, \qquad \ell, j \le 2,$$

without loss of radial Sobolev order. The actual stress supplies its H^9_6 observation jets.

We do not replace these with unprovided radial jets of $U_T^{-1}\mathsf{S}$.

For one full complementary contour across the compact observation interval use $\widetilde{B}_T = A_T - \lambda_{\mathrm{obs}}(T,k)I$. It differs from the stabilized B_T in the macro construction by the finite-rank $-d\Pi_T$ term, but their kernels after Q_T are identical.

Its selected pole is zero. After a decrease of c, its full unweighted complement lies to the left of $-4c$ with one strict gap. Select a fixed rectangle Γ_B around that complement with right edge $-2c$.

Put its other edges beyond all uniform operator bounds. Take $c < \min \Re\lambda_{\mathrm{obs}}/4$ and those edges sufficiently far that

$$|z + \lambda_{\mathrm{obs}}(T,k)| \ge c_0 > 0, \qquad z \in \Gamma_B.$$

The weighted core/tail proof applies with physical parameter $z + \lambda_{\mathrm{obs}}$.

It does not presume radial decay of the scalar shift. It also rules out additional weighted right spectrum on this family.

Resolvent derivatives use $\partial\widetilde{B}_T = \partial A_T - \partial\lambda_{\mathrm{obs}} I$. The identity terms cost no moments.

The pole contour supplies the related selected projection jets. Dunford on Γ_B proves (3.7.13).

The polynomial displayed there is a safe bound. The same fixed-chart pressure and Hodge equations apply to these T derivatives.

This is stronger than the weaker argument that two radial dilations of an output would leave only H^6_2.

Last all radial operators act on H^{10}_Y-valued data with the same bounds and commute with the fixed auxiliary-origin derivatives. Pointwise origin evaluation uses the different two-dimensional Sobolev loss.

This argument uses the actual complementary spectral gap and source tails. It is not a proof of a missing spectral winner or of a later nonlinear conclusion.

□

Lemma 3.7.5 (Exact sector exclusion and phase-gradient separation)**.** *Let α be an active source label and $j \in \mathbb{Z} \setminus \{0\}$ a relative harmonic. Write $n_\alpha = k_\ell p$. The estimates apply in particular to the finite set $|j| \le j_{\max}$ retained in Lemma 3.7.7.*

(a) For $\epsilon, \epsilon' \in \{+1, -1\}$, $\epsilon m + j n_\alpha \ne \epsilon' m$. Thus each nonzero relative carrier of a column whose low input lies in the sectors $\pm m$ has angular label outside $\{m, -m\}$.

(b) On the active label's portion of the fixed radial hull put $\mathfrak{s} = \sqrt{Q_\ell}$ and $\rho_\ell = Q_\ell^h$. The physical phase satisfies

$$|\nabla_{\mathrm{phys}}(j k_\ell \Phi_\alpha)| \;\ge\; c_n |j| k_\ell \,\mathfrak{s}^{-1} \;\ge\; c_n |j| \rho_\ell^{-1/2}\,\mathfrak{s}^{-1}.$$

On the prepared observation support $t/Q_\ell \in [c_-, c_+] \Subset (0,\infty)$, this gives the same lower bound with $\rho = t^h$ and a fixed comparison constant.

Proof. (a) The equality would force $jn_\alpha \in \{0, 2m, -2m\}$.

The first is excluded since $j \neq 0 \neq n_\alpha$.

The bound $|jn_\alpha| \geq |n_\alpha| \geq 2m+1$ excludes the other two values.

(b) Theorem 2(vii) gives $n = \sqrt{Q_\ell}\nabla_{\mathrm{phys}}\Phi_\alpha$, $|n| \geq c_n$, and $k_\ell = \lceil \rho_\ell^{-1/2} \rceil$. In each prepared carrier the right-ordered differential words act on a left-quantized scalar mask whose output has $|Z| = O(r)$ at mask radius r, by its kernel formula. Thus $Z = z/t^{1/2-h}$ is bounded there. The ratio $u = q/t \geq 1$ satisfies $u - Z^2u^{2h} = 1$, so u is bounded above since $2h < 1$. Active source bands have $Q_\ell \asymp \widetilde{q} \asymp q$. Hence $Q_\ell \asymp t$ on this chart and $\rho_\ell \asymp t^h$ there.

□

Lemma 3.7.6 (High-carrier duality for an operator column)**.** *On the prepared observation support of Lemma 3.7.5(b), put $\rho = t^h$ and let $X = e^{i\Psi}Af$, where $\Psi = jk_\ell\Phi_\alpha$ satisfies Lemma 3.7.5(b). Suppose*

$$\|Af\|_2 \leq P(S)\|f\|_2, \qquad \|\mathfrak{s}\nabla_{\mathrm{phys}}(Af)\|_2 \leq \rho^{-b}P(S)\|f\|_2, \qquad b < \alpha < 1/2.$$

If ϕ is a transported low test field and $w \in L^2$ satisfy $\|\phi\|_2 \leq \|w\|_2$ and $\|\mathfrak{s}\nabla_{\mathrm{phys}}\phi\|_2 \leq e^{cL}\rho^{-\alpha}\|w\|_2$ (for instance $\phi = L_\theta w$), and if $\varkappa \leq b$, then

$$|\langle X, \phi\rangle| \leq CP(S)(e^{cL}\rho^{1/2-\alpha} + \rho^{1/2-b})\|f\|_2\|w\|_2.$$

The constant is uniform over the fixed finite relative harmonics.

Proof. Put $\mathbf{e} = \nabla\Psi/|\nabla\Psi|^2$. The phase bounds give $|\mathbf{e}| \leq C\mathfrak{s}/(|j|k_\ell)$ and the related first coefficient derivative bound $C\rho^{-\varkappa}P(S)/(|j|k_\ell)$; the factor $\rho^{-\varkappa}$ is the cost of one evaluated radial derivative of the phase (Theorem 2(vii)).

Integration by parts, with the smooth zero extension at the hull, gives

$$|\langle e^{i\Psi}Af, \phi\rangle| \leq \frac{C}{|j|k_\ell}\left[(e^{cL}\rho^{-\alpha} + \rho^{-\varkappa}P(S))\|Af\|_2 + \|\mathfrak{s}\nabla_{\mathrm{phys}}(Af)\|_2\right]\|w\|_2.$$

Insert the two column bounds and $k_\ell \asymp \rho^{-1/2}$. □

Lemma 3.7.7 (Finite prepared column for the selected source)**.** *Fix the completed $p = 6/5$ source B_*, its selected simple $\pm m$ spectral pair, and the fixed finite source prefix and same label cover. Select the source jets and completed tail accuracy before decreasing the ancient-time threshold. The selected branch is centered at the pole, $\lambda_Z = \lambda_k = \lambda_{Zk} = 0$ (the centered complex phase data in Theorem 2(iv), used in (3.10.2)). This is used for the solvability $\ell A_1 e = 0$ of the first homological equation and for the absence of a $\lambda_{Zk}Zk$ term in B_2.*

Put $\varkappa = 10^{-5}$, $\theta = 2/5$, $\gamma = \theta - 128\varkappa = .39872$, $\nu = 1 - 128\varkappa = .99872$, and $p_0 = 3\gamma = 1.19616$. Let $k = -i\rho\partial_Z$, $\delta = \rho^\theta$, and let C_δ be the same shrinking phase mask on each scalar column.

There is a single global, real, solenoidal right-ordered column J_p and one scalar band operator

$$B_{\mathrm{band}} = \lambda_0 + B_2 + b_0(s), \qquad B_2 = \tfrac{1}{2}\lambda_{ZZ}Z^2 + i(\tfrac{1}{2} - h)Zk + \tfrac{1}{2}\lambda_{kk}k^2 + \rho c_0, \quad c_0 = c_1(0,0).$$

The products are left ordered. On the same smooth core, with A_* the full projected physical generator of this B_*,

$$\|(A_*J_p - \partial_s J_p - J_pB_{\mathrm{band}})C_\delta\|_{2\to L^2_{\mathrm{can}}} \leq C\rho^{p_0}P(S). \tag{3.7.27}$$

More precisely, for each radius r between δ and $r_{\mathrm{out}} = S_{\mathrm{mask}}^{-M}$, let C_r be a fixed-shape phase mask and put $a_\rho = \rho^{1/2-128\varkappa}$. With $R_p = A_*J_p - \partial_s J_p - J_pB_{\mathrm{band}}$ and the actual physical band row K, let Π_{zero} be the orthogonal projection onto the selected physical angular pair.

The full carrier-zero residual, with its radial complement, and the selected row obey

$$\|\Pi_{\mathrm{zero}} R_p C_r\| + \|K R_p C_r\| \le C(r^3 + \rho r + \rho^2) + P(S)\left[\rho^\nu r + \rho^{\nu+1/2-128\varkappa} + a_\rho (r + a_\rho)^2 + \rho^2\right], \tag{3.7.28}$$

$$\|(R_p)_{\mathrm{high}} C_r\| \le P(S)\left[(r + a_\rho)^3 + \rho^\nu (r + a_\rho)\right].$$

The leading radial profiles fix the first constant, and it does not grow with S. With the pole normalization (N_e) of Lemma 3.7.9, its retained m and $-m$ low column differs from the fixed physical reference column J_{ref} of Lemma 3.6.3 by

$$\|(\Pi_{\mathrm{zero}} J_p - J_{\mathrm{ref}}) C_r\|_{2 \to L^2_{\mathrm{can}}} \le C_T (r + \rho^{3/5}) + P(S)\rho^\nu, \qquad \delta \le r \le r_{\mathrm{out}}, \tag{3.7.29}$$

where C_T depends only on the leading profiles, their first correctors and the mask shape. After C_δ this is $O(\delta + \rho^\nu P(S))$. Lemma 3.7.9 proves (3.7.29). Remark 3.7.10 distinguishes this weaker comparison from the cubic primitive residual; no later step uses a stronger comparison.

Each nonzero-carrier output has angular label outside $\{m, -m\}$ and physical phase gradient bounded below as in Lemma 3.7.5(b) on its fixed radial hull. These assertions include each axial input admitted by C_δ.

They are operator bounds, not bounds on one Gaussian.

Proof. We give the cell equations and the power calculation.

The low physical velocity/pressure pair is (3.7.2)–(3.7.4). In particular its exact divergence chart acts on the horizontal Taylor pullback (3.7.3), not on the physical eigenvector Taylor polynomial itself. Lemma 3.7.1 cancels the full primitive Taylor equations through degree two and the constant subprincipal coefficient, with $c_0 = c_1(0,0)$. Its unremoved low residual on C_δ is $O(\delta^3 + \rho\delta + \rho^2)$, with a fixed leading constant. We keep all cutoff derivatives on the far right.

Every cell below, its accumulated pressure, the full matching tensor, the macro response, and the scalar b_0 are formed anew from this pair. They are not retained from a column with a different divergence chart. The degree-three word list, native H^{16}_5 bound, and number of cell steps are unchanged, so the finite gain and derivative counts below apply to these corrected inputs.

Canonical and source-box units. On the source box Q_j put $T = t/Q_j$, $d = 1/2 - h$, $c(T) = T^{-1-h}$ and $\rho_j = Q_j^h$. For the canonical axial input and velocity respectively the maps into this box are

$$D_T a(\mathsf{Z}) = a(\mathsf{Z}/T^d), \qquad U^{\mathrm{vel}}_T v(\mathsf{y}, \mathsf{Z}) = T^{-1/2-h} v(\mathsf{y}/\sqrt{T}, \mathsf{Z}/T^d).$$

Thus a velocity column J has box representative $J^{\mathrm{box}} = U^{\mathrm{vel}}_T J D_T^{-1}$. A canonical generator residual F has box representative $F^{\mathrm{box}} = c(T) U^{\mathrm{vel}}_T F D_T^{-1}$, since $Q_j^{1+h}\partial_t = c(T)\partial_s$ on physical samples. For pressure the amplitude factor is T^{-1-2h} with the same arguments: its box gradient is exactly $c(T) U^{\mathrm{vel}}_T \nabla_\rho \pi$. These residual conventions include the derivatives of the coordinate maps on both sides of a column. In box time they enter through $\rho_j \partial_T$; the spatial arguments give the usual radial and axial dilations. In particular $D_T Z D_T^{-1} = T^{-d}\mathsf{Z}$ and $D_T k D_T^{-1} = T^{1/2}(-i\rho_j \partial_{\mathsf{Z}})$. All scalar factors and their fixed slow derivatives are bounded on the observation interval. The radial dilations are exactly the observation derivatives counted in (3.7.6).

In the cell ODE, f_j and $V = J^{\mathrm{box}}_{\mathrm{low}}$ are already in box units. Equivalently, to apply $\mathcal{C}_{\mathrm{gen}}$ to any canonical high residual, first take F^{box} above, solve in the box, and pull the velocity back by $(U^{\mathrm{vel}}_T)^{-1}$ on the left and D_T on the right, with the corresponding pressure pullback.

In particular the derivative of the mask with respect to time is an annular $O(\rho)$ term, not discarded.

Write a high column as a finite sum of right-ordered $c_{ab}(R,Z,T,Y)Z^a k^b$, multiplied by the original source carrier phases. Let X_σ be a primary source coefficient with sign $\sigma = \pm 1$.

The first coefficient source is the actual signed fast derivative $f_{0,\sigma} = -i\sigma K(V\cdot n)X_\sigma$, $V = J_{\mathrm{low}}$, with the fixed angular Doppler imF_b. The minus sign comes from $-V\cdot\nabla B_*$ in the true-velocity generator (3.4.9): $-V\cdot\nabla(X_\sigma e^{i\sigma K\Phi}) = -i\sigma K(V\cdot n)X_\sigma e^{i\sigma K\Phi}$ at principal fast order.

The pressure applies the tangential projection P_n without a reversal of this sign.

It agrees with the raw velocity-pressure residual extraction defined below. The cell source in the displayed ODE is $+B_f^\ell P_n f_j$.

Thus, for the generator residual $\mathcal{E} = M - \partial_v$, the equation $z' = Mz + f$ gives $\mathcal{E}z = -f$, which cancels the residual. For each nonzero relative carrier j, solve the shifted principal normal-plane equation

$$z_j' = [\mathrm{diag}(\lambda,-\lambda) + E_f - j^2 d_p I - (\Lambda_{\mathrm{ref}} + imF_b)I]z_j + B_f^\ell P_n f_j, \quad z_j(0) = 0, \qquad t_j = B_f z_j,$$

where $P_n = I - n\otimes n/|n|^2$. The cell shift is

$$\Lambda_{\mathrm{ref}}(\mathsf{T}) = \lambda_0 \mathsf{T}^{-1-h}, \qquad \mathsf{T} = t/Q_\alpha.$$

Here λ_0 is the complex physical pole of B_{band}. The cell ODE holds T fixed. On the observation support $\mathsf{T}\in[c_-,c_+]\subset(0,\infty)$, so $\Re\Lambda_{\mathrm{ref}} \ge \lambda_* := \lambda_c c_+^{-1-h} > 0$. For $v \ge w$ and every fixed $a \ge 0$,

$$\left|\partial_{\mathsf{T}}^a e^{-(v-w)\Lambda_{\mathrm{ref}}(\mathsf{T})}\right| \le C_a(1+v-w)^a e^{-\lambda_*(v-w)}.$$

Thus slow derivatives of this factor have an integrable bound uniform in the pulse length. After physical sampling the additional derivative $\rho_\alpha\partial_{\mathsf{T}}$ acts on the entire cell output, as in the gain table below.

The primitive pressure is

$$\pi_j = \frac{i}{Kj|n|^2}[n\cdot K_b t_j - (\partial_v n)\cdot t_j - n\cdot f_j].$$

This pressure uses the same signed f_j as the cell ODE. We take the normal row of the principal momentum equation and differentiate $n\cdot t_j = 0$. This gives

$$-(\partial_v n)\cdot t_j + n\cdot K_b t_j + ijK|n|^2\pi_j = +n\cdot f_j.$$

The scalar shift and diffusion multiples of t_j vanish in this row.

We solve it to find the displayed pressure formula. The projected equation has source $+P_n f_j$.

The normal equation has source $+n\cdot f_j$. Thus with the negative leading residual above, the velocity and pressure coefficients cancel that residual at first fast order.

Thus t_j and π_j solve the full principal momentum and normal equations, with pressure. If V_j is the unshifted fundamental matrix of Theorem 2(vii), the shifted propagator is

$$e^{-\int_w^v(\Lambda_{\mathrm{ref}}+imF_b)\,d\eta}V_j(v,w).$$

Its norm is at most $CP(v)P(w)^{-1}e^{-\lambda_*(v-w)}$.

Duhamel thus bounds each fixed coefficient, parameter, and auxiliary-origin derivative by its source envelope times $P(S)$. Differentiation of this equation and induction gives the same bound for the finite mixed jets.

The shifted normal $n + me_\vartheta/(KjR)$ differs by $O_m(\rho^{1/2}P(S))$. We keep its differentiated frame, constraint and pressure terms in the residual. The exact physical velocity is the full curl of

$$\frac{i\,n \times t_j}{jK|n|^2} e^{ijK\Phi + im\vartheta};$$

in each step we use the full curl, not its tangent leading term.

Denote this coefficientwise cell operation by $\mathcal{C}_{\mathrm{gen}}(f)$. It is the shifted principal inverse of Theorem 2(vii) applied to $-f$, with its pressure, and thus cancels the generator residual f.

In this section write $\mathcal{C} = \mathcal{C}_{\mathrm{gen}}$.

Keep an accumulated primitive pressure column Π, with its right-input derivatives. With F_* the unprojected velocity generator, define

$$\mathcal{R}_0(H, \Pi) = F_* H - \partial_s H - H(\lambda_0 + B_2) - \nabla\Pi, \qquad \mathcal{E}_0(H) = \mathbb{P}\mathcal{R}_0(H, \Pi).$$

The second identity uses exact solenoidality.

Keep the exact tagged expression-tree decomposition $\mathcal{R}_i = L_i + H_i + F_i$. Here L_i is the retained zero-carrier part.

The term H_i is the retained Gaussian-weighted nonzero-carrier source. The term F_i is the declared output-flat endpoint/deletion/localization remainder.

Let $\mathsf{H}_{\mathrm{raw}}$ extract only H_i, and exclude the output-flat remainder.

It is a selection of retained raw coefficient terms, not a claim that each small physical residual is a small weighted cell input. We extract cell coefficients before the global Leray projection.

The pressure projection keeps angular sectors but does not keep the compact support of a label. We start with the actual Taylor pressure $(J^{[0]}, \Pi^{[0]}) = (J_{\mathrm{low}}, \Pi_{\mathrm{low}})$, define for $i = 0, 1, 2$

$$f_i = \mathsf{H}_{\mathrm{raw}}\mathcal{R}_0(J^{[i]}, \Pi^{[i]}), \quad (\mathcal{B}_i, \pi_i) = \mathcal{C}^{\mathrm{pair}}_{\mathrm{gen}}(f_i), \quad J^{[i+1]} = J^{[i]} + \mathcal{B}_i, \quad \Pi^{[i+1]} = \Pi^{[i]} + \pi_i,$$

where $\mathcal{B}_0 = B_0, \mathcal{B}_1 = B_1, \mathcal{B}_2 = B_{2,\mathrm{high}}$.

The scalar quadratic operator remains B_2.

The full-curl velocity/primitive-pressure cell has the exact identity

$$\begin{aligned} \mathcal{R}_0(\mathcal{B}_i, \pi_i) &= -H_i + \mathcal{D}_i^{\mathrm{high}} + \mathcal{D}_i^{\mathrm{zero}} + F_{\mathrm{cell},i}, \\ H_{i+1} = \mathcal{D}_i^{\mathrm{high}}, &\quad L_{i+1} = L_i + \mathcal{D}_i^{\mathrm{zero}}, \quad F_{i+1} = F_i + F_{\mathrm{cell},i}. \end{aligned}$$

We perform the finite gain calculation on the retained $\mathcal{D}_i^{\mathrm{high}}$ before projection. We estimate the F_i remainder separately in the simultaneous right-masked $L^2 \to H^1$ output norms of Lemma 3.9.4.

We do not apply another inverse to it in a Gaussian-weighted input norm. That operation could remove its exponential endpoint smallness.

We project only the last physical residual norm. We project raw carrier-zero tensor rows separately for the macro response, with its genuine noncompact pressure. We use the same stored velocity/pressure-pair convention for all re-excitation, feedback and time-partition cells below.

Each f_i is the full new coefficient source. We do not omit any favorable term when we freeze the scalar input.

The cell shift remains Λ_{ref} throughout. It is the conversion of the s-time scalar λ_0 to pulse time:

$$\partial_s + \lambda_0 = (t/Q_\alpha)^{1+h}\big[\partial_v + \Lambda_{\mathrm{ref}} + \rho_\alpha \partial_{\mathsf{T}}\big],$$

by $\partial_s = t^{1+h}\partial_t$ and $Q_\alpha^{1+h}\partial_t = \partial_v + \rho_\alpha\partial_{\mathsf{T}}$. This is the combination $-(\partial_s + \lambda_0)$ that occurs in $\mathcal{R}_0$; it produces the damping $-\Lambda_{\mathrm{ref}} I$ of the cell ODE, with $\Re\Lambda_{\mathrm{ref}} \geq \lambda_* > 0$. The last term is the row

"$\rho\partial_T$ of coefficients" of the gain table. Any other shift Λ' leaves the residual $(\Lambda_{\mathrm{ref}}-\Lambda')t_j$, of relative order $|\Lambda_{\mathrm{ref}}-\Lambda'|$.

For $\Lambda'=\lambda_0$ this order is one, because t/Q_α lies in a fixed compact interval and not in a shrinking neighborhood of one. Thus only Λ_{ref}, up to an $O(r+a_\rho)$ change, is compatible with the gain table and with p_0. No uniform claim is made for endpoint boxes with $t/Q_\alpha\to 0$. The pole λ_0 is complex, not replaced by its real part or by μ_D.

The canonical scalar operator keeps λ_0.

Thus the cell inverse hides no derivative of the next feedback b_0.

The coefficient norm. We define the norm that the raw step gain (3.7.30) uses. Fix the source label, its pulse interval $[0,L_p]$ and the Gaussian envelope $P(v)$ from Theorem 2(vii). Fix also these data:

- the compact observation box $\mathfrak{B}$ in (R,Z,T,Y) and the mask radius r;
- finite carrier and word sets $J\subset\mathbb{Z}\setminus\{0\}$ and $\Gamma\subset\mathbb{N}^2$;
- the representative data and rounded phase constants of this label;
- the slow input weight $\omega=\mathsf{W}^{1/4}$ on charts carrying a weighted input and $\omega=1$ on unweighted inputs.

A tagged formal right-ordered column is an exact tagged expression

$$\mathsf{h}=\sum_{j\in J}\sum_{(a,b)\in\Gamma} c^{j}_{ab}(v;R,Z,T,Y)\,Z^a k^b\,e^{ijK\Phi+im_j\vartheta}.$$

For $N\in\mathbb{N}$ we put

$$\|\mathsf{h}\|_{N,r}:=\max_{j\in J}\ \max_{(a,b)\in\Gamma}\ \max_{|I|\le N}\ \sup_{v\in[0,L_p],\,\mathfrak{B}}\ \frac{r^{a+b}\,|\partial^I c^{j}_{ab}|}{P(v)\,\omega}.$$

As in Theorem 2(vii), ∂^I denotes ordinary coefficient derivatives in (v,R,Z,T,Y) with the label, its representative data and its rounded carrier fixed. On a weighted chart the supremum is over $\mathsf{W}>0$. Equivalently the numerator is bounded pointwise by a constant times $P(v)\omega$, with the weighted coefficient jets extended by zero on the zero set. For each fixed D,

$$\sup_{0<w\le e^{-2}} w^{1/4}(1+\log(1/w))^{D}<\infty.$$

Thus both $\sqrt{\mathsf{W}}\mathcal{L}^D_W$ and $\mathsf{W}\mathcal{L}^D_W$ in Theorem 2(vii) are bounded by $C_D\omega$ for every derivative order used here. The derivatives in the norm act on the coefficient. At fixed slow variables W is independent of the auxiliary pulse variable v, so the same ω factors out of the Duhamel integral in (N5). On a region where $\mathsf{W}\le e^{-A}$, it retains the bound $\omega\le e^{-A/4}$. Here $P(v)$ is the pulse envelope and $P(S)$ denotes a polynomial loss. "Order ρ^a" means $\|\mathsf{h}\|_{N,r}\le C_N\rho^a P(S)$.

The norm of $\mathsf{H}_{\mathrm{raw}}\mathcal{D}$ is the norm of the sub-sum with the tag H. For $\rho\le\rho_0$, $\delta\le r\le r_{\mathrm{out}}$ and fixed finite index sets, the norm has these properties:

(N1) $\|\mathsf{h}C_r\|_{2\to L^2}(v)\le C_\Gamma\,P(v)\sup\omega\,\|\mathsf{h}\|_{0,r}$;

(N2) if $|\partial^I g|\le M_I P(S)$ for $|I|\le N$, then $\|g\mathsf{h}\|_{N,r}\le C_N M_N P(S)\|\mathsf{h}\|_{N,r}$;

(N3) $\|\mathsf{h}k\|_{N,r}\le r\|\mathsf{h}\|_{N,r}$ and $\|\mathsf{h}Z\|_{N,r}\le(r+C_\Gamma\rho/r)\|\mathsf{h}\|_{N,r}$, with $\rho/r\le\rho^{3/5}\le a_\rho$;

(N4) $\|k\mathsf{h}\|_{N-1,r} \le (r+\rho+C_\Gamma\rho/r)\|\mathsf{h}\|_{N,r}$;

(N5) for the shifted zero-data cell $\mathcal{C}_{\mathrm{gen}}$ with the cell shift Λ_{ref}, the velocity has $\|t\|_{N,r} \le C_N P(S)\|f\|_{N,r}$ and the pressure has $\|\pi\|_{N,r} \le C_N P(S)\rho^{1/2}\|f\|_{N,r}$;

(N6) For pointwise products of amplitudes, multiply the coefficients and add their carrier labels and word degrees. Denote this product of tagged expressions by $\mathsf{h}_1 \odot \mathsf{h}_2$. Then $\|\mathsf{h}_1 \odot \mathsf{h}_2\|_{N,r} \le C_N\|\mathsf{h}_1\|_{N,r}\|\mathsf{h}_2\|_{N,r}$, where C_N depends on the fixed index sets and on $\sup\omega$.

Item (N1) follows from $\|cZ^a k^b C_r\| \le \sup|c|\, C_{ab} r^{a+b}$. Items (N2)–(N4) act on the amplitude and its right word after the carrier phase is factored out. A derivative of the carrier gives its explicit phase-gradient term in the cell equation. On the amplitude, $[k,Z] = -i\rho$ and $[k,c] = -i\rho c_Z$ give $Z^a k^b Z = Z^{a+1}k^b - ib\rho Z^a k^{b-1}$ and $k(cZ^a k^b) = cZ^a k^{b+1} - i\rho(c_Z Z^a + acZ^{a-1})k^b$, which uses one derivative of c. Item (N5) follows from Duhamel's formula: since F_b is real and $\Re\Lambda_{\mathrm{ref}} \ge \lambda_*$, Theorem 2(vii) gives $\|e^{-\int_w^v(\Lambda_{\mathrm{ref}}+imF_b)}V_j(v,w)\| \le CP(v)P(w)^{-1}e^{-\lambda_*(v-w)}$ for $j \ne 0$, hence the zero-data cell velocity satisfies $|t(v)| \le C\lambda_*^{-1}P(v)\sup(|f|/P)$; parameter derivatives of t satisfy the same zero-data equation, with sources $\partial^J f$ plus the terms $(\partial^{J'}\mathcal{A})\partial^{J-J'}t$, $J' \ne 0$, from the coefficient matrix $\mathcal{A}$ of the cell equation, and induction gives the $P(S)$ losses; the pressure carries the factor $(Kj|n|^2)^{-1} = O(\rho^{1/2})$. Item (N6) follows from Leibniz's rule, $P(v)^2 \le P(v)$, and $r^{a+b}r^{a'+b'} = r^{a+a'+b+b'}$. In the interaction of a source wave with a column, only the column carries an input word. When an operator differentiates another coefficient, (N3)–(N4) account for the derivative and its cost.

Finite unprojected gain, with all base interactions. Use the accumulated velocity/pressure pair and the declared retained unprojected decomposition above. Let the incoming coefficient have order ρ^a, let $K \asymp \rho^{-1/2}$, and let $\delta \le r \le r_{\mathrm{out}} < 1$ be the right-mask radius.

The shifted zero-data inverse gives its principal velocity coefficient t at order a and its pressure π at order $a+1/2$. Each entry in the next table is a factor relative to the incoming coefficient norm.

We suppress a fixed polynomial $P(S)$. The derivative list is enlarged before the ancient threshold is decreased.

Actual row in the linear identity	Relative factor
Time derivative and principal matrix on the coefficient curl	$\rho^{1/2-\varkappa}$
$(K_{\mathrm{full}} - K_b)t$ and $\rho\partial_T$ of coefficients	ρ
Radial transport bD_R, with $b = O(\rho)$	$\rho^{1-\varkappa}$
$G_b\rho\partial_Z$ on coefficients. $G_b k$ on the right input	ρ. r
Phase defect $ijK\mathcal{E}_\Phi$, $\mathcal{E}_\Phi = O(\rho P(S))$	$\rho^{1/2}$
First viscous cross $-i\rho jKD_\Phi$	$\rho^{1/2-\varkappa}$
Coefficient viscosity $-\rho D_0$	$\rho^{1-2\varkappa}$
Coefficient primitive-pressure gradient	$\rho^{1/2-\varkappa}$
Axial input derivative in pressure or curl	$K^{-1}k = O(\rho^{1/2}r)$
First and second axial-input viscous rows	$\rho Kk = O(\rho^{1/2}r)$. ρr^2
Finite angular normal/frame/curl corrections	$O_m(K^{-1})$
Right B_2 action	$r^2 + \rho$
Normal ordering across an input word or a coefficient	$O_\Gamma(\rho/r)$ on a word; $O(\rho)$ on a coefficient

The last row follows from (N3)–(N4). A commutation $[k, Z^a] = -ia\rho Z^{a-1}$ removes one factor of weight r from the existing word. The relative factor is $O_\Gamma(\rho/r)$, whereas $[k, c] = -i\rho c_Z$ keeps the word degree and uses one coefficient jet. Since $r \ge \rho^{2/5}$, $\rho/r \le \rho^{3/5} \le a_\rho$. A right quadratic costs $O_\Gamma((r+\rho/r)^2) = O_\Gamma(r^2+\rho)$ because $\rho \le r^2$. These bounds give the $r + a_\rho$ step gain. The order-one angular Doppler imF_b is in the principal cell ODE.

The operators D_Φ, D_0 keep the cylindrical phase and vector-Laplacian connections, with $-R^{-2}\,\mathrm{diag}(1,1,0)$. The full curl also keeps the normal shifts $me_\vartheta/(jKR)$ and $ke_z/(jK)$.

For the base interactions use the two ordered products in the exact bilinear identity in Theorem 2(vii). A full primary wave X has order $1/2$, but only its principal coefficient is tangent.

For a full cell Y of order a,

$$n \cdot X = O(\rho^{1-\varkappa} P(S)), \qquad n \cdot Y = O(\rho^{a+1/2-\varkappa} P(S)).$$

Thus the fast terms $K[(X\cdot n)Y + (Y\cdot n)X]$ have order at least $a + 1/2 - \varkappa$. The coefficient transports and cylindrical connections have the same or better gain.

Higher finite source waves have order $1 - 3\varkappa$, so even the crude cost K leaves gain $1/2 - 3\varkappa$. Tangential means have order $1 - \varkappa$ and radial means order two.

Their worst gain is $1/2 - \varkappa$. We include means regardless of their auxiliary support.

Cross-label high products vanish where their actual enlarged high supports are disjoint. For the low input, take $J = J_{\mathrm{low}} C_r$ in (3.7.2). Its finite right-word expansion through degree three and weighted radial profiles give $\|J\|_{2\to H^1_*} \le CP(S)$: a normalized axial derivative adds one right k or the factor $-i\rho a Z^{a-1}$, and a horizontal derivative acts on a fixed radial profile. All these word norms are bounded by Lemma 3.7.13. The global slow estimate in clause (vii) of the completion, exact solenoidality and the L^2 contraction of the Leray projector give

$$\|\mathbb{P}\,\mathrm{div}_\rho(V_s \otimes J + J \otimes V_s)\|_{2\to L^2_{\mathrm{can}}} \le C(\|V_s\|_\infty \|\nabla_* J\|_{2\to 2} + \|\nabla_* V_s\|_\infty \|J\|_{2\to 2}) \le C\rho^2 P(S).$$

The estimate includes the entire radial tail of J. For a finite differentiated carrier with total loss at most $\rho^{-1/2-128\varkappa}$, the same product costs at most $\rho^{3/2-128\varkappa} P(S)$; $3/2 - 128\varkappa = 1.49872 > 1.19616$. Each occurrence in the high rows keeps its own coefficient and phase estimates. This accounts for the slow discrepancy once.

The principal inverse contains the actual slow background. We keep the completed localization remainder in its simultaneous physical output norms. We do not reclassify it as a finite harmonic input.

Thus, with $a_\rho = \rho^{1/2-128\varkappa}$ and the coefficient norm $\|\cdot\|_{N,r}$ defined above, the retained high part of the actual cell remainder satisfies

$$\|\mathsf{H}_{\mathrm{raw}} \mathcal{D}(h)\|_{N-n_*,r} \le P(S)(r + a_\rho)\|h\|_{N,r}. \tag{3.7.30}$$

Here $n_* \le 3$ is the derivative cost of one row of the gain table: two viscous derivatives and one commutator. Each row factor is at most $r + a_\rho$ for $\rho \le 10^{-1}$ and $\rho^{2/5} \le r < 1$. The three steps use $3n_* \le 9$ of the $J_{\mathrm{prep}} = 72$ reserved derivatives. All generated relative harmonics are retained in this finite list. High-high products keep the Gaussian envelope because $P^2 \le P$.

Mean-high products and the shifted inverse keep it as well. The three exact recurrence steps give the high factor $(r + a_\rho)^3$.

We accumulate primitive pressures at each step. Application of the global Leray projection only at the last norm estimate keeps the physical identity.

We use no compact support of a Leray-projected coefficient.

The different output remainder F_i contains the actual endpoint term $(1-\psi)h-\psi' t$, aggregate-deletion terms, and completed tails. An exponentially small physical endpoint term need not be small after division by the Gaussian input weight.

Thus we do not feed it into (3.7.30). On the prepared comparable-time charts, $S \asymp |\log \rho|^{6/5}$ makes these endpoint outputs smaller than each fixed requested power after the finite physical derivatives.

Lemma 3.9.4 supplies the simultaneous output norms.

Why the principal opposite-carrier tensor vanishes. The primary real cosine has $X_+ = X_- = X$. Its signed principal source is $f_{0,\sigma} = -i\sigma K(V\cdot n)X$.

The homogeneous matrix in its zero-data cell equation depends on σ only through σ^2, with the same fixed complex shift. Thus $z_- = -z_+$ by uniqueness of the linear ODE, and the principal velocity response obeys $(B_0)_- = -(B_0)_+$.

Right $G_b k$, right B_2, and ordinary coefficient/time derivatives are sign-independent linear operations. They keep this oddness, as does another inverse with that same homogeneous matrix and zero initial data.

Their B_1 rows thus satisfy

$$X\otimes(-B_1) + X\otimes B_1 + (-B_1)\otimes X + B_1\otimes X = 0.$$

This is an identity of the complete symmetric tensor for each right-input word, before divergence, radial differentiation or Leray projection. It does not require real-valued B_1.

Terms with $1/(jK)$, signed curl/pressure/viscous-cross factors or shifted normals do not appear in this zero identity. They have the additional half-order gain in the previous table and remain in the full matching stress.

Higher source harmonics have no assumed parity.

The remaining carrier-zero stress has order $\rho^{\nu}P(S)$. The $B_{2,\mathrm{high}}$ return is $\rho^{1/2+2\gamma-\varkappa}$, above order one.

We impose the cancellation on the full symmetric tensor before application of physical divergence or Leray projection. On a radius-r right mask, each explicit Z or k factor costs r.

A fixed-geometry curl, normal, or pressure correction costs at most the stated a_ρ.

The previous three cell equations thus give the high $(r+a_\rho)^3$ row of (3.7.28). The even matching return from $B_{2,\mathrm{high}}$ has one primary a_ρ factor and two remaining cell factors. This gives $a_\rho(r+a_\rho)^2$ in the low row.

All columns in the next macro calculation are the generator-canceling columns just constructed. We put

$$J^{[2]} = J_{\mathrm{low}} + B_0 + B_1,$$
$$F_{\mathrm{mac},0} = -\operatorname{div}_h(\mathsf{S}_{\mathrm{match}}[J^{[2]}] + \mathsf{S}_{\mathrm{mean}}), \qquad f_{\mathrm{mac}} = P_0 F_{\mathrm{mac},0}.$$

Here the tensors are formed from the box representatives of the source velocity and of $J^{[2]}$, so f_{mac} is in source-box units. To extract the scalar, let U_T be the radial restriction of U_T^{vel} at the center and put $\ell_T = \ell_0 U_T^{-1}$. For the degree-zero word evaluate the complete force at $Z=0$ and at the physical auxiliary sample, including its radial shear. Denote this radial vector by $f^{(0)}_{\mathrm{mac},j}$. The local canonical coefficient and its global time partition are

$$b_{0,j}(s) = c(T)^{-1}\ell_T f^{(0)}_{\mathrm{mac},j}, \qquad b_0(s) = \sum_j \omega_j(s) b_{0,j}(s).$$

Indeed the selected box projection is $U_T e_0 \ell_T$, so its center value is $(U_T e_0) c(T) b_{0,j}$. The complementary box equation below uses $Q_c f_{\mathrm{mac}}$ in the same units. Pairing is after physical sampling: equivalently apply ℓ_T to the sheared radial force at each fixed temporal torus origin, then evaluate that origin. Here $\mathsf{S}_{\mathrm{match}}$ is the full carrier-zero matching tensor we recompute from these columns and the full retained source carrier coefficient $Z_{\alpha,j} = X_{\alpha,j} + H_{\alpha,j}$:

$$\mathsf{S}_{\mathrm{match}} = \sum_{\alpha, j \neq 0} (Z_{\alpha,j} \otimes Y_{\alpha,-j} + Y_{\alpha,-j} \otimes Z_{\alpha,j}).$$

Here α includes the pulse-direction label, but j is the complex carrier harmonic. We do not identify their indices.

We keep Haar and non-Haar auxiliary components of the zero-angular-carrier mean. In particular we do not fold the leading Taylor defect into this tensor.

We include the direct carrier-zero tangential mean explicitly:

$$\mathsf{S}_{\mathrm{mean}} = (u_{\mathrm{M}} - u_{\mathrm{B}}) \otimes J_{\mathrm{low}} + J_{\mathrm{low}} \otimes (u_{\mathrm{M}} - u_{\mathrm{B}}).$$

Its finite projected-force norm is of order $\rho^{1-O(\varkappa)} P(S)$, covered by $\rho^{\nu} P(S)$, not by an $O(\rho^2)$ tail assertion. Lemma 3.7.2 supplies the actual compact $H^9_{\langle R \rangle^6} H^{10}_Y$ domain of this full tensor, with all additional retained finite carrier-zero contributions.

Its proof uses the strengthened H^{18}_9 leading ladder and H^{14}_3 low column after two observation derivatives. Compact multiplication on the interaction hull supplies weight six.

The weaker H^6/H^4 statements alone do not supply this domain. This is a coefficientwise pole forcing.

The actual physical force is $-P_\rho \operatorname{div}_\rho \mathsf{S}$, and we do not claim it to be a finite input-frequency polynomial.

Use the pole macro solution together with its genuine pressure Π_{mac}. The difference between its frozen and actual pressure gradients is $(0, \rho \partial_Z \Pi_{\mathrm{mac}})$.

The omitted axial stress divergence has the same form. The weighted scalar-pressure estimate and the right-word identity bound each by $C \rho^{\nu} r P(S)$ on a radius-r mask, globally with pressure tails.

We keep these terms in the off-pole residual. We do not identify P_ρ with P_0.

We keep nonzero-degree words and center displacement as residuals, not included in b_0. The complementary equation $(T_0 + \lambda_{\mathrm{obs}} - A_c) b = Q f_{\mathrm{mac}}$ uses a positive source, since its left side is minus the generator residual.

Thus its addition cancels $Q f_{\mathrm{mac}}$. All later $Y_Q, Y_b, C_{\mathrm{part}}$ use $\mathcal{C}_{\mathrm{gen}}$ with their actual residuals.

Form this full carrier-zero tensor from $J_{\mathrm{low}} + B_0 + B_1$, and use its coefficientwise pole force f_{mac} just defined. Its actual physical projection displacement remains in the $\rho^{\nu} r$ residual. Split it with the current radial Riesz projection $P_{\mathrm{band}} = e\ell$: $f_{\mathrm{mac}} = P_{\mathrm{band}} f_{\mathrm{mac}} + Q f_{\mathrm{mac}}$.

On each right-ordered coefficient word use the exact translated causal response of Lemma 3.7.3 for the Q part. Lemma 3.7.2 admits the input.

We do not assume its pressure compact. That lemma and Lemma 3.7.3 supply the selected-pole H^9 stress to H^8 response, four weighted radial derivatives, observation-T derivatives, clock sampling, divergence and pressure.

The change from the selected pole to the current chart contributes one explicit center displacement. The estimate below bounds this displacement by the right-mask radius.

The frozen kernel does not absorb it.

Its exact physical lift is $\mathcal{T}_\rho b$. The omitted right scalar evolution is the retained composition $b_{ab} B_2$, of order $\rho^{\nu+2\theta}$.

$\rho\partial_T\mathcal{K}_T$ has order $\rho^{\nu+1}$. The center band coefficient, with its sampled complete moment, is the one scalar $b_0(s)$, defined when we pair the full center $P_{\mathrm{band}}f_{\mathrm{mac}}$ with ℓ.

The nonconstant band remainder has the extra δ from a positive-degree right word or center displacement. The same coefficientwise construction controls its evaluated derivatives.

In particular the shared mean gauge cancels in the opposite primary product. For a general radius r, that displacement costs r. This gives $\rho^{\nu}r$ in the low row and $\rho^{\nu}(r+a_\rho)$ after one high re-excitation.

For the constant even matching row, the primary return costs $\rho^{1/2-128\varkappa}$. The matching row then has order $\rho^{\nu+1/2-128\varkappa}$. The low homological identities leave $r^3+\rho r+\rho^2$, with its fixed leading constant.

We make the low estimate before the band row: the vector homological equations cancel the whole radial Taylor defect through degree two. The macro equation cancels Qf_{mac} in the full radial complement, while the actual b_0 cancels its selected degree-zero part.

Off-pole generator and coefficient changes cost $\rho^{\nu}rP(S)$. The later $B_{2,\mathrm{high}}$ matching return is bounded physically by $a_\rho(r+a_\rho)^2P(S)$.

The macro/feedback re-excitation returns cost $\rho^{\nu}a_\rho P(S)$, and the partition low return costs $\rho a_\rho P(S)$, no larger. All higher mean-on-correction terms have the stated positive orders.

We estimate the global omitted tail on the actual full H2 column before projection. Thus we do not infer a same-angular radial-complement residual from a bound on KR.

These full vector equations cancel or estimate it and prove the Π_{zero} bound. The K bound follows from exact angular separation and its fixed operator norm.

This proves the two graded lines before we apply any annular inverse or output mask. In particular we include no unjustified $\rho^{1/2}r$ return.

Finite input-word degrees. We count the total degree in the right-input words Z^ak^b, after the complete physical divergence chart or curl. Source fields, frames and clock coefficients have degree zero. Normal ordering does not increase degree, since $[k,Z]=-i\rho$ and $[k,c]=-i\rho c_Z$. The physical J_{low} has degree at most three by Lemma 3.7.1. A coefficientwise cell inverse and its primitive pressure do not increase input degree; the final full curl increases it by at most one. A general raw residual increases velocity degree by at most two, from viscosity or the right action of B_2. Its pressure-gradient row is within this bound for the accumulated cell pressure.

For a zero-carrier input, its extracted high source has the sharper increase of at most one: only the first-order interaction with a nonzero-carrier source can change the carrier. Viscosity, the time derivative, the scalar band and the zero-carrier pressure stay in the zero-carrier sector. Consequently the initial high source has degree at most four, and

$$\deg B_0\le 5,\qquad \deg B_1\le 8,\qquad \deg B_{2,\mathrm{high}}\le 11.$$

The macro tensor is formed from $J_{\mathrm{low}}+B_0+B_1$ before divergence. Its other factor is an actual source coefficient, independent of the right scalar input. Thus both the full matching tensor and the direct mean tensor have degree at most eight. The pole macro equation uses exactly $F_{\mathrm{mac},0}=-\operatorname{div}_h\mathsf{S}$ and the coefficientwise operator P_0 at $k=0$. Neither adds an input word. The macro kernel likewise acts coefficientwise, so

$$\deg b\le 8,\qquad \deg(\mathcal{T}_\rho b)\le 9.$$

The omitted axial stress divergence and $(0,\rho\partial_Z\Pi_{\mathrm{mac}})$ have degree at most nine and remain in the off-pole residual estimated above. They are not inputs to this pole macro equation. This distinction is essential for the count.

The high re-excitation of $\mathcal{T}_\rho b$ has degree at most ten, and its full-curl cell Y_Q has degree at most eleven. The sources $-b_0 B_0$ and $-(\partial_s \omega_j) B_{0,j}$ have degree at most five, hence Y_b and C_{part} have degree at most six. The complete physical column therefore has degree at most eleven, its raw residual at most thirteen, and that residual with two graph input powers and one output derivative at most sixteen (fifteen without the last derivative). These are polynomial-word bounds. They add no spectral k jets, radial moments, or source-coefficient differentiation levels. The freely selected smooth scalar masks supply their finite word seminorms and any extra kernel integration index.

$Y_Q = \mathcal{C}(\mathsf{H}_{\mathrm{raw}} \mathcal{R}_0(\mathcal{T}_\rho b, \Pi_{\mathrm{mac}}))$ cancels the high re-excitation of $\mathcal{T}_\rho b$. Fix the sign of the scalar by $\mathcal{E}_0(J_{\mathrm{low}} + B_0 + B_1 + \cdots) = +b_0 J_{\mathrm{low}} +$ nonband terms.

The residual relative to the stated $B_{\mathrm{band}} = \lambda_0 + B_2 + b_0$ is $\mathcal{E}_0(J) - b_0 J$. Its low scalar cancels, but its actual high part contains $-b_0 B_0$.

The fixed-shift cell response $Y_b = \mathcal{C}(-b_0 B_0)$ uses the box source $-c(T) b_0(s) B_0^{\mathrm{box}}$ and cancels this residual. Equivalently, after this correction one may multiply the unweighted prepared column by g, which satisfies $g_s/g = b_0$, and evolve the scalar by $\lambda_0 + B_2$.

J_p in the theorem is the unmultiplied column that keeps b_0 in B_{band}, so it is counted once. Its coefficient lift is constant in the physical radial direction after evaluation, so its evaluated radial derivative is zero.

The fixed auxiliary-origin jets bound ordinary derivatives. These responses leave, in this order, $\rho^{\nu+\gamma}$ and $\rho^{\nu+1/2-\varkappa}$ high/low returns.

$b_0 Y_b$ and the remaining scalar products are $O(\rho^{2\nu} P(S))$.

Coefficient loss and radial regularity have different derivative counts. The full high residual uses at most eleven source/geometry levels before physical output.

Its H^3 and fixed parameter/chart checks use at most twenty-one. For the arbitrary-input carrier-zero stress use Lemma 3.7.2, with the explicit count

$$\underbrace{(2 + 3 \cdot 3 + 5)}_{16\ \text{RAW/curl/cell/pressure}} + \underbrace{9}_{\text{radial}} + \underbrace{10}_{\text{origin}} + \underbrace{16}_{Z} + \underbrace{2}_{\text{observation}} + \underbrace{2}_{\text{frozen k}} + \underbrace{4}_{\text{connections}} = 59. \tag{3.7.31}$$

The remaining raw stresses start at order $1 - 3\varkappa$, so this count gives $1 - 62\varkappa$.

The eight next return levels still leave $1 - 70\varkappa > 1 - 128\varkappa$ on the stated arbitrary-input stress domain.

Ordinary origin jets actually cost fixed polynomials in S. The allowance $\varkappa$ is an upper bound for their losses.

The global contour uses its different finite k and moment rectangle (3.7.13). Its kernel acts coefficientwise at $k = 0$, not as a newly created input-frequency operator.

The positive radial order is instead

$$\begin{aligned} &2\ (S_0 e) + 2\ (\text{observation dilation}) + 1\ (\text{initial source}) + 1\ (B_0\ \text{curl}) \\ &\quad + 2\ (B_0\ \text{viscosity}) + 1\ (B_1\ \text{curl}) + 9\ (\text{stress norm}) = 18. \end{aligned} \tag{3.7.32}$$

The actual $H_R^{18}(\langle R \rangle^9)$ ladder supplies it, not spare powers of ρ. The native low column has H_5^{16}.

Two observation derivatives leave H_3^{14}. Multiplication on the fixed compact interaction hull permits the stress weight six there, without a claim of compactness of the global low velocity or pressure.

These are (3.7.6) and (3.7.7). The longest coefficient path below uses sixty-nine levels.

Even if we charge the two source-band observation/shear connections separately, this gives at most seventy-one, under $J_{\mathrm{prep}} = 72$. The second output derivative of Lemma 3.7.14 adds one level, so the full count is $59 + 8 + 3 + 2 = 72 = J_{\mathrm{prep}}$, with zero margin. We reserve $J_{\mathrm{src}} = 80$ in the actual

ordinary source export, and this leaves eight additional levels between that export and the prepared reservation.

The fixed diagonal in Theorem 2(vi) includes this finite list before we fix its thresholds. Pure-auxiliary Gevrey control and the weighted radial ladder are different inputs. If we reserve unused higher jets, the actual operation count and its exponent loss stay the same. This reserve also does not reselect the physical source, activation or spectral pair.

The same exponent used in the operator estimate remains $\nu = 1 - 128\varkappa$. We fix the finite prefix, memory cutoff and global returns with the necessary output accuracy before we select the ancient threshold.

Last take the original locally finite source-label cover. The exact time/space chart conjugacies pull back all local coefficients.

If we join observation charts with a fixed partition $\sum_j \omega_j = 1$, then $|\partial_s \omega_j| \le C\rho$ and $\sum_j (\partial_s \omega_j) J_{\mathrm{low}} = 0$. One more full-curl cell response C_{part} cancels the remaining high partition source $-\sum_j (\partial_s \omega_j) B_{0,j}$. Each summand has box source $-c(T)(\partial_s \omega_j) B_{0,j}^{\mathrm{box}}$, with $c(T)\partial_s \omega_j = \rho_j \partial_T \omega_j$.

Its residual is $O(\rho P(S)(r + \rho^{1/2-128\varkappa}))$ on a radius-r mask. Its low return is $O(\rho^{3/2-128\varkappa} P(S))$.

Use the single canonical $b_0 = \sum_j \omega_j b_{0,j}$ and rebuild Y_b from it. This makes J_p one global physical column, with no block reset. For this cell lift the finitely many overlapping source levels to their common lowest torus cover as in Theorem 2(vii). At fixed T the sampled scalar is a function of the temporal origin. In a pulse chart with shear $a(R)$, insert that function at $Y - a(R)$; on the physical sample $Y = a(R) + Y_t$ it gives precisely $b_0(s)$, independently of R. Cover changes have bounded level difference on the fixed phase chart. Thus the lift uses the same auxiliary derivatives and shear factors as the macro force. Differentiating $c(T)^{\pm 1}$ introduces only bounded slow factors, and physical slow differentiation carries ρ_j.

The carrier rounding $|n_\alpha| \ge 2m + 1$ of Theorem 2(vii), finite relative-harmonic closure and Lemma 3.7.5 give the sector exclusion and phase-gradient separation that we assert. Cross-label products vanish by Theorem 2(vii).

Lemma 3.7.9 below proves (3.7.29). We take the minimum of the high remainder 3γ, the low Taylor 3θ, macro re-excitation $\nu + \gamma$, and high-return $1/2 + 2\gamma - \varkappa$ and get $p_0 = 1.19616$ in (3.7.27).

The fixed physical cutoff commutator remains explicitly in the annular equation used after this. We do not include it in the unmasked residual estimate.

□

Lemma 3.7.8 (Scaled kernel bound)**.** *Let H_1, H_2 be Hilbert spaces, let $r > 0$, and let $\sigma : \mathbb{R}^2 \to B(H_1, H_2)$ be measurable, with $\sigma(Z, \cdot) \in C^2(\mathbb{R})$ for every Z and $\sigma(Z, k) = 0$ for $|k| \ge 2r$. Put $A = \sup_{Z,k} \|\sigma(Z,k)\|$ and $B = \sup_{Z,k} \|\partial_k^2 \sigma(Z,k)\|$. Then for every $\rho > 0$*

$$\|\operatorname{Op}_\rho(\sigma)\|_{L^2(\mathbb{R};H_1)\to L^2(\mathbb{R};H_2)} \le \int_{\mathbb{R}} \sup_Z \|\widehat{\sigma}(Z,u)\| \, \mathrm{d}u \le \frac{4}{\pi}(A + r^2 B). \tag{3.7.33}$$

The bound uses no derivative in Z and does not depend on ρ.

Proof. By (3.6.1), $\operatorname{Op}_\rho(\sigma) f(Z) = \int \widehat{\sigma}(Z,u) f(Z - \rho u) \, \mathrm{d}u$ with $\widehat{\sigma}(Z,u) = (2\pi)^{-1} \int e^{iuk} \sigma(Z,k) \, \mathrm{d}k$. Minkowski's integral inequality and the translation invariance of the L^2 norm give the first inequality. Since $\sigma(Z,\cdot)$ is C^2 and vanishes for $|k| \ge 2r$, we have $\|\widehat{\sigma}(Z,u)\| \le (2\pi)^{-1} 4rA$, and two integrations by parts give $\|\widehat{\sigma}(Z,u)\| \le (2\pi)^{-1} 4rBu^{-2}$. We use the first bound for $|u| \le 1/r$ and the second for $|u| > 1/r$:

$$\int \sup_Z \|\widehat{\sigma}(Z,u)\| \, \mathrm{d}u \le \frac{2r}{\pi}\Big(\frac{2A}{r} + 2rB\Big) = \frac{4}{\pi}(A + r^2 B).$$

□

Lemma 3.7.9 (Low rows of the prepared column)**.** Normalization (N_e). *Let $P(z)$, $z=(Z,k)$, be the Riesz projection of the frozen physical generator $L(z)$ for its selected simple eigenvalue $\lambda(z)$ on the phase chart of Lemma 3.6.2. Let $e_0=e$ and $\ell_0=\ell$ be the pole profiles used in J_{low}, with $\ell_0 e_0=1$. On the rectangle U supplied by Theorem 2(iv), $c(z)=\ell_0 P(z) e_0$ satisfies $|c(z)-1|\le\frac12$. Put*

$$e(z)=c(z)^{-1}P(z)e_0,\qquad \ell(z)=\ell_0 P(z),\qquad v(z)=\ell(z)^*.$$

These are the right and adjoint profiles of $J_{\mathrm{ref}}, H_{\mathrm{ref}}$ in Lemma 3.6.3. On the conjugate member of the pair we use the conjugate formulas. Then $e(z)$ is a right and $\ell(z)$ a left eigenvector, $\ell(z)e(z)=1$ (so $v^*e=I_2$ on the real pair), $e(z)\ell(z)=P(z)$, $\ell_0 e(z)=1$, $e(0)=e_0$ and $\ell(0)=\ell_0$. The bounds (3.6.3) hold with new constants. The derivatives $e_Z=\partial_Z e(0)$, $e_k=\partial_k e(0)$ are obtained by differentiating this physical contour formula, including the k-dependence of the physical divergence constraint. They define the physical Taylor polynomial p_2 in Lemma 3.7.1; its horizontal pullback is formed only after these physical derivatives are taken.

Bounds. *Let $\Pi=\Pi_{\mathrm{zero}}$, let $\delta\le r\le r_{\mathrm{out}}$, and let $C_r=\mathrm{Op}_\rho(c_r)$, $c_r(z)=\chi(z/r)$, be a fixed-shape right column mask as in Lemma 3.7.13, with $\operatorname{supp}\chi$ in the unit box. We take the right column masks in this left convention; Lemma 3.7.13 allows either convention, and this fixes the choice. Then*

$$\Pi J_p - J_{\mathrm{low}} = \Pi\,\mathcal{T}_\rho b \qquad \textit{exactly,} \tag{3.7.34}$$

$$\|(\Pi J_p - J_{\mathrm{low}})C_r\|_{2\to L^2_{\mathrm{can}}} \le C_\Gamma\,\mathfrak{b}(s) \le P(S)\rho^\nu, \tag{3.7.35}$$

$$\|(J_{\mathrm{low}} - J_{\mathrm{ref}})C_r\|_{2\to L^2_{\mathrm{can}}} \le C_T(r+\rho^{3/5}). \tag{3.7.36}$$

Here $\mathfrak{b}$ is the macro coefficient size of input (M) below. The constant C_Γ depends only on the finite macro word list and the mask shape, and C_T only on the profile bounds and the mask shape. Neither depends on ρ, S, κ_0 or r. In particular (3.7.29) holds, and (3.9.17) holds in the stronger form (3.7.35).

Proof. Inputs.

(I1) *Column structure.* By (3.9.1), the global time-partition correction, Lemma 3.7.12 and Remark 3.9.3, $J_p=J_{\mathrm{low}}+\mathcal{T}_\rho b+H_p$. Here $\mathcal{T}_\rho b$ is the macro lift, and H_p is the finite sum of the terms $B_0, B_1, B_{2,\mathrm{high}}, Y_Q, Y_b, C_{\mathrm{part}}$, each with a single nonzero relative carrier, joined by the time partition. The completed localization, opposite-band and finite-prefix tails are terms of the residual, not of the column.

(I2) Lemma 3.7.5(a).

(M) *Macro coefficient size.* $b=\sum_{(a,\beta)\in\Gamma_b} b_{a\beta}Z^a k^\beta$ with a finite word list Γ_b of degree at most eight and horizontally solenoidal coefficients, and

$$\mathfrak{b}(s):=\max_{(a,\beta)\in\Gamma_b}\sup_Z\big(\|b_{a\beta}\|_{L^2_h}+\|Gb_{a\beta,z}\|_{L^2_h}+\|G\partial_Z b_{a\beta,z}\|_{L^2_h}\big)\le P(S)\rho^\nu.$$

This is proved below, from Lemmas 3.7.2 and 3.7.3 and (3.7.26).

(I3) Lemmas 3.7.13, 3.6.1 and 3.7.8, the bounds (3.6.3), and Lemma 3.6.3 in the form $J_{\mathrm{ref}}=\mathrm{Op}_\rho(e)+\rho\mathcal{J}$ with $\|\mathcal{J}C_r\|\le C$.

(I4) Fix $0<r_U\le 1/2$ with the closed box of radius r_U inside U. Take $\widetilde{\zeta}\in C_c^\infty(U)$ equal to one on that box. The fixed-gap tail of Lemma 3.9.5 gives $\|\mathrm{Op}_\rho((1-\widetilde{\zeta})e)C_r\|\le C_U(\rho/r)^3$ for $r\le r_{\mathrm{out}}$ once the symbol supports lie in the box of radius $r_U/2$.

Normalization. On U we have $|c| \geq \frac{1}{2}$, so c^{-1} has the stated finite phase derivatives of c, and e, ℓ inherit (3.6.3). Write the rank-one projection as $P(z) = a(z)\beta(z)$ with $\beta a = 1$. Then $c = (\ell_0 a)(\beta e_0)$, $e = a/(\ell_0 a)$ and $\ell = (\ell_0 a)\beta$. Hence $\ell e = \beta a = 1$, $e\ell = a\beta = P$ and $\ell_0 e = 1$. Since $P(0)e_0 = e_0$ and $\ell_0 P(0) = \ell_0$, we get $e(0) = e_0$ and $\ell(0) = \ell_0$. The principal shift symbol $d_0 \chi_{s,\pm} e\ell = d_0 \chi_\pm P$ is independent of the normalization. We use the displayed gauge for the corrected columns and their exact pairing inverse. The physical Taylor jets are obtained by differentiating this contour formula, including its moving divergence constraint. The horizontal pullback in (3.7.3) is taken before these jets are used inside $\mathcal{T}_\rho$.

Proof of (M). Fix one source chart; the joined column uses $b = \sum_j \omega_j b_j$ with time weights $\omega_j \geq 0$, $\sum_j \omega_j = 1$, so it suffices to bound each b_j. The macro force is $f_{\mathrm{mac}} = P_0 F_{\mathrm{mac},0}$ with $F_{\mathrm{mac},0} = -\operatorname{div}_h \mathsf{S}$, and S is the carrier-zero tensor of Lemma 3.7.2, formed from the words of $J^{[2]} = J_{\mathrm{low}} + B_0 + B_1$; hence it is a finite sum of right-ordered words of degree at most eight, by the tensor count in paragraph 3.7.3, and $\|\mathsf{S}_{a\beta}\|_{\mathcal{D}} \leq C\rho^{1-128\varkappa} P(S) = C\rho^\nu P(S)$ for each word. The response b solves the causal complementary clock equation word by word at $k = 0$ (Lemma 3.7.3), so Γ_b is this word list. Its frozen kernel obeys (3.7.8), and the response has H^8 and four weighted radial derivatives bounded by the H^9 norm of the stress. The clock variable $r \geq 0$ runs into the past, where ρ is smaller and $\log(1/\rho)$ grows at most linearly in r; hence $\rho(s_r)^\nu P(S(s_r)) \leq C(1+r)^C \rho(s)^\nu P(S(s))$, and the factor e^{-cr} makes the memory integral converge. The norm $\|\cdot\|_{\mathcal{D}}$ contains sixteen ordinary Z derivatives and ten auxiliary derivatives (two-dimensional Sobolev embedding gives the evaluated values), and the frozen kernel does not depend on Z, so $\partial_Z b$ is the response to $\partial_Z \mathsf{S}$. Finally (3.7.26) bounds G from H^8_{w+1} to H^8_w, and H^8 controls L^2_h. This gives $\mathfrak{b}(s) \leq C\rho^\nu P(S)$. The unlifted b is horizontally solenoidal (the paragraph containing (3.7.26)).

Proof of (3.7.34). J_{low} is built from the $\pm m$ profiles, and the chart $\mathcal{T}_\rho$ acts in each angular sector, so $\Pi J_{\mathrm{low}} = J_{\mathrm{low}}$. Each term of H_p is a full curl of a potential with one carrier $e^{ijK\Phi + im\vartheta}$, $j \neq 0$. Curl, Leray projection and the time partition (whose weights depend on time only) keep the angular Fourier label, and this label is $\pm m + jn_\alpha \notin \{m, -m\}$ by (I2). Hence $\Pi H_p = 0$, and (I1) gives the identity.

Proof of (3.7.35). Since Π is an orthogonal projection, it suffices to bound $\mathcal{T}_\rho b C_r$. For one word put $w = b_{a\beta} Z^a k^\beta C_r f$. Since $\rho\partial_Z = ik$ on functions of Z,

$$\rho\partial_Z w_z = \rho(\partial_Z b_{a\beta,z}) Z^a k^\beta C_r f + \rho a\, b_{a\beta,z} Z^{a-1} k^\beta C_r f + i\, b_{a\beta,z} Z^a k^{\beta+1} C_r f,$$

and $\mathcal{T}_\rho w = (w_h - G\rho\partial_Z w_z, w_z)$. For a coefficient $c(x_h, Z)$ and a function $g(Z)$, Fubini's theorem gives $\|cg\|_{L^2} \leq \sup_Z \|c(\cdot, Z)\|_{L^2_h} \|g\|_2$. Lemma 3.7.13 gives $\|Z^{a'} k^{\beta'} C_r\| \leq C_{a'\beta'} r^{a'+\beta'} \leq C_{a'\beta'}$ for $a' + \beta' \leq 9$, because $\rho \leq r^2 \leq 1$. The sum over the finitely many words gives $\|\mathcal{T}_\rho b C_r\| \leq C_\Gamma \mathfrak{b}$, and (M) gives the last inequality. The radius enters only through $r \leq 1$ and $\rho \leq r^2$.

Proof of (3.7.36).

(i) *The symbol of* J_{low}. The coefficients of p_2, z_2 and E in (3.7.2) are fixed radial profiles. Hence $J_{\mathrm{low}} = \mathrm{Op}_\rho(b_{\mathrm{low}})$ exactly, where b_{low} is a polynomial in (Z, k) of degree at most three with fixed radial profile coefficients. Its value at the center is $b_{\mathrm{low}}(0) = e_0 + \rho(E - C_0)$, by the full divergence correction in (3.7.2). Thus $b_{\mathrm{low}}(0) = e_0 + \rho\beta_0$ with the fixed profile $\beta_0 = E - C_0$, and $|\partial_k^j b_{\mathrm{low}}| \leq C$ for $j \leq 3$ on the box of radius one.

(ii) By (N_e), $e(0) = e_0$. So $d := b_{\mathrm{low}} - e$ satisfies $|d(z)| \leq C(|z| + \rho)$ and $|\partial_k^j d(z)| \leq C$ $(1 \leq j \leq 3)$ for $|z| \leq r_U$.

(iii) *Composition.* Since b_{low} is a polynomial in k and its coefficients act by multiplication in Z, the proof of Lemma 3.7.13 gives the exact finite formula $\mathrm{Op}_\rho(b_{\mathrm{low}}) C_r =$

$\mathrm{Op}_\rho(\sum_{\alpha\le 3}\frac{(-i\rho)^\alpha}{\alpha!}\partial_k^\alpha b_{\mathrm{low}}\,\partial_Z^\alpha c_r)$. Next, $\mathrm{Op}_\rho(e)C_r=\mathrm{Op}_\rho(\widetilde{\zeta}e)C_r+\mathrm{Op}_\rho((1-\widetilde{\zeta})e)C_r$, and the second term is $O((\rho/r)^3)$ by (I4). Lemma 3.6.1 gives $\mathrm{Op}_\rho(\widetilde{\zeta}e)C_r=\mathrm{Op}_\rho(\widetilde{\zeta}ec_r)-i\rho\,\mathrm{Op}_\rho(\partial_k(\widetilde{\zeta}e)\partial_Z c_r)+\mathcal{R}$ with $\|\mathcal{R}\|\le C(\rho/r)^{3/2}$. The factor $r^{-3/2}$ is the $\frac{1}{2}$-Hölder norm in Z of $\partial_Z c_r$; its Fourier envelope in k is dilation invariant. Since $\widetilde{\zeta}=1$ on $\operatorname{supp} c_r$ ($r\le r_{\mathrm{out}}\le\frac{1}{4}$),

$$(J_{\mathrm{low}}-\mathrm{Op}_\rho(e))C_r=\mathrm{Op}_\rho(\sigma_r)+O((\rho/r)^{3/2}),\quad \sigma_r=dc_r-i\rho(\partial_k d)\partial_Z c_r+\sum_{\alpha=2}^{3}\frac{(-i\rho)^\alpha}{\alpha!}\partial_k^\alpha b_{\mathrm{low}}\,\partial_Z^\alpha c_r.$$

(iv) $\sigma_r(Z,\cdot)$ vanishes for $|k|\ge 2r$. With $|\partial^\alpha c_r|\le Cr^{-|\alpha|}$ and $\rho/r\le 1$, we have $|\sigma_r|\le C(r+\rho+\rho/r)$ and $r^2|\partial_k^2\sigma_r|\le C(r+\rho+\rho/r)$. Lemma 3.7.8 gives $\|\mathrm{Op}_\rho(\sigma_r)\|\le C(r+\rho/r)\le C(r+\rho^{3/5})$, since $\rho/r\le\rho/\delta=\rho^{3/5}$.

(v) By (I3), $J_{\mathrm{ref}}-\mathrm{Op}_\rho(e)=\rho\mathcal{J}$ with $\|\mathcal{J}C_r\|\le C$. Together with (iii) and (iv) this proves (3.7.36).

Finally $(\Pi J_p-J_{\mathrm{ref}})C_r=(\Pi J_p-J_{\mathrm{low}})C_r+(J_{\mathrm{low}}-J_{\mathrm{ref}})C_r$, because $\Pi J_{\mathrm{ref}}=J_{\mathrm{ref}}$. This gives (3.7.29). □

Remark 3.7.10 (Scope of the low comparison). Only the displayed weaker comparison is proved and used here. The exact divergence chart differentiates the complete scalar input; the horizontal pullback and the compensating cubic term of Lemma 3.7.1 are therefore part of the column even for this weaker bound. The cubic primitive residual (3.7.5) is a separate statement: its finite differential calculation does not assert a cubic estimate for the nonlocal comparison $J_{\mathrm{low}}-J_{\mathrm{ref}}$. The uses of (3.7.29) are Lemma 3.7.15 and (3.7.39) (where it enters through the quantity δ of (3.4.22)), the normalization comparison of the shifted Gram estimate, and Lemma 3.9.15 (through (3.9.17)). Each needs only the displayed form.

Lemma 3.7.11 (The prepared residual on a bounded family of mask shapes)**.** *Let $\mathfrak{B}$ be a bounded subset of C_c^∞ of the box of radius sixteen, bounded in each C^N norm. For $\sigma\in\mathfrak{B}$ and $\delta\le r\le r_{\mathrm{out}}$ put $Y=\mathrm{Op}_\rho(\sigma(z/r))$. Take the ancient threshold so $32r_{\mathrm{out}}<r_U$, with the box norm used in (I4); if a Euclidean ball is used take $32\sqrt{2}\,r_{\mathrm{out}}<r_U$. This ensures the support of every such shape is within the $r_U/2$ chart. Then (3.7.27) (with $r=\delta$) and the two lines of (3.7.28) hold with C_r replaced by Y, and Lemma 3.9.4 holds for Y. The constants depend on $\mathfrak{B}$ only through finitely many C^N norms; in particular the leading constant of (3.7.28) stays independent of S.*

Proof. The proofs of Lemma 3.7.7 and Lemma 3.9.4 use the right mask only in the following places.

(a) The operator norm of a word, (N1): $\|cZ^ak^bC_r\|\le\sup|c|\,\|Z^ak^bC_r\|$ with $\|Z^ak^bC_r\|\le C_{ab}r^{a+b}$, for degrees up to sixteen (thirteen residual degrees, two graph powers of k and one output level). This includes the low homological remainder after (3.7.29) and the $\rho^\nu r$ displacement.

(b) The output support $|Z|=O(r)$ of the mask in the left-kernel convention (proof of Lemma 3.7.12), and the Schur decay $(\rho/r)^N$ of the mask kernel across a fixed Z gap (third OUTPUT type of Lemma 3.9.4).

(c) The exact graph composition $C_r\langle k\rangle^2=\mathrm{Op}_\rho(c_r(1+k^2))$ and $\langle k\rangle^2C_r=\mathrm{Op}_\rho((1+k^2)c_r-2i\rho kc_{r,Z}-\rho^2c_{r,ZZ})$.

The coefficient algebra (N2)–(N6), the cell inverses, the gain table and the macro construction act on the column coefficients and do not involve the mask. For Y: (a) holds by the proof of Lemma 3.7.13 with χ replaced by σ, whose constants use the fixed support and the first two frequency derivatives

of $z^a\eta^{b-\alpha}\partial^\alpha\sigma$, bounded on $\mathfrak{B}$; (b) holds because $\mathrm{Op}_\rho(\sigma(z/r))f(Z)$ vanishes unless $|Z| \le 16\sqrt{2}\,r$ (left quantization), and the kernel $r\widehat{\sigma}(Z/r, ru)$ decays like $(1 + r|u|)^{-N}$ with constants given by ∂_k^N-norms of σ; (c) is exact for every symbol. Hence every constant of those proofs is bounded on $\mathfrak{B}$. □

Lemma 3.7.12 (A differentiated finite prepared column)**.** *Write the nonzero-carrier part of the selected column after the right mask as a finite sum $e^{i\Psi_j}A_jC_\delta$. We sum active labels, and its coefficients satisfy*

$$\|A_jC_\delta f\|_2 \le CP(S)\|f\|_2, \qquad \|\nabla_*(A_jC_\delta f)\|_2 \le C\rho^{-b_{\mathrm{col}}}P(S)\|f\|_2, \quad b_{\mathrm{col}} = 129\varkappa = .00129. \tag{3.7.37}$$

We include the full-curl, macro-response and partition corrections. The completed localization, opposite-band and finite-prefix tails are not components of the column. They are terms F_i of the residual decomposition $\mathcal{R}_i = L_i + H_i + F_i$, and Lemma 3.9.4 estimates them as OUTPUT errors at $O(\rho^2P(S))$ in L^2 and in ∇_*.

Proof. The construction above is a finite sum of right-ordered words $c_{ab}(R, Z, T, Y)Z^ak^b$. Take the coefficient norms in radial H^1 (or the stronger radial spaces supplied by the macro kernel). Take them with one bound for all the slow variables.

Multiplication and Fubini, together with $\|Z^ak^bC_\delta\| \le C\delta^{a+b}$, give the zero-order operator norm from these coefficient norms. One normalized axial derivative is $k = -i\rho\partial_Z$, so

$$k(cZ^ak^bC_\delta f) = cZ^ak^{b+1}C_\delta f - i\rho c_Z Z^ak^bC_\delta f - i\rho acZ^{a-1}k^bC_\delta f.$$

We bound the first term and the commutator, since $\rho/\delta \le \delta$.

Radial differentiation acts on the coefficient. The residual angular derivative and cylindrical connection have fixed m and a fixed positive radial hull.

Here are the coefficient bounds necessary for that argument. The principal source KX_σ has order zero, since $K = O(\rho^{-1/2})$ and the primary wave has order $\rho^{1/2}$.

The mean and wave coefficient classes in Theorem 2(vii) keep order under each fixed ordinary coefficient derivative. An evaluated radial derivative loses at most $\varkappa$.

For a coefficient multi-index I, differentiation of the zero-data cell equation gives the same shifted homogeneous matrix with source

$$\partial^I f_j + \sum_{0<J\le I} \binom{I}{J} (\partial^J A_{\mathrm{cell}})\partial^{I-J}z_j.$$

The shifted Gaussian Duhamel estimate above thus closes the finite mixed jets by induction, and it adds only fixed powers of S. The full-curl remainder has an extra K^{-1}.

After one additional evaluated derivative it still gains $\rho^{1/2-2\varkappa}$. The next high responses gain ρ^γ at each cell. The macro, scalar-feedback and partition returns have the positive orders displayed in (3.7.28).

These spare powers bound the additional derivative. The coefficient conversion uses the fifty-nine-level stress bound (3.7.31).

At most eight return levels and two output-derivative or multiplication levels follow. The total is at most sixty-nine levels for the first derivative. The second derivative of Lemma 3.7.14 needs one further output level; with the two source-band connections it uses all seventy-two reserved levels ($59 + 8 + 3 + 2 = 72$), so J_{prep} has no spare level.

The prepared reservation is seventy-two and the ordinary source export is eighty, with the different connection margin above. The actual sixty-nine-level sequence stays below the existing $128\varkappa$ allowance.

We include the additional single evaluated derivative in $b_{\mathrm{col}} = 129\varkappa$. This comparison bounds only the coefficient powers.

The initial stress uses the independent eighteen-order radial ladder (3.7.32). The macro kernel's eight radial output derivatives and four weighted output derivatives separately supply the last single gradient.

The primary response is of order zero and later responses keep positive powers, so $P(S)$ still bounds their zero-order norms.

Last, C_δ has output support $|Z| = O(\delta)$ in the left-kernel convention. With $u = q/t$, the chart identity reads $u - Z^2u^{2h} = 1$, thus $q/t = 1 + O(\delta^2)$ there.

All active source bands in this estimate satisfy $Q_\alpha \asymp t$. Their number is polynomial in S and Theorem 2(vii) bounds their pointwise overlap.

Summation enlarges only $P(S)$. We fixed the finite-prefix and completed-tail accuracy in the same finite seminorms before the ancient threshold.

The macro tail uses its weighted radial norm, and the source hull multiplies high re-excitation. This proves (3.7.37) on the smooth core and then by density for each input.

□

Lemma 3.7.13 (Word bounds for the fixed-shape masks)**.** *Let $C_r = \mathrm{Op}^L_\rho(\chi_r)$ or $C_r = \mathrm{Op}^L_\rho(\chi_r)^*$, where $\mathrm{Op}^L_\rho(p)u(Z) = (2\pi\rho)^{-1}\iint e^{i(Z-Z')\xi/\rho}p(Z,\xi)u(Z')\,\mathrm{d}Z'\,\mathrm{d}\xi$ is the left quantization, $\chi_r(Z,\xi) = \chi(Z/r,\xi/r)$ and $\chi \in C^\infty_c(\mathbb{R}^2)$ is the fixed shape. If $\rho \le r^2 \le 1$, then for all $a, b \ge 0$*

$$\left\| Z^a k^b C_r \right\|_{L^2\to L^2} \le C_{a,b,\chi}\, r^{a+b}, \qquad k = -i\rho\partial_Z.$$

Proof. $Z^a k^b = \mathrm{Op}^L_\rho(Z^a\xi^b)$ exactly. Since $Z^a\xi^b$ is a polynomial in ξ, the composition formula is a finite and exact sum:

$$Z^a k^b\,\mathrm{Op}^L_\rho(\chi_r) = \sum_{\alpha\le b}\frac{(-i\rho)^\alpha}{\alpha!}\frac{b!}{(b-\alpha)!}\,\mathrm{Op}^L_\rho(Z^a\xi^{b-\alpha}\partial^\alpha_Z\chi_r) = \sum_{\alpha\le b} c_\alpha\,\rho^\alpha r^{a+b-2\alpha}\,\mathrm{Op}^L_\rho(\sigma_\alpha(Z/r,\xi/r)),$$

with $\sigma_\alpha(z,\eta) = z^a\eta^{b-\alpha}\partial^\alpha_z\chi(z,\eta) \in C^\infty_c$. The unitary dilation $u \mapsto r^{-1/2}u(\cdot/r)$ conjugates $\mathrm{Op}^L_\rho(\sigma(\cdot/r,\cdot/r))$ to $\mathrm{Op}^L_{\rho/r^2}(\sigma)$, whose norm is bounded uniformly in $\rho/r^2 \le 1$. Indeed, for either left or Weyl quantization with parameter δ, the modulus of its kernel is bounded by

$$\frac{C}{\delta}(1+|Z-Z'|^2/\delta^2)^{-1}\sup_x\int_{\mathbb{R}}(|\sigma(x,k)| + |\partial_k^2\sigma(x,k)|)\,\mathrm{d}k.$$

This follows by integration by parts in k twice. Integration of this majorant in either spatial variable gives the uniform L^2 bound by Cauchy–Schwarz. Since $\rho^\alpha r^{-2\alpha} \le 1$ the claim follows. For the adjoint convention write $Z^a k^b\,\mathrm{Op}^L_\rho(\chi_r)^* = (\mathrm{Op}^L_\rho(\chi_r)\,k^bZ^a)^*$ and expand $\chi_r\#(\xi^b\#Z^a)$. This is again a finite exact sum, because Z^a and ξ^b are polynomials. Each term has the form $r^{a+b}(\rho/r^2)^{\alpha+\gamma}\sigma(Z/r,\xi/r)$ with $\sigma \in C^\infty_c$, and the same scaling applies. □

Lemma 3.7.14 (Second derivatives of the prepared high amplitudes)**.** *Let $\delta \le r \le r_{\mathrm{out}}$ and let A_j be the nonzero-carrier amplitudes of Lemma 3.7.12, with the full-curl, macro-response, feedback and partition corrections. Let $\nabla_* = (D_{\mathsf{R}}, \mathsf{R}^{-1}\partial_\theta, \rho\partial_Z)$ act on cylindrical components with the cylindrical connection, and let ∇_a, ∇_b be any two of its components. Then*

$$\|\nabla_a\nabla_b(A_jC_rf)\|_{L^2_{\mathrm{can}}} \le C\rho^{-b_2}P(S)\,\|f\|_2\,, \qquad b_2 = 130\varkappa = .0013. \tag{3.7.38}$$

Thus input (C4) of Lemma 3.9.1 holds with $b_0 = 0$, $b_1 = 129\varkappa$, $b_2 = 130\varkappa$, and Lemma 3.9.1 gives $\|JC_r\|_{L^2_Z \to H^2_*} \le \rho^{-1} P(S)$ when (C2) and (C5) hold.

Proof. We use only the inputs of the proof of Lemma 3.7.12, taken one ordinary derivative deeper.

(A1) *Words.* $A_j = \sum_{(a,b)\in\Gamma} c^j_{ab} Z^a k^b$ with right-ordered words of degree $a + b \le 11$, C_r on the far right, and a number of words and labels at most $P(S)$ (the paragraph after (3.9.1)). The coefficients vanish outside the fixed radial hull $\mathsf{H} = \{\mathsf{R}_- \le \mathsf{R} \le \mathsf{R}_+\}$ of the source label (Lemma 3.7.7).

(A2) *Coefficient jets.* For $|I| \le 2$ ordinary derivatives in $(\mathsf{R}, \mathsf{Z}, y)$, $\sup |\partial^I c^j_{ab}| \le \rho^{-128\varkappa} P(S)$.

(A3) *Evaluated derivatives.* By the pulse-coordinate chain rule and the physical derivative bounds in Theorem 2(vii), $D_{\mathsf{R}} = \partial_{\mathsf{R}} + \lambda a_r(\mathsf{R}) v_r \cdot \partial_y$ with a constant vector v_r, a_r smooth on H, and $|\lambda| \le \rho^{-\varkappa} S^C$; the axial operator $\rho\partial_Z$ and the angular operator have no y part, and $D_{\mathsf{R}} v = \partial_{\mathsf{Z}} v = 0$. The identities from the pulse-coordinate chain rule in Theorem 2(vii) hold for every lifted coefficient, in particular for $D_{\mathsf{R}} f$, so they iterate exactly; the block/label change contributes only the constant factor $Q/Q_\gamma \asymp 1$.

(A4) *Masks.* Lemma 3.7.13 with $a + b \le 13$ ($\rho/r^2 \le \rho^{1/5}$).

Fix one word, put $g = Z^a k^b C_r f$ (a function of Z only) and $u = c\,g$, $c = c^j_{ab}$. Since the coefficients of D_{R} do not depend on Z,

$$\begin{aligned} D^2_{\mathsf{R}} u &= \big[c_{\mathsf{RR}} + 2\lambda a_r v_r \cdot \partial_y c_{\mathsf{R}} + \lambda a_r' v_r \cdot \partial_y c + \lambda^2 a_r^2 (v_r \cdot \partial_y)^2 c\big] g, \\ \rho\partial_Z D_{\mathsf{R}} u &= (\rho\partial_Z D_{\mathsf{R}} c)\, g + (D_{\mathsf{R}} c)\, (ikg), \\ (\rho\partial_Z)^2 u &= \rho^2 c_{ZZ}\, g + 2i\rho c_Z\, (kg) - c\,(k^2 g), \end{aligned}$$

because $\rho\partial_Z = ik$. With $[k, Z^a] = -i\rho a Z^{a-1}$,

$$kg = (Z^a k^{b+1} - i\rho a Z^{a-1} k^b) C_r f, \quad k^2 g = (Z^a k^{b+2} - 2i\rho a Z^{a-1} k^{b+1} - \rho^2 a(a-1) Z^{a-2} k^b) C_r f,$$

so (A4) gives $\|g\|_2 + \|kg\|_2 + \|k^2 g\|_2 \le C r^{a+b} (1 + r + \rho/r)^2 \|f\|_2 \le C \|f\|_2$. On H the coefficients depend on θ only through the fixed angular factor $e^{\pm im\vartheta}$ and the cylindrical frame, so each $\mathsf{R}^{-1}\partial_\theta$ and each connection term is multiplication by a matrix that is smooth and bounded with its derivatives on H (constants depend on the fixed m), and $[D_{\mathsf{R}}, \mathsf{R}^{-1}\partial_\theta] = -\mathsf{R}^{-2}\partial_\theta$ is of the same type. Hence every second derivative of u is a finite sum of terms $c'\,g'$ with $g' \in \{g, kg, k^2 g\}$ and $|c'| \le C(1 + |\lambda|)^2 \max_{|I|\le 2} |\partial^I c|$. By Fubini, $\|c'g'\|_{L^2_{\mathrm{can}}} \le C|\mathsf{H}|^{1/2} \sup|c'|\, \|g'\|_2$, with the bounded chart Jacobian on H already used in Lemma 3.7.12. By (A2) and (A3) each word gives $\rho^{-2\varkappa - 128\varkappa} P(S) \|f\|_2$. The sum over words and the bounded pointwise overlap of labels (Theorem 2(vii)) cost $P(S)$. This proves (3.7.38) on the smooth core, and closedness of $\nabla_a \nabla_b$ extends it to $f \in L^2$.

Verification of (A2). The classes the mean and wave coefficient bounds of Theorem 2(vii) and the norms $\|\cdot\|_{N,r}$ with (N2)–(N6) hold for each fixed derivative order with only $P(S)$ losses. The step gain (3.7.30) costs $n_* \le 3$ levels per cell. The prepared reservation already contains two output levels ((3.7.31), the paragraph after it, and the paragraph after (3.9.1)). The case $i = 1$ used one of them, and the second derivative uses the other. We count pessimistically, as if one of the two were a multiplication level, so that the second output derivative needs one new level. The pessimistic count is

$$\underbrace{59}_{(3.7.31)} + \underbrace{8}_{\text{returns}} + \underbrace{3}_{\text{output/multiplication}} + \underbrace{2}_{\text{source-band connections}} = 72 = J_{\mathrm{prep}}.$$

The reservation is therefore used with zero margin, and any further ordinary derivative level would exceed it. The exponent count gives $1-3\varkappa-70\varkappa = 1-73\varkappa > 1-128\varkappa$. The coefficient allowance $128\varkappa$ therefore does not change, and it keeps a margin of $55\varkappa$. The full-curl part $\nabla_*\times(i\,n\times t/(jK|n|^2))$ of an amplitude needs third derivatives of t, but it carries K^{-1} and contributes at most $\rho^{1/2-3\varkappa}P(S)$. The radial-regularity paths are as follows. The amplitudes $B_0, B_1, B_{2,\mathrm{high}}$ use at most $2n_*+1+2 \le 9$ derivatives of the low profiles, and H_5^{16} (in two horizontal variables) supplies 14 pointwise derivatives. The amplitude Y_Q uses at most one derivative of $\mathcal{T}_\rho b$ in the high interaction, one in the curl and two output derivatives, so at most 4. Lemma 3.7.3 supplies H^8, that is 6 pointwise derivatives. The amplitude Y_b has the scalar factor $b_0(s)$, and C_{part} has the factor $\partial_s\omega_j(s)$; neither is differentiated in space. □

Lemma 3.7.15 (The prepared shift in the two bands)**.** *Freeze a fixed phase chart and its positive shift gap before selection of $\delta = \rho^{2/5}$. Let J_r, K_r be the exact physical fixed reference and $J_* = J_r + (J_p - J_r)C_\delta$, $K_* = M_*^{-1}K_r$, $M_* = K_rJ_*$, with $K_*J_* = I_2$.*

Take the selected prepared column of Lemma 3.7.7. In particular its retained-angle low column satisfies (3.7.29): after C_δ it differs from J_r by $O(\delta+\rho^\nu P(S))$, $\nu = .99872$.

Each nonzero carrier of its high part has angular label outside $\{m,-m\}$ and phase gradient as in Lemma 3.7.5(b) on a fixed radial hull.

Then, for $D = S_p - S_{\mathrm{ref}}$ and the transported filters,

$$\|L_\theta D\|_{2\to 2} \le CP(S)(\rho^\nu + \delta + \rho + e^{cL}\rho^{1/2-\alpha}), \tag{3.7.39}$$

$$\|C_sK_*H_\theta v\|_2 \le CP(S)(e^{cL}N^{-1}+\delta)\,\|H_\theta v\|_2 + CP(S)\zeta\,\|v\|_2\,. \tag{3.7.40}$$

The high-output column may have order-one norm. Its weighted reverse size, together with the stretching term in (3.4.18), is bounded by $M_0 = B_a^C P(S) = \rho^{-o(1)}$, independently of L.

Proof. The low part of $(J_p - J_r)C_\delta$ is bounded by (3.7.29), that is by $C_T(\delta+\rho^{3/5}) + P(S)\rho^\nu \le 2C_T\delta + P(S)\rho^\nu$ (Lemma 3.7.9). The fixed row K_r acts on the sectors $\pm m$ only and thus annihilates nonzero carriers, by Lemma 3.7.5(a).

The completed opposite-band, finite-prefix and localization tails are residual OUTPUT terms (Lemma 3.7.12 and Remark 3.9.3), not components of J_*; they enter only the residual. Thus $M_* = I + E_\delta$ with $\|E_\delta\| \le \frac14$ by Lemma 3.9.15, and M_* has a bounded exact Neumann inverse.

Integration by parts along the phase gradient gives the inverse carrier frequency, by Lemmas 3.7.12 and 3.7.6. Take $\alpha = 1/4 > b_{\mathrm{col}}$.

The additional amplitude term $\rho^{1/2-b}$ then satisfies the bound $\rho^{1/2-\alpha}$.

Transported Bernstein costs $e^{cL}N$. Their product is $e^{cL}\rho^{1/2-\alpha}P(S)$.

This proves the first bound on whole input, not only low input.

Only C_sK_r has the necessary $H^{-1}\to L^2$ endpoint, since the uncut horizontal reference row admits arbitrary axial frequency. For a transported high input this endpoint gives $n_L^{-1} \le Ce^{cL}N^{-1}$, with the physical padded radius n_L of (3.4.10), rather than N^{-1}.

The threshold (3.4.24) ensures $n_L \ge 1$. Exact normalization and the retained Taylor remainder cost at most $\delta P(S)$.

We estimate the padded low leakage in (3.4.19) in a different calculation. This gives the second bound. Multiplication by the prepared column and the clock-normalized output cost $B_a^C P(S)$.

The reverse entry does not use transported derivatives of that column. The other dominant reverse term is $(l\cdot\nabla)W$, which was bounded by $P(S)\,\|l\|$ without e^{cL} in (3.4.18).

All terms with flow derivatives carry positive powers of ρ. This gives the claimed M_0. □

3.8 The prepared-shifted propagator and its Green operator

Main result. Theorem 3.8.2 gives a causal physical propagator and Green operator for the completed equation with its prepared shift. It uses the fixed leading reference and prepared-column bounds for the same selected source.

The result applies on the full physical space with the stated forcing profiles.

3.8.1 The fixed reference and the completed shift

The critical mode correction uses the full-space estimate in Theorem 3.8.2.

The unshifted Theorem 3.5.1 gives the propagator bound for the faster inverse. The shifted gap depends on the selected source.

We fix it before the ancient threshold.

Lemma 3.8.1 (Exact fixed physical leading reference)**.** *For the selected source, let S_{spec} be the real two-band physical leading shift of Theorem 2(iv). Let $S_{\mathrm{ref}} = d_0 J_r C_s K_r$ use the exact normalized fixed physical reference of Lemma 3.6.3.*

On all physical angular and axial frequencies,

$$\|S_{\mathrm{ref}} - S_{\mathrm{spec}}\|_{2\to 2} \le C\rho P(S) + \epsilon_{\mathrm{visc}}(\rho) + \epsilon_{\mathrm{quant}}(\rho) = o(1).$$

Thus the leading equation shifted by S_{ref} has a propagator bounded by $C_{\mathrm{ref}} e^{g_{\mathrm{ref}}(s-r)}$ with one fixed $g_{\mathrm{ref}} < \lambda_c$. The chart, the shift symbols $\chi_\pm$ and the height d_0 are those fixed in Theorem 2(iv).

Proof. On $\operatorname{supp} C_s$, the physical right and left principal symbols of J_r, K_r equal the current true Riesz profiles E, ℓ. These are the profiles of Theorem 2(iv), in the same gauge.

The horizontal extension outside that fixed support does not enter the shift. The left-kernel product of Lemma 3.6.1 gives $J_r C_s K_r = \mathrm{Op}_\rho(E\chi_{s,\pm}\ell) + O_{2\to 2}(\rho P(S))$.

Its first bracket and the physical divergence correctors have explicit ρ factors. The exact scalar pairing inverse is $I + O(\rho P(S))$ by Lemma 3.6.3.

Since $E\ell = P_{0,\pm m}$ on the mask supports and $\chi_{s,\pm} = \chi_\pm$, the inviscid principal symbol of S_{ref} is $S_{0,\pm m} = d_0 \chi_\pm P_{0,\pm m}$ on the whole phase plane. The anti-Wick and left quantizations of this compactly supported symbol differ by $\epsilon_{\mathrm{quant}}(\rho) = o(1)$ by the fixed-chart kernel comparison. The reference columns are solenoidal, so $P_\rho S_{\mathrm{ref}} P_\rho = S_{\mathrm{ref}}$. Sandwiching by the orthogonal projection P_ρ preserves the norm bound. The Gaussian analysis is an isometry, so replacing $S_{0,n}$ by $S_{\rho,n}$ in the anti-Wick operator costs at most

$$\epsilon_{\mathrm{visc}}(\rho) = \max_{n=\pm m} \sup_{Z,k} \|S_{\rho,n}(Z,k) - S_{0,n}(Z,k)\| = o(1)$$

by Theorem 2(iv).

Outside the selected pair the two shifts vanish by their angular definition. This proves the operator difference.

We use the rate $g_2 < \lambda_c$ from Theorem 2(iv). We select $g_{\mathrm{ref}} \in (g_2, \lambda_c)$ once.

Variation of constants for the bounded shift difference gives

$$\|U_{\mathrm{ref}}(s,r)\| \le Ce^{g_2(s-r)} + C\epsilon(\rho_0) \int_r^s e^{g_2(s-\tau)} \|U_{\mathrm{ref}}(\tau,r)\| \, \mathrm{d}\tau,$$

Here $\epsilon(\rho_0) \to 0$ with one convergence modulus on the ancient range as its threshold increases. Gronwall bounds this by $Ce^{(g_2 + C\epsilon(\rho_0))(s-r)}$.

We increase the threshold so that the exponent is below g_{ref}. This fixed leading gap does not bound a return from a shrinking mask.

□

Theorem 3.8.2 (Completed prepared auxiliary inverse)**.** *For the one last $p = 6/5$ source of Theorem 2, take the fixed physical shift chart and one mask C_s selected in the previous spectral construction. Its physical leading reference of Lemma 3.8.1 has, on all angular and axial frequencies, a propagator $\|U_{\mathrm{ref}}(\theta,\sigma)\| \le C_{\mathrm{ref}} e^{g_{\mathrm{ref}}(\theta-\sigma)}$ with a fixed $g_{\mathrm{ref}} < \lambda_c$.*

Select the prepared column of Lemma 3.7.7 and its normalized row as in Lemma 3.7.15. We select the fixed positive chart gap before $\delta = \rho^{2/5}$.

Then the actual completed prepared-shifted physical equation

$$v_s = (A_{\mathrm{lead}} + R - S_p)v + f, \qquad \operatorname{div} v = \operatorname{div} f = 0 \tag{3.8.1}$$

has a real causal propagator U_p on the full physical L^2 space. Its domain includes all angular sectors.

There are a fixed $g_{\mathrm{aux}} < \lambda_c$, an ancient threshold, and an output-time envelope $C_*(\rho) = \rho^{-o(1)}$ such that

$$\|U_p(s,r)\|_{2\to 2} \le C_*(\rho(s)) e^{g_{\mathrm{aux}}(s-r)}, \qquad r \le s. \tag{3.8.2}$$

For each fixed $\beta_c > \lambda_c$, real q, and fixed nonnegative integer j, take strongly measurable solenoidal forcings modulo equality almost everywhere in time and define

$$\|f\|_{\beta_c,q,j;T} = \operatorname*{ess\,sup}_{s\le -T} e^{-\beta_c s}\rho(s)^{-q}(1+\log(1/\rho(s)))^{-j}\,\|f(s)\|_2\,.$$

The causal Green

$$G_p f(s) = \int_{-\infty}^{s} U_p(s,r) f(r)\,\mathrm{d}r \tag{3.8.3}$$

converges in physical L^2 and satisfies the next estimate. Its constant depends on the displayed profile exponents but not on T:

$$\|G_p f(s)\|_2 \le C_{\beta_c,q,j} C_*(\rho(s)) e^{\beta_c s}\rho(s)^q (1+\log(1/\rho(s)))^j\,\|f\|_{\beta_c,q,j;T}\,. \tag{3.8.4}$$

Both (3.8.2) and (3.8.4) hold for the algebraic and dynamic fixed-reference rows of Lemma 3.6.3, with the same fixed C_s and g_{aux}. The Green estimate holds for every $\beta_c > g_{\mathrm{aux}}$, including $\beta_c = \lambda_c$.

It also holds with the weight $q_*\rho^{1+\sigma}$ of Section 3.9. By (3.8.2), the Duhamel ratio is at most $C_* \int_0^\infty e^{-(\lambda_c - g_{\mathrm{aux}} - \epsilon)u}(1+hu)^C du$, where $q_*(s) = \gamma(s) e^{\lambda_c s} T^b$ is the weight of Section 3.9; there $\gamma(s)$ is the center-gauge modulus, not the exponent $\gamma = \theta - 128\varkappa$ of Lemma 3.7.7. The bound holds since $(\log\gamma)' = o(1)$.

Proof. Theorem 2(v), with the same gauge and fixed-prefix/diagonal-tail proof, gives the actual completed-wave value and gradient estimates. Theorem 2(v) supplies the all-label clock and its normalized derivatives.

Theorem 2(iv) and Lemma 3.8.1 give the leading rate for S_{ref}. The same clause supplies the Gram metric for the extension (3.4.2) with its fixed smooth shift S_{app}. Lemma 3.4.2 estimates the work of $S_p - S_{\mathrm{app}}$ on the high input. Its prepared-column bounds come from Lemmas 3.7.7 and 3.7.15.

Thus each analytic input to the next block argument refers to this one completed source and this one physical mask.

For the algebraic reference columns the principal profiles on the shift support are the same e, ℓ as in Lemma 3.8.1. The proof there gives the same strict leading rate on $s \le -T$ for sufficiently

large $T > 0$. Omitting the first correctors and their divergence restorations preserves the masked smoothing and angular support used in Lemma 3.7.15. The additional low-column error is $O(\rho P(S))$. Since $0 < \nu < 1$ and $\rho \le 1$, it fits into the $O(\delta + \rho^{\nu} P(S))$ bound of (3.7.29) at radius δ. Select rates

$$\max(g_{\mathrm{ref}}, g_1) < g_{\mathrm{alg}} < g_{\mathrm{aux}} < \lambda_c.$$

Lemma 3.4.4 applied at g_{alg} gives $\|U_{\mathrm{alg}}(s,r)\| \le C(s) e^{g_{\mathrm{alg}}(s-r)}$ with $C(s) = \max\{1, C_*(\rho(s))\} = \rho(s)^{-o(1)}$.

Write $\Delta S = S_{p,\mathrm{dyn}} - S_{p,\mathrm{alg}}$ for the difference of the prepared shifts in (3.8.1). The right and adjoint fixed columns differ by $O(\rho)$ on L^2, since their first correctors and divergence restorations carry ρ and ρ^2, respectively, with bounded compact-chart kernels. The inverse pairing identity $M_d^{-1} - M_a^{-1} = M_d^{-1}(M_a - M_d)M_a^{-1}$ gives the same bound for their normalized fixed rows. In Lemma 3.7.15 the change of J_* is $(J_{r,d} - J_{r,a})(I - C_\delta)$, with d, a denoting the two fixed references. The bounds $\|J_*\| \le P(S)$ and $\|M_*^{-1}\| \le 2$ there give $O(\rho P(S))$ for the change of $K_* = M_*^{-1} K_r$, by the same inverse identity. Expanding $d_0 J_* C_s K_*$ with its fixed mask therefore gives

$$\|\Delta S(s)\|_{2\to 2} \le C\rho(s) P(S(s)), \qquad \epsilon_T := \sup_{\tau \le -T} C(\tau) \|\Delta S(\tau)\|_{2\to 2} \longrightarrow 0.$$

On each finite interval the bounded perturbation defines U_{dyn} by the Volterra equation

$$U_{\mathrm{dyn}}(s,r) = U_{\mathrm{alg}}(s,r) - \int_r^s U_{\mathrm{alg}}(s,\tau) \Delta S(\tau) U_{\mathrm{dyn}}(\tau,r)\, \mathrm{d}\tau.$$

The iterated integrals converge there by the factorial bound on the ordered time simplex. Put $v(s,r) = \|U_{\mathrm{dyn}}(s,r)\| / [C(s) e^{g_{\mathrm{alg}}(s-r)}]$. For $r \le s \le -T$ the algebraic estimate inside the integral has its prefactor at s; the normalized inequality is

$$v(s,r) \le 1 + \int_r^s C(\tau) \|\Delta S(\tau)\| v(\tau,r)\, \mathrm{d}\tau \le 1 + \epsilon_T \int_r^s v(\tau,r)\, \mathrm{d}\tau.$$

Grönwall gives $v(s,r) \le e^{\epsilon_T (s-r)}$. Choose T so that $\epsilon_T \le g_{\mathrm{aux}} - g_{\mathrm{alg}}$. This proves (3.8.2) for both two-time propagators with the same output-time envelope $C(s)$.

For either propagator, insert this bound in (3.8.3). Since $\rho(s) = 1/(h|s|)$, fixed powers of $\rho(r)/\rho(s)$ and ratios of logarithmic weights grow at most polynomially in $s - r$. Integrability against $e^{-(\beta_c - g_{\mathrm{aux}})(s-r)}$ for $\beta_c > g_{\mathrm{aux}}$ proves (3.8.4) and convergence of its Bochner integral. For the center weight choose $0 < \epsilon < \lambda_c - g_{\mathrm{aux}}$; on a sufficiently ancient interval $(\log \gamma)' = o(1)$ gives $\gamma(r)/\gamma(s) \le e^{\epsilon(s-r)}$. The other factors again have polynomial ratios. Finite-interval variation of constants gives the right-inverse identity. Letting the initial time tend to $-\infty$ in (3.8.2) gives uniqueness in the faster-decaying homogeneous class. The columns and masks preserve real conjugation. On each fixed weighted forcing space the same argument also gives $G_{p,\mathrm{dyn}} = G_{p,\mathrm{alg}}(I + \Delta S G_{p,\mathrm{alg}})^{-1}$: the norm of $\Delta S G_{p,\mathrm{alg}}$ is at most a profile-dependent constant times ϵ_T. □

3.9 Removal of the physical shift and an exact real mode

Main result. Proposition 3.9.34 removes the auxiliary shift for the selected completed source, in the stated critical forcing space. Proposition 3.10.4 then gives a nonzero real mode of the original completed equation, with the stated norm and energy bounds.

These results use the completed auxiliary propagation and the physical spectral data for that same member. The source construction, true-velocity spectral construction, and completed all-frequency auxiliary propagation precede this section.

They fix one completed base B_* and one conjugate pair of maximal growth $\pm m$. All the operators below are those of that same base.

In particular the completed generator keeps its waves and the pressure constraint. We give the finite-kernel and two-column argument necessary to remove the auxiliary shift, and then construct a real homogeneous solution of the unshifted linear equation.

Actual analytic domains. The physical spectral and completed-source inputs used here belong to one jointly selected member. The lemmas below prove the compact macro stress, typed output, graph-normalizer, and fixed-gap commutator domains where the proof uses them.

The scalar inverse, physical auxiliary inverse and Gaussian cell inverse keep their different forcing spaces, as specified in the lemmas below.

3.9.1 Typed OUTPUT bounds and finite graph localization

We fix the source and profile constants in this subsection before ancient thresholds. We always retain a right mask. We distinguish an OUTPUT error, a scalar graph output of an uncut reference row, and a SOURCE for the Gaussian cell inverse.

Lemma 3.9.1 (Column H^2 bound, conditional)**.** *Fix $\delta \le r \le r_{\mathrm{out}}$. Let ∇_* be the normalized physical derivative of Lemma 3.9.4 (axial part $\rho\partial_Z$), let ∇_*^2 denote two iterated components of ∇_*, and put $\|u\|_{H^2_*} = \sum_{i\le 2} \|\nabla_*^i u\|_{L^2_{\mathrm{can}}}$. Suppose the right column on the range of the mask splits as*

$$JC_r = J^0 C_r + \sum_{\iota\in I} e^{i\Psi_\iota} A_\iota C_r + J^{\mathrm{tl}} C_r,$$

with a zero-carrier part J^0, finitely many high-carrier terms and a localization tail, such that:

(C1) $\#I \le P(S)$;

(C2) $\|J^0 C_r f\|_{H^2_*} \le P(S)\,\|f\|_2$;

(C3) on the support of A_ι, $|\nabla_*\Psi_\iota| \le \rho^{-1/2}P(S)$ and $|\nabla_*^2\Psi_\iota| \le \rho^{-1}P(S)$;

(C4) $\|\nabla_*^i A_\iota C_r f\|_2 \le \rho^{-b_i} P(S)\,\|f\|_2$ for $i = 0,1,2$, with $b_0 = 0$, $b_1 \le \frac{1}{2}$ and some $b_2 \ge 0$;

(C5) $\left\|J^{\mathrm{tl}} C_r\right\|_{L^2\to H^2_*} \le P(S)$.

Then

$$\|JC_r\|_{L^2_Z \to H^2_*} \le \rho^{-\max(1,b_2)} P(S).$$

In particular, if $b_2 \le 1$ the bound is $\rho^{-1}P(S)$, which implies the bound $\rho^{-2}P(S)$ used in the proof of Lemma 3.9.4.

Moreover, suppose J^0 is a finite sum of right-ordered words $c(x_h, Z)Z^a k^b$ (after the exact chart $\mathcal{T}_\rho$), with

$$\sup_Z \sum_{l\le 3} \left\|\partial_Z^l c(\cdot, Z)\right\|_{H^3_1} \le C.$$

If

$$\left\|Z^a k^b C_r\right\|_{L^2\to L^2} \le C$$

for the finitely many (a,b) that occur with up to three extra powers of k, then (C2) holds with $P(S)$ replaced by C. For a smooth radial cutoff χ_Q to $\{R \ge cQ^{-1/2}\}$ with $|\nabla^i \chi_Q| \le CQ^{i/2}$, one also has

$$\left\|\chi_Q J^0 C_r\right\|_{L^2\to H^3_*} \le CQ^{1/2}.$$

Proof. For any first-order derivations ∇_a, ∇_b and a function F,

$$\nabla_a\nabla_b(e^{i\Psi}F) = e^{i\Psi}\big[-(\nabla_a\Psi)(\nabla_b\Psi)F + i(\nabla_a\nabla_b\Psi)F + i(\nabla_b\Psi)\nabla_a F + i(\nabla_a\Psi)\nabla_b F + \nabla_a\nabla_b F\big].$$

With $F = A_\iota C_r f$, (C3) and (C4),

$$\left\|\nabla_*^2(e^{i\Psi_\iota}A_\iota C_r f)\right\|_2 \le P(S)\big[\rho^{-1} + \rho^{-1} + 2\rho^{-1/2-b_1} + \rho^{-b_2}\big]\,\|f\|_2 \le \rho^{-\max(1,b_2)}P(S)\,\|f\|_2\,,$$

and the zero- and first-order terms are smaller. Summation over ι costs the factor $\#I \le P(S)$; add (C2) and (C5).

For the second part, $(c\,g)(x_h, Z) = c(x_h, Z)g(Z)$ with $g = Z^a k^b C_r f$, and $\|c\,g\|_{L^2(\mathrm{d}x_h\,\mathrm{d}Z)} \le \sup_Z \|c(\cdot, Z)\|_{L^2}\,\|g\|_2$. Horizontal derivatives fall on c; $\rho\partial_Z(cg) = \rho c_Z g + c\,(ikg)$ since $k = -i\rho\partial_Z$, and $ikg = iZ^a k^{b+1}C_r f + \rho a Z^{a-1}k^b C_r f$, since $i[k, Z^a] = \rho a Z^{a-1}$ (the second term vanishes for $a = 0$). After $j \le 3$ axial derivatives the reordered words are constant multiples of $\rho^i Z^{a-i}k^{b+j-i}C_r$, $0 \le i \le \min(a, j)$. Their norms are bounded by the stated $Z^a k^{b+j}C_r$ bound. Indeed, integration by parts against $(Z^{2l-1})'$ and Cauchy–Schwarz give $\|Z^{l-1}v\|_2 \le 2\|Z^l\partial_Z v\|_2/(2l-1)$ for $l \ge 1$. Iterate this on smooth masked inputs and extend by density. The cutoff estimate follows from $1 \le (c^{-1}Q^{1/2}\langle R\rangle)$ on $\operatorname{supp}\chi_Q$ and the weight one in H_1^3. □

Lemma 3.9.2 (The subprincipal row S_0)**.** *Write $S_0 = P_k F_1$ for the projected order-ρ primitive symbol of (3.6.5):*

$$S_0 v = P_k F_1(Z,k)v = P_k\Big[(\Delta_h - k^2 + (\tfrac12 + h)) + \tfrac12 y\cdot\nabla_h)v - R_h\cdot\nabla_h v - v_h\cdot\nabla_h(R_h, 0) - v_z\partial_Z\mathcal{B}_0\Big].$$

In the normalized chart, $\mathcal{B}_0 = (U_h, W) = (\Omega\, y^\perp, \mathcal{U})$ and $R_h = \mathcal{V}\,y/R$, with $\Omega, \mathcal{U}, \mathcal{V}$ in the similarity coordinates $y = x_h/\sqrt{t}$, $Z = z/t^{1/2-h}$ of the completed field. Since $B_0 = t^{-\frac12-h}(\mathcal{H}e_\theta + \mathcal{U}e_z) + t^{-1/2}\mathcal{V}e_r$ and $t^{-1/2} = \rho\, t^{-\frac12-h}$, the pair $(R_h, 0)$ is the order-ρ part of the leading field.

(a) $R_h(y, Z) = -y\int_0^1 \theta\, g(\theta y, Z)\,\mathrm{d}\theta$, *with* $g = \partial_Z W$.

(b) Suppose $W(\cdot, Z)$ is supported in $|y| \le R_W$ for $Z \in I_Z$. This is the axial support condition in Theorem 2(iv). Then $\left\|D^\beta R_h\right\|_\infty \le (R_W + |\beta|)\,\|g\|_{C^{|\beta|}}$ for $|\beta| \le 5$, and in particular $R_h \in C_b^5$. If instead only $|D^\beta g(y)| \le C_\beta\langle y\rangle^{-2}$ holds, then $R_W\left\|D^\beta g\right\|_\infty$ is replaced by $\frac{\pi}{2}C_\beta$.

(c) $\partial_Z\mathcal{B}_0 \in C_b^5$ uniformly for $Z \in I_Z$.

Consequently F_1 is a differential operator of order two, whereas S_0 includes the nonlocal projection P_k. The principal part of F_1 is Δ_h, with constant coefficients. Its first-order coefficients are $\frac12 y$ (exactly linear) and R_h (bounded). Its zeroth-order coefficients are $(\frac12 + h) - k^2$ (bounded on Λ), $\nabla_h R_h$ and $\partial_Z\mathcal{B}_0$ (in C_b^4). On the selected sectors $\mathsf{H}_{\pm m}$ this gives $\|S_0 v\|_{H_w^s} \le C\,\|v\|_{H_{w+1}^{s+2}}$ for $s \le 4$ and $\lceil w\rceil + 1 \le m - 1$. With $e \in H_6^6$ we obtain $S_0 e \in H_5^4$. The physical connection also contains the divergence-chart and pressure terms in (3.7.1); it is not obtained from $S_0 e$ alone. The corresponding full corrector bounds are those of Lemma 3.7.1.

Proof. (a) The leading field in Theorem 2(iv) is divergence-free. In the positive similarity chart $r = t^{1/2}R$ and $z = t^{\frac12-h}Z$. So $\operatorname{div}_x B_0 = t^{-1}[R^{-1}\partial_R(R\mathcal{V}) + \partial_Z\mathcal{U}]$, using $(\frac12 + h) + (\frac12 - h) = 1$ (the swirl part is divergence-free). Regularity at $R = 0$ gives $R\mathcal{V} = -\int_0^R s\,\partial_Z\mathcal{U}(s, Z)\,\mathrm{d}s$, and the substitution $s = \theta R$ gives (a). (b) Put $I(y) = \int_0^1 \theta g(\theta y)\,\mathrm{d}\theta$. Then $D^\beta(y_i I) = y_i D^\beta I + \beta_i D^{\beta-e_i}I$, and $D^\beta I = \int_0^1 \theta^{1+|\beta|}(D^\beta g)(\theta y)\,\mathrm{d}\theta$. Hence $|y||D^\beta I| \le \int_0^{|y|} |D^\beta g(s\hat{y})|\,\mathrm{d}s \le R_W\left\|D^\beta g\right\|_\infty$ and $|D^{\beta-e_i}I| \le$

$\|g\|_{C^{|\beta|-1}}$. (c) $\partial_Z U_h = (\partial_Z \Omega)\, y^\perp$, and $|\partial_Z \partial_r^j \Omega| \le C\langle r\rangle^{-2-2h-j}$ for $j \le 5$ (Theorem 2(iv)). Together with Cartesian regularity at the axis, this bounds five Cartesian derivatives by $C\langle r\rangle^{-1-2h}$. Also $\partial_Z W$ is smooth with compact support. For the mapping bound: Δ_h maps $H^{s+2}_w \to H^s_w$, $\frac{1}{2} y\cdot\nabla_h$ maps $H^{s+1}_{w+1} \to H^s_w$, the multiplications are bounded by the C^s norms of their coefficients (the coefficient bounds of Theorem 2(iv)), and P_k is bounded by the weighted Leray bound in Theorem 2(iv). □

Remark 3.9.3 (Application to the prepared column). For the uncut prepared column (3.9.1), including its time-partition correction, the decomposition in Lemma 3.9.1 has $J^{\mathrm{tl}} = 0$ and $J^0 = J_{\mathrm{low}} + \mathcal{T}_\rho b$. The low coefficients are in H^{16}_5 by Lemma 3.7.1; the macro coefficients are in H^8_{6-j} before G and H^8_{5-j} after it, by Theorem 2(iv). The word bounds of Lemma 3.7.13 give (C2).

The other terms $B_0, B_1, B_{2,\mathrm{high}}, Y_Q, Y_b, C_{\mathrm{part}}$ are full curls with nonzero carriers. Their number is at most $P(S)$ by the fixed cover and finite cell tree. The phase bounds $|\nabla_*\Psi| \le \rho^{-1/2}P(S)$ and $|\nabla_*^2\Psi| \le \rho^{-1/2-\varkappa}P(S)$ give (C3). Lemmas 3.7.12 and 3.7.14 give (C4) with $b_1 = 129\varkappa$ and $b_2 = 130\varkappa < 1$, for all admitted right masks. Thus $\|JC_r\|_{L^2\to H^2_*} \le \rho^{-1}P(S)$.

Endpoint, deletion, localization, opposite-band and finite-prefix errors, and any macro-memory truncation error, arise when the completed generator acts on this finite column. They belong to the residual F_i, not to J^{tl}, and are estimated in the simultaneous L^2 and ∇_* output norms of Lemma 3.9.4. No H^2 estimate on such residual tails is inferred. The optional fixed-physical-radius cutoff clause of Lemma 3.9.1 is unused for this uncut column.

Lemma 3.9.4 (Simultaneous OUTPUT bound)**.** *For each $\delta \le r \le r_{\mathrm{out}}$, the sum of actual OUTPUT errors satisfies*

$$\|F_{\mathrm{out}}C_r\|_{L^2_Z\to L^2_{\mathrm{can}}} + \|\nabla_* F_{\mathrm{out}}C_r\|_{L^2_Z\to L^2_{\mathrm{can}}} \le C\rho^2 P(S).$$

Here ∇_* is the isotropic normalized physical derivative, with axial part $\rho\partial_Z$. The same bound holds with the actual right graph factor $C_r\langle k\rangle^2$, $k = -i\rho\partial_Z$.

This does not give a bound for unmasked physical F_{out} on arbitrary H^{-2} input. We do not return an OUTPUT error to the Gaussian-weighted cell inverse.

Proof. There are five actual OUTPUT types. First, $CP(v)P(w)^{-1}e^{-\lambda_*(v-w)}$ bounds the shifted cell kernel.

A source $P(w)a(w)$ produces $CP(v)\sup|a|$. Differentiated coefficient equations form a finite triangular recurrence with the same kernel.

The differentiated coefficients thus cost only fixed powers of S. On $[0, L_p]$ the cutoff equals one on $[3L_p/10, 7L_p/10]$. The supports there of $1-\psi$ and ψ' lie in the Gaussian tails, where $P(v) \le e^{-cS}$. The two endpoint terms $(1-\psi)h - \psi' t$ therefore cost at most $\rho^{-M}P(S)e^{-cS}$ after finite curls, pressure, words and one output derivative. This is flat because $S \asymp \log^{6/5}(1/\rho)$.

Second, on the actual aggregate deletion and transition set the weight is $\mathsf{W} \le e^{-cS}$. We keep the exact cutoff curl. After each specified finite derivative, the source classes keep a positive W^β factor.

Other factors are logarithms, $P(S)$, and a finite negative ρ power. This is again flat.

We divided by uncut positive amplitudes, not by the aggregate cutoff.

Third, we insert the fixed spatial cutoff $\zeta(Z)$ in the raw coefficients as in Section 3.7.1. The macro kernel has no input-k dependence and keeps this support.

Lemma 3.7.4 applies to its frozen-parameter domain and physical pressure comparison only. It does not replace this coefficientwise kernel by a frequency-dependent one.

Across the fixed physical Z output gap, the freely selected scalar right-mask kernel has arbitrary finite Schur decay $(\rho/r)^N$. The actual coarse source $W^{2,\infty}$ and column H^2 output losses together are bounded by $\rho^{-4}P(S)$.

We select $N = 16$ after the finite word factors, or increase it by a finite amount. This leaves $\rho^{-4}(\rho/r)^{16} \le \rho^{5.6}$.

Only the scalar mask undergoes this many integrations by parts. We do not differentiate the spectral profile or macro resolvent this many times.

The oscillatory carrier has modulus one. The coarse output bound includes its finite physical derivatives.

We do not assume that its physical frequency translation is small. A frequency-gap argument applies only after the LOW row removes the high carrier.

If we truncate a macro memory at $K\log(1/\rho)$, its fixed reduced gap gives any prescribed power after selection of K. An untruncated memory has no invented tail.

Fourth, we select one finite source prefix with $h\beta_N \geq (\frac{1}{2}+h)+6$. The actual diagonal tail through two physical derivatives and the smooth off-tip localization field give, globally,

$$\|E_N(y)\|_{W^{2,\infty}_y} \leq CQ^{\frac{1}{2}+h}, \qquad E_N(y) = Q^{\frac{1}{2}+h}e_N(\sqrt{Q}y,t).$$

This includes trace labels $Q_\gamma \gg Q$.

We first construct the compact macro input by Lemma 3.7.2, then its response. Lemma 3.9.1 gives

$$\|JC_r\|_{L^2\to H^2_y} \leq \rho^{-\max(1,b_2)}P(S) = \rho^{-1}P(S) \leq \rho^{-2}P(S),$$

since $b_2 = 130\varkappa$ by Lemma 3.7.14.

The true product rule and whole-space Leray bound on H^1 now give

$$\|P\,\mathrm{div}(E_N\otimes J + J\otimes E_N)C_r\|_{H^1_y} \leq C\rho^{(\frac{1}{2}+h)/h-2}P(S), \qquad (\tfrac{1}{2}+h)/h-2 > 49.$$

We do not invert the remainder again. This order does not use the full-column bound to prove its own macro source domain.

Fifth, if we cut a noncompact column at a fixed physical radius, its transition lies at $R \asymp Q^{-1/2}$. Leading five-k and corrector four-k ladders keep two moments.

We use one moment for the actual divergence primitive. For the macro response and its finite mixed parameter jets, equation (3.7.26) uses one of the four remaining moments.

We do not assume a compact vertical tail or horizontal solenoidality for the k derivatives. Choose a smooth exterior cutoff $\chi_Q(R) = \chi_{\mathrm{ext}}(Q^{1/2}R)$ with $\chi_{\mathrm{ext}} = 0$ on $[0,c]$ and $\chi_{\mathrm{ext}} = 1$ on $[2c,\infty)$ for a fixed $c > 0$. The remaining weight $\langle R\rangle$ controls the H^3 norm on its support. Thus

$$\|\chi_Q JC_r\|_{H^3} \leq CQ^{1/2}\rho^{-2}P(S).$$

Indeed $\langle R\rangle^{-1} \leq CQ^{1/2}$ there, and differentiating the cutoff j times in the horizontal Cartesian variables costs at most $C_jQ^{j/2}$ for $1 \leq j \leq 3$. The product rule gives the estimate for $0 < Q \leq 1$.

Radial dilation of the cutoff stays bounded. Full-curl repair and one output derivative cost at most $\rho^{1/(2h)-2}P(S)$, with exponent greater than 48. We do not assert that any fixed normalized-radius cutoff has this property.

An uncut column has no such cutoff error. We use the uncut column. The fixed-radius cut is not used, so the full-curl repair of a cut column is not a column component, and input (C5) of Lemma 3.9.1 holds with $J^{\mathrm{tl}} = 0$.

For the graph statement, we use exact left quantization:

$$C_r\langle k\rangle^2 = \mathrm{Op}_\rho(c_r(1+k^2)), \qquad \langle k\rangle^2\,\mathrm{Op}_\rho(c_r) = \mathrm{Op}_\rho((1+k^2)c_r - 2i\rho k c_{r,Z} - \rho^2 c_{r,ZZ}).$$

Because $\rho/r \leq r$, these masks are bounded right masks with the same finite kernel estimates. Word degree thirteen becomes fifteen (and one output level can give sixteen).

This is a finite polynomial on compact input frequency. It does not require sixteen resolvent derivatives.

We increase the freely selected mask integration index to bound these factors. This proves the simultaneous assertion on arbitrary right-masked scalar L^2 input, not just one Gaussian.

First-symbol $O(\rho^{3/2})$ remainders, time-partition errors, $\rho^{\nu} r$ pressure displacement and high-to-low returns are NOT OUTPUT tails. They remain in their different residual rows.

□

Lemma 3.9.5 (Finite kernel and graph normalization)**.** *Write $H^{-2}_{\mathrm{ax},\rho}$ for the scalar graph space with norm $\|\langle k\rangle^{-2} f\|_2$. Fixed OUTER plateau separations in the actual row/column family have $O(\rho^{3/2} P(S))$ kernels, also from $H^{-2}_{\mathrm{ax},\rho}$ after the actual compact-output localization.*

For $E_j = K_{\mathrm{ref}} D_p C_j$, $M_j = I + E_j$, the exact inverse on this graph space is

$$M_j^{-1}|_{H^{-2}_{\mathrm{ax},\rho}} = I - (M_j^{-1}|_{L^2}) E_j. \tag{O5}$$

The inverse does not itself smooth.

Proof. Use the two-radius version of (SC2) in paragraph 3.9.2.1, with a fixed outer plateau and the actual right radius $r \geq \delta$. Here are the radial interfaces in that application. In each fixed angular sector put $\mathcal{H} = L^2_{\mathrm{rad}}$. The leading profiles, including their five k derivatives, lie in the common space $H^6_2 \subset \mathcal{H}$, with ordinary Z jets through seventeen. The first homological correctors, with four k derivatives, lie in $H^4_2 \subset \mathcal{H}$, with sixteen ordinary Z jets. Their contributions retain the prefactor ρ. The divergence primitive G in the displayed reference columns uses one moment: $G\partial_Z e_z, G\partial_Z v_z$ use the leading ladder, and $G\partial_Z E_{1,z}, G\partial_Z v_{1,z}$ occur with ρ^2. The latter have four k jets in H^4_1 and fifteen ordinary Z jets. These are bounded maps into $\mathcal{H}$; their adjoints are rows on $\mathcal{H}$, not unweighted Leray derivatives.

First apply every finite right-ordered word to C_r. Exact differentiation gives a column symbol s_r supported in $\operatorname{supp} c_r$, with

$$\|\partial_Z^l \partial_k^j s_r\|_{\mathcal{H}} \leq P(S) r^{-l-j}, \qquad l \leq 3, \quad j \leq 2.$$

These are the finite coefficient estimates of (3.9.1), after the reference row removes the nonzero angular carriers. They use the coefficient reservation, not additional spectral k derivatives. More explicitly, the prepared output path uses $59 + 8 + 3 + 2 = 72$ ordinary levels. Three further ordinary Z derivatives for separation, plus two for an axial graph placement, use at most $77 < 80 = J_{\mathrm{src}}$ levels of the already selected export (Theorem 2(vi)). The eleven input-word factors have acted on the smooth mask and add no eleven coefficient derivatives to this count. All these extra derivatives are on carrier-free coefficients, not on a fast phase. Apply the column version of (SC2) to the actual adjoint reference row and this symbol. Its leading term uses $n = 3$; each ρ corrector uses $n = 2$. The additional ρ^2 divergence correction is already of the required output size. Consequently the fixed-plateau errors are bounded by

$$CP(S)\left[(\rho/r)^3 + \rho(\rho/r)^2 + \rho^2\right] \leq CP(S)\rho^{9/5}.$$

Actual completed output tails have their separate $O(\rho^2 P(S))$ bound from Lemma 3.9.4. No polynomial spatial weight is applied to a rough adjoint row.

For the right graph norm replace s_r by $s_r(1 + k^2)$. This exact replacement keeps its support and scaled seminorms. For an output graph factor the identity in the proof of Lemma 3.9.4 spends two ordinary Z jets, not two radial moments or two further k derivatives. Thus the same argument

holds from $H^{-2}_{\mathrm{ax},\rho}$ after the stated compact-output localization. Pure smooth-mask errors alone may be taken to arbitrary finite order.

The uncut reference defect has axial order at most two after its common dilation cancels. Its radial differential terms are assigned to the adjoint reference profile in the physical pairing. They use at most two Sobolev derivatives and one radial moment for dilation. Thus the leading H^6_2 ladder still has H^4_1, the first corrector H^4_2 ladder has H^2_1, and the $\rho^2 G$ restoration retains at least unweighted H^2. The leading quantization-time term $h\rho k\partial_k v$ belongs to the ρ, $n = 2$ class: its four k derivatives use only the fifth leading derivative. Time derivatives of first-corrector terms have overall order ρ^2 and are estimated in the right-masked output norm. This gives the stated map into the scalar H^{-2} space without placing an unbounded differential operator on arbitrary physical L^2 input.

In particular $E_j : H^{-2}_{\mathrm{ax},\rho} \to L^2$ is bounded. Since E_j maps into L^2, the expression $I-(M_j^{-1}|_{L^2})E_j$ is well-defined and bounded on H^{-2}. Multiplication by $I + E_j$ on either side verifies (O5), using the ordinary L^2 inverse. Its identity part remains nonsmoothing. For fixed masks the exact identity

$$[F, M_j^{-1}] = -M_j^{-1}[F, E_j]M_j^{-1}$$

is therefore valid also on this graph extension. Localized rows such as $C_\chi M_j^{-1}$ are bounded $H^{-2} \to L^2$ by (O5) and the compact-frequency bound for C_χ. No Neumann-series truncation or additional inverse symbol class is used. □

Lemma 3.9.6 (Two fixed-gap scalar inverse commutators)**.** *Let $A = d_{\mathrm{old}} + d_0 C_s - B_{\mathrm{int}}$ be the fixed-gap SHIFTED scalar operator, and $G = A^{-1}$ on the gauged scalar forcing profile $q_*\rho^{1+\sigma}$, $\sigma = 3/20$. Its norm is fixed, not the physical auxiliary inverse's $\rho^{-o(1)}$ norm.*

Select nested fixed masks F_0, F_1, F_2, F_3. Each next mask equals one on a fixed neighborhood of the previous support.

The mask F_0 covers the full C_s support. Then

$$\|F_0 G(1 - F_3)\| \le C\rho^{3/2}P(S).$$

Proof. The fixed cubic is supported where the outer masks are constant.

Finite composition and Lemma 3.9.5 give $[A, F_i] = \rho L_i + R_i$, where L_i is output-localized on dF_i, $\|L_i\| \le C + \rho^c P(S)$ and $\|R_i\| \le \rho^{3/2}P(S)$. The fixed-gap scalar convolution keeps each of the finitely many profiles multiplied by $\rho^a P(S)$, since their logarithmic derivatives are $o(1)$.

On the ancient-boundary core $[F, G] = G[A, F]G$. For fixed smooth phase masks with the symbol of F' equal to one near the support of the symbol of F, finite nonstationary phase gives $F(1 - F') = O_N(\rho^N)$ for every fixed N; this is not an exact zero. We retain the exact identity

$$FG(1 - F') = F(1 - F')G + FG[A, F']G.$$

Use it with $(F, F') = (F_0, F_1)$ and with (F_2, F_3), retaining also $(1-F_1)(1-F_3) = (1-F_3)+O_N(\rho^N)$. The resulting formula is

$$F_0 G(1 - F_3) = F_0 G[A, F_1]F_2 G[A, F_3]G + R_{\mathrm{gap}} + R_{\mathrm{plat}},$$

where

$$R_{\mathrm{gap}} = F_0 G[A, F_1](1 - F_2)G(1 - F_3), \qquad \|R_{\mathrm{plat}}\| \le C_N \rho^N P(S).$$

The plateau remainder is a finite sum of products containing a smooth fixed-gap mask error and bounded fixed-gap inverses. Their convolution estimates preserve each of the finitely many weights

multiplied by ρ^N. Choose $N = 4$; the remainder remains smaller than $\rho^{3/2}P(S)$, including after the later single critical ρ^{-1} loss. By the fixed-gap calculus, we can multiply the first commutator on the right by F_2 with a fixed-gap remainder, so $\|[A, F_1](1 - F_2)\| \le C\rho^{3/2}P(S)$ and $\|R_{\mathrm{gap}}\| \le C\rho^{3/2}P(S)$. The displayed main term is $O(\rho^2[C + \rho^c P(S)]^2)$, by $[A, F_i] = \rho L_i + R_i$ and the fixed norm of G.

Each omitted term contains a plateau remainder or R_i and bounded FIXED scalar inverses. We first localize graph tails by Lemma 3.9.5.

We transport all masks and G together under N: $F_i' = NF_iN^{-1}$, $G' = NGN^{-1}$. Exact conjugacy keeps the identity without estimating N_s from smallness of $N - I$.

The difference between the physical mask and its conjugate is the fixed-gap commutator estimated. □

3.9.2 The finite profile algebra and the fixed masks

Write $T = -s = t^{-h}/h$, $\rho = (hT)^{-1} = t^h$, and $k = -i\rho\partial_Z$. Scalar amplitudes are in $L^2_Z(\mathbb{C}^2)$ with involution $(a_+, a_-) \mapsto (\overline{a_-}, \overline{a_+})$.

All phase masks below are a fixed finite family after the source and spectral pair have been selected. The outer shift chart and its strict scalar gap are frozen first. Its shift mask C_s is one on a fixed neighborhood of the supports of the two right-column masks $C_\delta, C_{\log}$ and the transitions necessary below. Here C_r is the fixed-shape phase mask of radius r of Lemma 3.7.7. The power mask is $C_\delta = C_r$ at $r = \delta$. The logarithmic-radius cell is $C_{\log} = C_r$ at $r = r_{\mathrm{out}}$, with $r_{\mathrm{out}} = S_{\mathrm{mask}}^{-M}$ defined below.

We then select the smaller cubic blend radius κ_0 strictly inside this plateau. It does not change C_s or its gap.

Choose the fixed masks nested in the order $C_s \prec C_0 \prec C_1 \prec C_\chi \prec C_b$ inside the eigenbundle chart, where the symbol of the next mask equals one on a fixed neighborhood of the preceding closed support. Thus $\operatorname{supp} d\chi$ has positive distance from the full shift and the inner masks. Choose the output pad C_{ann} around this transition inside the plateau of C_b, with its closed support still separated from the inner masks. We take $C_\chi = \mathrm{Op}_\rho(\chi)^*$ in the output-adjoint left-quantization convention of Lemma 3.6.5.

This fixes the localized-row cutoff orientation below. The inner power radius is $\delta = \rho^{2/5}$.

On the ancient range $0 < \rho < 1$ set

$$L(s) = 1 + \log(1/\rho(s)), \qquad S = S_{\mathrm{mask}}(s) = L(s)^{6/5}, \qquad r_{\mathrm{out}}(s) = S_{\mathrm{mask}}(s)^{-M}.$$

This is a smooth mask-design clock, distinct from the discrete source pulse scale $S_\ell = \ell^{6/5}$. On a prepared band $Q = 2^{-\ell} \asymp t$ we have $\rho = t^h \asymp \rho_Q = 2^{-h\ell}$, so $S_{\mathrm{mask}} \asymp S_\ell$.

Since $\rho_s = h\rho^2$, the exact derivatives are

$$(\log S_{\mathrm{mask}})_s = -\frac{6h\rho}{5L}, \qquad (\log r_{\mathrm{out}})_s = \frac{6Mh\rho}{5L}.$$

In particular $|\partial_s \log r_{\mathrm{out}}| \le C_M\rho/L = o(\delta^2)$. For each fixed M, $\delta \ll r_{\mathrm{out}}$ at sufficiently small ρ.

Here $P(S)$ denotes a polynomial of fixed degree, and it may change from line to line. The source clock estimate makes $P(S) = \rho^{-o(1)}$.

Lemma 3.7.7 gives the coefficientwise cell construction and its radial, angular and ordinary-jet estimates. On one source chart its prepared right column has the finite form

$$J_{\mathrm{prep}} = J_{\mathrm{low}} + B_0 + B_1 + B_{2,\mathrm{high}} + T_\rho b + Y_Q + Y_b. \tag{3.9.1}$$

The global column also includes the finite full-curl correction for the time-partition derivative of B_0.

This correction has the same high-carrier support and $O(\rho P(S)(r+a_\rho))$ radius-r residual, where $a_\rho = \rho^{1/2-128\varkappa}$. Each coefficient of the six correction terms to the right of J_{low} is a finite sum of right-ordered words $c_{ab}(R,Z,T,Y)Z^a k^b$.

The scalar input is on the far right.

The maximal physical input-word degree is eleven, with the separate degree-eight macro coefficient and degree-nine macro lift counted in paragraph 3.7.3. The primary cell inverses act on these coefficients and the auxiliary clock, not on an arbitrary input's time derivative.

The coefficients include full physical curl, divergence restoration and pressure. The source recursion provides ordinary coefficient derivatives through the selected source budget $J_{\mathrm{src}} = 80$.

Its prepared reservation $J_{\mathrm{prep}} = 72$ contains the fifty-nine-level stress sequence (3.7.31), eight return levels, and two output levels. These use sixty-nine levels in total and leave room for the two different source-band connections. With the second output derivative of Lemma 3.7.14 the count is $59+8+3+2 = 72 = J_{\mathrm{prep}}$, with zero margin.

The selected right and left radial profiles provide five k derivatives, sixteen ordinary Z derivatives and the requisite fixed weighted radial moments. These are finite-order assertions for the one selected member, with constants independent of ρ.

The high carriers have angular labels $m + jn_\gamma$ with $j \neq 0$.

Since $|n_\gamma| \geq 2m+1$, these labels lie outside $\{m, -m\}$ (Lemma 3.7.5), so they are orthogonal to the fixed $\pm m$ reference row. Matching opposite carriers are retained in the low macro stress before this projection.

Only these finite low words and the prescribed localization tails enter the row estimates.

Let $J_{\mathrm{ref}}, K_{\mathrm{ref}}$ be the dynamically corrected fixed reference maps, normalized so $K_{\mathrm{ref}} J_{\mathrm{ref}} = I_2$. Both right columns use the same difference $D_p = J_p - J_{\mathrm{ref}}$.

$$J_j = J_{\mathrm{ref}} + D_p C_j, \quad E_j = K_{\mathrm{ref}} D_p C_j, \quad M_j = I + E_j, \quad K_j = M_j^{-1} K_{\mathrm{ref}}, \qquad j = \delta, \log. \tag{3.9.2}$$

We estimate the E_j before we apply either inverse.

The actual row annihilates all nonzero high carriers in (3.9.1). The remaining low words have the just stated finite k moments and ordinary derivatives.

We keep the right mask in each word.

Lemma 3.9.7 (Finite-family same-mask localization)**.** *Let C be any fixed mask equal to one on the right-column supports and a fixed neighborhood. Let R_{raw} be the old-coordinate completed residual in (3.9.20).*

The actual finite profile estimates give

$$\begin{aligned} \|[C, E_j]\| + \|(I - C_b)E_j\| + \|E_j(I - C_b)\| &\leq C\rho^{3/2} P(S), \quad j = \delta, \log, \\ C_\chi K_{\log} R_{\mathrm{raw}} - B_{\mathrm{int}} C_\chi &= \rho C_{\mathrm{ann}} A_{\mathrm{ann}} + R_{\mathrm{sep}}, \\ \|R_{\mathrm{sep}}\| \leq C\rho^{3/2} P(S), &\qquad \|A_{\mathrm{ann}}\| \leq C + \rho^c P(S), \end{aligned} \tag{3.9.3}$$

where $B_{\mathrm{int}} = C_b K_{\log} R_{\mathrm{raw}} C_b$. Here C_{ann} is an output mask on the fixed transition of C_χ, and we fix $c > 0$. By Lemma 3.9.14, the display above holds with $A_{\mathrm{ann}} = 0$ and $\|R_{\mathrm{sep}}\| \leq C_{\kappa_0}\rho^{3/2}P(S)$; the general form is kept only for comparison with the text. The scalar B_{int} splits as $B_{\mathrm{int}} = C_b \operatorname{Op}_\rho(e_{\kappa_0}) C_b + B_{\mathrm{int}}^{\mathrm{nc}}$ with $\|\operatorname{Op}_\rho(e_{\kappa_0})\| \leq C_B \kappa_0^3$ and, after a κ_0-dependent ancient threshold, $\|B_{\mathrm{int}}^{\mathrm{nc}}\| \leq \omega_B(s) = C_b r_{\mathrm{out}}(s)^3 + C_{\kappa_0}\rho(s)^{2/5} P(S)$. The constants C_B, C_b do not depend on κ_0, S or ρ (Lemma 3.9.30). The upper bound $\omega_B(s)$ tends to zero as $s \to -\infty$. Lemma 3.9.14 gives the precise form of the first two lines of (3.9.3), with a proof.

Proof. The input-word counts are upstream of any localization result: paragraph 3.7.3 gives column degree eleven and residual degree thirteen; the two axial graph factors in Lemma 3.9.4 give degree fifteen. These counts establish the degree needed in (SC4). The physical operator bound at that degree is the separate condition in the paragraph on p. 697. The first line and the row factorization follow from the stronger estimates of Lemma 3.9.14: its proof uses the finite two-radius calculus, the pole normalization of Lemma 3.9.15, and the graph extension of Lemma 3.9.5. The normalizer proof uses the low-row identity and the kernel calculus, not the present lemma. Thus this forward reference is noncircular. In particular the row factorization holds with $A_{\mathrm{ann}} = 0$. The cubic decomposition and the stated noncubic bound are Lemma 3.9.30. All arbitrary-order remainders used there are products of smooth masks; leading and first-corrector separations retain their respective finite orders three and two, the latter with its actual factor ρ. □

3.9.2.1 Finite separated composition on the actual mask scales

The following kernel argument uses the left ordering (3.6.1). It precedes the graph and inverse-normalizer applications: no graph bound or row estimate is an input to this argument. Put $k = -i\rho\partial_Z$ and $\delta = \rho^{2/5}$. All radial operator norms below are between specified Hilbert spaces with compatible domains and ranges; an unbounded differential operator is not an admissible middle factor without its domain.

For a symbol b write

$$M_q(b) = \int |u|^q \sup_Z \|\widehat{b}(Z,u)\|\, du, \qquad L_q(b) = \int \sup_Z \|\partial_Z^q \widehat{b}(Z,u)\|\, du.$$

Fixed compact k support and $q+2$ bounded k derivatives give $M_q(b) \le C_q \max_{j\le q+2} \|\partial_k^j b\|_\infty$. For a fixed-shape smooth mask c at radius r, scaling gives $M_q(c) + L_q(c) \le C_q r^{-q}$. If d has k support in an interval of length $O(r)$, the absolute Fourier envelope used in Lemma 3.7.8 gives

$$\int \sup_Z \|\widehat{d}(Z,u)\|\, du \le C(\|d\|_\infty + r^2\|\partial_k^2 d\|_\infty). \tag{3.9.4}$$

These estimates follow by splitting the Fourier integral at $1/r$ and integrating twice by parts on its tail. They use operator norms directly, without an operator-norm-valued Plancherel assertion.

Lemma 3.9.8 (Finite left composition)**.** *If the displayed envelopes are finite, then*

$$\mathrm{Op}_\rho(b)\,\mathrm{Op}_\rho(c) = \sum_{j=0}^{n-1} \frac{(\rho/i)^j}{j!}\,\mathrm{Op}_\rho((\partial_k^j b)(\partial_Z^j c)) + R_n, \tag{3.9.5}$$

$$\|R_n\| \le \frac{\rho^n}{n!} M_n(b) L_n(c). \tag{3.9.6}$$

Proof. The exact product kernel applied to f is

$$\iint \widehat{b}(Z,u)\widehat{c}(Z-\rho u, v) f(Z-\rho(u+v))\, du\, dv.$$

Taylor's formula for the second factor has integral remainder

$$\frac{(-\rho u)^n}{(n-1)!}\int_0^1 (1-t)^{n-1}\partial_Z^n \widehat{c}(Z - t\rho u, v)\, dt.$$

Translation is an L^2 isometry. Taking the supremum of each multiplier's operator norm and applying Minkowski gives (3.9.6). Fourier moments give the displayed coefficients. The absolute envelopes justify Fubini and extension from a smooth core to L^2. □

Lemma 3.9.9 (Separated composition with finite rectangular jets)**.** *Let a, c be smooth fixed-shape scalar masks of radii $r_a, r_c \in [\delta, 1]$ with disjoint closed phase supports. The symbol c is compactly supported; a may be a plateau complement $1 - a_0$. The right symbol may also be a fixed finite sum of such masks with radii at least r_c and bounded coefficients; separation is required for the support of their full sum, not for its summands. This includes a fixed outer mask minus a shrinking inner plateau. Let b be supported in one fixed phase chart and define*

$$B_{n,d}(b) = \max_{\substack{0\le l\le n+d\\ 0\le j\le n+2}} \sup_{Z,k} \|\partial_Z^l \partial_k^j b(Z,k)\|.$$

Then, for each fixed nonnegative integer d and $\alpha + \beta \le d$,

$$\|Z^\alpha k^\beta \operatorname{Op}_\rho(a) \operatorname{Op}_\rho(b) \operatorname{Op}_\rho(c)\| \le C_{n,d} B_{n,d}(b) \left(\frac{\rho}{r_a r_c}\right)^n. \tag{3.9.7}$$

The constants use the fixed chart and finitely many mask seminorms, independently of the radii and ρ. Any $P(S)$ or physical ρ factor in the symbol norm remains on the right.

Proof. First expand the product of b, c through order $n-1$ by Lemma 3.9.8. Its remainder is $O(B_{n,0}\rho^n r_c^{-n})$, and the left mask is uniformly bounded. For $j < n$ put $d_j = (\partial_k^j b)(\partial_Z^j c)$ and $m = n - j$. Expand the product of a, d_j through order $m-1$. All local terms vanish, since derivatives of d_j remain supported in $\operatorname{supp} c$. Its remainder is bounded by

$$C\rho^m M_m(a) L_m(d_j) \le C B_{n,0} \rho^m r_a^{-m} r_c^{-n}.$$

Indeed, apply (3.9.4) to $\partial_Z^m d_j$. Leibniz uses Z orders at most $m \le n$ and k orders at most $j+2 \le n+1$ of b. The mask has at most $j + m = n$ ordinary Z derivatives; its two possible extra k derivatives are compensated by r_c^2 in that envelope. Thus $L_m(d_j) \le C B_{n,0} r_c^{-n}$. For a finite sum of right masks, apply the envelope bound to each summand at its own radius and sum. All local terms still vanish for the full d_j; they need not vanish for each summand separately. For $a = 1 - a_0$, treat the identity exactly; its Fourier delta mass has zero positive moments. Multiplication by $\rho^j/j!$ and summation prove the assertion for $d = 0$, since $r_a \le 1$.

For output words use the exact identities

$$Z^\alpha \operatorname{Op}_\rho(a) = \sum_{j=0}^{\alpha} \binom{\alpha}{j} (i\rho)^j \operatorname{Op}_\rho(\partial_k^j a) Z^{\alpha-j},$$

$$k^\beta \operatorname{Op}_\rho(a) = \sum_{t=0}^{\beta} \binom{\beta}{t} (-i\rho)^t \operatorname{Op}_\rho(\partial_Z^t a) k^{\beta-t}.$$

Move the differential powers through the left mask and the middle symbol to the right mask; move spatial powers through the left mask only, then multiply the middle symbol by Z^q. The resulting right symbols are

$$q_v = \sum_{j=0}^{v} \binom{v}{j} (-i\rho)^j k^{v-j} \partial_Z^j c, \qquad k^v \operatorname{Op}_\rho(c) = \operatorname{Op}_\rho(q_v).$$

They have the same support and bounded rescaled seminorms on the fixed chart, since $\rho/r_c \le 1$. Every left-mask derivative has an accompanying ρ and hence costs at most a bounded factor ρ/r_a. Multiplication by Z^q is bounded on the middle chart. This uses at most β additional ordinary Z derivatives of b and no additional rough k derivative. Apply the $d = 0$ estimate to the finite expansion. □

Corollary 3.9.10 (Separated pairs and polynomial parts)**.** *If b has fixed compact support disjoint from the radius-r symbol c, then*

$$\|\operatorname{Op}_\rho(b)\operatorname{Op}_\rho(c)\| \le C\rho^n M_n(b) r^{-n}.$$

The unweighted assertion uses no ordinary Z derivative of b. For an output word of degree d, the proof uses at most d additional ordinary Z derivatives.

For the separated pair and triple, let $n = 2$ or 3 and write the left-ordered symbol as $b = b_c + p$, where b_c has fixed compact phase support and

$$p(Z,k) = \sum_{h=0}^{J} p_h(Z)k^h, \qquad J \le n.$$

Fix a bounded interval I containing the Z-projection of the working chart in its interior. In the radial operator norm in use, put

$$P_{n,d} = \max_{0\le h\le J,\ 0\le l\le n+d} \sup_{Z\in I} \|\partial_Z^l p_h(Z)\|.$$

Assume these derivatives are continuous on I, and use $B_{n,d}(b_c) + P_{n,d}$ as the symbol bound, uniformly over any parameters in the estimate. For a pair, assume $\operatorname{supp} b$ *and* $\operatorname{supp} c$ *are disjoint and use the factor $(\rho/r_c)^n$. For a triple, the two masks have disjoint supports and the factor is $(\rho/(r_a r_c))^n$, as in (3.9.7). This includes a bounded constant operator as the exterior part of a horizontal reference profile.*

Proof. For a compact separated pair, the local terms of (3.9.5) vanish and its remainder gives the first bound. For the polynomial part, the differential product rule gives exactly

$$\operatorname{Op}_\rho(p)\operatorname{Op}_\rho(c) = \sum_{j=0}^{J} \frac{(\rho/i)^j}{j!} \operatorname{Op}_\rho(d_j), \qquad d_j = (\partial_k^j p)(\partial_Z^j c).$$

Each d_j is supported in $\operatorname{supp} c$. For $0 \le j \le J$ and $0 \le m \le n-j$, Leibniz's rule and (3.9.4) give $L_m(d_j) \le C P_{n,0} r_c^{-j-m}$. Indeed, k is bounded on the chart, the coefficients receive at most m derivatives in Z, and the r_c^2 in the Fourier bound pays for two additional k derivatives of the mask. For a finite sum of right masks, use this bound on each summand at its own radius.

For the pair, combine the polynomial and compact expansions at each order $j < n$. Their sum contains $(\partial_k^j b)\partial_Z^j c$ and vanishes by separation. The compact remainder is bounded by (3.9.6). If $J = n$, its polynomial term of order n costs at most $C P_{n,0}(\rho/r_c)^n$, by the $m = 0$ bound above. For the triple, apply Lemma 3.9.8 to a, d_j at order $m = n - j$ for $j < n$. The local terms vanish by separation of a, c. Including the factor ρ^j, the remainder is bounded by

$$C\rho^n r_a^{-(n-j)} P_{n,0} r_c^{-n} \le C P_{n,0}\big(\rho/(r_a r_c)\big)^n.$$

For $j = n$ use the uniform norm bound for the left mask and the same order-n term as for the pair. Lemma 3.9.9 bounds the compact middle part.

For $Z^\alpha k^\beta$, $\alpha+\beta \le d$, commute the differential powers through to the right mask as in Lemma 3.9.9. This differentiates p_h at most β further times. Spatial powers multiply the middle coefficient by bounded powers of Z on I. The resulting right symbols retain the mask support and its rescaled derivative bounds. Thus $P_{n,d}$ controls the same estimates with the output word. □

Corollary 3.9.11 (Adjoints, graph weights and actual radial rows)**.** *The unweighted separated estimate holds for an adjoint middle factor with the same $Z \le n$, $k \le n+2$ rectangle. Axial weights $\langle k\rangle^m$, $0 \le m \le 2$, on either outer edge require at most two additional ordinary Z derivatives and no extra rough k derivative. Smooth endpoint adjoints are allowed on the actual scales $r_a, r_c \ge \delta$.*

The right mask can instead be a radial column s_r on the same support with $\|\partial_Z^l \partial_k^j s_r\| \le P(S) r^{-l-j}$, $l \le n$, $j \le 2$, in its actual operator norm. This includes the right-masked finite columns $\mathcal{S}_j$ in the same-mask proof. For a right graph weight replace s_r exactly by $s_r(1+k^2)$.

Proof. The exact adjoint kernel contains $\widehat{b}(Z+\rho u, u)^*$. Taylor expansion gives

$$\mathrm{Op}_\rho(b)^* = \sum_{j=0}^{n-1} \frac{(\rho/i)^j}{j!} \mathrm{Op}_\rho(\partial_Z^j \partial_k^j b^*) + E_n, \qquad \|E_n\| \le C\rho^n B_{n,0}(b).$$

The remainder envelope is $\rho^n \int |u|^n \sup_Z \|\partial_Z^n \widehat{b}(Z,u)\|\, du$. Apply the preceding lemma at order $n-j$ to its jth symbol; total derivative orders stay $Z \le n$, $k \le n+2$. The graph identities are

$$(1+k^2)\,\mathrm{Op}_\rho(c) = \mathrm{Op}_\rho((1+k^2)c - 2i\rho k c_Z - \rho^2 c_{ZZ}),$$
$$\mathrm{Op}_\rho(c)(1+k^2) = \mathrm{Op}_\rho(c(1+k^2)).$$

Compact endpoints therefore absorb the graph weights on the same support. For a left complement commute k^2 through the mask and middle factor; differentiating the adjoint remainder kernel gives the same conclusion with two extra ordinary Z derivatives. Input k powers are absorbed by the right compact mask. Interpolation of the $m = 0, 2$ estimates gives $0 \le m \le 2$. In particular $\|T\|_{H^{-2}_{\mathrm{ax},\rho} \to L^2} = \|T\langle k\rangle^2\|_{L^2 \to L^2}$.

For a smooth endpoint adjoint, its order-N conversion remainder is $O((\rho/r^2)^N)$, not an asymmetric-radius remainder. Choose the order before use: since $r \ge \rho^{2/5}$, $N \ge 5n$ gives $O(\rho^n)$, which is no larger than the desired two-radius bound. For any fixed word/graph placement the same order is retained. To see this, dilate $Z = rx$, $k = r\xi$ and put $\epsilon = \rho/r^2$. In the unit-scale Taylor remainder, the differentiated mask is evaluated at $x + t\epsilon u$ in its fixed support, so $|x|^A \le C_A(1+\epsilon|u|)^A$. Transfer each output ξ derivative from the translated input by integration in u; it differentiates u^N, the smooth Fourier kernel, or its spatial argument. Every term retains ϵ^N. The resulting absolute moments are finite using, for example, Z derivatives through $N+B$ and k derivatives through $N+A+B+2$ for the word $Z^A k^B$. Scaling back adds $r^{A+B} \le 1$; bounded mask centers are handled by the finite binomial formula. Thus $N = 30$ also suffices for all pure-mask words of degree fifteen followed by SC4 and one ρ^{-1} Green loss: the remaining power is $\rho^{30/5-3-1} = \rho^2$. This argument uses the actual lower radius bound and does not extend it to $r = \sqrt{\rho}$ by assertion.

For s_r the same two Taylor remainders use $L_n(s_r)$ and (3.9.4). Products remain in their original operator order and the Hilbert domains are unchanged. □

Scope of the word estimate and finite products. Arbitrary finite spatial output words in (3.9.7) are asserted for a left-ordered middle symbol, or behind a compact smooth left endpoint. They are not asserted for an uncut adjoint profile with only finitely many k jets: its spatial tails need not have those moments. The rough scalar word applications below are left-ordered. The adjoint reference rows use only the stated axial graph weights.

The leading profile rectangle of (3.6.3) gives $n = 3$ with values in the common space H^6_2; the first corrector rectangle gives $n = 2$ in H^4_2, with its actual physical factor ρ. Both include the extra ordinary Z derivatives for graph weights. A scalar coefficient multiplier independent of k is treated

directly: its product with the right mask is exact, and the second Taylor expansion differentiates the coefficient only in Z.

For a fixed finite product of bounded radial maps, insert finitely many nested smooth plateau masks between the endpoints and telescope. Each off-plateau term is a single middle-factor estimate above, while the remaining maps are bounded on their specified intermediate spaces. The least finite order suffices, and physical coefficient factors are retained. A radial differential map must first be placed on a profile with the required Sobolev order. A Leray derivative must retain the moment loss in Theorem 2(iv); it is not a bounded arbitrary-input unweighted multiplier. Inverse normalizers are localized by $[C, M^{-1}] = -M^{-1}[C, M]M^{-1}$, not treated as unexplained members of the symbol family.

Pure smooth-mask errors have arbitrary finite order, including fixed polynomial output words and axial graph weights. The relevant denominators are $r_a r_c$: a fixed outer plateau gives $(\rho/r)^n$, an outer logarithmic plateau and inner radius r give $(\rho/(r_{\mathrm{out}} r))^n$, and two logarithmic radii give $(\rho/r_{\mathrm{out}}^2)^n$. These are the geometries used below. No uniform fourth-order assertion for a merely C_b^4 middle symbol, and no arbitrary-order assertion from a finite profile ladder, is used.

Residual identities before localization. The following identities are algebraic and are used before any row estimate. With $d_{\mathrm{old}} = \partial_s - B_{\mathrm{old}}$ and $D_p = J_p - J_{\mathrm{ref}}$, put

$$R_D = A_* D_p - (D_p)_s - D_p B_{\mathrm{old}}, \quad R_{\mathrm{ref}} = A_* J_{\mathrm{ref}} - (J_{\mathrm{ref}})_s - J_{\mathrm{ref}} B_{\mathrm{old}},$$

and $J_{\mathrm{raw}} = J_{\mathrm{ref}} + D_p C_{\log}$. Direct differentiation gives

$$R_{\mathrm{raw}} = R_{\mathrm{ref}} + R_D C_{\log} - D_p[d_{\mathrm{old}}, C_{\log}]. \tag{3.9.8}$$

For the physical scalar band B_f, define $T_* = K_{\mathrm{ref}} A_* + (K_{\mathrm{ref}})_s - B_f K_{\mathrm{ref}}$ and $F = B_f - B_{\mathrm{old}}$. Differentiating $K_{\mathrm{ref}} J_{\mathrm{ref}} = I$ gives

$$K_{\mathrm{ref}} R_{\mathrm{ref}} = F + T_* J_{\mathrm{ref}}. \tag{3.9.9}$$

Also $R_{p,\mathrm{old}} = R_p + J_p(B_{\mathrm{band}} - B_{\mathrm{old}})$ gives

$$R_{\mathrm{raw}} = R_{\mathrm{ref}}(I - C_{\log}) + R_{p,\mathrm{old}} C_{\log} - D_p[d_{\mathrm{old}}, C_{\log}].$$

These formulas do not import the estimates of the outer-row lemma.

Calculus used in the precise row lemmas. Lemmas 3.9.14, 3.9.24, 3.9.29, 3.9.30, 3.9.31 and 3.9.32 use, besides the lemmas they cite, only the following facts. "Tiny" is reserved for the uniformly smooth mask remainders: it means bounded by $C_N(\rho/r^2)^N$ at every fixed required order, also in the finite polynomial-word and graph norms explicitly used. Here $r \geq \delta$ is the smallest mask radius. The constants depend on the corresponding fixed smooth-mask seminorms. Order thirty suffices even after the degree-fifteen residual bound and one critical ρ^{-1} Green loss. Rough profiles and scalar coefficients instead use the finite powers in (SC2).

(SC1) Lemmas 3.7.8, 3.7.13 and 3.6.1.

(SC2) *Finite separated composition.* Lemmas 3.9.8, 3.9.9 and Corollaries 3.9.10, 3.9.11 give, for the actual disjoint masks of radii $r_a, r_c \geq \delta$,

$$\|X_1 X_2 X_3\| \leq C B_n(X_2) \left(\frac{\rho}{r_a r_c}\right)^n.$$

Here B_n is the stated finite rectangular symbol seminorm, in the actual radial operator spaces. A leading profile uses $n = 3$ and five k derivatives; a physical first corrector uses ρ times $n = 2$ and four k derivatives. Axial graph weights through order two are allowed as in Corollary 3.9.11. The left scalar word estimates through degree eleven use $n = 3$ for λ_a, e_{κ_0} and ρ times $n = 2$ for c_1, c_a, with the rectangular suppliers and explicit extension below. Global polynomial band terms use the exact polynomial clause of Corollary 3.9.10. An absent middle factor, or a pure smooth-mask product, has every required finite order. Finite products retain their typed radial interfaces and all coefficient factors $P(S)$. Exact inverse normalizers are handled by their commutator identity. No fourth-order estimate for a general C_b^4 coefficient, no unrestricted spatial words on uncut rough adjoints, and no arbitrary order from finite profile regularity is assumed. The finite bounds used below are proved in Section 3.9.2.1.

(SC3) *Graph bounds.* T_{ref} and T_* (defined in the proof of Lemma 3.9.29) map L^2_{can} into $H^{-2}_{\mathrm{ax},\rho}$ with norm at most $P(S)$. Each compact-frequency mask maps $H^{-2}_{\mathrm{ax},\rho}$ into L^2 with norm at most C. The operators E_j map $H^{-2}_{\mathrm{ax},\rho}$ into L^2, and M_j^{-1} extends to $H^{-2}_{\mathrm{ax},\rho}$ by (O5) of Lemma 3.9.5, with norm at most $P(S)$. [Lemma 3.9.5.]

(SC4) *Crude residual bound on the scalar domain.* Write $D_d(\rho)$ for the completion of $\mathcal{S}(\mathbb{R}_Z;\mathbb{C}^2)$ in $\|f\|_{D_d} = \sum_{a+b\le d} \|Z^a k^b f\|_2$, $k = -i\rho\partial_Z$. The unmasked estimate proved on p. 697 is

$$\|R_p f\|_{L^2_{\mathrm{can}}} \le C\rho^{-3} P(S) \|f\|_{D_{15}(\rho)} \qquad (f \in \mathcal{S}). \tag{Prepared}$$

The paragraph on p. 697 gives the corresponding bounds for $R_{\mathrm{ref}}, R_D, R_{\mathrm{raw}}$. For every bounded $Y : L^2_Z \to D_{15}(\rho)$ this yields $\|XY\| \le C\rho^{-3} P(S) \sum_{a+b\le 15} \|Z^a k^b Y\|$ for all four residuals by density and composition. The subsequent uses take Y to be a small mask remainder.

(SC5) *Prepared residual on a bounded family of mask shapes.* Let $\mathfrak{B}$ be a bounded subset of C_c^∞ of the box of radius sixteen (bounded in each C^N norm). For $\sigma \in \mathfrak{B}$ and $r \in [\delta, r_{\mathrm{out}}]$ put $Y = \mathrm{Op}_\rho(\sigma(z/r))$. Then the two lines of (3.7.28) hold with C_r replaced by Y, with constants that depend only on $\mathfrak{B}$; in addition $\|(I - \Pi_{\mathrm{zero}})R_p Y\| \le P(S)[(r + a_\rho)^3 + \rho^\nu(r + a_\rho) + \rho^2]$. [Lemma 3.7.11.]

(SC6) *Rows on the fixed chart.* For a fixed output mask C supported in the inner eigenbundle chart (in particular C_χ, C_b): (3.6.18) with $\theta = \frac{1}{2}$; the right-defect bound $\|(LJ_{\mathrm{ref}} - (J_{\mathrm{ref}})_s - J_{\mathrm{ref}}B)C\| \le C\rho^{3/2}P(S)$ of the right-corrector construction before (3.6.10); and the wave form

$$(A_* - L)v = -\mathbb{P}\,\mathrm{div}_*(W^\natural \otimes v + v \otimes W^\natural), \qquad \|W^\natural\|_\infty \le \rho^{1/2}P(S), \quad \|\nabla_* W^\natural\|_\infty \le P(S). \tag{3.9.10}$$

The identity in (3.9.10) holds because A_* and L are the Leray-projected linearizations of the same normalized operator about $B_* = B_0 + W$ and B_0, and $\mathrm{div}\, v = \mathrm{div}\, W = 0$ give $(W\cdot\nabla)v + (v\cdot\nabla)W = \mathrm{div}(W\otimes v + v\otimes W)$; the normalized completed-wave bounds are those in Theorem 2(v). Condition (V): $\|[C_\chi, Y_w]\| + \|(I - C_b)Y_w C_\chi\| \le C\rho^{3/2}P(S)$ for $Y_w = K_{\mathrm{ref}}(A_* - L)J_{\mathrm{ref}}$; it is proved in Lemma 3.9.12. The wave bound (W) $\|CK_{\mathrm{ref}}(A_* - L)\|_{L^2\to L^2} \le C\rho^{1/2}P(S)$ is proved in Lemma 3.9.32.

Reduction of the unmasked residual bounds. All operators below act initially on Schwartz functions. Write $D_j = D_j(\rho)$ for the scalar word space in (SC4). For a local coefficient $c(R, \theta, Z)$, Fubini gives $\|cf\|_{L^2_{\mathrm{can}}} \le \sup_Z \|c(\cdot, Z)\|_{L^2_{x_h}} \|f\|_2$. A sufficient test for (Prepared) is a representation

$R_p f = \sum_{a+b\le 15} T_{ab} Z^a k^b f$ with $\sum \|T_{ab}\|_{L^2_Z \to L^2_{\mathrm{can}}} \le C\rho^{-3} P(S)$. A Leray projection on the far left is a contraction.

Reference residual. By Lemma 3.6.3, $J_{\mathrm{ref}} f = e_\infty f + \mathrm{Op}^L_\rho(j) f$, where j has fixed compact phase support and consists of the leading compact difference, the first corrector and the two divergence restorations. Its symbol bounds control two physical horizontal derivatives and one horizontal dilation. Indeed only one radial moment is needed for $y_h \cdot \nabla_h$; the leading and first-corrector ladders still have that moment after two k derivatives and the explicit horizontal primitive. A compact k-symbol with these two k derivatives bounded in the indicated radial space has kernel bounded there by $C\rho^{-1}(1 + |Z - Z'|/\rho)^{-2}$, by two integrations by parts. Its scalar majorant is integrable in either axial variable. For an output k the symbol is $kj - i\rho j_Z$; the same formula iterates twice. A factor of Z on such an output is bounded on the left symbol support. Differentiating $\mathrm{Op}^L_\rho(j)$ at fixed input uses the ordinary s-derivative of the symbol plus $(\rho_s/\rho) k \partial_k j$, with $\rho_s = h\rho^2$; the extra k derivative is within the finite compact ladders, including the first corrector. The exterior term $e_\infty f$ uses the scalar words $1, k, k^2, Zk$. This proves

$$\|J_{\mathrm{ref}} f\|_{H^2_*} + \|y_h \cdot \nabla_h J_{\mathrm{ref}} f\|_2 + \|Zk J_{\mathrm{ref}} f\|_2 + \|(\partial_s J_{\mathrm{ref}}) f\|_2 \le C \|f\|_{D_2}.$$

The physical bound in Part 2(iv), with $\epsilon = h/4$ at derivative order one, gives $\|B^\natural_*\|_\infty \le C$, $\|\nabla_* B^\natural_*\|_\infty \le C\rho^{-3/4}$ globally since $\nabla_* = \sqrt{t}\,\nabla_x$ on physical samples. Thus each convection and strain term in the projected linearization costs at most $C(1 + \rho^{-3/4})\|f\|_{D_2}$. Diffusion has coefficient ρ; the two dilation terms and bounded zeroth-order terms are covered by the preceding display. Equivalently these bounds follow by transforming the physical projected equation, with the dilation acting on the transported solenoidal space. The scalar band B_{old} is the sum of the common Zk term, a bounded exterior constant, compact-phase symbols and the scalar feedback. Their $D_2 \to L^2_Z$ bound is $C_{\kappa_0} P(S)$ by the same kernel estimate. Altogether R_{ref} obeys (SC4) with room in the power of ρ.

Difference and raw residuals. Lemma 3.9.23 gives $\|J_p f\| + \|D_p f\| \le P(S)\|f\|_{D_{11}}$. Its scalar word estimate for a degree-two polynomial plus a compact-phase symbol bounds $\|(B_{\mathrm{band}} - B_{\mathrm{old}}) f\|_{D_{11}} \le C_{\kappa_0}\|f\|_{D_{13}}$. The exact identity $R_D = R_p + J_p(B_{\mathrm{band}} - B_{\mathrm{old}}) - R_{\mathrm{ref}}$ therefore leaves only (Prepared). In fact R_{raw} itself needs no unrestricted estimate for R_p. In (3.9.8) the term $R_D C_{\log}$ uses $R_p C_{\log}$ from (SC5), while $\|C_{\log} f\|_{D_j} \le C_j \|f\|_2$ for each fixed j by the smooth mask word estimate. For the last term, $\|[d_{\mathrm{old}}, C_{\log}] f\|_{D_{11}} \le C_{\kappa_0} P(S)\|f\|_{D_2}$. Indeed $C_{\log} B_{\mathrm{old}}$ uses the last scalar band bound. For $B_{\mathrm{old}} C_{\log}$, normal order its quadratic dilation and use the compact-symbol estimate of Lemma 3.9.23 with the mask on the right. For $\partial_s C_{\log}$, both ρ_s/ρ and $(r_{\mathrm{out}})_s / r_{\mathrm{out}}$ are $O(\rho)$, and the differentiated rescaled mask has uniformly bounded seminorms. These estimates and $\|D_p f\| \le P(S)\|f\|_{D_{11}}$ give the asserted raw bound. A factor C_{κ_0} multiplying a term with spare positive powers can be absorbed by the ancient threshold after κ_0 is fixed.

Prepared residual on unrestricted input words. Fix the finite prefix that defines the column and work at fixed canonical input $f \in \mathcal{S}(\mathbb{R}; \mathbb{C}^2)$. Put $d = \frac{1}{2} - h$, $r_* = S^{-M} = r_{\mathrm{out}}$, and write $L^2_h = L^2(\mathbb{R}^2_{y_h})$. Here and in the separated estimate P_M is a polynomial for fixed mask exponent M. We shall absorb it with a strict power of ρ, so the following argument imposes no lower bound on M.

First remove the right mask in the *coefficient* construction. For one tagged word $c_{ab} Z^a k^b$ in (3.9.1) the norm preceding (3.7.30) majorizes the individual quantity $r_*^{a+b} |\partial^I c_{ab}|$ divided by the pulse envelope and slow weight. Both weights are bounded above, with at most a polynomial in S. Since $a + b \le 11$, undoing this amplitude weight costs at most S^{11M}. This step uses the defining supremum before summation of the words. The column in (3.9.1) is the same expression at each radius. Shape-dependent scalar cutoffs occur on its far right when it is tested. The fixed spatial

cutoff $\zeta(Z)$ in the paragraph following Lemma 3.7.2, on the other hand, is part of the raw coefficients. All its derivatives have compact support, the coefficientwise pole kernel acts at fixed Z, and every high response has a local source or an interaction on that support. Thus the six corrections and C_{part} are evaluated on $|Z| \le C$. There $q = t\mathcal{Q}(Z) \asymp t$, all contributing bands satisfy $Q \asymp t$, and $T = t/Q$ stays in a fixed positive compact interval. The finite label sum costs $P(S)$. The polynomial column J_{low} is treated on all of $\mathbb{R}_Z$.

For clarity we verify the estimates on the three types of coefficient separately.

1. For J_{low}, Lemma 3.7.1 gives a polynomial of degree at most three with fixed H^{16}_5 radial coefficients and explicit nonnegative powers of ρ. Two horizontal derivatives or one radial dilation are bounded into L^2_h. Two axial derivatives are normal ordered using $[k, Z] = -i\rho$. The axial dilation is $Z\partial_Z$ with its generator factor ρ, so it uses Zk. At fixed input the time derivative of k^b is $bh\rho k^b$. The coefficients therefore satisfy the required bounds also on large Z, with the powers of Z left in the scalar domain.

2. For the macro term, undo the shear before taking the radial norm. In the notation of Lemma 3.7.2, a coefficient written $\mathcal{U}g(R, Y) = g(R, Y - a(R))$ samples to $g(R, Y_t)$ at $Y = a(R) + Y_t$. Consequently its sampled radial derivatives are fixed-origin radial derivatives of g. The same cancellation holds under a change of the observation radius. The projected pole stress has the two T, sixteen Z and ten origin derivatives specified in that lemma. The kernel estimate (3.7.8) and its weighted version (3.7.23) bound the resulting coefficient in H^8_{6-j} for the frozen derivatives $j \le 2$. Differentiation of the memory integral is dominated by $C(1+u)^C e^{-cu}$, as in the proof of (3.7.35). The physical lift takes $b_h - G\rho\partial_Z b_z$ and b_z, and a scalar k can also act to its right. The horizontal primitive G spends one moment. Even at $j = 2$ there remain three moments, enough for the one horizontal dilation. A time derivative at fixed canonical y_h, Z differentiates T, a bounded multiple of $Z\partial_Z$, the radial dilation, and the temporal origin. The origin derivative is bounded by the ten Hilbert origin derivatives by Sobolev embedding on the two-dimensional torus. These estimates give uniform L^2_h bounds for the two spatial derivatives and the one time derivative used here, with the common coefficient allowance $P_M(S)$. The weight ρ^ν in the stress even gives a positive power before the coarse estimate.

3. Each remaining term is a full curl on the bounded annulus of (A1) of Lemma 3.7.14. After the exponential has been factored out, (A2),(A3) bound two sampled amplitude derivatives by $\rho^{-130\varkappa}P_M(S)$. For a phase $\Psi = jK\Phi$ the bounds in Remark 3.9.3 give

$$|\nabla_*\Psi|^2 + |\nabla^2_*\Psi| \le \rho^{-1}P(S).$$

One time derivative of the amplitude uses one ordinary T, v, Y derivative in (N5) and the chart motion. Indeed at fixed canonical variables $\mathsf{R} = \sqrt{T}|y_h|$, $\mathsf{Z} = T^d Z$, and

$$T_s = \rho T, \quad \mathsf{R}_s = \tfrac{1}{2}\rho\mathsf{R}, \quad \mathsf{Z}_s = d\rho\mathsf{Z}, \quad (Y_t)_s = T^{1+h}c_{\mathrm{aux}}v_t.$$

The last coefficient is bounded, and on the compact annulus the radial shear motion is $O(\rho^{1-\varkappa}P(S))$. In the pulse dictionary $t_*v = 1$, $D_{\mathsf{R}}v = D_z v = 0$. Differentiating $\Phi = p\theta + p_z\mathsf{Z}/\rho_Q + x_0\mathsf{R} - v(pF_b + p_zG_b)$ costs $P(S)$ in canonical time. In the axial term one has $\mathsf{Z}_s/\rho_Q = O(1)$, since $\rho \asymp \rho_Q$. Therefore $|\Psi_s| \le \rho^{-1/2}P(S)$. Rounded quantities are held fixed within their smooth chart. To see the time estimate before sampling, write the cell as $t_v = At + g$, $t(0) = 0$ at fixed band data. An ordinary chart parameter derivative at fixed v solves $(\partial_\beta t)_v = A\partial_\beta t + (\partial_\beta A)t + \partial_\beta g$ with zero initial value. Applying the shifted kernel bound

in (N5) costs only $P(S)$ in the coefficient norm. The term from varying v is $At+g$ times v_s, with $v_s = T^{1+h}$ on the sampled pulse. The cell duration and the rounded constants are fixed for this differentiation. For Y_Q the differentiated source uses at most one macro derivative in the interaction, one for the potential curl and one for the time output. The mixed stress and kernel bounds of the preceding item allow this choice, including one observation derivative and a radial dilation on the bounded interaction annulus. For Y_b differentiate the scalar lift at the temporal origin using the formula for $b_{0,j}$ following (3.7.30) and its same stress estimate. For C_{part} use a fixed smooth time partition in the compact variable T. Since $T_s = \rho T$, its first and second canonical derivatives are $O(\rho)$ and $O(\rho^2)$. These differentiations preserve the same ordinary coefficient budget as two spatial outputs. The cell estimate (N5) allows ordinary parameter derivatives, and the two observation slots are already included in (3.7.31). The factors $c(T)^{\pm 1}$ and the finite overlap are bounded. Thus the high coefficients with their phases have two spatial derivatives bounded in L^2_h by $\rho^{-1-130\varkappa}P_M(S)$ and a time derivative bounded by $\rho^{-1/2-130\varkappa}P_M(S)$. One radial dilation on their support costs at most one spatial derivative.

For products with the input, use Fubini in Z and the identity $k(cZ^a k^b f) = cZ^a k^{b+1} f - i\rho(c_Z Z^a + acZ^{a-1})k^b f$. It follows that $\|J_p f\|_2 \le \rho^{-130\varkappa}P_M(S)\|f\|_{D_{11}}$, and that two spatial derivatives, $\rho Z\partial_Z$, one horizontal dilation, or one coefficient time derivative have norm at most $\rho^{-1-130\varkappa}P_M(S)\|f\|_{D_{13}}$. The stronger direct column estimate is also available from Lemma 3.9.23. The full curls and the physical macro lift make $J_p f$ solenoidal for every such input. The completed velocity enters only through the two physical convection terms. Use its global bounds $\|B_*^\natural\|_\infty \le C$ and $\|\nabla_* B_*^\natural\|_\infty \le C\rho^{-3/4}$ from the reference calculation above. The Leray projector is contractive. The generator has diffusion coefficient ρ, dilation coefficients $O(\rho)$ and a bounded scalar term. Hence these bounds apply equally to $A_* J_p$ including the completed velocity outside the packet hull. Last, B_{band} is a quadratic polynomial in Z, k with bounded coefficients (including the scalar b_0). Normal ordering maps D_{13} to D_{11} with norm $P(S)$. For the actual $\varkappa = 10^{-5}$ the resulting coarse bound, even charging the full derivative loss and the strain loss together, is

$$\|A_* J_p f\| + \|(\partial_s J_p)f\| + \|J_p B_{\mathrm{band}} f\| \le C\rho^{-2}P_M(S)\|f\|_{D_{13}}.$$

For fixed M, $\rho P_M(S)$ is bounded on the ancient tail. This proves (Prepared) before any scalar right mask is imposed, and the preceding identities give all the claims of (SC4).

Lemma 3.9.12 (The visible part of the wave row)**.** *Let $W = B_* - B_0$, in the normalization $W^\natural(y,t) = t^{1/2+h}W(\sqrt{t}\,y,t)$ from Theorem 2(v), and let V be the angular mean of its finite retained part $W - E$, where E is the completed diagonal and localization tail of (a). Put $A_V v = -\mathbb{P}\,\mathrm{div}_*(V\otimes v + v\otimes V)$, $Y_w = K_{\mathrm{ref}}(A_* - L)J_{\mathrm{ref}}$ and $Y_V = K_{\mathrm{ref}}A_V J_{\mathrm{ref}}$.*

(a) W has no component of angular label $\pm 2m$, apart from the tail E (diagonal tail and localization correction). For every fixed compact-frequency mask C, $\|C(Y_w - Y_V)\| + \|(Y_w - Y_V)C\| \le C\rho^{49}$.

(b) In canonical velocity units the finite multiplication field is $V = V_s + \mu^\natural$. It has no carrier phase, and $\|\partial_Z^j V\|_\infty + \|\partial_Z^j \nabla_* V\|_\infty \le \rho^{1-2\varkappa}P(S)$ for $j \le 4$. In particular $[k, V] = -i\rho\partial_Z V$ is bounded by $\rho^{2-2\varkappa}P(S)$. Frequency localization is the separated operator estimate in (c), not an assertion of compact Fourier support.

(c) For fixed masks F in the chart and every fixed mask F' equal to one on a neighbourhood of $\operatorname{supp} F$*,*

$$\|[F, Y_w]\| \le C\rho^{2-2\varkappa}P(S), \qquad \|FY_w(I-F')\| + \|(I-F')Y_w F\| \le C\rho^3 P(S).$$

In particular condition (V) holds: $\|[C_\chi, Y_w]\| + \|(I - C_b)Y_w C_\chi\| \le C\rho^{3/2}P(S)$.

(d) In the retained finite expansion, each wave–column product surviving Π_{zero} *has zero relative carrier. Its two fast phases cancel before divergence and projection. The diagonal and localization tail acting on the column satisfies the separate bounds of Lemma 3.9.4.*

Proof. Structure of W: two field types. By the construction, $W = (u_{\mathrm{B}} - B_0) + (B_* - u_{\mathrm{B}})$ (the decomposition stated before (3.4.1)), and $B_* - u_{\mathrm{B}}$ is produced by the operations listed in the finite construction of Theorem 2(vii). A field is of *type (A)* if it is a finite sum of terms $c(v; R, Z, T, Y)e^{ijK_\ell\Phi_\alpha}$ with one label α, $j \neq 0$, and c supported, with all fixed derivatives, in the enlarged auxiliary rectangles of α. It is of *type (B)* if it has zero relative carrier: angular label zero and no carrier phase in Z; it may depend on Y and be spread over the torus.

- *Products.* $(\mathrm{A})_\alpha \times (\mathrm{A})_\beta$ with $\alpha \neq \beta$ vanishes: by Theorem 2(vii), distinct labels whose slow supports meet have disjoint enlarged auxiliary preimages, also for every fixed derivative. $(\mathrm{A})_\alpha \times (\mathrm{A})_\alpha$ is of type $(\mathrm{A})_\alpha$, or of type (B) when $j + j' = 0$, since then the carrier phases cancel exactly. (A)×(B) is of type (A), with the same label and carrier, and keeps the rectangle support. (B)×(B) is of type (B).

- *Local operations.* Physical derivatives, curls, multiplication by the cutoffs (functions of the point) and finite matrix solves at a point keep each type. The zero-data pulse equations integrate along the pulse path inside the rectangle of their label (Theorem 2(vii)), so they keep type (A).

- *Operations that are nonlocal in Y.* These act only on type-(B) data. The Haar projection Π and the torus inverses T_0^{-1}, D_v^{-1} act on zero-Haar mean forces of the mean iteration: at initialization $v_0 = -T_0^{-1} f_\theta$, $\gamma_0 = -T_0^{-1} f_z$, as in Theorem 2(vii). The shifted radial integrals $I, J, \mathcal{L}$ act on mean-class inputs with $\Pi f = 0$ (Theorem 2(vii)). Their outputs are carrier-free. D_v^{-1} has one further use, the clock inverse; it acts on a carrier-free envelope and feeds only an analysis weight, not W.

- *Pressure and projection.* Rotation equivariance preserves the angular label under the Leray projection and the radial pressure inverse. The construction multiplies the local full-curl wave velocities before projection (Remark 3.9.3). Opposite carriers on one label therefore cancel their full phases in the raw matching tensor. The pressure enters linearly, and its gradient may have a nonlocal tail.

- *Box divergence inverse.* $\mathcal{B}_{\mathrm{div}}$ acts only on $g_{\mathrm{loc}} = \nabla\chi_{\mathrm{loc}} \cdot u_\infty$, which is supported on a fixed physical annulus $a \le |x| \le b$. On the fixed ball about the origin, the localized field equals u_∞ by Theorem 2(i). The operator $\mathcal{B}_{\mathrm{div}}$ may mix labels, but its correction is small after normalization: on the annulus the normalized field is bounded by $CQ^{\frac{1}{2}+h} = C\rho^{(\frac{1}{2}+h)/h}$ with $(\frac{1}{2}+h)/h > 50$ (the same normalization as for the diagonal tail below; the weights $\langle R\rangle^7$ alone do not cover the part of the annulus near the axis). So the localization correction, like the diagonal tail E_N ($\|E_N\|_{W^{2,\infty}} \le CQ^{\frac{1}{2}+h} = C\rho^{(\frac{1}{2}+h)/h}$, $(\frac{1}{2}+h)/h > 50$; Lemma 3.9.4, fourth type), enters Y_w only with norm at most $C\rho^{49}$. We call these two terms the tail E.

Hence $W = W_A + W_B + E$, where W_A is a sum of type-(A) fields over the labels and W_B is of type (B). Here $W_B = (u_{\mathrm{B}} - B_0) + \mu$, where μ is the zero-carrier mean given by Theorem 2(vii). It collects all carrier-free components, including the same-label returns with $j + j' = 0$. The auxiliary variable Y does not depend on ϑ (the angular operator has no y part; proof of Lemma 3.7.14, (A3)).

So a type-(A) term has angular label jn_α by the rounded phase formula in Theorem 2(vii), with $|jn_\alpha| \geq 2m+1$ for $j \neq 0$, and a type-(B) term has label zero.

(a). Since $K_{\mathrm{ref}} = K_{\mathrm{ref}}\Pi$, $J_{\mathrm{ref}} = \Pi J_{\mathrm{ref}}$, and multiplication, divergence and $\mathbb{P}$ keep angular labels, a component of W of label ℓ contributes to Y_w only if $\ell \pm m \in \{m, -m\}$, that is $\ell \in \{0, \pm 2m\}$. By the structure, the only such components are $V = W_B$ and the visible part of E. For the tail, move the divergence to the compact-frequency side, as in the proof of (W) in Lemma 3.9.32: the bound is $C\rho^{49}$, by the preceding paragraph.

(b). The label-zero part of W_A is zero, since $j \neq 0$. So in canonical units the finite carrier-free contribution to the angular mean is $V_s + \mu^\natural$, with $V_s = t^{1/2+h}(u_{\mathrm{B}} - B_0)$. The completed tail E is estimated in its own output norm in (a). The full-space slow estimate imported from Part 2 gives $O_j(\rho^2)$ in the tangential and axial components, $O_j(\rho^3)$ radially. The tangential components of $\mu^\natural$ have order $\rho^{1-\varkappa}$, and its radial one order ρ^2, with the fixed coefficient derivatives and $P(S)$ losses of Theorem 2(vii). On the finite carrier-free multiplication part one has exactly $[k, M_V] = -i\rho M_{\partial_Z V}$ on the smooth core. An evaluated horizontal derivative loses at most $\rho^{-\varkappa} S^C$, and the axial derivative has no Y part (proof of Lemma 3.7.14, (A3)). This gives the bounds and the exact commutator identity in (b). The same argument gives the additional two ordinary Z derivatives when needed for an axial graph factor; these are fixed coefficient derivatives within the source reservation.

(c). The divergence restorations in Lemma 3.6.3 make H_{ref} exactly physically solenoidal. Hence $H_{\mathrm{ref}}^* \mathbb{P} = H_{\mathrm{ref}}^*$ on the smooth core and by duality. Put $\mathcal{V}u = V \otimes u + u \otimes V$. The physical integration by parts identity is therefore

$$Y_V = M_{\mathrm{ref}}^{-1} (\nabla_* H_{\mathrm{ref}})^* \mathcal{V} J_{\mathrm{ref}}.$$

It uses the full gradient tensor and the actual tensor contraction. No derivative of the frozen projector P_k is inserted between unweighted spaces. Boundary terms vanish first for smooth compact tests; the profile Sobolev bounds extend this identity to the localized operators below.

On the fixed phase chart the leading gradient column has five k derivatives in H_2^5; the ρ corrector has four in H_2^3. The displayed G restorations spend one moment, leaving at least weight one, and the ρ^2 restoration is already smaller than the requested error. An axial derivative is exactly $ik + \rho\partial_Z$ and uses no radial moment. Multiplication by V is bounded on unweighted radial L^2; its ordinary Z derivatives through three obey (b). After the compact endpoint placement described next, the two profile interfaces are, explicitly, scalar $L_Z^2 \to L_Z^2(L_{\mathrm{rad}}^2)$, multiplication in that space, and its actual Hilbert-adjoint row. Ordinary derivatives through five suffice if an axial graph factor is present, and are supplied by the same fixed ordinary coefficient estimates used in (b). No new k derivative is required.

The fixed horizontal extension contributes the unbounded axial term ikv_0. We do not regard that global gradient column as L^2 bounded. Use the exact identities

$$k \operatorname{Op}_\rho(b) = \operatorname{Op}_\rho(b)k - i\rho \operatorname{Op}_\rho(b_Z), \qquad kV = Vk - i\rho V_Z.$$

For $(I - F')Y_V F$ move this k to the right compact endpoint; kF is a bounded compact symbol, and the commutator terms carry ρ and one ordinary Z derivative. For $FY_V(I - F')$ take the Hilbert adjoint and use its compact right endpoint, or equivalently keep the output derivative behind $FM_{\mathrm{ref}}^{-1} : H_{\mathrm{ax},\rho}^{-1} \to L^2$. The latter map follows from the graph endpoint bounds and the exact inverse identity. The same exact first-order calculation handles the constant extension in each intermediate plateau. More explicitly put $U = (\nabla_* H_{\mathrm{ref}})^* \mathcal{V} J_{\mathrm{ref}}$. The first-order identities above give $U : L^2 \to H_{\mathrm{ax},\rho}^{-1}$ with norm $O(\rho^{1-2\varkappa} P(S))$. Choose a fixed plateau P between F and F'. The exact split

$$\begin{aligned} FM_{\mathrm{ref}}^{-1} U(I - F') = {} & FM_{\mathrm{ref}}^{-1} PU(I - F') \\ & + F(M_{\mathrm{ref}}^{-1} - I)(I - P)U(I - F') + F(I - P)U(I - F') \end{aligned}$$

places the unnormalized separation behind the compact output P in the first term. In the second, the inverse leakage is estimated $H^{-2}_{\mathrm{ax},\rho} \to L^2$ by Lemma 3.6.4; the last term is a pure-mask error in the same graph placement. Thus the unbounded axial part is never multiplied merely by an $L^2 \to L^2$ leakage bound.

Choose finitely many nested fixed plateau masks between F and F'. Telescoping the three bounded factors in the preceding identity gives separated errors by (SC2): order three for a leading profile or the multiplication coefficient, and order two with its prefactor ρ for a corrector. Every term still contains V, whose norm is $\rho^{1-2\varkappa}P(S)$. The ρ^2 restoration needs only first-order separation. Consequently these unnormalized separated errors are $O(\rho^{4-2\varkappa}P(S))$. The normalizer is handled by $[F, M_{\mathrm{ref}}^{-1}] = -M_{\mathrm{ref}}^{-1}[F, E_{\mathrm{ref}}]M_{\mathrm{ref}}^{-1}$, not as an additional symbol. Lemma 3.6.4 gives its fixed-gap $O(\rho^3)$ leakage, so the off-plateau error contributes at most the same order after multiplication by V. This proves the two separated bounds in (c), including the stated weaker $O(\rho^3 P(S))$ bound.

On the padded compact chart the same three factors have a first-symbol product with an $O(\rho^{2-2\varkappa}P(S))$ remainder by Lemma 3.6.1. The scalar principal symbol and its first derivatives have size $\rho^{1-2\varkappa}P(S)$, so commutation with F costs one factor ρ. The exact inverse commutator contributes $O(\rho^2\rho^{1-2\varkappa}P(S))$. Thus $\|[F, Y_V]\| \le C\rho^{2-2\varkappa}P(S)$. Part (a) transfers these bounds to Y_w. Take $F = C_\chi$ and choose F' between C_χ and C_b to obtain (V), since $2 - 2\varkappa > 3/2$.

(d). A product of a label-α wave harmonic j with a column term of the same label and relative carrier j' has angular label $\pm m + (j + j')n_\alpha$. This lies in $\{m, -m\}$ only if $j + j' = 0$, because $|n_\alpha| \ge 2m + 1 > 2m$, and then the carrier phases cancel exactly. Products of distinct labels vanish, and products with $u_{\mathrm{B}} - B_0$, μ or B_0 keep the relative carrier. For the remaining tail E, the fourth OUTPUT estimate in Lemma 3.9.4 controls the full projected product on the right mask. □

Consequently condition (V) of (SC6) holds; it is part (c) of Lemma 3.9.12. The real point is not whether the visible part of $A_* - L$ vanishes (it does not: $V \neq 0$), but the size of its commutator and separated tails, quantified in (b)–(c). A component of label $\pm 2m$ would carry the combined Z phase of two labels and could move k by an amount of order one. Theorem 2(vii) excludes such components in the retained fields. Part (a) bounds their possible contribution from the tail by $C\rho^{49}$ on the fixed mask.

Lemma 3.9.13 (Reference residual on a fixed mask)**.** *Let $\widetilde{C}$ be a fixed mask with symbol supported in the inner eigenbundle chart. For every bounded operator Y on L^2_Z,*

$$\|R_{\mathrm{ref}}\widetilde{C}Y\|_{L^2_Z \to L^2_{\mathrm{can}}} \le C_{\kappa_0}P(S)\|Y\|, \qquad R_{\mathrm{ref}} = A_*J_{\mathrm{ref}} - (J_{\mathrm{ref}})_s - J_{\mathrm{ref}}B_{\mathrm{old}}.$$

Proof. Write $R_{\mathrm{ref}} = R^L_{\mathrm{ref}} + (A_* - L)J_{\mathrm{ref}} + J_{\mathrm{ref}}(B - B_{\mathrm{old}})$ with $R^L_{\mathrm{ref}} = LJ_{\mathrm{ref}} - (J_{\mathrm{ref}})_s - J_{\mathrm{ref}}B$. By (SC6), $\|R^L_{\mathrm{ref}}\widetilde{C}\| \le C\rho^{3/2}P(S)$. Put $u = J_{\mathrm{ref}}\widetilde{C}Ya$. It is solenoidal, $\|u\| \le C\|Ya\|$, and $\|\nabla_* u\| \le C\|Ya\|$: the horizontal derivatives fall on the radial profiles, and $\rho\partial_Z \operatorname{Op}_\rho(e)\widetilde{C} = \operatorname{Op}_\rho(\rho\partial_Z e)\widetilde{C} + i\operatorname{Op}_\rho(e)k\widetilde{C}$ with $\|k\widetilde{C}\| \le C$. By (3.9.10), $\operatorname{div}(W \otimes u) = (u \cdot \nabla_*)W$ and $\operatorname{div}(u \otimes W) = (W \cdot \nabla_*)u$, so $\|(A_* - L)u\| \le \|\nabla_* W^\natural\|_\infty\|u\| + \|W^\natural\|_\infty\|\nabla_* u\| \le P(S)\|Ya\|$. Finally $B - B_{\mathrm{old}} = \operatorname{Op}_\rho(e_{\kappa_0} + \rho(c_1 - c_a)) - b_0$ on the chart (the dilations cancel), so $\|(B - B_{\mathrm{old}})\widetilde{C}\| \le C_{\kappa_0}$ by (SC2) and the kernel bound in the proof of Lemma 3.7.13 applied to the compact chart symbols after subtracting their constant parts, and $\|J_{\mathrm{ref}}\| \le C$. □

Lemma 3.9.14 (Precise same-mask bounds)**.** *Let C be a fixed mask equal to one on a fixed neighbourhood of the supports of C_δ, $C_{\log}$ and their transitions (for instance $C_s, C_0, C_1, C_\chi, C_b$). For $\rho \le \rho_1$ and $j = \delta, \log$,*

$$\|(I - C)E_j\| + \|E_j(I - C)\| + \|[C, E_j]\| \le C'\rho^{9/5}P(S), \tag{3.9.11}$$

also as maps from $H^{-2}_{\mathrm{ax},\rho}$. *Moreover, after a* κ_0*-dependent threshold,*

$$C_\chi K_{\log} R_{\mathrm{raw}} - B_{\mathrm{int}} C_\chi = R_{\mathrm{sep}}, \qquad \|R_{\mathrm{sep}}\| \le C_{\kappa_0}\rho^{3/2}P(S), \tag{3.9.12}$$

and, for every fixed mask $F_\sharp$ *that equals one on a neighbourhood of the cubic blend box and of* $\operatorname{supp} C_{\log}$*, with* $C_b = 1$ *near* $\operatorname{supp} F_\sharp$*,*

$$\|[B_{\mathrm{int}}, F_\sharp]\| \le C_{\kappa_0}\rho^{3/2}P(S). \tag{3.9.13}$$

Thus (3.9.3) *holds with* $\rho^{9/5}$ *in its first line, its row factorization holds with* $A_{\mathrm{ann}} = 0$*, and the commutator hypothesis* $[A, F_i] = \rho L_i + R_i$*,* $\|R_i\| \le C_{\kappa_0}\rho^{3/2}P(S)$*, of Lemma 3.9.6 holds for* $A = d_{\mathrm{old}} + d_0 C_s - B_{\mathrm{int}}$ *and its nested masks* F_1, F_2, F_3 *(the term* ρL_i *comes from* d_{old} *alone).*

Proof. Exact form of E_j. By (3.7.34) and $K_{\mathrm{ref}} = K_{\mathrm{ref}}\Pi$, $E_j = K_{\mathrm{ref}}\Pi D_p C_j = K_{\mathrm{ref}}\mathcal{S}_j - C_j$ with $\mathcal{S}_j = (J_{\mathrm{low}} + \Pi\mathcal{T}_\rho b)C_j$, because $K_{\mathrm{ref}}J_{\mathrm{ref}} = I$. Each word of $J_{\mathrm{low}} + \Pi\mathcal{T}_\rho b$ is a coefficient in (x_h, Z) times $Z^a k^\beta$. Left multiplication by a function of Z and the finite exact expansion of $k^\beta C_j$ (proof of Lemma 3.7.13) show that $\mathcal{S}_j = \mathrm{Op}_\rho(s_j)$ with s_j supported in $\operatorname{supp} c_j$ and

$$\|\partial_Z^l \partial_k^q s_j\|_{L^2_{\mathrm{rad}}} \le P(S) r_j^{-l-q}, \qquad l \le 3, \quad q \le 2.$$

The right graph factor replaces s_j by $s_j(1+k^2)$ on the same support. The finite differential words have already acted on this mask; they do not act on an adjoint row's spatial tails.

Proof of (3.9.11). $(I - C)C_j$ and $C_j(I - C)$ are tiny by (SC2). Write $K_{\mathrm{ref}} = M_{\mathrm{ref}}^{-1}H_{\mathrm{ref}}^*$ and $M_{\mathrm{ref}} = I + \rho\widetilde{E}_{\mathrm{ref}}$. The upstream normalizer calculation, Lemma 3.6.4, gives

$$\|[C, M_{\mathrm{ref}}^{-1}]\|_{H^{-2}_{\mathrm{ax},\rho}\to L^2} \le C\rho^2.$$

The same estimate holds on L^2; the inverse is used as a bounded graph extension, not as a smoothing operator. Next $H_{\mathrm{ref}}^* = \mathrm{Op}_\rho(v)^* + \rho\mathcal{H}^*$, and the supports of $1 - c$ and s_j have a fixed distance. (SC2) gives $\|(I - C)H_{\mathrm{ref}}^*\mathcal{S}_j\| \le P(S)[(\rho/r_j)^3 + \rho(\rho/r_j)^2] \le P(S)\rho^{9/5}$. Hence $\|(I - C)E_j\| \le C\rho^{9/5}P(S)$. Also $E_j(I - C) = K_{\mathrm{ref}}(J_{\mathrm{low}} + \Pi\mathcal{T}_\rho b)C_j(I - C) - C_j(I - C)$, and the words applied to the tiny $C_j(I - C)$ give a tiny term. Finally $[C, E_j] = -(I - C)E_j + E_j(I - C)$. For inputs in $H^{-2}_{\mathrm{ax},\rho}$ use $\|C_j\langle k\rangle^2\| \le C$ and the weighted form of (SC2).

Proof of (3.9.12). Put $X = K_{\log}R_{\mathrm{raw}}$ and $Y_w = K_{\mathrm{ref}}(A_* - L)J_{\mathrm{ref}}$. Since $B_{\mathrm{int}} = C_b X C_b$, the exact identity

$$C_\chi X - C_b X C_b C_\chi = [C_\chi, X] + (I - C_b)XC_\chi + C_b X(I - C_b)C_\chi$$

holds. The last term is a smooth-mask error and is tiny by (SC2) and (SC4). We use the exact algebra in paragraph 3.9.2.1: $R_{\mathrm{raw}} = R_{\mathrm{ref}} + R_D C_{\log} - D_p[d_{\mathrm{old}}, C_{\log}]$, $K_{\mathrm{ref}}R_{\mathrm{ref}} = F + T_*J_{\mathrm{ref}}$ with $F = \mathrm{Op}_\rho(e_{\kappa_0} + \rho(c_1 - c_a))$, and $T_*J_{\mathrm{ref}} = T_{\mathrm{ref}}J_{\mathrm{ref}} + Y_w - b_0$.

(i) $[C_\chi, M_{\log}^{-1}]K_{\mathrm{ref}}R_{\mathrm{raw}} = -M_{\log}^{-1}[C_\chi, E_{\log}]M_{\log}^{-1}K_{\mathrm{ref}}R_{\mathrm{raw}}$. By (3.9.11) on $H^{-2}_{\mathrm{ax},\rho}$ and (SC3), this term is $O_{\kappa_0}(\rho^{9/5}P(S))$. Indeed, $F + T_*J_{\mathrm{ref}}$ maps into $H^{-2}_{\mathrm{ax},\rho}$ by (SC3) and the scalar symbol bound. The two remaining terms of $K_{\mathrm{ref}}R_{\mathrm{raw}}$ are bounded on L^2 by $C_{\kappa_0}P(S)$, as verified in (iv).

(ii) $[C_\chi, F]$. The symbol e_{κ_0} is supported where $c_\chi = 1$, so $[C_\chi, \mathrm{Op}_\rho(e_{\kappa_0})] = (C_\chi - I)\,\mathrm{Op}_\rho(e_{\kappa_0}) - \mathrm{Op}_\rho(e_{\kappa_0})(C_\chi - I)$ is $O(C_{\kappa_0}\rho^3)$ by the principal-symbol order-three case of (SC2). Lemma 3.6.1 gives $\|\rho[C_\chi, \mathrm{Op}_\rho(c_1 - c_a)]\| \le C_{\kappa_0}\rho^2$.

(iii) $[C_\chi, T_* J_{\mathrm{ref}}]$. The scalar b_0 commutes with C_χ. By (SC6), $\|C_\chi T_{\mathrm{ref}} J_{\mathrm{ref}}\| \le C\rho^{3/2}P(S)$, and $T_{\mathrm{ref}} J_{\mathrm{ref}} C_\chi = K_{\mathrm{ref}}(LJ_{\mathrm{ref}} - (J_{\mathrm{ref}})_s - J_{\mathrm{ref}}B)C_\chi$ is $O(\rho^{3/2}P(S))$ by the right-defect bound. The wave commutator $[C_\chi, Y_w]$ is $O(\rho^{2-2\varkappa}P(S))$ by Lemma 3.9.12(c).

(iv) Put $r = r_{\mathrm{out}}$, $Y_{\mathrm{ref}} = K_{\mathrm{ref}} R_{\mathrm{ref}}$, and let C be any of $C_\chi, C_b, F_\sharp$. Take the ancient threshold so that $8r \le \kappa_0$. On the scalar Schwartz core,

$$K_{\mathrm{ref}} R_D C_{\log} = K_{\mathrm{ref}} R_p C_{\log} + K_{\mathrm{ref}} J_p \operatorname{Op}_\rho(\sigma_B) C_{\log} - Y_{\mathrm{ref}} C_{\log}, \qquad \operatorname{Op}_\rho(\sigma_B) = B_{\mathrm{band}} - B_{\mathrm{old}}.$$

The common axial dilation and b_0 cancel, giving $\sigma_B = \lambda_{\mathrm{quad}} - \lambda_a + \rho(c_* - c_a)$. Both differences vanish on the fixed κ_0 box.

For the reference term, take fixed chart masks H, C with $C = 1$ near $\operatorname{supp} H$. The identity $Y_{\mathrm{ref}} = F + T_{\mathrm{ref}} J_{\mathrm{ref}} + Y_w - b_0$ gives

$$\|(I - C) Y_{\mathrm{ref}} H\| \le C_{\kappa_0} \rho^{3/2} P(S).$$

Indeed, (SC2) bounds $(I - C)FH$ by $C_{\kappa_0}\rho^3$ using orders three and ρ times two. The right-defect bound in (SC6) gives $\|T_{\mathrm{ref}} J_{\mathrm{ref}} H\| \le C\rho^{3/2}P(S)$. Lemma 3.9.12(c) bounds $(I - C)Y_w H$ by $C\rho^3 P(S)$, and $(I - C)H$ is a pure-mask error. Choose $H = 1$ on a fixed neighbourhood of $\operatorname{supp} C_{\log}$ inside the plateau of C. All words through degree fifteen on $(I - H)C_{\log}$ are tiny by (SC2). Thus (SC4) bounds $Y_{\mathrm{ref}}(I - H)C_{\log}$, even after its ρ^{-3} loss. Adding the term with $HC_{\log}$ gives the same $C_{\kappa_0}\rho^{3/2}P(S)$ bound for $(I - C)Y_{\mathrm{ref}} C_{\log}$. Lemma 3.9.13 on H and the same split give the global bound $\|Y_{\mathrm{ref}} C_{\log}\| \le C_{\kappa_0} P(S)$.

For the band difference write $\mathcal{W}_{11}(U) = \sum_{a+b\le 11} \|Z^a k^b U\|$. In both orders,

$$\begin{aligned} &\mathcal{W}_{11}\big(\operatorname{Op}_\rho(\sigma_B) C_{\log}\big) + \mathcal{W}_{11}\big(C_{\log} \operatorname{Op}_\rho(\sigma_B)\big) \\ &\qquad \le C_{\kappa_0}\big[(\rho/r)^3 + \rho(\rho/r)^2\big] \le C_{\kappa_0}\rho^{9/5}. \end{aligned}$$

For the first product this is Corollary 3.9.10, including the quadratic polynomial part. Words through degree eleven require at most 14 ordinary Z and five k derivatives in the principal symbol, and 13 and four in the connection, supplied by Lemma 3.9.19. For the reverse product, $Z^a k^b C_{\log} = \operatorname{Op}_\rho(d_{ab})$ has the same support and uniformly bounded rescaled seminorms. Expand its product with the compact part on the right by Lemma 3.9.8 at orders three and two, respectively. Here $M_n(d_{ab}) \le Cr^{-n}$. The right polynomial part has an exact expansion through degree two in the principal symbol and degree zero in the connection. The local terms cancel because each full difference vanishes near the mask. Finally $r \ge \rho^{2/5}$. The degree-eleven column bound (3.9.36), proved directly from paragraph 3.7.3, gives the same estimate times $P(S)$ after J_p or D_p.

Output away from the logarithmic support. For each of the fixed masks C in (iv) we prove

$$\|(I - C) K_{\mathrm{ref}} R_p C_{\log}\|_{L^2_Z \to L^2_Z} \le C_{\kappa_0}\rho^{9/5} P(S).$$

Only $r = r_{\mathrm{out}} = S^{-M}$ is needed here. In particular a fixed polynomial $P_M(S)$ in an intermediate coefficient bound is affordable. We verify which coefficients have to be differentiated.

Write $H = H_{\mathrm{ref}}$ for the unnormalized physical adjoint column and let Π be projection to the two angular sectors of the reference pair. Its divergence restorations give $H^*\mathbb{P} = H^*$ and $H^*\Pi = H^*$. Test the residual against H before computing its symbol. A physical pressure gradient pairs to zero, including the nonlocal gradient in the convection and diffusion

terms. The remaining unprojected velocity operator uses the local generator on the same solenoidal column. The time derivative and the dilation terms preserve angular sectors. Set $J^0 = J_{\mathrm{low}} + \mathcal{T}_\rho b$. The angular projection of the time, diffusion, dilation and scalar-band terms uses only J^0. In the convection term the retained carrier-zero field is the leading physical field plus the slow difference and the zero-carrier correction. Its product with J^0 survives. The only other retained products are the tensors between a source wave and a high column with the opposite harmonic on the same label. Distinct active labels have disjoint enlarged preimages. For a single label $|n_\alpha| > 2m$, so that $\pm m + (j + j')n_\alpha \in \{\pm m\}$ implies $j + j' = 0$. Consequently their exponentials cancel in the *tensor itself*. This is Lemma 3.9.12(d) applied before the single divergence. The completed output errors have their $O(\rho^2 P(S))$ norm after the actual right mask by Lemma 3.9.4. A bounded fixed mask and H^* preserve that bound. We use no derivative of their unmasked coefficients.

It remains to estimate the finite local part. Normal order its input words as $m_{ab}(y_h, Z)Z^a k^b$, leaving all factors of Z that came from the scalar input on the right. Their maximal degree is thirteen by (3.9.1) and the two generator derivatives. The following checks give

$$\max_{0\le l\le 3} \sup_{|Z|\le Cr} \|\partial_Z^l m_{ab}(\cdot, Z)\|_{L_h^2} \le C P_M(S). \tag{R}$$

Here C in the radius bound is the fixed mask shape constant.

(a) For J_{low}, its H_5^{16} coefficients support two physical derivatives and one dilation moment. Its axial dependence is polynomial in the right words. On $|Z| \le Cr$, the leading normalized multiplier and its first four axial derivatives and first horizontal derivative are bounded uniformly in y_h. On compact radial sets this follows from the smooth physical chart, and on the exterior the heat swirl and its fixed differentiated power bounds apply. The leading axial velocity has compact radial support on this Z-chart. The carrier-free source difference, including the slow part against the entire radial profile, satisfies Lemma 3.9.12(b). In the divergence form at most one derivative falls on either multiplier or column. All these terms have (R).

(b) For the macro contribution the pole kernel is independent of the input frequency and acts coefficientwise at a fixed axial variable. The domain of Lemma 3.7.2 gives the sixteen ordinary Z derivatives, including at the two observation derivatives. G commutes with ∂_Z. The lift costs at most one Z derivative, diffusion at most two, and (R) another three, at most six altogether. Time differentiation can introduce $Z\partial_Z$ instead of a diffusion derivative. For the radial estimates the unsheared sampling, the H_{6-j}^8 kernel, and the one-moment bound on G are exactly those used on p. 697. Alternatively even two evaluated radial derivatives charged at $\rho^{-2\varkappa}$ are paid for by the macro order $\rho^{1-128\varkappa}$. The Z derivatives do not differentiate the radial shear, the torus origin or a carrier in this term. The scalar $b_0(s)$ and the partition functions depend only on time. Multiplication by each polynomial band coefficient and normal ordering introduce bounded coefficients in (R).

(c) In each surviving wave tensor the source amplitude has size $\rho^{1/2}P(S)$, including a fixed number of ordinary axial jets, by Theorem 2(vi),(vii). For the high column work in the tagged coefficient norm preceding (3.7.30) and remove r^{a+b} at cost S^{11M}. Ordinary axial derivatives commute with the evaluated radial shear and preserve the label. The proof of (N5) differentiates a zero-data cell in these parameters: the extra sources are the differentiated input and the lower derivatives of the velocity multiplied by derivatives of

the same cell matrix. The interval, envelope and integration variable v are independent of Z. Thus its ordinary differentiated bound has the same polynomial loss and uses one ordinary source derivative per extra axial derivative. For $B_0, B_1, B_{2,\mathrm{high}}$ the three extra axial derivatives fall on local coefficients of at most three cells. They do not add three radial derivatives to the fixed low profile. For Y_Q, tracing the derivatives through its one interaction and curl needs at most seven ordinary axial derivatives of the macro stress, counting one each for the lift, interaction, curl and divergence in addition to the three derivatives in (R). The kernel commutes with them and its input supplies sixteen. The number of radial derivatives required of this macro response is at most four, as in (A2). For Y_b, C_{part} the scalar factors in the physical multiplier are independent of Z. Their pulse lifts have the ordinary origin and time estimates used on p. 697. In the conservative total source count, the three axial jets require at most $72+3$ ordinary levels, with $75 \le 80$ available on this same finite source. Even charging each additional jet a loss $\rho^{-\varkappa}$ gives amplitude size at most $\rho^{-131\varkappa} P_M(S)$. One evaluated radial derivative in the tensor divergence costs at most another $\rho^{-\varkappa} P(S)$. No factor K from either phase remains. The radial support of these tensors is a bounded annulus. The resulting L^2_h bound is at most $\rho^{1/2-132\varkappa} P_M(S)$, which implies (R).

Writing ξ for the symbol frequency and c_r for the left symbol of the right mask, the exact identity

$$k^b C_r = \mathrm{Op}^L_\rho \left(\sum_{j=0}^{b} \binom{b}{j} \xi^{b-j} (-i\rho)^j \partial_Z^j c_r \right)$$

shows that the finite residual applied to $C_{\log}$, in this pairing, is a column $\mathrm{Op}^L_\rho(s_r)$ supported in $\operatorname{supp} c_r$. This calculation puts the input words on the smooth mask. By (R) and $\rho/r^2 \le 1$,

$$\|\partial_Z^l \partial_\xi^q s_r\|_{L^2_h} \le C P_M(S) r^{-l-q}, \qquad 0 \le l \le 3, \quad 0 \le q \le 2.$$

All frequency derivatives in this display fall on scalar monomials and the smooth mask. Apply the adjoint form of the finite separated composition, exactly as in the proof of (3.9.11), to $H^* \mathrm{Op}^L_\rho(s_r)$. The leading row has the five frequency jets at order three and the first corrector has four at order two. The remaining second-order correction is bounded with its prefactor. Because $1-C$ vanishes on a fixed neighbourhood of this support the result is at most

$$C_{\kappa_0} P_M(S) \big[(\rho/r)^3 + \rho(\rho/r)^2 + \rho^2 \big].$$

To restore the inverse pairing, commute $1-C$ past M_{ref}^{-1} using Lemma 3.6.4. The commutator is $O(\rho^2)$, and (SC5) bounds the other factor $H^* R_p C_{\log}$ by $P(S)$ on L^2. This last estimate estimates the actual residual without differentiating its tail. Since $r^{-1} = S^M$ and M is fixed, the sum is $O_{\kappa_0}(\rho^{9/5})$ upon enlarging the ancient threshold. This proves the separated estimate for the same completed field and the stated cutoffs. On the input side $K_{\mathrm{ref}} R_D C_{\log}(I-C)$ is tiny by (SC2) and (SC4). Together the three terms of the split give $\|[C, K_{\mathrm{ref}} R_D C_{\log}]\| \le C_{\kappa_0} \rho^{3/2} P(S)$.

For the connection use the exact identity

$$[d_{\mathrm{old}}, C_{\log}] = [\partial_s - B_{\mathrm{band}}, C_{\log}] + [\mathrm{Op}_\rho(\sigma_B), C_{\log}].$$

The preceding two word bounds control the last commutator after $K_{\mathrm{ref}} D_p$ on all L^2 inputs. The first commutator is $\rho \,\mathrm{Op}_\rho(q_r)$, where q_r is supported in $\operatorname{supp} c_{\log}$ and has uniformly bounded rescaled seminorms. The time symbol is $\partial_s c_{\log} + h\rho k \partial_k c_{\log}$, with $|\partial_s \log r| = O(\rho)$.

Both products with the quadratic band have exact second-order expansions. Its first phase derivatives are $O(r)$ on the mask, and its second-order contribution is $O(\rho^2/r^2) \le O(\rho)$. The same bounds hold after rescaled derivatives. The proof of (3.9.11) applies to $\mathrm{Op}_\rho(q_r)$ because it uses only this support, these seminorms and $K_{\mathrm{ref}} J_{\mathrm{ref}} = I$. Thus $K_{\mathrm{ref}} D_p[\partial_s - B_{\mathrm{band}}, C_{\log}]$ has norm $O(\rho P(S))$, and multiplication on either side by $I - C$ gives $C\rho^{1+9/5}P(S)$ as an upper bound. Including the band difference gives $C_{\kappa_0}\rho^{9/5}P(S)$ on either side for the full connection term.

(v) $(I - C_b)XC_\chi$. Write $(I - C_b)M_{\log}^{-1} = M_{\log}^{-1}(I - C_b) + M_{\log}^{-1}[C_b, E_{\log}]M_{\log}^{-1}$ and use (i) with C_b for the commutator. For the reference part use the fixed-plateau estimate in (iv) with $H = C_\chi$, $C = C_b$. The remaining terms have the output bounds of (iv) with $C = C_b$, followed on the right by the bounded C_χ.

Together, $\|R_{\mathrm{sep}}\| \le C_{\kappa_0}\rho^{3/2}P(S)$.

Proof of (3.9.13). $B_{\mathrm{int}} = C_b X C_b$, and $[C_b, F_\sharp]$ is tiny because $C_b = 1$ near $\operatorname{supp} F_\sharp$. So it suffices to bound $[X, F_\sharp]$ on the range of C_b and before C_b. The argument for $[C_\chi, X]$ in (i)–(iv) uses only that C_χ is a fixed mask equal to one near the cubic blend box and near $\operatorname{supp} C_{\log}$, and that it lies in the chart of (SC6). It applies verbatim to $F_\sharp$ and gives $\|[F_\sharp, X]\| \le C_{\kappa_0}\rho^{3/2}P(S)$. □

3.9.3 Exact two-column algebra

Let $A_*(s)$ be the completed true-velocity generator and $D = \partial_s - A_*$. We normalize the dynamically corrected power pair (J_δ, K_δ). Its physical shift is

$$S_\delta = d_0 J_\delta C_s K_\delta, \qquad D_\delta = D + S_\delta, \qquad K_\delta J_\delta = I_2. \tag{3.9.14}$$

The completed auxiliary inverse G_δ solves $D_\delta G_\delta = I$ in the same ancient forcing classes.

We build the logarithmic right column J_{raw} with the same fixed reference and finite correction, but it has its own scalar operator $d_{\mathrm{old}} = \partial_s - B_{\mathrm{old}}$. Put

$$\begin{aligned} &N = K_\delta J_{\mathrm{raw}} = M_\delta^{-1} M_{\log}, && J = J_{\mathrm{raw}} N^{-1}, && K = K_\delta, \\ &B' = N B_{\mathrm{old}} N^{-1} + N_s N^{-1}, && d' = \partial_s - B' = N d_{\mathrm{old}} N^{-1}. \end{aligned} \tag{3.9.15}$$

Lemma 3.9.15 below gives $\|M_j^{-1}\| \le 4/3$ and bounded N, N^{-1}.

Lemma 3.9.15 (Bound for the column inverses)**.** *There are a constant C_E and a polynomial P, both fixed by the selected member, its prepared column of Lemma 3.7.7, the fixed reference of Lemma 3.6.3 and the finite list of mask shapes (thus independent of ρ, of S and of the later blend radius κ_0), such that for $j = \delta, \log$, with $r_\delta = \delta$ and $r_{\log} = r_{\mathrm{out}}$,*

$$\|E_j\|_{L^2_Z \to L^2_Z} \le C_E(r_j + \rho^{3/5}) + P(S)(\rho^\nu + \rho), \qquad \nu = 1 - 128\varkappa = .99872. \tag{3.9.16}$$

Consequently there is $\rho_1 > 0$, depending only on these data and on the exponent M of $r_{\mathrm{out}} = S^{-M}$, such that for $\rho(s) \le \rho_1$

$$\|E_j\| \le \tfrac{1}{4}, \qquad \|M_j^{-1}\| \le \tfrac{4}{3}, \qquad \|N\| \le \tfrac{5}{3}, \qquad \|N^{-1}\| \le \tfrac{5}{3}.$$

These operators act at one time, so the same bounds hold on every weighted space Y_α below. The bound $\|M_j^{-1}\| \le 4/3$ is the one used throughout; the weaker form $\|M_j^{-1}\| \le 2$ that appears in the proof of Lemma 3.9.27 is implied by it.

Proof. Inputs. (a) Lemma 3.7.5(a) (proved there). (b) The prepared column of Lemma 3.7.7: its low part is (3.7.2), with its pressure (3.7.4), built on the same normalized physical eigenprofile as J_{ref}. Its remaining zero-carrier part is the macro ρ^{ν} row; the physical connection is already included in J_{low}, while opposite-band and localization tails belong to the residual. These facts give, for every fixed-shape mask C_r with $\delta \le r \le r_{\mathrm{out}}$,

$$\|(\Pi J_p - J_{\mathrm{low}})C_r\|_{2\to L^2_{\mathrm{can}}} \le P(S)(\rho^{\nu} + \rho). \tag{3.9.17}$$

Here $\Pi = \Pi_{\mathrm{zero}}$ is the orthogonal projection onto the angular labels $\pm m$. Lemma 3.7.9 proves (3.9.17), in the stronger form (3.7.35), from the exact identity (3.7.34) and the macro size (M); its proof uses the radius only through $\rho \le r^2 \le 1$. The comparison (3.7.29) with J_{ref} and the residual bound (3.7.28) are not used. (c) Lemma 3.6.3: $J_{\mathrm{ref}} = \mathrm{Op}_{\rho}(e) + \rho\mathcal{J}$ and $H_{\mathrm{ref}} = \mathrm{Op}_{\rho}(v) + \rho\mathcal{H}$, where $\mathcal{J}C_r$ and $\mathcal{H}$ are bounded on L^2 with fixed constants; $K_{\mathrm{ref}} = M_{\mathrm{ref}}^{-1}H_{\mathrm{ref}}^{*}$ with $\|M_{\mathrm{ref}}^{-1}\| \le 1 + C\rho$ by (3.6.17); and $v(z)^{*}e(z) = I_2$ at every point $z = (Z, k)$ of the chart. The profile bounds (3.6.3) make all symbols below smooth on the chart, with S- and κ_0-independent jets. (d) The kernel formula (3.6.1) and Lemma 3.6.1.

Step 1: exact removal of the high carriers. The adjoint profiles carry the angular labels $\pm m$ only, so $H_{\mathrm{ref}}^{*} = H_{\mathrm{ref}}^{*}\Pi$ and $K_{\mathrm{ref}} = K_{\mathrm{ref}}\Pi$. Also $\Pi J_{\mathrm{ref}} = J_{\mathrm{ref}}$. Hence

$$E_j = K_{\mathrm{ref}}\Pi(J_p - J_{\mathrm{ref}})C_j.$$

Every nonzero-carrier term of J_p (including the time-partition correction and the carrier parts of Y_Q, Y_b) has an angular label outside $\{m, -m\}$ by input (a). Thus Π annihilates it exactly. We use no bound for the high part, whose norm may be of order one.

Step 2: splitting. We have

$$\Pi D_p C_j = (J_{\mathrm{low}} - \mathrm{Op}_{\rho}(e))C_j + (\Pi J_p - J_{\mathrm{low}})C_j - \rho\mathcal{J}C_j.$$

By (3.9.17) and input (c), the last two terms have norm at most $P(S)(\rho^{\nu} + \rho) + C\rho$.

Step 3: the symbol vanishes at the pole up to $O(\rho)$. Write $J_{\mathrm{low}} = \mathrm{Op}_{\rho}(b_{\mathrm{low}})$. The symbol b_{low} is a polynomial in (Z, k) of degree at most three. Its coefficients are the fixed physical jets, the reduced corrector E, and their horizontal primitives in (3.7.2). At the pole the cubic terms containing k vanish, while the full divergence chart contributes $-\rho C_0$. Hence, with $\beta_0 = E - C_0$,

$$b_{\mathrm{low}}(0) = e(0) + \rho\beta_0, \qquad \|\beta_0\| \le C.$$

Put $a = v^{*}(b_{\mathrm{low}} - e)$. Since $v(0)^{*}e(0) = I_2$, we get $a(0) = \rho v(0)^{*}\beta_0$. On the unit phase box all derivatives of a of order at most four are bounded by a fixed constant. Hence

$$|a(z)| \le C(|z| + \rho), \qquad |\partial^{\alpha}a(z)| \le C \quad (1 \le |\alpha| \le 4,\ |z| \le 1). \tag{3.9.18}$$

No cubic or quadratic structure of $b_{\mathrm{low}} - e$ is used. Only the vanishing of a at the pole is used, and this follows from the common pole profile and $v^{*}e = I_2$.

Step 4: operator bound. The mask C_j is supported in the box of radius $r_j \le r_{\mathrm{out}} < 1$. We multiply $b_{\mathrm{low}} - e$ and v by a fixed cutoff $\widetilde{\zeta}$ that equals one on a neighbourhood of the unit box. The resulting cutoff error is $O(\rho)$, which is sufficient here. Indeed b_{low} has k-degree at most three, and its coefficients are fixed polynomials in Z on the working chart. Corollary 3.9.10 applies with $n = 3, d = 0$, including the terminal cubic term $O((\rho/r_j)^3)$. The remaining compact leading symbols and adjoint profiles use (SC2) at order three, and their ρ corrections use order two. The fixed horizontal extension is treated exactly as a constant symbol. Since $r_j \ge \delta$, these errors are $O(\rho^{9/5})$ or smaller. The subsequent adjoint-to-left conversion has the separate $O(\rho)$ bound in (i). Three facts follow from the kernel formula (3.6.1).

(i) $\|\operatorname{Op}_\rho(\widetilde{\zeta}v)^* - \operatorname{Op}_\rho((\widetilde{\zeta}v)^*)\| \le C\rho$. The adjoint kernel and the kernel of the adjoint symbol differ by $\widehat{w}(Z+\rho u,u) - \widehat{w}(Z,u)$ with $w = \widetilde{\zeta}v$ and the variable $u = (Y-Z)/\rho$. The mean value theorem gives a majorant $C\rho|u|\langle u\rangle^{-3}$, and Schur's test applies.

(ii) By Lemma 3.6.1, $\operatorname{Op}_\rho(\widetilde{\zeta}v^*)\operatorname{Op}_\rho(\widetilde{\zeta}(b_{\mathrm{low}} - e)) = \operatorname{Op}_\rho(\widetilde{\zeta}^2 a) + O(\rho)$.

(iii) By the same lemma, $\operatorname{Op}_\rho(\widetilde{\zeta}^2 a)C_r = \operatorname{Op}_\rho(\widetilde{\zeta}^2 a c_r) - i\rho\operatorname{Op}_\rho(\partial_k(\widetilde{\zeta}^2 a)\partial_Z c_r) + O((\rho/r)^{3/2})$. The first-order term has norm at most $C\rho/r \le C\rho/\delta = C\rho^{3/5}$, since $|\partial_Z c_r| \le C/r$.

We also use $\|\operatorname{Op}_\rho(\sigma)\| \le \int_{\mathbb{R}} \sup_Z |\widehat{\sigma}(Z,u)|\,du$, which follows from (3.6.1) by Minkowski's inequality. This quantity is invariant under the dilation $\sigma(z) \mapsto \sigma(z/r)$. For $\tau(w) = (\widetilde{\zeta}^2 a)(rw)c(w)$, two integrations by parts in ξ and (3.9.18) bound it by $C\sum_{|\alpha|\le 2}\|\partial_w^\alpha \tau\|_\infty \le C(r+\rho)$, since $r^{|\beta|}|\partial^\beta a| \le Cr$ for $|\beta| \ge 1$. Thus $\|\operatorname{Op}_\rho(\widetilde{\zeta}^2 a c_r)\| \le C(r+\rho)$. Combining (i)–(iii) with $\|M_{\mathrm{ref}}^{-1}\| \le 1 + C\rho$ and the $\rho\mathcal{H}$ term of H_{ref} gives

$$\|K_{\mathrm{ref}}(J_{\mathrm{low}} - \operatorname{Op}_\rho(e))C_j\| \le C(r_j + \rho^{3/5}).$$

Step 5: conclusion. Steps 1–4 and $\|K_{\mathrm{ref}}\|_{L^2_{\mathrm{can}}\to L^2_Z} \le C$ give (3.9.16). Since $r_{\mathrm{out}} = S^{-M} \to 0$, $\rho^{3/5} \to 0$ and $P(S)\rho^\nu = \rho^{\nu - o(1)} \to 0$, there is ρ_1 with $\|E_j\| \le 1/4$ for $\rho \le \rho_1$ and $j = \delta, \log$. We have $r_\delta = \delta \le r_{\mathrm{out}}$, so one threshold covers both j. The Neumann series gives $\|M_j^{-1}\| \le \sum_n 4^{-n} = 4/3$. Finally $\|N\| = \|M_\delta^{-1}M_{\log}\| \le \frac{4}{3}\cdot\frac{5}{4} = \frac{5}{3}$, and $N^{-1} = M_{\log}^{-1}M_\delta$ has the same bound.

For $j = \delta$ this is the statement $M_* = I + o(1)$ in the proof of Lemma 3.7.15. The only input that is not proved in this section is (3.9.17). □

In particular $KJ = I_2$.

Lemma 3.9.16 (The literal-mask comparison)**.** *For the normalized columns in* (3.9.15)*,*

$$\Delta_s = d_0(C_s - NC_sN^{-1}), \qquad \|\Delta_s\| \le C\rho^{3/2}P(S). \tag{3.9.19}$$

The inverse of $d' + d_0C_s$ has the same fixed-gap bound as the conjugate inverse of $d_{\mathrm{old}} + d_0C_s$ for sufficiently ancient time. Its separated-mask estimates keep a positive power after one critical ρ^{-1} loss.

Proof. The two columns use the same D_p, so

$$N - I = M_\delta^{-1}K_{\mathrm{ref}}D_p(C_{\log} - C_\delta).$$

The last factor is a genuine right phase annulus between the power and logarithmic regions. By Lemma 3.9.7, the two $E_\delta, E_{\log}$ have $O(\rho^{3/2}P(S))$ left and right leakage outside the plateau of C_s.

Exact multiplication, rather than an assertion of pseudolocality of M_δ^{-1}, gives for $F = I - C_s$

$$FM_\delta^{-1}E_j = FE_j - FE_\delta M_\delta^{-1}E_j.$$

This bounds the left leakage of $N - I$. Its right leakage follows from the displayed right-annulus factor.

Thus $\|[C_s, N]\| \le C\rho^{3/2}P(S)$ and $C_s - NC_sN^{-1} = -[N, C_s]N^{-1}$ proves (3.9.19). The operator identity

$$d' + d_0C_s = N(d_{\mathrm{old}} + d_0C_s)N^{-1} + \Delta_s$$

permits a Neumann perturbation of the previously fixed scalar gap.

Each off-phase estimate uses the finite nested mask family and its commutator bounds in (3.9.3). Mere smallness of $N - I$ would not keep those estimates.

The one critical loss multiplies $\rho^{3/2}P(S)$ to give $\rho^{1/2}P(S) = o(1)$. □

We do not estimate the rapidly sampled derivative N_s from $N - I = o(1)$. Direct differentiation of (3.9.15) shows that, with

$$R_{\mathrm{raw}} = A_* J_{\mathrm{raw}} - (J_{\mathrm{raw}})_s - J_{\mathrm{raw}} B_{\mathrm{old}}, \tag{3.9.20}$$

$$R = A_* J - J_s - J B', \qquad T = K A_* + K_s - B' K, \tag{3.9.21}$$

one has the exact identities

$$R = R_{\mathrm{raw}} N^{-1}, \quad DJ = Jd' - R, \quad KD_\delta = (d' + d_0 C_s)K - T, \quad TJ = KR. \tag{3.9.22}$$

The N_s terms cancel in R.

On $Q = I - JK$, the scalar change in T also disappears because $KQ = 0$. These are identities on one fixed smooth core, then extend only through the localized bounds below.

The physical shift in (3.9.14) remains literally C_s. The scalar conjugacy does not change its evolution.

The dynamic fixed reference is essential here. If $S_{\delta,0}$ denotes the algebraic-reference shift, its actual dynamic correction obeys $\|S_\delta - S_{\delta,0}\| \le \rho P(S)$ on the stated profile spaces.

The constructed auxiliary inverse for the old reference thus transfers by the exact perturbation formula

$$G_\delta = G_{\delta,0}\bigl(I + (S_\delta - S_{\delta,0})G_{\delta,0}\bigr)^{-1}. \tag{3.9.23}$$

The factor inside the inverse differs from I by $\rho^{1-o(1)}P(S)$, with one bound after an increase of the ancient threshold. Formula (3.9.23) keeps causality and reality.

It is not a replacement of the power-window shift by a logarithmic one.

3.9.4 A right inverse of the unshifted completed operator

Define the exact retraction $Q_\delta = I - J_\delta K$ and the instantaneous forcing norm

$$|f|_* = \|Kf\|_{L^2_Z} + \|Q_\delta f\|_{L^2_{\mathrm{phys}}}. \tag{3.9.24}$$

It is equivalent to the physical norm with at most finite $P(S)\rho^{-o(1)}$ factors. Its exact identity $|J_\delta a|_* = \|a\|$ controls the fixed-small cubic term in the last error.

That term does not acquire a growing column norm. The energy argument does not take any derivative of (3.9.24).

Fix a finite reference time s_{ref} in the preparation interval. Put $g_+(s) = \exp(\int_{s_{\mathrm{ref}}}^{s} b_{0,+}(r)\,\mathrm{d}r)$, $g_- = \overline{g_+}$ and $\gamma = |g_+| > 0$. Let $\lambda_c = \Re\lambda_0 > 0$ and let b be the Gaussian polynomial exponent. For $\sigma = 3/20$ set

$$q_*(s) = \gamma(s)e^{\lambda_c s}T^b, \qquad \|f\|_{\mathcal{F}_\sigma} = \operatorname*{ess\,sup}_{s\le -s_0} q_*(s)^{-1}\rho(s)^{-1-\sigma}|f(s)|_*.$$

Here $\mathcal{F}_\sigma$ consists of strongly measurable canonical L^2 forcings in the solenoidal fiber at almost every s, modulo equality almost everywhere, with finite displayed norm. Put $W = q_*\rho^{1+\sigma}$. The map $f \mapsto W^{-1}(Kf, Q_\delta f)$ identifies this space with the closed subspace of the vector-valued L^∞_s product consisting of pairs (a, v) with $v(s)$ solenoidal and $K(s)v(s) = 0$ almost everywhere. Indeed the inverse is $W(J_\delta a + v)$, by $KJ_\delta = I$. The rows and columns are strongly measurable and bounded on each compact time interval. The fiber conditions are closed under almost-everywhere pointwise L^2 limits, so this is a Banach space. The scalar pair spaces use the same measurability convention. Timewise bounds for a forcing hold almost everywhere; a mild state has its continuous representative on finite intervals. The Gaussian curvature q_G is written q below.

A direct bound for the scalar band evolutions. In this paragraph B_{full} denotes the old scalar band operator $B_{\mathrm{old}} = B_a + b_0(s)I$ of (3.9.15), written on the conjugate pair. Hypotheses imported: On the real pair space $L^2_Z(\mathbb{C}^2)$ write $B_{\mathrm{full}}(s) = \mathrm{diag}(B_+(s), B_-(s)) + b(s)$, where

$$B_\pm(s) = \mathrm{Op}^L_\rho(\lambda_\pm(Z,k) + \rho c_\pm(s,Z,k)) + \rho(\tfrac{1}{2} - h)Z\partial_Z, \tag{3.9.25}$$

Op^L_ρ is the left quantization with $k = -i\rho\partial_Z$, and:

(H1) $\lambda_\pm \in C^6(\mathbb{R}^2)$ with all derivatives of order ≤ 6 bounded, $\lambda_\pm$ constant outside a fixed compact phase chart (the exterior extension of Lemma 3.9.21), and $\Re\lambda_\pm \le \lambda_c$ on $\mathbb{R}^2$. This is the stated property "principal real symbol at most λ_c" of the extended band. The jets of Lemmas 3.6.2 and 3.6.1 give this property.

(H2) $c_\pm(s,Z,k)$ are measurable in s at each (Z,k). Their spatial derivatives through order four are bounded uniformly in s.

(H3) For this old scalar operator, $b(s) = \mathrm{diag}(b_0(s), \overline{b_0(s)})$, with measurable b_0 satisfying $|b_0| \le \rho^{.99872}P(S) \to 0$ as $s \to -\infty$.

The remaining physical dynamic correctors belong to the intertwining residual, not to B_{old}. The critical inverse below removes this scalar feedback by its exact center gauge.

For the shifted operator the same hypotheses hold with $\lambda_\pm$ replaced by $\lambda_\pm - d_0\chi_{s,\pm}$, where $\Re(\lambda_\pm - d_0\chi_{s,\pm}) \le g_s < \lambda_c$ on $\mathbb{R}^2$ for the fixed d_0, by the gap estimate in Lemma 3.9.21.

Lemma 3.9.17 (Anti-Wick real-part bound)**.** *Let $a = a_\infty + a_c$, where $a_\infty \in \mathbb{C}$ is constant and $a_c \in C^6_b(\mathbb{R}^2)$ has support in a fixed compact phase set $\mathcal{K}$. This holds at every use below: by (H1) and its shifted version, the extended band, the shift symbol $d_0\chi_s$ and the compactly supported fills are constant outside a fixed chart. Assume $\Re a \le g$. Then for $0 < \rho \le 1$ and $u \in \mathcal{S}(\mathbb{R})$,*

$$\Re\langle \mathrm{Op}^L_\rho(a)u, u\rangle \le (g + C\rho\,\|a\|_{C^6_b})\|u\|_2^2,$$

with C depending only on $\mathcal{K}$.

Proof. (i) *Left to Weyl.* Constants have equal left and Weyl quantizations, so only a_c matters. With $\widehat{a}_c(Z,v) = (2\pi)^{-1}\int e^{ivk}a_c(Z,k)\,dk$, the kernel formula (3.6.1) and the Weyl kernel formula used in Lemma 3.9.20 give

$$(\mathrm{Op}^L_\rho(a_c) - \mathrm{Op}^W_\rho(a_c))u(Z) = \int [\widehat{a}_c(Z,v) - \widehat{a}_c(Z - \rho v/2, v)]\,u(Z-\rho v)\,dv.$$

Three integrations by parts in k over the compact set $\mathcal{K}$ and the mean value theorem in Z bound the bracket by $C_{\mathcal{K}}\rho|v|\langle v\rangle^{-3}\|a_c\|_{C^4_b}$. Since $|v|\langle v\rangle^{-3}$ is integrable, Schur's test gives $\|\mathrm{Op}^L_\rho(a) - \mathrm{Op}^W_\rho(a)\| \le C_{\mathcal{K}}\rho\|a_c\|_{C^4_b}$. We do not expand the operator $e^{-\frac{i\rho}{2}\partial_Z\partial_k}$ in a Taylor series; it is not bounded on C^k_b without loss of derivatives.

(ii) *Weyl real part.* $\mathrm{Op}^W_\rho(b)^* = \mathrm{Op}^W_\rho(\bar{b})$, thus $\Re\langle \mathrm{Op}^W_\rho(a)u,u\rangle = \langle \mathrm{Op}^W_\rho(\Re a)u,u\rangle$.

(iii) *Anti-Wick comparison.* With the coherent states φ_w, $w \in \mathbb{R}^2$, the anti-Wick quantization $\mathrm{Op}^{AW}_\rho(p) = (2\pi\rho)^{-1}\int p(w)\,|\varphi_w\rangle\langle\varphi_w|\,dw$ satisfies $\mathrm{Op}^{AW}_\rho(p) \le \sup p$ for real p, and $\mathrm{Op}^{AW}_\rho(p) = \mathrm{Op}^W_\rho(p * \Gamma_\rho)$ with Γ_ρ the centered Gaussian of covariance $\frac{\rho}{2}I$. Since Γ_ρ is even, $p*\Gamma_\rho - p = \rho r_2$ with derivatives of r_2 up to order two in each variable bounded by $C\|p\|_{C^6_b}$.

For $p = \Re a$, subtract its constant part. Taylor's formula with integral remainder for $p * \Gamma_\rho - p$, also applied after two k derivatives, gives

$$\sup_Z \int (|r_2(Z,k)| + |\partial_k^2 r_2(Z,k)|)\, \mathrm{d}k \le C_{\mathcal{K}} \|a_c\|_{C_b^4}.$$

Indeed the linear Gaussian moment vanishes, the second absolute moment is $O(\rho)$, and translation in k preserves the L_k^1 norms of the compactly supported derivatives. The Weyl kernel estimate in the proof of Lemma 3.7.13 therefore gives

$$\langle \mathrm{Op}_\rho^W(\Re a)u, u\rangle \le \langle \mathrm{Op}_\rho^{AW}(\Re a)u, u\rangle + C\rho\|a\|_{C_b^6}\|u\|^2 \le (g + C\rho\|a\|_{C_b^6})\|u\|^2.$$

The combination of (i)–(iii) proves the lemma. □

Lemma 3.9.18 (Scalar propagator bound)**.** *Assume (H1)–(H3) and fix $\epsilon > 0$. There is T_ϵ such that the evolutions $U^{(0)}, U^{(s)}$ of $\partial_s - B_{\mathrm{full}}$ and $\partial_s - B_{\mathrm{full}} + d_0 C_s$ exist on $L^2_Z(\mathbb{C}^2)$.*

For $r \le s \le -T_\epsilon$, they satisfy

$$\|U^{(0)}(s,r)\| \le e^{(\lambda_c+\epsilon)(s-r)}, \qquad \|U^{(s)}(s,r)\| \le e^{(g_s+\epsilon)(s-r)}.$$

Proof. Put $d(s) = (\frac{1}{2} - h)\rho(s)$ and $a(s,r) = \int_r^s d(\tau)\, \mathrm{d}\tau$. The unitary maps $V(s,r)f(Z) = e^{a(s,r)/2} f(e^{a(s,r)} Z)$ solve the dilation equation with generator $d(s)(Z\partial_Z + 1/2)$ on Schwartz functions. Write either full generator as this term plus $K(s)$, including $-d(s)I/2$ in $K(s)$. This family is locally uniformly bounded. Testing the left quantization against two Schwartz functions gives measurable matrix coefficients by (H2), since its symbol at $(Z, \rho(s)\xi)$ is measurable in s and the two test functions give an integrable majorant in (Z,ξ). Density, separability of L^2 and (H3) then give strong measurability of $K(s)f$ for each f. The strongly continuous unitary dilations preserve that property for $H(s) = V(r,s)K(s)V(s,r)$. The successive vector-valued integrals for $Y(s)f = f + \int_r^s H(\tau)Y(\tau)f\, \mathrm{d}\tau$ are bounded at order j by $\|f\|(\sup\|H\|\,|s-r|)^j/j!$ on each finite interval. Their sum is locally absolutely continuous for each f. Uniqueness gives the evolution law for $U(s,r) = V(s,r)Y(s)$. Since $\|U(s,r)f\| = \|Y(s)f\|$, for almost every s we have

$$\frac{d}{ds}\|U(s,r)f\|^2 = 2\Re\langle K(s)U(s,r)f, U(s,r)f\rangle.$$

Apply Lemma 3.9.17 to $a = \lambda_\pm$ alone.

$C\rho$ bounds the lower-order term $\rho\,\mathrm{Op}_\rho(c_\pm)$ with the stated finite C^4 symbol norm.

We do not assume two additional derivatives of $c_\pm$. Thus

$$\tfrac{d}{ds}\|u\|^2 = 2\Re\langle K(s)u, u\rangle \le 2(\lambda_c + C\rho(s) + |b_0(s)|)\|u\|^2.$$

Select T_ϵ such that $C\rho + |b_0| \le \epsilon$ for $s \le -T_\epsilon$. Integration gives the first bound.

In these old coordinates C_s is exactly the sectorwise left quantization of $\chi_{s,\pm}$. Applying the same form estimate to $\lambda_\pm - d_0\chi_{s,\pm}$, whose real part is at most g_s, gives the second bound. Lemma 3.9.16 transfers the shifted inverse to the normalized coordinates. □

Lemma 3.9.19 (Ordinary axial derivatives of the scalar symbols)**.** *On the fixed physical phase chart, the principal eigenvalue and the actual connection satisfy*

$$\begin{aligned} |\partial_Z^l \partial_k^j \lambda| &\le C_{l,j}, \quad l \le 17, \quad j \le 5, \\ |\partial_Z^l \partial_k^j c_1| &\le C_{l,j}, \quad l \le 16, \quad j \le 4. \end{aligned} \tag{3.9.26}$$

Smooth fixed-chart extensions preserve these rectangles. The quadratic blend λ_a and the compact cubic symbol $e_{\kappa_0} = \chi_{\kappa_0}(\lambda - \lambda_{\mathrm{quad}})$, equal to $\lambda - \lambda_a$ on the working chart, have the first rectangle with κ_0-dependent constants. A smooth blend of c_1 to its center value has the second rectangle. No fifth k derivative of a first corrector is asserted.

Proof. Write $\ell = v^*$ for the physical left eigenrow. Since $P_k e = e$, $\ell P_k = \ell$ and $\ell e = 1$, (3.6.6) gives

$$\lambda = \ell F_0 e - i(\tfrac{1}{2} - h)Zk, \qquad c_1 = \ell R_1.$$

The second identity is the solvability equation in the proof of Lemma 3.6.2. The operator F_0 in (3.6.5) is affine in k and uses one horizontal derivative. Leibniz's rule, the eighteen ordinary source jets and (3.6.3) give the first rectangle. At $j = 5$ the leading profiles still lie in H^6_2, so every radial pairing is bounded.

The displayed formula for R_1 in that proof spends at most one further Z or k derivative of a leading profile. Its pressure and divergence terms have the stated H^4_{6-j} bounds for $l \le 16$, $j \le 4$: the explicit e_Z, e_k and pressure derivative use the leading seventeenth Z and fifth k derivatives. Pairing with ℓ proves the second rectangle. Multiplication by the smooth extension and blend cutoffs preserves the indicated derivatives; only their constants depend on κ_0. □

Lemma 3.9.20 (Critical form bound for a fixed quadratic blend)**.** *Fix the selected $h > 0$, put $T = (h\rho)^{-1}$ and $k = -i\rho\partial_Z$. Let $\lambda_a \in C^6_b(\mathbb{R}^2)$ and $c_a \in C^4_b(\mathbb{R}^2)$ be the extensions used below, each equal to a constant outside a fixed phase chart.*

Suppose that, on a fixed phase ball of radius $\kappa_0 > 0$,

$$\lambda_a = \lambda_{\mathrm{quad}} = \lambda_0 + \tfrac{1}{2}\lambda_{ZZ}Z^2 + \tfrac{1}{2}\lambda_{kk}k^2, \qquad c_a = c_*,$$

and that $\Re(\lambda_0 - \lambda_a) \ge c\min(Z^2 + k^2, 1)$ globally. The c_a bounds may be uniform bounds for a time-dependent family.

We use no time derivative here. Assume $q > 0$, $\Re\lambda_{kk} < 0$ and

$$\lambda_{ZZ} = \lambda_{kk}q^2/h^2 + (1 + 2(\tfrac{1}{2} - h)/h)q.$$

Put $a = \lambda_{kk}/(2h^2)$, $b_d = (1 + 2(\frac{1}{2} - h)/h)/2$, $X = -\Re(a)q > b_d$, $\beta = -c_*/h - aq$, and

$$\eta_q = X - b_d/2 - \sqrt{X^2 - b_d X}, \qquad (\mathscr{U}_T u)(x) = T^{-1/4}u(x/\sqrt{T}).$$

For $B_a = \mathrm{Op}^L_\rho(\lambda_a + \rho c_a) + \rho(\frac{1}{2} - h)Z\partial_Z$, define

$$H_T = T\lambda_0 - \beta - \frac{x}{2}\partial_x - T\mathscr{U}_T B_a \mathscr{U}_T^{-1}.$$

There are finite constants C_{h,κ_0} and T_{h,κ_0}, for this fixed member and blend, such that

$$\Re\langle H_T u, u\rangle \ge -(\eta_q + C_{h,\kappa_0}\rho^{1/2})\|u\|_2^2 \qquad (T \ge T_{h,\kappa_0},\ u \in \mathcal{S}(\mathbb{R})).$$

In particular, if $\eta_q < \sigma$, an increase of the ancient threshold puts the error below any fixed fraction of $\sigma - \eta_q$.

We assert no uniformity as h or κ_0 tends to zero.

Proof. For the exact quadratic operator the definition of H_T gives

$$H_{\mathrm{quad}} = a\partial_x^2 - b_d x\partial_x - (aq^2 + b_d q)x^2 + aq.$$

Write $A_0 = -\Re a > 0$. Integration by parts gives

$$\Re\langle H_{\mathrm{quad}}u, u\rangle = A_0\|u'\|_2^2 + (A_0q^2 - b_dq)\|xu\|_2^2 + (b_d/2 - X)\|u\|_2^2.$$

The nonnegative square $\|\sqrt{A_0}u' + \sqrt{A_0q^2 - b_dq}\,xu\|_2^2$ expands to show the first two terms are at least $\sqrt{A_0(A_0q^2 - b_dq)}\|u\|_2^2$.

Thus the quadratic real form has a lower bound of $-\eta_q$.

For localization work in the original Z variable. Its bounded self-adjoint real-form representative is

$$A_\rho = \mathrm{Sym}\Big[T\,\mathrm{Op}_\rho^L(\lambda_0 - \lambda_a) - h^{-1}\,\mathrm{Op}_\rho^L(c_a)\Big] - \Re\beta + b_d/2, \qquad \mathrm{Sym}\,A = (A + A^*)/2.$$

Thus the uncut dilation has real part $b_d/2$.

It has not been estimated as a bounded transport operator. In particular $\|A_\rho\| \le C_{h,\kappa_0}T$ for $T \ge 1$.

Select real smooth phase cutoffs χ_0, χ_1 with $\chi_0^2 + \chi_1^2 = 1$, $\chi_0 = 1$ on the $\kappa_0/4$ ball and $\mathrm{supp}\,\chi_0$ inside the $\kappa_0/2$ ball. We can give them as the cosine and sine of a smooth step.

Put $Q_j = \mathrm{Op}_\rho^W(\chi_j) = Q_j^*$. $\chi_1 - 1$ has compact phase support.

We fix these masks before ρ tends to zero.

We record the symbol classes and the finite-order localization error. Subtract the constant exterior values. The differences are compact-phase symbols.

For such a symbol the Weyl kernel in the convention of (3.6.1) is

$$\mathrm{Op}_\rho^W(a)u(Z) = \int \widehat{a}(Z - \rho v/2, v)u(Z - \rho v)\,dv.$$

Taylor expansion at Z through first order has remainder bounded by $C\rho^{3/2}|v|^{3/2}$. Three k derivatives give the integrable Fourier envelope $(1 + |v|)^{-3}$.

A 1/2-Hölder first Z derivative of that envelope bounds the Taylor remainder. The principal symbol's C^6 bounds control these mixed derivatives and the Schur envelopes.

Application of the same calculation to a product, as in Lemma 3.6.1, gives its first Weyl bracket and an $O_{\kappa_0}(\rho^{3/2})$ operator remainder. The first Weyl bracket of a symbol with itself is zero.

A first commutator with a mask is $\rho\,\mathrm{Op}_\rho^W(c)$ plus $O(\rho^{3/2})$, with c a fixed compact symbol formed with only one derivative of the principal symbol. For its second commutator, a zeroth-order product estimate with $O(\rho^{1/2})$ error suffices.

It uses fewer derivatives. Twice that remainder times the mask norm bounds the commutator with the existing bounded remainder.

Thus

$$\sum_{j=0}^{1} Q_j^2 = I + R_\rho, \quad \|R_\rho\| \le C_{\kappa_0}\rho^{3/2}, \qquad \sum_{j=0}^{1}\|[Q_j, [Q_j, A_\rho]]\| \le C_{h,\kappa_0}T\rho^{3/2}.$$

For the order-ρ coefficient, use three k derivatives and one Z derivative. The first absolute Fourier moment and the mean-value formula give a zeroth-order product error $O(\rho)$.

Its four available derivatives suffice, and its prefactor makes this $O(T\rho^2)$, smaller than the displayed remainder. Constants outside the fixed chart commute.

Thus the proof uses no higher derivative of the spectral profile. The algebraic identity

$$A_\rho = \sum_j Q_j A_\rho Q_j - \tfrac{1}{2}(R_\rho A_\rho + A_\rho R_\rho) + \tfrac{1}{2}\sum_j [Q_j,[Q_j,A_\rho]]$$

is a phase-space IMS identity with error $O_{h,\kappa_0}(T\rho^{3/2}) = O_{h,\kappa_0}(\rho^{1/2})$.

On a neighborhood of $\operatorname{supp}\chi_0$ the principal and order-ρ symbols agree with the quadratic model. The zero and first product symbols of their localized difference thus vanish.

The inner mask has a fixed positive gap to the boundary of the exact-quadratic plateau. The polynomial part requires no bounded-symbol assumption.

For either polynomial Z^2 or k^2, the Weyl product with χ_0 stops at order two. Each coefficient in this expansion has compact phase support.

We compose once more with χ_0 and then use only the compact-symbol estimate above. In this way we treat the unbounded quadratic before we estimate the finite Schur remainder. The same calculation for $c_a - c_*$ uses its zero-order vanishing and $O(\rho)$ product error.

It follows that

$$\langle A_\rho Q_0 u, Q_0 u\rangle \geq -\eta_q \|Q_0 u\|_2^2 - C_{h,\kappa_0}\rho^{1/2}\|u\|_2^2.$$

This uses the exact oscillator form, not an anti-Wick conversion error at its minimum.

For the exterior piece select a nonnegative smooth fill f supported strictly inside $\{\chi_1 = 0\}$ such that $\Re(\lambda_0 - \lambda_a) + f \geq c_1\kappa_0^2$ everywhere, with a fixed $c_1 > 0$. Such a fill exists by the quadratic well bound.

The zero and first product symbols of $Q_1 \operatorname{Op}_\rho^L(f) Q_1$ vanish. Lemma 3.9.17, applied with the sign reversed to the filled principal symbol, and the bounded lower-order coefficients give

$$\langle A_\rho Q_1 u, Q_1 u\rangle \geq (Tc_1\kappa_0^2 - C_{h,\kappa_0})\|Q_1 u\|_2^2 - C_{h,\kappa_0}\rho^{1/2}\|u\|_2^2.$$

The anti-Wick conversion here costs $TO_{\kappa_0}(\rho) = O_{\kappa_0}(1/h)$. We keep this cost in the fixed constant, and an increase of T lets $Tc_1\kappa_0^2$ absorb it.

The interior and exterior bounds, the IMS identity, and $\|Q_0 u\|^2 + \|Q_1 u\|^2 = \|u\|^2 + O_{\kappa_0}(\rho^{3/2})\|u\|^2$ prove the claim. Unitary dilation transfers it back to H_T.

The conjugate component has the same real-form bound. □

Lemma 3.9.21 (Critical, fixed-gap and annular scalar Greens)**.** *Consider the scalar band of the selected B_*, in the same center gauge $g_s/g = b_0$. The old-coordinate critical equation $d_{\mathrm{old}}a = f$ has a real-pair-compatible inverse G_a.*

Its endpoint is the ancient end $s = -\infty$, or equivalently the future end of logarithmic ancient time $R = \log(-s) = +\infty$. Its domain is the scalar component of $\mathcal{F}_\sigma$.

Its pointwise cost is one ρ^{-1} factor. The equation $(d_{\mathrm{old}} + d_0 C_s)a = f$ has a causal fixed-gap inverse G_s with no such factor.

Take the finite family of fixed-shape output annuli A_r and inner cutoffs C_r used below. Their radius functions satisfy $\delta \leq r \leq 2\kappa_0$ on the relevant causal history and $|\partial_s \log r| \leq C\rho$. Set $\mathcal{A}_f(s) = q_*(s)\rho(s)^{1+\sigma}\|f\|_{\mathcal{F}_\sigma}$.

Then

$$\begin{aligned} \|A_r G_a f(s)\|_2 &\leq C r^{-2}\mathcal{A}_f(s), \\ \|[d_{\mathrm{old}}, C_r] G_a f(s)\|_2 &\leq C(\rho/r^2 + o(1))\mathcal{A}_f(s). \end{aligned} \tag{3.9.27}$$

In the first display we first read A_r, C_r, G_a in the old center-gauged scalar coordinates. In the normalized coordinates put

$$A_r' = NA_rN^{-1}, \quad C_r' = NC_rN^{-1}, \quad G_a' = NG_aN^{-1}.$$

The same two estimates hold with each primed mask, operator and Green in the display, with a constant independent of all dyadic $r \in [\delta, 2\kappa_0]$.

We use no assertion that an unprimed shrinking mask has the same bound against G'_a. The last estimate uses the row/column cutoff orientation of the parametrix. No reverse-order commutator assertion is necessary.

Proof. First construct the inverse in the old scalar coordinates.

On the closed rectangle $\overline{U}$ of Theorem 2(iv), the Hessian of $\Re\lambda$ is uniformly negative definite. Integrating twice along the segment from the centered pole gives $\Re(\lambda_0 - \lambda(Z,k)) \geq c(Z^2+k^2)$ on U. Let λ_{quad} be its centered quadratic Taylor polynomial.

Select a fixed χ_{κ_0} equal to one in the κ_0 box and zero outside the $2\kappa_0$ box. First define

$$\lambda_a = \lambda + \chi_{\kappa_0}(\lambda_{\mathrm{quad}} - \lambda).$$

Both terms of this convex blend satisfy the same quadratic lower bound for their real deficit on U.

Then extend its symbol to a fixed lower-real-part constant outside that chart. We use a cutoff equal to one on each working column and mask support.

The transition lies inside the strict well, so this finite-jet symbol λ_a obeys

$$p(Z,k) := \Re(\lambda_0 - \lambda_a(Z,k)) \geq c\min(Z^2+k^2, 1)$$

globally. Choose a smooth cutoff ζ_{chart} compactly supported in the physical chart and equal to one on all working column and mask supports. For the current order-ρ coefficient take

$$c_a = c_* + (1-\chi_{\kappa_0})\zeta_{\mathrm{chart}}(c_1 - c_*), \qquad c_* = c_1(0,0). \tag{3.9.28}$$

The constant is the physical center value of (3.7.1). This choice equals c_* on the inner neighborhood and outside the outer chart, and equals c_1 on the working region outside the blend. It preserves the second rectangle of (3.9.26), with κ_0-dependent constants. Choose the cutoffs real and use the conjugate formula on the other sector. The exterior extension changes no working column or mask support. The operator is the genuine left-ordered $B_a = \mathrm{Op}_\rho(\lambda_a + \rho c_a) + \rho(\frac{1}{2} - h)Z\partial_Z$, with the dilation left uncut.

In the old auxiliary scalar coordinates of (3.9.15), the completed center feedback is the diagonal scalar $b_0(s)$, so $B_{\mathrm{old}} = B_a + b_0(s)I$ on the conjugate pair. Here the symbol c_a in (3.9.28) is fixed in time, and the sampled cell coefficients defining $b_0 = \sum_j \omega_j b_{0,j}$ in Lemma 3.7.7 are measurable on their charts. The locally finite smooth partition therefore gives (H2)–(H3) for the actual time dependence. The remaining physical low/high coupling belongs to the intertwining residual R in (3.9.20).

We do not insert it into this auxiliary scalar Green. Use the scalar sixth phase derivative at the end of Lemma 3.6.2 and its selected ordinary jets.

These give the finite principal six-jet and lower-order Fourier moments used below.

The complex source curvature target in Theorem 2(iv) gives a positive real $q = a_m^2 C_q/\Delta$, $a_m = m/r_0$, and $\lambda_{ZZ} = (\lambda_{kk}/h^2)q^2 + (1 + 2(\frac{1}{2} - h)/h)q$. Put $a = \lambda_{kk}/(2h^2)$, $b_d = (1 + (1-2h)/h)/2$, $X = -\Re(a)q$.

Theorem 2(iv) gives $X > b_d$ and

$$\eta_q = X - \frac{b_d}{2} - \sqrt{X^2 - b_d X} \leq \frac{1}{16} < \frac{1}{8} < \sigma.$$

The extensions selected satisfy $\lambda_a = \lambda_{\mathrm{quad}}$ and $c_a = c_*$ on the fixed inner κ_0 box. Lemma 3.9.20 then applies to the normalized generator H_T in (3.9.29) below and gives

$$\Re\langle H_T u, u\rangle \geq -(\eta_q + C_{h,\kappa_0}\rho^{1/2})\|u\|_2^2.$$

We first fix the source and h, then the outer masks and their gap, and then the blend radius κ_0.

Only then is the ancient threshold increased to make this error smaller than the selected fraction of $\sigma - \eta_q$. We do not discard a generic $O(\rho)$ quantization error after multiplication by $T = (h\rho)^{-1}$.

We specify the endpoint and integral that define this inverse. We first use the plus component.

The minus component is its conjugate. Set $T = -s$, $R = \log T$, and $\widetilde{a} = g^{-1}a$, $\widetilde{f} = g^{-1}f$; this removes the exact center feedback from state and force: $g^{-1}d_{\mathrm{old}}(g\widetilde{a}) = (\partial_s - B_a)\widetilde{a} = \widetilde{f}$.

The map

$$(\mathscr{U}_T u)(x) = T^{-1/4}u(x/\sqrt{T})$$

is unitary on L^2. With $\beta = b_G$ as in (3.10.4), define $b(R) = e^{\lambda_0 T}T^{-\beta+1/4}\mathscr{U}_T\widetilde{a}(s)$.

Direct differentiation converts the pulled-back equation into the equation below. This includes $\partial_R s = -T$ and the derivative of the unitary dilation:

$$\partial_R b = H_T b + F(R), \qquad H_T = T\lambda_0 - \beta - \frac{x}{2}\partial_x - T\mathscr{U}_T B_a \mathscr{U}_T^{-1}, \qquad F = -Te^{\lambda_0 T}T^{-\beta+1/4}\mathscr{U}_T\widetilde{f}. \tag{3.9.29}$$

The $+1/4$ in the amplitude derivative cancels the $-1/4$ derivative of $\mathscr{U}_T$.

Thus the displayed generator has no unaccounted scalar Jacobian term.

By the definition of q_* and $T\rho = 1/h$,

$$\|F(R)\|_2 \le Ce^{-\sigma R}\|f\|_{\mathcal{F}_\sigma}. \tag{3.9.30}$$

The unitary dilation group and the bounded finite-symbol part of H_T build a two-direction evolution on each finite R-interval. The previous lower real-form bound gives a bound on its backward propagator $\mathcal{V}(R,U)$, $U \ge R$. We fix $\eta_q < \eta < \sigma$ and a sufficiently ancient threshold. Then this propagator satisfies $\|\mathcal{V}(R,U)\|_{2\to 2} \le e^{\eta(U-R)}$.

Define the critical inverse by the convergent Bochner integral

$$b(R) = -\int_R^\infty \mathcal{V}(R,U)F(U)\,\mathrm{d}U, \qquad (G_a f)(s) = g(s)\mathscr{U}_T^{-1}\big(e^{-\lambda_0 T}T^{\beta-1/4}b(R)\big). \tag{3.9.31}$$

Equations (3.9.30) and (3.9.31) give

$$\|b(R)\|_2 \le C(\sigma-\eta)^{-1}e^{-\sigma R}\|f\|_{\mathcal{F}_\sigma}, \qquad \|G_a f(s)\|_2 \le Cq_*(s)\rho(s)^\sigma\|f\|_{\mathcal{F}_\sigma}.$$

Splitting the integral at a finite U gives the finite-interval variation-of-constants identity. Testing it against smooth members of the adjoint dilation domain gives $d_{\mathrm{old}}G_a f = f$ in distributions for every forcing in the stated class: the forcing is locally Bochner integrable, and the tail converges by (3.9.30).

If a homogeneous solution has the same $O(e^{-\sigma R})$ normalized bound, propagation from U back to R and $U \to \infty$ make it zero. Thus the ancient-end condition is explicit and fixes this inverse uniquely in its output class.

The integral uses $U \ge R$, which means $s(U) \le s(R)$: it depends only on earlier physical fast time. It is not a terminal-zero condition at a finite upper endpoint of s.

Fix $b > 0$ so both shift symbols are one on $|(Z,k)| \le b$. There $\Re(\lambda_a - d_0\chi_s) \le \lambda_c - d_0$ for the original $d_0 > 0$. Outside this ball the global deficit for λ_a gives $\Re(\lambda_a - d_0\chi_s) \le \lambda_c - c\min(b^2,1)$ since $\chi_s \ge 0$. Thus one can take $g_s = \lambda_c - \frac{1}{2}\min\{d_0, c\min(b^2,1)\}$ for both sectors and all sufficiently small blend radii.

The finite Weyl/left conversion and exact dilation integration by parts give the same bound with an $o(1)$ error. Lemma 3.9.18 (bounded perturbation of the dilation group) then constructs the old causal G_s with rate g_s.

We first prove the annular bound in these old scalar coordinates and then apply the exact normalization (3.9.15).

We prove the fixed-radius extension and its radius-uniform constants in Lemma 3.9.27 below. It uses only the critical bound just given and a different core fill.

The argument below also gives the shrinking preparation range used here. It remains to prove the stronger annular output estimate.

For any selected radius r, let $V_r = \mathrm{Op}_\rho^{\mathrm{AW}}(r^2 v((Z,k)/r))$, where the nonnegative fixed v fills the smaller phase core. Then $p + r^2 v(\cdot/r) \geq cr^2$.

Anti-Wick positivity and the finite second Fourier moments give a Weyl comparison error $O(\rho) = o(r^2)$, with one bound for $r \geq \delta = \rho^{2/5}$. Apply the same exact center-gauge pullback to the filled old scalar operator $d_{\mathrm{ann}} = d_{\mathrm{old}} + V_r$.

It has a nonautonomous forward evolution with damping $\lambda_c - cr(s)^2$. Thus it has a causal inverse G_{ann} of pointwise cost Cr^{-2}.

To see this without a fixed value of r, note $|(\log r)'| = O(\rho) = o(r^2)$. For the dyadic family $r_j(s) = 2^j \rho(s)^{2/5}$ one has $\partial_s \log r_j = (2/5)h\rho$, independent of j.

For $r_{\mathrm{out}} = S_{\mathrm{mask}}^{-M}$ its logarithmic derivative is $6Mh\rho/(5L)$. Also

$$\partial_s \log(r_j/r_{\mathrm{out}}) = h\rho\left(\frac{2}{5} - \frac{6M}{5L}\right) > 0$$

after the threshold $L > 3M$.

Thus a dyadic radius inside the outer preparation chart at output time stays inside it at each earlier time in its causal history. We make the outer truncation of this family with a smooth fixed-shape cutoff $\omega(r_j/r_{\mathrm{out}})$.

Its time derivative is $O_M(\rho)$ on the transition. Only a bounded number of j meet that transition at each time. We thus never differentiate a discontinuous time-dependent last index. Since each active $r_j \geq \delta$, the $o(r_j^2)$ comparison is uniform even though the number of active indices grows like $O(\log(1/\rho))$.

We differentiate $e^{-c\int_u^s r(v)^2\,\mathrm{d}v} A(u)/r(u)^2$, for any of the fixed polynomial/log time profiles A, and we integrate from the ancient endpoint to get the $r(s)^{-2}$ factor. The ancient boundary vanishes since $\int_u^s r(v)^2\,\mathrm{d}v$ diverges as $u \to -\infty$.

Here G_a, G_{ann} denote these old center-gauged inverses for now, and the exact inverse identities are

$$G_a = G_{\mathrm{ann}} + G_{\mathrm{ann}} V_r G_a, \qquad [C_r, G_{\mathrm{ann}}] = G_{\mathrm{ann}}[d_{\mathrm{ann}}, C_r] G_{\mathrm{ann}}.$$

The two terms in the first identity have the same ancient-end condition. The boundary term in finite-interval Duhamel tends to zero.

Use the same g-pulled-back coordinates and divide by $e^{\lambda_c s}$. This bound is a fixed power/logarithm of $|u|$ times $\exp(-c\int_u^s r(v)^2\ \mathrm{d}v)$.

This tends to zero as $u \to -\infty$, since $r \geq \delta = \rho^{2/5}$ and $\int_{-\infty}^s \rho(v)^{4/5}\ \mathrm{d}v = \infty$. The commutator identity follows first for compactly supported forcing and then by the same boundary estimate for the weighted class.

For a mask C_r that separates the fill from the output annulus, the finite scaled-kernel calculus gives $\|[d_{\mathrm{ann}}, C_r]\| \leq C\rho$ and separated leakage $O((\rho/r^2)^2)$.

The Weyl-product remainder is $O(\rho^2 r^{-2})$. Insert C_r next to V_r in the first identity and use the second.

In the only nontrivial term the successive costs are

$$G_a : \rho^{-1}, \quad V_r : r^2, \quad G_{\mathrm{ann}} : r^{-2}, \quad [d_{\mathrm{ann}}, C_r] : \rho, \quad G_{\mathrm{ann}} : r^{-2};$$

their product is r^{-2}. The leakage contributes $(\rho/r^2)^2\rho^{-1} = (\rho/r^2)r^{-2} \le Cr^{-2}$.

This gives the first estimate in (3.9.27). For the second, let A_r equal one near the transition of C_r. The principal, dilation and time terms give an operator T_r of size $O(\rho)$, since the cutoff has fixed shape and $|\partial_s \log r| + \rho_s/\rho = O(\rho)$. The finite radius calculus of Lemma 3.9.26, applied on the right as in Lemma 3.9.27, gives

$$[d_{\mathrm{old}}, C_r] = T_r A_r + O_{\kappa_0}(\rho^{3/2}/r).$$

Thus $A_r G_a$ costs $O(r^{-2})$ in the main term. The global $O(\rho^{-1})$ bound on G_a costs $O_{\kappa_0}(\sqrt{\rho}/r)$ in the remainder, which tends to zero uniformly since $r \ge \rho^{2/5}$.

The two are on the same center-gauged scalar forcing class. Last the scalar conjugacy (3.9.15) transports the critical and annular inverses to d' without a radius-dependent commutator estimate on N.

In fact, for each dyadic radius separately, the exact identities are

$$A'_r G'_a = N A_r G_a N^{-1}, \qquad [d', C'_r]G'_a = N[d_{\mathrm{old}}, C_r]G_a N^{-1}.$$

The bounds $\|N\| + \|N^{-1}\| \le C$ from (3.9.15) are uniform in ρ, thus in the number and sizes of the radii. The old r^{-2} constant is thus unchanged up to one fixed factor.

These exact transported masks need not themselves be Weyl cutoffs. Separately, the fixed outer physical shift mask remains unprimed. By Lemma 3.9.7, the leakage of N, N^{-1} outside the C_s plateau gives $\|[C_s, N]\| \le C\rho^{3/2}P(S)$.

The exact identity

$$d' + d_0 C_s = N(d_{\mathrm{old}} + d_0 C_s)N^{-1} + d_0(C_s - N C_s N^{-1})$$

then transfers the old fixed-gap Green by a Neumann perturbation. The extra $\rho^{3/2}P(S)$ shift difference remains smaller after the one critical ρ^{-1} loss.

□

We use the physical carrier-zero bound of Lemma 3.7.7 here before application of K. Its proof cancels the full radial complement by the macro kernel, with the direct mean tensor.

The carrier-zero and complementary estimates control the full physical residual on the inner plateau. There the central box uses the global cost $O(\rho^{-1})$, and an annular piece with a right annular pad uses $O(r^{-2})$. On the logarithmic transition and the exterior piece the full residual has the coarser bound $O_{\kappa_0}(P(S))$ after its fixed chart mask. The corresponding Green cost is at most $O(r_{\mathrm{out}}^{-2}) = O(S^{2M})$. Lemma 3.9.31 combines these estimates for the full physical remainder Z_0.

The auxiliary G_δ of Theorem 3.8.2 has a pointwise $m(\rho) = \rho^{-o(1)}$ profile cost, as opposed to a uniform endomorphism bound on $\mathcal{F}_\sigma$.

Select fixed nested masks with positive plateau gaps such that

$$\operatorname{supp} C_s \subset \{C_0 = 1\}, \quad \operatorname{supp} C_0 \subset \{C_1 = 1\}, \quad \operatorname{supp} C_1 \subset \{C_\chi = 1\}, \quad \operatorname{supp} C_\chi \subset \{C_b = 1\}.$$

Such nested cutoffs exist inside U because the original supports $\operatorname{supp} \chi_\pm$ are compactly contained in U. Choose the cubic blend inside their unit plateaux and then take the ancient threshold large enough for both shrinking preparation supports.

It is not necessary to equal one on the larger parametrix supports. This covers the full shift support, not only the power window.

Transport the masks through N as $C'_i = N C_i N^{-1}$, and set $K'_\chi = C'_\chi K$. We transport the scalar Green in the same way, $G'_a = N G_a N^{-1}$.

Define

$$U = JC_1'G_a'C_0'K_\chi', \qquad Z_0 = I - DU, \qquad P_0 = U + G_\delta Z_0. \tag{3.9.32}$$

The ordered products are actual bounded maps in the prepared norms. We do not treat any of the masks as a projection.

Lemma 3.9.22 (Right defect and localized row)**.** *On the same core, then by the finite-profile bounds,*

$$\begin{aligned} DP_0 &= I - E, \qquad E = S_\delta G_\delta Z_0, \\ Z_0 &= I - JC_1'C_0'C_\chi'K - (J[d', C_1'] - RC_1')G_a'C_0'K_\chi', \\ K(I - JC_1'C_0'C_\chi'K) &= (I - C_1'C_0'C_\chi')K. \end{aligned} \tag{3.9.33}$$

Writing $A_\chi = [d', C_\chi']$,

$$K_\chi' D_\delta = (d' + d_0 C_s)K_\chi' - (C_\chi' T + A_\chi K) + d_0[C_\chi', C_s]K. \tag{3.9.34}$$

All terms in (3.9.34) *are either fixed-gap interior, output-annular or have a positive-power finite-kernel remainder as in* (3.9.3)*.*

Proof. Since $D_\delta G_\delta = I$ and $D = D_\delta - S_\delta$, $DP_0 = DU + (I - S_\delta G_\delta)(I - DU) = I - E$.

Apply $DJ = Jd' - R$, use $d'G_a' = I$ and commute d' past C_1' to get the second identity. We multiply its first term by $KJ = I$ to get the third.

For (3.9.34), multiply $KD_\delta = (d' + d_0C_s)K - T$ on the left by C_χ' and commute the scalar differential operator past the output mask. Its time derivative belongs to $[d', C_\chi']$.

We keep the last commutator. We do not conjugate the physical shift mask. □

For the error estimate one first applies the localized row identity, not the unbounded global row T, to G_δ. Lemma 3.6.5 gives the leading reference $O(\rho^{3/2}P(S))$ interior row and the explicit $\rho C_{\mathrm{ann}}A_{\mathrm{ann}}$ output-annular term.

The normalization and scalar connection terms in (3.9.34) keep that cutoff orientation. The completed wave part of its complementary row is $-K\mathbb{P}\,\mathrm{div}(W \otimes f + f \otimes W)$.

On a fixed output mask, its derivative is transferred to the H^1 adjoint reference test profile, giving $C\sqrt{\rho}P(S)\|f\|_2$. Exact normalization cancels its connection on Q, so no estimate of M_s or N_s is necessary there.

We absorb the old-coordinate scalar B_{int} in (3.9.3) before conjugation. Its normalized counterpart is $NB_{\mathrm{int}}N^{-1}$.

We keep the physical shift-mask comparison as in (3.9.38)–(3.9.39). We fix the gap before the independent choice of κ_0.

Lemma 3.9.6 performs the two inverse-commutator steps on the fixed-gap scalar inverse after we absorb B_{int}. It leaves $\rho^{3/2}P(S)$ fixed-gap tails, and it never charges the physical auxiliary inverse's subpower constant to the fixed cubic. Shrinking annuli keep their different radius-matched calculus.

Put $a_\rho = \rho^{1/2-128\varkappa}$ and $\nu = 1 - 128\varkappa$. The two rows of (3.7.28) hold for the prepared residual R_p at every $\delta \le r \le r_{\mathrm{out}}$. To pass to the logarithmic column, let A be a fixed-shape central or annular mask at radius r, supported as a symbol in the box of radius $4r$. Write $A' = NAN^{-1}$ and $\mathrm{Op}_\rho(\sigma_B) = B_{\mathrm{band}} - B_{\mathrm{old}}$. The exact residual identity of paragraph 3.9.2.1 gives

$$(R_{\mathrm{raw}} - R_p)A = (R_{\mathrm{ref}} - R_p)(I - C_{\log})A + J_p\,\mathrm{Op}_\rho(\sigma_B)C_{\log}A - D_p[d_{\mathrm{old}}, C_{\log}]A.$$

Suppose $\delta \le r \le \theta_\chi r_{\mathrm{out}}/8$, where $\theta_\chi r_{\mathrm{out}}$ is the plateau radius of $C_{\log}$. Then $\mathcal{W}_{15}((I - C_{\log})A) = O((\rho/r^2)^{30})$ by (SC2), with $\mathcal{W}_d(Y) = \sum_{a+b\le d}\|Z^a k^b Y\|$. Applying (SC4) to this error costs $\rho^{-3}P(S)$.

The last two terms have full physical norm $O_{\kappa_0}(P(S)\rho^{9/5})$ by the degree-eleven column estimate (3.9.36) and the separated word estimates in (a3)–(a4) of Lemma 3.9.24. Since $\rho/r^2 \le \rho^{1/5}$, the same bound holds for $(R_{\mathrm{raw}} - R_p)A$.

Now $RA' = R_{\mathrm{raw}}AN^{-1}$ and $K = M_\delta^{-1}K_{\mathrm{ref}}$ is uniformly bounded. With Π_{zero} the physical projection onto the two selected angular sectors, (SC5) consequently gives

$$\begin{aligned}\|\Pi_{\mathrm{zero}}RA'\| + \|KRA'\| &\le C(r^3 + \rho r + \rho^2) + C_{\kappa_0}P(S)\rho^{9/5}\\ &\quad + P(S)\big[\rho^\nu(r+a_\rho) + a_\rho(r+a_\rho)^2 + \rho^2\big],\\ \|(I-\Pi_{\mathrm{zero}})RA'\| &\le P(S)\big[(r+a_\rho)^3 + \rho^\nu(r+a_\rho) + \rho^2\big]\\ &\quad + C_{\kappa_0}P(S)\rho^{9/5}.\end{aligned} \tag{3.9.35}$$

The first constant is independent of S and κ_0. The ρ^ν terms come from the even-sign return after the primary odd stress cancels. The high $B_{2,\mathrm{high}}$ matching return contributes $a_\rho(r+a_\rho)^2$. On pieces meeting the logarithmic transition the reference term and the commutator must be retained. The scalar return there uses the output mask and the bound in part (b) of Lemma 3.9.24. The full physical return there uses the polynomial estimate of Lemma 3.9.31.

Lemma 3.9.23 (Direct column bound for scalar word errors)**.** *For a scalar operator Y put*

$$\mathcal{W}_d(Y) = \sum_{a+b\le d} \|Z^a k^b Y\|_{L^2_Z\to L^2_Z}.$$

For the selected prepared column and every Y with $\mathcal{W}_{11}(Y) < \infty$,

$$\|J_pY\|_{L^2_Z\to L^2_{\mathrm{can}}} \le P(S)\mathcal{W}_{11}(Y), \qquad \|D_pY\| \le P(S)\mathcal{W}_{11}(Y) + C\|Y\|. \tag{3.9.36}$$

For left-ordered scalar separated products, Lemma 3.9.9 therefore applies at order three to λ_a, e_{κ_0} and at order two, with their actual prefactor ρ, to c_a, c_1. The same applies to the separated pair of Corollary 3.9.10, including its specified polynomial part. For each such scalar symbol b, including a polynomial part of total degree at most two,

$$\mathcal{W}_{11}(\mathrm{Op}_\rho(b)Y) \le C_{\kappa_0}\mathcal{W}_{13}(Y). \tag{3.9.37}$$

Proof. Paragraph 3.7.3 counts every physical input word in J_p through degree eleven, including the degree-nine macro lift and the partition correction. The zero-output-derivative coefficient estimates in the proof of Lemma 3.7.12 are bounded by $P(S)$: the primary KX_σ has order zero and the later responses keep nonnegative powers of ρ. Multiplication and Fubini give the first inequality before applying any special right mask. Subtract the bounded J_{ref} to obtain the second. The loss $\rho^{-b_{\mathrm{col}}}$ belongs to an additional output gradient and is absent here; SC4's ρ^{-3} is a residual bound, not a column bound.

Exactly,

$$k^b\,\mathrm{Op}_\rho(a) = \sum_{t=0}^{b}\binom{b}{t}(\rho/i)^t\,\mathrm{Op}_\rho(k^{b-t}\partial_Z^t a).$$

Equivalently, move the remaining k powers onto the smooth right mask as in Lemma 3.9.9; this retains the degree of polynomial middle symbols. Thus eleven word degrees spend at most eleven ordinary Z derivatives. The lemma's order-three bill is $Z \le 14$, $k \le 5$, and its order-two bill is $Z \le 13$, $k \le 4$. Even two further ordinary derivatives for an axial graph placement fit (3.9.26). These finite orders suffice; no arbitrary-order estimate for a profile or connection is used.

For (3.9.37), split b into its fixed-chart compact part and its polynomial part (including any exterior constant). In the compact part, the preceding exact identity and left multiplication by Z^a give compact symbols with bounded Fourier L^1 envelopes, using only $Z \le 11$ and $k \le 2$ derivatives of b. Hence their operators are bounded before Y. For the polynomial part, exact normal ordering with $[k, Z] = -i\rho$ gives input words of degree at most $11 + 2 = 13$. This proves the inequality. Consequently applying a rough scalar symbol to an already separated pure-mask error preserves its smallness through these finite word norms; no additional integration order is spent on that symbol. □

Lemma 3.9.24 (The scalar row on radius-matched pieces)**.** *Let the right column masks be* $C_r = \mathrm{Op}_\rho(\chi(z/r))$ *with* $\chi = 1$ *on the box of radius* $\theta_\chi \in (0,1)$ *and* $\operatorname{supp}\chi$ *in the unit box, so that the symbol of* $C_{\log}$ *is one on the box of radius* $\theta_\chi r_{\mathrm{out}}$*. Let* ψ*,* $r_j = 2^{j+1}\delta$ *and* $r_J \in [2r_{\mathrm{out}}, 4r_{\mathrm{out}}]$ *be as in the proof of Proposition 3.9.33. Let* $\pi = \psi(z/r_0)$ *with* $r = r_0 = 2\delta$*, or* $\pi = \psi(z/2r_j) - \psi(z/r_j)$ *with* $r = r_j$*,* $j < J$*, and put* $\Pi' = Y\,\mathrm{Op}_\rho(\pi)$ *with* $Y \in \{C_b, C_bC_1\}$*. Assume* $8r_{\mathrm{out}} \le \kappa_0$*. Then, for* $s \le -s_1(\kappa_0)$*:*

(a) if $r \le \theta_\chi r_{\mathrm{out}}/8$*,*

$$\|C_bK_{\log}R_{\mathrm{raw}}\Pi'\| \le \mathcal{G}(r) + C_{\kappa_0}P(S)\rho^{9/5},$$
$$\mathcal{G}(r) = C_g(r^3 + \rho r + \rho^2) + P(S)[\rho^\nu r + \rho^{\nu+a} + a_\rho(r + a_\rho)^2 + \rho^2],$$

with $a = \frac{1}{2} - 128\varkappa$*;*

(b) if $\theta_\chi r_{\mathrm{out}}/8 < r \le r_J$*,*

$$\|C_bK_{\log}R_{\mathrm{raw}}\Pi'\| \le C'_g r^3 + C_{\kappa_0}a_\rho P(S), \qquad a_\rho = \rho^{1/2-128\varkappa}.$$

The constants C_g, C'_g *depend only on the leading profiles, the masks and* θ_χ*. To transport these scalar bounds, put* $C'_b = NC_bN^{-1}$ *and* $\widetilde{\Pi} = N\Pi'N^{-1}$*, where* Π' *is the old-coordinate product defined above. Since* $K = NK_{\log}$*,*

$$C'_bKR\widetilde{\Pi} = N(C_bK_{\log}R_{\mathrm{raw}}\Pi')N^{-1}.$$

Thus (a) and (b) bound this normalized scalar row with an additional factor of at most C_N^2*. The full physical plateau estimate is* (3.9.35)*.*

Proof. Inputs. (SC1)–(SC6), Lemma 3.9.15, the independent algebra of paragraph 3.9.2.1, and the centering $\lambda_Z = \lambda_k = \lambda_{Zk} = 0$, $c_0 = c_*$. The cubic estimate used in (b1) is only part (i) of Lemma 3.9.30; its proof is independent of the present lemma and the outer-row estimate. Part (ii) of that later lemma is used only after both row estimates have been established.

Preliminaries. By (SC2), $\Pi' = \mathrm{Op}_\rho(\pi) + \text{tiny}$, so $\|Z^ak^b\Pi'\| \le Cr^{a+b}$ for $a + b \le 15$, and Π' is supported in the box of radius $4r$ up to tiny terms. Put $R_{p,\mathrm{old}} = A_*J_p - (J_p)_s - J_pB_{\mathrm{old}} = R_p + J_p(B_{\mathrm{band}} - B_{\mathrm{old}})$. Since $D_p = J_p - J_{\mathrm{ref}}$, (3.9.51) reads

$$R_{\mathrm{raw}} = R_{\mathrm{ref}}(I - C_{\log}) + R_{p,\mathrm{old}}C_{\log} - D_p[d_{\mathrm{old}}, C_{\log}].$$

Since $\rho(\frac{1}{2} - h)Z\partial_Z = \mathrm{Op}_\rho(i(\frac{1}{2} - h)Zk)$ and b_0 occurs in both operators, $B_{\mathrm{band}} - B_{\mathrm{old}} = \mathrm{Op}_\rho(\sigma_B)$ with $\sigma_B = \lambda_{\mathrm{quad}} - \lambda_a + \rho(c_* - c_a)$. This symbol vanishes on the κ_0 box, which contains the box of radius $8r_{\mathrm{out}}$. Also $K_{\log} = M_{\log}^{-1}K_{\mathrm{ref}}$, $\|M_{\log}^{-1}\| \le \frac{4}{3}$, $K_{\mathrm{ref}} = K_{\mathrm{ref}}\Pi_{\mathrm{zero}}$, and $\|C_b\| \le C_m$.

(a). Here Π' lives in the box of radius $\theta_\chi r_{\mathrm{out}}/2$, at distance at least $\theta_\chi r_{\mathrm{out}}/2$ from the transition of $c_{\log}$.

(a1) $(I - C_{\log})\Pi'$ is tiny by (SC2). Then $C_b M_{\log}^{-1}(F + T_* J_{\mathrm{ref}})(I - C_{\log})\Pi'$ is tiny by (SC3), because $C_b M_{\log}^{-1}$ maps $H^{-2}_{\mathrm{ax},\rho}$ into L^2 with norm at most $P(S)$.

(a2) $C_{\log}\Pi' = \mathrm{Op}_\rho(\pi) + \text{tiny}$, and π is a fixed shape at radius r. By (SC5) for $\mathrm{Op}_\rho(\pi)$ and (SC4) for the tiny part,

$$\begin{aligned}\|C_b M_{\log}^{-1} K_{\mathrm{ref}} \Pi_{\mathrm{zero}} R_p C_{\log}\Pi'\| \le \tfrac{4}{3} C_m \|K_{\mathrm{ref}}\| \big[& C_{\mathrm{PG}}(r^3 + \rho r + \rho^2) \\ & + P(S)(\rho^\nu r + \rho^{\nu+a} + a_\rho (r + a_\rho)^2 + \rho^2)\big].\end{aligned}$$

Here C_{PG} is the constant of (SC5) for the finite family of shapes used below, and we set $C_g = \frac{4}{3} C_m \|K_{\mathrm{ref}}\| C_{\mathrm{PG}}$.

(a3) For $\mathrm{Op}_\rho(\sigma_B) C_{\log}\Pi'$, each of $\lambda_{\mathrm{quad}} - \lambda_a$ and $c_* - c_a$ vanishes near $\operatorname{supp} c_{\log}$. Corollary 3.9.10, with the polynomial part kept in the full principal symbol, and Lemma 3.9.23 give

$$\mathcal{W}_{11}\big(\mathrm{Op}_\rho(\sigma_B) C_{\log}\Pi'\big) \le C_{\kappa_0}\big[(\rho/r_{\mathrm{out}})^3 + \rho(\rho/r_{\mathrm{out}})^2\big] + \text{tiny}.$$

Since $r_{\mathrm{out}} \ge \delta$, the two powers are at most $\rho^{9/5}$ and $\rho^{11/5}$. Applying J_p, and then the bounded row and projection, gives $C_{\kappa_0} P(S) \rho^{9/5}$.

(a4) From $d_{\mathrm{old}} = \partial_s - B_{\mathrm{old}}$ we get $[d_{\mathrm{old}}, C_{\log}] = \partial_s C_{\log} - [B_{\mathrm{old}}, C_{\log}]$. The time derivative has a smooth transition symbol and its actual $O(\rho)$ prefactor. The scalar commutator $[B_{\mathrm{old}}, C_{\log}]$ equals

$$(I - C_{\log})\,\mathrm{Op}_\rho(\lambda_a + \rho c_a + i(\tfrac{1}{2} - h)Zk) - \mathrm{Op}_\rho(\lambda_a + \rho c_a + i(\tfrac{1}{2} - h)Zk)(I - C_{\log}).$$

The first term applied to Π' has outer radius r_{out} and inner radius r; the second contains the pure-mask error $(I - C_{\log})\Pi'$, to which (3.9.37) applies. Lemma 3.9.9 at orders three and ρ times two, with the polynomial dilation treated exactly, yields

$$\mathcal{W}_{11}\big([d_{\mathrm{old}}, C_{\log}]\Pi'\big) \le C_{\kappa_0}\big[(\rho/(r_{\mathrm{out}} r))^3 + \rho(\rho/(r_{\mathrm{out}} r))^2\big] + \text{tiny} \le C_{\kappa_0} P(S) \rho^{9/5}.$$

Here $r \ge \delta$ and $r_{\mathrm{out}}^{-1} = S^M$. The direct bound (3.9.36), without SC4's residual loss, gives the same bound after D_p.

(b). Now $r > \theta_\chi r_{\mathrm{out}}/8$, so $r_{\mathrm{out}} \le 8r/\theta_\chi$. Put $Y' = (I - C_{\log})\Pi'$; it satisfies $\|Z^a k^b Y'\| \le C r^{a+b}$.

(b1) *Reference part, F.* $C_b M_{\log}^{-1} F Y' = C_b F Y' - C_b M_{\log}^{-1} E_{\log} F Y'$, and $\|E_{\log}\| \le \frac{1}{4}$. Here $FY' = \mathrm{Op}_\rho(e_{\kappa_0})\Pi' - \mathrm{Op}_\rho(e_{\kappa_0}) C_{\log}\Pi' + \rho\,\mathrm{Op}_\rho(c_1 - c_a)Y'$. By Lemma 3.9.30(i) (whose proof applies verbatim to the mask $C_{\log}$ of radius r_{out}) the first two terms are at most $C_e(r^3 + r_{\mathrm{out}}^3) \le C_e(1 + 512\theta_\chi^{-3}) r^3$, and the third is at most $C_{\kappa_0}\rho$.

(b2) *Reference part, T_*.* $C_b M_{\log}^{-1} T_* J_{\mathrm{ref}} Y' = M_{\log}^{-1} C_b T_* J_{\mathrm{ref}} Y' - M_{\log}^{-1}[C_b, E_{\log}] M_{\log}^{-1} T_* J_{\mathrm{ref}} Y'$. By (SC6), $\|C_b T_* J_{\mathrm{ref}}\| \le \|C_b T_{\mathrm{ref}}\|\|J_{\mathrm{ref}}\| + \|C_b K_{\mathrm{ref}}(A_* - L)\|\|J_{\mathrm{ref}}\| + |b_0| C_m \le C\rho^{1/2} P(S)$. By (3.9.11) and (SC3), the second term is $O(\rho^{9/5} P(S))$.

(b3) *Prepared part.* $C_{\log}\Pi' = C_{\log}\,\mathrm{Op}_\rho(\pi) + \text{tiny}$, and $C_{\log}\,\mathrm{Op}_\rho(\pi) = \mathrm{Op}_\rho(\sigma(z/r_{\mathrm{out}}))$, where σ is the rescaled left-composition symbol of $c_{\log}\#\pi$. It is supported in the box of radius sixteen (its Z support is that of $c_{\log}$, its frequency support that of π, and $r \le r_J \le 4 r_{\mathrm{out}}$), and it lies in a bounded set of C_c^∞ uniformly in $r/r_{\mathrm{out}} \in [\theta_\chi/8, 4]$ (symbol calculus with $\rho/r_{\mathrm{out}}^2 \le 1$). By (SC5) at radius r_{out}, $\|C_b M_{\log}^{-1} K_{\mathrm{ref}} \Pi_{\mathrm{zero}} R_p C_{\log}\Pi'\| \le C_g^\sharp(r_{\mathrm{out}}^3 + \rho r_{\mathrm{out}} + \rho^2) + P(S) a_\rho$, which is at most $512\theta_\chi^{-3} C_g^\sharp r^3 + C\rho + P(S) a_\rho$. Here $C_g^\sharp = \frac{4}{3} C_m \|K_{\mathrm{ref}}\| C_{\mathrm{PG}}^\sharp$, and $C_{\mathrm{PG}}^\sharp$ is the constant of (SC5) for the shape family $\{\sigma\}$ of this step (box of radius sixteen, $r/r_{\mathrm{out}} \in [\theta_\chi/8, 4]$); it is fixed with the masks. The term with σ_B is $C_{\kappa_0} P(S) \rho^{9/5}$, as in (a3).

(b4) Split $[d_{\mathrm{old}}, C_{\log}] = [\partial_s - B_{\mathrm{band}}, C_{\log}] + [\mathrm{Op}_\rho(\sigma_B), C_{\log}]$. The first term is ρ times a smooth mask with bounded rescaled seminorms, by the exact quadratic products in the proof of Lemma 3.9.14(iv). Its time derivative term uses $\rho_s/\rho = h\rho$ and $|\partial_s \log r_{\mathrm{out}}| \le C_M \rho/L$. Both orders of the product in the second commutator have $\mathcal{W}_{11}$ norm at most $C_{\kappa_0}\rho^{9/5}$ by the two separated word estimates in that proof. The degree-eleven column bound (3.9.36) therefore gives $\|D_p[d_{\mathrm{old}}, C_{\log}]\| \le C_{\kappa_0}\rho P(S)$.

Summing (b1)–(b4) gives (b) with $C_g' = 2C_m(C_e + C_g^\sharp)(1 + 512\theta_\chi^{-3})$; the terms $C\rho^{1/2}P(S)$, $C_{\kappa_0}\rho$ and $C_{\kappa_0}P(S)\rho^{9/5}$ are at most $C_{\kappa_0}a_\rho P(S)$. □

3.9.4.1 The ordered scalar return

Main result. Proposition 3.9.33 bounds the complete ordered defect for the actual source and finite family in the stated retraction norm. Its hypotheses are the scalar estimates and physical finite-family bounds below.

We select the blend radius before the ancient threshold.

Coordinates and spaces. Put $W(s) = q_*(s)\rho(s)^{1+\sigma}$ and

$$\|a\|_{Y_\alpha} = \operatorname*{ess\,sup}_{s\le s_*} \frac{\|a(s)\|_{L^2_Z}}{W(s)\rho(s)^\alpha}, \qquad \|f\|_{\mathcal{F}_\sigma} = \operatorname*{ess\,sup}_{s\le s_*} \frac{|f(s)|_*}{W(s)}.$$

We write polynomial factors in $S = (1 + \log(1/\rho))^{6/5}$ explicitly when necessary. The old and normalized scalar spaces use these same weights. Their equivalence constants follow from the bounds for N, N^{-1}.

The pointwise identities $KJ = KJ_\delta = I$ imply $\|Kf(s)\|_2 \le |f(s)|_*$ and $|J_\delta a(s)|_* = \|a(s)\|_2$. The physical and retraction norms are equivalent with a factor $P(S)\rho^{-o(1)}$, which will occur only next to a positive power of ρ.

The normalization formulas give,

$$K_{\log} = N^{-1}K, \qquad R = R_{\mathrm{raw}}N^{-1}, \qquad B_0 = B_{\mathrm{int}} = C_b K_{\log} R_{\mathrm{raw}} C_b, \qquad B = NB_0N^{-1} = C_b' K R C_b'. \tag{3.9.38}$$

Thus R_{raw} is the old-coordinate residual throughout the row factorization with the same mask. Its unnormalized row is $K_{\mathrm{ref}}R_{\mathrm{raw}}$.

The mixed-coordinate product $K_{\log}R$ is not this row. We do not infer an estimate for N_s from $N - I$.

Write the old row factorization and its exact transport as

$$\begin{aligned} C_\chi K_{\log} R_{\mathrm{raw}} - B_0 C_\chi &= \rho C_{\mathrm{ann}} A_{\mathrm{ann}} + R_{\mathrm{sep}}, \\ L := \chi K R - B\chi &= N(\rho C_{\mathrm{ann}} A_{\mathrm{ann}} + R_{\mathrm{sep}})N^{-1}, \qquad \chi = C_\chi'. \end{aligned} \tag{3.9.39}$$

Here C_{ann} is an output pad on the fixed transition of C_χ. It is separated from the full shift support.

The remainder has norm $C_{\kappa_0}\rho^{3/2}P(S)$ and $\|A_{\mathrm{ann}}\| \le C + \rho^c P(S)$. By Lemma 3.9.14, both displays hold with $A_{\mathrm{ann}} = 0$. The fixed-gap inverse is

$$\widehat{G}_s = (d' + d_0 C_s - B)^{-1}.$$

Equivalently, before the physical-mask comparison it is the conjugate of $(d_{\mathrm{old}} + d_0 C_s - B_0)^{-1}$.

The comparison term is the Δ_s in 3.9.16, of size $C\rho^{3/2}P(S)$, and its fixed-gap Neumann series includes this term.

Lemma 3.9.25 (The complete ordered defect)**.** *Set $Q = I - JK$, $A_\chi = [d', \chi]$, and*

$$H = LK + \chi TQ + A_\chi K - d_0[\chi, C_s]K.$$

With the original masks in their original order,

$$\begin{aligned} Z_0 &= I - JC_1'C_0'\chi K - (J[d', C_1'] - RC_1')G_a'C_0'\chi K, \\ \chi K Z_0 &= \chi(I - C_1'C_0'\chi)K - \chi[d', C_1']G_a'C_0'\chi K + \chi KRC_1'G_a'C_0'\chi K. \end{aligned} \tag{3.9.40}$$

The full error $E = S_\delta G_\delta Z_0$ equals

$$\boxed{E = d_0 J_\delta \{C_s \widehat{G}_s \chi K Z_0 + C_s \widehat{G}_s H G_\delta Z_0 + C_s(I - \chi)K G_\delta Z_0\}.} \tag{3.9.41}$$

None of these identities treats a phase mask as an exact projection.

Proof. Use $DJ = Jd' - R$ to compute $Z_0 = I - DJC_1'G_a'C_0'\chi K$.

Then use $KJ = I$ to get (3.9.40).

The relations $KD_\delta = (d' + d_0C_s)K - T$ and $TJ = KR$ give

$$\chi K D_\delta = (d' + d_0C_s)\chi K - \chi T - A_\chi K + d_0[\chi, C_s]K.$$

Since $T = KRK + TQ$ and $\chi KR = B\chi + L$, this is $\chi K D_\delta = (d' + d_0C_s - B)\chi K - H$.

Apply this identity to $G_\delta f$ and use $D_\delta G_\delta f = f$. The function $y = \chi K G_\delta f$ is $O(q_*\rho^{1+\sigma-o(1)})$ as $s \to -\infty$ (Theorem 3.8.2), and the homogeneous equation for $d' + d_0C_s - B$ has no nonzero solution in this class: its propagator grows at most at the rate $g_s + \epsilon + \|B_0\| < \lambda_c$ (here $\|B_0\| \le C\kappa_0^3 + o(1)$), so a homogeneous solution with this bound vanishes after propagation from $r \to -\infty$. Thus $\widehat{G}_s$ is also a left inverse on y, and $\chi K G_\delta = \widehat{G}_s \chi K + \widehat{G}_s H G_\delta$. Last split $C_s K = C_s \chi K + C_s(I - \chi)K$ in $E = d_0 J_\delta C_s K G_\delta Z_0$.

□

Uniformity in the blend radius. Fix the leading band chart, the outer masks, h, the fixed scalar gap, and a reserve $0 < \eta_* < \sigma - \eta_q$ before selection of κ_0. Select a fixed upper bound $\kappa_* > 0$ such that each $8\kappa_*$ box lies in that chart.

All unindexed constants below are independent of $0 < \kappa_0 \le \kappa_*$ and of r, ρ. Constants with subscript κ_0 may enter only late thresholds or terms that tend to zero.

The critical form bound gives

$$\|G_a f(s)\|_2 \le C_* \rho(s)^{-1} W(s) \|f\|_{Y_0}, \tag{3.9.42}$$

with a constant independent of κ_0. Indeed fix $\eta = (\sigma + \eta_q)/2$ before choosing κ_0. For each κ_0, take the ancient threshold so the form error in the proof of (3.9.29) is at most $\eta - \eta_q$. That energy inequality gives $\|\mathcal{V}(R, U)\| \le e^{\eta(U-R)}$. For $f \in Y_0$, the exact center gauge in (3.9.30) cancels with the weight q_*; its remaining normalization depends only on h and the fixed exponent. Thus the integral in (3.9.31) is bounded by a fixed multiple of

$$\|f\|_{Y_0} \int_R^\infty e^{\eta(U-R) - \sigma U}\, dU = \frac{e^{-\sigma R}}{\sigma - \eta} \|f\|_{Y_0}.$$

Undoing the unitary dilation gives $q_* \rho^\sigma = \rho^{-1} W$ as asserted. Dependence on the blend radius enters only when choosing how far back in time the form error meets the fixed margin. For the separately shifted scalar inverse absorb the $O(\kappa_0^3) + o(1)$ perturbation inside its fixed gap.

Lemma 3.9.26 (Finite radius calculus used below)**.** *Let $z=(Z,k)$, $\epsilon=\rho/r^2\le 1$, and let $c(z/r)$ have fixed compact support and shape. The blend $\lambda_a=\lambda-\chi(z/\kappa_0)(\lambda-\lambda_{\mathrm{quad}})$ has, after subtraction of λ_0 and the dilation $z=ry$, the weighted bounds*

$$a_r(y)=r^{-2}(\lambda_a(ry)-\lambda_0),\qquad |\partial^\alpha a_r(y)|\le C_\alpha\langle y\rangle^{2-|\alpha|},\quad |\alpha|\le 6, \tag{3.9.43}$$

for $\delta\le r\le 2\kappa_0$.

The exterior extension is the constant one in the critical form lemma. With fixed compact pads, the finite left or Weyl product has its usual first-order term and an $O(\epsilon^{3/2})$ bounded-operator remainder for a_r against c.

For the unitary dilation $(U_rf)(x)=r^{1/2}f(rx)$ this gives

$$U_r[\mathrm{Op}^L_\rho(\lambda_a),\mathrm{Op}^L_\rho(c(z/r))]U_r^{-1}=\rho\,\mathrm{Op}^L_\epsilon(\ell_r)+O(\rho^{3/2}/r),\qquad \|\mathrm{Op}^L_\epsilon(\ell_r)\|\le C, \tag{3.9.44}$$

where ℓ_r has support on the fixed scaled transition of c. Two compact symbols with separated supports have product $O(\epsilon^{3/2})$ if their zero and first product symbols vanish.

For a bounded C^4 subprincipal symbol, the zero-order product remainder against a compact scaled mask is $O_{\kappa_0}(\epsilon^{1/2})$.

Proof. Taylor's formula gives $|\partial^\alpha(\lambda-\lambda_{\mathrm{quad}})(z)|\le C|z|^{3-|\alpha|}$ for $|\alpha|\le 3$.

We bound higher derivatives on the fixed chart. On a derivative of the blend cutoff one has $|z|\asymp\kappa_0$, so multiplication by $\kappa_0^{-|\beta|}$ keeps the related order-three estimate.

On the remaining fixed extension region $|z|$ stays bounded below independently of κ_0. For $|y|\le 1$, the critical point at the origin gives $|\lambda_a(ry)-\lambda_0|\le Cr^2|y|^2$ and $|\nabla\lambda_a(ry)|\le Cr|y|$. For orders 2 through 6 use the factor $r^{|\alpha|-2}$ in the differentiated symbol. On the blend transition $r\le 2\kappa_0$ absorbs each excess cutoff derivative. For $|y|\ge 1$ the same estimates with $|ry|=r|y|$ give (3.9.43).

The exterior constant has derivatives zero. The same argument gives one bound for the scaled C^6 norm of $r^{-3}e_{\kappa_0}(ry)c(y)$, where $e_{\kappa_0}=\chi(z/\kappa_0)(\lambda-\lambda_{\mathrm{quad}})$.

Work in the scaled phase plane with coordinate $y=(x,\xi)$ and parameter ϵ. Write $a=a_r$ and use the Fourier convention

$$c(y)=\int\widehat{c}(p,q)E_{p,q}(y)\,\mathrm{d}p\,\mathrm{d}q,\qquad E_{p,q}(y)=e^{i(px+q\xi)}.$$

Write $\#_W,\#_L$ for the Weyl and left symbol products at this parameter. On Schwartz tests their exact products with a plane wave are

$$\begin{aligned} a\#_W E_{p,q}&=E_{p,q}\,a(y+\tfrac{\epsilon}{2}(-q,p)),\quad & E_{p,q}\#_W a&=E_{p,q}\,a(y-\tfrac{\epsilon}{2}(-q,p)),\\ a\#_L E_{p,q}&=E_{p,q}\,a(x,\xi+\epsilon p),\qquad & E_{p,q}\#_L a&=E_{p,q}\,a(x+\epsilon q,\xi).\end{aligned}$$

Indeed $\mathrm{Op}^L_\epsilon(E_{p,q})u(x)=e^{ipx}u(x+\epsilon q)$, and the Weyl kernel evaluates the modulation at $x+\epsilon q/2$. Substitution in the product kernel gives the displayed translations. Fourier inversion against the smooth fixed mask is justified on test functions by the polynomial growth in (3.9.43).

For each translation v in these formulas subtract $a(y)+v\cdot\nabla a(y)$. The remaining factor is

$$\int_0^1(1-t)\,v^{\top}\nabla^2a(y+tv)v\,\mathrm{d}t.$$

The Hessian and its derivatives through order three are bounded on the whole scaled plane by (3.9.43). For either ordering and either quantization, the integrated remainder symbol b_ϵ therefore satisfies

$$\max_{|\gamma|\le 3}\|\partial_y^\gamma b_\epsilon\|_\infty\le C\epsilon^2\int|\widehat{c}(p,q)|\,(p^2+q^2)(1+|(p,q)|)^3\,\mathrm{d}p\,\mathrm{d}q\le C_c\epsilon^2.$$

This estimate also covers translated points outside the compact pad. Fourier inversion of the linear term gives $\epsilon(a_\xi c_x - a_x c_\xi)/(2i)$ for $a\#_W c$ and $\epsilon a_\xi c_x/i$ for $a\#_L c$.

We pass from these symbol bounds to the off-diagonal operator estimate. For $z = (z_x, z_\xi)$ use the normalized packets

$$g_z^\epsilon(x) = (\pi\epsilon)^{-1/4} e^{-(x-z_x)^2/(2\epsilon) + i z_\xi (x - z_x/2)/\epsilon}, \qquad \int |g_z^\epsilon\rangle\langle g_z^\epsilon| \frac{\mathrm{d}z}{2\pi\epsilon} = I.$$

For a symbol b with three bounded derivatives and $Q = W, L$, its matrix $\langle \mathrm{Op}_\epsilon^Q(b) g_w^\epsilon, g_z^\epsilon\rangle$ equals, up to a constant phase,

$$\int_{\mathbb{R}^2} b(m_Q + \sqrt{\epsilon}\, u)\, K_Q(u) e^{i\eta\cdot u}\, \mathrm{d}u, \qquad \eta = \frac{(w_\xi - z_\xi, z_x - w_x)}{\sqrt{\epsilon}}.$$

For Weyl quantization $m_W = (z + w)/2$ and $K_W(u) = \pi^{-1} e^{-|u|^2}$. These follow by taking the midpoint in the physical kernel and integrating the difference variable against the two Gaussians. For left quantization put $x = z_x + \sqrt{\epsilon}\, u_1$ and $\xi = w_\xi + \sqrt{\epsilon}\, u_2$ in the Fourier integral for the operator. Then $m_L = (z_x, w_\xi)$ and $K_L(u) = (\sqrt{2}\,\pi)^{-1} e^{-|u|^2/2 + i u_1 u_2}$. Both amplitudes and all their derivatives are integrable.

For $|\eta| > 1$, integrate three times in the direction $\eta/|\eta|$. A derivative falling on b carries the factor $\sqrt{\epsilon} \le 1$. For $|\eta| \le 1$ use the absolute integral directly. Thus for the matrix $\mathcal{R}_\epsilon(z, w)$ of either remainder,

$$|\mathcal{R}_\epsilon(z, w)| \le C \max_{|\gamma|\le 3} \|\partial^\gamma b_\epsilon\|_\infty \left\langle \frac{z - w}{\sqrt{\epsilon}} \right\rangle^{-3}. \tag{3.9.45}$$

Integrating the last factor in either center against the frame measure gives

$$(2\pi)^{-1} \int_{\mathbb{R}^2} \langle u\rangle^{-3}\, \mathrm{d}u = \int_0^\infty t(1 + t^2)^{-3/2}\, \mathrm{d}t = 1.$$

The frame resolution gives the L^2 bound $C_c\epsilon^2$, in particular $C_c\epsilon^{3/2}$. The cancellation took place in the exact translated symbol before the frame estimate.

For two compact C^6 symbols f, g on fixed pads, one can also allow different quantizations. Write $T_u = \mathrm{Op}_\epsilon^L(E_u)$ for $u = (u_1, u_2)$ and set $t_L = 0$, $t_W = 1/2$. The plane-wave actions above give

$$\mathrm{Op}_\epsilon^{Q_1}(E_u)\, \mathrm{Op}_\epsilon^{Q_2}(E_v) = e^{i\epsilon P(u,v)} T_{u+v}, \qquad P = t_{Q_1} u_1 u_2 + t_{Q_2} v_1 v_2 + u_2 v_1.$$

After Fourier inversion the constant and linear terms of the exponential are products of the symbols and their derivatives in left quantization. They vanish for separated supports. Since T_{u+v} is unitary and $|e^{it} - 1 - it| \le t^2/2$ for real t, the remainder norm is at most

$$C\epsilon^2 \int \langle u\rangle^4 |\widehat{f}(u)|\, \mathrm{d}u \int \langle v\rangle^4 |\widehat{g}(v)|\, \mathrm{d}v \le C\epsilon^2 \|f\|_{H^6} \|g\|_{H^6}.$$

The last inequality uses $\langle u\rangle^{-2} \in L^2(\mathbb{R}^2)$. The Sobolev norms are uniform on the fixed pads.

For the bounded C^4 subprincipal symbol against a smooth mask, subtract only the value at y. The first derivative integrated along the translation segment, with up to three further derivatives, gives $\|b_\epsilon\|_{C^3} \le C_{\kappa_0, c}\epsilon$. This implies the required $O_{\kappa_0}(\epsilon^{1/2})$ bound. Conjugating by U_r replaces $\mathrm{Op}_\rho^L(\lambda_a)$ by $\lambda_0 + r^2\, \mathrm{Op}_\epsilon^L(a_r)$ and the mask by $\mathrm{Op}_\epsilon^L(c)$. The first commutator coefficient is $\ell_r = (a_{r,\xi} c_x - c_\xi a_{r,x})/i$, supported on the transition of c and uniformly bounded through three derivatives there. The same frame bound gives $\|\mathrm{Op}_\epsilon^L(\ell_r)\| \le C$. Since $r^2\epsilon = \rho$ and $r^2\epsilon^{3/2} = \rho^{3/2}/r$, subtraction of the two left products gives (3.9.44).

□

Lemma 3.9.27 (Annular output up to the fixed blend radius)**.** *The first estimate in 3.9.27 holds with one bound for all the fixed-shape output annuli necessary below with $\delta \le r \le 2\kappa_0$:*

$$\|A_r G_a f(s)\|_2 \le C r(s)^{-2} W(s) \|f\|_{Y_0}. \tag{3.9.46}$$

For an inner cutoff $C_r = \mathrm{Op}_\rho(c(z/r(s)))$ of fixed smooth shape, with transition at this radius and $|\partial_s \log r| \le C\rho$,

$$\|[d_{\mathrm{old}}, C_r] G_a f(s)\|_2 \le C \left(\frac{\rho}{r^2} + C_{\kappa_0} \frac{\sqrt{\rho}}{r} \right) W(s) \|f\|_{Y_0}. \tag{3.9.47}$$

The same estimates hold with A_r, C_r, G_a simultaneously conjugated by N. Their leading constants are independent of κ_0.

Proof. Take $\delta(u) \le r(u) \le 2\kappa_0$ on the causal history $u \le s$ and $|\partial_u \log r| \le C\rho$. For a dyadic index active at output time s, continue that index back with $r(u) = 2^j \delta(u)$. Then $r'/r = (2/5)h\rho$ and $r(u) \le r(s)$ for $u \le s$.

Select a fixed-shape annular cutoff X_r which is one on the support of A_r. Select a nonnegative compact core fill $v(z/r)$ and separate its support from that of X_r.

The inner radius of this fill is a fixed fraction of r. By the uniform well inequality,

$$p(z) + r^2 v(z/r) \ge c_0 r^2, \qquad p = \Re(\lambda_0 - \lambda_a),$$

with $c_0 > 0$ independent of κ_0.

Put $V_r = \mathrm{Op}_\rho^W(r^2 v(z/r))$ and $d_{\mathrm{ann}} = d_{\mathrm{old}} + V_r$.

Anti-Wick comparison of its real form costs $C_{\kappa_0}\rho = o(r^2)$, since $\rho/r^2 \le \rho^{1/5}$. The order-ρ subprincipal and dilation real parts have the same bound.

We increase the ancient threshold, so the filled equation has damping $\lambda_c - c_0 r(s)^2/2$. Its inverse satisfies

$$\|G_{\mathrm{ann}} F(s)\|_2 \le C r(s)^{-2} W(s) \|F\|_{Y_0}.$$

This is an estimate for a radius that depends on time.

After removal of the same center gauge and $e^{\lambda_c s}$, the logarithmic derivatives of W and r^{-2} are $O(\rho)$. Compare the derivative of $e^{-(c_0/2)\int_u^s r(v)^2\,\mathrm{d}v} W(u)/r(u)^2$.

The ancient boundary vanishes because $\int_{-\infty}^s r(u)^2\,\mathrm{d}u = \infty$.

Write $v_a = G_a f$. The exact local equation is

$$d_{\mathrm{ann}}(X_r v_a) = X_r f + [d_{\mathrm{old}}, X_r] v_a + V_r X_r v_a.$$

This bound $C\rho + C\rho^{3/2}/r$ controls the principal-symbol commutator in Lemma 3.9.26, the exact dilation commutator, and the derivative of the cutoff that depends on time.

The lower-order coefficient contributes at most $C\rho + C_{\kappa_0}\rho^{3/2}/r$, where the leading C depends only on the one bound for its amplitude. Separation from the fill gives $\|V_r X_r\| \le C r^2 (\rho/r^2)^{3/2}$.

Thus (3.9.42) bounds the right side of this equation by $C(1 + C_{\kappa_0}\sqrt{\rho}/r) W \|f\|_{Y_0}$. Since $\sqrt{\rho}/r \le \rho^{1/10}$, its constant is uniform after one late threshold.

Apply G_{ann}. Last $A_r = A_r X_r + O((\rho/r^2)^{3/2})$.

The last error times (3.9.42) is at most $C r^{-2}(\sqrt{\rho}/r) W \|f\|_{Y_0}$. This proves (3.9.46).

For (3.9.47), let T_r denote any leading transition term of the principal, time or dilation commutator. Choose A_r equal to one near its symbol support. In the scaled variables T_r is ρ times a compact symbol with uniformly bounded derivatives through order four. The zero-order product estimate of Lemma 3.9.26 gives

$$T_r = T_r A_r + O(\rho \epsilon^{1/2}), \qquad \rho\epsilon^{1/2} = \rho^{3/2}/r.$$

Thus $T_r A_r G_a$ uses the annular output estimate for $A_r G_a$. The principal composition remainder also has size $C\rho^{3/2}/r$.

The subprincipal commutator, with the zero-order estimate in Lemma 3.9.26, has size $C_{\kappa_0}\rho^{3/2}/r$. Apply (3.9.46) to the padded main term and (3.9.42) to these remainders.

For normalization use only the exact identities

$$A_r' G_a' = N A_r G_a N^{-1}, \qquad [d', C_r'] G_a' = N [d_{\mathrm{old}}, C_r] G_a N^{-1}.$$

The bounds $\|M_j^{-1}\| \le 4/3$ of Lemma 3.9.15 give bounds for N, N^{-1} independent of κ_0 after the late threshold. We do not estimate any commutator of N with a shrinking mask here.

□

Lemma 3.9.28 (The actual ordered cubic return)**.** *For the same e_{κ_0},*

$$\| \operatorname{Op}_\rho^L(e_{\kappa_0}) G_a f(s)\|_2 \le \left[C\kappa_0 + C\rho^{1/5} + C\rho^{1/2}\log(1/\rho)\right] W(s) \|f\|_{Y_0}. \tag{3.9.48}$$

The fixed outer mask in the actual product $N \operatorname{Op}_\rho^L(e_{\kappa_0}) C_1 G_a N^{-1}$ adds only $C_{\kappa_0}\rho^{1/2} W \|f\|_{Y_0}$ to this estimate.

Proof. Take a smooth phase cutoff $\psi = 1$ on the unit box, supported in the twice-unit box.

With $r_j = 2^j\delta$, the exact symbol partition is

$$e_{\kappa_0} = e_{\kappa_0}\psi(z/\delta) + \sum_{j\ge 0} e_{\kappa_0}\{\psi(z/(2r_j)) - \psi(z/r_j)\}.$$

Each nonzero summand b_j is supported in $r_j \le |z| \le 4r_j$, and a nonzero summand necessarily has $r_j \le 2\kappa_0$. Its scaled C^6 norm is at most Cr_j^3.

There are at most $C\log(1/\rho)$ active indices at any time. Select an output annular pad A_j equal to one on a fixed neighborhood of this full shell.

Lemma 3.9.26 gives the ordered identity with an explicit norm error

$$\operatorname{Op}_\rho^L(b_j) = \operatorname{Op}_\rho^L(b_j) A_j + R_j, \qquad \|R_j\| \le C r_j^3 (\rho/r_j^2)^{3/2} = C\rho^{3/2}.$$

its zero and first product errors vanish on the plateau. Thus the main term after G_a has size $Cr_j W\|f\|_{Y_0}$, and its remainder has size $C\rho^{1/2} W \|f\|_{Y_0}$.

The inner term has size $C\delta^3\rho^{-1}W = C\rho^{1/5}W$. Sum $\sum r_j \le 4\kappa_0$ and the remainder count.

This proves (3.9.48). The outer C_1 is one on a fixed neighborhood of the blend support.

Thus $\operatorname{Op}(e_{\kappa_0})C_1 = \operatorname{Op}(e_{\kappa_0}) + O_{\kappa_0}(\rho^{3/2})$, which proves the last assertion. At no point do we identify $\operatorname{Op}(e_{\kappa_0} a_j)$ with $\operatorname{Op}(e_{\kappa_0})\operatorname{Op}(a_j)$ without its remainder.

Conjugate each factor together for the normalized estimate. □

Physical inputs for the remaining paths. The scalar lemmas above are finite estimates. The proof of $\|E\| < 1$ also uses the actual physical finite-family bounds.

The next estimates specify their domains and applications. They do not replace a physical estimate by a scalar estimate.

In (3.9.40), the full $RC_1' G_a' C_0' \chi K$ has a polynomial bound from $\mathcal{F}_\sigma$ to physical L^2/W. This bound precedes application of K.

On the plateau, (3.9.35) gives the two physical components, including the radial complement in the selected angular sectors. At $r = 2\delta$ the full bound is $O_{\kappa_0}(P(S)\rho^{6/5})$ and the global Green costs ρ^{-1}. On the other plateau pieces its annular cost is $O(r^{-2})$. On the bounded number of transition

pieces and the exterior piece, Lemma 3.9.31 uses the full $O_{\kappa_0}(P(S))$ chart bound and a Green cost of at most $Cr_{\mathrm{out}}^{-2} = CS^{2M}$.

To check this physical assertion directly, let $u = J_{\mathrm{ref}} C_1 a$ in the isotropic canonical coordinates.

The leading radial endpoint and the fixed k cutoff give

$$\|u\|_2 + \|\nabla_* u\|_2 \le CP(S)\|a\|_2, \qquad (\nabla_*)_Z = \rho \partial_Z.$$

The actual completed-wave bounds are $\|W^\natural\|_\infty \le \rho^{1/2} P(S)$ and $\|\nabla_* W^\natural\|_\infty \le P(S)$ by the normalized completed-wave bound in Theorem 2(v). These are values of the completed sum.

Thus the full physical perturbation satisfies

$$\|\mathbb{P}\,\mathrm{div}_*(W^\natural \otimes u + u \otimes W^\natural)\|_2 \le C(\|W^\natural\|_\infty \|\nabla_* u\|_2 + \|\nabla_* W^\natural\|_\infty \|u\|_2) \le CP(S)\|a\|_2.$$

The whole-space Leray projector has its L^2 bound. We use no unsupported commutator with it. The leading right-column defect is $O(\rho^{3/2} P(S))$ after this fixed right cutoff (the right-corrector construction before (3.6.10)).

The blend contribution is $J_{\mathrm{ref}}\,\mathrm{Op}(e_{\kappa_0})$ plus bounded lower-order terms. This proves the necessary $O(P(S))$ bound for the full unprepared $R_{\mathrm{ref}} C_1$, with the carrier-zero radial complement, without a scalar KR estimate in its place.

The same moving-mask commutators use (3.9.47). Thus Z_0 has a fixed polynomial physical norm, and $G_\delta Z_0$ has physical norm $P(S)\rho^{-o(1)}$ on this forcing profile.

We do not claim one bound for it as an endomorphism of $\mathcal{F}_\sigma$.

The term H has four explicit parts. The first and third have output support on the fixed C_χ transition, apart from $O_{\kappa_0}(\rho^{3/2} P(S))$ remainders.

The two fixed-gap inverse commutators in 3.9.6, with each mask transported together, place $C_s \widehat{G}_s$ on their left. The result is $o(1)$ even after the physical cost above.

For the second part, the dynamic-reference row on Q has its localized $\rho^{3/2} P(S)$ bound. The completed-wave row is $O(\rho^{1/2} P(S))$ after transfer of its one derivative to the fixed output adjoint.

The scalar normalization connection vanishes on Q. The fourth part and the last term in (3.9.41) are fixed-plateau remainders of order $\rho^{3/2} P(S)$.

All these paths tend to zero.

The first two terms of $\chi K Z_0$ in (3.9.40) are supported outside a fixed neighborhood of C_s, up to the same plateau remainders. They thus use the two fixed-gap commutators.

Their possible single global G_a costs only ρ^{-1}. Their total size is $O_{\kappa_0}(\rho^{1/2} P(S))$.

The sole remaining path is the explicitly ordered scalar product

$$d_0 J_\delta C_s \widehat{G}_s \chi K R C_1' G_a' C_0' \chi K.$$

Its fixed cubic component is $N\,\mathrm{Op}(e_{\kappa_0}) C_1 G_a N^{-1}$ and Lemma 3.9.28 covers it. It never passes through G_δ.

The last J_δ has norm equal to one in the retraction norm.

Lemma 3.9.29 (The old scalar row outside the prepared pad)**.** *Let $C_{\log}^{\mathrm{pad}} = \mathrm{Op}_\rho(\psi(z/r_J))$, with ψ and $r_J \in [2r_{\mathrm{out}}, 4r_{\mathrm{out}}]$ as in the proof of Proposition 3.9.33. It equals one on a neighborhood of the logarithmic column support and its transition. For $Y \in \{C_1, C_b\}$ put $R_o^Y = (I - C_{\log}^{\mathrm{pad}}) Y$, and $R_o = R_o^{C_1}$. Then, for $s \le -s_1(\kappa_0)$,*

$$\|(B_0 - C_b\,\mathrm{Op}(e_{\kappa_0}) C_b) R_o\| \le C_{\kappa_0} \rho^{1/2} P(S), \tag{3.9.49}$$

and, for $Y \in \{C_1, C_b\}$,

$$\|C_b(K_{\log} R_{\mathrm{raw}} - \mathrm{Op}(e_{\kappa_0})) R_o^Y\| \le C_{\kappa_0} \rho^{1/2} P(S). \tag{3.9.50}$$

The complementary output supplied to G_a is an annulus with inner radius comparable to r_{out}. We keep its outer radius fixed.

Proof. Inputs. (SC1)–(SC4) and (SC6); Lemma 3.9.15; (3.9.11); and the chart property: $\operatorname{supp} C_b$ lies in the fixed chart on which $\lambda_a = \lambda + \chi_{\kappa_0}(\lambda_{\mathrm{quad}} - \lambda)$ and on which Lemma 3.6.5 applies.

Step 1: exact algebra. Let $B = \mathrm{Op}_\rho(\mu + \rho c_1)$ be the band generator of Lemma 3.6.5, and let $B_f = B + b_0$ be the unblended reference scalar operator with the same dilation and center gauge. Then $F := B_f - B_{\mathrm{old}} = \mathrm{Op}_\rho(e_{\kappa_0} + \rho(c_1 - c_a))$ on the chart, since $\lambda - \lambda_a = e_{\kappa_0}$ there. Put

$$R_{\mathrm{ref}} = A_* J_{\mathrm{ref}} - (J_{\mathrm{ref}})_s - J_{\mathrm{ref}} B_{\mathrm{old}}, \quad R_D = A_* D_p - (D_p)_s - D_p B_{\mathrm{old}}, \quad T_* = K_{\mathrm{ref}} A_* + (K_{\mathrm{ref}})_s - B_f K_{\mathrm{ref}}.$$

(i) For $J_{\mathrm{raw}} = J_{\mathrm{ref}} + D_p C_{\log}$, the definition $R_{\mathrm{raw}} a = A_* J_{\mathrm{raw}} a - \partial_s(J_{\mathrm{raw}} a) + J_{\mathrm{raw}}(\partial_s - B_{\mathrm{old}})a$ and the product rule for $\partial_s(D_p C_{\log} a)$ give

$$R_{\mathrm{raw}} = R_{\mathrm{ref}} + R_D C_{\log} - D_p[d_{\mathrm{old}}, C_{\log}]. \tag{3.9.51}$$

(ii) Differentiation of $K_{\mathrm{ref}} J_{\mathrm{ref}} = I$ gives $(K_{\mathrm{ref}})_s J_{\mathrm{ref}} = -K_{\mathrm{ref}}(J_{\mathrm{ref}})_s$, hence $T_* J_{\mathrm{ref}} = K_{\mathrm{ref}} A_* J_{\mathrm{ref}} - K_{\mathrm{ref}}(J_{\mathrm{ref}})_s - B_f$ and $K_{\mathrm{ref}} R_{\mathrm{ref}} = F + T_* J_{\mathrm{ref}}$.

(iii) With T_{ref} of Lemma 3.6.5, $T_* = T_{\mathrm{ref}} + K_{\mathrm{ref}}(A_* - L) - b_0 K_{\mathrm{ref}}$.

Step 2: the fixed masks. $c_b = 1$ on a neighbourhood of $\operatorname{supp} c_1$, so $C_b R_o = R_o + \mathrm{tiny}$ by (SC2) (the factor $c_b - 1$ and c_1 have disjoint supports). Hence $(B_0 - C_b \operatorname{Op}(e_{\kappa_0}) C_b) R_o = C_b(K_{\log} R_{\mathrm{raw}} - \operatorname{Op}(e_{\kappa_0})) R_o + \mathrm{tiny}$, where the tiny terms are controlled by (SC4). Thus (3.9.49) follows from (3.9.50) with $Y = C_1$, which we now prove for both Y. (For $Y = C_b$ we do not claim $C_b R_o^{C_b} = R_o^{C_b}$, since $c_b^2 \neq c_b$ on the transition of c_b.)

Step 3: separated terms. The symbol of $C_{\log}$ is supported in the box of radius r_{out}, whereas $1 - \psi(z/r_J)$ vanishes on the box of radius $r_J \geq 2r_{\mathrm{out}}$. The pure-mask product has, with every needed word and axial graph weight,

$$\mathcal{W}_{15}(C_{\log} R_o^Y) \leq C_N(\rho/r_{\mathrm{out}}^2)^N.$$

For this term alone apply (SC4), taking $N = 4$:

$$\|K_{\log} R_D C_{\log} R_o^Y\| \leq C\rho^{-3} P(S)(\rho/r_{\mathrm{out}}^2)^4 = C\rho P(S) r_{\mathrm{out}}^{-8}.$$

For the other term use the direct column bound (3.9.36). The scalar commutator contains $\lambda_a + \rho c_a + i(\frac{1}{2} - h)Zk$, and $-\partial_s C_{\log}$ has a smooth transition symbol. Scalar factors applied to a pure-mask error are bounded by (3.9.37). To apply the compact-right version of Lemma 3.9.9, write

$$R_o^Y = \mathrm{Op}_\rho(y - \psi(z/r_J)) + \mathrm{tiny},$$

where y is the symbol of Y: the fixed plateau identity $C_{\log}^{\mathrm{pad}} Y = C_{\log}^{\mathrm{pad}} + \mathrm{tiny}$ proves this formula. The full difference is zero near $\operatorname{supp} c_{\log}$ and is the allowed sum of a fixed mask and a shrinking mask. Orders three for λ_a and two with prefactor ρ for c_a, with exact polynomial dilation, give

$$\mathcal{W}_{11}([d_{\mathrm{old}}, C_{\log}] R_o^Y) \leq C_{\kappa_0}[(\rho/r_{\mathrm{out}}^2)^3 + \rho(\rho/r_{\mathrm{out}}^2)^2] + \mathrm{tiny}.$$

The smooth time-derivative term is included in the pure-mask errors. Hence

$$\begin{aligned}&\|K_{\log}(R_D C_{\log} - D_p[d_{\mathrm{old}}, C_{\log}]) R_o^Y\| \\ &\quad \leq C_{\kappa_0} P(S)[\rho r_{\mathrm{out}}^{-8} + \rho^3 r_{\mathrm{out}}^{-6} + \rho^3 r_{\mathrm{out}}^{-4}] \leq C_{\kappa_0} \rho^{1/2} P(S)\end{aligned}$$

after the ancient threshold. In particular the connection term is never charged the crude ρ^{-3} residual loss.

Step 4: the reference term. By Step 1, $C_b K_{\log} R_{\mathrm{ref}} R_o^Y = C_b M_{\log}^{-1}(F + T_* J_{\mathrm{ref}}) R_o^Y$.

(a) We have $C_b M_{\log}^{-1} F R_o^Y = C_b F R_o^Y - C_b M_{\log}^{-1} E_{\log} F R_o^Y$ and $E_{\log} F R_o^Y = K_{\mathrm{ref}} D_p(C_{\log} F R_o^Y)$. Split $F = \mathrm{Op}_\rho(e_{\kappa_0}) + \rho\,\mathrm{Op}_\rho(c_1 - c_a)$. The same logarithmic separation as in Step 3 gives

$$\mathcal{W}_{11}(C_{\log} F R_o^Y) \le C_{\kappa_0}\left[(\rho/r_{\mathrm{out}}^2)^3 + \rho(\rho/r_{\mathrm{out}}^2)^2\right] + \mathrm{tiny}.$$

By (3.9.36), its contribution is $O(C_{\kappa_0}\rho^3 P(S))$. Also

$$C_b F R_o^Y = C_b\,\mathrm{Op}_\rho(e_{\kappa_0}) R_o^Y + \rho C_b\,\mathrm{Op}_\rho(c_1 - c_a) R_o^Y,$$

and the second term is bounded by $C_{\kappa_0}\rho$.

(b) $C_b M_{\log}^{-1} T_* J_{\mathrm{ref}} R_o^Y = M_{\log}^{-1} C_b T_* J_{\mathrm{ref}} R_o^Y - M_{\log}^{-1}[C_b, E_{\log}] M_{\log}^{-1} T_* J_{\mathrm{ref}} R_o^Y$. By Step 1(iii) and (SC6), $\|C_b T_* J_{\mathrm{ref}}\| \le C(\rho^{3/2} + \rho^{1/2} + \rho^{.99872})P(S)$. By (3.9.11) on $H^{-2}_{\mathrm{ax},\rho}$ and (SC3), the second term is $O(\rho^{9/5}P(S))$.

Step 5. Steps 3–4 give $C_b(K_{\log} R_{\mathrm{raw}} - \mathrm{Op}(e_{\kappa_0}))R_o^Y = O(C_{\kappa_0}\rho^{1/2}P(S))$, which is (3.9.50). No estimate of $(M_{\log})_s$ or N_s is used. □

Lemma 3.9.30 (Cubic and noncubic parts of the old scalar)**.** *Write* $B_0 = C_b\,\mathrm{Op}_\rho(e_{\kappa_0})C_b + B_0^{\mathrm{nc}}$.

(i) $\|\mathrm{Op}_\rho(e_{\kappa_0})\| \le C_B\kappa_0^3$. *For a mask* Π' *as in Lemma 3.9.24, of radius* r, $\|\mathrm{Op}_\rho(e_{\kappa_0})\Pi'\| \le C_e r^3$ *after a* κ_0*-dependent threshold.*

(ii) For $s \le -s_1(\kappa_0)$,

$$\|B_0^{\mathrm{nc}}\| \le \omega_B(s) := C_\flat r_{\mathrm{out}}(s)^3 + C_{\kappa_0}\rho(s)^{2/5}P(S).$$

The constants $C_B, C_e, C_\flat$ *do not depend on* κ_0, S *or* ρ. *Here* $r_{\mathrm{out}}(s) = S(s)^{-M}$ *and* $S(s)$ *are clocks, not parameters, so* $\omega_B(s) \to 0$ *as* $s \to -\infty$ *and* $\omega_B \le \gamma_{\mathrm{gap}}/8$ *is an ancient-threshold condition imposed after* κ_0.

Proof. (i). By the proof of Lemma 3.9.26, $|\partial^\alpha e_{\kappa_0}(z)| \le C_3|z|^{3-|\alpha|}$ for $|\alpha| \le 3$, uniformly in κ_0, and e_{κ_0} is supported in the box of radius $2\kappa_0$. Lemma 3.7.8 with $r = \kappa_0$ gives $\|\mathrm{Op}_\rho(e_{\kappa_0})\| \le \frac{4}{\pi}(C_3(2\sqrt{2}\kappa_0)^3 + \kappa_0^2 C_3\, 2\sqrt{2}\kappa_0) =: C_B\kappa_0^3$. For the second bound let $\widetilde{\psi} = \psi(z/8r)$. It is one on the box of radius $8r$, while $\operatorname{supp}\pi$ lies in the box of radius $4r$. Lemma 3.7.8 gives

$$\|\mathrm{Op}_\rho(e_{\kappa_0}\widetilde{\psi})\| \le Cr^3$$

with a constant independent of κ_0. First remove the fixed masks in $\Pi' = Y\,\mathrm{Op}_\rho(\pi)$: pure-mask localization gives $\Pi' = \mathrm{Op}_\rho(\pi) + O((\rho/r)^4)$, whose contribution is bounded by $C_{\kappa_0}\rho^4 r^{-5}$ since $r \le 1$.

For $b = e_{\kappa_0}(1 - \widetilde{\psi})$, use a smooth dyadic partition $b = \sum_R b_R$ into annuli with $R \gtrsim r$ and $R \lesssim \kappa_0$. Every b_R retains the factor $1 - \widetilde{\psi}$, hence vanishes in the box of radius $8r$ and is separated from π. Cubic vanishing for the first three derivatives and the supplied six scalar k derivatives give

$$\|\partial_k^j b_R\|_\infty \le C_{\kappa_0} R^{3-j} \quad (0 \le j \le 6), \qquad \int |u|^4 \sup_Z |\widehat{b}_R(Z,u)|\,\mathrm{d}u \le C_{\kappa_0} R^{-1}.$$

Derivatives of $\widetilde{\psi}$ occur only where $R \asymp r$. The Fourier bound follows from the envelope $C_{\kappa_0}R^4(1 + R|u|)^{-6}$. For the smooth right mask,

$$\int \sup_Z |\partial_Z^4 \widehat{\pi}(Z,v)|\,\mathrm{d}v \le Cr^{-4}.$$

In the fourth-order expansion of Lemma 3.9.8, all local terms vanish by the disjoint supports. Thus

$$\|\operatorname{Op}_\rho(b_R)\operatorname{Op}_\rho(\pi)\| \le C_{\kappa_0}\rho^4 R^{-1} r^{-4}.$$

Since $\sum_R R^{-1} \le C/r$, with no logarithmic loss, the total exterior error is at most

$$C_{\kappa_0}\rho^4 r^{-5} = C_{\kappa_0} r^3 (\rho/r^2)^4 \le C_{\kappa_0} r^3 \rho^{4/5}.$$

It is at most r^3 after a κ_0-dependent threshold. This proves the local bound with C_e independent of κ_0.

(ii). Use the exact partition $I = \operatorname{Op}_\rho(\pi_{\mathrm{in}}) + \sum_{j<J}\operatorname{Op}_\rho(\phi_j) + \operatorname{Op}_\rho(\pi_{\mathrm{ext}})$ of the proof of Proposition 3.9.33. For an inner or shell piece, $B_0^{\mathrm{nc}}\operatorname{Op}_\rho(\pi) = C_b(K_{\log}R_{\mathrm{raw}} - \operatorname{Op}_\rho(e_{\kappa_0}))\Pi'$ with $\Pi' = C_b\operatorname{Op}_\rho(\pi)$. Lemma 3.9.24 and (i) bound it by $\mathcal{G}(r) + C_m C_e r^3 + C_{\kappa_0}P(S)\rho^{9/5}$ for $r \le \theta_\chi r_{\mathrm{out}}/8$, and by $(C_g' + C_m C_e)r^3 + C_{\kappa_0}a_\rho P(S)$ for the at most $\log_2(32/\theta_\chi)+1$ transition pieces. For the exterior piece, $B_0^{\mathrm{nc}}\operatorname{Op}_\rho(\pi_{\mathrm{ext}}) = C_b(K_{\log}R_{\mathrm{raw}} - \operatorname{Op}_\rho(e_{\kappa_0}))C_b\operatorname{Op}_\rho(\pi_{\mathrm{ext}})$ and $C_b\operatorname{Op}_\rho(\pi_{\mathrm{ext}}) = R_o^{C_b} - [C_b, C_{\log}^{\mathrm{pad}}]$, where the commutator is tiny, so (3.9.50) gives $C_{\kappa_0}\rho^{1/2}P(S)$. Summing with $\sum_{j<J} r_j^3 \le \frac{1}{7}r_J^3 \le 10 r_{\mathrm{out}}^3$, $\sum_j r_j \le 8 r_{\mathrm{out}}$, $J \le \log(1/\rho)$ and $a_\rho \le \delta$ gives

$$\|B_0^{\mathrm{nc}}\| \le 10(C_g + C_g' + 2C_m C_e) r_{\mathrm{out}}^3 + C(\rho r_{\mathrm{out}} + \rho^2 \log\tfrac{1}{\rho}) + C_{\kappa_0}P(S)(\rho^\nu + a_\rho \log\tfrac{1}{\rho}).$$

This is at most ω_B with $C_\flat = 10(C_g + C_g' + 2C_m C_e)$, since $a_\rho \log(1/\rho) \le \rho^{2/5}$ for small ρ. □

Lemma 3.9.31 (Polynomial bound for the parametrix remainder)**.** *For $s \le -s_1(\kappa_0)$ and $f \in \mathcal{F}_\sigma$,*

$$\|Z_0 f(s)\|_{L^2_{\mathrm{can}}} \le C_{\kappa_0}P(S)W(s)\|f\|_{\mathcal{F}_\sigma},$$

where the polynomial P depends on M.

Proof. Inputs. (SC2), (SC4), (SC5); Lemma 3.9.4; the bounds (3.9.42), (3.9.46) and the exterior annular bound (A5) of the proof of Proposition 3.9.33; the column bounds $\|J_{\mathrm{ref}}\| \le C$ and $\|J_p Y\| \le P(S)\sum_{a+b\le 11}\|Z^a k^b Y\|$ (Lemmas 3.7.12 and 3.7.9); $\|[d_{\mathrm{old}}, C_1]\| \le C\rho$ ((A2) of the proof of Proposition 3.9.33); and the reference residual bound (R0) of Lemma 3.9.13: $\|R_{\mathrm{ref}}\widetilde{C}Y\| \le C_{\kappa_0}P(S)\|Y\|$ for a fixed mask $\widetilde{C}$ in the chart. Lemma 3.9.13 proves the assertion of the paragraph "Physical inputs for the remaining paths".

Recall $Z_0 = I - JC_1'C_0'\chi K - (J[d', C_1'] - RC_1')G_a'C_0'\chi K$.

(i) $|f|_* = \|Kf\| + \|Q_\delta f\|$ and $f = J_\delta K f + Q_\delta f$ give $\|f(s)\| \le (1 + \|J_\delta\|)|f(s)|_*$, and $\|J_\delta\| \le \|J_{\mathrm{ref}}\| + \|D_p C_\delta\| \le P(S)$. Also $\|J\| = \|J_{\mathrm{raw}}N^{-1}\| \le C_N(\|J_{\mathrm{ref}}\| + \|D_p C_{\log}\|) \le P(S)$.

(ii) $\|JC_1'C_0'\chi K f(s)\| \le P(S)|f(s)|_*$.

(iii) Put $g = C_0'\chi K f$, so $\|g\|_{Y_0} \le C\|f\|_{\mathcal{F}_\sigma}$. Exactly, $[d', C_1']G_a' = N[d_{\mathrm{old}}, C_1]G_a N^{-1}$, so (3.9.42) gives $\|J[d', C_1']G_a' g(s)\| \le P(S)C_N^2 C\rho\, C_a\rho^{-1}W\|g\|_{Y_0}$.

(iv) $RC_1'G_a'g = R_{\mathrm{raw}}C_1 G_a \widetilde{g}$ with $\widetilde{g} = N^{-1}g$. Insert the partition of I between C_1 and G_a, and pads X_j, X_o as in Step 4 of the proof of Proposition 3.9.33. For the pure-mask pad remainders, order 30 in the smooth-mask calculus gives at worst $(\rho/\delta^2)^{30} = \rho^6$ in the required degree-fifteen word norms. After (SC4)'s ρ^{-3} and the global Green's ρ^{-1}, a factor ρ^2 remains. For a piece $\Pi'' = C_1\operatorname{Op}_\rho(\pi)$ of radius r, use (3.9.51) in the form of the proof of Lemma 3.9.24: $R_{\mathrm{raw}}\Pi'' = R_{\mathrm{ref}}(I - C_{\log})\Pi'' + R_p C_{\log}\Pi'' + J_p\operatorname{Op}_\rho(\sigma_B)C_{\log}\Pi'' - D_p[d_{\mathrm{old}}, C_{\log}]\Pi''$.

- If $r \le \theta_\chi r_{\mathrm{out}}/8$, the first term is tiny by (a1) of that proof and (SC4), (R0). Its third and fourth terms are $O(C_{\kappa_0}P(S)\rho^{9/5})$ by the repaired word estimates (a3),(a4) and (3.9.36), without applying the crude residual loss to those scalar errors. Since $C_{\log}\Pi'' = \mathrm{Op}_\rho(\pi) + \text{tiny}$, (SC5) and (SC4) give $\|R_p C_{\log}\Pi''\| \le P(S)\mathcal{P}(r)$ with $\mathcal{P}(r) = (r+a_\rho)^3 + \rho^\nu(r+a_\rho) + r^3 + \rho r + \rho^2$.
- If $r > \theta_\chi r_{\mathrm{out}}/8$ or for the exterior piece, each term is at most $P(S)$: by (R0) (with $\widetilde{C} = C_b$, up to tiny terms), by (SC5) at radius r_{out} as in (b3) of that proof, by the word bounds of J_p, and by $\|[d_{\mathrm{old}}, C_{\log}]\| \le C\rho$ with the words of D_p.

The inner box costs $C_a\rho^{-1}$, a shell $4C_A r_j^{-2}$, and the exterior $16C_A r_J^{-2}$. Thus

$$\frac{\|R_{\mathrm{raw}}C_1 G_a \widetilde{g}(s)\|}{W\|\widetilde{g}\|_{Y_0}} \le P(S)\Big[\frac{\mathcal{P}(2\delta)}{\rho} + \sum_{r_j \le \theta_\chi r_{\mathrm{out}}/8} \frac{\mathcal{P}(r_j)}{r_j^2} + \frac{C}{r_{\mathrm{out}}^2}\Big] + C_{\kappa_0}P(S)\rho^{4/5}.$$

Here $\mathcal{P}(2\delta)\rho^{-1} \le C\rho^{1/5}$, and $\sum_j \mathcal{P}(r_j)r_j^{-2} \le C(r_{\mathrm{out}} + a_\rho^3\delta^{-2} + \rho^\nu\delta^{-1} + \rho^\nu a_\rho\delta^{-2} + \rho\delta^{-1} + \rho^2\delta^{-2}\log\frac{1}{\rho}) \le C$. The number of transition and exterior pieces is bounded, and $r_{\mathrm{out}}^{-2} = S^{2M}$.

Collecting (i)–(iv) proves the lemma. □

Lemma 3.9.32 (The complementary row)**.** *With $T = KA_* + K_s - B'K$ and $Q = I - JK$ as in* (3.9.20)*,*

$$\|\chi TQ\|_{L^2_{\mathrm{can}} \to L^2_Z} \le C\rho^{1/2}P(S).$$

Proof. Inputs. Lemma 3.6.5 ((3.6.18) with $\theta = \frac{1}{2}$), (SC2), (SC3), Lemma 3.9.15, and the wave bound (W) of (SC6), which we prove at the end from

(W1) the wave form (3.9.10) of (SC6), and

(W2) $\|\nabla_* H_{\mathrm{ref}} a\|_{L^2} \le P(S)\|\langle k\rangle a\|_2$ (radial H^1 profile bounds of Lemma 3.6.2 and $\rho\partial_Z = ik$).

Exact algebra. Since $KQ = 0$, $TQ = (KA_* + K_s)Q$. With $K = K_\delta = M_\delta^{-1}K_{\mathrm{ref}}$, $K_s = -M_\delta^{-1}(M_\delta)_s K + M_\delta^{-1}(K_{\mathrm{ref}})_s$, so $K_sQ = M_\delta^{-1}(K_{\mathrm{ref}})_s Q$. Also $K_{\mathrm{ref}}Q = M_\delta KQ = 0$, so for the band generator B of Lemma 3.6.5,

$$TQ = M_\delta^{-1}\big(K_{\mathrm{ref}}A_* + (K_{\mathrm{ref}})_s - BK_{\mathrm{ref}}\big)Q = M_\delta^{-1}XQ, \qquad X = T_{\mathrm{ref}} + K_{\mathrm{ref}}(A_* - L).$$

Since $\chi = NC_\chi N^{-1}$ and $N^{-1}M_\delta^{-1} = M_{\log}^{-1}$, we get $\chi TQ = NC_\chi M_{\log}^{-1}XQ$. By (O5), $M_{\log}^{-1}X = X - M_{\log}^{-1}E_{\log}X$ on $H^{-2}_{\mathrm{ax},\rho}$, and $E_{\log}X = K_{\mathrm{ref}}D_p(C_{\log}C_\chi X + C_{\log}(I - C_\chi)X)$.

Bounds. $\|C_\chi T_{\mathrm{ref}}\| \le C\rho^{3/2}P(S)$, and $\|C_\chi K_{\mathrm{ref}}(A_* - L)\| \le C\rho^{1/2}P(S)$ by (W). The pure smooth-mask product satisfies

$$\sum_{a+b\le 11} \|Z^a k^b C_{\log}(I - C_\chi)\langle k\rangle^2\| \le C_N(\rho/r_{\mathrm{out}})^N$$

for any fixed finite N, by the smooth-mask and graph forms of the separated calculus. Lemma 3.9.23 therefore makes $K_{\mathrm{ref}}D_pC_{\log}(I - C_\chi)$ tiny as a map from $H^{-2}_{\mathrm{ax},\rho}$ to L^2_Z. Here all high derivatives fall on the masks. The remaining factor obeys $\|X\|_{L^2\to H^{-2}} \le P(S)$ by (SC3) and (W1). Also $\|K_{\mathrm{ref}}D_pC_{\log}\| = \|E_{\log}\| \le \frac{1}{4}$, $\|M_{\log}^{-1}\| \le \frac{4}{3}$, $\|N\| \le \frac{5}{3}$ and $\|Q\| \le 1 + \|J\|\|K\| \le P(S)$. Hence $\|\chi TQ\| \le \frac{5}{3}(1 + \frac{1}{3}C_m)\|C_\chi X\|P(S) + \text{tiny} \le C\rho^{1/2}P(S)$.

Proof of (W). Let C be a fixed output mask in the chart, $f \in L^2_{\mathrm{can}}$ and $a \in L^2_Z$. Then $\langle CK_{\mathrm{ref}}(A_* - L)f, a\rangle = \langle (A_* - L)f, u\rangle$ with $u = H_{\mathrm{ref}}M_{\mathrm{ref}}^{-*}C^*a$, which is solenoidal. Since $\mathbb{P}u = u$, (W1) and one integration by parts give $|\langle (A_* - L)f, u\rangle| \le 2\|W^\natural\|_\infty\|f\|\|\nabla_* u\|$. By (3.6.17), $\|\langle k\rangle M_{\mathrm{ref}}^{-*}C^*a\| \le C\|a\|$, so (W2) gives $\|\nabla_* u\| \le P(S)\|a\|$. Hence $\|CK_{\mathrm{ref}}(A_* - L)\| \le C\rho^{1/2}P(S)$. □

Proposition 3.9.33 (Completion of the ordered defect estimate)**.** *Fix the actual source and finite family. Fix also the following, all before the blend radius (there κ_0 is called κ_{crit}):*

- *the masks $C_s \prec C_0 \prec C_1 \prec C_\chi \prec C_b$, where $X \prec Y$ means that Y equals one on a fixed neighbourhood of* $\operatorname{supp} X$*;*
- *the output pad C_{ann};*
- *the shift constant d_0 and the frozen scalar gap $\gamma_{\mathrm{gap}} = \lambda_c - g_s > 0$;*
- *the exponent M of $r_{\mathrm{out}} = S^{-M}$;*
- *the bound κ_* of the paragraph "Uniformity in the blend radius", decreased once so that (3.9.54) below holds.*

There are constants $\mathfrak{c}_1, \mathfrak{c}_2$, fixed by these data, with the following property. For each $\kappa_0 \in (0, \kappa_*]$ there are a threshold $s_1(\kappa_0)$ and a function ω_{κ_0} with $\omega_{\kappa_0}(s_0) \to 0$ as $s_0 \to \infty$. For $s_0 \geq s_1(\kappa_0)$, with all norms taken over $s \leq -s_0$,

$$\|E\|_{\mathcal{F}_\sigma \to \mathcal{F}_\sigma} \leq \mathfrak{c}_1\kappa_0 + \mathfrak{c}_2\, r_{\mathrm{out}}(-s_0) + \omega_{\kappa_0}(s_0), \qquad \omega_{\kappa_0}(s_0) \leq C_{\kappa_0} \sup_{s \leq -s_0} (\rho^{1/5} + P(S) C_*(\rho) \rho^{1/4}). \tag{3.9.52}$$

The constants $\mathfrak{c}_1, \mathfrak{c}_2$ do not depend on κ_0, on ρ or on s_0. If $\kappa_0 \leq \min\{\kappa_*, (4\mathfrak{c}_1)^{-1}\}$ and s_0 is then so large that $\mathfrak{c}_2 r_{\mathrm{out}}(-s_0) + \omega_{\kappa_0}(s_0) \leq \frac{1}{4}$, then $\|E\| \leq \frac{1}{2}$. In that case $I - E$ is invertible on $\mathcal{F}_\sigma$ by its Neumann series, and $\|(I-E)^{-1}\| \leq 2$.

Proof. Conventions. $W = q_* \rho^{1+\sigma}$, and Y_0 and $\mathcal{F}_\sigma$ are taken over $s \leq -s_0$. The letter C denotes a constant fixed by the data listed in the statement and by the finite list of mask shapes. It is independent of κ_0, ρ, s_0. C_{κ_0} may also depend on κ_0. $P(S)$ is a polynomial fixed by the same data and M. $C_*(\rho) = \rho^{-o(1)}$ is the envelope of Theorem 3.8.2, and $C_N = 5/3$. We fix $n = 30$ for the pure smooth-mask remainders. This choice does not increase any profile derivative count. For a scalar operator X we write $X' = NXN^{-1}$, and $\chi = C_\chi'$. Bounds for Volterra operators are pointwise in output time, as in (3.9.42).

Exact norm identities. For $f \in \mathcal{F}_\sigma$, $\|Kf(s)\|_2 \leq |f(s)|_* \leq W(s)\|f\|_{\mathcal{F}_\sigma}$. Also $|J_\delta a|_* = \|a\|_2$, because $KJ_\delta = I$ and $Q_\delta J_\delta = 0$. Hence an operator $J_\delta \mathcal{B}$ has norm on $\mathcal{F}_\sigma$ equal to $\sup_f \|\mathcal{B}f\|_{Y_0} / \|f\|_{\mathcal{F}_\sigma}$.

Inputs.

(A1) Lemma 3.9.15: $\|N^{\pm 1}\| \leq C_N$ once $\rho(-s_0) \leq \rho_1$. The estimate uses (3.9.17), which Lemma 3.7.9 derives from its macro size condition (M).

(A2) *Mask calculus.* Let X, Y be smooth fixed-shape masks.

- If $X \prec Y$, then $\|YX - X\| + \|XY - X\| \leq C\rho^n$.
- If $\operatorname{dist}(\operatorname{supp} X, \operatorname{supp} Y) > 0$, then $\|XY\| \leq C\rho^n$.
- If one factor shrinks with radius $r \geq \delta$ and the gap is fixed, the bound is $C(\rho/r)^n$.
- If both factors have radius $\asymp r$ and their supports are separated at scale r, the bound is $C(\rho/r^2)^n$.

Moreover $\|[d_{\mathrm{old}}, C_1]\| \leq C\rho$, and $[d_{\mathrm{old}}, C_1] = Y_1[d_{\mathrm{old}}, C_1] + O(C_{\kappa_0}\rho^{3/2})$ for a fixed pad Y_1 of the transition of C_1 with $\operatorname{dist}(\operatorname{supp} Y_1, \operatorname{supp} C_0) > 0$. [The first two assertions concern fixed masks; the next two give their shrinking-radius forms. They follow from Lemma 3.9.8 and the smooth-mask part of Section 3.9.2.1, including the specified word and graph bounds. The commutator statement follows from (3.9.44) with a fixed radius, the exact dilation commutator and $\partial_s \operatorname{Op}_{\rho(s)}$.]

(A3) *Fixed-gap inverse.* Let $G_s = (d_{\mathrm{old}} + d_0 C_s)^{-1}$ be the Duhamel inverse with the propagator $U^{(s)}$ of Lemma 3.9.18. Then $\|G_s\|_{Y_0 \to Y_0} \le 2/\gamma_{\mathrm{gap}}$ and $\|G_s\|_{Y_{-1} \to Y_{-1}} \le 2/\gamma_{\mathrm{gap}}$. Take $\epsilon = \gamma_{\mathrm{gap}}/8$ in Lemma 3.9.18. Since $W = \gamma e^{\lambda_c s} h^{-1-\sigma} T^{b-1-\sigma}$, $(\log \gamma)' = \Re b_0 = O(\rho^{.99872} P(S))$ by (H3), and $T(u) = T(s) + (s-u)$, we get $W(u) \le e^{-(\lambda_c - 2\epsilon)(s-u)} W(s)$ for $u \le s \le -s_0$ once $s_0 \ge |b-1-\sigma|/\epsilon$. Hence $\|G_s g(s)\| \le \int_{-\infty}^{s} e^{(g_s+\epsilon)(s-u)} W(u)\, du\, \|g\|_{Y_0} \le W(s)\|g\|_{Y_0}/(\gamma_{\mathrm{gap}} - 3\epsilon)$. The inputs of E_2, E_3 carry the extra weight ρ^{-1} of G_a, that is they lie in Y_{-1}. Since $\rho(u)^{-1} = \rho(s)^{-1} + h(s-u)$, the same integral is at most $\rho(s)^{-1} W(s) \|g\|_{Y_{-1}} [(\gamma_{\mathrm{gap}} - 3\epsilon)^{-1} + h\rho(s)(\gamma_{\mathrm{gap}} - 3\epsilon)^{-2}]$, which is at most $(2/\gamma_{\mathrm{gap}})\rho(s)^{-1} W(s) \|g\|_{Y_{-1}}$ after a threshold. The Neumann series of Step 2 and the comparison Δ_s keep both weights.

(A4) *Separated fixed-gap path.* For $\alpha \in \{0, -1\}$, $\|C_s \widehat{G}_s (I - C_0') g(s)\| \le C_{\kappa_0} \rho^{3/2} P(S) W(s) \rho(s)^{\alpha} \|g\|_{Y_\alpha}$. [Lemma 3.9.6, with $F_0 \succ C_s$, intermediate F_1, F_2 and $F_3 = C_0$, transported by N and combined with $\|[C_s, N]\| + \|\Delta_s\| \le C\rho^{3/2} P(S)$ from Lemma 3.9.16 and the Neumann formula in Step 2(a) below. Its hypothesis $[A, F_i] = \rho L_i + R_i$ with $\|R_i\| \le C_{\kappa_0} \rho^{3/2} P(S)$, for $A = d_{\mathrm{old}} + d_0 C_s - B_{\mathrm{int}}$, is verified: ρL_i comes from d_{old} (Lemma 3.9.26), $[C_s, F_i]$ is tiny, and $[B_{\mathrm{int}}, F_i]$ is bounded by (3.9.13), which uses Lemma 3.9.12 for the wave row. The fixed-gap inverse is used on Y_0 and Y_{-1} by (A3).]

(A5) *Critical and annular Greens.*

- (3.9.42), where C_a is the constant written C_* there: $\|G_a g(s)\| \le C_a \rho^{-1} W \|g\|_{Y_0}$.
- (3.9.46): $\|X G_a g(s)\| \le C_A r^{-2} W \|g\|_{Y_0}$ for every fixed-shape output annulus X with radius parameter $r \in [\delta, 2\kappa_0]$, uniformly in κ_0 after a κ_0-dependent threshold.
- The same bound for the exterior shape $X = \mathrm{Op}_\rho(1 - \psi(z/r))$.

[Lemmas 3.9.21 and 3.9.27. For the exterior shape the proof of Lemma 3.9.27 applies verbatim. It uses only the global well inequality $p + r^2 v(z/r) \ge c_0 r^2$, the separation of the output cutoff from the fill, and the commutator of the cutoff, which here is minus the commutator of the compact $\psi(z/r)$.]

(A6) *Scalar row.*

(a) Lemma 3.9.24. For the pieces $\Pi' = Y\,\mathrm{Op}_\rho(\pi)$ of Step 4, $Y \in \{C_b, C_b C_1\}$, of radius $r \in [2\delta, r_J]$,

$$\begin{aligned}
&\|C_b K_{\log} R_{\mathrm{raw}} \Pi'\| \le \mathcal{G}(r) + C_{\kappa_0} P(S) \rho^{9/5} \qquad (r \le \theta_\chi r_{\mathrm{out}}/8),\\
&\|C_b K_{\log} R_{\mathrm{raw}} \Pi'\| \le C_g' r^3 + C_{\kappa_0} a_\rho P(S) \qquad (\theta_\chi r_{\mathrm{out}}/8 < r \le r_J),\\
&\mathcal{G}(r) = C_g(r^3 + \rho r + \rho^2) + P(S)[\rho^\nu r + \rho^{\nu+a} + a_\rho (r + a_\rho)^2 + \rho^2].
\end{aligned}$$

Here $a = \frac{1}{2} - 128\varkappa$, θ_χ is the plateau fraction of the mask shape, and C_g, C_g' do not depend on S or κ_0. The second line covers the shells that meet the transition of $C_{\log}$ (up to $r_J \le 4 r_{\mathrm{out}}$), which (3.9.35) does not. This estimate uses (SC1)–(SC6), with (SC5) supplied by Lemma 3.7.11.

(b) Lemmas 3.9.30 and 3.9.14. $B_0 = C_b\,\mathrm{Op}_\rho(e_{\kappa_0}) C_b + B_0^{\mathrm{nc}}$ with $\|\mathrm{Op}_\rho(e_{\kappa_0})\| \le C_B \kappa_0^3$ and $\|B_0^{\mathrm{nc}}\| \le \omega_B(s) = C_\flat r_{\mathrm{out}}^3 + C_{\kappa_0} \rho^{2/5} P(S)$, with $C_B, C_\flat$ independent of κ_0. The logarithmic term r_{out}^3 in this upper bound tends to zero and enters the fixed-gap absorption in Step 2. The row factorization (3.9.39) holds with $A_{\mathrm{ann}} = 0$ and $\|R_{\mathrm{sep}}\| \le C_{\kappa_0} \rho^{3/2} P(S)$, the E_j bounds in the first line of (3.9.3) hold with $\rho^{9/5}$, and $\|[B_{\mathrm{int}}, F_i]\| \le C_{\kappa_0} \rho^{3/2} P(S)$ for the nested masks of (A4). The wave row needs care: $A_* - L$ has a visible part of angular

label 0 (the slow difference and the tangential mean), but it carries no carrier phase and moves k only by $O(\rho P(S))$; components of label $\pm 2m$, which could move k by $O(1)$, are absent from the retained fields because products of distinct source labels vanish. Their possible contribution from the tail is $O(\rho^{49})$ on a fixed mask (Lemma 3.9.12). These bounds use (SC1)–(SC6).

(A7) (3.9.49) and (3.9.50), where we take the pad $C^{\mathrm{pad}}_{\log} = \mathrm{Op}_\rho(\psi(z/r_J))$ fixed below. Lemma 3.9.29 uses (SC1)–(SC4), (SC6) and Lemma 3.9.15.

(A8) Lemma 3.9.28, including its last assertion, with constant C_{cub} in front of κ_0. C_{cub} is independent of κ_0, because the scaled C^6 norms of the shells and C_A are.

(A9) *Physical paths.*

(a) $\|Z_0 f(s)\|_{L^2} \le C_{\kappa_0} P(S) W(s) \|f\|_{\mathcal{F}_\sigma}$. Lemma 3.9.31 uses (SC2), (SC4), (SC5) and Lemmas 3.9.4 and 3.9.13.

(b) Theorem 3.8.2 with the weight WL^j:

$$\|G_\delta g(s)\|_{L^2} \le C\, C_*(\rho) W(s) L(s)^j \operatorname*{ess\,sup}_{u \le s} \frac{\|g(u)\|_{L^2}}{W(u)L(u)^j}.$$

(c) $\|K\|_{L^2 \to L^2_Z} \le C$, from Lemma 3.6.3 and (A1).

(d) $\|\chi T Q\|_{L^2 \to L^2_Z} \le C\rho^{1/2} P(S)$. Lemma 3.9.32 uses (3.6.18), (SC2), (SC3) and the wave form (3.9.10).

Step 1: exact decomposition. Insert $\chi K R = B\chi + L$ from (3.9.39) into the second line of (3.9.40). Then (3.9.41) becomes $E = \sum_{i=1}^{7} E_i$ with

$$\begin{aligned}
E_1 &= d_0 J_\delta C_s \widehat{G}_s\, \chi (I - C_1' C_0' \chi) K, & E_2 &= -d_0 J_\delta C_s \widehat{G}_s\, \chi [d', C_1'] G_a' C_0' \chi K, \\
E_3 &= d_0 J_\delta C_s \widehat{G}_s\, L C_1' G_a' C_0' \chi K, & E_4 &= d_0 J_\delta C_s \widehat{G}_s\, B(\chi - I) C_1' G_a' C_0' \chi K, \\
E_5 &= d_0 J_\delta C_s \widehat{G}_s\, N B_0 C_1 G_a C_0 C_\chi N^{-1} K, & E_6 &= d_0 J_\delta C_s \widehat{G}_s\, H G_\delta Z_0, \\
E_7 &= d_0 J_\delta C_s (I - \chi) K G_\delta Z_0.
\end{aligned} \tag{3.9.53}$$

In E_5 we used $BC_1' G_a' C_0' \chi = N B_0 C_1 G_a C_0 C_\chi N^{-1}$, which is exact by (3.9.38).

Step 2: the two outer factors.

(a) By (A6b), $\|B_0\| \le C_m^2 C_B \kappa_0^3 + \omega_B(s)$, where C_m bounds the fixed masks and $\omega_B(s) \to 0$ (Lemma 3.9.30). We require

$$C_m^2 C_B \kappa_*^3 \le \gamma_{\mathrm{gap}}/8. \tag{3.9.54}$$

After a threshold with $\omega_B \le \gamma_{\mathrm{gap}}/8$, $\|B_0\| \le \gamma_{\mathrm{gap}}/4$. Then $G_s^B = (d_{\mathrm{old}} + d_0 C_s - B_0)^{-1} = G_s \sum_k (B_0 G_s)^k$ has $\|G_s^B\|_{Y_0 \to Y_0} \le 4/\gamma_{\mathrm{gap}}$ by (A3).

(b) Lemma 3.9.16 gives $d' + d_0 C_s - B = N(d_{\mathrm{old}} + d_0 C_s - B_0) N^{-1} + \Delta_s$. With $\mathcal{G} = N G_s^B N^{-1}$ this means $\widehat{G}_s = \mathcal{G}(I + \Delta_s \mathcal{G})^{-1}$. Once $\|\Delta_s\| \le C\rho^{3/2} P(S) \le \gamma_{\mathrm{gap}}/(8C_N^2)$,

$$\|d_0 C_s \widehat{G}_s\|_{Y_0 \to Y_0} \le C_\Lambda := \frac{8|d_0| C_m C_N^2}{\gamma_{\mathrm{gap}}}. \tag{3.9.55}$$

(c) Every E_i has the form $J_\delta \mathcal{B}_i$. The input satisfies $\|C_0 C_\chi N^{-1} K f\|_{Y_0} \le C_m^2 C_N \|f\|$.

Step 3: separated and plateau paths E_1–E_4.

- E_1. We have $\chi(I - C_1'C_0'\chi) = (I - C_0')\chi + N(C_0C_\chi - C_\chi C_1 C_0 C_\chi)N^{-1}$. The last bracket is $O(\rho^n)$ by (A2). So (A4) and (3.9.55) give $\|E_1\| \le C_{\kappa_0}\rho^{3/2}P(S) + C\rho^n$.
- E_2. Write $\chi[d', C_1'] = (I - C_0')\chi[d', C_1'] + NC_0C_\chi[d_{\mathrm{old}}, C_1]N^{-1}$.
  - By (A2), $\|C_0C_\chi[d_{\mathrm{old}}, C_1]\| \le C_{\kappa_0}\rho^{3/2}$. Combined with (3.9.55) and the critical cost $C_a\rho^{-1}$, this part contributes $C_{\kappa_0}\rho^{1/2}$.
  - The first part has norm at most $C\rho$. By (A4) it is followed by the factor $C_{\kappa_0}\rho^{3/2}P(S)$, and G_a costs ρ^{-1}. Its contribution is $C_{\kappa_0}\rho^{3/2}P(S)$.

  Hence $\|E_2\| \le C_{\kappa_0}\rho^{1/2}P(S)$.
- E_3. By (A6b), $L = NR_{\mathrm{sep}}N^{-1}$ with $\|R_{\mathrm{sep}}\| \le C_{\kappa_0}\rho^{3/2}P(S)$ (Lemma 3.9.14). The path costs $C_\Lambda C_N^2 C_{\kappa_0}\rho^{3/2}P(S)\cdot C_a\rho^{-1}$, with $\widehat{G}_s$ applied on the weighted space of (A3). Hence $\|E_3\| \le C_{\kappa_0}\rho^{1/2}P(S)$.
- E_4. $B(\chi - I)C_1' = NB_0(C_\chi - I)C_1N^{-1} = O(P(S)\rho^n)$ by (A2), so $\|E_4\| \le CP(S)\rho^{n-1}$.

Step 4: the direct scalar return E_5. Put $g = C_0C_\chi N^{-1}Kf$. It remains to bound $\|B_0C_1G_ag(s)\|$. Fix $\psi \in C_c^\infty(\mathbb{R}^2)$ with $0 \le \psi \le 1$, $\psi = 1$ on the unit box and $\operatorname{supp}\psi$ in the box of side four. Assume, as we may by the choice of shape, that $\operatorname{supp} C_{\log}$ lies in the box of radius r_{out}. At each time s put $r_j = 2^{j+1}\delta$, and let J be the least index with $r_J \ge 2r_{\mathrm{out}}$, so $2r_{\mathrm{out}} \le r_J \le 4r_{\mathrm{out}}$. Define

$$\pi_{\mathrm{in}} = \psi(z/r_0), \qquad \phi_j = \psi(z/2r_j) - \psi(z/r_j)\ (0 \le j < J), \qquad \pi_{\mathrm{ext}} = 1 - \psi(z/r_J).$$

The sum telescopes to one, and Op_ρ is linear. Hence, exactly,

$$I = \mathrm{Op}_\rho(\pi_{\mathrm{in}}) + \sum_{j<J}\mathrm{Op}_\rho(\phi_j) + \mathrm{Op}_\rho(\pi_{\mathrm{ext}}).$$

Then $C_{\log}^{\mathrm{pad}} = \mathrm{Op}_\rho(\psi(z/r_J))$ equals one on a neighbourhood of the support and transition of $C_{\log}$, and $R_o = \mathrm{Op}_\rho(\pi_{\mathrm{ext}})C_1$. Let X_j be a fixed-shape annulus pad of radius parameter $r_j/2$ that equals one on $\operatorname{supp}\phi_j$. Let $X_o = \mathrm{Op}_\rho(1 - \psi(4z/r_J))$. We take $s_1(\kappa_0)$ so large that $8r_{\mathrm{out}} \le \kappa_0$. Then every radius used lies in $[\delta, 2\kappa_0]$, and every shell lies in the κ_0 box, where $\lambda_a = \lambda_{\mathrm{quad}}$. Split $B_0 = C_b\,\mathrm{Op}_\rho(e_{\kappa_0})C_b + B_0^{\mathrm{nc}}$.

(i) *Cubic part.* We have $C_bC_1 = C_1 + O(\rho^n)$ by (A2). Lemma 3.9.28 then gives

$$\|C_b\,\mathrm{Op}_\rho(e_{\kappa_0})C_bC_1G_ag(s)\| \le C_m\big[C_{\mathrm{cub}}\kappa_0 + C\rho^{1/5} + C\rho^{1/2}\log(1/\rho) + C_{\kappa_0}\rho^{1/2}\big]W\|g\|_{Y_0}.$$

(ii) *Noncubic part on a piece.* Let $\Pi \in \{\mathrm{Op}_\rho(\pi_{\mathrm{in}}), \mathrm{Op}_\rho(\phi_j)\}$ have radius r, and put $\Pi' = C_bC_1\Pi$, so that $B_0C_1\Pi = C_bK_{\log}R_{\mathrm{raw}}\Pi'$ and $B_0^{\mathrm{nc}}C_1\Pi = C_b(K_{\log}R_{\mathrm{raw}} - \mathrm{Op}_\rho(e_{\kappa_0}))\Pi'$. On the κ_0 box, $|\partial^\alpha e_{\kappa_0}| \le C|z|^{3-|\alpha|}$, and Lemma 3.9.30(i) gives $\|\mathrm{Op}_\rho(e_{\kappa_0})\Pi'\| \le C_er^3$ after the threshold. Together with (A6a),

$$\|B_0^{\mathrm{nc}}C_1\Pi\| \le \begin{cases} \mathcal{G}(r) + C_mC_er^3 + C_{\kappa_0}P(S)\rho^{9/5}, & r \le \theta_\chi r_{\mathrm{out}}/8, \\ (C_g' + C_mC_e)r^3 + C_{\kappa_0}a_\rho P(S), & \theta_\chi r_{\mathrm{out}}/8 < r \le r_J. \end{cases} \tag{3.9.56}$$

(iii) *Inner box,* $r = r_0 = 2\delta$. Since $\delta/r_{\mathrm{out}} = \rho^{2/5}S^M \to 0$, the ancient threshold ensures $2\delta \le \theta_\chi r_{\mathrm{out}}/8$. Use the first line of (3.9.56) and the global cost $C_a\rho^{-1}$. With $\delta = \rho^{2/5}$ the contribution is at most

$$C(\rho^{.2} + \rho^{.4} + \rho) + P(S)(\rho^{.39872} + \rho^{.49744} + 9\rho^{.29872} + \rho) + C_{\kappa_0}P(S)\rho^{4/5}.$$

(iv) *Shells.* Write $\mathrm{Op}_\rho(\phi_j) = \mathrm{Op}_\rho(\phi_j)X_j + \mathrm{Op}_\rho(\phi_j)(I - X_j)$. The second term is $O((\rho/r_j^2)^n) = O(\rho^{n/5})$ by (A2). So (A5) and (3.9.56) give, per shell, $4C_A r_j^{-2}$ times the right side of (3.9.56), plus $P(S)\rho^{n/5-1}$. For the interior shells ($r_j \le \theta_\chi r_{\mathrm{out}}/8$) sum using $\sum r_j \le 2r_J \le 8r_{\mathrm{out}}$, $\sum r_j^{-1} \le \delta^{-1}$, $\sum r_j^{-2} \le \delta^{-2}$, $J \le \log(1/\rho)$ and $a_\rho \le \delta$. There are at most $\log_2(32/\theta_\chi) + 1$ transition shells, each with $r_j^{-2} \le 64\theta_\chi^{-2}S^{2M}$; they add at most $4C_A(C_g' + C_mC_e)\sum r_j + C_{\kappa_0}a_\rho P(S)S^{2M}$. The total is

$$\mathfrak{c}_2' r_{\mathrm{out}} + C(\rho^{.6} + \rho^{1.2}) + P(S)(\rho^{.59872} + \rho^{.69744} + \rho^{.49872}\log(1/\rho) + \rho^{1.2} + \rho) + C_{\kappa_0}a_\rho P(S)S^{2M},$$

with $\mathfrak{c}_2' = 32C_A(C_g + 2C_mC_e + C_g')$. This constant is independent of κ_0.

(v) *Exterior.* We have $B_0^{\mathrm{nc}}C_1\,\mathrm{Op}_\rho(\pi_{\mathrm{ext}}) = B_0^{\mathrm{nc}}R_o + O(P(S)(\rho/r_J)^n)$, because $[C_1, \mathrm{Op}_\rho(\psi(z/r_J))] = O((\rho/r_J)^n)$. Moreover $R_o(I - X_o) = O((\rho/r_J^2)^n)$, by disjoint rescaled supports. By (A7) and the exterior case of (A5) at radius $r_J/4$, the contribution is at most $C_{\kappa_0}\rho^{1/2}P(S)\cdot 16C_A r_J^{-2} \le C_{\kappa_0}\rho^{1/2}P(S)S^{2M}$.

Multiply by $C_\Lambda C_N$ (Step 2) and $C_m^2C_N$. This gives

$$\|E_5\| \le \mathfrak{c}_1\kappa_0 + \mathfrak{c}_2 r_{\mathrm{out}} + C_{\kappa_0}\sup_{s\le -s_0}(\rho^{1/5} + P(S)\rho^{1/4}),$$

$$\mathfrak{c}_1 = C_\Lambda C_N^2 C_m^3 C_{\mathrm{cub}}, \qquad \mathfrak{c}_2 = C_\Lambda C_N^2 C_m^2 \mathfrak{c}_2'.$$

Step 5: physical paths E_6, E_7.

- H. By (A6b), (A9c), (A9d) and (A2), $\|H\|_{L^2\to L^2_Z} \le C_{\kappa_0}\rho^{1/2}P(S)$. Here $\|[d', \chi]\| \le C_{\kappa_0}\rho$. Also $[\chi, C_s] = N[C_\chi, C_s + N^{-1}[C_s, N]]N^{-1} = O(\rho^{3/2}P(S))$ by (A2) and Lemma 3.9.16.
- $G_\delta Z_0$. Choose j with $P(S) \le CL^j$. Then (A9a) and (A9b) give $\|G_\delta Z_0 f(s)\| \le C_*(\rho)P(S)W(s)\|f\|$.
- E_6. Hence $\|E_6\| \le C_\Lambda C_{\kappa_0}\sup_s \rho^{1/2}P(S)C_*(\rho)$.
- E_7. We have $C_s(I - \chi) = -[N, C_s]N^{-1} + NC_s(I - C_\chi)N^{-1} - [C_s, N]C_\chi N^{-1}$, which is $O(\rho^{3/2}P(S))$. Hence $\|E_7\| \le C\sup_s \rho^{3/2}P(S)C_*(\rho)$.

Step 6: summation. The worst positive powers are

- $\rho^{1/5}$, from the inner box and Lemma 3.9.28;
- $P(S)\rho^{.29872} \le P(S)\rho^{1/4}$, from the inner box;
- $\rho^{1/2}P(S)C_*(\rho)$, from the remaining paths.

Steps 3–5 therefore give (3.9.52), with ω_{κ_0} as displayed. The threshold $s_1(\kappa_0)$ collects the following conditions:

- $\rho \le \rho_1$ (Lemma 3.9.15);
- the conditions in (A3) and Step 2;
- $2\delta \le \theta_\chi r_{\mathrm{out}}/8$ and $8r_{\mathrm{out}} \le \kappa_0$;
- the uniformity threshold of (A5).

The constant $\mathfrak{c}_1$ is the product of the following factors.

- C_Λ depends on d_0, C_m, C_N and γ_{gap}. It is uniform in κ_0 because of (3.9.54).
- $C_N = 5/3$, by Lemma 3.9.15, whose E_j do not contain κ_0.
- C_m is the bound of the fixed masks, which are chosen before κ_0.
- C_{cub} is the per-shell bound $Cr_j^3 \cdot r_j^{-2}$ summed to $\sum r_j \le 4\kappa_0$. The scaled C^6 bound of the shells is uniform in κ_0 (proof of Lemma 3.9.26). The annular constant C_A is uniform in κ_0 because the convex blend keeps $p \ge c|z|^2$ with c independent of κ_0.

Hence $\mathfrak{c}_1$ is independent of κ_0. The same holds for $\mathfrak{c}_2$. The dependence on κ_0 enters only through C_{κ_0} in front of positive powers of ρ, and through $s_1(\kappa_0)$.

Once the completed field is fixed, we choose the remaining parameters in the following order.

1. the masks, d_0, γ_{gap}, M and κ_*;
2. $\kappa_0 = \kappa_{\mathrm{crit}} \le (4\mathfrak{c}_1)^{-1}$;
3. the ancient threshold $s_0 \ge s_1(\kappa_0)$ with $\mathfrak{c}_2 r_{\mathrm{out}}(-s_0) + \omega_{\kappa_0}(s_0) \le 1/4$.

This order does not change any early source, shift mask or scalar gap. Then $\|E\| \le 1/2$, and the Neumann series converges on $\mathcal{F}_\sigma$.

The finite graph and word bounds (SC3), (SC4) apply on their stated domains. The scalar rectangles of Lemma 3.9.19 and the column bound (3.9.36) give the instances of (SC2) used here. Pure-mask errors use order thirty, and rough scalar errors use orders three and ρ times two. The identities before the row estimates are those of paragraph 3.9.2.1. The cubic estimate of Lemma 3.9.30(i) enters the graded row. Its noncubic estimate in part (ii) follows from the row estimates. The partition and Green bounds enter through (A2) and (A5). The prepared residual and fixed-shape estimates are (3.7.27) and (3.7.28). The physical estimates use the completed-wave bound and fixed cover of Theorem 2(v), (vii), the completed-field decomposition in Lemmas 3.7.2, 3.7.3, 3.6.5, and 3.9.6, together with (A9b). □

Proposition 3.9.34 (Critical unshifted right inverse)**.** *For the one selected completed source B_*, fix the same masks and one $\kappa_0 > 0$ in the order above. There is a sufficiently ancient threshold and a real right inverse G_{crit} of the original completed D on $\mathcal{F}_\sigma$.*

Its scalar/column output for a source of profile $q_*\rho^{1+\sigma}$ is $O(q_*\rho^\sigma P(S))$. Its auxiliary output is $O(q_*\rho^{1+\sigma-o(1)})$.

The two statements are tame profile bounds. A uniform physical output norm may use any fixed exponent below σ.

Proof. Theorem 2(iv) fixes the completed member, its selected physical pair and the shifted leading propagation bound. Lemma 3.7.7 and Theorem 3.8.2 then give the auxiliary inverse on its stated domain.

The exact defect is (3.9.41). Proposition 3.9.33 gives $\|E\| \le C\kappa_0 + Cr_{\mathrm{out}} + o_{\kappa_0}(1)$ with a κ_0-independent leading constant.

Select κ_0 to put the first term below $1/4$, and then increase the ancient threshold to put the remaining terms below $1/4$. The Neumann series converges on the same forcing space. To see the right-inverse identity on this whole space, first read (3.9.33) in distributions on a compact time interval. The scalar and auxiliary states satisfy their variation-of-constants equations there. For the term U, integration by parts against a smooth test differentiates JC_1' and gives exactly $J[d', C_1'] - RC_1'$. Its spatial action extends by the localized column bounds in Lemma 3.9.31; the time integral is justified by the local L^2 bounds on states and forcings. Thus $DP_0 f = (I - E)f$ for locally integrable representatives of all $f \in \mathcal{F}_\sigma$. Each finite sum $P_0 \sum_{j=0}^{n} E^j f$ has derivative under D equal to $f - E^{n+1} f$. The source converges in $\mathcal{F}_\sigma$, and the states converge in local $L^1_s L^2$ by the two output bounds for P_0. Passing to distributions gives $DG_{\mathrm{crit}} f = f$ for $G_{\mathrm{crit}} = P_0(I - E)^{-1}$.

The scalar part requires one and only one critical ρ^{-1} factor. Positive-power source terms can absorb the finite $P(S)$ and auxiliary $\rho^{-o(1)}$ factors.

The fixed-small term does not. This gives the stated profile outputs.

The integral (3.9.31) shows that $G_a f(s)$ depends only on $f(u)$ with $u \le s$. The annular, fixed-gap and auxiliary inverses have the same physical-time dependence, while masks and normalizers act at one time.

Each power of E is thus causal. Its Neumann series has uniform convergence and keeps that property. Each term preserves conjugate-pair reality.

□

3.10 The centered Gaussian and a global physical packet

In the similarity variables $R = r/\sqrt{t}$ and $Z = z/t^{1/2-h}$, put $T = -s$, $\rho = t^h = (hT)^{-1}$ and $k = -i\rho\partial_Z$ when k acts on an axial profile. In estimates on a comparable-time band we write $S \asymp (1+\log(1/\rho))^{6/5}$ and $P(S)$ for a fixed polynomial bound. The selected simple branch is centered so that $\lambda_Z = \lambda_k = \lambda_{Zk} = 0$ and $\lambda_c = \Re\lambda_0 > 0$, with negative real axial curvature. Let e, ℓ be its normalized right and left radial profiles, $\ell e = 1$.

Normal ordering $kZ = Zk - i\rho$ in the finite low column gives the current scalar constant

$$c_* = c_1(0,0). \tag{3.10.1}$$

It includes the pressure, dilation and eigenbundle ordering terms. In the unscaled Z coordinate the center quadratic is

$$B_{\mathrm{quad}} = \lambda_0 + \tfrac{1}{2}\lambda_{ZZ}Z^2 + \tfrac{1}{2}\lambda_{kk}k^2 + i(\tfrac{1}{2} - h)Zk + \rho c_*. \tag{3.10.2}$$

The selected source controls make a real $q > 0$ solve the complex Riccati identity

$$\frac{\lambda_{kk}}{h^2}q^2 + \left(1 + \frac{2(\frac{1}{2} - h)}{h}\right)q - \lambda_{ZZ} = 0. \tag{3.10.3}$$

The spectral data retained in Theorem 2(iv) give the Gaussian width $q = q_G > 0$ and place the selected phase at $\lambda_Z = \lambda_k = \lambda_{Zk} = 0$. They give $\Re\lambda_{kk} < 0$ and $X_G = -q\Re\lambda_{kk}/(2h^2) > b_d$, where

$b_d = (h^{-1} - 1)/2$. Taking real parts in (3.10.3) now yields $\Re\lambda_{ZZ} = 2q(b_d - X_G) < 0$. The identity (3.10.3) must hold exactly: a mismatch ε leaves a packet residual of size $\varepsilon\rho q_*$, which is not in $\mathcal{F}_\sigma$.

Set

$$b_G = -\frac{c_*}{h} - \frac{\lambda_{kk} q}{2h^2}, \qquad g_+'(s) = b_{0,+}(s) g_+(s), \quad g_- = \overline{g_+}, \quad \gamma = |g_+|. \tag{3.10.4}$$

The completed scalar center feedback obeys $|b_{0,\pm}(s)| \le \rho^{.99872} P(S)$ and thus $\log\gamma(s) = o(T)$ and $(\log\gamma)' = o(1)$. The scalar norm has exponent $b = \Re b_G - 1/4$ and weight $q_*(s) = \gamma(s) e^{\lambda_c s} T^b$.

Lemma 3.10.1 (Exact paired Gaussian)**.** *Put*

$$\phi_+ = g_+(s) e^{\lambda_0 s} T^{b_G} e^{-qTZ^2/2}, \qquad \phi = 2^{-1/2}(\phi_+, \overline{\phi_+}). \tag{3.10.5}$$

Then ϕ is a real pair solution of the centered quadratic equation with the completed scalar feedback b_0. Its L^2_Z norm equals $c_q q_*(s)$ for a fixed $c_q > 0$.

Proof. Since $T = -s$ and $\rho = (hT)^{-1}$,

$$\frac{\partial_s \phi_+}{\phi_+} = \lambda_0 + b_{0,+} - \frac{b_G}{T} + \frac{q}{2} Z^2, \quad \frac{k\phi_+}{\phi_+} = \frac{iq}{h} Z, \quad \frac{k^2\phi_+}{\phi_+} = \frac{q}{h^2 T} - \frac{q^2}{h^2} Z^2.$$

Substitution in (3.10.2) shows that the Z^2 coefficient equals $q/2$ by (3.10.3), while its T^{-1} coefficient is $-b_G$ by (3.10.4). Thus $\partial_s \phi_+ = (B_{\mathrm{quad}} + b_{0,+})\phi_+$.

The minus component is the physical conjugate equation. Last $\int e^{-qTZ^2}\,\mathrm{d}Z = (\pi/(qT))^{1/2}$, so $\|\phi\|_2 = c_q \gamma e^{-\lambda_c T} T^{\Re b_G - 1/4} = c_q q_*(s)$.

□

Endpoint check on the exact center. For the quadratic equation of Lemma 3.10.1, let $d_{\mathrm{quad}} = \partial_s - (B_{\mathrm{quad}} + b_0)$. Since $\rho_s = h\rho^2$ and $d_{\mathrm{quad}}\phi = 0$,

$$f = d_{\mathrm{quad}}(\rho^\sigma \phi) = \sigma h \rho^{1+\sigma} \phi.$$

The normalized Gaussian is a constant vector ψ in (3.9.29).

Its normalized forcing is $F(R) = -\sigma\rho(R)^\sigma \psi$. Formula (3.9.31) on this center yields $b(R) = \rho(R)^\sigma \psi$, thus $G_{\mathrm{quad}} f = \rho^\sigma \phi$.

This exact center calculation agrees with the critical output weight and the ancient-end condition in (3.9.31).

Choose real even $\chi_x, \chi_k \in C_c^\infty(\mathbb{R})$ equal to one near zero, with supports sufficiently small that the product symbol of $C_{\mathrm{in}} = \chi_x(Z/\delta)\chi_k(k/\delta)$ lies inside both right-column plateaus. Here $k = -i\rho\partial_Z$ and $\delta = \rho^{2/5}$. This left-ordered mask preserves conjugate pairs.

We define

$$v_{\mathrm{app}} = J_{\mathrm{raw}} C_{\mathrm{in}} \phi. \tag{3.10.6}$$

The Gaussian's Z and semiclassical k widths are $O(\rho^{1/2})$, so their ratio to δ is $\rho^{1/10}$. Indeed $(C_{\mathrm{in}} - I)\phi = (\chi_x - 1)\phi + \chi_x(\chi_k - I)\phi$, with the scaled cutoffs just defined. The first term is a spatial Gaussian tail and the second uses a Fourier Gaussian tail. Each fixed number of spatial and frequency weights or derivatives costs at most a power of ρ^{-1} against the factor $e^{-c\delta^2/\rho}$.

This does not make a nonlocal scalar-symbol mismatch exponentially small only because its symbol vanishes on the inner box. We prove its correct finite four-k-derivative estimate below.

Lemma 3.10.2 (Residual of the completed packet)**.** *For the globally fixed completed source and its full curl and pressure reconstruction,*

$$\|Dv_{\mathrm{app}}(s)\|_{2,\mathrm{can}} + |Dv_{\mathrm{app}}(s)|_* \le Cq_*(s)\rho^{p_0}P(S), \qquad p_0 = 1.19616. \tag{3.10.7}$$

Here D is the fast-time generator. The full-vector norm is canonical. Under

$$\mathcal{U}_t v = t^{-\frac{1}{2}-h} v(x_h/\sqrt{t}, x_3/t^{\frac{1}{2}-h}),$$

velocity L^2 acquires $t^{1/4-3h/2}$. A genuine physical linearized force also acquires t^{-1-h}: $\mathcal{L}_{B_*}\mathcal{U}_t v = t^{-1-h}\mathcal{U}_t Dv$.

The next faster inverse uses physical forcing norms. The normalized logarithmic coordinates give the same physical packet: if $\phi' = N\phi$ and $C'_{\mathrm{in}} = NC_{\mathrm{in}}N^{-1}$, then $JC'_{\mathrm{in}}\phi' = v_{\mathrm{app}}$.

Proof. Insert the finite local column (3.9.1) and its global time-partition correction from Lemma 3.7.7 into the completed velocity-pressure equation. Keep the scalar input on the right.

The low degree-zero through degree-two operator identities cancel: the degree-one equation determines e_Z, e_k, and the reduced radial resolvent determines the degree-two correction. The ordering constant is (3.10.1).

On a radius δ mask, each remaining low Taylor word has one of three forms. It has three factors Z, k, one ρ and one such factor, or two ρ factors.

Their norms are, in this order, $O(\delta^3)$, $O(\rho\delta)$ and $O(\rho^2)$. The two finite high cell iterations leave a full high residual with gain $\rho^{3(2/5-128\varkappa)} = \rho^{1.19616}$.

The coefficientwise odd matching stresses cancel before divergence. The remaining zero-word macro return is $O(\rho^\nu)$ and its center displacement supplies an extra δ.

The distinct $B_{2,\mathrm{high}}$ matching return is of higher order. These finite word classes retain full curl, pressure, axial viscous and time-partition derivatives.

The largest partition correction is $O(\rho P(S)(\delta + a_\rho))$. We fixed opposite-band, finite-prefix completion and global localization tails at $O(\rho^2 P(S))$ before the mask choice.

Thus the smallest exponent is $p_0 = 1.19616$.

More explicitly, with d_{old} the full auxiliary scalar operator, the exact intertwining identity gives

$$Dv_{\mathrm{app}} = J_{\mathrm{raw}}C_{\mathrm{in}}d_{\mathrm{old}}\phi + J_{\mathrm{raw}}[d_{\mathrm{old}}, C_{\mathrm{in}}]\phi - R_{\mathrm{raw}}C_{\mathrm{in}}\phi.$$

Put

$$r_\rho(Z,k) = \lambda_a(Z,k) - \lambda_{\mathrm{quad}}(Z,k) + \rho(c_a(Z,k) - c_*).$$

The shared uncut dilation and the feedback cancel. This symbol vanishes on a fixed box $|Z| \le z_0, |k| \le k_0$ and satisfies $|\partial_k^j r_\rho| \le C_j(1 + Z^2 + k^2)$, $j \le 4$.

For the L^2-normalized Gaussian g_ρ, its unitary semiclassical Fourier transform obeys

$$\|(1+k^2)\partial_k^j \widehat{g}_\rho\|_1 \le C_j\rho^{1/4-j/2}, \qquad j \le 4.$$

On $|Z| \ge z_0/2$, four integrations in the left-quantized Fourier integral give

$$|\operatorname{Op}_\rho(r_\rho)g_\rho(Z)| \le C\rho^4\rho^{-1/2}\rho^{1/4-2}(1+Z^2)|Z|^{-4} = C\rho^{7/4}(1+Z^2)|Z|^{-4}.$$

This envelope is square integrable on that exterior. On the bounded inner Z interval only $|k| \ge k_0$ occurs, a Gaussian Fourier tail.

Thus the scalar mismatch is $O(q_*\rho^{7/4})$ in L^2_Z. The scalar cutoff commutator is the quadratic cutoff commutator plus the two compositions with this mismatch.

Write $C_{\mathrm{in}}\phi = \phi + (C_{\mathrm{in}} - I)\phi$. The finite Gaussian-tail graph norms bound the action of the order-two symbol on the second term.

It follows that the two scalar terms in the exact identity above have this bound, up to $P(S)$.

The lift is the actual bounded right-masked column $J_{\mathrm{raw}} = J_{\mathrm{ref}} + D_p C_{\log}$, not an uncut differential operator. For each finite word, $\|Z^a k^b C_r\| \le C_{a,b} r^{a+b}$.

Derivatives on a mask cost $\rho/r \le r$. Coefficient value bounds and the macro radial norms give $\|J_{\mathrm{raw}}\|_{L^2_Z \to L^2_{\mathrm{can}}} \le P(S)$, with its full curl and pressure lift.

Thus the lifted scalar error is $O(q_* \rho^{7/4} P(S))$, also in the retraction norm. It is smaller than the finite-column $p_0 = 1.19616$ bound by $7/4 - p_0 = .55384$.

The critical input is full-vector L^2. This argument gives no H^2 or H^3 norm of the packet residual.

After this, physical-time smoothing applies to the exact mode.

The last term has the finite-column bound just computed. The retraction norm adds only fixed $P(S)$ factors. The equality in normalized coordinates follows by direct substitution of $J = J_{\mathrm{raw}} N^{-1}$. □

Lemma 3.10.3 (Positive-time identification of the exact mode)**.** *Let $I = [a, b] \Subset (0, t_*)$. Suppose B is real and solenoidal, smooth on $I \times \mathbb{R}^3$, and $\sup_{t \in I} \|B(t)\|_{W^{3,\infty}} < \infty$.*

Let $V \in L^\infty(I; L^2_\sigma(\mathbb{R}^3))$ satisfy

$$\partial_t V - \Delta V + \mathbb{P}\,\mathrm{div}(B \otimes V + V \otimes B) = 0$$

in distributions on the interior of I. Then V has a unique weakly continuous L^2_σ representative on I.

With its weak trace $V(a)$ as datum, it agrees with the linear energy solution on I. In particular,

$$V \in C(I; L^2_\sigma) \cap L^2(I; H^1_\sigma).$$

Thus positive-time energy estimates and interior parabolic smoothing apply to this same distributional mode.

Proof. The equation and the order-zero boundedness of $\mathbb{P}$ give

$$\|\partial_t V\|_{H^{-2}} \le C(1 + \|B\|_\infty)\|V\|_2$$

almost everywhere. Thus V has a Lipschitz H^{-2} representative.

For a test in H^2, the pairing with this representative is continuous. We approximate an arbitrary L^2 test by H^2 tests and use the same essential L^2 bound.

This gives a weakly continuous L^2 representative at the two endpoints and throughout the interval. Its values remain in the same closed L^2 ball and in the solenoidal subspace.

We construct the linear energy solution U with datum $V(a)$ by spatial regularization or the usual Galerkin approximation. The transport term by B cancels, and the remaining term obeys

$$\left| \int U \cdot (U \cdot \nabla) B \, dx \right| \le \|\nabla B\|_\infty \|U\|_2^2.$$

This energy estimate gives $U \in C(I; L^2_\sigma) \cap L^2(I; H^1_\sigma)$.

We must identify V with U. We do not assume that V belongs to this energy class.

We set $w = V - U$ and fix $a < c \le b$. For a smooth compactly supported solenoidal terminal test ψ, we solve the adjoint equation on $[a, c]$:

$$-\partial_t \phi - \Delta \phi - \mathbb{P}(B \cdot \nabla \phi) + \mathbb{P}((\nabla B)^T \phi) = 0, \qquad \phi(c) = \psi, \qquad \mathrm{div}\,\phi = 0.$$

After time reversal this is a forward parabolic problem.

The stated $W^{3,\infty}$ bound gives differentiated energy estimates through order two. These estimates give an adjoint solution with

$$\phi \in L^\infty([a,c];H^2_\sigma), \qquad \partial_t\phi \in L^\infty([a,c];L^2_\sigma).$$

These estimates follow first for regularized coefficients and terminal tests and pass to the limit.

In particular, ϕ is strongly continuous in L^2.

The distributional equation for w extends by spatial density to H^2 test fields. Time mollification and the previous bounds thus justify the product identity

$$\langle w(c),\phi(c)\rangle - \langle w(a),\phi(a)\rangle = \int_a^c \left(\langle \partial_t w,\phi\rangle_{H^{-2},H^2} + \langle w,\partial_t\phi\rangle_{L^2}\right) dt = 0.$$

The two differential operators are adjoints on solenoidal fields.

Integration by parts changes $B\cdot\nabla$ to $-B\cdot\nabla$ and $(w\cdot\nabla)B$ to $(\nabla B)^T\phi$. The endpoint pairings follow from the weak L^2 continuity of w and the strong L^2 continuity of ϕ.

Since $w(a)=0$ in this weak trace, $\langle w(c),\psi\rangle = 0$. Such terminal tests are dense in L^2_σ, so $w(c)=0$ for each $c\in[a,b]$.

Thus $V=U$ on I, which proves the assertion. □

Proposition 3.10.4 (A real exact completed linear mode)**.** *The original completed physical linearization about B_* has a nonzero real solution V. It is smooth for positive time, strongly zero in L^2 at $t=0$, and has finite dissipation.*

It satisfies the separated bounds (3.2.1) of the branching theorem for some fixed M, C_V, c_V after we select a single ancient threshold.

Proof. Take $\sigma = 3/20 = .15$. The source exponent has the strict margin $p_0 - 1 - \sigma = .04616 > 0$.

Lemma 3.10.2 thus puts Dv_{app} in the same $\mathcal{F}_\sigma$ on which Proposition 3.9.34 is a right inverse. That margin absorbs finite subpower losses.

Set

$$w = G_{\mathrm{crit}}(Dv_{\mathrm{app}}), \qquad v = v_{\mathrm{app}} - w.$$

Then $Dv = 0$ and

$$\frac{\|w(s)\|_2}{q_*(s)} \le C\rho^{.15}P(S) + C\rho^{1.15-o(1)} \longrightarrow 0.$$

The first bound is a tame profile estimate. It is a uniform physical output statement with any fixed exponent below .15, for instance .14.

All operators keep the pair involution, thus v is real.

The spatial and Fourier Gaussian tails following (3.10.6) give $\|C_{\mathrm{in}}\phi\|_2 \ge (c_q/2)q_*$ for all sufficiently ancient s. On the conjugate pair, (3.9.15) gives $C_{\mathrm{in}}\phi = N^{-1}K_\delta v_{\mathrm{app}}$. Hence

$$\|v_{\mathrm{app}}\|_2 \ge \frac{c_q q_*}{2\|N^{-1}\|\,\|K_\delta\|} \ge cq_*,$$

by Lemma 3.9.15 and the uniform bound on K_δ. Since $\|w\|_2 = o(q_*)$, it follows that $\|v\|_2 \ge (c/2)q_*$ for all sufficiently ancient s. The column upper bound gives $\|v\|_2 \le P(S)q_*$.

Return to physical variables with $V(t,x) = t^{-\frac{1}{2}-h}v(s,y,Z)$, $y = x_h/\sqrt{t}$, and $Z = x_3/t^{\frac{1}{2}-h}$. The exact coordinate and divergence conjugacy gives

$$\partial_t V - \Delta V + \mathbb{P}\,\mathrm{div}(B_*\otimes V + V\otimes B_*) = 0, \qquad \mathrm{div}\,V = 0.$$

The physical Jacobian is $\mathrm{d}x = t^{\frac{3}{2}-h}\,\mathrm{d}y\,\mathrm{d}Z$, thus

$$\|V(t)\|_2 = t^{\frac{1}{4}-\frac{3}{2}h}\|v(s)\|_2 = t^{1/4-3h/2}\|v(s)\|_2. \tag{3.10.8}$$

Because $\log\gamma = o(T)$ and $q_* = \gamma e^{-\lambda_c T}T^{\Re b_G - 1/4}$, the upper and lower L^2 bounds have leading physical exponential $e^{-\Lambda_* t^{-h}+o(t^{-h})}$, where $\Lambda_* = \lambda_c/h$.

The separated rates $.9\Lambda_*$ and $1.1\Lambda_*$ absorb fixed polynomial factors and the $o(t^{-h})$ term. On each compact positive-time interval, the physical Jacobian and canonical bounds give $V \in L^\infty_t L^2_\sigma$.

The completed base has the necessary bounded spatial jets there. Lemma 3.10.3 thus identifies this distributional mode with its energy solution before we apply any energy estimate. Positive-time parabolic smoothing uses windows t^K, with K fixed from the finite spatial jets of B_*.

It raises the upper L^2 bound to H^3 with a fixed polynomial loss. We enlarge M once to get (3.2.1).

The exponential upper bound gives $V(t) \to 0$ strongly in L^2. On (ε, t_1) the actual physical equation has the energy estimate

$$\tfrac{1}{2}\|V(t_1)\|_2^2 + \int_\varepsilon^{t_1} \|\nabla V\|_2^2\,\mathrm{d}t \le \tfrac{1}{2}\|V(\varepsilon)\|_2^2 + \int_\varepsilon^{t_1} \|\nabla B_*(t)\|_\infty \|V(t)\|_2^2\,\mathrm{d}t.$$

The selected base has a finite polynomial bound on $\|\nabla B_*\|_\infty$, so the last integral converges at zero.

The limit $\varepsilon \downarrow 0$ gives finite physical dissipation and no initial distributional impulse. The previous positive-time energy identification and the parabolic smoothing property apply to this same mode and give the related whole-space pressure.

□

3.11 A faster inverse from the full propagator

Main result. Proposition 3.11.3 gives a causal Sobolev inverse under the base-jet and full propagator bounds the jet bound of Theorem 2(iv) and (3.3.1) for one physical background. Its constants remain fixed when the ancient threshold increases.

The rate $\beta = 3\Lambda_*/2$ exceeds the propagator rate $\Lambda_* + \epsilon$, where $0 < \epsilon < \Lambda_*/2$. Duhamel's formula first gives an L^2 inverse.

An energy estimate on a short physical-time interval gives the Sobolev gain for the quadratic term.

3.11.1 The L^2 inverse by Duhamel

Proposition 3.11.1 (Physical L^2 inverse at the faster rate)**.** *Assume* (3.3.1) *with some* ϵ*. Fix* $\beta > \Lambda_* + \epsilon$*,* $L_1 \ge 0$*, and let* $T \ge T_0 := \max(T_\epsilon, 1)$*.*

For measurable $F : (0, T^{-1/h}] \to L^2_\sigma$ *with* $\|F\|_{\beta,L_1} := \operatorname{ess\,sup}_{\tau\ge T} e^{\beta\tau}\tau^{-L_1}\|F(t)\|_2 < \infty$*, the causal Duhamel integral*

$$z(t) = \int_0^t U_*(t,t')F(t')\,\mathrm{d}t'$$

converges in L^2 *and satisfies* $z \in C((0, T^{-1/h}]; L^2)$*. Also,* $z(t) \to 0$ *in* L^2 *as* $t \downarrow 0$*.*

The function z *is a distributional solution of* $\mathcal{L}_{B_*} z = F$*, and*

$$\|z(t)\|_2 \le C\,\tau^{L_1+\epsilon}e^{-\beta\tau}\|F\|_{\beta,L_1}, \tag{3.11.1}$$

where $C = C_\epsilon C_{\beta-\Lambda_*-\epsilon,L_1}/h$ *is uniform for* $T \ge T_0$*.*

Proof. As t' increases from 0 to t, $\tau' = t'^{-h}$ decreases from $+\infty$ to τ, with $\mathrm{d}t' = -h^{-1}\tau'^{-1-1/h}\,\mathrm{d}\tau'$. Reversing the limits and using $\tau'^{-1-1/h} \le 1$ for $\tau' \ge T \ge 1$, we obtain from (3.3.1)

$$\int_0^t \|U_*(t,t')F(t')\|_2\,\mathrm{d}t' \le \frac{C_\epsilon \tau^\epsilon}{h} e^{-(\Lambda_*+\epsilon)\tau} \int_\tau^\infty e^{-(\beta-\Lambda_*-\epsilon)\tau'}\tau'^{L_1}\,\mathrm{d}\tau'\,\|F\|_{\beta,L_1}.$$

With $c = \beta - \Lambda_* - \epsilon > 0$, and $\tau \ge 1$, $\int_\tau^\infty e^{-c\tau'}\tau'^{L_1}\,\mathrm{d}\tau' \le C_{c,L_1}\tau^{L_1}e^{-c\tau}$ (substitute $\tau' = \tau + u$ and use $(\tau+u)^{L_1} \le \tau^{L_1}(1+u)^{L_1}$). This gives absolute convergence and (3.11.1), with one bound for all T, because the integral only uses $\tau' \ge \tau \ge T$.

For $t_0 > 0$, the function $z_{t_0}(t) = \int_{t_0}^t U_*(t,t')F(t')\,\mathrm{d}t'$ solves $\mathcal{L}_{B_*}z = F$ on $[t_0,t]$ with zero datum. It is the energy solution because the coefficients are smooth and bounded there.

The same bound gives $z_{t_0} \to z$ in $C([\epsilon_1, T^{-1/h}]; L^2)$ for each $\epsilon_1 > 0$. Thus the distributional equation passes to the limit.

Equation (3.11.1) gives $\|z(t)\|_2 \to 0$ as $t \downarrow 0$. □

3.11.2 Forced physical smoothing and one uniform Sobolev inverse

The previous inverse gives a physical L^2 solution. The nonlinear product requires H^3 output from H^2 forcing.

An estimate local in physical time gives this gain without an additional spectral inverse.

Lemma 3.11.2 (A unit-window forced estimate)**.** *Let U be a solenoidal energy solution on $0 < r \le 1$ of*

$$\partial_r U - \Delta U + \mathbb{P}\,\mathrm{div}(\mathcal{B}\otimes U + U\otimes\mathcal{B}) = \mathcal{F},$$

where $\mathrm{div}\,\mathcal{B} = 0$ and $\|\mathcal{B}\|_{L_r^\infty W_y^{4,\infty}} \le C_0$. If $U(0) \in L^2$ and $\mathcal{F} \in L_r^\infty H_y^2$, then

$$\|U(1)\|_{H^3} \le C(C_0)\big(\|U(0)\|_2 + \|\mathcal{F}\|_{L_r^\infty H_y^2}\big). \tag{3.11.2}$$

No temporal derivative of $\mathcal{B}$ or $\mathcal{F}$ is necessary.

Proof. We set $E_j = \|U\|_{H^j}^2$ and $D_j = \|\nabla U\|_{H^j}^2$.

For $0 \le j \le 3$, we differentiate the equation j times and pair with the same derivatives of U. The undifferentiated transport by $\mathcal{B}$ vanishes since it is solenoidal.

Each remaining Leibniz term places at most $j+1 \le 4$ spatial derivatives on $\mathcal{B}$. A small part of D_j plus $C\sum_{i\le j} E_i$ bounds each term.

The Leray projector is orthogonal and commutes with Cartesian derivatives. For $j \ge 1$, we move one derivative from $\partial^j\mathcal{F}$ to $\partial^j U$ in the dual pairing.

Young's inequality then bounds the forcing contribution by $C\|\mathcal{F}\|_{H^{j-1}}^2 + \frac{c}{4}D_j$. At $j = 0$, we use $\|\mathcal{F}\|_2^2$.

Thus

$$\frac{d}{dr}E_j + cD_j \le C\sum_{i\le j} E_i + C\|\mathcal{F}\|_{H^{\max(j-1,0)}}^2. \tag{3.11.3}$$

The $j = 0$ inequality gives the L^2 supremum and integrated H^1 bound. We multiply the jth inequality by r^j.

The dissipation in the $(j-1)$st weighted inequality bounds the extra $jr^{j-1}E_j$. Induction and Gronwall give

$$\sup_{0<r\le 1} r^j E_j(r) + \int_0^1 r^j\|U(r)\|_{H^{j+1}}^2\,\mathrm{d}r \le C_j\big(E_0(0) + \|\mathcal{F}\|_{L^\infty H^2}^2\big), \qquad j \le 3.$$

The weights vanish at the initial endpoint, so we use no higher-order initial trace. Approximation of the L^2 datum and force, followed by the energy uniqueness estimate, proves the assertion for the stated energy solution.

At $r = 1$ this is (3.11.2). □

Proposition 3.11.3 (Uniform physical $H^2 \to H^3$ inverse)**.** *Assume the jet bound of Theorem 2(iv) and (3.3.1), and let $\beta = 3\Lambda_*/2$. There are fixed T_0, L, C_G such that for each $T \ge T_0$ the physical causal solution operator G_T satisfies*

$$G_T : Y_\beta(T; H^2_\sigma) \longrightarrow X_{\beta,L}(T; H^3_\sigma), \qquad \mathcal{L}_{B_*} G_T F = F, \qquad \|G_T\| \le C_G. \tag{3.11.4}$$

Here

$$\|F\|_{Y_\beta(T)} = \operatorname*{ess\,sup}_{\tau \ge T} e^{\beta\tau} \|F(t)\|_{H^2}, \qquad \|u\|_{X_{\beta,L}(T)} = \operatorname*{ess\,sup}_{\tau \ge T} e^{\beta\tau} \tau^{-L} \|u(t)\|_{H^3}.$$

In particular F may contain arbitrary angular frequencies.

Increasing T does not make the constants grow.

Proof. For $0 \le j \le 4$, Theorem 2(iv) gives $\|\nabla_x^j B_*(t)\|_\infty \le C_j t^{-N_j}$ on the whole space. These four derivatives and the value bound suffice for the smoothing estimate.

We fix an integer K so that

$$K > 1 + h, \quad K > 1, \quad K(j+1)/2 \ge N_j \quad (0 \le j \le 4), \qquad \delta(t) = t^K. \tag{3.11.5}$$

We decrease the original positive-time interval so that $\delta(t) \le t/4$. On $I_t = [t - \delta, t]$, we set

$$r = (t' - t + \delta)/\delta, \quad y = x/\sqrt{\delta}, \quad U(r, y) = u(t', \sqrt{\delta} y),$$

and

$$\mathcal{B}(r, y) = \sqrt{\delta} B_*(t', \sqrt{\delta} y), \qquad \mathcal{F}(r, y) = \delta F(t', \sqrt{\delta} y).$$

The whole-space Leray projector commutes with this isotropic rescaling.

For $j \le 4$, differentiation of $\mathcal{B}$ gives $\delta^{(j+1)/2} \nabla_x^j B_*$. Since $t' \simeq t$, equation (3.11.5) gives a uniform bound for its $W^{4,\infty}$ norm.

Lemma 3.11.2 applies to the *same* physical solution supplied by Proposition 3.11.1. The L^2 energy uniqueness argument in the lemma identifies the distributional inverse solution with the regularized window solution.

The inverse scaling gives

$$\|u(t)\|_{H^3} \le C\delta^{-3/2} \left(\sup_{t' \in I_t} \|u(t')\|_2 + \delta \sup_{t' \in I_t} \|F(t')\|_{H^2} \right). \tag{3.11.6}$$

For $\delta \le 1$, the three scaling factors in this coarse estimate are

$$\begin{aligned} \|U(0)\|_2 &= \delta^{-3/4} \|u(t - \delta)\|_2, \\ \|\mathcal{F}\|_{H^2_y} &\le \delta^{1-3/4} \|F\|_{H^2_x}, \\ \|u(t)\|_{H^3_x} &\le C\delta^{3/4 - 3/2} \|U(1)\|_{H^3_y}. \end{aligned}$$

Proposition 3.11.1 with $L_1 = 0$ (admissible since $\beta - \Lambda_* = \Lambda_*/2 > \epsilon$) and $\|F\|_2 \le \|F\|_{H^2}$ give, for $\|F\|_{Y_\beta(T)} \le 1$,

$$\|u(t)\|_2 \le C\tau^\epsilon e^{-\beta\tau} \le C t^{-M_1} e^{-\beta t^{-h}}, \qquad M_1 = h\epsilon, \tag{3.11.7}$$

with one fixed ancient threshold.

Across I_t, $t'/t \in [3/4, 1]$, while $t'^{-h} - t^{-h} = O(\delta t^{-1-h}) = O(t^{K-1-h})$. Thus the exponential factor and all fixed physical powers are comparable with one constant throughout the interval.

We substitute (3.11.7) and the Y_β forcing bound into (3.11.6) to get

$$\|u(t)\|_{H^3} \le Ce^{-\beta\tau}(t^{-3K/2-M_1} + t^{-K/2})\|F\|_{Y_\beta(T)} \le C\tau^L e^{-\beta\tau}\|F\|_{Y_\beta(T)}$$

with, for example, $L = (3K/2 + M_1 + 1)/h$. We fixed K, M_1, L before the ancient cutoff.

The proof used no time derivative of F.

We define G_T by $G_T F = z$ from Proposition 3.11.1 on $(0, T^{-1/h}]$. Causality makes this definition independent of the future extension.

The same source, masks, K, L, and estimates apply for each later T. The operator remains real and solenoidal.

The Duhamel solution of Proposition 3.11.1 gives its distributional equation. This proves (3.11.4) with a single C_G.

□

Proposition 3.11.3 supplies the inverse used in the nonlinear proof. It does not supply the different exact nonzero homogeneous mode.

3.12 The abstract branching argument

Main result. Theorem 3.3.2 gives a real family with the same force and trace and a separation estimate at every positive time of one common interval. The argument uses one exact linear mode and one causal inverse at a faster exponential rate. The application must verify these inputs for the selected base.

Proof of Theorem 3.3.2. We fix one member (3.3.4). By Proposition 3.11.3, the hypotheses (3.3.5) and (3.3.8) give the inverse (3.3.9). We fix its constants and those in (3.3.7). Let $\lambda_U = 0.9\Lambda_*$, $\lambda_L = 1.1\Lambda_*$, and $\beta = 1.5\Lambda_*$. The available rate margins are

$$\lambda_L < \beta < 2\lambda_U, \qquad 2\lambda_U - \beta = 0.3\Lambda_*, \quad \beta - \lambda_L = 0.4\Lambda_*. \tag{3.12.1}$$

The canonical and physical rates satisfy the explicit identities: $\Lambda_* = \lambda_c/h$ and $\beta = \beta_c/h$ by (3.3.10).

For every real $|a| \le 1$ we seek

$$u_a = B_* + aV + w_a, \qquad w_a = -G_T\mathbb{P}\,\mathrm{div}[(aV + w_a) \otimes (aV + w_a)]. \tag{3.12.2}$$

For divergence-free $x, y \in H^3(\mathbb{R}^3)$, the three-dimensional H^3 product bound and the order-zero Leray multiplier give

$$\|\mathbb{P}\,\mathrm{div}(x \otimes y)\|_{H^2} \le C_3\|x\|_{H^3}\|y\|_{H^3}. \tag{3.12.3}$$

H^3 is an algebra, so one derivative of xy belongs to H^2. The multiplier is bounded on H^2.

We write $\|\cdot\|_X = \|\cdot\|_{X_{\beta,L}(T)}$ and define

$$A_T = C_3C_V^2 \sup_{\tau\ge T} \tau^{2M}e^{-(2\lambda_U-\beta)\tau},$$
$$B_T = C_3C_V \sup_{\tau\ge T} \tau^{M+L}e^{-\lambda_U\tau},$$
$$D_T = C_3 \sup_{\tau\ge T} \tau^{2L}e^{-\beta\tau}.$$

Each tends to zero as $T \to \infty$, by the positive rate margins. One factor V and one factor with X weight give the displayed B_T. After multiplication by the Y_β weight, the exponential factor is $e^{-\lambda_U \tau}$.

Choose $T \geq T_0$ beyond the mode threshold with $T^{-1/h} < T_b$. Independently of a, require

$$C_G(A_T + 2B_T + D_T) \leq 1, \qquad 2C_G(B_T + D_T) \leq \tfrac{1}{2}. \tag{3.12.4}$$

Increase T also to ensure

$$4C_G(A_T + B_T) \sup_{\tau \geq T} \tau^{L+M} e^{-(\beta - \lambda_L)\tau} \leq c_V/2.$$

This is possible by (3.12.1). We fix this T and the associated inverse G_T for the whole family. For the right side Φ_a of (3.12.2),

$$\begin{aligned} \|\Phi_a(w)\|_X &\leq C_G(a^2 A_T + 2|a|B_T\|w\|_X + D_T\|w\|_X^2), \\ \|\Phi_a(w) - \Phi_a(z)\|_X &\leq 2C_G(|a|B_T + D_T)\|w - z\|_X \end{aligned}$$

on the common unit ball. The first bound and (3.12.4) make that ball invariant for every a. The second gives contraction constant at most $1/2$. The closed real solenoidal subspace is invariant, so the unique fixed point w_a there is real and solenoidal. Comparing $\Phi_a(w_a)$ with $\Phi_a(0)$ gives

$$\|w_a\|_X \leq 2C_G a^2 A_T. \tag{3.12.5}$$

In particular $w_0 = 0$. Holding w_b fixed, expand the two tensors in $\Phi_a(w_b) - \Phi_b(w_b)$. Their difference is $(a - b)$ times $(a + b)V \otimes V + V \otimes w_b + w_b \otimes V$. Thus

$$\|\Phi_a(w_b) - \Phi_b(w_b)\|_X \leq C_G|a - b|(|a + b|A_T + 2B_T\|w_b\|_X).$$

The remaining difference $\Phi_a(w_a) - \Phi_a(w_b)$ has norm at most $\frac{1}{2}\|w_a - w_b\|_X$. Absorbing it gives

$$\|w_a - w_b\|_X \leq 4C_G(A_T + B_T)|a - b|. \tag{3.12.6}$$

Let $q_a = aV + w_a$. The fixed point and (3.3.6) imply the exact projected difference equation

$$\partial_t q_a - \Delta q_a + \mathbb{P}\,\mathrm{div}(B_* \otimes q_a + q_a \otimes B_* + q_a \otimes q_a) = 0. \tag{3.12.7}$$

We put

$$\pi_a = (-\Delta)^{-1}\partial_i\partial_j(B_{*,i}q_{a,j} + q_{a,i}B_{*,j} + q_{a,i}q_{a,j}). \tag{3.12.8}$$

For $t > 0$ the tensor in (3.12.8) lies in L^2 by the L^∞ bound on B_* and the H^3 bound on q_a. The Fourier multiplier $-\zeta_i\zeta_j/|\zeta|^2$ therefore defines a real L^2 pressure correction. The divergence identity gives $\mathrm{div}\, T + \nabla\pi_a = \mathbb{P}\,\mathrm{div}\, T$ for the tensor in (3.12.8). Addition of the base equation shows that $(B_* + q_a, p_* + \pi_a)$ solves the unprojected (3.3.3) with the same f_*.

On each compact positive-time subinterval the equations for q_a, V give $\partial_t q_a, \partial_t V \in L^\infty_t H^1_x$. Indeed the velocities are bounded in H^3 there and B_* has bounded spatial jets. Take their continuous L^2 representatives. For a fixed pair a, b and time t, approach t by times on the full-measure set for (3.12.5) and (3.12.6). Weak compactness in H^3 and strong L^2 continuity identify the weak limits with $w_a(t)$ and $w_a(t) - w_b(t)$. Lower semicontinuity yields the asserted weighted H^3 estimates at t. Hence for every pair and time,

$$\|u_a(t) - u_b(t)\|_2 \geq |a - b|\|V(t)\|_2 - \|w_a(t) - w_b(t)\|_2 \geq \tfrac{1}{2}c_V|a - b|\tau^{-M}e^{-\lambda_L\tau}. \tag{3.12.9}$$

The last inequality uses the common choice of T. Fix $0 < t_* < T^{-1/h}$ so that t_* lies in the interior of the construction. Each q_a tends strongly to zero in L^2 as $t \downarrow 0$. Thus $u_a(0) = u_{0,*}$ for every a. The exponential H^3 bounds give $\int_0^{t_*} \|\nabla q_a(t)\|_2^2 \,\mathrm{d}t < \infty$. The base energy class gives $B_* + q_a \in C_t L^2 \cap L_t^2 H^1$. On (ε, t), test (3.12.7) against q_a to get

$$\frac{1}{2}\frac{\mathrm{d}}{\mathrm{d}t}\|q_a\|_2^2 + \|\nabla q_a\|_2^2 = -\int_{\mathbb{R}^3} q_a \cdot (q_a \cdot \nabla) B_* \,\mathrm{d}x. \tag{3.12.10}$$

The B_* transport and q_a self-transport terms cancel by solenoidality.

The bound $\|\nabla B_*(t)\|_\infty \le C t^{-N_1}$ and the exponential decay of q_a make the right side integrable at zero. On compact positive-time intervals the H^3 bound, the smooth base and positive-time parabolic regularity give smooth velocity and pressure. Testing the full equation with spatial cutoffs and passing to their limit gives (3.1.1) there. The convection, pressure and viscosity cutoff errors are bounded as in Remark 3.13.1. Strong L^2 convergence to $u_{0,*}$, finite dissipation and integrable force work extend the identity to intervals starting at zero. □

3.13 Joining at the singular time and continuation on a regular interval

Use the physical time of the completion, with the singularity at zero. For each $a \in [-1, 1]$, extend q_a and π_a by zero to the negative time interval. The unprojected difference equation on positive times has velocity q_a, pressure π_a and zero force. Its time boundary term against a compactly supported smooth vector test tends to zero because $q_a(t) \to 0$ strongly in L^2. The mixed and quadratic tensors are locally integrable through zero by L^2 continuity of both velocities. The pressure correction is locally integrable there as well. In fact

$$\|\pi_a(t)\|_2 \le C(\|B(t)\|_\infty + \|q_a(t)\|_\infty)\|q_a(t)\|_2.$$

The polynomial bound on $B(t)$ and the exponential decay of $q_a(t)$ make this bound integrable at zero. Adding the extended difference equation to the background equation gives the full momentum identity through zero with the pressure $p_B + \pi_a$ and force f. For each interval straddling zero, add the background energy identity up to zero and the forward identity for $B + q_a$ from zero onwards. Their endpoint energies agree by the strong trace u_0.

Smooth joining away from the origin. Write $q = q_a = aV + w_a$ and $T_a = B \otimes q + q \otimes B + q \otimes q$ for $t > 0$ near zero. The mode estimate of Proposition 3.3.1 and (3.12.5) give $\|q(t)\|_{H^3} = O_N(t^N)$ for every $N \ge 0$, uniformly in $|a| \le 1$. The fixed spatial support and the spatial derivative estimates of Theorem 2(ii),(iv) give $\|B(t)\|_{H^s} = O_s(t^{-M_s})$ for every $s \ge 0$ and some M_s.

Suppose $\|q(t)\|_{H^s} = O_{s,N}(t^N)$ for all N, with $s \ge 3$. The H^s product estimate gives the same bounds for T_a, since each term has a factor q. On $[t/2, t]$, Duhamel's formula for (3.12.7) and the heat Fourier multipliers give, for $0 < t < \min(1, t_*)$,

$$\|q(t)\|_{H^{s+1/2}} \le C_s t^{-1/4}\|q(t/2)\|_{H^s} + C_s \int_{t/2}^{t} (t - v)^{-3/4}\|T_a(v)\|_{H^s} \,\mathrm{d}v.$$

The first term uses the bound at power $N + 1$, and the integral kernel has mass $O(t^{1/4})$. Induction in half-derivative steps yields $\|q(t)\|_{H^m} = O_{m,N}(t^N)$ for all integers $m, N \ge 0$.

For time derivatives use

$$\partial_t B = \Delta B - \mathbb{P}\,\mathrm{div}(B \otimes B) + \mathbb{P}f, \qquad \partial_t q = \Delta q - \mathbb{P}\,\mathrm{div}\, T_a.$$

The smooth force with fixed spatial support has bounded time derivatives in each H^m near zero. Induction on j, using the spatial estimates at all orders, gives polynomial bounds in t^{-1} for $\|\partial_t^j B(t)\|_{H^m}$ and $O_{j,m,N}(t^N)$ bounds for $\|\partial_t^j q(t)\|_{H^m}$ for every N. Indeed each term of $\partial_t^j T_a$ contains a time derivative of q of order at most j, including order zero. The order-zero Fourier multipliers in (3.12.8) give the same flat bounds for $\partial_t^j \pi_a$. Sobolev embedding and time difference quotients at zero show that the zero extensions of q_a, π_a are smooth, with all space-time derivatives zero on $t = 0$. At each $x \neq 0$ the joined pair therefore has the full jet of the smooth background (B, p_B) from Theorem 2(ii).

Remark 3.13.1 (Spatial boundary terms in the energy identity). On a compact positive-time slab the total velocity u is in H^3 and the pressure p is in L^2. In the Newtonian formula of Theorem 2(ii), the quadratic term is an L^2 Riesz transform, and the force term has multiplier of size $|\zeta|^{-1}$ applied to a smooth spatially compact force. Its square is integrable at zero frequency in three dimensions. The correction is an L^2 Riesz transform by (3.12.8). With a smooth cutoff on balls of radius R, the boundary terms from pressure, convection and viscosity are bounded respectively by

$$CR^{-1}\|p\|_2\|u\|_2, \qquad CR^{-1}\|u\|_3^3, \qquad CR^{-1}\|u\|_2\|\nabla u\|_2.$$

They tend to zero uniformly on the slab.

Lemma 3.13.2 (Uniform continuation on a regular terminal interval)**.** *Fix a regular time interval $[d, e] \Subset (0, T_b)$ and a family of real solenoidal data $v_a = q_a(d)$, indexed by a real interval. Suppose $\sup_a \|v_a\|_{H^3} \le K_d$ and, for all a, b,*

$$m_d|a - b| \le \|v_a - v_b\|_2, \qquad \|v_a - v_b\|_{H^3} \le M_d|a - b|, \qquad m_d > 0.$$

There is $0 < 2\delta < e - d$, depending only on these bounds, $e - d$ and $\sup_{[d,e]} \|B\|_{H^3}$, with the following property. For every smooth time cutoff $0 \le \chi \le 1$ equal to one near d, put $b_\chi = \chi B$. For all a there is a unique real mild perturbation $h_a \in C([d, d + 2\delta]; H^3_\sigma)$ solving

$$\partial_t h_a - \Delta h_a = -\mathbb{P}\operatorname{div} Q_\chi(h_a), \qquad h_a(d) = v_a, \qquad Q_\chi(h) = b_\chi \otimes h + h \otimes b_\chi + h \otimes h.$$

On $[d, d + \delta]$ it satisfies, simultaneously for all a, b,

$$\|h_a(t) - h_b(t)\|_2 \ge \tfrac{1}{2} m_d|a - b|, \qquad \|h_a(t) - h_b(t)\|_{H^3} \le 2M_d|a - b|.$$

Where the original regular perturbation exists and χ has remained one since d, it agrees with h_a. If $v_0 = 0$, then $h_0 = 0$.

Proof. On $[d, d + \ell]$ use the supremum H^3 norm. The heat multiplier gives $\|e^{r\Delta}\mathbb{P}\operatorname{div} Q\|_{H^3} \le Cr^{-1/2}\|Q\|_{H^3}$ for $r > 0$. The heat evolution of v_a has norm at most K_d. On the ball of radius $R = 2K_d + 1$ the Duhamel integral is Lipschitz with constant at most $C\sqrt{\ell}(\sup_{[d,e]} \|B\|_{H^3} + R)$ by the H^3 product estimate. It vanishes at $h = 0$. Choose $\ell < e - d$ to make this constant at most $1/2$. The resulting mild map preserves the ball and contracts there. On shorter subintervals the same difference estimate gives uniqueness among continuous H^3 solutions, by subdivision using their finite norms. This also gives agreement on the initial plateau. Comparing the two fixed points gives $\sup \|h_a - h_b\|_{H^3} \le 2M_d|a - b|$.

Set $D = h_a - h_b$. The equation for D gives $\|\partial_t D\|_2 \le C_*\|D\|_{H^3}$ from the Laplacian and the same product bound, with C_* depending only on R and the background bound. Thus $\|D(t) - D(d)\|_2 \le 2C_* M_d(t - d)|a - b|$. Choose $0 < 2\delta < \ell$ with $2C_* M_d\delta \le m_d/2$. Both the lifespan and the separation bound are independent of derivatives of χ.

On interior positive-time slabs the heat estimate from H^{k-1} to $H^{k+1/2}$ costs $O(r^{-3/4})$ for $0 < r \le 1$. Starting at $k = 3$, the product bound and iteration away from d give every spatial order. The equation then gives the time derivatives. In particular the continuation is smooth up to $d + \delta$. The pressure increment is $\pi_a = (-\Delta)^{-1}\partial_i\partial_j Q_\chi(h_a)_{ij}$, summed over i, j. It is in L^2 by the bounded Fourier multiplier and the product bound. Adding the equation for b_χ shows that $(b_\chi + h_a, \chi p_B + \pi_a)$ solves the full equation with common force $\partial_t b_\chi - \Delta b_\chi + \operatorname{div}(b_\chi \otimes b_\chi) + \nabla(\chi p_B)$. The H^3 velocity permits the global energy calculation on this regular interval. The pressure gradient is orthogonal to the solenoidal velocity and the convection term integrates to zero. □

3.14 Proof of the main statement

Proof of Theorem 3. Fix the completed background (B, p_B, f) of Theorem 2, including its common strong trace at zero and its pressure reconstructed from the two-sided leading field. The perturbations below are all taken about this one background. The domain estimate (Prepared) and the separated estimate on p. 705 hold for this same field. Proposition 3.3.1 gives the real mode V and the propagator estimate for this same B. Theorem 2(iv) supplies the spatial jet bounds for B. Apply Theorem 3.3.2 once. Denote its common positive endpoint by t_c and its perturbations by $q_a = aV + w_a$. Choose $0 < d < e < \min\{t_c, t_0, T_b\}$, using the regular existence interval and the mode interval of Proposition 3.3.1. Take $t_* = d$ in the main statement. The bounds at $t = d$ give

$$\sup_{|a|\le 1} \|q_a(d)\|_{H^3} < \infty, \qquad m_d|a-b| \le \|q_a(d) - q_b(d)\|_2, \qquad \|q_a(d) - q_b(d)\|_{H^3} \le M_d|a-b|$$

for some $m_d > 0$ and $M_d < \infty$. Here the lower bound is (3.12.9), and the upper bound follows by adding $|a-b|\,\|V(d)\|_{H^3}$ to the difference estimate for $w_a - w_b$. The smooth, spatially compact B has bounded H^3 norm on $[d, e]$. Lemma 3.13.2 thus fixes a length $\delta > 0$ before we choose the time cutoff.

Choose $0 < T_{\text{in}} < T_-$ and $-T_{\text{in}} < b_- < 0$, and put $T_{\text{out}} = d + \delta$. Take $\chi \in C_c^\infty((-T_{\text{in}}, T_{\text{out}}))$, $0 \le \chi \le 1$, equal to one on $[b_-, d + \delta/3]$ and zero for $t \ge d + 2\delta/3$. Define

$$\begin{aligned} &\widetilde{B} = \chi B, \qquad \widetilde{p} = \chi p_B, \\ &F = \chi f + \chi' B + (\chi^2 - \chi)\operatorname{div}(B \otimes B). \end{aligned} \tag{3.14.1}$$

The product rule in distributions gives $\partial_t \widetilde{B} - \Delta\widetilde{B} + \operatorname{div}(\widetilde{B} \otimes \widetilde{B}) + \nabla\widetilde{p} = F$, with $\operatorname{div}\widetilde{B} = 0$. Near the singular time $F = f$. Each additional term in (3.14.1) is supported where the original solution is smooth. The spatial support lies in K by Theorem 2. Extension by zero gives a smooth force supported in $\operatorname{supp}\chi \times K \Subset (-T_{\text{in}}, T_{\text{out}}) \times \mathbb{R}^3$. For the pressure normalization, taking the divergence of (3.14.1) gives

$$\operatorname{div} F - \partial_i\partial_j(\widetilde{B}_i\widetilde{B}_j) = \chi(\operatorname{div} f - \partial_i\partial_j(B_iB_j))$$

with summation over i, j. Spatial Newtonian convolution therefore gives χp_B.

Set each perturbation and its pressure correction to zero for $t \le 0$. On $0 < t \le d$ use q_a, π_a from the branching criterion. On $[d, d + \delta]$ use the perturbation h_a of Lemma 3.13.2 with $h_a(d) = q_a(d)$ and its pressure correction. Denote the resulting fields by $\widetilde{q}_a, \widetilde{\pi}_a$. On a compact positive-time slab containing d in its interior, the original q_a and B are bounded in H^3. Starting at an earlier time on that slab, the distributional difference equation gives the heat Duhamel formula with tensor $B \otimes q_a + q_a \otimes B + q_a \otimes q_a$ bounded in H^3. The heat estimate for $\mathbb{P}\operatorname{div}$ in Lemma 3.13.2 bounds the last ε units of its integral in H^3 by $C\sqrt{\varepsilon}$. The earlier part is continuous in H^3 by strong continuity of the heat semigroup. Thus q_a lies in the $C_t H^3$ uniqueness class of that lemma near d. While

$\chi = 1$ after d, uniqueness gives $h_a = q_a$. The pressure formulas there are identical. Thus the velocity and pressure are smooth across d. The zero-amplitude perturbation vanishes throughout. Estimate (3.12.9) separates every pair on $(0, d]$. On $[d, d + \delta]$ separation follows from the lower bound $\frac{1}{2} m_d |a - b|$ in Lemma 3.13.2.

On the smooth past each solution equals $(\widetilde{B}, \widetilde{p})$ and satisfies the classical energy identity with F. Near zero the cutoff is identically one, so Section 3.13 gives the unprojected equation across zero and the global energy identity. The flat extension on p. 752 gives joint smoothness of the velocity and pressure across $t = 0$ at every $x \neq 0$. On the regular terminal interval the same equation and identity follow from Lemma 3.13.2. The regular overlaps and common strong trace allow addition of the identities for arbitrary endpoints. The energy-class bounds on the closed interval follow from the bounds on these three pieces.

On $[-T_{\mathrm{in}}, T_{\mathrm{out}}]$ set

$$(u^{(a)}, p^{(a)})(t) = (\widetilde{B} + \widetilde{q}_a, \widetilde{p} + \widetilde{\pi}_a)(t).$$

The force vanishes near both endpoints, and the common velocity vanishes near $t = -T_{\mathrm{in}}$. The two-sided strong trace, its spatial singularity and the past L^∞ blow-up at $t = 0$ are those of Theorem 2(iii), since the common past equals B near that time. The mode and quadratic approximation on $0 < t \leq d$ follow from Proposition 3.3.1 and Theorem 3.3.2. □

Remark 3.14.1 (Initial velocity and trace at blow-up). Every member starts from zero at $t = -T_{\mathrm{in}}$ under the force F of (3.14.1). Restriction to $[0, t_*]$ gives the forward family from the compactly supported, essentially unbounded trace $B(0)$. On that interval $F = f$.

Bibliography

[1] Dallas Albritton, Elia Bruè, and Maria Colombo, *Non-uniqueness of Leray solutions of the forced Navier–Stokes equations*. Annals of Mathematics **196** (2022), 415–455. DOI.

[2] Dallas Albritton and Wojciech Ożański, *Linear and nonlinear instability of vortex columns*. Journal of the European Mathematical Society (2025), published online first. DOI.

[3] Levent Alpöge and Tristan Buckmaster, *Finite-time blow-up for the Navier–Stokes equations*. Manuscript, 20 November 2026. Authors' repository.

[4] Levent Alpöge and Tristan Buckmaster, *Blowup for the Euler equations with smooth forcing*. Preprint (September 2026). GitHub repository.

[5] Elia Bruè, Maria Colombo, and Anuj Kumar, *Flexibility of two-dimensional Euler flows with integrable vorticity*. Duke Mathematical Journal **175** (2026), 1593–1647. DOI.

[6] Tristan Buckmaster, Matei P. Coiculescu, and Chen Li, *Non-uniqueness of Leray–Hopf solutions to the unforced three-dimensional Navier–Stokes equations*. Hexagon manuscript 2611.00143v1 (2026).

[7] Tristan Buckmaster, Maria Colombo, and Vlad Vicol, *Wild solutions of the Navier–Stokes equations whose singular sets in time have Hausdorff dimension strictly less than 1*. Journal of the European Mathematical Society **24** (2022), 3333–3378. DOI.

[8] Tristan Buckmaster and Vlad Vicol, *Nonuniqueness of weak solutions to the Navier–Stokes equation*. Annals of Mathematics **189** (2019), 101–144. DOI.

[9] Matthieu Cadiot, Alexandru D. Ionescu, Hao Jia, and Stan Palasek, *On the non-uniqueness of solutions of the axi-symmetric swirl-free Navier–Stokes equations, II*. arXiv:2611.27984 (2026).

[10] Luis Caffarelli, Robert Kohn, and Louis Nirenberg, *Partial regularity of suitable weak solutions of the Navier–Stokes equations*. Communications on Pure and Applied Mathematics **35** (1982), 771–831. DOI.

[11] Jiajie Chen and Thomas Y. Hou, *Stable nearly self-similar blowup of the 2D Boussinesq and 3D Euler equations with smooth data I: Analysis*. arXiv:2210.07191 (2022).

[12] Jiajie Chen and Thomas Y. Hou, *Stable nearly self-similar blowup of the 2D Boussinesq and 3D Euler equations with smooth data II: Rigorous numerics*. arXiv:2305.05660 (2023).

[13] Alexey Cheskidov and Xiaoyutao Luo, *Sharp nonuniqueness for the Navier–Stokes equations*. Inventiones Mathematicae **229** (2022), 987–1054. DOI.

[14] Matei P. Coiculescu and Stan Palasek, *Non-uniqueness of smooth solutions of the Navier–Stokes equations from critical data*. Inventiones Mathematicae **244** (2026), 165–219. DOI.

[15] Peter Constantin, Mihaela Ignatova, and Vlad Vicol, *Regularity for axisymmetric Navier–Stokes with an Euler length*. arXiv:2609.20762 (2026).

[16] Peter Constantin, Mihaela Ignatova, and Vlad Vicol, *Regularity of asymptotically axisymmetric solutions to the 3D Navier–Stokes equations with analytic forcing*. arXiv:2609.20803 (2026).

[17] Diego Córdoba and Luis Martínez-Zoroa, *Blow-up for the incompressible 3D-Euler equations with uniform $C^{1,\frac{1}{2}-\epsilon} \cap L^2$ force*. Duke Mathematical Journal, to appear. arXiv:2309.08495 (2023).

[18] Diego Córdoba, Luis Martínez-Zoroa, and Fan Zheng, *Finite time blow-up for the hypodissipative Navier Stokes equations with a force in* $L^1_t C^{1,\epsilon}_x \cap L^\infty_t L^2_x$. Archive for Rational Mechanics and Analysis **250** (2026), article 38. DOI.

[19] A. D. D. Craik and W. O. Criminale, *Evolution of wavelike disturbances in shear flows: a class of exact solutions of the Navier–Stokes equations*. Proceedings of the Royal Society of London. Series A **406** (1986), 13–26. DOI.

[20] Joel Dahne and Vladimír Šverák, *Non-uniqueness for the complex Ginzburg–Landau equation*. arXiv:2609.08985v2 (2026).

[21] Camillo De Lellis and László Székelyhidi Jr., *The Euler equations as a differential inclusion*. Annals of Mathematics **170** (2009), 1417–1436. DOI.

[22] Tarek M. Elgindi, *Finite-time singularity formation for* $C^{1,\alpha}$ *solutions to the incompressible Euler equations on* $\mathbb{R}^3$. Annals of Mathematics **194** (2021), 647–727. DOI.

[23] Tarek M. Elgindi, Tej-Eddine Ghoul, and Nader Masmoudi, *On the stability of self-similar blow-up for* $C^{1,\alpha}$ *solutions to the incompressible Euler equations on* $\mathbb{R}^3$. Cambridge Journal of Mathematics **9** (2021), 1035–1075.

[24] Charles L. Fefferman, *Existence and smoothness of the Navier–Stokes equation*. In *The Millennium Prize Problems*, Clay Mathematics Institute, Cambridge, MA (2006), 57–67.

[25] Hiroshi Fujita and Tosio Kato, *On the Navier–Stokes initial value problem. I*. Archive for Rational Mechanics and Analysis **16** (1964), 269–315. DOI.

[26] Thierry Gallay and Didier Smets, *Spectral stability of inviscid columnar vortices*. Analysis & PDE **13** (2020), 1777–1832. DOI.

[27] Julien Guillod and Vladimír Šverák, *Numerical investigations of non-uniqueness for the Navier–Stokes initial value problem in borderline spaces*. Journal of Mathematical Fluid Mechanics **25** (2023), article 46. DOI.

[28] Eberhard Hopf, *Über die Anfangswertaufgabe für die hydrodynamischen Grundgleichungen*. Mathematische Nachrichten **4** (1950), 213–231. DOI.

[29] Thomas Y. Hou, Yixuan Wang, and Changhe Yang, *Nonuniqueness of Leray–Hopf solutions to the unforced incompressible 3D Navier–Stokes Equation*. arXiv:2509.25116v3 (2025, revised 2026).

[30] Thomas Y. Hou, Xiang Qin, Peicong Song, and Wenhan Zhang, *A viscous cascade construction of nonunique Leray–Hopf solutions to the unforced 3D Navier–Stokes equations*. arXiv:2611.06117 (2026).

[31] Alexandru D. Ionescu, Hao Jia, and Stan Palasek, *On the non-uniqueness of solutions of the axi-symmetric swirl-free Navier–Stokes equations, I*. arXiv:2606.07501 (2026).

[32] Philip Isett, *A proof of Onsager's conjecture*. Annals of Mathematics **188** (2018), 871–963. DOI.

[33] Hao Jia and Vladimír Šverák, *Local-in-space estimates near initial time for weak solutions of the Navier–Stokes equations and forward self-similar solutions*. Inventiones Mathematicae **196** (2014), 233–265. DOI.

[34] Hao Jia and Vladimír Šverák, *Are the incompressible 3d Navier–Stokes equations locally ill-posed in the natural energy space?* Journal of Functional Analysis **268** (2015), 3734–3766. DOI.

[35] Tosio Kato, *Strong* L^p*-solutions of the Navier–Stokes equation in* $\mathbb{R}^m$*, with applications to weak solutions*. Mathematische Zeitschrift **187** (1984), 471–480. DOI.

[36] Herbert Koch and Daniel Tataru, *Well-posedness for the Navier–Stokes equations*. Advances in Mathematics **157** (2001), 22–35. DOI.

[37] Zhen Lei and Xiao Ren, *Finite-time blowup for Navier–Stokes with smooth forcing, Part I: Construction of self-similar solutions with admissible stress and flat remainder*. arXiv:2609.35406 (2026).

[38] Zhen Lei and Xiao Ren, *Finite-time blowup for Navier–Stokes with smooth forcing, Part II: Residual correction via oscillatory pulses*. arXiv:2611.06869 (2026).

[39] S. Leibovich and K. Stewartson, *A sufficient condition for the instability of columnar vortices*. Journal of Fluid Mechanics **126** (1983), 335–356. DOI.

[40] Jean Leray, *Sur le mouvement d'un liquide visqueux emplissant l'espace*. Acta Mathematica **63** (1934), 193–248. DOI.

[41] Jindřich Nečas, Michael Růžička, and Vladimír Šverák, *On Leray's self-similar solutions of the Navier–Stokes equations*. Acta Mathematica **176** (1996), 283–294. DOI.

[42] OpenAI, *Finite time blowup for Navier–Stokes*. Preprint, 8 September 2026. Source PDF.

[43] OpenAI, *Finite time blowup for the Euler equation*. Preprint (September 2026). Source PDF.

[44] R. T. Seeley, *Extension of C^∞ functions defined in a half space*, Proc. Amer. Math. Soc. **15** (1964), 625–626. DOI.

[45] Tai-Peng Tsai, *On Leray's self-similar solutions of the Navier–Stokes equations satisfying local energy estimates*. Archive for Rational Mechanics and Analysis **143** (1998), 29–51. DOI.

[46] Misha Vishik, *Instability and non-uniqueness in the Cauchy problem for the Euler equations of an ideal incompressible fluid. Part I*. arXiv:1805.09426 (2018).

[47] Misha Vishik, *Instability and non-uniqueness in the Cauchy problem for the Euler equations of an ideal incompressible fluid. Part II*. arXiv:1805.09440 (2018).

[48] Yongji Wang, Mehdi Bennani, James Martens, Sébastien Racanière, Sam Blackwell, Alex Matthews, Stanislav Nikolov, Gonzalo Cao-Labora, Daniel S. Park, Martin Arjovsky, Daniel Worrall, Chongli Qin, Ferran Alet, Borislav Kozlovskii, Nenad Tomašev, Alex Davies, Pushmeet Kohli, Tristan Buckmaster, Bogdan Georgiev, Javier Gómez-Serrano, Ray Jiang, and Ching-Yao Lai, *Discovery of unstable singularities*. arXiv:2509.14185 (2025).